Geological Survey of Canada
Commission géologique du Canada

PAPER
ÉTUDE 86-1A

CURRENT RESEARCH PART A
RECHERCHES EN COURS PARTIE A

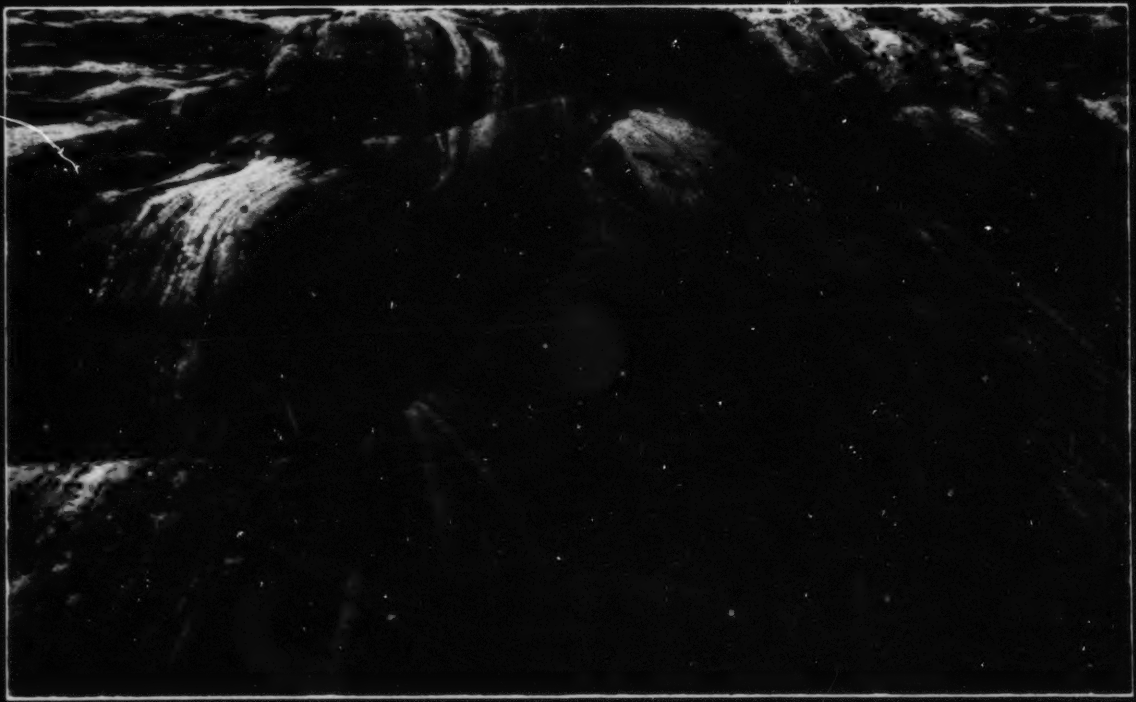

(Pages 1-384)

Canada

1986

86-02288/

Notice to Librarians and Indexers

The Geological Survey's twice-yearly *Current Research* series contains many reports comparable in scope and subject matter to those appearing in scientific journals and other serials. All contributions to Current Research include an abstract and bibliographic citation. It is hoped that these will assist you in cataloguing and indexing these reports and that this will result in a still wider dissemination of the results of the Geological Survey's research activities.

Avis aux bibliothécaires et préparateurs d'index

La série *Recherches en cours* de la Commission géologique paraît deux fois par année; elle contient plusieurs rapports dont la portée et la nature sont comparables à ceux qui paraissent dans les revues scientifiques et autres périodiques. Tous les articles publiés dans les Recherches en cours sont accompagnés d'un résumé et d'une bibliographie, ce qui vous permettra, nous l'espérons, de cataloguer et d'indexer ces rapports, d'où une meilleure diffusion des résultats de recherche de la Commission géologique.

GEOLOGICAL SURVEY OF CANADA
PAPER 86-1A

COMMISSION GÉOLOGIQUE DU CANADA
ÉTUDE 86-1A

CURRENT RESEARCH
PART A

RECHERCHES EN COURS
PARTIE A

Issued in two sections/Publiée en deux volumes:
pages 1-384 and/et pages 385-826

1986

© Minister of Supply and Services Canada 1986

Available in Canada through

authorized bookstore agents and other bookstores

or by mail from

Canadian Government Publishing Centre
Supply and Services Canada
Ottawa, Canada K1A 0S9

and from

Geological Survey of Canada offices:

601 Booth Street
Ottawa, Canada K1A 0E8

3303-33rd Street N.W.,
Calgary, Alberta T2L 2A7

100 West Pender Street
Vancouver, British Columbia V6B 1R8
(mainly B.C. and Yukon)

A deposit copy of this publication is also available
for reference in public libraries across Canada

Cat. No. M44-86/1AE Canada: $20.00
ISBN 0-660-11992-7 Other countries: $24.00

Sold in sets

Price subject to change without notice

Cover

Rotated competent amphibolite pod with drag-folded foliation on its margins, Wager Bay area, District of Keewatin.

This illustration appears in report 27, p. 173, by J.R. Henderson et al.

Page couverture

Masse minéralisée allongée d'amphibolite ayant été affectée par un mouvement de rotation, et dont la schistosité en bordure se caractérise par des plis d'entraînement; cette masse se situe dans la région de la baie Wager, district de Keewatin.

Cette illustration paraît à la page 173 du rapport 27 de J.R. Henderson et coll.

DIRECTOR GENERAL
DIRECTEUR GÉNÉRAL
R.A. Price

- Administrative Services / *Services administratifs* — Y. P. Claude
- Personnel Services / *Services du personnel*
- Financial Services / *Services financiers*
- Special Advisor / *Conseiller spécial* — J.A. Maxwell

CHIEF GEOLOGIST
GÉOLOGUE EN CHEF
J. G. Fyles

- International Relations Unit / *Services des relations internationales*
- Mineral Development Programs Unit / *Service des programmes de mise en valeur des ressources minérales*
- Program Office / *Bureau de planification* — D. G. Benson
- Special Projects / *Projets spéciaux*

CORDILLERAN GEOLOGY DIVISION (Vancouver, B.C.)
DIVISION GÉOLOGIE DE LA CORDILLÈRE (Vancouver, C.-B.)
R. B. Campbell

- Mainland Geology / *Géologie continentale*
- Pacific Marine Geology (Pacific Geoscience Centre) / *Géologie marine du Pacifique (Centre géoscientifique du Pacifique)*
- Information Services / *Services d'information*

PRECAMBRIAN GEOLOGY DIVISION
DIVISION GÉOLOGIE DU PRÉCAMBRIEN
J. C. McGlynn

- Bear-Slave / *Bear-Slave*
- Northern Churchill / *Churchill-Nord*
- Superior-Grenville / *Supérieur-Grenville*
- Paleomagnetism / *Paléomagnétisme*
- Geochronology / *Géochronologie*
- Petrology / *Pétrologie*
- Special Projects / *Projets spéciaux*

RESOURCE GEOPHYSICS AND GEOCHEMISTRY DIVISION
DIVISION GÉOPHYSIQUE ET GEOCHIMIE APPLIQUEES
A. G. Darnley

- Resource Geochemistry / *Géochimie appliquée*
- Resource Geophysics / *Géophysique appliquée*
- Regional Geophysics / *Géophysique régionale*
- Special Projects / *Projets spéciaux*
- Technical Services / *Services techniques*

TERRAIN SCIENCES DIVISION
DIVISION SCIENCE DES TERRAINS
J. S. Scott

- Paleoecology and Geochronology / *Paléoécologie et géochronologie*
- Geomorphic Processes / *Processus géomorphologiques*
- Sedimentology and Mineral Tracing / *Sédimentologie et détection des minéraux*
- Engineering Geology / *Géologie appliquée*
- Regional Projects / *Projets régionaux*

GEOLOGICAL INFORMATION DIVISION
DIVISION INFORMATION GÉOLOGIQUE
R. G. Blackadar

- Scientific Editing Publication Production / *Rédaction scientifique et publication*
- Data Systems / *Systèmes informatisés*
- Cartography / *Cartographie*
- Library Services / *Services de la bibliothèque*
- Technical Photography / *Techniques photographiques*
- Publications / *Publications*

INSTITUTE OF SEDIMENTARY AND PETROLEUM GEOLOGY (Calgary, Alta.)
INSTITUT DE GÉOLOGIE SÉDIMENTAIRE ET PÉTROLIÈRE Calgary, Alberta
W. W. Nassichuk

- Petroleum Geology / *Géologie pétrolière*
- Regional Geology / *Géologie régionale*
- Coal Geology / *Géologie du charbon*
- Paleontology (including Ottawa) / *Paléontologie (incluant Ottawa)*
- Geological Information / *Information géologique*
- Petroleum Resource Assessment Secretariat / *Secrétariat d'évaluation des ressources pétrolières*

ATLANTIC GEOSCIENCE CENTRE (Darthmouth, N.S.)
CENTRE GÉOSCIENTIFIQUE DE L'ATLANTIQUE - Dartmouth, N.-É.
M. J. Keen

- Eastern Petroleum Geology / *Géologie pétrolière de l'Est*
- Environmental Marine Geology / *Géologie du milieu marin*
- Regional Reconnaissance / *Recherche régionale*
- Program Support / *Planification*

ECONOMIC GEOLOGY AND MINERALOGY DIVISION
DIVISION GÉOLOGIE ÉCONOMIQUE ET MINÉRALOGIE
D. C. Findlay

- Mathematical Applications In Geology / *Mathématiques appliquées à la géologie*
- Mineral Deposits Geology / *Géologie des gîtes minéraux*
- Regional Metallogenic Studies / *Études de la métallogénèse régionale*
- Regional Mineral Resource Assessment / *Évaluation des ressources minérales régionales*
- Mineral Resource Information Services / *Services d'information sur les ressources minérales*
- Analytical Chemistry / *Chimie analytique*
- Mineralogy / *Minéralogie*

Separates

A limited number of separates of the papers that appear in this volume are available by direct request to the individual authors. The addresses of the Geological Survey of Canada offices follow:

601 Booth Street,
OTTAWA, Ontario
K1A 0E8

Institute of Sedimentary and Petroleum Geology,
3303-33rd Street N.W.,
CALGARY, Alberta
T2L 2A7

Cordilleran Geology Division
100 West Pender Street,
VANCOUVER, B.C.
V6B 1R8

Atlantic Geoscience Centre,
Bedford Institute of Oceanography,
P.O. Box 1006,
DARTMOUTH, N.S.
B2Y 4A2

When no location accompanies an author's name in the title of a paper, the Ottawa address should be used.

Tirés à part

On peut obtenir un nombre limité de "tirés à part" des articles qui paraissent dans cette publication en s'adressant directement à chaque auteur. Les adresses des différents bureaux de la Commission géologique du Canada sont les suivantes:

601, rue Booth
OTTAWA, Ontario
K1A 0E8

Institut de géologie sédimentaire et pétrolière
3303-33rd, St. N.W.,
CALGARY, Alberta
T2L 2A7

Division de la géologie de la Cordillère
100 West Pender Street
VANCOUVER, Colombie-Britannique
V6B 1R8

Centre géoscientifique de l'Atlantique
Institut océanographique de Bedford
B.P. 1006
DARTMOUTH, Nouvelle-Ecosse
B2Y 4A2

Lorsque l'adresse de l'auteur ne figure pas sous le titre d'un document, on doit alors utiliser l'adresse d'Ottawa.

SCIENTIFIC AND TECHNICAL REPORTS
RAPPORTS SCIENTIFIQUES ET TECHNIQUES

ECONOMIC GEOLOGY/GÉOLOGIE ÉCONOMIQUE

E. ZALESKI: Geology of the Linda volcanogenic massive sulphide deposit, Snow Lake, Manitoba 15

P.D. VAILLANCOURT and D.F. SANGSTER: Isotope and hydrocarbon studies of the Yava sandstone-lead deposit, Cape Breton Island, Nova Scotia: a progress report 133

A.L. SANGSTER: Willemite and native silver occurrences, Kirkmount, Pictou County, Nova Scotia 151

K.H. POULSEN, D.E. AMES, and A.G. GALLEY: Gold mineralization in the Star Lake pluton, La Ronge belt, Saskatchewan: a preliminary report 205

C.M. SAUNDERS and D.F. STRONG: Assessment of lead-zinc deposits of the western Newfoundland carbonate platform 229

A.E. WILLIAMS-JONES, I.M. SAMSON, and R.L. LINNEN: Preliminary results of a study of the ores, wall-rock alteration, and fluid inclusions at the Madeleine copper mine, Gaspé, Quebec 239

D.F. STRONG and C.M. SAUNDERS: Geological setting of sulphide mineralization at Tilt Cove, Newfoundland 319

A.D. PAKTUNC: St. Stephen mafic-ultramafic intrusion and related nickel-copper deposits, New Brunswick 327

S. CATTALANI and A.E. WILLIAMS-JONES: Geological and fluid inclusion studies at the Saint-Robert Ag, W, Bi deposit, eastern townships, Quebec 365

K. STEVENS: Metallogenic studies in the Candego and Madeleine mines area, Gaspesie, Quebec: a progress report 435

V. RUZICKA and G.M. LECHEMINANT: Developments in uranium geology in Canada, 1985 .. 531

GEOCHEMISTRY/GÉOCHIMIE

G.E.M. HALL and J.E. VAIVE: Analysis of in-house control reference samples by commercial laboratories using inductively-coupled plasma emission spectrometry 71

G.E.M. HALL and J.C. PELCHAT: The determination of boron and other refractory elements in geological materials by inductively-coupled plasma emission spectrometry 89

Y.T. MAURICE and M.M. MERCIER: A new approach to sampling heavy minerals for regional geochemical exploration 301

Y.T. MAURICE: Interpretation of a reconnaissance geochemical heavy mineral survey in the eastern townships of Quebec 307

M. ZENTILLI, M.C. GRAVES, T. MULJA, and I. MacINNIS: Geochemical characterization of the Goldenville-Halifax transition of the Meguma Group of Nova Scotia: preliminary report 423

GEOCHRONOLOGY/GÉOCHRONOLOGIE

M.J. FRAREY and T.E. KROGH: U-Pb zircon ages of late internal plutons of the Abitibi and eastern Wawa subprovinces, Ontario and Quebec 43

R.A. FRITH, W.D. LOVERIDGE, and O. VAN BREEMEN: U-Pb ages on zircon from basement granitoids of the western Slave Structural Province, northwestern Canadian Shield 113

A. ARCHER, R.T. BELL, and R.I. THORPE: Age relationships from U-Th-Pb isotope studies of uranium mineralization in Wernecke breccias, Yukon Territory 385

W.D. LOVERIDGE: U-Pb ages on zircon from rocks of the Lac de Morhiban map area, Quebec 523

M.T. BRANDON, M.J. ORCHARD, R.R. PARRISH, A. SUTHERLAND BROWN, and C.J. YORATH: Fossil ages and isotopic dates from the Paleozoic Sicker Group and associated intrusive rocks, Vancouver Island, British Columbia 683

MARINE GEOSCIENCE/ÉTUDES GEOSCIENTIFIQUES DU MILIEU MARIN

R.B. TAYLOR, R.W.G. CARTER, D.L. FORBES, and J.D. ORFORD: Beach sedimentation in Ireland: contrasts and similarities with Atlantic Canada 55

A.C. GRANT, E.M. LEVY, K. LEE, and J.D. MOFFAT: **Pisces IV** research submersible finds oil on Baffin Shelf 65

R.J. ROGERSON, H.W. JOSENHANS, and T. BELL: A 3.5 kHz acoustic survey of Nachvak Fiord, northern Labrador 221

J.V. BARRIE, W.T. COLLINS, J.I. CLARK, C.F.M. LEWIS, and D.R. PARROTT: Submersible observations and origin of an iceberg pit on the Grand Banks of Newfoundland 251

H.F.L. WILLIAMS: Depositional facies and evolution of Lulu Island topset deposits, Fraser Delta, British Columbia 559

R.A. KOSTASCHUK, J.L. LUTERNAUER, and T.H. MILLARD: Sediment transport during the 1985 freshet in the outer main channel of the Fraser River estuary, British Columbia 565

A. ROBERTS and J. LIEDTKE: Airborne definition of suspended surface sediment and intertidal environments in the Fraser River plume, British Columbia 571

MINERALOGY/MINÉRALOGIE

D.C. HARRIS: The minerals in the main Hemlo gold deposit, Ontario 49

I.M. SAMSON and A.E. WILLIAMS-JONES: Illite crystallinity studies in the Gaspé-Connecticut Valley synclinorium around Barnston, Quebec 359

G.M. WALLACE: The mineralogy of the McGerrigle plutonic complex, Gaspé, Quebec 507

PALEONTOLOGY/PALÉONTOLOGIE

M.J. DABROS and P.J. MUDIE: An automated microscope system for image analysis in palynology and micropaleontology 107

A.E.H. PEDDER: The Devonian rugose coral genera **Haplothecia, Kuangxiastraea** and **Scruttonia** 649

M.J. COPELAND: **Dioxycaris fritzi** sp. nov. (Arthropoda, Phyllocarida) from the Pika Formation (Middle Cambrian, **Bolaspidella** Zone), Jasper National Park, Alberta 663

PETROLEUM GEOLOGY/GÉOLOGIE PÉTROLIÈRE

M.P. AVERY, J.S. BELL, and K.D. McALPINE: Vitrinite reflectance measurements and their implications for oil and gas exploration in the Jeanne d'Arc Basin, Grand Banks, eastern Canada 489

K.G. OSADETZ and L.R. SNOWDON: Petroleum source rock reconnaissance of southern Saskatchewan 609

D.K. NORRIS and A.R. CAMERON: An occurrence of bitumen in the Interior Platform near Rengleng River, District of Mackenzie 645

QUATERNARY GEOLOGY/GÉOLOGIE DU QUATERNAIRE

Inventory mapping and stratigraphic studies/Inventaire cartographique et stratigraphique

W.W. SHILTS and S.L. SMITH: Stratigraphy of placer gold deposits; overburden drilling in Chaudière Valley, Quebec 703

S.A. EDLUND: Vegetation-geology-climate relationships of western Melville Island, District of Franklin 719

Sedimentology and geomorphology/Sédimentologie et géomorphologie

R.A. KLASSEN and A.M. BOLDUC: Ice flow trends and drift composition, Flowers River area, Labrador 697

F.J. THOMPSON and R.A. KLASSEN: Ice flow directions and drift composition, central Labrador 713

J.R. MACKAY: Fifty years (1935 to 1985) of coastal retreat west of Tuktoyaktuk, District of Mackenzie 727

J.D. ADSHEAD, B.D. BORNHOLD, and E.E. DAVIS: Indurated deposits and possible plume bands in a hydrothermal mound, northeast Pacific 737

M.T. KRAWETZ and S.B. McCANN: Coastal characteristics, east-central Ellesmere Island, District of Franklin 749

REGIONAL GEOLOGY/GÉOLOGIE RÉGIONALE

Appalachian region/Région des Appalaches

J.D. HILL: Granitoid plutons in the Canso area, Nova Scotia 185

H.S. SWINDEN and P.E. SACKS: Stratigraphy and economic geology of the southern part of the Roberts Arm Group, central Newfoundland 213

J.B. WHALEN and C. GARIÉPY: Petrogenesis of the McGerrigle plutonic complex, Gaspé, Quebec: a preliminary report 265

R.P. RAESIDE, S.M. BARR, C.E. WHITE, and F.A.R. DENNIS: Geology of the northernmost Cape Breton Highlands, Nova Scotia 291

J.B. WHALEN: A-type granites in New Brunswick 297

K.L. CURRIE: The boundaries of the Avalon tectonostratigraphic zone, Musquash Harbour-Loch Alva region, southern New Brunswick 333

M.R. CAUDILL and R.D. NANCE: Variscan tectonostratigraphy of the Mispec Group, southern New Brunswick: stratigraphy and depositional setting 343

E.J. ZWICKER and D.F. STRONG: The Great Bend ophiolite, eastern Newfoundland: field investigations 393

G.M. YEO and GAO RUIXING: Late Carboniferous dextral movement on the Cobequid-Hollow fault system, Nova Scotia: evidence and implications 399

T.L. HOPE and S.L. WOODEND: Geological mapping and igneous and metamorphic petrology, Queen's and Shelburne counties, Nova Scotia 429

B.H. O'BRIEN: Preliminary report on the geology of the Mahone Bay area, Nova Scotia 439

J.B. MURPHY: Geology of the western Antigonish Highlands, Nova Scotia 445

M. COYLE, D.F. STRONG, and D.B. DINGWELL: Geology of the Sheffield Lake group, west-central Newfoundland 455

D.J. FUREY and D.F. STRONG: Geology of the Harbour Breton Complex, Newfoundland 461

D.J. KONTAK and D.F. STRONG: The volcano-plutonic King's Point complex, Newfoundland 465

S. DUNSWORTH, T. CALON, and J. MALPAS: Structural and magmatic controls on the internal geometry of the plutonic complex and its chromite occurrences in the Bay of Islands Ophiolite, Newfoundland 471

M. COYLE and D.F. STRONG: Geology of the southern and northern margins of the Springdale Caldera, Newfoundland 499

J.V. OWEN: Geology of the Silver Mountain area, western Newfoundland 515

P.A. CAWOOD and H. WILLIAMS: Northern extremity of the Humber Arm Allochthon in the Portland Creek area, western Newfoundland, and relationships to nearby groups 675

H. WILLIAMS and P.A. CAWOOD: Relationships along the eastern margin of the Humber Arm Allochthon between Georges Lake and Corner Brook, western Newfoundland 759

Arctic Islands/Archipel Arctique

A.B. LANGILLE, E.T. BURDEN, W.B. SEARS, and D.C. HOLLOWAY: Geological investigation of Cretaceous? strata beneath Cape Dyer Basalts (Paleocene), Baffin Island, District of Franklin 483

Cordilleran region/Région de la Cordillère

M. JOURNEAY and R.L. BROWN: Major tectonic boundaries of the Omineca Belt in southern British Columbia: a progress report 81

E.W. MOUNTJOY and R. FOREST: Revised structural interpretation, Selwyn Range between Ptarmigan and Hugh Allan creeks, British Columbia – an antiformal stack of thrusts 177

K.R. McCLAY and M.W. INSLEY: Structure and stratigraphy of the Gataga fold and thrust belt, northeastern British Columbia 259

R.T. BELL: Megabreccias in northeastern Wernecke Mountains, Yukon Territory 375

T. KUBLI: Stratigraphy and structure of the Hadrynian Horsethief Creek Group in the northern Dogtooth Range south of Grizzly Creek, Purcell Mountains, British Columbia 553

D.B. HALWAS and P.S. SIMONY: The Castlegar Gneiss Complex, southern British Columbia 583

L.C. STRUIK: A regional east-dipping thrust places Hadrynian onto probable Paleozoic rocks in Cariboo Mountains, British Columbia 589

F. CORDEY: Radiolarian ages from the Cache Creek and Bridge River complexes and from chert pebbles in Cretaceous conglomerates, southwestern British Columbia 595

M.P. DUBORD, D.W. MORROW, and R.W. MACQUEEN: A shelf-to-basin transition in the Devonian Ogilvie Formation, Yukon Territory 603

M.R. MCDONOUGH and P.S. SIMONY: Geology of the northern Selwyn Range, western Main Ranges, Rocky Mountains, British Columbia: preliminary report 619

Canadian Shield/Bouclier canadien

M.R. ST-ONGE, S.B. LUCAS, D.J. SCOTT, and N.J. BÉGIN: Eastern Cape Smith Belt: an early Proterozoic thrust-fold belt and basal shear zone exposed in oblique section, Wakeham Bay and Cratère du Nouveau Québec map areas, northern Quebec 1

J.E. KING, M.E. VILLENEUVE, D. SPETHMANN, and K.H. WILCOX: Geology of the northwestern metamorphic-internal zone and an outlier of the eastern Great Bear Magmatic Zone of Wopmay Orogen, Big Bend area, District of Mackenzie 21

H.H. BOSTOCK: Reconnaissance geology of Precambrian rocks of the Fort Resolution, Taltson Lake, and Fort Smith areas, District of Mackenzie 35

J.P. GROTZINGER and Q. GALL: Preliminary investigations of Early Proterozoic Western River and Burnside River formations: evidence for foredeep origin of Kilohigok Basin, District of Mackenzie 95

F.W. CHANDLER: Sedimentology and paleoclimatology of the Huronian (Early Aphebian) Lorrain and Gordon Lake Formations and their bearing on models for sedimentary copper mineralization 121

J.R. HENDERSON, A.N. LeCHEMINANT, C.W. JEFFERSON, K. COE, and M.N. HENDERSON: Preliminary account of the geology around Wager Bay, District of Keewatin 159

P.H. THOMPSON, N. CULSHAW, J.R. BUCHANAN, and P. MANOJLOVIC: Geology of the Slave Province and Thelon Tectonic Zone in the Tinney Hills-Overby Lake (west half) map area, District of Mackenzie 275

J.B. HENDERSON and R.I. MACFIE: Artillery Lake map area, District of Mackenzie: a transect across the Thelon Front 411

D.T. JAMES: Geology of the Moraine Lake area, District of Mackenzie; Part 2: a transect across part of the Thelon Tectonic Zone 417

G.D. JACKSON: Notes on the Proterozoic Thule Group, northern Baffin Bay 541

M. SCHAU and M. BECKETT: High grade metamorphic rocks of northwestern Melville Peninsula, District of Franklin 667

R.F. EMSLIE, C. LEFEBVRE, B. KJARSGAARD, and R. SHERLOCK: Atikonak River massif, Labrador 755

STRATIGRAPHY/STRATIGRAPHIE

B. BEAUCHAMP, B.C. RICHARDS, E.W. BAMBER, and B.L. MAMET: Lower Carboniferous lithostratigraphy and carbonate facies, upper Banff Formation and Rundle Group, east-central British Columbia 627

STRUCTURAL GEOLOGY/GÉOLOGIE STRUCTURABLE

S.J. HAYNES, B.A. REILLY, and L.A. KIELY: Structural setting of the Mile Lake gold prospect, Guysborough County, Nova Scotia 141

C.R. VAN STAAL: Preliminary results of structural investigations in the Bathurst camp of northern New Brunswick 193

R.D. NANCE and J.B. WARNER: Variscan tectonostratigraphy of the Mispec Group, southern New Brunswick: structural geometry and deformational history 351

SCIENTIFIC AND TECHNICAL NOTES
NOTES SCIENTIFIQUES ET TECHNIQUES

B. MACLEAN and G. VILKS: Marine geological program in the Byam Martin Channel - Lougheed Island region, District of Franklin 769

P.J. KURFURST: Geotechnical investigation of seabottom sediments, Tuktoyaktuk area, District of Mackenzie 775

L.A. DREDGE and E. NIELSEN: Gold concentrations in till, Great Island, northern Manitoba 779

D.A. ST-ONGE and J.S. SCOTT: Notes on the geomorphology and Quaternary geology of northeastern Ungava Peninsula, Nouveau Québec 783

S.M. ROSCOE: Felsic volcanic rocks in the Nonacho Group near Whitefish Lake, District of Mackenzie 787

K.G. SHIH and R. MACNAB: Efficient algorithms for computing the gravitational effect of rectangular prisms 791

R.L. CHRISTIE: The Melville Project, 1984-85: progress report 795

D.K. NORRIS: Lower Devonian Road River Formation on the north flank of Romanzof Uplift, northern Yukon Territory 801

B.W. CHARBONNEAU and S.S. SWETTENHAM: Gold occurrence in radioactive calc-silicate float at Sandybeach Lake, Nueltin Lake area, District of Keewatin 803

CANADA-NOVA SCOTIA CO-OPERATIVE MINERAL PROGRAM 1981-84
CANADA-NOUVELLE-ÉCOSSE: PROGRAMME COOPÉRATIF SUR LES MINÉRAUX 1981-84 809

AUTHOR INDEX/INDEX DES AUTEURS 384a

Erratum 384b

SCIENTIFIC AND TECHNICAL REPORTS
RAPPORTS SCIENTIFIQUES ET TECHNIQUES

Eastern Cape Smith Belt: an early Proterozoic thrust-fold belt and basal shear zone exposed in oblique section, Wakeham Bay and Cratère du Nouveau Québec map areas, northern Quebec

Project 850003

M.R. St-Onge, S.B. Lucas [1], D.J. Scott [2], and N.J. Bégin [3]
Precambrian Geology Division

St-Onge, M.R., Lucas, S.B., Scott, D.J., and Bégin, N.J., Eastern Cape Smith Belt: an early Proterozoic thrust-fold belt and basal shear zone exposed in oblique section, Wakeham Bay and Cratère du Nouveau Québec map areas, northern Quebec; in Current Research, Part A, Geological Survey of Canada, Paper 86-1A, p. 1-14, 1986.

Abstract

Three distinct sets of structures are well developed in the eastern early Proterozoic Cape Smith Belt. Mesoscopic D1 tight south-facing folds of cover units are associated with a pervasive syn-metamorphic axial-planar schistosity in favourable lithologies at all structural levels, except in the area south of a frontal thrust zone. D1 thrust faults, documented by stratigraphic repetitions, splay upward from a basal décollement located at the Archean basement/Proterozoic cover interface. Hanging wall and footwall rocks of the décollement record high ductile strains over a zone of increasing thickness, from south to north towards the hinterland. Common in the lower structural levels is a transverse D1 stretching lineation which, considered with asymmetric D1 folds of bedding, indicates southward, top-side-over, movement of cover units. Syn- to late-D1 mineral assemblages in pelitic schists on the north margin of the belt, indicate metamorphic temperature of 550°C and minimum pressure of 5.5 kb, 200 m above the basement-cover contact. Mesoscopic, late- to post-metamorphic, chevron to rounded D2 folds of the D1 schistosity are co-axial with the D1 folds. The D2 folds have limb asymmetries suggestive of folds cascading off macroscopic basement-cored D2 antiforms. The distribution of the mesoscopic D2 folds with respect to first-order structures suggests diachronous development of the basement-cored antiforms. A major D3 cross fold with over 12 km of structural relief on its western limb provides the oblique section required to study the involvement of cover and basement in the two older D1 and D2 sets of structures.

Résumé

Trois ensembles distincts de structures caractérisent la partie est de la zone de Cape Smith qui date du début du Protérozoïque. Des plis mésoscopiques serrés, D1, dirigés vers le sud, déforment les unités de couverture et sont associés à une schistosité syn-métamorphique D1 de plan axial. Cette schistosité D1 est présente dans toutes les lithologies favorables, à tous les niveaux structuraux, exception faite de la région au sud d'une zone frontale de chevauchement. Les failles chevauchantes D1, définies par des répétitions stratigraphiques, ont leur origine dans un décollement de base situé au contact entre le socle d'âge archéen et la couverture d'âge protérozoïque. La zone de déformation dans la lèvre supérieure et la lèvre inférieure du décollement de base, devient progressivement plus importante du sud vers l'arrière-pays au nord. Aux niveaux structuraux inférieurs, une linéation d'allongement transversale D1 et des plis asymétriques D1 du litage, indiquent un mouvement de chevauchement à direction sud pour les unités de la couverture. Des associations minérales syn- à tardi-D1 dans les métapélites du côté nord de la zone de Cape Smith, indiquent une température métamorphique de 550°C et une pression minimum de 5,5 kb, à 200 m du contact socle-couverture. Des plis mésoscopiques D2, tardi- à post-métamorphiques avec charnière arrondie ou en chevron, déforment la schistosité D1. Les plis D2, co-axiaux avec les plis D1, sont caractérisés par une asymétrie de flancs qui rappelle des plis en cascade sur flanc d'antiformes macroscopiques D2 à noyaux de socle. La répartition des plis mésoscopiques D2 par rapport aux structures de premier ordre, semble indiquer un développement diachrone des antiformes à noyaux de socle. Un pli transverse D3 important, avec plus de 12 km de relief structural sur son flanc ouest, offre la coupe oblique requise pour l'étude du comportement à la fois du socle et de la couverture dans les ensembles de structures D1 et D2 plus anciennes.

[1] Department of Geological Sciences, Brown University, Providence, Rhode Island, U.S.A. 02912
[2] Department of Geology, McMaster University, Hamilton, Ontario L8S 4L8
[3] Department of Geological Sciences, Queen's University, Kingston, Ontario K7L 3N6

Introduction

The ca 1.9 Ga (Zindler, 1981) Cape Smith Belt is a thrust-fold belt (Hynes and Francis, 1982; Lamothe et al., 1984) which trends east-west across the northern part of the Superior craton (Ungava Peninsula, northern Quebec) between Hudson Strait and Hudson Bay. The thrust-fold belt contains well exposed volcanic and sedimentary units that were deformed and metamorphosed in the 1.9-1.8 Ga Trans-Hudson Orogen (Taylor, 1982). These units are now bounded on the north, south and east sides by granodioritic gneisses of Archean age (Taylor and Loveridge, 1981; Doig, 1983).

Although various areas of the Cape Smith Belt have been mapped at scales of 1:63 360 (Beall, 1959, 1960; De Montigny, 1959; Gélinas, 1962; Gold, 1962) or 1:126 720 (Bergeron, 1959) and the whole belt was mapped at a 1:250 000 scale by Taylor (1982), the structure and the tectonic evolution of the early Proterozoic belt have remained a subject of controversy (for a review see Hoffman, 1985). Significant progress was made in the understanding of the structural framework of Cape Smith Belt with the publication of a detailed stratigraphic, structural and petrological transect of the central belt by Hynes and Francis (1982) and Francis et al. (1983). The published transect is an excellent documentation of the stratigraphy and the structure of relatively high structural levels within the Cape Smith Belt. A study at high structural levels however cannot fully constrain the extent of basement involvement in the deformation of the cover rocks nor resolve the question of in situ (e.g. Baragar and Scoates, 1981; Hynes and Francis, 1982) versus allochthonous (Hoffman, 1985) derivation with respect to surrounding Archean basement.

Taylor (1982) published 1:250 000 scale geological maps for the Wakeham Bay (25E) and the cratère du Nouveau-Québec (35H) map areas that clearly show Archean basement continuously exposed from south side to north side around the eastern end of the Cape Smith Belt. These two map areas therefore hold the key to understanding the various structural features of the belt from low structural levels, where basement-cover relationships and the allochthonous nature of the belt can be evaluated (Hoffman, 1985), westward to the higher structural levels exposed in the vicinity of the Hynes and Francis transect.

A three-year 1:100 000 scale mapping project was initiated in the summer of 1985, to study the Cape Smith Belt and the adjacent Archean basement east of 72°20'W. West of

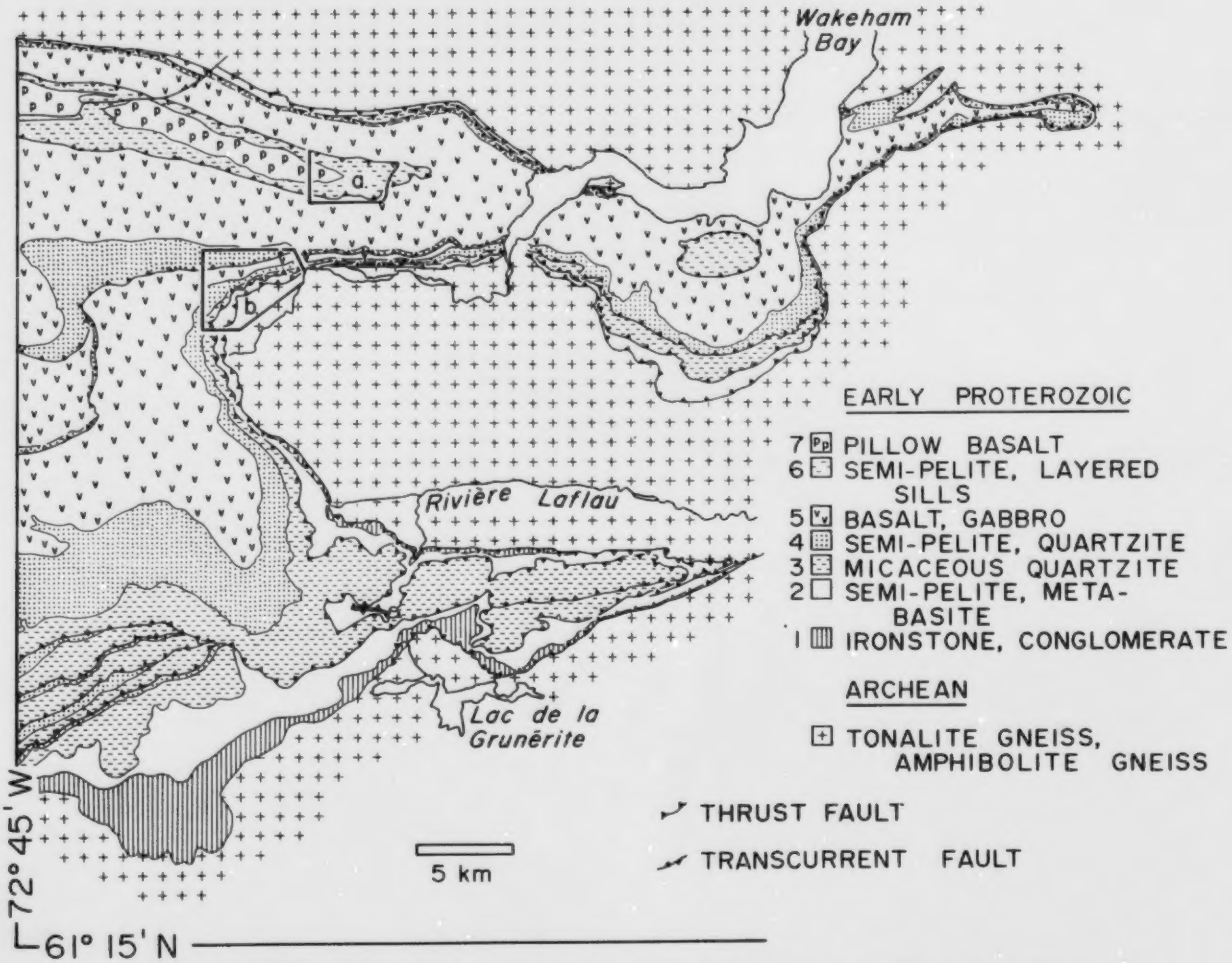

***Figure 1.1.** Geological map of the eastern Cape Smith Belt, Wakeham Bay-Grunérite Lake area. Descriptions of early Proterozoic formations 1 to 7 are given in text. Outlined areas "a" and "b" correspond to areas in Figures 1.8a and b.*

this longitude Daniel Lamothe (Ministère de l'Energie et des Ressources-Québec) is leading a major on-going long-term project that will yield full 1:50 000 scale coverage of the Cape Smith Belt west to Hudson Bay.

Within the framework of the regional GSC project, a study of the variations in structures on outcrop- to mineral grain-scale and deformation processes by Steve Lucas will form the basis of a Ph.D. thesis (Brown University). A study of the regional metamorphism at the various exposed structural levels in the Cape Smith Belt, with an emphasis on mineral-producing reactions in metabasites, by Normand Bégin will be the basis for an M.Sc. thesis (Queen's University). Lastly, a detailed petrological study of the metasediments in the Proterozoic basal shear zone by Dave Scott will form the basis of a B.Sc. thesis at McMaster University.

Summary of Results

Ten weeks of field work in the Wakeham Bay – Grunérite Lake area (Fig. 1.1) have documented that:

1. A thin autochthonous to paratochthonous low-strain sedimentary sequence on the south margin of the Cape Smith Belt rests directly on Archean basement showing no evidence of Proterozoic transposition.
2. The entire Proterozoic section in the eastern end of the Cape Smith Belt (with the exception of the sequence in 1) occurs in a series of thrust slices bounded by south-verging (D1) thrust faults defined by structural repetitions of stratigraphic units.
3. A basal décollement at the basement-cover interface is associated with the thrust system. The hangingwall and footwall rocks of the décollement record high ductile strains over a zone of increasing thickness, from south to north, towards the hinterland. Most of the thrusts root on a fault in the basal high strain zone. Late synmetamorphic thrust faults with relatively small displacements cut the basal décollement and associated shear zone and place basement gneisses over cover rocks.
4. Lensoid meta-ultramafic tectonic blocks occur locally within the basal shear zone, at or near the actual sheared basement-cover interface or décollement. The blocks have an anthophyllite-actinolite assemblage which suggests a composition different than that of the layered gabbro-peridotite sills characterized by serpentine-tremolite and found at higher structural levels.
5. Favourable lithologies at all structural levels with the exception of units from the southern autochthonous margin, have a penetrative synmetamorphic schistosity (S1) which is axial planar to south-facing tight to isoclinal folds of bedding (F1).
6. A transverse stretching lineation (L1) common in the lower structural levels and pervasive in the basal shear zone, when considered with the F1 fold asymmetry and overall thrust-ramp geometry, indicates southward movement of cover rocks during D1.
7. A pelitic interval above the basal décollement, on the north side of the Cape Smith Belt contains the metamorphic assemblage kyanite-staurolite-garnet-biotite-muscovite-plagioclase-quartz. The assemblage is indicative of metamorphic temperature of 550°C and minimum pressure of 5.5 kb.
8. Mesoscopic late- to postmetamorphic chevron to rounded parallel folds (F2) of the S1 fabric have a marked limb asymmetry suggestive of an origin as folds cascading off basement-cored D2 antiforms into pinched cover-rock synforms. The distribution of north-facing versus south-facing mesoscopic folds however is not always consistent with the mapped limbs of the macroscopic D2 basement-cored folds and continued first-order folding and/or doming following higher-order mesoscopic fold formation is proposed.
9. Macroscopic high-angle D3 cross folds affect both basement and cover in the eastern part of the Cape Smith Belt and provide a cumulative structural relief of 12-15 km. D3 fold hinges are readily documented by reversals in plunge azimuth of the F2 folds.

These observations are fully consistent with the regional tectonic framework proposed by Hoffman (1985).

Stratigraphy

The metasedimentary and metavolcanic rocks of the Cape Smith Thrust-Fold Belt have been divided by Bergeron (1959) into a lower Povungnituk Group and an upper Chukotat Group. West of the present study area, Hynes and Francis (1982) describe the Povungnituk Group as consisting of a lower part of marine, slope-facies, dominantly-siliciclastic sediments and an upper part of mixed siliciclastics, minor rhyolite and both extrusive and intrusive Fe- and Ti-rich tholeiites. In contrast, the Chukotat Group is almost devoid of sediments and consists of volcanic and intrusive rocks that range in composition from highly magnesian (komatiitic) basalts to low-Ti tholeiitic basalts (Hynes and Francis, 1982). Francis et al. (1983) interpreted the chemical changes in the igneous rocks of the section as reflecting various stages of on-going epicontinental rifting leading eventually to the formation of oceanic crust.

In order to fully unravel the structure of the Cape Smith Belt in the Wakeham Bay – Grunérite Lake area, a composite stratigraphy was established for the medium-grade rocks based on the consistent superposition (Fig. 1.1) of 7 informal formations designated as 1 to 7, from bottom to top.

Formation 1: ironstones and basal conglomerate

The ironstones found mostly on the autochthonous south margin of the belt, west of Grunérite Lake (Fig. 1.1) vary in thickness from 50 m to 500 m. In most localities the ironstones rest unconformably on more steeply-dipping Archean tonalitic gneisses that show no evidence of penetrative Proterozoic fabric. Locally, pockets of oligomictic garnetiferous metaconglomerate (Fig. 1.2) less than 0.5 m thick occur between the gneisses and the overlying ironstones.

Different units within the ironstones have been recognized in the Grunérite Lake area and also west of 74°20'W (J. Moorhead, personal communication, 1985). These consist of ferruginous sandstones, interbedded massive magnetite/grunerite schist carbonate-rich grunerite schist and garnet-biotite-Al amphibole-grunerite schist. These various units although strikingly different in their mineral assemblages are not very continous laterally within the ironstone formation and therefore the latter could not be subdivided at the present scale of mapping.

Formation 2: semi-pelites and metabasites

Overlying the ironstones are approximately 60 m to 340 m of semi-pelites and fine grained quartzites that grade laterally into mafic sediments, interlayered with metabasites. Individual beds range from millimetre thick in the semi-pelites to centimetre thick in the quartzites. Rounded to subrounded quartz grains with a minor amount of feldspar (plagioclase?) were the only clasts noted in the field. Metamorphic biotite and minor muscovite are found in the matrix and define a bedding-parallel schistosity.

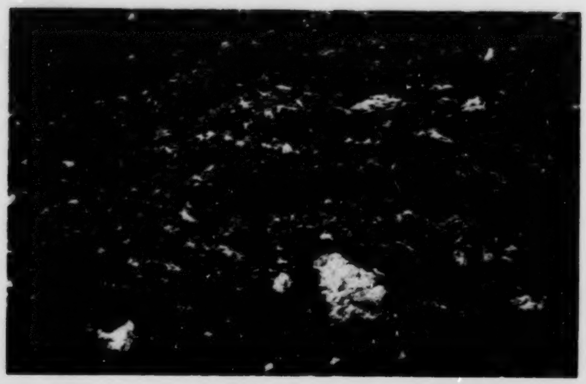

Figure 1.2. Basal garnetiferous conglomerate (formation 1) northwest of Grunérite Lake. GSC 204232-T.

Figure 1.3. Dolomite unit, top of formation 2. GSC 204232-W.

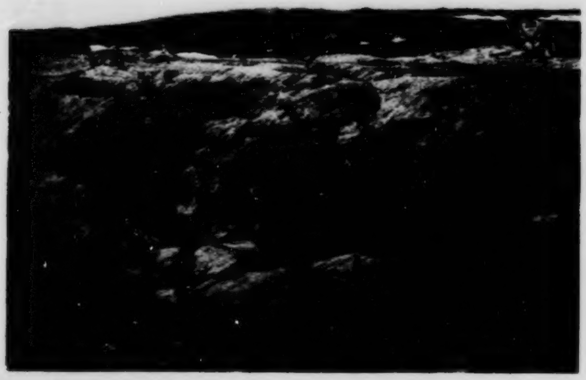

Figure 1.4. Micaceous quartzite (formation 3), north shore of Wakeham Bay, showing a well developed S1 schistosity and transverse stretching lineation (L1) defined by rodding of recrystallized quartz. GSC 204232-Z.

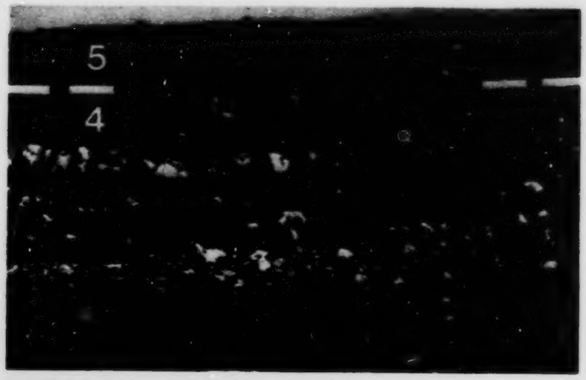

Figure 1.5. White orthoquartzite interbedded with dark semi-pelite in formation 4 overlain by basalts of formation 5. Outcrop is 15 m high. GSC 204233-A.

Figure 1.6. Relatively unstrained pillow basalt near the top of formation 5. GSC 204232-L.

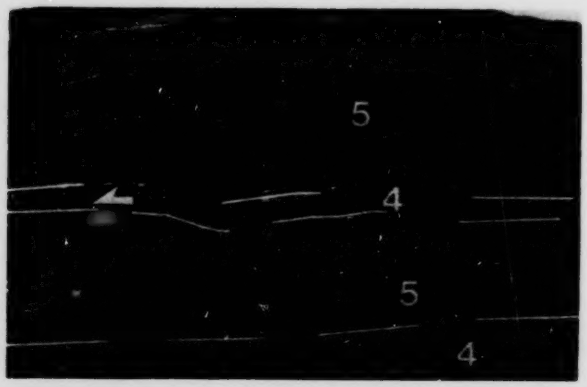

Figure 1.7. Thrust fault placing quartzites of formation 4 in hanging wall on metabasites of formation 5 in footwall. Cliff is 150 m high. GSC 204232-V.

The mafic sediments consist mostly of quartz-biotite beds that contain metamorphic actinolite and/or hornblende, indicative of a volcanogenic component in the clastic sediment. Associated with the mafic sediments are hornblende-plagioclase metabasite. No pillows or flow-top breccias were noted in these units and the amphibolite to upper amphibolite grade makes the distinction between massive flow or sill difficult.

In the Wakeham River valley a large boudinaged gabbro-peridotite sill has been mapped within the semi-pelites and mafic sediments of formation 2. The majority of the layered sills however are found within formations 6 and 7.

The top of formation 2 is marked by a discontinuous interval of mostly dolomite and associated calc-silicate units. The dolomite (Fig. 1.3) varies in thickness from 2 m to 5 m and shows no obvious internal sedimentary structures, other than shale interbeds.

Formation 3: micaceous quartzite

This massive, homogeneous, ridge-forming unit (Fig. 1.4) varies in thickness from 70 m to 270 m. The micaceous quartzite consists mostly of recrystallized quartz (>90%) and minor amounts of biotite and muscovite, the former giving the rock a dark grey colour on broken surfaces and the latter a whitish-silver sheen on S1 schistosity planes. The unit is also characterized by the common occurrence of discontinuous milky quartz veins and seggregations generally a few millimetres to 2-3 cm in width.

Formation 4: orthoquartzites and semi-pelite

Above the micaceous quartzites, formation 4 consists of clean white orthoquartzite interbedded with dark semi-pelite (Fig. 1.5); it varies in thickness from 240 m to 2200 m. The overall thickness of the formation is greatly inflated in the upper Laflau River area (Fig. 1.1) by emplacement of numerous gabbro sills. These are presumably the feeders to the overlying volcanic units. The semi-pelites are thin-bedded (1 cm scale) occasionally graded, and are characterized by parallel laminations at the top of beds. The semi-pelitic beds are quartz-rich with biotite as the principal metamorphic mineral.

The orthoquartzites commonly preserve graded bedding, with subrounded to rounded quartz clasts varying from sub-millimetre to several millimetres in diameter.

Associated with the gabbro sills, semi-pelities and orthoquartzite is a very small number of thin (1 m) rhyolitic lenses that show no marked lateral continuity.

Formation 5: basalts

Ridge-forming basalts conformably overlie or interfinger with the clastic sediments (top of Fig. 1.5). Formation 5 varies in thickness from 2100 m to 4100 m, the top of the formation corresponding, as far west as mapped to date, to a tectonic contact. The main volcanic pile consists of interlayered pillow lavas (Fig. 1.6), massive flows and numerous sills. Rare semi-pelite and fine grained quartzites are preserved between flows. The few top determinations in pillow lavas from less strained units, consistently indicate the units are upright.

Total penetrative strain (D1) in the volcanic rocks decreases up-section from the base of the formation and pillows near the top are flattened to low aspect ratios (1:1.5-2). This trend is reversed at the upper contact of formation 5, where several metres of highly strained metabasite are found in contact with overlying sediments. West of Wakeham Bay gabbro sills are cut-off against the upper contact. The high strain S1 fabric at the top of the basalt formation is developed parallel to the bedding in the sediments at the base of unit 6. In addition, a well developed stretching lineation defined by quartz smears and alignment of biotite is found in well foliated semi-pelite at the base of formation 6.

That the contact between formations 5 and 6 is a tectonic feature is indicated by the truncation of formation 5 units and the highly strained nature of rocks on both sides of the contact. Given that the foliation at the top of unit 5 is parallel to that in the overlying sediments it is proposed that a low angle fault separates formations 5 and 6.

Formation 6: semi-pelites

Structurally above the volcanic units of formation 5 are 400 m to 500 m of parallel-laminated semi-pelites interlayered with dark biotite-bearing impure quartzites and white orthoquartzites. Beds in the semi-pelites are several millimetres to 2.3 cm thick whereas individual quartzite beds average 0.25 to 0.5 m. Quartzite beds are discontinuous and seem to be restricted to channel structures. Graded bedding is noted in a few localities.

This sedimentary interval is host to numerous thick massive gabbro, peridotite and layered gabbro-peridotite sills. The layered sills give an indication of tops at time of emplacement, which is consistently top-side-up.

Formation 7: pillow basalts

Formation 7, the highest stratigraphic unit mapped to date in the eastern Cape Smith Belt, consists almost exclusively of little-deformed basalt pillow-lavas and a number of gabbro and peridotite sills. The formation conformably overlies the semi-pelites of formation 6 and has a minimum thickness of 300 m. No sediments occur in this section.

Stratigraphic correlation with Povungnituk and Chukotat groups

Although extrapolation of stratigraphic units over 50 km is tenuous, from rock unit descriptions of Hynes and Francis (1982) and some field observations, we propose a first-order correlation of the 7 formations mapped in this project with the Povungnituk and Chukotat groups of the central Cape Smith Belt. Formations 1, 2 and 3 would tentatively correspond to the lower Povungnituk Group, formations 4, 5 and the sediments of formation 6 to the upper Povungnituk Group and formation 7 plus the layered sills in formation 6 to the Chukotat Group.

The transition between the Povungnituk Group and the Chukotat Group as described in Francis et al. (1983) is a good match for the sedimentary-layered sill interval described in formation 6. The sheared contact between formations 5 and 6 is also reported by Francis et al. (1983) who elected not to consider the Chukotat Group as allochthonous with respect to the underlying volcanics on geochemical grounds. We feel that even if the extrusive and intrusive rocks can be related geochemically to the underlying basalts, the presence of a bedding-parallel high strain zone at the volcanic-sediment contact and the cut-offs of the volcanic rocks against the sediments indicate that the contact between formations 5 and 6 is tectonic.

Synmetamorphic D1 structures

Folds and thrust faults

In general, D1 structures are characterized by relatively rare, disharmonic, tight to isoclinal folds of

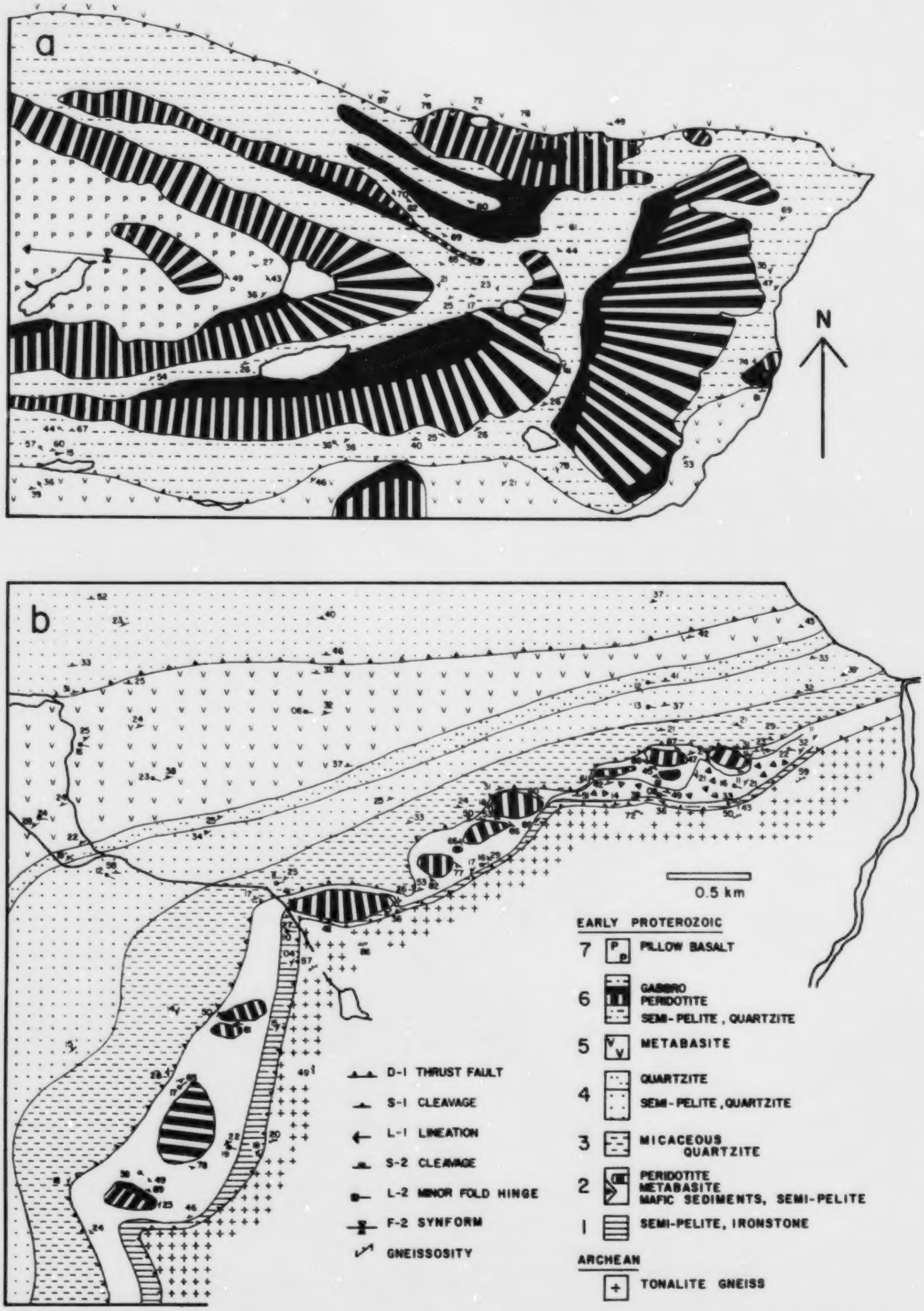

Figure 1.8. *Geological maps for areas "a" and "b" outlined in Figure 1.1. Peridotite sill at lower structural levels (Fig. 1.8b) is boudinaged and shows close to 100% extension in contrast to sills at higher structural levels (Fig. 1.8a) which show no D1 strain and are simply folded about an open F2 synform.*

bedding in formations 2 to 4, a strong bedding parallel synmetamorphic schistosity to mylonitic foliation that has a steep "down-dip" lineation decreasing in intensity going both up section and from north to south, and by relatively few thrust faults, each with significant displacement (kilometre-scale). F1 folds, commonly coaxially refolded by F2 folds producing a Type 3 interference pattern (Ramsay, 1967), are restricted to the sediments of formations 2 to 4; this is thought to reflect the importance of rheologic layering with sufficient competency contrast for the development of buckle folds (Johnson, 1980). In contrast, F1 folds are absent from formations 5 and 7 volcanics, which lack significant rheologic layering and closely spaced bedding planes.

The F1 folds in the basal shear zone are occasionally modified to mesoscopic sheath folds (Cobbold and Quinquis, 1980). Due to the paucity of F1 folds at higher structural levels, a transition from upright, parallel folds at high structural levels to the recumbent, similar folds near the décollement as in the Helvetic Nappes (e.g. Ramsay, 1981; Ramsay et al., 1983), Variscan fold belt of southwest England (Sanderson, 1979), and the nappes of Kilohigok Basin (Tirrul, 1985) is not observed.

The tectono-stratigraphic subdivision of the eastern Cape Smith Belt has enabled the recognition of inter-formational stratigraphic repetitions (e.g. Fig. 1.7) defining six thrust faults, each placing older stratigraphic units on top of younger units (Fig. 1.1). The approximately 20° westward plunge in the east end of the belt, the result of D3 cross-folding, allowed six thrust faults to be mapped from the basal shear zone along strike to higher structural levels. The thrusts all splay from a detachment at the top of formation 2, which itself ramps up from the basal décollement, located at the basement-cover interface, south-east of Wakeham Bay (Fig. 1.1). The thrust geometry is characterized by broad isostratigraphic flats that parallel the basal décollement and ultimately connect with ramps that cut up-section towards the south (Fig. 1.1). The thrust glide zone appears to have occurred in semi-pelite or micaceous quartzite showing a small change in stratigraphic level of the thrust in the hanging wall along strike (i.e. up structural section). Two lateral ramps have been inferred on the north-limb of the belt defining a kilometre-scale horse of formation 3 in the basal shear zone.

The presence of flat-ramp-flat geometries is characteristic of thrusted continental margin sediments (e.g. Price, 1981; Boyer and Elliot, 1982), and is found along the thrusts southwest of Wakeham Bay (Fig. 1.1). The presence of fault related folds (fault-bend folds of Suppe, 1983) in the hanging walls of these thrusts is consistent with the flat-ramp-flat geometries in the map area.

The polarity of the stratigraphic repetitions (older on younger from north to south on north dipping fault planes) and the sense of shear deduced from transverse lineations and fold asymmetry within the basal shear zone (see next section) all require southward directed movement during thrusting and imbrication of the Cape Smith Belt units.

The seventh thrust fault shown in Figure 1.1, separates formations 5 and 6. As previously discussed, field evidence suggests a tectonic contact parallel to bedding in formation 6, at the top of the volcanic section; given the documented sense of movement on the other six thrusts, south-directed reverse movement is inferred.

Field relationships between thrust slices and the faults themselves suggest that fault development proceeded in regular foreland-directed (southward) sequence, with piggy-back stacking (Butler, 1982; Boyer and Elliot, 1982). Although higher faults were not observed to be folded above ramps in structurally lower thrusts, folding of a thrust surface due to boudinage of an underlying peridotite sill about 20 m above the basal detachment was documented (Fig. 1.8b). This relationship suggests that the boudinage of the sill, a result of high shear strain in formation 2, occurred during movement along the basal detachment which followed movement on the overlying thrusts. It appears that the sole fault continued to propagate at the basement-cover interface to very close to the toe of the thrust belt.

Basal shear zone and décollement

West of the river flowing north from Grunérite Lake (Fig. 1.1), the conglomerates or ironstones of formation 1 rest directly, with an angular discordance, on the Archean tonalitic gneisses.

East of that river, the basement-cover contact is tectonic (the basal décollement or detachment for the D1 thrusting deformation), and can be mapped continuously around the east end of the belt to the northern margin. This east-to-west transition from a tectonic to an unconformable basement-cover contact north of Grunérite Lake corresponds to the stepping up of the basal décollement into the units of formation 1 at the toe of the thrust belt. The frontal thrust zone consists of several small faults, delineated by small-scale shear zones with <1 m-wide strain gradients in which a strong steeply-dipping S1 fabric is developed axial planar to asymmetric, south-verging folds of bedding.

The basal décollement, and the thrusts that parallel it along isostratigraphic flats for several kilometres (parallel to the transport direction) before ramping up section represent slip discontinuities in a basal shear zone. The basal shear zone decreases from a total width of over 240 m, of which 2-3 m involve basement gneisses on the north margin of the belt to a total thickness of only a few metres of sheared cover rocks and 1-2 cm of reworked basement gneisses on the south margin. The shear zone is developed in the siliciclastic, carbonate and volcanogenic sediments of formations 2 to 4 and in the mafic volcanics of formation 5, with D1 strain decreasing up-section in formation 5. The basal shear zone was defined for mapping purposes on several qualitative indicators of the amount of D1 strain, including demonstrable or inferred strain-induced grain size reduction, presence of a stretching lineation, intensity of the S1 fabric and its angular relationship to bedding (S1 parallel to bedding in the shear zone) and boudinaged competent bodies (e.g. quartz veins, peridotite sills).

The Archean basement rocks structurally underlying the basal shear zone consist of steep-to-moderately-dipping tonalitic gneisses, with the gneissosity defined by centimetre-scale alternating bands of tonalite and granodiorite vein material (Fig. 1.9). Two to three metres from the basement-cover contact on the north margin and a few centimetres from that contact on the south margin the Archean gneisses are progressively recrystallized exhibiting demonstrable strain-induced grain-size reduction (Fig. 1.10); in this zone any pre-existing fabric becomes completely transposed into parallelism with the basement/cover contact by progressive ductile reworking (Fig. 1.11). The transposed basement units are characterized by the growth of aligned muscovite and garnet in the synmetamorphic (S1) foliation plane which contains a well developed penetrative transverse stretching lineation (L1) defined by rodding of recrystallized quartz and feldspar (Fig. 1.12). Asymmetric, tight to isoclinal F1 folds occur in these transposed basement zones with E-W trending axes (Fig. 1.13). The sense of asymmetry of these folds is consistent with southward top-side-over movement in the transposed basement zone. Given the approximate orthogonality of the fold axes and the stretching lineation, we conclude that the finite extension direction closely parallels the transport direction for D1 deformation;

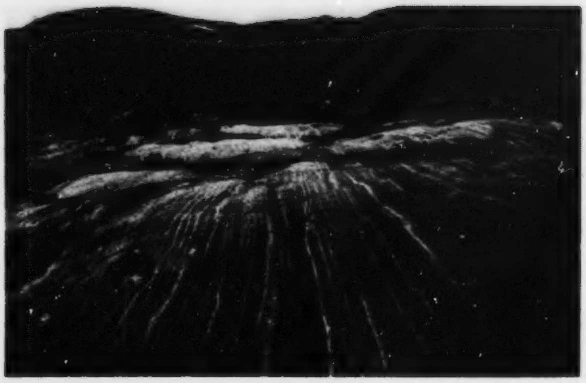

Figure 1.9. *Archean tonalite gneiss, east shore of Wakeham Bay. GSC 204233-H.*

Figure 1.10. *Archean tonalite gneiss showing marked grain-size reduction in transposed zone of basal décollement (left side of photo, under pen). GSC 204233-F.*

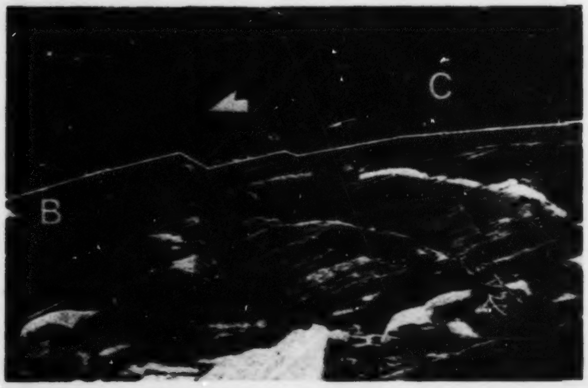

Figure 1.11. *Basal décollement with transposed Archean basement tonalite gneiss B in footwall and sheared Proterozoic cover units C in hanging wall. GSC 204233-G.*

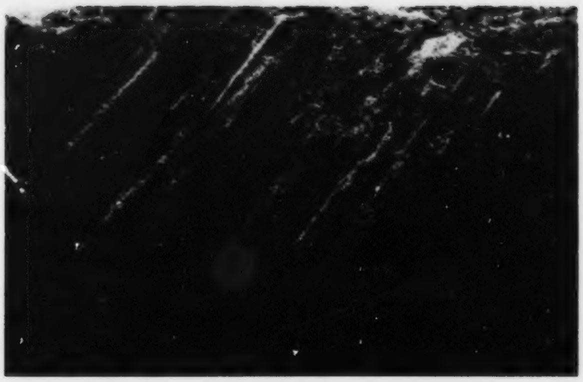

Figure 1.12. *Transverse stretching (L1) lineation defined by rodding of recrystallized quartz and feldspar in transposed basement gneisses. GSC 204233-J.*

Figure 1.13. *Asymmetric D1 fold of transposed basement, consistent with southward top-side-over (left-side-of-photo-down) movement. GSC 204233-E.*

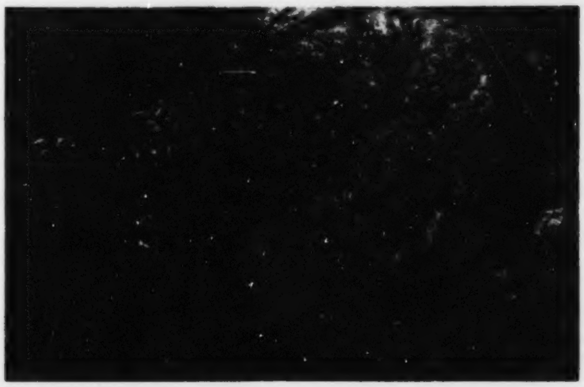

Figure 1.14. *Plagioclase-quartz "smears" defining the transverse stretching lineation in metabasites. GSC 204232-N.*

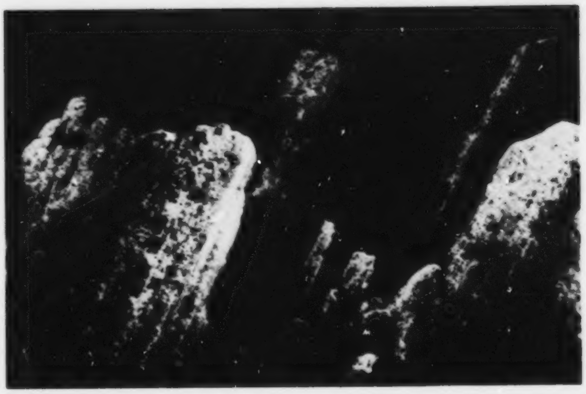

Figure 1.15. Quartz-"smears" defining the transverse stretching lineation in metasediments. GSC 204233-C.

Figure 1.16. D1 fold hinge in micaceous quartzite with axial-planar syn-metamorphic S1 schistosity (arrow). GSC 204232-R.

Figure 1.17. Late D1 thrust with Archean tonalite gneisses B on hanging wall and Proterozoic cover units C on footwall. GSC 204232-M.

this conclusion will be tested by microscopic examination of transposed basement samples in varying orientations, since evidence for non-coaxial strain and kinematic indicators should be found in the XZ plane (X>Y>Z) of the finite strain ellipsoid.

Proterozoic cover rocks in the basal shear zone show a variety of fabric elements and structural features indicative of high shear strains accommodated by continuous ductile strain. In orthoquartzites of formation 4, an inferred mylonitic foliation (by comparison with mesoscopically undeformed orthoquartzites at the same stratigraphic interval at higher structural levels) is developed. The highly strained quartzites are aphanitic suggesting complete recrystallization, contain quartz ribbons developed from vein material, and have a well developed transverse "quartz-smear" stretching lineation developed in S1 planes. Metabasites of formations 2, 4 and 5 are also L-S tectonites, with stretching lineations, defined by aligned metamorphic hornblende and/or actinolite and plagioclase-quartz smears, contained in synmetamorphic (S1) schistosity planes (Fig. 1.14). Other metasedimentary lithologies in the basal shear zone also contain transverse stretching lineations, defined by quartz smearing (Fig. 1.15) in synmetamorphic foliation planes that are axial planar to F1 folds of bedding (Fig. 1.16). The stretching lineations developed in the Proterozoic rocks are coaxial with the Proterozoic lineation in the transposed basement zones.

The basal shear zone, as described above, systematically decreases in thickness from north to south. This southward thinning is attributed to increasingly more displacement being accommodated at higher structural levels by discrete thrust faults, imbricating the early Proterozoic cover units.

Basement-involved thrusting

South of Laflau River (Fig. 1.1) at the east end of the belt, basement is thrusted on cover (Fig. 1.17). At the base of the thrusted basement, Archean gneisses are transposed with muscovite and garnet occurring in the S1 schistosity. Since the thrust carries not only basement units but also the basal shear zone of the belt and yet is characterized by metamorphic mineral growth, it is interpreted as late D1 in age. A similar fault, also associated with gneiss transposition and metamorphic mineral growth, has thrust basement on cover and offsets the basal shear zone in one of the Proterozoic outliers north of Laflau River. It is speculated that these late D1 faults developed after movement on the basal décollement had ceased, thus coupling the deformed cover and basement, but before north-south horizontal compression had abated.

D1 strain: low and high structural levels

As described in the previous section, a penetrative synmetamorphic S1 schistosity is well developed in all the units involved in the basal shear zone. This schistosity, which is in general parallel to bedding and axial planar to tight F1 folds, contains everywhere a well developed L1 transverse lineation (Fig. 1.18). Locally mesoscopic sheath folds can be identified within the basal shear zone. Bulk strain is thus high, and corroborated by the complete transposition of pre-existing fabrics in the basement gneisses within the basal shear zone.

At the higher structural levels, the strain state of all rock units is significantly lower. The penetrative synmetamorphic (S1) schistosity is no longer present in the more competent units such as gabbro or peridotite sills or thick quartzite beds, in contrast to lower structural levels. In the metasediments, an S1 slaty cleavage is well developed

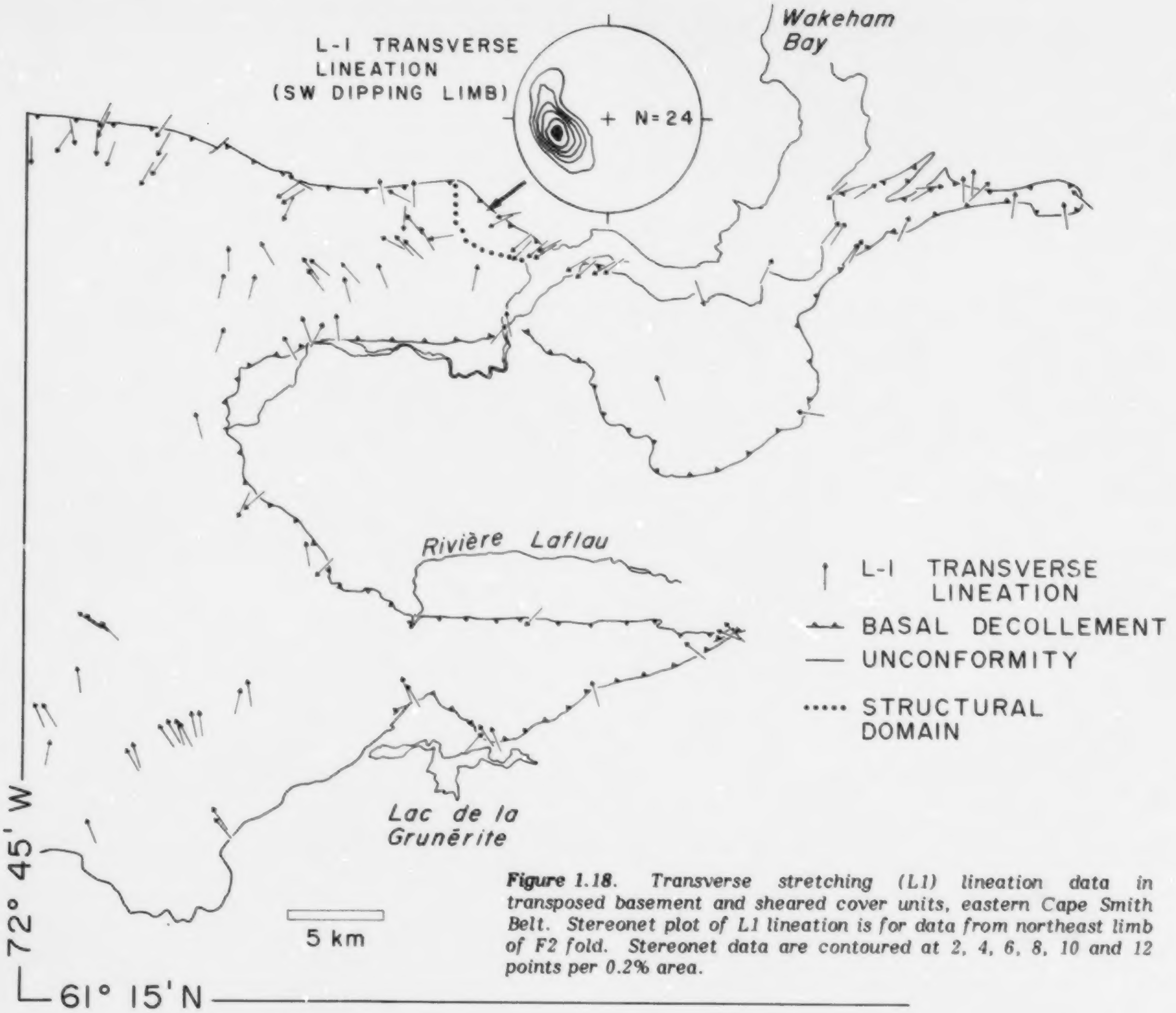

Figure 1.18. Transverse stretching (L1) lineation data in transposed basement and sheared cover units, eastern Cape Smith Belt. Stereonet plot of L1 lineation is for data from northeast limb of F2 fold. Stereonet data are contoured at 2, 4, 6, 8, 10 and 12 points per 0.2% area.

in the semi-pelitic layers but corresponds only to a weak spaced-cleavage in the more quartz-rich beds. In both cases, S1 is no longer parallel to bedding (Fig. 1.19) and refracts on passing between semi-pelite and quartzite layers. Round millimetre-size detrital quartz grains in higher structural level quartzites contrast with previously described aphanitic quartzites in the basal shear zone at the same stratigraphic position, providing a basis for concluding that the lower quartzites experienced strain-induced grain size reduction. A qualitative manifestation at the macroscopic scale of the contrast in bulk strain between low and high structural levels is the map pattern of peridotite sills (Fig. 1.8). A large layered gabbro-peridotite sill within the basal shear zone in the Wakeham River area is boudinaged into over 12 discrete blocks to which the S1 schistosity is largely conformable (Fig. 1.8b). In contrast, at the highest structural level mapped, similar layered gabbro-peridotite sills also emplaced in metasediments remain continuous (Fig. 1.8a) and relatively undeformed. If the deformation in the basal shear zone approximates simple shear with bedding as the shear plane, the sill in Figure 1.8b must have been initially oblique to bedding. Given that the sill now records close to 100%

Figure 1.19. Bedding S-0 and non-bedding-parallel, refracted D1 tectonic fabric S-1 in quartzites and semi-pelites of formation 4 (high structural levels). GSC 204233-B.

extension, and that its initial angle to bedding was probably small, high shear strains are implied for at least the lower section of the basal shear zone.

Late to postmetamorphic D2 structures

The present map pattern of the eastern Cape Smith Belt is in large part dominated by two westward-plunging macroscopic synforms of Proterozoic cover and one median basement-cored antiform (Fig. 1.1). Preliminary results from gravity modelling over the central part of the Cape Smith Belt in the Nuvilik Lake area indicates that the same first-order "W"-shaped basement fold-profile continues westward at least 50 km (T. Feininger, personal communication, 1985).

The macroscopic folds fold the basal shear zone, individual discrete thrusts (Fig. 1.1) and metamorphic isograds (Fig. 1.20). The formation of these folds clearly postdates the establishment of the D1 structures and therefore are considered as D2.

At a mesoscopic scale, the D2 folding is characterized by chevron folds (F2) of the synmetamorphic (S1) fabric in volcanogenic metasediments, metabasites and phyllosilicate-rich siliciclastic metasediments. F2 mesoscopic folds in quartzites, carbonates and transposed basement have a more rounded profile and are approximately parallel. On an outcrop scale, the F2 mesoscopic folds are demonstrably non-cylindrical and occur in fold trains continuous at outcrop scale and generally disharmonic between mechanically distinct units. The F2 minor folds are coaxial with the first order cover rock synclines (Fig. 1.21) and approximately coaxial with F1 folds.

The F2 folds are characterized by a marked limb asymmetry, ubiquitous development of crenulation microfolds in phyllosilicate- and amphibole-rich lithologies and by the sporadic development of a spaced pressure solution crenulation cleavage along steep microfold limbs (Fig. 1.22). Very rarely, a spaced cleavage defined by the alignment of biotite has been found axial planar to the F2 folds. If this is not solely due to mechanical rotation of biotite, it would suggest a late-metamorphic development for these folds. The F2 folds are easily distinguished from the everywhere tight to isoclinal F1 folds of bedding. Locally F1 folds can be seen refolded by the more open F2 folds (Fig. 1.23) resulting in mesoscopic Type 3 fold interference patterns (Ramsay, 1967).

In the northern macroscopic asymmetric D2 synform exposed at the northeast end of the belt, the well-developed mesoscopic F2 folds have in general different limb asymmetries on opposite limbs, with both asymmetries indicating relative movement of cover rocks off the basement-covered antiforms and into the pinched cover rock synforms. The amplitude of the basement antiforms may have been enhanced by buoyant rise of basement gneisses in the antiforms and consequent sinking of the Proterozoic allochthons in the synforms as a result of the gravitational instability set up by thrusting of relatively dense mafic-ultramafic sheets on a less dense tonalitic basement.

However, in the northern synform the change in limb asymmetry does not occur at the hinge (Fig. 1.21). The pattern of mesoscopic F2 folds on the limbs of the median antiform is not clearly related to the first-order F2 fold geometry; the mesoscopic F2 folds are all north-facing asymmetric structures except in a narrow zone on its southern limb. The present distribution of F2 minor folds suggests that initial first order F2 folds were probably modified by subsequent development of smaller wavelength folds coaxial with the initial F2 folds. Further work is required to completely understand the nature of the D2 deformation.

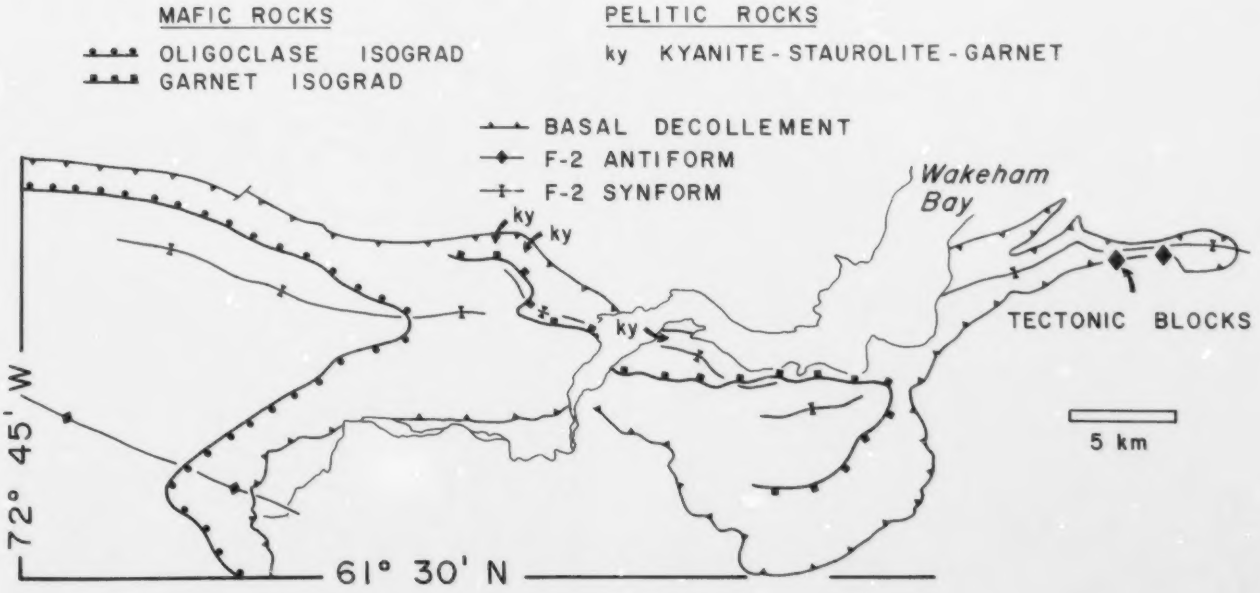

Figure 1.20. Mineral isograds and macroscopic F2 fold hinges, showing a normal (hot-side-down) metamorphic pattern for the eastern Cape Smith Belt. Oligoclase isograd is from Schimann (1978).

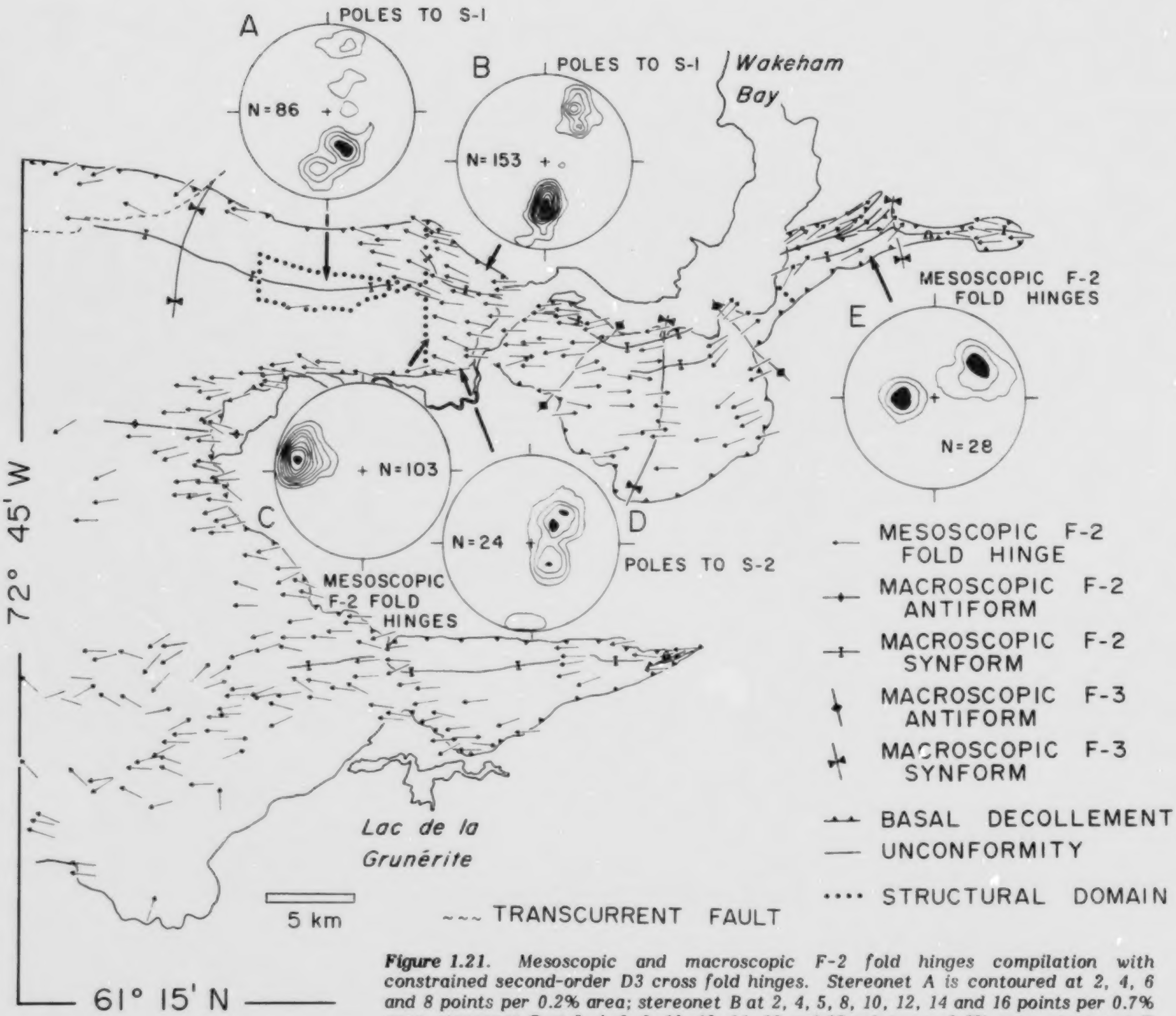

Figure 1.21. *Mesoscopic and macroscopic F-2 fold hinges compilation with constrained second-order D3 cross fold hinges. Stereonet A is contoured at 2, 4, 6 and 8 points per 0.2% area; stereonet B at 2, 4, 5, 8, 10, 12, 14 and 16 points per 0.7% area; stereonet C at 2, 4, 6, 8, 10, 12, 14, 16 and 18 points per 0.6% area; stereonet D at 2, 4, 6 and 8 points per 0.2% area; and stereonet E at 2, 4 and 6 points per 0.6% area.*

Figure 1.22. *North-facing F2 fold of synmetamorphic S1 schistosity S-1 with axial planar S2 spaced dissolution cleavage S-2. GSC 204232-U.*

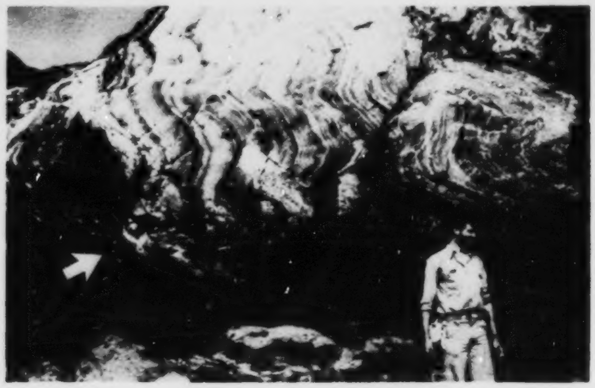

Figure 1.23. *North-facing mesoscopic F2 folds of quartzite on north-dipping limb of macroscopic basement-cored F2 fold. Arrow points to refolded early isoclinal F1 fold. GSC 204233-D.*

Metamorphism

Metabasites

Westra (1978) and in particular Schimann (1978) have shown that the eastern end of the Cape Smith Belt is characterized by greenschist to amphibolite facies mineral assemblages in mafic rocks. In the Wakeham Bay area, an isograd based on the first occurrence of garnet in metabasites of appropriate composition was mapped (Fig. 1.20). Above the isograd, diopside can occur instead of garnet, depending on the Fe/Mg ratio of the upper amphibolite facies rocks. The map trace of the garnet isograd (Fig. 1.20) indicates that it is folded by a postmetamorphic peak D2 macroscopic fold and that the isograd is hot-side-down or normal.

Also shown in Figure 1.20 is an isograd based on the albite-oligoclase transition, as determined in thin section by Schimann (1978). This isograd corresponds to the upper stability of actinolite + hornblende and to the boundary between transitional-greenschist-amphibolite and amphibolite facies in metabasites. West of this isograd, the amount of hornblende progressively decreases in the metabasites, but remains part of the mafic assemblages to the limit of the 1985 mapping.

Metapelites

Thin 1-5 m layers of metapelitic schist occur on the northern margin of the belt in the Wakeham Bay area in formation 4. The metapelites are characterized by a spectacular kyanite-staurolite-garnet-muscovite-biotite-plagioclase-quartz assemblage and field observations indicate that the garnets are poikiloblastic. The assemblage (plus H_2O) is univariant in the seven component system SiO_2-Al_2O_3-FeO-MgO-Na_2O-K_2O-H_2O and indicates metamorphic temperatures of 550-570°C and pressures of more than 5.5 kb (Fig. 1.24).

Tectonic blocks

The lower part of the basal shear zone, at or near the basal décollement (the basement-cover tectonic contact) is locally characterized (Fig. 1.20) by ultramafic tectonic blocks. The blocks are elliptical, vary in size from 0.5 m to just over 1.0 m and are sandwiched by transposed basement gneisses on the lower side and sheared semi-pelite cover on the top side or within highly strained semi-pelites a few metres above the basement-cover contact. The tectonic blocks seem to consist mostly of the assemblage actinolite-anthophyllite-enstatite(?)-carbonate. The assemblage is unlike that of the meta-periodotite sills found in formations 2, 6 and 7 which seems to be mostly diopside-serpentine-tremolite-carbonate. Thin section work is required to corroborate the exotic nature of the tectonic blocks at or near the basal décollement in the basal shear zone.

D3 cross folds

Macroscopic northerly trending (D3) cross folds affect both basement and cover units in the eastern Cape Smith Belt. These folds are developed on the west-dipping flank of a first order long wavelength D3 fold, considered to be responsible for exposing basement units continuously from south margin to north margin in the Wakeham Bay – Grunérite Lake area (Fig. 1.1). The macroscopic D3 second order cross folds occur to the south of Wakeham Bay in a fold train with wavelengths of 10 to 20 km. These folds hinges are accurately constrained by the reversal in plunge azimuths of the D2 mesoscopic fold hinges (Fig. 1.21). The interference of F2 and F3 folds has produced a map scale type I interference pattern (Ramsay, 1967) in the northern synform.

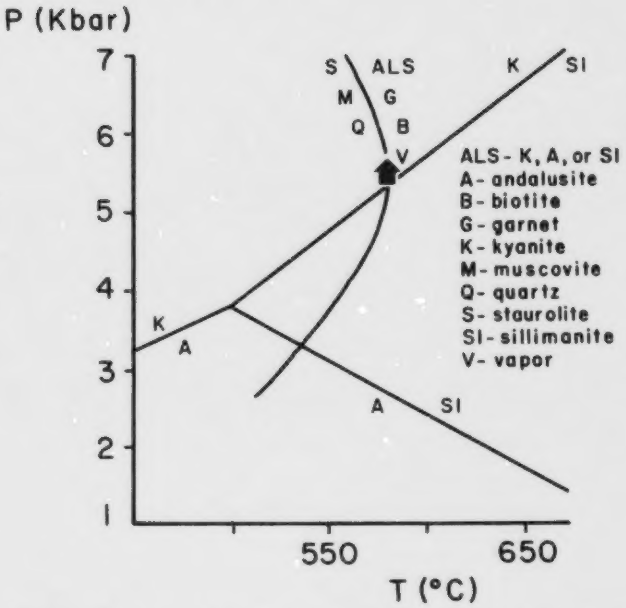

Figure 1.24. *Part of the P-T petrogenetic grid for pelites for the system SiO_2-Al_2O_3-FeO-MgO-Na_2O-K_2O-H_2O showing the staurolite-muscovite breakdown-curve and the Al_2SiO_5 phase diagram (for references see St-Onge, 1984).*

The oblique sections of the Cape Smith Belt resulting from the D3 cross folds correspond to a minimum of 12 km of structural relief. With continued mapping to the west, to document the stratigraphy, structure and metamorphism at anticipated higher structural levels and by making full use of the D3 related cumulative structural relief, it should be possible to construct a rigourous down-plunge cross-section of the eastern end of the Cape Smith Belt. This in effect will provide a unique, detailed profile of a mafic-volcanic-dominated thrust-fold belt, from amphibolite grade at low structural levels where layer parallel shear has produced a basal high strain zone containing several slip discontinuities, including the basal décollement at the exposed basement-cover interface, to greenschist grade higher structural levels where the bulk strain is accommodated by slip on discrete thrust faults and by development of pressure solution cleavages in incompetent lithologies.

Acknowledgments

It is our great pleasure to salute Janien Schwarz who managed to deal with the cooking needs of a crew of ten and still smile in the end. We are grateful to Daniel Lamothe (MER-Québec) for the exchange of scientific ideas during and after the summer. We thank Charlie Arngak, President of the Corporation of the Northern Village of Kangiqsujuak for his help among the ice flows of Wakeham Bay and Mark Tertiak for his hospitality in town. Finally our thanks to Peter Horsman of Trans-Québec Helicopters, Gaéthan Roby and Ken Stirmey of Air Inuit for co-operation with logistics.

Paul Hoffman, Rein Tirrul, Maurice Lambert and Simon Hanmer are gratefully acknowledged for critically reading earlier versions of the manuscript. SBL acknowledges financial support from the American Chemical Society in the form of a Petroleum Research Fund grant.

References

Baragar, W.R.A. and Scoates, R.F.J.
1981: The Circum-Superior belt: a Proterozoic plate margin?; in Precambrian Plate Tectonics, ed. A. Kroener, Elsevier, Amsterdam, p. 297-330.

Beall, G.H.
1959: Preliminary report on the Cross Lake area, New Québec; Québec Department of Mines, Preliminary Report 396, p. 9.

1960: Preliminary report on the La flamme Lake area, New Québec; Québec Department of Mines, Preliminary Report 435.

Bergeron, R.
1959: Povungnituk Range area, New Québec; Québec Department of Mines, Preliminary Report 392, p. 9.

Boyer, S.E. and Elliot, D.
1982: Thrust systems; Bulletin of the American Association of Petroleum Geologists, v. 66, p. 1196-1230.

Butler, R.W.H.
1982: The terminology of structures in thrust belts; Journal of Structural Geology, v. 4, No. 3, p. 239.

Cobbold, P.R. and Quinquis, H.
1980: Development of sheath folds in shear regimes; Journal of Structural Geology, v. 2, No. 12, p. 119-126.

De Montigny, P.A.
1959: Preliminary report on the upper Deception River area, New Québec; Québec Department of Mines, Preliminary Report 398, p. 8.

Doig, R.
1983: Rb-Sr isotopic study of Archean gneisses north of Ungava, Québec; Canadian Journal of Earth Sciences, v. 20, p. 821-829.

Francis, D., Ludden, J., and Hynes, A.
1983: Magma evolution in a Proterozoic rifting environment; Journal of Petrology, v. 24, Part 4, p. 556-582.

Gélinas, L.
1962: Watts Lake area, New Québec; Québec Department of Natural Resources, Preliminary Report 471.

Gold, D.P.
1962: Preliminary report on Lake Brisbois area, New Québec; Québec Department of Natural Resources, Preliminary Report 470.

Hoffman, P.F.
1985: Is the Cape Smith Belt (northern Québec) a klippe?; Canadian Journal of Earth Sciences, v. 22, p. 1361-1369.

Hynes, A. and Francis, D.M.
1982: A transect of the early Proterozoic Cape Smith foldbelt, New Québec; Tectonophysics, v. 88, p. 23-59.

Johnson, A.M.
1980: Folding and faulting of strain-hardening sedimentary rocks; Tectonophysics, v. 62, p. 251-278.

Lamothe, D., Picard, C., and Moorhead, J.
1984: Région du Lac Beauparlant, Bande de Cap Smith-Maricourt, Nouveau Québec; Ministère de l'Énergie et des Ressources, Québec, DP 84-39, scale 1:50 000.

Price, R.A.
1981: The Cordilleran Foreland thrust and fold belt in the southern Canadian Rocky Mountains; in Thrust and Nappe Tectonics, ed. K. McClay and N.J. Price, Geological Society of London Special Publication v. 9, p. 427-448.

Ramsay, J.G.
1967: Folding and fracturing of rocks; in McGraw-Hill, New York, p. 555.

1981: Tectonics of the Helvetic Nappes; in Thrust and Nappe Tectonics, ed. K. McClay and N.J. Price, Geological Association of London Special Publication, v. 9, p. 293-304.

Ramsay, J.G., Casey, M., and Kligfield, R.
1983: Role of shear in development of the Helvetic fold-thrust belt of Switzerland; Geology, v. 11, p. 439-442.

Sanderson, D.J.
1979: The transition from upright to recumbent folding in the Variscan fold belt of southwest England: a model based on the kinematics of simple shear; Journal of Structural Geology, v. 1, No. 3, p. 171-180.

Schimann, K.
1978: On regional metamorphism in the Wakeham Bay area, New Québec; in Metamorphism in the Canadian Shield, ed. J.A. Fraser and W.W. Heywood, Geological Survey Canada, Paper 78-10, p. 245-248.

St-Onge, M.R.
1984: The muscovite-melt bathograd and low-P isograd suites in north-central Wopmay Orogen, Northwest Territories, Canada; Journal of Metamorphic Geology, v. 2, p. 315-326.

Suppe, J.
1983: Geometry and kinematics of fault-bend folding; American Journal of Sciences v. 283, p. 648-721.

Taylor, F.C.
1982: Reconnaissance geology of a part of the Canadian Shield, northern Québec and Northwest Territories; Geological Survey of Canada, Memoir 399, 32 p.

Taylor, F.C. and Loveridge, W.D.
1981: A Rb-Sr study of a new Québec Archean granodiorite; in Current Research, Geological Survey of Canada, Paper 81-1C, p. 105-106.

Tirrul, R.
1985: Nappes in the Kilohigok Basin and their relation to the Thelon Tectonic Zone, District of Mackenzie; in Current Research, Geological Survey of Canada, Paper 85-1A, p. 407-420.

Westra, L.
1978: Metamorphism in the Cape Smith – Wakeham Bay area north of 61°N, New Québec; in Metamorphism of the Canadian Shield, Geological Survey of Canada, Paper 78-10, p. 237-244.

Zindler, A.
1981: Nd and Sr isotope studies of komatiites and related rocks; in Komatiites, ed. N.T. Arndt and E.C. Nisbet, Allen and Unwin, London, p. 399-420.

Geology of the Linda volcanogenic massive sulphide deposit, Snow Lake, Manitoba

Project 830014

Eva Zaleski [1]
Precambrian Geology Division

Zaleski, E., Geology of the Linda volcanogenic massive sulphide deposit, Snow Lake, Manitoba; in Current Research, Part A, Geological Survey of Canada, Paper 86-1A, p. 15-20, 1986.

Abstract

The Linda deposit is hosted by felsic volcanic rocks on the overturned limb of the Anderson Bay anticline. Volcanic rocks, hosting the Rod, Stall Lake and Anderson Lake deposits, on the northwest limb of the anticline are proposed to be lateral equivalents. At the Linda deposit, two synvolcanic alteration zones stratigraphically underlie the main pyritic body. A proximal, dominantly sericitic alteration zone, discordant to stratigraphy, occurs directly beneath the pyritic body and envelops subsidiary sulphide lenses and stringer mineralization. A distal, subconcordant, dominantly chloritic alteration zone underlies the proximal alteration as well as apparently unaltered felsic volcanic rocks. During regional metamorphism, the altered rocks were recrystallized to metamorphic assemblages which include staurolite, kyanite, magnetite, biotite, gahnite and garnet. Regional deformation resulted in a complex structure and overturned stratigraphy. Comparison with other deposits in the area suggests that the proximal alteration represents a pipe which was the locus of upwelling hydrothermal fluids, and that the distal alteration zone occurs in a reservoir rock of regional significance.

Résumé

Le gisement de Linda est encaissé dans des roches volcaniques felsiques sur le flanc retourné de l'anticlinal d'Anderson Bay. Des roches volcaniques contenant les gisements de Rod, de Stall Lake et d'Anderson Lake sur le flanc nord-ouest de l'anticlinal seraient des équivalents latéraux de ce gisement. Au gisement de Linda, deux zones d'altération synvolcanique sont stratigraphiquement sous-jacentes à la principale masse pyriteuse. Une zone d'altération proximale, de nature surtout séricíteuse et stratigraphiquement discordante, se manifeste directement sous la masse pyriteuse et entoure des lentilles secondaires de sulfure et des veinules minéralées. Une zone d'altération distale subconcordante, de nature surtout chloritique, repose sous la zone d'altération proximale et sous des roches volcaniques felsiques apparemment non altérées. Au cours d'un épisode de métamorphisme régional, les roches altérées ont été recristallisées en associations métamorphiques composées de staurolite, de cyanite, de magnétite, de biotite, de gahnite et de grenat. La déformation régionale a produit une structure complexe et une stratigraphie inversée. Une comparaison avec d'autres gisements dans la région semble indiquer que l'altération proximale correspond à une cheminée par où montaient des fluides hydrothermaux et que la zone d'altération distale se trouve dans une roche réservoir d'importance régionale.

[1] Department of Earth Sciences, University of Manitoba, Winnipeg, Manitoba R3T 2N2

Introduction

The Linda volcanogenic massive sulphide deposit is located within the Flin Flon-Snow Lake greenstone belt in the Churchill Province of the Canadian Shield (Figure 2.1). The belt is flanked on the north by the Kisseynew sedimentary gneiss belt and overlain to the south by Paleozoic sediments. Other economic and subeconomic massive sulphide deposits occur within the greenstone belt; those in the Snow Lake area include the Stall Lake, Rod, Anderson Lake, Ghost Lake/Lost Lake and Chisel Lake deposits, all currently producing Cu-Zn ore.

The deposit discussed in this paper has been designated as Linda II by Corporation Falconbridge Copper to distinguish it from Linda I, a deposit 1.3 km north of Linda II. The Linda I deposit is shown on the map of Froese and Moore (1980).

The Linda deposit was extensively drilled by Corporation Falconbridge Copper (CFC), mainly from 1978-1981. Core from drillholes, defining three composite cross-sections of the sulphide body and associated alteration has been examined and sampled by the author. This report incorporates data, maps, compilations and interpretations previously made by Corporation Falconbridge Copper geologists.

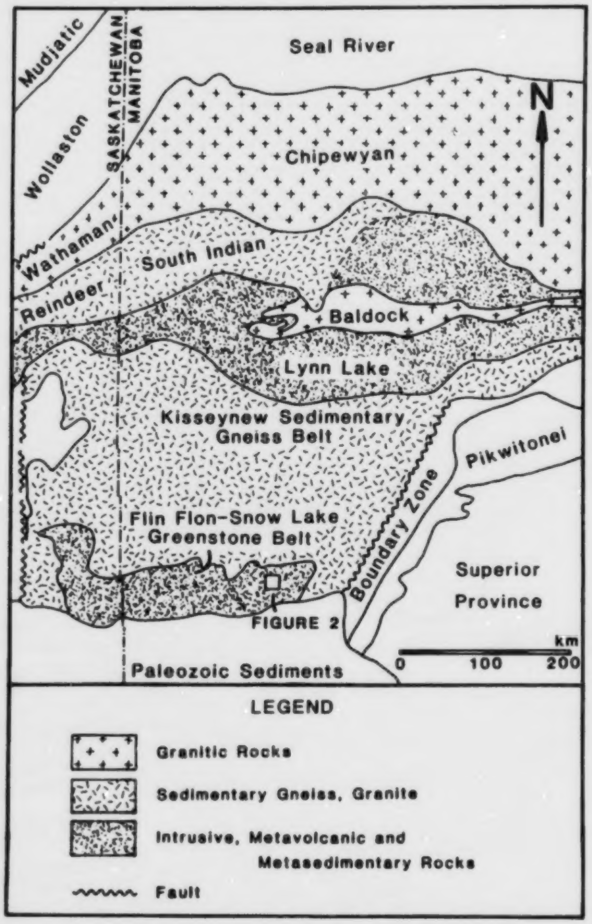

Figure 2.1. *Location of the Snow Lake area (Figure 2.2) in the Flin Flon-Snow Lake greenstone belt. Major tectonic subdivisions of Proterozoic age in the Churchill Province are ornamented. Adapted from Lenton (1981).*

General geology

Froese and Moore (1980) discussed the geology, structure and metamorphism of the Snow Lake area. Metavolcanic rocks of the Amisk Group, ranging from mafic to felsic in compostion, host the massive sulphide bodies and alteration zones (Figure 2.2). The Amisk Group also includes greywacke and shale, commonly overlying volcanic rocks. An intrusion of quartz-eye tonalite was interpreted as a synvolvanic sill (Walford and Franklin, 1982). Younger Missi Group metasediments, consisting of crossbedded lithic arenites, were deposited on Amisk Group rocks.

Three main deformational events were proposed by Froese and Moore (1980). Tight to nearly isoclinal F1 folding produced the earliest recognizable folds. The S1 schistosity, axial planar to F1 folds, is defined by mineral alignment and flattening of fragments subparallel to compositional layering. Possible L1 lineation is apparently subparallel to, and not distinguishable from, later L2 lineation. In the vicinity of Anderson and Stall lakes, F2 folding produced open northeasterly trending warps (Southeast Bay antiform, Whitefish Bay synform). S1 schistosity is commonly folded, but biotite in felsic volcanic rocks tends to be reoriented parallel to F2 axial planes. Numerous folds on all scales, and intense crenulation of alteration zone schists, were attributed to F2 folding. The prominent northeasterly plunging elongation of massive sulphide bodies was thought to be an expression of L2 lineation. D3 deformation mainly influenced the northern part of the area with the emplacement of gneiss domes and the tightening of F2 folds adjacent to the domes.

An early deformed thrust fault, the McLeod Road fault, was postulated to account for older Amisk volcanic rocks overlying younger Amisk and Missi sediments. The late Berry Creek fault forms a topographic lineament west of Wekusko Lake, but its eastward extension is obscure.

Metamorphic zones, showing the transition from the low-grade greenstone terrane in the south to the high-grade terrane of the Kisseynew gneiss belt, were recognized by Froese and Gasparrini (1975) and Froese and Moore (1980). Three isograds delineate the boundaries of four metamorphic zones characterized by the mineral assemblages: chlorite-biotite, chlorite-biotite-staurolite, biotite-staurolite-sillimanite, and biotite-sillimanite-almandine. Conditions of peak metamorphism were attained after the occurrence of most of the D2 deformation; this is reflected in the discordant position of the isograds relative to regional structure. The surface projection of the Linda deposit lies within the chlorite-biotite-staurolite zone.

Geology of the Linda deposit

The sulphide mineralization and alteration, associated with the Linda deposit, occur in Amisk volcanic and volcaniclastic rocks with very minor amounts of intercalated fine grained graphitic sediment. Northeasterly trends are due to structural transposition of primary structures and to superposition of D1 and D2 planar and linear fabrics. Primary layering strikes 40°-75° and dips 55°-70° northwest. The Linda deposit lies on the overturned flank of the F1 Anderson Bay anticline and on the eastern limb of the F2 Whitefish Bay synform (Figure 2.2). The inverted morphology of the deposit provides the evidence for the anticlinal closure, i.e. stringer sulphide zones and alteration zones overlie the massive sulphide body in its present configuration (Figure 2.3) and require stratigraphic topping to the southeast. Northwesterly topping directions from pillow basalts south of Anderson Creek indicate that the trace of the anticlinal axis passes through Anderson Bay (Jeffery, 1982). Mapping by Falconbridge geologists does not support the F1 fold (Anderson Lake anticline) shown south of Stall Lake by Froese and Moore (1980).

The Linda deposit and its alteration zones are hosted by felsic volcanic rocks, and the main massive sulphide body is closely associated with a quartz-phyric unit informally referred to as quartz porphyry. Falconbridge geologists tentatively correlated this unit with the quartz-phyric felsic rocks which host the Rod, Stall Lake and Anderson Lake deposits (Jeffery, 1982) on the northwestern flank of the Anderson Bay anticline (Figure 2.2).

Descriptions of units (Figure 2.3)

In the immediate vicinity of the Linda deposit, exposure is generally poor and neither the deposit, nor its associated alteration, outcrops on surface. The definition of both surface and subsurface stratigraphy and morphology has mainly depended on the interpretation and projection of drill core data. The rock units have been based on megascopic examination of core, and the rock names are intended as general field terms.

Unit 1: felsic volcanic and volcaniclastic rocks

The unit may include rocks of rhyolitic to dacitic affinity. Biotite is the most abundant ferromagnesian mineral, usually occurring in thin 0.1-1 mm layers at 0.5-10 mm intervals. The compositional layering variably has a planar or a lensoid anastomosing character, and the biotite shows a strong foliation oriented at an oblique angle to the layering. Some rock specimens are convincingly fragmental with well defined felsic clasts in a more mafic matrix. But contacts commonly are diffuse, making the identification of fragments ambiguous. Garnet, magnetite and amphibole are

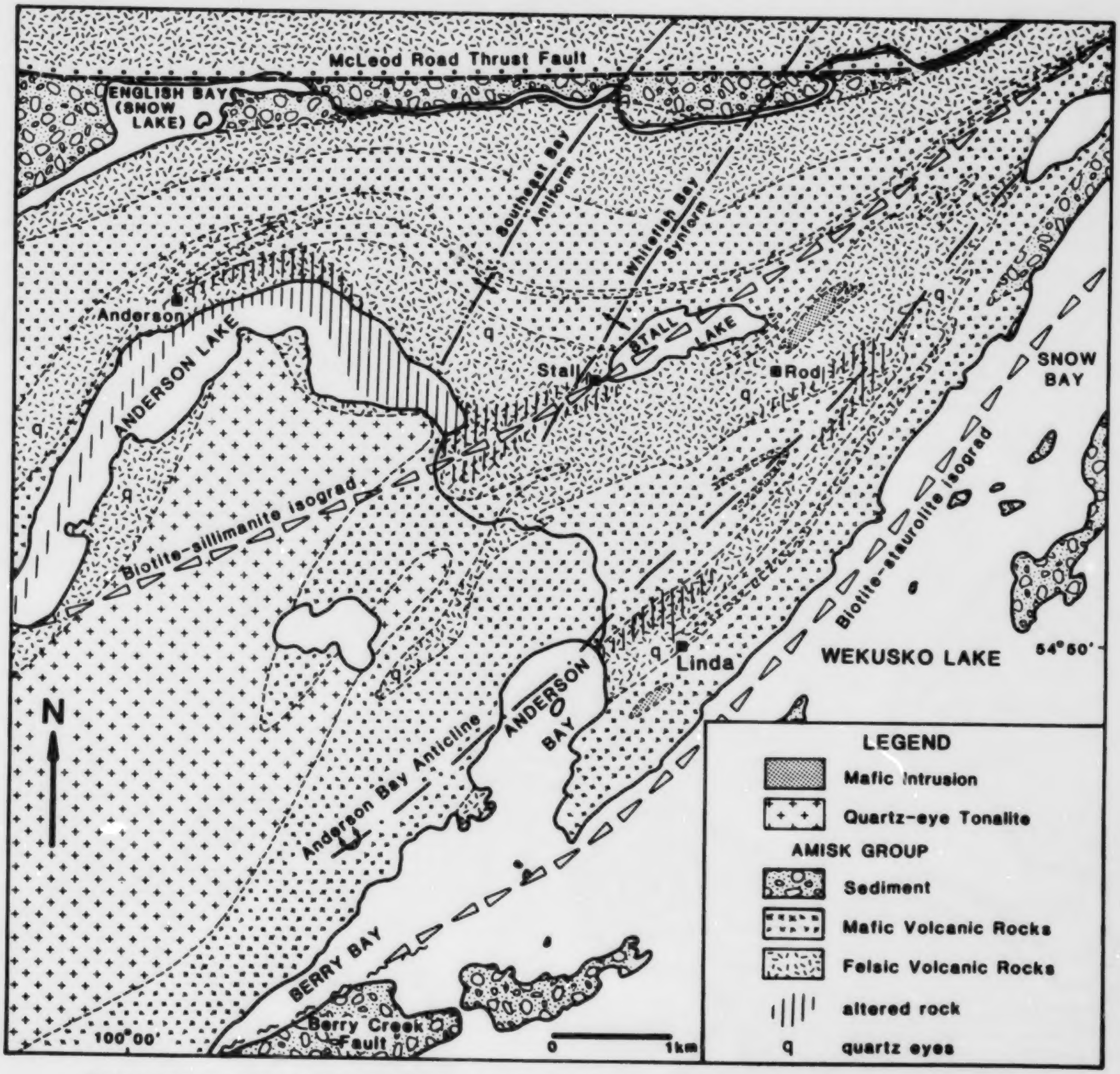

Figure 2.2. Geology of a part of the Snow Lake area in the vicinity of the Linda deposit. Modified from Jeffery (1982) and Froese and Moore (1980).

also found, with amphibole usually restricted to darker, more dacitic rocks. It commonly occurs in acicular clots up to 5 mm in diameter surrounded by a white siliceous corona suggestive of a depletion halo.

1a. Cherty felsic rocks. These are massive or brecciated milky-white to buff coloured, extremely fine grained to aphanitic rocks which occur within sections of felsic volcanic rock. Brecciation is most common adjacent to altered rock and often hosts pyritic stringer mineralization cemented by silica. The fragment margins are mutually conformable and interlocking as a pervasive fracturing or in situ fragmentation. Disseminated euhedral magnetite is sporadically present. The unit may include massive rhyolite and undetermined proportions of silicified basalt (unit 2) and silicified felsic volcanic rocks.

Unit 2: basalt

Hornblende is the most abundant mafic mineral and occurs as small needles defining a strong lineation in typically fine grained massive basalt. The unit has minor coarsely recrystallized variants, with coarse grained acicular hornblende, usually unoriented, growing in either a chloritic or a felsic matrix. Rare curviplanar structures, composed of finer grained, more mafic zones up to 1 cm in width, could be interpreted as pillow selvages.

Unit 3: sediment

Fine grained sediment occurs in lenses of limited lateral extent at two stratigraphic horizons, both within altered felsic volcanic rock. The unit is most commonly fine-bedded, dark, argillaceous, graphitic and abundantly mineralized with pyrite and pyrrhotite.

Unit 4: quartz porphyry

Blue quartz eyes of 3-5 mm diameter in a felsic matrix, generally constitute 5-25% of the rock. Aphyric or weakly porphyritic felsic volcanic rocks are interlayered with quartz-eye porphyry, especially at higher stratigraphic levels. The distinction between units may be ambiguous, due to gradational and rhythmic changes and to alteration. The unit is closely associated with the main massive sulphide body and is commonly altered to a quartz-eye sericite schist.

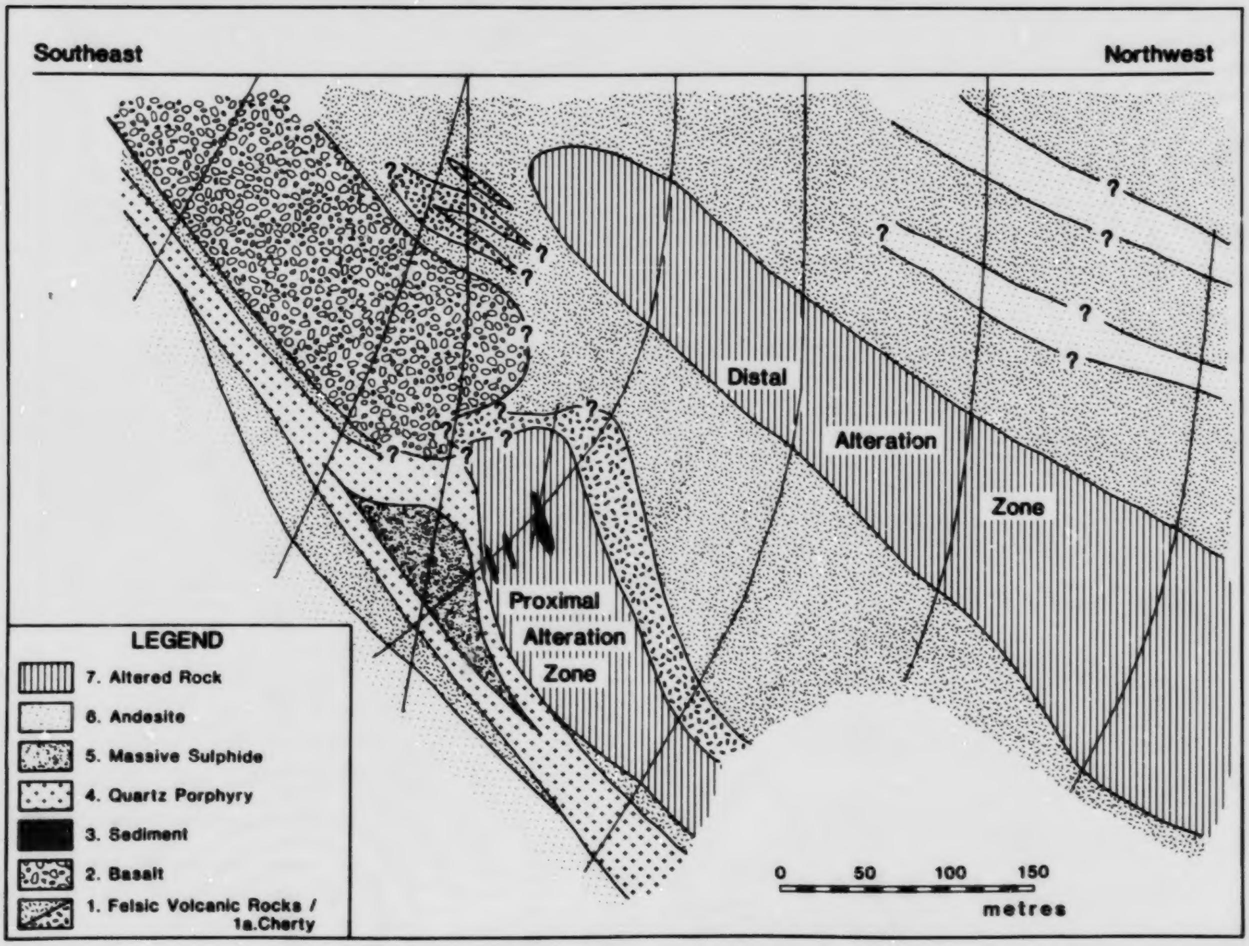

Figure 2.3. Schematic cross-section of the Linda deposit. Ambiguity in the correlation of contacts and rock units is highlighted by question marks. Logged portions of drillholes are shown. Horizontal and vertical scales are equal.

Unit 5: massive sulphide

A massive to semi-massive sulphide body occurs as a concordant thick lens, associated with quartz porphyry (unit 4). Medium- to coarse-grained granular pyrite is intergrown with abundant calcite or quartz. Pyrrhotite, sphalerite and chalcopyrite are present sporadically in minor amounts. Several smaller, less extensive sulphide lenses are associated with stringer and disseminated mineralization stratigraphically underlying the main sulphide body. These subsidiary lenses vary from dominantly pyrite-calcite, to pyrite with minor pyrrhotite-sphalerite-chalcopyrite and silicate alteration minerals.

Unit 6: andesite

Mafic and felsic layers on a scale of 0.5-5 cm constitute most of the unit. The layering in some rocks has a lensoid possibly fragmental aspect, but the contacts are generally diffuse as a result of recrystallization of amphibole to a medium to coarse grain size. Massive variants of the unit are rare. Abundant acicular amphibole, commonly unoriented, is found in a chloritic or a felsic matrix. Some zones also contain abundant biotite. Calcite pervades most of the unit, mainly occurring on partings parallel to the layering.

Unit 7: alteration zones

Two distinct schistose alteration zones have been delineated and are described in detail in a later section. A distal, mainly concordant zone occurs stratigraphically 200-250 m below the sulphide body. A proximal, discordant zone directly underlies the main sulphide body and encompasses the smaller sulphide lenses and the stringer and disseminated mineralization.

Alteration

Altered rocks are characterized by assemblages of metamorphic minerals resulting from regional metamorphism of synvolcanic hydrothermal alteration. Two discrete zones (distal and proximal) have been recognized, both developed in dominantly felsic volcanic rocks (Figure 2.3).

The distal alteration zone stratigraphically underlies the sulphide mineralization and proximal zone and is surrounded by apparently unaltered felsic volcanic rocks. The strike length is approximately 1000 m and the maximum width approximately 250 m. The thickness varies somewhat down-plunge but generally remains subconcordant to structural trends. Strongly deformed quartz veins are abundant and constitute a large proportion of some drillhole intersections over intervals of several metres. Immediately adjacent to veins, porphyroblastic minerals increase in abundance and grain size. The mineralogy of the altered rock is dominated by chlorite, with assemblages including staurolite, kyanite, sericite, magnetite and biotite. Garnet is present in the outer transitional margins of the zone. Hornblende in some rocks is associated with chlorite in more mafic portions, possibly reflecting a basaltic precursor. Sulphide minerals are rarely present in more than trace amounts. Internal zonation of mineral assemblages is not clearly defined and their distribution seems quite variable. Magnetite tends to be limited to more central areas of the zone.

The proximal alteration zone forms the footwall alteration beneath the main sulphide body and envelops minor sulphide lenses, stringer and disseminated mineralization, and mineralized graphitic sediment. Alteration affects felsic volcanic rocks and, to a lesser extent, quartz porphyry. Cherty rocks are common stratigraphically beneath the zone and in some localities recognizable within the zone. Minor sericitic or chloritic alteration extends into hanging wall felsic volcanic rocks and quartz prophyry. Quartz veins are less abundant than in the distal zone. The mineralogy is dominantly sericitic with assemblages including kyanite, staurolite, gahnite, biotite, chlorite, and rarely, magnetite, garnet and fuchsite(?). Internal structure has not been distinguished, and it seems likely that the lateral extent of the core examined has not given a good representation of the cross-sectional morphology. Structural repetition of sulphide lenses and enveloping alteration also cannot be ruled out at this time.

In addition to the two alteration zones, other minor alteration types were observed. Many contacts of basalt (unit 2) are silicified and gradational to cherty felsic rocks (unit 1a), particularly along the stratigraphic upper contact and along the down-dip truncation. Fine grained massive basalt is variably recrystallized to a heterogeneous rock with zones of coarse grained amphibole in a felsic matrix. This grades to fine grained cherty rock containing epidote and amphibole laths and euhedral magnetite. Biotite, garnet, chlorite and pyrrhotite may also be present in the transitional zone. The gradation from fine grained basalt occurs over 5-15 m; the basal finally merges into cherty felsic rock generally indistinguishable from typical cherty zones of unit 1a.

Calc-silicate minerals occur in felsic volcanic rocks mainly on the periphery of the distal alteration zone. Localized patches of up to 1 m in size have diffuse contacts with unaltered volcanic rock and some are associated with quartz veins. Alternatively, calc-silicate minerals occur as incipient alteration parallel to compositional layering. Minerals include epidote, tremolite, calcite and diopside(?), with habits varying from matted fibrous to coarse grained interlocking.

Angular discordant fractures occur sporadically, generally with a fine hairline filling of quartz, carbonate and more rarely hematite. Some fractures are densely distributed forming a network and pervasively altering the host rock.

Structure and morphology

The Linda deposit was subjected to regional deformation resulting in a complex structure. The absence of any well defined marker unit hinders unambiguous interpretation of morphology. In general, only broad rock units, such as felsic, or mafic, volcanic rocks, can be correlated with confidence between drillholes. Many variations are visible within any single drillhole. The main sulphide body has an ellipsoidal shape, exceeding 1500 m in length and plunging in the plane of layering at approximately 30°. Other megascopic structures, such as the elongation of the alteration zones and the down-dip truncation of basalt (unit 2), have comparable plunges. The proximal alteration zone is strongly discordant to the general structural trends, and is developed mainly in a volume directly down-dip of the truncated basalt (Figure 2.3). The distal alteration zone was interpreted as discordant (Jeffery, 1982), but this interpreation is poorly constrained and the zone is better described as subconcordant. The two alteration zones are separated by 75-150 m of unaltered or slightly altered felsic volcanic rocks. Drilling has not defined the down-plunge and down-dip extent of alteration, so that both zones remain open-ended.

Drill core commonly exhibits minor tight folding with a well developed axial planar fabric in felsic rocks, defined by mica and amphibole showing an alignment oblique to the compositional layering. An oblique alignment is commonly observed even in the absence of visible minor folding. In intensely altered rocks, phyllosilicates are strongly schistose,

commonly with a pronounced crenulation fabric. Most altered rocks also exhibit a layered structure, consisting of alternating phyllosilicate layers 1-4 mm in width and felsic layers 2-10 mm in width. The layers are common crenulated or corrugated and the phyllosilicates tend to be oriented parallel to the axial planes of the crenulation fabric. Porphyroblastic minerals such as staurolite, magnetite, kyanite, biotite and garnet occur with random orientations or aligned parallel to phyllosilicates.

Discussion

The structural complexity associated with polyphase regional dynamic metamorphism has been superimposed on the primary stratigraphy complexity of the volcanic terrane hosting the Linda deposit. Unambiguous correlation of individual flows or volcaniclastic units has not generally been possible near the deposit, however, on a regional scale, the stratigraphy is apparently quite continuous (Figure 2.2). In the vicinity of the Linda deposit, basalt (unit 2) pinches out downdip, and, although small scale folds are present sporadically throughout the section, the general continuity of rock units and the lack of major repetition suggests that the basalt does not occupy a fold nose. The silicified gradational contacts and the downdip position of the proximal alteration zone suggest that the basalt may continue downdip, but this would have to be in a completely altered form. This seems unlikely because the graphitic sediments also occur downdip, and some sections suggest the presence of felsic volcanic rocks on the downdip side of the proximal alteration zone. The most probable explanation at this time is the presence of a primary discontinuity such as a synvolcanic fault or a volcanic contact; for example, onlapping of basalt onto a felsic volcanic pile. This also provides an early structural control on the location of the proximal alteration zone. The presence of the graphitic sediment is still enigmatic, suggesting a hiatus in volcanic activity and accumulation in local basins.

The extent and significance of silicification at the Linda deposit remains unevaluated. Walford and Franklin (1982) reported a lack of evidence for silicification at the Anderson Lake mine, but proposed that the abundant quartz veins may reflect silica mobilized during hydrothermal alteration. Outcrops of silicified pillows are found near the Stall Lake mine, and extensive areas of silicified rock occur south of Chisel Lake, west of Anderson Lake (R. Skirrow, personal communication 1985). Given the textural and mineralogical similarity between silicified mafic rock and felsic rock, it may be difficult to recognize silicified rocks, particularly in drill core.

The general disposition of the alteration zones at the Linda deposit is similar to that reported for the Anderson Lake and Stall Lake mines (Walford and Franklin, 1982). Beneath the orebodies, an alteration pipe, hosting stringer mineralization, cuts stratigraphy at an oblique angle. The pipe extends down to intersect a lower conformable alteration zone. Walford and Franklin (1982) interpreted the lower zone as the location of a hydrothermal fluid reservoir of regional extent, intersected by several conduits which allowed fluid uprise and which are now manifested by the discordant alteration pipes. The correlation of stratigraphy as proposed in Figure 2.2 locates the distal alteration zone of the Linda deposit close to the same regional reservoir horizon. The proximal alteration zone of the deposit may represent an alteration pipe, but its intersection with the distal alteration zone has not been documented.

Ackowledgments

Corporation Falconbridge Copper provided access to drill core and to unpublished company reports, and allowed the use of office facilities at Snow Lake. B.D. Simmons and H.F. Keats discussed the Linda deposit and were particularly helpful in outlining the interpretations already arrived at by company geologists after many years of careful work. E. Froese initiated the project and my interest in the topic, and I look forward to many more stimulating conversations with him. J.M. Franklin pointed out analogies to the Anderson Lake mine. N.M. Halden provided guidance and discussion.

References

Coats, C.J.A., Clark, L.A., Buchan, R., and Brummer, J.J.
1970: Geology of the copper-zinc deposits of Stall Lake Mines Ltd., Snow Lake area, N. Manitoba; Economic Geology, v. 65, p. 970-984.

Froese, E. and Gasparrini, E.
1975: Metamorphic zones in the Snow Lake area, Manitoba; Canadian Mineralogist, v. 13, p. 162-167.

Froese, E. and Moore, J.M.
1980: Metamorphism in the Snow Lake area, Manitoba; Geological Survey of Canada, Paper 78-27.

Jeffery, B.D.
1982: Linda-McKayseff properties, Snow Lake, Manitoba; internal evaluation report, Corporation Falconbridge Copper.

Lenton, P.G.
1981: Geology of the McKnight-McCallum Lakes area; Manitoba Department of Energy and Mines, Mineral Resources Division, Geological Report GR 79-1.

Walford, P.C. and Franklin, J.M.
1982: The Anderson Lake mine, Snow Lake, Manitoba; in Precambrian Sulphide Deposits, H.S. Robinson Memorial Volume, ed. R.W. Hutchinson, C.D. Spence and J.M. Franklin, Geological Association of Canada, Special Paper 25, p. 481-523.

- 3 -

Geology of the northwestern metamorphic-internal zone and an outlier of the eastern Great Bear Magmatic Zone of Wopmay Orogen, Big Bend area, District of Mackenzie

Project 850006

J.E. King, M.E. Villeneuve [1], D. Spethmann [2], and K.H. Wilcox [3]
Precambrian Geology Division

King, J.E., Villeneuve, M.E., Spethmann, D., and Wilcox, K.H., Geology of the northwestern metamorphic-internal zone and an outlier of the eastern Great Bear Magmatic Zone of Wopmay Orogen, Big Bend area, District of Mackenzie; in Current Research, Part A, Geological Survey of Canada, Paper 86-1A, p. 21-33, 1986.

Abstract

In the northwestern metamorphic-internal zone of Wopmay Orogen, a severely deformed granitic gneiss containing Archean xenoliths is interpreted to have intrusive contacts with early Proterozoic (initial-rift facies) Akaitcho Group rocks. The Akaitcho Group in the area includes abundant basic flows and sills, semipelite, quartzite and marble that are generally correlative with Akaitcho units elsewhere in the orogen. The Akaitcho Group has been polyfolded and metamorphosed at upper amphibolite facies conditions.

The easternmost strata of the Great Bear Magmatic Zone (Dumas Group) comprise lacustrine to alluvial fan sequences with minor basalts. They are preserved in a north-trending, fault-bounded (?) syncline. These faults, together with nearby mylonite bands, may be a high structural level of the Wopmay Fault Zone.

Well developed breccias which occur in the internal zone below the unconformity of the late Proterozoic Hornby Bay Group are thought to be related to reactivation of a regional set of transcurrent faults. The breccias are associated with intense alteration and minor uranium mineralization.

Résumé

Dans la zone interne métamorphique nord-ouest de l'orogène de Wopmay, un gneiss granitique très déformé contenant des xénolites archéens aurait des contacts intrusifs avec les roches du groupe d'Akaitcho (faciès de la fosse initiale) du Protérozoïque ancien. Dans la région examinée, le groupe d'Akaitcho comprend de nombreux filons-couches et coulées basiques, de la semi-pélite, de la quartzite et du marbre, que l'on peut généralement mettre en corrélation avec les unités de ce groupe ailleurs dans l'orogène. Le groupe d'Akaitcho a été déformé en de nombreux plis et métamorphisé dans des conditions propres au faciès supérieur des amphibolites.

Les couches les plus à l'est de la zone magmatique de Great Bear (groupe de Dumas) comprennent des séquences lacustres et des cônes alluviaux avec de petites quantités de basalte. Ces couches sont conservées dans un synclinal à orientation nord qui est limité par des failles (?). Ces failles, de même que les zones voisines de mylonite, pourraient correspondre à un niveau structural élevé de la zone de failles de Wopmay.

La présence de brèches bien développées qui se manifestent dans la zone interne sous la discordance du groupe tardi-protérozoïque de Hornby Bay serait due à la réactivation de l'ensemble des décrochements régionaux. Ces brèches sont associées à une altération intense et à une faible minéralisation en uranium.

[1] Department of Earth and Planetary Sciences, Washington University, St. Louis, Mo., U.S.A. 63130
[2] Department of Geology, University of Ottawa, Ottawa, Ontario K1N 6N5
[3] Department of Geological Sciences, Queen's University, Kingston, Ontario K7L 3N6

Introduction

In the most northwestern exposed part of the Hepburn Metamorphic-Internal Zone of Wopmay Orogen (McGlynn, 1970; Fraser et al., 1972; Hoffman, 1980), early Proterozoic Akaitcho Group (initial-rift facies) (Easton, 1981b) gneisses and granitic gneisses (in part Archean) are almost entirely isolated from the rest of the internal zone by intervening, post-orogenic rocks of the Hornby Bay Group (Fig. 3.1, 3.2). Although the general geology has been mapped at the 1:100 000 scale (Hoffman, 1984), numerous questions concerning the area arose as work progressed in other parts of the orogen. Some of the questions are: what is the structural and stratigraphic significance of the gneisses which have yielded Archean ages?; is the basement gneiss allochthonous or autochthonous?; is the Akaitcho Group in the Big Bend area correlative with Akaitcho Group units in other areas of known Archean basement?; is the structural style of the Akaitcho Group similar to that farther south where thrust-nappes occur (St-Onge et al., 1982, 1983a, 1984; King, 1985)?; what is the nature of the boundary between the metamorphic-internal zone and the Great Bear Magmatic Zone?; and what is the nature and significance of the Wopmay Fault Zone (Easton, 1981a; St-Onge et al., 1984; King, 1985) and can it be recognized in the area?

In order to answer these questions, detailed mapping (1:25 000 to 1:50 000 scale) of the metamorphic-internal zone north of the Zephyr Fault (Fig. 3.2) was carried out in the latter half of the 1985 field season. A summary of results is as follows:

1. The gneisses dated as being Archean in age (Chamberlain et al., 1984; S.A. Bowring, personal communication) occur as xenoliths within a large, severely deformed body of granitic and amphibolitic gneiss which is interpreted to be intrusive into the Akaitcho Group.
2. The Akaitcho Group in the Big Bend area comprises an intimately mixed assemblage of amphibolite-facies metabasites, semipelite, marble and ironstones which is generally, but not specifically correlative with Akaitcho assemblages elsewhere in the orogen. These units have been affected by an early set of progressively refolded folds, probably recumbent in attitude. These folds are correlated with the main phase of the Calderian Orogeny. Upright, northeast-trending folds of uncertain origin affect all earlier structures.
3. The easternmost strata of the Great Bear Magmatic Zone (Dumas Group) occur in a fault-bounded, synclinal outlier. The stratigraphy of the outlier comprises a coarsening-upwards sequence of lacustrine, fluviatile, then distal-and proximal-alluvial fan deposits. Basaltic flows occur throughout the section. The western boundary fault of the outlier is intruded by Great Bear plutons. An isograd based on a reaction producing chlorite plus muscovite trends across the outlier.
4. The set of north-south trending faults which border the Dumas outlier, together with mylonitic shear zones which affect nearby units, may be the manifestation at a high structural level of late displacement on the Wopmay Fault Zone.
5. Polymictic breccias in the metamorphic-internal zone near the unconformable contact with the post-orogenic Hornby Bay Group (Bigbear fluvial system) are thought to be related to late reactivation of a regional set of transcurrent faults. Pronounced hydrothermal alteration and minor uranium mineralization has occurred along many of the fault surfaces. These breccias are very similar to breccias at the base of the Athabasca Basin.

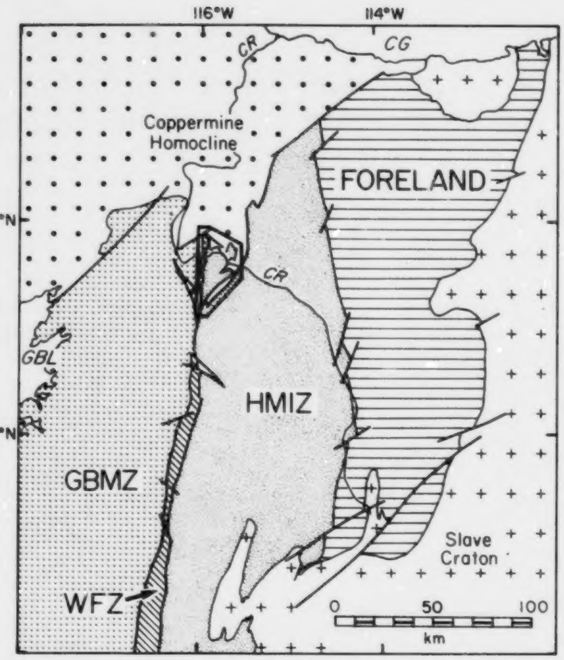

Figure 3.1. *General location map with the tectonic zones of Wopmay Orogen (after Hoffman and Bowring, 1984). Area covered by Figure 3.2 (Big Bend area) is outlined. GBMZ - Great Bear Magmatic Zone; HMIZ - Hepburn Metamorphic Internal Zone; WFZ - Wopmay Fault Zone. Bodies of water: CG - Coronation Gulf; CR - Coppermine River; GBL - Great Bear Lake.*

Previous Work

General stratigraphic relationships pertaining to the Big Bend area are presented by Hoffman (1978, 1980, 1984). Granitic gneisses which underlie much of the area (Fig. 3.2) were initially considered to be part of the composite Wentzel Batholith of the early Proterozoic (1.89-1.88 Ga) Hepburn Intrusive Suite (Hoffman et al., 1980), but were later interpreted to be part of a basement complex (Hoffman, 1984) on the basis of Archean (2.9-2.5 Ga) U-Pb (zircon) ages (Chamberlain et al., 1984; S.A. Bowring, personal communication, 1984). The granitic gneisses are flanked by an assemblage of amphibolite-grade metasediments and metabasic units is correlated with the ca. 1.9 Ga (Hoffman and Bowring, 1984; S.A. Bowring, personal communication, 1984) Akaitcho Group (Easton, 1981b, 1982) which was deformed during the ca. 1885 Ma Calderian Orogeny (Hoffman and Bowring, 1983; St-Onge et al., 1983b).

Greenschist-facies metasedimentary and calc-alkaline metavolcanic units of the Dumas Group occur mainly west of the Wopmay Fault Zone but in some areas onlap the Calderian internal zone. The Dumas Group, together with relatively undeformed granites which intrude it, belong to the Great Bear Magmatic Zone (Hoffman and McGlynn, 1977; Hoffman, 1978; Bowring, 1982).

Northeast (dextral)- and northwest (sinistral)-trending transcurrent faults displace all of the above units. These faults are part of a conjugate system that affects much of the northwest Canadian Shield (Hoffman, 1980).

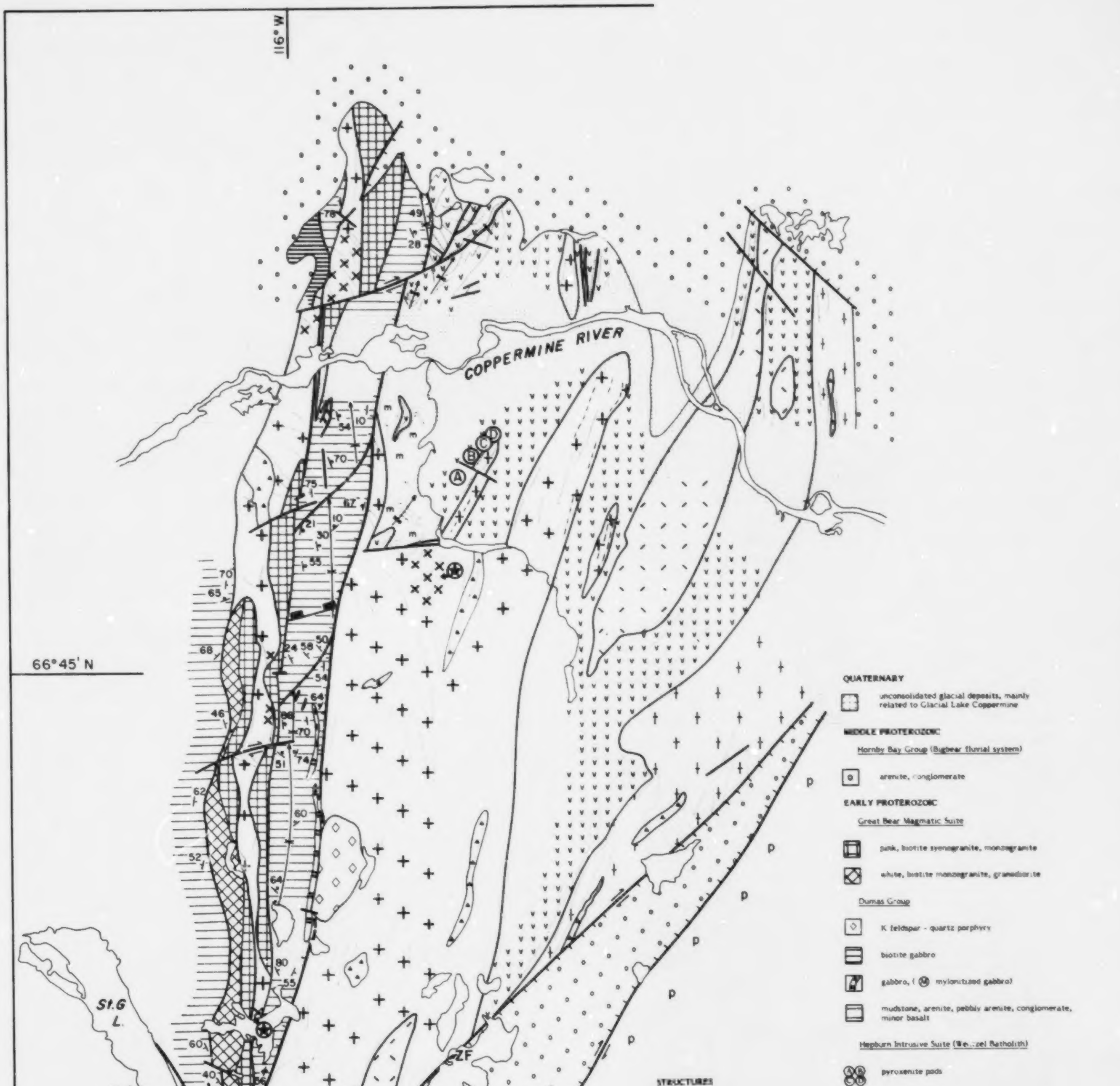

Figure 3.2 *Simplified geological map in the Big Bend area of the northwestern metamorphic internal zone of Wopmay Orogen. ZF - Zephyr Fault; circled stars - location of samples yielding Archean U-Pb zircon ages. Bodies of water: St. G.L. - St. Germain Lake; P.L. - Perrault Lake.*

Post-orogenic micaceous siltstones, feldspathic arenites and paraconglomerates, which occur in the north part of the map area and within grabens to the south (Fig. 3.2), are part of the Bigbear fluvial system of the middle Proterozoic Hornby Bay Group (Kerans et al., 1981).

Akaitcho Group

Stratigraphy

In the Big Bend area, Akaitcho Group stratigraphy is characterized by two distinct lithologic assemblages. Metabasites and semipelites with minor quartzite and marble are the dominant assemblage comprising over 80% of the initial-rift units. The metabasic units are 1 cm to tens of metres wide and consist of massive to finely layered amphibolitic gneisses which are commonly garnet-rich and are interpreted to be basic flows and/or intrusives. Semipelitic biotite (-hornblende -garnet) - quartz schists are the most common metasedimentary unit. Discontinuous ironstone is commonly intercalated with the semipelites and is composed primarily of layered quartz-rich and magnetite-rich bands 3 cm in width. The ironstone is also usually finely interlayered with hornblende-plagioclase-garnet schist (metatuff?) and dolomite marble and is associated with anomalous amounts or iron silicates, iron sulphides and graphite. The layering is commonly boudinaged or tectonically disrupted. Where ironstones are present, the associated semipelites contain an anomalous amount of iron silicates, iron sulphides and graphite. This type of ironstone corresponds to the mafic to felsic volcanic association of Algoman-type ironstone (classification of Shegelski, 1978, as quoted in R. Hall, personal communication, 1983). White, often fuchsitic, metaquartzites form distinctive units 10 cm to 15 m in width. Well defined, centimetre-scale layering in the quartzites may represent primary bedding. Numerous bands of marble, 1 cm to 10 m wide, are finely intercalated with the metabasic and metasedimentary units. The marbles are composed either of massive dolomite or of dolomite with calc-silicates (actinolite, tremolite, diopside or forsterite) arranged randomly or in well defined, narrow layers. Individual units within this mixed lithologic assemblage may be traced for up to 30 m. Further correlation is hampered by abrupt facies changes and by complex folding and faulting.

The second lithological assemblage is composed predominantly of marbles with only a minor (less than 5%) component of metabasic or siliciclastic units. The marbles are characterized by interlayered massive dolomite-marble and calc-silicate-laminated marble.

The variety of rock types in the Akaitcho Group of the Big Bend area is comparable with that south of 66°N (King, 1985) and with those reported by Easton (1981a) for other parts of the orogen, and is compatible with the interpretation of the Akaitcho Group as an initial-rift facies assemblage (Easton, 1981b, 1982). In the Big Bend area, however, marble, quartzite and ironstone units are more abundant than elsewhere and cannot be specifically correlated with any other part of the Akaitcho Group. Also, although Easton (1982) and King (1985) have used the occurrence of granite-and gneiss-bearing conglomerate to suggest that the Akaitcho Group was elsewhere deposited at least in part on granitic basement, no such conglomerates were documented in the Big Bend area. No other evidence

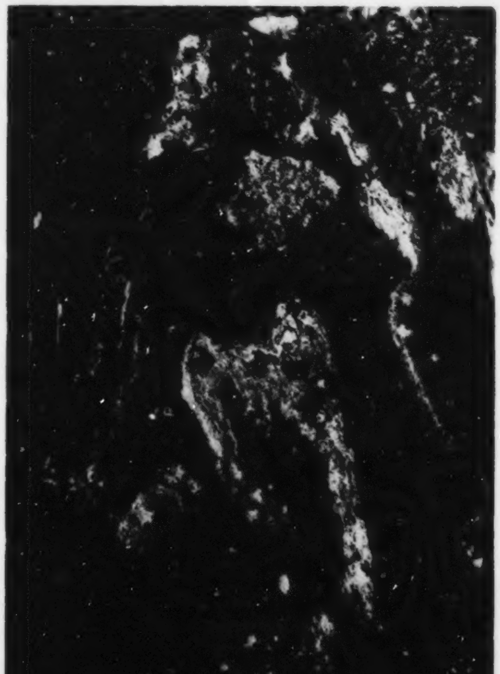

Figure 3.3a. *Type 2 interference pattern in Akaitcho Group layered dolomite-actinolite marble. Dark coloured layers are dolomite-marble; light coloured layers are actinolite-dolomite marble. Surface of exposure is nearly horizontal. Pen is 15 cm long. GSC 204307-M*

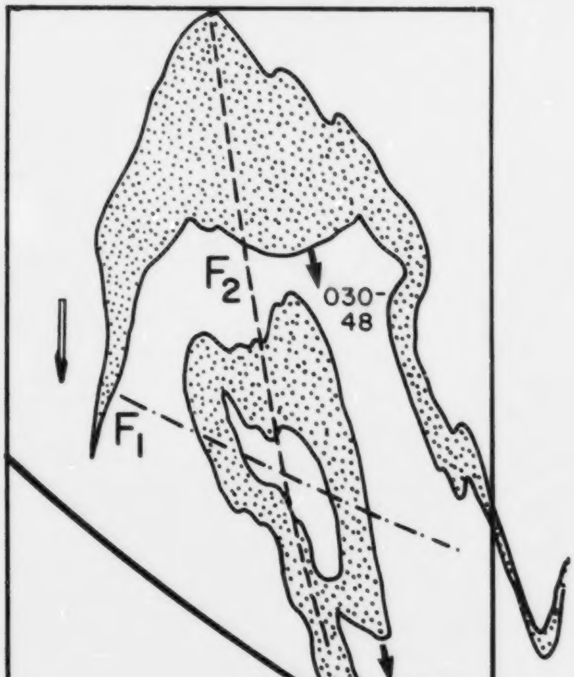

Figure 3.3b. *Line drawing and extension of photograph in Figure 3.3a. Actinolite-dolomite layers are highlighted by stipple pattern. Small arrows are measured F_2 axes. Pen is 15 cm long.*

which could be interpreted to indicate the composition of presence of nearby basement has been recognized in the Akaitcho Group stratigraphy in the Big Bend area.

Structure

The Akaitcho Group is characterized by a well-developed planar fabric which is defined by gneissic layering in plagioclase-rich amphibolites and in (sparse) pelites, by a biotite schistosity in the semipelites and by thin bands of calc-silicates in the marbles. The planar layering is involved in metre-scale to outcrop-scale isoclinal folds (F_{1a}). The axial surfaces of these folds are locally involved in a second phase of isoclinal coaxial folding (F_{1b}). All surfaces were subsequently involved in upright, open folds (F_2) about axes that plunges moderately (25-40°) to the northeast (Fig. 3.2). A few late, metre-scale, open folds (F_3), which trend and gently plunge to the southeast were observed on the limbs of the macroscopic F_2 folds. This polyphase folding history has resulted in a very complex fold interference pattern. The main pattern of Akaitcho structure is predominantly a type 2 interference pattern (Ramsay, 1967) formed by the interference of $F_{1a,b}$ folds by the F_2 folds (Fig. 3.3). Although type 2 patterns predominate, a variety of interference patterns can be observed in a single outcrop because of the variable orientation of the early, isoclinal fold axial surfaces due to their polyphase history. The dominant type 2 pattern suggests that the $F_{1a,b}$ axial surfaces initially dipped moderately to shallowly. Relatively local complexities occur where F_{1a} hinges are wrapped around F_{1b} folds. No axial planar cleavages were observed in folds of the F_1 generation.

Mesoscopic F_2 hinges were only clearly observed in the thick marble assemblage where compositions are not favourable for the development of a cleavage. The only significant linear fabric element consists of a pronounced alignment of the calc-silicate minerals parallel to the F_2 axes. An axial-planar crenulation cleavage is present in biotite schist layers at the hinge zone of the F_3 folds.

The F_1 folds are interpreted to have formed during the Calderian Orogeny because they are similar in style and intensity to Calderian folds of the Akaitcho Group farther south (St-Onge et al., 1982, 1983b, 1984; King, 1985). The authors realize that correlation by style can be problematic but believe it to be the most reasonable interpretation. The F_2 folds are interpreted to be part of the Tree River Deformation, a regional episode of crossfolds which affect all structures of the Calderian Orogeny (Hoffman et al., 1984).

Metamorphic grade

South of Zephyr Fault, a set of isograds in Akaitcho Group pelites marks the first appearance of andalusite, sillimanite and granitic pods + K-feldspar (Fig. 3.2). Metamorphic grade increases with proximity to the Wentzel Batholith. These are part of the western suite of regional isograds of St-Onge (1983). Although obscured by units of the overlying Hornby Group, the eastern margin of the Wentzel pluton and the concordant isograds are interpreted to be offset to the northeast along the Zephyr and nearby transcurrent faults. North of the fault the mineral assemblage in sparse Akaitcho Group pelites of granitic pods-K-feldspar-quartz-biotite-plagioclase indicates temperatures of over 650°C consistent with the assemblage hornblende, plagioclase and garnet in metabasic units. Unfortunately, the assemblages in the area are not favourable for determining metamorphic pressures.

Wentzel Batholith

Gneisses, which have been shown to be in part Archean and in part Proterozoic in age (Chamberlain et al., 1984; S.A. Bowring, personal communication, 1984), occur on the east and west side of an outlier of Dumas Group rocks (Fig. 3.2). On the east side, these gneisses constitute a large central body which has long prong-like extensions to the north and also occur as thin sheets (1 m-500 m wide) interlayered with Akaitcho Group units. Contacts are concordant with layering in the Akaitcho Group. Within both the thin sheets and the main body, rock types are very heterogeneous.

In some areas, the gneisses can be termed 'straight gneisses' (e.g. Fig. 3.4) (in the sense of Davidson et al., 1982). This field term is used to designate a very evenly layered gneiss whose layering is notably continuous even though it is often very fine. By analogy with Davidson et al. (1982) the straight gneisses are interpreted as tectonites which have undergone very high strain. Indeed, in the more finely layered straight gneiss, grain size is very small (to 0.5 mm), quartz is drawn out in leaves, and plagioclase has the form of millimetre-scale, rounded, grains. This unit can be termed 'protomylonite' in the terminology of Sibson (1977), or more precisely, 'homoclastic, mature protomylonite' in the terminology of Hanmer and Lucas (1985). No structures with which one could interpret a strain regime (e.g. pure shear vs. simple shear) or kinematic history were observed.

The eastern prong of the main body of gneisses (Fig. 3.2) is primarily pink-weathering, monzogranitic straight gneiss, with less than 5% amphibolite xenoliths. The gneisses tend to be coarser grained and more coarsely layered in the centre of the prong, and finer (to protomylonitic) on the margins. This textural variation infers a strain gradient which increases towards the margin of the prong.

Figure 3.4. 'Straight layered' quartztofeldspathic and amphibolitic gneiss. This layering is typical of units which underly much of the northern prongs of the main gneiss body, although the mafic component as shown in this photograph is unusually high. Pen is 15 cm long. GSC 204307-K

There is, however, no evidence of a tectonic discontinuity at the margin. The contact of the gneisses with Akaitcho units is sharp, although rare, thin (1 m wide) sheets (veins?) of granitic gneiss are present in Akaitcho units within a few hundered metres of the contact. There is no change in the degree of deformation of the Akaitcho Group with proximity to the contact or evidence of faulting at the contact. The character of this contact, whether intrusive or tectonic, therefore remains equivocal.

The western prong contains some straight gneisses, mainly at its northern and southern ends, but is primarily foliated to gneissic, syeno- to monzogranite. Pegmatite veins cut across layering at a high angle, and are themselves weakly foliated. At three localities where the contact with the adjacent Akaitcho Group units was exposed, it is characterized by sheeted veins of the granitic gneiss (20-100 cm wide) interlayered with the Akaitcho Group amphibolite gneisses, quartzites and siltstones. This contact, therefore, is interpreted to be intrusive.

Layering in both prongs trends parallel to their length, even in the tip zones, and dips are steep (60-90°). There are no domains of preferred easterly or westerly dips in either Akaitcho Group gneisses or granitic gneisses and there is therefore no evidence to support an interpretation of the prongs of granitic gneiss as cores of macroscopic antiforms (cf. Hoffman, 1984). No stratigraphic evidence is present to suggest that either of these prongs were local, syn-rifting basement highs.

The small sheets of granitic gneiss exterior to the main body are lithologically very similar to the gneisses described above and are both coarsely and finely (straight) layered. One sheet, east of the main body (Fig. 3.2), contains heterogeneously developed protomylonitic to mylonitic zones, parallel to the regional layering, although no structures which could provide information regarding the kinematic history of the rock (kinematic indicators) were observed.

The main body of gneisses is more heterogeneous than either of its prongs or nearby sheets. One area in particular, immediately south of the east-west fault which forms part of the northern boundary to the main body (cluster of x-pattern and star, Fig. 3.2), is extremely complex. In this area, coarse grained and coarsely interlayered, massive monzogranite, quartzo-feldspathic gneiss, amphibolitic gneiss, isolated boudins of amphibolite, and finely layered granitic to tonalitic and amphibolitic gneiss (straight gneiss?) are intricately intermixed (Fig. 3.5). Where very fine layering is present, it is involved in tight, usually polyphase, centimetre-scale folds (e.g. Fig. 3.5). Samples of a tonalitic gneiss from this area (starred location, Fig. 3.2) have yielded ages of 2.9 Ga (U/Pb in zircon, Chamberlain et al., 1984) indicating that at least part of this mixed assemblage is Archean. However, less than 1 km to the east, outcrop-scale inclusions of ironstone and metasiltstone are present. Because of the abundance of these rock types in adjacent Akaitcho group units, these inclusions are considered to be Proterozoic in age. The 2.9 Ga tonalitic gneiss is therefore interpreted to be part of a composite xenolith population within a main body of Proterozoic Wentzel Batholith gneiss.

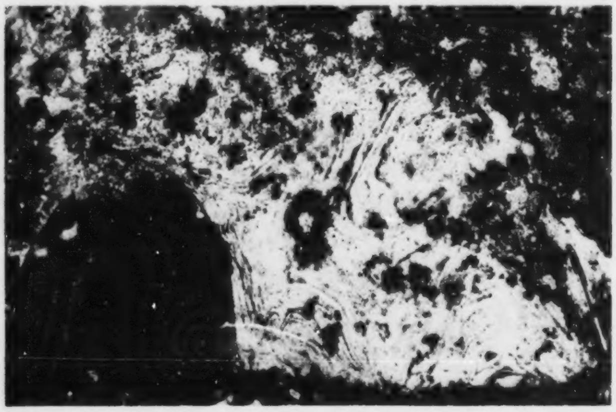

Figure 3.5. Finely layered, complexly folded quartzo-feldspathic gneiss and boudin of amphibolitic gneiss. This outcrop is near the location from which a 2.9 Ga date was derived (easternmost starred location, Fig. 3.2). Pen is 15 cm long. GSC 204307-L

Monzogranitic gneisses in the southern part of the main body are coarse grained and coarsely layered and contain abundant, large (1 m - 1 km diameter) xenoliths and layers of massive to heterogeneously strained amphibolite. Massive, pink-weathering syeno- to monzogranite is interspersed with the gneisses at the outcrop scale. The contact with Akaitcho Group units to the east is a poorly exposed zone of coarse grained and very coarsely interlayered to migmatitic granitic and amphibolitic gneisses. This zone could be either an intrusive contact with the adjacent Akaitcho Group units or a different phase of the main gneiss body whose contact relationships are indeterminate.

Rocks which are very similar to the coarse grained, coarsely layered gneisses described above also occur west of the Dumas outlier. These gneisses form a narrow band which is bordered mainly by intrusive Great Bear plutons. Where the gneisses are in contact with Dumas Group units, zones of brecciation are present with no clear unconformity preserved. The contact is therefore interpreted to be faulted. Within the band a distinct suite of coarsely layered migmatites, comprising biotite-rich, tonalitic gneisses and thick layers or boudins of amphibolite, occurs as outcrop-scale to kilometre-scale xenoliths. The tonalite component weathers white, a feature which, together with its migmatitic character, distinguishes it from the surrounding, more evenly layered, pink granitic gneisses. These migmatites must be older than the enclosing gneisses and may be another population of preserved Archean fragments within the Wentzel Batholith.

A large pluton of biotite syeno- to monzogranitic gneiss, which has a sheeted, intrusive contact with Akaitcho Group rocks, is present on the eastern side of the map area (Fig. 3.2). These gneisses bear a strong resemblance to the main body of well-layered, pink gneisses described above. South of Zephyr Fault, a sequence of isograds in adjacent Akaitcho Group pelites indicate increasing temperatures toward the offset extension of the pluton. The porphyroblasts are syntectonic with respect to the main Calderian deformation, suggesting that the gneissic pluton is Calderian in age. This interpretation has been corroborated by a U/Pb (zircon) date of 1890 Ma (S.A. Bowring, personal communication, 1984) from the southern extension of the pluton (south of the map area in Fig. 3.1).

In the northwestern metamorphic-internal zone the contact between granitic gneisses and adjacent metamorphosed Akaitcho Group units can be locally interpreted as intrusive. In places the gneisses are highly strained near their boundaries and do not show the unequivocally intrusive contact. Archean rocks do compose part of the assemblage, but obviously cannot account for the intrusive contacts. As a working model, we suggest that the bulk of the gneisses are part of the Proterozoic Wentzel Batholith and were severely deformed, especially in their narrow extensions and separate sheets, during the Calderian deformation. The distinct tonalitic migmatites and gneisses are Archean fragments which have been incorporated within the batholith. Whether their incorporation was a tectonic or igneous process remains an open question. This hypothesis

will be tested by MEV who will be conducting geochronological studies of several of the key units as part of his M.Sc. thesis.

Garnet granite

Three syeno- to monzogranite plutons, which contain greater than 5% garnet throughout most of their exposed area, occur in the northeastern and southern part of the map area (Fig. 3.2). The large, northern pluton typically contains megacrysts of K-feldspar, and locally plagioclase. This pluton is notable both for its homogeneous composition (except for slight changes in the feldspar ratio) and for its very evenly developed biotite foliation. The small northern pluton is very similar to its larger neighbour although it contains xenoliths of amphibolite and has a weaker foliation. The southern pluton is everywhere characterized by abundant, large, euhedral megacrysts of K-feldspar although and fabric can vary from a weak biotite foliation to a more gneissic texture due to the presence of locally abundant biotite, biotite schlieren or inclusions of metasedimentary rocks. The three plutons have sharp, sheeted or, locally, diffuse, intrusive contacts with their host rocks.

The plutons of garnet granite pose an interesting petrologic problem. The plutons strongly resemble peraluminous plutons of the Hepburn Batholith which intrudes garnet-bearing pelites to the east (Hoffman et al., 1980; Hoffman, 1984) yet intrude either mixed Akaitcho metabasites and semipelites which contain only minor garnet of variable size and colour, or older plutons of the Wentzel Batholith, in which garnets are only sparsely present in some amphibolite xenoliths or layers. It is difficult to consider the even sized, even coloured, extremely abundant garnets in the pluton as being xenocrysts derived from the relatively sparse and variable garnet component of the host units (Pattison et al., 1982). These problems will be examined by MEV as another aspect of his M.Sc. project.

Pyroxenites

Four pods of pyroxenite occur within Akaitcho Group units south of the Coppermine River (cf. Hoffman et al., 1980; Hoffman, 1984). The bodies range in size from 6x4 m to 200x100 m; their long axes parallel to gneissic layering in the adjacent Akaitcho units. They appear to dip parallel to adjacent gneissic layering. Their distinctive brownish-red, smooth weathering surface stands out clearly against the adjacent amphibolitic and quartzo-feldspathic gneisses of the Akaitcho Group.

The pyroxenite typically consists of euhedral, serpentinized clinopyroxenes, 0.5 cm in size, enclosed in a fine grained matrix of chlorite, actinolite and magnetite. The two smallest pyroxenite pods (localities A and B, Fig. 3.2) are massive bodies with a mainly homogeneous composition and grain size although the body at B contains minor grain-size layering. In contrast, the northern and western portion of the largest body of the cluster (locality D, Fig. 3.2) contains layers of hornblende, 0.5-1.0 cm wide and spaced at 5 cm intervals. This layering strikes north to northeasterly and dips steeply.

The pyroxenite body at locality C (Fig. 3.2) is the only one of the cluster which is characterized by compositional and grain-size heterogeneity. In this body a well defined layering is defined by continuous 0.5 cm wide bands of magnetite, apparently primary layering, spaced 20-30 cm apart. Unfortunately, most of the outcrop is frost heaved, so that the observed layering is not in its correct orientation. The general impression, however, was that layering was inclined steeply to moderately (approx. 60°) to the south.

A penetrative cleavage, defined by the alignment of actinolite occurs sporadically throughout the pyroxenite. The boundaries of the body are commonly characterized by a retrograde, talc-actinolite schist.

The age and tectonic significance of the pyroxenites are not known. They may be related to a large pyroxenite body which transgresses contacts within the Hepburn Batholith (Hoffman et al., 1980) in which case they would be late or post-Hepburn in age. The presence of a penetrative foliation in the pyroxenite pods distinguishes them from ultramafic units in the post-orogenic Muskox Intrusion.

Dumas Group

The easternmost Dumas Group units in Wopmay Orogen occur in an outlier bounded by faults and intrusions. The outlier contains mainly siliciclastic units although basalts, basic tuffs and gabbros are present. All units are cut by felsic porphyries.

The current mapping extended to the Dumas Group rocks immediately west of the outlier (Fig. 3.2) where S. Bowring of Washington University, Mo. has recently completed detailed field work.

Siliciclastic units

Four distinct facies associations have been identified within the Dumas outlier (Fig. 3.6):

1. North of the Coppermine River units include coarsely interlayered, polymictic, paraconglomerate, pebbly feldspathic arenite and feldspathic arenite. Although unequivocal bedding orientations in this area are rare, field observations suggest that the feldspathic arenite is at the base of the exposed section and is overlain by pebbly feldspathic arenite, then by interlayered paraconglomerate and pebbly arenite in an overall coarsening-upward sequence. The conglomerate is poorly bedded to massive and contains angular to sub-rounded clasts which have a continuous grain-size variation from 1 cm to over 20 cm in diameter. Clasts include felsic porphyries, vein quartz, amphibolitic and granitic gneisses and silicic, flow-layered volcanics. Porphyry fragments usually account for over 80% of the total population but very locally, gneissic fragments dominate. Evenly sized, 1-2 mm grains of quartz, plagioclase and K-feldspar compose the matrix. The feldspathic arenites are similar in composition to the matrix of the conglomerate and are massively bedded. Vaguely layered horizons within individual beds, or entire beds, may contain abundant pebbles, predominantly of quartz but also comprising igneous and gneissic fragments identical to those in the conglomerate facies.
2. Immediately south of the Coppermine River mudstones are interlayered with conspicuous, medium grained arkosic sandstone to pebbly feldspathic arenites. Although the sequence has been structurally disrupted by faulting, it appears to coarsen upward. The lower part of the section is composed of finely laminated mudstone, with minor siltstone laminae and quartz-arenite lenses. Normal grading, small flame structures, scours and trough cross-beds are common in the silty layers. Pebble-lag deposits occur at the base of some of the arenite lenses. The lowermost pebbly arenite beds form thin (1 m), laterally extensive sheets with sharp bases. In these, rounded quartz and subangular K-feldspar pebbles are evenly distributed through a well sorted, feldspathic arenite matrix; the grain-size distribution is continuous between pebbles and matrix. Sub-angular lithic fragments, similar in size to the quartz pebbles, are locally distributed evenly through the beds but often are concentrated at, or near, the basal contact.

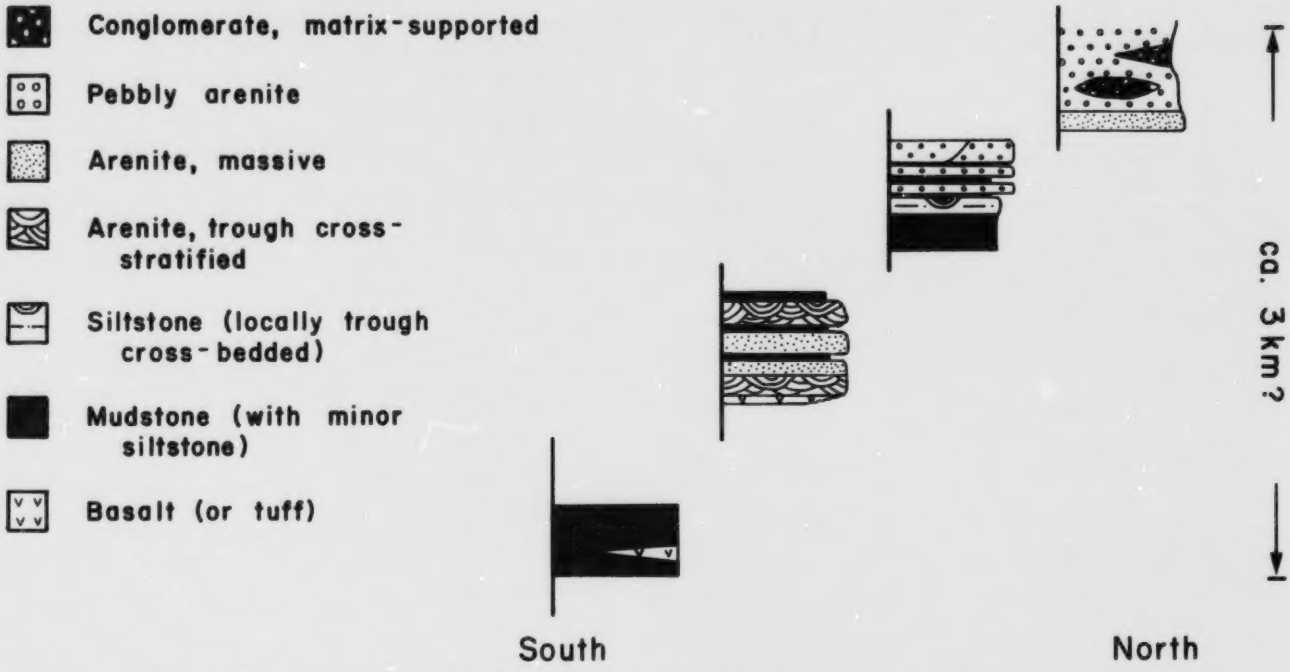

Figure 3.6. Schematic stratigraphic section of the Dumas Group at four localities in the outlier. Because the syncline plunges northward, progressively higher stratigraphic levels are preserved to the north. The number and thickness of beds are diagrammatic, and are meant to show relative abundances and thicknesses only.

The number and thickness of the pebbly arenite beds increases up-section to where thick-bedded (2 m) pebbly arenites dominate and only minor (less than 5%) mudstone interlayers are present. Here, the pebbly arenites fill wide (up to 1 km), thin (1-3 m) sheets which in places are seen to be composite beds.

3. The central part of the outlier is dominated by a sequence of interlayered arenites, 1 cm to several metres in thickness, and thin mudstone units. The arenites are generally well bedded, medium grained and are characterized by trough crossbedding outlined by biotite-rich and heavy-mineral(?)-bearing lamina. Where the arenite beds overlie mudstones, their basal contacts show pronounced scour features such as shallow scours, abrupt channels cutting though the mudstone, or rip-up clasts. The mudstones are characterized by well graded, centimetre-scale bedding and the siltstones are commonly trough crossbedded.

4. In the southernmost part of the outlier, poorly to well-graded mudstone rhythmites with rare siltstone lamina characterize the Dumas Group section.

Volcanic units

Discontinuous lenses of aphyric basalt, locally pillowed and commonly vesicular, interfinger conformably with the clastic sequence. The lenses are 5 m to 80 m thick and up to 1 km in strike length. Rare chloritic schists may be tuffaceous or volcaniclastic units.

Intrusive units

Small porphyry bodies with a wide range of composition intrude all units of the map area except for the Great Bear plutons (most porphyries are too small to be shown in Fig. 3.2). Felsic porphyries with phenocrysts of any or all of quartz, K-feldspar, or plagioclase are the most common of the suite. Mafic porphyries with K-feldspar, quartz, biotite and/or plagioclase phenocrysts in a matrix of plagioclase and hornblende are less common. One biotite-gabbro pluton and numerous gabbroic sills and dykes also intrude the Dumas Group units (Fig. 3.2).

Stratigraphic interpretation

The predominance of porphyry and volcanic fragments in the Dumas Group clastic units suggests that the provenance was a domain of eroding volcanoes. Since the porphyries which cut the internal zone (ie. feeders to a now-eroded, overlying sequence) decrease markedly in occurrence eastward and are abundant to the west, the clastic component is interpreted to have been derived mainly from the west. The outcrop areas where gneissic fragments dominate the clast population may represent local channelling from the Akaitcho terrain now exposed to the east but may also have been derived from the mafic gneisses, suspected to be Archean in age, exposed west of the outlier. There is no other evidence for a significant contribution of coarse clastic material from the unroofed internal zone. An analysis of the provenance and sedimentology of the clastic units of the Dumas Group within the outlier will form part of B.Sc. thesis by DS. The southernmost mudstone section represents a low-energy, perhaps lacustrine environment whereas the mudstone – feldspathic arenite section is interpreted as a fluvial deposit. The central sheets and composite beds of pebbly arenite are considered distal sheet (debris) flows which are locally channelled; the underlying and interlayered, graded mudstones and siltstones, into which the sheets flowed, are interpreted as lacustrine to interflow deposits. Farther north, conglomeratic debris flows are locally intercalated with the arenite sheet flows. If the outlier is a relatively coherent, north-plunging syncline (see below), the variation in facies assemblages from south to

north is a cross-section of a coherent stratigraphic section (Fig. 3.6) and records the filling in of a lacustrine to alluvial system by increasingly more proximal debris flows from an unroofing volcanic domain to the 'west'.

Contact relationships of the Dumas outlier

The west side of the outlier has been intruded by Great Bear plutons for most of its length. One kilometre south of the Coppermine River, where the Great Bear pluton pinches out, the outlier is adjacent to gneisses interpreted to be in part Archean (Fig. 3.2). The easternmost gneisses are affected by a 10 m wide zone of braided, steeply dipping cataclastic zones which have undergone extensive chloritic alteration. Because of the alteration, it was not possible to determine in the field whether Dumas Group units were involved in the cataclasite. It is hoped that cut slabs and thin sections will resolve this problem. Because the eastern boundary of the outlier truncates the hinge zone of the syncline cutting out much of the east limb of the syncline, it also is interpreted to be a fault. Zones of chlorite-bearing cataclasite were observed at several locations along the boundary.

Metamorphic grade and structure

The mudstones of the Dumas Group near the Coppermine River contain chlorite-muscovite-quartz and weather a silver-grey to green-black colour. Farther south the mudstones are purple, and, although no distinct minerals could be identified in the field, chlorite and metamorphic muscovite were apparently absent. An isograd marking a reaction which involves chlorite and muscovite therefore separates the two domains (Fig. 3.2). Because of locally limited exposure and the truncated width of the outlier, the orientation of the isograd and its relationship to the syncline (ie. folded or not?) could not be determined. Metabasic units contain chlorite-epidote assemblages in both domains.

The general form of the outlier of Dumas Group is that of a 'half-canoe'-shaped syncline which plunges moderately (25°) northward in its southern part and is horizontal near the Coppermine River (Fig. 3.2, 3.7). Near the Coppermine River a weak phyllitic cleavage defined by aligned chlorite and muscovite grains appears to be axial planar to the syncline, suggesting that folding was synchronous with equilibration of the chlorite-muscovite isograd. The hinge zone of the synform is dextrally offset and rotated counterclockwise by a set of northeast-trending faults that do not extend outside of the outlier. On the east side, they appear to root in the north-south trending boundary fault but on the west side they are truncated by a Great Bear pluton. The internal faults therefore predate this Great Bear pluton. Also, because the pluton and units farther west are not displaced, it is possible that the internal faults also root to the west in a north-south trending fault which now is obscured by the Great Bear pluton.

The interior of the outlier is characterized by an array of northeast, northwest and north-south trending small-scale faults whose vector of displacement could not be determined, even by detailed mapping. However, since the synclinal structure maintains its overall form, displacements probably are not large. If the amount of dip-slip displacement on the faults within the outlier is not great, over 3 km of obliquely-exposed stratigraphic section would be preserved within the outlier (Fig. 3.6). Northeast-trending transcurrent faults, part of the regional conjugate array, offset the north-south trending cataclastic boundary zones (Fig. 3.6).

Great Bear plutons

Plutons of the Great Bear Magmatic Suite in the map area correspond to the G_3 granites of Hoffman (1984). Two lithologic units are recognized (Fig. 3.2) but cannot be separated in time. The most abundant unit is a syeno- to monzogranite which weathers pink and commmonly contains coarse 'blebs' of quartz. Biotite is abundant and hornblende is locally present, especially near xenoliths of amphibolitic gneiss. The second unit, a white-weathering, leucocratic monzogranite to granodiorite, is mainly present as a narrow margin on the west side of the pink granites. In places, however, the two units are intimately intermixed. They appear to be concordant with the structural grain in the Dumas unit to the west, but crosscut bedding in the outlier. A foliation defined by flattened quartz grains and biotite parallels the length of the plutons.

The problem of the Wopmay Fault Zone

Eighty kilometres south of the present map area, the Wopmay Fault Zone (WFZ) is a 1-15 km wide belt of mylonites and brittle faults which form the boundary between

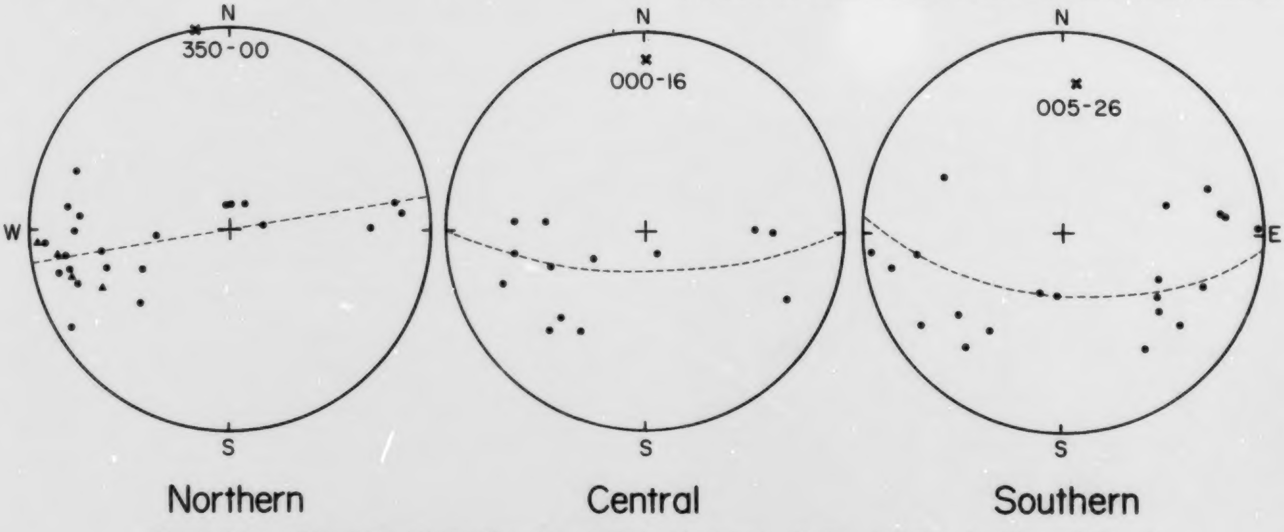

Figure 3.7. Stereonets illustrating the change of plunge of the syncline in the outlier of Dumas Group. Dots - poles to bedding; triangles - poles to cleavage; heavy 'x' - beta axis.

the Calderian internal zone and the Great Bear Batholith (Fig. 3.1) (Easton, 1981a; Hoffman, 1984; St-Onge et al., 1984; King, 1985). The fault system was active from late Calderian to late Great Bear time concurrent with decreasing temperatures (King, 1985). An array of kinematic indicators at all scales shows that displacement in the fault zone was predominantly dextral transcurrent, although some dip-slip (west-side-down) displacement occurred late in its evolution (King, 1985). Dumas units adjacent to the Wopmay Fault Zone south of 66°N (Fig. 3.1) experienced minor ductile strain and are displaced by dip-slip faulting along the north-south fault system. Near 66°N volcaniclastic units of the Dumas Group locally overlie the western part of the fault zone but a 1.5 km wide mylonite zone is preserved on the east side (King, 1985). Forty-five kilometres south of the present map area (Fig. 3.1), conglomerates derived from east of the Wopmay Fault Zone drape off a block of Archean granite, which is contained within the fault zone, and interfinger with Dumas mudstones to the west (Hoffman, 1978; Bowring, 1982). No mylonites have been recognized at this latitude.

In the Big Bend area, the boundary between the Calderian internal zone and the Great Bear Magmatic Zone is complex (Fig. 3.2). The boundary, however, does bear some of the attributes of the Wopmay Fault Zone as it is known to the south, although no major mylonite zones were recognized. A number of centimetre-scale shear zones which trend north-south and dip steeply, cut the Dumas Group and westernmost Akaitcho Group units near the boundary. In two locations where the internal schistosity of these shear zones was oblique to their margins, it was consistent with a dextral sense of displacement in the plane of view (horizontal). In one area immediately south of, but along strike with the Dumas outlier (Fig. 3.2, Location M), a braided array of steeply dipping shear zones, 2 mm to 10 cm wide and containing zones of protomylonite and mylonite, cut Dumas Group metagabbro (Fig. 3.8). The sense of displacement within the shear zones could not be unequivocally determined. These zones are crosscut by granitic dykes related to the Great Bear intrusions. Also, within the map area the Calderian internal zone - Great Bear Magmatic Zone boundary is associated with a set of north-south striking faults which have a component of dip-slip displacement (ie. the boundaries of the Dumas outlier) a situation similar to that of the Wopmay Fault Zone to the south. A final point that can be made involves the Great Bear plutons at the boundary. The plutons are relatively undeformed and crosscut Dumas Group stratigraphy and structures, and their very elongate form cannot therefore be attributed to deformation or to preferential intrusion along Dumas

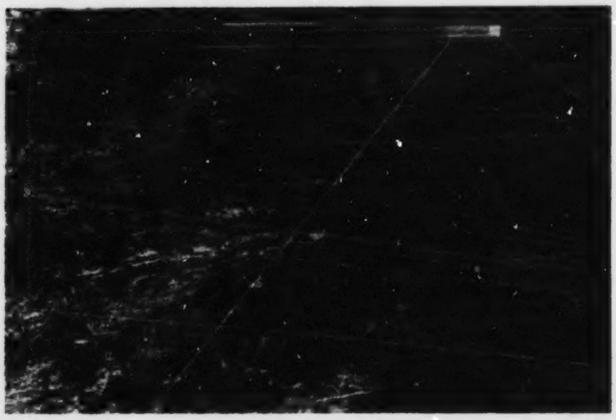

Figure 3.8. Mylonitic shear zone cutting metagabbro of the Dumas Group. Pen is 15 cm long. GSC 204307-W

Group structures. This leaves open the possibility that a pre-existing structure in the structural basement of the Dumas Group, controlled the locus of emplacement of the Great Bear plutons.

One possible interpretation of the boundary in the Big Bend area is that it is a high-level expression of late displacement in the Wopmay Fault Zone. The 5° northward tilt of the overlying Coppermine Homocline (Irvine and Baragar, 1972) indicates that at least the northern end of the exposed Wopmay Orogen has been flexed downward and higher structural levels of even the latest structures in the orogen should be exposed at these latitudes. In the Big Bend area, we may be seeing a greater thickness of Dumas than was preserved to the south straddling and obscuring the locus of the fault zone. The system of north-south faults on which the Dumas Group is down-faulted may be the high-level expression of late displacement taking place in the buried Wopmay Fault Zone. Carrying this interpretation further, it is possible that the faults which offset the synclinal axis within the outlier, and which are contained entirely within the outlier, are manifestations of dextral transcurrent displacement along the north-south fault system, similar to that documented for the Wopmay Fault Zone to the south (St-Onge et al, 1984; King, 1985). The north-south trend of the syncline within the outlier is not compatible with a fault-related genesis. Within the context of the suggested model this implies that the syncline was formed before displacement on the adjacent fault strands.

The timing of the postulated dextral transcurrent movement has important implications for features of the Great Bear Magmatic Zone. The displacement would certainly predate the Great Bear G_3 plutons but its relationships to the porphyries is uncertain. The eastern boundary fault of the Dumas Group outlier appears to be intruded by a large porphyry (Fig. 3.2). However, the exposure is such that it is possible, although difficult, that the fault continues between the Dumas Group rocks and the porphyry. An interpretation of a crosscutting relationship is therefore somewhat equivocal. If displacement on the boundary fault predates the Dumas porphyry, it must have been contemporaneous with the calc-alkaline magmatism of the Great Bear Magmatic Zone. If it postdates the porphyry but pre-dates the Great Bear (G_3) plutons it could be associated with regional, northwest-trending folding of Great Bear stratigraphy (which is interpreted to have occurred in a dextral transpressive tectonic regime (Hoffman, 1980).

Breccias and alteration seams

Well developed breccias and discrete zones of intense alteration occur in all units in the northern part of the map area. The breccias and alteration are most pronounced in Akaitcho Group gneisses near the unconformity at the base of the Hornby Bay Group (Bigbear fluvial system), but also occur in the Wentzel plutons and Dumas Group, and are found up to 8 km south of the unconformity.

The most striking of the breccias contain densely packed, randomly oriented clasts in a matrix of fine grained rock fragments and occur in irregular or planar zones (Fig. 3.9). The matrix fragments are a fine grained equivalent of the clast population. Most of the large fragments are rounded to subrounded whereas the matrix fragments tend to be angular to subangular. The range in size of the clasts varies with the size of the breccia body; the largest observed breccia body (10 m x 50 m) contains fragments up to 2 m in diameter. The smallest observed matrix fragments are less than 1 mm, although the true character and size range of the finer matrix component has not yet been determined. No penetrative fabric other than that already present in the country rock gneisses was obverved

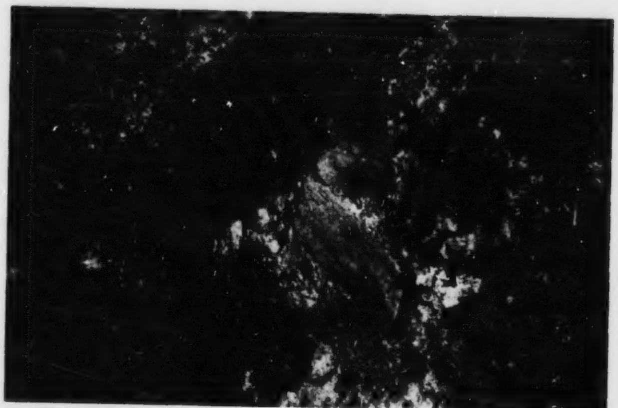

Figure 3.9a. Breccia in which elongate, subangular to subrounded clasts of Akaitcho Group gneisses are densely packed in a matrix of finer-grained rock fragments. There is a continuous range of grain sizes between matrix and the large clasts. Pen is 15 cm long. GSC 204307-G

Figure 3.10. Part of a carbonate-cemented breccia. Angular to subrounded clasts are correlative with adjacent Akaitcho Group units. The matrix is homogeneous, fine grained carbonate. Pen is 15 cm long. GSC 204307-J

Figure 3.9b. Line drawing outlining the large clasts in Figure 3.9a. Fine grained matrix occurs in areas left blank. Pen is 15 cm long.

in either the clasts or matrix. Most of the clasts within these breccia zones are similar to the adjacent rock although 'exotic' (with respect to the immediately adjacent units) clasts are commonly present. All of the 'exotic' clasts can be correlated with units within the map area which occur below the sub-Bigbear fluvial system unconformity; no Hornby Group or younger units were recognized in the clast populations.

A second type of breccia comprises lensoid or vein-like bodies of brecciated Akaitcho Group gneisses, similar to those described above, except that these lack the fine cataclastic matrix and are cemented by fine grained carbonate (Fig. 3.10). As above, the tectonic fragments are mainly derived from the adjacent rocks, although a small percentage are 'exotic' to the observed adjacent units. These breccia-carbonate veins range in width from 1 cm to several metres. All dip steeply to vertically. Iron and copper sulphide minerals commonly occur within the carbonate-cemented breccias.

Intense, hematitic and/or dark green chloritic alteration occurs along discrete fractures and within breccia bodies. Where most intense, the alteration produces seams and vein-like bodies of hematitic and chloritic clays in which the original rock type is obliterated. The thicker, more completely altered zones were devoid of any systematic structure. Narrower seams, however were locally characterized by a systematic planar alignment of the chlorite grains parallel to the margins of the seams. Fabric was oriented at an acute angle to the seam margins.

Where any of the breccias or alteration zones can be traced along strike, they narrow and pinch out. Usually a fracture, stained by hematitic or chloritic alteration, extends from their termination. In most instances neither a sense nor amount of displacement in the breccia zones can be determined; the host rock appears to be disaggregated and 'jumbled' at the outcrop scale. Locally there appears to have been no significant displacement, but commonly the wall rocks have been at least rotated relative to each other, and are not stratigraphically correlative across the breccia zones. Although this pattern of disaggregation is mimicked at the map scale, macroscopic structures such as the syncline within the Dumas Group outlier and the late synform of Akaitcho Group units north of the Coppermine River maintain their overall forms.

Fractures with pronounced chlorite-hematite alteration were documented to decrease in abundance from the Hornby unconformity to very sporadic zones 8 km south of the unconformity. This is equivalent to 700 m of true structural depth of penetration (after reconstruction of the 5° north tilt (Irvine and Baragar, 1972) of the northern part of Wopmay Orogen).

The Coppermine River breccias bear a strong resemblence to breccias within the basement rocks beneath the Athabasca Basin in Saskatchewan (Currie, 1969; Wallis et al., 1983; Pagel et al., 1985), where they are commonly associated with uranium mineralization. The Big Bend area has been intensely prospected for uranium (Department of Indian Affairs and Northern Development, 1981).

<u>Origin of the breccias and alteration</u>

Since similar breccias have not been reported in rocks of the Bigbear fluvial system, they are interpreted to have formed prior to its deposition. Their strong spatial association with the sub-Bigbear unconformity, however, suggests a genetic link between the two. Any model for the formation of the breccias must incorporate these time and spatial constraints and allow for some dilation (to open the carbonate-filled vein network) and for the brittle

deformation processes implied by the cataclastic character of the fault rocks. One explanation is that the breccias were formed by processes active during the reactivation of pre-existing transcurrent faults and fractures prior to and during Hornby sedimentation. The orientation of the breccias is similar to the orientations of a regionally developed fracture set. On the basis of orientation and small-scale offsets, the fracture set has been interpreted to be a component of the late conjugate transcurrent fault system. Also, syndepositional facies changes in the Bigbear system show that the northeast- and northwest-trending transcurrent faults were reactivated with dip-slip and oblique-slip displacement during deposition of the system (Kerans et al., 1981). Postdepositional faults which parallel the transcurrent set are also considered to be related to continuing activity on the fault set. The dilational extension of some of the zones may have been incurred as fault surfaces very near the paleo-erosion surface were reactivated. However, north-south orientations are more prevalent for breccias than for the fractures set and it may be significant that the two largest bodies of fragmental breccias trend north-south and are offset along small, southeast-trending faults. Possibly the formation of the north-south trending beccia zones is related to the late activity of the Wopmay Fault Zone postulated above and predates the conjugate transcurrent event.

The chlorite-hematite-carbonate alteration of basement is very similar to alteration beneath the Athabasca sandstone where is is ascribed to reduced, hydrothermal emanations derived from the basement (Wallis et al., 1983). Isotope studies would be required to determine the ultimate source of the fluids in the Big Bend area, although the close spatial association of the zones of alteration with the sub-Bigbear system unconformity point to meteoroic sources. In the Athabasca Basin, the interaction between the basement-derived reductant and a flow of oxidized, metal-bearing fluid moving though the overlying Athabasca sandstone acts to precipitate mineralization (Wallis et al., 1983). The relationship between the structure, alteration and mineralization of the Coppermine River breccias will be examined by KHW as part of a BSc thesis.

Acknowledgments

We would like to thank Martin Irving for his efficient expediting services. We also acknowledge with pleasure, the set-outs, cooking and good company provided by Lynn Riese of Trophy Lodge, Great Bear Lake. Paul Hoffman is thanked for his critical review, which resulted in a greatly improved text.

References

Bowring, S.A.
1982: Preliminary geologic map of the Kamut and Adam Lakes map areas (86K/9, 86K/8); Economic Geology Series map, Department of Indian Affairs and Northern Development, Yellowknife, N.W.T.

Chamberlain, V.E., Lambert, R.St.J., Bradley, M., and Marten, B.E.
1984: Archean zircon ages for tonalite gneisses, Coppermine River area, N.W.T.; Geological Association of Canada, Program with Abstracts, v. 9, p. 51.

Currie, K.L.
1969: Geological notes on the Carswell Circular Structure, Saskatchewan; Geological Survey of Canada, Paper 67-32, 60 p.

Davidson, A., Culshaw, N.G., and Nadeau, L.
1982: A tectono-metamorphic framework for part of the Grenville Province, Parry Sound region, Ontario; in Current Research, Part A, Geological Survey of Canada, Paper 82-1A, p. 175-190.

Department of Indian Affairs and Northern Development
1981: Index to Mining and Assessment Reports, Northern Affairs Program, Mining Division, 531 p.

Easton, R.M.
1981a: Geology of the Grant Lake and Four Corners map-areas, District of Mackenzie, N.W.T.; in Current Research, Part B, Geological Survey of Canada, Paper 81-1B, p. 83-94.

1981b: Stratigraphy of the Akaitcho Group and the development of an early Proterozoic continental margin, Wopmay Orogen, Northwest Territories; in Proterozoic Basins of Canada, ed. F.H.A. Campbell, Geological Survey of Canada, Paper 81-10, p. 79-95.

1982: Tectonic Significance of the Akaitcho Group, Wopmay Orogen, Northwest Territories; Ph.D. Thesis, Memorial University of Newfoundland, St. John's, Newfoundland, 432 p.

Fraser, J.A., Hoffman, P.F., Irvine, T.N. and Mursky, G.
1972: The Bear Province; in Variations in Tectonic Styles in Canada, eds. R.A. Price, R.J.W. Douglas, Geological Association of Canada, Special Paper 11, p. 453-503.

Hanmer, S. and Lucas, S.B.
1985: Anatomy of a ductile transcurrent shear: the Great Slave Lake Shear Zone, District of Mackenzie, N.W.T. (preliminary report); in Current Research, Part B, Geological Survey of Canada, Paper 85-1B, p. 7-22.

Hoffman, P.F.
1978: Geology of the Sloan River map-area (86K), District of Mackenzie; Geological Survey of Canada, Open File Map 535 (1:125,000 scale).

1980: Wopmay Orogen: A Wilson cycle of early Proterozoic age in the northwest of the Canadian Shield; in The Continental Crust and Its Mineral Deposits, ed. D.W. Strangway, Geological Association of Canada, Special Paper 20, p. 524-549.

1984: Geology, Northern Internides of Wopmay Orogen, District of Mackenzie, Northwest Territories; Geological Survey of Canada, Map 1576A, scale 1:250 000.

Hoffman, P.F. and Bowring, S.A.
1983: Extensive effects of three different collisions on the foreland of Wopmay Orogen, Northwest Canadian Shield; Geological Association of Canada, Program with Abstracts, v.8, p. A33.

1984: Short-lived 1.9 Ga continental margin and its destruction, Wopmay Orogen, Northwest Canada; Geology, v. 12, p. 68-72.

Hoffman, P.F. and McGlynn, J.C.
1977: Great Bear Batholith: A volcano-plutonic depression; in Volcanic Regimes in Canada, ed. W.R.A. Baragar, L.C. Coleman, J.M. Hall, Geological Association of Canada, Special Publication 16, p. 169-192.

Hoffman, P.F., St-Onge, M.R., Easton, R.M., Grotzinger, J., and Schulze, D.E.
1980: Syntectonic plutonism in north-central Wopmay Orogen (early Proterozoic), Hepburn Lake map-area (86J), District of Mackenzie; in Current Research, Part A, Geological Survey of Canada, Paper 80-1A, p. 171-177.

Hoffman, P.F., Tirrul, R., Grotzinger, J.P., Lucas, S.B., and Eriksson, K.A.
1984: The externides of Wopmay Orogen, Takijuq Lake and Kikerk Lake map areas, District of Mackenzie; in Current Research, Part A, Geological Survey of Canada, Paper 84-1A, p. 383-395.

Irvine, T.N. and Baragar, W.R.A.
1972: Muskox Intrusion and Coppermine River Lavas, Northwest Territories, Canada; XXIV International Geological Congress, Excursion A29, Montréal, Québec, 70 p.

Kerans, C., Ross, G.M., Donaldson, J.A., and Geldsetzer, H.J.
1981: Tectonism and depositional history of the Helikian Hornby Bay and Dismal Lakes Groups, District of Mackenzie; in Proterozoic Basins of Canada, ed. F.H.A. Campbell, Geological Survey of Canada, Paper 81-10, p. 157-182.

King, J.E.
1985: Structure of the metamorphic-internal zone, northern Wopmay Orogen, Northwest Territories, Canada; PhD Thesis, Queen's University, Kingston, Ontario, 207 p.

McGlynn, J.C.
1970: Bear Province; in Geology and Economic Minerals of Canada, ed. R.J.W. Douglas, Geological Survey of Canada, Economic Geology Report v. 1, Fifth ed., p. 77-84.

Pagel, M., Wheatley, K., and Ey, F.
1985: The origin of the Carswell Circular Structure; in The Carswell Structure Uranium Deposits, Saskatchewan, ed. R. Lainé, D. Alonso, and M. Svab, Geological Association of Canada, Special Paper 29, p. 213-223.

Pattison, D.R.M., Carmichael, D.M. and St-Onge, M.R.
1982: Geothermometry and geobarometry applied to early Proterozoic 'S- type' granitoid plutons, Wopmay Orogen, Northwest Territories, Canada; Contributions to Mineralogy and Petrology, v. 79, p. 394-404.

Ramsay, J.G.
1967: Folding and Fracturing of Rocks; McGraw-Hill, 568 p.

Shegelski, R.J.
1978: Stratigraphy and geochemistry of Archean iron formations in the Sturgeon Lake – Savant Lake greenstone terrain; Ph.D. Thesis, University of Toronto, Toronto, Ontario.

Sibson, R.H.
1977: Fault rocks and fault mechanism; Geological Society of London, Journal, v. 133, p. 191-213.

St-Onge, M.R.
1983: 'Normal' and 'inverted' metamorphic isograds and their relations to syntectonic Proterozoic batholiths in the Wopmay Orogen, Northwest Territories, Canada; Tectonophysics, v. 76, p. 295-316.

St-Onge, M.R., King, J.E. and Lalonde, A.E.
1982: Geology of the central Wopmay Orogen (early Proterozoic), Bear Province, District of Mackenzie: Redrock Lake and the eastern portion of Calder River map areas; in Current Research, Part A, Geological Survey of Canada, Paper 82-1A, p. 99-108.

1983a: The Calderian Orogeny of Wopmay Orogen, N.W.T.: Evolution of an early Proterozoic collision-generated metamorphic-plutonic zone; Geological Association of Canada, Program with Abstracts, v. 8, p. A66.

1984: Deformation and metamorphism of the Coronation Supergroup and its basement in the Hepburn Metamoprhic-Plutonic Zone of Wopmay Orogen: Redrock Lake and the eastern portion of Calder River map areas, District of Mackenzie; in Current Research, Part A, Geological Survey of Canada, Paper 84-1A, p. 171-180.

St-Onge, M.R., Lalonde, A.E. and King, J.E.
1983b: Geology, Redrock Lake and eastern Calder River map-areas, District of Mackenzie: The central Wopmay Orogen (early Proterozoic), Bear Province, and the western Archean Slave Province; in Current Research, Part A, Geological Survey of Canada, Paper 83-1A, p. 147-152.

Wallis, R.H., Saracoglu, N., Brummer, J.J. and Golightly, J.P.
1983: Geology of the McLean Uranium Deposits; in Uranium Exploration in Athabasca Basin, Saskatchewan, Canada, ed. E.M. Cameron, Geological Survey of Canada, Paper 82-11, p. 71-110.

ADDENDUM

M.E.V. Villeneuve has recently derived a preliminary date of 2.9 Ga (Pb-Pb, zircon) from the eastern prong of the main body of granitic gneisses. This extends the amount of known Archean rocks in the gneiss complex and suggests that a significant component of the complex is Archean. Since there is no evidence of an unconformity at the contact between the dated gneisses and the Akaitcho Group, the contact at this locality must be tectonic. The occurrence of thin (less than 1 m) sheets of granitic gneiss in Akaitcho Group units near the gneiss complex and the intrusive contact of the western prong indicate, however, that parts of the complex are Proterozoic intrusives.

Reconnaissance geology of Precambrian rocks of the Fort Resolution, Taltson Lake, and Fort Smith areas, District of Mackenzie

Project 850005

Hewitt H. Bostock
Precambrian Geology Division

Bostock, H.H., Reconnaissance geology of Precambrian rocks of the Fort Resolution, Taltson Lake and Fort Smith areas, District of Mackenzie; in Current Research, Part A, Geological Survey of Canada, Paper 86-1A, p. 35-42, 1986.

Abstract

In Fort Resolution area amphibolites and metasediments persist as outliers and inclusion-schlieren gneiss along the east margin of an unfoliated granodiorite batholith. The batholith is in strongly foliated northern contact with white quartz monzonite and both are crosscut by the Great Slave Lake Shear Zone. Quartzite near Taltson River is possibly correlative to Wilson Island Group.

In south-central Taltson Lake area scheelite occurs as minor stratabound disseminations and veins within high-grade gneiss remnants in megacrystic granite.

In southeast Taltson Lake area a prominent fault separates eastern fine grained gneisses from coarser gneisses to the west. Foliated megacrystic granite is faulted against the western gneisses whereas massive, coarse grained granite intrudes those to the east. Western outliers of Nonacho Group occur as lenses along the fault and as slices overlying and faulted against the western gneisses.

Late northwesterly trending mafic dykes intrude most of these rocks.

Résumé

Dans la région de Fort Resolution, les amphibolites et les métasédiments persistent sous forme d'avant-buttes et de gneiss à inclusions de schlieren le long de la marge est du batholite granodioritique non feuilleté. Au nord, le batholite forme un contact fortement feuilleté avec une monzonite quartzifère blanche; les deux sont recoupés par la zone de cisaillement de Great Slave Lake. Il existe peut-être une corrélation entre le quartzite trouvé près de la rivière Taltson et le groupe de Wilson Island.

Dans la partie centrale-sud de la région du lac Taltson, on trouve de la scheelite sous forme de disséminations et de filons peu importants à l'intérieur de strates observées dans des restes de gneiss fortement métamorphisés dans un granite mégacrystique.

Dans la partie sud-est de la région du lac Taltson, une faille proéminente sépare des gneiss à grains fins à l'est de gneiss plus grossiers à l'ouest. Le mouvement d'une faille a déplacé le granite mégacrystique feuilleté contre les gneiss de l'ouest tandis qu'un granite grossier de nature massive a fait intrusion dans les gneiss à l'est. À l'ouest, des avant-buttes du groupe de Nonacho se manifestent sous forme de lentilles le long de la faille et sous forme de tranches chevauchant les gneiss à l'ouest, ou reposant contre ces derniers.

Des filons mafiques récents, à orientation nord-ouest, font intrusion dans la plupart de ces roches.

Introduction

Mapping (1:250 000 scale) during the 1985 field season was concentrated in the Fort Resolution area (NTS 85H), but preliminary reconnaissance was carried out in the south-central part of the Taltson Lake area (NTS 75E) to search northward for indications of stratabound scheelite mineralization like those found in high grade gneisses farther south, and to examine the western contact of the Nonacho Group. Bedrock is exceptionally well exposed throughout these areas except where it merges along the west boundary of the Fort Resolution area with the Slave River floodplain.

The most extensive unit found in the Fort Resolution area is an unfoliated granodiorite-granite complex which intrudes the previously known plutonic, metasedimentary and volcanic rocks at Thubun Lakes. An isolated remnant of pebbly quartzite, possibly correlative to the Wilson Island Group and likely downfaulted within this complex, occurs near the junction of Rat and Taltson rivers. Two new occurrences of scheelite in pelitic gneiss are reported within the megacrystic granite batholith of the southern Taltson Lake area. Mylonites which follow the Allen Fault Zone through the Fort Smith area (NTS 75D) pass northward into fine grained gneisses in the southeastern Taltson Lake area. The western Nonacho outliers occur along and near the fault boundary between these fine grained gneisses and coarser gneisses farther west.

Ice movement, as indicated by glacial striae, was from the northeast. Eskers and sand plains are few, being found mostly in the eastern part of the Taltson Lake area. The whole of the Fort Resolution area has been covered by a veneer of laminated silty clay which commonly flanks even high lying outcrops, but which has presumably been washed from outcrops by wave action in glacial lakes and by subsequent erosion.

Fort Resolution area

Amphibolites and metasediments

The oldest rocks within the Fort Resolution area (Fig. 4.1) comprise amphibolites, metapelites, calc-silicate rocks and quartz-rich gneisses (unit 1a) that occur southwest of Thubun Lakes, on the east margin of the area near 61°15'N latitude, and along the northern shore of Deskenatlata Lake at the southeast corner of the area. Particularly near Thubun Lakes, amphibolites commonly show well developed lamination suggestive of high strain followed by recrystallization. In the northern region amphibolites are dark green, and fine grained with or without plagioclase-rich laminae, grading locally into dark fine grained biotite-bearing gneisses. Pelitic rocks are grey to rusty stained, fine- to medium-grained, commonly muscovite-bearing biotite gneisses cut by muscovite pegmatite. Calc-silicate gneisses are plagioclase-bearing and epidote-bearing to epidote-rich. In places, in zones of apparently lower strain, more massive amphibolite is preserved, and in one such zone lenticular structures with dark margins and epidote-rich cores are strongly suggestive of pillows.

Metasediments (unit 1b) which lie on the east boundary of the area, about 61°15'N latitude, are biotite-muscovite-quartz-feldspar gneisses, locally garnet-bearing, that are interleaved with granitic rocks. Locally andalusite is present and tourmaline was observed at several outcrops. Some bands within these gneisses are quartz-rich.

Metapelites and quartz-rich gneisses at northern Deskenatlata Lake (unit 1b) locally contain garnet and chloritic pseudomorphs possibly derived from cordierite. Sillimanite was observed in gneisses east of the lake and in inclusion-rich migmatite to the north.

Migmatites

Inclusion-schlieren gneiss. A discontinuous zone of inclusion-schlieren gneiss (unit 2a) extends along the east border of Fort Resolution area from Thubun Lakes to Deskenatlata Lake. This gneiss consists of foliated to massive amphibolite xenoliths and less abundant inclusions and schlieren of pelitic or biotite-rich gneiss in a predominantly white weathering, but locally pink, fine- to medium-grained granodiorite. The distribution and abundance of inclusions and schlieren vary widely. Pelitic rocks within the migmatite are commonly garnet bearing, and in the southern part of the area locally contain sillimanite.

Metamorphic grade in the migmatites reached at least middle amphibolite facies in the southern part of the area, but similarity of the southern gneisses to nearby high grade metasediments of the Fort Smith area (Bostock, 1982) suggests that they may have attained upper amphibolite or lower granulite facies. The presence of andalusite instead of sillimanite in pelitic gneiss along the central west margin of the area, and of muscovite-bearing biotite gneiss in the northeastern corner near Thubun Lakes suggests northward decreasing metamorphic grade. The coarse grained plutonic aspect and absence of sedimentary structures in the northern gneisses is consistent with retrogression of these rocks from high metamorphic grade, but the persistence of apparently pristine, low grade, epidote-rich cores in local pillows in the amphibolite is not readily reconciled with this interpretation. Microscopic examination of these rocks may settle this problem.

Hybrid plutonic rocks. Mafic gneisses comprising inclusions and schlieren of mafic plutonic rocks in medium-to coarse-grained, foliated to massive biotite or hornblende granodiorite (unit 2b) are present along Taltson River at the east margin of the Slave River floodplain. No inclusions of recognizable metasedimentary origin were observed, most being medium- to coarse-grained, and of hypidiomorphic texture. It seems likely therefore that these gneisses represent intermixing of mafic dykes or older mafic phases within the granodiorite.

Plutonic rocks

Two major plutonic complexes are present within the Fort Resolution area. North and northeast of Lake of the Rock on Thubun River a white weathering, mostly strongly foliated, medium grained biotite quartz monzonite bearing local zones of biotite migmatite is preserved (unit 3). South of Lake of the Rock a batholithic complex primarily composed of massive, megacrystic to equigranular granodiorite to quartz monzonite is exposed (unit 4). Coarse black locally poikilitic biotite is the typical mafic mineral in southern and western parts of the complex, but hornblende and chlorite are prominent elsewhere. This complex is extensively but variably intruded by dykes and small irregular bodies of pink leucocratic granite. In the contact zone between the two granite complexes both are strongly foliated, and although lenses of white granodiorite appear locally within the pink granodiorite, the age relations are obscured. Lithological similarity of the white weathering granodiorite to the Slave Granite and of some phases of the megacrystic granodiorite to the megacrystic granite of the Fort Smith area to the southeast (Bostock, 1982) may indicate that the white weathering rocks are the older.

Mylonite belts

Two northeasterly trending belts of mylonitic rocks (unit 5) are prominent within the Fort Resolution area and an additional north trending, likely older belt of high strain

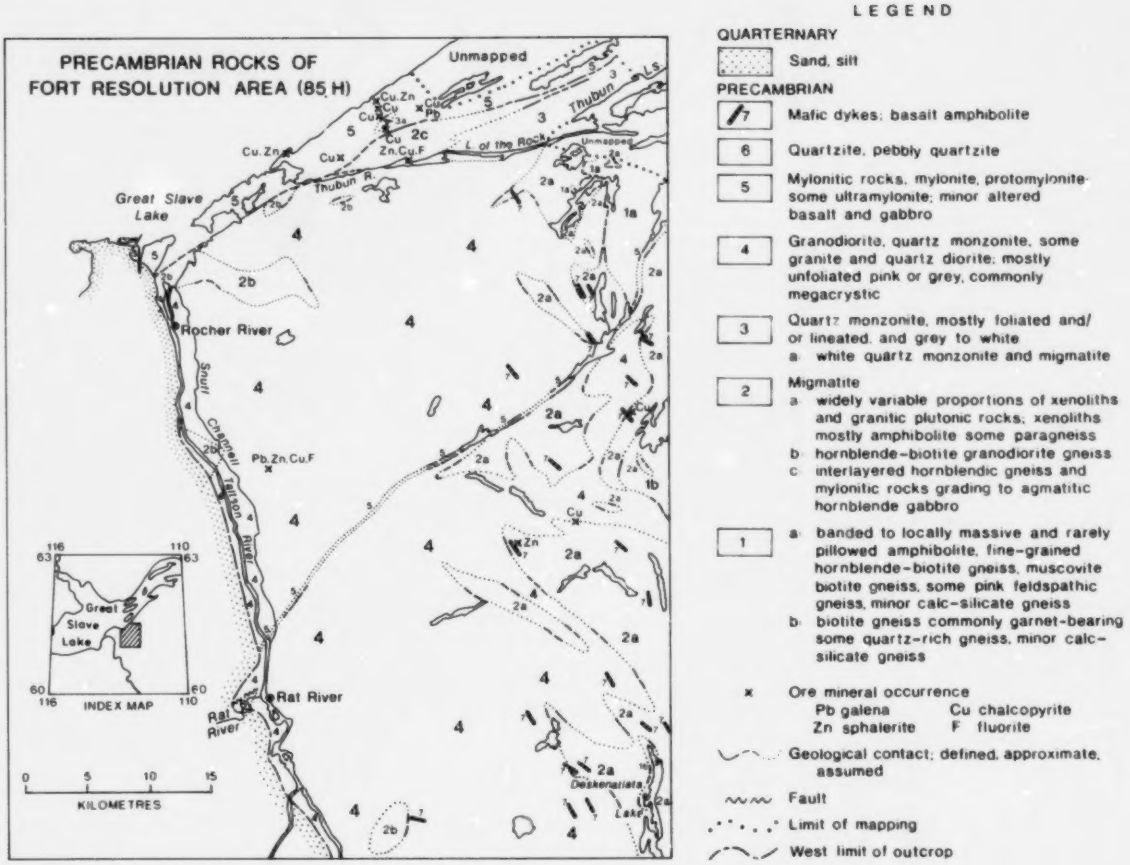

Figure 4.1. *Precambrian rocks of Fort Resolution area (NTS 85H).*

gneisses lies immediately to the east. The most prominent of these is the Great Slave Lake Shear Zone, (Hanmer and Lucas, 1985) the western end of which extends across the northern part of the area mapped.

Great Slave Lake Shear Zone. Rocks within this belt consist primarily of pink to locally yellow-green or grey mylonites, protomylonites and some ultramylonite. Foliation in the mylonites trends mostly parallel to the margins of the belt and dips steeply, mostly to the southeast. Lineations trend subparallel to the belt and plunge gently (up to 20°) in either direction. Locally these rocks are intruded by mafic dykes, but in places as along the northwestern edge of the belt just northeast of the estuary of Thubun River, substantial amounts of basaltic to gabbroic rocks have been deformed within the mylonite. Elsewhere, in zones of lower strain, strongly foliated white weathering granodiorite and migmatite, like that to the south, are recognizable within the margins of the belt.

Contacts between the mylonites and less deformed rocks along the southeast margin of the belt are gradational. Northeast of the estuary of Thubun River the gradational zone is broad and strong foliation extends far into the adjacent rocks. To the southwest the zone of foliated rocks shrinks and lenses of granodiorite appear to be sheared into the mylonite locally. Near the estuary of Taltson River discrete minor mylonite belts appear subparallel to the main belt within the granitic rocks.

Median mylonite belt. The median mylonite belt comprising mylonite to protomylonite stretches in a zone up to several hundred metres across from north of Rat River on Taltson River to Thubun Lakes. In places minor zones of mylonite up to a metre across were observed subparallel to the belt along its southeast margin. Foliation in the mylonite is steeply southeast dipping to vertical. Lineation is not well developed except at the northeast limit of mapping where it plunges eastward at about 40°. The northwest margin is less well exposed but at one place in the central part of the belt granitic rocks immediately adjacent to the belt are fractured and veined. Near Thubun Lakes where the belt intersects paragneisses, the mylonitic rocks are biotite-rich and more schistose. Smaller mylonite zones up to a metre wide and subparallel to the median belt locally penetrate the plutonic rocks within the foliated zone that extends for several kilometres south of Thubun River.

Sedimentary rocks

Quartzite at Rat River. An isolated hill of white weathering, pale purplish-white, clean, 1 mm grain size quartzite containing scattered pebbles and pebble clusters of white vein quartz, purple quartzite and rare grey flinty quartzite (unit 6) is present immediately north of Rat River and west of the village of Rat River. The outcrop shows very little variation or evidence of stratification. Locally the quartzite is cut by white quartz veins up to 5 cm thick showing cockscomb texture but no sulphide mineralization.

Red stained and sheared plutonic rock outcrops immediately to the northeast and north of Rat River village respectively suggesting that the quartzite may be down faulted against plutonic rocks to the north. The pebbly quartzite is not like any of the pre-Devonian Paleozoic rocks which underlie the Slave River floodplain to the west, but is possibly related to quartzites described by Stockwell (1933) on Stoney Island (off Slave River delta) which he compared to Wilson Island Group.

Et-Then Group. Purplish red-brown sandstone and conglomerate of the Et-Then Group occurs on some of the small islands immediately offshore along the south coast of Great Slave Lake (not shown in Fig. 4.1). A landing on one of these islands revealed sandstone with numerous conglomerate beds up to about 4 m thick containing a variety of granite, gneiss and vein quartz pebbles and cobbles. One cobble of finely homoclastic (Hanmer and Lucas, 1985) protomylonite like that in the adjacent mylonite belt to the south was seen. The beds have been tilted and faulted and now show various trends with dips of about 75°.

Late dykes

Thin, typically northwesterly trending, steeply dipping mafic dykes (unit 7) are scattered within the eastern part of the area, mostly within the migmatite but some intrude white weathering foliated quartz monzonite north of Lake of the Rock. These dykes tend to be slightly foliated along their margins parallel to contacts but do not show the foliation of the enclosing rocks which they cut. The dykes are commonly less than 1 m in width and may occur in swarms of four or five. A few reach 3 or 4 m wide and are medium-fine grained, ophitic, but most are fine to very fine grained. Partial alteration of pyroxene to hornblende is evident in the coarser grained dykes and rarely this alteration appears to be complete. Dykes commonly pinch and swell along strike and may be offset up to 1 or 2 m along minor faults. The predominent northwesterly trend suggests that these dykes may be part of the 1700 Ma Sparrow Dyke Swarm, McGlynn et al., 1974).

Economic geology

Mineralized quartz veins. Quartz veins showing cockscomb texture and bearing minor amounts of chalcopyrite are common within the mylonite belt of the Great Slave Shear Zone near Thubun River and at intervals in the same rocks along the coast of Great Slave Lake farther northeast. A similar vein bearing small amounts of galena and sphalerite in addition to minor chalcopyrite and fluorite occurs within granodiorite east of Snuff Channel on Taltson River. Most of these veins show brecciation suggesting minor fault movements during emplacement of quartz, but none seen during the present work appear to be of economically significant size. Similar but larger quartz veins containing substantially greater amounts of galena and sphalerite are present near O'Connor Lake immediately east of the Fort Resolution area (McGlynn, 1971).

Gossans. Minor gossans were observed in dark biotite gneisses associated with amphibolite and locally in association with amphibolite fragments in inclusion-schlieren migmatite. Minor sphalerite in association with one of these gossans within inclusion-schlieren migmatite about 19 km north-northwest of Deskenatlata Lake, remains to be confirmed by laboratory study. The amphibolite inclusions, forming 15% of the rock as a whole, occupy a zone of unknown dimensions along the shore of a small lake. Pyrite-pyrrhotite forms about 15% of its amphibolite host.

Scheelite-bearing gneiss, south Taltson Lake area

Reconnaissance of the shores and immediate hinterland about three lakes in the south-central part of the Taltson Lake area (Fig. 4.2) was done to follow up discovery of scheelite in gneisses within the Fort Smith area immediately to the south (Bostock and Thompson, 1983). In the Taltson Lake area these gneisses (unit 1) occupy one major lenticular belt and numerous small bodies of garnet-biotite-quartz-feldspar gneiss and schist that are engulfed within the regional megacrystic granite. Andalusite is recognized in some of the gneisses but sillimanite and cordierite are only rarely preserved. Chlorite and muscovite are now more common, indicating that the gneisses have been extensively retrograded from the upper amphibolite-lower granulite facies reached in the Fort Smith area immediately to the south.

Pink to buff, medium- to coarse-grained, strongly foliated to massive, biotite-chlorite granite with augen to euhedral megacrysts of potassium feldspar commonly up to 2 cm (unit 2a) intrudes and is interleaved with the gneisses. Garnet is common in the rock and altered cordierite less common. Bodies of granite within the schists commonly occupy ridge or hill tops with gently eastward dipping schist and gneiss between, but local zones of steep or reversed dip are also present. Quartz lineation is widely evident and plunges gently either northerly or southerly. In the central-western part of the area mapped (see Fig. 4.2) the granite is intermingled with medium grained hornblende granodiorite to diorite. In places these more mafic rocks form blocks within, and are veined by, the granite, but elsewhere age relations appear conflicting. Quartz-feldspar veins bearing black tourmaline are present locally in a poorly defined east trending zone through both granite and more mafic rocks. Granite and gneiss are intruded locally by northwesterly trending dykes (unit 3) of the Sparrow Dyke Swarm.

Small amounts of scheelite, in tiny veins and as minute grains disseminated within individual laminae in the gneisses were found at two places distributed approximately along regional strike within the major gneiss belt. These occurrences were not recognized in the field but were discovered during examination of rock specimens in ultraviolet light. Identification was confirmed by X-ray diffraction.

Reconnaissance of Precambrian rocks about the western margin of Nonacho Group

A preliminary reconnaissance of basement gneisses and Nonacho Group was made along Taltson River (Fig. 4.3) in the southeastern part of the Taltson Lake area. This area lies immediately north of the confluence of two prominent shear zones, the Allen Fault Zone (Godfrey and Langenberg, 1978) and a second shear zone through Hill Island Lake (Bostock, 1984).

Basement gneiss complex

The basement upon which Nonacho Group was deposited comprises two regional units separated approximately by Taltson River which flows from Taltson Lake through King and Lady Grey lakes. The western unit (unit 1b) comprises remnants of medium grained granodioritic rocks, commonly with amphibolite inclusions or schlieren, that have been more or less broken up, intruded by a more leucocratic host, and to varying degrees deformed and altered. Within these rocks are zones of stronger, northerly trending deformation which include amphibolite bodies (dykes ?) that are transposed parallel to banding, stretched, boudined and variably assimilated into the surrounding gneiss. Rarely,

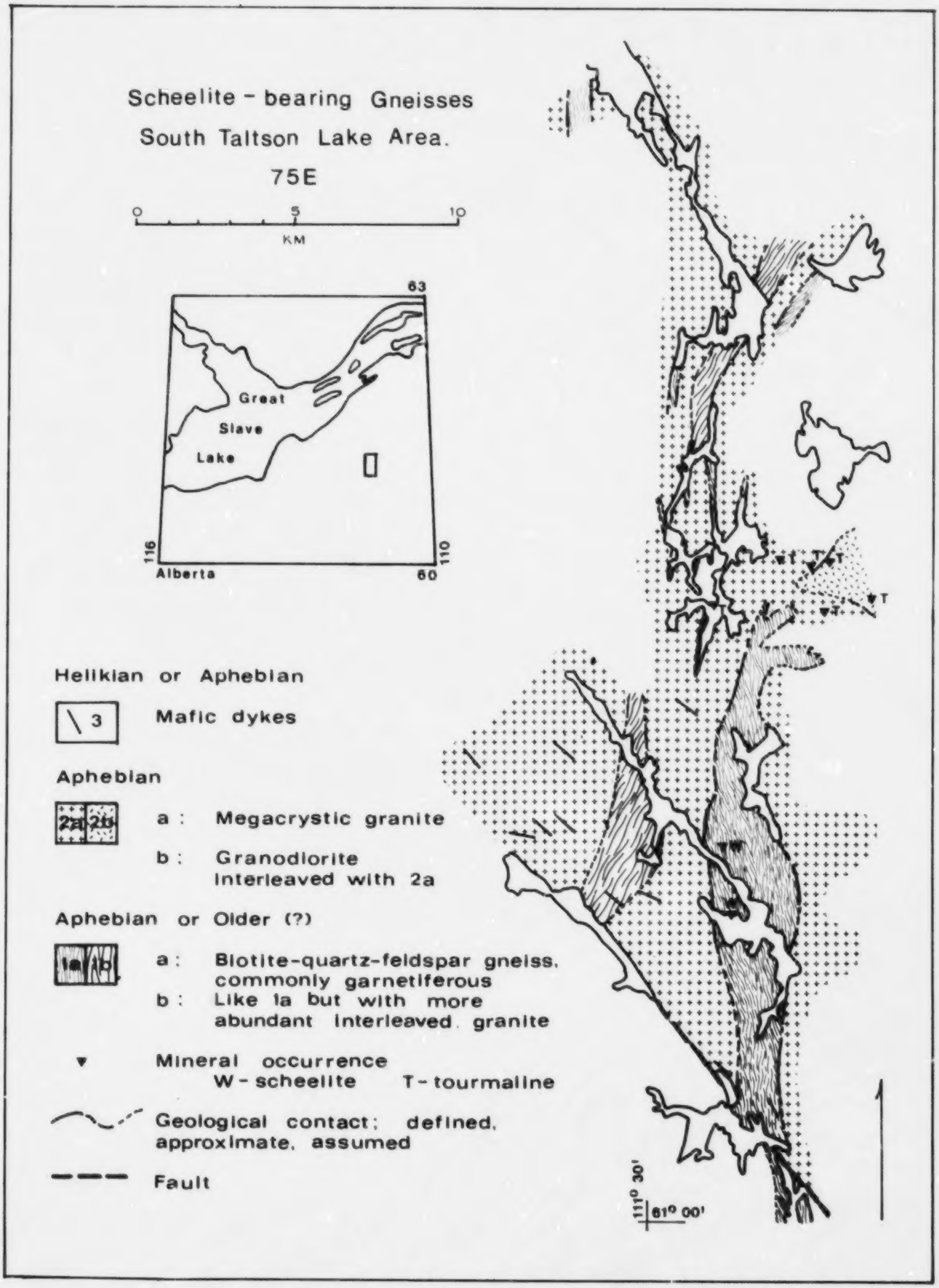

Figure 4.2. Scheelite-bearing gneisses, South Taltson Lake area (NTS 75D).

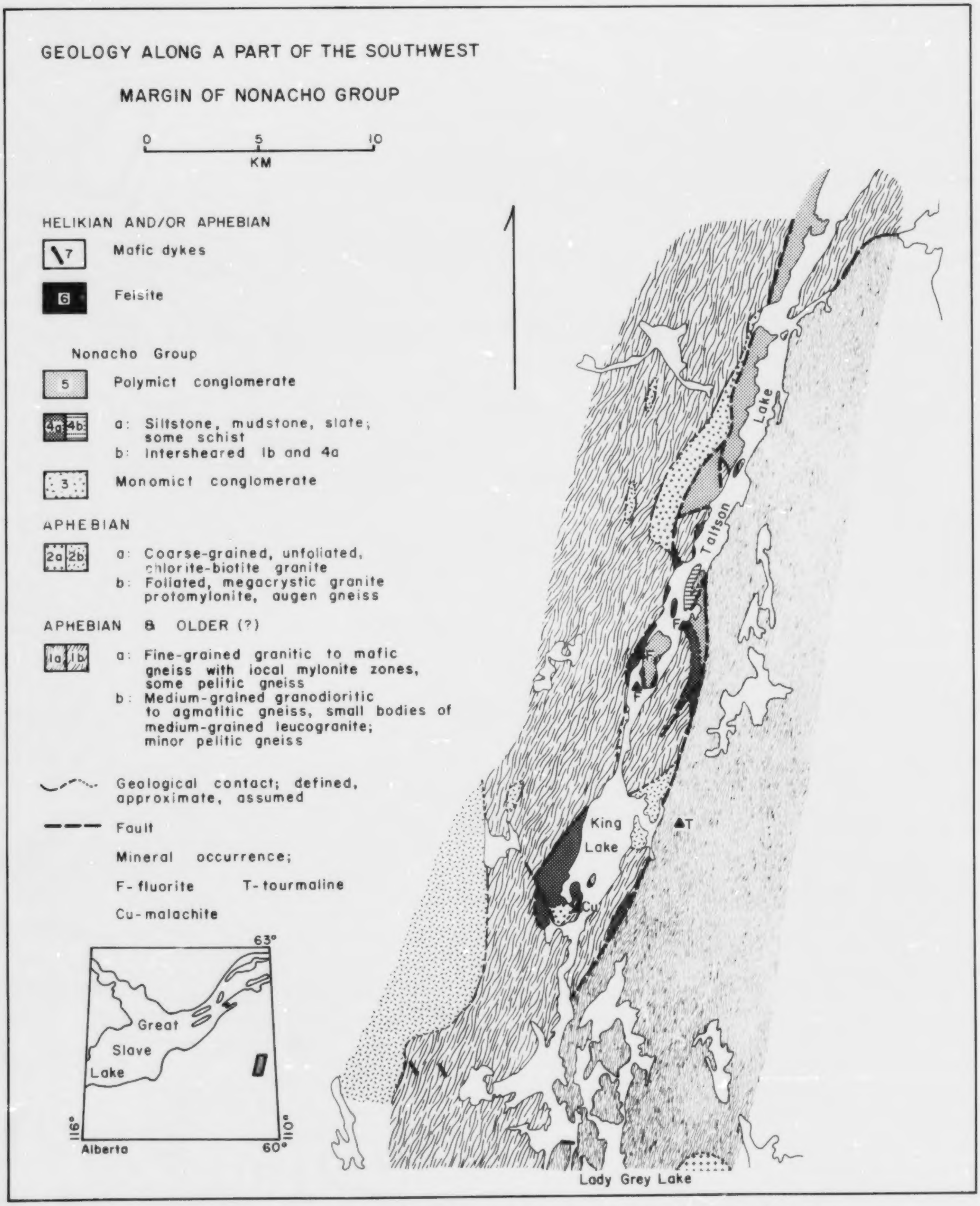

Figure 4.3. Geology along the southwest margin of a part of Nonacho Group (NTS 75D).

garnet-bearing amphibolite and paragneiss inclusions are present. Locally bodies of biotite, hornblende or chlorite augen gneiss (unit 2b), only some of which are of mappable size, are present. All of these rocks, except unit 2b, are variably intruded by dyke-like and irregular bodies of pink, leucocratic, predominantly fine grained but locally pegmatitic, granite.

The eastern gneiss (unit 1a) comprises fine grained biotite, chlorite and hornblende-bearing gneisses, commonly sucrosic, with still finer grained mylonitic zones. Narrow belts of pelitic gneiss, mostly muscovite-bearing but locally preserving garnet and sillimanite, are fairly common about Lady Grey Lake and east of the southern half of King Lake. None were recognized farther north where dark, fine grained, schistose biotite and biotite-hornblende-rich zones are more common. At one locality east of King Lake fine grained muscovite-chlorite-bearing granite gneiss contains scattered grey inclusions of quartz-rich, tourmaline-bearing rock up to several centimetres in length. Black tourmaline forms up to about 10% of these inclusions.

Megacrystic granite, protomylonite, and augen gneiss

West of the southern part of King Lake, pink granite (unit 2b) with potassium feldspar megacrysts up to 3 cm in length is in sheared contact with the gneisses of unit 1b. Mafic content (chlorite-biotite) is about 5%. The granite is strongly foliated to protomylonitic in the southern part of the region examined, but foliation is much weaker in the north. Lineated quartz in the strongly foliated region plunges about 25° south. Similar but commonly more mafic granite to granodiorite forms smaller bodies that range to augen gneiss within the gneisses of unit 1b. East of the north end of Lady Grey Lake coarse grained, equigranular, pink chlorite-biotite granite intrudes fine grained gneisses of unit 1a.

Nonacho Group

Unmetamorphosed to low grade sediments within the area mapped are outliers of the more extensively preserved parts of the Nonacho Basin immediately to the east. The entire basin within Taltson Lake area was mapped by Henderson (1939). Later work (McGlynn, 1978; Aspler and Donaldson, 1984) was of a less detailed nature about the southwestern Nonacho outliers described here.

Major bodies of unbedded basal conglomerate of Nonacho Group (unit 3) occur inland west of Taltson Lake and, west of central King Lake, and a few smaller bodies occur along the northwest shore of King Lake. The clasts are angular to rounded and of variable dimensions, mostly cobble to boulder size. The sparse matrix is typically coarse granitic sand. Clast lithologies are primarily plutonic like those found in the local basement, but vein quartz is also locally present. Megacrystic granite clasts like those of the batholith to the west (see Fig. 4.2) are rare and of uncertain correlation. No mylonite clasts were seen. The contact between conglomerate and basement gneiss is exposed at central King Lake where red weathering pegmatitic granitic rock appears among outcrops of conglomerate as the contact is approached, suggesting that the surface of unconformity is irregular. Farther northwest along the western margin of the overlying siltstone unit, wedges of conglomerate and siltstone are intersheared with basement along the contact.

Overlying the basal conglomerate, but not seen in direct contact with it, are interbedded grey to mauve and green siltstones (unit 4a) exposed at central King and southern Taltson lakes. Sandstones and scattered pebbles occur within the unit locally. Graded beds are evident locally. Moderately to strongly developed cleavage is widespread. On the first broad peninsula on the east shore of Taltson Lake and north of the outlet, rocks of this unit are intimately intersheared with basement gneiss (unit 4b). Greenish to dark grey schist with scattered quartz and granite pebbles occurs along the boundary fault between gneisses of units 1a and 1b east of King Lake. Crystallization of muscovite in pressure shadows about granite pebbles suggests that this outlier has reached lower greenschist metamorphic grade.

Polymict conglomerate and quartz sandstone (unit 5) occur intermittently along the shores of Taltson Lake. Clasts are mostly moderately to well rounded and comprise vein quartz, sandstones, siltstones, some granitic and gneissic rocks, and local concentrations of intermediate to mafic volcanic rocks. Some beds consist mostly of slate chips. Clasts are mostly loosely packed in sandy to silty matrix. Quartz sandstone occurs in thin beds interleaved with the conglomerate, but forms massive beds in the higher exposures on the large island at the outlet of Taltson Lake.

Massive flinty grey to green felsite (unit 6) is intrusive into sandstone of unit 5 along the east rapids at the outlet of Taltson Lake. On the east shore at the upper entrance to the western rapids, small bodies up to a few metres across of similar but coarser more suggary textured felsite intrude the basement gneiss.

Mafic dykes

West of Lady Grey Lake, northwest-trending slightly altered diabase dykes (unit 7) up to 5 m thick are found in groups of several dykes intrusive into the gneisses. These dykes are likely part of the Sparrow Dyke Swarm. Similar but commonly more fractured and altered dykes intrude units 3 to 5 of the Nonacho Group. These dykes trend more northerly to northeasterly parallel to faulting along Taltson River valley, and are substantially thicker, reaching up to 65 m in width. They occur in areas of fine detail on the map and are therefore not shown.

Faults

Taltson River valley lies along the projected trend of major mylonite zones present in the Fort Smith area (Bostock, 1982). These mylonites appear to peter out within the fine grained gneisses of unit 1a perhaps partly as a result of northward increasing grain growth. Northward increasing severity of retrogression of pelitic bands in the gneisses may have accompanied this recrystallization. From King Lake northward, basement gneisses particularly along the east shore of Taltson River are intensely broken up, brecciated and healed by chloritic material. West of the river many blocks of basement gneiss have been wedged up along oblique faults within the sediments. Likewise, evidence of shearing west of King Lake where north-northeasterly trending contacts are exposed, and omission of unit 4 between units 3 and 5 at Taltson Lake, suggest major faulting along the river valley. This faulting, though possibly younger than the most prominent mylonitization to the south, suggests a northward transition from ductile to brittle deformation. Shear bands seen locally in unit 1a and 1b gneisses east of King Lake suggest that movement along this zone had a sinstral slip component.

Economic geology

One occurrence of minor malachite stain was found along a fault separating unit 1b gneiss from Nonacho siltstone-mudstone on the west shore of central King Lake. Purple fluorite in minor quartz veins occurs in siltstone-mudstone of unit 4a at three localities near the south end of Taltson Lake.

References

Aspler, L.B. and Donaldson, J.A.
1984: The Nonacho Basin (Early Proterozoic) Northwest Territories, Canada: sedimentation and deformation in a strike-slip setting; Contribution 09-84 of Ottawa-Carleton Centre for Geoscience Studies, p. 1-61.

Bostock, H.H.
1982: Geology of the Fort Smith map area, District of Mackenzie, Northwest Territories (NTS 75D); Geological Survey of Canada, Open File 859, p. 1-52.

1984: Preliminary geological reconnaissance of the Hill Island Lake and Taltson Lake areas, District of Mackenzie; in Current Research, Part A, Geological Survey of Canada, Paper 84-1A, p. 165-170.

Bostock, H.H. and Thompson, D.L.
1983: Fluorescent minerals from the Fort Smith area, District of Mackenzie; in Current Research, Part B, Geological Survey of Canada, Paper 83-1B, p. 401-402.

Godfrey, J.D. and Langenberg, C.W.
1978: Metamorphism in the Canadian Shield of northeastern Alberta; in Metamorphism in the Canadian Shield, ed. J.A. Fraser and W.W. Heywood; Geological Survey of Canada, Paper 78-10, p. 129-138.

Hanmer, S. and Lucas, S.B.
1985: Anatomy of a ductile transcurrent shear: the Great Slave Lake Shear Zone, District of Mackenzie, N.W.T. (preliminary report); in Current Research, Part B, Geological Survey of Canada, Paper 85-1B, p. 7-22.

Henderson, J.F..
1939: Taltson Lake; Geological Survey of Canada, Map 525A with marginal notes.

McGlynn, J.C.
1971: Metallic mineral industry, District of Mackenzie, Northwest Territories; Geological Survey of Canada, Paper 70-17, p. 144.

1978: Geology of the Nonacho Basin, District of Mackenzie, Northwest Territories; Geological Survey of Canada, Open File 543 (map).

McGlynn, J.C., Hanson, G.N., Irving, E., and Park, J.K.
1974: Paleomagnetism and age of Nonacho Group sandstones and associated Sparrow Dykes, District of Mackenzie; Canadian Journal of Earth Sciences, v. 11, p. 30-42.

Stockwell, C.H.
1933: Great Slave Lake-Coppermine River area, Northwest Territories; in Geological Survey of Canada, Summary Report 1932, Part C, p. 37c-63c.

U-Pb zircon ages of late internal plutons of the Abitibi and eastern Wawa subprovinces, Ontario and Quebec

M.J. Frarey and T.E. Krogh [1]
Precambrian Geology Division

Frarey, M.J. and Krogh, T.E., U-Pb zircon ages of late internal plutons of the Abitibi and eastern Wawa subprovinces, Ontario and Quebec; in Current Research, Part A, Geological Survey of Canada, Paper 86-1A, p. 43-48, 1986.

Abstract

The ages of eleven felsic plutons widely distributed over a distance of 700 km within the greenstone terranes of the Abitibi and eastern Wawa subprovinces of the Canadian Shield have been precisely determined using U-Pb zircon techniques. With one exception, the ages fall between 2675 and 2700 Ma. The distribution and post-kinematic relationship of the intrusions indicates that the entire region from Lake Superior to the Grenville Front achieved tectonic stability by 2675 Ma. The range of ages evidently constitutes a discrete interval of regional granitic emplacement which, from scanty available ages of nearby volcanics, was separated from host volcanism by some 20 to 40 Ma.

Résumé

La datation du zircon par la méthode de l'U-Pb a permis de déterminer très précisement l'âge de 11 plutons felsiques répartis sur 700 km dans les terrains à roches vertes de la sous-province d'Abitibi et de la partie est de la sous-province de Wawa du Bouclier canadien. Les âges obtenus pour tous les plutons, sauf un, se situent entre 2 675 et 2 700 Ma. La répartition des intrusions et leurs liens post-tectoniques révèlent que toute la région du lac Supérieur jusqu'au front de Grenville avait atteint la stabilité tectonique il y a 2 672 Ma. La gamme d'âges représenterait donc un intervalle discrèt de mise en place régionale du granite qui, d'après les rares dates établies à partir des roches volcaniques voisines, a été séparé de l'épisode de volcanisme par une période de quelque 20 à 40 Ma.

[1] Royal Ontario Museum, 100 Queen's Park, Toronto, Ontario M5S 2C6

Introduction

In recent years an increasing number of U-Pb isotopic ages have been reported from the Abitibi and eastern Wawa Subprovinces of Superior Province, that is, the region between Lake Superior in the west to the Grenville Front near Chibougamau in the east (Fig. 5.1). The ages have been derived predominantly from felsic volcanic and plutonic rocks of these greenstone terranes which, though interrupted by the Kapuskasing Structural Zone, may be considered as a single belt; it is probably the world's largest exposed "greenstone belt". A compilation at 1:500 000 by Thurston and Franconi (1984) shows the general geology of most of the territory. While the number of ages has increased, systematic coverage is still lacking and in some important areas such as Matagami and Noranda in Quebec reliable and precise isotopic ages are needed. The scarcity of information (other than K-Ar ages) as of 1977 is illustrated by Figure 21 of Stockwell (1982), a compilation showing only six "orogenic"[1] ages in the region concerned, only one of which (Steiger and Wasserburg, 1969), is a U-Pb zircon determination. A general dearth in fact characterizes the whole of Superior Province, large tracts of which are devoid of other than K-Ar mineral dates, inhibiting the understanding and interpretation of the geological history of the province. This report presents eleven new zircon ages by the authors and briefly discusses their significance in the evolution of the region.

In an effort to increase the U-Pb age database of greenstone belts, the first author collected numerous samples from late or post-tectonic plutons over a wide area of Superior Province. For the region under discussion, thirteen were selected to provide geographic distribution, and of these, eleven contained suitable zircon populations, providing the results included herein. All isotopic analyses for these eleven were carried out at the Jack Satterly Geochronology Laboratory of the Royal Ontario Museum under the direction of T.E. Krogh. The analytical data are shown in Tables 5.1 and 5.2. In determining final precise age values, techniques developed by Krogh (1982, a, b) were applied. For all but one age, chords to the concordia curve were drawn using three or more points.

Most of the plutons are in districts that have been well-studied and described in various reports; brief site descriptions are given below, and their locations are shown in Figure 5.1.

Inasmuch as most of the plutons sampled are fresh, unfoliated or weakly foliated, discordant, and invade folded supracrustals of subgreenschist to upper amphibolite grade, and in some cases display narrow metamorphic aureoles, it might be argued that they are anorogenic rather than orogenic and unrelated to the magmatism and tectonism of the crustal cycle. On the other hand, the ages show that granite emplacement and host rock deposition and deformation within this belt are not separated by great time gaps like those characterizing Proterozoic anorogenesis and orogeny in North America (see Anderson, 1983, Fig. 1) and the intrusions are best described as post-kinematic, late-orogenic, or late-tectonic. No post-Archean granite plutons have been identified within the belt. In general, the plutons are probably cogenetic, but with few exceptions are not coeval, with the associated host volcanic rocks. Some may have been accompanied by mild local deformation. In any case, for the main purpose of this study the sampled plutons are important as evolutionary markers, providing a ready means of constraining the time of regional tectonism in the greenstone belts, and together with the ages of volcanism, where available, also providing numerical time brackets for the entire deposition-deformation-metamorphism-plutonism cycle.

Sample sites from east to west

1. Opemisca Pluton

This body is a discordant ovoid intrusion some 25 km in long dimension invading folded and metamorphosed volcanic and sedimentary strata of the Roy Group and associated

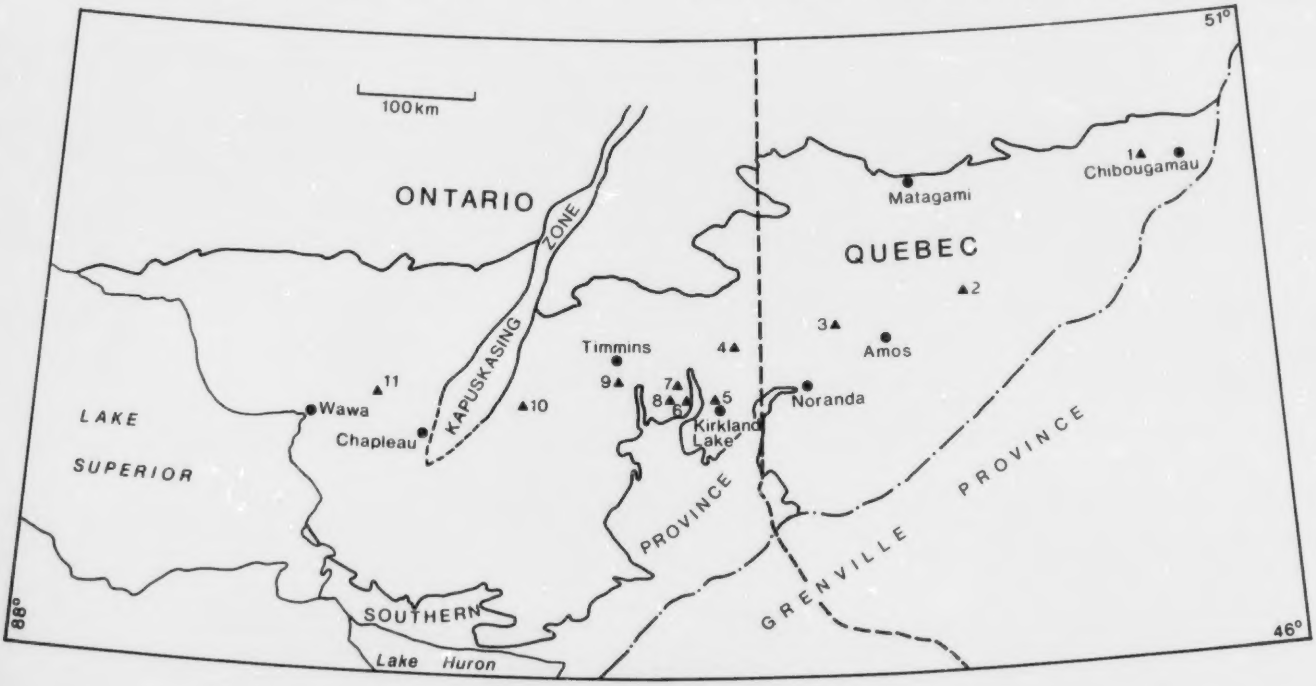

Figure 5.1. ***Distribution of plutons.***

[1] In this note "orogenic" refers to processes of deformation, metamorphism, and plutonism of the region, to the rocks involved and their isotopic ages.

mafic intrusions. Its setting and composition are described by Duquette (1970, 1972) and Durocher (1974, 1975) and its petrology and geochemistry are described by Wolhuter (1971). The pluton consists mainly of hornblende granodiorite and monzonite grading outward to marginal hornblende syenite. Where sampled in Levy Township (latitude 49°52'00"; longitude 174°48'30"), the rock is a coarse grained, pinkish, hornblende quartz monzonite consisting of hornblende, plagioclase, potassium feldspar, quartz, chlorite, and epidote with accessory sphene, zircon, opaques and apatite. It is unfoliated and equigranular. The Opemisca pluton has been studied isotopically by Dallmeyer et al. (1975) employing

Table 5.1. Calculated U-Pb zircon ages of internal plutons, Abitibi and eastern Wawa subprovinces

Pluton	Field sample	Age Ma	Error 2 sigma	Probability of fit per cent	Lower intersection Ma	No. of points
Opemisca	FC-2-76	2697.3	-1.7 + 1.9	44	367	3
Franquet	FC-3-76	2691.6	-3.4 + 3.6	77	1013	3
Taschereau	FC-6-76	2718.1	-2.2 + 2.3	13	650	4
Garrison Stock	FC-12-75	2678.9	-3.6 + 3.9	98 (3 points)	938	3
Winnie Lake	FC-7-75	2677.3	-2.4 + 2.5	100 (2 points)	556	2
Watabeag 1	FC-5-75	2681.3	-2.6 + 2.7	10	644	3
Watabeag 2	FC-9-75	2676.0	-2.1 + 2.2	46	570	3
Watabeag 3	FC-3-75	2699.0	-2.9 + 3.5	54	900	3
Adams Stock	FC-10-75	2686.4	-2.8 + 3.0	37	510	3
Hoodoo Lake	FC-8-76	2683.7	-3.0 + 3.2	22	977	4
Ash Lake	FC-9-76	2684.5	-2.6 + 2.7	16	495	3

Input errors, (2 sigma): ± 0.50% on all Pb-U ratios, ± 0.1% on $^{207}Pb/^{206}Pb$ ratios of abraded (top) point, ±0.15% on others for each line (except FC-9-76 which has 0.15% on all 3 points").

Table 5.2. U-Pb isotopic data (Abr. = abraded; N0° = non-magnetic at 0°)

Field Sample	Fraction Analyzed	Sample Weight mg.	Concentrations ppm U	Concentrations ppm Pb	Measured $^{206}Pb/^{204}Pb$	Atomic Ratios Corrected for Blank and Common Pb $^{206}Pb/^{238}U$	$^{207}Pb/^{235}U$	$^{207}Pb/^{206}Pb$
FC-3-75	N0° Abr.	1.22	75.1	46.0	11923	0.5202	13.278	0.18512
	N0° Bulk	2.56	107.4	62.5	11229	0.4918	12.362	0.18231
	N0° dup.	2.66	103.5	59.4	9996	0.4855	12.172	0.18187
FC-5-75	N0° Abr.	0.34	221.7	130.6	8706	0.5021	12.622	0.18231
	N0° Bulk	1.3	399.8	203.4	5418	0.4458	10.939	0.17800
	M1°	1.03	580.6	266.1	3692	0.4053	9.765	0.17476
FC-7-75	N0° Abr.	0.264	217.2	127.8	4993	0.5024	12.609	0.18203
	N0° Bulk	2.2	362.8	166.3	1258	0.3921	9.431	0.17444
FC-9-75	N0° Abr.	0.305	91.0	54.1	4424	0.5084	12.775	0.18223
	N0° Bulk	4.5	172.4	95.5	7775	0.4743	11.1780	0.18016
	M1°	2.0	317.7	148.8	1853	0.4109	9.957	0.17577
FC-10-75	N0° Abr.	0.62	229.8	124.0	256	0.4945	12.452	0.18265
	N0° Bulk	3.0	252.1	132.8	6645	0.4665	11.640	0.18096
	MO Bulk	2.29	293.0	143.2	5048	0.4341	10.724	0.17919
FC-12-75	N0° Abr.	0.244	247.7	141.3	421	0.5032	12.605	0.18166
	N0° Bulk	0.86	456.3	245.6	1487	0.4612	11.228	0.17709
FC-2-76	N0° Abr.	0.519	70.5	43.0	3247	0.5198	13.253	0.18493
	N0° Clear	0.77	89.4	51.6	5533	0.4914	12.456	0.18384
	M3° Clear	0.71	103.4	57.9	6393	0.4763	12.047	0.18344
FC-3-76	N0° Abr.	0.45	178.2	108.6	8336	0.5180	13.160	0.18426
	N0° Bulk	1.9	291.2	150.2	1756	0.4532	11.023	0.17639
	MO Bulk	0.56	767.0	359.7	562	0.4167	9.826	0.17103
FC-6-76	N0° Short Abr.	0.25	162.6	97.0	6307	0.5063	12.988	0.18606
	N0° Long Abr.	0.20	313.4	180.0	4691	0.4883	12.458	0.18505
	N0° Bulk	1.2	450.3	232.0	7398	0.4621	11.638	0.18267
	M1 Bulk	1.43	652.3	297.7	4204	0.4098	10.079	0.17838
FC-8-76	N0° Bulk	0.375	321.3	193.5	15308	0.5125	12.939	0.18310
	N0° Bulk	3.21	410.9	219.4	7985	0.4702	11.559	0.17832
	N0° Bulk dup.	1.27	400.6	212.6	5857	0.4700	11.532	0.17796
	M1 Bulk	1.3	504.7	240.8	1279	0.4112	9.653	0.17024
FC-9-76	N0° Bulk	0.65	494.9	259.3	8176	0.4777	11.950	0.18143
	N0° Bulk	1.16	486.1	253.1	7799	0.4737	11.857	0.18155
	M3° Bulk	0.53	1205.0	471.0	2649	0.3592	8.585	0.17332

Ar-Ar and K-Ar techniques on hornblende. Ar-Ar ages were 2692 ± 30 and 2656 ± 30 Ma respectively; K-Ar hornblende ages were 2653 ± 64 and 2647 ± 61 Ma. Neglecting error limits, three of these cooling ages are appreciably younger than the U-Pb zircon age determined in this study and all predate the estimated close of the Kenoran Orogeny by roughly 150-190 Ma.

Age: 2697.3 $^{+1.9}_{-1.9}$ Ma. This age is confirmed by a recent Pb-Pb age of 2695 ± 8 Ma (Gariépy, 1984).

2. Franquet pluton (informal name), Franquet Township, Quebec

A relatively small circular pluton a few kilometres across, this body was sampled at Mile 72 of provincial Highway 113, where the road is crossed by the Canadian National Railway line to Matagami. It is well exposed in an adjacent railway cut, but the sample was taken from fresh core from a large-diameter drillhole then in progress. Available maps show the body discordantly cutting folded volcanic rocks. The sample consists of salmon-red coarse grained massive quartz monzonite containing fresh plagioclase and microcline, quartz, about 5 per cent hornblende, and 10 per cent biotite. Accessories include allanite, sphene, zircon, apatite and opaques. The sample site is located at latitude 49°17'07", longitude 76°52'45".

Age: 2691.6 $^{+3.6}_{-3.4}$ Ma.

The larger Waswanipi Lake Pluton northeast of Franquet Township was also visited, but where observed it was strongly sheared and foliated and therefore was not sampled. Gariépy (1984) has obtained a Pb-Pb mineral age of 2616 ± 19 Ma from the intrusion.

3. Taschereau Stock, Launay Township, Quebec

The sample site is on Highway 111, 2.5 km west of Launay Station and about 43 km west of Amos (latitude 48°38'45"; longitude 78°33'50"). The intrusion is an irregular body about 20 km in long dimension cutting volcanic rocks and mafic intrusions of the La Sarre-Amos belt. The sample consisted of quartz monzonite containing about equal amounts of plagioclase and microcline, 25 per cent quartz, minor amounts of biotite and epidote and accessory zircon and sphene. A sample from a larger body to the east in Villemontel Township ("Villemontel pluton" or "Dalquier stock") proved to be extensively altered and was not processed.

Age: 2718.3 $^{+2.3}_{-2.2}$ Ma. This age is abnormally old relative to other plutons sampled and the Taschereau stock may be synvolcanic or syntectonic.

4. Garrison Stock, Garrison Township, Ontario

The intrusion is a subcircular body about 5 km across cutting folded volcanics and intercalated sediments some 35 km east of the town of Matheson. Garrison Township has been mapped in detail by Satterly (1951). Where sampled (latitude 48"28'30"; longitude 79°56'30") the rock is a weakly foliated pale pink to grey coarse grained granodiorite. It appears not to have been altered or sheared by a nearby fault crossing the stock.

Age: 2678.9 $^{+3.9}_{-3.6}$ Ma.

For comparison, zircons from volcanics of the Hunter Mine Group in Rand Township adjoining Garrison Township on the north, low in the stratigraphic succession, gave a U-Pb concordia age of 2710 ± 2 Ma (Nunes and Jensen, 1980), and volcanics to the south, high in the succession, were dated at 2703 ± 2 Ma (ibid), leaving an interval of 24 Ma between the younger age and the emplacement of the Garrison stock.

5. Winnie Lake Stock, Bernhardt, Maisonville, and Teck townships, Ontario

The Winnie Lake Stock lies 9 km north of the town of Swastika, mostly in Bernhardt Township (Rupert and Lovell, 1970; Pyke et al., 1973). It is approximately 8 km by up to 3 km in size. Its contacts appear to be subparallel with adjacent structural trends in the host volcanic rocks, which are mainly andesitic units of the Misema Subgroup, Blake River Group (Goodwin, 1977, Fig. 8, 9) or of the Kinojevis Group of Thurston and Franconi (1984). The stock is cut by one or more post-tectonic Matachewan diabase dykes. The sample was taken near the south end of the stock (latitude 48°11'00"; longitude 80°08'30") and consists of massive pink coarse grained biotite-rich quartz monzonite or granite. According to Thomson (1950) the intrusion becomes syenitic in Teck Township. The U-Pb age of invaded volcanics in the Swastika-Kirkland Lake area has not been determined.

Age: 2677.3 $^{+2.5}_{-2.4}$ Ma.

6. Watabeag Batholith, Dunmore Township, Ontario

Watabeag Batholith is a large irregular north-south mass lying west of provincial Highway 11 and north of the town of Matachewan. It extends for some 45 km across the regional trend of the invaded basalts of the Blake River Group (Pyke et al., 1973; Goodwin, 1977), later reclassified as Tisdale Group (Thurston and Franconi, 1984). The western margin is lobate into the volcanics whereas the eastern margin, although mainly covered by Huronian Supergroup strata, appears to be more linear. The batholith is cut by numerous north-trending Matachewan diabase dykes. Because of its size and easy access it was sampled at three sites. The Dunmore Township sample was obtained in the southeast, along a logging road in the central part of the township (latitude 48°08'35"; longitude 80°27'45"). Here the rock is a pink, biotitic, foliated, coarse grained sub-porphyritic quartz monzonite.

Age: 2681.3 $^{+2.7}_{-2.6}$ Ma.

7. Watabeag Batholith, McEvay Township

The second sample from this batholith was taken in one of the marginal lobes, at Sylvia Falls on the Watabeag River (latitude 48°18'30"; longitude 80°36'00") about 21 km north-northwest of the site in Dunmore Township. Here the rock is a salmon-red, massive, coarse grained, weakly foliated quartz monzonite. The sample site is a small outcrop area crossed by a diabase dyke. The determined age is 5 Ma younger than sample 6 and 23 Ma younger than that of sample 8 (below) from the same batholith, suggesting that the batholith is composite and was emplaced over a considerable time span.

Age: 2676.0 $^{+2.2}_{-2.1}$ Ma.

8. Watabeag Batholith, Baden Township

Sample site 8 is about 13 km southwest of site 6, located on a logging road leading to Radisson Lake in Michie Township (latitude 48°05'45"; longitude 80°41'45"). The sampled rock is a mottled buff and black, massive, medium- to coarse-grained quartz diorite. Its age indicates that it represents an early phase of the emplacement of the Watabeag Batholith or that it is an earlier intrusion. Lovell (1967), who mapped the township and environs, thought that diorite and quartz diorite of the area were early differentiates of the granitic magma, although he described the diorite and granite as gradational, implying no significant separation in time. The derived age, 23 Ma older than that given by sample 7, and about 18 Ma older than sample 6 from the main part of the batholith, suggests that the diorite is an appreciably earlier intrusion.

Age: 2699.0 $^{+3.5}_{-2.9}$ Ma.

In the Matachewan district, granitoid bodies such as the Watabeag Batholith are closely associated spatially with a suite of syenite and mafic syenite intrusions, but the age relationship between these two suites has not been conclusively established. Both suites are older than the Matachewan dyke swarm, crudely dated at 2643 ± 100 Ma (recalculated from Gates and Hurley, 1973). Samples of the Cairo-Holmes syenite body adjacent to the Watabeag Batholith were examined at one locality but field tests failed to show the presence of zircons. The syenite may be zircon-bearing elsewhere or alternatively, isotopic work on sphene, which is abundant in the syenite, might resolve the problem.

9. Adams Stock, Adams, Price, McArthur, Eldorado, Douglas and Fripp Townships, Timmins area

The Adams Stock, about 10 km south of Timmins, is the westernmost of several well-defined post-tectonic stocks south and southeast of the city. It and the nearby Geikie Stock were mapped by Pyke (1975, 1978a, b); they invade folded volcanic and minor sedimentary rocks of the Deloro, Redstone River and Blake River groups of Goodwin, (1977), the Deloro and Tisdale groups of Thurston and Franconi (1984), and associated mafic intrusions, and are cut by Matachewan and younger diabase dykes. According to Pyke (1975), the Adams Stock is granodioritic, containing small amounts of hornblende, biotite, epidote and chlorite, and accessory magnetite, sphene, zircon, apatite and pyrite. Outcrops are massive to weakly foliated, medium grained, grey to pink, and porphyritic (microcline). The sample came from a roadside outcrop in McArthur Township about 3 km west of Papakomeka Lake (latitude 48°15'30"; longitude 80°20'00").

From geological reasoning and analogy, Pyke (1978b) considered the granodioritic Adams and Geikie stocks to be younger than more sodic trondhjemitic intrusions of the nearby Peterlong Lake Complex that also intrude the volcanic complex. This relationship remains to be established by an isotopic age from the trondhjemite.

Age: 2686.4 $^{+3.0}_{-2.8}$ Ma.

Zircons from upper, intermediate, and lower parts of the volcanic pile in the Timmins area, including a location in Douglas Township not far from sample 8, have been dated at 2703, 2717, and 2725 Ma respectively (Nunes and Pyke, 1980, 1981), leaving a span of only 17 Ma between latest dated volcanism (Douglas Township sample) and emplacement of post-kinematic intrusion, as given by the age of the adjacent Adams Stock. Just northeast of the stock, a differentiated ultramafic intrusion cutting lower volcanics gave a concordia age of 2697 Ma (Nunes and Pyke,1980, 1981).

10. Hoodoo Lake Pluton, Keith Township, Ontario

This intrusion, about 10 km by 4 km in size, concordantly to discordantly cuts foliated mafic volcanics with sharp contacts (Breaks, 1978). According to Breaks (1978) the pluton in general is leucocratic, homogeneous, grey, medium grained, porphyritic (microcline) granodiorite. Accessory minerals are epidote, sphene, apatite, magnetite, allanite and zircon. The sample site (latitude 48°05'20"; longitude 82°20'45") is in the southeastern part of the body about 2 km west of Hoodoo Lake. There, the rock appears from the feldspar ratio to be quartz monzonite, characterized by pink potassic feldspar phenocrysts up to 2 cm long.

Age: 2683.7 $^{+3.2}_{-3.0}$ Ma.

11. Ash Lake Pluton, Copenace Township, Ontario

This irregular intrusion extends for some 16 km in north-south direction just east of Dog Lake, flanked by mafic and felsic volcanics of eastern Wawa Subprovince. It has been classed by Srivastava and Bennett (1978) as post-tectonic and is cut by numerous north-to northwest-trending diabase dykes. Those authors reported that the pluton in Riggs and West townships just north of the sample site is composed of massive to weakly foliated trondhjemite to granodiorite. The sample was obtained from a small quarry on Highway 651 about 7 km south of the village of Missinabie (latitude 48°17'00"; longitude 84°17'00") and consists of very coarse grained, pinkish, massive, biotitic quartz monzonite or granodiorite.

Age: 2684.5 $^{+2.7}_{-2.6}$ Ma

Discussion

The range of all ages in Table 1 is 42 Ma; excluding the Taschereau pluton, which may be synkinematic, the range is lowered to 24 Ma (2676 to 2699). The great majority of similar internal plutons of the Abitibi and Wawa subprovinces were probably intruded in this latter interval. In contrast, zircon ages of volcanism reported from various parts of the region (Nunes and Jensen, 1980; Nunes and Pyke, 1980, 1981; Turek et al., 1982) for the most part exceed 2700 Ma, indicating, like the geological relationships, that the plutons are not coeval with volcanism. From the sparse volcanic age data available, the two are separated by roughly 20-40 Ma. The post-kinematic nature and ages of the widespread plutons dated show that essentially the entire region became tectonically stabilized between 2675 and 2700 Ma, as has been established previously for local areas (e.g. Percival and Krogh, 1983). The origin and significance of much younger K-Ar and Rb-Sr mineral ages common to all districts remains uncertain.

References

Anderson, J.L.
1983: Proterozoic anorogenic granite plutonism; in Proterozoic Geology; selected papers from an international Proterozoic symposium (L.G. Medaris Jr. et al., ed.); Geological Society of America, Memoir 161, p. 133-154.

Breaks, F.W.
1978: Geology of the Horwood Lake area; Ontario Geological Survey, Report 169.

Dallmeyer, R.D., Maybin, A.H., and Durocher, M.E.
1975: Timing of Kenoran metamorphism in the eastern Abitibi belt, Quebec; evidence from ^{40}Ar-^{39}Ar ages of hornblende and biotite from post-kinematic plutons; Canadian Journal of Earth Sciences, v. 12, p. 1864-1873.

Duquette, G.
1970: Archean stratigraphy and ore relationships in the Chibougamau district; Quebec Department of Natural Resources, Special Paper 8.

1972: The Chibougamau-Chapais greenstone belt; in Precambrian geology and mineral deposits of the Noranda-Val d'Or and Matagami-Chibougamau greenstone belts, ed. G.O. Allard; 24th International Geological Congress, Montreal, Field Excursion Guidebook A41-C41, p. 51-69.

Durocher, M.E.
1974: Geology of parts of the northeast and northwest quarters of Opemisca Township, Abitibi-East County, Quebec; Quebec Department of Natural Resources, Mineral Deposits Service, Preliminary Report D.P. 204.

Durocher, M.E. (cont.)
1975: Geology of the southwest quarter of Opemisca Township, Abitibi-East County, Quebec; Quebec Department of Natural Resources, Mineral Deposits Service, Preliminary Report 298.

Gariépy, C.
1984: U-Pb isotopic evidence for the presence of pre-2.7 Ga sialic crust in the Abitibi greenstone belt, Quebec (abst.); Geological Association of Canada-Mineralogical Association of Canada Joint Annual Meeting, Program with Abstracts, p. 65.

Gates, T.M. and Hurley, P.M.
1973: Evaluation of Rb-Sr dating methods applied to the Matachewan, Abitibi, Mackenzie and Sudbury dike swarms in Canada; Canadian Journal of Earth Sciences, v. 10, p. 900-919.

Goodwin, A.M.
1977: Superior Province volcanism; in Volcanic regimes in Canada, ed. W.R.A. Baragar, L.C. Coleman and J.M. Hall; Geological Association of Canada, Special Paper 16, p. 205-241.

Krogh, T.E.
1982a: Improved accuracy of U-Pb ages by the creation of more concordant systems using an air abrasion technique; Geochimica and Cosmochimica Acta, v. 46, p. 637-649.

1982b: Improved accuracy of U-Pb ages by the creation of more concordant fractions using a high gradient magnetic separation technique; Geochimica and Cosmochimica Acta, v. 46, p. 631-635.

Lovell, H.L.
1967: Geology of the Matachewan area; Ontario Department of Mines, Geology Report 51, 61 p.

Nunes, P.D. and Jensen, L.S.
1980: Geochronology of the Abitibi metavolcanic belt, Kirkland Lake area – progress report; in Summary of geochronology studies 1977-1979, ed. E.G. Pye; Ontario Geological Survey, Miscellaneous Paper 92, p. 40-45.

Nunes, P.D. and Pyke, D.R.
1980: Geochronology of the Abitibi metavolcanic belt, Timmins-Matachewan area - progress report; in Summary of geochronology studies 1977-1979, ed. E.G. Pye; Ontario Geological Survey, Miscellaneous Paper 92, p. 34-39.

1981: Time-stratigraphic correlation of the Kidd Creek orebody with volcanic rocks south of Timmins, Ontario, as inferred from zircon U-Pb ages; Economic Geology, v. 176, p. 944-951.

Percival, J.A. and Card, K.D.
– Structure and evolution of Archean crust in central Superior Province, Canada; in Archean Supracrustal Sequences, ed. L.D. Ayres and P.C. Thurston; Geological Association of Canada, Special Paper. (in press)

Percival, J.A. and Krogh, T.E.
1983: U-Pb zircon geochronology of the Kapuskasing structural zone and vicinity in the Chapleau-Foleyet area, Ontario; Canadian Journal of Earth Sciences, v. 20, p. 830-843.

Pyke, D.R.
1975: Geology of Adams and Eldorado Townships; Ontario Division of Mines, Geoscience Report 121.

1978a: Geology of the Peterlong Lake area; Ontario Geological Survey, Report 171, 53 p.

1978b: Geology of the Redstone River area, District of Timiskaming; Ontario Division of Mines, Geoscience Report 161, 71 p.

Pyke, D.R., Ayres, L.D., and Innes, D.G.
1973: Timmins-Kirkland Lake; Ontario Division of Mines, Geological Compilation Series, Map 2205, 1:253,440.

Rupert, R.J. and Lovell, H.L.
1970: Geology of Bernhardt and Morrisette Townships; Ontario Department of Mines, Geology Report 84.

Satterly, J.
1951: Geology of Garrison Township; Ontario Department of Mines, Annual Report, v. 58, Pt. 4.

Srivastava, P. and Bennett, G.
1978: Geology of Riggs and West Townships, District of Algoma; Ontario Geological Survey, Report 174.

Steiger, R.H. and Wasserburg, G.J.
1969: Comparative U-Th-Pb systematics in $2.7x10^9$yr plutons of different geological histories; Geochimica et Cosmochimica Acta, v. 33, p. 1213-1232.

Stockwell, C.H.
1982: Proposals for time-classification and correlation of Precambrian rocks and events in Canada and adjacent areas of the Canadian Shield Part 1: A time classification of Precambrian rocks and events; Geological Survey of Canada, Paper 80-19.

Thomson, J.E.
1950: Geology of Teck Township and the Kenogami Lake area, Kirkland Lake gold belt; Ontario Department of Mines, Annual Report, v. LVII, Pt. V, p. 1-53.

Thurston, P.C. and Franconi, A. (ed.)
1984: Lithostratigraphic map of the Abitibi Subprovince; Ontario Geological Survey – Ministère de l'Énergie et des Ressources, Québec, Map 2484 (Ontario), DV83-16 (Quebec).

Turek, A., Smith, P.E., and Van Schmus, W.R.
1982: Rb-Sr and U-Pb ages of volcanism and granite emplacement in the Michipicoten belt – Wawa, Ontario; Canadian Journal of Earth Sciences, v. 19, p. 1608-1626.

Wanless, R.K.
1969: Isotopic age map of Canada; Geological Survey of Canada, Map 1256A, 1:5,000,000.

Wolhuter, L.E.
1971: The Opemisca Pluton; Quebec Department of Natural Resources, Special Paper 6, 113 p.

The minerals in the main Hemlo gold deposit, Ontario

Project 680023

D.C. Harris
Economic Geology and Mineralogy Division

Harris, D.C., Minerals in the main Hemlo gold deposit, Ontario; in Current Research, Part A, Geological Survey of Canada, Paper 86-1A, p. 49-54, 1986.

Abstract

The Hemlo gold deposit which is substantially enriched in Mo, Sb, As, Hg, Tl, V and Ba, contains a diverse assemblage of minerals. The most common ore minerals are pyrite, molybdenite, stibnite, tetrahedrite-tennantite, sphalerite, zinckenite, realgar, cinnabar and aktashite with minor to trace amounts of 36 other metallic minerals. Gold occurs principally as native gold that contains up to 22.1 wt.% Hg and up to 29.1 wt.% Ag. The average composition of 89 grains from various parts of the deposit gave Au 86.2, Hg 6.5, Ag 5.9 wt%. The gangue minerals are principally quartz, barite, sericite, vanadian muscovite, rutile and barian microcline.

Résumé

Le gisement aurifère d'Hemlo, très riche en Mo, Sb, As, Hg, Tl, V et Ba, contient une association variée de minéraux. Les minéraux métalliques les plus communs sont la pyrite, la molybdénite, la stibnite, la tétraédrite-tennantite, la sphalérite, la zinckénite, le réalgar, le cinnabar et l'aktashite; on y trouve également de petites quantités ou des traces de 36 autres minéraux métalliques. L'or se présente surtout sous forme d'or natif pouvant contenir jusqu'à 22,1 % en poids de Hg et 29,1 % en poids d'Ag. La composition moyenne de 89 grains provenant de différentes parties du gisement est la suivante: Au, 86,2 % en poids, Hg, 6,5 % en poids, Ag, 5,9 % en poids. La gangue se compose surtout de quartz, de barytine, de séricite, de muscovite à vanadium, de rutile et de microcline à baryum.

Introduction

The Hemlo gold deposit, discovered in 1982, is located near the northeast shore of Lake Superior, 35 km east of Marathon, adjacent to the Trans-Canada Highway (17). The deposit which is of Archean age occurs at the contact between felsic metavolcanics and metasedimentary rocks, north of the Hemlo fault. The ore-bearing rocks are sericite schists, siliceous metasedimentary and fragmental rocks.

The main ore zone strikes at an azimuth of 115° and dips north at 50° to 70°. The deposit consisting of several mineralized zones extends 2900 m in length, 1300 m vertically and ranges in thickness from 3 to 45 m with some surface exposure. The deposit is estimated to contain at least 76 million tonnes of ore with about 651 million grams of gold. The deposit is presently being mined by three companies, Teck-Corona Operating Corporation, Noranda Incorporated and Lac Minerals Limited. For more details on the geology of the Hemlo area the reader is referred to a field guide edited by McMillan and Robinson (1985).

The present study was initiated in 1983 to determine: the mineralogy of the deposit; the ore textures; the mineral zonation within the deposit; the effect of metamorphism and tectonic deformation on the minerals; and the genesis of the ore. This paper presents the minerals in the Hemlo deposit and the chemical nature of the ore.

Samples and method of investigation

For this study, split drill core samples of the mineralized zone were selected at 1 m intervals or less, from 25 drillholes. Sampling of the drill core was based, in part, on the gold assays and by visual logging of the core. Each sample consists of a piece of drill core measuring 5-10 cm in length. Over 800 polished sections and 110 polished thin sections were prepared from the samples. The sections were first examined under a polarizing microscope to identify the minerals using their optical properties, but most identifications had to be done using an electron microprobe equipped with an energy dispersive analyzer, by quantitative electron microprobe analyses and by X-ray powder diffraction techniques.

Mineralogy

The minerals identified in the main Hemlo ore horizon are listed in Table 6.1. They are grouped as common, less common, and rare, as determined by their frequency of occurrence in the samples examined. Because the Hemlo deposit is mineralogically zoned, this classification is not applicable to every part of the orebody. As well, ore minerals other than pyrite, which account for less than 1% of the deposit, are fine grained and difficult to recognize. Therefore, normal quantitative measuring techniques such as image analyzers are not practical. The simplified mineral formula (Fleischer, 1983) and chemical composition or elemental characteristic at Hemlo are also listed in Table 6.1.

The mineralogy and chemistry of the Hemlo deposit indicate a close association of Au with Mo, Sb, As, Hg, Tl, V and Ba. In Table 6.2, an elemental listing of minerals is presented with a relative estimate of their contribution for a particular element.

Pyrite is the most abundant sulphide and its mode of occurrence gives the ore a stratified appearance. It occurs in two modes, as coarse subhedral to anhedral deformed aggregates up to 3 mm in maximum dimension which are concentrated in "layers" up to 1 m thick and as fine grained euhedral grains less than 200 μm in maximum dimension which are finely disseminated throughout the silicate ground mass.

Native gold is the principal gold phase with minor to trace amounts of aurostibite and rarely as calaverite and unidentified Hemlo No. 1. Native gold occurs as free grains between 1 and 20 μm in size along quartz-feldspar grain boundaries, as inclusions in, or rimmed with, native arsenic, cinnabar, stibnite, sulphosalts and aurostibite and as inclusions in pyrite fractures. Megascopically, visible native gold is rare. The native gold contains up to 22.1 wt. % Hg and up to 29.1 wt. % Ag. It varies in composition from sample to sample and from grain to grain within the same polished section. The averaged composition of 89 grains from polished sections throughout the deposit gave Au 86.2, Hg 6.5, Ag 5.9 wt. %. Most gold grains are low in silver contents with the highest values obtained in samples collected from the northwest down plunge extension of the Lac orebody. There is no marked correlation between gold assays and pyrite-rich samples. The best indicator of gold is the presence of molybdenite. Some of the highest gold assays occur in zones that contain highly fractured boudinaged quartz veins enriched in a mineral assemblage of realgar-cinnabar-stibnite. These zones occur principally in the Noranda and Lac orebodies.

There is a close association between mercury and thallium minerals. The mercury minerals cinnabar and aktashite are the most abundant. These occur in the central and thickest part of the deposit which extends vertically from the surface outcrops on the Lac orebody to a depth of 1000 m in the northwest down-plunge extension and laterally along strike to the east on to the Teck-Corona orebody at a point slightly beyond hole 220W where the orebody narrows to 10 m and barite is absent. Other mercury-bearing minerals are sphalerite (up to 27.5% Hg), native gold and tetrahedrite-tennantite. These minerals occur outside, as well as within the central orebody. It is worth noting that the high mercury-bearing sphalerite has optical properties virtually the same as those of the iron-poor variety, varying in colour from pale yellow to colourless. Microprobe analysis shows that the mercury occurs as isomorphous substitution and X-ray determinations showed an increase in unit-cell dimension. A search of the literature indicates that the highest recorded mercurian sphalerite (19%) was found in the oxidation zone of the Belo-Osipovskoye deposit, USSR, associated with primary and secondary cinnabar in stockwork ore (Vasil'yev and Laurent'yev, 1969).

The thallium minerals, parapierrotite and routhierite are rare in the deposit and because of their similar optical properties to cinnabar, are difficult to recognize.

Molybdenite is widespread throughout the deposit and as noted earlier is the best indicator of gold. It occurs mainly in association with silicate minerals, but occasionally as inclusions in pyrite and less frequently in barite. Molybdenite occurs as individual euhedral crystals or as platy masses parallel to the foliation of the ore. A few finely disseminated grains of native gold (<2 μm) were found to occur as inclusions within molybdenite flakes and interstitial to the platy masses.

The antimony and arsenic minerals account for the majority of the ore minerals found within the deposit. There is isomorphous substitution between these two elements which contributes to a variable composition for the sulphosalt minerals. The formula listed in Table 6.1 is the most representative for a particular species in the Hemlo ore. Stibnite, zinckenite and tetrahedrite are the most widespread antimony phases. Stibnite is the most abundant and is readily visible in some hand specimens, particularly in boudinaged quartz veins where it occurs as disseminations and as masses concentrated along the peripherals of the quartz boudins. Realgar is the most abundant arsenic species and its presence gives an orange colour to quartz-rich hand specimens.

Tennantite is a minor phase, but in some drillholes, particularly from the northwest down plunge extension of the Lac orebody, it becomes a major arsenic mineral. Native arsenic and native antimony generally occur in the same samples, sometimes in association with aurostibite, berthierite, realgar, stibnite and gudmundite. As reported by Barton (1971), berthierite, gudmundite, and aurostibite are stable only under conditions of relatively low sulphur activity. These minerals in association with native arsenic and native antimony in the Hemlo ore clearly indicate conditions of sulphur-poor hydrothermal solutions.

The gangue minerals in the deposit are essentially quartz, mica, feldspar and barite. Barite is a major constituent and occurs in zones which range from massive (up to 40 per cent coarse barite) to thin fracture fillings and as disseminations. In some drillholes, barite only occurs in the lower part of the ore horizon, in other drillholes it occurs throughout the width of the ore horizon and in the east orebody of Teck-Corona it is nearly absent. Barite has also been identified in units below the ore horizon. Microprobe analyses of barite from holes W135 and W70 of Lac Minerals gave SrO values from 0.5 to 7.2 wt. %. The barite in the Hemlo deposit has been referred to as the first occurrence of stratiform barite in the Archean of North America (Cameron and Hattori, in press). This presence of massive barite and the enrichment of Sb, As, Hg and Tl have been some of the arguments for relating the Hemlo deposit to near surface syngenetic hot spring systems. The features observed in this

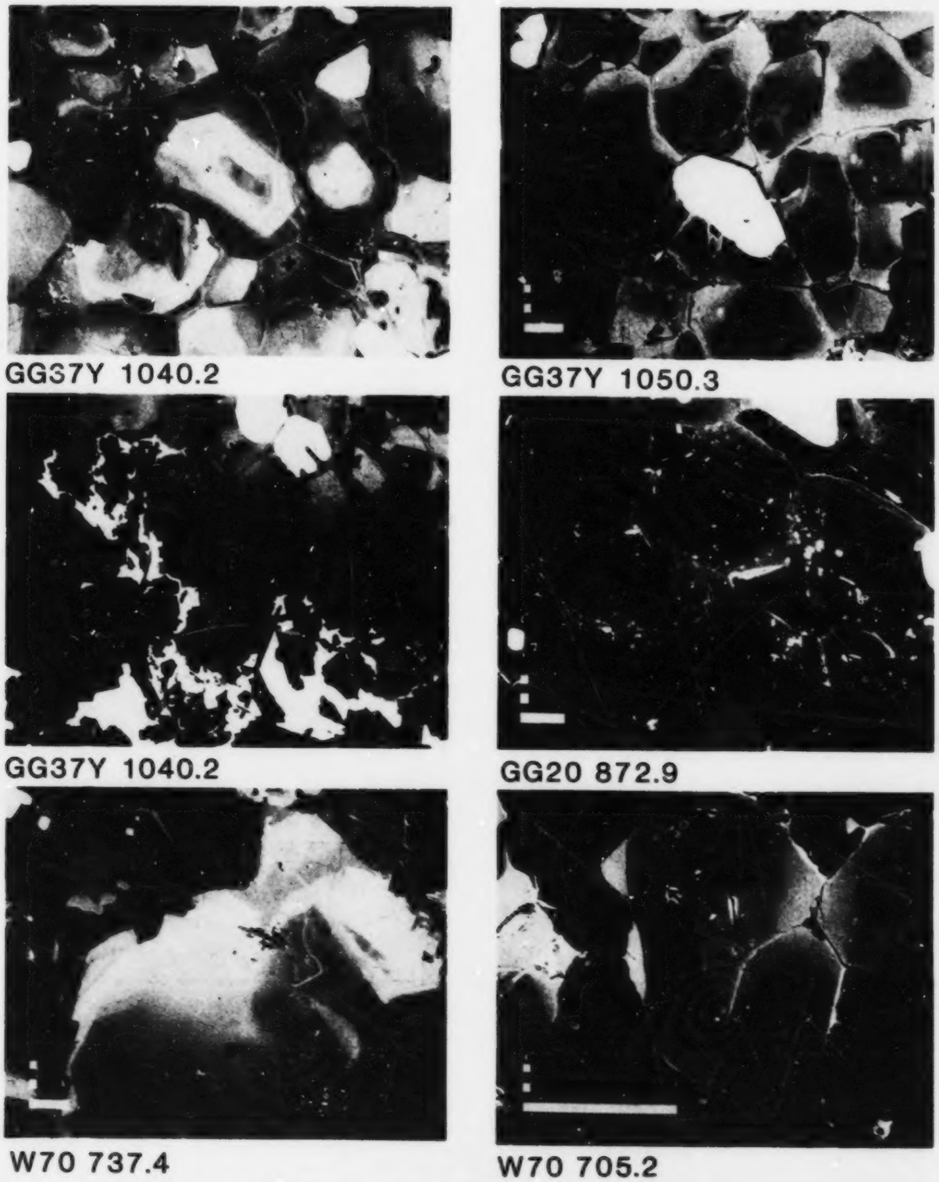

Figure 6.1. SEM back-scattered images of barium-containing microcline feldspar. The dark to light grey areas represent increasing barium content. In GG37Y 1050.3, the lightest grey areas contain 15.0% BaO. In W70 705.2, the barium varies from 4.5% BaO at the intersection of the three grains to 2.6% BaO in the cores. The white areas are pyrite and the black areas are quartz and mica. The labels represent the drill hole and metres. The scale bar is 100 μm.

Table 6.1. Minerals in the Hemlo gold deposit

Ore Minerals		
Common species	Simplified formula	Hemlo
Native Gold	Au	Hg0.0-22.1, Ag0.0-29.1
Pyrite	FeS_2	FeS_2
Molybdenite	MoS_2	MoS_2
Sphalerite	ZnS	Hg0.0-27.5, Fe0.0-1.9
Arsenopyrite	FeAsS	FeAsS
Stibnite	Sb_2S_3	As0.0-4.8
Tetrahedrite	$(Cu,Fe,Zn)_{12}Sb_4S_{13}$	Hg0.0-18.6, Ag0.0-8.9
Tennantite	$(Cu,Fe,Zn)_{12}As_4S_{13}$	Hg0.0-15.2, Ag0.0-8.3
Zinckenite	$Pb_6Sb_{14}S_{27}$	As0.0-11.5
Realgar	AsS	Sb0.0-0.5
Cinnabar	HgS	HgS
Aktashite	$Cu_6Hg_3As_4S_{12}$	$Cu_6Hg_3(As,Sb)_4S_{12}$
Less common species	Simplified formula	Hemlo
Aurostibite	$AuSb_2$	$AuSb_2$
Chalcopyrite	$CuFeS_2$	$CuFeS_2$
Pyrrhotite	$Fe_{1-x}S$	$Fe_{1-x}S$
Galena	PbS	PbS
Native antimony	Sb	As0.0-1.3
Berthierite	$FeSb_2S_4$	Mn0.0-13.4
Bournonite	$PbCuSbS_3$	As0.0-6.0
Boulangerite	$Pb_5Sb_4S_{11}$	As2.4-5.8
Native Arsenic	As	As
Gersdorffite	NiAsS	Fe1.4-14.9
Parapierrotite	$Tl(Sb,As)_5S_8$	$TlSb_5S_8$
Routhierite	$TlHgAsS_3$	$Cu_{1.0}Tl_{1.0}Hg_{2.0}(As_{1.4}Sb_{0.6})S_6$
Altaite	PbTe	PbTe
Twinnite	$Pb(Sb,As)_2S_4$	$Pb(Sb_{1.2}As_{0.8})S_4$
Orpiment	As_2S_3	Sb0.0-5.0
Geocronite	$Pb_{14}(Sb,As)_6S_{23}$	$Pb_{14}(Sb_{3.0}As_{3.0})S_{23}$
Rare species	Simplified formula	Hemlo
Native Silver	Ag	Ag
Hemlo No. 1	–	$Tl_{0.2}Ag_{0.4}Au_{0.6}Sb_{2.0}S_{2.0}$
Chalcostibite	$CuSbS_2$	$CuSbS_2$
Jamesonite	$Pb_4FeSb_6S_{14}$	$Pb_4FeSb_6S_{14}$
Gudmundite	FeSbS	FeSbS
Ullmannite	NiSbS	NiSbS
Coloradoite	HgTe	HgTe
Galkaite	$(Cs,Tl)(Hg,Cu,Zn)_6(As,Sb)_4S_{12}$	–
Melonite	$NiTe_2$	$NiTe_2$
Tvalchrelidzeite	$Hg_{12}(Sb,As)_8S_{15}$	$Hg_{12}(Sb_{4.7}As_{3.3})S_{15}$
Baumhauerite	$Pb_3As_4S_9$	$Pb_3(As_{2.2}Sb_{1.8})S_9$
Cubanite	$CuFe_2S_3$	$CuFe_2S_3$
Seligmannite	$PbCuAsS_3$	$PbCu(As_{.52}Sb_{.48})S_3$
Dufrenoysite	$Pb_2As_2S_5$	$Pb_2(As_{1.1}Sb_{0.9})S_5$
Calaverite	$AuTe_2$	$AuTe_2$
Pararealgar	AsS	not analyzed
Stibarsen	SbAs	SbAs
Breithauptite	NiSb	NiSb
Clausthalite	PbSe	PbSe
Wurtzite	(Zn,Fe)S	Fe4.8Hg6.2
Silicates, etc: Minerals		
Common species	Simplified formula	Hemlo
Quartz	SiO_2	SiO_2
Muscovite	$KAl_2(Si_3Al)O_{10}(OH,F)_2$	–
Vanadian muscovite	$K(Al,V)_2(Si_3Al)O_{10}(OH,F)_2$	V_2O_3 up to 8.5
Biotite	$K,(Mg,Fe^{+3})_3(Al,Fe^{+3})(Si_3O_{10}(OH,F)_2$	–
Phlogopite	$KMg_3Si_3AlO_{10}(F,OH)_2$	–
Microcline	$KAlSi_3O_8$	$KAlSi_3O_8$
Barian microcline	$KAlSi_3O_8$	BaO up to 16.6
Barite	$BaSO_4$	SrO up to 7.2
Titanite	$CaTiSiO_5$	$CaTiSiO_5$

Table 6.1 (cont.)

Less common species	Simplified formula	Hemlo
Plagioclase	$(Na,Ca)Al_2Si_3O_8$	An_0-An_{90}
Anhydrite	$CaSO_4$	$CaSO_4$
Calcite	$CaCO_3$	$CaCO_3$
Scheelite	$CaWO_4$	$CaWO_4$
Apatite	–	–
Clinozoisite	$Ca_2Al_3(SiO_4)_3(OH)$	–
Zoisite	$Ca_2Al_3(SiO_4)_3(OH)$	$Ca_2Al_3(SiO_4)_3OH$
Zircon	$ZrSiO_4$	–
Amphiboles	–	Tremolite, Actinolite, Hornblende
Tourmaline	–	var. dravite
Rare species	**Simplified formula**	**Hemlo**
Fluorite	CaF_2	–
Cafarsite	$Ca_8(Ti,Fe,Mn)_{6-7}(AsO_3)_{12} \cdot 4H_2O$	$Ca_6(Ti,Mn,V,Fe)_7(AsO_3)_{12} \cdot xH_2O$
Ferberite	$FeWO_4$	$Fe_{.67}Mn_{.18}Mg_{.15}15WO_4$
Monazite	$(Ce,La,Nd,Th)PO_4$	$(Ce,La,Nd,Th)PO_4$
Allanite	$(Y,Ce,Ca)_2(Al,Fe)_3(SiO_4)(OH)$	$(Ca,RE)_2(Al,Fe)_3(SiO_4)(OH)$
Stilbite	Zeolite Group	not analyzed
Chlorite	Chlorite Group	–
Vanadian grossular	$Ca_3Al_2Si_3O_{12}$	$Ca_{3.1}Al_{1.2}V_{0.8}Si_{2.9}O_{12}$
Vesuvianite	$Ca_{10}Mg_2Al_4(SiO_4)_5(Si_2O_7)_2(OH)_4$	not analyzed
Oxide Minerals		
Common species	**Simplified formula**	**Hemlo**
Rutile	TiO_2	$(Ti,Sb,V,W)O_2$
Tomichite	$(V,Fe)_4Ti_3AsO_{13}(OH)$	$(V,Fe,Ba,Al)_4Ti_3(As,Sb)O_{13}(OH)$
Less common species		
Magnetite	Fe_3O_4	Fe_3O_4
Ilmenite	$FeTiO_3$	MnO.0-4.7
Rare species		
Hematite	Fe_2O_3	$(Fe,V)_2O_3$
Chromite	$FeCr_2O_4$	$Fe_{.56}Zn_{.45}Al_{.99}Cr_{.95}V_{.04}O_4$
Pyrochlore group	$A_{1-2}B_2O_6(O,OH,F)$	$Ca_{2.5}Ti_{1.3}Sb_{1.5}O_6$

study, such as the textural relationships of interstitial barite with the quartz-feldspar gangue minerals, the lack of ore minerals in the barite itself, the near absence of barite in the Teck-Corona deposit and the crosscutting features of barite veins as found in the underground workings, all suggest non-syngenetic relationships between the barite and the ore minerals. Instead, the evidence more clearly supports later emplacement of the barite, probably as a result of tectonic deformation or hydrothermal activities.

Mica is widespread and occurs as sericite, muscovite, vanadium-bearing muscovite and less common as phlogopite-biotite. Sericitic alteration associated with the mineralization is developed in the hangingwall and more extensively in the footwall. In the ore horizon, sericite is widespread, but the feldspar in the ore shows very little sericitic alteration. Muscovite and vanadium-bearing muscovite are the most abundant with vanadium contents up to 8.5% V_2O_3. The vanadium-bearing muscovite (incorrectly referred to as roscoelite) is easily recognized by its light to dark grass green colour. The vanadium-bearing muscovite has been identified throughout the deposit but only occurs in the ore-bearing zones. Similar to molybdenite, the vanadium-bearing muscovite is an indicator of gold. Phlogopite and biotite occur in isolated thin zones and more work is necessary to determine whether they are primary or secondary in origin.

Feldspar, with barite and quartz, is a major gangue mineral. It occurs mainly as microcline, as a barium-bearing microcline and less common as albite. Most microcline is of the barian variety, containing up to 9.4% BaO in the mineralized horizon and up to 16.6% BaO in some samples from the hangingwall units. The barium content of microcline in the ore is quite variable and electron microprobe backscattered images (Fig. 6.1) show crystal growth zoning and irregular distribution of barium in the microcline. Next to barite, microcline is the second major barium-bearing species and in some zones, it is the principal mineral of barium. In thin section, some of the microcline is readily distinguished by its characteristic cross-hatch twinning, whereas others show no twinning and only microprobe analyses can determine if it is the barian variety. Albite is rare and occurs with microcline and quartz in narrow zones. All feldspar throughout the deposit exhibits very little sericitic alteration.

Rutile is widespread and it occurs as anhedral to subhedral grains which may be up to 2 mm in maximum dimensions, but most grains are less than 200 µm. Some partial to near complete alteration to titanite is present. Microprobe analyses show that rutile in the mineralized horizon contains as much as 5.6 V_2O_3, 6.5 Sb_2O_3 and 2.3 WO_2. The isomorphous substitution of V-Sb-W in rutile

Table 6.2. Elemental listing of minerals and their relative proportions in the Hemlo gold deposit

	Major	Minor	Trace
Gold	Native Gold	Aurostibite	Hemlo No. 1 Calaverite
Molybdenum	Molybdenite	-	-
Antimony	Stibnite Zinckenite Tetrahedrite	Native antimony Boulangerite Bournonite Chalcostibite Gudmundite Berthierite Aurostibite Ullmannite Rutile (up to 6.5 Sb_2O_3) Twinnite Parapierrotite Geocronite	Jamesonite Stibarsen Breithauptite Tvalchrelidzeite Pyrochlore-type
Arsenic	Realgar	Orpiment Native arsenic Gersdorffite Tomichite Arsenopyrite Routhierite Geocronite Aktashite Tennantite	Seligmannite Dufrenoysite Pararealgar Baumhauerite Cafarsite Stibarsen
Mercury	Cinnabar Aktashite	Tetrahedrite (up to 18.6) Tennantite (up to 15.2) Native gold (up to 22.1) Sphalerite (up to 27.5) Routhierite	Tvalchrelidzeite Coloradoite
Thallium	Parapierrotite Routhierite	-	Hemlo No. 1 Galkaite
Vanadium	Muscovite (up to 8.5 V_2O_3) Rutile (up to 5.6 V_2O_3)	Tomichite	Cafarsite Garnet Hematite
Barium	Barite Microcline up to 16.6 BaO)	Muscovite (up to 2.0 BaO)	Tomichite

appears to be the first reported and with regards to the Hemlo deposit, the rutile composition indicates the presence of the ore horizon.

Acknowledgments

The author is grateful to various personnel of Lac Minerals Limited, Noranda Inc. and Teck-Corona Operating Corporation, without whose assistance and cooperation, this mineralogical study of the main Hemlo gold deposit could not have been undertaken. Most of the polished sections were prepared by Y. Bourgoin, CANMET with a few prepared by R. Burke, GSC. Powder X-ray identifications were done by A.C. Roberts, GSC.

References

Barton, P.B., Jr.
1971: The Fe-Sb-S system; Economic Geology, v. 66, p. 121-132.

Cameron, E.M. and Hattori, K.
— The Hemlo gold deposit, Ontario: a geochemical and isotopic study; Geochimica et Cosmochimica Acta, v. 49. (in press)

Fleischer, M.
1983: Glossary of mineral species 1983. 4th edition. The Mineralogical Record Inc., Tucson.

MacMillan, R.H. and Robinson, D.J. (ed.)
1985: Gold and copper-zinc metallogeny within metamorphosed greenstone terrain, Hemlo-Manitouwadge-Winston Lake, Ontario, Canada; Guidebook, a joint publication; Geological Association of Canada and the Canadian Institute of Mining and Metallurgy, 91 p.

Vasil'yev, V.I. and Laurent'yev, Yu.G.
1969: A new mercury-bearing species of sphalerite; Akademiya Nauk SSSR, Doklady, Dokl. Acad. Sci. U.S.S.R. Earth Sciences Section 186, p. 137-139.

Beach sedimentation in Ireland: contrasts and similarities with Atlantic Canada

Project 820046

R.B. Taylor, R.W.G. Carter [1], D.L. Forbes, and J.D. Orford [2]
Atlantic Geoscience Centre, Dartmouth

Taylor, R.B., Carter, R.W.G., Forbes, D.L., and Orford, J.D., Beach sedimentation in Ireland: contrasts and similarities with Atlantic Canada; in Current Research, Part A, Geological Survey of Canada, Paper 86-1A, p. 55-64, 1986.

Abstract

The initial results of a collaborative project to examine sedimentation, evolution, and morphodynamic behaviour of coarse clastic beaches in the North Atlantic region are presented. Distinctive features of the Irish coast include the high crest elevations of exposed gravel beaches, large volumes of sand stored in coastal dune fields, and lateral and vertical segregation of sand and gravel in some of the larger beach systems. While littoral sedimentation at individual sites is closely linked to sediment supply conditions, major contrasts in beach characteristics between the Irish and Canadian Atlantic coasts may be attributed to clear differences in relative sea level history and contemporary climatic and oceanographic conditions.

Résumé

Le présent rapport résume l'étude de la sédimentation de plage entreprise à divers emplacements le long de la côte Atlantique découverte de l'Irlande. Les données représentent les premiers résultats d'un projet conjoint visant à étudier la sédimentation, l'évolution et le comportement morphodynamique des plages à fragments grossiers dans le nord de l'Atlantique. La côte irlandaise se caractérise par une forte élévation des crêtes des plages de gravier découvertes, de grandes quantités de sable contenues dans les champs de dunes littoraux et une ségrégation latérale et verticale du sable et du gravier dans certains des plus gros réseaux de plages. Bien que la sédimentation littorale à certains emplacements soit fonction des apports de sédiments, les caractéristiques contrastantes les plus frappantes des plages de la côte Atlantique de l'Irlande et du Canada sont peut être dues aux différences marquées de l'histoire du niveau relatif de la mer et aux conditions climatiques et océanographiques contemporaines.

[1] University of Ulster, Coleraine, Northern Ireland
[2] Queen's University, Belfast, Northern Ireland

Introduction

Beach deposits on both sides of the North Atlantic Ocean share some similarities of form and structure arising in part from an abundance of coarse grained glaciogenic source deposits and exposure to high-energy ocean wave conditions. There are, however, definable differences in terms of sea-level history and prevailing weather patterns, which give rise to distinctive subsets of morphological and sedimentological forms on the Irish and Canadian Atlantic coasts (Carter, 1983; Carter and Orford, 1984; Forbes, 1985; Forbes and Taylor, in press).

Recognition of these issues led to the establishment of a collaborative research project, designed to extend our understanding of gravel beach morphodynamics and sedimentology by combining observations from a more diverse set of environments than is available on one side of the Atlantic alone. The project has provided an opportunity to bring together several years of independent work, supplemented by joint field studies in Ireland (1984) and in eastern Canada (1985). This paper focusses on distinctive aspects of shore-zone sedimentation in Ireland and explores some of the similarities and differences between coastal sedimentary systems on opposite sides of the North Atlantic Ocean.

The Irish coast

The geological background to the Irish coast has been described by Stephens (1970, 1975) and by Davies and Stephens (1978). Carboniferous limestone covers the central lowlands and extends to the coast at the head of Galway Bay in the west, on parts of the northwest coast, and in the vicinity of Dublin in the east (Fig. 7.1). Resistant pre-Carboniferous rocks form discontinuous uplands adjacent to the coast in the southwest, west, northwest, and locally on the east coast, while Tertiary basalts play a similar role in the north. In contrast, much of the east and southeast coast is developed in areas of limited relief. The geological structure is dominated by northeast-southwest trending Caledonide features in the north and west whereas east-west Hercynian structures predominate in the south. Differential erosion of these rocks has produced a spectacular embayed coast along the entire western seaboard, where high rock cliffs alternate with large embayments in which substantial volumes of estuarine, beach, and windblown sediments have accumulated (Fig. 7.1, 7.2).

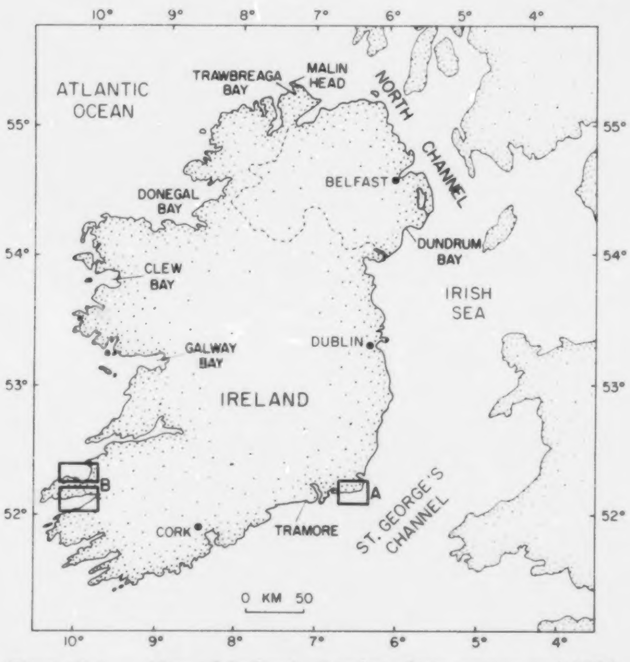

Figure 7.1. Map of Ireland, showing place names and 1984 study sites on the southeast coast in Co. Wexford (box A, Fig. 7.4) and in the southwest in Co. Kerry (box B, Fig. 7.5).

While the major features of the Irish coast are structurally controlled, much of the geomorphological detail is related to late Quaternary glaciation and associated postglacial changes in relative sea level (RSL). Both regional and local ice sheets covered most of Ireland at some time during the last 100 ka. The most recent glaciation (the Midlandian) occurred since 25 ka BP. Only the northern two thirds of the island was ice-covered, mainly from lowland ice basins in central and north central Ireland (Fig. 7.3). A thicker ice sheet of Scottish origin occupied the Irish and Malin seas, with occasional incursions inland, especially along the north coast (Davies and Stephens, 1978). During early deglaciation, local mountain ice centres became more active (Fig. 7.3). Ice is thought to have been largely clear of Ireland by 13 ka BP, although cirque glaciers persisted later in some areas (Davies and Stephens, 1978). Products of the various glaciations mantle the coast and tend to be thicker and more complex along the eastern seaboard. Few primary sediment sources remain along the west coast, but those that do influence the coastal planform. A notable example is the major drumlin field that extends seaward into Clew Bay (Fig. 7.1), forming an extensive archipelago (Guilcher, 1962; Davies and Stephens, 1978, fig. 6.2) analogous to the flooded Lunenburg drumlin field in Mahone Bay, Nova Scotia (Johnson, 1925; Piper et al., 1983).

Ice loading led to high RSL in Ireland in the late Pleistocene. Raised beaches and cliffs occur up to 20 to 25 m above present sea level in the north. All of Ireland, with the possible exception of the southeast, has undergone isostatic delevelling, although both magnitudes and rates have varied along a north-northeast-trending axis. However, regional and local neotectonic disturbances, plus non-linear surface warping, confuse any simple recovery patterns (Carter, 1982a; Devoy, 1983). The interaction of isostatic and eustatic factors has produced a variety of sea-level histories in different parts of Ireland (Fig. 7.3). The broad contrasts are between those areas, mainly in the north, where Pleistocene RSL was well above present, forming raised coastal landforms, and those locations where sea level 'peaked' in the mid-Holocene, circa 7 to 5 ka BP, due to interplay between eustatic and residual isostatic movements (Fig. 7.3).

Since about 5 ka BP (the exact timing varies: Mitchell and Stephens, 1974; Carter, 1982a; Shaw, 1985), RSL has been largely stable. This statement requires some qualification because slight but significant fluctuations in RSL may have taken place (Shaw, 1985). The effects on open coasts, however, have been masked within the normal range of tide and wave processes (Carter, 1983). The widespread use of beach-ridge heights as indicators of RSL on the Irish coast (e.g. Mitchell and Stephens, 1974) is open to question. Present sea-level trends are somewhat unclear. South of Ireland, in southwest England and northern France, sea level is rising by about 1.7 mm/a (Pugh and Farell, 1983). At Dublin, the overall rise since 1937 is 0.3 mm/a, but the trend has been variable and RSL has fallen slightly since 1960 (Carter, 1982b). Farther north, at Belfast, RSL remained stationary from 1917 to 1950, but has fallen since, possibly due to man-induced causes (Carter, 1982b). Only in the vicinity of Malin Head, the extreme northerly mainland peninsula, is there a clear trend of falling RSL, averaging 2.4 mm/a over the past 20 years.

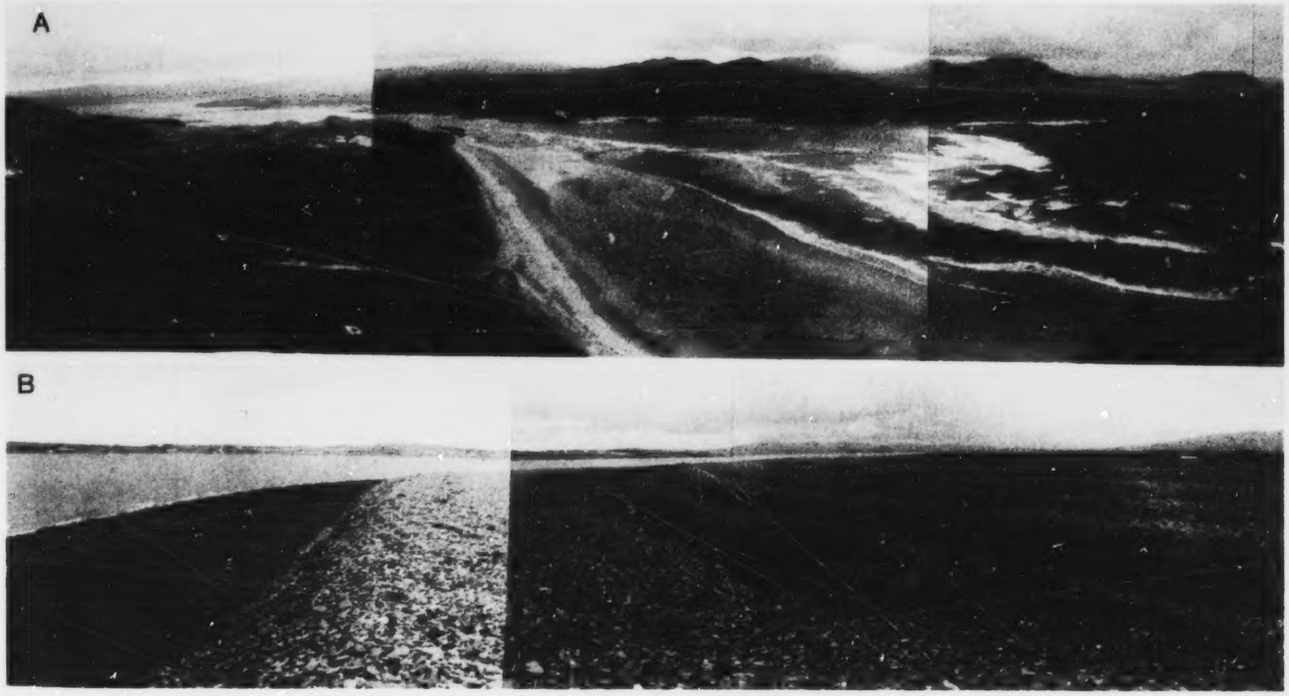

Figure 7.2. *Examples of contrasting coastal environments in the west of Ireland: (A) exposed sand-rich barrier with wide dissipative beachface and large scale dune field, Five Finger Strand at the mouth of Trawbreaga Bay (note person circled for scale); and (B) gravel beach-ridge deposit at Derrymore, formed in the sheltered wave environment of Tralee Bay.*

All coastal changes in Ireland must be viewed in the context of these sea-level trends. In addition, there are clear differences in coastal environment between the east and west coasts (Fig. 7.4, 7.5) in terms of planform, wave energy, and sediment economy. The west coast, exposed to Atlantic storm and swell, comprises a series of resistant headlands bounding sediment-accumulating bays and estuaries. With limited remaining primary sources, sediments within these embayments are well sorted, both horizontally (longshore) and vertically (beach-dune). For example, littoral deposits in Dingle, Brandon, and Tralee bays (Fig. 7.5) range from low-energy gravel beach deposits in sheltered locations (e.g. Cromane and Derrymore, Fig. 7.2B) to large sand and gravel features, some with major dune deposits resting on a gravel substrate, in exposed sites (e.g. Inch and Rossbehy strands). The east coast, by comparison, still has extensive stretches of eroding boulder-clay cliffs forming active sediment sources. The east is dominated by relatively high-frequency wave spectra issuing from cyclonic disturbances over the Irish Sea, although swell penetration from the Atlantic may be important in the secular evolution of beach plan (Carter, 1983). Beaches and barriers in the southeast (Fig. 7.4) appear to have migrated landward, losing contact with their original shelf and coastal sediment sources. This process has contributed to the development of closed drift (longshore transport) cells with very little new sediment input (Lowry and Carter, 1982). The 1984 field investigations reported in this paper focussed on coastal development and sedimentation processes in the west and southeast (Fig. 7.5).

Sites on the southeast coast

A series of fringing barrier beaches extending over 30 km along shore from Ballyteige to Carnsore Point (Fig. 7.4) has been the subject of detailed investigation by Carter and Orford (1980, 1981, 1984) and Orford and Carter (1982a,b, 1984, 1985). The Lady's Island, Tacumshin, and Ballyteige barriers are essentially single-crested features developed in mixed sand and gravel with a very thin cover of dune sand on the barrier crest, except at the east end of Ballyteige Bay where substantial dune deposits occur. Barrier crest elevations range up to 6 m or more above mean high water at ordinary spring tide (MHWOST) (Fig. 7.6).

Based on earlier work at these sites, Carter and Orford (1984) proposed concepts of barrier evolution involving seepage dominance, persistent transgressive behaviour, and new models for upper-beach sedimentation processes in coarse sands and gravels. Vertical facies sequences in back-barrier deposits suggest a switching of depositional loci from washover to crest locations (as a function of the amount of overwash) as the barrier aggrades vertically (Carter and Orford, 1984). They have argued that wave overwash is promoted by the reflective characteristics of steep beachface slopes, which result in amplification of storm wave runup and development of specific upper-beach features. At Carnsore, a berm or supratidal terrace over 30 m or more wide and 2 m above MHWOST (Fig. 7.6, 7.7) protects the dune front against erosion by storm waves during neap tides, but may transform erosional waves to constructional swash runup when storm-surge conditions coincide with spring tides. Swash ramp development (Fig. 7.7A,B) against eroded dune scarps is believed to occur under these conditions (Orford and Carter, 1985).

At the time of our visit to Carnsore in September 1984, the supratidal terrace was well developed, with a width of approximately 30 m. Sections in the upper beach revealed quasi-horizontally stratified sand and gravel with many coarsening-up units, some lenticularity, numerous low-angle truncations, and a large variance in the thickness of

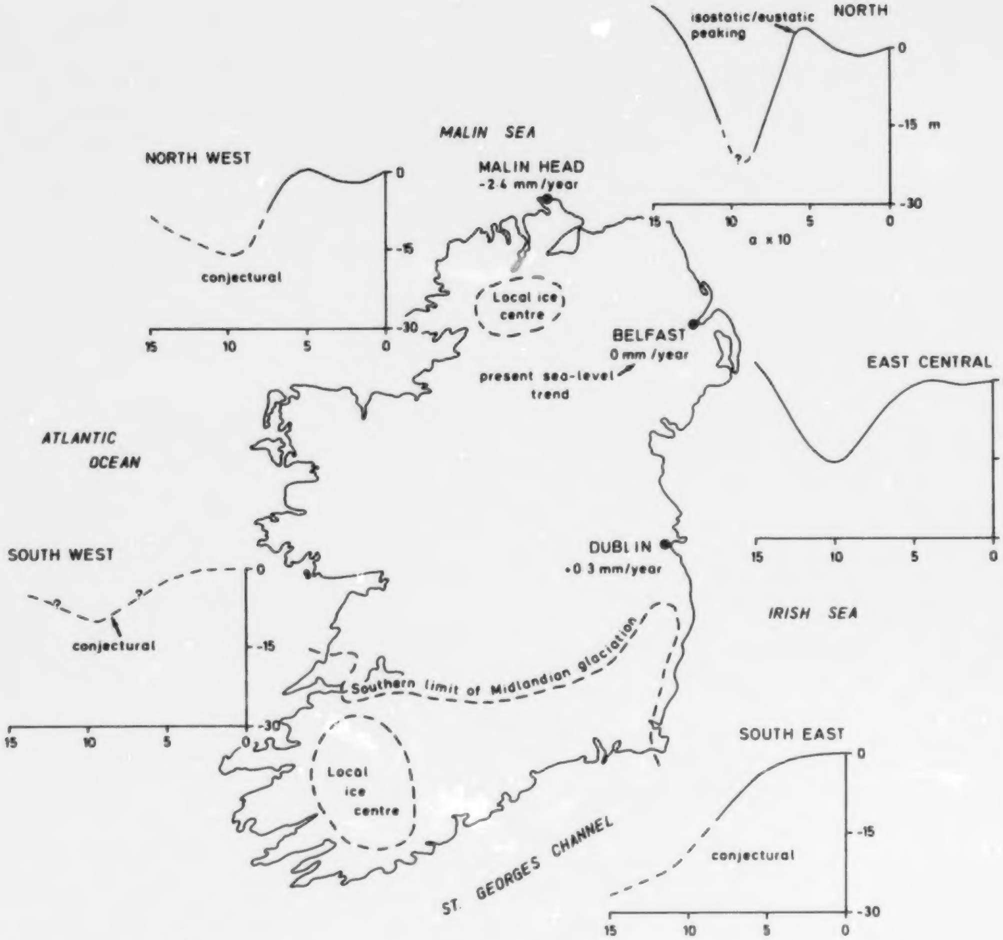

Figure 7.3. *General limits of Midlandian glaciation in Ireland and locations of local ice centres in the southwest (Co. Kerry) and northwest (Co. Donegal). Schematic representation of late Pleistocene and Holocene changes in relative sea level (RSL) around the Irish coast. RSL curves show a south to north transition from eustatic- to isostatic-dominated response. These gross differences may still be apparent in present sea-level trends, as indicated for Dublin, Belfast, and Malin Head.*

individual units (Fig. 7.7C,D). Above the supratidal terrace, swash ramps covered the seaward margin of thin discontinuous dunes overlying washover gravel. Low-angle seaward dips in the upper beachface section and repeated surveys since 1978 suggest that the supratidal terrace develops over several months by slow swash-ridge accretion during periods of wave approach from the southwest (Orford and Carter, 1985).

The Ballyteige barrier (Fig. 7.4) is distinguished from the Tacumshin and Carnsore beaches by a wider beachface developed in mixed sand and gravel and a sandy low-tide terrace (Fig. 7.6) near the tidal channel at the west end. Back-barrier gravels (pits A-C, Fig. 7.6), interpreted as inactive washover deposits, are overlain by a continuous dune and soil cover that decreases in thickness shoreward from the dune crest. Toward the east end of Ballyteige Bay, large volumes of sand are stored in an extensive dune field with crest elevations as high as 17 m O.D.

Coarse gravel beach deposits are characterized by high permeability and an absence of tidal inlets (Carter and Orford, 1984; Carter et al., 1984). This is a distinctive feature of the gravel barriers of southeast Ireland and of similar features at exposed sites on the Canadian Atlantic coast. The frequency of tidal breaching appears to increase with increasing sand/gravel ratios in the system. At Ballyteige (Fig. 7.4), a relatively sand-rich system, lower barrier permeability and higher average runoff from the terrestrial drainage basin have contributed to the development of an ebb-dominated tidal inlet at the west end of the beach. The inlet is bounded by a gravel-based ebb-delta structure that acts as a sediment reservoir for the beach. Observations here and in Dingle Bay (Fig. 7.5) have led to the suggestion that, in gravel-dominated systems, the absence of tidal inlets (which may act to recycle some sediment seaward) and of associated ebb-delta deposits (sediment reservoirs) may contribute to the landward migration of supply-limited barriers (Carter and Orford, 1984).

Sites on the west coast

Within Dingle Bay (Fig. 7.5), the two exposed outer barrier deposits are fronted by wide shoreface and beachface sands forming a broad highly dissipative surf zone. The larger of the two barriers is Inch Strand, which extends three

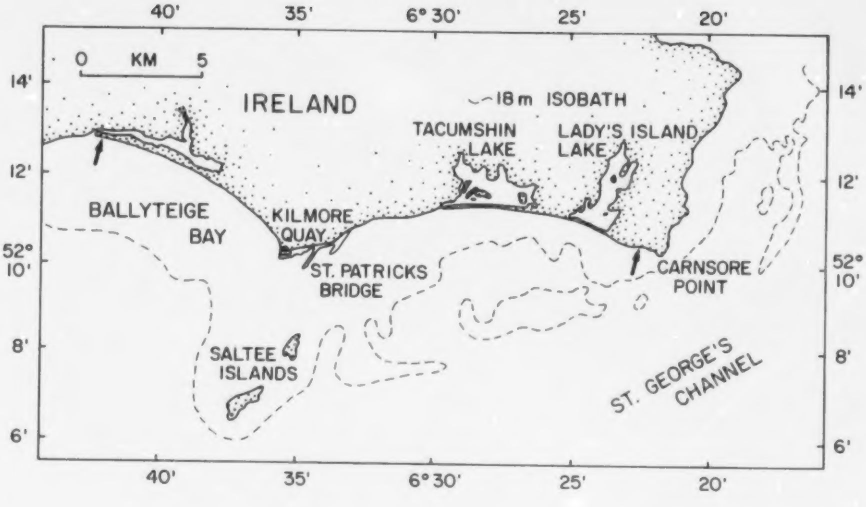

Figure 7.4.

Coarse-clastic fringing barriers extending west from Carnsore Point, Co. Wexford. The 1984 field surveys and sediment sampling were concentrated on the beach at Carnsore and barriers at Tacumshin and Ballyteige. Arrows denote locations of beach profiles in Figure 7.6. St. Patrick's Bridge is a pebble-cobble transverse ridge that may be a tombolo-remnant shoal (Orford and Carter, 1982b) analogous to transverse ridges described from the Nova Scotia coast (Taylor et al., 1985).

quarters of the way across the bay from the north shore. Our work was concentrated on Rossbehy Strand, a large gravel-based spit deposit on the south side of the bay. This feature, like Inch, is capped by a major dune field, with crest elevations ranging up to 16 m toward the distal end. The spit is attached to the cliffed perimeter of Dingle Bay by a narrow gravel barrier (Guilcher and King, 1961). At present, the gravel storm ridge (up to about 3 m above MHWOST) extends at least 1 km distally along-shore before disappearing beneath the dunes. Gravel is also exposed within runnels across the lower beach face and in features that may represent recurve-spit deposits beneath the dunes on the back-barrier shore. Basal cut at the front of the dunes exposes beach gravel overlain by dune sand (Fig. 7.8) and interstratified sand and gravel in places where gravel storm units, deposited over dune sand, have been buried subsequently by slumpling or dune progradation.

Inch Strand displays many similarities to Rossbehy Strand. The neck at Inch is wider and less starved of sand. Dunes extend almost the entire length of Inch Strand and are less stable toward the centre of the bay, where sand is funnelled landward across the barrier through large blowouts to form high slipface deposits prograding onto the back-barrier marsh (Guilcher and King, 1961). At both Rossbehy and Inch, the beach expands toward the tidal inlet, where it merges with a large ebb-tidal delta complex (Fig. 7.5). The latter is dominated by a central ebb channel, bounded on each side by a channel-margin bar and marginal flood channels. The significance of the close proximity of major dune fields to tidal inlets in several parts of Ireland is not clear. However, it appears that the large ebb-delta complex in Dingle Bay may act as a sediment reservoir and the ebb-tide flow as a mechanism by which wind-, wave- and flood-driven sediments are recycled to, or retained on, the seaward side of the barrier.

Another west-coast barrier showing vertical and horizontal segregation of sand and gravel is Bartraw Strand in Clew Bay. Bartraw Strand was originally composed of three beach segments separated by a small drumlin and an inlet. The only remaining evidence of the drumlin is a gravel lag shoal. At the south end, where the barrier is connected to the south shore of Clew Bay (Fig. 7.8), Bartraw Strand is characterized by low dunes in the backshore and a wide dissipative sand beachface. Gravel is restricted to swash lines and storm deposits at the base of the dunes. The north end of the beach is gravel-dominated with a steeper beachface slope. Sections in the dunes and inlet fill suggest intermittent gravel washover sedimentation over low-level dune sand on this part of the barrier (Fig. 7.8). Overall, however, superposition of dune sand on a gravel beach foundation is a major feature of the facies geometry at this site.

In some more sheltered inner-bay locations (in Dingle and Tralee bays, for example), sediment-starved gravel beach deposits show evidence of distal expansion by redistribution of sediment from the updrift end. Behind Rossbehy and Inch strands, Cromane foreland forms an inner barrier fronting Castlemaine Harbour. This feature has been described by Guilcher and King (1961) as a low moraine connected to the mainland by a gravel tombolo. Contemporary growth of low recurve spit features at the distal end of Cromane appears to be associated with longshore transport of gravel in pulses. Morphological evidence for this process is provided by a small ness of gravel storm ridges fronting a 19th-century seawall and coast-guard station opposite the Inch-Rossbehy tidal inlet.

In Tralee Bay, a spectacular compound recurved gravel spit deposit has developed at Derrymore (Fig. 7.2B, 7.5). Map and airphoto data document rapid northeastward progradation of Derrymore spit (Guilcher and King, 1961, fig. 16, 17). The beach ridges are composed of locally-derived pebble-cobble gravel. Sand cover on Derrymore is thin or absent, except at the southwest end of the beach where low dunes occur. Guilcher and King (1961) hypothesized that the main Derrymore complex developed at a time of greater wave exposure before formation of the tombolo between Fahamore and the mainland (Fig. 7.5). However, historical map evidence and observations in 1984 show that erosion of the neck and accretion of new ridges at the distal end of the spit are ongoing processes. Cross-shore profiles surveyed along the length of Derrymore (Fig. 7.9) indicate that the presently active storm ridges, although higher than the oldest ridges in the complex, are similar in height to features of intermediate age. At the neck, the barrier is transgressing rapidly by beachface erosion and washover transport. The observed formation of new ridges in recent years and similarity to active beach ridge deposits in other low-energy environments (Taylor, 1980; Forbes, 1985) suggest that the whole complex could have formed under sheltered wave conditions.

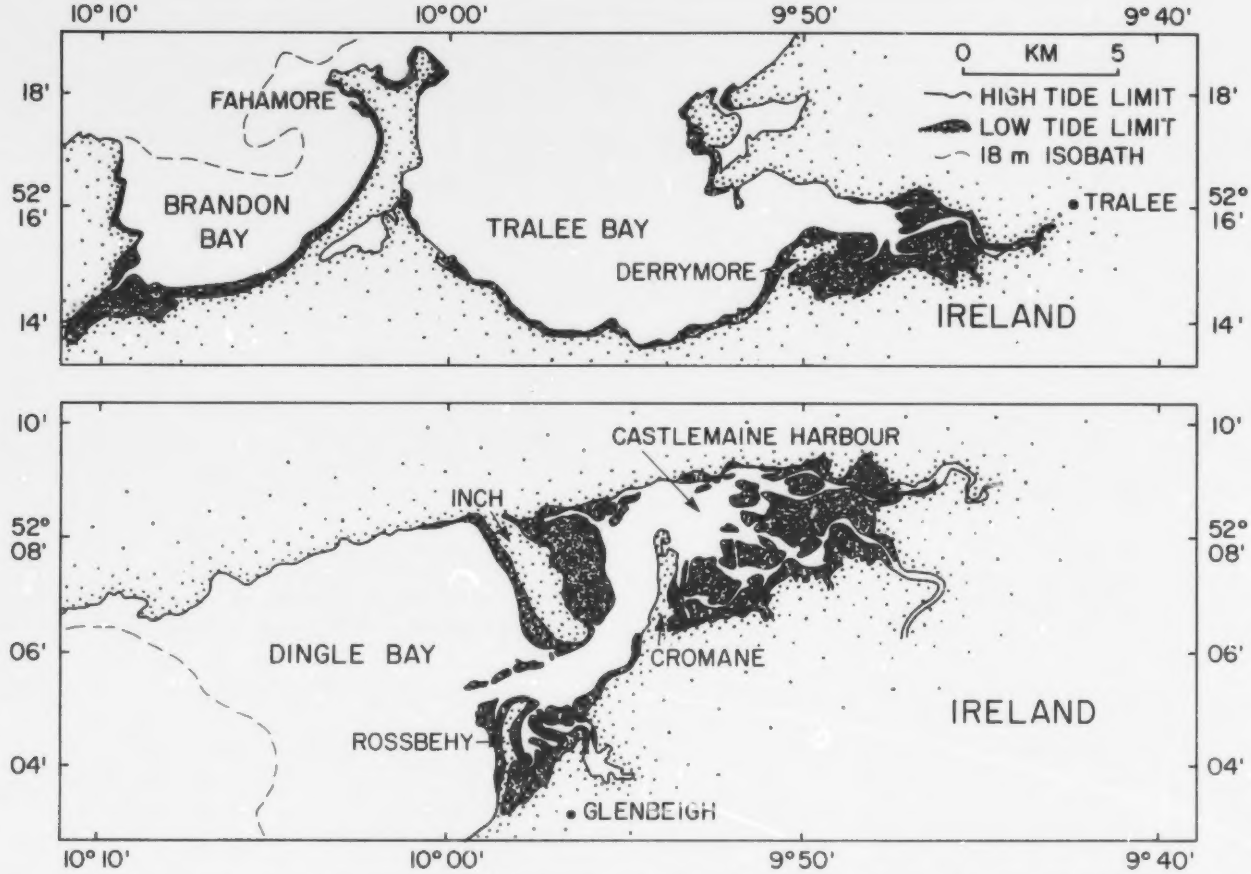

Figure 7.5. *Beaches examined on the southwest coast of Ireland in 1984. The exposed outer beaches (Inch, Rossbehy, and Brandon) are characterized by highly dissipative beachface sands and large dune fields. Smaller gravel beaches (Cromane and Derrymore) are developed in sheltered inner-bay environments.*

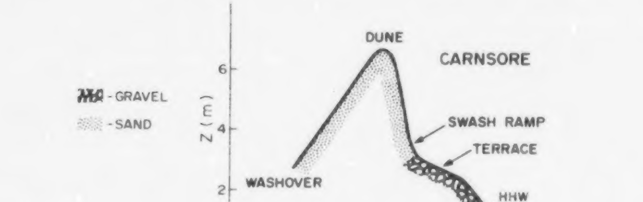

Figure 7.6. *Cross-shore profiles surveyed at Carnsore (October 1978, Orford and Carter, 1982a) and Ballyteige (September 1984); locations shown by arrows in Figure 7.4. Pits (A-C) in the back-barrier platform at Ballyteige show depth to relict gravels interpreted as washover deposits. Gravel overtopping (not shown) at the barrier crest and sand-gravel washover deposits are also present at Carnsore.*

Derrymore appears to have been sheltered by a large island at Fahamore throughout Holocene time. Bouldery till is exposed across the intertidal shoreface along the seaward side of Fahamore at the north end of Brandon Bay (Fig. 7.5). This is overlain in the upper foreshore by a compacted herbaceous peat with rooted stumps of **Salix** and **Betula** (Fig. 7.8B), which have yielded preliminary carbon-14 dates of 4.6-4.1 ka BP. Pollen data suggest that the peat is a back-barrier deposit dating from sometime in the interval 6.5-5.2 ka BP, between the expansion of **Alnus** and the appearance of substantial human activity (J. Shaw, personal communication, 1985). The peat is taken to indicate a relative sea level at least 1.5 m below present and its compressed condition is attributed to burial by onshore migration of the dune barrier.

Discussion

In comparison with coastal features of Atlantic Canada, distinctive features of the Irish coast include the high crest elevations of gravel beaches on the open southeast coast (Fig. 7.5; Carter and Orford, 1981) and in the north (Carter, 1982a), the very large volumes of sand stored in coastal dune fields in many parts of the island (Fig. 7.2A), and the distinct lateral and vertical separation of sand and gravel in the larger beach systems. Bedrock geology, coastal planform, wave exposure, and type and abundance of source sediments can lead to local variability of beach development in any coastal region. However, differences in climate, RSL history, and oceanographic conditions on opposite sides of the

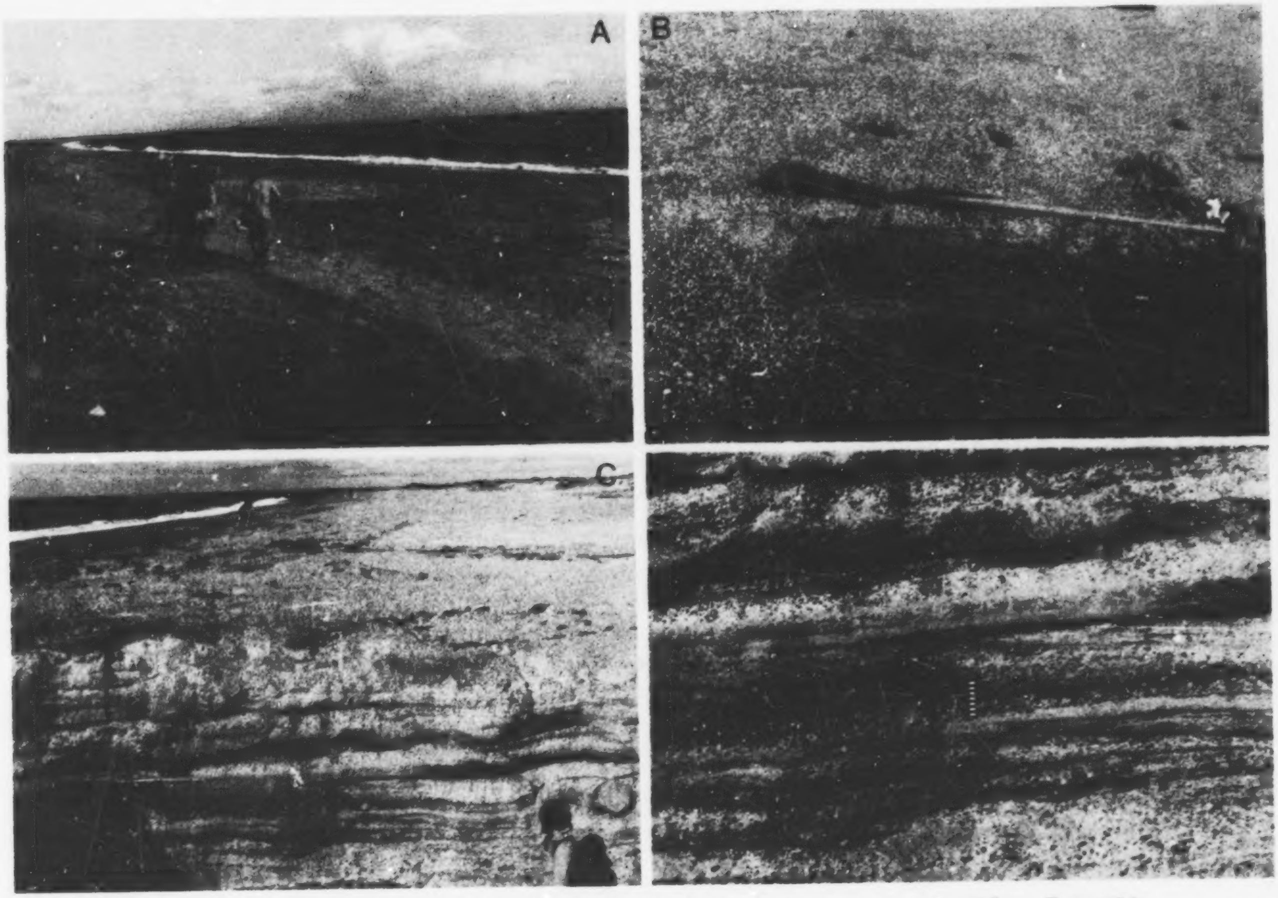

Figure 7.7. *Swash ramp (A) and section (B) showing internal structure, upper beachface, Tacumshin Barrier. Supratidal terrace (C) 2 m above MHWOST at Carnsore Beach, where sections cut through the terrace (D) reveal coarsening-up units of variable thickness (ocean to left). Landward-dipping terrace units are frequently truncated by low-angle seaward-dipping upper-beachface deposits.*

Atlantic account for a large proportion of the contrasts observed between coastal sites in eastern North America and Ireland.

The Atlantic coast of Ireland is dominated by onshore winds and storm waves generated by northeastward passage of extra-tropical cyclonic depressions. Ice is not a factor. The east coast of Canada is similarly storm-dominated, but with more marked seasonal variance in ice, wind, and wave conditions. Although strong onshore (easterly) winds accompany winter storms, the prevailing winds in the Canadian Maritime Provinces are offshore (southwest in summer and northwest in winter). Maximum annual significant wave heights in deep water range from 10 to 16 m off the west of Ireland in contrast to values of 8 to 11 m off Nova Scotia and Newfoundland (Neu, 1984). Post-storm decay swell commonly reaches 12- to 14-s period in both regions but periods in excess of 20 s may be important in the development of gravel beaches in western Britain and Ireland (Carter and Orford, 1984). Except for the Bay of Fundy, much of the Canadian Atlantic coast experiences spring tidal ranges (0.8-2.7 m) somewhat lower than values prevailing along the Irish coast (1.6-4.8 m). Although various parts of the Canadian Atlantic coast have experienced both falling and rising RSL during postglacial time, much of the region has been subject to rising water levels over the past few thousand years (Quinlan and Beaumont, 1981). Modern tide-gauge records reveal rates of increase in mean RSL of 4 mm/a and more (Grant, 1975; Forbes, 1984). This contrasts with conditions on much of the Irish coast, which has enjoyed approximately constant RSL over the past 5 ka (Fig. 7.3; Carter, 1982a; Devoy, 1983).

Despite long-term stability of RSL, the coarse grained barrier beaches of southeast Ireland are migrating onshore and display transgressive facies sequences similar to those observed in areas of rising RSL in eastern Canada. The ongoing marine transgression on the Canadian east coast results in exposure of new sediment sources to coastal erosion and locally abundant sediment supply conditions. Where large sediment sources are available, beach progradation has occurred despite rising RSL (Grant, 1975; Forbes, 1985; Forbes and Taylor, in press). At other sites where sediment supply is limited, wave runup and washover dynamics appear to be more important in the short term than RSL in determining high rates of landward migration of gravel barriers (Forbes, 1984). The greater incidence of washover activity on Canadian barriers (relative to conditions on the Irish coast) may be partly due to a different phase in the cycle of back-barrier deposition prompted by lower barrier crest elevations in Canada. Gravel barriers exceeding 6 m above MHWOST occur both in Ireland and eastern Canada (Orford and Carter, 1982b; Forbes, 1984), but most gravel beaches on the Canadian coast are lower and are either

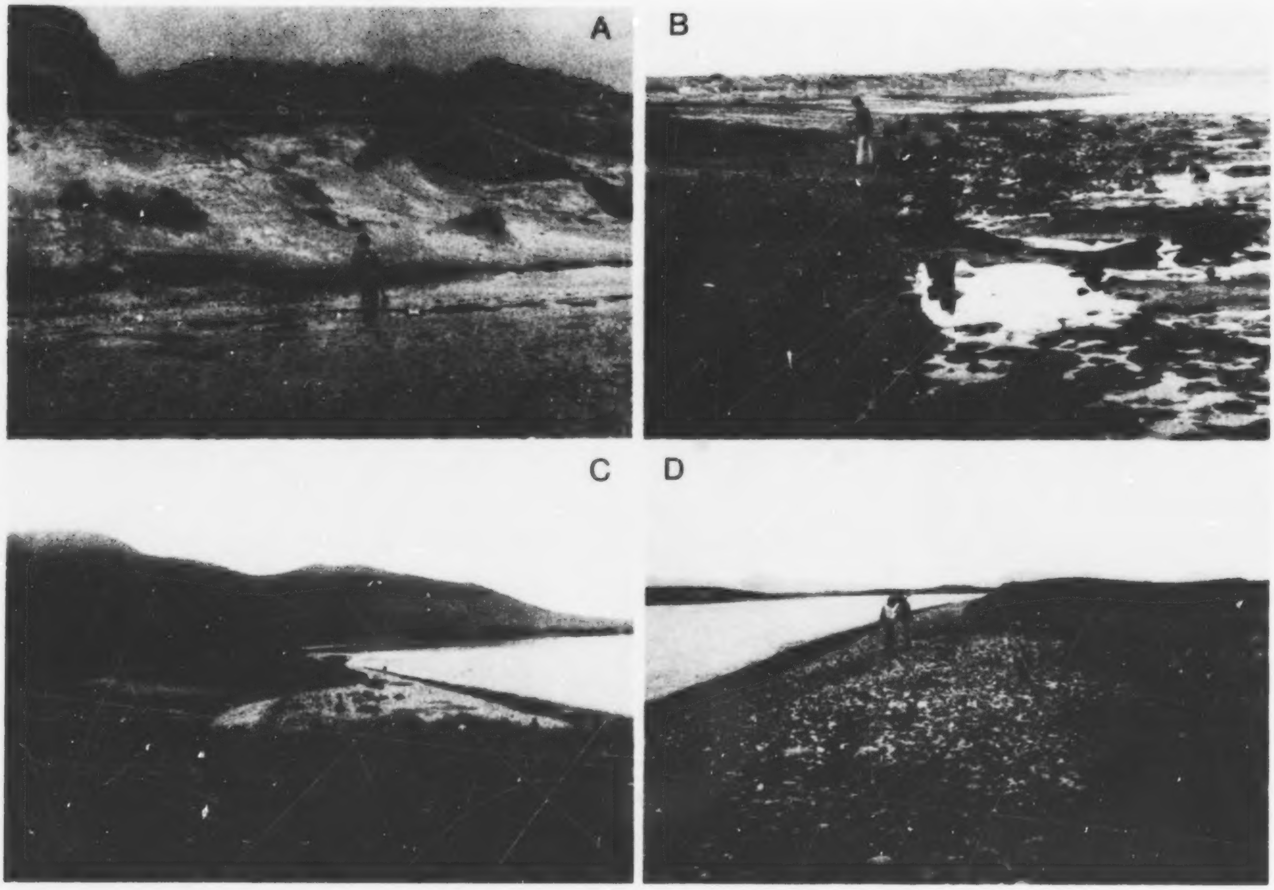

Figure 7.8. Views of (A) the seaward side of Rossbehy spit where a basal gravel unit is overlain by slumped dune deposits; (B) a foreshore exposure of herbaceous peat with tree stumps overlying bouldery till, overrun by an onshore-migrating barrier (in background), Fahamore, Brandon Bay; (C) general view of Bartraw Strand, Clew Bay, looking toward the south end of the barrier, with gravel inlet-fill in middle ground; (D) interstratified gravel overwash and dune sediments at barrier crest, north end of Bartraw Strand.

devoid of sand or topped with a low solitary dune line similar to that observed at Tacumshin and Carnsore (Fig. 7.6) in southeast Ireland. Although the supratidal terrace observed at Carnsore (Fig. 7.4, 7.6C) has few reported analogues elsewhere in Ireland or in eastern Canada, a superficially similar feature has been described from a site in southeast Newfoundland (Forbes, 1985). But whereas the terrace at Carnsore develops slowly by incremental swash-ridge accretion, the Newfoundland feature appears to have formed during a single late-winter storm and is associated with very large swash cusps. The origin and significance of upper beachface cusp, terrace, and ramp deposits in relation to barrier overtopping and stability are topics that require further study.

Impressive volumes of sand are stored in dune systems along the coast of Ireland (Fig. 7.2A). Wide dune belts with crest elevations up to 6-10 m are common features of the larger beaches and dune crest heights up to 30 m occur at Tramore. A distinctive feature of many large dune deposits on the Irish coast is their association with basal gravel beach sediments, as at Rossbehy Strand, Dundrum Bay, and Tramore. Such vertical separation of sand and gravel is uncommon on the Canadian Atlantic coast. Moreover, large-scale coastal dune deposits in general are less common in eastern Canada. The best-developed examples, with crest elevations up to 20 m, occur in Prince Edward Island and western Newfoundland (Armon and McCann, 1977; Owens, 1979; Forbes, 1984) (the largest dunes in eastern Canada, offshore on Sable Island, are unique by virtue of their location in an area of extensive sand on the outer continental shelf).

Radiocarbon dating of dune soils in Ireland indicates that the major dune complexes did not develop until after maximum marine transgression (since 5 ka BP) and that most dune systems were well developed by 3.5 ka BP (Carter, 1982a). In eastern Canada, Armon and McCann (1977), working along the north coast of western Prince Edward Island, have concluded that coastal dunes in that area were initiated since 2.5 ka BP. At another site on the central north coast of the island, airphoto evidence reveals formation of a major dune complex over a 40-year interval (Simmons, 1982), with transformation from extensive backbarrier washover sands in 1935 to large-scale dune development in 1974.

The abundance of sand at many coastal sites in Ireland may reflect characteristics of local paraglacial source materials, but the development and maintenance of large

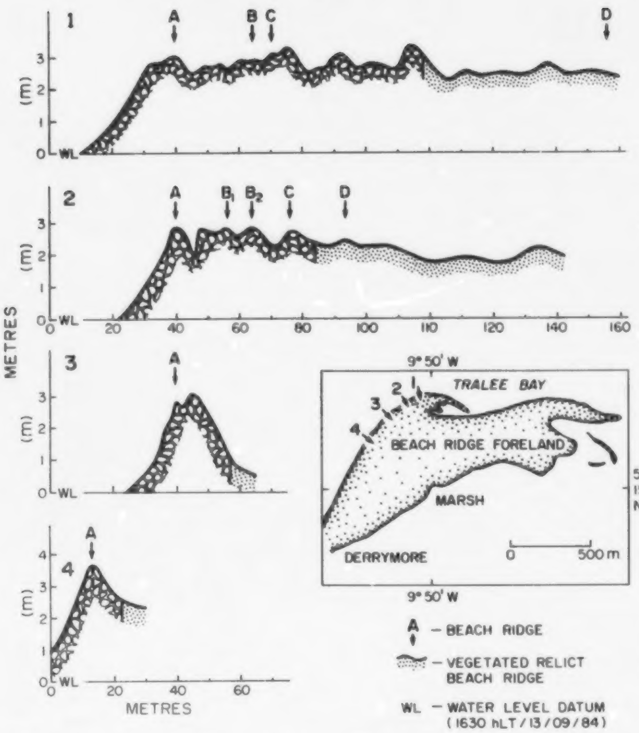

Figure 7.9. Cross-sectional profiles across Derrymore spit, Tralee Bay, illustrate changes in beach ridge size and spacing from the prograding distal end of the spit (profile 1) to the transgressive neck (profile 4). Figure 7.2B shows the beach ridges at profile 2.

dune deposits must be related to particularly favourable environmental conditions. In Ireland, these may include prevailing onshore winds that tend to feed the dunes from beachface or ebb-shoal sources, favourable growing conditions for dune grasses, and long-term stability of relative sea level. The limited development of beach dune systems on the outer Canadian Atlantic coast may be related to prevailing offshore winds that tend to return sand from dunes to beachface sinks, snow and ice covered (or ice-bonded) beach surfaces in winter, and rapidly rising relative sea level.

Barrier sedimentation processes are closely related to RSL behaviour and sediment supply regime. The implications of RSL adjustment for coastal dune development remain somewhat obscure, although evidence from Ireland suggests that limited RSL fluctuation about a stable mean datum may favour growth of large dune systems. A marked increase in dune building activity in the Canadian Great Lakes region has been related to rising lake levels after 1972 (R. Davidson-Arnott, personal communication, 1985). Thom et al. (1981), working in eastern Australia, have documented cessation of washover sedimentation and initiation of dune building as RSL stabilized at the end of the mid-Holocene transgression, a pattern similar to that observed in Ireland. They have also noted that mid and late Holocene intervals of dune instability in eastern Australia may have been associated with intensified wave and wind activity. In Atlantic Canada, most of the large coastal dunes occur in localities with ample sediment supply, in a zone through the southwest to northeast Gulf of St. Lawrence where the change in RSL over the past 2 ka has been very limited (Quinlan and Beaumont, 1982). Examples from Prince Edward Island also indicate that, under suitable circumstances, large dunes may develop very rapidly, on a time scale unrelated to RSL.

At present, much of Atlantic Canada is experiencing rapid sea-level rise comparable to that observed in Ireland in the early Holocene. Carter (1982a) has suggested that the transgression rate prior to 7 ka BP in Ireland may have exceeded the reaction time of some barriers, leaving them as submerged remnants. With comparable high rates of RSL rise prevailing in Atlantic Canada at the present time, many coastal barriers are subject to foreshore recession, landward migration, breaching or overstepping, and restricted dune development, except at sites with abundant sediment supply. The impact of sediment supply (including artificial extraction) and sea-level changes on the development and stability of gravel barriers remains a major focus of ongoing investigations under this project.

Acknowledgments

We are grateful to the Scientific Affairs Division of the North Atlantic Treaty Organization (grant 016/84) for funding this international project. Additional support was provided by the University of Ulster, Queen's University of Belfast, and the Geological Survey of Canada. J. Shaw participated in the Irish coastal surveys in 1984 and provided lively and thoughtful input to field discussions of issues raised in this paper. We also wish to record our thanks to R.J. Devoy for his hospitality and interest. P. Ricketts and R. Davidson-Arnott kindly reviewed the paper and offered some interesting and helpful discussion.

References

Armon, J.W. and McCann, S.B.
1977: Longshore sediment transport and a sediment budget for the Malpeque barrier system, southern Gulf of St. Lawrence; Canadian Journal of Earth Sciences, v. 14, p. 2429-2439.

Carter, R.W.G.
1982a: Sea level changes in Northern Ireland; Proceedings Geologists' Association, London, v. 93, p. 7-23.

1982b: Recent sea level variations on the north and east coasts of Ireland and associated shoreline response; Proceedings Royal Irish Academy, v. 82B, p. 177-187.

Carter, R.W.G. (cont.)
1983: Raised coastal landforms as products of modern process variations, and their relevance in eustatic sea level studies: examples from eastern Ireland; Boreas, v. 12, p. 167-182.

Carter, R.W.G. and Orford, J.D.
1980: Gravel barrier genesis and management: a contrast; Proceedings Coastal Zone 80, American Society of Civil Engineers, New York, p. 1304-1320.

1981: Overwash processes along a gravel beach in southeast Ireland; Earth Surface Processes, v. 6, p. 413-426.

1984: Coarse clastic barrier beaches: a discussion of the distinctive dynamic and morphosedimentary characteristics; in Hydrodynamics and Sedimentation in Wave-dominated Coastal Environments, ed. B. Greenwood and R.A. Davis, Jr.; Marine Geology, v. 60, p. 377-389.

Carter, R.W.G., Johnston, T.W., and Orford, J.D.
1984: Stream outlets through mixed sand and gravel coastal barriers: examples from southeast Ireland; Zeitschrift fur Geomorphologie, v. 28, p. 427-442.

Davies, G.L.H. and Stephens, N.
1978: The Geomorphology of the British Isles: Ireland; University Paperbacks, Methuen, London, 250 p.

Devoy, R.J.
1983: Late Quaternary shorelines in Ireland: an assessment of their implications for isostatic land movement and relative sea level changes; in Shorelines and Isostasy, ed. D.E. Smith and A.G. Dawson; Institute of British Geographers, Special Publication, No. 16, Academic Press, p. 227-254.

Forbes, D.L.
1984: Coastal geomorphology and sediments of Newfoundland; in Current Research, Part B, Geological Survey of Canada, Paper 84-1B, p. 11-24.

1985: Placentia Road and St. Mary's Bay: field-trip guide to coastal sites in the southern Avalon Peninsula, Newfoundland; in Proceedings Canadian Coastal Conference 1985, ed. D.L. Forbes; Associate Committee for Research on Shoreline Erosion and Sedimentation, National Research Council Canada, Ottawa, p. 587-605.

Forbes, D.L. and Taylor, R.B.
– Coarse-grained beach sedimentation under paraglacial conditions, Canadian Atlantic coast; in Glaciated Coasts, ed. D. Fitzgerald and P. Rosen; Academic Press. (in press)

Grant, D.R.
1975: Recent coastal submergence of the Maritime Provinces; Proceedings Nova Scotian Institute of Science, v. 27, Supplement 3, p. 83-102.

Guilcher, A.
1962: Morphologie de la baie de Clew (Comte de Mayo, Irelande); Bulletin Association Geographie Francaise, No. 303-4, p. 53-65.

Guilcher, A. and King, C.A.M.
1961: Spits, tombolos and tidal marshes in Connemara and west Kerry, Ireland; Proceedings Royal Irish Academy, v. 61B, No. 17, p. 283-338.

Johnson, D.W.
1925: The New England-Acadian Shoreline; John Wiley and Sons, New York, 608 p.

Lowry, P. and Carter, R.W.G.
1982: Computer simulation and delimitation of littoral drift cells on the south coast of Co. Wexford, Ireland; Journal of Earth Sciences, Royal Dublin Society, v. 4, p. 121-132.

Mitchell, G.F. and Stephens, N.
1974: Is there evidence for a Holocene sea-level higher than that of today on the coasts of Ireland?; Colloques Internationaux CNRS, No. 219, p. 115-125.

Neu, H.J.A.
1984: Interannual variations and longer-term changes in the sea state of the North Atlantic from 1970 to 1982; Journal of Geophysical Research, v. 89, p. 6397-6402.

Orford, J.D. and Carter, R.W.G.
1982a: Crestal overtop and washover sedimentation on a fringing sandy gravel barrier coast, Carnsore Point, southeast Ireland; Journal of Sedimentary Petrology, v. 52, p. 262-278.

Orford, J.D. and Carter, R.W.G. (cont.)
1982b: Geomorphological changes on the barrier coasts of south Wexford; Irish Geography, v. 15, p. 70-84.

1984: Models of longshore washover spacing on coarse clastic barriers; Marine Geology, v. 56, p. 207-226.

1985: Storm-generated dune armouring on a sand-gravel barrier system, southeastern Ireland; Sedimentary Geology, v. 42, p. 65-82.

Owens, E.H.
1979: Prince Edward Island: coastal environments and the cleanup of oil spills; Environmental Protection Service, Environment Canada, Economic and Technical Review Report EPS 5-EC-79-5, 167 p.

Piper, D.J.W., Letson, J.R.J., de Iure, A.M., and Barrie, C.Q.
1983: Sediment accumulation in low-sedimentation, wave-dominated, glaciated inlets; Sedimentary Geology, v. 36, p. 195-215.

Pugh, D.T. and Farell, H.E.
1983: Tides, surges and mean sea level trends; in Shoreline Protection; Institution of Civil Engineers, Thomas Telford, London, p. 59-69.

Quinlan, G. and Beaumont, C.
1981: A comparison of observed and theoretical post-glacial relative sea level in Atlantic Canada; Canadian Journal of Earth Sciences, v. 18, p. 1146-1163.

1982: The deglaciation of Atlantic Canada as reconstructed from the postglacial relative sea-level record; Canadian Journal of Earth Sciences, v. 19, p. 2232-2246.

Shaw, J.
1985: Aspects of Holocene coastal evolution, Co. Donegal, Ireland; unpublished Ph.D. dissertation, University of Ulster, Coleraine, 278 p.

Simmons, M.D.
1982: Have catastrophic storms shaped P.E.I.'s North Shore?; Proceedings Workshop on Atlantic Coastal Erosion and Sedimentation; Associate Committee for Research on Shoreline Erosion and Sedimentation, National Research Council Canada, Ottawa, p. 23-36.

Stephens, N.
1970: The coastline of Ireland; in Geographical Studies, ed. N. Stephens and R.E. Glasscock; Queen's University, Belfast, p. 125-145.

1975: The coastline of Ireland; Geoscience and Man, v. 14, p. 105-111.

Taylor, R.B.
1980: Coastal environments along the northern shore of Somerset Island, District of Franklin; in The Coastline of Canada, ed. S.B. McCann; Geological Survey of Canada, Paper 80-10, p. 239-250.

Taylor, R.B., Wittmann, S.L., Milne, M.J., and Kober, S.M.
1985: Beach morphology and coastal changes at selected sites, mainland Nova Scotia; Geological Survey of Canada, Paper 85-12, 59 p.

Thom, B.G., Bowman, G.M., and Roy, P.S.
1981: Late Quaternary evolution of coastal sand barriers, Port Stephens-Myall Lakes area, central New South Wales, Australia; Quaternary Research, v. 15, p. 345-364.

Pisces IV research submersible finds oil on Baffin Shelf

Projects 760015, 740003

A.C. Grant, E.M. Levy [1], K. Lee [1], and J.D. Moffat [1]
Atlantic Geoscience Centre, Dartmouth

Grant, A.C., Levy, E.M., Lee, K., and Moffat, J.D., **Pisces IV** research submersible finds oil on Baffin Shelf; in Current Research, Part A, Geological Survey of Canada, Paper 86-1A, p. 65-69, 1986.

Abstract

Evidence of natural seepage of petroleum from the seabed off the coast of Baffin Island was first reported in 1976. Chemical analyses of samples from the oil slick on the sea surface, and geological and geophysical studies of the Baffin Shelf supported this interpretation. Liquid oil recovered from the sea floor off Scott Inlet in October, 1985, by the research submersible **Pisces IV**, confirms the existence of natural oil seeps, and indicates that source rocks for petroleum are present in the Baffin Bay region.

Résumé

Des traces de suintement naturel de pétrole provenant du fond de la mer au large de la côte de l'Île Baffin ont été signalées pour la première fois en 1976. L'analyse chimique des échantillons de la nappe d'hydrocarbures trouvée à la surface de la mer ainsi que l'étude géologique et géophysique de la plate-forme continentale de Baffin ont appuyé cette interprétation. La récupération du pétrole liquide du fond de la mer au large de l'Inlet Scott en octobre 1985 par le submersible PISCES IV confirme l'existance de suintements naturels de pétrole et indique la présence, aux alentours de la baie de Baffin, de roches mères pétrolifères.

---

[1] Atlantic Oceanographic Laboratory, Dartmouth

Introduction

Evidence of natural seepage of petroleum from the seafloor off the northeast coast of Baffin Island was first recognized in 1976 (Loncarevic and Falconer, 1977; Levy, 1977). The evidence consisted of an oil slick on the sea surface and eruption of gas bubbles and oil droplets within the area of the slick. Several detailed studies were subsequently undertaken of the background levels of petroleum residues in the surface slick, water column, and surficial bottom sediments, and of the geology of the area (Levy, 1978, 1979a, b; MacLean, 1978; MacLean and Falconer, 1979; Levy and MacLean, 1981). A comprehensive review of all previous investigations was published by MacLean et al. (1981).

In 1981 the research submersible **Pisces IV**, operating from the support vessel **Pandora II**, was used to investigate the sea bottom northeast of Scott Inlet in the area where seepage appears to be most active. No seepage of oil or gas from the seafloor was found at that time, but a number of patches of white "fuzzy slime", which were interpreted as evidence of bacterial growth associated with emission of hydrocarbons, were observed. With the return of **Pandora** and

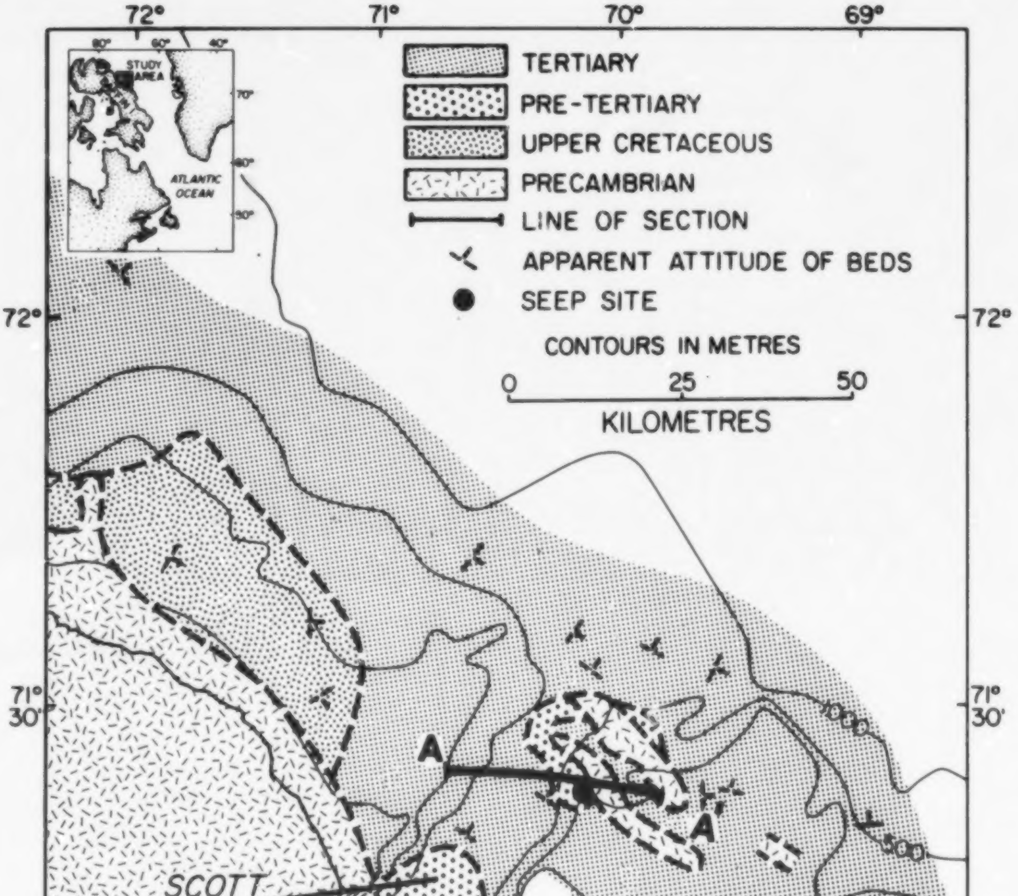

Figure 8.1. Geological map of Baffin Shelf off Scott Inlet (modified after MacLean et al., 1981). Line A-A¹ is location of cross section in Figure 8.2.

Pisces to the east coast of Canada for the 1985 field season, a joint cruise (BIO cruise 85-063) to the seep area was organized by the Chemical Oceanographic Division of the Atlantic Oceanographic Laboratory and the Atlantic Geoscience Centre of the Geological Survey of Canada. This work (September 23 to October 5) was the final phase of the **Pisces** program in Arctic waters for 1985. This paper is a preliminary report of the results from this cruise, with emphasis on geological observations.

Regional geology and morphology of the seep area

The principal features of the submarine geology and morphology of the continental shelf off Scott Inlet, Baffin Island, are indicated in Figure 8.1. Scott Trough is a deep, erosional depression trending northeast across the shelf, with depths as great as 800 m. Oil slicks have been observed on many occasions on the sea surface over Scott Trough and the bank area to the southeast. The most persistent slick is near a basement high on the southeast flank of the outer part of Scott Trough (Fig. 8.1), and seepage in that area appears to originate within sedimentary strata flanking the northwest-southeast trending basement high (Fig. 8.2).

Cruise program

The objectives of the 1985 cruise to the seep area were to obtain samples of the white slime observed previously; to collect samples of the gas emanating from the seafloor in the areas of the slime; to collect samples of dissolved or dispersed seep material from the overlying water column; to measure the rate and direction of ascent of oil released from the seabed; and to carry out additional geological reconnaissance of the area.

The first dives in the seep area were used to emplace gas samplers in the area of white slime. The samplers were in the form of pyramids, constructed from aluminum, with and open bottom and a chamber for trapping gas at the apex. Two of these units were successfully deployed and subsequently recovered. Both traps contained small amounts of methane, ethane and hydrogen sulphide gas.

Samples of the white slime, generally observed as coatings on the surface of pebbles and cobbles on the seafloor, were obtained at several locations with a suction sampler and a robotic arm, operated from the submersible. The predominant slime material has been tentatively identified as filamentous bacteria of the genus **Beggiatoa**. Samples of the bacterial mat were incubated on board ship with radioisotopes to determine the rates of dark CO_2-fixation and heterotrophic potential. Bacterial standing stock will be determined by scanning electron and epifluorescence microscopy of fixed samples.

As the final procedure of two dives, samples of dyed diesel fuel were released from the seafloor to measure the rate and direction of ascent of oil droplets. From a release depth of 400 m, the oil reached the surface in slightly over one hour. One sample came to the surface about 400 m south of the point of release; the second came up almost directly over the release point. Although the properties of the diesel fuel no doubt differ from those of the natural oil, and recognizing that water currents in the area vary in direction and strength, this simple experiment nonetheless indicates that the slicks observed on the sea surface at Scott Trough lie fairly close to the location from which the material escapes from the seafloor.

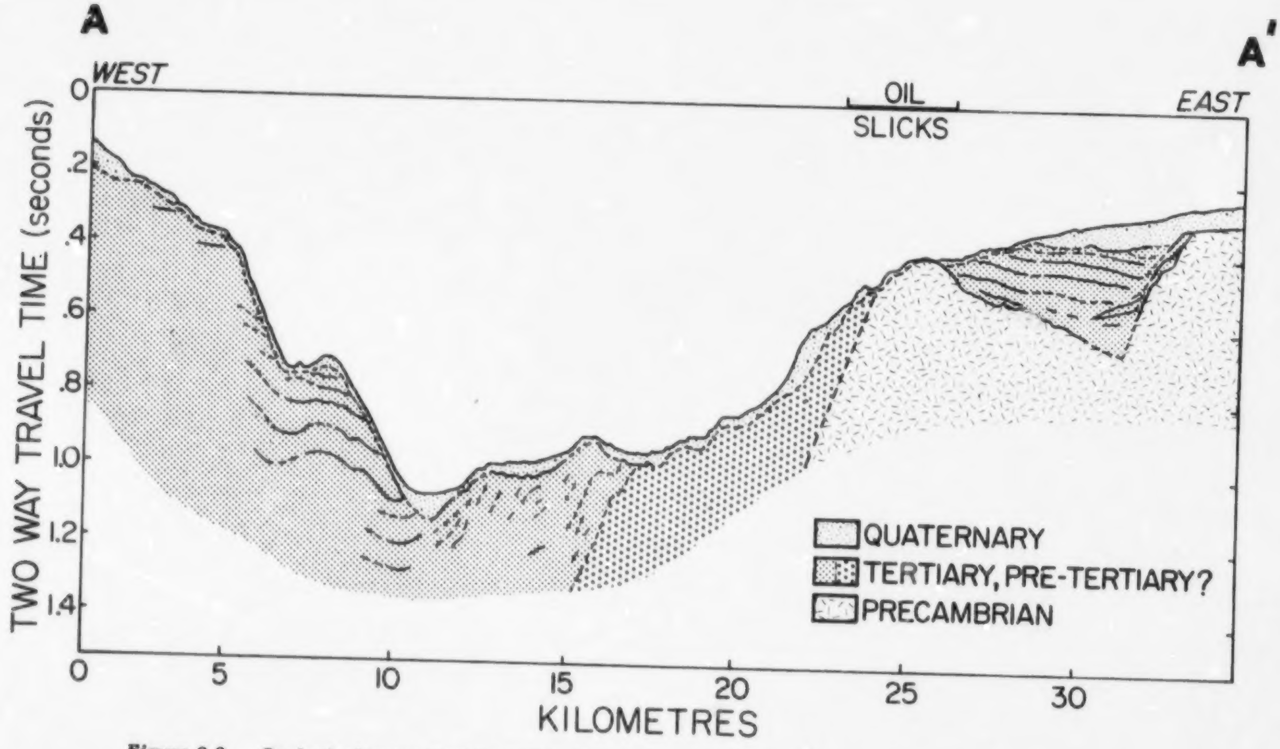

Figure 8.2. Geological cross section across the outer part of Scott Trough showing the sedimentary sequences adjoining the basement high (modified after MacLean et al., 1981). Extent of oil slick along the line at the time of the survey (September 24, 1978) is indicated.

Figure 8.3. *Photograph of sample of crust formed around fissure in the seafloor (by R. Belanger).*

Sampling of the water column was carried out during periods when the **Pisces** was not deployed and the **Pandora** could remain on station for periods of several hours (usually overnight). The in situ sampler pumps seawater through a filter and a cartridge containing XAD-2 resin to extract particulate and dissolved organic compounds. The samples collected by this device are being analyzed.

Several dives were devoted primarily to geological reconnaissance of the seep area, with a principal objective of recovering samples of bedrock. Two dives were carried out on the southeast wall of Scott Trough, southwest of the seep area. An escarpment with outcropping bedrock was encountered approximately 20 km southwest of the seep site, at a depth of about 100 m. However, because of a strong current at the time of the dive it was not possible to obtain a sample from this location.

The final dive of the cruise was a traverse of about 3 km, south from Precambrian basement across the main seep area (Fig. 8.1). Extensive esposures of bedrock, strewn with numerous boulders, were observed in the area mapped as Precambrian by MacLean et al. (1981). The surfaces of the outcrops were smooth and rounded, presumably due to the action of glacial ice. The contact of the Precambrian with overlying "Pre-Tertiary" strata was covered with overburden and was not directly observed, but the transition to these younger rocks was expressed by a general decrease in the irregularity of the seafloor. The bottom deposits along the survey track consist of mud, gravel and boulders. Because the boulders are concentrated in low ridges, and linear areas of the seafloor are devoid of gravel, it is considered that the bottom morphology and sediment distribution have been modified by the effects of iceberg scouring. The water depth in this area ranges from 360 to 430 m.

Shortly after reaching the Pre-Tertiary zone (Fig. 8.1) occasional small patches of filamentous bacteria were observed. The area of earlier sampling dives on the seep site was recognized by the presence of **Pisces IV** skid marks in the bottom sediment. A short distance to the south of this area, it was noted that the surface layer of sediments in some of the white slime patches was hardened into a weakly cemented crust, and a sample was collected with the robotic arm of the **Pisces**. Continuing to the south, after passing over a low ridge on the seafloor, several prominent patches of bacteria were observed, with obvious crusts in two of the patches. A general impression of the setting of this concentration of bacterial mats was that they lie within a roughly circular, saucer-like depression, estimated to be about 30 m in diameter and 2 to 3 m deep. The two areas of crust appeared to be undermined and partially collapsed. Closer inspection revealed narrow fissures extending into the seafloor at these locations, and probing with the robotic arm indicated that the "crust" around the fissures was very hard. Two fragments of the crust were secured with the robotic arm and placed in the storage tray; one of these fragments (Fig. 8.3) exuded droplets of oil that floated upward. When this specimen was brought to the surface it was placed on a sheet of plastic, and several cubic centimeters of dark brown, medium viscosity oil dripped from it and were collected.

Further sampling and inspection of the fissures was precluded because the **Pisces** battery power was nearly exhausted and the dive was terminated. A follow-up dive was planned for the next day – the final day of the cruise, but it was cancelled because of bad weather.

Discussion of results

The discovery of oil in the indurated crust within an area of white, "fuzzy slime" confirms that these bacterial mats are related to the seepage of petroleum from the seafloor. As mentioned, laboratory analyses are in progress on the bacteria, gas, and oil samples recovered during this cruise.

The specimen of crust that has yielded oil appears to be composed of indurated bottom sediment, since it consists of pebbles of igneous rock cemented in a fine matrix. The matrix reacts readily with acid, and therefore has an appreciable carbonate content. A carbonate cement has been reported for crusty material collected at the site of a gas seep in the North Sea (Hovland et al., 1985). The surface of the specimen has a corroded aspect; the pits may express both dissolution of the matrix material and the imprints of igneous pebbles. The oil that drained from this rock was trapped in the downward concave pits on its under surface; the "crust" itself is not the source rock for the oil. The fissures in the seafloor within the patches of indurated sediment are assumed to be the routes of egress of the oil from a deeper source. No flow of oil from these fissures was noted during the brief time that they were under observation. It is anticipated that analyses of the oil may provide some indication of its geological age, and suggest whether it was derived from Tertiary or Mesozoic strata, or from older, Paleozoic rocks.

The dimensions of the saucer-like depression in which the crust, fissures and oil were found are within the size ranges reported for "pock marks", which are circular depressions on the seafloor believed to be due to flowage of gas from the underlying sediments (e.g. Josenhans et al., 1978; Hovland, 1981; Hovland et al., 1985; Nelson and Healy, 1984). The presence of pock marks on the seafloor could be documented by side-scan sonar surveys, and these should be included in future investigations of this area. Future studies should also include additional submersible work directed at locating the active fissure(s) in the seafloor. Active fissures may be the sites of enhanced biological activity, as reported from the Gulf of Mexico, the North Sea and Santa Barbara Channel (Kennicutt II et al., 1985; Hovland et al., 1985; Spies and DesMarais, 1983).

Acknowledgments

We were much impressed by the expert operation and handling of the **Pisces IV** submersible, and we are grateful to the **Pisces** diving team and the Captain, officers and crew of the **M.V. Pandora II** for their extensive assistance and hospitality throughout the cruise. We thank J.S. Bell and K.D. McAlpine for helpful review of this manuscript.

References

Hovland, M.
1981: Characteristics of pock marks in the Norwegian Trench; Marine Geology, v. 39, p. 103-117.

Hovland, M., Judd, A., and Maisey, G.
1985: North Sea gas feeds the North Sea fishes; New Scientist, August 8, no. 1468, p. 26.

Josenhans, H.W., King, L.H., and Fader, G.B.
1978: A side-scan sonar mosaic of pock marks on the Scotian Shelf; Canadian Journal of Earth Sciences, v. 15, p. 831-840.

Kennicutt II, M.C., Brooks, J.M., Bidigare, R.R., Fay, R.R., Wade, T.L., and Macdonald, T.J.
1985: Vent-type taxa in a hydrocarbon seep region on the Louisiana Slope; Nature, v. 317, p. 351-353.

Levy, E.M.
1977: Scott Inlet slick: an Arctic oil seep?; Spill Technology Newsletter, v. 2, no. 6, p. 21-27.

1978: Visual and chemical evidence for a natural seep at Scott Inlet, Baffin Island, District of Franklin; in Current Research, Part B, Geological Survey of Canada, Paper 78-1B, p. 21-26.

1979a: Concentration of petroleum residues in the waters and sediments of Baffin Bay and the Eastern Canadian Arctic – 1977; Bedford Institute of Oceanography Report Series, BI-R-79-3, January 1979.

1979b: Further chemical evidence of natural seepage on the Baffin Island shelf; in Current Research, Part B, Geological Survey of Canada, Paper 79-1B, p. 379-383.

Levy, E.M. and MacLean, B.
1981: Natural hydrocarbon seepage at Scott Inlet and Buchan Gulf, Baffin Island shelf: 1980 update; in Current Research, Part A, Geological Survey of Canada, Paper 81-1A, p. 401-404.

Loncarevic, B.D. and Falconer, R.K.
1977: An oil slick occurrence off Baffin Island; in Report of Activities, Part A, Geological Survey of Canada, Paper 77-1A, p. 523-524.

MacLean, B.
1978: Marine geological-geophysical investigations in 1977 of the Scott Inlet and Cape Dyer, Frobisher Bay areas of Baffin Island continental shelf; in Current Research, Part B, Geological Survey of Canada, Paper 78-1B, p. 13-20.

MacLean, B. and Falconer, R.K.
1979: Geological-geophysical studies in Baffin Bay and Scott Inlet – Buchan Gulf and Cape Dyer – Cumberland Sound areas of the Baffin Island shelf; in Current Research, Part B, Geological Survey of Canada, Paper 79-1B, p. 231-244.

MacLean, B., Falconer, R.K., and Levy, E.M.
1981: Geological, geophysical and chemical evidence for natural seepage of petroleum off the northeast coast of Baffin Island; Canadian Petroleum Geology, v. 29, p. 75-95.

Nelson, C.S. and Healy, T.R.
1984: Pockmark-like structures on the Poverty Bay sea bed – possible evidence for submarine mud volcanism; New Zealand Journal of Geology and Geophysics, v. 27, p. 225-230.

Spies, R.B. and DesMarais, D.J.
1983: Natural isotope study of trophic enrichment of marine benthic communities by petroleum seepage; Marine Biology, v. 73, p. 67-71.

Analysis of in-house control reference samples by commercial laboratories using inductively-coupled plasma emission spectrometry

Project 580175

G.E.M. Hall and J.E. Vaive
Resource Geophysics and Geochemistry Division

Hall, G.E.M. and Vaive, J.E., Analysis of in-house control reference samples by commercial laboratories using inductively-coupled plasma emission spectrometry; in Current Research, Part A, Geological Survey of Canada, Paper 86-1A, p. 71-79, 1986.

Abstract

In-house reference samples were distributed to major commercial Canadian laboratories for major, minor and trace element determination by inductively-coupled plasma emission spectrometry (ICP-ES). The results reported are compared to values obtained by X-ray fluorescence (XRF) and atomic absorption spectrometry (AAS).

Ca, Al, Fe, Mg, Mn, and Ti exhibit acceptable precision and accuracy by ICP-ES but the precision obtained for silicon is significantly inferior compared to XRF. P can be determined at low levels by ICP-ES, provided attention is given to spectral interferences. Flame emission should be urged for Na and K below about 1% as these elements are normally measured under less than optimum conditions by ICP-ES or XRF. Reproducibility across ICP-ES and XRF laboratories for Ba is poor, owing to lack of available calibrating standards and solubility problems. Cu, Zn, Mo, Co, Ni, Cr, and V can be determined with good accuracy and precision by ICP-ES. Atomic absorption spectrometry is the preferred technique for the determination of cadmium and lead below 20 ppm as ICP-ES is too insensitive.

Résumé

Des échantillong de référence de la Division ont été distribués aux principaux laboratoires commerciaux canadiens à des fins d'analyse des éléments majeurs, mineurs et des oligo-éléments, effectuée au moyen de la spectroscopie par émission de plasma. On compare ici les résultats aux chiffres obtenus par fluorescence des rayons X et par spectrométrie par absorption atomique.

La spectroscopie par émission de plasma donne des résultats d'une précision acceptable pour le Ca, l'Al, le Fe, le Mg, le Mn et le Ti; cependant, dans le cas du Si, les résultats ainsi obtenus sont bien moins précis que ceux obtenus par fluorescence aux rayons X. La spectroscopie par émission de plasma permet de déterminer la présence de faibles quantités de P pourvu que l'on tienne compte du brouillage spectral. La méthode de l'émission de flamme est préférée pour analyser le Na et le K lorsque les teneurs sont inférieures à environ 1 % car ces éléments sont normalement mesurés par spectroscopie par émission de plasma ou par fluorescence des rayons X dans des conditions laissant souvent à désirer. La reproductibilité des résultats de l'analyse du Ba par spectroscopie par émission de plasma et par fluorescence des rayons X est pauvre d'un laboratoire à l'autre étant donné les problèmes de solubilité et la pénurie des normes d'étalonnage. La spectroscopie par émission de plasma donne des résultat exacts et précis dans le cas du Cu, du Zn, du Mo, du Co, du Ni, du Cr et du V. La spectrométrie par absorption atomique est la méthode préférée pour déterminer les teneurs en Cd et en Pl inférieures à 20 ppm car la spectrométrie par émission de plasma est trop peu sensible.

Introduction

Most commercial laboratories in Canada now have the capability to analyze geological samples for major, minor and trace elements by inductively-coupled plasma emission spectrometry (ICP-ES). Comprehensive publications describing this technique applied to geological material have been written by: Floyd et al. (1980); Walsh and Howie (1980); Brenner et al. (1980); Church (1981); and McLaren et al. (1981). The precision, sensitivity and speed of ICP-ES, together with its low susceptibility to concomitant interferences, have led to rapid acceptance by environmental scientists and geochemists. Usually, 30 to 40 elements are determined on a simultaneous spectrometer in a matter of 1 to 2 minutes and calibrations are linear over at least three orders of magnitude. Much of the data used by Govindaraju (1984) in his compilation of working values for 170 international reference samples of silicate rocks and minerals were obtained by this technique.

In-house controls were prepared in large quantities in 1980 to be used in monitoring precision and accuracy of data produced by contract and Geological Survey of Canada laboratories. These eight samples reflect well the varied composition of rocks collected from sediment-hosted Zn-Pb deposits in the Yukon Territory. These are described later. Six controls were interspersed amongst samples submitted to one 'ICP' laboratory over a three-month period for major and minor element determinations to assess the precision obtained. These controls were later sent to five other 'ICP' laboratories and a 'DCP' (Direct-Current Plasma) laboratory for the same analyses, but not in replicate. X-Ray fluorescence data were also obtained from two sources for comparison purposes. All eight control samples were sent to seven 'ICP'/'DCP' laboratories for analysis of trace elements by whatever 'total' or 'partial' decomposition was usually recommended. Atomic absorption (AA) spectrometry was then used for comparison.

Sample description

All samples were ball-milled to minus 200-mesh in the final preparation stage.

XY29 – A composite sample of a high grade stratigraphic section of mineralization (sphalerite-galena-pyrite) from the Howards Pass (XY) deposit, Yukon Territory. Matrix comprises carbonaceous cherty mudstone with occasional limestone interbeds and concretions.

XY03 – A composite prepared from outcropping Devonian carbonaceous cherty mudstone, Howards Pass, Yukon Territory.

XYPC – A composite sample from adit material mined from hanging wall phosphatic chert, Howards Pass (XY) deposit, Yukon Territory.

CHRT – Near-massive to finely laminated carbonaceous chert collected from outcrop of the hanging wall of the Howards Pass (XY) deposit, Yukon Territory. Minor additions of W, Mo were made to the sample before crushing and blending.

SLBA – Blend of weakly baritic massive sulphide (sphalerite, galena) from the Tom deposit, MacMillan Pass and cherty mudstones from the same area, with carbonaceous shale from Howards Pass, Yukon Territory.

BASL – Similar to SLBA, but a different blend with more barite from Tea property to give a higher BaO content.

GNO1 – Composite outcrop samples were collected from a stratigraphic section of the Gary No.

NSH – Black carbonaceous siliceous shale collected from drillholes through the Road River Group, Howards Pass deposit, Nahanni map area (NTS 105I), Yukon Territory.

Sample decomposition

Major and minor elements

The preparation of a stable solution containing the total content of all the elements of interest is a prerequisite of this method. For major element determination, the lithium metaborate ($LiBO_2$) fusion introduced by Suhr and Ingamells (1966) is often used. A known weight of sample is mixed with a fixed weight of $LiBO_2$ (high purity) in a graphite or platinum crucible, fused at about 1000°C for 20 minutes and dissolved in a fixed volume of dilute nitric acid. Many schemes incorporate use of an internal standard, such as scandium (Brenner et al., 1980) or lanthanum (Walsh and Howie, 1980) to improve precision by compensating for changes in nebulisation efficiency and plasma fluctuations. The sample solution is usually quite dilute to minimize the total dissolved solids (1 to 2%) introduced to the ICP, since sensitivity is not normally a problem. Calibration standards are treated similarly. The five laboratories employing the $LiBO_2$ decomposition used flux:sample ratios in the range 4 to 7 and dilution factors of 200 to 2500.

The use of hydrofluoric acid, in combination with perchloric, hydrochloric and nitric acid is a well-established procedure for the dissolution of silicates. If the evaporation is carried out in an open vessel, then Si is lost as SiF_4, precluding its determination. However, the decomposition is often preferred in that flux reagents are not introduced into solution, allowing a lower dilution factor and analysis of more elements at acceptable detection limits. A number of rock-forming minerals will not be completely dissolved by this procedure: zircon, chromite, spinel, cassiterite, rutile, kyanite and barite. Two laboratories reported results after an $HF-HClO_4-HNO_3$ decomposition. A lengthy but efficient decomposition procedure is to fuse (with $LiBO_2$) the residue remaining after an $HF-HClO_4-HNO_3$ attack and combine the solutions prior to analysis. This generates a solution suitable for major (except Si) and trace element determination with low salt content and dilution factor. Decomposition in Parr bombs with HF where Si is not lost is avoided in high production work as it is so time-consuming and costly.

A fused disc of the sample is prepared for XRF analysis, often with the aid of a Claisse automatic fluxer operated under well-controlled conditions. Typically, 1 g of sample powder is mixed with a mixture of 5 g lithium tetraborate and 0.3 g lithium fluoride and fused over a burner with automated mixing to achieve homogeneity.

Trace elements

Trace elements are often determined after an $HF-HClO_4-HNO_3$ attack or a faster partial decomposition such as aqua regia ($HCl-HNO_3$) or $HClO_4-HNO_3$. The dilution factor is normally 100 or less to achieve adequate sensitivity. ICP-ES is not capable of determining Rb and Cs to satisfactory levels in geological materials owing to excessive ionization and lack of sensitivity. Some laboratories report element values which will likely be in error on partial decompositions due to incomplete dissolution, precipitation or volatilization loss; these elements include Cr, V, Be, Ti, W, Ba and B. Warnings are sometimes issued with these numbers. Four laboratories determined the traces off a 'total' acid attack and five off a 'partial' acid attack.

Results and discussion

Major and minor elements

Tables 9.1 to 9.6 present data obtained for controls XY29, XY03, CHRT, NSH, SLBA and BASL, respectively. Labs 1, 2, 3, 4 and 10 reported ICP (or DCP) analyses after a $LIBO_2$ usion, Labs 7 and 8 after a $HF-HClO_4-HNO_3$ attack, and Labs 5 and 6 reported XRF data. A comparison of precision by the two techniques can be made by studying replicate analyses of XY29, XY03 and NSH (Tables 9.1, 9.2 and 9.4). Two sets of data are shown for NSH and XY29 by Lab 6 as the samples were submitted one year apart. The element Ba is included in these tables as it becomes a major constituent of some of the controls (BASL, SLBA in particular).

Chemical interferences are rare in ICP-ES, the major interference being spectral (line overlap, molecular emission, stray light). This interference can be avoided in major element determination as a wide choice of lines is available, sensitivity not being a limiting factor in this case. Calibration standards and sample solutions must be matched in terms of flux reagent content to avoid viscosity changes.

SiO_2
Concentration range examined: 26 to 73%
Range in Relative Standard Deviation (RSD)
obtained by Lab 10: 1.3% (XY29) to 3.1% (NSH)

Although XY29 gave the least amount of variation when analyzed by Lab 10, it showed the poorest interlaboratory (ICP/DCP) precision at 7.7% RSD. No bias is evident

Table 9.1. Analytical results for major and minor elements, Control XY29

Decomposition	Method	Laboratory Number	Number of Determinations	SiO_2 %	Al_2O_3 %	Fe_2O_3 %	CaO %	MgO %	Na_2O %	K_2O %	MnO %	TiO_2 %	P_2O_5 %	Ba %
$LiBO_2$	ICP	1	1	62.7	2.25	6.59	13.0	0.22	0.02	0.85	0.48	0.10	1.03	0.13
$LiBO_2$	ICP	2	1	65.4	2.31	6.05	13.8	0.28	0.01	1.01	0.43	0.10	0.92	0.02
$LiBO_2$	ICP	3	1	55.7	2.02	6.18	12.7	0.23	<0.01	0.71	0.41	0.08	0.99	0.06
$LiBO_2$	DCP	4	1	54.5	1.85	5.85	12.5	0.24	0.07	0.71	0.40	0.08	1.07	0.06
$LiBO_2$	ICP	10	9	59.2±.8	2.10±.05	6.08±.17	12.7±.2	0.25±.01	0.07±.01	0.70±.06	0.39±.01	0.10±.01	1.02±.06	0.05±.01
$LiBO_2$	XRF	5	1	$\overline{54.3}$	$\overline{1.82}$	$\overline{5.31}$	$\overline{12.3}$	$\overline{0.30}$	$\overline{0.44}$	$\overline{0.70}$	$\overline{0.38}$	$\overline{0.07}$	$\overline{0.94}$	$\overline{0.09}$
$LiBO_2$	XRF	6	1	56.5	2.15	5.70	12.0	0.27	0.01	0.65	0.40	0.10	0.97	0.06
$LiBO_2$	XRF	6	20	56.8±.4	1.97±.12	6.00±.09	12.1±.1	0.20±.06	<0.01	0.69±.02	0.40±.01	0.10±.01	0.99±.01	0.06±.06
$HF-HClO_4-HCl-HNO_3$	ICP	7	1		2.28	6.40	13.0	0.25	0.04	0.80	0.40	0.07	1.03	0.03
$HF-HClO_4-HNO_3$	ICP	8	1		2.02	6.43	13.9	0.29	0.04	0.68	0.37	0.08	1.07	0.12

Table 9.2. Analytical results for major and minor elements, Control XY03

Decomposition	Method	Laboratory Number	Number of Determinations	SiO_2 %	Al_2O_3 %	Fe_2O_3 %	CaO %	MgO %	Na_2O %	K_2O %	MnO %	TiO_2 %	P_2O_5 %	Ba %
$LiBO_2$	ICP	1	1	64.2	8.41	3.39	6.10	0.73	0.13	2.57	0.01	0.48	0.14	3.26
$LiBO_2$	ICP	2	1	65.8	8.80	3.21	6.19	0.81	<0.01	2.93	0.01	0.45	0.10	3.75
$LiBO_2$	ICP	3	1	61.8	8.63	3.42	6.33	0.96	0.30	2.58	0.01	0.43	0.10	4.37
$LiBO_2$	DCP	4	1	61.5	8.35	3.23	6.04	0.82	0.13	2.45	<0.01	0.47	0.18	3.60
$LiBO_2$	ICP	10	11	63.1±1.6	8.58±.26	3.31±.19	6.12±.21	0.82±.04	0.19±.02	2.46±.15	0.01±.003	0.53±.03	0.11±.02	4.09±.17
$LiBO_2$	XRF	5	1	$\overline{64.3}$	$\overline{8.38}$	$\overline{3.24}$	$\overline{6.35}$	$\overline{0.82}$	$\overline{0.31}$	$\overline{2.36}$	$\overline{0.02}$	$\overline{0.50}$	$\overline{0.14}$	$\overline{4.46}$
$LiBO_2$	XRF	6	1	63.2	8.60	3.15	6.20	0.75	0.10	2.50	0.02	0.50	0.14	3.85
$LiBO_2$	XRF	5	6		8.29±.14	3.34±.06	6.09±.19	0.70±.06	0.06±.03	2.42±.10	0.02±.005	0.44±.02	0.14±.01	4.52±.20
$HF-HClO_4-HCl-HNO_3$	ICP	7	1		9.97	3.47	7.16	0.89	0.12	2.90	0.01	0.36	0.14	0.11
$HF-HClO_4-HNO_3$	ICP	8	1		9.27	3.32	9.96	0.81	0.13	2.63	0.01	0.47	0.10	>1.0

Table 9.3. Analytical results for major and minor elements, Control CHRT

Decomposition	Method	Laboratory Number	Number of Determinations	SiO_2 %	Al_2O_3 %	Fe_2O_3 %	CaO %	MgO %	Na_2O %	K_2O %	MnO %	TiO_2 %	P_2O_5 %	Ba %
$LiBO_2$	ICP	1	1	72.1	7.85	3.89	2.02	0.73	0.14	2.49	0.30	0.34	0.25	2.12
$LiBO_2$	ICP	2	1	72.7	9.13	4.19	2.18	0.91	0.12	2.78	0.30	0.36	0.40	1.99
$LiBO_2$	ICP	3	1	72.1	8.20	4.22	2.62	1.18	1.04	2.42	0.28	0.30	0.24	2.42
$LiBO_2$	DCP	4	1	70.2	8.00	3.97	1.92	0.85	0.28	2.40	0.26	0.35	0.22	2.36
$LiBO_2$	ICP	10	11	73.5±1.5	8.16±.15	4.03±.12	2.00±.14	0.86±.02	0.42±.02	2.46±.12	0.27±0.01	0.39±.02	0.27±.03	2.64±.09
$LiBO_2$	XRF	5	1	$\overline{73.9}$	$\overline{8.06}$	$\overline{3.95}$	$\overline{2.21}$	$\overline{0.82}$	$\overline{0.48}$	$\overline{2.35}$	$\overline{0.27}$	$\overline{0.38}$	$\overline{0.26}$	$\overline{2.93}$
$LiBO_2$	XRF	6	1	75.0	8.05	4.00	2.17	0.75	0.01	2.40	0.29	0.37	0.26	2.50
$HF-HClO_4-HCl-HNO_3$	ICP	7	1		9.20	4.06	2.42	0.91	0.34	2.69	0.28	0.28	0.25	0.16
$HF-HClO_4-HNO_3$	ICP	8	1		9.40	4.35	2.32	0.92	0.45	2.60	0.28	0.35	0.32	>1.0

Table 9.4. Analytical results for major and minor elements, Control NSH

Decomposition	Method	Laboratory Number	Number of Determinations	SiO_2 %	Al_2O_3 %	Fe_2O_3 %	CaO %	MgO %	Na_2O %	K_2O %	MnO %	TiO_2 %	P_2O_5 %	Ba %
$LiBO_2$	ICP	1	1	70.2	7.48	2.15	4.00	1.62	0.02	2.56	0.02	0.41	0.34	1.05
$LiBO_2$	ICP	2	1	69.8	8.56	2.24	4.27	1.95	0.04	3.05	0.01	0.42	0.27	0.70
$LiBO_2$	ICP	3	1	67.3	7.92	2.17	4.41	2.02	0.49	2.64	0.01	0.32	0.27	1.16
$LiBO_2$	DCP	4	1	65.5	7.24	2.03	3.84	1.81	0.14	2.44	0.01	0.41	0.29	1.11
$LiBO_2$	ICP	10	14	70.2±2.2	7.92±.34	2.13±.14	3.98±.69	1.81±.11	0.25±.15	2.47±.15	0.02±.004	0.45±.05	0.34±.12	1.33±.12
$LiBO_2$	XRF	5	1	71.5	7.79	2.07	4.26	1.79	0.30	2.63	0.02	0.44	0.35	1.42
$LiBO_2$	XRF	6	1	71.6	7.85	2.05	4.31	1.84	<0.01	2.60	0.01	0.44	0.35	1.22
$LiBO_2$	XRF	6	34	69.3±.7	7.70±.16	1.96±.04	4.15±.05	1.81±.06	0.05±.03	2.51±.03	0.01±.004	0.41±.01	0.36±.01	1.10±.02
$HF-HClO_4-HCl-HNO_3$	ICP	7	1		8.91	2.13	4.71	1.95	0.20	3.11	0.01	0.28	0.34	0.03
$HF-HClO_4-HNO_3$	ICP	8	1		9.35	2.10	4.89	1.92	0.11	2.12	0.01	0.40	0.45	>1.0

Table 9.5. Analytical results for major and minor elements, Control SLBA

Decomposition	Method	Laboratory Number	Number of Determinations	SiO_2 %	Al_2O_3 %	Fe_2O_3 %	CaO %	MgO %	Na_2O %	K_2O %	MnO %	TiO_2 %	P_2O_5 %	Ba %
$LiBO_2$	ICP	1	1	62.4	5.26	3.72	6.58	2.50	0.12	1.06	0.24	0.22	0.19	6.16
$LiBO_2$	ICP	2	1	62.9	5.29	3.55	6.52	2.69	0.01	1.06	0.20	0.19	0.24	7.00
$LiBO_2$	ICP	3	1	62.0	5.35	3.87	6.56	2.88	0.16	0.82	0.20	0.18	0.07	8.92
$LiBO_2$	DCP	4	1	58.1	5.00	3.59	6.41	2.65	0.08	0.80	0.20	0.20	0.12	7.80
$LiBO_2$	ICP	10	11	59.7±1.1	5.36±.16	3.71±.16	6.42±.28	2.66±.14	0.18±.03	0.79±.04	0.19±.03	0.23±.02	0.37±.10	9.25±.44
$LiBO_2$	XRF	5	1	59.2	5.03	3.47	6.46	2.69	0.50	0.77	0.19	0.25	0.14	8.56
$LiBO_2$	XRF	6	1	57.7	4.70	3.50	6.32	2.55	0.01	0.72	0.21	0.23	0.13	7.76
$HF-HClO_4-HCl-HNO_3$	ICP	7	1		5.95	3.90	7.27	2.90	0.12	0.86	0.24	0.17	0.14	3.6
$HF-HClO_4-HNO_3$	ICP	8	1		5.42	3.43	6.66	2.83	0.11	1.18	0.18	0.19	0.09	>1.0

Table 9.6. Analytical results for major and minor elements, Control BASL

Decomposition	Method	Laboratory Number	Number of Determinations	SiO_2 %	Al_2O_3 %	Fe_2O_3 %	CaO %	MgO %	Na_2O %	K_2O %	MnO %	TiO_2 %	P_2O_5 %	Ba %
$LiBO_2$	ICP	1	1	26.3	1.87	1.77	7.45	0.68	0.08	0.41	0.04	0.08	0.10	25.4
$LiBO_2$	ICP	2	1	25.9	1.74	1.87	7.16	0.73	0.01	0.37	0.06	0.07	0.09	34.0
$LiBO_2$	ICP	3	1	25.8	1.79	1.74	7.30	0.77	0.08	0.27	0.03	0.07	0.07	35.9
$LiBO_2$	DCP	4	1	25.6	1.73	1.65	7.63	0.73	<0.01	0.29	0.03	0.08	0.15	36.3
$LiBO_2$	ICP	10	4	26.3±.8	1.96±.08	1.88±.20	7.52±.42	0.68±.04	0.10±.02	0.38±.03	0.03±.01	0.07±.01	0.07±.04	40.8±4.0
$LiBO_2$	XRF	5	1	25.9	1.85	1.50	7.83	0.66	0.37	0.28	0.03	0.26	0.09	34.7
$LiBO_2$	XRF	6	1	25.4	1.35	1.70	7.48	0.44	<0.01	0.25	0.03	0.17	0.09	34.2
$HF-HClO_4-HCl-HNO_3$	ICP	7	1		2.07	1.80	8.47	0.77	0.04	0.34	0.03	0.69	0.07	8.37
$HF-HClO_4-HNO_3$	ICP	8	1		1.68	1.54	7.55	0.66	0.04	0.36	0.03	0.07	0.06	>1.0

between XRF and ICP results, but XRF tends to produce superior precision on the same sample. No interference problems for Si determined in rocks by ICP-ES have been reported. However, low Si values can be obtained when care is not taken to prevent hydrolysis after $LiBO_2$ fusion. This possibility, together with omission of an internal standard, could explain the erratic data shown by ICP laboratories.

Al_2O_3

Concentration range examined: 1.9 to 8.6%
Range in RSD obtained by Lab 10: 1.8% (CHRT) to 4.3% (NSH)

Results obtained by the 'total' acid attack ($HF-HClO_4-HNO_3$) tend to be noisier and higher than those obtained by $LiBO_2$ fusion. Rather than being subject to spectral interferences itself, aluminum causes interference on elements whose analytical lines lie below 220.0 nm by a broad-band emission. Interlaboratory precision for the ICP labs is much worse than that for the XRF labs for samples CHRT (7.9 to 9.1% ICP; cf. 8.1% XRF) and NSH (7.2 to 8.6% ICP; cf. 7.7 to 7.9% XRF). Precision and mean data are comparable for the other standards.

Fe_2O_3

Concentration range examined: 1.8 to 6.0%
Range in RSD obtained by Lab 10: 1.1% (BASL) to 6.6% (NSH)

Again, XRF produced slightly better precision than ICP-ES but the average values are virtually the same. Note the excellent reproducibility for XY29 by Lab 6 (XRF) when the standards were analyzed within one large sample batch compared to the value obtained when submitted at a different time (5.70% cf. 6.00%).

CaO
Concentration range examined: 2.0 to 12.7%
Range in RSD obtained by Lab 10: 1.6% (CHRT) to 17.0% (NSH)

Lab 10 obviously had a problem with NSH and BASL; the RSD obtained from the results of 5 laboratories (ICP/DCP) for NSH is a much more acceptable 5.6% (cf. 17.0% by Lab 10). Thompson and Walsh (1983) have reported that calcium, unlike most other elements, is extremely sensitive to power fluctuations, as low as 0.1%. Average values obtained by the two techniques are comparable and precision slightly superior by XRF.

MgO
Concentration range examined: 0.2 to 2.6%
Range in RSD obtained by Lab 10: 2.3% (CHRT) to 6.1% (NSH)

Results by XRF and ICP-ES are very comparable, with the exception of a low result for BASL by Lab 6 (XRF).

Na_2O
Concentration range examined: 0.01 to 0.4%
Range in RSD obtained by Lab 10: 4.8% (CHRT) to 60.0% (NSH)

Both ICP and XRF sets of results for Na are very poor indeed. The above precision for CHRT within one laboratory is good; however, the precision obtained across ICP/DCP and XRF laboratories after a $LiBO_2$ fusion is a shocking 94%! Lab 5 (XRF) appears to have problems with the determination of sodium on all samples. The sodium atom emission line lies at about 589 nm, a different wavelength area from most other elements. Often an outrigger monochromator is used to monitor Na because of the limited range of the grating chosen for the polychromator. The optimum region in the plasma to provide the best sensitivity for the alkali metals differs from most other elements in being higher in the flame, in the cooler region where ionization is lower. Thus, if an ICP system has been optimized for major elements such as Si and Al, the determination of Na using an atom and not an ion line will be degraded.

K_2O
Concentration range examined: 0.3 to 2.5%
Range in RSD obtained by Lab 10: 4.8% (CHRT) to 8.6% (XY29)

Data for K_2O are much better than that for Na_2O above, probably owing to the generally higher content in the samples. XRF and ICP-ES results compare favourably although the latter technique is not favoured for potassium at low levels (<0.2%) because of its poor detection limit.

MnO
Concentration range examined: 0.01 to 0.39%
Range in RSD obtained by Lab 10: 2.5% (XY29) to 33% (BASL)

Data presented for MnO are good by all laboratories and methods. The RSD understandably rises at low levels, as seen for BASL.

TiO_2
Concentration range examined: 0.07% to 0.53%
Range in RSD obtained by Lab 10: 5.1% (CHRT) to 14.3% (BASL)

Results by both techniques were generally good, the two exceptions being Lab 5 (XRF) and Lab 7 (ICP) for BASL.

P_2O_5
Concentration range examined: 0.07 to 1.02%
Range in RSD obtained by Lab 10: 5.9% (XY29) to 57% (BASL)

XRF data for P_2O_5 are much more consistent than ICP-ES; the RSD for Lab 10 (ICP) on NSH is 35% compared to 3% for Lab 6 (XRF). SLBA results across the ICP/DCP laboratories are particularly noisy (58%). This comparison is probably rather unfair to ICP-ES as it was evident that Lab 10 was experiencing calibration difficulties at the time of analysis. A vacuum or purged spectrometer is normally used for phosphorus as the preferred line is at 178.29 nm. The 213.62 nm line is subject to interference by high concentrations of Cu and Al which must be corrected for.

Ba
Concentration range examined: 0.05 to 38%
Range in RSD obtained by Lab 10: 3.4% (CHRT) to 10.9% (NSH)

Barite is not appreciably attacked by $HF-HClO_4-HNO_3$ which explains the very low results shown in the tables. Often a carbonate fusion is used, followed by dissolution in HCl, or $LiBO_2$ is the flux reagent. Care must be taken to prevent Ba from precipitating out as $BaSO_4$. EDTA is often added to complex Ba and hence keep the element in solution. The two highly baritic samples (BASL, SLBA) show a 'tolerable' precision of 13%, not unexpected as many laboratories may not have calibration standards to match.

The sample with the poorest overall RSD for the above elements by ICP-ES (Lab 10) is undoubtedly NSH. This is not attributable to particularly low or uncommon levels of these elements. One might question the homogeneity of the sample but the XRF results (Lab 6) indicate good reproducibility. On the other hand, results by XRF and ICP-ES for samples XY29 and CHRT agree well and reproducibility is generally good.

Trace elements

Tables 9.7 to 9.14 present the trace element results obtained for XY29, XY03, XYPC, CHRT, NSH, SLBA, BASL and GNO1 respectively. Labs 3, 4, 7, 8 reported data from a 'total' attack and Labs 1, 2, 7, 8, 9 from 'partial' acid attacks. Lab 4 also reported results by AAS on 'total' and 'partial' acid decompositions for XY03, CHRT and SLBA. Precision within a laboratory using ICP-ES was not measurable at this time and, therefore, only the range of values across the laboratories can be discussed. A good indication of reproducibility obtained by AA within one lab (Lab 11) is given by Table 9.11 (NSH). The elements listed comprise the 'core' package offered by most companies; other data were received but not included for the sake of clarity.

Spectral lines used for a particular element will vary, dependent upon the array of each spectrometer and its resolving power. Corrections for spectral interferences, especially by major elements such as Fe, Al, Ca and Mg, become very important for the trace elements. These interferences are manifest as direct spectral overlap, spectral wings and broadband spectral shifts. Predictions of interfering elements are made with the help of wavelength tables (Winge et al., 1979; Brenner and Eldad, 1984) and correction coefficients, often more than 200, are established and inserted into the computer software. The usefulness of short wavelength scans in the vicinity of analyte wavelengths is of paramount importance in characterizing the spectroscopic interference, especially for samples of different and difficult matrices such as these.

Table 9.7. Analytical results for trace elements, Control XY29

Decomposition	Method	Laboratory Number	Number of Determinations	Cu Ppm	Pb %	Zn %	Mo Ppm	Co Ppm	Ni Ppm	Cr Ppm	Cd Ppm	V Ppm
$HF-HClO_4-HNO_3$	ICP	3	1	97	1.00	3.08	385	<5	170	152	109	399
$HF-HCl-HNO_3-HClO_4$	ICP	7	1	87	0.89	3.02	361	8	185	163	117	386
$HF-HClO_4-HNO_3$	ICP	8	1	92	0.94	>1.0	400	8	193	200	114	400
$HF-HCl-HNO_3-HClO_4$	DCP	4	1	102	0.96	>2.0	364	8	208	207	103	396
$HCl-HNO_3-H_2O$	ICP	1	1	82	0.80	2.44	306	5	139		79	75
$HCl-HNO_3-H_2O$	ICP	9	1	88	0.77	2.22	263	5	139		77	65
$HCl-HNO_3$	ICP	7	1	89	0.87	2.89	345	7	166	140	109	176
$HClO_4-HNO_3$	ICP	8	1	105	0.91	>1.0	415	6	193		110	
$HClO_4-HNO_3$	ICP	2	1	95	0.80	3.11	336	12	182		113	157
$HCl-HNO_3$	AA	4	11	114 ± 15	1.02 ± .28	3.71 ± .54	481 ± 57	10 ± 2	237 ± 31		134 ± 20	184 ± 29

Table 9.8. Analytical results for trace elements, Control XY03

Decomposition	Method	Laboratory Number	Number of Determinations	Cu Ppm	Pb Ppm	Zn Ppm	Mo Ppm	Co Ppm	Ni Ppm	Cr Ppm	V Ppm
$HF-HClO_4-HNO_3$	ICP	3	1	34	30	107	<20	<5	22	70	234
$HF-HCl-HNO_3-HClO_4$	ICP	7	1	30	10	123	19	5	18	65	187
$HF-HClO_4-HNO_3$	ICP	8	1	37	42	135	8	6	16	89	230
$HF-HCl-HNO_3-HClO_4$	DCP	4	1	33	49	113	8	3	19	84	207
$HCl-HNO_3-H_2O$	ICP	1	1	31	38	97	7	3	12	15	66
$HCl-HNO_3-H_2O$	ICP	9	1	31	34	94	6	3	12	8	56
$HCl-HNO_3$	ICP	7	1	31	6	273	9	4	34	22	250
$HClO_4-HNO_3$	ICP	8	1	32	41	120	7	6	14		
$HClO_4-HNO_3$	ICP	2	1	32	32	99	14	5	11	7	96
$HF-HClO_4-HNO_3$	AA	4	11	36 ± 6	27 ± 4	117 ± 12		4 ± 2	16 ± 3		255 ± 26
$HCl-HNO_3$	AA	4	8	34 ± 6	34 ± 6	86 ± 21	12 ± 3	7 ± 3	17 ± 5		106 ± 23

Table 9.9. Analytical results for trace elements, Control XYPC

Decomposition	Method	Laboratory Number	Number of Determinations	Cu Ppm	Pb Ppm	Zn Ppm	Mo Ppm	Co Ppm	Ni Ppm	Cr Ppm	Cd Ppm	V Ppm
$HF-HCl-HNO_3-HClO_4$	ICP	3	1	951	6500	7980	<20	<5	102	127	34	388
$HF-HCl-HNO_3-HClO_4$	ICP	7	1	846	5300	7310	30	8	107	124	38	411
$HF-HClO_4-HNO_3$	ICP	8	1	1010	6600	8130	33	8	100	160	30	465
$HF-HCl-HNO_3-HClO_4$	DCP	4	1	875	6960	8121	32	7	115	184	34	449
$HCl-HNO_3-H_2O$	ICP	1	1	846	5149	6802	22	5	70	47	25	155
$HCl-HNO_3-H_2O$	ICP	9	1	889	5197	6827	22	5	72	38	25	125
$HCl-HNO_3$	ICP	7	1	906	5010	7280	24	7	86	79	35	314
$HClO_4-HNO_3$	ICP	8	1	1025	6300	8340	32	6	100		32	
$HClO_4-HNO_3$	ICP	2	1	959	5490	8070	32	9	93	22	46	251

Table 9.10. Analytical results for trace elements, Control CHRT

Decomposition	Method	Laboratory Number	Number of Determinations	Cu Ppm	Pb Ppm	Zn Ppm	Mo Ppm	Co Ppm	Ni Ppm	Cr Ppm	V Ppm
$HF-HCl-HNO_3-HClO_4$	ICP	3	1	30	1100	899	30	<5	35	65	266
$HF-HCl-HNO_3-HClO_4$	ICP	7	1	32	654	883	36	7	23	64	252
$HF-HClO_4-HNO_3$	ICP	8	1	33	1210	1090	25	8	34	88	275
$HF-HCl-HNO_3-HClO_4$	DCP	4	1	30	1170	921	23	5	35	74	249
$HCl-HNO_3-H_2O$	ICP	1	1	25	1087	848	18	3	15	16	80
$HCl-HNO_3-H_2O$	ICP	9	1	30	1144	902	18	4	17	13	74
$HCl-HNO_3$	ICP	7	1	28	1030	884	20	6	18	26	161
$HClO_4-HNO_3$	ICP	8	1	28	1260	1075	22	11	22		
$HClO_4-HNO_3$	ICP	2	1	32	1190	1010	24	8	23	4	117
$HF-HClO_4-HNO_3$	AA	4	9	26 ± 2	791 ± 177	822 ± 52	20 ± 1	5 ± 1	27 ± 2		258 ± 45
$HCl-HNO_3$	AA	4	8	31 ± 5	1108 ± 135	796 ± 206	26 ± 6	6 ± 3	23 ± 3		163 ± 25

Table 9.11. Analytical results for trace elements, Control NSH

Decomposition	Method	Laboratory Number	Number of Determinations	Cu Ppm	Pb Ppm	Zn Ppm	Mo Ppm	Co Ppm	Ni Ppm	Cr Ppm	Cd Ppm	V Ppm
$HF-HCl-HNO_3-HClO_4$	ICP	3	1	30	140	654	20	<5	40	79	5.0	517
$HF-HCl-HNO_3-HClO_4$	ICP	7	1	30	121	666	17	5	42	76	4.4	494
$HF-HClO_4-HNO_3$	ICP	8	1	30	131	880	21	8	37	100	1.0	580
$HF-HCl-HNO_3-HClO_4$	DCP	4	1	28	145	657	16	3	38	86	5.2	463
$HCl-HNO_3-H_2O$	ICP	1	1	24	132	623	15	3	23	11	3.0	79
$HCl-HNO_3-H_2O$	ICP	9	1	28	128	633	14	3	25	7	3.0	68
$HCl-HNO_3$	ICP	7	1	27	121	636	15	4	30	30	4.1	254
$HClO_4-HNO_3$	ICP	8	1	28	154	805	19	5	38		1.5	
$HClO_4-HNO_3$	ICP	2	1	31	159	755	30	6	36	19	10.1	143
$HF-HClO_4-HNO_3$	AA	11	34	32 ± 2	113 ± 22	696 ± 29	15 ± 3	4 ± 1	44 ± 2		4.7 ± 1.0	531 ± 30

Table 9.12. Analytical results for trace elements, Control SLBA

Decomposition	Method	Laboratory Number	Number of Determinations	Cu Ppm	Pb Ppm	Zn Ppm	Mo Ppm	Co Ppm	Ni Ppm	Cr Ppm	Cd Ppm	V Ppm
$HF-HCl-HNO_3-HClO_4$	ICP	3	1	1840	3500	5865	830	733	87	78	45	198
$HF-HCl-HNO_3-HClO_4$	ICP	7	1	1690	4520	5240	733	715	91	70	44	182
$HF-HClO_4-HNO_3$	ICP	8	1	1960	5900	5625	750	760	84	89	32	170
$HF-HCl-HNO_3-HClO_4$	DCP	4	1	1880	5080	5764	809	750	105	88	38	182
$HCl-HNO_3-H_2O$	ICP	1	1	1811	5110	5348	680	517	76	18	33	64
$HCl-HNO_3-H_2O$	ICP	9	1	1857	4730	5035	525	503	75	15	31	55
$HCl-HNO_3$	ICP	7	1	1780	4570	5360	752	519	88	26	43	115
$HClO_4-HNO_3$	ICP	8	1	2055	4430	5810	740	750	80		35	
$HClO_4-HNO_3$	ICP	2	1	1750	4780	5820	724	685	98	9	146	102
$HF-HClO_4-HNO_3$	AA	4	11	1798 ± 121	4263 ± 119	6085 ± 283		742 ± 47	91 ± 7		44 ± 2	198 ± 16
$HCl-HNO_3$	AA	4	4	1976 ± 62	5113 ± 375	5653 ± 401	924 ± 66	850 ± 50	105 ± 6		48 ± 2	108 ± 5

Table 9.13. Analytical results for trace elements, Control BASL

Decomposition	Method	Laboratory Number	Number of Determinations	Cu Ppm	Pb Ppm	Zn Ppm	Mo Ppm	Co Ppm	Ni Ppm	Cr Ppm	V Ppm
$HF-HCl-HNO_3-HClO_4$	ICP	3	1	180	448	472	30	323	149	28	88
$HF-HCl-HNO_3-HClO_4$	ICP	7	1	159	724	474	27	332	152	29	85
$HF-HClO_4-HNO_3$	ICP	8	1	187	630	560	26	345	145	35	81
$HF-HCl-HNO_3-HClO_4$	DCP	4	1	186	365	546	23	302	170	30	52
$HCl-HNO_3-H_2O$	ICP	1	1	191	754	504	20	235	125	6	60
$HCl-HNO_3-H_2O$	ICP	9	1	174	686	475	13	267	130	5	50
$HCl-HNO_3$	ICP	7	1	169	721	481	24	313	138	13	69
$HClO_4-HNO_3$	ICP	8	1	210	450	580	27	380	158		
$HClO_4-HNO_3$	ICP	2	1	170	621	482	23	300	137	11	67
$HCl-HNO_3$	AA	4	4	196 ± 7	683 ± 29	534 ± 14	29 ± 2	376 ± 21	168 ± 4		92 ± 6

Table 9.14. Analytical results for trace elements, Control GN01

Decomposition	Method	Laboratory Number	Number of Determinations	Cu Ppm	Pb Ppm	Zn Ppm	Mo Ppm	Co Ppm	Ni Ppm	Cr Ppm	Cd Ppm	V Ppm
$HF-HCl-HNO_3-HClO_4$	ICP	3	1	28	10	285	<20	6	39	41	5.0	376
$HF-HCl-HNO_3-HClO_4$	ICP	7	1	26	13	284	10	8	37	39	4.5	373
$HF-HClO_4-HNO_3$	ICP	8	1	31	12	320	12	32	38	49	0.5	375
$HF-HCl-HNO_3-HClO_4$	DCP	4	1	26	14	276	8	4	32	41	4.8	310
$HCl-HNO_3-H_2O$	ICP	1	1	25	11	292	7	1	33	22	4	192
$HCl-HNO_3-H_2O$	ICP	9	1	40	46	312	9	32	33	14	3	169
$HCl-HNO_3$	ICP	7	1	24	6	273	9	7	34	24	3.8	250
$HClO_4-HNO_3$	ICP	8	1	24	9	320	10	30	36		1.5	
$HClO_4-HNO_3$	ICP	2	1	30	20	319	10	29	35	4	4.7	264
$HCl-HNO_3$	AA	4	8	28 ± 3	4 ± 3	300 ± 12	9 ± 3	6 ± 3	39 ± 4		5.6 ± 1.7	288 ± 16

Cu
Range of concentration examined: 30 to 1800 ppm
Lower determination limit quoted
by ICP labs: 0.5 to 1 ppm

The reproducibility of results obtained by AA and ICP-ES are similar, the RSD being about 7% at the 30 ppm level. There is no increase in Cu found following an acid attack with HF rather than without, as evidenced by both AAS and ICP-ES results. The two sets of AAS results obtained by Lab 4 after different decompositions show poor agreement (1798 ppm cf. 1976 ppm); no explanation could be found. Excellent results for Cu by ICP-ES can be expected.

Pb
Range of concentration examined: 10 to 10 000 ppm
Lower determination limit quoted
by ICP labs: 2 to 5 ppm

The sensitivity for lead by ICP-ES is not really adequate for non-mineralized samples. Another problem encountered in this analysis is that $PbSO_4$ can precipitate out following dissolution in oxidizing acids and consequently lead to low apparent concentration. For this reason, in the Geochemistry Laboratory, sulphides are attacked initially by HCl alone to drive off the sulphur as H_2S and then HNO_3 is used to dissolve the sample.

Poor results at low Pb levels are evidenced for GNO1 where the RSD for the nine values is 76%, with a mean of 16 ppm. The spread of values after a 'total' attack for BASL is 365 to 724 ppm, the low value being reported by Lab 4 who obtained a very different 683 ppm of a 'partial' attack and AAS finish! Further problem-ridden data are shown for SLBA and CHRT by Lab 4 where AAS values after a 'total' attack are low by about 25%. Sample XY29, containing 1.0% Pb, gave a good RSD of only 9% for the nine values, compared with 27% obtained by Lab 4 using AA. Thus, below about 30 ppm, the poor reproducibility of results by ICP-ES can be attributed to inadequate sensitivity and, at higher concentrations of Pb, the wide scatter is attributed to different dissolution procedures, inadequate in the presence of sulphate.

Zn
Range of concentration examined: 100 to 30 000 ppm
Lower determination limit quoted
by ICP labs: 1 ppm

The sensitivity for Zn by ICP-ES is adequate, though not quite as good as AA. The 213.86 nm line has a minor Cu interference and Mg interferes on the 202.55 nm line. Results by Lab 8 tend to be high, particularly with NSH and Lab 7's value for XY03 by HCl-HNO_3 is obviously in error. Typical RSD values are given by SLBA (5.4% at 5540 ppm) and BASL (8.3% at 508 ppm).

Mo
Range of concentration examimed: 10 to 800 ppm
Lower etermination limit quoted
by ICP labs: 1 to 5 ppm

The detection limit for Mo by ICP-ES is significantly better than AA. The commonly used 202.03 nm line lies in the region of the Al recombination band which must be corrected for. The analytical wavelength used by Lab 3 was not the most sensitive and hence shows a high detection limit. The RSDs obtained by both techniques are comparable (about 13% at 350 ppm, 20% at 20 ppm), although Lab 4 shows a high mean by AA following an HCl-HNO_3 attack.

Co
Range of concentration examined: 4 to 700 ppm
Lower determination limit quoted
by ICP labs: 1 ppm

The 228.62 nm line is sensitive and interference-free. The precision obtained by AA and ICP-ES is comparable. Results by Lab 4 using AA on the HCl-HNO_3 attack appear high. The noise at low levels ($\sim$10 ppm) is acceptable for all samples except GNO1 where values range from 1 to 32 ppm!

Ni
Range of concentration examined: 15 to 200 ppm
Lower determination limit quoted
by ICP labs: 1 ppm

Nickel behaves similarly to cobalt in the ICP. GNO1 shows remarkably good reproducibility with a RSD of 7% at 35 ppm. Results for XY29 by Lab 4 by AA after an HCl-HNO_3 attack appear high.

Cr
Range of concentration examined: 30 to 200 ppm
Lower determination limit quoted
by ICP labs: 1 ppm

Chromium determination is sensitive and interference-free by ICP-ES. Problems arise not from the analysis but from incomplete dissolution of the mineral chromite which is often unsuccessfully dissolved by HF-$HClO_4$-HNO_3. This does not appear to be a problem with these samples which contain rather low levels of Cr. Acid attack without HF for breakdown of silicates is ineffective.

Cd
Range of concentration examined: 5 to 110 ppm
Lower determination limit quoted
by ICP labs: 0.5 ppm

Above 20 ppm, the precision by ICP-ES is acceptable. Lab 2 obviously had a contamination problem with the analysis of SLBA, also evident to a lesser extent in the analysis of NSH. At the 5 ppm level (NSH, GNO1), the results are very noisy and inferior to AAS. The laboratories are probably quoting too low a determination limit for this element by ICP-ES.

V
Range of concentration examined: 80 to 500 ppm
Lower determination limit quoted
by ICP labs: 1 ppm

Vanadium has a number of good, sensitive emission lines from which to choose and does not suffer a decomposition problem with HF-$HClO_4$-HNO_3 as chromium does. Again, HF is required to recover 'total' V. The results for CHRT after a total acid dissolution show a mean of 260 ppm with a good RSD of 4.7%.

Results for CHRT, NSH and SLBA by AAS and ICP-ES after a total attack compare well, whereas the mean for XY03 by AAS is high by about 20%.

Conclusions

The objective of this study was to gain an appreciation for the range of values to be expected when laboratories are requested to analyze 'difficult' samples by ICP-ES on a routine basis without replication. It should be kept in mind that the precision shown across laboratories analyzing by ICP-ES, or by any other technique for that matter, is bound

to be inferior to that obtained within one laboratory. Caution must also be observed in forming conclusions with respect to comparison of XRF and ICP-ES. XRF is a well-established technique whose limitations and interferences are thoroughly documented; atomization and ionization processes in ICP-ES are still being studied. Only two 'XRF' laboratories were used. There tends to be much more variation in sample preparation procedures in ICP-ES than XRF and dissolution problems are likely to be encountered in ICP-ES with samples such as these, containing high concentrations of sulphur and barite.

In reviewing the data obtained for major elements, one would find acceptable the values reported by ICP-ES for calcium, iron, magnesium, manganese and titanium. The inter- and intra-laboratory precision shown by XRF for silicon is certainly superior to that obtained by ICP-ES and most spectroscopists (Thompson and Walsh, 1983) would agree that precision must be improved for this element. The aluminum results by ICP-ES are poor for two samples (CHRT and NSH) and, with these exceptions, the data are acceptable. Sodium shows appalling variability by both techniques and this element by XRF is known to be difficult to determine below 1% unless counting time is increased to improve sensitivity. The authors would recommend flame emission for determination of the alkali metals below 1% concentration. The baritic samples (BASL and SLBA) show problems in reproducibility for phosphorus by ICP-ES; this perhaps is due to inadequate spectral correction at low levels in a troublesome region of the spectrum.

Variability in the barium data is quite high for both techniques; this is hardly surprising as few laboratories would have standards at these levels with which to calibrate. Again, maintaining the barium in solution in the presence of sulphate would pose an added complexity to the ICP-ES technique. The elements copper, zinc, molybdenum, cobalt, nickel and vanadium can be determined with good precision and accuracy by ICP-ES. The authors would recommend using AAS to determine cadmium and lead at low concentration levels (<20 ppm). The dissolution problems encountered for lead are present with both AAS and ICP-ES. Chromium is determined well by ICP-ES, provided a fusion is carried out if chromite is present.

Acknowledgements

The authors wish to thank I.R. Jonasson and W.D. Goodfellow for collection and preparation of the control reference samples. The authors also wish to thank W.D. Goodfellow and G.R. Lachance for critical reading of this manuscript.

References

Brenner, I.B., Watson, A.E., Russell, G.M., and Goncalves, M.
1980: A new approach to the determination of the major and minor constituents in silicate and phosphate rocks; Chemical Geology, v. 28, p. 321-330.

Brenner, I.B. and Eldad, H.
1984: A spectral line atlas for miltitrace and minor element analysis of geological and ore mineral samples by ICP-AES; ICP Information Newsletter, 10, p. 451-508.

Church, S.E.
1981: Multi-element analysis of fifty-four geochemical reference samples using inductively coupled plasma-atomic emission spectrometry; Geostandards Newsletter, v. V, p. 133-160.

Floyd, M.A., Fassel, V.A., and D'Silva, A.P.
1980: Computer-controlled scanning monochromator for the determination of 50 elements in geochemical and environmental samples by inductively coupled plasma-atomic emission spectrometry; Anaytical Chemistry, v. 52, p. 2168-2173.

Govindaraju, K.
1984: 1984 Compilation of working values and sample description for 170 international reference samples of mainly silicate rocks and minerals; Geostandards Newsletter, v. VIII, p. 3-85.

McLaren, J.W., Berman, S.S., Boyko, V.J., and Russell, D.S.
1981: Simultaneous determination of major, minor, and trace elements in marine sediments by inductively-coupled plasma atomic emission spectrometry; Analytical Chemistry, v. 53, p. 1802-1806.

Suhr, N.H. and Ingamells, C.O.
1966: Solution technique for the analysis of silicates; Analytical Chemistry, v. 38, p. 730-734.

Thompson, M. and Walsh, J.N.
1983: A handbook of inductively coupled plasma spectrometry; Blackie and Son Ltd., Glasgow, p. 92.

Walsh, J.N. and Howie, R.A.
1980: An evaluation of the performance of an inductively coupled plasma source spectrometer for the determination of the major and trace constituents of silicate rocks and minerals; Mineralogical Magazine, v. 43, p. 967-974.

Winge, R.K., Peterson, V.J., and Fassel, V.A.
1979: Inductively-coupled plasma-atomic emission spectroscopy: prominent lines; Applied Spectroscopy, v. 33, p. 206-219.

Major tectonic boundaries of the Omineca Belt in southern British Columbia: a progress report

EMR Research Agreement 129

Murray Journeay[1] and Richard L. Brown[2]
Cordilleran Geology Division

Journeay, M. and Brown, R.L., Major tectonic boundaries of the Omineca Belt in southern British Columbia: a progress report; in Current Research, Part A, Geological Survey of Canada, Paper 86-1A, p. 81-88, 1986.

Abstract

Large scale overthrusting and regional extension are both known to have been operative within the southern Omineca Belt. This project addresses the problem of how these two tectonic processes have interacted in both space and time, and the extent to which each may have influenced the structural and thermal histories of the southern Omineca hinterland. Our focus for the 1985 field season has been to identify major tectonic boundaries along the west flank of the Omineca Belt (between latitudes 50 and 52 degrees north), with particular emphasis on their kinematics, relative timing and tectonic signature. Data collected this summer confirm existing models for a two-stage history of northeasterly-directed overthrusting along the Monashee décollement, and has established the existence of a major down-to-the-west detachment zone along the northwest flank of the Shuswap Complex.

Résumé

D'importants mouvements de chevauchement et d'extension régionale ont eu lieu dans la partie sud de la zone d'Omineca. La présente étude examine la façon dont ces deux processus tectoniques ont agi l'un sur l'autre dans le temps et dans l'espace et jusqu'à quel point chacun des processus a pu influer sur l'histoire structurale et l'histoire thermique de la partie sud de l'arrière-oays de la zone d'Omineca. Lors de la campagne sur le terrain de 1985, on s'est surtout efforcé de reconnaître les principales limites tectoniques du flanc ouest de la zone d'Omineca (entre les latitudes de 50 et de 52 degrés nord), en insistant surtout sur leur cinématique, leur synchronisme relatif et leur signature tectonique. Les données recueillies cet été confirment le bien-fondé des modèles existants de chevauchement en deux phases, en direction nord-est, le long du décollement de Monashee, et établissent l'existence d'une importante zone de décollement vers l'ouest, le long du flanc nord-ouest du complexe de Shuswap.

[1] Department of Geology, Middlebury College, Middlebury, Vermont 05753
[2] Department of Geology, Carleton University, Ottawa, Ontario K1S 5B6

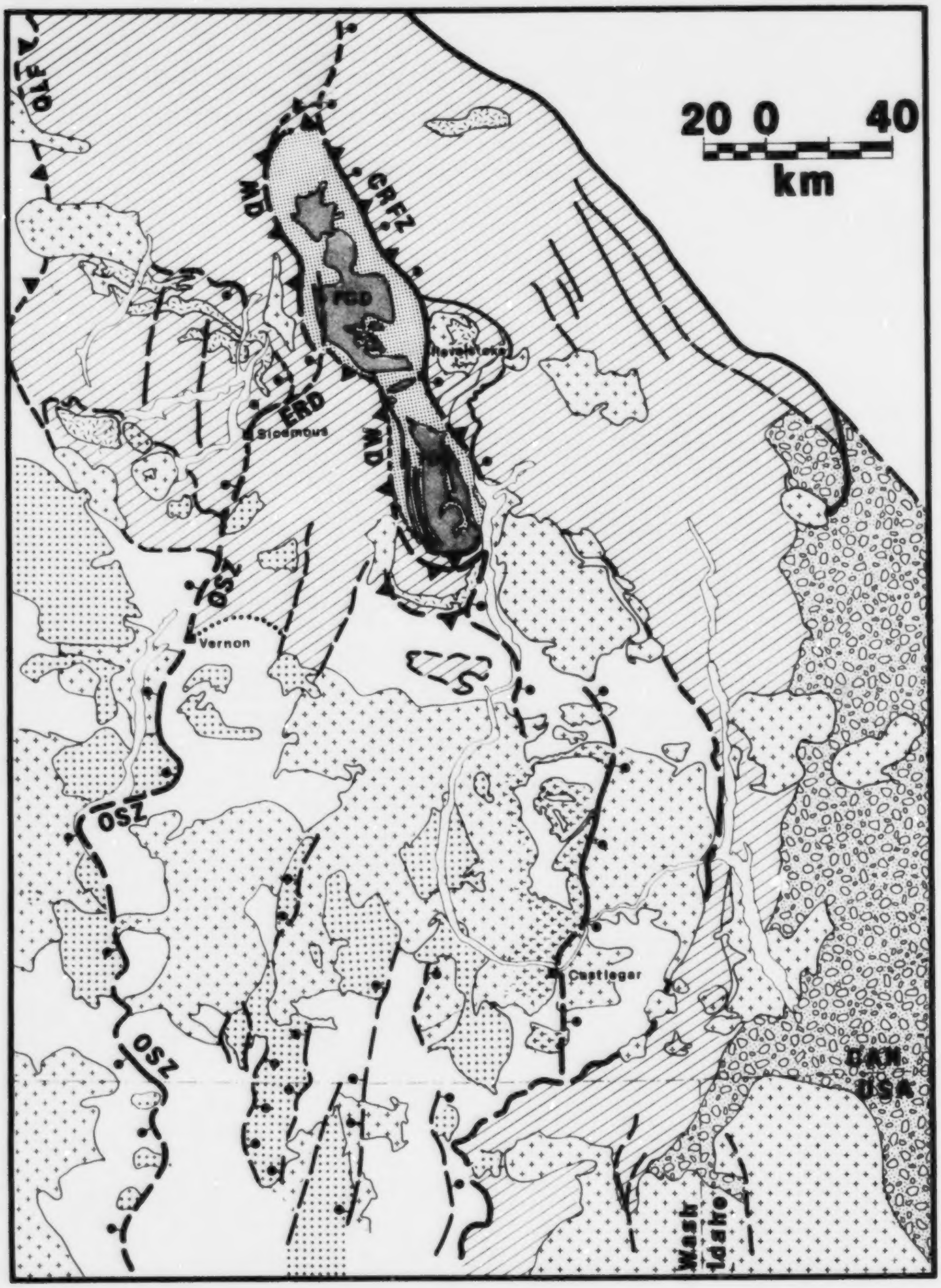

Figure 10.1. Regional tectonic map of major tectonic elements and their bounding faults within the southern Omineca Belt; southeastern British Columbia and adjacent parts of Washington and Idaho. Modified from Parrish et al. (1985). Bounding Faults include: the Quesnel Lake fault (QLF), Monashee décollement (MD), Okanagan shear zone (OSZ), Eagle River detachment (ERD), and the Columbia River fault zone (CRFZ). Map units: upper Proterozoic and Mesozoic units of uncertain provenance and accreted terranes (blank), Proterozoic and lower Paleozoic continental margin sequences of the Selkirk Allochthon (ruled) and Proterozoic Belt-Purcell Group (pebble pattern), Proterozoic platform sequence of the Monashee Complex (light shading), Aphebian basement terrane of the Monashee Complex (dark shading), undifferentiated Paleozoic plutonic rocks (ticking), undifferentiated Mesozoic rocks (large crosses) and their deformed equivalents (asymmetric crosses), and undifferentiated Cenozoic plutonic and related volcanic rocks (small crosses).

Introduction

The origin and tectonic significance of metamorphic core complex terranes (see Crittenden et al., 1980), and their role in the evolution of adjacent thrust and fold belts of the Rocky Mountain Foreland, have become topics of considerable debate in recent years (see reviews of Coney, 1980 and Armstrong, 1982). A key to the understanding of these core complex terranes has been the recognition that they may evolve either by means of progressive shortening and tectonic thickening, or by large scale regional extension and thinning of the crust. Each of these tectonic processes is capable of generating significant components of differential shear and uplift, and hence similar patterns of deformation and regional metamorphism.

Objectives

This study focuses on the structural, thermal and tectonic evolution of the Monashee Complex and overlying Selkirk Allochthon of southeastern British Columbia, (Fig. 10.1). Primary objectives of the study are: 1) to document field evidence for large scale overthrusting and/or extensional faulting within the southern Omineca Belt, between latitudes 50 and 52 degrees north, 2) to evaluate the extent to which these two tectonic processes may have influenced the structural and thermal histories of rocks exposed within the Monashee Complex and overlying Selkirk Allochthon, and 3) to utilize this information to test the validity of specific compressional and extensional models for this part of the southen Omineca Belt.

The field area for the 1985 season encompasses those parts of the Anstey and Seymour ranges east of the Shuswap Lakes, and the western Jordan and Ratchford ranges between Hoskins Creek and Eagle River Pass (Fig. 10.2). In addition, reconnaissance mapping (1:50,000 scale) was carried out along the Okanagan Valley between Vernon and Sicamous, and along both north and south flanks of Thor-Odin dome in the vicinity of Mt. English and Gates Ledge, respectively. Details of the mapping results are shown in Figure 10.2, and are discussed below.

Regional tectonic setting

The stacking order and internal deformation histories of thrust sheets that comprise the southern half of the Omineca Belt indicate a piggyback style of emplacement, whereby tectonically thickened portions of the evolving hinterland were successively detached and displaced eastward toward the craton along foreland stepping zones of crustal shear. In order of emplacement, these imbricate thrust sheets are the Quesnel Lake Sheet (which carries terranes accreted to North America), the Selkirk Allochthon, and the Monashee Complex (see Fig. 10.1). The boundaries between these tectonic assemblages are defined by the Quesnel Lake Fault and the Monashee décollement. These low angle zones of crustal shear are believed to have linked shortening and thickening of the Omineca Belt with thin-skinned thrusting and eastward telescoping of the adjacent Rocky Mountain foreland (Brown and Read, 1983; Brown et al., in press).

The Monashee Complex (Read and Brown, 1981) is well exposed in a tectonic window within the lower plate of the Monashee décollement (Fig. 10.1). It is cored by Aphebian basement gneiss (2.2 Ga; Armstrong, 1983) and unconformably overlying metasedimentary cover rocks of probable late Proterozoic age, and represents the oldest and deepest known tectonic element of the southern Omineca Belt. Basement and cover sequences of the Monashee Complex both share a polyepisodic history of deformation and regional metamorphism, and are interpreted to be the shortened and thickened equivalents of attenuated continental crust and early platform sediments that initially extended westward beneath pericratonic sequences of the Cordilleran miogeocline. Structurally, the Monashee Complex is a doubly plunging antiformal system of basement-cored fold nappes and associated tectonic slivers, that is believed to have been assembled in the Mesozoic and unroofed sometime in the early Tertiary (Brown and Read, 1983; Journeay, 1983; Monger et al., in press; Brown et al., in press). Frenchman Cap and Thor-Odin domes are second-order structural culminations along the northwest-trending axis of the Monashee Complex, and are believed to be the products of superposed folding (Read and Klepacki, 1981; Journeay, 1981; Duncan, 1984).

Major tectonic boundaries

The Monashee décollement (Read and Brown, 1981) is a fundamental lithological, metamorphic and tectonic boundary within the southern Omineca Belt. It is defined by a wide zone (500-750 m) of mylonitic rocks that separate Aphebian basement gneiss and mantling metasedimentary rocks of the Monashee Complex from deep level metasedimentary and related metaplutonic rocks (Shuswap Complex) of the overlying Selkirk Allochthon. Along its length, the décollement is characterized by recrystallized and annealed mylonitic fabrics, sheath folds, intense transposition, and the attenuation of stratigraphy within both its hanging wall and immediate footwall.

Along the east flank of the Monashee Complex, the décollement is coincident with the surface trace of down-to-the-east shears of the Columbia River Fault zone (Wheeler, 1965; Brown and Psutka, 1979; Read and Brown, 1981; Brown and Murphy, 1982; Lane, 1984). The zone is an east-dipping detachment fault of uncertain displacement which extends the length of the Columbia River, from upper Arrow Lake to the Big Bend (Fig. 10.1). The fault cuts older mylonitic rocks of the Monashee décollement, and in slices of its upper plate carries low-grade metamorphic rocks of variable age, which have been downdropped from shallow tectonic levels of the overlying Selkirk Allochthon.

Mapping this past summer has confirmed the existence of a low-angle, west-side-down detachment zone along the Eagle River valley, and of minor down-to-the-west ductile shears within mylonitic rocks along the west flank of the Monashee Complex. The shear zone, here named the Eagle River Detachment, is a major lithological, structural and metamorphic discontinuity which separates the high-grade metamorphic infrastructure of the Selkirk Allochthon (Shuswap Complex) from relatively low-grade metasedimentary rocks of the Mt. Ida Group and related plutonic rocks of the Seymour Range (Wheeler, 1965; Fig. 10.2). Preliminary results suggest that the Eagle River detachment may be the breakaway zone for an imbricate stack of down-to-the-west listric normal faults along the west flank of the Omineca Belt. The detachment extends southwest into Sicamous, and may be part of the Okanagan Shear zone.

Monashee Décollement

Detailed studies of the Monashee décollement along the northwest flank of Frenchman Cap dome have shown it to be a zone of episodic crustal shear that records both an early high pressure and a late, low pressure history of displacement and uplift (Journeay, 1983, 1985, in prep.). The high pressure shear zone is here referred to as MD_1 and the low pressure shear zone as MD_2. The two shear zones coincide along the west-dipping flank of the Monashee Complex, but diverge along both the north margin of Frenchman Cap dome and along the south flank of Thor-Odin dome (see Fig. 10.1). The west-dipping mylonite zone along the branchline of these two

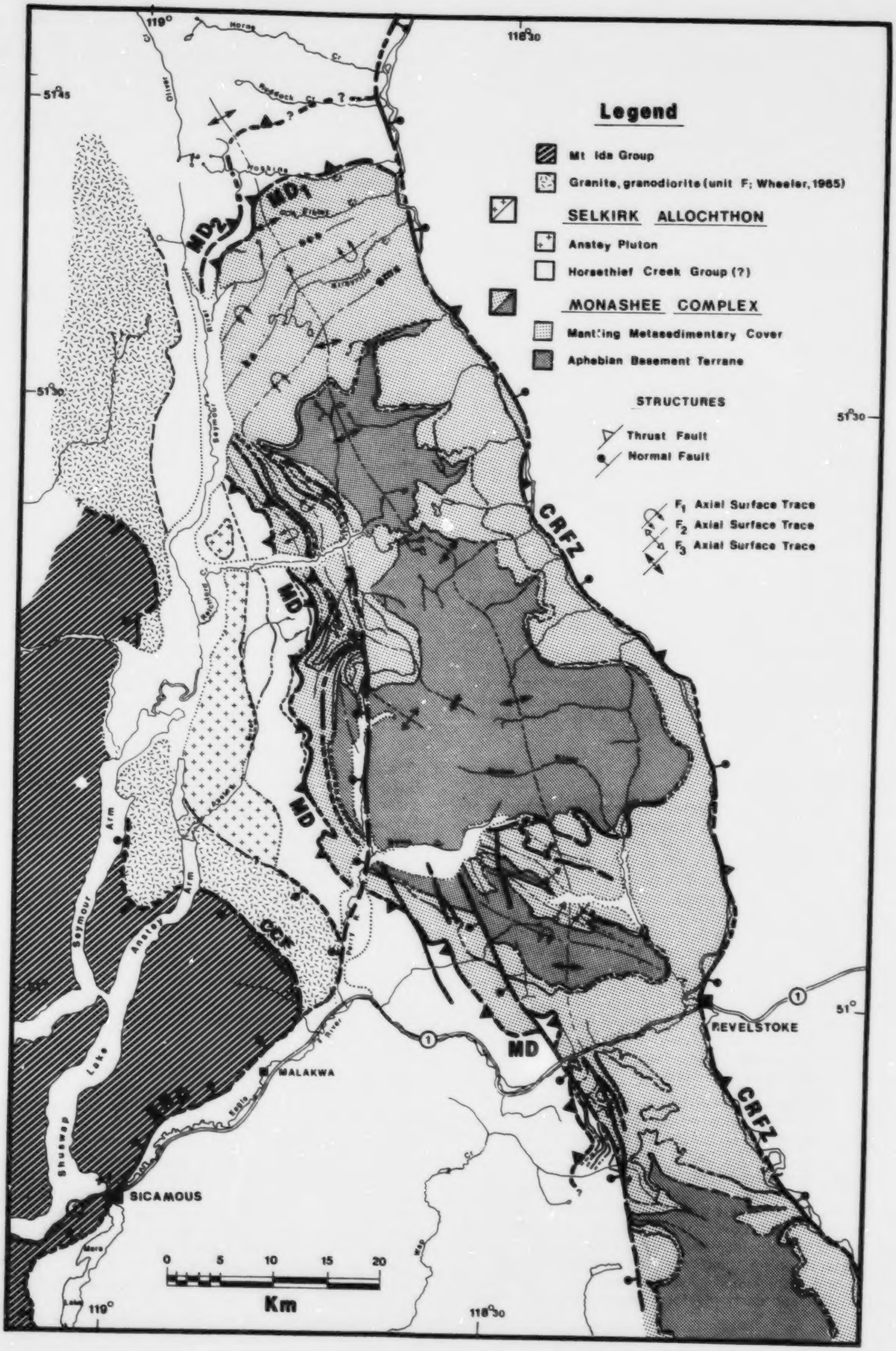
Legend
Mt Ida Group
Granite, granodiorite (unit F; Wheeler, 1965)
SELKIRK ALLOCHTHON
Anstey Pluton
Horsethief Creek Group (?)
MONASHEE COMPLEX
Mantling Metasedimentary Cover
Aphebian Basement Terrane
STRUCTURES
Thrust Fault
Normal Fault
F1 Axial Surface Trace
F2 Axial Surface Trace
F3 Axial Surface Trace
MD1
MD2
MD
CRFZ
CCF
REVELSTOKE
MALAKWA
SICAMOUS
Km
0 5 10 15 20

shear zones extends nearly 250 m into footwall rocks of the Monashee Complex, and as much as 500-750 m into the overlying Selkirk Allochthon. Structures that occur within this zone of high strain become increasingly less flattened and more variable in orientation away from the shear zone, and have been mapped well into both upper and lower plates (Brown, 1980; Journeay, 1981, 1983; Scammell, pers. comm).

High pressure MD_1 shear zone

The surface trace of the high-pressure MD_1 shear zone is defined in the field by the truncation of footwall stratigraphy and early to pre-metamorphic isoclinal folds. Along the north flank of Frenchman Cap dome, the shear zone cuts metasedimentary cover sequences of the Monashee Complex and folds along the overturned limb of the Sibley Creek syncline (Scammell, 1985, and personal communication, 1985). Along the northwest and west flanks of the dome, MD_1 cuts across the axial surfaces of at least three pre-metamorphic folds; the Sibley Creek syncline, Kirbyville anticline and Grace Mountain syncline (Fig. 10.2). The Kirbyville anticline and Grace Mountain syncline reappear within the footwall of MD_1 along the south flank of Frenchman Cap dome, and are believed to be correlative with fold closures mapped farther south within Thor-Odin dome (Journeay, in prep.). Together, these relationships suggest the development of a structural culmination within the northern Monashee Complex sometime after the development of early F_1 folds and associated thrust faults, but before detachment and eastward displacement of the Selkirk Allochthon along MD_1.

Kinematics. Kinematic indicators within the MD_1 shear zone are well preserved along both north and south flanks of the Monashee Complex. In both areas, mylonitic rocks contain a strong WSW trending stretching lineation and a variety of inclined planar fabric elements. Kinematic indicators that were used in the field to determine a sense of shear include a combination of shear and inclined secondary flattening foliations (S-C surfaces; Berthé et al., 1979), shear bands, asymmetric feldspar porphyroclasts, rotated boudins, and inclined pressure shadows.

Kinematic indicators were considered reliable if two or more of these structures could be identified within a single outcrop, and their mechanism of formation specified. In all locations, secondary flattening fabrics and pressure shadows were found to be east-verging with respect to the boundaries of individual shear domains. Shear bands, on the other hand, were found to be west-verging, listric in geometry, and asymptotic to individual shear zone boundaries. Together, these mylonitic fabrics record an upper plate to-the-east sense of shear during early emplacement of the Selkirk Allochthon. The abundance and reliablitiy of these kinematic indicators decreases toward the branch line of MD_1 and MD_2, presumably due to low pressure reheating within the upper carapace of the Monashee Complex during renewed thrusting of the Selkirk Allochthon.

Relative timing. Early displacement along MD_1 postdates the development of westerly-verging, synmetmorphic folds within the Selkirk Allochthon between latitudes 51 and 52° north, and pre-dates the quenching of high pressure (M_1) isograds within the Monashee Complex. These west-verging folds of the upper plate are coeval with prograde regional metamorphism within the Selkirk Allochthon, which on the basis of crosscutting relationships established elsewhere in the Omineca Belt (Armstrong, 1982; Archibald et al., 1983), is thought to have quenched sometime between 166 and 156 Ma. High pressure metamorphic zones of the underlying Monashee Complex cut across the trace of MD_1 along both north- and south-dipping flanks of the complex, and are themselves cut by MD_2. These isograds are inferred to have quenched sometime between 157 and 155 Ma. Together, these relationships imply that early overthrusting of the Selkirk Allochthon (along MD_1) must have occurred sometime between 165 and 155 Ma. Pressure sensitive mineral assemblages within the shear zone indicate that MD_1 evolved at depths in excess of 25-30 km, and was uplifted at least 10-12 km prior to renewed overthrusting of the Selkirk Allochthon along MD_2 (Journeay, 1985, and in prep.).

Figure 10.2 (opposite). Major bounding faults of the northern Monashee Complex and adjacent Selkirk Allochthon. Bounding faults include: high and low pressure shear zones of the Monashee décollement (MD_1 and MD_2, respectively), Eagle River detachment (ERD), Craigellachie Creek fault (CCF), and the Columbia River Fault zone (CRFZ).

Low pressure MD_2 shear zone

MD_2 is defined by a network of interlocking ductile shears of variable width that extend throughout the zone of high strain. Where coincident with MD_1, these younger shear zones typically envelop lozenge-shaped domains of mylonitic gneiss in which pre-existing fabrics are either less intensely developed, or have been recrystallized. The locus of displacement for MD_2 appears to have been near the base of a thick intercalated sequence of semipelitic and pelitic schists, and ultramafic-bearing amphibolites. These upper plate lithologies are contiguous with, and presumed to be at least in part correlative with Hadrynian sequences of the Horsethief Creek Group exposed within the northern Monashee and adjacent Selkirk Mountains (Brown, 1981).

The zone of detachment for MD_2 diverges from MD_1 along the north and south flanks of the Monashee Complex, and is defined along its length by abrupt discontinuities in metamorphic grade. Upper plate rocks consistently lie on the high temperature side of the second sillimanite isograd, and contain a high volume (> 50%) of in situ granitic melt. Local occurrences of matrix kyanite within migmatitic sillimanite-alkali feldspar schists imply that these rocks most likely quenched at pressures in excess of 7.1 kb. Lower plate assemblage zones are cut at moderate to high angles by MD_2, and are inferred to have quenched at pressures of between 6.4 and 7.1 kb. High pressure M_1 isograds within the lower plate of MD_2 are overprinted by a sequence of low pressure (2-3.4 kb) assemblage zones that range in grade from upper amphibolite facies in the immediate footwall of the shear zone to lower greenschist facies within the core of Frenchman Cap dome. These low pressure assemblage zones define an inverted metamorphic gradient within the lower plate of MD_2, that is interpreted to have been produced during renewed overthrusting and thermal relaxation of the overlying Selkirk Allochthon (Journeay, 1985, and in prep.).

Kinematics. Mylonitic fabrics and associated structures that formed during the development of MD_2 are recognized primarily within localized shear zones, attenuated layers of migmatitic gneiss, and within coarse grained pegmatites that crosscut pre-existing mylonitic rocks of MD_1. They include both flattening and shear foliations, stretching and mineral lineations, shear bands, and variably inclined to reclined asymmetric folds. Except for their timing and degree of recrystallization, these structures are virtually indistinguishable from those observed within

mylonitic rocks of MD_1. The inclination of these structures consistently records an upper plate to-the-east sense of shear. The juxtaposition of 7.1 (+) kb upper plate assemblages with 2.0-3.4 kb assemblages of the lower plate implies a large component of horizontal displacement along MD_2; absolute displacements have yet to be determined. These relationships require MD_2 to be a westerly-rooted thrust fault.

Relative timing. Reactivation of the Monashee décollement along MD_2 postdates the quenching of high pressure M_1 isograds within the northern Monashee Complex (157-155 Ma), and is known to have occurred sometime before low pressure reheating, and the quenching of inverted low pressure (M_2) isograds within the immediate footwall of MD_2. The timing of this low pressure reheating event has not yet been firmly established, but is believed to be no older than 80-95 Ma (Journeay, in prep.). The upper age for the reheating event is constrained by conventional K-Ar cooling dates on micas of between 60 and 40 Ma. Direct dating of both high and low pressure metamorphic events is in progress.

Down-to-the-west shears

Down-to-the-west ductile shears are postmetamorphic features developed along the west flank of the Monashee Complex. They are typically less than 2-3 m in width, unannealed, and record only minor amounts of displacement within both upper and lower plate mylonites of the Monashee décollement. Without exception, these late shears were found to postdate up-to-the-east mylonitic fabrics associated with MD_2, and to predate northerly trending extension and shear fractures of probable Eocene age. The cumulative offset across these listric normal shears along the west flank of Frenchman Cap dome is unknown. However, the continuity of stratigraphy and metamorphic grade across the upper plate of MD_2 suggests that total displacement along any individual shear zone is not likely to have been more than a few tens of metres. The relationship between these down-to-the-west shears and the Eagle River detachment has not yet been firmly established.

Eagle River detachment

The contact between high grade metamorphic and related plutonic rocks of the Selkirk Allochthon (Shuswap Complex) and overlying low grade metasedimentary rocks of the Mt. Ida Group along the west flank of the Omineca Belt has previously been interpreted as: 1) an intrusive contact (Brock, 1934; Cairnes, 1932), 2) a high angle fault contact (Jones, 1959), 3) a steep but continuous metamorphic gradient reflecting the infrastructure-suprastructure transition (Fyson, 1970), and 4) as a possible southern extension of the Monashee décollement (Read and Brown, 1981; Okulitch, 1984). Mapping this past summer suggests that this boundary is more likely a low angle, down-to-the-west detachment fault which has downdropped low grade rocks of the Mt. Ida Group from shallower tectonic levels. Evidence in support of this hypothesis includes the discovery of down-to-the-west mylonitic fabrics along the boundary between these two metamorphic terranes and the juxtaposition of upper plate rocks that are inferred to have quenched at lower pressures and temperatures than their footwall counterparts.

On the basis of these criteria, the Eagle River detachment has been mapped northeast from Mara Lake, through Sicamous and along the north side of the Eagle River valley, as far east as Craigellachie Creek (Fig. 10.2). At Craigellachie Creek, the detachment splays northward into a listric, west-dipping brittle shear zone, here named the Craigellachie Creek fault (CCF). This fault separates low grade Mt. Ida Group metasediments from underlying granitic and granodioritic plutonic rocks of the southern Anstey Range (Unit F, Wheeler, 1965) and can be traced northwestward along the east bank of Craigellachie Creek into Four mile Creek (Fig. 10.2). It has not yet been studied in detail. Rock units within both upper and lower plates of the fault are highly fractured, and in many localities have been reduced to chaotic breccia and gouge zones, similar to those observed within the Columbia River Fault zone. Conjugate shear fractures are locally well developed within the fault zone. Their inclination records a normal or down-to-the-west sense of shear. The magnitude of displacement along this fault is unknown.

Preliminary results suggest that the Eagle River detachment may extend eastward from Craigellachie Creek as a low angle shear zone separating an upper plate plutonic complex of weakly deformed granite and granodiroite from underlying high grade metamorphic rocks of the Shuswap Complex. The boundary is poorly exposed, but can be traced eastward into the Perry River valley, where it joins the surface trace of the Perry River fault. From here, it probably extends northwest across the southern Anstey Range, into the Shuswap Lake area, and then north along the west side of the Seymour River valley along the boundary between units E and F of Wheeler (1985) (Fig. 10.2).

Mapping of the boundary east of Craigellachie Creek has revealed a gradual increase in the intensity of deformation toward the base of the plutonic complex. It is not yet known, however, whether this boundary is everywhere a fault contact, or whether displacement across the detachment dies out to the north along an intrusive contact between shallow level plutonic rocks and uplifted high grade metamorphic rocks of the Shuswap Complex.

Discussion and conclusions

The Monashee Complex has previously been interpreted as an exhumed antiformal duplex system of basement cored horses that evolved during shortening and tectonic thickening of the continental margin in mid-Jurassic to Late Cretaceous time (Brown and Read, 1983; Brown et al., 1984; Journeay, 1985, and in prep.; Monger et al., in press; Brown et al., in press). In this model, the Monashee décollement is interpreted to be a westerly-rooted blind thrust that originated at depths in excess of 25 km, and which fed eastward into shallower tectonic levels of the adjacent Rocky Mountain Foreland. In the early stages of its development, the décollement served as a floor thrust to the Selkirk Allochthon. In the latter stages of its evolution, it became a roof thrust to foreland-stepping shear zones within the underlying Monashee Complex (Journeay, in prep.). Throughout its evolution, the décollement acted as a kinematic link between shortening and tectonic thickening within the Omineca hinterland and thin-skinned thrusting within the adjacent Rocky Mountain Foreland (Brown et al., in press). Data collected this summer confirm a two-stage history of uplift and overthrusting along the Monashee décollement, and are consistent with a model of basement duplexing.

Recent studies have documented the existence of a major west-dipping detachment zone within the Okanagan Valley (Templeman-Kluit, 1984; Bardoux, 1984; Parkinson, 1985; Parrish et al., 1985). It is interpreted as a low-angle extensional fault, and is believed to have been active in the Eocene. Cumulative displacement along the fault is unknown. Regional geochronometry of gneissic rocks within the footwall of the fault, however, suggest a minimum uplift component of at least 10 km over a time period of approximately 10 Ma (Parkinson, 1985).

The trace of the Okanagan Shear zone extends north along the Okanagan Valley to Enderby (Bardoux, personal communication, 1985), and is believed to continue either as a

single detachment surface, or as an imbricate fan of low-angle normal faults, at least as far as Mara Lake. The Eagle River detachment is here interpreted to be part of this extensional fault system. The geometry of the Eagle River shear zone and related listric normal faults along the west flank of the Omineca Belt implies that this may be the break-away zone for the Okanagan detachment. Testing of this hypothesis will be carried out during the 1986 field season.

Acknowledgments

Mapping of the MD_1 and MD_2 boundaries along the north flank of Frenchman Cap dome was carried out in the company of Rob Scammell and Chris Rees. We thank them for stimulating discussions and logistical support.

References

Archibald, D.A., Glover, J.K., Price, R.A., Farrer, E., and Carmichael, D.M.
1983: Geochronology and tectonic implications of magmatism and metamorphism, southern Kootenay Arc and neighbouring regions, southern British Columbia. Part I: Jurassic to mid-Cretaceous; Canadian Journal of Earth Sciences, v. 20, p. 1891-1913.

Armstrong, R.L.
1982: Cordilleran metamorphic core complexes – from Arizona to southern Canada; Annual Review of Earth and Planetary Sciences, v. 10, p. 129-154.
1983: Cordilleran S- and I-type granites: indicators of lithosphere thickness; in Geological Association of Canada, Annual Meeting, Victoria, British Columbia.

Bardoux, M.
1984: The Kelowna detachment zone, Okanagan Valley, south-central British Columbia; in Current Research, Part A, Geological Survey of Canada, Paper 84-1A, p. 333-348.

Berthé, D., Choukroune, P., and Jegouzo, P.
1979: Orthogneiss, mylonite, and non-coaxial deformation of granites: the example of the South Armorican shear zone; Journal of Structural Geology, v. 1, p. 31-44.

Brock, R.B.
1934: The metamorphism of the Shuswap terrane of British Columbia; Journal of Geology, v. 42, p. 673-699.

Brown, R.L.
1980: Frenchman Cap dome, Shuswap Complex, British Columbia: a Progress report; in Current Research, Part A, Geological Survey of Canada, Paper 80-1A, p. 47-51.
1981: Metamorphic core complex of southeastern Canadian Cordillera and relationship to foreland thrusting; in Thrust and Nappe tectonics, ed. K. McClay and N.J. Price; Geological Society of London, Special Publication 9, p. 463-474.

Brown, R.L. and Murphy, D.C.
1982: Kinematic interpretation of mylonitic rocks in part of the Columbia River fault zone, Shuswap terrane, British Columbia; Canadian Journal of Earth Sciences, v. 19, p. 456-465.

Brown, R.L. and Psutka, J.F.
1979: Stratigraphy of the east flank of Frenchman Cap dome, Shuswap Complex, British Columbia; in Current Research, Part A, Geological Survey of Canada, Paper 79-1A, p. 35-36.

Brown, R.L. and Read, P.B.
1983: Shuswap terrane of British Columbia: a Mesozoic "core complex"; Geology, v. 11, p. 164-168.

Brown, R.L., Journeay, J.M., Lane, L.S., Murphy, D.M., and Rees, C.J.
– Obduction, backfolding, and piggyback thrusting in the metamorphic hinterland of the southeast Canadian Cordillera; Journal of Structural Geology. (in press)

Cairnes, C.N.
1932: Mineral resources of the northern Okanagan Valley, British Columbia; in Summary Report 1931, Part A, Geological Survey of Canada, p. 66-109.

Coney, P.J.
1980: Cordilleran metamorphic core complexes: an overview; in Cordilleran Metamorphic Core Complexes, ed. M.D. Crittenden, Jr., P.J. Coney, and G.H. Davis; Geological Society of America, Memoir 153, p. 4-34.

Crittenden, M.D., Coney, P.J., and Davis, G.H.
1980: Cordilleran Metamorphic Core Complexes; Geological Society of America, Memoir 153, 490 p.

Duncan, I.J.
1984: Structural evolution of the Thor-Odin gneiss dome; Tectonophysics, v. 101, p. 87-130.

Fyson, W.K.
1970: Structural relations in metamorphic rocks, Shuswap Lake area, British Columbia; in Structure of the Southern Canadian Cordillera, ed. J.O. Wheeler; Geological Association of Canada, Special Paper 6, p. 107-122.

Jones, A.G.
1959: Vernon map-area British Columbia; Geological Survey of Canada, Memoir 296, p. 116.

Journeay, J.M.
1981: Basement/cover relationships and structural evolution of north-central Frenchman Cap dome, Shuswap complex, southeastern British Columbia; in Geological Association of Canada, Program with abstracts, p. 29.
1983: Progressive deformation and inverted regional metamorphism associated with Mesozoic emplacement of the Shuswap-Monashee complexes, SE British Columbia; in Geological Society of America, Programs with Abstracts, v. 15, p. 606.
1985: Thermo-tectonic evolution of the Monashee Complex; a basement duplex, Omineca Belt, B.C.; in Geological Society of America, Abstracts with Programs, Cordilleran Section, v. 17, p. 364.
– Stratigraphy, internal strain and thermo-tectonic evolution of northern Frenchman Cap dome; an exhumed basement duplex structure, Omineca hinterland, SE Canadian Cordillera, (82 M/7); unpublished PhD dissertation, Queen's University, Kingston, Ontario. (in preparation)

Lane, L.S.
1984: Brittle deformation in the Columbia River fault zone near Revelstoke, southeastern British Columbia. Canadian Journal of Earth Sciences, v. 21, p. 584-598.

Monger, J.W.H. (principal compiler), Woodsworth, G.H., Price, R.A., Clowes, R.N., Riddihough, R.P., Currie, R., Hoy, T., Preto, V.A.G., Simony, P.S., Snavely, P.D., and Yorath, C.J.
– Transect B2. southern Canadian Cordillera, North American continent-ocean transects. Geological Society of America, Decade of North American Geology Program. (in press)

Okulitch, A.V.
1984: The role of the Shuswap metamorphic complex in Cordilleran tectonism; a review; Canadian Journal of Earth Sciences, v. 21, p. 1171-1193.

Parkinson, D.
1985: Geochronology of the western side of the Okanagan metamorphic core complex, southern B.C.; Geological Society of America, Cordilleran Section, Abstracts with Programs, p. 399.

Parrish, R., Carr, S., and Parkinson, D.
1985: Metamorphic complexes and extensional tectonics, southern Shuswap complex, southeastern British Columbia; Geological Society of America, Cordilleran Section Guidebook, p. 12-1 to 12-15.

Read, P.B. and Brown, R.L.
1981: Columbia River fault zone: southeast margin of the Shuswap and Monashee complexes, southern British Columbia; Canadian Journal of Earth Sciences, v. 18, p. 1127-1145.

Read, P.B. and Klepacki, D.W.
1981: Stratigraphy and structure: northern half of Thor-Odin nappe, Vernon east-half map area, southern British Columbia; in Current Research, Part A, Geological Survey of Canada, Paper 81-1A, p. 169-173.

Scammell, R.J.
1985: Stratigraphy and structure of the northwestern flank of Frenchman Cap Dome, Monashee Complex, British Columbia: preliminary results; in Current Research, Part A, Geological Survey of Canada, Paper 85-1A, p. 311-316.

Templeman-Kluit, D.
1984: Meteoric water model for gold veins in a detached terrane; Geological Society of America, Abstracts with Programs, p. 674.

Wheeler, J.O.
1965: Big Bend map area, British Columbia; Geological Survey of Canada, Paper 64-32, 37 p.

The determination of boron and other refractory elements in geological materials by inductively-coupled plasma emission spectrometry

Project 580175

G.E.M. Hall and J.C. Pelchat
Resource Geophysics and Geochemistry Division

Hall, G.E.M. and Pelchat, J.C., The determination of boron and other refractory elements in geological materials by inductively-coupled plasma emission spectrometry; in Current Research, Part A, Geological Survey of Canada, Paper 86-1A, p. 89-94, 1986.

Abstract

The determination of boron, together with molybdenum, vanadium, chromium, tungsten and phosphorus in international geochemical reference materials by inductively-coupled plasma emission spectrometry is described. These elements are measured as their oxyanions in solution after a Na_2CO_3:$NaNO_3$ fusion and water leach. Precision and accuracy data are presented for nine international standards. The limits of determination achieved by this procedure are as follows: B: 2 $\mu g\ g^{-1}$; Mo: 4 $\mu g\ g^{-1}$; V: 6 $\mu g\ g^{-1}$; Cr: 4 $\mu g\ g^{-1}$; W: 10 $\mu g\ g^{-1}$; and P: 50 $\mu g\ g^{-1}$.

Résumé

Le présent rapport décrit le processus de détermination, par spectroscopie par émission de plasma, du bore, du molybdène, du vanadium, du chrome, du tungstène et du phosphore dans les matériaux de référence géochimique de nature internationale. Ces éléments sont mesurés sous forme d'oxyanions en solution à la suite d'une fusion au Na_2CO_3:$NaNo_3$ et d'une lixiviation à l'eau. Des données sur l'exactitude et a précision sont présentées pour neuf solutions de référence internationales. Les limites de détermination par cette méthode sont les suivantes: B: 2 $\mu g\ g^{-1}$; Mo: 4 $\mu g\ g^{-1}$; V: 6 $\mu g\ g^{-1}$; Cr: 4 $\mu g\ g^{-1}$; W: 10 $\mu g\ g^{-1}$; et P: 50 $\mu g\ g^{-1}$.

Introduction

Boron is an important accessory constituent of rocks associated with certain types of gold vein mineralization (tourmaline, axinite). It is also commonly used as a paleosalinity indicator in black shales and mudstones; consequently it is an important constituent of evaporites, being one of the last elements to crystallize out; it is also important as a geothermal heat indicator (hot springs, geysers solfataras) in the form of colemanite, borax, etc.

The boron content of geological materials has been determined almost exclusively in the past by one of two techniques: emission spectrography using a DC arc (Dale, 1979) and colorimetry based on formation of the boron-curcumin complex (Dible et al., 1954). Recently, Baucells et al. (1984) have improved upon the emission spectrographic method to achieve a minimum detectable concentration of 11 $\mu g\ g^{-1}$ B; and Troll and Sauerer (1985) have combined extraction of boron by ethylhexane-1, 3-diol (after carbonate fusion) with spectrophotometry of the carminic acid complex to determine boron in the 1 - 1000 $\mu g\ g^{-1}$ range. In 1982, Owens et al. (1982) were the first to publish a paper describing a method to determine boron specifically in geological reference materials by inductively-coupled plasma emission spectrometry (ICP-ES). A carbonate fusion was carried out, the solution neutralized and measured against similarly prepared synthetic standards using a Perkin-Elmer ICP/5000 spectrometer. A detection limit of 5 $\mu g\ g^{-1}$ was achieved. Borsier and Garcia (1983) later described an automated ICP method to determine major and trace elements, including boron, in geological samples after a sodium peroxide fusion. Detection limit and precision were somewhat poorer here. Din (1984) described a procedure to separate the boron from potentially interfering iron by successive fusions with potassium dihydrogenphosphate and potassium hydroxide prior to ICP emission measurement at 249.68 nm. Thompson and Walsh (1983) commented on the lack of exploitation of ICP emission spectrometry for boron by analysts in geochemistry in their excellent handbook on the subject. It was therefore decided to evaluate the performance of the high resolution ICP sequential emission spectrometer, recently purchased by the Geological Survey of Canada, with respect to boron determination.

A strong attack is required for boron-bearing minerals such as tourmaline, so fusions with alkali metal carbonates, alone and with oxidants, were examined. Potassium carbonate was thought to be desirable because the potassium could be precipitated later as its perchlorate salt; sodium carbonate, however, has a lower melting point (853°C cf. 903°C) and is not hygroscopic. The temperature and time of fusion were both optimized once the preferred decomposition was found.

Since the major portion of analytical time is often spent on the decomposition itself, other elements of interest which would also be brought into solution were determined; these elements comprised molybdenum, vanadium, chromium, tungsten and phosphorus (as their oxyanions). A thorough study was made of all emission lines of suitable sensitivity for each element, checking for spectral interferences by scanning a 0.08 nm window centred on each line while aspirating high concentrations of likely interferents. Found to be useful in planning this interference study was the spectral line atlas compiled by Brenner and Eldad (1984).

Experimental factors

Reagents

Deionized, distilled water was used throughout. Carbonates and nitrates were 'Baker analyzed' reagent grade. Individual standard stock solutions were obtained from Spex Industries Inc., Metuchen, U.S.A. All linear polyethylene labware was washed in 30% nitric acid and repeatedly rinsed with deionized, distilled water.

Instrumentation

A Jobin-Yvon (ISA, Metuchen, New Jersey, U.S.A.) 38 high resolution sequential ICP emission spectrometer was used. Details of the instrumentation and operating conditions used are given in Tables 11.1 and 11.2 respectively. The path from the viewing zone of the argon plasma to the entrance of the spectrometer was flushed with nitrogen as was the spectrometer itself, allowing emission measurement in low ultra-violet region of the spectrum. Both Meinhard and GMK nebulisers were tested. The sample gas flow was mass-flow controlled for better precision and a humidifer was used with the nebuliser to improve high salt tolerance.

Sample decomposition

A 200 mg sample, ground to at least -100 mesh, was placed in a 25 mL nickel crucible and thoroughly mixed with 1 g of the flux, a 5:1 mixture of N_2CO_3: $NaNO_3$. The crucible was placed in a muffle furnace and the temperature raised to 900°C and maintained there for 15 minutes following the melting stage. After cooling, the contents of the crucible were leached with water and warmed on a hot plate, stirring to ease dissolution. The contents (~20 mL) were transfered to a 50 mL polyethylene test-tube and warmed for several hours. After cooling, the solution was

Table 11.1. Instrumentation

RF generator:	2.5 kW, frequency 27.12 MHz
Monochromator:	1 metre Czerny-Turner, nitrogen-purged for low UV wavelengths
Grating:	holographic 3600 grooves/mm, resolution of 0.01 nm first order
Torch:	JY demountable quartz with argon sheathing gas
Nebuliser:	Meinhard concentric, Type C high salt (TR-30-C2) with Scott-type spray chamber
Pump:	Gilson, peristaltic, Model Minipuls II
Computer:	Columbia Commander Micro, 96 k bytes memory; dual floppy disc; sotfware by J-Y

Table 11.2. Operating conditions

RF forward power:	1.05 kW (<10 W reflected)
Plasma gas flow rate:	13 L min^{-1}
Auxiliary gas flow:	0.15 L min^{-1}
Sample gas flow:	0.6 L min^{-1}
Nebuliser pressure:	38 psi
Sample uptake rate:	1.35 mL min^{-1}
Slit widths:	entrance 40 μm exit 40 μm height 7 mm
Photomultiplier tube:	1200 volts
Observation zone:	10 mm above initial radiation zone

Table 11.3. Spectral lines and calibration standards

Element	Analytical wavelength	Background position		Calibration standards		
		low	high	low	medium	high
	nm	nm		μg mL^{-1}		
P	178.225 I	-	0.020	Reagent Blank	10	50
Mo	202.030 II	0.016	0.019	"	1.0	3.0
W	207.911 II	-	0.024	"		
B	249.773 I	-	0.020	"	1.0	3.0
Cr	267.716 II	-	0.019	"	1.0	3.0
V	311.838 II	-	0.016	"	1.0	3.0

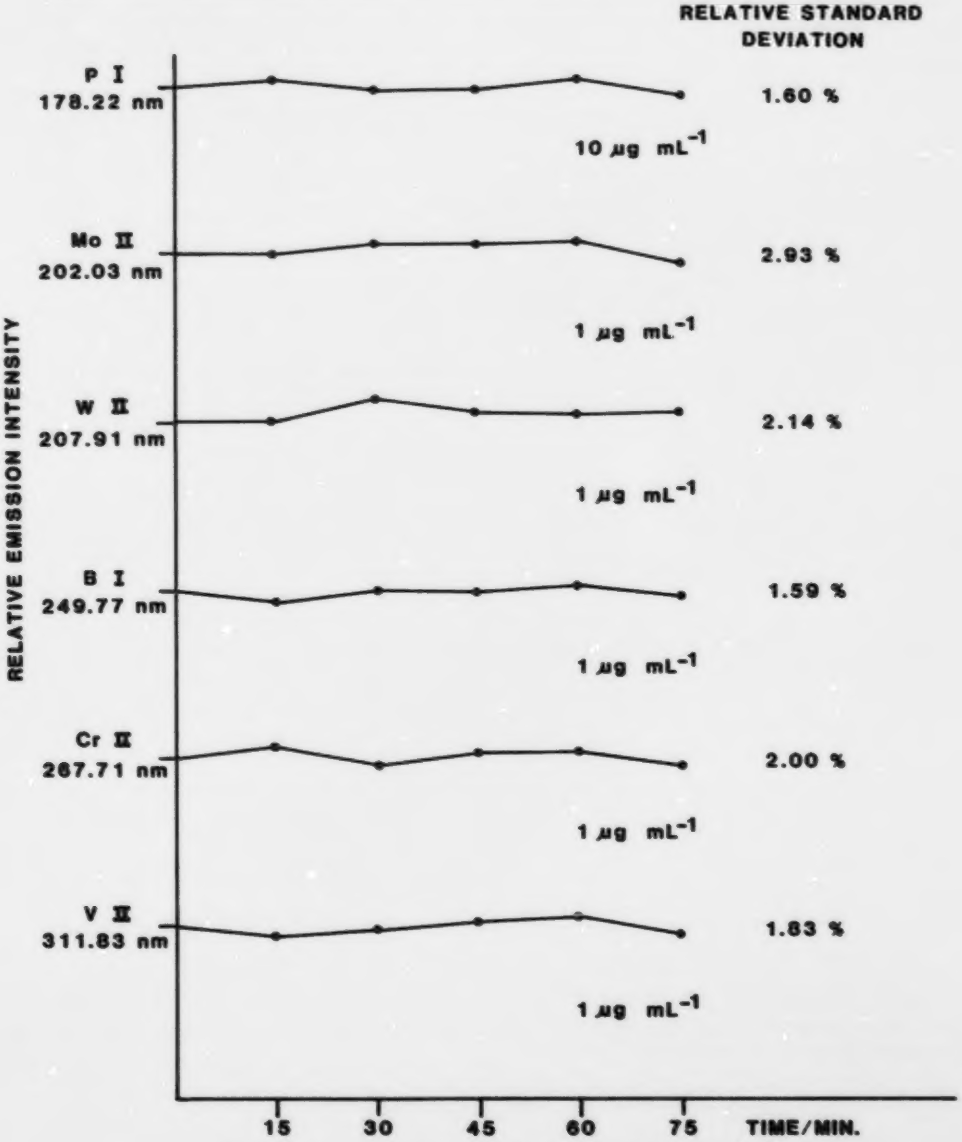

Figure 11.1. Variation in emission signal with time.

centrifuged and the clear supernatant liquid transfered to a 25 mL polyethylene volumetric flask and made up to the mark with water. The pH of this solution was 12.

Blanks and calibration standards were taken through a similar procedure using Eppendorf uL pipettes to deliver accurate amounts of standard stock solutions.

Calibration

Analyte spectral wavelengths were chosen to be the most sensitive available with the least amount of interferences likely to be encountered with typical sample material. The positions for background correction measurement were determined by studying spectral line atlases and by scanning the analyte lines while nebulising samples particularly high in concentrations of potential interferences. These wavelengths are shown in Table 11.3 together with the standard concentrations used for calibration. There is an aluminum recombination interference on the Mo 202.03 nm line, necessitating correction on both sides of the line. Correction coefficients were found to be unnecessary with the chosen wavelengths. An integration time of 500 ms was chosen as optimum for each measurement. Recalibration was carried out after 10 samples.

Analysis

Nine reference materials from the United States Geological Survey (USGS), the Canadian Certified Reference Materials Project (CCRMP), Group International de Travail (GIT-IWG) and the Institute of Geophysical and Geochemical Prospecting, China (IGGE) were subjected to the proposed method. All solutions were analyzed for one element before proceeding to the next; this was found to be more efficient than analyzing each solution at once for all 6 elements as the scan speed of the JY38 is slow.

Results and discussion

Prior to deciding upon the final flux mixture of 5:1 Na_2CO_3:$NaNO_3$, various fusions and sinters were examined. International reference materials were used to test the accuracy and precision of these decompositions. Potassium carbonate alone and a 5:1 mixture of K_2CO_3:KNO_3 were tested in a muffle furnace at 950-1050°C. Potassium, rather than sodium as the cation, appeared beneficial because perchloric acid could be added after the dissolution, resulting in precipitation of insoluble potassium perchlorate. This would drastically decrease the dissolved salt content of the analyte solution at the ICP and hence reduce the problem of nebuliser clogging and drift. It was found that platinum crucibles were attacked by the flux very seriously, especially in the presence of a sample containing a high concentration of Fe(II). Nickel crucibles were then used but occasional creeping up and over the walls would occur. Decomposition by sintering over a flame was attempted, followed by $HClO_4$ addition. Low results were obtained for Mo, V, Cr and W; these were attributed to incomplete attack. A salt build-up was seen to occur at the top of the torch and clogging was evident with both the Meinhard and GMK nebulisers. It was then decided to test Na_2CO_3 with $NaNO_3$ as added oxidant as the flux and to establish the salt tolerance level of the ICP for alkaline sodium solutions. A 4% Na_2CO_3 solution could be nebulized all day without clogging. Figure 11.1 depicts the variation in the signal intensity of each analyte standard with time. The relative standard deviation ranges from 1.6% for B to 2.9% for Mo.

The solution detection limit for each analyte, defined as that concentration generating a signal equal to 3 times the standard deviation of the blank signal (10 readings), is shown in Table 11.4. The corresponding real detection limits in the samples themselves (factor of 125) are somewhat degraded by the presence of the analytes, especially boron, in the flux reagents. These determination limits are specific for this procedure. The sensitivity for molybdenum and tungsten is

Table 11.4. Detection, determination limits and precision data obtained by the described method of analysis

Element	Detection limit in solution[a] $\mu g\ mL^{-1}$	Determination limit in sample[b] $\mu g\ g^{-1}$	Typical coefficient of variation (n = 5)	Concentration range in igneous and sedimentary rocks[c] $\mu g\ g^{-1}$
B	.002	2.0	1.7% at 17 $\mu g\ g^{-1}$ (MA-N)	3 - 100
Mo	.006	4.0	14% at 8 $\mu g\ g^{-1}$ (GSD-6)	0.2 - 2.6
V	.005	6.0	2.2% at 90 $\mu g\ g^{-1}$ (GXR-4)	20 - 250
Cr	.004	4.0	6% at 13 $\mu g\ g^{-1}$ (GXR-1)	4 - 2980
W	.015	10	7% at 28 $\mu g\ g^{-1}$ (GSD-6)	0.1 - 1.8
P	.05	50	1.1% at 615 $\mu g\ g^{-1}$ (GXR-1)	170 - 1100

[a] Defined as the concentration of an element in 4% $Na_2CO_3/NaNO_3$ solution which gives an emission signal equal to three times the standard deviation of the blank.

[b] Based on a 0.2 g sample with 1.0 g flux, diluted to 25 mL final volume.

[c] As published by Rose et al. (1979)

Table 11.5. Analyte concentrations in geological reference materials determined by ICP emission spectrometry

Reference material	B	Mo	V	Cr	W	P
GXR-1 (Jasperoid)	15.1 ± 0.6 (15.5)[a]	17.8 ± 2.2 (15)[a]	81 ± 2 (79)[a]	13.2 ± 0.8 (13)[a]	203 ± 6 (210)[a]	615 ± 7 (610)[a]
GXR-4 (Copper Mill-head)	4.0 ± 1.1 (4.3)[c]	311 ± 4 (310)[a]	90 ± 2 (90)[a]	68 ± 3 (64)[a]	31 ± 4 (32)[a]	1364 ± 18
GXR-5 (Soil)	19.8 ± 0.4 (20)[a]	30.2 ± 1.4 (28)[a]	57 ± 4 (66)[a]	108 ± 3 (106)[a]	<10 (1.1)[a]	311 ± 6 (305)[a]
SGR-1 (Oil shale)	50.3 ± 1.4 (50)[b]	35 ± 2 (36)[a]	124 ± 4 (125)[a]	32 ± 2 (33)[a]	<10	1030 ± 14 (1265)[a]
SCo-1 (Cody shale)	68.4 ± 1.8 (66)[a]	<4 (1.4)[a]	129 ± 3 (135)[a]	73 ± 2 (71)[b]	<10	857 ± 15 (960)[a]
MAG-1 (Marine mud)	132 ± 3 (130)[a]	<4 (1)[a]	138 ± 3 (140)[a]	107 ± 3 (105)[b]	<10	780 ± 12 (785)[a]
MA-N (Granite)	17.2 ± 0.3 (17)[a]	<4	<6 (4.6)[b]	<4 (3)[a]	66 ± 2 (70)[a]	6012 ± 40 (6065)[a]
FeR-2 (Iron formation)	59.5 ± 1.2 (61)[a]	<4 (3)[a]	29 ± 2 (37)[a]	44 ± 3 (47)[b]	<10	1158 ± 16 (1178)[b]
GSD-6 (Stream sediment)	48.2 ± 2.1 (50)[b]	8.1 ± 1.1 (7.7)[b]	140 ± 3 (142)[b]	192 ± 4 (190)[b]	28 ± 2 (25)[b]	1026 ± 22 (1003)[b]

[a] Numbers in parentheses are proposed values given by Govindaraju (1984).
[b] Numbers in parentheses are recommended values given by Govindaraju (1984).
[c] Numbers in parentheses are recommended values given by Gladney et al. (1979).

not adequate for many geological samples as indicated by a comparison of the determination limits and concentration ranges found in rocks (Table 11.4); however, it is thought useful to include these two elements in this 'package' for geochemical exploration purposes. The determination limit established for molybdenum is twice that obtained by atomic absorption spectrometry on a routine basis in the Geochemistry Laboratories and that for tungsten is 2.5 times higher than that obtained by the standard colorimetric dithiol method (Stanton, 1966).

The results obtained for 5 separate determinations (over a period of 4 months) of boron and other refractory elements in 9 geological reference materials are given in Table 11.5 together with the consensus literature values. The general accuracy of the method is indicated by the good agreement between the concentrations found and recommended (or proposed), the mean ratio of found/recommended values being 0.98 with a standard deviation of 0.07 ($n = 42$). The sample SGR-1 was treated slightly differently in that it was ashed at 300°C for 2 hours to reduce its high organic content. Three values appear to be low: vanadium in GXR-5, and phosphorus in the two shales, SGR-1 and SCo-1. Gladney et al. (1979) recommended a value for V in GXR-5 of 60 ± 20 ppm which indicates that there is a high degree of variation in published data. The low P results in the shales is currently under evaluation. Analytical reproducibility for the elements studied in the work, as indicated by the standard deviations shown in Table 11.5, was mostly in the range 2-8% coefficient of variation, except at levels approaching detection limits.

Iron did not pose a problem as a potential spectral interferent as most of the element remains in the carbonate/oxide residue in agreement with Bock (1979) who found less than 0.1% solubilized iron after a carbonate fusion. GXR-1 which contains about 25% Fe yielded a solution for analysis containing only 5 $\mu g\ mL^{-1}$ Fe. Thus, the lengthy sample preparation procedure described by Din (1984) proved unnecessary.

This method is now in routine use and the study is being expanded to include the possible determination of gallium, germanium and aluminum by the same decomposition. The recovery of vanadate and tungstate in the presence of high concentrations of TiO_2 in the solid residue (Bock, 1979) will also be investigated. Use of the outboard H-20 monochromator on the JY38 to monitor an internal standard chosen to compensate for changes in plasma conditions is currently being examined.

Acknowledgments

The authors wish to thank I.R. Jonasson and G.R. Lachance for critical review of this manuscript.

References

Baucells, M., Lacort, G., Roura, M., and Rauret, G.
1984: Determination of boron in silicate geological material by an emission spectrographic method; Applied Spectroscopy, v. 38, p. 572-574.

Bock, R.
1979: A handbook of decomposition methods in analytical chemistry; The Blackie Group, Glasgow, p. 111.

Borsier, M. and Garcia, M.
1983: Analyse automatique d'echantillons geologiques par plasma ICP; Spectrochimica Acta, v. 38B, p. 123-127.

Brenner, I.B. and Eldad, H.
1984: A spectral line atlas for multitrace and minor element analysis of geological and ore mineral samples by ICP-AES; ICP Information Newsletter, v. 10, p. 451-508.

Dale, L.S.
1979: The emission spectrographic determination of boron in silicate materials; Applied Spectroscopy, v. 33, p. 404-409.

Dible, W.T., Truog, E., and Berger, K.C.
1954: Boron determination in soils and plants; Analytical Chemistry, v. 26, p. 418-421.

Din, V.K.
1984: The preparation of iron-free solutions from geological materials for the determination of boron (and other elements) by inductively-coupled plasma emission spectrometry; Analytica Chimica Acta, v. 159, p. 387-391.

Gladney, E.S., Perrin, D.R., Owens, J.W., and Knab, D.
1979: Elemental concentrations in the United States Geological Survey's Geochemical Exploration Reference Samples - A review; Analytical Chemistry, v. 51, p. 1557-1569.

Govindaraju, K.
1984: 1984 Compilation of working values and sample description for 170 international reference samples of mainly silicate rocks and minerals; Geostandards Newsletter, v. VIII, p. 3-85.

Owens, J.W., Gladney, E.S., and Knab, D.
1982: Determination of boron in geological materials by inductively-coupled plasma emission spectrometry; Analytica Chimica Acta, v. 135, p. 169-172.

Potter, N.M. and Lovelace, R.R.
1984: Determination of boron in engine coolants by direct current plasma atomic emission spectrometry; Analytica Chimica Acta, v. 162, p. 419-422.

Rose, A.W., Hawkes, H.E., and Webb, J.S.
1979: Geochemistry in mineral exploration; Academic Press, London, p. 553-557.

Stanton, R.E.
1966: Rapid methods of trace analysis for geochemical application; Arnold, London, p. 86-87.

Thompson, M. and Walsh, J.N.
1983: A handbook of inductively coupled plasma spectrometry; Blackie and Son Ltd., Glasgow, p. 99.

Troll, G. and Sauerer, A.
1985: Determination of trace amounts of boron in geological samples with carminic acid after extraction with 2-ethylhexane-1, 3-diol; Analyst, v. 110, p. 283-286.

Preliminary investigations of Early Proterozoic Western River and Burnside River formations: evidence for foredeep origin of Kilohigok Basin, District of Mackenzie

Project 810021

J.P. Grotzinger [1] and Q. Gall [2]
Precambrian Geology Division

Grotzinger, J.P. and Gall, Q., Preliminary investigations of Early Proterozoic Western River and Burnside River formations: evidence for foredeep origin of Kilohigok Basin, District of Mackenzie; in Current Research, Part A, Geological Survey of Canada, Paper 86-1A, p. 95-106, 1986.

Abstract

In the Kilohigok Basin, the Western River and Burnside River formations comprise three successively overlying tectono-stratigraphic sedimentary units of regional extent: a basal shallow water siliciclastic/carbonate platform, overlain by deepwater flysch, in turn overlain by shallow marine and fluvial molasse. This stratigraphy represents an initial stable shelf (passive margin?) whose outer, southerly edge rapidly subsided contemporaneous with arching and subaerial exposure of its interior. Shelf drowning represents the onset of foredeep subsidence subparallel to the trend of Thelon Tectonic Zone. Arching and subsidence were perpendicular to the tectonic transport direction of intrabasinal nappes, indicating that convergence and uplift along Thelon Tectonic Zone were probably responsible for foredeep subsidence within Kilohigok Basin. Following drowning, the platform was buried by deepwater deposits (flysch); with progressive uplift and basin filling, the foredeep entered the molasse phase and fluvial sediments prograded towards the foreland. The foredeep model places constraints on the origin of Thelon Tectonic Zone and provides a more comprehensive understanding of the tectonic evolution of the Slave Province and its relation to the Wopmay Orogen.

Résumé

Dans le bassin de Kilohigok, les formations de Western River et de Burnside River se composent de trois unités sédimentaires tectono-stratigraphiques respectivement sus-jacentes et d'étendue régionale: à la base, une plate-forme silicoclastique et carbonatée d'eau peu profonde recouverte par un flysch d'eau profonde lui-même, à son tour, recouvert par une molasse fluviale et marine peu profonde. Il s'agit, stratigraphiquement, d'une plate-forme primaire stable (marge passive?) dont l'affaisement rapide du bord externe sud a eu lieu en même temps que le bombement et la mise à nu subaérienne de sa partie intérieure. L'inondation de la plate-forme a marqué le début de l'affaisement de l'avant-fosse subparallèlement à l'orientation de la zone tectonique de Thelon. Le bombement et l'affaisement ont eu lieu perpendiculairement à la direction du transport tectonique des nappes intrabassinales, phénomène qui indique que la convergence et le soulèvement le long de la zone tectonique de Thelon auraient provoqué l'affaisement de l'avant-fosse à l'intérieur du bassin de Kilohigok. Après avoir été inondée, la plate-forme a été enfouie sous des sédiments d'eau profonde (flysch). Le soulèvement progressif et le comblement du bassin ont marqué le début d'une phase d'accumulation de molasse dans l'avant-fosse et de progradation des sédiments fluviatiles vers l'avant-pays. Ce modèle d'avant-fosse apporte certaines restrictions en ce qui à trait à l'origine de la zone tectonique de Thelon et fournit des renseignements plus complets sur l'évolution tectonique de la province des Esclaves et ses liens avec l'orogène de Wopmay.

[1] Lamont-Doherty Geological Observatory. Palisades, N.Y. 10964
[2] McGill University, Department of Geological Sciences, Montreal, Quebec H3A 2A7

Introduction

Parts of Kilohigok Basin, Northwest Territories, (Fig. 12.1) are currently being studied to document the timing and cause of basin subsidence, the relation of the basin to the contemporaneous Thelon Tectonic Zone, and the possible correlation of stratigraphic units with those in the foreland of Wopmay Orogen. The present study includes extensive measuring of detailed stratigraphic sections and limited 1:50 000 scale mapping of selected areas. This preliminary report summarizes observations and interpretations made during the 1985 field season. Further investigations are planned for the 1986 field season.

Previous and current research

Initial reconnaissance mapping of Kilohigok Basin was done by O'Neill (1924). This was followed by a second generation of mapping, including subdivision and description of the major stratigraphic units (Wright, 1957; Fraser, 1964; Tremblay, 1967; Fraser and Tremblay, 1969; Tremblay, 1971). Subsequently, 1:500 000 scale mapping of the basin was completed by Campbell and Cecile (1976), with special emphasis on the sedimentology of specific units (Cecile, 1976; Cecile and Campbell, 1977, 1978; Campbell and Cecile, 1981). Most recently, nappes were discovered in the southeast part of the basin during detailed 1:50 000 scale mapping (Tirrul, 1985).

Hoffman (1973) interpreted Kilohigok Basin as an aulacogen. Campbell and Cecile (1981) interpreted the basin as a northwest-trending intracratonic trough, developed as a splay off of an inferred aulacogen, to the north of Kilohigok basin; the aulacogen was believed to open westward into the passive margin of Wopmay Orogen. More recently, reconnaissance work by Hoffman et al. (1984) and regional stratigraphic work by Grotzinger (1985) suggested that large volumes of siliciclastic sediment were being derived from a region east of Kilohigok Basin and entering the passive margin of Wopmay. Such an observation is inconsistent with the interpretation of Kilohigok Basin as a rift, which might have trapped sediment, preventing its transport across the stable craton. In addition, revised correlations based on more accurate time lines of Wopmay-Kilohigok strata indicate a major west-to-east thickening toward the east edge of Kilohigok Basin, and it was speculated that sediments were being derived from unroofing of the Thelon Tectonic Zone, located southeast of Kilohigok Basin. Contemporaneous work in the Thelon Tectonic Zone suggested that it might have been a site of major crustal-scale thrusting with a westerly transport component (Thompson and Ashton, 1984; Thompson et al., 1985). Support for this model was obtained independently by Tirrul (1985), who discovered northwest-verging nappes in the southeast corner of Kilohigok basin. These nappes probably represent a higher structural level of the Thelon Tectonic Zone, which contains metamorphic assemblages (staurolite-kyanite) suggesting 12 to 15 km of syn- to post-tectonic uplift (Tirrul, 1985; Thompson, personal communication, 1985).

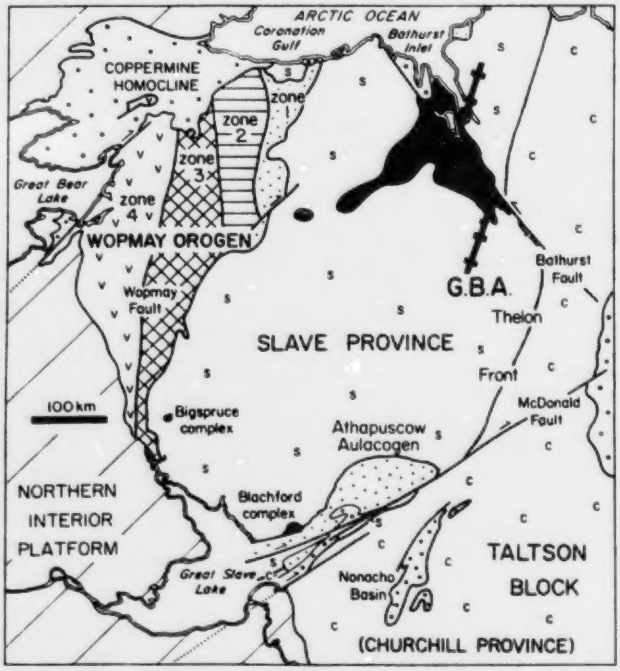

***Figure 12.1.** Location of Kilohigok Basin (black) relative to other tectonic elements in northwest Canadian Shield. G.B.A.; Gordon Bay Arch. "Thelon Front"; eastern edge of Thelon Tectonic Zone. Modified after Hoffman (1980).*

If sediments of Kilohigok Basin were derived from unroofing the Thelon Tectonic Zone, then basin subsidence may have been related to flexure of the lithosphere in response to convergence and crustal thickening along the Thelon Tectonic Zone, rather than extension in a region adjacent to an inferred aulacogen. The present study is designed to test this model by: 1) establishing the detailed facies relationships in key areas of the basin, 2) determining provenance of siliciclastic sediments, 3) documenting locations and trends of major depocentres and arches, and 4) evaluating the major stages of basin evolution.

Foredeeps are characteristically elongate, rapidly subsiding basins that form as "moats" adjacent to orogenic belts, where crustal thickening causes downwarping of the adjacent lithosphere (Beaumont, 1981). Facies are arranged asymmetrically so that shallow water facies near the foreland pass abruptly into deep water facies filling the basin axis. Most foredeeps display three fundamental stages of evolution: 1) initial, rapid submergence or drowning of an earlier, slowly subsiding platform (possibly passive-margin carbonates), 2) deep water sedimentation in a narrow axial trough; submarine fan and related deposits are common, and show longitudinal sediment dispersal patterns, and 3) shallow marine to fluvial sedimentation associated with final filling of the foredeep, with sediment dispersal towards the foreland. Initial foredeep subsidence may be preceded by up-arching and subaerial exposure of older platform sediments, generating an unconformity along the exposure surface. This is a consequence of the flexural origin of foredeeps, and the elastic properties of the lithosphere (cf. Beaumont, 1978). Finally, the trend of foredeep basins and related arches commonly is parallel to the trend of the load (commonly stacked thrusts) that generates the basin. Consequently, in ancient orogenic belts, foredeep basins and arches should be approximately parallel to related thrust-fold belts, and perpendicular to tectonic transport indicators (eg. stretching lineations).

Preliminary work conducted during the 1985 field season strongly suggests that the Kilohigok Basin formed by flexure of the early Proterozoic lithosphere, in response to convergence along the Thelon Tectonic Zone. Evidence for this includes identification of an early stable shelf sequence (Kimerot Platform; 500 m thick), which underwent drowning along its outer edge and up-arching within its interior to produce a karstic unconformity before it was deeply submerged. Overlying sediments (2 to 2.5 km thick) are deep water submarine fan and interfan deposits, with paleocurrents indicating sediment dispersal parallel (axial) to Gordon Bay Arch. Overlying deposits (1 to 2 km thick) are shallow marine shelf sediments with complex sediment

dispersal patterns, succeeded by a major, southeastward thickening (up to 1.5 km thick) wedge of fluvial coarse sands and conglomerates. Conglomerates contain clasts of most underlying lithologies, supplementing a dominant population of intraformational clasts. Such a mixture is common in migrating foredeeps that ultimately cannibalize themselves in advanced stages of development. Paleocurrents within fluvial sediments indicate sediment dispersal across the foredeep axis and arch, toward the foreland.

Kimerot Platform

The Kimerot Platform occurs in the southeastern part of Kilohigok Basin, where it is 0 to 500 m thick (Fig. 12.2, 12.3). Platform sediments are also preserved in several outliers, located east of Kilohigok Basin. The Kimerot Platform contains a transgressive siliciclastic part (0 to 250 m thick), and overlying carbonate part (0 to 250 m thick). Several detailed sections across the platform reveal major facies relations within the preserved outcrop belt (Fig. 12.3, 12.4). Unfortunately, most of the platform is no longer preserved within the present basin limits, so the trend of major facies belts cannot be reliably determined. However, changes in thickness and facies within the preserved outcrop belt (Fig. 12.3, 12.4) suggest that the platform probably faced southwest, south or southeast, and that the preserved cross-section is at a high angle to the trend of facies belts. This is supported by north-south elongation of platform stromatolites which were probably elongate approximately perpendicular to shelf trend.

Kimerot siliciclastics

Description. The siliciclastic part of Kimerot Platform (Fig. 12.3, 12.4) contains a basal transgressive lag overlain by a unit of trough crossbedded, coarse grained to pebbly

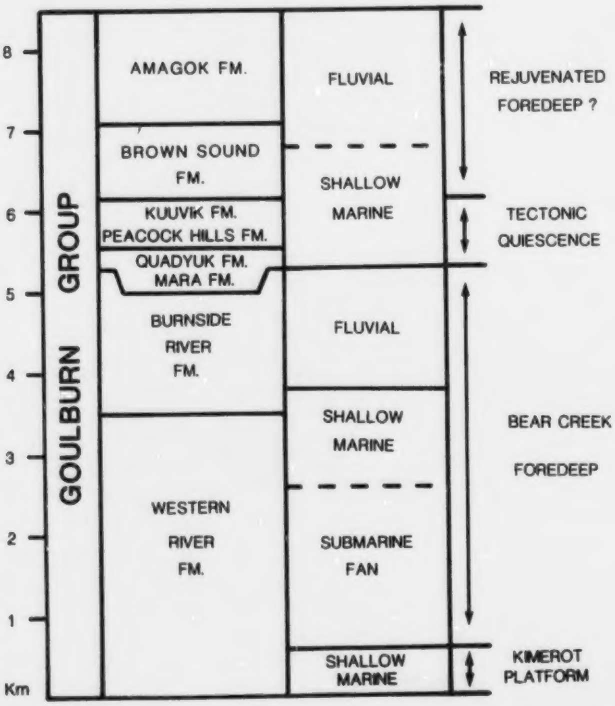

Figure 12.2. *Stratigraphy of Goulburn Group, Kilohigok Basin, in thickest (axial) part of basin. Also shown are major depositional environments and tentative tectono-stratigraphic subdivisions.*

sandstone, overlain by a unit of fine- to medium-grained hummocky cross-stratified sandstone with minor dolomites, (collectively unit 1a of Tirrul, 1985) in turn overlain by a siltstone/dolomite unit with small scale hummocky cross-stratification and interbedded stromatolitic and clastic textured dolomites (unit 1c of Tirrul, 1985). In part, the upper two units are laterally equivalent to a laminated mudstone/siltstone unit, (unit 1b of Tirrul, 1985) only developed near section 1 (Fig. 12.4). The basal lag (0 to 3 m thick) is generally a clast-supported conglomerate with sand matrix. Clasts are dominantly vein quartz, with minor amounts of metagreywacke, iron formation and granitoids, all derived locally by weathering of basement rocks. Clasts are subangular to subrounded, and units generally fine upward into overlying trough crossbedded sandstones.

Trough crossbedded sandstones (0 to 80 m thick) contain sets of troughts 5 to 20 cm thick, that form laterally continuous (> 50 m) beds with scoured bounding surfaces. Sands are medium to very coarse, locally pebbly, subrounded to well rounded, and contain 10 to 15% feldspar. Paleocurrent data (Fig. 12.4) indicate sediment transport to the northwest, southeast and southwest, and suggest that sands may have been transported along shore in some areas (data with NW/SE trends) but offshore in others (data with SW trend).

Hummocky cross-stratified sandstones form a unit 0 to 140 m thick that is typically fine- to medium-grained, and thinly bedded. Beds contain low angle truncation surfaces defining hummocks and uncommon swales, with wavelengths of 1 to 3 m, and amplitudes of 10 to 30 cm. Thicker beds up to 50 cm commonly have scoured, trough crossbedded bases which flatten upwards into hummocky strata. Between sections 3 and 6, hummocky sandstones contain biostromal mounds 1.5 m high and 150 m long (Fig. 12.5). Biostromes are composed of very irregular, dolomitic columns, separated by inter-column quartz sands which are crosslaminated. Internal stromatolitic lamination also is irregular and poorly preserved. At section 5, intermound sands are trough crossbedded channel deposits, scouring underlying hummocky cross-stratified sands and adjacent biostromes. Channel sands are overlain by hummocky cross-stratified sands. Upwards, hummocky cross-stratified sandstones pass into laminated siltstones.

The siltstone/dolomite unit (0 to 130 m thick) contains abundant small scale hummocky cross-stratification (wavelengths a few tens of centimetres, amplitudes < 10 cm), abundant clastic-textured and biohermal dolomites, and uncommon hummocky cross-stratified medium grained sandstones. Siltstones contain some thick laminae to thin beds of very fine grained sandstone with planar lamination, bundles of asymmetric wave ripples, and graded laminae. These layers may have load structures. Dolomite beds are 0.3 to 2 m thick, and increase in abundance upwards. Stromatolitic units are biohermal, but clastic-textured beds are sheets that extend for tens of kilometres.

The laminated mudstone/siltstone unit (0 to > 200 m) is only developed southeast of section 1. It is dominated by graded and nongraded laminae of mudstone and siltstone, with uncommon wave ripples and rare, scour-and-drape structures less than 20 cm wide and 1 to 2 cm deep. Also, rare, thin clastic-textured dolomite beds are present. This unit probably is laterally equivalent to the hummocky cross-stratified sandstone unit and the siltstone/dolomite unit.

Interpretation. The lower siliciclastic part of Kimerot Platform is best accommodated in a transgressive shoreface model (cf. Spearing, 1975). The sequence progresses upwards from trough crossbedded coarse and pebbly sandstones, through medium sands with large scale hummocky cross-stratification, up to siltstones with small scale hummocky cross-stratification and abundant dolomites. This is

consistent with a gradual northward shift in deposition environments from upper shoreface through lower shoreface, to the offshore. The onset of carbonate sedimentation would result from decreased siliciclastic influx, as a result of continued transgression of exposed basement. Such deposits characterize the Cretaceous Gallup sandstone of western North America (Spearing, 1975). Although the Gallup is progradational, and the stratigraphy is inverted relative to that in the Kimerot, troughed sands are interpreted as upper shoreface deposits, hummocky sands are interpreted as lower shoreface deposits, and laminated siltstones represent offshore deposits.

In the Kimerot siliciclastic sequence, troughed sands are sheets that were spread over the shelf during probable longshore dune migration. There are no recognizable composite bed forms in these sheeted sandstones to suggest that they represent discrete offshore bars or sand ridges as documented by Brenner (1980), Schurr (1984) or Walker (1984). Hummocky cross-stratified sands probably formed over the deeper part of the shoreface by storm reworking and resedimentation of inner shoreface troughed sands (Hamblin and Walker, 1979). Stromatolite bioherms may have caused channeling of storm-surge return or geostrophic currents, producing trough crossbedding in an otherwise hummocky regime. As transgression continued, siliciclastic influx was decreased resulting in deposition of siltstones and carbonates. The laminated mudstone/siltstone unit probably formed on the distal shelf, generally below storm wave-base, as shown by the dominance of graded and nongraded laminae, and common lack of any hummocky cross-stratification (cf. Reineck and Singh, 1972; Soegaard, 1984). Eventually, continued transgression and/or decreased siliciclastic influx allowed a major stromatolitic reef complex to develop, as the lower unit in the overlying carbonate part of Kimerot Platform.

Kimerot carbonates

Description. The carbonate part of Kimerot Platform contains three units; a lower reef unit (0 to 80 m thick), a middle cyclic unit (0 to 130 m thick), and an upper reef/rhythmite unit (0 to 30 m) (units 1d-g, Tirrul, 1985). The lower reef unit thins northward and may in part, pass laterally into siltstones and dolomites of the underlying siliciclastic part of the platform (Fig. 12.3). The overlying cyclic unit also thins northward; its upper boundary is probably isochronous, but the lower part of the unit may be laterally equivalent to the upper part of the underlying reefal unit. In the upper reef/rhythmite unit, reefal facies thin southward and pass laterally into probably time-equivalent

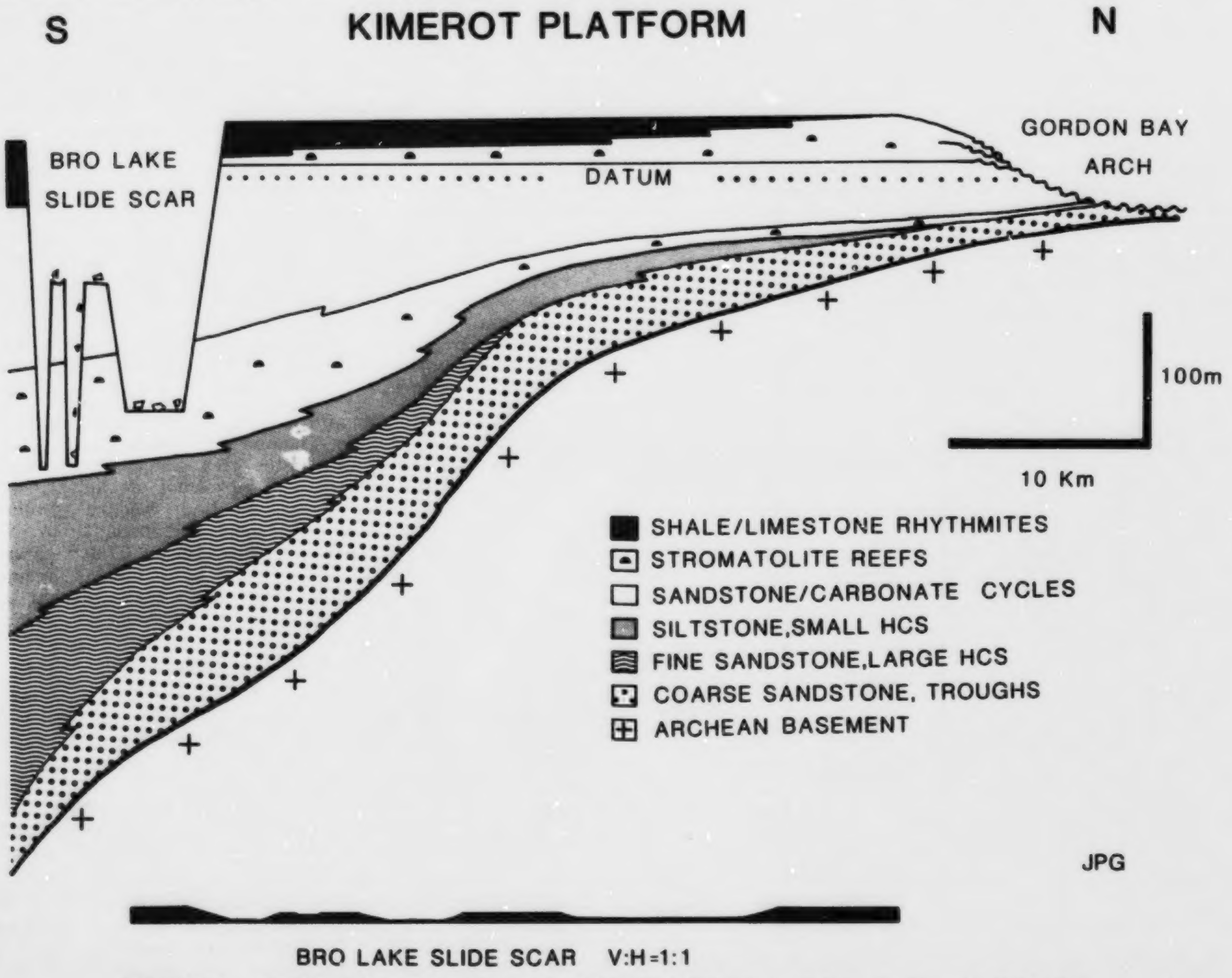

Figure 12.3. *Stratigraphic cross-section of Kimerot Platform. Datum is top of distinctive shallowing-upward cycle. Note 1:1 V:H reconstruction of Bro Lake Slide Scar at bottom of diagram. Distribution of measured sections is similar to that shown in inset of Figure 12.4.*

rhythmite facies (Fig. 12.3). Northward, reefal facies contain a few layers of tepee and tidal flat facies. The datum used in reconstructing Figure 12.3 is the top of a distinctive shallowing-upward cycle that can be correlated across the outcrop belt. Such contacts are very nearly isochronous in both Phanerozoic and Proterozoic cyclic sequences (Fischer, 1964; Anderson et al., 1984; Grotzinger, 1985, in press; Read et al., in press).

The upper part of Kimerot Platform is conformable over much of its width, but becomes a major erosional unconformity northwestward toward Gordon Bay, where underlying units are progressively cut out all the way down to Archean basement. Locally the unconformity is karstic, and residual topographic relief of several metres can be seen. "Valleys" between erosional remnants commonly are filled with rounded pebbles and cobbles of eroded lithologies. Similar relationships are observed in the northern part of Beechy Lake area, south of Bathurst Fault, where carbonates and basal clastics of Kimerot Platform are successively cut out to the northwest by an intraformational unconformity. These truncations define a northeast trend of 130-140 km if left-slip is accepted for the displacement on the Bathurst Fault (Campbell and Cecile, 1981; Tirrul, 1985). A positive area corresponding to this trend is herein termed the Gordon Bay Arch which supersedes the "Hanimok High" of Campbell and Cecile (1981) for which a trend was not confidently established (F.H.A. Campbell, personal communication, 1985).

The Kimerot Platform is everywhere mantled by dark laminated mudstone. Near section 3 (Fig. 12.4) units at the top of the platform are locally missing, probably due to sliding of parts of the platform (Tirrul, 1985). Megabreccias line the flanks and bases of possible slide scars (Fig. 12.3).

The lower reefal unit (Fig. 12.3) consists of large, strongly elongate stromatolite mounds, 0.5 to 3 m wide and 0.3 to 2 m high. Groups of mounds are separated by channels (1 to 50 m wide, 0.5 to 3 m deep containing trough cross-bedded sandstone. Mounds are composed of smaller, branching columnar stromatolites which also are strongly elongate. All stromatolites are elongate approximately north-south. Mounds become smaller northwestward and are eventually cut out over the Gordon Bay Arch. Mounds are dolomitized except for thin beds of limestone. To the southeast, penetrative strain is extremely high (Tirrul, 1985), preventing accurate facies reconstruction. It appears however, that the reefal unit passes gradually into fine grained siliciclastics, suggesting a low gradient transition

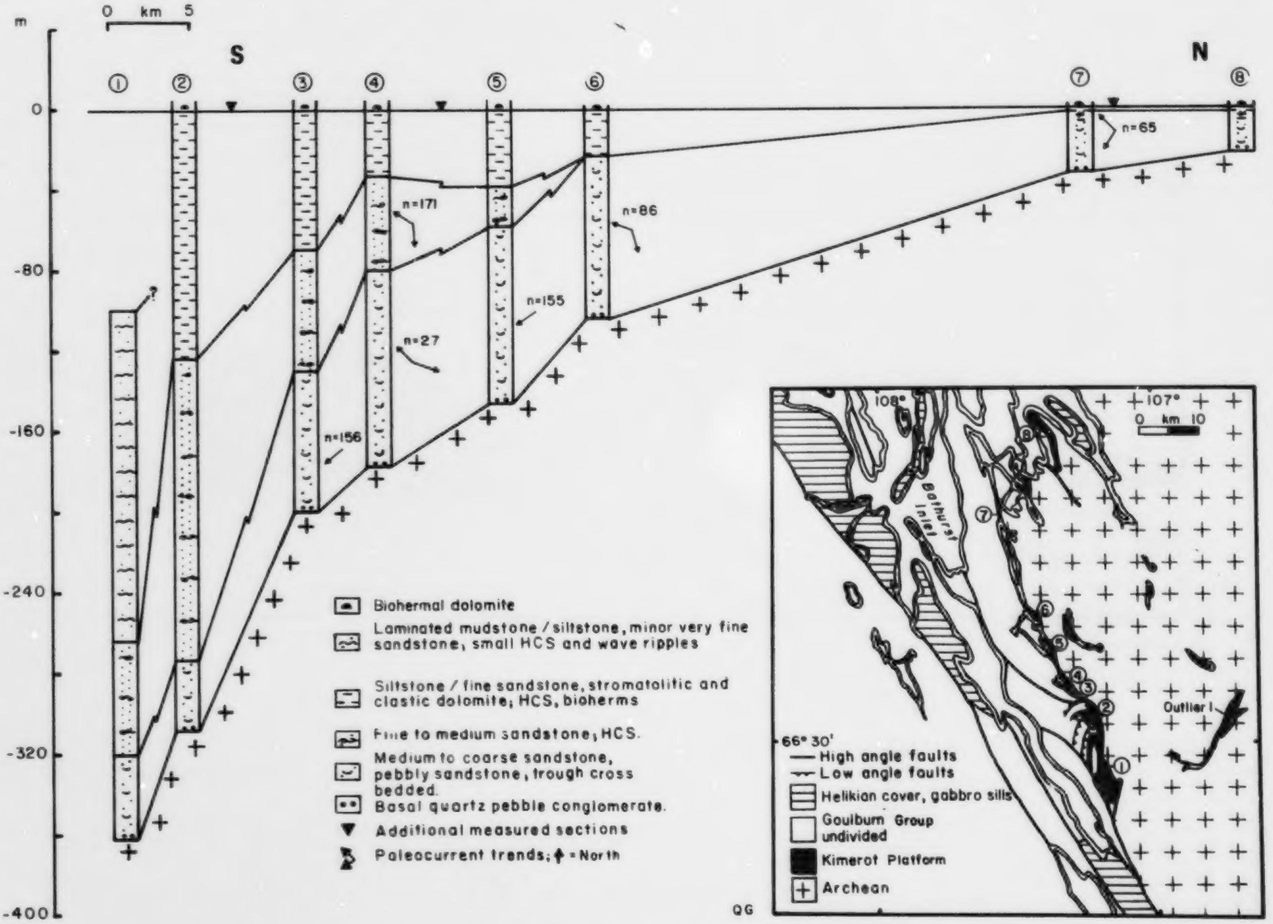

***Figure 12.4.** Stratigraphic cross-section of siliciclastic part of Kimerot Platform. Location of sections shown on inset map. Note that data from section 1, are not used in reconstructing cross-section of Figure 12.3. This is because of extreme strain in overlying carbonates.*

into the deeper basin (ramp?), rather than a rim which would be associated with an abrupt change into deeper water facies containing slope and allodapic breccias. In most areas the lower reefal unit is overlain by 1 to 10 m of trough crossbedded quartz-rich sandstone, which forms a regionally extensive blanket.

The overlying cyclic unit (Fig. 12.3) consists of 50 to 75 shallowing-upward cycles, 0.5 to 2 m thick. Lower parts of most cycles contain trough crossbedded siliciclastic/carbonate sands, with abundant intraclasts derived from underlying cycle caps. Upper parts of cycles contain cryptalgalaminites and tufas; stromatolites are uncommonly developed as transitional facies between the lower and upper parts of cycles. Cycle caps are commonly erosional, with well developed tepee structures and locally developed pisolite. To the southeast, troughed sands at bases of cycles pass laterally into hummocky cross-stratified fine sands, and cryptalgalaminites and tufas of cycle caps pass laterally into stromatolites. Although most of the cyclic unit lacks distinctive marker beds, several occur near the top and can be correlated for over 50 km at a high angle to depositional strike.

The upper reef/rhythmite unit is marked by a sharp lower contact, exactly parallel to underlying cycle boundaries (Fig. 12.3). On this basis, it is inferred to be approximately chronostratigraphic. Reefal facies comprise large, strongly elongate mounds (1 to 2 m wide, 0.5 to 1 m high), cored by smaller, branching columnar stromatolites, also elongate. All mounds are dolomitized. Channels are present and filled with crossbedded sands. Adjacent to Gordon Bay Arch, mounds contain brecciated horizons, associated with tidal flat facies. Some breccias are locally filled with botryoidal fibrous marine cements, that are well preserved despite pervasive dolomitization. To the southeast, reefs pass laterally into probably time-equivalent rhythmite facies that consist of thickly interlaminated dark mudstone and limestone (Fig. 12.3). Where rhythmites overlie reefal facies, the contact often contains 0.5 to 1.0 m of mounded edgewise conglomerate; clasts are derived from adjacent stromatolites.

Interpretation. The lower reefal unit was probably a ramp, deepening to the south or southeast, and may have formed during continued rise in sea level, which would have reduced siliciclastic influx. Large stromatolite mounds indicate subtidal water depths that were shallow enough to allow strong elongation by wave and/or tidal-produced currents. Channels filled with crossbedded sands may represent tidal channels. Mounds decrease in size to the north-northwest, suggesting a decrease in water depths where subsidence rates were lower (indicated by thinning of section). A relative drop in sea level may be indicated by the blanket of sandstone capping the reefal unit. On other

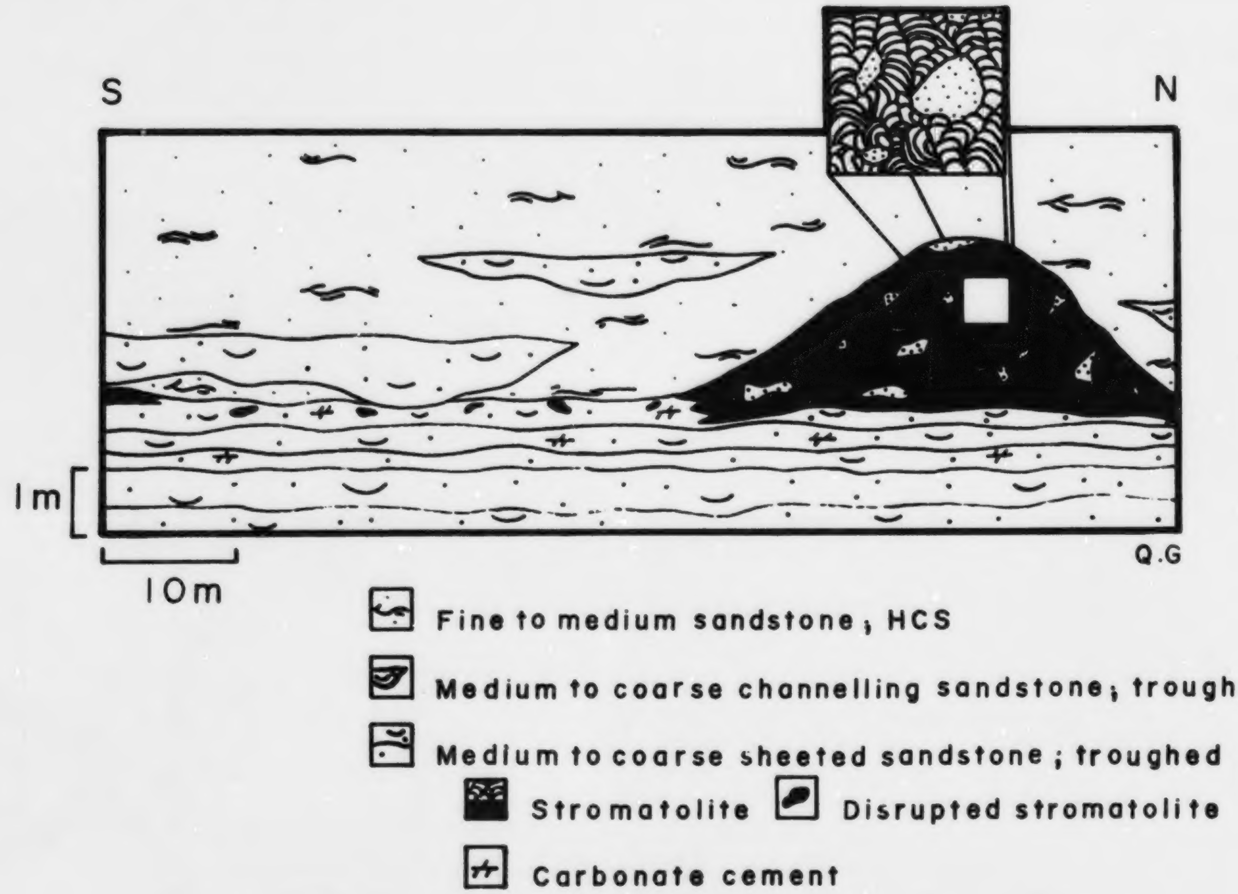

***Figure 12.5.** Relationship between stromatolite biostromes and siliciclastic facies of hummocky cross-stratified sandstone unit.*

platforms, clastics were spread out as sheets during low stands in sea level (e.g. "Hawke Bay Event"; Palmer and James, 1979; Read, personal communication, 1985).

Development of the cyclic unit represents stabilization of the platform. Pinch out of tidal-flat facies within cycles to the south-southeast suggests that cycles formed by progradation of flats in that direction. Cycles probably formed in response to small changes in sea level (few metres), indicated by the brecciated, erosional cycle caps (cf. Grotzinger, 1985, in press; Read et al., in press). Siliciclastic sands forming bases of cycles (subtidal) may in part represent reworked eolian sediments which would have migrated across flats during low stands in sea level. However, sands may also have been imported by longshore transport during subtidal sedimentation. Evidence for extensive transport of subtidal sands is supported by ubiquitous trough crossbedding in sands.

The transition from cyclic unit to overlying reef/rhythmite unit represents an abrupt change to greater water depths where open-marine reefs and/or rhythmites were deposited. This transition was nearly isochronous as indicated by parallelism of the contact between the cyclic unit and reef/rhythmite unit, and underlying cycle boundaries (Fig. 12.3). This abrupt facies change at the top of Kimerot Platform is identical to the transition between cyclic sediments of the early Proterozoic Rocknest Platform and its overlying reefal veneer (Grotzinger, 1985). Initial increase in water depth over Kimerot Platform was followed by diachronous drowning of the platform, as shown by progressive northwest onlap of rhythmite facies over reefal facies (Fig. 12.3). During drowning of the outer platform, uplift of the inner platform over Gordon Bay Arch occurred (Fig. 12.3). Arching was probably synchronous with drowning because both drowning and arching postdate deposition of the cyclic unit, and predate deposition of deep water dark mudstones which cover the platform in all areas. This relationship is of great importance because it strongly suggests that drowning was caused by tectonic flexure of the platform, rather than a eustatic rise in sea level. Eustatic drowning is not likely because it does not account for simultaneous uplift of the inner shelf and drowning of the outer shelf. Support for a hypothesis of flexural tectonic drowning is found in the orthogonal relationship between the trend of Gordon Bay Arch, and the trend of finite extension lineations within nappes (Tirrul, 1985). Most likely, the northeast trend of Gordon Bay Arch is a product of northwest tectonic transport of thrust-nappes, which would have emplaced a load on the lithosphere.

Further evidence for tectonic drowning of the platform is the Bro Lake Slide, which scalloped the upper platform during drowning. Sliding and drowning probably were synchronous because both postdate deposition of the cyclic unit, and predate deposition of overlying deep water dark mudstones. Sliding of platform sediments is known to occur along the shelf break of rimmed platforms, simply due to gravitational instability (e.g. Mullins and Neumann, 1979). The Bro Lake Slide Scar however, is located well back on the platform, away from the probable shelf-to-slope transition zone. Furthermore the platform was probably a low-gradient ramp and lacked slopes that would allow sliding to occur. Thus, sliding probably occurred in response to steepening of the platform during tectonic flexure.

In sum, tectonic rather than eustatic submergence of the platform is supported by the coincidence of rapid outer platform drowning with flexural uparching of the platform interior, and simultaneous sliding of parts of the platform down tectonically steepened slopes. Diachronous southeast-to-northwest drowning of the platform is probably related to decreasing rates of tectonic subsidence (and thus relative sea level rise) towards the Gordon Bay Arch; such a systematic decrease in subsidence rate would be a direct consequence of flexural downwarping (e.g. Beaumont, 1978). Drowning of Kimerot Platform heralds the onset of foredeep subsidence and sedimentation in Kilohigok Basin.

At this stage in the study, it is not possible to determine whether Kimerot Platform formed on a passive continental margin, or in an intracratonic basin. If it did form on a passive margin, then it was destroyed at a very early age; subsidence rates should have been large, and this is not in agreement with the unusually thin cycles of the cyclic unit.

Bear Creek Foredeep

The "Bear Creek Foredeep" includes sediments of the Burnside River Formation and parts of the Western River Formation that overlie the Kimerot Platform (Fig. 12.2). These sediments are superbly exposed in the Bear Creek Hills area, east of Bathurst Inlet. The foredeep sequence (5.5 km thick) is subdivided spatially into a thicker axial sequence (3.0 to 5.5 km) developed above the outer part of Kimerot Platform, and a thinner shelf sequence (1.5 to 3.0 km) developed over the Gordon Bay Arch (Fig. 12.6). The axial sequence consists of submarine fan and related deposits (up to 1.5 km thick), that pass up into continuous mudstones (1 km thick), overlain by shelf sandstones and mudstones (up to 1.5 km thick), in turn overlain by an upper sequence of fluvial sandstones and conglomerates (1.5 km thick).

The shelf sequence was developed synchronously with the axial sequence, but generally under much lower subsidence rates (Fig. 12.6). Shelf sediments (0.5 to 2 km thick) are dominated by shallow marine sandstones and mudstones, with minor carbonates, and pass upwards into fluvial sandstones and conglomerates (0 to 1 km thick). Most shelf sands contain unconformities which pass into conformable contacts southeastward, toward the basin axis (Fig. 12.6). Shelf sands are generally laterally separated from deep water axial sands by a zone devoid of sands, probably representing the slope and area of bypassing.

Because of the great thickness and aerial extent of Bear Creek Foredeep deposits, only a limited number of sections were measured during the 1985 season. Of sections measured in marine deposits (Western River Formation), most were in the axial sequence, and only two were measured in the fluvial sequence (Burnside River Formation). Enough data however, were collected so that when used in combination with documentation by Campbell and Cecile (1981), it allows a preliminary cross-section of the foredeep to be constructed (Fig. 12.6).

Axial sequence, lower part

Description. The lower part of the axial sequence consists of interbedded dark mudstones and fine to coarse sandstones (10-15% feldspar), locally containing carbonate blocks (units 2a-f, Tirrul, 1985). Sandstones occur as large lenses, tens of kilometres wide and hundreds of metres thick. The lowermost lens (unit 2b, Tirrul, 1985) consists of amalgamated sand layers, separated by occasional mudstones. Sands are massive or normally graded, rarely trough crossbedded, and occasionally contain large blocks of clastic-textured or stromatolitic dolomite and limestone. Dolomite blocks appear to be derived from the siltstone/dolomite unit of the siliciclastic part of Kimerot Platform, but limestone blocks are of uncertain origin. Where present, blocks are reverse graded.

Overlying sandstone lenses are composed of interbedded sandstones and dark mudstones. These may be arranged in thinning-upward fining-upward sequences, 30 to 70 m thick. Sandstones are fine- to very coarse-grained, and beds commonly are trough crossbedded or massive, and pinch out within 50 to 100 m along strike. Rarely, sandstone beds

contain classical Bouma sequences, and many beds consist of a single set of trough foresets. Beds are 0.1 to 3 m thick, with scoured bases and flute casts. Thin mudstones may separate sand beds that are otherwise amalgamated. Paleocurrent measurements of crossbed foresets and flutes show longitudinal transport to the southwest, parallel to the basin axis and Gordon Bay Arch.

Interpretation. A deep water submarine fan origin for sandstone lenses in the lower part of the axial sequence is supported by several features that compare with other well documented submarine fan sequences (cf. Howell and Normark, 1982). These are: large sand lenses on the scale tens of kilometres by hundreds of metres, completely enclosed in finely laminated dark mudstones; individual sand beds that are channelized and discontinous over 50 to 100 m; sand beds form thinning-upward fining-upward sequences; sand beds contain trough crossbedding, graded bedding, massive bedding, rare Bouma sequences, and have scoured or channeled bases with flute casts; sediment transport is strongly unimodal, consistent with transport in a narrow trough. In the lower sand lens, coarse, amalgamated sands containing blocks with inverse grading may reflect a setting on the inner-fan channel or channelized portion of suprafan lobes (Eriksson, 1982; Howell and Normark, 1982; Walker, 1984). In the upper sand lenses, discontinuous sand beds form thinning-upward fining-upward sequences which may reflect deposition on the channelized or braided portion of suprafan lobes.

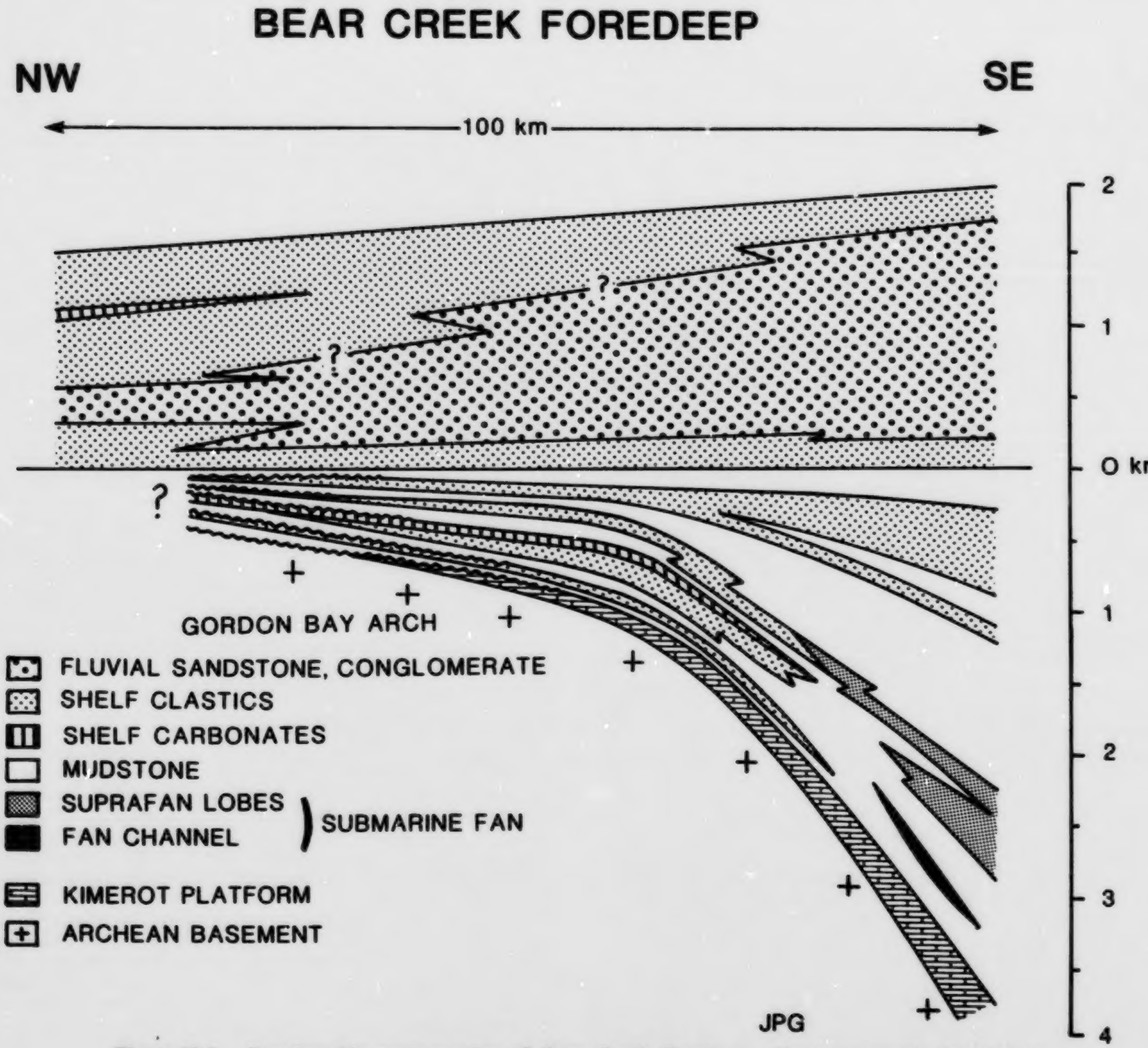

Figure 12.6. Stratigraphic cross-section of Bear Creek Foredeep. Note systematic increase in thickness to southeast, which reflects differential subsidence; location of submarine fan facies (axial zone) over outer part of Kimerot Platform; progressive shallowing of foredeep axis with time. Lower "shelf carbonate" unit is Beechy Platform; upper "shelf carbonate" unit is Bd member of Burnside River Formation.

In the stratigraphically highest sand "lens", apparent submarine fan facies in the axial sequence pass laterally into shelf sands of the shelf sequence. The reason for this is not yet clear, although it may have to do with the evolving geometry of the foredeep allowing lateral migration of fan deposits toward the foreland, at the same time the basin was filling.

Paleocurrents in sand beds with troughs and/or flutes show remarkably unimodal sediment dispersal, parallel to the basin axis and Gordon Bay Arch. Longitudinal sediment dispersal is a classical feature of foredeeps (McBride, 1962; Potter and Pettijohn, 1963; Mutti, 1985), and is a product of the narrowly confined and linear geometry of the basin.

Axial sequence, middle part

Description. The middle part of the axial sequence is dominated by shallow marine shelf sandstone and mudstone units (units 3a-B_1, Tirrul, 1985). All units are within the Western River Formation, except for the uppermost shelf sand unit, which forms the lowermost member of the Burnside River Formation. Sandstone units are 70 to 600 m thick, and laterally continuous for over 100 km, unlike underlying fan deposits. Intervening mudstones are 30 to 300 m thick. Internally, sandstone units contain sequences dominated by trough crossbedded sheet sands with polymodal paleocurrent patterns, that pass laterally and vertically into units dominated by hummocky cross-stratification, and then into units dominated by mudstone with uncommon thin sand layers. Some sand units are maroon, with abundant mudchips within crossbeds, and rare possible desiccation cracks.

Interpretation. The middle part of the axial sequence represents filling and shallowing of the foredeep, and the onset of widespread shallow shelf sedimentation. Variations in relative sea level probably produced alternation of shallow shelf sandstones (with hummocky crossbedding and trough crossbedding) with deeper shelf mudstones. Maroon, trough crossbedded sandstones with mud chips may be shallow subtidal to lowest intertidal sediments, or possibly even fluvial. However, in the absence of fossils, distinguishing trough crossbedded shallow marine facies from braided fluvial facies is difficult. Well documented fluvial sequences (Campbell and Cecile, 1981) in the upper part of the axial sequence, however, have strongly unimodal paleocurrent patterns, unlike inferred marine units described here which have complex polymodal patterns.

Axial sequence, upper part

Description. This unit was examined during reconnaissance, and descriptions rely heavily on those already published (e.g. Campbell and Cecile, 1981). The unit (Burnside River Formation) generally consists of fluvial sandstone and conglomerate in a thick wedge that thins northwestward. A characteristic feature is the development of fining-upward cycles (0.2 to 2.5 m thick) which have conglomeratic scoured bases that pass upward into trough crossbedded sandstones, overlain by planar-laminated sandstones, and capped by mudstone layers. Conglomerates are dominated by clasts of vein quartz and intraformational quartzite, but also contain clasts of many underlying lithologies, including granitic and metasedimentary basement. All paleocurrents indicate sediment dispersal to the northwest (Campbell and Cecile, 1981), across and perpendicular to the trend of Gordon Bay Arch.

Interpretation. Fluvial facies of the upper part of the axial sequence have been interpreted as braided river deposits (Campbell and Cecile, 1981). In the foredeep model presented here, they represent final basin filling, and transport of sediment across the basin, directly towards the foreland. Campbell and Cecile (1981) interpreted conglomerate composition to reflect intrabasinal processes. The abundance of intraformational quartzite clasts and vein quartz clasts was inferred to represent early, synsedimentary cementation of clastics and silcrete development on floodplains, throughout deposition of the unit. Vein quartz was believed to have been precipitated in fractures related to shallow dewatering and compaction. Subsequent rapid subsidence in the basin would have fractured the early cemented floodplains, resulting in instantaneous fluvial capture and production of intraformational boulders by rapid channel downcutting (Campbell and Cecile, 1981).

The interpretation presented here differs significantly from that of Campbell and Cecile (1981). Burnside sediments were examined for evidence of early cementation or silcrete development and, if present, it is not abundant. Fractures filled with vein quartz are rare in general, and most occurrences could be related to a system of conjugate transurrent faults which postdates the Burnside River Formation (Tirrul, 1985). Furthermore, most vein quartz is formed during deep burial to levels much greater than floodplains. Finally, many intraformational quartzite boulders contain fractures not present in the host rock, indicating fracturing at depth prior to resedimentation.

Foredeeps migrate in front of prograding thrust-fold belts (Beaumont, 1978, 1981). Thus, initial foredeep deposits may be incorporated into thrust wedges advancing toward the foreland. Sediments are delaminated by propagating thrusts, uplifted, eroded and recycled back into the foredeep. Such cannibalization of the Jurassic/Cretaceous foredeep adjacent to the Cordilleran thrust wedge occurred during deposition of the Paleocene Paskapoo Formation (Bally et al., 1966). In the Bear Creek Foredeep, intraformational quartzite boulders in fluvial facies probably reflect a similar history of early foredeep sedimentation, cannibalization during progressive migration of the thrust wedge, and recycling of quartzites back into the foredeep. Vein quartz would have been formed during fracturing associated with thrusting. Other clast lithologies indicate that the early axial part of the foredeep, as well as basement were also being reworked.

Shelf sequence

Description. The shelf sequence in Bear Creek Foredeep contains a lower shallow marine part, and upper fluvial part (Fig. 12.6). All marine units except for the uppermost shelf sand (Burnside River Fm.) are in the Western River Formation. Fluvial sediments (Burnside River Fm.) are distal equivalents of facies described above and are not discussed here.

The lower marine sequence contains alternating sequences of sandstones (40 to 100 m thick) and mudstones (10 to 80 m thick), with uncommon carbonates (1 to 30 m thick). Most shelf sandstones are dominated by hummocky cross-stratification, but some contain abundant trough cross-stratification, and one unit is dominated by large scale, tabular-planar crossbedding with sets up to a few metres thick. The tabular-planar crossbedded sands are overlain by 1 to 30 m of stromatolitic carbonate (Beechy Platform; Fig. 12.6). The Beechy Platform contains large stromatolite mounds that are locally up to 3 m wide, 1 to 2 m high, and 100 m long.

The Beechy Platform and many sand units within the foredeep shelf sequence have unconformable upper contacts, some erosional (Fig. 12.6). Unconformities are marked by scoured surfaces overlain by layers containing pebbles or cobbles of underlying sands; siliciclastic mudstones and siltstones may contain layers of patchy carbonate cementation and poorly developed tepee profiles. Locally, zones of complex brecciation several metres thick are developed below unconformities, particularly where clastic carbonate was deposited in addition to siliciclastic sands. Above the Beechy Platform, well developed pisolitic profiles

are locally developed on scalloped solution surfaces. Tepees and breccias are also present, as are layers (10 to 100 cm thick) of fibrous dolomite cement. Cements are composed of botryoids (originally aragonite?) up to several centimetres wide, and have well preserved prismatic crystals with square terminations.

Interpretation. Shelf sandstones and mudstones were deposited over the Gordon Bay Arch, where subsidence rates were greatly reduced relative to the axial part of Bear Creek Foredeep. Consequently, water depths were generally much shallower, as shown by the abundance of hummocky cross-stratification, wave ripples, and crossbedding with complex polymodal patters.

The presence of unconformities capping shelf sand and carbonate units indicates large fluctuations in relative sea level. Because these sequences are, in part, located over the Gordon Bay Arch, it is not yet possible to determine whether relative sea level oscillations were tectonic- or eustatic-induced. A eustatic origin, however, is suggested by their possible lateral extent beyond the influence of arching, as well as the direct juxtaposition of deep water mudstone facies on many of the surfaces, without intervening paralic sediments. If eustatic, sea level oscillations would have been third- to fourth-order cycles (cf. Vail et al., 1977).

If the Bear Creek unconformities separate offlap-onlap sequences, then they are sequence boundaries and time lines in the sense that the unit below the surface is everywhere older than the unit above the surface (Vail et al., 1977). This has important implications for the Bear Creek Foredeep as well as other Precambrian siliciclastic sequences where, in the absence of fossils, only tuff beds (easily reworked in shelf settings) are presently available for time correlation. Therefore, Bear Creek unconformities must be thoroughly investigated during future research in order to ascertain whether they are tectonic or eustatic, and if they extend into the Coronation Supergroup of Wopmay Orogen.

Regional correlations

Preliminary correlations between the Western River and Burnside River formations of Bear Creek Foredeep, and Coronation Supergroup of Wopmay Orogen suggest that Bear Creek Foredeep may have initiated and culminated during the rift and passive margin stages of Wopmay Orogen, respectively. At this point in the study, the best time line used in making correlations is the lateral extension of the Rocknest Formation (intraclastic member) from Wopmay Orogen into Kilohigok Basin. The Rocknest Formation correlates with the K4 member of Cecile and Campbell (1978) in the Peacock Hills area, which in turn correlates with the Bd member of Campbell and Cecile (1981), a regionally extensive carbonate unit in the central and western parts of the Burnside River Formation. The Rocknest K4-Bd unit probably formed during a eustatic sea level high, an event that was probably nearly isochronous over the Rocknest Platform (Grotzinger, 1985). These relations indicate that Burnside sedimentation was coeval with Rocknest sedimentation, and thus the Bear Creek Foredeep was in an advanced stage of development during the carbonate phase of passive margin sedimentation in Wopmay.

Another possible time line may be the correlation of deep water shales at the base of the Odjick Formation (lowermost passive margin strata, Wopmay Orogen) with one or more of the possible sequence boundaries in the shelf sequence of Bear Creek Foredeep. It should be emphasized that this correlation is speculative, although easily testable due to excellent exposures. If correct, then it suggests that Kimerot Platform and overlying marine sequences in Bear Creek Foredeep may have been deposited during rifting in Wopmay Orogen.

Possible foredeep reactivation

Development of a regional carbonate platform up to 600 m thick (Peacock Hills and Kuuvik formations; Fig. 12.2) over Bear Creek Foredeep clastics probably signifies the end of convergence and uplift along Thelon Tectonic Zone. However, reactivation of Thelon Tectonic Zone at a later time may be indicated by deposition of the Brown Sound and Amagok formations. These units comprise an eastward-thickening wedge (up to 2 km) of mudstones, immature sandstones and conglomerates, in which fluvial facies (Amagok Fm.) have unimodal westward-directed paleocurrents.

Unlike the underlying fluvial wedge of Bear Creek Foredeep (eastern facies of Burnside River Fm.), the Brown Sound/Amagok wedge contains a significant volume of felsic to intermediate volcanic and hypabyssal plutonic clasts with minor coarser grained diorite clasts (Campbell and Cecile, 1981). These clasts may be undeformed, which contrasts with other vein quartz and quartzite clasts, granitic and gneissic clasts, and mylonites. Significantly, the undeformed suite of clasts may comprise a consanguineous arc-related volcanic-plutonic suite, that developed on top of, or adjacent to, the Thelon Tectonic Zone. This hypothetical arc may have been a high level equivalent of some intrusive rocks in the Thelon Tectonic Zone (Thompson, personal communication, 1985). If so, then the arc has been subsequently completely eroded. This hypothesis has an obvious testable prediction in that the age of volcanic clasts in the Amagok Formation should agree closely with the ages of some granites in the Thelon Tectonic Zone. Arc volcanism should predate an inferred collision at about 1.9 Ga along the Thelon Tectonic Zone. However, this would not explain why volcanic clasts are limited to the Brown Sound/Amagok wedge and absent from the underlying foredeep strata, as high level volcanic rocks should be the first to be eroded. Alternatively the volcanism might be related to crustal melting consequent to the collision, in which case their stratigraphic restriction could be explained and their predicted age would fall between about 1.9 and 1.85 Ga.

Initial conclusions

Preliminary investigations during the 1985 field season permit several tentative conclusions. These will be scrutinized during future research.

1. The Kilohigok Basin is probably a major foredeep, related to convergence along the Thelon Tectonic Zone. Apparent stages of development mimic those seen in younger foredeeps and include tectonic drowning of a stable platform (Kimerot Platform) and formation of a flexural "outer swell" (Gordon Bay Arch). This was followed by rapid subsidence of the platform and depositon of axial submarine fan sediments followed by shallow marine shelf sands and muds, overlain by fluvial sands and gravels shed toward the foreland. The composition of fluvial conglomerates suggests foreland-directed migration of the foredeep axis with time.
2. The trend of Gordon Bay Arch is perpendicular to finite extension lineations in nappes described by Tirrul (1985). Nappes are probably the highest preserved structural level of the Thelon Tectonic Zone, which suggests that flexure of the lithosphere to produce Bear Creek Foredeep was caused by crustal-scale thrusting in the Thelon Tectonic Zone. More generally, the development of Gordon Bay Arch indicates that the early Proterozoic lithosphere was capable of elastic flexure in response to emplacement of crustal-scale thrust loads.
3. Intrabasinal unconformities are developed within shelf sequences proximal to the foreland. Unconformities may relate to flexure over the Gordon Bay Arch, or alternatively, to eustatic fluctuations in sea level.

If eustatic, unconformities are probably time lines, and provide a superb opportunity to precisely correlate events in Bear Creek Foredeep with those in Wopmay Orogen.

4. Preliminary regional correlations suggest that Bear Creek Foredeep subsidence probably was synchronous with rifting in Wopmay Orogen. If so, then it suggests that rifting in Wopmay occurred during convergence along the Thelon Tectonic Zone. A Phanerozoic analogue of this is present in north Alaska where, during the Jurassic to Cretaceous, convergence in the Brooks range (foredeep) occurred synchronously with rifting and initial passive margin subsidence of the Beaufort shelf (Grantz and May, 1982). The two zones are separated by approximately 300 km, and a flexural high (Barrow Arch) intervenes. Not surprisingly, the Prudhoe Bay giant oil fields are located over the Barrow Arch.

Acknowledgments

We gratefully acknowledge the Geological Survey of Canada for logistical support and the opportunity to work in Kilohigok Basin. Barry Cadigan and Gary Luffman are thanked for field assistance. Martin Irving, based in Yellowknife, provided excellent expediting services. Echo Bay Mines, Ltd. is thanked for use of their helicopter. S.A. Bowring visited us and participated in valuable discussions, and sampling of siliciclastic sediments for detrital zircon provenance studies. Critical reviews by R. Tirrul and P.F. Hoffman substantially improved an earlier version of the manuscript..

References

Anderson, A.K., Goodwin, P., and Sobieski, T.
1984: Episodic accumulation and the origin of formation boundaries in the Helderberg Group of New York State; Geology, v. 12, p. 120-123.

Bally, A.W., Gordy, P.L., and Stewart, G.A.
1966: Structure, seismic data and orogenic evolution of southern Canadian Rockies; Bulletin of Canadian Petroleum Geology, v. 14, p. 337-381.

Beaumont, C.
1978: The evolution of sedimentary basins on a visco-elastic lithosphere: theory and examples; Royal Astronomical Society, Geophysical Journal, v. 55, p. 471-498.

1981: Foreland basins; Royal Astronomical Society, Geophysical Journal, v. 65, p. 291-329.

Brenner, R.
1980: Construction of process-response models for ancient epicontinental seaway depositional systems using partial analogs; American Association of Petroleum Geologists, Bulletin, v. 64, p. 1223-1244.

Campbell, F.H.A. and Cecile, M.P.
1976: Geology of the Kilohigok Basin; Geological Survey of Canada, Open File 332, 1:500 000 scale map.

1981: Evolution of the early Proterozoic Kilohigok Basin, Bathurst Inlet-Victoria Island, Northwest Territories; in Proterozoic Basins of Canada, ed. F.H.A. Campbell; Geological Survey of Canada, Paper 81-10, p. 103-131.

Cecile, M.P.
1976: Stratigraphy and depositional history of the Upper Goulburn Group, Kilohigok Basin, Bathurst Inlet, N.W.T.: unpublished Ph.D. thesis, Carleton University, Ottawa.

Cecile, M.P. and Campbell, F.H.A.
1977: Large-scale stratiform and intrusive sedimentary breccias of the lower Proterozoic Goulburn Group, Bathurst Inlet, N.W.T.; Canadian Journal of Earth Sciences, v. 14, p. 2364-2387.

1978: Regressive stromatolite reefs and associated facies, middle Goulburn Group (lower Proterozoic), in Kilohigok Basin, N.W.T.: an example of environmental control of stromatolite form; Bulletin of Canadian Petroleum Geology, v. 26, p. 237-267.

Eriksson, K.A.
1982: Geometry and internal characteristics of Archean submarine channel deposits, Pilbara block, Western Australia; Journal of Sedimentary Petrology, v. 52, p. 383-393.

Fischer, A.G.
1964: The Lofer cyclothems of the Alpine Triassic; in Symposium on Cyclic Sedimentation, ed. D.F. Merriam; State Geological Survey of Kansas, Bulletin 169, v. 1, p. 107-149.

Fraser, J.A.
1964: Geological notes on the northeastern District of Mackenzie, N.W.T.; Geological Survey of Canada, Paper 64-40.

Fraser, J.A. and Tremblay, L.P.
1969: Correlation of Proterozoic strata in the northwestern Canadian Shield; Canadian Journal of Earth Sciences, v. 6, p. 1-9.

Grantz, A. and May, S.D.
1982: Rifting history and structural development of the continental margin north of Alaska; in Studies in Continental Margin Geology, ed. J.S. Watkins and C.L. Drake; American Association of Petroleum Geologists, Memoir 34, p. 77-102.

Grotzinger, J.P.
1985: Evolution of early Proterozoic passive-margin carbonate platform, Rocknest Formation, Wopmay Orogen, N.W.T., Canada; unpublished Ph.D. thesis, Virginia Polytechnic Institute and State University, Blacksburg.

– Cyclicity and paleoenvironmental dynamics of an early Proterozoic carbonate platform, Rocknest Formation, Wopmay Orogen, N.W.T., Canada; Geological Society of America, Bulletin. (in press)

Hamblin, A.P. and Walker, R.G.
1979: Storm-dominated shallow marine deposits: the Fernie-Kootenay (Jurassic) transition, southern Rocky Mountains; Canadian Journal of Earth Sciences, v. 16, p. 1673-1690.

Hildebrand, R.S. and Roots, C.F.
1985: Geology of the Riviere Grandin map area (Hottah Terrane and western Great Bear Magmatic Zone), District of Mackenzie; in Current Research, Part A, Geological Survery of Canada, Paper 85-1A, p. 373-383.

Hoffman, P.F.
1973: Evolution of an early Proterozoic continental margin: the Coronation geosyncline and associated aulacogens of the northwestern Canadian Shield; Royal Society of London, Philosophical Transactions, series A, v. 273, p. 547-581.

Hoffman, P.F. (cont.)
1980: Wopmay Orogen: a Wilson cycle of early Proterozoic age in the northwest of the Canadian Shield; in The Continental Crust and its Mineral Deposits, ed. D.W. Strangway; Geological Association of Canada, Special Paper 20, p. 523-549.

Hoffman, P.F., Tirrul, R., Grotzinger, J.P., Lucas, S.B., and Eriksson, K.A.
1984: The externides of Wopmay Orogen, Takijuq Lake and Kikerk Lake map areas, District of Mackenzie; in Current Research, Part A, Geological Survey of Canada, Paper 84-1A, p. 383-395.

Howell, D.G. and Normark, W.R.
1982: Sedimentology of submarine fans; in Sandstone Depositional Environments, ed. P.A. Scholle and D. Spearing; American Association of Petroleum Geologists, Memoir 31, p. 365-404.

McBride, E.F.
1962: Flysch and associated beds in the Martinsburg Formation (Ordovician), Central Appalachians; Journal of Sedimentary Petrology, v. 32, p. 39-91.

Mullins, H.T. and Neumann, A.C.
1979: Carbonate slopes along open seas and seaways in the northern Bahamas; in Geology of Continental Slopes, ed. L.A. Doyle and O.H. Pilkey; Society of Economic Paleontologists and Mineralogists, Special Publication 27, p. 165-192.

Mutti, E.
1985: Turbidite systems and their relations to depositional sequences; in Provenance of Arenites, ed. G.G. Zuffa, p. 65-93.

O'Neill, J.J.
1924: The geology of the Arctic Coast of Canada, west of Kent Peninsula. In Report of the Canadian Arctic Expedition 1913-1918, v. XI, Part A., King's Printer, Ottawa, 107 pp.

Palmer, A.R. and James, N.P.
1979: The Hawke Bay event: a circum-Iapetus regression near the lower to middle Cambrian boundary; in Proceedings, Caledonides in the U.S.A., ed. D.R. Wones; Virginia Polytechnic Institute and State University, Department of Geological Sciences, Memoir 2.

Potter, P.E. and Pettijohn, F.J.
1963: Paleocurrents and Basin Analysis; Academic Press Inc., New York.

Read, J.F., Grotzinger, J.P., Bova, J.A., and Koerschner, W.F.
– Models for generation of carbonate cycles; Geology. (in press)

Reineck, G. and Singh, I.
1972: Genesis of laminated sand and graded rhythmites in storm-sand layers of shelf mud; Sedimentology, v. 18, p. 123-128.

Shurr, G.
1984: Geometry of shelf-sandstone bodies in the Shannon sandstone of southern Montana; in Siliciclastic Shelf Sediments, ed. R. Tillman and C. Siemers; Society of Economic Paleontologists and Mineralogists, Special Publication 34, p. 63-84.

Soegaard, K.
1984: Sedimentological constraints on Precambrian crustal evolution in northern New Mexico; unpublished Ph.D. thesis, Virginia Polytechnic Institute and State University, Blacksburg.

Spearing, D.
1975: Shallow marine sands; in Depositional Environments as Interpreted from Primary Sedimentary Structures and Stratification Sequences, ed. J. Harms, J. Southard, D. Spearing, and R. Walker; Society of Economic Paleontologists and Mineralogists, Short Course 2, p. 103-132.

Tirrul, R.
1985: Nappes in the Kilohigok Basin, and their relation to the Thelon Tectonic Zone, District of Mackenzie; in Current Research, Part A, Geological Survey of Canada, Paper 85-1A, p. 407-420.

Thompson, P.H. and Ashton, K.
1984: Preliminary report on the geology of the Tinney Hills-Overby Lake (west half) map area – a look at the Thelon Tectonic Zone northeast of Bathurst Fault; in Current Research; Part A, Geological Survey of Canada, Paper 84-1A, p. 415-423.

Thompson, P.H., Culshaw, N., Thompson, D.L., and Buchanan, J.R.
1985: Geology across the western boundary of the Thelon Tectonic Zone in the Tinney Hills-Overby Lake (west half) map area, District of Mackenzie; in Current Research, Part A, Geological Survey of Canada, Paper 85-1A, p. 555-572.

Tremblay, L.P.
1967: Contwoyto Lake map-area, District of Mackenzie (74 E/14); Geological Survey of Canada, Paper 66-28 and Map 10-1966.

1971: Geology of the Beechy Lake map-area, District of Mackenzie; Geological Survey of Canada, Memoir 365, 56 p.

Vail, P.R., Mitchum, R.M., and Thompson, S., III
1977: Seismic stratigraphy and global changes of sea level, Part 3: Relative changes of sea level from coastal onlap; in Seismic Stratigraphy – Applications to Hydrocarbon Exploration; ed. C. Payton; American Association of Petroleum Geologists, Memoir 26, p. 63-81.

Walker, R.G.
1984: Shelf and shallow marine sands; in Facies Models, Second Edition, ed. R.G. Walker; Geoscience Canada, Reprint Series 1, p. 141-170.

Wright, G.M.
1957: Geological notes on the eastern District of Mackenzie, N.W.T.; Geological Survey of Canada, Paper 56-10 and Map 17-1956.

An automated microscope system for image analysis in palynology and micropaleontology

Project 820044

M. Jean Dabros and Peta J. Mudie
Atlantic Geoscience Centre, Dartmouth

Dabros, M.J. and Mudie, P.J., An automated microscope system for image analysis in palynology and micropaleontology; in Current Research, Part A, Geological Survey of Canada, Paper 86-1A, p. 107-112, 1986.

Abstract

This report describes an automated image analysis system (AIAS) developed at AGC for computerized identification and counting of palynomorphs and opaline microfossils. Other uses of the system being tested are size and shape analysis of floc camera suspended particulates and of gravel beds in photographs of the seafloor. Future uses may include quantitative analysis of a) vitrinite reflectance and kerogen colour; b) morphometry of foraminifera, and c) ice crystal volume and sediment deformation in slabbed sediment cores.

Résumé

Un système automatisé d'analyse d'images a été développé au Centre géoscientifique de l'Atlantique afin d'identifer et de compter par ordinateur des palynomorphes et des microfossiles opalins. D'autres sujets d'études tentés avec ce système comprennent l'analyse de la taille et la forme des particules en suspension montrées par la caméra à floculats et des graviers photographiés par caméra sous-marine. Quelques usages futures pourraient inclure des analyses quantitatives a) de la réflectance de la vitrinite et de la couleur du kérogène; b) de la morphométrie des foraminifères; et c) du volume des crystaux de glace et des déformations de la structure des sédiments.

Introduction

The Atlantic Geoscience Centre (AGC) has developed a new automated image analysis system (AIAS) for computerized micropaleontology, including identification, counting, and analysis of volume, density and shape of palynomorphs and siliceous microfossils. The system was initially acquired (January, 1985) for automation of palynological microscopy. The success of this application led to further development of the system for other micropaleontological applications, including size and shape analysis of microfossils in Cretaceous biosiliceous sediment, volume analysis of fossilizable micro-organisms in plankton tow samples (S. McClatchie, personal communication, 1985), and for analysis of particulate matter in floc-camera photonegatives (Kranck, 1984).

This report describes the main features of computerized image analysis microscope system and its method of operation; describes the micropaleontological applications that have been developed during the past year; and outlines other potential applications that might be useful in geological research. In order to explain the unique features of the system, however, we shall first give a brief account of other automated image analysis systems that have been used for processing of geological data and we shall compare the AGC system with some other types of image analysis systems.

AGC's system basically consists of a Leitz TAS PLUS system for automated processing and evaluation of microscopic optical images. The TAS PLUS is the youngest generation of computerized microscopes which Wild Leitz Ltd. (Toronto) developed for applications in biomedical research (Vrolijk et al., 1981), in coal petrology, and for industrial uses requiring microscope inspection of materials, e.g. location of cracks in microchip circuits or defects in textile fibres. Fabbri (1984) gave examples of the most common uses of the system in geology: digitizing graphic displays (e.g. maps and photographs), quantifying grain area or geometry by scanning of thin sections or micrographs, mapping grains in thin sections or polished mounts, and automatic counting of α-particle tracks on radiographs. All these uses are basically the same as those that could be performed by the TAS PLUS. The salient difference is that most of these applications require use of either a large mainframe computer, or a dedicated microcomputer, and all except the GSC GIAPP (Geological Image Analysis Program Package) have limited user interactive programming options. This means that software cannot be modified easily to accomodate a variety of applications or changes in the composition of material from one sample to another, e.g. as encountered in analysis of borehole samples.

The automated image analysis system developed for quantification of coal facies and diagenetic changes (Chao et al., 1982) uses hardware modules that are basically the same as the TAS PLUS but have a more limited user interaction capability. The Joyce-Loebl MAGISCAN system used by Chao, and the updated MAGISCAN II, have fewer hardware programmed morphometric functions and a more limited range of user interactive options than the TAS PLUS; their operation, therefore, is slower and much more time is needed to modify a software program for a specific purpose or type of material. For example, it took about 12 months to develop the PASCAL language program described by Chao et al. (1982), yet this has more limited capabilities than AGC's FOSLOC-2 program which took only about four weeks to develop for palynological applications.

Another automated image analysis system that performs essentially the same operations for palynological analysis was built by the University of South Carolina (Erlich, 1985). This system cost about three times more than AGC's system and it took more than two years to develop for dedicated use in petrology. The Zeiss KONTRON can perform light microscopic as well as SEM image analysis functions; however, it has a spot scanner for user interaction and it cannot easily be programmed by a user; also, at present this system has a limited capability for adjusting to fluctuations in grey levels (brightness of the image) and this drift cannot be automatically controlled by the user, which is one of the most powerful and useful functions of the TAS PLUS. Finally, Leico Ltd. is developing a new microscopy system using an Olympus microscope with an automated stage, but at present this system has no automatic focusing capability which is another very powerful function of the TAS PLUS.

AGC's automated image analysis system

AGC's system is based on a Leitz TAS PLUS modular, interactive automated image analysis system (Fig. 13.1). The optical module of the system consists of a Leitz Orthoplan microscope with a digitally-controlled hologen lamp, a microprocessor-driven scanning stage and a software-operated rotating optical prism for automatic focusing. Mounted on the microscope is a Bosch TV camera with special circuitry for image measurement, and a Plumbicon tube, selected for its low geometrical distortion and good uniformity of light distribution. The camera scans specimens placed on the microscope stage and the TV signal is sent through a video amplifier to a DEC PDP 11 minicomputer interfaced with a DEC LS-II microcomputer where it is processed in six real time binary image memories with Boolean interconnection between images and/or bit-planes. The TAS PLUS has a power supply regulator for voltage stabilization and circuit protection which eliminates possible electrical failure chain reactions. The system has dual 8 inch floppy disk drives for software programs and temporary data storage, a 3-colour video monitor with ASCII keyboard, and a keypad for manual control of grey level, image edge detection, lamp intensity focus and stage movement. Hard-copy of data is obtained from an Epson 150 cps dot matrix printer/plotter. The 14 inch video monitor has 68 sensefields on the edge of the screen which can be used for complete image analysis by means of a light pen module.

The TAS PLUS operates on binary images. This is a two-step process involving the conversion of grey image to a binary image and the consequent processing of the binary image. There are two methods available for converting grey image to binary image. The first method is "Thresholding" which involves setting upper and lower limits for grey level detection and any part of the image that falls within this prescribed grey level range is defined as "ON" while all other intensities are defined as "OFF". TAS PLUS detection is in 1% steps, giving a possible resolution of 100 grey levels. The second method is "Edge detection" which is capable of discerning particles on a background of varying light intensity or matrix density.

Once a binary image has been obtained, processing can be performed by both hardware and software operations. TAS PLUS processing is based on a hexagonal raster (picture point array) in which each point is equidistant from its 6 neighbours. Hardware processing of the binary image includes: 1) elementary two-dimensional logic which performs erosion, dilation, particle reconstruction, separation of touching particles and hole closing; 2) "mini-ring" programmable two-dimensional logic which allows the user to selectively operate on specific positions within the raster. This enables operations such as skeletonization and related operations e.g. thinning, end point detection, linear transformations and connection of broken boundaries. For example, skeletonization can successively locate those pixels in an image which are maximally distant and hence, the

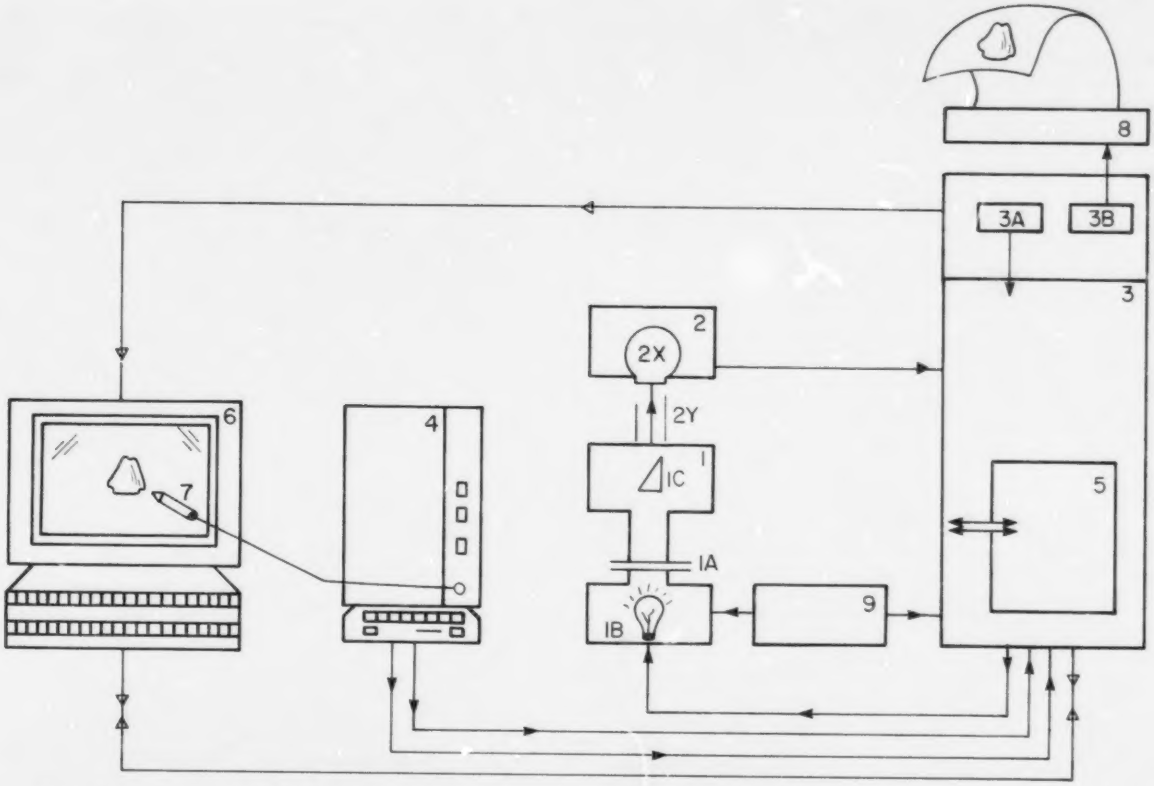

Figure 13.1. Simplified flow diagram of AGC's automated image analysis system operations. No. 1-9 denote the hardware modules. 1 – microscope; 1A – automated stage holding slide-mounted specimens; 1B – digitally controlled light source; 1C – rotating optical prism; 2 – camera; 2X – videocamera tube; 2Y – light path; 3 – minicomputer; 3A – software master program files; 3B – operating program files; 4 – manual operations box; 5 – microcomputer; 6 – video monitor and keyboard; 7 – light pen; 8 – printer/plotter; 9 – power supply.

image outline can be reconstructed very precisely. Line thinning and related processes can be used to reconstruct outlines by iterative "turning off" of pixel sets within the image. Measurements of individual particles can be made by sending perimeter trace points under software control to the PDP 11. Possible measurements include particle area, equivalent diameter, perimeter, shape, centre of gravity, elongation, largest diameter, position of extreme points, number and area of holes, reflectance, convexity and perimeter angularity (Feret diameter).

Programming is done in TASIC via the keyboard or by light pen control of the video monitor sense fields. TASIC is an interpretive FORTRAN-type computer language. TASIC statements range from simple labels to complex commands which can perform complete analysis sequences like FORTRAN subroutines. TASIC statements can be executed immediately by typing them on the keyboard or they can be entered in a user program and executed later as part of a complete program. TASIC includes a text editor for program entry, storage and retrieval. TASIC programs execute similarly to BASIC, providing easy program modification and on-line debugging. At present, permanent data files are stored on the PDP 11 which has a 32 Kbyte memory, and the image data are temporarily stored in the LS-II which has a 64 Kbyte memory. If required, the data in the microcomputer can be recorded in FORTRAN and stored in a PROM (Programmable Read Only Memory) for on-line transfer to a large mainframe computer such as the Cyber 730 at Bedford Institute of Oceanography. The PDP 11 may also be used independently for other data processing, e.g. to run the CABFAC program for factor analysis of palynomorph distributions (Mudie, 1982).

The light pen, in addition to image editing, is used for interactive programming. Each of the sensefields on the video monitor represents one or a group of TASIC commands and the user can call any of these by touching the appropriate sensefield with the light pen. Once a correct image processing sequence has been determined, this sequence is incorporated into a complete program which then performs processing designed to optimize analysis of a particular sample, particle or microfossil type.

Current applications of the AGC system

An example of this type of interactive programming is our FOSLOC-2 program which was initially developed in collaboration with Leitz programmer, Christopher Kay, of Wild Leitz Ltd., Toronto. FOSLOC is a general program that we designed to scan a slide, locate microfossils and record their co-ordinates. The output is a table of the co-ordinates for all identified objects, after which the program returns to each individual microfossil, centres it on the video screen, then focuses it on the microscope and monitor for verification of correct identification by the micropaleontologist. The authors substantially modified this program with respect to field processing and specimen selection criteria, e.g. area, shape and density, in developing FOSLOC-2 which is designed to locate and list the

co-ordinates of specified types of pollen, spores and dinoflagellate cysts. One the system has completed its search, the user then checks the identifications by recalling each of the specimens onto the video screen, and deleting those that were misidentified. We also added an optional subroutine whereby the identified specimens may be displayed as dot-print pictures on hard copy from the printer/plotter (Fig. 13.2).

FOSLOC-2 is particularly useful for counting abundant well-preserved pollen types, e.g. **Picea** and **Pinus**, in Holocene sediments, and for checking the distribution of counting control material e.g. **Eucalyptus** gains or plastic microspheres (J.G. Ogden, personal communication, 1985); in fact, FOSLOC-2 was used on AGC's system in order to test the precision of visual counts when Ogden was developing the microsphere counting method. FOSLOC-2 is also extremely useful for locating rare palynomorphs in nearly barren samples such as those characterizing most late glacial lake sediments, Arctic Ocean sediments (Mudie and Blasco, 1985), and pelagic sediments seaward of continental margins (Mudie, 1982, 1985).

At present, the time required for the system to scan about 300 palynomorphs in a pollen-rich sample is about 40 minutes after which another 20 minutes are required for the user to check the palynomorph identifications. This is about the same total time needed to perform the task visually, without recording the specimen co-ordinates (an additional time of ca. 0.5 h). With the automated image analysis system, however, the user need only be at the microscope for 20 minutes, i.e. the system decreases labour-intensive tasks by about 60 – 125%. The time needed for the system to scan a whole 22 x 30 mm slide, however, is 2 to 4 hours, depending on the palynomorph frequency; hence, scanning for rare specimens is presently an unacceptably long procedure for routine work. One way of alleviating this problem would be to install a video memory which would provide storage of the identified images on a disc. The system could then be set up to scan overnight and store the results to be played back at the user's convenience. Addition of a second video monitor on which all identified palynomorphs could be displayed simultaneously would also speed up verification procedures. Another improvement would be the addition of a large, high speed printer/plotter.

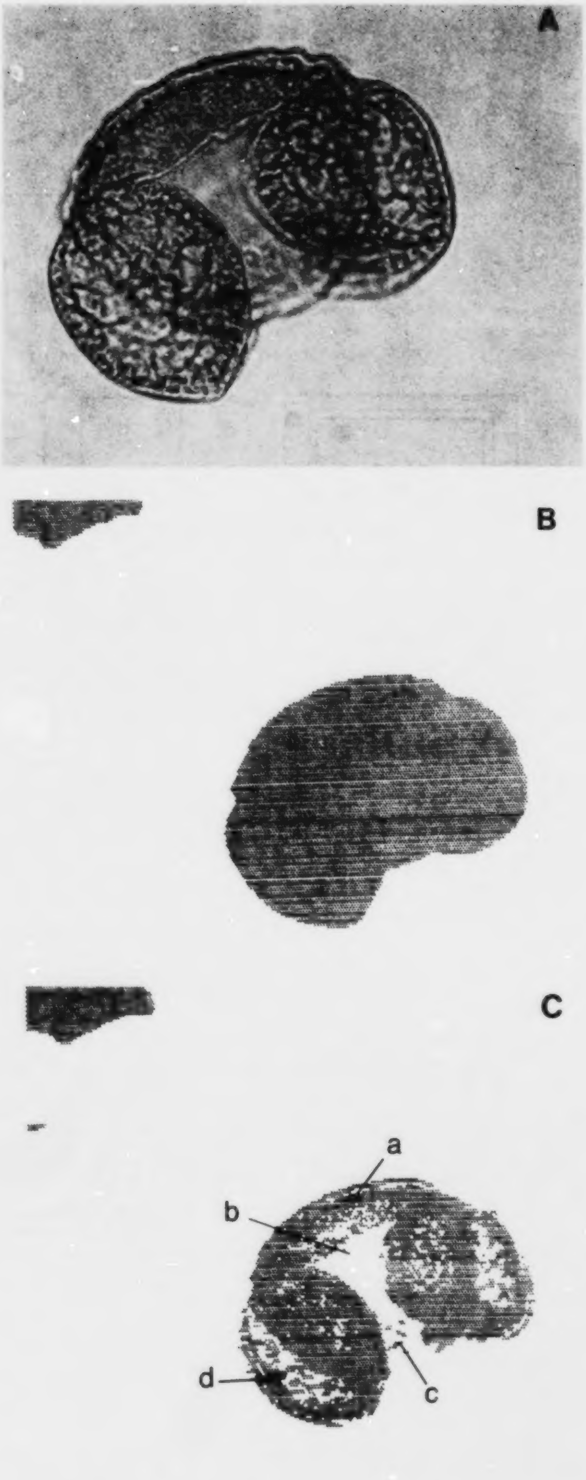

Figure 13.2

*A) Light microphotograph of **Pinus resinosa** pollen grain, magnification x 1000.*

B) Dot matrix printout of the image of this grain as identified by the system during a routine scan at a magnification of x 200.

C) Printout of grain in B) after adjustment of grey levels to enhance micromorphological features. Note that the system has accurately recorded the density difference between cappa (a) and corpus (b), including "belly wart" granules (c) which are typical of this pollen species, and the reticulate nature of the sacci (d).

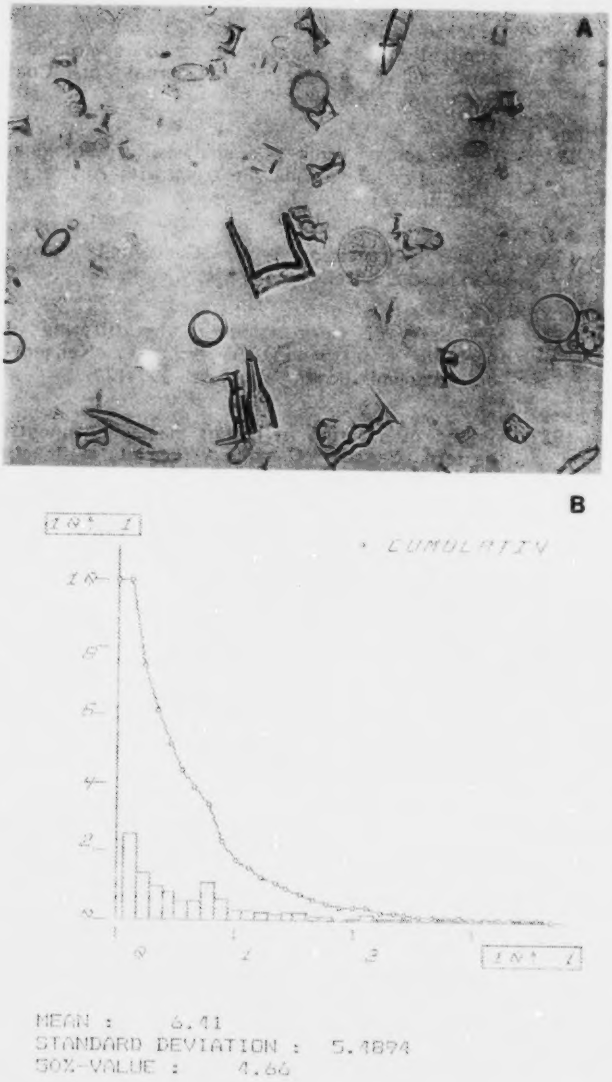

Figure 13.3

A) Light micrograph of opaline microfossils in a strewn-mount slide of laminated biosiliceous ooze from CESAR Core 6; magnification x 400.

B) Graphs of microfossil size distribution produced by the system operating at x 200 magnification

The other application we have successfully developed for AGC's system is the program DIAT.SIZ which identifies diatoms, silicoflagellates and archeomonads in smear slides of biosiliceous ooze, measures the diameter of each specimen, sorts the data into size classes, and plots a histogram and cumulative curve of microfossil size distribution (Fig. 13.3). DIAT.SIZ was developed by the authors in about 10 days after receiving a copy of the Leitz software programs TASSEP.ENG and TASSEP.PLU which were written in 1982 for grain size analysis of microscopic particles. The Leitz programs were first tested on a reference smear slide of diatomaceous mud for which visual counts of grain size distribution had been reported (Piper, 1976). The automated image analysis system gave a result of 41% clay, 59% silt and <1% sand on a count of 8492 particles, whereas the standard slide count estimated 46% clay, 54% silt, 0.5% sand from 10 random traverses. This agreement was considered good enough to warrant further development for special uses in micropaleontology.

DIAT.SIZ was subsequently developed in order to quantify the range of size and shape of opaline microfossils in light-dark lamina couplets of Upper Cretaceous sediment from the Arctic Ocean (Mudie and Blasco, 1985). This task was previously attempted by visual methods in order to estimate whether the couplets represent changes in bottom current speed (contourites), distal turbidites or changes in water chemistry and/or productivity (varves). The time needed for visual inspection of 10 fields, measuring and plotting the data was about 4 hours which was prohibitively long; furthermore, the reproducibility of results was extremely poor due to the difficulty of measuring particles with a wide range of shapes and orientations. The system takes about 15 minutes to perform these operations on at least 20 random fields containing a minimum of 300 specimens, and it takes about 10 minutes to display the results on the printer/plotter (Fig. 13.3). An F-test on the variance of 3 separate runs showed no statistical difference in the automated image analysis system results at the 90.0% confidence level.

Possible future applications

In addition to the add-on modules and hardware described above, we are in the process of developing several other geological applications of AGC's automated image analysis system. First, we plan to develop a Leitz program, CRIMP, for precise quantification of the number and shape of angular projections on a particle. This should greatly expand the ability of the system to discriminate among species of cavate and proximo-chorate dinocysts, to routinely quantify archeopyle geometry, angularity of sand grains or grain surfaces, and to quantify the size and shape of any microfossil less than 50 µm thick. Replacement of the present incident light source with a reflected light source is possible and hardware can be obtained for automated vitrinite reflectance studies. We are also testing the use of low power objectives on the microscope for quantifying the shape and size of sediment flocs from floc camera photonegatives. This capability might also be used to increase the speed and analytical power of AGC's VSA, an optical grain size analysis system (Syvitski and Swinbanks, 1980). This development might also be used to quantify the range of pebble/boulder size and shape in bottom camera photonegatives, or with addition of a larger stage, for pebble counts of sediment core X-radiographs. We are also investigating the possible use of our automated image analysis system for quantification of videocamera images to allow computer analysis of SEM data, morphometric analysis of foraminifera, and palynological video-libraries.

Other possible developments would require the acquisition of new optical modules and corresponding computer hardware. For example, replacement of the Orthoplan microscope with a fluorescence microscope and a suitable videocamera would allow rapid, very precise

quantification of kerogen maturation colour. Use of a stereoscopic "Macroboard" optical system with a zoom camera lens would permit automated counting of foraminifera and coarse sediment particles (> 63 μm). Combined with reflected light and a temperature controlled stage, a "Macroboard" could also be used for quantitative study of ice crystal deformation in slabbed cores of marine sediment. Ice formation in permafrost soils significantly alters both the geotechnical and geochemical properties of marine sediments, both of which are of considerable importance to the drilling industry.

Summary

1. AGC's automated image analysis system consists of a light microscope and videocamera with automated stage, focusing and light source controls, a programmable video monitor which can be operated using either a keyboard or a light pen, and a minicomputer coupled with a microcomputer for image processing.
2. For palynology and micropaleontology, AGC's system is better than most other systems because of its powerful hardware functions for automated image viewing and morphometric analysis of microscopic objects, and because of its user interactive programming capabilities.
3. The system is now fully operational for automated identification, counting and data display of pollen, dinoflagellate cysts and siliceous microfossils. It operates at a saving of 60 – 125% of the person-hours required for manual and visual performance of microscope studies.
4. The potential range of the system's applications includes automated smear slide analysis, quantification of vitrinite reflectance and kerogen maturation colour, analysis of data recorded on photonegatives or videotape, and measurement of ice crystal morphology in permafrost soil samples.

Acknowledgments

We thank Patricia Stoffyn Egli and Aubrey Fricker, Atlantic Geoscience Centre for their critical reviews of this paper; we also thank Dr. Stoffyn Egli for many hours of useful discussion about automated image analysis systems.

References

Chao, E.C.T., Minkin, J.A., and Thompson, C.L.
1982: Application of automated analysis to coal petrography; International Journal of Coal Geology v. 2, p. 113-150.

Erlich, R.
1985: Petrographic image analysis; Geological Association of Canada, Program with Abstracts, v. 10, p. 32.

Fabbri, A.
1984: Image Processing of Geological Data; Van Nostrand Reinhold Co., New York, 244 p.

Kranck, K.
1984: The role of flocculation in the filtering of particulate matter in estuaries; in V.S. Kennedy, ed., Academic Press, Orlando, p. 159-175.

Mudie, P.J.
1982: Pollen distribution in recent marine sediments, eastern Canada; Canadian Journal of Earth Sciences, v. 19, p. 729-747.

1985: Palynology and dinoflagellate biostratigraphy of DSDP Leg 94, Sites 607 and 611, North Atlantic Ocean; in Initial Reports of the Deep Sea Drilling Project, ed. W.T. Ruddiman and R. Kidd; v. 94; Government Printing Office, Washington, D.C.

Mudie, P.J. and Blasco, S.M.
1985: Lithostratigraphy of the CESAR cores; in Initial Geological Report on CESAR – the Canadian Expedition to Study the Alpha Ridge, Arctic Ocean, ed. H.R. Jackson, P.J. Mudie and S.M. Blasco; Geological Survey of Canada, Paper 84-22, p. 59-99.

Piper, D.J.W.
1976: A Manual of Sedimentological Techniques; Dalhousie University Printers, Halifax, Nova Scotia, 76 p.

Syvitski, J.P.M. and Swinbanks, D.D.
1980: VSA: a new fast size analysis technique for low sample weight based on Stokes settling velocity; Canadian Geotechnical Journal v. 17, p. 304-312.

Vrolijk, J., Pearson, P.L., and Pleom, J.S.
1981: TAL: an interpretive language for the Leyden Television Analysis System; in Languages and Architectures for Image Processing, ed. M.J.B. Duff and S. Levialdi; Academic Press, London, p. 125-137.

U-Pb ages on zircon from basement granitoids of the western Slave Structural Province, northwestern Canadian Shield

Project 750052

R.A. Frith, W.D. Loveridge, and O. Van Breemen
Precambrian Geology Division

Frith, R.A., Loveridge, W.D., and Van Breemen, O., U-Pb ages on zircon from basement granitoids of the western Slave Structural Province, northwestern Canadian Shield; in Current Research, Part A, Geological Survey of Canada, Paper 86-1A, p. 113-119, 1986.

Abstract

A 3 point U-Pb concordia intercept age of 2989 +6/-5 Ma was obtained on zircon separated from a basement granitoid that underlies Yellowknife Supergroup metavolcanic rocks in the Grenville Lake region of the Indin Lake map area (NTS 86B). This result which is supported by the more scattered U-Pb results on zircon from a second sample 12 km distant along strike, dates the age of zircon crystallization of the tonalite pluton protolith. Monazite separated from the second sample dates the peak of Kenoran thermal metamorphism in the area at 2596 +/-3 Ma.

Résumé

On a obtenu un âge de 2989 +6/-5 Ma à partir de trois points d'intersection sur une courbe concordia de l'U-Pb pour du zircon prélevé dans un socle granitoïde sous-jacent aux roches métavolcaniques du supergroupe de Yellowknife dans la région du lac Grenville de la carte Indin Lake (SNRC 86B). Ce résultat, appuyé par les résultats plus diffus des courbes concordias de l'U-Pb pour du zircon d'un deuxième échantillon prélevé 12 km plus loin, suivant la direction, établit l'âge de la cristallisation de la roche-mère, un pluton de tonalite. L'analyse de la monazite prélevée dans le deuxième échantillon attribue à la phase maximale du thermométamorphisme du Kénorien un âge de 2596 +/-3 Ma.

Introduction

Since Stockwell's (1933) discovery of basal conglomerate overlying granitoid basement in the Point Lake area, the Yellowknife Supergroup has been considered by many to be ensialic (Baragar, 1966; Heywood and Davidson, 1969; McGlynn and Henderson, 1970; Frith and Roscoe, 1980). The first geochronological confirmation of pre-Yellowknife ages was a Rb-Sr whole-rock isochron on rocks interpreted as basement to the supergroup, from the Grenville Lake area of the Indin Lake map area, by Rosaline Frith (Frith et al., 1974, 1977). An age of 2939 +/-50[1] Ma was obtained, which proved to be older than ages measured on Yellowknife Supergroup volcanic rocks from elsewhere in the Slave Structural Province (Frith and Loveridge, 1982). However, microclinization of plagioclase and migmatization in the basement gneiss of the Grenville Lake area suggested that the Rb-Sr date represented a time of K and Rb metasomatism. The present study establishes both a more precise value for the age of intrusion and, from a concordant U-Pb age determination on monazite, the age of Kenoran thermal metamorphism in the region.

Geological considerations

The basement rocks of the area are typified by those at Grenville Lake. They are metasomatized by potassic-rich migmatite. The least altered rock (square, Fig. 14.1) is a medium grained, biotite, plagioclase, quartz tonalite gneiss. The gneiss is cut by secondary aplite veins related to the migmatization and by undeformed muscovite pegmatite of younger age. The tonalite gneiss is also cut by easterly trending gneissic amphibolite dykes that may have been feeders to the overlying pillow basalts (Frith et al., 1977). The foliation of the dykes is common with that of the host gneiss, but the degree of gneissosity is more apparent toward the margins of the dykes. Near their centres ophitic textures are preserved.

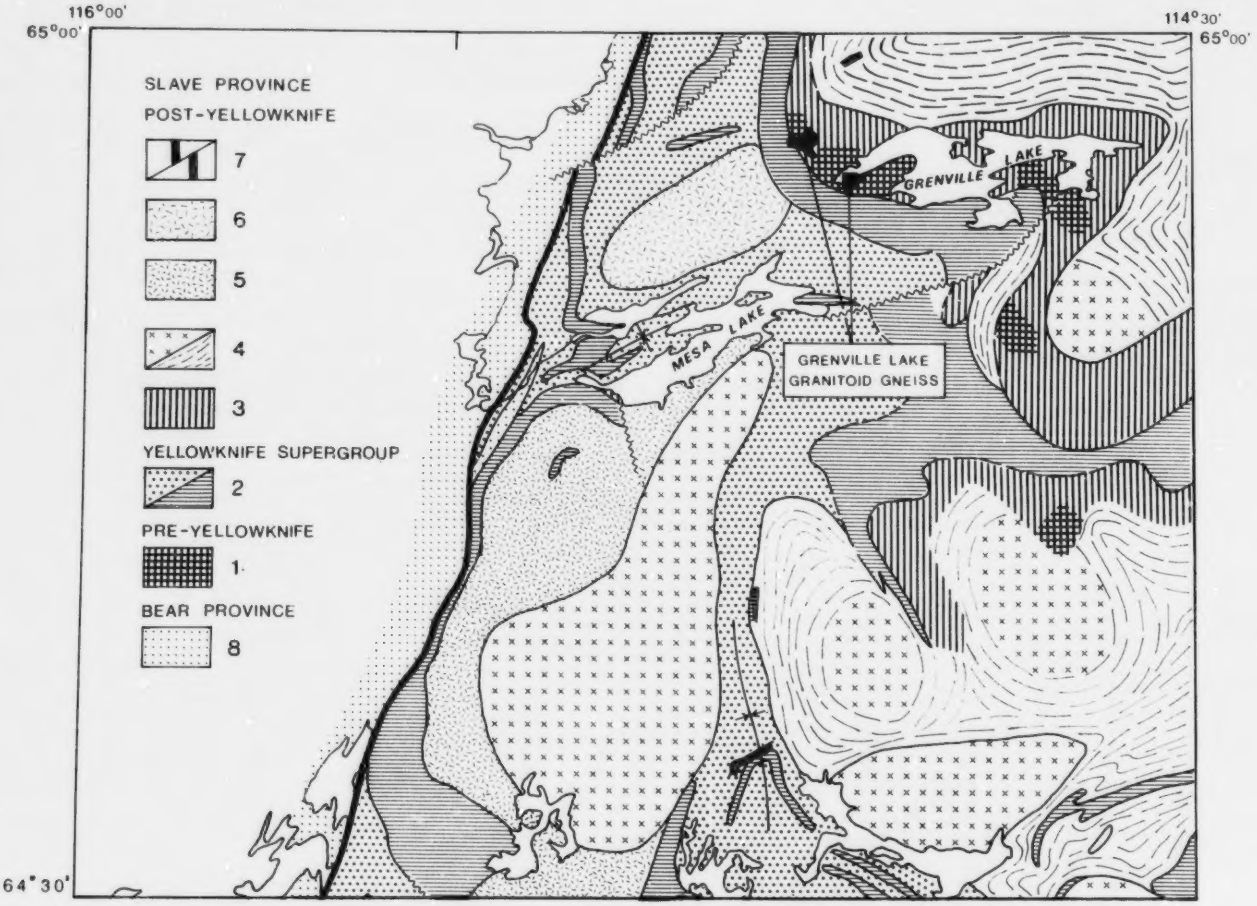

Figure 14.1. *Regional geology of the north Indin Lake map area (NTS 86B, N/2) showing sample localities for FYR-274 (solid dot) and FYT-905 (solid square) in the Grenville Lake area.*

1 = tonalite-granodiorite basement gneiss;
2 = Yellowknife Supergroup metasediments/pillow basalts;
3 = migmatite and gneiss derived in part from unit 1;
4 = granite/migmatite terrain derived in part from unit 2;
5 = Origin Lake granodiorite-tonalite;
6 = Mesa Lake granodiorite;
7 = Bear-Slave boundary fault/muscovite granite pegmatite

[1] Recalculated using ^{87}Rb decay constant = 1.42×10^{-11} a^{-1}

The adjacent pillow basalts have been tectonically thinned parallel to the foliation in the basement gneiss. The deformation is greatest near the basement contact, but is still evident in the gneiss 3 km to the north. The contact is intensely sheared and primary relationships are obliterated. Since the deformation affects both the basement rocks and the volcanics but not the crosscutting muscovite pegmatite, it is likely related to the Kenoran Orogeny, the close of which was marked by the intrusion of orogenic and anorogenic plutonic rocks in the region (units 5 and 6, Fig. 14.1). It is not known if any appreciable displacement occurred between the pillow basalts and the basement gneiss.

Rocks from locality FYT-905 are homogeneous, medium grained, grey gneisses of tonalite and granodiorite composition. The rocks, which have a slight gneissosity defined by biotite, have been locally discoloured to light salmon pink by deformed quartzofeldspathic veins which cut in seemingly random orientations. The degree of deformation increases toward the contact with the volcanic rocks but is overprinted by later shearing at the contact.

Rocks from locality FYR-274 (Fig. 14.1) are similar to those on the peninsula at Grenville Lake (FYT-905), except for a greater degree of discolouration due to replacement of plagioclase by microcline (deduced from cobalti-nitrate staining of smooth outcrop surfaces). The rocks are cut by large, simple granite pegmatites containing K-feldspar, muscovite and quartz.

Geochronology

Previous work

Other U-Pb zircon studies have suggested that basement gneiss may underlie significant areas of the Slave Structural Province. In the Yellowknife area metamict zircon from a tonalite diatreme in the Con Mine gave discordant $^{207}Pb/^{206}Pb$ ages between 3210 and 3030 Ma (Nikic et al., 1980). U-Pb zircon dating of basal granitoids in the Point Lake area gave an age of 3152 ± 2 Ma (Krogh and Gibbons, 1978; Krogh, personal communication, cited in Henderson et al., 1982) and single zircon age determinations from the same rocks suggest that some zircon in the overlying metasediments may be as old as 3.2 to 3.5 Ga (Scharer and Allegre, 1982). A U-Pb study of zircon from these rocks by Henderson et al., (1982) yielded results in general agreement with the 3152 ± 2 Ma age of Krogh and Gibbons (1978).

Regional mapping has shown that the Slave Craton extends westward into the Bear Structural Province and structurally underlies much of the Proterozoic metasediments (Frith et al., 1977; St-Onge et al., 1984) which were thrust over the craton from the west (Hoffman, 1973, 1980). Zircon from granitoid gneiss in the Coppermine River area yielded discordant U-Pb ratios with $^{207}Pb/^{206}Pb$ ages ranging from 2700 to 2890 Ma (Chamberlain et al., 1984). Similar rocks in the southwest part of the Redrock Lake area, 60 km northwest of Grenville Lake, gave a U-Pb age on zircon of 3.5 Ga (Bowring and van Schmus, 1984).

In the Cotterill Lake area 85 km to the south, intrusive granitic plutons were dated at 2532 ± 126 Ma (Frith, 1980) by the Rb-Sr whole-rock isochron method.

Analytical procedures and results

U-Pb studies were carried out on zircon from two samples of the basement gneisses in the Grenville Lake area. The first, FYR-274, was collected in 1972 from the same rock on which Rosaline Frith et al. (1977) measured the

Table 14.1. Analytical data, zircon and monazite from samples FYT-905 and FYR-274.

Size and characteristics	Weight mg	U ppm	Pb* ppm	Measured $^{206}Pb/^{204}Pb$	Isotopic abundances, ^{206}Pb=100 ^{204}Pb	^{207}Pb	^{208}Pb	Isotopic ratios $^{206}Pb/^{238}U$	$^{207}Pb/^{235}U$	Age, Ma $^{207}Pb/^{206}Pb$
FYT-905, zircon										
+105, abr	0.314	323.9	196.0	1371	0.0612	22.076	20.007	0.50396	14.847	2934
-105 +74, abr	0.540	342.5	205.1	2263	0.0399	21.785	17.964	0.50396	14.816	2930
-105 +74, abr	0.288	828.8	406.8	1285	0.0756	21.325	14.505	0.43027	12.127	2862
FYR-274, zircon										
+93, abr	[1]-	-	-	1720	0.0487	22.692	14.590	0.53263	16.254	2990
+93, hp	3.53	927.7	459.4	535	0.1821	22.462	20.471	0.42559	11.932	2853
-74 +64	14.29	999.0	502.3	594	0.1637	21.737	21.505	0.42858	11.708	2811
-44	0.27	1323.4	707.9	329	0.2064	21.126	42.710	0.39896	10.270	2713
+74, nm, hp	1.55	914.2	390.2	299	0.3163	22.999	28.782	0.35810	9.509	2764
FYR-274, monazite										
+74, hp	0.96	321.7	2349	40.39	0.1828	19.651	1544.5	0.49673 (2600 Ma)	11.911 (2597 Ma)	2596

[1] Weight of +93 abraded zircon fraction not measured, hence U and Pb ppm not calculated; see text.

Grain size is in µm, abr = hand picked and abraded, hp = hand picked nm = non magnetic, Pb* = radiogenic Pb, isotopic abundances of Pb presented after subtraction of Pb blank.

2939 ± 50 Ma, Rb-Sr isochron (initial $^{87}Sr/^{86}Sr$ = 0.700 ± 0.001). The second sample, FYT-905, was collected 12 km along strike to the east, in 1984, from a location where secondary introduction of granitic material was less evident. Analysis of U and Pb in zircon from the latter sample yielded a definitive upper concordia intercept age. The FYR-905 results also provided the key to interpretation of the disparate earlier results obtained from FYR-274.

Analysis of U and Pb in three zircon fractions from FYR-905 took place in 1985; FYR-274 analyses started in 1974 and continued sporadically until 1983. Analytical procedures were generally similar to those described by Loveridge (1986) except for zircon fraction weights (see Table 14.1). The monazite was dissolved and processed in 1981 using the same procedures as for zircon.

U-Pb ages have been calculated using the uranium decay constants and isotopic composition recommended by Steiger and Jaeger (1977). Linear regression of the U-Pb data and error estimation are based on Davis (1982).

FYT-905. Zircon was sparse in this rock and the concentrate obtained was very small. The largest, clearest components of zircon were hand picked (Table 14.1) but no separation based on magnetic properties was made due to the small amount available. Four morphologies were noted (see Appendix) and clear members of all four were included in the three fractions analyzed. Dark, fractured, possibly metamict grains were omitted; these are similar to the total zircon population from FYR-274. The three fractions were lightly abraded (Krogh, 1982) in order to remove surficial zircon which is more susceptible to lead loss by environmental influences.

Analytical results are listed in Table 14.1 and displayed on a concordia diagram (Fig. 14.2). The three data points from FYT-905 are collinear within analytical uncertainty, defining a chord which cuts the concordia curve at 2989 +6/-5 Ma and 804 Ma. The uranium content of these three zircon fractions ranges from 324 to 829 ppm with the higher uranium data point being the most discordant. Since the two -105 +74 μm fractions were picked sequentially from the same bulk material, the higher U content (829 vs. 342 ppm) of the second fraction is probably due to inclusion of more material of marginal quality.

FYR-274. Five zircon and one monazite fraction were separated for U-Pb analysis. Zircon and monazite morphologies are described in the Appendix. The zircon grains in these fractions were darker and more heavily fractured internally than the relatively clear zircon selected from FYT-905.

The U and Pb contents of the +93 μm, abraded fraction were not obtained, as the precision of the balance in use at the time was insufficient to accurately weigh the very small amount of zircon used. (The quantities (nanograms) of lead and uranium in this fraction were precisely determined,

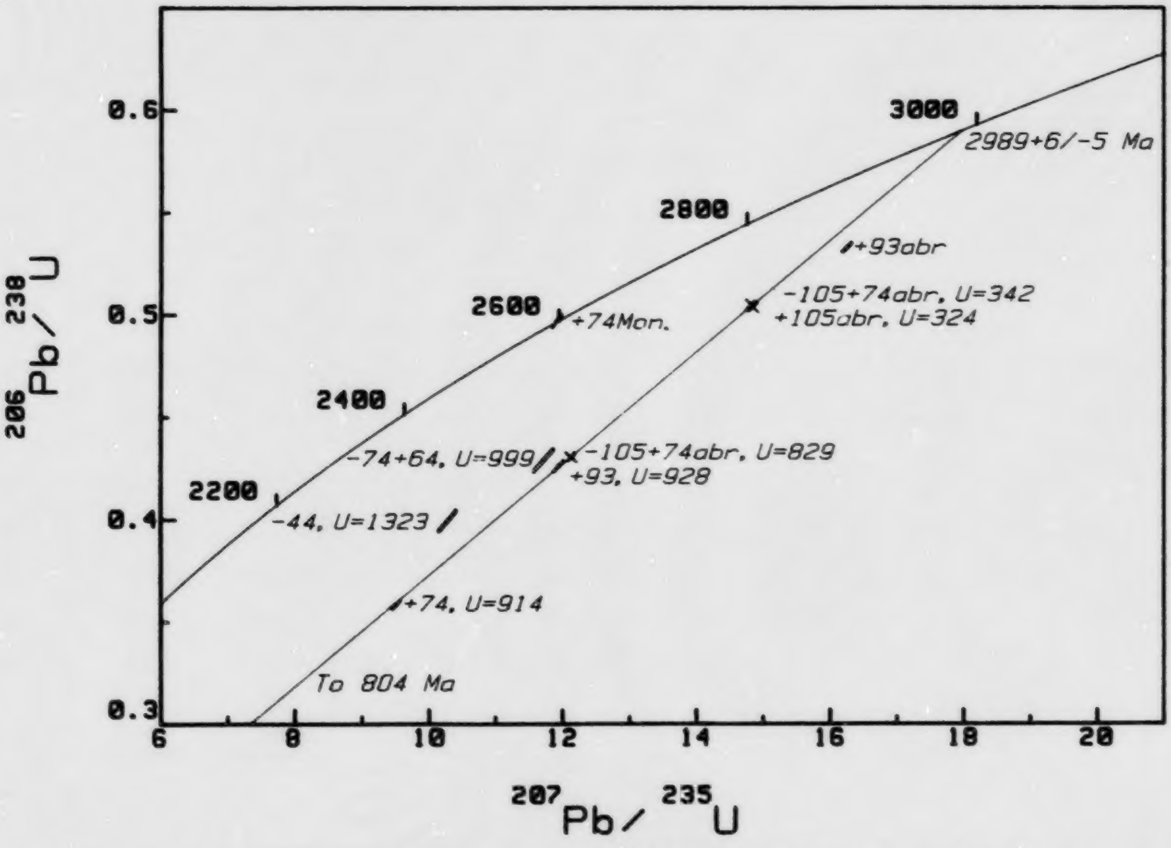

***Figure 14.2.** Concordia diagram showing the results of U-Pb analyses of zircon and monazite (Mon.) from samples FYT-905 and FYR-274. Cross symbols indicate FYT-905 results. Note that the FYT-905, +105 abr and upper, -105 +74 abr points are superimposed.*

yielding an accurate Pb/U ratio; the lack of precision of the balance prevented only the contents (ppm) of U and Pb in the zircon to be obtained).

Analytical results are presented in Table 14.1 and depicted on a concordia diagram (Fig. 14.2). Only the data point for the +93 μm, unabraded fraction falls on the chord defined by the FYR-905 results although the +74 μm data point is just slightly below this chord. Measured uranium contents are very high, 914 to 1323 ppm, suggesting that mechanical effects associated with radioactive decay may be responsible for the highly fractured structure of the FYR-274 zircons.

The monazite data point is concordant within analytical uncertainty at 2596 ± 3 Ma, the calculated ages agreeing within 0.2% (Table 14.1). The $^{207}Pb/^{206}Pb$ age, being the most accurately measured, is the stated result.

Discussion

The age of the basement gneiss is defined by the three collinear data points from FYT-905 (Fig. 14.2), which have a 17% probability of fit to a chord which cuts concordia at 2989 +6/-5 and 804 +13/-12 Ma (Davis, 1982). The zircon morphology suggests that this is the primary age of an igneous precursor to the gneiss. Faint euhedral zoning is present in the prismatic zircon crystals, indicative of igneous magmatic genesis, while the sharp terminations and absence of overgrowths or corrosion attest to the lack of metamorphic alteration. Thus the zircon of FYT-905 apparently grew in an igneous environment but was not visibly affected by subsequent development of gneissosity. This age agrees with the Rb-Sr whole-rock isochron age of 2939 ± 50 Ma within analytical uncertainty.

The data point for the +93 μm unabraded zircon fraction of FYR-274 falls on the FYT-905 chord (Fig. 14.2); regression of the four points yields an upper intercept age of 2990 +6/-5 Ma with an improved (23%) probability of fit. The +74 μm data point from FYR-274 falls slightly below either of the above chords.

The data points for the two finest zircon fractions from FYR-274, -74 +64 and -44 μm, lie above the FYT-905 chord. Two alternative explanations may be given for this.

1. Due to the very high U contents of these fractions (Table 14.1), primary lead loss may have occurred earlier than in FYT-905 zircon (ca. 804 Ma), thus establishing these points on lead loss chords above that of FYT-905.
2. Some lead loss may have occurred from these high U zircons at ca. 2596 Ma, at the peak of thermal metamorphism as indicated by the concordant monazite result. The observed systematics would then have resulted from a two stage (2596, 804 Ma) lead loss process with minor recent lead loss also a possibility.

The data point for the +93 μm abraded fraction falls to the right of the FYT-905 chord. Two alternative explanations are suggested for the position of this point.

1. A small component of centrally located inherited radiogenic lead may be present in the +93 μm zircon. This fraction was heavily abraded leaving only the very central portion of the original zircon grains extant. A small amount of 3150 Ma zircon Pb for example (Krogh and Gibbins, 1978), would be sufficient to cause the point to fall to the right of the chord. No cores were seen within the zircon grains analyzed but work in this laboratory has indicated that a small proportion of cores may not be easily visible under transmitted light.
2. Alternatively, the heavy abrasion might have concentrated central zircon material that did not lose lead until recent time. The $^{207}Pb/^{206}Pb$ age of this fraction, 2990 Ma, is essentially indentical to the FYT-905 upper intercept age. The location of the data point would be explained by recent lead loss from 2989 Ma zircon. For this explanation to apply, however, the central portion of all the abraded grains must have avoided lead loss at ca. 800 Ma. As this occurrence is unlikely, and since the +93 μm unabraded fraction shows no indication of inherited lead, the authors do not find either explanation entirely satisfactory.

The concordant 2596 ± 3 Ma monazite age dates the peak of Kenoran thermal metamorphism in this area. The FYT-905 and coarser grain size FYR-274 zircon results show no evidence of lead loss due to this event despite the high U contents (greater than 800 ppm in some instances).

Petrogenesis

Models for the evolution of the Slave Structural Province include either simatic or ensialic volcanism. Folinsbee et al. (1968) suggested that simatic island-arc volcanism, which in a present day setting would be attributed to crustal subduction, was the mode of volcanism in the Archean Slave Province. However, Pettijohn (1970) and Henderson (1972) have pointed out that the quartz content of the Yellowknife Supergroup metasedimentary greywackes-mudstones are too high to have a simple basic volcanic provenance. This promoted other workers (McGlynn and Henderson, 1970; Henderson, 1981; Frith and Roscoe, 1980) to support an ensialic model. The results of this study, and the mounting accumulation of data giving ages older than the Yellowknife Supergroup (at least in the western regions of the Slave craton), support this viewpoint.

Acknowledgments

The authors thank R.D. Stevens for the initial zircon separations and morphological descriptions and R.W. Sullivan for helping with the analytical work. Janet King kindly reviewed the manuscript.

References

Baragar, W.R.A.
1966: Geochemistry of the Yellowknife Supergroup volcanic rocks; Canadian Journal of Earth Sciences, v. 3, no. 1, p. 9-30.

Bowring, S.A. and van Schmus, W.R.
1984: U-Pb zircon constraints on evolution of Wopmay Orogen, NWT; in 1984 Joint Annual Meeting of the Geological Association of Canada and the Mineralogical Association of Canada, Volume of Abstracts, London 1984, p. 47.

Chamberlain, V.E., Lambert, R. St. J., Bradley, M., and Marten, B.E.
1984: Archean zircon ages for tonalite gneisses, Coppermine River area, N.W.T.; in 1984 Joint Annual Meeting of the Geological Association of Canada and the Mineralogical Association of Canada, Volume of Abstracts, London 1984, p. 51.

Davis, D.W.
1982: Optimum linear regression and error estimation applied to U-Pb data; Canadian Journal of Earth Sciences, v. 19, no. 11, p. 2141-2149.

Folinsbee, R.E., Baadsgaard, H., Cumming, G.L., and Green, D.C.
1968: A very ancient island arc; in The Crust and Upper Mantle of the Pacific Area, ed. L. Knopoff, C.L. Drake, and P.J. Hart; American Geophysical Monograph, v. 12, p. 441-449.

Frith, R.A.
1980: Rb-Sr age of the Cotterill Lake granites, Indin Lake area, District of Mackenzie; in Rubidium-strontium and uranium-lead isotopic age studies, Report 3; in Current Research, Part C, Geological Survey of Canada, Paper 80-1C, p. 234-236.

Frith, R.A., Frith, R., Hemstaedt, H., Hill, J.D., and Leatherbarrow, R.
1974: Geology of the Indin Lake area (NTS 86B) District of Mackenzie, in Report of Activities, Part A, Geological Survey of Canada, Paper 74-1A, p. 165-171.

Frith, R. and Loveridge, W.D.
1982: Ages of Yellowknife Supergroup volcanic rocks, granitoid intrusive rocks and regional metamorphism in the northeastern Slave Structural Province; in Current Research, Part A, Geological Survey of Canada, Paper 82-1A, p. 225-237.

Frith, R.A. and Roscoe, S.M.
1980: Tectonic setting and sulphide deposits of the Hackett River Belt, Slave Province; Canadian Mining and Metallurgical Bulletin, v. 73, no. 815, p. 143-153.

Frith, R., Frith, R.A., and Doig, R.
1977: The geochronology of the granitic rocks along the Bear-Slave Province boundary, northwest Canadian Shield; Canadian Journal of Earth Sciences, v. 14, no. 6, p. 1356-1353.

Henderson, J.B.
1972: Sedimentology of Archean turbidites at Yellowknife, Northwest Territories; Canadian Journal of Earth Sciences, v. 9, no. 7, p. 882-902.

1981: Archean basin evolution in the Slave Province, Canada; in Precambrian Plate Tectonics, ed. A. Kroner; Elsevier, Amsterdam, p. 213-235.

Henderson, J.B., Loveridge, W.D., and Sullivan, R.D.
1982: A U-Pb study of zircon from granitic basement beneath the Yellowknife Supergroup, Point Lake, District of Mackenzie; in Rb-Sr and U-Pb Isotopic Age Studies, Report 5, in Current Research, Part C, Geological Survey of Canada, Paper 82-1C, p. 173-178.

Heywood, W.W. and Davidson, A.
1969: Geology of Benjamin Lake map-area, District of Mackenzie; Geological Survey of Canada, Memoir 361.

Hoffman, P.
1973: Evolution of an early Proterozoic continental margin; the Coronation Geosyncline and associated aulacogens of the Northwestern Canadian Shield; Royal Society of London, Philosophical Transactions, Part A, v. 273, p. 547-581.

1980: Wopmay Orogen: a Wilson cycle of early Proterozoic age in the northwest of the Canadian Shield; in The Continental Crust and its Mineral Deposits, ed. D.W. Strangway; Geological Association of Canada, Special Paper 20, p. 523-549.

Krogh, T.E.
1982: Improved accuracy of U-Pb zircon ages by the creation of more concordant systems using an air abrasion technique; Geochimica et Cosmochimica Acta, v. 46, p. 637-649.

Krogh, T.E. and Gibbons, W.
1978: U-Pb isotopic ages of basement and supracrustal rock in the Point Lake area of the Slave Structural Province, Canada; in 1978 Joint Annual Meeting of the Geological Association of Canada, Mineralogical Association of Canada and the Geological Association of America, Volume of Abstracts, Toronto 1978, p. 438.

Loveridge, W.D.
1986: U-Pb ages on zircon from rocks of the Lac de Morhiban map area, Quebec; in Current Research, Part A, Geological Survey of Canada, Paper 86-1A, Report 63.

McGlynn, J.C. and Henderson, J.B.
1970: Archean volcanism and sedimentation in the Slave Structural Province; in Symposium on Basins and Geosynclines of the Canadian Shield, ed. A.J. Baer; Geological Survey of Canada, Paper 70-40, p. 31-44.

Nikic, Z., Baadsgaard, H., Folinsbee, R.E., Krupicka, J., and Payne-Leech, A.
1980: Boulders from the basement, the trace of an ancient crust; Geological Society of America, Special Paper 182, p. 169-174.

Pettijohn, F.J.
1970: The Canadian Shield – a status report; in Symposium on Basins and Geosynclines of the Canadian Shield, ed. A.J. Baer; Geological Survey of Canada, Paper 70-40, p. 239-255.

Scharer, U. and Allègre, C.J.
1982: Investigation of the Archean crust by single grain dating of detrital zircon: a greywacke of the Slave Province, Canada; Canadian Journal of Earth Sciences, v. 19, no. 10, p. 1910-1918.

Steiger, R.H. and Jaeger, E.
1977: Subcommission on Geochronology: convention on the use of decay constants in geo- and cosmochronology; Earth and Planetary Science Letters, v. 36, p. 359-362.

Stockwell, C.H.
1933: Great Slave Lake-Coppermine area, Northwest Territories; Geological Survey of Canada, Summary Report for 1932, p. 37-63.

St-Onge, M.R., King, J.E., and Lalonde, A.E.
1984: Deformation and metamorphism of the Coronation Supergroup and its basement in the Hepburn metamorphic-plutonic zone of Wopmay Orogen: Redrock Lake and the eastern portion of Calder River map areas, District of Mackenzie; in Current Research, Part A, Geological Survey of Canada, Paper 84-1A, p. 171-180.

Appendix

Zircon and Monazite Morphology

FYT-905: Zircon from FYT-905, consists predominantly of euhedral, doubly terminated crystals. Two morphologies were noted:

Prismatic crystals with length to breadth ratios of 2 to 4 made up about 20% of the total. The crystals are mostly clear and prismatic with faint growth zoning, especially evident under crossed-nicols. No overgrowths were observed. Some twinning crystals were noted in 'v' and 'x' configuration. Grain sizes varied but were not much greater than 105 μm.

Equidimensional crystals – three sub-types were noted:

a. Buttons; these grains are pink to buff, clear as a gem with no overgrowths and well faceted.

b. Short, clear prisms; these grains are short and stubby, light brown and are mostly inclusion-free. Faint zoning is evident in crossed-nicols.

c. Short, transluscent prisms; These grains are similar in shape to (b) but are more opaque, fractured with goethite staining and commonly have a dark brown to black overtone. These were possibly more metamict and mostly discarded.

Assessment: Although two distinct type were noted, there were gradations between both types. It is noteworthy that neither type had overgrowths and that metamictization only affected some of the equidimensional type.

FYR-274: The initial zircon concentrate from this sample contained more than 90% golden to amber zircon crystals, generally euhedral with blunt to rounded terminations. Concentric zoning was clearly visible in most crystals and internal fractures were abundantly present, a major characteristic that partially obscures other internal structure. Small dark equidimensional inclusions are visible in most grains. Thin overgrowths of pale pink clear zircon are present on some grains and rare grains appear to be composed of the same clear pink, less fractured zircon. No cores ascribable to pre-existing zircon crystals were seen. Most grains exhibited corroded and pitted surfaces and parallel growth twins were observed. Length to breadth ratios ranged from 1.2:1 to 3.4:1.

Monazite from FYR-274 consisted of rounded equant to egg-shaped grains with roughly pitted to granular earthy brown surfaces. A few of the grains appeared to be sheathed in a lighter brown envelope but most were opaque except for smaller sizes which were translucent. Internal fractures and dark nucli were observed in many of the translucent grains.

Sedimentology and paleoclimatology of the Huronian (Early Aphebian) Lorrain and Gordon Lake Formations and their bearing on models for sedimentary copper mineralization

Project 760027

F.W. Chandler
Precambrian Geology Division

Chandler, F.W., Sedimentology and paleoclimatology of the Huronian (Early Aphebian) Lorrain and Gordon Lake formations and their bearing on models for sedimentary copper mineralization; in Current Research, Part A, Geological Survey of Canada, Paper 86-1A, p. 121-132, 1986.

Abstract

The Early Aphebian Cobalt Group consists in ascending order of the Gowganda, Lorrain, Gordon Lake and Bar River formations. Quartz arenite of the upper part of the Lorrain is alluvial in origin and achieved its mineralogical maturity through diagenetic leaching. Red, fine grained sandstone at the base of the Gordon Lake Formation was deposited in a coastal sabkha. Relict anhydrite inclusions and various evaporite-related forms of silica minerals are evidence of the origin of the replacement products even in metamorphosed rocks.

The bulk of the Gordon Lake Formation consists of turbidite-like units that are deposited as upward-fining, flat laminated storm cycles of varied scales on a storm-dominated marine shelf. Glauconite and pyritized chamosite are widespread through the formation but do not define an inshore-offshore zoning.

During deposition of the upper part of the Lorrain Formation, and of the Gordon Lake formation, the paleoclimate was probably warm and relatively dry. Stratabound, disseminated copper mineralization, at the boundary of the Lorrain and Gordon Lake formations may have been leached from the upper part of the Lorrain Formation.

Résumé

Le groupe de Cobalt de l'Aphébien inférieur est constitué dans l'ordre ascendant des formations de Gowganda, de Lorrain, de Gordon Lake et de Bar River. L'arénite quartzifère de la partie supérieure de la formation de Lorrain est d'origine alluviale; elle a atteint sa maturité minéralogique par lixiviation diagénétique. Un grès rouge, à grains fins, situé à la base de la formation de Gordon Lake, a été mis en place dans une sebkha littorale. Des inclusions résiduelles d'anhydrite et diverses formes, apparentées aux évaporites, de minéraux siliceux sont la preuve de l'origine des produits de substitution, même dans les roches métamorphisées.

La majeure partie de la formation de Gordon Lake se compose d'unités ressemblant à des turbidites dont la sédimentation s'effectue sous forme de cycles de tempête de différentes échelles caractérisés par des couches plates affinées vers l'amont et se produisant sur une plate-forme marine fouettée par des tempêtes. On trouve de la glauconite et de la chamosite pyritisée réparties dans toute la formation, mais elles ne caractérisent pas une zonation littorale au large.

Au cours de la sédimentation de la partie supérieure de la formation de Lorrain et de la formation de Gordon Lake, le paléoclimat était probablement chaud et relativement sec. Une minéralisation en cuivre disséminée et limitée par les strates, située à la limite des formations de Lorrain et de Gordon Lake, peut avoir été lixiviée depuis la partie supérieure de la formation de Lorrain.

Introduction

This paper is the second progress report (Chandler, 1984) on the geological setting of stratabound copper mineralization in the Huronian Cobalt Group. The Huronian Supergroup consists of up to 10 km of mainly clastic sediments 2.3-2.45 Ga old (Frarey et al., 1982; Krogh et al., 1984) the youngest group of which, the Cobalt Group, is the most widespread (Fig. 15.1), overlapping north over the Archean granitic basement.

Sparse, sabkha-related stratabound copper mineralization lies at the boundary between the Lorrain and Gordon Lake formations in the Flack Lake area (defined as north of the Flack Lake Fault). Common association of this type of mineralization with evaporites (Gustafson and Williams, 1981) suggests a hot and at least seasonally dry paleoclimate. In the Flack Lake area, however, the Lorrain Formation has been interpreted as deposited under a hot wet (bauxite-forming) climate and the overlying Gordon Lake Formation under a dry periglacial climate (Wood, 1973). This indicates a new climatic variant for the above form of mineralization. Casshyap's (1969) suggestion that the Gordon Lake Formation is a distal equivalent of the Lorrain, and more generally Walther's Law would seem to disagree with this drastic climate change. Any attempt to resolve the above question would be bedevilled by marked disagreement on the depositional environments of the Lorrain Formation, especially the upper quartz arenite member and of the Gordon Lake Formation. The present study was undertaken in part to resolve these inconsistencies.

Information was drawn from some of the better exposed parts of the Gordon Lake Formation; near Flack Lake, in Narrow Bay and from some previously unstudied exposures at Welcome Lake (Fig. 15.1). Diamond drill core from the Flack Lake area, at present stored by the Ontario Ministry of Natural Resources at Sault Ste. Marie was also examined. This consists of material submitted by Canadian Johns Manville Ltd. (hole no. 157-68-1), by Sutherland and Associates from Stag Lake and some core drilled over the winter 1983-1984 by Canamax Resources Ltd.

This report features (a) a description of the exposures of the Gordon Lake Formation at Welcome Lake; (b) a new interpretation of the sedimentology of the Gordon Lake Formation; and (c) a new, simpler and internally consistent paleoclimatic model for the Lorrain and Gordon Lake formations.

Previous work

The Cobalt Group consists of four mutually conformable formations in ascending order, the Gowganda, Lorrain, Gordon Lake and Bar River (Fig. 15.1). The Gowganda Formation has a mainly ortho- and paraconglomeratic lower part and an upper part comprises mainly sandstone and argillite. It is generally believed to have been deposited in a range of glacially-related environments (Lindsey, 1969; Young, 1970).

The Lorrain Formation can be divided regionally into a lower feldspathic sandstone member, a middle quartz or jasper pebble conglomerate-bearing member and an upper quartzite member (Wood, 1973; Young, 1973). Its depositional environments have been much disputed and opinions range from alluvial fan, fluvial and eolian to beach and shallow marine. Assignment of depositional environments for the quartz arenite member has rested on interpretations of textural and mineralogical maturity and on cross-bed paleocurrent patterns.

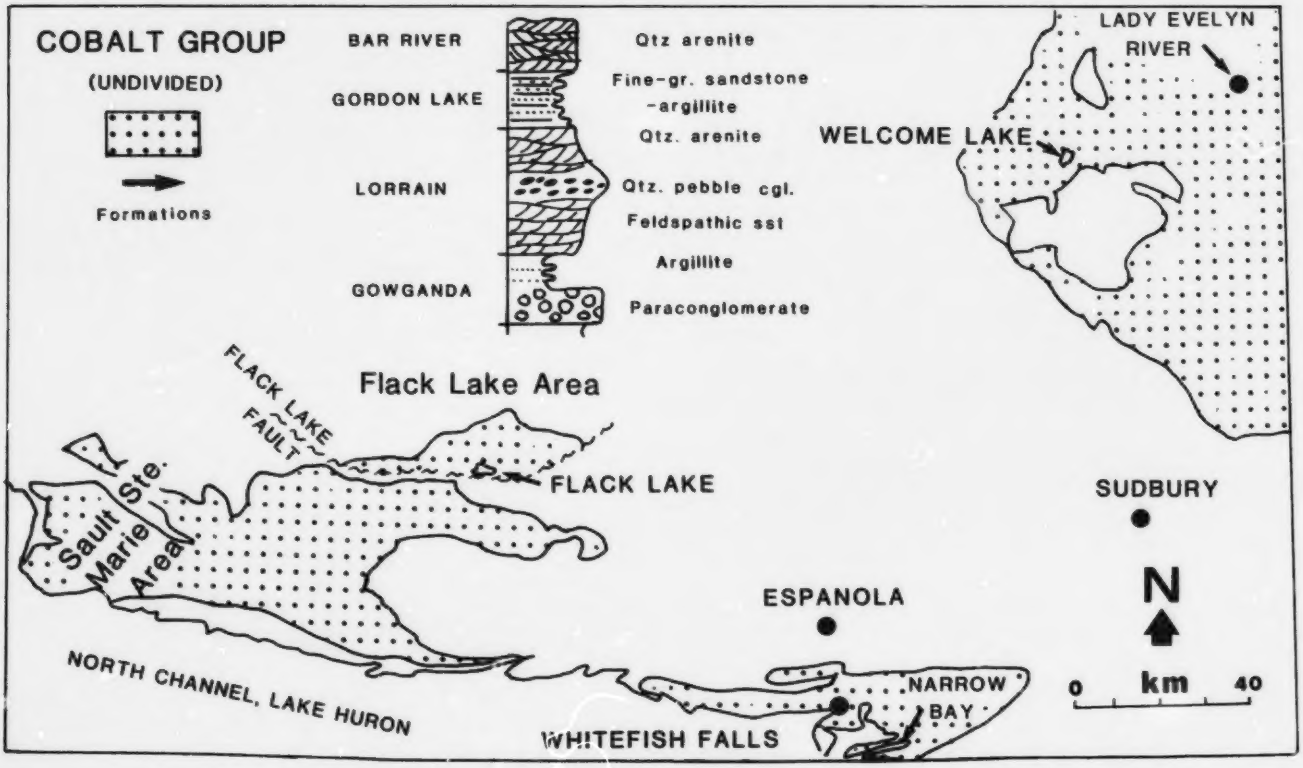

Figure 15.1. Location map for part of the Cobalt Group, Ontario, with generalized stratigraphic column.

From textural maturity Card (1970, 1978), Hadley (1968), Siemiatkowska (1977) and Young (1973) suggested beach or shallow marine environments. There is however evidence that the upper member is, in some places at least, texturally immature. Wood (1970) commented that in the Flack Lake area iron oxide dust trains on detrital quartz grains indicate a lower sphericity and roundness than would be expected from the mineralogical maturity. Siemiatkowska (1977) showed in her Table 6, samples from about 50 km west of Flack Lake of the upper member that are not texturally mature. Also, Chandler (1984) found angular zircon heavy mineral grains in quartz arenite from the top of this member as well as very angular quartz grains from drill core, both from the Flack Lake area. It might be significant that the Whitefish Falls area (south of Espanola) studied by Card (1978) is metamorphosed and deformed (e.g. Chandler, 1969, Plate 24) and is an area of which Casshyap (1971) wrote "that deformation and widespread pressure solution produced a highly condensed framework in which the original roundness of the detrital quartz is completely obscured".

Shallow marine and beach environments have been assigned to the upper member of the Lorrain Formation (Card, 1970, 1976; Casshyap, 1971; Hadley, 1968; Pettijohn, 1970a; Young, 1973) from evidence of high mineralogical maturity. There was, it seems, a general view at the time, typified by Pettijohn (1970b) who stated "All the known alluvial sands are immature – poorly rounded, generally arkosic or lithic sands". There were however some critics of this general concept. For example Frarey and Roscoe (1970) and Roscoe and Frarey (1970) regarded the Lorrain formation as alluvial and derived from a highly weathered source in which most feldspar had already been destroyed.

Pettijohn's (1970b) view is no longer held (Chandler, 1984, p. 190). However locally at least Frarey and Roscoe's conclusion requiries modification because feldspathic sandstone with fresh feldspars has been found by the writer at the top of the Lorrain Formation at Welcome Lake. Thus it is possible that the upper member of the Lorrain was feldspathic on deposition (see below).

Reports of sedimentary structures diagnostic of depositional environments from the upper member of the Lorrain Formation are conspicuously lacking. One example of opposed crossbeds was discovered by D. Long in 1985 at Welcome Lake. Although commonly taken as indicative of tidal marine influence, a single occurrence should be treated with circumspection especially as opposed crossbeds are known from fluvial environments (Alam et al., 1983).

Lowey (1985) who also used facies analysis, Frarey (1977), and Hadley (1968), all employed a unimodal paleocurrent pattern to infer that the Lorrain Formation is alluvial, a conclusion similarly derived by Wood (1970) for the upper member. Card (1978) thought the paleocurrent pattern from the upper member south of Espanola to be distinctly polymodal and therefore evidence of marine deposition. Card's data were taken from a deformed and metamorphosed area, an area from which Young (1966) has doubted the validity of paleocurrent patterns based on crossbeds, suggesting that deformation would impose collection bias. Although Siemiatkowska (1977) reported polymodal paleocurrents from the upper member 50 km west of Flack Lake, her Figure 10 that illustrates the point, shows a strongly unimodal pattern similar to that of Wood (1970). New data bearing on the depositional environment of the upper member of the Lorrain Formation are discussed below.

The Gordon Lake Formation is a sequence of thinly interbedded flat-bedded sandstone and graded and rippled siltstone and mudstone. From drill core Eisbacker and Bielenstein (1969) divided it into three members at Flack Lake, a lower unit of reddish, mottled quartz sandstone and siltstone, a middle unit of green argillite and chert and an upper unit of reddish-buff, mudcracked siltstone, argillite and rare chert. From exposure south of Espanola, Card (1978) divided the 1100 m thick formation into three intergradational units, a lower upward-fining sandstone-rich unit up to 90 m thick, a middle pelite-rich unit up to 900 m thick and an upper sandstone-rich unit up to 90 m thick.

From sedimentary structures including mudcracks and sedimentary breccia Frarey (1977) suggested a shallow marine to supratidal environment for the formation. Card (1976) and Siemiatkowska (1978) used desiccation cracks to advance a tidal flat origin, a view supported by Wood (1970, 1973) from the presence of sulphate nodules in the lower part of the formation and an occurrence of hematite oolites. Although Wood (1970) reinterpreted the abundant "mudcracks" of the formation as syneresis cracks, Card (1978) interpreted small scale sedimentary cycles as turbidites deposited entirely in deep water. Chandler (1984) agreed with Wood (1973) that the sulphate-bearing lower part of the formation was deposited on a sabkha but reinterpreted Card's (1978) small scale cycles as storm beds deposited on a storm-dominated marine shelf (Chandler, 1985), separating them from Bouma cycles by the presence, only in the storm beds of symmetrical wave ripples (Allen, 1982).

The Bar River Formation consists of up to 900 m of white or hematite-stained quartz arenite with minor siltstone (Card, 1976) with some subarkose at the top (Wood, 1970). Crossbeds and ripple marks have been widely reported from the formation (e.g. Card, 1978; Siemiatkowska, 1978; Wood, 1970).

Polymodal paleocurrents have been inferred from undivided sedimentary structures (Card, 1976; Wright, 1985), from crossbeds (Wood, 1970) and from ripple marks (Wright, 1985). These data, with the high maturity of the formation (Card, 1976; Pettijohn, 1970a), suggested a marine environment with recycling of sedimentary rocks (Card, 1976). Bimodal grain size, truncation of crossbed tops and northeast trend of linear ripple crests coupled with southward paleoflow in the upper member of the Lorrain Formation indicated to Wood (1970) that the Bar River Formation was deposited on an east-west oriented beach with eolian influence. Roscoe and Frarey (1970) however, finding no evidence of reversing currents, suggested that the spheroidal grains of the formation could have been inherited from a sub-Huronian regolith and argued for fluvial deposition of the Bar River Formation.

More recently Chandler (1984) found zircon concentrates from the Bar River Formation to be more mature than some from the top of the Lorrain Formation, suggesting a more intense abrasion history. He also reported apparent herringbone crossbeds and wave miniripples (Singh and Wunderlich, 1978), from the Flack Lake and the Welcome Lake (Fig. 15.2) areas. The above, with mudcracks, also noted by Wood (1970) suggested to Chandler (1984) a tidal marine environment with emergence of sand shoals. Wright (1985), from the first regional study of the formation found multidirectional ripple crests, herringbone crossbeds with reactivation surfaces, both supporting a tidally influenced marine environment.

Sedimentology

Sedimentary sequences and structures

The present study supports the division of the Gordon Lake Formation into three parts. Brecciation of mudstone layers, previously mentioned in the basal member is so

pronounced that few coherent layers remain. Brecciation, however, is also present intermittently throughout the middle member. Eisbacher and Bielenstein (1969) described the middle member as composed of argillite and chert but packets of fine sand beds are present at random throughout the member both in the Narrow Bay and Welcome Lake areas.

A syncline, centred on Welcome Lake, 80 km north of Sudbury, contains previously unstudied good exposures of the Gordon Lake and Bar River formations. A measured partial section on the northwest shore of the lake (D. Long, personal communication, 1985) allows for a thickness of 900 m of the Gordon Lake, similar to that of other areas (Frarey and Roscoe, 1970). The Welcome Lake area is of interest because unusual lithologies occur at the contact with the Lorrain Formation. Their composition sheds light on the paleoclimatic interpretation of the two formations.

Exposures of white-weathering sandstone at the top of the Lorrain Formation on the northwest shore of Welcome Lake are texturally immature, medium grained and contain abundant fresh microcline and plagioclase and some quartz and carbonate cement. Between this white unit of the Lorrain Formation and typical sandstone-mudstone cycles of the Gordon Lake Formation there is an unexposed stratigraphic thickness of about 105 m if there is no structural interference.

Farther west, on some offshore islands, two unusual units occupy this unexposed interval, a barite-cemented sandstone and an overlying red siltstone. The barite cemented sandstone, dips homoclinally into the lake and could be up to 100 m thick. It is a coarse- to very coarse-grained texturally immature subarkose, pink to red, with bleached layers 30-50 cm thick. The bleached layers are crowded with recessive patches of barite-cemented sandstone. The unit is crossbedded and contains one occurrence of herringbone crossbeds (Fig. 15.3). The red siltstone unit consists mainly of purple- to red quartz-rich very fine sandstone to siltstone with sericite or carbonate cement and irregular clots of hematite laths. Other minor lithologies associated with the red siltstone include impure carbonate and sandstone. The carbonate contains up to 25% of quartzofeldspathic silt and was seen only as a few isolated blocks on the shoreline. The sandstone is orange-red, light green-purple and light pink. It is crossbedded with about 20% of light grey to green wave-rippled siltstone. The red siltstone

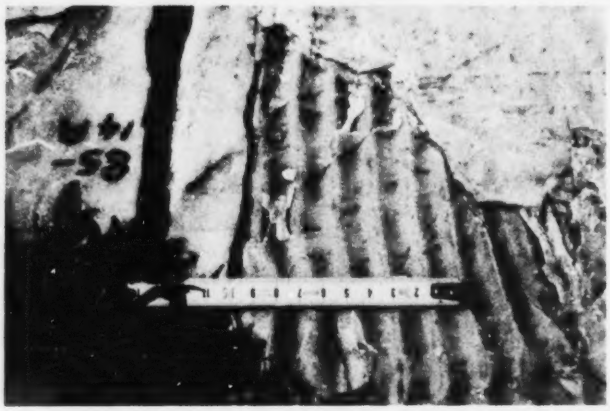

Figure 15.2. *Wave mini ripples in the Bar River Formation, Welcome Lake, indicative of near emergency. (203989D)*

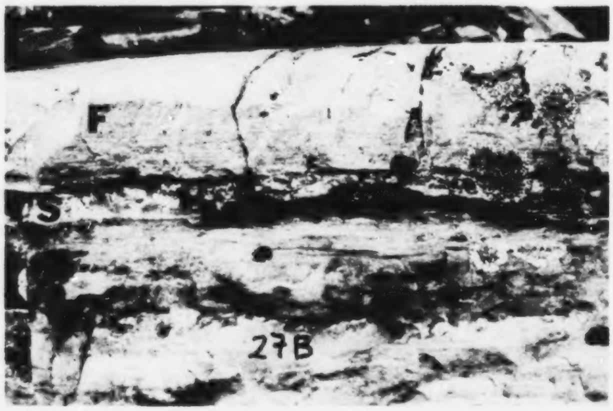

Figure 15.4. *Flat laminated storm bed, 15 cm thick (F), Gordon Lake Formation, Welcome Lake, overlying with scoured base, syneresis – cracked siltstone(s). (203989I)*

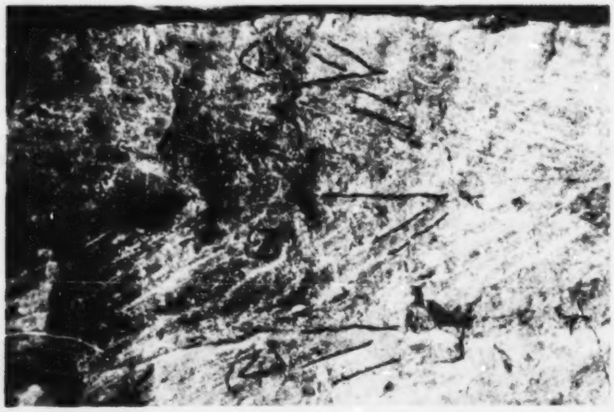

Figure 15.3. *Opposed crossbeds in barite-cemented feldspathic sandstone at the top of the Lorrain Formation, Welcome Lake. Sets are marked 1 to 4. Forsets are picked out by black magic marker. (203989C)*

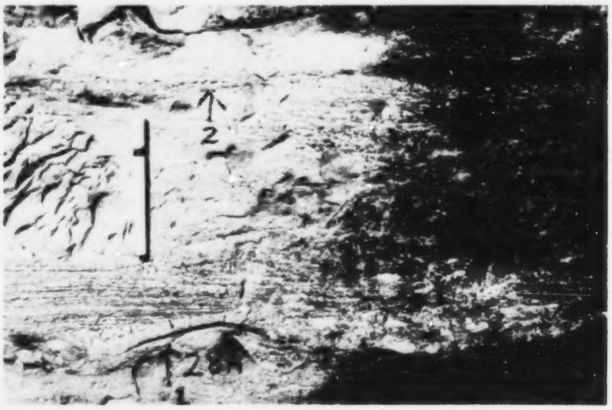

Figure 15.5. *Nested storm beds of mixed fine grained laminated sandstone and mudstone-pebble breccia, Gordon Lake Formation, Welcome Lake. Arrows mark scoured base and top of a 22 cm-thick bed. Concave-up laminae near the top of the bed on right side of figure could be hummocky or swaley crossbedding. (203989R)*

unit is arranged in a gently dipping syncline and its top is not exposed, but from information above the unit is likely quite thin.

The drab, variably pyritic middle member of the formation is dominated by interstratified siltstone flat-bedded fine sand beds, and graded, laminated, rippled and brecciated and syneresis-cracked siltstone and mudstone.

The thickest sand beds are generally 10-50 cm thick and, where complete, fine upward to pale green mudstone. The base may be scoured and overlain by angular pebbles of green mudstone eroded from previous bed tops. The lower part of the bed is commonly horizontally laminated (Fig. 15.4) or may contain low angle (about 5°) crossbedding. Where not truncated by erosion the upper part of the sand unit may contain symmetrical or assymetrical linear wave ripples, current ripples, interference or climbing ripples, the last rare. The rippled interval is terminated by a graded green mudstone layer with syneresis cracks. These sand beds are present throughout the formation and can dominate intervals up to 25 m thick even in the middle of the formation where they can be stacked due to syndepositional erosion and brecciation of the upper part of each cycle (Fig. 15.5). At Narrow Bay these units are drab, but at Welcome Lake where the rocks are unmetamorphosed the sand beds are coloured red up to 300 m into the formation. The upper and lower margins of the sand beds appear to have been reduced to the pale green-grey colour of the contiguous sediments. In some cases the bed has a pinch and swell appearance (Fig. 15.6). Inspection of bedding surface exposure shows this pinch and swell form to have an amplitude of about 10 cm, a wavelength of about 2 m and to be hummocky in form (Fig. 15.7). The sand beds are interpreted to be storm beds transported offshore from the oxidized nearshore zone, by storm-related bottom currents. The pinch-and-swell structure is interpreted as hummocky crossbedding, caused by storm waves. Water escape structures (Fig. 15.8) in some of the sand beds are evidence of loose grain packing caused by rapid deposition. Although commonest in turbidites they have also been recognized from shallow water sediments (Collinson and Thompson, 1982). The above sand beds are the thickest of a series of upward fining units deposited by powerful storms. At its thinnest the upward-fining unit may be represented by units 3-5 cm thick

Figure 15.6. Pinch and swell structure defining top and base of sand bed (arrow points up), Gordon Lake Formation, Narrow Bay. Bed is about 25 cm thick. Structure interpreted as hummocky crossbedding. (203989F)

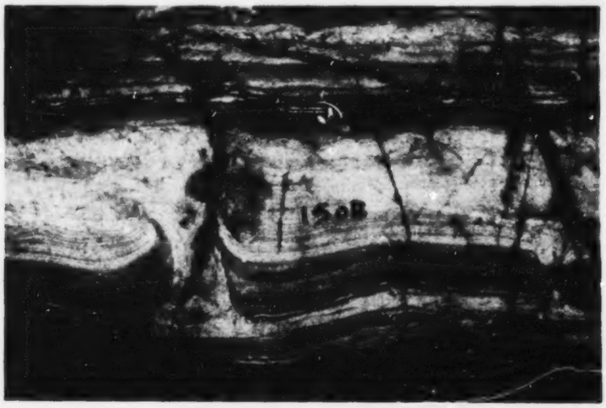

Figure 15.8. Water escape structure in fine grained laminated sandstone, Gordon Lake Formation, Narrow Bay. Thin graded storm beds (T) overlie deformed bed. (203989E)

Figure 15.7. View along bedding surface of nested storm beds, Gordon Lake Formation, Welcome Lake, shows hummocky surface of beds, believed to have been formed by storm waves. (203989G)

Figure 15.9. Thin storm beds, Gordon Lake Formation, Narrow Bay. Irregular white discordant laminae in upper mudstone part of thicker (upward pointing arrows) beds are syneresis cracks. Note some beds have broken into load casts(L). (203989K)

Figure 15.10. Rippled unit, Gordon Lake Formation, Narrow Bay. Wave ripples of lenticular bedded fine sand are separated by syneresis-cracked mud layers. Upper half of figure is composed of base of flat-laminated sandstone storm bed. (203989H)

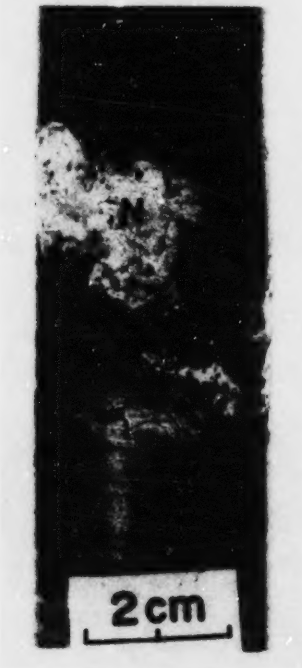

Figure 15.11. Quartz-rimmed, enterolithic calcite nodules (N) in drill core, Gordon Lake Formation, Flack Lake area, believed to have replaced anhydrite nodules. (4303A)

with thin rippled or laminated sand base overlain by graded, syneresis cracked green mudstone (Fig. 15.9). These thinner units are regarded as deposited by weaker storms. They strongly resemble similarly interpreted recent units from the North Sea (Allen, 1982, Fig. 12-10). Intervals are rarely more than 20 cm thick and are composed of lenticular bedded current or wave-rippled fine sand. Mud laminae separating the ripples are commonly syneresis cracked (Fig. 15.10). These units are probably caused by weak waves and currents with a variety of origins.

Fine- to medium-grained crossbedded sandstone occurs throughout the Gordon Lake Formation. With green mudstone-pebble layers, it is common in the anhydrite-nodule bearing lower part of the formation. Within the storm bed-dominated middle part of the formation it is rare and usually restricted to single beds. An upward-coarsening sequence of mainly crossbedded sandstone is transitional to the overlying Bar River Formation.

Sulphate nodules and their replacement products

Sulphate nodules are characteristic of coastal tidal flats (coastal sabkhas) in hot dry regions such as the Persian Gulf, where they occur through the evaporative concentration of interstitial groundwater (Kinsman, 1969). Because stratabound marine transgression-related copper mineralization commonly occurs with evidence of evaporites (Gustafson and Williams, 1981), presence of such nodules in a sequence is a useful exploration guide.

Nodular anhydrite in the Cobalt Group has so far only been reported from drill core from the Flack Lake area (Eisbacher and Bielenstein, 1969). It has been regarded as a strictly local phenomenon (Sims et al., 1981). Wood (1973) found chert nodules with the anhydrite nodules in the Flack Lake core and was unable to establish a genetic connection between them. Examination of three drill cores from the Canamax drilling showed that 18-22 separate nodule horizons are present over a stratigraphic interval of 35-40 m, most apparently siliceous. In the core drilled by Canadian Johns Manville 28 anhydrite nodule zones and 8 zones of siliceous nodules occur over 60 m. Some of the nodules are enterolithic (Fig. 15.11) and one nodule zone showed chickenwire texture.

There are many reported examples of the replacement of sulphate nodules by carbonate, quartz and microcrystalline silica in both Phanerozoic (Milliken, 1979) and Proterozoic (Muir, 1979) rocks. Apart from the stratigraphic association with anhydrite nodules there are several features in the siliceous nodules of the above drill core that suggest that they have formed by replacement of the anhydrite nodules. These include the presence of length-slow chalcedony (Folk and Pittman, 1971), relict laths and rounded and orthogonal granules of anhydrite in the replacing quartz crystals (Fig. 15.12) (identification by electron microprobe and petrographic microscope) and presence of flamboyant megaquartz (Milliken, 1979; Tucker, 1976; Young, 1979). Pure calcite (electron microprobe analysis) associated with the silica minerals may have been formed by solution of the anhydrite.

Realization that the siliceous nodules in drill core at the base of the Gordon Lake Formation are silicified evaporite nodules prompted a search for similar nodules in exposure. They were found at Welcome Lake, on the Lady Evelyn River (Fig. 15.13) 200 m east of the west boundary of McGiffin Township and in Narrow Bay (Fig. 15.14). In all cases they contain anhydrite relicts (Fig. 15.15). The occurrence in Narrow Bay is of interest because the nodules have survived deformation and regional metamorphism to the upper greenschist facies (Card, 1976).

Chamosite and glauconite

Another feature of the Gordon Lake Formation is the presence of likely chamosite oolites and altered glauconite peloids. Crudely oolitic chamosite in the Gordon Lake Formation from the Sault Ste. Marie area suggested to Pirie (1961) a marine environment for all or part of the formation. One exposure in the Flack Lake area (Wood, 1970) yielded hematite oolites and pellets of muscovite-sericite and of a colourless mineral of low birefringence, possibly chamosite.

Oolites and peloids are present as minor constituents of sandstone beds from drill core and from outcrop of the Gordon Lake Formation, from the Flack Lake and Lady Evelyn River and Welcome Lake areas. In the upper and lower redbeds transitional to the Bar River and Lorrain formations they consist of limonite and hematite, but in the drab pyritic middle member of the Gordon Lake Formation they consist of two types: (a) pyritized chamosite oolites in which the internal concentric structure (Fig. 15.16) is defined by almost submicroscopic pyrite grains (Fe and S determined by electron microprobe) and (b) botryoidal grains composed of K-mica (electron microprobe) that is structureless, colourless to brown and very fine grained. The K-mica peloids possess irregular shrinkage cracks (Fig. 15.17) reminiscent of the shrinkage cracks that are common in glauconite (McRae, 1972).

The writer has found that the chamosite and glauconite-like grains both occur throughout the formation apart from the thin upper and lower oxidized members. Therefore there is no apparent separation in the middle member into an inshore chamosite zone and an offshore glauconite zone, such as are found on modern marine shelves (Van Houten and Purucker, 1984).

Chamosite and glauconite are most common on marine shelves (Van Houten and Purucker, 1984). Their presence throughout the bulk of the Gordon Lake Formation is interpreted as evidence of a marine shelf environment for the bulk of the formation. Presence of hematite oolites in red

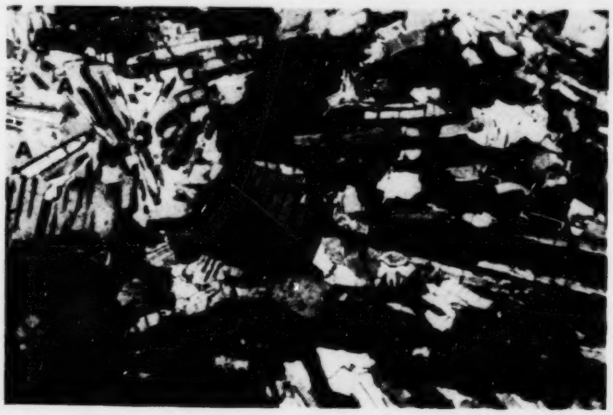

Figure 15.12. Partial silicification of anhydrite nodule, Gordon Lake Formation, Flack Lake area. Lightly grey equant quartz grain (A) near margin of nodule (out of figure to the left) encloses early laths of anhydrite. To the right, anhydrite laths are being replaced by granular anhydrite (B). (203989O)

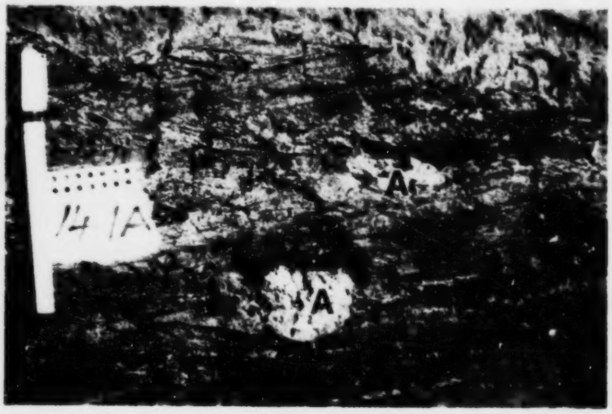

Figure 15.14. Quartz nodules (A) containing relict anhydrite (see Fig. 15.15), in Gordon Lake Formation, Narrow Bay, at upper greenschist facies of regional metamorphism. (203989M)

Figure 15.13. Jasper nodules, about 15 cm long (dark) rimmed by common white granular quartz (arrowed) in green mudstone of Gordon Lake Formation. Near Lady Evelyn River nodules contain relict crystals of anhydrite. (203989L)

Figure 15.15. Recrystallized chert? in quartz nodule of Figure 15.14, Gordon Lake Formation, Narrow Bay. Relict square inclusions of anhydrite (arrowed). Grain at centre is 0.05 mm across.

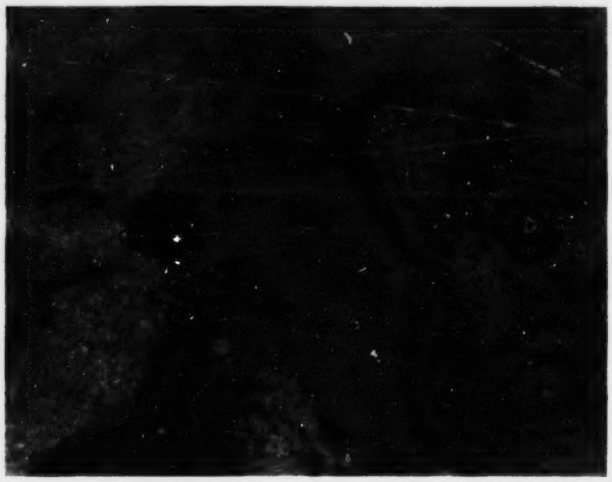

Figure 15.16. *Chamosite oolite in sandstone, 0.26 mm long, Gordon Lake Formation, from drill core, Flack Lake area. Concentric structure in grain is traced by fine grained pyrite crystals (black). (85-46)*

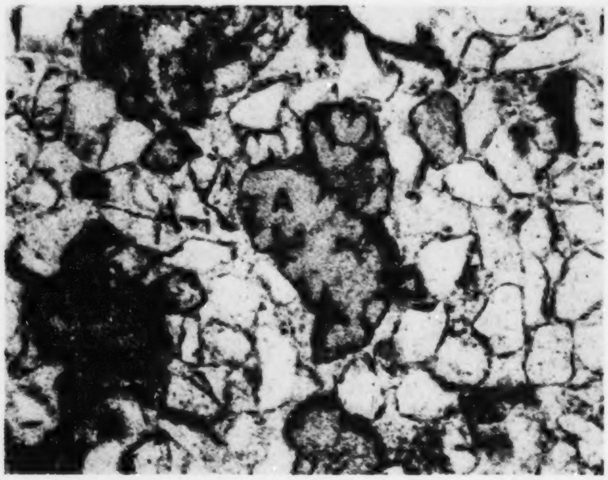

Figure 15.17. *Altered glauconite ? grains (mid-grey) in sandstone storm bed, Gordon Lake Formation, Welcome Lake. Grain in centre (A) 0.44 mm long, has botryoidal outline and cracks reminiscent of glauconite. Grains are now composed of K-mica. (85-12)*

storm beds in the lower middle member of the formation with reduced margins at Welcome Lake can be easily explained under Allen's (1982, p. 505) model for offshore transport of sand and during storms.

If the hematite oolites reported by Wood (1970) did not come from the upper or lower members it is also possible that they formed during Phanerozoic uplift and erosion, from either chamosite or glauconite grains.

Stable Isotopes

Pyritic beds in the Gordon Lake Formation

Pearson (1980) suggested that the reason for the weak stratabound copper mineralization at the base of the Gordon Lake Formation is the lack of suitable reductants. Examination of core drilled by Canamax Resources Ltd. indicated that the bulk of the formation is pyritic, some parts markedly so. One bed traced over a strike length of 3.8 km and about 1 m thick contains hand specimens with about 50% of pyrite. The sulphide examined under the microscope appears either ideomorphic or has the appearance of rounded clasts. Petrographic evidence indicates that some of the pyrite at least has acquired its form from chamosite pellets which it has replaced (Fig. 15.16). Hartmann and Nielsen (1969) presented isotopic and other evidence that pyrite in marine sediments commonly forms in the upper few tens of centimetres of newly deposited material by the activity of sulphate reducing bacteria. This process leaves as its signature a spread in the ratio of light and heavy sulphur isotopes with a concentration of the light isotope if the system is not closed. Monster et al. (1979) reasoned that the process has been in force for at least 2.75 Ga.

Hattori et al. (1983) in a study of atmospheric evolution found pyrite of the Gordon Lake Formation to have a spread of $^{34}\delta$ S of -10.6 to +7.6, in keeping with the above concepts. The pyrite-rich bed mentioned above was sampled because it is possible that the stratabound copper sulphide mineralization in the Gordon Lake Formation is related to the Nipissing diabase sills that cut the Cobalt Group. Over a strike length of 3.8 km it yielded $^{34}\delta$ S values of +3.4, +4.2, +4.6, +4.6, +4.9 and +6.0. A sample from a pyritic sandstone bed 12 m above gave a value of +6.0. The very narrow spread of these values does not support a biological mechanism of pyrite formation. The average of the first 5 data at +4.2 is very close to the value for the Nipissing diabase that intrudes the formation and coincides with the value for mafic igneous rocks of Holser and Kaplan (1966).

At this early stage of the investigation the writer can only suggest that the pyrite did not have a simple biogenic origin and that the bed was an open system. Possible sources include unmodified igneous sulphur or a mixture of biogenic sulphur and sulphur derived from dissolved anhydrite nodules.

Direction of movement of (ore forming?) groundwater

The cupriferous basal beds of the Gordon Lake Formation have been interpreted as sabkha in origin (Wood, 1973). The sabkha is a zone of mixing for solutions of continental and marine origin (Patterson and Kinsman, 1981). In modelling sabkha-related copper deposits Renfro (1974) suggested that evaporative updraw pulled copper-bearing solutions from terrestrial redbeds up into contact with reducing sabkha environments. It is therefore important in trying to model the sabkha-related copper mineralization at the base of the Gordon Lake Formation to determine the source and flow direction of the solutions potentially involved in depositing the copper. Cameron (1983) analyzed the Sr and S isotope ratios from 5 anhydrite nodules from the base of the Gordon Lake Formation in the Flack Lake area. The Sr isotope values $^{87}Sr/^{86}Sr$ range from 0.7365 to 0.7459 and were interpreted to mean derivation of the Sr from a continental brine. Sulphur isotope values $^{34}\delta S$ from +12.3 to +15.6 suggested minimum marine values with contamination from continental and other sources.

At Welcome Lake feldspathic sandstone at the top of the Lorrain Formation is cemented by barite. The sandstone is overlain by red siltstone at the base of the Gordon Lake Formation. General stratigraphic data, i.e. presence of an underlying alluvial formation and an overlying marine formation and the principle that Ba is immobile in sulphate rich environments, together suggest that Ba ought to have reached its present environment from below.

Sr and S isotope ratios were taken from two samples of the barite of the barite-cemented sandstone at the top of the Lorrain Formation. The $^{87}Sr/^{86}Sr$ ratio was 0.7131 and 0.7134 (preliminary analytical results, W.D. Loveridge). The $^{34}\delta S$ was +4.99 and +4.95.

Seawater of 2.3 Ga age was interpreted (Veizer and Compston, 1976) as having a $^{87}Sr/^{86}Sr$ ratio of 0.703. The $^{87}Sr/^{86}Sr$ of the barite, therefore, is too high to reflect marine derivation and could be explained, as in the case of Cameron (1983), by derivation from the underlying Archean granitic terrane or from feldspathic sandstones derived from them – i.e. the barite of the sandstone could be explained by diagenetic destruction of arkosic feldspar in the Lorrain Formation.

The uniform sulphur isotope ratios are lighter than those of Cameron (1983) and fit well with the mean value for continental igneous and metamorphic rocks of +4 from Holser and Kaplan (1966).

In summary, the strontium and sulphur isotope data suggest a basement source for the barite, i.e. an upward movement of groundwater. The heavier sulphur values than those of Cameron (1983) are consistent with the barite-cemented sandstone being lower in the stratigraphic column than the nodules sampled by Cameron and farther from the influence of marine sulphate.

Discussion: inferences for paleoclimate of the Cobalt Group

The evidence presented here suggests that data in support of a marine origin for the Lorrain Formation are suspect and that the formation is alluvial. Contrary to Wood's (1973) suggestion that the entire Gordon Lake Formation is a tidal flat deposit, the sedimentological evidence indicates that only the basal oxidized, mudstone-breccia and crossbed rich, sulphate nodule-bearing part was so deposited, the bulk of the formation being laid down on a fairly deep marine shelf, below the influence of currents that would transport sand as dune fields, but within the reach of storm waves and currents.

The Bar River Formation, a texturally mature quartz arenite with evidence of tidal currents and of emergence probably reflects a partial regression to an inner shelf environment. Its compositional and textural uniformity suggest deposition as an aggradational sand body (Galloway and Hobday, 1983, p. 164). Thus the sequence Lorrain-Gordon Lake-Bar River probably reflects marine transgression from the alluvial environment to outer shelf, followed by partial regression to inner shelf.

The glacigene origin of the Gowganda Formation (Young, 1970) is not seriously questioned. The succeeding Lorrain Formation consists of a lower feldspathic part overlain by quartz arenite in which the place of the feldspar has been taken by a range of aluminous minerals (Chandler et al., 1969; Wood, 1973; Young, 1973). This upward maturation has been explained by marine reworking (e.g. Card, 1976), by weathering in the source area (Roscoe and Frarey, 1970) or by synsedimentary bauxitization (Wood, 1973). Textural evidence discredits the first of these models. Wood (1973) used petrographic evidence including feldspar pseudomorphs in the lower part of the formation and intact framework and kaolinite grain coatings in the upper part of the formation to suggest that feldspar had not been deposited with the quartz arenite of the upper part. Chandler et al. (1969) however found that some of the kaolinite is postmetamorphic. Also sericite patches in the quartz arenite are the same size as quartz clasts. The presence of crushed feldspars indicates that some component of intact framework was caused by late compaction. Pearson (1980) reported feldspar from the upper part of the Lorrain Formation in the Flack Lake area. Further the writer found abundant fresh feldspar in the upper part of the formation in the Welcome Lake area. Presence of barite cement in this feldspathic sandstone is more consistent with diagenetic leaching than bauxitization. Examination of the bauxite literature has yielded no reference to formation of barite cemented arkose under bauxite-forming conditions. Thus weathering at source or during deposition seem less likely to have removed feldspar than diagenetic solution.

Casshyap (1969) regarded the Gordon Lake Formation as a distal facies equivalent of the Lorrain, a view consistent with Walther's Law and followed by the writer. Because sandstone of the Gordon Lake Formation contains a significant amount of feldspar and because of its immature suite of clay minerals relative to the upper part of the Lorrain Formation, Wood (1973) rejected it as a distal facies equivalent of the Lorrain. Instead, because of the fine grain size of the Gordon Lake Formation he concluded that it must have formed from glacial loess and that the formation was deposited under a periglacial climate.

The fine grain size of the formation can be explained by deposition as storm beds which characteristically are of fine sand to silt size (Kreisa, 1981; Dott and Bourgeois, 1982), a conclusion independently reached by the writer from facies sequence analysis. The immature suite of clay minerals can be explained by incomplete maturity of its proximal facies equivalent – the upper part of the Lorrain Formation.

The sabkha evaporites at the base of the Gordon Lake Formation suggest a hot, relatively dry but not necessarily arid climate. When considered with Wood's (1973) tropical model for the upper Lorrain Formation a drastic climate change is required. If however the two formations are facies equivalents, the presence of fresh feldspar in the Gordon Lake suggests that there ought to have been feldspar in the upper Lorrain quartz arenite when it was deposited. Diagenetic alteration of feldspar to produce quartz arenite is not unknown from the Proterozoic (Ramaekers, 1981). Also, quartz rich alluvium can be formed under a relatively dry climate. For example in the Sudan, with a Savanna climate of 650 mm rainfall mainly as seasonal thunderstorms and a mean average temperature of 28.5°C, granite debris surrounding an inselberg is being reduced to quartz gravel (up to 96% quartz) by solution of feldspar and eluviation of derived clay minerals by flushing, after thunderstorms (Ruxton, 1958).

In conclusion, a warm relatively dry, possibly seasonal climate is favoured for the upper Lorrain Formation and Gordon Lake Formation for the following reasons. (1) Unlike previous models drastic shifts in paleoclimate are not required. (2) There is evidence that at least some of the sandstone of the upper part of the Lorrain Formation was feldspathic on deposition and that feldspar was lost by diagenetic leaching. In consequence it is not necessary to involve a wet-climate model for the stratabound copper mineralization in this sequence. Contrary to Pearson (1980) sufficient sulphur is present as pyrite in the sequence to form a copper orebody. It is suggested that the cause of the weak mineralization be either insufficient transport of copper or a copper-poor source. It is probably significant that there are no mafic volcanic rocks in the Cobalt Group.

Acknowledgments

During the summers of 1984 and 1985, Gerry Bennett and Jerry Jeff Donald and their staff provided welcome support at the core-storage warehouse of the Ontario Ministry of Natural Resources at Sault Ste. Marie. Professor Darryl Long of Laurentian University provided logistical support at Welcome Lake. Stable isotope analyses were provided by W.D. Loveridge of the Geological Survey of Canada and by the Duncan Derry Laboratory at Ottawa University. Stuart Roscoe, who also critically read the manuscript, Eoin Cameron, and W.D. Loveridge, of the Geological Survey of Canada are thanked for enlightening discussion.

References

Alam, M.M., Crook, K.A.W., and Taylor, G.M.
1985: Environmental and tectonic implications of herring-bone cross-stratification in modern fluvial sands; Lithosphere Dynamics and Evolution of Continental Crust, in Geological Society of Australia, Abstracts Series No. 9, 6th Annual Geological Convention, Canberra, 1983, p. 210.

Allen, J.R.L.
1982: Sedimentary structures, their character and physical basis; Developments in Sedimentology, v. 30B, Elsevier.

Cameron, E.M.
1983: Evidence from early Proterozoic anhydrite for sulphur isotopic partioning in Precambrian oceans; Nature, v. 304, no. 5921, p. 54-56.

Card, K.D.
1970: Discussion of: The Huronian Supergroup north of Lake Huron, by Frarey, M.J. and Roscoe, S.M., in Symposium on basins and geosynclines of the Canadian Shield, ed. A.J. Baer; Geological Survey of Canada, Paper 70-40, p. 157.

1976: Geology of the McGregor Bay-Bay of Islands area, Districts of Sudbury and Manitoulin, Ontario; Ontario Division of Mines, Geological Report GR138.

1978: Geology of the Sudbury-Manitoulin area, Districts of Sudbury and Manitoulin; Ontario Geological Survey, Report 166.

Casshyap, S.M.
1969: Petrology of the Bruce and Gowganda formations and its bearing on the evolution of Huronian sedimentation in the Espanola-Willsville area, Ontario (Canada); Paleogeog., Paleoclim., Paleoecol., v. 6, p. 5-36.

1971: Petrology and sedimentation of Huronian arenites, south of Espanola, Ontario; Canadian Journal of Earth Sciences, v. 8, p. 20-49.

Chandler, F.W.
1969: Geology of the Huronian Rocks of Harron Township and surrounding areas, North Shore of Lake Huron, Ontario; unpublished Ph.D. thesis University of Western Ontario.

1984: Sedimentary setting of an Early Proterozoic copper occurrence in the Cobalt Group, Ontario: preliminary assessment; in Current Research, Part A, Geological Survey of Canada, Paper 84-1A, p. 185-192.

1985: Geology of the Early Aphebian copper and gold-bearing Gordon Lake Formation, Ontario, Canada; in Precambrian Exogenetic Processes, International Correlation Project 160, Symposium, Carleton University, Ottawa, Canada, Aug. 17-18, 1985, Abstracts, p. 2-4.

Chandler, F.W., Young, G.M., and Wood, J.
1969: Diaspore in early Proterozoic quartzites (Lorrain Formation) of Ontario; Canadian Journal of Earth Sciences, v. 6, p. 337-340.

Collinson, J.D. and Thompson, D.B.
1982: Sedimentary Structures; George Allen and Unwin.

Dott, R.H., Jr. and Bourgeois, Joanne
1982: Hummocky stratification: significance of its variable bedding sequences; Geological Society of American Bulletin, v. 93, p. 663-680.

Eisbacher, G.H. and Bielenstein, H.U.
1969: The Flack Lake Depression, Elliot Lake Area; in Report of Activities, Part B, Geological Survey of Canada, Paper 69-1B, p. 58-60.

Folk, R.L. and Pittman, J.S.
1971: Length-slow chalcedony: a new testament for vanished evaporites; Journal of Sedimentary Petrology, v. 41, p. 1045-1058.

Frarey, M.J.
1977: Geology of the Huronian Belt between Sault Ste Marie and Blind River, Ontario; Geological Survey of Canada, Memoir 383.

Frarey, M.J. and Roscoe, S.M.
1970: The Huronian Supergroup North of Lake Huron; in Symposium on Basins and Geosynclines of the Canadian Shield, ed. A.J. Baer; Geological Survey of Canada, Paper 70-40, p. 143-158.

Frarey, M.J., Loveridge, W.D., and Sullivan, R.W.
1982: A U-Pb Age for the Creighton Granite, Ontario; in Rb-Sr and U-Pb isotopic studies, Report 5, in Current Research, Part C, Geological Survey of Canada, Paper 82-1C, p. 129-132.

Galloway, W.E. and Hobday, D.K.
1983: Terrigenous clastic depositional systems, applications to petroleum, coal and uranium exploration; Springer.

Gustafson, L.B. and Williams, Neil
1981: Sediment-Hosted stratiform Deposits of Copper, Lead and Zinc; Economic Geology, 75th Anniversary volume, p. 139-178.

Hadley, D.G.
1968: Sedimentology of the Huronian Lorrain Formation, Ontario and Quebec, Canada; unpublished Ph.D thesis, Johns Hopkins Univ., Baltimore, Md., 301 p.

Hartmann, M. and Nielsen,
1969: δ^{34}S-Werte in rezenten Meeressedimenten und ihre Deutung am Beispiel einiger Sedimentprofile aus der westlichen Ostsee; Geoloyische Rundschau, v. 58, p. 621-655, abstracted in Faure, Gunter, 1977; Principles of Isotope Geology, Wiley and Sons.

Hattori, K., Krouse, H.R., and Campbell, F.A.
1983: The start of sulfur oxidation in continental environments about 2.2 x 10^9 years ago; Science, v. 221, p. 549-551.

Holser, W.T. and Kaplan, I.R.
1966: Isotope geochemistry sedimentary sulphates; Chemical Geology, v. 1, p. 93-135.

Kendall, A.C.
1984: Evaporites; in Facies Models, second edition, ed. R.G. Walker; Geoscience Canada Reprint Series, 1, p. 259-296.

Kinsman, D.J.J.
1969: Modes of formation, sedimentary associations and diagnostic features of shallow-water and supratidal evaporites; American Association of Petroleum Geologists Bulletin, v. 53, p. 830-840.

Kreisa, R.D.
1981: Storm-generated sedimentary structures in subtidal massive faces with examples from the Middle and Upper Ordovician of southwest Virginia, Journal of Sedimentary Petrology, v. 51, p. 823-848.

Krogh, T.E., Davis, D.W., and Corfu, F.
1984: Precise U-Pb zircon and Baddeleyite Ages for the Sudbury Area; in The Geology and Ore Deposits of the Sudbury structure, ed. E.G. Pye et al.; Ontario Geological Survey, Special Volume 1, p. 431-446.

Lindsey, D.A.
1969: Glacial sedimentology of the Precambrian Gowganda Formation, Ontario, Canada; Geological Society of America Bulletin, v. 80, p. 1685-1701.

Lowey, G.W.
1985: Stratigraphy and sedimentology of the Lorrain Formation, Huronian Supergroup (Aphebian), between Sault Ste. Marie and Elliot Lake, Ontario, and implications for stratiform gold mineralization; Geological Survey of Canada, Open File 1154.

McRae, S.G.
1972: Glauconite, Earth-science Reviews, v. 8, p. 397-440.

Milliken, K.L.
1979: The silicified evaporite syndrome – two aspects of silicification history of former evaporite nodules from southern Kentucky and Northern Tennessee; Journal of Sedimentary Petrology, v. 49, p. 245-256.

Monster, J., Appel, P.W.U., Thode, H.G., Schidlowski, M., Carmichael, C.M., and Bridgwater, D.
1979: Sulphur isotope studies in early Archean sediment from Isua, W. Greenland: implications for the antiquity of bacterial sulphate reduction, Geochimica et Cosmochimica, Acta, v. 43, p. 405-413.

Muir, M.D.
1979: A sabkha model for the deposition of part of the Proterozoic McArthur Group of the Northern Territory and its implications for mineraliation; Bureau of Mines Journal, Australian Geology and Geophysics, v. 4, p. 149-162.

Patterson, R.J. and Kinsman, D.J.J.
1981: Hydrologic framework of 2 sabkhas along the Arabian Gulf; American Association of Petroleum Geologists Bulletin, v. 65, p. 1457-1475.

Pearson, W.N.
1980: Copper Metallogeny, North shore region of Lake Huron, Ontario, Ph.D. thesis (unpub.) Queen's Univ.

Pettijohn, F.J.
1970a: The Canadian Shield, a status report 1970; in Symposium on Basins and Geosynclines in the Canadian Shield, ed. A.J. Baer; Geological Survey of Canada, Paper 70-40, p. 239-255.

Pettijohn, F.J. (cont.)
1970b: Response to comment by Roscoe S.M. and Frarey, M.J. on The Canadian Shield – A status report; in Symposium on Basins and Geosynclines of the Canadian Shield; Geological Survey of Canada, Paper 70-40, p. 239-255.

Pirie, R.G.
1961: The general geology of the Upper Cobalt Group, Bruce Mines District, Ontario, Canada, M.A., (unpub.) Indiana Univ., 117 p.

Ramaekers, R.
1981: Hudsonian and Helikian Basins of the Athabasca Region, Northern Saskatchewan, p. 219-233; in Proterozoic Basins of Canada, Geological Survey of Canada, Paper 81-10.

Renfro, A.R.
1974: Genesis of evaporite-associated stratiform metalliferous deposits: a sabkha process; Economic Geology, v. 69, p. 33-45.

Roscoe, S.M. and Frarey, M.J.
1970: Comments on: The Canadian Shield-A status report, 1970, by Pettijohn, F.J., in Symposium on Basins of the Canadian Shield, ed. A.J. Baer; Geological Survey of Canada, Paper 70-40, p. 255-262.

Ruxton, B.P.
1958: Weathering and subsurface erosion in granite of the piedmont angle, Balos, Sudan; Geological Magazine, v. 95, p. 353-377.

Siemiatkowska, K.M.
1977: Geology of the Wakomata Lake area, District of Algoma, Ontario Division of Mines, Geoscience Report 151.

1978: Geology of the Endikai Lake Area, District of Algoma; Ontario Geological Survey, Report 178.

Sims, P.K., Card, K.D., and Lumbers, S.B.
1981: Evolution of early Proterozoic basins of the Great Lakes region; in Proterozoic Basins of Canada, ed. F.H.A. Campbell; Geological Survey of Canada, Paper 81-10, p. 379-397.

Singh, I.B. and Wunderlich, Friedrich
1978: On the terms wrinkle marks, (runzelmarken), millimetre ripples and mini ripples; Senchenbergiana Maritima, v. 10, p. 31-37.

Tucker, M.E.
1976: Replaced evaporites from the Late Precambrian of Finnmark, Arctic Norway, Sedimentary Geology, v. 16, p. 193-204.

Van Houten, F.B. and Purucker, M.E.
1984: Glauconitic Peloids and Chamositic ooids – favorable factors, constraints and problems; Earth-Science Reviews, v. 20, p. 211-243.

Veizer, J. and Compston, W.
1976: $^{87}Sr/^{86}Sr$ in Precambrian carbonates as an index of crustal evolution, Geochimica et Cosmochimica Acta, v. 40, p. 905-914.

Wood, John
1970: The stratigraphy and sedimentation of the Upper Huronian Rocks in the Rawhide Lake-Flack Lake Area, Ontario; unpublished M.Sc. thesis, University of Ontario.

Wood, John (cont.)
1973: Stratigraphy and deposition environments of upper Huronian rocks of the Rawhide Lake-Flack Lake area, Ontario; in Huronian Stratigraphy and Sedimentation, Geological Association of Canada, Special Paper 2, p. 73-95.

Wright, D.J.
1985: Preliminary Report on the stratigraphy and sedimentology of the Huronian Bar River Formation, Ontario; in Current Research, Part B, Geological Survey of Canada, Paper 85-1B, p. 111-116.

Young, G.M.
1966: Huronian stratigraphy of the MacGregor Bay Area, Ontario: Relevance of the Paleogeography of the Lake Superior Region; Canadian Journal of Earth Sciences, v. 3, p. 203-210.

Young, G.M.
1970: An extensive Early Proterozoic glaciation in North America?; Paleogeography, Paleoclimatology, Paleoecology, v. 7, p. 85-101.

1973: Tillites and aluminous quartzites as possible time markers for middle Precambrian (Aphebian) rocks of North America; Geological Association of Canada, Special Paper 12, p. 97-127.

Young, H.R.
1979: Evidence of former evaporites in the Cambro-Ordovician Durness Group, Northwest Scotland; Sedimentary Geology, v. 22, 287-303.

Isotope and hydrocarbon studies of the Yava sandstone-lead deposit, Cape Breton Island, Nova Scotia: a progress report[1]

Project 650056

P.D. Vaillancourt and D.F. Sangster
Economic Geology and Mineralogy Division

Vaillancourt, P.D. and Sangster, D.F., Isotope and hydrocarbon studies of the Yava sandstone-lead deposit, Cape Breton Island, Nova Scotia: a progress report; in Current Research, Part A, Geological Survey of Canada, Paper 86-1A, p. 133-140, 1986.

Abstract

The Yava deposit occurs in an Upper Carboniferous fluviatile sandstone above an unconformity on lower Carboniferous sedimentary rocks and a Devonian intrusion. Yava is located along the southeast margin of Salmon River Basin within Fundy Basin. The deposit consists of three zones of disseminated galena each overlying a basement depression and separated from the adjacent zones by an intervening basement high.

Reflectance values of vitrinite are higher in the Yava area than in the rest of the Salmon River Basin. Sulphur isotope values show a wide spread similar to other continental sandstone-hosted deposits. Lead isotopes indicate that ore leads are homogeneous whereas rock leads are heterogeneous.

The initial findings, together with other evidence not reported here, support a groundwater genetic model for Yava. The high vitrinite values are considered to be formed from oxidation of coal, the sulphur isotope patterns are typical of deposits formed by the circulation of meteoric groundwaters and the lead isotope values in ore galenas suggest derivation of lead from feldspars in the adjacent quartz feldspar porphyry.

Résumé

Le gisement de Yava se trouve dans un grès fluviatile du Carbonifère supérieur, au-dessus d'une discordance entre des roches sédimentaires du Carbonifère inférieur et une intrusion du Dévonien. Il longe la bordure sud-est du bassin de Salmon River dans le bassin de la baie de Fundy. Le gisement consiste en trois zones de galène disséminée, occupant des dépressions du socle et séparées l'une de l'autre par des soulèvements de ce dernier.

La réflectance de la vitrinite est plus élevée dans la région du Yava que dans le reste du bassin de Salmon River. Les valeurs des isotopes du soufre sont très variées et s'apparentent à celles d'autres gisements continentaux logés dans des grès. Les isotopes du plomb indiquent que les plombs du minerai sont homogènes, alors que les plombs de la roche sont hétérogènes.

Les premiers indices, ainsi que d'autres non signalés dans la présente communication, soutiennent l'hypothèse d'un modèle génétique des eaux souterraines pour le gisement de Yava. Les valeurs élevées de vitrinite seraient dues à l'oxydation du charbon; la répartition des isotopes du soufre est caractéristique des gisements formés par la circulation des eaux souterraines de nature météorique; et, les valeurs des isotopes du plomb dans les galènes semblent indiquer que le plomb provient des feldspaths logés dans le porphyre quartzo-feldsparthique voisin.

[1] Contribution to Canada-Nova Scotia Mineral Development Agreement 1984-89. Project carried by Geological Survey of Canada.

Introduction

This project was initiated after the closing of the Yava mine in 1981 when the Nova Scotia Department of Mines and Energy invited the second author to conduct a research project in the mine area. Since the project began, several aspects of the geology at Yava have been investigated (Vaillancourt and Sangster, 1984; Vaillancourt, 1985). This paper reports on studies of coal alteration, sulphur and lead isotopes, and the relevance of these results to the genetic history of the deposit.

Regional geology

Yava is located in the Salmon River Basin portion of the Fundy Basin system of the Appalachian orogen (Figure 16.1). The deposit is at the southeast margin of the basin, where upper Carboniferous strata form an asymmetric syncline with beds dipping gently to the northwest. The sedimentary rocks rest nonconformably on the Loch Lomond plutonic complex (Figure 16.2). The Salmon River Basin includes a mixed Carboniferous succession dominated by marginal continental alluvial, fluvial and marine (including evaporite) sediments. At Yava, the stratigraphic succession above the quartz-feldspar porphyry is made up of the Uist, the MacKeigan Lake and the ore-hosting Silver Mine formations followed by conglomerates of the Big Barren formation and coal-bearing sandstone of the Glengarry Valley Formation. There is an overstep of sedimentary strata on basement rock to the northeast from the Loch Lomond Basin to the Salmon River Basin.

Yava deposit

The deposit consists of three zones, each of which are located over a paleotopographic depression in the underlying Lower Devonian quartz-feldspar porphyry. Ore grade mineralization is confined to a 3-7 m thick zone, which transgresses bedding as it follows the basement profile. Galena occurs in bands or disseminations between rounded to subrounded quartz grains in grey sandstone (Fig. 16.3). The West zone originally contained 5.6 million tonnes of ore at 5.2% Pb (Bonham, 1982).

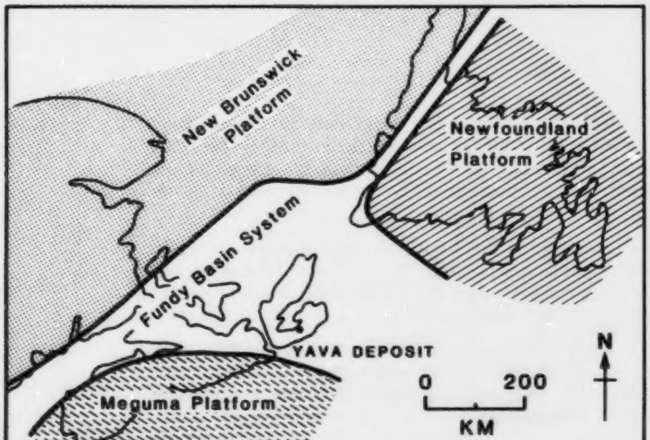

***Figure 16.1.** Generalized map of the Fundy Basin area and adjoining platforms (from McCabe and Schenk, 1982).*

The genetic model currently proposed is of a groundwater migration where meteoric waters moving along sandstone aquifers leach Pb from basement-derived feldspars in the sediment and precipitate galena under reducing conditions in intergranular pore space (Fig. 16.4).

Organic alteration

A very special aspect of Yava is the presence of coaly fragments in sandstone at the base of the Silver Mine Formation, commonly in silicified form and well mineralized (Fig. 16.5). To better understand the thermal history of coal and its relationship to mineralization, vitrinite reflectance studies were undertaken on mineralized and unmineralized samples to determine coal rank and degree of alteration. Vitrinite determinations were carried out by P. Hacquebard and M. Avery at the Atlantic Geoscience Centre of the Geological Survey of Canada and by contract at the Atlantic Coal Institute, Sydney, Nova Scotia.

Vitrinite reflectance is used on coal samples to assess conditions of burial and metamorphism of organic material. Usually, an increase in reflectance is the result of higher rock temperature as a result of burial. Samples of coaly material from sandstone were taken from drillcore northeast, southwest and northwest of Yava and from the Terra Nova district just west of the Salmon River Basin (Fig. 16.2). Reflectance values for coaly material in sandstone at Yava are notably higher than elsewhere in the Salmon River Basin. At Yava, reflectance values are in the range 0.7-1.4, with a median value of 1.15, whereas the values for samples taken from the rest of the basin are between 0.6 and 1.3 with a median value of 0.85 (Fig. 16.6). In an earlier study by Hacquebard and Donaldson (1970), an average reflectance value of 0.8 was assigned to the Salmon River Basin.

The higher reflectance values have previously been interpreted to be the result of an ore-related thermal event (Scott, 1980; Bonham, 1982) because Ro values increase with depth and proximity to Pb mineralization. In Figure 16.7, the highest vitrinite reflectance values are close to, or in, zones of highest Pb mineralization in the grey sandstone. As a further test of thermal history, M.S. Barss of the Atlantic Geoscience Centre analyzed thermal alteration of kerogen from shales interlayered with mineralized and silicified coal to determine the extent of alteration in the surrounding rocks. The results from shale were found to be in conflict with those from coal. Thermal alteration indices for kerogen in shales are generally low, with values between -2 and 2, corresponding to reflectance values between 0.47 and 0.9 which are significantly lower than those recorded for coal fragments at the same depths.

The difference in reflectance values between shales and coal fragments suggests that a thermal event was probably not responsible for the high coal rank at Yava. If high temperature affected the coal, it should have also affected nearby shale. Oxidation can, under some circumstances, also produce high reflectance values and, in the case of Yava, is considered a more likely process than thermal maturation because of the disparity between the coal and shale studies. High reflectance values of coal in sandstone could have resulted from the passage of oxidized meteoric water through the sandstone aquifer. The shale bands, in contrast, would preserve the original reflectance values (and therefore record the true thermal history) because of the exclusion of meteoric water from the shale aquiclude.

Sulphur isotopes

A total of 44 samples, mostly of galena and pyrite from the sandstone and coal fragments, were submitted for sulphur isotope analysis. Additional samples from dolostone of the Uist Group in the Big Glen and Rock Elm areas and gypsum from the MacKeigan Lake Group were also analyzed. Although there are exceptions, most values fall between -30 and +30‰. Sandstone-hosted sulphides, consisting mainly of galena, have heavier values, ranging from -15 to +30‰ while the lighter values, ranging from -30 to +15‰, are in coal-hosted sulphides, mostly pyrite (Fig 16.8). The difference in values between galena and pyrite is opposite to that expected for normal sulphide fractionation patterns (Sangster, 1976). Gypsum values are between +10 and +25‰; the average of +16.7‰ compares well with +17‰ seawater average for the early Carboniferous Period (Claypool et al., 1980).

Sulphur isotopes of other sandstone-hosted deposits are compared with those of Yava in Figure 16.9. The Scandinavian ones of Cambrian age with a marine affiliation (Laisvall, Vassbo, Osen, Galaa) are generally more positive (Bjørlykke, 1983) than Yava. The German deposits of Triassic age with a continental affiliation (Mechernich, Maubach) are more negative. Tertiary continental sandstone-hosted copper deposits in the southwest United States, the Warnock, Happy Jack and Ady are also more negative. The Maybell and Amarillo sandstone-uranium deposits (Sangster, 1976) are most similar to Yava in terms of total range of values.

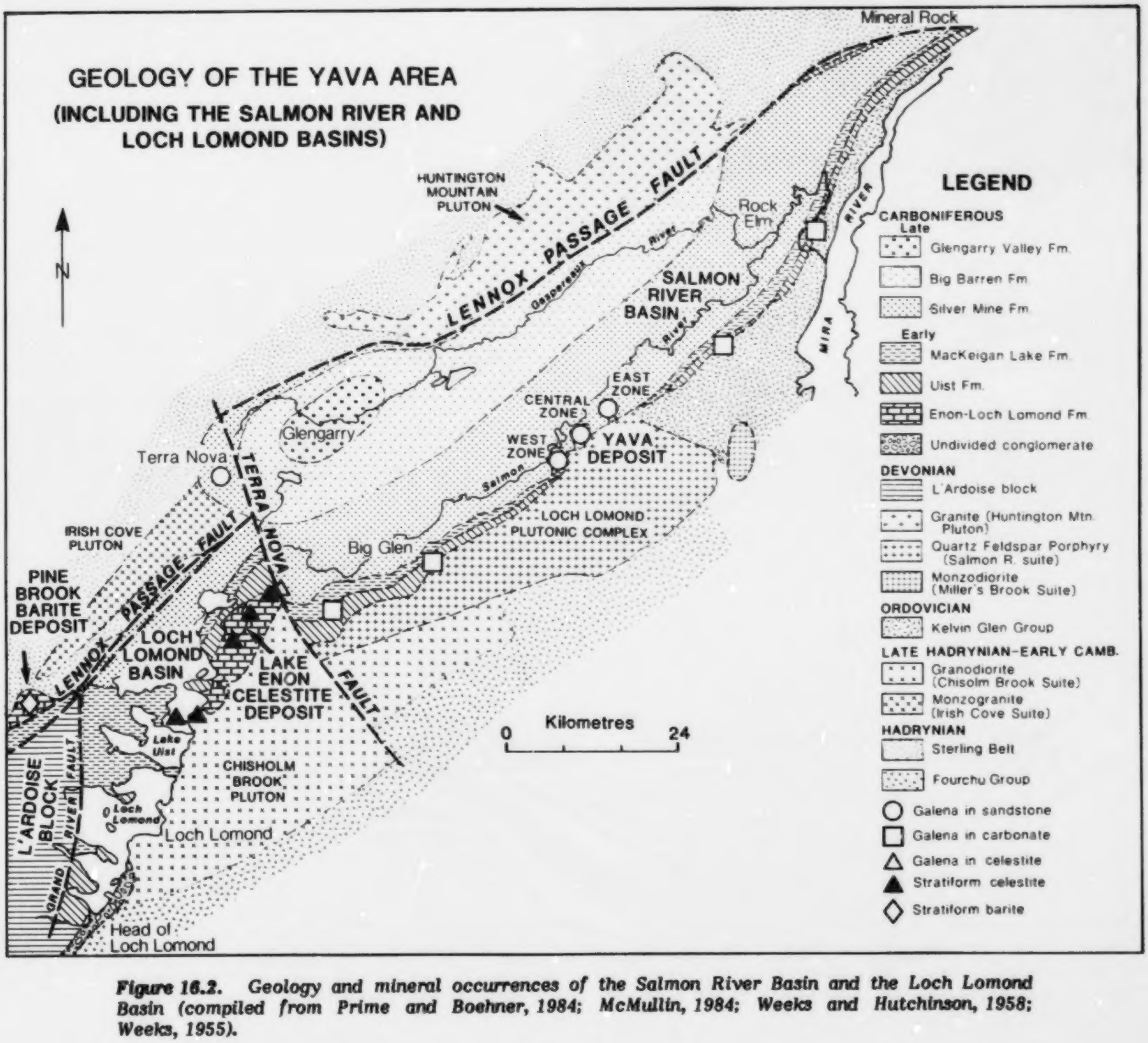

Figure 16.2. *Geology and mineral occurrences of the Salmon River Basin and the Loch Lomond Basin (compiled from Prime and Boehner, 1984; McMullin, 1984; Weeks and Hutchinson, 1958; Weeks, 1955).*

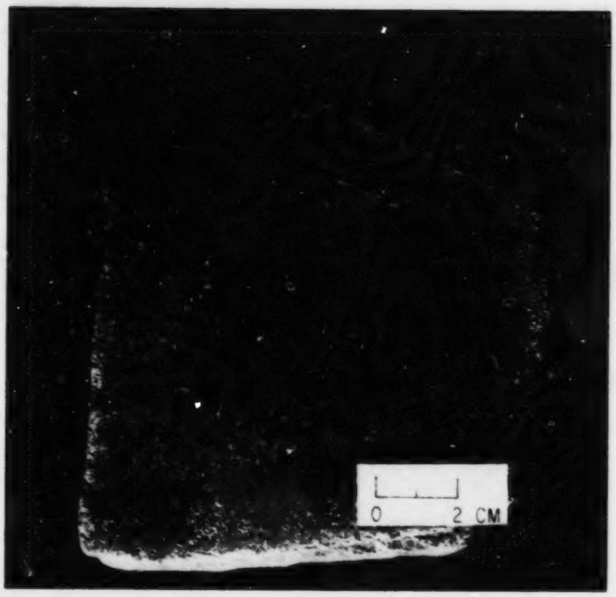

Figure 16.3

Mature grey sandstone with galena-rich bands. (GSC 204077-M)

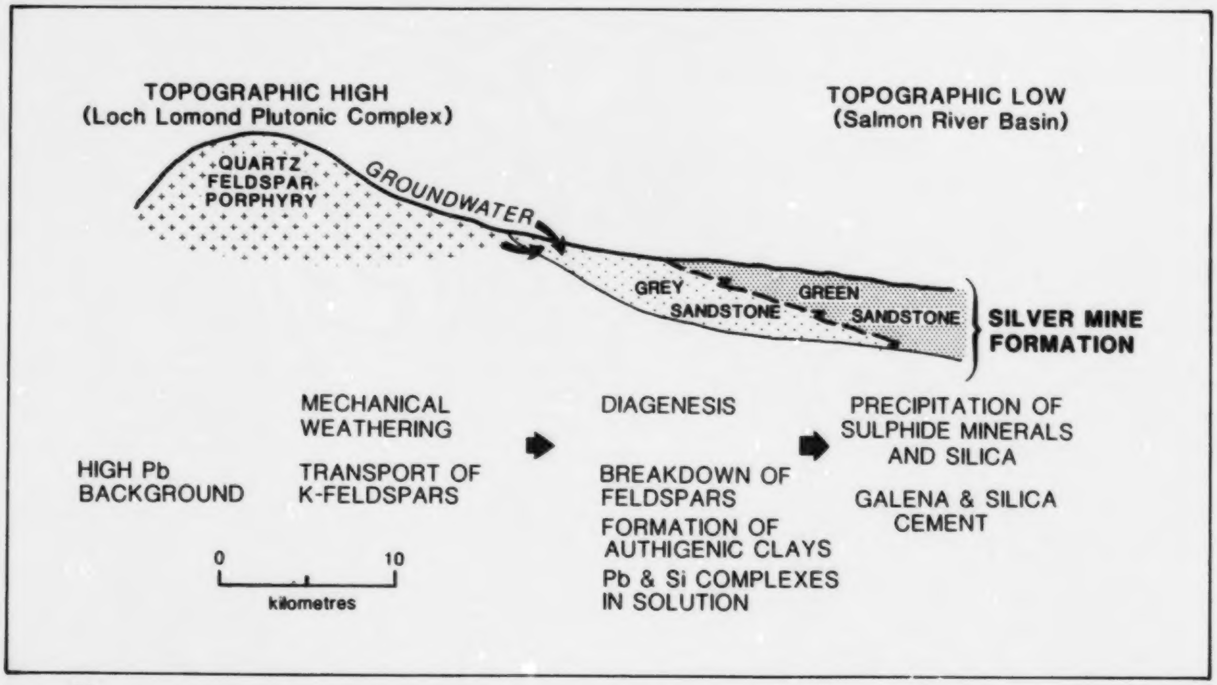

Figure 16.4. *Schematic representation of a genetic model for the Yava deposit.*

Figure 16.5

Silicified and mineralized coal fragment, base of grey sandstone, Yava mine. (GSC 204007-N)

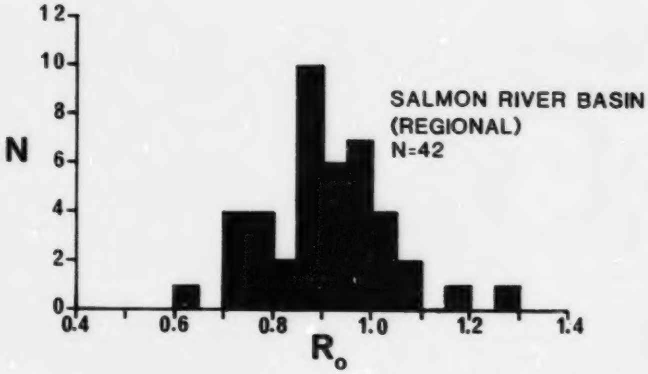

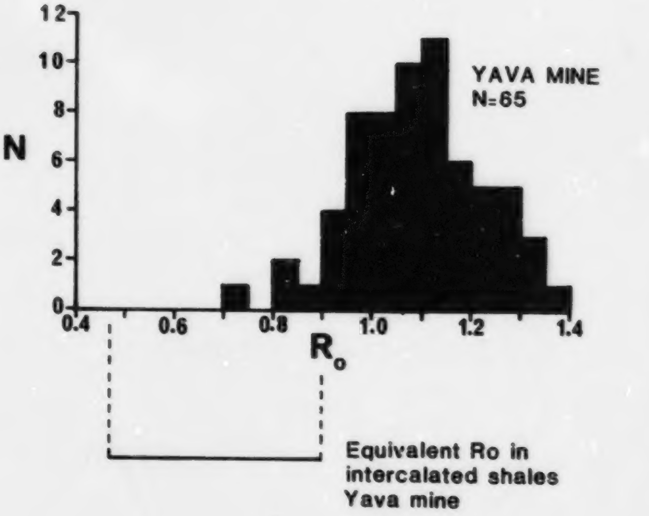

Figure 16.6

Vitrinite reflectance data for coaly material in sandstone of the Salmon River Basin (top) and Yava mine area (bottom). Also shown are equivalent reflectance values of kerogen in shales intercalated with the sandstone.

Lead isotopes

Two types of material were analyzed for Pb isotopes: galena from sandstone in the Yava deposit and quartz-feldspar porphyry from the Loch Lomond plutonic complex. Ore leads are relatively homogeneous compared to the rock leads (Fig. 16.10). The three rock leads from the quartz-feldspar porphyry closest to the values for the Yava mine are from samples highest in Pb content and closest to the mine and may be transitional in composition. The ore leads are not particularly radiogenic, permitting an interpretation of a probable source in potassium feldspar of the Loch Lomond basement complex. This concept is further supported by higher than normal Pb content in the quartz-feldspar porphyry (54 ppm; Barr et al., 1984) compared with average lead content in granites (22 ppm; Wedepohl, 1974).

Conclusion

Each of these areas of research supports the groundwater model for the genesis of Yava in the following manner:

1. A thermal origin for the vitrinite values in coal fragments is not favoured because of the discrepancy with the shale thermal alteration indices. In situ oxidation by meteoric waters may instead be responsible for the high reflectance values and is considered to be a plausible alternative.
2. The sulphur isotope values, with their wide range, are most like those from sandstone uranium deposits which are commonly considered to form on the continent from the migration of meteoric groundwaters.
3. The lead isotope values in ore galenas are very similar to those from underlying basement. This is permissible evidence for the concept that Pb-bearing feldspars, derived from the quartz-feldspar porphyry, were the immediate source of lead. Under diagenetic conditions in the sandstone, the feldspar grains could have been broken down by groundwater moving through the sandstone aquifer. Diagenetic destruction of potassium feldspar would have released Pb into the groundwater followed by precipitation of galena in reduced zones of the sandstones.

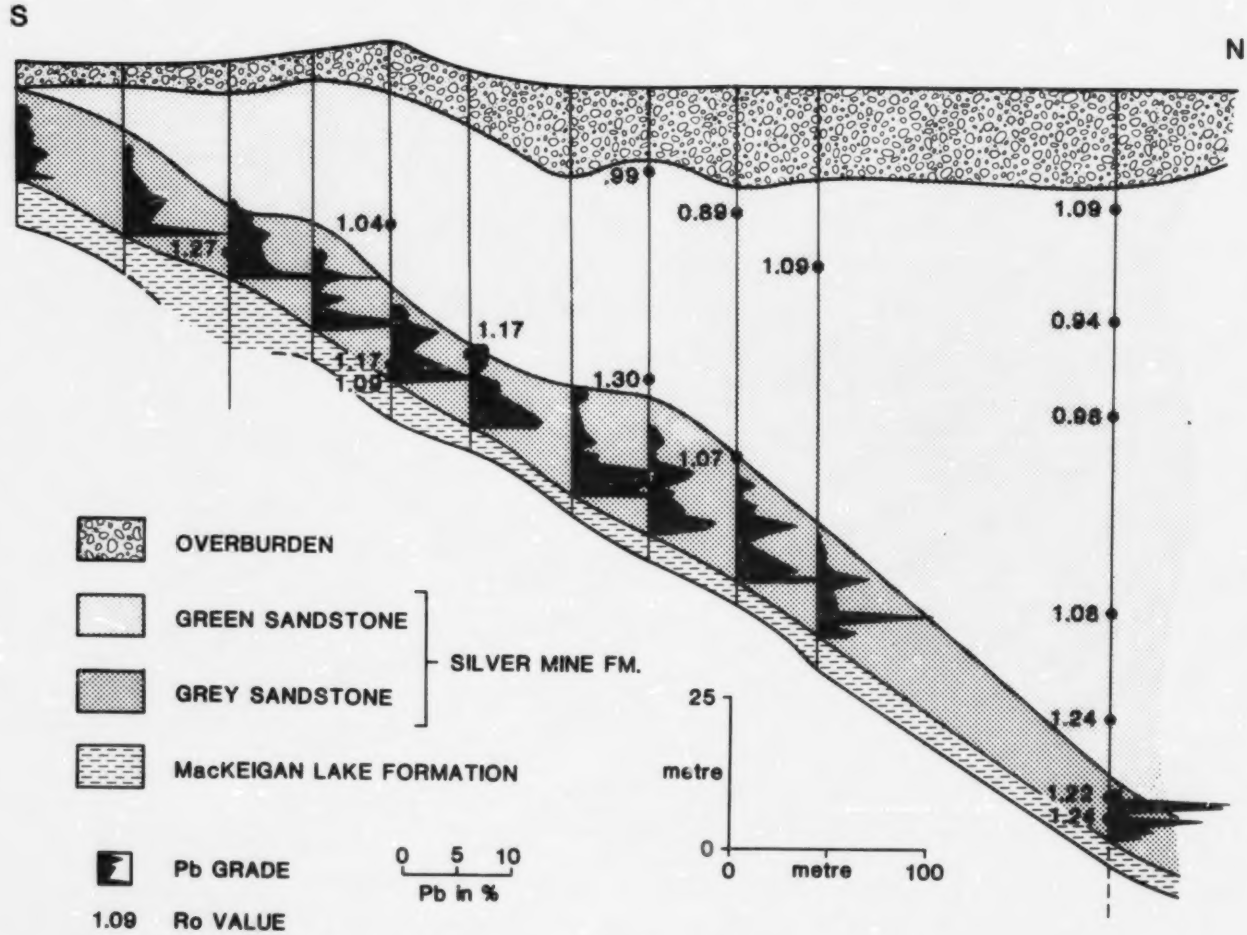

Figure 16.7. Vitrinite reflectance values for coaly material in selected drillholes, with associated Pb grades, along a north-south section through the West Zone, Yava mine.

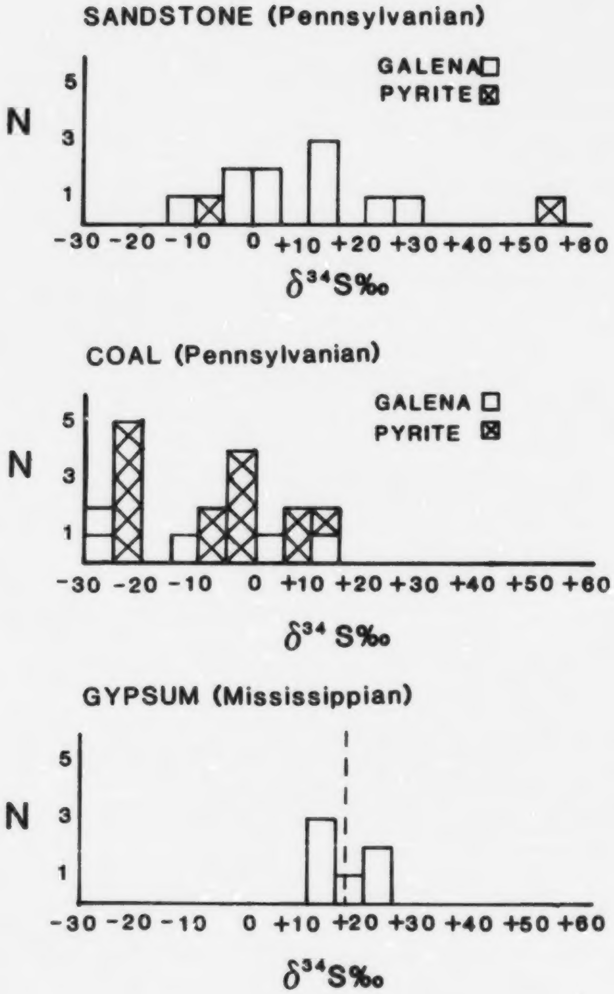

Figure 16.8. Histograms of sulphur isotope data, Yava mine area. Dashed line in gypsum histogram indicates composition of sulphate-sulphur in Mississippian ocean (from Claypool et al., 1980).

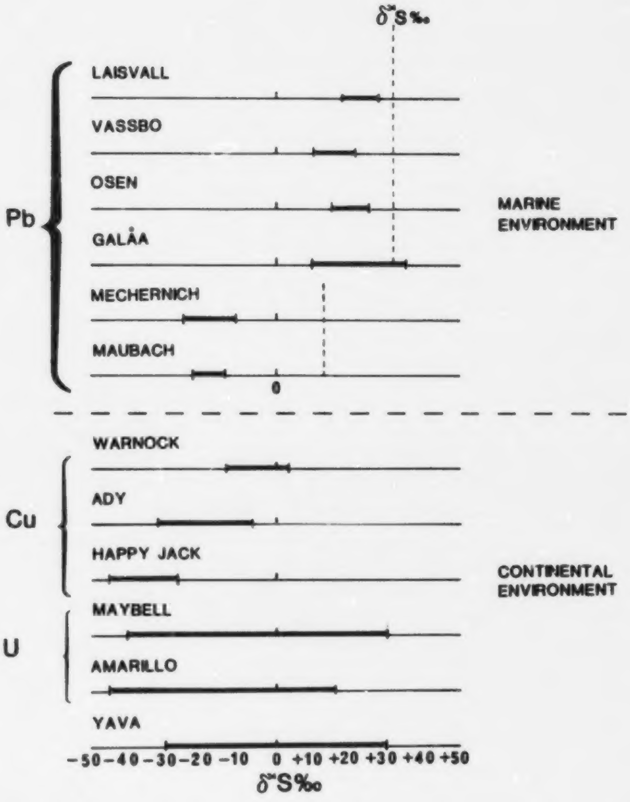

Figure 16.9. Sulphur isotope ranges for sandstone-lead (including Yava), sandstone-copper, and sandstone-uranium deposits (from Sangster, 1976). Note similarity of Yava to sandstone-uranium data. Vertical dashed lines represent isotopic compositions of contemporaneous seawater sulphate.

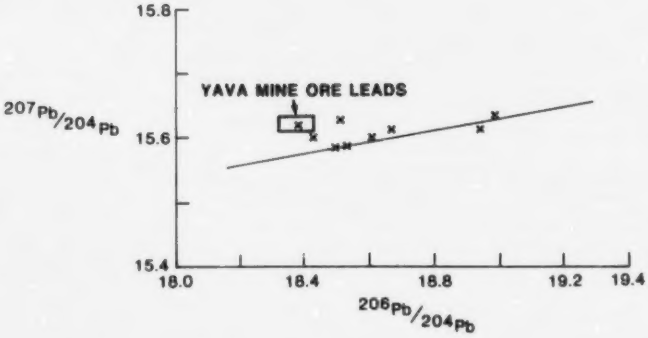

Figure 16.10. Lead isotope data for quartz-feldspar porphyry and ore leads, Yava mine area. Rock leads are indicated by crosses; ore leads plot within the box.

References

Barr, S.M., Sangster, D.F., and Cormier,R.F.
1984: Petrology of Early Cambrian and Devono-Carboniferous intrusions in the Loch Lomond complex, southeastern Cape Breton Island, Nova Scotia; in Current Research, Part A, Geological Survey of Canada, Paper 84-1A, p. 203-211.

Bjørlykke, A.
1983: Sulphur isotope composition of the sandstone lead deposits in southern Norway; Norges Geologiske Undersokelse, v. 300, p. 143-158.

Bonham, O.J.
1982: Geology of the Yava sandstone-lead deposit, Cape Breton, Nova Scotia; unpublished MSc. thesis, Dalhousie University, Halifax, Nova Scotia, 181 p.

Claypool, G.E., Holser, W.T., Kaplan, I.R., Sakai, H., and Zak, I.
1980: The age curves of sulfur and oxygen isotopes in marine sulfate and their mutual interpretation; Chemical Geology, v. 28, p. 199-260.

Hacquebard, P.A. and Donaldson, J.R.
1970: Coal metamorphism and hydrocarbon potential in the Upper Paleozoic of the Atlantic provinces, Canada; Canadian Journal of Earth Sciences, v. 7, p. 1139-1163.

McCabe, P.J. and Schenk, P.E.
1982: From sabkha to coal swamp – the Carboniferous sediments of Nova Scotia and New Brunswick: Field Excursion Guidebook, Excursion 4A; International Association of Sedimentologists, 11th International Congress on Sedimentology, McMaster University, Hamilton, Ontario.

McMullin, D.W.
1984: Geology and geochemistry of the granitoid rocks of the Loch Lomond Irish Cove area, Cape Breton Island; unpublished M.Sc. thesis, Acadia University, Wolfville, Nova Scotia, 239 p.

Prime, G. and Boehner, R.C.
1984: Preliminary report on the geology of the Glengarry Half-Graben and vicinity, Cape Breton Island, Nova Scotia; in Mines and Minerals Branch, Report of Activities, 1983, Nova Scotia Department of Mines and Energy, Report 84-1, p. 61-69.

Sangster, D.F.
1976: Sulphur and lead isotopes in strata-bound deposits; in Handbook of Strata-bound and Stratiform Ore Deposits, ed. K.H. Wolf; Elsevier Scientific Publishing Company, Amsterdam, p. 219-266.

Scott, P.
1980: Geochemistry and petrography of the Salmon River lead deposit, Cape Breton Island, Nova Scotia; unpublished MSc. thesis, Acadia University, Wolfville, Nova Scotia, 111 p.

Vaillancourt, P.D.
1985: Sandstone lithology in the Silver Mine formation and its relation to galena occurrence in the Yava deposit, Cape Breton Island, Nova Scotia; in Current Research, Part A, Geological Survey of Canada, Paper 85-1A, p. 743-751.

Vaillancourt, P.D. and Sangster, D.F.
1984: Petrography of mineralization at the Yava sandstone-lead deposit, Nova Scotia; in Current Research, Part A, Geological Survey of Canada, Paper 84-1A, p. 345-352.

Wedepohl, K.H.
1974: Lead; abundance in common magmatic rock types; crustal abundance; in Handbook of Geochemistry, ed. K.H. Wedepohl; Berlin, Springer-Verlag, ch. 82E, v. II-5, 18 p.

Weeks, L.J.
1955: Grand Narrows, Cape Breton Island, Nova Scotia; Geological Survey of Canada, Map 1040A, with marginal notes, scale 1"=1 mile.

Weeks, L.J. and Hutchinson, R.D.
1958: Mira, Cape Breton Island, Nova Scotia; Geological Survey of Canada, Map 1056A, with marginal notes, scale 1"=1 mile.

- 17 -

Structural setting of the Mile Lake gold prospect, Guysborough County, Nova Scotia[1]

Contract 14SQ.23233-4-0798

S.J. Haynes[2], B.A. Reilly[2], and L.A. Kiely[2]

Haynes, S.J., Reilly, B.A., and Kiely, L.A., Structural setting of the Mile Lake gold prospect, Guysborough County, Nova Scotia; in Current Research, Part A, Geological Survey of Canada, Paper 86-1A, p. 141-150, 1986.

Abstract

Combined regional and detailed mapping of the Mile Lake area indicates that the early Paleozoic Meguma Group has suffered polyphase deformation and metamorphism. A comparison of regional geological studies with recent airborne vertical magnetic gradient maps confirmed the presence of a major synclinorium of Meguma Group sediments, and several parallel fold structures, that join the Forest Hill and Country Harbour gold districts in an area previously considered to be occupied by a large granitoid pluton.

Mineralogical studies indicate that gold at Mile Lake is restricted to microscopic inclusions in arsenopyrite-rich areas of the quartz veins. Crystalloblastic arsenopyrite grains were fractured during a D_3 deformation event, while gold, pyrrhotite, chalcopyrite, sphalerite and galena were deformed by ductile flow.

Résumé

Un levé géologique régional et détaillé de la région du lac Mile indique que le groupe de Meguma du Paléozoïque inférieur a subi des épisodes de métamorphisme et de déformation polyphasés.

En comparant des études géologiques régionales et des cartes récentes de gradients magnétiques verticaux, obtenues par levé aérien, on a pu confirmer la présence d'un important synclinorium constitué de sédiments du groupe de Meguma et de plusieurs plis parallèles qui relient les districts aurifères de Forest Hill et de Country Harbour dans une région auparavant réputée occupée par un important pluton granitoïde.

Des études minéralogiques indiquent que l'or du lac Mile se manifeste uniquement en inclusions microscopiques, dans des zones riches en arsénopyrite des veines de quartz. Des grains cristalloblastiques d'arsénopyrite ont été fracturés lors de la déformation D_3, alors que l'or, la pyrrhotite, la chalcopyrite, la sphalérite et la galène ont été déformés par écoulement ductile.

---

[1] Contribution to the Canada-Nova Scotia Mineral Development Agreement 1984-1989. Project carried by the Geological Survey of Canada, Economic Geology and Mineralogy Division, Project 850052.
[2] S. Haynes Consulting Ltd., P.O. Box 397, Fonthill, Ontario L0S 1E0

Introduction

The Mile Lake gold prospect is located in the Meguma domain of eastern Nova Scotia about 3 km south of the Guysborough County Fault (Fig. 17.1). This fault is a major structure that represents the southern margin of an east-west graben (the Glooscap Fault System) separating the Meguma domain from the Avalon domain to the north (Schenk, 1978).

The Meguma domain of Nova Scotia (Schenk, 1978) comprises a thick Lower Paleozoic metasedimentary sequence (Meguma Group) intruded by Devonian granitoid plutons. The Meguma Group comprises more than 5400 m of flyschoid wackes with thin siltstone and slate interbeds (Goldenville Formation) overlain by about 3500 m of slate with minor sand units (Halifax Formation). The Meguma Group is considered to be turbiditic in origin but exact details of deposition and facies diachroneity are controversial (Phinney, 1961; Schenk, 1970, 1971; Harris and Schenk, 1975; Smith, 1981; Stow, 1982; Waldron, 1983). Amalgamated sandstone units and both partial and complete Bouma sequences are present (Waldron, 1983).

The Mile Lake gold prospect forms part of the Forest Hill Gold District, Guysborough County (Faribault, 1935). Gold is associated with quartz veins in the Goldenville Formation, as are all the gold deposits in the Meguma domain; however, the Forest Hill district is unusual in that the rocks have been elevated to the staurolite-andalusite ± cordierite grade of regional Pyreneean metamorphism and have suffered ductile-shear that postdates Acadian folding (Haynes, 1984).

The purpose of this research project was to determine both the regional structural setting of the Mile Lake Gold Prospect and structural controls on the auriferous quartz veins.

Regional setting

Previous mapping by Faribault (1935) and Schiller (1961) indicated that the Forest Hill district was bounded to the south and west by a large body of granite extending to Country Harbour (Fig. 17.2). However, regional mapping at a scale of 1:10 000 has revealed that this area is dominated by a major synclinorium (Country Harbour-Forest Hill Synclinorium), cored by highly deformed schists of the Halifax Formation, and that large granitoid plutons are restricted to the area north of Forest Hill (Fig. 17.2). Elsewhere in the area, granitoid intrusions are present as small stocks (some tourmaline-bearing), sills, or dykes. In addition, anticlinal structures are present both to the north (Mile Lake Anticlinorium) and south (Howlett Brook Anticline) of the major synclinorium.

Interpretation of the geology is hampered by the extensive cover of glacial overburden. However, comparison of the known geology with the recent vertical magnetic gradient maps by the Geological Survey of Canada (1984) suggests that the Forest Hill and Mile Lake anticlines are, in fact, separate structures, separated by a syncline, and that a major northwesterly-trending fault, west of the Forest Hill mine, dextrally offsets the fold structures and granite north of the Forest Hill camp (Fig. 17.3).

In the greenschist facies to the southwest of the study area, the earliest recognized deformation (D_1) is a flat-lying grain alignment cleavage (S_1) attendant to step-like monoclinal folds (O'Brien, 1983). Although D_1 fabrics were not recognized at Mile Lake, deformed S_1 cleavages are present at Forest Hill (Smith et al., 1985). These monoclines were refolded during the main period of Acadian upright folding and development of attendant upright sub-axial planar S_2 cleavages: slaty cleavage in pelites and spaced cleavage

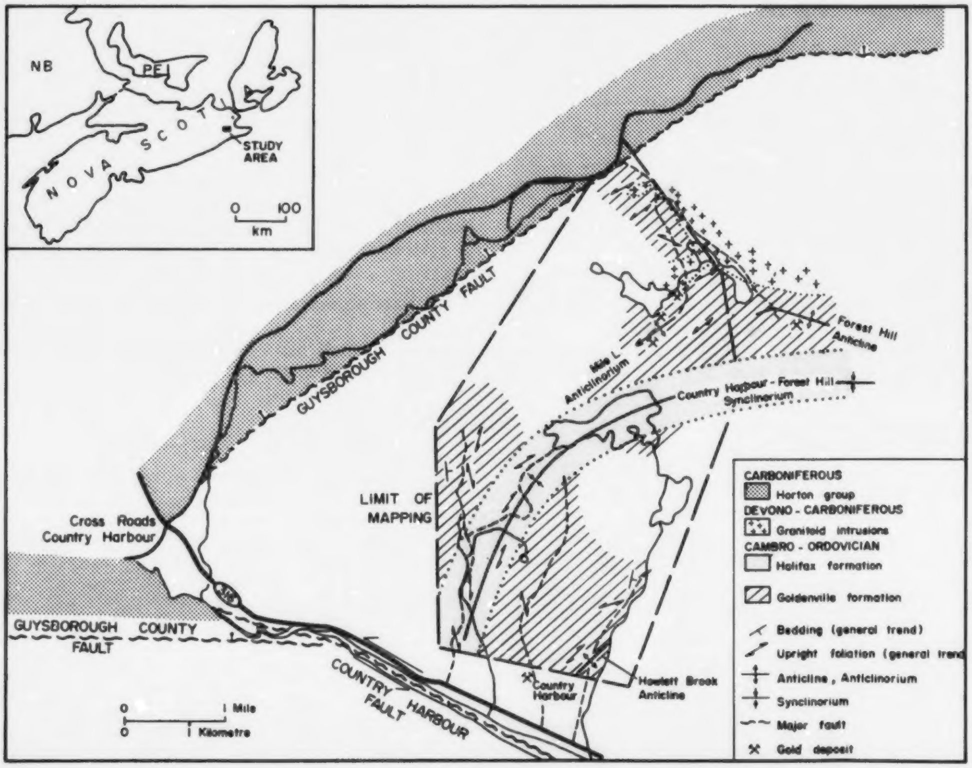

Figure 17.1. *Location and regional geology of the Mile Lake area. Blank areas within mapped area indicate no outcrop (from 1:10 000 scale mapping).*

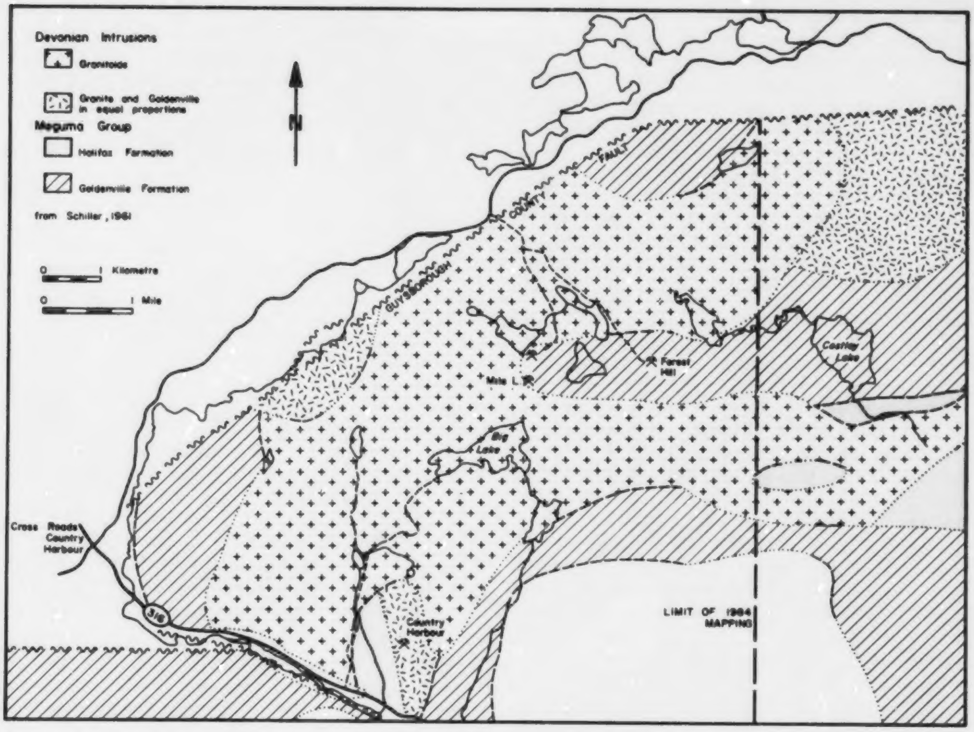

Figure 17.2. Previous geological interpretation after Schiller (1961) from 1:50 000 scale mapping.

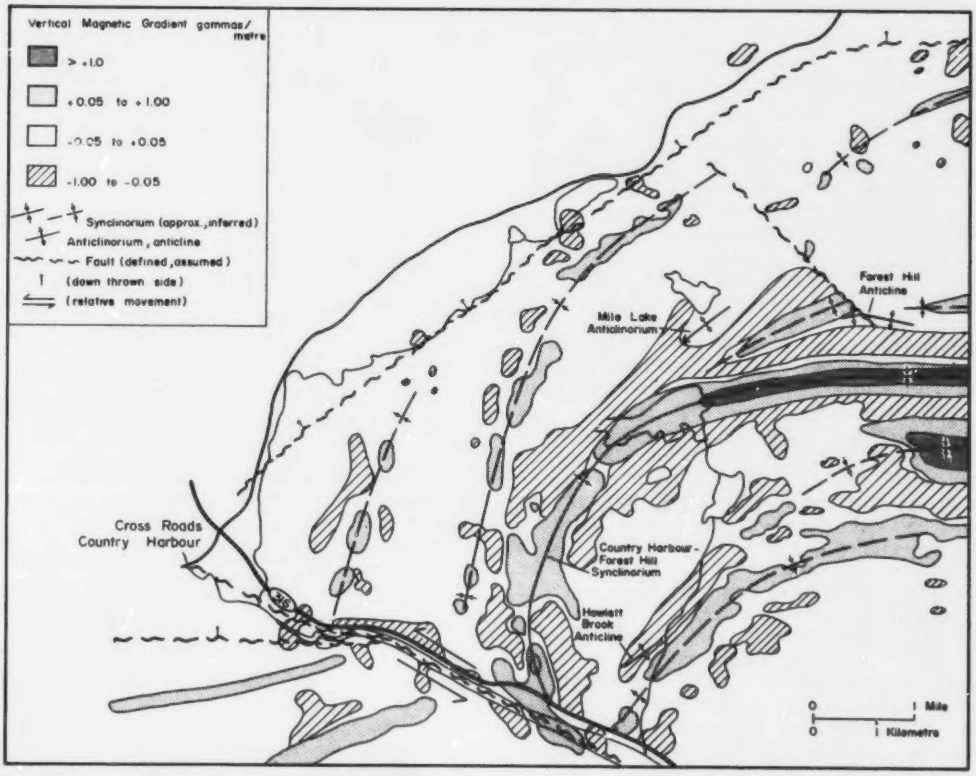

Figure 17.3. Correlation of geology with 1:50 000 scale airborne gradiometer survey by the Geological Survey of Canada (1984).

(pressure solution cleavage) in psammites. In the eastern Meguma domain, these Acadian fabrics are overprinted by randomly-oriented porphyroblasts that increase in metamorphic grade from greenschist (muscovite-chlorite) in the south to amphibolite facies (andalusite-staurolite-biotite-garnet ± cordierite) in the north. These porphyroblastic mineral assemblages have been related to a period of static regional metamorphism by Smith (1981). Although granitoid plutons may locally overprint the regional mineral isograds, ^{39}Ar-^{40}Ar dating by Dallmeyer and Keppie (1984) suggests that both granitoid intrusion and static regional metamorphism in the eastern Meguma domain may be related to the same thermal event at 365-375 Ma.

In the Country Harbour-Forest Hill area structural mapping (Fig. 17.4) revealed that the static thermal event was followed by transcurrent ductile-shear deformation (D_3). This deformation appears to be related to movements on the Guysborough County Fault as a northward increase in strain is apparent: S tectonites occur in the southeast, L, S tectonites nearer the Guysborough County Fault (Fig. 17.4). Deformation is controlled by lithology and thickness of units. In the Goldenville Formation, thick arenaceous psammite units appear to have acted as semi-rigid blocks, often preserving earlier fabrics and vein orientations. In some semi-pelite units an earlier flat-lying crenulation cleavage may be preserved, while earlier structures in argillaceous schist units are transposed bedding-parallel. At low strains in the southern part of the area, D_3 is represented by an upright F_3 fold of bedding and early slaty and spaced cleavages (S_2) in Goldenville metasediments (Fig. 17.5). The relationships of bedding to both S_2 and S_3 cleavages in the hinge of this fold indicates that bedding is not overturned and that the fold is an anticline (Howlett Brook Anticline, Fig. 4). This anticline is attended by development of steep biotite foliation (S_3), best developed in pelitic units where very small F_3 minor folds of S_2 cleavage are present. Along Howlett Brook (Fig. 17.4) asymmetric ripple marks and current bedding are preserved at the top of a thick sand unit that exhibits no evidence of cleavage. As strain increases northward towards Mile Lake, the upright S_3 biotite flattening-foliation becomes more intense and is oriented subparallel to bedding. This is accompanied by rotation of porphyroblasts in argillaceous units. At higher strains, earlier fabrics in pelites are transposed parallel to the upright S_3 foliation, which becomes bedding-parallel, while earlier fabrics in psammites are folded into tight F_3 isoclinal multiple folds with axial surfaces parallel to the steep S_3 foliation. In many granitoids (Fig. 17.6) and some argillaceous schist units, a spaced shear fabric has developed (C-plane) rotating the flattening foliation (S-plane). This dual fabric (shear and flattening planes) has been defined by Berthe et al. (1979), and Ponce deLeon and Choukroune (1980), as a C-S fabric and is characteristic of mylonite zones formed by ductile shear. The orientation of the S-plane relative to the C-plane gives the sense of shear (dextral in the Forest Hill-Mile Lake area), while slickensides on the C-plane give the direction of shear (subhorizontal in the study area). At lower strains the plane of flattening (S-plane) formed. As strain increased, the rocks yielded and were sheared along spaced parting-planes (the C-plane). Movement on the C-planes resulted in a lineation in the direction of movement (slickensides on the C-plane), and rotation of the S-planes between each adjacent C-plane. As strain increased, the angle between the C and S-planes decreased from 45°, and the C-planes became more numerous and spaced closer together. This C-S fabric is represented in Figure 17.4 by a new map symbol that allows the dip and strike of the C-plane, the angle between the C and S-planes, the rake of slickensides on the C-plane, and the sense of shear (dextral or sinistral) to be read directly. In some small granitoid bodies S-planes are parallel to the S_3 biotite flattening foliations in the enclosing metasediments (the C-S map symbols indicate the location of granitoid outcrops in Fig. 17.4). However, in many cases S_3 foliations in psammites strike at an orientation intermediate between the azimuths of C and S in adjacent granitoids. This is probably due to a combination of the effects of ductility contrasts and rotation of the S-planes in the C-S fabrics. Except for one outcrop, the sense of D_3 ductile shear is dextral.

North of Mile Lake, outcrop is sparse. The limited exposures near the Guysborough County Fault (Fig. 17.4) reveal complex structural relationships where several strongly hematized granitoid bodies have intruded Goldenville metasediments. C-S fabrics are apparent in both granitoids and metasediments but S-planes may be locally transposed to parallelism with C-planes. C-planes in granitoids are curved, while C-planes and S_3 foliations in the metasediments are tightly folded about complex vertically-plunging fold axes (Fig. 17.7). In some granitoids, C-planes are tightly spaced and linear rodding of quartz and feldspar has developed parallel to slickensides on the C-planes. Metasomatic blastic plagioclase is present in all rock types but has developed as large rounded porphyroblastic masses in schistose metasediments, overgrowing S_3 foliations (Fig. 17.7). These fabrics and metasomatic minerals are considered to represent peak conditions of progressive ductile-shear during final movement on the Guysborough County Fault.

The last tectonic movement (D_4) was large scale ductile displacement during sinistral movement along the strike-slip Country Harbour Fault. Adjacent to the fault, brittle deformation resulted in the formation of breccias and fractures filled with chlorite-carbonate (Haynes, 1984); northeast and southwest of the fault, structures are bent through about 140° forming the present arcuate shape of the Country Harbour-Forest Hill Synclinorium (Fig. 17.4). Small-scale evidence of these movements is present at Mile Lake as local bending of the ductile shear fabrics toward the south. The duration of displacement on the Country Harbour Fault is unknown but final movement must be later than the Guysborough County Fault and the Carboniferous sediments (Horton Group) infilling the St. Marys graben in the north.

Mile Lake deposit

Gold production from the original Sinclair and McGrath shafts (Fig. 17.8) at Mile Lake is unclear as available figures, listed by the Nova Scotia Department of Mines and Energy, are given for the whole Forest Hill Gold District. Between 1892 and 1916 this amounted to 20 792 ounces of gold at a grade of 0.49 oz Au/ton. Subsequent records are poor but intermittent production continued until the 1930s for a total of 25 102 ounces of gold from 56 613 tons of ore milled. The Mile Lake property is presently under investigation by the Mile Lake Mining Company who used material from the "M" Zone for on-site recovery tests in their pilot mill.

Outcrop at Mile Lake is limited to a 60 m by 90 m stripped area. This area was washed down, surveyed and geologically mapped at a scale of 1:100 (Fig. 17.8).

Within this area, the Mile Lake Anticlinorium comprises two F_3 isoclinal antiforms, striking approximately N45°E. These F_3 folds have axial surfaces parallel to upright ductile-shear S_3 biotite flattening-foliation fabrics and have tightly folded both bedding and early S_2 spaced cleavage.

Between the two antiforms a central belt of psammite is flanked by schists. Within the psammites several zones of thin (1 to 3 cm) calc-silicate interbeds are present (Fig. 17.8). These may represent D_3 ductile shear transposition of the carbonate pods commonly present in psammites at chlorite grade to the southwest (Haynes, 1983). This central area is

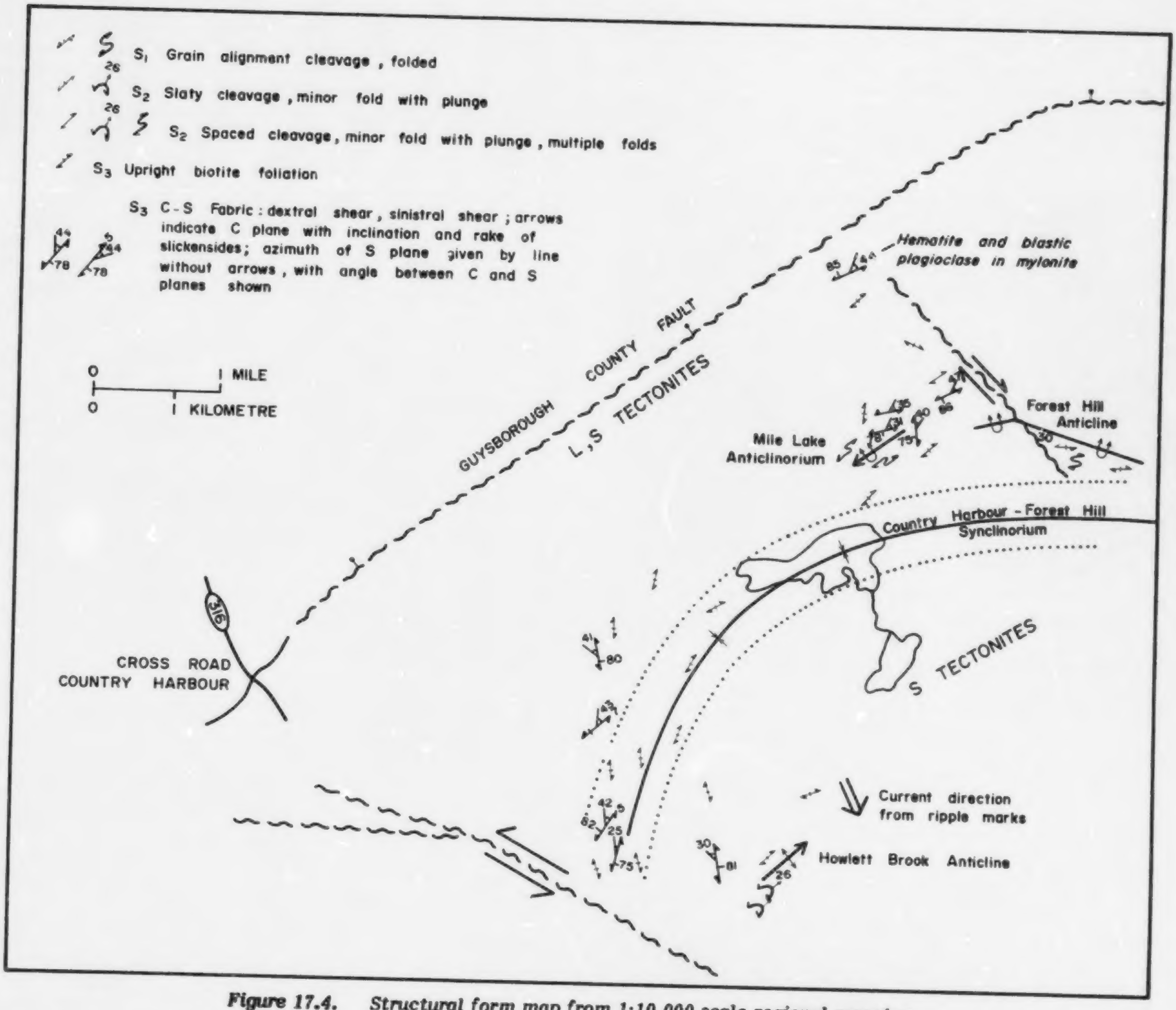

Figure 17.4. *Structural form map from 1:10 000 scale regional mapping.*

Figure 17.5. *Bedding-cleavage relationships, northwest limb of the Howlett Brook Anticline (F_3), 3 m northwest of fold hinge (to right of photograph). Upright S_3 biotite foliation in pelitic unit attends very small upright minor folds of S_2 slaty cleavage.*

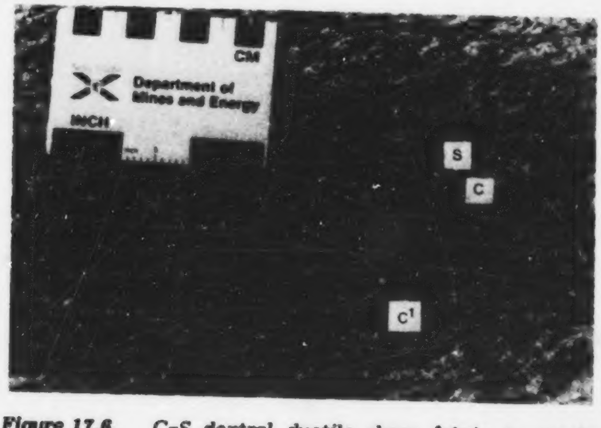

Figure 17.6. *C-S dextral ductile shear fabric in granite, Mile Lake area. Locally, a second shear plane (C^1) dextrally deforms the initial C-S fabric.*

also marked by the presence of several bedding-parallel "sills" of granite and pegmatite. These occur along strike of the metasediments commonly as tadpole-shaped forms with their "heads" commonly facing northeast (Fig. 17.9); although some "heads" also face southwest. These tadpole-shapes are probably the result of boudinage of granitoid sills during D_3 dextral ductile shear.

Figure 17.7. Complex folding of S_3 fabrics about vertically plunging fold axes, 300 m south of the Guysborough County fault. White areas are rounded masses of metasomatic plagioclase overgrowing S_3 foliation.

The Southeastern Antiform comprises three small antiforms and two small synforms (Fig. 17.8), all of which are doubly-plunging at shallow angles. Numerous S and Z minor folds of S_2 spaced cleavage are developed on the flanks of these small F_3 folds (Fig. 17.10). The McGrath and Sinclair leads are located on the northwest limb of the Southeastern Antiform.

To the southeast of Southeastern Antiform an undeformed body of coarse granite is partly exposed (Fig. 17.8). Several small randomly-oriented zenoliths are present, some of which contain S_2 spaced cleavage. This intrusion appears either to have been emplaced after S_3 foliation or to have remained rigid during D_3 deformation as, on its northeast side, S_3 fabrics in the enclosing metasediments are deformed around the granite as small folds with vertical axes; also, a shear plane, with slickensides raking 30°SE, has developed at the granite contact. Metasediments to the north and west of this granite display deformed current-bedding and S_2 spaced cleavages, transposed by upright S_3 biotite flattening-foliation.

The Sinclair Lead is exposed as a quartz vein in a trench to the southeast of the shaft (Fig. 17.8). This vein is parallel to bedding (dipping 60° to 70°NW) and pinches and swells from 20 cm to 50 cm. On the northwest wall of the trench, the vein contains a small pod of leucocratic pegmatite. The vein is enclosed by both arenaceous and argillaceous schists containing abundant arsenopyrite euhedra and, locally, leaves of pyrite.

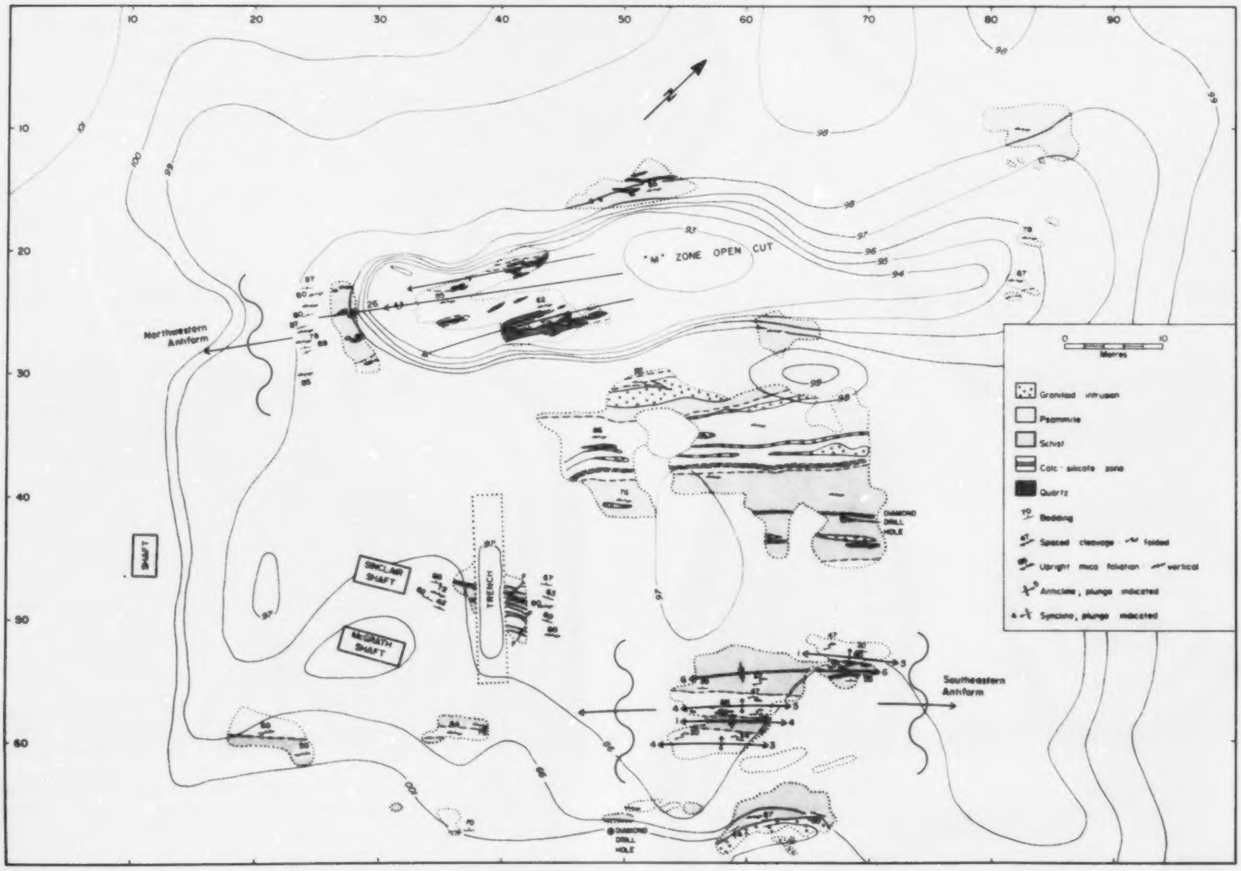

Figure 17.8. Topography and geology of the Mile Lake prospect based on 1:100 scale mapping.

The northeastern antiform is present in a 60 m x 8 m open cut excavated to a depth of about 3 m into the "M" zone series of auriferous quartz veins (Fig. 17.8). Mapping at a scale of 1:20 (Fig. 17.11) indicates that these comprise a complex en-echelon series of tight isoclinal S and Z folds of boudinaged quartz veins and their enclosing schists and metawackes, generally plunging 10° to 40° southwest. Many folds are rootless and the limbs of subsidiary minor folds commonly coalesce to form thickened multiple veins of quartz in their hinge zones. Larger minor folds display bulbous masses up to 2 m across strike of coalesced veins in their hinge zones; in places, with their limbs bending inward in the form of sheath folds (Fig. 17.11). Several mineralogically-different vein typomorphs are apparent within the coalesced masses. However, due to the structural complexity and transposition these cannot be traced more than a few metres and their structural relationships to each other are unclear. Three quartz-vein typomorphs have been distinguished in the field: 1. massive; 2. banded, often with quartz fibres perpendicular to the walls of individual bands (bands being 1 to 3 cm thick); 3. plagioclase-rich. Coarse arsenopyrite (up to 6 cm) is abundant in the host sediments, particularly at vein contacts and as folded septa within thickened masses of coalesced quartz veins (Fig. 17.6). Within individual quartz veins arsenopyrite appears to be most abundant about zenoliths (dislocated septa?) of country rock.

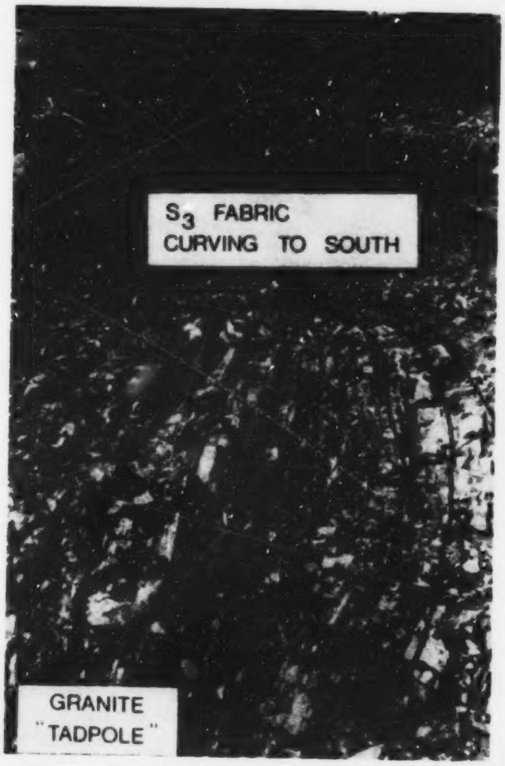

Figure 17.9. Granite "tadpole" with head facing northeast, Mile Lake (notebook is 17 cm high). Bedding and S_3 fabric in Goldenville metasediments curves southward to the Sinclair Shaft (in background).

At the southwestern end of the "M" zone open cut, the hinge of the Northwestern Antiform is exposed (Fig. 17.8). At this locality the two multiply-folded limbs of the antiform (Fig. 17.8, 17.11) merge together down plunge to form a tight F_3 isoclinal fold hinge with an axial plane dipping about 80-87°NW. This hinge is cored by an argillaceous schist unit containing quartz masses that exhibit isoclinal rootless minor sheath folds. The plunge at the argillaceous schist/arenaceous schist contact at the top of the hinge is 33°SW but this is only local. By comparison with the plunge of the hinge on the northwest wall of the open cut (10°SW) and minor fold plunges on the southeastern wall (26°SW), and extrapolation of the plunges of the two major limbs of the antiform, an overall plunge of about 26 ± 10° was calculated.

The northwest wall of the open cut forms the hinge of a flat-lying southeast facing fold structure plunging 10°SW. On the upper part of the wall bedding dips 76°SE, at the bottom 87°NW. The upper part of the wall displays unusual markings that may be "tool marks" or fossil tracks. If so, bedding on this fold is right-way-up and the antiform would be an upright anticline. By relation to the adjacent geology this fold is interpreted as the southeastern limb of an upright F_3 sheath fold. Several minor F_3 folds are present in quartz veins and metasediments in the outcrop at the base of the northwest wall (upper part of Fig. 17.11).

A flat-lying fracture filled with clay is present on the southwest and southeast walls of the open cut. Its origin is in question but it may represent a post-glaciation unloading feature as no obvious horizontal displacement could be ascertained.

Figure 17.10

S and Z minor folds of S_2 spaced cleavage about one of the small F_3 antiforms comprising the Southeastern Antiform, Mile Lake.

Figure 17.11. Detailed geology of exposure in the floor of the "M" Zone Open Cut based on 1:20 mapping.

General character and mineralogy of ore, Mile Lake open cut

Sulphide minerals in host metasedimentary rocks

Abundant arsenopyrite and minor pyrrhotite are present in all metasedimentary rocks in the "M" zone but are enriched in schist units (Fig. 17.11), in which arsenopyrite may locally constitute several per cent of the rock. In schist units S_3 biotite foliation wraps around blocky arsenopyrite grains, which also display quartz pressure shadows, whereas the pyrrhotite grains or aggregates are flattened parallel to this foliation. This indicates that both these sulphides were formed prior to ductile shear deformation.

No gold was observed in the host metasedimentary rocks. Ilmenite is present, but is also a common constituent of Goldenville rocks throughout the eastern Meguma domain.

Quartz vein mineralogy

Most veins in the "M" zone consist of massive quartz. Commonly, arsenopyrite is present at the vein margins with the host rocks and the vein quartz has been recrystallized parallel to the S_3 biotite foliation in the schists.

The plagioclase-rich veins contain rounded plagioclase grains, enveloped by a matrix of randomly-oriented biotite and epidote, adjacent to quartz layers in which the individual quartz grains have recrystallized parallel to the S_3 foliation.

Small actinolite-rich veins are present in the bulbous quartz masses of the "M" zone but are of very limited extent and distribution. They comprise randomly-oriented actinolite grains that poikiloblastically enclose rounded quartz inclusions and are set in a matrix of recrystallized quartz (S_3). Rare 1 mm idiomorphic grains of sphene are present in some veins. Actinolite-sericite bands have been isoclinally folded by F_3 microfolds that are associated with the S_3 recrystallized quartz fabric. Thus, actinolite must have formed prior to S_3, possibly during the M_3 static metamorphism.

The principal sulphide mineral in the quartz veins is arsenopyrite, which occurs as idiomorphic crystals as much as 5 cm across, and as crystalline aggregates as much as 15 cm in diameter. In polished section fine grained pyrrhotite is common as: poikilitic inclusions in large arsenopyrite grains; fillings of the interstices between idiomorphic arsenopyrite grains; fracture-fillings in arsenopyrite; and as rims to small idiomorphic arsenopyrite crystals.

Other sulphide minerals are rare. One grain of marcasite was observed as a rounded inclusion in pyrrhotite. Chalcopyrite occurs as a very minor constituent, usually either as inclusions contained within pyrrhotite and arsenopyrite or as rims on arsenopyrite grains. Sphalerite was observed in only one section, in which it occurs with biotite rimming arsenopyrite. Galena is present as very small poikilitic inclusions in arsenopyrite, sometimes with associated gold.

Although native gold is not uncommon in the quartz veins, it is restricted to microscopic inclusions, only visible under high magnification, in either pyrrhotite or arsenopyrite. Gold is present in pyrrhotite as solitary rounded grains in the poikilitic inclusions of pyrrhotite in arsenopyrite, as blebs in the pyrrhotite that is interstitial to idiomorphic arsenopyrite grains, and as blebs within pyrrhotite fracture-fillings in arsenopyrite. In arsenopyrite, gold occurs as: isolated inclusions in large arsenopyrite crystals (Fig. 17.12), as elongated blebs connected to hairline fracture-fillings, and as isolated hairline fracture-fillings which in some cases contain minor pyrrhotite. The greatest accumulations of gold occur in specimens in which several textural varieties of gold are present.

The textural relationships of the sulphides and gold suggest that they may have been deposited, or recrystallized, at the same time. Because of its high crystalloblastic strength, arsenopyrite preferentially develops idiomorphic forms while softer sulphides (pyrrhotite, chalcopyrite, sphalerite and galena) and gold are usually anhedral. Thus, the rims and interstitial fillings of the softer sulphides around idiomorphic grains can result from contemporaneous, rather

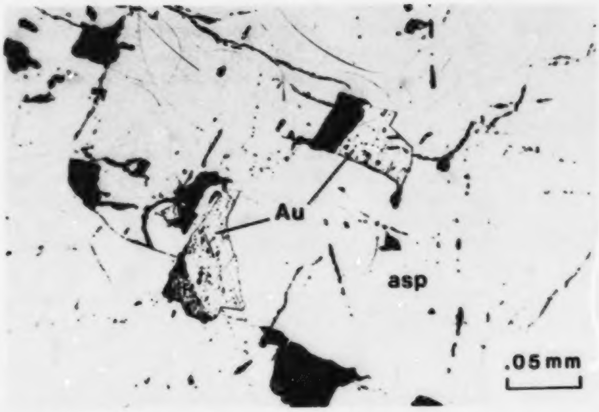

Figure 17.12. *Isolated grains of gold (Au) and gangue poikilitically enclosed by arsenopyrite (asp).*

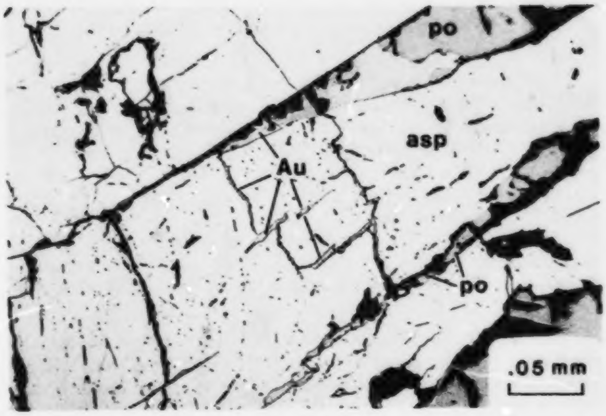

Figure 17.13. *High grade gold ore. Larger blebs of gold (Au) occur with pyrrhotite (po) filling interstices between arsenopyrite grains (asp); these blebs are connected by two sets of gold-filled fractures in the arsenopyrite.*

than later, deposition of the soft sulphides. In fact, the poikilitic inclusions of soft sulphides and gold suggest that they were deposited continuously during arsenopyrite growth and/or earlier-formed grains were incorporated by crystalloblastic arsenopyrite. Although the textural relations of the sulphides to quartz and biotite (see above) indicate that the sulphides predate D_3 ductile shear fabrics, it is impossible to ascertain from the sulphide textures their relationship to the different periods of deformation and metamorphism. The one exception is the gold- and sulphide-filled fractures in arsenopyrite. These probably represent the mechanical effect of the brittle failure of arsenopyrite, and the accompanying ductile flow of incompetent sulphides and gold into the resultant fractures, due to the intense strains of D_3 shear in the "M" zone. Evidence for this is that many of the gold-filled fractures terminate at elongated inclusions of gold (Fig. 17.13). Furthermore, it is possible that the soft sulphides may have ductilely flowed into the interstices between idiomorphic arsenopyrite grains during this same deformation.

Geochemical data

Chemical data have been obtained for numerous whole rock and vein specimens from the immediate vicinity of the Mile Lake deposit. Trace analyses for gold and 18 other elements were carried out on 43 quartz vein specimens and 68 metasedimentary rocks. For 19 granites in this area a similar suite of trace element analyses has been obtained, in addition to standard whole rock analyses and a suite of 9 "lithophile" elements (F, B, Be, Li, Sn, Pb, Rb, Zr and Sr).

Discussion and conclusions

Both the ductile-shear fabrics and the Guysborough County fault parallel the southward swing of the Country Harbour-Forest Hill synclinorium as it approaches the northwest-southeast trending Country Harbour fault. West of Country Harbour, the northern boundary of the Meguma domain continues as the east-west trending St. Mary's fault. This arcuate feature appears to result from large-scale ductile tectonic displacement during sinistral movement along the strike-slip Country Harbour fault. The duration of this displacement is unknown but final movements must be younger in age than the Early Carboniferous sediments to the north which are displaced. Small-scale evidence of these movements is present at Mile Lake as local bending of the upright ductile shear fabrics toward the south.

Field studies in the Mile Lake area have revealed that the structures present in the northeastern part of the Meguma domain are far more complex than previous geological mapping indicated. In particular, fold structures are so tight and abundant that 1:100 or even 1:20 scale mapping is required in order to deduce true relationships. This implies that 1:50 000 scale mapping of the northern Meguma domain may be of dubious value and that even 1:10 000 scale mapping may only reveal parts of the tectonic and structural history. However, of great importance to regional studies is that the Mile Lake structure appears as a small fold closure on the 1:50 000 scale vertical magnetic gradiometer maps (Geological Survey of Canada, 1984). This could indicate that the numerous small closures, observed elsewhere on the magnetic gradiometer maps of eastern Nova Scotia, may represent folds in the Meguma metasediments. Of particular interest is that the gradiometer maps indicate that the Devonian granitoid intrusions are of limited extent in the area between Country Harbour and Forest Hill.

Gold at Mile Lake is restricted to microscopic inclusions in arsenopyrite-rich areas of the quartz veins. Based on their textural relationships, gold, arsenopyrite, pyrrhotite, chalcopyrite, sphalerite and galena appear to have formed at essentially the same time. However, the textures are interpreted to have been modified by: 1. pre-D_3 crystalloblastic growth of arsenopyrite, and; 2. syn-D_3 fracturing of arsenopyrite accompanied by ductile flow of gold and soft sulphides. The extremely fine grained nature of the gold indicates that the ore may require very fine grinding in order to optimize gold recovery.

The relationship of gold to different quartz-vein typomorphs, regional structure and granitoid intrusion is presently unknown. However, field mapping indicates that D_3 deformation postdates quartz-vein deposition. All the quartz veins are deformed by D_3 ductile shear fabrics, and none of the veins display geometric arrays that would suggest progressive ductile deformation of an initial en-echelon fracture filling related to the D_3 ductile shearing.

The presence of pegmatite in the quartz of the Sinclair lead suggests the possibility that at least some of the quartz (and gold) may have been derived from the Devonian granitoid intrusions. Relationships at Forest Hill (Haynes, 1984) indicate that deposition of gold and quartz was polygenetic: with the earliest deposition of auriferous quartz veins occurring pre- or syn-D_1, and the latest deposition related to the Devonian intrusions. By inference,

the gold and quartz may have a similar polygenetic origin at Mile Lake, although there is no direct structural evidence for this.

From the viewpoint of gold exploration, this study indicates the potential for additional gold-quartz mineralization in the area previously thought to be granite between Country Harbour and Mile Lake. Exploration should concentrate on the northern and southern flanks of the Country Harbour-Forest Hill Synclinorium along the Goldenville-Halifax contacts (Fig. 17.1). In addition, the gradiometer data (Fig. 17.3) indicate several parallel fold structures to the west of this synclinorium. As outcrop is sparse in this area, a regional geochemical program along these structures is suggested.

This work indicates that the Mile Lake deposit is the most severely deformed of all the Meguma gold deposits and that the specific location of gold veins near the Guysborough County Fault is complicated by boudinage, transposition and multiple sheath folding related to D_3 ductile shear. This implies that exploration for gold deposits in this area must take account of the local structures present.

Several different types of granitoids are present in the Mile Lake camp. Adjacent to the southern contact of the Cameron lead (the gold deposit immediately north of Mile Lake in Fig. 17.1) a prominent mass of tourmaline-garnet aplogranite (in part greisenized?) is present. This indicates potential for economic lithophile elements (Sn, W, Be, etc.) as well as gold in this area of the Meguma domain.

References

Berthe, P., Choukroune, P., and Jegouzo, P.
1979: Orthogneiss, mylonite and non coaxial deformation of granites: the example of the South Amorican Shear Zone; Journal of Structural Geology, v. 1, p. 31-42.

Dallmeyer, R.D. and Keppie, J.D.
1984: Geochronological constraints on the accretion of the Meguma Terrane with North America; Geological Society of America, Northeastern Section Annual Meeting, Rhode Island, Program with Abstracts.

Faribault, E.R.
1935: Forest Hill Gold District, N.S.; Geological Survey of Canada Map, Scale 500 feet = 1 inch.

Geological Survey of Canada
1984: High resolution aeromagnetic total field and vertical gradient maps of Guysborough County, Nova Scotia; Geological Survey of Canada, Open File 1048 (1:50 000 scale).

Harris, I.M. and Schenk, P.E.
1975: The Meguma Group; in Ancient Sediments of Nova Scotia: Eastern Section, I.M. Harris (editor); Economic Paleontologists and Mineralogists, Guidebook.

Haynes, S.J.
1983: Typomorphism of turbidite-hosted auriferous quartz veins, southern Guysborough County; Report of Activities, Nova Scotia Department of Mines and Energy, Report 83-1, p. 183-224.

Haynes, S.J. (cont.)
1984: Polygenesis of gold deposits, Eastern Meguma domain; Report of Activities, Nova Scotia Department of Mines and Energy Report 84-1, p. 215-223.

O'Brien, B.H.
1983: The structure of the Meguma Group between Gegogan Harbour and Country Harbour, Guysborough County; Report of Activities, Nova Scotia Department of Mines and Energy, Report 83-1, p. 145-181.

Phinney, W.C.
1961: Possible turbidity-current deposit in Nova Scotia; Geological Society of America Bulletin, v. 72, p. 1453-1454.

Ponce deLeon, M.I. and Choukroune, P.
1980: Shear zones in the Iberian Arc; Journal of Structural Geology, v. 2, p. 63-68.

Schenk, P.E.
1970: Regional variation of the flysch-like Meguma Group (Lower Paleozoic) of Nova Scotia, compared to recent sedimentation off the Scotian Shelf; Geological Association of Canada, Special Paper 7, p. 127-153.

1971: Southeastern Atlantic Canada, northwestern Africa and continental drift; Canadian Journal of Earth Sciences, v. 8, p. 1218-1251.

1978: Synthesis of the Canadian Appalachians; Geological Survey of Canada, Paper 78-13, p. 111-136.

Schiller, E.
1961: Geology map, Sheet 11F/5, Guysborough County, Nova Scotia; Geological Survey of Canada, Map 27-1961, Scale 1 inch to 1 mile.

Smith, P.K.
1981: Geology of the Sherbrooke area, Guysborough County, Nova Scotia; Report of Activities, Nova Scotia Department of Mines and Energy Report 81-1, p. 77-94.

Smith, P.K., Haynes, S.J., and Reilly, B.A.
1985: Turbidite-hosted gold deposits, Meguma domain, eastern Nova Scotia; R.M. Pickerill, C.K. Mawer and L.R. Fyffe (editors), "Fredericton 85"; Geological Association of Canada/Mineralogical Association of Canada, Guidebook Excursion 11, 67 p.

Stow, D.A.V.
1982: Toward an anatomy of fine-grained sediments; Episodes, v. 1982, no. 2, p. 3-4.

Waldron, J.W.F.
1983: Sedimentary features of some Goldenville Formation sandstones, Sherbrooke area, Eastern Nova Scotia; Report of Activities, Nova Scotia Department of Mines and Energy, Report 83-1, p. 257-261.

Willemite and native silver occurrences, Kirkmount, Pictou County, Nova Scotia[1]

Project 700059

Alan L. Sangster
Economic Geology and Mineralogy Division

Sangster, A.L., Willemite and native silver occurrences, Kirkmount, Pictou County, Nova Scotia; in Current Research, Part A, Geological Survey of Canada, Paper 86-1A, p. 151-158, 1986.

Abstract

Willemite and native silver have been identified in calcite veins cutting Precambrian James River Formation argillite and greywacke near Kirkmount in the Antigonish Highlands. Both of these occurrences are unusual, not only for Nova Scotia, but elsewhere. They are thought to be related to relatively young (late Paleozoic to early Mesozoic) faults that might be part of the Cobequid-Chedabucto fault system. The willemite-ferruginous-manganiferous carbonate assemblage is similar to assemblages elsewhere that are considered to be of supergene origin.

Résumé

On a identifié de la willémite et de l'argent natif dans des veines de calcite qui pénètrent des argilites et des grauwackes de la formation précambrienne de James River, à proximité de Kirkmount dans les hautes-terres d'Antigonish. Ces deux manifestations sont inhabituelles, non seulement en Nouvelle-Écosse, mais ailleurs aussi. On pense qu'elles sont associées à des failles relativement jeunes (du Paléozoïque supérieur au Mésozoïque inférieur) qui pourraient faire partie du réseau de failles de Cobequid-Chedabucto. L'association de carbonates willémitifères, ferrugineux et manganésifères ressemble à d'autres associations qui auraient une origine supergène.

---

[1] Contribution to Canada-Nova Scotia Mineral Development Agreement 1984-1989. Project carried by Geological Survey of Canada.

Introduction

Willemite (Zn_2SiO_4) occurs in carbonate veinlets in the Precambrian James River Formation found in core from a hole drilled in 1980 by St. Joseph Explorations Limited at Kirkmount, Nova Scotia (Fig. 18.1). Native silver was found associated with brecciated quartz-carbonate veins during recent surface mapping near the drillhole. These unusual occurrences are about 8 km southeast of Stellarton, Nova Scotia, in the western part of the Antigonish Highlands. This paper is a preliminary report on these occurrences.

A stream geochemical survey carried out by Bingley (1977) indicated the presence of zinc in the Kirkmount area. The area was staked by St. Joseph Explorations Limited[1] and subsequent surveys (Sangster, 1978; Sangster et al., 1979; and Wowkodaw, 1979) outlined two drill targets (Sangster, 1980). Hole 326-2 intersected 9100 ppm Zn (in sludges) over 99 m (325 ft). A 21 m (68.3 ft) section of core assayed 1.66% Zn. The zinc occurs despite the apparent absence of sulphides and sludge analyses indicate low copper (30 to 143 ppm) and lead (7 to 83 ppm) contents.

General geology

The willemite- and native silver-bearing veinlets occur in argillite and greywacke which are the oldest exposed rocks of the Antigonish Highlands (Murphy, 1985a). These rocks were first described by Fletcher (1886) and named the James River Formation. Later they were assigned an Ordovician age (Williams, 1914). The James River Formation near Kirkmount has been described by Bell (1940) and Maehl (1961). Benson (1974) completed the first detailed mapping of its distribution just west of Kirkmount. Work by Keppie (1978) and mapping by Murphy et al. (1979, 1982), Murphy (1985a, b) and Yeo and Murphy (1985) has redefined the James River Formation as late Precambrian in age.

In the vicinity of the Kirkmount Zn and Ag occurrences, the James River Formation consists of argillite and greywacke (Figure 18.2). Apart from the section provided by the core from the St. Joseph hole 326-2, rocks of the James River Formation are observable only in a few small roadside outcrops and a small quarry 150 m west of the drillhole, owned by Mr. Lawrence Campbell of MacLellan's Brook. The James River Formation is being quarried for road metal.

The argillite is grey-green to pale or medium olive green, fine grained and varies from massive to well laminated, the latter showing millimetre-scale graded beds. Bedding laminations are accentuated by red hematite stains. The rocks are commonly highly fractured and jointed with surfaces coated by brown-red iron oxides, black manganese oxides and minor specular hematite.

The greywacke is a fine- to medium-grained, grey, grey-green or red brown mottled rock. Fracturing is less abundant than in the argillite but the greywacke contains similar iron and managenese stains. Minor barite was seen in small fractures in the greywacke.

Bedding is visible only in the argillite. Local attitudes are highly variable but strikes are generally about east-west with moderate to steep north dips.

Willemite occurrence

Hole 326-2 cut an extensive zone of brecciated argillite and greywacke which hosts a complex network of calcite veinlets. The willemite-bearing sections of the breccia are easily recognized by the bright green fluorescence of the mineral under short wave U.V. radiation (confirmed by X-ray diffraction). The fluorescence is a result of the substitution of manganese for zinc and the fluorescent variety is named troostite (Berry and Mason, 1959; Ford, 1964). Calcite in the hole shows a variety of fluorescence characteristics. These features are described below and illustrated in Figure 18.3.

Calcite-willemite breccias

The calcite-willemite mineralization is hosted by two types of breccia. The more important breccia consists of gash vein networks with 1 to 10 mm wide fractures with

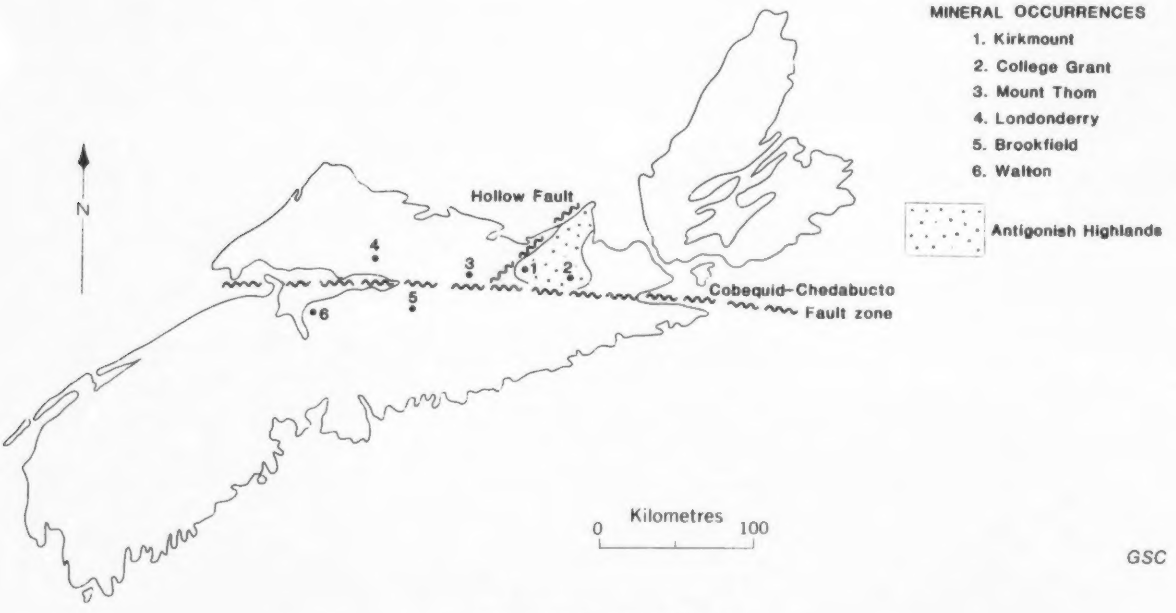

Figure 18.1. *Location Map.*

[1] Now Sulpetro Minerals Limited.

carbonate (Fig. 18.4) and/or willemite (Fig. 18.5) filling fractures or occurring in hairline seams around breccia clasts (Fig. 18.6). Minor chlorite and hematite alteration is associated with some of the more intensely veined areas (Fig. 18.5).

The second breccia type consists of 1 to 5 cm greywacke and argillite fragments set in a matrix of 1 to 3 mm argillite fragments cemented by argillite (Fig. 18.7). Superficially, this breccia is similar to some syn-sedimentary breccias in clastic rocks but the presence of veins in larger fragments indicates that brecciation post-dates the calcite veining. This breccia type hosts minor interstitial calcite mineralization but does not appear to host extensive willemite.

Willemite

Most willemite occurs in greywacke breccia between 56 m (183 ft) and 71 m (234 ft) in the hole but other minor occurrences are present as well. Megascopically, willemite occurs as 1 to 3 mm white, prismatic to equant crystals which are commonly attached to the vein wall as a coating between the calcite vein filling and wall rock. Where the layers are thicker (3 mm) a colloform-like structure is outlined by varying intensities of green fluorescence. Where veins are less than one millimetre thick, the willemite-bearing gash veins are monomineralic.

Calcite

Calcite veinlets are ubiquitous in the hole to a depth of 86.5 m (284 ft). The calcite is white to buff or pink in colour and fine- to medium-grained. It occurs most commonly as a vein filling and less commonly as interstitial grains. The calcite shows three fluorescent varieties. The most striking variety shows a strong red fluorescence and occurs sporadically to 50 m (165 ft) in the hole but not below that depth. The second variety fluorescesses dull red. Its occurrence is roughly equivalent to the bright red fluorescent calcite but it extends deeper into the willemite sections. A third, nonfluorescent variety, which shows rusty oxidation on the core surface, occurs throughout the hole. X-ray diffraction analyses on one specimen of each type indicates all are calcite but with major peaks shifted due to probable trace element substitution. McGowan (1980) indicated that bright red fluorescence in calcite results from the presence of 3 to 5 per cent manganese substituting for calcium. On the other hand since iron quenches fluorescence, it is probable that the fluorescent characteristics of Kirkmount calcite are a result of varying substitutions of iron and manganese for calcium.

Chemical analyses

Geochemical analyses by St. Joseph Explorations Limited (Sangster, 1980) demonstrated a wide zone of geochemically anomalous rocks in hole 326-2 (Fig. 18.3). This was confirmed by assays of 21 m (68.3 ft) of core, representing the higher sludge analyses (24 m (80 ft) at 14 900 ppm Zn), which returned a value of 1.66% Zn. The writer assayed 20 core samples (5 to 15 cm each) for six elements. The results are presented in Table 18.1 with the following comments.

1. The Zn values show no clear relationship to fluorescence with the exception of sample KQS-85-39 (abundant green fluorescence) which returned 11.2% Zn. Samples KQS-85-35, 43, and 45 contained 0.30 to 1.05% Zn even though they contained neither veins nor fluorescent minerals. Zinc in an unidentified form is widespread in both argillites and greywackes. Very fine grained nonfluorescent willemite or white iron free sphalerite may be present.

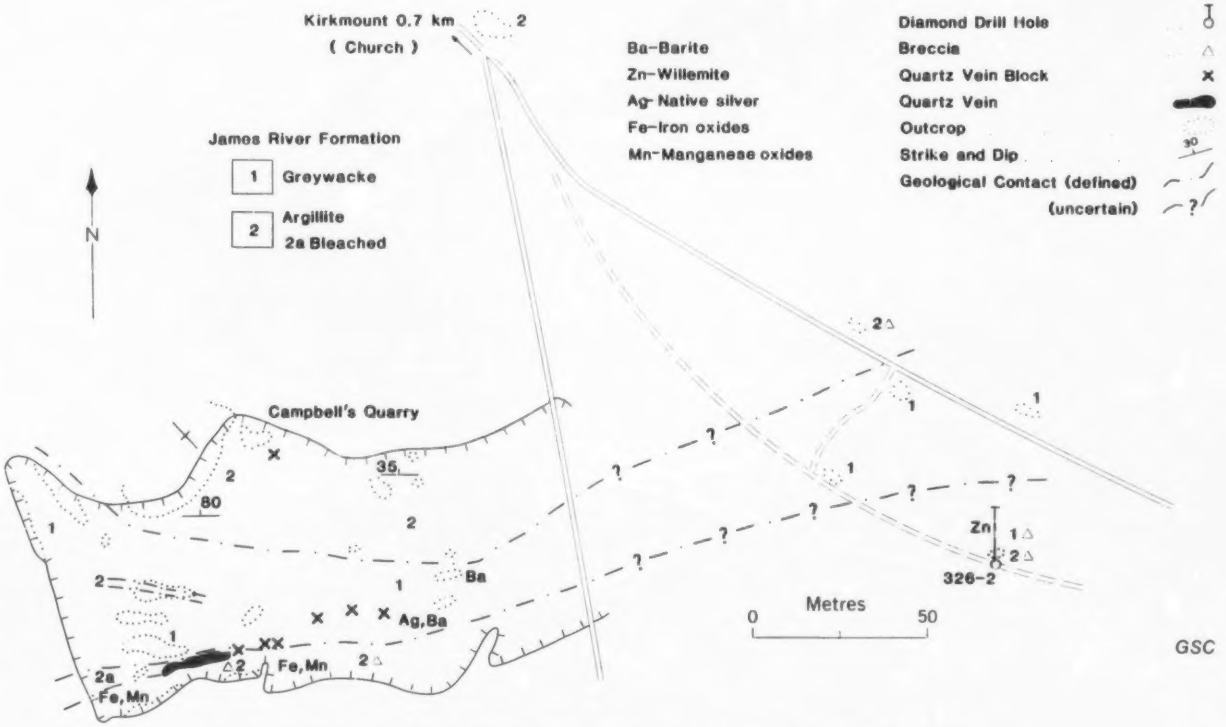

Figure 18.2. Geology of the Campbell Quarry area, Kirkmount, Nova Scotia.

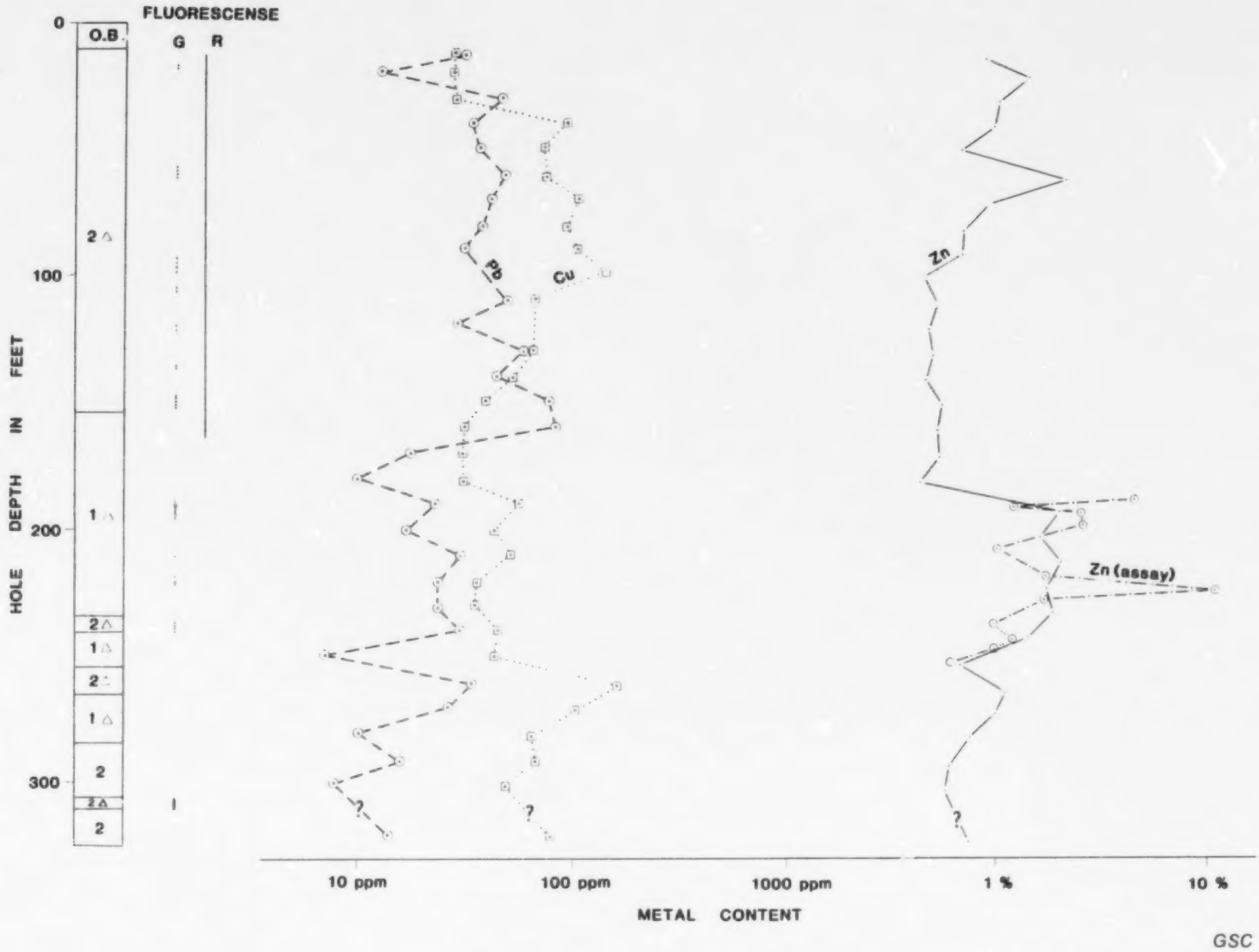

Figure 18.3. Lithologic log of hole 326-2 with chemical profiles from Sangster (1980). Cu, Pb and Zn and geochemical analyses of continuous sludges. Samples represent 10 foot intervals. Zn (assay) is the result of assay of 68.3 feet of core. G – green fluorescence, R – red fluorescence. See Figure 18.2 for legend.

Figure 18.4. Brecciated greywacke (grey) with pink calcite veins (KQS-85-32, Hole 326-2, 147 ft). (GSC 204321-B)

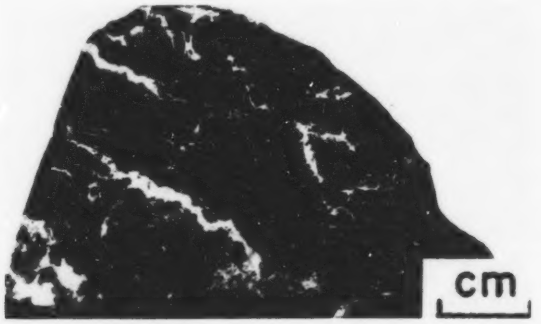

Figure 18.5. Brecciated chloritic greywacke (grey) with hematitic alteration (darker grey to black) containing 1 to 7 mm veinlets of willemite (white) (Sample KQS-85-41, Hole 326-2, 219 ft). (GSC 204321-F)

Figure 18.6. Hairline fracture fillings of willemite (white) in greywacke (grey) (Sample KQS-85-39, Hole 326-2, 194 ft). (GSC 204321-E)

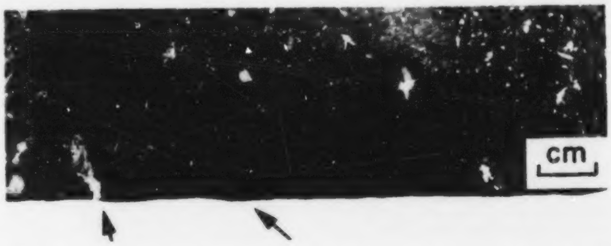

Figure 18.7. Breccia containing larger greywacke clast (dark grey) with truncated calcite veinlets (arrows) in a matrix of smaller argillite clasts with a granular argillite matrix. (Sample KQS-85-22, Hole 326-2, 49.5 ft). (GSC 204321)

2. The contents of Cu, Pb, Ag, Sr, and Ba are all within normal background ranges with the exception of slightly anomalous leads in samples KQS-85-27, 33 and 39 and 0.46 oz/t Ag in sample 28. Barium values are low considering the presence of trace amounts of barite in veinlets on surface.

Native silver occurrence

Native silver was found in a fractured and brecciated quartz-carbonate vein in Campbell's rock quarry while investigating the area near the zinc occurrence (Fig. 18.2). The small quarry measuring 70 by 150 m contains interbedded and highly fractured grey-green and green argillite and grey to grey-green greywacke similar to that in the drillhole but less brecciated. Irregular quartz and carbonate veins and vein networks occur scattered throughout the quarry. Near quartz veins along the south side of the quarry, the argillites have been brecciated and invaded by ferruginous calcite and siderite. The Fe-bearing carbonates have been oxidized, forming an extensive Fe- and Mn-stained area. Near the quartz veins, the argillites have been altered and bleached to a pale grey-green colour.

The native silver occurs as blebs up to 1 cm in length (Fig. 18.8) in a 50 cm-diameter block of brecciated bull quartz vein material containing a dark brown-weathering white carbonate matrix. A 5 cm barite rosette was present in the same block but not near the silver. The block was found at the east end of the quarry and was probably derived from the southwest corner of the quarry. The native silver is hosted by the carbonate in fractured quartz vein material and is associated with a dark green chlorite. Extensive prospecting and slabbing of quartz-carbonate vein material indicates that the silver is not widespread and to date is only of mineralogical interest.

Table 18.1. Assays on selected core samples from hole 326-2 (per cent except silver in oz/T)[1]

Sample No.	Depth (ft)	Cu	Pb	Zn	Ag	Sr	Ba	Fluorescence*
KQS-85-20	21.5	0.003	0.005	1.04	0.04	0.001	0.037	T-r
KQS-85-21	26.5	0.001	0.005	0.07	0.04	0.001	0.023	T-G, r
KQS-85-22	49.5	0.006	0.008	0.52	0.02	0.002	0.022	T-R
KQS-85-23	53.0	0.016	0.004	1.97	0.05	0.002	0.072	T-R, r
KQS-85-24	55.5	0.003	0.007	0.89	0.01	0.003	0.061	T-r
KQS-85-25	59.0	0.002	0.007	0.67	0.01	0.003	0.053	T-R
KQS-85-26	75.5	0.001	0.004	0.73	0.01	0.001	0.060	T-G, M-r
KQS-85-27	73.0	0.003	0.042	0.93	0.02	0.003	0.057	M-R
KQS-85-28	119.0	0.002	0.006	0.40	0.46	0.003	0.047	M-G, A-R
KQS-85-29	134.5	0.002	0.002	0.56	0.01	0.001	0.040	T-R
KQS-85-30	139.0	0.002	0.002	0.56	0.02	0.003	0.054	T-r
KQS-85-31	144.0	0.001	0.002	0.33	0.02	0.002	0.041	M-R
KQS-85-33	151.0	0.001	0.021	0.46	0.04	0.002	0.055	M-R
KQS-85-34	158.5	0.001	0.004	0.91	0.01	0.005	0.031	N
KQS-85-35	172.0	0.001	0.003	1.03	0.01	0.002	0.022	T-r
KQS-85-36	177.0	0.002	0.002	0.43	0.02	0.006	0.004	T-r
KQS-85-39	194.0	0.005	0.016	11.20	0.02	0.001	0.031	A-G
KQS-85-43	229.0	0.002	0.004	0.30	0.01	0.012	0.026	N
KQS-85-44	273.0	0.004	0.006	1.36	0.01	0.001	0.005	M-r
KQS-85-45	201.0	0.002	0.006	1.05	0.01	0.004	0.062	N

* Fluorescence symbols: R-bright red, r-dull red, G-green, N-none, T-trace, M-moderate concentration, A-abundant fluorescent variety

[1] Assays by Bondar-Clegg & Company Ltd.

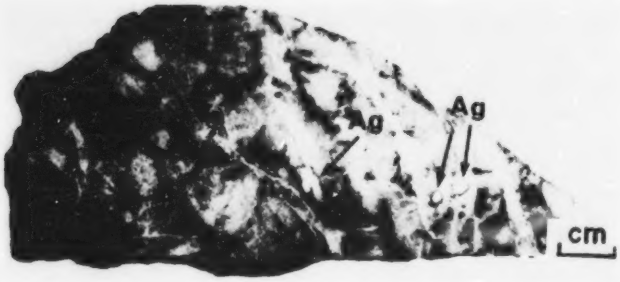

Figure 18.8. Native Silver in calcite veins (white) cutting quartz (med grey) and chlorite (dark grey to black) (Sample KQS-85-55, Campbell Quarry). (GSC 204321-A)

Possible interrelationship of willemite and silver

Although the willemite and native silver occurrences are separate localities a close genetic association is possible. The minerals occur about 200-300 m apart in similar gash veins in similar host rocks. The Zn soil geochemical anomaly outlined by St. Joseph Explorations Limited extends from east of the drillhole to an area near the quarry. However, it apparently does not extend into the quarry (Sangster et al., 1979; Wowkodaw, 1979). The position of the anomaly suggests that the willemite extends to within 100 m of the silver and is roughly on strike. Also, minor Ag values were reported in drillhole sample KQS-85-28.

Discussion

Willemite at Kirkmount is associated with ferruginous and manganiferous carbonates, hematite and specularite on surface joints and fractures, and silver. Minor siderite is present and further investigation may show that siderite and/or ankerite are more widespread than is currently apparent.

A literature survey on willemite indicates that it occurs most commonly as a supergene mineral in arid climates in the oxidized zones of Zn deposits. Lindgren (1908) reported willemite in association with calcite, smithsonite, calomine and hydrozincite from the supergene zone at Tres Hermanas, Mexico. It occurs in the oxidized zone at Balmat, New York with hematite, specularite, secondary (white) sphalerite, galena and chlorite (Brown, 1936). At Beltana, Australia, colloform willemite occurs with smithsonite and a complex suite of secondary lead and zinc arsenates, phosphates, manganates and vanadinates (Muller, 1972). At the Teneginskii deposit, Russia, Okhapkin et al. (1981) documented a large number of associated supergene minerals with willemite including goethite, hydrogoethite, hydromica, calcite, dolomite, ankerite, quartz and sericite. Many willemite occurrences are described by Pough (1941) who considered that the supergene environment is the normal habitat for willemite and that other occurrences, such as in high grade metamorphic rocks at Franklin Furnace, N.J. (Brown, 1968) and in alkaline intrusions (Metcalf-Johansen, 1977; Chao et al., 1967) are unusual. Pough pointed out that willemite forms under oxidizing conditions which favour the production of hematite rather than limonite (when hemimorphite is produced).

Much remains to be documented about the Kirkmount occurrence before its origin can be demonstrated. However, as a preliminary comment, the Kirkmount mineral assemblages are compatible with those referred to above; the presence of hematite and specularite in joints and fractures is in agreement with the observation of Pough (1941) stated above; and the colloform textures exhibited in specimen KQS-85-41 are similar to those described by Muller (1972). These data support a supergene origin for the willemite at Kirkmount, perhaps related to a Carboniferous or Cretaceous arid climate.

On the other hand, with the exception of the presence of willemite, the Kirkmount occurrence bears a strong resemblance to a series of carbonate-dominant, fracture-controlled mineral occurrences which are spatially related to the Cobequid-Chedabucto fault zone (Fig. 18.1). The Londonderry supergene limonite-hematite deposits result from the weathering of ferruginous carbonates (Weeks, 1948; Wright, 1975) which are within breccia zones along the Cobequid fault. Barite, sphalerite, galena, chalcopyrite and silver are minor constituents of these breccias (Felderhof, 1978; Chatterjee, 1983). At Brookfield, siderite and barite-siderite bodies occur in late faults cutting Horton sediments (Wright, 1975) and at Walton, massive barite-siderite and complex lead-zinc-copper-silver deposits are associated with late faults cutting Windsor and Horton Group sedimentary rocks (Boyle, 1972). Chalcopyrite is found in association with ankerite, pyrite and sphalerite in fault breccias at Mount Thom (Ponsford and Lyttle, 1984). East of Kirkmount, at College Grant, chalcopyrite occurs in small veins with siderite, hematite, calcite, specular hematite and pyrite (Nova Scotia Department of Mines and Energy, Mineral Index File). Except at Walton no research has been done on these deposits but all are generally considered to be of hydrothermal origin (Boyle, 1972; Weeks, 1948; Wright, 1975) within faults and fault related breccias of the Cobequid-Chedabucto fault zone. Major strike-slip movement on this fault is believed to have continued from Siluro-Devonian to Carboniferous with dip-slip movement continuing into the Upper Triassic and Lower Jurassic (Donohoe and Wallace, 1979). Since mineralization at Mount Thom, Walton and Brookfield cuts Carboniferous sedimentary rocks, the mineral occurrences could range anywhere in age from Carboniferous to Jurassic. The Kirkmount deposits have many features in common with these hydrothermal deposits and the possible presence of primary hydrothermal willemite can not be ruled out.

The occurrence of willemite as a possible source of soil and rock geochemical zinc anomalies should be noted, with the realization that in follow-up prospecting, the presence of the usual limonitic surficial alteration normally associated with Fe-bearing sphalerite decomposition may be absent. The use of commercially available Zn test solution (Zinc ZAP) and extensive rock geochemical analyses are essential to the effective prospecting of this type of occurrence. At Kirkmount it was noted that Zn test solution gave a positive response when applied to managanese oxide coatings on joint surfaces within the geochemically anomalous area when no Zn minerals could be seen. The scavenging of Zn by manganese is detectable and this test may prove effective in prospecting areas of anomalous Zn.

Acknowledgments

Confirmation of the identification of native silver was made by D.C. Harris on the electron microprobe. X-ray diffraction identifications of willemite and calcite were made by R.N. Delabio. K.V. Kirkham and D.F. Sangster reviewed the manuscript and made helpful suggestions. The writer thanks the Nova Scotia Department of Mines and Energy for the use of their rock preparation facilities at the Core Library in Stellarton, Nova Scotia.

References

Bell, W.A.
1940: The Pictou Coalfield, Nova Scotia; Geological Survey of Canada, Memoir 225, 161 p.

Benson, D.G.
1974: Geology of the Antigonish Highlands, Nova Scotia; Geological Survey of Canada, Memoir 376, 92 p.

Berry, L.G. and Mason, B.
1959: Mineralogy; W.H. Freeman and Company, San Francisco, 612 p.

Bingley, J.M.
1977: Stream sediment geochemical reconnaissance program – New Glasgow area; Nova Scotia Department of Mines, Open File Report 325, 15 maps.

Boyle, R.W.
1972: Geology, geochemistry and origin of the barite, manganese, lead-zinc-copper-silver deposits of the Walton-Cheverie area, Nova Scotia; Geological Survey of Canada, Bulletin 166, 181 p.

Brown, J.S.
1936: Supergene sphalerite, galena and willemite at Balmat, N.Y.; Economic Geology, v. 31, no. 4, p. 331-354.

1968: Ore deposits of the northeastern United States; in Ore deposits in the United States, Graton-Sales Volume; (ed) John D. Ridge, American Institute of Mining, Metallurgical and Petroleum Engineers, Inc., p. 1-19.

Chao, C.Y., Harris, D.C., Hounslow, A.W., Mandarino, J.A., and Perrault, G.
1967: Minerals from the nepheline syenite, Mont St. Hilaire, Quebec; The Canadian Mineralogist, v. 9, pt. 1, p. 109-123.

Chatterjee, A.K.
1983: Metallogenic map of the Province of Nova Scotia; Nova Scotia Department of Mines and Energy.

Donohoe, H.V. and Wallace, P.I.
1979: Anatomy of the Cobequid fault and its relation to the Glooscap and Cabot Fault Systems, in Mineral Resources Division Report of Activities 1978, Nova Scotia Department of Mines, p. 162.

Felderhof, G.W.
1978: Barite, celestite and fluorite in Nova Scotia; Nova Scotia Department of Mines, Bulletin No. 4, 463 p.

Fletcher, H.
1886: Report on geological surveys and explorations in the counties of Guysborough, Antigonish and Pictou; Geological Survey of Canada, Annual Report for 1885, v. 2, p. 5-128.

Ford, W.E.
1964: Dana's Textbook of Mineralogy, Fourth Edition; John Wiley and Sons, 851 p.

Keppie, J.D.
1978: Browns Mountain Group, Antigonish Highlands, Nova Scotia – preliminary reassessment; Geological Society of America, Northeastern Section, Program with Abstracts, p. 50.

Lindgren, W.
1908: New occurrence of willemite and anhydrite; Science, v. 18, p. 933.

Maehl, R.H.
1961: The older Palaeozoic rocks of Pictou County, Nova Scotia; Province of Nova Scotia, Department of Mines, Memoir No. 4, 112 p.

McGowan, D.
1980: Fluorescence; Canadian Rockhound, v. 24, no. 4, p. 24-28.

Metcalf-Johansen, J.
1977: Willemite from the Ilimaussage alkaline intrusion; Mineralogical Magazine, v. 41, no. 1, p. 71-75.

Muller, D.W.
1972: Geology of the Beltana willemite deposits; Economic Geology, v. 67, no. 8, p. 1146-1167.

Murphy, J.B.
1985a: Geology of the southwestern Antigonish Highlands, Nova Scotia; in Current Research, Part B, Geological Survey of Canada, Paper 85-1B, p. 519-530.

1985b: Geological maps of the central and southern Antigonish Highlands, Nova Scotia; Geological Survey of Canada, Open File 1181.

Murphy, J.B., Keppie, J.D., and Hynes, A.J.
1979: Geology of the northern Antigonish Highlands; in Nova Scotia Department of Mines, Report of Activities, Report 79-1, p. 105-107.

1982: Geological map of the northern Antigonish Highlands, Nova Scotia; Nova Scotia Department of Mines and Energy, Map 82-3.

Okhapkin, N.A., Miroshnikou, A.E., and Strimzha, T.P.
1981: Geological and mineralogical features of the ancient mature zone of oxidation of the Teneginskii lead-zinc deposit; Soviet Geology and Geophysics, v. 22, no. 1, p. 47-52.

Ponsford, M. and Lyttle, N.A.
1984: Metallic mineral occurrence map and data compilation, Central Nova Scotia – Map Sheets 11D and 11E; Nova Scotia Department of Mines and Energy, Open File Report 599, 12 p.

Pough, F.H.
1941: Occurrence of willemite; American Mineralogist, v. 26, no. 2, p. 92-102.

Sangster, A.L.
1978: Report on a drainage geochemical survey, Kirkmount area, Pictou County, Nova Scotia; Nova Scotia Department of Mines and Energy, Mineral Assessment File 07-M-39(01).

1980: Report on diamond drilling, Kirkmount – Project 1326; Nova Scotia Department of Mines and Energy, Mineral Assessment File 07-M-39(04).

Sangster, A.L., Brown, D., and St. George, T.
1979: Geology and soil geochemistry survey maps; Nova Scotia Department of Mines and Energy, Mineral Assessment File 07-M-39(02).

Weeks, L.J.
1948: Londonderry and Bass River map areas, Colchester and Hants Counties, Nova Scotia; Geological Survey of Canada, Memoir 245, 86 p.

Williams, M.Y.
1914: Arisaig-Antigonish district, Nova Scotia; Geological Survey of Canada, Memoir 60, 173 p.

Wowkodaw, O
1979: Report on geochemical soil survey, Kirkmount, Pictou County, Nova Scotia; Nova Scotia Department of Mines and Energy, Mineral Assessment File 07-M-39(03).

Wright, J.D.
1975: Iron deposits of Nova Scotia; Nova Scotia Department of Mines, Economic Geology Series 75-1, 154 p.

Yeo, G. and Murphy, B.
1985: Preliminary Geological map of the New Glascow – Toney River area; (NTS 11E10, 15 in prep).

Preliminary account of the geology around Wager Bay, District of Keewatin

Projects 850004, 840003

J.R. Henderson[1], A.N. LeCheminant[1], C.W. Jefferson[2], K. Coe[3], and M.N. Henderson[2]

Henderson, J.R., LeCheminant, A.N., Jefferson, C.W., Coe, K., and Henderson, M.N., Preliminary account of the geology around Wager Bay, District of Keewatin; in Current Research, Part A, Geological Survey of Canada, Paper 86-1A, p. 159-176, 1986.

Abstract

In the northern coastal area of Wager Bay, banded orthogneiss and amphibolite grade supracrustal rocks of Archean or Early Proterozoic age are multiply deformed, attenuated and intruded by Early Proterozoic calc-alkaline I-type plutons which were subsequently weakly deformed. In the southern, east-trending part of Wager Bay, the same rock types are mylonitized in a zone at least 25 km wide.

Preliminary results of the mapping are presented here in three parts: 1) Megacrystic granite and granodiorite, Ford Lake; 2) Geology north of the Wager Bay Shear Zone; 3) Geology of the Wager Bay Shear Zone.

Résumé

Dans la zone côtière nord de la baie Wager, des orthogneiss rubannés et roches supracorticales de faciès amphibolite, d'âge archéen ou protérozoïque sont déformées plusieurs fois et atténuées. Au début du Protérozoïque, des plutons calco-alcalins de type I y sont intrusifs et sont par la suite faiblement déformés. Au sud, dans la partie de la baie Wager d'orientation est-ouest, les mêmes types de roches sont mylonitisés dans une zone large d'au moins 25 km.

Les résultats préliminaires des levés sont présentés ici en trois parties: 1) granite et granodiorite mégacrystiques, lac Ford; 2) géologie au nord de la zone de cisaillement de la baie Wager; 3) géologie de la zone de cisaillement de la baie Wager.

[1] Precambrian Geology Division
[2] Economic Geology and Mineralogy Division
[3] University of Exeter

Introduction

The bedrock geology of Wager Bay region interests us for the following reasons: (1) a composite batholith with a distinctive aeromagnetic anomaly pattern north of Ford Lake provides insight into the character of late Hudsonian granitic magmatism in the central Churchill Province in the Baker Lake-Repulse Bay region; (2) a belt of supracrustal rocks on the southwest coast of Wager Bay outlined by helicopter reconnaissance (Heywood, 1967) needs more detailed mapping for the purpose of mineral resource assessment prior to the establishment of a national park; (3) aeromagnetic anomaly maps of the central Churchill Province indicate that a major shear zone occurs along the south coast of Wager Bay.

Acknowledgments

The resource assessment aspect of this project was partially funded by contributions from Environment Canada and the Department of Indian and Northern Affairs. Polar Continental Shelf Project provided rotary-wing support and Parks Canada loaned fuel to C.W.J. that helped us over the break-up period in early July. We are extremely grateful to Subhas Tella for many expediting services in Rankin Inlet. With his gracious help many potential problems were avoided. Our student assistants, Isabelle Derome, Nick Vallinakis, Diane Brent, Jim Shaver, Paula MacKinnon and Robin Wyllie were eager and able to carry out all their assignments, and their efforts are greatly appreciated. We thank Jon Scoates for spending ten days helping us to sort out the rocks in the beginning of the season.

PART 1: MEGACRYSTIC GRANITE AND GRANODIORITE, FORD LAKE

A.N. LeCheminant

Introduction and geological setting

A broad spectrum of coarse grained granitic rocks are well exposed in rugged country at the head of Wager Bay (area 1, Fig. 19.1). Ford Lake is a tidal lake joined to Wager Bay by a reversing falls. Five weeks mapping in 1985 was limited to areas accessible by boat or foot traverses from Ford Lake or from a Y-shaped lake to the northeast (Fig. 19.2).

North of Ford Lake three major units of coarse grained porphyritic to megacrystic granitic rocks coalesce to form a composite batholith exceeding 300 km^2 in area. This batholith, informally named the Ford Lake batholith, comprises a discrete 140 km^2 pluton of magnetite-sphene-biotite monzogranite in contact to the north with a coarser grained fluorite-biotite syenogranite. The syenogranite is bounded to the northwest by hornblende-biotite granodiorite. At all external contacts, the batholith intruded amphibolite-grade granitic and granodioritic gneiss that locally contain sheets of foliated leucocratic granite.

The batholith is part of an extensive northeast-trending belt of Early Proterozoic massive to slightly foliated biotite and biotite-hornblende granite and granodiorite mapped and briefly described by Heywood (1961, 1967). The plutonic belt extends more than 300 km from the Wager Bay Shear Zone to Committee Bay and consists of at least 12 discrete bodies. Aeromagnetic and radiometric maps (Geological Survey of Canada 1974, 1977, 1984a, b) were published after the reconnaissance geological mapping. Preliminary reinterpretation of the combined data suggests that many of the bodies are composite plutons, elliptical to subcircular in plan, consisting of magnetite-rich plutons and closely associated, less magnetic, K-Th-U-enriched granites. The Ford Lake batholith is a well exposed example of one of these composite bodies. Heywood (1967) and Wanless et al. (1967) report an age for the batholith of 1630 ± 50 Ma (K-Ar, biotite). The age recalculated with revised decay constants (Steiger and Jager, 1977) is 1635 ± 50 Ma.

Pre-batholith rocks

Pre-batholith rocks have been subdivided into four lithological packages: (1) banded grey biotite and biotite-hornblende granodiorite and quartz diorite gneiss with enclaves of supracrustal rocks; (2) augen granite and granodiorite gneiss; (3) migmatitic granite and granodiorite gneiss with sheets of foliated leucocratic granite; and (4) weakly porphyritic foliated granite.

Enclaves of supracrustal rocks enclosed within banded gneiss include biotite paragneiss, feldspathic quartzite, sillimanite schist, and thin discontinuous boudinaged units of amphibolite and ultramafic rocks. An orthogneiss unit of microcline augen granite and granodiorite gneiss is in gradational contact with banded gneiss. Both units contain bands of protomylonite gneiss with a prominent L-S fabric. Regional foliation trends are southwesterly with moderate to shallow northwesterly dips. Mineral lineations consistently plunge shallowly to the west.

Sheets of foliated leucocratic biotite and biotite-hornblende granite intruded migmatized equivalents of the banded gneiss/paragneiss unit south and east of the batholith. Migmatized granitic gneiss is also exposed in the steep walls of the drift-covered valley west of the Y-shaped lake.

The fourth pre-batholith unit is a discrete body of foliated pink biotite granite that underlies at least 12 km^2 and forms rubbly, frost-heaved outcrops. It intruded banded gneiss but is found as xenoliths in the batholith. The weakly porphyritic magnetite-biotite granite is fine- to medium-grained and has a colour index of 2-5. Adjacent to its eastern contact the granite contains irregular crosscutting veins and crude bands of syenogranite with coarse biotite and magnetite crystals. This veining is probably a contact effect of the monzogranite intrusion.

Ford Lake batholith

Magnetite-sphene-biotite monzogranite

The southernmost pluton in the Ford Lake batholith is a homogeneous 140 km^2 body of coarse grained porphyritic to megacrystic monzogranite. Internal foliation within the body, largely defined by pink tabular 1-3 cm microcline crystals, is nearly concordant with mineral foliation and gneissosity in adjacent country rocks (Fig. 19.2). The pluton contains enclaves of fine- to medium-grained meta-sedimentary rocks including microcline-rich quartzite, sillimanite-cordierite schist, and garnet-diopside, wollastonite and scapolite-diopside calc-silicate and marble. Enclaves typically range from a few metres to a few tens of metres, however, several attain widths of at least 60 m and one has been traced for more than 1 km. Screens of granitoid gneiss are preserved near the southeastern contact of the pluton and rare xenoliths of foliated biotite granite occur along its western contact.

Mineralogically the monzogranite is characterized by tabular phenocrysts (1-3 cm) and some megacrysts (4-5 cm) of Carlsbad-twinned perthitic microcline set in a coarse grained matrix of oligoclase, microcline and quartz. Thin rims of albite or myrmekite occur along microcline-oligoclase boundaries. Mafic minerals include fresh biotite (8-15%) and up to 2% magnetite and 2% sphene. Euhedral rhombs of sphene up to 6 mm form partial or complete coronas around magnetite. Hornblende is rare or absent. Accessory minerals are pyrite, apatite, allanite, and zircon. Zircon crystals are large and abundant, many have discrete cores and zoned rims. Samples from this pluton and the

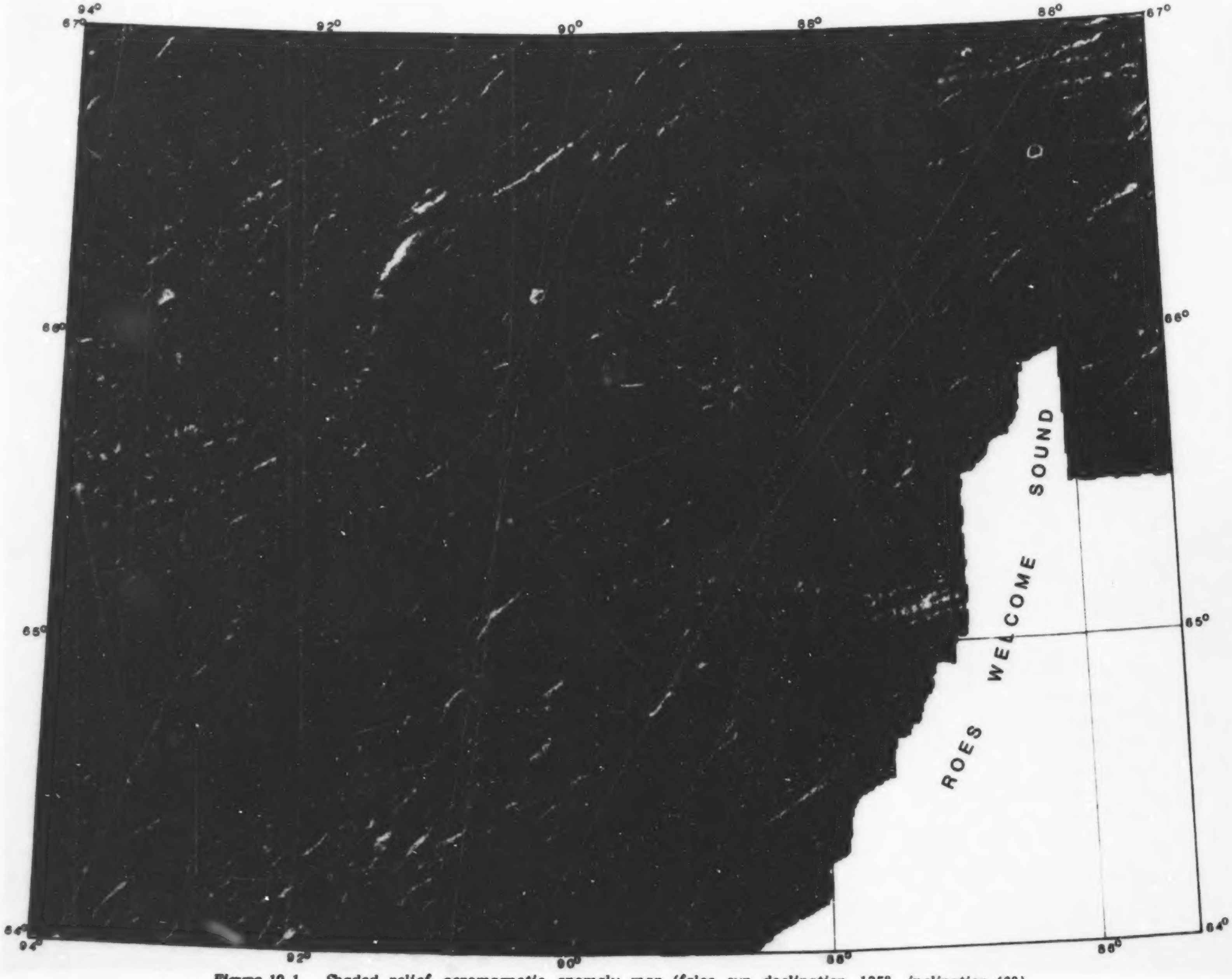

Figure 19.1. Shaded relief aeromagnetic anomaly map (false sun declination 135°, inclination 40°) showing the outlines of the regions discussed in Part 1 (area 1), Part 2 (areas 2 and 3), and Part 3 (area 4).

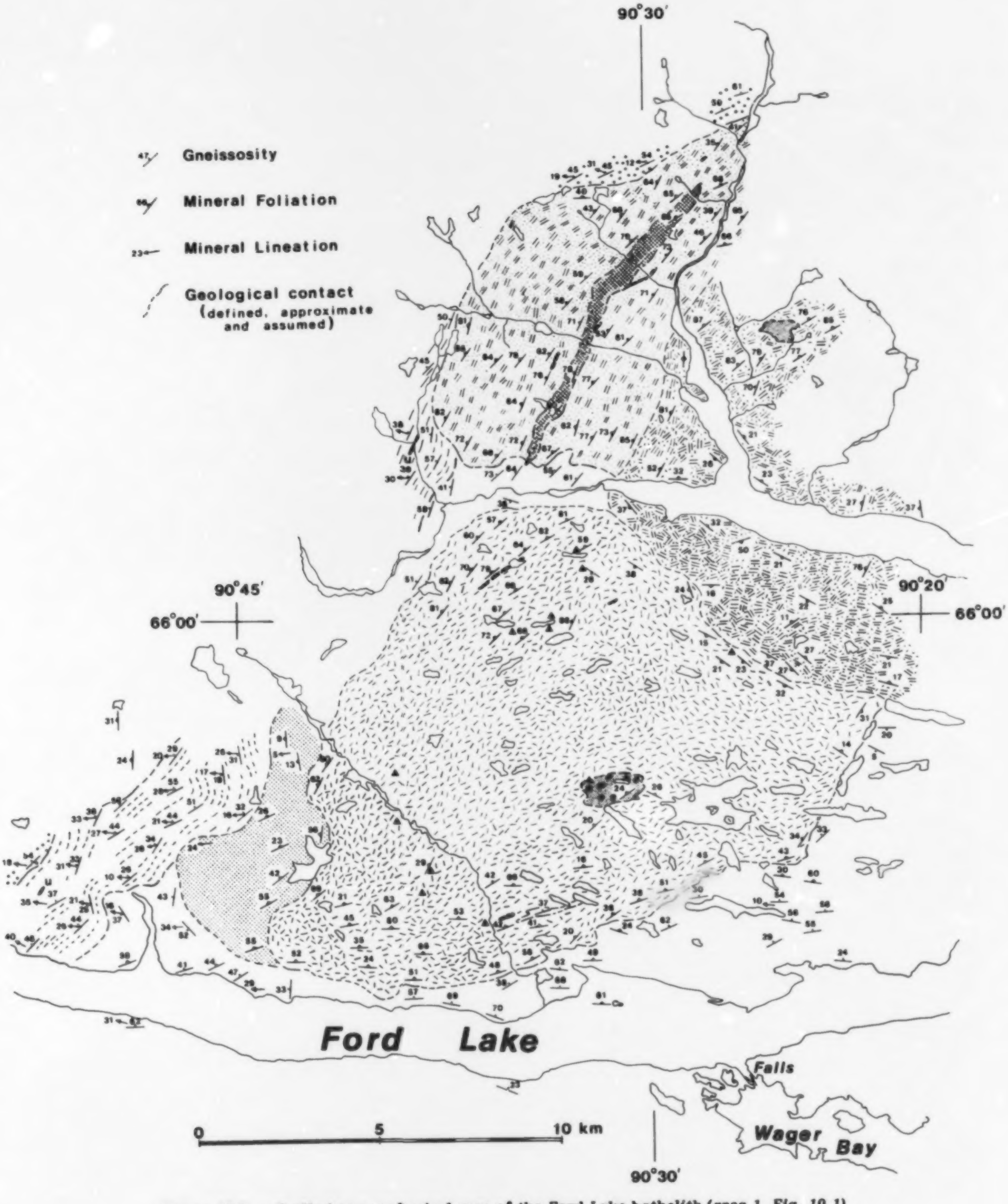

Figure 19.2. Preliminary geological map of the Ford Lake batholith (area 1, Fig. 19.1).

syenogranite will be dated by U-Pb zircon chronology for comparison with ages obtained for plutonic rocks within and immediately adjacent to the Wager Bay Shear Zone.

Fluorite-biotite syenogranite

Deeply weathered, pink to red, megacrystic syenogranite is exposed in steep cliffs up to 400 m high along both arms of the Y-shaped lake. The eastern and northern contacts of the body have not yet been mapped but its extent exceeds 80 km^2. Weak foliation defined by microcline megacrysts is shallow-dipping and erratic within the pluton but along its southern and western contacts the foliation is subparallel to foliations in the structurally overlying monzogranite and granodiorite. Xenoliths are extremely rare. Only one area with garnet-bearing metasedimentary enclaves was noted. Ubiquitous but minor small dykes and veins of fine grained pink aplite and leucocratic medium grained biotite granite are probably genetically related to the host syenogranite. Some dykes are dismembered and contain a contact parallel foliation and/or compositional zoning. These dykes probably are the result of late-stage fluids emplaced in fractures when crystallization of the pluton was almost complete.

Megacrysts of perthitic microcline make up 50% or more of the syenogranite. They typically range from 2-4 cm but crystals to 6 cm are not unusual and in exceptional cases tabular crystals reach 9-10 cm in length. Inclusions of plagioclase and biotite within some megacrysts define concentric zones parallel to crystal faces suggesting several growth stages. The matrix consists of coarse-grained quartz, plagioclase and microcline with 5-10% clots of biotite, hornblende and allanite. High radioelement content in the abundant euhedral allanite has produced hydrated metamict crystals. Colour variations visible microscopically show the original crystals were complexly zoned. Quartz grains adjacent to the hydrated allanites contain radial patterns of microfractures and adjacent biotites are kink-banded. Accessory minerals (fluorite, sphene, iron oxides, apatite, and zircon) are spatially associated with clusters of ferromagnesian minerals. Sulphides are rare although a few grains of molybdenite were noted.

Hornblende-biotite monzogranite/granodiorite

The 4.5 km wide northeast-trending monzogranite to granodiorite body underlies more than 50 km^2. Textural and mineralogical similarities to the megacrystic syenogranite indicate this granodiorite may be a comagmatic border phase. The pluton has sharp near concordant external contacts except along its southern contact (Fig. 19.2). The strong internal foliation trends 210-220° and dips moderately to steeply northwest. Thin dykes and veins of biotite leucogranite and aplite are less abundant than in the syenogranite. A few veins up to 4 cm wide containing coarse allanite crystals were emplaced into minor shear zones.

The granodiorite is coarse grained with tabular microcline megacrysts to 6 cm and smaller zoned plagioclase phenocrysts. Biotite (5-11%) and hornblende (3-6%) are the principal ferromagnesian minerals. They are concentrated in clusters with accessory sphene, magnetite, allanite, apatite and abundant zircon.

Legend for Figure 19.2

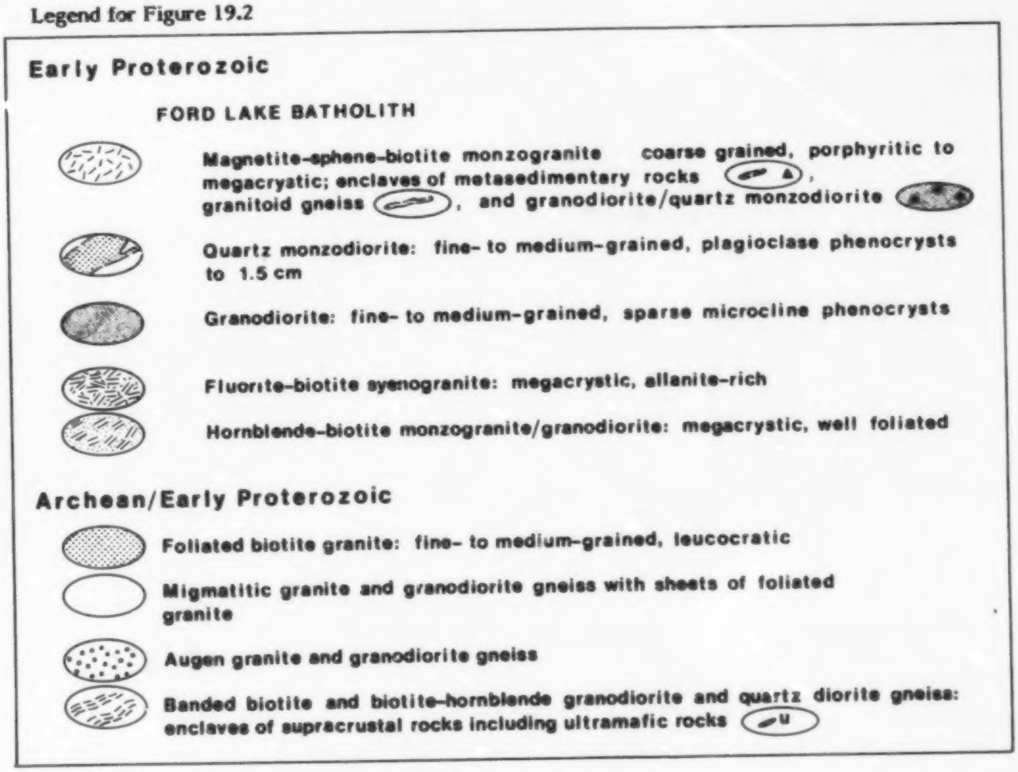

Minor intrusions

The syenogranite was intruded by small (<1 km^2) irregular bodies of fine- to medium-grained weakly foliated granodiorite with a colour index of 15-20. The granodiorite contains sparse microcline phenocrysts to 1 cm and is slightly finer grained adjacent to contacts and in small offshoot dykes. The stock shown in Figure 19.2 is the only mapped intrusion of several inferred from air photo interpretation.

The magnetite-sphene-biotite monzogranite contains a small body of foliated porphyritic granodiorite or quartz monzodiorite similar to the intrusion described above. The granodiorite contains enclaves of fine grained metasedimentary rocks especially along its outer contacts. Veins and sheets of monzogranite along the outer contacts are associated with porphyroblastic microcline in the granodiorite. These observations suggest both metasedimentary rocks and granodiorite are enclaves within the monzogranite.

A northeast-trending dyke of dark grey porphyritic quartz monzodiorite intruded the hornblende-biotite granodiorite. The 9 km long dyke has a fine grained chilled zone along both margins. The rock contains 15-20% uniformly distributed plagioclase phenocrysts to 1.5 cm and scattered rare microcline xenocrysts. The matrix comprises plagioclase, subequal proporations of biotite and hornblende totalling about 25%, and a fine grained vermicular intergrowth of alkali feldspars and quartz. Accessory minerals are opaques (3%), probably mainly magnetite, apatite (1%), and trace sphene, allanite, epidote and carbonate. Branching subparallel dykes along the southeastern side of the main dyke resemble the chill margin of the main dyke throughout. At both ends of the dyke and locally along its northwestern margin a thin unit of medium grained biotite monzogranite or quartz monzonite separates megacrystic granodiorite from the chill margin of the dyke.

Irregular dykes and lensoid bodies of granite pegmatite up to one metre wide are common around the margins of the Ford Lake batholith. Less abundant pegmatites cut all units of the batholith. Both simple pegmatites and zoned pegmatites with quartz cores contain large crystals of graphic-textured microcline, minor biotite and muscovite and rare magnetite and allanite.

Discussion

Megacrystic granite and granodiorite are common rock types in calc-alkaline batholiths related to plate margin igneous activity (Bateman and Chappell, 1979; Kawachi and Sato, 1978; Reesor, 1958). High modal magnetite, hornblende and sphene in the Ford Lake batholith are characteristic of I-type plutons (Chappell and White, 1974). Most batholith rocks retain original igneous textures although prominent planar internal fabric and minor shear zones indicate some strain. These features probably result from deformation during final stages of crystallization rather than primary flow in the magma or deformation with subsolidus growth. Petrofabric and megacryst zoning studies are required to better understand the origin of the planar fabric and its relationship to megacryst formation.

Lineaments that control drainage and the shape of major lakes within the Ford Lake batholith relate primarily to prominent fracture sets within the plutonic rocks. No substantial fault offset of units within the batholith has been mapped. Preliminary work along Ford Lake suggests its southern shoreline is controlled by an east-west brittle fault.

The high magnetite content of the monzogranite and granodiorite units of the batholith causes well defined aeromagnetic anomalies that closely match the mapped contacts. The anomaly pattern on the east side of the monzogranite implies northeast-trending structural control of the pluton margin although exposed monzogranite-gneiss contacts are intrusive. The aeromagnetic anomaly over the pluton is asymmetric. A linear high on the west side suggests the pluton has a northeast-trending keel beneath its western half aligned with the quartz monzodiorite dyke to the north.

The syenogranite has a low magnetic expression compared to other units in the Ford Lake batholith. A strong K-Th-U radiometric anomaly over the pluton distinguishes it clearly from magnetically low gneisses west of the batholith. Occurrence of purple fluorite, large zoned zircons and abundant allanite indicates the syenogranite has high radioelement and REE content. Allanite-rich veins in granodiorite suggest REE and Th were mobile in hydrothermal fluids perhaps released during late crystallization of nearby syenogranite. The presence of other radioactive and REE-bearing accessory minerals is likely. Evidence for Cu-Mo mineralization sometimes associated with I-type plutons such as the Ford Lake batholith is limited to rare crystals of molybdenite within the batholith and one occurrence of chalcopyrite and malachite in migmatitic gneiss on the north shore of Ford Lake.

PART 2: THE SUPRACRUSTAL BELT NORTH OF THE WAGER BAY SHEAR ZONE

C.W. Jefferson

Introduction

A belt of supracrustal gneisses originally outlined by Heywood (1967) cropping out on the southwest coast of Wager Bay was the focus of mapping at 1:60 000 and 1:30 000 scales (areas 2 and 3, Fig. 19.1). Preliminary results of this mapping are shown in Figures 19.4 and 19.5. Figure 19.3 summarizes fourteen rock units in relative chronological order. It also is a legend for Figures 19.4 to 19.6. Figure 19.6 is a detailed map of an excellent coastal exposure that contains most of the elements discussed below. The following account describes the fourteen map units from oldest to youngest.

Supracrustal rocks (Fig. 19.3, unit 14)

Supracrustal rocks are most abundant on the mainland from north of Paliak Islands to the northern boundary of Figure 19.5, yet account for less than 30% of the bedrock outcrop. They are recessive, usually rusty weathering units dominated by semipelites (biotite-quartz-feldspar gneiss). They range in thickness from several metres to 300 m and in length from several metres to kilometres. Many continuous supracrustal units also contain remarkably continuous feldspathic sillimanite quartzite layers, but amphibolites, ultramafics, iron formation and calc-silicates are boudinaged.

The contact relationships of the supracrustal rocks are generally enigmatic. No conglomerates but common mylonitic zones define contacts of supracrustal map units. Lenticular bodies of pelitic gneiss, amphibolite and iron formation decrease in apparent abundance away from the main supracrustal units. The lenticular bodies can be interpreted as xenoliths or they can be boudins. Commonly there is evidence that the supracrustal rocks were deformed prior to their inclusion in the tonalite gneisses; as might be expected, boundaries are generally concordant with the gneisses (Fig. 19.4, 19.5 and 19.6) but internal fabrics are more complex than those external to the xenoliths.

Semipelite is medium grey and locally rusty. It usually contains layers a few centimetres to metres thick of 1-3 mm garnets. Pyrrhotite is more uniformly disseminated. Other variants include sillimanite and cordierite. Discontinuous iron formation comprises alternating magnetite and quartz laminae with minor garnet-biotite quartzite layers 1 to

10 cm thick. Locally sulphide facies are present. Quartzite units up to 100 m thick and kilometres long are feldspathic, and contain sillimanite and disseminated pyrrhotite. Calc-silicates (calcite-diopsite ± epidote, garnet, scapolite) are minor but common constituents of the supracrustal gneisses. They generally are very poddy and discontinuous. Some contain abundant pyrrhotite.

Small amphibolite boudins are common in supracrustal map units and also occur in trains within the tonalitic gneiss (Fig. 19.3, unit 13). Pillow structures are not preserved. Most boudins are less than 2 m in diameter but range up to 650 m long and 150 m wide. Foliation in the boudins is commonly rotated as much as 90° with respect to the regional gneissosity whereas the long axes of the boudins are approximately parallel to regional trends.

Ultramafic enclaves are frequently associated with the amphibolites. Hornblendites probably represent mineral variations in the basalt parent. Some ultramafic rocks are deeply altered and metamorphism was followed by hydration so that assemblages are of serpentine, chlorite, talc and amphibole, but in some examples olivine and clinopyroxene survive and the rock is lherzolite or wehrlite.

Chronological relationships are unclear in most places but in Fig. 19.6 ultramafics constitute pods in an early pegmatite dyke (Fig. 19.3, unit 9). Relationships are consistent with their being cumulates related to gabbroic intrusions. Anorthosite to gabbro enclaves range in grain size from medium to aggregates in which plagioclase crystals are tennis ball size. Anorthosite bodies more commonly have high grade, deep crustal associations and hence these enclaves may not be part of the supracrustal suite.

Pink and grey granite-tonalite gneiss (Fig. 19.3, unit 13)

The most abundant unit north of the Wager Bay Shear Zone is banded biotite granite and tonalite gneiss. Lithologically, this banded gneiss is typical of those from many late Archean terranes all known or assumed to be orthogneiss. It is logically part of the major crust-forming event that took place in the late Archean in all continental nucleii, and may yield magmatic and metamorphic ages of 2.7 to 2.9 Ga. The major granitic gneiss unit was accompanied by minor anastamosing sheet injections mainly of aplite and pegmatite from which it cannot be separated in time.

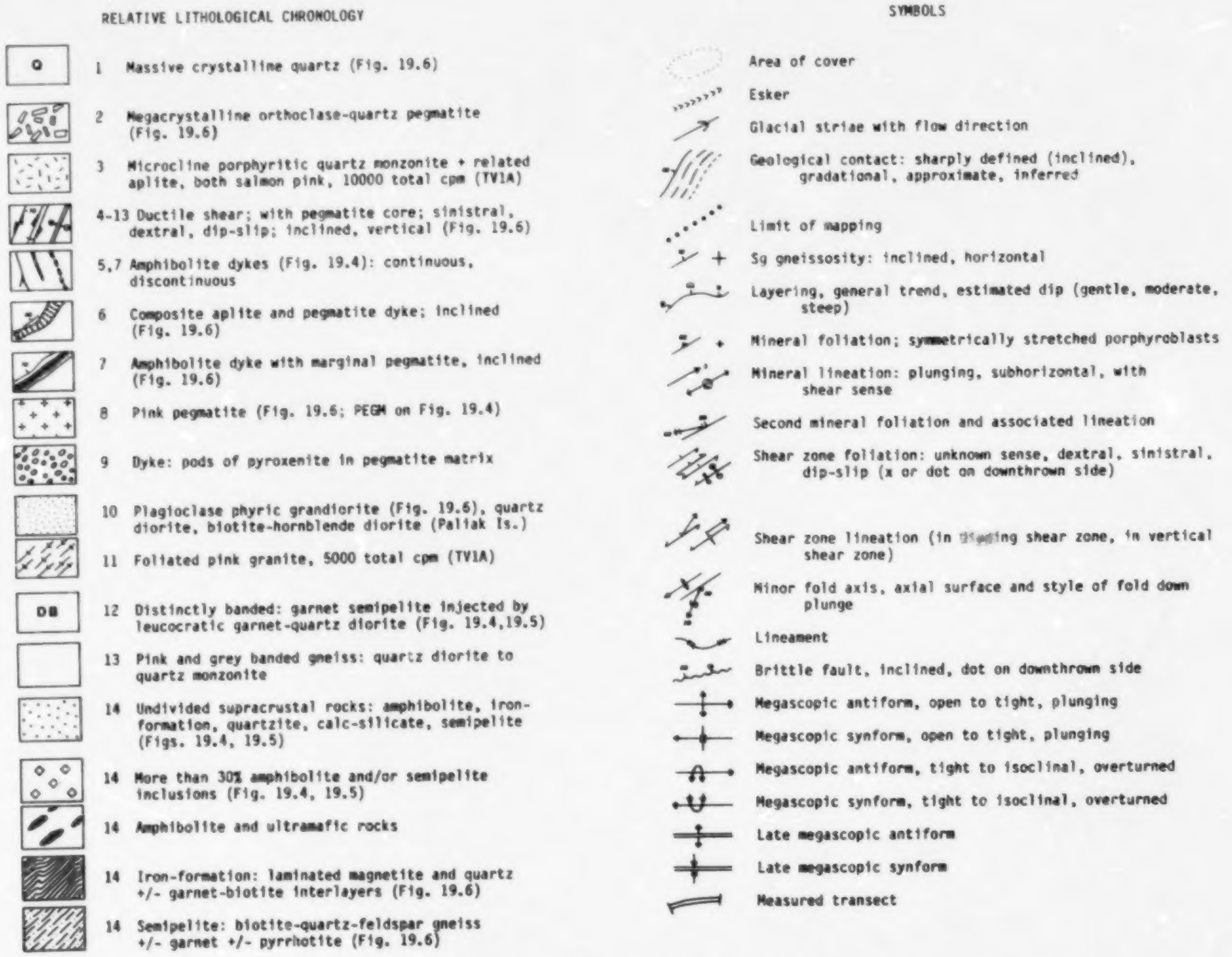

Figure 19.3. *Rock types and symbols used in Figures 19.4, 19.5 and 19.6. The rock types are arranged in relative chronological order and keyed to text by number.*

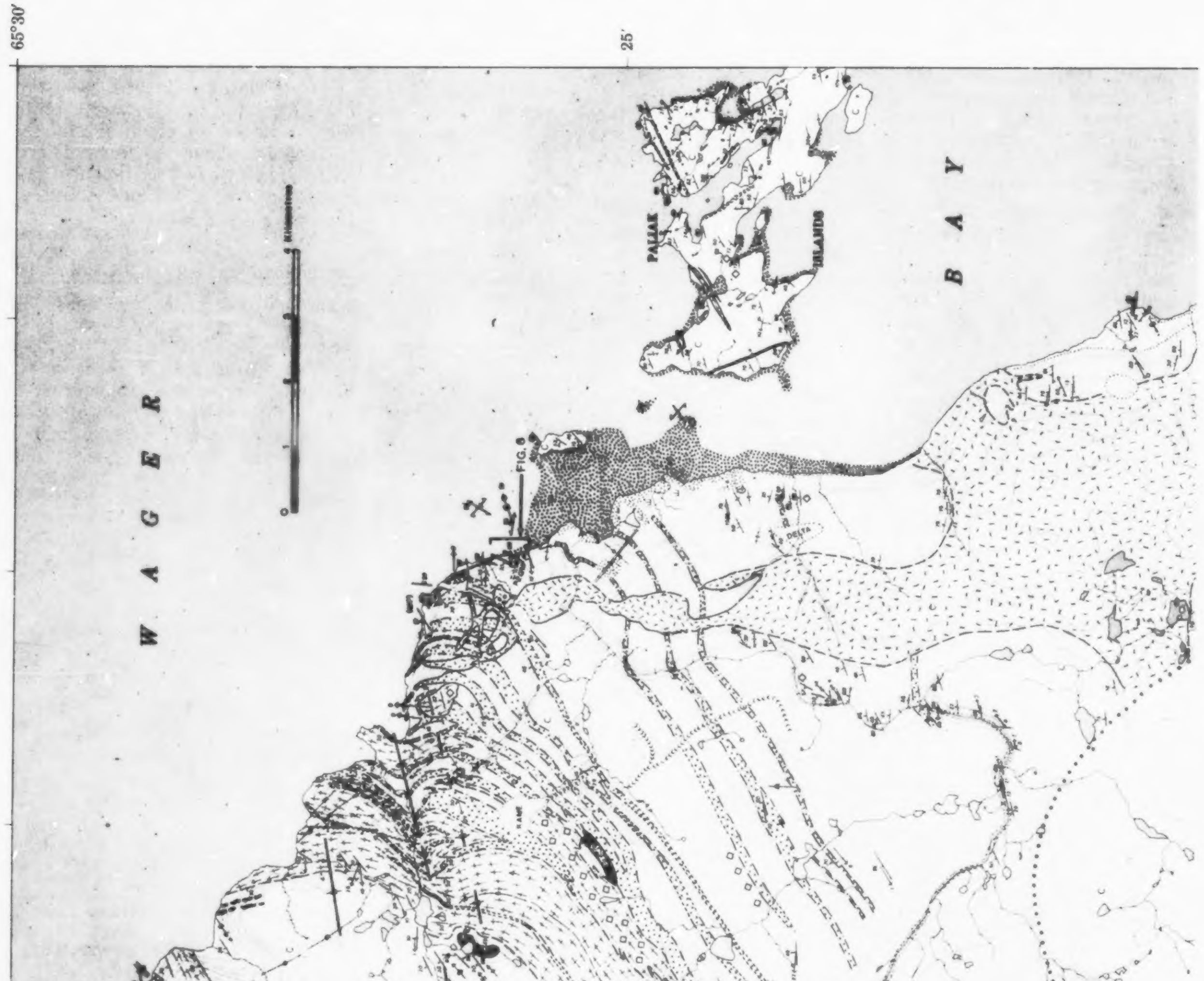
65°30'
25'
WAGER
BAY
PAALAK
ISLANDS
FIG. 8
DELTA

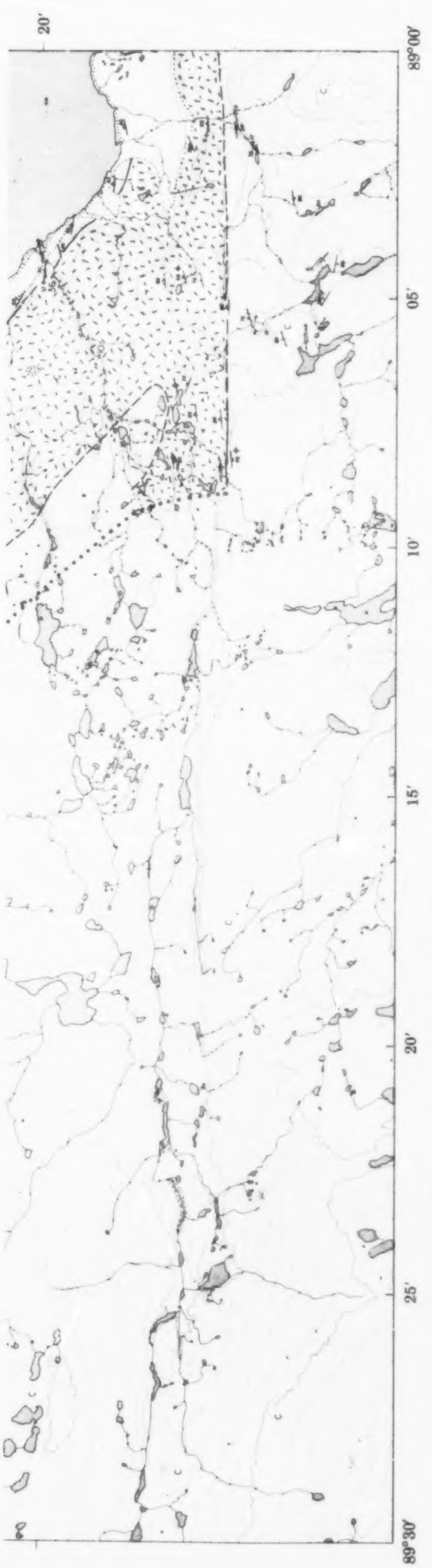

Figure 19.4. *Preliminary geological map of area 3 (Fig. 19.1), contiguous with Figure 19.5. Legend in Figure 19.3. Geology by C.W.J., K.C., J.R.H., A.N.LeC., M.H.; compiled by C.W.J.; drafted by K. Nguyen.*

Foliated intrusive rocks (Fig. 19.3, units 12 to 10)

A distinctive migmatitic paragneiss (unit 12) comprises dark brown and white to pale tan interlayers which are centimetres to decimetres thick. The dark layers are biotite paragneiss containing generally abundant garnets. The light layers are leucocratic quartz diorite with diagnostic but sparse garnets. The more feldspathic interlayers pinch, swell and anastomose. In detail the quartz diorite component intrudes and truncates biotite foliation in the paragneiss.

Weakly foliated, weakly radioactive (avg. 5000 counts-per-minute total gamma radiation on McPhar TV-1A spectrometer) pink granitic sheets (unit 11) are spatially associated with the supracrustal rocks, but they are absent from monotonous pink and grey gneisses to the northwest. Quartz diorite and more mafic biotite-hornblende-diorite (unit 10) form similar but smaller sheets on Paliak Island and the adjacent mainland. Granite sheets greater than 500 m in map width produce positive aeromagnetic responses of up to 750 gammas on regional aeromagnetic maps (Geological Survey of Canada, 1984a). The sheets intrude both orthogneiss and paragneiss map units, most frequently at the contacts between paragneiss and tonalitic gneiss. The sheets and their internal weak biotite foliation trend parallel to regional gneissosity but are crosscutting in detail.

Some granodiorites (unit 10) are medium to small, irregularly shaped bodies with well developed L-S fabrics that are apparently parallel to gneissic layering and lineation. They contain abundant phenocrysts of plagioclase and K-feldspar in a medium- to fine-grained groundmass of plagioclase, microcline, biotite, with accessory magnetite, sphene and apatite. The phenocrysts are strongly rodded (see Fig. 19.6).

Pegmatite, aplite, ductile amphibolite, granite and quartz veins (Fig. 19.3, units 9 to 1)

A variety of pegmatites intrude the paragneiss belt. The detailed map shown in Fig. 19.6 outlines two ages of large-pegmatite formation as well as numerous narrow pegmatite aplite and ductile amphibolite dykes associated with shear zones. The largest and oldest pegmatite (Fig. 19.3, unit 8) is a complex anastomosing dyke about 40 m wide and trending approximately east across area 4. Parts, if not all of it, are associated with vertical as well as horizontal ductile shears. It is a biotite granite with irregularly distributed allanite grains, and a weak east-west vertical foliation.

A discontinuous, very discordant, unfoliated pegmatite dyke up to 3 m wide (Fig. 19.3, unit 2) trends northerly across area 4 and is the youngest intrusion noted in the area. This dyke is composed of megacrystalline pink orthoclase and quartz with local myrmekitic texture. The core of the dyke contains pods of massive quartz. Patches of massive quartz occur elsewhere within area 4 away from the pegmatite and also appear to be relatively young.

At least four ages of amphibolite dykes intrude the region. The earliest are preserved as thin sheets of amphibolite (Fig. 19.3, unit 14) which have only a short trace

Figure 19.5. *Preliminary geological map of area 2 (Fig. 19.1), contiguous with Figure 19.4. Legend in Figure 19.3. Geology by C.W.J.; west half based on coastal traverse and air photo interpretation. Drafted by K. Nguyen.*

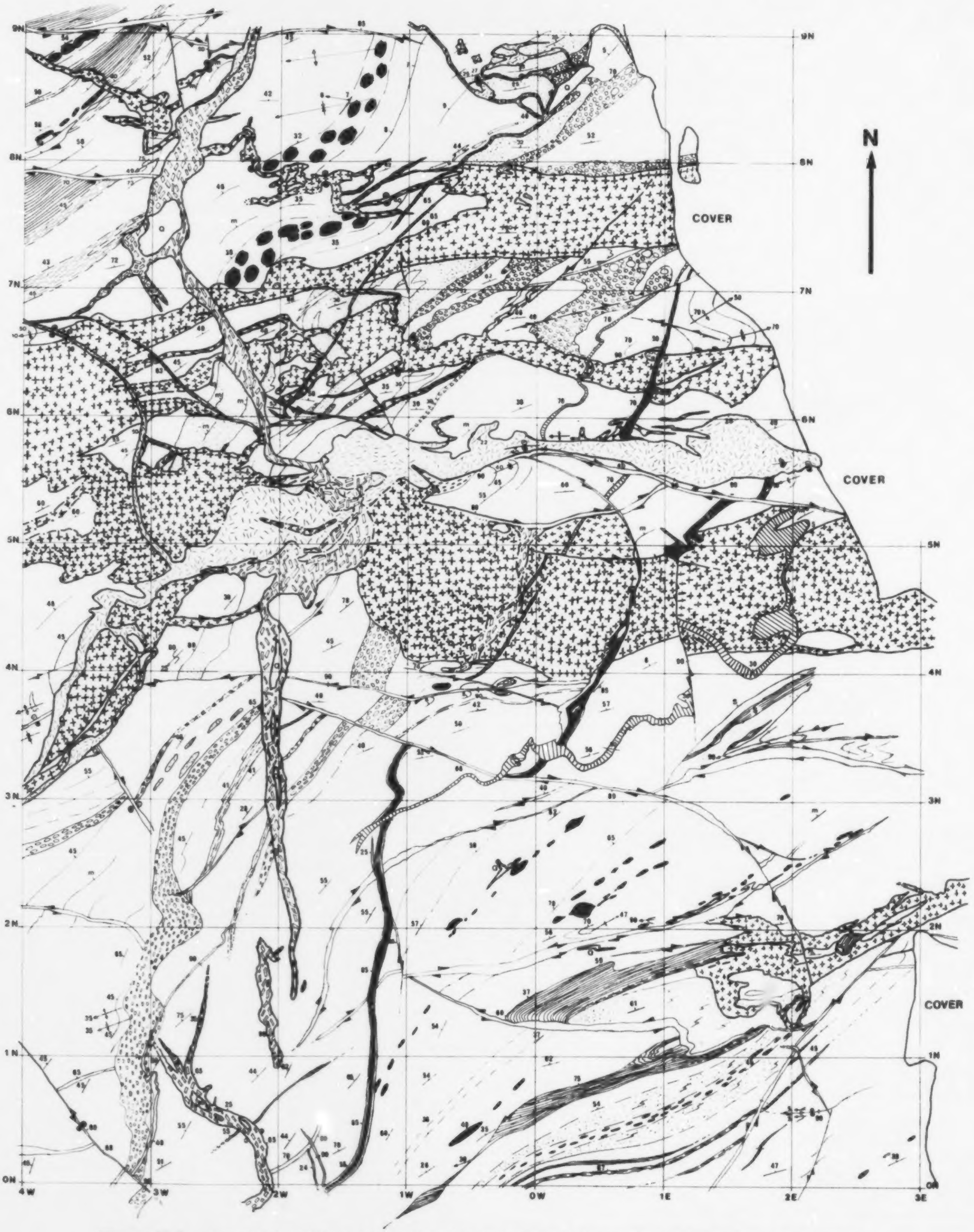

Figure 19.6. Detail of tonalitic gneiss, location indicated in Figure 19.4. Grid spacing is 10 metres; legend in Figure 19.3. Geology by C.W.J. and J. Shaver; drafting by L. McGuire.

and cut the gneissossity at a low angle (e.g. Fig. 19.6, 0.3N/1.7E). These dykes indicate a protracted and complicated history to the gneisses before and subsequent to their injection. Members of the second suite (Fig. 19.3, unit 7) are 1-3 m wide, occupy dilatant planar structures, and trend northwesterly. As shown in Figure 19.6 they include a pegmatitic border phase. Where they cross an older pegmatite (unit 8) the border phase is absent and lobes of pegmatite project into the pegmatite. These relationships suggest that the border phase on the dyke resulted from partial melting of hot country rocks by the basic magma, that the pegmatite body (unit 8) was still molten when it was intruded by the dyke, and that during deformation the mafic rock was more ductile than the felsic rock. Members of the third suite (Fig. 19.3, unit 5) also occupy planar dilatant fractures but appear to be less deformed than the second, and trend north-northwesterly. They are also composite with two or more mafic phases, one of which forms crescumulate margins to the dykes. The fourth suite is represented by one or possibly two gently dipping amphibolite dykes occupying sinistral ductile shear zones (Figure 19.5, 65°34'N, on the coast).

Two minor felsic dykes (Fig. 19.3, unit 6) are shown on Figure 19.6. These are composite with aplite and pegmatite phases, and contain distinctive large blue apatites.

A porphyritic granite with related aplites (Fig. 19.3, unit 3; Fig. 19.5, 19.6) trends 14 km south-southeasterly from the coast, and are cut-off by the east-west Wager Bay Shear Zone. The granite has a positive aeromagnetic response up to 750 gammas (Geological Survey of Canada, 1984a). Contacts are invariably sharp but irregular. Microcline phenocrysts in the main body just southwest of area 4 are aligned parallel to a weak matrix foliation trending southeasterly and dipping moderately to the northeast. Near its margins the granite is locally foliated and contains abundant, large, generally unrotated xenoliths of gneiss and paragneiss. Around the north end of the main body and on Paliak Islands, numerous related dykes and sills of porphyritic granite and nonporphyritic aplite are present. All of these acid bodies give total count gamma ray responses on McPhar TV1-A scintillometers of about 10 000 cpm. Petrographically, the granite consists of large microcline phenocrysts in a matrix of quartz, minor plagioclase and biotite.

Structure

Structure is described in approximate chronological order. Mylonitic fabrics are among the oldest and youngest structures observed. Old mylonitic fabrics trending subparallel to gneissossity mark the contacts between many of the paragneiss belts and the pink and grey gneisses. Some belts mapped as undivided unit 14 (Fig. 19.3) are uniformly fine grained grey mylonites with well developed microcline porphyroclasts, and with subhorizontal extension lineations recording sinistral shear. The porphyroclasts range up to 30 cm in diameter and appear to have originated as pegmatitic microcline crystals. Extensive tails of finer grained feldspar are strung out along the mylonitic lineation. In washed coastal exposures the mylonites are grey, whereas inland they are rusty and weather recessively, not unlike semipelitic gneisses. Many of the mylonites include boudinaged lenses of iron formation and garnet-bearing biotite gneiss. They may also have orthogneiss components.

Fabric patterns in the banded granite-tonalite gneiss (unit 13, Fig. 19.3) indicate a complex structural history. The earliest preserved phase of deformation was isoclinal folding followed by asymmetric folding with S folds forming on both limbs of the earlier isoclines. The next stage was of flattening, which in places produced shears and the removal of the short limb of the S folds. Further flattening tightened existing folds and produced small local straight zones. Subsequently, the new fabric of the straight zones was itself folded asymmetrically. Surviving mineral lineations are parallel with axes of the latest folds. Figure 19.7 summarizes the macroscopic geometry of the planar and linear fabrics of the region just north of the Wager Bay Shear Zone, including Paliak Islands, the coastal region west of the islands, and Savage Islands. Note that planar elements tend to dip northwest at low angles, and linear elements are dispersed in a great circle coincident with the mean foliation orientation.

The macroscopic structures in the supracrustal belt are open to isoclinal folds which have no axial planar fabric. Axial surface traces of large folds are shown by single lines in Figures 19.4 and 19.5. The majority of these folds are upright, but some verge toward the southeast, and some overturned isoclines verge to the northwest. Their axial surface trends curve from about 010° at the extreme northwest edge of the supracrustal belt towards parallelism with the 090° Wager Bay Shear Zone in the south. Plunges are gentle, and adjacent trains of synforms and antiforms commonly plunge in opposite directions. These folds involve all map units from 14 to 9 inclusive (Fig. 19.3).

The large folds are warped by gentle, poorly defined folds shown as double lines on Figures 19.4 and 19.5. These folds are interpreted where abrupt changes in the trends of map unit are not explainable by topography, and are well expressed west of the mylonite in Figure 19.5 where interference patterns are developed on the gently dipping crest of an earlier antiform.

Economic geology

Wager Bay and northern Southampton Island have been proposed by Parks Canada as national park areas. Economic Geology and Mineralogy Division has been charged with the assessment of the mineral resource potential of this large

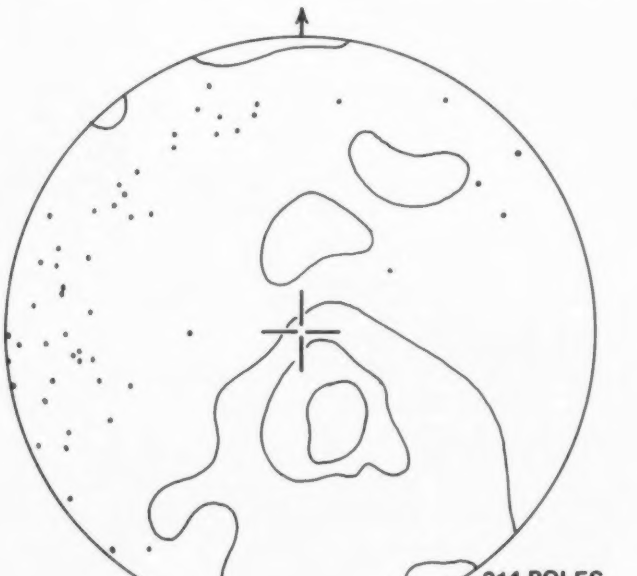

Figure 19.7. Lower hemisphere, equal area plot of foliation poles (contoured) and lineations from the mainland east of the radioactive granite, Paliak Islands and Savage Islands (Fig. 19.8).

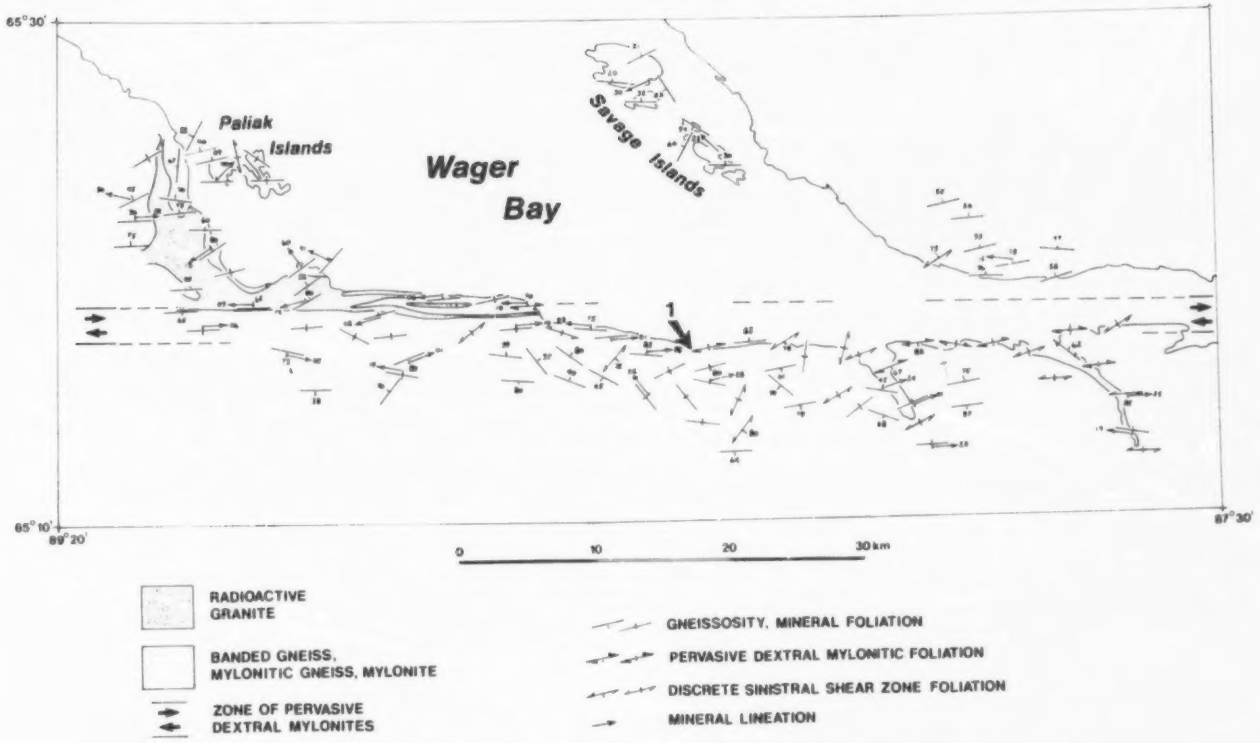

Figure 19.8. *Geological map showing part of the Wager Bay Shear Zone (area 4, Fig. 19.1).*

area over a two year period. The supracrustal belt was chosen for detailed study because of its greater economic potential relative to the pink and grey tonalitic gneisses apparent elsewhere around Wager Bay. The supracrustal rocks are complexly deformed, extremely attenuated, and are dominated by metasedimentary assemblages with few amphibolites of possible volcanic origin. Although supracrustal gneisses are mappable as continuous units, their internal geometry is complex (Fig. 19.6) and not readily mappable on a scale that would be encouraging for an exploration program.

Pyrrhotite is abundant in most of the paragneisses. Some sulphide iron formation was observed, and trace amounts of chalcopyrite and molybdenite were identified from five scattered localities. All gossan areas were sampled for lithogeochemical analysis, and these samples are now being processed. The northernmost thick supracrustal unit is marked by extensive gossans (Fig. 19.4) and will be examined in detail in the summer of 1986.

PART 3: GEOLOGY OF THE WAGER BAY SHEAR ZONE

J.R. Henderson, M.N. Henderson and K. Coe

Introduction

Our main purpose is to examine the east striking linear aeromagnetic anomaly zone extending from the south coast of Wager Bay, westward to Woodburn Lake; a distance of more than 400 km (see Fig. 19.1 and Geological Survey of Canada, 1984a). Inspection of the regional aeromagnetic

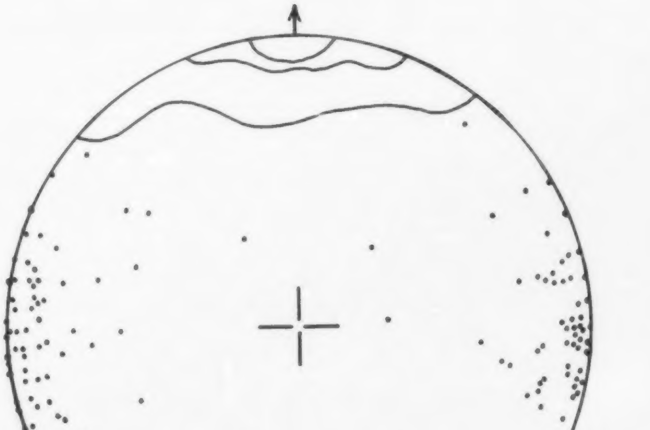

Figure 19.9. *Lower hemisphere, equal area plot of foliation poles (contoured) and lineations (dots) from the belt of pervasive dextral mylonites on the south coast of Wager Bay.*

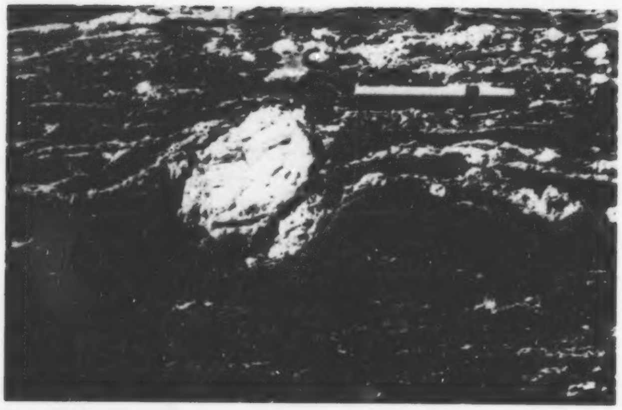

Figure 19.10

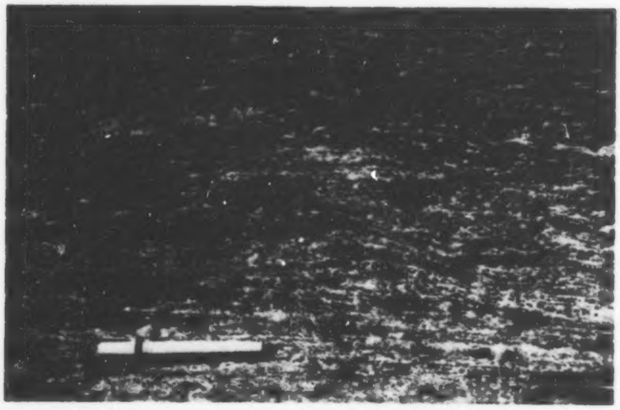

Figure 19.11

Figure 19.12A

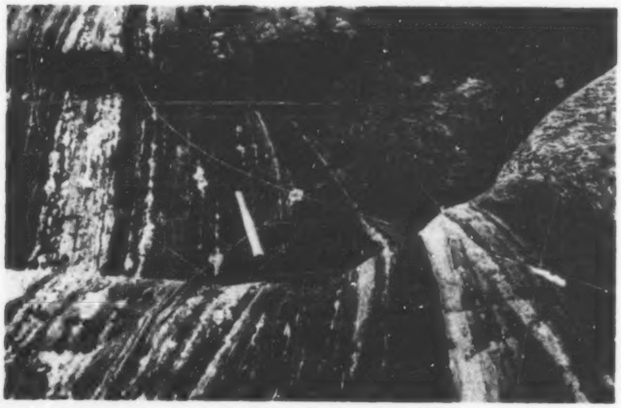

Figure 19.12B

Figure 19.13

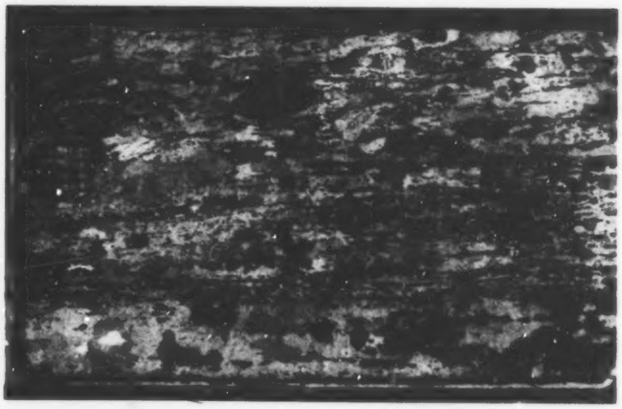

Figure 19.14

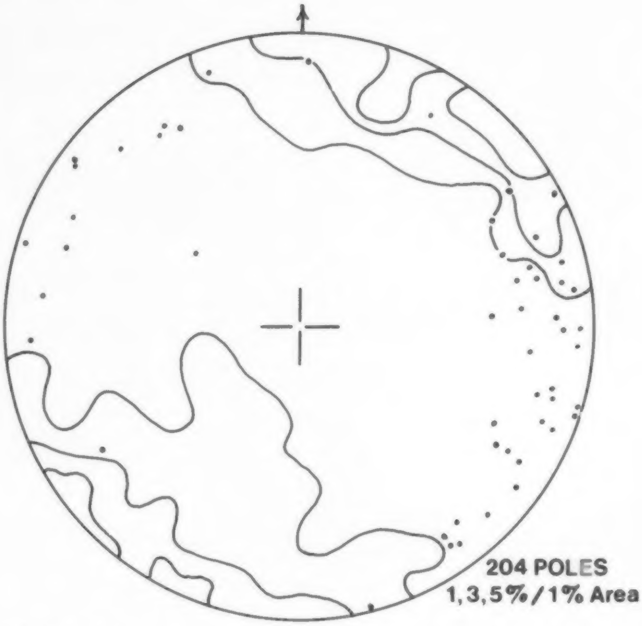

Figure 19.15. Lower hemisphere, equal area plot of foliation poles (contoured) and lineations (dots) from the region south of the east-west zone of pervasive dextral mylonites.

*Figure 19.10. A microcline porphyroclast exposed in a plane parallel to the **XZ** section of the finite strain ellipsoid. The porphyroclast and its lenticular "wings" of fine microcline grains have rotated clockwise due to dextral shear in the mylonite matrix. GSC 204259-U.*

*Figure 19.11. An amphibole-rich layer exposed in a plane parallel to the **XZ** section of the finite strain ellipsoid, extended by several shear bands and consistent with dextral shear in the mylonite matrix. GSC 204259-M.*

*Figure 19.12. A competent amphibolite pod exposed in a plane parallel to the **XZ** section of the finite strain ellipsoid showing clockwise rotation due to dextral shear in the mylonite matrix.*

A. Overall view of the pod looking east (geological pick for scale). GSC 204259-Y.

B. Close-up view of the pod margin showing drag-folded internal foliation, and a rotated feldspar porphyroclast in the matrix mylonite (at the point of the pick) that has been rotated clockwise in response to pervasive dextral shear (cf. Fig. 19.10) GSC 204259-T.

*Figure 19.13. An inhomogeneously extended pegmatite dyke exposed in a plane parallel to the **XZ** section of the finite strain ellipsoid. The pegmatite was emplaced at a larger angle to the mylonitic foliation and was subsequently rotated and extended clockwise. GSC 204259-J.*

Figure 19.14. Photomicrograph (partly-crossed polarizers) of a granite mylonite viewed in the plane parallel to the XZ section of the finite strain ellipsoid. Note the quartz ribbons composed of amoeboid quartz grains enclosing trains of much finer grained feldspar and mica (bottom of photo). Width of photo is 3.5 cm. GSC 203884-Q.

anomaly patterns is strongly suggestive of a component of dextral ductile shear across a 25 km wide zone to the west of Wager Bay. Along the south coast of Wager Bay (where we worked during 1985) the magnetics show a marked asymmetry with a prominent magnetic high to the south and a magnetic low to the north situated on the shear zone.

From our mapping (Fig. 19.1 area 4, and Fig. 19.8), we defined three zones from north to south on the basis of their characteristic structural fabric and geometry: (1) a zone north of the dextral mylonites composed of banded pink and grey gneisses intruding older supracrustal components and intruded by younger radioactive granitic rocks; (2) a zone of pervasive dextral mylonites 2-3 km wide paralleling the south coast of Wager Bay; and (3) a zone south of the dextral mylonite belt composed of folded dextral mylonitic gneisses commonly displaced by discrete sinistral shears.

The latter two zones will be described in the following sections. Observations in the zone north of the pervasive dextral myonites are included in the preceding description of the supracrustal belt which may contain the parent rocks composing the mylonitic zones to the south.

Geology of the zone of pervasive dextral mylonites

Flanking the south coast of Wager Bay is a very strong 2.5 km wide east-west shear zone. In this zone there is such a convergence of lithotypes that lithological mapping becomes almost impossible. Within the zone, however, bands

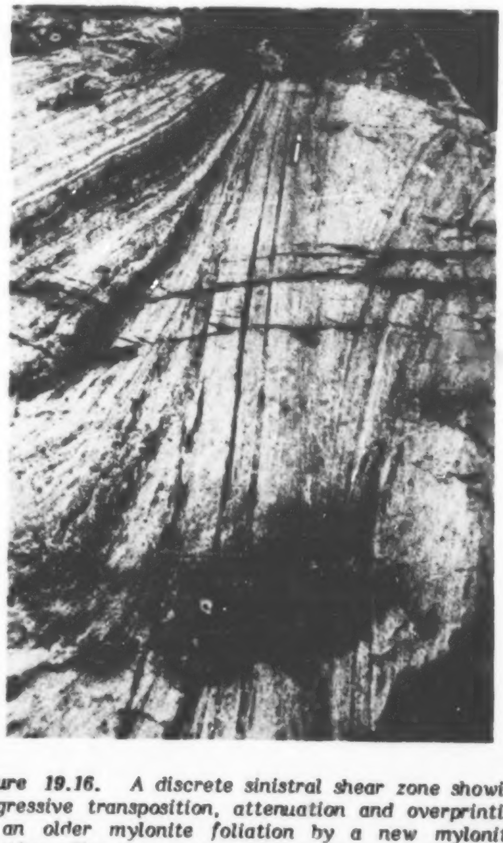

Figure 19.16. A discrete sinistral shear zone showing progressive transposition, attenuation and overprinting of an older mylonite foliation by a new mylonitic foliation. The view is east subparallel to the horizontal mineral lineation on the mylonitic foliation. GSC 204259-O.

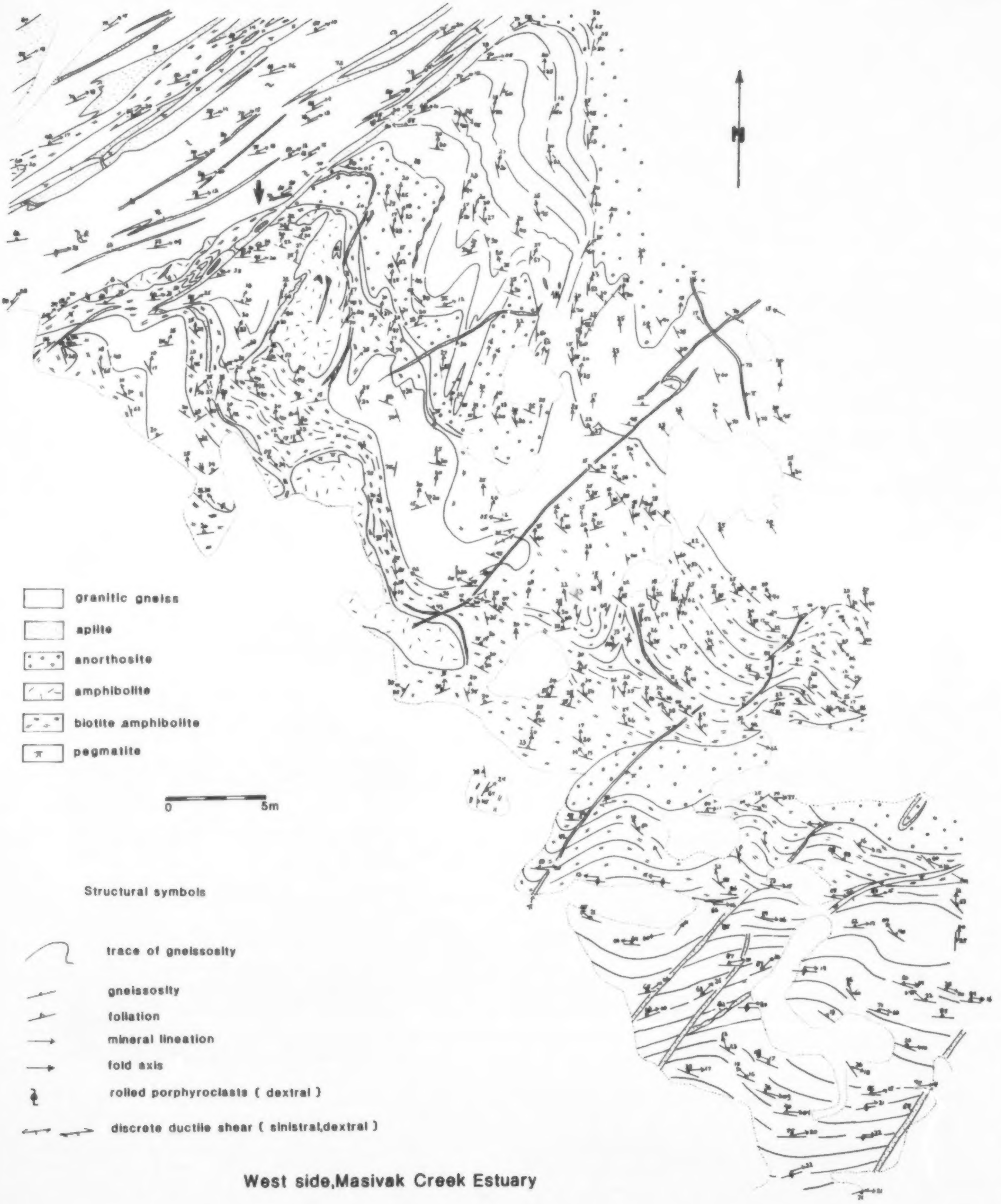

Figure 19.17. *Geological map illustrating the nature of the transition out of the east-west belt of pervasive dextral mylonites into the mylonitic gneisses to the south. (Located on the west side of Masivak Creek inlet at the bold arrowhead in Fig. 19.8). Surveyed and mapped by J.R.H. and Paula MacKinnon.*

Figure 19.18. View south in the direction of the arrow on Figure 19.17 across the discrete sinistral shear zone on the border of the pervasive dextral mylonites showing a progressively bent mineral lineation on the surfaces of a gently northeast-dipping mylonitic foliation. GSC 204259-1

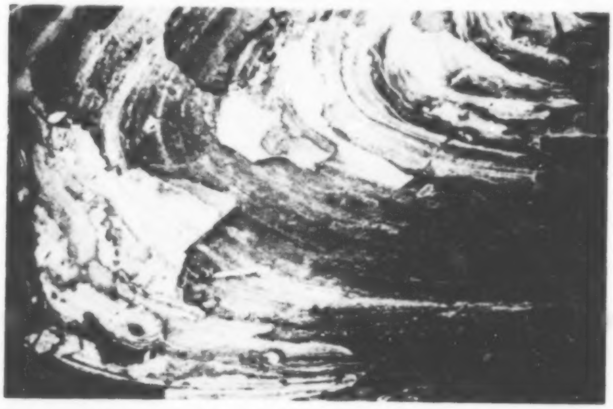

Figure 19.19. Gently dipping mylonitic foliation showing feldspar-aggregate mineral lineations progressively transposed and overprinted by a new lineation related to sinistral ductile shearing. Located at tip of arrow on Figure 19.18. GSC 204259-V.

of distinctive lithology can be traced, in some cases for several kilometres. The best example is of two feldspathic quartzites which nearly extend over the length of the zone mapped. These formations are at most 5 m thick and usually about 15 m apart, separated by feldspathic mylonite of undetermined parentage. These are very planar lenses, tapering gradually to a few centimetres thickness before being disrupted. They show no mesoscopic boudinage, a feature very regularly developed in hornblende and feldspathic enclaves in the mylonite. The kinematic sense in the east-west belt is everywhere dextral, the mylonitic foliation is steep and the mineral lineation generally plunges at a low angle, (Fig. 19.9). Whilst a range of kinematic indicators was used, it should be admitted that most are variations on the rule of Z folds indicating dextral and S folds indicating sinistral movement. Rotated microcline porphyroclasts (Fig. 19.10) are the most commonly observed kinematic indicator (cf. Davidson, 1984, Fig. 6E, F), but shear bands (Fig. 19.11) were also noted (cf. White, 1979, Fig. 1), as well as rotated competent rock pods with drag-folded foliation on their margins (Fig. 19.12A, B). In addition all discordant aplite and pegmatite dykes within the zone lie in the acute angle to the right of a line drawn normal to the

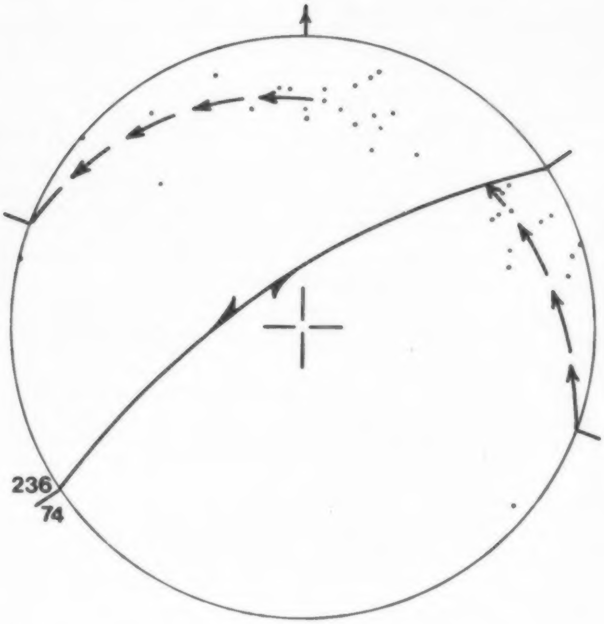

Figure 19.20. Lower hemisphere, equal area plot of structural fabric elements measured in the region south of the sinistral shear zone shown in Figures 19.17-19.19. Dots are mineral lineations, the unbroken great circle oriented 236/74 is the sinistral shear zone, and the arrows define the great circle rotation path of the mineral lineations.

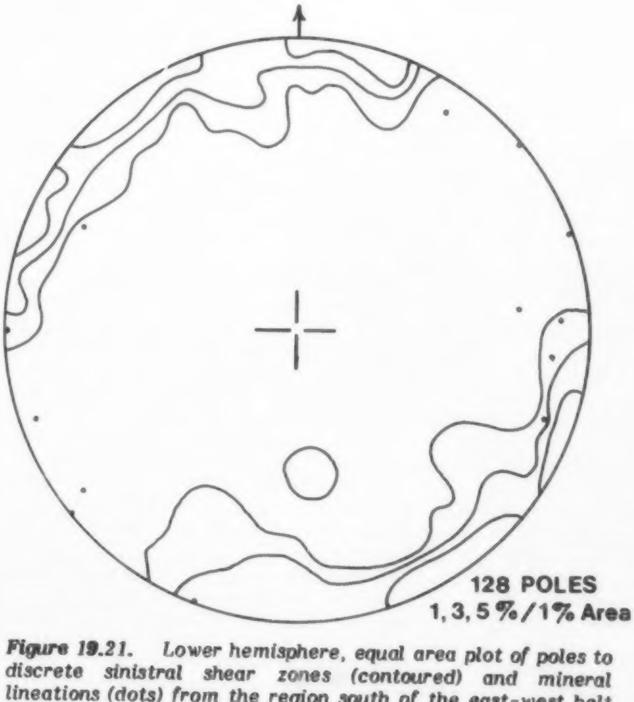

Figure 19.21. Lower hemisphere, equal area plot of poles to discrete sinistral shear zones (contoured) and mineral lineations (dots) from the region south of the east-west belt of pervasive dextral mylonites.

horizontal trace of the mylonitic foliation (Fig. 19.13), which is consistent with dextral rotation in noncoaxial bulk shear. At a few localities feldspar porphyroclasts indicating dextral movement have become involved in discrete sinistral shear zones. It is significant that they retain their original sense of rotation. From this it follows that at least in the east-west zone the net movement is dextral transcurrent.

On the microscopic scale asymmetrical fabrics seem rare. Although to date only 20 thin sections have been given cursory examination none show obvious fabric asymmetries. Thin sections do show that quartz commonly has grown to very large size relative to other minerals; engulfing much smaller aligned grains of feldspar and mica (Fig. 19.14).

Geology south of the zone of pervasive dextral mylonites

In contrast to the abrupt transition into the dextral mylonite belt from the north, the transition out of the belt to the south is much less apparent or abrupt. The characteristic feature of the southern zone is the disruption of the very regular east-west, vertical dextral mylonitic fabrics. Figure 19.15 shows the regional dispersion of the east-west foliation and lineation pattern; note the general tendency of the foliation to strike southeast. Another characteristic structural feature of this southern zone is the appearance of numerous discrete sinistral ductile shear zones (Fig. 19.16) which attenuate the older mylonitic fabric.

The boundary between the east-west dextral mylonites and the zone to the south is illustrated in Figure 19.17, a detailed survey done on a 25 m^2 grid. The edge of the pervasive dextral mylonite belt is shown in the northwest corner of the figure; note that the mylonitic foliation strikes east-northeast rather than the dominant east-west trend for the belt in general. There is a tendency for the dextral fabric to assume large, low amplitude wave forms near the transition into the southern zone, where the dextral mylonites are bent into much smaller folds, commonly with northeast striking discrete sinistral shears forming the short limbs of the folds.

A very interesting feature illustrated in Figure 19.17 is a discrete northeast striking sinistral shear on the boundary between the straight mylonites in the northwest corner of the map and the rocks to the south. The bending of the fabrics to the left into the shear from the south indicates the sinistral sense-of-shear. Note that an aplite dyke is emplaced within the shear zone, and immediately north of the aplite microcline porphyroclasts are rotated clockwise in the mylonite matrix. Mineral lineations south of the discrete shear become progressively rotated to the left into parallelism with the shear zone over a distance of about two metres. Figure 19.18 is a view south from the dextral mylonite, across the discrete sinistral shear (direction and location indicated by bold arrow on Fig. 19.17) showing feldspar-aggregate lineations bent 140° on the gently north-northeast dipping mylonitic foliation. Figure 19.19 is a close-up view of the sinistral shear (location indicated at arrow head in Fig. 19.18) showing the sinistral transposition of the older feldspar-aggregate lineation, and its overprinting by a new feldspar-aggregate lineation within 0.5 m of the discrete shear. The old mylonitic foliation is overprinted by new steeply north-dipping mylonitic foliation out of the field of view, but immediately north of the area shown in Figure 19.19. This geometry is summarized in Figure 19.20 which shows the distribution of feldspar-aggregate lineations on the surface of the dextral mylonite foliation. The original mean trend and plunge of the lineations is about 010/25. They are bent about 140° in the direction of the arrows on the 290/25 great circle to an intersection with the 236/74 sinistral shear zone, and define the shearing direction at 050/22 (cf. Ramsay, 1960). Figure 19.21 summarizes on a stereonet all of the sinistral shear planes and mineral lineations measured in the southern zone. The shear planes are all vertical or nearly so and strike in the northeast-southwest quadrants.

Our mapping of this zone is not complete; we believe that we have not yet defined the southern margin of the Wager Bay Shear Zone, and we plan to continue work, south and north of Wager Bay along the Hudson Bay coast in 1986.

References

Bateman, P.C. and Chappell, B.W.
1979: Crystallization, fractionation, and solidification of the Tuolumne Intrusive Series, Yosemite National Park, California; Geological Society of America, Bulletin, v. 90, p. 465-482.

Chappell, B.W. and White, A.J.R.
1974: Two contrasting granite types; Pacific Geology, v. 8, p. 173-174.

Davidson, A.
1984: Identification of ductile shear zones in the southwestern Grenville Province of the Canadian Shield; in Precambrian Tectonics Illustrated, ed. A. Kroner, and R. Greiling; E. Schweizer bart'sche Verlagsbuchhandlung (Nagele U. Obermiller), Germany, Stuttgart, p. 263-279.

Geological Survey of Canada
1974: Geophysical series (Aeromagnetic), Map 7629G, Wager Bay, scale 1:250 000.

1977: Geophysical series (Aeromagnetic), Map 7651G, Walker Lake, scale 1:250 000.

1984a: Magnetic Anomaly Map, Map NQ 15-16-17-M, Quoich River, scale 1:1 000 000.

1984b: Open File 1053, Radioactivity Maps, Map NQ 15-16-A, Quoich River, scale 1:1 000 000.

Heywood, W.W.
1961: Geological notes, northern District of Keewatin; Geological Survey of Canada, Paper 61-18, 9 p.

1967: Geological notes, northeastern District of Keewatin and southern Melville Peninsula, District of Franklin, Northwest Territories (Parts of 46, 47, 56, 57); Geological Survey of Canada, Paper 66-40, 20 p.

Kawachi, Y. and Sato, T.
1978: Orthoclase megacrysts in the Yakushima granite, southern Kyushu, Japan; Neues Jahrb Mineral Abh, v. 132, p. 136-152.

Ramsay, J.G.
1960: The deformation of early linear structures in areas of repeated folding, Journal of Geology, v. 68, p. 75-93.

Reesor, J.E.
1958: Dewar Creek map-area with special emphasis on the White Creek Batholith, British Columbia; Geological Survey of Canada, Memoir 292, 78 p.

Steiger, R.H. and Jager, E.
1977: Subcommission on geochronology: convention on the use of decay constants in geo- and cosmochronology; Earth and Planetary Science Letters, v. 36, p. 359-362.

Wanless, R.K., Stevens, R.D., Lachance, G.R., and Edmonds, C.M.
1967: Age determinations and geological studies, K-Ar isopic ages, report 7; Geological Survey of Canada, Paper 66-17, p. 67-68.

White, S.
1979: Large strain deformation; report on a Tectonic Studies Group discussion meeting held at Imperial College, London, November 14, 1979; Journal of Structural Geology v. 1, p. 333-339.

Revised structural interpretation, Selwyn Range between Ptarmigan and Hugh Allan creeks, British Columbia — an antiformal stack of thrusts

EMR Research Agreement 53/04/85

E.W. Mountjoy [1] and R. Forest [1]
Cordilleran Geology Division

Mountjoy, E.W. and Forest, R., Revised structural interpretation, Selwyn Range between Ptarmigan and Hugh Allan creeks, British Columbia – an antiformal stack of thrusts; in Current Research, Part A, Geological Survey of Canada, Paper 86-1A, p. 177-183, 1986.

Abstract

Fieldwork in 1985 resolved most of the major structural problems and slightly modified the stratigraphic thickness of the Miette Group as follows; upper Miette 1500 + m, middle Miette 2500 + m and lower Miette 4000 + m (2000 m upper pelite and 2000 + m lower grit), giving a total thickness of more than 8000 m for the Miette Group.

The structure of the Chatter Creek thrust sheet consists of a doubly plunging, 50-km-long antiform, the Fraser River antiform. Thrust imbricates that duplicate the lower Miette grits can be traced from the west limb of the antiform around the southeast plunge of the structure where they cut upsection and duplicate and disappear into the lower Miette pelite of the east limb. Thus the structure is a duplex consisting of a stack of folded imbricates or an anitformal stack of thrusts. At the surface the floor thrust is the Ptarmigan thrust which eastward must join with the underlying Chatter Creek thrust at depth. Two minor, late stage normal faults have a southwest side down sense of displacement.

Résumé

En 1985, les travaux sur le terrain ont permis de résoudre la plupart des principaux problèmes structuraux et de modifier légèrement la puissance statigraphique du groupe de Miette: la partie supérieure du groupe de Miette a plus de 1500 m, la partie moyenne plus de 2500 m et la partie inférieure plus de 4000 m (2000 m de pélite sur plus de 2000 m de grès grossier), donnant ainsi une puissance totale de plus de 8000 m pour le groupe de Miette.

La nappe de charriage de Chatter Creek est un anticlinal à double plongement de 50 km de long, que l'on nomme anticlinal du fleuve Fraser. Les écailles qui sont la répétition des grès grossiers de la partie inférieure du groupe de Miette peuvent être suivies à partir du flanc ouest de l'anticlinal, puis autour du plongement sud-est de la structure où elles obliquent vers la section supérieure, se superposent et disparaissent dans la pélite de la partie inférieure du groupe de Miette située sur le flanc est. La structure forme ainsi un duplex constitué d'une superposition d'écailles plissées ou de chevauchements à structure anticlinale. En surface, le chevauchement de fond, appelé chevauchement de Ptarmigan, doit rejoindre à l'est, en profondeur, le chevauchement sous-jacent de Chatter Creek. Deux petites failles normales de la phase tardive présentent un déplacement vers le bas du côte sud-ouest.

[1] Department of Geological Sciences, McGill University, 3450 University St., Montreal, Quebec H3A 2A7

Introduction

During the summer of 1985 problem areas near the head of Blackman and Hugh Allan creeks were investigated in detail, and the northern extension of the Ptarmigan thrust was examined near the head of Yellowjacket Creek. A preliminary summary of the structure and stratigraphy of the area based on 1983 and 1984 fieldwork was published by Mountjoy et al. (1984, 1985) and the metamorphism studied in detail by Leonard (1984, 1985) and Forest (1985). More detailed information on the structure and stratigraphy are in the M.Sc. theses of Leonard (1985) and Forest (1985) but some parts require revision. We have included unpublished information from the Geological Survey of Canada Bow-Athabasca project (Price and Mountjoy, 1970; Mountjoy and Price, 1984). The area to the northwest near Bulldog Creek was mapped by McDonough (1984); and summarized in McDonough and Simony (1984). To the west the gneissic rocks in the Purcell thrust sheet and related structures have been studied by Chamberlain et al. (1979, 1985) and by Oke and Simony (1981).

This report revises the structure of Mountjoy et al. (1985). Previously, the Ptarmigan thrust sheet was mapped as a series of thrust imbricates on the west flank of the Fraser River antiform that appeared to reflect considerable displacement. We experienced difficulties in extending the Ptarmigan thrust southwards and the thrust displacements appeared to decrease very rapidly towards the south. In addition, some unusual normal faults were inferred (see Fig. 58.1, Mountjoy et al., 1985, revised here as Fig. 20.1). The lack of obvious fault traces in the lower Miette pelites on the east limb of the Fraser River antiform, and the extensive ice cover and glacial deposits in the valleys prevented us from determining the correct structure from the initial mapping.

In the summer of 1985 individual grit units were walked out on the nose of the structure (Fig. 20.1, 20.2). The data gained in this more detailed mapping help resolve most of the difficulties encountered in the earlier work and allow a more coherent and satisfactory interpretation of the structure. Around the nose of the antiform a series of thrust imbricates duplicates the upper part of the lower Miette grits and the basal part of the overlying lower Miette pelites, and cuts up section from grits into the pelites. Where these thrusts place lower Miette pelite over lower Miette pelite they can no longer be mapped, except where grit units in the lower Miette pelite (see stratigraphy) are duplicated, indicating that a thrust fault occurs somewhere within the intervening pelites. Two of the main thrust imbricates are inferred to occur beneath the glacier between the heads of Ptarmigan and Blackman creeks (Fig. 20.2).

Stratigraphy

The area is underlain by strata of the Hadrynian Miette Group. The Miette Group is divisible into three informal mappable units; upper, middle and lower on the basis of stratigraphy established on 1:50 000 scale maps in the Jasper area (Mountjoy, 1976; Mountjoy and Price, 1984, 1985). The upper Miette consists of a predominantly pelitic sequence up to 2000 m thick. The middle Miette is more than 2500 m thick and consists of a composite series of graded, pebbly sandstones (grits) in cliff-forming units 50 to 100 m thick which alternate with somewhat thicker dark grey to greenish grey pelites. The lower Miette comprises two distinct units, an upper dark grey to black pelite, 2000 to 2500 m in maximum thickness (not true thickness due to folding), and a lower grit sequence more than 1500 m thick. The upper black pelite is similar to the lower Miette of the McBride area (Carey and Simony, 1985), but contains black carbonate in its lower part rather than in its upper part as in the McBride region.

Determination of the correct stratigraphic sequence is essential for mapping the structure. The most complete, continuous and best exposed section of the lower and middle Miette occurs on the west limb of the Fraser River antiform in the hanging wall of the Ptarmigan thrust on the ridges north of Ptarmigan Creek (52°51'N, 118°40'W). The intensity of the folding and the number of thrust imbricates gradually decrease upwards in the lower Miette so that the upper part of these grits and the overlying lower Miette pelites and middle Miette grits are homoclinally southwest dipping and little deformed. These three units can be traced more-or-less continuously between Hugh Allan and Bulldog creeks (for stratigraphic details of the upper and middle Miette see Mountjoy et al., 1985). The upper Miette Group pelites outcrop only in the Ptarmigan thrust sheet. Minimum thickness is 1000 m.

The middle Miette consists of a series of composite, graded, poorly sorted pebble conglomerates and rare boulder conglomerates interbedded with thick dark grey to black pelites. It has a minimum thickness of 2500 m on the west limb of the antiform. The base is gradational and is arbitrarily selected at the base of the lowest thick mappable grit unit.

The lower Miette pelites form a monotonous sequence of dark grey- to rusty-weathering outcrops with rare silty and sandy intervals, and occasional thick lenticular grit units. This quartzite units 80 to 100 m thick occur 560 to 800 m below the top of the lower Miette pelite in the Ptarmigan thrust sheet. Dark grey to black micritic limestones in units 10 to 30 m thick occur near the base of the lower Miette pelite. In the hanging wall of the Ptarmigan thrust north of Ptarmigan Creek, the lower Miette pelite is 2000 to 2500 m thick, much thinner than the tectonically thickened lower Miette pelites on the east limb of the Fraser River antiform (Fig. 20.1, 20.2).

Two units (20 to 100 m thick) of coarse and conglomerate grit (G1 and G2; Fig. 20.2, 20.3) form locally mappable markers within the lower Miette pelite. The lower grit (G1) occurs about 1000 m above the base and locally splits into two mappable grit units. The upper grit (G2) occurs 300 to 500 m above the first and about 500 m below the base of the middle Miette (Fig. 20.2, 20.3). Both grit units thicken and thin rapidly along strike and both disappear northwards on the east limb of the antiform near latitude 52°38', south of Ptarmigan Creek. Two similar grits occur on the southwest limb of the antiform above the roof thrust (Fig. 20.2, 20.3). Northwest of Ptarmigan Creek a prominent grit repeated by an east dipping thrust occurs on the east limb of the antiform. It appears to be stratigraphically equivalent to the lower grit (G1). It is possible that the two grits may be the same unit. This would, however, necessitate additional thrust faults on the east limb of the Fraser River antiform thus thinning the lower Miette pelite by about 300 m.

A lower grit sequence, the lower Miette grits, lies conformably beneath the lower Miette pelites. The base is not observed. About 800 m is exposed within the antiform, 1500 to 2000 m in the hanging wall of the Ptarmigan thrust, and in the cross-sections it is up to 2500 m. All of these thicknesses represent tectonically thickened sequences and its true thickness will not be known until more detailed work is carried out in the core of the antiform. The lower Miette grits are superficially similar to grit units in the middle Miette, except that: 1) the grit units are generally thinner (up to 50 m thick), 2) they are more calcareous and contain brown weathering carbonate throughout, and 3) the thickness of the interbedded pelite sequences is more variable. Dark grey to black carbonates also occur in the lower part of these grits. This more carbonate-rich sequence is similar to the Horsethief Creek Group (?) in the Purcell thrust sheet, that overlies the Mount Blackman Gneiss (Leonard, 1984, 1985).

Thus the upper clastic, carbonate and slate units of Simony et al. (1980) and Oke and Simony (1981) are upper Miette Group and the underlying grit is middle Miette, as originally mapped by Price and Mountjoy (1970) and Craw (1977). They are not equivalents of the Horsethief Creek Group west of the Rocky Mountain Trench but rather are equivalents of the stratigraphically higher Yankee Belle, Cunningham, and Isaac formations, and the upper Kaza Group of the Cariboo Mountains. If the stratigraphic sequence and interpretations of Pell and Simony (1982, 1984) are correct, the Proterozoic units are reasonably consistent on both sides of the Rocky Mountain Trench in terms of overall thickness

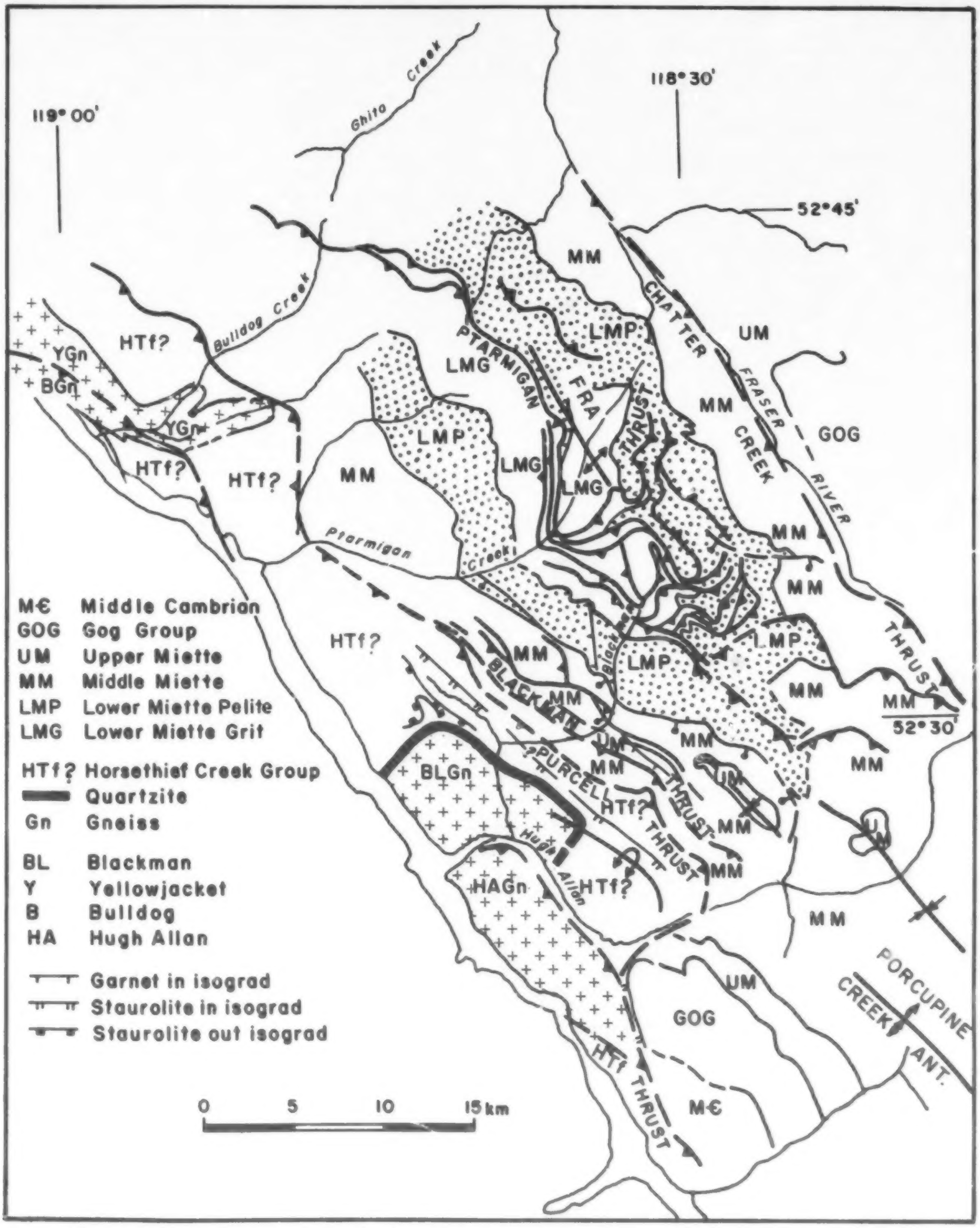

Figure 20.1. Geological map of the Ptarmigan – Hugh Allan Creek region, Selwyn Range (revised from Fig. 58.1 in Mountjoy et al., 1985). Geology around Bulldog Creek from McDonough (1984) and McDonough and Simony (1984).

and the vertical arrangement of similar lithologic sequences. In summary, in the region mapped, the total composite thickness of the Miette Group is a minimum of 8000 m (upper Miette 1500+, middle Miette 2500+ and lower Miette 4000 m). The thickness of the upper and middle Miette are stratigraphic whereas the lower Miette represents tectonic thicknesses.

Structure

Three major thrust faults occur in the area, from northeast to southwest, the Chatter Creek, Blackman and Purcell thrust faults (Fig. 20.1). The gneisses and their cover of Hadrynian strata of Horsethief Creek Group(?) form the most westerly Purcell thrust sheet. The Fraser River antiform dominates the Chatter Creek thrust sheet (Fig. 20.1, 20.2).

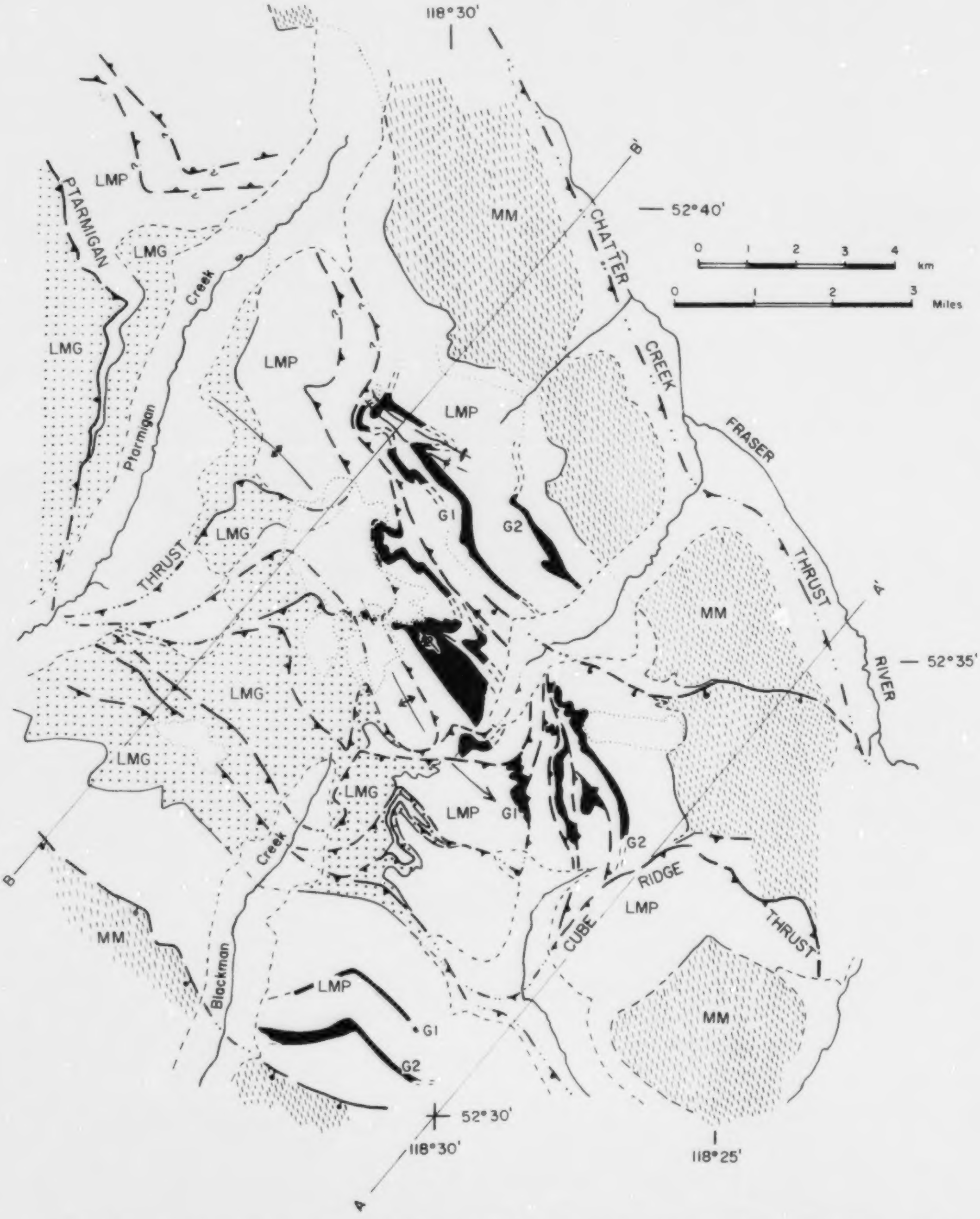

Figure 20.2. Geological map of Ptarmigan Creek area. Legend: LMG: Lower Miette Grits, LMP: Lower Miette Pelite, G1, G2: grit units within LMP, MM: Middle Miette Grits; AA' location of cross-section in Figure 20.3 and BB' location of cross section in Figure 20.4.

Chatter Creek thrust and Fraser River antiform

The Chatter Creek thrust sheet contains a major anticlinal or antiformal structure, the Fraser River antiform, a large, open, upright doubly-plunging structure which extends for about 50 km from the head of Hugh Allan Creek to Yellowjacket Creek. Its axis trends at approximately 135° with a shallow plunge of 15 to 20 degrees southeast. It exposes the lowest part of the stratigraphic sequence, with lower Miette pelites occurring in the core of the structure along most of its length. The lowest unit, the lower Miette grits, is exposed where Ptarmigan Creek has cut across the antiform.

The Fraser River antiform is bounded on the northeast by the Chatter Creek thrust which underlies it at depth (Fig. 20.2, 20.3, 20.4). The trace of the Chatter Creek thrust is covered in the upper Fraser River valley. The fault places middle Miette strata on the west side of the valley over east-dipping Gog Group and upper Miette strata of the Simon syncline to the northeast (Mountjoy and Price, 1984).

Although the core of the antiform is not well exposed, horses (imbricates) of the west limb can be traced around the southeast closure of the structure until they disappear into and duplicate the lower Miette pelite on the east limb or are offset by a small normal fault. Only the structurally highest horses can be observed. The lowest horses are largely hidden beneath an extensive ice sheet. The structure is clearly a duplex consisting of a stack of folded imbricates (Fig. 20.1 to 20.4) or an antiformal stack of thrusts using the terminology of Boyer and Elliott (1982). The cross-sections (just south of Ptarmigan Creek, Fig. 20.4, and just north of Hugh Allan Creek, Fig. 20.3) show the folded nature of these imbricates. These cross-sections are drawn conservatively, utilizing the smallest displacements and the thinnest stratigraphic sequence. These constraints require that the Chatter Creek thrust underlies the antiformal stack at a low angle (Fig. 20.4).

The Ptarmigan thrust represents the floor thrust of the horses at the head of Ptarmigan Creek. Some of the faults merge in a southeast direction and also appear to die out to the northwest. The Ptarmigan Creek thrust occurs about 2 km above the Chatter Creek thrust (Fig. 20.4). The intervening lower Miette grits may also be imbricated but this is not evident from our field observations.

All the fault imbricates cut up section from a glide zone in the lower Miette grits to a higher glide zone in the lower Miette pelites, forming a step or a ramp. Each fault successively from west to east cuts off part of the ramp. The successive development of these horses produced the antiform, with the folding dying out downwards. Further steepening of the flanks of the Fraser River antiform may have been caused by additional compression accompanied by crenulation-cleavage development. Northward, towards the antiformal culmination, the dip of the Chatter Creek thrust is inferred to decrease and flatten (Fig. 20.4). This is typical of many antiformal stacks of thrusts in which the floor thrust is often flat or gently folded (Boyer and Elliott, 1982). Thus, where each higher horses (imbricate) is folded by and about the lower ones, folding dies out downwards and provides clear evidence that the higher horses formed first and the lower ones last.

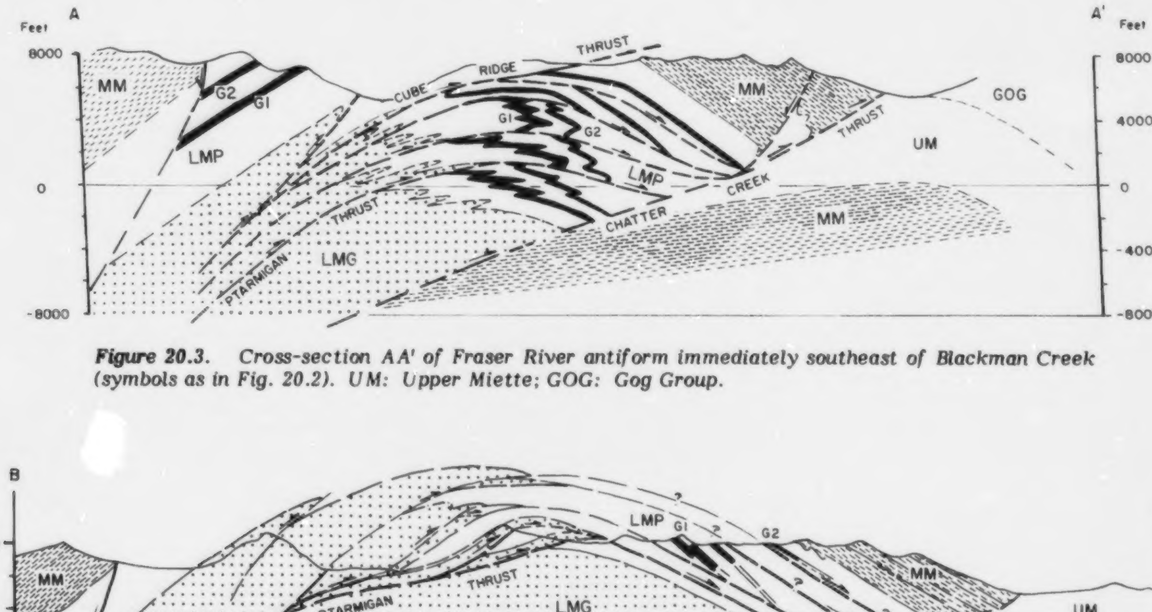

Figure 20.3. Cross-section AA' of Fraser River antiform immediately southeast of Blackman Creek (symbols as in Fig. 20.2). UM: Upper Miette; GOG: Gog Group.

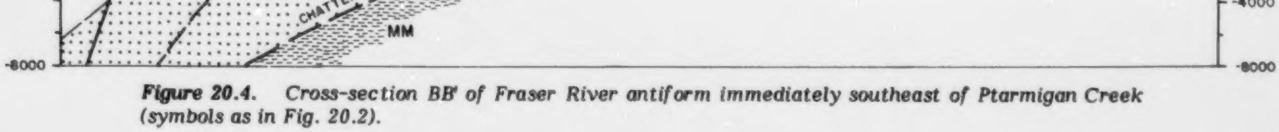

Figure 20.4. Cross-section BB' of Fraser River antiform immediately southeast of Ptarmigan Creek (symbols as in Fig. 20.2).

The Cube Ridge thrust and a splay from it cannot be traced into east dipping faults around the southeast closure of the antiform. Because they are not folded, they appear to represent later faults that utilized the roof thrust and displace the west limb of the antiform upwards like back limb thrusts in the Foothills and Front Ranges.

The Fraser River antiformal stack of thrusts is generally similar in overall structure and scale to the Mount Crandell duplex in the Lewis thrust in Waterton National Park (Douglas, 1952, Dahlstrom's (1970) type example of a duplex; see also Fig. 17 in Boyer and Elliott (1982)).

Folds

Two sets of colinear folds are recognized throughout the area. The first was formed early, during the main episode of thrusting. The second (F2) is characterized by axial planar crenulation cleavages developed by crenulation of S1.

Macroscopic and mesoscopic F1 folds vary from tight to isoclinal, inclined to recumbent with wavelengths up to 200-300 m. These folds are syn-thrusting and pre- to syn-metamorphic and only occur close to the Ptarmigan thrust and associated splays.

On the west side of the Fraser River antiform, axial planes dip steeply to the southwest; near the crest they are flat and on the east limb they dip to the northeast. F1 folds always have a northeastern vergence.

Macroscopic F2 folds are developed on the east limb of the antiform and locally in the Ptarmigan thrust sheet. These folds are open to gentle, with upright or steeply inclined axial planar crenulation cleavage, and wavelengths similar to those of the F1 folds. F2 folds generally overprint the long limbs of F1 folds.

Normal faults

Previously a major normal fault (Hugh Allan) was inferred along much of Hugh Allan Creek, but this is incorrect. There is no need to infer such a fault (Fig. 20.1, 20.2), because the geological relationships near the head of the north fork of Hugh Allan Creek require two thrust faults, the Cube Ridge thrust and the thrust farther southeast (Fig. 20.2). Previously we had incorrectly interpreted that the lower Miette pelites on the east had been downdropped by a normal fault against lower Miette grits to the west (see Fig. 58.1, Mountjoy et al., 1985) and we extended this fault down Hugh Allan Creek to join the normal fault that occurs farther southwest. This latter normal fault downdrops and offsets part of the Porcupine Creek syncline. Delineation of its southeastern continuation will have to await mapping southeast of Hugh Allan Creek. There is no connection between these structures and the previously inferred 4 to 6 km offset of the Purcell thrust along Hugh Allan Creek (Fig. 20.1). The offset may represent a lateral tear fault or a re-entrant in the Purcell thrust sheet (e.g. like the Pine Mountain overthrust in the southern Appalachians, or the Lewis thrust at North Kootenay Pass). To the northeast another normal fault of small displacement occurs on the east limb of the antiform near 52°34' latitude and also has a southwest-side-down sense of displacement. Presumably these faults resulted from extension during the middle Tertiary.

Discussion and interpretation

Mountjoy et al. (1985) recognized two different colinear sets of folds, which they interpreted as due to the progressive migration of strain within a thrust sheet during its emplacement as in a model proposed by Sanderson (1982). However, we now believe that the second set of folds is due either to a progressive deformation or to a discrete deformation event unrelated to that in which the first set was produced.

Folds of the first set are syn-thrusting and are restricted to a deep structural level associated with the Ptarmigan thrust and its imbricates. These F1 folds are sometimes unrooted and are believed to have resulted from extensive shearing along the fault plane during the main episode ot thrusting. The second deformation (upright folds and crenulation-cleavage) could be a result of progressive deformation. However, the second set of folds also could be the product of a second and separate phase of deformation. If this is correct F1 and F2 folds of the Selwyn Range would correlate with the F2 and F3 folds observed in the Selkirk and Monashee mountains (see Simony et al., 1980). The F2 and F3 folds of the Selkirks (Simony et al., 1980) have the same morphology and relative timing of metamorphism to the two sets of folds (F1 and F2) of the Selwyn Range.

Conclusions

Mapping of a series of thrust imbricates around the southeast closure of the Fraser River antiform within the Chatter Creek thrust sheet resolves the main structural problems encountered in our earlier work and provides a more coherent and satisfactory interpretation of the structure.

The duplex structure consisting of an antiformal stack of thrusts resulted from the successive development of a series of imbricates that cut up section from a glide zone in the lower Miette grits to a higher glide zone in the lower Miette pelites. The movement of each imbricate over this step or ramp folded the overlying structures. Thus the structurally highest imbricates have been folded the most and the floor thrust is only gently folded. A second and probably a separate deformation resulted in the cleavage that crenulated S1.

The presence at the surface of an antiformal stack of thrusts provides a structural model for interpreting similar antiforms which form structure culminations elsewhere in the Rocky Mountains. It is especially helpful for interpreting the deeper portions of these structures. The antiformal stack of thrusts has application to interpreting the deeper structure of the Porcupine Creek anticlinorium and the structure beneath the Simpson Pass thrust near Lake Louise.

More fieldwork is needed in the core, and along the east flank, of the antiform to determine if additional east dipping thrusts cut the lower Miette pelites and grits to check the structural relationships between the two phases of deformation, and the thickness and lithology of the lower Miette grits. Mapping south of Hugh Allan Creek is necessary to determine the southeast extent of the normal faults and the Blackman thrust.

Acknowledgments

Forest was supported by a Natural Science and Engineering Research Council postgraduate scholarship. In addition to EMR research support, financial support for field work and laboratory analyses came from Mountjoy and Hynes' NSERC grant A2128 and A7983. The authors are grateful to A. Hynes and R. Dechesne for counsel, helpful discussions and critical review of the manuscript. J.O. Wheeler also provided a helpful review. We deeply appreciate the field support and logistics provided by Yellowhead Helicopters of Valemount.

References

Boyer, S.E. and Elliot, D.
1982: Thrust Systems; American Association of Petroleum Geologists Bulletin, v. 66, p. 1196-1230.

Carey, J.A. and Simony, P.S.
1985: Stratigraphy, sedimentology and structure of Late Proterozoic Miette Group, Cushing Creek area, B.C.; Bulletin Canadian Petroleum Geology, v. 33, p. 184-203.

Chamberlain, V.E., Lambert, R. St. J., Baadsgaard, H., and Gale, N.H.
1979: Geochronology of the Malton Gneiss complex of British Columbia; in Current Research, Part B, Geological Survey of Canada, Paper 79-1B, p. 45-50.

Chamberlain, V.E., Lambert, R.St. J., and Holland, J.G.
1985: Geochemistry and geochronology of the gneisses east of the southern Rocky Mountain trench, near Valemount, British Columbia; Canadian Journal of Earth Sciences, v. 22, p. 980-991.

Craw, D.
1977: Metamorphism, structure and stratigraphy of the Southern Park Ranges (Western Rocky Mountains), British Columbia; unpublished M.Sc. thesis, University of Calgary, Calgary.

1978: Metamorphism, structure and stratigraphy in the southern Park Ranges, British Columbia; Canadian Journal of Earth Sciences, v. 15, p. 86-98.

Dahlstrom, C.D.A.
1970: Structural geology in the eastern margin of the Canadian Rocky Mountains; Bulletin Canadian Petroleum Geology, v. 18, p. 332-406.

Douglas, R.J.W.
1952: Preliminary map, Waterton, Alberta; Geological Survey of Canada, Paper 51-22.

Forest, R.C.
1985: Structure and metamorphism of Ptarmigan Creek area, Selwyn Range B.C.; unpublished M.Sc. thesis, McGill University, Montreal.

Leonard, R.
1984: Metamorphism, structure and stratigraphy around the Mount Blackman Gneiss, British Columbia; in Current Research, Part A, Geological Survey of Canada, Paper 84-1A, p. 121-124.

1985: Variable structural style, stratigraphy, total strain and metamorphism adjacent to the Purcell thrust near Blackman Creek B.C.; unpublished M.Sc. thesis, McGill University, Montreal.

McDonough, M.R.
1984: Structural evolution and metamorphism of basement gneisses and Hadrynian cover, Bulldog Creek area, British Columbia; unpublished M.Sc. thesis, University of Calgary, Calgary.

McDonough, M.R. and Simony, P.S.
1984: Basement gneisses and Hadrynian Metasediments near Bulldog Creek, Selwyn Range, British Columbia; in Current Research, Part A, Geological Survey of Canada, Paper 84-1A, p. 99-102.

Mountjoy, E.W.
1976: Edson to Valemount – the Rocky Mountain Front and Main Ranges along highway 16 in the Jasper area; in Geological Association of Canada, Edmonton, Field Trip C-11 Guidebook, p. 4-42.

Mountjoy, E.W. and Price, R.A.
1984: Amethyst Lakes 83 D/9 geological map and cross-sections 1:50 000 scale; Geological Survey of Canada, Open File 1075.

1985: Jasper (83 D/16) geological map and cross-sections 1:50 000 scale; Geological Survey of Canada, Map 1611A.

Mountjoy, E.W., Forest, R., and Leonard, R.
1984: Non-basement involvement in the western Main Ranges, Jasper-Valemount, Alberta and B.C.; Geological Society of America, Abstracts with programs, v. 16, no. 6, p. 602.

1985: Structure and stratigraphy of the Miette Group, Selwyn Range, between Ptarmigan and Hugh Allan creeks, British Columbia; in Current Research, Part A, Geological Survey of Canada, Paper 85-1A, p. 485-490.

Oke, C. and Simony, P.S.
1981: Basement gneisses of the Western Rocky Mountains, Hugh Allan Creek area, British Columbia; in Current Research, Part A, Geological Survey of Canada, Paper 81-1A, p. 181-184.

Pell, J. and Simony, P.S.
1982: Hadrynian Horsethief Creek Group/Kaza Group correlations in southern Cariboo Mountains, British Columbia; in Current Research, Part A, Geological Survey of Canada, Paper 82-1A, p. 305-308.

1984: Stratigraphy of the Hadrynian Kaza Group between the Azure and North Thompson rivers, Cariboo Mountains, British Columbia; in Current Research, Part A, Geological Survey of Canada, Paper 84-1A, p. 95-98.

Price, R.A. and Mountjoy, E.W.
1970: Geological structure of the Canadian Rocky Mountains between Bow and Athabasca Rivers, a progress report; Geological Association of Canada, Special Paper 6, p. 7-26.

Sanderson, D.J.
1982: Models of strain variation in Nappes and Thrust sheets: a review; Tectonophysics, v. 88, p. 201-233.

Simony, P.S., Ghent, E.D., Craw, D., Mitchell, W., and Robins, D.B.
1980: Structural and metamorphic evolution of northeast flank of the Shuswap Complex, southern Canoe River area, British Columbia; Geological Society of America Memoir 153, p. 445-461.

Granitoid plutons in the Canso area, Nova Scotia[1]

Project 850016

J.D. Hill
Precambrian Geology Division

Hill, J.D., Granitoid plutons in the Canso area, Nova Scotia; in Current Research, Part A, Geological Survey of Canada, Paper 86-1A, p. 185-192, 1986.

Abstract

The Canso area is underlain by metasedimentary rocks of the Meguma Group and numerous granitoid plutons of probable Devonian age. Deformation and metamorphism that reached amphibolite grade affected the Meguma Group during the Acadian Orogeny whereas a younger heterogeneous dextral shearing event (or events) affected both the Meguma Group and the granitoid plutons in most of the area.

The granitoid plutons, ranging in composition from biotite tonalite to muscovite granite, were emplaced in a relatively stable tectonic environment after the Acadian Orogeny. At least seven stages of magma emplacement have been recognized, which resulted in the intrusion of more than twenty plutons. The lack of correspondence between pluton age and composition indicates that magmas were generated during more than one phase of partial melting.

Résumé

Le sous-sol de la région de Canso est constitué de roches métasédimentaires du groupe de Meguma et de nombreux plutons granitoïdes probablement d'âge dévonien. La déformation et le métamorphisme, qui ont atteint le faciès des amphibiolites, ont altéré le groupe de Meguma lors de l'orogenèse de l'Acadien, alors qu'une ou plusieurs phases plus récentes de cisaillement dextre de nature hétérogène ont altéré le groupe de Meguma et les plutons granitoïdes dans la majeure partie de la région.

Les plutons granitoïdes, dont la composition varie de la tonalite à biotite au granite à muscovite, sont apparus dans un milieu tectonique relativement stable après l'orogenèse de l'Acadien. On a reconnu au moins sept phases de magma qui ont donné lieu à l'intrusion de plus de 20 plutons. L'absence de corrélation entre l'âge des plutons et leur composition indique que les magmas sont le produit de plusieurs phases de fusion partielle.

[1] Contribution to Canada-Nova Scotia Mineral Development Agreement 1984-1989. Project carried by Geological Survey of Canada.

Introduction

Recent discoveries of Sn-W and U mineralization in rocks associated with the South Mountain batholith and its satellitic plutons have emphasized the need for more information on the geology of Acadian granitoid intrusions in Nova Scotia. Consequently, a mapping and petrological project has been initiated on the granitoid plutons in the Meguma terrane east of Halifax. The initial phase of this project, reported herein, involved mapping of the Chedabucto peninsula east of longitude 61°13'W at a scale of 1:25 000 during the summer of 1985.

The area was first mapped by Faribault (1893) and later remapped, in part, by Weeks (1959) and Stevenson (1964). Since the early 1950s, considerable mineral exploration has been carried out by several companies, particularly in the northern half of the area. Details and data relating to this work are available in the files of the Nova Scotia Department of Mines and Energy (NSDME) in Halifax. McKenzie and MacGillivary (1974) have described samples of granitoid plutons collected from roadside exposures. An $^{40}Ar/^{39}Ar$ plateau age of 368 ± 8 Ma was obtained on granite in the Whitehead area (Reynolds et al., 1981). The distribution of airborne gamma ray anomalies has been investigated by Ford and Ballantyne (1983). University theses have been completed by Schiller (1959) on the petrology of andalusite schist north of Whitehead, Nichols (1976) on the metamorphism and structure of the Whitehead area, Shaw (1983) on the Lazy Head tungsten showing and Poole (1984) on the structure of the Halifax Formation north of Whitehead. Keppie (1985) has described the structural evolution of rocks in the southeast corner of Durells Island.

Highways and trails provide good access to about half the area. However, numerous islands and most of the south coast can only be reached by boat. Wind and fog limited mapping in these areas to the latter part of July and August. Bedrock exposures are magnificent along the coast but diminish in number and quality inland, becoming almost nonexistent in some areas. For this reason, field work was concentrated on coastal areas and inland traverses were confined to well exposed barrens, roads, lake shores and power lines. These limitations are reflected in the reliability of geological data shown in Figure 21.1.

The project is part of the Canada-Nova Scotia Mineral Development Agreement. Assistance by J.M. Hill was instrumental in completing the field work. Discussion with W.H. Poole in the field helped to elucidate and resolve several problems. The manuscript was reviewed by F.W. Chandler and C.R. van Staal.

Geological setting

The area lies in the extreme eastern part of the Meguma terrane, immediately south of the Minas Geofracture (Keppie, 1982). The rocks can be grouped into two main divisions.

(i) Meguma Group – Cambro-Ordovician metasedimentary rocks which are divided into the older psammitic Goldenville Formation and the younger pelitic Halifax Formation. These rocks were deformed and metamorphosed during the Acadian Orogeny.

(ii) Granitoid plutons – Numerous mica-bearing intrusions ranging in lithology from tonalite to granite (igneous rock names used are those recommended by Streckeisen, 1976). They are believed to be similar in age to other Acadian granitoid plutons in the Meguma terrane, as suggested by the 368 ± 8 Ma date obtained by Reynolds et al. (1981) on granite near Whitehead.

One or more events of shearing affected all of the rocks in the northern two thirds of the area. Thus, many of the granitoid rocks have one or more tectonic fabrics, ranging from a weakly developed mineral foliation to a strong augen gneissosity.

Meguma Group (Units 1, 2)

The Goldenville Formation is divided into laminated (Unit 1a) and relatively massive (Unit 1b) subunits. These are not separated by geological boundaries in Figure 21.1 because of scale limitations and the fact that they locally pass from one to the other along strike. Overall, Unit 1a is dominant in the southern half of the map area whereas Unit 1b is mainly restricted to the northern half.

Unit 1a – Consists mainly of fine grained laminated metawacke (beds 0.5-2.0 m thick) intercalated with relatively massive metawacke (beds 0.5-4.0 m thick) and minor metapelite (beds 1-50 cm thick). Meta-arenite is rare but locally occurs as elongate lenses up to 10 cm thick. Unit 1a contains numerous primary and penecontemporaneous structures including grading, crossbedding, groove and load casts, slump folds and breccia, rip-up clasts and flame structure, all of which are well displayed along the south coast of Sheep Island.

Unit 1b – Relatively massive metawacke in beds up to 10 m thick. Thin horizons of metapelite, and variations in the degree of weathering or intensity of the foliation are commonly the only indications of bedding. However, faintly laminated beds and discontinuous lenses enriched in amphibole and garnet occur locally.

In most places, the character of the Goldenville Formation changes in the upper 50 to 200 m. As the contact with th Halifax Formation is approached, beds become thinner and the proportion of metapelite increases. Similar transition zones have been recognized elsewhere in the Meguma Group (McBride, 1978; O'Brien, 1985). The contact between the Goldenville and Halifax formations has been drawn in Figure 21.1 using a 1:1 ratio of psammite to pelite.

The Halifax Formation is divided into muscovite-biotite-chlorite phyllite and schist (Unit 2a), andalusite schist (Unit 2b) and black graphitic schist (Unit 2c). Unit 2c represents a specific facies within the Halifax Formation whereas the distinction between Units 2a and 2b seems to reflect differences in grade of metamorphism as much as composition. A 5 m thick sill of rhyolite containing quartz and feldspar phenocrysts was found in the Halifax Formation in three places along the northwest shore of Whitehead Harbour.

Unit 2a – Light to dark grey muscovite-biotite-chlorite phyllite and schist is locally interbedded with thinner layers of metawacke and meta-arenite. The pelitic beds range from 1 cm to 3 m thick and commonly contain discontinuous laminae of more siliceous material. Repeated beds (1 to 5 cm thick) of buff to orange meta-arenite containing abundant garnet (termed coticules by Schiller, 1963) are characteristic of the Halifax Formation north of Whitehead. They typically form up to 10% of each outcrop and in places, occur as numerous concretion-like bodies within 30 cm thick beds of metapelite. Small porphyroblasts of garnet and cordierite are common in the more pelitic horizons.

Unit 2b – Two bands of andalusite schist occur northwest of Whitehead Harbour. They consist of up to 35% euhedral porphyroblasts of andalusite in laminated beds which are locally intercalated with thin meta-arenite beds identical to those described above for Unit 2a. This observation, coupled with the fact that Unit 2b grades westward into Unit 2a northwest of Whitehead, suggests that the presence of andalusite is at least partly controlled by grade of metamorphism.

Unit 2c – Graphitic schist is the dominant lithology in the Halifax Formation along the north coast. It also forms a few thin beds in Unit 2a north and west of Whitehead. It is typically rusty due to the presence of up to 50% pyrite and pyrrhotite as disseminated grains and tiny veinlets. Although graphitic schist is the dominant lithology in Unit 2c, it is typically interbedded with thinner beds of grey schist and metawacke. Andalusite and cordierite porphyroblasts up to 12 cm in length are common in both pelitic lithologies.

Plutonic rocks (Units 3 to 8)

More than 20 larger plutons and numerous smaller bodies ocur in the map area. Although many of these are the result of discrete pulses of magma, others are obviously segments of individual plutons that have become disrupted by the intrusion of younger magmas. Xenoliths of metasedimentary rocks, all of which appear to be correlative with the Meguma Group, are widespread and locally abundant. Plutons along the south coast commonly possess a subhorizontal flow foliation defined by alignment of phenocrysts, mica-enriched layers and lensoid xenoliths. Farther north, the primary foliation is obliterated and supplanted by a steeply-dipping tectonic foliation.

The plutons are divided into six units based on differences in composition, texture and age. All but one of the interplutonic contacts observed in the field are intrusive. Typically, they are marked by zones of agmatite ranging from a few metres to a few kilometres in width. Dyke-host and xenolith-host contacts in the agmatite zones commonly follow two or more planes within individual outcrops, suggesting that they are at least partly controlled by pre-existing fractures. The one exception is the contact between Units 6b and 8 north and south of Admiral Lake (Fig. 21.1). There, the contact appears to be gradational. Distinguishing the two lithologies, however, is not always easy and diligent search in the future may reveal an intrusive relationship.

The complete sequence of magmatic events was not determined, although in general, the units are arranged in chronological order. The reader should remember that several plutons of similar lithology may be included in each unit, whereas age relationships may have been determined for only one or two of those plutons.

Unit 3 – Medium grained foliate biotite tonalite. Only remnants of what was once a much larger tonalite intrusion (or intrusions) are preserved, with the greatest concentration of tonalite shown as a single body in the northeast corner of Dover Bay. It consists of plagioclase, 10-20% biotite and 10-25% quartz. A characteristic feature is the ubiquitous occurrence of 1-5% disc-shaped metasedimentary xenoliths up to 50 cm in length oriented parallel to the foliation. Tonalite is crosscut by dykes of Units 5, 6 and 8.

Unit 4 – Fine grained biotite-muscovite granite outcrops at the north end of Dover Bay and at Big Branch Lake. Exposures of Unit 4 along the west side of Dover Bay are slightly coarser grained (grain size = 1-3 mm) and the two textural phases appear to be sharply gradational in outcrops at the head of Dover Bay. Both phases are relatively massive and contain 3-5% muscovite and 1-3% biotite. The exact age of this unit is uncertain. Dykes of Units 6b and 8 crosscut Unit 4 at the head of Dover Bay. Xenoliths of aplitic granite similar to Unit 4 were found in adjacent plutons of Units 5 and 7.

Unit 5 – Coarse grained seriate biotite granodiorite to granite. This unit is characterized by 20-35% subhedral phenocrysts of alkali feldspar which range from 3 to 15 cm long. Groundmass quartz and feldspar grains are commonly 0.5-1.0 cm in diameter and there is little demarcation in size between phenocrysts and groundmass. Biotite is 3-7% and muscovite is typically less than 2% except in minor altered zones. Unit 5a carries ubiquitous accessory garnet whereas Unit 5b lacks garnet. Unit 5 is cut by dykes of Units 6b and 8 and contains xenoliths of Unit 3 and what appears to be Unit 4.

Unit 6 – Medium grained biotite-muscovite and muscovite-biotite granite. This unit dominates the northern half of the map area. Mica forms 4-7% of the rock with biotite dominating in Unit 6a and muscovite dominating in Unit 6b. Unit 6c is similar in composition to Unit 6b but is slightly coarser grained with feldspar augen approaching 2 cm in length. Unit 6c is restricted to the northeast corner of the map area where it is marked by the presence of 1 to 30% lensoid xenoliths of Unit 1. The internal structure of Unit 6 is not well known because of lack of exposure in many areas. Dykes(?) of Unit 6a appear to crosscut Unit 6b southwest of Hazel Hill Lake. The contact relationship between Units 6b and 6c is unknown, although the significant difference in grain size suggests it is intrusive. Unit 6b is cut by dykes of Unit 8 northwest of Andrew Island. Xenoliths of Unit 5 were found in Unit 6 in the same area.

Unit 7 – Medium grained muscovite granite. This unit is characterized by the presence of 4-10% muscovite and less than 1% biotite. It is the only plutonic phase in which miarolitic cavities were found. The pluton of Unit 7 on the west side of Dover Bay contains 2-5 cm wide spherules of mica-free granite which locally form up to 30% of the rock. The age of Unit 7 is unknown, although several xenoliths of granite similar to Unit 4 were found in one outcrop.

Unit 8 – Medium- to coarse-grained seriate biotite granodiorite to granite. This unit is virtually identical to Unit 5b except that it contains only 1-10% alkali feldspar phenocrysts that range up to 3-4 cm long. Unit 8 contains numerous xenoliths of Unit 5, some of which exceed 100 m in width. Dykes of Unit 8 crosscut Units 5 and 6b northwest of Andrew Island.

Miscellaneous plutonic lithologies

Several other igneous lithologies occur as xenoliths and dykes too small to be shown on Figure 21.1. The most widespread of these is granite pegmatite, carrying one or more of muscovite, biotite, garnet and tourmaline, which is associated with nearly every pluton. Although several ages of pegmatite were recognized, it was not possible to relate specific compositional varieties to individual plutons or units.

Aplite is also common, occurring as small dykes and larger irregular masses in some plutons. The most abundant type is a grey weathering aplite containing 2-3% biotite which is a late phase associated with Unit 5.

Several other textural and compositional varieties of granite occur as isolated dykes and xenoliths throughout the plutonic terrane. In general they appear to represent intrusions that are not exposed at the current level of erosion or that have been destroyed by the invasion of younger magmas.

Mixed rocks (Units Agm, Mig)

A highly variable mixture of Meguma Group metasedimentary rocks, granite and granite pegmatite form a large, poorly exposed zone of agmatite (Unit Agm) in the central part of the map area. The granite and granite pegmatite intimately inject the metasedimentary rocks at all scales ranging from small dykes to undefined masses up to 50 m across. Either metasedimentary or granitoid rocks may dominate individual or groups of outcrops. The agmatite passes into adjacent plutons by gradual decrease in the proportions of both pegmatite and metasedimentary enclaves.

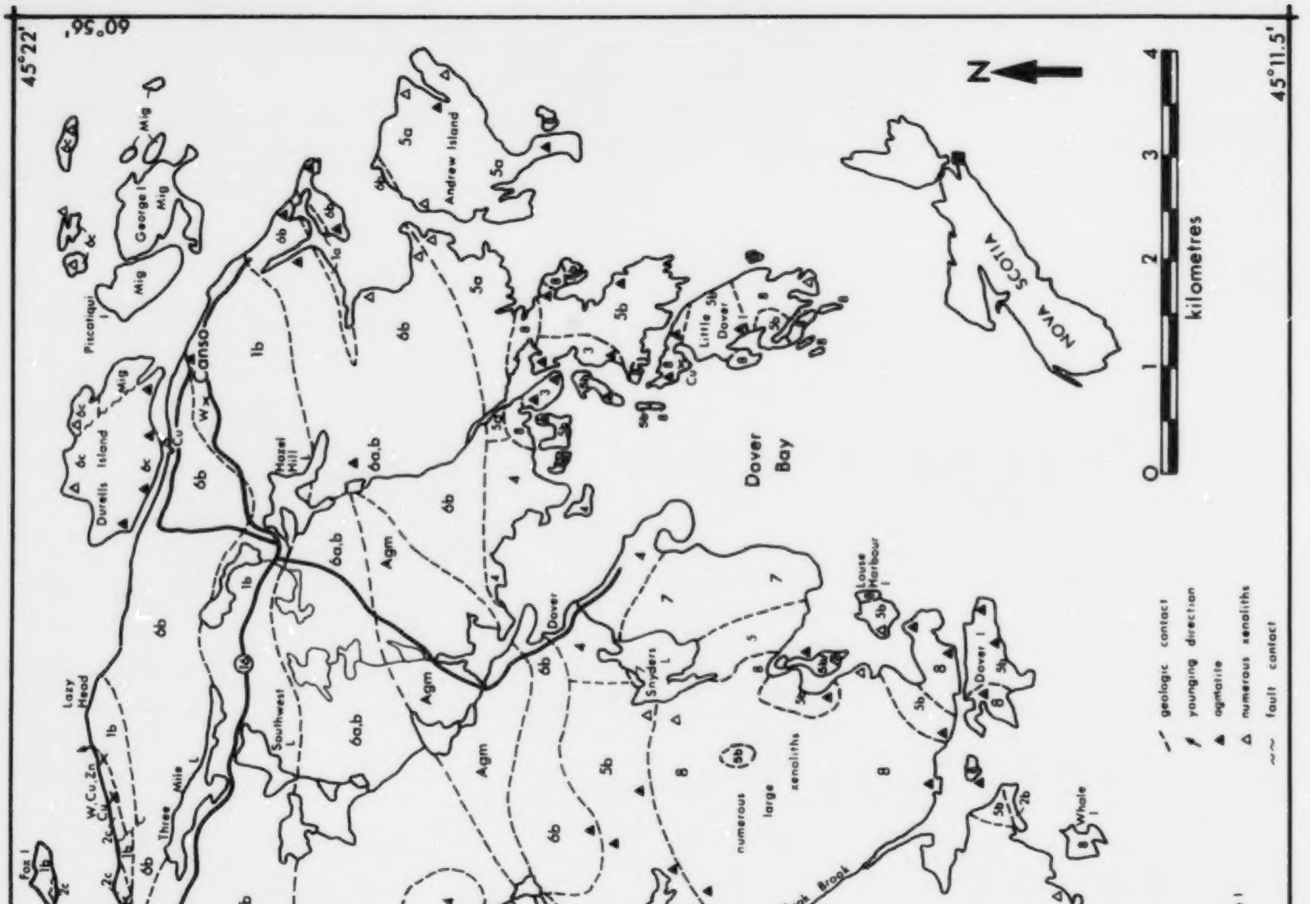
45°22'
60°56'
45°11.5'
61°13'
N
0 1 2 3 4
kilometres
NOVA SCOTIA
Dover Bay
Andrew Island
George I
Durells Island
Piscatiqui I
Canso
Hazel Hill
Lazy Head
Three Mile L
Southwest L
Fox I
Black Pt
Half Island Cove
Big Branch L
Otter Bk
Coerycoff L
Whitehead
Whitehead Harbour
Sheep Island
Admiral L
White Head I
Millstone I
Whale I
Kyak Brook
Snyders L
Dover
Little Dover
Dover I
Louse Harbour
numerous large xenoliths
geologic contact
younging direction
agmatite
numerous xenoliths
fault contact

LEGEND

DEVONIAN(?)

8 - Medium- to coarse-grained seriate biotite granodiorite to granite

7 - Medium grained muscovite granite

6 - Medium grained granite of more than one age. a - biotite > muscovite; b - muscovite > biotite; c - medium- to coarse-grained, muscovite > biotite

5 - Coarse grained seriate biotite granodiorite. a - with accessory garnet; b - without garnet

4 - Fine grained biotite-muscovite granite

3 - Medium grained tonalite

CAMBRO-ORDOVICIAN (Meguma Group)

2 - Halifax Formation. a - muscovite-biotite-chlorite phyllite and schist, locally porphyroblastic; b - andalusite schist; c - graphite schist, commonly porphyroblastic

1 - Goldenville Formation. a - thinly bedded laminated metawacke and minor metapelite; b - massive metawacke

Agm - Agmatite, with mixed outcrops of Meguma Group, granite and granite pegmatite

Mig - Banded migmatite containing layers and lenses of metawacke (Unit 1), contaminated tonalite gneiss and metagranite (Unit 6c)

Figure 21.1. *Sketch map showing the general geology of the Canso area, Nova Scotia.*

A large zone of migmatite (Unit Mig) outcrops in a series of islands north and east of Canso. It is composed of lenticular layers, 1 mm to 5 m thick, of three main lithologies:

i. The dominant phase is medium grained tonalite (or granodiorite?) gneiss which contains small clots of mica as well as rounded knots, less than 25 cm in diameter, of coarse grained alkali feldspar with minor quartz and muscovite.

ii. Layers and lenses of metawacke (Unit 1), commonly containing 1-10 mm thick streaks of granitic material, are intimately mixed with the tonalite gneiss. All gradations in texture and composition between metasedimentary and tonalite gneiss bands occur. In many places, metawacke forms xenolith-like bodies in the tonalite gneiss.

iii. Bands and lenses of medium- to coarse-grained biotite-muscovite metagranite intrude phases (i) and (ii). The metagranite appears to represent dykes of Unit 6c that have been transposed during subsequent deformation.

Structure and deformation

Structural and metamorphic events can be grouped into those that occurred prior to intrusion of the granitoid plutons (i.e. Acadian Orogeny) and those that occurred after intrusion (i.e. dextral shearing). All of the dominant structures trend approximately east to northeast, making it difficult to recognize older foliations and folds.

The oldest tectonic structure observed is a slaty cleavage or schistosity (S_1) which is generally parallel or subparallel to bedding (S_0) in the Meguma Group. It is defined by a preferred dimensional orientation of muscovite, biotite and chlorite and is axial planar to tight, gently to moderately plunging mesoscopic folds. Although no macroscopic F_1 folds were observed, repetition of the Goldenville and Halifax formations at map scale indicates the presence of a series of synclines and anticlines. Structural data indicate that the macroscopic F_1 folds are tight to isoclinal, gently plunging to the east and west, and slightly overturned to the north and south.

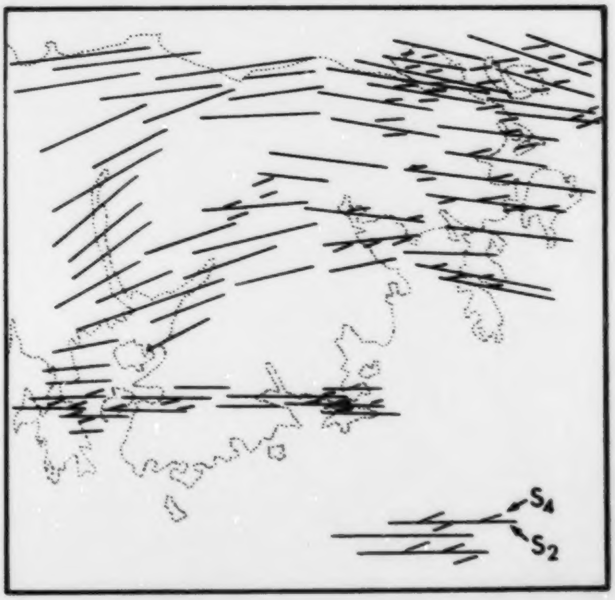

Figure 21.2. ***Distribution of S_2 and S_4 in the Canso area. Line spacing reflects the intensity of deformation.***

a. S_2 (parallel pencil) and S_4 (parallel pen cap) in granite (unit 5) west of Andrew Island.

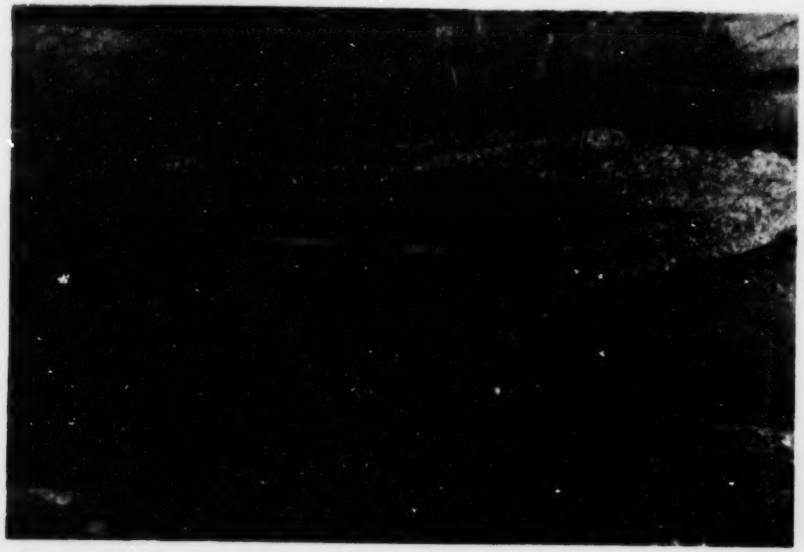

b. F_2 with S_2 axial plane foliation parallel pen, Durells Island.

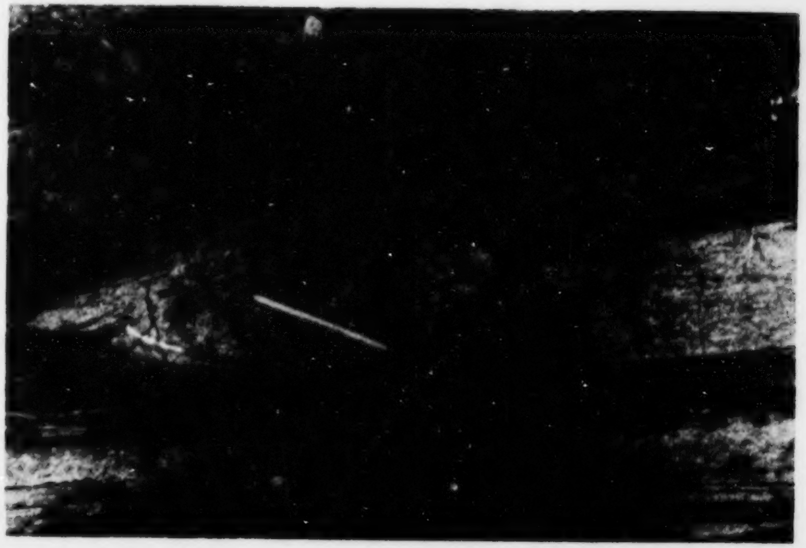

c. F_3 with S_2 folded around. Pen is parallel S_4 which crosscuts both limbs. Durells Island.

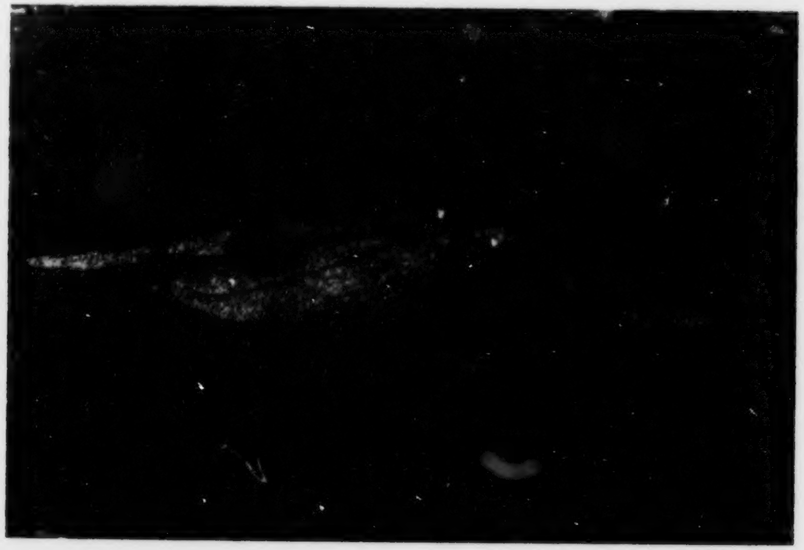

d. Boudinaged dyke of granite in metawacke of Meguma Group shows dextral drag along S_4. Pen is parallel to S_2. Durells Island.

Figure 21.3. *Structures related to late stage dextral shearing in the Canso area.*

Porphyroblasts of andalusite, cordierite, garnet and rare staurolite overgrow S_1 in many pelitic beds of the Meguma Group. They are believed to have formed during regional metamorphism that reached amphibolite grade after F_1 folding had ceased.

Contact metamorphic aureoles associated with the granitoid plutons were not recognized in the field, mainly because of later deformation and retrograde metamorphism. However, Schiller (1963) reported the existence of a cordierite-bearing aureole, about 400-900 m wide, around the western side of Unit 6b north of Whitehead. Obvious thermal metamorphic effects were found in xenoliths of Unit 2b in granite plutons along the south coast. What were once andalusite schists are now well indurated hornfels containing intergrown masses of fibrolite.

At least three stages of ductile shearing postdate granite emplacement. Keppie (1985) has ascribed these to a single event of progressive deformation related to late Carboniferous-early Permian transcurrent movements along the Minas Geofracture. The oldest and most widespread structure is a foliation (S_2) which varies from a weak mineral alignment to a strong augen gneissosity. Its distribution is illustrated in Figure 21.2. S_2 is defined by very fine grained muscovite, biotite and chlorite in all rocks as well as ribbon quartz and feldspar augen in granite (Fig. 21.3a). It is axial planar to numerous Z-shaped folds (Fig. 21.3b). Subsequent (or continued?) deformation resulted in the formation of coaxial Z-shaped F_3 folds which lack an axial plane foliation (Fig. 21.3c). Finally, a spaced mylonitic foliation (S_4) developed at a small angle to S_2 (Fig. 21.3a). Dextral shear of older structures is ubiquitous along S_4 planes (Fig. 21.3d). Substantial movement during this period is indicated by the common occurrence of subhorizontal slickensides on S_2 and S_4 planes and the extreme flattening of xenoliths in deformed granite.

Several types and ages of late, minor structures were recognized in various places. Kink bands occur in all units, especially in the northern half of the map area. Discrete planes of brittle shear showing variably developed crush zones and both dextral and sinistral displacements are common in the northern part of the map area as well. They may be related to strike-slip faults recognized along the north coast. Crenulation and spaced cleavages that postdate S_2 were found in the restricted areas, but their significance is unknown.

Economic geology

The most important economic mineral showing is the Lazy Head prospect which lies about 2 km west of Durells Island. It consists of 2-5 cm thick quartz veins containing scheelite, chalcopyrite, sphalerite, pyrite and pyrrhotite. The veins crosscut a 1.5 m thick bed of manganiferous garnet-quartz rock which is interlayered with phyllite and minor metawacke. Shaw (1983) placed the mineralized horizon in the upper part of the Goldenville Formation. However, using a 1:1 ratio of psammite to pelite to separate the Goldenville and Halifax formations puts the mineralized bed in the lower Halifax Formation, about 60 m above the Goldenville-Halifax contact. Scheelite and pyrite also occur in garnet-quartz rock in the Goldenville Formation 0.5 km west of Canso (MOD card 28, NSDME files). Similar garnet-quartz beds lacking mineralization have been found in the Halifax Formation 2.1 km west of Black Point and in numerous places north of Whitehead.

Several other mineral showings of minor importance are scattered throughout the map area. Pyrite and pyrrhotite are abundant in graphitic schist (Unit 2c) in the Halifax Formation, forming up to 50% of the rock in some places. Accessory chalcopyrite is associated with the pyrite and pyrrhotite in two outcrops of this unit. Chalcopyrite has also been found as thin coatings on foliation planes in pyritiferous graphite-andalusite schist (Unit 2c) in the bottom of the narrow channel south of Durells Island (Mod card 21, NSDME files). Three lenses of muscovite-garnet-tourmaline granite pegmatite intrude the Goldenville Formation near Cole Harbour River. Each of these contains one or more of beryl, molybdenite, chalcopyrite and pyrite in accessory amounts. Very small amounts of pyrite and chalcopyrite occur in vuggy micaceous clots in biotite granite xenoliths (Unit 5) trapped in Unit 8 on Little Dover Island.

Discussion and summary

The Canso area is underlain by metasedimentary rocks of the Cambro-Ordovician Meguma Group and granitoid plutons that are believed to be middle to late Devonian. The Meguma Group consists of an older Goldenville Formation and a younger Halifax Formation separated by a thin transitional zone. Only rocks stratigraphically within about 2 km of the Goldenville-Halifax contact are exposed in the Canso area.

The Meguma Group was deformed into east-trending subhorizontal folds during the Acadian Orogeny. Greenschist facies regional metamorphism accompanied deformation. Metamorphism culminated at amphibolite grade after deformation waned with the growth of post-S_1 porphyroblasts of andalusite, cordierite, garnet and staurolite.

Numerous granitoid plutons ranging in composition from tonalite to granite were emplaced during the Devonian. They intruded after formation of the late Acadian porphyroblasts, as shown by thermal overprinting of andalusite in hornfels xenoliths. The highly variable orientation of planar plutonic-metasedimentary contacts within individual outcrops suggests that emplacement took place in a relatively stable tectonic environment. The presence of rare miarolitic cavities limits the depth of emplacement to shallow to moderate crustal levels. Although stoping appears to have played a dominant role in creating space, individual plutons also appear to have caused forceful deflection of Meguma strata in some places. At least seven magmatic phases have been recognized. The lack of correlation between composition and age of each phase indicates that more than one cycle of partial melting – uprise and differentiation – intrusion occurred. The prevalence of planar interplutonic contacts which appear to be fracture-controlled suggests that each pluton had sufficient time to cool and crack prior to intrusion of the next magma. This observation suggests that the 10-12 Ma time span interpreted for emplacement of the Nova Scotia batholith (Clarke and Halliday, 1980) may be too small for the granitoid plutons in the Canso area.

The northern part of the area was subjected to a complex history of dextral shearing under greenschist facies conditions. Deformation affected both the Acadian structures in the Meguma Group as well as the previously undeformed granitoid plutons. It produced several generations of Z-shaped folds, mylonitic foliations and lineations, all compatible with large amounts of dextral, subhorizontal movement along the Minas Geofracture (Keppie, 1982). High strain is recorded by metasedimentary xenoliths which have length to width ratios that vary from 1:1 in undeformed granite to 100:1 in deformed granite.

The most significant economic mineral showings are scheelite occurrences in garnet-quartz rocks in the Meguma Group. The widespread development of similar garnet-quartz beds in the Whitehead area provide additional targets for future exploration. Although no significant mineralization or alteration zones were found in the granitoid plutons, the

common occurrence of mineralization in similar rocks associated with the South Mountain batholith should provide suitable stimulus for exploration. The most favourable sites for mineralization are believed to be the muscovite-enriched granites (Units 4, 6, 7) which have the highest airborne radiometric eU/eTh ratios (Ford and Ballantyne, 1983).

References

Clarke, D.B. and Halliday, A.N.
1980: Strontium isotope geology of the South Mountain batholith, Nova Scotia; Geochimica et Cosmochimica Acta, v. 44, p. 1045-1058.

Faribault, E.R.
1893: Whitehaven Sheet, Nova Scotia; Sheet No. 26, Geological Survey of Canada.

Ford, K.L. and Ballantyne, S.B.
1983: Uranium and thorium distribution patterns and lithogeochemistry of Devonian granites in the Chedabucto Bay area, Nova Scotia; in Current Research, Part A, Geological Survey of Canada, Paper 83-1A, p. 109-119.

Keppie, J.D.
1982: The Minas Geofracture; in Major Structural Zones and Faults of the Northern Appalachians, ed. P. St-Julien and J. Béland; Geological Association of Canada, Special Paper 24, p. 263-280.

1985: Geology and tectonics of Nova Scotia; in Appalachians Geotraverse (Canadian Mainland); Geological and Mineralogical Associations of Canada Annual Meeting, guidebook to excursion 1, p. 23-108.

McBride, D.E.
1978: Geology of the Ecum Secum area, Halifax and Guysborough Counties, Nova Scotia; Nova Scotia Department of Mines and Energy, Paper 78-1, 12 p.

McKenzie, C. and MacGillivary, J.
1974: Eastern Nova Scotia granites project; unpublished report for the Department of Geology, Dalhousie University, Halifax, Nova Scotia.

Nichols, D.
1976: The metamorphic and structural evolution of the metasediments and granites in the Whitehaven area, Guysborough County, Nova Scotia; unpublished B.Sc. thesis, Dalhousie University, Halifax, Nova Scotia.

O'Brien, B.H.
1985: Preliminary report on the geology of the LaHave River area, Nova Scotia; in Current Research, Part A, Geological Survey of Canada, Paper 85-1A, p. 789-794.

Poole, J.
1984: An example of structural deformation of the Halifax Formation in the Whitehead area, Meguma terrain, eastern Nova Scotia; unpublished B.Sc. thesis, St. Francis Xavier University, Antigonish, Nova Scotia, 89 p.

Reynolds, P.H., Zentilli, M., and Muecke, G.K.
1981: K-Ar and $^{40}Ar/^{39}Ar$ geochronology of granitoid rocks from southern Nova Scotia. Its bearing on the geological evolution of the Meguma Zone of the Appalachians; Canadian Journal of Earth Sciences, v. 18, p. 386-394.

Schiller, E.A.
1959: Petrography and petrology of the andalusite schists, Port Felix, Nova Scotia; unpublished M.Sc. thesis, Michigan State University.

1963: Mineralogy and geology of the Guysborough area, Nova Scotia, Canada; unpublished Ph.D. thesis, University of Utah, 162 p.

Shaw, W.G.
1983: A geological investigation of the Lazy Head tungsten prospect, Guysborough County and a comparison with the Moose River deposit, Halifax County, Nova Scotia; unpublished M.Sc. thesis, Dalhousie University, Halifax, Nova Scotia, 217 p.

Stevenson, I.M.
1964: Chedabucto Bay, Nova Scotia; Geological Survey of Canada, Map 1156A.

Streckeisen, A.
1976: To each plutonic rock its proper name; Earth Science Reviews, v. 12, p. 1-33.

Weeks, L.J.
1959: Cape Canso, Guysborough and Richmond Counties, Nova Scotia; Geological Survey of Canada, Map 1074A.

Preliminary results of structural investigations in the Bathurst camp of northern New Brunswick[1]

Project 850018

Cees R. van Staal
Precambrian Geology Division

van Staal, C.R., Preliminary results of structural investigations in the Bathurst camp of northern New Brunswick; in Current Research, Part A, Geological Survey of Canada, Paper 86-1A, p. 193-204, 1986.

Abstract

The earliest structures include two generations of folds (F_{1A} and F_{1B}) due to a single progressive deformation (D_1). Later generations of folds are labelled F_2 to F_5. The first four groups of folds have an important influence on the regional distribution of rock types in the Bathurst camp, though the present horseshoe-shaped outcrop pattern of the felsic volcanics is mainly a product of F_4. D_1 deformation is responsible for transposition of bedding in layer-parallel movement zones and high strain zones in volcanic rocks. Primary igneous and sedimentary structures are well preserved locally due to the varying degree of D_1 deformation, which also controls development of subsequent structures.

Deformation and accompanying alteration change the appearance and nature of the rocks, making correlation difficult. The banded iron formation and the red hematitic and manganiferous slates are potential structural markers, but their use is hindered by poor exposure. Both rock types are associated with massive sulphides but are not lateral equivalents, as other workers have suggested.

Résumé

Les structures les plus anciennes comprennent deux générations de plis (F_{1A} et F_{1B}) dus à une seule déformation progressive (D_1). Des générations plus récentes de plis ont été désignées par les termes F_2 à F_5. Les quatre premiers groupes de plis influent beaucoup sur la répartition régionale des types de roches dans le camp de Bathurst, bien que le patron actuel semi-circulaire des affleurements de roches volcaniques felsiques soit surtout un produit de F_4. La déformation D_1 a transformé la structure stratifiée des roches volcaniques en zones de mouvements parallèles aux couches et en zones de fortes tensions. Les structures ignées et sédimentaires primaires ont été bien conservées par endroits.

La déformation et l'altération résultante modifient l'apparence et la nature des roches, rendant toute corrélation difficile. La formation ferrifère rubanée et les ardoises hématitiques et manganésifères rouges sont des horizons structuraux repères possibles, mais difficiles à utiliser en raison de leur mauvaise exposition. Les deux types de roches sont associés à des sulfures massifs, sans toutefois en être des équivalents latéraux, comme l'ont suggéré d'autres géologues.

[1] Contribution to Canada-New Brunswick Mineral Development Agreement 1984-89. Project carried by Geological Survey of Canada.

Introduction

This paper reports some of the progress made during structural studies in the Bathurst camp in northern New Brunswick (Fig. 22.1). The Bathurst camp comprises the northern part of the Miramichi Massif of Fyffe et al. (1981), which is underlain by rocks of the Cambro?-Ordovician Tetagouche Group (Helmstaedt, 1971, 1973; Skinner, 1974).

A complex sequence of felsic metavolcanic rocks makes up the bulk of the Tetagouche Group in the northern part of the Miramichi Massif. The felsic volcanic rocks define a large horseshoe-shaped outcrop pattern, that has been interpreted to outline a more-or-less circular caldera (Davies, 1966; Harley, 1979).

Numerous massive sulphide deposits including the large Brunswick No. 12 orebody, are closely associated with the felsic volcanic rocks. Deformation played an important role in concentrating the sulphides in the Brunswick No. 6 and No. 12 deposits (van Staal and Williams, 1984). Because of the intense multiple deformation, stratigraphic relationships between the various volcanic and sedimentary rock units are puzzling. One of the aims of this study is to decipher these stratigraphic relationships through a detailed structural analysis. Better understanding of the regional structural and stratigraphic history is important to mineral exploration in the Bathurst camp.

Lithologies, age and stratigraphic relationships

The base of the Tetagouche Group consists of a sequence of alternating greenish-grey quartzites and dark grey-black phyllites. The phyllites are locally carbonaceous. This rock unit can be traced throughout the Miramichi Massif into southwestern New Brunswick (Poole, 1967; Rast et al., 1980; Fyffe, 1982) and adjacent parts of Maine, where it is in part known as the Grand Pitch Formation (Neuman, 1968). Neuman assigned a Cambrian age to the Grand Pitch Formation on the basis of the occurrence of **Oldhamia smithi** Reudemann. Arenig fossils in calcareous rocks near the top of this unit in northern and central New Brunswick (Neuman, 1968; Fyffe, 1976), and Tremadocian graptolites found in intercalated black slates in west-central New Brunswick (Fyffe et al., 1983) indicate a Cambrian to early Ordovician age for the lower Tetagouche Group. Poole (1967) and Helmstaedt (1971) suggested that the quartzite-phyllite unit represents platformal deposits, while Skinner (1974) and Fyffe (1982) interpreted these rocks as quartzose turbidites. Preservation of thin, tabular, graded beds, local cross-stratified quartzite beds intercalated with phyllites, and poor sorting in the quartzose beds favour the latter interpretation.

The quartzite-phyllite unit is structurally overlain by felsic metavolcanic rocks in the Brunswick Mines area (Boyle and Davies, 1964; Stockwell and Tupper, 1966). The felsic metavolcanic rocks comprise both porphyritic and aphanitic types and were previously interpreted as meta-ash-flow tuffs (Davies, 1972; Skinner, 1974), mainly on the basis of their large areal extent. The porphyritic types are generally transformed into augen schists by deformation. Primary features other than phenocrysts, such as pumice, shards and welding are generally either absent or were destroyed by subsequent deformation and metamorphism, though Juras (1981) observed shards and fiamme in a few rocks at Brunswick No. 12 mine. Field work this summer showed that bedding (cm to m scale) and grading are rather common in the quartz-feldspar augen schist. This confirms a pyroclastic origin for these. Sorting is relatively well developed locally, suggesting that at least part of these rocks are pyroclastic fall rather than pyroclastic flow deposits (Fig. 22.2). Some augen schists probably represent thin porphyritic dykes or sills as is indicated by their presence as massive boudins, occasionally with crosscutting relationships in bedded and graded augen schists . Pisolitic felsic volcanic rocks found between the Brunswick Mines area and Nine Mile Brook, north of road 430, are tentatively interpreted as epiclastic rocks.

The bulk of the felsic metavolcanics is massive and aphanitic. Locally the aphanites grade into porphyritic rocks with phenocrysts of K-feldspar and albite and occasional chert-filled gas-escape pipes. The origin of these rocks is problematic, but conchoidal fractures and rare flow banding, as well as the absence of fragments, suggest that they are in part probably rhyolite flows.

Quartzite pebbles in an agglomerate or conglomerate within the felsic metavolcanic rocks just west of Austin Brook open pit (Davies, 1972), and pelecypod fossils of probable Middle or Upper Ordovician age, in a silicic sulphide-bearing tuff at Taylor Brook (Gummer et al., 1978), suggest that the felsic metavolcanic rocks are, in general, younger than the underlying quartzite-phyllite unit. The presence of tuffaceous layers in the quartzite-phyllite unit close to the contact with the felsic metavolcanic unit suggests a gradual change from siliciclastic to volcaniclastic sedimentation. This is consistent with the findings of Poole (1963), Neuman (1968), Fyffe (1982) and Fyffe et al. (1983) in the southwestern parts of the Miramichi Massif and indicates that felsic volcanic activity may have started as early as late Arenig.

The economically important Brunswick No. 6 and No. 12 massive sulphide deposits, which form an integral part of an extensive Algoma type iron formation unit, are enclosed by the felsic metavolcanic rocks.

The felsic metavolcanic unit is structurally overlain by greyish quartzose sedimentary and mafic metavolcanic rocks. In the western parts of the investigated area (Fig. 22.1) the metasediments are locally absent and the mafic volcanics directly overlie the felsic volcanics. The sediments consist mainly of thin (cm scale) beds of rhythmically alternating quartzose, or locally feldspathic, greywackes and phyllites. The phyllites are locally graphitic. Occasionally there are intercalations of conglomerates and tuffaceous layers. Ubiquitous grading, and the presence of crosslamination locally, suggests that the rhythmites represent distal turbidites. Younging direction indicators in these turbidites at the contact with the basalt, as well as their inclusion of detritus of the felsic volcanics (but not of the mafic volcanics) suggest that these turbidites are older than the basalts. This is opposite to the stratigraphic division proposed by Davies (1979). The turbidites generally show a rusty staining on surface outcrops due to accessory amounts of sulphides. Locally there are small intercalations of massive sulphide deposits and red manganiferous phyllite or slate.

The mafic metavolcanic unit comprises mainly pillow basalts, although pillows are locally deformed beyond recognition. Amygdules and shelves occur occasionally and were used in conjunction with pillow stems for way-up determinations (Sawyer et al., 1983). Hyaloclastite and flow breccias occur locally. Fragments may have been rounded and stretched to such an extent by deformation that these autoclastic rocks are difficult to distinguish from conglomerates. Thin, centimetre-scale, greenish tuffaceous turbidites are interlayered with and overlie the basalts, suggesting that turbidite deposition continued during and after extrusion of the basalts.

On the basis of field relations Helmstaedt (1971, 1973) and Fyffe (1982) assigned a younger age to the basalt than the felsic volcanics, in contast to the interpretations of Skinner (1974) and Whitehead and Goodfellow (1978). Felsic volcanic clasts in rare agglomerates or conglomerates in the

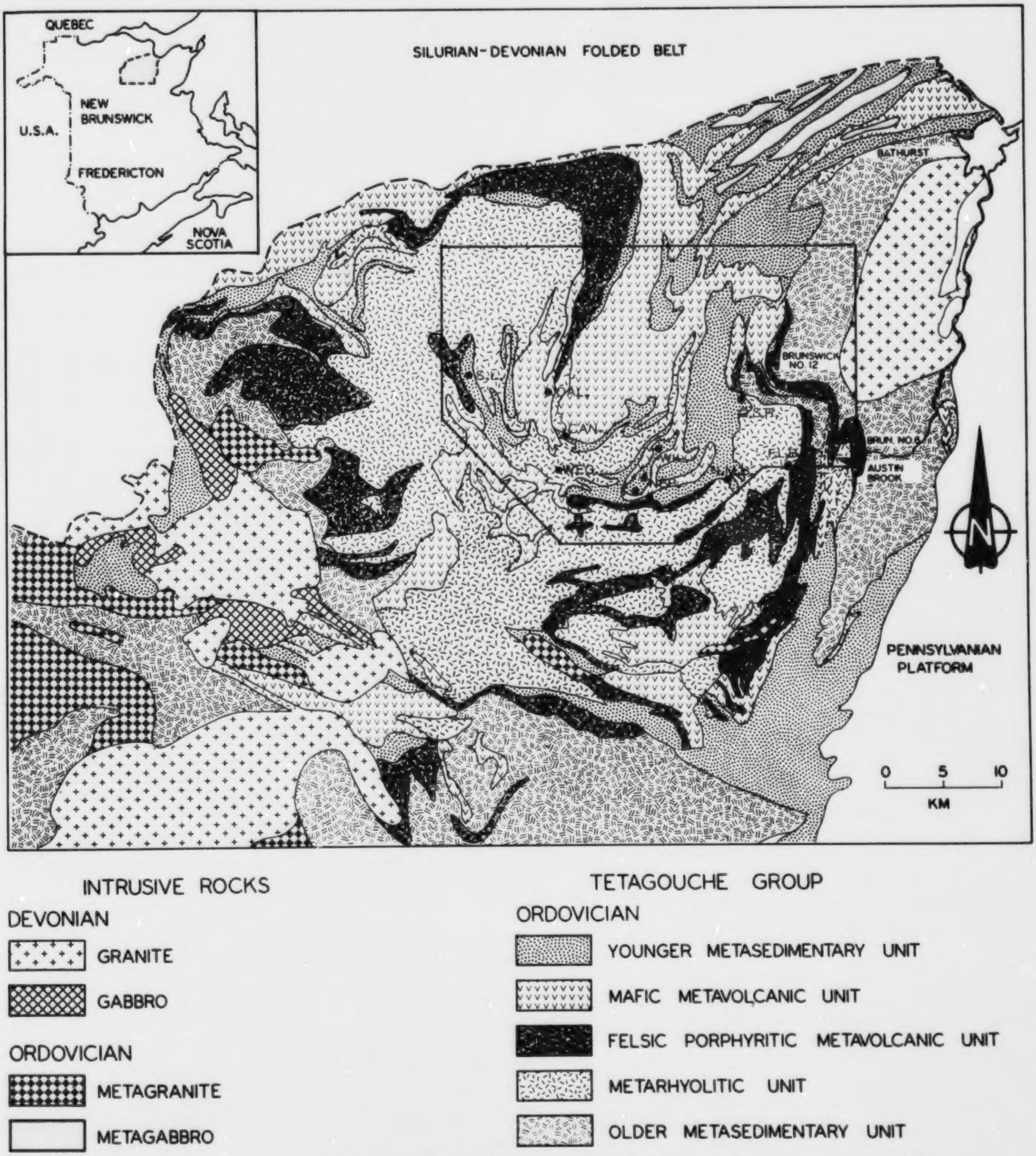

Figure 22.1. *Geology of the northern part of the Miramichi Massif, adapted from Davies (1979). Outlined area was focus of investigation this summer. Black dots are known occurrences of massive sulphide deposits. Abbreviations refer to their names in common use; S.L. – Strachens Lake, CaL – California Lake, Can – Canoe Landing Lake, Weg – Wedge, Wil – Willet, Nep – Nepisiquit A,B,C, N.M.B. – Nine Mile Brook, F.L.B. – Flat Landing Brook, Q.S.R. – Quebec Smelting and Refining.*

Figure 22.2. Example of an air-fall crystal tuff. Large euhedral crystals are phenocrysts of feldspar.

basalts west of Brunswick No. 12 mine (van Staal, 1985) and a few top determinations close to the contacts with underlying rock units are consistent with the interpretations of Helmsteadt (1971, 1973) and Fyffe (1982). If the few fossil localities in intercalated limestone (Kennedy et al., 1979; Nowlan, 1981) and associated graptolitic black shale (Skinner, 1974) are representative, then the basalts are mainly Caradoc. This would set an upper limit to the felsic volcanic activity. The felsic volcanic rocks and basalts are not necessarily in normal stratigraphic contact, however, since highly strained rocks (stretched pillows) are common in the basalts, particularly close to these contacts. This might also explain the problematic lenses of basalts enclosed within the felsic volcanics. More work (e.g. radiometric dating) is necessary to solve this problem.

Mesocopic structure

Five groups of folds have been recognized in the Brunswick Mines area (van Staal and Williams, 1984). They are subdivided on the basis of overprinting relationships and symmetry arguments into six generations of folds (van Staal and Williams, in press; van Staal, 1985). The first two generations of folds (F_{1A} and F_{1B}) have been interpreted as the result of one progressive deformation (Fig. 22.3) (van Staal, 1985).

The same structural history which is more complex than that of previous workers (Helmstaedt, 1971, 1973), is recognized in the rest of the investigated area. Overprinting relationships between folds of the first group are very rare but there is additional evidence that D_1 represents a complex progressive deformation.

Problems with the use of style in the structural analysis of the Bathurst camp

The most common approach to the analysis of structurally complex areas with poor exposure and relatively few overprinting relationships is to group structures mainly on the basis of style (Turner and Weiss, 1963; Hobbs et al., 1976). Use of this method, however, is dangerous since one style group can contain more than one generation of folds (see Williams, 1970). Nevertheless, continuous exposure underground and in the open pits provided enough overprinting relationships to demonstrate that such an approach is justified in the Brunswick Mines area (van Staal and Williams, 1984), although the first style group contains two generations of folds (F_{1A} and F_{1B}).

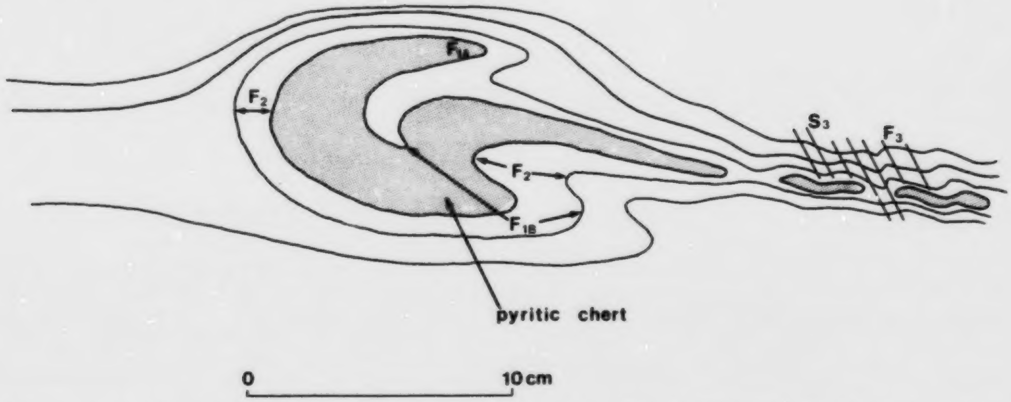

Figure 22.3. Overprinting relationship between F_{1A},F_{1B} and F_2 folds. East ore zone, Brunswick No. 12 mine.

The distinction between the intrafolial F_1 and F_2 folds is important for mineral exploration, since it was shown that the Brunswick No. 6 and No. 12 orebodies are concentrated in structural basins formed by the interference of large F_1 and F_2 folds (van Staal and Williams, 1984). Such interference patterns may be found by carefully mapping the small, mesoscale, F_2 folds (see van Staal and Williams, in press). However, there is some overlap in style between F_1 and F_2 folds. F_2 folds are generally tight structures with interlimb angles on the order of 20-40° degrees. They are rarely isoclinal. Exceptions occur in the less competent rocks such as the Pb-Zn rich, massive sulphides. F_1 folds are generally isoclinal, but are locally tight or even close structures. F_1 structures also fold the strong bedding parallel foliation in the sedimentary rocks and there is thus the potential of misclassification of tight intrafolial folds in areas that lack continuous outcrop and sufficient overprinting relationships. A differentiated, axial plane crenulation cleavage accompanies tight F_2 folds in phyllosilicate-rich rocks, but is generally lacking in tight F_1 folds. Locally, there is a differentiated layering (S_1) in the felsic metavolcanics that is axial planar to rare F_1 folds (van Staal and Williams, 1984). Despite their mesoscopically domainal nature, the S_1 foliation is penetrative or continuous within both domains (viz. microlithon and septum) whereas the S_2 differentiated crenulation cleavage is domainal on all scales. Cleavage morphology therefore constitutes a style criterion. Furthermore, M_1-related porphyroblasts are syn- or post-D_1 structures, but are consistently overprinted by F_2 structures. Microstructures and metamorphic criteria are therefore important in grouping F_1 and F_2 structures.

Another overlap in style occurs between F_3 and F_4 structures. F_4 structures are represented by kinkbands in more competent rocks and kinks or chevron folds in less competent phyllites. F_3 folds are generally also kinks in phyllites and therefore easily confused with F_4 (Fig. 22.4). However, in the Brunswick Mines area F_3 folds are generally accompanied by a crenulation cleavage (S_3) whereas S_4 is represented by kinkbands or microfractures. Furthermore, F_4 kinked micas are still strained whereas F_3 kinked micas have serrated kinkband boundaries (Etheridge and Hobbs, 1974), and locally there is also new growth by nucleation instead of by grain boundary migration alone. A preliminary examination of microstructures in rocks investigated this summer indicates that these criteria appear to be consistent and therefore are important in grouping.

High-strain zones

All rocks found in the Tetagouche Group show evidence of polyphase ductile deformation, although there is a marked variation in intensity. Primary igneous and sedimentary structures are well preserved locally, but are obliterated beyond recognition elsewhere within the same unit. Lack of recognition or understanding of this type of heterogeneous deformation has resulted in speculative interpretations of the timing of deformation (cf. McBride, 1976). Steeply dipping, narrow zones of high strain coincide with repetitions in lithology in the Brunswick Mines area and were interpreted as D_1 related ductile thrusts (van Staal, 1985); their present steep dip is due to F_2 refolding.

Mapping elsewhere in the Bathurst camp reveals the heterogenous character of D_1, which is particularly evident in rocks containing strain markers, such as pillows, phenocrysts, pebbles and volcanic fragments. For instance, the thick sequence of mafic volcanic rock that occupies the core of the Nine Mile synform (see below), is supposed to contain an alternating sequence of pillow basalts and banded tuffs (Jones, 1962). Locally, however, there is relatively good continuity of outcrop and in such areas weakly deformed pillow lavas can be traced into narrow zones, a few hundred metres thick at the most, that consist of dark green slates or banded phyllites. Vague lenticular layering and preserved pillow selvages (Fig. 22.5) mark the outlines of strongly elongated pillows in some of the less deformed parts of the zones. Compositionally layered rock found in more deformed zones could be interpreted as a mafic tuff if it were not continuous with the pillowed volcanics. These zones are parallel to the lithological contacts and bedding. Bedding in boudins, or lenticular inclusions of sediment are locally truncated at a small angle, suggesting that these structures are the sites of shear strains. The presence of monoclinic sets of shearbands (White, 1979) and the occasional presence of sheath folds in similar zones in the sediments are consistent with such a noncoaxial strain history. Although high-strain zones occur in all rock units, they are most difficult to recognize in the sediments because of the lack of good strain markers. Strong attenuation and complete transposition in the fashion described by Knopf and Ingerson (1938) and Turner and Weiss (1963) are the best indicators for their existence here. These structures are interpreted to mark the sites of ductile thrusts, although poor exposure generally prevents a full determination of their regional extent.

Alteration accompanying D_1 deformation transformed the volcanics into phyllonites and/or mylonites in these high-strain zones. Not surprisingly, post-D_1 folding is generally confined to these well foliated zones as well. Localized softening of the volcanics during D_1 is thus also responsible for at least part of the heterogeneous distribution of the later structures.

Nine Mile structure

The dominant structure in the study area (Fig. 22.1) is the Nine Mile fold (Fig. 22.6). This was previously interpreted as a southerly plunging antiform (Skinner, 1974; Fyffe, 1982).

However, a plot of bedding (S_0) and bedding parallel foliation (S_1) in the domain of the Nine Mile structure on the lower hemisphere of an equal area projection (Fig. 22.7a) defines a vertical fold with a slight tendency towards a steeply plunging synform rather than an antiform. The dips of S_0/S_1 are steep and change frequently through the vertical, within short distances. Locally, where there is good continuity of outcrop, it can be shown that this is due, at least in part, to the presence of tight intrafolial, and shallow plunging F_2 folds. This regional distribution of S_0/S_1 suggests, therefore, that F_2 folds are probably quite abundant, although F_1 folds may also be responsible in part for this. Deep drilling by Brunswick Mining & Smelting on the Canoe Landing Lake massive sulphide deposit in the hinge area of this structure (Fig. 22.1) shows that this structure is a steeply plunging synform in this area (Fig. 22.8). The contacts between the various units dip steeply towards the north. Consequently the plunge must also be northerly.

The relative age of the Nine Mile fold is problematic. This structure folds and redistributes S_2 and must therefore be younger. Fyffe (1982) classified this structure as an F_3 fold but F_3 structures are dominantly S-shaped instead of the Z-folds expected on the east limb (Fig. 22.9). This is best illustrated by the large F_3 Pabineau folds (Fig. 22.6; van Staal and Williams, 1984). This indicates that F_4 or a younger deformation are more probably the cause of this structure. F_4 kinkfolds have the required Z-shape on the east limb and S_4 is statistically parallel to the axial surface of the Nine Mile Synform (Fig. 22.7b). Moreover the steep plunge of the Nine Mile synform, as deduced from drill holes, is consistent with the vertical or steep plunge common to the mesoscopic F_4 folds. A problem is the common Z-shape of

F_4 folds on the west limb of the Nine Mile synform. This limb of the Nine Mile synform is shared with the Tetagouche antiform (Fig. 22.6; Helmstaedt, 1970; Skinner, 1974). Helmstaedt (1970) observed that D_2 folds (=F_3 in this study) have a consistent S-shape on both limbs of the Tetagouche antiform. He explained this feature to result from refolding by F_4. The author confirms the observations of Helmstaedt that F_3 folds are dominantly S-shaped; thus there is a similar relationship between F_3 folds and the Nine Mile synform (Fig. 22.9). The Tetagouche antiform and Nine Mile synform were probably formed during the same event. However, the Z-shape of F_4 kinkbands, or folds on the west limb of the Nine Mile synform, needs explanation. There are three possible explanations:

1. The Nine Mile synform and Tetagouche antiform are actually F_4 folds. The anomalous Z-shaped kinkbands on the west limb of the Nine Mile synform represent the conjugate part of S-shaped kinkbands. The latter did not develop because of the already existing presence of the S-shaped F_3 folds.
2. These structures are younger than F_4.

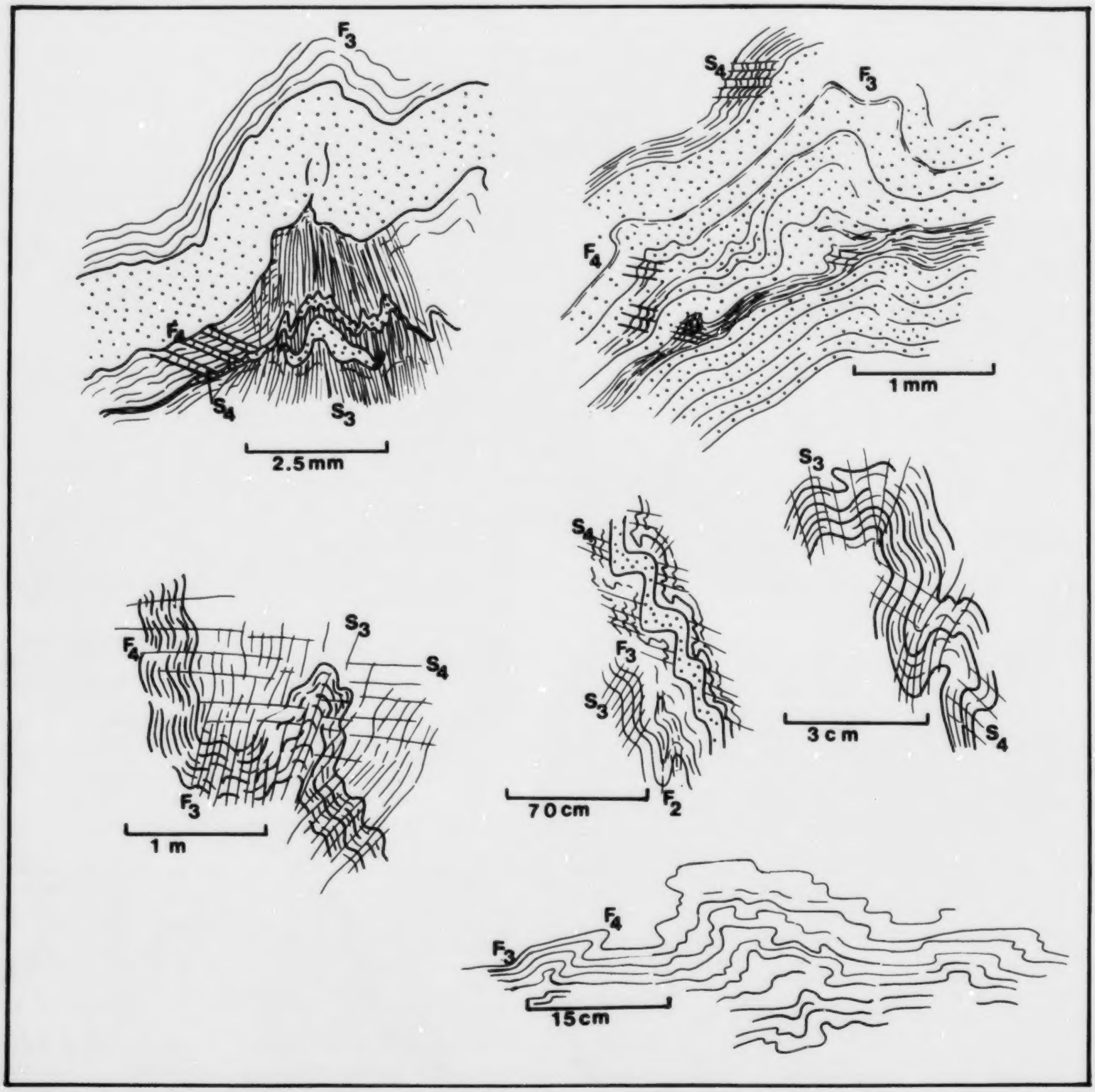

Figure 22.4. *Overprinting relationships at various scales between F_3 and F_4 folds.*

3. F_3 and F_4 represent a conjugate pair of structures with one of the sets more strongly developed than the other on the different limbs.

Although F_3 and F_4 are locally found in a boxfold or conjugate configuration, overprinting relationships and metamorphic criteria (see above) show that F_3 and F_4 represent two different generations. The third explanation can thus be rejected. The second explanation is possible, but to date there is no mesoscopic evidence for a younger generation of folds that could be related to these structures. F_5 structures have shallow dipping axial planes and result from vertical shortening rather than the horizontal shortening required to have formed the Nine Mile synform and Tetagouche antiform. This leaves the first explanation as the most likely. It is also consistent with the observation that F_4 folds are relatively rare on the west limb of the Nine Mile synform. The young age of the Nine Mile structure shows that the horseshoe outcrop pattern of felsic volcanic rocks that defines the Bathurst camp structure (Fig. 22.6) is a secondary feature and does not reflect the shape of a caldera (cf. Davies, 1966; Harley, 1979). This conclusion is also evident from the fact that at least one tectonic foliation is folded around the Bathurst camp structure (Smith, 1957; Helmstaedt, 1970, 1971, 1973; Skinner, 1974). Nevertheless the great volume of felsic volcanic rocks does suggest that such a feature may have existed here in Ordovician times.

Economic geology

The Bathurst camp is well known for its numerous massive sulphide occurrences, especially the giant Brunswick No. 12 orebody. The Brunswick No. 6, No. 12 and Austin Brook deposits (Fig. 22.1) form an integral part of an extensive Algoma type iron formation (Gross, 1967; Davies, 1972) that can be traced along strike for tens of kilometres (Stockwell and Tupper, 1966; van Staal and Williams, in press) on the basis of sparse outcrop, drillhole and geophysical data. The intimate relationship between iron formation and sulphides is well displayed at the Brunswick No. 6 and Austin Brook deposits, where massive hematite-magnetite-jasper rocks directly overlie the massive sulphides. The important Flat Landing Brook (Troop, 1984) and Heath Steele deposits (Fig. 22.1) are also associated with this type of iron formation, suggesting that these and the Brunswick orebodies occur in the same stratigraphic horizon. The close relationship between iron formation and massive sulphides was used extensively as an exploration tool in the Bathurst camp during the sixties and seventies. Not all iron formation is magnetic, however, and structural attenuation (van Staal and Williams, in press) as well as folding and thrusting complicates tracing this horizon into areas of poor outcrop. Additional information concerning the distribution of the iron formation is therefore important in understanding the structure, the exact relationships between the various sulphide deposits, and the complex felsic volcanic stratigraphy.

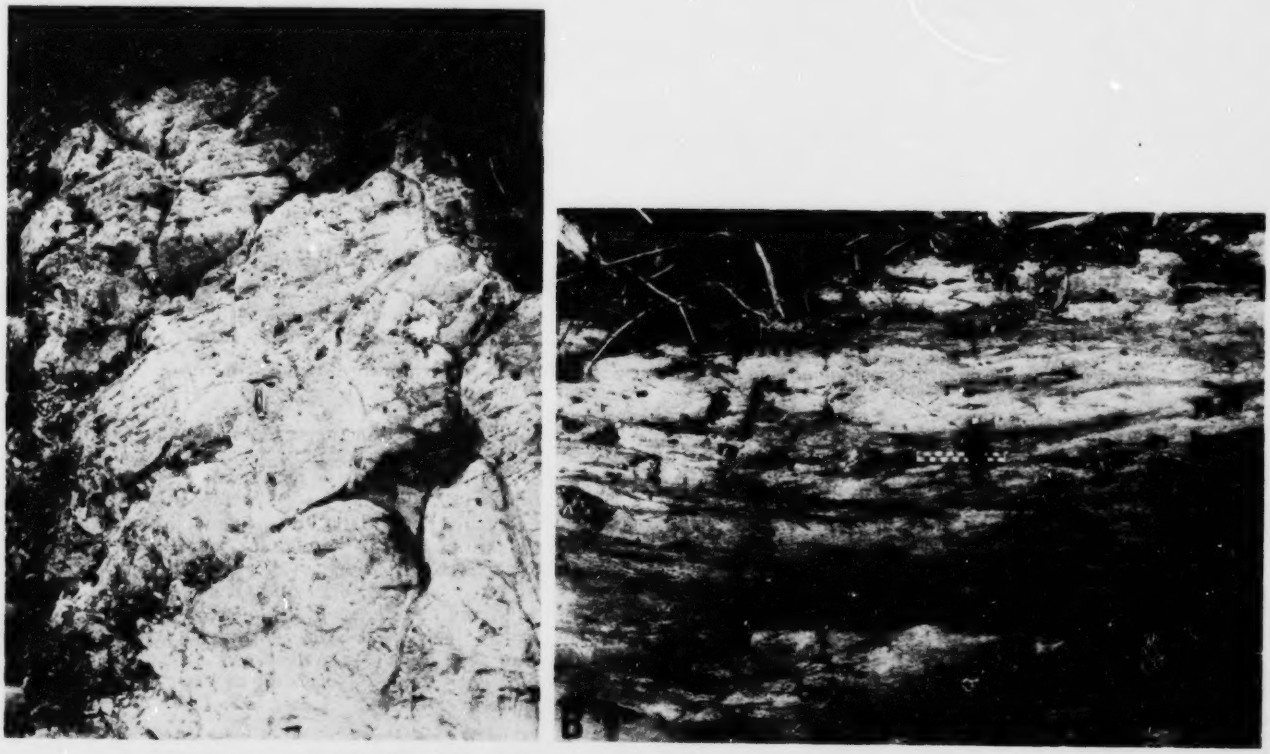

Figure 22.5. a. Relatively weakly deformed pillow basalt. A foliation is present only in the softer pillow selvages. b. Same rock transformed into phyllonite.

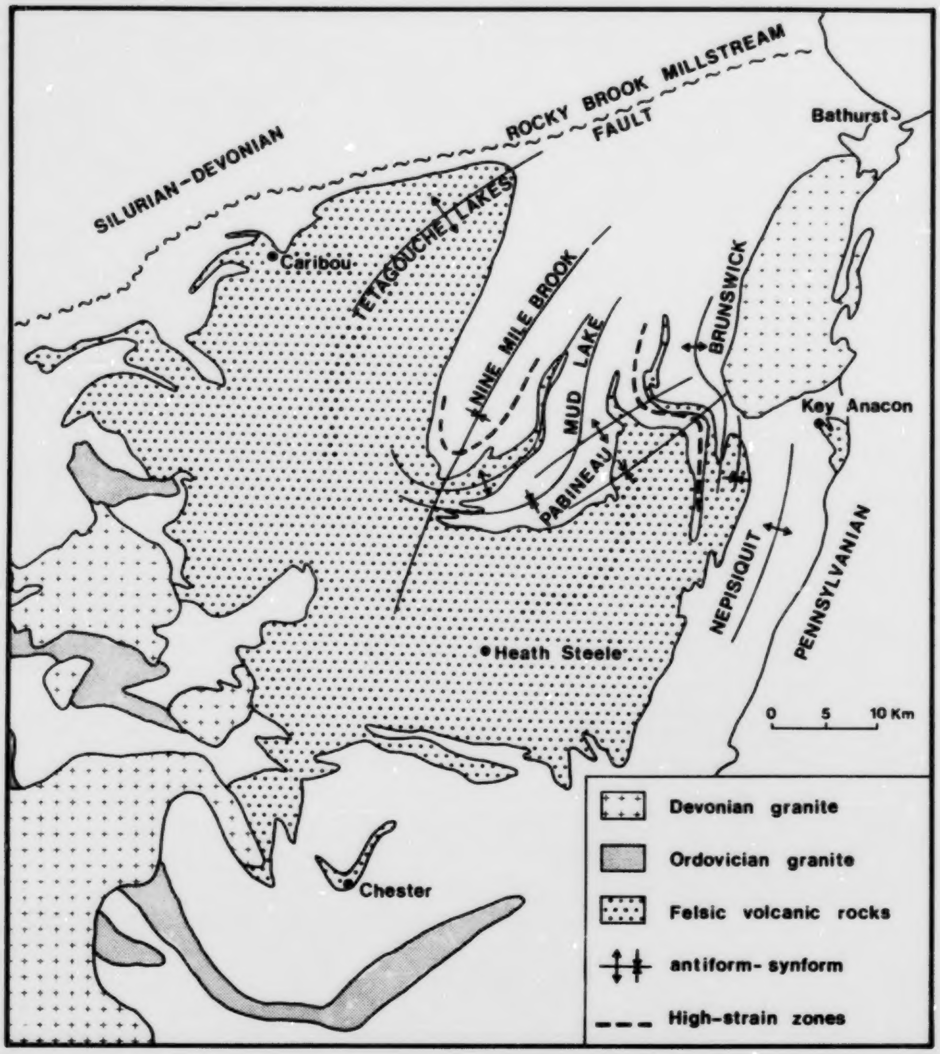

Figure 22.6. Simplified geological map of Bathurst camp with the important large scale structures.

Contrary to the common view, massive base metal sulphide deposits in the Bathurst camp are not always hosted by felsic volcanic rocks. In the domain of the Nine Mile synform (Fig. 22.1) there are at least eight small massive sulphide deposits that are hosted by thin bedded distal turbidites. These turbidites, however, are locally tuffaceous and the sulphides generally occur close to the contact with the underlying felsic volcanics, suggesting a relationship to felsic volcanic activity here also.

Crossbedding and grading in relatively weakly deformed quartzose turbidites in the footwall of the abandoned Wedge Mine (Fig. 22.1) suggest that tops are to the south, away from the felsic volcanics. This is consistent with top determinations based on metal zoning in the massive sulphide body (Les Davies personal communication, 1985). The Wedge deposit is overlain by black graphitic phyllites. Graphitic phyllites commonly occur close to the other deposits as well. Red hematitic and manganiferous slates or phyllites are also associated with these sulphides, but are generally more distal to these deposits. This red slate-sulphide horizon forms another important structural marker (cf. Helmstaedt, 1973). The regional distribution of this unit defines several large and tight to isoclinal folds, such as the Mud Lake synform and antiform (Fig. 22.6). An important question for regional geometrical interpretations is whether the red hematitic slate horizon is a distal time stratigraphic equivalent of the iron formation as suggested by Helmstaedt (1973) or another sulphide bearing horizon. In the Brunswick Mines area red hematitic slates occur at the contact between the felsic and mafic volcanic rocks. They can be traced by means of a few outcrops and numerous drillholes from the No. 12 mine property to the Nepisiquit River west of the Austin Brook open pit (van Staal, 1985). It is significant that the red slates structurally overlie the Brunswick iron formation-sulphide unit, from which they are separated by clastic sediments and a thick sequence of felsic volcanic rocks.

Although Helmstaedt's (1973) interpretation cannot be ruled out as a possibility, the simplest solution is that the red slates and iron formation represent two distinct stratigraphic horizons, that were formed in two different geological environments. The association of sulphides with turbidites suggests relatively rapid ore deposition at a time when there was abundant erosion of felsic volcanic rocks, perhaps as a result of resurgent doming of the caldera block, if the caldera hypothesis of Harley (1979) is applicable. Absence of

Figure 22.7.

a. Lower hemisphere equal area projection of 450 poles to S_0/S_1 in the domain of the Nine Mile structure: contours 1,2,3 and 4, 5% per area.

b. Lower hemisphere equal area projection of F_4 and poles to S_4 in hinge area of Nine Mile structure.

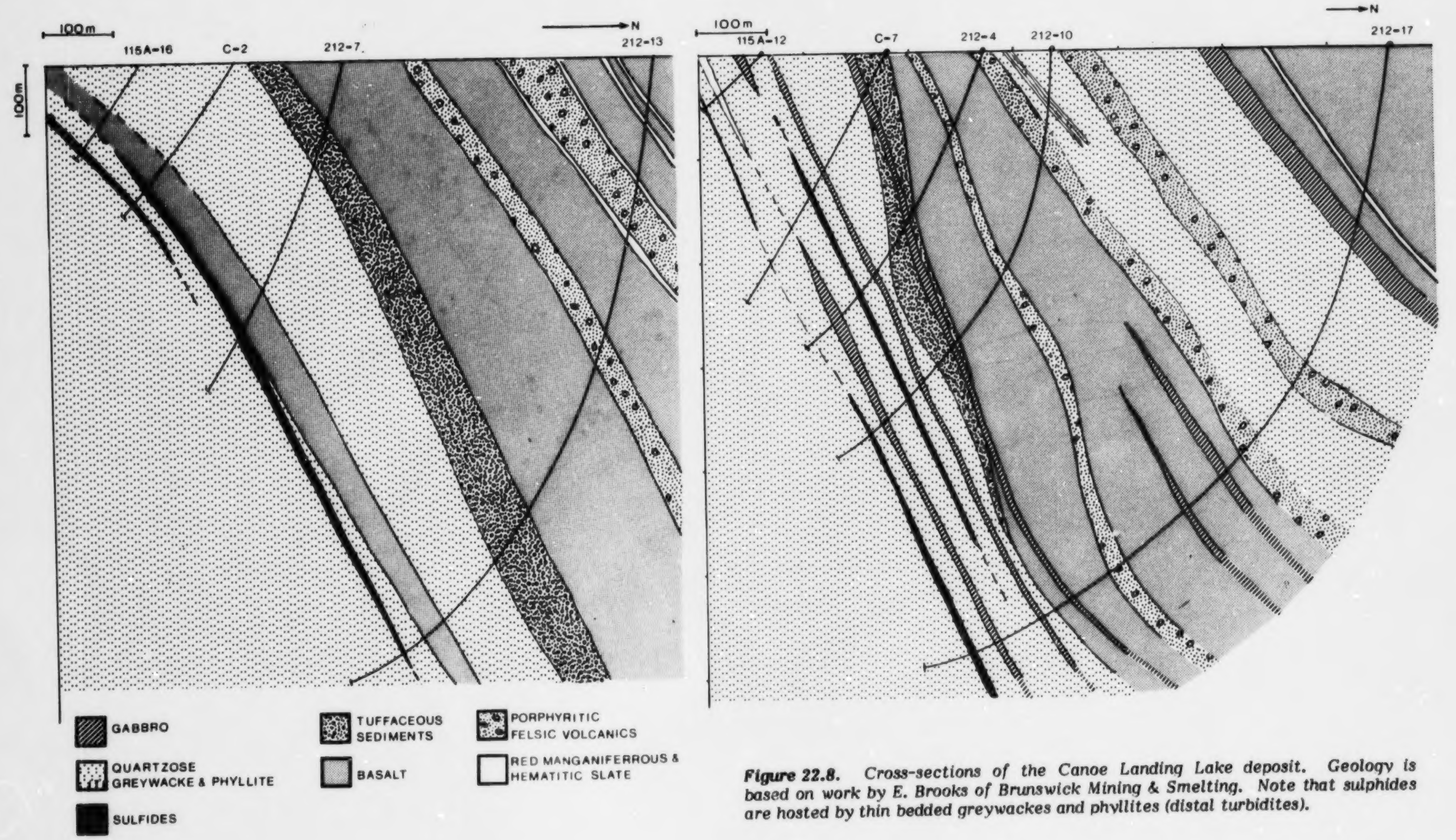

Figure 22.8. *Cross-sections of the Canoe Landing Lake deposit. Geology is based on work by E. Brooks of Brunswick Mining & Smelting. Note that sulphides are hosted by thin bedded greywackes and phyllites (distal turbidites).*

Figure 22.9. *Map of Nine Mile structure with schematic distribution of F_3/S_3 and F_4/S_4.*

sedimentary structures other than bedding in the sediments associated with the Brunswick orebodies, particularly where the deformation is relatively weak, suggests a lower energy environment than for the turbidite-hosted sulphides. Stromatolites discovered in carbonate facies iron formation at Brunswick No. 12 mine (van Staal, 1985) suggest that the Brunswick orebodies were deposited in relatively shallow water as well. This observation is consistent with the presence of pelecypod fossils discovered in a sulphide-bearing felsic tuff at Taylor Brook (Gummer et al., 1978).

Acknowledgments

I am very grateful to my field assistants John Langton and Steve Marston whose endurance and initiative were a great asset during this summer's field work. Field trips and discussions with Ernie Brooks, Les Davies, Les Fyffe, Bill Poole and Gary Yeo in particular were helpful and educational. Logistic support and the hospitality provided by Sharon McKinnon and other personnel of the Mines Branch in Bathurst is greatly appreciated. Gary Yeo critically read this manuscript.

References

Boyle, R.W. and Davies, L.J.
1964: Geology of the Austin Brook and Brunswick No. 6 sulphide deposits, Gloucester County, New Brunswick; Geological Survey of Canada, Paper 63-64, 23 p.

Davies, L.J.
1966: Geology of parts of the Atlantic Provinces; Geological Association of Canada, Guidebook, p. 33-43.

1972: The geology and geochemistry of the Austin Brook area, Gloucester County, New Brunswick, with special emphasis on the Austin Brook iron formation; unpublished Ph.D. thesis, Carleton University, 254 p.

Davis, L.J. (cont.)
1979: Geological map of northern New Brunswick; New Brunswick Department of Natural Resources, Mineral Resources Branch, Map NR-3, 1979.

Etheridge, M.A. and Hobbs, B.E.
1974: Chemical and deformational controls on recrystallization of mica; Contributions to Mineralogy and Petrology, v. 43, p. 111-124.

Fyffe, L.R.
1976: Correlation of geology in the southeastern and northern parts of the Miramichi zone; in 139th Annual Report of the Department of Natural Resources of New Brunswick, p. 137-141.

1982: Taconian and Acadian structural trends in central and northern New Brunswick; in Major Structural Zones and Faults of the Northern Appalachians, ed. P. St-Julien and J. Béland; Geological Association of Canada, Special Paper 24, p. 117-129.

Fyffe, L.R., Pajari, G.E., Jr., and Cherry, M.E.
1981: The Acadian plutonic rocks of New Brunswick; Maritime Sediments and Atlantic Geology, v. 17, p. 23-36.

Fyffe, L.R., Forbes, W.H., and Riva, J.
1983: Graptolites from the Benton area of west-central New Brunswick and their regional significance; Maritime Sediments and Atlantic Geology v. 19, p. 117-125.

Gross, C.A.
1967: Geology of iron deposits in Canada II. Iron deposits in the Appalachian and Grenville regions of Canada; Geological Survey of Canada, Economic Geology Report 22.

Gummer, P.K., Von Guttenberg, R., and Ferguson, L.
1978: A recent fossil discovery in the Ordovician Tetagouche volcanic complex of New Brunswick; unpublished paper presented at the New Brunswick Annual Meeting of the Canadian Institute of Mining and Metallurgy, Bathurst, N.B., 9 p.

Harley, D.N.
1979: A mineralized Ordovician resurgent caldera complex in the Bathurst-Newcastle mining district, New Brunswick, Canada; Economic Geology, v. 74, p. 786-796.

Helmstaedt, H.
1970: Geology of map area 0-6, Head of Middle River and Wildcat Brook; Mineral Resources Branch, Department of Natural Resources, New Brunswick, Map Series 70-1, 18 p.

1971: Structural geology of Portage Lakes area, Bathurst-Newcastle district, New Brunswick; Geological Survey of Canada, Paper 70-28, 42 p.

1973: Structural geology of the Bathurst-Newcastle district; New England Intercollegiate Geological Conference, 65, Field guide to excursion, trip 5-A, p. 34-46.

Hobbs, B.E., Means, W.P., and Williams, P.F.
1976: An outline of structural geology. John Wiley and Sons, New York, 571 p.

Jones, R.A.
1962: Parts of Forty and Nine Mile Brooks; New Brunswick Mines Branch, P.M. 61-1, 13 p.

Juras, S.J.
1981: Alteration and sulphide mineralization in footwall felsic metapyroclastic and metasedimentary rocks, Brunswick No. 12 deposit, Bathurst, New Brunswick, Canada; unpublished M.Sc. thesis, University of New Brunswick, 208 p.

Kennedy, D.J., Barnes, C.R., and Uyeno, T.T.
1979: A middle Ordovician conodont faunule from the Tetagouche Group, Camel Back Mountain, New Brunswick; Canadian Journal of Earth Sciences, v. 16, p. 540-551.

Knopf, E.B. and Ingerson, E.
1938: Structural Petrology; Geological Society of America, Memoir 6, 270 p.

McBride, D.E.
1976: Tectonic setting of the Tetagouche Group, host to the New Brunswick polymetallic massive sulphide deposits; in Metallogeny and Plate Tectonics, ed. D.F. Strong; Geological Association of Canada, Special Paper 14, p. 473-485.

Neuman, R.B.
1968: Paleogeographic implications of Ordovician shelly fossils in the Magog belt of the northern Appalachians region; in Studies of Appalachian Geology Northern and Maritime, ed. E-An. Zen, W.S. White, J.B. Hadley, and J.B. Thompson; Interscience, New York, p. 35-48.

Nowlan, G.S.
1981: Some Ordovician conodont faunules from the Miramichi Anticlinorium, New Brunswick; Geological Survey of Canada, Bulletin 345, 35 p.

Poole, W.H.
1963: Geology, Hayesville, New Brunswick; Geological Survey of Canada, Map 6-1963.

1967: Tectonic evolution of the Appalachian region of Canada; Geological Association of Canada, Special Paper 4, p. 9-51.

Rast, N., Lutes, G.G., and St. Peter, C.
1980: The geology and deformation history of the southern part of the Matapedia zone and its relationship to the Miramichi zone and the Canterbury basin; in The Geology of Northeastern Maine and Neighboring New Brunswick, ed. D.C. Roy and R.S. Naylor; 72nd Annual Meeting of the New England Intercollegiate Geological Conference, p. 191-201.

Sawyer, E.W., Barnes S.J., and Buck, M.J.
1983: Pillow shelves: determination of bedding direction and structural facing direction from shelves in deformed pillow lavas; Canadian Journal of Earth Sciences, v. 20, p. 1483-1487.

Skinner, R.
1974: Geology of the Tetagouche Lakes, Bathurst and Nepisiquit Falls map-areas, New Brunswick; Geological Survey of Canada, Memoir 371, 133 p.

Smith, C.H.
1957: The Bathurst-Newcastle area; Geological Survey of Canada, Map 1-1957.

Stockwell, C.H. and Tupper, W.M.
1966: Geology of the Brunswick No. 6 and No. 12 mining area, Gloucester County, New Brunswick; Geological Survey of Canada, Paper 65-13, 8 p.

Troop, D.G.
1984: The petrology and geochemistry of Ordovician banded iron formations and associated rocks at the Flat Landing Brook massive sulphide deposit, northern New Brunswick; unpublished M.Sc. thesis, University of Toronto, 217 p.

Turner, F.J. and Weiss, L.E.
1963: Structural Analysis of Metamorphic Tectonites, McGraw-Hill, New York, 545 p.

van Staal, C.R.
1985: Structure and metamorphism of the Brunswick Mines area, Bathurst, New Brunswick, Canada; unpublished Ph.D. thesis, University of New Brunswick, 483 p.

van Staal, C.R. and Williams, P.F.
1984: Structure, origin and concentration of the Brunswick No. 12 and No. 6 orebodies; Economic Geology, v. 79, p. 1669-1692.

– Structural analysis of the Brunswick orebodies; Institute of Mining and Metallurgy, Transactions. (in press)

White, S.
1979: Large strain deformation: report on a tectonic studies group discussion meeting held at Imperial College, London; Journal of Structural Geology v. 1, p. 333-339.

Whitehead, R.E.S. and Goodfellow, W.D.
1978: Geochemistry of volcanic rocks from the Tetagouche Group, Bathurst, New Brunswick, Canada; Canadian Journal of Earth Sciences, v. 15 p. 207-219.

Williams, P.F.
1970: A criticism of the use of style in the study of deformed rocks; Geological Society of America, Bulletin, v. 81, p. 3283-3296.

Gold mineralization in the Star Lake pluton, La Ronge belt, Saskatchewan: a preliminary report[1]

Project 840018 and MDA 102-5-3-5

K.H. Poulsen, D.E. Ames, and A.G. Galley
Economic Geology and Mineralogy Division

Poulsen, K.H., Ames, D.E., and Galley, A.G., Gold mineralization in the Star Lake pluton, La Ronge belt, Saskatchewan: a preliminary report, in Current Research, Part A, Geological Survey of Canada, Paper 86-1A, p. 205-212, 1986.

Abstract

Gold-quartz veins in the Aphebian Star Lake granitoid pluton are localized in NE-striking shear zones containing protomylonitic to mylonitic rocks. Mineralized veins are composed mainly of quartz with pyrite and pyrrhotite with common accessory calcite, scheelite, tourmaline, molybdenite and chalcopyrite. Gold occurs principally as inclusions or fracture fillings in iron sulphides. The gold mineralization is restricted to elongate shoots which plunge SW within the shear zones parallel to the intermediate strain axis. These deposits are perhaps distinctive in that they have formed in a very ductile environment with minimal associated wall rock alteration.

Résumé

Les filons de quartz aurifère dans le pluton granitique aphébien de Star Lake sont localizées dans des zones de cisaillement protomylonitiques et mylonitiques. Les veines minéralisées se composent surtout de quartz, de pyrite et de pyrrhotite, et de quantités variables de clacite, scheelite, tourmaline, molybdénite et chalcopyrite. L'or se trouve principalement dans des inclusions et des fractures des sulfures de fer. La minéralisation aurifère est confinée à des cheminées étirées plongeant vers le sud-ouest dans les zones de ciscaillement, parallèlement à l'axe intermédiaire de déformation. Ces gisements sont peut-être distincts parce qu'ils se sont formés dans un environnement très ductile et que l'altération des épontes est très faible.

---

[1] Contribution to Canada-Saskatchewan Mineral Development Agreement 1984-1989. Project carried by Geological Survey of Canada.

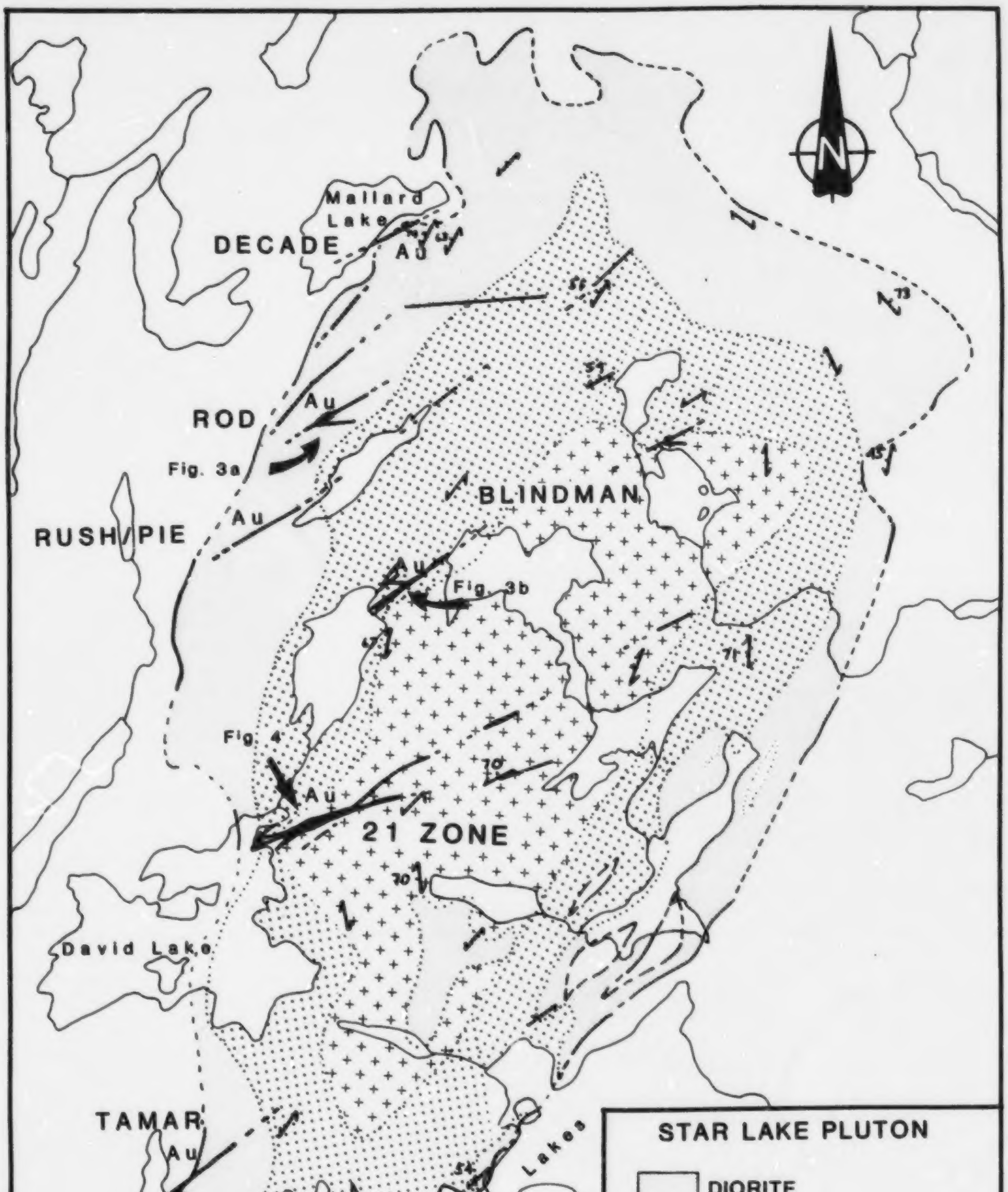

Figure 23.1. *Geology and gold deposits of the Star Lake pluton.*

Introduction

The Star Lake granitoid pluton, located 150 km northeast of La Ronge, Saskatchewan, intrudes metavolcanic rocks of the Aphebian La Ronge granite-greenstone domain. Gold was discovered in the intrusion in 1944 (Coombe, 1984) and subsequent exploration culminated in the discovery of the 21 Zone deposit in 1983. This small but rich deposit, with drill indicated reserves of 230 000 tons grading .5 oz Au per ton (Murphy, 1985) is scheduled for production at the rate of 220 tons per day (Northern Miner, Aug. 1, 1985, p. 1).

We initiated a study of gold mineralization in the Star Lake pluton in 1984 under the Canada-Saskatchewan Mineral Development Agreement. The objective is to investigate structural controls on mineralization at all scales to improve exploration models for this type of deposit and to gain a better understanding of the processes of formation. This report summarizes our results to date.

General Geology

The Star Lake pluton is crudely elliptical in plan, approximately 6 km by 3 km, with its long axis oriented north-northeast (Fig. 23.1). Thomas (1984) demonstrated the compositional zonation of the intrusion from dioritic margin, through quartz monzonite to granitic (sensu stricto) core; our mapping confirms, with some modification, the pattern of zonation (Fig. 23.1). The contacts between compositional types are commonly abrupt but locally appear to be transitional rather than intrusive. The granitoid rocks are commonly xenolithic and locally display a faint compositional layering of probable igneous origin.

The pluton is transected by swarms of dykes which strike north-northeast. They vary in width from a few centimetres to a few metres and in composition from mafic to felsic. Dykes of all compositions within a particular swarm are generally subparallel in strike but local crosscutting relationships are preserved. The oldest dykes consist of coarse amphibolite which is likely derived from a rock of gabbroic to pyroxenitic composition. These are cut by grey dykes composed of finer grained hornblende/feldspar porphyritic rock of basaltic composition, in turn cut by dykes of more intermediate granitoid composition and finally, all rocks are cut by aplite dykes.

Structural Geology

Metamorphic foliation (S_1)

The rocks of the Star Lake pluton have been metamorphosed and variably deformed. Biotite within the intrusion is of metamorphic origin and formed along with epidote at the expense of original hornblende. Most of the rocks in the pluton display a weak to moderate metamorphic foliation which is recognized by the alignment of biotite grains and aggregates. Long axes of deformed xenoliths are subparallel to this. While no rigorous strain study has been undertaken, aspect ratios of such xenoliths appear to be nearly equal on surfaces which are variably oriented at a high angle to the foliation; this indicates a tectonic flattening. This metamorphic foliation, here termed S_1, varies significantly in orientation from place to place (Fig. 23.1) but on average strikes N15°E, subparallel to the long axis of the intrusion, and dips 60° west-northwest. S_1 tends to parallel the contacts of the pluton near its margins (Fig. 23.1).

Mylonitic foliation (Sm)

An intense protomylonitic to locally mylonitic foliation superposes the weaker metamorphic foliation within relatively narrow discrete shear zones. The modern mylonite terminology (Sibson, 1977; White, 1982) is appropriate for these rocks because a transition from least deformed to most deformed rocks can be demonstrated with attendant intensification of foliation and of degree of grain-size reduction. The quartz monzonites adjacent to the 21 Zone show that transition clearly. Four states of deformation are identified and illustrated in Figure 23.2:

a) The host quartz monzonite is an equigranular rock typically containing 18% quartz, 47% plagioclase (An_{16}), 26% microcline and 9% mafic minerals, principally biotite and epidote. Even the least deformed specimens contain undulose and polygonized quartz, minor recrystallized microcline at igneous grain boundaries and a weak orientation of biotite grains (S_1).

b) Specimens which possess a readily visible metamorphic foliation (S_1) are identified by a consistent planar orientation of biotite grains and aggregates. The size and shape of feldspars are not appreciably changed though a weak planar orientation of these minerals is common. At the microscopic scale, leucocratic minerals have recrystallized at grain boundaries.

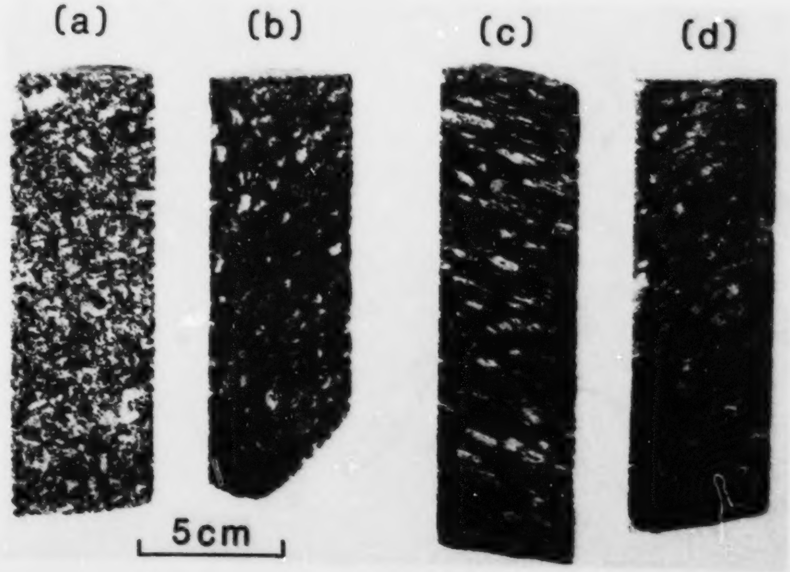

Figure 23.2

Four states of increased deformation (a through d) in quartz monzonite in and near the 21 Zone Shear.

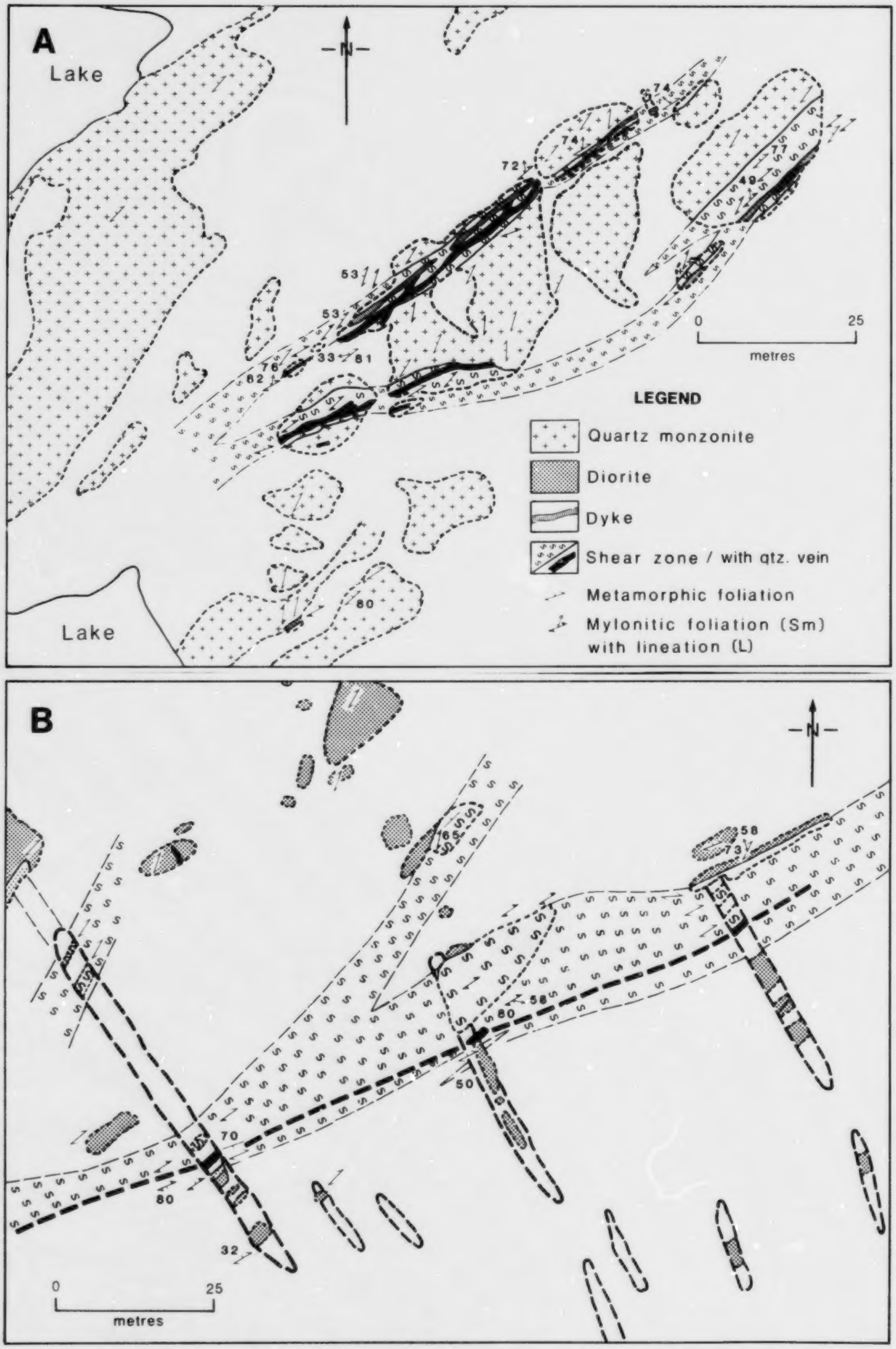

Figure 23.3. (a) Geology of part of the shear zone at Blindman Lake; (b) Geology of part of the Rod Shear Zone.

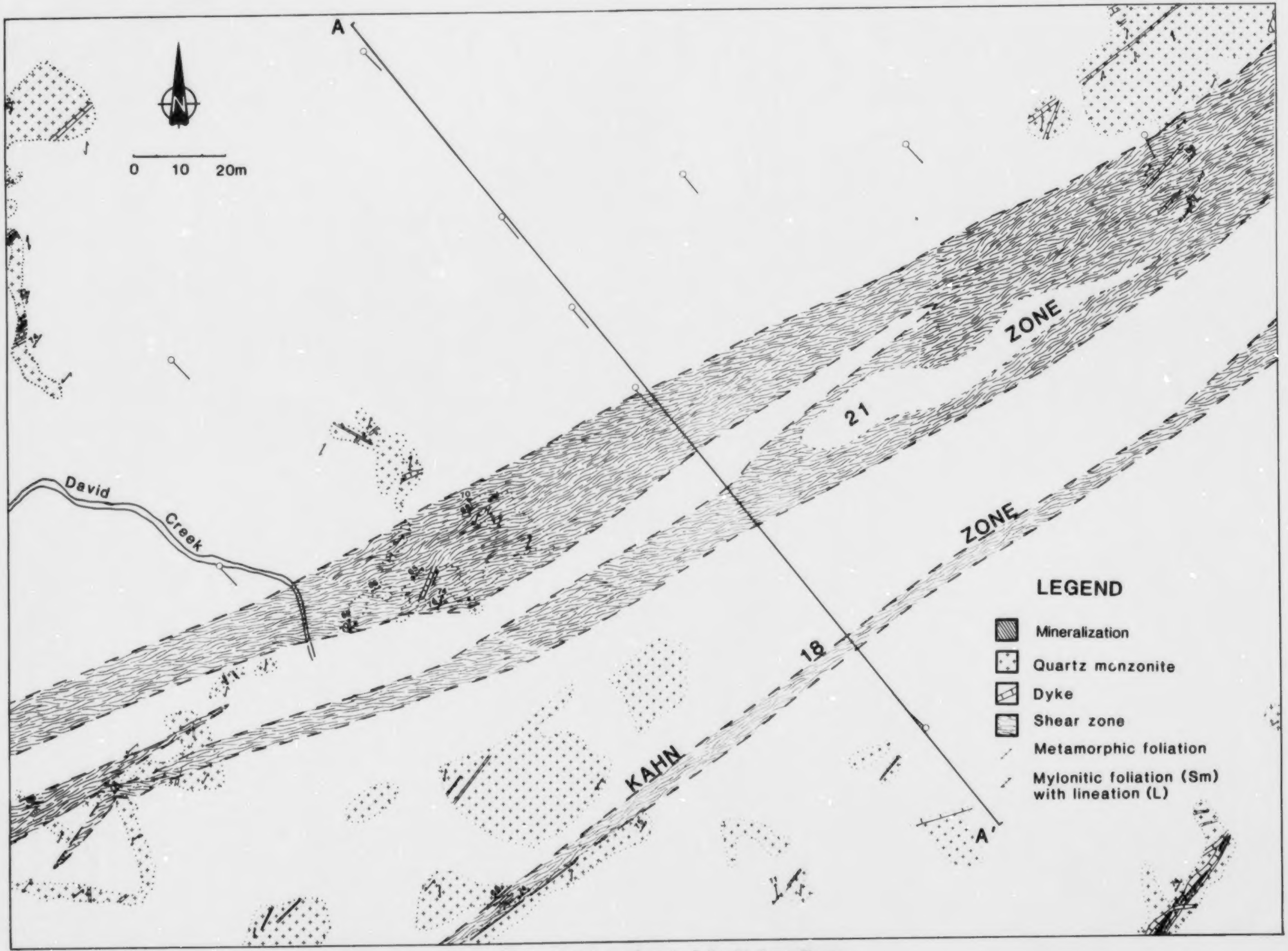

Figure 23.4. *Geology of part of the 21 Zone Shear.*

c) The protomylonitic rocks have a strong undulose foliation (Sm). Much of the quartz, feldspar and biotite has been substantially reduced in size to form a fine grained matrix which comprises 10 to 50% of the rock. Original quartz grains which have not been completely reduced in size occur as lenticular polycrystalline aggregates while feldspar porphyroclasts, though dimensionally oriented, remain tabular to slightly rounded. Modest quantities of muscovite and calcite appear as newly generated minerals in the matrix.

d) The most intense deformation of the granitoid rocks is represented by mylonite containing greater than 50% matrix grains with a strong foliation. Elongate quartz ribbons are common. Porphyroclasts of microcline and plagioclase tend to be asymmetric in shape and locally fractured, extended and rotated in a consistent sense at the scale of a hand specimen.

Shear zone geometry

The protomylonitic and mylonitic foliations, here termed S_m, are restricted to shear zones which are up to 30 m wide but most commonly comprise several anastamosed branches, each of which is 1-5 m wide. The shear zones typically strike N60°E though there is some dispersion about this mean (Fig. 23.1); the shear zones have a steep dip to the northwest.

While the shear zones are mapped on the basis of intensity of deformation of the granitoid rocks, they also affect, and may have been localized by, the various dyke rocks. Many dykes are themselves intensely foliated whereas adjacent dykes are not. Those which are not completely foliated, however, commonly share with the host granitoid at least one "sheared" contact across which both rocks are affected by the deformation. Thus in some cases small shear zones are coincident with a dyke or dyke margin. Where the shear zones affect larger volumes of granitoid rock, the dykes play a much more passive role and are merely incorporated into the shear zone. Note that in a case such as this, foliation in dykes is a spatial rather than temporal matter; foliated dykes are not necessarily older than those which are not foliated; simply put, dykes are more likely to be foliated if they are near or within shear zones which involve the granitoid rocks.

In detail, geometry of the shear zones is quite complex. They may be cored by dykes or depart from them (Fig. 23.3). Rapid changes in shear zone width occur along strike and branching of individual shears to form anastamosed networks can be demonstrated both in plan (Fig. 23.3, 23.4) and in section (Fig. 23.5).

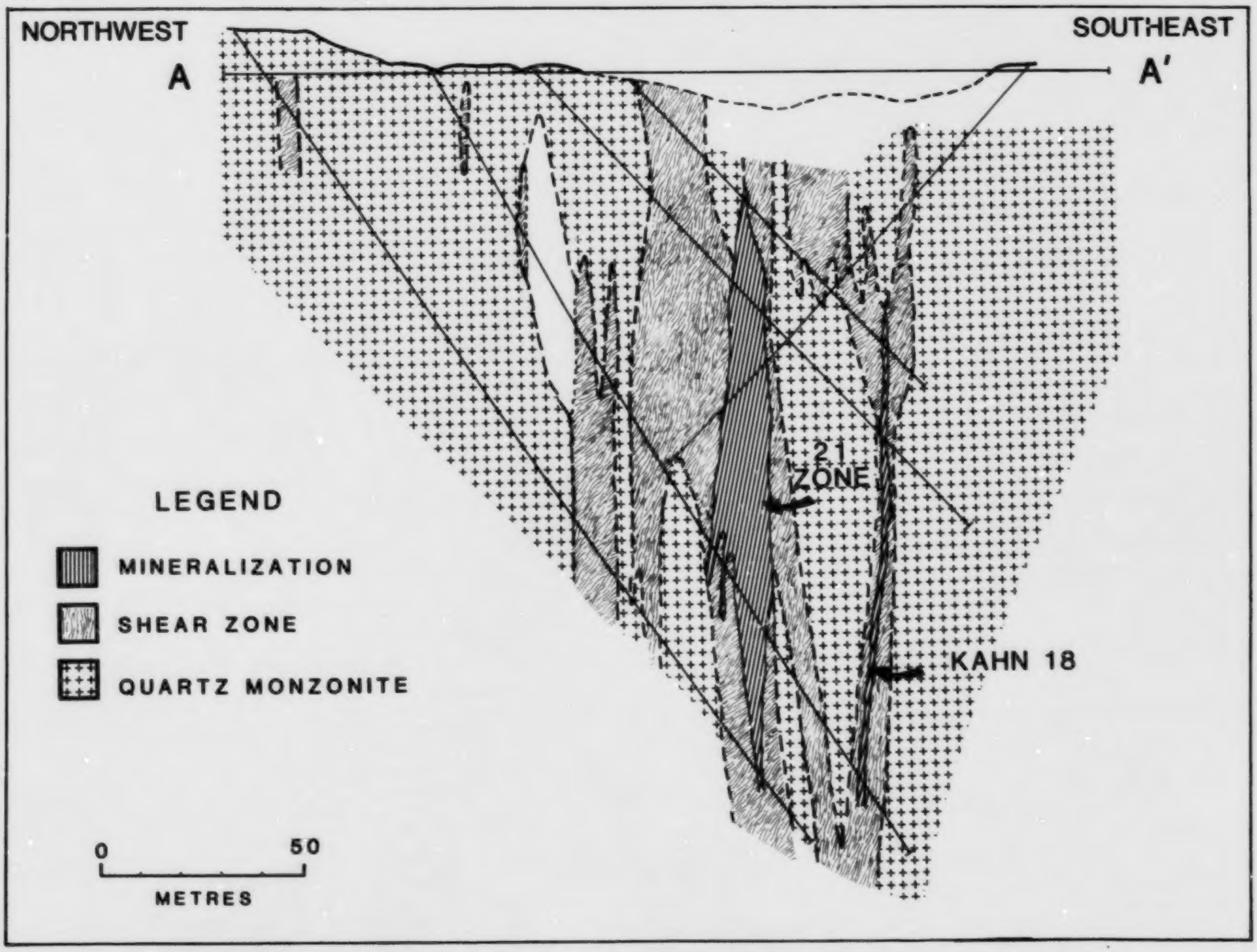

Figure 23.5. Cross-section through the 21 Zone Shear; see Figure 23.4 for the line of section.

Shear zone kinematics

This study is directed towards kinematic interpretation of the shear zones in addition to establishing their geometry. Several observations warrant a first order kinematic interpretation:

i) The mylonitic foliation (Sm) contains a prominent mineral lineation (Fig. 23.6) formed by extended, rod-shaped porphyroclasts. This lineation pitches approximately 75° to the northeast in the foliation plane.

ii) The mylonitic foliation is oblique to the mapped boundaries of the shear zones (Fig. 23.3, 23.4, 23.5); strike of foliation is more northerly and dip is shallower than that of the shear zones.

iii) Shear zones, as viewed in plan, tend to deflect S_1 and create observable offsets of transected dykes in a "dextral" sense.

iv) A secondary foliation is visible locally on surfaces which are normal to Sm and parallel to the mineral lineation (Fig. 23.6b). This shear band or extensional crenulation cleavage superposes Sm and is held to be a reliable kinematic indicator (White et al., 1980).

All of the above observations are consistent with shear zones having an inclined component of shear displacement with the northwest side of a zone directed down and to the northeast (Fig. 23.7). This gives the impression of a "normal" fault geometry for these shear zones, a result which is understandable, however, if we consider the possibility that shear zone kinematics may be related to the more pervasive strain associated with S_1. In this case, the "extensional" nature of the shear zones is dictated by the direction of shortening associated with S_1 (Fig. 23.7, inset). This interpretation also allows for the possibility that shallower conjugate shear zones could also be present in the Star Lake pluton; these have not been observed to date. Note that in the present discussion, it is not implicit that S_1 and Sm are strictly coeval and continuous; the field relations favour a superposition of Sm on S_1.

Economic Geology

Mineralogy

Gold mineralization in the Star Lake pluton is clearly localized in quartz veins in the ductile shear zones described above (Fig. 23.1). The veins are commonly central to shear zones and discordant to the mylonitic foliation at the local scale, even though they, too, show some evidence of ductile deformation. Individual veins may be long and continuous or short and lenticular or irregular quartz masses containing wall rock inclusions. Gold occurs with iron sulphides in the veins; coarse pyrite is the principal sulphide at the 21 Zone deposit whereas pyrrhotite with lesser pyrite is typical in the northern part of the intrusion. Visible gold is rare, particularly at 21 Zone, and calcite, scheelite, tourmaline, molybdenite and chalcopyrite occur in amounts which are variable from vein to vein. Ore specimens from the 21 Zone deposit were examined microscopically by D.C. Harris (Economic Geology and Mineralogy Division sample examination report M84-145). The coarse pyrite crystals (1 to 2 cm) were found to poikilitically enclose small composite inclusions of calaverite ($AuTe_2$), tellurobismuthite (Bi_2Te_3), hessite (Ag_2Te), rare chalcopyrite and native gold. Aside from this common site within the pyrite crystals, native gold occurs locally in fractures in the pyrite or rarely with tellurides in the gangue. Chalcopyrite, commonly intergrown with bornite, covellite and wittichenite (Cu_3BiS_3), occurs mainly in gangue minerals or in fractures in pyrite. Magnetite, marcasite and most pyrrhotite occur adjacent to pyrite in gangue. Melonite ($NiTe_2$) was identified as a single euhedral crystal in pyrite.

Alteration

Extensive hydrothermal alteration is generally absent from the wall rocks adjacent to gold mineralization in the Star Lake pluton. The mylonitic and protomylonitic rocks within the 21 Zone shear are chemically indistinguishable from the less deformed quartz monzonites even when the most common "mobile" elements are considered (Fig. 23.8). The only alteration directly related to gold is a pale green coloration imparted to otherwise pink to grey mylonitic rocks within a metre or two of veins in the 21 Zone deposit; the green coloration results from the sericitization of otherwise fresh microcline by simple hydration.

Hematite alteration is more common but does not appear to be distributed with a specific relationship to ore. The hematite occurs, locally with green clay minerals (kaolin-montimorillonite, x-ray diffraction) in brittle post-mylonitic fractures. Many of these fractures are enveloped by penetratively hematized granitoid rocks which may be either intensely or little deformed.

Plunge of ore shoots

Diamond drill results show that the mineralization within the shear zones occurs in ore shoots with their long axis plunging moderately to shallowly to the southwest (i.e. Fig. 23.4, 23.5). Our kinematic analysis implies a

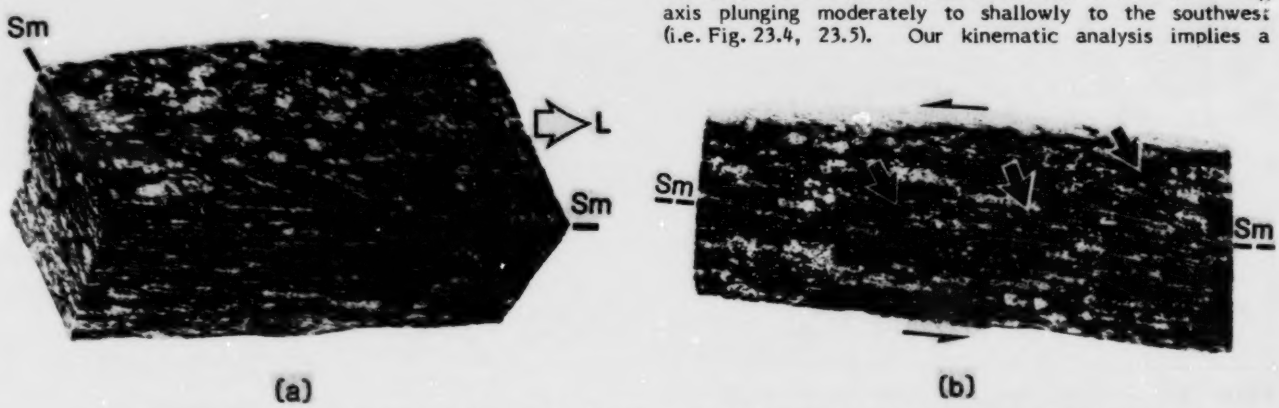

Figure 23.6. *(a) Lineation in protomylonite, 21 Zone area; (b) Polished slab cut parallel to lineation and normal to foliation as in (a). Note extensional crenulation cleavage (arrowed) and inferred shear sense.*

northeasterly plunging tectonic transport direction, so that the plunge of ore shoots is closer to parallelism with the intermediate rather than major axis of strain within the shear zone. This intermediate axis also coincides roughly with the line of intersection of Sm and S_1 and likely also represents the intersection of individual branches in the shear zones.

Discussion

The Star Lake shear zones are relatively small geological targets and the mineralization within them much smaller still. Geological exploration for gold within them is difficult, particularly in the absence of extensive hydrothermal alteration. Two aspects of our work have applicability in this area. First, the shear zones which are the first order targets in this area can be located successfully, whether they contain gold or not, by recognition and mapping of anomalous foliation (Sm). We have applied the modern mylonite terminology in doing so but this is not essential; it is simply necessary to distinguish the intensely deformed equivalents of the less deformed granitoid rocks. Second, the preliminary kinematic analysis shows a correlation between ore shoot plunge and the inferred intermediate strain axis for individual shear zones; this suggests some potential for plunge prediction at an early stage of a drill program for deposits of this type. A third exploration aspect, one which we have not resolved, is what factors control the localization of gold within a particular shear zone. At this stage, we are considering several possibilities including intersection of shear zone branches, involvement of dykes as inhomogeneities within zones or a control by post-mylonitic brittle fractures.

From the point of view of process, the observed association of shear zones and gold is not uncommon and the Star Lake deposits have counterparts elsewhere in the Canadian Shield but these rarely display extremely "ductile" mylonitic rocks unique to Star Lake shear zones. In addition, the lack of extensive metasomatic change of the bulk composition of the granitoid rocks also suggests higher temperature processes than are common for most auriferous shear zones (Kerrich et al., 1977). Despite the early ductile history of the Star Lake shear zones, they subsequently hardened to result in formation of extensional crenulation cleavage and brittle fractures which are the locus for quartz veins.

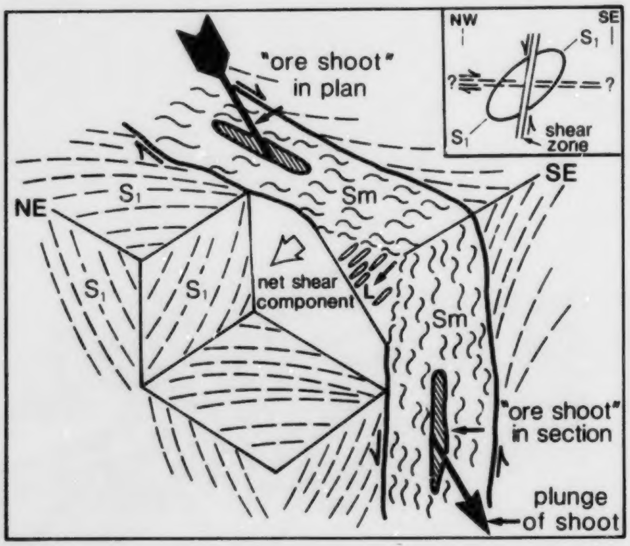

Figure 23.7. Schematic diagram illustrating the relationship of mylonitic foliation (Sm) to other geometric elements in a typical Star Lake Shear zone. Inset shows the possible relationship of shear zone orientation and kinematics to S_1.

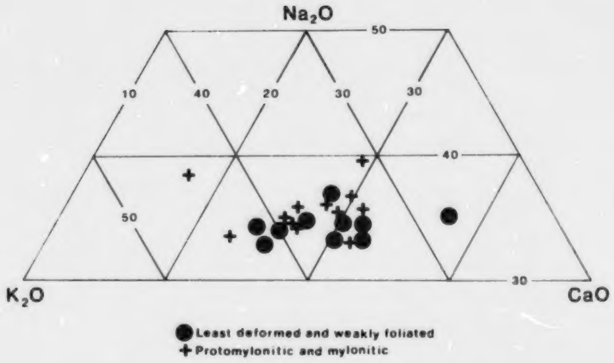

(Ternary plotting points based on weight per cent analyses)

Figure 23.8. Part of a ternary plot showing the similarity of Na_2O, K_2O and CaO contents of mylonitic versus least deformed rocks from the 21 Zone area.

Acknowledgments

Our studies have benefited greatly from the co-operation of industry and provincial geologists working in the Star Lake area. Don Harris provided microscopic and microprobe analyses of the ore specimens and G.M. Lecheminant provided x-ray diffraction support. Patti Tirschman and James Scoates provided able field assistance.

References

Coombe, W.
1984: Gold in Saskatchewan; Saskatchewan Geological Survey, Open File Report 84-1.

Kerrich, R., Fyfe, W.S., Gorman, B.E., and Allison, I.
1977: Local modification of rock chemistry by deformation; Contribution to Mineralogy and Petrology, v. 65, p. 183-190.

Murphy, W.
1985: Geology and exploration history of the gold mineralization in the Star Lake area; p. 23-25 in Extended Abstracts, Technical Program for "Gold in the Western Shield"; Canadian Institute of Mining and Metallurgy Symposium booklet, 46 p.

Sibson, R.H.
1977: Fault rocks and fault mechanisms; Geological Society of London, Journal, v. 133, p. 191-213.

Thomas, D.J.
1984: Geological mapping, Star Lake area; in Summary of Investigations 1984, Saskatchewan Geological Survey, Miscellaneous Report 84-4, p. 21-31.

White, S.
1982: Fault rocks of the Moine Thrust zone: a guide to their nomenclature; Textures and Microstructures, v. 4, p. 211-221.

White, S.H., Burrows, S.E., Carreras, J., Shaw, N.D., and Humphreys, F.J.
1980: On mylonites in ductile shear zones; Journal of Structural Geology, v. 2, p. 175-187.

Stratigraphy and economic geology of the southern part of the Roberts Arm Group, central Newfoundland[1]

Project 840059

H. Scott Swinden[2] and Paul E. Sacks[3]
Economic Geology and Mineralogy Division

Swinden, H.S. and Sacks, P.E., Stratigraphy and economic geology of the southern part of the Roberts Arm Group, central Newfoundland; in Current Research, Part A, Geological Survey of Canada, Paper 86-1A, p. 213-220, 1986.

Abstract

The Roberts Arm Group is a sequence of Ordovician marine volcanic, subvolcanic, and volcaniclastic rocks, in fault contact to the east with strongly deformed metasedimentary rocks and intruded by Acadian granitoid rocks. In the west the group is cut by outliers of the Topsails Intrusive Suite.

Five west facing lithostratigraphic units have been traced from Great Gull Pond south to Lake Bond, informally designated from east to west Baker Brook Basalt, Gull Hill sediments, Burnt Island Basalt, Gullbridge felsic volcanics, South Brook basalt. These units are tentatively correlated with similar stratigraphic units in the Handcamp area.

Volcanogenic mineralization occurs mainly in the Burnt Island basalt and Gullbridge volcanics. The polymetallic Handcamp prospect contains significant amounts of precious metals, hosted in a unit interpreted as equivalent to the Gullbridge felsic volcanics. Exhalative products of the alteration systems have not been identified; however exhalative sulphides if present, may occur only above the highest recognized alteration in the South Brook basalt.

Résumé

Le groupe de Roberts Arm, une séquence de roches volcaniques, volcanoclastiques et sous volcaniques de nature marine et d'âge ordovicien, est en contact de faille, à l'est, avec des roches métasédimentaires fortement déformées et pénétrées par des roches granitoïdes d'âge acadien. À l'ouest, le groupe est pénétré par des avant-buttes de la suite intrusive de Topsails.

Cinq séquences lithostratigraphiques orienteés vers l'ouest ont été suivies vers le sud, de l'étang Great Gull jusqu'au lac Bond. Celles-ci sont officieusement designées, de l'ouest à l'est, le basalte de Baker Brook, les sédiments de Gull Hill, le basalte de Burnt Island, les roches volcaniques felsiques de Gullbridge, et le basalte de South Brook. Ces unités sont provisoirement corrélées avec une séquence stratigraphique similaire dans la région de Handcamp.

Des minéralisations volcanogènes se manifestent surtout dans le basalte de Burnt Island et les roches volcaniques de Gullbridge. Le dépot polymétallique de Handcamp, qui contient des concentrations importantes de métaux précieux, se trouve dans une unité stratigraphiquement équivalente aux roches volcaniques felsiques de Gullbridge. Les produits exhalatifs associés aux systèmes d'altération n'ont pas été identifiés, mais peuvent exister, le cas échéant, au dessus de l'altération stratigraphiquement la plus haute reconnue à date dans le basalte de South Brook.

[1] Contribution to the Canada-Newfoundland Mineral Development Agreement 1984-1989. Project carried by Geological Survey of Canada.
[2] Department of Mines and Energy, P.O. Box 4750, St. John's, Newfoundland A1C 5T7
[3] 15 South Ten Eyck Ave., Cazenovia, New York, 13035, U.S.A.

Introduction

This report summarizes the initial results of a project to investigate the metallogeny of the "Buchans-Roberts Arm Belt", a sequence or Ordovician volcanic, volcaniclastic and subvolcanic rocks in the north-central part of the Dunnage Terrane, central Newfoundland. The belt includes the Buchans, Roberts Arm, Cottrell's Cove, Chanceport and Frozen Ocean groups (Fig. 24.1) and hosts numerous volcanogenic sulphide occurrences including the well known Buchans orebodies and former producers at Gullbridge and Pilley's Island. Field work was carried out during 1985 in the southern part of the Roberts Arm Group between Lake Bond and the Handcamp prospect (Fig. 24.2).

Hayes (1951) and Kalliokoski (1955) first mapped this area at a scale of 1 inch to 1 mile. Hayes (1951) mapped the area northwest of Burnt Pond and was the first to correlate volcanic and sedimentary rocks in this area with the "Roberts Arm volcanics" mapped by Espenshade (1938) in the Pilley's Island area to the north. Kalliokoski (1955) mapped the Gull Pond sheet to the south and also recognized correlatives of Espenshade's "Roberts Arm volcanics" which he termed the "Roberts Arm Formation". Kalliokoski (1955) also correlated volcaniclastic rocks immediately east of the volcanic rocks with the Crescent Lake Formation, a sequence of chert and argillite mapped by Espenshade (1938) near Roberts Arm. Following Espenshade (1938), he assigned the Roberts Arm volcanics and Crescent Lake Formation to the "Badger Bay Series". Kalliokoski (1955) was the first to record the thermal metamorphism of sedimentary rocks east of Great Gull Pond and in the Powderhorn Lake area, which he attributed to nearby granite intrusion. Neale and Nash (1963) included the present project area in their 1 inch to 4 mile scale mapping of the Sandy Lake (12H) area. They retained Hayes' and Kalliokoski's correlations with the Roberts Arm volcanics and the Crescent Lake Formation but dropped the term "Badger Bay Series" in favour of the "Exploits Group", first defined by Heyl (1936) in central Notre Dame Bay. Williams (1964) was the first to define the Roberts Arm Group as it is presently constituted, including in it Espenshade's (1938) Roberts Arm volcanics and Crescent Lake Formation. Dean and Strong (1976), in their compilation of Notre Dame Bay geology, extended this revised nomenclature to the southern part of the Roberts Arm Group. They retained Kalliokoski's correlation of metasedimentary rocks east of Gull Pond with the Crescent Lake formation and assigned metasediments in the Powderhorn Lake area to the Silurian Sansom Greywacke. Recent compilations of the geology of this area (e.g. Kean et al., 1981; Hibbard et al., 1984) have followed Dean and Strong's (1976) nomenclature and correlations.

Volcanogenic mineralization was first reported in the southern part of the Roberts Arm Group in 1905 when prospectors discovered rusty, copper-bearing outcrops on the west shore of Gull Pond. These outcrops, which sparked considerable exploration activity into the middle part of the century (see review in Upadhyay, 1972), proved to be the surface expression of the Gullbridge orebody. A somewhat smaller Zn-Cu deposit was discovered in Reid Lot 50 on the northwest shore of Lake Bond in the early 1950s which was extensively drilled but proved to be subeconomic. There are many small volcanogenic mineral occurrences in the area; in most cases, the stratigraphic, structural and genetic

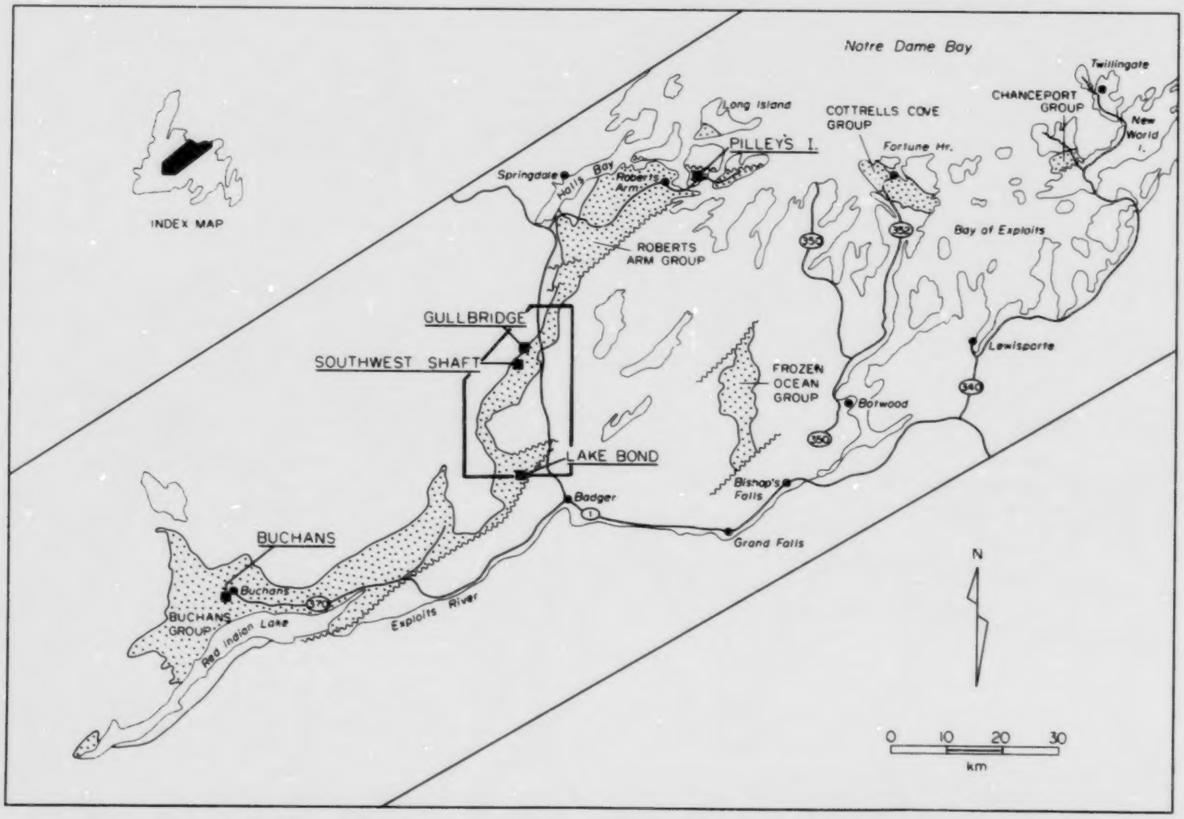

Figure 24.1. *Location of the Buchans-Roberts Arm belt. Heavy solid line outlines 1985 field area. Volcanogenic sulphide deposits indicated by half filled squares.*

relationships between these occurrences and the larger, better known deposits have not been well documented. One showing of particular interest is the Handcamp Prospect 10 km northeast of Gullbridge which has yielded significant gold values and is the only showing in the Roberts Arm Group which is primarily a gold target.

During the 1985 field season, all previously reported mineral occurrences were examined and mapped in detail where exposure warranted. Geological units were traced between the known mineralized areas and representative samples taken for assay and whole rock geochemical studies.

Regional geology

The Roberts Arm Group consists of Ordovician marine volcanic, subvolcanic and volcaniclastic rocks. The group can be traced from Notre Dame Bay to the southern boundary of the Great Gull Lake map area (Fig. 24.1), a distance of approximately 60 km. It attains a maximum thickness of approximately 4 km in the area south of Roberts Arm but towards the south, the section is considerably thinner and the rocks more deformed and metamorphosed due to the intrusion of large Acadian granitoid bodies to the east and west (the Twin Lakes Complex and the Topsails Intrusive Suite respectively). Correlative volcanic and sedimentary rocks to

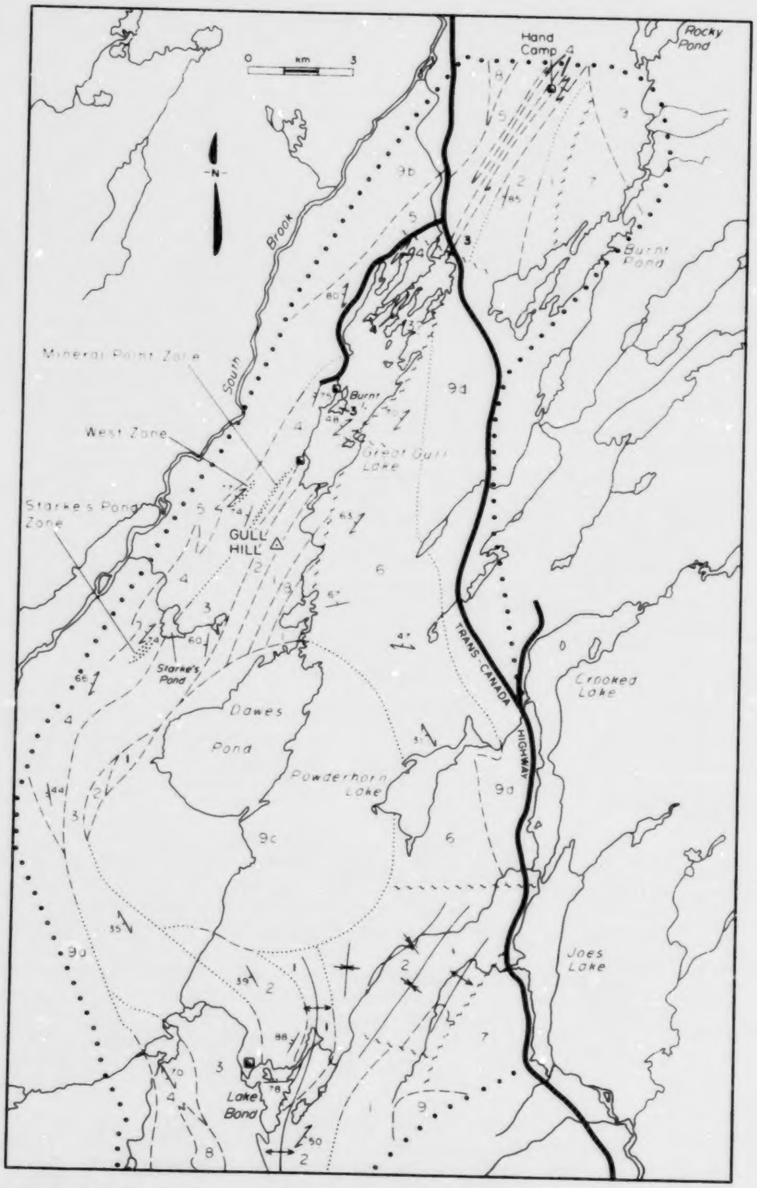

Figure 24.2. Geology of the southern part of the Roberts Arm Group. Heavy dots outline the 1985 field area. Labelled stippled areas north of Dawes Pond are alteration zones (see text for description). Half-filled squares are principal volcanogenic sulphide occurrences; from south to north: Lake Bond, Southwest Shaft, Gullbridge, Handcamp.

DEVONIAN AND YOUNGER

9 - Granitoid intrusive rocks: 9a - Skull Hill Quartz Syenite; 9b - Topsails Intrusive Suite; 9c - Dawes Pond Granite; 9d - Twin Lakes Complex.

8 - Mafic intrusive rocks; gabbro, diorite, diabase, pyroxenite

ORDOVICIAN-SILURIAN

7 - Sansom Greywacke; greywacke, fine grained conglomerate with volcanic provenance

ORDOVICIAN-SILURIAN (?)

6 - Metamorphic rocks; quartzite, andalusite and staurolite-bearing pelite, carbonaceous shale of uncertain derivation

ORDOVICIAN

Roberts Arm Group

5 - South Brook basalt* - pillow lava, massive basalt

4 - Gullbridge felsic volcanics* - rhyolitic ash flow tuff, lesser rhyolite flows, minor mafic schist

3 - Burnt Island basalt* - pillow basalt, mafic tuff, chloritic schist

2 - Gull Hill sediments* - volcaniclastic chert, ferruginous chert, sandy and fine conglomeratic sedimentary rocks

1 - Baker Brook basalt* - pillow baalt, massive basalt

* - informal names.

Geologic contact; approximate, assumed.

Strike and dip of bedding; tops known, tops unknown.

Strike and dip of principal foliation.

Anticlinal axis; synclinal axis

Principal volcanogenic mineral occurrences.

the south of the project area, most recently mapped by Kean and Jayasinghe (1982) are referred to the Buchans Group. The distinction between the Buchans and Roberts Arm groups across the map junction which forms the southern boundary of the present project area is one of nomenclature and has no geological significance.

The nature of the eastern contact of the Roberts Arm Group in this area is of some regional importance. It has previously been interpreted as a west facing, conformable contact between basal Roberts Arm Group (Crescent Lake Formation sediments) and the underlying Upper Ordovician to Silurian Sansom Greywacke (Dean and Strong, 1976; Dean, 1978; Kean et al., 1981). This interpretation requires that the Roberts Arm Group be at least Late Ordovician in age. An alternative viewpoint, based on radiometric age dating, regional geological relationships and fossil evidence, holds that the Roberts Arm Group is Middle Ordovician or older (e.g. Bostock et al., 1979; Nelson and Kidd, 1979; Nowlan and Thurlow, 1984). Our mapping shows that most rocks east of Great Gull Pond contain a pronounced but inhomogeneous penetrative fabric which trends northeast to north and varies from a schistosity in pelitic rocks to a strongly linear foliation in others. Cataclastic textures are locally well developed and mylonite is present in some areas. This deformation is interpreted as evidence for a major fault along the east shore of Great Gull Lake separating metasedimentary rocks to the east (previously mapped as Crescent Lake Formation) from mafic volcanics of the Roberts Arm Group to the west. Although conflicting interpretations of the age of the Roberts Arm Group are not yet satisfactorily resolved, there is little likelihood that a stratigraphic succession from Roberts Arm Group to Sansom Greywacke is present in this area.

A thermal metamorphic event postdates the principal deformation of sedimentary rocks to the east of the fault. Andalusite and staurolite porphyroblasts are common in pelitic units and some outcrops near the east end of Powderhorn Lake are migmatized with net veins of plagiogranite cutting amphibolite fragments in a breccia. It is not yet clear whether the metamorphism is a late regional event or a thermal aureole around the Twin Lakes Complex (e.g. Kalliokoski, 1955) although the latter seems more likely.

The affinity of this metamorphic terrane is unclear at present. In the area east of Great Gull Lake, where some exposures are relatively unstrained, the rocks consist of fine to medium grained greywacke and pebbly conglomerate locally interbedded with siltstone and argillite and minor quartzite. These are lithologically similar to Sansom Greywacke exposed to the north in Notre Dame Bay and quite unlike the volcaniclastic green and red chert and argillite which characterize the Crescent Lake Formation in its type area to the north. We think it unlikely that any rocks east of Great Gull Lake are correlative with the Crescent Lake Formation. The metasediments near Powderhorn Lake include staurolite-bearing carbonaceous meta-shales interbedded with quartz-rich sandy beds and these are unlike Sansom Formation lithologies elsewhere. It is possible that these are metamorphosed Caradocian shale, known to underlie the Sansom Greywacke elsewhere in Notre Dame Bay (Dean, 1978; Dean and Meyer, 1982).

The faulted eastern margin of the Roberts Arm Group is locally cut by later granite intrusions. Near Dawes Pond, it is intruded by the Dawes Pond Granite consisting mainly of coarse grained biotite granite, quartz monzonite and granodiorite. North of Burnt Pond, near the northern limit of mapping, it is intruded by diorite and granodiorite probably related to the Twin Lakes Complex (Kean et al., 1981).

The western contact of the Roberts Arm Group, obscured by a large bog throughout the central part of the project area, has been interpreted by previous workers as partly an intrusive contact with granitic rocks related to the Topsails Intrusive Suite and partly a stratigraphic or faulted contact with Silurian volcanic rocks of the Springdale Group (Dean and Strong, 1976). Farther south, an intrusive contact can be demonstrated between Roberts Arm Group volcanic rocks and the Skull Hill Quartz Syenite, an outlier of the Topsails Intrusive Suite. To the north, west of the northern end of Great Gull Lake, there is a similar intrusive contact with an outlier of the Topsails Intrusive Suite (Kean and Jayasinghe, 1982) and with a more mafic intrusive body of unknown affinity (Kalliokoski, 1955; Dean and Strong, 1976).

Geology of the Roberts Arm Group

Detailed mapping of the Roberts Arm Group between Great Gull Lake and Lake Bond (Fig. 24.2), has defined a stratigraphic succession which can be recognized throughout the present project area. We have identified five lithostratigraphic units within the southern part of the Roberts Arm Group which we have designated with informal names in the following section and in Figure 24.2 for purposes of description and discussion.

The stratigraphy is best exposed and most complete in the area south and southeast of Great Gull Lake. Sparse top indications from pillows and volcaniclastic sediments indicate that this is a generally west-facing sequence. In the following discussion, the stratigraphy is described from bottom (east) to top (west).

Baker Brook basalt. The Baker Brook basalt, consisting of variably deformed and locally sheared pillow lava and lesser massive basalt, is the basal unit of the Roberts Arm Group. It outcrops in the islands at the south end of Great Gull Lake and to the south along Baker Brook. South of Baker Lake, it is cut off by the Dawes Pond Granite but emerges again in the area east of Lake Bond in the core of a major anticline surrounded by overlying volcaniclastic sediments. Farther east, this unit again outcrops in the core of another anticline, the east limb of which is faulted against younger Sansom Greywacke (Fig. 24.2). A small lens of Baker Brook basalt is inferred to be present near the southwest end of Dawes Pond based on correlation of overlying felsic rocks with the Gull Hill sediments (see below).

East of the Trans-Canada Highway, basalts at the bottom of the Roberts Arm Group between Burnt and Rocky ponds are stratigraphically equivalent to and therefore tentatively correlated with the Baker Brook basalt.

Gull Hill sedimentary rocks. The Gull Hill sediments, in the type area between Gull Hill and Dawes Pond, consist predominantly of bedded, commonly dark green, volcaniclastic rocks which are very fine grained to aphanitic and have the aspect of chert. Beds of red to maroon ferruginous chert are abundant and locally there are graded beds of sandy volcaniclastic material. Near the bottom of the unit, adjacent to its contact with the underlying Baker Brook basalt, the chert is laminated, deep red in colour and up to 10 m thick. Stratigraphically higher ferruginous chert is generally 1 to 10 m thick and pale shades of red and maroon.

The Gull Hill sediments are absent from the section between the southwest end of Great Gull Lake and the Trans-Canada Highway. To the south, they strike into the Dawes Pond Granite but outcrop again southwest of Dawes Pond as a small lens of bedded volcaniclastic chert.

Sedimentary rocks which outcrop on the shores of Lake Bond have previously been assigned to the Crescent Lake

Formation (Kalliokoski, 1955; Dean and Strong, 1976). They comprise a folded but dominantly west-facing sequence consisting of dark green volcaniclastic chert with minor dark red to maroon mudstone and shale at the base overlain by volcaniclastic sandstone, pebbly sandstone, fine conglomerate and minor volcaniclastic chert. The basal green cherty beds are strikingly similar to those outcropping on Gull Hill and the ubiquitous red chert and mudstone suggest a similar depositional environment. The correlation with the Gull Hill sediments is further supported by the stratigraphic position of these rocks below the Burnt Island basalt (see below). Folding has repeated parts of the sequence several times between Lake Bond and Catamaran Brook (Fig. 24.2).

East of the Trans-Canada Highway, where the stratigraphy of the Roberts Arm Group appears to be more complete, a silicic volcaniclastic unit consisting of sandy and pebbly turbidites interbedded with green volcaniclastic chert overlies the basal basalt. Previous workers have assigned these rocks to the Crescent Lake Formation (e.g. Kalliokoski, 1955; Dean and Strong, 1976). Lithologically, these rocks resemble the Gull Hill sediments at Lake Bond and, to a lesser extent, the volcaniclastic cherts characteristic of the Gull Hill area although the ferruginous cherts are absent. The stratigraphic position of these rocks further supports their correlation with the Gull Hill unit.

Burnt Island basalt. The Burnt Island basalt hosts the Gullbridge and Lake Bond sulphide deposits and is therefore of considerable economic interest. It is the only lithostratigraphic unit which outcrops continuously between Great Gull Lake and Lake Bond and is therefore also an important stratigraphic marker. Near Gullbridge it consists principally of massive pillow basalts. However, southwest of Great Gull Lake where the unit is quite thin, highly sheared and generally schistose mafic rocks which are at least in part clastic and probably tuffaceous are prevalent. A marked thickening of the unit in the area of Starke's Pond is accompanied by the return of recognizable pillow lavas which are also abundant in the Lake Bond area.

It is difficult to assign the mafic volcanics in the northern part of Great Gull Lake to either the Burnt Island or Baker Brook basalts because of the absence of the Gull Hill sediments. However, geophysical data suggest that red chert-bearing silicic rocks in this area are along strike with the Gullbridge felsic volcanics (see below) implying that at least some of the volcanics east of them belong to the Burnt Island basalt. East of the Trans-Canada Highway, basalt which outcrops between the correlatives of the Gull Hill sediments and the Gullbridge felsic volcanics (see following section) are tentatively correlated with the Burnt Island basalt on the basis of stratigraphic position.

Gullbridge felsic volcanics. The Gullbridge felsic volcanics, as the host to many of the smaller showings in the project area, are of economic interest. Their main outcrop is an approximately 1 km wide belt which can be traced continuously from Gullbridge to the area southwest of Dawes Pond where it is cut off by the Skull Hill Quartz Syenite (Fig. 24.2). The dominant lithology is fine grained rhyolitic ash flow tuff which is remarkably uniform in character. Locally, coarse pyroclastic rocks with lithic clasts up to 5 cm long are present; these are particularly abundant in the area west of the south end of Great Gull Lake. Massive to porphyritic rhyolite outcrops immediately west of the Gullbridge Mine and also near Starke's Pond; these bodies are interpreted as small, extrusive, rhyolite domes. Between Gullbridge and the area west of Gull Hill, the felsic volcanics are characterized by two distinctive features: 1) the ubiquitous presence of thin interbeds and lenses of red to maroon ferruginous chert, and 2) an inhomogeneously developed but extensive quartz-sericite (+/- pyrite) hydrothermal alteration. Both of these features are of economic significance and will be further considered later in this report.

Although the Gullbridge felsic volcanics strike into the Skull Hill Quartz Syenite southwest of Dawes Pond, they reappear near Skull Pond west of Lake Bond where they consist of massive to porphyritic rhyolitic ash flow tuff. Interbedded red chert is absent but locally, quartz-sericite-pyrite alteration is present.

Northeast of Gullbridge, silicic volcanic and volcaniclastic rocks with interbedded ferruginous chert occur as thin, discontinuous units in the bays at the north end of Great Gull Lake. The most easterly prominent unit is on strike with and lies along geophysical trends with the Gullbridge felsic volcanics. We interpret this unit to be equivalent to at least part of the Gullbridge felsic volcanics although it is possible that the Gullbridge felsic volcanics actually feather out into a series of thin lenses at the north end of Great Gull Pond. In this case, the several thin silicic units in the western and central bays as well as the mafic rocks between them could all be distal lateral equivalents of the Gullbridge felsic volcanics.

East of the Trans-Canada Highway, a prominent felsic volcanic and silicic volcaniclastic unit which outcrops beside the highway can be traced northeast for over 4 km to the Handcamp area where it hosts the Handcamp prospect (Fig. 24.2). This unit is relatively thin and contains considerably more volcaniclastic material than the Gullbridge felsic volcanics in the mine area. The abundance of red chert and the widespread hydrothermal alteration which characterizes the mineralized area at Handcamp are very similar to those at Gullbridge and these are the only two areas in which these features occur together. On this basis, we tentatively correlate the Handcamp mineralized horizon with the Gullbridge felsic volcanics although we recognize that this correlation, in view of its economic significance, requires further substantiation.

South Brook basalt. The South Brook basalt is the uppermost unit in the southern part of the Roberts Arm Group. Basalts in this unit are most commonly massive although pillows are locally present west of the Gullbridge Mine and in the area west of Starke's Pond. The South Brook basalt can be traced continuously throughout the northern and central parts of the project area but disappears under the bog west of Starke's Pond. Southwest of Lake Bond, it emerges from the Skull Hill Quartz Syenite, where it consists of massive basalt interbedded with bedded mafic pyroclastic rocks.

The western (upper) contact west of Great Gull Lake and Dawes Pond is obscured by the large bog which forms the South Brook valley. To the north and in the southwestern corner on the project area, it is intruded by granitoid rocks related to the Topsails Intrusive Suite.

Economic geology

More than 30 mineral occurrences and prospects have previously been documented in the southern part of the Roberts Arm Group (Hibbard et al., 1984). Most consist of stringer and disseminated pyrite with minor chalcopyrite associated with hydrothermal alteration of the host volcanic rocks. Sphalerite is a major component of the Lake Bond deposit. Precious metals and galena are present only at the Handcamp prospect which also contains significant sphalerite. Most showings occur in either the Burnt Island

basalt or the Gullbridge felsic volcanics although locally, hydrothermal alteration and associated mineralization are present in the South Brook basalt as well. For descriptive purposes, the numerous showings can be grouped into three broad areas: 1) Lake Bond; 2) Gullbridge-Dawes Pond, and 3) Handcamp. Mineralization in each area is briefly described below.

Lake Bond

The Lake Bond deposit (Fig. 24.2) consists of disseminated and stringer pyrite, chalcopyrite and sphalerite hosted by intensely altered pillow lavas of the basal part of the Burnt Island basalt. The mineralization and associated alteration is well exposed on the northwest shore of Lake Bond in a series of trenches which date from the early 1970s. Chlorite and pyrite are the principal alteration products in the mineralized zone; epidote is not commonly associated with mineralization although it is a principal component of alteration assemblages elsewhere in the Lake Bond area. The deposit is particularly zinc rich relative to other prospects in this part of the Roberts Arm Group. Exploration activity in the early 1950s and sporadic efforts since that time have outlined reserves of approximately 1.1 million tonnes grading 0.3% Cu and 2.12% Zn (Consolidated Morrison Explorations Ltd., 1976).

Hydrothermal alteration related to this mineralizing event is not restricted to the immediate area of the deposit. An anomalous alteration, characterized by epidote which forms irregular patches and veinlets and locally a prominent boxwork of interlocking veinlets is developed in the Burnt Island basalt over an area of more than 2 km^2 southwest of Lake Bond. The altered rocks are generally pervasively chloritized and locally they contain ragged patches and anastamosing veinlets of black chlorite. Several minor pyrite (+/- chalcopyrite) occurrences in this area constitute sulphide-rich, generally black chlorite-bearing, facies of this alteration.

Gullbridge-Dawes Pond

Disseminated and stringer pyrite with lesser chalcopyrite is associated with alteration of the upper part of the Burnt Island basalt and the Gullbridge felsic volcanics between Gullbridge and the area west of Dawes Pond (Fig. 24.2). The mineralized alteration is mainly confined to three linear zones, which for convenience in the following discussion, are termed the "Mineral Point", "West" and "Starke's Pond" zones (see Fig. 24.2).

The Mineral Point zone is the most extensive of the three and continues more than 4.5 km between Gullbridge and the area west of Gull Hill. North of Gullbridge, it is under the water of Great Gull Lake and at its southern end disappears under thick drift. At its northern end, this alteration zone includes the Mineral Point (Gullbridge) orebody, a sulphide-rich stockwork in variably altered mafic volcanic rocks which has been metamorphosed to a cordierite-anthophyllite bearing assemblage by a nearby granite intrusion (Upadhyay and Smitheringale, 1972; Swinden, 1984). This orebody produced approximately 3 million tonnes of ore grading 1.1% Cu between 1967 and 1972 (Upadhyay and Smitheringale, 1972). Approximately 2 km southwest of Gullbridge, this alteration zone hosts the Southwest Shaft deposit, a small pyrite-chalcopyrite stockwork which apparently traverses the contact between the Burnt Island basalt and the Gullbridge felsic volcanics. Between Gullbridge and the Southwest Shaft, the alteration is dominantly within the Burnt Island basalt and is characterized by a chlorite-biotite-andalusite (+/- cordierite) assemblage. However, it appears to crosscut the stratigraphy at a shallow angle and between the Southwest Shaft and the area west of Gull Hill, is primarily within the overlying Gullbridge felsic volcanics where the alteration is characterized by quartz-sericite-pyrite assemblage. The alteration zone is not homogeneously mineralized throughout its exposed extent. Disseminated pyrite, which generally imparts a rusty appearance to weathered surfaces, is common and stringers up to 2 cm wide and 50 cm long locally occupy particularly sulphide-rich zones. Minor amounts of chalcopyrite are present in several locations, although not in economically interesting quantities.

The fact that the Mineral Point alteration zone apparently cuts across the stratigraphy, coupled with abundant evidence for both flattening and shearing, suggests that the zone may be an originally orthogonal alteration zone which has been transposed approximately into the plane of the stratigraphy by deformation. This process has been successfully modeled, for example, by Sundblad (1980), who showed that given a sufficient degree of combined pure and simple shear, a volcanogenic sulphide system would approach the shape of a disk with boundaries at a shallow angle to stratigraphic contacts. In the case of the Mineral Point zone, detailed structural analysis is needed to determine whether the strain can be shown to be sufficient to produce the observed geometry.

The "West zone" underlies a 1.3 km long belt on the northwest side of the Gullbridge felsic volcanics (Fig. 24.2). This zone of intense silicification, sericitization and pyritization is wholly within the felsic volcanic rocks. Pyrite is disseminated in rusty, cross cutting zones and rare patches and stringers of massive pyrite up to 1 m long are present at the northeast end of the zone. Minor chalcopyrite is present at a few localities. Although it is possible that this is a structural repetition of the Mineral Point alteration zone, there is no structural or stratigraphic evidence for such repetition. In view of the abundant evidence throughout the area for hydrothermal alteration at several different levels of the volcanic pile, we tentatively interpret these alteration zones as separate and distinct, either recording different hydrothermal events or different levels of a single episode of hydrothermal activity.

The "Starke's Pond zone" can be traced for approximately 2 km southwest of Starke's Pond (Fig. 24.2). It is similar in most respects to the West zone, consisting of disseminated and stringer pyrite which locally cut highly sericitized and silicified Gullbridge felsic volcanics. No chalcopyrite was seen. The Starke's Pond zone does not appear to be continuous with either of the previously mentioned zones although it occupies approximately the same stratigraphic position as the southwest end of the Mineral Point zone.

As previously noted, the Gullbridge felsic volcanics contain abundant small lenses of red and maroon chert between Gullbridge and the area northwest of Gull Hill. One particularly extensive bed, termed the "Gullbridge ferruginous chert" by Swinden (1976), overlies the Mineral Point alteration zone and can be traced for approximately 2 km along strike from Gullbridge to immediately northwest of the Southwest Shaft. This unit, as well as other smaller ferruginous chert units in this area, may have resulted from exhalative activity associated with the waning stages of the hydrothermal system(s) which are recorded by the alteration zones. No other exhalative deposits have been identified in the area.

The South Brook basalt contains evidence of local hydrothermal activity as well. Zones of anomalous epidote-black chlorite alteration are locally present and a small, disseminated pyrite (chalcopyrite)-bearing stockwork occurs in this unit northwest of Starke's Pond. Alteration associated

with this prospect can be recognized through an area of more than 0.5 km^2 southeast of the showing. The relationship, if any, between this alteration and that in the lower parts of the stratigraphy is not known.

Handcamp prospect

The Handcamp prospect, discovered in 1928, is the only significant gold prospect in the Buchans-Roberts Arm belt. In view of the present exploration emphasis on gold, the Handcamp prospect assumes some importance, not only as a potentially economic deposit but also as a case study of processes of gold concentration that may characterize similar undiscovered mineralization elsewhere in the belt.

The mineralization at Handcamp consists of pyrite, chalcopyrite, sphalerite and minor galena hosted by altered volcanic, volcaniclastic and chemical sedimentary rocks. Precious metals are present in varying amounts; peak values of 587 g/t Ag and 74 g/t Au have been recorded from selected, high grade, grab samples and although concentrations are normally much lower, ore grades of Au and Ag over narrow widths have been recorded in several locations (Franc de Ferriere, 1978). The mineralized zone has been extensively sampled in several trenches and also by four generations of diamond drilling dating from 1941. According to the assay data, the mineralization is sporadic and restricted to a stratigraphic interval characterized by felsic volcanic and silicic volcaniclastic rocks, abundant red chert and ferruginous chert which is approximately 50 m wide.

A widespread hydrothermal alteration is recorded not only in the mineralized zone but also in the adjacent mafic volcanic rocks. The most intense alteration has locally produced a quartz-sericite-pyrite assemblage which has obliterated all original textures in the rock. This alteration facies carries the Cu-Zn-Pb sulphide mineralization which locally is Au- and Ag-bearing. Magnetite is a common late alteration product and locally forms lenses and anastamosing stringers within the alteration zone. All of the altered rocks are highly flattened and sheared. Mafic rocks adjacent to the mineralized zone contain abundant epidote, occurring as veinlets, patches and pervasively epidotized domains up to 50 cm in diameter. Chlorite is ubiquitous, both as a pervasive alteration product and as local black chlorite veinlets. Magnetite is also common in this alteration facies; it forms veinlets and is locally delicately interbanded with epidote in pillow interstices and open space fillings. The alteration gradually dies out to the east of the mineralized horizon.

The unit which hosts the mineralization has been traced in outcrop and diamond drillholes for more than 1200 m along strike and regional mapping suggests that it can be correlated with the mixed felsic volcanic-volcaniclastic-chert outcrops on the Trans-Canada Highway north of Little Gull Pond. Hydrothermal alteration and erratic disseminated pyrite and chalcopyrite are locally associated with this zone east of the Trans-Canada Highway, although no precious metals have been detected in this area to date. Correlation of the Handcamp horizon with outcrops as far west as the Trans-Canada Highway raises the possibility that it can also be correlated with the Gullbridge stratigraphy farther to the southwest. Our data suggest that such a correlation is at least feasible. The overall stratigraphic succession of the Roberts Arm Group in the Handcamp area is similar to that exposed at the south end of Great Gull Lake although the thickness and facies of some units are different. Such a correlation is supported by the similarity between host rocks (particularly the abundance of ferruginous chert) and the associated alteration in the two areas.

Conclusions

The southern part of the Roberts Arm Group consists of a mixed assemblage of volcanic, volcaniclastic and chemical sedimentary rocks. Hydrothermal alteration is widespread in some units and is associated with all of the mineralization known to date in the area. The field work summarized in this report has led to several new conclusions concerning the stratigraphy and economic geology of this part of the Roberts Arm Group. These are summarized briefly below:

1. Contrary to previous workers, we believe there is a relatively simple stratigraphy which can be traced throughout the southern part of the Roberts Arm Group. Five lithostratigraphic units have been identified and informally named; stratigraphic relationships between them are defined in the area south and southwest of Great Gull Lake. All elements of the stratigraphic succession are present in most areas, although facies changes do occur along strike.

2. Sedimentary rocks east and southeast of Great Gull Lake, assigned by previous workers to the Crescent Lake formation and the Sansom Greywacke, are inhomogeneously but locally strongly deformed and thermally metamorphosed. We interpret the deformation as evidence for a major, northeast trending fault along the east shore of Great Gull Lake separating these rocks from the Roberts Arm Group to the west. The metamorphism we interpret as a contact metamorphic effect related to intrusion of Acadian granitoid rocks. The affinity of the metasedimentary rocks is unclear although they do not appear to be typical of the Crescent Lake formation in its type area.

3. Most volcanogenic mineralization is hosted by the Burnt Island basalt and the Gullbridge felsic volcanics. The two principal deposits in the area are mineralogically and stratigraphically distinct. Gullbridge occurs near the top of the Burnt Island basalt and is primarily a metamorphosed, Cu-rich stockwork associated with a laterally extensive alteration zone. The Lake Bond deposit occurs at the base of the Burnt Island basalt and is primarily a Zn-rich stockwork with lesser Cu. Although the two are not stratigraphically equivalent, they may have formed during the same period of alteration and mineralization.

4. Alteration associated with the Gullbridge orebody can be traced for more than 4.5 km along strike. The alteration zone crosscuts the stratigraphy at a small angle and is interpreted as a flattened and sheared, originally crosscutting, alteration zone. The two other similar but smaller alteration zones are present in the area between Great Gull Lake and Starke's Pond.

5. Precious metal mineralization is present at the Handcamp prospect, approximately 10 km northeast of Gullbridge. The mineralization is associated with hydrothermal alteration similar to but generally more magnetite-rich than that in the central and southern parts of the area. The presence of galena and precious metals in this area also distinguish it from other mineralization in the area. Regional stratigraphic considerations indicate that the mineralized horizon at Handcamp may be stratigraphically equivalent to the Gullbridge felsic volcanics.

6. Exhalative sulphide mineralization has not been identified in the project area although the widespread hydrothermal alteration and stockwork-type mineralization strongly suggests that such mineralization could be present. The numerous lenses of ferruginous chert in the Gullbridge felsic volcanics may be an exhalative facies of the hydrothermal systems. Alternatively, discharge may have

occurred at stratigrphically higher levels and massive sulphide bodies may be present, for example, in the upper parts of the Gullbridge felsic volcanics or in the South Brook basalt. The latter possibility is supported by the presence of alteration and minor mineralization in this unit.

Acknowledgments

Paul Deering provided capable assistance during the field work. John O'Sullivan of ESSO Minerals Ltd. discussed aspects of the geology with us and loaned us some critical air photos. We thank Baxter Kean, Paul Dean and Dave Strong for critical comments on an early version of the manuscript.

References

Bostock, H.H., Currie, K.L., and Wanless, R.K.
1979: The age of the Roberts Arm Group, north-central Newfoundland; Canadian Journal of Earth Sciences, v. 16, p. 599-606.

Consolidated Morrison Exploration Ltd.
1977: Diamond drill records for Lake Bond property with accompanying report; unpublished company report, 1 p.

Dean, P.L.
1978: The volcanic stratigraphy and metallogeny of Notre Dame Bay; Memorial University of Newfoundland, Report 7, 204 p.

Dean, P.L. and Meyer, J.R.
1982: Metallogenic study of Mid-Ordovician cherts and shales of central Newfoundland; Newfoundland Department of Mines and Energy, Mineral Development Division, Report 82-1, p. 175-187.

Dean, P.L. and Strong, D.F.
1976: Geological compilation maps for Notre Dame Bay; Newfoundland Department of Mines and Energy, Mineral Development Division, Open File 947.

Espenshade, G.H.
1938: Geology and mineral deposits of the Pilley's Island area; Newfoundland Department of Natural Resources, Geological Section, Bulletin No. 6, 56 p.

Franc de Ferriere, A.
1978: Report on geological, geophysical and geochemical investigations, 1978 season (Handcamp Property); unpublished report for Falconbridge Nickel Mines Ltd., 30 p.

Hayes, J.J.
1951: Preliminary map, Marks Lake; Geological Survey of Canada, Paper 51-20.

Heyl, G.R.
1936: Geology and mineral deposits of the Bay of Exploits area; Geological Survey of Newfoundland, Bulletin No. 3, 66 p.

Hibbard, J.P., Hill, J., Hyde, R., Barry, J., and Green, R.
1984: Sandy Lake (12H), Newfoundland Mineral Occurrence Map; Newfoundland Department of Mines and Energy, Mineral Development Division, Map 83-60.

Kalliokoski, J.
1955: Gull Pond, Newfoundland; Geological Survey of Canada, Preliminary Map 54-4.

Kean, B.F. and Jayasinghe, N.R.
1982: Geology of the Badger area (12A/16), Newfoundland; Newfoundland Department of Mines and Energy, Mineral Development Division, Report 81-2, 37 p.

Kean, B.F., Dean, P.L., and Strong, D.F.
1981: Regional geology of the central volcanic belt of Newfoundland; Geological Association of Canada, Special Paper 22, p. 65-78.

Neale, E.R.W. and Nash, W.A.
1963: Sandy Lake (east half), Newfoundland; Geological Survey of Canada, Paper 62-28, 40 p.

Nelson, K.D. and Kidd, W.S.F.
1979: The age of the Roberts Arm Group, north-central Newfoundland: Discussion; Canadian Journal of Earth Sciences, v. 16, p. 2068-2070.

Nowlan, G.S. and Thurlow, J.G.
1984: Middle Ordovician conodonts from the Buchans Group, central Newfoundland, and their significance for regional stratigraphy of the Central Volcanic Belt; Canadian Journal of Earth Sciences, v. 21, p. 284-296.

Strong, D.F.
1977: Volcanic regimes of the Newfoundland Appalachians; Geological Association of Canada, Special Paper 16, p. 61-90.

Sundblad, K.
1980: A tentative 'volcanogenic' formation model for the sediment-hosted Ankarvattnet Zn-Cu-Pb deposit, Central Swedish Caledonides; Norges Geologiske Undersokelse, Bulletin 57, p. 211-228.

Swinden, H.S.
1976: Chemical sedimentation associated with mid-Paleozoic volcanism in central Newfoundland; unpublished M.Sc. thesis, Memorial University of Newfoundland, St. John's, 234 p.

1984: The Gullbridge Mine; Newfoundland Department of Mines and Energy, Mineral Development Division, Report 84-3, p. 131-140.

Upadhyay, H.D.
1970: The geology of the Gullbridge copper deposit, Newfoundland; unpublished M.Sc. thesis, Memorial University of Newfoundland, 134 p.

Upadhyay, H.D. and Smitheringale, W.D.
1972: The Gullbridge copper deposit, Newfoundland: volcanogenic sulphides in cordierite-anthophyllite rocks; Canadian Journal of Earth Sciences, v. 9, p. 1061-1073.

Williams, H.
1964: Botwood map area; Geological Survey of Canada, Map 60-1963.

A 3.5 kHz acoustic survey of Nachvak Fiord, northern Labrador

Project 810037

R.J. Rogerson[1], H.W. Josenhans, and T. Bell[1]
Atlantic Geoscience Centre, Dartmouth

Rogerson, R.J. Josenhans, H.W., and Bell, T., A 3.5 kHz acoustic survey of Nachvak Fiord, northern Labrador; in Current Research, Part A, Geological Survey of Canada, Paper 86-1A, p. 221-228, 1986.

Abstract

Nachvak Fiord contains four basins between Tasiuyak Arm and Nachvak Bay. The basins are up to 214 m deep and contain up to 55 m of stratified sediment overlying unstratified tills. The total sediment package can be divided into four units which probably represent a complete cycle of deglaciation from lodgement till through ice-contact, ice-proximal and ice-distal facies. Two moraine-like features are identified between the basins, and sediment thicknesses change greatly on either side of them, suggesting they were the sites of tillstands in recession, or stadial maxima. Thus, the sediment units in the basins are not likely synchronous in formation. Lodgement till was probably being formed in the westernmost basin while ice-proximal, or even ice-distal sediments were being emplaced in the outer basin.

Résumé

Le fjord de Nachvak comprend quatre bassins entre le bras de Tasiuyak et la baie de Nachvak. Les bassins atteignent 214 m de profondeur et renferment 55 m de sédiments stratifiés recouvrant des tills non stratifiés. L'ensemble des sédiments peut être divisé en quatre unités qui représentent probablement un cycle complet de déglaciation, soit de bas en haut: le faciès de till de fond, le faciès de contact glaciaire, le faciès le plus rapproché de la glace et le faciès le plus éloigné de la glace. Entre les bassins, on a pu identifier deux entités morainiques, de part et d'autre desquelles les puissances des sédiments varient considérablement, phénomène qui semble indiquer qu'il doit s'agir d'emplacements correspondant à des arrêts dans le mouvement de retrait ou à des maxima stadiaires. Ainsi, les unités sédimentaires des bassins n'ont probablement pas été mises en place en même temps. Le till de base s'accumulait probablement dans le bassin le plus occidental alors que l'accumulation des sédiments les plus proches ou même les plus éloignés de la glace avait lieu dans le bassin extérieur.

[1] Departments of Geography and Earth Sciences, Memorial University of Newfoundland, St. John's, Newfoundland A1B 3X5

Introduction

3.5 kHz and sidescan sonar surveys of Nachvak Fiord, Labrador, sediments were made in July and August 1984 as part of a co-operative program between the Atlantic Geoscience Centre and the Canadian Hydrographic Service. The surveys provide preliminary information on bathymetry and subbottom sediments between the fiord threshold in Nachvak Bay and the Townley Basin, including Tallek Arm: a total fiord length of about 30 km (Fig. 25.1). The length of acoustic traverses within the fiord exceeded 125 km: the main centre profile, line 19, is shown on Fig. 25.1. In 1985 the three-man submersible **Pisces IV** provided actualistic observations of fiord-bottom features.

The southern portion of the fiord hinterland has been the subject of glacial geology investigations between the Selamiut Range (Evans and Rogerson, 1985) and the Gulch Peninsula (Bell and Rogerson, 1985). The marine acoustic data, herein, provide an independent check on the deglacial model proposed (Rogerson and Evans, 1984) and permit some correlation with the offshore stratigraphy. In this paper, fiord-bottom morphostratigraphy is examined and a tentative deglaciation sequence is proposed from subbottom stratigraphy alone.

Nachvak Fiord

Nachvak Fiord lies at latitude 59°N and cuts 45 km inland through the Selamiut Range, the highest range in the Torngat Mountains in northern Labrador. The fiord is 2 to 4 km wide, increasing gradually eastwards until it meets Nachvak Bay which opens to the Labrador Sea. The sidewalls of the fiord are steep, even vertical, in parts, rising 1000 m from sea level at Kutyaupok Mountain. The upper part of the fiord divides into Tallek Arm which cuts due south for 12 km, and Tasiuyak Arm which trends generally westward for an equivalent distance. At the head of Tasiuyak Arm, Nachvak Lake continues the same glacial valley trend for a farther 10 km.

A number of small coves occur on the southern side of the fiord east of Tallek Arm. Ivitak Cove, at the mouth of the McCornick River, is the largest of these. Tinutyarvik Cove and Naksaluk Cove to the east are fed by smaller streams issuing from smaller valleys.

Bathymetry in the fiord reveals a succession of basins, four of which occur between Tasiuyak Arm and Nachvak Bay. From west to east, these are the Townley, Koktortoaluk, Ivitin and Outer basins. East of the Outer Basin, the water of Nachvak Bay is very shallow with frequent shoals and an average channel depth of 50 m.

Maximum water depths in the four basins are 89, 168, 170, and 214 m from west to east. The acoustic basement of crystalline and metasedimentary rocks lies approximately 120, 230, 230, and 310 m below sea level.

The four basins are separated by shallow barriers, between 50 and 180 m below sea level. Two of these, at Kogarsok and Tinutyarvik, have many of the characteristics of riegeln or glacier steps covered with till-like sediments and typical end moraine form.

Subbottom sediment units

Five acoustic units are recognized, termed A, B, C, D, and E from bottom to top. They are reproduced in three sections on Figure 25.2, and represented along the approximate centre line of the fiord in Figure 25.3.

Total stratified sediment thickness is over 50 m in the Outer Basin, over 30 m in the Ivitin and Koktortoaluk basins and over 10 m in the Townley Basin (Fig. 25.4). Over the shallow barriers between the basins there are no stratified

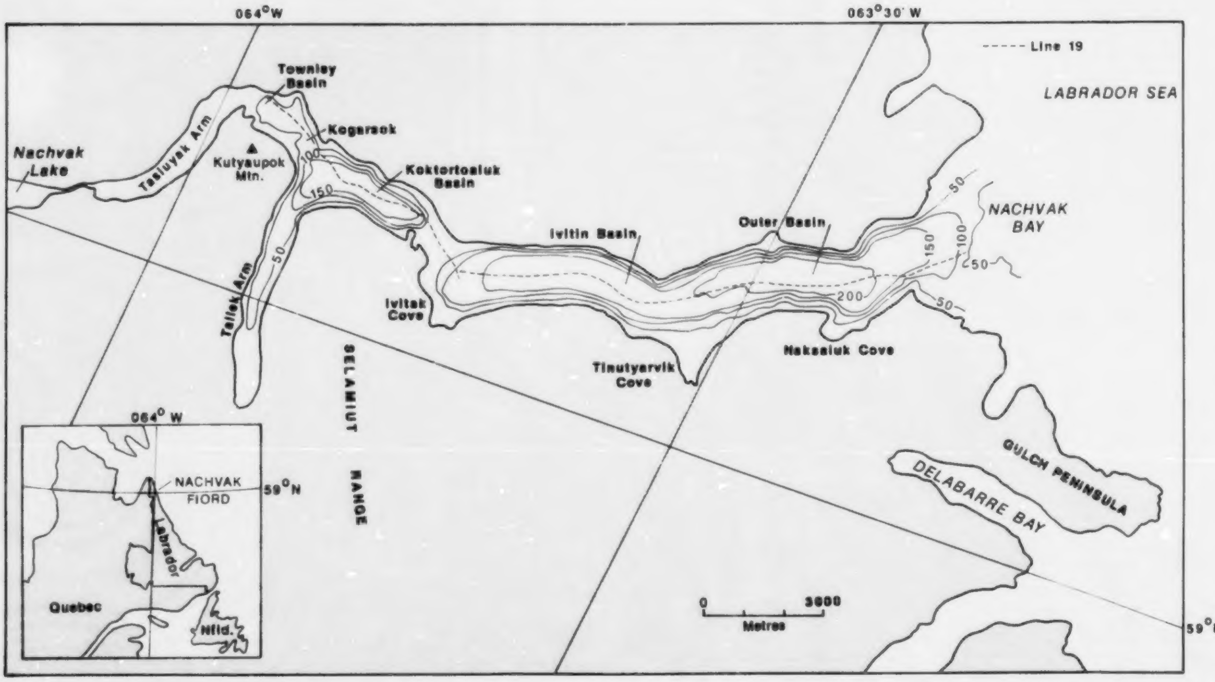

Figure 25.1. Nachvak Fiord: location, place names and bathymetry. The dotted line represents the position of the section shown in Figure 25.2.

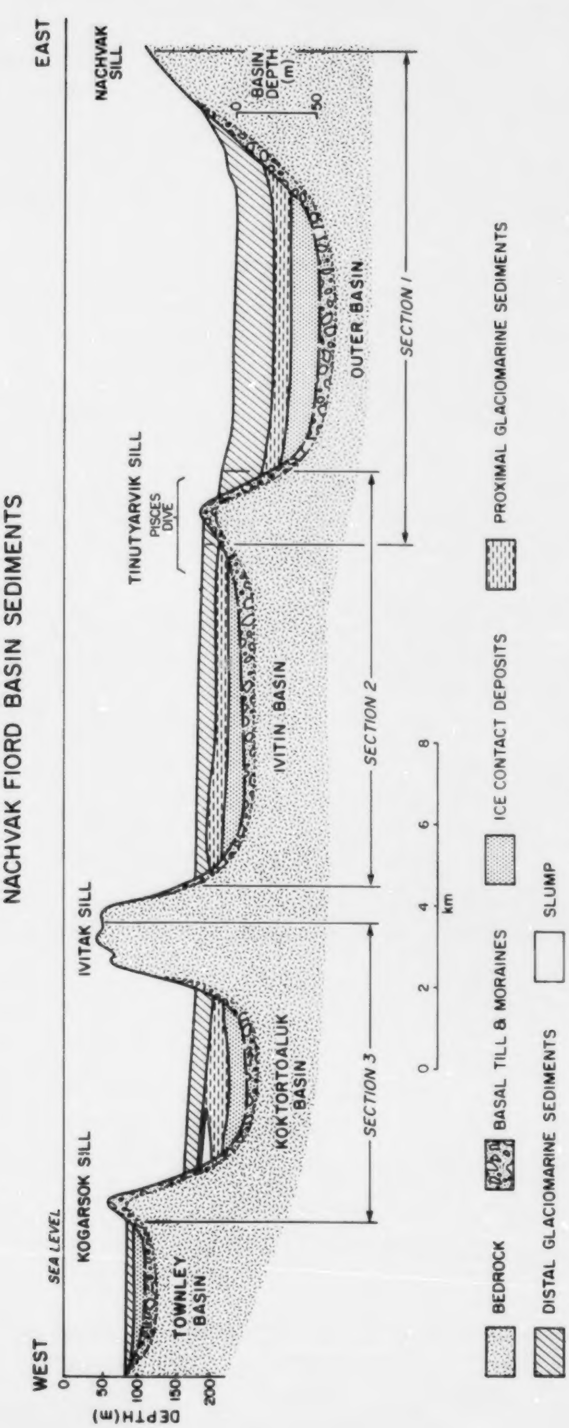

Figure 25.2. *Diagrammatic-interpreted section along line 19 from Nachvak Bay to the Townley Basin. Interpretations are based on analysis of 3.5 kHz acoustic data and one submersible transect.*

sediments, although two of the barriers may be heavily covered with till, or largely formed of till. The 3.5 kHz system does not have sufficient energy to penetrate and clearly differentiate the basal till from underlying bedrock, thus the differentiation of the lowest units as shown on Figure 25.2 is purely interpretive.

Unit A. This is the impenetrable base of the fiord. It appears to be covered in most areas by acoustic reflectors, but is exposed at the submarine surface in the shallow area west of Ivitak Cove, and may also outcrop in the shallow mouth of the fiord.

Unit B. The upper surface of unit B is basin-like in form and underlies stratified sediments. In some areas parallel to subparallel reflectors appear beneath unit B, suggesting it is composed of bedded sediments rather than bedrock. The areas of the fiord bed where unit B is not covered by sediments contain some interesting morphologies. The barrier at Kogarsok, between the Townley Basin and the Koktortoaluk Basin is particularly distinctive, consisting of a steeply sloping, narrow ridge oriented across the fiord (Fig. 25.5). Similarly, the barrier at Tinutyarvik, between the Ivitin and Outer basins is a narrow ridge sloping down both upfiord as well as downfiord (Fig. 25.6). Both features have the geomorphic characteristics of end-moraine ridges.

Unit C. In the Outer Basin at least three reflectors are present within unit C, often separating acoustically transparent beds which appear to be massive and up to 5 m thick. The unit is at least partly stratified. The upper surface of the unit in all the basins is relatively flat to wavy, while the lower surface appears to be more irregular. Shallow hollows in the lower surface appear to be filled with lenses of ponded sediment, while hummocks are also present. Immediately west of Tinutyarvik, unit C is poorly defined where the reflection pattern is one of hummocky clinoforms. This may be due to disturbance by either submarine slumping or by some glacial process.

Unit D. This unit is over 25 m thick in the outer basin, but only 10 to 15 m thick in the Ivitin and Koktortoaluk basins, and less than 5 m thick in the Townley Basin. It contains several acoustic reflectors of variable strength with configurations varying from parallel to wavy to subparallel. It contains some discontinuities, minor gas pockets and lens-shaped ponded features.

In the Koktortoaluk Basin, a separate subunit exists within unit D. It consists of a wedge of sediment, over 10 m thick on its western margin immediately north of Tallek Arm (Fig. 25.7). The unit, which is internally reflection-free, extends through a significant portion of unit D, thinning to a single reflector within it.

Unit E. Unit E contains several sharp reflectors in a parallel configuration which probably indicate a flat-lying fine grained sediment. In the Outer Basin it averages 25 m, increasing to >30 m towards the eastern end. In the Ivitin and Koktortoaluk basins it is between 12 and 15 m, while in the westernmost Townley Basin, it is only 5 m thick. The flat reflectors are interrupted occasionally by irregular forms which indicate gas pockets. Where they form broad chaotic features near the basin margins, they may indicate sediment slumps or slides. Where no slumps border the margin, the unit forms a slightly mounded onlap facies over basement. Unit E is continuous with modern sediments which are presently being deposited on the fiord bottom in basin locations.

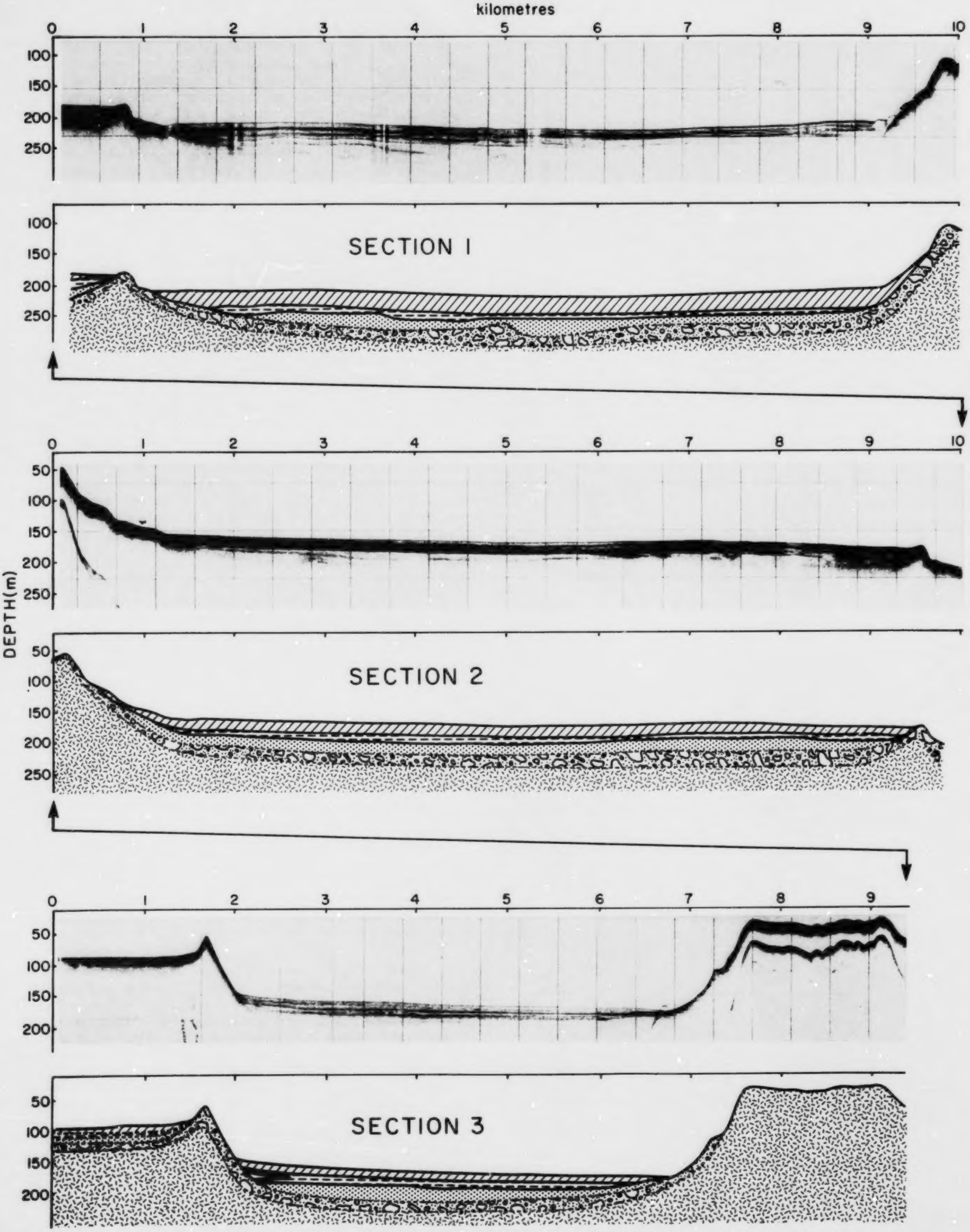

***Figure 25.3.** Acoustic units in Nachvak Fiord taken from the 3.5 kHz record. (see Fig. 25.2 for location of sections 1-3).*

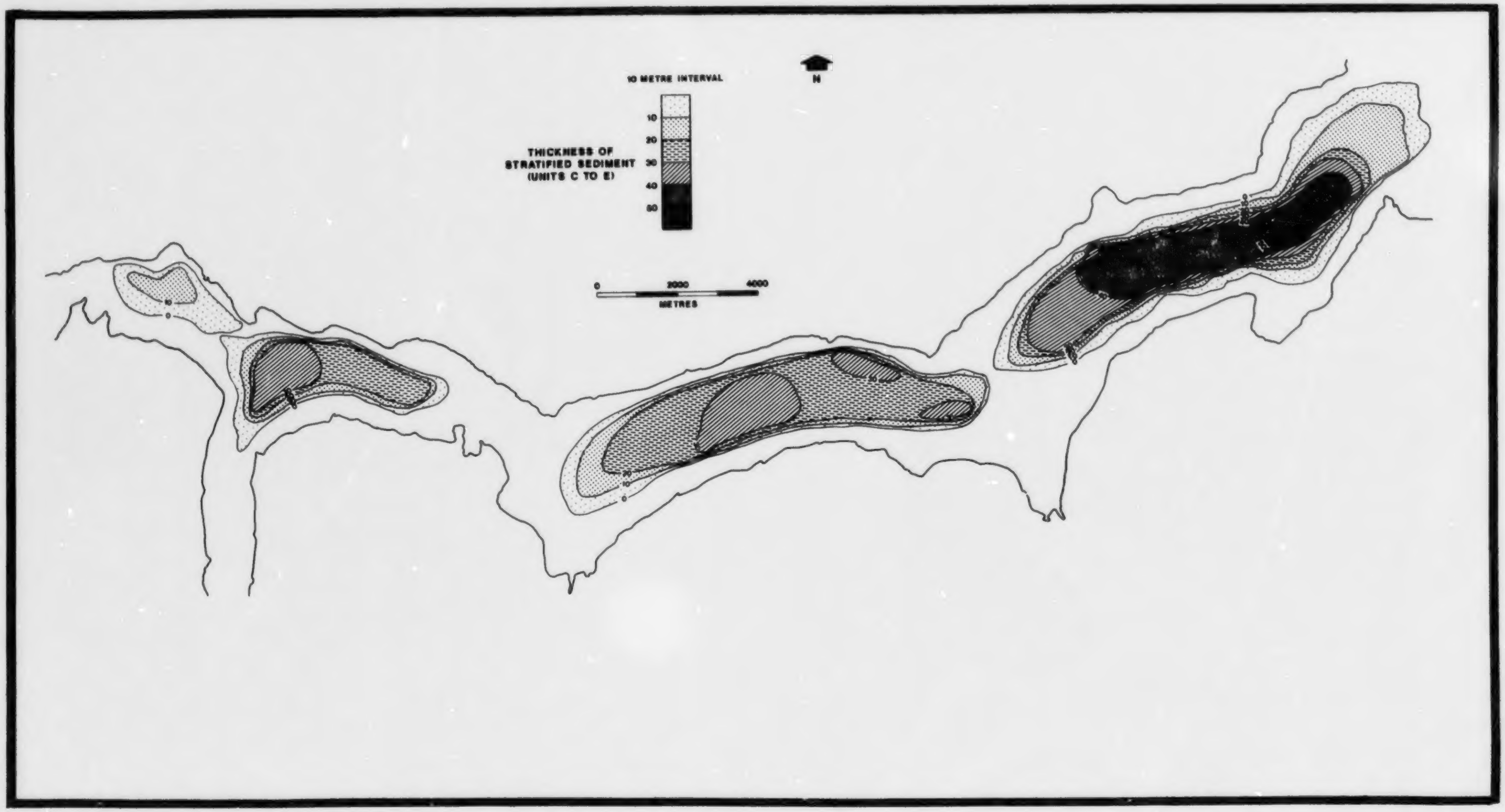

Figure 25.4. Isopach map of stratified sediments (units C to E) in Nachvak Fiord.

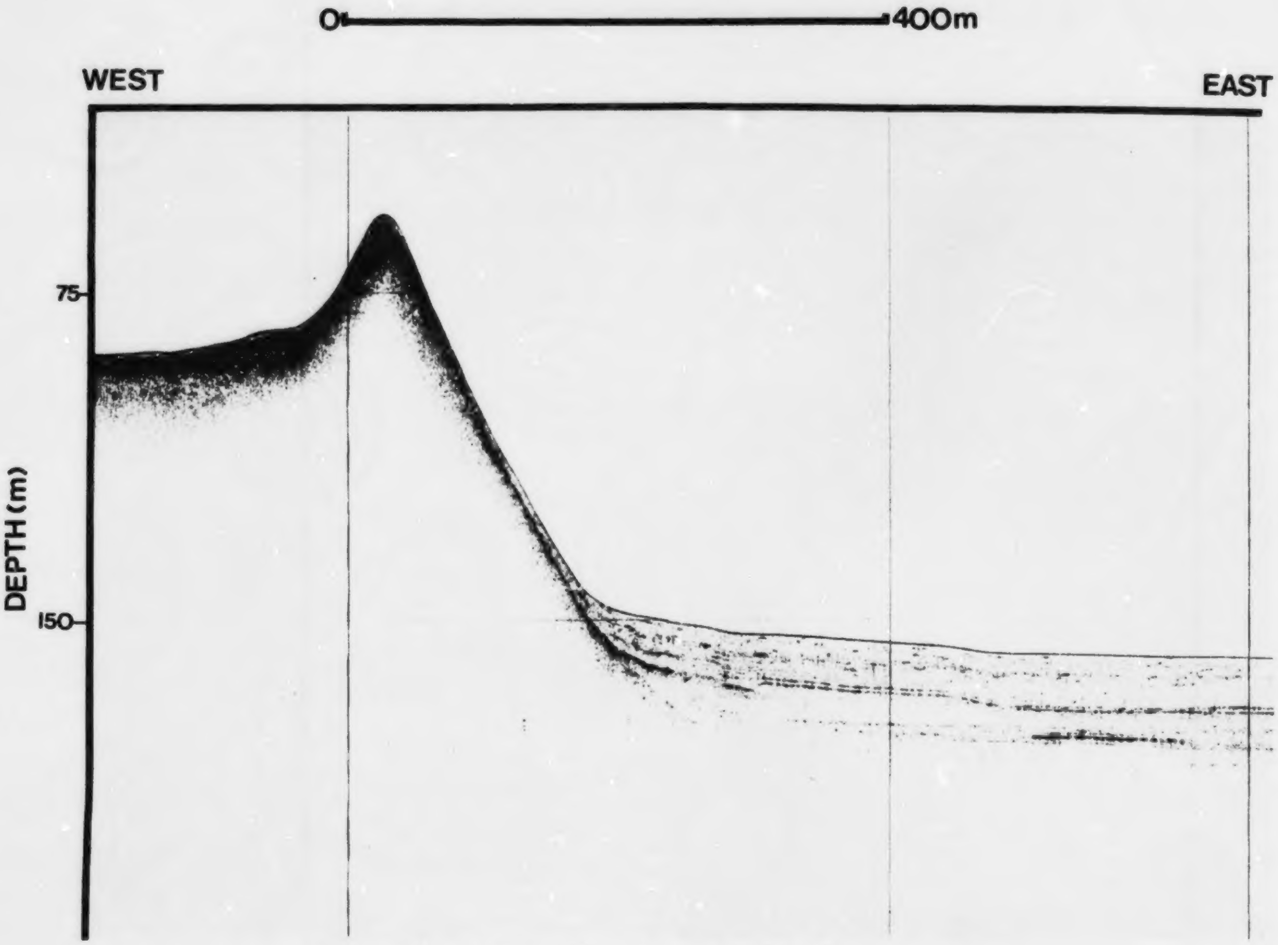

Figure 25.5. *3.5 kHz profile of the moraine-like ridge at Kogarsok.*

Interpretation and discussion

The acoustic data presented show a locally complex, but regionally consistent pattern which is interpreted to represent the complete stepwise deglacial sequence of Nachvak Fiord. Total sediment thickness increases towards the Outer Basin, suggesting longer ice-free period(s) towards the sea to trap progressively more sediments. The acoustic units are tentatively associated with specific deglacial environments.

Unit A is interpreted as glacially smoothed and over-deepened bedrock of crystalline gneisses, anorthosites and metasediments, subaqueously exposed at the fiord threshold in Nachvak Bay and the sill to the west of Ivitak. Tills, fanglomerates and talus may also occur within this unit where they are composed of coarse blocks which are impenetrable to the acoustic signal.

Unit B is interpreted as representing basal till and frontal moraine complexes. The classic moraine shapes at Kogarsok and Tinutyarvik probably represent frontal deposition at ice margins during still-stands in recession. This interpretation is confirmed by traverses in 1985 in the **Pisces IV** which revealed that the Tinutyarvik feature is a steep bouldery ridge with no evidence of exposed bedrock.

Unit C is interpreted as composed of ice-contact sediments. Several reflectors in the unit dip upfiord, suggesting a western sediment source. The material is interpreted to comprise coarse grained sand with laterally extensive silt. Lack of stratification suggests deposition within the complex setting found at the immediate ice margin.

Unit D is interpreted as glaciomarine sediments which contain stratification due to settling in the water column. It owes its acoustic variability to changes in the amount and type of sediment derived from the calving ice margin.

Unit E is interpreted as comprising ice-distal sediments. It is typically well stratified and the lateral continuity of individual reflectors suggests it is formed by a uniform rain out of fine grained material. Some increase in thickness of the unit towards the western end of the basins also suggests a source from the retreating ice margin. The sedimentary texture is interpreted as fine muds.

Units B-E appear therefore to comprise a complete deglacial cycle, ranging from basal till through ice-contact to ice-distal sediments. The units B through the earliest part of E would appear to have been completely emplaced in the Outer Basin at a time when the ice margin stood still at the end moraine-like feature at Tinutyarvik (Fig. 25.8).

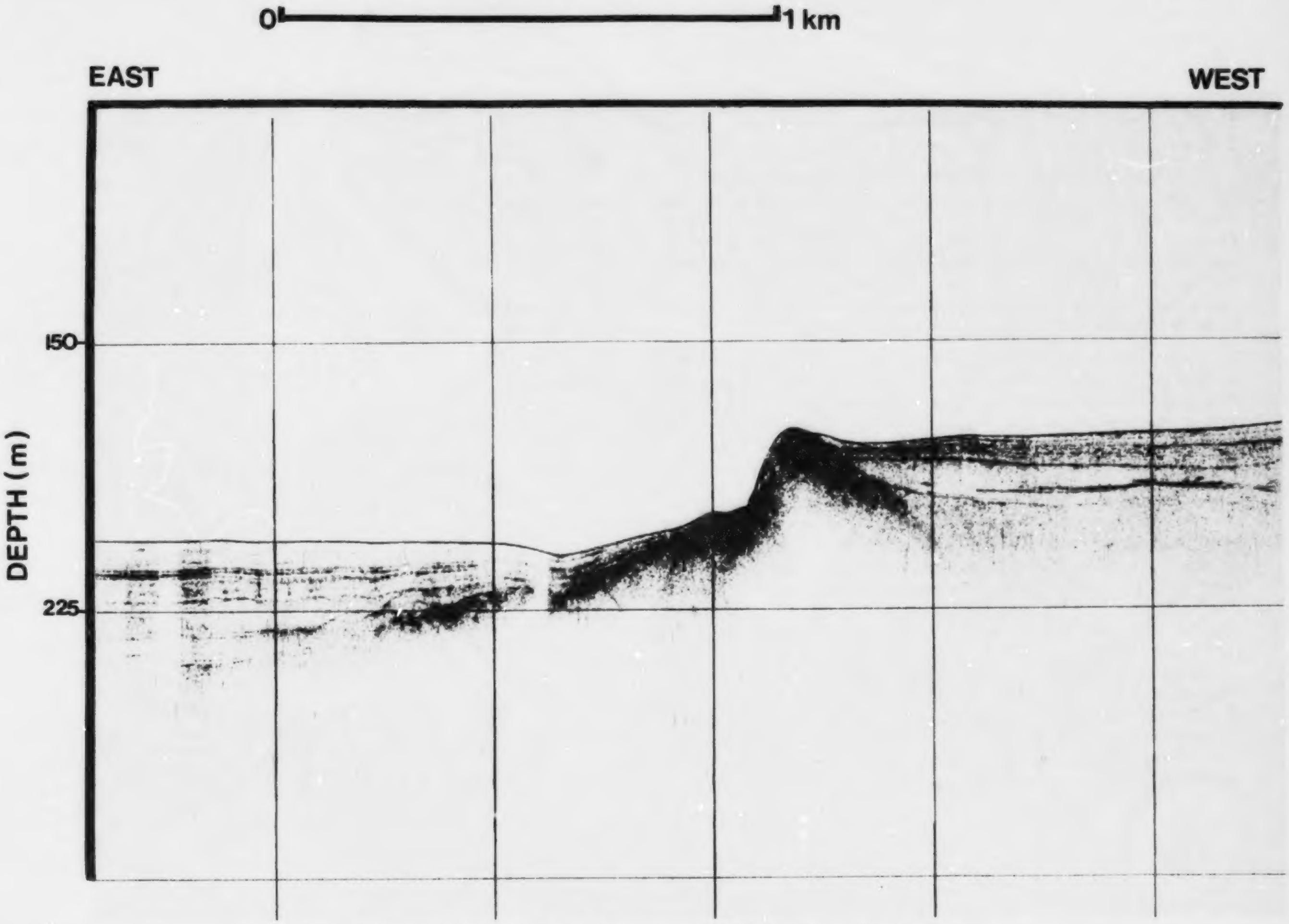

Figure 25.6. *3.5 kHz profile of the moraine-like ridge at Tinutyarvik.*

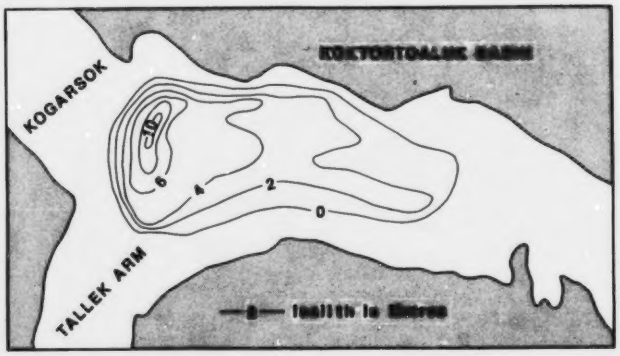

Figure 25.7. *Isoliths on the subunit within unit D interpreted as a slump.*

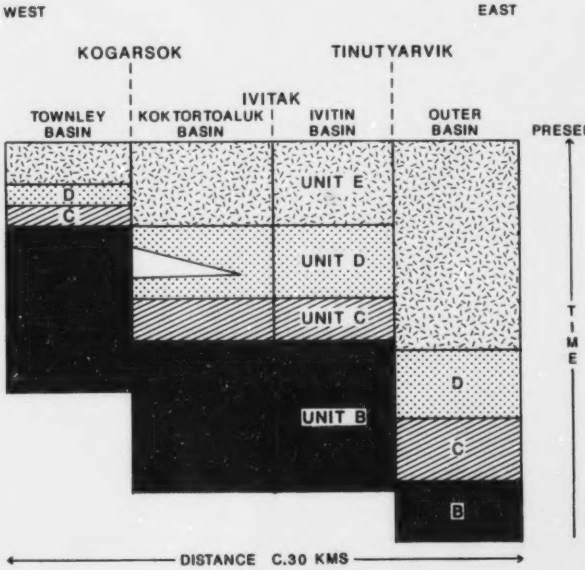

Figure 25.8. *Time/distance diagram on deposition of acoustic (sediment) units in Nachvak Fiord.*

Subsequent to the Tinutyarvik still stand, the ice is interpreted as having rapidly retreated to a later still stand at the moraine-like feature at Kogarsok. During this time a complete, but younger deglacial sequence would have been deposited in the Koktortoaluk and Ivitin basins. Following a still stand at Kogarsok, a much denuded ice tongue must have rapidly retreated from Townley Basin since only a thin deglacial sequence is in evidence there.

The relationship of the Tallek Arm tributary system to the overall Nachvak Fiord sediments is not clear since the stratigraphic section in the Arm was not completely penetrated by the acoustic source. Within the resolution of the 3.5 kHz system, the Arm is dominated by sediments discharged from the local rivers. Underlying these prodelta sequences may be some stratified sediments, possibly related to an ice-dammed condition at the northern end.

Perhaps related to circumstances in Tallek Arm is the wedge-like subunit within unit D in the Koktortoaluk Basin (Fig. 25.7). This latter may have been deposited while ice was grounded at, and constructing, the Kogarsok moraine. The sediment may have issued from Tallek Arm, or may be a slump unit from the face of the moraine.

The significance of the Tinutyarvik and Kogarsok ice margins is uncertain from this record and justifies further examination of the fiord. The Tinutyarvik moraine may represent a Late-Wisconsinan maximum, or be formed at some still stand during recession from the maximum. Evidence exists in the terrestrial record in the form of raised beaches, marine limits and soils-dated moraines, that the Late Wisconsinan maximum did indeed terminate between 20 Ka and 10 Ka BP in the Tinutyarvik area (Evans and Rogerson, 1985). Acoustic similarities suggest that the basal unit B may be linked to the upper till on the outer shelf, interpreted as Late Wisconsinan in age. Such an interpretation would reduce the Tinutyarvik still stand to a recessional event rather than a stadial or glacial maximum.

Acknowledgments

This research was supported primarily by GSC project 810037 under DSS Contract OSC84-00671, although groundwork for the study of the glaciation of Nachvak Fiord was aided by Energy, Mines and Resources Research Agreements 283 (1983) and 257 (1984), and Natural Sciences Engineering Research Council Operating Grants A6105 to R.J. Rogerson. The authors thank Capt. Adams, Officers and Crew of the CCGS **Labrador** for their help while the data were being collected, and D. Locke who helped rig and run the equipment. E. Comeau, B.W. MacGowan, and B. MacIntyre of the Canadian Hydrographic Service surveyed the fiord water depths and made their results available to us. Ali Aksu of Memorial University provided assistance during the interpretation of the acoustic record, and Sandra Halliday drew the maps and diagrams.

References

Bell, T. and Rogerson, R.J.
1985: Drift pebble lithology and glaciation of Gulch Peninsula, Nachvak Fiord, northern Labrador; Schedule and Abstracts, 1985 Annual Meeting, Canadian Association of Geographers, University of Trois-Rivières, Quebec, p. 29.

Evans, D.J.A. and Rogerson, R.J.
1985: The use of soils in dating successive glacial/deglacial phases in a low-Arctic mountain environment; in International Geomorphology 1985, ed. T. Spencer, p. 168.

Rogerson, R.J. and Evans, D.J.A.
1984: Glaciation of the northern Selamiut Range and part of Nachvak Fiord, Torngat Mountains, northern Labrador; Abstract, 13th Annual Arctic Workshop, Institute of Arctic and Alpine Research, Boulder, Colorado, p. 49.

Assessment of lead-zinc deposits of the western Newfoundland carbonate platform[1]

Contract 34SZ. 23233-5-0350

Cynthia M. Saunders[2] and D.F. Strong[2]

Saunders, C.M. and Strong, D.F., Assessment of lead-zinc deposits of the western Newfoundland carbonate platform; in Current Research, Part A, Geological Survey of Canada, Paper 86-1A, p. 229-237, 1986.

Abstract

Sixty-one mineral occurrences in the carbonate platform of western Newfoundland were examined and sampled. The occurrences are found in Cambrian to Mississippian limestones and dolostones which outcrop from Port au Port to the tip of the Great Northern Peninsula. The occurrences can be grouped into two broad types. Type I is sphalerite ± galena mineralization associated with white dolomite spar gangue – "Mississippi Valley type". The amount of sulphides and gangue is a function of the secondary porosity of the rocks which decreases with their age. Type II mineralization is vein/open-space filling associated with calcite and barite gangue and is dominantly of Mississippian age. The mineralization is confined to veins in less permeable Cambrian and Ordovician strata and tends to fill open spaces in more permeable Mississippian rocks.

Résumé

Soixante et une venues minérales ont été étudiées et échantillonnées dans la plate-forme de roches carbonatées, de l'ouest de Terre-Neuve. Ces venues se trouvent dans des calcaires et des dolomies d'âge cambrien à mississippien et affleurent de Port-au-Port jusqu'à la pointe de la péninsule Great Northern. Ces venues peuvent être regroupées en deux grands types. La minéralisation du type I est constituée de sphalérite ± galène dans une gangue de cristaux blancs de dolomite; il s'agit du type <<Mississippi Valley>>. Les proportions de sulfures et de gangue sont fonction de la porosité secondaire des roches qui décroît avec l'âge de ces dernières. La minéralisation du type II renferme des matériaux de remplissage de filons et d'espaces libres dans une gangue de calcite et de barytine; elle est principalement d'âge mississippien. La minéralisation est restreinte aux filons se trouvant dans des couches moins perméables du Cambrien et de l'Ordovicien et a tendance à remplir les espaces libres dans les roches plus perméables du Mississippien.

---

[1] Contribution to the Canada-Newfoundland Mineral Development Agreement 1984-89. Project carried by Geological Survey of Canada, Economic Geology and Mineralogy Division, Project 650056.

[2] Department of Earth Sciences, Memorial University of Newfoundland, St. John's, Newfoundland A1B 3X5

Introduction

This report concerns fieldwork carried out during the summer of 1985 under contract between Canewf Resources Ltd. and the Geological Survey of Canada. The objectives of the field component of the project were as follows.

1. Document relevant qualitative and quantitative information concerning the selected mineral occurrences/showings in the study area (Fig. 26.1) and record the following information.

   i) Unique identification code or number.

   ii) Exact location.

   iii) Lithological description, strike and dip and formation name(s) of host rocks.

   iv) Detailed description of the nature of mineralization.

   v) Detailed description of the observed minerals.

   vi) Detailed description of any diagnostic features such as zoning, alteration or any unique textural relationships.

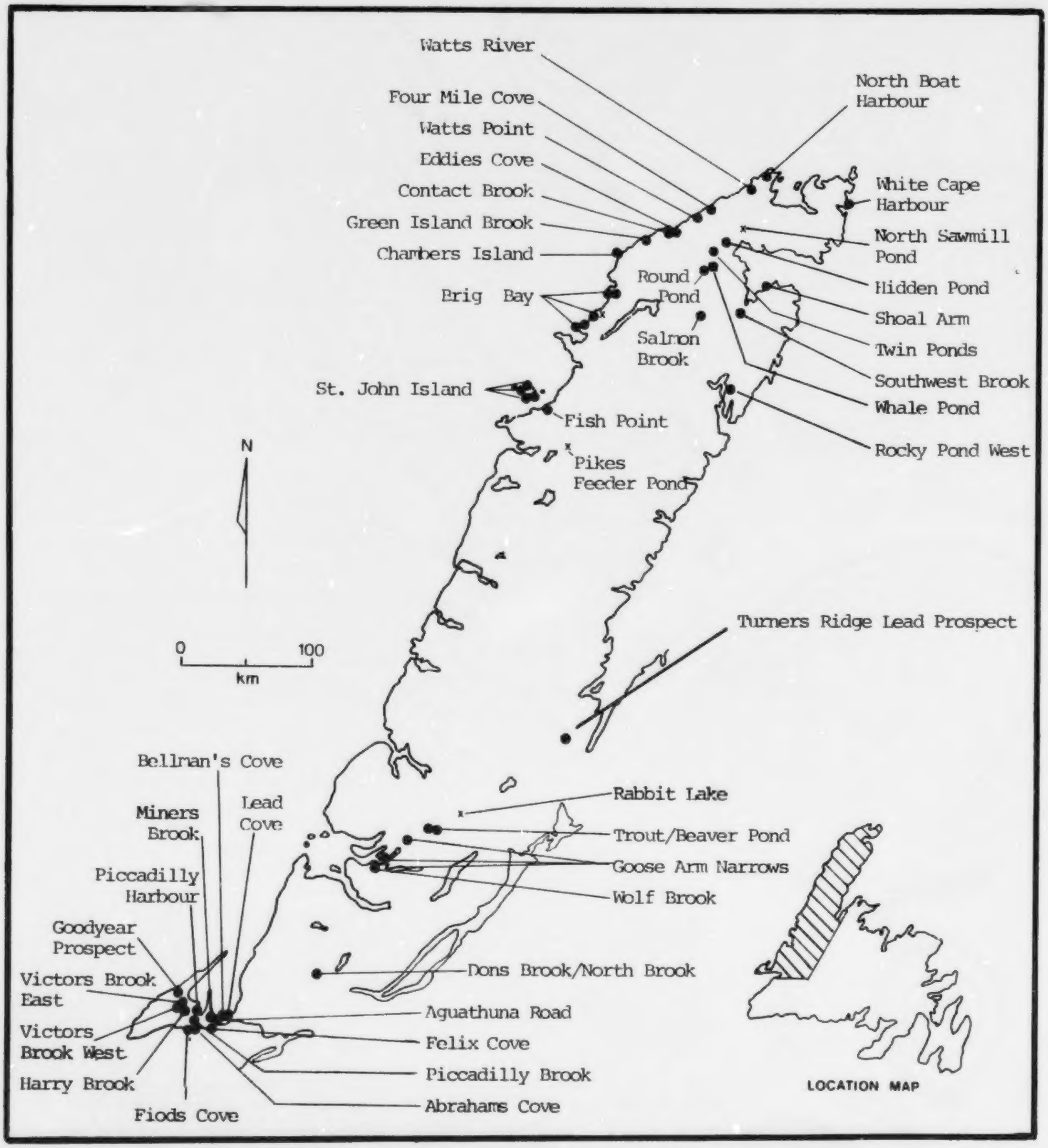

***Figure 26.1.** Mineral occurrences studied in this project. Dots show occurrences sampled, crosses show occurrences not sampled due to inaccessibility or non-availability of core.*

vii) Strike and dip of the mineralized zone.

viii) Physiographic description and a detailed geological sketch map of the occurrence.

2. Collect and document rock samples from selected mineral occurrences/showings (Fig. 26.1).

General geology

The generalized stratigraphy of the autochthonous carbonate platform of western Newfoundland is summarized in Table 26.1. The March Point Formation, of upper Middle Cambrian age, is the oldest unit of concern to this study. It consists of bioturbated, dolomitized micritic limestone, locally with a basal unit of grey shale and rusty weathering sandstone (Knight, 1977). The burrows tend to be preferentially dolomitized, but near the top of the formation bioturbation is less frequent and dolomitization is well developed throughout (Knight, 1977). Fossils in the formation are brachiopods, trilobites and gastropods. The formation was laid down in a predominantly subtidal low energy environment (Knight, 1977).

The Petit Jardin Formation, of Upper Cambrian age, overlies the March Point Formation. Knight (1980) has divided it into four members; in ascending stratigraphic order they are: Lower Dolostone Member, Stromatolite Member, Upper Dolostone Member and Cherty Dolomite Member. Thinly-stratified dolostones, dolomitic shales, mottled dolostones, stromatolitic dolostones and intraclastic and oolitic dolarenites are commonly found throughout the formation (Knight, 1980). The Stromatolite Member contains large flat domal stromatolites up to one metre high and two or more metres across (Knight, 1977). The Lower Dolostone Member contains trilobites and inarticulate brachiopods (Knight, 1977). Shallow water features such as mudcracks, mudflake breccias, ripple marks and crossbedding are common, and suggest that the formation was deposited mainly in a shallow water carbonate flat environment during a regression (Knight, 1980).

The Watts Bight Formation (Table 26.1) consists mainly of dark grey to black coarsely crystalline stromatolitic dolostone which was originally a bioturbated lime mud with large stromatolite mounds (Knight, 1978; 1980). A horizon of micritic and dolomitic limestone occurs in the middle of the formation. Coiled gastropods and orthocone cephalopods are abundant (Knight, 1977). The Watts Bight Formation was deposited during a transgressive period, for the most part in relatively deep quite water (Knight, 1977).

The overlying Boat Harbour Formation represents a return to shallower water conditions. The lower part of the formation consists of shallowing upwards sequences containing bioturbated lime mudstone, and thinly laminated dolostone. This is overlain by bioturbated lime mudstone with abundant stromatolites (Knight, 1980). Dolomite pseudobreccia locally replaces bioturbated limestone (Knight, 1978). A pebble bed near the top of the formation represents a widespread sedimentological and faunal break (Knight, 1978). Fauna include conodonts and abundant trilobites.

The Catoche Formation is composed dominantly of extensively bioturbated, well bedded blue-grey micritic limestone. Fossils are abundant and include trilobites, brachiopods, ostracods, gastropods, cephalopods and sponges (Knight, 1977). Locally, small sponge "patch" reefs and stromatolite-sponge mounds are developed (Knight, 1977, 1980). The formation was deposited in a subtidal shelf environment during a transgressive period. The upper part of the Catoche Formation is intensively dolomitized. White dolomite spar pseudobreccia and dolomite collapse breccia zones (described in more detail below) are common. These host the Newfoundland Zinc deposit.

The overlying Aguathuna Formation consists of thinly laminated siliceous dolostones and shales which formed in a carbonate flat environment (Knight, 1980). Macrofossils are absent but conodonts have been used to date the formation as Lower Ordovician (Stouge, 1982).

The Middle Ordovician Table Head Group has been divided into the Table Point, Table Cove, Black Cove and Cape Cormorant Formations (Klappa et al., 1980). The Table Point Formation, of most concern to this study, consists of bioturbated, rubbly weathering, massive grey limestones and zones of interbedded limestone-dolostone (Klappa et al., 1980). Fossils include ostracods, gastropods, orthocone cephalopods, trilobites, bryozoa and brachiopods (Klappa et al., 1980; James and Stevens, 1982).

Table 26.1. Generalized stratigraphy of western Newfoundland (after Knight, 1977, 1978, 1980; Klappa et al., 1980; James and Stevens, 1982; and Stouge, 1982)

AGE	GROUP	FORMATION
Mississippian	Codroy Group	
---unconformity---		
Middle Ordovician	Table Head Group	Cape Cormorant Fm. Black Cove Fm. Table Cove Fm. Table Point Fm.
Lower Ordovician	St. George Group	Aguathuna Fm. Catoche Fm. Boat Harbour Fm. Watts Bight Fm.
Upper Cambrian Middle Cambrian	Port au Port Group	Petit Jardin Fm. March Point Fm.
Cambrian	Lower Group	Labrador Hawke Bay Fm. Forteau Fm. Bradore Fm.

Results

Occurrences which were examined and sampled are shown in Figure 26.1. Each occurrence was assigned a National Mineral Inventory number (e.g. 12B/9-Pb001). The first part of this number denotes the National Topographic Survey code for the 1:50 000 scale map on which the occurrence is located. In some instances (e.g. Eddies Cove, East Trenches, and Twin Ponds Quarry) where the particular occurrence visited is not listed with the NMI, it was assigned the NMI code for the nearest listed occurrence. The status given each occurrence is that assigned by the NMI with a few changes based on observations made during this study. Status categories are as follows: 1. Producer; 2. Developed prospect; 3. Past producer – dormant; 4. Past producer – exhausted; 5. Prospect; 6. Showing; 7. Indication.

The occurrences can be grouped into two basic types:

I) "Mississippi Valley type" open space filling associated with secondary white dolomite and

II) Vein/open space filling associated with calcite with or without barite.

Within type I there exists a gradation between two end-members: (a) mineralization restricted to fractures, veinlets, small clots and disseminations in low porosity/permeability dolostones predominantly of Cambrian age. (b) mineralization found in open spaces and in the matrix to dolomite pseudobreccias and collapse breccias developed in predominantly Ordovician strata. Type II can be further subdivided into three categories: (a) vein/open space-filling mineralization hosted by Mississippian rocks of the Codroy Group, which are characterized by high porosity and permeability; (b) vein mineralization hosted by relatively impermeable Cambro-Ordovician rocks of the Port au Port, St. George or Table Head groups, but of the same age and type as (a) and part of the same overall mineralizing system; (c) vein mineralization of unknown age or affinity. As space is too limited for descriptions of all occurrences, only representative examples of each type are presented.

Type Ia

Type Ia occurrences are those that show similarities to the mineralization at the Newfoundland Zinc Mine, Daniels Harbour, especially the association of sphalerite with dolomite pseudobreccia zones. "Pseudobreccia" (Cumming, 1968) is a term given to a distinctive rock developed in burrowed lime mudstone (Knight, 1980) which contains 5 to 80% white dolomite spar (Lane, 1984). The dolomite spar in part replaces original dolostone or limestone and in part fills open spaces formed by in situ dissolution of the original rock (Crossley and Lane, 1984). Relict isolated rounded patches of dolostone resemble breccia fragments, hence the term "pseudobreccia". True spar breccias (collapse breccias) are also associated with the ore at Daniels Harbour (Lane, 1984). These breccias are characterized by angular fragments, commonly only slightly rotated, set in a white dolomite spar matrix, and are formed by disruption of strata due to faulting or collapse as a result of dissolution (Lane, 1984). Stratabound true spar breccias occur on a small scale; these are cogenetic with pseudobreccias. Large (10-30 m by 100 m) linear spar breccias which crosscut the stratigraphy are generally later than the pseudobreccias (Lane, 1984). The white dolomite spar found in both types of breccia represents the latest phase of dolomitization in the diagenetic history of the rocks (Haywick and James, 1984). The sphalerite generally precedes the white dolomite spar and tends to line fragments in both pseudobreccia and collapse breccia. It also occurs as botryoidal growths filling cavities in pseudobreccia (Crossley and Lane, 1984). The ore-bearing horizons occur within the upper 50 m of the Lower Ordovician Catoche Formation.

The Salmon River #6 showing, 12P/1-Zn006, (Fig. 26.2a) exhibits many similarities to the mineralization at the Daniels Harbour deposit. Sphalerite and galena occur as clots and disseminations in dolomite pseudobreccia zones which are developed in grey micritic limestone of the Catoche Formation. Contacts between the limestone and the pseudobreccia zones are abrupt and irregular. The "fragments" in the pseudobreccia are fine grained black dolostone. Sphalerite ranges from green to yellow to red. At one trench green sphalerite forms clots up to 4 cm and forms up to 20% of the rock. At another trench fine grained yellow sphalerite is disseminated in black dolostone and red sphalerite crystals up to 3 mm are associated with clots of calcite spar. Locally, galena in aggregates up to 3 cm is found with the sphalerite. At Daniels Harbour red sphalerite and calcite generally occur late in the paragenesis (T. Lane, personal communication, 1985).

At St. John Island (12I/14-Zn004) white dolomite spar pseudobreccia zones replace Middle Ordovician Table Point Formation limestone (Fig. 26.2b). The spar zones take the form of vertical pillars with an overall trend of about 60°. The contact between the limestone and the pseudobreccia is characterized by a 10-20 cm border of brown porous dolostone. "Fragments" in the pseudobreccia are fine grained black dolostone. Reddish-brown to yellow sphalerite occurs as 1-2 cm botryoidal clots filling voids within the pseudobreccia. Minor galena occurs as 1 mm cubes. Calcite spar locally fills voids in the pseudobreccia.

Type Ib

Type Ib mineralization is found in Cambrian dolostones of the March Point and Petit Jardin formations. It consists of sphalerite and galena occurring on a relatively limited scale as clots, disseminations, veinlets and fracture coatings with associated white dolomite spar which tends to form 1-3 cm rounded clots. Minor quartz tends to be associated with the dolomite especially in the Petit Jardin Formation. The host rocks are typically massive dolostones with no development of pseudobreccia or collapse breccia. A gradation does, however, exist between this end-member and the Type Ia end-member. The gradation is exhibited by such features as local and/or poor development of pseudobreccia and collapse breccia in Cambrian rocks, e.g. at Green Island Brook #1 and Chambers Island.

The occurrences at Eddies Cove East are hosted by Cambrian rocks of the March Point and Petit Jardin Formations. Several occurrences in the area were examined. The area was trenched and drilled by Cominco in 1979. In the area of the trenches, 12P/8-Pb002 (not shown) galena occurs as clots and in thin (<0.5 cm) veinlets with white dolomite spar. The host rock is bluish-grey very fine grained thinly laminated dolostone of the Petit Jardin Formation. The occurrences along Eddies Cove Brook, 12P/8-Zn004, Zn005 and Zn006, (Fig. 26.3a) consist of sphalerite and/or galena, hosted by fine- to medium-grained black dolostone of the March Point Formation. The sphalerite occurs intergrown with white dolomite in 1 cm rounded clots. Galena occurs in clots and veinlets with white dolomite spar. At North Eddies Cove, 12P/8-Pb001 (not shown) no mineralization was found, but white dolomite spar occurs in 1 to 2 cm rounded clots. At all of the Eddies Cove occurrences the dolostone is massive and there is little development of pseudobreccia or secondary porosity. White dolomite spar is restricted to thin veinlets and 1 to 2 cm clots, as is mineralization which is sparse and is associated with the dolomite.

The Green Island Brook occurrences, (Green Island Brook 1, 3 and 4) 12P/7-Zn002, Zn004 and Pb001 also occur in black to brown very fined grained dolostones of the March Point Formation. At Green Island Brook 1 (not shown) the occurrence has characteristics intermediate between Type Ia and Ib, i.e. there is local development of dolomite pseudobreccia. Sphalerite occurs as 1 mm greenish crystals disseminated in a small area of the outcrop. Minor disseminated pyrite occurs with the sphalerite. The host rock is black fine grained dolostone with poorly developed pseudobreccia texture. Very fine grained (< 1 mm) crystals of white dolomite are disseminated through the black dolostone. The other two Green Island Brook occurrences, 3 and 4 are most typical of the Type Ib end-member. At these occurrences sphalerite occurs in sparse rounded dolomite-quartz clots in fine grained, bioturbated, dark brown dolostone. Rare galena occurs as disseminated 0.5 mm cubes and as fracture coatings. Minor calcite is found in some of

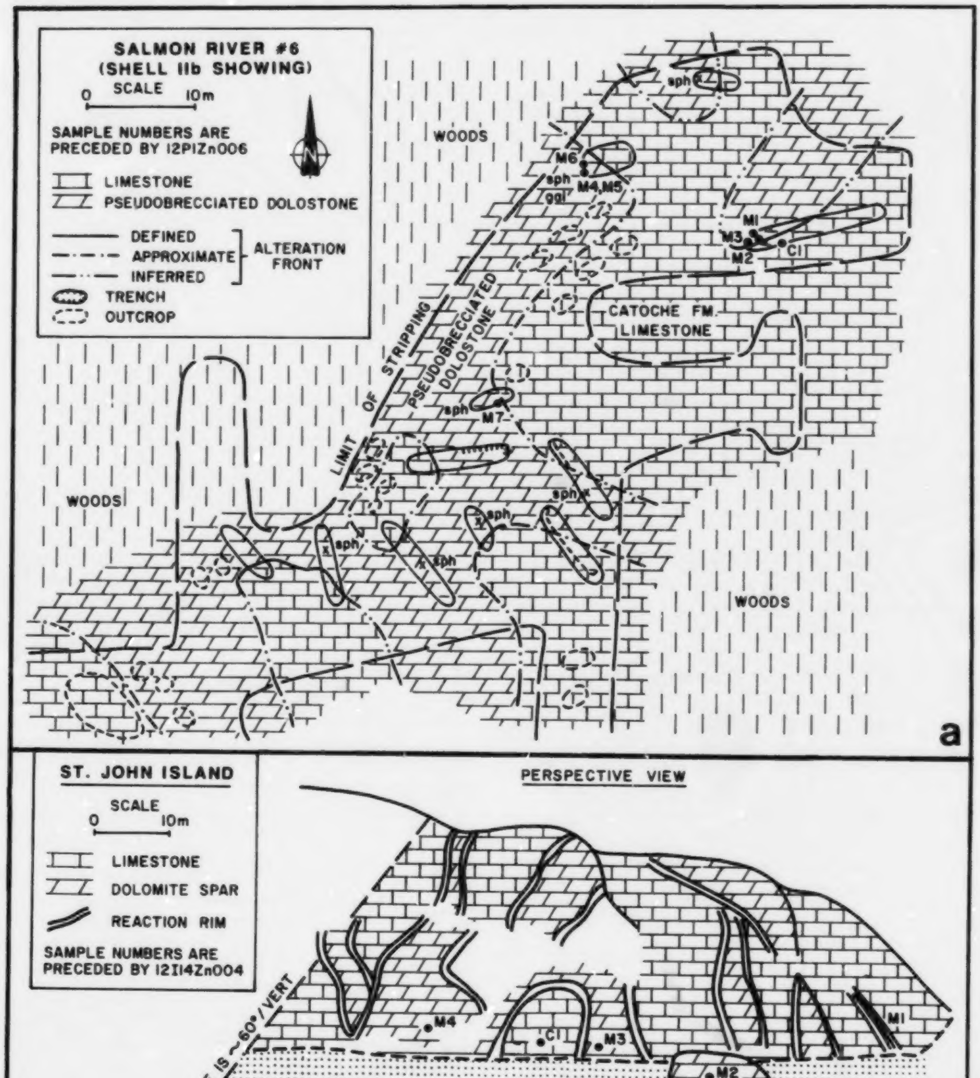

Figure 26.2. *a. Plan view of trenches at Salmon River 6 showing, hosted by the Catoche Formation. b. Perspective view of dolomite spar pillars cutting Table Point Formation at St. John Island showing.*

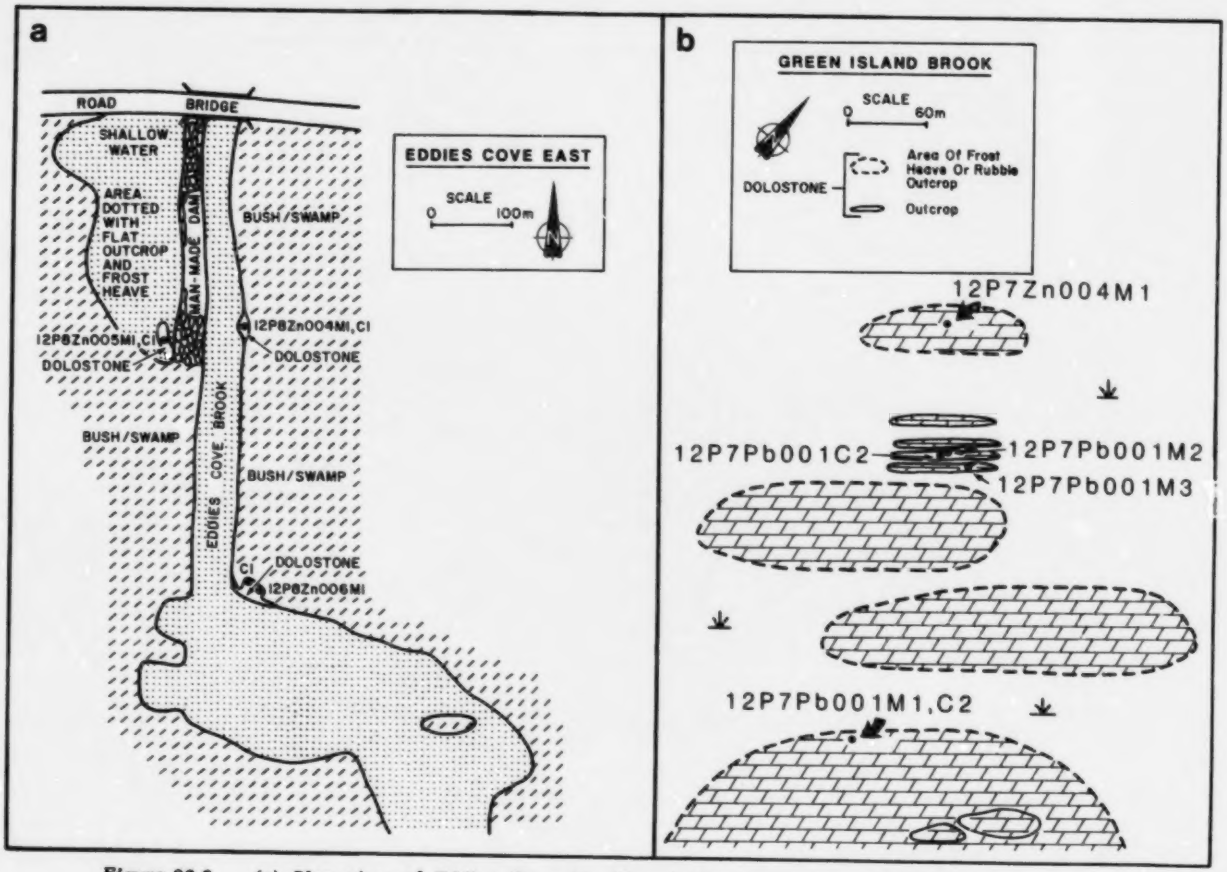

Figure 26.3. *(a) Plan view of Eddies Cove 11, 12 and 13 occurrences. (b) Plan view of Green Island Brook 3 and 4 occurrences. Host unit for both areas is the March Point Formation.*

the gangue clots. Zoning is dolomite-calcite-quartz. Sphalerite is found in the centre of clots and appears to postdate the dolomite.

Type II

Type II occurrences are vein/open space filling mineralization associated with calcite plus or minus barite. These can be subdivided into three subgroups as described previously. All occurrences of Type IIa and IIb are found on the Port Au Port Peninsula. Type IIc occurrences are found over a wide area, from the Dons Brook area between Stephenville and Corner Brook to White Cape Harbour at the tip of the Great Northern Peninsula.

Type IIa

The mineralization at Lead Cove, Bellmans Cove, Aguathuna Quarry, Miners Brook and, in part, at Piccadilly Brook occurs as open-space fillings and replacements in Codroy Group limestones which occur in north-trending paleokarst valleys. The Codroy Group unconformably overlies Table Head Formation limestone at these localities. The limestone is in places brecciated and consists of angular limestone fragments up to several centimetres long set in a micritic matrix which is commonly replaced by calcite spar. The limestones are very fossiliferous and contain brachiopods, gastropods and oncolites. Marcasite, galena, sphalerite, pyrite, calcite and barite fill voids and surround limestone fragments and fossils replacing a micritic matrix. Mineralization also occurs in 1-10 cm wide, generally vuggy veins which are randomly oriented. Most veins are zoned, but the zoning varies for each occurrence.

At Bellmans Cove, 12B/10-Pb003 (Fig. 26.4a) mineralization in the Codroy Group consists of pyrite, marcasite and sphalerite associated with calcite and barite. Sphalerite is found on the east side of the cove in vugs with calcite and less commonly with marcasite and barite. It occurs as black euhedral to subhedral crystals up to 2 cm across. Marcasite is abundant especially near the unconformable contact between the Codroy Group and the Table Head Group where a heavy gossan is developed. Here marcasite and calcite spar surround limestone breccia fragments and, in places, completely replace the matrix. Marcasite forms up to 30% of the rocks. On the west side of the cove pyrite is the dominant sulphide and sphalerite was not found. Pyrite occurs as massive lenses up to 40 x 20 cm in vugs. It also occurs in veins with calcite and barite. Zoning is pyrite-calcite-barite. No galena was found on either side of the cove.

At Lead Cove, 12B/10-Pb002 (Fig. 26.4b) galena and marcasite occurs in veins and vugs in brecciated Codroy Group limestone. Zoning is marcasite-galena-calcite or marcasite-calcite or galena-calcite. Galena-calcite veins cut disseminated marcasite mineralization. Minor barite was found in vuggy coarsely crystalline calcite veins. Marcasite replaces the matrix surrounding oncolites and is found surrounding limestone fragments. No sphalerite was found.

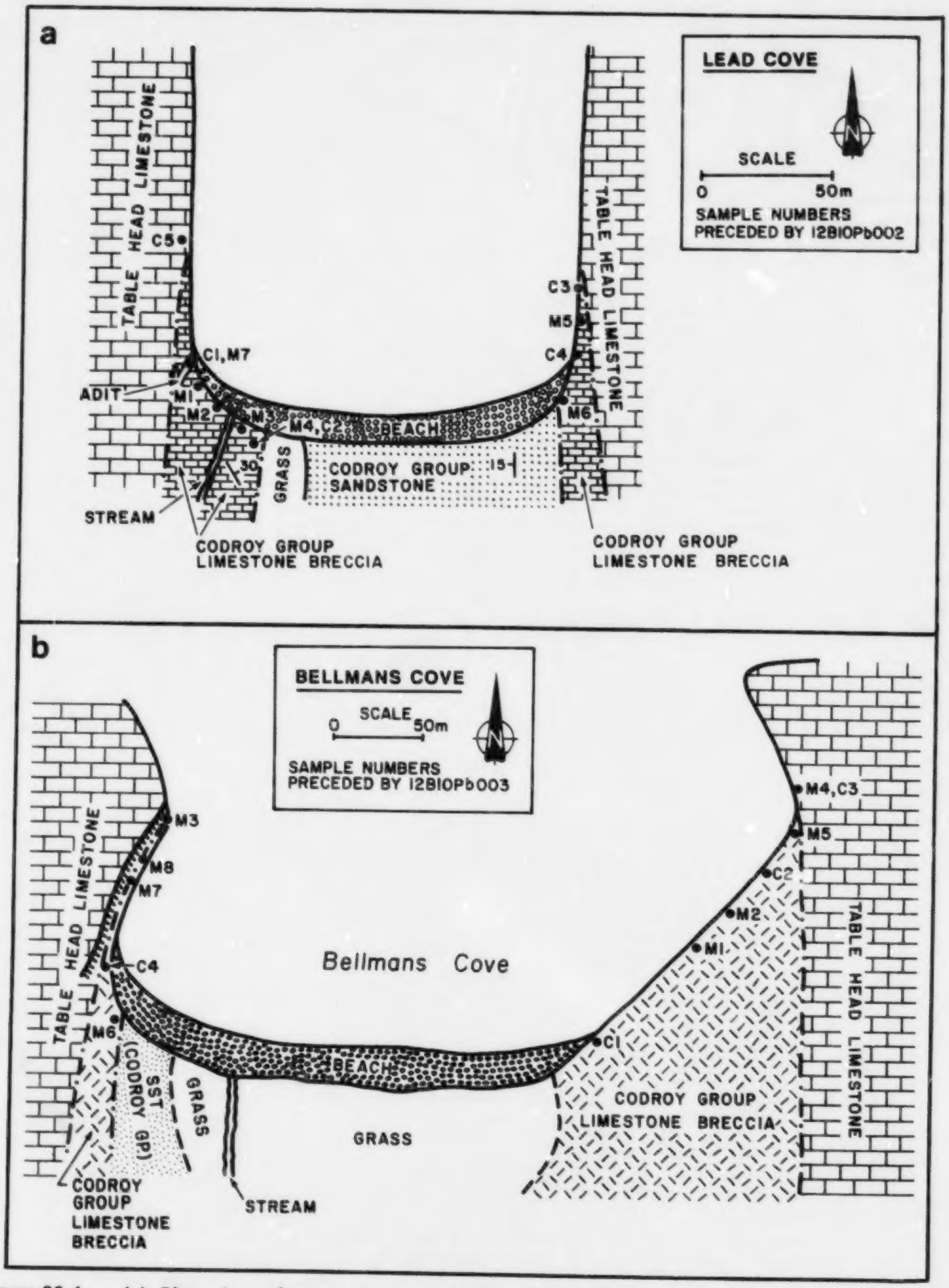

Figure 26.4. *(a) Plan view of showing at Lead Cove. (b) Plan view of showing at Bellmans Cove. Host unit for both areas is the Codroy Group.*

Type IIb

Type IIb mineralization takes the form of vertical to subvertical calcite veins which cut through limestones of the Port au Port, St. George and Table Head groups. At Piccadilly Harbour and the Goodyear Prospect, where these veins cut the Table Head Group, they contain abundant galena, sphalerite and marcasite. Veins which cut Port au Port and St. George Group limestone at Felix Cove, Abrahams Cove and Fiods Cove are barren or contain minor mineralization. The veins are commonly cored by voids lined with dogtooth calcite spar and in places minor barite. They appear to have been emplaced along pre-existing faults or zones of weakness. The overall mineralogy of the veins suggests that they may be of the same age and type as the mineralization hosted by Codroy Group rocks (Type IIa).

At Piccadilly Harbour, 12B/10-Pb001, (Fig. 26.5a) a swarm of heavily mineralized calcite veins cuts through Table Head limestone. Veins strike from 100 to 130°. Mineralization includes coarse blue galena (cubes and rounded crystals up to 1 cm), euhedral 1 mm dark blue to black sphalerite crystals, brown anhedral sphalerite, marcasite,

and minor bladed pink barite. Zoning in the largest vein (about 10 cm wide) is as follows: calcite-marcasite-calcite-intergrown galena + brown sphalerite-calcite-intergrown marcasite, black and blue sphalerite and galena. Smaller veins are zoned as calcite-intergrown marcasite, sphalerite, galena, or calcite-marcasite. Other veins contain only calcite. One calcite-marcasite-barite vein was sampled.

At Fiods Cove, 12B/10-Pb005, (Fig. 26.5b) vertical to subvertical calcite veins cut limestone of the St. George Group. They strike 85 to 110°. Most veins contain only calcite – variably coloured and cored by dogtooth calcite veins. One such vein is cored by bladed marcasite crystals. Codroy Group limestone boulder conglomerates occur in several paleokarst valleys. These conglomerates contain limestone boulders up to 1.5 m across, set in a red muddy matrix. They are not heavily mineralized, in contrast to Codroy Group rocks at Lead Cove and Bellmans Cove. They are, however, cut by calcite veinlets indicating that the veinlets postdate the conglomerate formation.

Type IIc

Type IIc veins are widespread and differ from each other in mineralogy. The vein at Dons Brook, 12B/9-Pb001, contains black resinous anhedral sphalerite and minor galena

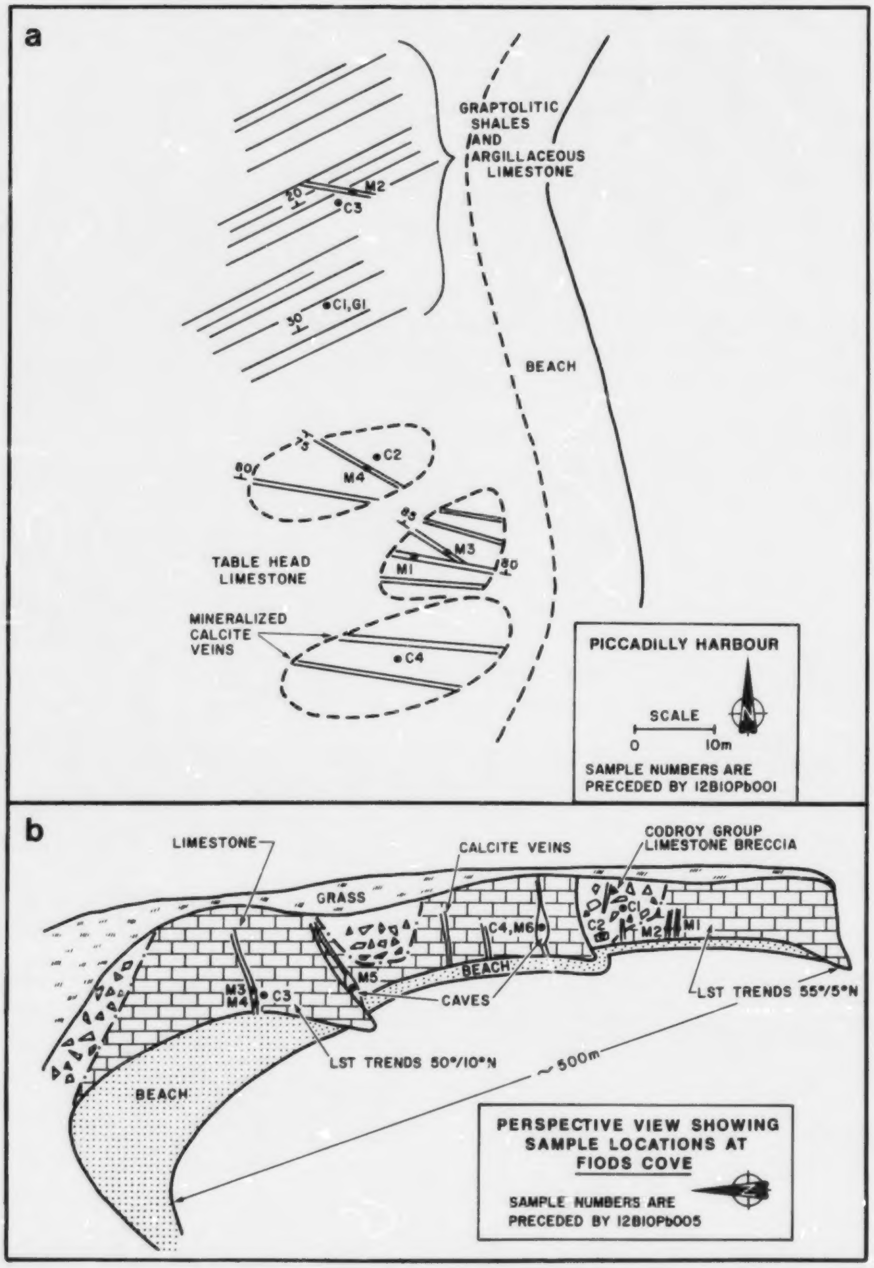

Figure 26.5. (a) Plan view of showing at Piccadilly Harbour; mineralized calcite veins cut Table Head Group. (b) Perspective view of occurrence at Fiods Cove; mineralized calcite veins cut limestone of St. George Group.

in a gangue of quartz and calcite. At Wolf Brook, 12H/4-Pb003, the vein is zoned galena-sphalerite-calcite and resembles the veins at Piccadilly Harbour. At Goose Arm Brook, 12H/4-Pb003, a crusty pyrite gossan zone outcrops. Only minor sphalerite was found in calcite veins, but there are reports of abundant galena and sphalerite vein mineralization. These three showings are found in Cambrian rocks of the Petit Jardin Formation and the largely equivalent Hughes Brook Formation. It is possible that these veins may be part of the widespread post-Mississippian mineralizing system that affected the Port au Port Peninsula, but at the present time there is no conclusive evidence for or against this idea.

The other Type IIc veins outcrop on the Great Northern Peninsula. At Shoal Arm Island, 2M/4-Zn001, calcite veins up to 30 cm thick cut limestone of the Table Head Group. Minor sphalerite has been reported from these veins, but none was found during this study. At White Cape Harbour, 2M/11-Zn001, mineralized veins were reported to cut Table Head limestones on a small island in the harbour. The outcrop on this island is highly deformed argillite and sandstone, possibly of the Goose Tickle Formation. Numerous barren quartz-calcite veins cut these rocks.

Conclusions

Lead-zinc occurrences in autochthonous carbonate rocks of western Newfoundland can be grouped into two broad types. Type I occurrences are "Mississippi Valley type" open space filling associated with secondary white dolomite. Within type I there exists a gradation between two end-members: (a) mineralization found in open spaces and in the matrix to dolomite pseudobreccias and collapse breccias developed in predominantly Ordovician strata. (b) mineralization restricted to fractures, veinlets, small clots and disseminations in low porosity/permeability dolostones predominantly of Cambrian age; Type II occurrences are vein/open space filling associated with calcite plus or minus barite. These can be further subdivided into three categories: (a) vein/open space-filling mineralization hosted by Mississippian rocks of the Codroy Group, which are characterized by high porosity and permeability; (b) vein mineralization hosted by relatively impermeable Cambro-Ordovician rocks of the Port au Port, St. George and Table Head groups, but of the same age and type as (a) and part of the same overall mineralizing system; (c) vein mineralization of unknown age or affinity.

Acknowledgments

We are grateful to D.F. Sangster, Geological Survey of Canada, for suggesting this study, and I. Knight of the Newfoundland Department of Mines and Energy for sharing his knowledge of the carbonates of western Newfoundland. S. Cochrane of the Newfoundland Department of Mines and Energy assisted in the sampling of drill core at the Core Storage Facility in Pasadena. Geologists from exploration companies including Brinco, Teck, Noranda and Westfield gave permission for sampling of core from various showings. C. Anstey provided valuable field assistance.

References

Crossley, R.V. and Lane, T.E.
1984: A Guide to the Newfoundland Zinc Mines Limited ore bodies, Daniels Harbour; in Mineral Deposits of Newfoundland – 1984 Perspective, ed. H.S. Swinden; Newfoundland Department of Mines and Energy, Report 84-3, p. 45-51.

Cumming, L.M.
1968: St. George-Table Head disconformity and zinc mineralization, western Newfoundland; Canadian Institute of Mining and Metallurgy, Bulletin, v. 61, p. 721-725.

Haywick, D.W. and James, N.P.
1984: Dolomites and dolomitization of the Lower Ordovician St. George Group of western Newfoundland; in Current Research, Part A, Geological Survey of Canada, Paper 84-1A, p. 531-536.

James, N.P. and Stevens, R.K.
1982: Anatomy and evolution of a Lower Paleozoic continental margin, western Newfoundland; Eleventh International Congress on Sedimentology, Field Excursion Guidebook 2B, 75 p.

Klappa, C.F., Opalinski, P.R., and James, N.P.
1980: Middle Ordovician Table Head Group of western Newfoundland: A revised stratigraphy; Canadian Journal of Earth Sciences, v. 17, p. 1007-1019.

Knight, I.
1977: The Cambrian-Ordovician platformal rocks of the Northern Peninsula; Newfoundland Department of Mines and Energy, Report 77-6, 27 p.

1978: Platformal sediments on the Great Northern Peninsula: stratigraphic studies and geological mapping of the North St. Barbe district; Newfoundland Department of Mines and Energy, Report 78-1, p. 140-150.

1980: Cambro-Ordovician carbonate stratigraphy of western Newfoundland; sedimentation, diagenesis and zinc-lead mineralization; Summary of a paper given at the 82nd Annual General Meeting of the Canadian Institute of Mining and Metallurgy, Toronto, Ontario, April 20-24, 1980, Newfoundland Department of Mines and Energy, Open File NFLD. 1154, 34 p.

Lane, T.E.
1984: Preliminary classification of carbonate breccias, Newfoundland Zinc Mines, Daniels Harbour, Newfoundland; in Current Research, Part A, Geological Survey of Canada, Paper 84-1A, p. 505-512.

Stouge, S.
1982: Preliminary conodont biostratigraphy and correlation of Lower to Middle Ordovician carbonates of the St. George Group, Great Northern Peninsula, Newfoundland; Newfoundland Department of Mines and Energy, Report 82-3, 59 p.

Preliminary results of a study of the ores, wall-rock alteration, and fluid inclusions at the Madeleine copper mine, Gaspé, Quebec[1]

Contract 14SQ.23233-3-1966

A.E. Williams-Jones[2], I.M. Samson[3], and R.L. Linnen[2]

Williams-Jones, A.E., Samson, I.M., and Linnen, R.L., Preliminary results of a study of the ores, wall-rock alteration, and fluid inclusions at the Madeleine copper mine, Gaspé, Quebec; in Current Research, Part A, Geological Survey of Canada, Paper 86-1A, p. 239-249, 1986.

Abstract

The Madeleine mine exploited stockwork copper ores in biotite hornfels adjacent to the McGerrigle Mountains granitic complex, Gaspé. The deposit is zoned from bornite in the core to chalcopyrite-pyrrhotite at the edge.

The mineralization is in quartz-biotite veins or sulphide stringers associated with local biotitization and, less commonly, in calc-silicate veins. Muscovite-chloritic alteration and veining and later quartz-carbonate veining postdated the main mineralizing event.

High salinity Na-K-Fe-Ca-bearing fluids with temperatures $\geq$350°C dominated the ore stage. CO_2/CH_4 fluids were important in calc-silicate veins. Lower salinity, lower temperature fluids circulated during muscovite-chlorite alteration and veining. High salinity fluids were also present during late quartz-carbonate veining.

A model is presented tracing the evolution of the hydrothermal system from an early orthomagmatic and synmetamorphic ore stage to postmetamorphic, meteoric water-dominated stages. Explanations for the sulphide zonation involve increasing water/rock ratios into the deposit and/or a sedimentary source for iron and sulphur.

Résumé

Dans la mine Madeleine, on a exploité des minerais de cuivre en stockwerk, logés dans des cornéennes à biotite adjacentes au complexe granitique des monts McGerrigle, à Gaspé. Le gisement est zoné; du noyau de bornite, on passe à de la calcopyrite et pyrhotite en bordure.

La minéralisation se trouve dans des filons de quartz et biotite ou dans des veinules de sulfure associés à une biotisation locale et, moins souvent, dans des filons de silicate calcaire. L'altération en muscovite et chlorite et la formation de filons de ces minéraux, ainsi que plus tard la formation de filons de quartz et de carbonate, sont plus récentes que la minéralisation principale.

Des fluides de forte salinité, contenant du Na-K-Fe-Ca et dont les températures atteignent $\geq$350°C, ont dominé la phase de formation du minerai. Des quantités importantes de fluides de CO_2/CH_4 occupaient des filons de silicate calcaire. Des fluides de plus faible salinité et à plus faible température ont circulé pendant la phase d'altération en muscovite et chlorite et de formation de filons de ces minéraux. Il y avait aussi des fluides de forte salinité pendant la formation des derniers filons de quartz et de carbonate.

Les auteurs présentent un modèle qui retrace l'évolution du système hydrothermal à partir d'une première phase orthomagmatique et synmétamorphique jusqu'à des phases postmétamorphiques, dominées par l'eau météorique. Ils expliquent la zonation des sulfures par l'accroissement des rapports eau/roche dans le gisement ou par la présence d'une source sédimentaire de fer et de soufre, ou les deux.

---

[1] Contribution to the Canada Economic Development Plan for Gaspé and Lower St. Lawrence Mineral Program 1983-88. Project carried by Geological Survey of Canada, Economic Geology and Mineralogy Division, Project 650056.

[2] Department of Geological Sciences, McGill University, Montreal, Quebec H3A 2A7

[3] Mineral Exploration Research Institute, P.O. Box 6079, Sta. A, Montreal, Quebec H3C 3A7

Introduction

The Madeleine copper deposit is a small bornite/chalcopyrite stockwork located within the contact metamorphic aureole of the late Devonian McGerrigle Mountains granitic complex (Fig. 27.1). The deposit contained approximately 8.7×10^6 tonnes of ore grading 1.15% Cu and 7 gm/tonne Ag, and was mined from 1969 until 1982.

This study of the Madeleine mine is part of a larger project designed and funded by the Federal Government to investigate the metallogeny of the Gaspé region, Quebec. The work was carried out under a contract administered by the Mineral Exploration Research Institute, Montreal.

Geological setting

The mineralization occurs as an en echelon array of five, steeply plunging, chimney-shaped orebodies that are located within 200 m of the main McGerrigle intrusive mass. The orebodies, which are all hosted by metasediments, intersect bedding at a low angle and bottom out against the intrusion at depth (Fig. 27.2).

Over 80% of the ore was contained in the Main orebody which is hosted by a 100 m thick biotite-cordierite hornfels (Main Hornfels). One other orebody is hosted by this unit and the remainder by the compositionally similar 75 m thick Footwall Hornfels that lies 30 m stratigraphically below the Main Hornfels. Both units contain thin calc-silicate hornfels beds (2-5 cm) and thicker lenticular marble beds (0.1-1.5 m). The mine succession represents part of the Cambro-Ordovician Quebec Group and underwent deformation and low grade regional metamorphism during the Taconic and Acadian orogenies prior to its hornfelsing by the McGerrigle intrusive complex.

Intrusive rocks are, with the exception of a few dykes, restricted to the confines of the McGerrigle pluton and mainly comprise older mafic inclusion-rich syenites and granodiorites in the north and younger granites, monzonites and granodiorites in the south. The complex also contains three small bodies of nepheline syenite, and numerous late felsic, pegmatitic and diabasic dykes.

The ores

Introduction

The mineralization occurs mainly as closely spaced sulphide and quartz-sulphide veins and stringers (1 mm to 1 cm thick) and less commonly as blebby disseminations. The veins and stringers are of several generations as evidenced by their degree of deformation, crosscutting relationships and by their vein and alteration minerals. Early veins are commonly folded and boudinaged and are cut by later planar veins.

Biotite veins

The earliest veins and stringers are characterized by the mineral assemblages quartz-biotite ± sulphide ± feldspar ± tourmaline and sulphide ± biotite. These veins occur both within, and obliquely to, the plane of the principal foliation (Fig. 27.3a). Many veins are boudinaged and most are only continuous over a few centimetres. A small number of sulphide stringers were observed to be flattened as part of the foliation about cordierite porphyroblasts or cut by cordierite porphyroblasts (Fig. 27.3b). These veins are of particular interest as they suggest that this veining event occurred prior to, or synchronous with, the contact metamorphism. Most of the minerals in the early veins have been altered. The most common indications of this are the replacement of biotite by chlorite or muscovite and the sericitization of feldspar. In some cases later mineral assemblages, e.g. chlorite-calcite, occur along microfractures within the veins. These microfractures also appear to have acted as sites for the precipitation/remobilization of the sulphide minerals (Fig. 27.3c). Such precipitation/remobilization does not, however, appear to have changed the nature of the original sulphide assemblages.

Calc-silicate veins

Biotite veins are succeeded by veins containing the assemblage quartz-tremolite-epidote ± diopside ± calcite ± sulphides. Additional minerals that occur in the calc-silicate veins are calcite, muscovite, biotite, sphene, and apatite. These veins are quite similar in their form and mode of occurrence to the biotite veins but postdate them. They are also commonly chloritized and/or sericitized.

Muscovite-chlorite veins

Veins containing the assemblages quartz-muscovite ± chlorite ± sulphides ± calcite and quartz-chlorite ± muscovite ± calcite ± sulphides are the most widely encountered in the deposit. Most of these represent early biotite veins in which biotite has been replaced by chlorite or muscovite. Some are later veins in which the above minerals were precipitated directly from solution. These later veins are generally planar and commonly cut the earlier biotite and calc-silicate veins.

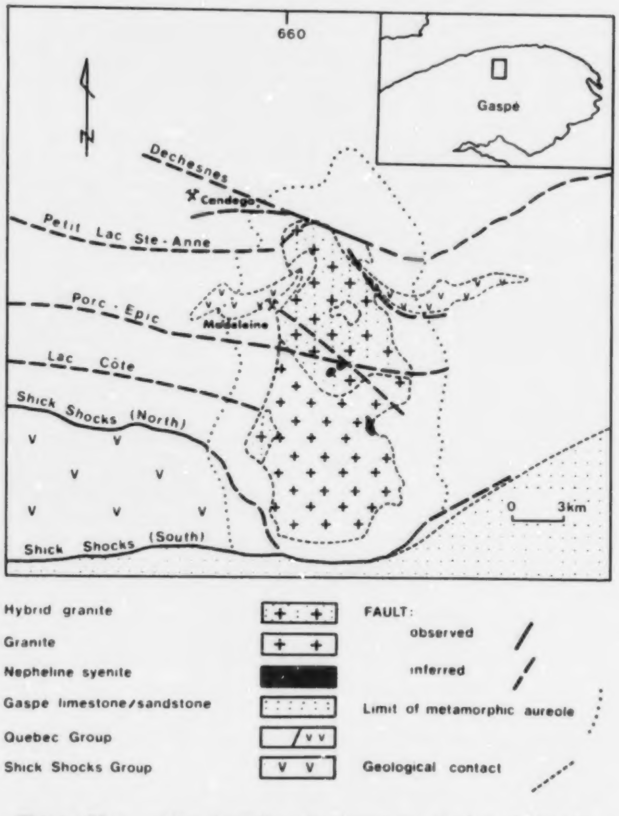

Figure 27.1. Map showing the location of the Madeleine deposit. Geological information is modified from de Romer (1977) and Lachance and Duquette (1977).

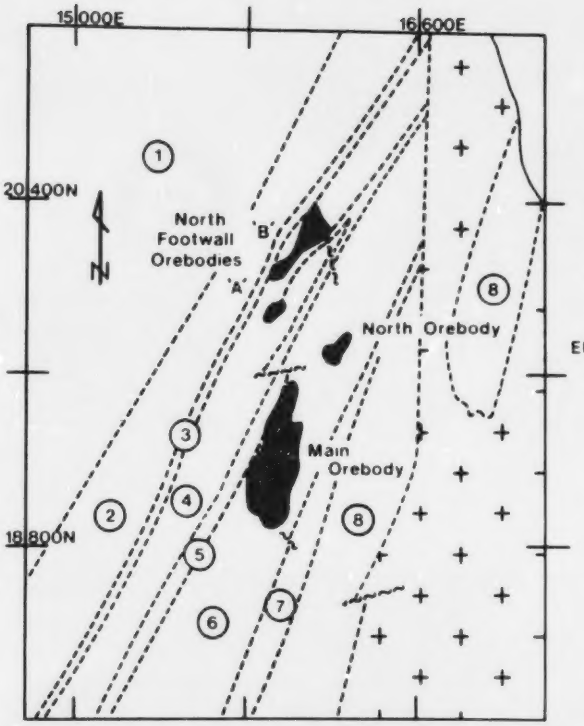

Figure 27.2a. *A geological plan of the 2900 foot level of the Madeleine mine from Girard (1971).*

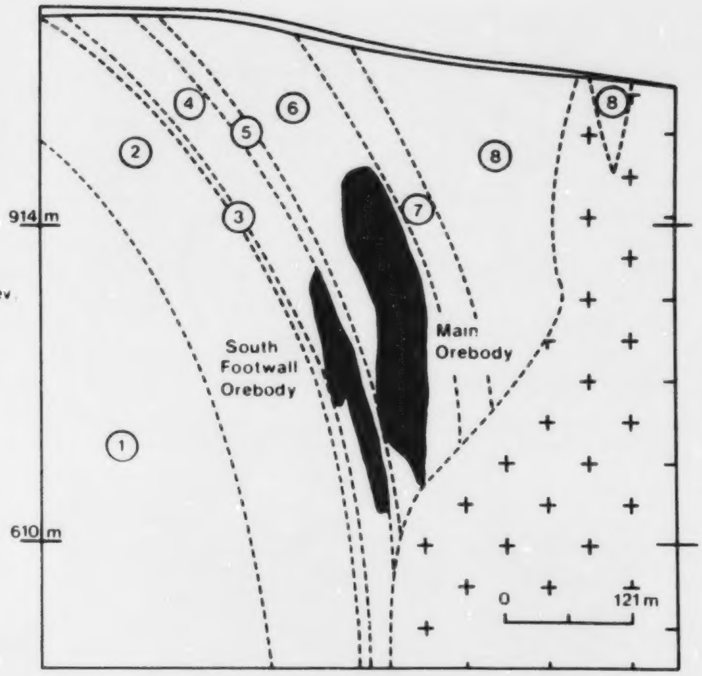

Figure 27.2b. *A geological cross-section along line 53.00 of the Madeleine deposit from Girard (1971).*

Late quartz-carbonate veins

The youngest set of veins contains the assemblage quartz-ankerite-calcite, with or without minor galena and/or sphalerite and/or chalcopyrite. These veins are planar, typically thicker (1-5 cm) than the earlier vein sets, and relatively uncommon.

Sulphide mineralogy

Each orebody is zoned with respect to the main sulphide minerals from pyrrhotite at the rim through chalcopyrite-pyrrhotite, chalcopyrite, chalcopyrite-bornite to bornite in the core. The zonation is independent of vein type, which suggests that most of the ore deposition was early and that ore minerals in later veins are the products of fairly local remobilization.

Minor proportions of the following additional sulphide minerals are common: digenite, covellite, safflorite-lollingite, and cobaltite. Girard (1971) also reported rare occurrences of breithauptite, cubanite, djurleite, linnaeite, niccolite, pararammelsbergite, and rammelsbergite.

Pyrrhotite occurs as anhedral grains of variable size. In the pyrrhotite-chalcopyrite zone it commonly embays or even veins chalcopyrite.

Chalcopyrite is the main sulphide mineral in the deposit, and is similar in its mode of occurrence to pyrrhotite. In the chalcopyrite-bornite zone it may be myrmekitically intergrown with bornite (Fig. 27.3d), vein the bornite, rim the bornite, or occur as flames and triangular lamellar grids within bornite. These textures may represent exsolution of chalcopyrite from bornite, possibly catalyzed by the later veining. Alternatively some of the textures may be what they appear to be, i.e. replacements of bornite by chalcopyrite.

Bornite is similar in form to chalcopyrite and pyrrhotite and is generally mauve. Rare crystals of an orange variety are present in some early biotite-bearing veins.

The arsenide minerals are found in all of the main sulphide zones described above. They commonly show euhedral forms and were clearly deposited early, as evidenced by embayments filled with chalcopyrite, bornite, or pyrrhotite.

Sphalerite occurs as anhedral crystals in chlorite/muscovite and carbonate-bearing veins. The sphalerite commonly contains small inclusions of bornite, chalcopyrite, or pyrrhotite. Fine blebby exsolutions of chalcopyrite are common.

Covellite, digenite, and djurleite occur as thin feathery, grain boundary, or fracture-associated replacements of bornite and are interpreted to represent very late alteration.

Alteration

The host rocks have been altered both pervasively and locally, the latter being manifest most commonly as vein haloes.

Biotitization

The earliest veins commonly, but not always, have narrow haloes, up to twice the vein width, of biotite ± tourmaline (Fig. 27.3e). The biotite of the halo is

Figure 27.3. Photomicrographs

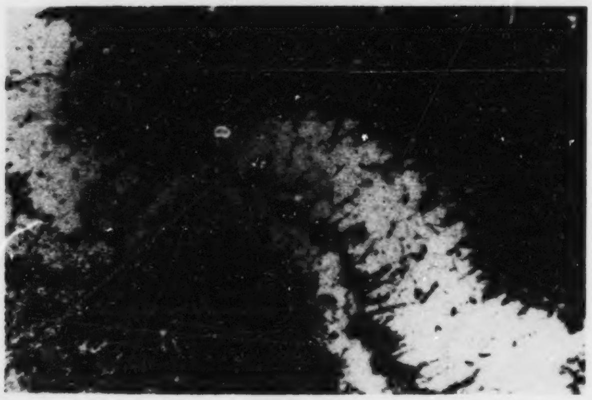

a. In transmitted light (32X) showing an early folded quartz-biotite vein (S18-395).

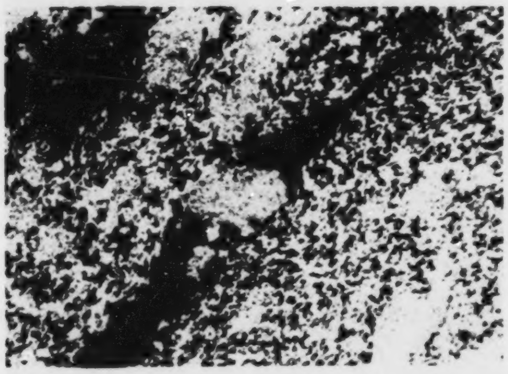

b. In transmitted light (40X) of an early chalcopyrite-bornite stringer in the plane of the foliation cut by porphyroblast of cordierite (U39-167C).

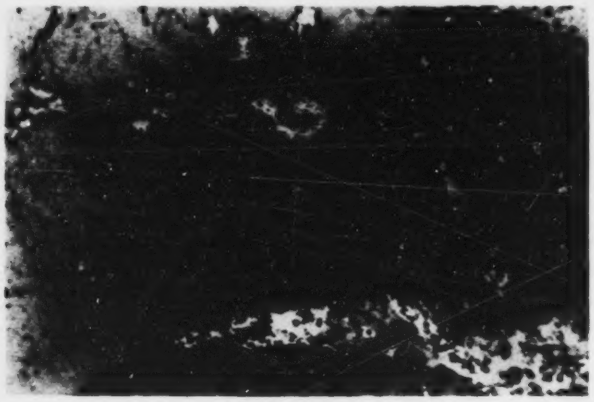

c. In reflected light (32X) showing bornite and chalcopyrite filling fractures in a quartz vein (U28-241).

d. In reflected light (32X) showing graphic intergrowth of bornite and chalcopyrite. Bornite is the darker phase (S43-57 1).

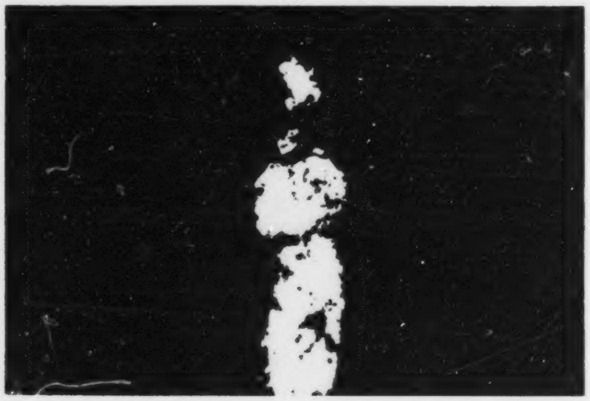

e. In transmitted light (40X) of a boudinaged quartz-biotite-chalcopyrite vein with biotite halo (U39-150).

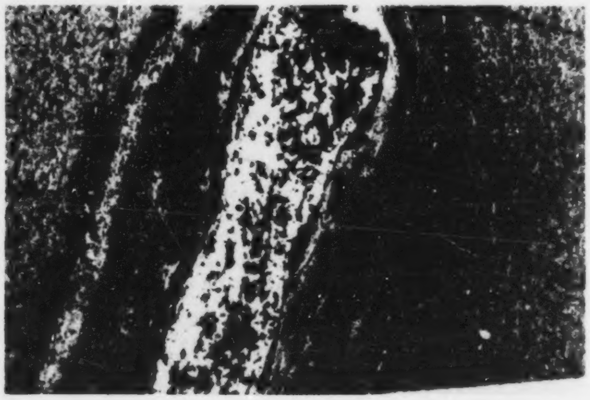

f. In transmitted light (crossed nicols; X2) showing a boudinaged calc-silicate vein with an alteration envelope zoned outwards from the vein with bands of epidote, tremolite and chlorite.

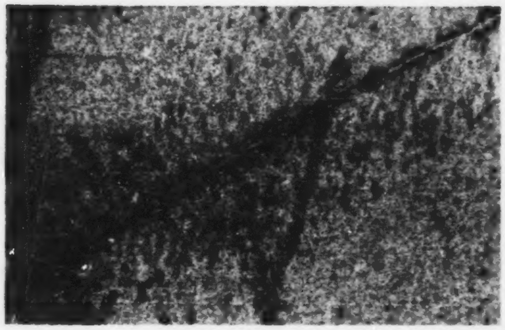

g. In transmitted light (6X) of a late chlorite-chalcopyrite vein cutting early chalcopyrite stringers. Note that the chlorite vein is only mineralized where it intersects an early chalcopyrite stringer. The chlorite vein is associated with a narrow halo of intense chloritization and a broader halo in which cordierite porphyroblasts are chloritized but the biotite of the groundmass is unaffected (U39-124).

indistinguishable from that of the host rock, except by its coarser grain. Coarse grained biotite and tourmaline also occur along cleavages and fractures and as isolated segregations. In some cases the biotite in these haloes and segregations has been altered partially or completely to chlorite, muscovite, or a mixture of these minerals.

Whether or not there has been pervasive biotitization is still an open question. As noted earlier, the host is a biotite hornfels, and thus such pervasive alteration might be difficult to distinguish from contact metamorphism, in which case the biotitization is simply a part of that metamorphism.

Calc-silicate alteration

The calc-silicate veins, almost without exception, have haloes. These are commonly zoned, generally with the following sequence of mineral assemblages occurring away from the vein: epidote; epidote-tremolite; tremolite; tremolite-chlorite; and chlorite (Fig. 27.3f). In some cases, however, the inner zone is missing and in others a diopside zone is developed between the vein and the epidote zone. Several of the haloes also display lateral variations in the zoning, generally through the omission of minerals. In one extreme case a fully zoned calc-silicate halo was seen to pass over 2-3 cm along the vein into a chloritic envelope.

Muscovite-chlorite alteration

Veins containing muscovite and/or chlorite are commonly surrounded by envelopes of muscovite and/or chlorite, according to the relative importance of the two minerals in the veins. The alteration envelopes of these veins are generally wider than those of earlier stages, typically from two to ten times vein width (Fig. 27.3g). Muscovite and/or chlorite are also common as a pervasive alteration.

Fluid inclusions

Fluid inclusions are common in all quartz-bearing veins. The inclusions are generally small ($\leq$10 μm in diameter), but may range up to 30 μm in diameter. Most inclusions are either secondary or pseudosecondary; very few are unquestionably primary. They generally have simple regular shapes, although some, notably larger inclusions are quite irregular.

Fluid inclusion types

Four basic types of fluid inclusions can be distinguished on the basis of their appearances at room temperature (Fig. 27.4): 1) liquid-vapour (liquid-rich; LV); 2) vapour-liquid (vapour-rich; VL); 3) liquid-liquid-vapour (LLV); and 4) liquid-vapour-solids (LVS). VL and LLV inclusions, as will be shown below, contain variable proportions of CO_2 and CH_4. LVS inclusions contain from 1 to 5 solid phases. These solids include an isotropic cubic mineral, assumed to be halite, that occurs in virtually all the LVS inclusions, and a reddish rod-shaped mineral that is also very common.

Distribution of fluid inclusion types

The distribution of fluid inclusion types amongst the various vein stages is given in Table 27.1 and is based on 360 inclusions from 23 vein samples. The data show: 1) that the highest proportions of LVS inclusions occur in the biotite veins; 2) that CO_2-CH_4-bearing inclusions are relatively uncommon in these veins; 3) that the highest proportion of CO_2-CH_4-bearing inclusions occur in the calc-silicate veins; 4) that these veins also contain high proportions of LVS inclusions; 5) that muscovite-chlorite veins contain much larger proportions of LV inclusions than the earlier veins, but also contain large proportions of VL, LLV and LVS inclusions; and 6) that the later quartz-carbonate veins contain the highest proportions of LV inclusions, significant proportions of LVS inclusions, but no VL or LLV inclusions.

Low temperature microthermometry

Microthermometric measurements were made on 100 μm doubly polished rock sections using an S.G.E. Model III heating/freezing stage which has been calibrated between -90 and +500°C by melting a selection of organic compounds and native elements whose melting temperatures are well known.

Frozen LV inclusions generally exhibit signs of first melting at temperatures between -50 and -20°C. This indicates the presence of dissolved salts other than NaCl and KCl (Crawford, 1981). Final ice melting occurs at temperatures between -40 and 0°C with maxima at -25 and -5°C (Fig. 27.5A). These maxima point to high and low salinity fluids of separate origin.

Many inclusions, classified as VL at room temperature, develop an additional fluid phase on cooling. Most frozen VL inclusions begin to melt at temperatures between -108 and -85°C. Most VL and all LLV inclusions exhibit final melting of the inner phase between -80 and -56°C (Fig. 27.5B). These data indicate that the vapour phase in many VL inclusions and all LLV inclusions and the inner liquid phase in LLV inclusions is composed of a mixture of CO_2 and CH_4 which varies in composition from CH_4-rich to CO_2-rich (Burruss, 1981). CH_4 and CO_2 have been independently identified in these inclusions using laser induced Raman spectroscopy. These species, and several heavier hydrocarbons, were also detected in mass-spectrometric analyses of bulk fluids extracted from Madeleine vein quartz.

LVS inclusions generally begin to melt between -70 and -60°C. Final ice-melting temperatures are difficult to discern because of the crystallization of various hydrate phases, some of which are optically indistinguishable from ice. The low initial melting temperatures are considered to reflect eutectic temperatures for a complex H_2O-salt system, that may include calcium and iron chlorides.

a) liquid-vapour.

d) liquid-vapour-halite.

b) vapour-liquid.

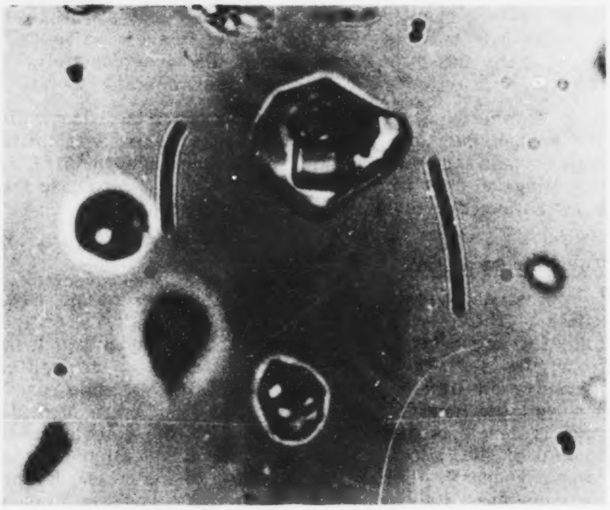

e) liquid-vapour-halite-other salts.

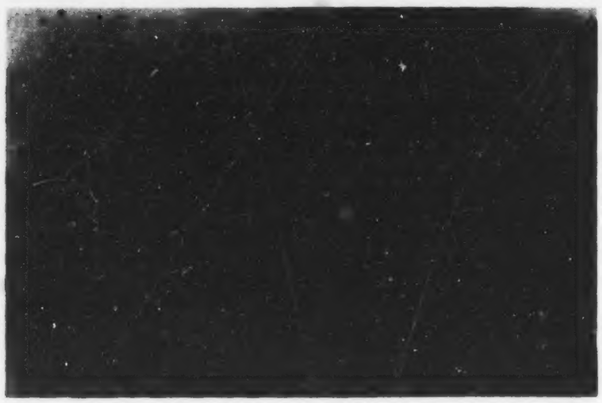

c) H_2O liquid-CO_2 liquid-CO_2 vapour (from edge to centre).

Figure 27.4. *Photomicrographs of the principal fluid inclusion types recognized in quartz from the Madeleine veins.*

Table 27.1. Percentages of the principal types of fluid inclusions in each of the four mineralogically distinctive vein stages. The table is based on 360 fluid inclusions from 23 samples that were studied during the course of the investigation.

Vein stage	LV	Inclusions VL, LLV	LVS
Biotite	6	9	85
Calc-silicate	16	32	52
Musc-chlorite	38	18	44
Qtz-carbonate	71	0	29

High temperature microthermometry

Most LV inclusions homogenize between 200 and 400°C with the largest numbers of inclusions homogenizing at about 250 and 330°C. This statement refers mainly to muscovite-chlorite veins and to a lesser extent to calc-silicate veins (Fig. 27.6A, B). There are insufficient data to draw any conclusions about homogenization temperatures for LV inclusions in biotite veins, and those in late quartz-carbonate veins yield a narrow range of homogenization temperatures: 240 ± 40°C (Fig. 27.6C).

Few homogenizations were obtained for VL and LLV inclusions because most of them decrepitated on heating owing to the high coefficient of thermal expansion of CO_2. Homogenizations were, however, obtained for 10 inclusions at temperatures ranging between 300 and 400°C.

Vapour disappearance temperatures for LVS inclusions generally occur in the range 160 to 400°C. There is also an indication that these temperatures may be bimodally distributed. Biotite veins are clearly represented by low and high temperature LVS inclusions with vapour disappearance temperature maxima centred on 230 and 350°C (Fig. 27.7A). In the case of calc-silicate veins there is a single maximum at approximately 250°C (Fig. 27.7B). The data for the muscovite-chlorite veins resemble those for the biotite veins except that the higher temperature maximum is centred on 300°C, which corresponds to the low between the peaks for the biotite veins (Fig. 27.7C). Only one vapour disappearance temperature was obtained for an LVS inclusion from a quartz-carbonate vein. The temperature, 236°C, is consistent with the data for the LV inclusions.

Solid phase dissolution temperatures were obtained only for halite, except in a small number of cases where a second mineral was also dissolved. Halite dissolution occurs over roughly the same range of temperature as vapour disappearance, but generally at lower temperatures than the latter (Fig. 27.8). In only 1 of 23 samples studied (S18-446; a quartz-biotite vein) was the temperature of halite dissolution (8 of 9 inclusions) consistently greater than the temperature of vapour disappearance. The modal difference between the two temperatures in the sample was 62°C (the range was -6 to -99°C, and -56 to -74°C for 5 inclusions); the modal vapour disappearance temperature was 231°C (the range for 8 of the inclusions was 212 to 240°C). These data are used below to obtain an estimate of fluid pressure. A second solid was dissolved in 10 inclusions. In 3 cases dissolution occurred at temperatures below 65°C; the phase was small, round and isotropic, and may be sylvite. In the other cases dissolution occurred at temperatures above those of vapour phase disappearance and halite dissolution; the second dissolved phase was represented by at least two minerals, including the reddish rod-shaped mineral referred to earlier.

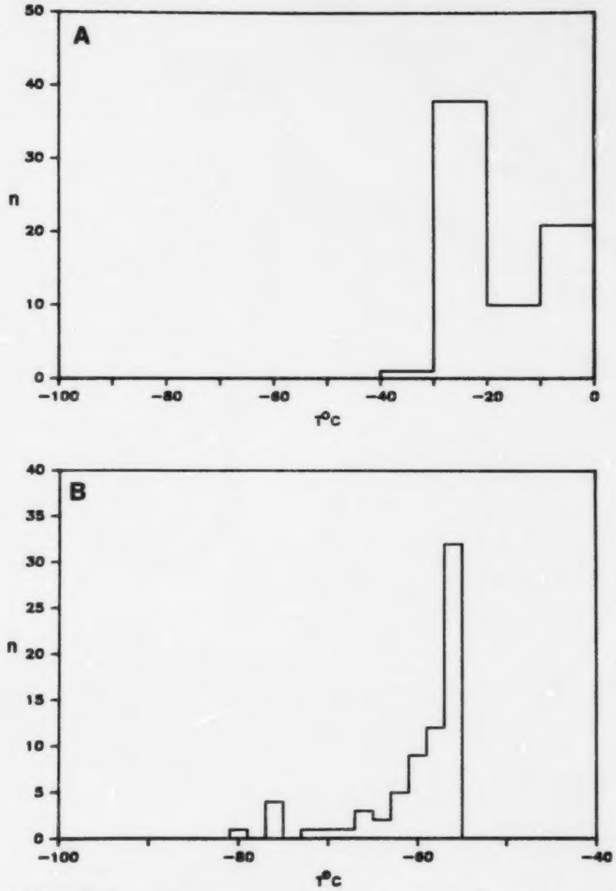

Figure 27.5. Histograms showing the distributions of A) final ice melting temperatures of LV inclusions and B) final melting temperatures of solid CO_2/CH_4 in LLV inclusions. The bimodality of final ice melting temperatures in B (-25 and -5°C) indicates that there were separate high and low salinity fluids. The strong maximum in B at -56°C shows that the incondensible phase in a large proportion of VL and LLV inclusions is CO_2. The skewness of the distribution to lower melting temperatures indicates, however, that an equally large proportion of these inclusions consist of varying mixtures of CO_2 and CH_4, some with over 50% methane.

Salinity-homogenization relations for LV inclusions

Figure 27.9 is a plot of freezing point depressions versus homogenization temperatures for LV inclusions. The diagram shows that these inclusions trapped separate high and low salinity fluids which homogenize at similar temperatures of between 200 and 350°C.

Solid phase identification

Freshly broken fragments of a limited number of quartz veins were examined using a scanning electron microscope equipped with an energy dispersive spectrometer to aid identification of the solid phases in LVS inclusions. Only a small number of the opened inclusions were found to contain solid phases, presumably because, in most instances, the solids were lost during rupture of the inclusions or during subsequent sample preparation and analysis. By far the most

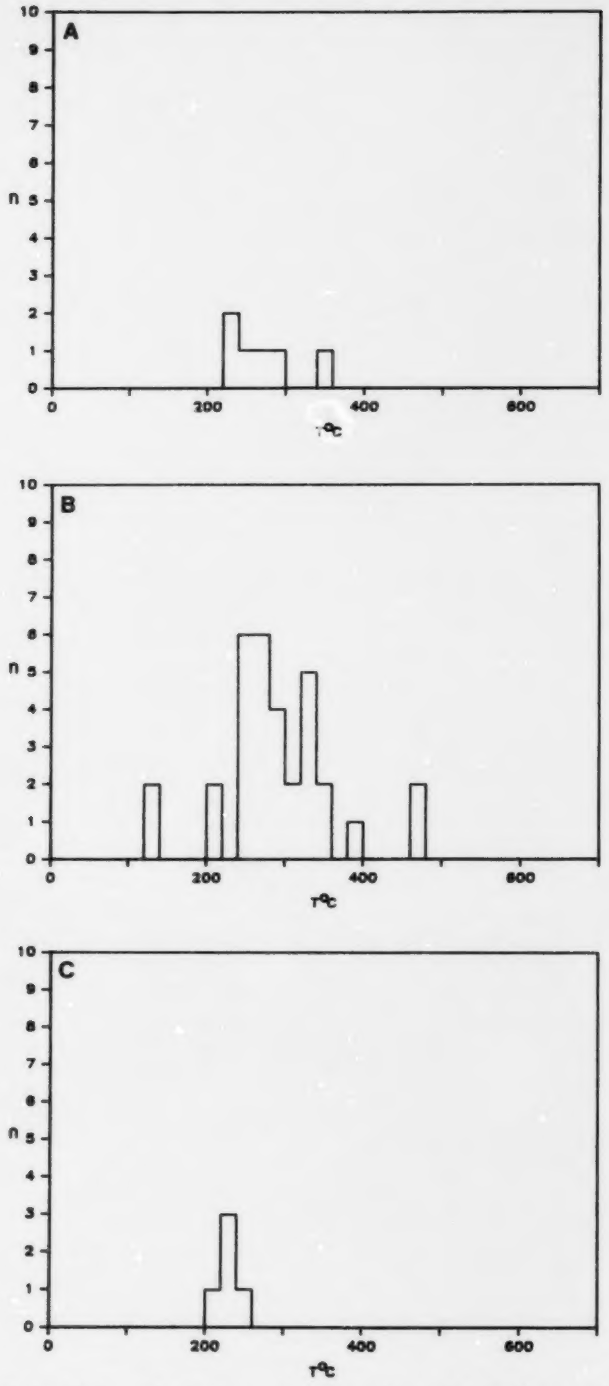

Figure 27.6. *Histograms showing the distributions of homogenization temperatures for LV fluid inclusions in A) calc-silicate veins, B) muscovite-chlorite veins, and C) quartz-carbonate veins. Note that in B there is a clearly defined maximum at 260°C and a weaker maximum at 330°C suggesting that the muscovite/chlorite veins trapped separate higher and lower temperature LV fluids; and that in C there is a single sharp maximum at 230°C.*

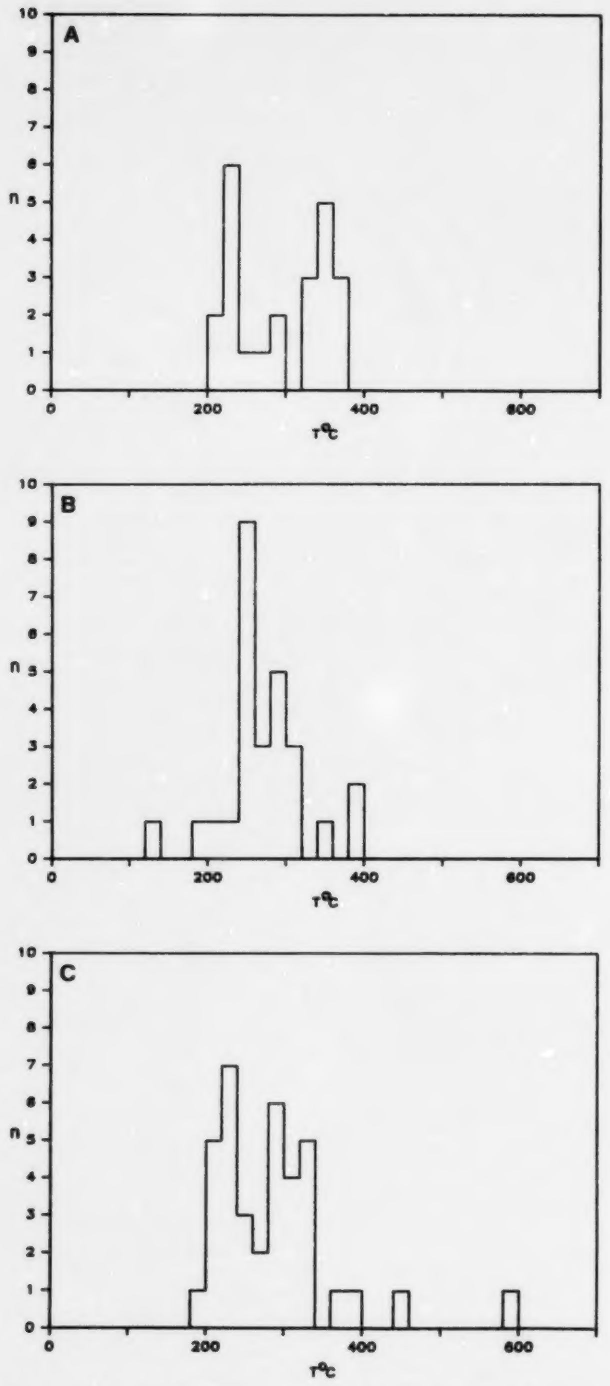

Figure 27.7. *Histograms showing the distributions of vapour disappearance temperatures in LVS fluid inclusions for A) biotite veins, B) calc-silicate veins and C) muscovite/chlorite-bearing veins. In A there are sharp maxima at 230 and 350°C; in B there is a strong maximum at 250°C and possibly a second maximum at 290°C; in C there is a sharp maximum at 230°C and a second compound peak centred on 310°C. These data suggest that there were three temperature intervals in which major fluid entrapment occurred. The lowest temperature interval is represented in each of the stages; the intermediate temperature interval is reflected in the calc-silicate veins and muscovite-chlorite veins but not in the biotite veins; and the high temperature interval in the biotite-bearing veins.*

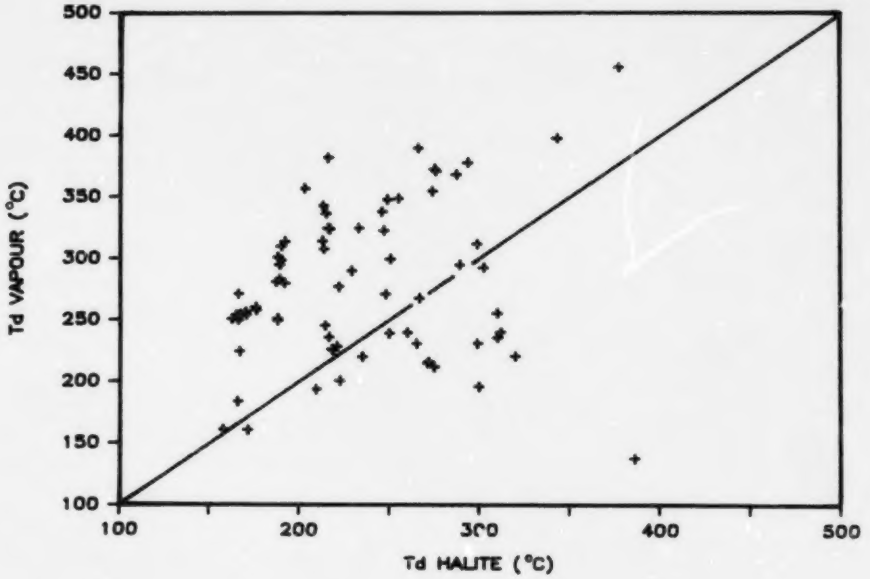

Figure 27.8

A diagram showing halite dissolution temperatures (Td) versus vapour disappearance temperatures (Tv) for LVS inclusions. The line separates inclusions with Tv > Td from those in which Td > Tv. It can be seen that Tv < Td in the great majority of inclusions. Moreover 7 of the 11 inclusions in which Td ≫ Tv come from a single sample S18-446.

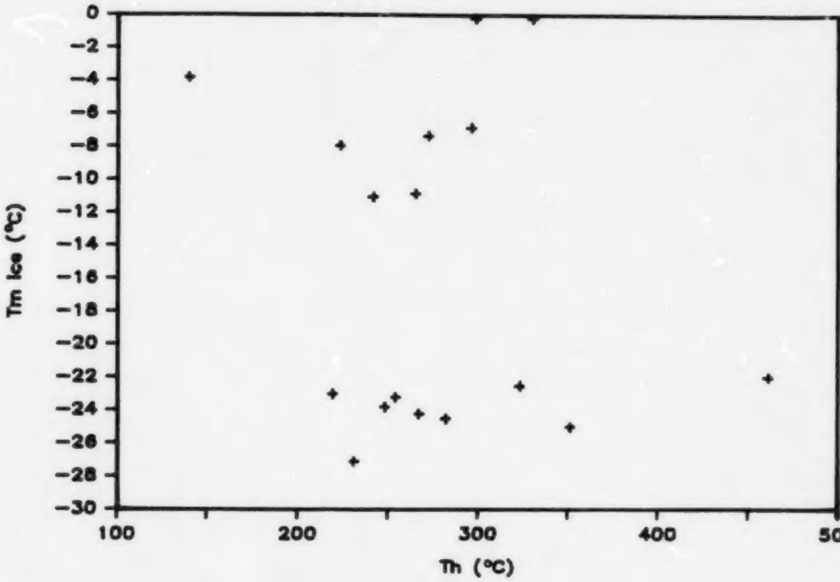

Figure 27.9

A diagram showing final ice melting temperatures versus homogenization temperatures for LV fluid inclusions. It can be seen that there are clearly separable low and high salinity groups (high and low ice melting temperatures).

commonly observed solid was a prismatic hexagonal iron chloride mineral (Fig. 27.10). This solid probably represents the reddish, rod-shaped mineral that was referred to in the section dealing with fluid inclusion types. Halite and/or sylvite were identified in only a few specimens. They undoubtedly escaped more easily than the iron chloride mineral owing to their equant shapes and lower densities. Other solid phases include bornite, chalcopyrite, biotite, a calcium mineral, probably calcite, and an iron-manganese mineral, possibly a rhodochrosite-siderite solid solution. It can probably be assumed, on the basis of frequency of occurrence, that halite and the iron chloride phases are daughter minerals. The origin of the other solids is less clear. In some cases they may be daughter minerals but, in most cases, they were probably trapped with the fluid.

Discussion

The data presented in the preceding sections provide some interesting clues about the history of the Madeleine deposit and some important initial constraints on the physico-chemical conditions that operated on the ore-forming fluids.

Timing

Several lines of evidence suggest that the early veins and associated biotitic alteration reflect a hydrothermal event that occurred prior to, or synchronous with, the development of the McGerrigle thermal aureole. Most of the early veins and stringers are parallel to the principal foliation (hornfelsing must have proceeded contemporaneously with deformation); discordant veins are folded about this foliation;

Figure 27.10. An S.E.M. photomicrograph of an opened fluid inclusion containing a prismatic crystal of an iron-chloride daughter mineral in quartz from a biotite vein.

and concordant sulphide stringers are flattened with it about cordierite porphyroblasts or disrupted by them (Fig. 27.3a, b). There is also evidence that the bulk of the mineralization was introduced at this time. The sulphide minerals are zonally distributed with bornite in the core of the deposit and chalcopyrite-pyrrhotite at its margins. This zonation is discernible in all except the late carbonate veins, which suggest that it was established early and was unaffected by later veining/alteration. Indeed, the textural evidence presented earlier shows that the volumetrically important muscovite-chlorite event probably produced little veining, but instead, served mainly to overprint early veins and remobilize the sulphides contained in them.

Pressure-temperature conditions

The most useful estimate of pressure at this time is provided by data from a set of LVS inclusions from sample S18-446 (biotite-bearing vein; see section dealing with high temperature microthermometry) in which the modal halite dissolution temperature exceeds the modal vapour disappearance temperature (231°C) by 62°C. A minimum pressure of 365 bars was calculated for these data using the method of Roedder and Bodnar (1980). Minimum pressure estimates based on vapour disappearance temperatures range from 15 to 195 bars.

The homogenization temperatures of the various inclusion types give minimum estimates of the temperatures of entrapment. These data suggest that large quantities of high and lower salinity fluids were trapped at minimum temperatures of approximately 350, 300, and 250°C (see Fig. 27.6, 27.7). CO_2/CH_4 fluids were generally trapped at minimum temperatures of between 300 and 400°C.

The temporal distribution of the fluids is, unfortunately, not at all clear. Low temperature, high salinity fluids are, for example, abundantly preserved in all stages of veining. The high temperature, high salinity group, however, is abundant only in the early biotite veins; the intermediate temperature high salinity group is dominant in the muscovite-chlorite veins and to a lesser extent in the calc-silicate veins, but is absent from the biotite veins; the CO_2/CH_4-bearing fluids are mainly trapped in the calc-silicate veins; and only low temperature, high and low salinity, fluids occur in the late quartz-carbonate veins (Fig. 27.6, 27.7 and Table 27.1). This would seem to suggest that: the highest temperatures were attained in the early fluids which deposited biotite veins; fluid temperatures were lower during subsequent calc-silicate and muscovite-chlorite veining; and lowest during the emplacement of the late-stage quartz-carbonate veins. The interpretation assumes that the low temperature, high and lower salinity, inclusions represent overprinting in all except the late quartz-carbonate veins, and that the high temperature inclusions in many muscovite-chlorite veins are there because these veins represent altered early veins.

Fluid-rock interaction

The evidence from this study is that the early fluids were high temperature, saline, and contained significant concentrations of sodium, iron, and potassium. The origin of these fluids is uncertain. The geological setting and their similarity, however, in terms of temperature and composition, to typical porphyry fluids suggests that they were probably orthomagmatic (Nash, 1976). These fluids caused biotitic alteration and extensive deposition of quartz and Cu-Fe sulphides, possibly through reactions of the form:

$$CH + QZ + 4K^+ + 2MgFe^{2+} = BI + 8H^+$$

(This and other alteration reactions presented below are balanced for constant alumina.)

$$H_4SiO_4 = QZ + H_2O$$

$$4CuCl^+ + 4FeCl^{2+} + 8H_2S = 4CP + 16\ H^+ + 16\ Cl^-$$

The result, as may be seen from the above reactions, is that the fluids probably became more acidic.

Some of the relatively early fluids undoubtedly passed through calcareous beds that are present in the ore horizon and overlying units. If acid, they would have reacted with the calcite in these rocks and, in the process, dissolved significant calcium and some CO_2. Most of the CO_2 produced by the reaction would not have dissolved because CO_2 is relatively insoluble in brines (Bowers and Helgeson, 1983), but could have become physically entrained with the saline fluid and subsequently entrapped with the latter in the calc-silicate veins as separate VL/LLV and LVS inclusions. The presence of significant CH_4 in many CO_2-bearing inclusions suggests, in addition, that conditions were relatively reducing. The high calcium ion activity developed in the brines undoubtedly explains the precipitation of calc-silicate minerals in veins and the alteration of the host biotite hornfelses to calc-silicate minerals. The zonation of the latter, from epidote at the vein margin outwards through tremolite-epidote and tremolite to chlorite, conforms with the expected gradient of decreasing calcium ion activity away from the vein. Calcium ion activities were not, however, uniformly high, as is evidenced by the fact that some of the alteration envelopes about calc-silicate veins do not contain epidote and others contain only chlorite. An important consequence of the alteration is that the acidity of the fluids was increased as is indicated by the following idealized reaction:

$$BI + 8H_2O + 10Ca^{2+} + O_2 + 2MgFe^{2+} + 20QZ = 2EP + 4TR + 6K^+ + 18H^+$$

The volumetrically important muscovite-chlorite stage occurred when temperatures had fallen to about 300°C. This temperature also corresponds roughly with the upper limit of low salinity LV inclusion homogenizations (Fig. 27.8). It is thus probable that this stage marks the collapse of the orthomagmatic system and the influx of large volumes of meteoric waters. Although the origin of the fluids that were

active during the muscovite-chlorite stage is unknown, it is clear they were more acidic than in the preceding stages. This can be seen from the following idealized reaction in which biotite breaks down through hydrogen ion metasomatism to muscovite and chlorite.

$$15Bi + 44H^+ = MU + 3CH + 24QZ + 15MgFe^{2+} + 14K^+ + 12H_2O$$

The very late stage quartz-carbonate veins clearly postdated the formation of the ore deposit. They do, however, have in common with the earlier veins sets, the fact that they contain a small proportion of high salinity fluid inclusions. The significance of this and the fact that all vein stages contain sets of low temperature fluid inclusions is not understood. It may indicate that there was late stage boiling or alternatively, that late stage fluids tapped high salinity sources.

Ore deposition

Factors which are typically called upon to account for mineral deposition are drop in temperature, boiling, wall-rock alteration, and dilution of the ore fluids. Temperature drop may certainly have been a factor, particularly as the temperature range indicated by the fluid inclusion data corresponds closely with that in which the solubility of Cu-Fe sulphides changes most sharply (Crerar and Barnes, 1976). There is no evidence of there having been a major boiling event. Effervescence of incondensible gases, however, was apparently extensive and may well have been a factor in ore deposition: it would have increased pH in the residual fluids and thereby reduced the solubility of the ore minerals. Alteration of the host rock probably did not directly cause sulphide precipitation because it would seem to have increased the acidity of the fluids during the main ore stage. It may, however, have contributed to the generally reducing conditions that would have favoured sulphide deposition, as evidenced by the presence of methane-bearing fluid inclusions and iron sulphide in the form of pyrrhotite. Dilution, which occurred mainly during the post-ore muscovite-chlorite altering event, is likewise not considered to have been an important cause of sulphide deposition.

One feature of the ores that is undoubtedly an important key to understanding how the deposit was formed is the zonation of the sulphides from bornite in the core of the deposit through bornite-chalcopyrite and chalcopyrite to chalcopyrite-pyrrhotite at the margins. The zonation also appears to coincide with the paragenetic sequence of sulphide deposition as indicated by ore textures. The most obvious explanation for this sequence is that it mirrors the relative solubility of these minerals and reflects a change in some parameter such as temperature or pH from the centre to the edge of the deposit. In fact it is known that, if transport of the metals is via chloride complexes (probable in the case of the Madeleine deposit because of the high salinity of the fluids), the observed sequence will be produced by trends of decreasing temperature and/or pH (Barnes, 1975). Such trends would have been present, if, as is likely, the water/rock ratio was highest in the core of the deposit. A high water/rock ratio in the core would have led to lower heat loss and a higher fluid temperature in this zone. The pH would likewise, have been higher because dissolved ionic species are more associated at higher temperatures, and also because wall-rock alteration has less effect on fluid composition at higher water/rock ratios. An alternative explanation for the zoning may be that the iron and sulphur contents of the solution changed from core to rim of the deposit, possibly as a function of the outwardly decreasing water/rock ratio. The mineral sequence reflects a continuous decrease in Cu/Fe and (Cu+Fe)/S from the core to the rim which could be explained by postulating that iron and sulphur came in large part from the sediments, whereas the copper had a dominantly orthomagmatic origin. Much of the future work on the deposit will be directed to examining in detail some of the ideas that have been presented in this and the preceding paragraph.

References

Barnes, H.L.
1975: Zoning of ore deposits: types and causes; Royal Society of Edinburgh, Transactions, v. 69, p. 295-311.

Bowers, T.S. and Helgeson, H.C.
1983: Calculation of the thermodynamic and geochemical consequences of non-ideal mixing in the system H_2O-CO_2-NaCl on phase relations in geologic systems: equation of state for H_2O-CO_2-NaCl fluids at high pressures and temperatures; Geochimica et Cosmochimica Acta, v. 47, p. 1247-1275.

Burruss, R.C.
1981: Analysis of phase equilibria in C-O-H-S fluid inclusions; in Short Course in Fluid Inclusions: Applications to Petrology, ed. L.S. Hollister and M.L. Crawford; Mineralogical Association of Canada, p. 39-74.

Crawford, M.L.
1981: Phase equilibria in aqueous fluid inclusions; in Short Course in Fluid Inclusions: Applications to Petrology, ed. L.S. Hollister and M.L. Crawford; Mineralogical Association of Canada, p. 75-100.

Crerar, D.A. and Barnes, H.L.
1976: Ore solution chemistry V. Solubilities of chalcopyrite and chalcocite assemblages in hydrothermal solution at 200° to 350°C; Economic Geology, v. 71, p. 772-794.

de Romer, H.S.
1977: Région des McGerrigle; Ministère des Richesses Naturelles, Rapport géologique 184, 233 p.

Girard, P.
1971: The Madeleine copper mine, Gaspé, Quebec: a hydrothermal deposit; unpublished Ph.D. thesis, McGill University, 243 p.

Lachance, S. and Duquette, G.
1977: Région de Boisbuisson (NW); Ministère des Richesses Naturelles, Québec, Rapport géologique 187, 78 p.

Nash, J.T.
1976: Fluid inclusion petrology – data from porphyry copper deposits and applications to exploration; U.S. Geological Survey, Professional Paper 907-D, 16 p.

Roedder, E. and Bodnar, R.J.
1980: Geologic pressure determinations from fluid inclusion studies; Annual Review of Earth and Planetary Sciences, v. 8, p. 263-301.

Submersible observations and origin of an iceberg pit on the Grand Banks of Newfoundland

Projects 790018, 830056

J.V. Barrie [1], W.T. Collins [1], J.I. Clark [1], C.F.M. Lewis, and D.R. Parrott
Atlantic Geoscience Centre, Dartmouth

Barrie, J.V., Collins, W.T., Clark, J.I., Lewis, C.F.M., and Parrott, D.R., Submersible observations and origin of an iceberg pit on the Grand Banks of Newfoundland; in Current Research, Part A, Geological Survey of Canada, Paper 86-1A, p. 251-258, 1986.

Abstract

An elongated seabed depression 125 by 80 m and 10 m deep was investigated using a manned submersible in October, 1984 and again in August, 1985 on the Grand Banks of Newfoundland. This pit in 87 m of water is typical of a small population of depressions found that indent the seabed up to seven times deeper than the deepest iceberg furrows in the same area and in similar water depths. This feature, although not associated with a typical iceberg furrow, is interpreted as a seabed response to impact and loading by a rolling and grounding iceberg. Side berms up to 2.5 m above the seabed were formed as the iceberg was displaced in a southward direction where it came hard aground. Subsequent failure of the underlying silt and clay Tertiary beds resulted in an overdeepened pit. This enlargement was probably the result of combined vertical loading with an increased iceberg draught, and current or wave-induced horizontal loading causing passive failures. The iceberg pit appears to be of recent origin.

Résumé

Une dépression marine allongée de 175 m sur 80 m, profonde de 10 m, a été étudiée à l'aide d'un sous-marin piloté en octobre 1984 et en août 1985, sur les Grands bancs de Terre-Neuve. Cette fosse, par 87 m d'eau, est caractéristique d'un petit ensemble de dépressions qui s'enfoncent dans le fond marin sept fois plus profondément que les sillons d'icebergs les plus profonds dans la même région et dans des profondeurs d'eau semblables. Cette dépression, bien qu'elle ne soit pas associée à un sillon creusé par un iceberg, proviendrait de la réaction du fond marin au choc et au poids d'un iceberg qui aurait roulé pour ensuite venir s'échouer. Des gradins latéraux s'élevant à 2,5 m au-dessus du fond marin se seraient formés lors du déplacement de l'iceberg vers le sud, où il s'est brutalement échoué. L'affaissement ultérieur des couches sous-jacentes de limon et d'argile du Tertiaire a approfondi la dépression. Cet agrandissement est probablement le résultat de l'action combinée d'une charge verticale liée à un tirant d'eau accru de l'iceberg et d'une charge horizontale due aux vagues, ce qui a causé les affaissements passifs. La dépression semble être d'origine récente.

[1] Centre for Cold Ocean Resources Engineering (C-CORE), Memorial University of Newfoundland, St. John's, Newfoundland A1B 3X5

Introduction

Pits or circular depressions in the seafloor have a similar density of distribution as modern iceberg scours and were first defined by Fader and King (1981) as "iceberg pits" because of their often close association with linear iceberg scours. The maximum reported penetration of all measured iceberg pits into the underlying sediments on the Grand Banks of Newfoundland is 8.0 m (Mobil Oil Ltd., 1985). (Pits can be up to seven times deeper than the deepest iceberg scour within the 80 to 120 m bathymetric corridor.)

Depressions or pits in the seabed have been documented in numerous site specific and regional geological and geophysical survey lines on the Grand Banks of Newfoundland (Amos and Barrie, 1980; Fader and King, 1981; Lewis and Barrie, 1981; Fader et al., in press; Barrie et al., in press). These features range in width from 30 to 350 m and in depth from 0.5 to 8.0 m with an average of depth 3.0 m (Mobil Oil, 1985). Based on observations by manned submersible, the pits are elliptical to circular in shape and the sub-bottom profiler records commonly show a V-shaped depression.

Linear to curved iceberg scour marks (furrows) also occur over the northeastern Grand Banks region and can be broken down into two distinct age populations (Fader and King, 1981; Lewis and Barrie, 1981). Recent scours occur in water depths to at least 200 m with the greatest density of occurrence at approximately 150 m (Lewis and Barrie, 1981; d'Apollonia and Lewis, in press). In water depths less than 120 m, on the Grand Banks, iceberg scours are rarely deeper than 1.5 m whereas in water depths greater than 120 m the

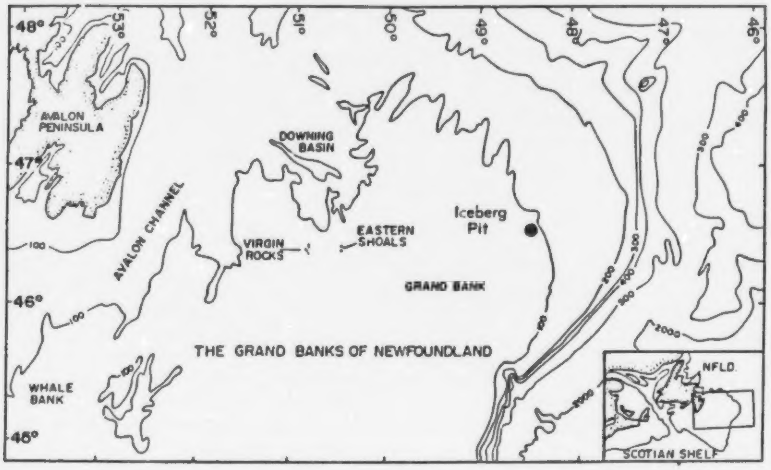

Figure 28.1

Map showing general bathymetry of Grand Banks of Newfoundland and location of iceberg pit.

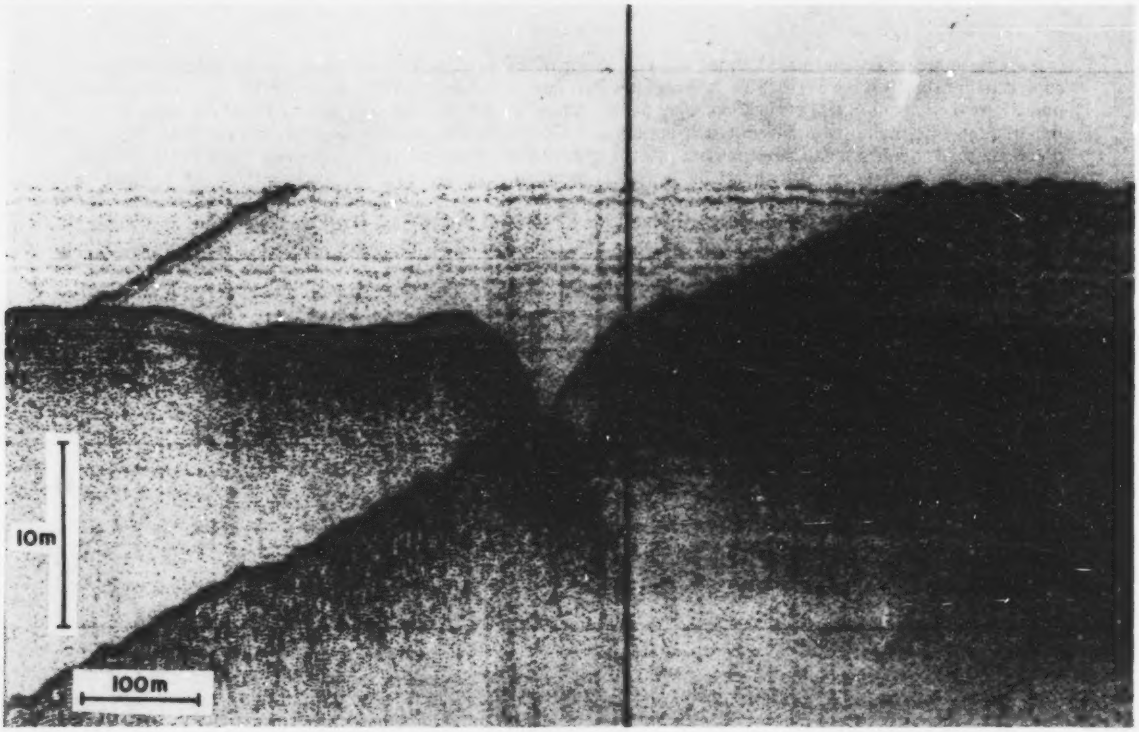

Figure 28.2. *High resolution seismic profile (Huntec DTS) and sidescan sonar record of the pit. The inclined reflectors on the seismic profile are superimposed interference patterns and should be ignored. Sidescan image courtesy of G.B. Fader and R.O. Miller, Atlantic Geoscience Centre.*

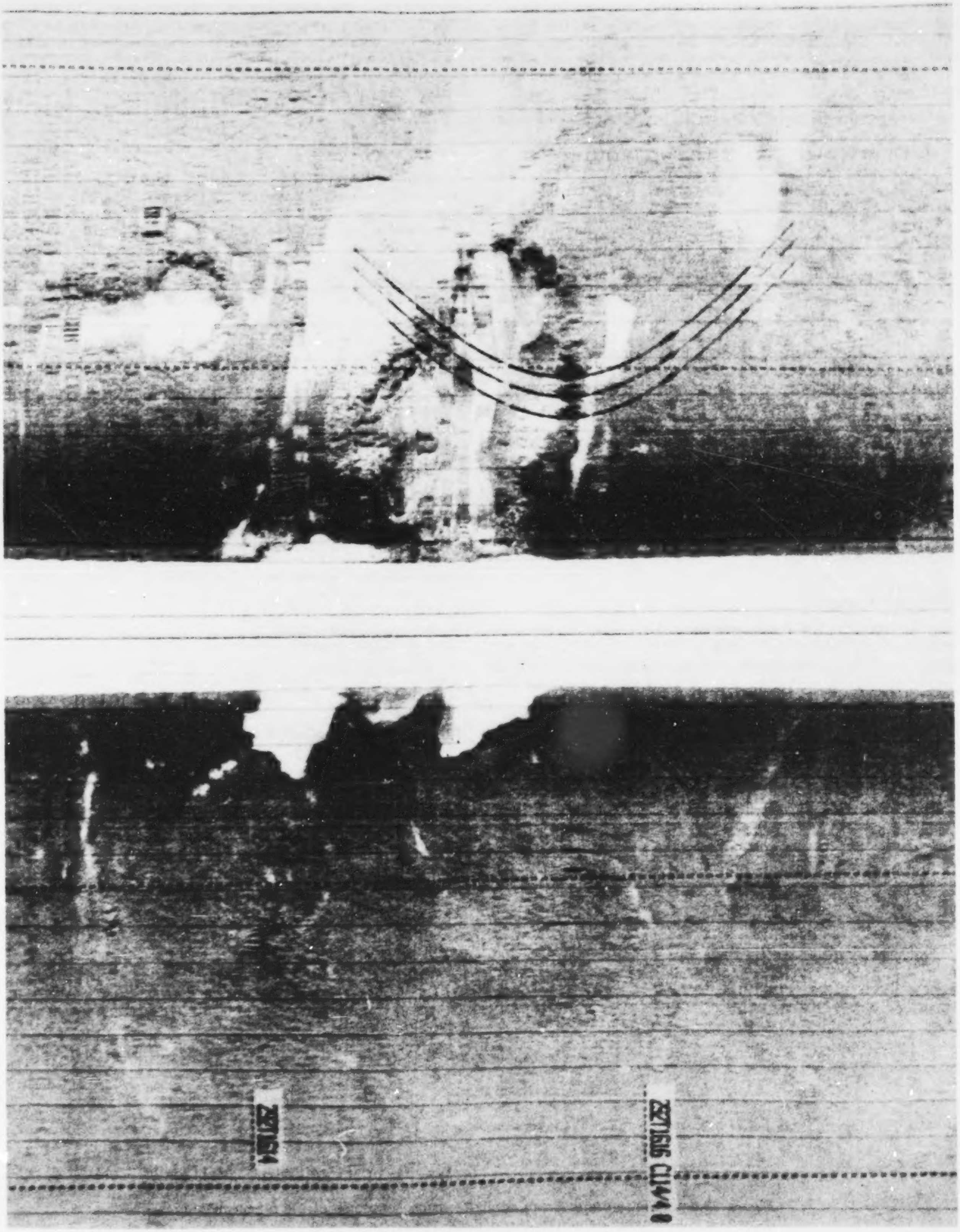

Figure 28.2 (cont.)

maximum iceberg scour depth in the region is 7.0 m (Lewis and Barrie, 1981; d'Apollonia and Lewis, 1981; Mobil Oil, 1985). These deeper scour marks are associated with a degraded network of iceberg furrows thought to be related to Pleistocene low sea levels (Fader and King, 1981) and are therefore relict.

The origin of these iceberg pits has been a subject of controversy. The profiles show a low amplitude berm, commonly associated with iceberg scouring mechanisms. It has also been suggested that these features could be "pockmarks" originating from the erosion of underlying clays initiated by the ascension of gas or water (gasturbation) (e.g. King and MacLean, 1970; Josenhans et al., 1979; Hovland, 1981). However no shallow gas has been detected in the Hibernia area (Mobil Oil Ltd., 1985). Another possible mechanism suggested has been related to thermokarst (Mobil Oil, 1985) but there is no evidence to support this interpretation.

In October 1980 a circular depression 5.4 m deep and 100 m wide was identified from Huntec DeepTowed Seismic (DTS) sub-bottom profiler data 11 km east-southeast of the Hibernia P-15 discovery well (Fig. 28.1). This pit along with two other such pits were discovered during a co-operative C-CORE/Mobil Oil geophysical cruise. In order to explain the origin and significance of these pits, a manned submersible program was dedicated to their study. The 5.4 m deep pit was chosen as a primary target because of its well-developed and fresh character and its proximity to the Hibernia oil field. The following discussion describes this particular feature and proposes a mechanism of formation for this type of depression found on the northeastern Grand Banks of Newfoundland.

Field investigations

In October 1984, and August 1985, C-CORE and the Department of National Defence undertook a joint program using the **SDL-1** submersible and its support vessel **HMCS Cormorant**. Scientists from C-CORE, Geological Survey of Canada, Mobil Oil Ltd. and the Biology Department of the Memorial University of Newfoundland participated in both investigations. In addition to the submersible observations a 100 kHz sidescan sonar system with an integral 3.5 kHz sub-bottom profiler was used to survey the size and shape of the pit. Two additional visits to this area were made in 1985 by **MV Pandora II** with the **Pisces IV** submersible (Bedford Institute of Oceanography). Although no dives were attempted due to poor weather conditions useful sidescan sonar survey data were collected over the pit (Fig. 28.2).

Regional setting

The pit described is located at 46°43.3'N, 48°37.5'W on the nearly flat terrace-like northeastern margin of Grand Bank in 87 m of water. The seabed gradient steepens perceptibly just below the site and flattens into a second terrace between the 100 m and 110 m bathymetric contours before steepening again toward the shelf edge at approximately 200 m. This inter-terrace slope is interpreted to define the late Pleistocene low stand of sea level (Fader and King, 1981; Barrie et al., 1984).

The cold Labrador Current flows southward closely following the 200 m isobath (Petrie and Anderson, 1983) and brings icebergs into the area seasonally (Murray, 1969; Dinsmore, 1972; Markham, 1981). Some icebergs are carried southward onto Grand Bank across the general pit location by storm winds and currents (Lewis and Barrie, 1981). The orientation of sand waves and megaripples above 110 m water depth reflect southward migration possibly associated with storm driven currents or enhanced bottom currents (Barrie et al., 1984). Calculations of orbital velocity at the seabed show that wave base for the Hibernia winter wave climate (Neu, 1982) extends to the 100 m isobath (Barrie et al., in press).

Surficial sediments in the locale of the pit consist of the gravel facies of the Grand Banks Sand and Gravel Formation (Barrie et al., 1984; Fader et al., in press). It is an acoustically highly reflective surface composed of gravelly sand or sandy gravel. The gravel often occurs as a pebble armour over the sand. The surficial sediments (Quaternary) are less than 0.5 m thick and unconformably overlie seaward-dipping silts and clays of probable late Tertiary to early Pleistocene age.

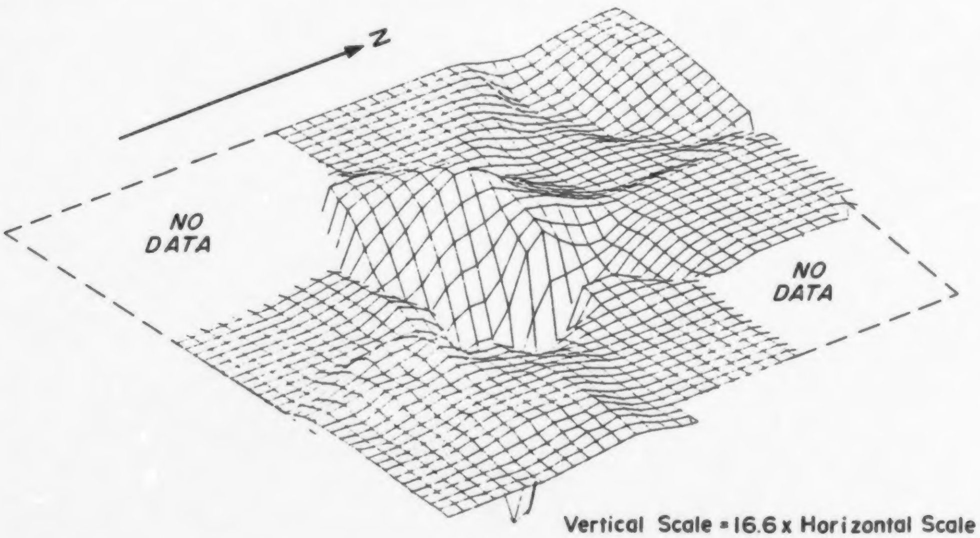

Figure 28.3. Three dimensional computer representation of the pit morphology (based on unprocessed geophysical profiles).

Pit description

Two high resolution seismic reflection (Huntec DTS) and numerous 100 kHz sidescan sonar surveys, including 3.5 kHz sub-bottom profiler, have been carried out across the pit area since 1980 (Fig. 28.2). Another feature interpreted to be a small pit occurs 20 m to the west of the main disturbance. Two distinct patches of low reflectivity on the sidescan sonograms, to the southwest of the pit, are interpreted to be silt and clay sediments. These features measure 35 m and 60 m in their longest axis which is oriented parallel to the direction of scour. To the north of the pit, the sonograms show areas of low reflectivity interpreted to be sand. The Huntec DTS sub-bottom profiles over the pit show a V-shaped depression between 5.4 and 6.5 m deep. Continuous reflections, interpreted to be Tertiary strata, appear flat lying and intersect the walls of the depression. A synthesis of pit morphology based on all available geophysical information is displayed in Figure 28.3 as a 3-D reconstruction.

An interpretation of the pit was produced from direct submersible observations, including the use of an on-board sector scanning sonar, and numerous sidescan sonar surveys (Fig. 28.4). Its overall shape exhibits an entrance ramp, two side walls, and a back wall creating an amphitheater-like appearance. The long axis is oriented north-northeast and measures 125 m. The short axis is perpendicular to the long axis and measures 45 m. All measurements refer to the edges defined by the intersection of the undisturbed seabed and the walls of the pit.

Measurements by the depth gauge of the submersible indicate the undisturbed seabed is 87 m below sea level and the pit floor at its deepest point is 97 m below sea level giving a maximum pit depth of 10 m. The discrepancy between this depth and depths of 5.4 and 6.5 m measured by geophysical methods clearly illustrates the benefits of direct observation and measurements. In order to properly measure the dimensions of the pit using a sub-bottom profiler it is necessary to run numerous closely spaced lines with the tow fish placed near the seafloor to optimize the horizontal and vertical resolution of the system. Since any single line is not guaranteed to cross a pit (or any other feature) at its widest or deepest point caution should be exercised when feature dimensions must be based on limited coverage.

For purposes of description the pit is divided into three zones. These are berm, pit walls and pit floor.

From submersible observations a berm (raised rim) occurs on all sides of the depression except to the north (Fig. 28.4, 28.5). The berm is variable in width and height. Above the backwall, the berm is a discontinuous series of isolated mounds up to 2.5 m high, 4 m long, and 3 m wide. The poorly sorted berm material consists of boulders, gravel, sand, and blocks of underlying Tertiary sediment (Fig. 28.4, 28.5). Some of the blocks show intense bioturbation. The in situ Tertiary silt and clay sediments underlying the berm (Fig. 28.5a) show signs of deformation. Breakage surfaces and in one case doming of the previously flat lying sediments occurs. The sidewall berms are up to 2 m in height, are better sorted, and consist largely of gravel and sand

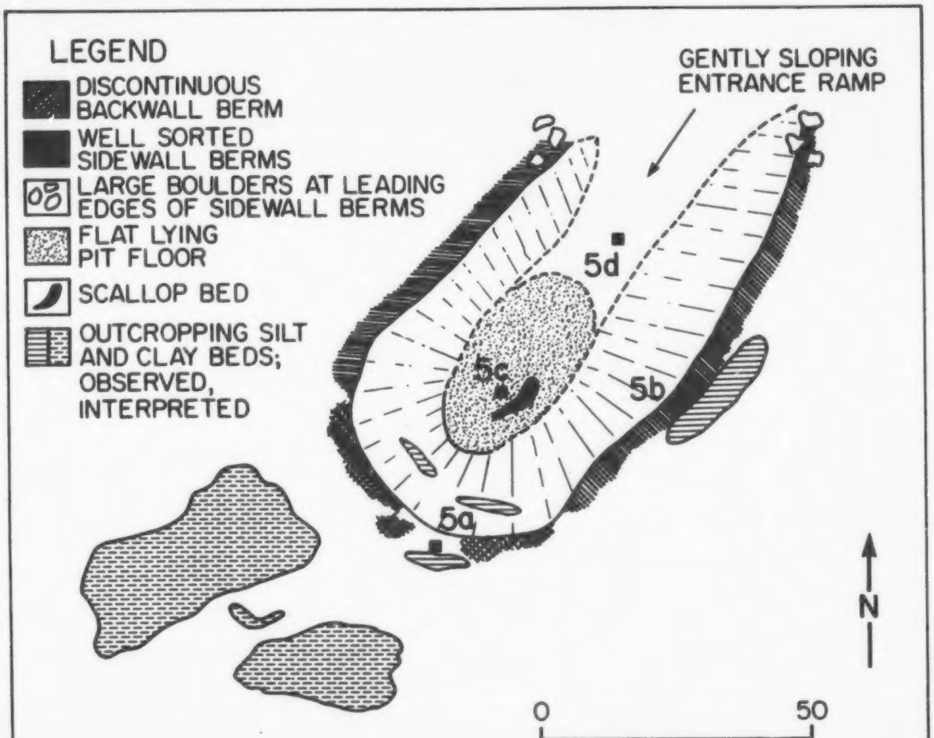

Figure 28.4. Schematic plan view of the iceberg pit based on submersible observations, showing the locations of the bottom photographs presented in Figures 28.5a-28.5d. Diagram prepared by Bedford Institute of Oceanography, Drafting and Illustrations.

Figure 28.5a. *Photograph showing the backwall berm and underlying silt and clay beds of probable Tertiary age.*

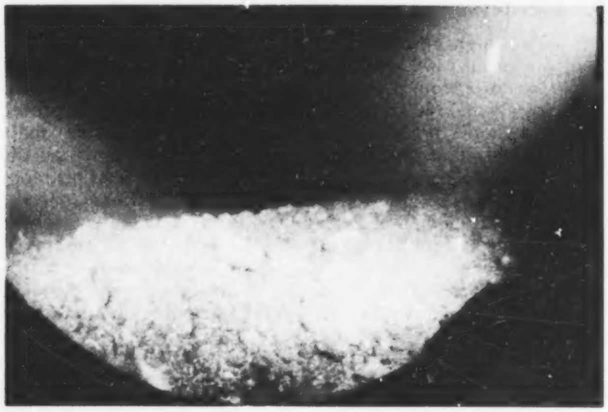

Figure 28.5b. *Photograph showing the sidewall berm.*

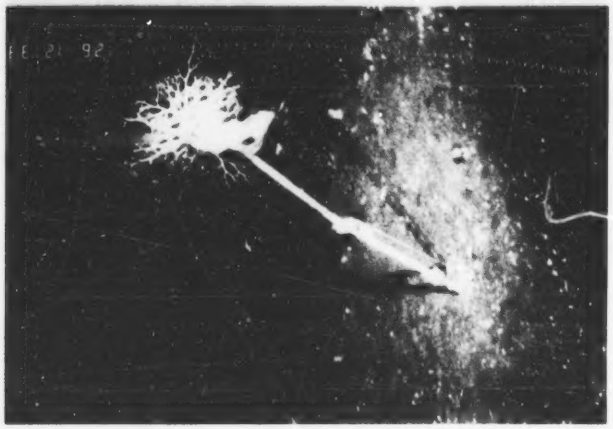

Figure 28.5c. *Photograph showing a 'depth of disturbance' rod in the sand of the pit floor.*

Figure 28.5d. *Photograph of parallel troughs on the entrance 'ramp' to the pit.*

(Fig. 28.5b). Boulders 1.5 to 2 m in diameter occur at the leading edge of each sidewall berm (Fig. 28.4). At the gently sloping "entrance" to the north there is a smooth slope break into the pit and no berm.

The walls of the pit have a thin veneer of gravel and sand overlying silt and clay sediments. Boulders are also present on the slope. The silt and clay beds outcrop in numerous places on the walls but are best exposed along the backwall where broken beds appear to be deformed and dip towards the centre of the pit. The wall slopes are variable. The maximum slope occurs at the backwall and ranges to 25 degrees. One slope measurement of 18 degrees was made near the base of the east sidewall using the inclinometer of the submersible. In general the slope angles average 20 degrees except to the north where the "entrance" ramp slopes less than 10 degrees.

The flat-lying pit floor measures 40 m by 25 m with its long axis perpendicular to the back wall (Fig. 28.4). Sediment on the floor consists of medium to fine olive grey sand (Fig. 28.5c) and scattered boulders are also found on the pit floor. A crescent shaped bed of Icelandic scallops (Chlamys Icelandicus) (Fig. 28.5c) is situated just east of the centre of the floor and shells are scattered throughout. The scallop bed was unchanged over the 10 month period between observations. A depth of disturbance rod implanted at the centre of the pit in October 1984 was still erect in August 1985 (Fig. 28.4, 28.5c). The rod showed an increase of 3-4 mm of fine grained sand deposited at this location.

Few sedimentary bedforms were associated with the pit. Wave induced ripples, with 30 cm wavelength and amplitudes of 2-3 cm were found on the floor of the pit. Low relief linear gravel troughs, approximately 50 cm wide, 15 cm deep with 1.5 m separation were observed on the shallow sloped north 'entrance' (Fig. 28.5d). These features were oriented towards the centre of the pit, parallel to the slope dip.

Pit origin and age

The overall shape of the pit describes a very short deep iceberg scour ending in an amphitheater-like depression. The steep back wall to the south and side walls surrounded by a berm and the shallow-sloped scour trough to the north, suggest that the depression was formed by a grounding iceberg trenching in a southerly direction. Similar depression and berm morphology have been described for undoubted ice scour marks from submersible and diving observations by Josenhans and Barrie (1982) on the Labrador Shelf, by Syvitski et al. (1983) for the eastern Canadian continental shelf and by McLaren (1982) in Byam Martin Channel.

To account for the depth of the depression, which is 8.5 m greater than the average iceberg scour depth for this water depth on the Grand Banks, a mechanism different from the dragging of an ice keel appears to be necessary.

It is suggested that the pit formation process began when an iceberg's centre of buoyancy changed due to calving or splitting. This resulted in the iceberg rolling to a new stable position, increasing its draught and impacting the seabed. Theoretical studies by Bass and Peters (1984) and Bass et al. (in press) have shown that such a scenario may occur with an increased draught of up to 50 per cent. More recently iceberg splitting and rotation with seabed grounding has been observed on the Labrador shelf (Lewis et al., 1985). The impact and subsequent deceleration due to grounding of the iceberg on the seabed produces a vertical dynamic load on the sediment. Inclined loading could possibly be accounted for by combination of the vertical load with horizontal loads related to initial direction of momentum decline of the iceberg, or to wave action and current drag on the grounded iceberg. A bearing capacity failure typically produces pressures exceeding the passive earth pressure (Terzaghi, 1943). Typical of the passive failure mode is heave of the seabed some distance away from the pit. Heave was observed at the pit as two zones of low reflectivity on the sidescan sonogram south of the pit. Further refinement of the seabed failure mechanism is required through calculation of forces produced by waves and currents on the iceberg, the determination of the sediment failure criteria, and the influence of wave loading on the seabed.

The age of the pit is not known but is considered to be measurable in tens of years. Its location above the lowest stand of sea level (Fader and King, 1981; Barrie et al., 1984), dates the feature within the post-transgressive age (<10 000 years). The exposure of the underlying silt and clay beds in an environment of active sediment transport indicates a short exposure time. No other fine grained sediments have been identified on the seabed of the area. The pit has little noticeable infill as seen by the depth of disturbance rod over one year and the pit walls show fresh bioturbated silt and clay beds and a fresh talus slope at the base of the wall. In addition, encrusting biological growth on talus boulders was sparse compared to growth on boulders on the surrounding seabed indicating recent disturbance (R. Hooper, personal communication). Finally, a nearby man-made pit, the Hibernia B-08 experimental glory hole which is only five years old, exhibits a similar character to that of the pit. Further work, including sampling, detailed acoustic profiling and comparison with other pits is required to confirm its origin and age.

Summary

Elongated depressions up to 10 m in depth found on the northeastern Grand Banks of Newfoundland are considered to be iceberg formed pits where the iceberg loading results in a bearing capacity failure and subsequent pit overdeepening. The 10 m deep depression examined by manned submersible observations in 87 m water depth is probably less than 100 years old. The processes that formed this iceberg pit and created sediment failure may be unique to areas of the continental shelf that consist of unlithified sediments and are influenced by grounding icebergs and an active wave regime.

Acknowledgments

The research presented here would not have been possible without the support of the Department of National Defence and in particular Commander Rick Bowers, for whom we have named the pit, the pilots of **SDL-1** and crew of the **HMCS Cormorant**. We would like to thank Bob Hooper of the Memorial University of Newfoundland who contributed his biological expertise to this project. In addition we thank Jørn Landva, C-CORE, and Steve d'Apollonia, Geological Survey of Canada, who assisted our study in many ways. Review of the manuscript and helpful suggestions were given to the authors by G.B. Fader, H.W. Josenhans, K. Moran, and C.M.T. Woodworth-Lynas. The work was supported by an OERD (Office of Energy Research and Development – Offshore Geotechnics Program) funding contract to C-CORE through the federal Department of Energy, Mines and Resources.

References

Amos, C.L. and Barrie, J.V.
1980: Hibernia and Ben Nevis seabed study – Polaris V cruise report, June 1980; C-CORE Data Report 30-17, 40 p.

d'Apollonia, S.J. and Lewis, C.F.M.
1981: Iceberg scour data maps for the Grand Banks of Newfoundland between 46°N and 48°N; Geological Survey of Canada, Open File Report, No. 819, 13 p.
– A numerical model for calculating long term spatial distribution and mean frequency of iceberg grounding events; Ice Scour Workshop, Feb. 5-6, 1985, Calgary, Alberta. (in press)

Barrie, J.V., Lewis, C.F.M., Fader, G.B., and King, L.H.
1984: Seabed processes on the north-eastern Grand Banks of Newfoundland: modern reworking of relict sediments; Marine Geology, v. 27, p. 209-227.

Barrie, J.V., Collins, W.T., Segall, M.P., and Lewis, C.F.M.
– Holocene development and sediment stability of the northeastern Grand Banks of Newfoundland; Geological Survey of Canada, Open File Report, 155 p. (in press)

Barrie, J.V., Collins, W.T., and Parrott, D.R.
– Grand Banks pits: description and postulated Origin; Proceedings of Ice Scour Workshop, Feb. 5-6, 1985, Calgary, Alberta. (in press)

Bass, D., Gaskill, H.S., and Carter, W.
– Iceberg generated pits: theoretical study; 5th International Symposium on Offshore Mechanics and Arctic Engineering, Tokyo, Japan. (in press)

Bass, D. and Peters, G.R.
1984: Computer simulation of iceberg instability; Cold Regions Science and Technology, v. 9, p. 163-169.

Dinsmore, R.P.
1972: Ice and its drift into the North Atlantic Ocean; International Commission for the Northwest Atlantic Fisheries Special Publication No. 8, p. 89-127.

Fader, G.B.
– Surficial and bedrock geology of the Grand Banks; Bedford Institute of Oceanography, Review 1985. (in press)

Fader, G.B. and King, L.H.
1981: A reconnaissance study of the surficial geology of the Grand Banks of Newfoundland; in Current Research, Part A, Geological Survey of Canada, Paper 81-1A, p. 45-56.

Fader, G.B., Lewis, C.F.M., Barrie, J.V., Parrott, D.R., Collins, W.T., Miller, R.O., and d'Apollonia, S.J.
– Quaternary geology of the Hibernia area of Northeast Grand Bank; Geological Survey of Canada, Open File. (in press)

Hovland, M.
1981: Characteristics of pockmarks in the Norwegian Trench; Marine Geology, v. 39, p. 103-111.

Josenhans, H.W., King, L.H., and Fader, G.B.
1979: A sidescan mosaic of pockmarks on the Scotian Shelf; Canadian Journal of Earth Sciences, v. 15, p. 1082-1092.

Josenhans, H.W. and Barrie, J.V.
1982: Preliminary results of submersible observations on the Labrador Shelf; in Current Research, Part B, Geological Survey of Canada, Paper 82-1B, p. 269-276.

King, L.H. and MacLean, B.
1970: Pockmarks on the Scotian Shelf; Bulletin of the Geological Society of America, v. 81, p. 3141-3148.

Lewis, C.F.M. and Barrie, J.V.
1981: Geological evidence of iceberg grounding and related seafloor processes in the Hibernia discovery area of Grand Bank, Newfoundland; in Symposium on Production and Transportation Systems for the Hibernia Discovery; Newfoundland Petroleum Directorate, St. John's, Newfoundland, p. 146-177.

Lewis, C.F.M., Parrott, D.R., Lever, J.H., Diemand, D., Dyke, M., Carter, W.J., and Stirbys, A.F.
1985: DIGS-85: dynamics of iceberg grounding and scouring: iceberg and seabed mapping observations; 14th Arctic Workshop: Arctic Land-Sea Interaction, Dartmouth, N.S., Nov. 6-8, 1985.

MacLaren, P.
1982: The coastal geomorphology, sedimentation and processes of eastern Melville and western Byam Martin Islands, Canadian Arctic Archipelago; Geological Survey of Canada, Bulletin 333, 39 p.

Markham, W.E.
1981: Ice Atlas, eastern Canadian seaboard; Atmospheric Environment Service, Environment Canada, Toronto, Ontario, 96 p.

Mobil Oil Canada Ltd.
1985: Hibernia Development Project Environmental Impact Statement; v. IIIa Biophysical Assessment; Mobil Oil Canada Ltd., St. John's, Newfoundland, 258 p.

Murray, J.E.
1969: The drift, deterioration and distribution of icebergs in the North Atlantic Ocean; in Canadian Institute of Mining and Metallurgy Special Volume 10, The Ice Seminar, p. 3-18.

Neu, H.J.A.
1982: 11-year deep-water wave climate of Canadian Atlantic waters; Canadian Technical Report of Hydrography and Ocean Sciences, No. 13, 41 p.

Petrie, B. and Anderson, C.
1983: Circulation on the Newfoundland Continental Shelf; Atmosphere-Ocean, v. 21, p. 207-226.

Syvitski, J.P.M., Fader, G.B., Josenhans, H.W., MacLean, B., and Piper, D.J.W.
1983: Seabed investigations of the Canadian east coast and Arctic using PISCES IV; Geoscience Canada, v. 10, p. 59-68.

Terzaghi, K.
1943: Theoretical Soil Mechanics; John Wiley and Sons, p. 26-41.

Structure and stratigraphy of the Gataga fold and thrust belt, northeastern British Columbia

K.R. McClay and M.W. Insley [1]
Cordilleran Geology Division and Economic Geology and Mineralogy Division

McClay, K.R. and Insley, M.W., Structure and stratigraphy of the Gataga fold and thrust belt, northeastern British Columbia; in Current Research, Part A, Geological Survey of Canada, Paper 86-1A, p. 259-264, 1986.

Abstract

In the Gataga River area of the Kechika Trough, western Rocky Mountains of northeastern British Columbia, strata ranging from Hadrynian to Late Devonian form a northwest-striking fold and thrust belt. The Kechika Trough consists of highly deformed Ordovician-Early Devonian Road River and mid-Late Devonian Lower Earn Group rocks. These argillites, cherts and siltstones are bounded on the west and east by platformal, shallow water carbonates. Stratiform barite-lead-zinc deposits occur in the Upper Devonian of the Lower Earn Group. Three phases of deformation are recognized. Phase 1 comprises asymmetric folding on northeast-trending axes. Mesozoic phase-2 deformation produced a complex pattern of southerly and northeasterly verging thrusts and folds with intense cleavage. The northwesterly striking structures of phase-2 are locally deformed by phase-3 dextral kink folds. During deformation the siliciclastic Road River and Earn Group rocks formed a weak plastic buffer zone between the more competent carbonate units that bound the trough to the east and west.

Résumé

Dans la région de la rivière Gataga de la dépression de Kechika, dans l'ouest des Rocheuses, dans le nord-est de la Colombie-Britannique, des couches allant de l'Hadrynien au Dévonien supérieur forment une zone de plis et de chevauchements d'orientation nord-ouest. La dépression de Kechika est constituée de roches très déformées de la formation de Road River datant de l'Ordovicien et du Dévonien inférieur et de la partie inférieure du groupe d'Earn datant du milieu du Dévonien supérieur. Ces argilites, cherts et pélites sont limités à l'ouest et à l'est par des carbonates de plate-forme mis en place en eaux peu profondes. Des dépôts stratiformes de barytine, plomb et zinc gisent dans le Dévonien supérieur de la partie inférieure du groupe d'Earn. On reconnaît trois phases de déformation. La phase 1 consiste en des plis dyssymétriques sur des axes de direction nord-est. La déformation de la phase 2, d'âge mésozoïque, a produit un réseau complexe de plis et de chevauchements de direction sud et nord-est, donnant lieu à un clivage intense. Les structures de direction nord-ouest de la phase 2 sont déformées par endroits par des plis en chevrons dextres de la phase 3. Durant la déformation, les roches silicoclastiques de Road River et du groupe d'Earn ont formé une zone tampon plastique et fragile entre les unités de carbonates plus compétentes qui limitent la dépression à l'est et à l'ouest.

[1] Department of Earth Sciences, University of London Goldsmiths' College, London SE8 3BU England

Introduction

Gataga River area (Fig. 29.1), a complex northwest-trending fold and thrust belt in the western Rocky Mountains of northeastern British Columbia, contains intensely folded, faulted and cleaved strata that range from Hadrynian to Late Devonian. The area contains part of the Kechika Trough – a narrow, long linear belt of Ordovician-Devonian, dominantly fine grained siliciclastic rocks that are the southern extension of the Selwyn Basin (Fig. 29.1).

The Kechika Trough contains significant stratiform Ba-Pb-Zn deposits in the Devonian Lower Earn Group siliciclastic rocks – e.g. Driftpile Creek, Cirque, Elf and Fluke deposits (MacIntyre, 1983; Carne and Cathro, 1982).

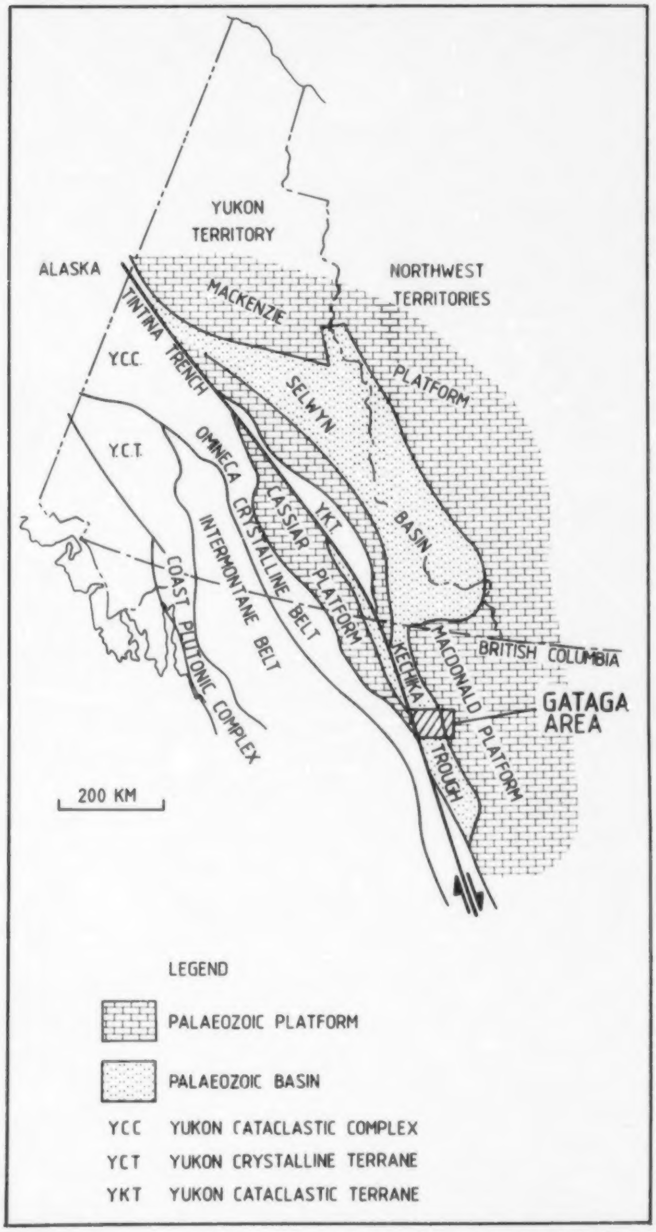

Figure 29.1. Location of the Gataga area in the Kechika Trough of northeastern British Columbia.

The regional and local geology of the Gataga region has received little detailed study and the tectonic and stratigraphic setting of the Driftpile Creek stratiform Ba-Pb-Zn deposits (MacIntyre, 1983) is poorly understood.

The present study was initiated in 1985 as part of an ongoing research program on the tectonics, stratigraphy and sedimentology of stratiform clastic-hosted lead-zinc deposits in the Canadian Cordillera (McClay, 1983a,b). The 1985 program included both detailed and regional mapping of the Driftpile Creek (Fig. 29.1) in the Gataga River district (NTS sheets 94E/16, 94F/14, 94K/4, 94L/1), and detailed structural and stratigraphic analysis. During 1985 mapping was concentrated on the area of Driftpile Creek and northwards to Braid Creek (94L/1).

Previous work in the Gataga area included regional 1:250 000-scale reconnaissance mapping by Taylor and Stott (1973), Gabrielse (1962) and MacIntyre (1981, 1983). Detailed mapping of the Driftpile Creek Ba-Pb-Zn deposit, carried out by Archer Cathro and Associates (Carne and Cathro, 1982), recognized the existence of a belt of highly folded and faulted Ordovician-Devonian fine grained siliciclastic rocks in the Gataga district. In this study we aim to establish a detailed stratigraphy for the Gataga district and to determine the sedimentological and structural evolution of the area focusing in particular on the stratiform Ba-Pb-Zn deposits.

Stratigraphy

Stratigraphic nomenclature adopted in this paper follows that of Fritz (1980), Gabrielse (1962), MacIntyre (1983) and Taylor and Stott (1973). Strata in the study area range from Hadrynian through to Late Devonian. They form a northwest-striking fold and thrust belt (Fig. 29.2). Generally recessive weathering Ordovician through Devonian shales, siltstones, cherts, thin limestones and lensoidal bodies of chert-pebble conglomerates form a highly deformed core of the thrust belt (Fig. 29.2, 29.3). These siliciclastic rocks are flanked on the west by generally resistant, west-dipping thrust panels of Cambrian through Early Ordovician limstone, dolomites, dolomitic siltstones and phyllites (Fig. 29.2), and on the east by thick, resistant, steeply dipping panels of folded and thrust Proterozoic argillites, sandstones, Cambrian quartzites and limestones (Fig. 29.2, 29.3). Stratigraphic columns which incorporate data from both the eastern and western parts of the map area are shown in Figure 29.4. Accurate thickness determinations are hampered by the intense deformation and cleavage.

Late Proterozoic (Hadrynian)

The lowermost strata exposed in the map area are a thick succession of green slates, phyllites and brown sandstones which are interpreted to be Late Proterozoic (Hadrynian) (Taylor and Stott, 1973). These form the cores of anticlines and the hanging-wall panels of thrust sheets at the eastern margin of the map (Fig. 29.4).

Gog Group (Lower Cambrian)

Grey-brown weathering quartzites and thin siltstones of Gog Group equivalents (Fritz, 1980) form resistant cores to anticlines at the eastern boundary of the map area (Fig. 29.2, 29.3). The quartzites, typically medium- to thick-bedded with abundant crossbedding, were assigned to the late Lower Cambrian **Bonnia-Oleneluss** by Fritz (1980). He suggested that these rocks may be correlative with the Gog Group of the southern Rocky Mountains.

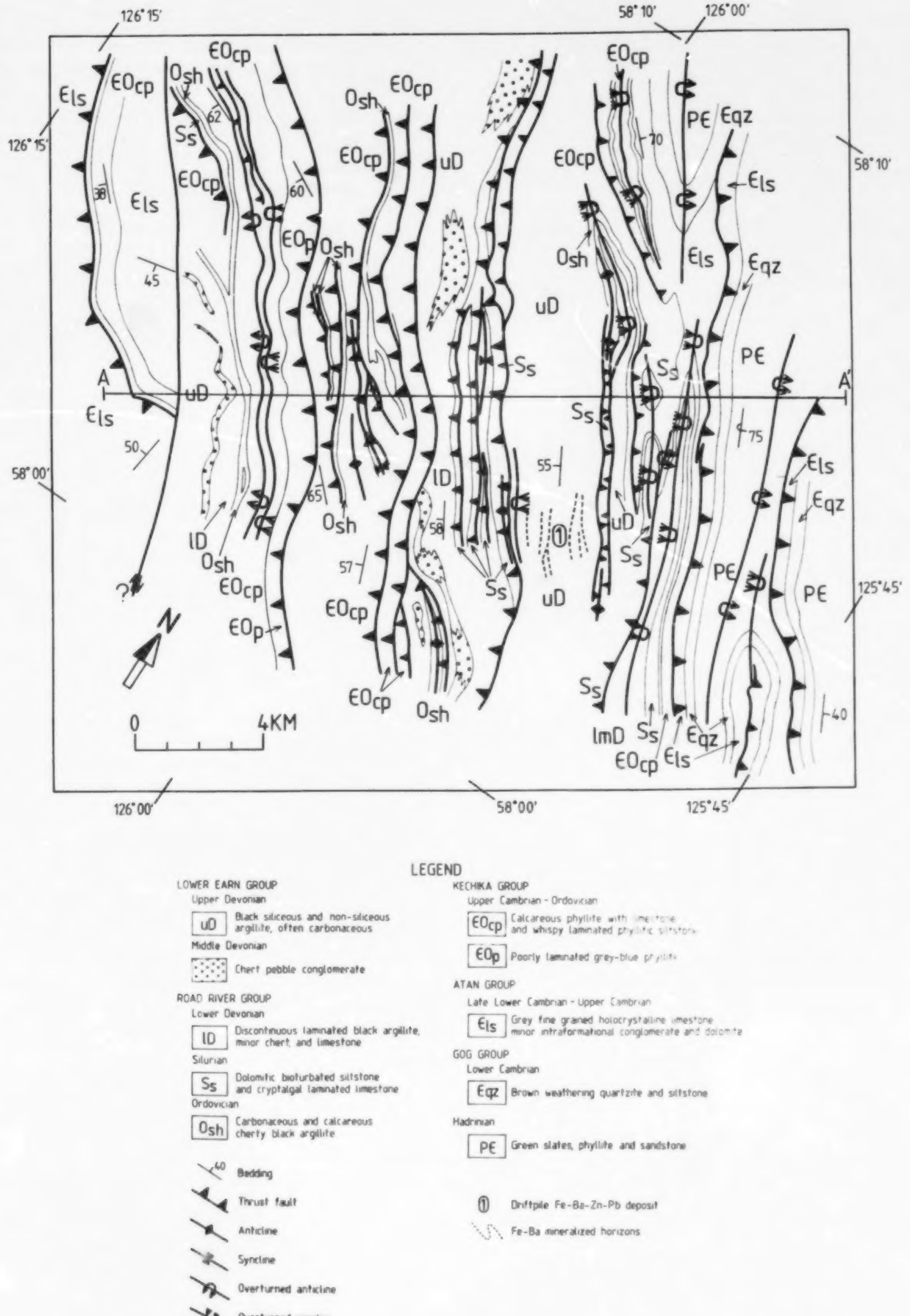

Figure 29.2. ***Preliminary geological map of the Gataga area. (1) is the Driftpile Creek barite-lead-zinc deposit.***

Atan Group (Late Lower Cambrian to Upper Cambrian)

The eastern panel of resistant carbonate units (Fig. 29.2, 29.3) consists of approximately 360 m of predominantly thin- to thick-bedded pale grey weathering, fine grained holocrystalline limestones, minor intraformational limestone conglomerates and pale cream-coloured dolomites (Fig. 29.4). These units are thrust westward over the Ordovician-Devonian siliciclastic sequences (Fig. 29.2, 29.3); a calcitic mylonite is developed at the base of the thrust units. In the western part of the map area possible Atan Group equivalents are resistant, highly deformed alternating thin- to medium-bedded limestones and dolomites (Fig. 29.2, 29.3). Further work is required to define the Cambrian stratigraphy in the western part of the map area.

Kechika Group (Upper Cambrian-Ordovician)

The Kechika Group rocks appear to conformably overlie the Atan carbonates in the map area. In the east the Kechika Group consists of approximately 150 m of grey-brown-weathering calcareous phyllites with intercalated thin bedded limestones and is apparently conformably or paraconformably overlain by the Ordovician black argillites and cherts. In the west approximately 400 m of poorly laminated grey-blue phyllites pass upwards into grey-brown phyllites with intercalated medium bedded grey limestones. In this part of the map area the intercalated limestone beds are more abundant than in the east. The calcareous phyllites and limestones are overlain by 200 m of bioturbated wispy argillites containing **zoophycos** and irregular burrow trace fossils. This upper unit of the Kechika Group is characterized by distinctive orange-weathering ferroan dolomitic beds up to 12 m thick.

Road River Group (Ordovician-Middle Devonian)

Ordovician through Devonian Road River rocks conformably overlie the Kechika Group. In the Gataga area the basal Road River rocks are a thin (approximately 30-60 m) succession of recessive, graptolitic carbonaceous black argillites, cherts and minor thin limestones. This in turn is overlain by 130 m of resistant, distinctive orange weathering dolomitic micaceous siltstones which contain Silurian graptolites and abundant burrow and grazing trail trace fossils. This Silurian siltstone is a unique map unit in the Gataga area; it is overlain by recessive, silver-grey weathering black argillites, black cherts and minor limestones of presumed Lower Devonian age. They are found at the western margin of the 'central fold and thrust belt' (Fig. 29.2, 29.3). The intense deformation of the fine grained siliciclastics of the Road River Group makes both thickness determinations and stratigraphic correlations difficult.

Lower Earn Group (Middle to Late Devonian)

The Road River Group is succeeded by a highly deformed sequence of Lower Earn Group (sensu lato after Gordy et al., 1982) 'black clastics'. In the 'western thrust belt' (Fig. 29.2, 29.3) the base of the Lower Earn Group is characterized by tongues of resistant, thick bedded chert-pebble conglomerates and chert grits which interdigitate with thin bedded laminated siltstones and silty banded argillites. This is overlain by several hundred metres of recessive, unlaminated to thinly laminated silver-grey-weathering black argillites, cherty argillites and cherts which range from Frasnian to Fammenian (Orchard, personal communication, 1985). This Late Devonian unit (informally called the 'Gunsteel Formation' farther south at the Cirque deposit (Jefferson et al., 1983)) contains at least two horizons of stratiform barite and barite-lead-zinc mineralization (Fig. 29.2). These horizons have been traced for at least 10 km along strike and are repeated by folding and thrust fault (Fig. 29.2). This unit is the uppermost formation exposed in the map area.

Structure

The map area consists of three distinct tectono-stratigraphic packages which exhibit complex polyphase folding and thrust faulting (Fig. 29.2, 29.3). The dominant structural features are northwest-striking thrust-bounded packages of chevron- to tightly-folded and cleaved strata. In the west the fault-bounded panels of the 'western thrust belt' (Fig. 29.3) are resistant units of Atan carbonates, highly deformed Kechika Group phyllites and Road River siliciclastics which have been thrust northeastwards on steeply west-dipping thrust faults (Fig. 29.3). The 'central fold and thrust belt' consists of tightly folded and faulted recessive-weathering Earn Group strata (Fig. 29.3). Fold axial planes and thrust planes are generally upright to very steeply dipping. The 'eastern thrust belt' consists predominantly of resistant Cambrian carbonates and younger strata which are thrust westwards over the Earn Group strata of the 'central fold and thrust belt' (Fig. 29.3).

A preliminary detailed structural analysis of the Gataga area has indicated at least three deformation phases:

1. An early, prethrusting and pre-main-cleavage phase of folding on northeast-trending fold axes. A local early cleavage is found around Phase-1 fold hinges.
2. Dominant northwest-striking, northeasterly-verging folding and thrusting with the accompanying development of a penetrative cleavage. The folds are tight to chevron style and generally plunge gently either to the northwest or to the southeast. The southwesterly verging folds and thrusts in the 'eastern thrust belt' (Fig. 29.3) may have

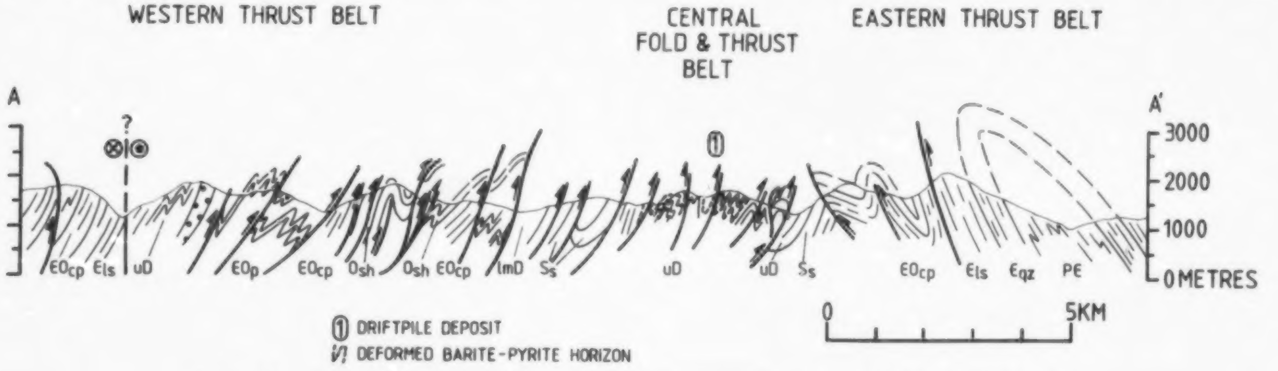

***Figure 29.3.** Southwest-northeast cross-section through the Gataga fold and thrust belt.*

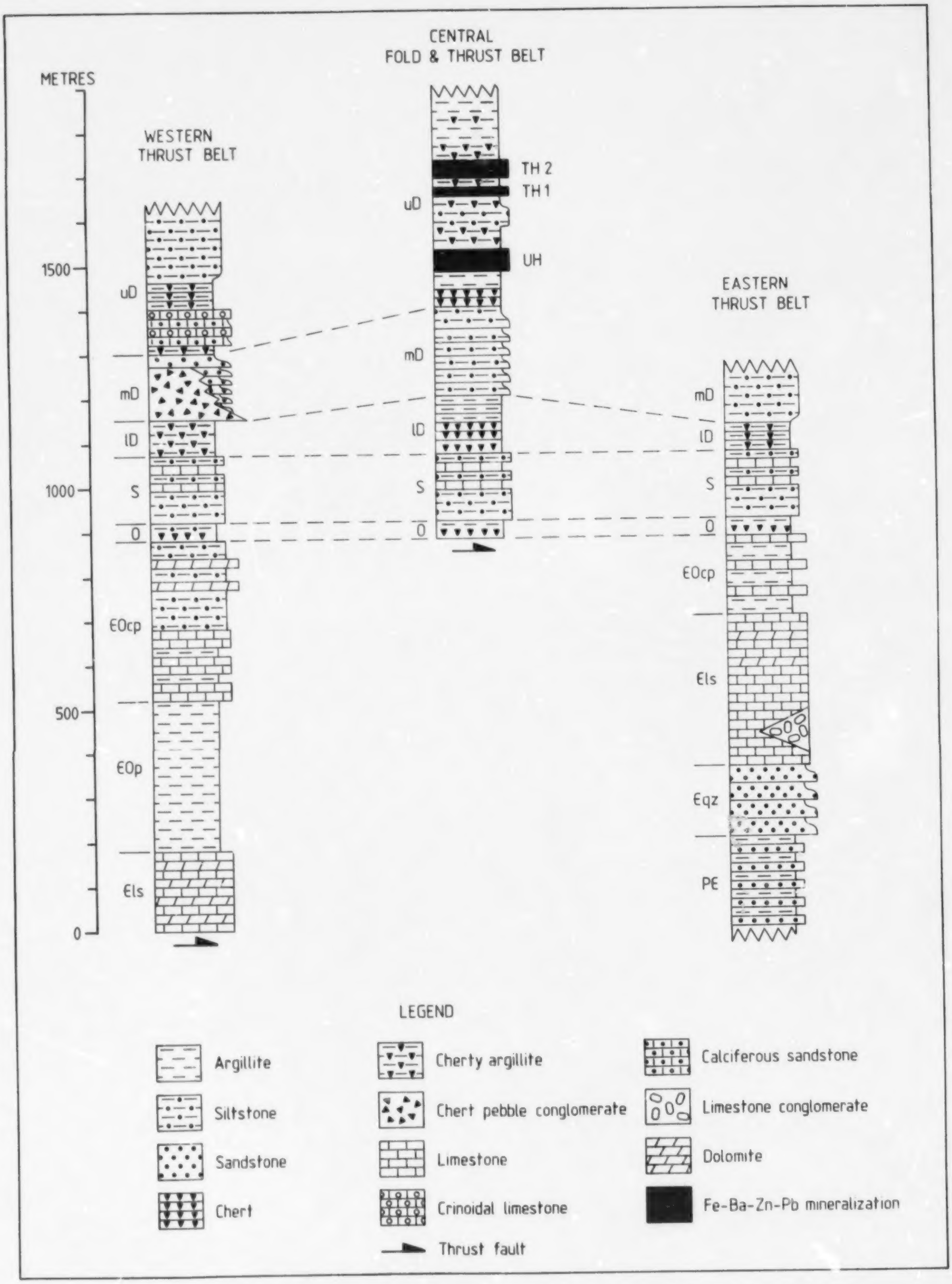

Figure 29.4. *Compilation stratigraphic sections through the Gataga fold and thrust belt.*

formed early in the Phase-2 deformation and have been subsequently rotated and steepened by later northeasterly directed thrusting. All thrust faults are now steeply dipping, having been rotated to that attitude by movement on underlying thrusts.

3. Late northeast- to east-striking dextral reverse kink-folding produced minor folds, dilatant vein systems and minor reorientation of earlier structures. To date only one important fault with possible strike-slip movement has been identified in the westen part of the map area (Fig. 29.2, 29.3).

Mineralization

The Lower Earn Group siliciclastics of the Gataga area host at least three occurrences of stratiform barite (±lead, zinc) mineralization. The most important of these is the Driftpile Creek deposit (Fig. 29.2) held by the Gataga Joint Venture. This deposit consists of at least two stratiform intervals of barite-pyrite-galena-sphalerite mineralization. Preliminary biostratigraphic analysis using conodonts indicates a Frasnian to Fammenian (Late Devonian) age (M. Orchard, personal communication, 1985) for the barite-lead-zinc deposits.

The barite mineralization is typically rhythymically interbedded massive, laminated and blebby barite and siliceous, cherty argillites ranging from 5 to 50 m in thickness. Local concentrations of pyrite, galena and sphalerite in the barite units have been drilled by the Gataga Joint Venture exploration group.

Discussion and conclusions

The first season's field work enabled us to establish a preliminary tectonic history and a lithostratigraphy for the Gataga area. Further biostratigraphic studies using conodonts are being undertaken. The deformation patterns in the Gataga area are more complicated than hitherto recognized. The identification of an early fold-event which may possibly be related to early- or syn-depositional tectonics could have had a significant effect on the distribution of the barite deposits within the Kechika Trough.

The dominant Mesozoic thrusting and folding of Phase-2 deformation produced both southwestward and northeastward tectonic transport on the margins of the Kechika Trough. There is a strong lithostratigraphic control on deformation style; the massive competent carbonate units form thick thrust panels whereas the fine-grained siliciclastics are tightly folded, cleaved and faulted in the 'central fold and thrust belt'. This 'palaeo-triangle zone' of 'soft' Road River and Earn group rocks in the Kechika Trough acted as a buffer zone between the two opposing thrust complexes to the northeast and southwest (Fig. 29.2, 29.3). Continued deformation on underlying 'blind thrusts' beneath the exposed section rotated and steepened the thrust sheets at the present surface.

Phase-3 deformation may be interpreted as a dextral-shear couple associated with Late Cretaceous dextral-strike-slip faulting along the Rocky Mountain Trench (Gabrielse, 1985). To date only one major possible strike-slip fault (Fig. 29.2) has been mapped in the Gataga area.

Acknowledgments

This project is supported by a Natural Environment Research Council Grant to K.R. McClay. Logistic assistance was provided by Archer Cathro and Associates and the Gataga Joint Venture, and by the Geological Survey of Canada through H. Gabrielse and D. Sangster. N. Way and J. Purcell gave able assistance in the field. R. Carne is thanked for valuable assistance and discussions on the geology of the Driftpile Creek area.

References

Carne, R.C. and Cathro, R.J.
1982: Sedimentary exhalative (sedex) zinc-silver-lead deposits, northern Canadian Cordillera; Canadian Institute of Mining and Metallurgy Bulletin, v. 75, p. 66-78.

Fritz, W.H.
1980: Two Cambrian stratigraphic sections near Gataga River, northern Rocky Mountains, British Columbia; in Current Research, Part C, Geological Survey of Canada, Paper 80-1C, p. 113-119.

Gabrielse, H.
1962: Kechika, British Columbia; Geological Survey of Canada Map 42-1962.

1985: Major dextral transcurrent displacements along the Northern Rocky Mountain Trench and related lineaments in north-central British Columbia; Geological Society of America Bulletin, v. 96, p. 1-14.

Gordy, S.P., Abbott, J.G. and Orchard, M.J.
1982: Devono Mississippian (Earn Group) and younger strata in east-central Yukon; in Current Research Part B, Geological Survey of Canada, Paper 82-1B, p. 92-100.

Jefferson, C.W., Kilby, D.B., Pigago, L.C. and Roberts, W.J.
1983: The Cirque barite-lead-zinc deposits, northeastern British Columbia; in Sediment hosted stratiform lead-zinc deposits, ed. D.F. Sangster; Mineralogical Association of Canada Short Course Notes, v. 9, p. 121-140.

McClay, K.R.
1983a: Structural evolution of the Sullivan orebody, Kimberly, British Columbia; Economic Geology, v. 78, p. 1398-1424.

1983b: Deformation of stratiform lead-zinc deposits; in Sediment hosted stratiform lead-zinc deposits, ed. D.F. Sangster; Mineralogical Association of Canada Short Course Notes, v. 9, p. 283-309.

MacIntyre, D.G.
1981: Geology of the Akie River Ba-Pb-Zn mineral district; British Columbia Ministry of Energy, Mines and Petroleum Resources, Preliminary Map 44.

1983: Geology and stratiform barite sulphide deposits in northeastern British Columbia; in Sediment hosted stratiform lead-zinc deposits, ed. D.F. Sangster; Mineralogical Association of Canada Short Course Notes, v. 9, p. 85-120.

Taylor, G.C. and Stott, D.F.
1973: Tuchodi Lakes map-area, British Columbia, Geological Survey of Canada, Memoir 373.

Petrogenesis of the McGerrigle plutonic complex, Gaspé, Quebec: a preliminary report[1]

Project 840021

J.B. Whalen and C. Gariépy[2]
Precambrian Geology Division

Whalen, J.B. and Gariépy, C., Petrogenesis of the McGerrigle plutonic complex, Gaspé, Quebec: A preliminary report; in Current Research, Part A, Geological Survey of Canada, Paper 86-1A, p. 265-274, 1986.

Abstract

The McGerrigle plutonic complex consists of a relatively compositionally homogeneous granite suite and a compositionally diverse (gabbro to granite) hybrid suite. Excellent field evidence for acid-basic magma mixing suggests that the granite suite is contemporaneous with or slightly younger than the hybrid suite. The complex contains a large spectrum of compositions (45-77 wt% SiO_2) which display generally smooth but nonlinear distribution patterns on Harker diagrams. The pluton has alkaline affinities and exhibits relatively similar chondrite normalized REE patterns (La/Yb = 5 to 22) for the mafic to felsic compositions. K-feldspar lead isotopic compositions show a considerable spread and variations which are independent of rock lithology.

Different petrologic processes worth consideration are fractional crystallization, multiple separate magmas, magma mixing and crustal and/or fluid phase interaction. Further work, now in progress, is required before a quantitative petrogenic model is possible.

Résumé

Le complexe plutonique McGerrigle comporte une suite granitique de composition relativement homogène et une suite hybride de composition variée (gabbroïque à granitique). Sur le terrain, on observe des phénomènes de mélange entre le magma acide et le magma basique qui semblent indiquer que la suite granitique est contemporaine ou légèrement plus jeune que la suite hybride. Le complexe contient des roches de composition très variable (45 à 77 % de SiO_2) qui montrent des patrons de répartition réguliers, mais non linéaires, sur les diagrammes de Harker. Le pluton est d'affinité alcaline et les patrons de répartition des terres rares sont semblables (La/Yb = 5 à 22) aussi bien dans les roches mafiques que dans les roches felsiques. Les mesures de la composition isotopique de plomb, faites sur des feldspaths potassiques, montrent de très grandes distributions et variations qui ne sont pas liées à la lithologie des roches.

Les processus pétrogénétiques dignes de mention sont la cristallisation fractionnée, l'existence de magmas multiples, le mélange de magmas et l'interaction du magma avec les matériaux de la croûte ou une phase fluide, ou les deux. Les résultats de travaux en cours permettront d'élaborer un modèle pétrogénétique quantitatif.

---

[1] Contribution to the "Plan de dévelopment économique Canada/Gaspésie et Bas Saint-Laurent, Volet Mines 1983-1988

[2] Department des Sciences de la Terre; Université du Québec à Montréal, Casse Postale 8888, Succursale "A", Montréal, P.Q. H3C 3P8

Introduction

The McGerrigle plutonic complex covers a rugged area of about 100 km^2 in the Gaspé segment of the north-central Appalachian orogenic belt (Fig. 30.1). The heterogeneous nature of the intrusive complex and spectacular evidence for the coexistence and mixing of mafic and felsic magmas have been previously documented (Whalen, 1985). In this paper we report on preliminary petrological, geochemical and isotopic data collected to date and we constrain the petrogenetic models for the intrusive complex to a few possible cases. Studies of the mineral chemistry, the isotopic geochemistry (O and Pb) and the geochronology (U/Pb on accessory minerals and K-Ar on mafic silicates) have been initiated and they should allow us to better understand and quantify the genesis of the complex.

General Geology

The McGerrigle plutonic complex can be roughly subdivided into granite and hybrid suites. The bulk of the granite suite occurs in the southern portion of the pluton (Fig. 30.1). The hybrid suite, though mainly restricted to the northern half of the pluton, does outcrop to the north and southeast of Mount Richardson and to the east of Les Cones. The hydrid suite includes a component lithologically identical to the granite suite rocks but the contact relationships between the hybrid and granite suites are ambiguous: contacts appear to be gradational in many areas, being marked by the appearance of mafic indlusions in the granite. However, there are also examples of sharp intrusive relationships between younger granite and hybrid suite rocks. Based on their outcrop area, granitic rocks form about 75% of the complex, basaltic rocks about 5% and hybrid rocks (dioritic to syenitic composition) about 20%. A modal quartz-plagioclase-K-feldspar plot (Fig. 30.2) and modal data for representative samples (Table 30.1) illustrate the range of rock types present in the McGerrigle plutonic complex.

The radiometric age of the pluton is at present controversial. K/Ar whole-rock ages on two granite samples from the northern portion of the pluton gave ages of 356.4 ± 4 Ma and 346.2 ± 7 Ma (de Romer, 1977). Work in progress using Rb/Sr systematics on whole-rock samples suggests distinct periods of intrusion in the northern and the southern portion of the complex, separated by a time gap of some 25 Ma (C. Laroque, personal communication 1985). Altogether, this suggests the complex was intruded during Devonian time, but further work will be required to fine-tune the history of the plutonic suite.

The relatively compositionaly homogeneous granite suite has been subdivided into different intrusive phases on the basis of grain size, feldspar mineralogy and equigranular or porphyritic character. Contacts between the phases, which are not shown in Figure 30.1, appear to be mainly gradational. The granitic rocks vary in colour from scarlet red to white and their main mafic mineral is biotite with local hornblende ± pyroxene. Magnetite, apatite, zircon, titanite and allanite are minor accessory phases.

The hybrid suite consists of geologically complex and compositionally diverse mixtures of gabbro, basalt, diorite, quartz diorite, granodiorite, monzodiorite, quartz monzonite, syenite, and granite. Although some portions of the hybrid suite have been subdivided into homogeneous intrusive units on a scale of 1:25 000, the most striking feature of the bulk of the suite is its heterogeneity on both map and outcrop scale. Variations in texture and composition commonly are very rapid such that it is often difficult to decide whether such variants represent large inclusions or contemporaneous or younger intrusions. In the case of mafic-felsic mixtures, contact relationships described by Whalen (1985) such as chilled margins on mafic inclusions, pillow-like structures of chilled basaltic rock in granite and broken-up mafic dykes cutting granite, indicate the coexistence of mafic and felsic magmas. On an outcrop scale there is evidence for intermediate or hybrid rocks produced by mixing, but the field relationships are complex and indicate multiple injection and hybridization.

The mafic portion of the hybrid suite ranges in grain size from fine- to coarse-grained and forms small bodies scattered over the northern half of the pluton. In some areas mafic rocks form abundant inclusions in more felsic hybrid suite rocks. The finer grained variants often occur in close proximity to felsic rocks and exhibit evidence of potassium metasomatism in the form of fine grained secondary biotite. The mineralogy is titanaugite, plagioclase (labradorite), kaersutitic amphibole, titaniferous manganiferous biotite, apatite, ilmenite, magnetite and sulphides (G.M. Wallace, personal communication). A main feature which distinguishes felsic portions of the hybrid suite from the granite suite is a lower content of quartz (<10%) and the common presence of patchy mafic mineral aggregates derived from partially digested mafic xenoliths. Such aggregates vary in colour from grey to reddish, are fine- to medium-grained and range in texture from hypidiomorphic granular to porphyritic. Mafic mineral content ranges to as high as 30%, the main phase being hornblende, commonly with salitic clinopyroxene cores, and less abundant biotite. Opaques, zircon, titanite, apatite and allanite are common accessory phases. Associated with the two southern areas of hybrid suite rocks are metasomatized gabbros which vary from fine- to coarse-grained and form areas up to 0.5 km across. Primary calcic plagioclase has been replaced by untwinned plagioclase and the mafic minerals are pseudomorphed by diopside plus rutile and titanite.

In the northern portion of the pluton near Mount Passe, there are a number of pod-shaped bodies of miaskitic nepheline syenite which have irregular, probably gradational contacts with hybrid suite rocks. They are porphyritic with perthitic alkali feldspar, biotite and aegerine-augite phenocrysts in a trachytic textured matrix of similar mineralogy plus nepheline, apatite, titanite, zircon and oxides (sample WXMG16 in Table 30.1). Relationships suggest that this undersaturated magma was contemporaneous with the magmas that produced the hybrid suite. Also, cutting hydrid suite rocks in the northern part of the pluton, are rare, thin (up to 3 m wide) peralkaline nepheline syenite dykes or sills which contain trachytic textured alkali feldspar, nepheline, sodalite, aegerine, arfvedsonite, aenigmatite and accessory minerals (sample WXMG37 in Table 30.1).

Geochemistry

Analytical methods

The geochemical analyses were completed at the Université de Montréal, using the following techniques: major element analyses were carried out on glass discs using an automated X-ray fluorescence (XRF) spectrometer; the CO_2 and H_2O+ contents were measured by gas chromatography using the method outlined by Brooks et al. (1969); trace element analyses were completed by XRF on pressed powder pellets (Schroeder et al., 1980) except for Sc, Cs, Hf, Ta, Th, U, and the REE which were determined by instrumental neutron activation analysis using the method of Bergerioux et al. (1979).

Initial Pb isotopic compositions were determined on K-feldspar separates which were severely leached in order to remove all Pb of a secondary origin (Gariépy and Allègre, 1985). The measurements were completed at the Institut de Physique du Globe de Paris using the techniques described by Manhès et al. (1984).

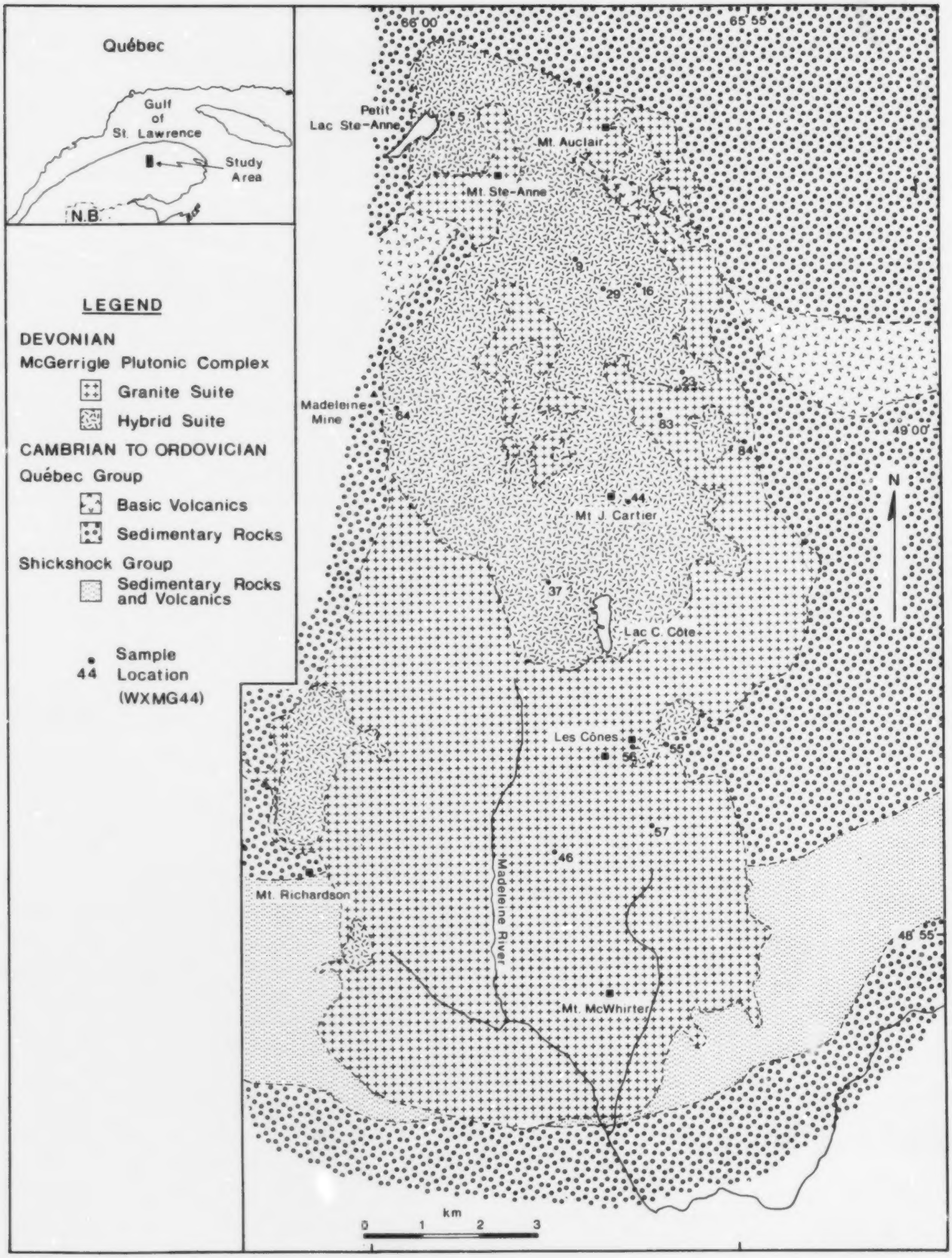

Figure 30.1. Location of the McGerrigle plutonic complex, Gaspe, Quebec and a generalized geological map of the area giving locations of some studied samples.

General Features

Representative analyses from the different suites present in the McGerrigle complex are listed in Table 30.2 and the sample locations are shown in Figure 30.1. The salient features of the geochemical data collected to date are illustrated in Figures 30.3 to 30.7 and described below.

1. A very large spectrum of compositions covering a large range in silica content (45 to 77 wt%) is present in the complex.
2. With the exception of the metasomatized rocks and the Quebec Group metabasalts, all samples display low water contents and negligible amounts of CO_2, indicating that the rocks were probably not affected by secondary alteration processes.

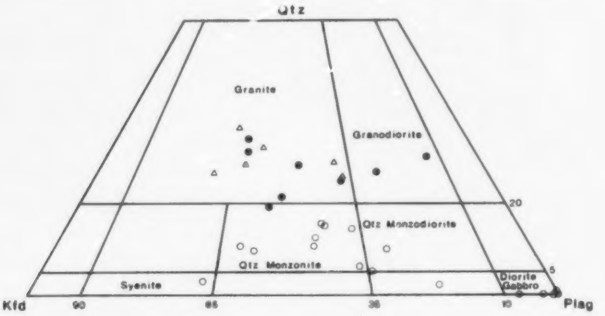

Figure 30.2. *Modal composition of representative samples of the McGerrigle plutonic complex; nomenclature after Streckeisen (1973): (O) hybrid suite; (●) granite suite samples from the northern portion of the complex; (Δ) granite suite.*

3. On Harker diagrams (Fig. 30.3) the suite exhibits generally smooth but non-linear distribution patterns. These are of two main types: (a) negative correlations, slightly to strongly curved and (b) concave upward type distributions. The negative correlations with SiO_2 are exhibited by FeO, MgO, CaO, P_2O_5, Sc, Cr, Ni, Cu, and Zn which are elements entering the major mineral phases; the existence of a negative trend between P^{205} and SiO_2 suggests that apatite is a liquidus phase. The concave upward distribution is exhibited by two major elements (Na_2O and Al_2O_3) and by trace elements such as Zr, REE, Hf, Th and U. In granitoid systems, the latter trace elements are mainly controlled by accessory phases such as zircon, sphene or allanite (Exley, 1980; Fourcade and Allègre, 1982) and the concave upward type distributions indicate that such accessory phases became insoluble at some point in the history of the magmas. Compared to both types of distribution, the nepheline syenites and some of the hybrid suite syenites plot outside the main trends, at a point opposite to the maximum curvature of the trends, suggesting an unusual formational process. Elements which are mainly controlled by the feldspar minerals and biotite, such as K_2O and Rb, exhibit positive, somewhat scattered, correlations with SiO_2 whilst Sr (Fig. 30.3e) has a complex negative correlation. Within the granite suite K_2O, Rb, and Sr, exhibit variations.
4. The suite has alkaline affinities as indicated by a Na_2O+K_2O versus SiO_2 diagram (Fig. 30.4) and by very high contents of large-ion lithopile elements. Also, when compared to alkaline (A-type) granitoids throughout the world (Whalen et al., in preparation), the suite has moderate Zr and high Nb contents (Fig. 30.5).

Table 30.1. Representative modal data* for the McGerrigle plutonic complex

	Hybrid suite								Granite suite				Nepheline syenite	
Symbols[1]	0	0	s	X	o	o	*	*	a	a	+	+	N	N
WXMG No.	64	23	55	5	9	29	87	44	56	57	46	83	16	37
Quartz	0.0	1.8	0.0	2.2	0.3	0.0	8.0	8.8	25.5	27.4	27.2	27.1	0.0	0.0
K-feldspar	0.0	15.0	0.0	1.8	0.2	20.3	21.9	46.5	49.2	42.4	25.4	33.5	78.3	61.8
Plagioclase	52.1	54.1	64.9	47.6	63.7	42.7	49.2	33.6	21.1	25.6	40.3	35.3	0.0	0.0
Nepheline	0.0	0.0	0.0	0.0	0.0	0.0	0.0	0.0	0.0	0.0	0.0	0.0	9.2	19.3
Sodalite	0.0	0.0	0.0	0.0	0.0	0.0	0.0	0.0	0.0	0.0	0.0	0.0	0.0	2.8
Biotite	12.4	6.9	0.0	9.3	28.9	23.1	0.1	1.6	2.2	2.3	4.0	2.0	4.6	0.2
Amphibole	25.3	10.7	0.0	33.2	1.4	0.7	14.2	6.7	1.6	1.0	2.3	1.7	0.5	3.5
Clinopyroxene	6.1	3.4	25.1	tr	1.6	8.4	2.2	tr	0.0	0.0	0.0	0.0	2.5	11.9
Aenigmatite	0.0	0.0	0.0	0.0	0.0	0.0	0.0	0.0	0.0	0.0	0.0	0.0	0.0	0.6
Titanite	0.0	0.9	7.3	0.0	2.7	0.9	0.9	0.1	0.3	tr	0.0	0.2	1.9	0.0
Zircon	0.0	tr	0.1	0.0	0.1	0.1	0.1	0.1	tr	tr	tr	tr	2.2	0.0
Apatite	0.9	1.5	2.6	2.4	1.0	1.4	0.6	tr	tr	0.1	tr	tr	0.0	tr
Allanite	0.0	0.1	0.0	0.0	0.0	0.0	0.0	0.0	0.1	0.0	tr	tr	0.0	0.0
Opaques	3.2	5.6	0.0	3.5	tr	2.4	2.8	2.7	0.1	1.1	0.9	0.2	0.8	0.0
Fluorite	0.0	0.0	0.0	0.0	0.0	0.0	0.0	0.0	0.0	0.0	0.0	0.0	0.0	tr

* Modes are the product of 2 000 points on a 16 by 10 cm rock slab stained using the methods of Norman (1974) and 1 200 points on a thin section except for the fine grained sample WXMG5 which is a thin section point count only.

[1] Symbols as used in Figures 30.3, 30.4 and 30.8.

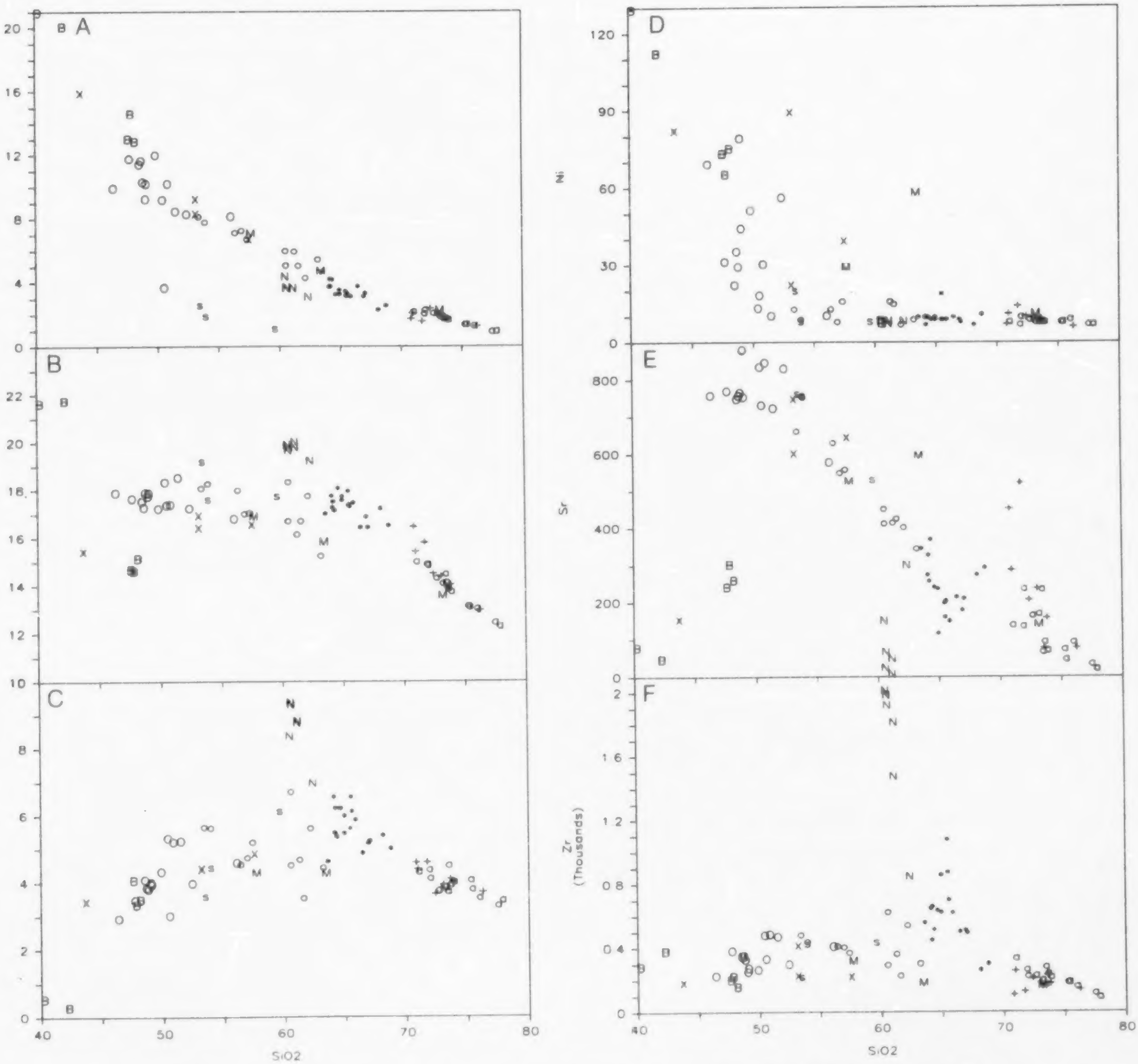

Figure 30.3. *Representative Harker variation diagrams for the McGerrigle plutonic complex.*

(N) nepheline syenites
Granite Suite
(a) K-feldspar dominant granites
(+) two-feldspar granites
Hybrid Suite
(*) quartz monzodiorites to syenites (o) diorites and hybrid rocks

(O) gabbros and diabases
(X) mafic xenoliths
(M) mixed samples
(s) metasomatized gabbro

(B) Quebec Group basalt

Table 30.2. Representative chemical analyses from the McGerrigle plutonic complex

	Hybrid suite								Granite suite				Nepheline syenite	
Symbols[1] WXMG	0	0	s	X	o	o	*	*	a	a	+	+	N	N
No.	64	23	55	5	9	29	87	44	56	57	46	83	16	37
SiO_2	47.83	55.46	53.97	57.03	51.91	59.56	61.14	66.78	73.41	72.40	72.49	73.65	61.21	59.58
TiO_2	1.85	2.10	2.90	1.46	1.98	0.94	1.13	0.52	0.25	0.29	0.36	0.25	0.67	0.29
Al_2O_3	17.29	16.59	17.63	16.38	17.60	18.06	16.61	16.75	13.67	13.66	14.53	14.00	18.85	19.31
Fe_2O_3	2.33	2.93	0.36	1.92	2.76	1.70	1.94	1.10	1.01	0.82	0.99	0.81	1.79	2.98
FeO	6.90	5.40	1.60	4.90	5.50	3.50	3.30	2.00	0.80	1.00	1.50	1.00	1.40	0.90
MnO	0.17	0.15	0.05	0.14	0.18	0.15	0.1	0.08	0.06	0.05	0.04	0.05	0.15	0.27
MgO	6.98	2.95	4.03	3.80	3.39	1.46	2.48	0.54	0.28	0.32	0.56	0.33	0.49	0.07
CaO	8.23	5.21	13.74	6.11	5.11	2.54	5.89	1.43	0.72	1.01	1.93	1.30	1.29	0.90
Na_2O	3.89	4.53	4.46	4.80	5.52	6.61	3.53	5.10	3.99	3.88	3.66	3.99	6.83	9.21
K_2O	1.67	3.03	0.32	1.70	2.54	3.59	3.05	5.38	5.06	4.78	3.96	4.30	5.49	4.99
P_2O_5	0.54	0.72	1.09	0.52	0.90	0.40	0.24	0.16	0.11	0.11	0.13	0.11	0.16	0.09
H_2O	1.33	0.61	0.56	0.97	0.98	0.45	0.50	0.16	0.31	0.20	0.21	0.22	0.60	0.75
CO_2	0.15	0.12	0.12	0.19	0.14	0.14	0.04	0.07	0.30	0.16	0.07	0.16	0.13	0.08
C_1	0.06	0.04	0.04	0.06	0.07	0.03	0.05	0.03	0.02	0.06	0.03	0.02	0.01	0.19
F	0.07	0.10	0.16	0.06	0.12	0.07	0.06	0.06	0.06	0.06	0.05	0.04	0.04	0.05
TTE	0.17	0.16	0.17	0.14	0.20	0.17	0.12	0.15	0.10	0.10	0.09	0.08	0.20	0.34
Total	99.46	100.10	101.20	100.18	98.90	99.37	100.18	100.31	100.15	98.90	100.60	100.31	99.31	100.00
Trace Elements (ppm)														
Rb	37	89	11	51	156	102	86	138	190	172	148	130	152	188
Sr	879	575	758	642	662	413	426	174	72	96	207	158	300	23
Zr	249	405	427	217	486	626	230	498	218	240	206	177	845	1979
Nb	53	69	79	62	103	104	48	97	69	61	36	46	202	362
Y	31	50	78	31	48	33	37	65	57	54	39	32	32	62
Cr	44	5	6	33	6	4	11	5	3	3	1	2	0	5
Ni	79	10	8	39	13	7	15	8	8	8	10	8	8	7
Cu	43	24	6	15	16	9	14	4	3	2	7	4	4	3
Zn	86	50	14	70	116	83	50	40	28	33	30	23	61	134
Sc	17.0	12.2	20.9	13.6	10.6	3.7	15.4	4.1	2.3	2.9	3.7	2.5	1.6	0.8
Cs	1.5	1.2	NA	0.9	3.9	1.9	1.2	1.5	2.8	2.2	1.9	1.8	2.5	2.0
Hf	5.3	8.8	10.6	5.3	9.8	12.4	6.5	13.1	7.1	8.0	6.7	5.5	14.6	34.6
Ta	3.0	4.8	4.1	3.2	5.8	6.8	3.5	6.5	5.7	6.7	4.5	5.0	10.8	17.9
Th	4.7	15.3	5.3	10.3	11.2	19.9	18.7	34.2	33.1	25.3	21.1	26.0	17.5	59.4
U	1.3	3.8	2.3	2.5	3.3	4.2	3.6	4.2	5.5	4.5	3.7	3.6	4.6	14.0
La	47.7	69.9	42.4	56.3	86.5	63.6	54.2	156.5	99.0	68.9	52.5	47.4	93.5	155.1
Ce	86.7	130.8	128.1	99.9	162.7	134.0	93.5	215.3	126.8	116.2	92.2	81.9	155.2	248.5
Nd	31.5	48.7	67.1	34.3	55.2	36.6	32.4	61.2	43.4	34.0	27.7	24.1	34.8	54.0
Sm	7.37	10.90	16.40	7.15	11.60	7.22	6.84	11.10	8.79	7.50	6.02	4.81	6.49	9.39
Eu	2.07	2.63	3.71	1.69	2.75	1.73	1.48	1.39	0.80	0.92	0.94	0.86	1.08	0.63
Tb	1.11	1.57	2.29	0.98	1.49	0.91	1.05	1.47	1.23	1.07	0.87	0.76	0.89	1.38
Yb	2.24	3.71	5.17	2.24	3.77	3.23	2.85	4.62	4.44	4.71	3.15	2.59	3.76	7.25
Lu	0.34	0.59	0.83	0.37	0.63	0.51	0.37	0.73	0.68	0.72	0.50	0.40	0.67	1.22

Analyst C. Gariépy

[1] Symbols as used in Figures 30.3, 30.4 and 30.8.

5. Chondrite normalized REE patterns for the various intrusive types present in the complex are presented in Figure 30.6. Within the hybrid suite, mafic rocks (including gabbros, mafic xenoliths, and diabase dykes), diorites, and mixed rocks show normalized La/Yb ratios in the range of 4.9 to 21.8 and are indistinguishable on the basis of their REE patterns. The metasomatically altered gabbros are similar to the other mafic hybrid suite rocks (Fig. 30.6a) but with slightly flatter chondrite normalized patterns. The quartz monzodiorites and quartz monzonites are essentially similar except that some quartz monzonites and syenites (Fig. 30.6c) have slight to moderate negative Eu anomalies with Eu/Eu* values of 0.77 to 0.91. Though the granite suite (Fig. 30.6d, 30.6e) exhibits considerable variation in REE abundance and La/Yb ratios (9.7 to 16.5), and the K-feldspar dominant granites have strong negative Eu anomalies (Eu/Eu* = 0.66-0.74), most granite samples have patterns similar to

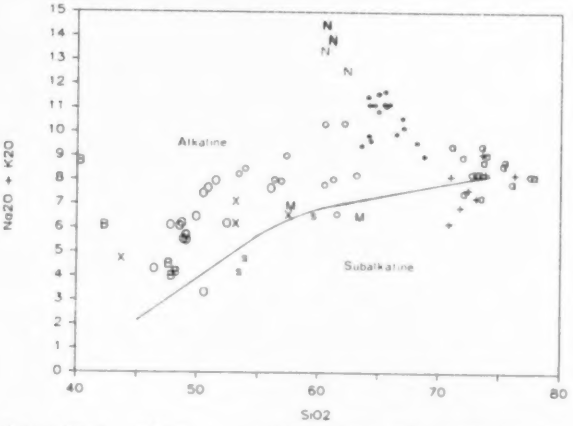

Figure 30.4. *(K_2O + Na_2O) versus SiO_2 plot for the McGerrigle plutonic complex showing the boundary between alkalic and subalkalic rocks (Miyashiro, 1978) (symbols as in Fig. 30.3).*

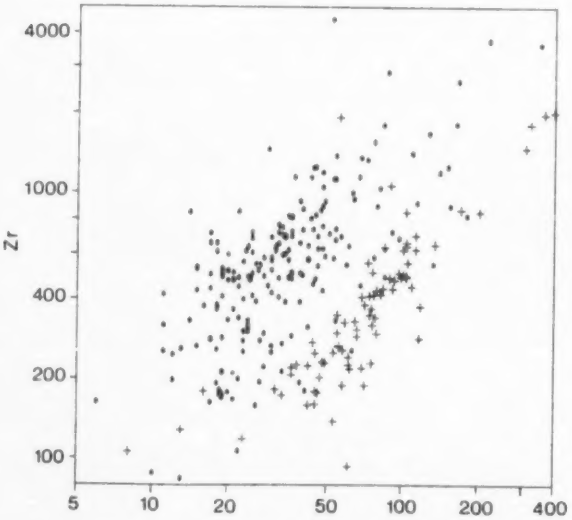

Figure 30.5. *Zr versus Nb plot for the McGerrigle plutonic suite (+ symbols) and A-type granitic rocks from elsewhere in the world (* symbols) (data from Whalen and Currie, in prep.).*

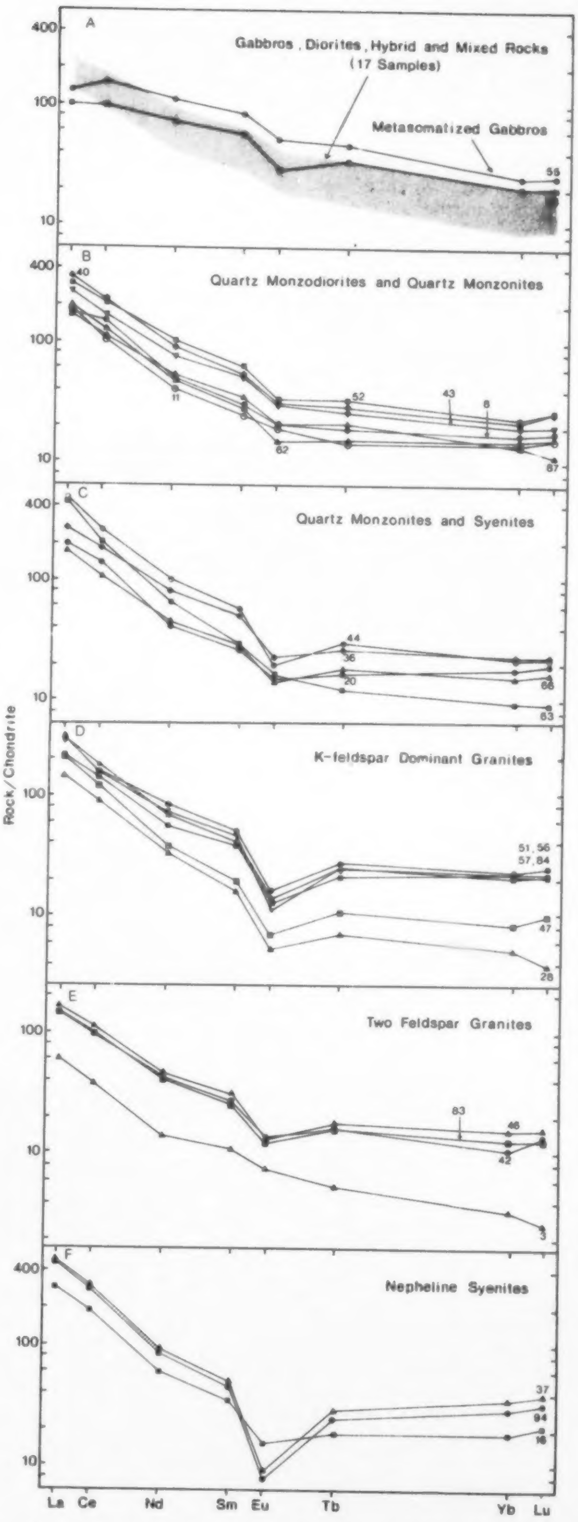

Figure 30.6. *Whole rock REE data normalized to chondritic abundances of Taylor and Gorton (1977) for the various intrusive rock types of the McGerrigle plutonic complex.*

hybrid suite rocks. The two analyzed peralkaline syenite dykes (samples WXMG-37 and 94 in Fig. 30.6f) have identical strong negative Eu anomalies (Eu/Eu* = 0.57) and greater LREE enrichment than other intrusive rocks in the pluton. In contrast, the miaskitic nepheline syenite pattern (sample WXMG-16 in Fig. 30.6f) is almost identical to some of the hybrid suite quartz monzonites.

6. From their bulk chemical composition, there is no apparent evidence that the granite or the hybrid suite rocks in the southern portion of the pluton are distinct from lithologically similar rocks located in the northern sector of the complex. Within the granitic suite, there are important trace element variations but these show no clear geographical systematics and are most likely related to the crystallization of the granitic samples. Granitic samples which have a higher plagioclase content (Fig. 30.2) and higher CaO and Sr content (eg. WXMG-5 in Table 30.2) appear to be ones which are closely associated with mafic hybrid suite rocks.

7. The initial Pb-isotopic composition of some 40 representative samples from the McGerrigle complex, determined directly on uranium-free K-feldspar separates, is illustrated in Figure 30.7. There are several features on this diagram. Firstly, the initial Pb-isotopic compositions show a considerable spread with $^{206}Pb/^{204}Pb$, $^{207}Pb/^{204}Pb$ and $^{208}Pb/^{204}Pb$ ratios ranging from 18.02 to 19.04, 15.52 to 15.63, and 37.80 to 39.10 respectively. When compared to the field occupied by Hercynian granitoid rocks from Western Europe (Michard-Vitrac et al., 1981), the McGerrigle complex alone displays an even wider range of variations. Secondly, when examined in terms of lithologic type, the data do not define any apparent grouping: for example, the granitic suite rocks display both the lowest and the highest initial Pb-isotopic compositions. Thirdly, relative to the field occupied by north Atlantic mid-ocean ridge basalts, the McGerrigle samples are more radiogenic, showing higher $^{207}Pb/^{204}Pb$ and $^{208}Pb/^{204}Pb$ isotopic compositions for comparable $^{206}Pb/^{204}Pb$ ratios.

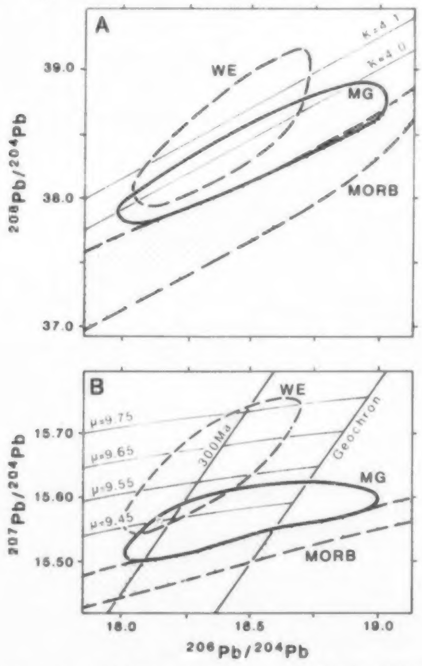

Figure 30.7. *(a) $^{206}Pb/^{204}Pb$ versus $^{207}Pb/^{204}Pb$ correlation diagram summarizing the results obtained on K-feldspars from the McGerrigle complex (solid line field labelled MG). The composition of Hercynian granitoid intrusives (Michard-Vitrac et al., 1981) from Western Europe (WE) and the composition of North Atlantic mid-ocean ridge basalts (stippled) Dupré and Allègre, 1980) corrected 350 Ma backwards are shown for comparison. Single stage growth curves for closed-system evolution using Stacey and Kramers (1975) data are shown for reference together with the present-day and the 300 Ma old geochrons.* ***(b)*** *$^{206}Pb/^{204}Pb$ versus $^{208}Pb/^{204}Pb$ correlation diagram comparing the McGerrigle data to Western Europe (WE) and to MORB.*

Discussion

The geochemical and isotopic characteristics observed to date in the McGerrigle plutonic complex most likely result from a combination of various magmatic processes. These are individually considered below.

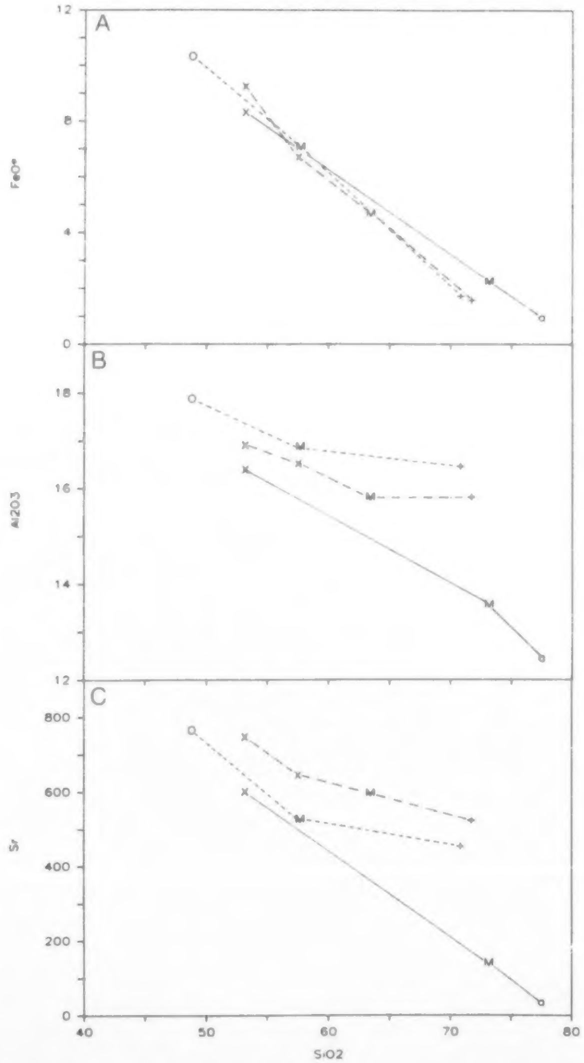

Figure 30.8. *Representative Harker variation diagrams illustrating the chemical variations of granite-mixed sample-mafic sample suites from three locations in the northern portion of the McGerrigle pluton; samples from the same site are joined by tie lines and symbols are as in Figure 30.3.*

1. Fractional crystallization

Features of the complex are not compatible with the fractional crystallization of a single magma to generate the suite of igneous rock types present in the complex. Firstly, fractional crystallization alone cannot generate variations of the Pb-isotopic composition; the observed spectrum requires at least the presence of a second component. Secondly based on outcrop area, the largest proportion (~75%) of the complex is granitic and only a small proportion (~5%) is basaltic, this is contrary to what would be expected from fractional crystallization of one magma.

At a smaller scale, there is evidence for limited crystal fractionation. For example, the correlation between the compatible elements and the SiO_2 content could result from fractionation of the major mineral phases. Also, some of the variations in Rb and Sr contents coupled with the existence of important Eu anomalies in granitic rocks (Fig. 30.6d, 30.6e) are most readily explained by feldspar fractionation. In addition, the fact that incompatible elements such as Zr, Nb, Hf, Ta, and the REE do not show consistent and large increases throughout the suite could be explained by fractionation of accessory phases. Consequently, fractionation of separate parent magmas, fractionation coupled with magma mixing or assimilation induced fractional crystallization are reasonable possibilities to generate the different portions of the complex.

2. Multiple separate magmas

One possibility is that the complex formed from a number of distinct separate magmas (heterogeneous source areas) which have undergone some crystal fractionation. If geochronological work indicates significant time gaps between different portions of the complex coupled with the presence of isotopically distinct domains, then considerable support would be provided for such a model. However, the fact that there is a compositional continuum within the suite characterized by fairly smooth chemical variations, the exception being the nepheline syenites, and a lack of distinctive groupings of lithological types on Pb-isotopic plots weigh against this model.

3. Magma mixing

Field evidence from this complex documented by Whalen (1985) indicated the presence of contemporaneous acid and mafic magmas. As in the case of the Topsails Igneous Terrane (Whalen and Currie, 1984), it was thought that interaction or hybridization between these two end members might be responsible for the range of intrusive rock types present in the complex. To help test this hypothesis, a suite of samples was collected from each of three locations where textural evidence for coexisting acid-basic magmas was best exposed. From each location a granitic, a mafic and a mixed (mafic inclusions in granite) sample was analyzed. The mixed samples do fall on or close to lines joining their two component rock types for many elements (Fig. 30.8) but the relationships are not, based on the work of Whalen and Currie (1984), as linear as was expected. The mixed samples do not bear a close chemical resemblance to the hybrid rocks as they should if the hybrid rocks are the products of mixing of these same two components (compare Fig. 30.3 and Fig. 30.8). Also, the markedly nonlinear distribution patterns on Harker diagrams of the suite for many elements is incompatible with a simple two component mixing model. It should be noted that in the plots which are nonlinear (Fig. 30.3), the nepheline syenites consistently plot opposite the curve or inflection point in the trends. This feature suggests the possibility of a three component mixing model involving a granitic, a basaltic and an intermediate undersaturated magma. One possible problem which such a model is the observed volume of undersaturated rocks present in the complex. As these rocks are rather difficult to distinguish in the field from the other syenites, this may be more an apparent rather than a real problem.

4. Crustal interaction

One straightforward explanation for the observed Pb-isotopic patterns observed in the complex is a mixture of an unradiogenic (mantle-derived?) component with various components from the continental crust. Once again, however, simple binary mixing with a crustal contaminant is ruled out by the data as single lithological suites (e.g. the granitic rocks) yield both unradiogenic and very radiogenic compositions. More complex scenarios will have to be considered such as, for example, crustal contamination coupled with fractional crystallization or injection of mantle-derived mafic magma(s) inducing partial melting at lower crustal depths.

Similarly a possibility, suggested by de Romer (1977), is that the hybrid suite mafic component represents altered basalts which may be equivalent to Quebec Group wall rocks. Contamination of a granitic magma with these wall rocks might have produced the hybrid suite. Although this model does not explain the origin of the alkaline gabbroic rocks, this possibility was tested for the hybrid suite and a number of samples of Quebec Group metabasalts were analyzed. The results indicate that the mafic component associated with the hybrid suite is distinct from the Quebec Group metabasalts; however, some of the mafic xenoliths in the granites are similar to the basalts, suggesting that some assimilation did occur, at least in the granitic suite rocks.

5. Effects of an aqueous fluid phase

In addition to the magmatic mechanisms discussed above, some of the complex could be the product of interaction with, or loss of, an aqueous fluid phase. Massive pervasively altered gabbros associated with the hybrid suite supports an active role for an aqueous fluid phase. Also, the existence of undersaturated alkaline rocks within the complex, igneous rocks often characterized by fluid generated alteration (fenetization), indicates this process needs to be seriously considered. In addition, the distribution of the hybrid rocks, their fine grained nature and their associated granitic rocks as well as the coarser grained nature of the granitic rocks in the southern part of the complex are compatible with the hybrid suite being a roof-zone complex. Unusual behavior of major and trace elements, in part due to the activity of an aqueous fluid phase, has been documented in the roof-zones of other granitic plutons (e.g. Whalen, 1983).

Conclusions

The above discussion of several magma-modifying processes allow us to eliminate some simple petrogenetic models for the evolution of the McGerrigle complex and stress the need for careful interpretation and chemical modelling of the existing data base. It is clear that the genesis of the complex is the result of a combination of the processes considered above. Consequently, further work is required to constrain these processes to a few plausible cases. In particular, dating of the different suites could help decipher the intrusion sequence as a function of time and oxygen isotopic tracing should constrain the processes of crustal interaction and the effects of a fluid phase.

Acknowledgments

We acknowledge C.J. Allègre and J.N. Ludden for allowing access to their geochemical facilities and G. Gauthier and R. Lapointe for their skilled technical help.

References

Bergerioux, C., Kennedy, G., and Zikovsky, L.
1979: Use of the semi-absolute method in neutron activation analysis; Journal of Radioanalytical Chemistry, v. 50, p. 229-234.

Brooks, C., Hart, S.R., Krogh, T.E., and Davis, G.L.
1969: Carbonate contents and $^{87}Sr/^{86}Sr$ ratios of calcites from Archean meta-volcanics; Earth and Planetary Science Letters, v. 6, p. 35-38.

de Romer, H.S.
1977: McGerrigle Mountains area; Quebec Ministry of Natural Resources, Geological Report 174, 233 p.

Dupré, B. and Allègre, C.J.
1980: Pb-Sr-Nd isotopic correlation and the chemistry of the North Atlantic mantle; Nature, v. 286, p. 17-22.

Exley, R.A.
1980: Microprobe studies of REE-rich accessory minerals; implications for Skye granite petrogenesis and REE mobility in hydrothermal systems; Earth and Planetary Science Letters, v. 48, p. 97-110.

Fourcade, S. and Allègre, C.J.
1981: Trace element behavior in granite petrogenesis: a case study. The calc-alkaline plutonic association from the Qerigut complex (Pyrenees, France); Contributions to Mineralogy and Petrology, v. 76, p.177-195.

Gariépy, C. and Allègre, C.J.
1985: The lead isotope geochemistry and geochronology of late-kinematic intrusives from the Abitibi greenstone belt, and the implications for late Archean crustal evolution; Geochimica et Cosmochimica Acta, v. 49

Manhès, G., Allègre, C.J., and Provost, A.
1984: U-Th-Pb systematics of the eucrite "Juvinas": Precise age determination and evidence for exotic lead; Geochimica et Cosmochimica Acta, v. 48, p. 2247-2264.

Michard-Vitrac, A., Albarede, F., and Allègre, C.J.
1981: Lead isotopic composition of Hercynian granitic K-feldspars constrains continental genesis; Nature, v. 291, p. 460-464.

Miyashiro, A.
1978: Nature of alkalic volcanic rock series; Contributions to Mineralogy and Petrology, v. 66, p. 91-104.

Norman, B.
1974: Improved techniques for selective staining of feldspars and other minerals using Amaranth; United States Geological Survey Journal of Research, v. 2, p. 73-79.

Schroeder, B., Thompson, G., Sulanowski, M., and Ludden, J.N.
1980: Analysis of geological materials using an automated X-ray fluorescence system; X-ray Spectrometry, v. 9, p. 198-205.

Stacey, J.C. and Kramers, J.D.
1975: Approximation of terrestrial lead isotope evolution by a two-stage model; Earth and Planetary Science Letters, v. 26, p. 207-221.

Streckeisen, A.L.
1973: Classification and nomenclature of plutonic rocks, recommendations; Geotimes, v. 18, no. 10, p .26-30.

Taylor, S.R. and Gorton, M.P.
1977: Geochemical application of spark source mass spectrometry – III element sensitivity, precision, and accuracy; Geochimica et Cosmochimica Acta, v. 41, p. 1375-1380.

Whalen, J.B.
1983: The Ackley City batholith, southeastern Newfoundland; evidence for crystal versus liquid-state fractionation; Geochimica et Cosmochimica Acta, v. 47, p. 1443-1457.

1985: The McGerrigle plutonic complex, Gaspé, Quebec: evidence of magma mixing and hybridization; in Current Research, Part A, Geological Survey of Canada, Paper 85-1A, p. 795-800.

Whalen, J.B. and Currie, K.L.
1984: The Topsails igneous terrane, Western Newfoundland: evidence tor magma mixing; Contributions to Mineralogy and Petrology, v. 87, p. 319-327.

– Geochemical characteristics of A-type granites. (in preparation)

Geology of the Slave Province and Thelon Tectonic Zone in the Tinney Hills-Overby Lake (west half) map area, District of Mackenzie

Project 830010

Peter H. Thompson, Nicholas Culshaw, J.R. Buchanan[1], and P. Manojlovic[2]
Precambrian Geology Division

Thompson, P.H., Culshaw, N., Buchanan, J.R., and Manojlovic, P., Geology of the Slave Province and Thelon Tectonic Zone in the Tinney Hills-Overby Lake (west half) map area, District of Mackenzie; in Current Research, Part A, Geological Survey of Canada, Paper 86-1A, p. 275-289, 1986.

Abstract

In the Thelon Tectonic Zone and the Slave Province adjacent to the west, a late Archean straight belt has been overprinted by an early Proterozoic event. These events are expressed by a NNE-SSW zonation. The westernmost zone preserves a record of an Archean crust segmented into a relatively stiff superstructure separated from a more ductile infrastructure along the sillimanite zone within which occurs the limit of granite migration and one or more tectonic slides. High grade metasediments of the Yellowknife Supergroup in the eastern Bathurst Terrane underlie a central zone of high grade Archean strain overprinted by staurolite-chlorite and lower grade tectonites. The lower grade tectonites are associated with basement-involved deformation of the Goulburn Group and a possible ductile phase of the Bathurst fault. The easternmost zone, the Ellice River Terrane, is dominated by a straight belt formed in quartzofeldspathic gneisses. Dextral transcurrent motion was important in forming this zone.

Résumé

La zone tectonique de Thelon a été formée par un événement majeur qui s'est superposé, au début du Protérozoïque, à une déformation antérieure (Archéen?) de la croûte d'ampleur régionale. L'événement du Protérozoïque a laissé sa trace dans le socle cristallin sous la forme d'une zonation qui est dirigée du nord-nord-est au sud-sud-ouest. La zone la plus à l'est englobe le terrain d'Ellice River, dominé par la présence d'une zone rectiligne dans des gneiss quartzo-feldspathiques. Un mouvement de décrochement dextre a contribué pour beaucoup à la formation de cette zone. Sur des sédiments très métamorphisés du supergroupe de Yellowknife, dans l'est du terrain de Bathurst, repose une zone centrale dans laquelle des staurolites-chlorites et des tectonites de métamorphisme moins avancé trahissent une certaine compression. Les tectonites moins métamorphisées sont associées à une déformation postnappe du groupe de Goulbourn qui a également affecté le socle. (La faille de Bathurst a peut-être connu une phase ductile à cette époque.) La zone d'extrême ouest constitue, par rapport à la zone tectonique de Thelon, un avant-pays relativement peu déformé, où s'est préservé un témoin d'une croûte archéenne qui comprend une superstructure assez cassante séparée d'une infrastructure plus ductile par des gradients de métamorphisme qui constituent la limite de la migration des granites et le site de glissements tectoniques.

[1] Department of Geology, University of Ottawa, Ottawa, Ontario K1N 6N5
[2] Department of Geology, Carleton University, Ottawa, Ontario K1S 5B6

Introduction

The map area includes part of the Thelon Tectonic Zone (TTZ), a 75-100 km wide feature having variable but distinctive topographic, geophysical, and geological characteristics that occurs along the eastern boundary of the Slave Structural Province of the northwestern Canadian Shield (Thompson and Henderson, 1983; Thompson et al., 1985). With a complex history spanning more than one billion years and including at least two orogenic episodes, one late Archean and the other early Proterozoic, the poorly known and imperfectly defined Thelon Tectonic Zone is important to an understanding of both provinces and may provide useful insight into other major Precambrian structural boundaries. Furthermore, the extent to which the geology of the Slave Province, with its demonstrated economic potential for gold and base metal deposits, is continuous into and across the Thelon Tectonic Zone is of prime interest. The main emphasis of this project is the crystalline rocks that make up 98% of the area mapped. The remainder includes rocks of the early Proterozoic Goulburn Group which unconformably overlie the Archean along the western limit of mapping and contain a clear record of parts of the latest event of the polyorogenic history evident in the crystalline rocks of the area.

Part 1 of this report includes completed versions of the preliminary lithologic, dyke, and metamorphic maps published by Thompson et al. (1985), summarizes the lithology and metamorphism, and considers briefly the significance of the map area for the Thelon Tectonic Zone in general. Part 2 (N.C.) describes the structural aspects of the regional mapping completed this summer and highlights of the local structural studies.

Mapping at 1:250 000 scale of the crystalline rocks and a thin fringe of sedimentary cover in the Tinney Hills (76J) and Overby Lake (76I, W/2) map areas was completed this year. Otto van Breemen (GSC) sampled extensively for geochronology and Nicholas Culshaw (GSC) studied a number of structural problems evident from last year's mapping. Dan Thompson (Princeton) finished the 1:50 000 scale mapping that will provide the geological basis for a Ph.D. study of the polymetamorphic regional metamorphism across the western boundary of the Thelon Tectonic Zone in the southern part of the area. Work continued on a petrographic/X-ray diffraction/microprobe study of the low grade metamorphism of the Goulburn Group (Martin Frey, Basel), mineral chemistry and geothermobarometry of Archean pelitic migmatites (Michael Brown, Kingston, U.K.), petrology of basic dykes (Randy Buchanan, University of Ottawa), and compilation and analysis of structural geology of the area (N.C.). Detailed work on a sillimanite grade ductile shear zone (Normand Bégin, Laval) is complete and samples were collected for B.Sc. theses on part of the kyanite-staurolite overprint present in Archean migmatites (David Corrigan, University of Ottawa) and on the petrochemistry of a pluton in the Ellice River Terrane (Mark Newman, McMaster).

Acknowledgments

With pleasure we acknowledge the enthusiastic, hardworking and cheerful assistance of David Corrigan, Francine Gaudard, Melanie Haggart, Mark Newman and Marc Tremblay. A first class job of cooking, baking, ordering and running the kitchen was done by Robyn Brown. Martin Irving, once again, did an excellent job of expediting for us. Logistical assistance provided by Bill Padgham and the Geology Office of the Department of Indian Affairs and Northern Development was much appreciated. Ptarmigan Airways provided high quality fixed wing support. John Henderson and Maurice Lambert constructively reviewed the manuscript.

PART 1. LITHOLOGY, METAMORPHISM AND THE THELON TECTONIC ZONE

P.H. Thompson, J.R. Buchanan, and P. Manojlovic

Lithology

The current project has refined and extended the Archean and Proterozoic geological framework outlined in the region so ably by Fraser (1964, 1968, 1978).

A pronounced angular unconformity separates the early Proterozoic clastic and carbonate rocks of the Goulburn Group (Campbell and Cecile, 1976, 1981) from Archean metasedimentary rocks and granite along the western limit of the area mapped. These rocks were deformed and metamorphosed (Thompson and Ashton, 1984; Thompson and Frey, 1984) at low grade during an event that produced thrusts and folds in the cover (Tirrul, 1985) which were subsequently, locally, tightly folded and interlayered with basement thrusts (see below) that in some cases may be rooted in reactivated Archean structures. The sedimentology of these rocks has been linked to events in Wopmay Orogen to the west (Campbell and Cecile, 1981) and to a rising source area in the direction of the Thelon Tectonic Zone (Hoffman et al., 1984; Grotzinger and Gall, 1986). The late phase metamorphic assemblages overprinted on the Archean rocks of the map area imply 12-15 km of Proterozoic uplift and erosion either during or after deposition of the Goulburn Group.

Thompson et al. (1985) divided the crystalline rocks into the Bathurst and Ellice River terranes west and east, respectively (Fig. 31.1), of the "main boundary zone", a line which, in the south half of the area, coincides with a marked change in lithology, a relatively low grade transcurrent shear zone, a characteristic aeromagnetic expression, and a swarm of metamorphosed and variably deformed diabase/gabbro dykes. The boundary was taken to be the western limit of the Thelon Tectonic Zone, that is -the Thelon Front. The boundary was drawn along the contact between the "pink" gneiss/migmatite/granitoid unit and the main mass of metamorphosed supracrustal rocks of the Yellowknife Supergroup. In the north half of the map area this relationship is maintained but the lithologic contact diverges from the other features and overall lithologic contrast between the two terranes is greatly reduced. While division into two terranes is a convenient way to deal with the geology in the map area, this year's mapping has shown that the approach may not work to the north. It must be noted that the term "terrane" is not meant to imply that the particular entity is "suspect" (or not). The term is simply intended to denote the gross geological contrasts between the two areas of the map sheet.

Bathurst Terrane

Most of the Bathurst Terrane is made up of aluminosilicate-bearing migmatites derived from associated pelitic schist and metagreywacke of the Yellowknife Supergroup. Thin zones or lenses of a highly variable lithologic package, including layered amphibolite,

fine grained quartzofeldspathic gneisses, pelitic schist/psammite, migmatite, marble/calc-silicate gneiss and metagabbro are scattered across the metasedimentary terrane and associated with the migmatitic/plutonic complex to the north. These rocks, in part of volcanic origin, are most prominent along or just east of the boundary with the Ellice River Terrane and in the southwest corner of the map area. The felsite unit is present as layers or lenses in the metasediments west of Gordon Bay. Equivalents of this unit already removed by erosion may be the source of felsic volcanic clasts in the Amagok Formation of the Goulburn Group noted by Campbell and Cecile (1981) and Grotzinger and Gall (1986).

Garnet-amphibole-quartz gossan rocks (meta-iron formation) occur within the metasedimentary rocks at all metamorphic grades (Fig. 31.1). Ten samples of the silicate-rich part of these features were assayed for gold with results ranging from <5 to 420 ppb. All the occurrences noted by Thompson and Culshaw (1985) have been staked. Several more were found this year in the Yellowknife Supergroup east of the Hiukitak River and one west of Overby Lake (Fig. 31.1).

The metaplutonic rocks that comprise about 15 per cent of the terrane are grouped into leucogranite/granodiorite and tonalite/diorite suites. White weathering two mica granites and associated white tourmaline-bearing pegmatites, locally containing sillimanite, garnet and/or cordierite, are compositionally similar to migmatite leucosomes and commonly contain abundant metasedimentary inclusions. The field relations are compatible with their derivation from the surrounding metasedimentary rocks at some point below the present erosion surface. Three of the pegmatites have Late Archean ages (van Breemen, personal communication, 1985). The syntectonic nature of most of these plutons and their occurrence in the sillimanite zone near the migmatite isograd, which is in part a high grade shear zone or slide, supports the conclusion they are part of the late Archean main phase tectono-metamorphic event in the map area. The other more mafic suite ranges from biotite-hornblende granodiorite to tonalite. These rocks are foliated, metamorphosed, and, locally, migmatized. They are limited in their distribution to the northern part of the Bathurst Terrane and as small plutons along the boundary with the Ellice River Terrane, where they are associated with the heterogeneous supracrustals. A thin layer of tonalite and a string of smaller bodies outlines the major fold in the central part of the terrane. Occurrences of garnet-amphibole-quartz gossan rocks associated with zones (too thin to show on the map) of felsic and hornblende bearing gneisses follow the same trend.

North of the Hiukitak River (Fig. 31.1), rocks of the granodiorite-tonalite suite are part of a heterogeneous complex of variably migmatized and foliated plutonic rocks, hornblende migmatite/gneiss, thin belts of layered amphibolite, pelitic migmatite and at one locality a garnet granite. This association is similar to that in the northern part of the Ellice River Terrane, although the fine grained straight gneisses are absent. Reconnaissance mapping (Fraser, 1964) indicates the predominant metasedimentary character of the Bathurst Terrane does not continue to the north.

Several swarms of basic dykes intrude the Bathurst Terrane. The youngest dykes, part of the Mackenzie swarm (~1200 Ma) are characteristically fresh and highly magnetic. Pre-Goulburn Group dykes (Fig. 31.2), both discordant and concordant with respect to structure and layering in the country rock, can be divided into four types.

(a) Discordant porphyritic or amygdaloidal metadiabase dykes localized in the western part of the Bathurst Terrane; trend 340-000°, known to intrude type (b).

(b) Massive metadiabase/gabbro, 340-090° moderately to strongly discordant to high grade country rock fabrics; grade ranging from lowest greenschist to amphibolite facies; distributed right across the map area but most common in the western Bathurst Terrane.

(c) Masses of metadiabase/gabbro commonly with relict igneous features and coarser grain size than (b); degree of amphibolitization ranging from low (pyroxene preserved) to complete transformation to amphibole schist in shear zones; in general, conformable to country rock fabric (N to NNE), but locally crosscutting; occur mainly within a zone up to 30 km wide that is slightly oblique to the boundary between the Bathurst and Ellice River terranes (Fig. 31.2). That is, in the south these bodies are common on both sides of the terrane boundary but to the north they are mainly found in the Ellice River Terrane gneisses.

(d) Completely recrystallized, relatively coarse grained, garnet amphibolite boudins and conformable layers lacking igneous textures that occur in Yellowknife Supergroup migmatites are prominent west and north of Beaulac (Fig. 31.2) and are similar to Archean garnet amphibolite boudins and layers in the Yellowknife Supergroup 100-200 km to the south southwest (Frith, 1982; Henderson and Thompson, 1981).

The discordant metamorphosed basic dykes separate the late Archean main phase metamorphism and deformation (including north-northeast oriented layering and foliation in high-grade metasedimentary rocks and sillimanite grade ductile shear zones) from post-dyke, post-Goulburn Group late phase events.

Ellice River Terrane

Both the "pink" gneiss/migmatite/granitoid and pyroxene migmatite/gneiss/charnockite units that underlie most of the Ellice River Terrane are characterized by textural variations ranging from homogeneous metaplutonic rocks through migmatized plutonic rocks to gneisses and layered migmatite, and compositions varying from granite to tonalite, but a relatively simple and unchanging mineralogy comprising quartz, plagioclase, K-feldspar, biotite and hornblende. Clinopyroxene and/or orthopyroxene are present in the granulite facies zones. Superimposed on these variations and in part the cause of them are at least two regional metamorphic gradients and variable strain gradients which modify the rocks to straight gneisses, protomylonite and mylonite. This lithologic package is a mappable entity that can be distinguished from the other units or lithologic packages across several thousand square kilometres in the Ellice River Terrane and in the northernmost part of the Bathurst Terrane where, although present, it is not the predominant association. Partial melting of intermediate plutonic rocks and the common occurrence of hornblende and/or pyroxene in leucosomes requires temperatures of the upper amphibolite and granulite facies. The rare occurrences of garnet-clinopyroxene in these rocks may reflect moderate pressures. In many outcrops there is a history of crystallization, remelting, recrystallization and deformation, but except for granitic pegmatitic bodies clear-cut intrusive relations are rare. Basic gneiss and migmatite of probable supracrustal origin and hornblendite occur as inclusions in both units; no pelitic or marble inclusions are known. The "homogeneity of the heterogeneity" of these rocks, the granitoid appearance, and the inclusions support the conclusion that the ultimate protolith was mainly plutonic.

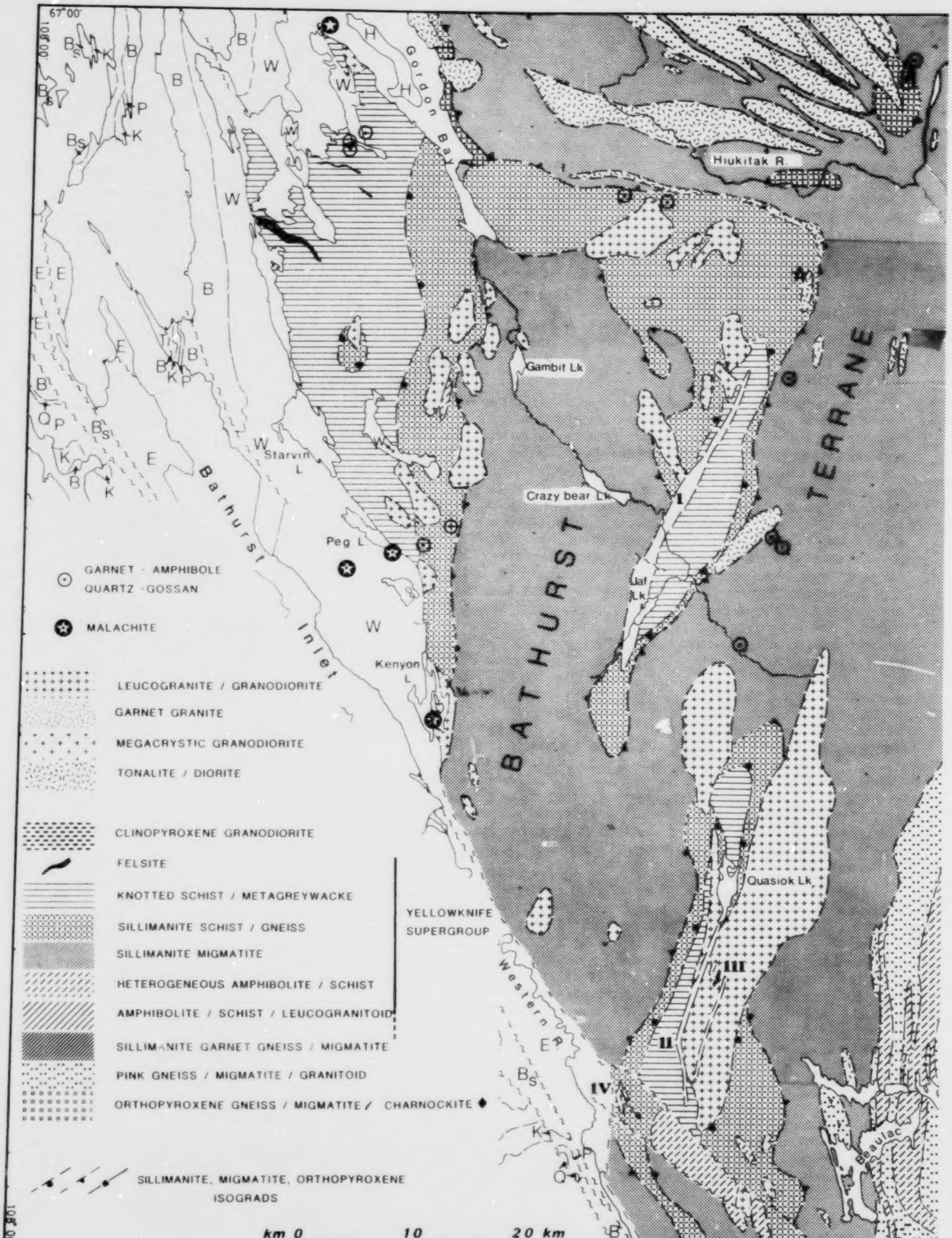
67°00'
108°00'
Gordon Bay
Hiukitak R.
Gambit Lk
Crazy bear Lk
Jaf Lk
Starvin L
Peg L
Kenyon L
Quasiok Lk
Beaulac
Bathurst Inlet
Western
BATHURST TERRANE
I
II
III
IV
66°00'
106°00'
GARNET - AMPHIBOLE QUARTZ - GOSSAN
MALACHITE
LEUCOGRANITE / GRANODIORITE
GARNET GRANITE
MEGACRYSTIC GRANODIORITE
TONALITE / DIORITE
CLINOPYROXENE GRANODIORITE
FELSITE
KNOTTED SCHIST / METAGREYWACKE
SILLIMANITE SCHIST / GNEISS
SILLIMANITE MIGMATITE
HETEROGENEOUS AMPHIBOLITE / SCHIST
AMPHIBOLITE / SCHIST / LEUCOGRANITOID
SILLIMANITE GARNET GNEISS / MIGMATITE
PINK GNEISS / MIGMATITE / GRANITOID
ORTHOPYROXENE GNEISS / MIGMATITE / CHARNOCKITE
YELLOWKNIFE SUPERGROUP
SILLIMANITE, MIGMATITE, ORTHOPYROXENE ISOGRADS
km 0 10 20 km

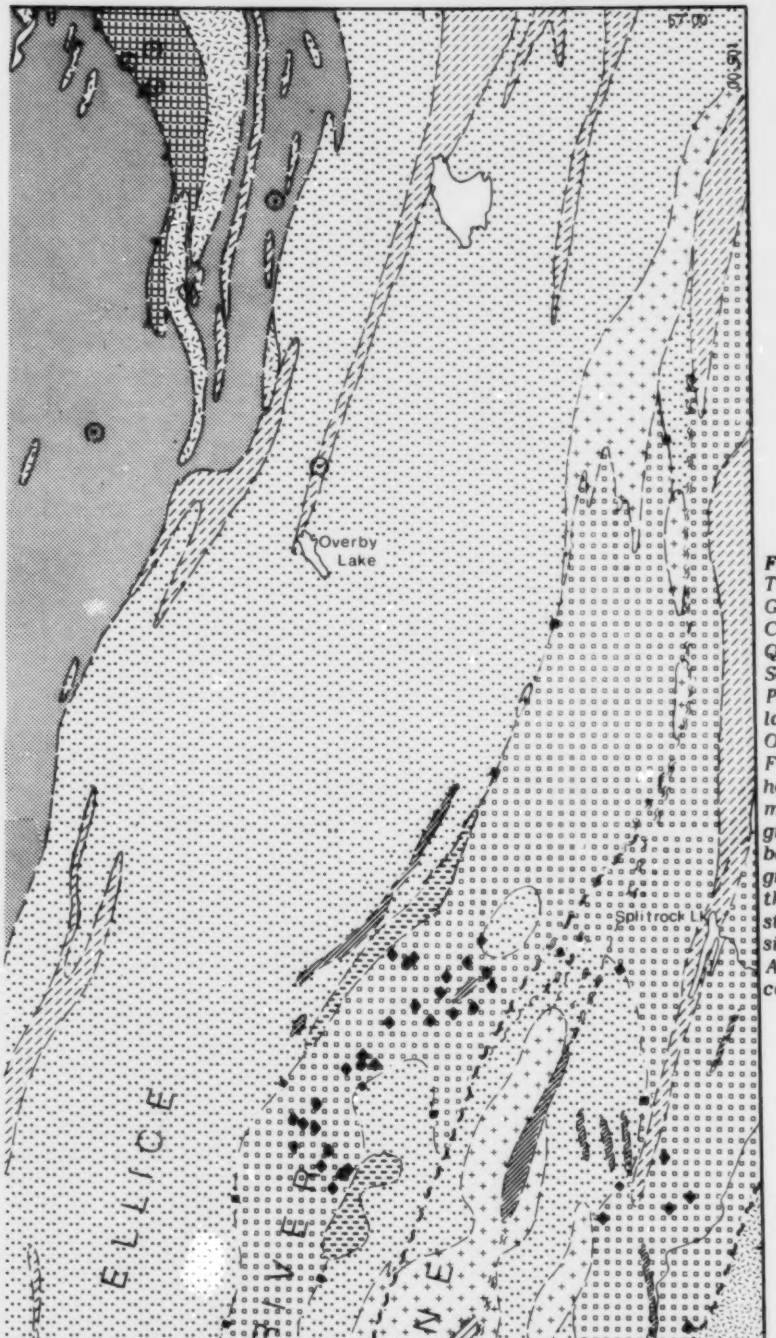

Figure 31.1. *Preliminary lithologic map of the Tinney Hills-Overby Lake map area. Subdivision of Goulburn Group (not patterned) after Campbell and Cecile (1976); Western River (W), Burnside (B), Quadyuk (Q), Peacock Hills (P), Kuuvik (K), Brown Sound (BS) and Amagok (A) formations; also late Proterozoic Ellice Formation (E) and undifferentiated late Proterozoic sediments and volcanics (H). Outliers I-IV are correlated with the Western River Formation. In the Ellice River Terrane the heterogeneous amphibolite/schist unit contains migmatitic hornblende and pyroxene-bearing gneisses. The boundary between terranes is taken to be the western contact of the main mass of "pink" gneiss/migmatite/granitoid with supracrustal rocks of the Yellowknife Supergroup. There is no stratigraphic significance to Legend. Open star is site of pegmatite containing muscovite yielding late Archean Age (Rb/Sr, van Breemen, personal communication, 1985).*

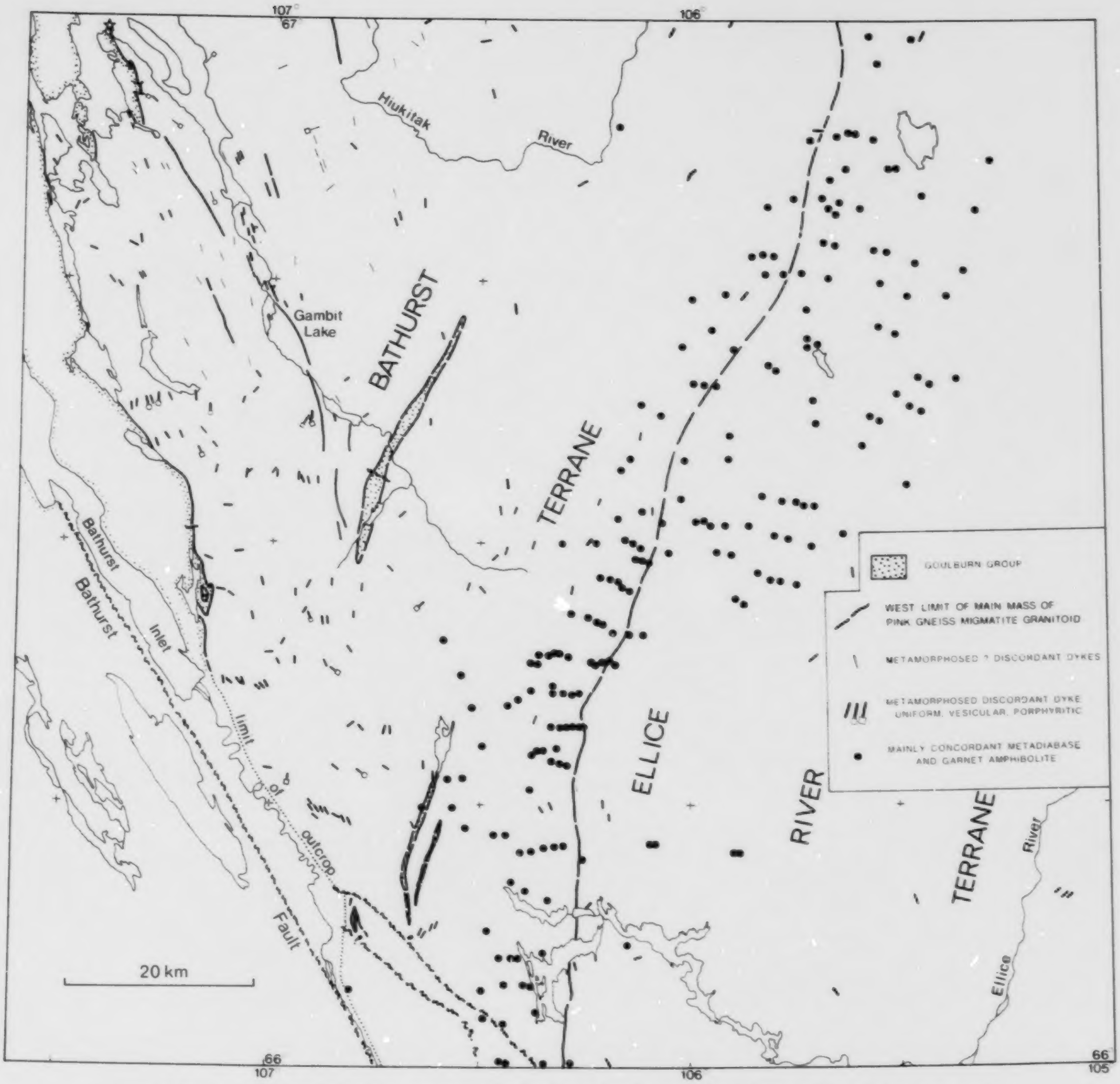

Figure 31.2. *Preliminary map showing distribution of dykes in the Tinney Hills-Overby Lake map area. Mackenzie dykes are not shown. The main boundary between the Bathurst and Ellice River terranes is shown as a heavy dashed line; outliers of Goulburn Group are stippled.*

The striking lithologic similarities between this unit and the crystalline complex considered to be basement to the Yellowknife Supergroup in the Healey Lake area persist throughout the map area.

Rock units considered to have been supracrustal rocks originally but now range in grade from middle amphibolite to granulite facies (heterogeneous amphibolite schist, sillimanite garnet gneiss/-migmatite, amphibolite/schist/leucogranitoid, Fig. 31.1) are limited to long narrow zones a few metres to several kilometres wide and up to tens of kilometres long. These zones are made up of various combinations of pelitic schist/psammite or migmatite, layered amphibolite, rusty gneiss/meta-iron formation, fine grained quartzofeldspathic gneiss, and marble or calc-silicate gneiss. Pink pegmatites are quite common. At Splitrock Lake, aplitic granite and garnet granite are associated with these rocks. In the supracrustal belt between Ragged Lake and the Ellice River two mica granodiorite is present. Contacts with adjacent megacrystic biotite metagranodiorite, pink gneiss/migmatite granitoid and pyroxene migmatite/gneiss are invariably covered or strongly tectonized. In view of the similar associations of similar lithologies, these rocks are considered, for the present, to be equivalent to the heterogeneous supracrustal package that is part of the Yellowknife Supergroup in the Bathurst Terrane.

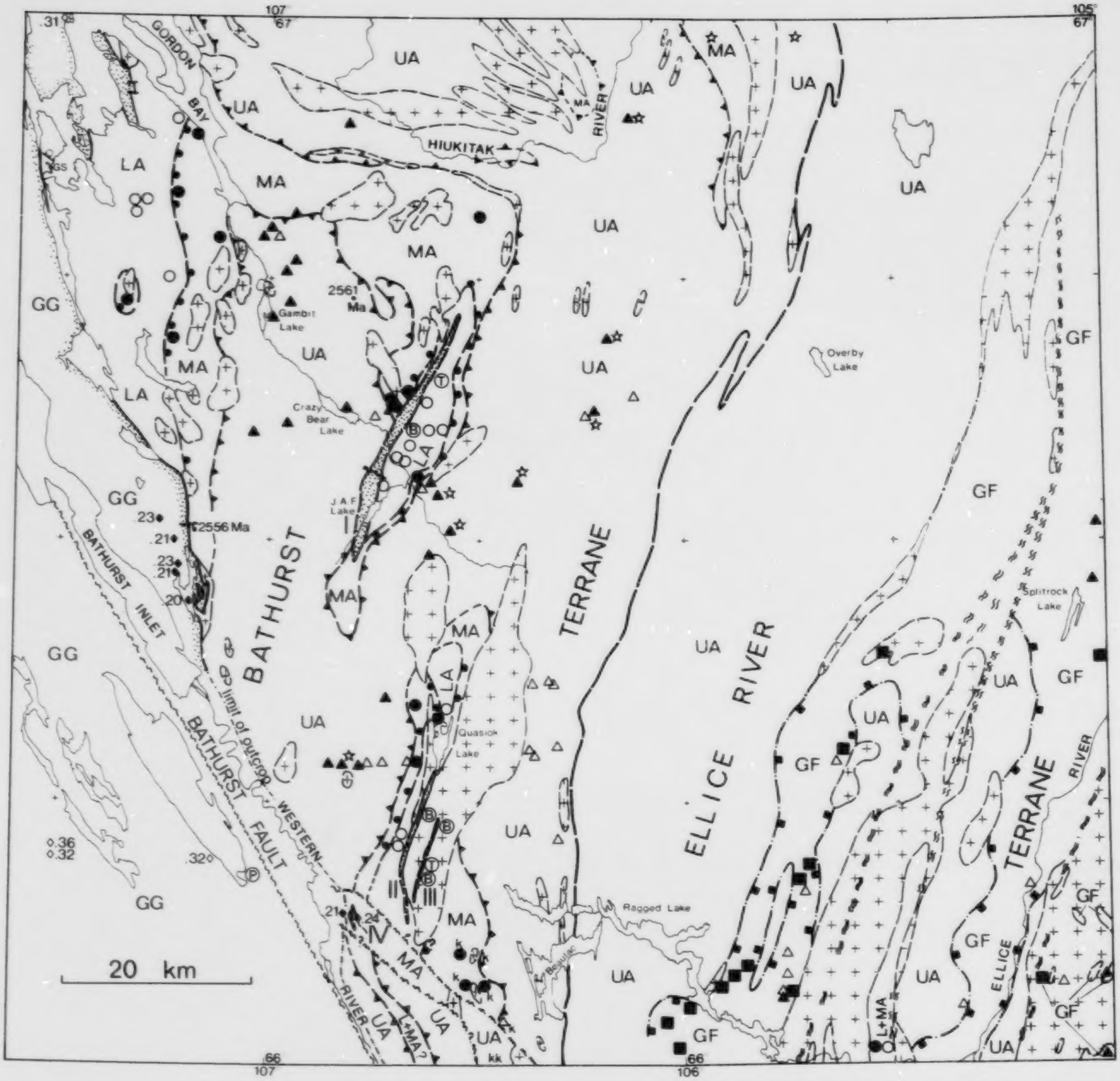

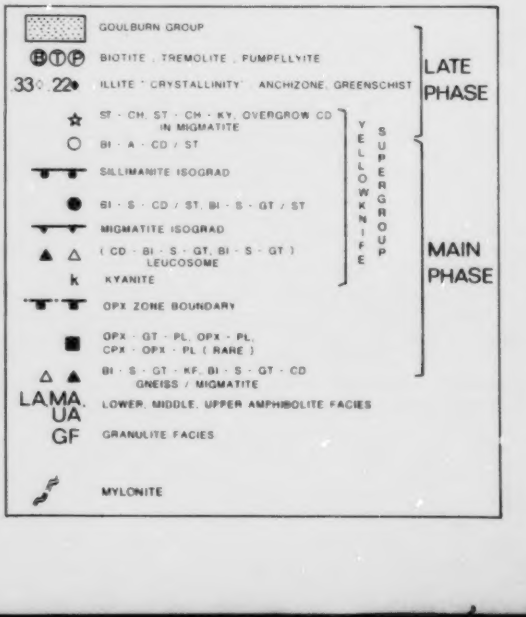

Figure 31.3. *Preliminary metamorphic map of part of the Tinney Hills-Overby Lake map area. Illite crystallinity data from Martin Frey (personal communication, 1984). Note addition of small patch of greenschist facies (sub-cordierite grade) (GS) rocks adjacent to unconformity in northwest corner of the map. The implication that the main phase high grade rocks are the same age right across the map area may not be supported by subsequent petrologic and geochronological study. Some of the high grade rocks in the Ellice River Terrane may have formed before or after the Yellowknife Supergroup.*

Four relatively homogeneous metaplutonic bodies have been outlined in the Ellice River Terrane. In the southeast corner, a garnet granite, locally sillimanite-bearing, intrudes granulite facies supracrustal rocks that, locally, show protomylonitic fabrics while the granite itself has been foliated/lineated, folded and locally mylonitized at high grade. A lense-shaped, relatively weakly foliated, unmigmatized, porphyritic and homogeneous clinopyroxene granodiorite occurs along the western limit of the central granulite facies zone. Hornblende rims on clinopyroxene and late biotite show it has been metamorphosed. The megacrystic biotite metagranodiorite east of Ragged Lake was described by Thompson et al. (1985). In the north half of the Ellice River Terrane there is another batholith of megacrystic biotite metagranodiorite. Where it is strongly foliated, this unit is a spectacular pink and grey weathering rock with an augen texture made up of dark fine grained biotite-rich matrix anastomosing around pink feldspar phenocrysts 0.5-10 cm long. Several smaller bodies occur like strings of beads along shear zones which bound the main batholith to the northwest and southeast and the granulite facies rocks along strike to the south-southwest. The batholith does not appear to have been subjected to such high grade itself. Scattered outcrops of this distinctive rock occur near Ragged Lake. In the map area adjacent to the south, Frith (1982) described a large batholith of similar composition and texture. James (1985) and Henderson and MacFie (1985) have mapped a similar lithology 200 and 300 km farther south in the Thelon Tectonic Zone.

On the basis of composition, structure and metamorphism, the plutonic rocks of the Ellice River Terrane cannot be distinguished from those characteristic of the domains of the Slave Province made up mainly of plutonic rocks and gneiss/migmatite/granitoid complexes (see e.g. Henderson et al., 1982; Frith, 1982). In view of the evidence for a major Proterozoic orogenic event in the Thelon Tectonic Zone, however, the possibility that some or all of these rocks are Proterozoic is considered and zircon samples were collected with the intention of determining the age of plutonic events in the area.

The swarm of metamorphosed basic intrusions near the western boundary is another important element in the history of the Ellice River Terrane. Further study is required to determine the extent to which basic intrusions near the terrane boundary are syntectonic with respect to both Archean main phase deformation and later Proterozoic events.

Considering both terranes together, particularly in the northern part of the map area, it is evident that Archean lithologies and main phase metamorphism are continuous across the western boundary of the Thelon Tectonic Zone. As in the Healey Lake map area 200 km to the south-southwest (Henderson et al., 1982) there is no evidence of a geosuture along the Thelon Front. Such a feature, if it does exist, would lie farther to the east.

Regional metamorphism

Most of the observations in the supracrustal rocks in the map area (Fig. 31.3) can be accounted for by a two-stage metamorphic history. The predominant high grade rocks formed during a "main phase" event that was followed by intrusion of basic dykes and deposition of the Goulburn Group before a "late phase" event metamorphosed these rocks and overprinted the main phase assemblages. Main phase mineral assemblages and isograds are, for the most part, typical of the low pressure andalusite/sillimanite type metamorphism characteristic of the last major orogenic event in the Slave Province at 2600 Ma (Thompson, 1978). The volume of migmatite derived from the Yellowknife Supergroup, however, is unusually high. As is the case along the western boundary of the Thelon Tectonic Zone, farther south (Henderson and Thompson, 1981; Frith, 1982) main phase kyanite occurs in the south-central part of the area near the boundary. These rocks are considered to represent a greater degree of post-metamorphic uplift and erosion than has occurred over most of the rest of the Slave Province farther west. Late phase assemblages indicate a narrower range of metamorphic conditions that begins in the anchizone (subgreenschist) and does not exceed lower amphibolite facies. Presence of both andalusite and kyanite in staurolite-bearing overprint assemblages means low to intermediate pressures.

Late Archean Rb-Sr ages of coarse grained muscovite from white pegmatites in sillimanite schist and pelitic migmatite in the Bathurst Terrane (van Breemen, personal communication, 1985) provide a minimum age for the main phase metamorphism and deformation (Fig. 31.1). The distribution, mineralogy and contact relations of the pegmatites indicate they are part of the metamorphic process and syntectonic with respect to main phase deformation. The ages are, therefore, probably close to the age of metamorphism.

In the Bathurst Terrane main phase grade ranges from greenschist facies through cordierite-andalusite (staurolite) and sillimanite schist to anatectic garnet-cordierite-sillimanite biotite migmatites of the upper amphibolite facies. Migmatization of granodiorite/tonalite has occurred in the northern part of the terrane. Garnet-cordierite-bearing leucosomes suggest temperatures (~675°C) sufficient to involve biotite in the melting reactions. The common occurrence in sillimanite migmatites of garnets rimmed by cordierite may be explained by decreasing pressure at high temperature (Hollister, 1977). Maximum pressures probably did not exceed 6-7 kb.

The wide distribution of pelitic rocks in the Bathurst Terrane provides good control on a regional isograd pattern that records the distribution of pressure and temperature during an important stage in the evolution of the area. Textures in thin sections, outcrop scale relations between fabric elements and metamorphic minerals, and the form of the isograd pattern demonstrate the synchroneity of deformation and main phase metamorphism. This is evident not only during the heating of the terrane but during cooling and uplift of the rocks as well. Preferred orientation of sillimanite knots is an example of the former while the grain size reduction observed in sillimanite grade ductile shear zones that has occurred in the migmatites during or soon after solidification of the leucosomes is an example of the latter. Furthermore, relations between structure and metamorphic grade imply that the latter, to a certain extent, controlled the structural evolution.

In the Bathurst Terrane (Fig. 31.3), evidence of the late phase metamorphic event is found in Archean sillimanite schist (NE corner) and metasedimentary migmatite, in the post-Archean, pre-Goulburn basic dykes and in the Goulburn Group. More illite crystallinity data (Martin Frey, personal communication, 1985) have further documented the eastward increase in metamorphic grade of the cover sequence from middle anchizone west of Bathurst Fault to upper anchizone/greenschist facies east of the fault and greenschist facies in outliers I-IV. The grade of discordant dykes increases eastward as well, with greenschist facies assemblages west of outlier I and greenschist to lower amphibolite facies rocks between outlier II and the eastern boundary of the terrane. Field observations and preliminary petrography show that staurolite-chlorite-andalusite/kyanite replace cordierite in migmatites of the Bathurst Terrane within a zone bounded to the west by a north to north-northeast line through outlier I and to the east by the main boundary in north half of the area. At present, in the

south half, these assemblages are limited to a zone bounded by lines through outliers I and II. Greenschist facies retrogression of variable intensity is widespread. In the absence of Goulburn Group or basic dykes, differentiation between late main phase, late phase and post-late phase retrogression is not always possible.

Main phase metamorphism in the Ellice River Terrane is predominantly upper amphibolite and granulite facies. Partial melting is widespread in rocks ranging in composition from granite to tonalite in both the pink gneiss/migmatite/granitoid and the pyroxene gneiss/migmatite/charnockite. Hornblende and/or pyroxene are commonly found in the leucosomes of these rocks. Migmatitic pelitic rocks typically contain sillimanite, garnet, cordierite and spinel, with cordierite separating the other three minerals from the matrix quartz and feldspar. The low biotite and high K-feldspar content suggest higher temperatures than were attained in the pelitic migmatites to the west, but once again, the cordierite coronas are compatible with decreasing pressure at high temperature. K-feldspar-orthopyroxene is quite common in felsic granulites and orthopyroxene-plagioclase and clinopyroxene-plagioclase in mafic granulites. Two pyroxene rocks also occur. Since garnet has only been seen in pelitic rocks or in the layered amphibolites of the heterogeneous supracrustal sequence, and pyroxene and plagioclase are stable together, pressures were probably in the intermediate range. Between the central and eastern granulite facies zones in the southern Ellice River Terrane, bounded as far as is known by relatively low grade high strain zones and mylonites, there is a segment composed of lower to middle amphibolite facies metasedimentary and metavolcanic rocks and two mica granite surrounded by a metamorphosed megacrystic biotite granodiorite.

Late phase assemblages in the Ellice River Terrane are greenschist to lower amphibolite facies and are primarily associated with high strain zones and mylonites. Away from these zones the effects of retrogression are much reduced. In the western third of the Ellice River Terrane pelitic migmatite is reduced to tectonoclastic schist composed of biotite, chlorite, white mica, garnet (rarely) and porphyroclasts of feldspar, but farther east, fresh cordierite is preserved and staurolite-kyanite overgrowth textures such as occur in the eastern Bathurst Terrane are absent. In many granulites pyroxene has hornblende and/or biotite rims, while others are completely free of coronas. Biotite rims also grow on hornblendes in the pink gneiss unit. Wherever grain size reduction has been accompanied by water, retrogression has been moderate to severe. Some orthopyroxene-bearing rocks, however, show flow textures and broken pyroxene grains with minimal retrogression. Obviously, as is the case in the metamorphosed dykes, the extent to which water is available during strain determines the degree of retrogression.

In the absence of evidence to the contrary at present, the main and late phases of metamorphism in the Ellice River Terrane are correlated with the late Archean and post-Goulburn events, respectively, in the Bathurst Terrane. Testing of this correlation and the alternative hypotheses that parts of the Ellice River Terrane high grade rocks are either older or younger than the western main phase event, or both, is in progress.

Thelon Tectonic Zone

The change from irregular and west- to northwest-oriented structures and irregular lithologic patterns in the Slave Province to the linear lithologic pattern with a pronounced N to NNE preferred orientation typical of the Thelon Tectonic Zone is one of the original criteria for the Thelon Front, the eastern boundary of the Slave Province as defined by Wright (1967). In the Healey Lake area, the change is considered to be Archean (Henderson and Thompson, 1981). A late Archean age determined from a pegmatite cutting north-trending high-grade, high strain fabrics in the Bathurst Terrane (Fig. 31.1), metamorphosed dykes discordant to N to NNE fabrics, and the syndeformation nature of the main phase metamorphism indicate the change is also Archean in the Tinney Hills-Overby Lake map area. The concordance of the tectonic history in the two areas supports the idea that a major north to north-northeast straight belt formed along the eastern edge of the Slave province at the end of the Archean. Proterozoic events recorded in both areas including major crustal overthrusting and transcurrent shear zones likely represent reactivation of the old structure (Thompson and Henderson, 1983).

The mapping this year revealed that, typical of the development of knowledge of the Thelon Tectonic Zone (Henderson and Thompson, 1981; Henderson et al., 1982; Henderson and Macfie, 1985), the coincidence of a marked lithologic change, a low grade, higher strain zone, a basic dyke swarm and a change in the aeromagnetic anomaly map that was the basis for defining the western boundary of the Thelon Tectonic Zone in the south part of the map area (Thompson et al., 1985), does not continue to the north edge of the map. The lithologic contrast is much less prominent. The proportion of supracrustal rocks decreases west of the boundary and increases slightly to the east and the "pink" gneiss/migmatite/granitoid characteristic of the Ellice River Terrane occurs in the northern Bathurst Terrane. The foliation in deformed migmatites and the western limit of the main mass of pink gneiss/migmatite/granitoid follow a north-south trend and begin to bend to the northwest, while the fine grained, thin layered, high strain straight gneiss maintain a north-northeast orientation. The swarm of variably amphibolitized basic dykes shifts eastward into the Ellice River Terrane and follows the straight gneiss trend (Fig. 31.2). A linear trough in the aeromagnetic anomaly map also follows this trend, while a prominent positive anomaly just to the west broadens and bends to the northwest.

The reconnaissance mapping (Fraser, 1964) shows that north of Bathurst Terrane the proportion of metasedimentary rocks remains relatively low and foliations bend around to the northwest, and that along strike from the Ellice River Terrane (Fig. 31.1) there is a north-south preferred orientation continuous to the Arctic Coast which is limited to the west by the Thelon Front as defined by Stockwell (1969, 1982). The western limit of this zone also marks the eastern end of a swarm of discordant basic dykes. This line is a more appropriate western boundary of the Thelon Tectonic Zone than the tentative one indicated by Thompson and Ashton (1984) which parallels the western limit of straight ribby "topography" on the aeromagnetic anomaly map.

In the Tinney Hills-Overby Lake map area, the western boundary of the Thelon Tectonic Zone, the Thelon Front cannot be defined on the basis of any one characteristic. With similar high grade lithologies on both sides, it is not a lithologic or metamorphic boundary. Structural orientation is not conclusive either, for N to NNE oriented structures occur up to 35 km west of the preferred boundary in southern part of the area but these features die out to the NNE where they encounter structural trends bending around into the Thelon Tectonic Zone orientation. Although it is relatively easy to draw a western limit to the Thelon Tectonic Zone at 1:1 000 000 scale, at 1:250 000 the boundary is a composite feature with a gradational nature and the relative importance of geological and geophysical criteria change along strike (see also Henderson and Thompson, 1981; Frith, 1982; Henderson and Macfie, 1985). These aspects of the boundary reflect in part the superposition of two or more orogenic events.

PART 2. SUMMARY OF FIELD WORK IN STRUCTURAL GEOLOGY

N. Culshaw

Introduction

This section summarizes structural aspects of this summer's field work and presents a brief, preliminary structural overview of the Tinney Hills-Overby Lake map area. The section is divided into an outline of the results of local studies conducted in order to improve understanding of problems previously identified and a description of structures mapped this summer in the regional program. The simple tectonic zonation of the map area presented in the overview is interpreted to record mainly Proterozoic events and does not deal with the problem of pre-existing Archean features and their possible influence on Proterozoic structures. As such it reflects the bias of the author of this section. The idea of an Archean transprovincial mobile belt as the original Thelon Tectonic Zone is not dismissed.

Local studies - highlights

Archean tectonics in the western Bathurst Terrane. The nature and interrelationships of several important Archean structures have been clarified. These are well exposed structures in the northwest far removed from the Proterozoic(?) reworking which characterizes the eastern part of the map area. Their importance is that they give a clear picture of local Archean tectonics which formed the architecture on which the reworking was imposed. The structures imply that this part of the Archean crust was subdivided along slide/shear zones which coincide with metamorphic isograds such that a mobile lower level was overlain by a less ductile roof. The possibility is entertained that a nappe of lower level migmatites was emplaced along a slide/shear zone which is well exposed in the northwest of the area. The best exposed structures are upright folds with subvertical axes and fingerprint-like profiles (fingerprint-structures) situated within the sillimanite schists and adjacent knotted schists west of Gambit Lake (Fig. 31.1 and Domain 1, Fig. 68.6, Thompson et al., 1985). The axial surface of the westernmost fold is subvertical and trends N to NNE parallel to a zone situated on the east side of the fold, of strong deformation, transposition and transcurrent motion which is bounded on its west side by the sillimanite isograd and marks the appearance of plentiful granite and pegmatite. This fold and transposition zone is itself transposed at its northern end by a steeply dipping zone of high transcurrent shear strain and folding which trends 340° along the western shore of southern Gordon Bay (Gordon Bay Zone) and extends inland several kilometres to the southeast. The western boundary of the Gordon Bay Zone also appears to be close to the sillimanite isograd. A zone of high strain dipping shallowly NNE and striking ESE from Gordon Bay has been interpreted as a ductile thrust zone (Hiukitak Zone) which separates overlying migmatites from the sillimanite schists below, which lie to the east of Gordon Bay and north of Gambit Lake (Fig. 31.1 and Domains 2 and 3 in Fig. 68.6, Thompson et al., 1985). This zone is warped by the Gordon Bay Zone such that it swings NNW along the eastern shore of Gordon Bay. At the southeastern extremity of the Hiukitak Zone high strain rocks have been rotated to a southerly trend about subvertical axes (see below).

These structures are all formed in the interval of main phase metamorphism, within which they form a sequence of progressive deformation. There is abundant evidence that the Archean biotite-muscovite granites and pegmatites were emplaced syntectonically within the structures.

A general framework of Archean tectonics within the western Bathurst Terrane can be made from the pattern of metamorphism, deformation and magmatism. An overall controlling factor of the framework appears to be the distribution of metamorphic grade. For example, the N to NNE fingerprint structures are on the flank of a transposition/shear zone, are bordered by the sillimanite isograd and mark the structurally upward limit of syntectonic granite migration. It could be argued that both the limit of transposition and the limit of granite motion are the result of the lesser ductility of the superincumbent lower grade knotted schists compared to the sillimanite schists. The roof of this ductile infrastructure may be traced by following the belt of sillimanite schists and granites from the fingerprint structures clockwise around the migmatites of Gambit Lake (Fig. 31.1). In accord with this model the migmatites above the Hiukitak ductile thrust zone may be regarded as allochthonous infrastructure rooting somewhere to the north or northwest.

Basement involved deformation of Goulburn Group. Tirrul (1985) documented a thin-skinned thrust and fold belt exposed in oblique cross-section in the Goulburn Group east of the southern part of Bathurst Inlet at Bear Creek Hills. He considered the belt to be the highest structural level of the Thelon Tectonic Zone. His study was restricted to the Goulburn Group and not the basement. At several localities within relatively narrow zones, structures were formed which involved both basement and cover:

1. Kenyon Lake. A zone of variably deformed and retrograde (greenschist facies) steeply foliated basement extends from near Kenyon Lake to the vicinity of Gordon Bay (Fig. 68.6, Thompson et al., 1985) lying within the migmatites close to their western boundary. It is very well developed in the south where it contains abundant foliated mafic dykes and is greater than 2 km wide. Southward it is continuous along strike into the trace of the axial surface of folds of basement and cover (see Fig. 51.4, Tirrul, 1985) and several syn-folding steeply dipping thrusts of granitic basement over cover. These folds and associated cleavage have been assigned to D_2 by Tirrul (1985). If this is correct then the basement structures formed during or shortly after thin-skinned thrusting in the cover which also was assigned to D_2 by Tirrul (1985).
2. Peg Lake to Starvin' Lake. In this region and farther to the northeast, narrow zones of retrogression and fabrics indicative of NW transport are sporadically developed confined to pelitic horizons in low dipping knotted schist. A tiny Goulburn remnant is associated with one of these.
3. Goulburn Group outlier I. Within the southern quarter of this outlier, structures responsible for its geometry postdate thin-skinned décollement thrusting which occurs here within the lower Western River Formation at a similar level to the décollement in the Bear Creek Hills (J. Grotzinger, personal communication, 1985). Basement, cover and décollement are folded about steeply dipping axial surfaces and subhorizontal axes which trend parallel to the length of the belt. This folding is accompanied by thrusting on steeply dipping surfaces. The foliation in an intensely deformed retrograde basement slice which lies within the outlier may be traced without break into the fabric of the overlying folded basal conglomerate. The planar-linear basement fabric is similar to those in zones of steeply dipping retrograde basement tectonites to east and south of the outlier (Fig. 68.6 and 68.8, domain 6, Thompson et al., 1985).

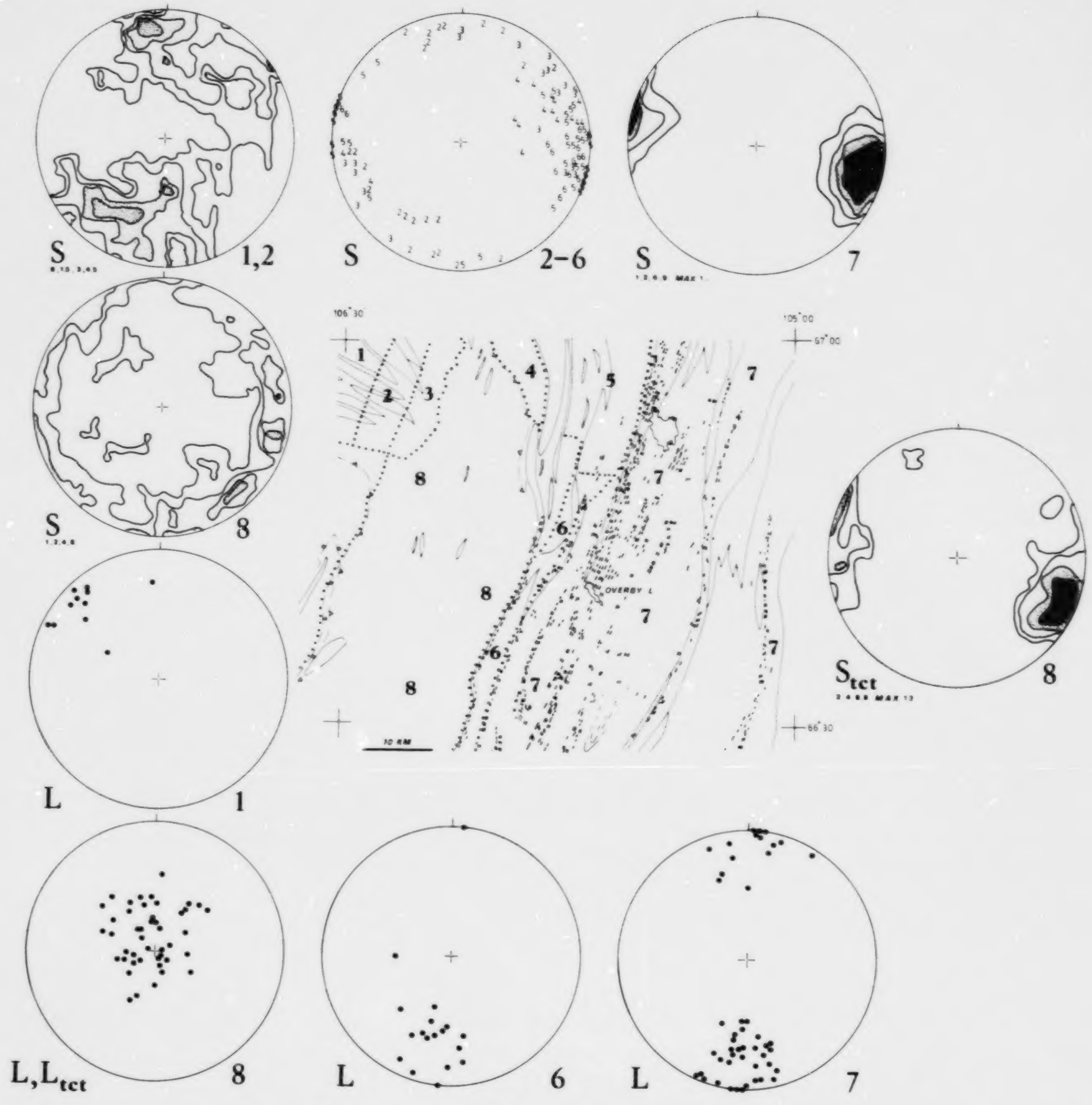

Figure 31.4. Macroscopic geometry of north part of Ellice River Terrane and northeast part of Bathurst Terrane (outlined in Fig. 31.1). Equal area plots; mineral lineations (L) shown as dots; foliation poles (S) contoured (with values indicated) except for domains 2 to 6, which are numbered to illustrate extent of sympathetic rotation of lithological boundaries and foliations. Only SE part of domain 1 is shown. For domain 8 very strong to tectonoclastic foliations from migmatites are separated (see text for metamorphic grade of these) and are dominant contributor to lineation diagram. Straight gneiss and mylonitic rocks - dashes.

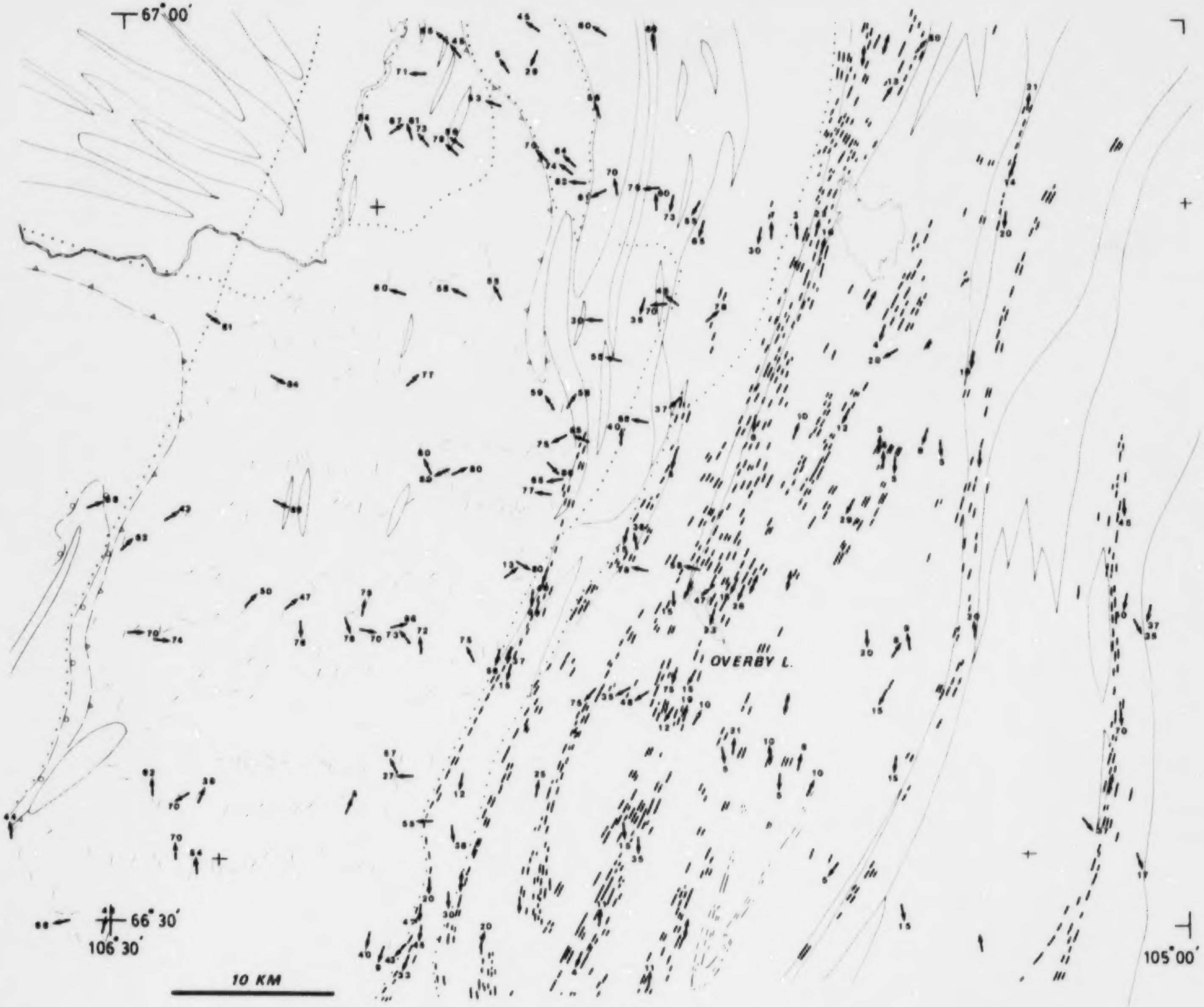

Figure 31.5. *Distribution of mineral lineations (dark arrows) in northern part of Ellice River Terrane and northeast part of Bathurst Terrane (outlined in Fig. 31.1). Straight gneiss and mylonitic rocks - thick grey dashes; foliation in Bathurst Terrane migmatites - thin grey dashes.*

The western margin of the outlier is formed of overturned shallowly west dipping basal Western River Formation overlain by a shallowly dipping greenschist facies mylonite zone formed from superincumbent basement migmatites which were transported towards the southeast. This thrust is likely correlative with that observed east of the outlier (op. cit. Fig. 68.10a), with recumbent folds within the outlier and flattish crenulations within and adjacent to the outlier, both of which are coaxial with the earlier upright folds.

The westward basement over cover thrusting at outliers II and III (Thompson and Ashton, 1984), the basement-cover relations at all three outliers and Kenyon Lake, and the possible synchroneity with these events of a ductile Bathurst Fault may be interpreted to be the result of wrench fault related tectonics (Wilcox et al., 1973; Harding, 1974). In this interpretation, the outliers and the Kenyon Lake folds and thrusts are compressional structures of the type characteristically associated with major strike slip faults. Thus the passage of a northwest migrating deformation front is envisaged accompanying basement compression concentrated along pre-existing basement structures at the NW advancing tip of the propagating ductile Bathurst Fault. This scheme is critically dependent on the synchroneity of the Kenyon Lake-outlier structures with the ductile phase of the Bathurst Fault. An alternate view is that the Kenyon Lake-outlier structures are simply late expressions of the type of compressional structures which are developed across the map sheet in a wide belt between outlier 1 and the main boundary zone (Fig. 31.1 and see below). The distance from the trace of the Bathurst Fault to outlier 1 is evidence in favour of the latter view.

Ductile phase of the Bathurst Fault. It is important to recognize and characterize any ductile expression of the Bathurst Fault within the Tinney Hills-Overby Lake map area since regarding the fault system simply as a brittle phenomena does not account for several observations. For example, Tirrul (1985) contrasted low estimates of slip based on offset of magnetic carriers with high estimates based on matching stratigraphy of the Goulburn Group across the fault. He suggested that the lower values, accounted for by the discrete (brittle) slip, may be reconciled with the higher by postulating a ductile component of slip, implied also by north trending fault related folds.

Mylonites indicative of a ductile phase have already been mapped to the SE in the Beechey Lake area (Frith, 1982). In the Tinney Hills-Overby Lake map area the ductile phase may be recorded in the southwesternmost basement exposure (Fig. 31.1 and Thompson et al., 1985, Fig. 68.6) where foliations generally trend NW-SE parallel to the local isograd pattern (Fig. 1 and op. cit. Fig. 68.2, 68.5). Within this zone migmatites, sillimanite schists and mafic dykes are zonally deformed and retrogressed at greenschist facies. These relations resemble those displayed by NNE trending zones of basement retrogression within the Bathurst Terrane which can be related to post-thin-skinned-thrusting deformation of Goulburn Group cover (see below). On account of these similarities of deformation and metamorphism, the NW trending tectonites may therefore be of similar age to the NNE trending zones and be either zones of original NW trend, reoriented NNE trending zones, or NNE zones reoriented to NW and reoriented subsequently accommodating strike-slip motion. The presence of "augen" containing NNE zones within this domain favours the two latter alternatives.

Structural relations in the northeast Tinney Hills-Overby Lake map area

The area mapped this summer is divisible into two zones which are continuations of similar zones to the SSW (Fig. 68.6, Thompson et al., 1985). In these northern segments, however, the problems of relating probable Proterozoic structures to known Archean structures are highlighted. The dominant structure in the east of the map area is a wide straight belt/transcurrent shear zone which underlies most of the Ellice River Terrane (Fig. 31.2). This is separated from the well preserved Archean structures which lie west of the Hiukitak River and outlier 1, by a NNE trending zone in which main phase (Archean) fabrics and trends of lithological units are preserved but in which there are numerous dominantly second phase (staurolite-chlorite grade in north) shear zones which imply compression across the belt in the Proterozoic. A moot point is whether these zones and the Proterozoic straight belt were imposed on a similarly oriented Archean straight belt. The evidence supports the existence of north trending Archean structures in the NNE trending Proterozoic zone of compression but an Archean shear zone cannot be delineated with confidence within this zone.

The eastern part of the area, which is a continuation of the Ellice River Terrane, may be described as a straight belt in the sense of Watson (1973) since it comprises a 30 km wide zone of NNE striking steeply west dipping gneiss of exceedingly constant orientation (Fig. 31.4). It is a continuation of zones of predominantly highly strained gneiss which in western Ellice River Terrane run NNE from Ragged Lake in a 20 km wide strip, in central Ellice River Terrane form a narrower belt including and along strike from the megacrystic granodiorite (Fig. 31.1; and 10 and 13 in Fig. 68.6, Thompson et al., 1985), converging at the northern tip of an augen of granulite-rich more irregular gneiss (Fig. 31.1 and domain 12, Fig. 68.6, op. cit.) and which evidently continues north of the map area. The straight belt is composed of zones comprising straight gneiss (sensu Davidson et al., 1982) and subordinate mylonite and protomylonite ranging from hundreds of metres to two or three kilometres in width which are interleaved with zones of coarser grained gneiss of equally constant orientation (Fig. 31.4). Lineations are well represented in type 2a mafic bodies and are for the most part very shallowly plunging (Fig. 31.4, 31.5) as in the equivalent terrane to the south (Fig. 68.9, Thompson et al., 1985). For the whole belt a dextral transcurrent shear strain is inferred. Large scale steeply (Fig. 68.6, op. cit.) and shallowly plunging (Fig. 31.4) tight folds of unknown age are present in the straight belt.

The zone immediately west of the straight belt which includes all the Bathurst Terrane east of outlier 1 and the Hiukitak River is different from the straight belt in several important respects, including lithology (Fig. 31.1, 31.4 and see domains 6-9, Fig. 68.6, op. cit.). Along the northwestern and northern margin of the zone NW-SE Archean structural trends are deflected into more northerly trends, on the east side apparently feeding into the straight belt. This deflection is evident both from foliation and lithological boundary trends and results from folding about subvertical axes (Fig. 31.4). Rb-Sr dating of muscovite from an unfoliated pegmatite give a late Archean minimum age for rotation to a N-S direction (Fig. 31.1; van Breemen, personal communication, 1985). Farther south in the monotonously migmatitic area foliations are generally steep but do not form readily discernible map-scale patterns (Fig. 31.5). There is a similarity, however, between the gross geometry of the main phase foliations from within the migmatites of the eastern Bathurst Terrane (domain 8, Fig. 31.4) and that of the foliations from domains showing map scale deflections of Archean trends of lithological units (domains 2-6, Fig. 31.4).

This suggests that there are several unrecognized small scale domains which record this deflection within the migmatites. Fabric variations in the eastern Bathurst terrane are prominent, for example, the migmatites are cut by many discontinuous zones of tectonite (as illustrated in Fig. 68.3b, op. cit.). These comprise mostly staurolite-chlorite grade rocks and are correlated with those of predominantly lower grade to the SSW (east of outlier 1 in Fig. 31.1 and domains 6 and 8, Fig. 68.8, op. cit.), including those forming the basement slice in the Goulburn outlier I (see above). The tectonite zones are all predominantly steeply dipping and have a somewhat variable trend but are dominated by NNE strikes (Fig. 31.4). In contrast to those in the straight belt, to the east stretching lineations in these tectonites have a uniformly steep near down-dip plunge (Fig. 31.4, 31.5). These second phase fabrics are interpreted to record an episode of compression across this part of the Bathurst terrane. Among this population of tectonites is a significant group of both higher grade sillimanite-bearing rocks and those in which lower grade assemblages appear to have overprinted higher grade tectonites. It is not clear whether these trends are original, or reoriented Archean structures.

A plausible interpretation of all the structures described in this section is that they represent at minimum three kinematically and temporally distinct events: (1) the deflection of Archean NW-SE trends at least to N-S (and possibly to NNE) in the late Archean; (2) the overprinting, probably dominantly in the Proterozoic, of migmatites by narrow shear zones with steep shear directions. These appear to record a phase of crustal compression which is pervasive east of outlier I and west of the straight belt and is related in part to folding and thrusting of the cover, which postdated thin-skinned thrusting of the cover; (3) formation in the east of a wide ductile transcurrent shear zone, the straight belt (not necessarily younger than (2)) which itself abuts probable thrust bound terranes to the east (Thompson et al., 1985).

Overview

These results allow the division of the basement rocks of the Tinney Hills-Overby Lake map area into three NNE trending zones. The easternmost zone corresponds to the Ellice River Terrane (Fig. 31.1). This is dominated by a wide Proterozoic (?) straight belt/transcurrent shear zone in which displacement is believed to be dextral. Further characteristics of this belt are "augen" or resisters, in the sense of Watson (1973), for example the granulite gneiss and charnockite in central Ellice River Terrane, variably foliated non-migmatitic granitoids which are elongate parallel to the length of the zone and mafic dykes along the Ellice River Terrane boundary. In the southeastern corner of the Ellice River Terrane steeply dipping LS tectonites and mylonites, both with a down dip stretching lineation (Thompson et al., 1985, Fig. 68.9c) probably mark the initiation of a thrust regime. The second zone lies within the eastern Bathurst Terrane, east of outlier 1 (corresponding to domain 8 and its SSW extension in Fig. 31.4) where structures are present indicative of compression across the zone. These appear to be dominantly second phase (Proterozoic) and both basement and Goulburn Group (Proterozoic) cover were shortened together in the latest (lowest grade) episode of this phase. The Archean structure of this zone is a cause of debate, however to the west of this zone, west of outlier 1 (Fig. 31.1), Archean structures are well preserved within the Bathurst Terrane metasediments. This last zone would then constitute the relatively undeformed foreland beneath the Bear Creek Hills thin-skinned thrust belt formed in the Goulburn Group cover. Perhaps the décollement of these thrusts root in the zone of compression east of outlier 1. In the southwest corner of the basement block, rocks are ductilily deformed along the Bathurst Fault trend, the aforementioned shortening of basement and cover may in part be related to movement on this wrench fault.

References

Campbell, F.H.A. and Cecile, M.P.

1976: Geology of the Kilohigok Basin; Geological Survey of Canada, Open File Map 332, 1:500 000 scale.

1981: Evolution of the early Proterozoic Kilohigok Basin, Bathurst Inlet-Victoria Island, Northwest Territories; in Proterozoic Basins of Canada, ed. F.H.A. Campbell; Geological Survey of Canada, Paper 81-10, p. 103-131.

Coward, M.P., James, P.R. and Wright, L.I.

1976: The northern margin of the Limpopo mobile belt, southern Africa; Geological Society of America Bulletin, 87, p. 601-611.

Davidson A., Culshaw, N.G., and Nadeau, L.

1982: A tectono-metamorphic framework for part of the Grenville Province, Parry Sound region, Ontario; in Current Research, Part A, Geological Survey of Canada, Paper 82-1A, p. 175-190.

Fraser, J.A.

1964: Geological notes on northeastern District of Mackenzie, Northwest Territories (Report and Map 45-1963); Geological Survey of Canada, Paper 63-40, 16 p.

1968: Geology across Thelon Front, District of Mackenzie (76I, J); in Report of Activities, Part A, Geological Survey of Canada, Paper 68-1A, p. 134.

1972: Artillery Lake map area, District of Mackenzie; Geological Survey of Canada, Paper 71-38, 17 p.

1978: Metamorphism in the Churchill Province, District of Mackenzie; in Metamorphism in the Canadian Shield, ed. J.A. Fraser and W.W. Heywood; Geological Survey of Canada, Paper 78-10, p. 195-202.

Frith, R.A.

1982: Second preliminary report on the geology of the Beechey Lake-Duggan Lakes map areas, District of Mackenzie; in Current Research, Part A, Geological Survey of Canada, Paper 82-1A, p. 203-211.

Frith, R.A. and Loveridge, W.D.

1982: Ages of Yellowknife Supergroup volcanic rocks and regional metamorphism in the northeastern Slave Structural Province; in Current Research Part A, Geological Survey of Canada, Paper 82-1A, p. 225-237.

Grotzinger, J.P. and Gall, Q.

1986: Preliminary investigation of early Proterozoic Western River and Burnside River formations: evidence for foredeep origin of Kilohigok Basin, District of Mackenzie; in Current Research, Geological Survey of Canada, paper 86-1A, report 12.

Harding, T.P.

1974: Petroleum Traps Associated with Wrench Faults; The American Association of Petroleum Geologists Bulletin, v. 58, p. 1290-1304.

Henderson, J.B. and Thompson, P.H.

1980: The Healey Lake map area (northern part) and the enigmatic Thelon Front, District of Mackenzie; in Current Research, Part A, Geological Survey of Canada, Paper 80-1A, p. 165-169.

1981: The Healey Lake map area and the enigmatic Thelon Front, District of Mackenzie; in Current Research, Part A, Geological Survey of Canada, Paper 81-1A, p. 175-180.

Henderson, J.B. and Thompson, P.H. (cont.)
1982: Geology of Healey Lake map area (1:125 000 scale map and marginal notes); Geological Survey of Canada, Open File 860.

Henderson, J.B. and Macfie, R.I.
1985: The northern Artillery Lake map-area: a transect across the Thelon Front, District of Mackenzie in Current Research, Part A, Geological Survey of Canada Paper 85-1A, p. 441-448

Henderson, J.B., Thompson, P.H., and James, D.T.
1982: The Healey Lake map area and the Thelon Front problem, District of Mackenzie; in Current Research, Part A, Geological Survey of Canada, Paper 82-1A, p. 191-195.

Hill, J.D. and Frith, R.A.
1982: Petrology of the Regan Intrusive Suite, in the Nose Lake-Beechey Lake map area, District of Mackenzie; Geological Survey of Canada, Paper 82-8, 26 p.

Hoffman, P.F., Tirrul, R., Grotzinger, J.P., Lucas S.B., and Eriksson, K.A.
1984: The externides of Wopmay Orogen, Takijuq Lake and Kikerk Lake map areas, District of Mackenzie; in Current Research, Part A, Geological Survey of Canada, Paper 84-1A, p. 383-395.

Hollister, L.S.
1977: The reaction forming cordierite from garnet, The Khtada Lake metamorphic complex, British Columbia; Canadian Mineralogist, v. 15, p. 217-229.

James, D.T.
1985: Geology of the Moraine Lake area and the Thelon Front, District of Mackenzie; in Current Research, Part A, Geological Survey of Canada, Paper 85-1A, p. 449-454.

Korstgard, J.
1979: Nagssugtoquidian Geology; Gronlands Geologiske Undersogelse Rapport 89, 146 p.

Nash, D.
1979: Nagssugtoquidian tectonics at the western end of the Itivdleq shear zone, West Greenland; Gronlands Geologiske Undersogelse Rapport 89, p. 43-46.

Stockwell, C.H.
1969: Tectonic map of Canada (1:5 000 000); Geological Survey of Canada, Map 1251A.

1982: Proposals for time-classification and correlation of Precambrian rocks and events in Canada and adjacent areas of the Canadian Shield Part 1: A time classification of Precambrian rocks and events; Geological Survey of Canada, Paper 80-19, 135 p.

Thompson, P.H.
1978: Archean regional metamorphism in the Slave Province - A new perspective on some old rocks; in Metamorphism of the Canadian Shield, ed. J.A. Fraser and W.W. Heywood; Geological Survey of Canada, Paper 78-10, p. 85-102.

Thompson, P.H. and Ashton, K.
1984: Preliminary report on the geology of the Tinney Hills-Overby Lake (W 1/2) map area, District of Mackenzie: a look at the Thelon Tectonic Zone northeast of the Bathurst Fault; in Current Research, Part A, Geological Survey of Canada, Paper 84-1A, p. 415-423.

Thompson, P.H. and Culshaw, N.
1985: Tinney Hills map area, District of Mackenzie; Geological Survey of Canada, Open File 1155.

Thompson, P.H. and Frey, M.
1984: Illite "crystallinity" in the Western River Formation and its significance regarding the regional metamorphism of the early Proterozoic Goulburn Group, District of Mackenzie; in Current Research, Part A, Geological Survey of Canada, Paper 84-1A, p. 409-414.

Thompson, P.H. and Henderson, J.B.
1983: Polymetamorphism in the Healey Lake map area - implications for the Thelon Tectonic Zone; in Current Activities Forum, 1983, Program with Abstracts, Geological Survey of Canada, Paper 83-8, p. 2.

Thompson, P.H., Culshaw, N., Thompson, D.L., and Buchanan, J.R.
1985: Geology across the western boundary of the Thelon Tectonic Zone in the Tinney Hills-Overby Lake (west half) map area, District of Mackenzie; in Current Research, Part A, Geological Survey of Canada, paper 85-1A, p. 555-572.

Tirrul, R.
1985: Nappes in the Kilohigok Basin and their relation to the Thelon Tectonic Zone, District of Mackenzie; in Current Research, Part A, Geological Survey of Canada, Paper 85-1A, p. 407-420.

Van Biljon, W.J. and Legg, L.H.
1983: The Limpopo Belt; Geological Society of South Africa Special Publication 8, 203 p.

Watson, J.V.
1973: Effects of reworking on high-grade gneiss complexes; Philosophical Transactions of the Royal Society of London, Series A, v. 273, p. 443-455.

Wilcox, R.E., Harding, T.P., and Seely, D.R.
1983: Basic Wrench Tectonics; American Association of Petroleum Geologists Bulletin, v. 57, p. 74-96.

Wright, G.M.
1967: Geology of the southeastern barren grounds, parts of the Districts of Mackenzie and Keewatin (Operations Keewatin, Baker, Thelon); Geological Survey of Canada, Memoir 350.

Geology of the northernmost Cape Breton Highlands, Nova Scotia[1]

Contract 27ST.23233-5-0009

Robert P. Raeside[2], Sandra M. Barr[2],
Chris E. White[2], and Frank A.R. Dennis[2]

Raeside, R.P., Barr, S.M., White, C.E., and Dennis, F.A.R., Geology of the northernmost Cape Breton Highlands, Nova Scotia; in Current Research, Part A, Geological Survey of Canada, Paper 86-1A, p. 291-296, 1986.

Abstract

Geological mapping in the northernmost Highlands of Cape Breton Island during the summer of 1985 has shown that the area can be divided into two zones of different lithologic character but both consisting mainly of rocks of inferred Precambrian age. The bulk of the area, west of a fault zone in the valleys of Wilkie and Grays Hollow brooks, is composed of felsic and mafic gneisses and varied plutonic rocks, including anorthosite, monzodiorite, syenite and granite. East of the fault zone the diversity of lithologic types is less extreme and the rocks consist predominantly of felsic gneisses and schists (characterized by high-pressure regional metamorphic mineral assemblages indicating bathozone 5), and felsic granitoid rocks. Other units in the map area include volcanic and sedimentary rocks of the Devono-Carboniferous Fisset Brook Formation and sedimentary rocks of the Carboniferous Horton and Windsor groups.

Résumé

Le levé géologique effectué dans la partie la plus septentrionale des hautes terres de l'île du Cap-Breton au cours de l'été de 1985 a révélé qu'il est possible de diviser cette région en deux zones à lithologies différentes, mais néanmoins principalement constituées de roches qui dateraient du Précambrien. Le gros de la région, à l'ouest d'une zone faillée dans les vallées des ruisseaux Wilkie et Grays Hollow, est constitué de gneiss felsique et mafique et de diverses roches plutoniques dont l'anorthosite, la monzodiorite, la syénite et le granite. A l'est de la zone faillée, la région présente des types lithologiques moins variés et les roches sont surtout des schistes et des gneiss felsiques (caractérisés par des paragenèses métamorphiques de haute pression à caractère régional, indiquant la zone bathyale 5) ainsi que des granitoïdes felsiques. La région étudiée contient aussi des unités de roches volcaniques et sédimentaires de la formation de Fisset Brook du Dévono-Carbonifère et des unités de roches sédimentaires des groupes de Horton et de Windsor du Carbonifère.

---

[1] Contribution to the Canada-Nova Scotia Mineral Development Agreement 1984-89. Project carried by the Geological Survey of Canada, Precambrian Geology Division, Project 760027.
[2] Department of Geology, Acadia University, Wolfville, Nova Scotia B0P 1X0

Introduction

Geological mapping at a scale of 1:50 000 in the northernmost Highlands of Cape Breton Island during 1985 continued a project which involves mapping and analysis of the Precambrian and Paleozoic crystalline rocks of the entire Highlands (Raeside et al., 1984; Barr et al., 1985a). The Cape Breton Highlands occupy a significant position in the Appalachian Orogen and make up one of the largest sections of basement rocks in Atlantic Canada. Figure 32.1 presents the general geology of the study area which is bounded by the Gulf of St. Lawrence and Atlantic Ocean on the west, north and northeast, by the Aspy Fault on the southeast and the Grande Anse valley in the south. Approximately 30% of the area is underlain by Upper Paleozoic sedimentary rocks of the Horton and Windsor groups (Neale and Kelley, 1960; Bradley and Bradley, 1984) which were not mapped in detail.

Previous maps of the area (Neale, 1963a, 1964a, b) provided detail of the Upper Paleozoic sedimentary rocks, but were of a reconnaissance nature for the crystalline rocks, and serve only to outline the approximate position of most of the major rock types. No detailed analyses of stratigraphy, structure, metamorphism or plutonic sequences were provided. In a regional compilation of the geology of Nova Scotia, Keppie (1979) showed much of the area to be underlain by mafic gneiss and schist of uncertain affinity, a series of questionably Hadrynian plutons (anorthosite, gabbro and syenite), and a number of smaller felsic plutons and felsic gneiss and schist units. The studies by Macdonald and Smith (1980) and Smith and Macdonald (1981, 1983) focussed on smaller areas in the northern Cape Breton Highlands and have been incorporated into this study.

Acknowledgments

The authors gratefully acknowledge financial support from the Department of Energy, Mines and Resources, Geological Survey of Canada, and the Natural Sciences and Engineering Research Council of Canada.

Overview

The area can be subdivided into two zones of different lithologic character. The bulk of the area, west of the informal Wilkie Brook fault system recognized in the valleys of Wilkie and Grays Hollow brooks, is composed of an undivided package of felsic and mafic gneisses, and a series of plutonic rocks of variable composition and development of foliation. East of the fault zone the diversity of lithologic types is less extreme, and the rocks consist of predominantly felsic gneisses and schists and felsic granitoid rocks.

Lithologic units, west of Wilkie Brook fault system

Western gneissic complex

The main components of the western gneissic complex are quartzofeldspathic gneiss, amphibolite and granitic gneiss. These lithologies occur intimately intermixed with each other and it has not been possible to separate them on a 1:50 000 scale map. Smaller amounts of calcareous rocks were also noted.

The dominant lithology is a quartzofeldspathic gneiss of variable appearance, ranging from medium to coarse grained, mildly to strongly foliated, and unsheared to severely sheared. The abundance of mafic minerals varies from less than 2% to more than 40%. Typically these are biotite, hornblende and opaque minerals; rarely they include garnet. No aluminosilicate minerals have as yet been noted in the western gneissic complex. Most of the samples sectioned, and especially those which have been more strongly sheared, have been intensely altered to quartz-chlorite-epidote-saussurite assemblages.

Amphibolitic rocks occur throughout the western gneissic complex and make up about 30% of the unit. Typically these are thoroughly recrystallized medium to coarse grained mesocratic amphibolites with accessory ilmenite mantled by retrograde sphene. Biotite is also present in more leucocratic varieties. Less commonly some fine grained amphibolites preserve relict compositional banding implying they are derived from layered volcanic (or pyroclastic) rocks. A relict gabbroic texture was also noted in some specimens.

Calcareous rocks have been noted at only two localities. A tremolite-phlogopite-diopside schist unit occurs in Polletts Cove Brook and marble xenoliths with calc-silicate skarn margins occur in a syenitic pluton in the northwest of the map area. The marble xenoliths are assumed to be derived from a calcareous horizon in the western gneissic complex.

Mildly to strongly foliated intrusive rocks are intimately mixed with the gneissic rocks. These range in composition from granite to anorthosite, but do not appear to show any spatial relationship to the plutonic bodies described below. In some cases the foliation is the result of recrystallization under high grade regional metamorphic conditions, along with the surrounding gneisses, in other cases the foliation is a shear foliation which is also pervasive through the gneisses. In addition, a variety of unfoliated intrusive rocks occur as dykes and sills in the western gneiss complex. These include granite and granite pegmatite which are presumed to be related to post-tectonic plutons described below, and basaltic dykes.

Anorthosite

Anorthosite occurs as small plutons and dykes within the gneissic complex in the central and western parts of the map area. Some of these anorthosite bodies were identified by earlier workers (Neale, 1963a, b) and have been the subject of petrologic studies (Jenness, 1966; Mitchell, 1979; Smith and Macdonald, 1983). Our mapping has redefined the distribution of previously mapped anorthosite, identified the presence of a major additional body, and established the intrusive relationship between anorthosite and the gneissic complex.

The anorthosite consists mainly of unzoned or weakly zoned plagioclase of approximately An_{50} composition with accessory apatite. Grain size ranges from fine to coarse, and primary texture is allotriomorphic granular. Alteration is generally moderate to intense, with abundant epidote, sericite, zoisite, chlorite, and sphene. Many samples are strongly sheared. Primary mafic minerals are rare, but Smith and Macdonald (1983) reported the presence of relict pyroxene and amphibole.

Monzodiorite and related rocks

Mappable bodies of monzodiorite occur in apparent close association with anorthosite in the southern part of the map area. These are intruded by abundant dykes and small plutons of syenite and granite. Locally the monzodiorite appears to grade to diorite, and may be correlative with dioritic rocks within the western gneissic complex which could not be mapped as separate bodies.

Although variable in composition, typical monzodiorite is a medium grained, foliated, red and black rock consisting of plagioclase, clinopyroxene, and amphibole with minor amounts of K-feldspar and quartz. Alteration and shearing are widespread.

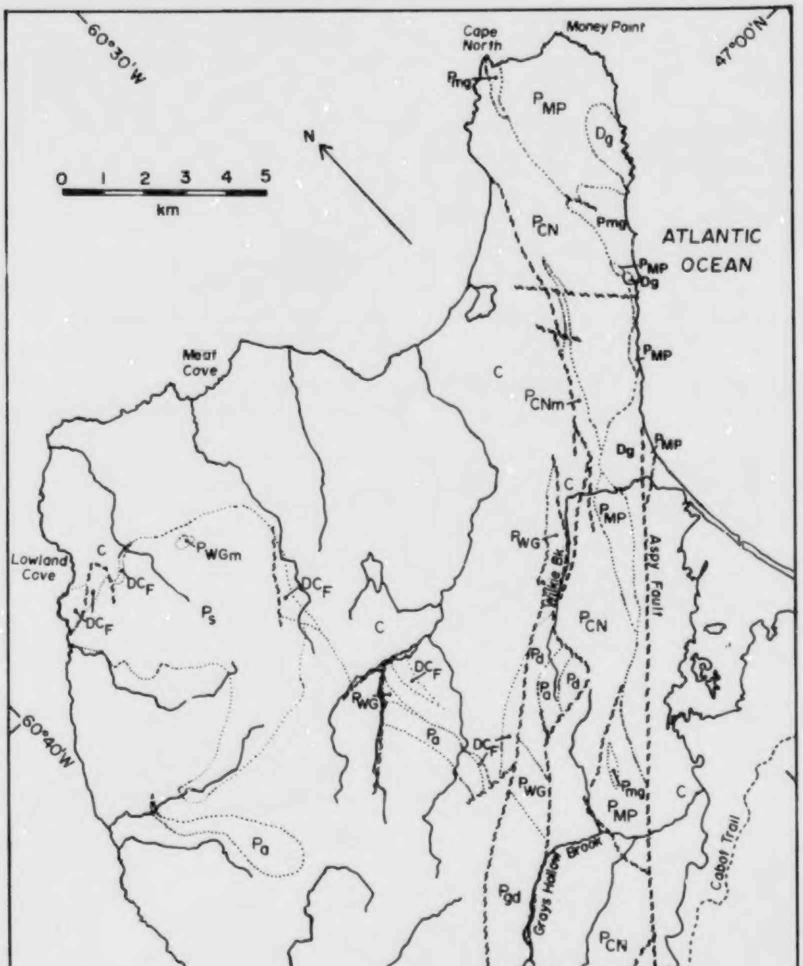

Figure 32.1

Geological map of the northernmost Cape Breton Highlands, Nova Scotia.

LEGEND

Carboniferous

C — undivided sedimentary rocks of the Horton and Windsor Groups

Devono-Carboniferous

DC_F — Fisset Brook Formation; rhyolite, basalt, andesite, conglomerate, sandstone, siltstone

D_g — Unfoliated granites

Precambrian (?)

P_a — anorthosite

P_d — monzodiorite, diorite, dioritic gabbro; P_{dm}, mylonitized equivalent

P_{gd} — granodiorite

P_{mg} — microgranite

P_s — syenite

P_{MP} — Money Point Group; pelitic, semipelitic or psammitic schists, amphibolites, metavolcanics

P_{CN} — Cape North Group; semi- pelitic and pelitic gneiss, amphibolites, marble, calc-silicate gneiss; P_{CNm}, mylonite zones

P_{WG} — Western gneissic complex; semipelitic and psammitic gneiss, amphibolite, granitoid gneiss, calc-silicate schist; P_{WGm}, marble

Symbols

contact (defined, approximate, assumed)

fault (defined, approximate, assumed)

highway

Syenite

Syenite forms a large intrusion in the northern part of the map area and also occurs as small bodies and dykes within the gneissic complex and in association with monzodiorite and anorthosite bodies. Although relations are not clear, the syenite apparently intruded all of the above units. This unit is particularly significant because the Meat Cove zinc deposit (Chatterjee, 1979) as well as other sulphide showings, occur in association with marble xenoliths within the syenite.

The syenite is typically medium to coarse grained and pink to dark pink. It ranges from equigranular to strongly foliated, the latter apparently the result of shearing. Recrystallized textures are typical. The syenite consists mainly of strongly perthitic alkali feldspar, with minor amounts of albitic plagioclase, quartz, amphibole, and pyroxene. Apatite, zircon, and opaque oxides are abundant accessory minerals.

Lithologic units, east of Wilkie Brook fault system

Two major units of stratified rocks are recognized between the Wilkie Brook and Aspy fault systems: the predominantly gneissic Cape North Group and the predominantly schistose Money Point Group. These groups were originally identified by Macdonald and Smith (1980) in the Cape North peninsula and can be traced south from the peninsula in a continuous belt for 15 km. As in the area described by Macdonald and Smith (1980), the exact nature of the contact between the two lithologies is uncertain. A faulted contact can be recognized in at least two localities in Grays Hollow Brook, but it is uncertain if there is significant displacement on these faults. North of Grays Hollow Brook, the contact, although poorly exposed, appears conformable.

Cape North Group

The rocks of the Cape North Group include a wide variety of lithologies, but are characterized by the ubiquitous presence of gneissic semipelitic and pelitic lithologies. In addition, there are substantial amounts of amphibolitic rocks, and smaller amounts of psammitic and calcareous lithologies. All of these lithologies are abundantly intruded by granitoid sheets and lenses.

Semipelitic gneisses are the most common rock types. These are typically medium to coarse grained quartz-plagioclase-biotite-hornblende gneisses and may also contain garnet and K-feldspar. The intensity of gneissic banding ranges from negligible to moderately well developed. Pelitic gneisses are interlayered with the semipelitic gneisses and commonly contain kyanite, garnet and orthoclase in addition to quartz, plagioclase, biotite and hornblende. Relict staurolite was also noted in one sample. Pelitic gneisses tend to exhibit a more pronounced compositional layering than semipelitic gneisses.

Metamorphosed mafic rocks are common in the Cape North Group. These range from hornblende-biotite gneisses (more micaceous varieties are schists) to massive amphibolites. No examples of cross-cutting relationships were recorded and it is assumed that the mafic rocks represent metamorphosed concordant igneous layers.

Calc-silicate lithologies are a minor constituent of the Cape North Group. Commonly these are pure calcite marbles, but rare calc-silicate gneisses are also developed.

A broad band of mylonite recognized by Macdonald and Smith (1980) in the Cape North peninsula disappears under Carboniferous sedimentary rocks north of Wilkie Brook. It is inferred to pass into the Wilkie Brook fault system, where the zone of movement is much narrower (up to 10 m wide) and is shown in Figure 32.1 as a single fault.

Money Point Group

The Money Point Group comprises low to medium grade pelitic and semipelitic rocks with minor amounts of psammitic and mafic rocks. The predominantly volcanic sections identified by Macdonald and Smith (1980) do not occur in the area to the south. All the rock types in the group are closely interbedded and it has not been further subdivided.

Metasedimentary rocks make about 90% of the Money Point Group in the map area, and of these, semipelitic lithologies are most abundant. Typically they contain quartz, muscovite, biotite, garnet and opaque minerals, and many also have K-feldspar and amphibole. The ubiquitous presence of amphibole (hornblende) in these schists implies that the protolith probably was in part volcanogenic. Metamorphic grade generally increases to the west, and has produced rare staurolite or kyanite in the semipelitic rocks. Pelitic rocks occur as thinly interbedded layers and in addition commonly contain staurolite and kyanite – some specimens have up to 50% aluminosilicate minerals. In the higher metamorphic grade sections of the Money Point Group, the more pelitic lithologies have developed migmatites. Psammitic rocks are relatively uncommon in the Money Point Group, and occur as thick isolated layers and as thin layers interbedded with more aluminous lithologies. They are composed of quartz, feldspar and micas.

Metavolcanic rocks make up about 10% of the Money Point Group. These occur as layers of mafic schists ranging up to 20 m in thickness, but are more commonly closely interlayered with the metasedimentary rocks. They occur as amphibolites and are composed of pale hornblende and calcic plagioclase with abundant ilmenite or sphene.

All rock types in the Money Point Group have been intruded by numerous granitic and granodioritic sheets, some of which have undergone regional deformation and metamorphism along with the stratified rocks.

Granodiorite

Apparently intruded into the rocks of the Cape North Group in the central part of the eastern belt is a strongly sheared granodioritic body. This unit lies within the Wilkie Brook fault system and is extensively deformed by it. In most outcrops, the granodiorite occurs as a strongly foliated, sheared chlorite schist with lenses of less altered and sheared red and black granodiorite. In the less sheared areas it is a mildly foliated to massive grey granodiorite bearing small xenoliths of diorite. Throughout most of its outcrop area it is cut by abundant brick red syenogranite dykes – commonly these comprise up to 30% of the outcrop area, and have undergone the same shearing event as the host granodiorite. Neither the syenogranite nor the granodiorite extends as dykes into the country rocks. Overall lithologic similarity suggests that this unit may be correlative with the monzodiorite body west of the Wilkie Brook fault system.

In thin section, the unsheared granodiorite displays an equilibrium allotriomorphic-granular texture with medium- to coarse-grained coarsely antiperthitic plagioclase and fine- to medium-grained perthitic microcline, quartz, hornblende and clinopyroxene.

Other lithologic units

In addition to the lithologies described above, other crystalline rock types in the map area include small granitic plutons, granitic and mafic dykes, and rhyolites of the Fisset Brook Formation.

Granite

Granite forms a series of small plutons along the eastern and southern margins of the map area, but it also occurs abundantly in dykes and small plutons throughout the area except in the Fisset Brook Formation and younger units.

The most common type of granite is medium- to coarse-grained and red in colour due to iron oxide staining in both plagioclase and alkali feldspar. These rocks are locally foliated, and typically show variable effects of shearing and cataclasis. Quartz typically forms about 40% of the rocks, most of which are leucogranites containing only very minor amounts of chloritized biotite. They range from monzogranite (in which plagioclase is equal to or more abundant than alkali feldspar) to syenogranite and alkali feldspar granite. The monzogranites are similar to the Relay Station granite of Macdonald and Smith (1980) which has given a Carboniferous Rb-Sr age (Cormier, 1980). These granites are also similar in character to the North River granite to the south which has yielded a Devonian age (Barr et al., 1985b).

Also widespread in the area are medium- to fine-grained microgranite and aplite dykes and small plutons showing a range in composition similar to that in the coarser grained granites described above. These are normally foliated, and may predate the coarser granites.

In the southeastern part of the area, muscovite-biotite granites occur locally. These also are typically foliated. They are similar to the granites of the Devonian White Point pluton to the south (Barr et al., 1982).

Fisset Brook Formation

Discontinuous occurrences of volcanic and sedimentary rocks around the periphery of the crystalline rocks of the map area have been correlated with the Devono-Carboniferous Fisset Brook Formation by most earlier workers (MacKasey, 1963; Kelley and MacKasey, 1965; Smith and Macdonald, 1981). This is based on lithological similarity and the presence of poorly preserved trilete spores from the Lowland Cove section in the northwestern part of the map area (Smith and Macdonald, 1981). Cormier and Kelley (1964), however, reported a whole rock Rb-Sr isochron age of 491 +/- 25 Ma (values recalculated using current decay constant by Keppie and Smith, 1978) from the volcanic rocks at Lowland Cove.

The present mapping shows these rocks to be somewhat more extensive than previously mapped. Rhyolite, interpreted by Smith and Macdonald (1981) to be the basal unit, is in faulted or inferred unconformable contact with the syenite and western gneissic complex in the northwest and east. Although variable in groundmass grain size and texture and proportion of phenocrysts, the rhyolite is characterized by the presence of resorbed quartz and sanidine in spherrulitic, microcrystalline, or cryptocrystalline quartz and K-feldspar groundmass.

Rhyolitic units were previously identified in the western part of the map area by Neale (1963a). These units are composed of discontinuous rhyolitic flows, pyroclastic deposits and conglomerates with rhyolitic clasts. In the Eastern Brook area, the unit lies unconformably on granite and granitic gneiss of the western gneissic complex, and consists of a thin basal amygdaloidal basalt, a massive variably porphyritic rhyolite and a series of interbedded rhyolites and conglomerates, with conglomerate making up approximately 40% of the upper section.

Discussion

The Cape Breton Highlands, west of the Aspy Fault, can be separated into two belts. Between the Aspy and Wilkie Brook faults metamorphic and igneous lithologies can be correlated from Cape North to the southern part of the map area, including those areas mapped by Macdonald and Smith (1980) and Smith and Macdonald (1983). This belt is characterized by high pressure regional metamorphism (Bathozone 5) and felsic granitoid intrusion. West of the Wilkie Brook fault system, the metamorphic lithologies do not display suitably pelitic compositions to determine the pressure of metamorphism. In this area intermixed semipelitic gneisses and amphibolites are intruded by a number of anorthosite, granite and gabbroic or dioritic plutons and sheets, and syenite plutons.

The nature of the boundary (the Wilkie Brook fault system) between the eastern and western sections has not been fully established. The fault mainly occurs as a branching fault system ranging from 15 m to 300 m wide. In some areas it occurs as a broad mylonite zone, in others as an intense shear zone, and in a granodioritic body it appears to dissipate into a 1500 m wide zone of strongly to intensely foliated rock.

References

Barr, S.M., O'Reilly, G.A., and O'Beirne, A.M.
1982: Geology and geochemistry of selected granitoid plutons of Cape Breton Island; Nova Scotia Department of Mines and Energy, Report 82-1, 176 p.

Barr, S.M., Raeside, R.P., and Macdonald, A.S.
1985a: Geology of the southeastern Cape Breton Highlands, Nova Scotia; in Current Research, Part B, Geological Survey of Canada, Paper 85-1B, p. 103-109.

Barr, S.M., Jamieson, R.A., and Raeside, R.P.
1985b: Igneous and metamorphic geology of the Cape Breton Highlands; Geological Association of Canada/Mineralogical Association of Canada, Excursion 10, Frederiction, New Brunswick, 48 p.

Bradley, D.C. and Bradley, L.M.
1984: Age and development of structural relief between basement and Carboniferous, northern Cape Breton Island, Nova Scotia; Geological Society of America, Northeastern Section, Abstracts with Programs, vol. 16, p. 5.

Chatterjee, A.K.
1979: Geology of the Meat Cove Zinc deposit, Cape Breton Island, Nova Scotia; Nova Scotia Department of Mines and Energy, Paper 79-3, 27 p.

Cormier, R.F.
1980: New rubidium/strontium ages in Nova Scotia; Nova Scotia Department of Mines, Mineral Resources Division, Report of Activities, Report 80-1, p. 223-233.

Cormier, R.F. and Kelley, D.G.
1964: Absolute age of the Fisset Brook Formation and the Devonian-Mississippian boundary, Cape Breton Island, Nova Scotia; Canadian Journal of Earth Sciences, v. 1, p. 159-166.

Jenness, S.E.
1966: The anorthosite of northern Cape Breton Island, Nova Scotia; a petrological enigma; Geological Survey of Canada, Paper 66-21.

Kelley, D.G. and MacKasey, W.O.
1965: Basal Mississippian volcanic rocks in Cape Breton Island, Nova Scotia; Geological Survey of Canada, Paper 64-34.

Keppie, J.D.
1979: Geological map of the Province of Nova Scotia; Nova Scotia Department of Mines and Energy, scale 1:500 000.

Keppie, J.D. and Smith, P.K.
1978: Compilation of isotopic age data of Nova Scotia; Nova Scotia Department of Mines and Energy, Report 78-4.

Macdonald, A.S. and Smith, P.K.
1980: Geology of the Cape North area, northern Cape Breton Island, Nova Scotia; Nova Scotia Department of Mines and Energy, Paper 80-1, 60 p.

MacKasey, W.O.
1963: Petrography and stratigraphy of a Lower Mississippian, Pre-Horton volcanic succession in northwest Cape Breton Island; unpublished M.Sc. thesis, Carleton University, Ottawa, Ontario.

Mitchell, P.L.
1979: A study of rare earth element geochemistry and mineral chemistry of the anorthosites and related rocks near Pleasant Bay, Cape Breton Island, Nova Scotia; unpublished B.Sc. thesis, Dalhousie University, 88 p.

Neale, E.R.W.
1963a: Geology, Pleasant Bay, Cape Breton Island, Nova Scotia; Geological Survey of Canada, Map 1119A.

1963b: Geology, Dingwall, Cape Breton Island, Nova Scotia; Geological Survey of Canada, Map 1124A.

Neale, E.R.W. (cont.)
1964a: Geology, Cape St. Lawrence, Cape Breton Island, Nova Scotia; Geological Survey of Canada, Map 1149A.

1964b: Geology, Cape North, Cape Breton Island, Nova Scotia; Geological Survey of Canada, Map 1150A.

Neale, E.R.W. and Kelley, D.G.
1960: Stratigraphy and structure of Mississippian rocks of northern Cape Breton Island; Proceedings Geological Association of Canada, v. 12, p. 79-96.

Raeside, R.P., Barr, S.M., and Jong, W.
1984: Geology of the Ingonish River--Wreck Cove area, Cape Breton Island, Nova Scotia; Nova Scotia Department of Mines and Energy, Mines and Minerals Branch, Report of Activities, Report 84-1, p. 249-258.

Smith, P.K. and Macdonald, A.S.
1981: The Fisset Brook Formation at Lowland Cove, Inverness County, Nova Scotia; Nova Scotia Department of Mines and Energy, Paper 81-1, 18 p.

1983: The geology of the Red River Anorthosite Complex, Inverness and Victoria Counties, Nova Scotia; Nova Scotia Department of Mines and Energy, Paper 83-1.

A-type granites in New Brunswick[1]

Project 850019

Joseph B. Whalen
Precambrian Geology Division

Whalen, J.B., A-type granites in New Brunswick; in Current Research, Part A, Geological Survey of Canada, Paper 86-1A, p. 297-300, 1986.

Abstract

Anorogenic or alkaline (A-type) granites have not been widely recognized in New Brunswick. A number of occurrences were identified during the 1985 field season, including subalkaline A-types which contain significant granite-related W-Sn-Mo-F mineralization.

Résumé

Les géologues n'ont pas reconnu de granites anorogéniques ou alcalins (de type A) sur une grande échelle au Nouveau-Brunswick. Ils ont cependant observé un certain nombre au cours de la campagne de mai 1985, notamment des granites subalcalins de type A qui sont le siège d'une minéralisation importante en W-Sn-Mo-F.

[1] Contribution to the Canada-New Brunswick Mineral Development Agreement 1984-89.

Introduction

Among recent attempts to classify the plutonic rocks in New Brunswick, Fyffe et al. (1981) used structure, texture, field relationships, mineralogy and chemical characteristics to subdivide them into eight main groups (types a to h). In metallogenic summaries of the New Brunswick Appalachians, Ruitenburg and Fyffe (1982, 1983 and 1985), subdivided the granites according to the classification of Chappell and White (1974) into I- and S-types. A summary paper on Canadian Appalachian granites (Currie, personal communication, 1985) will employ the classification scheme of Pitcher (1983) to subdivide the granites into I-, IC-, S-, M- and A-types. However, the economically and tectonically important anorogenic or alkaline (A-type) granites have not been widely recognized in New Brunswick.

Granite classifications and A-type granites

Initially Chappell and White (1974) proposed a genetic subdivision of granitic rocks into those derived from sedimentary sources (S-types) and those from igneous sources (I-types). Subsequently tectonic factors which imply that I-type granites are the product of Cordilleran and postorogenic uplift regimes and S-types the product of continental collision (e.g. Beckinsale, 1979; Pitcher, 1983) were added to this initial concept. Further genetic-tectonic granite subdivisions were made by the addition of A-types (Loiselle and Wones, 1979; Collins et al., 1982) and M-types (White, 1979) to encompass the granites of anorogenic and oceanic arc settings, respectively. The presence of common, quite felsic I-type granite in the Appalachian-Caledonian belt led Pitcher (1983) to suggest an IC-granite subtype. Felsic granites (SiO_2>74 wt.%) can be difficult to classify, because the ability of major element criteria (i.e. Al/(Ca/2+Na+K) and K/Na ratios) to distinquish S- and I-types is thought to reflect a signature given to the magma by the restite (refractory melt residue) component. In felsic granites the restite component is minimal or nonexistent so the I- and S-type criteria based on major element chemistry break down and more sophisticated trace element data must be used. Recently serious attempts, similar to those so popular for basic volcanic rocks (e.g. Pearce and Cann, 1973; Floyd and Winchester, 1975), have been made using trace elements to characterize plutonic rocks of different tectonic environments (Pearce et al., 1984; Brown et al., 1984). These classifications recognize the existence of anorogenic or within-plate granites (A-types of Loiselle and Wones (1979)).

A-type granites are characterized by high SiO_2, Na_2O+K_2O, Fe/Mg, F, Zr, Nb, Ga, Sn, Y, and REE (except Eu) and low CaO, Ba, and Sr (Loiselle and Wones, 1979; Collins et al., 1982; White and Chappell, 1983). They are interpreted to have originated by partial melting of a protolith (felsic granulite) from which an orogenic granite magma had previously been extracted, and which was therefore enriched in F- and/or Cl-rich refractory ferromagnesian and accessory minerals. If the A-type melt is enriched in F, amphibole can be stabilized early and a peraluminous composition may be produced by amphibole fractionation, but if the melt is enriched in Cl, Ca-rich plagioclase may be the dominant fractionating phase and a peralkaline A-type may result (Collins et al., 1982). Mineralization associated with A-types includes Sn, Mo, Bi, Nb, W, Ta, and F (Collins et al.,1982; Pitcher, 1983). It has been noted in Nigeria that Sn mineralization is only associated with the sub-alkaline A-types not with the peralkaline granites (Imeokparia, 1985). A-type granites represent both the rift-associated magmatism of shield areas and the final plutonic event in orogenic belts. Such granites have been recognized in Proterozoic (Anderson, 1983) and Paleozoic orgenic belts (e.g. the Lachlan Fold Belt of Australia (Collins et al., 1983); the Newfoundland (Taylor, 1979; Whalen and Currie, 1983) and U.S. Applalachians (Buma et al., 1971) and the Nigerian rift valleys (Bowden and Whitley, 1974)).

A-type granites in New Brunswick

Current field work combined with a literature search has defined a number of possible occurrences of A-type granites in New Brunswick (see Fig. 33.1).

1. At the northern end of the St. George Batholith the Welsford complex has long been known to be peralkaline (Jackson, 1968) and therefore an A-type granite. Examination of this body by the author indicated that the granitic portion is lithologically identical to the main granite phase of the Topsails Terrane in Newfoundland (Whalen and Currie, 1983, 1984). Though a 383 Ma Rb/Sr age has been obtained from the Welsford (Fyffe et al., 1981), extrusive phases of this body are interbedded with the Silurian Jones Creek Formation (Currie, personal communication, 1985), so it is probably of similar age to the Early Silurian (Whalen et al., in press) Topsails A-type granites.
2. In the Popple Depot area Fyffe et al. (1981) thought that the Mount Elizabeth Granite varied from a biotite granite in the east to a hornblende granite in the western extremity. Mapping this past summer by the author demonsrated the presence of a medium- to coarse-grained, two-feldspar, biotite granite in the east and a one-feldspar, hastingsite-fayalite granite with associated hastingsite-hedenbergite-fayalite syenite in the west. These two distinct granite types are separated by a zone of complex interaction between mafic magma (probably equivalent to the West Portage Brook Troctolite) and felsic magma (probably equivalent to the A-type "portion" of the Mount Elizabeth Granite). Features of this zone, which contains mixtures of felsic aplite, quartz monzonite, diorite and syenite, are very similar to those described from the McGerrigle plutonic complex in the Gaspé (Whalen, 1985; Whalen and Gariépy, 1986) and the Topsails Terrane, Newfoundland (Whalen and Currie, 1984). Further geological mapping and chemical work is required to better understand this area.
3. The bulk of the eastern lobe of the St. George Batholith (Mount Douglas pluton) (Fig. 33.1) exhibits highly variable textural features with gradational and intrusive relationships between different high-level very felsic granitic phases. At the southwest margin of the eastern lobe, a fine- to medium-grained granophyric arfvedsonite-aegirine granite phase has been identified by the author. Age relationships between this phase and the rest of the Mount Douglas pluton, which is considered to be of Early Carboniferous age (Ruittenberg and Fyffe, 1985), are unclear at present. This A-type granite may be equivalent to the Welsford complex or contemporaneous with the other high level phases of the Mount Douglas pluton. In this regard, it is notable that this pluton exhibits a close lithological resemblance to the A-type marginal subalkaline to peralkaline phases of the Topsails Terrane (Whalen and Currie, 1983, 1984) and the Ackley City Batholith (Whalen, 1980, 1983). These features, and also the sparse geochemical data of Ruitenberg and Fyffe (1982), which indicates high Zr, Ce and Nb contents in the St. George, suggest that the whole eastern lobe and perhaps also the western lobe (Lake Utopia pluton, excluding the Magaguadavic pluton) might be better classified as A-type rather than S-type, as has been done by Ruitenberg and Fyffe (1985). Associated with the Mount Douglas pluton, and also with stocks of similar age and composition to the north (e.g. Mt. Pleasant Stock),

are significant W, Sn, Mo, F, Be ± Cu, Pb and Zn bearing quartz and greissen veins (Ruitenberg and Fyffe, 1985). Work on these adjacent stocks by Taylor et al. (1985) has indicated that they too are of A-type.

4. The Burnt Hill stocks (Fig. 33.1) are postorogenic, early Carboniferous, equidimensional, porphyritic and equigranular biotite ± muscovite granite intrusions which commonly display high-level characteristics such as granophyre and/or miarolites and moderate to low grade metamorphic aureoles (Fyffe et al., 1981). These bodies have significant associated W, Sn, Mo, F, Be ± Cu, Pb and Zn in greissen and endogranitic veins and disseminations and have been classified as S-type (Ruitenberg and Fyffe, 1985). The sparse available chemical data (Martin, 1966; Ruitenberg and Fyffe, 1982), in particular low CaO, Sr and Ba and high SiO_2, F, Zr, Ce and Nb in these granites indicates that they are probably A-type not S-type granites. The fact that they may be muscovite-bearing does not preclude them being A-type for muscovite-bearing A-types have been recognized elsewhere (Anderson, 1985).

5. In their classification of New Brunswick Acadian granites, Fyffe et al. (1981) distinguished two granite types or groupings which appear to have characteristics of A-type granites: a medium-grained equigranular biotite ± hornblende granite (type g) and a coarse-grained equigranular biotite granite characterized by minor porphyritic and granophyric phases (type h). Subsequently, Ruittenberg and Fyffe (1985) classified most of these granites as S-type. All the above discussed examples of A-type granites have been recognized from granites within the type g and h groups and it is quite possible that other granites of these groups are also of A-type. It has been noted earlier that it is difficult to classify such felsic granites without sophisticated trace

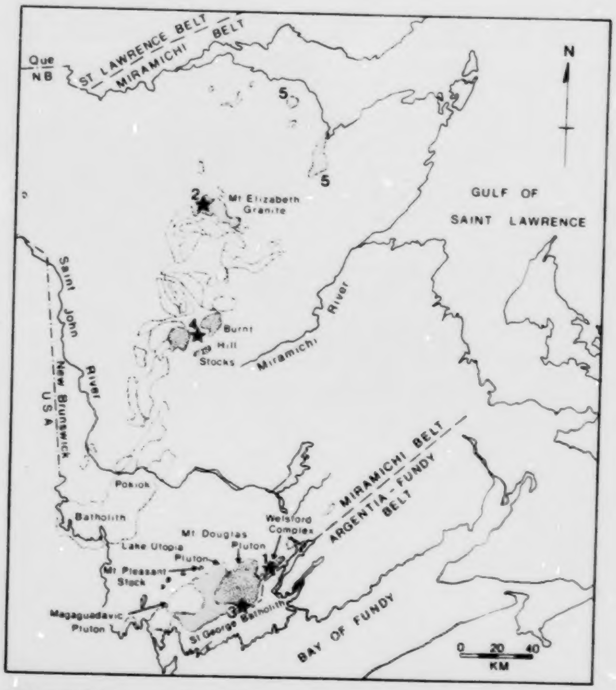

Figure 33.1. *Distribution of Acadian and Ordovician granites in New Brunswick (from Currie, personal communication, 1985) showing the location of possible occurrences of A-type granites numbered 1 to 5 as discussed in the text.*

element data. Geochemical work in progress will help resolve whether any of the other g and h group granites are A-types.

Conclusions

A-type granites appear to be much more abundant in New Brunswick than previously recognized. The significant granite-related mineralization (e.g. Burnt Hill and St. George-Mt. Pleasant area deposits) are associated with non-peralkaline A-type granites not with the abundant clearly S-type granites (e.g. most of the Pokiok Batholith). Work in progress on New Brunswick granites by the author should better resolve the age, chemical signature and tectonic setting of these granites.

Acknowledgments

The author would like to thank L.R. Fyffe for advice and insights into granites in New Brunswick. Field assistance was provided by A. Butler.

References

Anderson, J.L.
1983: Proterozoic anorogenic granite plutonism of North America; in Proterozoic Geology, ed. Medaris et al.; Geological Society of America, Memoir 161, p. 133-154.
1985: Proterozoic anorogenic two-mica granites: Silver Plume and St. Vrain Batholiths of Colorado; Geology, v. 13, p. 177-180.

Beckinsale, R.D.
1979: Granite magmatism in the tin belt of south-east Asia; in Origin of Granite Batholiths: Geochemical Evidence, ed. M.P. Atherton and J. Tarney; Shiva Publishing Ltd; p. 34-44.

Bowden, P. and Whitley, J.D.
1974: Rare Earth patterns in peralkaline and associated granites; Lithos, v. 7, p. 15-21.

Brown, G.C., Thorpe, R.S., and Webb, P.C.
1984: The geochemical characteristics of granitoids in contrasting arcs and comments on magma sources; Journal Geological Society of London, v. 141, p. 413-426.

Buma, G., Frey, F.A., and Wones, D.R.
1971: New England granites: trace element evidence regarding their origin and differentiation; Contributions to Mineralogy and Petrology; v. 31, p. 300-320.

Chappell, B.W. and White, A.J.R.
1974: Two contrasting granite types; Pacific Geology, v. 8, p. 173-174.

Collins, W.J., Beams, S.D., White, A.J.R., and Chappell, B.W.
1982: Nature and origin of A-type granites with particular reference to southeastern Australia; Contributions to Mineralogy and Petrology, v. 80, p. 189-200.

Floyd, P.A. and Winchester, J.A.
1975: Magma type and tectonic setting discrimination using immobile elements; Earth and Planetary Science Letters, v. 27, p. 211-218.

Fyffe, L.R., Pajari, G.E., and Cherry, M.E.
1981: The Acadian plutonic rocks of New Brunswick; Maritime Sediments and Atlantic Geology, v. 17, p. 23-36.

Imeokparia, E.G.
1985: Mesozoic granite magmatism and tin mineralization in Nigeria; in Granite – Related Mineral Deposits – extended abstracts of papers, ed. R.P. Taylor and D.F. Strong; Canadian Institute of Mining and Metallurgy Conference, Halifax, Nova Scotia, p. 137-141.

Jackson, E.V.
1968: Geological report, Welsford granite study; New Brunswick Department of Natural Resources, Map Series 68-2.

Loiselle, M.C. and Wones, D.R.
1979: Characteristics and origin of anorogenic granites; Geological Society of America Abstracts With Program, v. 11, p. 468.

Martin, R.F.
1966: A chemical and petrographic study of the granitic rocks of New Brunswick, Canada; M.Sc. thesis, Pennsylvania State University, 120 p.

Pearce, J.A. and Cann, J.R.
1973: Tectonic setting of basic volcanic rocks investigated using trace element analysis; Earth and Planetary Science Letters, v. 19, p. 290-300.

Pearce, J.A., Harris, N.B.W., and Tindle, A.G.
1984: Trace element discrimination diagrams for the tectonic interpretation of granitic rocks; Journal of Petrology, v. 25, p. 956-983.

Pitcher, W.S.
1983: Granite type and tectonic enviornment; in Mountain Buiding Processes, ed. K. Hsu; Academic Press, London, p. 19-40.

Ruitenberg, A.A. and Fyffe, L.R.
1982: Mineral deposits associated with granitoid intrusions and related subvolcanic stocks in New Brunswick and their relationship to Appalachian tectonic evolution; Canadian Institute of Mining and Metallurgy Bulletin, v. 75, p. 83-97.

1983: Metallic mineral zonation related to tectonic evolution of the New Brunswick Appalachians; in Regional Trends in Geology of the Appalachian – Caledonian – Hercynian – Mauritanide Orogen, ed. P.E. Schenk; Reidel Publishing Company, p. 363-373.

1985: Characteristics and tectonic setting of granitoid related mineral deposits in New Brunswick; in Granite-Related Mineral Deposits – extended abstracts of papers, ed. R.P. Taylor and D.F. Strong; Canadian Institute of Mining and Metallurgy Conference, Halifax, Nova Scotia, p. 205-210.

Taylor, R.P.
1979: Topsails igneous complex – further evidence of middle Paleozoic epeirogeny and orogenic magmatism in the northern Appalachians; Geology, v. 10, p. 488-490.

Taylor, R.P., Sinclair, W.D., and Lutes, G.
1985: Geochemical and isotopic characterization of granites related to W-Sn-Mo mineralization in the Mount Pleasant area, New Brunswick; in Granite – Related Mineral Deposits – extended abstracts of papers, ed. R.P. Taylor and D.F. Strong; Canadian Institute of Mining and Metallurgy Conference, Halifax, Nova Scotia, p. 265-273.

Whalen, J.B.
1980: Geology and geochemistry of the molybdenite showings of the Ackley City Batholith; Canadian Journal of Earth Sciences, v. 17, p. 1246-1258.

1983: The Ackley City Batholith, southeastern Newfoundland: evidence for crystal versus liquid-state fractionation; Geochimica et Cosmochimica Acta, v. 47, p. 1443-1457.

1985: The McGerrigle plutonic complex, Gaspé, Quebec: evidence of magma mixing and hybridization; in Current Research, Part A, Geological Survey of Canada, Paper 85-1A, p. 796-800.

Whalen, J.B. and Currie, K.L.
1983: The Topsails igneous terrane of western Newfoundland; in Current Research, Part A; Geological Survey of Canada, Paper 83-1A, p. 15-23.

1984: The Topsails igneous terrane, Western Newfoundland: evidence for magma mixing; Contributions to Mineralogy and Petrology, v. 83, p. 319-327.

Whalen, J.B., Currie, K.L., and van Breeman, O.
– Episodic Ordovician – Silurian plutonism in the Topsails igneous terrane, Western Newfoundland; Canadian Journal of Earth Sciences. (in press)

Whalen, J.B. and Gariépy, C.
1986: Petrogenesis of the McGerrigle plutonic complex, Gaspé, Quebec: a preliminary report; in Current Research, Part A, Geological Survey of Canada, Paper 86-1A, Report 30.

White, A.J.R
1979: Sources of granite magmas; Geological Society of America Abstracts with Program, v. 11, p. 539.

White, A.J.R. and Chappell, B.W.
1983: Granitoid types and their distribution in the Lachlan Fold Belt, southeastern Australia; Geological Society of America, Memoir 159, p. 21-34.

A new approach to sampling heavy minerals for regional geochemical exploration[1]

Project 840052

Y.T. Maurice and M.M. Mercier[2]
Resource Geophysics and Geochemistry Division

Maurice, Y.T. and Mercier, M.M., A new approach to sampling heavy minerals for regional geochemical exploration; in Current Research, Part A, Geological Survey of Canada, Paper 86-1A, p. 301-305, 1986.

Abstract

A procedure for rapid and economical extraction and concentration of heavy minerals from alluvial deposits is described. The technique is ideal for systematic geochemical surveys in areas of relatively easy access. It is carried out in two stages.

1. A heavy mineral preconcentrate is obtained at the sample site using a portable suction dredge, and
2. A final heavy mineral concentrate is produced in the laboratory with a spiral concentrator.

By processing a large volume of alluvium at each sample site, the method ensures that a sufficient quantity of heavy minerals is collected to perform chemical analyses for several elements including gold. The suction dredge also enables the sampling of underwater deep layers of stream sediments thus increasing the likelihood of collecting particles of precious metals and of other high density minerals if they are present.

Résumé

Le texte décrit une méthode rapide et économique d'extraire et de concentrer les minéraux lourds alluvionnaires. La méthode s'applique particulièrement aux levés géochimiques systématiques dans des régions relativement faciles d'accès. La procédure s'effectue en deux étapes:

1. on produit d'abord un préconcentré de minéraux lourds au site d'échantillonnage au moyen d'une drague à sluice portative,
2. on prépare ensuite en laboratoire un concentré final de minéraux lourds avec un séparateur à spirales.

Le traitement d'un volume important d'alluvions à chaque site d'échantillonnage assure une quantité suffisante de minéraux lourds pour permettre d'effectuer des analyses chimiques pour plusieurs éléments incluant l'or. Le fonctionnement par succion de la drague à sluice permet également d'échantillonner, sous l'eau, des couches profondes de sédiments alluvionnaires ce qui augmente les chances de récolter des particules de métaux précieux où d'autres minéraux très denses s'ils sont présents.

---

[1] Contribution to the Federal Asbestos Initiatives Geoscience Research Program 1984-1987
[2] Géorex, Sherbrooke, Québec J1L 1Y1

Introduction

In 1984 the Geological Survey of Canada undertook a heavy mineral survey of alluvial deposits at a reconnaissance scale in the Eastern Townships of Quebec. Sampling was conducted during the 1984 and 1985 field seasons over an area of approximately 13 000 km^2. This work was carried out in an effort to stimulate mineral exploration in the area, including gold exploration, by providing new data on the distribution of a variety of metals of economic importance. The present paper deals only with the sampling and concentration techniques used. The analytical data and interpretation of the 1984 portion of the survey can be found in Maurice and Mercier (1985) and Maurice (1986).

The study is based primarily on chemical analyses of heavy mineral concentrates rather than on the identification of mineral species. This produces numerical data that are easily and conveniently represented on geochemical maps. The method requires that, at each sample site, a sufficient quantity of heavy minerals be collected to allow for several chemical analyses plus a small amount to be stored for future mineralogical studies. The preferred sample contains from 30 to 40 grams of minus 0.85 mm, nonmagnetic heavy minerals. A minumum of five grams is required.

Sampling pattern

Sample sites were selected prior to the field operations and marked on 1:50 000 topographical maps. Each map was divided into 25 km^2 cells using the UTM grid printed on the maps. For the 1984 survey, the basic sampling design was one site per cell selected on the basis of ease of access, generally at a road-stream intersection. If a choice of sites existed, then preference was given to the one for which the surface area of the drainage basin upstream from the sample site was closest to the surface area of the cell. When a higher order stream intersected a cell, however, an additional sample was collected on it. In 25% of the cells, a special sampling design was adopted to enable the study of the geochemical variance at various levels using the method described by Garrett and Goss (1980). In the cells chosen for this study, two streams in two different drainage basins were selected. On one of them, one sample was collected normally. On the other, three samples were collected: two from the same site and a third one about one kilometre from the other two. In 1984, a regular stream sediment sample was also collected at every site for comparison with the heavy minerals. The resulting sample site density in 1984 was one site per 14.5 km^2.

In 1985, two sites per 25 km^2 cells were selected according to the same criteria of accessibility and representativity of drainage basins as in 1984. In some cells that were less accessible, only one and sometimes no samples could be collected; however, in order to maintain an average sample density of one sample per 12.5 km^2, some sample sites were added to the more accessible cells. Neither the higher order streams nor the regular stream sediments were sampled in 1985 because the results of the 1984 survey did not show this practice to be useful (Maurice, 1986). Sampling for the purpose of studying the geochemical variance was discontinued in 1985.

Heavy mineral sampling and concentration procedures

In order to collect an adequate amount of heavy minerals, it is necessary to process a rather large volume of alluvium. It is also essential that the sampling operation be rapid so that an economical rate of progress can be maintained. The traditional method of sampling heavy minerals with a gold pan was judged to be too slow and too arduous to be used in this project.

A special technique was developed for the Eastern Townships project; it is carried out in two stages:

1. A heavy mineral preconcentrate is obtained at the sampling site using a portable suction dredge.
2. A final heavy mineral concentrate is obtained in the laboratory using a spiral concentrator.

Sampling with a portable suction dredge

Several models of portable suction dredges are available commercially. The one used in the Eastern Townships (Fig. 34.1) comes equipped with a 25 x 132 cm sluice box, a 500 lpm centrifugal water pump, a 3 hp gasoline engine, suction and pressure hoses, a tubular steel frame mounted on a truck tube for flotation. Its assembled weight is 32 kg. A backpack model weighing about half the full size model was used to access hard-to-reach sample sites.

The dredge operates as follows: the gasoline engine drives the water pump which circulates a high-speed water jet inside a nozzle attached to the suction hose. This generates a vacuum inside the nozzle which is used to suck gravel from the bottom of the stream. The water-gravel mixture is driven through the suction hose to the sluice box where the heavy minerals together with a substantial amount of lighter material, including rock fragments, are retained.

The suction dredge has an advantage over other methods because it enables, on the one hand, processing of a large volume of gravel in a relatively short time, and on the other, sampling underwater deep layers of stream sediments which increases the likelihood of collecting particles of precious metals and of other high-density minerals if they are present.

At each sample site, the precise spot where the sample is to be collected is chosen after careful examination of stream bed and local physiographic features in order to maximize heavy mineral recovery. For example, sampling is carried out on the downstream side of large boulders or other obstacles. A sudden widening of the stream channel or, in meandering streams, the upstream portions of gravel bars are also favoured spots. Unwanted effects from road building materials are avoided by always collecting the sample several tens of metres upstream from the road-stream intersection.

In order to reach the deeper layers of alluvium, the gravel is dredged as much as possible from one spot rather than from a large area. Ideally, bedrock should be reached

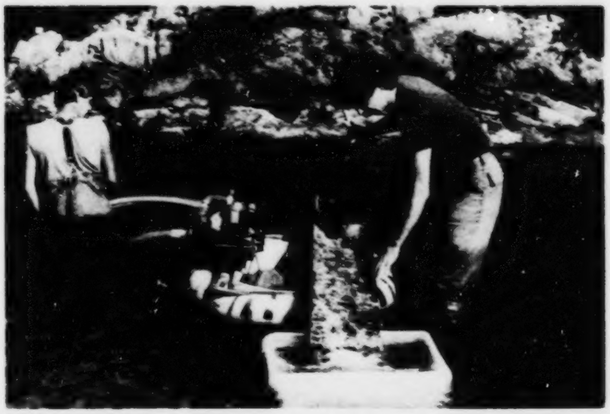

Figure 34.1. *Suction dredge in operation. At this site, the volume of gravel was being measured using the plastic tub behind the dredge. This was not normally done.*

but this is rarely possible. Often, clay layers are encountered which may act as barriers to the downward penetration of the heavy mineral grains.

When the dredging operation is complete, a series of manoeuvres is carried out to bag the sample. This includes sieving the content of the sluice box to minus 2 mm and washing thoroughly all parts of the dredge, not only to ensure total heavy mineral recovery at each site but also to prevent contaminating the subsequent samples.

The amount of preconcentrate collected is fairly constant at about 4 to 5 kg which corresponds to the maximum capacity of the sluice box. The proportion of heavy minerals in the preconcentrate, however, is quite variable and is related to the volume of stream gravel dredged, to the characteristics of the stream bed and physiographic features at the sample site, and to the nature and composition of the rocks and surficial deposits in the region. With regards to the volume of gravel dredged, the manufacturer claims that the dredge has a capacity of 1.5 to 3.0 m^3 per hour. In practice, however, the rate is much lower and varies with the nature of the alluvium (presence of large boulders, clay, degree of compaction, etc.), interruptions due to clogging of the suction hose or nozzle, the amount of water in the stream, the flow rate, etc. A few volume measurements made on site (Fig. 34.1) indicated that about 0.2 m^3 or about 250 to 300 kg of alluvium of particle size inferior to 6.4 cm (diameter of nozzle opening) is dredged on average to collect a sample. The dredge is usually allowed to run for about one half hour which means that the processing rate is about 0.4 m^3/hour.

Production of the final concentrates

Final heavy mineral concentrates are prepared from the preconcentrates obtained from the suction dredge. Figure 34.2 is a flowchart outlining the procedure followed in the present survey.

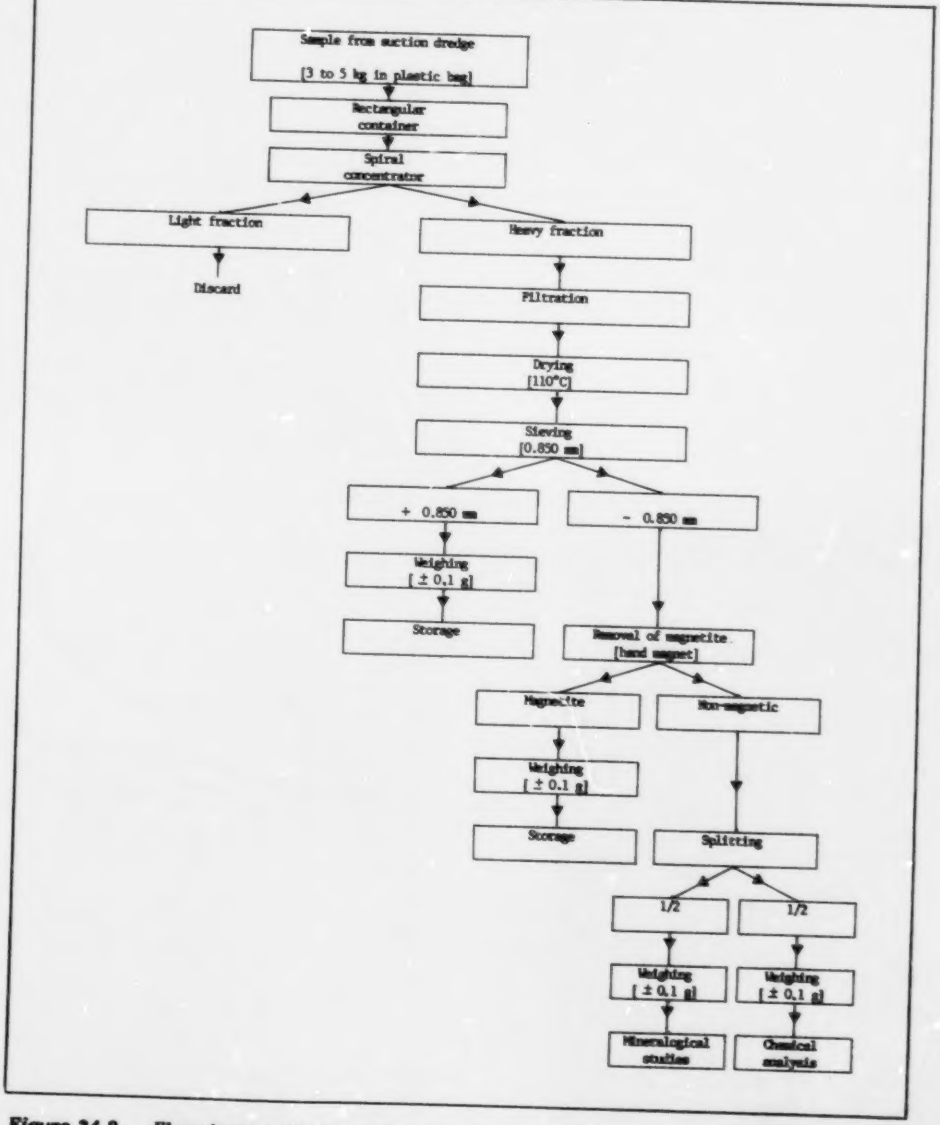

Figure 34.2. *Flowchart outlining the procedure for preparing heavy mineral concentrates.*

Because of the amount of material involved, 4 to 5 kg, it would not be practical to separate the heavy minerals in the preconcentrates with heavy liquids. A spiral concentrator, on the other hand, can accomplish this conveniently and economically.

The main components of the spiral concentrator, also known as a gold wheel or gold screw (Fig. 34.3) are: a stainless steel bowl with a central opening towards which converge four rubber ribs forming spirals, a small container located behind the bowl for collecting the heavy minerals, a perforated wash tube with a faucet located radially in front of the bowl, a water pump attached to the wash tube, an overflow apron to collect excess water and the light minerals, and an electric motor. All except the pump are mounted on a tubular steel A-frame with a mechanism to adjust the pitch angle of the bowl. There are several models; the one used in the Eastern Townships comes equipped with a 12V DC motor and the bowl has a diameter of 47.5 cm.

The electric motor drives the bowl at a speed of about 25 rev./minute. The preconcentrate is introduced gradually near the bottom of the rotating bowl and the mineral grains work their way up the ribs towards the central opening. Simultaneously, the cascading water from the perforated tube washes down the light minerals so that only the heavies are able to reach the central opening. The water jet from the hole in the perforated tube nearest the centre of the bowl is adjusted to wash the heavy minerals through the central opening into the small container behind the bowl where they accumulate.

The separation of the heavy minerals occurs in decreasing order of their specific gravity: the black oxides and the sulphides are followed by silicates such as garnet and pyroxene. Gold and other dense minerals are extracted early but other useful minerals such as goethite or limonitized sulphides may be recovered later in the sequence because their high porosity reduces their density. It is important to monitor progress of the heavy mineral separation with a binocular microscope in order to determine when to stop the apparatus once the heavy minerals above a pre-established density have (nearly) all been recovered. Generally, when the recovery of common garnet (specific gravity = 3.2 to 4.2) is nearly complete, one can assume that most useful heavy minerals have been exhausted.

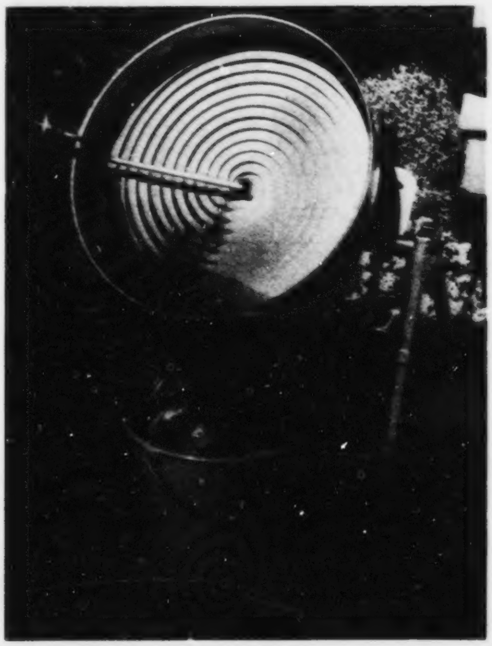

Figure 34.3. Spiral concentrator

Subsequent steps in the procedure (Fig. 34.2) include filtration to remove excess water, drying in an oven at 110°C, sizing at ± 0.85 mm (20 mesh in the Tyler designation), removal of magnetite with a hand magnet, and splitting the nonmagnetic fraction into two equal portions, one for chemical analyses and the other to be stored for future mineralogical studies.

Figure 34.4 shows the results of grain size analyses of two nonmagnetic concentrates obtained from suction dredge preconcentrates treated in the spiral concentrator. These are regular samples from two different areas of the 1985 survey that were sieved to minus 0.85 mm following the standard preparation procedure (Fig. 34.2). Note that the bulk of the heavy minerals in both samples have a grain size ranging from 105 to 425 microns (150 to 35 mesh in the Tyler designation). Research is currently underway to compare grain size distributions and mineralogical composition of concentrates obtained using this procedure with the grain size distribution and mineralogy of the total heavy mineral content of stream gravel obtained by heavy liquid separation.

Figure 34.5 gives the total (a) and nonmagnetic (b) weight distribution of all 703 heavy mineral concentrates (-0.85 mm) produced during the 1985 survey. The figure shows that the amount of heavy minerals recovered is quite variable. The medians (that separate the number of samples in two halves) are situated at 43 and 32 g respectively. In the case of some samples containing less than 10 g of nonmagnetic heavy minerals, the volume of stream gravel dredged (and the time required to do it) was increased significantly to ensure that the minimum 5 g required for the chemical analyses would be obtained. In a few cases it was necessary to return to the site and operate the dredge for one hour or more. These sites were situated in regions exceptionally deficient in heavy minerals.

Discussion

When the pitch angle of the bowl and the flow of water from the wash tube are well adjusted, the spiral concentrator produces a good quality heavy mineral concentrate at a

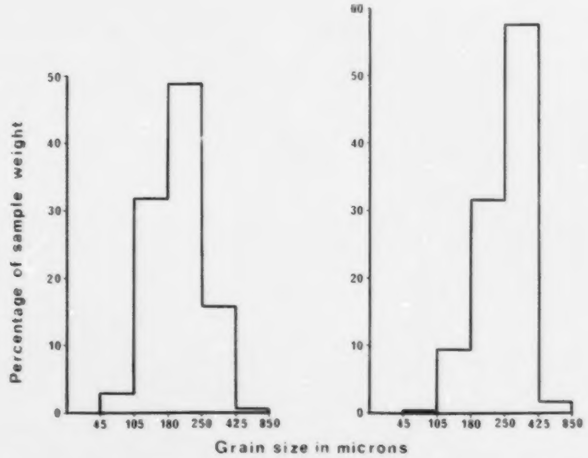

Figure 34.4. Histograms showing grain size distribution of two samples of nonmagnetic, -0.85 mm, heavy mineral concentrates obtained from suction dredge preconcentrates treated in the spiral concentrator.

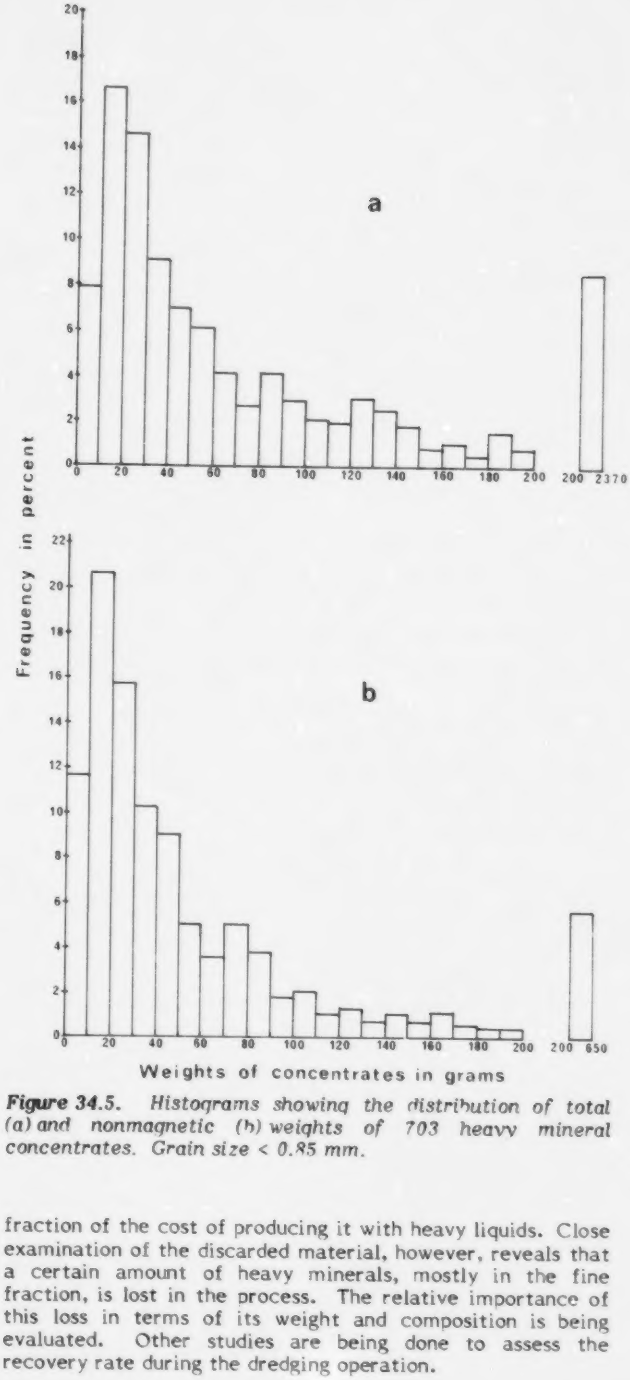

Figure 34.5. Histograms showing the distribution of total (a) and nonmagnetic (b) weights of 703 heavy mineral concentrates. Grain size < 0.85 mm.

fraction of the cost of producing it with heavy liquids. Close examination of the discarded material, however, reveals that a certain amount of heavy minerals, mostly in the fine fraction, is lost in the process. The relative importance of this loss in terms of its weight and composition is being evaluated. Other studies are being done to assess the recovery rate during the dredging operation.

It should be remembered that the objective of the sampling operation is to collect economically sufficient heavy minerals to perform chemical analyses and, in that context, the loss of some heavy minerals is not critical. Consistency in the sampling and concentration procedures ensures that the data are perfectly interpretable but it is recognized that the portion of heavy minerals that is lost could have a somewhat different geochemical signature from the recovered portion.

Heavy mineral losses during sampling and concentration should also be taken into consideration when attempting to convert element concentrations in heavy mineral concentrates to element concentrations in original stream gravel. It should be pointed out, however, that our data (Maurice and Mercier, 1985) were not intended to be converted in this way because neither the volumes nor the weights of original stream gravel were measured during the dredging operation. Our study is based on metal concentrations in heavy mineral concentrates which has the advantage of being independent of fortuitous variations in the actual abundance of heavy minerals in stream gravel which can be considerable, even locally (see Fig. 34.5).

For an order of magnitude, if we assume that 250 kg of gravel are dredged at a site, the proportion of heavy minerals in the gravel (conversion factor) would be 1/1000 if 250 g of concentrate are recovered and 1/10 000 if only 25 g are recovered. These can be considered as minimum conversion factors because any heavy mineral loss (that contains mineral grains of the element to be converted) during the sampling and concentration operations, plus the coarse (+0.85 mm) fraction which is not taken into account in the proportions above, will contribute to increase the conversion factor. On the other hand, the 250 kg used in this example include only the sand and gravel that can pass through the 6.4 cm diameter suction nozzle. Stream gravel usually contains an abundance of much coarser (bouldery) material and, when this is taken into account, the real proportion of heavy minerals in the total stream gravel drops considerably. For these reasons, data obtained by the methods described here are unsuitable to estimate grades for placer development, for example.

In summary, the procedures developed in the field and in the laboratory are fully satisfactory for regional geochemical exploration purposes. Research currently in progress on various aspects of the technology, including testing different apparatus, mineralogical studies of grain size fractions etc., will likely lead to improvements in the technique.

References

Garrett, R.G. and Goss, T.I.
1980: UANOVA: A Fortran IV program for unbalanced nested analysis of variance; Computers and Geosciences, v. 6, p 35-60.

Maurice, Y.T.
1986: Interpretation of a geochemical reconnaissance heavy mineral survey in the Eastern Townships of Quebec; in Current Research, Part A, Geological Survey of Canada, Paper 86-1A, Report 35.

Maurice, Y.T. et Mercier, M.
1985: Méthode d'échantillonnage et résultats d'un levé géochimique de minéraux lourds en Estrie, Québec (21E 3, 4, 5, 6, 12); Commission géologique du Canada, Dossier publique 1145.

Interpretation of a reconnaissance geochemical heavy mineral survey in the Eastern Townships of Quebec[1]

Project 840052

Y.T. Maurice
Resource Geophysics and Geochemistry Division

Maurice, Y.T., Interpretation of a reconnaissance geochemical heavy mineral survey in the Eastern Townships of Quebec; in Current Research, Part A, Geological Survey of Canada, Paper 86-1A, p. 307-317, 1986.

Abstract

Multi-element distribution patterns obtained from the analyses of heavy mineral concentrates collected in streams at an approximate sample density of 1 sample per 13 km^2 reveal widespread southeastward glacial dispersion. Glacial processes, rather than alluvial transport, appear to be the dominant dispersal mechanism for the heavy minerals.

Chromium, which originates from an ophiolite belt to the north of the study area, is uniformly enriched throughout the region showing occasional lows in the shadow of prominent topographical features. The chalcophile elements, originating from sulphide deposits, show ribbon-like dispersal trains parallel to the direction of glaciation, but their intensity is somewhat attenuated as a result of oxidation and leaching. The gold patterns in some cases coincide with those of the chalcophile elements and are more persistent, suggesting that alluvial gold in the Eastern Townships derives in part, if not entirely, from the glacial erosion of sulphide deposits. Tungsten displays strong anomalies in the vicinity of Devonian granites providing targets for mineral exploration.

Résumé

Les distributions d'éléments obtenues à partir d'analyses de concentrés de minéraux lourds provenant d'alluvions et cueillis au taux d'environ un échantillon à tous les 13 km^2, révèlent une dispersion glaciaire régionale vers le sud-est. Les processus glaciaires, plutôt que le transport alluvionnaire, semblent constituer le mécanisme dominant de dispersion des minéraux lourds.

Le chrome, qui provient d'une bande d'ophiolites au nord de la région étudiée, est enrichi uniformément sur tout le territoire couvert par l'étude. On retrouve par endroits des teneurs en chrome plus basses à l'ombre de certaines protubérances topographiques. Les éléments chalcophiles, qui proviennent des gisements de sulfures, montrent des traînées de dispersion allongées parallèlement à la direction d'écoulement glaciaire. Leurs intensités sont souvent atténuées suite aux effets des processus d'oxydation et de lessivage. Les motifs de dispersion de l'or coïncident par endroits avec ceux des éléments chalcophiles tout en étant plus continus. Ce phénomène semble indiquer que l'or alluvionnaire de l'Estrie provient en partie ou en totalité de l'érosion glaciaire des gisements de sulfures. Le tungstène affiche de fortes anomalies au voisinage des granites dévoniens délimitant ainsi des cibles d'exploration.

[1] Contribution to the Federal Asbestos Initiatives Geoscience Research Program 1984-87.

Introduction

In this paper, the analytical results of the heavy mineral geochemical survey are interpreted, the technical aspect of which is described by Maurice and Mercier (1986).

The project was undertaken on the one hand, to develop a rapid and economical method of sampling and concentrating alluvial heavy minerals and, on the other, to document the regional distribution of several metals of economic importance including gold. The area has long been known for its placer gold deposits but no one has ever attempted to produce a geochemical distribution map for gold in this region. It was hoped that such data would help explain the origin of the placer deposits.

Sampling was carried out over two consecutive field seasons. Figure 35.1 shows the area sampled during each of the 1984 and 1985 compaigns. Most of the results of the 1984 campaign have already been published by the Geological Survey of Canada (Maurice and Mercier, 1985). The present paper is mostly concerned with the data from the 1984 survey because the analytical results of the 1985 samples are not available at the time of writing. However, some preliminary observations made in 1985 are included.

Sampling and analytical techniques

The reader is referred to Maurice and Mercier (1986) for details on every aspect of heavy mineral sampling and concentration related to this project. The same article also discusses sampling patterns, sample density, selection of sample sites, etc.

Gold in the heavy mineral concentrates was analyzed by a special technique known as Metallic Sieves Analysis. This method ensures representative analyses of samples containing coarse particulate gold. A ring and puck type pulverizer is used to grind the total sample designated for analysis (see Maurice and Mercier, 1986, Fig. 35.2). Unlike the disc type, which can cut or smear the gold particles, the ring and puck pulverizer acts like a 'rolling pin' and flattens the gold grains thereby increasing their surface area. The pulverizing time is controlled to minimize breakage of the gold grains. The pulverized sample is then sized to ±100 µm. The total coarse fraction, that contains the flattened gold grains, and a subsample of the fine fraction, usually 20 grams, are analyzed by fire assay lead collection and flame atomic absorption. The gold content of the minus 100 µm subsample is taken to be representative of the entire fine fraction as it is assumed that fine gold will be evenly distributed throughout that fraction. The gold content of the plus 100 µm fraction is then mathematically redistributed over the original weight of the sample. In the present survey, high chromium in many samples required that only 5 grams of minus 100 µm material be used.

As indicated by Maurice and Mercier (1986), regular stream sediments were also collected at every sample site. Those samples were sieved to minus 100 µm, and a 20 g subsample of the fine fraction was analyzed for gold using the same fire assay-atomic absorption technique as for the heavy minerals.

The other elements in the heavy mineral concentrates were analyzed by the following methods: wavelength dispersive X-ray fluorescence using pressed pellets (Cr, Ba, Nb, Sb, Sn, Ta); atomic absorption spectrophotometry using a $HCl:HNO_3$ (1:3) sample decomposition (Cu, Pb, Zn, Bi, Ni, Mo, Ag, Fe); colorimetry using a $HNO_3:HClO_4$ extraction (As); colorimetry using a carbonate sintering/hot water extraction (W); DCP-ES using a persulphate fusion (total Fe).

Ti, Y, and S were not analyzed in 1984 samples but will be in the 1985 samples.

Note on concentrations

The reader is reminded that, with the exception of the gold in regular stream sediment data (see Fig. 35.7), the concentrations presented in the figures and text of this article represent concentrations of elements in heavy mineral concentrates and that no attempt was made to recalculate the concentrations in the original alluvial deposits. As indicated by Maurice and Mercier (1986), these concentrations are of the order of 10^3 to 10^4 times greater than they would be, had they been converted to concentrations in the original sediments. This approach has the advantage of eliminating geochemical variations that are due solely to variation in the abundance of heavy minerals in the alluvial deposits. Such variations reflect largely the hydraulic conditions at the sample site and are unwanted when the purpose is to compare metal concentrations between sites as in the present study.

Characteristics of heavy mineral surveys

Alluvial geochemical surveys based on the analyses of heavy mineral concentrates produce anomalies and dispersal patterns that may not be detected in regular stream sediment surveys particularly for those elements which occur in the stream sediments in concentrations close to the limit of analytical detection. Also, heavy mineral anomalies are mostly related to clastic dispersions because the sampling process eliminates most of the species that are normally enriched hydromorphically (clay minerals, organic matter, hydroxide coatings, etc.). This is particularly significant for the chalcophile elements such as Cu and Zn which occur in streams mostly in hydromorphic forms. When these elements are found in a detrital form (e.g. as sulphide grains), even in low concentrations, this may be indicative of the existence of a mineralized bedrock source.

The sampling technique utilized in this project should be regarded as a convenient method for sampling glacial deposits. These deposits, rather than the underlying bedrock,

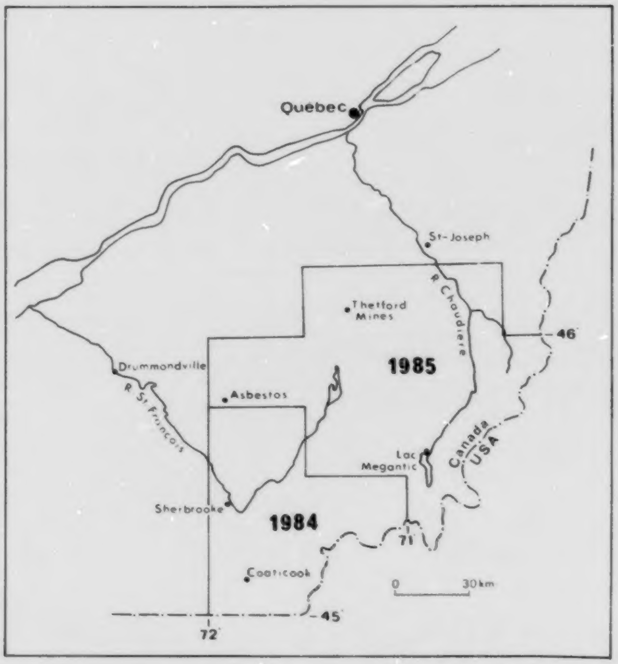

Figure 35.1. *Regions sampled in 1984 and in 1985.*

are the main source of heavy minerals in the streams. Furthermore, at the scale at which the survey was conducted, it does not appear that any significant alluvial transport of heavy minerals took place. For example, when a segment of a main stream is enriched in a given element causing a geochemical anomaly, the tributaries of that stream in the same region are generally also anomalous. This situation could not result simply from the alluvial transport along the main stream of mineral grains originating from a distant source upstream from the anomaly. Rather, the two-dimensional geometry of the anomaly requires that the deposits through which the anomalous streams flow, be themselves anomalous. Also, the heavy mineral grains, as observed under the binocular microscope, are mostly angular further suggesting limited alluvial transport of heavy minerals in that region.

The role of glaciation in geochemical dispersion

The importance of glacial transport in geochemical dispersion in southern Quebec has been well documented by Shilts (1973, 1974, 1975, 1976, 1984), Rencz and Shilts (1980) and McDonald and Shilts (1971). These articles describe, among others, surveys that were carried out in the Thetford Mines and Lac Mégantic regions and show dispersal trains defined by erratics, specific minerals, and geochemical anomalies that extend over 50 km from their sources. These dispersal trains are generally oriented towards the southeast which corresponds to the well established predominant glacial transport direction in the region.

Data on heavy mineral dispersal in the 1984 survey are in full agreement with previous observations. Figure 35.2 shows the dispersal of Cr, which derives largely from the

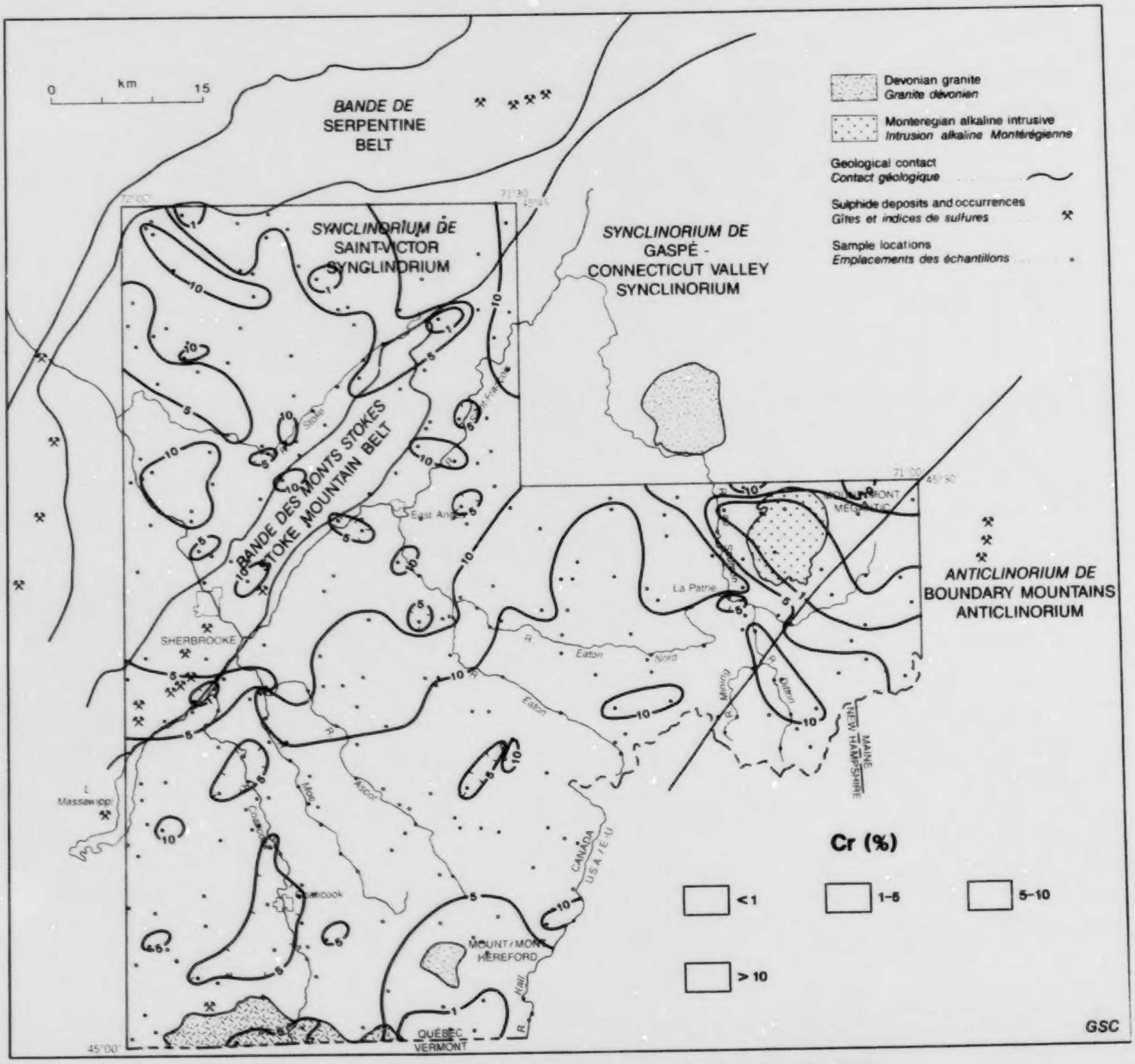

Figure 35.2. *Distribution of chromium in heavy mineral concentrates.*

Serpentine Belt located north and northwest of the study area. The background, at 5 to 10% Cr, is uniformely high throughout the area. A zone of much lower values (<1% Cr) can be seen forming a shadow to the southeast of the Mount Mégantic intrusive, probably as a result of dilution of the chromite by a large quantity of other heavy minerals derived from the intrusive rocks. This zone was found to be very rich in magnetite and ilmenite with an abundance of characteristically large glassy zircons. Niobium is enriched along the same trend (Fig. 35.3).

Other areas of low Cr occur to the south of Mount Hereford and near the Serpentine Belt. The latter probably reflects Quaternary deposits composed chiefly of material that originated from sedimentary rocks to the north of the Serpentine Belt and relatively defficient in Cr. The crest of high Cr values (>10% Cr) oriented NE-SW in the central part of the study area corresponds to the position of an active glacial front (McDonald, 1969). Chromite may have accumulated in the terminal zone of the glacier as a result of a "conveyor-belt" type of transport mechanism.

Dispersal of the chalcophile elements

The heavy mineral concentrates were analyzed for a number of chalcophile elements including Cu, Pb, Zn, Bi, As, Sb, and Ag. These elements occur mostly as sulphides which oxidize more or less rapidly when exposed to the atmosphere. When oxidation occurs, the metals are released as ions in solution although some may be retained in goethite, a product of sulphide oxidation, or as other secondary minerals. Interpretation of dispersal patterns and anomalies for these elements should therefore be attempted with caution.

Sulphide grains are commonly found in heavy mineral concentrates from Eastern Townships streams. Pyrite is found fresh or oxidized in a majority of the samples and, in

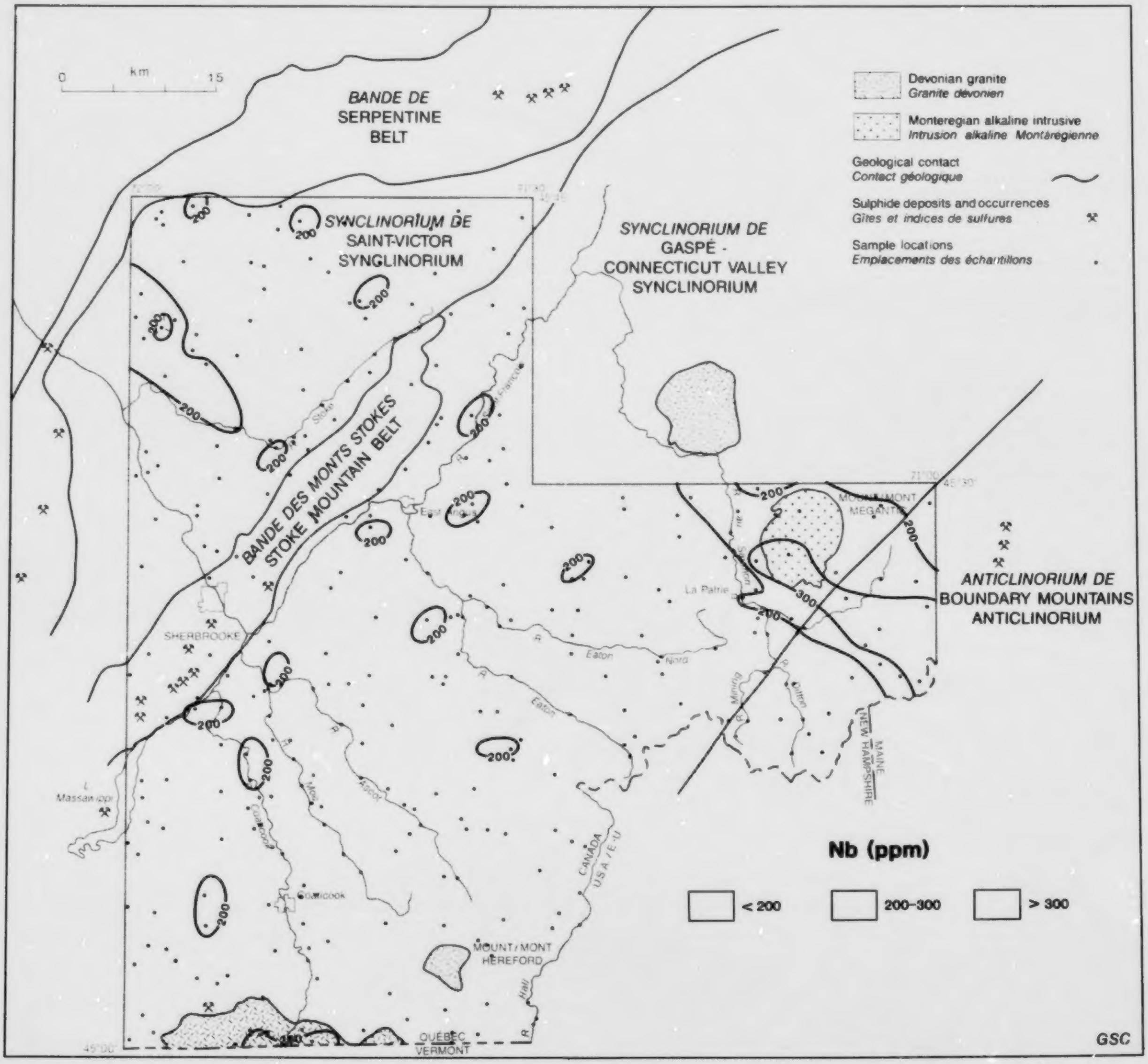

Figure 35.3. *Distribution of niobium in heavy mineral concentrates.*

some, it constitutes the predominant phase. The sulphides are thought to derive from unoxidized layers of glacial deposits. Therefore, in interpreting the data, it is important to bear in mind that sulphides will only occur in stream alluvium if such deposits are being actively eroded by the stream. Any protection of the sulphide grains from oxidation while in the stream will also increase the likelihood of sulphides being present in the samples. For example, fresh sulphide grains were often recovered from clay-rich layers on the stream bed. The grains are imbedded in the clay which isolates them, retarding their oxidation.

Chalcophile elements are, therefore, expected to generate relatively weak heavy mineral anomalies and the absence of an anomaly is not conclusive evidence that an anomaly would not occur should the surficial conditions be different.

Figure 35.4 shows the distribution of Ag. A large anomaly trending parallel to the direction of glaciation occurs in the Coaticook, Moe and Ascot river basins in the southwestern part of the survey area, and appears to originate from the mineralized district south of Sherbrooke. Cu (Fig. 35.5), Pb, and Zn (Maurice and Mercier, 1985) show similar patterns which support the view that the metals were glacially transported from the deposits. According to Harron (1976), these deposits contain massive pyrite, chalcopyrite, sphalerite, galena, barite, tetrahedrite-tennantite, pyrrhotite, arsenopyrite, tellurides and recoverable quantities of gold and silver. The heavy mineral data show some enrichment in Bi, Sb, Mo, and Ba at the source, but these elements do not form detectable dispersal trains.

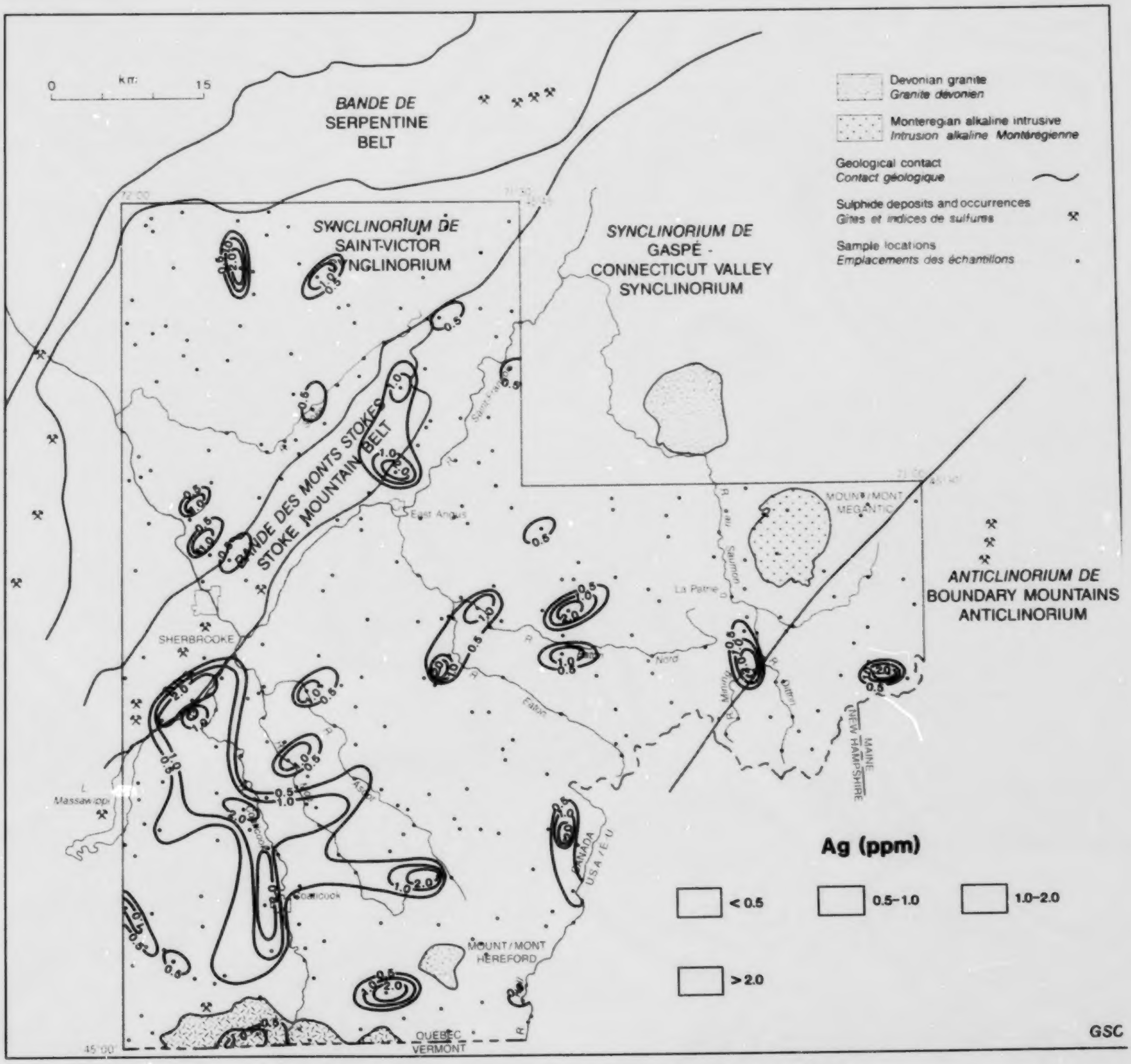

***Figure 35.4.* Distribution of silver in heavy mineral concentrates.**

Other chalcophile element anomalies occur throughout the survey area and most are considered to be part of glacial dispersal trains that are not always obvious.

Gold distribution

Gold is found in measurable quantities (>0.01 ppm) in 85% of the heavy mineral concentrates collected in 1984. In 27 samples, the gold particles were sufficiently coarse to be observed in the dredge during sampling or in the laboratory during preparation of the concentrates. Studies are in progress to determine whether gold in the heavy mineral concentrates is always in the form of free native gold particles or whether other minerals such as pyrite contribute to the apparent gold content.

Figure 35.6 shows the distribution of gold in heavy mineral concentrates in the 1984 survey area. A series of anomalies occur in the Coaticook, Moe and Ascot river basins forming a dispersal train which is oriented similarly to, and coincides largely with the dispersal patterns of the chalcophile elements in that area. These were interpreted as having been formed by glacial transport of detritus originating from the massive sulphide district south of Sherbrooke. This suggests that those deposits, which are auriferous (Harron, 1976), are also the source of the gold anomalies. Prior to glaciation, extensive auriferous gossans may have formed over the sulphide bodies. This material, along with base metal sulphides, would have been eroded by the advancing ice sheet and incorporated in the till along a southeastward path. Subsequent destruction and leaching of the auriferous minerals in the till would have freed the gold, probably allowing it to agglomerate into particles of various sizes which are now found in the streams. McDonald (1966) reported having found fine angular gold flakes in the oxidized zone of tills in the same general area and suggested that gold in recent alluvium is washed from the till.

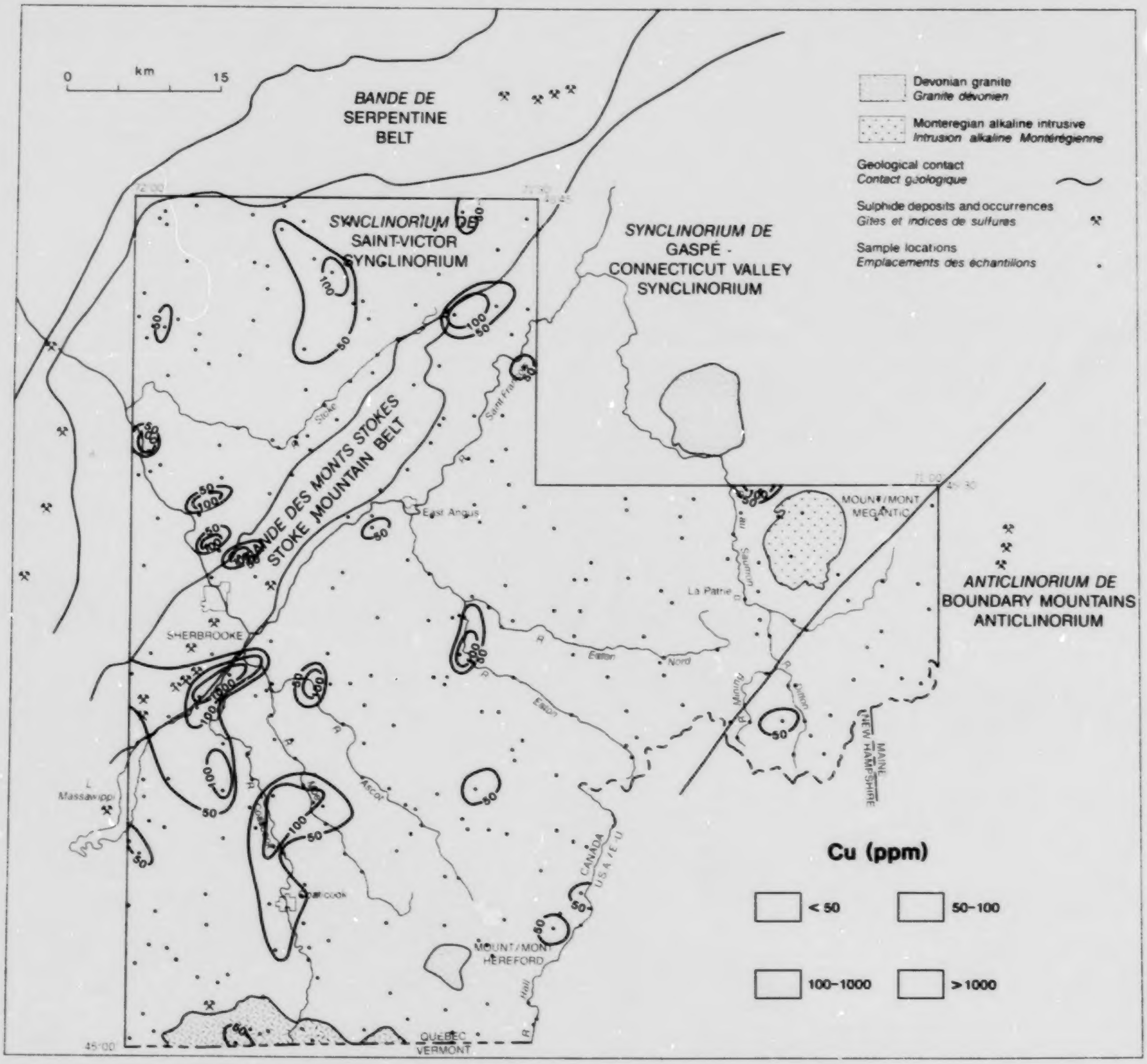

Figure 35.5. *Distribution of copper in heavy mineral concentrates.*

It is interesting to note that the heavy mineral sampling and analytical methods utilized in this project were successful in outlining nearly all of the known placers in the survey area (Chalmers, 1898; McGerrigle, 1935; Boyle, 1979; LaSalle, 1980). Other gold anomalies of similar intensity to those related to known placers were outlined in areas where alluvial gold had never been reported before. This is the case for anomalies located south of Lake Massawippi and to the northwest of Stoke Mountains. In contrast, the gold distribution as outlined by the minus 100 μm fraction of regular stream sediments (Fig. 35.7) shows much weaker anomalies and no clear pattern.

The gold anomalies outlined to the northwest of Stoke Mountains, those located along the Eaton and Eaton Nord rivers, and the wide anomaly north of East Angus (Fig. 35.6) appear to form a dispersal train oriented parallel to the predominant direction of ice movement. This train is 60 km long and may be longer if the anomalies to the east, in the Mining Brook and Ditton River, are considered to be part of it. The advancing ice sheet may have deviated eastward on approaching the high ground along the international boundary causing the eastward deflection in the dispersal train.

The analytical results of the 1985 survey are not available at the time of writing but Figure 35.8 shows the location of all samples collected in 1984 and 1985 in which native gold particles were observed in the field during sampling and/or in the laboratory as the heavy mineral concentrates were being prepared. The dispersal trends thus defined in the 1985 survey area are tentative and may be modified when the analytical results become available. Nevertheless, the patterns appear consistent with a glacial dispersal mechanism.

The Chaudière and Linière river basins are well known alluvial gold districts but new auriferous areas seem to be emerging from the 1985 survey. In the Thetford Mines area, all of the concentrates in which native gold was observed

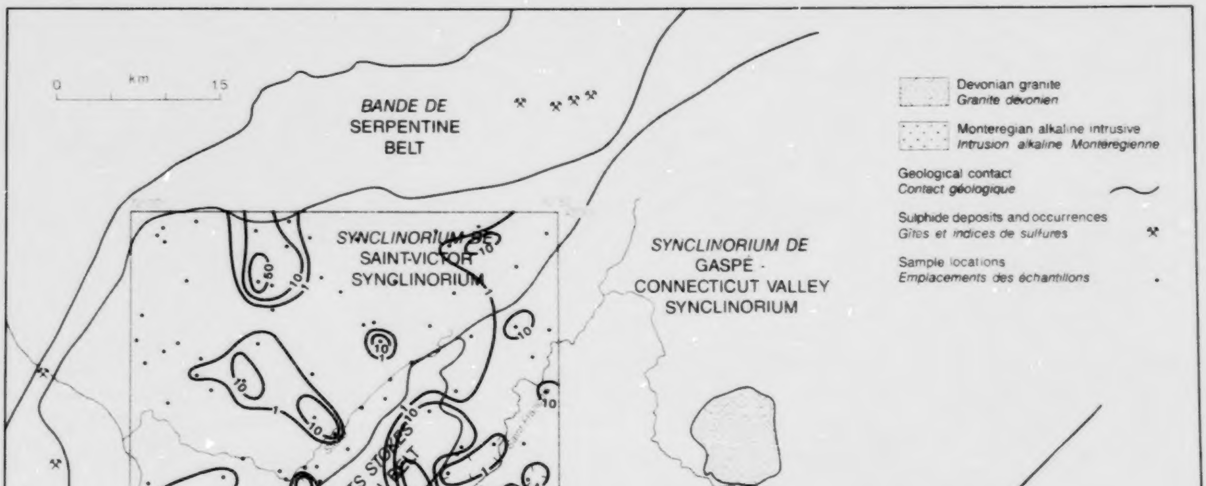

Figure 35.6. *Distribution of gold in heavy mineral concentrates.*

contain over 50% magnetite. The dispersal pattern for magnetite (not shown) appears to indicate the source to be associated with the Tibbit Hill volcanics (unit 10, Fig. 35.8), but other sources are possible especially since a northward ice movement has been postulated for that region (Lamarche, 1971). Dispersal patterns for other elements such as Cr and Ti may shed some light on this question.

Near Lake Mégantic, along the international boundary, gold particles were seen in several samples. This area is overlain by an extensive morainic complex deposited in part by ice moving southwest up the Upper Chaudière Valley (Gadd et al., 1972). Alluvial gold in this area may well be related to these deposits.

Some samples collected in 1985 to the northwest of Mount Mégantic also contain gold particles. These link two anomalous zones outlined by the 1984 survey. The long dispersal train described earlier, which extends from the Ditton River to the northwest corner of the 1984 survey area, may in fact extend north of the Serpentine Belt as shown on Figure 35.8.

In addition to the southeast trending dispersal trains, Figure 35.6 shows a background for gold that is uniformly high (from 1 to 10 ppm) to the southeast of the Stoke Mountain Belt forming a northeast oriented band over the Gaspé-Connecticut Valley Synclinorium. The background for gold is considerably lower (<1 ppm) to the northwest of the Stoke Mountain Belt, over the Saint-Victor Synclinorium. Research is in progress to determine whether these differences can be attributed to differences in the compositions of the rocks forming the two synclinoria or, to the southeastward dispersal of auriferous detritus from the Stoke Mountain Belt. Gauthier (1985) reported that intrusive and pyritiferous volcanic rocks in that belt are enriched in gold.

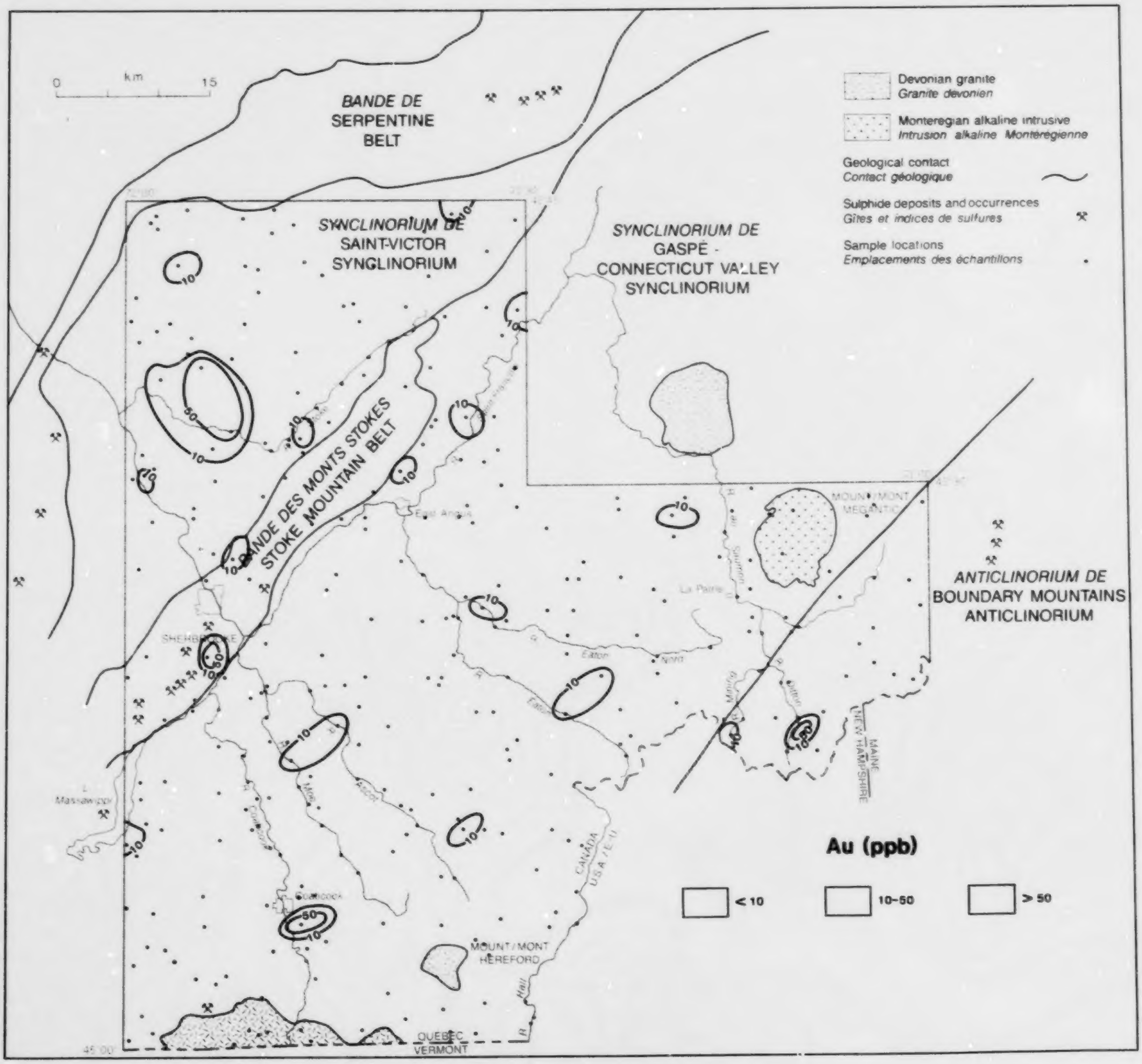

Figure 35.7. *Distribution of gold in minus 100 μm fraction of regular stream sediments.*

Tungsten anomalies

A spectacular tungsten anomaly occurs in the area surrounding Mount Hereford and the granites to the southwest of it, near the Quebec-Vermont border (Fig. 35.9). The 10 ppm W contour line may correspond to the outer limit of the thermal metamorphic halo around the intrusives judging from scant field observations made at the time of sampling. The intense part of the anomaly to the south of Mount Hereford may be partly the result of this zone having been protected from glacial erosion. The relatively low Cr concentrations (Fig. 35.2) in this area support this view. Nevertheless, it is recommended that this zone be examined carefully for tungsten deposits.

The characteristic heavy mineral assemblage of this anomaly consists of fluorescent scheelite grains, commonly large and angular, remarkably well preserved euhedral garnet crystals, and lamellar ilmenite. At one site, near the Coaticook River, a signifiant concentration of monazite crystals was seen under the binocular microscope. In another sample, collected south of Mount Hereford on the stream that flows along the international boundary, a few grains of cassiterite and of an unidentified lead-antimony mineral were observed.

In the Mount Mégantic area, tungsten also occurs as scheelite. The anomaly appears to be part of a dispersal train, perhaps originating from a thermal metamorphic zone

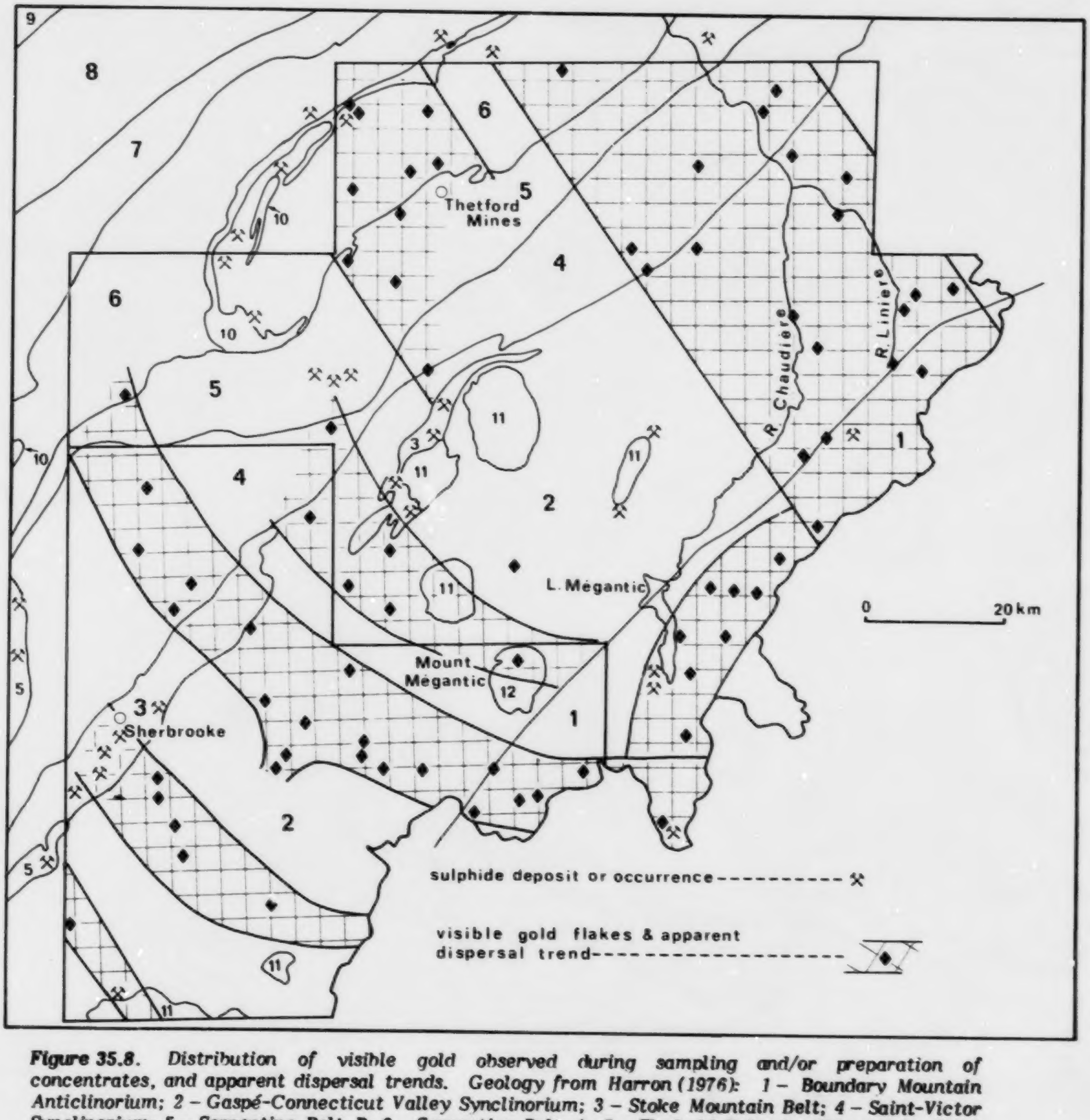

Figure 35.8. Distribution of visible gold observed during sampling and/or preparation of concentrates, and apparent dispersal trends. Geology from Harron (1976): 1 – Boundary Mountain Anticlinorium; 2 – Gaspé-Connecticut Valley Synclinorium; 3 – Stoke Mountain Belt; 4 – Saint-Victor Synclinorium; 5 – Serpentine Belt-B; 6 – Serpentine Belt-A; 7 – Flyshoid Belt; 8 – Klippen; 9 – Saint Lawrence Lowlands; 10 – Tibbit Hill Volcanics; 11 – Devonian granite; 12 – Monteregian Intrusion.

around a granite body to the northwest of Mount Mégantic. The apparent westerly deviation of the main trend near La Patrie could be the result of late ice movements.

Discussion

The heavy mineral survey has outlined dispersal patterns and anomalies for a variety of metals. These appear to have all been shaped, to a lesser or greater extent, by glacial action. In the case of the chalcophile elements, post glacial oxidation and leaching have also contributed to attenuate the anomalies.

Mineral exploration should now be directed towards finding the sources of the metals. Massive sulphide deposits have been shown to be the probable source of a gold and base metal dispersal train south of Sherbrooke and it is likely that detailed examination of other dispersal trains outlined by this survey will reveal other metalliferous sources, known or unknown. This is not to say that these sources are necessarily concentrated deposits in every case. It is possible that rock types containing only slight enrichment of certain metals over wide areas could have generated similar patterns. However, the presence of specific ore minerals in the anomalous samples restricts the type of metal enrichment that can be expected at the source.

The geometry of the dispersal trains is likely to be related to the geometry of the ice lobes rather than to that of the source. The intensity of the anomalies within the dispersal trains may also be (inversely) related to the rate of advance of the ice. The position of meltwater channels within and under the ice may also have had a role to play in locating individual anomalies.

In the specific case of gold, there is another possible source. The richest placer deposits in the Chaudière River valley occur in limonite-cemented stream gravels in buried valleys or under thick layers of more recent Quaternary deposits. They are believed by some to be preglacial

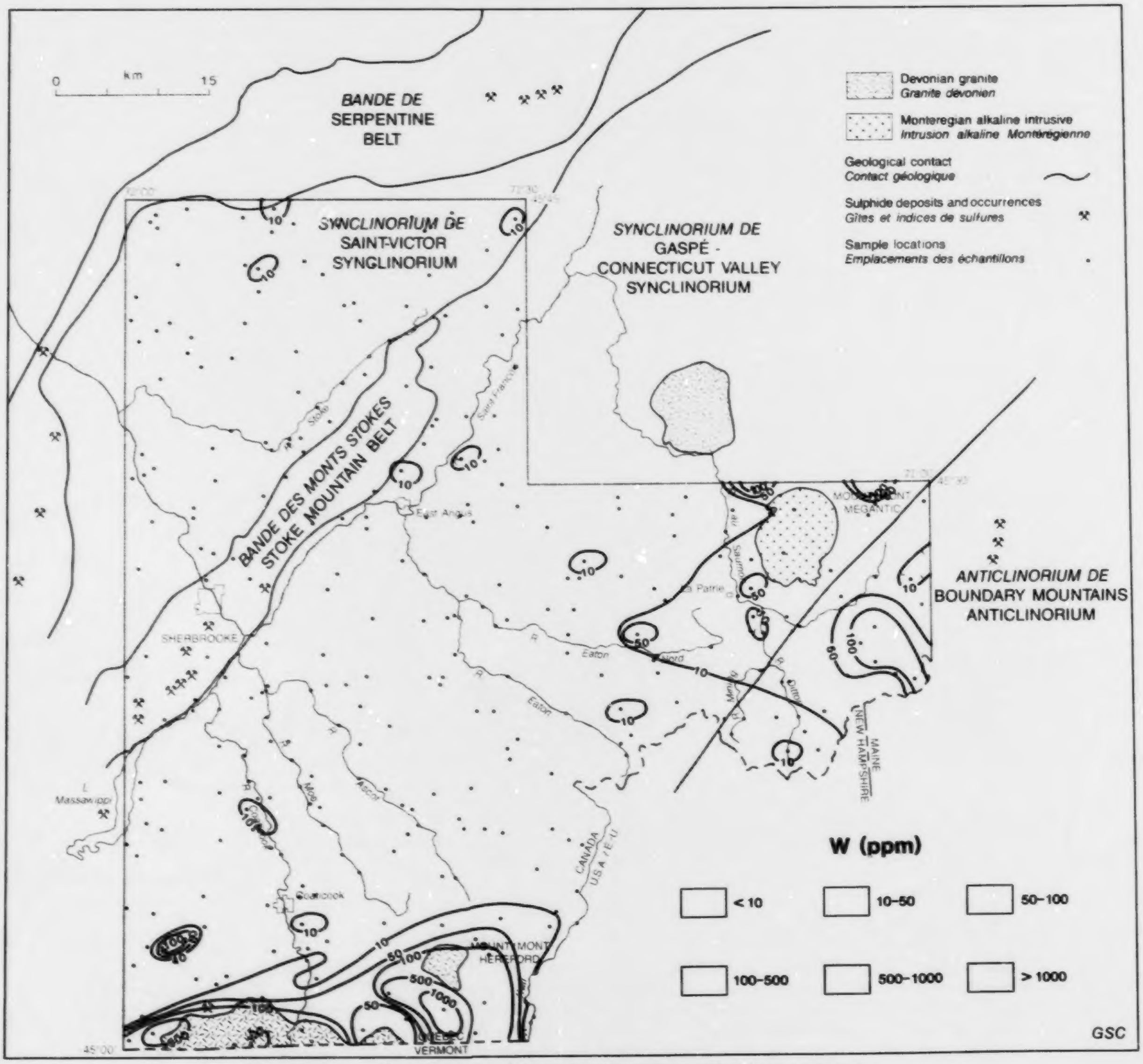

Figure 35.9. *Distribution of tungsten in heavy mineral concentrates.*

(possibly Tertiary), deriving from deep weathering and erosion of local bedrock (MacKay, 1921), and by others to be interglacial or interstadial (Gadd, 1964). If the latter interpretation is the correct one, the gold could have been transported from outside the placer area during an early glaciation. Regardless of how they were formed, these placers were likely an important source of gold in the till and recent alluvium; anomalies outlined in the present survey may help locate the buried valleys in which they occur.

Acknowledgments

The writer thanks R.W. Boyle and N.R. Gadd for reviewing the manuscript and for providing many useful suggestions.

References

Boyle, R.W.
1979: The geochemistry of gold and its deposits; Geological Survey of Canada, Bulletin 280, 584 p.

Chalmers, R.
1898: Report on the surface geology and auriferous deposits of south-eastern Quebec; Geological Survey of Canada, Annual Report, new series v. 10, rep. J, 160 p.

Gadd, N.R.
1964: Surficial geology, Beauceville map-area Quebec; Geological Survey of Canada, Paper 64-12, 3 p.

Gadd, N.R., McDonald, B.C., and Shilts, W.W.
1972: Deglaciation of southern Quebec; Geological Survey of Canada, Paper 71-47, 19 p.

Gauthier, M.
1985: Synthèse métallogénique de l'Estrie et de la Beauce (secteur sud); Ministère de l'Énergie et des Ressources du Québec, MB85-20, 186 p.

Harron, G.H.
1976: Métallogénèse des gîtes de sulfures des Cantons de l'est; Ministère des Richesses Naturelles du Québec, rapport ES-27, 42 p.

Lamarche, R.Y.
1971: Northward moving ice in the Thetford Mines area of southern Quebec; American Journal of Science, v. 271, p. 383-388.

LaSalle, P.
1980: L'or dans les sédiments meubles – formation des placers, extraction et occurrences dans le sud-est du Québec; Ministère de l'Énergie et des Ressources, DPV-745, 26 p.

MacKay, B.R.
1921: Beauceville map area, Quebec; Geological Survey of Canada, Memoir 127, 105 p.

Maurice, Y.T. and Mercier, M.
1985: Méthode d'échantillonnage et résultats d'un levé géochimique de minéraux lourds en Estrie, Québec (21 E3, 4, 5, 6, 12); Geological Survey of Canada, Open File 1145.

1986: A new approach to sampling heavy minerals for regional geochemical exploration; in Current Research, Geological Survey of Canada, Paper 86-1A, Report 34.

McDonald, B.C.
1966: Auriferous till in the Eastern Townships, south-eastern Quebec; Geological Survey of Canada, Paper 66-2, p. 51-53.

1969: Surficial geology of La Patrie-Sherbrooke area, Quebec, including Eaton River watershed; Geological Survey of Canada, Paper 67-52, 21 p.

McDonald, B.C. and Shilts, W.W.
1971: Quaternary stratigraphy and events in south-eastern Quebec; Geological Society of America Bulletin, v. 82, p. 683-698.

McGerrigle, H.W.
1935: Mount Megantic area, southeastern Quebec, and its placer gold deposits; Quebec Bureau of Mines, Annual Report, Part D, p. 63-104.

Rencz, A.N. and Shilts, W.W.
1980: Nickel in soils and vegetation of glaciated terrains; in Nickel in the Environment, ed. J.O. Nriagu; John Wiley & Sons Inc.

Shilts, W.W.
1973: Glacial dispersal of rocks, minerals and trace elements in Wisconsinian till, southeastern Quebec, Canada; Geological Society of America, Memoir 136, p. 189-219.

1974: The wealth the glaciers left behind; GEOS, (Fall 1974) Energy, Mines and Resources, Canada, p. 8-9.

1975: Principles of geochemical exploration for sulphide deposits using shallow samples of glacial drift; Canadian Mining and Metallurgical Bulletin, v. 68, no. 757, p. 73-80.

1976: Glacial till and mineral exploration; in Glacial Till, ed. R.F. Legget; Royal Society of Canada, Special Publication 12, p. 205-223.

1984: Till geochemistry in Finland and Canada; Journal of Geochemical Exploration, v. 21, p. 95-117.

Geological setting of sulphide mineralization at Tilt Cove, Newfoundland[1]

Contract DSSOSZ85-00010

D.F. Strong[2] and C.M. Saunders[2]

Strong, D.F. and Saunders, C.M., Geological setting of sulphide mineralization at Tilt Cove, Newfoundland; in Current Research, Part A, Geological Survey of Canada, Paper 86-1A, p. 319-325, 1986.

Abstract

Three main stratigraphic units are recognized in the Tilt Cove area; the Betts Cove ophiolite and the Bobby Cove Formation of the Snooks Arm Group, both Lower Ordovician, and the Silurian Cape St. John Group. Massive sulphide mineralization occurs in the ophiolite pillow lava unit close to its base, as at Betts Cove. The Cape St. John Group unconformably overlies the ophiolite, but is also tectonically interleaved with it. Magnetite-bearing cherts are associated with both the basalt and sandstones at the base of the Cape St. John Group, and locally contain Au as well as Cu mineralization. Metasomatic gain or loss of silica has produced a silica-rich and a silica-poor group from the relatively less altered pillow lavas, which exhibit chemical variation related to advanced partial melting of the upper mantle.

Résumé

Trois principales unités stratigraphiques se trouvent dans la région immédiate de Tilt Cove: l'ophiolite de Betts Cove et la formation de Bobby Cove, les deux appartenant au groupe de Snooks Arm et datant de l'Ordovicien inférieur, et le groupe silurien de Cape St. John. Des minéralisations de sulfures massifs sont localisées dans les laves en coussins près de la base de cette unité, comme à Betts Cove. Le groupe de Cape St. John repose en discordance sur l'ophiolite, mais est également tectoniquement interstratifié avec ce dernier. Des cherts renfermant de la magnétite sont associés aux basaltes et grès à la base du groupe de Cape St. John, et contiennent par endroits des minéralisations en Au et Cu. Des gains et pertes métasomatiques de silice ont produit des roches enrichies et appauvries en silice à partir des laves en coussins moins alterées qui, elles-mêmes, témoignent de changements chimiques liés à la fusion avancée du manteau supérieur.

---

[1] Contribution to the Canada-Newfoundland Mineral Development Agreement 1984-89. Project partly carried by Geological Survey of Canada, Economic Geology and Mineralogy Division, Project 840059.

[2] Department of Earth Sciences, Memorial University of Newfoundland, St. John's, Newfoundland A1B 3X5

Introduction

This report describes the results of mapping carried out by the first author in 1980, funded by Newmont Exploration of Canada Ltd., and the second author in 1984, funded by the Geological Survey of Canada under the Canada-Newfoundland Mineral Development Agreement. Mapping was controlled by cut lines, spaced at 100 m, which were chained and flagged at 25 m intervals. The Tilt Cove area of north-central Newfoundland on the eastern coast of the Baie Verte Peninsula (Fig. 36.1), is of economic importance because of the Rambler copper mines, the Advocate asbestos mine, and the Tilt Cove copper mines. In tectonic terms the geology of the peninsula represents a complex suture zone between ancient oceanic crust (of which the Betts Cove ophiolite forms a part) and the eastern continental margin of ancient North America. Previous work in the Tilt Cove area has been reviewed by Strong (1984).

Geological setting

The Lower Ordovician Snooks Arm Group forms an arcuate belt extending over 15 km between Betts Cove in the southwest to Tilt Cove in the northeast (Fig. 36.1). Upadhyay (1973) was the first to describe and interpret the group clearly as an ophiolite suite conformably overlain by volcanic and sedimentary rocks of presumed island arc affinity, and his stratigraphic subdivisions are shown in Figure 36.2. Upadhyay and Neale (1979) subdivided the pillow lava member of the ophiolite in the Betts Cove area into a lower komatiitic unit which is in sharp contact with an overlying unit similar to typical mid-ocean ridge basalts. Mineralization at Betts Cove is associated with the lowermost pillow lava unit, near the sheeted diabase-pillow lava contact (Upadhyay and Strong, 1973).

The Betts Cove ophiolite, as exposed in the Betts Cove area, is typical of ophiolites throughout the world. From the base upwards it includes Ultramafic, Gabbroic, Sheeted Diabase, and Pillow Lava members, all with transitional contacts. The Ultramafic Member, with a maximum thickness of about 750 m, is typically layered harzburgite-dunite-pyroxenite with graded and crossbedded layers dipping about 50° to the southeast. Ultramafic rocks also occur as intrusive gas breccia dykes, serpentinites, and talc-carbonate and pegmatitic veins and dykes of pyroxenite.

The Gabbroic Member, reaching a maximum thickness of 330 m, has a transitional contact with the underlying Ultramafic Member, but is faulted out throughout most of the ophiolite belt. The gabbro ranges from pegmatitic to fine grained, and displays cumulate bands ranging from anorthosite to clinopyroxenite. Towards its top the Gabbro Member is cut by abundant diabase dykes, marking the transitional contact with the overlying Sheeted Diabase Member. The latter, reaching 1.6 km thick and striking perpendicular to the igneous cumulate layering, consists of almost 100% dykes with minor ultramafic or gabbroic screens.

The Pillow Lava Member, the most extensive of the ophiolite, occurs throughout its 15 km length, with a thickness up to 1.5 km, but is thinned to less than 50 m along the south shore of Long Pond (Fig. 36.3). This Member includes a nearly continuous argillaceous unit about 60 m thick. The pillows are typically mafic in composition, variolitic, and close-packed with minor interpillow chert. Ultramafic pillows, observed near the base of the Member near Partridge Pond, pass transitionally into sills along strike. Pillow breccias are common near the base, and in the eastern (Tilt Cove) end of the belt, are typically variolitic and have

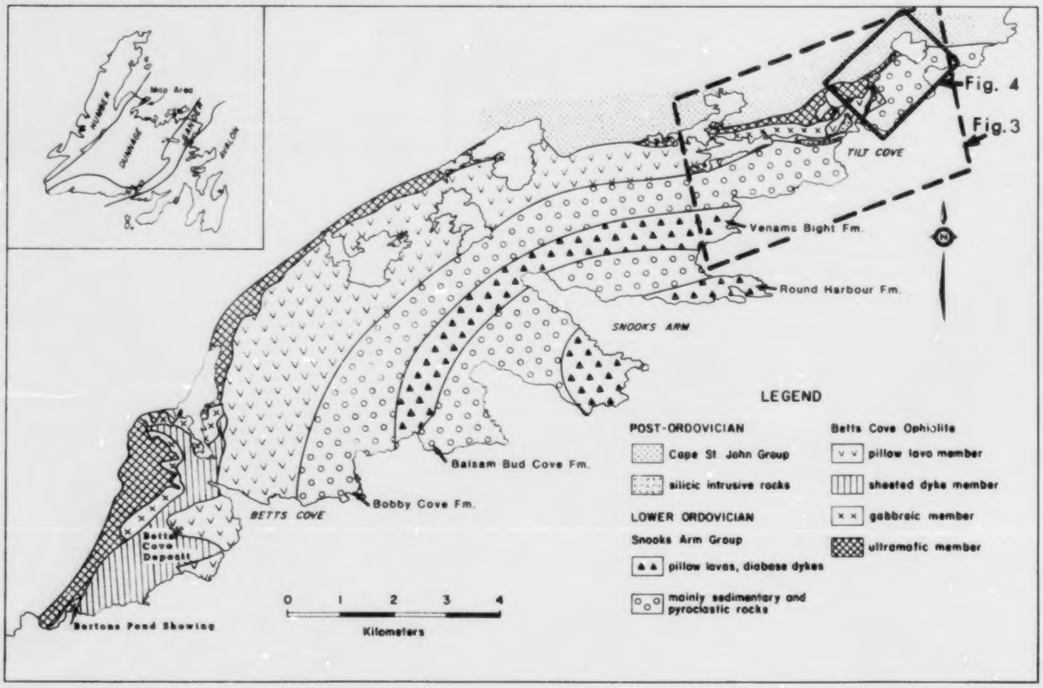

Figure 36.1. *Geology of the Betts Cove-Tilt Cove area (after Upadhyay, 1973).*

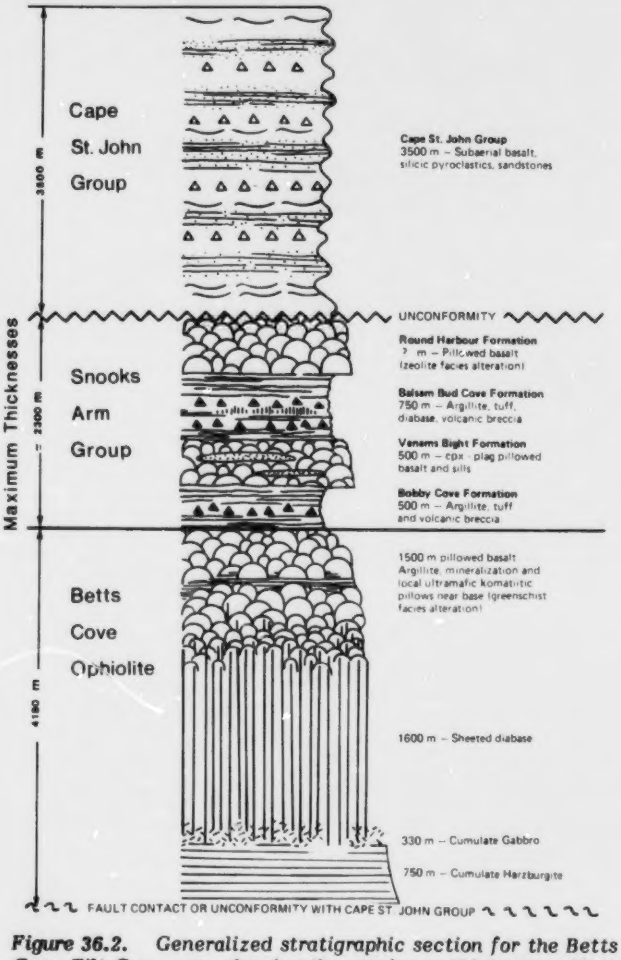

Figure 36.2. *Generalized stratigraphic section for the Betts Cove-Tilt Cove area, showing the maximum thicknesses (data from Upadhyay, 1973).*

abundant red chert. The units overlying the ophiolitic rocks (Fig. 36.2) are not related to the massive sulphide mineralization. Descriptions of these can be found in Upadhyay (1973).

The present study focussed on the geology of the Tilt Cove area between Beaver Cove Pond and Long Pond; the most important features are shown on Figure 36.3. The following descriptions of rocks in the Windsor Lake-Beaver Cove Pond area (Fig. 36.4) are given in the order of decreasing age, based upon the sequence shown in Figure 36.2.

Ultramafic rocks occupy a belt ranging from about 350 to 100 m wide, over a distance of 3 to 4 km. They range from black massive serpentinite, which appears to have been derived from harzburgite, to strongly foliated rusty-weathering yellow talc-carbonate. On its northwest boundary the belt is in contact with the overlying rocks of the Cape St. John Group. The contact can be seen as clearly unconformable in the cliffs north of Windsor Lake, but in general it is faulted.

The southern contact of the ultramafic belt is not exposed, but it is assumed to be a fault for a number of reasons. It traverses a variety of the "overlying" rocks from both the pillow lavas and Bobby Cove Formation and is everywhere strongly foliated parallel to the contact. Furthermore, the absence of the gabbroic and sheeted diabase units, which typically separate ophiolitic pillow lavas from ultramafic rocks, might be explained by their removal through faulting.

The ophiolitic pillow lavas occupy a 400 m thick block about 500 m long, bounded by a fault on the NE and the cliffs of Tilt Cove on the SW, and continue west of Tilt Cove (Fig. 36.3). Their northern contact is a steep scarp which appears to be a fault separating them from the (underlying) talc-carbonates and serpentinites (Fig. 36.4). The upper two-thirds of the pillow lavas are grey green and variolitic, with abundant pillow breccia which is cemented by calcite and silica, and locally is well bedded and gradational into aquagene tuff. In several cases they also contain large clasts of rhyolitic quartz porphyry. Wedges of the variolitic pillow lavas occur as three large fault-bounded blocks in the northeastern part of Figure 36.4.

A thin (about 1 m) discontinuous band of red tuff-argillite-jasper extends northeastwards from the Tilt Cove cliffs. These sedimentary rocks are similar to those of the overlying Bobby Cove Formation, which consists of about equal proportions of sedimentary rocks and diabase dykes and sills. The sedimentary rocks are of three main types, coarse green greywackes, fine grained green siltstones, and very fine grained red to chocolate laminated cherts and argillites. These all consist of essentially volcanic components, and are locally gradational but generally occur as distinct units.

Diabase of the Bobby Cove Formation forms both sills and dykes which, in many areas, disrupt the sedimentary rocks indicating intrusion before their lithification. They are typically green grey and fine grained, although coarse grained varieties and rare plagioclase-phyric types are seen. They are extremely hard, reflecting their relatively unaltered nature, although disseminated pyrite is not uncommon. Contacts are rarely traceable for any great distance.

The Cape St. John Group may be in either unconformable or fault contact with the ophiolitic rocks. The unconformable relation is exposed in the cliffs north of Windsor Lake, and is readily followed northeastwards to the shoreline where it was described by Neale et al. (1975). The Group can be divided into three main interbedded lithological groups in the map area, subaerial silicic pyroclastics, their water-lain equivalents (sandstones), and subaerial basalts. The sandstones are thin bedded to massive, typically with a flaggy bedding plane cleavage, crossbedded, of variable thickness up to a metre, and gently northward-dipping near the unconformity but steeper towards the north. They are consistently fine to medium grained, yellow green, and contain grey-green clasts of fuchsite, derived from the ultramafic rocks of the ophiolite, in a calcareous matrix. A breccia soil zone is locally developed on basalt at the base of coarsely crossbedded sandstones. Magnetite-rich iron formation, associated with chalcopyrite-bearing massive pyrite, is seen close to the base of the group.

The basaltic rocks of the Cape St. John Group are massive, green purple, fine grained, nonporphyritic (although DeGrace et al., 1976 mention plagioclase phenocrysts), and highly vesicular. The vesicles are filled with calcite and chlorite, and their concentration and alignment in some areas give a bedding orientation parallel to that of the sandstones.

Coarsely porphyritic grey-green intrusive quartz-feldspar-porphyries traverse the stratigraphic sequence from the cliffs west of Tilt Cove northwards towards Beaver Cove Pond. They are best exposed between the two open pits of the East Mine, and west of there they show a flow-banded chilled margin where they intrude the pillow breccias. Between these two open pits the porphyry is somewhat altered, but elsewhere it appears to be less so.

Mineralization

The main mineral deposits of the Snooks Arm Group are the massive pyrite-chalcopyrite (± Au ± Ag) orebodies which were mined at Betts Cove and Tilt Cove. Between 1875 and 1878 the Betts Cove mine shipped 95 999 tons of ore said to have averaged greater than 10% Cu. Grab samples from dumps on the property yielded 4.148 Zn, 0.39 to 1.83% Cu, 6 dwts. (9 g) Au and 18 dwts. (28 g) Ag, per long ton (Snelgrove and Baird, 1953). A third dump was similarly sampled and yielded 9.42% Cu with only traces of Zn and Au.

Upadhyay and Strong (1973) showed that the Betts Cove deposits occur at a stratigraphic position close to the base of the ophiolite sequence, near the sheeted diabase-pillow lava contact. They suggested that a similar stratigraphic control is found at Tilt Cove, as well as in other ophiolite sequences, and would be expected if the ore deposits formed early in the history of the ophiolite, i.e. at oceanic spreading centres.

The Tilt Cove deposits occur at the opposite end of the ophiolite belt from Betts Cove, a distance in excess of 15 km (Fig. 36.3). The following summary is taken from DeGrace et al. (1976, p. 46). The Tilt Cove Mine opened in 1864 and operated continuously until 1917, reportedly producing 1 491 136 tons of Cu ore, 78 015 tons of regulus (matte) and 5416 tons of Cu ingots. The total amount of Cu recovered from these products was estimated at over 61 000 short tons. The West mine contained 8 to 12% Cu and the East mine about 4%. Some Au, Ag and much sulphur were recovered at Swansea, Wales, where most of the ore was shipped for smelting. In 1954 First Maritime Mining Corporation Ltd. commenced development and rehabilitation of the mine, and production resumed in 1957 at 2000 tons of Cu ore per day. Operating ceased in 1967, and total production over the ten-year period amounted to 183 597 125 pounds of Cu and 42 425 ounces of Au from approximately 7 400 000 tons of ore.

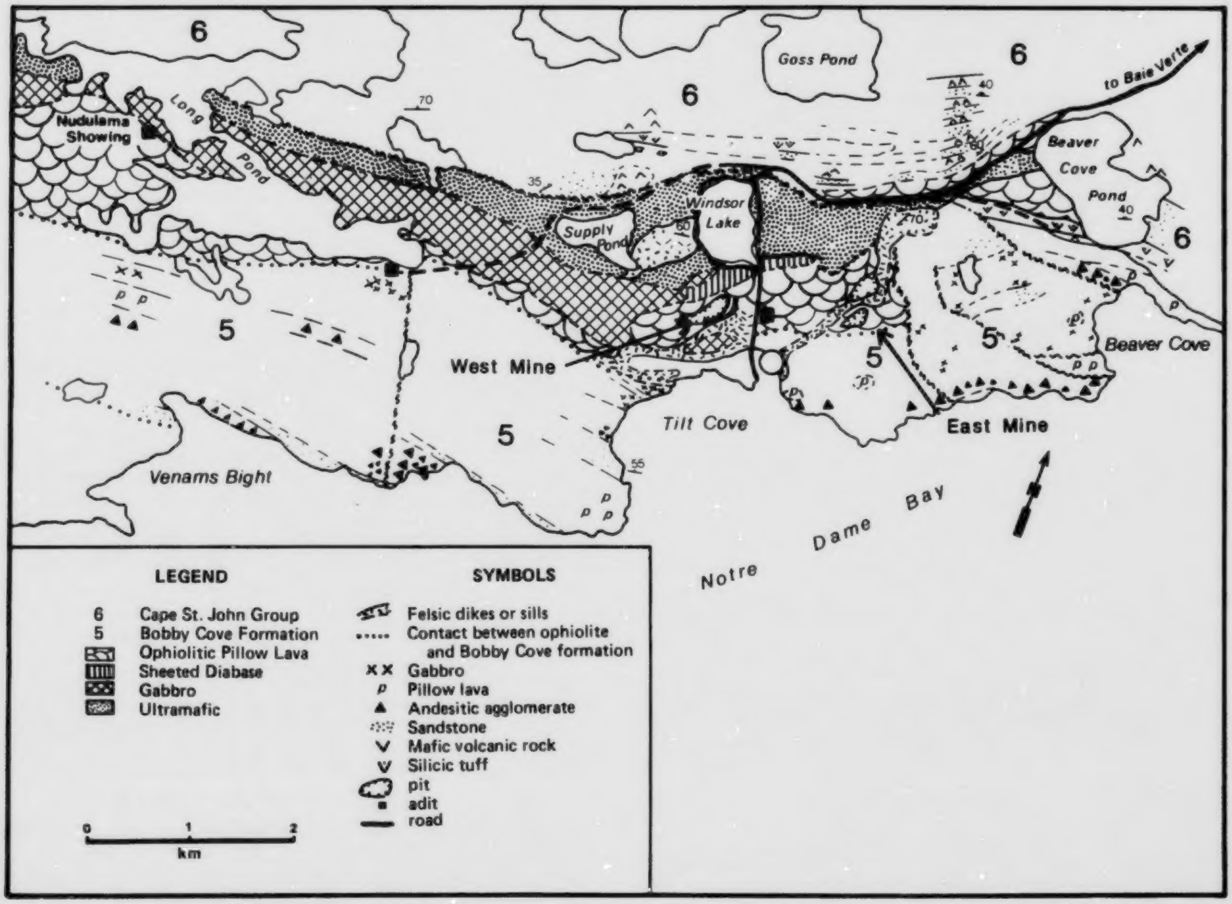

Figure 36.3. Geological setting of massive sulphide deposits and showings in the Tilt Cove-Long Pond area (modified from Upadhyay, 1973).

This study has confirmed the clear stratigraphic control of all massive sulphide mineralization near the base of the ophiolite sequence. It occurs in the variolitic pillow lava and calcite-cemented pillow-breccia unit which extends from the East mine to the Nudulama showing (Fig. 36.3). The West mine and the Nudulama showing occur at the base of this unit, in contact with the sheeted diabase, while the East mine orebodies are found higher up in the unit. All mineralization is accompanied by intense black chloritization as well as more restricted stockwork pyrite and silica.

The mineralization is mainly pyrite and chalcopyrite, with lesser amounts of sphalerite, as well as traces of galena at Nudulama. Magnetite is common in the ores of Tilt Cove, and is especially evident, along with coarse specular hematite, in the East mine main lode. A curious occurrence of massive to disseminated pyrite-chalcopyrite is found near Mud Pond in the schistose talc-carbonate rocks derived from ultramafic rocks. The sulphide minerals exhibit the same tectonic fabrics as the host-rocks, indicating their pre-deformation origin.

Magnetite-bearing cherts are common throughout the volcanic sequence, and are not always associated with sulphide mineralization. These rocks, the Goss Pond sediments of Douglas et al. (1940), are associated with both the basalt and sandstones at the base of the Cape St. John Group, and locally contain Au as well as Cu mineralization.

Numerous small pits, shafts and adits are seen throughout the area, especially near the East and West mines but also in the same horizon at the east end of Long Pond and around the Nudulama showing where there are two shafts about 20 m apart and two adits (possibly connected) on opposite sides of the hill. The adits were driven on stockwork mineralization in the sheeted diabase unit, while the main shaft was sunk on more massive ore in the pillow lava-pillow breccia unit.

Geochemistry

Eighty-four rocks were analyzed for major element oxides, 17 trace elements, and 9 rare-earth elements at Memorial University, and a further 69 analyses of major and some trace elements were provided by Newmont Exploration of Canada Ltd. The aim of these geochemical studies is to clarify features such as the primary compositions of the ore horizon basalts, their magmatic affinities and tectonic significance, and how their chemistry might relate to mineralization and provide a guide to exploration.

As Saunders (1985) described, the mineralization at Betts Cove is typically associated with footwall zones of intense quartz-chlorite alteration within a background greenschist assemblage of actinolite-epidote-chlorite-albite-quartz. Actinolite and epidote are much less abundant at Tilt Cove, with background alteration characterized by chlorite,

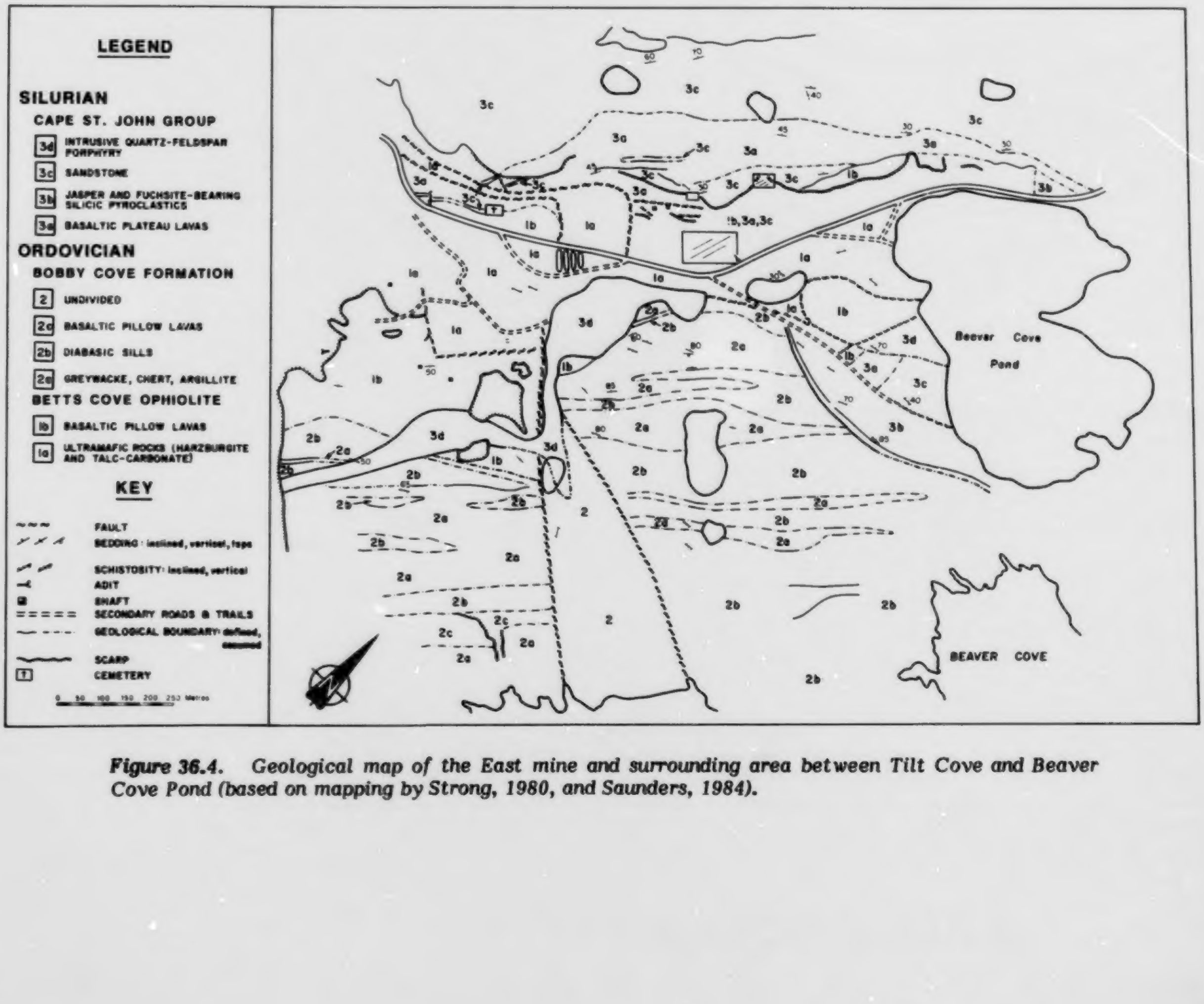

Figure 36.4. Geological map of the East mine and surrounding area between Tilt Cove and Beaver Cove Pond (based on mapping by Strong, 1980, and Saunders, 1984).

quartz and albite. As noted above, however, the mineralization at Tilt Cove is found within a broader scale stratigraphic unit characterized by strong chloritization and in some cases consisting almost totally of chlorite, despite excellent preservation of pillow structures and textures.

Since the main variance of the Tilt Cove data is contributed by MgO and SiO_2, these oxides are plotted in Figure 36.5a at a full scale from 100% SiO_2 to 100% MgO, in which the "zero" corner is actually the apex of a triangular plot representing all of the remaining components. This gives some idea of the total variation in the data, although only the two oxides would generally be considered explicitly in such a plot, as in Figure 36.5b. Also plotted are some of the primary and secondary minerals found in these rocks. The main trend of variation in Figure 36.5a can be related to gain or loss of silica producing a silica-rich and a silica-poor group on either side of the main body of data.

Rocks in the low-silica field of Figure 36.5b are those described above as characterized by abundant chlorite (black in hand specimen), and it can be seen that the rocks approach the compositions of chlorites. It might thus be suggested that they reflect a process involving chloritization, which in this case at least is just the opposite result of the same process of silica transport. There are, however, other processes which must be taken into account to explain the full data variation.

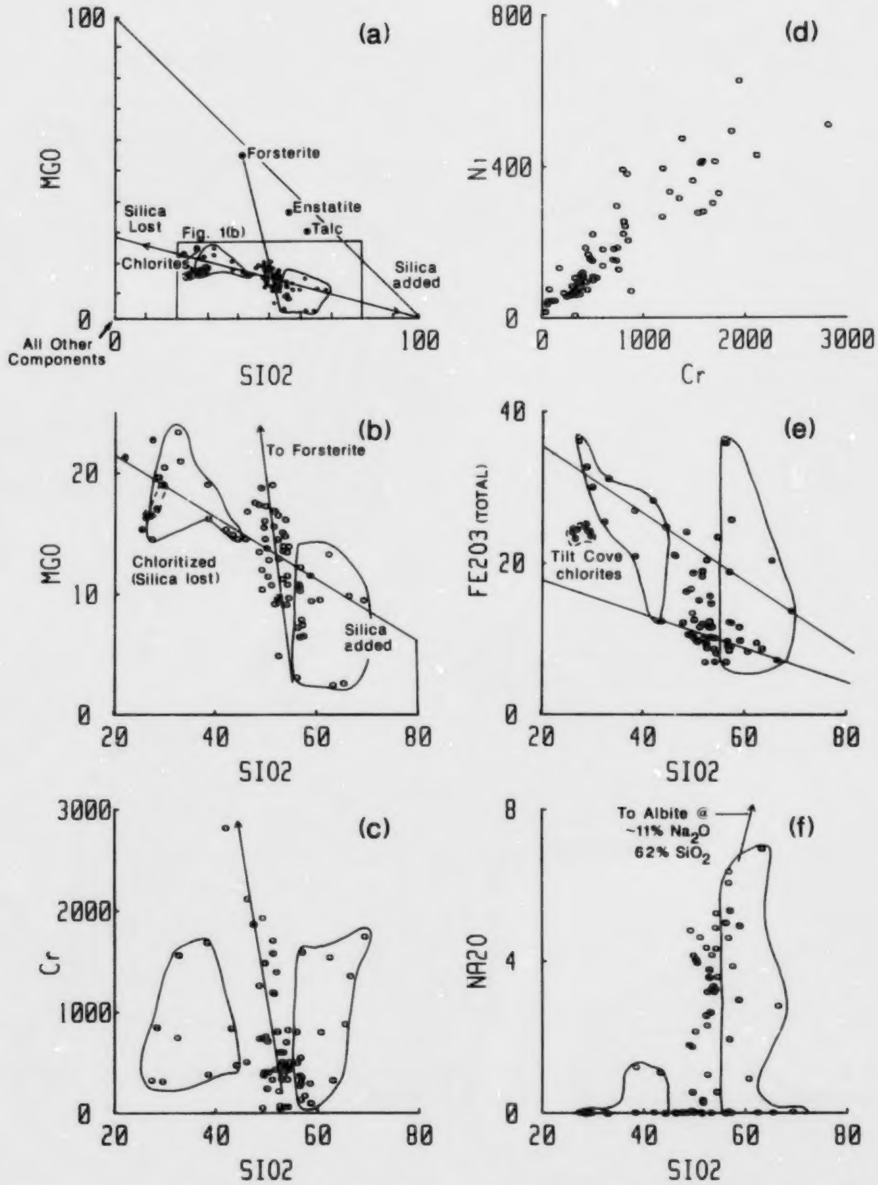

Figure 36.5. *Variation of some major and trace elements in selected rocks of the Betts Cove ophiolite in the Tilt Cove area.*

The central cluster of data in Figure 36.5b exhibits a separate trend which can be related to magmatic processes involving the addition of olivine through either advanced partial melting of the upper mantle or magmatic accumulation of olivine. The former is preferred because of the aphanitic textures, i.e. lack of evidence for any phenocrysts, in the pillow lavas. Such a primary process is necessary because no observed secondary minerals would produce the same trends, nor would they be expected to concentrate elements such as Cr. Figure 36.5c shows that there is a Cr-enrichment trend which parallels that of MgO in Fig. 36.5b, and there are other equally consistent "magmatic" correlations such as Ni-Cr (Fig. 36.5d) which cannot be related to secondary processes.

It can be seen from Figure 36.5e that the silica-poor group is somewhat richer in total iron than can be accounted for by the chlorite compositions, as are some samples from the other two groups. While some of these high iron contents can again be explained in terms of silica loss from the central group of primary compositions, some iron values are too high, particularly in those samples which are also silica-enriched. These are readily related to the addition of iron as both sulphides and hematite, both of which are common in these rocks. The presence of secondary albite in Tilt Cove rocks is reflected in the high sodium concentrations, as seen in Figure 36.5f. It is noteworthy that sodium is not high in the chlorite-rich, silica-poor samples, but that it is enriched in the silica-rich group as well as the central cluster of relatively less altered samples.

Summary

Geological mapping in the Tilt Cove area has shown that most massive sulphide showings occur within a pillow lava-pillow breccia unit traceable over a distance of 5 km at the base of the extrusive portion of the Betts Cove ophiolite. Other showings occur in intensely deformed and altered (talc-carbonate) ultramafic rocks of the ophiolite, and within flows and sediments at the base of the Cape St. John Group. The geochemical studies indicate a magmatic trend relating to variation in the proportion of forsteritic olivine, and a dominant alteration trend relating to addition or loss of silica. Ancilliary variations result from albitization and from iron addition as both sulphides and oxides. Detailed studies are in progress to assess other elemental variations and to relate these trends to specific showings and orebodies.

Acknowledgments

We are grateful to J.A. Coope for permission to use the data of Newmont Exploration of Canada Ltd., to Tyson Birkett for help during the study, and to S.J.P. Burry for field assistance. The study was funded by Newmont, the Geological Survey of Canada, and the Natural Sciences and Engineering Research Council of Canada Operating Grant no. A7975 to D.F. Strong.

References

DeGrace, J.R., Kean, B.F., Hsu, E., and Green, T.
1976: Geology of the Nippers Harbour map area (2E/13), Newfoundland; Newfoundland Mineral Development Division, Report 76-3, 73 p.

Douglas, G.V., Williams, D., Rove, O.N., and others
1940: Copper deposits of Newfoundland; Newfoundland Geological Survey, Bulletin 20.

Neale, E.R.W., Kean, B.F., and Upadhyay, H.D.
1975: Post-ophiolite unconformity, Tilt Cove-Betts Cove area, Newfoundland; Canadian Journal of Earth Sciences, v. 12, p. 880-886.

Saunders, C.M.
1985: Controls of mineralization in the Betts Cove Ophiolite; unpublished M.Sc. thesis, Memorial University of Newfoundland, 200 p.

Snelgrove, A.K. and Baird, D.M.
1953: Mines and mineral occurrences in Newfoundland; Newfoundland Department of Mines and Energy, Information Circular, No. 4, 149 p.

Strong, D.F.
1984: Geological Relationships of alteration and mineralization at Tilt Cove, Newfoundland; in Newfoundland Department of Mines and Energy, Mineral Development Division, Report 84-3, p. 81-90.

Upadhyay, H.D.
1973: The Betts Cove ophiolite and related rocks of the Snooks Arm Group, Newfoundland; unpublished Ph.D. thesis, Memorial University of Newfoundland.

Upadhyay, H.D. and Neale, E.R.W.
1979: On the tectonic regimes of ophiolite genesis; Earth and Planetary Science Letters, v. 43, p. 93-102.

Upadhyay, H.D. and Strong, D.F.
1973: Geological setting of the Betts Cove copper deposits, Newfoundland: an example of ophiolite sulfide mineralization; Economic Geology, v. 68, p. 161-167.

St. Stephen mafic-ultramafic intrusion and related nickel-copper deposits, New Brunswick[1]

A. Dogan Paktunc

Paktunc, A.D., St. Stephen mafic-ultramafic intrusion and related nickel-copper deposits, New Brunswick; in Current Research, Part A, Geological Survey of Canada, Paper 86-1A, p. 327-331, 1986.

Abstract

Geological mapping of the St. Stephen mafic-ultramafic intrusion and logging of the available diamond-drill core were carried out during summer 1985. The intrusion appears to have been synorogenically emplaced into the lower Ordovician Charlotte Group sedimentary rocks during the Acadian Orogeny. Pelitic hornfelses containing mineral assemblages indicative of medium grade metamorphism were developed around the intrusion. The intrusion consists of peridotite, troctolite, gabbro, norite and anorthosite between which the contacts appear to be gradational. Nickel-copper mineralization occurs in the form of massive, semimassive and disseminated varieties. Textures such as matrix sulphides occupying the interstices between cumulus olivine grains and immiscible sulphide blebs indicate a magmatic origin for the deposits. Presence of abundant sulphidic country rock fragments within the intrusion suggests that assimilation of crustal rocks played an important role in the formation of immiscible sulphides.

Résumé

Le levé géologique de l'intrusion mafique-ultramafique de St. Stephen et les diagraphies des carottes des sondages au diamant ont été réalisés au cours de l'été de 1985. Il semble s'agir d'un phénomène syntectonique survenu dans les roches sédimentaires du groupe de Charlotte de l'Ordovicien inférieur pendant l'orogenèse de l'Acadien. Des cornéennes pélitiques qui renferment des associations minérales caractérisées par un degré de métamorphisme moyen se sont développées autour de l'intrusion. Cette dernière se compose de péridotite, de troctolite, de gabbro, de norite et d'anorthosite entre lesquels les contacts semblent progressifs. On observe également une minéralisation en nickel et cuivre tant massive et semi-massive que disséminée. Des textures comme celle des sulfures de la gangue qui occupent les interstices entre les grains d'olivine amoncelés et les bulles de sulfure immiscibles indiquent que les gisements sont d'origine magmatique. La présence de fragments de roche encaissante sulfurée dans l'intrusion semble indiquer que l'assimilation des roches de la croûte a joué un rôle important dans la formation de sulfures immiscibles.

[1] Contribution to Canada-New Brunswick Mineral Development Agreement 1984-1989.
Project funded by Geological Survey of Canada, Economic Geology and Mineralogy Division.

Introduction

About five weeks during the 1985 field season were spent mapping the St. Stephen intrusion and logging the diamond-drill core. Due to poor exposure geological contacts were drawn arbitrarily with the aid of ground geophysical and diamond-drill data. Core from about 66 holes drilled by the Atlantic Nickel Mines, and Boliden and Hanna Mining Companies, was logged and sampled, with particular attention being devoted to the nickel-copper mineralization.

The St. Stephen intrusion underlies an area of approximately 24 km^2 and is located in the southwestern corner of New Brunswick (Fig. 37.1). The southern half of the intrusion is within the town limits of St. Stephen and of Calais (Maine, U.S.A.).

Nickel-copper deposits in the St. Stephen area have been intermittently explored since their discovery about 1870. Various exploration activities and development work carried out by companies such as Atlantic Nickel Company and Boliden, continued until the early seventies. By this time, total reserves from the three deposits (namely Rogers Farm, Hall-Caroll and C-zone) were estimated to be 1 000 000 tons at 0.53% Cu and 1.05% Ni. Because of metallurgical problems in recovering Ni from the pyrrhotite-rich ore and low tonnage of the deposits, no further exploration was carried out by the companies in the area.

This preliminary report summarizes the work completed to the end of the 1985 field season.

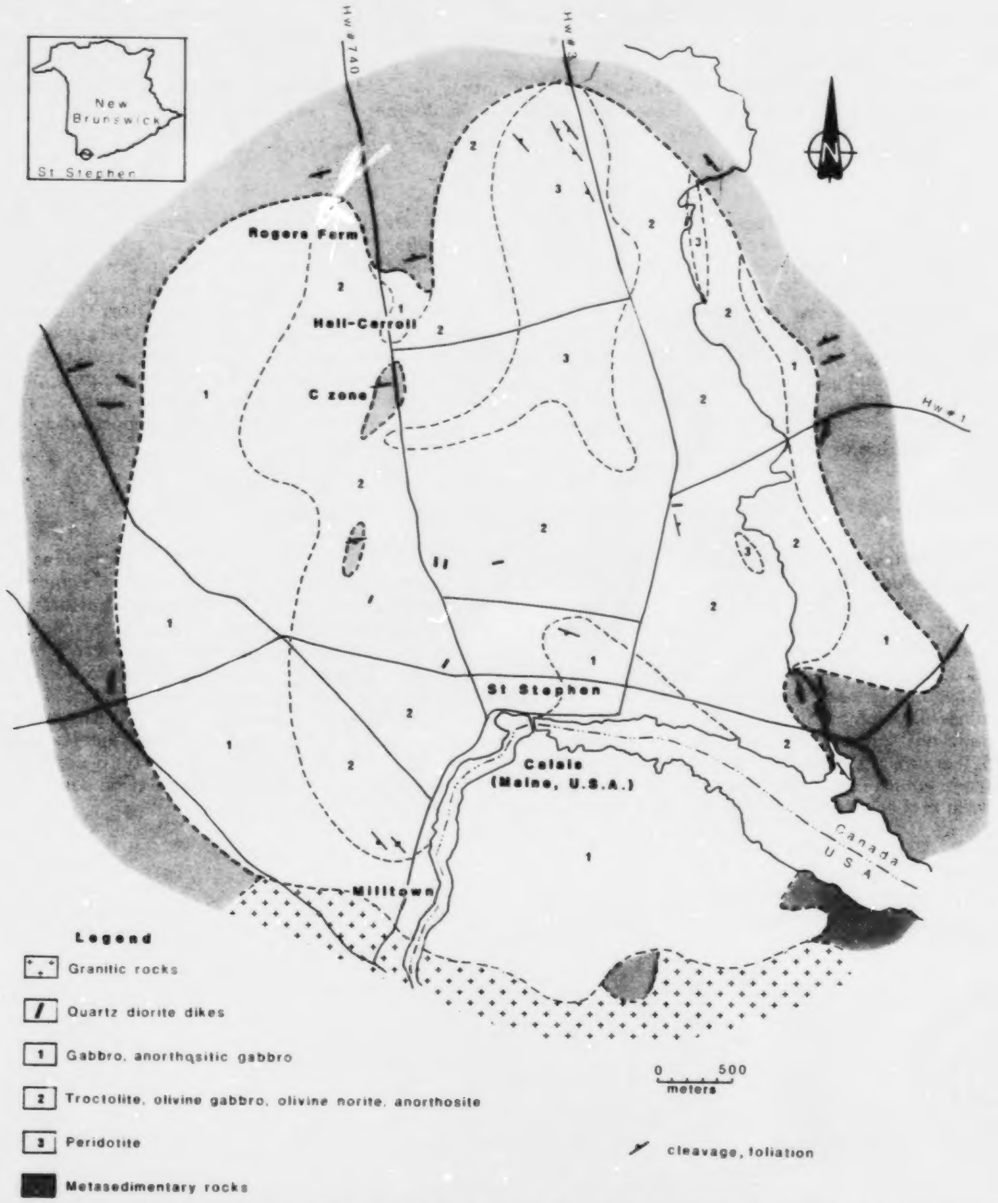

Figure 37.1. Geology of the St. Stephen intrusion. Geological boundaries in the U.S.A. portion of the intrusion are after Ludman (1985).

General geology

The southwestern part of New Brunswick is underlain by strongly folded lower Ordovician Charlotte Group sedimentary rocks. These include carbonaceous black shale, siltstone, sandstone and their metamorphosed equivalents, slates and schists. The sedimentary rocks were intruded by the St. Stephen mafic-ultramafic complex (Ruitenberg, 1972). Two K-Ar ages on hornblendes are of 415 ± 19 and 401 ± 20 Ma, whereas 350 ± 15 and 364 ± Ma were obtained from biotites in the same samples (see Wanless et al., 1973). Pajari et al. (1974) interpreted the hornblende ages as representing the emplacement of the intrusion and the biotite ages as an updating due to a later thermal event. According to them, the St. Stephen intrusion is postorogenic, emplaced following the last phase of the Acadian deformation, but before the intrusion of the St. George batholith at 394 ± 20 Ma. Since the error limits on the ages of the two intrusions overlap and the "similarity" of the St. George pluton and the granitic rocks on the south of the St. Stephen intrusion is not well documented, the age relationship between them remains uncertain. A postorogenic interpretation of the age of the St. Stephen intrusion is not clear either, since northeasterly trending penetrative foliation, although not well developed, is present in rocks of the intrusion. Thus the intrusion may be considered synorogenic. According to Ruitenberg (1972), the St. Stephen intrusion postdates at least the early folding of the Acadian Orogeny. Several mafic intrusions in the Maine Appalachians were reported to have been deformed by late Acadian events (Westermann, 1972; Newell, 1978). Moreover, according to Ludman (1982, 1985), plutonism in the Calais area has occurred between the two periods of penetrative deformation corresponding to the Acadian Orogeny.

St. Stephen intrusion

The intrusion basically consists of peridotite, troctolite, anorthosite, gabbro, and norite. These lithologies are transitional amongst one another. Layering is not observed, but may exist undetected because of scarcity and small size of outcrop, and lack of exposure showing the third dimension.

Peridotite occurs in the northern half of the intrusion. It is best observed along Highway No. 3. Although it outcrops only in the northeastern portion of the intrusion, its abundance at depth in the Rogers Farm area and other parts

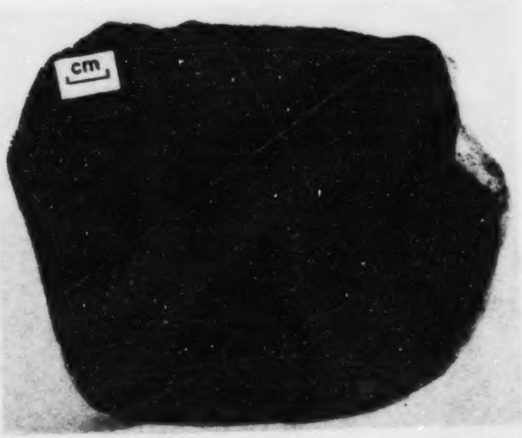

Figure 37.2. Polished slab of peridotite (olivine cumulate). Olivine, dark grey cumulus mineral; plagioclase, white intercumulus mineral; clinopyroxene, black in the form of oikocrysts.

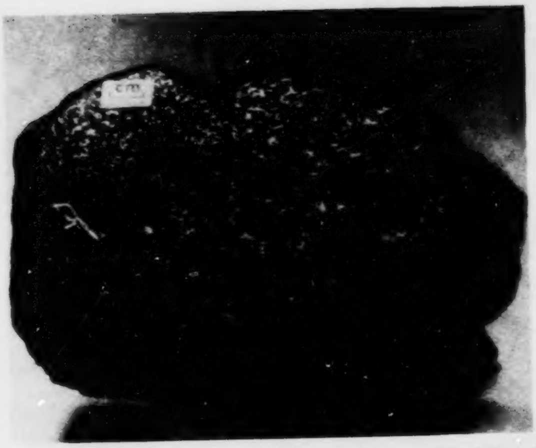

Figure 37.3. Polished slab of peridotite with interstitial sulphide (net-textured sulphide).

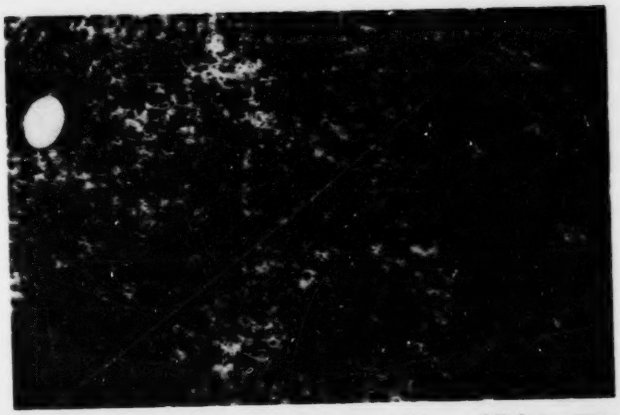

Figure 37.4. Medium grained troctolite. Olivine, grey; plagioclase, white.

of the intrusion is defined by logging of the diamond-drill cores. The peridotite is medium grained and displays cumulus textures (Fig. 37.2). Olivine forms the cumulus phase whereas plagioclase is intercumulus. Locally, clinopyroxene forms coarse oikocrysts. Sulphides, where present, occur as disseminated droplets or matrix-filling in the interstices between olivine crystals, forming net-textured sulphide (Fig. 37.3). Minor chromian-spinel is also present as euhedral-subhedral grains, some being enclosed in early formed olivine. Medium- to course-grained troctolite appears to be the most abundant rock type in the intrusion (Fig. 37.4). It shows a wide range from olivine-rich, near peridotite to plagioclase-rich varieties. Olivine is the cumulus phase in olivine-rich troctolites whereas plagioclase becomes the cumulus phase in the plagioclase-rich varieties. Troctolite is also present in the form of patchy pegmatitic phases in other rock types (Fig. 37.5). Minor clinopyroxene may be present as an intercumulus phase. With increasing amounts of clinopyroxene, the rock grades into olivine gabbro. Textural features similar to those of troctolites are present in olivine gabbro. The only difference is the presence of intercumulus clinopyroxene. Anorthosite is a minor unit. Its contact relations, where seen, are highly irregular. The rock is medium grained and consists of euhedral-subhedral plagioclase laths that are usually zoned. Norite consists of equigranular euhedral-subhedral orthopyroxene and

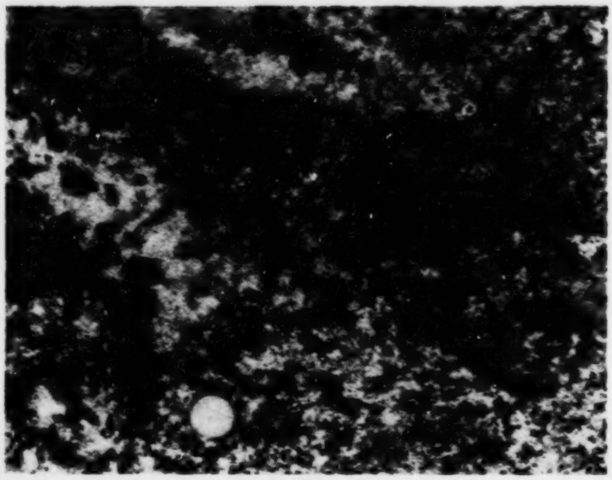

Figure 37.5. Pegmatitic troctolite in olivine gabbro. Olivine, coarse black grains; plagioclase, white. Fine grained black material in olivine gabbro is intercumulus clinopyroxene.

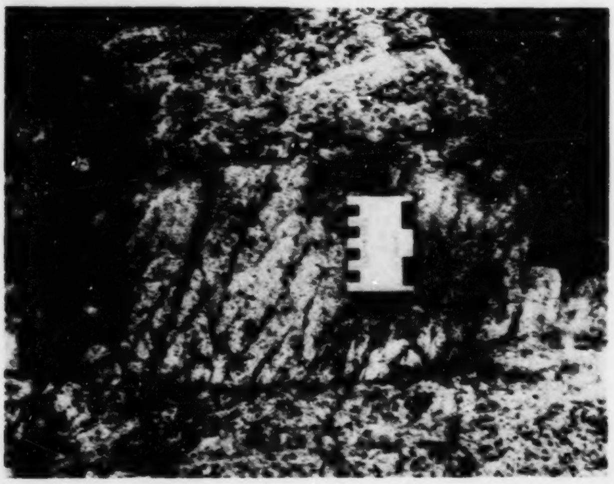

Figure 37.6. Aplitic quartz diorite dyke cutting olivine gabbro.

plagioclase grains. It also contains abundant disseminated ilmenite grains usually associated with minor magnetite. Gabbro occurs in the southern and western part of the intrusion and as a marginal phase near the eastern margin. Its abundance is not as great as indicated by previous investigators since it appears that troctolites and olivine gabbros have been in part mapped as gabbros. The gabbro is medium- to coarse-grained and displays considerable mineralogical and textural variation. Northeasterly to easterly trending quartz diorite dykes cut the rocks of the intrusion (Fig. 37.6). Their thickness is around 20 cm. They are fine- to medium-grained and equigranular. A 60 cm thick diabase dyke was observed in the central part of the intrusion. It is fine grained and displays typical ophitic texture.

Generally speaking the rocks of the intrusion are fresh. Locally developed alteration is intense in the Rogers Farm area and the Hall-Carroll zone and appears to be associated with brecciation. Original textures and mineralogy in such zones have largely been obliterated, making positive identification of the rocks extremely difficult.

Contact metamorphism

Due to the scope of the project, the metasedimentary country rocks around the intrusion were examined only in the scattered exposures within a few kilometres of the contacts. In general, the assemblage cordierite-andalusite-biotite-muscovite-quartz in pelitic hornfelses is indicative of medium grade metamorphism near the contact. In one location the assemblage cordierite-andalusite-sillimanite-biotite-muscovite-K-feldspar-quartz may suggest high grade metamorphism if muscovite is not primary. Contact metamorphism appears to be absent at the southeastern contact, near the mouth of Dennis Stream at the St. Croix River, suggesting a possible fault contact.

Mixed rocks

Metasedimentary and igneous rock fragments are present in the intrusion. Their abundance, distribution and character vary greatly from place to place. The fragments display irregular outlines and range in size from 5 mm to 5 cm. In part they are aligned along certain directions which are believed to represent magmatic currents (Fig. 37.7). Margins of the inclusions tend to be sharp, although some fragments appear to have been partially melted. Both barren and mineralized fragments may be present in the same rock.

Ore deposits

The orebodies occur in the northern half of the intrusion where the area is underlain predominantly by peridotites and olivine-rich mafic rocks. With one exception the southern half of the intrusion, which consists predominantly of gabbros, appears to be barren; a massive pyrrhotite body is found near the western shore of the St. Croix River, immediately north of Milltown.

About 14 mineralized zones were defined by Atlantic Nickel Company in the northern half of the intrusion. Of the 14 zones, the Rogers Farm, the Hall-Carroll zone, and the C-zone are the most important on which detailed exploration activities were carried out by Atlantic Nickel and Boliden. One common feature of these zones is that they appear to

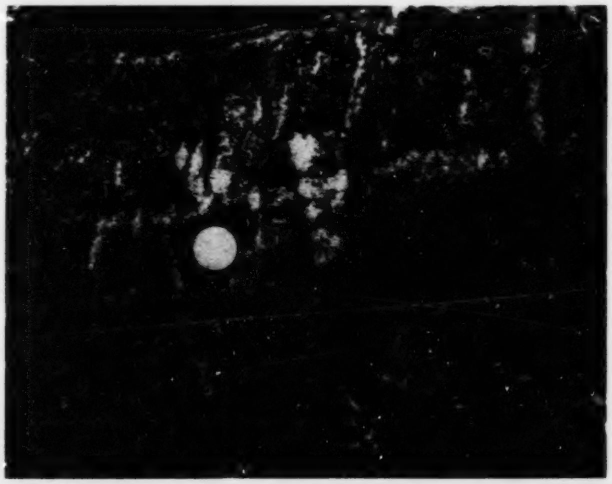

Figure 37.7. Xenoliths showing preferred orientation in olivine gabbro.

follow north-northeasterly-trending structures. This led MacKenzie (1940) and Houston (1956) to interpret the ore deposits as being controlled by north-northeasterly-trending faults/shear zones. According to G.M. Archibald (1964, Atlantic Nickel Mines Ltd. report), however, the mineralization is controlled by a northeasterly trending sediment horizon in the Rogers Farm, the Hall-Carroll and the C-zones.

The mineralization is not confined to a particular rock type but occurs in various lithologies and has different forms and textures. Excluding minor amounts of disseminated sulphide that are found in almost every rock unit, sulphides occur in four textural forms: massive, matrix, blebby, and remobilized. The first three forms, in a general way, represent magmatic sulphides whereas the fourth is associated with late stage magmatic and/or deformational events. Massive sulphides seen in the diamond-drill cores over intervals up to 4 m long, are found in association with variably altered mafic-ultramafic rocks. In most cases, alteration is so intense that the original rock type is difficult to identify. In several locations, the massive sulphide is associated with fresh peridotite carrying varying amounts of matrix sulphides. Matrix sulphides are made up of a network of sulphides usually occupying the interstices between cumulus olivine crystals in peridotite (Fig. 37.3). The amount of sulphides varies from 10 to 40% (by volume). Immiscible sulphide blebs are found in various rock types. They are usually subrounded and range from 3 to 10 mm. The smaller ones coalesce to form larger blebs; in places, they form very large blebs up to 4 cm across with irregular outlines. The sulphides become progressively mobilized by alteration and/or deformation. It is common to see sulphide forming small apophyses/veins extending from a sulphide bleb. They occur along fractures and cleavages in more altered and deformed rocks.

Ore genesis

According to MacLean (1969), Shamazaki and Clark (1973) and Haughton et al. (1974) sulphides can be separated immiscibly from a basaltic magma by 1) decreasing pressure and temperature, 2) increasing sulphur and oxygen fugacities, 3) increasing SiO_2, Na_2O, K_2O, MgO, Al_2O_3 activities and decreasing FeO activity. Among these, 2) and 3) are believed to have played important roles in the formation of immiscible sulphides in the St. Stephen magma.

Since the surrounding metasedimentary rocks are sulphidic, the presence of abundant country rock fragments within the intrusion implies that they may have been incorporated into the magma; therefore, they could be a major source of sulphur. This is not, however, necessarily supported by the sulphur isotope analyses carried out by GSC in 1966 (Wanless, 1966, unpublished data). The $\delta^{34}S$ values obtained from the intrusion are relatively homogeneous, ranging from -2.00 to +0.44‰ with the exception of two anomalous results (-4.89 and -9.33‰) from the central part of the intrusion. The range corresponds to chondritic values, suggesting a mantle source for the sulphur. The country rock sulphides on the other hand display a great variation in their $\delta^{34}S$ values (-10.44 to +7.11‰). Thus, the interpretation that the two anomalous values result from contamination, although possible, is not certain.

As mentioned above, increases in the activity of certain elements, causing decreased sulphur solubility can be produced by contamination of the magma with the surrounding pelitic and quartzitic metasediments. These along with the other factors (i.e. fO_2, T, P) merit further consideration.

Occurrence of abundant immiscible sulphide blebs in a variety of mafic to ultramafic rocks representing different depths at the Rogers Farm may indicate nucleation of sulphides at different levels in the chamber and/or at different times. An early separation of magmatic sulphides from the magma is apparent from the matrix sulphides in peridotite. They probably accumulated before the crystallization of plagioclase from the intercumulus liquid.

Acknowledgments

I am grateful to O.R. Eckstrand for suggesting the topic and for his supervision. Review of the manuscript by D.C. Findlay and O.R. Eckstrand was greatly appreciated.

References

Haughton, D.R., Roeder, P.L., and Skinner, B.J.
1974: Solubility of sulfur in mafic magmas; Economic Geology, v. 69, p. 451-467.

Houston, R.S.
1956: Genetic study of some pyrrhotite deposits of Maine and New Brunswick; Maine Geological Survey, Bulletin.

Ludman, A.
1982: Bedrock geology of the Fredericton 2-degree quadrangle, Maine; Maine Geological Survey, Open File 82-30.

1985: Pre-Silurian rocks of eastern and southeastern Maine; Maine Geological Survey, Open File 85-78.

MacKenzie, G.S.
1940: The St. Stephen map area, Charlotte County, New Brunswick; New Brunswick Department of Lands and Mines.

MacLean, W.H.
1969: Liquidus phase relations in the FeS-FeO-Fe_3O_4-SiO_2 system, and their application in geology; Economic Geology, v. 64, p. 865-884.

Newell, W.R.
1978: Stratigraphy, structure and petrology of the Bingham quadrangle, west central Maine; unpublished M.Sc. thesis, Syracuse University, 80 p.

Pajari, G.E., Jr., Trembath, L.T., Cormier, R.F., and Fyffe, L.R.
1974: The age of the Acadian deformation in southwestern New Brunswick; Canadian Journal of Earth Sciences, v. 11, p. 1309-1313.

Ruitenberg, A.A.
1972: Metallization episodes related to tectonic evolution, Rolling Dam and Mascarene-Nerepis Belts, New Brunswick; Economic Geology, v. 67, p. 434-444.

Shamazaki, H. and Clark, L.A.
1973: Liquidus relations in the FeS-FeO-SiO_2-Na_2O system and geological implications; Economic Geology, v. 68, p. 79-96.

Wanless, R.K., Stevens, R.D., Lachance, G.R., and DeLabio, R.N.
1973: Age determinations and geological studies, K-Ar isotopic ages, Report 11; Geological Survey of Canada, Paper 73-2.

Westermann, D.S.
1972: Petrology of the Pocomoonshine gabbro-diorite, Big Lake quadrangle, Maine; unpublished Ph.D. thesis, Leigh University, 287 p.

The boundaries of the Avalon tectonostratigraphic zone, Musquash Harbour-Loch Alva region, southern New Brunswick

Project 730044

K.L. Currie
Precambrian Geology Division

Currie, K.L., The boundaries of the Avalon tectonostratigraphic zone, Musquash Harbour-Loch Alva region, southern New Brunswick; in Current Research, Part A, Geological Survey of Canada, Paper 86-1A, p. 333-341, 1986.

Abstract

The Avalon zone, characterized by a Late Precambrian volcano-plutonic episode and a faunally distinctive Cambrian section, lies between the Belleisle fault and a transcurrent fault along the shore of the Bay of Fundy. Right-hand transcurrent motion on the latter fault in Carboniferous time produced en echelon structures with local low angle thrusting and intense deformation. Thrust allochthons, confined to a zone no more than a km wide, consist entirely of deformed equivalents of nearby autochthonous rocks. Local kinematic indicators suggest latest right-hand movement on the Belleisle fault, but there is a large left-hand step in the fault trace. An unusual bimodal sheeted dyke complex in the step region (Kingston complex) hints that left-hand motion may have occurred in Late Precambrian time. The combined motion on the faults produced relative northeast translation of the Avalon zone in Carboniferous time. Carboniferous deformation appears to be mainly of high level type, with minor associated magmatism and metamorphism.

Résumé

La zone d'Avalon, caractérisée par un épisode volcano-plutonique de la fin du Précambrien et d'une section cambrienne qui se distingue par sa faune, s'étend entre la faille de Belleisle et un décrochement qui longe la rive de la baie de Fundy. Cette dernière faille a été affectée au Carbonifère par un mouvement de décrochement dextre qui a produit des structures en gradins avec, par endroits, un charriage à angle faible et une déformation intense. Les allochtones, confinés dans une zone d'au plus un kilomètre de largeur, sont entièrement constitués d'équivalents déformés des roches autochtones avoisinantes. D'après des indicateurs tectoniques locaux, un mouvement dextre aurait affecté ultérieurement la faille de Belleisle, mais la trace de la faille présente un large gradin senestre. La présence inhabituelle, dans la région des gradins, d'un groupe bimodal de dykes en strates (complexe de Kingston) laisse supposer qu'un mouvement senestre s'est peut-être produit à la fin du Précambrien. Les mouvements combinés des failles ont produit une translation relative nord-est de la zone d'Avalon au Carbonifère. Le Carbonifère semble avoir déformé surtout les niveaux supérieurs, le magmatisme et le métamorphisme y étant peu importants.

Introduction

The Avalon tectonostratigraphic zone in Canada can be recognized by presence of Late Precambrian (550-650 Ma) volcano-plutonic complexes and a Cambrian sedimentary section with a distinctive fauna (Williams, 1979). The zone consists of several separated terranes (Keppie, 1984), but little is known about the relation of these terranes to each other, to the Devono-Carboniferous basins separating the terranes, or to neighbouring tectonostratigraphic zones. Most workers assume the Avalon tectonostratigraphic zone is bounded by major transcurrent faults (Keppie, 1982; Hanmer, 1981), but the time of origin of these faults and their movement history remain poorly understood. The region around Saint John, New Brunswick, exhibits both margins of a well exposed terrane within the Avalon zone (Currie, 1984). A study of this area should yield information on the nature of the boundaries of the Avalon tectonostratigraphic zone.

General geology

Figure 38.1 shows the geology of the Musquash Harbour-Loch Alva region. The geological units resemble those in the Saint John region (Currie et al., 1981; Currie and Nance, 1983; Currie, 1984), but some difficulty was experienced in distinguishing between similar lithologies of differing age (see Table 38.1). Other recent workers in the southern (Musquash Harbour) part of this area appear to have encountered similar difficulties, leading to drastic divergences in stratigraphy and structure among the several recent maps. I found the map of McCutcheon (1984) to be the most lithologically reliable, although I disagree with some details of his structural interpretation. The northern part of the area in the Long Reach-Loch Alva area has received little systematic work since the mapping of Alcock (1959) and MacKenzie (1948), although a recent preliminary map covers this region (McCutcheon and Ruitenberg, 1984).

The oldest lithological unit in the mapped region, the Brookville gneiss (unit Ab, Fig. 38.1) of Aphebian age (Currie et al., 1981) does not outcrop west of Musquash Harbour. Hybrid granodiorite with large blue quartz eyes and a pervasively chloritized mafic matrix, which forms part of the Lepreau pluton (unit Hd), strongly resembles hybridized Brookville gneiss in the Rockwood Park area of Saint John (Currie et al., 1981). The presence of this rock in the Lepreau pluton may indicate that Brookville gneiss is present at depth, or formed part of the protolith of the pluton.

Metasedimentary rocks of the Green Head Group (unit Hgh) unconformably overlie the Brookville gneiss in the Saint John region, although the unconformity is much modified by remobilization. Grey to buff marble of the Green Head group appears in major amount on the east side of Musquash Harbour, but only in thin tectonized smears to the west. Pervasive carbonatization of some plutonic rocks on the west side of the harbour suggests that Green Head marble may have reacted with them. For many years the Green Head marble was thought to be the only major carbonate unit in this region, but McCutcheon (1981, 1984) demonstrated the presence of a basal carbonate unit in the Carboniferous section (Parleeville Formation). The two carbonate units can be distinguished by (a) coarse grain size of the Green Head (generally >1 mm), (b) grey-blue to buff colour of the Green Head compared to red, grey-green or black shades in the Parleeville, and (c) the local presence of fossils in the Parleeville. Both units locally contain spectacularly developed stromatolites. The quartzite member of the Green Head Group, a fine grained, resistant olive to pale grey psammite occurs in major amount east of Musquash Harbour, but mainly as abundant inclusions in

Legend

QUATERNARY

Qt till, boulder clay, sand and gravel

--unconformity--

TRIASSIC

Tl LEPREAU FORMATION: chocolate brown cobble conglomerate and crossbedded sandstone

--unconformity--

CARBONIFEROUS

Cl LANCASTER FORMATION: Grey sandstone, quartz pebble conglomerate, black siltstone

--gradational contact--

Cbl BALLS LAKE FORMATION: red polymict conglomerate, sandstone and shale

--conformable contact--

Cp PARLEEVILLE FORMATION: red to grey-green limestone, basal black cryptalgal laminite

--relations unknown--

Ck KENNEBECASIS FORMATION: red-brown conglomerate and crossbedded sandstone

--unconformity--

DEVONIAN

Dmd McDOUGALL LAKE PLUTON: pink quartz and feldspar porphyritic, rapakivi biotite granite

--intrusive contact (to units Sw and Sjc)--

SILURIAN

Sw WELSFORD COMPLEX: riebeckite granite and syenite, granophyre, rhyolite

--intrusive contact (to unit Sjc)--

Sjc JONES CREEK FORMATION: thin bedded calcareous shale and siltstone; hornfels

--relations unknown, probably tectonic--

Slr LONG REACH FORMATION: basalt flows, minor calcareous siltstone and chert

--relations unknown, probably tectonic--

CAMBRO-ORDOVICIAN

COsj SAINT JOHN GROUP: grey-green siltstone, black shale, basal quartzite and red sandstone

--disconformity--

EOCAMBRIAN

Ed Red feldspathic sandstone, tuff, arkose, conglomerate; basalt flows

--unconformity or disconformity--

PRECAMBRIAN

Hc COLDBROOK GROUP: basalt, rhyolite, ignimbrite red laharic breccia, minor chert and siltstone

--gradational contact--

GOLDEN GROVE SUITE (no time relations implied)

Hk KINGSTON COMPLEX: alternating salic and mafic dykes, 10 cm to 20 m wide

He Epidote alaskite, leucogranite and quartz porphyry (Lingley pluton)

Hh Granite and granodiorite: hornblende-dominant quartz-rich rocks (Ludgate Lake pluton)

Hd Diorite, monzonite; minor gabbro, hornblendite complex mixed plutonic rocks (Musquash pluton)

--intrusive contact--

Hm MARTINON FORMATION: grey to black siltstone, basal debris flow; hornfels, basalt sills

--unconformity--

Hgh GREEN HEAD GROUP: grey to buff marble (m), olive to pale grey psammite (q)

--mobilized unconformity--

Ab BROOKVILLE GNEISS: hornblende+/-biotite tonalitic gneiss and migmatite

Contact, approximate or assumed

Fault, high-angle, wrench or normal

Fault, thrust, teeth on thrust block

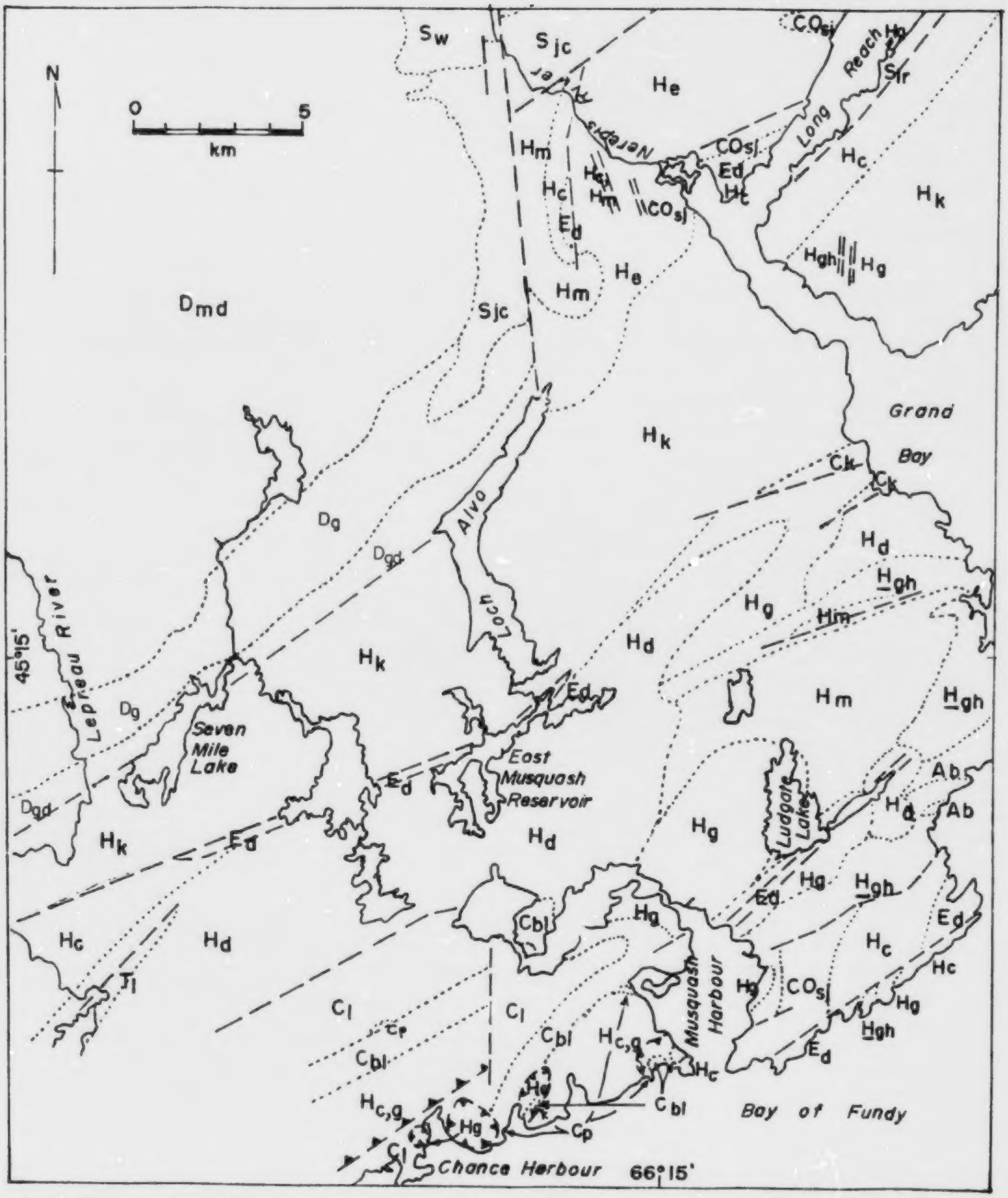

Figure 38.1. Geological sketch of the Musquash Harbour-Loch Alva area. Geology in part modified from McCutcheon, 1984; Parker, 1984; Currie, 1984; Alcock, 1959; Mackenzie, 1948; and McCutcheon and Ruitenberg, 1984.

Table 38.1. Distinction of lithologically similar units

Units	Similarities	Diagnostic criteria
Green Head Group (Hgh)	Major carbonate	Coarse, buff to blue grey
Parleeville Fm. (Cp)		fine, red to green, fossils
Martinon Fm. (Hm)	Black to grey siltstone,	Massive, no bedding
Jones Creek Fm. (Sjc)	siltstone, hornfels	Layered, skarn, fossils
Coldbrook Group (Hc)	Basalt	Associated rhyolite, lahars
Eocambrian (Ed)		Associated red volcanogenic sediments
Long Reach Fm. (Slr)		Associated grey fossil-bearing siltstone
Eocambrian (Ed)	Red conglomerate, sandstone	Feldspathic, associated basalt, soft deformation
Balls Lake Fm. (Cbl)		Quartz pebbles, red shale rip-ups
Saint John Gp. (COsj)	Grey sandstone	Greenish, thick black siltstone-shale
Lancaster Fm. (Cl)		Quartz-pebble beds, thin black plant-bearing beds

plutons on the western side of the Harbour. Because of their olive colour and fine grain, such inclusions superficially resemble boudined dykes.

The Martinon Formation (unit Hm), a debris flow and turbidite sequence invaded by basalt sills, lies on the Green Head Group with unconformity. Much of the Martinon Formation consists of fine grained, homogeneous, dark brown to black siltstone without bedding or other recognizable primary features. This homogeneous character offers a valuable diagnostic criterion in the northeastern corner of the region where the Martinon Formation is found juxtaposed to the lithologically similar Silurian Jones Creek Formation. The latter virtually always exhibits bedding, even when hornfelsed. Greenish calc-silicate bands produced from calcareous beds are particularly diagnostic. South of the mouth of the Nerepis River along the hydro line and in new highway cuttings, the Martinon Formation can be observed to underlie red lahars and flows of the Coldbrook Group approximately conformably, and to be intruded by presumed late Precambrian plutons. The observed relations suggest that the Martinon Formation is more closely related to the Coldbrook Group than to the Green Head Group as previously supposed (Wardle, 1977). In the east-central part of the mapped area the Martinon Formation separates the Ludgate Lake and Lepreau plutons.

In the Saint John region, older units are overlain by volcanogenic rocks of the Coldbrook Group and intruded by a coeval, presumably cogenetic suite of plutons (Golden Grove suite). Within a central core the plutons exhibit a deep-seated character with migmatized, metasomatized aureoles (Currie et al., 1981), whereas elsewhere they are relatively high-level plutons (Currie, 1984). West of Saint John relations between the Coldbrook Group and Golden Grove suite appear to be gradational along the Bay of Fundy. More deep-seated plutonic rocks appear north of Highway 1, substantially offset in a right-hand sense from the deep-seated core previously mapped. The intricate relations among the plutonic rocks and Coldbrook Group suggest that they are roughly of the same age, and probably genetically related. The mixed Rb-Sr isochron age of 526 Ma reported by Poole (1980) for these rocks is therefore probably significant.

A large mass of relatively quartz-poor rocks stretches across much of the central part of the mapped area (unit Hd, Lepreau pluton). The composition of this pluton varies from monzonitic, with significant potassium feldspar, through various varieties of diorite (essentially hornblende-plagioclase rocks) to hornblendite. Despite the generally quartz-poor character of the complex, it exhibits abruptly gradational transitions to internal masses of coarse quartz-feldspar rock. In appearance these masses, characterized by large blue quartz eyes, resemble porphyries of the Coldbrook Group. The textural and compositional inhomogeneity of the Lepreau pluton are extreme. Even within compositionally homogeneous zones, variations in grain size produce striking swirling or schlier-like patterns in outcrop. Typically the rock exhibits a grey-green to jade green fresh surface due to pervasive epidotization. Epidote may also be present in football-sized masses. Many outcrops west of the head of Musquash Harbour exhibit complex relations between dark and light phases ranging from agmatite to interdigitating relations in which both phases exhibit marginal chilling. The Lepreau pluton contains few mafic dykes relative to other Golden Grove plutons. Contact relations of the complex can be examined in road cuts. The complex appears to exhibit mutually chilled margins against the Ludgate Lake pluton and against quartz-feldspar porphyries along Musquash Harbour.

Granite and granodiorite (unit Hg) characterized by abundant visible quartz occur east of Ludgate Lake. The plutons consist of homogeneous, essentially massive, medium- to fine-grained, pale pink rocks whose dominant mafic is hornblende, but which consistently contain biotite. The plutons contain recognizable Green Head xenoliths and rather abundant altered mafic dykes. Mutually chilled contacts between the Ludgate Lake pluton and the Lepreau pluton are well exposed in a road cut west of Ludgate Lake. The Ludgate Lake pluton probably provided the samples yielding a Rb-Sr isochron age of 615 Ma (Olszewski et al., 1980).

Epidote alaskite, leucogranite and quartz porphyry (unit He) form one of the most characteristic units of the Saint John region. The rocks consist essentially of large quartz and feldspar grains with interstitial epidote. Depending on the amount of epidote the rocks may appear pink, tan or pale green. Much of this material appears to be

subvolcanic to the Coldbrook Group, and difficult to reliably distinguish from it. The coast of the Bay of Fundy between Musquash Harbour and Chance Harbour exposes the upper levels of a volcano-plutonic complex, subvolcanic leucogranite along the coast, and extrusive in the coves.

The Kingston complex (unit Hk) consists essentially exclusively of north- to north-northwest-trending, alternating salic and mafic dykes (Currie, 1984) ranging in width from 10 cm to 20 m. Mafic dykes range from fine grained, slightly altered basaltic material, massive or with blobby plagioclase phenocrysts, to medium grained dioritic (hornblende-plagioclase) rocks with small micropegmatite patches. Salic dykes consist of pink, fine grained felsite, feldspar-porphyritic rhyolite, locally spherulitic, or pale grey chloritized microgranite. Intrusive relations demonstrate that all of the varieties locally intrude one another, and hence must be of similar age. Small fault slivers of granite, Green Head Group and Coldbrook Group occasionally occur in the complex parallel to the dykes. The Kingston complex has now been mapped more than 50 km across the trend of the dykes, from Hampden to Loch Alva, without change in essential character. The length along strike of the dykes appears to remain relatively constant at about 10 km. Within the mapped area the complex contacts the Lingley epidote alaskite pluton on one side and the Lepreau pluton on the other. No contacts are exposed; no dykes have been observed in the plutons and no inclusions of the plutons have been recognized in the dyke complex. The lithologies exposed in the Kingston complex strikingly resemble those in the Coldbrook Group and the Golden Grove suite, particularly the plagioclase-porphyritic, slightly altered diorite and the epidote leucogranite. The mechanism which could produce a bimodal sheeted dyke complex of these dimensions is at present unknown.

Southeast of Seven Mile Lake is a mafic-dominated sequence which exhibits volcanic phenomena near its northern margin (ignimbrites, fragmentals) but becomes hypabyssal to the south and resembles the Kingston complex. This sequence differs from the Kingston complex in two important respects. (a) The bulk of the rocks are mafic (80-90%) although salic rocks are always present. (b) The rocks trend northeast, parallel to the regional tectonic "grain", while the dykes of the Kingston complex trend at right angles to this grain. The similarity in style and lithology between the Kingston complex and this mafic-dominated sequence is sufficiently close that they are considered to demonstrate a transition from Coldbrook Group to Kingston complex.

Rocks assigned to the Coldbrook Group (unit Hc) underlie a large area along the Bay of Fundy and a smaller region northwest of the Lepreau pluton. The material along the Bay of Fundy comprises about 80% salic component and 20% mafic component. Along the sea cliffs the rocks consist of quartz-eye leucogranite with mafic dykes, but in the coves both salic and mafic rocks become fragmental (tuffs, agglomerates, ignimbrites) and even laharic material is locally present. Mafic rocks commonly form dykes in salic ones, but the reverse relation is locally observed, and some examples exhibit very complex interfingering relations suggestive of mutual intrusion. This region clearly formed the upper parts of a volcano-plutonic edifice whose original top now faces northwest. Poole (1980) used samples from this region to obtain a composite Rb-Sr isochron age of 526 Ma, but Rast et al. (1978) considered the rocks Carboniferous. McCutcheon (1984) showed the volcano-plutonic rocks were unconformably overlain by the Carboniferous section, and considered them to be late Precambrian. A zircon concentrate is now being prepared from these rocks which will hopefully settle the question.

Currie (1984) and Tanoli et al. (1985) defined and described a sequence of volcanogenic redbeds and basalts younger than the Coldbrook Group, but older than the Cambro-Ordovician Saint John Group (unit Ed). The abundance of volcanic detritus and association with basalt readily distinguish this sequence from Carboniferous redbeds (Balls Lake Formation) which typically contain a high proportion of quartz cobbles. The Eocambrian sequence in the north-central part of the mapped area consists of coarse red cobble to boulder conglomerate with clasts entirely composed of Coldbrook porphyries and leucogranites. The abundance of conglomerate suggests a local unconformity between the Coldbrook Group and the Eocambrian section. The thin slivers of Eocambrian rocks west of Loch Alva consist of red sandstones with pebbly beds, clearly representing a more distal facies than the conglomerates.

Recognition of the Eocambrian section forms a key to the correct interpretation of the stratigraphy and structure of this region. Alcock (1938) mapped these rocks partly as Coldbrook Group and partly as Carboniferous, leading to confusion over the "Mispec Group" which took more than 40 years to sort out (Currie and Nance, 1983). Mackenzie (1948) consistently mapped these rocks as part of the Saint John Group, leading to unnecessary complications in stratigraphy. Rast et al. (1978) and Parker (1984) considered the occurrences in Saint John city as Carboniferous, which required a complicated series of nappes to explain their emplacement. All these complications disappear when the rocks are returned to their correct stratigraphic position.

The Cambro-Ordovician Saint John Group (unit COsj) outcrops within the mapped area only on Musquash Harbour (Currie, 1984) and in two small fault-bounded slivers south of Nerepis River. The new lithological zonation of the Saint John Group proposed by Pickerill and Tanoli (1985) permits much more accurate stratigraphic assignment of this material.

The Silurian Long Reach Formation (unit Slr) does not outcrop west of Saint John River according to the present interpretation. Three outcrops on Grand Bay shown by Mackenzie (1948) as Long Reach Formation, have been assigned to the Coldbrook Group. These outcrops differ in no respect from surrounding material long regarded as part of the Coldbrook Group. Correct assignment of isolated basaltic rocks, however, is notably difficult because moderately altered basaltic rocks have been observed in the Coldbrook Group and equivalent rocks (dykes in the Green Head Group and Golden Grove suite, Kingston complex) in the Eocambrian section and in the Long Reach Formation. Coldbrook basalts appear more deformed and metamorphosed, but no reliable diagnostic criteria are known for distinguishing between these basalts.

The Silurian Jones Creek Formation (unit Sjc) comprises grey-green siltstone, shale and calcareous shale, commonly fossiliferous. Much of the Jones Creek Formation within the mapped area has been hornfelsed. These flinty hornfelses can be distinguished from similar rocks in the Martinon Formation by the common occurrence of colour banding and deep green skarn bands. The Jones Creek Formation does not form part of the Avalon zone, but lies within the terrane to the north.

The Welsford complex (unit Sw) consists of alkali granite, syenite and granophyre, readily distinguished from other granitoid rocks by the presence of blue alkaline amphibole. A number of phases can be distinguished in this high-level pluton (Currie, 1984). The Welsford complex gave an early Devonian (380 Ma) Rb-Sr age (Fyffe et al., 1981), but the occurrence of apparently correlative rhyolite porphyries within the Silurian section northeast of the

mapped area (I. Patel, personal communication, 1983) suggests that the true age may be Silurian. Like the Jones Creek formation, the Welsford complex does not form part of the Avalon zone.

The third component, the region lying north of the Avalon zone is the McDougall Lake pluton (unit Dmd) of the Saint George batholith (Fyffe et al., 1981). This pluton consists of quartz and plagioclase porphyritic biotite granite. Toward the margins of the pluton the grain size decreases to less than 1 mm, but granophyric or chilled phases appear to be absent. The central part of the pluton contains rapakivi feldspars up to 3 cm across which are riddled with fine inclusions of matrix minerals ("megacrysts"). These large feldspars may be either roughly euhedral, or ovoid to blobby. The McDougall Lake pluton gave a Rb-Sr age of 345 Ma (Fyffe et al., 1981). The pluton appears to be completely undeformed except for narrow (30 cm), dyke-like zones of greenish mylonite which are rarely seen in the southern part of the pluton.

The Carboniferous stratigraphic section in the Saint John region has provoked controversy for more than 100 years. The stratigraphy may be divided into northern and southern divisions. The northern division, the Kennebecasis Formation, occurs only as small fault slivers west of the Saint John River. This formation consists of locally derived, red to brown conglomerate and sandstone of Fammenian to Westphalian age (Currie, 1984). The Kennebecasis Formation is a distal equivalent to several formations in the Moncton basin to the northeast.

The southern division, traditionally termed the Mispec Group, consists of three well defined formations. The basal unit, the Parleeville Formation (unit Cp), rests unconformably on Coldbrook Group and related rocks. An undisturbed unconformity can be seen on the east shore of Musquash Harbour. The Parleeville Formation consists of basal black, stromatolitic, cryptalgal laminite overlain by pale green, thinly bedded limestone or calcareous shale, and capped by thick bedded red limestone or calcareous shale. These rocks occur as local lenticles commonly associated with faults. (Green Head carbonate exhibits similar allochthonous intrusive character in Saint John city, see Currie et al., 1981.) The Visean to Namurian Parleeville Formation is absent east of Musquash Harbour (McCutcheon, 1981).

Red conglomerate, siltstone and shale of the Balls Lake Formation (unit Cbl) rests on Parleeville Formation, or unconformably on Coldbrook Group and equivalent plutons. The thickness of the Balls Lake Formation decreases northward from roughly 300 m near Chance Harbour to less than 100 m near Musquash. Nance et al. (1985) showed that the Balls Lake Formation exhibits a basal, pale green sandstone-siltstone sequence which forms an important marker horizon. This marker demonstrates that the west shore of Musquash Harbour corresponds closely to the base of the Balls Lake Formation. As originally pointed out by Currie and Nance (1983), and refined by Nance et al. (1985), the Balls Lake-Lancaster sequence represents alluvial fan deposits. Much of the material in the Musquash Harbour-Chance Harbour region represents proximal to mid-fan deposits.

The Lancaster Formation (unit Cl), which gradually overlies the Balls Lake Formation, consists of pale grey to almost black, near massive lithic sandstone with pebble conglomerate lenses, and black, fossiliferous, carbonaceous lenses which are locally coal-bearing (Alcock, 1959). In favourable exposures the Lancaster Formation exhibits cross stratification, climbing ripples and grading. The age of the Lancaster Formation is Westphalian (see Currie and Nance, 1983 for references), but the formation appears to become younger from northeast to southwest, passing from Westphalian A to D in a distance of about 30 km. As pointed out by Currie and Nance (1983) and Nance et al. (1985), the Lancaster Formation represents distal alluvial deposits from a fan complex which created the Balls Lake Formation as proximal and mid-fan deposits.

Chocolate massive torrential conglomerate of the Triassic Lepreau Formation (unit Tl) occurs as a mass about 5 m across and 4 m high just west of Musquash Harbour. This material can readily be distinguished from the deformed Balls Lake Formation by lack of cleavage. The large, crumbly character of the exposure suggests that it is not a boulder, but an outlier of Triassic rocks known to occur on the west edge of the mapped area (Alcock, 1959) and offshore (Currie, 1984).

Quaternary cover (unit Qt) is locally very thick in the mapped area. Bedded sand and gravel deposits of presumed alluvial origin rise to 25 m above sea level, and to 60 m or higher along the Nerepis River. This material has been overridden by ubiquitous till and boulder clay.

Structure of the southern margin of the Avalon terrane

The ground along the northwest shore of the Bay of Fundy has been the subject of extensive studies by N. Rast and colleagues during the past 15 years. Since the now classic paper by Rast and Grant (1973), it has been proposed in several publications (Rast et al., 1978; Parker, 1984) that essentially all of this ground consists of far-travelled nappes of Carboniferous rocks transported toward the northwest. Improved knowledge of Carboniferous stratigraphy, as well as the present remapping, make it clear that this view is no longer tenable.

The Carboniferous section in the Musquash Harbour-Chance Harbour region forms a well defined, southwest-plunging synclinorium divided into two branches by a central block of Coldbrook Group. This overall W-shaped pattern, opening to the southwest, is complicated by smaller north-trending cross structures and by local faulting. The northern arm of the synclinorium, termed the Lepreau syncline by Rast et al. (1978) forms an isoclinal syncline slightly overturned toward the northwest. The style and scale of folding and associated cleavage resemble that of the Saint John syncline (Wardle, 1977). The basal Balls Lake Formation contains abundant locally derived cobbles, and the unconformity at its base is exposed on the south side of the syncline. On the north side of the syncline, the unconformity is not exposed, and a high angle reverse fault may be present, as it is in the Saint John syncline (Currie, 1984). The plunge of the structure, about 15°, is well defined in the very well exposed hinge region east of the head of Musquash Harbour.

The hinge region of the main synclinorium can be examined along the west shore of Musquash Harbour. Thanks to the improved stratigraphy of the Balls Lake Formation introduced by Nance et al. (1985), a complete, well ordered stratigraphic section can be measured here, and a totally undisturbed unconformity between basal Carboniferous and late-Precambrian volcano-plutonic rocks can be examined on the east side of the Harbour. This contact can be traced all the way to Chance Harbour. As usual in this region, this southeastern limb of the fold is overturned although the stratigraphy is not significantly disturbed.

These observations make it clear that most of the ground between Musquash Harbour and Chance Harbour is underlain by autochthonous material which forms a natural extension of the Saint John city region (Currie, 1984) in both lithology and structural style. However Rast and Grant (1973) drew attention to spectacular, westerly transported allochthons along the Bay of Fundy with

essentially flat-lying bases. Such allochthons clearly could not be produced by the simple folding described above. In addition to the allochthons two other structural features require explanation. One is the eastern and southeastern end of the volcanic-plutonic block north of Chance Harbour. The other is the north-northwest-trending syncline, overturned to the southwest, running up the west side of Musquash Harbour.

Four allochthons occur between Chance Harbour and Musquash Harbour (Fig. 38.1). All these allochthons consist mainly of volcano-plutonic rocks apparently identical to the Coldbrook Group or Golden Grove intrusions although rocks of the allochthons are much more internally shattered than the autochthonous rocks. Two of the allochthons contain a thin (<10 m) section of Balls Lake Formation overlying the granitoid rocks. No exotic lithologies appear in any of the allochthons. Indeed no exotic slices have been recognized anywhere in the Saint John region. Currie (1984) suggested that intensely deformed rocks near Coleson Cove might contain exotic slices, but R.D. Nance (personal communication, 1985) has since shown that all these rocks can be assigned to known units.

The central volcano-plutonic block north of Chance Harbour terminates abruptly against a north-south scarp, at the foot of which Lancaster Formation exhibits strong north-trending, west-dipping cleavage. On its southeast side this block contacts very deformed Lancaster Formation on the shore of Chance Harbour. The Lancaster Formation here exhibits two cleavages, the earlier of which has been recumbently folded about a gently southeast-dipping cleavage. However the exposed (faulted) contact between the Lancaster Formation and the volcano-plutonic block dips moderately northwest, and the straightness of this contact across tens of metres of vertical relief suggests a moderate to steep dip on a regional scale. I propose that the volcano-plutonic block has been transported south and east on high-angle reverse faults.

The north-trending syncline on the east shore of Musquash Harbour can be minutely examined on sea cliffs. The structure extends north more than 2 km where it produces a marked warp in the outcrop of Carboniferous units. Like the east edge of the volcano-plutonic block, it indicates some element of east-west compression.

On the west side of Musquash Harbour this compression was associated with significant northeast over southwest transport and development of strong axial planar cleavage.

Several seasons of field work along the Bay of Fundy in the Saint John region suggest the following generalizations. (1) Strong deformation and structures tend to be discontinuous, and are always en echelon to the right. Examples include zones of strong deformation (Chance Harbour offset to Musquash Head-Negro Head offset to Cape Spencer), folds in the Saint John Group (Currie, 1984), and deep-seated plutonic rocks of the Golden Grove suite. (2) Visible faulting generally trends northeast, dips at relatively steep angles and may have transport directions from southeast to northwest or vice versa. (3) Low angle faults occur only along the shore of the Bay of Fundy, and are associated with intense deformation. (4) Transported rocks are all of types well known in the Saint John region.

These observations strongly suggest major wrenching in a right-hand sense with a master fault lying just offshore in the Bay of Fundy. This fault could be a westward extension of the Cobequid Fault system (Keppie, 1982). Wrenching produces local compression depending on the curvature of the fault, and local configuration of the wall rocks. Hence both north- and south-dipping cleavage could develop, in accordance with observations of domainal distribution of cleavage (Nance et al., 1985). Strong compression must occur in zones connecting the ends of small splays of the master fault. This could explain the overturned cross structure at Musquash Harbour. The configuration of the volcanic-plutonic block north of Chance Harbour could be explained by clockwise rotation due to right-hand wrenching. The presence of allochthons along the Fundy coast indicates expulsion of material due to shortening, but does not necessarily indicate large transport distance. Since the transported blocks appear to be locally derived, their observed horizontal base may result from small horizontal transport of blocks brought up from deeper levels (termed "flower structure" by Nance et al. (1985).

Structure of the northern margin of the Avalon terrane

The southern margin of the Avalon terrane in southern New Brunswick has been extensively discussed in the literature in recent years, but the northern margin has attracted little attention (but see Garnett and Brown, 1973). Northeast of the mapped area this boundary can be easily recognized by a shatter zone (Wheaton Brook fault) which separates the Silurian Jones Creek Formation from Coldbrook Group and related rocks (Currie, 1984). This shatter zone can be traced as far west as a prominent lineament running north from Loch Alva. Northwest of the Wheaton Brook fault the stratigraphic column appears to be essentially continuous and well-ordered. To the southeast the rocks form a multitude of small fault slivers, some no more than 10 m across, which trend north, north-northeast, or northeast. These slivers contain various combinations of Martinon, Coldbrook and Eocambrian lithologies. Where the Wheaton Brook fault meets the north-trending lineament, the Jones Creek Formation makes a sharp bend toward the south and pinches out within a few kilometres. Along the lineament the Jones Creek Formation exhibits unusual cusp-shaped small folds that mimic the large scale distribution of the formation. The Welsford complex exhibits a left hand offset of several hundred metres on this lineament which appears to mark a major structure against which the Wheaton Brook fault is offset.

According to Mackenzie (1948), a fault parallel to the Wheaton Brook fault lies in the southwestern part of Loch Alva, and extends from there toward the southwest. This region was not mapped in detail in 1985. Reconnaissance observations established the following points. (1) The McDougall Lake pluton is undeformed except for rare dyke-like mylonitic bands. (2) South of the McDougall Lake pluton the units, from north to south, are (a) massive diorite or gabbro with rounded felsic blebs (possibly part of the Saint George batholith), (b) an epidotized rhyolite-felsite-granite complex with strong northeast-trending foliation (units Dg and Dgd). These rocks were mapped by McCutcheon and Ruitenberg (1984) as Devonian, but they resemble late Precambrian granitoids of the Avalon terrane. (c) a mafic-dominated dyke complex in which dykes and local mylonitization trend northeast and dip steeply (Kingston complex?), (d) a narrow northeast-trending zone of red volcanogenic sandstone and conglomerate (Eocambrian), and (e) mylonitic grey-green felsite and granite (Lepreau pluton?). These five units occupy a zone 7 to 10 km wide between undoubted McDougall Lake pluton and undoubted Lepreau pluton. The observations suggest three possibilities. (1) Units (c) to (e) belong to the Avalon terrane, and the terrane boundary follows the fault from Loch Alva to Seven Mile Lake. (2) Some or all of units (a) to (e) are fault slices of uncertain age and origin analogous to the Long Reach Formation, and the terrane boundary is an anastamosing fault system. (3) The McDougall Lake pluton truncates the zone boundary in the same fashion as the Ackley City batholith truncates the Gander-Avalon zone boundary of Newfoundland (Hanmer, 1981).

Possibility (3) seems improbable. Eastward and westward extensions of this fault system (Belleisle fault system) certainly cut Carboniferous rocks (Garnett and Brown, 1973; Pickerill et al., 1985). Possibility (2) may be supported by the numerous shears, shatter zones and fault slivers in this region (Grand Bay, East Musquash Reservoir, Ludgate Lake) but the significance of these structures is not well known. Possibility (1) approximates current "conventional wisdom" but there is little positive observational evidence in its favour. More detailed mapping is obviously required.

Local kinematic indicators in the Seven Mile Lake-Lepreau River area suggest latest right hand movement on the Belleisle fault system. However the major deformation zone is clearly offset in a left hand sense at the head of Loch Alva. The presence of a large exotic slice (Long Reach Formation) in this offset suggests large post-Silurian but pre-Carboniferous left hand offset. The Kingston complex offers an interesting clue to a very extended movement history in the same sense. In the present configuration, left hand movement would produce spreading across the lineament extending north from Loch Alva. Such spreading could provide a mechanism for emplacement of north-trending dykes, and by appropriate adjustment of the spreading rate could provide a mechanism to produce a bimodal dyke swarm by injection of mantle- and crustal-derived melts. On this mechanism the width across strike of the dyke complex would provide an estimate of late Precambrian strike slip on the fault.

Discussion

Field evidence strongly suggests major right-hand transcurrent movement along the southeastern margin of the Avalon terrane in southern New Brunswick, and major left-hand movement along the northwestern boundary. The net effect of such motion would be northeasterly transport of the Avalon zone relative to its boundaries, rather like a cork popped from a bottle. Such motion would result in significant shortening across tectonic strike southwest of Saint John. These deductions are compatible with the observed disappearance of the Avalon zone southwest of Saint John.

The timing and kinematics of deformation remain incompletely known. Latest deformation postdates Westphalian D, the youngest paleontologically labelled strata involved in folding. The deformation history may go back to Precambrian time. The disposition of the Kingston complex suggests late Precambrian faulting similar to Carboniferous faulting. At present there seems no way of deciding whether this similarity indicates long-lived deformation, or a return to an older pattern at a later time. Resolution of the possibilities will require substantial advances in the understanding of the stratigraphy and tectonic setting of the Coldbrook Group and related rocks. Detailed petrochemical studies now in progress may provide the necessary clues.

The nature of basement, that is pre-Carboniferous, involvement in Carboniferous deformation remains unclear. Stratified rocks of the Saint John Group and Carboniferous rocks exhibit isoclinal folding, but this does not prove isoclinal folding of underlying crystalline rocks. Extensive observations of the crystalline complex along the Bay of Fundy suggest that it is only locally plastically deformed, and is more commonly block faulted. Shortening by high angle block faulting could be combined with isoclinal folding of stratified cover.

The relation of the "southern" Carboniferous section, lacking Fammenian and Tournaisian strata and very poor in Visean and Namurian strata, to the "northern" Carboniferous section which has thick, widespread deposits of these ages, is not presently understood. The northern section is thought to have been deposited in fault-bounded basins deriving sediment from a southern source. Provenance studies have shown that much of this sediment came from the Avalon terrane (Pickerill et al., 1985), of which the Saint John region forms a part. The southern Carboniferous section did not derive sediment from the Avalon terrane but from some source still farther to the south, now faulted away, or hidden beneath the Bay of Fundy. The Caledonian block, including the Saint John region must have been topographically neutral during the Westphalian so that neither deposition nor strong erosion occurred. Close study of Carboniferous stratigraphy should illuminate the structure and evolution of the margin of the Avalon terrane.

References

Alcock, F.J.

1938: Geology of the Saint John region, New Brunswick; Geological Survey of Canada, Memoir 216, 65 p.

1959: Geology, Musquash, New Brunswick; Geological Survey of Canada, Map 1084A.

Currie, K.L.

1984: A reconsideration of some geological relations near Saint John, New Brunswick; Geological Survey of Canada, Paper 84-1A, p. 193-201.

Currie, K.L. and Nance, R.D.

1983: A reconsideration of the Carboniferous rocks of Saint John, New Brunswick; Geological Survey of Canada, Paper 83-1A, p. 29-36.

Currie, K.L., Nance, R.D., Pajari, G.E., and Pickerill, R.K.

1981: A reconsideration of the pre-Carboniferous geology of Saint John, New Brunswick; Geological Survey of Canada, Paper 81-1A, p. 23-30.

Fyffe, L.R., Pajari, G.E., and Cherry, M.E.

1981: The Acadian plutonic rocks of New Brunswick; Maritime Sediments and Atlantic Geology, v. 17, p. 23-26.

Garnett, J.A. and Brown, R.L.

1973: Fabric variations in the Lubec-Belleisle zone of southern New Brunswick; Canadian Journal of Earth Sciences, v. 10, p. 1591-1599.

Hanmer, S.K.

1981: Tectonic significance of the Gander zone, Newfoundland: an Acadian ductile shear zone; Canadian Journal of Earth Sciences, v. 18, p. 121-135.

Keppie, J.D.

1982: The Minas Geofracture; Geological Association of Canada, Special Paper 24, p. 263-280.

1984: The Appalachian collage; in The Caledonide orogen, Scandinavia and related areas, ed. D.G. Gee and B. Sturt; John Wiley and Sons, New York.

Mackenzie, G.S.

1948: Geology, Saint John, New Brunswick; Geological Survey of Canada, Map 1113A.

McCutcheon, S.R.

1981: Stratigraphy and paleogeography of the Windsor Group, southern New Brunswick; New Brunswick Department of Natural Resources, Mineral Resources Division, Open File 81-31, 210 p.

1984: Geology of the gold-bearing rocks in the Lorneville-Lepreau area; New Brunswick Department of Natural Resources, Mineral Resources Division, Information Circular 84-2.

McCutcheon, S.R. and Ruitenberg, A.A.
1984: Geology, Saint John; New Brunswick Department of Natural Resources, Mineral Resources Division, Plate 84-17.

Nance, R.D., Warner, J.B., and Caudill, M.R.
1985: The Mispec Group, Saint John: a tectonostratigraphic record of the Alleghenian (Variscan) event in southern New Brunswick; Geological Association of Canada, Abstracts with Program, v. 10, p. A43.

Olszewski, W.J., Gaudette, H.E., and Poole, W.H.
1980: Rb-Sr whole rock and U-Pb zircon ages from the Greenhead Group, New Brunswick; Geological Society of America, Abstracts with Program, v. 12, p. 76.

Parker, J.S.D.
1984: Geological relationships of basement to cover, Musquash Harbour to Black River, Saint John area, southern New Brunswick; unpublished M.Sc. thesis, University of New Brunswick, Fredericton.

Pickerill, R.K. and Tanoli, S.K.
1985: Revised lithostratigraphy of the Cambro-Ordovician Saint John Group, southern New Brunswick – a preliminary report; in Current Research, Part B, Geological Survey of Canada, Paper 85-1B, p. 441-449.

Pickerill, R.K., Carter, D., and St. Peter, C.
1985: The Albert Formation – oil shale, lakes, fans and deltas; Geological Association of Canada Annual Meeting, Fredericton, Excursion Guide 6.

Poole, W.H.
1980: Rb-Sr age of some granitic rocks between Ludgate Lake and Negro Harbour, southwestern New Brunswick; in Current Research, Part C, Geological Survey of Canada, Paper 80-1C, p. 170-173.

Rast, N. and Grant, R.H.
1973: Trans-Atlantic correlation of the Variscan-Appalachian orogeny; American Journal of Science, v. 273, p. 572-579.

Rast, N., Grant, R.H., Parker, J.S.D., and Teng, H.C.
1978: The Carboniferous deformed rocks west of Saint John, New Brunswick; in Guidebook for field trips in southeastern Maine and southwestern New Brunswick, ed. A. Ludman; Geological Bulletin 6, p. 162-173, Queens College Press, Flushing, New York.

Tanoli, S.K., Pickerill, R.K., and Currie, K.L.
1985: Distinction of Eocambrian and Lower Cambrian red-beds, Saint John area, New Brunswick; in Current Research, Part A, Geological Survey of Canada, Paper 85-1A, p. 699-702.

Wardle, R.J.
1977: The stratigraphy and tectonics of the Greenhead Group: its relationship to Hadrynian and Paleozoic rocks, southern New Brunswick; unpublished Ph.D. thesis, University of New Brunswick, Fredericton.

Williams, H.
1979: The Appalachian Orogen in Canada; Canadian Journal of Earth Sciences, v. 16, p. 792-807.

Variscan tectonostratigraphy of the Mispec Group, southern New Brunswick: stratigraphy and depositional setting

Project 730044

Michael R. Caudill[1] and R. Damian Nance[1]
Precambrian Geology Division

Caudill, M.R. and Nance, R.D., Variscan tectonostratigraphy of the Mispec Group, southern New Brunswick: stratigraphy and depositional setting; in Current Research, Part A, Geological Survey of Canada, Paper 86-1A, p. 343-350, 1986.

Abstract

The enigmatic Carboniferous Mispec Group of coastal southern New Brunswick is redefined to include the sedimentologically related Balls Lake and Lancaster formations based on detailed measured sections from coastal and river exposures southeast of Saint John. The West Beach Formation although formally included in the Mispec Group must remain a descriptive field term until its stratigraphic status is better defined. The purple to green lithic wackes and polymict conglomerates of the Balls Lake Formation are the product of alluvial fan sedimentation and display facies denoting deposition in proximal to mid-fan, mid-fan and distal fan settings. The grey lithic arenites of the Westphalian Lancaster Formation are largely the product of a major meandering stream system but partially represent overbank sediments influenced by the distal fan. Fluctuations in the relief of the fan source area produced interfingering and occasional lateral equivalency of these formations, while deformational fabrics within Balls Lake conglomerates imply syntectonic sedimentation. As paleocurrents indicate northwestward progradation of the Balls Lake fan into the basin drained by the Lancaster fluvial system in response to uplift of a southeasterly source, deposition of the Mispec Group is attributed to documented Variscan transpression at the western terminus of the dextral Cobequid Fault.

Résumé

Les auteurs ont redéfini l'énigmatique groupe carbonifère de Mispec, sur la côte sud du Nouveau-Brunswick. Ils y ont inclus les formations sédimentologiquement apparentées de Balls Lake et de Lancaster, en se fondant sur les résultats des mesures détaillées exécutées sur des sections d'affleurements côtiers et fluviaux au sud-est de Saint John. La formation de West Beach, bien que faisant officiellement partie du groupe de Mispec, continuera d'appartenir au domaine descriptif tant que son statut stratigraphique ne sera pas mieux défini. Les wackes lithiques et conglomérats hétérogènes pourpres à verts de la formation de Balls Lake résultent d'une sédimentation en cônes de déjection, et on y distingue un faciès proximal à intermédiaire, un faciès intermédiaire et un faciès distal. Les arénites lithiques grises de la formation westphalienne de Lancaster ont été produites en grande partie par un important réseau de fleuves à méandres, mais y sont également représentés des sédiments alluviaux d'inondation sous l'influence du cône de déjection distal. Les variations du relief de la source des cônes de déjection ont donné naissance à des interdigitations et, parfois aussi, à des équivalents latéraux de ces formations; d'un autre côté, la texture résultant de la déformation des tectonites à l'intérieur des conglomérats de Balls Lake font croire à une sédimentation syntectonique. D'après l'étude des paléocourants, il semble que le cône de Balls Lake a progressé vers le nord-ouest jusque dans le bassin arrosé par le réseau fluvial de Lancaster, en réponse au soulèvement d'une source située au sud-est; le dépôt du groupe de Mispec est attribué à une transpression connue qui se serait produite au cours de l'orogenèse de Variscan à l'extrémité ouest du décrochement dextre de Cobequid.

[1] Department of Geological Sciences, Ohio University, Athens, Ohio, 45701

Introduction

The Mispec Group of coastal southern New Brunswick constitutes an ill-defined succession of clastic sediments and volcanics that are traditionally considered to be of Carboniferous age and have been variably involved in late Paleozoic (Variscan) deformation (Hayes and Howell, 1937; Alcock, 1938; Rast et al., 1978; Ruitenberg et al., 1979). Beyond this, the stratigraphy, provenance, depositional environment and tectonic setting of the Mispec Group remain largely unresolved.

Variscan deformation in southern New Brunswick takes the form of basement-involved thrust sheets that define an east-northeast trending belt bordering the Bay of Fundy. North of this belt, Carboniferous sediments are essentially undeformed and were largely deposited in pull-apart basins produced by Variscan right-lateral displacements on major strike-slip faults (e.g. Bradley, 1982). The Mispec Group, in contrast, lies within the thrust belt and, west of Saint John, is involved in large-scale overturned structures that Rast et al. (1978) attribute to its northwestward emplacement as an allochthonous unit along the Variscan front of Rast and Grant (1973). However, in a preliminary study east of Saint John, Currie and Nance (1983) concluded that the Mispec Group was essentially flat-lying and parautochthonous, and reflected sedimentation under proximal fan and more distal fluvial conditions. Accordingly, they proposed that deposition and subsequent deformation of the Mispec Group occurred in response to uplift and emplacement of an allochthonous Variscan terrane farther south.

In order to substantiate this model, a detailed examination of the Mispec Group has been undertaken southeast of Saint John where the group straddles a Variscan front along which mildly deformed autochthonous units to the north are overthrust by their polydeformed stratigraphic equivalents to the south. In addition to more or less continuous coastal sections, the area consequently provides an opportunity to examine both the depositional and deformational history of the Mispec Group and hence establish their potential interrelationship. This report documents the stratigraphy and sedimentology of the Mispec Group as recorded in autochthonous units along the eastern shore of Saint John Harbour (Fig. 39.1) where the effects of deformation have been established (Nance, 1985). A complementary study of the structural geometry and deformational history of the group, as recorded in allochthonous units to the south, is presented by Nance and Warner (1986).

Stratigraphy

The Mispec Group is traditionally subdivided into the West Beach, Balls Lake, and Lancaster formations, although a consensus for this ascending stratigraphy has only recently been achieved (Wardle, 1978; Currie and Nance, 1983; Parker, 1984), and the status of the West Beach Formation is presently in question.

The Lancaster Formation conformably overlies the Balls Lake Formation and consists of grey to grey-brown lithic arenites with occasional thin conglomeratic pebble lags, substantial amounts of grey-green siltstones, and grey to dark grey shales. Common but generally poorly preserved plant fossils within Lancaster shales range in age from Westphalian B in Saint John (Stopes, 1914) to Westphalian C in the vicinity of Lepreaux (Rast, personal communication, 1985). Currie and Nance (1983) estimated a maximum thickness for the Lancaster Formation in excess of 400 m.

The Balls Lake Formation unconformably overlies the West Beach Formation and comprises grey-purple lithic wackes that often contain subrounded pebbles and thin conglomeratic horizons; grey-purple, moderately sorted, bimodal, and polymict orthoconglomerates; red to red-grey, unsorted, polymodal, and polymict paraconglomerates; and sporadic red siltstones. Vertical and lateral transitions from typical Balls Lake redbed lithologies to grey-green units similar to those of the Lancaster Formation suggest lateral equivalence of these two units in some areas. A Westphalian A to C time range for the Balls Lake Formation therefore seems probable. The formation attains an estimated thickness of 200 m east of the Mispec River and thins westward to a few metres near Saint John (Currie and Nance, 1983).

The West Beach Formation comprises a bimodal volcanic assemblage of basaltic and rhyolitic flows, hyaloclastites, ignimbrites, tuffs and agglomerates that are interbedded with maroon siltstones, sandstones, and polymict conglomerates. Although demonstrably older than the Balls Lake Formation, the age of the West Beach Formation

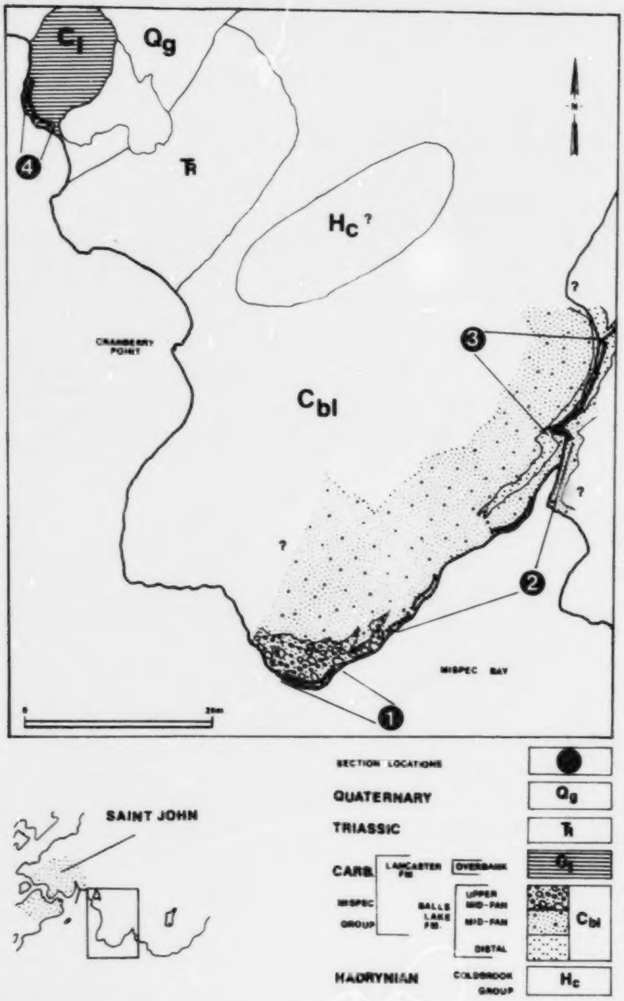

Figure 39.1. *Simplified geological map of east Saint John illustrating the distribution of facies and exposures encompassed by the synoptic stratigraphic sections of Figure 39.2 (modified after Currie, 1984 and Currie and Nance, 1983).*

is uncertain. Parker (1984) placed an Upper Devonian to Carboniferous age on the formation based on the absence of pre-Variscan deformational fabrics, although equivalent rocks had previously been assigned to the Namurian (Rast et al., 1978). However, Currie and Nance (1983) and Ruitenberg and McCutcheon (1985) correlate much of the West Beach Formation with the bimodal late Precambrian and Eocambrian (Currie, 1984; Tanoli et al., 1985) volcanics and volcaniclastics of the Coldbrook Group. As this would establish the West Beach Formation as a junior synonym, the validity of the Mispec Group has itself been questioned. While the group is perhaps best redefined to include only the sedimentologically related Lancaster and Balls Lake formations, intrusive relationships within the former at the Saint John Dry Dock and the latter south of Mispec Bay (Nance and Warner, 1986), clearly demonstrate the existence of Carboniferous volcanism as young as Westphalian. The West Beach Formation is consequently retained in the following discussion although it must remain a descriptive field-term until its stratigraphic position is better defined.

Section descriptions and interpretation

Detailed measured sections of the Mispec Group from coastal and river exposures bordering Mispec Bay (Fig. 39.1) are represented as idealized synoptic stratigraphic sections in Figure 39.2. These summarize the principal lithologic relationships for each of the major section locations, three of which lie within the Balls Lake Formation, while the fourth is separated by intervening Triassic sediments and lies within the Lancaster Formation some 6 km to the west.

Location 1

The stratigraphically highest units of the Balls Lake Formation exposed within the study area are represented by Location 1 at Mispec Point. The uppermost unit of this section is erosively based, has a channel-like geometry and fines upward from a thin clast-supported and moderately sorted pebble conglomerate to medium-fine sandstones with interspersed pebbly layers. Contained sedimentary structures generally equate to a decreasing flow regime. Somewhat lower in the section, coarse to medium sandstones preserve large-scale trough crossbedding, some of which is defined by pebble stringers presumably deposited on the slip face of the parent dune during its migration downstream.

Such fining-upward channel-fill deposits containing structures associated with declining flow regimes are commonly associated with the widening and shoaling of low sinuosity rivers as the system aggrades before changing course (Moody-Stuart, 1966). Furthermore, rapidly changing channel patterns are typical of low sinuosity streams and result from the equally rapid downstream migration of major sandbanks which produce large-scale trough cross-stratification similar to that defined by pebble stringers towards the base of Section 1 (Moody-Stuart, 1966). Fining upward channel-fills also develop due to deposition from waning flow following flooding events. Consequently, the absence of Epsilon crossbedding and lithologies representative of overbank deposition, coupled with the relatively common occurrence of large-scale trough crossbedding and the presence of several erosively based, fining-upward channel-fill sequences, point toward deposition of this portion of the Balls Lake Formation within a low sinuosity, braided fluvial system.

Towards the base of the section at Location 1, unusually coarse, broadly tabular conglomerates, 1 to 2 m thick with clasts up to 1 m in length are interbedded with fluvial sandstones and pebble conglomerates typical of those higher in the section. These unsorted, ungraded, matrix-supported polymict conglomerates comprise clasts of various lithologies, are void of any current stratification, and clearly reflect deposition by a gravity-driven mechanism. As they also contain a greater proportion of large clasts relative to matrix fines and obviously reflect deposition from a viscous medium, they are interpreted as subaerial debris flows (Renick and Singh, 1980).

This interpretation is supported by the textural inversion exhibited by these conglomerates. Pebbles contained within the debris flows characteristically display a significantly greater degree of rounding than larger cobble and boulder-sized clasts. For the most part the larger clasts are calcareous, commonly crossbedded sandstones lithologically similar to the interbeds of fluvial origin. In contrast, the smaller clasts are similar in size, degree of rounding and lithologic variety to those of fluvial conglomerates within fining upward sequences. These anomalous grain-size/roundness relationships may imply initiation of the debris flow in an area where associated fluvial sediments were available for entrainment.

The interbedding of debris flows with braided fluvial sediments is commonly held to be an indication of deposition within an alluvial fan setting. Furthermore, the distinctive lateral change in grain size and bedding thickness from Location 1 to Locations 2 and 3 as described below, is characteristic of facies transitions within alluvial fans. The lithologic similarity of the larger debris-flow clasts to interbedded fluvial sandstones, and of smaller clasts to pebbles contained in associated fluvial conglomerates, implies an origin for the debris flows on the contemporary fan surface. Interestingly, a number of the debris flows overlie erosional surfaces (Fig. 39.2) and hence have a concave-upward base and channel-like morphology. This is presumably the result of partial diversion of impinging debris flows along topographic lows created by stream channelization on the fan surface. The absence of soft-sediment deformation in units underlying these channel scours suggests the debris flows were redirected into long abandoned, inactive channel segments. This, together with the large volume of fluvial sediments relative to debris flow deposits, and the small average grain size of units at Location 1 relative to that associated with proximal fan sediments, is taken to indicate deposition of the Balls Lake Formation at Mispec Point in the upper reaches of the mid-fan region.

Finally, despite a lack of current stratification, boulder-sized calcareous sandstone clasts within the debris flow conglomerates are strongly aligned parallel to a distinctive cleavage preferentially developed in the siltstones of Location 3 (Fig. 39.1). The lack of internal deformation and associated rotational features suggest clast alignment occurred prior to conglomerate lithification as a result of syndepositional deformation, and hence supports the proposal of Currie and Nance (1983) that deposition of the Balls Lake Formation was contemporaneous with Variscan deformation.

Location 2

The Balls Lake Formation lying down-section to the northeast at Location 2 is lithologically similar to that of Location 1, except for the absence of interbedded debris flows. Fluvial conglomerates, ranging to 1 m in thickness, show horizontal to very low angle stratification and are associated with peripheral medium to coarse sandstone wedges (Fig. 39.2), in a fashion similar to that noted by Rust (1972) for modern bar deposits. Interbedded with these packages are a limited number of relatively thin, fining-upward sequences that presumably represent deposition from waning flow as topographically higher channels are abandoned.

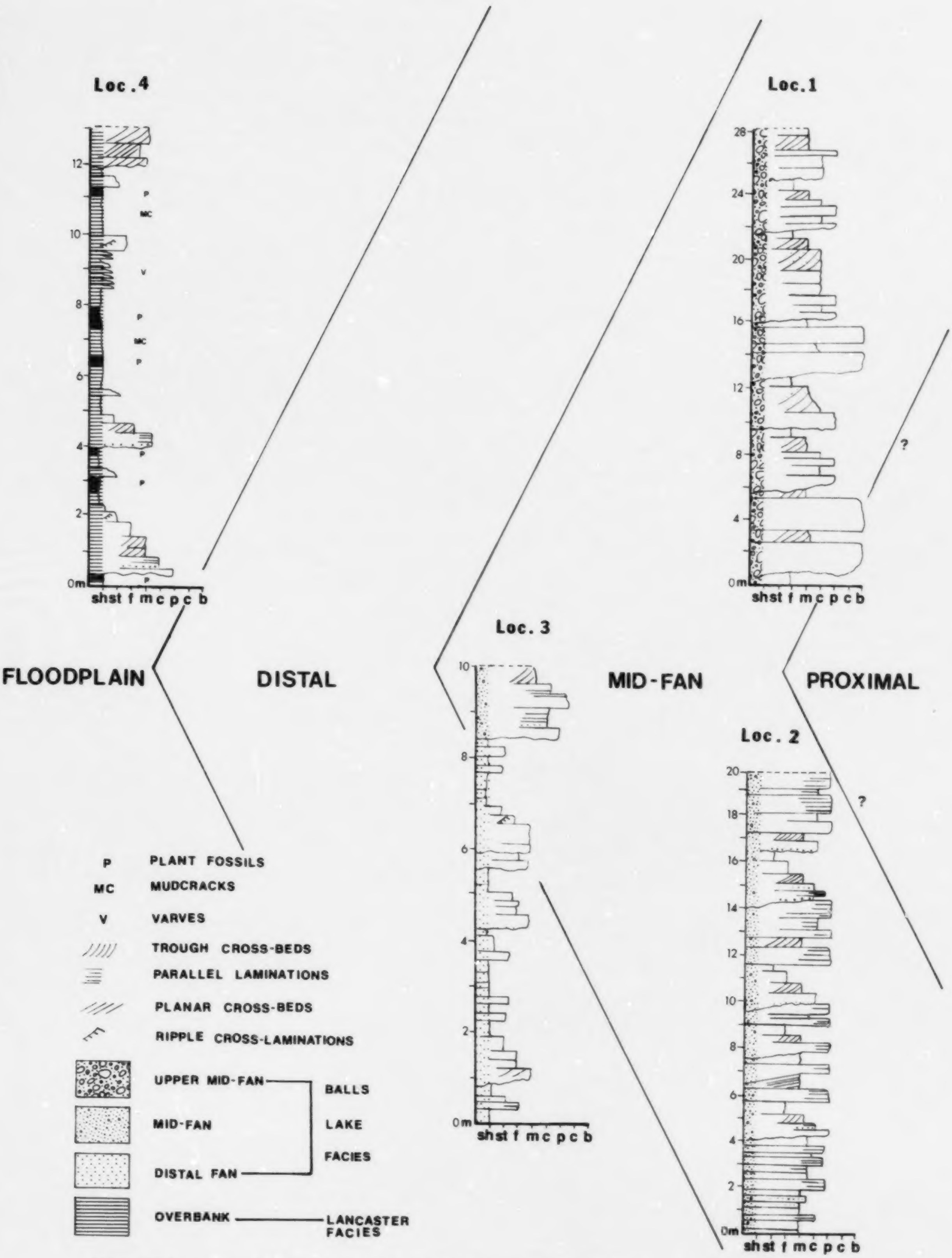

Figure 39.2. Correlation of synoptic stratigraphic sections showing a vertical distribution of facies suggestive of fan progradation.

Continuing down-section, fluvial conglomerate becomes thinner and siltstones are more common such that the section is dominated by laterally extensive, parallel-laminated and medium grained sandstones representing sheet-flood deposition during periods of high runoff.

The absence of debris flow deposits coupled with a general decrease in bedding thickness and a lack of thick, incised, fining-upward channel deposits, suggest deposition down-fan from Location 1 where channels were generally broader and shallower, and flow was less confined. Although both locations represent deposition within the mid-fan, the thick, incised channel fills at Location 1 suggest deposition above the fan intersection point, while features at Location 2 are characteristic of deposition below this point.

Location 3

Exposures along Mispec River at Location 3 (Fig. 39.1) occupy a stratigraphic position between those of Locations 1 and 2 (Fig. 39.2). The section exposes the greatest volume of siltstone and medium-to-thick shale observed within the Balls Lake Formation, but largely comprises laterally extensive, medium- to fine-grained, grey-green sandstones that are thin-to-medium bedded and of tabular form. Medium grained sandstones commonly possess low-relief erosional bases, while thinner, fine grained sandstones and siltstones show abrupt bases and grade upward to transitional contacts with shales.

Although evidence of current stratification is largely obscured, the marked decrease in bedding thickness and grain size relative to Locations 1 and 2 must reflect deposition in more distal regions of the fan. In the absence of diagnostic characteristics, the favoured interpretation is that of fluvial deposition related to flooding of the network of small streams draining the fan toe.

Distal fan regions are subjected to lower sedimentation rates than more proximal portions, and are hence more conducive to plant growth which is typically stifled by rapid sedimentation. Reduction of iron by decaying organic matter disseminated in fine grained distal sediments would account for the bedding-congruent green coloration of Location 3 sediments. Furthermore, vegetation in areas susceptible to flooding produces a baffling effect, which decreases flow velocity and encourages deposition of fines. This, in turn, fosters streambank stability and floodplain development, resulting in confined flow and channels that are narrower, deeper, and more sinuous than those typical of braided streams. As a result, deposits more typical of meandering streams are produced whereby laterally extensive, erosively based sandstones are interbedded with finer grained overbank deposits. Since the thickness of laterally accreted channel sands reflects stream size and depth, erosively based, medium bedded sandstones of Location 3 are taken to indicate channel deposition in small meandering streams which drain distal portions of the fan. Similarly, flooding of this small fluvial system results in the interbedding of small-scale vertical and lateral accretionary deposits.

Higher in the section at Location 3, fining-upward channel fills of thin grey-purple conglomerates and medium-to-fine sandstones, record the progradation of mid-fan facies over the distal fan. In contrast, sediments down-section take on characteristics similar to those of the Lancaster Formation, with occasional dark grey, carbonaceous shaly horizons. These ultimately give way to grey lithic arenites typical of meandering channel-fills within the Lancaster Formation (Currie and Nance, 1983). Units exposed north of Location 3 are therefore considered to represent a transitional zone between the distal reaches of the Balls Lake alluvial fan and floodplain sediments associated with the meandering system of the Lancaster Formation.

Location 4

This section lies within the Lancaster Formation some 6 km west of Locations 1, 2, and 3 (Fig. 39.1). The lowest unit is a small channel deposit scoured into underlying dark-grey shales containing disseminated plant fragments (Fig. 39.2). The channel fill grades upward from a pebble conglomerate containing shale rip-ups into coarse parallel-laminated sandstone, and illustrates deposition of coarse material in small streams incised into floodplain sediments.

Up-section, thick dark grey shales containing poorly preserved plant fragments are interbedded with thin fining-upward channel fills. Thin, varve-like graded couplets higher

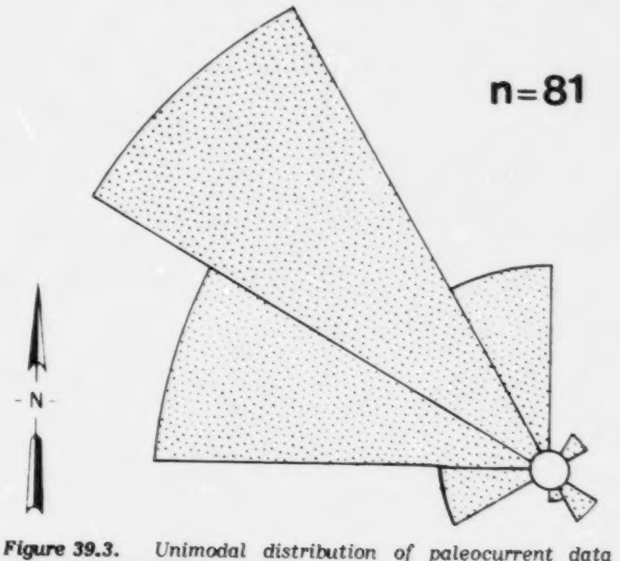

Figure 39.3. *Unimodal distribution of paleocurrent data indicating northwest paleoflow for units of the Balls Lake Formation.*

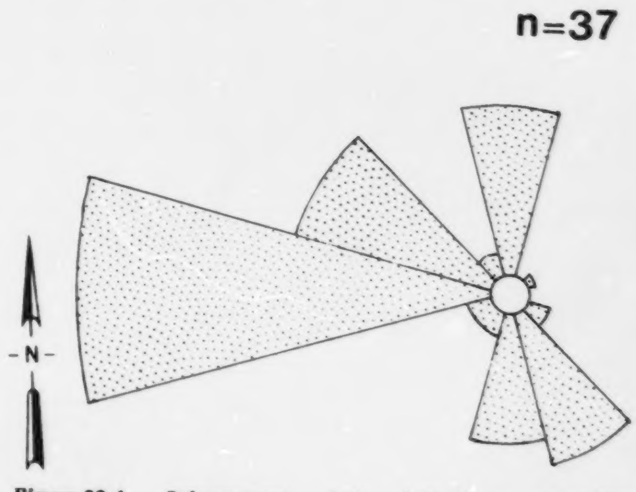

Figure 39.4. *Paleocurrent data indicating generally westerly paleoflow for units of the Lancaster Formation at Location 4.*

in the section form a composite, 1-m unit of limited lateral extent that is believed to indicate accumulation of fines in a shallow pond-like setting. The association of these sediments with sandstones and shales, some of which preserve sand-filled mudcracks, is highly indicative of subaerially exposed floodplains.

In the uppermost portion of the section, distinctly finer sandstones exhibiting both trough and planar crossbedding as well as parallel laminations, provide evidence for deposition through fluctuating flow velocities in small fluvial channels.

Location 4 is interpreted to reflect deposition in the overbank area of a large meandering stream system represented by the Lancaster Formation to the north. Thus, coarser channel-fill deposits near the base of the section are taken to represent proximity to the Balls Lake fan toe where flood events deliver coarse sediments to the adjacent Lancaster floodplain, while finer grained sandstones near the top of the section are attributed to stream deposition on an encroaching Lancaster floodplain at progressively greater distances from the receding fan toe. Nevertheless, the preponderance of shales at Location 4 in comparison to Location 3 indicates that sedimentation was controlled principally by flooding of the larger Lancaster system rather than the stream network draining the fan toe. The section is consequently the product of both the Lancaster fluvial system and the Balls Lake alluvial fan. In contrast, the shales characteristic of Location 3 were deposited beyond the influence of the Lancaster system and reflect overbank deposition during flooding of the distal fan streams.

Paleocurrent determinations

Paleoflow within the Balls Lake Formation (Fig. 39.3) is based largely on foreset inclination in trough crossbedding. Measurements are unimodal predominantly toward the northwest, and show a radial dispersal pattern, which is characteristic of alluvial fans (Bull, 1972). This implies broadly northwestward fan growth and a sediment source area that was located to the southeast.

Paleoflow within the Lancaster Formation (Fig. 39.4) shows a somewhat greater dispersion and was predominantly westward. However, rather than reflecting the major meandering stream responsible for the overbank sequence at Location 4, this delineates the flow direction of smaller streams draining the distal portions of the adjacent Balls Lake alluvial fan.

Section correlations

When placed in their relative stratigraphic positions (Fig. 39.2), the four sections show an encroachment of the mid-fan facies into areas initially and finally occupied by the distal facies. This progradational event terminates a coarsening-upward trend, which appears to give way to a fining-upward sequence initialized in the upper portion of Location 1. These large cycles record the response of the fan to changing local relief, and hence erosion rates, in the source area. This relationship emerges despite the fact that the structurally separated section at Location 4 is not vertically constrained.

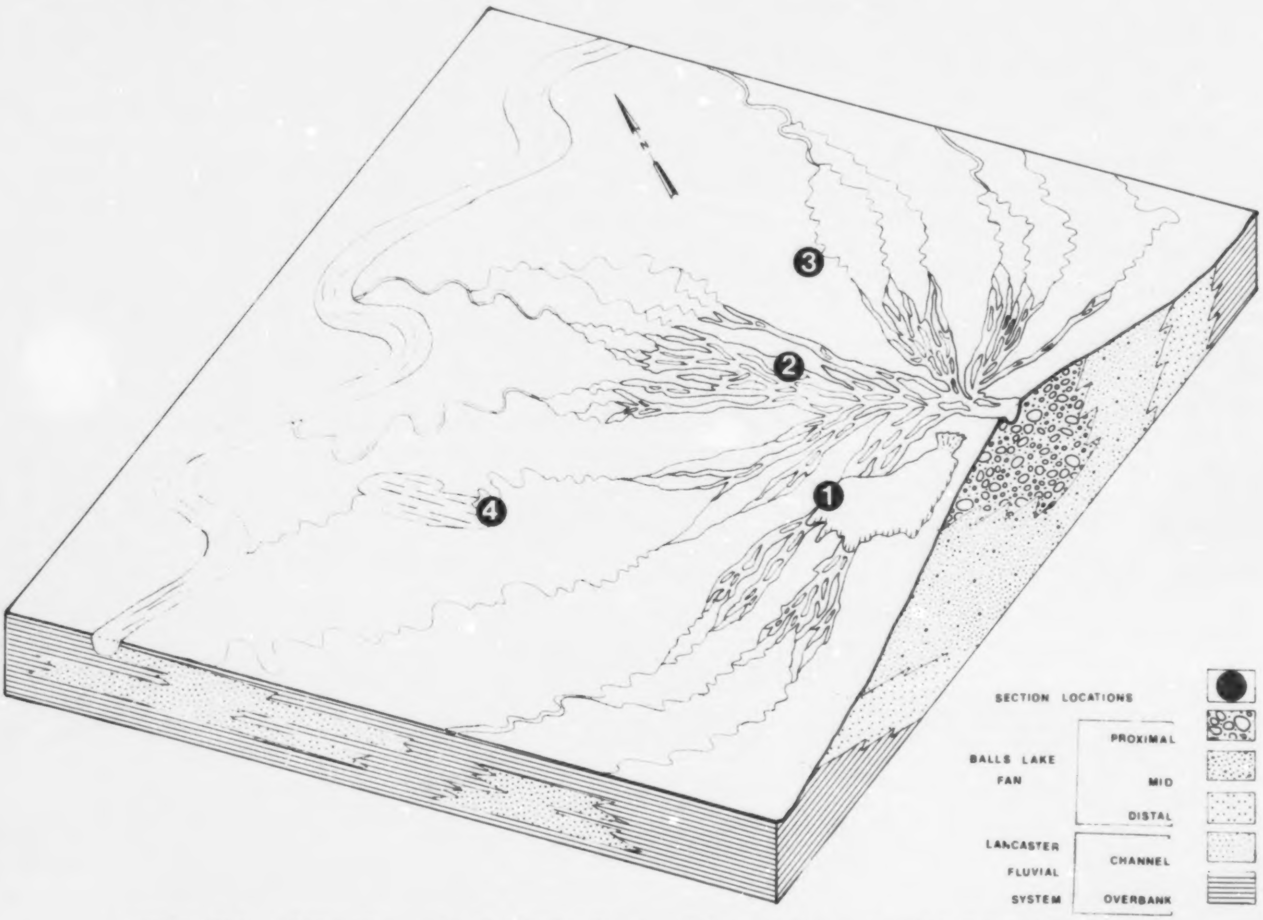

Figure 39.5. *Schematic model illustrating the depositional setting and spatial distribution of the Balls Lake and Lancaster Formations and their respective facies.*

Summary and discussion

A schematic model illustrating the depositional setting and spatial distribution of the Lancaster and Balls Lake formations, as dictated by the relative positions of the described field localities, is shown in Figure 39.5.

The debris flows and braided stream deposits which typify the Balls Lake Formation at Location 1 reflects alluvial fan sedimentation in the mid-to-proximal fan region. Here, deposition was dominantly fluvial but periodic debris flows developed on the contemporary fan surface and were diverted into low-lying abandoned stream channels as they moved down-fan. The Balls Lake Formation of Location 2 is similarly situated in the mid-fan area, although the lack of debris flows and abundance of fluvial bar deposits suggest that this section was located further down-fan and nearer to active braided channels. Location 3 represents the distal portion of the Balls Lake fan where sedimentation was controlled by small meandering streams draining the fan toe. Flooding of this stream network resulted in deposition of the overbank fines that characterize the sediments at this locality. In contrast, the Lancaster Formation at Location 4 comprises sediments deposited on the floodplain of a major fluvial system draining the basin in which both the Lancaster and Balls Lake formations were deposited. Here sedimentation was primarily influenced by flooding of the major stream system, although flood waters from the nearby Balls Lake fan affected deposition in smaller streams crossing the floodplain. Thin varve-like beds are attributed to the development of small pond-like features in the topographic lows on the floodplain.

Paleocurrent indicators from the Balls Lake Formation indicate a source area for the fan to the southeast, while those from the Lancaster Formation reflect the generally westerly flow of small sinuous streams draining across the Lancaster floodplain from the distal region of the adjacent Balls Lake fan.

Fluctuations of the rate of sedimentation in the respective depositional systems produced an interfingering of the Lancaster and Balls Lake formations as the fan prograded northwestward into the basin drained by the Lancaster river system (Fig. 39.5). Development of marked relief in a southerly source area is required for the development of the fan which, coupled with the syndepositional nature of at least part of the structural fabric within the Balls Lake Formation (Bradley, 1984; Nance and Warner, 1986), lends support to the model of Nance et al. (1985) in which uplift of the source area is attributed to Variscan transpression at the western terminus of the dextral Cobequid Fault. Structural telescoping within the Mispec Group, which intensifies south of Mispec Bay, has been interpreted in terms of a northward-propagating positive flower structure typical of convergent wrench zones (Nance and Warner, 1986). Development of the Balls Lake fan would therefore appear to reflect deposition that occurred ahead of, and was subsequently overridden by, an advancing Variscan allochthon as suggested by Currie and Nance (1983).

Acknowledgments

The authors greatly benefited from discussions with Tony Socci, Jim Warner and Saifullah Tanoli. Financial support for field work was provided by the Ohio University Research Council (OURC 9710) to Nance and a Sigma Xi Grant-in-Aid to Caudill. These are gratefully acknowledged. Kimberly Sorrell is thanked for her assistance in field annotation and sample collection.

References

Alcock, F.J.
1938: Geology of the Saint John region, New Brunswick; Geological Survey of Canada, Bulletin 210, 65 p.

Bradley, D.C.
1982: Subsidence in late Paleozoic basins in the northern Appalachians; Tectonics, v. 1, p. 107-123.

Bull, B.B.
1972: Recognition of alluvial-fan deposits in the stratigraphic record; Society of Economic Paleontologists and Mineralogists, Special Publication 19, p. 290-303.

Currie, K.L.
1984: A reconsideration of some geological relations near Saint John, New Brunswick; in Current Research, Part A, Geological Survey of Canada, Paper 84-1A, p. 193-201.

Currie, K.L. and Nance, R.D.
1983: A reconsideration of the Carboniferous rocks of Saint John, New Brunswick; in Current Research, Part A, Geological Survey of Canada, Paper 83-1A, p. 23-30.

Hayes, A.O. and Howell, B.G.
1937: Geology of Saint John, New Brunswick; Geological Society of America, Special Paper 5, 146 p.

Moody-Stuart, M.
1966: High and low-sinuosity stream deposits, with examples from the Devonian of Spitsbergen; Journal of Sedimentary Petrology, v. 36, p. 1102-1117.

Nance, R.D.
1985: Alleghenian deformation in the Mispec Group, Saint John Harbour, New Brunswick; in Current Research, Part A, Geological Survey of Canada, Paper 85-1A, p. 7-13.

Nance, R.D. and Warner, J.B.
1986: Variscan tectonostratigraphy of the Mispec Group, southern New Brunswick: structural geometry and deformational history; in Current Research, Part A, Geological Survey of Canada, Paper 86-1A, Report 40.

Nance, R.D., Warner, J.B., and Caudill, M.R.
1985: The Mispec Group, Saint John: A tectonostratigraphic record of the Alleghenian (Variscan) event in southern New Brunswick; Geological Association of Canada/Mineralogical Association of Canada, Program with Abstracts, v. 10, p. A43.

Parker, J.S.D.
1984: Geological relationships of the basement to cover Musquash Harbour to Black River, Saint John area, southern New Brunswick; unpublished Ph.D. thesis, University of New Brunswick, Fredericton, New Brunswick, 326 p.

Rast, N. and Grant, R.H.
1973: Transatlantic correlation of the Variscan-Appalachian orogeny; American Journal of Science, v. 273, p. 572-579.

Rast, N., Grant, R.H., Parker, J.S., and Teng, H.C.
1978: The Carboniferous deformed rocks west of Saint John, New Brunswick; in Guidebook for field trips in southeastern Maine and southwestern New Brunswick, ed. A. Ludman; New England Intercollegiate Geological Conference 70th Annual Meeting, Queens College Press, Flushing, New York, p. 162-173.

Renick, H.E. and Singh, I.B.
1980: Depositional sedimentary environments; 2nd edition, Springer-Verlag, New York, 431 p.

Ruitenberg, A.A., Giles, R.S., Venugopal, D.V., Buttimer, S.M., and McCutcheon, S.R.
1979: Geology and mineral deposits, Caledonia area; Mineral Resources Branch, New Brunswick Department of Natural Resources, Memoir 1, 213 p.

Ruitenberg, A.A. and McCutcheon, S.R.
1985: Excursion 8. Gold deposits of the Bay of Fundy coastal zone; in "Fredericton 85", Field Excursions, ed. R.K. Pickerill, C.K. Mawer, and L.R. Fyffe; Geological Association of Canada/Mineralogical Association of Canada, v. 11, 15 p., University of New Brunswick.

Rust, B.R.
1972: Structure and process in a braided river; Sedimentology, v. 18, p. 221-245.

Stopes, M.C.
1914: The "Fern Ledges" Carboniferous flora of Saint John, New Brunswick; Geological Survey of Canada, Memoir 14.

Tanoli, S.K., Pickerill, R.K., and Currie, K.L.
1985: Distinction of Eocambrian and Lower Cambrian redbeds, Saint John area, southern New Brunswick; in Current Research, Part A, Geological Survey of Canada, Paper 85-1A, p. 699-702.

Wardle, R.J.
1978: The stratigraphy and tectonics of the Greenhead Group: Its relationship to Hadrynian and Paleozoic rocks, southern New Brunswick; unpublished Ph.D. thesis, University of New Brunswick, Fredericton, New Brunswick.

Variscan tectonostratigraphy of the Mispec Group, southern New Brunswick: structural geometry and deformational history

Project 730044

R. Damian Nance [1] and James B. Warner [1]
Precambrian Geology Division

Nance, R.D. and Warner, J.B., Variscan tectonostratigraphy of the Mispec Group, southern New Brunswick: structural geometry and deformational history; in Current Research, Part A, Geological Survey of Canada, Paper 86-1A, p. 351-358, 1986.

Abstract

Variscan deformation southeast of Saint John, New Brunswick, strongly influenced Westphalian sedimentation within the penecontemporaneous Carboniferous Mispec Group and reflects sustained NW-SE compression developed in response to dextral transpression at the western termination of the Cobequid fault system.

In conjunction with the sedimentary record of the Mispec Group, present structures are attributed to Variscan transpression along downward-steepening en echelon thrust faults subparallel to the present Fundy shore. Thrust uplift during initial transpression is proposed to account for the southeasterly source area recorded in syntectonic alluvial fan and meandering stream sediments of the Mispec Group. Structural inversion through continued displacement produced the present structural geometry in which mildly deformed units of the Mispec Group are overthrust, in turn, by their highly deformed equivalents, older volcano-sedimentary sequences of the West Beach Formation and, finally, by the ?Hadrynian Cape Spencer granite.

Résumé

Les déformations survenues au cours de l'orogenèse de Variscan au sud-est de Saint John (Nouveau-Brunswick) ont fortement influencé la sédimentation westphalienne à l'intérieur du groupe carbonifère de Mispec (pénécontemporain); elles traduisent une compression NW-SE soutenue engendrée par un phénomène de transpression dextre à l'extrémité ouest du système de failles de Cobequid.

Les archives sédimentaires du groupe de Mispec permettent d'attribuer les structures actuelles à un régime de transpression qui se serait imposé au cours de l'orogenèse de Variscan le long de failles de poussée en gradins dont l'inclinaison s'accentue vers le bas et qui sont presque parallèles à la rive de la baie de Fundy. Les auteurs invoquent un soulèvement des nappes de charriage au début du régime de transpression pour expliquer la source sud-est relevée dans les sédiments syntectoniques de cônes de déjection et de fleuves à méandres du groupe de Mispec. Le déplacement s'est poursuivi, et une inversion structurale a produit la géométrie structurale actuelle de la région, dans laquelle des unités légèrement déformées du groupe de Mispec sont recouvertes en partie par leurs équivalents très déformés, par des séquences volcano-sédimentaires plus anciennes de la formation de West Beach et, finalement, par le granite de Cape Spencer (Hadrynien?).

[1] Department of Geological Sciences, Ohio University, Athens, Ohio 45701

Introduction

The effects of Late Paleozoic (Variscan) deformation in coastal southern New Brunswick, as recorded in sediments of the Carboniferous Mispec Group, appear as a narrow, east-northeast trending belt of basement-involved thrusting in sharp contrast to the regional strike-slip faulting that is the main deformational response to the Variscan event in Maritime Canada. In much of Maritime Canada, Variscan deformation reflects dominantly dextral movement on major wrench faults while penecontemporaneous Carboniferous sedimentation records the development of pull-apart basins (e.g. Bradley, 1982). In southern New Brunswick, however, the relationship of Carboniferous sedimentation to tectonics is less clear as the region has been interpreted as a major overthrust terrane (Rast and Grant, 1973) in which the Mispec Group formed an entirely allochthonous member of the overriding plate (Rast et al., 1978). The provenance, depositional setting and tectonic significance of the Mispec Group have consequently remained uncertain.

Recently, however, Currie and Nance (1983) have shown that the Mispec Group is, in part, authochtonous and have suggested that it records syntectonic alluvial and fluvial sedimentation developed in response to the uplift and emplacement of a major Variscan thrust sheet. In addition, Mosher and Rast (1984) have suggested that development of the overthrust terrane in southern New Brunswick reflects termination of dexral motion on the Cobequid-Chedabucto fault of Nova Scotia which would, in turn, provide a link between the regionally contrasting styles of Variscan deformation.

In order to test these proposals and refine the depositional and tectonic setting of the Mispec Group, a detailed study has been made of the area southeast of Saint John where tectonic juxtapositioning of autochthonous and allochthonous units permit the sedimentary record of the group to be examined in conjunction with its deformational history. This report documents the structural geometry of the Mispec Group as recorded in strongly deformed allochthonous units along the eastern shore of Mispec Bay, and forms a complementary study of that of Caudill and Nance (1986) which describes the stratigraphy and depositional setting of the group in autochthonous units to the north.

Unit descriptions

The bulk of lithologies southeast of Mispec Bay (Fig. 40.1) have long been included in the poorly defined Carboniferous Mispec Group (Hayes and Howell, 1937; Alcock, 1938). This assemblage is conventionally subdivided into bimodal volcanics ($?C_{wbv}$) and maroon to green volcanogenic sediments ($?C_{wbs}$) of the West Beach Formation (see Fig. 40.1); purple to green polymict conglomerates, sandstones and siltstones of the Balls Lake Formation (C_{bl}); and grey lithic arenites, pebble conglomerates and plant-bearing shales of the Westphalian Lancaster Formation (C_l). However, agreement on this ascending stratigraphy has only recently been achieved (e.g. Wardle, 1978; Currie and Nance, 1983; Parker, 1984; Ruitenberg, 1984), and the stratigraphic status of the West Beach Formation remains uncertain since its age (latest Precambrian or Carboniferous) is a matter of current debate. Caudill and Nance (1986) redefine the Mispec Group to include only the sedimentologically related Balls Lake and Lancaster formations, but suggest that the West Beach Formation be retained as a field term until its stratigraphic position is clarified. This approach is adopted in the following discussion. Additional units within the field area include the Cape Spencer granite ($?H_g$, Fig. 40.1) of uncertain but probable late Precambrian age (Currie and Nance, 1983; Ruitenberg, 1984), and small irregular aplite bodies (C_a, Fig. 40.1) that intrude the Balls Lake Formation.

Cape Spencer granite (Unit $?H_g$)

Extending northeastward from Cape Spencer (Fig. 40.1) is a series of strongly deformed granitic to quartz dioritic klippen that presently occupy the highest structural position and collectively constitute the Cape Spencer granite. These pink to green granitoid orthomylonites bearing porphyroclasts of quartz, orthoclase and plagioclase (An_{5-25}), are heterogeneously recrystallized to muscovite-chlorite schists and have been thrust northwestward over volcanic and sedimentary units of the West Beach Formation. The southeast-dipping basal thrust surface separating mylonitic grante from similarly deformed arkosic metasediments is spectacularly exposed at Cape Spencer. A late Hadrynian age for the granite best accounts for its structural and contact relationships, and is supported by textural and compositional similarities to Hadrynian plutons described by Currie et al. (1981) to the north.

West Beach Formation (units $?C_{wbv}$ and $?C_{wbs}$)

Tectonically underlying the Cape Spencer granite north and east of Cape Spencer is an allochthonous suite of deformed, grey to green volcaniclastic sandstones and siltstones, epidotized intermediate to mafic volcanics, fragmental pyroclastics, and occasional green, laharic conglomerates that have been collectively allocated to the West Beach Formation ($?C_{wbv}$, Fig. 40.1). The volcaniclastics show a pervasive orthomylonitic foliation, schistosity or slaty cleavage with porphyroclasts of quartz, feldspar and volcanic fragments, and abundant chlorite and calcite. More massive volcanics are similarly deformed with primary features preserved only as calcic plagioclase and minor quartz porphyroclasts that have escaped complete epidotization and chloritization. Fine grained protoliths of both volcanic and sedimentary origin are represented by chlorite-calcite schists.

Owing to the level of deformation, a Precambrian versus Carboniferous age for these rocks cannot be ascertained on the basis of field relationships, although they contain no fabric that is demonstrably pre-Variscan. However, they are believed to be younger than the Cape Spencer granite which, further northeast, is cut by probable West Beach mafic cykes (Currie and Nance, 1983), and must be older than the Balls Lake Formation to which they contribute clasts.

Structurally beneath and tectonically separated from the West Beach volcanics lies an allochthonous sequence of clastic and volcanogenic sediments ($?C_{wbs}$, Fig. 40.1) that has previously been assigned to both the Balls Lake Formation (Alcock, 1938; Ruitenberg et al., 1979; Parker, 1984) and the West Beach Formation (Hayes and Howell, 1937; Currie and Nance, 1983). Polyphase deformation and aplite intrusion have greatly obscured the original character of this lowest allochthonous unit, which has been transported northwest over strongly deformed but parautochthonous units of the Balls Lake and Lancaster formations. Light green, pyrite-bearing calcareous siltstones and purple to grey, tourmaline-bearing sandstones are similar to those of the Balls Lake Formation despite a pervasive cleavage or orthomylonitic foliation. However, they are not associated with the coarse lithic arenites and polymict conglomerates characteristic of this formation, but rather are interbedded with green and pink, volcanogenic chlorite-calcite schists resembling those of the West Beach Formation. The unit may therefore be transitional between

the West Beach and Balls Lake formations but is tentatively assigned to the former as its age and stratigraphic position are uncertain.

Balls Lake Formation (Unit C_{bl})

Deformed, purple to green polymict conglomerates, lithic wackes, siltstones and shales that form much of the coastal zone north of Ploughshare Rock, are assigned to the Carboniferous Balls Lake Formation (C_{bl}, Fig. 40.1) and closely resemble the mid-fan facies described by Caudill and Nance (1986). Light-green calcareous siltstones similar to their distal fan facies on Mispec River, are exposed southeast of Connoly Head (Fig. 40.1). However, southeast of Mispec Beach, primary structures are largely obliterated by a strong crenulated deformational fabric that varies from a solution cleavage in conglomerates and sandstones to a closely spaced slaty cleavage in finer lithologies. Abundant multiply oriented quartz veins are preferentially developed in coarser lithologies.

Lancaster Formation (Unit C_l)

Stratigraphically overlying the Balls Lake Formation at Ploughshare Rock and occupying much of the area between Mispec Bay and Millican Lake, are grey to tan, crossbedded lithic and quartz arenites, thin pebble conglomerates and black shales, that are occasionally plant bearing and are assigned to the Lancaster Formation (C_l, Fig. 40.1). These quartz-rich lithologies typically possess only a moderately developed solution cleavage but show a strong deformational gradient southward towards Ploughshare Rock and Millican Lake where they are overthrust by units of the West Beach Formation.

Aplite bodies (Unit C_a)

Sill-like masses of fine-grained aplite and smaller felsic dykes (C_a, Fig. 40.1) have been observed to intrude the Cape Spencer granite and sediments of the West Beach and Balls Lake formations. These comprise quartz, orthoclase,

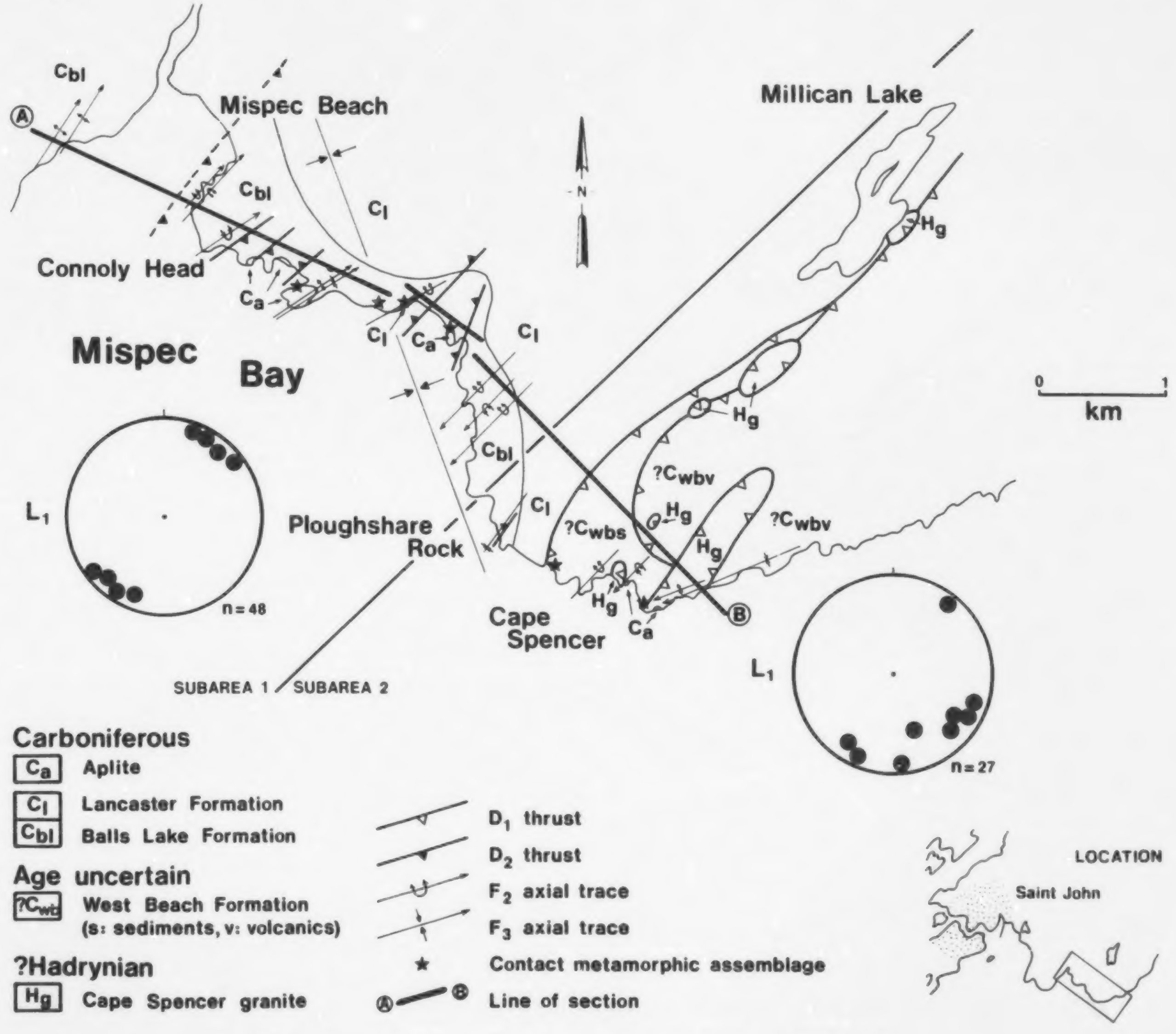

Figure 40.1. Geological sketch map of the eastern shore of Mispec Bay.

plagioclase (An_{5-15}) and calcite, and are associated with retrogressed andalusite-cordierite spotted slates which additionally affect the Lancaster Formation. Emplacement of these bodies is demonstrably syntectonic as both aplites and their associated contact metamorphic minerals crosscut the principal deformational fabric of their host rocks, but are themselves folded by later stages of Variscan deformation.

Structural fabrics and geometry

Three phases of Variscan deformation, two of which were major fabric-forming events, affect all units of the Mispec Group and have been designated D_1 to D_3 on the basis of overprinting. In addition, variation in the form and intensity of the first and principal fabric, as it intensifies towards the allochthonous slices of the Cape Spencer region, have been used to define two structural sub-zones arbitrarily separated by a gradational boundary north of Ploughshare Rock (Fig. 40.1).

D_2 Structures

The earliest recognizable phase of Variscan deformation (D_1) occurred in response to regional northwestward-directed thrusting that emplaced the Cape Spencer allochthons on surfaces now represented by the mylonitized basal contacts of the Cape Spencer granite and both units of the West Beach Formation. At this time, regional greenschist facies metamorphism accompanied the development of a pervasive but variably expressed, southeast-dipping tectonic fabric (S_1) that can contain a strong mineral lineation (L_1). S_1 is axial planar to rare, isoclinal minor folds (F_1) that plunge gently northeast and southwest (Fig. 40.2a). Large-scale, northwest-vergent overturned structures, such as those that accompany D_1 west of Saint John (Rast et al., 1978), have not been observed.

Subzone 1. In competent lithologies of the Balls Lake and Lancaster formations within subzone 1, S_1 is a widely spaced, protomylonitic solution cleavage defined by elongate, dissolution-modified, detrital quartz and feldspar porphyroclasts; dark, discontinuous dissolution cleavage folia; and fine quartz overgrowths and mica beards. In finer lithologies S_1 is a closely spaced slaty cleavage defined by syntectonically recrystallized muscovite and chlorite, and well-developed mica beards on small, dissolution-modified porphyroclasts. Elongate porphyroclasts and mica beards may also define an L_1 mineral lineation that, in subzone 1, plunges gently northeast and southwest parallel to F_1 axes, and has been attributed to both tectonic and sedimentary influences (Bradley, 1984). The latter is supported by the mutually perpendicular orientation of this lineation with respect to paleocurrent directions within the host Balls Lake and Lancaster formations (Caudill and Nance, 1986).

Based on axial ratios of porphyroclasts and conglomerate pebbles that average 1.5:1:0.7, the principal axis of strain (X) in subzone 1 parallels L_1 and F_1 axes, while the XY plane of strain lies within a broadly flat-lying S_1. Derived strain ellipsoids plot in both the constrictional and flattening fields. Although these are purely qualitative and ignore volume loss associated with development of the S_1 solution cleavage, their orientations relative to minor structures are similar to those of the classical Bygdin conglomerate (Hossack, 1968) and suggest flattening during thrust emplacement coupled with extension parallel to contemporary fold axes.

Subzone 2. Within klippen of the Cape Spencer granite and allochthonous units of the West Beach Formation which correspond to subzone 2 (Fig. 40.1), deformation is markedly more intense. In contrast to the protomylonitic solution cleavage of competent lithologies in subzone 1, S_1 in competent subzone 2 lithologies is an orthomylonitic foliation reflecting substantial ductile shearing, thrust-related flattening and post-tectonic annealing in addition to pressure solution. Less common ultramylonites and fine-grained schists similarly signal the southward intensification of S_1. Furthermore, the orientation of L_1 within subzone 2 is more variable and includes a southeast-plunging maxima that may represent the stretching direction during thrust transport.

Within the Cape Spencer granite, protomylonitic fabrics preserving primary granitic textures progressively give way to orthomylonites and ultramylonites within discrete shear zones and towards the basal thrusts of individual klippen. In protomylonitic granites S_1 is defined by microshears occupied by host mineral subgrains and syntectonically recrystallized muscovite. These separate S_1-parallel bands of dimensionally oriented quartz and feldspar porphyroclasts in which alignment has been achieved by rotation, dissolution normal to S_1, and crystallographic slip. In orthomylonitic granites, isolated sigmoidal porphyroclasts indicating top-to-northwest shear according to the criterion of Simpson and Schmid (1983), are enveloped by syntectonically recrystallized muscovite, chlorite, calcite and quartz, strain-free annealed quartz, and dissolution cleavage folia. Ultramylonitic granites are fine muscovite schists in which porphyroclasts are reduced to discontinuous patches of recrystallized and annealed quartz.

S_1 in metasediments is variably expressed as a solution cleavage, slaty cleavage and orthomylonitic foliation. In the protomylonitic Lancaster Formation at Ploughshare Rock, S_1 is a solution cleavage reflecting a combination of dissolution and shearing. In contrast to subzone 1, dissolution cleavage folia are more closely spaced and envelope sigmoidal, solution-modified porphyroclasts that exhibit a higher degree of strain and quartz pressure shadows of top-to-northwest shear sense. Subisotropic fabrics with core and mantle structures occur with pronounced post-tectonic annealing of quartz. In competent West Beach sediments, S_1 is commonly an orthomylonitic foliation defined by elongate, optically continuous quartz ribbons whose long axes define L_1. Dimensionally oriented subgrain development reflects significant mylonitization-related reduction in grain size, while the optical continuity of quartz ribbons and lack of pressure solution features, suggest that strain was accompanied by crystallographic slip. In finer lithologies S_1 is lithologically controlled and ranges from a slaty cleavage produced by syntectonic recrystallization of muscovite, to a closely spaced solution cleavage in which fine, solution-modified detrital prophyroclasts indicate top-to-northwest shear sense. Zones of post-tectonic annealed quartz may represent areas where high shear stresses were concentrated. Elongate porphyroclasts, quartz pressure shadows and mica beards that define L_1, plunge gently northeast, southwest and southeast.

Qualitative strain estimates again plot in both the constrictional and flattening fields, with prolate ellipsoids showing southeast-plunging axes of maximum elongation (X). However, observed strain in subzone 2 is complex and probably reflects the temporal and spatial overlap of various thrust-related processes such as shearing, flattening and pressure solution. In addition, deformation involved significant mass transfer, particularly in the Cape Spencer granite where the conversion of a quartzofeldspathic protolith to muscovite-rich mylonites requires a net loss of SiO_2, a portion of which is now represented by ubiquitus S_1-parallel quartz veins that locally achieve thicknesses of over 5 m (Alcock, 1938). Oblate strain ellipsoids in the granite suggest that porphyroclast extension parallel to X could not keep pace with shortening parallel to Z and normal

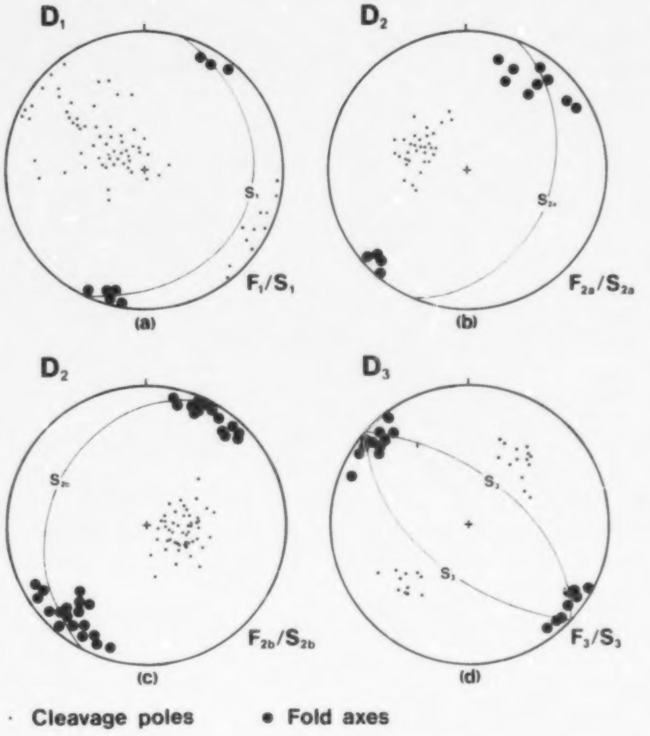

Figure 40.2. Stereographic projections of Variscan minor structures. (a) D_1 cleavage and fold axes, (b) D_2 cleavage and fold axes for northwest-verging structures, (c) D_2 cleavage and fold axes for southeast-verging structures, (d) D_3 fold axes and kink bands.

to S_1 through dissolution and crystallographic slip. Subzone 2 mylonitic fabrics are consequently attributed to the interaction of flattening and shear. Thus, shearing during initial northwestward thrusting produced southeast-plunging prolate ellipsoids, and was followed by flattening due to a component of subvertical overburden stress that became increasingly important as thrust imbrication progressed. However, variable amounts of shearing along discrete zones appears to be the dominant control of the degree of mylonitization. Northeast- and southwest-plunging lineations are attributed to local manifestations of subzone 1 strain geometry.

D_2 Structures

The second phase of Variscan deformation (D_2) is broadly coaxial with D_1 and produced asymmetric fold trains that verge both northwest (F_{2a}) and, more commonly, southeast (F_{2b}). Associated axial planar crenulation cleavages (S_2) range from barely perceptible to intense fabrics that locally transpose S_1. The resultant fold belt (Fig. 40.3) is superimposed on the D_1 thrust terrane at Cape Spencer, is geometrically conjugate in profile, and is mimicked on all scales. However, it is quite narrow since D_2 fold closures in the Mispec Group rapidly become less frequent and more gentle north of Mispec Bay (Nance, 1985). Associated D_2 thrusts are marked by an intensification of the S_2 cleavage and strong F_2 folding along S_2-parallel shear zones, but do not juxtapose different units and are likely to be of modest displacement relative to those of D_1.

F_{2a} folds, distinguished only by their northwest vergence, plunge gently northeast and southwest (Fig. 40.2b) and are confined to the northern portion of the field area. Upright to strongly overturned F_{2a} closures possess a variably expressed, axial planar cleavage (S_{2a}) that dips southeast and is principally the result of realignment of S_1 folia and dissolution along the steep limbs of F_{2a} microfolds in S_1. Less commonly, it is defined by top-to-northwest microshears and syntectonically recrystallized muscovite and chlorite. S_{2a} rapidly intensifies northeastward towards Mispec Bay where it is associated with overturned F_{2a} structures developed above a significant, southeast-dipping D_2 thrust at Mispec Beach. As a similar tectonic gradient in S_1 is absent, we differ from Parker (1984) who places a major, north-dipping D_1 thrust at this location.

F_{2b} folds are upright to recumbent structures that are coaxial with F_{2a} but show southeast vergence (Fig. 40.2c). They are absent in areas of F_{2a} folding and become more abundant to the southeast where they form mesoscopic chevrons in S_1 with near-vertical steep limbs and a top-to-southeast sense of shear. The axial planar S_{2b} crenulation cleavage dips northwest subparallel to minor D_2 thrusts and in texturally indistinguishable from S_{2a}, to which it is considered conjugate, as nowhere are the two fabrics observed together. D_2 is therefore considered a folding/backfolding response to renewed or continued northwest-southeast compression that earlier produced D_1.

D_3 Structures

A final phase of presumably Variscan deformation (D_3) produced upright, open folds, asymmetric kinks and conjugate kink sets that are equally dispersed across the entire field area. Fold and kink axes (F_3) plunge gently northwest and southeast (Fig. 40.2d), while locally developed axial surfaces (S_3) defined by quartz- or clacite-filled kink-band boundaries, dip steeply northeast and southwest. On an outcrop scale, interference of F_2 and F_3 folds produces dome and basin patterns, while the regional dispersion of F_2 axes suggests that the field area is transected by a broad F_3 synclinal flexure as shown in Figure 40.1. The tectonic significance of the minor northeast-southwest compression responsible for D_3 is presently unclear.

Metamorphism

Variscan deformation within the Mispec Group is associated with both regional and contact metamorphism. The first and most significant period (M_1) was a lower greenschist event that accompanied D_1. As a result, syntectonically recrystallized muscovite and chlorite define S_1 in pelitic and psammitic lithologies, while mylonitization of the Cape Spencer granite was accompanied by the breakdown of igneous feldspar to muscovite. Similarly, basalts of the West Beach Formation contain lower greenschist chlorite-epidote-calcite assemblages. Rare occurrences of extremely fine-grained brown mica may indicate the local attainment of biotite zone conditions.

A second period of metamorphism (M_2) accompanied the intrusion of aplite bodies (unit C_a) and resulted in the thermal recrystallization of calcite, cordierite, andalusite, chlorite and muscovite. Unfoliated but F_2 folded aplites associated with cordierite, andalusite and calcite porphyroblasts that overgrow S_1 but show dissolution and rotation along S_2, time this event as late or post-D_1 and pre-D_2. The coexistence of chlorite with cordierite and andalusite, coupled with the shallow nature of the intrusions, suggest temperatures for M_2 in the vicinity of 400°C (Turner, 1981). Partially retrogressed cordierite form fine aggregates within equant, composite porphyroblasts of

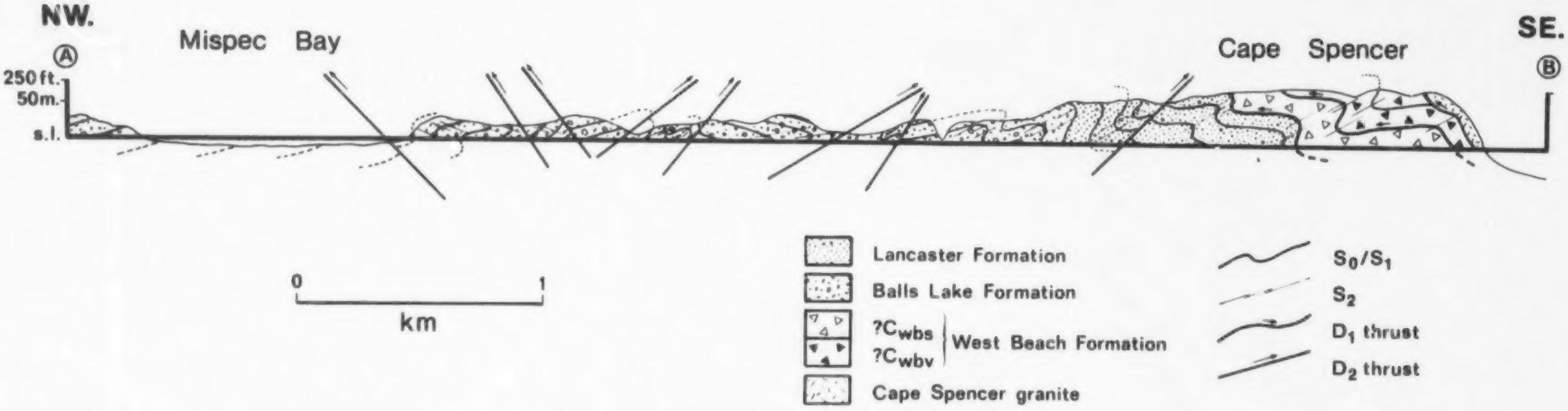

Figure 40.3. Schematic cross section, Mispec Bay to Cape Spencer (see Fig. 40.1 for location).

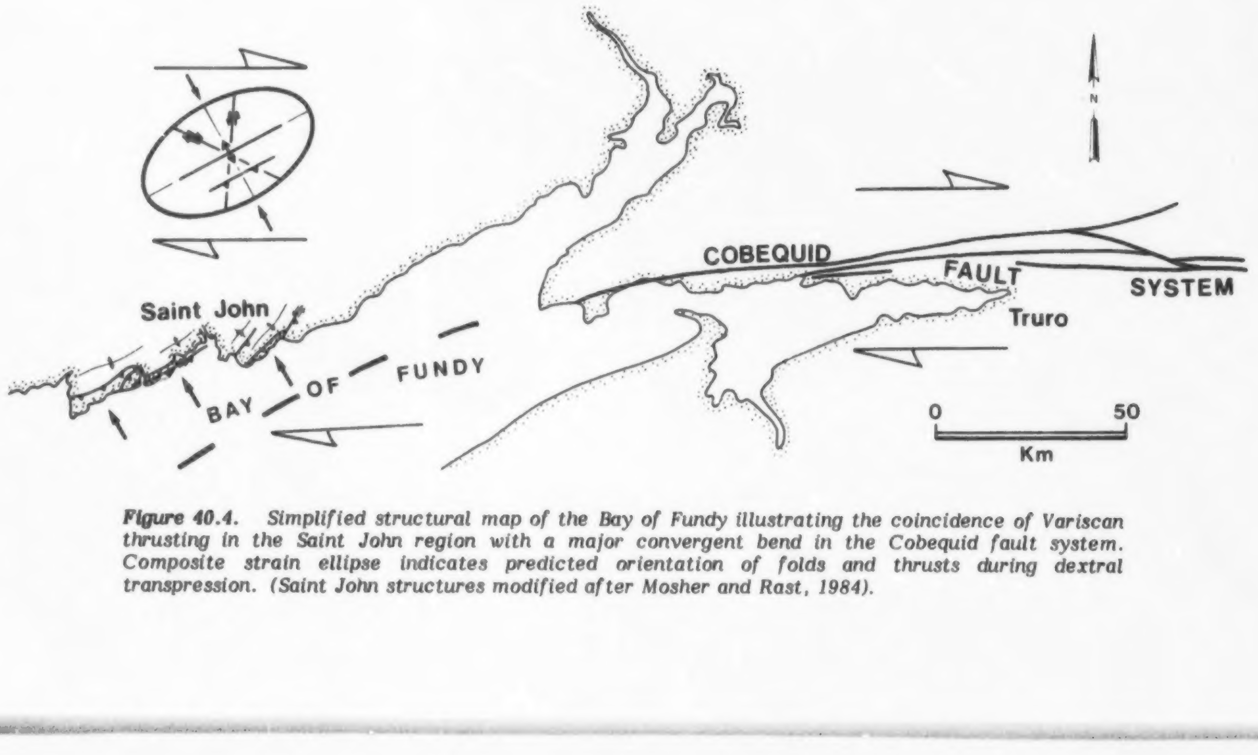

Figure 40.4. Simplified structural map of the Bay of Fundy illustrating the coincidence of Variscan thrusting in the Saint John region with a major convergent bend in the Cobequid fault system. Composite strain ellipse indicates predicted orientation of folds and thrusts during dextral transpression. (Saint John structures modified after Mosher and Rast, 1984).

randomly oriented chlorite, muscovite, quartz and calcite. Andalusite occurs as inclusion-filled cores to rounded, retrogressed porphyroblasts of randomly oriented muscovite. Calcite porphyroblasts include both clear, euhedral rhombs that overgrow S_1 and equant, inclusion-filled grains with clear rims and syntectonic rotational cores. Muscovite clots typical of spotted slates also overgrow finer muscovites that define S_1.

A final period of metamorphism (M_3) may have accompanied D_2 as some S_2-defining muscovite and chlorite appears to have been recrystallized rather than realigned during the D_2 event.

Discussion and interpretation

The principal phases of Variscan deformation within the Mispec Group southeast of Saint John reflect sustained northwest-southeast compression that was initially responsible for structural inversion of part of the stratigraphy during basement-involved, northwest-directed thrusting (D_1), and was later accommodated by conjugate folding and backthrusting (D_2). Syntectonic sedimentary fabrics within the Balls Lake Formation, coupled with its lateral equivalence to part of the Lancaster Formation (Caudill and Nance, 1986), constrains this Variscan deformation to the Westphalian. A strong tectonic control in the deposition of the Mispec Group is indicated by facies relationships, pebble lithologies that match allochthonous units to the southeast, and northwesterly paleocurrent directions aligned perpendicular to D_1 and D_2 fold axes (Caudill and Nance, 1986). Taken together, these features lend strong support to the proposal of Currie and Nance (1983) that the Mispec Group represents a sedimentary response to Variscan compressional uplift to the southeast, and hence provides a depositional and deformational record of the Variscan event in southern New Brunswick.

Carboniferous sedimentation in much of Maritime Canada has been successfully modeled in terms of pull-apart basins adjacent to major Variscan wrench faults (e.g. Bradley, 1982). While this is potentially consistent with the calc-alkaline volcanic assemblage of the West Beach Formation (Strong et al., 1979), assuming the latter is of Carboniferous age, it is clearly inconsistent with the demonstrably Carboniferous Balls Lake and Lancaster formations where sedimentation accompanied compressive deformation. Furthermore, the coincidence of Variscan deformation in southern New Brunswick with a major compressive bend at the western end of the Cobequid fault system (Fig. 40.4), which records significant right-lateral Westphalian displacement (Keppie, 1982), strongly suggests that the coaxial D_1 and D_2 events reflect convergent or transpressional wrenching. As illustrated by the experimentally derived, composite strain ellipse (insert Fig. 40.4), dextral transpression under these conditions would be accompanied by a northeast-southwest component of compression that would produce folds and thrusts whose orientation closely matches those of the Mispec Group.

A transpressional origin for Variscan deformation in southern New Brunswick might also account for the significant on-strike variation in its intensity and style. The regional, northwest-verging overturned structures produced during D_1 southwest of Saint John (Rast et al., 1978; Parker, 1984) and the post-tectonic greenschist facies metamorphism that culminates in the occurrence of garnet on Lorneville peninsula (Mosher and Rast, 1984) are absent southeast of the city, where D_1 folds are small and uncommon, while metamorphism is syntectonic and lies largely, if not entirely, within the chlorite zone. Furthermore, the allochthonous zones themselves are not laterally persistent but show en echelon trends. Thus, the intensely deformed belt of the Lorneville peninsula (Currie, 1984) does not extend east of Saint John but rather appears to side-step to that of Cape Spencer, which also terminates to the northeast and may again side-step seawards. Finally, in the vicinity of Musquash Harbour at the western end of the Lorneville belt, D_1 and D_2 structures trend northwest (Parker, 1984). Such trends are not observed elsewhere, but would be the predicted consequence of the thrust termination of dextral shear. These relationships are difficult to resolve within a simple overthrust system but are readily accommodated within a framework of transpression, where on-strike structural discontinuity and closely spaced contrasts in deformational intensity can be attributed to differing degrees of convergence along short, en echelon and right-stepping, synthetic wrench faults.

We therefore propose the conceptual model for Variscan deposition and deformation of the Mispec Group cartooned in Figure 40.5. In this scenario, Variscan thrusting is attributed to the development of a positive flower structure over a synthetic convergent wrench fault subparallel to the present Fundy shore. Such structures are characterized by high angle, upward-splaying faults that shallow into near-surface thrusts, and are typical of convergent wrench settings (Harding and Lowell, 1979). Uplift and structural inversion over the wrench fault would provide the southeasterly source area for the Balls Lake alluvial fans and meandering streams of the Lancaster Formation that are believed to feed a trunk meandering stream further north. However, with progressive displacement on the wrench system, the Mispec Group itself became involved in deformation. This resulted in the area's present structural geometry in which floodplain facies of the Lancaster Formation and transitional fan facies of the Balls Lake Formation are overthrust, in turn, by their deformed equivalents, units of the West Beach Formation and, finally, by the Cape Spencer granite.

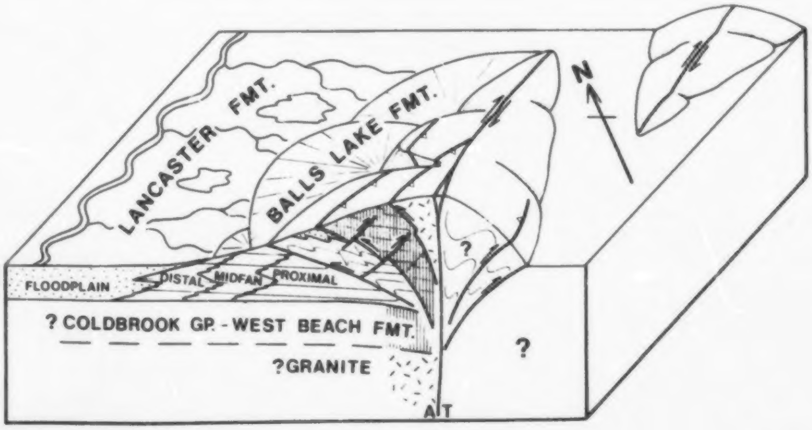

Figure 40.5

Conceptual model for the Variscan deposition and deformation of the Mispec Group through syndepositional, wrench-related thrusting during regional dextral transpression.

Acknowledgments

The authors greatly benefited from field discussions with Mike Caudill, Tony Socci, and Saifullah Tanoli. Financial support for field work was provided by the Ohio University Research Council (OURC 9710) to Nance and a Geological Society of America Grant-in-Aid to Warner. These are gratefully acknowledged.

References

Alcock, F.J.
1938: Geology of Saint John region, New Brunswick; Geological Survey of Canada, Memoir 216, 65 p.

Bradley, D.C.
1982: Subsidence in late Paleozoic basins in the northern Appalachians; Tectonics, v. 1, p. 107-123.

Bradley, L.M.
1984: Structural analysis of deformed Carboniferous strata, Mispec Beach, southern New Brunswick; unpublished M.S. thesis, State University of New York, Albany, New York, 134 p.

Caudill, M.R. and Nance, R.D.
1986: Variscan tectonostratigraphy of the Mispec Group, southern New Brunswick: Part I: Stratigraphy and depositional setting; in Current Research, Part A, Geological Survey of Canada, Paper 86-1A, Report 39.

Currie, K.L.
1984: A reconstruction of some geological relations near Saint John, New Brunswick; in Current Research, Part A, Geological Survey of Canada, Paper 84-1A, p. 193-201.

Currie, K.L. and Nance, R.D.
1983: A reconsideration of the Carboniferous rocks of Saint John, New Brunswick; in Current Research, Part A, Geological Survey of Canada, Paper 83-1A, p. 29-36.

Currie, K.L., Nance, R.D., Pajari, G.E., Jr., and Pickerill, R.K.
1981: Some aspects of the pre-Carboniferous geology of Saint John, New Brunswick; in Current Research, Part A, Geological Survey of Canada, Paper 81-1A, p. 23-30.

Harding, T.P. and Lowell, J.D.
1979: Structural styles, their plate tectonic habitats, and hydrocarbon traps in petroleum provinces; American Association of Petroleum Geologists Bulletin, v. 63, p. 1016-1058.

Hayes, A.O. and Howell, B.G.
1937: Geology of Saint John, New Brunswick; Geological Society of America, Special Paper 5, 146 p.

Hossack, J.R.
1968: Pebble deformation and thrusting in the Bygdin area (southern Norway); Tectonophysics, v. 5, p. 315-339.

Keppie, J.D.
1982: The Minas Geofracture; in Major structural zones and faults of the northern Appalachians, ed. P. St.-Julien and J. Beland; Geological Association of Canada, Special Paper 24, p. 265-280.

Mosher, S. and Rast, N.
1984: The deformation and metamorphism of Carboniferous rocks in Maritime Canada and New England; in Variscan tectonics of the North Atlantic region, ed. D.H.W. Hutton and D.J. Sanderson; Geological Society of London, Special Publication 14, Blackwell Scientific Publications, Oxford, p. 233-243.

Nance, D.
1985: Alleghenian deformation in the Mispec Group, Saint John Harbour, New Brunswick; in Current Research, Part A, Geological Survey of Canada, Paper 85-1A, p. 7-13.

Parker, J.S.D.
1984: Geological relationships of basement to cover, Musquash Harbour to Black River, Saint John area, southern New Brunswick; unpublished M.Sc. thesis, University of New Brunswick, Fredericton, New Brunswick, 326 p.

Rast, N. and Grant, R.H.
1973: Transatlantic correlations of the Variscan-Appalachian orogeny; American Journal of Science, v. 273, p. 572-579.

Rast, N., Grant, R.H., Parker, J.S.D., and Teng, T.C.
1978: The Carboniferous deformed rocks west of Saint John, New Brunswick; in Guidebook for fieldtrips in southeastern Maine and southwestern New Brunswick, ed. A. Ludman; New England Intercollegiate Geological Conference 70th Annual Meeting, Queens College Press, Flushing, New York, p. 162-173.

Ruitenberg, A.A.
1984: Geology and mineralogy of gold deposits in the Cape Spencer-Black River area; in Ninth Annual Review of Activities, ed. B.M.W. Carroll; Mineral Resources Division, New Brunswick Department of Natural Resources, Information Circular 84-2, p. 7-15.

Ruitenberg, A.A., Giles, R.S., Venugopal, D.V., Buttimer, S.M., McCutcheon, S.R., and Chandra, J.
1979: Geology and mineral resources, Caledonia area; Mineral Resources Branch, New Brunswick Department of Natural Resources, Memoir 1, 213 p.

Simpson, C. and Schmid, S.
1983: An evaluation of criteria to deduce the sense of movement in sheared rocks; Geological Society of America Bulletin, v. 94, p. 1281-1288.

Strong, D.F., Dickson, W.L., and Pickerill, R.K.
1979: Chemistry and prehnite-pumpellyite facies metamorphism of calcalkaline Carboniferous volcanic rocks of southeastern New Brunswick; Canadian Journal of Earth Sciences, v. 16, p. 1071-1085.

Turner, F.J.
1981: Metamorphic petrology: Mineralogical, field and tectonic aspects, 2nd Edition; McGraw-Hill, New York, 524 p.

Wardle, R.J.
1978: The stratigraphy and tectonics of the Greenhead Group: Its relationship to Hadrynian and Paleozoic rocks, southern New Brunswick; unpublished Ph.D. thesis, University of New Brunswick, Fredericton, New Brunwick, 294 p.

Illite crystallinity studies in the Gaspé-Connecticut Valley synclinorium around Barnston, Quebec[1]

Contract 12ST.23233-4-0780

Iain M. Samson[2] and Anthony E. Williams-Jones[3]
Economic Geology and Mineralogy Division

Samson, I.M. and Williams-Jones, A.E., Illite crystallinity studies in the Gaspé-Connecticut Valley synclinorium around Barnston, Quebec; in Current Research, Part A, Geological Survey of Canada, Paper 86-1A, p. 359-364, 1986.

Abstract

Illite crystallinity patterns in the sedimentary rocks of the Gaspé-Connecticut Valley synclinorium, in the vicinity of Barnston, Quebec, do not support the theory that a buried pluton is responsible for a magnetic anomaly in the same area. Anomalously low illite crystallinity indices fall within a NE-trending elliptical zone which, in part, overlaps with the magnetic anomaly. Samples with background illite crystallinity indices occur in the same area. If this zone of low illite crystallinity indices reflects a buried intrusive, the intrusive does not have a magnetic expression.

Intrusion of the Stanhope granite, exposed in southern part of the area, appears to have affected the clay mineralogy of the country rocks. Rocks within the Stanhope metamorphic aureole are characterized by a mixed-layer montmorillonite-mica mineral, possibly rectorite, which results in XRD peak interference, and produces anomalously high illite crystallinity indices. High, as well as low, illite crystallinity indices may be indicative of nearby intrusives.

Résumé

Les configurations critallines de l'illite dans les roches sédimentaires du synclinorium de Gaspé – vallée de Connecticut dans la région de Barnston, Québec, ne concorde pas avec l'hypothèse qu'un pluton en profondeur fut la cause d'une anomalie magnétique dans cette région. Des indices de cristallinité de l'illite de faible anomalie indiquent une zone ellipsoïde orientée vers le nord-est qui coïncide, en partie, avec l'anomalie magnétique. Des échantillons d'indices de cristallinite de l'illite normale se trouvent dans cette région. Si la zone de faibles indices de cristallinité de l'illite reflète la présence d'un amas intrusif en profondeur, celui ci n'a pas d'expression magnétique.

L'emplacement du granite de Stanhope, affleurant dans le sud de la région, semble avoir affecté les minéraux argileux dans les roches encaissantes. Dans la zone de métamorphisme de contact du granite, les roches se caractérisent par un minéral (de type illite-montmorillonite), probablement la rectorite, qui produit une interférence dans les pics XRD et ainsi augmente de façon significative la cristallinité de l'illite. Des indices élevés, aussi bien que faibles, de la cristallinité de l'illite, peuvent indiquer la présence d'amas intrusifs.

---

[1] Contribution to the Federal Asbestos Initiatives Geoscience Research Program 1984-87. Project carried by Geological Survey of Canada, Economic Geology and Mineralogy Division, Project 840059.

[2] Mineral Exploration Research Institute, C.P. 6079, Succ. A, Montreal, Quebec H3C 3A7

[3] Department of Geological Sciences, McGill University, 3450 University Street, Montreal, Quebec H3A 2A7

Introduction

This study deals with the clay mineralogy of sedimentary rocks in the Gaspé-Connecticut Valley synclinorium around Barnston, Eastern Townships, Quebec (Fig. 41.1). The principal objective of the study was to use variations in clay mineralogy as indicators of low grade thermal effects occurring as a result of contact metamorphism caused by a hidden intrusive underlying the area. Such an intrusion is suggested by a magnetic anomaly in the area and by several small intrusives exposed at the surface (Fig. 41.2).

Geology

The rocks of the Gaspé-Connecticut Valley synclinorium in this area are part of the Siluro-Devonian St. Francois Group, comprising a miogeoclinal sequence of interbedded, shales, slates, limestones, quartzites, greywackes and conglomerates which increase in metamorphic grade to marbles, phyllites, schists and hornfels towards the Stanhope granite pluton (Fig. 41.2).

The St. Francois Group may be subdivided in the study area into a western member dominated by argillaceous limestones and an eastern member comprising quartzites and greywackes (Fig. 41.2) (Cooke, 1957). The beds strike northeast and north-northeast and dip northwest at 50° to vertical. Cooke (1957) and Erdmer (1981) considered most of the sequence to be overturned, as evidenced by inverted crossbedding and graded-bedding. A regional penetrative cleavage is almost ubiquitous in argillaceous units. Its strike is subparallel to bedding, but it generally dips to the northwest at a lower angle (30 to 60°). In contact metamorphic rocks, a second penetrative cleavage or a crenulation cleavage may be present. Two styles of folding are recognized. The first set is isoclinal, with axial planes that approximately parallel bedding. These are mostly seen on a small scale in laminated limestones but may also form much larger structures (Cooke, 1957). The second is a more open S-type fold with a subhorizontal axial plane.

These sedimentary rocks have been intruded in the south of the area by the Acadian Stanhope granite (Averill pluton in Vermont) and by numerous related dykes which range from granites through quartz-porphyries to felsites (Cooke, 1957). A biotite K-Ar age for the pluton gave 346 ± 4 Ma (Erdmer, 1981).

Thin camptonite dykes trending east to southeast also intrude the sequence (Cooke, 1957; Poitevin and Cooke, 1946) and are presumably part of the Cretaceous Monteregian event.

Metamorphism

The degree of metamorphism varies significantly throughout the area. The development of coarse grained and porphyroblastic textures, visible in hand specimen, extends 3 to 5 km from the contact of the Stanhope pluton, with a protrusion of contact metamorphosed rock extending about 8 km northwards from the contact, west of the Coaticook River Valley (Fig. 41.2). Outside of this zone, argillaceous rocks remain fine grained, ranging from low grade fissile shales to relatively indurated, competent slates. Metamorphism of arenaceous and calcareous rocks is less obvious.

Erdmer (1981) reported a regional biotite-grade metamorphism for the area and Cooke (1957) reported alteration of ferromagnesian minerals to biotite and chlorite. However, de Romer has described an assemblage of calcite, quartz, sericite, and clay minerals for calcareous units in the St. Francois and Glenbrooke groups to the west, implying a lower diagenetic-metamorphic grade for the sequence.

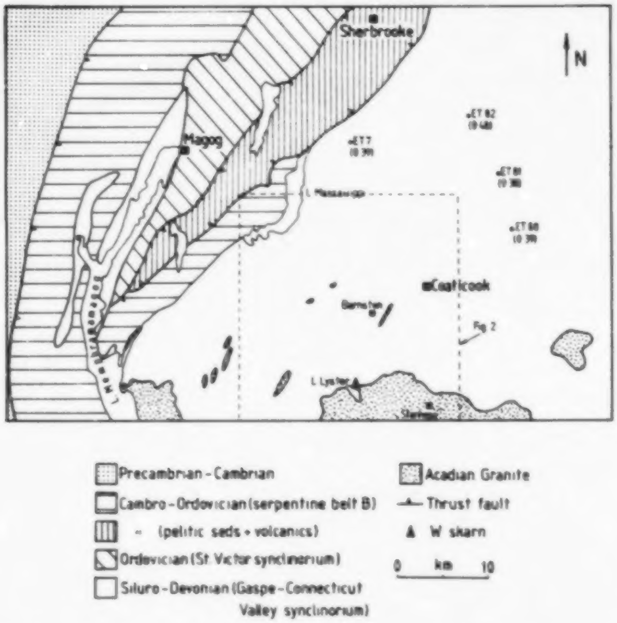

Figure 41.1. Simplified geological map of the south-western Eastern Townships. Based on Quebec Department of Natural Resources map no. 1866 (1:250 000). Sample locations and their illite crystallinity indices outside of the main study area are also shown.

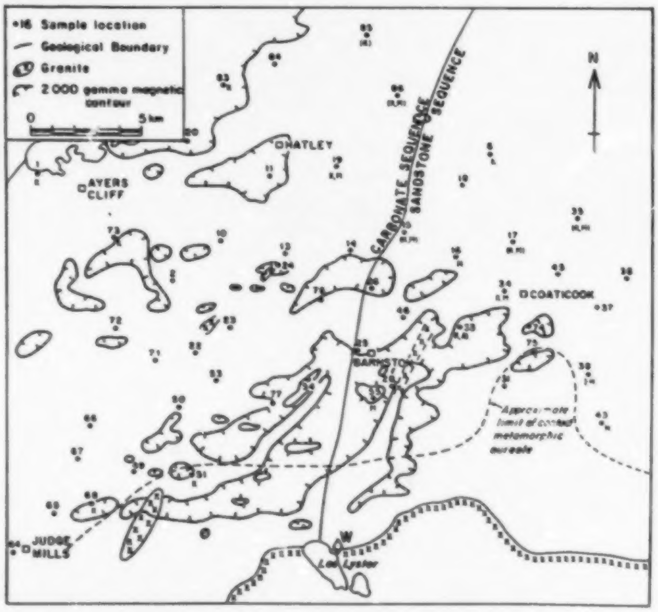

Figure 41.2. Geology and sample locations in the study area, position of 2000 gamma magnetic contour and location of samples containing montmorillonite (M), kaolinite (K) and mixed-layer montmorillonite-illite (I-M).

The contact metamorphic zones around the pluton are characterized by the first appearance of andalusite, staurolite and sillimanite in the pelites and by tremolite, K-feldspar, clinozoisite and diopside in the calc-silicate schists (Erdmer, 1981). Within one kilometre of the granite, metamorphic temperatures and pressures were estimated at 400 to 600°C and 2 to 3 kb respectively (Erdmer, 1981).

Sampling and analysis

Exposures in the study area are, in general, scarce owing to a thick cover of glacial drift. Fortunately, most of the rocks are argillaceous with few clean limestones and quartzites. In any exposure, the most argillaceous, least weathered rocks were sampled. Details of the clay mineralogy separation technique are given in Duba (1982).

Mineralogy of the >2 μm fraction

X-ray diffraction analysis shows the >2 μm fraction of rocks outside the high grade aureole to be dominated by illite, quartz, chlorite and feldspar (mostly plagioclase with some K-feldspar) (Fig. 41.3). Cooke (1957) reported the presence of secondary (diagenetic?) albite in the greywackes. Many of the rocks analyzed were calcareous. However, carbonates were not present in the >2 μm fraction due to their prior removal by acid dissolution. Biotite has not been identified in the >2 μm fraction.

Montmorillonite and kaolinite are present in many of the rocks in the area. Montmorillonite is indicated by the presence of a wide peak at about 7° 2θ (12.6 angstrom) which, on glycolation, shifts to about 5° 2θ (17.7 angstrom) (Fig. 41.3). Samples containing these clay minerals do not have a close spatial relationship with the magnetic anomaly and only one is close to a known intrusive (Fig. 41.2). In one sample (ET 38), from about 1 km outside of the aureole, a mixed-layer illite-montmorillonite was detected. This mineral is characterized by peaks at about 7° and 3.2° 2θ (Chen, 1977). Along strike, in the Gaspé peninsula, montmorillonite bearing rocks were found only in intrusion-related alteration zones (Duba and Williams-Jones, 1983a). It is possible that the observed clay mineral assemblages in this area are also related to hydrothermal alteration, but their wide distribution may be indicative of low temperature weathering. Although some of the montmorillonite-kaolinite bearing rocks are weathered, particularly along fracture surfaces, many appear very fresh. Alunite was also tentatively identified in one sample from about 1 km from a small intrusive (Fig. 41.2).

X-ray diffractograms of most samples from within the metamorphic aureole are characterized by a broad peak between 7.5 and 8.5° 2θ (Fig. 41.4). This appears either as a shoulder on the 001 mica peak or produces a composite, artificially broad mica peak. On glycolation, this interference effect disappears and a 'clean' mica peak remains. In two glycolated samples, new peaks appeared at 4 and 5.5° 2θ (Fig. 41.4). The change in lattice spacing on glycolation indicates the presence of expandable montmorillonite-type layers in the structure. This mineral is probably rectorite (allevardite), a sodium mica with a 1:1 mix of

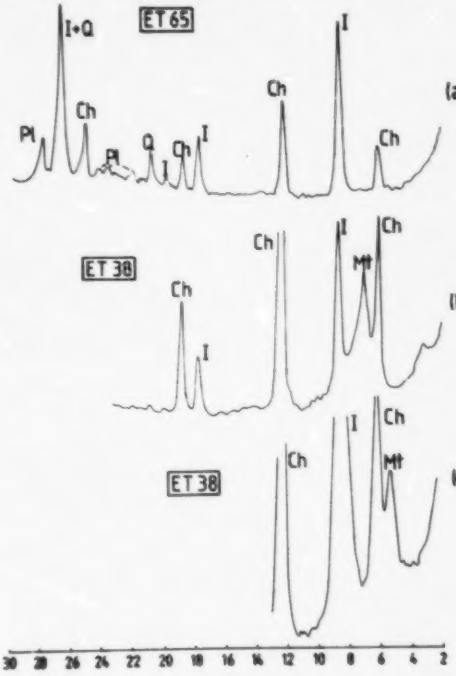

Figure 41.3. X-ray diffractograms of samples from outside of the aureole showing (a) a typical greywacke; (b) an untreated montmorillonite bearing slate; and (c) the same sample after glycolation. Q = quartz; Ch = chlorite; I = illite; Mt = montmorillonite; Pl = plagioclase.

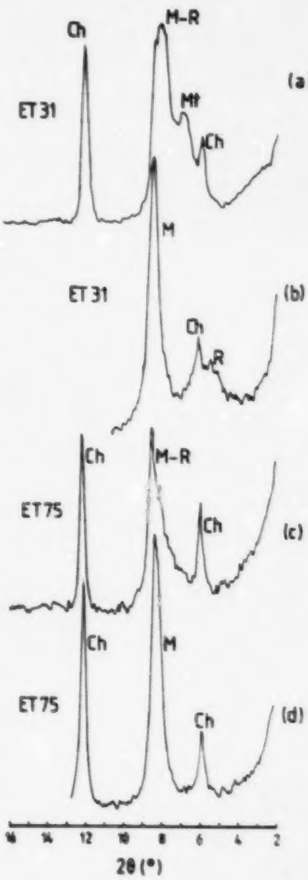

Figure 41.4. X-ray diffractograms of samples from within the metamorphic aureole showing the presence of a montmorillonite-type mineral (rectorite? = R). (a) and (c) are untreated. (b) and (d) are glycolated. M = mica.

montmorillonite and mica (paragonite) layers (Kisch, 1983). During normal burial, rectorite forms at the upper boundary of diagenesis (incipient metamorphism) (Kisch, 1983); however it is also found in active hydrothermal systems (Eslinger and Savin, 1973). Inasmuch as the metamorphic grade within the Stanhope aureole is relatively high, the rectorite in the study area probably has a hydrothermal origin.

Illite crystallinity index (IC)

Introduction

Illite is a mixed-layer clay mineral composed dominantly of dioctahedral muscovite layers with a small proportion of montmorillonite layers (Warshaw and Roy, 1961). With increasing diagenetic grade, the proportion of montmorillonite layers decreases, and the illite structure becomes more ordered, eventually transforming to well ordered muscovite. This progressive ordering is reflected in a narrowing of the 001 X-ray diffraction peak (10 angstrom basal reflection). The illite crystallinity index is measured as the width of the 001 peak at half its height and expressed in terms of the Bragg angle, 2θ. This ordering is very strongly influenced by temperature but can also be affected by fluid and host rock compositions. Owing to its response to elevated temperatures, illite crystallinity can be a useful guide to hidden intrusions (Duba and Williams-Jones, 1983a; Williams-Jones, in press). Such IC anomalies normally extend much farther from the heat source than the visible alteration.

Results

IC values of Barnston samples from outside the visible contact metamorphic zone range from 0.26 to 0.56° 2θ with most in the range 0.35 to 0.45° 2θ (Fig. 41.5). These values are comparable to those found in equivalent rocks of the Gaspé-Connecticut Valley synclinorium in the Gaspé Peninsula (Duba and Williams-Jones, 1983b) and suggest diagenetic conditions within the late diagenetic to anchizone stages (Ogunyomi et al., 1980; Frey et al., 1980). The width of the 001 peak of samples from within the aureole is typically quite large (0.4 to 2.0° 2θ). As discussed above, these values are anomalous and are due to peak interference, probably caused by the presence of rectorite.

Repeat analysis (from initial crushing onwards) of several samples with a range of IC values show excellent reproducability, to within 0.01° 2θ, in all cases.

Anomalously high and low IC indices are somewhat erratically distributed in the study area (Fig. 41.6). Low indices are concentrated in a broad northeast trending zone extending from the edge of the Stanhope granite some 15 km northeastwards. · However, a significant number of the samples in the zone yielded 'background' IC indices.

In this rock suite, there is no general correlation between rock type and IC index except that the four lowest values (>0.31) (Fig. 41.5), were all obtained from argillaceous limestones. However, this is the opposite to what would be expected if the low values were reflecting host rock composition. Because K^+ is required for the montmorillonite to illite and illite to muscovite transitions, argillaceous limestones should, if anything, have higher IC indices than the other sedimentary rock types (shales and greywackes) which are richer in potassium.

Discussion

As was noted in the previous section, anomalously low IC indices fall within a broad northeast-trending zone. However, this zone does not coincide with the position of the observed magnetic anomaly, although it does overlap with it to some extent. Therefore, although it is possible that the IC anomaly has resulted from the intrusion of a pluton or plutons, such igneous bodies do not appear to be related to

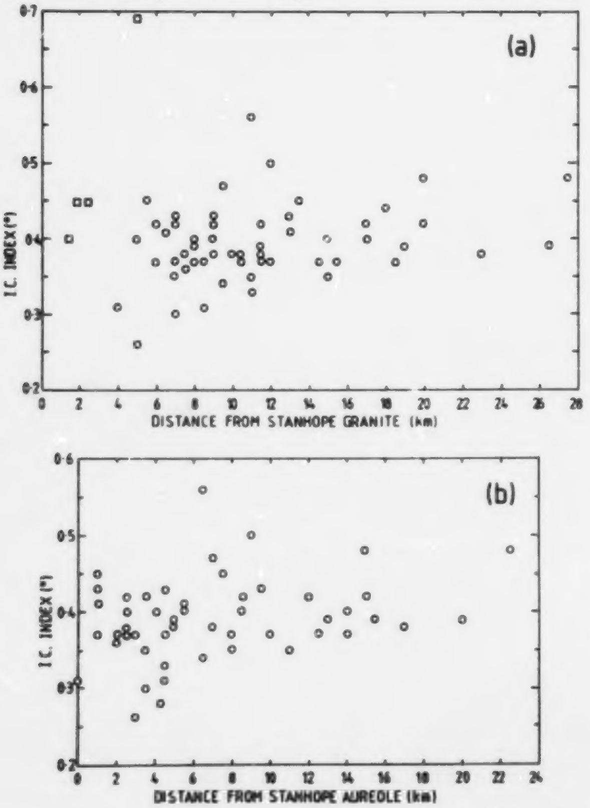

Figure 41.5. Variation of illite crystallinity with distance from (a) the Stanhope pluton contact and (b) the Stanhope metamorphic aureole. o = samples from outside the aureole; □ = samples from inside the aureole.

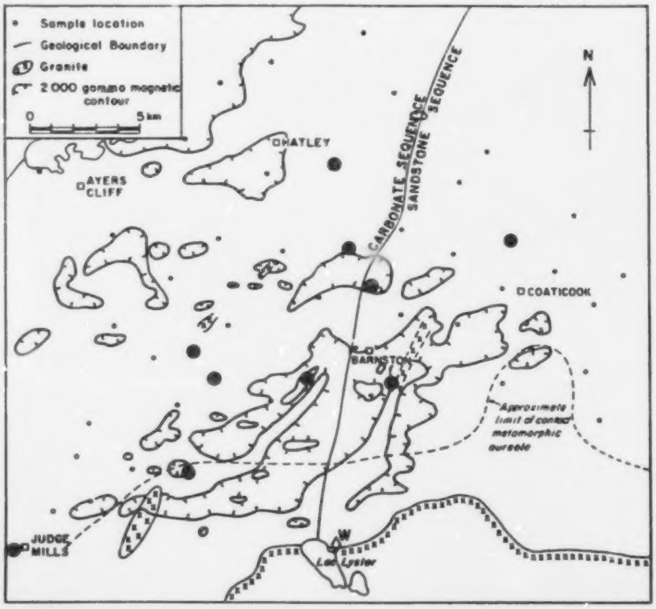

Figure 41.6. Distribution of anomalously low illite crystallinity indices (large dots) outside of the Stanhope metamorphic aureole.

the magnetic anomaly. Unfortunately, most of the area underlain by the magnetic anomaly has come under the thermal influence of the Stanhope granite, resulting in modification of the clay mineral assemblage, and making the interpretation of illite crystallinity indices in this area somewhat ambiguous (see below).

In the simplest model for the area, where only the Stanhope pluton caused contact metamorphism of the sequence, the IC index should decrease towards the contact. Although there is a general decrease in minimum IC index as the pluton is approached, there is a large degree of variability throughout the area (Fig. 41.5). With the exception of sample ET 51, which lies within the aureole, the lowest IC values typically occur 3 to 5 km from the edge of the aureole (Fig. 41.5, 41.6). One sample with a low IC index (ET 28) lies close to a small intrusive body (Fig. 41.6), but the other samples with low IC indices are unrelated to known intrusions. Within about 3 km of the aureole, IC indices increase to values comparable to those from more than 8 km from the aureole (<0.35) (Fig. 41.5).

There are two obvious models that may explain this overall pattern: 1. The low IC indices may have been produced by an intrusion that postdates the Stanhope pluton, implying that there was originally little variation in IC values with distance from the aureole. However, if this postulated intrusion is causing the magnetic high, as was already noted, low IC indices do not generally coincide with the magnetic anomaly; or 2. That there was originally an overall decrease in IC index towards the Stanhope pluton and that the high IC indices around the aureole are anomalous, due to the presence of rectorite.

The two high IC values in the area away from the pluton (Fig. 41.6) could also be due to contact metamorphic effects. However, rectorite is apparently absent from these rocks. One of the high values is relatively close to a small intrusive. The others are not but may be indicating the presence of intrusives nearby.

Conclusions

The pattern of anomalously low illite crystallinity indices obtained from the sediments of the study area cannot be clearly related to the large magnetic anomaly present in the area. Thus, the magnetic anomaly may not in fact indicate the presence of an intrusion at depth or, if there is an intrusion, it did not affect the IC indices of the overlying rocks. It is however possible that the zone in which the low IC indices are concentrated is underlain by a hidden intrusive, but that this intrusive does not have a magnetic expression.

The intrusion of the Stanhope granite probably imposed an IC gradient on the surrounding sediments, with IC indices decreasing towards the contact. However, close to the metamorphic aureole, IC indices increase, probably due to the presence of a mixed-layer mica-montmorillonite mineral (rectorite?) interfering with, and widening the 001 illite peak. Such a mineral is present in rocks within the aureole and presumably has a late hydrothermal origin. It may therefore be that high IC indices, and/or low indices, are indicative of hidden intrusives in certain sequences where a rectorite-type mineral develops.

Montmorillonite and kaolinite are relatively common in apparently unweathered rocks from outside of the aureole and, as with the IC anomalies, cannot be clearly related to either known intrusives or the magnetic anomaly. The montmorillonite in these rocks has a different structure (and composition?) from the rectorite within the aureole rocks.

References

Chen, P-Y.
1977: Table of key lines in X-ray powder diffraction patterns of minerals in clays and associated rocks; Geological Survey Occasional Paper 21, Indiana Department of Natural Resources, Bloomington, Indiana, 68 p.

Cooke, H.C.
1957: Région de Coaticook-Malvina; Rapport Géologique 69, Ministère des Mines, Province de Québec, Canada, 42 p.

Duba, D.
1982: The application of illite crystallinity, organic matter reflectance and isotopic techniques to the exploration for sedimentary-hosted hydrothermal ore deposits, south-western Gaspé; unpublished M.Sc. thesis, McGill University, 142 p.

Duba, D. and Williams-Jones, A.E.
1983a: The application of illite crystallinity, organic matter reflectance, and isotope techniques to mineral exploration: A case study in south-western Gaspé, Québec; Economic Geology, v. 78, p. 1350-1363.

1983b: Studies of burial metamorphism in the post-Taconic stage of the Appalachian orogen, south-western Gaspé; Canadian Journal of Earth Sciences, v. 20, p. 1152-1158.

Erdmer, P.
1979: Metamorphism in the Stanhope pluton aureole, Québec Appalachians: An estimate of conditions from mineral reactions in pelite and calc-schist; unpublished M.Sc. thesis, Queen's University.

1981: Metamorphism of the northwest contact of the Stanhope pluton, Québec Appalachians: Mineral equilibria in interbedded pelite and calc-schist; Contributions to Mineralogy and Petrology, v. 76, p. 109-115.

Eslinger, E.V. and Savin, S.M.
1973: Mineralogy and oxygen isotope geochemistry of the hydrothermally altered rocks of the Ohaki-Broadlands, New Zealand geothermal area; American Journal of Science, v. 273, p. 240-267.

Frey, M., Teichmuller, M., Teichmuller, R., Mullis, J., Kunzi, B., Breitschmid, A., Gruner, U., and Schwizer, B.
1980: Very low-grade metamorphism in external parts of the central Alps: Illite crystallinity, coal rank, and fluid inclusion data; Eclogae Geologicae Helvetiae, v. 73, p. 173-203.

Kisch, H.J.
1983: Mineralogy and petrology of burial diagenesis (burial metamorphism) and incipient metamorphism in clastic rock: chapter 5 in Larsen, G. and Chilingar, G.V. (eds.); Diagenesis in sediments and sedimentary rocks, 2; Developments in sedimentology, v. 25B; Elsevier, p. 289-493.

Ogunyomi, O., Hesse, R., and Heroux, Y.
1980: Pre-orogenic and synorogenic diagenesis and anchimetamorphism in Lower Paleozoic continental margin sequences of the northern Appalachians in and around Québec City, Canada; Bulletin of Canadian Petroleum Geologists, v. 28, p. 559-557.

Poitevin, E. and Cooke, H.C.
1946: Camptonite dykes from Sherbrooke district, Quebec; Royal Society of Canada, Transactions, Series 3, v. XL, p. 87-92.

Warshaw, C.M. and Roy, R.
1961: Classification and a scheme for the identification of layer silicates; Geological Society of America Bulletin, v. 72, p. 1455-1492.

Williams-Jones, A.E.
– Low temperature metamorphism of the rocks surrounding les Mines Gaspé, Québec: Implications for mineral exploration; Economic Geology. (in press)

Appendix

Clay mineralogy results (>2 µm fraction)

Abbreviations:

I:	Illite	Ch:	Chlorite
Q	Quartz	Pl:	Plagioclase
F:	Feldspar	Kf:	K-feldspar
M:	Montmorillonite	K:	Kaolinite
Al:	Alunite	G:	Graphite
gwke.:	greywacke	lmst.:	limestone
siltst.:	siltstone	argill.:	argillaceous
calc.:	calcareous	phyll.:	phyllite
qzite.:	quartzite	graph.:	graphitic
I-M:	mixed-layer illite-montmorillonite		
IC:	Illite crystallinity index		

Sample No.	Grid Reference	Lithology	Mineralogy (<2 µm)	IC (°2θ)
ET 1	307 063	argill. lmst.	I,K,Q	0.37
ET 2	648 019	gwke.	Ch,I,Q,Pl	0.37
ET 6	790 072	argill. lmst.	I,Q,K,M	0.40
ET 7	719 185	argill. lmst.	I,Q,Pl,M	0.39
ET 10	668 036	argill. lmst.	I,Q,Pl,Ch	0.43,0.43
ET 11	689 063	slate	I,Q,Ch,Pl	0.37
ET 13	694 029	argill. lmst.	I,Q,Ch	0.50
Et 14	721 031	calc. gwke.	I,Q,Pl,Ch	0.35,0.34
ET 15	743 038	black shale	I,Ch,Q,M,K	0.38,0.39
ET 16	765 029	gwke.	Q,I,Ch,Pl,M	0.38
ET 17	792 034	gwke.	I,Q,Ch,Pl	0.33
ET 18	768 059	gwke.	I,Q,Ch,Pl,K,(M)	0.45
ET 19	715 067	argill. lmst.	I,Q,K,M	0.35
ET 20	655 077	argill. lmst.	I,Q,Pl,G	0.40
ET 22	658 987	argill. lmst.	I,Q,Kf	0.31
ET 23	672 998	calc. phyll.	I,Ch,Q,Pl	0.40
ET 24	691 025	calc. phyll.	I,Ch,Q,Pl	0.42
ET 25f	724 987	argill. lmst.	Ch,I,Q,Pl	0.37
ET 26	731 015	argill. lmst.	Q,I,Pl	0.34
ET 28	738 972	argill. lmst.	I,Q,Pl	0.26,0.27
ET 33	767 998	shale	I,Ch,Q,Pl,K,Al	0.38,0.39
ET 34	786 013	argill. siltst.	I,Ch,Q,Pl,K,M	0.38
ET 35	816 044	shale	I,Ch,Q,K,M	0.41
ET 36	837 018	argill. qzite.	I,Ch,Q,Pl	0.37
ET 37	825 006	slate	Q,I,Ch,Pl	0.38
ET 38	822 973	calc. slate	Ch,I,Q,Pl,I-M	0.43
ET 43	826 956	gwke.	Q,I,Pl,Ch,M?	0.45
ET 45	808 021	graph. schist	Ch,I	0.37
ET 46	743 002	argill. siltst.	Ch,I,Q,Pl	0.39
ET 49	357 937	argill. lmst.	I,Q,Pl	0.37
ET 50	652 965	slate	Q,I,Ch,Pl	0.42
ET 51	656 935	argill. lmst.	I,Q,Pl,Kf,K,G	0.31
ET 53	666 977	slate	I,Q,Pl,Ch,G	0.35
ET 54	703 976	argill. lmst. (schistose)	I,Ch,Q,Pl	0.30
ET 55	731 967	calc. gwke.	I,Ch,Pl,M	0.40
ET 64	309 899	shale	I,Ch,Q,Pl	0.36
ET 65	324 916	calc. gwke.	I,Ch,Q,Pl	0.37
ET 66	337 955	argill. lmst.	I,Q,Ch,Pl	0.42
ET 67	332 940	argill. lmst.	I,Q,Ch,Pl	0.37
ET 68	340 922	argill. lmst.	I,Q,K,Kf	0.41
ET 71	641 985	gwke.	I,Ch,Q,Pl	0.43
ET 72	344 997	argill. lmst.	I,Q,Ch,Pl	0.56
ET 73	341 038	argill. lmst.	I,Q,K	0.37
ET 74	796 988	argill. phyll.	I,Ch,Q,Pl	0.40
ET 76	709 010	gwke.	I,Ch,Q	0.47
ET 77	688 966	argill. lmst.	I,Q,Pl,G	0.42
ET 80	888 081	slate	I,Ch,Pl,Q	0.39
ET 81	873 143	phyll.	Ch,I,Pl,Kf,G,A!?	0.38
ET 82	841 206	phyll.	I,Q,Ch,Pl	0.48
ET 83	668 100	argill. lmst.	I,Q,K	0.39
ET 84	691 111	argill. lmst.	I,Q,Kf	0.42
ET 85	728 123	gwke.	Ch,I,Q,Pl,K	0.48
ET 86	741 097	shale	I,Ch,M,K	0.42

Geological and fluid inclusion studies at the Saint-Robert Ag, W, Bi deposit, Eastern Townships, Quebec[1]

Contract 03SQ.23233-4-0447

Sergio Cattalani[2] and Anthony E. Williams-Jones[2]

Cattalani, S. and Williams-Jones, A.E., Geological and fluid inclusion studies at the Saint-Robert Ag, W, Bi deposit, Eastern Townships, Quebec; in Current Research, Part A, Geological Survey of Canada, Paper 86-1A, p. 365-374, 1986.

Abstract

Silver-tungsten mineralization at Saint-Robert-Bellarmin Eastern Townships, Quebec, occurs in high level quartz veins. These veins comprise an early, discordant silver-bearing set in the south and later concordant tungsten and bismuth-bearing sets in the centre and north respectively. The deposit is associated with granodioritic and lamprophyric dyke swarms. A 2.5 km x 400 m thermal metamorphic aureole indicates a larger intrusive stock at depth. The aureole is overprinted by fault-controlled alteration of proximal argillic and distal phyllic facies. Early, low salinity, liquid H_2O-liquid CO_2-vapour CO_2, and later, low salinity, post-ore, aqueous fluids are trapped as inclusions in quartz. Homogenization data indicate that the early CO_2-bearing fluids were trapped at approximately 200°C, and the later aqueous fluids between 150-200°C. Highly variable CO_2 contents in the early fluid suggest heterogeneous entrapment of immiscible CO_2-rich and H_2O-rich phases. Mineralization is attributed to CO_2 effervescence from initially acid meteoric solutions.

Résumé

La minéralisation en argent et tungstène à Saint-Robert-Bellarmin en Estrie, au Québec, se trouve dans de riches veines de quartz. Ces dernières renferment un ensemble argentifère inférieur discordant au sud et des ensembles supérieurs concordants, contenant du tungstène et du bismuth, au centre et au nord respectivement. Le gisement est associé à des nuées de dykes granodioritiques et lamprophyriques. Une auréole de thermométamorphisme de 2500 sur 400 m indique la présence d'un plus grand massif intrusif en profondeur. Un faciès argileux proximal et un faciès phylliteux distal d'altération contrôlée par des failles se surimposent à l'auréole. Au début, un mélange de H_2O liquide, CO_2 liquide et CO_2 vapeur de faible salinité et, plus tard, des fluides aqueux de faible salinité, postérieurs à la minéralisation, ont été piégés sous forme d'inclusions dans le quartz. Des données d'homogénéisation indiquent que les premiers fluides contenant du CO_2 ont été piégés à 200°C environ, et les fluides aqueux postérieurs, entre 150 et 200°C. Des teneurs très variables en CO_2 dans les premiers fluides semblent indiquer qu'il y a eu piégage hétérogène des phases immiscibles riches tant en CO_2 qu'en H_2O. On attribue la minéralisation à l'effervescence du CO_2 provenant de solutions météoriques de nature à l'origine acide.

---

[1] Contribution to the Federal Asbestos Initiatives Geoscience Research Program 1984-87. Project carried by Geological Survey of Canada, Economic Geology and Mineralogy Division, Project 770071.

[2] Department of Geological Sciences, McGill University, 3450 University St., Montreal, Quebec H3A 2A7

Introduction

The J.A.G. Mines, Saint-Robert deposit is located about 2 km east of the town of Saint-Robert-Bellarmin, in the Eastern Townships of Quebec (Fig. 42.1). Silver and tungsten-bearing veins have been known to be present in the area since the late 19th century. It was not however until the 1950s that serious exploration of these veins was undertaken.

The first extensive exploration of the deposit was conducted by the St. Robert Metals Corporation (1951-1958). This program delineated a zone of scheelite-bearing veins outcropping at surface and precious metal mineralization at depth. Drilling intersections of the latter included 14.14 oz/t Au over 1 foot, 11.8 oz/t Au and 6.58 oz/t Ag over 0.9 feet, and 25.00 oz/t Au and 5.8 oz/t Ag over 0.3 feet. Two adits, the Lacombe adit and the Lee tunnel were driven to exploit the mineralized zones. The property was brought briefly into production as a tungsten mine in 1958. Unfortunately, the Lee tunnel, which was to exploit the precious metal zone, had to be abandoned before it reached its target.

Subsequent exploration of the property by Nouvelle Mining (1970-1974), and J.A.G. Mines (1977-present), has focused on its precious metal potential. Neither company has however been able to reproduce the drilling results of the St. Robert Metals Corporation. The best recent intersections by J.A.G. Mines have been 37.8 oz/t Ag and 8.8% Zn over 1.2 feet, and 27.81 oz/t Ag and 3.16% Pb over 2.1 feet.

Geological setting

The Saint-Robert-Bellarmin property is largely underlain by sedimentary rocks of the Frontenac Formation, a miogeoclinal sequence of possible Early Ordovician age (Harron, 1976). These rocks were deformed during the Middle

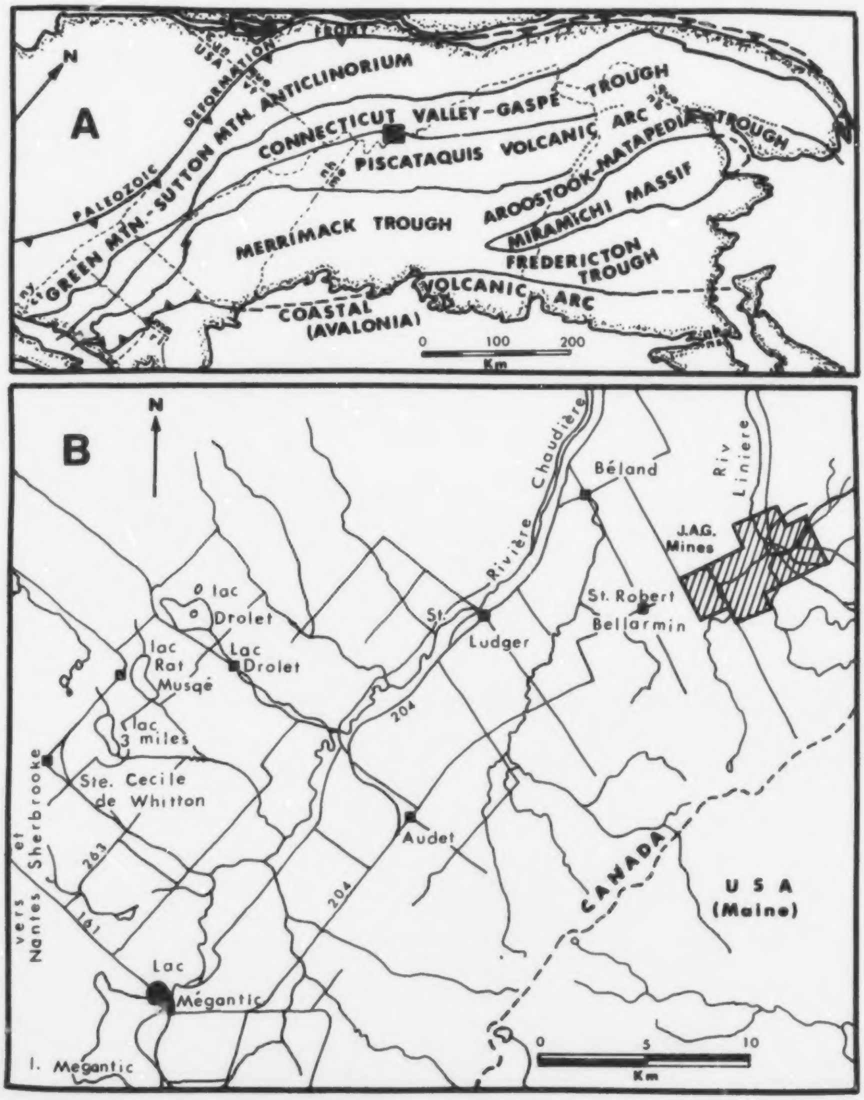

Figure 42.1. Location map for the J.A.G. Mines, Saint-Robert property: A – within the tectonic subdivisions of the northern Appalachians, after Bradley (1983); B – locally.

Ordovician Acadian orogeny and are exposed in the Boundary Mountain anticlinorium, a structure of the same age (St. Julien and Beland, 1982). The property is located immediately to the south of the fault-bounded contact between the Boundary Mountain anticlinorium, and the more northerly Gaspé-Connecticut Valley synclinorium. A swarm of Acadian dykes and possibly younger dykes cut the Frontenac Formation within the property limits.

Sedimentary rocks

The sedimentary rocks consist of a sequence of clastic turbiditic sediments comprising alternating quartzites, slates, and calcareous greywackes. These are overlain by unconsolidated Pleistocene glacial till, and recent alluvium, that together locally reach thicknesses in excess of 70 m.

Igneous rocks

The intrusive rocks consist of subparallel felsic dykes and later, mafic dykes. The felsic igneous rocks can be divided into two distinct types.

The first type is a fine- to medium-grained, leucocratic to mesocratic rock exhibiting porphyritic to glomeroporphyritic textures. This rock type is characterized by abundant relict quartz and plagioclase (An_{0-15}) phenocrysts, with smaller proportions of relict hornblende and biotite phenocrysts, set in a quartzofeldspathic groundmass containing accessory apatite. Much of the present mineralogy and texture of this rock is due to extensive hydrothermal alteration: the quartz and feldspar phenocrysts are overgrown by later quartz; the groundmass contains abundant patches of granophyric quartz; and, the mafic minerals are largely pseudomorphosed by chlorite, calcite, sericite, rutile, and leucoxene. Other secondary mineral phases include sphene and epidote. Dykes of this type measure up to 20 m in width and make up the bulk of the intrusive rocks on the property.

The second felsic igneous rock type consists of an aphanitic to medium grained, leucocratic, green, porphyritic rock, which contains relict phenocrysts of quartz and plagioclase set in a quartzofeldspathic groundmass of metasomatic texture. This rock type is distinguished from the first type by the absence of mafic phases, a light greenish colour, and a conchoidal fracture. The alteration mineralogy is qualitatively equivalent to that mentioned above. This rock generally forms narrower dykes (up to 6-7 m in width), that may commonly show a banded texture near one or both dyke/wall rock contacts.

Both felsic rock types are classified using the scheme of Streckeisen (1976) (Fig. 42.2). The first felsic type ranges from granodiorite to quartz-rich granite depending on the extent of alteration, while the second type is restricted to granodiorite compositions. These classifications are however tentative because alteration may have changed the chemical compositions of these rocks significantly. Based on their macroscopic appearance, as well as for reasons of clarity, the second felsic rock type will be hereafter referred to as an intrusive rhyolite.

The mafic igneous rocks are narrow (less than 2 m wide) dykes that commonly crosscut the felsic dykes at relatively high angles, and therefore represent a younger intrusive event. This rock type occurs as a fine- to medium-grained, melanocratic porphyritic variety containing relict phenocrysts of plagioclase, green hornblende and/or biotite, with smaller proportions of relict phenocrysts of diopsidic augite, and accessory apatite. In a significant proportion of the dykes, plagioclase occurs in the groundmass. Alteration is extensive, and consists of abundant rounded calcite patches, as well as biotite, chlorite, rutile, and minor sericite. Normative calculations from whole rock X-ray fluorescence analyses indicate up to 11% modal olivine. No olivine relicts were however detected optically. Based on the scheme for lamprophyres of Streckeisen (1979), these rocks are tentatively classified as spessartites and/or kersantites.

The dykes may be genetically related to a stock at depth, the presence of which is suggested by a broad regional positive magnetic anomaly under the central part of the property (Fig. 42.3).

Structure and metamorphism

The sedimentary strata on the property dip steeply to the north and south forming a number of tight, upright isoclinal folds trending east-northeast (Fig. 42.4b). A subvertical schistosity or penetrative cleavage (F_1) is consistent with folding throughout the area, and is generally indistinguishable from bedding. In addition to this major cleavage, there is a weaker, subparallel cleavage (F_2), which shows a maximum departure of 10-15° from F_1, resulting in a strong crenulation in the shaly units. A third, minor phase of deformation is represented by gentle, open folds, whose axial traces lie nearly normal to the first two. This event caused the F_1 and F_2 fold axes to dip locally at shallow angles either east-northeast or west-southwest.

Both the granodiorite porphyry dykes and the intrusive rhyolite dykes have intruded along the penetrative cleavage, and therefore are sill-like in the fold limbs. Some rhyolites have intruded along the cores of the granodiorite porphyry dykes, i.e. they were subjected to the same structural controls as the porphyry dykes.

A major system of vertical faults, referred to as the Main Fault system, with a strike length of at least 2.5 km, cuts through the centre of the property, parallel to the penetrative cleavage (Fig. 42.4b). Displacement appears to be dominantly dip-slip in character, with the downthrow to the north. Because vertical faults cut near-vertically dipping strata it is impossible to estimate the amount of displacement. Less numerous, seemingly subvertical, late minor faults occur nearly normal to the Main Fault system in the western and central parts of the property (Fig. 42.4b).

The regional metamorphic grade is lower greenschist to greenschist facies. Thermally metamorphosed brownish biotite hornfels occurs in an elongated oval zone whose long axis is coincident with the Main Fault system. This zone measures at least 2.5 km along strike and is about 400 to 500 m wide (Fig. 42.4a).

Alteration

The various lithotypes described above have undergone moderate to intense hydrothermal alteration in a zone which is roughly coincident with the biotite hornfels zone (Fig. 42.4b). Alteration is generally phyllic in character, resulting in pale greyish-green rocks that consist mainly of quartz, sericite, calcite, pyrite, and rutile. The degree of alteration and quartz veining increase visibly with proximity to the Main Fault system.

Adjacent to, and within faults of the Main Fault system however, the rocks are white and extremely friable and soft. X-ray diffraction analysis reveals that these rocks are mainly kaolinite. The overall pattern of alteration is clearly fault-controlled and may be described as consisting of narrow proximal argillic facies within a broad halo of distal phyllic facies.

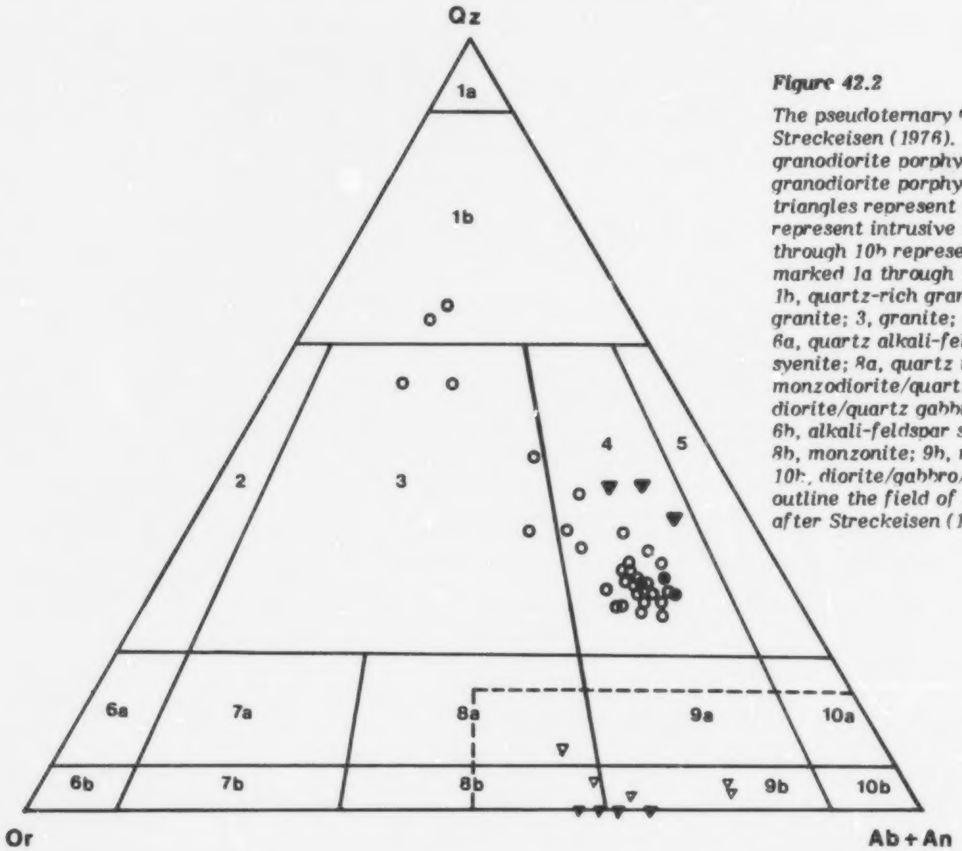

Figure 42.2

The pseudoternary Qz-Ab+An-Or diagram, after Streckeisen (1976). Open circles represent granodiorite porphyry, closed circles represent granodiorite porphyry chilled margins, open triangles represent mafic dykes, closed triangles represent intrusive rhyolites. Fields marked 1a through 10b represent intrusive rhyolites. Fields marked 1a through 10b represent: 1a, quartzolite; 1b, quartz-rich granitoids; 2, alkali-feldspar granite; 3, granite; 4, granodiorite; 5, tonalite; 6a, quartz alkali-feldspar syenite; 7a, quartz syenite; 8a, quartz monzonite; 9a, quartz-monzodiorite/quartz-monzogabbro; 10a, quartz diorite/quartz gabbro/quartz anorthosite; 6b, alkali-feldspar syenite; 7b, syenite; 8b, monzonite; 9b, monzodiorite/monzogabbro; 10b, diorite/gabbro/anorthosite. Dashed lines outline the field of spessartites and kersantites, after Streckeisen (1979).

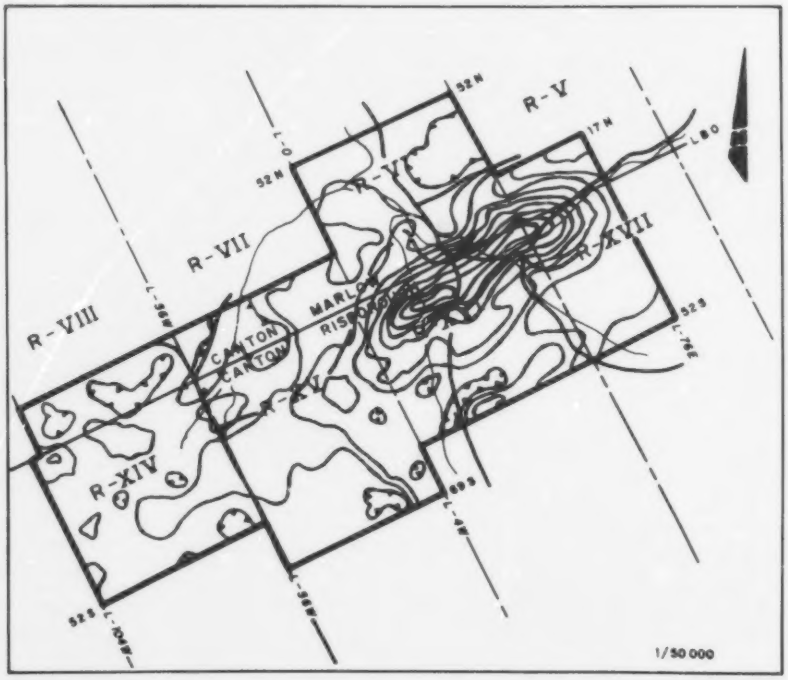

Figure 42.3

Regional magnetic anomaly map for the J.A.G. Mines, Saint-Robert property. Reproduced from Le Ministère d'Énergie et des Ressources de Québec.

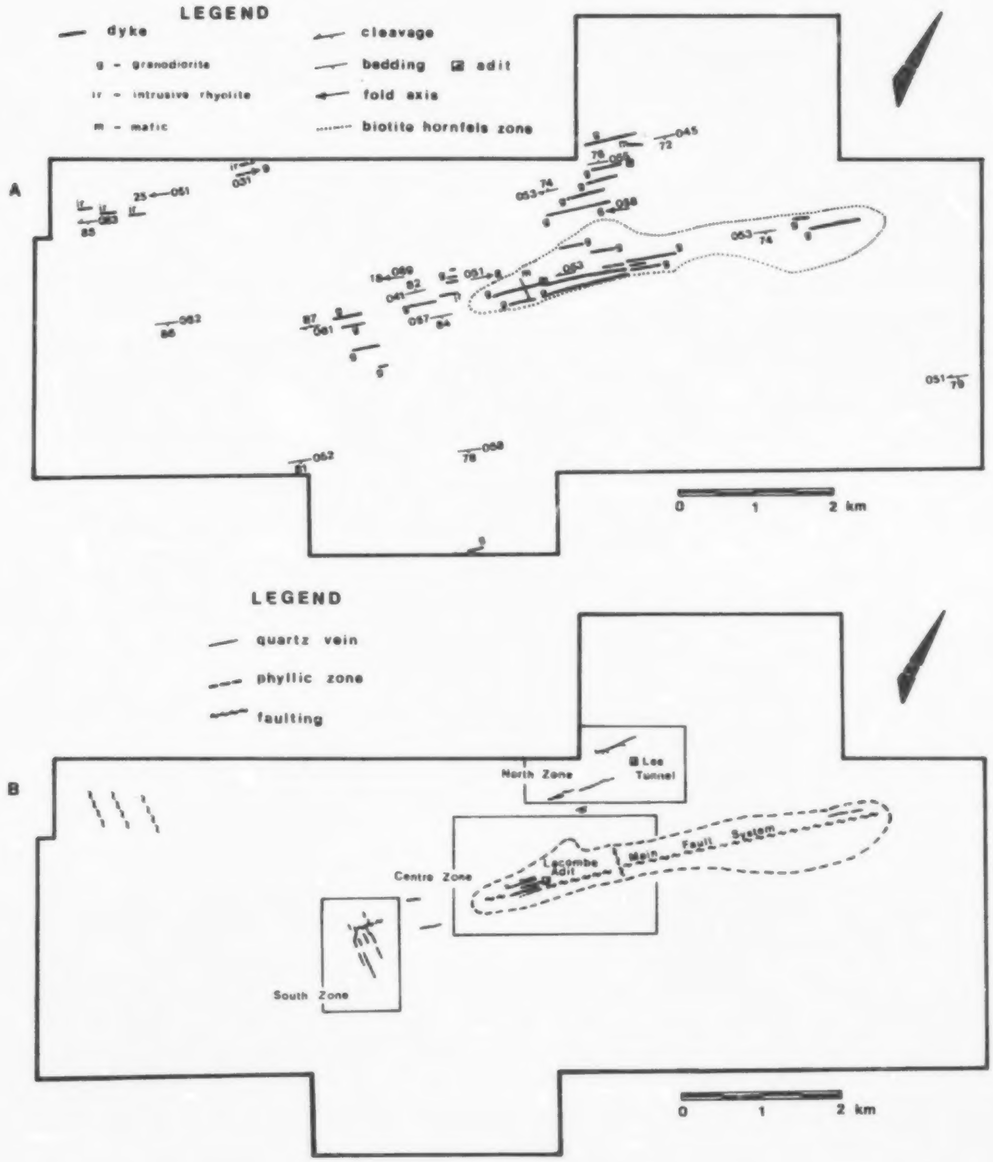

Figure 42.4. *Local geologic maps of the J.A.G. Mines, Saint-Robert property: A – map showing structure, intrusives, and thermal metamorphic halo; B – map showing quartz veining, faulting, and zone of phyllic alteration.*

A second smaller zone of phyllic alteration occurs to the northwest of the Main Fault system, in the North zone of the property (Fig. 42.4b). Unfortunately, the smaller number of drillholes and scarcity of outcrops in the area make it difficult to accurately delineate the extent of this zone.

Mineralization

The bulk of the mineralization on the property is contained within massive quartz veins which can reach up to 1 m in width, and up to about 150 m in length. These veins contain various Bi, Pb, Ag, Zn, Cu sulphides, as well as abundant scheelite. Vein formation postdates emplacement of all major geologic units in the Saint-Robert-Bellarmin area.

The major veins have been subdivided into three sets termed the North zone, South zone, and Central zone vein sets on the basis of their location (Fig. 42.4b). The North zone and Central zone vein sets occupy tensional fractures concordant to cleavage, striking approximately 060° and dipping subvertically. Evidence for a tensional environment during formation of these veins includes branching of the veins, variation in strike along individual veins, and the common occurrence of vugs. The South zone vein set, strikes almost normal to schistosity and dips 40-50° northeast. It is clearly crosscut by granodiorite porphyry dykes, to which the North zone and Central zone vein sets are parallel, and may therefore represent an earlier veining event.

The North zone quartz veins contain abundant pyrite and cosalite with minor argentiferous galena, sphalerite, and scheelite. The cosalite occurs as long (up to 10 cm), acicular needles, which in places radiate in from the vein/wall rock contacts in a fan-like fashion. More commonly, the cosalite occurs together with the other sulphides in fracture-filling stringers throughout the veins.

The Central zone veins contain abundant pyrite and scheelite, with lesser argentiferous galena, sphalerite, and minor cosalite. The sulphides generally occur as fracture-filling stringers in the cores of the veins, whereas scheelite commonly occurs as distinct euhedral crystals restricted to vein/wall rock contacts. The result is a visible zonation of the ore minerals within these veins. This is particularily well displayed in the Lacombe Adit, where in addition to the major veins, a stockwork-like array of smaller quartz veins of similar mineralogy is present.

The South zone vein set contains abundant argentiferous galena, sphalerite, and pyrite, as well as minor scheelite. The ore minerals are generally distributed erratically throughout the veins, and form small patches or aggregates. The South zone veins carry the richest silver grades found to date on the property. However, the occurrence of patches of massive sulphide greater than about 8-10 cm is rare. In addition, these veins have a tendency to suddenly pinch out both along strike and down dip.

The deposit may thus be described as consisting of an earlier, southern, silver-rich zone, with later contemporaneous central tungsten, and northern bismuth-rich zones.

Preliminary fluid inclusion results

A total of 120 fluid inclusions were investigated microthermometrically using an S.G.E. Model III, heating-freezing stage. The sample material in all cases was quartz from various scheelite and sulphide-bearing quartz veins, spanning all three zones of the Saint-Robert-Bellarmin property. The inclusions studied can generally be divided into two categories, here referred to as Type 1 and Type 2.

Type 1 inclusions

Type 1 inclusions are early stage, 3 phase (liquid H_2O, liquid CO_2, CO_2 vapour) inclusions with highly variable CO_2/H_2O volume ratios (estimated visually at a constant temperature of 40°C) ranging from 1:20 to almost pure CO_2 (Fig. 42.5). Such variability can commonly be seen within 100 to 200 μm^2 areas. Type 1 inclusions vary from a few micrometres up to almost 100 micrometres in diameter. Their morphology is in most cases that of equant to slightly elongated negative crystals, although they may be irregularly shaped. Type 1 inclusions predominate in all sample material studied and occur as isolated, pseudosecondary inclusions, as well as in inclusion trains of clearly secondary origin.

Type 2 inclusions

Type 2 inclusions are later, two-phase aqueous (liquid, vapour) inclusions with high liquid/vapour ratios from 9:1 to 99:1. They range from a few micrometres to well over 100 micrometres in diameter. They are commonly irregularily shaped, and generally occur along healed fractures of secondary origin. They are rarely seen as isolated pseudosecondary inclusions, although in a few crystals, large negative crystal-shaped, two-phase inclusions are present. They typically occur proximal to morphologically similar Type 1 inclusions, of which one or more may consist entirely of CO_2.

Eutectic melting and fluid composition

Final melting temperatures of liquid CO_2 (Tm CO_2) for most Type 1 inclusions correspond to the liquid-solid-vapour invariant point (-56.6°C) for the pure CO_2 system, indicating that it is a comparatively pure CO_2 phase (see Appendix, Table 42.1). However, in a number of inclusions, Tm CO_2 occurs significantly below -56.6°C. This suggests the presence of variable amounts of another component dissolved in the CO_2 liquid and gas. A likely candidate is CH_4, (Swanenberg, 1979). The mole fraction of CH_4 present in the CO_2-rich phase in Type 1 inclusions that would explain the observed range of melting temperatures for solid CO_2 (4.0°C), varies from 0.00 to about 0.15 X_{CH_4}, with a mean at about 0.02 X_{CH_4} (Swanenberg, 1979). Another possibly important contaminant of carbonic inclusions is N_2 (Roedder, 1972). At present though, very little is known about the effect of N_2 on the melting of CO_2.

A marked difference between the eutectic temperatures (Te) of liquid H_2O in Type 1 inclusions and of Type 2 inclusions is evident from data presented in Table 42.1 (Appendix). Type 1 inclusions show a range of Te from -40°C to -25°C, with a mean of -32.9°C, whereas Type 2 inclusions show a range of Te from -30.3°C to -20°C, with a mean of -24.7°C. The fluid composition for Type 2 inclusions is assumed to be one in which NaCl is the dominant ionic species present, as the range of initial melting temperatures is mainly between the stable and metastable eutectic points (-20.8°C and -28°C respectively) in the NaCl-H_2O system (Crawford, 1981). The lower initial melting temperatures of liquid H_2O in Type 1 inclusions suggest the presence of additional dissolved species. Candidates for these extra species include $MgCl_2$, and $CaCl_2$ (Crawford, 1981), and CO_2 (Higgins, 1985).

Salinity data

Salinities for Type 1 inclusions were calculated using the method outlined in Bozzo et al. (1973), in which the depression of CO_2 clathrate melting temperature is related to the salt content of the fluid by the following equation:

$$\text{Wt\% NaCl} = 0.05286\,(10-Tm_{clath})\,(Tm_{clath}+29.361)$$

This equation indicates that the salinity of Type 1 inclusions ranges from 0.00 to 7.92 equivalent Wt% NaCl, with a mean salinity of 3.83 equivalent Wt% NaCl.

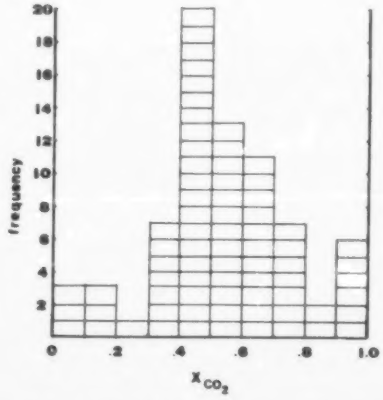

***Figure 42.5.** Diagram showing frequency versus X_{CO_2} for Type 1 inclusions.*

The salinities of Type 2 inclusions were determined using the equation developed by Potter et al. (1978), which relates the melting point depression of H_2O ice (Tm_{ice}), to the concentration of dissolved salts:

$$\text{Wt\% NaCl} = 1.76958Tm_{ice} - 3.2384\times10^{-2}Tm_{ice}^{2} + 5.2778\times10^{-4}Tm_{ice}^{3} + 0.028$$

The calculated range of salinity for Type 2 inclusions is from 0.53 to 9.47 equivalent Wt% NaCl, with a mean salinity of 4.92 equivalent Wt% NaCl.

Temperatures of final CO_2 clathrate melting (Tm_{clath}) for Type 1 inclusions and final ice melting (Tm_{ice}) for Type 2 inclusions are presented in Table 42.2 (Appendix).

Homogenization data

The homogenization data for this study are presented in Table 42.3 (Appendix), and as histograms of frequency versus homogenization temperature and frequency versus decrepitation temperature (Fig. 42.6a and 42.6b respectively). Although there are no significant peaks, it is clear that Type 1 inclusions generally homogenize at higher temperatures than Type 2 inclusions. Although a large majority of Type 1 inclusions decrepitated prior to homogenization, they did so at temperatures higher than the homogenization temperatures of any Type 2 inclusions. Decrepitation of Type 1 inclusions is attributed to the high coefficient of thermal expansion of CO_2 (Burruss, 1981).

All Type 1 inclusions homogenized to liquid or decrepitated after the vapour bubble size had decreased significantly. This indicates a relatively high density fluid.

Conditions of entrapment

Figure 42.7 is a diagram showing the distribution of Type 1 inclusions in terms of temperatures of decrepitation and homogenization versus mole fraction of CO_2. It should be noted that although most Type 1 inclusions decrepitated prior to complete homogenization, decrepitation in most cases occurred after a significant decrease in the vapour bubble size. This suggests that homogenization would have occurred at temperatures only slightly higher than those of decrepitation. The diagram indicates that X_{CO_2} of Type 1 fluid inclusions varies widely but that there is a negative correlation of X_{CO_2} with homogenization temperature. In fact, the distribution appears to define the high X_{CO_2} limb of an H_2O-CO_2 solvus. This suggests entrapment of a fluid in which the H_2O and CO_2 existed as separate immiscible phases (Ramboz et al., 1982). Such immiscible fluids could be trapped either homogeneously or heterogeneously.

Fluid inclusions formed by homogeneous entrapment of an immiscible fluid at constant P and T will homogenize on the solvus defined for the specific composition of the fluid at the pressure of trapping (Pichavant et al., 1982). This will result in a narrowly defined bimodal distribution of points corresponding to the intersections of the appropriate solvus with the temperature of trapping. In order to explain the observed distribution in terms of homogeneous entrapment, it is necessary that both temperature and pressure varied significantly. By contrast, heterogeneous entrapment of immiscible H_2O and CO_2-rich phases could produce the same distribution at constant P and T. The mixtures of H_2O and CO_2-rich fluids thus trapped by each inclusion would yield erroneously high homogenization temperatures and pressure where the true temperature of trapping would correspond to

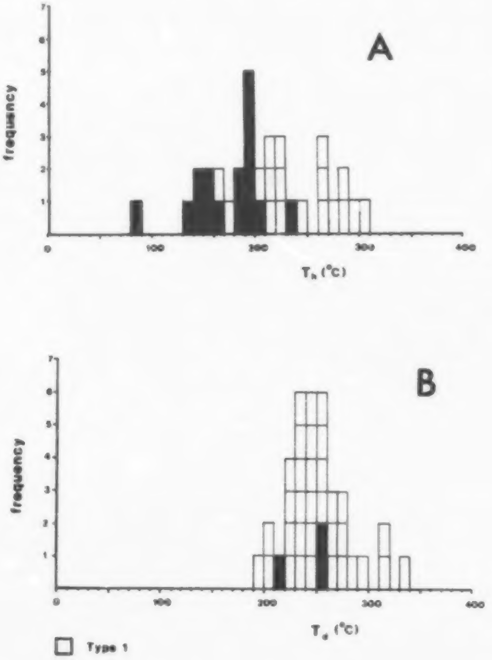

Figure 42.6. Homogenization data histograms: A – frequency versus homogenization temperature; B – frequency versus decrepitation temperature.

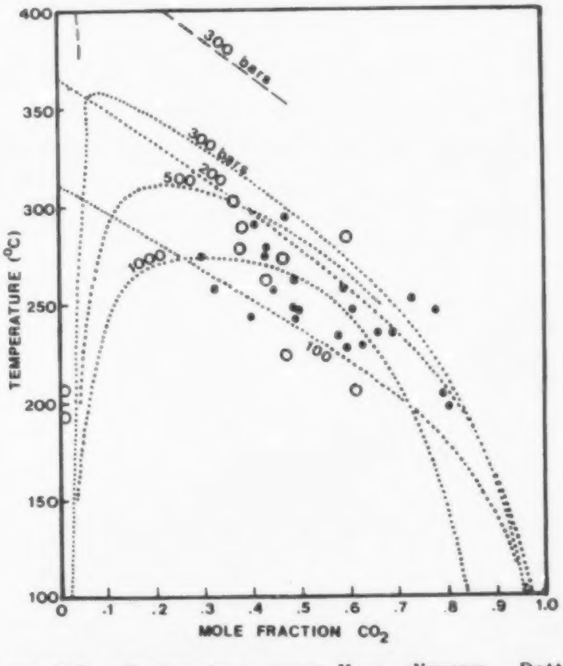

Figure 42.7. Temperature versus X_{CO_2} diagram. Dotted lines are for the pure CO_2-H_2O system taken from Takenouchi and Kennedy (1964), dashed lines are for the CO_2-H_2O-6 Wt% NaCl system. The 300 bar solvus is taken from Takenouchi and Kennedy (1965). Closed circles represent decrepitation temperatures, open circles represent homogenization temperatures.

the lowest homogenization temperature. This mode of entrapment is favoured over one of homogeneous entrapment, requiring variable P and T, for the reason that a distribution such as is seen on Figure 42.7 can be generated by inclusions existing within a very restricted area in a single crystal of quartz, the formation of which can be assumed to have occurred under relatively constant P and T conditions. Entrapment temperatures of approximately 200°C are thus proposed for Type 1 inclusions.

Pressures of entrapment for Type 1 inclusions cannot be reliably estimated from the data, but considering the abundant evidence of vein emplacement into wide open tension fractures, it is probable that entrapment pressures were relatively low and largely hydrostatic.

The entrapment temperatures for Type 2 inclusions have not been estimated but would have been within 15°C of the homogenization temperatures for pressures up to 500 bars (Roedder and Bodnar, 1980). This suggests that Type 2 inclusions were trapped at temperatures in the range 150-200°C.

Discussion

The study shows that the Saint-Robert-Bellamin Ag-W-Bi mineralization was emplaced at comparatively low pressures and at temperatures of approximately 200°C. The association of the deposit with dyke swarms, and its location within a thermal metamorphic aureole, suggest that it is related to an unexposed pluton at depth. It is proposed that this pluton provided a heat engine to drive a meteoric water-dominated hydrothermal system. The low temperature, low salinity, and presence of CO_2 in the early fluid are consistent with it having such a meteoric origin. The nature of the alteration (phyllic and argillic), suggests that this fluid was mildly to strongly acidic. It was probably also oxidizing.

A possible model for the deposit, is one in which downwelling groundwaters gained CO_2 and metals from interaction with country rocks (including calcareous sediments) and granite, and subsequently deposited their metals through a process of CO_2 effervescence and wall rock alteration as they moved into overlying tension fractures.

As noted earlier, the nature of the X_{CO_2}-temperature distribution of the early fluids along a solvus suggests that there was heterogeneous entrapment of immiscible CO_2 and H_2O-bearing fluids at the level of mineralization. This could indicate the unmixing of a formerly miscible H_2O-CO_2 fluid as it moved up to higher level, lower pressure regimes. If this was into tension fractures, as appears to have been the case at Saint-Robert-Bellarmin, the pressure drop would have been particularily sharp as it would have been accompanied by a change from near-lithostatic to near-hydrostatic conditions.

The effervescence of CO_2 and the wall rock alteration would have increased the pH of the residual H_2O-rich fluid, and thereby provided a mechanism for mineralization. It is possible that carbonate ligands were responsible for transport of tungsten (cf. Higgins, 1985), in which case the role of CO_2 effervescence in scheelite deposition would have been to reduce the activities of these ligands in the solution.

References

Bozzo, A.T., Chen, J.R., and Barduhn, A.J.
1973: The properties of the hydrates of chlorine and carbon dioxide; in 4th International Symposium on Fresh Water from the Sea, ed. A. Delyannis and E. Delyannis; v. 3, p. 437-451.

Bradley, D.C.
1983: Tectonics of the Acadian orogeny in New England and adjacent Canada; Journal of Geology; v. 9, p. 381-400.

Burruss, R.C.
1981: Analysis of phase equilibria in C-O-H-S fluid inclusions; in Short Course in Fluid Inclusions: Applications to Petrology, ed. L.S. Hollister and M.L. Crawford; Mineralogical Association of Canada, p. 39-69.

Crawford, M.L.
1981: Phase equilibria in aqueous fluid inclusions; in Short Course in Fluid Inclusions: Applications to Petrology, ed. L.S. Hollister and M.L. Crawford; Mineralogical Association of Canada, p. 75-100.

Harron, G.A.
1976: Metallogeny of sulphide deposits in the Eastern Townships; Ministère des Richesses Naturelles, Québec, Paper ES-27, 42 pp.

Higgins, N.C.
1985: Wolframite deposition in a hydrothermal vein system: The Grey River tungsten prospect, Newfoundland, Canada; Economic Geology, v. 80, p. 1297-1327.

Pichavant, M., Ramboz, C., and Weisbrod, A.
1982: Fluid immiscibility in natural processes: Use and misuse of fluid inclusion data; I. Phase equilibria analysis – a theoretical and geometrical approach; Chemical Geology, v. 37, p. 1-27.

Potter, R.W., II, Clynne, M.A., and Brown, D.L.
1978: Freezing point depression of aqueous sodium chloride solutions; Economic Geology, v. 73, p. 284-285.

Ramboz, C., Pichavant, M., and Weisbrod, A.
1982: Fluid immiscibility in natural processes: Use and misuse of fluid inclusion data; II. Interpretation of fluid inclusion data in terms of immiscibility; Chemical Geology, v. 37, p. 29-48.

Roedder, E.
1972: Composition of fluid inclusions; in Data of Geochemistry, (sixth edition), chap. JJ, techn. ed. M. Fleischer; U.S. Geological Survey Professional Paper 440-JJ.

Roedder, E. and Bodnar, R.J.
1980: Geologic pressure determinations from fluid inclusion studies; Earth and Planetary Science Annual Reviews; v. 8, p. 263-301.

St. Julien, P. and Beland, J.
1982: Major structural zones and faults of the Northern Appalachians; in Geological Association of Canada Special Paper 24, ed. P. St. Julien and J. Beland, p. 1-11.

Streckeisen, A.
1976: To each plutonic rock its proper name; Earth Science Reviews, v. 12, p. 1-33.

1979: Classification and nomenclature of volcanic rocks, lamprophyres, carbonatites, and melilitic rocks: Recommendations and suggestions of the IUGS subcomission on the systematics of igneous rocks; Geology, v. 7, p. 331-335.

Swanenberg, H.E.C.
1979: Phase equilibria in carbonic systems, and their application to freezing studies of fluid inclusions; Contributions to Mineralogy and Petrology, v. 68, p. 303-306.

Takenouchi, S. and Kennedy, G.C.
1964: The binary system H_2O-CO_2 at high temperatures and pressures; American Journal of Science, v. 262, p. 1055-1074.

1965: The solubility of carbon dioxide in NaCl solutions at high temperatures and pressures; American Journal of Science, v. 263, p. 445-454.

Table 42.1. Temperatures of final melting of CO_2 (Tm CO_2) for Type 1 inclusions, and temperatures of initial melting of liquid H_2O (Te) for Type 1 and Type 2 inclusions

Sample No.	Type 1 Te (°C)	Type 1 Tm CO_2 (°C)	Type 2 Te (°C)
	-29.4	-59.2	
R 5		-60.4	
		-56.6	
R 6	-36	-56.9	-25
		-56.6	-20
	-30.3	-56.5	-24
		-56.3	-23.2
		-56.5	-24.6
	-30	-56.7	-24.6
		-56.3	-25
		-56.4	-26
		-56.5	-26.7
		-56.3	-28
		-56.5	-25.6
	-30	-56.7	-24.8
		-56.6	-25.7
		-56.5	-24.2
		-56.5	-23.8
		-56.7	-25
		-56.3	-30.3
		-56.4	-27
		-56.3	-28
		-56.6	-28.2
	-28	-56.7	-25
		-56.6	-27
	-28	-58	-20
	-28.7		
	-33.4	-58.7	
	-29		
R 9	-29.6		-30
	-34.3		-29
	-30.6		
	-32.6		
	-36.5		
	-36		
	-36		
	-33.6		
	-36.6		
R 10		-58.7	
		-58.6	
		-58.7	
		-58.8	
		-58.9	
		-58.5	
		-58.5	
R 10A		-58.8	
	-37	-58.7	
R 11	-36.7		-26.7
	-35.6		
	-40		
	-39		
	-35.2		
	-27.8		
	-34		
	-33.4		
	-35.9		
	-36.8		
	-35		

Table 42.2. Temperatures of final CO_2 clathrate melting (Tm_{clath}) for Type 1 inclusions, and temperatures of final ice melting (Tm_{ice}) for Type 2 inclusions

Sample No.	Type 1 Tm_{clath} (°C)	Type 2 Tm_{ice} (°C)
R 6	7.3	-2.6
	7.4	-2.2
	8.4	-1.7
	7.8	-2.5
	9.0	-2.9
	8.6	-3.0
	8.6	-3.0
	8.2	-2.5
	8.1	-3.2
	8.4	-2.8
	8.3	-4.2
	8.5	-2.8
	8.4	-2.8
	8.7	-2.0
	9.6	-2.2
	8.3	-2.0
	7.0	-2.7
	9.1	-2.8
	9.0	-2.9
	8.7	-2.6
	8.0	-0.3
	8.5	-3.7
	8.9	-4.0
	8.6	-3.6
	8.5	-3.8
	8.6	-3.0
	8.9	
	8.3	
R 9	5.7	
	6.0	
	6.0	
	6.6	
	6.5	
	6.7	
	6.8	
	10.2	
	9.1	
	9.1	
	8.2	
	9.1	
	9.3	
	8.4	
	8.2	
R 10	6.6	
	6.2	
	6.8	
R 10A	6.0	
	8.0	

Table 42.3. Temperatures of final homogenization and decrepitation for Type 1 and Type 2 inclusions (Th and Td), and temperatures of homogenization of CO_2 liquid and vapour for Type 1 inclusions (Th CO_2)

Sample No.	Th (°C)	Type 1 Td (°C)	Th CO_2 (°C)	Type 2 Th (°C)	Type 2 Td (°C)
R 5	288	295	15.9		
	301.3		12.4		
		262	15.5		
		201			
		315	15.2		
			15.5		
		225			
		248	10.4		
			17.2		
		230	15.2		
		258	14.4		
	284				
		315			
R 6			7.7	150.2	
			-0.5	184.8	
			5.2	86	
		205		143.4	
	295.1			205.7	260
		230			220
		230		194.5	260
		260		151.3	
		290	5.4		
			21.3		
		235			
			17.7		
			21.6		
			11.9		
			13.6		
			19.5		
			8.8		
			19.6		
			17.6		
			19.5		
			2.6		
			1.1		
			21.6		
			2.1		
			0.4		
			1.4		
			11.0		
			19.5		
			21.5		
			5.0		
			20.5		
			23.8		
			21.6		
			2.8		
	221	260			
R 9		225	-1.5	165	
		245	18.3	198.7	
		273	11.8		
		257.6	5.9		
		221			
		222	10.4		
		230	6.3		
		230	10.5		
			11.3		
			20.3		
		245	7.9		
		251	13.0		
		248	20.8		
		242	10.7		
	248.7				
	269				
		235	11.5		
		195	6.3		
		243	14.8		
	166.8		4.7		
	204.7		7.7		
R 10		260	6.3		
	263	276	13.6		
			18.7		
			4.8		
	279		7.2		
R 10A		284	15.5	186	
	268		12.6	191	
	211	250		194	
	215	254		197	
	218	245			
R 11		255	18.6	130.2	
			20.2	148.6	
			8.9		
			11.1		
	224	228	14.2		
		273	15.1		
	274		17.9		
			9.8		

- 43 -

Megabreccias in northeastern Wernecke Mountains, Yukon Territory

Project 750069

R.T. Bell
Economic Geology and Mineralogy Division

Bell, R.T., Megabreccias in northeastern Wernecke Mountains, Yukon Territory; in Current Research, Part A, Geological Survey of Canada, Paper 86-1A, p. 375-384, 1986.

Abstract

In northeastern Wernecke Mountains megabreccias occur in an arcuate complex roughly 25 km wide and at least 80 km long. The breccia complex includes shattered and megabreccia units (mainly of fine grained Fairchild Lake Group strata) together with strongly disrupted elements of the Fairchild Lake Group. Although exact processes for the main phase of breccia formation are not clear, structural and stratigraphic relationships indicate clearly that the breccias are intrusive, terminate usually at the base of Gillespie Lake Group, and that they began to form during deposition of the Middle Proterozoic Wernecke Supergroup. There are striking metallogenic and lithological similarities with breccias in South Australia, an area of significant Cu-U ± Au deposits.

Résumé

Dans le nord-est des monts Wernecke, on peut observer des mégabrèches dans un complexe arqué qui mesure approximativement 25 km de largeur sur au moins 80 km de longueur. Le complexe bréchique renferme des unités de brèches de dislocation et de mégabrèches (constituées surtout de strates à grains fins du groupe de Fairchild Lake), ainsi que des éléments fortement disloqués du groupe de Fairchild Lake. On ne sait pas exactement par quels processus a eu lieu la phase principale de la formation des brèches, mais les relations structurales et stratigraphiques observées indiquent clairement que les brèches sont intrusives, qu'elles se terminent habituellement à la base du groupe de Gillespie Lake et qu'elles ont commencé à se former durant le dépôt du supergroupe de Wernecke au milieu du Protérozoïque. Ces unités présentent des similitudes métallogéniques et lithologiques frappantes avec des brèches découvertes en Australie du Sud, région où l'on trouve également des gisements importants de cuivre et d'uranium avec ou sans or.

Introduction

This report presents an interpretive geological map of the rock units in northeastern Wernecke Mountains. Field work to 1985 is incorporated in Figures 43.2, 43.3 and 43.4. Figure 43.2 is based on scattered field observations, local detailed mapping and discussions with others working in the area and published maps and airphoto interpretation. It is an interim compilation of published maps (Green, 1972; Blusson, 1974; Laznicka, 1977b, Norris, 1982a,b) for which field work was done before the extensive nature of the breccias was identified. It provides a basis for more detailed systematic remapping of this area. Such remapping is already in progress in the Dawson area, one hundred kilometres to the west.

A second purpose of this report is to provide additional data for comparison with other megabreccias such as those in South Australia. Jefferson (1978) and Bell (1982) have suggested that a connection once existed between the Proterozoic of South Australia and of the Yukon. If true then there are very important implications for mineral resources potential of the Proterozoic in northwestern Canada, as speculated in the last part of this report.

Figure 43.1 shows the general distribution of groups in the Wernecke Supergroup and location for the more detailed map (Fig. 43.2) which straddles four published map sheets: Wind River (Norris, 1982a); Snake River (Norris, 1982b); Nash Creek (Green, 1972) and Nadaleen (Blusson, 1974). Only the maps by Norris show the approximate location of some breccias. Figures 43.3 and 43.4 show detail in section and enlarged plan of the geology.

Stratigraphy

The region is underlain by Phanerozoic rocks and by three major Precambrian successions. Quaternary, Lower Paleozoic and the two lower Precambrian successions are present in the area of Figure 43.2. The uppermost Precambrian succession lies immediately to the east and together with the middle succession, the 'Pinguicula' Group, is described by Eisbacher (1977, 1978b, 1981). The lowest succession, the Wernecke Supergroup (Delaney, 1981) comprises as much as 14 km of sedimentary rocks divided into three groups.

Fairchild Lake Group

The lowest group of the Wernecke Supergroup as defined and described by Delaney (1981) is made up of at least 4 km of light to dark grey, laminated, commonly dolomitic, siltstone, mudstone and fine-grained sandstone, with minor black shale and light grey carbonate and quartzite. Pale greenish grey phyllites are locally distributed. On Figure 43.2 the Fairchild Lake Group is shown as three units.

Unit 1 comprises successions of mainly laminated dolomitic siltstone and mudstone with shattered zones and monolithic breccia dykes. It is interpreted to be part of the breccia complex because of: (1) internal disruption and the presence of breccia dykes; (2) stratigraphic disruption of the entire unit (see unit 2 below); and (3) heterolithic breccias adjacent to or bordering the unit. Unit 1 also contains thick successions of pale green phyllite and of light grey limestone.

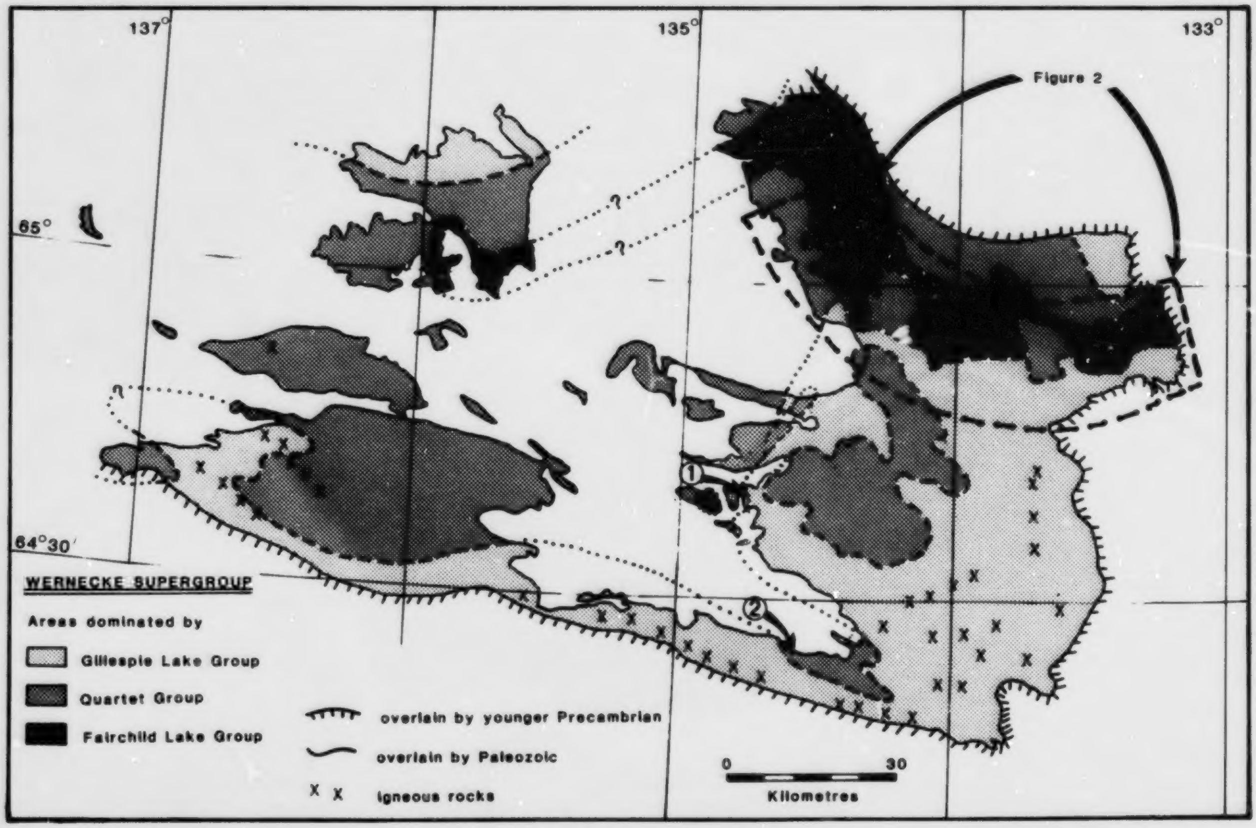

Figure 43.1. Distribution of Wernecke Supergroup in Northeastern Wernecke Mountains and locations referred to in text. After Bell (1978), Green (1972), Delaney (1978) and Norris (1982a,b).

Unit 2 comprises successions of mainly dolomite, laminated siltstone and fine sandstone but appears to lack internal shatter zones and significant internal breccias. Importantly it is usually very steeply dipping to overturned (for example see unit F-1 of Delaney, 1981). Rocks of Unit 2 are not easily ranked in stratigraphic order with the remaining Fairchild Lake Group. Unit 2 is accordingly designated a 'disrupted unit'. It is assigned with less certainty than unit 1 to the breccia complex, and is a target requiring more detailed mapping.

Unit 3 comprises mainly mudstone and siltstone with minor carbonate, quartzite, and black mudstone (shale, slate) markers. It is traced into and includes the transitional facies (F-TR of Delaney, 1981) of the Fairchild Lake Group. Accordingly it is intact with respect to stratigraphic order. With more detailed mapping undoubtedly parts of unit 2 will be assigned to unit 3.

Quartet Group

Overlying the Fairchild Lake Group, the Quartet Group, as defined by Delaney (1981) is characterized by a monotonous succession of black to dark grey siltstone, mudstone and sandstone. The transition to the overlying, orange-weathering Gillespie Lake Group rocks is gradational upwards through grey, dolomitic, thinly layered siltstone and sandstone. The Quartet Group is estimated to be at least 5 km thick, but in some cases it appears to be considerably thinner. Locally, faulting has created this apparent thinning but as discussed below some of the thinning is primary. Together with stratigraphic anomalies, it has implications for the timing and origin of the megabreccia development.

As noted above the Quartet Group is generally monotonous. This monotony is interrupted at locality 1 (Fig. 43.1) on an eastern tributary of Bond Creek where a radioactive gossan zone is hosted by black turbidites. Immediately east of the gossan, graded rudite beds (010° strike, 60° east dip, upright) are characterized by conglomeratic basal beds that grade sharply upward into dark grey laminated mudstones. These turbidite layers range from 10 cm to 3 m in thickness. The pebbles (maximum size 2 cm) are characterized by siltstone, siliceous mudstone and fine sandstone fragments that resemble parts of the Quartet Group or the upper Fairchild Lake Group. The pebbles are usually well rounded but about 10 per cent are angular in the thicker units. These turbidites are less than 200 m (stratigraphic thickness) below the base of the Gillespie Lake Group as exposed on the ridge immediately southeast. All units including the Gillespie Lake Group are cut by an east-trending, subvertical dolerite dyke. The interval between the turbidites and the Gillespie Lake Group is covered largely by talus or moraine, but heaved outcrops together with talus indicate that this interval is Quartet Group: mainly black mudstone, siltstone and fine sandstone with more dolomitic siltstone near the base of the Gillespie Lake Group. If these turbidites are truly within the Quartet Group and particularly within the upper part, they constitute a local departure from the generally coarsening upward aspect of the black clastics in the Quartet Group and they also reflect the first reported occurrence of conglomerates.

Massive zones of brownish, manganese- and iron-oxide-stained coarse homolithic breccias occur about 8 km west of locality 2. The fragments are of similar lithology to those in the turbidites, but they are larger (mainly centimetre size to a maximum of 15 cm) and lack apparent internal layering other than a weak subvertical north-trending foliation (cleavage). The fragments are both round and angular. In 1976 I thought these breccias were vent-breccia. However, the mixture of rounded and angular but homolithic fragments, similar to those in graded beds 8 km east, suggests they may be proximal slump zones. Heterolithic breccias, that crosscut overturned altered siltstones of the Fairchild Lake Group, occur about one kilometre farther west of the massive homolithic breccias. The host sequence contains green, grey and bleached (pinkish), siliceous dolomitic argillites and phyllites identical with altered zones in sediments of the Fairchild Lake Group around Fairchild Lake. None of the breccias contain unequivocal magmatically derived rocks; if volcanic they are the product of explosive gas-venting.

Slump folded beds are common in the upper two-thirds of the Quartet Group throughout the area; they may in part represent the distal response to doming and/or explosive venting that formed breccias such as those at Bond Creek (locality 2).

At the headwaters of Bond Creek thicknesses of possibly less than 1000 m but certainly not more than 2000 m of Quartet Group strata are estimated. In any case, here the Quartet Group is considerably thinner than the estimated thickness of 5 km quoted above.

The above stratigraphic anomalies are interpreted as responses to doming and explosive venting associated with emplacement of the breccia complex. Figure 43.5 presents a model which may explain these phenomena by breccia intrusion during Quartet Group time. Doming above sea level with venting should provide the breccias and coarse turbidites described above. Doming, not above sea level should provide areas of high freeboard, more or less starved of terrigenous sediments and could cause early initiation of carbonate deposition. Doming, in both cases could explain anomalous thinning of the Quartet Group. This hypothesis should be considered in future interpretations of thickness and paleocurrent direction data from the Quartet and Gillespie Lake groups.

Gillespie Lake Group

The Gillespie Lake Group, as defined by Delaney (1981), is characterized by grey, buff and brown weathering dolomite and minor epiclastic rocks showing both rapid lateral and vertical facies changes. Delaney (1981) estimated the unit to be at least 4 km thick. In Dolores Creek area it is truncated by an erosional unconformity and overlain by red and green siltstones of basal Pinguicula Group (Eisbacher, 1981). A 5-m-thick green andesitic flow overlies breccias at location 1 (Fig. 43.4) and is in turn overlain conformably by red and green siltstones. Farther south and along the south edge of the Wernecke Mountains there are volcanics and associated clastic rocks in the basal Pinguicula strata.

Pinguicula Group

The only published details on Pinguicula Group stratigraphy are in Eisbacher (1981) following what was essentially an informal regional usage by earlier workers. The group is correlated with the pre-Windermere (pre-Rapitan) Mackenzie Mountain Group and possibly Coates Lake Group (Jefferson and Ruelle, in press). For discussions on the Pinguicula Group see Eisbacher (1978a, 1979), Yeo et al. (1978), and Bell (1982).

During 1985 a single small exposure of coarse to fine feldspathic sandstone, pebbly sandstone and cobble conglomerate was discovered east of Mount Williams at locality 2 (Fig. 43.1). The basal cobble layer dips gently southwesterly, is about one metre thick, and lies on steeply southwest-dipping black siltstones of the Quartet Group. At the south end of the outcrop area a massive greenstone is likely a dyke within the Quartet Group (alternatively it may be a down-faulted sill or flow). The cobbles are light brown (weathered) to light green (unweathered), well rounded

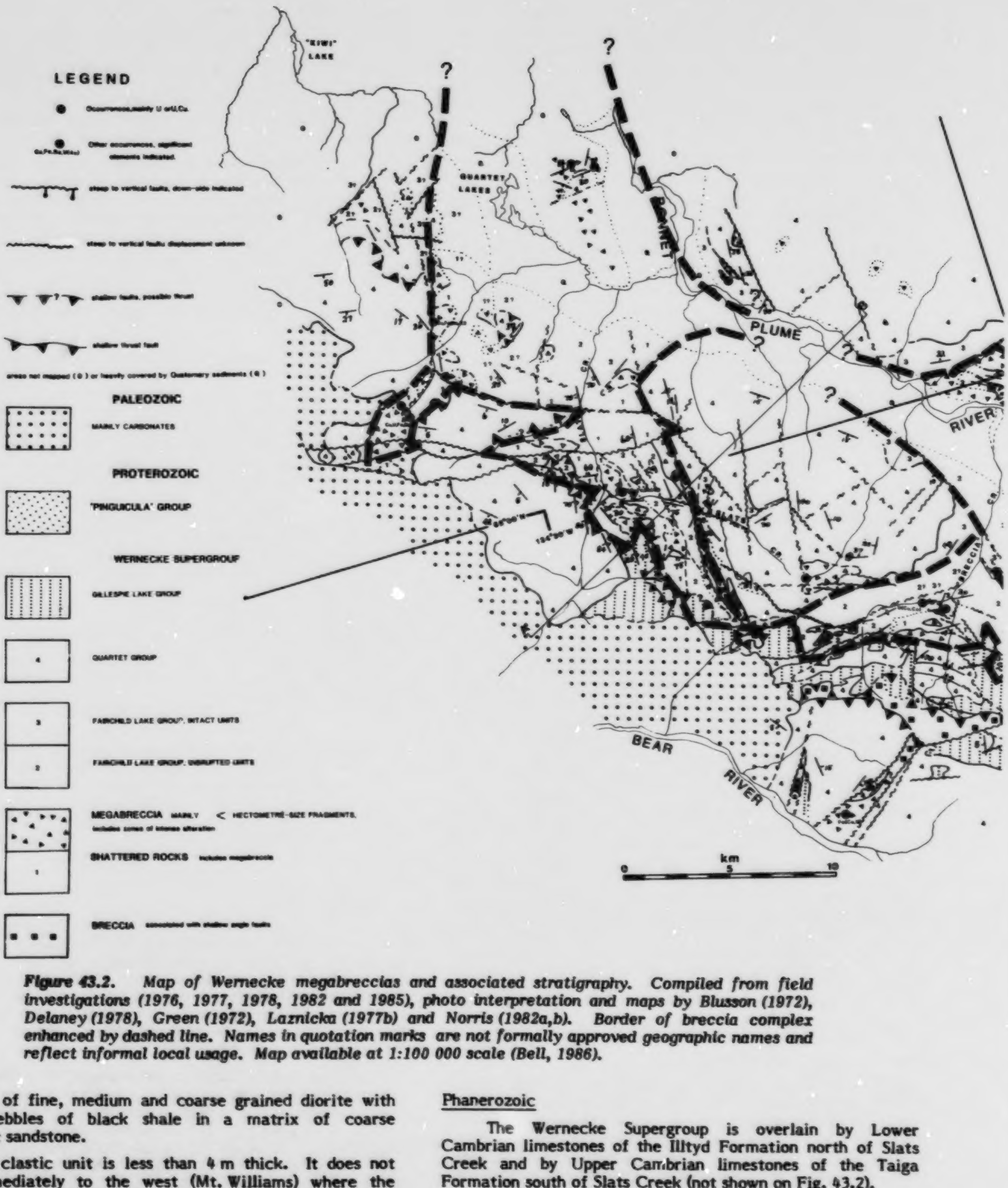

Figure 43.2. *Map of Wernecke megabreccias and associated stratigraphy. Compiled from field investigations (1976, 1977, 1978, 1982 and 1985), photo interpretation and maps by Blusson (1972), Delaney (1978), Green (1972), Laznicka (1977b) and Norris (1982a,b). Border of breccia complex enhanced by dashed line. Names in quotation marks are not formally approved geographic names and reflect informal local usage. Map available at 1:100 000 scale (Bell, 1986).*

fragments of fine, medium and coarse grained diorite with angular pebbles of black shale in a matrix of coarse feldspathic sandstone.

This clastic unit is less than 4 m thick. It does not occur immediately to the west (Mt. Williams) where the Gillespie Lake Group outcrops nor on the ridge to the east where Quartet Group rocks outcrop and therefore it is probably fault bounded. The unit is tentatively assigned to the Pinguicula Group but it may be younger.

Phanerozoic

The Wernecke Supergroup is overlain by Lower Cambrian limestones of the Illtyd Formation north of Slats Creek and by Upper Cambrian limestones of the Taiga Formation south of Slats Creek (not shown on Fig. 43.2).

Quaternary glacial and alluvial sediments cover much of the lowest valleys, particularly along Bonnet Plume River.

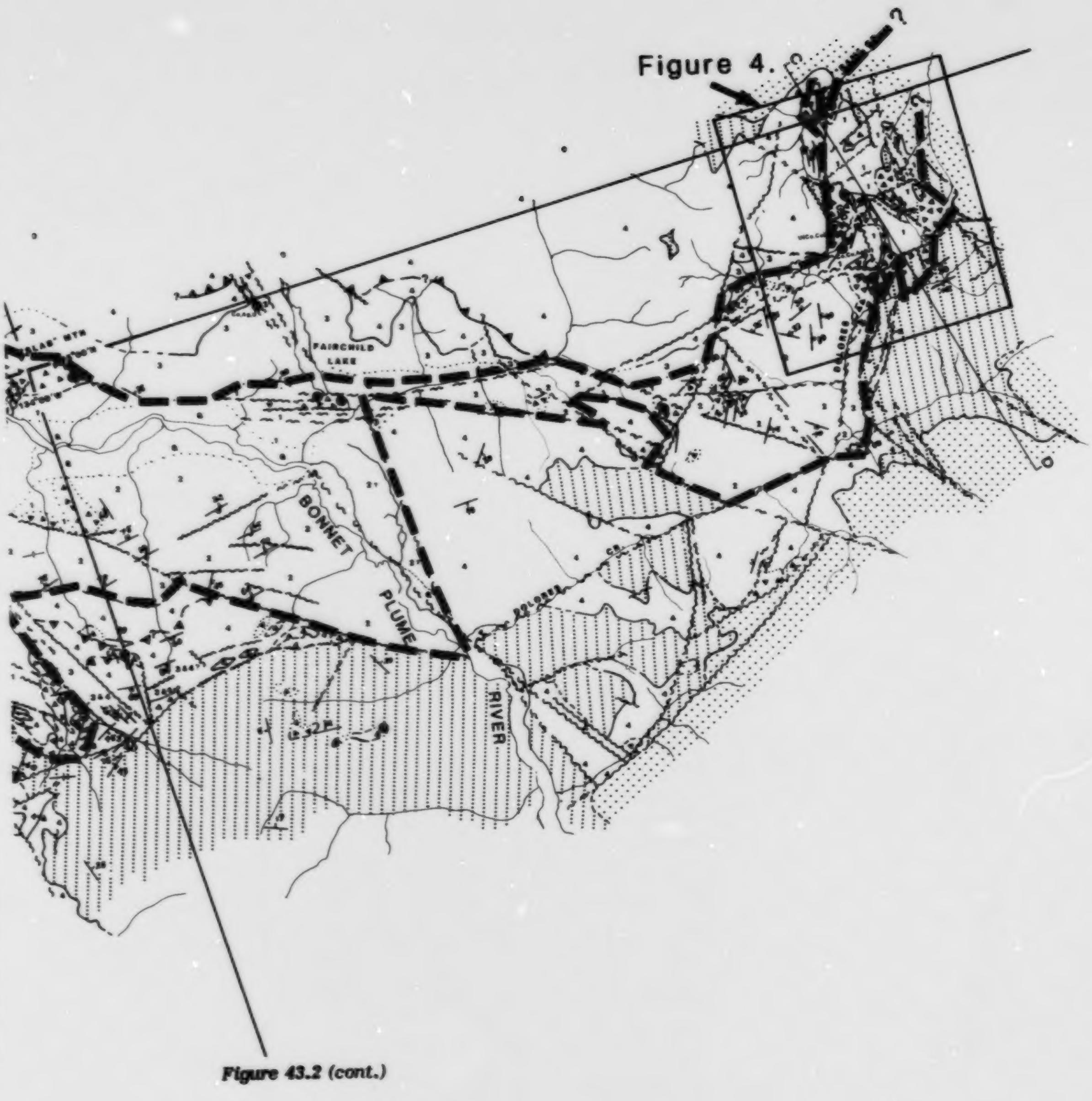

Figure 43.2 (cont.)

Structure

Away from the breccia zones bedding in all units shows shallow to moderate dips as shown on Figure 43.2. Tight folds occur along a portion of the breccia contact at 'Ram' Creek and parallel with the southeast branch of 'Breccia' Creek on the northeast side. In the upper part of the Fairchild Group to the northeast this latter zone is on strike with irregular folds that increase in amplitude downwards.

Only a few of the high-angle to vertical faults are shown on the maps. West-northwest-trending faults affect rocks as young as lower Cambrian. Northeast- and north-northeast-trending faults affect mainly Wernecke Supergroup rocks. North- and northwest-trending faults cut both Wernecke and Pinguicula strata. The drainage patterns in the region strongly reflect the northeast- and west-northwest-trending faults.

Northerly dipping thrust faults near Fairchild Lake increase the apparent thickness of Quartet Group rocks. A shallow southwest-dipping fault with mechanical characteristics of a 'thrust' occurs along the trend from the headwaters of 'Breccia' Creek to Slats Creek (Fig. 43.2, 43.3). A segment of this fault, described earlier (Bell, 1978), has been tentatively traced to the northwest. The notable feature is that overturned strata of the basal Gillespie Lake

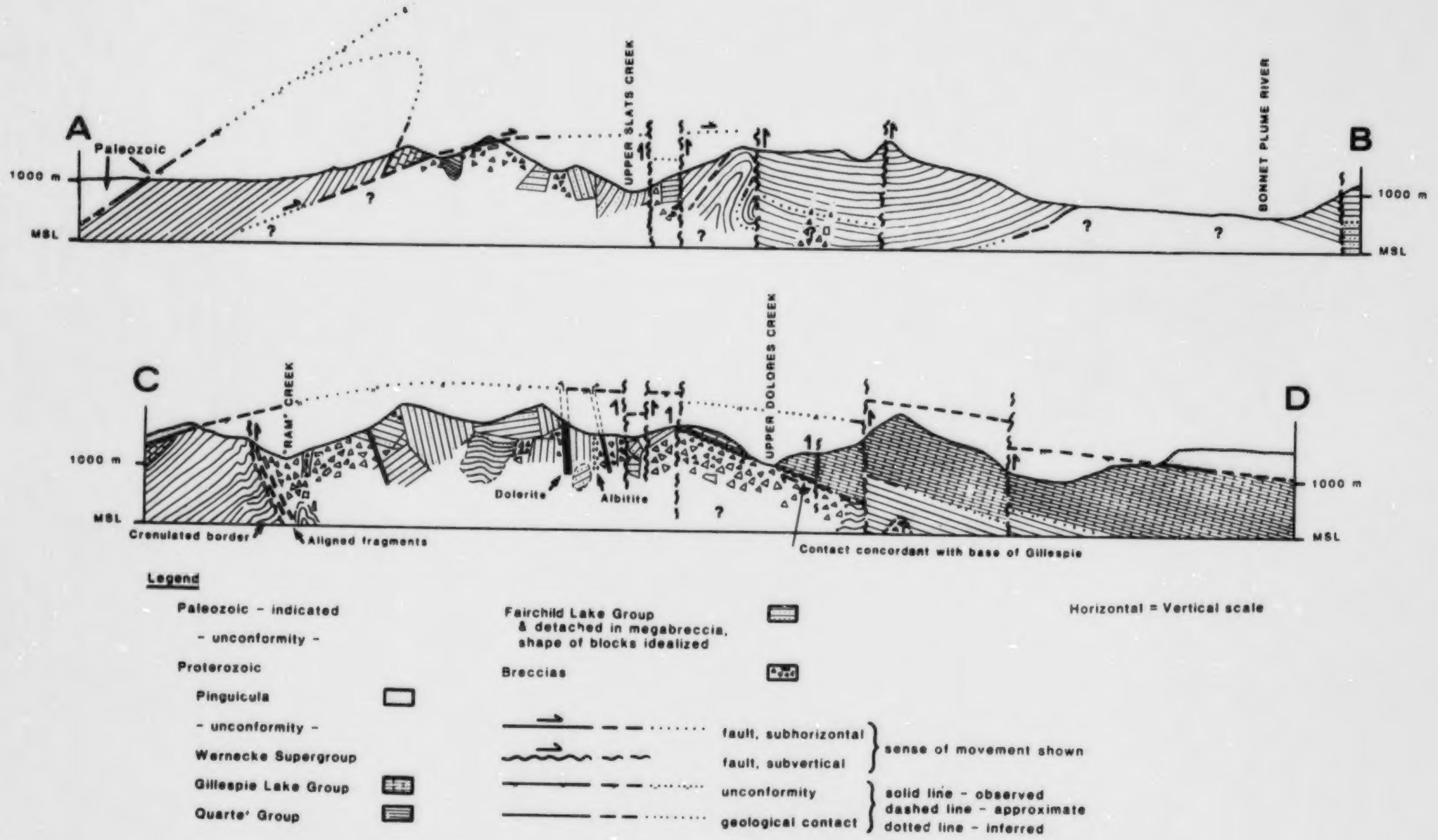

Figure 43.3. *Cross-sections through Wernecke megabreccias, with more detail on lithology.*

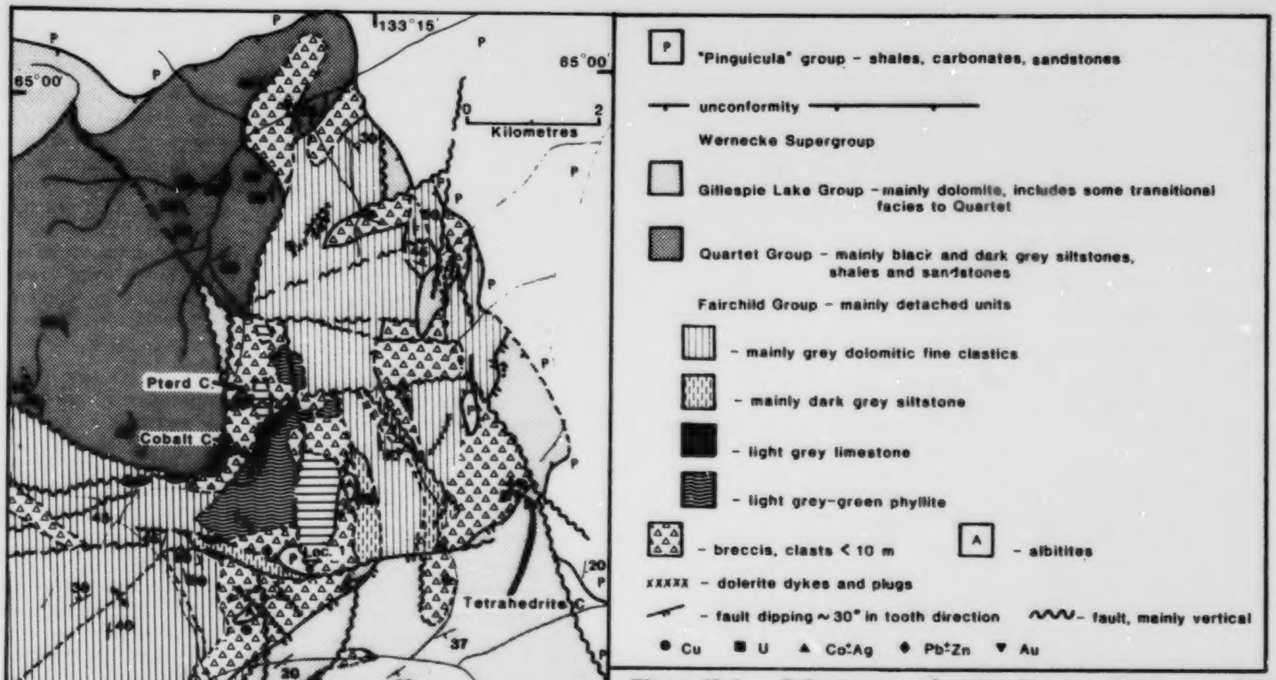

Figure 43.4. *Enlargement of upper Dolores Creek area from Figure 43.2 with more detail on lithology of detached units.*

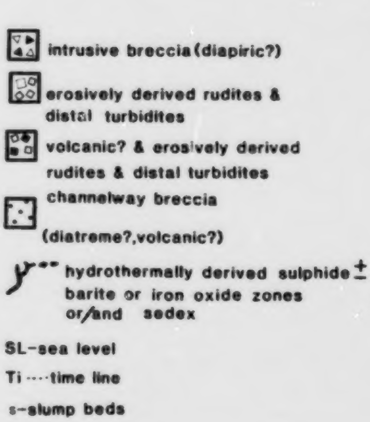

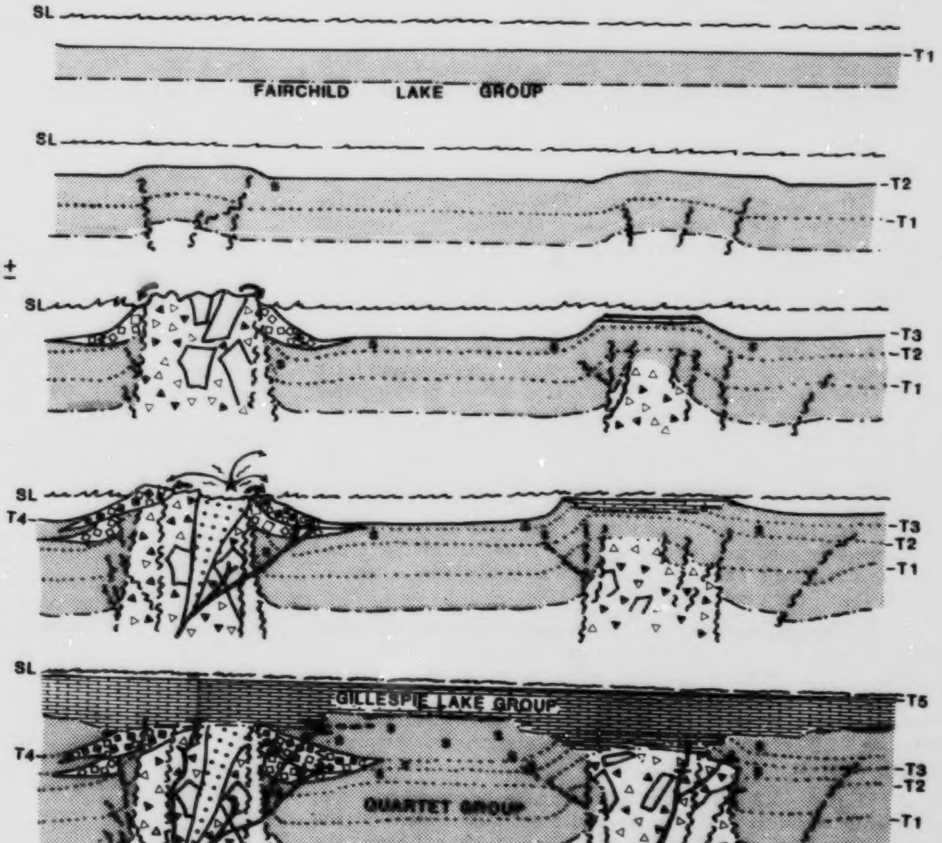

Figure 43.5

Speculative model for progressive intrusion of Wernecke breccias during deposition of Quartet and Gillespie Lake groups proposed to explain anomalous thicknesses of Quartet Group and presence of turbidites.

Group have been thrust over breccias dominated by fragments of Fairchild Lake Group at Slats Creek. The heterolithic breccias have a crude layering and fabric for 200 m beneath the fault that suggests they have been sheared subsequent to emplacement. At the head of 'Breccia' Creek the footwall zone is mainly brecciated (homolithic) upper Quartet Group rocks and in turn overlies folded upper Quartet and lower Gillespie Lake Group rocks. This fault, here termed the Slats Creek Fault, is cut by west-northwest-trending faults which in turn affect Lower Cambrian rocks. As neither Pinguicula nor Rapitan units occur in the area the age of this fault is not known with respect to these units.

The contact on the south side of the Dolores Creek breccia suggests constraints on the timing of brecciation (Fig. 43.3, 43.4). Lower Gillespie Lake Group strata are concordant with the breccia contact which dips about 30° southerly. Commonly the breccias are heterolithic but at one location west of 'Tetrahedrite' Creek they grade into homolithic breccias of dolomitic, laminated siltstone and sandstone similar to those in the transitional zone between Quartet and Gillespie Lake units. These homolithic breccias show both brittle and plastic deformation, the matrix is of smeared muddy and sandy silt(stone) and the fragments vary from angular with sharp contacts, to rounded with nebulous contacts grading into the matrix. In addition some fragments are strongly bent. Coarsening of grain-size (recrystallization) and obvious metasomatic alterations are absent. These and similar breccias in 'Pterd' Cirque both contain uranium minerals and anomalous copper and cobalt contents.

The above features suggest that a phase of brecciation occurred before the transitional Gillespie Lake rocks were fully lithified. The south contact suggests an intrusion of the main breccias that terminated (top-out) against lower Gillespie Lake Group strata. The northeastern contact is discordant with Quartet Group rocks; the border breccias have tabular fragments aligned with the contact.

The breccias

Mineral exploration in the 1950s and 1960s identified copper associated with breccias. However the regional distribution of these breccias was not recognized until Archer, Cathro and Associates (1981) Limited discovered uranium mineralization in these breccias in the mid 1970s.

Company reports from the 1960s suggested a volcanic origin for the breccias. Bell (in Bell and Delaney, 1977) suggested mainly diatreme and volcanic connections and later (1978) largely discounted these, and suggested a more passive process relating to faulting. However Tempelman-Kluit (1981) gave impressive evidence concerning a diatreme origin for the NOR breccia. Laznicka and Edwards (1979) suggested association with intrusive bodies. Delaney et al. (1982) proposed dividing the breccias into three varieties: fault, stope and channelway breccias. The channelway breccias may approach diatremes in the broad sense but in any case these are not laterally very extensive (less than 1 per cent).

To complicate matters the strongly iron-enriched zones beg a connection with Rapitan iron-formation (Bell, 1978, 1982; Gross, 1965). In addition, a few mineralized zones show elevated thorium contents (but still less than one tenth uranium content) and one associated with calcite veins shows strong REE enrichment which may suggest a connection with carbonatites.

Figure 43.2 shows the breccias as a whole to be huge, laterally extensive bodies. In this area, independent of the inclusion of disrupted units of Fairchild Lake Group, the breccia bodies are laterally connected and follow an arcuate pattern coalescing with the Richardson Fault Array (see Norris and Hopkins, 1977; Delaney, 1981; Bell, 1978, 1982). The breccia bodies contain clasts in the kilometre-size range, but commonly less than hectometre-size. Some of the smaller exotic clasts are of lithologies not represented in the intact Fairchild Lake Group (e.g. jaspilite and iron-formation clasts in swarms, gabbro-diorite, albitite). Some of the kilometre-size blocks have apparent stratigraphic thicknesses that are very much greater than lithologically similar units in the Fairchild Lake Group. Their association with other blocks which were definitely derived from lower levels, and with structures indicating upward movement imply that these very thick blocks are also exotic and derived from below.

Other features, including complex mineralogy have been summarized by Bell (1982) and compared with breccias in South Australia. Bell's (1982) comparison is further strengthened in this regard because parts of the spectacular Olympic Dam (Roxby Downs) deposit have been identified as being discordant heterolithic breccias (D. Roberts, personal communication, 1984); rather than entirely flat lying breccias as earlier proposed (Roberts and Hudson, 1983).

The term diapir is widespread in application to the South Australian breccias (Dalgarno and Johnson, 1968; Lemon, 1985) but it suffers from the same shortcoming in connection with interpretation of the Wernecke breccias; namely, the lack of known extensive evaporites. Dalgarno (1983) reviewed the differing hypotheses of origin for the South Australian breccias including: carbonatitic intrusions, structurally deformed horst blocks, mud islands, megaslumps, and syn- to post-depositional diapirism. It is plain that both the Adelaide Geosyncline of South Australia and the Wernecke Mountains of Yukon share similar, thick, Proterozoic records (Jefferson, 1978; Bell, 1982) and show evidence for extensional tectonism throughout their history (see for example Eisbacher, 1977, 1978b, 1981) which implies a deep crustal cause. Therefore it should not be surprising that faulting should be so pervasive. Igneous-like features (carbonatites, albitites, mafic-intermediate dykes and volcanics) and strong alteration effects (albitization, carbonatization, and especially mineralization) could be direct and indirect responses to deep-seated movements.

In the Wernecke Mountains the age of main brecciation event(s) appears to be older than the Pinguicula Group. Laznicka and Edwards (1979) provide evidence that albitites grade into breccias, implying a metasomatic origin for these albitites. This in turn implies that the breccias at Dolores Creek are older than or syngenetic with the albitization event. However, in 1985 large angular fragments of albitite were also found in the heterolithic breccias in this area. This implies that either another period of brecciation followed the formation of the albitites or there was an earlier generation of albitites.

Farther west in the Ogilvie Mountains, evidence exists for multiple phases of brecciation (Fig. 3, in Bell, 1978) and brecciation involving younger rocks (Lefebvre, 1980). In this area the cores of some of the smaller breccia bodies are intruded by dolerite dykes and some of the breccias are spatially associated with faults. Therefore it is concluded that several periods of breccia formation occurred in the Wernecke and Ogilvie mountains during the Late Proterozoic but that the main phase of breccia formation was completed in the Wernecke Mountains before deposition of the Pinguicula Group. The ages of uranium mineralization are discussed in an accompanying paper (Archer et al., 1986).

Conclusions

This paper together with earlier papers by Bell, Delaney and Laznicka demonstrates the size and complexity of the Wernecke megabreccias and provides some constraints on their genesis. The breccias have provided significant conduits for mineralizing fluids until at least the middle Cambrian.

The host stratigraphy, size, age and mineralogy of the Wernecke megabreccias are comparative with breccias in the Adelaide Geosyncline and Stuart Shelf of Australia. They also have in common diverse interpretations of origin (see for example: Lambert et al., 1982; Youles, 1984; Lemon, 1985) although the Adelaidean breccias have been studied for several decades. The Adelaidean breccias host numerous mineral deposits including the world class Olympic Dam (Roxby Downs) deposit. Closer comparison of the deposits and re-investigation of mineral occurrences of both areas are important. For example, when Olympic Dam was found some surprise was expressed at the hematite (± magnetite) and copper sulphide association although many of the occurrences farther east (for example Mount Painter (Youles, 1984)) also have this association. The discovery that intrusive breccias are important at Olympic Dam reveals the potential for more world class deposits in the Adelaide Geosyncline. By analogy, the same may be true for the Wernecke Mountains and adjacent areas.

As an aid to exploration, more detailed mapping is necessary in the Wernecke Mountains. Mapping is being done by the Geological Survey of Canada (see Thompson and Roots, 1982), and by students of P. Laznicka (University of Manitoba) sponsored by the Department of Indian and Northern Affairs. Regional aeromagnetic and gravity surveys have proven useful for exploration of the Australian breccias. The former would be very useful in the Wernecke Mountains area but gravity surveys would be somewhat impractical due to topographic relief.

Acknowledgments

Al Archer introduced me to the Wernecke breccias and together with K.M. Dawson, D.K. Norris and S.L. Blusson introduced me to the regional geology. A.T. Cross (1982), G. Delaney (1976), L.D. Jones (1977, 1978) and P. Ruck (1977) ably assisted during field seasons. L.D. Jones assisted in initial map compilation and W. Donaldson and G. Young assisted in drafting. I am very grateful for cooperation and courtesies extended by personnel from companies working in this area, particularly Archer, Cathro and Associates (1981) Limited, Eldorado Resources Limited, Esso Minerals Canada, Pamicon and Cordilleran Engineering. Access to various deposits and discussions on field relationships provided by these companies are invaluable. I gratefully acknowledge the enthusiastic support of my colleagues, particularly H. Gabrielse and C.W. Jefferson who critically reviewed an earlier draft of this paper.

References

Archer, A., Bell, R.T., and Thorpe, R.
1986: Age relationships from U-Th-Pb isotope studies of uranium mineralization in Wernecke breccias, Yukon Territory; in Current Research, Part A, Geological Survey of Canada, Paper 86-1A, Report 44.

Bell, R.T.
1978: Breccias and uranium mineralization in the Wernecke Mountains, Yukon – a progress report; in Current Research, Part A, Geological Survey of Canada, Paper 78-1A, p. 317-322.

Bell, R.T. (cont.)
1982: Comments on the geology and uraniferous mineral occurrences of the Wernecke Mountains, Yukon and District of Mackenzie; in Current Research, Part B, Geological Survey of Canada, Paper 82-1B, p. 279-284.

1986: Geological map of northeastern Wernecke Mountains, Yukon Territory; Geological Survey of Canada, Open File No. 1207.

Bell, R.T. and Delaney, G.D.
1977: Geology of some uranium occurrences in Yukon Territory; in Current Research, Part A, Geological Survey of Canada, Paper 77-1A, p. 33-37.

Blusson, S.L.
1974: Nadaleen River map-area of Operation Stewart; Geological Survey of Canada, Open File No. 205.

Dalgarno, C.R.
1983: Adelaide geosyncline sedimentary environments and tectonic settings symposium; Australian Geological Society Abstracts 10, 80 p.

Dalgarno, C.R. and Johnson, J.E.
1968: Diapiric structures and Late Precambrian-Early Cambrian sedimentation in Flinders Ranges, South Australia; in Diapirism and Diapirs, a Symposium, ed. J. Braunstein and G.D. O'Brian; American Association of Petroleum Geologists, Memoir 8, p. 301-314.

Delaney, G.D.
1978: A progress report on stratigraphic investigations of the lowermost succession of Proterozoic rocks, northern Wernecke Mountains, Yukon Territory; Department of Indian and Northern Affairs, Open File EGS 1978-10, 12 p., plus 3 figures.

1981: The mid-Proterozoic Wernecke Supergroup, Wernecke Mountains, Yukon Territory; in Proterozoic Basins of Canada, ed. F.H.A. Campbell; Geological Survey of Canada, Paper 81-10, p. 1-23.

Delaney, G.D., Jefferson, C.W., Yeo, G.M., McLennan, S.M., Aitken, J.D., and Bell, R.T.
1982: Some Proterozoic sediment-hosted metal occurrences of the northeastern Canadian Cordillera; in Idaho Bureau of Mines and Geology, Bulletin 24, p. 97-116.

Eisbacher, G.H.
1977: Tectono-stratigraphic framework of the Redstone Copper Belt, District of Mackenzie; in Report of Activities, Part A, Geological Survey of Canada, Paper 77-1A, p. 229-234.

1978a: Two major Proterozoic unconformities, northern Cordillera; in Current Research, Part A, Geological Survey of Canada, Paper 78-1A, p. 53-58.

1978b: Redefinition and subdivision of the Rapitan Group, Mackenzie Mountains; Geological Survey of Canada, Paper 77-35, 22 p.

1979: Comment 'Middle and late Proterozoic evolution of the northern Canadian Cordillera and Shield'; Geology, v. 7, p. 329.

1981: Sedimentary tectonics and glacial record in the Windermere Supergroup, Mackenzie Mountains, northwestern Canada; Geological Survey of Canada, Paper 80-27, 40 p.

Green, L.H.
1972: Geology of Nash Creek, Larsen Creek and Dawson map-areas, Yukon Territory; Geological Survey of Canada, Memoir 364, 157 p.

Gross, G.A.
1965: Geology of iron ore deposits and iron-formations of Canada; in Report of Activities, Field 1964, Geological Survey of Canada, Paper 65-1, p. 142-143.

Jefferson, C.W.
1978: Correlation of middle and upper Proterozoic strata between northwestern Canada and south and central Australia; Geological Association of Canada, Program with Abstracts, v. 3, p. 429.

Jefferson, C.W. and Ruelle, J.C.L.
– The Late Proterozoic Redstone Copper Belt, Mackenzie Mountains, N.W.T.; in Mineral Deposits of Northern Cordillera, ed. J.A. Morin; CIM Special Volume. (in press)

Lambert, I.B., Drexal, J.F., Donnelly, T.H., and Knutson, J.
1982: Origin of breccias in the Mount Pointer area, South Australia; Journal Geological Society of Australia, v. 29, p. 115-125.

Laznicka, P.
1977a: Geology and mineralization in the Dolores Creek area, Bonnet Plume Range, Yukon; in Current Research, Part A, Geological Survey of Canada, Paper 77-1A, p. 435-439.

1977b: Geology and mineralization in the Dolores Creek area, Yukon; Department of Indian and Northern Affairs, Open File, May 1977, 87 p.

Laznicka, P. and Edwards, R.J.
1979: Dolores Creek, Yukon – a disseminated copper mineralization in sodic metasomatites; Economic Geology, v. 74, p. 1352-1370.

Lefebvre, J.J.
1980: A propos de l'existence d'un "Wildflysch Katangien"; Annales de la Société géologique de Belgique, T. 103, p. 1-13.

Lemon, N.M.
1985: Physical modelling of sedimentation adjacent to diapirs and comparison with Late Precambrian Oratunga breccia body in central Flinders Ranges, South Australia; American Association of Petroleum Geologists Bulletin, v. 69, no. 9, p. 1327-1338.

Norris, D.K.
1982a: Wind River, Yukon; Geological Survey of Canada, Map 1528A.

1982b: Snake River, Yukon and N.W.T.; Geological Survey of Canada, Map 1529A.

Norris, D.K. and Hopkins, W.S.
1977: The geology of the Bonnet Plume Basin, Yukon Territory; Geological Survey of Canada, Paper 76-8, 20 p.

Roberts, D.E. and Hudson, G.R.T.
1983: The Olympic Dam copper-uranium-gold deposit, Roxby Downs, South Australia; Economic Geology, v. 78, p. 799-822.

Tempelman-Kluit, D.J.
1981: NOR, summary of assessment work and description of mineral properties; in Yukon, Geology and Exploration 1979-80, Geology Section, Department of Indian and Northern Affairs, p. 300-301.

Thompson, R.I. and Roots, C.F.
1982: Ogilvie Mountains project, Yukon; Part A: a new regional mapping program; in Current Research, Part A, Geological Survey of Canada, Paper 82-1A, p. 403-411.

Yeo, G.M., Delaney, G.D., and Jefferson, C.W.
1978: Two Proterozoic unconformities, northern Cordillera: discussion; in Current Research, Part B, Geological Survey of Canada, Paper 78-1B, p. 225-230.

Youles, I.P.
1984: The Olympic Dam copper-uranium-gold deposit, Roxby Downs, South Australia – a discussion; Economic Geology, v. 79, p. 1941-1944.

Author Index/Index des auteurs

Name	Page
Adshead, J.D.	737
Ames, D.E.	205
Archer, A.	385
Avery, M.P.	489
Bamber, E.W.	627
Barr, S.M.	291
Barrie, J.V.	251
Beauchamp, B.	627
Beckett, M.	667
Bégin, N.J.	1
Bell, J.S.	489
Bell, R.T.	375, 385
Bell, T.	221
Bolduc, A.M.	697
Bornhold, B.D.	737
Bostock, H.H.	35
Brandon, M.T.	683
Brown, R.L.	81
Buchanan, J.R	275
Burden, E.T.	483
Calon, T.	471
Cameron, A.R.	645
Carter, R.W.G.	55
Cattalani, S.	365
Caudill, M.R.	343
Cawood, P.A.	675, 759
Chandler, F.W.	121
Charbonneau, B.W.	803
Christie, R.L.	795
Clark, J.I.	251
Coe, K.	159
Collins, W.T.	251
Copeland, M.J.	663
Cordey, F.	595
Coyle, M.	455, 499
Culshaw, N.	275
Currie, K.L.	333
Dabros, M.J.	107
Davis, E.E.	737
Dennis, F.A.R.	291
Dingwell, D.B.	455
Dredge, L.A.	779
Dubord, M.P.	603
Dunsworth, S.	471
Edlund, S.A.	719
Emslie, R.F.	755
Finck, P.W.	809
Forbes, D.L.	55
Forest, R.	177
Frarey, M.J.	43
Frith, R.A.	113
Furey, D.J.	461
Gall, Q.	95
Galley, A.G.	205
Gao Ruixing	399
Gariépy, C.	265
Grant, A.C.	65
Graves, M.C.	423
Grotzinger, J.P.	95
Hall, G.E.M.	71, 89
Halwas, D.B.	583
Harris, D.C.	49
Haynes, S.J.	141
Henderson, J.B.	411
Henderson, J.R.	159
Henderson, M.N.	159
Hill, J.D.	185
Holloway, D.C.	483
Hope, T.L.	429
Insley, M.W.	259
Jackson, G.D.	541
James, D.T.	417
Jefferson, C.W.	159
Josenhans, H.W.	221
Journeay, M.	81
Kiely, L.A.	141
King, J.E.	21
Kjarsgaard, B.	755
Klassen, R.A.	697, 713
Kontak, D.J.	465
Kostaschuk, R.A.	565
Krawetz, M.T.	749
Krogh, T.E.	43
Kubli, T.	553
Kurfurst, P.J.	775
Langille, A.B.	483
LeCheminant, A.N.	159
LeCheminant, G.M.	531
Lee, K.	65
Lefebvre, C.	755
Levy, E.M.	65
Lewis, C.F.M.	251
Liedtke, J.	571
Linnen, R.L.	239
Loveridge, W.D.	113, 523
Lucas, S.B.	1
Luternauer, J.L.	565
Macfie, R.I.	411
MacInnis, I.	423
Mackay, J.R.	727
MacLean, B.	769
Macnab, R.	791
Macqueen, R.W.	603
Malpas, J.	471
Mamet, B.L.	627
Manojlovic, P.	275
Maurice, Y.T.	301, 307
McAlpine, K.D.	489
McCann, S.B.	749
McClay, K.R.	259
McDonough, M.R.	619
Mercier, M.M.	301
Millard, T.H.	565
Moffat, J.D.	65
Morrow, D.W.	603
Mountjoy, E.W.	177
Mudie, P.J.	107
Mulja, T.	423
Murphy, J.B.	445
Nance, R.D.	343, 351
Nielsen, E.	779
Norris, D.K.	645, 801
O'Brien, B.H.	439
Orchard, M.J.	683
Orford, J.D.	55
Osadetz, K.G.	609
Owen, J.V.	515

	Page
Paktunc, A.D.	327
Parrish, R.R.	683
Parrott, D.R.	251
Pedder, A.E.H.	649
Pelchat, J.C.	89
Poulsen, K.H.	205
Raeside, R.P.	291
Reilly, B.A.	141
Richards, B.C.	627
Roberts, A.	571
Rogerson, R.J.	221
Roscoe, S.M.	787
Ruzicka, V.	531
St-Onge, D.A.	783
St-Onge, M.R.	1
Sacks, P.E.	213
Samson, I.M.	239, 359
Sangster, A.L.	151
Sangster, D.F.	133
Saunders, C.M.	229, 319
Schau, M.	667
Scott, D.J.	1
Scott, J.S.	783
Sears, W.B.	483
Sherlock, R.	755
Shih, K.G.	791
Shilts, W.W.	703
Simony, P.S.	583, 619
Smith, S.L.	703
Snowdon, L.R.	609
Spethmann, D.	21
Stea, R.R.	809
Stevens, K.	435

	Page
Strong, D.F.	229, 319, 393, 455, 461, 465, 499
Struik, L.C.	589
Sutherland Brown, A.	683
Swettenham, S.S.	803
Swinden, H.S.	213
Taylor, R.B.	55
Thompson, F.J.	713
Thompson, P.H.	275
Thorpe, R.I.	385
Vaillancourt, P.D.	133
Vaive, J.E.	71
van Breemen, O.	113
van Staal, C.R.	193
Vilks, G.	769
Villeneuve, M.E.	21
Wallace, G.M.	507
Warner, J.B.	351
Whalen, J.B.	265, 297
White, C.E.	291
Wilcox, K.H.	21
Williams, H.	675, 759
Williams, H.F.L.	559
Williams-Jones, A.E.	239, 359, 365
Woodend, S.L.	429
Yeo, G.M.	399
Yorath, C.J.	683
Zaleski, E.	15
Zentilli, M.	423
Zwicker, E.J.	393

Erratum

Geological Survey of Canada, Paper 85-1B

Current Research, Part B

Report 16: Regional sedimentology of the Namewaminikan Group, northern Ontario: Archean fluvial fans, braided rivers, deltas, and an aquabasin: J.R. Devaney and P.W. Fralick.

p. 132: The following references were omitted.

Goodwin, A.M.
1977: Archean basin-craton complexes and the growth of Precambrian shields; Canadian Journal of Earth Sciences, v. 14, p. 2737-2759.

Hyde, R.S.
1980: Sedimentary facies in the Archean Timiskaming Group and their tectonic implications, Abitibi greenstone belt, northeastern Ontario, Canada; Precambrian Research, v. 12, p. 161-195.

Kehlenbeck, M.M.
1983: Structural studies in the Beardmore-Geraldton area; in Summary of Field Work, 1983, by the Ontario Geological Survey, ed. J. Wood et al.; Ontario Geological Survey, Miscellaneous Paper 116, p. 201-203.
1984: Use of stratigraphic and structural-facing directions to delineate the geometry of folded folds near Thunder Bay, Ontario; Geoscience Canada, v. 11, p. 23-32.

Langford, G.B.
1929: Geology of the Beardmore-Nezah gold area, Thunder Bay District; Ontario Department of Mines Annual Report, v. 37, part 4, 1928, p. 83-108.

Mackasey, W.O.
1975: Geology of Dorothea, Sandra, and Irwin Townships, District of Thunder Bay; Ontario Division of Mines, Geological Report 122, 83 p.
1976: Geology of Walters and Leduc Townships, District of Thunder Bay; Ontario Division of Mines, Geoscience Report 149, 48 p.

Mackasey, W.O., Edwards, G.R., and Cape, D.F.
1976: Legault Township, District of Thunder Bay; Ontario Division of Mines, Preliminary Map P 1191, Geological series, scale 1:15 840.

Geological Survey of Canada
Commission géologique du Canada

PAPER
ÉTUDE 86-1A

CURRENT RESEARCH PART A
RECHERCHES EN COURS PARTIE A

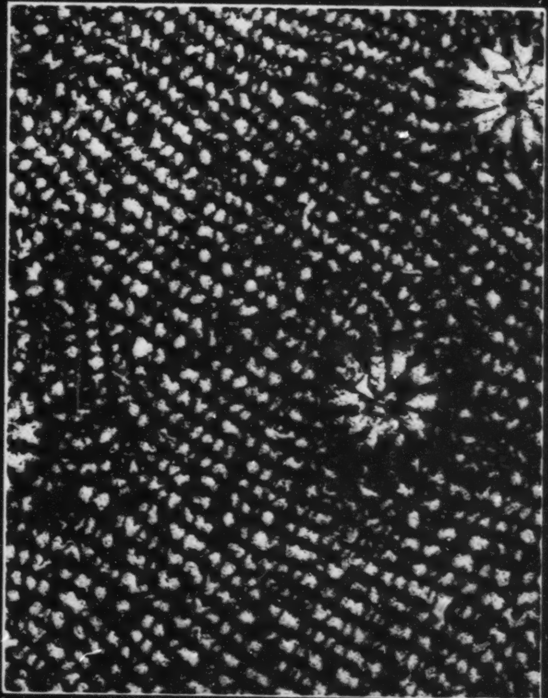

(Pages 385-826)

Canada

1986

Notice to Librarians and Indexers

The Geological Survey's twice-yearly *Current Research* series contains many reports comparable in scope and subject matter to those appearing in scientific journals and other serials. All contributions to Current Research include an abstract and bibliographic citation. It is hoped that these will assist you in cataloguing and indexing these reports and that this will result in a still wider dissemination of the results of the Geological Survey's research activities.

Avis aux bibliothécaires et préparateurs d'index

La série *Recherches en cours* de la Commission géologique paraît deux fois par année; elle contient plusieurs rapports dont la portée et la nature sont comparables à ceux qui paraissent dans les revues scientifiques et autres périodiques. Tous les articles publiés dans les Recherches en cours sont accompagnés d'un résumé et d'une bibliographie, ce qui vous permettra, nous l'espérons, de cataloguer et d'indexer ces rapports, d'où une meilleure diffusion des résultats de recherche de la Commission géologique.

GEOLOGICAL SURVEY OF CANADA
PAPER 86-1A

COMMISSION GÉOLOGIQUE DU CANADA
ÉTUDE 86-1A

CURRENT RESEARCH PART A

RECHERCHES EN COURS PARTIE A

Issued in two sections/Publiée en deux volumes:
pages 1-384 and/et pages 385-826

1986

© Minister of Supply and Services Canada 1986

Available in Canada through

authorized bookstore agents and other bookstores

or by mail from

Canadian Government Publishing Centre
Supply and Services Canada
Ottawa, Canada K1A 0S9

and from

Geological Survey of Canada offices:

601 Booth Street
Ottawa, Canada K1A 0E8

3303-33rd Street N.W.,
Calgary, Alberta T2L 2A7

100 West Pender Street
Vancouver, British Columbia V6B 1R8
(mainly B.C. and Yukon)

A deposit copy of this publication is also available
for reference in public libraries across Canada

Cat. No. M44-86/1AE Canada: $20.00
ISBN 0-660-11992-7 Other countries: $24.00

Sold in sets

Price subject to change without notice

Cover

Left Gravity corer being recovered with a marine sediment core in the plastic barrel, Byam Martin Channel, Lougheed Island region, District of Franklin. See note by MacLean and Vilks (p. 769-774) for details.

Right Transverse thin section, enlarged X10, of **Scruttonia** sp. cf. **S. bowerbanki** (Milne Edwards and Haine). See report 78, p. 649-661, by A.E.H. Pedder for details of Devonian rugose corals.

Page couverture

Gauche Recouvrement d'un carottier gravimétrique dont le tube de plastique contient un échantillon de sédiment marin prélevé dans le chenal Byam Martin, dans la région de l'île Lougheed, district de Franklin. Voir la note de MacLean et Vilks (p. 769-774) pour des détails plus précis.

Droite Lame mince transversale, aggrandie X10, de **Scruttonia** sp. cf. **S. bowerbanki** (Milne Edwards et Haine). Les détails relatifs aux tétracoralliaires se trouvent dans le rapport 78 de A.E.H. Pedder, p. 649-661.

- **DIRECTOR GENERAL** / *DIRECTEUR GÉNÉRAL* — R.A. Price
  - Administrative Services / *Services administratifs* — Y. P. Claude
  - Personnel Services / *Services du personnel*
  - Financial Services / *Services financiers*
  - Special Advisor / *Conseiller spécial* — J.A. Maxwell
  - **CHIEF GEOLOGIST** / *GÉOLOGUE EN CHEF* — J. G. Fyles
    - International Relations Unit / *Services des relations internationales*
    - Mineral Development Programs Unit / *Service des programmes de mise en valeur des ressources minérales*
    - Program Office / *Bureau de planification* — D. G. Benson
    - Special Projects / *Projets spéciaux*
  - **CORDILLERAN GEOLOGY DIVISION** (Vancouver, B.C.) / *DIVISION GÉOLOGIE DE LA CORDILLÈRE (Vancouver, C.-B.)* — R. B. Campbell
    - Mainland Geology / *Géologie continentale*
    - Pacific Marine Geology (Pacific Geoscience Centre) / *Géologie marine du Pacifique (Centre géoscientifique du Pacifique)*
    - Information Services / *Services d'information*
  - **PRECAMBRIAN GEOLOGY DIVISION** / *DIVISION GÉOLOGIE DU PRÉCAMBRIEN* — J. C. McGlynn
    - Bear-Slave / *Bear-Slave*
    - Northern Churchill / *Churchill-Nord*
    - Superior-Grenville / *Supérieur-Grenville*
    - Paleomagnetism / *Paléomagnétisme*
    - Geochronology / *Géochronologie*
    - Petrology / *Pétrologie*
    - Special Projects / *Projets spéciaux*
  - **RESOURCE GEOPHYSICS AND GEOCHEMISTRY DIVISION** / *DIVISION GÉOPHYSIQUE ET GÉOCHIMIE APPLIQUÉES* — A. G. Darnley
    - Resource Geochemistry / *Géochimie appliquée*
    - Resource Geophysics / *Géophysique appliquée*
    - Regional Geophysics / *Géophysique régionale*
    - Special Projects / *Projets spéciaux*
    - Technical Services / *Services techniques*
  - **TERRAIN SCIENCES DIVISION** / *DIVISION SCIENCE DES TERRAINS* — J. S. Scott
    - Paleoecology and Geochronology / *Paléoécologie et géochronologie*
    - Geomorphic Processes / *Processus géomorphologiques*
    - Sedimentology and Mineral Tracing / *Sédimentologie et détection des minéraux*
    - Engineering Geology / *Géologie appliquée*
    - Regional Projects / *Projets régionaux*
  - **GEOLOGICAL INFORMATION DIVISION** / *DIVISION INFORMATION GÉOLOGIQUE* — R. G. Blackadar
    - Scientific Editing / Publication Production / *Rédaction scientifique et publication*
    - Data Systems / *Systèmes informatisés*
    - Cartography / *Cartographie*
    - Library Services / *Services de la bibliothèque*
    - Technical Photography / *Techniques photographiques*
    - Publications / *Publications*
  - **INSTITUTE OF SEDIMENTARY AND PETROLEUM GEOLOGY** (Calgary, Alta.) / *INSTITUT DE GÉOLOGIE SÉDIMENTAIRE ET PÉTROLIÈRE* (Calgary, Alberta) — W. W. Nassichuk
    - Petroleum Geology / *Géologie pétrolière*
    - Regional Geology / *Géologie régionale*
    - Coal Geology / *Géologie du charbon*
    - Paleontology (including Ottawa) / *Paléontologie (incluant Ottawa)*
    - Geological Information / *Information géologique*
    - Petroleum Resource Assessment Secretariat / *Secrétariat d'évaluation des ressources pétrolières*
  - **ATLANTIC GEOSCIENCE CENTRE** (Darthmouth, N.S.) / *CENTRE GÉOSCIENTIFIQUE DE L'ATLANTIQUE - Dartmouth, N.-É.* — M. J. Keen
    - Eastern Petroleum Geology / *Géologie pétrolière de l'Est*
    - Environmental Marine Geology / *Géologie du milieu marin*
    - Regional Reconnaissance / *Recherche régionale*
    - Program Support / *Planification*
  - **ECONOMIC GEOLOGY AND MINERALOGY DIVISION** / *DIVISION GÉOLOGIE ÉCONOMIQUE ET MINÉRALOGIE* — D. C. Findlay
    - Mathematical Applications In Geology / *Mathématiques appliquées à la géologie*
    - Mineral Deposits Geology / *Géologie des gîtes minéraux*
    - Regional Metallogenic Studies / *Études de la métallogénèse régionale*
    - Regional Mineral Resource Assessment / *Évaluation des ressources minérales régionales*
    - Mineral Resource Information Services / *Services d'information sur les ressources minérales*
    - Analytical Chemistry / *Chimie analytique*
    - Mineralogy / *Minéralogie*

Separates

A limited number of separates of the papers that appear in this volume are available by direct request to the individual authors. The addresses of the Geological Survey of Canada offices follow:

601 Booth Street,
OTTAWA, Ontario
K1A 0E8

Institute of Sedimentary and Petroleum Geology,
3303-33rd Street N.W.,
CALGARY, Alberta
T2L 2A7

Cordilleran Geology Division
100 West Pender Street,
VANCOUVER, B.C.
V6B 1R8

Atlantic Geoscience Centre,
Bedford Institute of Oceanography,
P.O. Box 1006,
DARTMOUTH, N.S.
B2Y 4A2

When no location accompanies an author's name in the title of a paper, the Ottawa address should be used.

Tirés à part

On peut obtenir un nombre limité de "tirés à part" des articles qui paraissent dans cette publication en s'adressant directement à chaque auteur. Les adresses des différents bureaux de la Commission géologique du Canada sont les suivantes:

601, rue Booth
OTTAWA, Ontario
K1A 0E8

Institut de géologie sédimentaire et pétrolière
3303-33rd, St. N.W.,
CALGARY, Alberta
T2L 2A7

Division de la géologie de la Cordillère
100 West Pender Street
VANCOUVER, Colombie-Britannique
V6B 1R8

Centre géoscientifique de l'Atlantique
Institut océanographique de Bedford
B.P. 1006
DARTMOUTH, Nouvelle-Ecosse
B2Y 4A2

Lorsque l'adresse de l'auteur ne figure pas sous le titre d'un document, on doit alors utiliser l'adresse d'Ottawa.

SCIENTIFIC AND TECHNICAL REPORTS
RAPPORTS SCIENTIFIQUES ET TECHNIQUES

ECONOMIC GEOLOGY/GÉOLOGIE ÉCONOMIQUE

E. ZALESKI: Geology of the Linda volcanogenic massive sulphide deposit, Snow Lake, Manitoba 15

P.D. VAILLANCOURT and D.F. SANGSTER: Isotope and hydrocarbon studies of the Yava sandstone-lead deposit, Cape Breton Island, Nova Scotia: a progress report 133

A.L. SANGSTER: Willemite and native silver occurrences, Kirkmount, Pictou County, Nova Scotia 151

K.H. POULSEN, D.E. AMES, and A.G. GALLEY: Gold mineralization in the Star Lake pluton, La Ronge belt, Saskatchewan: a preliminary report 205

C.M. SAUNDERS and D.F. STRONG: Assessment of lead-zinc deposits of the western Newfoundland carbonate platform 229

A.E. WILLIAMS-JONES, I.M. SAMSON, and R.L. LINNEN: Preliminary results of a study of the ores, wall-rock alteration, and fluid inclusions at the Madeleine copper mine, Gaspé, Quebec 239

D.F. STRONG and C.M. SAUNDERS: Geological setting of sulphide mineralization at Tilt Cove, Newfoundland 319

A.D. PAKTUNC: St. Stephen mafic-ultramafic intrusion and related nickel-copper deposits, New Brunswick 327

S. CATTALANI and A.E. WILLIAMS-JONES: Geological and fluid inclusion studies at the Saint-Robert Ag, W, Bi deposit, eastern townships, Quebec 365

K. STEVENS: Metallogenic studies in the Candego and Madeleine mines area, Gaspesie, Quebec: a progress report 435

V. RUZICKA and G.M. LECHEMINANT: Developments in uranium geology in Canada, 1985 .. 531

GEOCHEMISTRY/GÉOCHIMIE

G.E.M. HALL and J.E. VAIVE: Analysis of in-house control reference samples by commercial laboratories using inductively-coupled plasma emission spectrometry 71

G.E.M. HALL and J.C. PELCHAT: The determination of boron and other refractory elements in geological materials by inductively-coupled plasma emission spectrometry 89

Y.T. MAURICE and M.M. MERCIER: A new approach to sampling heavy minerals for regional geochemical exploration 301

Y.T. MAURICE: Interpretation of a reconnaissance geochemical heavy mineral survey in the eastern townships of Quebec 307

M. ZENTILLI, M.C. GRAVES, T. MULJA, and I. MacINNIS: Geochemical characterization of the Goldenville-Halifax transition of the Meguma Group of Nova Scotia: preliminary report 423

GEOCHRONOLOGY/GÉOCHRONOLOGIE

M.J. FRAREY and T.E. KROGH: U-Pb zircon ages of late internal plutons of the Abitibi and eastern Wawa subprovinces, Ontario and Quebec 43

R.A. FRITH, W.D. LOVERIDGE, and O. VAN BREEMEN: U-Pb ages on zircon from basement granitoids of the western Slave Structural Province, northwestern Canadian Shield 113

A. ARCHER, R.T. BELL, and R.I. THORPE: Age relationships from U-Th-Pb isotope studies of uranium mineralization in Wernecke breccias, Yukon Territory 385

W.D. LOVERIDGE: U-Pb ages on zircon from rocks of the Lac de Morhiban map area, Quebec 523

M.T. BRANDON, M.J. ORCHARD, R.R. PARRISH, A. SUTHERLAND BROWN, and C.J. YORATH: Fossil ages and isotopic dates from the Paleozoic Sicker Group and associated intrusive rocks, Vancouver Island, British Columbia 683

MARINE GEOSCIENCE/ÉTUDES GEOSCIENTIFIQUES DU MILIEU MARIN

R.B. TAYLOR, R.W.G. CARTER, D.L. FORBES, and J.D. ORFORD: Beach sedimentation in Ireland: contrasts and similarities with Atlantic Canada 55

A.C. GRANT, E.M. LEVY, K. LEE, and J.D. MOFFAT: **Pisces IV** research submersible finds oil on Baffin Shelf 65

R.J. ROGERSON, H.W. JOSENHANS, and T. BELL: A 3.5 kHz acoustic survey of Nachvak Fiord, northern Labrador 221

J.V. BARRIE, W.T. COLLINS, J.I. CLARK, C.F.M. LEWIS, and D.R. PARROTT: Submersible observations and origin of an iceberg pit on the Grand Banks of Newfoundland 251

H.F.L. WILLIAMS: Depositional facies and evolution of Lulu Island topset deposits, Fraser Delta, British Columbia 559

R.A. KOSTASCHUK, J.L. LUTERNAUER, and T.H. MILLARD: Sediment transport during the 1985 freshet in the outer main channel of the Fraser River estuary, British Columbia 565

A. ROBERTS and J. LIEDTKE: Airborne definition of suspended surface sediment and intertidal environments in the Fraser River plume, British Columbia 571

MINERALOGY/MINÉRALOGIE

D.C. HARRIS: The minerals in the main Hemlo gold deposit, Ontario 49

I.M. SAMSON and A.E. WILLIAMS-JONES: Illite crystallinity studies in the Gaspé-Connecticut Valley synclinorium around Barnston, Quebec 359

G.M. WALLACE: The mineralogy of the McGerrigle plutonic complex, Gaspé, Quebec 507

PALEONTOLOGY/PALÉONTOLOGIE

M.J. DABROS and P.J. MUDIE: An automated microscope system for image analysis in palynology and micropaleontology 107

A.E.H. PEDDER: The Devonian rugose coral genera **Haplothecia, Kuangxiastraea** and **Scruttonia** 649

M.J. COPELAND: **Dioxycaris fritzi** sp. nov. (Arthropoda, Phyllocarida) from the Pika Formation (Middle Cambrian, **Bolaspidella** Zone), Jasper National Park, Alberta 663

PETROLEUM GEOLOGY/GÉOLOGIE PÉTROLIÈRE

M.P. AVERY, J.S. BELL, and K.D. McALPINE: Vitrinite reflectance measurements and their implications for oil and gas exploration in the Jeanne d'Arc Basin, Grand Banks, eastern Canada 489

K.G. OSADETZ and L.R. SNOWDON: Petroleum source rock reconnaissance of southern Saskatchewan 609

D.K. NORRIS and A.R. CAMERON: An occurrence of bitumen in the Interior Platform near Rengleng River, District of Mackenzie 645

QUATERNARY GEOLOGY/GÉOLOGIE DU QUATERNAIRE

Inventory mapping and stratigraphic studies/Inventaire cartographique et stratigraphique

W.W. SHILTS and S.L. SMITH: Stratigraphy of placer gold deposits; overburden drilling in Chaudière Valley, Quebec 703

S.A. EDLUND: Vegetation-geology-climate relationships of western Melville Island, District of Franklin 719

Sedimentology and geomorphology/Sédimentologie et géomorphologie

R.A. KLASSEN and A.M. BOLDUC: Ice flow trends and drift composition, Flowers River area, Labrador 697

F.J. THOMPSON and R.A. KLASSEN: Ice flow directions and drift composition, central Labrador 713

J.R. MACKAY: Fifty years (1935 to 1985) of coastal retreat west of Tuktoyaktuk, District of Mackenzie 727

J.D. ADSHEAD, B.D. BORNHOLD, and E.E. DAVIS: Indurated deposits and possible plume bands in a hydrothermal mound, northeast Pacific 737

M.T. KRAWETZ and S.B. McCANN: Coastal characteristics, east-central Ellesmere Island, District of Franklin 749

REGIONAL GEOLOGY/GÉOLOGIE RÉGIONALE

Appalachian region/Région des Appalaches

J.D. HILL: Granitoid plutons in the Canso area, Nova Scotia 185

H.S. SWINDEN and P.E. SACKS: Stratigraphy and economic geology of the southern part of the Roberts Arm Group, central Newfoundland 213

J.B. WHALEN and C. GARIÉPY: Petrogenesis of the McGerrigle plutonic complex, Gaspé, Quebec: a preliminary report 265

R.P. RAESIDE, S.M. BARR, C.E. WHITE, and F.A.R. DENNIS: Geology of the northernmost Cape Breton Highlands, Nova Scotia 291

J.B. WHALEN: A-type granites in New Brunswick 297

K.L. CURRIE: The boundaries of the Avalon tectonostratigraphic zone, Musquash Harbour-Loch Alva region, southern New Brunswick 333

M.R. CAUDILL and R.D. NANCE: Variscan tectonostratigraphy of the Mispec Group, southern New Brunswick: stratigraphy and depositional setting 343

E.J. ZWICKER and D.F. STRONG: The Great Bend ophiolite, eastern Newfoundland: field investigations 393

G.M. YEO and GAO RUIXING: Late Carboniferous dextral movement on the Cobequid-Hollow fault system, Nova Scotia: evidence and implications 399

T.L. HOPE and S.L. WOODEND: Geological mapping and igneous and metamorphic petrology, Queen's and Shelburne counties, Nova Scotia 429

B.H. O'BRIEN: Preliminary report on the geology of the Mahone Bay area, Nova Scotia 439

J.B. MURPHY: Geology of the western Antigonish Highlands, Nova Scotia 445

M. COYLE, D.F. STRONG, and D.B. DINGWELL: Geology of the Sheffield Lake group, west-central Newfoundland 455

D.J. FUREY and D.F. STRONG: Geology of the Harbour Breton Complex, Newfoundland 461

D.J. KONTAK and D.F. STRONG: The volcano-plutonic King's Point complex, Newfoundland 465

S. DUNSWORTH, T. CALON, and J. MALPAS: Structural and magmatic controls on the internal geometry of the plutonic complex and its chromite occurrences in the Bay of Islands Ophiolite, Newfoundland 471

M. COYLE and D.F. STRONG: Geology of the southern and northern margins of the Springdale Caldera, Newfoundland 499

J.V. OWEN: Geology of the Silver Mountain area, western Newfoundland 515

P.A. CAWOOD and H. WILLIAMS: Northern extremity of the Humber Arm Allochthon in the Portland Creek area, western Newfoundland, and relationships to nearby groups 675

H. WILLIAMS and P.A. CAWOOD: Relationships along the eastern margin of the Humber Arm Allochthon between Georges Lake and Corner Brook, western Newfoundland 759

Arctic Islands/Archipel Arctique

A.B. LANGILLE, E.T. BURDEN, W.B. SEARS, and D.C. HOLLOWAY: Geological investigation of Cretaceous? strata beneath Cape Dyer Basalts (Paleocene), Baffin Island, District of Franklin 483

Cordilleran region/Région de la Cordillère

M. JOURNEAY and R.L. BROWN: Major tectonic boundaries of the Omineca Belt in southern British Columbia: a progress report 81

E.W. MOUNTJOY and R. FOREST: Revised structural interpretation, Selwyn Range between Ptarmigan and Hugh Allan creeks, British Columbia – an antiformal stack of thrusts 177

K.R. McCLAY and M.W. INSLEY: Structure and stratigraphy of the Gataga fold and thrust belt, northeastern British Columbia 259

R.T. BELL: Megabreccias in northeastern Wernecke Mountains, Yukon Territory 375

T. KUBLI: Stratigraphy and structure of the Hadrynian Horsethief Creek Group in the northern Dogtooth Range south of Grizzly Creek, Purcell Mountains, British Columbia 553

D.B. HALWAS and P.S. SIMONY: The Castlegar Gneiss Complex, southern British Columbia 583

L.C. STRUIK: A regional east-dipping thrust places Hadrynian onto probable Paleozoic rocks in Cariboo Mountains, British Columbia 589

F. CORDEY: Radiolarian ages from the Cache Creek and Bridge River complexes and from chert pebbles in Cretaceous conglomerates, southwestern British Columbia 595

M.P. DUBORD, D.W. MORROW, and R.W. MACQUEEN: A shelf-to-basin transition in the Devonian Ogilvie Formation, Yukon Territory 603

M.R. MCDONOUGH and P.S. SIMONY: Geology of the northern Selwyn Range, western Main Ranges, Rocky Mountains, British Columbia: preliminary report 619

Canadian Shield/Bouclier canadien

M.R. ST-ONGE, S.B. LUCAS, D.J. SCOTT, and N.J. BÉGIN: Eastern Cape Smith Belt: an early Proterozoic thrust-fold belt and basal shear zone exposed in oblique section, Wakeham Bay and Cratère du Nouveau Québec map areas, northern Quebec 1

J.E. KING, M.E. VILLENEUVE, D. SPETHMANN, and K.H. WILCOX: Geology of the northwestern metamorphic-internal zone and an outlier of the eastern Great Bear Magmatic Zone of Wopmay Orogen, Big Bend area, District of Mackenzie 21

H.H. BOSTOCK: Reconnaissance geology of Precambrian rocks of the Fort Resolution, Taltson Lake, and Fort Smith areas, District of Mackenzie 35

J.P. GROTZINGER and Q. GALL: Preliminary investigations of Early Proterozoic Western River and Burnside River formations: evidence for foredeep origin of Kilohigok Basin, District of Mackenzie 95

F.W. CHANDLER: Sedimentology and paleoclimatology of the Huronian (Early Aphebian) Lorrain and Gordon Lake Formations and their bearing on models for sedimentary copper mineralization 121

J.R. HENDERSON, A.N. LeCHEMINANT, C.W. JEFFERSON, K. COE, and M.N. HENDERSON: Preliminary account of the geology around Wager Bay, District of Keewatin 159

P.H. THOMPSON, N. CULSHAW, J.R. BUCHANAN, and P. MANOJLOVIC: Geology of the Slave Province and Thelon Tectonic Zone in the Tinney Hills-Overby Lake (west half) map area, District of Mackenzie 275

J.B. HENDERSON and R.I. MACFIE: Artillery Lake map area, District of Mackenzie: a transect across the Thelon Front 411

D.T. JAMES: Geology of the Moraine Lake area, District of Mackenzie; Part 2: a transect across part of the Thelon Tectonic Zone 417

G.D. JACKSON: Notes on the Proterozoic Thule Group, northern Baffin Bay 541

M. SCHAU and M. BECKETT: High grade metamorphic rocks of northwestern Melville Peninsula, District of Franklin 667

R.F. EMSLIE, C. LEFEBVRE, B. KJARSGAARD, and R. SHERLOCK: Atikonak River massif, Labrador 755

STRATIGRAPHY/STRATIGRAPHIE

B. BEAUCHAMP, B.C. RICHARDS, E.W. BAMBER, and B.L. MAMET: Lower Carboniferous lithostratigraphy and carbonate facies, upper Banff Formation and Rundle Group, east-central British Columbia 627

STRUCTURAL GEOLOGY/GÉOLOGIE STRUCTURABLE

S.J. HAYNES, B.A. REILLY, and L.A. KIELY: Structural setting of the Mile Lake gold prospect, Guysborough County, Nova Scotia 141

C.R. VAN STAAL: Preliminary results of structural investigations in the Bathurst camp of northern New Brunswick 193

R.D. NANCE and J.B. WARNER: Variscan tectonostratigraphy of the Mispec Group, southern New Brunswick: structural geometry and deformational history 351

SCIENTIFIC AND TECHNICAL NOTES
NOTES SCIENTIFIQUES ET TECHNIQUES

B. MACLEAN and G. VILKS: Marine geological program in the Byam Martin Channel - Lougheed Island region, District of Franklin 769

P.J. KURFURST: Geotechnical investigation of seabottom sediments, Tuktoyaktuk area, District of Mackenzie 775

L.A. DREDGE and E. NIELSEN: Gold concentrations in till, Great Island, northern Manitoba 779

D.A. ST-ONGE and J.S. SCOTT: Notes on the geomorphology and Quaternary geology of northeastern Ungava Peninsula, Nouveau Québec 783

S.M. ROSCOE: Felsic volcanic rocks in the Nonacho Group near Whitefish Lake, District of Mackenzie 787

K.G. SHIH and R. MACNAB: Efficient algorithms for computing the gravitational effect of rectangular prisms 791

R.L. CHRISTIE: The Melville Project, 1984-85: progress report 795

D.K. NORRIS: Lower Devonian Road River Formation on the north flank of Romanzof Uplift, northern Yukon Territory 801

B.W. CHARBONNEAU and S.S. SWETTENHAM: Gold occurrence in radioactive calc-silicate float at Sandybeach Lake, Nueltin Lake area, District of Keewatin 803

CANADA-NOVA SCOTIA CO-OPERATIVE MINERAL PROGRAM 1981-84 809
CANADA-NOUVELLE-ÉCOSSE: PROGRAMME COOPÉRATIF SUR LES MINÉRAUX 1981-84 809

AUTHOR INDEX/INDEX DES AUTEURS 825

Erratum 826

Age relationships from U-Th-Pb isotope studies of uranium mineralization in Wernecke breccias, Yukon Territory

Projects 750069, 780032

A. Archer [1], R.T. Bell, and R.I. Thorpe
Economic Geology and Mineralogy Division

Archer, A., Bell, R.T., and Thorpe, R.I., Age relationships from U-Th-Pb isotope studies of uranium mineralization in Wernecke breccias, Yukon Territory; in Current Research, Part A, Geological Survey of Canada, Paper 86-1A, p. 385-391, 1986.

Abstract

Pb-U ± Th isotope analyses for 17 specimens of uraniferous breccia from the northeastern Wernecke Mountains reveal several apparent ages for mineralization. The oldest date, 1194 Ma, reflects either initial emplacement of the breccias or their modification by effects of the Rackla orogeny. The 731 to 631 Ma dates are interpreted to reflect mineralization at the time of deposition of Rapitan (Windermere) thick clastic wedges and iron formation. The 510 Ma date reflects mid-Cambrian mineralization roughly coincident with regional uplift (and attendant karstification) and development of thick clastic wedges. This was also an important period for Pb-Zn mineralization. Younger dates resulted from continuing remobilization, and all isotopic ages for mineralized breccia reflect movements associated with the Richardson Fault array.

Résumé

Les datations par les isotopes du plomb et de l'uranium avec ou sans thorium réalisées sur 17 spécimens de brèches uranifères provenant du nord-est des monts Wernecke attribuent plusieurs âges apparents aux minéralisations. La date la plus ancienne, 1194 Ma, s'applique soit à la mise en place initiale des brèches, soit à leur modification sous l'action de l'orogenèse de Racklan. Dans l'intervalle 731-631 Ma, on inscrit la minéralisation qui s'est effectuée à l'époque du dépôt des couches clastiques épaisses (clastic wedges) de la formation de Rapitan (système de Winderemere), de même que la formation du fer. Par ailleurs, l'âge de 510 Ma est attribué à une minéralisation du Cambrien moyen qui coïncide approximativement avec un soulèvement régional (et la karstification qui l'accompagne) et à la formation de couches clastiques épaisses. Ce fut également une période importante pour la minéralisation plombo-zincifère. Les âges plus récents s'expliquent par le fait que les dépôts ont été constamment remobilisés. Tous les âges isotopiques des brèches minéralisées rendent compte des mouvements associés au système de failles de Richardson.

---

[1] Archer, Cathro & Associates (1981) Limited, Vancouver

Introduction

In an attempt to clarify age relationships in mineralized megabreccias in the Wernecke Mountains, the authors collaborated to publish all pertinent data on Pb-U ± Th isotopes from these occurrences. One of us (A.A.) has been active in mineral exploration in the area for the past two decades and collected and submitted the first six specimens to be dated. Another (R.B.) has studied the uranium mineralization as part of a program of uranium resource assessment in Canada and collected the remaining specimens. The other (R.T.) has studied these as part of a program of Pb-isotope studies of mineral deposits in Canada. The interpretations presented are tentative and are in part intended to provide stimulation for further studies.

Background discussions of the geology of the Wernecke megabreccias are given by Archer and Schmidt (1978), Bell (1978, 1982, 1986), Bell and Delaney (1977), Delaney (1981) and Delaney et al. (1982). In addition useful data and conclusions are provided on Pb-isotopes of other deposits in the area by Godwin et al. (1982).

The breccias in the northeastern Wernecke Mountains form an arcuate complex more than 80 km long and about 15 to 25 km wide along the Bonnet Plume River. They intrude the lowermost sedimentary Proterozoic Wernecke Supergroup. The main development of breccias ceased before deposition of the two succeeding Proterozoic sedimentary successions. These Precambrian rocks were affected by faulting in late Proterozoic and middle Cambrian time and certainly also by orogenies affecting the eastern Cordillera during the rest of the Phanerozoic. The main breccias are bounded by and are a continuation of a major fault system called the Richardson Fault array (Norris and Hopkins, 1977). Some breccias have been severely altered (silicification, albitization, chloritization, or carbonatization, often accompanied by hematite ± magnetite, or iron-rich carbonates) but others are only slightly altered. The main minerals of economic interest are chalcopyrite, brannerite and pitchblende.

Significant, similar breccias occur farther west within the Wernecke Mountains and in the Ogilvie Mountains. Some of these may represent younger (associated with mafic igneous intrusion, and thrust faulting) phases of brecciation than those under discussion.

Data

Table 44.1 gives the location and nature of the mineralized specimens used in this study. All but one come from specific mineral zones in the megabreccias near the Bonnet Plume River in northeastern Wernecke Mountains. The exception is from breccia in a Proterozoic window in the southern Richardson Mountains described by Tempelman-Kluit (1981).

Eisbacher (1981) summarized age relationships for the three Precambrian groups in the area: Wernecke Supergroup – older than 1200 Ma; Mackenzie Mountains Supergroup and Pinguicula Group – between 1200 and 800 Ma; and Windermere Supergroup (including Rapitan Group) – between 800 and 570 Ma. Interpretation of Pb-isotopes on galena from massive stratiform Pb-Zn-Cu sulphides near the top of the Wernecke Supergroup at Hart River suggests deposition at about 1280 Ma (Morin, 1979). The Wernecke megabreccias cut only the Wernecke Supergroup in the northeastern Wernecke Mountains (Bell, 1986). Two K/Ar dates on phlogopite and on biotite-rich argillite in or adjacent to these breccias give dates of 1510 and 1040 Ma respectively (Archer et al., 1977; Godwin et al., 1982). Godwin et al. (1982) presented Pb isotopes data for galenas from various Pb-Zn deposits in the area and developed a model that indicates a basement source for lead of about 1890 Ma with major remobilization at 520 Ma for a group of Pb-Zn deposits. These dates and age relationships therefore provide a background for studies on uraniferous deposits associated with the breccias.

The spatial association of these breccias with the Richardson Fault array must also be taken into account. The nearby thick clastic wedges in the Windermere (Eisbacher, 1977, 1978, 1981) are witness to intense faulting in this area. Farther south in the MacDonald Platform (94 K NTS) conglomerate wedges beneath carbonates of late (?) Early Cambrian age suggest periods of faulting at least twice during latest Precambrian or during earliest Cambrian time. In the Northern Cordillera there are also Middle Cambrian conglomeratic wedges, one of which is about 70 km west of the sample area.

Analytical results

The U/Pb analyses for 17 specimens from the Bonnet Plume-Wernecke breccia bodies are presented in Table 44.2. The analyses for specimens from the Quartet, Gnuckle, Otis N, Otis E, Igor and Pterd CW uranium occurrences were done in 1976 by Teledyne Isotopes Inc. under contract for Archer, Cathro and Associates Limited (now Archer, Cathro & Associates (1981) Limited). On the basis of galena lead isotope analyses contracted with Teledyne Isotopes Inc. in 1976 by the Geological Survey of Canada, the analytical uncertainty limits (2σ) on the lead isotope analyses are about 0.85% for the $^{206}Pb/^{204}Pb$ and $^{207}Pb/^{204}Pb$ ratios, 0.95% for the $^{208}Pb/^{204}Pb$ ratio, and 0.17% for the $^{207}Pb/^{206}Pb$ ratio. The analytical uncertainties for the quantitative U and Pb analyses are not known, but for purposes of calculating concordia intercept ages these uncertainty limits for the calculated $^{207}Pb/^{235}U$ and $^{206}Pb/^{238}U$ values have been assumed to be 1.5% (2σ). The remaining analyses were done by Geospec Consultants Ltd. in 1982, 1983 and 1985. The uncertainty limits (2σ) for these lead isotope analyses are approximately 0.042%, 0.052%, 0.058% and 0.014% for the ratios $^{206}Pb/^{204}Pb$, $^{207}Pb/^{204}Pb$, $^{208}Pb/^{204}Pb$ and $^{207}Pb/^{206}Pb$, respectively. For the calculated $^{207}Pb/^{235}U$ and $^{206}Pb/^{238}U$ ratios, uncertainty limits of 0.5% have been used (G.L. Cumming, personal communication) for concordia intercept calculations.

The analyses (Table 44.2) indicate a range of ages for the radioactive breccia specimens, generally from 400 to 730 Ma with one age at about 1200 Ma. The projection of lines defined by the isotopic analyses for Loon (9,10) and NOR (13), for Loon (11) and Pterd (6,14,15) and for Iota (12) and Otis (3,4) indicate that the best choice for a common lead is probably one with a comparatively low $^{207}Pb/^{204}Pb$ ratio in relation to many other late Proterozoic-early Paleozoic ore leads. Consequently, a common lead with $^{206}Pb/^{204}Pb$, $^{207}Pb/^{204}Pb$ and $^{208}Pb/^{204}Pb$ ratios at 17.287, 15.411 and 37.085, respectively, was chosen. This composition is intermediate between that for galena from Long Lake, Ontario (Thorpe, 1982) and from Catchers Pond, Newfoundland (Swinden and Thorpe, 1984).

The analytical results are shown on a concordia diagram (Fig. 44.1). The Igor (5) specimen yields a $^{207}Pb/^{206}Pb$ (radiogenic) age of about 1194 Ma, best interpreted as a minimum age. This specimen has such high lead isotope ratios that the choice of a more primitive common lead does not significantly change the calculated age; more precise concordia intercept calculations could not be made.

An analysis for the Deer-Fox (17) occurrence indicates a $^{207}Pb/^{206}Pb$ minimum age of 731 Ma.

The Iota (12), Otis N (4) and Gnuckle (2) specimens yield comparable $^{207}Pb/^{206}Pb$ ages. A linear regression of the data for these specimens, assuming correlated errors

(York, 1969), and calculation of the concordia intercepts for this regression line, yields an age of 631 ± 7 Ma with a mean square of Weighted Deviates (M.S.W.D.) value of 1.47. It should be noted, however, that this line is largely controlled by the Iota data point, which is nearly concordant. The line passes, within error limits, through the origin. The analyses for the Quartet (apparent $^{207}Pb/^{206}Pb$ ages of 663 Ma) and Otis E (apparent $^{207}Pb/^{206}Pb$ minimum age of 549 Ma) occurrences plot roughly within their uncertainty limits of the Iota-Otis N-Gnuckle line, and thus could be of similar age.

A suite of specimens that are apparently younger and generally comparable to each other in age are the Loon (11), Pterd (6,14,15), and perhaps Otis E (3). These yield a calculated concordia intercept age of 510 ± 8 Ma with an M.S.W.D. of 1.44 and a lower intercept of -12.4 ± 10.2 Ma. A slight expansion of the assumed analytical uncertainty limits would result in the regression line passing, within error, through the origin. An additional Pterd specimen (16) yields an apparently younger age of about 469 Ma ($^{207}Pb/^{206}Pb$ minimum age). This younger age result is consistent with the fact that this pitchblende-bearing specimen is from one of a set of radioactive veins that cut the mineralized breccia represented by the other Pterd specimens.

Although one specimen (11) from the Loon occurrence, as noted above, is in accord with an age of about 510 Ma, two other specimens from this property, analyzed as impure mineral concentrates (7,8) and as radioactive whole rock specimens (9,10), yield a younger age. The data points are nearly collinear and result in calculated concordia intercepts of 422 ± 7 Ma and 22 ± 5 Ma at M.S.W.D. = 2.05.

The specimen (13) from the NOR property, which consists of brannerite and monazite in a carbonate-rich breccia, yields a slightly discordant $^{207}Pb/^{206}Pb$ age of about 400 Ma. This is nearly within uncertainty limits of the 422 ± 7 Ma age for the Loon specimens.

Table 44.1. Short description and location of specimens

No	Occurrence	Location	Comment
1	Quartet	65°08'N 134°24'W	Brannerite separate from heterolithic breccia, outcrop
2	Gnuckle	64°56'N 134°16'W	Brannerite separate from deeply weathered breccia, frost heaved outcrop
3	Otis E	65°02'N 134°24'W	Brannerite from E trending veins system in heterolithic breccia, outcrop
4	Otis N	65°02'N 134°24'W	Brannerite from N trending veins system in heterolithic breccia, outcrop
5	Igor	65°02'N 134°38'W	Pitchblende-chalcopyrite-rich deformed breccia, outcrop
6	Pterd CW	64°57'N 133°17'W	Pitchblende-rich carbonate rich breccia from cirque wall, outcrop
7	Loon A-1	65°12'N 134°28'W	Brannerite separate from quartz-veins in breccia, outcrop
8	Loon B-1	65°12'N 134°28'W	Brannerite separate from quartz vein cutting Loon A outcrop
9	Loon A-2	65°12'N 134°28'W	Whole rock, siliceous heterolithic breccia containing brannerite, outcrop
10	Loon B-2	65°12'N 134°28'W	Whole rock, quartz vein containing coarse brannerite, outcrop
11	Loon C	65°12'N 134°28'W	Whole rock, chloritic breccia dyke, outcrop
12	Iota	64°56'N 133°15'W	Whole rock, homolithic grey argillite breccia, near contact with Gillespie Lake Group, outcrop
13	NOR	66°15'N 133°23'W	Whole rock, monzonite and brannerite bearing carbonate phase of breccia, frost heaved outcrop
14	Pterd A	64°58'N 133°18'W	Whole rock, brannerite margins to quartz veins in brecciated dolerite, boulder train on glacier
15	Pterd B-1	64°58'N 133°18'W	Whole rock, homolithic grey argillite breccia cut by pitchblende veins; boulder train on glacier
16	Pterd B-2	64°58'N 133°18'W	Pitchblende from vein separated from #15
17	Deer-Fox	65°13'N 134°50'W	Whole rock, brannerite and uraninite margins to quartz vein in argillite;felsenmeer

Table 44.2. Analytical data for radioactive specimens from Bonnet Plume-Wernecke breccia bodies. The radiogenic isotopes are indicated by asterisks. The common lead used for correction purposes had the composition $^{206}Pb/^{204}Pb$ = 17.287, $^{207}Pb/^{204}Pb$ = 15.411 and $^{208}Pb/^{204}Pb$ = 37.085.

							Calc. Daughter/Parent Ratios			Calculated Ages (Ma)		
No.	Occurrence	$^{206}Pb/^{204}Pb$	$^{207}Pb/^{204}Pb$	$^{208}Pb/^{204}Pb$	U%	Pb%	$^{207}Pb^*/^{206}Pb^*$	$^{206}Pb/^{238}U$	$^{207}Pb/^{235}U$	$^{206}Pb/^{238}U$	$^{207}Pb/^{235}U$	$^{207}Pb/^{206}Pb$
Analyses by Teledyne Isotopes Inc. (1976)												
1	Quartet	7553	480.3	299.2	34.69	1.286	.061685	.03900	.33170	246.6	290.9	663
2	Gnuckle	4425	281	293.3	34.84	0.442	.060259	.013006	.10806	83.3	104.2	613
3	Otis E	8790	528.6	680.5	22.24	0.438	.05850	.020092	.16206	128.2	152.5	548.6
4	Otis N	1699.8	117.9	104.4	25.97	0.641	.060915	.025115	.21094	159.9	194.3	636
5	Igor	10215	829.9	65.0	4.986	0.886	.079869	.18976	2.0897	1120.1	1145.4	1194
6	Pterd C W	2645.4	166.9	43.86	14.86	0.695	.057642	.048614	.38637	306.0	331.7	516
Analyses by Geospec Consultants Ltd. (1982, 1983, 1985)												
7	Loon A-1 (Mineral)	879.78	6.983	89.123	47.34	0.8892	.053997	.018254	.135904	116.6	129.4	371
8	Loon B-1 (Mineral)	1661.2	105.75	145.21	29.10	1.048	.054953	.037221	.28202	235.6	252.3	410
9	Loon A-2 (Whole Rock)	797.66	58.004	89.588	6.066	0.2034	.054581	.032149	.24194	204.0	220.0	395
10	Loon B-2 (Whole Rock)	2178.1	134.08	173.18	6.875	0.2605	.054919	.038294	.28997	242.3	258.5	409
11	Loon C	1426.2	96.615	51.449	0.2075	0.007779	.057457	.039005	.30997	246.7	274.2	509
12	Iota (Whole Rock)	429.37	44.269	38.993	0.03659	0.003984	.060743	.104314	.87365	639.6	637.5	630
13	N O R	616.43	48.164	58.568	2.684	0.1638	.054666	.058709	.44251	367.8	372.0	399
14	Pterd A	3912.9	239.91	40.743	1.158	0.0546	.057628	.050953	.40486	320.4	345.2	516
15	Pterd B-1 (Breccia)	3960.7	243.24	43.155	1.681	0.07562	.057775	.048589	.38706	305.9	332.2	521
16	Pterd B-2 (Mineral)	15256	875.33	48.631	2.722	0.1065	.056429	.042878	.33361	270.6	292.3	469
17	Deer-Fox	728.29	60.689	59.930	0.6740	0.04196	.063681	.060560	.53174	379.0	433.0	731

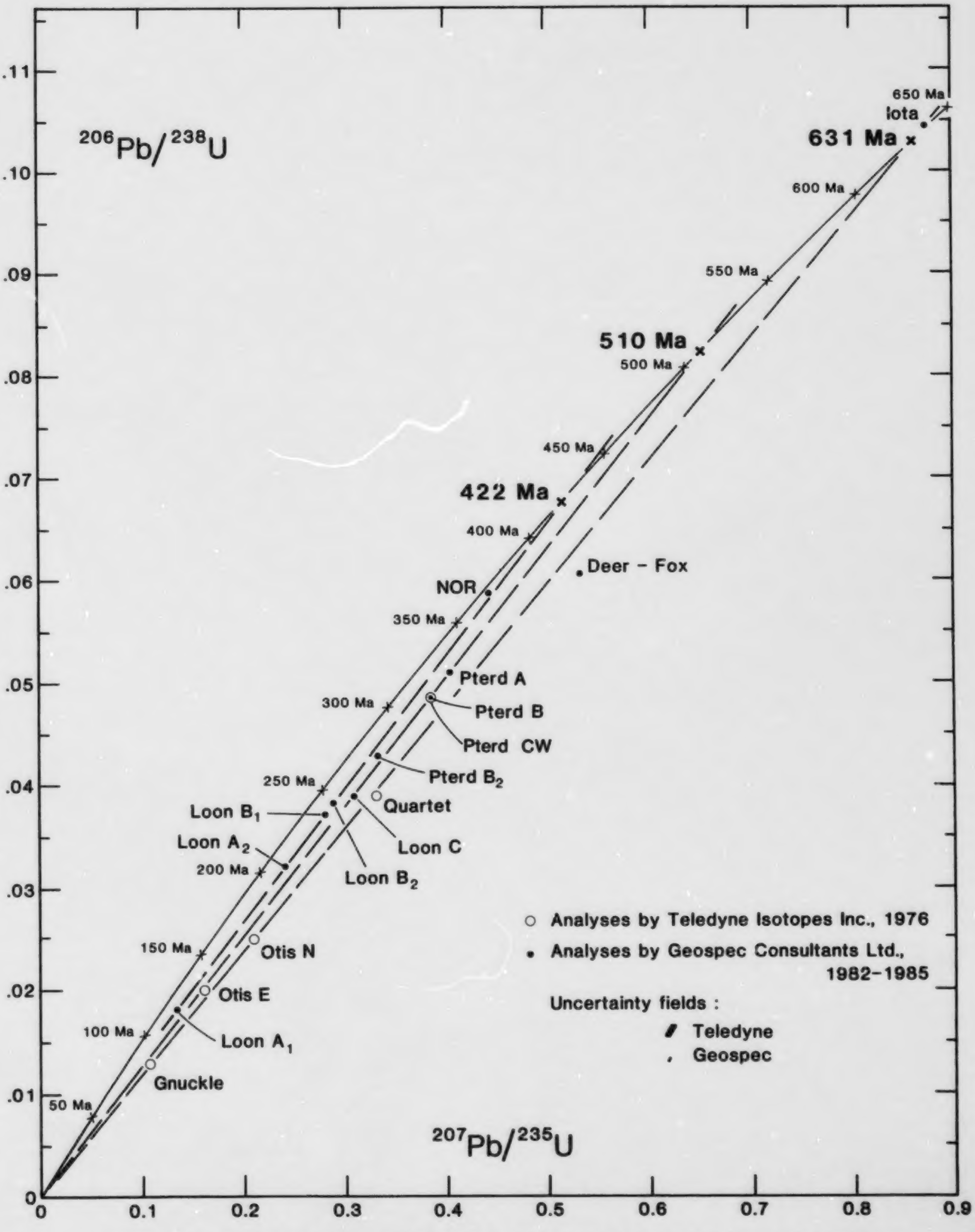

Figure 44.1. Concordia plot for uraniferous specimens from Wernecke breccia. Igor (5) data point is not on this diagram. The concordia intercept for Deer–Fox is 731 Ma.

Table 44.3. Thorium contents for four of the radioactive specimens, and calculated values based on these data

No.	Occurrence	Th(ppm)	$^{208}Pb/^{232}Th$	Calc. Th/Pb age
11	Loon C	31.00	0.025761	514 Ma
12	Iota	5.954	0.024917	497.5 Ma
14	Pterd A	7.938	0.067549	1321 Ma
17	Deer-Fox	699.3	0.018151	363.6 Ma

The thorium contents of four specimens were measured (Table 44.3), and for these $^{208}Pb/^{232}Th$ ages have been calculated. These ages are, however, unlikely to be very useful because there is no way to compensate for loss of lead from the system, and for most specimens loss of radiogenic lead is indicated by the concordia plot (Fig. 44.1). The 1321 Ma Pb/Th age for Pterd (14) is no doubt incorrect because the measured $^{208}Pb/^{204}Pb$ ratio of 40.743 is close to the assumed common lead ratio of 37.085, and an increase in this ratio for the common lead assumed would greatly reduce the calculated age.

Discussion

A date of 1194 Ma for the Igor occurrence (5) probably represents the time of origin of the breccias at this locality. However the breccias have been modified by deformation along the Slats Creek Fault (Bell, 1986), and thus the age may reflect the Rackla orogeny.

Deer-Fox (17) with a date of 731 Ma may represent mineralization or remobilization associated with another stage of faulting during early stages of deposition of the Windermere Supergroup. Similarly Iota (12), Otis N (4), Gnuckle (2), Quartet (1) and possibly Otis E (3) may have been mineralized in response to faulting late during deposition of the Windermere Supergroup at about 631 Ma.

Loon C (11), Pterd (6,14,15) and perhaps Otis E (3), three widely separated localities, together give a concordia intercept date of 510 ± 8 Ma. This date is interesting in that it is close to the middle Cambrian stage of widespread development of clastic wedges in the northeastern Cordillera as well as karstification indicated by a model proposed by Godwin et al. (1982). It indicates mobilization of uraniferous mineralizing fluids at that time as well. Otis E (3) is on trend with faults that cut Lower Cambrian strata but not nearby Upper Cambrian strata.

Loon (7,8,9,10) and NOR (13) together give a concordia intercept suggesting mobilization of uraniferous fluids at approximately 400-430 Ma. The Loon C breccia apparently cuts the breccia represented by specimens Loon A and B.

The 1194 Ma, 731-631 Ma and 510 Ma dates are felt to be of greatest relevance to mineralizing processes in the Wernecke breccias. More specimens from the Igor site should be studied to determine the timing of uranium mineralization with respect to local deformation thought to be associated with the Slats Creek Fault.

Both Otis specimens (3,4) are near massive hematite ± magnetite breccias. Their isotopic ages in the 631 Ma range reinforce the suggested relationship with iron mineralization in the area (Bell, 1982; Gross, 1965). To further test this relationship, uraniferous samples from iron-rich breccias (e.g. Pagisteel) should be analyzed. Samples collected to date are only weakly uraniferous.

Samples from breccias outboard (westerly) of the Richardson Fault array should be analyzed to more precisely fix the age of main brecciation. The best site is near the head of Bond Creek although most material here is out of radioactive equilibrium, thus suggesting very recent uranium and daughter-element mobility.

The pitchblende-bearing Iota and Pterd (6,14,15) samples come from least altered breccias marginal to the breccia complex which terminates against the lower Gillespie Lake Group, the uppermost unit of the Wernecke Supergroup. The breccia complex at these sites is unconformably overlain by basal strata of the Pinguicula Group. If these uraniferous breccias are related to unconformity-style accumulations, then the isotopic data suggest a very late Proterozoic (Iota, only weakly uraniferous) and a strong mid-Cambrian mineralization (Pterd 6,14,15). This mid-Cambrian mineralization is also in the same period as that determined for Pb-Zn mineralization (karst-related) in the eastern Cordillera by Godwin et al. (1982).

Acknowledgments

Teledyne Isotopes Inc., and Geospec Consultants Limited did isotopic analyses of the specimens. Access to many of the sites was provided to one of us (R.B.) by Archer, Cathro & Associates, Eldorado Nuclear Ltd. (Eldor), Cordilleran Engineering and Pamicon. J.C.M. Roddick provided computer programs for treatment of all the data in the final stages. K.M. Dawson collected specimen Loon C (11). Critical and constructive comments by C.W. Jefferson and S.M. Roscoe are gratefully acknowledged.

References

Archer, A., Bell, R.T., and Godwin, C.I.
1977: Mineralogical breccias of Wernecke Mountains; in Geological Association of Canada 1977 Annual Meeting, Vancouver, Abstracts, p. 4.

Archer, A. and Schmidt, U.
1978: Mineralized breccias of early Proterozoic age, Bonnet Plume River district, Yukon Territory; Canadian Institute Mining and Metallurgy Bulletin, v. 71, no. 796, p. 53-58.

Bell, R.T.
1978: Breccias and uranium mineralization in the Wernecke Mountains, Yukon – a progress report; in Current Research, Part A, Geological Survey of Canada, Paper 78-1A, p. 317-322.

1982: Comments on the geology and uraniferous mineral occurrences of the Wernecke Mountains, Yukon and District of Mackenzie; in Current Research, Part B, Geological Survey of Canada, Paper 82-1B, p. 279-284.

Bell, R.T. (cont.)
1986: Megabreccias in northeastern Wernecke Mountains, Yukon Territory; in Current Research, Part A, Geological Survey of Canada, Paper 86-1A, Report 43.

Bell, R.T. and Delaney, G.D.
1977: Geology of some uranium occurrences in Yukon Territory; in Report of Activities, Part A, Geological Survey of Canada, Paper 77-1A, p. 33-37.

Delaney, G.D.
1981: The mid-Proterozoic Wernecke Supergroup, Wernecke Mountains, Yukon Territory; in Proterozoic Basins of Canada, ed. F.H.A. Campbell, Geological Survey of Canada, Paper 81-10, p. 1-23.

Delaney, G.D., Jefferson, C.W., Yeo, G.M., McLennan, S.M., Aitken, J.D., and Bell, R.T.
1982: Some Proterozoic sediment-hosted metal occurrences of the northeastern Canadian Cordillera; in Idaho Bureau of Mines and Geology, Bulletin 24, p. 97-116.

Eisbacher, G.H.
1977: Tectono-stratigraphic framework of the Redstone Copper Belt, District of Mackenzie; in Report of Activities, Part A, Geological Survey of Canada, Paper 77-1A, p. 229-234.

1978: Redefinition and subdivision of the Rapitan Group, Mackenzie Mountains; Geological Survey of Canada, Paper 77-35, 22 p.

1981: Sedimentary tectonics and glacial record in the Windermere Supergroup, Mackenzie Mountains, northwestern Canada; Geological Survey of Canada, Paper 80-27, 40 p.

Godwin, C.I., Sinclair, A.J., and Ryan, B.D.
1982: Lead isotope models for the genesis of carbonate-hosted Zn-Pb, shale-hosted Ba-Zn-Pb, and silver-rich deposits in the northern Canadian Cordillera; Economic Geology, v. 77, p. 82-94.

Gross, G.A.
1965: Geology of iron ore deposits and iron-formations of Canada; in Report of Activities, Field 1964, Geological Survey of Canada, Paper 65-1, p. 142-143.

Morin, J.
1979: A preliminary report on Hart River – a Proterozoic massive sulphide deposit, Yukon Territory; in Mineral Industry Report, Department of Indian and Northern Affairs, 1979-9, p. 22-24.

Norris, D.K. and Hopkins, W.S.
1977: The geology of the Bonnet Plume Basin, Yukon Territory; Geological Survey of Canada, Paper 76-8, 20 p.

Swinden, H.S. and Thorpe, R.I.
1984: Variations in style of volcanism and massive sulphide deposition in Early to Middle Ordovician island-arc sequences of the Newfoundland Central Mobile Belt; Economic Geology, v. 79, no. 7, p. 1596-1619.

Tempelman-Kluit, D.J.
1981: NOR, summary of assessment work and description of mineral properties; in Yukon, Geology and Exploration 1979-80, Geology Section, Department of Indian and Northern Affairs, p. 300-301.

Thorpe, R.I.
1982: Lead isotope evidence regarding Archean and Proterozoic metallogeny in Canada; Revista Brasileira de Geociencias, v. 12, no. 1-3, p. 510-521.

York, D.
1969: Least squares fitting of a straight line with correlated errors; Earth and Planetary Science Letters, v. 5, p. 320-324.

The Great Bend ophiolite, eastern Newfoundland: field investigations[1]

Contract 58SZ.23233-5-0246

Edward J. Zwicker and D. F. Strong[2]

Zwicker, E.J. and Strong, D.F., The Great Bend ophiolite, eastern Newfoundland: field investigations; in Current Research, Part A, Geological Survey of Canada, Paper 86-1A, p. 393-397, 1986.

Abstract

Geological mapping of the ultramafic and gabbroic rocks of the Great Bend area, at 1:5000 scale, has substantially revised previous interpretations. In particular, a belt of sedimentary rocks has been found to separate the gabbroic from the ultramafic rocks, which allows for the possibility that the two suites of igneous rocks may have separate emplacement histories and even separate origins. The area contains several types of mineralization of economic interest. The mapping has significantly increased the extent of the known talc-magnesite zones, but substantiates the suggestion of earlier workers that the mineralization is controlled by fault and shear zones. Chromite lenses and pods are common throughout the serpentinized harzburgites and dunites. Pyrite and arsenopyrite are associated with quartz veins and also occur as disseminated zones in sedimentary rocks surrounding the ophiolite, and these have some gold potential.

Résumé

La cartographie géologique à 1/5 000 des roches ultramafiques et gabbroiques de la région de Great Bend a commandé une revision de certaines interprétations antérieures. En particulier, on a observé qu'une zone de roches sédimentaires sépare les roches gabbroïques des ultramafiques, d'où des époques différentes et à partir de sources différentes. La région renferme plusieurs types de minéralisation qui présentent un intérêt économique. Par suite de ces travaux, on a considérablement augmenté l'étendue des zones connues de talc-magnésite, mais on conclue, comme l'ont fait d'autres auteurs antérieurement, que la minéralisation se trouve sous l'influence de zones de failles et de cisaillement. Les dunites et harzburgites serpentinisées abondent en lentilles et en "pods" de chromite. La pyrite et l'arsénopyrite sont associées à des veines de quartz, et on en trouve également sous forme de zones disséminées dans des roches sédimentaires qui entourent l'ophiolite, où elles ont un certain potentiel aurifère.

[1] Contribution to the Canada-Newfoundland Mineral Development Agreement 1984-1989. Project carried by Geological Survey of Canada, Economic Geology and Mineralogy Division, Project 770063.

[2] Department of Earth Sciences, Memorial University of Newfoundland, St. John's, Newfoundland A1B 3X5

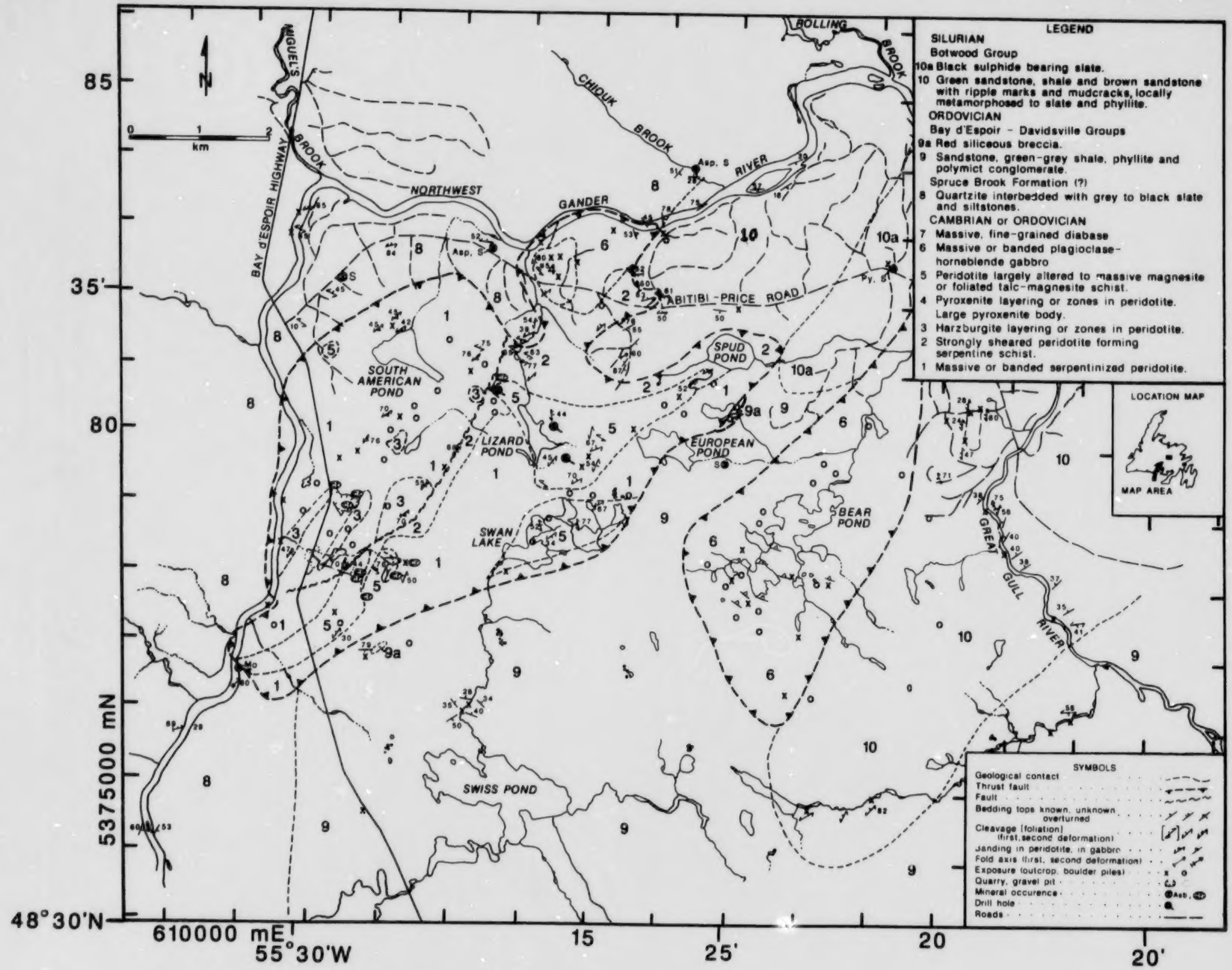

Figure 45.1. *Simplified geological map of the Great Bend ultramafic and associated rocks, central Newfoundland.*

Introduction

The Great Bend ophiolite is situated in central Newfoundland between latitude 48°30' and 48°37'N and between longitude 55°20' and 55°32'W (Fig. 45.1). For present purposes the ultramafic and gabbroic rocks and their alteration products are referred to as the Great Bend ophiolite, although not all features of a full ophiolite suite are seen. It has been depicted on maps as a roughly circular area about 10 km in diameter, that consists of ultramafic and gabbroic rocks. Access is provided by the Baie D'Espoir highway (route 360), and the Abitibi-Price logging road which extends 15 km east of the highway and crosses the northern edge of the ophiolite. The eastern and southeastern parts can be reached by traverses through the bush or along rivers and streams. Bedrock exposure in the area is locally good, with large intervening areas of swamp and thick overburden.

The area has been of continuing interest to mineral exploration companies due to its showings of magnesite, talc, chromite and asbestos. The present work documents the geological context of the ultramafic and mafic rocks of the Great Bend area, and the nature, extent and genetic controls of mineralization of potential economic interest. This paper reports on the first stage of the study which involved mapping of the ophiolite at a scale of 1:5000.

Previous work

The ultramafic and mafic rocks of the Great Bend area in Central Newfoundland (Fig. 45.1) form part of the Gander River ultramafic belt. These rocks have been interpreted as an ophiolite derived from a main ocean basin (e.g. Dewey and Bird, 1971) or, alternatively, from a back arc basin (e.g. Strong, 1973). Coleman-Sadd and Swinden (1984) suggested that the ultramafic rocks are tectonically underlain by sedimentary rocks and that the various ophiolites, including Great Bend, are part of a major allochthon. It has also been thought that some of the ultramafic bodies could be peridotite mantle diapirs (Stevens et al., 1974). Although the economic potential of the area has attracted much exploration interest, only a few investigators have examined the ophiolite in any detail, viz. Grady (1953), Coleman (1954), Kean (1973), and Coleman-Sadd (1982).

Grady (1953) reported that quartzitic sandstone, siltstone and shale, of possible Ordovician age made up the bulk of the sedimentary rocks surrounding the ultramafic body, which he suggested to be a layered laccolithic intrusion tilted towards the east. He observed that serpentinized dunite makes up its central areas, and that magnesite-quartz rock derived from serpentine occurs in a shear zone that extends northeastward for 6.5 km across the centre of the laccolith. Grady suggested that an outer rim of gabbro, anorthosite and norite extends around the eastern half of the body, and that a stock of pyroxenite about 1 km in diameter occurs at one place on its northern edge. He felt that there was a genetic relationship between this pyroxenite body and the other ultramafic rocks, with both probably being intruded during the Taconic Orogeny.

Coleman (1954) described four igneous rock types in the Great Bend area, viz. dunite, peridotite (harzburgite), gabbro and anorthosite-granophyre, and the surrounding sedimentary rocks as being highly siliceous and metamorphosed. He recognized abundant magnesite of varying purity as an alteration product of peridotite, and suggested that it was confined to zones of shearing and brecciation that controlled fluid circulation. Coleman considered the igneous rocks to be younger than the sedimentary rocks of the Great Bend area, forming a differentiated ultramafic complex of Bushveld or Stillwater type with dunite at the base and anorthosite-granophyre at the top. According to him the orientation of layering suggests that the complex was gently folded about a synclinal axis which plunges steeply to the southeast. Coleman noted three components of economic interest in the rocks of the Great Bend area, viz. magnesite, chromite and asbestos.

Kean (1973) examined the Great Bend and nearby Pipestone Pond ultramafic bodies and the surrounding metasedimentary rocks. He observed that the eastern contact between the Great Bend gabbro and the metasediments was faulted, resulting in brecciation and shearing of the gabbro. He suggested that the western contact of the ophiolite showed no evidence of shearing, although shearing and brecciation within the ultramafic body was common. Kean reported that where the siltstones are in contact with the dunite they appeared to have been baked to a hard black basalt-like rock, leading him to suggest that the dunite was intrusive. He also noted that localized zones of magnesite enrichment were controlled by faulting and brecciation.

Coleman-Sadd (1982) traversed the area around Great Bend, producing a revised geological map.

Current work

The first objective of the present investigation was to produce a geological map of the Great Bend ophiolite showing greater detail than has hitherto been available. This was done by systematic traverses spaced no more than 500 m apart across strike in an east-west or northwest-southeast direction, or by following streams, logging roads and lake shores to areas where outcrop could be recognized on aerial photographs. A simplified version of this map is shown in Figure 45.1.

Sedimentary rocks

The sedimentary rocks exposed along the Northwest Gander River in the southwestern part of the area (unit 8, Fig. 45.1), which Coleman-Sadd (1982) assigned to the Lower to Middle Ordovician Spruce Brook Formation, consist of quartzite and dark grey to black slate. Quartzite beds are 30-40 cm and beds about 10-20 cm thick. The sedimentary rocks overlie the peridotites, and numerous small thrust faults in both lithologies suggest that they have been thrust into this position. Sulphide-bearing quartz veins are relatively common in these rocks, with pyrite and chalcopyrite in both the veins and sedimentary rocks. To the north of the ultramafic rocks, e.g. along the Abitibi-Price road or along Chioux Brook, this unit is marked by intense arsenopyrite-pyrite mineralization.

Rocks of unit 9, which might be assigned to either the Davidsville or Baie d'Espoir Group, are seen in only a few localities in the map area. Along the Great Gull River and in the one exposure seen along the highway west of Swiss Pond the rocks are dominantly quartz pebble conglomerates. To the north of Swiss Pond they are shaly siltstones with a greenish colour reminiscent of unit 10 along the Great Gull River. This may imply that the location of the contact between units 9 and 10 along the Great Gull River requires some modification.

Greenish-purplish sandstones, siltstones and shales of the Botwood Group (unit 10) are exposed at a number of localities along the Abitibi-Price logging road and the Great Gull River. At the latter locality primary depositional features such as mud cracks, mud volcanoes and crossbedding indicate that the section is upright and the bedding strikes 95° and dips ~ 50°S. Nevertheless, folds were observed in this section, with axes plunging 75° to the NNW, which together with kinking of quartz veins, indicate significant deformation. Approximately 400 m north of Spud Pond, the

Table 45.1. Analytical data for selected samples from the Great Bend area, central Newfoundland. Sample descriptions are given in the text. (Analyses by X-Ray Assay Laboratories Ltd. by neutron activation).

Sample	Au ppb	As ppm	Ag ppm	Sb ppm	Te ppm	W ppm	Hg ppb
GB.85.415a	3	47	<0.5	16.0	0.1	1	1040
GB.85.415b	1	160	<0.5	32.0	<0.1	<1	1080
GB.85.345	1900	24000	<0.5	47.0	<0.1	<3	54
GB.85.346	3	48	<0.5	4.5	<0.1	7	< 5
GB.85.347	1	21	<0.5	4.5	<0.1	1	12

sedimentary rocks of unit 10 are cut by many quartz veins with well developed quartz crystals. Iron staining is especially abundant around the sulphide-bearing quartz veins, and several larger quartz veins show signs of brecciation.

Samples of sulphide mineralization from several areas have been analyzed for selected elements (Table 45.1). Samples GB.85.415a and 415b are both from the intensely folded black, locally graphitic, slates of unit 10a exposed north of Spud Pond (Fig. 45.1). These rocks contain abundant quartz and calcite veins, and the sulphides (mainly pyrite) are found in the veins, along cleavage and bedding planes, and as nodules.

Samples GB.85.345, 346, and 347 were collected along Chiouk Brook about 600 m north of its confluence with the NW Gander River, in our unit 8, or the Spruce Brook Formation of Coleman-Sadd and Swinden (1984). Sample GB.85.345 is from pyrite-arsenopyrite-rich grey-black brecciated slate exposed in the brook over about 100 m. The arsenopyrite occurs as very fine needles disseminated within the sediment, along with abundant pyrite and possible chalcopyrite. The zone strikes 098° and dips about 30°NE, parallel to both bedding and cleavage. Samples GB.85.346 and 347 are of highly weathered and iron-stained dark grey to black pyritic slates interbedded with more competent siltstones and quartzites that strike 062° and dip 78°SE. The low metal concentrations in these two samples compared to GB.85.345, may be due to leaching during the intense weathering. The gold concentration of nearly 2 grams/ton (ppm) in sample GB.85.345, together with elevated concentration of metals commonly associated with gold deposits (As, Hg) in other samples, warrants further evaluation of the sulphide-bearing sedimentary rocks of the Great Bend area for their economic gold potential.

Ultramafic rocks

The ultramafic rocks of the area are separated in Figure 45.1 on the basis of both primary and secondary characteristics. The peridotite (unit 1, Fig. 45.1) typically exhibits a brown weathered surface and contains disseminated chromite and multidirectional (usually in three mutually perpendicular directions) serpentine veins. The serpentine veins typically follow joint or fracture sets. On a fresh surface the peridotite is very fine grained and dark green to black. Layering is common in the peridotite, especially in the westernmost outcrops, and is most obvious where it is emphasized by orthopyroxenes in harzburgite (unit 3), or bands of chromite. Harzburgite is always present where there are chromite bands but the reverse is not always true. Away from the margins of the peridotite and shear zones the layering has an average strike of 040° and dips 60°ESE. The harzburgite layers (unit 3) appear to be more numerous within about 200 m of the talc-carbonate fault or shear zones (unit 5), and they contain asbestos veins at some localities.

The mapping of the known and newly discovered magnesite occurrences has delineated a trend which supports the suggestion of earlier workers that most of the talc-carbonate is associated with a large shear zone. The main shear zone and the associated talc-carbonate alteration strikes about 040° and transects the ultramafic body from its southwestern limit to the Abitibi-Price logging road in the north. Other outcrops in the ultramafic body that do not line up with this trend might be associated with a parallel shear zone or they may represent displacements of the main talc-carbonate zone along fault zones or the shallow dipping schistosity of the area.

On the weathered surfaces the carbonate is red and contains prominent quartz stringers. The unweathered rock is grey-green and commonly contains disseminated chromite. Two or more generations of quartz veins are generally present, with thin veins (about 2 mm) cut by thicker (about 5 mm) veins. Exposures within the main fault zone tend to show a progressive development of these quartz veins as fillings of tension gashes which have been continuously rotated, brecciated, and cut by new tension gash veins during shearing.

Pyroxenites occur locally as transitional facies from the harzburgites, but are most abundant in a semicircular area (unit 4) about 1 km in diameter at the northern extremity of the ultramafic body. The pyroxenite of this "plug" is a strongly serpentinized orthopyroxenite. On weathered surfaces it is similar to the harzburgites in colour and texture, but is typically finer grained and lacks primary structures. It is rich in magnetite and forms a strong anomaly on the aeromagnetic maps.

The gabbro associated with this pyroxenite is generally medium- to coarse-grained and contains biotite in addition to plagioclase and amphibole. There is a weak planar fabric in the gabbro, but boulders of the same lithology in the Northwest Gander River are strongly banded. In the Bear Pond area, banding in the gabbro is oriented consistently about 125°. Here the gabbro is medium- to coarse-grained, but no evidence was seen for the anorthosites or granophyres mentioned by Coleman (1954). An intriguing feature of this area is the occurrence of pods or blocks (xenoliths?) up to 2 m across of biotite-rich fine grained rocks within the gabbro. If these are confirmed as xenoliths of sedimentary origin, they would indicate that the gabbro was intrusive into sedimentary rocks, and thus would negate any interpretation of its origin as part of the ophiolite suite. An intrusive origin would also explain the apparently complete separation of the gabbro from the ultramafic rocks, and imply a separate origin for the two.

Discussion

One of the most important results of this work is the difference between the geological map shown in Figure 45.1 and those produced by previous workers. Of particular significance is the complete spatial separation of the

gabbroic from the ultramafic rocks, which had not been previously recognized, and thus the possibility that the gabbro might have a separate origin from the ultramafic rocks.

Of potential economic importance is the fact that the area of talc-magnesite mineralization has been demonstrated to be significantly more extensive than previously thought, although it has been confirmed that most of it is controlled by a major shear zone which extends in a northeasterly direction across the entire width of the ultramafic body. Detailed studies are in progress to establish the mineralogical, chemical and isotopic changes which accompany this alteration. The ultramafic rocks, particularly those with significant chromite mineralization, are also being assessed for platinum group elements. Also of significant economic interest is the fact that gold is enriched in some of the sedimentary rocks surrounding the ophiolite. The former are also mineralized by pyrite and arsenopyrite. The initial indications of significant gold concentrations associated with arsenopyrite would appear to warrant a more detailed and systematic investigation of the controls and extent of this type of mineralization.

Acknowledgments

We are grateful to Gayle Zwicker and Paul Roberts for field assistance and T. Calon, J. Lydon, H. Prichard and D. Wilton for stimulating discussion, and also to J. Lydon for critical reading of the manuscript. We thank Allan Huard for help with literature review and Larry Nolan for drafting Figure 45.1. The study was funded by contract between the Geological Survey of Canada and Canewf Resources Ltd. and partly by Operating Grant No. A7975 to D.F. Strong from the Natural Sciences and Engineering Research Council of Canada.

References

Coleman, L.C.
1954: The Great Bend area Northwest Gander River; Report for Newfoundland and Labrador Corporation; Newfoundland Department of Mines and Energy, File No.: Nfld. 20/11(27).

Coleman-Sadd, S.P.
1982: West Gander River (2D/11), west part, Newfoundland; Newfoundland Department of Mines and Energy, Mineral Development Division, Open File Map 82-59.

Coleman-Sadd, S.P. and Swinden, H. S.
1984: A tectonic window in central Newfoundland? Geological evidence that the Appalachian Dunnage Zone may be allochthonous; Canadian Journal of Earth Sciences, v. 21, p. 1349-1367.

Dewey, J. F. and Bird, J. M.
1971: Origin and emplacement of the ophiolite suite. Appalachian ophiolites in Newfoundland; Journal of Geophysical Research,v. 76, p. 3179-3206.

Grady, J.C.
1953: The geology of the southern half of the Serpentine Belt in east-central Newfoundland; Geological Survey Report, Newfoundland Department of Mines and Energy File No. Nfld. 20/11(5).

Kean, B.F.
1973: Notes on the geology of the Great Bend and Pipestone Pond ultramafic bodies; Newfoundland Department of Mines and Energy, Mineral Development Division, Report of Activities 1973, p. 33.

Strong, D. F.
1973: Plate tectonic setting of Appalachian-Caledonian mineral deposits, as indicated by Newfoundland examples; Society of Mining Engineering AIME, Transactions v. 256, p. 121-128.

Stevens, R. K., Strong, D. F., and Kean, B. F.
1974: Are some Eastern Appalachian ultramafic rocks mantle diapirs produced above a subduction zone?; Geology, v. 2, p. 175-178.

Late Carboniferous dextral movement on the Cobequid-Hollow fault system, Nova Scotia: evidence and implications[1]

Project 840045

Gary M. Yeo and Gao Ruixing [2]
Precambrian Geology Division

Yeo, G.M. and Gao Ruixing, Late Carboniferous dextral movement on the Cobequid – Hollow fault system, Nova Scotia: evidence and implications; in Current Research, Part A, Geological Survey of Canada, Paper 86-1A, p. 399-410, 1986.

Abstract

The offset of Devonian volcanics along the Cobequid Fault and Silurian strata along the Hollow Fault indicates a displacement of 20 to 35 km. Deformation and orientation of secondary faults and folds within Stellarton Graben are indicative of a large-scale, dextral, Riedel shear pattern. In response to movement on these fault systems, the Stellarton Graben developed as a synsedimentary rhomb graben in late Westphalian B-C time. Since the deposition of the Stellarton Group was contemporaneous with graben subsidence, it is unlikely that the coal seams known within the graben ever extended outside it (with the possible exception of the Thorburn coals). Juxtaposition of predominantly fluvial facies belonging to the Pictou Group against time-correlative, predominantly lacustrine facies belonging to the Stellarton Group can be explained by dextral faulting. Since the Stellarton Graben was probably not in existence in early Westphalian B time, it could not have been an obstacle to derivation of the New Glasgow Conglomerate from a southern source area.

Résumé

Le décalage des roches volcaniques dévoniennes le long de la faille de Cobequid et des strates siluriennes le long de la faille de Hollow est de l'ordre de 20 à 35 km. La déformation et l'orientation des failles et des plis secondaires à l'intérieur du fossé tectonique de Stellarton sont caractéristiques d'une faille de Riedel dextre à grande échelle. Sous l'action du mouvement de ces systèmes de failles, le fossé synsédimentaire et rhomboïdal de Stellarton s'est développé à la fin du Westphalien (B-C). Comme le dépôt du groupe de Stellarton est contemporain de l'affaissement qui a donné naissance au graben, il est peu probable que les couches de charbon connues à l'intérieur du fossé se soient déjà prolongées à l'extérieur (à l'exception peut-être des charbons de Thornburn). La juxtaposition d'un faciès à prédominance fluviatile appartenant au groupe de Pictou et d'un faciès chronostratigraphique à prédominance lacustre appartenant au groupe de Stellarton pourrait s'expliquer par un faillage à décrochements dextres. Étant donné que le fossé de Stellarton n'existait probablement pas encore au début du Westphalien B, il ne peut avoir fait obstacle à la dérivation du conglomérat de New Glasgow en provenance du sud.

---

[1] Contribution to Canada-Nova Scotia Mineral Development Agreement 1984-1989. Project carried by Geological Survey of Canada.
[2] Geology Department, University of New Brunswick, P.O. Box 4400, Fredericton, New Brunswick, E3B 5A3

Introduction

Between the Cobequid and Antigonish highlands of northern Nova Scotia lies the Stellarton Gap, a broad, northeast-trending trough underlain by Carboniferous strata. The pre-Carboniferous highland areas are bounded to the south and northwest respectively by the Cobequid and Hollow fault systems (Fig. 46.1). These faults subtend one another to form the Stellarton Graben, in which the productive seams of the Pictou Coalfield lie (Bell, 1940; Hacquebard and Donaldson, 1969). Rapid facies changes and coarsening of clastics towards these faults and localization of thick conglomerates adjacent to them indicates that the faults were the major control on Carboniferous sedimentation within the Stellarton Graben. This summary of field observations on the structural geology of Stellarton Gap and their stratigraphic implications is a sequel to a review of the regional stratigraphy of the area (Yeo, 1985).

Stellarton Gap has been the subject of more than 150 years of geological investigation (see Bell, 1940). Nevertheless, key structural and stratigraphic problems remain unsolved. These include: (1) comprehension of the relationship between the Cobequid and Hollow faults, (2) discernment of the original distribution of the coal-bearing strata preserved in the Stellarton graben, and (3) explanation of the present proximity of two distinctly different facies assemblages of the same age (Westphalian C): predominantly coarse grained fluvial clastics of the "Merigomish Formation" (name proposed for the lower Pictou Group in Stellarton Gap) north of Stellarton Graben, and predominantly fine grained lacustrine clastics of the Stellarton Formation within the graben, separated by the easternmost segment of the Cobequid Fault System and the New Glasgow Conglomerate (Westphalian B). A clear understanding of the basic structural elements of Stellarton Graben, the tectonic keystone of Stellarton Gap (Yeo, 1985) should help to resolve these problems.

Hypotheses for the origin of Stellarton Graben may be categorized according to whether dip-slip or strike-slip faulting are considered to have been predominant, and whether the faulting occurred at the same time as sedimentation or afterwards. Mechanisms by which grabens may be formed in response to dip-slip and strike-slip faulting are summarized schematically in Figure 46.2.

Bell (1940) followed earlier interpretations in considering the graben to be bounded by postdepositional normal faults (Fig. 46.2a). He interpreted folds within the graben to be evidence for an episode of north-south or northwest-southeast shortening prior to the time of faulting. Although Haites (1956) recognized that facies distributions in the Pictou Coalfield might be controlled by structure, he too considered the Stellarton Graben to be a postdepositional feature. He interpreted the north boundary faults (i.e. eastern extension of the Cobequid Fault) to have a reverse sense, however. Hacquebard and Donaldson (1969) recognized that graben subsidence was syndepositional. They inferred that the bounding faults had normal displacements.

Eisbacher (1967, 1969) demonstrated that significant dextral movement took place on the western Cobequid Fault in late Carboniferous time. This has been corroborated by the work of Donohoe and Wallace (1978; 1985) and White (1983). Eisbacher and other workers (Webb, 1967; Benson, 1974; Dewey and Fyson, in Boucot et al., 1974) suggested that the same stress regime might have acted on the Hollow Fault. Assuming such dextral movement, Fralick (1980) and Fralick and Schenk (1981) presented two possible interpretations for the Stellarton Graben. In the first, Fralick suggested that the north boundary fault system of the graben was a dextral splay from the Hollow Fault. This interpretation combines elements of both fault termination and divergent fault mechanisms (Fig. 46.2d,f). In the second, he suggested that Stellarton Graben formed at a sharp bend in a braided wrench fault system. This interpretation combines elements of the curved fault trace and side-stepping fault models (Fig. 46.2c,g).

Evidence for the sense of movement on the eastern Cobequid and Hollow faults has not been documented, however. Consequently, models proposed for the origin of Stellarton Graben, such as those outlined above, have remained speculative. Field observations and structural analyses presented below demonstrate that late Carboniferous movement on both these faults was dextral. This places important constraints on the tectonic and stratigraphic interpretation of Stellarton Gap.

Eastern Cobequid – Alma Fault

Several workers have suggested that movement on the Cobequid Fault was related to the development of the late Devonian to Carboniferous "Maritime Basin" (Belt, 1968; Bradley, 1982; and others). In a detailed study of systematic fractures in pebbles within Carboniferous conglomerates, and tectonic fabric studies of mylonite zones, Eisbacher (1967, 1969) demonstrated that dextral movement took place on the western Cobequid Fault during Westphalian B to Stephanian time. Stress field analyses at several localities south of the Cobequid Highlands showed that the principal stress axes of compression varied from 133 to 150 degrees (Eisbacher, 1967; 1969). Through comparison of deformation patterns in shear zones within the fault zone with displaced marker horizons on the Cobequid Fault at Greville Bay, and experimental gouge studies, White (1983) showed that dextral slip was pervasive along the shear zones. Until now, however, no evidence for the nature of deformation has been reported along the fault trace east of Truro. A minimum dextral displacement of 20 km on the Cobequid Fault is suggested by the offset of late Devonian rhyolites in the Parrsboro area (Donohoe and Wallace, 1978; 1985).

The ENE-trending segment of the Cobequid Fault from Lower Mount Thom to Alma can be traced into the E-trending Fletcher and New Glasgow faults, which form the northern boundary of Stellarton Basin (Fig. 46.1). The fault system dies out north of Thorburn, as the New Glasgow Fault cannot be traced across Sutherlands River. Intensive fracturing and shearing associated with the fault is visible in outcrops of Carboniferous conglomerate, sandstone, siltstone, or shale in Steele Run brook near Upper Mount Thom, in the West River valley near Salt Springs, and beside the Trans Canada Highway at Alma and north of Coalburn. Three tectonic rock types cam be distinguished in the fault zone: fault gouge, shear lenses, which are defined by at least two fractures and coated by the gouge, and fault breccia. The youngest rocks observed to be affected by the Cobequid Fault in Stellarton Gap belong to the upper Stellarton Formation (Westphalian C).

Field observations at three localities on the Lower Mount Thom – Alma segment of the Cobequid Fault are summarized in Figure 46.3. The long axes of the sandstone and siltstone shear lenses trend ENE to NE, parallel to the orientation of the fault zone. Two sets of shear fractures are well developed in shear bands within the fault zone. A discrete domain defined by one set of shear fractures indicates that the set trends 110 ± 10 degrees, and dips steeply. These fracture surfaces commonly show dextral offset. Another domain is defined by a steeply dipping set of fractures trending 330 ± 10 degrees. With few exceptions, the sense of displacement on these fracture surfaces is sinistral. The first set of shear fractures intersects the main shear trend at 25 ± 10 degrees, and the second set intersects it at 65 ± 10 degrees. These low and high angle conjugate

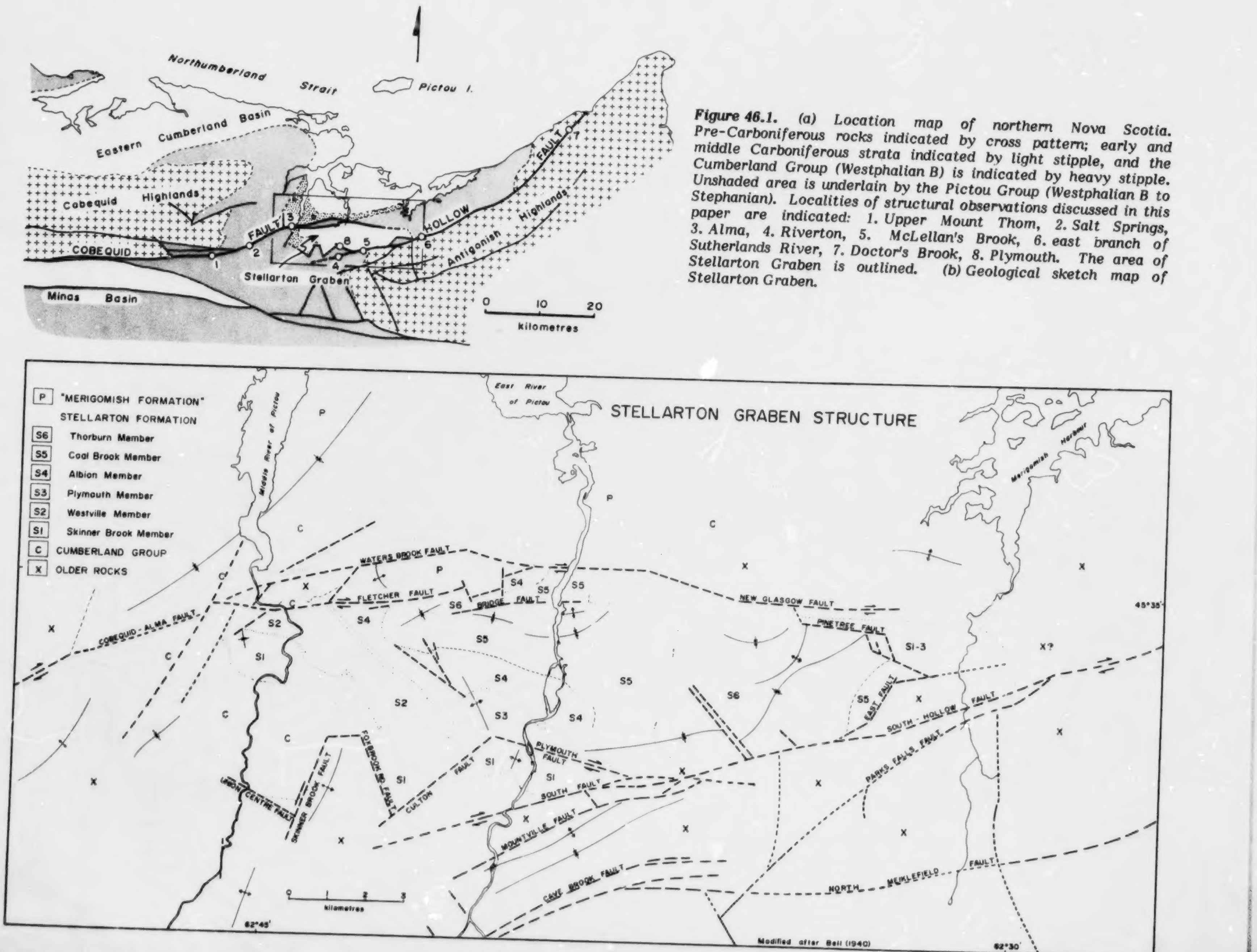

Figure 46.1. *(a) Location map of northern Nova Scotia. Pre-Carboniferous rocks indicated by cross pattern; early and middle Carboniferous strata indicated by light stipple, and the Cumberland Group (Westphalian B) is indicated by heavy stipple. Unshaded area is underlain by the Pictou Group (Westphalian B to Stephanian). Localities of structural observations discussed in this paper are indicated: 1. Upper Mount Thom, 2. Salt Springs, 3. Alma, 4. Riverton, 5. McLellan's Brook, 6. east branch of Sutherlands River, 7. Doctor's Brook, 8. Plymouth. The area of Stellarton Graben is outlined. (b) Geological sketch map of Stellarton Graben.*

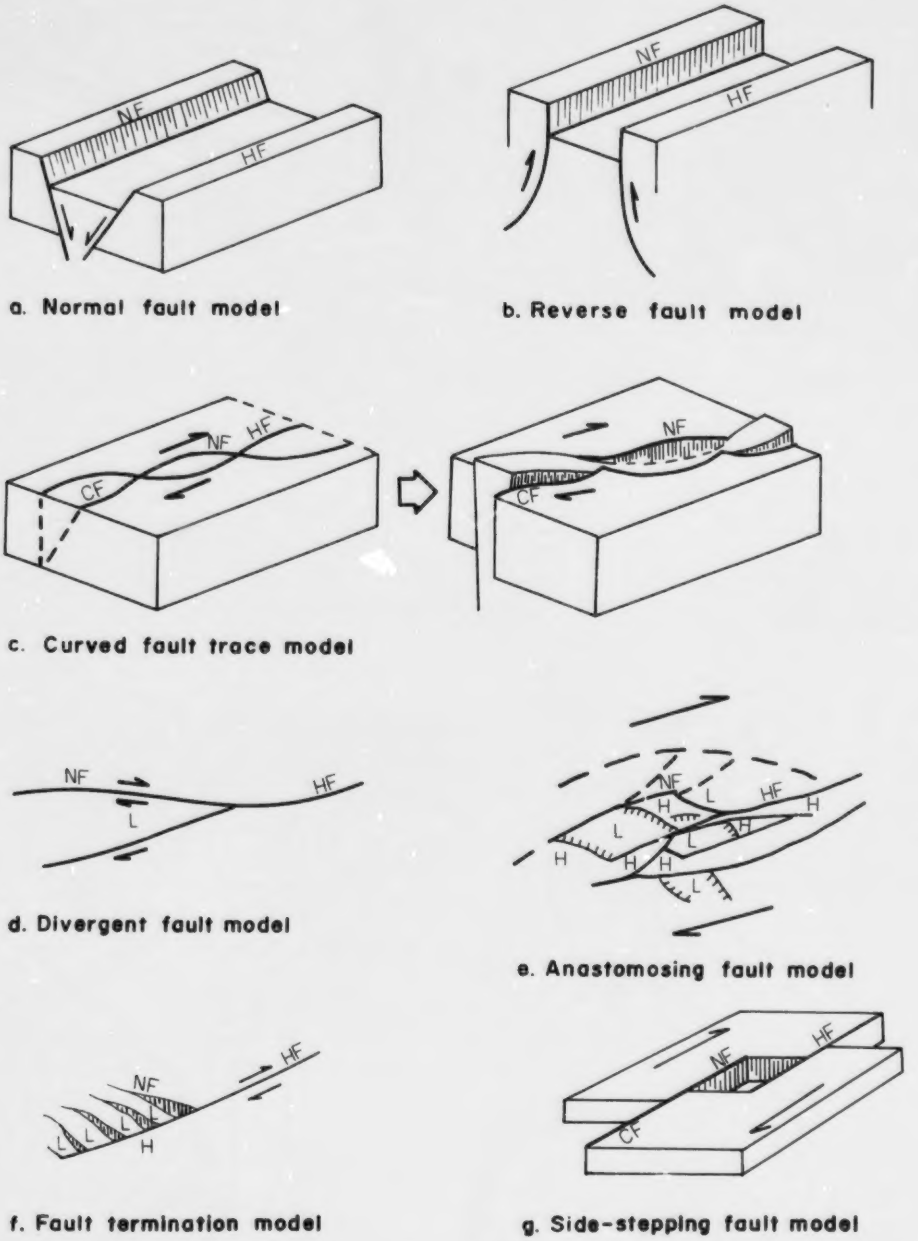

Figure 46.2. Mechanisms for graben development. Figures a and b are grabens formed by dip-slip faulting. Figures c to g are grabens formed by strike-slip faulting (after Reading, 1980). Fault systems are indicated: CF: Cobequid Fault, NF: North faults (eastern extension of Cobequid Fault), HF: Hollow Fault. Areas underlain by late Carboniferous strata (Pictou Group) are stippled. (a) Classic extensional graben bounded by normal faults. (b) Graben bounded by reverse faults, formed by compression. (c) Graben produced by strike-slip along intersecting, curved fault traces. (d) "Wedge graben" produced by divergent strike-slip faults. H and L are high and low areas respectively. (e) Graben produced by complexly anastomosing faults. (f) Half-graben due to secondary faulting (Riedel shears) at the termination of a strike-slip fault. (g) "Rhomb graben" produced by side-stepping transfer of movement from one strike-slip fault to another. This interpretation, suggested by Fralick (1980), is supported by the observations discussed in this paper.

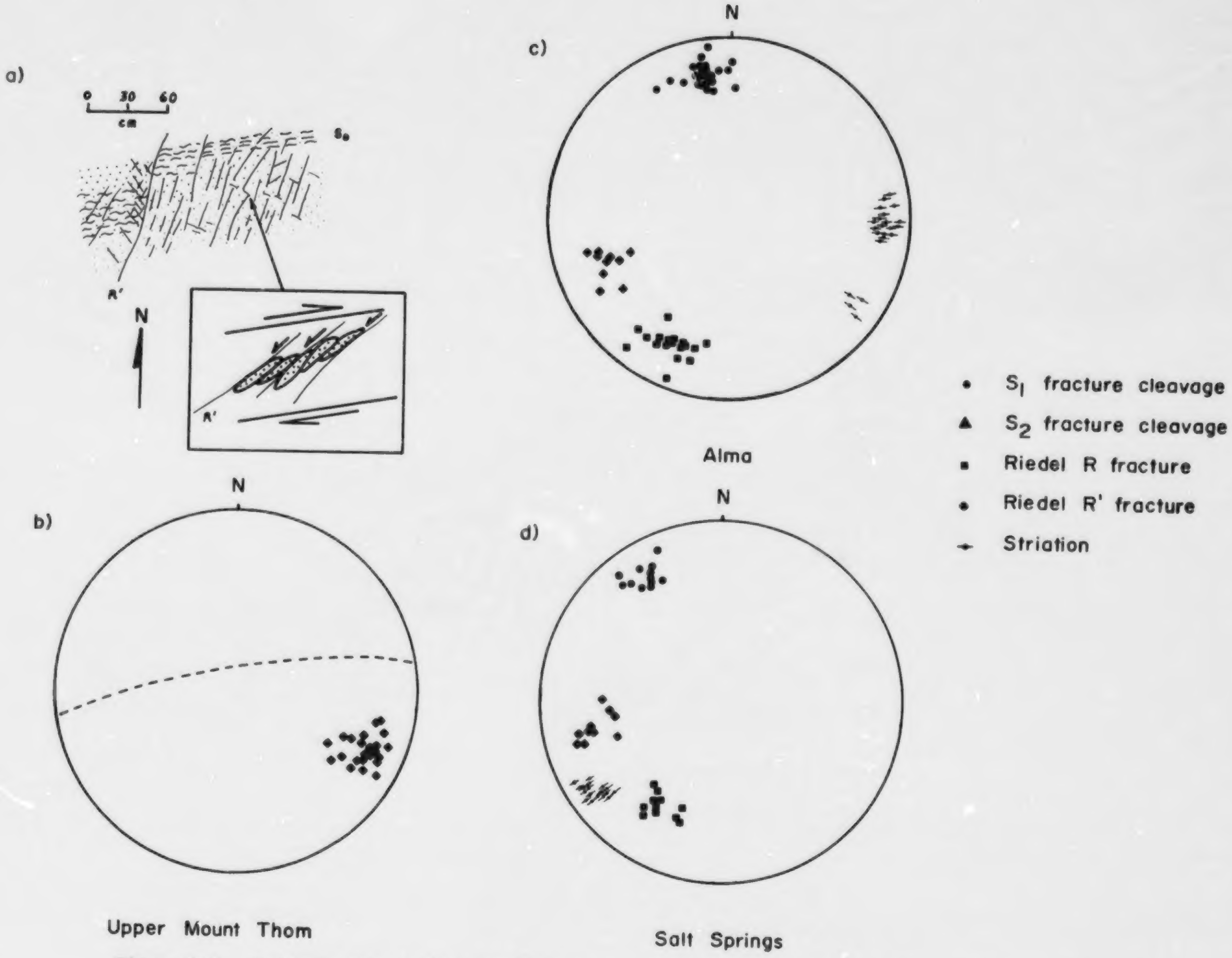

Figure 46.3. *Evidence for dextral displacement on the eastern Cobequid Fault. Locations of observations are shown in Figure 46.1.*

(a) Sketch of Riedel fracture pattern on fault near Upper Mount Thom. Sandstone lenses are bounded by bedding (S_0) and sinistral Riedel fracture surfaces (R') developed at a large angle oblique to the overall dextral shear sense.

(b) Equal-area lower hemisphere projection of poles to Riedel R' fracture cleavages (n = 24) from the fault zone near Upper Mount Thom. Great circle represents the fault zone.

(c) Plot of poles to fracture surfaces on the fault at Alma. S_1 surfaces (n = 24) strike subparallel to the fault. Striations on S_1 surfaces (n = 19), Riedel R (n = 18), and Riedel R' (n = 10) fracture surfaces are all consistent with dextral movement on the fault.

(d) Plot of poles to fracture surfaces on the fault at Salt Springs: S_1 surfaces (n = 12) strike subparallel to the fault. Striations on S_1 surfaces (n = 19), Riedel R (n = 11), and Riedel R' (n = 10) fracture surfaces indicate dextral fault movement.

shear fractures are Riedel shears (Tchalenko and Ambraseys, 1970; Freund, 1974). The acute angle of intersection of the two fracture sets is bisected by the direction of maximum compression (G_1), whose value is 140 ± 10 degrees.

Striations, plunging easterly at 10 to 25 degrees, are found on the NE- to ENE-striking fault planes (Fig. 46.3). Stepped mineral fibre growths and grooves on these polished surfaces are indicators of lateral movement. The sense of displacement along fractures that define lensoid bodies was obtained from subhorizontal slickensides in sheared rocks (Fig. 46.3c,d). These show that displacement on the R surfaces was dextral, with dip component of 10 to 28 degrees.

The observations described above are consistent with dextral movement along this segment of the Cobequid Fault.

Hollow Fault

Hollow Fault separates the Carboniferous sedimentary basins to the northeast from older rocks of the Antigonish Highlands. Its western extension forms part of the southern

boundary of the Stellarton Graben. Along much of its length, the fault zone is marked by a prominent topographic break. As noted above, late Carboniferous dextral movement on the Hollow Fault has been suggested by several workers (Eisbacher, 1967; 1969; Webb, 1969; Benson, 1974; Dewey and Fyson in Boucot et al., 1974; Fralick, 1980; Fralick and Schenk, 1981). Such an interpretation is supported by an apparent dextral offset of about 35 km shown by Silurian strata on the Hollow Fault. No direct evidence for the sense of fault movement, however, has been reported.

The Hollow Fault Zone itself is exposed at only a few localities: Doctors Brook, the east branch of Sutherlands River, McLellans Brook, and on the East River at Riverton (Fig. 46.4, 46.5). The youngest rocks directly observed to be deformed by the fault belong to the Canso Group (Namurian A).

An intensely foliated and deformed shear zone, about 250 m wide, is spectacularly exposed at Riverton, on the East River south of Stellarton (Fig. 46.4). The shear zone comprises foliated siltstone and sandstone blocks containing gouge zones, breccia and cataclasite (Sibson, 1977). In contrast with correlative rocks outside the shear zone, primary sedimentary features are poorly preserved. Form surface mapping in this shear zone reveals its deformation characteristics (Fig. 46.4b,c,e). The orientation of the penetrative S_1 cleavage surfaces, which are partly planar and partly curved, is nearly parallel to the strike of the shear zone. S_1 cleavage surfaces commonly show a dextral sense of offset. Bedded carbonate concretions in deformed reddish-brown siltstone are offset to the right by S_1 surfaces (Fig. 46.4d). In addition, asymmetrical, rotated concretions in siltstone are local indicators of internal rotation during deformation. The nodules appear to have undergone about 30 degrees of rotation with respect to original bedding. The axes of maximum elongation of the deformed concretions are now parallel to the trend of the S_1 cleavage surfaces.

S_2 cleavage surfaces, which overprint the S_1 cleavage, show evidence of sinistral offset (Fig. 46.4c,e,f). The sense of shear along the S_2 surfaces, which are oriented at a high angle oblique to the main shear couple, is predominantly sinistral, opposite to the overall sense of shear in the rocks (c.f. Lister and Williams, 1979; Simpson and Schmid, 1983).

Stretching lineations are of significance to the kinematic interpretation of these deformed rocks. Most lineations, measured in the gouge zones and on S cleavage surfaces nearly parallel to the major shear zone, trend 80 ± 10 degrees, and plunge 10 to 30 degrees (Fig. 46.4f). The sense of displacement on the fault indicated by the attitudes of the lineations is consistent with that indicated by the dextral offsets observed on the main (S_1) foliation surfaces.

Riedel R' shear fractures were also recognized in the Hollow Fault Zone on the East River (Fig. 46.4a,b). Internally undeformed blocks of sandstone, defined by the bedding and R' fractures, were rotated 20 to 30 degrees clockwise. The hanging wall of each fracture plane shows a sinistral displacement with a plunge of less than 45 degrees. This rotation is interpreted to be due to the overall dextral sense of movement acting on the shear zone boundary.

A well-developed fold observed in the shear zone was formed by folding of S_1 surfaces (Fig. 46.4e). Overprinted S_2 cleavage surfaces are axial planar to the fold. It plunges towards the NE at 50 degrees. We interpret it to result from right lateral simple shear within the fault zone.

Well-developed conjugate reverse kink bands can be seen on the East River in the area between the Hollow and Mountville faults, where interbedded shale and siltstone are deformed into an asymmetrical fold with a steep plunge towards the NE. The Z-shaped set of kink bands is better developed. Its axial planes strike NE to ENE, and it dips steeply northward. The less well-developed, S-shaped set has axial planes striking NW, and dips steeply southward. Their geometry suggests two possible interpretations: 1) conjugate kink bands were produced by dominantly dextral slip involved in dextral movement on both faults, or 2) NE-trending kink bands developed first due to dextral slip, while NW-trending kink bands developed later as the result of local stress adjustments.

Observations to document the Riedel shear fracture pattern in some shear bands within the Hollow Fault zone where it crosses McLellans Brook, Sutherlands River, and Doctor's Brook are shown in Figure 46.5. At each locality, a P fracture set (which can also be considered a set of curved S_1 surfaces) intersects the main shear band boundaries at 5 to 10 degrees. R fracture sets intersect the main shear planes at 20 to 30 degrees. Marker horizons (thin-bedded, greenish, fine grained sandstone) and P surfaces are displaced to the right by the R fracture set.

All of the observations made on the exposures of the Hollow Fault zone discussed above are consistent with late Carboniferous (late Visean to Westphalian C) dextral movement on the Hollow Fault.

Secondary structures within Stellarton Basin

Stellarton Graben is characterized by secondary NE- to ENE-trending en echelon folds and faults (see Bell, 1940). The orientation of faults intersected during coal mining operations and exploratory drilling can be used for structural analysis (Fig. 46.6). Three sets of faults may be distinguished clearly: a dominant set striking SSE, one subordinate set striking NE to ENE, and another subordinate set striking ESE. Comparison of faults found during coal mining operations with parallel faults exposed at the surface suggests that faults belonging to the first set (SSE) commonly have sinistral offsets. These faults can be interpreted as Riedel R' shear faults with a large dip-slip component (the plunge of lineations on these fault surfaces is about 45 degrees.). The second set (NE-ENE) is subparallel with the boundary faults. They are associated with other major faults or secondary faults. The third set (ESE) has dextral displacement with few exceptions. A good example is a shear zone near the Plymouth Fault, where the minor fold profiles give unequivocal evidence that dextral shear occurred on this fault (Fig. 46.7). The Plymouth Fault can be interpreted as a Riedel R shear fault.

A fourth set of low angle faults are observed in outcrop and core. These support Haites (1956) arguments for thrust faulting within the graben.

The folds and faults and the large-scale pattern of Riedel shears seen in Stellarton Graben were probably produced by dextral movement on the boundary faults.

Other structural features of Stellarton Gap

Outside Stellarton Graben, the structural geology of Stellarton Gap is relatively simple. The Scotsburn Anticline is a gentle fold plunging ENE from the Cobequid Highlands through the late Carboniferous "Merigomish Formation". It separates the Merigomish Sub-basin (Fralick, 1980) from the main part of Cumberland Basin. Between the easternmost segment of the Cobequid Fault and the Scotsburn Anticline lies the Trenton Syncline. Sediment dispersal patterns in the Pictou Group (Yeo, 1985) suggest that this regional fold pair developed during Westphalian time, concurrently with dextral movement on the Cobequid and Hollow faults. Thus, they probably formed in response to the same NW-SE compression.

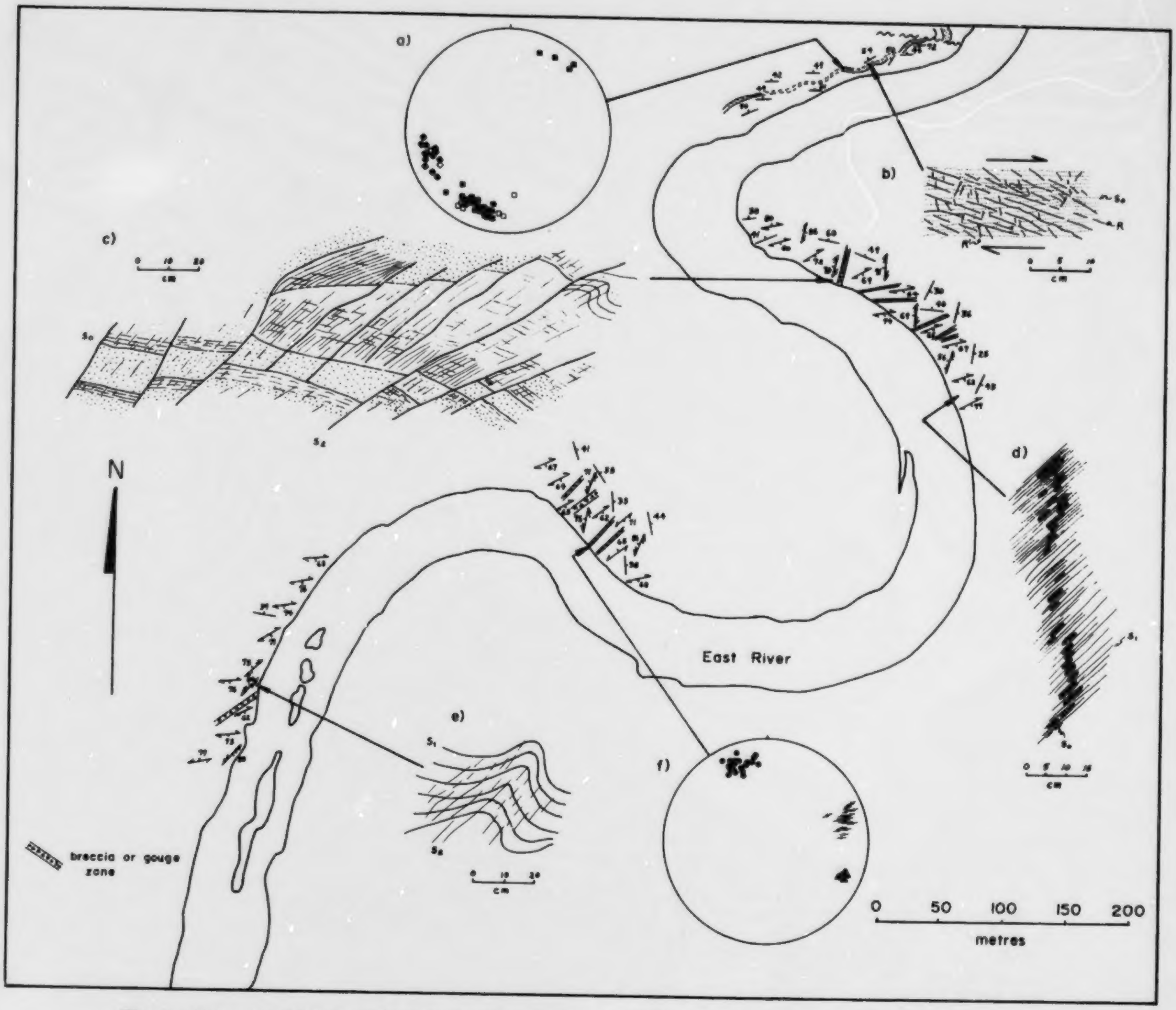

Figure 46.4. *Simplified geological sketch map of the Hollow Fault zone in Canso Group siltstones and minor sandstones near Riverton on the East River (see Fig. 46.1). Symbols for structural elements same as those in Figure 46.3.*

(a) Equal-area lower hemisphere plot of poles to Riedel R (n = 34) and R' (n = 15) fracture surfaces. Open symbols respectively indicate R surfaces with dextral offset (n = 7) and R' surfaces with sinistral offset (n = 2). The overall sense of shear is dextral.

(b) Sketch of Riedel fracture pattern demonstrating dextral shear on the northern edge of the Hollow Fault zone.

(c) Sketch of fracture pattern in the fault zone. Sandy lenses are defined by bedding (S_0) and clockwise-rotated S_2 cleavage surfaces with sinistral offset resulting from dextral shear.

(d) Sketch showing dextral offset of carbonate concretions (defining S_0) along S_1 cleavage surfaces in siltstone.

(e) S_1 cleavage surfaces folded in response to dextral shear and overprinted by axial planar S_2 cleavage.

(f) Plot of S_1 (n = 21) and S_2 (n = 5) fracture cleavages from the Hollow Fault. Gently ENE-plunging striations (n = 18) on the S_1 surfaces suggest dextral strike-slip.

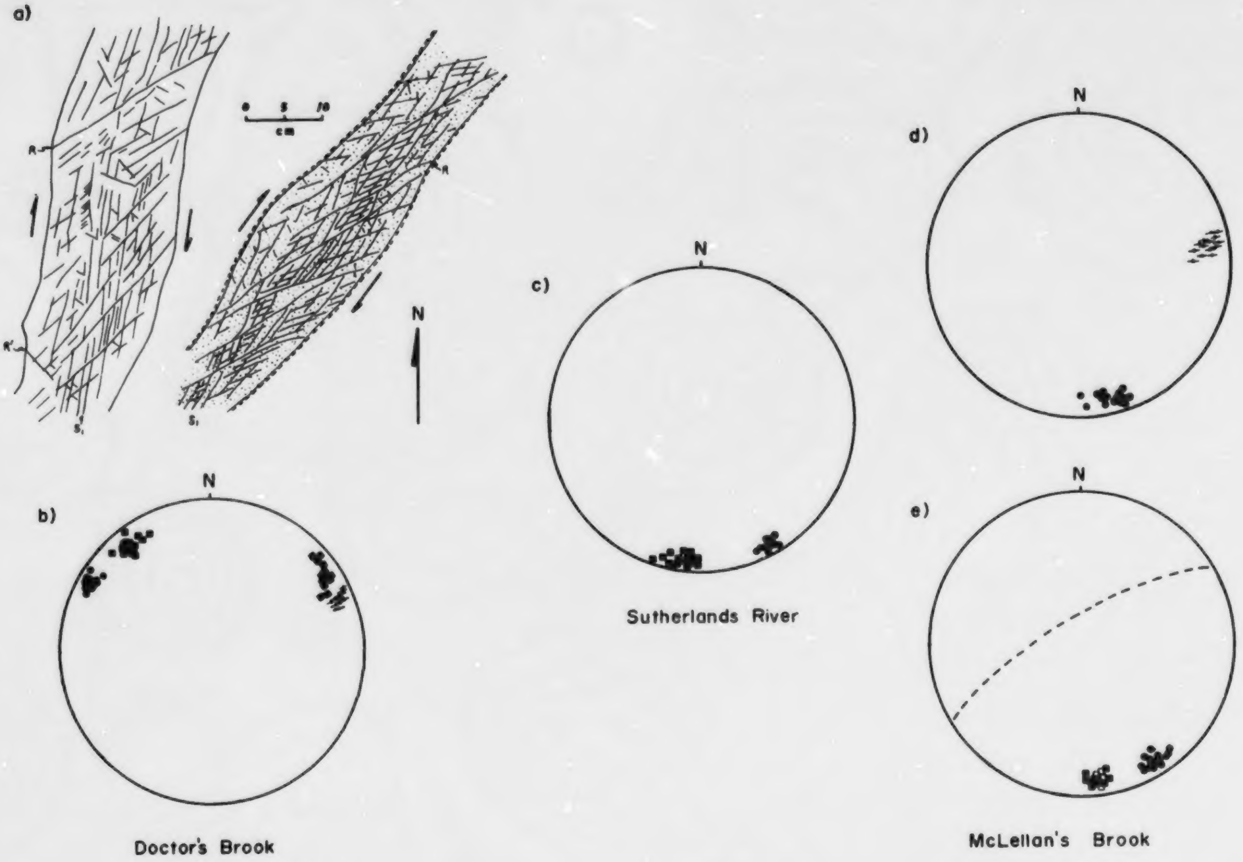

Figure 46.5. *Evidence for dextral displacement on the Hollow Fault. Locations of observations are shown in Figure 46.1. See Figure 46.3 for explanation of structural element symbols.*

(a) Sketches of two meso-scale shear zones in Windsor Group siltstones at Doctor's Brook. In the left-hand sketch, S_1 fracture surfaces strike 30-32 degrees and dip 85-87 degrees NW, and R' fracture surfaces strike 130-140 degrees and dip 74-84 degrees SW. In the right-hand sketch, S_1 surfaces strike 23-30 degrees and dip 80-87 degrees NW, and R fracture surfaces strike 50-54 degrees and dip 75-80 degrees NW. Dextral offset on R surfaces and sinistral offset on R' surfaces indicate overall dextral shearing.

(b) Equal-area lower hemisphere plot of poles to fracture surfaces from the Hollow Fault zone at Doctor's Brook. S_1 surfaces (n = 15) strike NNE subparallel to the fault. Riedel R (n = 22), Riedel R' (n = 15), and striations on the R surfaces (n = 11) are all consistent with dextral movement on the fault.

(c) Plot of poles to S_1 (n = 11) and R (n = 18) fracture surfaces on Hollow Fault on the east branch of Sutherlands River. The relationship between the two sets of fracture surfaces indicates dextral movement on the fault.

(d) Plot of poles to S_1 cleavage (n = 16) and gently plunging striations on these surfaces (n = 16) from the Hollow Fault at McLellan's Brook. The striations indicate dextral strike-slip.

(e) Plot of poles to S_1 cleavage (n = 17) and Riedel R fracture surfaces (n = 18) from the Hollow Fault at McLellan's Brook. R surfaces showing dextral offset (n = 6) are indicated by open symbols. The attitude of the fault zone is indicated by the great circle. Fault movement must have been dextral.

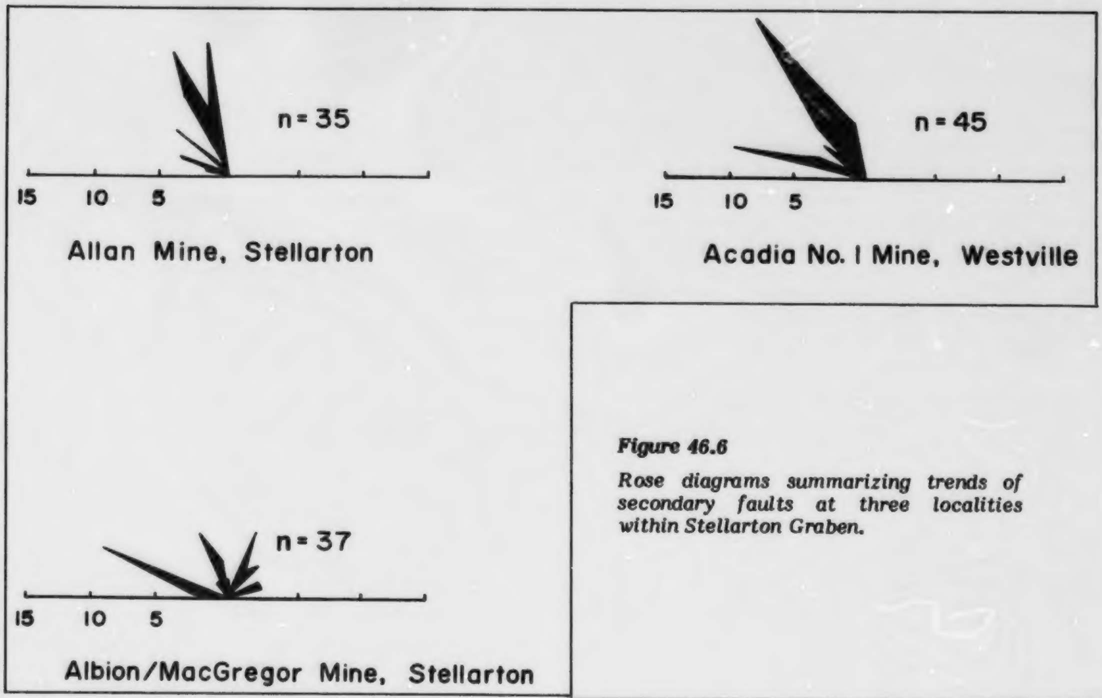

Figure 46.6

Rose diagrams summarizing trends of secondary faults at three localities within Stellarton Graben.

A small anticline trending easterly along the axis of Pictou Island is a postdepositional feature most likely caused by doming of Windsor Group evaporites. The dispersal pattern of "Merigomish Formation" sandstones exposed on the island is unaffected by this fold.

A few normal faults trending N to NNE appear to postdate all of the other structures. Displacement on these may locally be considerable, as indicated by the 120 m scarp visible along the west side of Green Hill. Movement on similar late faults cutting the western Cobequid Fault is post-early Jurassic (Donohoe and Wallace, 1985).

Evolution of Stellarton Gap

Movement on the Cobequid and Hollow faults likely began in the middle Devonian in response to regional crustal extension, indicated by emplacement of the Fountain Lake and McAras Brook volcanics (Bradley, 1982; and others). These faults may have developed on a much older zone of crustal weakness, however (B. Murphy, personal communication).

Re-activation of the Hollow Fault in late Visean time is indicated by deposition of the Hollow Conglomerate along the Hollow Fault zone (Fralick, 1980; Fralick and Schenk, 1981). This faulting episode punctuated a marine transgression in the northern Appalachians which resulted in deposition of the Windsor Group, the oldest strata exposed in Stellarton Gap. This marine incursion represents the culmination of a period of tectonic quiescence between the Acadian and Hercynian orogenies. It was probably terminated by the onset of the Permo-Carboniferous glaciation of Gondwanaland, as global sea levels dropped abruptly in response to the growth of

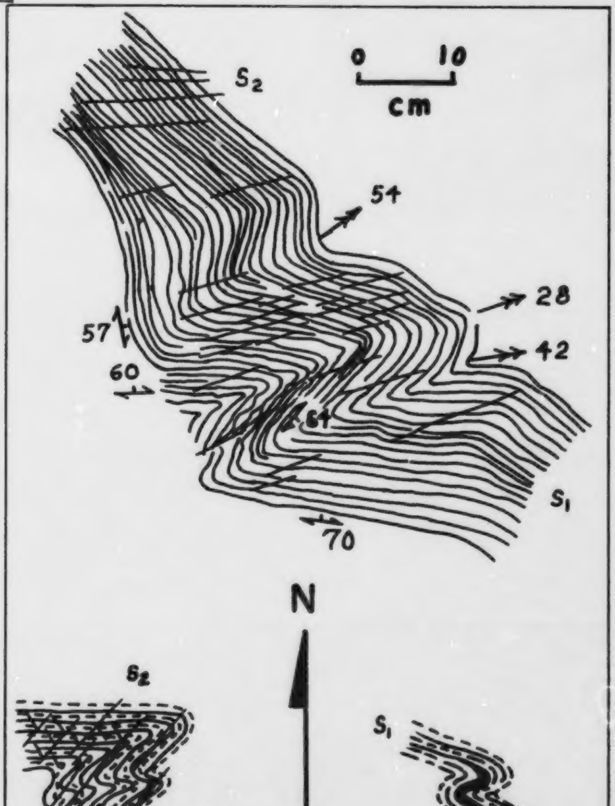

Figure 46.7. *Sketches of three fold profiles in Stellarton Formation siltstones from the Plymouth Fault zone on the East River (see Fig. 46.1). S_1 cleavage has been folded in response to dextral shear and overprinted by the S_2 cleavage. The Plymouth Fault can be regarded as a large-scale Riedel R fracture with dextral offset.*

ice sheets. Meandering river deposits of the Canso Group reflect continued quiescence in Stellarton Gap after this period of faulting.

Uplift of the Cobequid Highlands in late Namurian time resulted in shedding of coarse clastics of the Riversdale Group northward into Cumberland Basin and eastward into Stellarton Gap (Fig. 46.8a).

Both Cobequid and Hollow faults were re-activated in Westphalian B time as the New Glasgow Conglomerate was deposited in the centre of Stellarton Gap. Fault movement was probably dextral as sedimentation was essentially continuous from this time until the completion of infilling of Stellarton Graben (Fig. 46.8b).

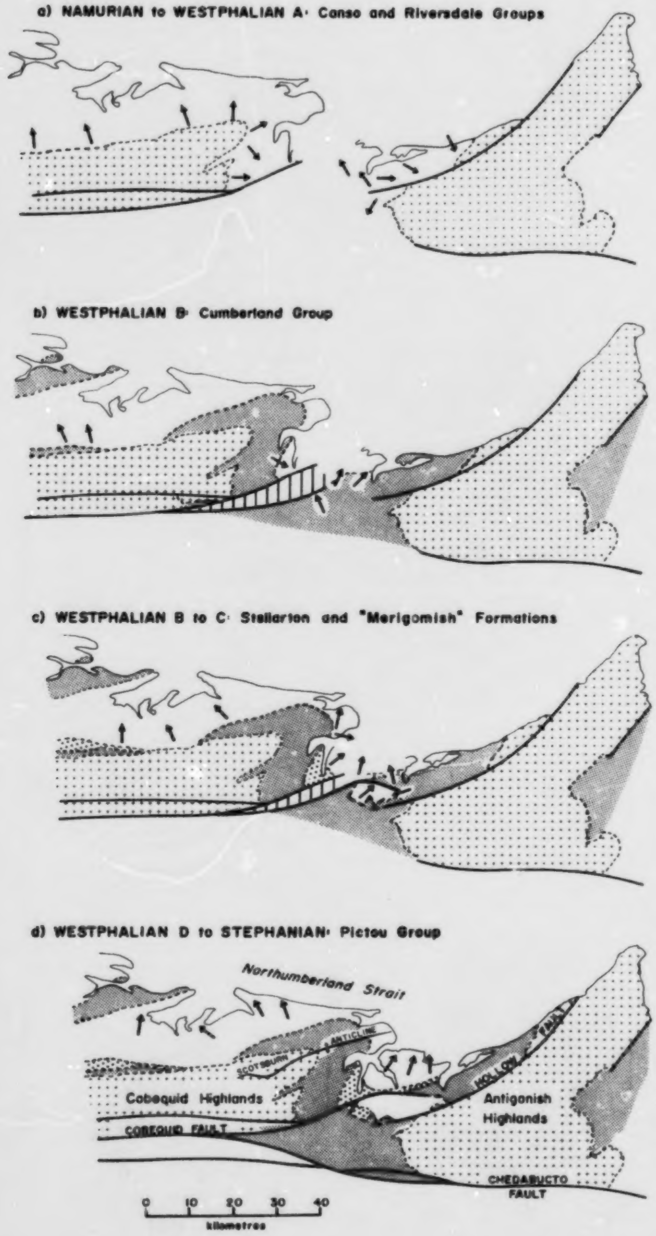

As strike-slip faulting continued, a rhomb graben developed between the Cobequid and Hollow faults: Stellarton Graben (Fig. 46.2g, 46.8c). The length of Stellarton Graben, about 20 km, may provide an approximation to the amount of strike-slip movement required for its formation. This corresponds with the amount of dextral displacement estimated for the Cobequid Fault in the Parrsboro area (Donohoe and Wallace, 1985). Lateral movement of the fault blocks may have been facilitated by sliding on evaporites of the underlying Windsor Group. The thick sequence (<2600 m) of fine grained, grey, lacustrine clastics which comprise the bulk of the Stellarton Formation indicates that sedimentation nearly kept up with subsidence (and basin extension). Hence, fault movement must have been generally gradual and continuous from late Westphalian B through Westphalian C time. Development of some marginal relief and either consequently increased rates of sedimentation or lower rates of subsidence are indicated by intervals of coarse grained clastics, coarsening of facies towards the graben margins, and development of redbed sequences. By Westphalian D time, subsidence of Stellarton Graben had ended, in response to cessation of strike-slip faulting. Clastics continued to be shed into Stellarton Gap until the Permian, however.

Conclusions

Field observations and structural analyses at several localities along the eastern Cobequid and Hollow faults consistently reveal that late Carboniferous movement was dextral. This is in agreement with the findings of Eisbacher (1967; 1969) and White (1983) from the western Cobequid Fault. The problems outlined in the introduction to this paper can therefore be resolved.

Stellarton Graben most likely formed as a simple rhomb graben in response to dextral movement on the Cobequid and Hollow fault systems, caused by NW-SE compression during Westphalian B and C time. Within Stellarton Graben, the orientation of secondary faults and en echelon right hand folds suggests a large-scale Riedel shear pattern consistent with regional dextral shear.

Figure 46.8. *Development of the Stellarton Graben in response to dextral movement on the Cobequid and Hollow faults in the late Carboniferous. Arrows indicate generalized sediment dispersal in eastern Cumberland basin and Stellarton Gap. The lacuna indicated by vertical bars across the eastern Cobequid Fault may be eliminated by progressive NW-SE shortening as the Scotsburn Anticline and Trenton Syncline developed.*

(a) Canso and Riversdale strata were deposited in Namurian to Westphalian A time. These sediments undoubtedly lapped farther onto the highland areas than their present boundary as shown.

(b) The Cumberland Group was deposited in Westphalian B time. Active subsidence of Stellarton Graben due to strike-slip faulting probably began during this time.

(c) Stellarton Formation sedimentation began in late Westphalian B in response to strike-slip movement and graben subsidence. Deposition of the "Merigomish" Formation (Pictou Group) in the northern part of Stellarton Gap began in Westphalian C time, while Stellarton Formation sedimentation continued.

(d) Subsidence of Stellarton Graben (and significant strike-slip on the Cobequid-Hollow Fault system) ended by Westphalian D time, but Pictou Group sedimentation continued into the Stephanian. Younger Pictou strata may have blanketed part of the Stellarton Graben.

If Stellarton Graben is a synsedimentary strike-slip basin, it is unlikely that the coal seams known within the graben ever extended outside it (with the possible exception of the Thorburn coals, the highest in the Stellarton Formation).

The juxtaposition of unlike facies belonging to the partly time-correlative "Merigomish" and Stellarton formations resulted from relative dextral strike-slip movement. The core area of the Trenton Syncline, which now lies north of the Stellarton Graben initially lay northwest of the site of the latter. Stellarton Graben could not have been an obstacle to derivation of the New Glasgow Conglomerate from a southern source area since it did not exist in early Westphalian B time.

Many problems still remain. The tectonic framework outlined above for the development of Stellarton Gap provides a context for detailed studies of the upper Carboniferous stratigraphy, currently in progress. The field work described here forms a basis for further study of the microstructure and kinematics of brittle deformation on the eastern Cobequid-Hollow fault system.

Acknowledgments

We thank Brendan Murphy and J.C. White for enthusiastic discussions and advice in the field, and Cees van Staal for critical comments on this paper. The field work reported here is part of a MSc study by Gao Ruixing at the University of New Brunswick, supported as part of the Stellarton Basin Analysis Project. This project is part of the Canada-Nova Scotia Mineral Development Agreement 1984-89.

References

Bell, W.A.
1940: The Pictou Coalfield, Nova Scotia; Geological Survey of Canada Memoir 225, 161 p.

Belt, E.S.
1968: Post-Acadian rifts and related facies, Eastern Canada; in Studies of Appalachian Geology: Northern and Maritime, Interscience Publishers, p. 95-113.

Benson, D.G.
1974: Geology of the Antigonish Highlands, Nova Scotia; Geological Survey of Canada, Memoir 376, 92 p.

Bradley, D.C.
1982: Subsidence in late Paleozoic basins in the northern Appalachians; Tectonics, v. 1, p. 107-123.

1983: Tectonics of the Acadian Orogeny in New England and adjacent Canada; Journal of Geology, v. 91, p. 381-400.

Boucot, A.J., Dewey, J.F., Dineley, D.L., Fletcher, R., Fyson, W.K., Griffin, J.G., Hickox, C.F., McKerrow, W.S., and Ziegler, A.M.
1974: Geology of the Arisaig area; Geological Society of America, Special Paper 139, 191 p.

Donohoe, H. and Wallace, P.
1978: Anatomy of the Cobequid Fault and its relation to the Glooscap and Cabot Fault Systems (abstract); Geological Society of America. Abstracts with Programs, v. 10, no. 7, p. 391.

Donohoe, H. and Wallace, P. (cont.)
1985: Repeated Orogeny, Faulting, and Stratigraphy in the Cobequid Highlands, Avalon Terrain of Northern Nova Scotia; Geological Association of Canada Annual Meeting 1985 (Fredericton), Fieldtrip Guidebook No. 3, 77 p.

Eisbacher, G.H.
1967: Tectonic Analysis in the Cobequid Mountains, Nova Scotia, Canada; unpublished Ph.D. thesis, Geology Department, Princeton University, Princeton, New Jersey, 108 p.

1969: Displacement and stress field along part of the Cobequid Fault, Nova Scotia; Canadian Journal of Earth Science, v. 6, p. 1095-1104.

Fralick, P.W.
1980: Tectonic and Sedimentological Development of a Late Paleozoic Wrench Basin: The Eastern Cumberland Basin, Maritime Canada; unpublished M.Sc. thesis, Dalhousie University, 188 p.

Fralick, P.W. and Schenk, P.E.
1981: Molasse deposition and basin evolution in a wrench tectonic setting: The late Paleozoic Eastern Cumberland Basin, Maritime Canada; in Sedimentation and Tectonics in Alluvial Basins, ed. A.D. Miall; Geological Association of Canada, Special Paper 23, p. 77-98.

Freund, R.
1974: Kinematics of transform and transcurrent faults; Tectonophysics, v. 21, p. 93-134.

Hacquebard, P.A. and Donaldson, J.R.
1969: Carboniferous coal deposits associated with flood plain and limnic environments in Nova Scotia; Geological Society of America, Special Paper 114, p. 143-191.

Haites, T.B.
1956: Some geological aspects of the Pictou Coalfield with reference to their influence on mining operations; in Third Conference on the Origin and Constitution of Coal (Crystal Cliffs, Nova Scotia), Nova Scotia Department of Mines and Nova Scotia Research Foundation, Halifax. p. 283-297.

Lister, G.S. and Williams, P.F.
1979: Fabric development in shear zones: Theoretical controls and observed phenomena; Journal of Structural Geology, v. 1, p. 283-297.

Ramsay, J.G.
1967: Folding and Fracturing of Rocks; McGraw-Hill, New York, 568 p.

1980: Shear zone geometry: A review; Journal of Structural Geology, v. 2, p. 83-99.

Reading, H.G.
1980: Characteristics and recognition of strike-slip fault systems; in Sedimentation in Oblique-Slip Mobile Zones, ed. P.F. Ballance and H.G. Reading; International Association of Sedimentologists, Special Publication 4, p. 7-26.

Sibson, R.H.
1977: Fault rock and faulting mechanisms; Journal of the Geological Society of London, v. 133, p. 191-213.

Simpson, C. and Schmid, S.M.
1983: An evaluation of criteria to deduce the sense of movement in sheared rocks; Geological Society of America Bulletin, v. 94, p. 1281-1288.

Tchalenko, J.S. and Ambreseys, N.N.
1970: Structural analysis of the Dasht-e Bayez (Iran) earthquake fractures; Geological Society of America Bulletin, v. 81, p. 41-60.

Webb, G.W.
1967: Paleozoic wrench faults in the Canadian Appalachians; American Association of Petroleum Geologists, Memoir 12, p. 754-786.

White, J.C.
1983: Structural development along a segment of the Cobequid Fault, Nova Scotia (abstract); Journal of Structural Geology, v. 5, p. 553.

Yeo, G.M.
1985: Upper Carboniferous sedimentation in northern Nova Scotia and the origin of Stellarton Basin; in Current Research, Part B, Geological Survey of Canada, Paper 85-1B, p. 511-518.

Artillery Lake map area, District of Mackenzie: a transect across the Thelon Front

Project 840005

John B. Henderson and Robert I. Macfie
Precambrian Geology Division

Henderson, J.B. and Macfie, R.I., Artillery Lake map area, District of Mackenzie: a transect across the Thelon Front; in Current Research, Part A, Geological Survey of Canada, Paper 86-1A, p. 411-416, 1986.

Abstract

The boundary between the Slave Province and the Thelon Tectonic Zone of the western Churchill is represented in three fault-bounded domains. A narrow central domain is intermediate in character between the western domain (Slave Province) with its curvilinear structural trends and patchy greenschist to amphibolite metamorphic pattern and the eastern domain which is dominated in the northwest by linear north-northeasterly structural trends with abundant mylonite zones and parallel upper amphibolite to granulite zones. This pattern is less pronounced to the east and south. The eastern domain contains migmatitic supracrustal rocks that increase in abundance to the south and are intruded by Proterozoic granite. The migmatites are similar in some respects to the Slave Yellowknife Supergroup although the relationship remains to be defined. Throughout the area are a series of northeasterly dextral faults, with some vertical component, that are splays off the master McDonald Fault that transects the southeastern third of the area.

Résumé

La frontière entre la province des Esclaves et la zone tectonique de Thelon (partie ouest de la province de Churchill) est représentée dans trois domaines limités par des failles. Entre un domaine Ouest (province des Esclaves) caractérisé par des directions structurales curvilinéaires et un métamorphisme variant entre le faciès des schistes verts tachetés et celui des amphibolites, et un domaine Est dominé dans le nord-ouest par des directions structurales linéaires nord-nord-est et contenant des zones mylonitiques abondantes et des zones parallèles de métamorphisme passant de la limite supérieure des amphibolites au faciès des granulites, s'interpose un domaine étroit accusant des caractéristiques intermédiaires. Cette configuration est moins prononcée à l'est et au sud. Le domaine Est renferme des roches supracorticales migmatitiques dont l'abondance augmente vers le sud et dans lesquelles fait intrusion du granite protérozoïque. Les migmatites ressemblent à certains égards au supergroupe de Yellowknife (province des Esclaves), quoique les relations restent encore à définir. Toute la région est parcourue de failles à décrochements dextres de direction nord-est qui ont une certaine composante verticale et qui sont, en fait, des projections de la faille principale de McDonald qui recoupe le tiers sud-est de la région.

Introduction

The Artillery Lake map area is diagonally divided by the central segment of the Thelon Front which separates the Slave Province with its curvilinear structural trends, relatively massive plutonic bodies and mainly low to intermediate metamorphic grade metasediments and metavolcanics of the Archean Yellowknife Supergroup, from the linear trends, strongly foliated granitoids and high grade gneisses and schists of the Thelon Tectonic Zone of the northwestern Churchill Province. This boundary was originally recognized during 1:1 000 000 scale regional helicopter reconnaissance mapping of the northwestern Shield (Wright, 1957, 1967; Fraser, 1964) and is currently the subject of more detailed investigations at 1:250 000 scale in its northern (Thompson et al., 1986), central (Frith, 1982a,b; Henderson et al., 1982; Henderson and Thompson, 1982; Henderson and Macfie, 1985) and southern sections (Bostock, 1986) south of Great Slave Lake. In addition, structural and metamorphic studies at 1:50 000 scale are currently ongoing in the central (James, 1985, 1986) and southern (Hanmer and Lucas, 1985) parts of the Thelon Tectonic Zone.

The current mapping of the Artillery Lake area at 1:250 000 scale was started in 1984 (Henderson and Macfie, 1985) with a transect across part of the northern third of the area and represents a continuation of the recent mapping of the Healey Lake area immediately to the north (Henderson et al., 1982; Henderson and Thompson, 1982). The Artillery Lake area was originally mapped at 1:1 000 000 scale as part of Operation Thelon (Wright, 1957, 1967) and the eastern half of the area was mapped at 1:250 000 scale by Fraser (1972). Gandhi (1985) recently studied the geology and mineral deposits in the southwest part of the area at Artillery Lake. Work this past field season was concentrated in the central to southeastern part of the area. The more detailed structural-metamorphic study across the Thelon Front and into the Thelon Tectonic Zone in the vicinity of the boundary between the Artillery Lake and Healey Lake map areas (James, 1985), continued to the east of these two map areas (James, 1986).

General geology

On the basis of the northern transect completed in 1984, the area was divided into 3 structural domains (Henderson and Macfie, 1985). It was found that these three domains are still generally applicable in the central transect across the area completed this year although little work was done in the central domain. The western domain, bounded on the east by north-northeasterly-trending faults between Ptarmigan and Deville Lakes (Fig. 47.1), has geology typical of the Slave Province with abundant, well preserved metasediments and metavolcanics of the Yellowknife Supergroup that have been intruded by massive lobate granitoid to diorite plutons. Structural trends are generally northerly to northwesterly but locally conform to the outline of the intrusions and are typically steep. Metamorphic grade is in the low pressure facies series and ranges from greenschist in a northerly trending zone between Ptarmigan and Clinton-Colden lakes to migmatite locally in septa between plutonic lobes. The central domain is a transitional zone intermediate between the western and eastern domains and includes some characteristics of both. Structural trends are generally northerly with local variations and are typically steep. The rock units consist primarily of heterogeneous, ill defined granitoid units, augen and migmatitic granitoids and a heterogeneous gneissic unit. Yellowknife metasedimentary units are present but only as relatively small bodies and are everywhere highly migmatitic. The domain presumably represents a relatively deeper structural level than that of the western domain. It is bounded on the east by a major belt of Yellowknife migmatites that contains within it a wide shear zone that has been traced well into the Healey Lake area to the north. The eastern domain consists of rock units similar to many in the central domain including units of migmatitic metasedimentary and metavolcanic rocks that become particularly abundant to the southeast and are extensively intruded by sheets of a younger but well foliated granite. Their relationship to the Yellowknife Supergroup rocks that occur in the western two domains remains to be determined. The rocks are strongly deformed with a very pronounced north-northeasterly trend and steep easterly dip particularly in the northwestern part of the domain. To the southeast the structural trends in the domain are more varied and dips generally more moderate and locally even flat. In the northern part of the domain are a series of discrete mylonite zones parallel to the regional trend that tend to die out in the southern part of the area mapped. A zone of granulite grade metamorphism is present in the west-central part of the domain but granulite grade rocks are only sporadically developed to the east and southeast. The McDonald Fault, a major dextral fault with displacement on the order of 100 km (on the basis of correlation of distinctive aeromagnetic anomalies (Henderson and Macfie, 1985, Fig. 54-1), passes through Mary Frances Lake. The geology mapped thus far south of the fault does not appear to differ significantly from much of that in the eastern domain.

Yellowknife Supergroup

In the western domain a rather large area of Yellowknife metasediments was outlined at Ptarmigan Lake. It extends north to join the extensive metasedimentary terrane that underlies much of Clinton-Colden Lake and continues north into the Healey Lake area. The metasediments are greywacke-mudstone turbidites so characteristic of much of the Slave Province to the west and northwest. Much of the metasediment is at amphibolite grade (assemblages of quartz, plagioclase, biotite, muscovite, cordierite, andalusite, sillimanite, staurolite) with a northerly trending zone of greenschist grade material in the central part of the area. On the east side of Ptarmigan Lake is a major unit of amphibolite grade mafic metavolcanics with well preserved primary features such as pillowed flows and volcanic breccia. It is bordered on the east by an elongate sill of texturally and compositionally varied anorthositic gabbro that is presumably related to a similar 4 km wide plutonic body southeast of Clinton-Colden Lake (Henderson and Macfie, 1985). The metavolcanics are thought to be related to the major mafic volcanic complex that occurs on the east side of Clinton-Colden Lake and extends north into the Healey Lake area but have been interrupted by the emplacement of the large granodiorite plutonic complex. The volcanics at Clinton-Colden Lake have been the target of extensive mineral exploration in the past. Unfortunately, only the northern part of the volcanics at Ptarmigan Lake are even moderately well exposed.

In the central domain only thin screens of migmatitic equivalents of the Yellowknife metasediments with a high proportion of white leucosome are present and are intruded by granitic to granodioritic rocks. This represents a continuation of the pattern seen previously north of Deville Lake. The major highly metamorphosed Yellowknife supracrustal belt containing the shear zone that marks the eastern boundary of the domain was traced south from Sifton Lake through the southwest side of Smart Lake where there are some small units of amphibolite in the otherwise migmatitic to porphyroclastic metasediments. Although much thinner than in the north and broken by cores of granitoid gneisses, the belt can probably be traced on the basis of its magnetic signature (Geological Survey of Canada, 1968) more or less continuously to the McDonald Fault. This belt can also be traced to the north where it is

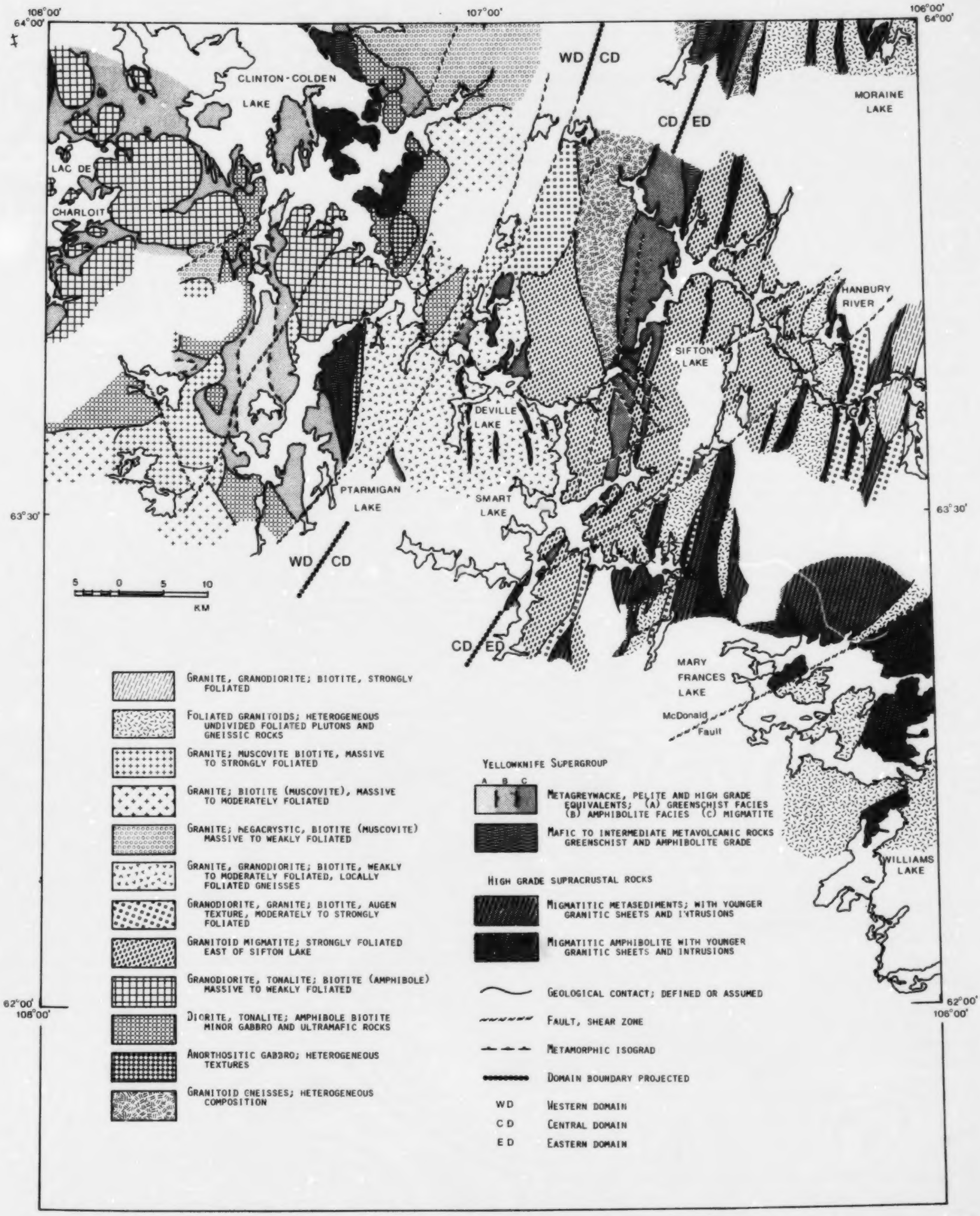

Figure 47.1. *Geological map of a transect across the Thelon Front, Artillery Lake map area.*

continuous with an extensive Yellowknife Supergroup terrane that opens to the northwest in the Slave Province proper (Henderson et al., 1982).

The southern part of the eastern domain is underlain by a much higher proportion of highly metamorphosed supracrustal rocks. As in the central domain, these supracrustal rocks are everywhere highly migmatitic and consist of either biotite rich migmatite with abundant coarse white leucosome or amphibolitic migmatite with typically less abundant white leucosome. Both varieties are intruded by thin sheets to elongate bodies of foliated, medium grained, biotite-poor granite. The proportion of the younger intrusive phase to the migmatic is highly varied. In places the granite is dominant. The amphibolitic migmatites are similar to the migmatitic Yellowknife metavolcanics east of Tourgis Lake in the Healey Lake area (Henderson and Thompson, 1980), whereas the biotite-rich migmatites are similar in many respects to the Yellowknife metasedimentary migmatites seen to the west in the central domain and to the north in the Healey Lake area (Henderson et al., 1982, Fig. 31.2). Metamorphic mineral assemblages in the biotite-rich migmatites, however, differ in that aluminosilicates rarely were identified in the field. Also, the local occurrence of hornblende and clinopyroxene implies a more calcic composition. The determination with any degree of confidence of the relationship of these migmatitic supracrustal rocks in the eastern domain with the Yellowknife Supergroup to the west will require further study.

Southeast of the McDonald Fault, at the east end of Mary Frances Lake and the northern part of Williams Lake to the south is a large area of similar supracrustal rocks but in which the amphibolitic migmatites dominate. These rocks have been translated into the area along the McDonald Fault over a distance of as much as 100 km, as interpreted from the displacement of distinctive aeromagnetic anomalies (Henderson and Macfie, 1985). Of particular interest is the contact between the amphibolitic and biotitic migmatites at one locality near the shore of Mary Frances Lake. Although the exposure is less than ideal and much of the area is frost heaved, the amphibolitic gneisses are separated from the biotitic migmatites by a narrow zone of carbonate, calc-silicate rocks and rusty sulphide-bearing silicate and oxide iron formation. The association of carbonate and iron formation at the contact between metavolcanics and metasediments of the Yellowknife Supergroup can be seen at several localities in the Slave Province, notably at the headwaters of the Back River and in the High Lake region (Henderson, 1975). This may be evidence that these migmatitic rocks are also related to the Yellowknife Supergroup or at least represent similar volcanic and sedimentary associations as seen in the Yellowknife of the Slave Province.

Intrusive and gneissic rocks

Most of the intrusive and gneissic rock units described previously from the northern transect across the area (Henderson and Macfie, 1985) are found in the central part of the area as well. A brief summary of additional information available as a result of subsequent work along a transect across the central part of the area follows.

In the western domain, the muscovite-bearing granites have been subdivided into two types. The first is a two mica granite in which the muscovite and biotite are both major components, either of which can be dominant. This granite is similar to the two mica granite that is so abundant in the Healey Lake area to the north. The second type has muscovite as a relatively minor phase. It is present east of Clinton-Colden Lake where it grades north into a coarsely megacrystic biotite dominant granite, and also southwest of Ptarmigan Lake where it appears to grade into the megacrystic granite that underlies much of the Artillery Lake terrane (Gandhi, 1985). East of Ptarmigan Lake, a long marrow body of anorthositic gabbro similar in many respects to that described previously east of Clinton-Colden Lake (Henderson and Macfie, 1985) occurs at the base of the volcanic sequence. Its contact relations with the volcanic unit is not well exposed. Like the previously described anorthositic gabbro, the unit is characterized by very heterogeneous composition and texture although nowhere does it have the extremely coarse crystal size seen in some phases of the northern body. It contains a magnitite-rich zone that has a pronounced aeromagnetic expression (Geological Survey of Canada, 1968). At one locality, coarse magnetite makes up more than half the rock.

The distinctive red and black augen textured granodiorite to granite that occurs in both the central and eastern domains was recognized at several localities east of Smart Lake where, because of its distinctive appearance and occurrence as narrow sheets that can be traced many kilometres along strike, is a useful marker for determining apparent displacement on faults. This augen granite is closely associated with metasedimentary migmatites in the region. The rather large, fairly homogeneous, well foliated, biotite-poor, granite to granodiorite reported previously to occur on the Hanbury River in the eastern part of the domain, and considered to be Archean, (Henderson and Macfie, 1985) has been dated at about 1920 Ma (U-Pb zircon and monazite, O. van Breemen, personal communication, 1985). Thin sheets to small plutons of similar granite occur within the supracrustal migmatites throughout much of the eastern domain. Many of the granitoid and gneissic rocks of this domain have been placed in an undivided unit for the time being. These are a heterogeneous assemblage of rocks ranging from diatexites derived from the supracrustals through complex granulite grade gneisses to homogeneous but well foliated megacrystic granites that amongst them presumably represent a variety of ages.

Structural geology

The geology of the area has been discussed thus far in terms of three domains that were defined on the basis of structural criteria (Henderson and Macfie, 1985). The domains become increasingly deformed from west to east and represent increasingly deeper structural levels at the present erosion level. The domain boundaries are north-northeasterly trending faults or shear zones. The two western domains seem to be extant only within the Artillery Lake area. To the north in the Healey Lake area the boundary faults disappear and the difference between the domains becomes less apparent.

The straight zone, a shear zone of porphyroclastic Yellowknife metasediments several kilometres wide that forms the boundary between the central and eastern domains has been mapped south from the Healey Lake area where it was concluded to be a good candidate as a single feature to mark the Thelon Front, the western margin of the Thelon Tectonic Zone (Henderson et al., 1982). South of Sifton Lake the shear zone becomes significantly narrower as does the belt of Yellowknife supracrustal rocks that contain it. The zone does, however, continue through to Smart Lake where its trend changes from southerly to southwesterly before continuing on to the south-southwest beyond Smart Lake. Although it is a much less impressive looking structure in the vicinity of Smart Lake compared with its appearance in the north, it is not clear whether the amount of strain accommodated by the structure has changed significantly. The changed aspect may be more a reflection of the thinning of the supracrustal rocks in which it occurs. On the other hand, the locus of inflection of the large paired gravity

anomaly (Earth Physics Branch, 1969a,b) that is in part coincident with the straight zone and which presumably reflects major deep crustal influences, departs from the straight zone south of Sifton Lake and shifts to the west across the central domain to its western boundary shear zone (Henderson and Macfie, 1985) suggesting the straight zone may be of lesser importance south of Sifton Lake.

In addition to the domain boundary structures, several other faults with similar generally northeasterly trends have been mapped. They occur in two sets. Although representatives of both sets are everywhere present, those in the western part of the area tend to trend north-northeasterly in contrast to the more northeasterly trends of most faults in the eastern part of the area. The most prominent of the latter set is the McDonald Fault which passes through Mary Frances Lake. The faults have a dextral horizontal component of movement that ranges from about 100 km in the case of the McDonald Fault to only a metre or so on some of the other faults, most of which are too small to portray at the scale of the map. It is suspected that the faults may have a significant component of vertical movement. This is indicated by the previously mentioned change in structural level across the domain boundaries in the case of the north-northeasterly set. In the eastern domain there is a change in the base level and magnetic intensity of aeromagnetic anomalies that can be traced across the northeast-trending faults. This together with the increasingly positive gravity gradient from south to north in the domain (Earth Physics Branch, 1969a) might be an argument for a vertical component on the faults with north side up. Of perhaps more direct significance is the occurrence of moderately southwesterly plunging stretching lineations in ductile fault zones associated with the McDonald Fault and with several nearby relatively minor parallel faults implying a vertical component during at least part of the history of the fault. Across the area, the faults of the two sets have increasingly ductile characteristics towards the east.

Also present in the area are a few faults that have a north-northwesterly trend and a sinistral sense of displacement and are thus similar to the Bathurst Fault, the major fault set through Bathurst Inlet that offsets a major part of the Thelon Tectonic Zone north of the Healey Lake area. These faults are best developed east of Smart Lake and like the other faults in the area have ductile characteristics. This is best shown in the fault zone north of the southeast arm of Smart Lake where the regional north-northeasterly trends are transposed to the north-northwest over a width of several hundred metres.

The eastern domain shows considerably more variety in structural style than was originally apparent from the northern transect across the area (Henderson and Macfie, 1985). In the northern part of the domain, particularly in the west, the structural trends are very straight and the dips steep. Abundant north-northeasterly trending closely spaced mylonite zones are expressed as prominent linears. To the south, however, the trends are curvilinear on a regional scale as shown by the large structural closure north of Mary Frances Lake. North of Williams Lake and in the southeast part of Mary Frances Lake, the structure in the migmatitic supracrustal rocks is very gentle to flat.

Metamorphism

The greenschist grade Yellowknife Supergroup rocks of the western domain that underlie a large part of Clinton-Colden Lake were found to extend well south, east of Ptarmigan Lake. The metamorphic gradient appears to be rather steep, the change from rocks containing coarse sillimanite pseudomorphs after andalusite to chlorite-biotite phyllites taking place over as little as a few hundred metres. The metamorphic pattern in the western block is thus more like the pattern in the central Slave Province, such as near Yellowknife where the pattern is that of local thermal domes or ridges commonly cored by intrusions (Henderson, 1985) as opposed to the broad regional southeasterly increasing metamorphic gradient observed in the Healey Lake area to the north. There is a strong metamorphic contrast between the greenschist and lower amphibolite grades of the western domain and the high grade migmatites of the central domain.

In the Healey Lake area a narrow zone of high pressure metamorphism within and somewhat west of the straight zone was inferred from the presence of kyanite (Henderson et al, 1982; James, 1985). The kyanite in the belt of migmatitic to porphyroclastic Yellowknife metasedimentary rocks east of Sifton Lake indicates that this zone continues into the Artillery Lake area. Although no kyanite has been recognized south of Sifton Lake, examination of thin sections of specimens from this area has not been completed. The disappearance of kyanite signalling the end of the high pressure zone would correspond approximately with the translation of the previously mentioned locus of inflection between the paired gravity anomalies from the straight zone between the eastern and central domains, to the west.

In the eastern domain, a zone of granulite grade metamorphism occurs about 7 km east of the main belt of migmatitic supracrustal rocks at the boundary of the domain. The western boundary of the granulite zone is quite sharply defined and is consistently parallel with the domain boundary. The zone itself is about 10 km wide and corresponds approximately to a north-northwesterly trending positive gravity anomaly. The eastern boundary of the zone is less clearly defined. East of the zone north of Mary Frances Lake are small sporadic occurrences of granulite grade rocks in what are mainly upper amphibolite rocks.

Acknowledgments

The enthusiastic assistance and good company of Sarah Bohan, Alain Dube, Scott Green and Daniel Roach greatly facilitated the field work. Martin Irving and Craig Robinson provided excellent expediting services using the facilities of the Geology Office of Indian and Northern Affairs Canada. The report has been significantly improved by critical reviews by J.A. Fraser and M.B. Lambert.

References

Bostock, H.H.
1986: Reconnaissance geology of Precambrian rocks of the Fort Resolution (85H), Taltson Lake (75E) and Forth Smith (75D) areas, south of Great Slave Lake; in Current Research, Part A, Geological Survey of Canada, Paper 86-1A, Report 4.

Earth Physics Branch
1969a: Artillery Lake, Northwest Territories; Earth Physics Branch, Department of Energy Mines and Resources, Canada, Gravity Map Series no. 89.

1969b: Upper Back River, Northwest Territories; Earth Physics Branch, Department of Energy, Mines and Resources, Canada, Gravity Map Series no. 92.

Fraser, J.A.
1964: Geological notes on northeastern District of Mackenzie, Northwest Territories; Geological Survey of Canada, Paper 63-40 (Map 45-1963).

1972: Artillery Lake map area, District of Mackenzie; Geological Survey of Canada, Paper 71-38, 17 p.

Frith, R.A.
1982a: Secondary preliminary report on the geology of the Beechey Lake – Duggan Lake map area, District of Mackenzie, Northwest Territories; in Current Research, Part A, Geological Survey of Canada, Paper 82-1A, p. 203-211.

1982b: Geology of Beechey Lake – Duggan Lake map area; Geological Survey of Canada, Open File 851.

Gandhi, S.S.
1985: Geology of the Artillery Lake Pb-Zu-Cu district, Northwest Territories; in Current Research, Part A, Geological Survey of Canada, Paper 85-1A, p. 359-363.

Geological Survey of Canada
1968: Artillery Lake, District of Mackenzie, Northwest Territories; Geological Survey of Canada, Aeromagnetic Series, Map 7192G, Geophysics Paper 7192.

Hanmer, S. and Lucas, S.B.
1985: Anatomy of a ductile transcurrent shear: the Great Slave Lake Shear Zone, District of Mackenzie, Northwest Territories (preliminary report); in Current Research, Part B, Geological Survey of Canada, Paper 85-1B, p. 7-22.

Henderson, J.B.
1975: Sedimentological studies of the Yellowknife Supergroup in the Slave Structural Province; in Report of Activities, Part A, Geological Survey of Canada, Paper 75-1A, p. 325-330.

1985: Geology of the Yellowknife-Hearne Lake area, a segment across an Archean basin; Geological Survey of Canada, Memoir 414, 132 p.

Henderson, J.B. and Macfie, R.I.
1985: The northern Artillery Lake map area: a transect across the Thelon Front, District of Mackenzie; in Current Research, Part A, Geological Survey of Canada, Paper 85-1A, p. 441-448.

Henderson, J.B. and Thompson, P.H.
1980: The Healey Lake map area (northern part) and the enigmatic Thelon Front, District of Mackenzie; in Current Research, Part A, Geological Survey of Canada, Paper 80-1A, p. 165-169.

1982: Geology, Healey Lake, District of Mackenzie, Northwest Territories; Geological Survey of Canada, Open File 860.

Henderson, J.B., Thompson, P.H., and James, D.T.
1982: The Healey Lake map area and the Thelon Front problem, District of Mackenzie; in Current Research, Part A, Geological Survey of Canada, Paper 82-1A, p. 191-195.

James, D.T.
1985: Geology of the Moraine Lake area and the Thelon Front; in Current Research, Part A, Geological Survey of Canada, Paper 85-1A, p. 449-454.

1986: The geology of the Moraine Lake area part two; a transect across part of the Thelon Tectonic Zone, District of Mackenzie; in Current Research, Part A, Geological Survey of Canada, Paper 86-1A, Report 48.

Thompson, P.H., Culshaw, N., Buchanan, J.R., and Manojlovic, P.
1986: Geology of the Slave Province and Thelon Tectonic Zone in the Tinney Hills – Overby Lake (west half) map area, District of Mackenzie; in Current Research, Part A, Geological Survey of Canada, Paper 86-1A, Report 31.

Wright, G.M.
1957: Geological notes on eastern District of Mackenzie, Northwest Territories; Geological Survey of Canada, Paper 56-10.

1967: Geology of the southeastern barren grounds, parts of the Districts of Mackenzie and Keewatin (Operations Keewatin, Baker, Thelon); Geological Survey of Canada, Memoir 350, 91 p.

Geology of the Moraine Lake area District of Mackenzie; Part 2: a transect across part of the Thelon Tectonic Zone

Project 840005

Donald T. James[1]
Precambrian Geology Division

James, D.T., Geology of the Moraine Lake area, District of Mackenzie; Part 2: a transect across part of the Thelon Tectonic Zone; in Current Research, Part A, Geological Survey of Canada, Paper 86-1A, p. 417-421, 1986.

Abstract

The eastern half of a transect was mapped in 1985 across part of the Thelon Tectonic Zone. The transect is divided into two parts separated by a north-northeasterly trending ductile shear zone east of Moraine Lake, that marks significant changes in lithology and structural style. Nevertheless the previously defined boundary zone 15 km west of Moraine Lake, between the Slave Province proper and the Thelon Tectonic Zone, marks the most significant changes in lithology, structural style and metamorphic grade. The shear zone east of Moraine Lake marks lithological and structural changes of regional improtance, and may mark the trace of a major, westerly directed thrust.

Résumé

En 1985, on a levé la carte de la moitié est d'un transect qui recoupe une partie de la zone tectonique de Thelon. Ce transect est divisé en deux sections séparées par une zone de cisaillement ductile de direction nord-nord-est qui se trouve à l'est du lac Moraine et qui marque des variations lithologiques et structurales importantes. Néanmoins, c'est encore la zone frontière déjà circonscrite 15 km à l'ouest du lac Moraine, entre la province des Esclaves et la zone tectonique de Thelon, qui montre les changements les plus importants des points de vue de la lithologie, du style structural et du degré de métamorphisme. La zone de cisaillement située à l'est du lac Moraine signale des variations lithologiques et structurales d'importance régionale et porte peut-être la trace d'une faille de poussée majeure de direction ouest.

[1] Department of Geological Sciences, Queen's University, Kingston, Ontario K7L 3N6

Introduction

This project is part of a continuing program to map and gain a better understanding of the Thelon Tectonic Zone (Fig. 48.1), the boundary region between the Slave and Churchill structural provinces. This report summarizes the 1985 field season. Mapping for this study is a continuation of work started in 1984 (James, 1985) and completes a 50 km long transect across part of the Thelon Tectonic Zone at 1:50 000 scale. This is in contrast to the 1:250 000 scale projects at Artillery Lake (Henderson and Macfie, 1986), Healey Lake (Henderson et al., 1982), the Beechey-Duggan Lakes area (Frith, 1982) and the Tinney Hills-Overby Lake area (Thompson et al., 1986). Most of the area mapped is contained within the Hanbury River map sheet (NTS 75 P) although parts of the Artillery Lake (NTS 75 O) and Baillie River (NTS 76 A) map sheets are also covered. (Throughout this report "transect" refers to the entire 50 km long transect and "map area" refers to the area east of Moraine Lake mapped in 1985, see Fig. 48.2).

The objectives of this field season were to examine in detail the geological characteristics of the area east of Moraine Lake and to compare and contrast the lithological units, metamorphic grade and structural style between the eastern and western parts of the transect. The most prominent features of the 1985 map area are a compositionally heterogenous unit of gneisses, the Darrell River gneiss, and a structural style which is quite different from that in the western part of the transect. The Darrell River gneiss is believed to be in part derived from supracrustal rocks. They are not Yellowknife Supergroup gneisses typical of the Slave Province. The area also contains late, foliated granite-granodiorite which is no where present west of Moraine Lake. The western part of the transect is divided into blocks separated by north-northeasterly trending ductile shear zones. The shear zones, with the exception of the easternmost zone, are marked by subhorizontal mineral lineations and have dextral, strike slip senses of shear. The most eastern of these shear zones and the gneisses to the east of it contain moderate to steep easterly plunging stretching lineations.

The map area also contains foliated and gneissic pyroxene-bearing granitoid rocks, distinctive from the Darrell River gneiss, which underlie the eastern edge of one of the largest, positive magnetic anomalies in the Canadian Shield (Geological Survey of Canada, 1967).

Lithology

Darrell River gneiss

The Darrell River gneiss is a diverse group of compositionally heterogenous gneisses including pink and grey gneisses (interlayered pink and grey gneisses of James, 1985), rusty quartzofeldspathic gneisses, foliated granitoids and granitoid gneisses of granodioritic composition, and biotite-garnet gneisses. This unit also contains 1-2 m thick layers of marble and calc-silicate gneiss which are interlayered with the rusty quartzofeldspathic gneisses and the biotite-garnet gneisses. West of Maze Lake individual layers of marble can be traced for up to 4 km. Occurrences of marble and calc-silicate are less common in the eastern part of the area. Mafic gneisses and mafic-block gneisses form a minor part of this unit but are common throughout the area. Quartz-rich gneisses are rare.

The pink and grey gneisses, rusty quartzofeldspathic gneisses, foliated and gneissic granitoids and biotite-garnet gneisses are the most abundant rock types in this unit. Outcrops typically have light coloured weathered surfaces and have maple-sugar-bronze or black-olive-green fresh surfaces. The pink and grey gneisses and the rusty quartzofeldspathic gneisses are characteristically well layered. Orthopyroxene appears to be relatively common in all rock types. Garnet is less common and restricted to the biotite-garnet gneisses and the pink and grey gneisses. Garnet may make up to 25% of the biotite-garnet gneisses.

Narrow zones of black or dung-brown mafic gneisses, mafic dykes and boudinaged mafic dykes are common throughout the Darrell River gneiss. Mafic-block gneisses are composed of randomly oriented, metre-sized to centimetre-sized mafic blocks separated by white granitoid. Orthopyroxene is a common constituent in mafic rocks.

Biotite-garnet migmatite gneiss

Brown, rusty-brown and grey biotite-garnet migmatite gneisses and garnetiferous diatexites form a north-trending belt in the Maze Lake area. This unit is well foliated and layered on all scales with gneissosity defined by white plagioclase and quartz leucosome layers and pods and brown or rusty-brown biotite-rich restite layers. Large areas of white, fine- to medium-grained plagioclase and quartz diatexite are common east of Maze Lake. Commonly the diatexites contain up to 10% fine, lilac garnets. West and north of Maze Lake the unit is quite homogeneous, however, towards the east it becomes extremely heterogeneous and in part consists of thinly interlayered biotite gneisses and mafic gneisses, mafic-ultramafic dykes, amphibolite gneisses and a small amount of pink granitoid migmatite gneiss. Some of these rock types closely resemble lithologies found within the Darrell River gneiss.

The restite portion of the biotite-garnet migmatite gneisses contains approximately 20% biotite with up to 10% garnet and rare sillimanite. No potassium feldspar was identified in the field from the restite or leucosome portions. Rare occurrences of orthopyroxene have been found in mafic gneisses northeast of Maze Lake.

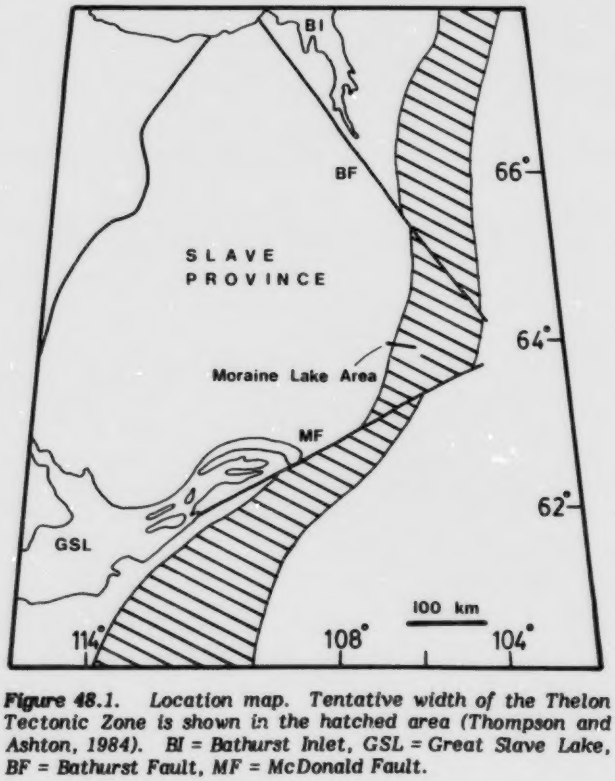

Figure 48.1. Location map. Tentative width of the Thelon Tectonic Zone is shown in the hatched area (Thompson and Ashton, 1984). BI = Bathurst Inlet, GSL = Great Slave Lake, BF = Bathurst Fault, MF = McDonald Fault.

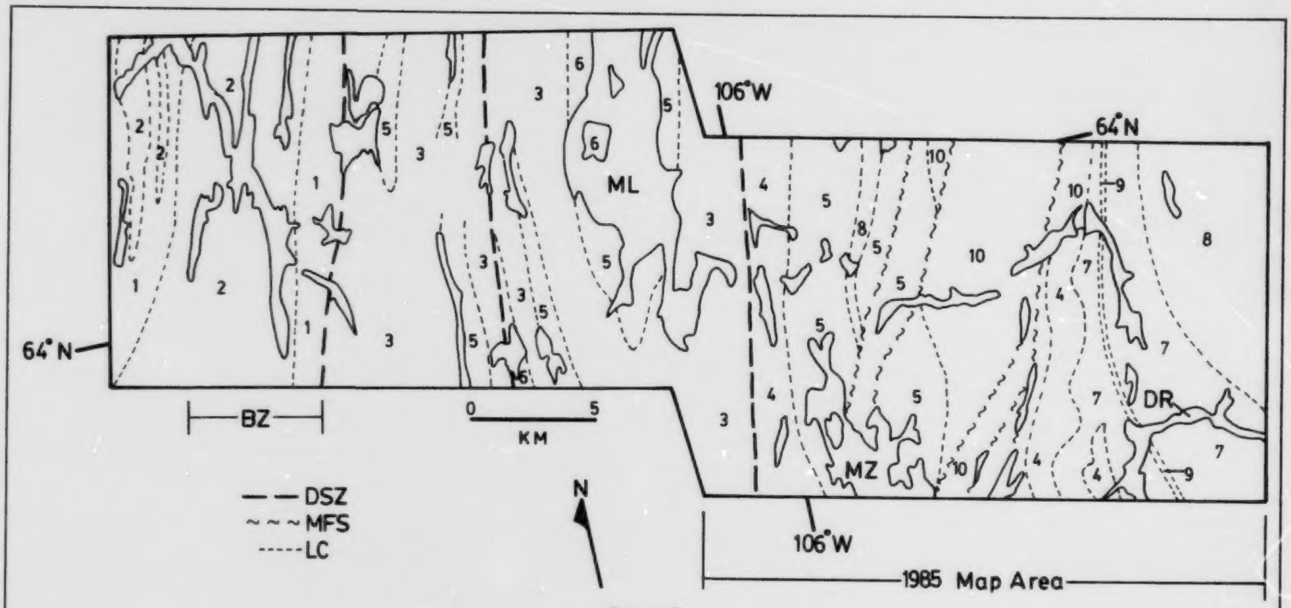

Legend

10 – Hornblende-biotite granodiorite-granite
9 – Hornblende granite
8 – Foliated megacrystic granite
7 – Granitoid gneiss-pyroxene bearing granitoid rocks
6 – Garnetiferous granite
5 – Biotite-garnet migmatite gneiss
4 – Darrell River gneiss
3 – Heterogeneous granitoid gneiss and migmatite gneiss
2 – Yellowknife Supergroup gneiss
1 – Migmatitic granitoid gneiss

ML – Moraine Lake
MZ – Maze Lake
DR – Darrell River

BZ – Boundary Zone
DSZ – Ductile Shear Zone
MFS – Fault (presumed splay fault from the McDonald Fault)
LC – Lithological contact, approximate

Figure 48.2. *Geology of a transect across part of the Thelon Tectonic Zone, Moraine Lake area.*

The age of these gneisses is unknown. Their composition is certainly suggestive of a sedimentary origin and in many outcrops they resemble biotite gneisses of the Yellowknife Supergroup. This correlation is extremely tentative especially in view of the very heterogeneous gneisses that are part of this unit northeast of Maze Lake, and which compositionally appear to be more closely related to the Darrell River gneiss.

Foliated granitoids and granitoid gneiss

Pink and tan granitoid gneisses, grey dioritic gneisses and foliated pyroxene-bearing granitoids outcrop east and north of Darrell River. A well layered gneiss of granodioritic composition is the most abundant member of this unit. These gneisses contain common, narrow (100 m wide) zones of grey dioritic gneisses and locally grade into pink or grey, massive to foliated, pyroxene-bearing granodiorite-quartz monzodiorite. Magnetite is relatively abundant and may make up to 5% of the rock. These gneisses underlie the western edge of the highest magnetic anomaly in the region and are believed to be the deformed and metamorphosed equivalents of plutonic rocks which intruded the Darrell River gneiss. The presence of orthopyroxene within the orthogneisses indicates that these rocks must have intruded the Darrell River gneiss early in the metamorphic history.

The extreme western part of the area mapped is underlain by a heterogeneous mixture of foliated and gneissic granitoid rocks (heterogeneous granulite gneiss of James, 1985). In this area this unit consists of grey, foliated diorites; pink, migmatitic granodiorite-granite gneisses and tan, foliated granodiorites that contain abundant mafic xenoliths. Hornblende and biotite are the most common mafic minerals although orthopyroxene has been identified in a few outcrops.

Foliated, potassium feldspar megacrystic granites and granodiorites underlie the northeastern part of the map area and form narrow belts west of Darrell River and northeast of Maze Lake. These rocks are always well foliated and commonly the flattening is strong enough to produce a gneissic fabric defined by pink feldspar streaks. Outcrops contain up to 35% coarse potassium feldspar and up to 15% hornblende and biotite combined. Locally the coarse megacrystic rocks grade into medium grained and equigranular rocks. West of Darrell River the contacts of this unit are poorly defined as it is mixed on all scales with foliated pink granites and granodiorite gneisses. These megacrystic granites are intrusive to the granitoid gneisses northeast of Darrell River. The apparent absence of orthopyroxene and the development of a strong foliation may indicate that these rocks were intruded after the metamorphic peak and that the deformation extended beyond the regional growth of orthopyroxene.

A narrow (750 m wide) body of pink, foliated hornblende granite outcrops east and north of Darrell River. This granite is fine grained, commonly strongly foliated and lineated and contains less than 10% hornblende. This granite has sharp, well defined contacts and can be traced from the northern to the southern boundaries of the map area.

The central part of the map area is underlain by a mixture of granite, granodiorite and locally, granitoid gneiss. Most outcrops are pink to tan, medium to coarse grained, foliated to locally weakly gneissic and have a granitic to granodioritic composition with up to 20% hornblende and/or biotite. Also contained within this unit are grey, hornblende and biotite granodiorite gneisses and a pink, massive to foliated biotite granite. In the northern part of the area these rocks contain xenoliths of amphibolite and rusty brown biotite gneiss. The hornblende-biotite assemblages, poor fabric development and presence of biotite gneiss xenoliths indicate that these rocks were intruded well past the metamorphic peak and late in the deformation history.

A pink, massive to foliated granite outcrops within the biotite-garnet migmatite gneisses at Maze Lake. These fine- to medium-grained leucogranites are mixed with the biotite-garnet migmatite gneisses on all scales forming foliation parallel layers and lenses of granite within the gneisses. This unit is characteristically homogeneous with respect to texture and composition. It is rarely strongly foliated and contains less than 10% biotite.

Structure and metamorphism

The structure in the map area is markedly different from the structure west of Moraine Lake where the region is subdivided by north-northeasterly trending Proterozoic ductile shear zones (James, 1985). Structural trends and lithological contacts in the map area are north-northeasterly, similar to the area west of Moraine Lake, however, the most prominent structural lineaments are north-northeasterly trending faults related to the much younger McDonald Fault.

The easternmost shear zone mapped in 1984 outcrops near the western boundary of the 1985 map area and separates foliated and gneissic granitoid rocks from Darrell River gneiss. The shear zone is less than 25 m wide and is marked by occurrences of mylonitic and protomylonitic granitoid gneiss. Fabrics dip steeply to the east with strong, down-dip stretching lineations. The zone is also marked by a thin interlayering of granitoid gneiss and a pink, fine grained and foliated/sheared granite. These thin granite sheets are only present within the shear zone. (This interlayering is also common in some of the smaller, discontinuous shear zones in the eastern part of the map area.) This is in marked contrast to the other three shear zones mapped in 1984 which all had subhorizontal mineral lineations and dextral, strike-slip senses of shear. Many other outcrops in the western and northeastern parts of the map area display shear fabrics that are not part of continuous shear zones. In all cases the fabrics contain stretching lineations that plunge steeply to moderately towards the east. West of Darrell River many narrow (<1 m) and apparently discontinuous shear zones are present. These zones have variable strikes from east-west to north-south and contain moderate to vertical down-dip mineral lineations. These structures are interpreted to be a reflection of a highly constrictive strain environment with a vertical to moderately east plunging maximum elongation direction. The development of these shear fabrics is believed to postdate the growth of orthopyroxene and predate the intrusion of the granitoid bodies that outcrop in the central part of the map area.

A second, much later shearing event is associated with another set of north-northeasterly trending faults that are splays from the McDonald Fault whose main trace is approximately 50 km to the south. The main trace of the McDonald Fault trends east-northeasterly and faults which splay off of it have curving traces that become more northerly trending away from the main trace towards the north. Deformation associated with each of these faults is in most cases confined to a few metres on either side of the fault traces. Porphyroclastic textures, shallow south plunging mineral lineations and slight deflections in the regional foliation are the common strain features.

Field observations of metamorphic assemblages indicate that the entire area is contained within the granulite facies. Orthopyroxene-clinopyroxene and orthopyroxene-biotite are common assemblages within the Darrell River gneiss and the granitoid gneisses. The biotite-garnet migmatite gneisses at Maze Lake contain the assemblage biotite-garnet and rarely biotite-garnet-sillimanite. The high degree of migmatization in these gneisses is further confirmation of the high metamorphic grade. No orthopyroxene has been identified within the biotite-garnet migmatite gneisses with the exception of two occurrences in mafic dykes northeast of Maze Lake.

There is no evidence from the field observations that there is more than one metamorphic episode in the map area, or that more than one has been preserved. Geochronological studies on granulites at Moraine Lake indicate an age of about 1970 Ma for presumed metamorphic zircons and monozite (Otto van Breemen, personel communication 1985). The 1984 mapping showed that at least in the area west of and including the boundary zone that two phases of metamorphism were present: a low pressure facies Archean metamorphism and a medium pressure facies Proterozoic metamorphism. Geothermometry-geobarometry will be required to help in the determination of the pressure facies of these granulitic rocks and may ultimately permit the correlation of the granulite facies metamorphism for the area east of Moraine Lake with one of the metamorphisms seen to the west.

Discussion

In view of the 1985 mapping, the boundary zone (James, 1985) still appears to be the most significant structural feature in this region marking discontinuities in structural style, lithology and metamorphic grade. However, the shear zone east of Moraine Lake which cuts the entire transect into two roughly equal parts also marks important changes in structural style and lithology. West of this line, shear zones contain subhorizontal mineral lineations and show dextral, strike-slip senses of shear. The shear zone east of Moraine Lake and the area to the east of it are marked by moderate to steep, easterly plunging stretching lineations. Significant lithological changes are also recognized. The Darrell River gneiss, a heterogeneous group of well layered pink and grey gneisses, rusty quartzofeldspathic gneisses, biotite-garnet gneisses, marbles, calc-silicate gneisses and granitoid gneisses of presumed supracrustal origin are very different from the Yellowknife Supergroup gneisses of the Slave Province.

One possible interpretation of the structural and lithological changes that are observed east of the shear zone, that is east of Moraine Lake, is that this area is entirely within the hanging wall of a westerly directed thrust. Emplacement of the granites and granodiorites which outcrop in the central part of the map area probably occurred after the thrusting but before the cessation of east-west regional shortening.

The age of the granulite facies metamorphism is uncertain. It appears from field observations that deformation outlasted the growth of orthopyroxene.

Geothermometry-geobarometry determinations on rocks from east and west of Moraine Lake will be used in an attempt to derive the regional temperature-pressure environment. Results may help to give some estimate of the amount of displacement on the thrust and give some ideas as to the age of the granulite facies metamorphism east and west of Moraine Lake. It is very possible that there are two ages of granulite facies metamorphism, one Archean and the other Proterozoic, represented in the Moraine Lake transect.

Acknowledgments

Sarah Bohan, Alain Dube, Scott Green and Dan Roach are thanked for their excellent help and fine company. John B. Henderson, Rob Macfie and Simon Hanmer made a visit to the field area. The field work for this study is supported as part of the adjacent and concurrent mapping of the Artillery Lake area by John B. Henderson. Expediting was provided by Martin Irving and Craig Robinson with the support of the Geology Office, Indian and Northern Affairs Canada in Yellowknife. John B. Henderson read an earlier version of this report. Otto van Breemen is thanked for permitting the use of unpublished geochronological data.

References

Frith, R.A.
1982: Second preliminary report on the geology of the Beechey-Duggan Lake map areas, District of Mackenzie, N.W.T.; in Current Research, Part A, Geological Survey of Canada, Paper 82-1A, p. 203-211.

Geological Survey of Canada
1967: Aeromagnetic Series, Maps 3564G, 3565G, 3568G, 3576G.

Henderson, J.B. and Macfie, R.I.
1986: The Artillery Lake map area: a transect across the Thelon Front, District of Mackenzie; in Current Research, Part A, Geological Survey of Canada, Paper 86-1A, report 47.

Henderson, J.B., Thompson, P.H., and James, D.T.
1982: The Healey Lake map area and the Thelon Front problem, District of Mackenzie; in Current Research, Part A, Geological Survey of Canada, Paper 82-1A, p. 191-195.

James, D.T.
1985: Geology of the Moraine Lake area and the Thelon Front, District of Mackenzie; in Current Research, Part A, Geological Survey of Canada, Paper 85-1A, p. 449-454.

Thompson, P.H. and Ashton, K.E.
1984: Preliminary report on the geology of the Tinney Hills-Overby Lake (W 1/2) map area. District of Mackenzie; a look at the Thelon Tectonic Zone northeast of the Bathurst Fault; in Current Research, Part A, Geological Survey of Canada, Paper 84-1A, p. 415-423.

Thompson, P.H., Culshaw, N., Buchanan, J.R., and Manojlovic, P.
1986: Geology of the Slave Province and Thelon Tectonic Zone in the Tinney Hills-Overby Lake (west half) map area, District of Mackenzie; in Current Research, Part A, Geological Survey of Canada, Paper 86-1A, report 31.

Geochemical characterization of the Goldenville-Halifax transition of the Meguma Group of Nova Scotia: preliminary report[1]

Contract 27ST.23233-5-0402

M. Zentilli[2], M.C. Graves[2], T. Mulja[2], and I. MacInnis[2]

Zentilli, M., Graves, M.C., Mulja, T., and MacInnis, I., Geochemical characterization of the Goldenville-Halifax transition of the Meguma Group of Nova Scotia: preliminary report; in Current Research, Part A, Geological Survey of Canada, Paper 86-1A, p. 423-428, 1986.

Abstract

The Moshers Island Member of the transition between the sandy Goldenville and shaly Halifax formations of the Cambro-Ordovician Meguma Group appears to be a significant control for metal concentration. In the LaHave River area it is preferentially enriched in Mn, Ba, Pb, Cu and Zn over other members of the Goldenville-Halifax transition zone. This paper characterizes the lithochemistry of the transition zone and gives credence to the concept that metal enrichment at this horizon may be a regional phenomenon with metallogenetic and exploration significance.

Résumé

Le niveau de Moshers Island, qui fait partie de la zone transitoire entre la formation sableuse de Goldenville et la formation schisteuse de Halifax, toutes deux du groupe cambro-ordovicien de Meguma, semble présenter des conditions favorables à la concentration des métaux. Dans la région de la rivière LaHavre, il est davantage enrichi en Mn, Ba, Pb, Cu et Zn que les autres niveaux de la zone transitoire de Goldenville-Halifax. Les auteurs de ce rapport établissent les caractéristiques lithochimiques de la zone transitoire et ajoutent foi à l'idée selon laquelle l'enrichissement en métaux de cet horizon est peut-être un phénomène régional qui présente beaucoup d'intérêt sur le plan des études métallogénétiques et sur le plan de l'exploration.

---

[1] Contribution to the Canada-Nova Scotia Mineral Development Agreement 1984-89. Project carried by Geological Survey of Canada, Economic Geology and Mineralogy Division, Project 700059.

[2] Department of Geology, Dalhousie University, Halifax, Nova Scotia B3H 3J5.

Introduction

The bedrock for most of Nova Scotia south of the Glooscap Fault as well as the foundation of the offshore Scotian Shelf to the south, and presumably the Bay of Fundy to the northwest, are made up of what is known as the Meguma Terrane (Williams and Hatcher, 1982). The Meguma Terrane, at least until the Carboniferous, is unlike the adjacent Avalon Terrane in metallogenesis (Zentilli and Graves, 1977), plutonism, tectonism, and sedimentation (Schenk, 1983). It consists predominantly of Lower Paleozoic strata, representing sedimentation from the Cambrian through Early Devonian with an estimated thickness of clastic metasedimentary rocks of over 14 km (Schenk and Lane, 1983) and of granitoid rocks.

It is found that, when one analyzes the patterns of mineral resource distribution (Zentilli and Graves, 1977; Graves and Zentilli, 1982; Zentilli et al., 1984), disproportionately large numbers of occurrences of gold, tungsten, arsenic, antimony, and the occurrence of lead and zinc mineralization hosted by non-igneous rocks of the terrane can perhaps be ascribed to less than 10 % of the apparent stratigraphic thickness, and more specifically to the transition between the older, coarser grained, Goldenville Formation and the overlying, shaly, Halifax Formation, referred to here as Goldenville-Halifax transition or the GHT. Both Halifax and Goldenville formations are Cambro-Ordovician.

The GHT is marked in several documented localities by a finely laminated, manganiferous unit, locally rich in calcareous calc-silicate nodules, spessartine quartzites (coticules of Keenan and Kennedy, 1983), carbon, and sulphides. This marker unit is overlain by a basal black, bituminous slate of the Halifax Formation (Zentilli and MacInnis, 1983). Recent work on lead-zinc occurrences (Binney et al., 1983; Cameron, 1985), manganese (Hingston, 1985), tungsten (Shaw, 1982; Fisher, 1984), and tin occurrences (Wolfson, 1983) indicates that the GHT and its associated manganiferous enrichment constitute a significant metallogenic control.

The spatial relationship between mineral occurrences and the GHT points to many questions which this project is addressing. Did the GHT serve as a source bed for metals? Is the present composition a reflection of its primary nature or is it due to diagenetic or metamorphic processes? How did the different physical properties of its constituents affect the behaviour of this unit to fluids during brittle and ductile deformation? Did it serve as a source bed or a barrier to flow of, or as a precipitator of, ore minerals? The location and definition of the GHT should provide not only a guide to potential mineral occurrences in southern Nova Scotia but also provide insight into mineralizing processes in pelitic sequences elsewhere (Graves and Zentilli, 1976). Preliminary data reported here allow a better definition of the nature of the transition lithologies, and may yield insight into the controls of mineralization in the GHT.

Field work was carried out in June, July, and August 1985 by M. Graves and T. Mulja. Crushing and powdering of samples for analysis is being done at Dalhousie University, Halifax, Nova Scotia.

Scope of research on the Goldenville-Halifax transition

The rocks of the GHT were sampled at twelve localities shown in Figure 49.1, on transects selected on the basis of good stratigraphic and structural control, excellent exposure, and different metamorphic grade. The following localities were sampled: (1) Sanford, (2) Cranberry Point, (3) Chebogue Point, (4) Broad River, (5) Dublin Shore, (6) Tancook Island, (7) Lake Charlotte, (8) Ship Harbour, (9) Liscomb Harbour, (10) Lundy, (11) Fogerty Head, and (12) Queensport Harbour.

The samples are being analyzed for major, minor, and selected trace elements including gold, organic, and volatile components. Representative samples of Goldenville metawackes and Halifax slates away from the GHT are being analyzed for comparison. Every fifth sample is being analyzed in duplicate, and internationally recognized rock standards are being used for control of precision and accuracy.

The contact between the Goldenville Formation and the Halifax Formation is not always clearly defined. Bailey (1898), when first mapping in the southwestern part of the Meguma Terrane, divided the rocks of the Meguma Group into three units. His quartzite division and black slate division are easily recognized today as Goldenville and Halifax lithologies. His transitional "banded argillite division", however was discarded by later workers as unmappable, especially in the eastern parts of Nova Scotia (see Taylor, 1967, for discussion).

The upper contact of the Goldenville Formation has been historically difficult to define. Faribault (1914), for example, used the highest exposed bed of greywacke as the position for the contact. This choice was also followed by Taylor (1967, 1969). Alternatively, sand/shale ratios have been used; the coarser grained rocks being Goldenville and the finer grained Halifax, though the precise ratio chosen has often not been stated. The two methods lead to similar contact location in places of sharp change from alternating large sandstone beds in thinly bedded shale but to very different locations in areas of gradational lithological change. In inland portions of the outcrop area, the contact is not exposed in many areas and the mapping problem is simplified as choosing the map unit best to describe individual outcrops. In the eastern portion of the outcrop area, the contact, where observable, is generally quite sharp but commonly it is not exposed; whereas in the central and western part of the province, contacts tend to be better exposed and more gradational. Colour changes often accompany this lithological change at the contacts. Goldenville rocks are typically grey and lower Halifax rocks typically black. Transition rocks at the top of the Goldenville Formation are in many places green. Unfortunately, some areas exhibit green slates in the lower Halifax Formation and colour classification can be misleading as a unique criteria for locating the contact.

Recent mapping (O'Brien, 1985a, b) has refined the knowledge of the stratigraphy of the transition lithologies of the Meguma Group in the central portion of Nova Scotia where the exposure is good and the regional metamorphic grade is low. This is a logical place to start in understanding the geochemical nature of the GHT but geochemical background data on the units are sparse (see Liew, 1979, for background geochemical data of the Goldenville Formation).

Mappable lithologies, that occur in this part of Nova Scotia, as described by O'Brien (1986), are given below:

Halifax Formation:	Cunard Member
Green Bay Formation:	Moshers Island Member, West Dublin Member, Rissers Beach Member
Goldenville Formation:	New Harbour Member

The New Harbour Member of the Goldenville Formation consists of thickly bedded, buff-weathered metawacke with thin interbeds of slate and slaty metawacke. The Rissers Beach Member of the Green Bay Formation consists of pervasively crosslaminated metawacke of variable width.

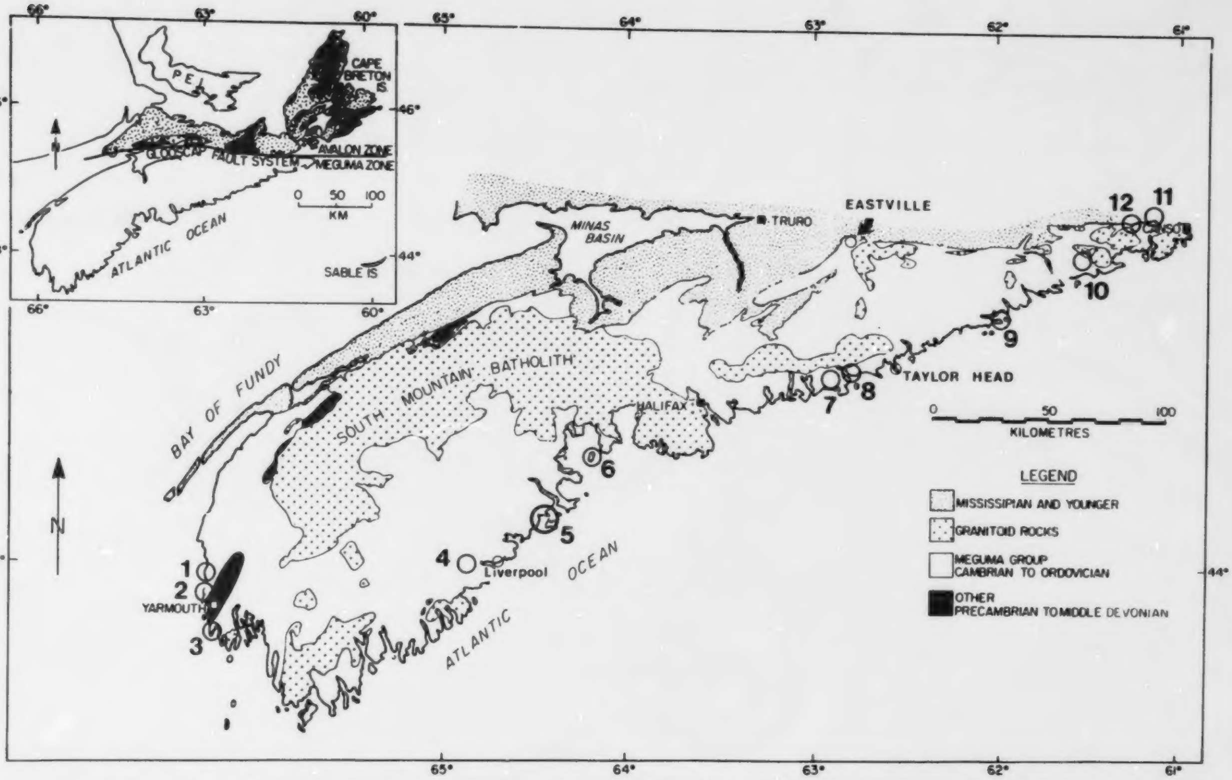

Figure 49.1. *Location map of sample transects: (1) Sanford, (2) Cranberry Point, (3) Chebogue Point, (4) Broad River, (5) Dublin Shore, (6) Tancook Island, (7) Lake Charlotte, (8) Ship Harbour, (9) Liscomb Harbour, (10) Lundy, (11) Fogerty Head, (12) Queensport.*

The West Dublin Member of the Green Bay Formation is similar to the New Harbour Member of the Goldenville Formation. The Moshers Island Member of the Green Bay Formation consists of green to grey-green, parallel-laminated argillite. The Cunard Member of the Halifax Formation consists of black slate interbedded with thinly bedded pyritiferous metasiltstone.

Large carbonate concretions commonly occur in the thicker metawacke beds of both the New Harbour and the West Dublin members. Small manganiferous concretions occur in layers within the Moshers Island Member. Variably-sized early diagenetic septarian nodules occur in the Cunard slates.

Lithogeochemical sampling

Transects for sampling were selected on the basis of good stratigraphic and structural control. Most of the transects are in coastal sections providing good exposure and access. Each transect contains a well mapped contact between the Goldenville Formation and the Halifax Formation. One end of the transect was located in unambiguous Halifax slates. The other end of the transect was several hundred metres down section in the Goldenville Formation.

Each transect was sampled at stations consisting of 10 to 30 m of vertical stratigraphic section. Fresh rock was collected at each station bed-by-bed to obtain samples representing the lithological variation of that portion of the transect. Some attempt was made to sample for horizontal variation but sections rarely outcropped more than 50 m along strike. Twenty to 50 samples were collected from each sample station. The spacing between sample stations was dictated by the quality and quantity of the outcrop and the variation within the transect. One station was located on either side of the mapped contact. Further stations were distributed to test the lithological variation of the transect. Stations at each end were governed by the limits of outcrop or were selected to represent rocks typical of Halifax or Goldenville formations. Most of the stations were in rock previously mapped as Goldenville Formation.

Over 400 samples were collected and the sample preparation and analyses are in progress. A preliminary summary of lithogeochemical results based on the major and trace element analyses of fifty samples from the LaHave River area is presented here (location 5, Fig. 49.1).

Analyses completed are for major elements performed by standard wet chemical methods at Dalhousie University, Halifax, Nova Scotia. Trace element analyses were done by standard XRF methods at St. Mary's University, Halifax, Nova Scotia. Every fifth sample was run as a duplicate and recognized international standards were used in both laboratories for control purposes.

Samples reported (Fig. 49.2) are from five sample stations, representing each of the five stratigraphic units.

The New Harbour Member was sampled within 50 m of its contact with the Rissers Beach Member at the headland to the west of the village of Green Bay (location A, Fig. 49.2). The Rissers Beach Member was sampled at the landward end of Crescent Beach in the middle of the unit (location B, Fig. 49.2). The West Dublin Member was sampled on the east shore of Bush Island in the upper third of the unit (location C, Fig. 49.2). The Moshers Island Member was sampled within

Table 49.1. Summary of major and trace element analyses of Meguma Group rocks of the LaHave River area

	(1)	(2)	(3)	(4)	(5)	(6)	(7)	(8)	(9)	(10)	(11)	(12)	(13)	(14)
SiO_2	76.52	62.21	70.07	79.29	59.81	48.32	59.46	73.21	62.31	72.08	62.00		60.25	69.00
Al_2O_3	11.97	19.10	15.20	10.54	20.88	4.68	18.63	14.14	22.88	12.27	18.40		15.55	13.45
Fe_2O_3	4.17	7.45	6.49	4.00	8.97	1.23	9.11	6.14	5.42	4.90	5.92		8.05	5.23
MgO	1.28	2.35	1.94	1.22	2.70	0.35	2.12	2.30	2.48	1.88	2.30		3.86	1.66
CaO	0.28	0.50	0.72	0.53	0.29	42.04	2.04	0.07	0.07	0.92	0.86		5.81	2.00
Na_2O	2.88	2.36	2.65	2.05	2.25	1.05	1.10	1.10	1.61	3.42	1.47		3.18	2.59
K_2O	2.03	4.52	1.85	1.60	3.74	0.82	2.98	1.88	3.43	1.63	5.23		2.52	1.78
TiO_2	0.59	0.96	0.65	0.48	0.83	0.23	1.01	0.77	1.25	0.53	0.77	0.77	0.95	0.56
MnO	0.05	0.09	0.18	0.10	0.23	1.03	3.08	0.22	0.25	0.10	0.09	0.11	0.12	0.08
P_2O_5	0.10	0.24	0.12	0.10	0.10	0.13	0.18	0.03	0.10	0.07	0.14			0.17
Ba	518	1234	356	321	840	151	1562	552	934			700	425	
Rb	74	153	78	58	148	24	112	78	145			140	90	
Sr	182	182	260	81	117	557	112	115	276			300	375	
Y	22	35	34	23	31	36	47	33	36			25	30	
Zr	201	223	239	220	200	226	185	185	173			160	165	
Nb	13	19	17	10	22	6	18	14	20			20	20	
Th	6	12	7	7	11	0	13	6	8		10	12	10	7
Pb	15	17	23	20	18	11	112	28	21			20	12	
Ga	15	27	19	13	28	6	24	22	30			20	15	
Zn	60	98	95	60	121	16	120	148	91		88	100	70	79
Cu	14	19	17	6	18	4	83	50	3		16	50	55	19
Ni	20	47	35	16	48	10	66	27	12		34	70	75	26
V	82	154	101	60	144	22	197	106	196		105	130	135	55
Cr	74	125	104	64	116	25	121	74	146		145	100	100	72
Total	100.00	100.00	100.00	100.00	100.00	100.00	100.00	100.00	100.00	97.75	97.14		100.45	96.55
n	4	4	9	6	2	1	10	2	2					

(1) Metawackes, New Harbour Member, Goldenville Fm: Green Bay.
(2) Slates, New Harbour Member, Goldenville Fm: Green Bay.
(3) Metawackes, Rissers Beach Member, Green Bay Fm: Crescent Beach.
(4) Metawackes, West Dublin Member, Green Bay Fm: Bush Island.
(5) Slates, West Dublin Member, Green Bay Fm: Bush Island.
(6) Carbonate concretion within metawacke, West Dublin Member, Green Bay Fm: Bush Island.
(7) Argillites, Moshers Island Member, Green Bay Fm: Bells Cove
(8) Metasiltstones, Cunard Member, Halifax Fm: Bells Cove.
(9) Slates, Cunard Member, Halifax Fm: Bells Cove.
(10) Metawackes, Goldenville Fm: Taylor Head (Liew, 1979).
(11) Slates, Goldenville Fm: Taylor Head (Liew, 1979).
(12) Average trace element content shale as compiled from various sources by Levinson (1974).
(13) Average continental crust from Taylor (1964).
(14) Paleozoic greywacke analyses from various sources as compiled by Liew (1979).

Note: Major oxides reported as weight per cent recalculated volatile-free to equal 100%; trace elements reported in ppm; total Fe reported as Fe_2O_3; and n = number of samples.

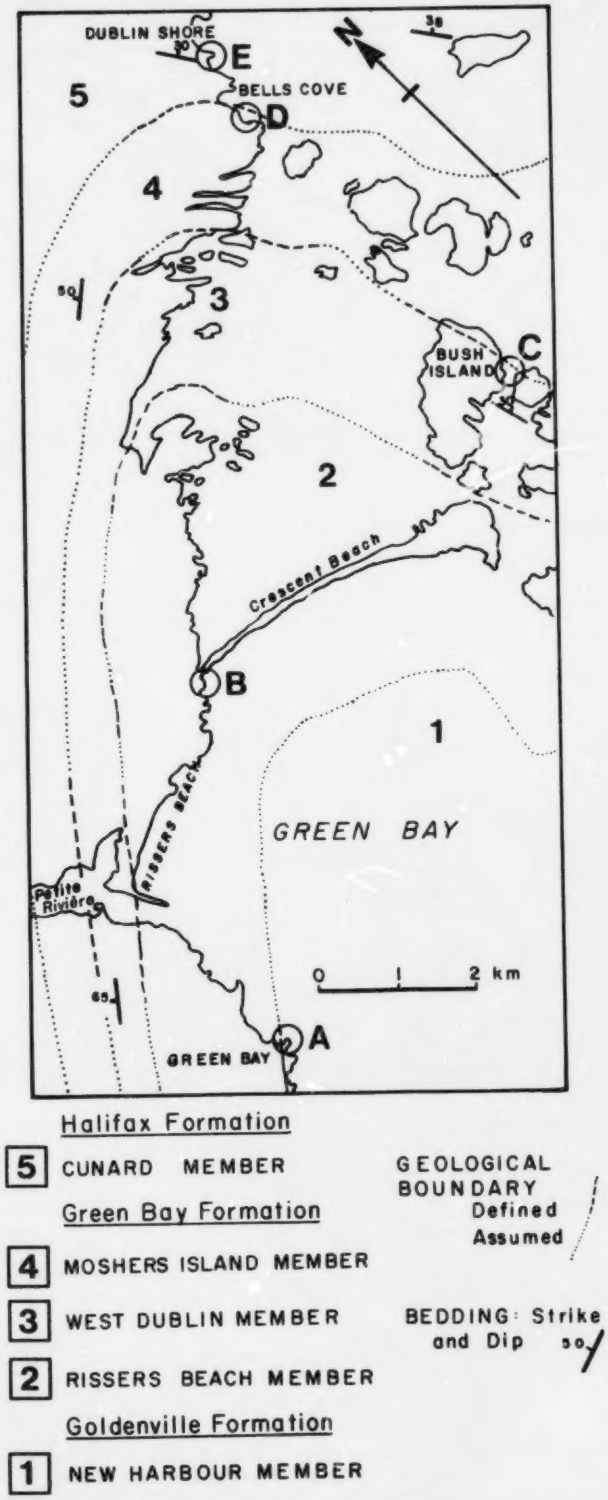

Figure 49.2. Location map of sample stations in the LaHave River area. Geology modified from O'Brien (1985b). Stratigraphic units from O'Brien (1986). See text for descriptions of lettered sample stations.

20 m of the top of the unit on the south side of Bells Cove (location D, Fig. 49.2), and the Cunard Member of the Halifax Formation was sampled on the north side of Bells Cove within the bottom 50 m of the unit (location E, Fig. 49.2). All sample sections are considered to be representative of the lithological character of the respective units sampled.

Results

Table 49.1 summarizes the preliminary results of this study. Results are presented for each lithology in the section mapped by O'Brien on the Dublin Shore of the LaHave River map area (O'Brien, 1985b).

The data of Table 49.1 show the similarity of the New Harbour and the West Dublin rocks. The sandstone beds and the shale beds differ from each other significantly and essentially all of this difference can be ascribed to mineral fractionation by normal sedimentary processes as shown by the sedimentary structures of these units. Little postsedimentation effect is seen in the distribution of elements. We hope to refine our view of diagenetic effects by studying in detail a series of large carbonate concretions that occur in the thicker sandstone beds of both these units (see Purves, 1974, for discussion of the metamorphism of these concretions). Sandstone and shale of the lower unit are very similar in their geochemical character.

The intervening Rissers Beach Member is geochemically intermediate between the sandstone and the shales of the surrounding two units. Current sedimentological work being done on this unit by P. Schenk, P. Adams, and J. Waldron provides a sedimentological mechanism to explain this intermediate behaviour. Pervasive crossbedding of the Rissers Beach sandstone indicates very rapid proximal deposition. Thus the geochemical and mineralogical fractionation of the more mature depositional mechanisms represented by the New Harbour and West Dublin Members is not evident in the Rissers Beach Member which appears to represent a mixture of the components which comprise the better sorted sandstone and shale of the enclosing units.

The Moshers Island Member is enriched in manganese with (volatile-free) values ranging from 1.68 wt.% to 12.02 wt.% and averaging 3.08 wt. % oxide as compared with values below 0.25 wt. % for the other units in the section (Table 49.1). The Moshers Island Member is also enriched in other trace elements, notably Pb (112 ppm average for 10 samples), Cu (83 ppm), and Zn (120 ppm). Values to 580 ppm Pb, 505 ppm Cu, and 154 ppm Zn were obtained. Average values of Ba are also enriched when compared to adjoining lithologies.

Preliminary conclusions

(1) Geochemistry is useful in characterizing lithological divisions in the Meguma metasedimentary rocks. (2) The Moshers Island Member of the Green Bay Formation in the LaHave Island area is anomalously enriched in Mn, Ba, and many trace metals such as Pb, Cu, and Zn. (3) The Moshers Island Member metal enrichment indicated by this study (Table 49.1) lends credence to the concept that metal enrichment at the GHT may be a widespread regional phenomenon that may have important metallogenic and exploration significance. Analytical studies currently in progress under this project will permit a comparison of the LaHave River results with regionally distributed transects across the GHT.

Studies of this kind are not only useful as a guide to mineral exploration but are necessary in establishing baselines for regional geochemical surveys and environmental studies.

Acknowledgments

Brian O'Brien graciously directed us to superb outcrops of the transition zone lithologies. John Waldron assisted in the systematizing of sedimentological and structural observations. Paul Schenk and Peter Adams added detail to the sedimentological and stratigraphic descriptions in the Dublin Shore sections. S.M. Parikh provided prompt wet geochemical analyses. J. Dostal and K. Cameron provided XRF trace element analyses. The advice of Craig Miller of the Nova Scotia Department of Mines and Energy and Al Sangster of the Geological Survey of Canada were especially appreciated.

References

Bailey, L.W.
1898: Report on the geology of southwest Nova Scotia; Geological Survey of Canada, Annual Report, v. 9, pt. M.

Binney, W.P., Sangster, A.L., and Zentilli, M.
1983: A lead-zinc deposit in metasediments of the Meguma Group, Eastville, Colchester County, Nova Scotia; International Geological Correlation Program, CCSS Symposium on Stratabound Sulphides of the Appalachian Caledonian Orogen, Project 60; Ottawa, September 16-17, 1983. Program and Abstracts, p. 8.

Cameron, B.
1985: The contact metamorphic effects of a granitoid pluton on zinc-lead mineralization in the manganiferous metasediments of the Meguma Group, Eastville, Colchester County, Nova Scotia; unpublished B.Sc., Dalhousie university, 104 p.

Faribault, E.R.
1914: Greenfield and Liverpool Town map-areas, Nova Scotia; Geological Survey of Canada, Summary Report, 1912, p. 334-340.

Fisher, B.E.
1984: A regional investigation of scheelite occurrences in the Meguma Group of Nova Scotia; unpublished B.Sc., Dalhousie University, 106 p.

Graves, M.C. and Zentilli, M.
1976: Gold-bearing quartz veins formed during continental collision; Geological Association of Canada/Mineralogical Association of Canada, Program with Abstracts, p. 57.

1982: A review of the geology of gold in Nova Scotia; in Geology of Canadian Gold Deposits; Canadian Institute of Mining and Metallurgy, Special Paper 23, p. 233-242.

Hingston, R.W.
1985: The manganiferous slates of the Cambro-Ordovician Meguma Group at Lake Charlotte, Halifax County, Nova Scotia; unpublished B.Sc. thesis, Dalhousie University, Halifax, Nova Scotia, 67 p.

Keenan, P.S. and Kennedy, M.J.
1983: Coticules – a key to correlation along the Appalachian Caledonian Orogen?; in Regional Trends in the Geology of the Appalachian-Caledonian-Hercynian-Mauritanide Orogen, ed. P.E. Schenk; NATO ASI Series C, v. 116, p. 355-362.

Levinson, A.A.
1974: Exploration Geochemistry; Applied Publishing Ltd., Maywood, Illnois, 614 p.

Liew, M.
1979: Geochemical studies of the Goldenville Formation at Taylor Head, Nova Scotia; unpublished M.Sc. thesis, Dalhousie University, Halifax, Nova Scotia.

O'Brien, B.H.
1985a: Preliminary report on the geology of the LaHave River area, Nova Scotia; in Current Research, Part A, Geological Survey of Canada, Paper 85-1A, p. 785-794.

1985b: Geology map of the LaHave area; Geological Survey of Canada, Open File Map 1156.

1986: Preliminary report on the geology of the Mahone Bay area, Nova Scotia; in Current Research, Part A, Geological Survey of Canada, Paper 86-1A, report 52.

Purves, M.F.
1974: Metasomatism of calcareous concretions of the Goldenville Formation; unpublished B.Sc. thesis, Dalhousie University, Halifax, Nova Scotia, 61 p.

Schenk, P.E.
1983: The Meguma terrane of Nova Scotia, Canada – an aid to trans-Atlantic correlation; in Regional Trends in the Geology of the Appalachian-Caledonian-Hercynian-Mauritanide Orogen; ed. P.E. Schenk; NATO ASI Series C, v. 116, p. 121-130.

Schenk, P.E. and Lane, T.E.
1983: Pre-Acadian sedimentary rocks of the Meguma Zone, Nova Scotia – a passive continental margin juxtaposed against a volcanic island arc; Excursion 5B, International Association of Sedimentologists Congress, Hamilton, 85 p.

Shaw, W.G.
1982: A geological investigation of the Lazy Head and Moose River tungsten deposits, Meguma Zone, central Nova Scotia; unpublished M.Sc. thesis, Dalhousie University.

Taylor, F.C.
1967: Reconnaissance geology of Shelburne map-area, Queens, Shelburne, and Yarmouth Counties, Nova Scotia; Geological Survey of Canada, Memoir 349, 83 p.

1969: Geology of the Annapolis-St. Marys Bay map-area, Nova Scotia; Geological Survey of Canada, Memoir 358, 65 p.

Taylor, S.R.
1964: Abundance of chemical elements in the continental crust: a new table; Geochimica et Cosmochimica Acta, v. 28, p. 1273-1284.

Williams, H. and Hatcher, R.D.
1982: Suspect terranes and accretionary history of the Appalachian orogen; Geology, v. 10, p. 530-536.

Wolfson, I.K.
1983: A study of the tin mineralization and litho-geochemistry in the area of the Wedgeport Pluton, southwestern Nova Scotia; unpublished M.Sc. thesis, Dalhousie University, 396 p.

Zentilli, M. and Graves, M.C.
1977: Evolution of metallogenic domains in Nova Scotia; Canadian Institute of Mining and Metallurgy Bulletin, v. 70, p. 69 (abstract).

Zentilli, M. and MacInnis, I.
1983: Geochemical investigation of manganiferous beds associated with stratabound lead-zinc mineralization in the Meguma Group; Nova Scotia Department of Mines and Energy, Information Series No. 6, p. 65-68.

Zentilli, M., Wolfson, I., Shaw, W., and Graves, M.C.
1984: The Goldenville-Halifax transition of the Meguma Group as control for metallic mineralization; Geological Society of America, Abstracts with Programs, v. 16, no. 1, p. 73.

Geological mapping and igneous and metamorphic petrology, Queen's and Shelburne counties, Nova Scotia[1]

Contract 27ST.23233-5-0019

T.L. Hope[2] and S.L. Woodend[3]

Hope, T.L. and Woodend, S.L., Geological mapping and igneous and metamorphic petrology, Queen's and Shelburne counties, Nova Scotia; in Current Research, Part A, Geological Survey of Canada, Paper 86-1A, p. 429-433, 1986.

Abstract

The Cambro-Ordovician turbiditic Meguma Group has been deformed and regionally metamorphosed during the Acadian Orogeny producing upper greenschist to middle amphibolite facies schists and granofels. The intrusion of the Devonian Port Mouton pluton further increased metamorphic grade around its margins to sillimanite zone assemblages. The pluton contains at least nine identifiable units which range in composition from tonalite to granite, and display abundant crosscutting relationships.

Résumé

Le groupe turbiditique cambro-ordovicien de Meguma a été déformé et régionalement métamorphisé au cours de l'orogène acadien, produisant des schistes et des granofels dont le métamorphisme varie de la limite supérieure du faciès des schistes verts au faciès moyen des amphibolites. L'intrusion du pluton de Port Mouton au Dévonien a augmenté le métamorphisme en bordures, conduisant à des assemblages de zones de sillimanite. Le pluton contient au moins neuf unités distinctes dont la composition varie de la tonalite au granite et laisse voir d'abondantes relations de recoupement.

[1] Contribution to the Canada-Nova Scotia Mineral Development Agreement 1984-1989 Project carried by Geological Survey of Canada, Precambrian Geology Division, Project 760027.

[2] Acadia University, Wolfville, Nova Scotia B0P 1X0
[3] Dalhousie University, Halifax, Nova Scotia B3H 3J5

Introduction

The project area lies in Queen's and Shelburne counties, southwestern Nova Scotia (Fig. 50.1). It covers approximately 1100 km^2 and includes all of NTS maps 20 P/10 and 15 and parts of 20 P/11 and 14. The southern part of the region is readily accessible by major highways and secondary roads to small villages. In the northern part of the area, access is from logging roads and an abandoned railway line.

The region is marked by low hills and valleys near the shore but the interior is flatter with large swamps. Outcrops inland are largely restricted to the major rivers. Exposure is good along the deeply incised coastline.

The study area includes the Devono-Carboniferous Port Mouton pluton which has intruded low to medium grade metasedimentary rocks of the Cambro-Ordovician Meguma Group.

Extensive cover of glacial till is present. The exact thickness is unknown but along a logging road west of Broad River, 6-8 m are exposed. Eskers are present near Sable River and west of Jordan River. Within the vicinity of the Port Mouton pluton, large granitic boulders up to 10 m across are common.

Geological maps of the area have been published by Gesner (1836), Bailey (1896), Faribault (1915) and Taylor (1967). Albuquerque (1977) described the geochemistry and evolution of the plutonic rocks in southwestern Nova Scotia, which included the Port Mouton pluton. West of the present study area, where contact and regional metamorphic effects on the Meguma Group cannot be distinguished, Rogers (1985) described the geology of the igneous-metamorphic complex in Shelburne and eastern Yarmouth counties.

The Port Mouton pluton appears to have been intruded in the Devonian but away from the metamorphic culmination in Roger's area. The purpose of the study by T.L. Hope is to identify the characteristics of contact metamorphism and compare them to the metamorphic effects developed around the Shelburne Pluton. A detailed study of the Port Mouton pluton involving mapping, geochemistry, isotopic dating and comparison of the pluton with the plutons of southwestern Nova Scotia is also being undertaken by S.L. Woodend. These topics form the basis of M. Sc. theses.

Acknowledgments

The field work for this project was supported by the Geological Survey of Canada and National Scientific and Environmental Research Council of Canada operating grants to R. Raeside (Acadia University) and D.B. Clarke (Dalhousie University).

Metasedimentary lithologies

Two major stratigraphic groups are recognized, the lower Goldenville Formation and the overlying Halifax Formation. In addition, a unit between the two can be recognized along the Broad River where the contact is well exposed. This unit is informally referred to as the Green Bay formation (O'Brien, personal communication, 1985).

Goldenville Formation

The Goldenville Formation is the most extensive unit in the area. The lower contact is not exposed in any part of the Meguma Zone, thus estimates of thickness are minimal. Taylor (1967) reported a thickness of 4400 m from the centre of the Lockeport syncline to the crest of the anticline along Green Harbour. Faribault (1915) estimated a thickness of 5592 m at Liverpool Bay, Queen's County, just north of the eastern limit of the area.

This formation consists of thickly bedded psammite locally containing calc-silicate lenses, psammite interbedded with semi-pelitic schists and minor slate and conglomerate.

The psammite is light to medium grey, fine- to medium-grained and throughout the area contains metamorphic biotite. The beds range in thickness from 1 cm to 10 m but average 2 m. Various sedimentary structures are preserved in the psammitic rocks. Small scale crossbedding, load casts and ripple marks are most common. Calc-silicate lenses, presumed to be metamorphosed calcareous concretions are found along the bedding planes. These lenses are typically elliptical in cross-section and elongate parallel to bedding, but some very irregular lenses were noted. They vary from 3 cm to 2 m in diameter.

Aluminous semipelitic schists occur as layers ranging in thickness from 4 cm to 3 m in the Goldenville Formation. Locally these rocks contain porphyroblasts of biotite, garnet, andalusite, cordierite and/or staurolite. Andalusite ranges in grain size from 2 to 30 cm and cordierite and staurolite grains are 1 to 3 cm wide. Biotite and garnet are 2 to 3 mm in diameter.

Andalusite weathers pink and displays a sieve texture, with inclusions of biotite, muscovite and quartz. Cordierite and staurolite contain fewer inclusions and are, respectively, light green and brown.

Reverse graded bedding of metamorphic origin is best displayed along Sandy Bay where andalusite porphyroblasts have crystallized in the originally argillaceous upper portions of the beds. The beds are typically separated by more biotite-rich layers.

A quartz pebble (granule) conglomerate with rare randomly distributed 3 to 4 cm long quartz pebbles (<0.5%) is exposed along the west side of Lockeport Harbour, near Western Head. it occurs in two 25 m wide zones separated by psammite beds and is interbedded with a biotite-garnet schist. Both the conglomerate and schist have been extensively folded. This conglomeratic and argillaceous sequence may have been deposited in a proximal turbidite environment. The source of the material is unknown.

Green Bay formation

The Green Bay formation is recognized between the Goldenville and overlying Halifax formations in the Broad River (Fig. 50.1). This unit was also recognized in the LaHave River area (O'Brien, personal communication, 1985) where it has been divided into three subunits. At the base, a rhythmically laminated green and grey-green sandstone is found. It is overlain by thinly to thickly bedded buff weathered, quartz-rich sandstone interstratified with grey-green and green sandstone. The uppermost unit consists of grey-green and green fine grained rhythmically laminated sandstones with concretions in Mn-rich beds (O'Brien, 1985). In the Broad River, the base is defined by the disappearance of 1 to 2 m wide beds of psammite of the Goldenville Formation and the top is defined by the appearance of grey-black slate of the Halifax Formation. The formation is 750 m thick. It can be subdivided into a lower and upper member.

The lower member is composed of 15 to 20 cm wide beds of psammite interbedded with finely laminated (1 to 2 cm) psammite and andalusite ± staurolite schist. Quartz-andalusite-muscovite-molybdenite veins ranging in width from 10 to 50 cm and pseudotachylyte veins (1 to 3 mm wide) are common.

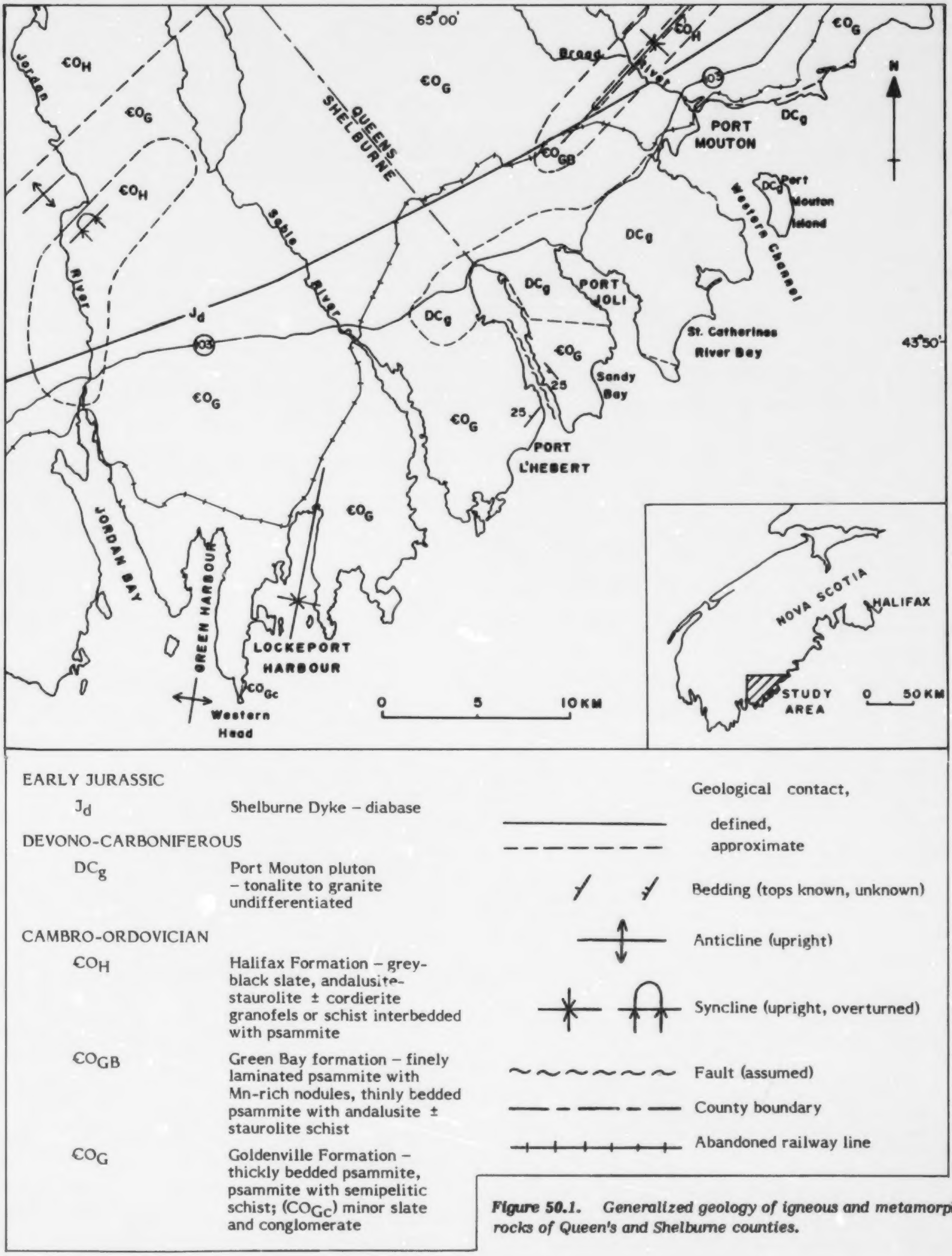

Figure 50.1. *Generalized geology of igneous and metamorphic rocks of Queen's and Shelburne counties.*

The upper member is composed of finely bedded (1 to 2 cm) psammite with interbeds of andalusite schist. Within these beds, pink coticule nodules (2 to 3 cm in diameter) are found. The nodules are elliptical where interbedded with the psammite but are typically stretched parallel to schistosity where interbedded with schist. They range from 3 mm to 5 cm in width and are composed of spessartine garnet and quartz. This unit has been associated with stratabound lead-zinc mineralization elsewhere in the Meguma Zone (Zentilli and MacInnis, 1983).

Halifax Formation

The Halifax Formation ranges from a grey-black slate exposed along the Broad River to an andalusite-cordierite-staurolite granofels or schist with interbedded psammite exposed along the Jordan River (Fig. 50.1). This variation is a product of both different metamorphic grades and protoliths.

In the Broad River about 250 m of Halifax Formation is exposed in the core of a syncline. The grey-black slate is finely laminated with bedding almost parallel to cleavage. Iron staining is prominent along cleavage planes.

At the western margin of the map area, the Halifax Formation is exposed along the Jordan River valley extending to the areas mapped by White (1984) and Rogers (1985). Correlation with these areas is difficult because of extensive glacial drift and limited outcrop. In the Jordan River area, the Halifax Formation consists of andalusite, staurolite ± cordierite granofels or schist. In the north part of the Jordan River section, pale green biotite slate and interbedded psammite is found. White (1984) noted crossbedding, convolute bedding and slump structures throughout the unit.

Igneous lithologies

Introduction

The Port Mouton pluton is roughly ellipitical with its 20 km long axis trending northeast, and its short axis approximately 9 km. Two small plugs reported by Taylor (1967) west-northwest of the main Port Mouton pluton were not located during this study. The Port Mouton pluton appears to be a very complex intrusion with at least nine distinct crosscutting units. The correlation between the units from the western section of the pluton (Port Joli and St. Catherines River Bay areas) and the eastern section of the pluton (Western Channel, Port Mouton Island) is proving difficult at this preliminary phase of investigation.

The Port Mouton pluton was dated (prior to detailed geological work) by the Rb-Sr and $^{40}Ar-^{39}Ar$ methods. Ages of between 349 and 340 Ma were obtained (Cormier and Smith, 1973; Reynolds et al., 1981; Elias, personal communication, 1985).

Lithologies

The mappable units in the western block of the Port Mouton pluton are listed in order from oldest to youngest.

Unit 1. Coarse grained mafic biotite tonalite to coarse grained mesocratic biotite-muscovite granodiorite. This unit is equigranular and locally subporphyritic. It contains inclusions of country rock of varying abundance and degree of assimilation.

Unit 2. Coarse grained leucocratic biotite-muscovite granitoid. This unit is equigranular and quartz-rich. It is a relatively minor unit which so far has only been observed to cut unit 1. Its relationship to other units is unknown.

Unit 3. Medium grained leucocratic biotite-muscovite granitoid to medium grained leucocratic granitoid with minor pegmatite.

Unit 4. Medium grained mesocratic biotite-muscovite granitoid to a medium grained mafic biotite granitoid. This is the predominant lithology in the Port Mouton pluton. The contacts between unit 3 and unit 4 are indistinct in places. Unit 3 can be found interbanded with unit 4 and as inclusions in unit 4. The contacts between units 3 and 4 are convoluted in places.

Unit 5. Fine grained mafic biotite (minor muscovite) granitoid breccia. This unit contains up to 50% angular to subrounded inclusions of quartz lenses, country rock and unit 1. Clasts range from 5 cm to approximately 50 cm.

Unit 6. Fine grained mesocratic to mafic biotite (minor muscovite) granitoid. This unit appears as dyke-like bodies. Rounded inclusions of leucocratic granitoid (unit 3?), country rock and biotite-rich 'xenoliths' comprise up to 25% of this unit.

Unit 7. Fine- to medium-grained leucocratic biotite-muscovite granitoid to a fine- to medium-grained leucocratic granitoid. In places this unit contains inclusions of unit 1 and country rock. Some fine- to medium-grained leucocratic biotite-muscovite granitoid dykes are distinctly banded. This unit is commonly associated with pegmatite dykes.

Unit 8. Fine-grained garnet aplite to quartz-muscovite-feldspar pegmatite dykes. The pegmatites typically contain traces of garnet and beryl and to a lesser extent tourmaline and biotite.

Unit 9. Amphibole and biotite-rich mafic dykes. This dyke contains approximately 35% biotite and 45% amphibole. Plagioclase makes up less than 10% of the rock. Trace minerals include sphene and apatite. This unit is found in two localities as dykes less than 60 cm wide. This mafic dyke is younger than unit 4 (medium grained mesocratic biotite-muscovite granitoid) but its relationship to units 5 through 8 is unknown.

The eastern section of the Port Mouton pluton is more complex than the western section. In a single 10 m^2 outcrop up to six granitoid phases can be distinguished. A new unit, not seen in the western section of the pluton is a medium- to coarse-grained (mesocratic equigranular) biotite-muscovite granitoid. It contains rounded inclusions 30 to 100 cm in diameter, of fine grained mesocratic biotite-muscovite granitoid (unit 6), which in turn contains country rock fragments. This unit although similar in appearance to unit 4, is distinct as it contains inclusions of unit 6.

The granite has intruded parallel to the bedding of the Goldenville Formation. Contacts with the country rock appear to be sharp. Exceptions occur near Hunts Point and White Point where migmatites have formed, and along the southern contact in the vicinity of St. Catherines River Bay where Meguma Group fragments and in situ beds are very ductile and show evidence of partial melting. Extensive pegmatite dykes occur at most of the Meguma Group-granite contacts. They intrude both the Port Mouton pluton and the Goldenville Formation.

The Shelburne Dyke outcrops at one locality, just east of Jordan River (Fig. 50.1). Boulders of diabase were noted at two other localities. The dyke consists of a green to black medium grained diabase.

Structure

Folding of the Cambro-Ordovician Meguma Group occurred during the Middle to Late Devonian Acadian Orogeny (Reynolds, et al., 1973). F_1 folds are tight to isoclinal, trending north to northeast with a plunge of 0 to 20°. These folds possess axial planar cleavage or schistosity (S_1). D_2 deformation is visible as crenulation cleavage at a few localities. A fault in Port L'Hebert is responsible for the reorientation of bedding, but the displacement is not known.

Metamorphism

Within the study area, the metamorphic facies range from upper greenschist to middle amphibolite. A garnet zone, staurolite-andalusite-cordierite zone and a sillimanite zone have been identified, but the precise nature and position of the isograds separating them have not yet been defined.

Development of porphyroblasts within the Goldenville Formation is best along the west side of Port Joli, near Sandy Bay and the west side of Port L'Hebert near its mouth. Andalusite ranges from 10 to 30 cm long, cordierite is 3 to 4 cm wide and staurolite is 1 to 2 cm wide. The coarse nature of the porphyroblasts may be related to the close proximity of the Port Mouton pluton. At a greater distance from the pluton, porphyroblasts tend to be smaller.

Large porphyroblasts are also developed within the Halifax Formation along the Jordan River Valley. In the Green Bay formation in the Broad River, andalusite (1 to 3 cm long) and staurolite 2 to 3 mm wide) porphyroblasts exist.

Mineralization

Pyrite, chalcopyrite and magnetite occur along schistosity planes in a biotite-muscovite schist in Jordan Bay. The zone is 0.5 m wide and 3 m long and may extend farther to the northeast.

Molybdenite and beryl are present in minor amounts in pegmatite veins cutting the Goldenville Formation and the Port Mouton pluton. Molybdenite is also present in quartz-muscovite-andalusite veins cutting the Green Bay formation.

Mn-rich nodules and beds occur in the Green Bay formation, the Mn occurring in spessartine garnet.

Gold in quartz veins has been reported along the Broad River (Faribault, 1915).

References

Albuquerque, C.A.R. de
1977: Geochemistry of the tonalitic and granitic rocks of the southern plutons; Geochemica et Cosmochimica Acta, v. 41, p. 1-13.

Bailey, L.W.
1896: Report on the geology of southwest Nova Scotia embracing the counties of Queen's, Shelburne, Yarmouth, Digby and part of Annapolis; Geological Survey of Canada, Annual Report, New Series, v. 19, pt. M, p. 1-154.

Cormier, R.F. and Smith, T.E.
1973: Radiometric ages of granitic rocks, southwestern Nova Scotia; Canadian Journal of Earth Sciences, v. 10, p. 1201-1210.

Faribault, E.R.
1915: Geology of the Port Mouton map-area, Nova Scotia; Geological Survey of Canada, Summary Report 1913, p. 251-258.

Gesner, A.
1836: Remarks on the Geology and Mineralogy of Nova Scotia; Halifax, Nova Scotia, Gossip and Coade, 272 p.

O'Brien, B.H.
1985: Preliminary report on the geology of the LaHave River area, Nova Scotia; in Current Research, Part A, Geological Survey of Canada, Paper 85-1A, p. 789-794.

Reynolds, P.H., Kublick, E.E., and Muecke, G.K.
1973: Potassium-argon dating of slates from the Meguma Group, Nova Scotia; Canadian Journal of Earth Sciences, v. 10, p. 1059-1067.

Reynolds, P.H., Zentilli, M., and Muecke, G.K.
1981: K-Ar and $^{40}Ar/^{39}Ar$ geochemistry of granitoid rocks from southern Nova Scotia: its bearing on the geological evolution of the Meguma Zone of the Appalachians; Canadian Journal of Earth Sciences, v. 18, p. 386-394.

Rogers, H.D.
1985: Geology of the igneous-metamorphic complex of Shelburne and eastern Yarmouth counties, Nova Scotia; in Current Research, Part A, Geological Survey of Canada, Paper 85-1A, p. 773-777.

Taylor, F.C.
1967: Reconnaissance geology of Shelburne map area, Queens, Shelburne and Yarmouth counties, Nova Scotia; Geological Survey of Canada, Memoir 349, 82 p.

White, C.E.
1984: Structure and metamorphism of the Jordan River Valley, Shelburne County, Nova Scotia; unpublished B.Sc. thesis, Acadia University, Wolfville, Nova Scotia, 74 p.

Zentilli, M. and MacInnis, I.
1983: Geochemical investigations of manganiferous beds associated with stratabound lead-zinc mineralization in the Meguma Group; Nova Scotia Department of Mines and Energy, Seventh Annual Open House and Review of Activities, Program and Summaries, p. 65-68.

Metallogenic studies in the Candego and Madeleine mines area, Gaspésie, Quebec: a progress report[1]

Contract 34SZ.23233-5-0438

K. Stevens[2]

Stevens, K., Metallogenic studies in the Candego and Madeleine mines area, Gaspésie, Quebec: a progress report; in Current Research, Part A, Geological Survey of Canada, Paper 86-1A, p. 435-437, 1986.

Abstract

Vein mineralization in a 100 km^2 area northwest of the McGerrigle Mountain granitic complex revealed the following: (1) quartz (transparent, white, and milky varieties), calcite (transparent, white, yellow, and black varieties) and tan to medium brown dolomite are the most abundant vein minerals; (2) sulphides, occurring in much lesser abundance, are composed of sphalerite, galena, chalcopyrite, pyrite, and pyrrhotite.

Studies of mineral zoning have revealed the presence of two quartz-rich, carbonate-poor "corridors" within the otherwise carbonate-dominated veins of the region. Chalcopyrite, pyrite, and pyrrhotite are present throughout the area but sphalerite and galena are present only locally.

Résumé

L'étude d'une minéralisation filonienne dans une région de 100 km^2 au nord-ouest du complexe granitique de McGerrigle Mountain a révélé ce qui suit: (1) les minéraux filoniens les plus abondants sont le quartz (variétés transparente, blanche et laiteuse), la calcite (variétés transparente, blanche, jaune et noire) et la dolomite ocre à brun moyen; (2) les sulfures, beaucoup moins abondants, sont constitués de sphalérite, de galène, de chalcopyrite, de pyrite et de pyrrhotite.

L'étude de la zonation minérale a révélé la présence de deux "corridors" riches en quartz et pauvre en carbonates dans les veines où dominent généralement les carbonates. La chalcopyrite, la pyrite et la pyrrhotite sont présentes dans toute la région, mais la sphalérite et la galène ne se trouvent que par endroits.

[1] Contribution to Canada Economic Development Plan for Gaspé and Lower St. Lawrence Mineral Program 1983-88. Project carried by Geological Survey of Canada, Economic Geology and Mineralogy Division, Project 650056.

[2] Mineral Exploration Research Institute, Montreal, Québec

Introduction

The region covered by this study occupies about 100 km^2 in the westernmost corner of Boisbuisson Township in the Gaspé Peninsula (Lachance and Duquette, 1977). It contains the Candego Mine, mined for Pb-Zn-Ag between 1948 and 1954, and the Madeleine copper mine, exploited from 1969 to 1982. This region is underlain by the Cambro-Ordovician Quebec Supergroup, immediately northwest of the Devonian McGerrigle Mountain granitic complex. Base and precious-metal-bearing sulphides occur in veins and/or in altered rocks at about 200 separate localities, including the sites of the Candego and Madeleine mines. Mineralized sites containing Cu-Fe sulphides (including the Madeleine Mine) occur relatively near the granite-sedimentary rock contact, whereas Pb-Zn-Ag sulphide sites (including the Candego Mine) occur relatively farther away from this contact.

This project was conceived as a two-year investigation into selected aspects of the metallogeny of the Candego and Madeleine mines map area. In year one (the year with which this report deals), the author is studying regional zoning of vein mineralogy, homogenization temperatures, and salinities of fluid inclusions in vein crystals. It is hoped that these techniques will prove effective in delimiting hydrothermal centres. In year two, the possible origins of the mineralizing fluids will be investigated with the aid of stable isotope analyses made on the fluid inclusion samples. A structural/tectonic analysis of the field area will be made, incorporating vein and bedding attitude data collected in year one.

Summary of work, summer 1985

A total of 151 samples of vein material were collected from 118 sites. Sample material included quartz, calcite, dolomite, siderite, sphalerite, galena and pyrite. Samples of vein quartz were also obtained from sphalerite-galena-bearing veins at two sites situated about 10 km west of the Candego Mine, in neighbouring Tourelle Township.

At each sample site vein mineralogy and textures were noted, along with vein widths and styles (e.g. stockworks, fissures, etc.). At about one-third of the sites it was possible to measure the attitudes of veins and of the enclosing sediments. Alteration features were qualitatively described (e.g. type, intensity).

An integral part of the vein mineral zoning study is the examination of vein mineralogy reported in diamond drill hole logs by exploration companies. The writer's work involved plotting selected holes on a base map, followed by the plotting of the summarized vein mineralogy intersected at various elevations. Seventy-four logs were selected from the Madeleine Mine property and the immediately surrounding area. All available logs from the Madeleine Mine itself were also perused (about 1000 logs). Although approximately 55 logs were available from the Candego area, little useful information is provided by these logs since they are too shallow and/or not favourably spaced for a mineral zoning study (most of them are clustered around the old mill and tailings dump). Four logs from the Mineral Creek area were included in the survey.

Preliminary results

Vein mineralogy

The most common vein minerals found in the study area are quartz (transparent, white and milky varieties) and carbonate minerals. The carbonates comprise calcite (transparent, white, yellow and black varieties) and dolomite (tan to medium brown). Siderite occurs rarely in the Candego and Cromar areas. The most common vein sulphides are sphalerite (chocolate brown to black), galena, chalcopyrite, pyrite and pyrrhotite. In the Cromar area arsenopyrite was noted in one vein and tetrahedrite in another.

Quartz ranges from fine- to coarse-grained, and from anhedral to euhedral to massive. Vugs are common and growth banding is not rare. Quartz often occurs as masses of drawn-out, fibrous-looking acicular crystals. It is possible that this distinctive texture might be the result of stresses applied to the crystals during or following deposition. At no site was this type of quartz found in an unmetamorphosed outcrop.

At least three quartz types occur in more than one part of the map area. White, anhedral, coarse grained quartz with a slightly waxy lustre has been encountered in the Madeleine Mine area, in the region between the Madeleine Mine property and the Cromar vein, in the Cromar and Candego areas, and to the northwest of Candego. Another distinctive quartz type is white to transparent, medium grained, anhedral and commonly displays the fibrous, drawn-out-looking crystal texture described above. This type of quartz occurs at sites between the Madeleine Mine property and the Cromar area, in the Cromar and Candego areas, and to the northwest of Candego. A third distinctive quartz type is grey to transparent, fine- to medium-grained and anhedral to euhedral. It occurs between the Madeleine Mine property and the Cromar area, and in the Cromar and Candego areas.

Vein carbonates and sulphides occur as streaks, blebs, masses or crystals which range from fine- to coarse-grained and from anhedral to euhedral.

Suitability of vein minerals for fluid inclusion studies

Quartz is the only mineral which has a widespread occurrence and which commonly has a transparency which makes it amenable to fluid inclusion studies. It therefore promises to be the most useful mineral for thermal mapping purposes and for comparing homogenization temperature and salinity data from different sample sites.

Calcite is locally of the right transparency and could be a source of some fluid inclusion heating-freezing data. Since, however, its occurrence is largely restricted to certain zones (described below) it is less useful than is quartz in terms of permitting the fulfillment of the aims of this study.

The relatively low abundance of sphalerite in this area (compared to that of quartz) likewise makes it a less useful mineral than quartz in this study. In any case, the opacity of sphalerite would render fluid inclusion detection difficult if not impossible. The writer, however, has previously obtained homogenization temperatures (but not salinity data) from fluid inclusions in dark sphalerite.

Mineral zones

Only the gangue mineral zoning has been evaluated in detail and zones have been defined on the basis of relative abundances of quartz and carbonate minerals.

Two quartz-rich zones have been delineated. One strikes west from the Madeleine Mine and the other occupies a northwest-striking corridor extending from Petit Lac Ste-Anne to beyond the Candego area. Both zones appear to be widest (and may in fact merge) near McGerrigle Mountains, and narrow with increasing distance from the latter. Carbonate is rare in these corridors; where present it makes up less than 10% of the gangue.

Almost all the veins situated outside of these quartz-rich corridors have a gangue containing from 10 to 100% carbonate minerals. Rarely, they contain quartz only.

Diamond drill hole log data suggest that the quartz-rich zones overlie the carbonate-rich zones.

Opaque mineral zoning studies are in progress. A cursory examination of the sample site data reveals that whereas chalcopyrite, pyrite and pyrhhotite are present throughout the field area, sphalerite and galena are of much more local occurrence. It is possible that they become more common with increasing distance from the McGerrigle Mountains. It is hoped that integration of the field and drill log data will permit the definition of distinct opaque mineral zones. Following this stage of the work, the writer will attempt to define regional vein types based on distinctive sulphide-gangue mineralogies.

Structural data

Most of the veins in the map area have widths of from 1 cm to about 2 m although, at one site, an 11 m wide vein was observed. In some cases, veins fill sets of parallel fracture planes, in other cases crackle breccias or stockworks and, in others, relatively wide fissures. The data concerning vein attitudes, widths and fracture types have been plotted on a base map but no attempt has yet been made to interpret them.

Alteration

There is evidence of wallrock alteration associated with veining at numerous sites. Alteration features, with respect to those of unaltered rocks, typically take the form of increased degrees of brittleness or compactness, colour changes and pyritization/rusting.

Contrasting styles of mineralization

Two different types of mineralized occurrence are present in this area. In one, quartz ± pyrite ± pyrrhotite ± chalcopyrite occur in veinlets 1 cm wide and/or disseminated in narrow zones or lenses parallel to the bedding of the sedimentary host rock. The wallrocks of such mineralized occurrences are typically rusted/pyritized and show other signs of alteration (e.g. increased brittleness, colour changes). In the second mineralization type, 0.1 to 1.0 m wide veins contain quartz, sphalerite, galena and, usually, carbonate minerals. The wallrocks of these veins in some cases exhibit increased hardness or brittleness, or colour changes, with respect to rocks distal to the veins, but no obvious pyritization or rusting.

At one site, west of the Madeleine Mine property, examples of both these mineralization types occur in an area about 100 m square. Here, they are not spatially associated, i.e. one sees either one type or the other in a given exposure.

Other evidence suggestive of more than one generation of veins/mineralization is present eleswhere in the area. About 2 km southwest of the Madeleine Mine buildings, non-mineralized black calcite veinlets cut hornfelsed sediments which contain pyrite and chalcopyrite in hairline fractures and disseminated along bedding plane laminations. At another locality, sphalerite-galena-bearing white quartz veins up to a metre wide and non-mineralized black calcite veinlets 2-3 cm wide occur in the same outcrop. There is no evident spatial association between the white quartz veins and the black calcite veinlets.

Reference

Lachance, S. and Duquette, G.
1977: Région de Boisbusson (NW); Québec Ministère des Richesses Naturelles, Rapport Géologique 187, 78 p.

Preliminary report on the geology of the Mahone Bay area, Nova Scotia[1]

Contract 14SQ.23233-5-0006

Brian H. O'Brien[2]

O'Brien B.H., Preliminary report on the geology of the Mahone Bay area, Nova Scotia; in Current Research, Part A, Geological Survey of Canada, Paper 86-1A, p. 439-444, 1986.

Abstract

The Mahone Bay area in Lunenburg County, Nova Scotia is underlain by Cambro-Ordovician metasediments, Lower Carboniferous limestones and evaporites and Devono-Carboniferous granitoids. The Cambro-Ordovician Meguma Group is separated into three formations and six members. Together they are approximately 13 km thick. Lateral facies variations and stratigraphical thickening and thinning of map units are however, common.

Rocks of the Meguma Group are folded about variably plunging, NE trending major folds. Individual folds are mapped for many tens of kilometres and change their shape in different units along the axial trace. Fractures are present in Meguma Group metasediments, Windsor Group limestones and Devono-Carboniferous granitoids. Some are occupied by veins or intrusions.

Regional metamorphism of the Meguma Group is in the lower greenschist facies but contact metamorphism near the granitoids produces an amphibolite facies hornfels.

Quartz veins at various structural and stratigraphical positions in the Meguma Group contain Au, W and Cu. Stratiform laminae in the Moshers Island Member are rich in Mn.

Résumé

La région de la baie Mahone, dans le comté de Lunenburg, Nouvelle-Écosse, repose sur des métasédiments cambro-ordoviciens, des calcaires et des évaporites du Carbonifère inférieur et des granitoïdes dévono-carbonifères. Le groupe cambro-ordovicien de Meguma se subdivise en trois formations et six niveaux (membres) qui ont ensemble environ 13 km d'épaisseur. Par ailleurs, il n'est pas rare d'observer des variations de faciès latérales et des variations d'épaisseur dans les unités cartographiées.

Les roches du groupe de Meguma sont déformées par des plis majeurs d'inclinaison variable et de direction nord-est. Certains plis s'étendent sur plusieurs dizaines de kilomètres, changeant de forme le long de la direction axiale. On observe des fractures dans les métasédiments du groupe de Meguma, les calcaires du groupe de Windsor et les granitoïdes dévono-carbonifères. Certaines renferment des veines ou des intrusions.

Le métamorphisme régional du groupe de Meguma est représenté par la limite inférieure du faciès des schistes verts, mais un métamorphisme de contact à proximité des granitoïdes a produit des hornfels qui présentent le faciès des amphibolites.

À divers niveaux structuraux et stratigraphiques du groupe de Meguma, des veines de quartz renferment Au, W et Cu. Le niveau de Moshers Island contient des lamines stratiformes riches en Mn.

---

[1] Contribution to the Canada-Nova Scotia Mineral Development Agreement 1984-89. Project carried by Geological Survey of Canada, Precambrian Geology Division, Project 760027.

[2] Hi-Tec Geoconsultants Ltd., R.R. #1, Hubbards, P.O. Box 244, Lunenburg County, Nova Scotia B0J 1T0

Introduction

The Mahone Bay area is located in south-central Lunenburg County, Nova Scotia (Fig. 52.1). It is mostly underlain by metasedimentary rocks of the Cambro-Ordovician Meguma Group in which eight new stratigraphic units are named (Fig. 52.2). Lower Carboniferous Windsor Group rocks are present, however, in coastal regions at the head of Mahone Bay (Fig. 52.2). Devono-Carboniferous granitoids and associated contact hornfels are found in the north of the map area.

The Mahone Bay area comprises approximately 1000 km^2 of ground mapped during the 1985 field season. Four provisional 1:25 000 scale maps were drawn to complement GSC Open File Map 1156 of the LaHave River area (O'Brien, 1985). Data from all of these maps have been compiled on the 1:250 000 scale map illustrated in Figure 52.2.

Lithostratigraphy

In the Mahone Bay area the Meguma Group is separable into three formations. From oldest to youngest, they are termed (1) the Goldenville Formation, (2) the Green Bay Formation (new unit) and (3) the Halifax Formation (Fig. 52.2). Exposures of the basal contact of the Green Bay Formation with the Goldenville Formation show it to be sharp and conformable. Likewise, the Halifax Formation-Green Bay Formation boundary is conformable and notably sharp. Neither the base of the Goldenville Formation nor the top of the Halifax Formation outcrops in the Mahone Bay area. Estimates of the exposed stratigraphical thicknesses are 1 km for the Goldenville Formation, 2 km for the Green Bay Formation and 10 km for the Halifax Formation. All three formations are mappable on 1:250 000 scale (Fig. 52.2). In general, the Goldenville Formation is typified by massive, buff-weathered sandstones, the Green Bay Formation characterized by rhythmically interbedded, green and grey-green sandstones, and the Halifax Formation identified by black and blue-grey slates interbedded with pyritiferous sandstones.

The Goldenville Formation

The uppermost part of the Goldenville Formation outcrops in the Mahone Bay area. This kilometre thick succession is locally called the New Harbour Member (new unit) and it is best exposed on the tip of the Aspotogan Peninsula (Fig. 52.2). The New Harbour Member is the equivalent of the Long Point Sandstone in the LaHave River area (Table 52.1).

Figure 52.1. *Location of Mahone Bay area Nova Scotia.*

The New Harbour Member is typically composed of 1-3 m thick, buff-weathered, quartz-rich sandstones (e.g. Fig. 3, O'Brien, 1985). In some locations 1-10 cm thick, green slates separate the sandstones. In the upper 500 m of this member slate is rare however. Where the New Harbour beds are succeeded by the Tancook Member (new unit), the uppermost part of the New Harbour succession contains 2-3 m thick, buff sandstones, with green beds notably absent. Where the New Harbour beds are overlain by the West Dublin Member (new unit), the New Harbour sequence of 2-3 m thick, buff sandstones passes vertically into 25-50 cm thick, buff sandstones some 200 m below its upper contact. Green slates are absent throughout this transition.

In the lower parts of the New Harbour Member green slates and strongly cleaved green sandstones become more common, although they are still dominated by massive to thickly bedded, quartz sandstones. Rhythmically interbedded green beds lithologically similar to those in the Green Bay Formation are found on the Aspotogan Peninsula in a 30 m interval about 700 m stratigraphically below the top of the New Harbour Member.

The Green Bay Formation

The Green Bay Formation is widely distributed throughout the Mahone Bay area and probably varies between 1-2 km in thickness. It is locally composed of three members; namely, the West Dublin Member (approximately 200-300 m thick), the Tancook Member (approximately 600-800 m thick) and the Moshers Island Member (new unit; approximately 150-300 m thick). The Moshers Island Member gradationally overlies both the Tancook and West Dublin members. By comparison with the Green Bay Formation in the LaHave River area, the Moshers Island Member is the equivalent of the Snug Harbour Sandstone and the West Dublin Member the same as the West Dublin Sandstone (Table 52.1). The basal Rissers Beach Member (new unit) of the Green Bay Formation (Table 52.1) is absent in the Mahone Bay area and does not intervene between the West Dublin and New Harbour members as it does in the LaHave River area.

In the Mahone Bay area strata of the Green Bay Formation resting sharply upon the Goldenville Formation and gradationally below the Moshers Island Member are separated into two members. Therefore, the West Dublin and Tancook members may be, in part, lateral equivalents. Where such strata are assigned to the West Dublin Member, the map unit has a thickness and an internal stratigraphy similar to that observed in the section at West Dublin (see GSC Open File Map 1156). Where the strata are assigned to the Tancook Member, the map unit is considerably thicker. Whereas the upper part of the Tancook Member is similar to the West Dublin Member, the basal part is quite distinctive. It is noteworthy that the uppermost 200 m of the New Harbour Member is thinly bedded only where it is in contact with the West Dublin Member.

The Tancook and West Dublin members of the Green Bay Formation are lithologically characterized by buff-weathered, quartz-rich sandstones interstratified with fine grained, rhythmically interbedded, green and grey-green sandstones. The buff sandstones are similar to those seen in the Goldenville Formation except they are generally thinner and contain abundant internal sedimentary structures. The green rhythmites are like those described from the LaHave River area (O'Brien, 1985). Buff sandstone beds range from 25 cm-1 m in thickness in the West Dublin Member but from 25 cm-3 m in thickness in the Tancook Member. In the latter member buff sandstones show relatively abundant signs of thixotropic deformation. Stratigraphical sections composed solely of fine grained, green rhythmites are found

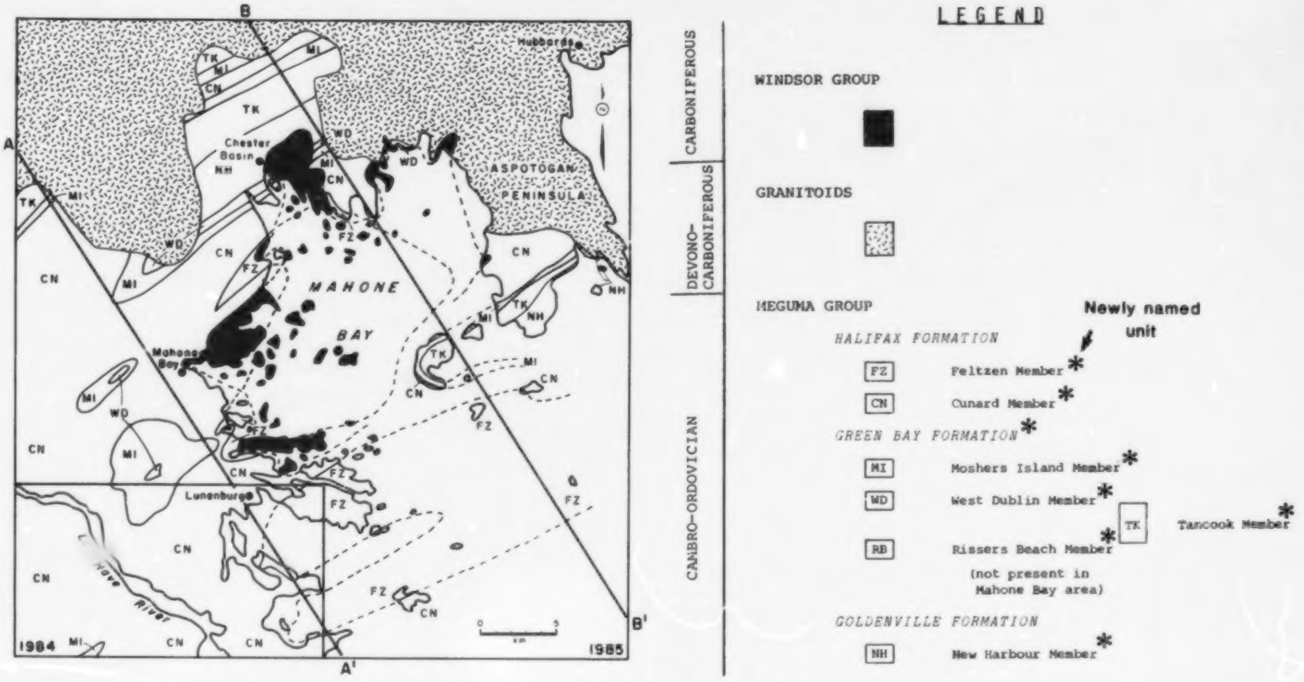

Figure 52.2. *Geological sketch map of the Mahone Bay area, Nova Scotia.*

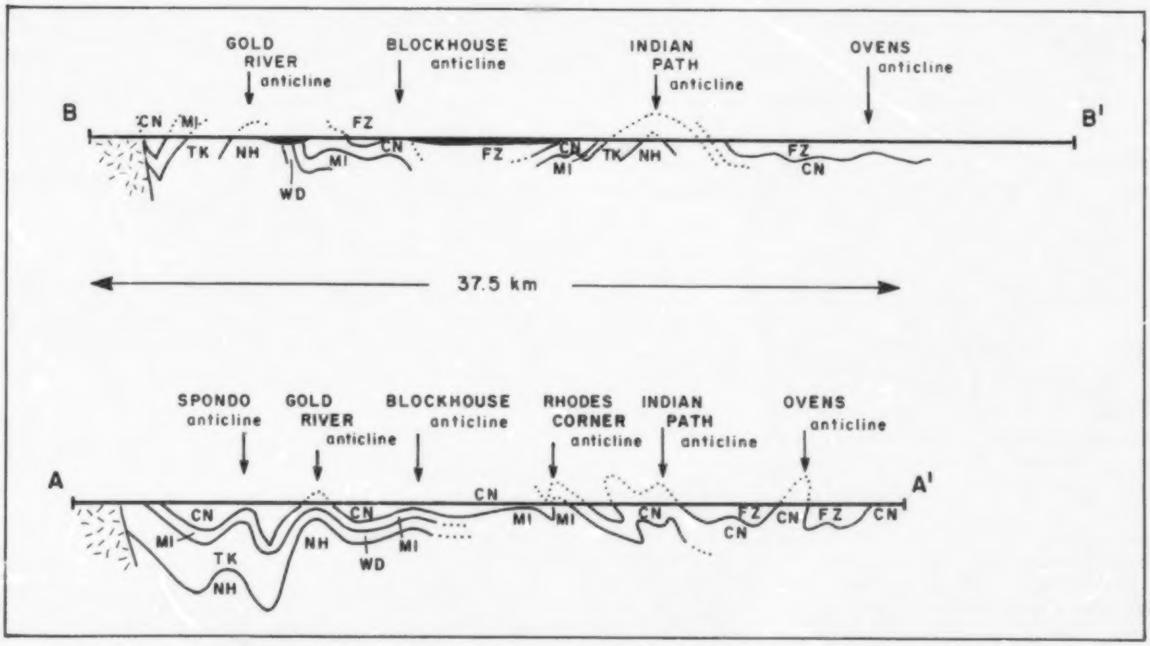

Figure 52.3. *Geological sections across the Meguma Group in the Mahone Bay area. For locations and identification of units see Figure 52.2.*

Table 52.1. Stratigraphical nomenclature in the Meguma Group of Lunenburg County, Nova Scotia

GSC Open File Map 1156	This report	
Feltzen Slate	Feltzen Member	HALIFAX FORMATION
Cunard Slate	Cunard Member	
Snug Harbour Sandstone	Moshers Island Member	GREEN BAY FORMATION
West Dublin Sandstone	West Dublin Member/Tanook Member (in part)	
Rissers Beach Sandstone	Rissers Beach Member (absent in Mahone Bay area)	
Long Point Sandstone	New Harbour Member	GOLDENVILLE FORMATION

up to 20 m thick in parts of the Tancook Member. They may be useful in future work for correlation purposes or for mapping the internal stratigraphy of the Tancook Member.

The Moshers Island Member of the Green Bay Formation comprises rhythmically laminated and rarer crosslaminated, green and grey-green, fine grained sandstones (e.g. Fig. 6, O'Brien, 1985). The rhythmic layering is on millimetre and centimetre scales. Pink and brown laminae are especially rich in Mn-bearing minerals. Mineralogically zoned concretions have grown in particular laminae in the upper parts of the Moshers Island Member. They define an excellent marker horizon. Buff sandstones of Goldenville type are conspicuously absent in the map unit.

The Halifax Formation

The Halifax Formation underlies most of the ground in the Mahone Bay area (Fig. 52.2) and represents about 75% of the total thickness of the Meguma Group in south-central Lunenburg County. Locally, the Halifax Formation is separated into two conformable and gradational members. The older Cunard Member (new unit) is well displayed near Cunard Cove (The Ovens) and the younger Feltzen Member (new unit) nearby at South Feltz or Blue Rocks. These map units are the equivalents of the Cunard Slate and the Feltzen Slate in the LaHave River area (Table 52.1). The Cunard Member varies dramatically in thickness from approximately 0.5 to 8 km. A minimum thickness estimate for the Feltzen Member is 1 km, but it is probably at least 2 km thick. The Feltzen Member outcrops in the central part of the map area in two regional basins largely obscured under the waters of Mahone Bay (Fig. 52.2). The Cunard Member appears regionally to encircle the Feltzen Member and is thinnest in the narrow area separating the two Feltzen basins.

Lithologically, the Cunard Member is composed of black slates interbedded with pyritiferous, grey, cross-stratified sandstones (e.g. Fig. 7, O'Brien, 1985). These fine grained sandstones have bed thicknesses from approximately 20-50 cm and they commonly contain giant nodules made up of chlorite, carbonate and sulphide.

The Feltzen Member comprises light grey, dark grey, and blue-grey slate rhythmically interbedded with laminated to thinly bedded, buff-weathered, grey sandstones (e.g. Fig. 8, O'Brien, 1985). Sandstone beds are bioturbated in places and are generally poorer in sulphides than those from the Cunard Member. Secondary carbonate is particularly common.

The Windsor Group

Outcrop of the Lower Carboniferous Windsor Group in the map area is restricted to the coastal regions of the northern part of Mahone Bay (Fig. 52.2). There, it rests with angular unconformity on folded strata of the Goldenville, Green Bay and Halifax formations, and on contact hornfels. In places, the Windsor Group lies nonconformably on Devono-Carboniferous granitoids. Given these relationships it is noteworthy that the Windsor basin is approximately the same size and shape as the northern Feltzen basin (Fig. 52.2).

In the Mahone Bay area the Windsor Group generally consists of limestones, gypsum, marls and shales. Lithostratigraphical units have been mapped by Faribault (1924, 1929) and the local stratigraphy discussed in detail by Sage (1954) and Giles (1981). The Windsor Group is preserved as a relatively thin cover sequence lying on a variety of basement rocks (Fig. 52.3). Its total thickness may be in the order of 150 m. Exposures relocated during the 1985 field season were few and, for the most part, occur immediately above the unconformity with the basement.

Structure

Structures of tectonic origin occur in the Windsor Group, the contact hornfels and the Meguma Group outside the aureoles.

The Meguma Group

In the Mahone Bay area the disposition of lithostratigraphical units in the Meguma Group is explained by the presence of large scale, NE-trending folds (Fig. 52.2). These folds display variable wavelengths and amplitudes, the fold

shapes changing considerably along the axial surface (e.g. contrast AA' and BB' in Fig. 52.3). The axial traces of some fold structures extend across the LaHave River and Mahone Bay areas and can be mapped for at least 55 km. The circular or elliptical outcrop patterns of some of the map units result from doubly plunging regional folds. The fold plunges are generally shallow but steep plunges are locally recorded along the axial traces. Where the regional folds are open and the plunge is steep, the strata strike NW and dip subvertically. In some mesoscopic folds the steeply plunging fold axes are observed to pass through the vertical. In doing so, the NW striking strata become inverted and the folds locally become downward-facing. Structures of this type are associated with ductile shear zones that are particularly well developed in the Feltzen-cored synclines.

The axial surfaces of most of the major folds are steep. Notable exceptions occur near the overturned Rhodes Corner Anticline (Fig. 52.3) where the Feltzen Member is regionally inverted.

Certain map units are observed to thicken or thin across particular folds (e.g. the Gold River Anticline and the Rhodes Corner Anticline in Fig. 52.3). Significant structural thickening or thinning is unlikely largely because this effect is normally seen in only one of several members affected by the folding. It does suggest, however, that some anticlines are sited on areas that may have been isostatically unstable during deposition.

Several types of foliation are developed in Meguma Group rocks. Subvertical slaty cleavage is the most widely distributed and commonly encountered. In some beds it is a crenulation cleavage. Where folds show notable cleavage fans, slaty cleavage dips moderately. Slaty cleavage is axial planar to steeply plunging, isoclinal folds in the ductile shear zones.

Spaced cleavage occurs in some sandstones. Considering the Mahone Bay Meguma succession as a whole, however, it is uncommon and weakly developed in comparison to exposures in eastern Nova Scotia (O'Brien, 1983). Subvertical fracture cleavage is associated with steeply plunging kink folds that deform the slaty cleavage. It is locally pervasive and axial planar to tight folds in the hangingwall and footwall of large faults.

Faults and joints are common throughout the Meguma Group in the Mahone Bay area. They have little effect on the regional outcrop pattern however. Systematic fracture patterns are present in Lower Carboniferous cover rocks and Cambro-Ordovician and Devonian basement rocks. A variety of igneous intrusions and hydrothermal veins are emplaced along these fractures or are offset by them.

The contact hornfels

The structure of the contact hornfels is exceedingly complex. Members of the Goldenville, Green Bay and Halifax formations are regionally folded and strike discordantly into the outer zone of the aureole. Here slaty cleavage is still recognizable and porphyroblast growth is seen to predate and postdate cleavage development. In the inner zone of the aureole the three Meguma formations become highly strained and recrystallized approaching the contact of the granitoids. Some 50 m from the granitoids highly strained, partially melted, Meguma Group schists and gneisses are folded and reorientated so that they are concordant to the contact trace. The structurally oldest pegmatites in the inner aureole are commonly found in rootless isoclinal folds whose axial surfaces lie parallel to the steep bedding planes. The structurally youngest pegmatites are underformed and are highly discordant to the bedding planes. Unfoliated granitoids contain xenoliths and large enclaves of the highly strained schists and gneisses.

The Windsor Group

The regional structure of the Windsor Group is hard to decipher because of poor exposure. Folds and faults are locally observable however. Some synclines in the Windsor Group are sited on Meguma Group synclines (Fig. 52.2), although the axial traces of the latter do not cross the unconformity. In contrast, some fractures in Meguma metasediments and Devono-Carboniferous granitoids traverse the basal Windsor contact and can be mapped in overlying strata.

Time of deformation

Most of the ductile deformation of the Meguma Group occurred after the deposition of the Halifax Formation (post-Tremadocian) and before the deposition of the Windsor Group (pre-Visean). Brittle deformation of the Meguma Group occurred before the emplacement of certain pegmatites and aplites, after the deposition of the Windsor Group and during and after the emplacement of the Mesozoic Shelburne dyke.

Metamorphism

In the Mahone Bay area the Meguma Group has been regionally metamorphosed probably to chlorite grade. Macroscopic porphyroblasts are not developed but chlorites and white micas are discernible along the foliations. Nodules and concretions are present in all map units. They are commonly augened and distorted by the slaty cleavage. Most are rich in carbonate relative to the host metasediments but those in the Moshers Island Member are particularly rich in garnet.

Contact metamorphism produces an approximately kilometre wide zone of spotted hornfels in the aureole of the Devono-Carboniferous granitoids in the northern part of the Mahone Bay area. Andalusite and cordierite are the common silicates, whereas pyrite and magnetic pyrrhotite are the common sulphides. In places, calc-silicate pods show relics of concretionary zoning.

Hydrothermal alteration is present in Meguma Group metasediments near pegmatites, sulphide-bearing quartz veins and mineral-filled joints.

Mineral commodities

The three past-producing gold mines located in the Mahone Bay area are situated on the Gold River, Blockhouse and Spondo anticlines (Fig. 52.3). Quartz veins in the New Harbour, West Dublin, Moshers Island and Cunard members have been reported to contain Au, W and Cu. In general, fissure veins associated with faults are more common than the saddle reef veins associated with folds.

Thin stratiform laminae in the concretionary beds of the Moshers Island Member are especially rich in Mn. The Rhodes Corner manganese occurrences are found in these beds in fractures and along bedding planes.

References

Faribault, E.R.
1924: Chester Basin; Geological Survey of Canada, Map 87.

1929: Mahone Bay; Geological Survey of Canada, Map 88.

O'Brien, B.H.
1983: The structure of the Meguma Group between Gegogan Harbour and Country Harbour, Guysborough County; Nova Scotia Department of Mines and Energy, Report 83-1, p. 145-181.

1985: Preliminary report on the geology of the LaHave River area, Nova Scotia; in Current Research, Part A, Geological Survey of Canada, Paper 85-1A, p. 789-794.

Giles, P.S.
1981: The Windsor Group of the Mahone Bay area, Nova Scotia; Nova Scotia Department of Mines and Energy, Paper 81-3, 51 p.

Sage, N.M.
1954: The stratigraphy of the Windsor Group in the Antigonish Quadrangle and the Mahone Bay-St. Margarets Bay area, Nova Scotia; Nova Scotia Department of Mines, Memoir 3, 168 p.

Geology of the western Antigonish Highlands, Nova Scotia[1]

Contract 14SQ.23233-5-0007

J.B. Murphy[2]
Precambrian Geology Division

Murphy, J.B., Geology of the western Antigonish Highlands, Nova Scotia; in Current Research, Part A, Geological Survey of Canada, Paper 86-1A, p. 445-453, 1986.

Abstract

The western Antigonish Highlands are underlain by two sequences; Precambrian turbidites and minor volcanics of the Georgeville Group unconformably overlain by Upper Ordovician to Lower Devonian successions consisting of bimodal volcanics and fossiliferous siliciclastics. These sequences are similar to those described in the southern Antigonish Highlands. Upper Ordovician-Lower Devonian rocks belong to the Arisaig Group and constitute an overstep sequence onto the Antigonish Terrane.

Faults are common. They comprise northeast (dextral) and northwest (sinistral) conjugate transcurrent faults and associated thrusts that are probably due to the interaction of the Chedabucto Fault to the south and the Hollow Fault to the north. Movement on these is thought to be Middle to Late Devonian in age, and they may reflect the docking of the Meguma Terrane along the Chedabucto Fault.

Résumé

La partie ouest des hautes-terres d'Antigonish repose sur deux séquences. La première, précambrienne, constituée de turbidites et de roches volcaniques en faible quantité du groupe de Georgeville, est recouverte en discordance de successions de l'Ordovicien supérieur et du Dévonien inférieur qui se composent de roches volcaniques bimodales et de roches silicoclastiques fossilifères. Ces séquences sont semblables à celles qui ont été circonscrites dans la partie sud des hautes-terres d'Antigonish. Les roches ordo-dévoniennes appartiennent au groupe d'Arisaig et forment une discordance transgressive (overstep) sur le terrain d'Antigonish.

Il n'est pas rare de rencontrer des failles dans la région. Il s'agit de décrochements de direction nord-est (dextres) et nord-ouest (senestres) et des failles de poussée associées, qui résultent probablement de l'interaction de la faille de Chedabucto au sud et de celle de Hallow au nord. Les mouvements ayant affecté ces failles se seraient produits au Dénovien moyen ou supérieur, peut-être sous l'effet de l'accostage du terrain de Meguma contre la faille de Chedabucto.

[1] Contribution to the Canada-Nova Scotia Mineral Development Agreement, 1984-89. Project carried by the Geological Survey of Canada, Precambrian Geology Division, Project 760027.
[2] Department of Geology, Saint Francis Xavier University, Antigonish, Nova Scotia B2G 2L3

Introduction and previous work

The Antigonish Highlands lie in northeastern mainland of Nova Scotia (Fig. 53.1) and consist of about 1500 km^2 of late Precambrian to lower Devonian, moderately to mildly metamorphosed sedimentary and volcanic rocks. The boundaries of the Antigonish Highlands are defined by the Hollow Fault to the north and west, by the Chedabucto Fault to the south and by the Antigonish Basin of Devono-Carboniferous age to the east (Fig. 53.1).

The Antigonish Highlands lie within the Avalon "Composite" Terrane, a terrane that stretches the entire length of the southeastern margin of the Canadian Appalachians (Williams and Hatcher, 1982; Keppie, 1983). This terrane reflects diverse Precambrian histories, but broadly similar lower Paleozoic histories, suggesting that the terrane amalgamated by earliest Cambrian (e.g. Keppie, 1983).

Mapping in the northern Antigonish Highlands was initiated in 1978, by the Nova Scotia Department of Mines and Energy (Murphy et al., 1982) and continued in 1983 in the southern highlands under the Canada-Nova Scotia Mineral Development Agreement (Murphy, 1984, 1985a,b). As a result of this mapping the stratigraphy and interpretation of the geological history has been completely revised (Fig. 53.2, Table 53.1). Much of the highlands is underlain by late Precambrian rocks of the Georgeville Group. This group consists of subaerial mafic to felsic volcanic rocks at the base (Keppoch Formation-Frasers Brook Member) overlain by volcanic rocks with interlayered marbles (Chisholm Brook Formation) or interlayered slates and greywackes (Keppoch Formation-Moose River Member) and in turn by a thick sequence of turbidites and minor mafic volcanics. The stratigraphy documents the progressive development of a sedimentary basin. In general, younger rocks occur in the centre of the Antigonish Highlands with older rocks to the north and south (Fig. 53.2).

In the northern highlands the Georgeville Group was complexly deformed in the late Precambrian, whereas in the southern highlands, the Georgeville Group is monoclinal and shows no evidence of regional folding. Cambrian-lower Ordovician(?) rocks unconformably overlie the Georgeville Group. They only occur in the extreme north of the area (Fig. 53.2) and consist of the MacDonald Brook Group (which is dominated by bimodal volcanics and red clastic sediments) and the Iron Brook Group, which is dominated by red clastic

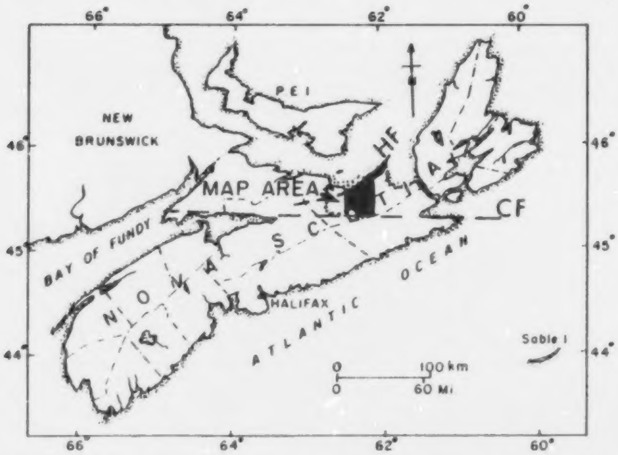

Figure 53.1. Location map of the Antigonish Highlands. Dotted area is shown in Figure 53.3. A composite map of the highlands (including the darkened area) is shown in Figure 53.2. HF - Hollow Fault, CF - Chedabucto Fault.

sediments, limestones, ironstones and calcareous tuffs (Murphy et al., 1982). These rocks were polydeformed probably in the middle Ordovician. Upper Ordovician(?)-Lower Devonian rocks were deposited unconformably on top of the Cambro-Ordovician rocks. They belong to the Arisaig Group and consist of red clastic sediments, bimodal volcanics and fossiliferous green to grey siltstones and shales. This report deals with the geology of the western part of the Antigonish Highlands and makes comparisons with the rest of the highlands.

Present work, Western Antigonish Highlands

The age and distribution of lithologies in the western highlands is shown in Figure 53.3, and its relationship to the rest of the highlands in Figure 53.2. In general, two distinct sequences are represented in Figure 53.3; late Precambrian metagreywackes, slates and metavolcanics of the Georgeville Group and uppermost Ordovician(?), lowermost Silurian to lower Devonian rocks of the Arisaig Group.

In some cases, stratigraphic interpretation of the western highlands is hindered by the presence of abundant faults. Independent evidence establishing the age of these rocks within the map area was difficult. Many interpretations are based on lithologic comparisons with the rest of the highlands, rather than on an extrapolation of established contacts. In general, Precambrian sediments are characterized by greywackes and plane-laminated slates, whereas Silurian rocks are abundantly fossiliferous, are dominated by siltstones and commonly contain detrital mica. Subdivision was not attempted in Precambrian rocks unless there was continuity with known relationships. Lower Silurian lithologies are distinctive and readily mappable (i.e. Beechill Cove and Ross Brook formations). Middle Silurian to lower Devonian rocks can be readily distinguished in the field only when the stratigraphic context is known. Failing this, the simplest way to distinguish these rocks is by paleontological data. At present, Ron Pickerill from the University of New Brunswick is identifying many of the fossils collected in the western highlands.

Georgeville Group

Precambrian volcanic lithologies are difficult to distinguish from Ordovician-Silurian volcanic rocks. However, the age of the rocks may be readily interpreted by the character of interlayered sediments. For example, in the southeastern highlands (Murphy, 1984), late Precambrian volcanics of the Keppoch Formation underlie or are interlayered with Precambrian greywackes; Upper Ordovician-Lower Silurian volcanics are associated with arkosic conglomerates and consistently underlie or are interlayered with lower Silurian fossiliferous rocks. However, in the southwestern highlands, most contacts are faulted and an assignment is usually based on the nature of the associated sediments.

Precambrian rocks are best exposed in streams and road sections north of the Browns Mountain Fault (BMF, Fig. 53.3) and to the east of the north-striking fault near Sunnybrae. The James River Formation (unit 3G), consists of green to grey feldspathic greywackes and green to grey slates with very minor volcanic rocks. Clasts within the greywackes are dominated by feldspars and by mafic intermediate and felsic volcanics. Greywacke units vary from 2 m to 2 cm in thickness. The thinner units commonly display slump structures. The slates display distinctive planar microlaminations with few sedimentary structures. One of the best exposures of the greywacke is in a quarry near Kirkmount, northwest of the map area. They are moderately cleaved except near faults where locally, schistose surfaces are developed. The assignment of this rock to the

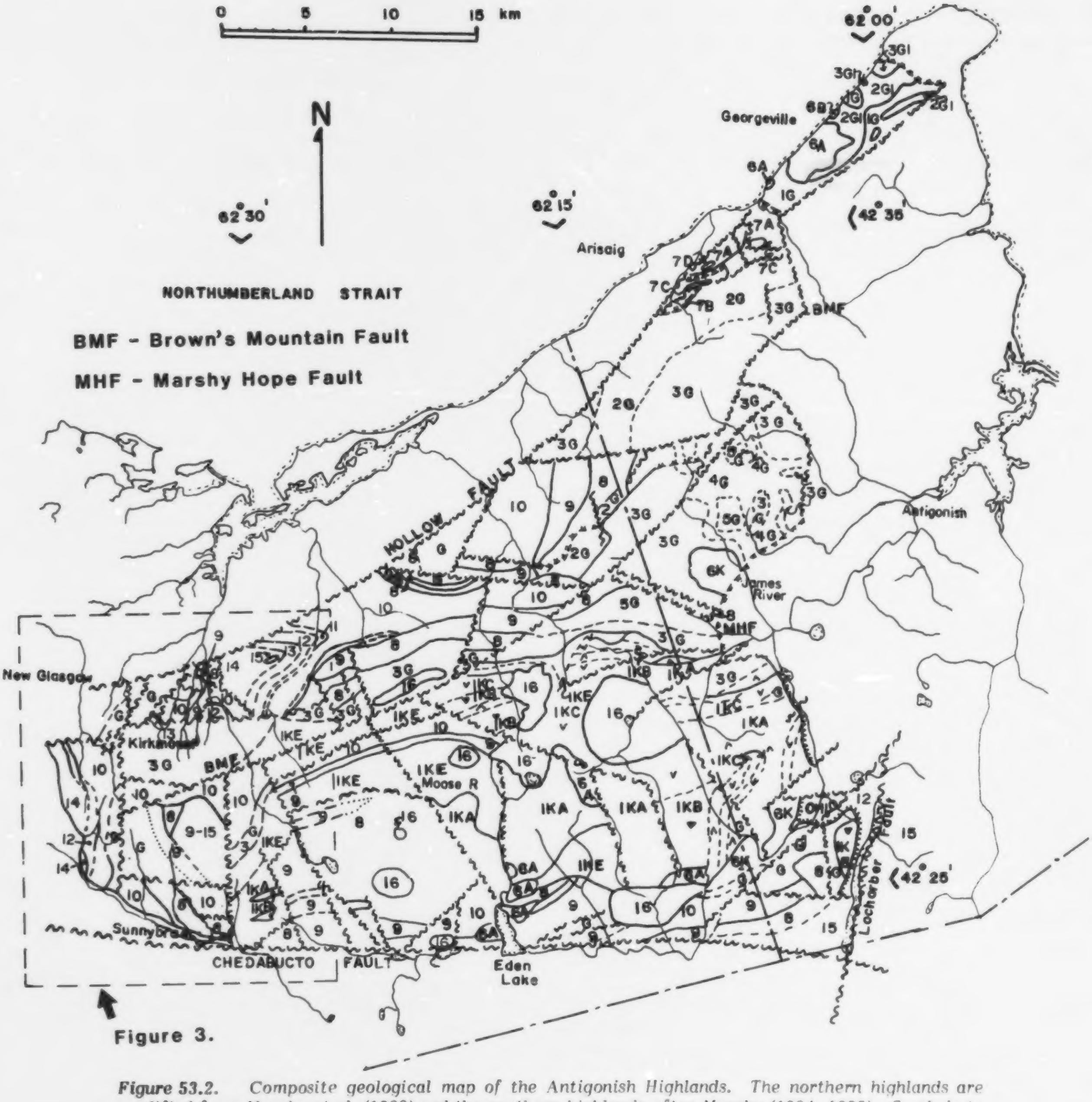

Figure 53.2. Composite geological map of the Antigonish Highlands. The northern highlands are modified from Murphy et al. (1982) and the southern highlands after Murphy (1984, 1985). Symbols to this map are given in the legend (Table 53.1).

James River Formation is based on lithologic comparison and on its broad continuity with James River turbidites to the east (see Fig. 53.3). Other areas where similar lithologies are exposed may also belong to the James River Formation but their relationships to other Precambrian rocks of the Antigonish Highlands are obscured by faulting or by overlying Silurian rocks and are classified as "Georgeville undivided" (unit G).

Precambrian volcanic rocks in the map area belong to the Keppoch Formation of the Georgeville Group. This formation has been subdivided using the presence (Moose River Member, IKE) or absence (the underlying Frasers Brook Member, IKA,B,C) of interlayered plane-laminated slates and greywackes with basalts (Murphy, 1985a). These slates and greywackes are similar to those of the overlying James River Formation.

In the western highlands, the Moose River member is best exposed on stream sections between the Browns Mountain and Miekelfield faults (Fig. 53.3). The Frasers Brook Member is best exposed on road sections east of the Sunnybrae-Websters Corner Fault. These rocks have been described in detail in previous reports and their descriptions are summarized here.

Table 53.1. Generalized stratigraphy of the Antigonish Highlands

F = Fossils Λ, ∇, (V), V, felsic, intermediate, mafic volcanic. X sediments, (Py) pyrite-bearing.

	NORTH		CENTRAL	SOUTH and WEST
Devono-Carb.			Undivided (see Boehner and Giles, 1982)	
	unconformity		16 Granite	16 Granite
U. Ordovician-L. Devonian			ASISAIG GROUP:	(see Boucot et al., 1974)
			10 Ross Brook Formation	15 Knoydart Formation
			9A, 9B Beechill Cove Formation (sediment, volcanic)	14 Stonehouse Formation
				13 Moydart Formation
			8a, 8b, 8 Bears' Brook Formation (sediment, volcanic, undivided)	12 McAdam Formation
				11 French River Formation
				10 Ross Brook Formation
				9 Beechill Cove Formation
				8 Bears' Brook Formation
	unconformity			
Cambrian-L. Ordovician		7D Granite, Syenite		
	7B IRON BROOK GROUP:	7A MACDONALD BROOK GROUP:		
	Ferrona Fm.	Arbuckle Fm.		
	Little Hollow Fm.		absent	absent
	Black John Fm.	Malignant Cove Fm.		
	unconformity		6K Granite	6K Granite
		H?,C?		
Hadrynian	6B Akaskite			
	6A Greendale Appinite Complex			6A Eden Lake Appinite Complex
			GEORGEVILLE GROUP:	
			G Georgeville Group Undivided (sediments)	
			5G South Rights Formation	
			4G Clydesdale Formation	
	3G1 Livingstone Cove Formation		3G James River Formation	Keppoch Formation
	2G1 Morar Brook Formation		2G Maple Ridge Formation	1KE Moose River Member
	1G Chisholm Brook Formation			1KA, 1KB, 1KC Fraser's Brook Member (felsic, intermediate, mafic)

Volcanic rocks consist of basalt, basaltic andesites, and rhyolite with minor volcanogenic sediments. Basalts are dark green, massive and generally aphyric. More rarely, they contain phenocrysts of augite (partly altered to chlorite) and quartz-chlorite amygdules.

Basaltic andesites are green to pale green in colour and contain phenocrysts of plagioclase (now albite) up to 1 cm long. Rhyolites within the Frasers Brook Member are commonly ignimbrites and are pink to red in colour. They display banding on weathered surfaces. This banding is usually defined by stretched and flattened pumice. Some rhyolites contain quartz eyes and/or plagioclase (now albite) phenocrysts. Felsic rocks in the Moose River Member, are not banded. The rocks are generally massive and pale to apple green in colour. Lahars are reddish green and contain poorly sorted, angular to subangular fragments of mafic to felsic volcanics, supported in a matrix of chlorite, sericite and quartz.

The volcanic rocks generally do not display a cleavage, except near faults, where the cleavage is locally intense and often penetrative. Two fabrics occur, one parallel to bedding and one at an acute angle to bedding (30° or less). Mafic rocks contain spots of chlorite (up to 2 cm). Felsic rocks are altered to sericite schists.

Arisaig Group

In contrast to Precambrian sequences, Upper Ordovician, Silurian to lower Devonian rocks are abundantly fossiliferous, micaceous and are characterized by arkosic sandstones, massive siltstones, and by laminated and bioturbated shales. It is difficult to distinguish between Precambrian and Silurian rock units adjacent to faults, where pervasive shearing has obscured some of the primary features.

These rocks, the Arisaig Group, are the oldest rocks that occur both to the north and south of Hollow Fault and may constitute an overstep sequence onto the Antigonish Highlands. The extrapolation of these formations across Hollow Fault is based on lithologic, stratigraphic, paleontological and geochemical similarities. These rocks consist of (in ascending order) the Bears Brook,

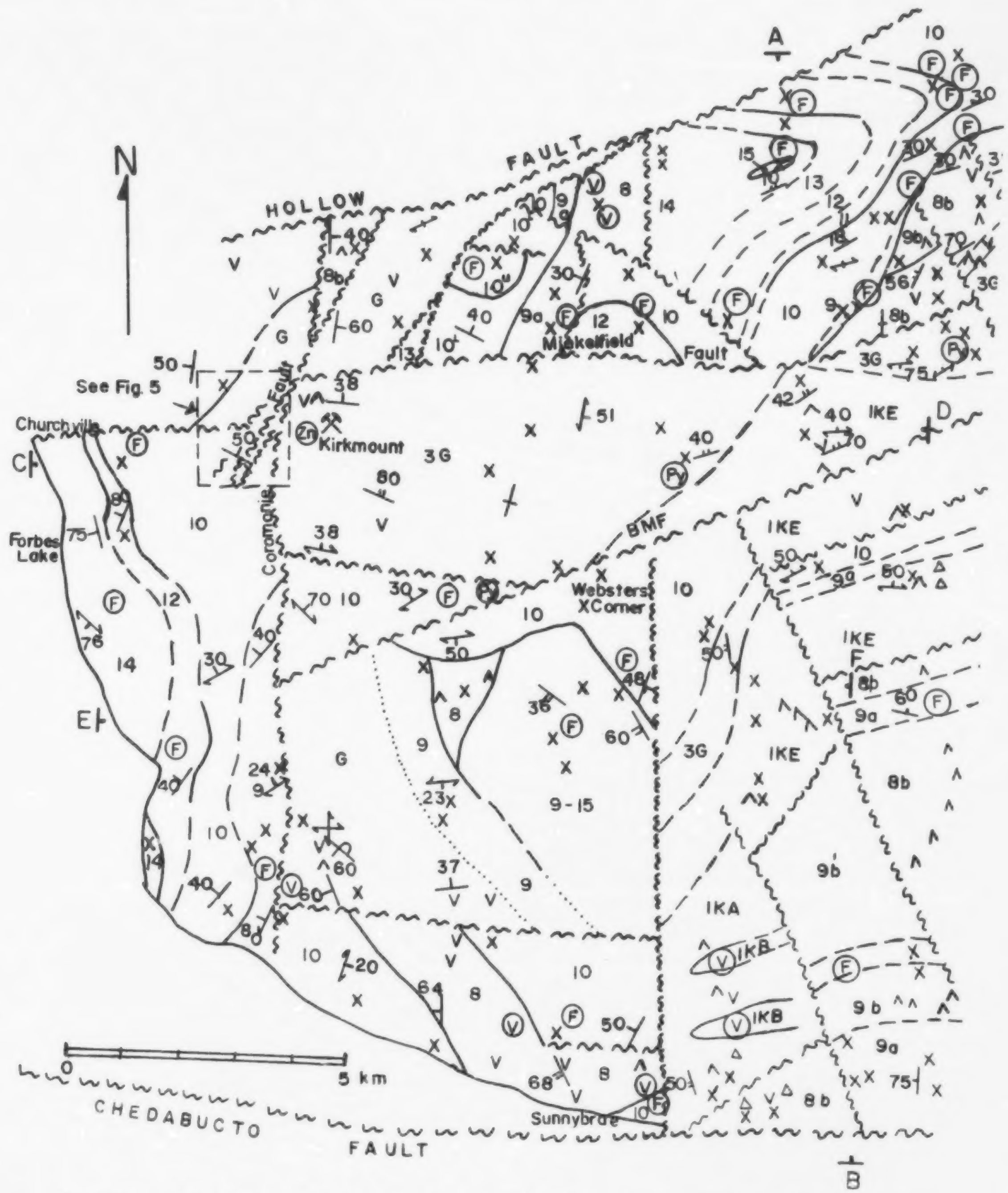

Figure 53.3. Geological map of the western Antigonish Highlands. Symbols are given in Table 53.1.

Beechill Cove, Ross Brook, French River, McAdam, Moydart, Stonehouse and Knoydart formations. Most of these have their type sections in the Arisaig area north of the Antigonish Highlands and all have been described in Boucot et al. (1974) and Maehl (1961).

The volcanic rocks of the lowermost formation of the Arisaig Group (see Table 53.1), the Dunn Point Formation to the north and the Bears Brook Formation to the south, display a similar and distinctive geochemical evolution. The mafic volcanic rocks have transitional alkalic-tholeiitic affinities, and the felsic volcanics consist of peraluminous rocks overlain by late stage SiO_2-rich differentiates (compare Keppie et al., 1979; Murphy and Cormier, in preparation).

The Bears Brook Formation (unit 8) consists of interlayered mafic and felsic volcanics, arkosic sandstones, conglomerates and minor red shales. Mafic volcanic rocks are aphyric, dark green, massive and may contain amygdules

filled with calcite, quartz or zeolites. Felsic volcanics consist of purple to pink banded ignimbrites, crystal and lithic tuffs. Arkoses are generally fine grained, contain abundant clasts of granite, diorite, mafic, intermediate and felsic volcanics, red slates, feldspar and quartz, in a hematite-quartz-rich matrix. They are also characterized by "rip-up" clasts of red shale and they are deposited in channels up to 5 m across. The Bears Brook Formation is best exposed near Sunnybrae in the south (Fig. 53.2).

The contact between the Bears Brook Formation and the overlying Beechill Cove Formation (unit 9) is placed at the uppermost volcanic rock that is stratigraphically underneath fossiliferous siltstones. The Beechill Cove Formation in the Antigonish Highlands may be subdivided into two members; a lowermost arkosic member similar to that of the Bears Brook Formation and an upper green fossiliferous member which consists of massive sandstone, siltstone and shales. Weathered surfaces display a limonitic staining. Fossils in the western highlands consist of brachiopods and crinoids. In the southeastern highlands, the Beechill Cove Formation has also yielded corals and trilobites (see Smith, 1979). This formation is best exposed in the west of the map area (Fig. 53.3) in a road section near the Corromonie Fault.

The Ross Brook Formation (unit 10), overlying the Beechill Cove Formation, consists of black to grey-black fossiliferous bioturbated shales (lower member, unit 10ℓ) overlain by an interlayered sequence of grey-black cleaved shales and massive, grey fossiliferous, crossbedded siltstones (unit 10u). Boucot et al. (1974) made a similar distinction in the type section in the type area near Arisaig. Fossils in the Ross Brook Formation consist of brachiopods, crinoids, graptolites and gastropods (Maehl, 1961). Near Sunnybrae, the Ross Brook Formation oversteps the Beechill Cove Formation and rests on the Bears Brook Formation. There is evidence of reworking of the Bears Brook Formation at the contact. This provides further evidence that lower Silurian rocks form part of a transgressive sequence (see also Murphy, 1985).

In the type area at Arisaig, the Ross Brook Formation is overlain by the French River, Doctors Brook and McAdam formations respectively. The contact between these was defined on the thickness of individual units and on ratios of sandstone-siltstone beds (Boucot et al., 1974). The age of these formations (Boucot et al., 1974; Maehl, 1961) is either upper-lower Silurian or middle Silurian.

The French River Formation (see Maehl, 1961) is exposed in only one locality in the area covered by Figure 53.3. The type section in French River consists of

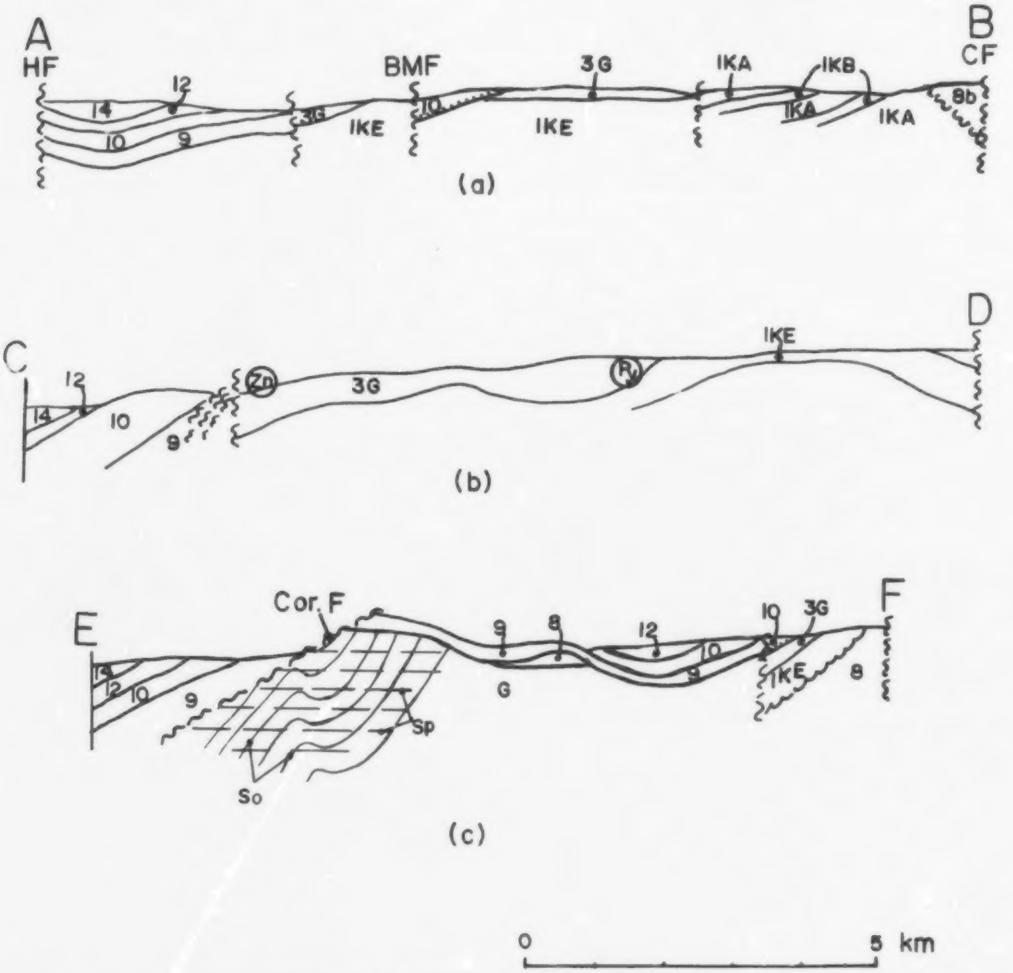

Figure 53.4. Selected cross-sections through the western Antigonish Highlands. Locations are given in Figure 53.3, symbols as in Table 53.1. Cor F - Corromonie Fault.

about 50 m of fossiliferous, grey to blue, fissile, micaceous siltstone, and interbedded grey shales. The basal contact with the Ross Brook Formation is defined by a sharp change in colour (Boucot et al., 1974).

In the northeastern part of the map area, the McAdam Brook Formation overlies the French River Formation with the Doctors Brook Formation absent (Fig. 53.3). In the west of the map area (Forbes Lake, Fig. 53.3) the McAdam Brook Formation overlies the Ross Brook Formation, with both the Doctors Brook and French River formations absent. The McAdam Formation consists of fossiliferous green-grey, to dark grey laminated micaceous siltstone and more massive sandstone.

The McAdam Formation is overlain by the Moydart Formation, which may be divided into a lower green and an upper red member (Maehl, 1961). The green member consists of sandstones and laminated siltstones. The red member consists of red shales and siltstones interlayered with green siltstones. The Moydart Formation is best exposed within thrust slices on McLellans Brook (Fig. 53.5). Since the Moydart Formation conformably underlies the Upper Silurian-Lower Devonian Stonehouse Formation it is probably Upper Silurian in age. The contact with the Stonehouse Formation is placed at the uppermost red unit. The Stonehouse Formation consists of fossiliferous, micaceous, fissile, blue-grey to green-grey laminated shales, siltstones and more massive, green sandstone. Some of the shales are calcareous and most siltstones display crossbedding. This formation is best exposed in the Forbes Lake area at the western extremity of the map area. The Knoydart Formation is exposed in a thrust slice on McLellans Brook (Fig. 53.5) and consists of red siltstones, shales and minor conglomerate. Pink to green calcareous lenses occur within the finer grained sediments. This relationship to older rocks is not exposed in the map area, although Maehl (1961), suggested that the contact with the underlying Stonehouse Formation is transitional. If this is true, then the Knoydart Formation should also be considered part of the Arisaig Group.

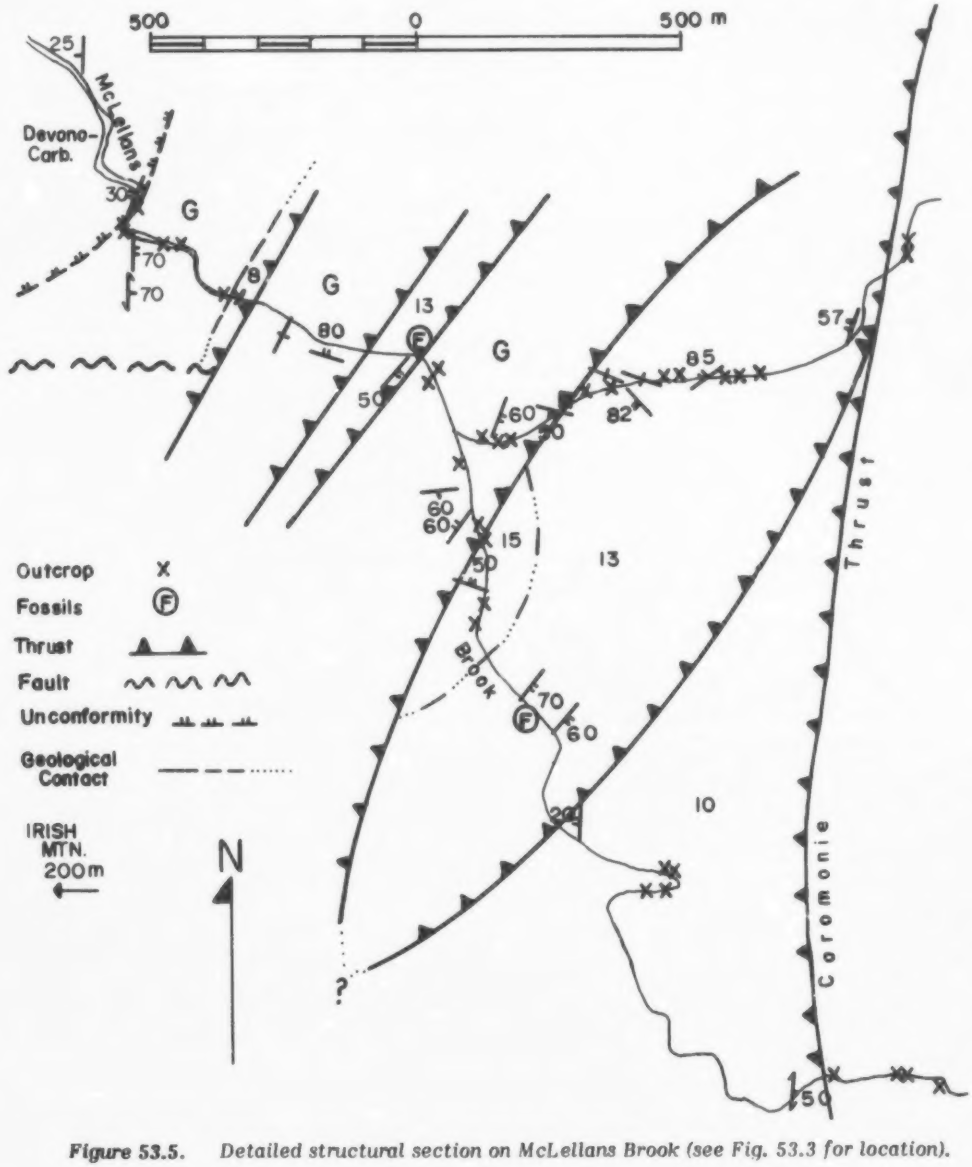

Figure 53.5. Detailed structural section on McLellans Brook (see Fig. 53.3 for location).

Intrusive rocks

Plutonic rocks are absent from the western highlands and diabase dykes are rare. This is in contrast to the southwestern highlands where granites, ranging in age from Precambrian to Devono-Carboniferous, are common and diabase dykes, probably of various ages intrude all lithologies from Precambrian to Carboniferous. Diabase dykes are dark green, massive, generally amygdaloidal and may be up to 5 m thick (e.g. McLellans Brook). In thin section they consist of an ophitic intergrowth of augite (partially altered to chlorite) and plagioclase (altered to albite) with abundant opaques. Amygdules are filled with quartz or calcite; minor epidote and zeolites also occur.

Deformation

The style of deformation is extremely varied. The rocks are monoclinal or gently folded (e.g. Fig. 53.4), except near major faults. Precambrian rocks show no evidence of regional folding. Their attitudes are probably considerably modified by faulting. Silurian rocks exhibit gentle open folding (e.g. Fig. 53.4a).

Deformation in the area is dominated by faulting in contrast to the southeastern highlands (Fig. 53.2, 53.3). The intensity and abundance of faults in the western highlands, precludes interpretations of the geometry of earlier structures. In general faults may be divided into two categories; those that are subparallel to the Hollow or Chedabucto faults (e.g. the Meikelfield (Fig. 53.3) and Browns Mountain faults (Fig. 53.2, 53.3)) and those that are at a high angle to these faults (the Corromonie Fault (Fig. 53.3)).

The Hollow and Chedabucto faults have long histories of repeated movements (e.g. Keppie, 1985). Penetrative fabrics generally occur within 300-700 m from these faults. Recrystallization to sericite and chlorite, commonly occurs along the cleavage planes. Two cleavages generally at 30 degrees or less may be recognized. These are interpreted as CS fabrics (Berthe et al., 1979) where C represents the shear plane and S the plane of flattening. These cleavages are gently to moderately dipping, except immediately adjacent to the faults where they are vertical. These relationships suggest that thrusting may be associated with the faults, thrusting that was probably localized resulting in local, rather than regional discontinuities.

Faults that are at high angles to Hollow and Chedabucto faults are northeast and northwest trending and are either vertically dipping transcurrent faults or low-angle thrusts. The transcurrent faults predominate and occur as conjugate sets. Northeast trending faults have dextral displacement while northwest trending faults have sinistral displacement. These faults are common throughout the entire southern highlands deforming Precambrian to lower Devonian rocks and are best exposed at Lochaber Lake (northeast-dextral) and Moose River (northwest-sinistral) (Fig. 53.2). These faults also contain well developed CS fabrics.

In the western highlands, many of the faults at a high angle to the Hollow and Chedabucto faults such as the Corromonie Fault are probably westwardly-dipping thrusts (Fig. 53.4b), thrusting Siluro-Devonian rocks onto Precambrian greywackes, slates and volcanics. No exotic stratigraphy occurs and the thrusts probably have limited movement. Immediately to the west of the Corromonie fault, an intense shallow to moderate westward dipping cleavage occurs in Siluro-Devonian rocks. In the Precambrian rocks east of the fault, cleavage is generally subhorizontal despite local changes in the attitude of the bedding. This suggests that this cleavage (and therefore the thrusting) postdates earlier folding of Precambrian rocks (e.g. Fig. 53.4c).

Imbricate northwestwardly dipping thrusts and reverse faults associated with the Corromonie Thrust occur on McLellans Brook (Fig. 53.5). The age of deformation is uncertain, but the youngest unit involved in thrusting in this area is the lower Devonian Knoydart Formation. Similar relationships are observed at Lochaber Lake in the southeastern highlands (Fig. 53.2). The association of thrusts with faults suggests that this area was under regional compression.

Although faulting and shearing of Carboniferous rocks is described in the "Stellarton Gap" (Yeo and Gao, 1986) these faults are thought to be extensional in origin. These relationships suggest that the thrusting is probably mid-upper Devonian in age (i.e. Acadian).

Economic geology

Murphy (1985) divided the occurrences of economically interesting areas in the southern and southwestern highlands into four categories.

1. Near the contact between subaerial and submarine Precamrian volcanic rocks.
2. As discontinuous stratabound lenses in Precambrian or Silurian age felsic volcanic rocks.
3. Quartz-eyed intrusive porphyries adjacent to the Browns Mountain Fault
4. Adjacent to northwest trending faults.

Two interesting localities occur in the western highlands (see Fig. 53.2). One is in an altered (sericitized) quartz-eyed porphyry which intrudes Silurian rocks and is adjacent to the Browns Mountain Fault. Thus it fits category 3.

The other is a Zn prospect at Kirkmount which is hosted in the turbidites of the James River Formation of the Georgeville Group (see Sangster, 1986, for further details). Previously, the Kirkmount Zn prospect was thought to be hosted in Silurian rocks (Maehl, 1961). The occurrence does not fit any of the above categories, but is particularly interesting in view of anomalously high Zn found associated with Morar Brook and Livingstone Cove formations of the Georgeville Group in the northern Antigonish Highlands (see Fig. 53.2, and Table 53.1, see also Chatterjee, 1982).

These observations suggest that the turbidites of the Georgeville Group may warrant a more detailed study than that previously considered.

Summary

The rocks of the western Antigonish Highlands are dominated by Precambrian turbidites, unconformably overlain by an Upper Ordovician to Lower Devonian sequence of bimodal volcanics and abundantly fossiliferous siliciclastic sediments. Interpretation of the relationship between these sequences is complicated by abundant faults and relationships are extrapolated from the southern highlands (Murphy, 1984). As such, a study of the western highlands adds little to the understanding of the geological history of the Antigonish terrane.

In general, lithological, paleontological and geological similarities of Upper Ordovician-Lower Devonian rocks to those of the type area at Arisaig, suggest that the Arisaig Group constitutes an overstep sequence onto the Antigonish Highlands. In the simplest sense, this would limit cumulative post-Lower Devonian movement on the Hollow Fault to about 30 km.

The faults are brittle shear zones with typical CS fabric and associated local thrusting. These faults affect rocks of Precambrian to Lower Devonian ages and are probably middle or upper Devonian in age, though some of the faults may be reactivated in the Carboniferous (see Yeo and Gao, 1986). The abundance of faults in the western highlands is probably due to the interaction between the Hollow and Chedabucto faults. The age of movement on these faults is approximately synchronous with the docking of the Meguma Terrane along the Chedabucto Fault (e.g. Keppie, 1983) and the geometry may reflect the docking procedure.

The Zn occurrence at Kirkmount is hosted by the James River Formation of the Georgeville Group and is therefore at a similar stratigraphic level to a Zn occurrence in the Georgeville area. Another example of an intrusive quartz-eyed felsic porphyry with associated pyrite has been found adjacent to the Browns Mountain Fault (see Murphy, 1985) providing further evidence of the economic potential of the fault.

Acknowledgments

I thank F. Chandler for organizational support and for visiting me in the field; J.D. Keppie, R.F. Cormier, K.L. Currie, R.D. Nance, G. Yeo and R. Gao, for their continuing interest in the Antigonish Highlands project; A. Sangster for introducing me to the Zn occurrence in the Kirkmount area; R. Pickerill for help with fossil identification; K. Bellefontaine, P. Campbell, D. Hatchette, E. Myketyn and S. Sears of St. Francis Xavier University who assisted in various parts of this project. The manuscript benefited considerably from reviews by F. Chandler and C. Larocque. Funding for this project, provided by the Geological Survey of Canada, is gratefully acknowledged.

References

Berthe, D., Choukroune, P., and Jegouzo, P.
1979: Orthogneiss, mylonite and non-coaxial deformation of granites, the example of the south Armorican Shear Zone; Journal of Structural Geology, v. 1, p. 31-42.

Boehner, R.C. and Giles, P.S.
1982: Geological map of the Antigonish Basin, Nova Scotia, scale 1:50 000; Nova Scotia Department of Mines and Energy, Map 82-2.

Boucot, A.J., Dewey, J.F., Dineley, D.L., Fletcher, R., Fyson, W.K., Griffin, J.G., Hiskox, C.F., McKerrow, W.S., and Zeigler, A.K.
1974: Geology of the Arisaig area, Antigonish County, Nova Scotia; Geological Society of America Special Paper 139, 191 p.

Chatterjee, A.K.
1982: Metallogenic map of the Province of Nova Scotia; Nova Scotia Department of Mines and Energy, Map 82-2.

Keppie, J.D.
1983: The Appalachian Collage; ed. by D.G. Gee and B. Sturt; International Geological Correlation Program, Caledonide Orogen Volume, Uppsala meeting, J. Wiley & Sons.

Keppie, J.D. (cont.)
1985: Itinerary of the Meguma Terrane; in Keppie et al. Appalachian Geotraverse, GAC/MAC Field Trip Guide Book, p. 48-7.

Keppie, J.D., Dostal, J., and Zentilli, M.
1978: Petrology of the Early Silurian Dunn Point and McGillivray Brook Formations, Arisaig, Nova Scotia; Nova Scotia Department of Mines, Paper 78-5, 20 p.

Maehl, R.H.
1961: The older Paleozoic of Pictou County, Nova Scotia; Nova Scotia Department of Mines, Memoir 4, 112 p.

Murphy, J.B.
1984: Geology of the southern Antigonish Highlands, Nova Scotia; in Current Research, Part A, Geological Survey of Canada, Paper 84-1A, p. 587-595.

1985a: Geology of the southwestern Antigonish Highlands, Nova Scotia; in Current Research, Part B, Geological Survey of Canada, Paper 85-1B, p. 519-530.

1985b: Geological map of central and southern Antigonish Highlands; Geological Survey of Canada, Open File 1181.

Murphy, J.B. and Cormier, R.F.
– Upper Ordovician to Lower Silurian rocks of the Antigonish Highlands, Nova Scotia. (in preparation)

Murphy, J.B., Keppie, J.D., and Hynes, A.J.
1982: Geological map of the Antigonish Highlands; Nova Scotia Department of Mines and Energy, Map 82-5.

Sangster, A.L.
1986: A willemite (Zn_2SiO_4) and a native silver occurrence, Kirkmount, Pictou County, Nova Scotia; in Current Research, Part A, Geological Survey of Canada, Paper 86-1A, report 18.

Smith, P.K.
1979: Note on the geology and new Silurian fossil occurrences, south and east of Kenzieville, Antigonish Highlands; Nova Scotia Department of Mines, Report of Activities, Report 79-1, p. 89-94.

Williams, H. and Hatcher, R.D., Jr.
1982: Suspect terranes and accretionary history of the Appalachian Orogen; Geology, v. 10, p. 497-560.

Yeo, G. and Gao, R.
1986: Late Carboniferous dextral movement on the Cobequid Fault system; in Current Research, Part A, Geological Survey of Canada, Paper 86-1A, report 46.

Geology of the Sheffield Lake group, west-central Newfoundland

Project 730044 and Contract 14SQ.23233-5-0076

Marylou Coyle [1], D.F. Strong [1], and D.B. Dingwell [2]
Precambrian Geology Division

Coyle, M., Strong, D.F., and Dingwell, D.B., Geology of the Sheffield Lake group, west-central Newfoundland; in Current Research, Part A, Geological Survey of Canada, Paper 86-1A, p. 455-459, 1986.

Abstract

The rocks of the Sheffield Lake group are inferred to unconformably overlie foliated mafic and intermediate rocks which form a basement to the region. The group is dominated by variably welded ash flow tuffs which, in contrast to most of the Springdale Group, are fine grained and dominated by crystals of quartz and alkali feldspar, with less abundant lithic clasts. On high peaks in the area the Sheffield Lake group is capped by aphanitic vitric tuffs which tend to be flow-banded and reminiscent of rheoignimbrites. The Sheffield Lake group is interbedded with mafic to intermediate flows, and intruded by a variety of granitoid rocks, including a peralkaline quartz-K-feldspar porphyry characterized by metasomatic oikocrysts of reibeckite which are also superimposed on the volcanic rocks which they intrude. The youngest rocks of the area are clastic sediments of presumed Carboniferous age occurring along the north shore of Sheffield Lake and on a small island within it.

Résumé

Les auteurs déduisent des résultats de leurs travaux que les roches du groupe de Sheffield Lake reposent en discordance sur des roches mafiques et intermédiaires foliées qui servent de socle à la région. Le groupe renferme surtout des tufs résultant de coulées de cendres et variablement soudés qui, contrairement à la majeure partie du groupe de Springdale, sont à grains fins et renferment surtout des cristaux de quartz et de feldspath alcalin, les pyroclastes lithiques y étant moins abondants que dans l'autre groupe. Sur les plus hauts sommets de la région, le groupe de Sheffield Lake est coiffé par des tufs vitreux aphanitiques qui, de façon générale, ont un aspect lité et font penser à des rhéoignimbrites. Le groupe de Sheffield Lake est interstratifié de coulées mafiques à intermédiaires; y font intrusion diverses roches granitoïdes, notamment un porphyre peralcalin à quartz-K-feldspath caractérisé par la présence de critaux poecilitiques de riébeckite qui sont également superposées aux roches volcaniques dans lesquelles ils font intrusion. Les roches les plus récentes de la région sont des sédiments clastiques dont on présume qu'ils remontent au Carbonifère; on les observe le long de la rive nord du lac Sheffield et sur un îlot de ce lac.

[1] Department of Earth Sciences, Memorial University of Newfoundland, St. John's, Newfoundland A1B 3X5
[2] Carnegie Geophysical Laboratory, 1401 Upton Street, N.W., Washington, D.C.

Introduction

The Birchy Lake valley, running along the trace of the Cabot Fault in western Newfoundland, is bounded on the east by high peaks such as Mounts Sykes and Seemore which are capped and underlain by a variety of welded ash flow tuffs and other volcanic rocks of probable Silurian age, referred to informally as the Sheffield Lake group. We introduce this term for the volcanic and intrusive rocks exposed between Sheffield Lake and Birchy Lake, although we anticipate that more detailed geochemical and geochronological studies will demonstrate that they are at least in part outflow deposits of the adjacent Springdale caldera, and hence should more strictly be included within the Springdale Group.

The Sheffield Lake group is under investigation as part of our continuing studies of the Silurian-Devonian volcanic and plutonic rocks extending throughout much of western Newfoundland (Coyle et al., 1985; Coyle and Strong, 1986). It is also of interest because of the abundance of peralkaline compositions, and in particular those with spectacular reibeckite oikocrysts as in the Mount Seemore area. Taylor et al. (1980) sampled the volcanic and intrusive rocks at Mount Seemore, as part of a more regional petrochemical study of the Topsails Complex, and showed them to have a composition similar to peralkaline continental comendites, strongly enriched in Zr and a number of other trace elements. They attributed this character to metasomatism by peralkaline magmatic fluids of probable mantle origin, an interpretation which was further refined and supported by Taylor et al. (1981). A detailed study of the oikocryst compositions, however, showed them to have formed from relatively oxidizing fluids, leading Strong and Taylor (1984) to suggest that meteoric hydrothermal fluids were also involved. Because of the importance of these questions to the genesis of peralkaline rocks in general, it was decided to map the nature and distribution of oikocrysts in some detail, with further geochemical, isotopic and experimental studies in an attempt to determine the nature of the fluids involved and the conditions under which they formed. Their abundance and lack of alteration also make these K-rich amphiboles ideal material for radiometric dating by the $^{40}Ar/^{39}Ar$ method.

Description of map units

In general, rock exposure is moderate on ridges, which are surrounded by areas of poor exposure, although there are some excellent river sections. Access to the area is good, with many gravel roads provided by foresting operations. The different geological units recognized in the area are shown in Fig. 54.1. The oldest, unit 1, are rocks which (Whalen et al., 1983) correlated with the Hungry Mountain Complex of Thurlow (1981), and include a complex array of rocks with probable origins ranging from Precambrian continental crust to Cambro-Ordovician ophiolitic and island arc material. In the map area these rocks are mainly foliated amphibolite and gabbro occurring as large screens and xenoliths in foliated diorite and granodiorite. These may be intruded by variably deformed tonalite and amphibole-biotite granite.

Unit 2 is the most extensive in the area, and is most similar to parts of the Springdale Group to the east. It is dominated by felsic ash flow tuffs of different compositions and degrees of welding, and includes minor areas of mafic volcanics too small for separation at the scale of Figure 54.1. Sheffield Brook has excellent exposure with a complex assemblage of at least eight rock types recognized. Five of these are included in unit 2, two in unit 3a, and one in unit 7 on Fig. 54.1. Purple to brown, densely welded crystal-rich, ash flow tuff is seen along the eastern end of the brook. The crystals in it are euhedral quartz and feldspar locally concentrated in streaky zones, and the tuff ranges from massive sections with curvilinear and columnar jointing to zones marked by internal shear planes and autobrecciation. Flattened vitric clasts are also seen along strike. This lithology can be tentatively correlated with unit 7 of Coyle et al. (1985).

The central parts of Sheffield Brook exposures unwelded tuff with a very ashy matrix having finely graded laminations with quartz-rich horizons, which can easily be mistaken for a fine red sandstone. This lithology is quite extensive and repeated several times along Sheffield Brook, and may represent either a well sorted ash flow unit or an ash fall into a lake or other water body. At present tentative correlation is made with parts of unit 8 in Coyle et al. (1985).

Several distinctive horizons of autobrecciated rhyolite clasts ranging from pebble to boulder size in a quenched purple matrix, are found within the above two lithologies. The orientation of these horizons can be undulose or network-like when they occur on a small scale, although the larger sections or "beds" of breccia have more consistent orientations.

The ignimbrite at the eastern end of Sheffield Brook is overlain by a complex red to green muddy to ashy lahar with local cherty horizons. The red muds are often silty with rounded clasts of rhyolite supported by the matrix silt. The green represents reduction spots and zones, preferentially focussed on mudballs and layers. These lahars are strongly deformed along the Sheffield Brook Fault, but also have abundant primary penecontemporaneous fold and slump features, along with channeled lenses typical of sedimentary or reworked volcanic deposits. These lithologies are cut by a number of dykes that pass westwards into a chaotically flow-banded maroon rhyolite, commonly aphyric but with concentrations of quartz and feldspar, which is interpreted to be a domical intrusion. Along the Sheffield Brook Fault the dykes are brecciated, leached and altered to a yellow green, with clots of pyrite and sericite. Large veins of calcite and fluorite cut the ignimbrite along the eastern end of Sheffield Brook.

These different lithologies are generally representative of unit 2, but other varieties are also seen. For example along Oxford Brook two-feldspar quartz crystal tuffs are interbedded with aphyric and plagioclase-phyric basalts. In other areas such as along the road just south and west of Mount Sykes the vitric tuffs are strongly devitrified, with large chalcedony-filled lithophysae and veins cutting the tuffaceous banding and flattening. In general the flattening is gently dipping but locally may be disrupted and steep.

Unit 3 is a distinctive fine grained welded ash flow tuff with sparsely distributed phenocrysts of quartz and K-feldspar. It is typically maroon and massive on the fresh surface, but weathers to a light colour in which the darker fiamme and flow-banding stand out. In general the flattening and flow-banding are gently dipping, as at Mount Sykes, but in some areas such as on the peak north of Sheffield Lake (Point E on section 1, Fig. 54.1) the banding is intense and steeply dipping, comparable to that seen in rhyolite domes and rheoignimbrites of the Springdale Group. In this area and elsewhere, as around Mount Sykes, the matrix of unit 3 may be marked by finely dispersed riebeckite needles, although no riebeckite oikocrysts are visible. The intensity of this metasomatism increases in areas where these glassy tuffs are near the peralkaline porphyries of unit 7, as at Mount Seemore, where they are marked by large reibeckite oikocrysts and strong albitization of the matrix. These areas are distinguished as unit 3a on Fig. 54.1. Along Sheffield Brook unit 3a is a massive oikocrystic rhyolite with local concentrations of quartz and feldspar. The rhyolite is quite glassy and weathers to a pale greenish white, with some "ghosty" fiamme upon which the riebeckite oikocrysts tend

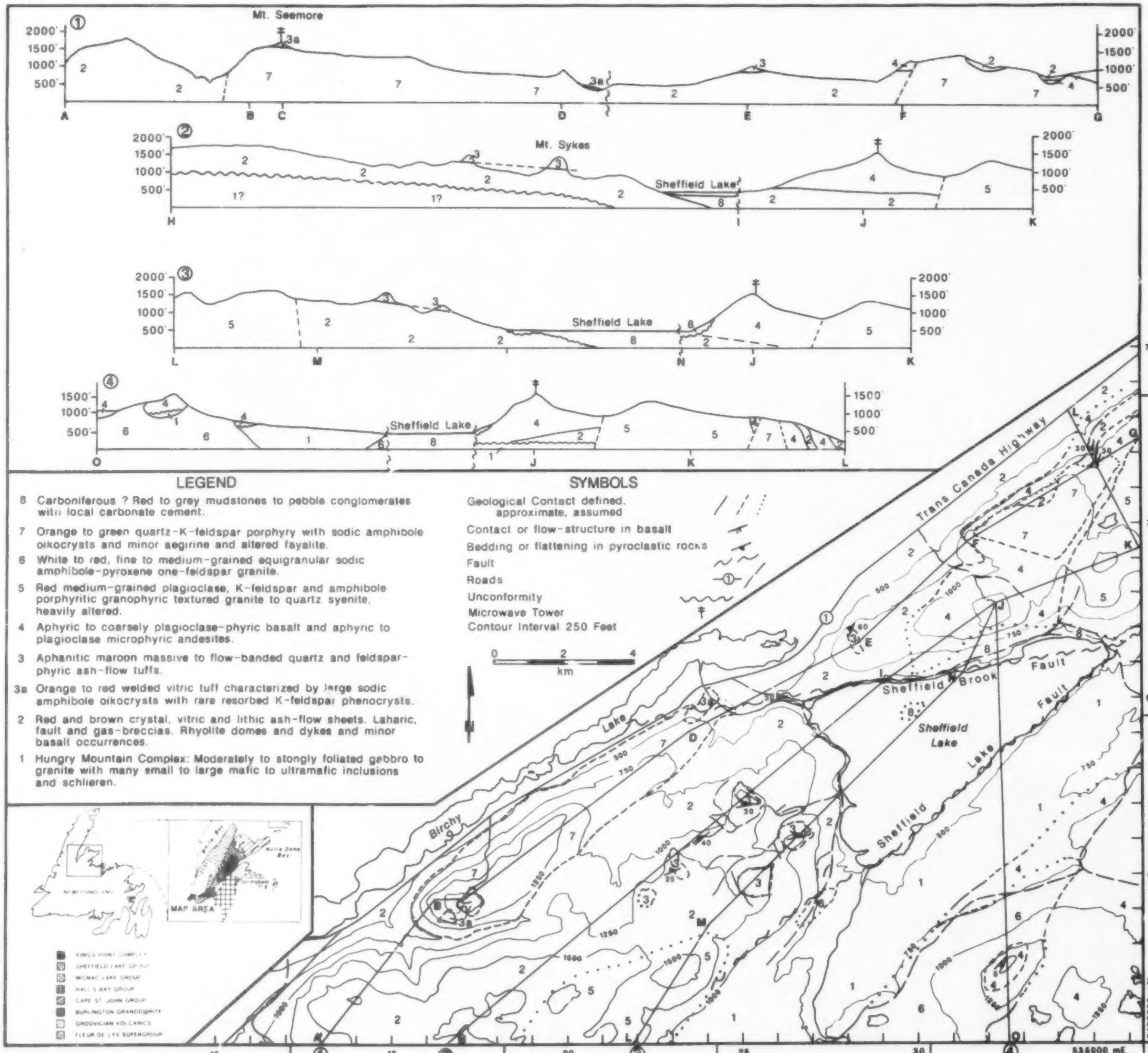

Figure 54.1. General geological map of Sheffield Lake-Birchy Lake area, western Newfoundland.

to concentrate. The oikocrysts range from 1 mm to almost 1 cm in size. As at Mount Seemore, bands and veinlets of reibeckite are also seen, some of which may be focused along pre-existing laminations or welding surfaces.

Unit 4 includes basalts and basaltic andesites. In the southeastern corner of the map area it is mainly basaltic flows which are gently dipping, even where found as roof pendants in granitic intrusions (Fig. 54.1). Although the contacts are not seen, the flows in this area are inferred to unconformably overlie the basement rocks of unit 1. Black aphyric rocks, probably of basaltic andesite composition are found in the area surrounding the microwave tower north of Sheffield Lake (Fig. 54.1). Although they are inferred to be underlain by the pyroclastic rocks of unit 2, they show no primary structures which can be used for orientations, and indeed might even be intrusive. Possible support for this interpretation is seen in an inclusion of pink granite, about 25 cm across, found about 50 m to the southwest of the microwave tower. Beneath the woods-road bridge on Oxford Brook, however, similar rocks are seen to be interlayered with welded tuffs of unit 2. Also seen along Oxford Brook are local zones of strongly plagioclase-phyric basalts, with phenocrysts up to 1 cm long sporadically distributed as zones within aphyric basalt. Small areas of basalt are also exposed within unit 2 at several localities southwest of Sheffield Lake.

Unit 5 is described by Whalen et al. (1983; their unit 17a) as red and medium grained with phenocrysts of K-feldspar, as well as amphibole and biotite, and ranging from quartz syenite to granite. We have not examined this granite in any detail other than to confirm this description in a few locations.

Unit 6 was only superficially examined in the present study, and the boundaries shown in Figure 54.1 are taken mostly from Whalen et al. (1983; their unit 20g). It is clearly seen to intrude the basaltic rocks of unit 4, which in several places are found as strongly hornfelsed roof pendants exposed only on the highest peaks (e.g. on section 4 of Fig. 54.1). The pendant shown on section 4 of Figure 54.1 is cut by intimately mixed composite dykes of felsic and mafic composition which appear to be derived from the granitic intrusion exposed only a few metres down-slope. In the areas that we examined there appear to be two granitic phases within unit 6. One is generally medium- to coarse-grained and pink, and characterized by quartz and pink feldspar with finer grained crystals of black amphibole. This is intruded by finer grained whitish-grey granite which has local zones of reibeckite pegmatite and abundant amphibole-lined miarolitic cavities and fractures. Whalen et al. (1983) also described parts of this unit as amphibole-sodic pyroxene one-feldspar granite which they designated as their unit 20g, intruding both the basalt and the Hungry Mountain Complex (unit 1 on Fig. 54.1). Fault breccias of granitoid rock, somewhat similar to that of unit 6, are seen along the trace of the Sheffield Lake Fault near the inferred contact with unit 1. Most previous workers (e.g. Taylor et al., 1980; Whalen et al., 1983) considered the granites of both units 5 and 6 to be offshoots of the Topsails Complex.

Unit 7 ranges from a quartz-feldspar-amphibole porphyry with reibeckite oikocrysts into a quartz syenite to a true syenite. The porphyries represent the chilled margins of, and are mutually gradational with, the coarser grained holocrystalline rocks, and in general is distributed around their margins. The porphyry is chilled against its contact with the oikocrystic rhyolites of unit 3. Along Sheffield Brook offshoots of this intrusion are also seen as radial dykes, some of which have chilled margins. This unit is similar to the porphyries of the King's Point area described by Kontak and Strong (1986).

Unit 8 has been seen during the present investigation only as a number of loose blocks of poorly consolidated yellow-brown sandstone along the hillside north of Sheffield Lake. However, they were previously exposed in outcrop during slumping of the overburden, as observed during mineral exploration by Brinco Ltd. in the 1960's (H.R. Peters, personal communication, 1985). During this same period outcrops of flat-lying grey flaggy sandstone-siltstone were mapped on the small island which is exposed in Sheffield Lake during times of low water. All these rocks can be compared to the younger Carboniferous rocks of western Newfoundland, particularly those of the Deer Lake Group found just to the southwest of Figure 54.1.

Structure

The lack of sedimentary rocks in the Sheffield Lake group make it necessary to rely upon regional stratigraphic relationships and volcanic features for indications of overall structure. The former are not always reliable on a local scale, since flattening and flowage features can be influenced by underlying topography and other factors, especially in rheoignimbrites where welding is intense and flow-banding strongly developed. In general, however, the flattening of fiamme in welded ash flow tuffs is paralleled by lithological boundaries, lithophysae zones, vesicle and crystal alignment in basalts, etc. On the regional scale these are gently dipping to horizontal, as can be seen on the sides of most high peaks in the area and shown on the cross-sections in Fig. 54.1. The main exception to this pattern is seen along Oxford Brook, where the ash flows and interbedded basalts range in dip from 20 to 60°. Nevertheless, no penetrative cleavage is seen here or elsewhere in the Sheffield Lake group, and this orientation may be related to the broad open folding seen in the Springdale Group to the east, or possibly to local tilting due to intrusion of units 5 or 7.

The two major faults recognized in the area are termed the Sheffield Lake Fault and the Sheffield Brook Fault. The former marks the straight eastern boundary of the lake, and is marked by small outcrops of granite fault breccia along its trace to the southwest of the lake (Fig. 54.1). Its main effect in the area seems to have been uplift and exposure of the basement rocks of unit 1. The Sheffield Brook Fault marks the northern boundary of the lake, and its effects are clearly seen in the brook where ignimbrites, mudstones and rhyolite dykes are strongly brecciated. There does not appear to have been much displacement along this fault, however, since lithologies such as those of units 3a and 7 extend across the brook at its western end. The age of these faults is not known, but it is reasonable to correlate them with faults that affected and controlled the development of Carboniferous pull-apart basins and sedimentation such as that of the Deer Lake Group (Hyde, 1984). The presumed Carboniferous sediments in Sheffield Lake suggest that it may represent a smaller version of these basins.

Discussion

Two striking questions are posed from the geology seen in the Sheffield Lake-Birchy Lake area. One is the stratigraphic and structural relationships of the Sheffield Lake group units to those of the Springdale Group, both in terms of original physical volcanology and subsequent deformational history. Second is that of the relationships between the peralkaline rocks of the Sheffield Lake group and those of the Springdale Group.

The answer to the former question will depend, along with the field relationships described above, upon radiometric dating of the units in both groups, and this will be done as part of the present investigation. The latter question is perhaps more fundamental in that it depends upon an

understanding of the processes involved in development of the oikocrysts. For example it is necessary to establish whether such processes affected rocks genetically related to the Springdale Group. If so, why only some parts of it and not others? If not, are the oikocrystic rhyolites of the Sheffield Brook area distinctly unrelated to the Springdale Group (i.e. indicating a separate magma chamber and separate caldera(?). The same questions might be asked for similar rocks of the King's Point Complex (Kontak and Strong, 1986). Detailed geochemical studies which are in progress may answer this question, as may experimental studies which are being planned to try and establish the conditions and mechanisms of oikocryst growth.

Acknowledgments

We thank K.L. Currie for his continuing support of this project, Phillipe Erdmer and J. Van Berkel for sharing helicopter time, David Healey and Joan Burry for field assistance, John O'Sullivan and Esso Minerals Ltd. for logistic support, and Larry Nolan for drafting Figure 54.1. We are especially grateful to the Newfoundland and Labrador Department of Forestry at Pynns Brook and Springdale for the use of their aerial photographs.

References

Coyle, M. and Strong, D.F.
1986: Geology of the southern and northern margins of the Springdale caldera, Newfoundland; in Current Research, Part A, Geological Survey of Canada, Paper 86-1A, Report 60.

Coyle, M., Strong, D.F., Gibbons, D., and Lambert, E.
1985: Geology of the Springdale Group, central Newfoundland; in Current Research, Part A, Geological Survey of Canada, Paper 85-1A, p. 157-163.

Hyde, R.
1984: Geological history of the Carboniferous Deer Lake basin in west central Newfoundland, Canada; in Atlantic Coast Basins, Paleogeography and Paleotectonics, Sedimentary and Geochemistry, v. 3, ed. H.J. Geldsetzer, W.W. Nassichuck, E.S. Belt, and R.W. MacQueen; Southern Illinois University Press, p. 85-104.

Kontak, D.J. and Strong, D.F.
1986: The King's Point volcano-plutonic complex, Newfoundland; in Current Research, Part A, Geological Survey of Canada, Paper 86-1A, Report 56.

Strong, D.F. and Taylor, R.P.
1984: Magmatic-subsolidus and oxidation trends in composition of amphiboles from silica-saturated peralkaline igneous rocks; Tschermaks Mineralogische und Petrographische Metteilungen, v. 32, p. 211-222.

Taylor, R.P., Strong, D.F., and Fryer, B.J.
1981: Volatile control of contrasting trace element distributions in peralkaline granitic and volcanic rocks; Contributions to Mineralogy and Petrology, v. 77, p. 267-271.

Taylor,R.P., Strong, D.F., and Kean, B.F.
1980: The Topsails igneous complex: Silurian-Devonian peralkaline magmatism in western Newfoundland; Canadian Journal of Earth Sciences, v. 17, p. 425-439.

Thurlow, J.G.
1981: The Buchans Group: its stratigraphic and structural setting; Geological Association of Canada, Special Paper 22, p. 79-90.

Whalen, J.B., Currie, K.L., and others
1983: Geology of the Topsails Igneous Terrane, Western Newfoundland; Geological Survey of Canada, Open File 923 (map).

Geology of the Harbour Breton Complex, Newfoundland

Project 730044 and Contract 14SQ.23233-5-0076

D.J. Furey [1] and D.F. Strong [1]
Precambrian Geology Division

Furey, D.J. and Strong, D.F., Geology of the Harbour Breton Complex, Newfoundland; in Current Research, Part A, Geological Survey of Canada, Paper 86-1A, p. 461-464, 1986.

Abstract

The Devonian Harbour Breton Complex comprises two granitoid plutons which intrude late Precambrian to Devonian volcanic and sedimentary rocks in the Avalon Zone of southern Newfoundland. Both plutons are elongated in a northeasterly direction, with the Main Stock about 30 km long and 6 km wide and the Old Woman Stock about 12 km long by 6 km wide. Both are zoned from an outer contact zone of miarolitic biotite-hornblende-bearing microgranite passing inward through alkali feldspar granite, medium grained biotite-hornblende granite, plagioclase-phyric monzogranite to a core of K-feldspar-phyric granite and microgranite. A number of Mo-Cu-F showings are found along the eastern margins of the Old Woman Stock.

Résumé

Le complexe dévonien de Harbour Breton est constitué de deux plutons granitoïdes qui font intrusion dans des roches volcaniques et sédimentaires de la fin du Précambrien et du Dévonien, dans la zone d'Avalon, dans le sud de Terre-Neuve. Les deux plutons s'allongent en direction nord-est, le stock Main mesurant environ 30 km de longueur sur 6 km de largeur, et le stock Old Woman, environ 12 km de longueur sur 6 km de largeur. Les deux sont bordés par une zone de métamorphisme de contact constituée de microgranite miarolitique à biotite et hornblende, qui passe successivement à travers un granite feldspathique alcalin, un granite à biotite-hornblende à grains moyens, un monzogranite à plagioclase et porphyre, pour finalement atteindre un noyau constitué de granite et de microgranite à K-feldspath-porphyre. Un certain nombre de minéralizations de Mo-Cu-F se rencontrent sur la bordure est du stock Old Woman.

[1] Department of Earth Sciences, Memorial University of Newfoundland, St. John's, Newfoundland A1B 3X5

Introduction

The Harbour Breton Complex forms part of a mid-Paleozoic postorogenic suite of granitoid intrusions in the Fortune Bay area of southern Newfoundland. The term complex is used here because the former term (Harbour Breton Granite) does not convey the fact that there are two separate intrusive bodies and that there are a number of rock types which are not strictly granitic. The two plutons are here termed the Main Stock and the Old Woman Stock, and their main lithological characteristics are shown in Figure 55.1. Six bodies of about 1 km^2 have been recognized outside the complex to the west of the Main Stock in the Harbour Breton area.

Both plutons are elongated in a northeasterly direction. The Old Woman Stock occupies a roughly elliptical area about 12 km long and 6 km wide, while the Main Stock has the same width but is about 30 km long. They intrude metapelites and hornfelses of the Precambrian-Cambrian Chappel Island Formation and quartz-pebble conglomerates, sandstones and pelites of the Devonian Pools Cove Formation. The Old Woman Stock is in fault contact with foliated granitoid rocks of the Precambrian Simmons Brook Batholith and the Devonian Cinq Isles Formation. The Main Stock intrudes the Simmons Brook Batholith.

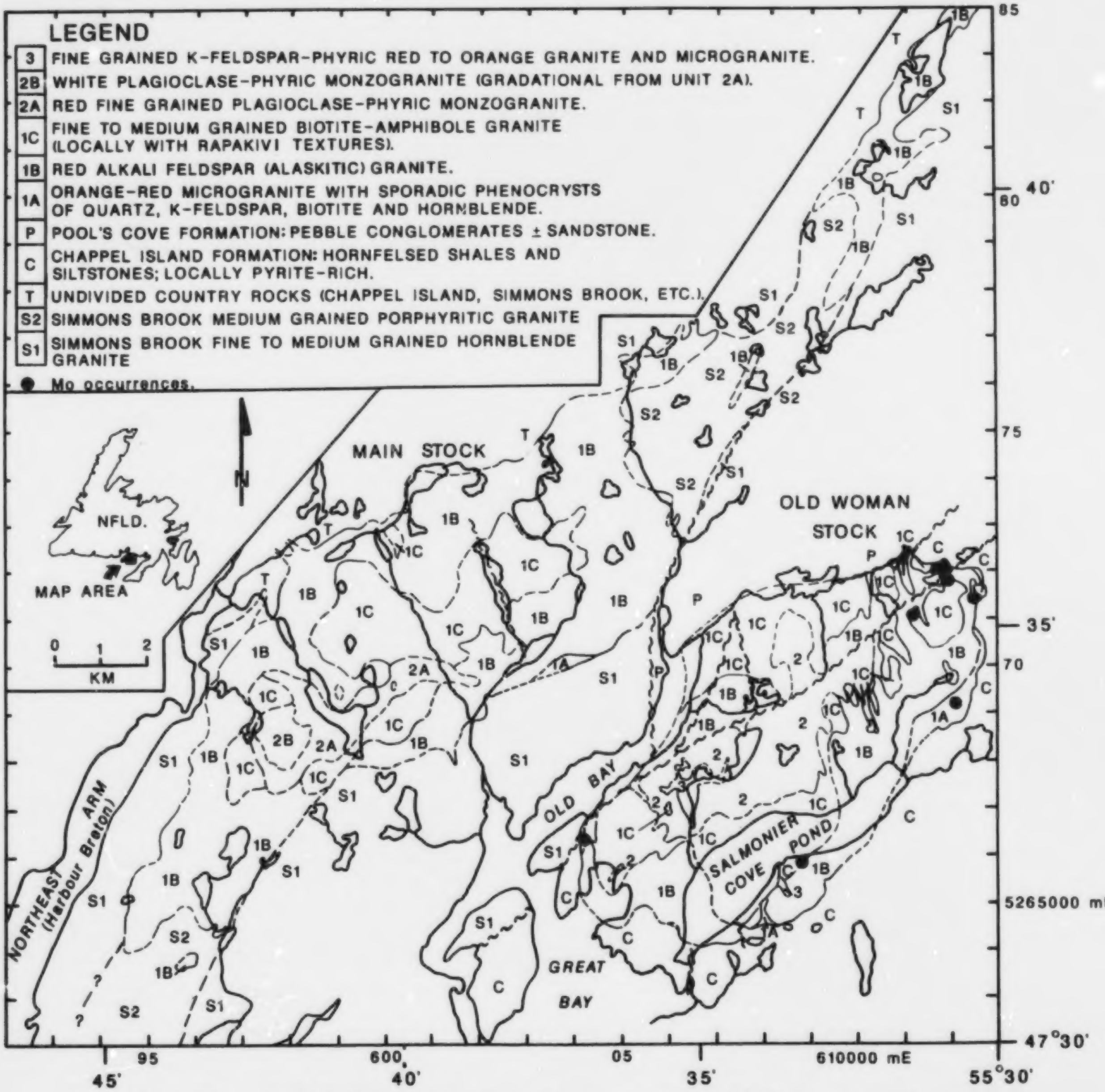

Figure 55.1. Simplified geological map of the Main Stock and Old Woman Stock of the Harbour Breton Complex, southern Newfoundland.

Lithological description of the stocks

Although they can be subdivided in more detail, based mainly on variations in the relative proportions of K-feldspar and plagioclase, both stocks can be seen in Figure 55.1 to consist of a number of roughly concentric zones. The outermost zone (unit 1) comprises a border/contact phase (unit 1A), followed inward by an extensive zone of medium grained alkali feldspar to adamellitic granite (unit 1B), fine- to medium-grained granite (unit 1C), red fine grained plagioclase-phyric monzogranite (unit 2A) transitional into white plagioclase-phyric monzogranite (unit 2B), and a core of fine grained K-feldspar-phyric red-orange granite and microgranite (unit 3).

Unit 1A consists of an alkali-feldspar granite (alaskite) which locally loses its granitic texture to appear as a microgranite with quartz, K-feldspar, biotite and rare hornblende phenocrysts. The constant order of distribution of these phenocrysts is quartz adjacent to contacts, giving way inwards to K-feldspar, followed by hornblende and biotite with rare plagioclase. The biotite may occur in patches or schlieren, and appears to be inversely proportional in abundance to hornblende. Plagioclase is rare, and its presence in unit 1C distinguishes it from unit 1B. Miarolitic cavities are common, lined by crystals of quartz, K-feldspar and amphibole, with local occurrences of zeolites. These cavities disappear inwards from the intrusive contacts.

Unit 1A is generally marked by zones of bleaching up to 50 m^2 with associated quartz veins, clay minerals, epidote, and molybdenite. The Chappel Island Formation typically contains disseminated pyrite near the contact. Unit 1A is almost completely lacking in the Main Stock, seen only at the contact northwest of Old Bay (Fig. 55.1). The boundaries between units 1A and 1B are locally sharp but generally gradational. In transition zones, where the distinction is somewhat vague, there are sporadic occurrences of pink K-feldspar with rapakivi texture.

Unit 1B consists of red alaskitic alkali feldspar granite which is divisible into four subtypes. Subtype 1 contains phenocrysts of quartz, K-feldspar and biotite in orange-red alaskite gradational from unit 1A. In the Old Woman Stock it is found mainly in valleys separating ridges of unit 1C, and shows some evidence of resulting from K-metasomatism along major joints. In the Main Stock it outcrops as high plateaus separated by river valleys and lowlands. It is readily recognized in the field by a distinctive joint pattern striking 170-180°, with no crosscutting joints. In subtype 2 hornblende is seen instead of biotite phenocrysts along the north contact of the Main Stock where it is deep red. A rare subtype 3 contains phenocrysts of only hornblende and K-feldspar along the north and eastern contacts of the Main Stock. Only one small outcrop of subtype 4 was observed, near the western end of the Main Stock. It has phenocrysts of only K-feldspar and is characterized by up to 20% pyrite. There does not appear to be any gradation between these subtypes, i.e. no occurrence of all four phenocryst phases together.

Unit 1C is fine- to medium- (locally coarse) grained pink to white granite gradational from unit 1B. Unlike units 1A and 1B, it does not contain any miarolitic cavities. It has up to 85% exposure, as pavements and at the tops of hills in the Old Woman Stock while in the Main Stock it is found on plateaus with the alaskite. It exhibits normal jointing in three directions. It contains 5-10% biotite and less than 1% amphibole. Plagioclase is typically altered to clay minerals.

Unit 2 consists of grey-purple saccharoidal granite with white-red plagioclase phenocrysts. The intrusive contact is well exposed near the tops of hills, e.g. between Long Pond and Red Cove, north of Salmonier Cove Pond. The contacts are sharp, with a chilled margin of approximately 10 cm, while the intruded unit 1 may be "alaskitized". Unit 2 is generally homogeneous, but in the Main Stock it can be divided into subunits 2A and 2B, red and white respectively. There is a gradation from 2A to 2B towards the centre of each stock, accompanied by an increase in grain size such that the plagioclase phenocrysts are not differentiated from the coarser matrix. Because subunits 2A and 2B show a comparable evolution to that of units 1A and 1B, it may be that their analogous development reflects second intrusions from similar magma chambers.

In the core of the Old Woman Stock unit 2 is cut by unit 3, a red-orange K-feldspar-phyric granite and microgranite. It is also found in a small outcrop just to the south of Salmonier Cove Pond. Unit 3 resembles unit 2 for which it may be mistaken if the contacts are not evident. Such contacts have been observed for those units identified as unit 3 on Figure 55.1 where they are sharp with a narrow chill zone less than 2 m wide. The northern part of unit 3 is a collection of 2-5 m wide dykes intruding unit 2B. Unit 3 is fractured and well jointed such that it outcrops as small hills surrounded by piles of rubble. Unit 3 has been correlated with local microgranite dykes which may extend outward from it through unit 1.

Diabase dykes

Diabase dykes are oriented NNE in the Old Woman Stock and NE to ENE in the Main Stock. Along Old Bay Stream, the K-feldspar-phyric megacrystic granite of the Main Stock is cut by a mafic dyke swarm of at least 3 generations. The first generation is invariably oriented ENE, is fine grained and generally contains aligned plagioclase crystals in the cores of dykes less than 1 m wide. A similar second generation cuts the first and appears to meander through the granite. The third generation is diabasic, aphanitic and grey black as opposed to greenish. These dykes occur either along the margins of the earlier generated dykes or in N-S fractures. Diabase dykes in both stocks are generally about 0.5 m or less wide, with sharp contacts with the granite. Those in the Main Stock typically host centimetre-sized pyrite crystals but they are rare in the Old Woman Stock.

Quartz veins

The western half of the Main Stock is host to ENE-trending quartz and quartz-K-feldspar veins which range from <2 to 50 cm in width and are traceable in outcrop for up to 200-300 m. They are generally spaced at 200 to 300 m. The quartz may be white to clear, fine grained at contacts with the granite but coarse in the vein centres. Pink K-feldspars may be seen in some veins and in some parts of a single vein. These veins are younger than and cut the diabase dykes. Similar veins are not as common but they are present throughout the rest of the Main Stock. In the Old Woman Stock they are most common in the areas of Mo mineralization along the eastern margin.

Structures

The axes of plutons and all phases and subdivisions are oriented northeasterly, which is taken to reflect a regional NW-SE compressional stress during intrusion, since neither stock shows any evidence of deformation to explain these orientations. The Chappel Island Formation is locally folded into tight isoclinal and recumbent folds to the south of the Old Woman Stock, with a resulting NE-striking cleavage. These structures are cut by the intrusive contacts.

Units 1, 2, and 3 are cut by NW-trending faults which have been cut by major ENE-trending faults. These faults are marked by a number of features.

1. Sheared hydrothermally-generated alaskite in deep valleys separating different blocks of granite.
2. Blocks of alaskite, such as that between Red Cove and Salmonier Cove Pond, which do not correspond to the intrusive scheme.
3. Minor displacements on the ENE-trending faults.
4. 5 to 15 m wide alternating bands of granite and albitized granite which suggest a zone of shearing and faulting.

All major structural blocks are well defined by these faults. The major WSW-ENE fault which extends from the NE corner of the Old Woman Stock to Old Bay bounds much of unit 2 and may have exerted some control on its intrusion. The faults appear to have been pre-diabase dykes and quartz veins, and appear to have exerted some control on mineralizing fluids. Joint patterns are generally consistent at 020, 080, 120, 170-180° and are steeply dipping. The latter orientation seems to be representative of the alaskite of unit 1. Local changes in joint patterns define faults in some alaskite blocks.

Mineralization

There are two kinds of mineralization associated with the Old Woman Stock, quartz-fluorite-molybdenite ± bornite ± pyrite, and pyrite within the contact zone. Pyrite occurs as small crystals and blebs/pods within the hornfels where the microgranite chill zone (unit 1A) is developed within the pluton. Where this zone is absent, and the alaskite is in contact with hornfels, the pyrite occurs in the alaskite. The F-Mo-Cu mineralization is associated with quartz veins, generally 2-10 cm wide, which may be traced for up to 5 m after which the veins appear to be unmineralized. At one locality within a gravel pit, four 8-10 cm wide quartz-fluorite-bornite veins occur with a 2-3 cm spacing. Similar but much less abundant mineralization is associated with the Main Stock.

Discussion

Detailed petrographic and chemical studies are necessary to provide explanation for the variations in composition, textures and colours which outline the concentric pattern of zonation seen in Figure 55.1. The fact that the same patterns are repeated in both stocks implies that they have a similar history, i.e. that they were both produced from the same magma chamber at the same time. The sequence of intrusion from granitic to monzonitic compositions may indicate that both stocks arose from progressively deeper levels within a larger magma chamber which was zoned with decreasing silica contents downwards. If the nearby Belleoram Pluton (Furey, 1985) was derived from the same magma chamber, its abundant mafic xenoliths and enclaves and even lower silica contents may indicate that it came from even deeper levels. Although no chemical data are yet available, it appears that the Mo-Cu-F mineralization is related to the highest silica rocks of the plutons, as would be expected for such a zoned magma chamber.

Acknowledgments

We are grateful to Kevin Hartley for field assistance and Larry Nolan for drafting of Figure 55.1. The study was funded by a contract between the Geological Survey of Canada and Canewf Resources Ltd., and partly by Operating Grant No. A7975 to D.F. Strong from the Natural Sciences and Engineering Research Council of Canada.

Reference

Furey, D.J.
1985: Geology of the Belleoram Pluton, southeast Newfoundland; in Current Research, Part A, Geological Survey of Canada, Paper 85-1A, p. 151-156.

The volcano-plutonic King's Point complex, Newfoundland

Project 730044 and Contract 14SQ.23233-5-0076

D.J. Kontak[1] and D.F. Strong[1]
Precambrian Geology Division

Kontak, D.J. and Strong, D.F., The volcano-plutonic King's Point Complex, Newfoundland; in Current Research, Part A, Geological Survey of Canada, Paper 86-1A, p. 465-470, 1986.

Abstract

The Silurian King's Point Complex represents part of an extensive suite of postorogenic, metaluminous to peralkaline granitoid and volcanic rocks in western Newfoundland. The complex evolved as a volcano-plutonic structure, now represented by a central granite-syenite intrusion enveloped by intrusive and extrusive rhyolite porphyries, all cut by abundant mafic dykes. The presence of an arcuate ring dyke, vent structures, and a variety of pyroclastic volcanic deposits suggest a cauldron subsidence origin for the complex. Petrological data indicate that magma-mixing processes were important in the petrogenesis of the granite-syenite suite. This involved both felsic and mafic liquids, represented now by the rhyolite porphyries and mafic dyke rocks, respectively. Extensive, postmagmatic fluid-rock interaction modified the primary mineralogy and chemistry of the igneous rocks to a peralkaline assemblage. This is represented by the presence of conspicuous riebeckite oikocrysts in the rhyolite porphyry units.

Résumé

Le complexe silurien de King's Point représente une partie d'une suite étendue de roches granitoïdes et volcaniques postorogéniques de composition métalumineuse à peralcaline, dans l'ouest de Terre-Neuve. Le complexe a évolué en une structure volcano-plutonique, maintenant représentée par une intrusion centrale de granite-syénite enveloppée par des porphyres rhyolitiques intrusifs et extrusifs, tous recoupés par d'abondants dykes mafiques. La présence d'un dyke annulaire arqué, d'évents et de divers dépôts volcaniques pyroclastiques donne à penser que ce complexe serait le résultat d'une subsidence annulaire. Les données pétrologiques indiquent que des processus de mélange de magmas ont joué un rôle important dans la pétrogenèse de la suite de granite-syénite. Y ont participé notamment des liquides felsiques et mafiques, représentés aujourd'hui par les porphyres rhyolitiques et les dykes mafiques respectivement. L'interaction postmagmatique des fluides et des roches, sur une grande échelle, a modifié la minéralogie et la chimie primaires des roches ignées, donnant un assemblage peralcalin, comme en fait foi la présence de cristaux poecilitiques de riébeckite bien visibles dans les unités de porphyre ryolitique.

[1] Department of Earth Sciences, Memorial University of Newfoundland, St. John's, Newfoundland A1B 3X5

Introduction

The King's Point Complex (Mercer et al., 1985) represents part of an extensive suite of metaluminous to peralkaline silicic granitoid and volcanic rocks in western Newfoundland (Fig. 56.1). This suite of rocks occurs near the structural boundary of the ancient continental margin of eastern North America and the Iapetus Ocean, represented today by the Humber and Dunnage zones, respectively, of Williams (1978, 1979). Neale et al. (1960), Neale and Nash (1963), and Neale (1962) first documented the extent of this postorogenic igneous suite, but its regional tectonic significance has only recently been discussed (Taylor, 1979). More recently the petrological features of correlative rocks in the Topsails Complex have been the subject of several studies (e.g. Taylor et al., 1980, 1981; Strong and Taylor, 1984; Whalen and Currie, 1984), which have focused on the extensive postmagmatic peralkaline metasomatism and the importance of magma mixing in the petrogenesis of this suite. This investigation represents a continuation of the field studies reported by Mercer et al. (1985), which are part of a larger scale study of postorogenic magmatism by Strong and co-workers at Memorial University of Newfoundland (e.g. Coyle et al., 1985, 1986; Coyle and Strong, 1986; Furey, 1985).

The term King's Point Complex was first introduced by Mercer et al. (1985) to include a large area of silicic plutonic rocks and their overlying volcanic equivalents which occupy an area of ca. 350 km^2 in the central part of the Baie Verte Peninsula. It occupies a large part of the King's Point map sheet (NTS 12 H/9) and the southern part of the Baie Verte map sheet (NTS 12 H/16). Possible correlative units are the La Scie Granite and Cape St. John Group (DeGrace et al., 1976) to the north, and the Topsails Complex (Whalen and Currie, 1983) and Sheffield Lake group (Coyle et al., 1986) to the south (see Fig. 56.1 inset).

This paper presents the results of two months of 1:12 500 scale geological mapping, conducted during July and August, 1984, around the northern half of the King's Point Complex (Fig. 56.1). This work complements the previous mapping of Mercer et al. (1985) in the southern part of the complex.

Extensive commercial logging operations and a recent (July-August, 1984) forest fire have considerably improved the access and exposure in the area. As a consequence of this and the detailed mapping scale numerous changes were made to the earlier map of Neale et al. (1960; reproduced in Hibbard, 1983), although the general features of the complex have remained unchanged.

The Burlington Granodiorite, for which a preferred age of 460-465 Ma has been assigned by Hibbard (1983), forms the local basement rock. The King's Point Complex itself remains undated, although a Middle to Late Silurian age has been assigned on the basis of apparent ages of 404 ± 25 Ma to 435 ± 14 Ma for units of presumed equivalent age (see Mercer et al. (1985) for a review).

Map units

Seven lithologies, some of which are further divided into additional subunits, have been recognized in the area, but only five are indicated in Figure 56.1. The sixth and seventh, represented by felsic and mafic dykes, respectively, are too small and localized to portray at this scale, but their field characteristics and distribution are discussed below.

Unit 1 - Burlington Granodiorite

The Burlington Granodiorite underlies the northern and western parts of the area, occupying the topographically low-lying regions. It is a medium- to coarse-grained, hornblende-, hornblende-biotite, or biotite granodiorite (nomenclature of Streckeisen, 1976, is used throughout), with lesser amounts of two-mica granite, leucogranite and pegmatitic segregations. The rock is variably altered with chlorite replacing the mafic minerals and plagioclase saussuritized. A penetrative S-fabric may be locally developed with associated shear zones, both with orientations of 055-075°.

More mafic varieties of this lithology occur just east of Burlington where Epstein (1983) has mapped diorites. We note also that in the northernmost portion of the map area, just south of the ring dyke, the granodiorite contains abundant mafic and ultramafic inclusions which record high grade metamorphic assemblages and intense deformation. These inclusions were probably derived at depth from Pacquet Harbour Group equivalent lithologies, the main outcrop of this unit being immediately north of the map area (Hibbard, 1983).

Unit 2 - porphyritic syenite

The porphyritic syenite occupies the central part of the area, forming several prominent topographic highs, with some smaller plugs of the same lithology around this central intrusion. The unit is quite heterogeneous, although no attempt was made to subdivide it.

The rock is generally a coarse grained, red to greenish-red, K-feldspar megacrystic (<3-4 cm; up to 30%) syenite, alkali syenite, alkali granite or syenogranite depending on the modal proportion of quartz (<1 cm; up to 20%). There appears to be a gradational relationship between increasing quartz content and proximity of the quartz-feldspar porphyry (unit 5) which envelopes the syenite (Fig. 56.1). Due to this phenomenon it was difficult at times to actually map a definitive boundary between the syenitic and rhyolitic units and, instead, we refer to the contact more appropriately as a transition zone. It may vary in width from a few metres to tens of metres, although in some cases the syenite has a chilled margin against the rhyolite.

The syenite contains variable amounts (0-5%) of dark green matrix amphibole which has an inverse relationship with the amount of quartz. This unit is also characterized by rounded to subrounded mafic inclusions from 0.5 cm to several metres across. Dark patches of partially assimilated material are interpreted as vestiges of mafic liquid (cf. Whalen and Currie, 1984). There appears to be an increase in the proportion of the mafic inclusions and dark patches towards the southern part of the large intrusion. It may be significant that this area is characterized by a higher frequency of mafic dyke rocks (see below) compared to the northern half of the intrusion.

The smaller plugs of syenite are similar to the larger intrusion, although they are more silicic with alkali granite and alkali syenite the dominant lithologies.

Unit 3 - equigranular alkali syenite

The equigranular alkali syenite contrasts with unit 2 by having an equigranular, medium grained texture and absence of mafic inclusions. The unit is restricted to the southeast part of the map area and its relationship to the porphyritic syenite remains unresolved at present.

The syenite shows a systematic compositional change in a vertical dimension commencing on the shores of Middle Arm and progressing northwards (up section) towards its contact with the overlying rhyolite porphyry, a distance of approximately 2 km. At its apparent base, the syenite is barren of quartz and contains a few miarolitic cavities, however, towards the top of this intrusion quartz consistently increases and miarolitic cavities are more abundant. Near its top the unit is rich enough in quartz to be called an

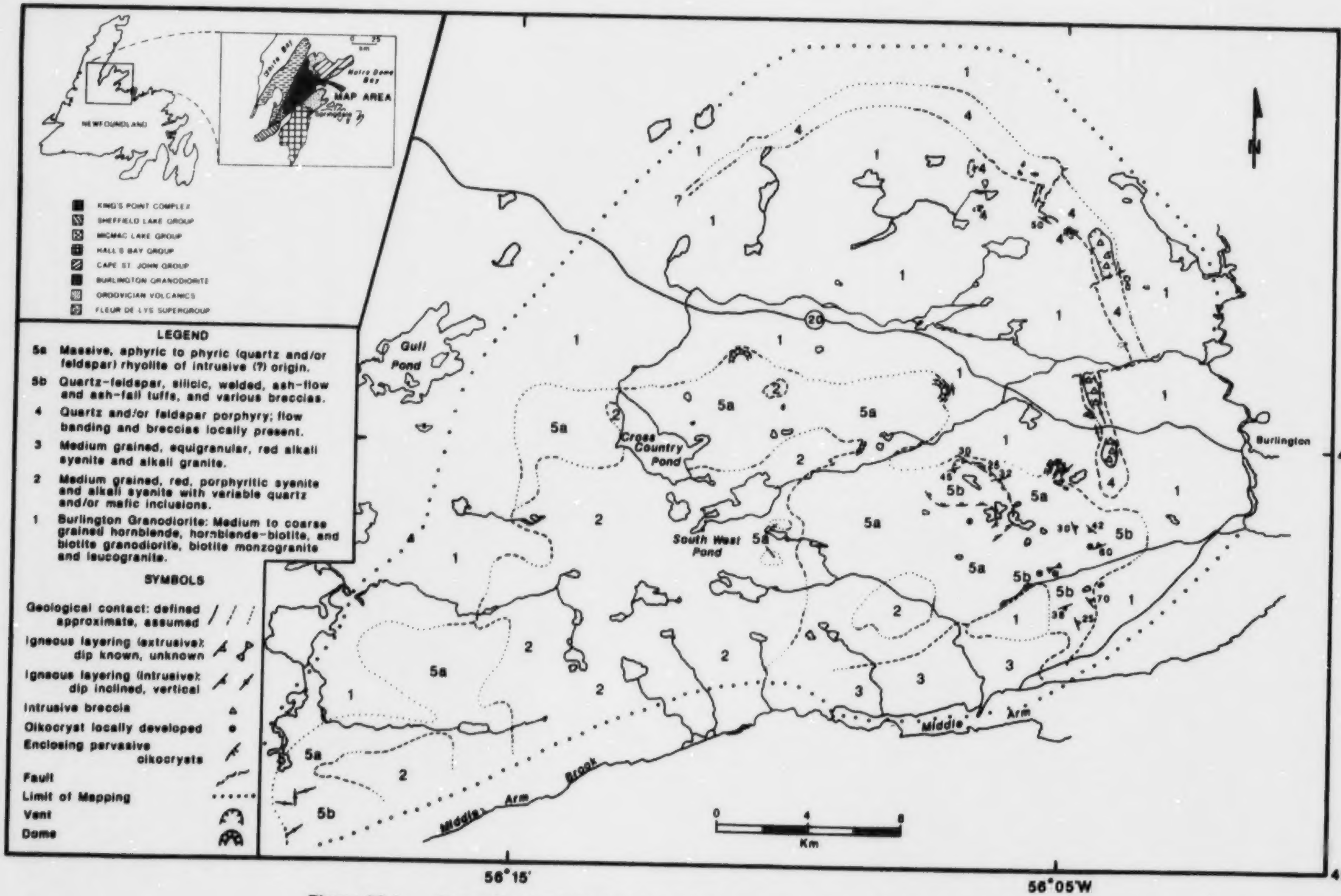

Figure 56.1. *Generalized lithological map of the northern part of the King's Point Complex.*

alkali granite. The unit contains minor amounts (<1%) of a chloritized mafic mineral, and pyrite locally occurs disseminated throughout. Miarolitic cavities are lined with an assemblage of quartz-pyrite-chlorite and fluorite was observed at one locality.

Unit 4 - intrusive rhyolite porphyry

An intrusive rhyolite porphyry unit forms an arcuate "ring dyke" which delineates the northern extent of the King's Point Complex. Mapping has somewhat modified the shape and extent of this unit (cf. Neale et al., 1960; Hibbard, 1983) and we have documented its southerly extension across the Burlington road (highway 20). Although faults are indicated, these are interpreted to have been active prior to emplacement of the ring dyke and to have controlled the locus of intrusion(s). There is no field evidence in the form of breccias or fault gouges to support post-emplacement offsets. In fact, at one locality a chilled margin with flow banding oriented perpendicular to the trend of the ring dyke (see Fig. 56.1) was observed.

The ring dyke forms a prominent topographic expression except along its northern and southwestern extensions where the lack of outcrop precludes extending the structure. We are thus not sure whether it pinches out here or continues farther (cf. Neale et al., 1960).

The ring dyke is internally composite and although we have not attempted to map individual units, areas characterized by extensive brecciation are indicated on Figure 56.1. The dyke consists of red and grey rhyolite porphyry with variable (<1 to 50%) amounts and proportions of quartz and alkali feldspar. Porphyry units may be chilled against earlier units, and where observed the intrusive margins are always chilled. Flow banding is ubiquitous, invariably convoluted, and fluidal textures are abundant near areas of brecciation. In several places one can observe an increase in fragment size and intensity of brecciation in a vertical dimension. Zones of hydrothermal alteration (pyrite ± hematite ± chlorite ± epidote ± sericite) are locally developed in such areas.

The areas of fragmentation generally consist of monolithic breccias with clasts of up to a metre across, but rare exotic xenoliths may include granodiorite and/or mafic rocks, both of which represent basement lithologies.

In one locality the ring dyke consists of syenite, similar to the quartz-rich varieties described above in unit 2. This is considered to represent a separate, small intrusion and best exemplifies the composite nature of the ring dyke.

Numerous other rhyolitic intrusions occur as dykes or, more rarely, as small, subcircular plugs cutting the granodiorite basement. They are variably porphyritic (0 to 30%) and have flow banding and chilled margins. Where they occur as dyke-like intrusions they have preferred orientations of 050-080°.

Unit 5 - intrusive/extrusive rhyolites

The most extensive unit of the King's Point Complex is represented by an intrusive/extrusive rhyolite. This lithology consists of numerous subunits, but for simplification only intrusive and extrusive members have been denoted on Figure 56.1. In the present investigation we have reserved the term extrusive for those lithologies where there exists indisputable field evidence (e.g. fiamme, pumice, bedding) indicating their origin. Using these criteria we have recognized three areas which consist of pyroclastic deposits, the remainder is presently considered to represent subvolcanic equivalents. In this context it is interesting to note that the volcanic units occur only at the perimeter of unit 5, possibly representing deposits on the flanks of a large domal structure. The upper part of this structure may also have consisted of various volcanic deposits, but subsequent erosion has removed all evidence.

The intrusive rhyolite (unit 5a) consists of massive and flow banded, aphyric to crystal (quartz and feldspar)-rich (up to 40%) lithologies. Where this unit is in contact with the porphyritic syenite (unit 2) it is noticeably coarser grained, contains larger crystals and quartz becomes the dominant phenocryst. Locally this unit may contain mafic clasts. Where the unit is in contact with the granodiorite the rhyolite is glassy, nearly aphyric (<1% crystals) and flow banding is parallel to the contact. Several small plugs exhibiting these features are indicated in Figure 56.1. We also note that inwards away from the contact there is an increase in both size and abundance of phenocrysts and the matrix is less glassy.

The extrusive rhyolites (unit 5b) consist of a variety of crystal-rich and crystal-poor ash-flow and ash-fall tuffs. In the easternmost extent of this unit there is a well preserved succession, several hundred metres thick, of volcanic breccias and welded ash-flow and ash-fall tuffs. This represents the greatest accumulation of extrusive rocks in the region mapped. In at least one area such rocks can be traced back to a possible vent which consists of very coarse (up to 1 m) autolithic breccia of dacitic to rhyodacitic composition.

In many parts of unit 5 the rocks are clearly peralkaline, marked by the abundance of fine to coarse (up to 1 cm), green to blue-green secondary amphibole similar to the riebeckite-arfvedsonite described by Strong and Taylor (1984). The megascopically conspicuous occurrences of this mineral have been indicated in Figure 56.1 and it is noted that there appears to be no obvious relationship of their distribution to any of the geological units (e.g. porphyritic syenite), although there is a concentration of the occurrences in the eastern part of the unit. Preliminary petrographic study indicates that this metasomatism is areally much more widespread, with extensive development of fine grained needles of amphibole in the matrices of most rocks, concomitant with albitization and perthitization of alkali feldspars and recrystallization of the groundmass.

Unit 6 - silicic dykes

Silicic dyke rocks cut the porphyritic syenite and equigranular syenite in a few localities. These dykes have unusual features which distinguish them from unit 4. They consist of convoluted, banded, spherulitic rhyolite-quartz-aplite-pegmatite composite dykes up to 20 m wide and 200 m long. They are oriented at 050-090°, similar to the other mafic and felsic dyke rocks in the region. In one locality mafic dykes were observed cutting this unit.

Unit 7 - mafic dykes

Numerous mafic dykes of variable length (up to 300 m) and width (<10 m) cut all the previously described units. The dykes, oriented 050-075°, invariably contain chilled margins and range from fine grained, aphyric varieties to plagioclase (up to 8-10 cm) ± pyroxene phyric (<10-15%) types. The dyke rocks are very similar to the mafic inclusions found in the porphyritic syenite unit.

In areas where exposure permits detailed mapping the dykes appear as swarms with up to a dozen parallel intrusions found within 200 m. Presumably this may be a widespread feature as indicated by the presence of isolated outcrops of this lithology over the entire map area.

Structure

There are no deformation-related structures in the King's Point lithologies, but the Burlington Granodiorite does record an earlier orogenic event (see Hibbard, 1983). These structures were important in controlling the orientation of the dyke rocks described above.

Neale et al. (1960) and Hibbard (1983) showed several large faults transecting the King's Point Complex. The results of present mapping indicated that there is no field evidence to support the presence of such faults, although we do note that in most cases they correlate with topographic and aerial photographic lineaments.

Geological relationships and development of the King's Point Complex

The field relationships documented above indicate that the King's Point Complex evolved as a volcano-plutonic complex with the initial development of a silicic volcanic carapace and subsequent emplacement of granitoid rocks, represented by the intrusive rhyolites and various syenites. The volcanic and plutonic suites are, however, not petrologically equivalent, except for the intrusive rhyolites.

Although geochemical data for this study are not yet available, we do have preliminary results for nine fine grained granites (unit 3 of this study), eleven quartz-feldspar porphyries (unit 5 of this study), and three rhyolitic dykes from the adjoining area mapped by Mercer et al. (1985). These data (Fig. 56.2) indicate that there exists a sharp geochemical distinction between the granites and other rocks. The granites are characterized by Rb contents between 150 and 200 ppm, while the porphyries all contain less than 125 ppm. The granites have much lower Nb contents than the porphyries and dykes and this is also mirrored by Y, Zr, Zn, Ga and other elements. These correlate with the peralkaline nature of the porphyries, reflected by agpaitic indices >1.00 and presence of riebeckite oikocrysts, versus the nonperalkaline nature of the granites with agpaitic indices <1.00 and modal biotite. Thus, it appears that there are at least two magmatic suites in the King's Point Complex, one peralkaline and the other metaluminous, directly analogous with those seen in the Topsails Complex to the south (Taylor et al., 1980).

We interpret the syenitic units as reflecting the mixing of two magmas, represented in the field by the intrusive/extrusive silicic rocks and mafic dykes. Although no evidence has been documented in this area for the coexistence of mafic and felsic magmas, we note that composite rhyolite-diabase dykes have been observed along the Middle Arm Ridge immediately south of the map area (Hibbard, 1983), at the western extent of the King's Point Complex (Mercer et al., 1985), and in the Topsails igneous terrane (Whalen and Currie, 1984). Coyle et al. (1985) have also observed mixed magmas within both volcanic and intrusive rocks of the Springdale Group. A magma-mixing origin for the syenites is also consistent with many of the features described above, such as the amount of modal quartz and amphibole, mafic inclusions, and contact relationships with the intrusive rhyolite unit. An obvious extension of this interpretation is that the silicic rocks represent the products of crustal fusion which resulted from injection of mafic magma into the continental crust. The widespread occurrence of mafic dykes cutting all the lithologies may also indicate that most of the area beneath the King's Point Complex was underlain by such a magma chamber of mafic composition.

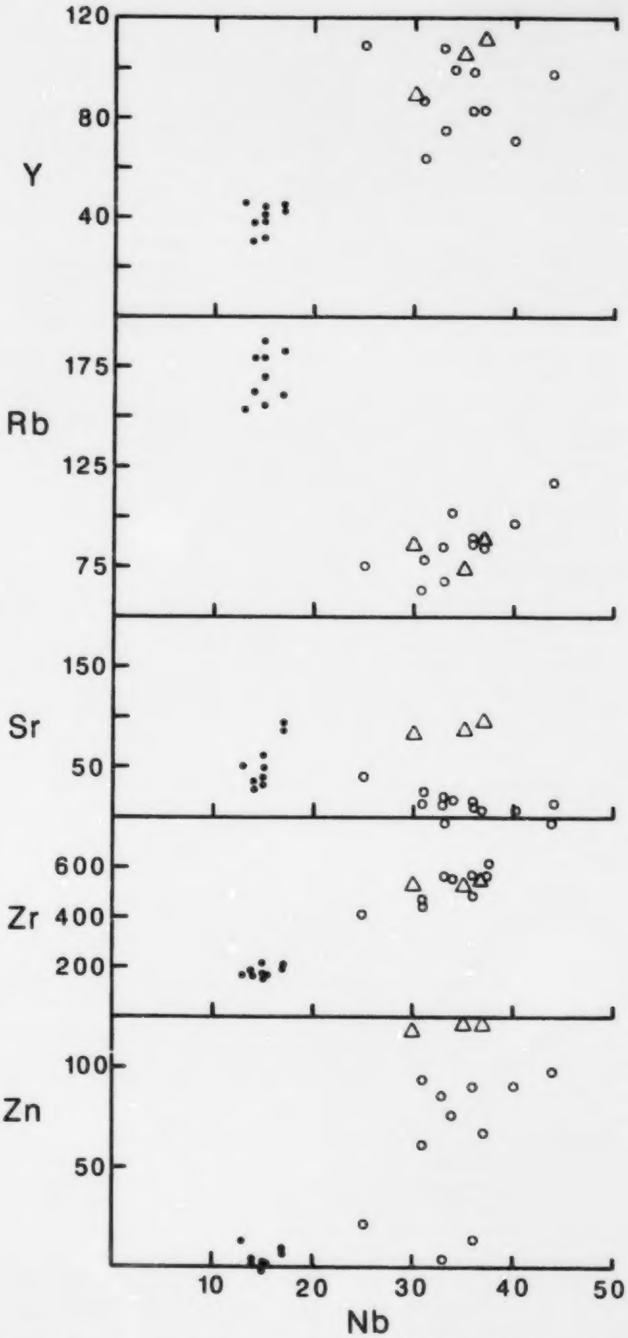

Figure 56.2. Plot of trace element data (ppm) for rocks of the King's Point Complex. Symbols are for the following rock units: fine grained granites (filled circles); quartz-feldspar porphyries (open circles); and rhyolite dykes (triangles).

Metasomatism

Although chemical data have not yet been obtained for the rocks under discussion, many of the samples appear to be peralkaline based on the presence of megascopically conspicuous sodic amphiboles. Preliminary petrographic study also reveals this to be a far more widespread phenomenon than initially suspected from observations in the field, with fine grained amphiboles present in most specimens examined. This metasomatic feature is also associated with extensive development of: (i) secondary albite (matrix and after K-feldspar), chlorite, carbonate, sphene, opaques (including pyrite) and sericite; (ii) coarse perthitic textures in alkali feldspars (cf. Parsons, 1980); and (iii) recrystallization of the matrix, and in some cases chemical corrosion of the phenocrystic phases. The development of peralkalinity as a late-stage, postmagmatic phenomenon has recently been addressed by several people (Taylor et al., 1980, 1981; Strong and Taylor, 1984), and this investigation again indicates the close spatial association between an intrusive peralkaline phase (i.e. the porphyritic syenite) and peralkaline silicic rocks. The initial petrographic studies are consistent with the ideas advanced by Strong and Taylor (1984) with the full spectrum of their magmatic and subsolidus textures present.

Acknowledgments

We are grateful to D. Taylor for capable field assistance, M. Coyle and D.B. Dingwell for discussion, and S.A. Blagdon for providing accommodation in Baie Verte. The Springdale office of the Newfoundland Department of Forestry kindly provided aerial photographs. This project was partly funded by the Geological Survey of Canada under contract (a study of postorogenic magmatism in Newfoundland) with Canewf Resources Ltd. and partly by the Natural Sciences and Engineering Research Council of Canada Operating Grant A7975.

References

Coyle, M. and Strong, D.F.
1986: Geology of the southern and northern margins of the Springdale caldera, Newfoundland; in Current Research, Part A, Geological Survey of Canada, Paper 86-1A, report 60.

Coyle, M., Strong, D.F., and Dingwell, D.B.
1986: Geology of the Sheffield Lake group, west-central Newfoundland; in Current Research, Part A, Geological Survey of Canada, Paper 86-1A, report 54.

Coyle, M., Strong, D.F., Gibbons, D., and Lambert, E.
1985: Geology of the Springdale Group, central Newfoundland; in Current Research, Part A, Geological Survey of Canada, Paper 85-1A, p. 157-163.

DeGrace, J.R., Kean, B.F., Hsu, E., and Green, T.
1976: Geology of the Nippers Harbour map area (2E/13); Newfoundland Department of Mines and Energy, Report 76-3, 73 p.

Epstein, R.S.
1983: The eastern margin of the Burlington Granodiorite, Newfoundland; unpublished M.Sc. thesis, University of Western Ontario, London, Ontario, 188 p.

Furey, D.J.
1985: Geology of the Belleoram pluton, southeast Newfoundland; in Current Research, Part A, Geological Survey of Canada, Paper 85-1A, p. 151-156.

Hibbard, J.
1983: Geology of the Baie Verte Peninsula, Newfoundland; Newfoundland Department of Mines and Energy, Memoir 2, 279 p.

Mercer, B., Strong, D.F., Wilton, D.H.C., and Gibbons, D.
1985: The King's Point Complex, western Newfoundland; in Current Research, Part A, Geological Survey of Canada, Paper 85-1A, p. 737-741.

Neale, E.R.W.
1962: King's Point area, Newfoundland; unpublished manuscript.

Neale, E.R.W. and Nash, W.A.
1963: Sandy Lake (east half), Newfoundland; Geological Survey of Canada, Paper 62-28, 40 p.

Neale, E.R.W., Nash, W.A., and Innes, G.M.
1960: King's Point, Newfoundland; Geological Survey of Canada, Map 35-1960.

Parsons, I.
1980: Alkali-feldspar and Fe-Ti oxide exsolution textures as indicators of the distribution and subsolidus effects of magmatic water in the Klokken layered syenite intrusion, south Greenland; Royal Society of Edinburgh, Transactions, Earth Sciences, v. 71, p. 1-12.

Streckeisen, A.L.
1976: To each plutonic rock its proper name; Earth Science Reviews, v. 12, p. 1-33.

Strong, D.F. and Taylor, R.P.
1984: Magmatic-subsolidus and oxidation trends in composition of amphiboles from silica-saturated peralkaline igneous rocks; Tschermaks Mineralogische und Petrographische Mitteilungen, v. 32, p. 211-222.

Taylor, R.P.
1979: Topsails igneous complex – further evidence of middle Paleozoic epeirogeny and anorogenic magmatism in the northern Appalachians; Geology, v. 7, p. 488-490.

Taylor, R.P., Strong, D.F., and Fryer, B.J.
1981: Volatile control of contrasting trace element distributions in peralkaline granitic and volcanic rocks; Contributions to Mineralogy and Petrology, v. 77, p. 267-271.

Taylor, R.P., Strong, D.F., and Kean, B.F.
1980: The Topsails igneous complex: Silurian-Devonian peralkaline magmatism in western Newfoundland; Canadian Journal of Earth Sciences, v. 17, p. 425-439.

Whalen, J.B. and Currie, K.L.
1983: The Topsails igneous terrane, western Newfoundland – 1:100 000 map and marginal notes; Geological Survey of Canada, Open File 923.

1984: The Topsails igneous terrane, western Newfoundland: evidence for magma mixing; Contributions to Mineralogy and Petrology, v. 87, p. 319-327.

Williams, H.
1978: Tectonic-lithofacies map of the Appalachian orogen; Memorial University of Newfoundland, Map 1.

1979: Appalachian Orogen in Canada; Canadian Journal of Earth Sciences, v. 16, p. 792-807.

Structural and magmatic controls on the internal geometry of the plutonic complex and its chromite occurrences in the Bay of Islands Ophiolite, Newfoundland[1]

Contract 27ST.23233-5-0247

S. Dunsworth[2], T. Calon[2], and J. Malpas[2]

Dunsworth, S., Calon, T., and Malpas, J., Structural and magmatic controls on the internal geometry of the plutonic complex and its chromite occurrences in the Bay of Islands Ophiolite, Newfoundland; in Current Research, Part A, Geological Survey of Canada, Paper 86-1B, p. 471-482, 1986.

Abstract

Detailed mapping in the Springers Hill area of the Lewis Hills Massif illustrates a complex history of synkinematic multiple intrusion and ductile deformation for the Bay of Islands Ophiolite Complex. The plutonic sequence is divided into an earlier deformed ophiolite and later synkinematic, heterogeneously deformed, ultramafic to gabbroic plutons which intrude the earlier sequence. Structural overprinting of the regional mantle tectonite fabric (S_1) by a broad, high temperature shear zone with an $L_2 \geq S_2$ mylonitic fabric is documented. Three unique types of chromite concentrations in the Springers Hill, Stowbridge and Bluff Head areas are recognized on the basis of their petrological setting and structural controls.

A simple, single, steady-state magma chamber model is inadequate to explain the evolution of the Bay of Islands plutonic complex. Our data show a complicated history of high temperature deformation and syn- to post-kinematic multiple intrusion which progressively modified the original geometry of the plutonic sequence and its chromitiferous bodies.

Résumé

Les cartes de détails établies dans la région de Springers Hill où se situe le massif Lewis Hills montrent que le complexe ophiolitique de Bay of Islands a connu une évolution compliquée, faite de multiples intrusions syntectoniques et de déformation ductiles. La séquence plutonique comprend une sous-séquence ophiolitique déformée et une sous-séquence postérieure constituée de plutons ultramafiques à gabbroïques syntectoniques, déformées de façon hétérogène, qui fait intrusion dans la première. Les auteurs montrent comment une vaste zone de cisaillement à haute température de texture (S_1) molynotique $L_2 \geq S_2$ s'est superposée à la structure tectonitique du manteau régional. On distingue trois types de concentrations de chromite dans les régions de Springers Hill, de Stowbridge et de Bluff Head, d'après des facteurs pétrologiques et structuraux.

L'évolution du complexe plutonique de Bay of Island ne saurait s'expliquer uniquement par un simple modèle de chambre magmatique à l'état stable. Les données recueillies par les auteurs mettent plutôt en évidence une série compliquée de déformations à haute température et de multiples intrusions syntectoniques et post-tectoniques qui ont peu à peu modifié la géochimie originale de la séquence plutonique et de ses massifs chromitifères.

---

[1] Contribution to the Canada-Newfoundland Mineral Development Agreement 1984-89. Project carried by Geological Survey of Canada, Economic Geology and Mineralogy Division, Project 770063.

[2] Department of Earth Sciences, Memorial University, St. John's, Newfoundland A1B 3X5

Introduction

The present study has two principal objectives. First, to map transects through the plutonic complex of the Bay of Islands Ophiolite in order to evaluate magma chamber models (eg. Casey and Karson, 1981; Casey et al., 1983), in light of new concepts regarding the effects of magmatism and ductile deformation on formation of ophiolitic complexes (Calon and Malpas, 1985; Calon, 1984; Dunsworth and Calon, 1984); and second, to evaluate structural control on the form and distribution of selected chromitiferous bodies within the plutonic sequence of the Bay of Islands Ophiolite Complex.

For the purposes of this study, three selected areas in the Bay of Islands ophiolite were mapped in detail on a 1:6250 colour airphoto base during the 1985 field season. Efforts were concentrated on a 16 km^2 area within the Springers Hill region of the Lewis Hills massif. In addition, two smaller areas (2-3 km^2) were mapped at Bluff Head, in the Lewis Hills, and at Stowbridge, on North Arm Mountain (Fig. 57.1).

The following report presents the main results of the field mapping component of the project which was carried out by S. Dunsworth, M. Warzkow and T. Calon.

Geological setting of the Bay of Islands Ophiolite

The Bay of Islands Ophiolite Complex, western Newfoundland, is exposed in four massifs. These include, from north to south; Table Mountain, North Arm Mountain, Blow Me Down Mountain and the Lewis Hills (Fig. 57.1). This north-northeast trending belt of mafic to ultramafic igneous rocks represents the remnants of a once cohesive slice of oceanic lithosphere which was obducted westward over the autochthonous Cambro-Ordovician continental margin during the Taconic Orogeny (Church and Stevens, 1971; Dewey and Bird, 1971; Williams, 1975).

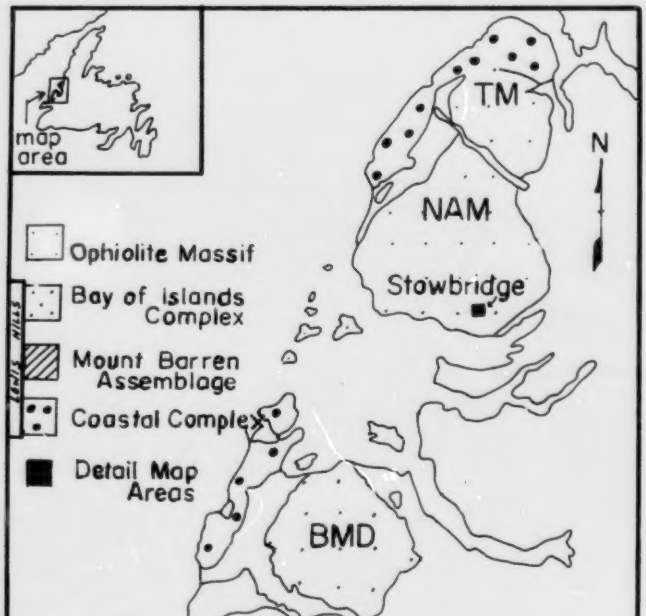

Figure 57.1. Bay of Islands region. Ophiolite Massifs; T.M. = Table Mountain, N.A.M. = North Arm Mountain, B.M.D. = Blow Me Down Mountain, L.H. = Lewis Hills.

The Lewis Hills Massif has been divided into three structural assemblages which are separated by steeply dipping, north-south trending contacts; from west to east, these assemblages include the Little Port Complex, the Mount Barren Assemblage and the Bay of Islands Complex (Karson, 1979). The two western assemblages, collectively referred to as the Coastal Complex, are thought to represent 500 Ma old (Mattison, 1975; Jacobsen and Wassenberg, 1979) oceanic crust accreted at a fossil oceanic fracture zone, near a ridge-transform intersection (Karson and Dewey, 1978; Karson, 1979; Karson et al., 1983). Deformation, amphibolite grade metamorphism and syn-to post-kinematic magmatism are concentrated within the 3 km wide Mount Barren Assemblage. The Bay of Islands Complex is interpreted to represent a cumulate sequence of younger oceanic crust and its underlying mantle peridotite accreted at an active ridge segment along the eastern margin of the Coastal Complex (Karson and Dewey, 1978).

Multiple magmatism has previously been recognized only within the Coastal Complex of the Lewis Hills Massif (Karson and Dewey, 1978; Karson et al., 1983). A number of syn- to post-kinematic intrusive bodies exhibiting two petrologically distinct peridotite suites have been documented. Karson et al. (1983) have suggested that the later intrusive suite was produced in the fossil fracture zone environment.

Magma chamber models for the formation of the Bay of Islands ophiolite have been presented by Casey and Karson (1981) and Casey et al. (1983) based upon the geometrical pattern of primary fine scale igneous layering (Fig. 57.2). The magma chamber profile for the Lewis Hills Massif as defined by Casey and Karson (1981) on the basis of the arcuate pattern of igneous layering, is orientated normal to that of the three northern massifs. This anomalous feature was interpreted by Casey et al. (1983) to represent possible pinching of the magma chamber at the intersection of the transform fault with the Coastal Complex (Fig. 57.2).

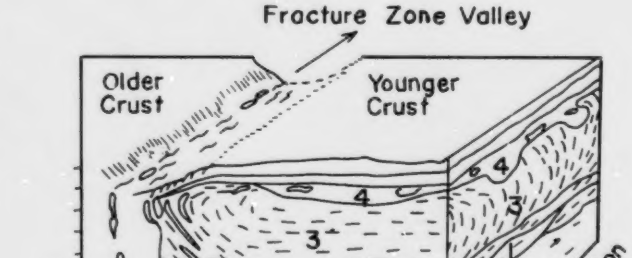

Figure 57.2. Block diagram of the magma chamber profile for the Lewis Hills Massif in which the arcuate pattern of the fine scale igneous layering is attributed to primary cumulate processed (after Casey and Karson, 1981). Symbols: H = mantle peridotite, 1 = dunite, 2 = ultramafic cumulates, 3 = layered gabbro, 4 = high level gabbro.

Springers Hill area

A generalized geological map of the Springers Hill area, covering approximately 16 km^2, is shown in Figures 57.3A and 57.3B. Only the deeper plutonic levels of the Bay of Islands ophiolite complex are exposed. These include an extensive section of polydeformed mantle peridotite tectonites in the southern to central part of the map area and variably deformed ultramafic to gabbroic cumulate sequences in the central to northern portion of the map area. The plutonic complex can be subdivided into two distinct magmatic suites. An earlier plutonic ophiolite "stratigraphy" (Penrose Conference Participants, 1972) has been intruded by later, synkinematic, heterogeneously deformed plutons. The contact between the two magmatic suites was mapped on the basis of xenolith bearing margins, truncation of structural fabrics and textural criteria. Because of the complex nature of multiple intrusion and deformation, the lithological descriptions of the two suites will be discussed first, followed by a characterization of the deformation patterns.

The early suite

The early suite consists of harzburgite, minor amounts of massive, variably chromitiferous dunite, a variety of ultramafic cumulates, layered olivine and hypersthene gabbro and massive gabbroic rocks with minor amounts of trondhjemite. Diabase dykes intrude both the layered ultramafic and mafic cumulates.

Harzburgite, representing the mantle component of the ophiolite, is characterized by a strong S_1 or L_1-S_1 fabric defined by the preferred dimensional orientation of elongate orthopyroxene and rare chromite grains. The harzburgite has been intruded by swarms of discontinuous dunite dykes, which usually range from a few centimetres to more than 3 m in width and are traceable along strike for up to 8 m. Because of the apparent lack of continuity to individual dykes, they are referred to here as "dykelets". The dunite dykelet orientations are dominantly oblique, but also parallel and highly discordant, to the harzburgite foliation. Synkinematic multiple intrusion of the dunite dykelets is indicated by the truncation of folded dykelets by younger, variable deformed dykelets. Regions which contain up to 65 volume per cent of discontinuous dunite dykelets exhibit an overall layered and interleaved appearance (Fig. 57.6A). The proportion of chromitiferous dunite dykelets hosted by harzburgite increases southward, and reaches a maximum in the main Springers Hill chromite showing. Mapping of zones with major dykelet concentrations delineated the form surface trace of a fold structure which, on the basis of orientation data for the dykelets, is interpreted as a synform (see Structure). A distinct absence of large bodies of massive, early suite dunite, either within or bordering the harzburgite, is noted for the area.

The nature of contacts between harzburgite and the ultramafic cumulate lithologies in the northern map area is unclear. Transposed interlayering of large (250 m x 75 m) boudinaged blocks of ultramafic cumulates occur within the northeastern exposure of the harzburgite tectonites at Carol Mountain (Fig. 57.3A). A large scale, low angle fault of unknown displacement has obliterated the exact nature of the transition to the overlying layered gabbro cumulates in the east. However, orientation of transposed primary layering and both planar and linear structural elements in the layered gabbro cumulates are concordant with those of the underlying ultramafic cumulates and harzburgite. Towards the northwestern part of the map area, harzburgite tectonite occurs infolded with the ultramafic to mafic cumulate units.

The ultramafic cumulates include wehrlite, troctolite, pyroxenite and pyroxene and/or hornblende flaser gabbro. All are characterized by a strong, $L_2 \geq S_2$ fabric, resulting in a rodded appearance of mineral aggregates in the foliation plane. Primary igneous layering is transposed into the foliation plane (Fig. 57.6B). Strain partitioning in the ultramafic cumulates is extremely heterogeneous resulting in the development of mylonite zones with strong planar/linear fabrics. These mylonites contain rotated pyroxene and hornblende porphyroclasts, and envelope variably sized boudins which exhibit complex fold patterns in their necks (Fig. 57.6C, 57.6D).

Within the Carol Mountain and northwestern map areas, the medium-fine grained layered olivine-hypersthene gabbros also show the strong $L_2 > S_2$ fabric. This fabric is defined by stretched and flattened mineral aggregates, as well as rotation of the primary cumulate layering to an orientation parallel to the regional S_2 fabric. Isoclinal folds with an axial planar foliation were frequently observed in the layered gabbro (Fig. 57.6E).

Diabase dykes are spatially associated with the early suite and intrude both layered gabbro with interlayered ultramafic zones, and more massive pyroxene gabbro. These syn- to post-kinematic, fine grained dykes range from 4 to 35 cm in width, outcropping for up to 10 m along strike.

The later suite

The later suite outcrops as massive bodies within the central, northeastern and northwestern parts of the map area and as two small exposures within harzburgite to the south (Fig. 57.3A).

The plutons show a wide range in modal composition, from chromitiferous dunite (<10% spinel), feldspathic dunite and feldspathic wehrlite to clinopyroxenite and lesser amounts of pyroxene and olivine-pyroxene gabbro. Faint traces of layering with variable orientations occur in isolated regions of the plutons. Grain size is highly variable and textures are commonly poikilitic with clinopyroxene oikocrysts ranging up to 4 cm in diameter. Pegmatitic wehrlite, pyroxenite and gabbroic dykes cut the plutons internally and show mutually crosscutting relationships. These dykes also intrude the harzburgite country rock, mainly along the northern and eastern margins of the central pluton. The close spatial association of the various rock types within the plutons as well as some compositional grading suggest that crystal fractionation processes yielded the lithogical variations.

The rocks of the later plutons are generally massive and structurally isotropic with intense $L_2 > S_2$ shear zones (Fig. 57.6F) that are randomly developed and occur predominantly along the northern and eastern margins of the central pluton. These shear zones range from a few centimetres to over 3 m in width and are traceable up to 15 m along strike. The concordance of the lineation trend of the later suite shear zones with the regional linear L_2 trend of the host rock demonstrates the ongoing nature of synkinematic intrusion during deformation (D_2) of the early suite.

A gradual transition from undeformed, poikilitic wehrlite of the late suite to a highly deformed facies, which is indistinguishable from the early suite, is exposed near Carol Mountain. In areas such as this, where continued ductile deformation has led to the progressive obliteration of criteria, such as truncated fabrics, xenolithic margins (Fig. 57.6G) and textural characteristics, used to distinguish multiple intrusion within the plutonic complex, the recognition of intrusive contacts may be very difficult.

Difficulties also arise in assigning the numerous pods and dykes of orthopyroxenite and clinopyroxenite, which syn- and post-kinematically intrude the early suite harzburgite, to a particular suite on the base of field criteria. They are provisionally interpreted to represent later phases of the early suite pending completion of geochemical work.

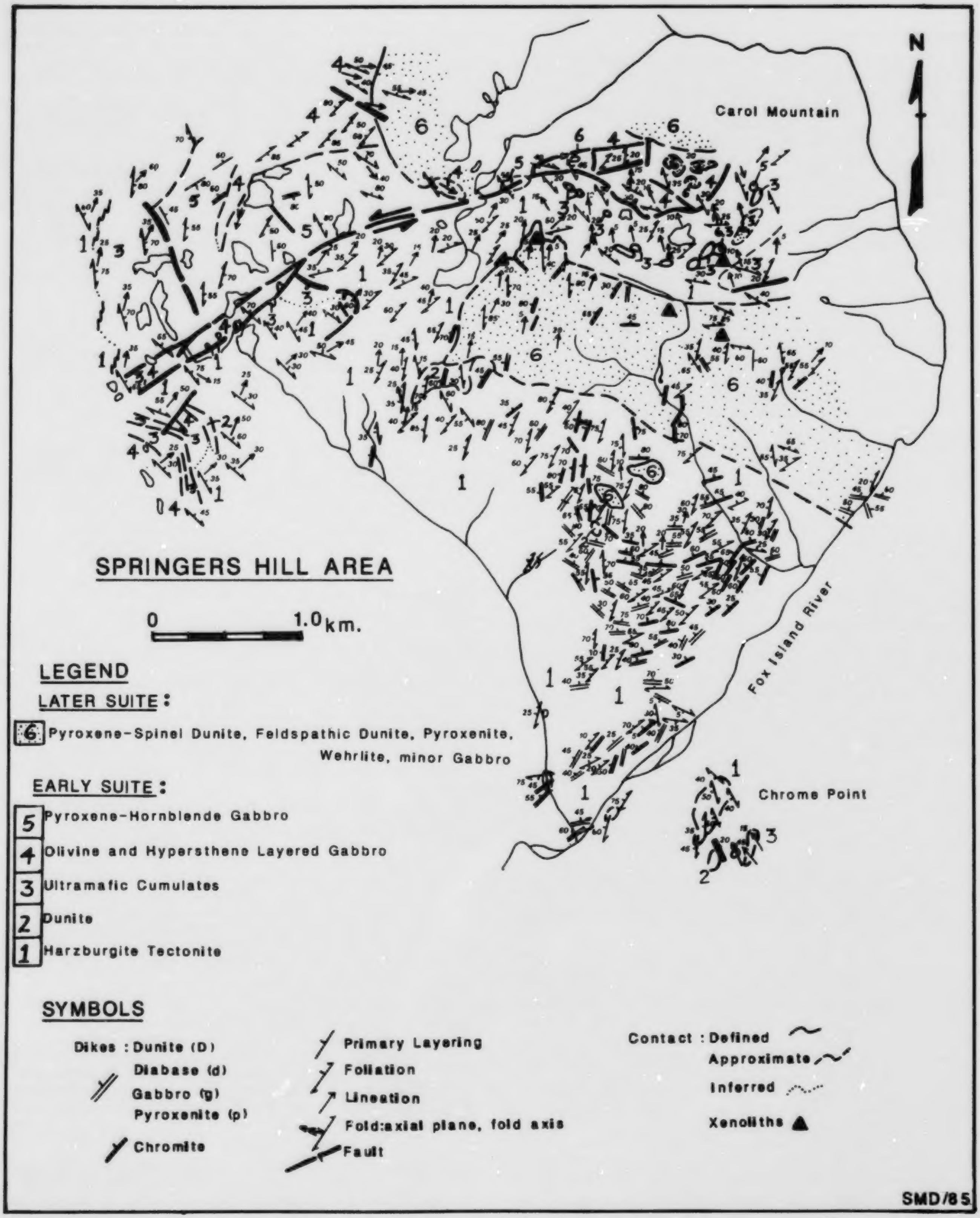

Figure 57.3A. *Springers Hill area showing main structural elements.*

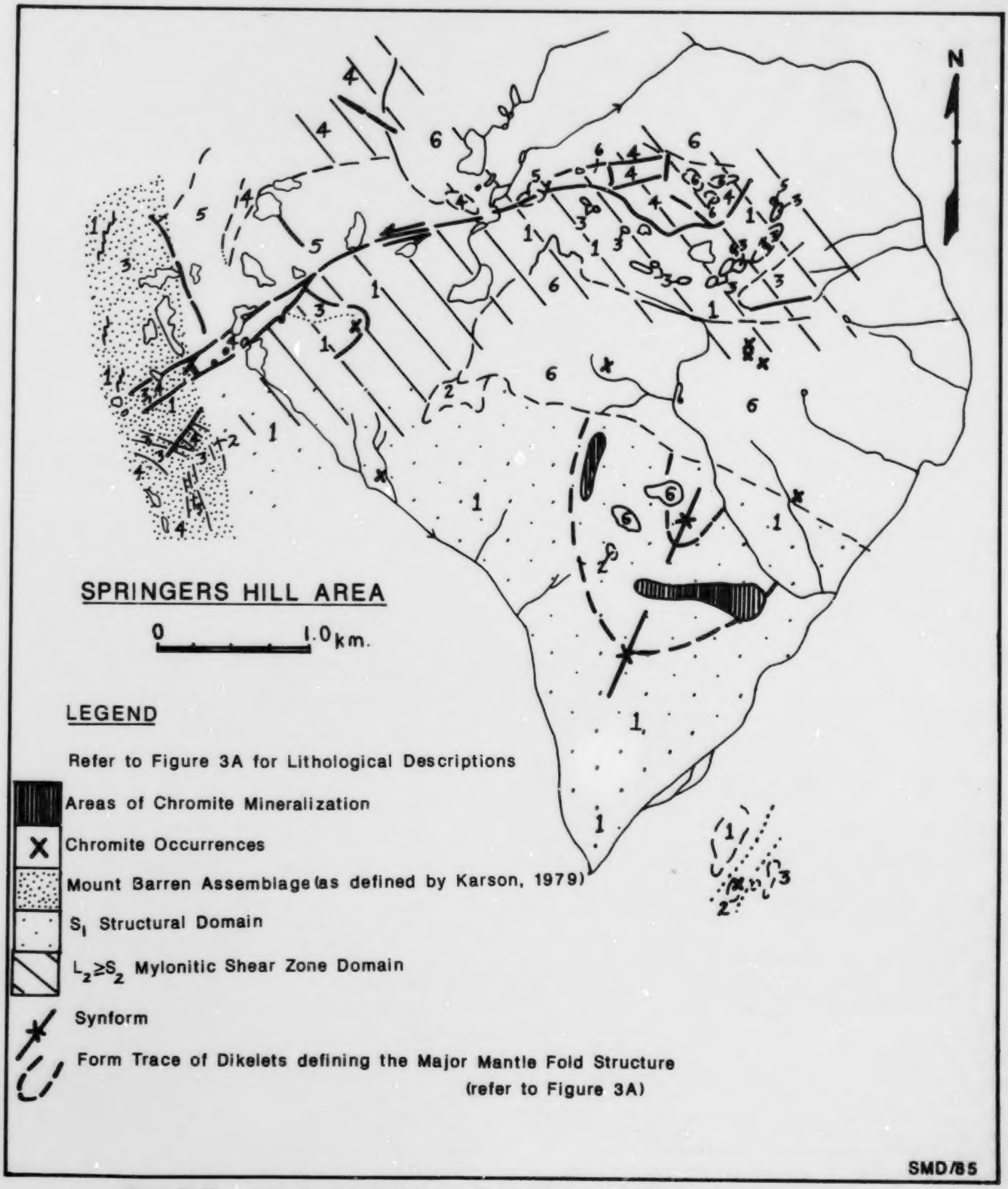

Figure 57.3B. Generalized geological map of the Springers Hill area showing distribution of main lithological units and structural domains.

Structure

The Springers Hill map area can be divided into two broad structural domains on the basis of structural overprinting and orientation patterns of the ductile deformational fabrics (Fig. 57.3B). To a large extent, the primary mineral assemblages show evidence of syntectonic recrystallization but no low temperature, retrograde mineral assemblages that are associated with the regional L-S fabrics. This indicates that the plastic deformation occurred at high temperatures. The earlier S_1 harzburgite tectonite fabric and the preferred orientation pattern of chromitiferous dunite dykelets have been overprinted, along the northern half of the map area, by a broad shear zone with a strong $L_2 \geq S_2$ fabric. This latter, intensely mylonitized zone variably affects all lithological units of both the early suite and later plutons (Fig. 57.3B).

The earlier harzburgite tectonite exhibits a strong regional S_1 foliation striking 000° to 045° and dipping steeply 60° to 85° NW. This mantle tectonite shows a range in textures from protogranular through porphyroclastic to coarse equigranular. A weak, moderately north-plunging lineation defined by the preferred dimensional orientation of elongate orthopyroxene and chromite phases was noted locally within the harzburgite. A major, inclined, northeast-plunging, synform within the harzburgite was delineated using the form trace of variably transposed dunite dykelets (Fig. 57.3A, 57.3B). The regional S_1 fabric is axial planar to this major fold structure. Small scale, isoclinal, parasitic folding of the dunite dykelets occur along the major fold limbs (Fig. 57.6H). A number of small scale ductile shear zones of unknown displacement occur both parallel to and crosscutting the regional S_1 fabric.

Towards the northern part of the mantle section, a gradual overprinting of the S_1 foliation by a major mylonitic shear zone ($L_2 \geq S_2$) was mapped. The harzburgites and cumulate rocks of the early suite show a strong $L_2 \geq S_2$ fabric orientated parallel to the transposed primary layering, while sections of the later plutons exhibit concordant $L_2 > S_2$ fabrics developed in localized ductile shear zones (see previous section). Beautifully exposed, small scale F_2 folds with axial planar S_2 surfaces were observed in harzburgite, and in ultramafic and mafic cumulates of the early suite.

In the Carol Mountain area, a north-northwest trending, shallow ($\leq$25°) east dipping S_2 is dominant. Local variations in strike attitudes result from disruption of the fabric by abundant small scale faults. The intensely developed stretching lineation plunges gently (< 20°) to the north. It is defined by rodding of pyroxene veins (Fig. 57.6I) and preferred dimensional mineral orientations. Rootless boudinaged lenses of dunite occur within the harzburgite mylonite (Fig. 57.6J). Parasitic asymmetrical F_2 folds are frequently exposed within the harzburgite-dunite tectonite (Fig. 57.6K).

Within the northwestern part of the map area, the S_2 fabric of the mylonite shear zone strikes northeast, dipping shallowly to the northwest, while the L_2 plunges gently to the north-northeast. This present pattern of S_2 orientation for the main shear zone can be explained by doming during the synkinematic intrusion of the later pluton (Fig. 57.3B). Local variation in the $L_2 > S_2$ fabric orientation is thought to most commonly reflect heterogeneous strain within the major mylonitic belt, but may also be due to rotation related to late faulting. The lithological and structural features within the northwestern sector of the S_2 shear zone belt are strikingly similar to those exposed in the Carol Mountain area.

The main S_2 mylonite shear zone appears to die out westward against a region which is along the eastern margin of the Mount Barren assemblage (Fig. 57.3B) as defined by Karson (1979). This area is characterized by a north-striking, moderate to steeply dipping planar structural fabric and steeply eastward-plunging lineation. These structures are developed within strongly infolded harzburgite and ultramafic to mafic cumulate lithologies that underwent high temperature, plastic deformation.

A major 070° trending lineament, in the northern part of the map area, is the locus of intense brittle deformation. Sinistral offset of the northwestern metacumulate sequence from its counterpart exposed in the Carol Mountain area, occurs along this major, vertical fault (Fig. 57.3A).

Stowbridge area

A 3 km^2 transect of the plutonic complex was mapped in the Stowbridge area of the North Arm Mountain Massif (Fig. 57.4). This transect contains a 2 km sequence of harzburgite, feldspathic pyroxene-dunite to wehrlite, pyroxenite, chromitiferous dunite, massive dunite and layered olivine and hypersthene gabbro. It also includes massive rodingitized gabbro and one north-trending fine grained diabasic dyke. Outcrop exposure of the ultramafic cumulates indicates progressively widening of this unit towards the north.

Structurally, the area is situated within a broad, northeast trending ductile mantle shear zone. Cumulate layering and major lithological contacts are transposed parallel to the regional S_1 fabric, which has a consistent 030° strike and a dip of 90°-60° W. A strong $L_1 > S_1$ fabric is developed locally with the lineation showing a northward plunge of 25° to 50°. Boudinaged orthopyroxenite veins occurs within both mantle and cumulate lithologies. Isoclinal folds with S_1 axial planar fabric are exposed mainly within the ultramafic cumulates. An abundance of small scale "Z", "M" and "S" minor folds in the southernmost exposure of the ultramafic cumulates suggests the presence of a major fold closure in this area (Fig. 57.4).

A few minor features indicating syn- to post-kinematic, multiple intrusion were observed within the area. These include irregular dyke intrusions of massive pyroxenite into the layered/foliated pyroxenite-dunite zone and intrusion of weakly lineated, coarse to poikilitic pyroxene-dunite into the strongly foliated, layered olivine gabbro sequence.

The position of the transition from cumulate to mantle peridotite lithologies is difficult to establish on the basis of mapping criteria alone, due to the concordance of S-L fabrics, the lack of any distinct textural change in the rocks over the mapped section, and the presence of minor clinopyroxene- and plagioclase-bearing veinlets parallel to S_1 for up to 700 m within the harzburgite.

Similarities between the Stowbridge and Springers Hill areas include the structural style and fabric intensity, the presence of abundant, rarely chromitiferous, dunite dykelets within the harzburgite, and multiple intrusive features.

Bluff Head area

A 2 km^2 area of the Bluff Head region was mapped in the immediate vicinity of the main chromite occurrence (Fig. 57.5). This area is in general poorly exposed. The distribution of lithologies appears to be controlled, at least to some extent by north-, east- and northwest-striking, steeply dipping faults. The lack of exposure and disruption by faulting hindered attempts to reconstruct the form trace of either transposed primary layering or structural fabrics between the various lithological units.

Harzburgite with a strong east trending, subvertical S_1 fabric outcrops in fault contact with layered gabbro in the northeastern part of the map area. The heterogeneously deformed, layered pyroxene gabbro exhibits north- to

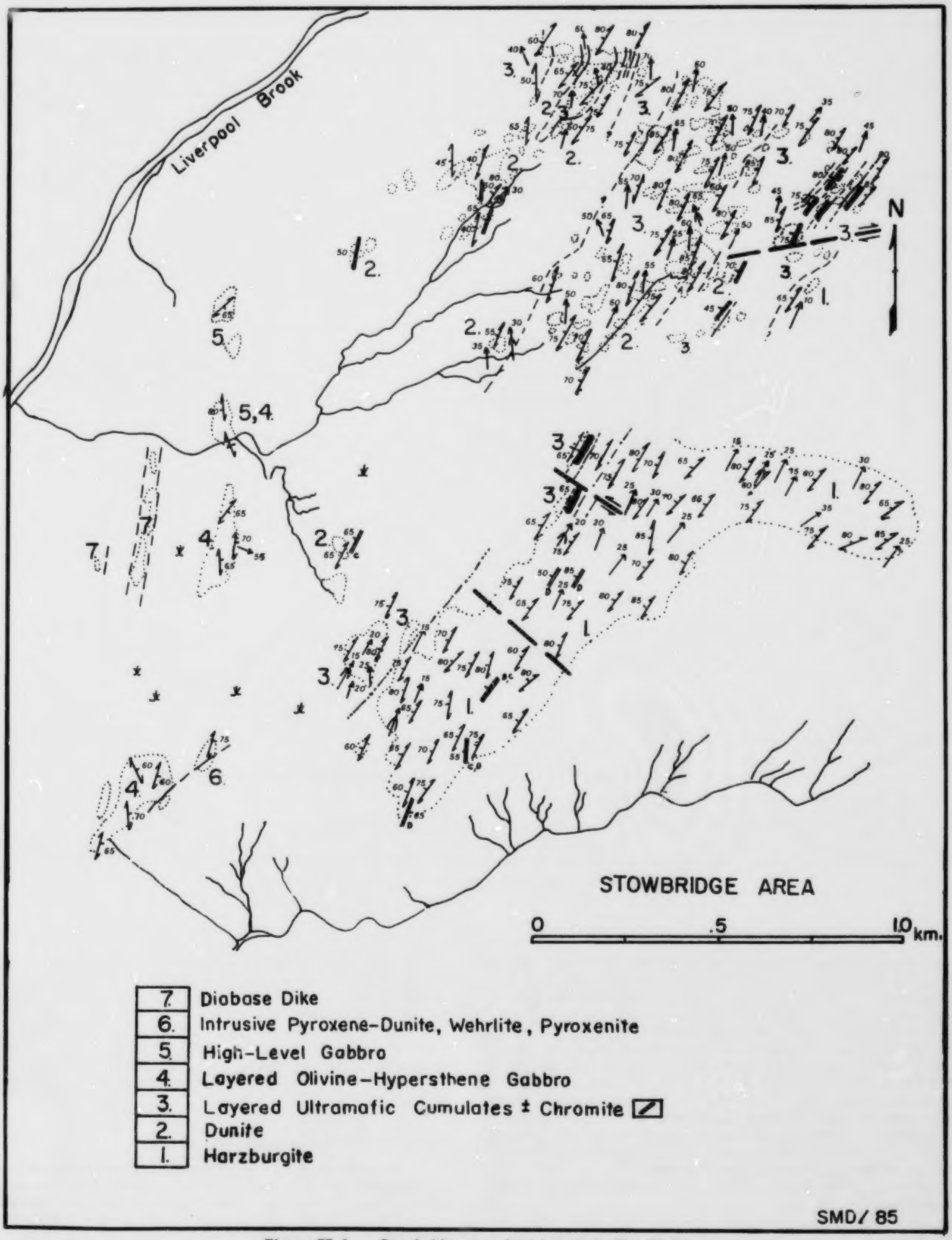

Figure 57.4. *Stowbridge area (symbols as in Fig. 57.3).*

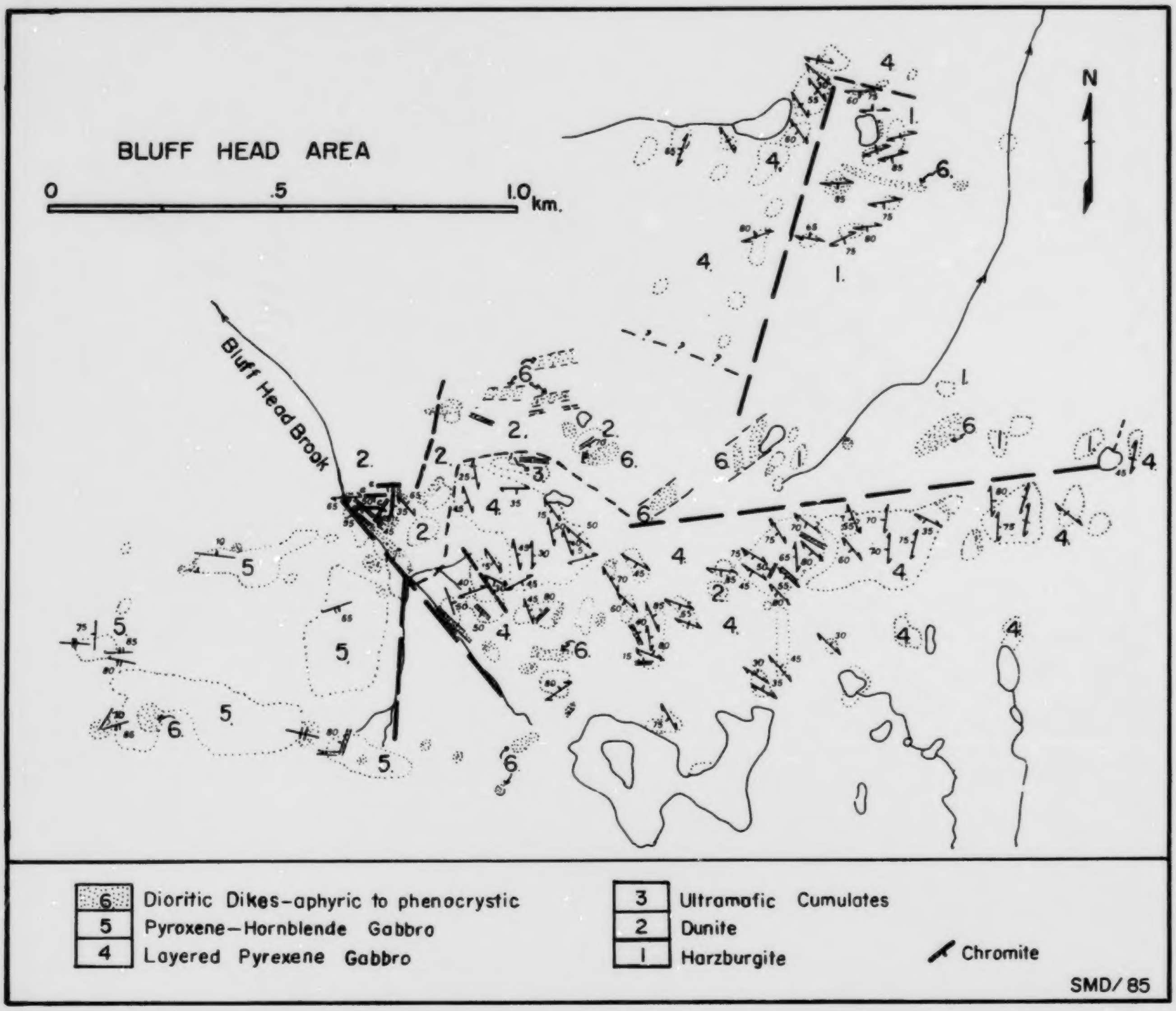

Figure 57.5. *Bluff Head area (symbols as in Fig. 57.3).*

northwest-striking, vertical to steeply east and west dipping layering (S_0), tectonite fabric (S_1) and rare F_1 fold closures. Massive, fine- to coarse-grained, pyroxene-hornblende gabbro outcrops along the western map margin. The massive dunite unit, which hosts the main chromite occurrence, is truncated to the west by a major northwest striking fault and to the northwest by the Bay of Islands sole thrust which runs along the 150 m elevation contour. To the north and east, contact relations of the dunite with the surrounding layered gabbro units are unclear. The rare occurrence of in situ (?) boulders of layered and foliated ultramafic cumulates in this contact zone may indicate the presence of an originally continuous sequence from dunite to layered gabbro. The presence of a structural discontinuity along the contact is, however, probable.

A prominent feature of the area are northeast to east striking dioritic dykes which crosscut all other units. The dykes exhibit a wide textural range, from aphyric to coarse (≤1 cm) plagioclase phyric. The dykes are undeformed, except for one which intrudes dunite at the main chromite showing and exhibits an intense east striking, 65°S dipping foliation. Minor dyke and pod-shaped intrusions of clinopyroxenite and sulphide bearing tonalite outcrop within dunite.

Comparison of the chromite occurrences

Chromite exploration within the Bay of Islands ophiolite commenced in the late 1890s. Since 1977 work by exploration companies has concentrated on detailed

prospecting, geophysics, geochemistry and diamond drilling of the major mineralization zones, notably Springers Hill and Bluff Head.

A comparison of the petrological setting and structural controls on chromite mineralization forms part of the present study. The major chromite concentrations are hosted within three unique settings, the main features of which are described in the following section.

Springers Hill chromite

Chromite concentrations in the Springers Hill area are spatially associated with both the early and later suites (Fig. 57.3B). The main Springers Hill deposit consists of numerous, discontinuous layers of disseminated to massive chromite contained within dunite dykelets hosted by the early suite mantle tectonite (Fig. 57.3B). The main zone containing chromitiferous dykelets has an east-west strike length of over 700 m, dipping 45 to 70° NW. Additional chromite concentrations discovered downslope, southeast of the main zone, indicates an approximate total thickness of 160 m for the east end of the mineralized zone. The dunite dykelets in this eastern region show a swing in strike to the northeast and a uniform 60° NW dip.

Within the main showing, euhedral to subhedral, <2 mm chromite grains are concentrated as discontinuous layers, pinched lenses and schlieren (Fig. 57.6M). Small scale folds in the chromite are common (Fig. 57.6L) and rare, moderately north-northeast plunging lineations are defined by elongate chromite grains. Small dunite dykelets crosscut and truncate chromite layers. Small scale, sinistral and dextral shear zones of limited displacement offset the chromitiferous zone in places.

Structurally, the deposit is situated along the southeast limb of the major synform as previously described. A second chromite occurrence, with identical lithological and textural features, is located 900 m north-northwest of the main showing (Fig. 57.3B). We interpret this to represent an extension of the main zone of chromitiferous dykelets, situated along the northwest limb of the synform. It thus appears that the main Springers Hill chromite occurrences are situated within an, as yet poorly defined planar zone of transposed parallel and occasionally crosscutting chromitiferous dunite dykelets which were folded during progressive mantle flow. It is also important to note that the chromitiferous zones should not be interpreted as a stratiform deposit. The internal structure of the main mineralized zone is presently being investigated by R. Dalh and D. Watkinson, of Carleton University.

The Chrome Point showing, south of Fox Island River (Fig. 57.3A), consists of a number of thin (2 to 6 cm), 150° striking, discontinuous chromitiferous layers hosted within massive and rubbly dunite. The geological setting of the chromite contrasts to that of the main Springers Hill deposit. Not only is the chromite at Chrome Point hosted by massive dunite (as opposed to dunite dykelets in harzburgite at Springers Hill), but dunite dykelets, whether chromitiferous or not, are absent from the spatially associated harzburgite in the area. The contact between dunite and harzburgite is not exposed in the Chrome Point area.

Minor chromite occurrences of two distinct forms occur within the plutons of the later magmatic suite (Fig. 57.3B). Randomly orientated bands of disseminated chromite occur within chromitiferous and clinopyroxene bearing dunite. Rare, angular and folded, massive chromite fragments, up to 35 cm in length and possibly xenolithic in origin, occur within variable deformed clinopyroxene bearing dunite and wehrlite, often in the vicinity of intrusive contact margins and harzburgite xenoliths.

Stowbridge chromite

The Stowbridge showing consists of a 4 to 8 m wide zone of thin (0.5 to 3 cm) discontinuous chromite layers hosted by dunite within an intensely deformed, 030° striking layered sequence of ultramafic cumulates (Fig. 57.4). The chromitiferous horizon dips consistently 65° to 70° to the northwest and is exposed discontinuously for more than 1000 m along strike. The chromite layers are concordant with the penetrative, regional S_1 fabric. A number of structurally concordant, chromitiferous dunite dykelets occur within the harzburgite.

Although there are lithological and structural similarities between the Springers Hill and Stowbridge areas the main chromite concentrations in the latter are hosted by the ultramafic cumulate sequence rather than the mantle peridotite, as is the case in Springers Hill.

Bluff Head chromite

Two chromite occurrences were examined in the Bluff Head area. The southern occurrence (Fig. 57.5) consists of thin, disseminated to massive chromite layers hosted within massive dunite. These discontinuous layers strike east-west and dip 45 to 65° south except near the eastern edge of the cliff face where the layering trends north and dips 35° east. This swing in orientation is attributed to the intense late faulting affecting the entire area.

Texturally, the showing is unusual in that it appears to exhibit a mixture of primary magmatic, structural and metamorphic textures. Large (up to 1 cm) euhedral, randomly orientated olivine laths occur interstitial to massive chromite and show a pseudo-crescumulate texture. Similar olivine textures developed during syntectonic, high temperature metamorphic growth have been described by Christiansen and Roberts (1985) from the Semail ophiolite, Oman and the Vourinos Complex, Greece. Shearing of chromite grains parallel to the layering and two small scale folds of chromite were observed locally.

The second chromite occurrence consists of in situ dunite boulders, located 3 km north of the southern exposure. These chromitiferous boulders show a strong schlieren texture with abundant minor folds. A strong, planar-linear alignment of elongate chromite grains occurs locally. Evidence of multiple intrusion was noted. One boulder of schlieren chromite shows abrupt truncation of the chromite layering by intrusion of an undeformed wehrlite unit (Fig. 57.6N). Xenoliths of dunite within isotopic wehrlite were observed in outcrops just south of the chromitiferous boulders.

Conclusions

As a result of the our detailed mapping in the Springers Hill, Stowbridge and Bluff Head areas, a number of important conclusions can be drawn regarding the magmatic and structural evolution of the Bay of Islands plutonic complex and its associated chromite bodies.

1. A multiple intrusive history for the Bay of Islands plutonic complex is indicated by the fact that an early, deformed ophiolite sequence is intruded by later, synkinematic, heterogeneously deformed ultramafic to gabbroic plutons. Thus, the simple plutonic stratigraphy of a single, steady-state magma chamber model as presented by Casey and Karson (1981) is inadequate for the Bay of Islands Complex.

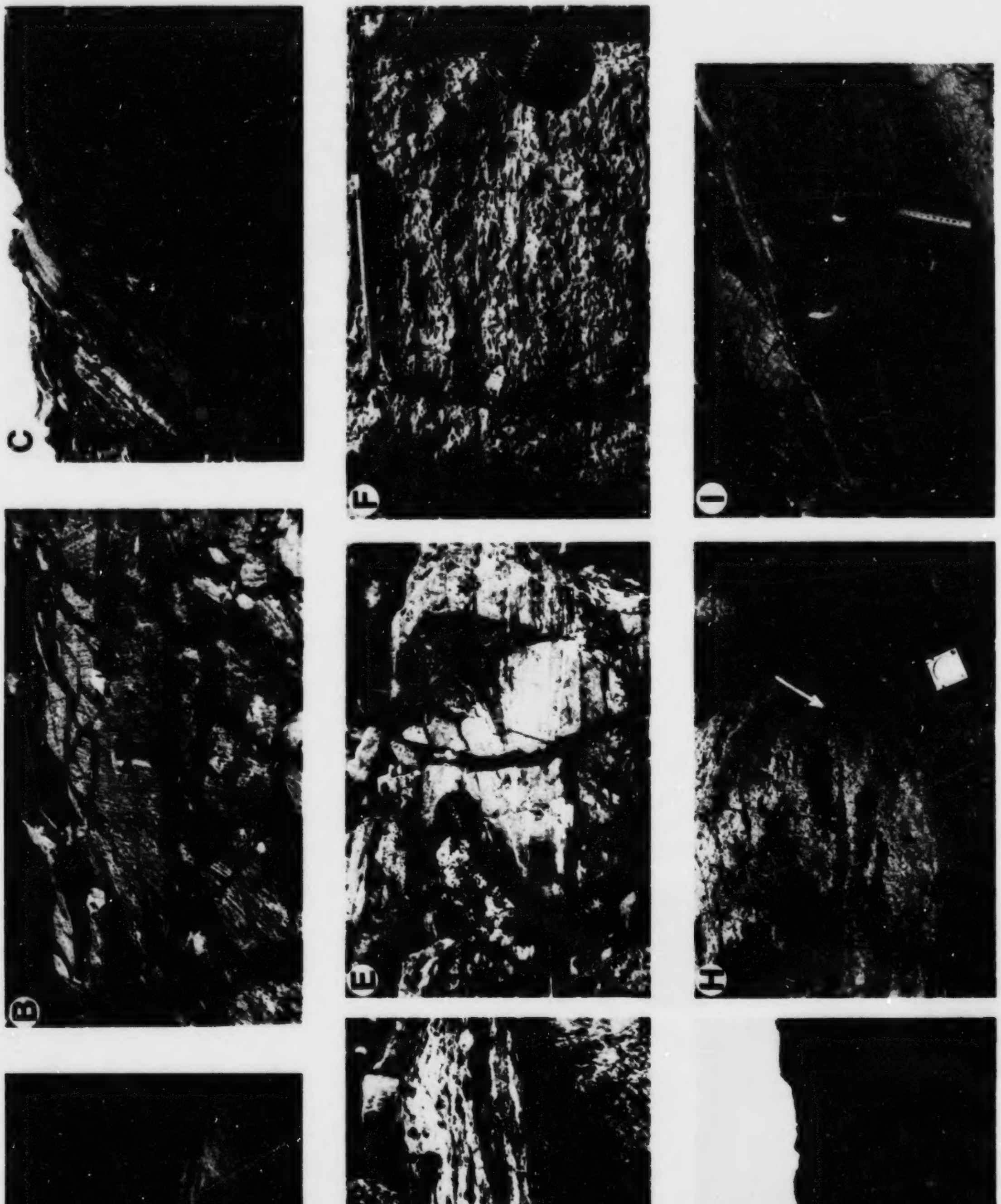
A
B
C
D
E
F
G
H
I

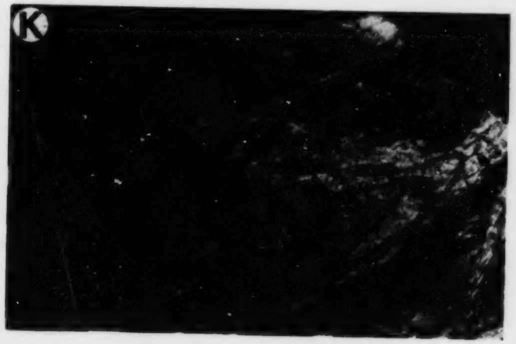

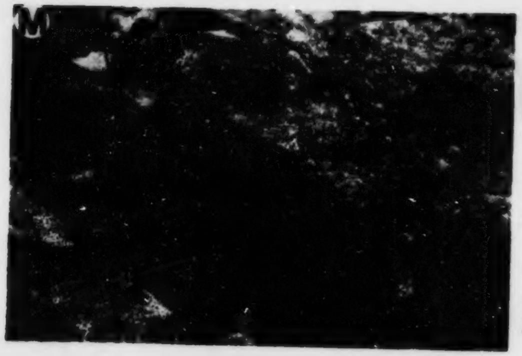

Figure 57.6

A. Chromitiferous dunite dykelets occuring interlayered with harzburgite, 100 m south of the main Springers Hill chromite deposit.

B. The intense $L_2 \geq S_2$ fabric of the ultramafic cumulates within the S_2 mantle shear zone belt. The shallow, northward plunging L_2 lies parallel to the hammer handle, in the foliation/layering plane.

C. Intense strain partitioning with flaser gabbro enveloping a boudinaged lens of less deformed gabbro and ultramafic cumulate.

D. Typical flaser gabbro with roated pyroxene-hornblende porphyroclasts.

E. An isoclinal F_2 fold closure in layered gabbro with a shallow dipping, axial planar S_2.

F. Heterogeneously developed $L_2 \geq S_2$ fabric defined by the alignment of elongated chromite and clinopyroxene grains with the later suite pluton.

G. Angular xenoliths of harzburgite and dunite hosted by later suite clinopyroxene-dunite and wehrlite along the northern intrusive margin of the central pluton.

H. Small scale, isoclinal folding of a dunite dykelet and host harzburgite, 75 m north of the main Springers Hill chromite deposit.

I. Intense boudinage of orthopyroxenite veins in the S_2 mantle shear zone. Outcrop surface orientation lies perpendicular to S_2 and oblique to L_2.

J. Large boudinaged lens of dunite within mylonitized harzburgite in the S_2 shear zone belt at Carol Mountain.

K. Parasitic, asymmetrical F_2 "S" folds in harzburgite-dunite tectonite of the S_2 shear zone belt.

L. Fold hinge of chromitiferous dunite and harzburgite, 150 m south of the main Springers Hill deposit. An axial planar S_1 is defined by chromite stringers and orthopyroxene grains, as marked on the outcrop.

M. Schlieren Chromite of the main Springers Hill showing.

N. Abrupt truncation of chromite and dunite bands by the later suite wehrlite intrusion in the Bluff Head area.

2. The high temperature, ductile deformation we have documented throughout the plutonic complex has resulted in the transposition of primary magmatic layering into the regional foliation planes (S_1 and S_2). As a result, the geometries of the fine scale igneous layering and major lithological boundaries reflect the patterns of plastic flow in the cumulate pile, (Nicolas and Violette, 1982), rather than the deposition pattern of the primary cumulate layering (Casey and Karson, 1981).

3. The major chromite concentrations within each of the study areas exhibit a unique petrologic setting, as well as a profound structural control on their present distribution. The harzburgite-hosted Springers Hill chromite deposit occurs as discontinuous chromite layers within swarms of dunite dykelets. The present orientation pattern of the dykelets defines a major synform whose origin is related to solid state flow in the mantle. Due to the transposition of dykelets during the high temperature plastic deformation, the original orientation of the dykelets cannot be reconstructed. Banded chromite of the Stowbridge area occurs interlayered with ultramafic cumulates in an intensely, plastically deformed sequence transposed parallel to the regional orientation of the mantle foliation. Dunite hosted layered chromite of the Bluff Head area exhibit both primary magmatic and secondary structural and metamorphic textures, but the deposit as a whole has suffered late-stage brittle disruption.

4. Striking similarities in lithology and structural style exist between the Bay of Islands Complex and a small area mapped within the Mount Barren Complex. Of particular interest is the down dip orientations of the extension lineation in foliation planes of the Mount Barren Assemblage. This geometry is difficult to reconcile with the kinematics of a "typical" transform regime as suggested by (Karson, 1979). In combination with the history of synkinematic multiple intrusive for the Bay of Islands Complex, it indicates the need to re-investigate the presently accepted division of structural and kinematic domains as outlined by Casey and Karson (1981) and Casey et al. (1983) for the Lewis Hills Massif.

Acknowledgments

The conscientious mapping by M. Wawrzkow is greatfully acknowledged. R. Talkington, R. Dahl and G. Suhr are thanked for the numerous, enjoyable discussions during the fieldwork. We would also like to thank J. Lydon and J. Scoates for their critical reading of the manuscript. W. Marsh and J. Hiscock are acknowledged for photo reproduction and draft typing of the manuscript, respectively. Finally, the prompt and efficient field support of Viking Helicopters and D. Mercer, Pasadena Expedition and Warehousing, contributed to the enjoyable and successful field season.

References

Calon, T.J.
1984: Patterns of high-temperature, plastic deformation in the plutonic sections of ophiolites; Geological Association of Canada, Mineralogical Association of Canada, Program with Abstracts, v. 9, p. 50.

Calon, T.J. and Malpas, J.G.
1985: Role of deformation in the evolution of the plutonic complex, Bay of Islands Ophiolite, Newfoundland, Geological Association of Canada, Mineralogical Association of Canada, Program with Abstracts, v. 10, p. A8.

Casey, J.F. and Karson, J.A.
1981: Magma chamber profiles from the Bay of Islands Ophiolite Complex: Implications for crustal level magma chambers of ocean ridges; Nature, v. 292, p. 295-301.

Casey, J.F., Karson, J.A., Elthon, D., Rosencrantz, E., and Titus, M.
1983: Reconstruction of the geometry of accretion during formation of the Bay of Islands Ophiolite Complex; Tectonics, v. 2, p. 509-528.

Christiansen, F.G. and Roberts, S.
– Formation of olivine pseudo-crescumulates by syntectonic axial planar growth during mantle deformation; Geology. (in press)

Church, W.R. and Stevens, R.K.
1971: Early Paleozoic ophiolite complexes of the Newfoundland Appalachian as mantle – ocean crust sequences; Journal of Geophysical Research v. 76, p. 1461-1466.

Dewey, F.J. and Bird, J.M.
1971: Origin and emplacement of the ophiolite suite: Appalachian ophiolites in Newfoundland; Journal of Geophysical Research v. 76, p. 3179-3206.

Dunsworth, S.M. and Calon, T.J.
1984: Relationships between deformation and magmatism in the plutonic complex, Troodos Ophilite, Cyprus; Geological Association of Canada, Mineralogical Association of Canada, Program with Abstracts, v. 9, p. 59.

Jacobsen, S.B. and Wasserburg, G.J.
1979: Nd and Sr isotopic study of the Bay of Islands ophiolite complex and the evolution of the source of mid-ocean ridge basalts; Journal of Geophysical Research, v. 84, p. 7429-7445.

Karson, J.A.
1979: Geological map (1:25 000) and descriptive notes on the Lewis Hills massif, Western Newfoundland; Geological Survey of Canada, Open File 628.

Karson, J.A. and Dewey, J.F.
1978: Coastal Complex, Western Newfoundland: An early Ordovician oceanic fracture zone; Geological Society America Bulletin, v. 89, p. 1037-1049.

Karson, J.A., Elthon, D.L., and DeLong, S.E.
1983: Ultramafic intrusions in the Lewis Hills Massif, Bay of Islands ophiolite complex, Newfoundland: Implications for igneous processes at oceanic fracture zones; Geological Society of America Bulletin, v. 94, p. 15-129

Mattinson, J.M.
1975: Early Paleozoic ophiolite complexes of Newfoundland: Isotopic ages of zircon; Geology, v. 3, p. 181-183.

Nicolas, A. and Violette, J.F.
1982: Mantle flow at oceanic spreading centres: models derived from ophiolites; Tectonophysics, v. 81, p. 319-339.

Penrose Conference Participants
1972: Ophiolites; Geotimes, v. 17, No. 12, p. 24-25

Williams, H.
1975: Structural succession, nomenclature and interpretation of transported rocks in western Newfoundland; Canadian Journal of Earth Sciences, v. 12, p. 1874-1894.

Geological investigation of Cretaceous? strata beneath Cape Dyer Basalts (Paleocene), Baffin Island, District of Franklin

Project 740003

A.B. Langille[1], E.T. Burden[1], W.B. Sears[1], and D.C. Holloway[2]
Atlantic Geoscience Centre, Dartmouth

Langille, A.B., Burden, E.T., Sears, W.B., and Holloway, D.C., Geological investigation of Cretaceous? strata beneath Cape Dyer Basalts (Paleocene), Baffin Island, District of Franklin; in Current Research, Part A, Geological Survey of Canada, Paper 86-1A, p. 483-488, 1986.

Abstract

Mesozoic and Cenozoic strata on the coast of Baffin Island near Cape Dyer provide (1) information about the potential for offshore hydrocarbons and (2) evidence to constrain the timing of rifting of Baffin Bay. Questionable megafloral evidence in deltaic sand bodies suggests the assignment of outliers to the Paleocene. In contrast, palynology suggests an Albian age.

Résumé

Les couches mésozoïques et cénozoïques sur la côte de l'île de Baffin près du cap Dyer fournissent (1) des renseignements sur les possibilités de trouver des hydrocarbures au large de la côte et (2) des preuves permettant d'établir la chronologie de la formation de fossés d'effondrement dans la baie de Baffin. Des indices mégafloraux discutables trouvés dans des masses de sable deltaïque portent à croire que les avant-buttes dateraient du Paléocène. Par opposition, la palynologie semble indiquer un âge albien.

[1] Memorial University of Newfoundland, St. John's, Newfoundland A1B 3X5
[2] Present address: Gulf Canada Resources Inc., Gulf Canada Square, P.O. Box 130, Calgary, Alberta T2P 2H7

Introduction

A rekindling of interest in Mesozoic and Cenozoic strata exposed along the coast of Baffin Island from Cape Dyer to Quqaluit Island was generated when, in 1976, scientists on the C.S.S. Hudson discovered hydrocarbon slicks from oil seeps off Scott Inlet (Loncarevic and Falconer, 1977). This discovery led to an increase in exploration on the Baffin Island shelf and subsequent discovery of additional slicks farther south in Buchan Gulf (Maclean and Falconer, 1979).

In the past, Mesozoic and Cenozoic outliers on southeastern Baffin Island contributed in a significant way to the ongoing debate over the timing of Baffin Bay rifting and seafloor spreading (Clarke and Upton, 1971). At present, the geological setting is explained by invoking one of two seafloor spreading models. The most widely accepted model is that of Clarke and Upton (1971), Keen et al. (1972, 1974), Srivastava (1978) and Jackson et al. (1979). According to this model, Baffin Bay formed as Paleogene seafloor spreading along the western arm of the Mid-Atlantic Ridge separated Labrador and Baffin Island from Greenland.

The opposing view stipulates that Baffin Island and Greenland did not drift apart to form Baffin Bay, but that continental crust is continuous from Baffin Island, across Baffin Bay and onto Greenland. This view states that Baffin Bay formed by foundering of continental blocks due to extensional forces which resulted in little new oceanic crust being produced (Grant, 1975, 1980; Umpelby, 1979; Kerr, 1980).

One of the cornerstones of these models is a presumed similarity of Baffin Island outliers with contemporaneous but much thicker outliers on western Greenland. To assess this similarity, a program to examine sections along the coast of Baffin Island for lithostratigraphy and biostratigraphy was undertaken.

Field Work

Sections of unconsolidated sand, shale, coaly shale and coal on Padloping, Durban and Quqaluit islands were measured and sampled for sedimentology and palynology (Fig. 58.1). Strata on these islands were found in small fault bounded basins on Precambrian basement. Sections were not well exposed; post-depositional faulting and soft-sediment deformation obscured many lateral relationships and cryogenic activity in the soft, unconsolidated sands distorted sedimentary structures. Where field relations could be determined with confidence, the sampling interval for detailed paleoenvironmental interpretations was very close (0.5 m or less). Preliminary observations are outlined for each of the islands.

Quqaluit Island

A northeasterly dipping section on the north side of the island at a location approximately equadistant between two projecting headlands was measured and sampled for sedimentology and palynology (Fig. 58.2). The lower contact with intensely weathered, friable and kaolinitic? Precambrian gneiss is scoured. Above this, is 52 m of cyclical coarsening upward shale and sandstone beds. Above 52 m, sandstones are uniformly thick bedded and fining upward cycles with tabular crossbeds, ironstone concretions, rip-up clasts and thin shale beds (Fig. 58.3). The top of the section at 115 m consists of interbedded sandstone and volcanic breccia beds.

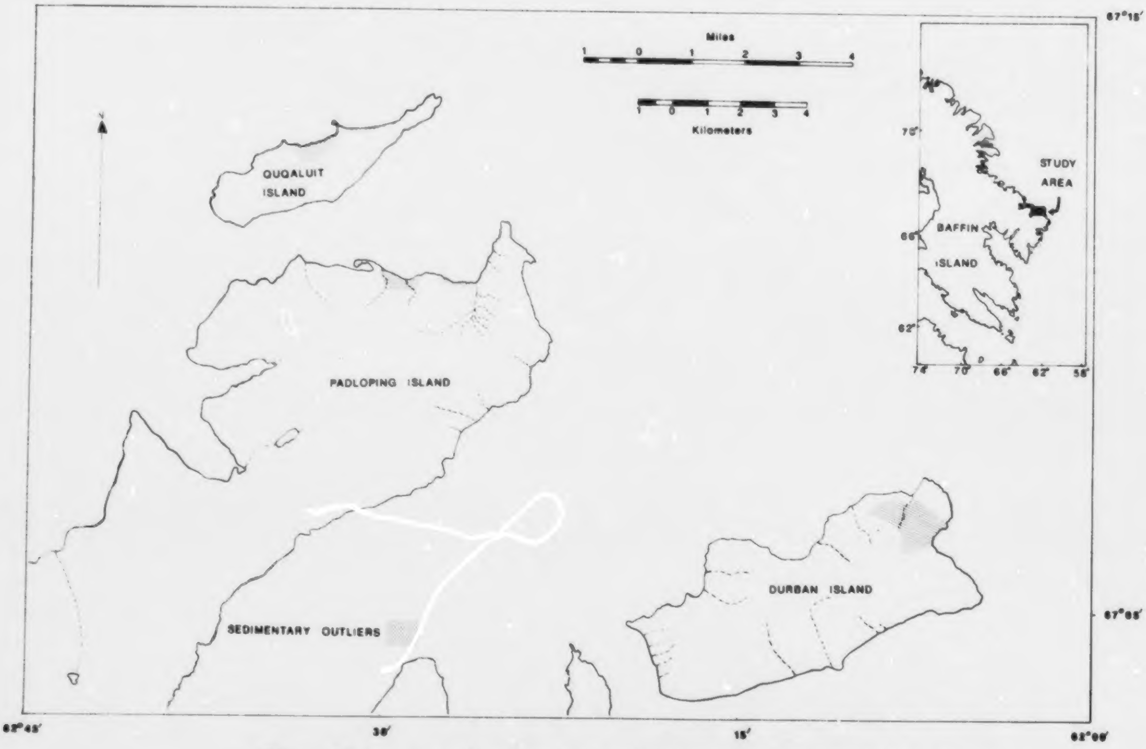

Figure 58.1. Map of sedimentary outliers examined in this study.

Padloping Island

The section at Padloping Island is a composite 180 m thick, derived from sections measured at two localities along the north coast of the island, east of a prominent sand spit (Fig. 58.2). Strata are deformed in a complex manner; a large Late or Post-glacial slump which dropped and rotated sediments and volcanics is superimposed on pre and post-depositional structures in this small basin (Fig. 58.4).

The lower contact with Precambrian gneiss is not directly observed. Periglacial debris consisting of intensely weathered gneiss occurs west of the outcropping strata; if projected onto the section, the Precambrian is approximately 40 m below the lowest sandstone outcrop.

The lower 30 m of measured section consists of coarsening upward trough crossbedded sandstones with thin shale lamina (Fig. 58.5). The interval from 30 to 70 m consists of thinly bedded sandstones containing concretions and shales containing Metasequoia needles. Above 70 m to the covered interval at 110 m the beds consist of shale with thin sandstones containing concretions.

The upper part of the section outcrops approximately 500 m farther east. Here, beds from 126 to 150 m consist of thinly stratified sandstone with concretions, coaly shale and coal. Above 150 m sandstone beds are thick bedded and fining upward cycles with trough cross stratification. The contact with overlying volcanics at 170 m is gradational; nevertheless, sandstone and shale beds are characterized by large mineralized logs on the contact with the volcanics.

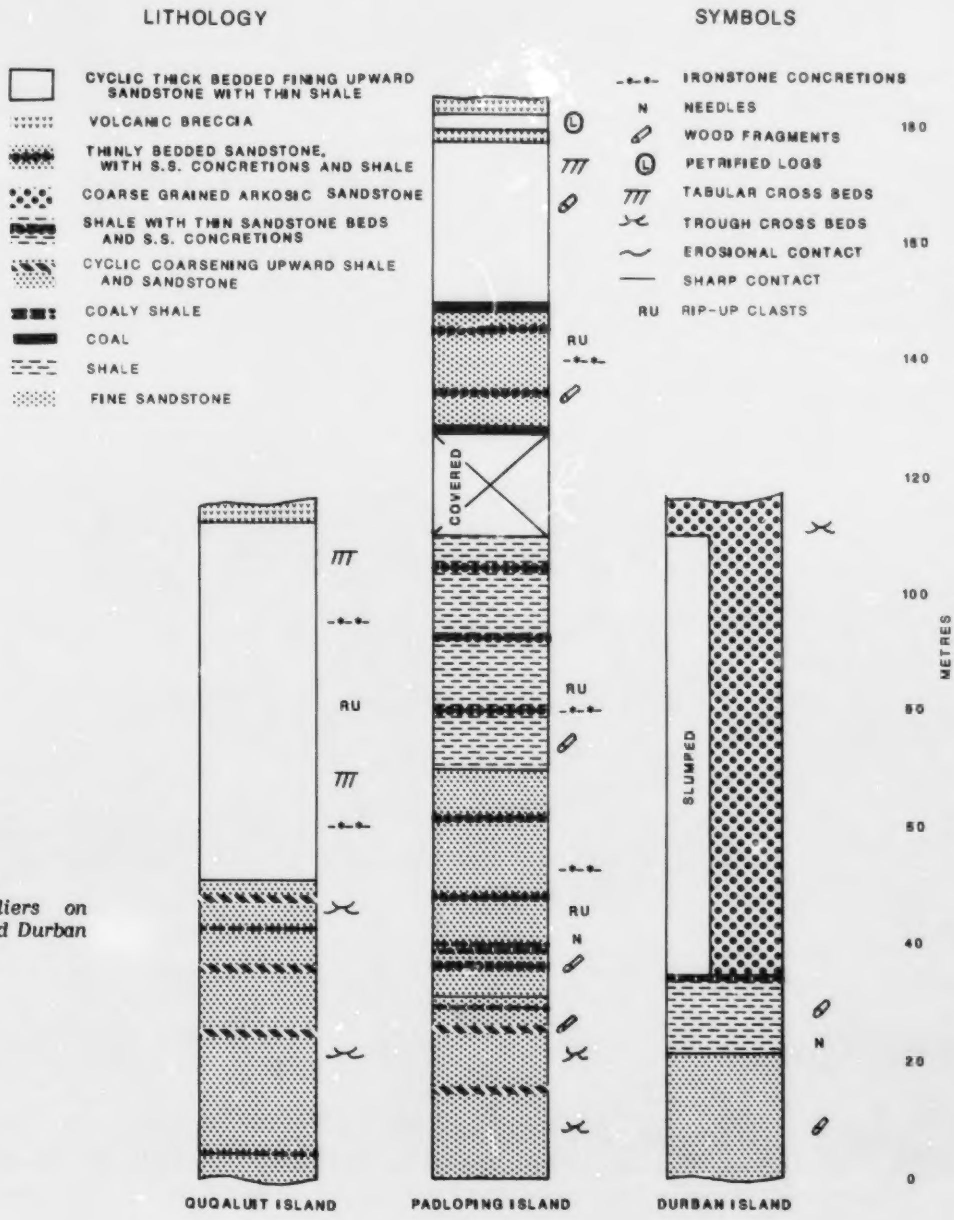

Figure 58.2

Stratigraphy of outliers on Quqaluit, Padloping and Durban islands.

Figure 58.3. Tabular crossbeds separated by thin shale partings.

Figure 58.4. Faulted, slumped and rotated strata of the lower part of the Padloping Island section.

Figure 58.5. *Trough crossbedded sandstones at the top of a coarsening upward cycle.*

Durban Island

Strata on Durban Island occur in a small fault bounded basin on the northeast corner of the island. Here, 22 m of thick bedded, fine grained sandstone overlies weathered Precambrian gneiss. This is overlain by 10 m of shale capped with 2 m of coaly, micaceous shale. The interval from 37 through 115 m is slumped sandstone covered with blocks of lithified granular sandstone. From a nearby hillside it can be seen that beds are close to the surface and that most of the slumped debris is locally derived. Above 115 m is an outcrop of indurated, coarse grained, trough crossbedded sandstone. Clarke and Upton (1971) indicated that this sandstone is 250 m thick; from our fieldwork, we could not reach this conclusion. A nearby hillside covered with blocks of indurated sandstone may be an up-faulted repeat section.

Palynology

Eight samples (GSC collection numbers 18461-18468) collected in 1980 from unspecified localities on Quqaluit, Padloping and Durban islands during a reconnaissance survey by the Geological Survey of Canada have been analysed. Slides and residues are at the Atlantic Geoscience Centre, Dartmouth.

All samples contain abundant woody material with minor amounts of cuticle and resin. Palynomorph assemblages are dominated by **Alisporites bilateralis** Rouse, 1959, **Cedripites canadensis** Pocock, 1962, **Parvisaccites radiatus** Couper, 1958, **Podocarpidites multesimus** (Bolkhovitina) Pocock, 1962 and **P. canadensis** Pocock, 1962. Biostratigraphically useful species include **Appendicisporites matesovai** Bolkhovitina, 1968, **Cicatricosisporites auritus** Singh, 1971, **Clavifera** sp. cf. **C. rudis** Bolkhovitina, 1968, **Concavissimisporites parkinii** Pocock, 1962, **Densoisporites microrugulatus** Brenner, 1963, **Foveogleicheniidites confossus** (Hedlund) Burger, 1976, **Foveosporites canalis** Balme, 1957, **Impardecispora marylandensis** (Brenner) Venkatachala, Kar and Raza, 1968, **Retitricolpites promiscuus** Laing, 1975 and **Saxetia scurrandus** (Norris) Srivastava, 1975.

Discussion

The age and depositional environment of outliers exposed along the coast of Baffin Island near Cape Dyer is by no means clear. Floral remains described by McMillan (1910) and Bell (in Clarke and Upton, 1971) from Durban Island were compared with the west Greenland sequence and to infer a nonmarine deposit of Paleocene age. In contrast, Deutsch and Patzold (1984) have paleomagnetic evidence suggesting an age older than Paleocene for basalts overlying strata on Durban Island and MacLean and Williams (1983) have nonmarine strata with Albian affinities off the coast of Padloping Island. Farther north, Choi et al. (1984) have evidence to suggest Tertiary plants evolved in the Arctic during the Cretaceous and Burden and Holloway (in press) have reassigned Cretaceous-Paleogene? outliers at Scott Inlet to the Quaternary.

In our study of the strata beneath Cape Dyer Basalts we have evidence indicating a period of intense weathering of Precambrian gneisses prior to the onset of clastic sedimentation. Deposits overlying gneisses are believed to represent deltas and shallow shelf sands. Where observed, the contact with subaqueous breccia beds is gradational. Nevertheless, with abundant wood at the contact, one or more catastrophic eruptions must have marked the onset of volcanism. Palynomorphs recovered from samples analysed to date indicate a nonmarine deposit of Albian or Cenomanian age. This is consistent with the age and depositional environments assigned to Albian through

Campanian deposits found in Greenland (Henderson et al. 1981). However, we cannot rule out the possibility that older strata have been reworked into Paleocene deltas and shelf deposits.

Conclusion

Preliminary investigations on our part indicate that the sediments beneath the Cape Dyer basalts represent deltas and shelf deposits. Palynology indicates that the outliers are nonmarine Albian or Cenomanian deposits correlative with similar strata in Greenland. The abundance of woody material in palynomorph preparations suggests that these sediments may, with sufficient burial, be gas prone.

Acknowledgments

Accommodations provided by both Parks Canada (Broughton Island) and the Department of Indian Affairs and Northern Development (Frobisher Bay), while travelling to and from the field were appreciated. Discussions with E. Deutsch and R. Patzold on paleomagnetism of Cape Dyer outliers were helpful and very informative. Our guide, Lymeckee Kakee, was invaluable and without his enthusiastic support the project could not have been as successful. Financial and logistical support was provided by the Geological Survey of Canada, Natural Sciences and Engineering Research Council and Polar Continental Shelf Project (E.B.), a Texaco Research Grant (A.L.), and Department of Indian Affairs and Northern Development – Northern Scientific Training Program Grants (A.L. and B.S.).

References

Burden, E.T. and Holloway D.C.
– Scott Inlet Inliers (Baffin Island, Northwest Territories), Cretaceous-Paleogene? Now Quaternary; Canadian Journal of Earth Sciences. (in press)

Choi, D.K., Traverse A., and Hickey L.J.
1984: Eureka Sound Formation (Late Cretaceous – Paleogene) Palynofloras from the Canadian Arctic, in relation to Angiosperm Migration; Sixth International Palynological Conference, Calgary, 21 p.

Clarke, D.B. and Upton, B.G.
1971: Tertiary basalts of Baffin Island: Field relations and tectonic setting; Canadian Journal of Earth Sciences. v. 8, pp. 248-258.

Deutsch, E. and Patzold, R.R.
1984: A discordant Early Tertiary pole position from the Cape Dyer Lavas, Canadian Arctic; E.O.S., v. 65, p. 200.

Grant, A.C.
1975: Geophysical results from the continental margin off southern Baffin Island; In Canada's continental margins and offshore Petroleum Exploration. Ed. by C.J. Yorath, E.R. Parker and D.J. Glass; Canadian Society of Petroleum Geologists Memoir No. 4, p. 411-413.

1980: Problems with plate tectonics: Labrador Sea; Canadian Society of Petroleum Geologists Bulletin, v. 28, p. 252-278.

Henderson, G., Schiener, E.J., Risum, J.B., Croxton, C.A., and Anderson, B.B.
1981: The West Greenland Basin; In Geology of the North Atlantic Borderlands, ed. by J.W. Kerr and A.J. Fergusson; Canadian Society of Petroleum Geologists Memoir No. 7, p. 399-428.

Jackson, H.R., Keen, C.E., Falconer, R.K., and Appleton, K.P.
1979: New geophysical evidence for sea floor spreading in central Baffin Bay; Canadian Journal of Earth Sciences, v. 11, p. 2122-2135.

Keen, M.J. and Clarke, D.B.
1974: Tertiary basalts of Baffin Bay: Geochemical evidence for a fossil hotspot; in Geodynamics of Iceland and the North Atlantic area, ed. L. Kristjansson and D. Reidal; (Dordrecht-Holland) Publishers, p. 127-137.

Keen, M.J., Johnson, J., and Park, I.
1972: Geophysical and geological studies in eastern and northern Baffin Bay and Lancaster Sound; Canadian Journal of Earth Sciences, v. 9, p. 689-708.

Kerr, J.Wm.
1980: Evolution of the Canadian Arctic Islands – A transition between the Atlantic and Arctic oceans, in The oceans basins and margins, 5, The Arctic Ocean. Ed. A.E.M. Naire, F.G. Stehli, and M. Churkin, Jr.; Plenum Press Publishing Company.

Loncarevic, B.D. and Falconer, R.K.
1977: An oil slick occurrence off Baffin Island; in Current Research, Part A, Geological Survey of Canada, Paper 77-1A, p. 523-524.

MacLean, B. and Falconer, R.K.
1979: Geological/Geophysical studies in Baffin Bay and Scott Inlet-Buchan Gulf and Cape Dyer-Cumberland Sound areas of the Baffin Island Shelf; in Current Research, Part B, Geological Survey of Canada, Paper 79-1B, p. 231-244.

MacLean, B. and Williams, G.L.
1983: Geological Investigations of Baffin Island Shelf in 1982; in Current Research, Part B, Geological Survey of Canada, Paper 83-1B, p. 309-315.

MacMillan, J.G.
1910: Geographical Report, in Report of the Dominion of Canada Government Expedition to the Arctic Islands and Hudson Strait on board the D.G.S. "Arctic" by J.E. Bernier; Government Printing Bureau, Ottawa.

Srivastava, S.P.
1978: Evolution of the Labrador Sea and its bearing on the early evolution of the North Atlantic; Geophysical Journal, Royal Astronomical Society, v. 52, p. 313-357.

Umpelby, D.C.
1979: Geology of the Labrador Shelf; Geological Survey of Canada, Paper 79-13, 39 p.

Vitrinite reflectance measurements and their implications for oil and gas exploration in the Jeanne d'Arc Basin, Grand Banks, eastern Canada

Projects 720103, 810034, 840083

M.P. Avery, J.S. Bell and K.D. McAlpine
Atlantic Geoscience Centre, Dartmouth

Avery, M.P., Bell, J.S., and McAlpine K.D., Vitrinite reflectance measurements and their implications for oil and gas exploration in the Jeanne d'Arc Basin, Grand Banks, eastern Canada; in Current Research, Part A, Geological Survey of Canada, Paper 86-1A, p. 489-498, 1986.

Abstract

Organic maturation profiles, based on vitrinite reflectance measurements, are reported for eight oil exploratory wells drilled in the Jeanne d'Arc Basin, offshore Newfoundland. Results suggest that the thickness of the oil generative window is controlled by the structural configuration of the basin which was established prior to Late Cretaceous. This oil window has migrated upward through the basin fill during the last 100 Ma due to burial beneath a regionally accreting blanket of Late Cretaceous and Tertiary sediments. The thickest part of the oil window, where the Upper Jurassic oil source rock had the best opportunity to generate hydrocarbons, lies adjacent to the majority of the significant oil discoveries, including the giant Hibernia field. Discovered gas may have been sourced in gas prone Lower Cretaceous shales or may be an overmature product of deeply buried oil source rocks.

Résumé

Sont presentés ici les profiles de maturation organique, basés sur des mesures de "vitrinite réflectance" provenant de huit sondages d'exploration pétrolière perforés dans le bassin Jeanne d'Arc, au large de Terre-Neuve. Les résultats montrent que la "fenêtre" de génération de pétrole est contrôlée par la configuration structurale du bassin qui a été formé avant le Crétacé supérieur. Cette "fenêtre" c'est deplacée vers le haut à travers les sédiments du bassin pendant les derniers 100 Ma, à cause de l'accumulation d'une couche régionale de sédiments d'âge crétacé supérieur et tertiaire. La partie plus épaisse de cette "fenêtre", où la roche-réservoir du Jurassique supérieur avait les meilleurs conditions pour produire des hydrocarbures, s'étend près de la majorité des plus importantes découvertes de pétrole, y compris l'énorme gisement d'Hibernia. Le gaz découvert peut avoir été formé dans des schistes argileux d'âge crétacé inférieur, susceptibles d'en produire, ou il peut être un produit "supermature" de roches-réservoirs profondément enfouies.

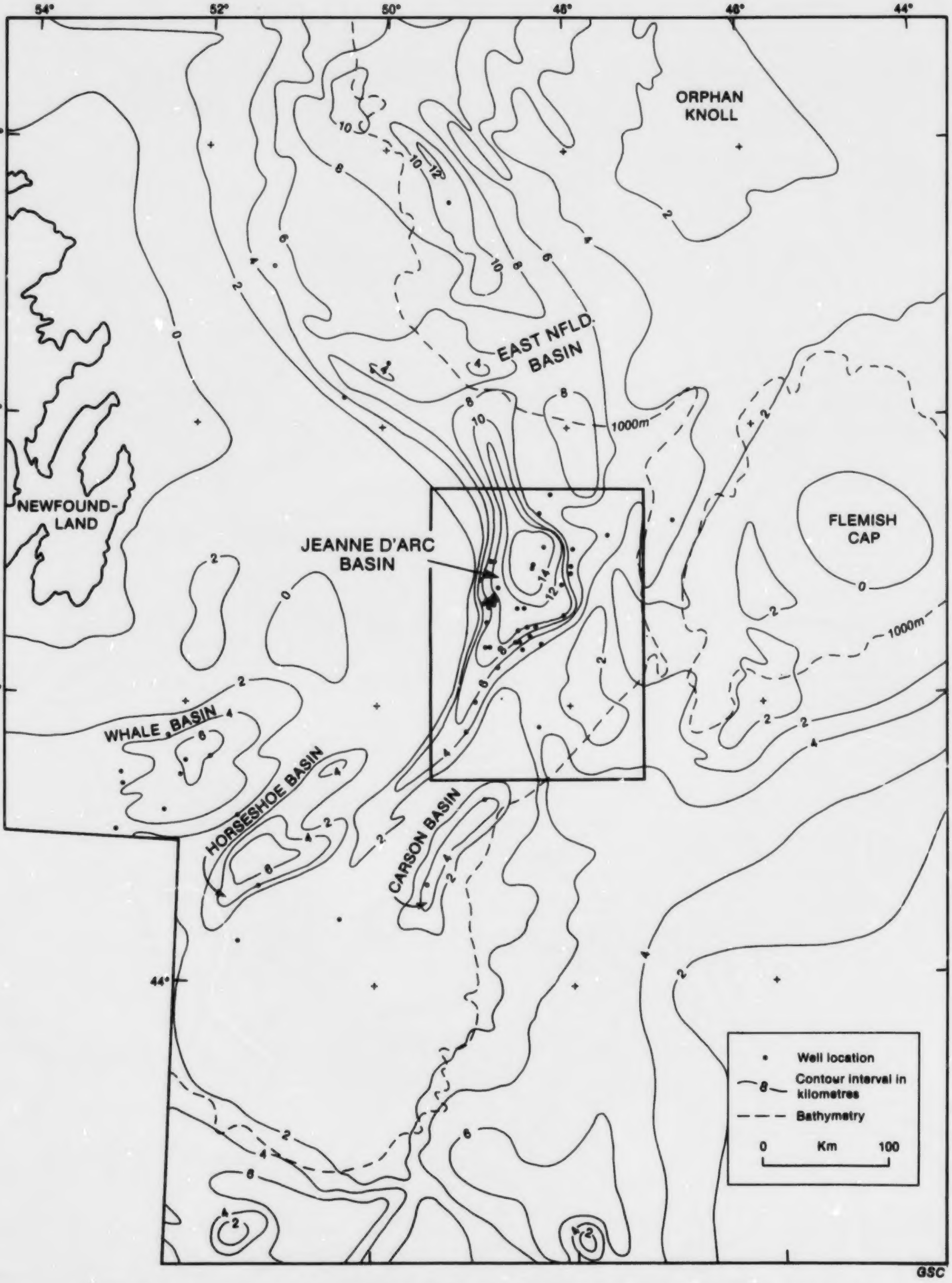

Figure 59.1. *Sediment thickness, Grand Banks area, showing locations of Mesozoic sedimentary basins and exploratory wells (after Grant et al., in press). Rectangle in centre outlines area of Figure 59.2.*

Introduction

Kerogen, the precursor of hydrocarbons, is formed during the early diagenesis of organic matter deposited with sediments. Further burial, accompanied by increased temperature and pressure, matures the kerogen to generate oil and gas. One method of determining the organic maturity of sediments and their ability to source hydrocarbons is to measure the light reflectance properties of vitrinite particles in kerogen.

The purpose of this paper is to report vitrinite reflectance measurements made on ditch-cutting samples obtained from eight oil exploratory wells drilled in the oil-bearing Jeanne d'Arc Basin on the Grand Banks of Newfoundland, eastern Canada, and to consider the regional implications of their organic maturation profiles in terms of the depth ranges over which hydrocarbons can be generated. This study is part of an ongoing program of basin analysis and hydrocarbon resource assessment of Canada's eastern continental margins in progress at the Atlantic Geoscience Centre.

Geological setting

The Grand Banks of Newfoundland are underlain by a series of fault-bounded Mesozoic sedimentary basins, separated by "basement" highs (Fig. 59.1). Basin forming tectonics ceased during late Lower Cretaceous time and the

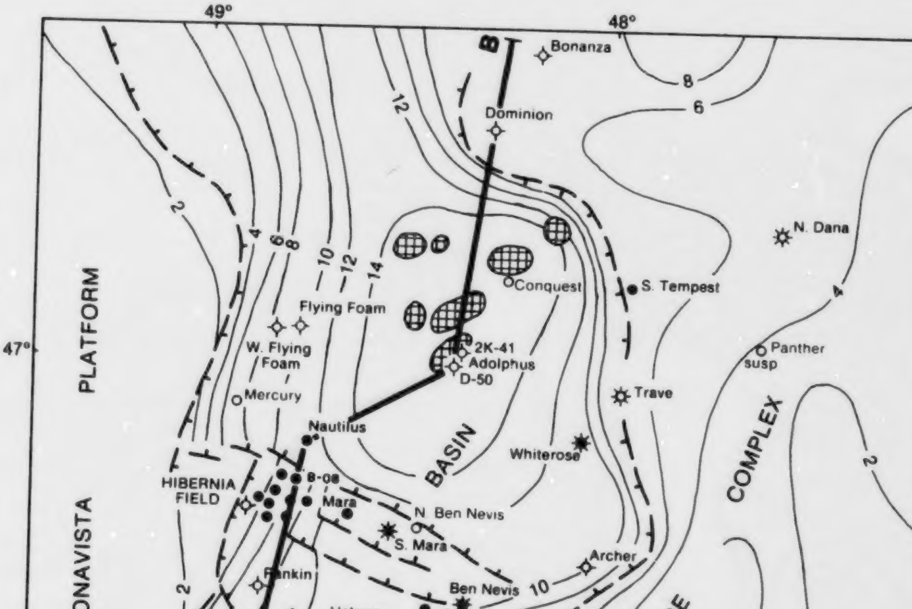

Figure 59.2. *Diagrammatic structure and sediment thickness map of the Jeanne d'Arc Basin (after Grant et al., in press).*

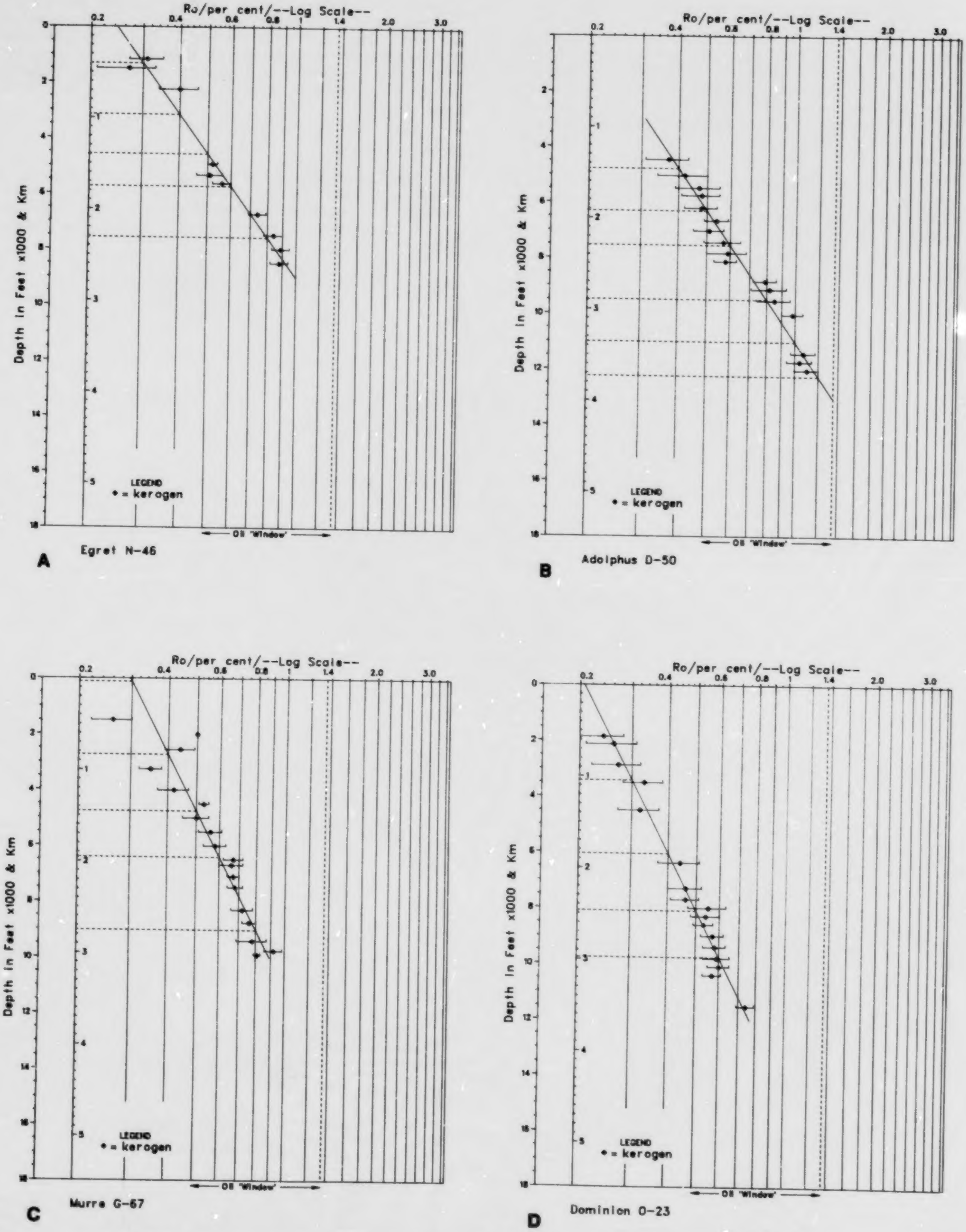

Figure 59.3. *Maturation profiles based on vitrinite reflectance (Ro) measurements made on samples from the Egret N-46, Adolphus D-50, Murre G-67 and Dominion O-23 wells.*

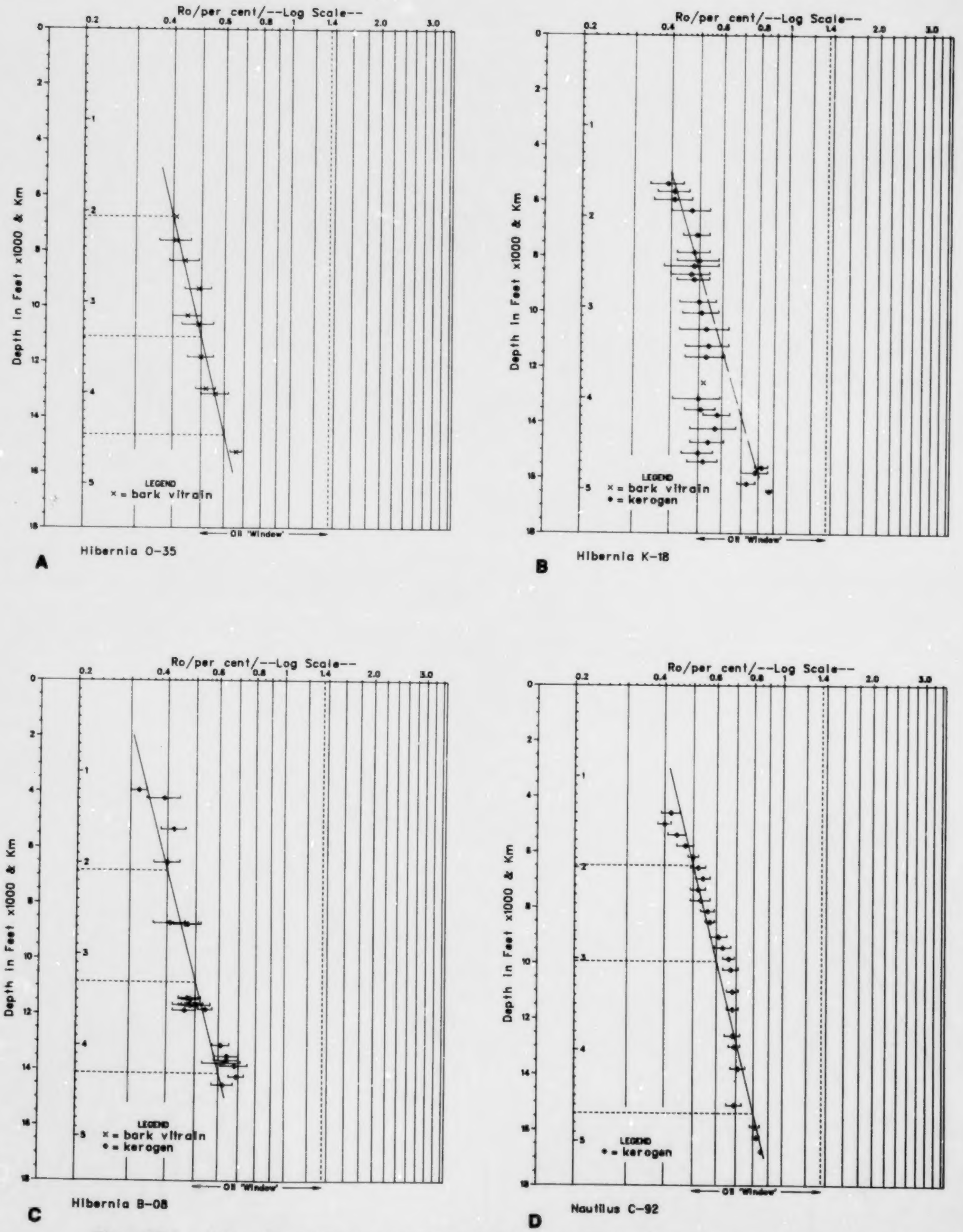

Figure 59.4. *Maturation profiles based on vitrinite reflectance (Ro) measurements made on samples from the Hibernia O-35, Hibernia K-18, Hibernia B-08 and Nautilus C-92.*

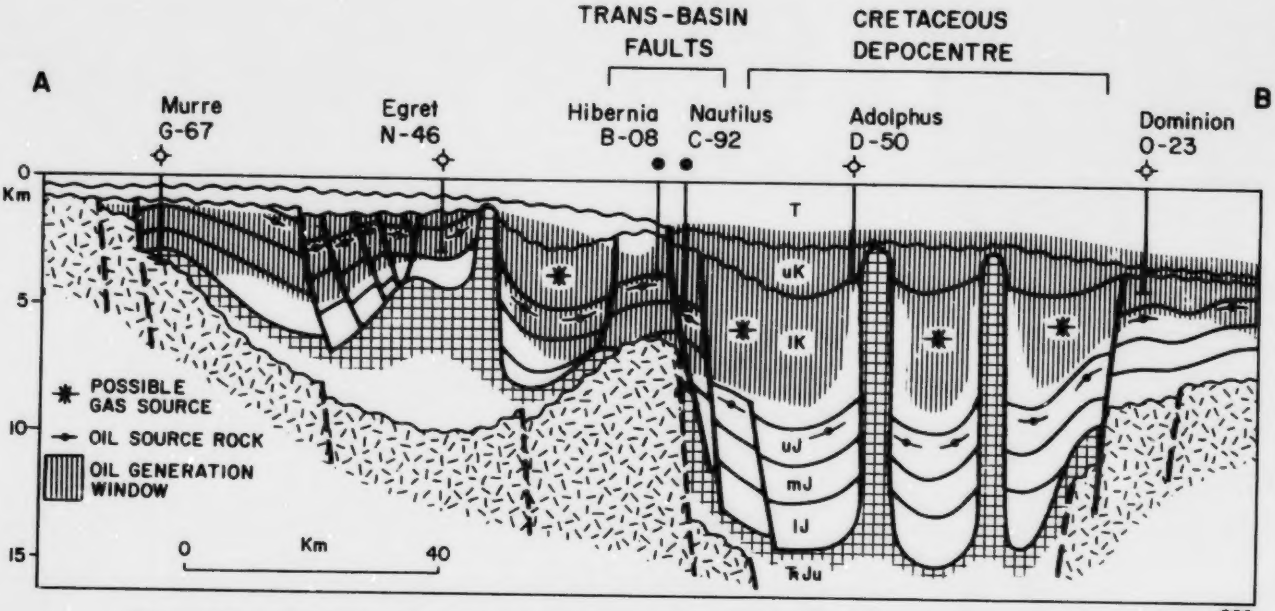

Figure 59.5. Schematic cross-section of the Jeanne d'Arc Basin showing the oil window in relation to source rock distribution (see location in Fig. 59.2). TrJu – Triassic/Jurassic undifferentiated, 1J – Lower Jurassic, mJ Middle Jurassic, uJ – Upper Jurassic, 1K – Lower Cretaceous, uK – Upper Cretaceous, T – Tertiary.

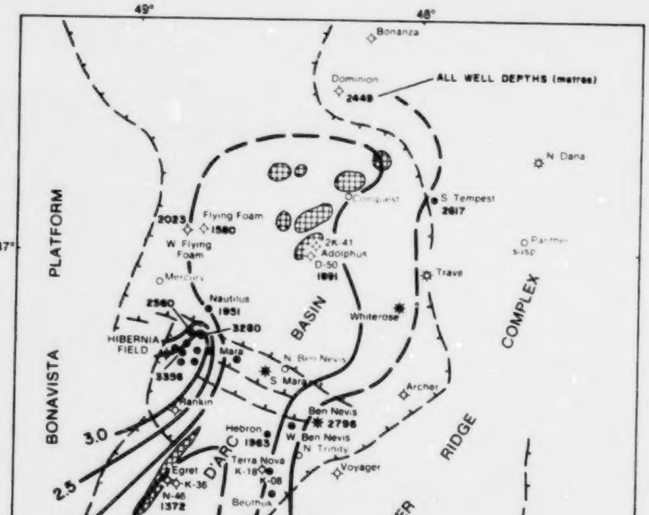

Figure 59.6. Preliminary map showing depth below sea level to top of oil window (0.5 Ro) in the Jeanne d'Arc Basin.

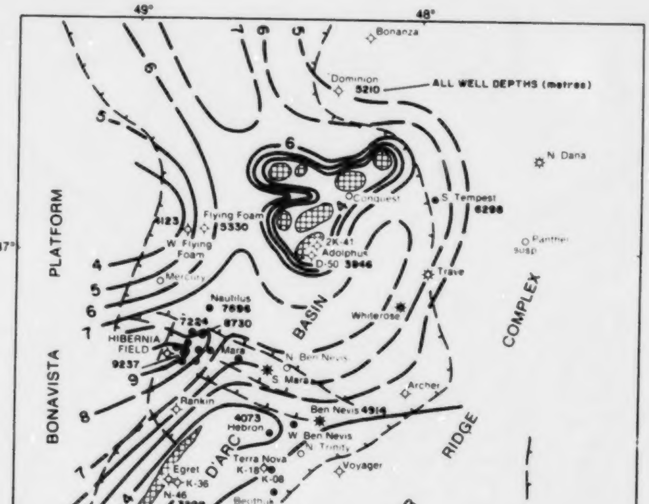

Figure 59.7. Preliminary map illustrating extrapolated depth below sea level to base of oil window (1.35 Ro) in the Jeanne d'Arc Basin.

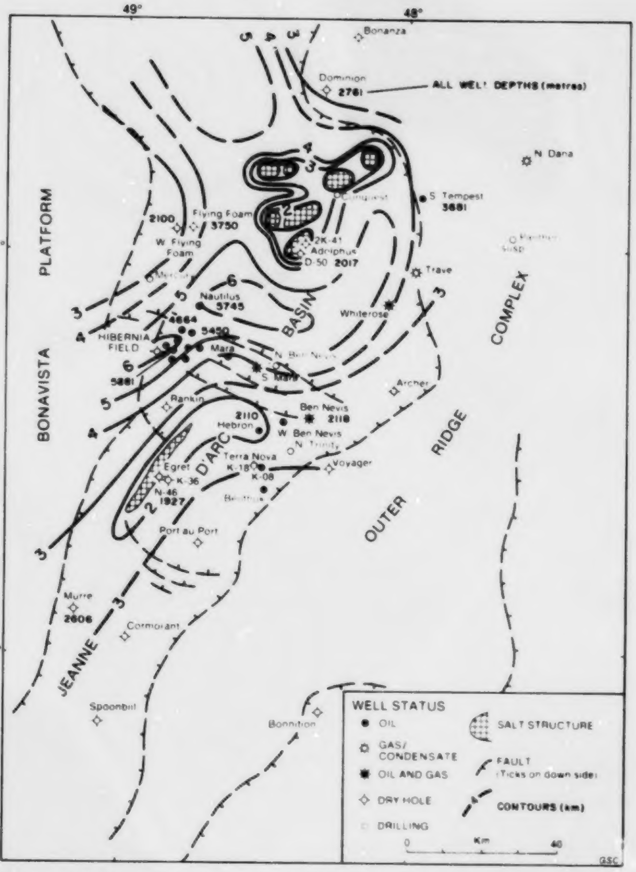

Figure 59.8. *Preliminary map illustrating inferred thickness of oil window in the Jeanne d'Arc Basin.*

surface of these two structural elements underwent peneplanation which gave rise to the Avalon Unconformity. Subsequently, the truncated basinal and basement rocks were overlain by a seaward thickening wedge of latest Mesozoic and Tertiary sediments.

The Jeanne d'Arc Basin is a southerly extension of the East Newfoundland Basin. It is a fault-bounded depocentre containing at least 14 km of sediments and lies between the stable Bonavista Platform, composed of metamorphosed Precambrian and Paleozoic rocks, and the Outer Ridge Complex which contains highly faulted Mesozoic sediments stratigraphically equivalent to the basal portion of the basin-fill sequence (Fig. 59.2).

The Jeanne d'Arc Basin and Outer Ridge Complex have been the site of all the significant hydrocarbon discoveries on the Grand Banks to date, including the giant Hibernia oil field.

Methods

Vitrinite reflectance in oil (Ro) was measured on samples obtained from kerogen residues collected during routine sample preparation for palynology (Davies and Avery, 1984). Polished grain mounts were prepared from residues derived from ditch cuttings, and a Zeiss Photomultiplier III incident light microscope system was used to identify vitrinite grains and measure their reflectance. A fully integrated Zonax microcomputer linked to the microscope provided direct shutter control, data acquisition, manipulation and display. With this system, basic statistical information can be updated as readings are made, and a continuous histogram can be displayed to monitor the range of values being recorded. Ideally, approximately one hundred reflectance readings should be made on each sample.

Ditch cutting residues often contain indigenous, reworked, caved and oxidized vitrinite grains and may include other vitrinite-like macerals which can be misidentified. In addition, petrographic criteria cannot easily be applied to identify the primary indigenous population. Therefore, it is necessary to assess the reflectance values obtained for each sample and select the primary population on which the mean Ro value will be determined. This involves comparing histograms of reflectance values measured on successive samples. In many cases there is a unimodal population and the choice is straightforward. Where multimodal populations are present, the values identified as primary are those which most closely fit the sequence established from adjacent samples. The data were plotted log normally and a maturation profile fitted by linear regression (Dow, 1977).

Results

In this report, we present vitrinite reflectance values and maturation profiles from eight wells in the Jeanne d'Arc Basin (Fig. 59.3, 59.4 and Appendix) for which there was good sample coverage and where the kerogen residues contained enough vitrinite for reliable reflectance measurements (Avery, 1981a, 1984, 1985a, b, c; Ervine, 1984a; Harrison, 1984a, b). The results from these eight wells have been used to interpret the maturation configuration of the basin (Fig. 59.5), and this interpretation has been augmented by vitrinite reflectance values from five other, less sampled, wells (Avery, 1981b, 1985d; Ervine, 1984b, c; Harrison, 1984c). Data coverage is biased by a concentration of wells in and around the Hibernia oil field, which reflects both recent drilling activity and information release.

The maturation profiles of the eight wells reveal significant variations in the rate of increase of maturation with depth, which appear to be related to their structural setting within the Jeanne d'Arc Basin. Adolphus D-50 and Egret N-46 are located near salt diapir structures and exhibit overall maturation gradients in the order of 0.2 log Ro/km. These high maturation gradients imply that the oil window is compressed at these locations. If we assume that oil can be generated from suitable source rocks between maturation levels corresponding to 0.5 Ro and 1.35 Ro, the oil window is approximately 2000 m thick at Adolphus D-50 and Egret N-46 and their tops are at 1891 and 1372 m below sea level respectively (Fig. 59.6, 59.7, 59.8).

Murre G-67 and Dominion O-23 are located on the basin margins. Stratigraphically the two wells are quite different. Murre G-67 encountered a relatively thin Cenozoic section overlying a much truncated Mesozoic section before bottoming in Devonian basement at 3337 m K.B. Dominion O-23 penetrated 2.5 km of Tertiary clastics before bottoming in Lower Cretaceous shales at 3998 m K.B. Nevertheless, both wells exhibit overall maturation gradients of 0.15 log Ro/km. Extrapolating the maturation/depth profiles indicates a 2606 m thick oil window between 1464 and 4070 m in Murre G-67 and 2761 m thick oil window between 2449 and 5210 m in Dominion O-23 (Fig. 59.6, 59.7, 59.8). These oil windows are believed to be representative of the basin margins.

The other four wells lie within or close to the Hibernia oil field and all have steep overall maturation profiles in the 0.07 log Ro/km range. These wells therefore exhibit thick oil windows. Due to their steep maturation gradients, 1.35 Ro oil floor values have to be obtained by projecting well below

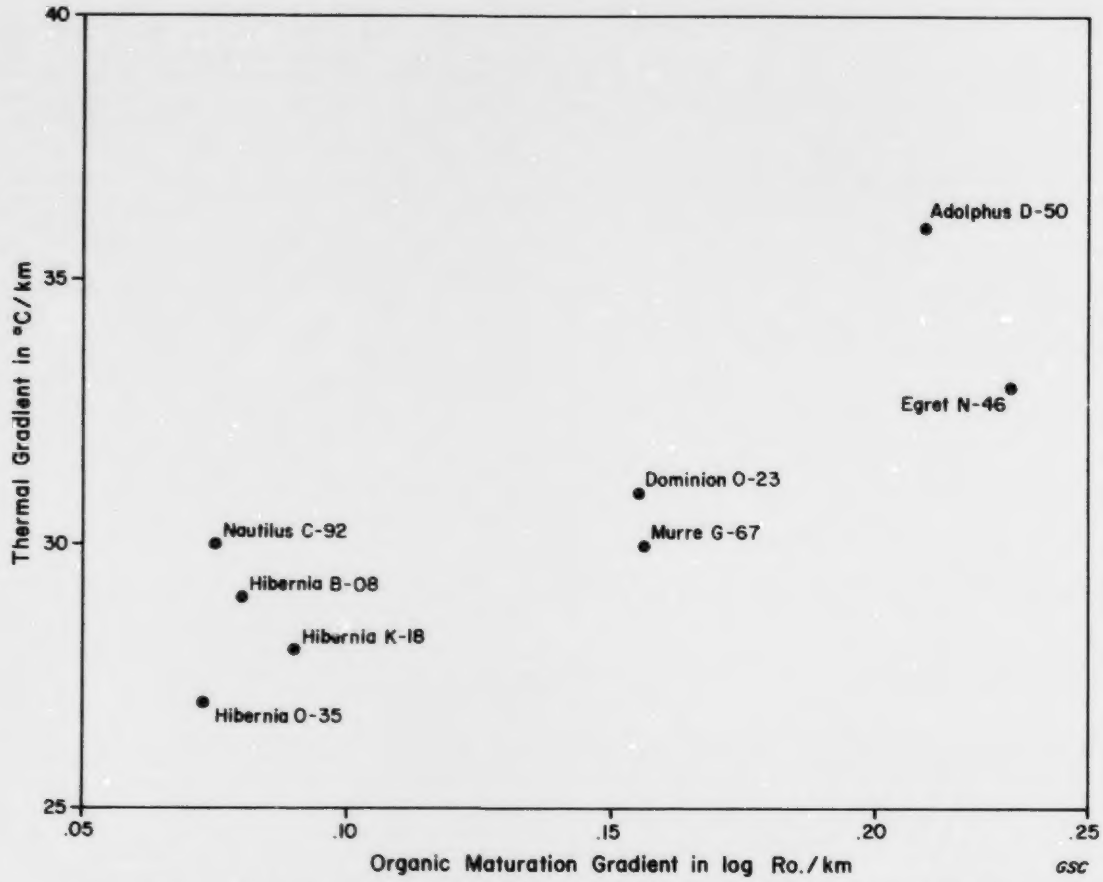

Figure 59.9. *Relationship between thermal and maturation gradients in the Jeanne d'Arc Basin.*

the sample intervals for Hibernia B-08, Hibernia K-18, Hibernia O-35 and Nautilus C-92. They indicate oil windows 4.5-6 km thick (Fig. 59.5, 59.8). It should be noted that the maturation values obtained from samples from Hibernia K-18 do not exhibit a regular increase with depth. This may be due to the presence of cavings or, possibly, absorbed oil may have suppressed vitrinite reflectance levels (Avery, 1984).

Although these eight wells do not adequately cover the whole Jeanne d'Arc Basin, they do allow a preliminary model of the maturation configuration to be outlined. This model is summarized in Figure 59.5, in which the cross-section illustrates our interpretation of maturation around salt diapirs, trans-basin faults, the main depocentre and the basin margins.

Maturation gradients in the Jeanne d'Arc Basin are closely related to present day thermal gradients. High maturation gradients clearly characterize wells with high thermal gradients and vice versa (Fig. 59.9). The correspondence between high thermal gradients at Adolphus D-50 and Egret N-46 and their relatively high maturation gradients is particularly noteworthy, as are the low thermal and maturation gradients at the three Hibernia wells and Nautilus C-92 (Fig. 59.9). It is worthwhile to consider the possible reasons for the present day variation in thermal gradients across the Jeanne d'Arc Basin. The conductivity contrast between the salt (high) and the adjacent sediments (low) allows salt diapirs to funnel heat upward into surrounding sediments but this effect alone may not raise temperatures in the sediments enough to cause significant increases in maturation levels (Keen, 1983). According to Keen (1983), upward migration of hot fluids around the Primrose diapirs on the Scotian Shelf may have caused the observed local enhancement of thermal maturity. We believe similar factors may be involved in the Jeanne d'Arc Basin. For instance, the small amount of oil recovered in a drill stem test at Adolphus 2K-41 has been shown to have been sourced in Upper Jurassic shales (Powell, 1984). This source rock now lies about 7 km below the reservoir, so conduits for significant vertical fluid migration must exist. We suspect that high maturation gradients will only characterize sediments immediately surrounding salt diapirs, and that the phenomenon will be local. The low thermal gradients of wells in the Hibernia area appear to characterize the trans-basin fault trend and the deeper parts of the Jeanne d'Arc Basin, and are believed to reflect the relatively low thermal conductivities of the thick Mesozoic clastic section. The median thermal gradients of the basin margin wells are thought to reflect the higher conductivities of the Pre-Mesozoic basement compared to the relatively thin Mesozoic-Cenozoic section. Present day thermal gradients therefore appear to be structurally controlled and reflect conductivity contrasts, as do maturation gradients.

Implications and conclusions

The structural configuration of the Jeanne d'Arc Basin was established prior to Late Cretaceous time (Grant et al., in press). Over the last 100 million years minor adjustments on faults and around diapirs have occurred, but the dominant process has been burial beneath a continuously accreting blanket of prograding latest Mesozoic and Tertiary sediments. Today's thermal gradient configuration is therefore likely to have existed throughout the last

100 million years. If so, the maturation configuration we can now map is likely to have had a similar form since Late Mesozoic time and a similarly shaped oil window can be assumed to have risen stratigraphically through the section during this period.

Bujak et al. (1977a, b), Swift and Williams (1980) and Powell (1984) recognized oil-prone Upper Jurassic source rocks in the Jeanne d'Arc Basin and Powell (1984) showed that these Kimmeridgian shales had sourced the oil reservoired at Hibernia and several other discoveries in the basin. Time Temperature Index calculations at the Nautilus C-92 location (Ervine, 1985) suggest that the Kimmeridgian shales reached the threshold for oil generation (Ro-0.5) during Albian time and that peak oil generation (Ro-0.8) occurred during Early Eocene time. No other wells studied by Ervine (1985) showed potential for earlier generation of hydrocarbons, although this may have occurred in the deeper parts of the basin. What is clear is that all the traps beneath the Avalon Unconformity were in existence approximately 100 million years ago and, from that period onwards, an oil window existed which is likely to have had a three-dimensional geometry very similar to its present configuration. Today the oil window is thickest in the Lower Cretaceous depocentre downdip of the trans-basin fault trend and the giant Hibernia oil field. This is the area, therefore, where the oil-prone Kimmeridgian shales spent the longest period within the oil window, and where oil generation should have been the most efficient. It is probably no coincidence that much oil has been found updip from this zone of high oil generative potential (Grant et al., in press).

The Lower Cretaceous shales in the Jeanne d'Arc Basin are rich in gas-prone kerogen (Ervine, 1985), and Grant et al. (in press) have suggested that the gas discovered at the North Dana I-43 and Trave E-87 locations may have been sourced from them. Alternatively, this gas may have been generated in the deeper part of the basin from Kimmeridgian shales which are now probably overmature for oil generation.

Acknowledgments

The authors are most grateful to B.J. Crilley and W.C. MacMillian for preparing the kerogen residues, and to G.M. Grant for drafting the figures. Suggestions from A.C. Grant and B.C. MacLean have improved the text.

References

Avery, M.P.

1981a: Vitrinite reflectance measurements of coals in Mobil et al. Hibernia O-35 well; Atlantic Geoscience Centre, Report EPGS-DOM.8-80PAH.

1981b: Vitrinite reflectance measurements of coals in the Mobil et al. Ben Nevis I-45; Atlantic Geoscience Centre, Report EPGS-DOM.7-81PAH.

1984: Vitrinite reflectance (Ro) on the dispersed organics and coaly inclusions in core samples in Mobil et al. Hibernia K-18; Atlantic Geoscience Centre, Report EPGS-DOM.3-84MPA.

1985a: Vitrinite reflectance (Ro) on the dispersed organics in the Mobil Gulf Adolphus D-50; Geological Survey of Canada, Open File 1199.

1985b: Vitrinite reflectance (Ro) on the dispersed organics in the Mobil Gulf Dominion O-23; Geological Survey of Canada, Open File 1200.

1985c: Vitrinite reflectance (Ro) of the dispersed organics and coaly matter from Mobil et al. Hibernia B-08 (revised report); Geological Survey of Canada, Open File 1201.

Avery, M.P. (cont.)

1985d: Preliminary report on vitrinite reflectance (Ro) of dispersed organics in Mobil-Gulf Flying Foam I-13; Atlantic Geoscience Centre, Report EPGS-DOM.6-85MPA.

Bujak, J.P., Barss, M.S., and Williams, G.L.

1977a: Offshore eastern Canada – Part I. Organic type and colour and hydrocarbon potential; Oil and Gas Journal, v. 75, no. 14, p. 198-202.

1977b: Offshore eastern Canada – Part II. Organic type and colour and hydrocarbon potential; Oil and Gas Journal, v. 75, no. 15, p. 96-100.

Davies, E.H. and Avery, M.P.

1984: A system for vitrinite reflectance analysis on dispersed organic matter for offshore eastern Canada; in Current Research, Part A, Geological Survey of Canada, Paper 84-1A, p. 367-372.

Dow, W.G.

1977: Kerogen studies and geological interpretations; Journal of Geochemical Exploration, v. 7, p. 79-99.

Ervine, W.B.

1984a: Vitrinite reflectance (Ro) on the dispersed organics in Mobil et al. Nautilus C-92 well; Atlantic Geoscience Centre, Report EPGS-DOM.21-84WBE.

1984b: Vitrinite reflectance (Ro) on the dispersed organics in Mobil Hebron I-13; Atlantic Geoscience Centre, Report EPGS-DOM.11-84WBE.

1984c: Vitrinite reflectance (Ro) on dispersed organics in Mobil et al. South Tempest G-88 well; Atlantic Geoscience Centre, Report EPGS-DOM.19-84WBE.

1985: A synthesis of hydrocarbon maturation data for the East Newfoundland Basin; Geological Survey of Canada, Open File 1178.

Grant, A.C., McAlpine, K.D., and Wade, J.A.

– Offshore geology and petroleum potential of Eastern Canada; in Energy Exploration and Exploitation; Elsevier, England. (in press)

Harrison, P.H.

1984a: Vitrinite reflectance (Ro) on the dispersed organics in the Amoco Imperial Skelly Egret N-46; Geological Survey of Canada, Open File 1170.

1984b: Vitrinite reflectance (Ro) on the dispersed organics in the Amoco-IOE A-1 Murre G-67; Geological Survey of Canada, Open File 1168.

1984c: Vitrinite reflectance (Ro) on the dispersed organics in the Mobil et al. West Flying Foam L-23; Atlantic Geoscience Centre, Report EPGS-DOM.27-84PHH.

Keen, C.E.

1983: Salt diapirs and thermal maturity, Scotian Basin; Bulletin of Canadian Petroleum Geology, v. 31, no. 2, p. 101-108.

Powell, T.G.

1984: Hydrocarbon-source relationships, Jeanne d'Arc and Avalon Basins, offshore Newfoundland; Geological Survey of Canada, Open File 1094.

Swift, J.H. and Williams, J.A.

1980: Petroleum source rocks, Grand Banks area: in Facts and Principles of World Petroleum Occurrence, ed. A.D. Miall; Canadian Society of Petroleum Geologists, Memoir 6, p. 567-588.

APPENDIX

Vitrinite reflectance data from eight wells drilled in the Jeanne d'Arc Basin

Depth range below K.B.	Mean Ro (SD) non-rotated	Number of readings Total	Number of readings Edited
ADOLPHUS D-50			
(feet)*			
4440-4470	.37(±.06)	50	31
5010-5040	.42(±.08)	45	30
5460-5490	.47(±.08)	46	32
5730-5760	.48(±.07)	47	33
6180-6210	.48(±.06)	44	36
6630-6660	.54(±.05)	56	45
6990-7020	.51(±.06)	44	36
7410-7440	.57(±.08)	45	27
7800-7830	.59(±.09)	80	60
8100-8130	.58(±.05)	45	38
8800-8830	.79(±.07)	61	10
9100-9130	.82(±.11)	51	9
9500-9530	.85(±.11)	58	12
10000-10030	.98(±.08)	74	47
11400-11430	1.07(±.10)	83	45
11700-11730	1.04(±.10)	18	11
12000-12030	1.10(±.10)	44	24
EGRET N-46			
(feet)*			
1140-1170	.31(±.04)	35	27
1470-1500	.27(±.06)	60	22
2220-2250	.40(±.06)	33	33
4910-4940	.52(±.02)	99	13
5310-5340	.51(±.05)	39	8
5610-5640	.56(±.04)	51	5
6710-6740	.74(±.05)	28	12
7470-7500	.84(±.06)	87	26
7970-8000	.89(±.06)	59	15
8470-8500	.88(±.06)	50	12
HIBERNIA O-35			
(metres)*			
2055-2065	**.41(±.01)	10	10
2310-2320	**.41(±.05)	27	27
2535-2545	**.44(±.05)	16	16
2845-2855	**.49(±.05)	4	4
3140-3150	**.45(±.05)	42	42
3235-3245	**.49(±.06)	7	7
3593-3605	**.50(±.05)	7	7
3945-3955	**.52(±.04)	50	50
4000-4010	**.56(±.06)	44	44
4640-4650	**.66(±.03)	13	13
DOMINION O-23			
(feet)*			
1830-1860	.24(±.04)	32	17
2100-2130	.26(±.05)	29	22
2850-2880	.27(±.05)	30	17
3480-3510	.33(±.05)	54	36
4470-4500	.32(±.05)	33	24
6360-6390	.44(±.07)	39	25
7270-7300	.46(±.06)	65	40
7670-7700	.46(±.05)	28	20
7970-8000	.55(±.08)	75	47
8270-8300	.54(±.06)	38	28
8570-8600	.53(±.04)	39	22
8970-9000	.57(±.05)	42	31
9370-9400	.58(±.05)	34	21
9770-9800	.59(±.06)	33	29
10070-10100	.60(±.05)	43	29
10380-10410	.57(±.04)	54	41
11490-11520	.74(±.05)	99	22
HIBERNIA B-08			
(metres)*			
1165-1205	.32(±.02)	14	9
1255-1295	.39(±.05)	40	35
1495-1635	.42(±.04)	33	30
1985-1995	.40(±.04)	54	22
2659.0	.41(±.05)	32	29
2669.2	.46(±.05)	32	31
2672.0	.47(±.05)	35	31
3482.4	.47(±.03)	21	21
3483.0	.47(±.03)	24	24
3488.0	.48(±.04)	31	31
3496.0	.48(±.03)	17	17
3554.3	**.50(±.03)	46	46
3556.6	**.47(±.05)	50	50
3557.0	**.49(±.04)	44	44
3559.1	.48(±.03)	20	20
3562.0	.50(±.06)	32	32
3606.7	.54(±.03)	22	20
3618.0	.46(±.04)	19	19
3990-4000	.61(±.04)	42	28
4110-4120	.64(±.06)	25	13
4155-4165	.64(±.06)	35	16
4185-4195	.62(±.09)	30	23
4245-4255	.68(±.07)	13	6
4335-4345	.69(±.04)	15	3
4425-4435	.62(±.05)	21	8
HIBERNIA K-18			
(metres)*			
1630-1640	.39(±.05)	20	17
1715-1725	.41(±.05)	39	39
1805-1815	.41(±.06)	18	18
1925-1935	.47(±.07)	30	30
2195-2205	.49(±.05)	16	16
2385-2395	.48(±.06)	37	33
2475-2485	.50(±.08)	58	53
2535-2545	.48(±.10)	50	50
2625-2635	.47(±.07)	71	70
2685-2695	.48(±.06)	30	30
2930-2940	.50(±.07)	61	61
3050-3060	.51(±.07)	43	43
3230-3240	.53(±.10)	78	78
3415-3425	.54(±.09)	99	98
3535-3545	.53(±.08)	99	97
3820-3820	**.52(±.01)	50	50
3995-4005	.50(±.09)	56	56
4115-4225	.51(±.06)	21	14
4175-4185	.58(±.06)	41	37
4325-4335	.57(±.10)	23	17
4475-4485	.54(±.07)	42	36
4595-4605	.50(±.06)	41	33
4690-4700	.52(±.06)	29	19
4750-4760	.82(±.04)	18	10
4810-4820	.78(±.08)	23	10
4930-4940	.73(±.05)	54	10
5015-5025	.87(±.02)	26	3
MURRE G-67			
(feet)*			
1470-1500	.26(±.04)	36	4
1980-2010	.50(±.01)	16	2
2530-2560	.44(±.05)	80	3
3230-3260	.35(±.03)	50	13
3980-4010	.42(±.05)	99	19
4480-4510	.53(±.02)	42	3
4980-5010	.50(±.05)	99	32
5480-5510	.56(±.05)	99	28
5980-6010	.58(±.05)	99	43
6470-6500	.67(±.05)	99	94
6610-6640	.66(±.06)	77	73
7070-7100	.67(±.03)	57	53
7470-7500	.68(±.04)	99	94
8270-8300	.72(±.06)	84	22
8730-8760	.76(±.04)	55	15
9380-9410	.78(±.09)	54	18
9730-9760	.92(±.06)	99	26
9880-9910	.81(±.02)	44	8
NAUTILUS C-92			
(metres)*			
1395-1405	.42(±.03)	62	61
1515-1525	.40(±.02)	85	83
1635-1645	.44(±.03)	84	79
1755-1765	.47(±.03)	99	96
1875-1885	.50(±.02)	99	94
1995-2005	.52(±.03)	99	93
2115-2125	.54(±.03)	21	17
2235-2245	.52(±.03)	21	21
2355-2365	.53(±.04)	14	10
2475-2485	.56(±.03)	39	39
2595-2605	.57(±.02)	22	22
2755-2765	.61(±.04)	44	39
2875-2885	.63(±.04)	36	35
2995-3005	.66(±.03)	24	22
3115-3125	.67(±.04)	69	63
3355-3365	.68(±.03)	72	71
3550-3560	.68(±.03)	36	35
3840-3850	.68(±.04)	99	95
3960-3970	.69(±.03)	74	74
4200-4210	.71(±.04)	44	42
4600-4610	.69(±.04)	11	8
4835-4845	.81(±.03)	36	33
4955-4965	.82(±.02)	7	5
5105-5115	.85(±.01)	4	4

NOTES

* Depth units are given in original measurement units for accuracy

**Vitrinite reflectance measurements for these samples were taken on larger coaly particles obtained from cores and ditch cuttings.

(SD) denotes standard deviation

Geology of the southern and northern margins of the Springdale Caldera, Newfoundland

Contract 14SQ.23233-5-0076

Marylou Coyle[1] and D.F. Strong[1]
Precambrian Geology Division

Coyle, M. and Strong, D.F., Geology of the southern and northern margins of the Springdale Caldera, Newfoundland; in Current Research, Part A, Geological Survey of Canada, Paper 86-1A, p. 499-506, 1986.

Abstract

Further evidence is presented that the Springdale Group represents a caldera-fill sequence, on a scale equal to that only of continental-scale calderas of areas such as the southwestern U.S.A. Geochemical studies of samples collected last year show that the group comprises a calc-alkaline series from basalts to rhyolites, with the exception of a silica gap for the basaltic andesite range from 52 to 56% SiO_2. The rhyolites exhibit a silica gap at 73-74% SiO_2 which separates them into a high-silica and a low-silica group, the latter of which is comparable to those generally considered to have been derived from large layered magma chambers. Such rocks are often economically mineralized, and may indicate that the Springdale Group has some economic potential.

Résumé

De nouveaux indices portent à croire que le groupe de Springdale représente une séquence de remblais de caldeira qui n'a d'égale que celle des caldeiras continentales trouvées, entre autres, dans le sud-ouest des États-Unis. L'étude géochimique des échantillons prélevés l'an dernier montre que le groupe comprend une série calco-alcaline dont la composition varie des basaltes aux rhyolites, la seule exception étant une lacune de silice dans la gamme des andésites basaltiques variant de 52 à 56 % de SiO_2. La lacune de silice des rhyolites oscille entre 73 et 74 % de SiO_2, phénomène qui permet de les répartir en deux groupes, soit l'un à forte teneur et l'autre à faible teneur en silice, ce dernier étant comparable aux rhyolites vraisemblablement dérivées de vastes chambres magmatiques stratifiées. Ces roches minéralisées ont souvent une valeur commerciale et leur présence ici pourrait indiquer que le groupe de Springdale se prêterait peut-être à des travaux d'exploitation rentables.

[1] Department of Earth Sciences, Memorial University of Newfoundland, St. John's, Newfoundland A1B 3X5

Introduction

The Springdale Group occurs along the western margin of Newfoundland's Lower Paleozoic central volcanic belt, where the underlying crust is transitional between the Iapetus oceanic and arc-related material and the older continental crust of North America. In the first stage of this study (Coyle et al., 1985), we described the Springdale Group as it is seen on the Springdale map sheet, and tentatively interpreted it as a caldera-fill sequence. The present paper forms a continuation of that work to the south (Fig. 60.1) where the group is exposed on the Gull Pond, Topsails and Sheffield Lake map sheets and to the north (Fig. 60.2) on the King's Point sheet.

The group is made up of a series of interbedded basaltic flows, silicic and intermediate ash flow tuffs, and fluviatile red sandstones and conglomerates derived mainly from the volcanic rocks. In general these rocks occur in a northeast-trending synformal basin throughout the central Springdale sheet, but to the south they are more gently dipping and strike across this trend, and are intruded by younger or cogenetic granitoid rocks of the Topsails Complex. In the area between the Little Bay and Kings Point roads to the north they exhibit some local lithological and structural differences from the main parts of the group, possibly indicating deposition in a local subbasin.

Despite their great extent and potential importance to understanding postorogenic magmatic activity in the Appalachians, no geochemical studies have previously been done on rocks of the Springdale Group, although data available for the correlative Cape St. John Group were interpreted by Strong (1977) as essentially calc-alkaline. We have now completed the first stage of our geochemical studies of the Springdale Group, and demonstrate that they are similarly calc-alkaline, and comparable to orogenic calc-alkaline suites of circum-Pacific regions (Ewart, 1982). We further show that the group includes a series of high-silica rhyolites, which are similar to the high-silica rhyolites derived from large layered siliceous magma chambers of continental regions such as the Basin and Range area of southwest U.S.A. (cf. Lipman et al., 1978). The Springdale caldera is unlike any found with orogenic calc-alkaline suites in that its large size, representing a minimum eruption volume between 10^3 and 10^4 km^3, is matched only by the largest epicontinental calderas such as those of the southwestern U.S.A. This implies a similar Silurian-Devonian tectono-thermal environment for western Newfoundland, as do the high-silica ash flow compositions.

Description of map units

Tentative correlations with units described by Coyle et al. (1985) have been attempted in this report, based on field evidence alone. More precise evaluation of these distinctions are currently underway (i.e. petrography and geochemistry) as part of the first author's post-graduate thesis research at Memorial University of Newfoundland.

Unit 1 is located along the east and western margins of the map area, and extends as elongate lenses toward the south. Along the eastern margin the lens is roughly 15 km long with a maximum width of 3 km, while exposures of this unit along the western margin form two belts interbedded with other lithologies of the Springdale Group. Three smaller lenses of this unit are found near the south-central margin of the map area.

Unit 1 is in contact with older basement rocks along its eastern margin (units A and B) and is interbedded with various units of the Springdale Group (units 2,3,4,6,7,8,E and F). Unit 1 is tentatively correlated with unit 2 of Coyle et al. (1985), consisting of a distinctive laharic and explosion breccia composite unit. Unit 1 is dominated by laharic flows, with tuffites and peperites, volcanic conglomerates and local red sandstones, and volcanic explosion breccias. In general the volcaniclastic lithologies are characterized by poor sorting and massive to very coarse bedding. The lahars have dominantly subangular blocks, in a locally vesicular muddy or ashy matrix. Both the coarse and fine fractions of these deposits are compositionally variable from basalt to rhyolite. Bedding is commonly absent in the lahars, but where present it is reversely graded, with the finer basal horizon much thinner than the overlying coarse beds. The fabric of the laharic flows is isotropic, with local imbrication of elongate clasts.

The tuffites are composed of predominantly pyroclastic debris and reworked volcanic clasts, and could be further subdivided into tuffaceous conglomerates and tuffaceous breccias. Boulders in these units are not as large as those of the lahars, but are also commonly subangular to subrounded. The composition of the larger clasts ranges from basaltic scoria and bombs to rhyolitic tuffs of varied texture. The matrix is dominated by shards and broken crystals with minor lithic fragments, and is locally vesicular. The peperites are composed of fine- to medium-grained volcanogenic sandstones which have been "burrowed into" by basaltic and intermediate flows. These may include variable detritus, including cobbles and pebbles of underlying flows and/or breccias, pyroclastic deposits etc.

Volcanic conglomerates differ from the above in that they have been more extensively reworked and redeposited as a clastic sedimentary rock. They contain large, subrounded to rounded boulders and cobbles in a sand-sized matrix, with an absence of any clay-sized fraction. Most of the clasts are silicic volcanics, with fewer of andesitic and basaltic compositon, and pumaceous material is absent. Sorting in these units ranges from poor to good. Bedding is common, and may be thick and structureless, thin and finely laminated, or crossbedded. These deposits commonly show normal grading, especially obvious in scour fills or channel deposit horizons which are represented by red arkosic sandstones interbedded with the more silicic and well bedded conglomerate horizons of this unit.

Explosion breccias are very similar to monomict lahars with a microbrecciated matrix, commonly composed of intermediate or basaltic volcanic material as both clasts and matrix. Bedding is commonly absent and the fabric is isotropic or shows "streaming" from a gas brecciation process. Unit 2 was produced by a number of physical mechanisms. The predominant feature in all of it's subunits is the large size of the clasts, carried in a finer matrix, i.e. with a strongly bimodal size distribution. These units represent facies developed during volcanic activity, ranging from near-source explosion deposits, to more distal, fluvially reworked deposits. Some debris flows may have been activated on unstable slopes and rapidly deposited, whereas others could have had long periods of reworking.

This unit is important as a marginal facies marker for the caldera. Similar units occur at caldera margins in modern environments.

Unit 2 includes intermediate flows, flow breccias, and intrusions, distributed along the eastern border of the volcanics in a lens about 6 km long and 1.5 km wide and an isolated exposure is also found in the central portion of the map area with a roughly circular dimension of 2 km across. Unit 2, which is interbedded with units 1, 3 and 4, and in part intrudes them, consists of nonvesicular dacite and andesite flows, commonly very aphanitic, locally with phenocrysts of flow-aligned plagioclase. The massive to heavily flow-foliated flows are typically brecciated. Intrusions of massive andesite are also found. Coyle et al. (1985) described a minor

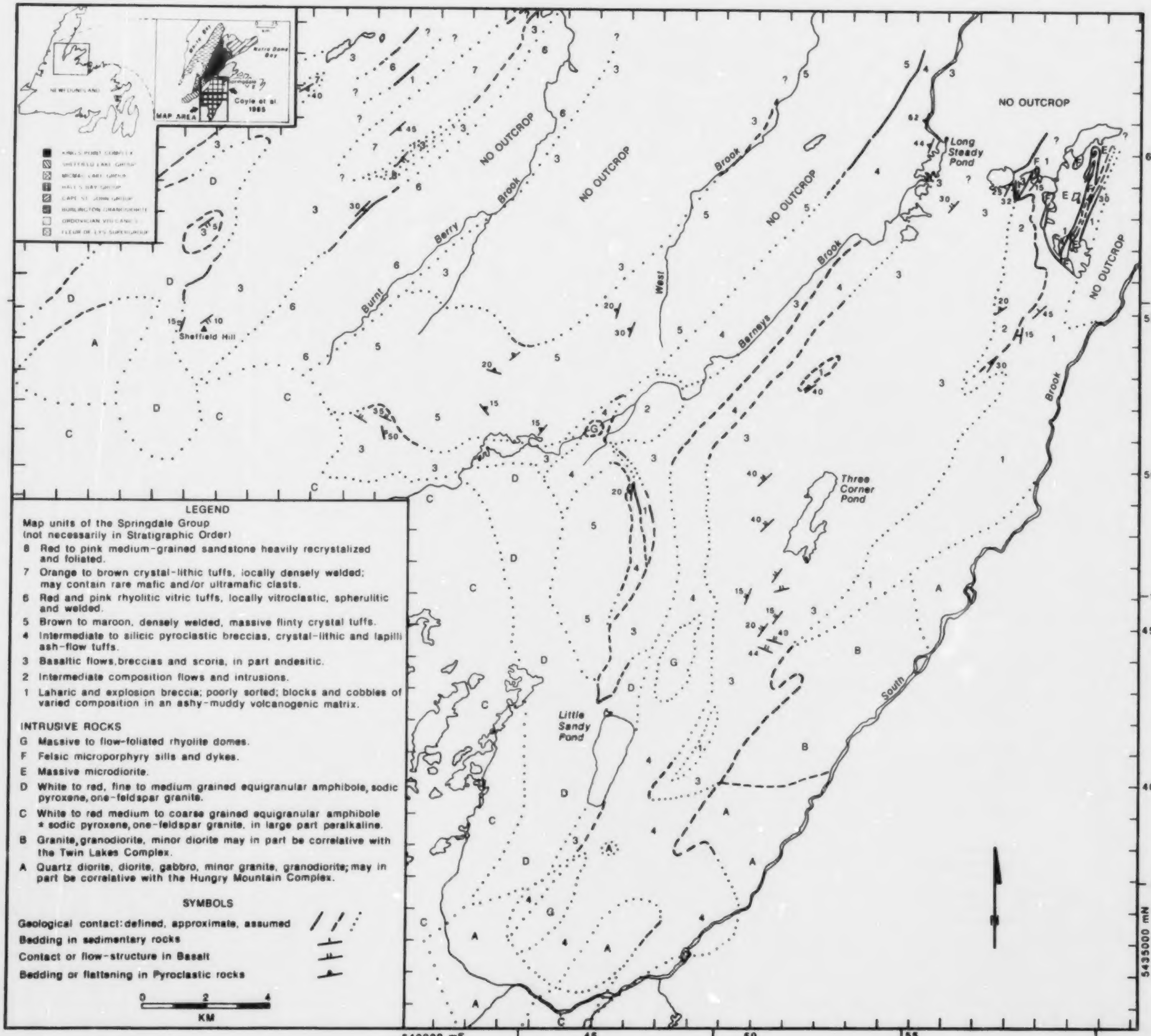

Figure 60.1. *Generalized geology of the southern parts of the Springdale caldera, Newfoundland.*

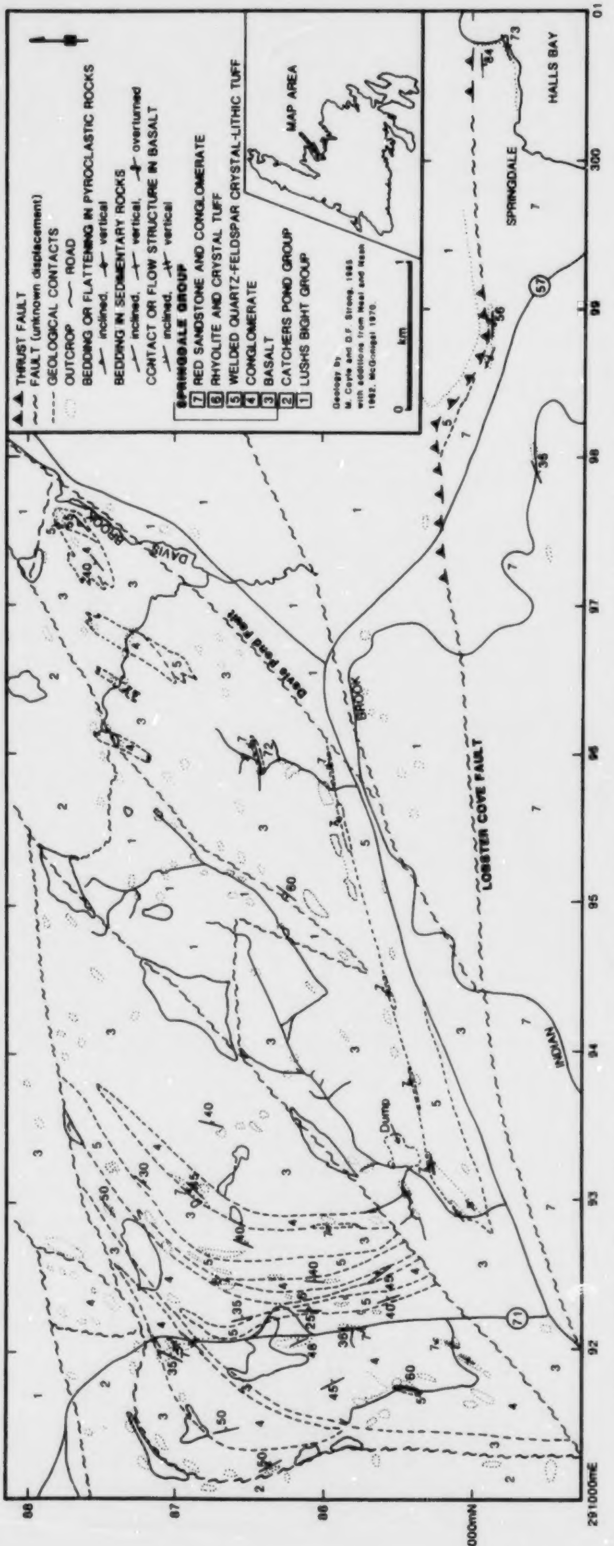

Figure 60.2. *Generalized geology of the Springdale Group between the Kings Point and Little Bay roads, Newfoundland.*

phase of this unit (on the northeastern Springdale sheet, unit 3), consisting of interbanded silicic and mafic compositions on the scale of centimetres and smaller.

The flows and intrusions of unit 2 represent a period of volcanism dominated by intermediate chemistry, unlike the other major lava flows, which are of basaltic composition. These intermediate rocks show some evidence of mixing of more mafic and silicic magmas, and it is expected that further study of the sequence of eruption of these units from their subjacent chamber should provide some indication of it's geometry and extent.

Unit 3 consists mainly of basaltic flows. Field evidence does not allow for a clear distinction of the compositional variation in the aphanitic and commonly hornfelsed flows. They are distributed throughout the entire area, best represented north of Three Corner Pond, along lower Barney's Brook and to the southwest on flat-topped ridges such as Sheffield Hill. This unit is found interbedded with units 1,2,4,5,6,7 and 8,is intruded by younger granitoid rocks of the Topsails Complex (units C and D), and rests disconformably upon, or is faulted against units A and B.

These flows are typically aphanitic, with local notable concentrations of plagioclase phenocrysts. They range from nonvesicular to highly vesicular, with amygdules of quartz, calcite and chlorite. The flows are variably altered throughout the entire Springdale Group and the secondary assemblages show no systematic geographic variation except along the eastern margins of the caldera where they have the greatest diversity of secondary minerals.

Unit 4 consists of silicic ash-flow tuffs, exposed continuously along Barney's Brook, in conformable contact with basaltic flows of unit 3, over a strike length of 14 km with a maximum width of 3 km on the Springdale sheet (unit 6, Coyle et al., 1985). They have been extended south an additional 22 km with maximum width of 6 km in the extreme southeast of the map area. These "Barney's Brook ash flows" are reddish brown to grey and display varying proportions of crystals, lithic fragments, and vitroclasts. On the Springdale sheet the basal part of the unit is a thick lithophysae-rich horizon resting on irregular flow tops of the basaltic unit 3. The individual lithophysae may be as large as 10 cm in diameter, with central cavities partially or completely filled with quartz crystals, radiating microlites, and chalcedony. This horizon grades up into a partially welded ashy crystal-lithic lapilli tuff. The phenocrysts are plagioclase, K-feldspar and quartz, commonly broken and concentrated in the matrix in preference to the pumice vitroclasts. A crude "bedding" is defined by flattening of the lapilli during welding.

The partially welded zone is vertically succeeded by a vitroclastic breccia tuff. Pumice bombs are flattened and can be as long as a metre. Concentrations of the large vitroclasts define a bedding which can be either normal or reversely graded. Throughout the partially welded zones, lithic fragments occur as local concentrations. They range from silicic volcanics to basalt and commonly define a bedding which is normally graded. These horizons are constant along strike, in terms of both their thickness and continuity along Barney's Brook.

A densely welded equivalent of the more northerly tuffs is found along the southern section of Barney's Brook and farther south, where the welding extends to its basal contact with underlying unit 3. The densely welded portions of unit 4 are maroon to brown lithic+vitric+crystal ash-flow tuffs. A welding lamination is seen on weathered surfaces, but on fresh surfaces they look massive and structureless. Phenocrysts are plagioclase, K-feldspar and quartz, which vary in relative proportions in a streaky manner.

Along the southeastern margin of Figure 60.1 unit 4 includes a strongly welded crystal-lithic tuff which has been brecciated during emplacement of a number of dome-like rocks (unit G). Unit 4 represents a number of pyroclastic flow units, each characterized by different proportions of lithics, vitroclasts, etc.

Unit 5 is found along West Brook and across the south central portion of the map. This unit is dacitic to rhyolitic, contains massive, vitric, strongly welded ash-flow tuffs, vitroclastic breccia and domes. Welding can be observed on weathered surfaces and is apparently flat lying in the southern exposures of this unit and becomes more steeply inclined on the Springdale sheet. Curvilinear joint surfaces are very common in the massive portions of the unit, internal plastic shear zones or local brecciation can been seen as well as flow folds. These features are indicative of domes and it is apparent from thin sections and geochemistry that there is at least one dome associated with this unit. The massive tuffs are locally porphyritic, with small euhedral flow-aligned plagioclase and rare quartz phenocrysts in a brown to maroon glassy matrix.

Petrographic studies have shown that the welded vitroclastic breccia described for unit 7 of Coyle et al. (1985), with very angular variably flow-folded and chaotically oriented "pumice fragments" represents the autobrecciated debris of cooling domal intrusions in the vicinity of contacts with their syngenetic pyroclastic veneer.

Unit 6 comprizes a sequence of silicic ash-flow tuffs and is intruded by high-silica dome rocks (unit B of Coyle et al., 1985). It extends throughout the central portion of the Springdale synform to the north and is mapped along the northwestern edge of this map as two NE-trending belts seen in Figure 60.1.

This unit includes an assemblage of dominantly devitrified, welded, pink and red rhyolitic K-feldspar-phyric, ash-flow tuffs and breccias, displaying a variety of features which represent processes of flow, autobrecciation, and devitrification in viscous rhyolitic flow tuffs. Since this ash-flow tuff grades into a sandstone at a few localities on the Springdale sheet, it may be part of a complex cooling unit rather than a simple cooling unit. Certain parts of this unit are very massive due to intense welding, and others consist of unwelded vitroclastic tuffs with large individually devitrified shards, each showing independent development of spherules. Other phases of the ash-flow breccias are not strongly devitrified, all with internal auto- or gas-brecciation textures. These breccias have clasts of plastically deformed rhyolitic lava and pumice. The vesicles are commonly infilled with pink to milky quartz.

The finer tuffs comprise a simple cooling unit with a sequence of massive welded ash flows, a partially welded horizon with lithophysae and spherulitic zones, and an upper breccia horizon. In the upper unit, mixed magmas are found within the breccias, with alternating thin basaltic and silicic bands. Near central Burnt Berry Brook the silicic tuffs are intruded by a rhyolitic plug or dome (unit B; see Coyle et al., 1985). These high silica rhyolite intrusions and flows have been studied geochemically during the past year and the results are discussed below.

Unit 7 occurs as an orange to brown densely welded crystal-lithic tuff in the interior of the central syncline of the Springdale Group (Coyle et al., 1985). Two areas of exposure are found in the northwestern extremity of this map area and extend as NE-trending exposures with a maximum length of 6 km and width of 2 km. This crystal tuff is very massive and because of the strong welding and obvious phenocrysts, it can have the appearance of an intrusive porphyry. It differs from unit 6 in that it has large obvious phenocrysts of quartz and feldspar, clasts of mafic and rare ultramafic lithologies, and does not demonstrate many of the fluidal characteristics of the other. The feldspars are often zoned and fractured, and together with the quartz can constitute up to 60% of the rock. The crystals are found in a red, brown or orange vitric aphanitic matrix. The lithics are commonly angular, and may have reaction haloes, especially the ultramafic clasts.

Unit 8 is found in one small ridge of exposure in the northwestern corner of the area (Fig. 60.1). It appears to be a sedimentary rock which has been deformed, possibly along a major axial fault which runs through the Springdale synform. The lithology is pink to red and has a sugary texture with foliated alignment of abundant pebbles. The range of more typical Springdale Group sedimentary facies is not mapped in this area, but until further study this lithology will be tentatively correlated with the sedimentary rocks.

Intrusive units

The intrusive rocks around the margins of the Springdale caldera have not been mapped as separate units. They have been sampled and their approximate contacts with the volcanic units have been delineated in the field so as to assess their diversity, relative ages and structural setting. Some of the information about these units (A,B,C, and D) has been compiled from Whalen et al. (1983), Thurlow (1981), Kalliokoski (1953, 1955) and Coyle et al. (1985) as well as aeromagnetic maps of the area.

Units E, F and G are genetically related to the Springdale volcanic sequences. The first two were mapped during the 1984 field season, and a few contact relationships were refined this year. They are found in the northeastern corner of the map area and have dimensions of 2.5 by 5 km. Unit E is a black fine grained microdiorite which is generally massive and is intruded by dykes and sills of unit F which is a pink massive aphanitic microporphyry. The porphyry is aphyric and in thin section is seen to contain finely disseminated bluish-green amphibole. We interpret this lithology to represent dykes and sills from a high-silica dome.

Unit G is found as three separate roughly oval exposures in the southern and central parts of the map. They are seen to intrude unit 4 and represent domes which have a common composition and array of textural features. They

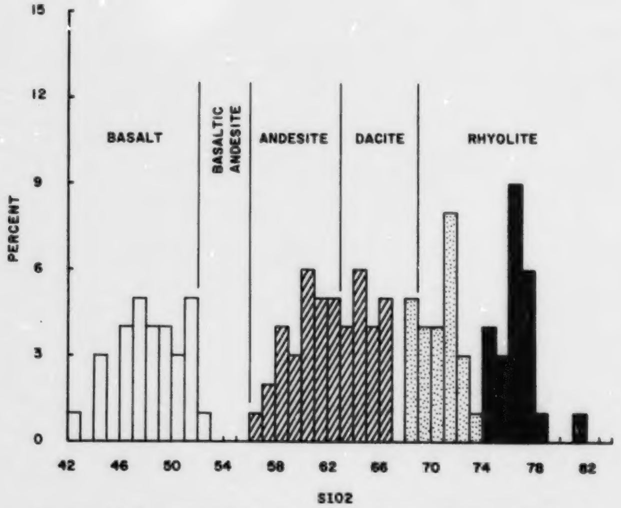

Figure 60.3. *Histogram of silica distribution in 133 volcanic rock samples of the Springdale Group. Classification boundaries are after Peccerillo and Taylor (1976).*

are flow-foliated with extreme convolution seen as fluidal folds and disruption of flow banding, autobrecciated and contain zones of intense development of spherules and other indications of gas-streaming. Autobrecciated aprons composed of disrupted fragments of the dome are considered as part of this unit. They are not reworked clasts in any sense and are commonly found in a glassy matrix which represents magma injected into the cooled rind along the margins of the intrusions.

King's Point Road area

This area was studied in some detail so as to clarify the geological relationships along the northwestern margin of the Springdale Group where it is bounded by older volcanic rocks of the Lushs Bight and Catchers Pond groups. Because this area occupies the edge of the basin where the Springdale Group is presumably thinnest, major changes in lithology can be caused by only very minor vertical movement along the numerous faults in the area. The result is a complex map (Fig. 60.2) with the various units having a limited strike length and being bounded by faults, more or less as shown by previous workers such as Neale and Nash (1960) and McGonigal (1970). We note, however, that the units appear to be distributed in a distinctly synformal pattern, not recognized by previous workers, with a NE-trending axial plane which is marked by one of the main faults shown on Figure 60.2.

The dominant unit of the Springdale Group on Figure 60.2 is the thickly bedded conglomerate (unit 4) which bounds the western part of the area and forms a series of upstanding ridges. It is best exposed in rock cuts along the King's Point road, where it is characterized by a wide variety of rounded clasts up to tens of centimetres across. They are mainly felsic and mafic volcanic rocks of local provenance within the Springdale Group, but some are of a granitic variety, the source of which has not been identified. The clasts are typically "floating" in a sand-sized matrix of volcanic derivation. The conglomerate is interbedded with air-fall tuffs towards the western edge of this unit, and basaltic flows along the King's Point road, both of which attest to its synvolcanic nature.

These rocks were clearly deposited by fluviatile and debris flow mechanisms traversing the full variety of rock types within the Springdale Group, and presumably deeper into the subvolcanic granitoid plutons. An obvious interpretation of these conglomerates is that they are roughly volcanologically equivalent to the coarse basaltic conglomerates/lahars which mark other margins of the Springdale caldera. Another interptetation is that they may represent a small sedimentary subbasin fill which has been moved to it's current position along the Lobster Cove Fault. They may in that case be a down-plunge facies of the synformally disposed Springdale Group which trends NNE and plunges toward the same direction.

The basaltic rocks (unit 3) in the area of Figure 60.2 are typical of those of the Springdale Group in general, with a purple to black colour, aphyric to coarsely plagiophyric, with large vesicles filled with quartz, calcite and chlorite. In many cases the vesicles are aligned so as to give a rough indication of bedding which is otherwise not seen in much of the area. Thin lenses of red sandstone are locally interbedded with the pyroclastics and the basalts, and may show some evidence of incorporation into the unconsolidated basaltic flows.

The felsic pyroclastic rocks of the area (Fig. 60.2) range from aphyric rhyolitic vitric tuffs or intrusions (on hills to the east of the King's Point road) to welded quartz-feldspar crystal-lithic tuffs (same area) to vitric coarse pyroclastic breccias grading into leached unwelded ash fall tuff (Springdale highway and north along power lines and dump road). Lithophysae-rich welded ash flows are seen along the King's Point road and to the east and west of it.

Unit 5 is orange to brown welded quartz and feldspar-phyric lithic tuff. The lithic fragments have a full range of volcanic compositions, but are dominantly basaltic. Welding textures help to demonstrate the orientation and stratigraphy of these units. A tentative correlation of this unit with unit 4 (Fig. 60.1) is suggested.

Unit 6 is found as a thin band interbedded with units 4 and 5. It is typically a pink to maroon ashy to glassy rhyolitic tuff and possible intrusions. The ashy parts of this unit may represent air fall which occurred at various periods during

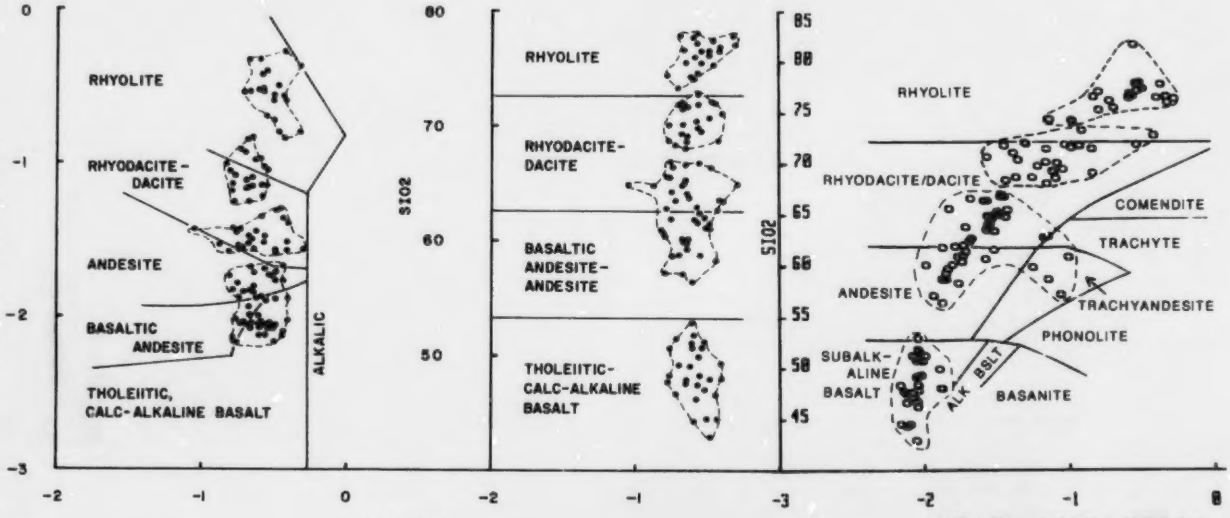

Figure 60.4. Classification of volcanic rocks of the Springdale Group in terms of silica and a number of "immobile" trace elements (boundaries after Winchester and Floyd, 1977).

the volcanism of the Springdale Group and thus is not easily correlated with a specific unit. The unit as a whole is like unit 4 (Fig. 60.1), although because of it's limited extent, less textural diversity is seen.

The sediments of unit 7 are typical of the Springdale Group in the vicinity of the town. They are fine- to medium-grained red and maroon sandstones, commonly graded, with local caliche horizons near the finer tops of beds. The sandstones are typically interbedded with pebble conglomerates which can represent the basal part of discrete sandy "cycles" of sedimentation. For further details on these lithologies see Wessel (1975).

Two groups of rocks are found in the map area which are not related to the Springdale Group; they are the Lushes Bight Group (unit 1) and the Catchers Pond Group (unit 2). In this study they were not mapped, but they were sampled and critical locations checked for structural information. McGonigal (1970) provided descriptions of these diverse and complex units in this region.

Geochemistry

Of some 622 samples collected during the 1984 field season, 133 have so far been analyzed for the major element oxides and 18 trace elements. Of these, 123 are of volcanic and associated subvolcanic rocks, and the others are from a variety of intrusive and other lithologies not directly related to the Springdale Group. Care was taken to exclude any rocks containing xenoliths or lithic clasts or amygdules, or which showed evidence of alteration. Other samples from both the 1984 and 1985 collections are being selected to provide a comprehensive geochemical data base for the Springdale Group. While the available data await a thorough assessment in conjunction with detailed petrographic studies, they do reveal a number of patterns which can be presented at this time.

A histogram of silica distribution (Fig. 60.3) confirms our earlier suggestion (Coyle et al., 1985), based on field and petrographic observations, that intermediate compositions are well represented in the Springdale Group. In fact one can see from Figure 60.3 that there are four groups separated by silica gaps between 53-56%, 67-68%, and 73-74% SiO_2. Using the terminology of Peccerillo and Taylor (1976), the lowest-silica group would be termed basalts, the intermediate group andesites-dacites, and both of the higher-silica groups would be termed rhyolites. For present purposes, the latter are termed low-silica and high-silica rhyolites. Only basaltic andesites are missing from making up the full calc-alkaline suite.

Using the Peccerillo and Taylor (1976) plot of K_2O vs. SiO_2, these rocks would be classified as a clearly calc-alkaline suite ranging from calc-alkaline basalts through andesites, dacites and the low-silica rhyolites. However the high-silica rhyolites show a much wider scatter to above 6% K_2O, and would thus be termed high-K rhyolites. Although this dispersion of K and other elements is a characteristic primary feature of high-silica magmas, and in many cases is associated with economic mineralization (see review by Tuach et al., 1985), there may have been some secondary redistribution of alkalis.

Other less mobile elements may provide more reliable classification, and some are shown in Figure 60.4 (after Winchester and Floyd, 1977). These elements also indicate that the Springdale Group is calc-alkaline. In this case, however, the rocks are grouped in different combinations from those seen in Figure 60.3, with the silica gap at basaltic andesites now spanned by the basaltic rocks, the andesites-dacites now classed as dacites, and the low-silica rhyolites now classed as rhyodacites-dacites. It can be seen from Figure 60.4 that this question is simply resolved by the fact that the Winchester and Floyd boundaries based on SiO_2 content are different from those of Peccerillo and Taylor. Since there is no significant variation in the Nb/Y ratio for any of these rocks, it is most useful to compare the data in terms of the parameters which are most variable in these classifications, i.e. Zr/Ti vs. SiO_2, as in Figure 60.4. Although the different groups are separated by silica on this diagram, there is a continuum in Zr/Ti ratio throughout the whole suite, confirming its truly calc-alkaline nature. More detailed studies are needed to identify and explain interesting

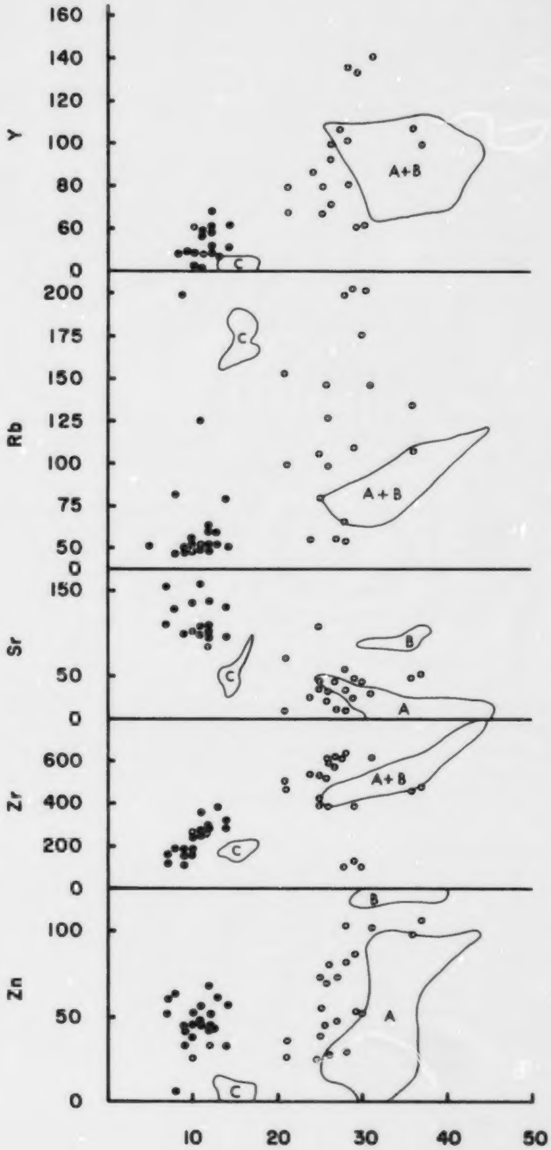

Figure 60.5. Variation of selected elements with niobium in the high-silica (circles) and low-silica (dots) rhyolites of the Springdale Group. Fields from the Kings Point area are shown for ignimbrites and porphyries (A), quartz-feldspar dykes (B), and granitic rocks (C), from Kontak and Strong (1986).

deviations from the calc-alkaline trend, such as the intermediate samples which have high Zr/Ti ratios on Figure 60.4.

The distinctive group of high-silica rhyolites merits further comment from both a petrogenetic and an economic viewpoint. With regard to the latter, they correspond precisely with those "specialized" volcanic and plutonic rocks which host economic deposits of Sn, W, Mo and other granophile elements, and are well known in both eastern Canada and western Europe. These rocks are most readily recognized by their high silica content, and indeed Tuach et al. (1985) have recently shown that 74% SiO_2 appears to be a critical minimum value for mineralization. In the case of the Springdale high-silica rhyolites, we further note that most of them are associated with small domes and their pyroclastic aprons, such as that exposed along the Burnt Berry Brook, and appear to have been emplaced late in the sequence.

The high-silica and low-silica rhyolites are compared in Figure 60.5, where a number of distinctive trace elements are plotted against niobium. It is clear that there is virtually a complete separation of the two types in terms of their Nb contents, as well as Zr, Sr and Y. The high-silica rhyolites also tend to have higher concentrations of Rb and Zn, but there is some overlap of the two groups. These differences in trace element concentrations are like those which distinguish peralkaline from metaluminous suites, and fields for two such suites from the probably correlative King's Point Complex (KPC) (Kontak and Strong, 1986) are drawn for comparison. Although the two groups from each area do not precisely overlap, it is clear that the same types of differences can be seen in both groups. The Springdale high-silica rhyolites are comparable to the peralkaline volcanics and dykes of the KPC, and the low-silica Springdale rhyolites are comparable to the KPC non-peralkaline intrusive rocks. An exception is seen for Rb, which is substantially enriched in the non-peralkaline KPC rocks but depleted in the Springdale low-silica rhyolites. These and other comparisons indicate that similar geochemical trends can be recognized in both volcanic and plutonic rocks from different parts of the Silurian-Devonian terranes of western Newfoundland, and may ultimately provide a means of precisely linking the volcanics with their intrusive source rocks. In this regard we note that in areas of well understood caldera type volcanism (e.g. Steven and Lipman, 1976), individual ash flow sheets can be traced to individual calderas, and this may well turn out to be the case for units of the Springdale and correlative groups.

Acknowledgments

We thank K.L. Currie for his continuing support of this project, P. Erdmer and J. Van Birkle for sharing helicopter time, J. Burry, D. Dingwell, D. and L. Kontak, P. Roberts, D. Taylor for field asistance, John O'Sullivan and Esso Minerals Ltd. for logistic support, G. Andrews, D. Press and G. Veinott for chemical analyses, and L. Nolan for drafting. We are especially grateful to the Newfoundland and Labrador Department of Forestry at Pynns Brook and Springdale for the use of their aerial photographs.

References

Coyle, M., Strong, D.F., Gibbons, D., and Lambert, E.
1985: Geology of the Springdale Group, central Newfoundland; in Current Research, Part A, Geological Survey of Canada, Paper 85-1A, p. 157-163.

Ewart, A.
1982: The mineralogy and petrology of Tertiary-Recent orogenic volcanic rocks: with special reference to the andesitic-basaltic compositional range; in Andesites, ed. R.S. Thorpe; John Wiley & Sons, p. 25-95

Kalliokoski, J.
1953: Springdale, Newfoundland: Geological Survey of Canada, Paper 53-5, 4 p.

1955: Gull Pond, Newfoundland (Second Preliminary Map); Geological Survey of Canada, Paper 54-4.

Kontak, D.J. and Strong, D.F.
1985: The volcano-plutonic King's Point Complex, Newfoundland; in Current Research, Part A, Geological Survey of Canada, Paper 86-1A, report 56.

Lipman, P.W., Doe, B.R., Hedge, C.E., and Steven, T.A.
1978: Petrologic evolution of the San Juan volcanic field, southwestern Colorado: Pb and Sr isotope evidence; Geological Society of America, Bulletin, v. 89, p. 59-82.

McGonigal, M.H.
1970: Geology of the Springdale Group west of the Little Bay Road, northwest central Newfoundland; unpublished B.Sc. thesis, Memorial University of Newfoundland, 37 p.

Neale, E.R.W. and Nash, W.
1960: Kings Point, Newfoundland; Geological Survey of Canada, Map 35-1960.

Peccerillo, A. and Taylor, S.R.
1976: Geochemistry of Eocene calc-alkaline volcanic rocks from the Kastamonu area, northern Turkey; Contributions to Mineralogy and Petrology v. 58, p. 63-81.

Steven, T.A. and Lipman, P.W.
1976: Calderas of the San Juan volcanic field, southwestern Colorado; U.S. Geological Survey, Professional Paper 958, p. 1-35.

Strong, D.F.
1977: Volcanic regimes of the Newfoundland Appalachians; in Volcanic Regimes in Canada, ed. W.R.A. Baragar, L.C. Coleman and J.M. Hall; Geological Association of Canada, Special Paper 16, p. 61-90

Thurlow, J.G.
1981: The Buchans Group: its stratigraphic and structural setting; Geological Association of Canada, Special Paper 22, p. 79-90.

Tuach, J., Davenport, P.H., and Dickson, W.L., and Strong, D.F.
1985: Geochemical enrichment/depletion trends in the Ackley Granite, southeast Newfoundland: their relevance to magmatic/metallogenic processes in high-silica granitoid systems; Canadian Journal of Earth Sciences.

Wessel, J.M.
1975: Sedimentary petrology of the Springdale and Botwood Formations, Central Mobile Belt, Newfoundland, Canada; unpublished Ph.D. thesis, University of Massachussetts, 216 p.

Whalen, J.B., Currie, K.L., and others
1983: Geology of the Topsails Igneous Terrane, Western Newfoundland; Geological Survey of Canada, Open File Map 923.

Winchester, J.A. and Floyd, P.A.
1977: Geochemical discrimination of different magma series and their differentiation products using immobile elements; Chemical Geology, v. 20, p. 325-343.

The mineralogy of the McGerrigle plutonic complex, Gaspé, Quebec[1]

Contract 12ST.23233-4-0044

G.M. Wallace[2]

Wallace, G.M., The mineralogy of the McGerrigle plutonic complex, Gaspé, Quebec; in Current Research, Part A, Geological Survey of Canada, Paper 86-1A, p. 507-514, 1986.

Abstract

The McGerrigle plutonic complex is a complex polyphase intrusive body that includes both under- and over-saturated rock types. Field relationships, petrography and mineralogy indicate that more than one type of petrogenetic process is responsible for variations between and within different rock types. Magma mixing is locally important; however, it is unlikely to be the most important process in the evolution of the volumetrically most abundant rock, granite. Many of the mafic to intermediate rocks exhibit evidence for metasomatism and recrystallization related to the intrusion of the more evolved felsic rocks. The undersaturated lithologies present in the pluton are alkali gabbro, small volumes of miaskitic nepheline syenite and tinguaite dykes. The tinguaites exhibit a complex mineralogy that varies with agpaitic index. The presence in this Devonian pluton of lithologies normally indicative of ensialic rifts is confirmed.

Résumé

Le complexe plutonique McGerrigle est une intrusion polyphasée qui comprend des roches sous- et sursaturées. Les relations de terrain, la pétrographie et la minéralogie indiquent que plusieurs processus pétrogénétiques sont responsables des variations entre les différents types de roches. Le mélange de magmas est important par endroits; cependant, il est peu probable que ce soit le processus le plus important dans l'évolution des roches granitiques qui prédominent dans le pluton. Plusieurs des roches mafiques à intermédiaires montrent des signes de métasomatisme et de recristallisation liés à l'intrusion des lithologies les plus felsiques. Les roches sous-saturées du pluton sont des gabbros alcalins, de faibles volumes de syénite miaskitique à néphéline et des dykes à tinguaïte. Les tinguaïtes présentent une minéralogie complexe qui varie selon leur index agpaïtique. On confirme la présence dans ce pluton dévonien de lithologies que l'on interprète couramment comme indices de rifts ensialiques.

[1] Contribution to the Canada Economic Development Plan for Gaspé-Lower St. Lawrence Mineral Program, 1983-88.

[2] Department of Geological Sciences, McGill University, Montreal, Quebec H3A 2A7

Introduction

The McGerrigle plutonic complex is a Middle to Late Devonian polyphase intrusive complex in the Gaspé Peninsula, Québec. The pluton forms a plateau approximately 100 km^2 in size that includes Mont Jacques-Cartier, the highest peak of the Canadian Appalachians. For a description of the general geology of the pluton, see Whalen (1985). This paper is based on a study of the petrography and mineralogy of a representative suite of 25 samples collected during the summer of 1984. The samples have been subdivided into five categories according to their chemistry, mode and mineralogy. Representative mafic mineral compositions are listed in Tables 61.1 to 61.4. The rocks assigned to a specific category are not necessarily petrogenetically related; the Rb/Sr data collected by C. Larocque (1985, personal communication) indicate the possibility of two distinct ages of intrusion in the map area during Devonian times. The work presented here is part of a broader project that includes studies of the whole-rock major and trace-element geochemistry (Whalen and Gariépy, 1986), lead-isotope geochemistry (C. Gariépy, in progress) and oxygen-isotope geochemistry.

Granite

Granite is the dominant rock-type of the McGerrigle plutonic complex. The complex has been subdivided into a granite and a hybrid suite (Fig. 61.1; Whalen and Gariépy, 1986). Small amounts of granite are also present in the hybrid suite. The hybrid granite contains many fine grained mafic inclusions that have been interpreted as evidence of a coexisting mafic magma (Whalen, 1985). Typically, the granites are medium- to coarse-grained, equigranular to porphyritic, and plot in the granite field in the IUGS classification scheme for plutonic rocks. Granite porphyry and alkali feldspar granite are also present.

Red-brown, perthitic alkali feldspar is typically subhedral to partly interstitial. Phenocrysts up to 1.5 cm in size may exhibit a rapakivi texture. In the granite porphyry, alkali feldspar forms a fine grained interlocking matrix with quartz and minor unzoned plagioclase. Low sanidine is typical, rather than microcline.

Plagioclase typically forms subhedral to euhedral, complexly zoned laths which, in some samples, are mantled by alkali feldspar. Its composition is sodic, typically

Table 61.1. Selected pyroxene compositions

SAMPLE	MG64[a] Av*(3)	MG64[b] Av(6)	MG6 Av(7)	MG25 Av(2)	MG23 Av(2)	MG40 Av(3)	MG8 Av(3)	MG90 Av(4)	Mg37[a] Av(2)	MG37[b] Av(5)	MG94 Av(4)	MG16 Av(3)
SiO_2	49.58	46.98	47.70	51.69	51.02	51.67	51.22	52.22	52.54	52.71	50.91	51.10
TiO_2	1.68	2.57	2.23	0.51	1.32	0.51	0.20	0.05	3.48	1.74	0.46	0.50
Al_2O_3	3.97	6.44	6.45	1.35	2.54	1.16	0.30	0.51	1.12	1.35	1.16	1.50
Fe_2O_3	**3.98	3.90	3.80	3.54	2.72	2.11	4.10	2.02	24.41	26.14	19.25	12.33
Cr_2O_3	0.02	0.00	0.01	0.02	0.00	0.00	0.00	0.00	0.00	0.00	0.00	0.00
MgO	14.47	12.97	13.45	10.94	15.22	12.50	8.18	11.59	0.37	0.27	1.45	6.48
FeO	3.56	4.26	4.17	9.04	6.03	9.42	13.48	8.98	2.50	2.94	6.43	5.94
MnO	0.22	0.15	0.18	0.50	0.37	0.95	1.39	0.92	0.54	0.38	2.09	1.55
ZrO_2	n.d.	n.d.	n.d.	n.d.	n.d.	n.d.	n.d.	n.d.	1.65	0.02	0.57[x]	0.24[y]
CaO	22.10	22.14	21.20	21.56	20.28	20.60	19.20	23.34	0.98	1.59	10.20	16.35
Na_2O	0.64	0.57	0.78	1.22	0.59	0.70	1.60	0.47	12.96	12.68	7.94	4.63
TOTAL	100.22	99.98	99.97	100.37	100.09	99.62	99.67	100.10	100.55	99.82	100.46	100.62
Si	1.834	1.753	1.772	1.950	1.891	1.955	1.988	1.974	2.004	2.014	1.978	1.981
AlZ	0.166	0.247	0.228	0.050	0.109	0.045	0.012	0.026	0.000	0.000	0.022	0.019
AlY	0.007	0.035	0.054	0.010	0.002	0.007	0.001	0.000	0.050	0.061	0.031	0.043
Ti	0.047	0.072	0.062	0.014	0.037	0.014	0.006	0.001	0.100	0.050	0.013	0.014
Fe^{3+}	0.111	0.109	0.106	0.100	0.076	0.060	0.120	0.058	0.700	0.751	0.562	0.482
Cr	0.001	0.000	0.000	0.001	0.000	0.000	0.000	0.000	0.000	0.000	0.000	0.000
Mg	0.797	0.720	0.744	0.614	0.840	0.704	0.473	0.652	0.021	0.015	0.084	0.115
Fe^{2+}	0.110	0.133	0.129	0.285	0.187	0.298	0.437	0.284	0.080	0.094	0.209	0.266
Mn	0.007	0.005	0.006	0.016	0.012	0.030	0.046	0.029	0.017	0.012	0.069	0.070
Zr	0.000	0.000	0.000	0.000	0.000	0.000	0.000	0.000	0.031	0.000	0.011	0.014
Ca	0.875	0.884	0.843	0.870	0.805	0.834	0.798	0.944	0.040	0.065	0.424	0.462
Na	0.046	0.041	0.056	0.089	0.042	0.051	0.120	0.034	0.957	0.438	0.597	0.535
$Mg/Mg+Fe^{2+}$	0.879	0.844	0.852	0.683	0.818	0.703	0.520	0.697	0.209	0.141	0.287	0.302

* Average of (n) analyses

** Fe_2O_3 and formula calculated by normalizing to 4 cations and then adjusting Fe^{3+} content so total number of oxygen atoms is equal to six following the recommendations of Robinson (1980).

x one determination only

y based on 3 analyses (not considered in the average composition).

Nomenclature after Poldervaart and Hess (1951) and Deer et al. (1978). MG64 low-Ti sector of titansalite (alkali gabbro), MG64b high-Ti sector of titansalite (alkali gabbro) MG6 titansalite (mafic inclusion), MG 25 secondary salite (alkali gabbro), MG23 titaniferous augite (syenodiorite), MG40 augite (monzonite), MG8 sodic ferroaugite (syenite), MG90 salite (diorite), MG37a titanaegirine (rim of phenocryst in peralkaline tinguaite) MG37b aegirine (core of 37a), MG94 aegirine-augite (intermediate tinguaite), MG16 aegirine-augite (miaskitic nepheline syenite).

Table 61.2. Selected amphibole compositions

SAMPLE	MG40 Av(5)	MG66 Av(4)	MG57 Av(5)	MG42 Av(3)	MG6 Av(4)	MG97 Av(5)	MG64 Av(8)	MG37 Av(7)
SiO_2	46.78	47.13	46.06	46.29	49.76	43.65	41.96	50.77
Al_2O_3	5.13	6.14	5.95	9.29	5.25	10.05	11.68	1.16
TiO_2	1.40	1.34	1.11	1.72	1.08	1.87	4.72	0.93
FeO	20.19	14.22	18.84	8.64	10.21	13.63	10.24	27.54
Fe_2O_3	4.4*	4.1*	4.4**	3.7**	5.0**	4.1**	1.8**	1.5**
MnO	1.21	0.69	0.98	0.26	0.36	0.32	0.23	2.81
MgO	7.69	11.24	8.20	14.35	13.66	10.81	13.15	1.74
CaO	9.43	10.60	10.74	11.32	11.47	11.58	11.26	1.09
Na_2O	2.16	1.82	1.94	2.64	0.88	2.04	2.76	7.96
K_2O	0.71	0.64	1.02	0.34	0.50	0.95	1.03	2.87
F^-	0.83	0.61	1.62	0.94	0.11	0.19	0.13	1.01
Cl	0.19	0.18	0.31	0.09	0.95	0.12	0.05	0.02
Total	99.74	98.40	99.97	98.80	97.86	98.75	98.77	98.78
O=F,Cl	0.39	0.30	0.75	0.41	0.07	0.03	0.00	0.13
Si	7.091	7.015	6.965	6.674	7.210	6.467	6.129	8.055
AlZ	0.909	0.985	1.035	1.326	0.790	1.533	1.871	0.000
Fe^{3+}Z	0.000	0.000	0.000	0.000	0.000	0.000	0.000	0.000
AlY	0.008	0.092	0.024	0.254	0.106	0.222	0.138	0.217
Ti	0.160	0.150	0.126	0.187	0.118	0.208	0.518	0.111
Fe^{2+}	2.560	1.770	2.382	1.042	1.238	1.689	1.252	3.653
Fe^{3+}	0.502	0.459	0.495	0.403	0.545	0.453	0.201	0.175
Mn	0.155	0.087	0.126	0.032	0.044	0.040	0.028	0.378
Mg	1.738	2.495	1.847	3.084	2.949	2.388	2.863	0.411
XOct	0.122	0.053	0.000	0.000	0.000	0.000	0.000	0.000
Ca	1.531	1.691	1.749	1.748	1.781	1.838	1.762	0.185
NaM_4	0.347	0.256	0.251	0.252	0.219	0.162	0.238	1.815
NaA	0.289	0.268	0.319	0.486	0.029	0.423	0.543	0.633
K	0.138	0.121	0.197	0.063	0.093	0.180	0.191	0.581
ΣA	0.427	0.389	0.516	0.549	0.122	0.604	0.734	1.214
F	0.398	0.285	0.776	0.428	0.051	0.089	0.059	0.504
Cl	0.049	0.045	0.080	0.021	0.036	0.030	0.012	0.005
Fe/Fe+Mg	0.638	0.472	0.609	0.319	0.377	0.473	0.336	0.102
Mg/Mg+Fe^{2+}	0.404	0.585	0.437	0.748	0.705	0.585	0.681	0.498

* Fe_2O_3 from wet-chemical data, formula based on 23 oxygen atoms.
** Fe_2O_3 and formula calculated by the method of Laird and Albee (1981) using a computer program written by A. Hynes.
Nomenclature of amphiboles after Leake (1978). MG40 ferro-hornblende (monzonite), MG46 magnesio-hornblende (granite), MG57 ferro-edenite (granite), MG42 edenitic hornblende in core of zoned grain (granite porphyry), MG6 magnesio-hornblende (fine-grained mafic inclusion), MG97 magnesio-hastingsitic hornblende (mafic inclusion), MG64 kaersutite (alkali gabbro), MG37 arfvedsonite (peralkaline tinguaite).

Table 61.3. Selected biotite compositions

SAMPLE	MG40 Av(8)	MG46 Av(6)	MG57 Av(5)	MG6 Av(6)	MG64 Av(6)	MG94 Av(4)	MG39 Av(1)	MG16 Av(5)
SiO_2	36.92	36.64	38.67	37.51	37.98	35.67	41.74	37.39
Al_2O_3	11.83	12.92	11.71	13.90	14.65	11.50	12.88	12.82
TiO_2	3.64	4.03	3.52	4.27	3.85	3.74	2.60	2.71
FeO	24.05	18.01	22.30	19.66	13.13	30.37	9.27	16.34
Fe_2O_3	3.3*	4.7*	0.0**	0.0**	2.6*	0.0**	0.0**	6.6*
MnO	0.47	0.20	0.45	0.16	0.14	3.07	4.40	1.77
MgO	7.19	10.42	10.33	11.79	14.81	2.50	14.63	9.46
CaO	0.01	0.01	0.01	0.02	0.01	0.00	0.00	0.01
Na_2O	0.04	0.14	0.09	0.14	0.79	0.10	0.17	0.13
K_2O	9.72	9.85	9.84	9.77	8.41	9.75	9.53	9.18
F	1.64	1.33	3.11	0.10	0.05	0.13	2.99	1.25
Cl	0.33	0.39	0.44	0.42	0.17	0.02	0.02	0.02
TOTAL	98.42	97.99	99.06	97.40	97.08	96.79	96.96	97.16
O=F,Cl	0.76	0.65	1.41	0.14	0.06	0.06	1.26	0.53
Si	2.871	2.786	2.951	2.819	2.779	2.889	3.067	2.852
AlZ	1.804	1.158	1.049	1.181	1.221	1.101	0.933	1.149
Fe^{3+}Z	0.046	0.057	0.000	0.000	0.000	0.000	0.000	0.000
AlY	0.000	0.000	0.005	0.050	0.042	0.001	0.183	0.003
Ti	0.213	0.230	0.202	0.241	0.212	0.229	0.144	0.156
Fe^{3+}	0.147	0.210	0.000	0.000	0.143	0.000	0.000	0.379
Mg	0.833	1.181	1.175	1.320	1.615	0.303	1.602	1.076
Fe^{2+}	1.564	1.148	1.423	1.223	0.837	2.060	0.570	1.042
Mn	0.031	0.013	0.029	0.010	0.008	0.211	0.274	0.115
NaY	0.000	0.002	0.000	0.000	0.000	0.015	0.000	0.000
ΣY	2.789	2.785	2.834	2.844	2.857	2.822	2.772	2.770
K	0.964	0.956	0.958	0.936	0.785	1.011	0.894	0.893
NaA	0.013	0.019	0.014	0.020	0.112	0.000	0.025	0.020
Ca	0.001	0.001	0.001	0.002	0.001	0.000	0.000	0.001
ΣA	0.978	0.976	0.972	0.958	0.898	1.011	0.918	0.914
F	0.403	0.320	0.750	0.024	0.011	0.034	0.695	0.301
Cl	0.044	0.050	0.057	0.053	0.021	0.002	0.002	0.002
Fe/(Fe + Mg)	0.678	0.545	0.548	0.481	0.378	0.872	0.262	0.569
Mg/(Mg + Fe^{2+})	0.348	0.507	0.453	0.519	0.658	0.128	0.738	0.508

*Fe O from wet-chemical data, formula based on 11 oxygens.
** formula based on 22 oxygens.
Nomenclature of biotites after Rock (1982). MG40 titaniferous biotite (monzonite), MG46 titaniferous biotite (granite), MG57 titaniferous biotite (granite), MG6 titaniferous biotite (mafic inclusion), MG64 titaniferous biotite (alkali gabbro), MG94 manganiferous titaniferous lepidomelane, MG39 manganiferous titaniferous phlogopite, MG16 manganiferous titaniferous lepidomelane.

Table 61.4. Selected accessory mineral compositions

SAMPLE #	MG63 Av(2)	MG40 Av(2)	MG37[a] Av(5)	MG37[b] Av(4)	MG37[c] Av(2)	MG37[d] Av(4)
SiO_2	31.55	20.25	35.87	42.49	56.75	40.19
TiO_2	2.27	16.41	11.05	9.16	0.51	0.01
Al_2O_3	11.95	0.52	1.19	0.34	0.08	34.23
ZrO_2	n.d.	n.d.	0.34	0.00	12.69	n.d.
Nb_2O_5	n.d.	n.d.	1.40	0.29	1.17	n.d.
MgO	1.50	0.30	0.60	0.29	0.00	0.00
FeO	15.85	10.14	26.36	34.34	5.57	0.18
MnO	0.44	0.30	7.97	5.22	2.50	0.03
La_2O_3	9.26	13.39	n.d.	n.d.	n.d.	n.d.
CaO	9.26	3.92	1.89	0.05	12.19	0.00
Na_2O	0.05	0.01	2.04	7.62	2.94	17.44
K_2O	0.00	0.00	6.64	0.00	0.31	0.03
Ce_2O_3	12.68	20.74	n.d.	n.d.	n.d.	n.d.
Y_2O_3	0.01	0.47	n.d.	n.d.	n.d.	n.d.
ThO_2	0.64	0.98	n.d.	n.d.	n.d.	n.d.
P_2O_5	0.03	0.07	n.d.	n.d.	n.d.	n.d.
F	n.d.	n.d.	1.47	0.10	0.22	8.24
Cl	n.d.	n.d.	0.02	0.01	0.76	0.14
TOTAL	95.49	87.49	96.84	99.91	95.69	100.49

MG63 allanite (quartz monzonite), MG40 chevkinite (monzonite), MG37a astrophyllite, MG37b aegnimatite, MG37c zirconium silicate (eucolite ?), MG37d sodalite (all from peralkaline tinguaite).

oligoclase (An_{11-15}), but the core of zoned grains may be as calcic as labradorite. Quartz is typically anhedral and dominantly interstitial.

Dark brown titaniferous biotite (Table 61.3, analyses MG46, MG57) is the dominant mafic phase present (except in the alkali feldspar granites) and is ubiquitous. In habit it varies from subhedral to interstitial and is locally intergrown with (and possibly replaces) amphibole. Incipient alteration to chlorite and titanite is visible in some samples. Brownish green, subhedral to euhedral amphibole varies in composition from magnesio-hornblende to ferro-hornblende and ferro-edenite (Table 61.2). One sample of granite porphyry contains zoned amphibole (brown edenitic hornblende core, magnesio-hornblende rim). Pyroxene is only observed in one sample of alkali feldspar granite, where it occurs as prismatic light green to colourless grains occasionally rimmed by amphibole. Accessory minerals identified are apatite, allanite, titanite, zircon, magnetite and ilmenite.

The Fe/(Fe+Mg) ratio of both biotite (0.50 to 0.60) and amphibole (0.32-0.62) in the granites exhibits a generally positive but irregular increase if plotted versus differentiation index (Fig. 61.1). The change in Fe/(Fe+Mg) of the amphibole is reflected in the compositional evolution from magnesio-hornblende to ferro-hornblende and finally, ferro-edenite in the most evolved granite studied. The existence of a general trend of increasing Fe/(Fe+Mg) ratio in the mafic silicates is consistent with the results from zoned crystals of amphibole which have a magnesium-rich core and an iron-rich rim. Increasing Fe/(Fe+Mg) of the mafic silicates suggests that chemical evolution of the magma, possibly through fractional crystallization rather than increasing oxygen fugacity, was the chief control of the chemistry of the mafic silicates. An increase in oxygen fugacity would result in either a decreasing or constant Fe/(Fe+Mg) ratio (e.g., Lalonde and Martin, 1983; Czamanske et al., 1981). Both biotite (1.2-3.1 wt.%) and amphibole (0.7-1.7 wt.%) have high fluorine content, indicating that fluorine must have been an important volatile constituent. Minor interstitial fluorite is found in the most evolved granites. High fluorine contents are typical of A-type granites (Collins et al., 1982).

Quartz monzonites

Small areas of quartz monzonite are found in both the northern and the southern half of the pluton and form part of the hybrid suite. This rock type exhibits a mineralogy similar to that of the granites; however, it is characterized by a lower quartz and a higher mafic mineral content than the granites. Amphibole is usually the dominant mafic mineral present; it is euhedral to partly interstitial and has a composition similar to that in the granites (Table 61.2, analysis MG40). Red-brown titaniferous biotite and, in some samples, a colourless pyroxene (salite composition) that is usually rimmed by amphibole are the other mafic minerals present. In the quartz monzonites, biotite and amphibole do not form a coherent trend if Fe/(Fe+Mg) is plotted versus differentiation index (Fig. 61.1). Some plot on or near the same trend as the granitic rocks whereas others plot away from this trend. This is consistent with multiple origins for the quartz monzonites, some possibly representing cumulates related to the granites whereas others may represent hybrid rocks produced by mixing of granite with more primitive magmas (see below).

Monzonites and syenites

Monzonite and syenite are the dominant felsic rock-types in the hybrid suite, though granodiorite, quartz monzonite, quartz syenite and granite are also present. They are typically fine grained to medium grained and generally porphyritic, with plagioclase the dominant phenocryst phase. Red-brown perthitic alkali feldspar (low sanidine) forms anhedral to subhedral interlocking grains. Quartz is interstitial. Plagioclase typically forms subhedral to euhedral, complexly zoned phenocrysts (xenocrysts?) that are commonly mantled by alkali feldspar. Compositions of the phenocrysts vary from andesine (An_{31}) in the core to albite (An_3) at the rim. Unzoned albite (An_0) is found in the groundmass. Green to brownish green, principally interstitial, amphibole is the dominant mafic mineral in most samples. It varies in composition from ferro-hornblende in the monzonite to actinolitic hornblende in the syenite. Dark brown titaniferous biotite is typically subhedral to interstitial and also occurs with amphibole in mafic clots. Incipient alteration to titanite and chlorite is visible in some samples. Pyroxene occurs as colourless to pale green, subhedral to euhedral grains that commonly are rimmed by amphibole and range in composition from augite to sodian ferroaugite. Accessory minerals identified include zircon, allanite, apatite, titanite, chevkinite, monazite (?), ilmenite and magnetite.

The limited number of samples studied in detail makes generalizations about the mineralogical evolution of the monzonites and syenites difficult. There is no evidence that the mafic silicates follow a trend of increasing Fe/(Fe+Mg) ratio with increasing compositional evolution (Fig. 61.1). The monzonites contain the highest Fe/(Fe+Mg) ratio for biotite and amphibole of all the oversaturated rocks studied, possibly reflecting the late crystallization of magnetite due to a low fugacity of oxygen. The high $Fe^{2+}/(Fe^{2+}+Fe^{3+})$ (0.78: J. Whalen, personal communication) ratio of the bulk rock and in the mafic silicates is consistent with this explanation.

In the syenite sample, the pyroxene present, sodian ferroaugite, exhibits a higher Fe/(Fe+Mg) ratio than the pyroxene in the monzonites, biotite and amphibole and the bulk rock $Fe^{2+}(Fe^{2+}+Fe^{3+})$ (0.50) exhibit much lower values than their counterparts in the monzonites. Amphibole and biotite are interstitial, whereas pyroxene in the syenite appears to have crystallized early, as it forms euhedral prismatic crystals. Therefore, as the syenite crystallized, saturation in water may have occurred. The water could then act as an oxidizing medium through dissociation and loss of hydrogen (Czamanske and Wones, 1973). The presence of interstitial titanite in the syenite is consistent with a relatively high fugacity of oxygen at a late stage (e.g. Wones, 1966).

Alkali gabbros

Alkali gabbro occurs in small (<200 m) scattered bodies within the hybrid suite. These are typically medium- to coarse-grained, massive and crosscut by felsic veins. The samples examined exhibit evidence that postmagmatic recrystallization has occurred to varying degrees. They consist of subhedral to euhedral laths of labradorite (An_{62-66}) that occasionally exhibit normal zoning. A secondary untwinned, unzoned, anhedral plagioclase of andesine composition (An_{33}) replaces the primary plagioclase and is interpreted to be postmagmatic. Pink brown titansalite (Table 61.1, samples MG25, 64, 646) exhibits sector zoning and defines a subophitic texture. In some cases only remnants of the initial titansalite are left in the core zone of amphibole. A pale green salitic pyroxene occurs in these samples as well and is interpreted to have a postmagmatic origin. Red-brown kaersutite rims and partially replaces titansalite, as well as forming interstitial grains. Replacement of the kaersutite by a brownish green low-titanium calcic amphibole is usually incomplete. There are also relatively small amounts of pale green secondary actinolitic amphibole, and along with chlorite these are likely the result of a low-temperature deuteric alteration. Reddish brown to dark brown titaniferous biotite occurs interstitially as well as in a rim around the amphibole and, in some cases, pyroxene. In all samples studied the biotite exhibits alteration to chlorite, titanite or epidote. The dominant accessory phase is apatite; it occurs as needles up to 2.2 mm in length some with a hollow core. The acicular habit of apatite is usually interpreted to indicate that rapid growth occurred (e.g. Wyllie et al., 1962). The presence of sector zoning within the pyroxene is a disequilibrium phenomenon (Dowty, 1976) and therefore also indicates that rapid growth occurred. Other accessory minerals, some of which are secondary, are oxides, sulphides, titanite, epidote, calcite, zircon and monazite(?). A mafic plagioclase-phyric dyke of a chemical composition similar to that of the alkali gabbros crosscuts quartz monzonite near the Madeleine mine. Even though the dyke rock exhibits a strong hydrothermal overprint, it still preserves remnants of red-brown titanium-rich amphibole in the matrix. In rare cases the amphibole is cored by pink-brown titanium-rich pyroxene.

Inclusions

Inclusions of variable composition and size occur throughout the hybrid suite and are of two types. The first are derived from the country rock, principally hornfels and metavolcanic rocks of the Quebec Group (De Romer, 1977); they will not be discussed here. The second group consists of mafic, intermediate and rare felsic inclusions that are considered genetically related to the McGerrigle pluton.

The fine grained mafic inclusions may exhibit both chilled and cuspate margins. These have been interpreted as evidence for the coexistence of a mafic magma with a felsic magma (Whalen, 1985). Such inclusions occur within granite and granodiorite, principally in the northern half of the pluton. They are generally porphyritic with a groundmass consisting of untwinned oligoclase (An_{21}), olive-green magnesio-hornblende, dark brown titaniferous biotite, titanite and acicular apatite. The presence of remnants of magnesian hastingsitic hornblende with anhedral titanite and the high content of oxide granules in the groundmass amphibole are interpreted to indicate that the primary amphibole was likely rich in titanium. Phenocrysts of zoned plagioclase (An_{29-45}) with a discontinuous rim of oligoclase (An_{21}) and of unzoned calcic plagioclase (up to An_{56}) are present. The former exhibit complex oscillatory zoning similar to that found within the host granodiorite and, therefore, may represent xenocrysts derived from the granodiorite. Subhedral phenocrysts of pink-brown pyroxene give compositions ranging from augite, titaniferous augite to titansalite and are usually rimmed and, to varying degrees, replaced by amphibole. Titansalite occurs as large (up to 1 cm), corroded and occasionally composite grains (with labradorite) and are interpreted as xenocrysts possibly derived from a cumulate pile at depth. A corona texture (actinolitic amphibole core and biotite rim) results from the pseudomorphism of pyroxene. Small round to oval, coarse grained areas consisting of sodic plagioclase, subhedral to euhedral magnesian hornblende, titanite, calcite, apatite, biotite, oxide and alkali feldspar possibly represent infilled

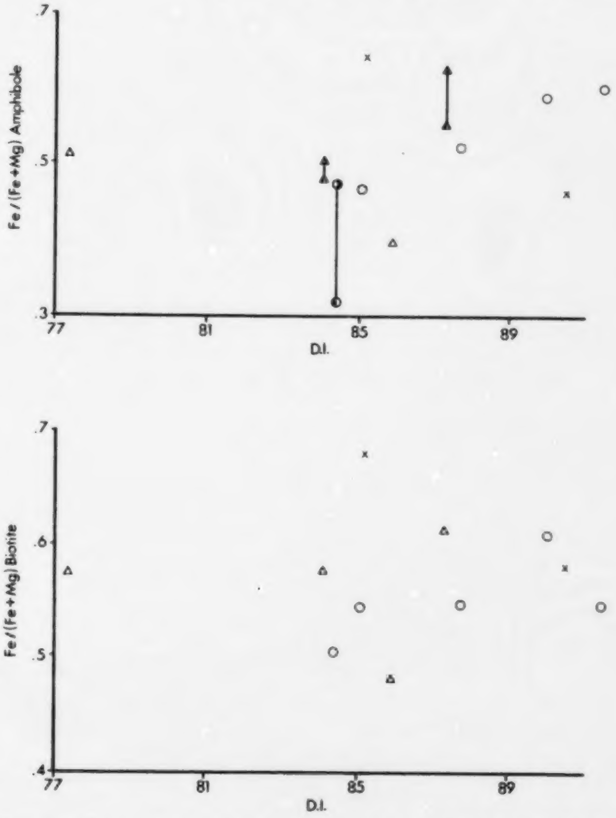

Figure 61.1. *Plot of Fe/(Fe+Mg) in biotite and amphibole versus differentiation index (normative quartz + orthoclase + albite + nepheline + kalsilite + leucite). Triangles quartz monzonites, circles granites and x syenites and monzonite. Half-filled symbols represent zoned grains (infilled right half indicates rim, infilled left half indicates core). Normative values used to calculate differentiation index were supplied by C. Gariépy.*

amygdules. The host-inclusion contact zone of samples exhibiting a chilled margin is characterized by a decrease in grain size, increase in biotite content (indicating that K metasomatism has occurred), and appearance of a pale green salitic pyroxene as well as skeletal and platy oxides.

Samples of diorite, monzodiorite and quartz monzonite have also been studied. Only the most important rock-forming minerals and textures can be discussed here. All samples studied contain two generations of plagioclase; the first subhedral, commonly zoned laths with a calcic core (An_{27-53}). Anhedral, untwinned oligoclase (An_{10-18}) which is compositionally similar to that found in the granites, rims and replaces the primary feldspar to varying degrees. In samples where it is a major mineral, alkali feldspar occurs as anhedral to subhedral, occasionally perthitic grains commonly mantling plagioclase. Pale green to colourless salite is present in most of the samples. In one sample it coexists with pale brown titaniferous augite which is extensively replaced by amphibole. The salite in this sample is interpreted to have a secondary origin. Textural and compositional data indicate that the salite has undergone recrystallization and is unlikely to preserve a primary igneous composition. Green, predominantly interstitial amphibole varies from magnesio- to actinolitic hornblende and, in some samples, occurs only as a late-stage replacement of pyroxene. Compositionally, the amphibole is similar to that in the enclosing granitic rocks though the Fe/(Fe+Mg) ratio, sodium and fluorine contents are typically lower and calcium is typically higher. Red brown to dark brown titaniferous biotite, generally exhibiting sutured contacts with feldspar, is present in all the inclusions studied. The range of Fe/(Fe+Mg) values of the biotite in the inclusions (0.43 to 0.57) is nearly identical to that found in the granites (0.46 to 0.61). Biotite occasionally exhibits alteration to chlorite, titanite and epidote. An enigmatic texture visible in many samples is the presence of elongate to oval colourless material along the cleavage in biotite. This material typically exhibits a low birefringence and in some cases is made up of a fibrous mineral (sillimanite?). An interesting possibility is that it represents devitrified glass formed by the partial melting of the biotite (e.g. Tindle and Pearce, 1983; Nédélec and Paquet, 1981). Apatite, the most common accessory mineral, occurs as acicular crystals commonly exhibiting a hollow core. In one sample studied the apatite occurs in linear trains of small grains that in some cases, crosscut grain boundaries. This is interpreted to indicate that apatite crystallized along microfractures or cleavages, possibly from a volatile phase. Many of the features mentioned above indicate that metasomatism, recrystallization and possibly even partial melting of the inclusions have occurred. This most likely resulted in modification of their primary igneous geochemistry (Bédard, 1985; Tindle and Pearce, 1983).

Nepheline syenites

Small volumes of nepheline syenite occur within the hybrid suite in the northern half of the pluton. They occur predominantly as thin tinguaite dykes (up to 2 m) whose agpaitic coefficient (Na+K)/Al ranges from 0.97 to 1.06. Miaskitic nepheline syenite (agpaitic coefficient of 0.93) occurs as small (<10 m) pod-shaped bodies north of Mont Jacques-Cartier.

The tinguaites are typically grey, fine grained, generally porphyritic and exhibit a complex mineral assemblage and texture that varies from dyke to dyke. Some dykes consist of a framework of unoriented tablets of alkali feldspar, whereas others are porphyritic with laths of alkali feldspar exhibiting a trachytic texture. One sample contains an extremely fine grained, anhedral felsic groundmass with scattered unoriented needles of pyroxene. Medium grained cogenetic inclusions (cumulates?) and rare metasomatized xenoliths (<4 cm) are found in some dykes.

Grey, perthitic alkali feldspar, low sanidine, occurs as subhedral to euhedral laths, both in the groundmass and as phenocrysts (occasionally exhibiting a glomeroporphyritic texture) in the dykes. Nepheline is present in all samples studied and is predominantly interstitial. Anhedral to subhedral phenocrysts of nepheline are present in some of the porphyritic peralkaline dykes. Sodalite is present only in the peralkaline tinguaites. It is predominantly interstitial, but the peralkaline porphyritic dykes contain anhedral to subhedral phenocrysts, and possibly resorbed (?) phenocrysts as well.

Pyroxene is present in all the samples studied and varies in habit from subhedral to euhedral phenocrysts to fine grained slender needles. Pyroxene and astrophyllite occasionally form radial aggregates. In the intermediate tinguaites (Na+K=Al), aegirine-augite is present, whereas in the peralkaline tinguaites grass-green aegirine to blue-green titan-aegirine (Ti>0.1 atoms per formula unit: Ronsbro et al., 1977) are found. Titan-aegirine typically rims aegirine. Along with a high titanium content, it also contains up to 1.83 wt.% ZrO_2 (Table 61.1, analysis MG37a). These enrichments likely reflect substitution of a Fe-NAT ($NaTi_{.5}Fe^{2+}{}_{.5}Si_2O_6$) component in the pyroxene (Nielsen, 1979). The low magnesium content of the pyroxene (0.23-0.37 wt.%) indicates that Mg-NAT ($NATi_{.5}Mg_{.5}Si_2O_6$) is unimportant.

Greenish blue to black arfvedsonitic amphibole is found in some dykes. It may form subhedral to euhedral, locally poikilitic, grains, or it may be interstitial. In only one dyke is amphibole dominant over pyroxene. The distribution of amphibole in this dyke is uneven. Some areas contain only aegirine whereas others contain only amphibole or amphibole replacing aegirine, possibly reflecting an uneven volatile distribution within the dyke. Generally, however, amphibole and aegirine appear to coexist at equilibrium with little evidence of mutual replacement.

A dark brown manganiferous titaniferous lepidomelane that exhibits orange pleochroism is present in most of the dykes. It commonly exhibits an interstitial to poikilitic texture, though subhedral to euhedral phenocrysts are also observed. Biotite is very iron-rich, with a Fe/(Fe+Mg) ratio of up to 0.87. In one peralkaline porphyritic dyke, a dark brown manganiferous titaniferous phlogopite is present. This mica occurs as scattered anhedral to interstitial flakes that may be rimmed by aegirine, indicating a possible reaction relationship. The relatively low totals on electron microprobe analysis (93-94%) possibly reflect the presence of lithium.

Astrophyllite occurs as orange acicular prisms in most, but not all, of the peralkaline dykes. In one sample, astrophyllite appears to be replacing biotite. It has a composition within the range of astrophyllite reported from other undersaturated rocks (Macdonald and Sanders, 1973).

Dark red to black aenigmatite forms anhedral to subhedral phenocrysts in some of the peralkaline dykes. It has a composition similar to the ideal formula ($Na_2Fe_5TiSi_6O_{20}$), with the principal substitution present being Mn^{2+} for Fe^{2+}. Recalculation in terms of 14 cations and 20 anions indicates that the Fe^{3+} content is nearly 0. This composition is typical of aenigmatite coexisting with aegirine (Larsen, 1978). In some peralkaline dykes, instead of aenigmatite a, manganese-rich (8 wt.% MnO) titanium-poor (0.03 wt.% TiO_2) magnetite is present, instead of aenigmatite. This likely indicates that the dykes were characterized by varying levels of oxygen fugacity.

Aenigmatite formed only where the oxygen fugacity (and temperature) were within the no-oxide field inferred by Marsh (1975) to delimit the stability field of aenigmatite coexisting with aegirine. A colourless, low-birefringence, high-relief, occasionally zoned zirconium silicate (eucolite?) is interstitial in some of the more strongly peralkaline dykes. Other accessories identified include apatite, poikilitic to interstitial zircon, titanite (replacing magnetite) and fluorite.

The miaskitic nepheline syenite is medium grained and porphyritic with grey subhedral perthitic low sanidine, subhedral apple green aegirine-augite and subhedral dark greenish brown manganiferous titaniferous lepidomelane. The groundmass exhibits a trachytic texture and consists of low sanidine, minor albite with interstitial biotite, aegirine-augite and nepheline. Accessories identified include titanite, apatite, zircon and magnetite.

The exact relationship of the miaskitic nepheline syenite to the tinguaites is still open to debate. There are two possibilities: 1) the peralkaline nepheline syenites represent liquids derived from a miaskitic magma through fractional crystallization, dominantly of alkali feldspar with a calcic component (plagioclase effect of Bowen, 1945) or 2) the miaskitic nepheline syenites may represent hybrid rocks derived through mixing of a peralkaline melt with small amounts of evolved (low Ca, Al>(Na+K) and low degree of silica saturation) felsic magma. Work under way will perhaps clarify this relationship.

Discussion

Whereas there is clear evidence for the coexistence of magmas (Whalen, 1985) and for hybridization on a small scale, the question on how important magma mixing is for the pluton as a whole is still open (Whalen and Gariépy, 1986). Textural and mineralogical data can be used as convincing evidence for magma mixing (e.g., Eichelberger, 1978; Hibbard, 1981; Vernon, 1983). The presence of phases that are totally out of chemical equilibrium with the magma, and of more than one population of a specific mineral within a single rock-type, mantling of one feldspar on another (rapakivi and antirapakivi textures), presence of mafic clots and of patchy cores in plagioclase have all been attributed to magma mixing. An alternative interpretation for some of these features is that they represent xenocrysts and microxenoliths (restite) derived from the source region of the magma (e.g. Chappell, 1978).

The granite suite is characterized by a relatively homogeneous composition and it rarely contains mafic inclusions. Some granites contain complexly zoned plagioclase; the highly calcic core in plagioclase may represent xenocrysts derived from the wall rock or source area of the granite. They could conceivably form by very early mixing of the granite with a more mafic magma. However, the fact that such cored plagioclase is only present in some samples and that the textural criteria for magma mixing or hybrid granites (see above and Didier, 1974) are generally absent indicates that other processes such as fractional crystallization probably controlled the evolution of the granites.

Some quartz monzonites appear to represent accumulations of crystals likely derived from the granites; others exhibit evidence of a hybrid origin. In these possible hybrids the higher mafic index, lower quartz content, presence of remnants of salitic pyroxene, mantling of zoned calcic plagioclase by alkali feldspar and presence of mafic clots are all characteristics of contaminated granitic magmas (Didier, 1974). The presence of acicular apatite exhibiting a hollow core is usually interpreted in terms of rapid growth. This may be due to supersaturation resulting from mixing of a mafic or intermediate magma (with a moderate to high P_2O_5 content reflecting the high level of saturation of P_2O_5: 4 to 12 wt.% according to Watson, 1979) with a felsic magma with a low level of saturation (0.04 to 0.28 wt.%: Watson and Capobianco, 1981). The common association of the quartz monzonites with areas characterized by a high content of inclusions is again consistent with hybridization.

The monzonites and syenites exhibit many of the same textures as the hybrid quartz monzonites, including mantled zoned plagioclase phenocrysts, mafic clots, acicular apatite occasionally with a hollow core, and zircon exhibiting irregular shapes which may be caused by resorption. These features are best developed and most common within the monzonites.

The intermediate rocks are more problematical as they have been metasomatized and recrystallized by their volumetrically dominant host-rocks; therefore more than one explanation is possible for their textural and mineralogical characteristics. The rocks rich in K-feldspar, such as the monzodiorites, are the most likely candidates for an origin by mixing. The presence of mantled zoned plagioclase and mafic inclusions in these samples is consistent with a hybrid origin.

The presence of low sanidine instead of low microcline, as would be expected of the slow cooling of a large plutonic complex like this one, is anomalous. One possibility is that the mixing of batches of magma led to enhanced flow of fluids through the solidifying mixture, which, in turn, led to relatively rapid cooling through the field of microcline (<450°C).

In light of the preliminary findings presented here, it seems obvious that the magmatic evolution of the Gaspé Peninsula in Devonian times is considerably more complicated than anticipated. In particular, igneous rocks normally considered rift-related are prominent so that the involvement of truly calc-alkaline magmatic suites remains to be established.

Acknowledgments

The author would like to acknowledge the help and encouragement given this work by C. Gariépy, J. Van Bosse, R. Wares and J. Whalen. J. Whalen was responsible for collecting a large number of the samples studied here and much of the interpretation of the field relationships. The author would like to thank Scott Green and Luciano Vendittelli for help in the field. This manuscript was significantly improved by R.F. Martin who also contributed some of the data and interpretation presented.

References

Bédard, J.H.
1985: La pétrogenèse et mécanisme de différenciation des magmas anorogéniques: exemples de la Gaspésie, de la Nouvelle-Angleterre et des collines Montérégiennes; Thèse de doctorat, Université de Montréal, Québec.

Bowen, N.L.
1945: Phase equilibria bearing on the origin and differentiation of the alkaline rocks; American Journal of Science, v. 243A, p. 75-89.

Chappell, B.W.
1978: Granitoids from the Moonbi district, New England batholith, eastern Australia; Journal of the Geological Society of Australia, v. 25, p. 267-283.

Collins, W.J., Beams, S.D., White, A.J.R., and Chappell, B.W.
1982: Nature and origin of A-type granites with particular reference to Southeastern Australia; Contributions to Mineralogy and Petrology, v. 80, p. 189-200.

Czamanske, G.K., Ishihara, S., and Atkin, S.A.
1981: Chemistry of rock-forming minerals of the Cretaceous-Paleocene batholith in southwestern Japan and implications for magma genesis; Journal of Geophysical Research, v. 86, B11, p. 10431-10469.

Czamanske, G.K. and Wones, D.R.
1973: Oxidation during magmatic differentiation, Finnmarka Complex, Oslo area, Norway: II. The mafic silicates; Journal of Petrology, v. 14, p. 349-380.

Deer, W.A., Howie, R.A., and Zussman, J.
1978: Rock-forming minerals; Vol. 2A, Single-chain silicates; 2nd ed., Longman Group Limited, London, 668 p.

De Romer, H.S.
1977: Région des Monts McGerrigle area; Ministère des Richesses Naturelles, Rapport Géologique 174, 233 p.

Didier, J.
1973: Granites and their enclaves: the bearing of enclaves on the origin of granites; Elsevier Scientific Publishing Company, New York, 393 p.

Dowty, E.
1976: Crystal structure and crystal growth: II. Sector zoning in minerals; American Mineralogist, v. 61, p. 460-469.

Eichelberger, J.C.
1978: Andesitic volcanism and crustal evolution; Nature, v. 275, p. 21-27.

Hibbard, M.J.
1981: The magma mixing origin of mantled feldspars; Contributions to Mineralogy and Petrology, v. 76, p. 158-170.

Laird, T. and Albee, A.L.
1981: Pressure, temperature and time indicators in mafic schists: their implication to reconstructing the polymetamorphic history of Vermont; American Journal of Science, v. 281, p. 97-126.

Lalonde, A.E. and Martin, R.F.
1983: The Baie-Des-Moutons syenitic complex, La Tabatière, Québec: II. The ferromagnesian minerals; Canadian Mineralogist, v. 21, p. 81-91.

Larsen, L.M.
1977: Aenigmatites from the Ilimaussaq intrusion, south Greenland: chemistry and petrological implications; Lithos, v. 10, p. 257-270.

Leake, B.E.
1978: Nomenclature of amphiboles; Canadian Mineralogist, v. 16, p. 501-520.

Macdonald, R. and Saunders, R.
1973: Chemical variation in minerals of the astrophyllite group; Mineralogical Magazine, v. 39, p. 97-111.

Marsh, J.S.
1975: Aenigmatite stability in silica-undersaturated rocks; Contributions to Mineralogy and Petrology, v. 50, p. 135-144.

Nédélec, A. and Paquet, J.
1981: Biotite melting in high-grade metamorphic gneisses from the Haut Allier (French Massif Central); Contributions to Mineralogy and Petrology, v. 77, p. 1-10.

Nielsen, T.F.D.
1979: The occurrence and formation of Ti-aegirines in peralkaline syenites; Contributions to Mineralogy and Petrology, v. 69, p. 235-244.

Poldervaart, A. and Hess, H.H.
1951: Pyroxenes in the crystallization of basaltic magma; Journal of Geology, v. 59, p. 472-489.

Robinson, P.
1980: The composition space of terrestrial pyroxenes – internal and external limits; in Pyroxenes, ed. C.T. Prewitt; Reviews in Mineralogy, v. 7, Mineralogical Society of America, Washington.

Rock, N.M.S.
1982: Chemical mineralogy of the Monchique alkaline complex, southern Portugal; Contributions to Mineralogy and Petrology, v. 81, p. 64-78.

Rønsbro, J.G., Pedersen, A.K., and Engell, J.
1977: Titan-aegirines from early Tertiary ash layers in northern Denmark; Lithos, v. 10, p. 193-204.

Tindle, A.G. and Pearce, J.A.
1983: Assimilation and partial melting of continental crust: evidence from the mineralogy and geochemistry of the autoliths and xenoliths; Lithos, v. 16, p. 185-202.

Vernon, R.H.
1983: Restite, xenoliths and microgranitoid enclaves in granites; Journal and Proceedings, Royal Society of New South Wales, v. 116, p. 77-103.

Watson, E.B.
1979: Apatite saturation in basic to intermediate magmas; Geophysical Research Letters, v. 6, p. 937-940.

Watson, E.B. and Capobianco, C.J.
1981: Phosphorus and the rare earth elements in felsic magmas: an assessment of the role of apatite; Geochimica et Cosmochimica Acta, v. 45, p. 2349-2358.

Whalen, J.B.
1985: The McGerrigle plutonic complex, Gaspé, Quebec: evidence of magma mixing and hybridization; in Current Research, Part A, Geological Survey of Canada, Paper 85-1A, p. 795-800.

Whalen, J.B. and Gariépy, C.
1986: Petrogenesis of the McGerrigle plutonic complex, Gaspé, Quebec: a preliminary report; in Current Research, Part A, Geological Survey of Canada, Paper 86-1A, Report 30.

Wones, D.R.
1966: Mineralogical indicators of relative oxidation states of magmatic systems; American Geophysical Union Transactions, v. 47, p. 216 (abstr.).

Wyllie, P.J., Cox, K.G., and Biggar, G.M.
1962: The habit of apatite in synthetic systems and igneous rocks; Journal of Petrology, v. 3, p. 238-243.

Geology of the Silver Mountain area, western Newfoundland[1]

J.V. Owen
Precambrian Geology Division

Owen, J.V., Geology of the Silver Mountain area, western Newfoundland; in Current Research, Part A, Geological Survey of Canada, Paper 86-1A, p. 515-522, 1986.

Abstract

The geology of the Silver Mountain area of the northern Long Range Mountains of western Newfoundland is dominated by crystalline Precambrian rocks which record an extended history of metamorphism, deformation and intrusion. The oldest rocks are granulite-facies quartzofeldspathic gneisses of inferred igneous parentage, and include (quartz) dioritic to granitic variants, and spatially associated anatectic(?) biotite granite. Biotite ± garnet ± sillimanite ± spinel ± graphite-bearing migmatitic gneisses, of uncertain age relative to the orthogneiss, are associated with quartzite and metacarbonate bands, and are inferred to be paragneisses. The gneissic rocks are intruded by a large pluton of mafic rocks, including mesocratic to leucocratic, pyroxene ±olivine ± amphibole-bearing metagabbro, and pegmatitic metagabbro, and by a variety of massive to foliated granites and granodiorites. Quartz-rich mica schist with quartzite interbands, banded marble, massive to foliated felsic porphyry, and mafic schist occurring in the southwestern portion of the map area are considered to be lower Paleozoic (Cambro-Ordovician?). The schistose rocks have been thrust westward over the Precambrian gneisses and intrusive rocks, and are partly overlain by undeformed conglomerates and redbeds of the Deer Lake basin.

Résumé

La géologie de la région du Mont Silver dans la partie nord des monts Long Range, dans l'ouest de Terre-Neuve, présente surtout des roches cristallines précambriennes dont les antécédents de métamorphisme, de déformation et d'intrusion remontent à un passé très lointain. Les plus anciennes de ces roches sont des gneiss quartzofeldspathiques d'origine présumémant ignée, appartenant au faciès des granulites et comprenant des variantes dioritiques (quartziques) à granitiques; un granite anatectique(?) à biotite y est géographiquement associé. Des gneiss migmatiques à biotite ± grenat ± sillimanite ± spinelle ± graphite, dont l'âge est incertain par rapport à l'orthogneiss, sont associés à des intercalations de quartzite et de métacarbonates et laissent supposer qu'il s'agit de paragneiss. Les roches gneissiques ont été traversées par un vaste pluton de roches mafiques, notamment un métagabbro mésocrate ou leucocrate à pyroxène ± olivine ± amphibole et un métagabbro pegmatitique, et par une gamme de granites et de granodiorites massifs ou feuilletés. Du schiste à mica riche en quartz contenant des intercalations de quartzite, un marbre rubané, un porphyre felsique massif ou feuilleté et un shiste mafique trouvé dans la partie sud-ouest de la région cartographique dateraient du Paléozoïque inférieur (cambro-ordovicien?). Ces roches schisteuses ont été déplacées vers l'ouest pour chevaucher les gneiss et les roches intrusives précambriennes et sont partiellement recouvertes par des conglomérats et des couches rouges non déformées du bassin de Deer Lake.

[1] Contribution to the Canada-Newfoundland Mineral Development Agreement 1984-1989. Project carried by Geological Survey of Canada, Project 850017

Introduction

This report summarizes field data collected in 1985 during 1:100 000 mapping of the Silver Mountain map sheet (12H/11). Mesoscopic aspects of major rock units and their relative chronologies, both observed and inferred, are outlined, and the focus of ongoing research in this area is described.

The Silver Mountain area is some 50 km north-northeast of Deer Lake, Newfoundland, and forms the southern portion of the northern Long Range Mountains of the Great Northern Peninsula (Fig. 62.1). The Long Range Mountains are predominantly underlain by Precambrian rocks, flanked to the east and west by miogeoclinal rocks of the Appalachian orogen. The similarity of medium- to high-grade crystalline rocks and a variety of mafic to felsic intrusive rocks in the Long Range Mountains to rocks in the Grenville Province of southern Labrador has led to the often repeated assertion that the Long Range forms an inlier of the Grenville Province. This hypothesis is supported by a 1130 ± 90 Ma age (Rb-Sr, whole rock) obtained for a megacrystic granite in the Long Range (Pringle et al., 1971). Various workers (e.g. Bostock, 1983; Erdmer, 1984) have noted that portions of the Precambrian terrane of the Long Range Mountains, particularly in the east, show widespread retrogression to greenschist facies, interpreted to record Grenvillian and(or) Paleozoic reworking of earlier, higher grade rocks.

Lithology

Rock units mappable at 1:100 000 scale may be conveniently subdivided into five "groups" according to their lithology and inferred age relative to major tectono-metamorphic and(or) intrusive events. These are: (A) gneissic rocks; (B) diorite-gabbro and their metamorphosed equivalents; (C) granite, granodiorite; (D) metasedimentary schist, marble, and massive to foliated felsic porphyry and metadiorite and (E) undeformed conglomerate and sandstone. Groups A, B and C are considered to be Precambrian in age, while D and E are inferred to be Paleozoic.

Precambrian terrane

A. Gneissic rocks. Gneissic rocks are dominant in the central and western parts of the map area. Although pelitic and calc-silicate gneiss occurs locally, most gneisses are biotite ± hornblende-bearing quartzofeldspathic rocks inferred to have been derived from an igneous protolith. Three quartzofeldspathic gneissic units have been identified. All locally contain orthopyroxene and quartz, demonstrating that granulite-facies conditions were prevalent over much of the area (see Fig. 62.1).

Unit 1 is a buff-brown, medium grained, biotite-bearing quartz dioritic to tonalitic gneiss. Brown orthopyroxene is generally present, and dark green hornblende is a common accessory mineral. This unit is homogeneous on both a hand sample and outcrop scale; gneissic layering, where present, is defined by thin, biotite-rich septa.

Unit 2 is a white-weathering, green-grey, medium grained quartz diorite gneiss. Both dioritic and granodioritic variants have been observed, and biotite (with or without hornblende) is the dominant mafic mineral. Hornblende-mantled orthopyroxene, and magnetite may occur as accessory minerals. The mafic minerals typically occur as 5-10 mm ovoid aggregates, which impart a "flecky" texture

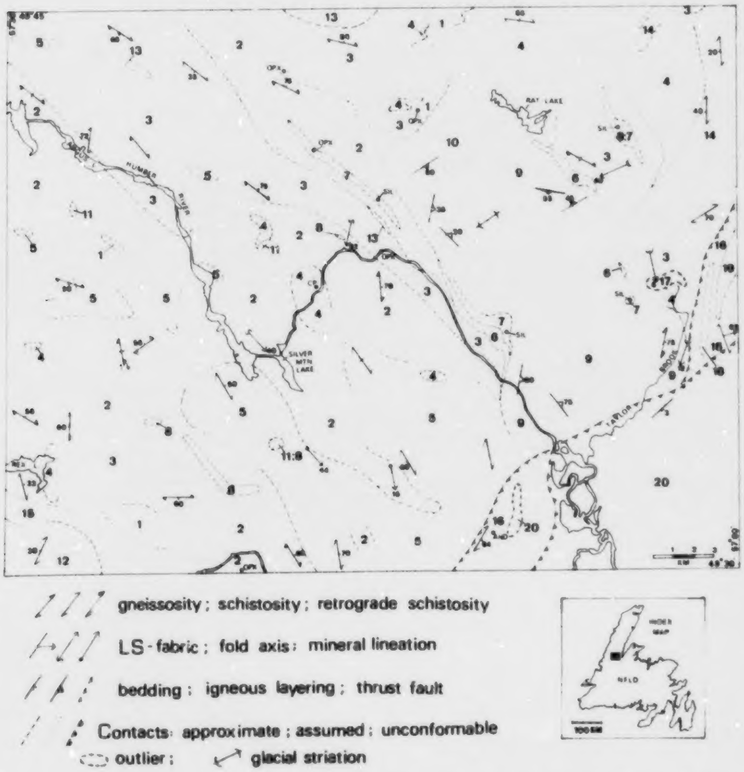

LEGEND

CARBONIFEROUS

20 Polymict conglomerate, red sandstone

CAMBRO-ORDOVICIAN (?)

19 Felsic porphyry
18 Metadiorite; mafic schist
17 Tremolite(?)-bearing marble
16 Metasedimentary schist; quartzite

NEOHELIKIAN (?) OR OLDER

15 Biotite granite-granodiorite
14 Ksp-megacrystic biotite granite
13 Ksp-megacrystic biotite ± hornblende granodiorite-granite
12 Biotite + hornblende granodiorite
11 Subophitic metagabbro
10 Pegmatitic metagabbro
9 Pyroxene ± olivine ± amphibole bearing metagabbro

PALEOHELIKIAN (?) OR OLDER

8 Massive quartz; quartzite
7 Bi ± gt ± sil ± gp quartzofeldspathic gneiss
6 Marble; calcsilicate rock
5 Biotite granite
4 Amphibolite; dioritic gneiss
3 Bi ± hbl ± opx granitic-granodioritic gneiss
2 Bi ± hbl ± opx (quartz) dioritic-granodioritic gneiss
1 Bi ± hbl ± opx quartz dioritic-tonalitic gneiss

Figure 62.1. *Simplified geological map of the Silver Mountain area, western Newfoundland. Lake names follow local nomenclature. Abbreviations: opx-orthopyroxene; cp-chalcopyrite; sil-sillimantie; and-andalusite; bi-biotite; gt-garnet; gp-graphite; hbl-hornblende; Ksp-K feldspar.*

to the rock, and which weather recessively, giving the weathered surface a distinctive pitted appearance. In places, biotite ± hornblende-seamed, relatively coarse grained granitic veins up to 10 cm wide impart a migmatitic character to the rock. The quartz diorite gneiss locally contains centimetre- to metre-scale mafic enclaves and layers consisting of hornblende, plagioclase, and, in places, biotite ± clinopyroxene (Fig. 62.2). This is the dominant gneissic unit in the map area. it is inferred to be derived from a variably quartz-bearing(?) gabbroic protolith.

Pink to grey, fine- to medium-grained, granitic to granodioritic gneiss (unit 3) occurs as metre- to kilometre-scale layers in the quartz diorite gneiss (unit 2; see Fig. 62.1). The granitic gneiss contains biotite, with rare hornblende ± orthopyroxene. In contrast to the quartz dioritic to tonalitic gneisses (units 1 and 2), unit 3 is typically migmatitic, with biotite-seamed, granitic leucosome veins up to 15 cm in width (Fig. 62.3). Where deformed, these are buff coloured, and extensive grain-size reduction has accompanied recrystallization. In low strain domains, however, the leucosomes are pink and are coarser grained than the adjacent gneiss. The unstrained leucosome contains grey or blue quartz, and is similar in appearance to medium grained, pink biotite granite (unit 5; see below) which is spatially associated with the quartzofeldspathic gneisses (Fig. 62.1).

Unit 4 comprises a variety of massive to foliated, amphibole-bearing mafic rocks, chiefly amphibolite. The massive to schistose amphibolite typically consists of dark green to black amphibole, plagioclase, and locally contains biotite. Gneissic to migmatitic amphibolite is mineralogically similar, but commonly contains clinopyroxene which in places occurs as 1 cm porphyroblasts in quartz- and plagioclase-rich leucocratic segregrations in the rock (Fig. 62.4). The amphibolites are more melanocratic than units 1 and 2, and are distinguished from other mafic rocks (units 9, 10, 11; see below) by the absence of primary igneous textures. Different textural varieties of the amphibolites could not be readily depicted at the scale of mapping. Both schistose and gneissic variants have been observed among the foliated amphibolites, and the unit probably comprises several ages of mafic rock. The amphibolite occurs as enclaves and layers in units 1, 2 and 3, and in younger plutonic rocks, and flanks the northeastern margin of the gabbroic pluton southeast of Rat Lake (Fig. 62.1).

Pink biotite granite (unit 5) is associated with quartz dioritic and granitic gneiss (units 2, 3) in the western and southern parts of the map area (Fig. 62.1). The granite is massive to foliated. Although generally containing biotite as the principal ferromagnesian mineral, the granite locally also contains amphibole. Where undeformed, the granite is medium grained and typically contains bluish quartz. Grain-size reduction accompanies the development of schistose to gneissose fabrics in the unit. The granite in part postdates the gneiss; dykes of massive, blue quartz-bearing biotite granite crosscut quartz diorite gneiss (unit 2; see Fig. 62.5) and migmatitic granite gneiss (unit 3) at several localities. However, gradational contacts between the granitic gneiss and coarser grained (1-5 mm), massive to weakly foliated biotite granite have been noted in several outcrops. Together with the similarity of the granite with the abundant leucocratic segregations in the granitic gneiss (unit 3), and the close spatial association with the quartzofeldspathic gneisses in general, this suggests that the granite may have been derived by partial melting of the granitic gneiss during early, high-grade metamorphism in the area.

Both clastic and chemical metasedimentary rocks occur in the central part of the map area. Pelitic and semi-pelitic rocks are represented by narrow ($\leq$ 1 km wide) bands of rusty-weathering, grey to green-brown coloured, biotite ± garnet ± sillimanite ± spinel ± graphite-bearing gneiss (unit 7) infolded with quartz dioritic gneiss (unit 2) north of Silver Mountain Lake, and associated with marble and calc-silicate rocks (unit 6) along the southwestern flank of the gabbroic pluton (unit 9, see below) south of Rat Lake (Fig. 62.1). The calcareous rocks, which flank the intrusion at three localities, consist of massive to layered, medium grained, buff, grey or white marble, in places with layers of dark grey calc-silicate rock up to a few metres wide. A one-metre-wide band of buff orthoquartzite occurs in the marble immediately southeast of Rat Lake. The marble is fairly pure except for the local presence of finely disseminated graphite and(or) olivine. Layering in the marble is defined by colour and(or) grain-size banding considered here to coincide with primary bedding. Mafic minerals in the calc-silicate layers include phlogopite, variably serpentinized olivine, diopside, garnet, and rare green spinel. P. Erdmer (personal communication 1985) has noted chondrodite in a thin section of the unit.

Unit 8 comprises medium grained, grey, layered quartzite, and massive, grey, white, or blue quartz. The layered quartzite is best exposed on a south-flowing tributary of the Humber River, approximately 7 km north-northeast of Silver Mountain Lake. At this locality, a band of grey quartzite at least 75 m wide (exclusive of a 30 m wide, subconcordant band of felsic porphyry (unit 19, see below)) is infolded with granitic gneiss (unit 3) in a sequence of quartzofeldspathic rocks dominated by quartz dioritic gneiss (unit 2). Layering in the quartzite is defined by grain-size variations and by light/dark grey colour banding on a centimetre- to metre-scale. Some layers contain magnetite and(or) biotite, and outline tight to isoclinal folds.

Massive quartz occurs principally in three localities: (1) to the northeast of Rat Lake; (2) to the northeast of Rex Lake; and (3) to the south of Silver Mountain Lake. The massive quartz near Rat Lake is white, medium grained, and contains layers of rusty, biotite- and sillimanite-bearing metapelitic gneiss (unit 7) up to at least 50 cm wide. The quartz at this locality is thus inferred to have a metasedimentary origin despite the absence of obvious sedimentary structures.

The band of massive quartz near Rex Lake is white, and contains traces of fine grained grey hematite. The origin of this band of quartz is uncertain, since no relict sedimentary features were observed. It is noteworthy, however, that graphite occurs in bands of otherwise similar, massive to layered, hematite-bearing white quartz to the north of the Silver Mountain area (P. Erdmer, personal communication, 1985). This may indicate a metasedimentary origin for massive white quartz in the map area.

Massive blue quartz occurs associated (and in places rhythmically interlayered) with medium grained, amphibole-bearing, subophitic metagabbro (unit 11, see below) in a 500-600 m wide body to the south of Silver Mountain Lake. The occurrence of rhythmically disposed, 1-100 cm wide layers of the quartz in the metagabbro suggest that it developed as a late, highly silicious fractionate of the mafic body. Similar blue quartz occurs as veins crosscutting various gneissic rocks in this, and other, localities in the Silver Mountain area.

B. Mafic rocks. An oblong pluton of medium- to coarse-grained metagabbro (unit 9) occurs to the south of Rat Lake. The dominant rock type is a mesocratic pyroxene ± olivine ± amphibole-bearing metagabbro (Fig. 62.6). Medium grained, grey leucogabbro occurs locally. One sample of subophitic leucogabbro sampled west of Taylor Brook contains olivine enclosed by both brown (titaniferous?) hornblendic amphibole and clinopyroxene. Orthopyroxene noted in some thin sections is largely replaced by an unidentified orange ferruginous(?) mineral. Erdmer (1984) reported monzonitic rocks associated with the gabbro;

Figure 62.2. *Refolded clinopyroxene-bearing mafic interband in flecky quartz diorite gneiss (unit 2). The mafic aggregates in the gneiss are reoriented parallel to the axial surface of the F2 folds.*

Figure 62.3. *Migmatitic biotite-bearing granitic gneiss, with 1-3 cm wide leucocratic segregations. Humber River, northwest of Birchy Dam.*

Figure 62.4. *Migmatitic amphibolite, with clinopyroxene-bearing leucocratic segregations. Same location as Figure 62.3.*

Figure 62.5. *Biotite granite (unit 5) crosscutting quartz diorite gneiss (unit 2). Humber River, northwest of Silver Mountain Lake.*

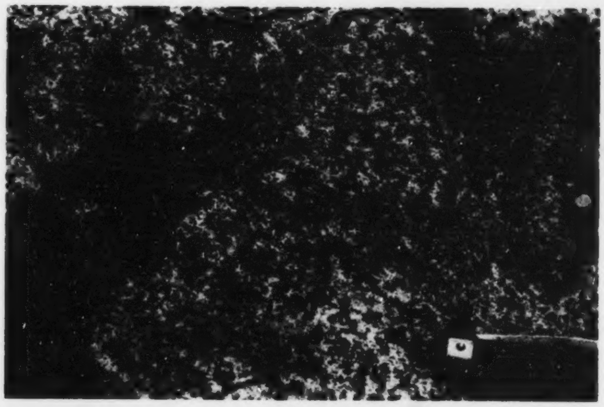

Figure 62.6. *Clinopyroxene- and olivine-bearing mesocratic metagabbro (unit 9), south of Rat Lake.*

Figure 62.7. *Pegmatitic metagabbro (unit 10), with amphibole-mantled, brown ortho(?) pyroxene.*

however, no K feldspar-bearing lithologies associated with the pluton were observed in the map area. The gabbro locally contains inclusions of quartzofeldspathic gneiss (unit 1?), and amphibolite (unit 4). Diverse, fine- to medium-grained, subophitic metagabbro inclusions are inferred to be early-crystallized fractions of the body.

The gabbro typically is massive, however, igneous layering defined by phase and(or) grain-size variations is locally developed on a centimetre- to metre-scale. The limited available data indicate that the primary layering dips moderately toward the centre of the intrusion (see Fig. 62.1). Primary layering in the metagabbro is crosscut by rectiplanar dykes of pegmatitic metagabbro (unit 10), which forms a mappable body south of Rat Lake. The pegmatitic metagabbro contains medium to dark green amphibole which in places encloses brown pyroxenes up to 15 cm in diameter (Fig. 62.7). Unit 10 is inferred to be a late, comagmatic phase of the intrusion.

Unit 11 comprises amphibole-bearing, subophitic metagabbro which occurs as relatively small bodies in quartzofeldpathic gneiss principally to the south and west of the gabbro intrusion of unit 9. The relative age of the two mafic units is unknown. Unit 11 may in part include satellites of the principal pluton, however, in contrast to the latter, pyroxene has not been observed in hand samples of the unit. This may reflect a higher degree of hydration of the smaller mafic bodies during regional metamorphism. Only the larger bodies of subophitic metagabbro are depicted in Figure 62.1. The geometry of these is unknown, although some mafic intrusions west of Rat Lake cap hills underlain by quartzofeldspathic gneiss and probably were emplaced as shallow-dipping sheets.

North-northeast-trending rectiplanar mafic dykes crosscut the mafic rocks of units 4, 9, 10, and 11, as well as quartzofeldspathic gneiss (units 1 to 3) and various granitoid rocks (e.g. unit 5). The dykes all contain amphibole, and have well-defined chilled margins. They are tentatively correlated with the ca. 600 Ma Long Range dyke swarm (Stukas and Reynolds, 1974). In contrast to Long Range dykes farther to the north which typically range up to several tens of meters in width, north-northeast trending mafic dykes in the Silver Mountain area are < 5 m wide, and may not be depicted at 1:100 000 scale.

C. Granite-granodiorite. Three categories of felsic intrusive rocks have been identified exclusive of the biotite granite (unit 5) spatially associated with the quartzofeldspathic gneisses. It is emphasized that the relative ages of these granitoids is unknown.

Unit 12 is a medium grained, grey, hornblende- and biotite-bearing granodiorite outcropping to the south of Rex Lake. The rock is massive to foliated, and contains saussuritized plagioclase, a feature typical of quartzofeldspathic rocks in this portion of the map area.

Two K feldspar-megacrystic granitoid rock types have been distinguished. Unit 13 is a grey to pink, medium grained, massive to foliated, megacrystic granite to granodiorite which occurs in the north-central and western part of the map area. The rock contains elongated K feldspar megacrysts up to 15 mm long. P. Erdmer (personal communication, 1985) reported that the northerly continuation of the intrusion in the north-central portion of the map area (see Fig. 62.1) also includes more mafic, non-megacrystic members, such as hornblende ± garnet metadiorite.

Unit 14 is a rose, medium to coarse grained, foliated, variably megacrystic biotite granite occurring in the northeastern corner of the map area. Tabular to lens-shaped K feldspar megacrysts are up to 3 cm long, and are set in a plagioclase-, quartz-, and biotite-rich, variably epidotized groundmass (Fig. 62.8). In places, the rock is coarse grained and is not distinctly megacrystic. The southern portion of the pluton includes pink, medium grained biotite granite not distinguished in Figure 62.1. Since this granite has not been seen in contact with the megacrystic granite, it is not known whether it is part of the same, or part of an unrelated intrusive complex.

Unit 15 is a grey to pink, fine to medium grained, massive to foliated, biotite-bearing granite. Only the body of granite immediately to the south of Rex Lake is depicted in Figure 62.1. The rock at this locality is well foliated, leucocratic, and has been extensively epidotized, a feature also noted in the quartzofeldspathic gneisses in the vicinity. Its age relative to the adjacent biotite + hornblende granodiorite (unit 12), and the biotite granite (unit 5) farther to the east, is unknown. Smaller granitic bodies (and associated granitic pegmatite veins) possibly correlative with unit 15 are seen to crosscut metagabbro (unit 9) and megacrystic granite-granodiorite (unit 13) to the northwest of Rat Lake.

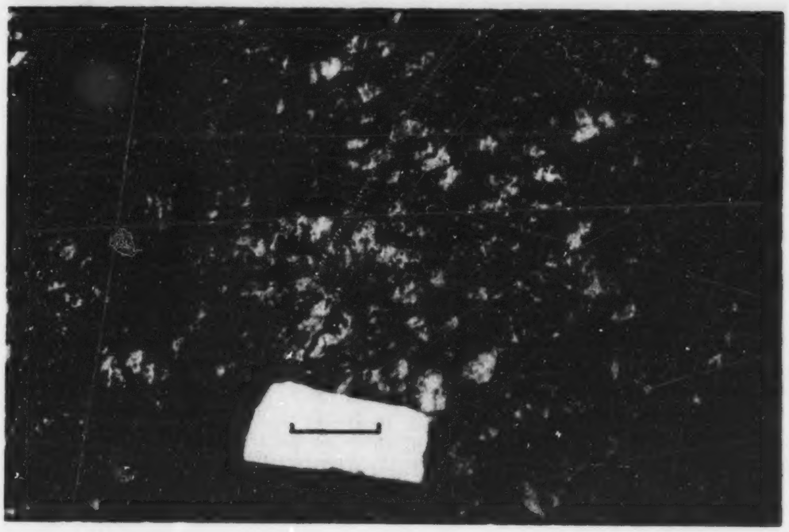

Figure 62.8

Foliated K feldspar-megacrystic biotite granite (unit 14), northeast of Rat Lake. Length of bar is 2 cm.

Paleozoic terrane

D. Cambro-Ordovician(?) metasedimentary and intrusive rocks. North-northeast trending schists along Taylor Brook are inferred to be metamorphosed Cambro-Ordovician sedimentary and igneous rocks. The age of the igneous rocks relative to the metasedimentary units is unknown. Both predate deposition of Carboniferous conglomerates and redbeds (unit 20, see below) of the Deer Lake Basin.

Unit 16 is a grey to tan, fine to very fine grained, quartz-rich schistose rock consisting chiefly of quartz, plagioclase, biotite and white mica. The presence of fine grained, centimetre-scale quartzose bands, and of medium grained, laminated quartzite interbeds up to at least 2 m wide demonstrate a sedimentary protolith for the schist. Unit 16 is tentatively correlated with parts of the middle Ordovician Coney Arm Group (Smyth and Schillereff, 1982), which occurs along strike to the north-northeast of the map area (see Erdmer, 1984, Fig. 2). Andalusite has been identified in the metasedimentary schist at one locality (Fig. 62.1).

Unit 17 is a tan weathering, laminated, fairly pure grey marble. It is finer grained, and lacks the calc-silicate layers and medium- to high-grade mineralogy of unit 6. Although the rock is lacking in "impure" horizons conducive to the development of metamorphic indicator minerals, white fibrous tremolite(?) has been noted in some hand samples. The marble shows a well defined, light/dark grey colour banding developed on a millimetre- to metre-scale. The marble is portrayed as a fault-bounded band of Paleozoic metacarbonate rocks of the Coney Arm Group on the revised geological map of Newfoundland compiled by Hibbard (1983). This correlation must be regarded as speculative, since the possibility that unit 17 is the retrograded equivalent of the calcareous rocks of unit 6 cannot at present be excluded. Furthermore, since the contact of the marble with the other schistose rocks along Taylor Brook was not observed, the nature of the contact, i.e. stratigraphic or structural, is unknown. Since unit 17 appears to be surrounded by granitic-granodioritic gneiss (unit 3) and amphibolite (unit 4), it is portrayed simply as an outlier in Figure 62.1.

Unit 18 is a 400-500 m wide north-northeast trending band of mafic rocks within the metasedimentary schist of unit 16. The centre of the band consists of a medium grained metadioritic rock consisting of amphibole and plagioclase; the margins have been highly strained, and consist of chlorite ± epidote-bearing mafic schist. Contact relations of these mafic rocks with unit 16 have not been observed, consequently it is not certain whether the mafic rocks are intrusive, or are mafic flows within a sedimentary-volcanic rock sequence.

Unit 19 is a tan to rose, very fine grained rock, containing well formed, 1-4 mm quartz and K feldspar phenocrysts. Locally, plagioclase and biotite also occur as phenocrysts. The phenocrysts are set in a very fine grained spherulitic groundmass consisting chiefly of plagioclase, with lesser quartz and traces of white mica. The rock has an overall mineralogy approximating that of a dacite or latite (possibly trachy-andesite). East of Taylor Brook, the rock is well foliated; farther to the west, minor (a few tens of metres wide) massive intrusions of the porphyry crosscut the gabbro pluton of unit 9. The presence of the porphyry as dykes in the gabbro precludes an extrusive origin for the rock despite the presence of quench textures (e.g. spherulites) in the groundmass. Rather, unit 19 is considered to be a hypabyssal intrusive rock. Erdmer (1984) suggested that the porphyry is Hadrynian or younger, and postulated that it may correlate with part of the Silurian Sops Arm Group described by Smyth and Schillereff (1982).

E. Conglomerate, redbeds. A few small outcrops of flat-lying, very coarse grained polymict conglomerate with interbeds of reddish-brown sandstone (unit 20) were observed in the southeastern corner of the map area. The conglomerate contains cobble- to boulder-size clasts of uncorrelated, pink, medium- to coarse-grained, massive biotite granite, and a variety of smaller, less abundant rock fragments. Gravel-sized rock fragments in the conglomerate include metadiorite, and pale grey cherty clasts. The mafic rock fragments commonly have well developed, reddish weathering rinds. Unit 20 is correlated with the Carboniferous North Brook Formation (Hyde, 1982). The North Brook Formation is the basal unit of the Deer Lake Basin, and includes grey to pink limestone in addition to the conglomerate and redbeds. The contact between the North Brook Formation and the underlying, schistose lower Paleozoic rocks (units 16 to 19) is inferred to be an unconformity, since the conglomerates and redbeds are undeformed.

Structure

The Precambrian terrane is dominated by a regional, northwest-trending, moderately to steeply dipping structural fabric defined by gneissic and schistose S-planes. This structural trend developed, at least in part, after the emplacement into the gneisses of various foliated intrusive rocks, including biotite granite (units 5, 15), K feldspar megacrystic granite and granodiorite (units 13, 14), and various mafic rocks (e.g. unit 9). Northwest-trending S-planes are associated with second(?) generation folds (F2), which deform early, open to tight folds (F1) in the gneisses about moderately south-southeast to southwest plunging axes. The axial surface schistosity (S2) is defined by oriented biotite flakes. S2 is readily discernible in the hinge area of open F2 folds in the gneisses (Fig. 62.9), but roughly parallels the gneissic layering in tight F2 folds.

The pre-D2 orientation of F1 folds is unknown, and no pre-F1 folds have been identified. Although predominantly trending toward the northwest, S2 shows some range in orientation. Since fold sets deforming S2 have not been identified on an outcrop scale, this may tentatively be attributed to contrasting rheological characteristics between different major rock units, to the effects of pre-S2 structures, and(or) to local variations in the strain field.

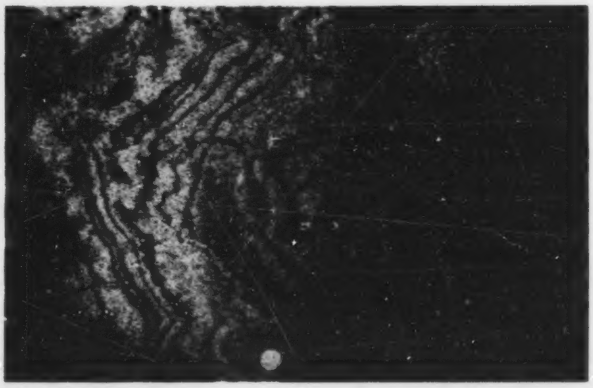

***Figure 62.9.** S2 developed along the axial surface of an F2 fold, which deforms an isoclinal F1 fold, both outlined by leucocratic veins in granitic gneiss (unit 3). Photo of a displaced block along the Humber River.*

Shallowly to moderately south-southwest plunging, upright folds are locally preserved in the lower Paleozoic(?) rocks (units 16 to 19) flanking Taylor Brook. These folds deform tight, small scale folds, and have a well defined, east-dipping axial planar schistosity. Evidence of polyphase Paleozoic deformation in pre-Carboniferous rocks straddling Taylor Brook is also provided by a mafic dyke, which crosscuts an east-dipping schistosity in megacrystic biotite granite (unit 14), and contains a non-penetrative schistosity oblique to the first. The younger schistosity is crenulated within 7 cm of the dyke borders, and shows the development of microlithons.

The schistose fabric developed in units 16, 18 and 19 commonly has a well-developed, east-plunging mineral lineation defined by mica-rich streaks alternating with elongate aggregates of quartz and feldspar. This is considered to be a stretching lineation, which contrasts with a subhorizontal intersection lineation ($So \wedge Sn$) seen locally in the metasedimentary schist of unit 16. CS-fabrics developed locally in the felsic porphyry (unit 19) indicate west-directed thrusting of the schistose rocks flanking Taylor Brook.

Metamorphism

Previous workers in the region noted that high-grade rocks were dominant in the western portion of the Long Range Mountains, whereas lower grade rocks occurred farther to the east (Bostock, 1983; Erdmer, 1984). Erdmer (1984) noted that granulite-facies rocks in Gros Morne National Park (immediately west of Angus Lake) were flanked to the east and west by compositionally similar gneisses exhibiting amphibolite-facies mineralogy. He found that the granulite-amphibolite transition in the area was largely gradational, except in one location, where a fault separates the granulites from the amphibolite-facies rocks. Mapping in the Silver Mountain area has demonstrated that granulite-facies rocks occur farther to the east than previously suggested.

Evidence for the attainment of high-grade metamorphism over much of the Silver Mountain area is provided by the widespread presence of orthopyroxene in the orthogneissic rocks of units 1, 2 and 3. Although variably replaced by amphibole, orthopyroxene has been observed in both the paleosome and leucosome components of migmatitic gneisses at several locations in the western half of the map area. The easternmost position of orthopyroxene in the gneisses observed during reconnaissance mapping is depicted in Figure 62.1. This is not intended to outline the approximate location of the orthopyroxene isograd, since orthopyroxene may occur in quartzofeldspathic gneisses still farther to the east. Rather, the preservation of orthopyroxene in this area demonstrates the sporadic nature of retrogression to amphibolite facies of the granulites.

Mafic enclaves oriented parallel to the regional, northwest-trending schistosity (S2) developed in granitoid rocks intruding the gneisses contain amphibole (hornblende?) and biotite. The partial retrogression of the granulites is thus inferred to have occurred during the development of south-plunging F2 folds.

Bostock (1983) suggested that two episodes of greenschist-facies metamorphism occurred in Precambrian gneisses and intrusive rocks in the eastern part of the northern Long Range Peninsula. He attributed the earlier episode, which predates emplacement of the Long Range dyke swarm, to the Grenvillian orogeny, and suggested that the younger episode, which postdates the dykes, occurred between late Lower Cambrian and late Ordovician times. Two orientations of greenschist-facies, ductile high-strain zones have been noted locally in the Silver Mountain area. The high-strain zones strike to the north, and to the east or northeast. Their age relative to the Long Range dykes is unknown, consequently they cannot be readily attributed to either Grenvillian or lower Paleozoic metamorphism.

Schistose fabrics defined by greenschist-facies minerals (chlorite, epidote) locally overprint the gneisses and intrusive rocks along narrow (centimetre- to metre-scale), steep, north-trending zones across the Precambrian terrane, and particularly in the westermost 10-12 km of the map area. Epidotization of quartzofeldspathic gneisses and granitoid rocks outside of these zones is also evident in this area, but may be attributed to the same retrogressive event.

Minerals developed along the greenschist-facies high-strain zones in the Precambrian terrane include chlorite and epidote in quartz diorite gneiss (unit 2), epidote and(or) white mica in granitic gneiss (unit 3), and biotite in the metagabbro pluton of unit 9. These north-trending fabrics are tentatively attributed to lower-middle Paleozoic orogenesis, since the orientation of these greenschist-facies fabrics approximately coincides with the north- to northeast-trending greenschist-facies schistose rocks flanking Taylor Brook. The significance of these low-grade fabrics is uncertain, however it is noteworthy that one north-trending greenschist-facies high-strain zone south of Angus Lake truncates the gneissic fabric in unit 2, which shows a horizontal dextral offset of a few metres. On this basis, the north-trending greenschist-facies shear zones present in the Precambrian terrane are considered to have a strike-slip displacement component.

East- to northeast-trending, moderately north-dipping mylonites transecting quartz diorite gneiss (unit 2) were observed at two locations south of Angus Lake. The relation of these to the north-trending high-strain zones is unknown; they may be analgous to either the Grenvillian or lower Paleozoic shear zones described by Bostock (1983) farther to the north.

Economic geology

Chalcopyrite occurs with biotite, quartz, and carbonate in vugs and fractures in amphibolite (unit 4) in a prospect on the woods road adjacent to the Humber River to the northeast of Silver Mountain Lake (see Fig. 62.1). In this outcrop, chalcopyrite comprises $\leq$ 1% of the rock, and is exposed in vugs and fractures developed in a zone < 5 m wide.

Masses of grey, white and blue quartz (unit 8), which in places exceed 100 m in width, represent a potential source of industrial stone. It should be noted that the quartz is rarely pure; hematite is a common accessory mineral.

Acknowledgments

I thank D. Machin for his enthusiastic assistance in the field. K. Currie and P. Erdmer are thanked for numerous discussions during the 1985 field season. The manuscript has benefitted from critical reviews by K. Currie, P. Erdmer, and C.F. Gower.

References

Bostock, H.H.
1983: Precambrian rocks of the Strait of Belle Isle area; in Geology of the Strait of Belle Isle Area, northwestern insular Newfoundland, southern Labrador and adjacent Quebec; Geological Survey of Canada, Memoir 400, p. 1-73.

Erdmer, P.
1984: Summary of field work in the northern Long Range Mountains, western Newfoundland; in Current Research, Part A. Geological Survey of Canada, Paper 84-1A, p. 521-530.

Hibbard, J. (compiler)
1983: Geology of the Island of Newfoundland (1:1 000 000 scale) Newfoundland; Department of Mines and Energy, Mineral Development Division, Map 83-106.

Hyde, R.S.
1982: Geology of the Carboniferous Deer Lake Basin; Newfoundland Department of Mines and Energy, Mineral Development Division, Map 82-7.

Pringle, I.R., Miller, J.A., and Warrell, D.M.
1971: Radiometric age determinations from the Long Range Mountains, Newfoundland; Canadian Journal of Earth Sciences, v. 8, p. 1325-1330.

Smith, W.R. and Schillereff, H.S.
1982: The pre-Carboniferous geology of southwest White Bay; in Current Research; Newfoundland Department of Mines and Energy, Mineral Development Division, Report 82-1, p. 78-98.

Stukas, V. and Reynolds, P.H.
1974: $^{40}Ar/^{39}Ar$ dating of the Long Range dykes of Newfoundland; Earth and Planetary Science Letters, v. 22, p. 256-266.

U-Pb ages on zircon from rocks of the Lac de Morhiban map area, Quebec

Project 760020

W.D. Loveridge
Precambrian Geology Division

Loveridge, W.D., U-Pb ages on zircon from rocks of the Lac de Morhiban map area, Quebec; in Current Research, Part A, Geological Survey of Canada, Paper 86-1A, p. 523-530, 1986.

Abstract

U-Pb age measurements on zircon were made on samples from four rock units of the Lac de Morhiban map area in the eastern Grenville Province of Quebec. The results are as follows:

Gneissic rock complex from the northern part of the map area; oldest rock unit investigated in this study, primary ages of rocks making up the gneiss complex are early Paleohelikian/late Aphebian or older.

Rhyolitic metavolcanic rock belonging to the Wakeham Group, from the southern part of the map area; age of volcanic deposition 1271 +13/-3 Ma.

Augen gneiss surrounding the Romaine River anorthosite; age of zircon crystallization, 1079 ± 5 Ma; zircon may be of igneous or metamorphic origin.

Late plutonic rocks intruding the three above units; age of intrusion 993 ± 3 Ma.

Résumé

On a effectué la datation à l'U-Pb du zircon trouvé dans des échantillons provenant de quatre unités lithologiques de la région cartographique du lac de Morhiban, dans l'est de la province de Grenville du Québec. Les résultats sont les suivants:

- le complexe de roches gneissiques dans la partie nord de la région cartographique représente la plus ancienne des unités rocheuses étudiées; les roches formant le complexe gneissique datent du Paléohélikien ancien ou Aphébien récent, ou même d'avant.
- les roches métavolcaniques rhyolitiques du groupe de Wakeham, dans la partie sud de la région cartographique, ont été mises en place il y a environ 1271 +13/-3 Ma.
- le gneiss oeillé qui entoure l'anorthosite de Romaine River s'est cristallisé il y a 1079 ± 5 Ma; il se peut que le zircon soit d'origine ignée ou métamorphique.
- des roches plutoniques récentes font intrusion dans les trois unités susmentionnées; l'intrusion daterait de 993 ±3 Ma.

Introduction

In 1976, geological reconnaissance was carried out in the Lac de Morhiban and Natashquan River map areas of the eastern Grenville Province of Quebec. A description of the major rock types in this area and a tentative sequence of events were published by Bourne et al., 1977. Samples were submitted to the Geochronological Laboratory of the Geological Survey of Canada with a view to establishing a time framework for these events. U-Pb ages on zircon from four of these samples are presented in this paper.

Geology

The following brief descriptions of the rock units investigated in this study are drawn from Bourne et al., 1977 and from additional material supplied by Bourne, who also provided lithological descriptions and chemical analyses of the rock samples (Table 63.1).

Table 63.1. Chemical analyses and sample locations for samples discussed in this report

BRA-76-	182	1305	55	28
	major elements (weight %)			
SiO_2	64.1	62.3	70.9	67.0
TiO_2	.37	1.13	.57	1.14
Al_2O_3	16.7	15.7	12.5	14.5
Fe_2O_3	2.6	1.8	.8	2.7
FeO	2.7	3.3	4.2	2.5
MnO	.09	.10	.05	.08
MgO	1.22	1.30	.69	.67
CaO	4.29	3.00	1.05	2.83
Na_2O	3.9	3.9	2.6	2.2
K_2O	2.55	5.46	5.33	5.58
P_2O_5	.54	.61	.15	.88
CO_2	0	0	.6	0
H_2Ot	.20	.40	.60	.20
Total	99.8	99.4	100.3	100.7
	trace elements (p.p.m.)			
Rb	60	130	300	280
S	300	300	0	0
Zn	60	140	20	100
	normative minerals (weight %)			
Q	21.1	11.2	31.2	28.0
or	15.4	32.9	32.1	33.0
ab	33.0	33.0	22.0	18.6
an	17.7	9.2	0.4	8.3
il	0.7	2.1	1.1	2.2
mt	3.8	2.6	1.2	3.9
en	3.0	3.0	1.7	1.7
fs	2.4	2.2	6.2	0.6
wo	0	1.4	0	0
co	1.0	0	2.8	1.8
	sample location			
Zone	20	20	20	20
Northing (km)	5760.2	5695.4	5672.5	5698.0
Easting (km)	503.7	515.0	546.4	568.4
N.T.S.	12M/15W	12M/7W	12M/1W	12M/8E

Gneissic rocks (map unit 1; Bourne et al., 1977)

Gneissic rocks are restricted to the northern parts of the map area. This structurally and lithologically complex unit comprises a varied assemblage ranging from pink gneisses of granitic composition to light grey gneisses of tonalitic to dioritic composition. Their precursors are not known although the presence of rare sillimanite-bearing gneiss suggests that some are sedimentary in origin. Wherever encountered, this rock unit appears to have been subjected to partial melting. A quartz-biotite-garnet-sillimanite assemblage observed in one outcrop suggests that middle amphibolite facies or higher metamorphic conditions were attained. Orthopyroxene, present locally as preserved cores rimmed by hornblende, may be either igneous or metamorphic in origin. It has not been found in any rocks of possible sedimentary origin from these gneisses but the scarcity of such rocks limits the significance of this observation. It is probable that the formation of orthopyroxene is associated with the period of partial melt development, which in turn would be related to an early episode of upper amphibolite, locally granulite, facies metamorphism. This would accord with the zircon morphology (Appendix) and with the metamorphic grade of the rocks mapped by Stevenson (1969) to the north.

The sample analyzed was collected from gneiss along the shore of Lac Mabille in the northwestern corner of the map area, less than 1 km south of the Labrador border. This gneiss is fine- to medium-grained, medium grey, granodioritic in composition and constitutes about 70 per cent of the outcrop. The remainder of the outcrop consists of mafic rock in layers and pink pegmatite of several generations.

Anorthosite and spatially related plutonic rocks (map units 3, 4a and 4d, Bourne et al., 1977)

Anorthosite and spatially related plutonic rocks are exposed along the west margin of the area. The anorthosite, unit 3, is part of the Romaine River complex which in turn is a lobe of the huge Havre St. Pierre anorthosite (Sharma and Franconi, 1975). The anorthosite has been completely recrystallized to a snow-white, massive, polygonal aggregate of plagioclase.

Foliated diorite, unit 4d, is restricted to the perimeter of the anorthosite mass and is clearly younger than the anorthosite, as blocks of anorthosite about one metre across are found within the diorite near the contact between the two rock types.

Foliated monzogranite (unit 4a), the rock dated in this study, appears on large scale as a "rind" wrapping around the anorthosite mass (Sharma and Franconi, 1975). It is a medium grained, foliated, augen granitoid rock which is pink on both weathered and fresh surfaces. Polycrystalline aggregates of potassium feldspar form aligned lenticular augen that define a prominent foliation. Members of this unit are commonly weathered; the analyzed sample comes from the least weathered outcrop of this unit. The sample site is approximately 16 km north of Lac Saumer on top of a broad hill. The foliated monzogranite grades into the foliated diorite unit, the boundary having been placed by Bourne et al. (1977) where the augen of potash feldspar make their appearance.

The metamorphic grade of units 3 and 4 appears to be middle amphibolite facies or higher; however, in contrast to unit 1, no evidence of partial melting was observed in units 3 and 4.

Metavolcanic rocks

Metavolcanic rocks of predominantly intermediate composition (unit 6v, Bourne et al., 1977) occur in the southern half of the map area. Deposited as flows and pyroclastic rocks, they range in composition from quartz latite porphyry to latite porphyry and may be traced into coarser grained rocks of quartz monzonitic composition (unit 6h, ibid.). No intrusive relationships were seen between the volcanic rocks and the hypabyssal quartz monzonite, the contact being defined only by the large difference in grain size between the two units. Both units are at a lower metamorphic grade (middle to upper greenschist facies) than the amphibolitic facies rocks previously described.

Members of the metavolcanic unit typically have high Zr content (average of 33 Wakeham Group volcanic analyses is 657 ppm). Some samples of this unit bear evidence of a tuffaceous origin, and although there is no direct evidence of this in the dated sample since the greenschist facies metamorphism which has overprinted these rocks has obliterated all primary textures of this nature, it is believed by Bourne to also have been a tuff.

Sharma and Jacoby (1973) considered similar metavolcanic rocks to the south to be part of the Wakeham Group. Bourne concurs (personal communication) and assigns to the Wakeham Group both the metavolcanic and the metasedimentary rocks (unit 5, Bourne et al., 1977) of the map area. The rock dated is considered by Bourne to be a typical and representative metarhyolite member of the Wakeham Group.

Plutons of monzogranite to quartz monzonite composition (unit 8, Bourne et al., 1977)

Plutons of monzogranite to quartz monzonite composition intrude the previously described rock units. These plutons are coarse grained and massive except at the margins where there is a strong concordant alignment of quartz and mafic minerals.

The rock dated in this study (pluton c, group 1, ibid.) is from the belt of northeast trending plutons exhibiting characterstically strong positive circular aeromagnetic signatures. The analyzed sample is a medium to coarse grained, pink monzogranite (BRA-76-28, Table 63.1), which is very weakly foliated. Potassium feldspar and plagioclase crystals are up to 2 cm in length and the quartz has a distinctive blue-grey colour. A second group of spatially associated plutons (not dated in this study) is believed by Bourne to be older, as northwest trending aeromagnetic patterns associated with these plutons suggest mild deformation related to northwest trending folding that has not affected the group 1 plutons.

Analytical procedures

Approximately 50 kg of rock were collected from each of the four sites considered in this report. The sample of granodioritic gneiss (unit 1) yielded only a few grams of zircon; the other three yielded tens of grams. The initial U-Pb analyses on these zircon concentrates were made in 1978 and were supplemented by additional analyses in 1983. Chemical analyses and sample locations for these samples are given in Table 63.1.

Procedures used for concentration and preparation of zircon fractions, chemical extraction of U and Pb from zircon, and isotopic analysis of U and Pb evolved over this period for which a general description is given in Sullivan and Loveridge (1980). Exceptions to this description are as follows. In 1978, zircon fractions were not handpicked to ensure 100% purity. Sieving and magnetic separation procedures were employed to ensure that the purity of the fractions analyzed was greater than 90%. Weights of zircon fractions analyzed, 5-20 mg in 1978, decreased to 1-4 mg in 1983. All fractions analyzed in 1983 were handpicked and some were abraded (Krogh, 1982) in generally successful attempts to obtain more concordant data points. Fractions analyzed in 1983 are designated in Table 63.2 by the letters "h" (handpicked) or "a" (handpicked and abraded); others were analyzed in 1978.

Mass spectrometric procedures in use in 1978 were those described by Sullivan and Loveridge (1980) whereas analyses undertaken in 1983 were performed on a Finnigan MAT-261 mass spectrometer in the multicollector mode. In this mode, ion beams composed of each of the four lead isotopes are collected and measured simultaneously in four separate Faraday cups. A more accurate measure of the miniscule ^{204}Pb abundance is obtained, at essentially the same time, by stepping the magnetic field in order to measure the ^{204}Pb/^{207}Pb ratio on an associated electron multiplier.

Lead contamination introduced during the chemical extraction procedures was generally less than 2% of the zircon lead present. The common lead component of the zircon lead itself, was also generally less than 2%. The isotopic composition assumed for the common lead component was that of a Stacey and Kramers (1975) model lead, the age of which was defined by the zircon upper concordia intercept age.

U-Pb ages were calculated using the uranium decay constants and isotopic compositions recommended by Steiger and Jaeger (1977). Linear regression of the U-Pb data and error estimation is based on Davis (1982). Davis' model for nonlinear data (op. cit.) was used when the data points formed a linear trend but were not collinear within analytical uncertainty. As this model is applicable only when the data include a point that is concordant within a few percent, the method of York (1969) was used for the regression of data for the granodioritic gneiss sample. Potassium argon age measurements on hornblende and/or biotite from this gneiss, the quartz monzonitic augen gneiss unit and the late intrusive quartz monzonite have been published previously (Wanless et al., 1979) and are presented for reference in Table 63.3 with a previously unpublished Rb-Sr age on biotite from the granodiorite gneiss.

Results and Discussion

Gneissic rocks (unit 1)

Sample BRA-76-182 was collected from the unit of gneissic rocks that occur in the northern one third of the map area. Five zircon fractions were separated for uranium and lead analysis (Table 63.2). Zircon morphology is described in the Appendix. The resultant data points form a linear trend (Fig. 63.1) but are not collinear within analytical uncertainty. Regression analysis of all five data points yields upper and lower concordia intercept ages of 1665 + 58/-40 and 860 +139/-150 Ma. However, it is pertinent that the two smallest (-37 μm) size fractions contain the highest U contents, 494 and 531 ppm. This combination of high U content and small grain size would have rendered these fractions highly susceptible to secondary lead loss in recent time. Furthermore, the calculated lower intercept age is unlikely to represent the time of primary lead loss. This would almost certainly have occurred during the prograde stage of the Grenville Orogeny (cf. Gebauer and Grunenfelder, 1976) for which a reasonable age might be 1150 Ma. Fitting a chord constrained at the lower end to intersect concordia at 1150 Ma to the data points representing the three coarser zircon fractions results in an upper intercept age of approximately 1790 Ma.

Table 63.2. Analytical data, U-Pb analyses of zircon

Size fractions are given in μm; N = non magnetic, M = magnetic at given angle; H = handpicked; A = handpicked and abraded; L/S = larger/smaller component of abraded zircon; Pb*(ppm) denotes the radiogenic Pb content; Pb isotopic abundances are presented after subtraction of Pb blank.

Sample Size fraction	Weight (mg)	U (ppm)	Pb* (ppm)	Measured $^{206}Pb/^{204}Pb$	Isotopic abundance, ^{206}Pb=100 ^{204}Pb	^{207}Pb	^{208}Pb	$^{206}Pb/^{238}U$	$^{207}Pb/^{235}U$	$^{207}Pb/^{206}Pb$ age(Ma)
Unit I. BRA-76-182										
+105, N-0°	10.66	434.7	117.2	2745	0.0112	9.873	15.710	0.25062	3.3587	1571
-105+74, A, N-1°	3.06	416.4	119.9	57794	0.0008	9.877	16.368	0.26525	3.6088	1599
-105+74, H, N-1°	0.84	258.6	69.51	6453	0.0089	9.771	13.959	0.25339	3.3708	1557
-37, N-2°	7.63	494.3	122.0	2077	0.0168	9.528	14.969	0.23192	2.9723	1487
-37, M-2°	4.32	531.5	132.3	4343	0.0152	9.587	16.709	0.23031	2.9776	1503
Unit III. BRA-76-1305										
+149, A, N-0°	4.42	89.30	17.39	3880	0.0120	7.706	18.602	0.18003	1.8705	1078
+149, N-1°	18.86	114.5	21.52	986.4	0.0196	7.827	16.626	0.17650	1.8370	1081
-44+37, N-1.5°	14.23	160.2	29.75	5587	0.0058	7.594	15.576	0.17564	1.8191	1071
-37, H	1.05	221.3	40.55	2853	0.0131	7.720	18.064	0.17017	1.7675	1077
Unit IV. BRA-76-55										
-149+88, A, N+0.5°	1.00	237.2	54.82	2221	0.0373	8.825	17.686	0.21536	2.4645	1269
-149+88, N+0.5°	18.58	230.3	50.43	1147	0.0789	9.387	16.803	0.20789	2.3726	1264
-62+44, N+1°	11.82	230.9	49.74	2819	0.0117	8.487	14.362	0.20474	2.3495	1274
-62+44, M+1°	3.50	311.7	64.09	1398	0.0416	8.776	16.165	0.19438	2.1955	1243
Unit V. BRA-76-28										
+149, N-1°	8.81	487.7	72.77	1880	0.0118	7.333	10.055	0.14855	1.4675	976
-149+105, A, L, N-1.5°	0.94	233.4	38.22	2999	0.0024	7.238	12.435	0.15927	1.5819	987
-149+105, A, S, N-1.5°	0.61	118.7	19.58	775.6	0.0038	7.260	11.934	0.16094	1.5990	988
-159+105, H, N-1.5°	3.03	201.5	32.30	2411	0.0249	7.551	13.197	0.15599	1.5474	985

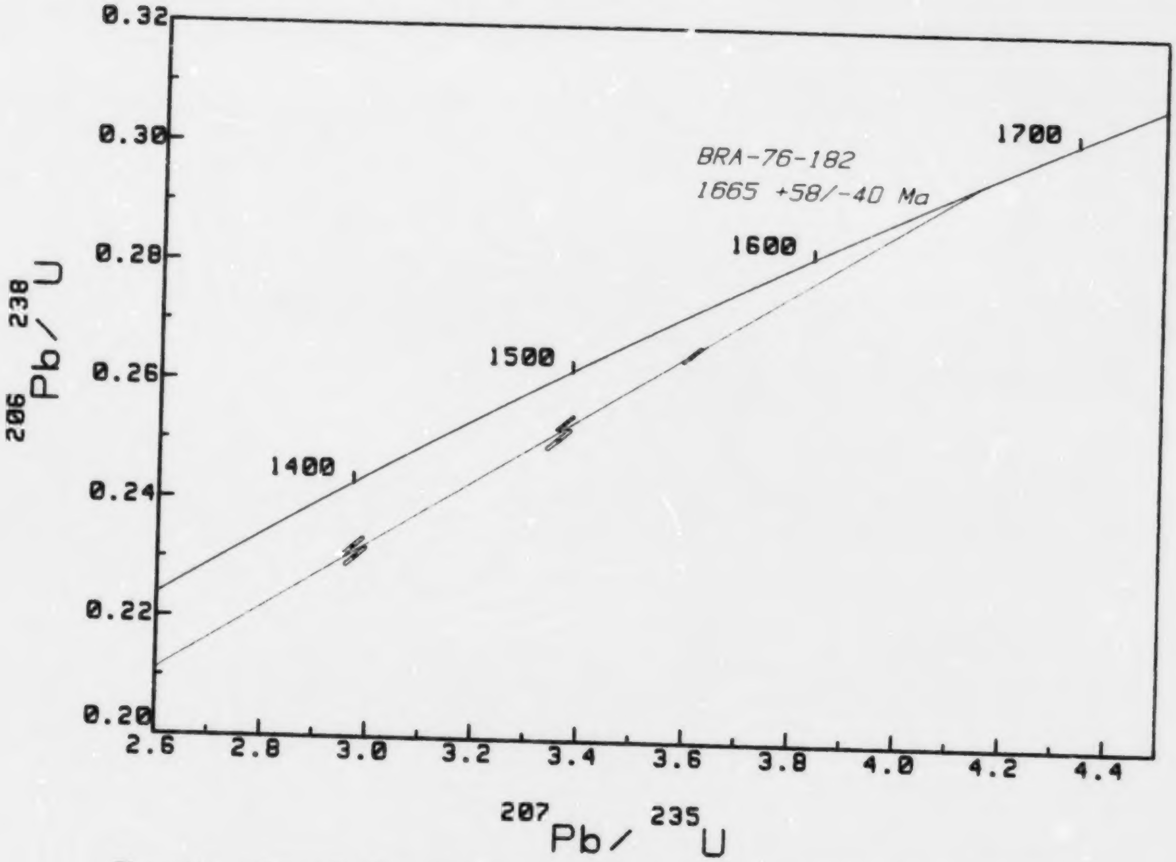

Figure 63.1. *Concordia diagram showing the results of U-Pb analyses of zircon from BRA-76-182.*

The majority of zircon grains are zoned throughout suggesting a magmatic origin (Jocelyn and Pidgeon, 1974). Most zoned grains show rounding of the euhedral tips to rounding of the whole crystals, suggesting overgrowth and/or corrosion of the crystal shape during metamorphic processes (op. cit.). Rare, clear ellipsoidal zircon with rounded crystal facets suggests some new zircon growth under conditions of granulite facies metamorphism (Pidgeon and Aftalion, 1972). It is concluded that the sampled gneiss had an igneous origin and was subsequently affected by a high grade metamorphic disturbance with new growth of metamorphic rims.

The age of this high grade metamorphic period is not directly known but is probably not much younger than the age of crystallization of igneous zircon in the sample studied, since the alignment of data points does not appear to have been perturbed by the addition of metamorphic zircon substantially younger than 1600-1700 Ma. The gneissic complex probably includes rocks of several different primary ages; it follows that all the gneissic rocks affected by the high grade metamorphic disturbance have primary ages comparable to or older than that of the sample studied. The igneous zircon may have originated as early as 1790 Ma although this date is not clearly defined. Later influences may have included corrosion and/or zircon growth during high grade metamorphism, primary lead loss associated in time with the Grenvillian Orogeny, and secondary lead loss from the finer zircon component in recent time. Further work would be required to quantify each of these influences. For the present we suggest that the northern gneiss unit is at least early Paleohelikian and possibly late Aphebian in age.

As such it is clearly older than the other units included in this study and is comparable in age with granulite gneiss from the north shore of Wilson Lake 250 km to the north (1699 ± 3 Ma, Currie and Loveridge, 1985) and gneiss of granodioritic composition 300 km to the northeast (1680 Ma, Krogh, 1983, cited in Erdmer, 1984).

Foliated monzogranite, unit 4a

Four zircon fractions from sample BRA-76-1305 were analyzed and results are listed in Table 63.2 and presented in Figure 63.2. Zircon morphology is described in the Appendix. Specific zircon fractions were chosen to closely define the U-Pb systematics. Two fractions of the least magnetic, largest grains were analyzed and one of these was abraded (Krogh, 1982) to minimize the content of surficial zircon that is more prone to lead loss. Two fine size fractions were also analyzed; these might be expected to have lost a relatively greater amount of lead in recent time due to the larger surface to volume ratios.

Data points from these four fractions are not collinear within analytical uncertainty but form a relatively concordant linear trend. Regression analysis using Davis' (1982) model for nonlinear data results in upper and lower intercept ages of 1079 +17/-11 and 62 Ma with the uncertainty associated with the lower intercept age being a factor of ten greater than age itself; ie. the lower intercept age is indistinguishable from zero.

The $^{207}Pb/^{206}Pb$ ages of three of the four fractions differ from the 1079 Ma upper intercept age by 2 Ma or less. The +149 µm abraded fraction yields a data point only

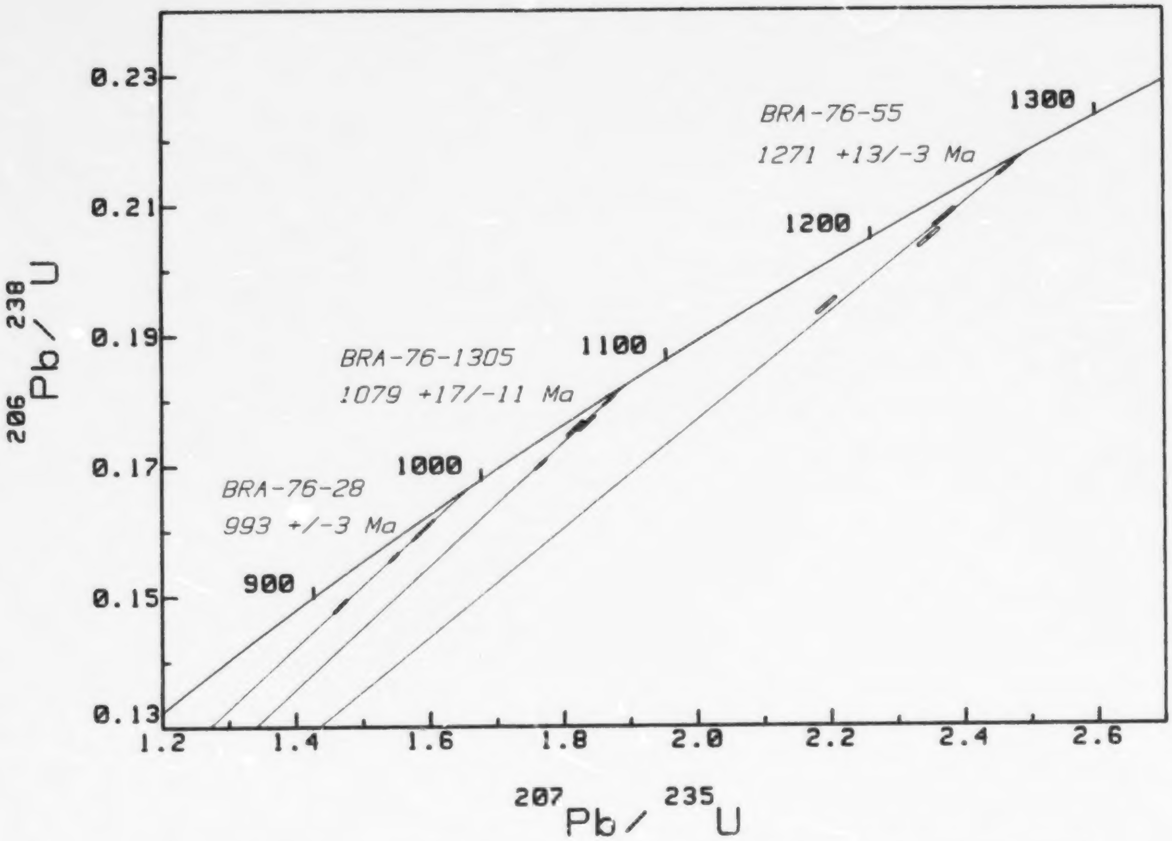

Figure 63.2. *Concordia diagram showing the results of U-Pb analyses of zircon from BRA-76-55, BRA-76-1305 and BRA-76-28.*

about 1% discordant with a $^{207}Pb/^{206}Pb$ age of 1078 Ma. The -44 + 37 µm nonmagnetic fourth fraction which does not fit this pattern, was analyzed prior to the introduction of handpicking zircon grains in our laboratories. Although impurities were less than 5%, they may have been sufficient to account for the slightly lower (1071 Ma) $^{207}Pb/^{206}Pb$ age. The average $^{207}Pb/^{206}Pb$ age defined by the remaining three fractions is 1079 ± 5 Ma and we adopt this result based on the assumption that the small amount of lead loss seen occurred at zero Ma.

The near concordance of these data points may be attributed to the low U contents of the zircon. The +149µm abraded fraction for which the data point is 1% discordant has the lowest U content, 89 ppm, whereas the data point for the -37µm fraction (U = 221 ppm) is still only 7% discordant. It is noted that the data point for the abraded +149µm fraction shows no evidence of a component of lead inherited from an earlier regime, despite the occurrence in many zircon grains of what appear to be miniscule inherited zircon crystals.

The origin of these zircons is not specifically indicated by their morphological features; the clear zircon of which they are composed may be formed by either igneous or metamorphic processes. The lack of internal euhedral zoning suggests that these zircons were not formed under magmatic conditions but Silver (1969) noted that randomly oriented needle and rod inclusions, which are ubiquitous in these grains, are typical of magmatic zircons. Surface irregularities indicate zircon resorption during the high grade metamorphic conditions whereas rare, clear, oval shaped grains with rounded facets in the finest size fractions suggest minor secondary zircon growth at near granulite facies conditions (cf. Pidgeon and Aftalion, 1972). Since the high grade metamorphic processes appear to have produced zircon corrosion rather than growth in the larger grains, the 1079 ± 5 Ma age is attributed to the time of primary zircon growth but it is uncertain whether this was in an igneous or earlier metamorphic environment.

Metavolcanic rocks, unit 6v, Wakeham Group

Sample BRA-76-55 is from an outcrop of dark grey, porphyritic, volcanic rock of rhyolitic composition (Table 63.1) located at a rapids on the Aguanus River, approximately 6 km northeast of Lac Arthur. In the zircon concentrate (Appendix) the regular zoning, euhedral shape, and presence of relatively large (+149µm) crystals suggest a slow development under magmatic conditions prior to extrusion.

The four analyzed fractions (Table 63.2, Fig. 63.2) yielded data points which are not collinear within analytical uncertainty but form a relatively concordant linear trend. Regression analysis (Davis, 1982) yielded upper and lower concordia intercept ages of 1271 + 13/-3 and 161 Ma. The ratios from the abraded -149 +88µm fraction are only 1% discordant and yield a $^{207}Pb/^{206}Pb$ age of 1269 Ma, in close agreement with the 1271 Ma concordia intercept. This age is interpreted as being the age of formation of the volcanic precursor.

Late intrusive rocks (unit 8)

Sample BRA-76-28 was collected from a young quartz monzonite intrusion exposed at the shore of Lac la Galissonnière. Four zircon fractions were selected for U-Pb analysis. Results are presented in Table 63.2 and Figure 63.2; zircon morphology is described in the Appendix. The +149 µm nonmagnetic fraction sampled the bulk concentrate and was not hand-picked but was of greater than 90% purity. Two -149 µm nonmagnetic fractions were hand-picked from the clear members of the population and one of these was abraded. Larger and smaller size fractions were picked from the abraded zircon. The data points for these four fractions are collinear and relatively concordant, defining a chord of upper and lower intercept ages 993 ± 3 and 184 +52/-50 Ma. The 993 ± 3 Ma upper intercept age is interpreted as the age of intrusion of the quartz monzonite.

Potassium-argon and rubidium-strontium ages

K-Ar and Rb-Sr ages on mineral separates are presented in Table 63.3. The Rb-Sr age of 926 ± 20 Ma for biotite for sample BRA-76-182 (unit 1) was determined on a small remaining portion of the concentrate used for the K-Ar age measurement. It is in closer agreement with the (K-Ar) ages on hornblende from samples BRA-76-1305 (unit 4a) and BRA-76-28 (unit 8) than is the 963 ± 27 Ma K-Ar age on the same biotite. Because the primary age of the gneiss is relatively old as indicated by the U-Pb zircon result, it is possible that the K-Ar age may reflect a small component of excess argon in the biotite. Thus the Rb-Sr age of 926 ± 20 Ma is to be prefered for BRA-76-182. Although this age is in good agreement with the K-Ar hornblende ages from BRA-76-1305 and BRA-76-28 it is significantly higher than the K-Ar age of 868 ± 25 Ma on biotite from BRA-76-28. This pattern is consistent with a differential cooling history with earlier attainment of argon blocking temperatures to the north but the data are too few to be conclusive.

Conclusions

1. The gneissic complex located in the northern part of the map area is the oldest rock unit dated in this study. U-Pb, zircon results indicate a primary early Paleohelikian/late Aphebian age or older for rocks of this complex. K-Ar (963 ± 27) and Rb-Sr (926 ± 20) age measurements on biotite indicate Grenvillian updating.
2. U-Pb measurements on zircon from a volcanic rock of rhyolitic composition provide an age of 1271 +13/-3 Ma for this member of the Wakeham Group.
3. The age of crystallization of zircon from the augen gneiss which forms an envelope surrounding the Romaine River anorthosite was found to be 1079 ± 5 Ma by the U-Pb, zircon method. It is uncertain whether this zircon is of igneous or metamorphic origin. A K-Ar date of 919 ± 41 Ma on hornblende from this sample indicates later Grenvillian updating.
4. The above rocks were intruded by a number of plutons, one of which was dated at 993 ± 3 Ma by the U-Pb, zircon method. K-Ar ages of 900 ± 41 and 868 ± 25 Ma were determined on hornblende and biotite from the same sample.

Table 63.3. K-Ar and Rb-Sr dates from mineral concentrates

Sample no.	Mineral	Age (Ma)	Publication no. (Wanless et al., 1979)	Method
BRA-76-182	Biotite	963 ± 27	GSC 78-205	K-Ar
	Biotite	926 ± 20	This report	Rb-Sr
BRA-76-1305	Hornblende	919 ± 41	GSC 78-202	K-Ar
BRA-76-28	Hornblende	900 ± 41	GSC 78-204	K-Ar
BRA-76-28	Biotite	868 ± 25	GSC 78-203	K-Ar
BRA-76-182: Rb 456.6 ppm		$^{87}Rb/^{86}Sr$	75.29 ± 1.13	
common Sr 17.53 ppm		$^{87}Sr/^{86}Sr$	1.7019 ± 0.0004	

References

Bourne, J.H., Stott, G., Borduas, B., and Lalonde, A.
1977: Lac de Morhiban and Natashquan River map area; Geological Survey of Canada, Paper 77-1A, p. 199-204.

Currie, K.L. and Loveridge, W.D.
1985: Geochronology of retrogressed granulites from Wilson Lake, Labrador; in Current Research, Part B, Geological Survey of Canada, Paper 85-1B, p. 191-197.

Davis, D.W.
1982: Optimum linear regression and error estimation applied to U-Pb data; Canadian Journal of Earth Sciences, v. 19, no. 11, p. 2141-2149.

Erdmer, P.
1984: Precambrian geology of the Double Mer-Lake Melville region, Labrador; Geological Survey of Canada, Paper 84-18, 37 p.

Gebauer, D. and Grünenfelder, M.
1976: U-Pb zircon and Rb-Sr whole rock dating of low-grade metasediments; example: Montagne Noire (Southern France); Contributions to Mineralogy and Petrology, v. 15, p. 13-32.

Jocelyn, J. and Pidgeon, R.T.
1974: Examples of twinning and parallel growth in zircons from some Precambrian granites and gneisses; Mineralogical Magazine, v. 39, p. 587-594.

Krogh, T.E.
1982: Improved accuracy of U-Pb zircon ages by the creation of more concordant systems using an air abrasion technique; Geochimica et Cosmochimica Acta, v. 46, p. 637-649.

Pidgeon, R.T. and Aftalion, M.
1972: The geochronological significance of discordant U-Pb ages of oval-shaped zircons from a Lewisian gneiss from Harris, outer Hebrides; Earth and Planetary Science Letters, v. 17, p. 269-274.

Sharma, K.N.M. and Franconi, A.
1975: Magpie, Saint-Jean and Romaine Rivers area; Ministère des Richesses Naturelles du Québec, geological report no. 163, 73 p.

Sharma, K.N.M. and Jacoby, R.
1973: Jérémie and Gaudreault Lake area, Duplessis County, Quebec; Ministère des Richesses Naturelles du Québec, open file report No. GM-28442, 16 p.

Silver, L.T.
1969: A geochronologic investigation of the Adirondack Complex, Adirondack Mountains, New York; in Origin of anorthosite and related rocks, ed. Y.W., Isachsen; Memoir 18, New York State Museum and Science Service.

Stacey, J.S. and Kramers, J.D.
1975: Approximation of terrestrial lead isotope evolution by a two stage model; Earth and Planetary Science Letters, v. 26, p. 207-221.

Steiger, R.H. and Jaeger, E.
1977: Subcommission on Geochronology: convention on the use of decay constants in geo- and cosmochronology; Earth and Planetary Science Letters, v. 36, p. 359-362.

Stevenson, I.M.
1969: Lac Brûlé and Winokapau Lake map areas, Newfoundland and Quebec; Geological Survey of Canada, Paper 67-69, 16 p.

Sullivan, R.W. and Loveridge, W.D.
1980: Uranium-lead age determinations on zircon at the Geological Survey of Canada: current procedures in concentrate preparation and analysis; in Loveridge, W.D., Rubidium-strontium and uranium-lead isotopic age studies, Report 3; in Current Research, Part C, Geological Survey of Canada, Paper 80-1C, p. 161-246.

Wanless, R.K., Stevens, R.D., Lachance, G.R., and Delabio, R.N.
1979: Age determinations and geological studies, K-Ar isotopic ages, Report 14; Geological Survey of Canada, Paper 79-2.

York, D.
1969: Least squares fitting of a straight line with correlated errors; Earth and Planetary Science Letters, v. 5, p. 320-324.

Appendix

Zircon morphology

Unit 1, BRA-76-182: This concentrate comprises a mixed population of zircon grains. The majority (c. 90%) are translucent, rounded-euhedral to rounded, with evident euhedral zoning. Tubes, rods and dark blebs are common internal features and some grains have cores. Numerous examples of parallel growth and necking (Jocelyn and Pidgeon, 1974) are seen and length to breadth ratios range from 1.5:1 to 4:1.

The minor component consists of clear colourless euhedral crystals with rounded tips and length to breadth ratios generally in the range 3:1 to 4:1. Zoning is generally absent from this population except for zoned overgrowths which are evident on the tips of some grains. A few clear zircon grains are more equidimensional, ellipsoidal in shape with rounded facets similar to those attributed by Pidgeon and Aftalion (1972) to having grown during granulite facies metamorphism. Small bubble inclusions are visible in most clear grains.

Unit 4a, BRA-76-1305: The zircon in this concentrate consists of clear to pale golden grains with irregular surfaces ranging from subhedral to irregular in shape, essentially transparent with no visible cores. Zoning is absent but many dark blebs, needles and tube like internal structures are evident. Some inclusions, primarily in the larger grain sizes, appear to be very small randomly oriented zircon and/or other crystals. Length to breadth ratios in the whole zircon grains range from 1:1 to 4:1 but broken grains form the majority in the coarser size fractions. Minor (10%) clear, ellipsoidal, grains with rounded facets are present in the finest size fractions.

Unit 6v, BRA-76-55: This concentrate consists of clear to translucent, euhedral zircon crystals. Some are regularly zoned while others display no zoning. Length to breadth ratios range from 2:1 to (rarely) 4:1 with many broken pieces. Colour varies from colourless to pale yellow and many crystals have bubble, rod and tube like internal structures. A few rounded grains were noted.

Unit 8, BRA-76-28: This zircon concentrate consists of a heterogeneous mixture of shapes and sizes. The major component (c. 75%) is made up of translucent euhedral crystals, mostly broken, with length to breadth ratios of the whole crystals ranging from 1.5:1 to 4:1. Zoning is often seen in the translucent population and many inclusions are evident. This population appears to grade into a clear population of euhedral to rounded-euhedral lath like crystals, mostly broken. Length to breadth ratios are similar to the above but zoning is absent. The clear component is more prevalent in the finer grain sizes approaching 50%. More rounded zircons are also more prevalent in the finer grains sizes, typically ellipsoidal with length to breadth ratios 1.5:1 or less, translucent, and containing only small bubble inclusions.

Developments in uranium geology in Canada, 1985

Project 750010

V. Ruzicka and G.M. LeCheminant
Economic Geology and Mineralogy Division

Ruzicka, V. and LeCheminant, G.M., Developments in uranium geology in Canada, 1985; in Current Research, Part A, Geological Survey of Canada, Paper 86-1A, p. 531-540, 1986.

Abstract

Field and laboratory investigations of uranium occurrences and deposits indicate that (1) the formation of the world's largest high grade uranium deposit at Cigar Lake, Saskatchewan, at 1.3 Ga was apparently contemporaneous with thermal events associated with intrusion of the Mackenzie dyke swarms; (2) localization of the recently discovered polymetallic mineralization at Close Lake and Natona Bay, Saskatchewan is controlled by similar structural and lithological factors as the Cigar Lake deposit; (3) elements and assemblages associated with polymetallic mineralization at Sand Lake, and Key Lake in Saskatchewan, and at Long Lake, in New Brunswick; (4) the chemical properites of carbon in uranium and gold bearing seams of the Elliot Lake deposits are consistent with kerogen and similar to kerogen from the Vaal Reef, Witwatersrand, South Africa.

Résumé

Les études sur le terrain et en laboratoire des venues et des gisements d'uranium révèlent que (1) la formation, il y a environ 1,3 milliard d'années, du plus grand dépôt au monde d'uranium à forte teneur à Cigar Lake, en Saskatchewan, a vraisemblablement eu lieu en même temps que les événements thermiques associés à l'intrusion de l'essaim de filons de Mackenzie; (2) l'emplacement de la minéralisation polymétallique récemment découverte à Close Lake et à Natona Bay, en Saskatchewan, manifeste des facteurs structuraux et lithologiques similaires à ceux du gisement de Cigar Lake; (3) les éléments et les associations minérales associés à la minéralisation polymétallique à Sand Lake et à Key Lake en Saskatchewan, à Otish Basin au Québec et à Long Lake au Nouveau-Brunswick; (4) les propriétés chimiques du carbone trouvées dans l'uranium et dans les filons aurifères des gisements d'Elliot Lake sont comparables à celles du kérogène et semblables à celles du kérogène provenant de Vaal Reef, Witwatersrand, en Afrique du Sud.

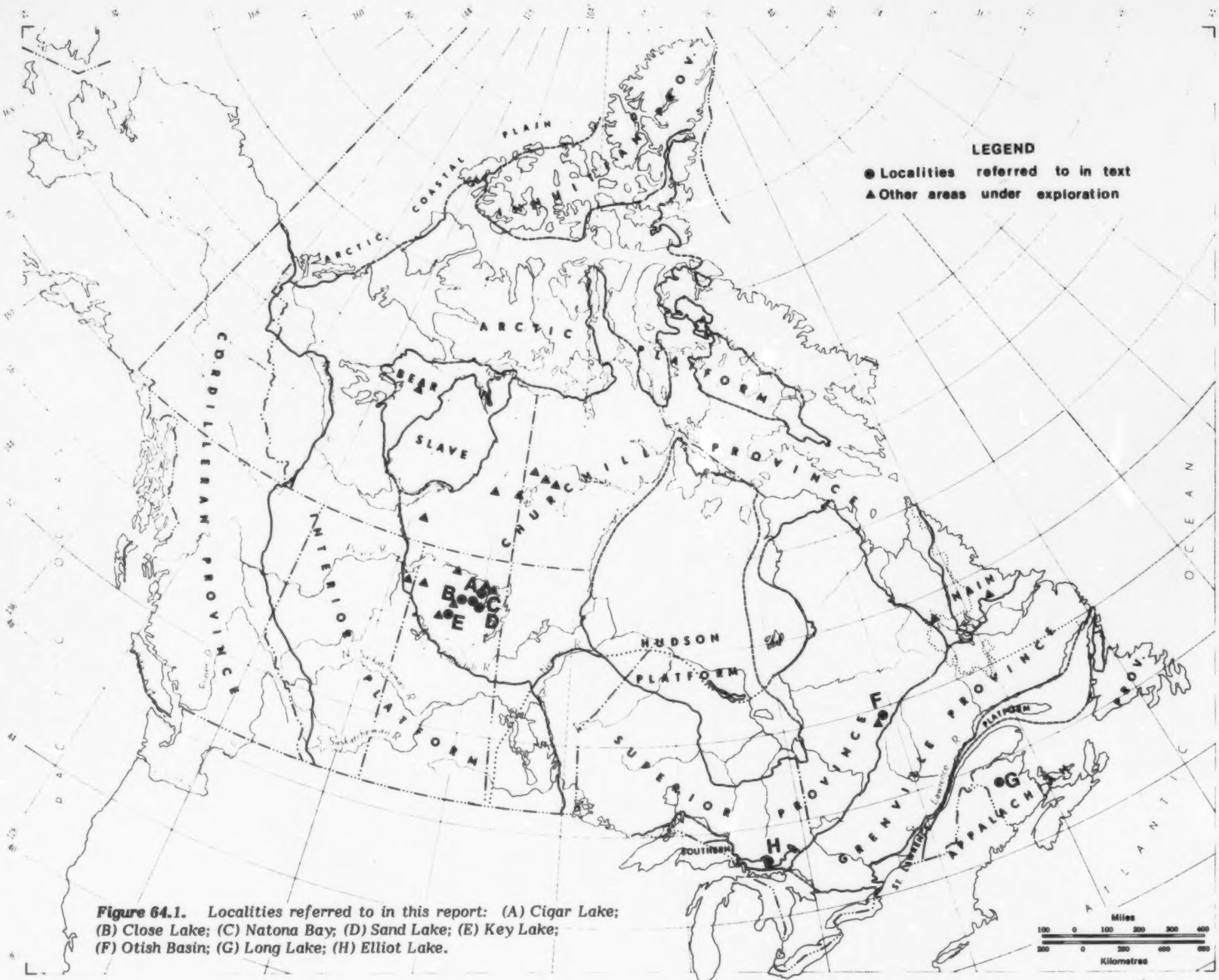

Figure 64.1. Localities referred to in this report: (A) Cigar Lake; (B) Close Lake; (C) Natona Bay; (D) Sand Lake; (E) Key Lake; (F) Otish Basin; (G) Long Lake; (H) Elliot Lake.

Introduction

In 1985 studies of the economic geology of Canadian uranium resources were focussed on recently discovered occurrences, as well as on deposits under development and on producing mines.

As in previous years, exploration for uranium was concentrated mainly in the Athabasca Basin region of Saskatchewan and Alberta; in the Baker Lake-Thelon Basin, District of Keewatin; Nonacho Basin and Bear Geological Province, District of Mackenzie; Otish Basin, Quebec; Labrador Trough, Quebec and Labrador; and in the Central Mineral Belt of Labrador (Fig. 64.1). The occurrences at Close Lake and Natona Bay are apparently the most important recent discoveries. Deposits under development include the Cigar Lake orebody at Waterbury Lake and the 'B' Zone at Collins Bay, Saskatchewan.

In 1985 uranium concentrates were produced in Saskatchewan by the Key Lake Mining Corporation, from the Key Lake mine; by Eldorado Resources Limited, from stockpiles at the Rabbit Lake mine; by Cluff Mining from the Cluff Lake deposits (Claude, Dominique-Peter); and from Elliot Lake, Ontario, mines by Rio Algom Ltd. from the New Quirke, Panel, and Stanleigh mines, and by Denison Mines Ltd. from the Denison mine.

In New Brunswick, an inventory survey of uranium occurrences was carried out under contract to the Geological Survey under the Canada – New Brunswick Mineral Development Agreement.

In the course of regional mineral resource assessment by the EMR Uranium Resource Appraisal Group, key deposits and areas were selected for detailed study. Some results are presented in this paper. Locations of the deposits and prospects examined are shown in Figure 64.1.

Cigar Lake deposit, Saskatchewan

The Cigar Lake deposit is the world's largest known high grade uranium deposit, estimated at present to contain 110 000 tonnes of uranium metal in material grading on average 12 per cent U (Alsthom et al., 1985, p. 15).

Uranium-lead isotope analyses on three pitchblende samples from the Cigar Lake deposit (Fig. 64.2), collected from drillcore from different parts of the main high grade pod, revealed ratios as shown in Table 64.1. Using the $^{206}Pb/^{238}U$ and $^{207}Pb/^{235}U$ ratios the concordia intercept (Fig. 64.3) is at 1.3 Ga. It thus appears that the crystallization of pitchblende is contemporaneous with the thermal event associated with intrusion of the Mackenzie dyke swarms (Fahrig and Wanless, 1963).

The pitchblende in sample 'A' occurs as massive botryoidal grains associated with fine grained granular gersdorffite, chalcopyrite and pyrite embedded in fine grained green chlorite and surrounding anhedral grains of dolomite (Fig. 64.4). Pitchblende in sample 'B' is associated with rammelsbergite, galena, Fe-carbonate and chlorite. Pitchblende in sample 'C' is associated with gersdorffite and rammelsbergite and intergrown with nickeline. As reported previously (Ruzicka and LeCheminant, 1985) this euhedral U-Ni-Co mineralization belongs to the earliest phase of the ore-forming process.

Locally, pitchblende replaces the kaolin matrix of the sandstone and surrounds needles of rutile, botryoidal rings of gersdorffite, and aggregates of siderite (Fig. 64.5). This pitchblende belongs to the second phase of mineralization. The second phase also includes coffinite. Within the clay matrix, a nearly amorphous potassium-rich, yellow-green (glauconite-celadonite) mica and rosettes of siderite, enclosing a dark grass-green very low birefringent amorphous mineral Fe, Si (Mg, Al, K, Mn), (apparently a mixture of siderite and chamosite, Fig. 64.6), accompany the pitchblende. The clay in the vicinity of the mineralization is commonly soft and in some places contains carbon (kerogen ?) nodules a few millimetres in diameter (Fig. 64.7).

Selected core samples from a drillhole penetrating the high grade portion of the Cigar Lake deposit were analyzed for U, Ni, As, Co, Al, Zr, Th, Pb, Zn, K, Cu, Ag, Mo and Y. The best correlation ($r > 0.8$) was observable between the following pairs of elements: U-Pb: 1.00, U-Zn: 0.98; Ni-As: 0.93; Ni-Cu: 0.99; Ni-Ag: 0.81; Ni-Mo: 0.99; Ni-Y: 0.94; As-Cu: 0.93; As-Ag: 0.88; As-Mo: 0.92; As-Y: 0.91; Pb-Zn: 0.99; Cu-Mo: 0.99; Cu-Y: 0.91 and Mo-Y: 0.93. Al, K and Zr exhibit the lowest correlation coefficients with the other elements.

In respect to vertical distribution of the principal constituents, uranium occupies two intervals: between 395 and 407 m and between 427 and 441 m with a peak at 437.8 m (Fig. 64.8a). Arsenic has a somewhat similar distribution with a peak at 434.4 m (Fig. 64.8b). Nickel is concentrated in a relatively narrow interval at the base of the ore body with a peak at 434.4 m (Fig. 64.8c). Cobalt exhibits a distribution pattern similar to that of nickel with a peak at 432.6 m (Fig. 64.8d).

Field and laboratory observations of the Cigar Lake deposit in 1985 indicate: (a) the U ± Ni ± Co ± As mineralization was deposited in several phases; (b) the main episode of uranium mineralization took place at about 1.3 Ga; (c) the ascending hydrothermal fluids caused corrosion or dissolution of quartz grains in sandstone and produced clay alteration haloes along fault or fracture zones in both the basement rocks and in the sandstone; (d) siderite and other carbonates were introduced by hydrothermal fluids; (e) certain clays, not necessarily directly associated with pitchblende, were enriched in Al, Mg and K; (f) carbon (kerogen ?) nodules were formed in soft clays in the vicinity of the unconformity; (g) within the mineralization good correlation ($r > 0.8$) was observed between elements in the two groups, U-Pb-Zn and Ni-Cu-Mo-As-Y-Ag; (h) uranium and arsenic exhibit the broadest vertical distribution, whereas nickel and cobalt show the narrowest range.

Close Lake and Natona Bay occurrences, Saskatchewan

Intimate knowledge of the geological environment and an appropriate exploration technique led Cogema Canada Limited to the discovery of uranium-polymetallic mineralization near Close Lake, some 16 km to the west of Cigar Lake (North American Gold Mining Industry News, 1985; Fig. 64.2). The mineralization is associated with the sub-Athabasca unconformity, which separates basement rocks, including a graphitic metapelite layer, from clastic sedimentary rocks of the Manitou Falls Formation. The unconformity occurs at a depth exceeding 600 m below the present surface. It is believed that the Close Lake mineralization is associated with the same structural trend as the Cigar Lake deposit.

The Natona Bay occurrence was discovered by Saskatchewan Mining Development Corporation about 22 km northeast of the Cigar Lake deposit (Fig. 64.2). The U-Ni-As-Zn-Pb mineralization occurs mainly in altered rocks of the Manitou Falls Formation, near its base and in altered graphitic semipelite just below the sub-Athabasca unconformity. In this area the unconformity occurs about 250 m below the present surface. The basement rocks include, in addition to the semipelite, cordierite gneiss, meta-arkose, calc-silicate rocks and tourmaline pegmatite. The principal types of hydrothermal alteration are hematization, chloritization, illitization, kaolinization, bleaching and silicification. In addition to massive pitchblende, the principal components of the mineralization are gersdorffite, nickeline, sphalerite, jordisite, galena,

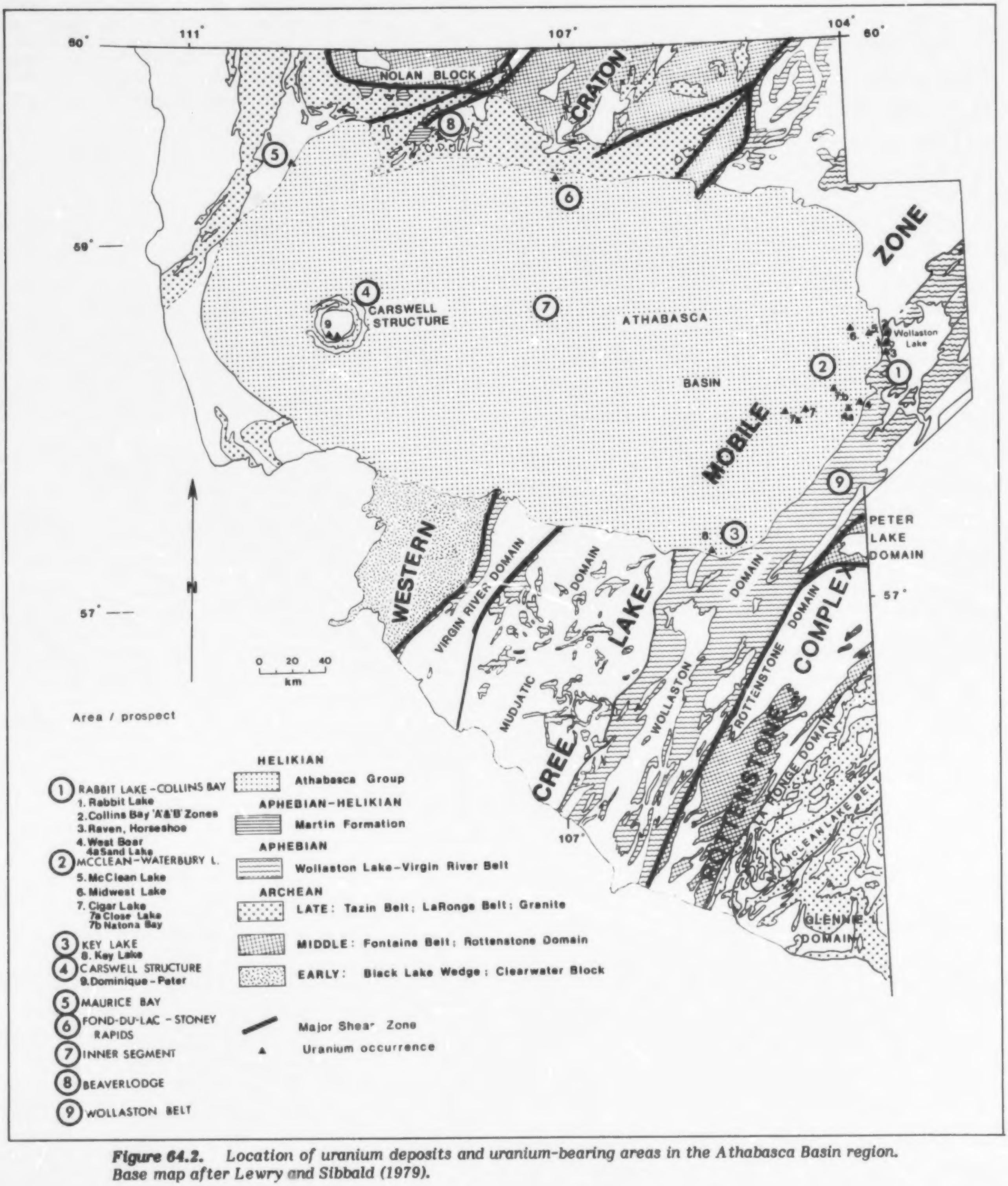

Figure 64.2. Location of uranium deposits and uranium-bearing areas in the Athabasca Basin region. Base map after Lewry and Sibbald (1979).

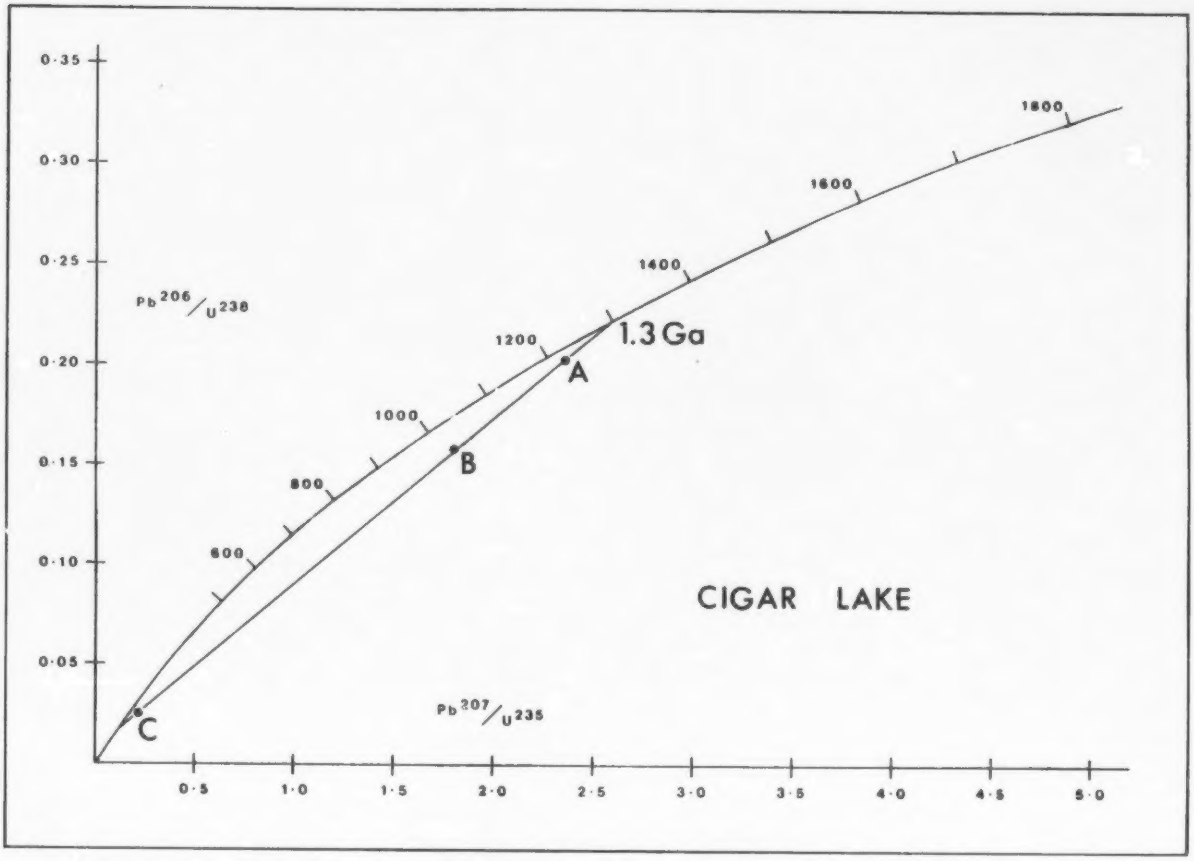

Figure 64.3. Concordia plot of U-Pb isotope analyses of pitchblende samples from the Cigar Lake deposit, Saskatchewan.

Table 64.1. U-Pb isotope ratios, Cigar Lake deposit

Sample/depth in m	$^{207}Pb/^{206}Pb$	$^{206}Pb/^{238}U$	$^{207}Pb/^{235}U$
B/420.6	0.08261	0.1586	1.806
A/426.1	0.08547	0.2012	2.372
C/434.75	0.07711	0.02173	0.2310

NB. Analyses by Geospec Consultants Ltd., Edmonton, Alberta.

chalcopyrite and pyrite. The Natona Bay mineralization is apparently controlled by the same structural and lithological features as Cigar Lake.

Sand Lake occurrence, Saskatchewan

The Sand Lake uranium-polymetallic occurrence (Fig. 64.2) is associated with a northeast-trending fault system which is apparently a continuation of the Collins Bay thrust fault. The occurrence was discovered in 1983 by Agip Canada Limited using a conceptual genetic model for the unconformity-related deposits in the Athabasca Basin region, namely lithology of the basement rocks and style and intensity of clay alteration. Mineralization at Sand Lake is most intense in the faulted and altered basement rocks, but also occurs in the sandstone cover. The mineralization extends between 170 and 200 m below present surface. The basement rocks consist of graphitic metapelites, garnetiferous granite pegmatite dykes and calc-silicate rocks.

In addition to uranium (in massive pitchblende and finely disseminated boltwoodite) lead, molybdenum, vanadium, titanium, cobalt, nickel and arsenic are present in association with chlorite, V-phyllosilicates and Fe-rich illite. Molybdenite is present in very fine grains replacing vanadian mica (Fig. 64.9). Vanadium and titanium form an anisotropic oxide locally associated with cobaltite. Microprobe analysis of the titanium vanadate (Fig. 64.10) indicated Ti (17.8 %), V (18.7 %), O (63.5 %), (ATOM. %) / TiO_2 (46.1 %), V_2O_3 (45.6) (WT. %). Boltwoodite $[K_2(UO_2)_2(SiO_3)_2(OH)_2 \cdot 5H_2O]$ is finely intergrown with the phyllosilicates.

Some observations on mineralization of the Gartner orebody, Key Lake deposit, Saskatchewan

In order to study the vertical distribution of mineral assemblages in the basement rocks of the Key Lake Gartner orebody, core was sampled from a drillhole located approximately in the centre of the open pit. The samples, each representing a megascopically distiguishable unit, were collected from the section below the unconformity which occurs at 478.0 m above the sea level at the drillhole collar.

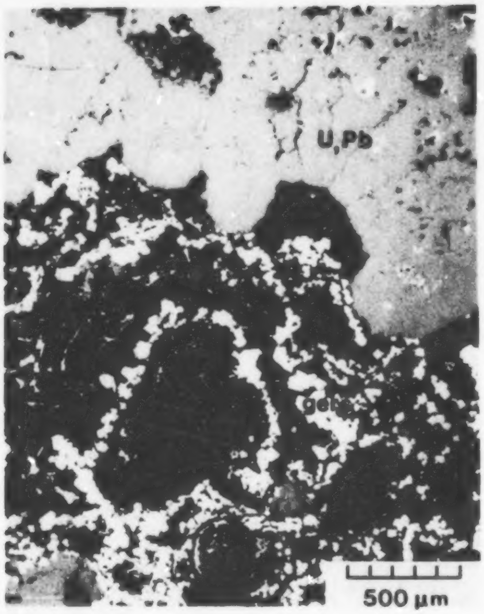

Figure 64.4. Pitchblende (U, Pb), associated with gersdorffite (gers), chalcopyrite (cpy) and pyrite (py) surrounding grains of dolomite (dol), Cigar Lake deposit, Saskatchewan. (Reflected light).

Figure 64.6. Rosettes of siderite (sid) enclosing a dark grass-green mineral (C ?), apparently a mixture of siderite and chamosite, are embedded in [K, Fe, Al, Si, (Mg)] clay-mica ('clay'). Cigar Lake deposit, Saskatchewan. (Transmitted light).

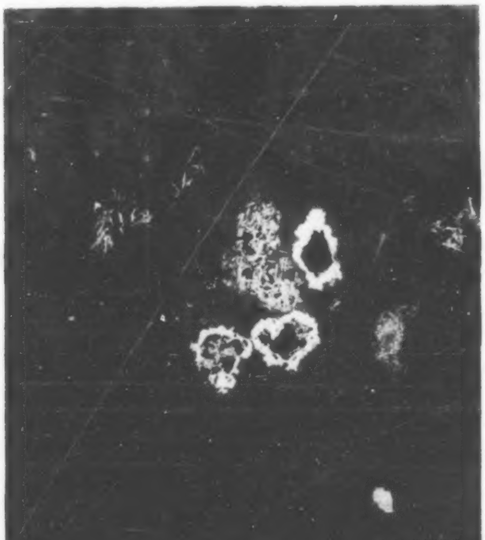

Figure 64.5. Pitchblende (U) replacing clay matrix of sandstone and surrounding needles of rutile (Ti) and botryoidal rings of gersdorffite (gers), which in turn surrounds aggregates of siderite; Cigar Lake deposit, Saskatchewan. (Reflected light).

Figure 64.7. Carbon nodules in soft clay; Cigar Lake deposit, Saskatchewan.

At the top of the section (15.7 m below the unconformity) quartz-muscovite-graphite schist contains a few grains of rutile associated with phyllosilicates. Below this unit (17.7 m below the unconformity) graphitic gneiss is kaolinized, chloritized, altered to Mg-rich clay and cut by veinlets of dravite. Mineralization consists of euhedral rutile and pyrite-bravoite aggregates (Fig. 64.11) testifying to low temperatures of crystallization (about 135°C). At 18.2 m, massive pitchblende is intimately intergrown with gersdorffite and nickeline and embedded in an illite-chlorite-hematite matrix (Fig. 64.12). The host rock is entirely argillic. At 21.3 m the abundance of nickel minerals increases, the host rock is illitized and graphite in the graphitic gneiss is depleted. The pitchblende is associated with nickel arsenides (Fig. 64.13). At 24.3 and 26.45 m the chloritized and illitized migmatitic gneiss hosts pyrite-bravoite and some anatase with traces of uranium. At 51.0 m, slightly altered, foliated biotite-plagioclase granitic gneiss carries no mineralization, but contains only accessory zircon and apatite.

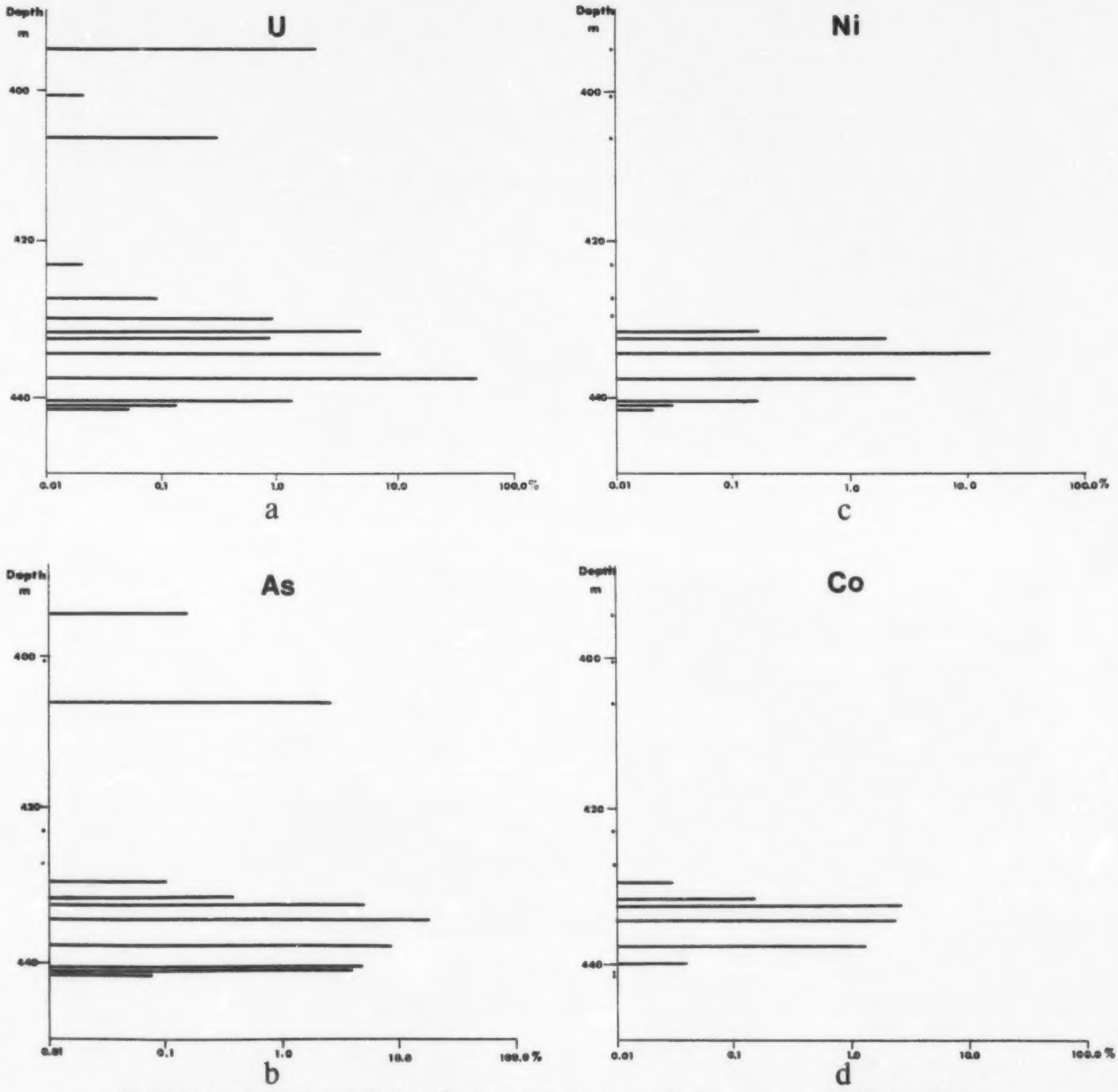

Figure 64.8. Vertical distribution of selected elements in selected core samples from a drillhole penetrating the Cigar Lake deposit, Saskatchewan; contents of constituents in percent and in a logarithmic scale; (a): U, (b): As, (c): Ni, (d): Co.

The above observations can be summarized as follows: 1. The most favourable host rock for U-Ni mineralization below the unconformity is graphitic schist or gneiss. 2. Mineralization increases with increasing chloritization and illitization. 3. Mineralization took place at or below about 135°C as indicated by the presence of bravoite (Ramdohr, 1980). 4. The crystalline basement rocks were affected by extensive magnesium and boron metasomatism as attested by the presence of dravite, chlorite and Mg-rich clays. 5. Graphite in the host rock was depleted by varying amounts depending upon intensity of the alteration processes.

Figure 64.9. *Phyllosilicates (mica) replaced by molybdenite (moly); Sand Lake occurrence, Saskatchewan. (Transmitted light).*

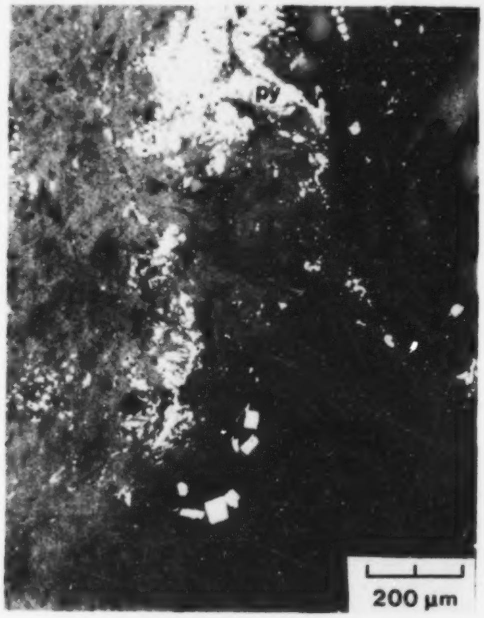

Figure 64.11. *Pyrite-bravoite aggregates (py, br) and euhedral rutile in chlorite-kaolin matrix; Gartner orebody, Key Lake deposit, Saskatchewan. (Reflected light).*

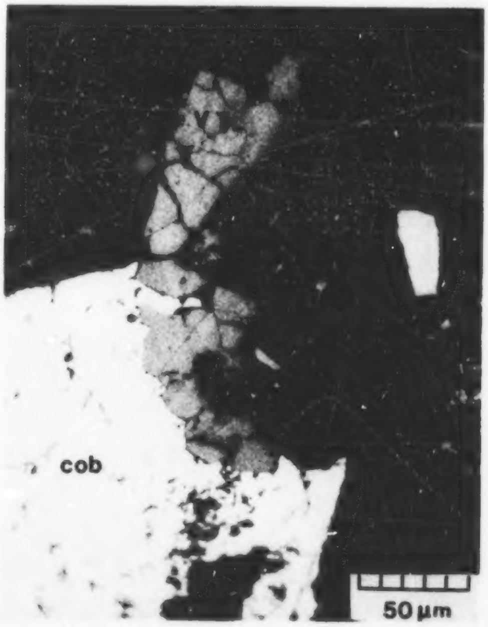

Figure 64.10. *Bright grain of anhedral cobaltite (cob) associated with an anisotropic V-Ti oxide; Sand Lake occurrence, Saskatchewan. (Reflected light).*

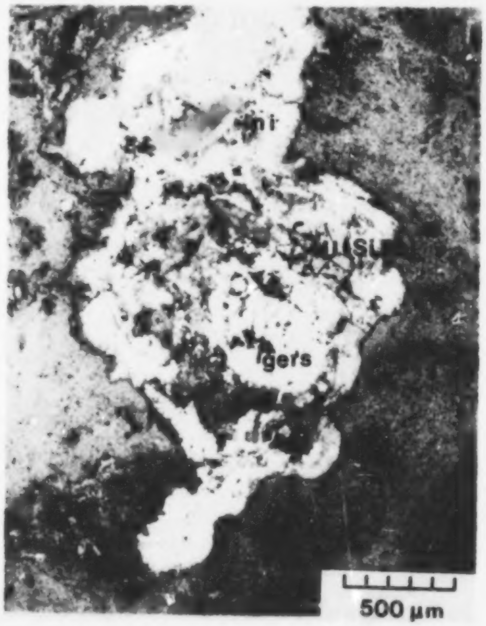

Figure 64.12. *Pitchblende [U (Si, Pb)] intergrown with gersdorffite (gers) and nickeline (ni) in an illite-chlorite-hematite mass. Gartner orebody, Key Lake deposit, Saskatchewan (Reflected light).*

Polymetallic mineralization in Otish Basin, Quebec

Continuing studies of uranium occurrences in the Otish Group, Quebec (Ruzicka and LeCheminant, 1984) revealed that the epigenetic mineralization spatially related to gabbroic intrusions represents a regional metallogenic feature associated with hydrothermal activity at about 1.7 to 1.8 Ga. Host rocks are deuterically and hydrothermally altered gabbroic rocks and hydrothermally altered sedimentary rocks of the Indicator and Peribonca formations. The polymetallic mineralization was controlled by regional faults parallel to the long axis of the Otish Basin, by gabbroic dykes and sills, by permeability barriers in the host rocks, and by zones of sodic and carbonate metasomatism.

Figure 64.13. Pitchblende U (+ Ni, As, Pb) surrounding a core of nickeline (ni). Associated minerals are gersdorffite, millerite, Co-bearing nickel sulphides and anatase in a kaolin matrix. Gartner orebody, Key Lake deposit, Saskatchewan. (Reflected light).

Figure 64.15. A U-Ti phase ('brannerite') in chlorite, (chl). Otish Basin, Quebec (Transmitted light).

Figure 64.14. Joseite-like mineral Pb Bi Te Se (S) with exsolved clausthalite (claus) intergrown with a Bi-Te-(Se) phase in quartz and chlorite gangue. Otish Basin, Quebec. (Reflected light).

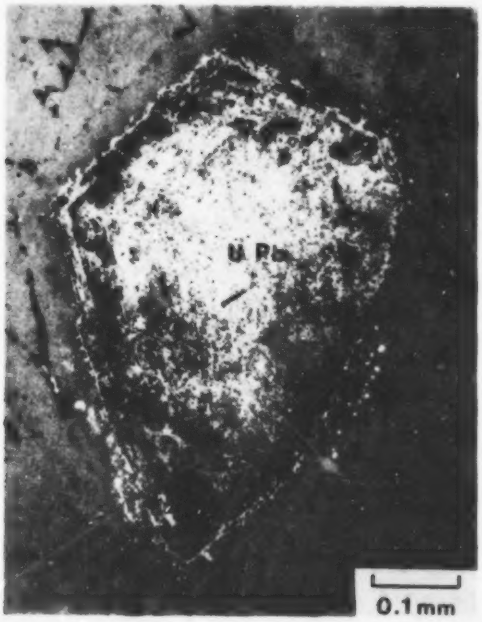

Figure 64.16. Pb-rich uraninite (U, Pb) with small satellitic grains of galena and pyrite. Otish Basin, Quebec. (Reflected light).

Uranium occurs in veins and irregular bodies in several paragenetic assemblages. These include: (a) uraninite veinlets accompanied by selenides ('joseite', clausthalite), tellurides and sulphides (galena, chalcopyrite, pyrite) associated with chlorite in carbonate host rocks (Mn bearing calcite or dolomite) (Fig. 64.14); (b) U-Ti phase ('brannerite') associated with anatase/rutile in chlorite (Fig. 64.15); (c) euhedral uraninite with associated pyrite, chalcopyrite, galena and chlorite in calcite (Fig. 64.16); (d) pitchblende in anhedral patches or intergrown with chalcocite and accompanied by a U-Ti phase ('brannerite'), galena, wittichenite, covellite, bornite, chalcopyrite and pyrite in albite-calcite gangue. Similar paragenetic assemblages are observed in occurrences at Romanet River-Romanet Lake in the Labrador Trough, Quebec (Bell and Ruzicka, 1985). Native gold was identified in one of the samples from this area.

Uranium - polymetallic mineralization in the Miramichi Zone, New Brunswick

Metallogenic studies conducted under the Canada – New Brunswick Mineral Development Agreement revealed similarities between the geological environment which hosts the recently discovered Swanson deposit in Pittsilvania County, Virginia, and the uranium-polymetallic mineralization at Long Lake, Victoria County, New Brunswick.

The U-Pb-Cu-Zn-Mo-Sn-Ag-Au mineralization at Long Lake is associated with brecciated and strongly hydrothermally altered Devonian granitoids and with adjacent sedimentary country rocks of the Miramichi Zone. The area was explored in the past and several occurrences of polymetallic mineralization have been tested by trenching and drilling (Crouse, 1977; Fyffe and Pronk, 1985). Values up to 0.34% U over 0.15 m; 15.3 % Zn over 0.30 m; 0.2% Mo over 0.30 m; and 670 ppm Au over 0.37 m were reported by Fyffe and Pronk (Fyffe and Pronk, 1985, p. 29).

This area deserves a more detailed metallogenic study.

Carbon in the Elliot Lake deposits, Ontario

Five GSC samples of uraniferous quartz-pebble conglomerates from the Elliot Lake deposits contain carbon seams and nodules commonly referred to as thucholite (Ruzicka, 1981; Ruzicka and LeCheminant, 1984). The samples have recently been studied by T.O. Willingham, B. Nagy and L.A. Nage at the Laboratory of Organic Chemistry, University of Arizona, Tucson, Arizona; by D.H. Krinsley at the Department of Geology, Arizona State University, Temple, Arizona; and by D.J. Mossman at the Department of Geology, Mount Allison University, Sackville, New Brunswick (Willingham et al., in press). Their investigations using combined high vacuum pyrolysis-gas chromatography-mass spectrometry, neutron activation and electron microscopy revealed that the stratiform carbon is essentially uraniferous and auriferous kerogen that resembles carbon seam kerogens of the Witwatersrand, South Africa.

Two samples, (RAD 74-11, Denison Mine and RAD 83-01, Stanleigh Mine), were studied in detail by mass spectrometry. The kerogen pyrolyzates analyses of the first sample contained 25, and the second sample contained 9 of the 28 compounds identified in the carbon seams of the Vaal Reef, Witwatersrand.

Acknowledgments

The authors acknowledge the co-operation of geologists and management personnel from the following companies: Cogema Canada Limited, Saskatchewan Mining Development Corporation, Agip Canada Limited, Key Lake Mining Corporation, Ecological and Resources Consultants Ltd., Rio Algom Limited and Denison Mines Limited.

References

Alsthom, Cea, Cogema, Edf and Framatom
1985: Brief News; French Nuclear Newsletter; No. 2 – July, 1985.

Bell, R.T. and Ruzicka, V.
1985: Uranium in the Circum-Ungava Belt, northern Quebec and Labrador: new information from the central Labrador Trough; in Current Research, Part A, Geological Survey of Canada, Paper 85-1A, p. 145-149.

Crouse, G.
1977: Geological notes, Long and Trousers Lakes (map area K-11), New Brunswick; New Brunswick Department of Natural Resources, Mineral Resources Division, P.M. 77-191, 16 p. (map revised 1982).

Fahrig, W.F. and Wanless, R.K.
1963: Age and significance of diabase dyke swarms of the Canadian Shield; Nature, v. 200, p. 934-937.

Fyffe, L.R. and Pronk, A.G.
1985: Bedrock and surficial geology – rock and till geochemistry in the Trousers Lake area, Victoria County, New Brunswick; Mineral Resources Division, Department of Natural Resources, New Brunswick, Report of Investigation No. 20, 74 p.

Lewry, J.F. and Sibbald, T.I.I.
1979: A review of pre-Athabasca basement geology in Northern Saskatchewan; in Uranium Exploration Techniques, Proceedings of a Symposium held in Regina, 1978, November 16-17, edited by G.R. Parslow, Saskatchewan Geological Society, Special Publication 4, p. 19-58.

North American Gold Mining Industries News
1985: Significant uranium found by Imperial joint venture; v. 3, No. 10, May 10, 1985.

Ramdohr, P.
1980: The ore minerals and their intergrowths; Pergamon Press, 1207 p.

Ruzicka, V.
1981: Some metallogenic features of the Huronian and Post-Huronian uraniferous conglomerates; in "Genesis of Uranium- and Gold-bearing Precambrian Quartz-Pebble Conglomerates" United States Geological Survey, Professional Paper 1161-V, p. V1-V8.

Ruzicka, V. and LeCheminant, G.M.
1984: Uranium deposit research, 1983; in Current Research, Part A, Geological Survey of Canada, Paper 84-1A, p. 39-51.

1985: Summary on uranium in Canada, 1984; in Current Research, Part A, Geological Survey of Canada, Paper 85-1A, p. 15-22.

Willingham, T.D., Nagy, B., Nagy, L.N., Krinsley, D.H., and Mossman, D.J.
– Uranium-bearing stratiform organic matter in paleoplacers of the Lower Huronian Supergroup, Elliot Lake – Blind River region, Canada; Canadian Journal of Earth Sciences. (in press)

Notes on the Proterozoic Thule Group, northern Baffin Bay

Project 770013

G.D. Jackson
Precambrian Geology Division

Jackson, G.D., Notes on the Proterozoic Thule Group, northern Baffin Bay; in Current Research, Part A, Geological Survey of Canada, Paper 86-1A, p. 541-552, 1986.

Abstract

Tide-dominated shelf sedimentation prevailed during deposition of that part of the Wolstenholme Formation seen by the writer, and was interrupted twice by meandering stream sedimentation and once by plateau basalt volcanism. Prodelta-type sediments occur locally at two stratigraphic positions. Part of the Dundas Formation was deposited in a subtidal restricted basin while the overlying Narssârssuk Formation contains coastal sabkha deposits. Abrupt changes in lithologies and environments may be due to syndepositional faulting.

Easterly sedimentary transport prevailed in southeast Ellesmere Island and southwesterly transport prevailed in western Greenland. A nearby land source probably lay immediately west of the Thule Group on Ellesmere Island.

The Thule Group and Bylot Supergroup were probably deposited, at least in part, as a continuous deposit in a single basin during opening of the Poseidon Ocean at 1200-1250 Ma.

Résumé

Une sédimentation dominée par des marées et ayant lieu sur une plateforme a caractérisé la mise en place de la partie de la formation de Wolstenholme examinée par l'auteur; elle a été interrompue deux fois par l'accumulation de sédiments de cours d'eau à méandres et une fois par des épisodes de volcanisme associé aux basaltes de plateau. Des sédiments de type prodeltaïques sont trouvés par endroits à deux emplacements stratigraphiques. Une partie de la formation de Dundas a été mise en place dans un bassin subtidal à circulation restreinte tandis que la formation susjacente de Narssârssuk contient des sédiments de sabkha côtier. Les brusques changements de lithologie et de milieu porraient être le résultat de la formation de failles synsédimentaires.

Le transport des sédiments s'est fait surtout vers l'est dans le sud-est de l'île Ellesmere et vers le sud-ouest dans l'ouest du Groenland. Une source terrestre de sédiments se trouvait vraisemblablement à proximité, soit just à l'ouest du groupe de Thule dans l'île Ellesmere.

Le groupe de Thule et le supergroupe de Bylot ont probablement été mis en place, du moins en partie, sous forme de dépôt continu dans un seul bassin au cours de l'ouverture de l'océan Poséidon il y a de 1200 à 1250 Ma.

Introduction

Neohelikian Thule Group strata outcrop in southeast Ellesmere Island and northwest Greenland about the northern tip of Baffin Bay (Fig. 65.1). These multicoloured strata are well displayed in picturesque cliffs adjacent to numerous glaciers along the coast. Recent studies of the Thule Group have been made by Dawes (1972, 1975, 1976a,b), Dawes et al. (1973, 1982), Frisch and Christie (1982), and Frisch et al. (1978). Earlier work on Greenland is referred to by Davies et al. (1963). Distribution of formations is provided by Davies et al. (1963), Dawes (1976b, 1979) and Frisch and Christie (1982).

In July 1982 the writer accompanied W.F. Fahrig and K.W. Christie during their examination of the Thule Group for paleomagnetic studies at Clarence Head, Goding Bay, Northumberland Island and Dundas.

This report presents new paleocurrent and stratigraphic data that add to the understanding of Thule Group deposition and enable a better comparison to be made with the penecontemporaneous and similar Bylot Supergroup of northern Baffin Island (Jackson and Iannelli, 1981).

The Thule Group overlies nonconformably an Archean-Aphebian granulite grade basement complex. In Greenland, retrograde amphibolite facies rocks are also present in the basement complex (Dawes et al., 1982; Frisch, 1983; Frisch et al., 1978). Locally at Clarence Head and on the north shore of western Northumberland Island the Thule strata are in fault contact with the basement (Fig. 65.1). At both localities the seaward, basement block has moved up relative to the landward block; a feature also noted by Dawes et al. (1982). Steeply dipping mylonite and zones of shattered rock up to one metre thick transect the gneisses at Clarence Head. Regolithic material has not been identified below the Thule Group. Davies et al. (1963) described a red platy gneiss at the base as containing large quantities of green to yellowish rounded to angular quartz in a sericitic matrix, and suggested it may be fault gouge. The description, however, resembles that of regolithic material underlying the Bylot Supergroup on northern Baffin Island (Fig. 65.1).

Thule Basin strata are about 4500 m thick in Greenland where three formations have been differentiated (Davies et al., 1963; Dawes, 1976b). The lowermost Wolstenholme Formation consists of chiefly light coloured

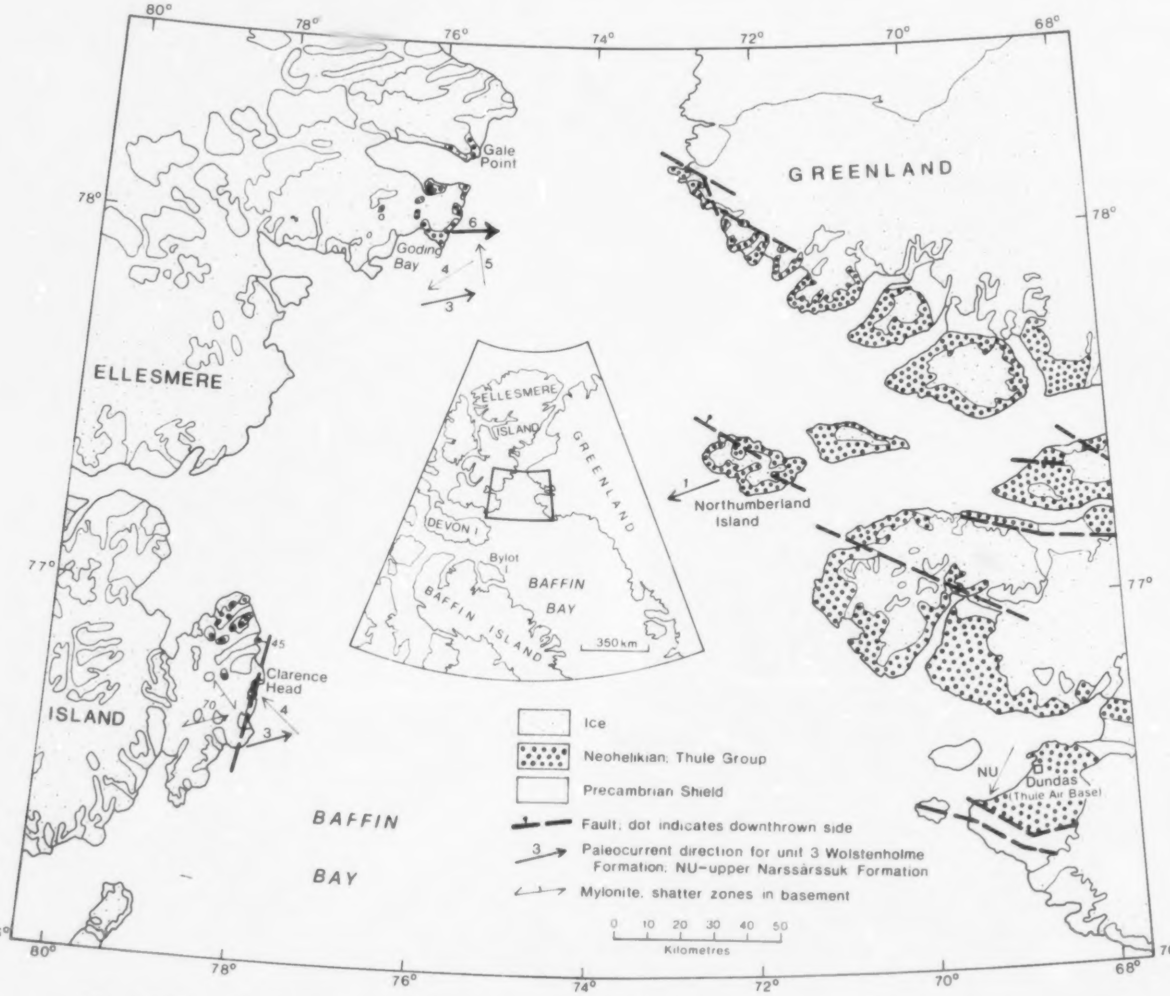

Figure 65.1. Location diagram showing the distribution of the Thule Group. Weight of arrows showing paleocurrent directions is in proportion to the number of readings involved.

quartzarenite with massive basalt flows and sills in the lower part. The overlying Dundas Formation is dominated by thinly interbedded black shale and siltstone. The uppermost Narssârssuk Formation is a variegated cyclically deposited carbonate-clastic sequence. Only about 1100 m of the lowermost Wolstenholme Formation are preserved on Ellesmere Island (Dawes et al., 1982; Frisch and Christie, 1982). Basic sills intrude the two lower formations and basic dykes intrude all three formations and some of the sills. (Davies et al., 1963; Dawes et al., 1973; Frisch and Christie, 1982). Thule strata are commonly baked adjacent to intrusive bodies and the lower contacts of volcanic flows.

The age of the Thule Group has been discussed by Dawes et al. (1973, 1982) and by Frisch and Christie (1982). They concluded, after assessing whole-rock K-Ar ages and the presence of acritarchs in unit 4 that units 1-3 of the Wolstenholme Formation may be about 1200 Ma, and units 4 and above may be as young as Hadrynian. Considering the intergradational nature of units 1-6 the writer suggests that the Thule Group may be 1200-1300 Ma.

Thule Group strata are flat lying to gently dipping and some broad flexures are present (Dawes et al., 1982). Numerous faults cut the Thule strata, such that some of the sections are in tilted fault blocks. Local folding has also occurred adjacent to some faults.

The following basic descriptions refer to the localities visited by the writer and are intended to augment descriptions already provided in the publications noted above. Differences in thickness have been obtained for the same unit in the same general area by different persons. These differences may represent variations in primary thickness as well as repetition or ommission of strata by unrecognized faults. All of the writer's sections were measured except for subunit 1D of the Wolstenholme Formation.

Wolstenholme Formation

This formation ranges from about 500 m in thickness near Dundas to more than 2000 m on Northumberland Island. About 1100 m of strata on southeast Ellesmere Island are truncated by the present erosion surface. Six major units have been differentiated within the Wolstenholme Formation by Dawes et al. (1982), and by Frisch and Christie (1982) and their terminology is used below.

Unit 1: basal sandstone

Clarence Head. About 10-24 m of the uppermost part of this unit were seen at Clarence Head downfaulted along an exposed fault against basement gneisses to the east (Fig. 65.1, 65.2). Frisch and Christie (1982) have reported a thickness of 40 m for this unit at Gale Point. Slickensides and 50 cm of fault gouge containing clasts up to 2.5 cm in diameter occur along the fault. Basal white sugary thin- to very thick-bedded quartzarenite is overlain by a similar thickness of laminated to thin bedded pale pink, green and grey quartzarenite that is pebbly in its lower part. Interbeds of red to green and grey-black shale increase in abundance upward toward unit 2. Three coarsening up cycles, 1.5-5 m thick, were noted in this unit. Cross laminations, mud cracks, symmetrical ripple marks, load structures and reduction spots are present also.

Northumberland Island. Only unit 1 was examined on Northumberland Island where according to Dawes et al. (1982) it is about 200 m thick. The writer obtained 386 m including 65 m of gabbro sills (Fig. 65.2) along the east side of Cadogan Glacier (westernmost large valley glacier on the north side of Northumberland Island). Unit 1 at this locality is divided into 4 intergradational subunits (A-D; Fig. 65.2).

Subunit A, about 180 m thick, is mostly buff to orange, laminated to medium bedded quartzarenite with a few local red, maroon and green interbeds. Medium to very thick beds predominate in the lowermost strata, and bedding thins upward. Several fining-thinning upward cycles up to 2 m thick occur in the upper part. Crossbeds are abundant (Fig. 65.3) and are up to 1 m high. Compound crossbedding characterized by low angle surfaces, and hummocky bedding is well displayed in some outcrops. Mudcracks, symmetrical ripples and small channels occur locally. Secondary false colour banding resembling liesegang bands is common and may be related to water table activity.

Subunit B is gradational with both the underlying and overlying subunits. The thickness increases from 36-72 m southward over a distance of about 1.5 km. Pale green to grey very thin-to medium-bedded quartzarenite and subarkose with green shaly interbeds and partings predominate. Pink, brown and white beds are also present. The beds of the top 15-20 m are discontinuous, more shaly, and contain shale chips and balls and some wavy to lumpy beds. Red beds appear near the top of the subunit and increase in abundance upward. Crossbeds (Fig. 65.3) and symmetrical ripple marks are less abundant than in subunit A.

Subunit C, 57 m thick, is composed almost entirely of red to reddish brown strata consisting of very thin- to thin-bedded sandstone interbedded with laminated to very thin-bedded shale and siltstone. Some pale grey sandstone beds occur in the basal part. Some medium bedded strata, in the upper part of the subunit are discontinuous and lumpy bedded. Green shaly partings and red and green beds to 8 cm thick composed of mud balls to 6 cm in diameter are also present in the upper part. Subunit C contains relatively few crossbeds (Fig. 65.3), but they increase in abundance at the top of the subunit where a few ripple marks are also present.

Subunit D, planar, medium- to very thick-bedded quartzarenite is estimated to be about 75 m thick, and is gradational and conformable with the underlying strata. The basal 4 m is pale greenish grey with a few red sandstone beds to 40 cm thick. Above this are several metres of buff weathered strata, but the bulk of the subunit is white. Crossbeds are either rare or difficult to see.

Depositional environment. Much of subunit A on Northumberland Island displays well developed compound crossbedding. Crossbeds (Fig. 65.3) abundant and up to 1 m high, are west-directed with only a minor easterly bimodal component in most of the submembers, but are strongly bimodal (NE-SW) in the upper part. The abundance and nature of the crossbeds indicate that sediment deposition was probably in sand ridges and waves in a tidally influenced shallow shelf environment (Johnson, 1978; Walker, 1984). The thinning upward of the bedding and the fining upward cycles in the upper part may indicate shallowing water and an approaching shoreline. Paleocurrents in subunit B are similar to those in the underlying subunit and tidally influenced deposition probably predominated. The top part (15-20 m), however, was probably deposited in a relatively protected area, possibly behind a barrier island or in a lagoon (Elliot, 1978a; Reinson, 1984). The lower part of subunit C is considered to contain some beach deposits, but most of the subunit is probably a mixture of meandering stream channel and overbank deposits formed in a low energy environment (Collinson, 1978; Walker and Cant, 1984). Relatively clean shelf sandstones were then deposited in subunit D. Three crossbeds from uppermost subunit C suggest southerly transport and four from basal subunit D northerly to westerly transport (Fig. 65.3).

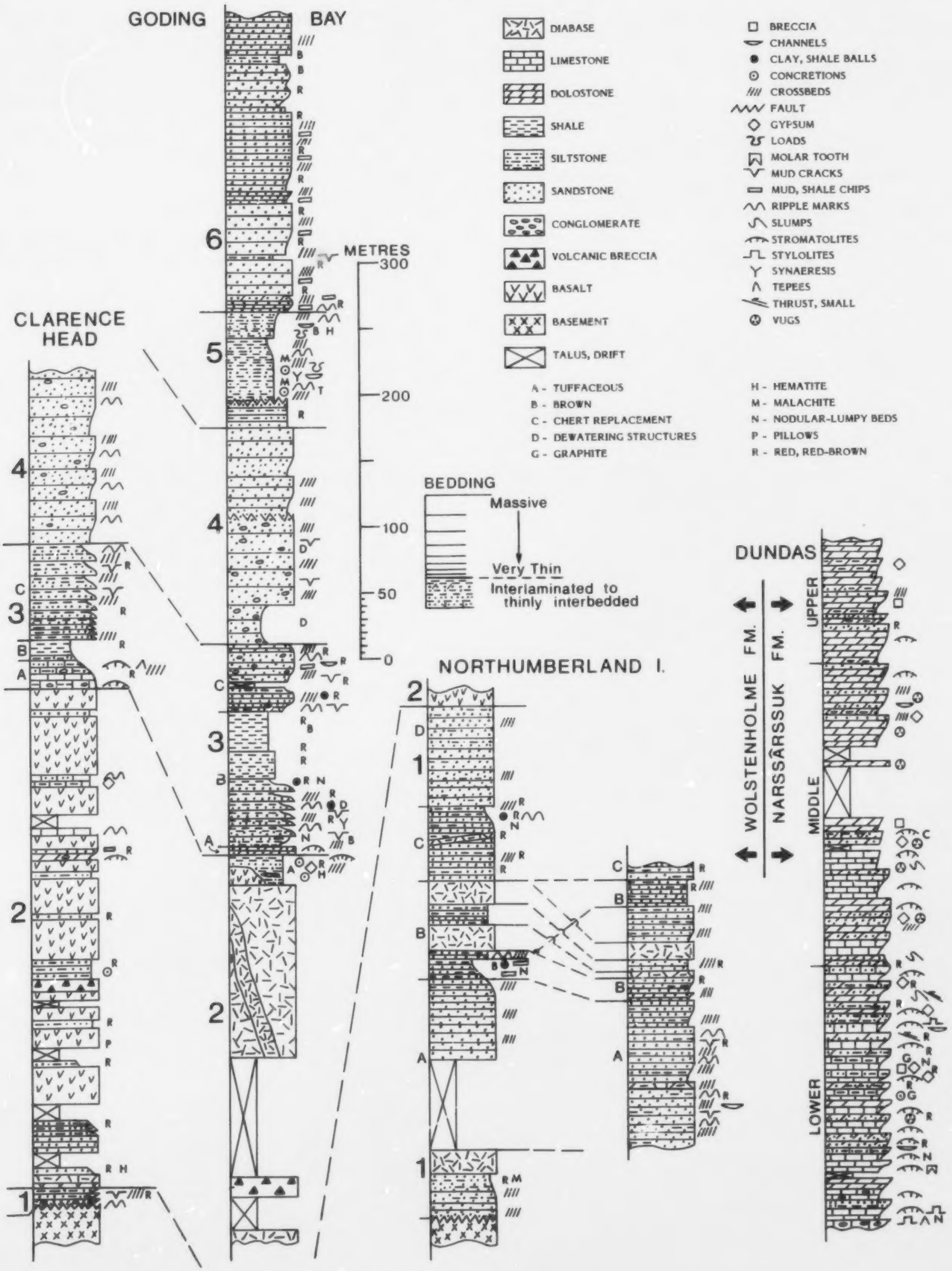

Figure 65.2. Stratigraphic sections of the Thule Group. The section on the right is of the Narssârssuk Formation. The rest are of the Wolstenholme Formation.

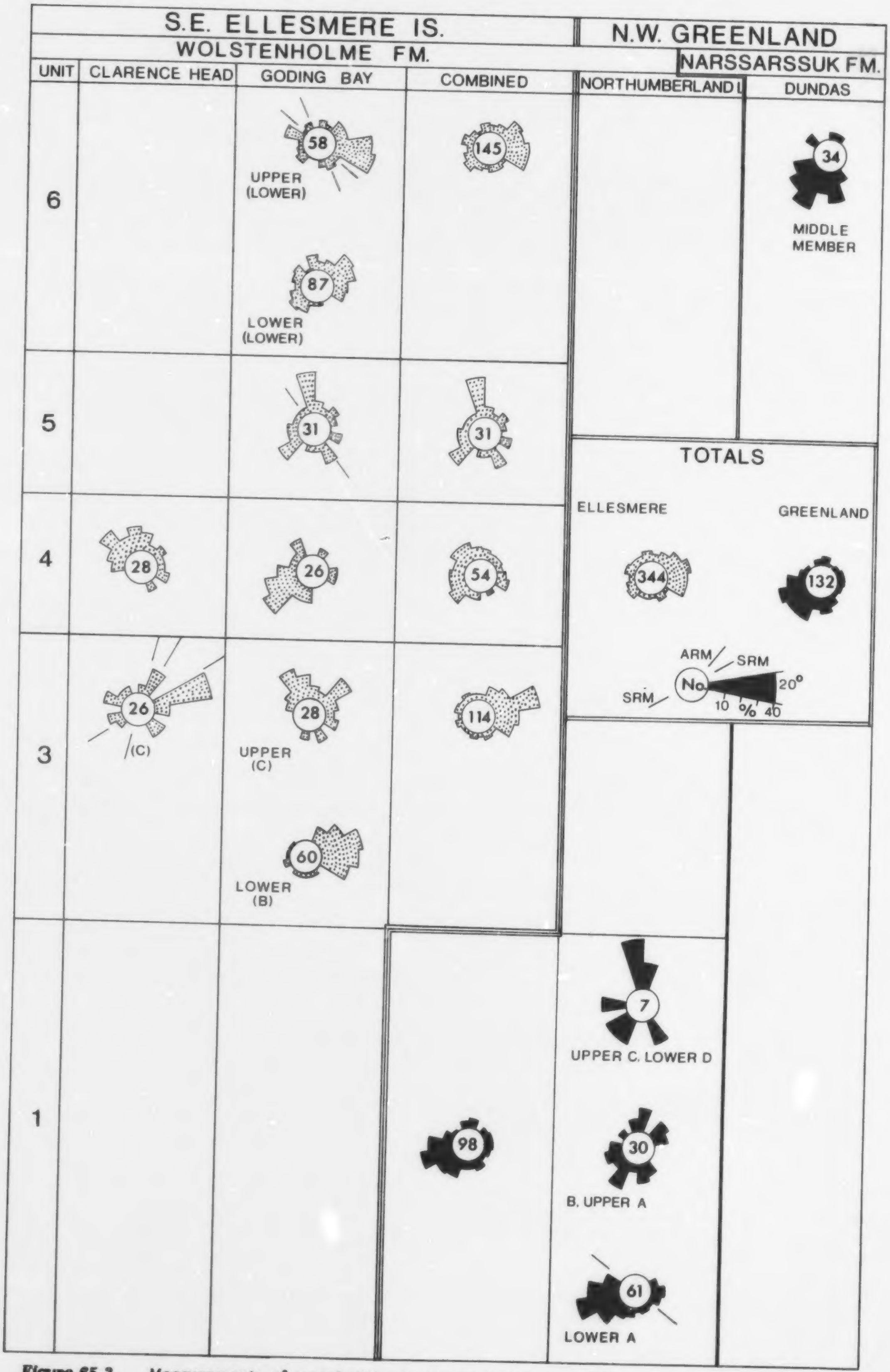

Figure 65.3. *Measurements of crossbedding in the Thule Group. SRM = symmetrical ripple marks. ARM = asymmetrical ripple marks.*

At Clarence Head, the presence of coarsening up cycles suggests a regressive beach environment, which is in agreement with the conclusions of Frisch and Christie (1982) for Gale Point.

Unit 2: basalt - red bed

Clarence Head. The writer obtained a thickness of 374 m for this unit while Frisch and Christie (1982) estimated 218 m for a nearby section. This difference may be due to the difficult nature of the terrain, the variable nature of the stratigraphy in this unit, and the arbitrary placing of the lower contact at the base of the lowermost flow. Only minor amounts of sediment is interbedded with the basalt flows and sills. The flows are difficult to differentiate from the sills, but probably predominate. They have a maximum individual flow thickness of 43 m (Fig. 65.2). Flows are massive, dark grey green to grey and reddish grey, commonly have brecciated, amygdaloidal to locally vesicular tops, and are vuggy locally. Pillow-like features occur at the base of one flow and bent columnar jointing occurs in another flow adjacent to a breccia zone. Volcanic breccia up to 9 m thick and containing rounded to angular volcanic clasts as much as 1.2 m in diameter was seen at two localities. Agglomerate lenses, laminated tuff, and red sandstone and shale lenses are also present in the breccia. Tops of some flows contain sediment fragments. Others contain sedimentary dykes and calcite veining.

Sedimentary sequences as much as 25 m thick are displaced abruptly along strike by flows at the same stratigraphic level in the lower part of the sequence.

Between-flow sedimentary sequences have a maximum thickness of 15 m except for a thicker basal sequence (Fig. 65.2) that contains fining up sequences in its upper part. Most lower-unit sediments are red, laminated to very thick bedded, arkosic sandstone and minor interbedded shale and siltstone. Hematite-rich laminae are common. A few small pebble conglomerate lenses, sandstone beds composed of shale grains, and rare buff to green quartzarenite beds are also present. The upper parts of some thin beds in the middle of the sequence are full of small spherical bodies (pisolites or concretions?). Abundant reduction spots are also present. Concretions and mud chips occur locally. Crossbeds are exceptionally rare.

Carbonate, chiefly grey laminated to very thin bedded shaly to siliciclastic limestone, is the predominant sediment in the upper part of the unit. A few limestone-clast granule conglomerate beds, 25 cm volcanic clasts in limestone, symmetrical and asymmetrical ripple marks, cryptalgal laminites, and gypsum nodules are present.

Goding Bay. About 293 m in unit 2 was measured at Goding Bay, but the lower part of the section was mostly drift covered. Frisch and Christie measured 312 m and obtained a thickness of about 200 m at Gale Point 30 km to the north. A similar thickness has been inferred for unit 2 on Northumberland Island (Dawes et al., 1982). According to Frisch and Christie (1982) sediments make up a relatively large part of the unit at Goding Bay which includes a 130 m thick gabbro sill.

A 15 m thick volcanic breccia in the lower part of unit 2 contains faintly rimmed angular to rounded clasts, bombs and pillow-like bodies up to 75 x 12 cm.

A complex 23 m sequence, its basal part baked by the underlying thick gabbro sill, is the uppermost subunit of unit 2. It is composed mostly of dark grey-green, thickly laminated to very thin bedded slate, shale and siltstone with minor locally crossbedded sandstone and tuff, and rare stromatolitic siliceous dolostone. Reddish-grey rocks occur mostly in the upper part of this subunit. Bedding is planar to undulose.

Within the shale subunit numerous basalt flows and dyklets, up to 60 cm thick, have altered margins. Olive-green spherical to ellipsoidal to nodular concretions up to 25 cm in diameter, composed of chlorite, iron carbonate, siliceous material containing hematite crystals and possibly gypsum, occur both in the sediments and flows.

Immediately to the west the large sill is overlain by a basalt flow and only the upper 9 m of this shale subunit is present.

Depositional environment. The flows are typical tholeiitic plateau basalts (Frisch and Christie, 1982) deposited in a terrestrial environment. Fining up cycles suggest fluvial deposition for sediments in the lower part of the unit. Local basal-flow pillows and interbedded carbonate in the upper part indicate the sea was nearby. The abundance of iron-rich concretions in the 23 m concretionary shale unit at Goding Bay and the presence of rare turbidite-like quartzarenite beds suggests the shale unit probably represents prodelta or offshore muds (Elliot, 1978b). The small concretion-bearing thin flows or tuffaceous units are probably related to the adjacent flow immediately to the west, which may have flowed from a westerly direction, based on the orientation of its frontal margin.

Unit 3: carbonate-shale

This unit overlies unit 2 conformably, and at both Clarence Head and Goding Bay may be divided into three conformable subunits: a basal carbonate subunit A, a middle cyclic subunit B and an upper sandstone subunit C.

Clarence Head. Unit 3 is 107 m thick at Clarence Head (79 m - Frisch and Christie, 1982). The basal carbonate subunit (A) varies from 13-22 m thick. Where seen by Frisch and Christie (1982) it is chiefly brown dolostone while at a nearby locality the writer found mostly grey limestone. At one locality subunit A is grey, thinly laminated to medium bedded, finely- to coarsely-crystalline limestone and silty limestone, and calcareous siltstone. Basal conglomeratic lenses contain limestone and quartz granules and small pebbles. Cryptalgal laminites, laterally linked columnar stromatolites up to 10 cm high, small ellipsoidal stromatolites to 3 cm in diameter and a few 15 cm high tepee structures occur in the lower part of the limestone. The upper part of the submember is relatively silty and contains some very fine grained sandstone and flat limestone-clast conglomerate.

The middle subunit (B) is only 15 m thick at Clarence Head and consists of interbedded red shale and red and buff sandstone overlain by 12 m of red shale. The lower cyclic part of this subunit, so well developed at Goding Bay (below), seems to be largely missing at Clarence Head.

The upper subunit (C) is 70 m thick and consists of quartzarenite beds up to 50 cm thick interbedded with red shale beds up to 40 cm thick. Quartzarenite increases upward from 60 to 90% of the rock. The quartzarenite is mostly grey in the first 16 m but above this is predominantly white. Minor green shaly partings and laminae are common. Locally, laminated to medium bedded red and white sandstone is interbedded in layers up to 1 m thick in the upper 12 m. Crossbeds are abundant throughout, and include some herringbone crossbeds (Fig. 65.3). Mudcracks are common and a few ripple marks and hematite-rich laminae were seen in the upper part. The contact between units 3 and 4 is placed where red sandstone and shale interbeds give way to mauve quartzarenite.

Goding Bay. Unit 3 is 158 m thick at Goding Bay as measured in a composite section (little more than 100 m – Frisch and Christie, 1982). It is about 140 m thick on Northumberland Island (Dawes et al., 1982).

Subunit A is 5-6 m thick and is composed of light brown thinly laminated siliceous dolostone in beds to 1 m thick with thin interbeds of green argillaceous rock. Cryptalgal laminites occur in the dolostone.

Subunit B is 102 m thick. Its lower part is composed of cyclically interbedded sandstone and shale. About 7 m of the lowermost cycle, a coarsening up cycle, is exposed. Lumpy bedded, brown, locally green shale beds decrease in thickness from 80 to 2 cm upward. The shale is interbedded with very thin- to medium-bedded light grey green subarkose in which planar to wavy bedded subarkose alternates with, and commonly overlies planar crossbedded subarkose.

The rest of the lower part of subunit B consists of several fining up cycles composed of lower light green and red-green sandstone in beds up to 3 m thick but mostly less than 60 cm, and upper red shale in beds to 7 m thick but mostly less than 1 m. The sandstone beds are composed of alternating crossbedded (Fig. 65.3) and planar to wavy bedded sandstone in thicknesses up to 10 cm, commonly with crossbedded sandstone at the base. Sandstone in upper cycles commonly contains shale chips and carbonate-rich laminae. Crossbeds in the lower part of the subunit commonly contain shaly laminae. Basal sandstone beds are in sharp irregular contact with the underlying shale into which shallow channels have been cut. The shale beds are planar bedded and are in irregular but conformable contact with underlying sandstone. Tops of shale beds are commonly mudcracked and some have a bleached conglomeratic regolithic zone containing sandstone clasts. Some sandstone tops are also mudcracked. Symmetrical ripple marks are common. Synaeresis cracks and small pisolites or oncolites were seen at single locations.

The upper part of subunit B contains 51 m of reddish-brown shale with disseminated well rounded quartz grains and granules and a few widely interspersed sandstone beds in the lower part.

Subunit C is 50 m thick at Goding Bay. Its lower part is composed of layers 3-10 m thick alternating from interbedded red sandstone and shale in beds 50 cm to 1 m thick, to sandstone layers containing only minor shale laminae and partings. The sandstone changes composition upward from subarkose to quartzarenite. The irregular bedding varies from thick laminated to thin bedded. White, light green and mauve sandstone, and carbonate cemented sandstone, occur locally. Green shale partings increase in abundance upward.

The upper part of subunit C is composed of red granular to fine pebbly sandstone with green shale partings. A layer of grey, locally red quartzarenite caps the subunit and in it the bedding changes upward from irregular to even.

Crossbeds (Fig. 65.3) are abundant in the subunit which also contains a few symmetrical ripple marks, mudcracks, channels and rare clay balls.

Depositional environment. The basal carbonates of subunit A are probably intertidal to supratidal deposits upon which fluvial deposition was again encroaching.

A single, basal coarsening-up cycle of subunit B at Goding Bay probably represents a regressive beach environment and was preserved under the overlying fining up cycles at both Clarence Head and Goding Bay which are meandering stream and overbank deposits. The stream deposits contain relatively thin active channel and abandonment sandstones that possess characteristic internal structures, and which are overlain by thicker vertical accretion shales. The thick red shale at the top of the subunit changes thickness over short distances, and probably represents stacked vertical accretion fines (Collinson, 1978; Walker and Cant, 1984). Crossbeds are strongly easterly directed at Goding Bay (Fig. 65.3), suggesting the shore lay in that direction.

Subunit C is considered to represent either interbedded tidal flat shale and intertidal sandstone, or possibly estuarine deposits, in which sandstone increases in proportion upward. Crossbeds are variable, chiefly directed to the northeast at Clarence Head and northwesterly at Goding Bay.

Unit 4: white sandstone

Clarence Head. Only 132 m of this unit were examined at Clarence Head. Lack of time prevented the overlying strata, including units 5 and 6, from being studied here. Frisch and Christie (1982) remarked on the wedge-shaped nature of this unit and reported thicknesses ranging from less than 100 to more than 200 m. Tilting and erosion of a fault block may be a contributing factor to this wedge shape.

The lower contact is gradational with unit 3, and the lower 57 m consists of thinly to very thickly interbedded white (to 1.5 m) and mauve (to 20 cm) quartzarenite and minor subarkose. A few red sandstone beds and hematite laminae occur in the lower part of this sequence. Overlying strata consist of white, cream and light grey quartzarenite in 25-50 m thick sequences.

Crossbeds (Fig. 65.3) and symmetrical ripple marks are abundant throughout the unit, while quartz pebbles and reduction spots occur locally.

Goding Bay. Unit 4 was found to be 164 m thick while Frisch and Christie (1982) reported thicknesses of a little more than 180 m and 265 m. Thicknesses of up to 260 m occur on Northumberland Island (Dawes et al., 1982). A few strike faults are associated with units 4 and 5 at Goding Bay along which vertical displacements of up to 20 m occur.

The strata are chiefly white medium- to very thick-bedded (1.5 m) quartzarenite, similar to those at Clarence Head. Buff and grey sandstones, containing internal laminae to medium beds within thicker beds are common. Orange beds occur locally. In the lower part of unit 4, mauve colours are common and red sandstone and hematite laminae are present as well. Quartz and sandstone pebbles to 3 cm in diameter are concentrated locally. Crossbeds (Fig. 65.3) are abundant throughout the unit and mudcracks, dewatering structures and reduction spots, although less common, are also present. Ubiquitous false bedding or liesegang rings, discolouration layering at various angles to the sedimentary layering, may be related to ground water.

Depositional environment. The colour, thick bedded nature and abundance of crossbeds indicate deposition occurred on a shallow intertidal shelf. Crossbeds are northwesterly directed at Clarence Head, southwesterly directed at Goding Bay, and are only slightly bimodal (Fig. 65.3). Longshore currents, however, cannot be ruled out as a method of transport and the crossbed directions may be indicative of an inlet or channel way to the west between Clarence Head and Goding Bay.

Unit 5: red sandstone-shale

This unit was seen by the writer only at Goding Bay where a thickness of 87 m was obtained. The actual contact with underlying unit 4 was observed only from a distance on nearby cliffs where it seemed to be sharp but conformable.

Frisch and Christie (1982) reported thicknesses of 84 and possibly 180 m at Goding Bay, and 120 m at Clarence Head where the lower contact is abrupt but gradational. More than 300 m of the red sandstone-shale unit outcrop on Northumberland Island where the lower contact is described as sharp (Dawes et al., 1982).

The basal 20 m consists of laminated to medium bedded, poorly exposed, crossbedded red sandstone, siltstone and lensitic shale. Minor buff to white sandstone occurs in the lower part of this sequence.

The middle 48 m of unit 5 is composed of very thin to thinly interbedded green shale and siltstone and green to pale greenish-white, very fine grained, equigranular quartzarenite arranged in a large number of thin, chiefly fining-up cycles. The strata are commonly planar to wavy laminated with abundant ripple drift lamination. Quartzarenite forms about 15% of the lower part of the sequence, where it occurs in beds about 1.5 m apart, and decreases in abundance upward. Lenticular bedding is more common in quartzarenite than in shale beds. The quartzarenite beds have a maximum thickness of 20 cm, are lensitic to locally discontinuous, almost always have sharp contacts with the underlying shale or siltstone, and have been channelled and loaded into the underlying strata (Fig. 65.4). The tops of underlying beds commonly have ripplemarked surfaces while loadcasts occur chiefly at the bottom of the quartzarenite beds. The tops of most quartzarenite beds are conformable and are in sharp to gradational contact with overlying siltstone and shale. Some quartzarenite tops, however, are capped by a ripplemarked erosion surface and some shale has been channelled into the quartzarenite. The quartzarenite beds themselves are commonly crossbedded (Fig. 65.3) and may be massive as well as laminated. A few thin conglomeratic lenses contain quartz granules up to 1.5 cm in diameter. In addition to structures already noted, interference ripples, climbing ripples and synaeresis are common. Flutes are also present. Dark green weathering, coarse grained carbonate lenses and concretions up to 25 cm thick occur sporadically in the middle part of this sequence. Malachite staining was seen at two horizons.

The upper part of unit 5 consists of 19 m of interbedded, thinly laminated to very thin bedded, brown, fissile shale, siltstone and very fine grained sandstone. Massive siltstone beds up to 35 cm thick occur at the base and up to 14 cm thick at the top. Hematite-rich layers up to 15 cm thick occur sporadically. Load structures, interference ripples and channel fillings are common. The lithologies of this upper sequence are interbedded with the middle sequence lithologies for a thickness of as much as 3 m in which brown siltstone is channelled into green shale. A few green shale and siltstone lenses and beds up to 30 cm thick also occur at the top of this upper sequence.

Depositional environment. The basal red beds probably represent an influx of fluvial material into the basin by a stream readvancing into the depositional basin. The overlying 48 m green shale unit is almost unique and is similar only to the 23 m sequence at the top of unit 2 at Goding Bay. Contained structures in the white lenticular quartzarenite beds and their relationship to adjacent strata suggest they may have been deposited by turbidity currents. The quartzarenite beds and iron-rich concretions suggest the 48 m green shale subunit may be a prodelta or offshore basin deposit (Elliott, 1978b). The variable nature of the crossbeds (Fig. 65.3) may favour an offshore deposit. The overlying brown shale subunit may represent a deltaic or beach deposit. The abrupt vertical changes in lithologies and possibly in depositional invironment may be related to syndepositional faulting.

Unit 6: uppermost sandstone

The uppermost unit of the Wolstenholme Formation is truncated by the present erosion surface on southeast Ellesmere Island. A partial section 227 m thick was examined by the writer at Goding Bay where Frisch and Christie (1982) measured about 330 m of strata. They report 24 m of strata for unit 6 at Clarence Head, while several hundred metres are present on Northumberland Island and 900 m on the adjacent island to the east (Dawes et al., 1982).

Unit 6 seems conformable with unit 5 at Goding Bay, although there is a sharp change in lithology, basal unit 6 strata consisting of red to light grey sandstone with crossbeds to 20 cm high. The lower 151 m of unit 6 is mainly pale to dark dusky red sandstone interbedded with considerable white, light grey, buff and light pink sandstone in thicknesses up to about 10 m. The sandstones are mostly very thin to medium bedded, rarely thick bedded (to 1 m), quartzarenite. Green laminae and partings together with red and green mud and shale chips are disseminated throughout the lower 151 m. A few carbonate laminae occur near the base of the sequence and 3 m of laminated to very thin bedded, mudcracked,

Figure 65.4

Nature of bedding in prodelta-type sediments of subunit 5B at Goding Bay. The light coloured beds are quartz arenite turbidites. A dark iron-carbonate lense lies just left of the 1.5 m long rod.

red shale and siltstone occur 40 m above the base. Crossbeds (Fig. 65.3) are abundant throughout the sequence and herringbone crossbeds are common in the lower part, chiefly below the 3 m shale unit (Fig. 65.3: lower-lower). Symmetrical and interference ripples are common.

The upper 76 m seen at Goding Bay are composed mostly of pale brown laminated to thin bedded quartzarenite with minor light green to pale red interbeds. Extensive white and red quartzarenites were not seen. A 7 m section of thinly laminated shale, siltstone and sandstone occurs in the middle of the 76 m sequence. The lower strata are mauve, and the upper brown and the weathered surface is bluish. Structures seem less varied and common in the 76 m sequence than in the 151 m sequence, and fewer crossbeds were seen.

This subdivision of unit 6 seems in agreement with that of Frisch and Christie (1982), although the 3 m bed of dolomitic subarkose used by them as a dividing point was not seen.

Depositional environment. The abundance of crossbedding suggests that lower unit 6 sandstones were probably deposited in a shallow shelf tide-dominated environment. Crossbeds are weakly bimodal and herringbone crossbeds are present. The major indicated current direction changes upward from northeast to southeast (Fig. 65.3). A decrease in abundance of crossbedding suggests storm dominated deposition may have prevailed during deposition of upper unit 6 strata.

Dundas Formation

Seen only briefly at Dundas, the Dundas Formation is noted here to complete the stratigraphic picture. Except for some personal notes, the following comments are taken from Davies et al. (1963), Dawes (1979) and Dawes et al. (1982).

The Dundas Formation is at least 1000 m thick (730 m minus 120 m for diabase sills at Dundas - Davies et al., 1963) and is composed mostly of black fissile shale interbedded with pale grey quartzarenite, some siltstone and minor dark grey to black stromatolitic dolostone, chiefly in the upper part. The contact with the underlying Wolstenholme Formation is gradational, but the contact with the overlying Narssârssuk Formation is not exposed. Davies et al. (1963) concluded that the latter formation overlies the Dundas. Dawes (1979) in noting that gypsum, chert, and stromatolitic dolostone were common to both upper Dundas and lower Narssârssuk strata concluded that the Narssârssuk Formation is all or in part of younger age than the Dundas.

Most of the formation seen at Dundas consists of three alternating lithological packages up to 14 m thick namely: predominantly black shale, quartzarenite, and interbedded shale and quartzarenite sequences in which the lithologies occur in beds commonly 0.3 to 1 m (max. 3 m) thick. Although, in general, quartzarenite decreases in abundance upward in the formation, it increases upward in abundance within some of the interbedded sequences. The quartzarenite beds are commonly very fine grained and thin laminated to medium bedded. Minor dolostone increases upward in abundance. Mudcracks are abundant in the formation and ripple marks are common. Crossbeds, however, are very rare. Pyrite increases in amount adjacent to diabase sills.

According to Dawes et al. (1982) the Dundas Formation has been interpreted as a shallow water deltaic to coastal plain deposit. The strata seen in the Dundas area may be largely subtidal, and the quartzarenite beds may have been deposited by turbidity currents formed during storms or times of flood. The change from Wolstenholme shelf to Dundas basinal deposition may have been accompanied by syndepositional faulting.

Narssârssuk Formation

According to previous work (Davies et al., 1963; Dawes, 1975, 1976b, 1979) the Narssârssuk Formation consists of at least 1000 m of variegated, well layered carbonates, shale, siltstone and sandstone deposited in cycles in which the lithologies are laterally gradational as well as interbedded. Some of the strata are gypsiferous and cherty. Davies et al. (1963) subdivided the formation into three carbonate-dominated, vertically gradational members: lower red member, middle Aorfêrneq dolomite member, and upper red member. The Narssârssuk Formation occurs only in a small area south of Dundas and on an island immediately to the west (Fig. 65.1). About 520 m of strata along the mainland coast southwest of Dundas were examined by the writer (Fig. 65.2).

Lower red member

According to Davies (1963) the top of the member is at the top of the highest red beds in the lower part of the formation. Above this position red beds are absent for well over 100 m. For this study about 198 m of strata were measured below this position. Davies et al. (1963) reported about 310 m based primarily on well data. Several small thrusts were noted in the coastal section with overthrusting of up to a few metres to the north and northwest.

Most of the lower red member is grey limestone deposited in sequences up to 10 m thick, but mostly less than 6 m. Individual beds range from beds a few metres thick to thin laminations. Thick beds commonly show faint interval layering and the laminated varieties include both evenly laminated limestone and wavy cryptalgal laminites (Fig. 65.2). Most of the strata are calcisiltite to calcilutite, but coarsely recrystallized limestone occurs locally. Lumpy bedded limestone, pockets of flat clast conglomerate and vuggy limestone are common. Brecciated limestone is minor. Broad domal stromatolites, commonly 30 cm in diameter, are abundant and range up to 1.5 m in diameter; a few ellipsoidal types to 10 cm are also present. Thin gypsum seams and graphite occur sporadically. Structures present in addition to those already mentioned include: stylolites, sulphate casts, small channels and locally, tepee and molar tooth structures (Fig. 65.2).

Dolostone is a minor lithology in the lower red member, but increases upward in abundance (Fig. 65.2). Buff to grey colours predominate but light green is common and a few beds are pale pink. Most dolostone is very fine grained, and is not as thickly bedded as the limestone but otherwise contains the same types of beds. One bed contains flattened shaly dolostone nodules. The stromatolites are also similar to those in the limestone but a smaller variety of minor structures are present.

Red to green-grey and buff siliciclastic strata include arkose, subarkose, siltstone and shale. Pebble intraclasts occur sporadically. Thin gypsum seams and scattered pink gypsum ellipsoids up to 8 cm across occur at a few horizons. The strata are chiefly thick bedded to thin laminated, contain carbonate, and occur interbedded and intermixed with one another in packages, overlain and underlain by carbonates, and commonly less than 6 m thick, but as much as 10 m thick. Few structures were noted but include small channels, stylolites and rare crossbeds.

Lower member strata described above are interbedded in about 16 shallowing up sequences (James, 1984; Kendall, 1984) that range from 6 to 17 m in thickness (Fig. 65.2). Sequences begin at a sharp, commonly erosional base, and are truncated by the base of the overlying sequence. Siliciclastics, where present, are commonly gradational with underlying carbonates and are considered to

cap the sequences although some are overlain and underlain by erosional intervals. Examples of some of the sequences that are present are:

i) Several limestone sequences, especially in the lower part of the member consist of lower very thick to thin bedded limestone overlain by evenly laminated and/or cryptalgal laminites.

ii) Thick bedded limestone grading up to laminated limestone grading up to siliciclastic gypsum.

iii) Limestone, grading up to dolostone grading up to siliciclastics.

iv) Thin bedded dolostone grading up to shaly dolostone grading up to siliciclastics.

Middle Aorfêrneq dolostone member

A thick succession of dolostones and limestones lies between the lower and upper red bed members for which Davies et al. (1963) reported a thickness of about 134 m. About 227 m of strata were measured along the coast between red bed horizons, although this includes 55 m of covered section in the middle of the member (Fig. 65.2). Dolostone and limestone are equally abundant in the lower half of the member, but limestone is negligible in the upper half.

The carbonates are similar to those in the underlying member although vuggy dolostone is more abundant in the middle Aorfêrneq dolostone member. Flinty dolostone and chert replacement is also present whereas lumpy bedded carbonate and flat clast conglomerate are rare. As in the lower member, disseminated mud, silt and sand are more widespread in the dolostone than in the relatively clean limestone. Minor structures are somewhat less varied and abundant than in the lower member although stromatolites seem about as common. Oolites are also present (Davies et al., 1963). Carbonate strata occur in relatively thick sequences, differentiated chiefly by bedding differences. These sequences are up to 23 m thick, although most are 7 m or less.

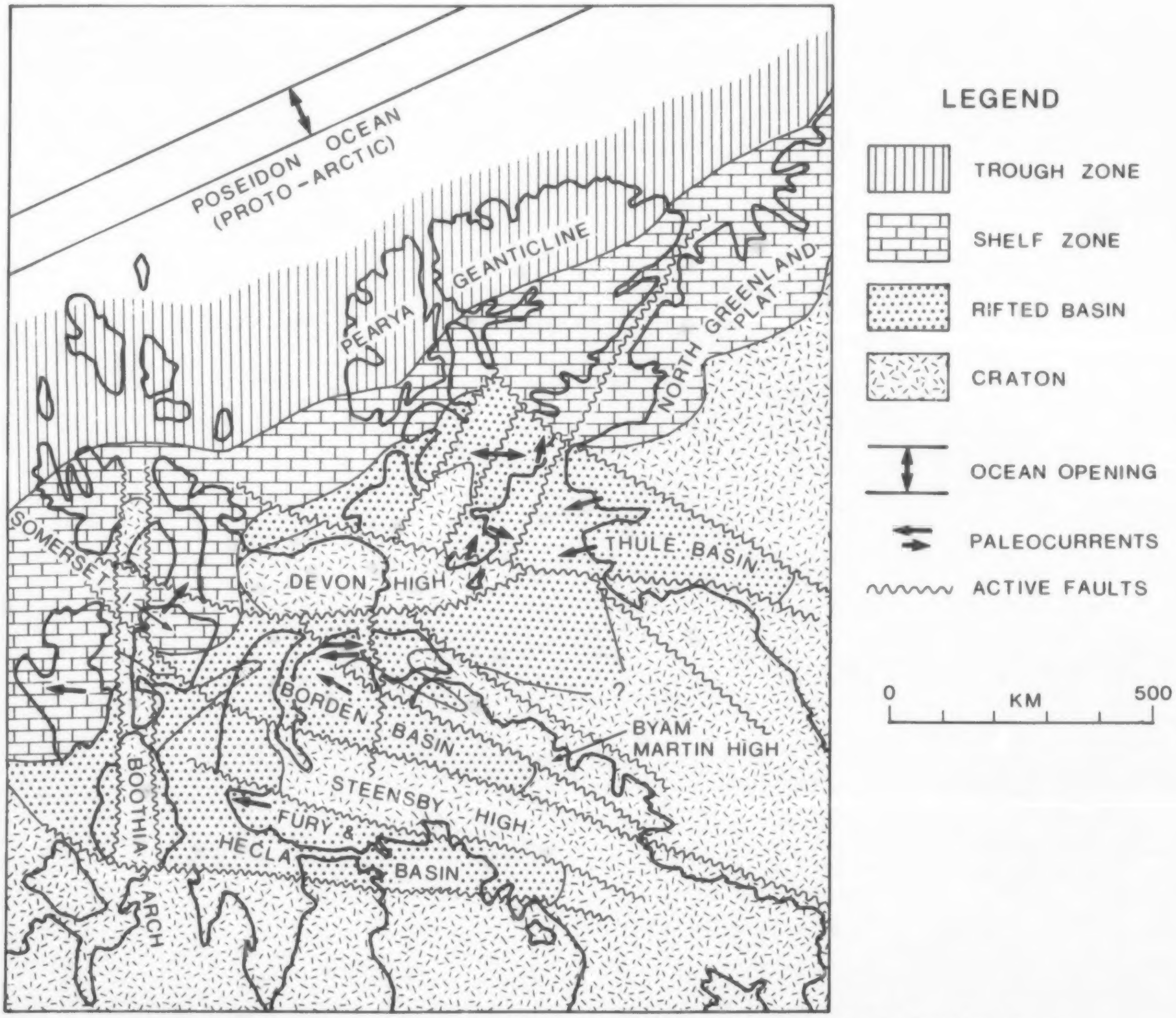

Figure 65.5. Schematic reconstruction for the 1200-1250 Ma opening of the Poseidon Ocean. Position of Greenland relative to Canada is modified from Le Pichon et al. (1977); see also Jackson and Iannelli (1981). Pearya Geanticline is from Trettin et al. (1972).

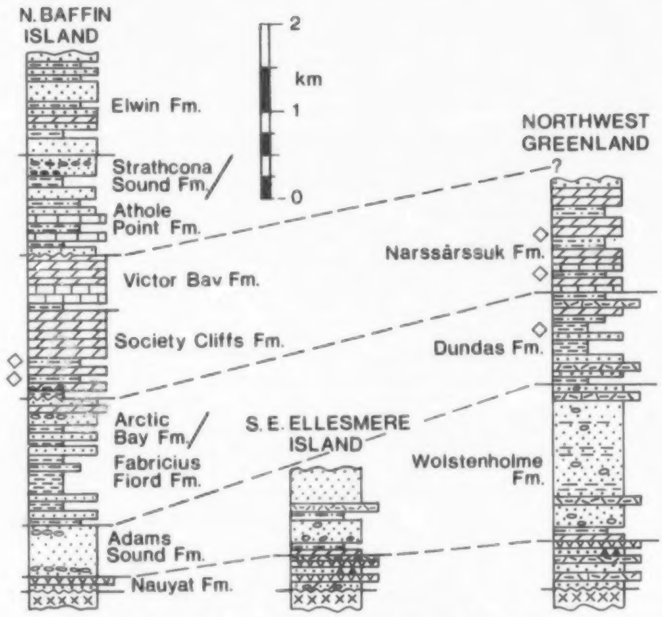

Figure 65.6. *Correlation of Neohelikian strata in Borden and Thule basins. Modified from Davies et al. (1963), Dawes et al. (1982), Frisch and Christie (1982), Jackson and Iannelli (1981), Jackson et al. (1985).*

The middle member was deposited in 8 or 10, 8-23 m thick shallowing up sequences similar to, but thicker than those in the lower member. They include:

i) Very thick bedded limestone, grading up into interbedded laminated limestone and dolostone grading up into sandstone.

ii) Laminated vuggy dolostone grading up into shaly and crossbedded sandstone.

iii) Thin bedded dolostone, grading up into laminated dolostone and calcareous dolostone, grading up into crossbedded quartzarenite.

Thick bedded to laminated quartzarenite, shale and minor siltstone and subarkose occur interbedded and intergradational, commonly with carbonate, in sequences up to 7 m thick. Buff, brown, light grey, and light green colours predominate and the strata are better sorted and less abundant than in the underlying member. Some coarsening-up beds are present and crossbedding occurs in several places (Fig. 65.2, 65.3).

Upper red member

The lowermost 100 m of the 460 m present (Davies et al., 1963) were examined. The observed strata are mostly buff to light grey thin bedded to thin laminated clean dolostone, deposited in sequences up to 14 m thick. Relatively few structures were seen (Fig. 65.2). Thin bedded to laminated and crossbedded dolomitic sandstone (arkose quartzarenite) and shale occur in a few red, buff and green sequences up to 4 m thick. The strata were deposited in 5-6 shallowing up cycles similar to previous ones. The basal cycle is about 32 m thick but the overlying one is of comparable thickness to those in the lower member.

Depositional environment. Narssârssuk strata were probably deposited in a series of shallowing up coastal sabkha sequences in a low energy environment (James, 1984; Kendall, 1984; Till, 1978). The minor amount of sedimentary breccia and conglomerate present, suggests protected deposition such as in a lagoon. The very thick to thin bedded carbonates may represent subtidal deposits while the cryptalgal laminites represent the intertidal deposits. The siliciclastics in the lower and upper redbed members represent the supratidal deposits. The relatively thick clean sequences of the middle Aorfêrneq dolomite member represent relatively stable conditions when the siliciclastic beds were deposited in an intertidal environment.

Summary, regional tectonics

That part of the Wolstenholme Formation seen by the writer consists chiefly of quartzarenites deposited in a tide-dominated shelf environment. A meandering stream redbed sequence occurs in the middle of unit 1 on Wolstenholme Island and in the lower part of unit 3 on southeast Ellesmere Island. Unit 2 is composed mostly of tholeiitic plateau basalt flows and sills (Frisch and Christie, 1982; Dawes et al., 1982). Strata resembling prodelta deposits occur at Goding Bay at the top of unit 2 and in the middle of unit 5. Some of the Dundas Formation was probably deposited in a subtidal basin while the overlying Narssârssuk Formation occurs in shoaling up sabkha cycles.

On southeast Ellesmere Island easterly directed fluvial and marine crossbeds in unit 3 (Fig. 65.3), and emplacement from the west of a flow in unit 2, suggest the presence of a land area immediately to the west (Fig. 65.5). R. Thorsteinsson (personal communication, 1985) reached a similar conclusion for early Paleozoic time. If the westerly directed marine crossbeds in unit 4 represent currents parallel to a shoreline then an embayment or a channel may have existed to the west between Goding Bay and Clarence Head during unit 4 deposition (Fig. 65.2, 65.3). Frisch and Christie (1982) indicated chiefly westward transport for unit 4 at Goding Bay and easterly transport at Clarence Head.

Dawes et al. (1982) noted that the main transport directions for the Thule Group in Greenland are to the south and southwest which is similar to the Greenland data presented here (Fig. 65.3). Therefore, southwesterly transport predominated on Greenland and easterly transport on southest Ellesmere. This may also suggest the presence of a land area to the west (Fig. 65.5) contrary to the open sea area depicted by Jackson and Iannelli (1981).

Many correlations of the Thule Group and Bylot Supergroup have been attempted (see Jackson and Iannelli, 1981), and many close similarities exist (Fig. 65.6). The volcanics that have redbed and carbonate strata associated with them yield similar K-Ar ages (Jackson and Iannelli, 1981) and are very similar chemically (Galley et al., 1983). The Dundas Formation and the Arctic Bay Formation of the Bylot Supergroup have closely similar stratigraphies. The Society Cliffs and Victor Bay formations of the Bylot Supergroup on Bylot Island (Jackson et al., 1985) are also similar to the Narssârssuk Formation. Dawes et al. (1982) have reported that syndepositional faulting occurred during deposition of the Thule Group. This is also the case with the Bylot Supergroup (Fig. 65.6; Jackson and Iannelli, 1981). The latter show no sign of thinning on northern Bylot Island. Therefore, the deposition of some strata, such as the carbonates, may have been continuous from one basin to the next (Fig. 65.5; Jackson et al., 1985).

Figure 65.5, depicting relationships during the Neohelikian opening of the Poseidon Ocean at 1200-1250 Ma, has been modified from Jackson and Iannelli (1981). In considering the abundant evidence of faulting and rifting related to this ocean opening (Fahrig, 1985; Jackson and Iannelli, 1981), it seems likely that some displacement of Greenland relative to Baffin Island and/or Ellesmere occurred at that time.

Acknowledgments

The author is grateful to the Ministry for Greenland and the Commission for Scientific Research for permission to carry out the studies described above. Logistical support was received from the Canadian Polar Continental Shelf Project, the Greenland Geological Survey and from W.F. Fahrig. Both P.R. Dawes and T.O. Frisch were most helpful, and discussed the geology of the Thule Group with the writer. The manuscript was critically read by J.B. Henderson who made many improvements.

References

Collinson, J.D.
1978: Alluvial sediments; in Sedimentary Environments and Facies, ed. H.G. Reading; Elsevier, New York, p. 15-60.

Davies, W.E., Krinsley, D.B., and Nicol, A.H.
1963: Geology of the North Star Bugt area, northwest Greenland; Meddeleser om Gronland, bd. 162, n. 12, 68 p.

Dawes, P.R.
1972: Precambrian crystalline rocks and younger sediments of the Thule district, North Greenland; Gronlands Geologiske Undersogelse, Rapport 45, p. 10-15.

1975: Reconnaissance of the Thule Group and underlying basement rocks between Inglefield Bredning and Melville Bugt, western North Greenland; Gronlands Geologiske Undersogelse, Rapport 75, p. 34-38.

1976a: 1:500 000 mapping of the Thule district, North-West Greenland; Gronlands Geologiske Undersogelse, Rapport 80, p. 23-28.

1976b: Precambrian to Tertiary of northern Greenland; in Geology of Greenland, ed. A.E. Escher and W.S. Watt; Geological Survey of Greenland, Copenhagen, p. 248-303.

1979: Field investigations in the Precambrian terrain of the Thule district, northwest Greenland; Gronlands Geologiske Undersogelse, Rapport 95, p. 14-22.

Dawes, P.R., Frisch T., and Christie, R.L.
1982: The Proterozoic Thule Basin of Greenland and Ellesmere Island: importance to the Nares Strait debate; in Nares Strait and the Drift of Greenland: a Conflict in Plate Tectonics, ed. P.R. Dawes and J.W. Kerr; Meddeleser om Gronland, Geoscience 8, p. 89-104.

Dawes, P.R., Rex, D.C., and Jepsen, H.F.
1973: K/Ar whole rock ages of dolerites from the Thule district, western North Greenland; Gronlands Geologiske Undersogelse, Rapport 55, p. 61-66.

Elliott, T.
1978a: Clastic shorelines; in Sedimentary Environments and Facies, ed. H.G. Reading; Elsevier, New York, p. 143-177.

1978b: Deltas; in Sedimentary Environments and Facies, ed. H.G. Reading; Elsevier, New York, p. 97-142.

Fahrig, W.F.
1985: The tectonic settings of continental diabase dyke swarms: failed arm and early passive margin; International Conference Mafic Dyke Swarms; University of Toronto, Erindale Campus, p. 42-43 (abstract).

Frisch, T.
1983: Reconnaissance geology of the Precambrian Shield of Ellesmere, Devon and Coburg islands, Arctic Archipelago: a preliminary account; Geological Survey of Canada, Paper 82-10, 11p.

Frisch, T. and Christie, R.L.
1982: Stratigraphy of the Proterozoic Thule Group, southeastern Ellesmere Island, Arctic Archipelago; Geological Survey of Canada, Paper 81-19, 13 p.

Frisch, T., Morgan, W.C., and Dunning, G.R.
1978: Reconnaissance geology of the Precambrian Shield on Ellesmere and Coburg islands, Canadian Arctic Archipelago; in Current Research, Part A, Geological Survey of Canada, Paper 78-1A, p. 135-138.

Galley, A.G., Jackson, G.D., and Iannelli, T.R.
1983: Neohelikian subaerial basalts with ocean-floor type chemistry, northwestern Baffin Island; Geological Association of Canada, program with abstracts, v. 8, p. A25 (abstract).

Jackson, G.D. and Iannelli, T.R.
1981: Rift-related cyclic sedimentation in the Neohelikian Borden Basin, northern Baffin Island; in Proterozoic Basins of Canada, ed. F.H.A. Campbell; Geological Survey of Canada, Paper 81-10, p. 269-302.

Jackson, G.D., Iannelli, T.R., Knight, R.D., and Lebel, D.
1985: Neohelikian Bylot Supergroup of Borden Rift Basin, northwestern Baffin Island, District of Franklin; in Current Research, Part A, Geological Survey of Canada, Paper 85-1A, p. 639-649.

James, N.P.
1984: Shallowing-upward sequences in carbonates; in Facies Models, 2nd ed., ed. R.G. Walker; Geoscience Canada, Reprint 1, p. 213-228.

Johnson, H.D.
1978: Shallow siliciclastic seas; in Sedimentary Environments and Facies, ed. H.G. Reading; Elsevier, New York, p. 207-258.

Kendall, A.C.
1984: Evaporites; in Facies Models 2nd ed., ed. R.G. Walker; Geoscience Canada, Reprint 1, p. 259-296.

Le Pichon, X., Sibnet, J.C., and Francheteau, J.
1977: The fit of the continents around the North Atlantic Ocean; Tectonophysics, v. 38, p. 169-209.

Reinson, G.E.
1984: Barrier island and associated strand-plain systems; in Facies Models, 2nd ed., ed. R.G. Walker; Geoscience Canada Reprint 1, p. 119-140

Till, R.
1978: Arid shorelines and evaporites; in Sedimentary Environments and Facies, ed. H.G. Reading; Elsevier, New York, p. 178-206.

Trettin, H.P., Frisch, T.O., Sobczak, L.W., Weber, J.R., Niblett, E.R., Law, L.K., de Laurier, I., and Whitham, K.
1972: The Innuitian Province; in Variations in Tectonic Styles in Canada, ed. R.A. Price and R.J.W. Douglas; Geological Association of Canada, Special Paper 11, p. 83-181.

Walker, R.G.
1984: Shelf and shallow marine sands; in Facies Models, 2nd ed., ed. R.G. Walker; Geoscience Canada, Reprint 1, p. 141-170

Walker, R.G. and Cant, D.J.
1984: Sandy fluvial systems; in Facies Models, 2nd ed., ed. R.G. Walker; Geoscience Canada, Reprint 1, p. 71-89.

Stratigraphy and structure of the Hadrynian Horsethief Creek Group in the northern Dogtooth Range south of Grizzly Creek, Purcell Mountains, British Columbia

EMR Research Agreement 139

Thomas Kubli [1]
Cordilleran Geology Division, Vancouver

Kubli, T., Stratigraphy and structure of the Hadrynian Horsethief Creek Group in the northern Dogtooth Range south of Grizzly Creek, Purcell Mountains, British Columbia; in Current Research, Part A, Geological Survey of Canada, Paper 86-1A, p. 553-558, 1986.

Abstract

The Hadrynian Horsethief Creek Group in the Dogtooth Range of the northernmost Purcell Mountains can be subdivided into a grit, slate, carbonate and upper clastic division. A stratigraphic section 1500 m thick was measured in detail from the lowermost grits exposed in the hanging wall of the Goat Ridge thrust to the upper part of the slate division. At the base of the succession, slates, marbles, limestones and calcareous sandstones and grits, represent a phase of slow sedimentation either at the base or possibly in the middle of the grit division. The middle part of the section shows typical thinning and fining-upward cycles of a submarine fan assemblage. The boundary between the grit and slate divisions is gradational in an interbedded sandstone-pelite succession. Estimated thicknesses are 1000 m and perhaps 1500 m for the grit division, 800 m for the slate division and a minimum of 200 m for the carbonate division.

Résumé

On peut diviser le groupe de Horsethief Creek de l'Hadrynien, dans les monts Dogtooth de la partie la plus septentrionale des chaînons Purcell, en grès grossiers, en ardoises, en carbonates et en roches clastiques supérieures. On a mesuré en détail une coupe stratigraphique de 1500 m de puissance depuis les grès grossiers inférieurs qui affleurent dans la lèvre supérieure du chevauchement de Goat Ridge jusqu'à la partie supérieure des ardoises. À la base de la série, les ardoises, les marbres, les calcaires ainsi que les grès et les grès grossiers calcaires constituent une phase de sédimentation lente soit à la base, soit probablement au milieu des grès grossiers. Le milieu de la coupe est caractérisé par les cycles ascendants d'amincissement et d'affinement d'un assemblage en éventail d'origine sous-marine. La limite entre les grès grossiers et les ardoises est progressive et se trouve dans une série de grès et de pélites interstratifiés. Les puissances estimées atteignent 1000 m et peut-être même 1500 m pour les grès grossiers, 800 m pour les ardoises et au moins 200 m pour les carbonates.

[1] Department of Geology and Geophysics, University of Calgary, Calgary, Alberta T2N 1N4

Introduction

The stratigraphy of the Hadrynian Horsethief Creek Group was established for the Dogtooth Range by Evans (1933) and by Wheeler (1963). A detailed description and interpretation of the Horsethief Creek strata in the Dogtooth Range north of Grizzly Creek was given by Poulton (1970) and Poulton and Simony (1980).

During the summer of 1985 the Copperstain Mountain – Moonraker Peak area was mapped at a scale of 1:20 000 from the Dogtooth thrust in the east to Bald Ridge in the west (Fig. 66.1). Several stratigraphic sections were measured, one in great detail. Bedding attitude, cleavage, cleavage-bedding relationships, fold axes of megascopic and mesoscopic folds and stratigraphic tops were used to construct a preliminary cross-section through the area. Oriented samples were taken to provide information about strain and stress regimes in the vicinity of thrust faults in a later stage of this study.

Structure

The Dogtooth Range consists of a series of imbricate thrust sheets between the Beaver River normal fault and the Purcell thrust. A minimum tectonic shortening of 50% was estimated by Simony and Wind (1970). Thrust faults are northeasterly direted and some are overturned north of the study area (Fig. 66.1).

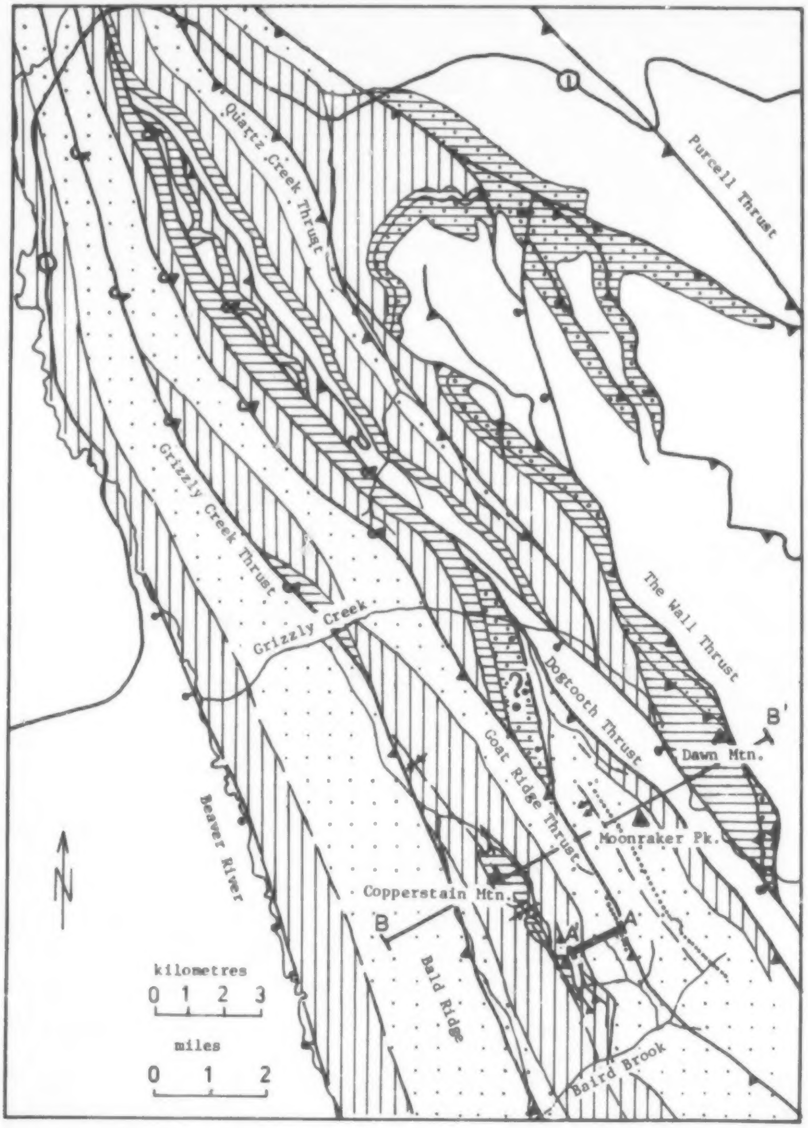

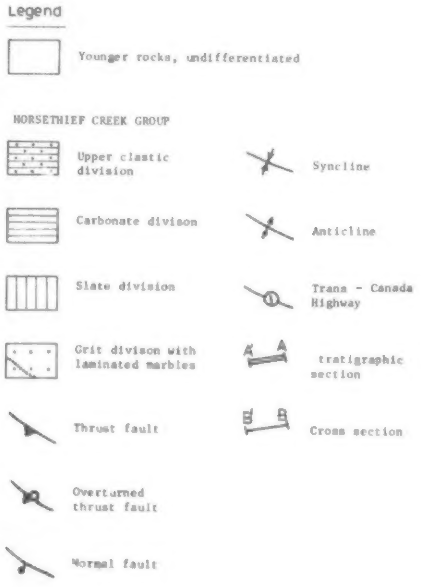

The two major mappable structures between Bald Ridge and the Dogtooth thrust are a broad, slightly overturned anticline in the grits west of Moonraker Peak and the Copperstain Mountain syncline.

Axial trends of major and associated minor folds range from 310 to 340 degrees. Plunges are gentle, up to 15 degrees. Pervasive axial planar cleavage is best developed in pelitic layers and is generally southwest dipping in the hanging wall of the Dogtooth thrust. West of the Goat Ridge thrust this earlier (F1) cleavage is crosscut at low angles by a west dipping, more northerly striking fracture cleavage (Fig. 66.2) which may be related to a late stage of thrust faulting. Strain slip cleavage, as described by Poulton (1970), was observed only in the vicinity of the Grizzly Creek thrust. Slightly deformed

***Figure 66.1.** Geological map of the northern Dogtooth Mountains, using data from field season 1985, Wheeler (1963), Poulton and Simony (1980) and showing locations of stratigraphic section and cross-section.*

axial planes of early (F1) isoclinal folds could be found in the hanging wall of the Dogtooth thrust immediately above the thrust zone.

The Moonraker anticline is exposed for at least 8 km and can be traced farther to the south. Pervasive vertical axial planar cleavage, abundant minor faults and a complex folding style characterize its core zone.

The Copperstain syncline, outlined by yellow weathering dolomite lenses and dark grey limestones, has an almost vertical to steeply west-dipping axial plane in the study area. Farther south it is overturned to the east.

Numerous minor thrust and normal faults of different generations complicate the map pattern of this structure. One of these thrusts in the eastern limb of the syncline displaces a dolomite lens by approximately 100 m and can be traced for 8 km.

Stratigraphy

Four distinguishable stratigraphic units of the Horsethief Creek Group were mapped in the study area.

The grit division is the lowermost unit and is characterized by coarse sandstones and fine pebble conglomerate interbedded with pelitic layers and a few thin limestone layers. Estimated maximum thickness in the area is approximately 1500 m.

The second unit, the slate division, comprises pelitic rocks interbedded with minor coarser clastics and carbonate layers. Characteristic are graded and ripple crosslaminated silt and sand laminae, dominant light to dark steel-grey or blue-grey colour, high mica content and pyrite and siderite porphyroblasts (Poulton and Simony, 1980). Maximum estimated thickness is 900 to 1000 m.

The measured stratigraphic section shown in Figures 66.3 and 66.4 reaches from the Goat Ridge thrust up to a set of minor thrust faults within the slate division (see Fig. 66.1 for location).

The lowest unit exposed in this section consists of grey slates and phyllites overlain by green and purple weathering slates.

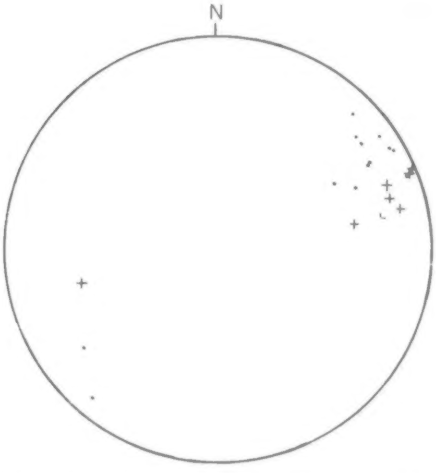

Figure 66.2. Pervasive axial planar cleavage (.) and more northerly striking fracture cleavage (+) in the hanging wall of the Goat Ridge thrust.

The overlying 40 m are characterized by grey limestones and sandy limestones. At their base a very prominent green laminated marble is exposed. It consists of 2-5 cm thick layers of green phyllite alternating with greenish grey recrystallized limestone beds of the same thickness. Individual beds can be traced at least several hundreds of metres. The thickness of this unit changes from 5 to 15 m due to variations with position within major folds.

The 150 m of the succession overlying the limestones consist of pelitic slates and phyllites interbedded with sandy yellow weathering limestones, calcareous grits and sandstones as well as fine grained red sandstones. In the lower part sandy limestones are predominant and crosslamination occurs. Towards the top red sandstone beds become predominant.

The middle part of the measured section (240 to 1050 m) is characterized by typical thinning and fining upward cycles of grit sedimentation as described in Poulton and Simony (1980). Thicknesses of individual cycles can vary from 50 to 90 m. Crossbedding is very rare, as are small scale channels but graded beds are common. According to Poulton and Simony (1980), all observed features are consistent with deposition in a "proximal exotic" situation in

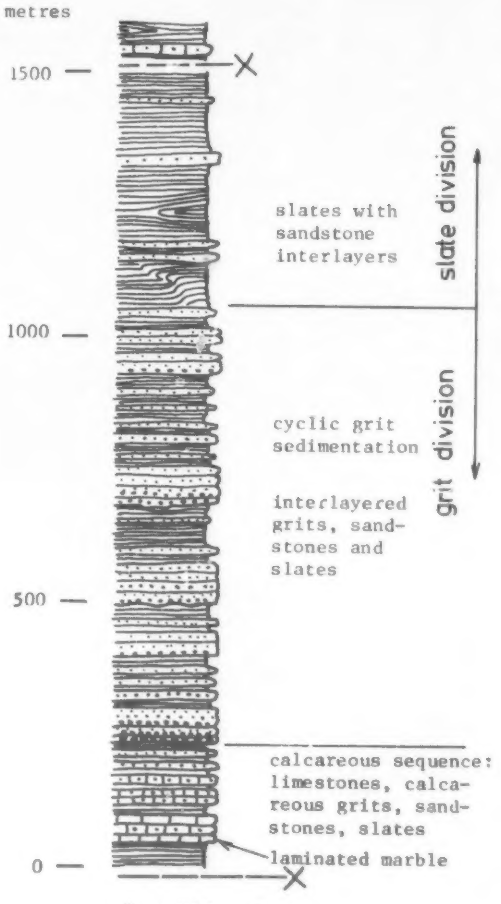

Figure 66.3. Stratigraphic section of the grit and slate divisions in the hanging wall of the Goat Ridge thrust.

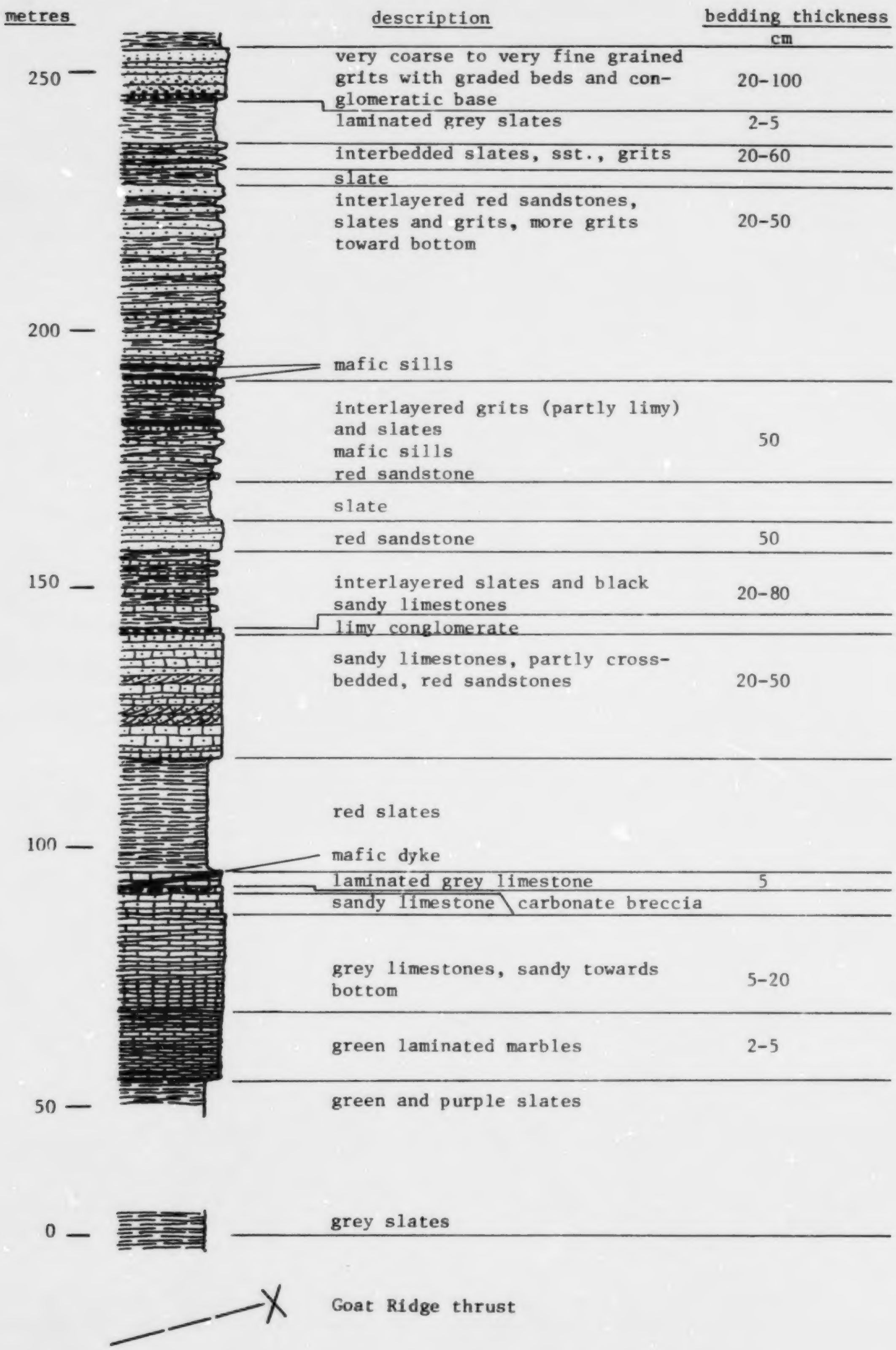

Figure 66.4. ***Bottom part of the stratigraphic section shown in Figure 66.3.***

a channelled (upper) submarine fan. The lower boundary of the overlying slate division is gradational in an interbedded sandstone – pelite succession. Red sandstone beds become very common in the upper grit and lower slate division whereas calcareous yellow weathering sandstones are characteristic for the latter. The boundary is chosen where the pelite/grit ratio exceeds 1:1. As the slate division in the area is disturbed by many minor faults, no complete section could be measured. The estimated thickness for this unit is 800 m.

The overlying carbonate division consists mainly of massive limestones and dolomites in the footwall of the Dogtooth thrust, reaching thicknesses of approximately 200 m. West of the Dogtooth thrust in the Copperstain Mountain syncline (western facies area of Poulton, 1972) the carbonate division is characterized by large massive, partly stromatolitic dolomite lenses embedded in a succession of slates of various composition, sandstones calcareous sandstones and thin grey limestones beds. Lateral transitions from limestone to dolomite can be observed.

The upper clastic division overlying the carbonates could not be found in outcrop west of the Dogtooth thrust.

Conclusions

Compared to the middle part of the measured section, the base represents a stage of overall low sedimentation rates. The monotonous sequence of laminated pelitic slates and the lack of coarse detritus at the base of the measured section indicate sedimentation in deep water during a phase of subsidence or transgression and/or very low relief in the source area. The overlying laminated marbles must have been deposited in shallow water in a very "quiet" environment with low sedimentation rates during a regressive phase. The consistent cyclicity of the marble-shale layering may be the result of either cyclic sea level changes or cyclic influx from the sediment source into a shallow basin. Increasing deposition of sands, represented by the overlying sequence of calcareous sandstones and grits can be explained by uplift of the source area and/or subsidence in the basin.

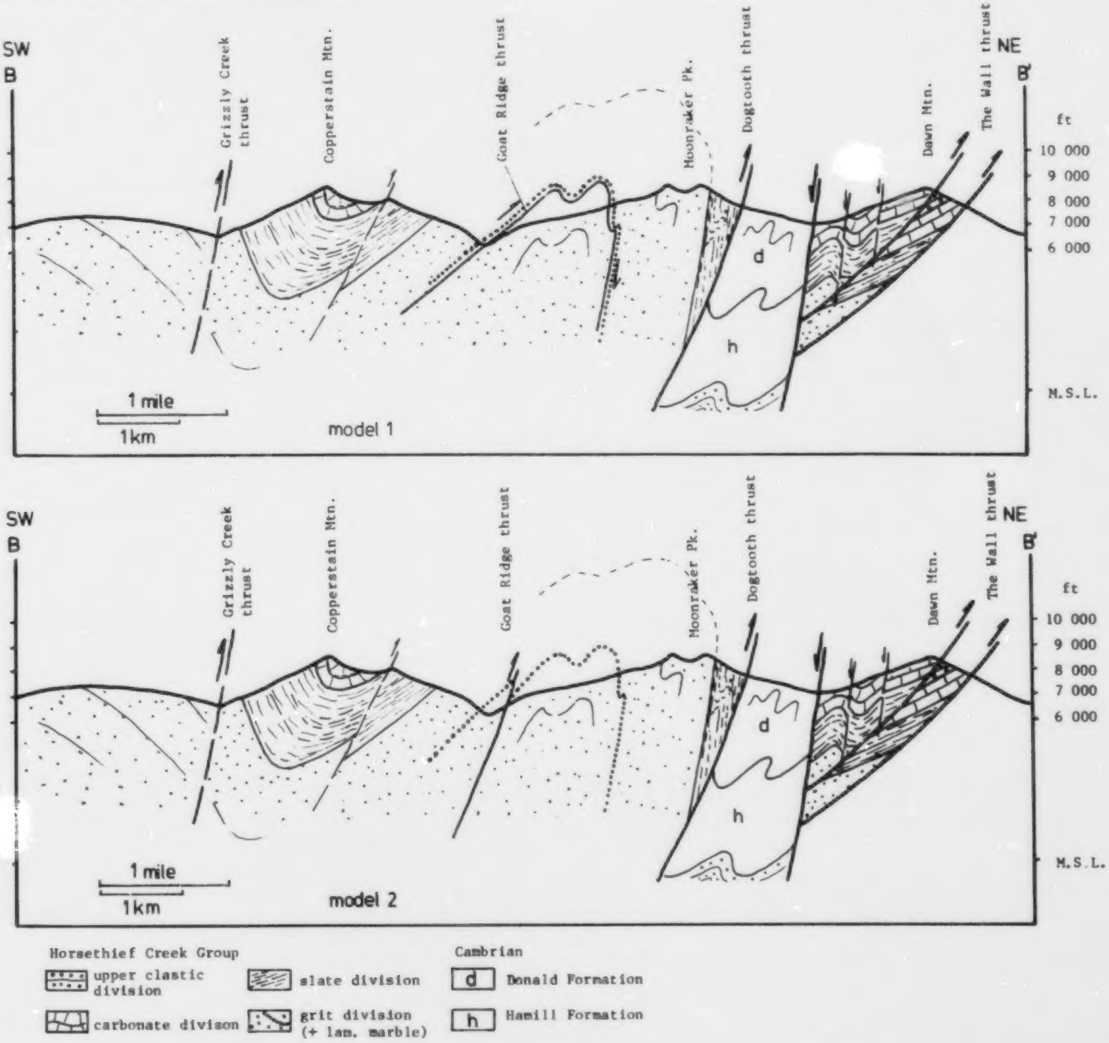

Figure 66.5. *Schematic cross-sections using two different stratigraphic models.*

Following model 1 used in Figure 66.5, the assumption can be made that the slate and laminated limestone sequence is a previously unrecognized stratigraphic unit which underlies the grit division and that the base of the grit division has been observed in the measured section. Consequently the measured section must be separated from the underlying grits by a fault which is the Goat Ridge thrust. The laminated marble occurs on both limbs of the Moonraker anticline, at equal distances from the fold core and everywhere shows high compressive and shear strain, suggesting that a fault underlies it. This leads to the conclusion that the Goat Ridge thrust is an early bedding parallel folded thrust. Using model 1 the thickness estimated for the grit division west of the Goat Ridge thrust is approximately 1000 m.

In model 2 of Figure 66.5 the assumption is made that the shale-limestone sequence represents only a phase of low sedimentation within the grit division and the Goat Ridge thrust is presumed to be a minor fault, younger than the major folds. Consequently the intensive deformation of the laminated marbles and associated limestones is due only to minor detachment within the stratigraphic sequence. Considering the fact that the shale-limestone sequence outcrops only once in the footwall of the Goat Ridge thrust, a maximum displacement of only about 100 m is possible in model 2 (Fig. 66.5). The thickness of the grit division derived from this model is 1500 m, which corresponds to thicknesses measured by Poulton (1970) and Poulton and Simony (1980).

References

Evans, C.S.

1933: Brisco-Dogtooth map-area, British Columbia; Geological Survey of Canada, Summary Report 1932. Pt.AII, p. 106-176.

Poulton, T.P.

1970: Stratigraphy and sedimentology, Horsethief Creek Formation, northern Dogtooth Mountains, British Columbia; M.Sc. thesis, University of Calgary, Alberta.

1972: Upper Proterozoic 'Limestone Unit', Northern Dogtooth Mountains, British Columbia; Canadian Journal of Earth Sciences, v. 10, p. 292-305.

Pouton, T.P. and Simony, P.S.

1980: Stratigraphy, sedimentology, and regional correlation of the Horsethief Creek Group (Hadrynian, Late Precambrian) in the northern Purcell and Selkirk Mountains, British Columbia; Canadian Journal of Earth Sciences, v. 17, p. 1708-1724.

Simony, P.S. and Wind, G.

1970: Structure of the Dogtooth Range and adjacent portions of the Rocky Mountain Trench; Geological Association of Canada, Special Paper 6, p. 41-51.

Wheeler, J.O.

1963: Rogers Pass map-area, British Columbia and Alberta (82N W1/2); Geological Survey of Canada, Paper 62-32.

Depositional facies and evolution of Lulu Island topset deposits, Fraser Delta, British Columbia

EMR Research Agreement 275-04-84 and Project 790006

Harry F. L. Williams[1]
Cordilleran Geology Division

Williams, H.F.L., Depositional facies and evolution of Lulu Island topset deposits, Fraser Delta, British Columbia; in Current Research, Part A, Geological Survey of Canada, Paper 86-1A, p. 559-564, 1986.

Abstract

Preliminary interpretation of depositional facies encountered in a series of boreholes on Lulu Island B.C. provides, for the first time, direct evidence of a buried 'proto-delta' underlying the eastern part of the Fraser Delta. Deposits formed during the 12 m (ca.) rise in sea level between approximately 7700 and 4700 BP suggests that vertical accretion of the delta's facies (floodplain, tidal marsh, intertidal silts and sands) kept pace with the rising sea level. The prevalence of tidal marsh and/or floodplain deposits overlying the former subaerial surface of the 'proto-delta' indicates that no major submergence and subsequent landward migration of sandy tidal facies occurred.

A model of the progradation rate of Lulu Island based on the seaward migration of the tidal-marsh zone, and consistent with the concept of progressive reduction in the rate of deltaic progradation, was developed.

The finding that vertical accretion may occur in response to a rise in sea level has important implications for research concerned with coastal depositional environments.

Résumé

L'interprétation préliminaire des faciès de sédimentation, observés dans une série de sondages effectués dans l'île Lulu en Colombie-Britannique, a fourni pour la première fois une preuve directe de l'existence d'un <<proto-delta>> enfoui sous la partie est du delta du fleuve Fraser.

Les dépôts qui se sont accumulés pendant l'élévation de 12 m (ca) du niveau de la mer il y a environ 7700 à 4700 ans, semblent indiquer que la superposition verticale des faciès deltaïques (plaine d'inondation, marais littoral, limons et sables intertidaux) a suivi la montée du niveau de la mer. La prédominance des dépôts de marais littoraux ou de plaines d'inondation, ou les deux, reposant sur l'ancienne surface subaérienne du <<proto-delta>> indique qu'il n'y a pas eu de submersion de grande amplitude et de migration ultérieure vers les terres des faciès sableux de nature littorale.

On a mis au point un modèle de la vitesse de progradation de l'île Lulu basé sur la migration de la zone de marais littoraux vers la mer, et compatible avec la notion de réduction progressive dans le processus de progradation deltaïque.

La constatation du fait que la superposition verticale peut être le résultat d'une élévation du niveau marin présente des répercussions importantes au niveau de la recherche portant sur les milieux de sédimentation littoraux.

[1] Department of Geography, Simon Fraser University, Burnaby, B.C. V5A 1S6

Introduction

The Fraser Delta (Fig. 67.1) has been growing into the Strait of Georgia from its apex at New Westminster for about 10 000 years (Mathews and Shepard, 1962; Johnson, 1921; Clague and Luternauer, 1983). This period encompassed a rise in sea level of about 12 m from approximately 7700 to 4700 BP (Clague et al., 1982; Styan, 1981; Styan and Bustin, 1984; see Fig. 67.2).

Clague et al. (1983) proposed that a substantial Fraser 'proto-delta', graded to the -12 m sea level, developed prior to 7700 BP and was subsequently buried beneath more recent deltaic deposits. Such a proposal remains speculative, however, since direct evidence of a buried alluvial surface within the Fraser Delta has not been found. The effects of the rise in sea level on the character of deltaic deposits and on the growth of the delta during the period 7700 to 4700 BP also remain largely unknown.

This preliminary report describes the first attempt, based on detailed borehole data, to determine the effect of the change in sea level on the nature and growth of the Fraser Delta's topset deposits.

Methods

As part of an ongoing research program on the structure and evolution of the Fraser Delta, eight boreholes were drilled on Lulu Island, B.C. (Fig. 67.1). Data were obtained from a combination of core and auger samples. Field logging of cores involved the visual assessment of grain size, organic matter content and sedimentary structures.

The borehole data were used in conjunction with a number of borehole records provided by the B.C. Department of Highways to construct a stratigraphic section along the east-west axis[1] of Lulu Island. It is assumed that this axis parallels the direction of progradation of this part of the Fraser Delta. All elevations were adjusted to geodetic datum (approximates mean sea level).

A second aspect of this research was the characterization of present-day depositional environments on the Lulu Island tidal flats (Fig. 67.1) which was required for the interpretation of the drill cores. Information from sedimentological and biogeographical studies of the tidal flats (Hutchinson, 1982; Luternauer, 1980; Luternauer and Murray, 1973) was combined with data collected on several field surveys, to develop a generalized model of the biosedimentological characteristics of tidal flat depositional environments.

Results

The stratigraphic section along the east-west axis of Lulu Island is presented in Figure 67.3. At this stage no attempt has been made to correlate between boreholes. Microscopic examination of the apparent tephra layer in

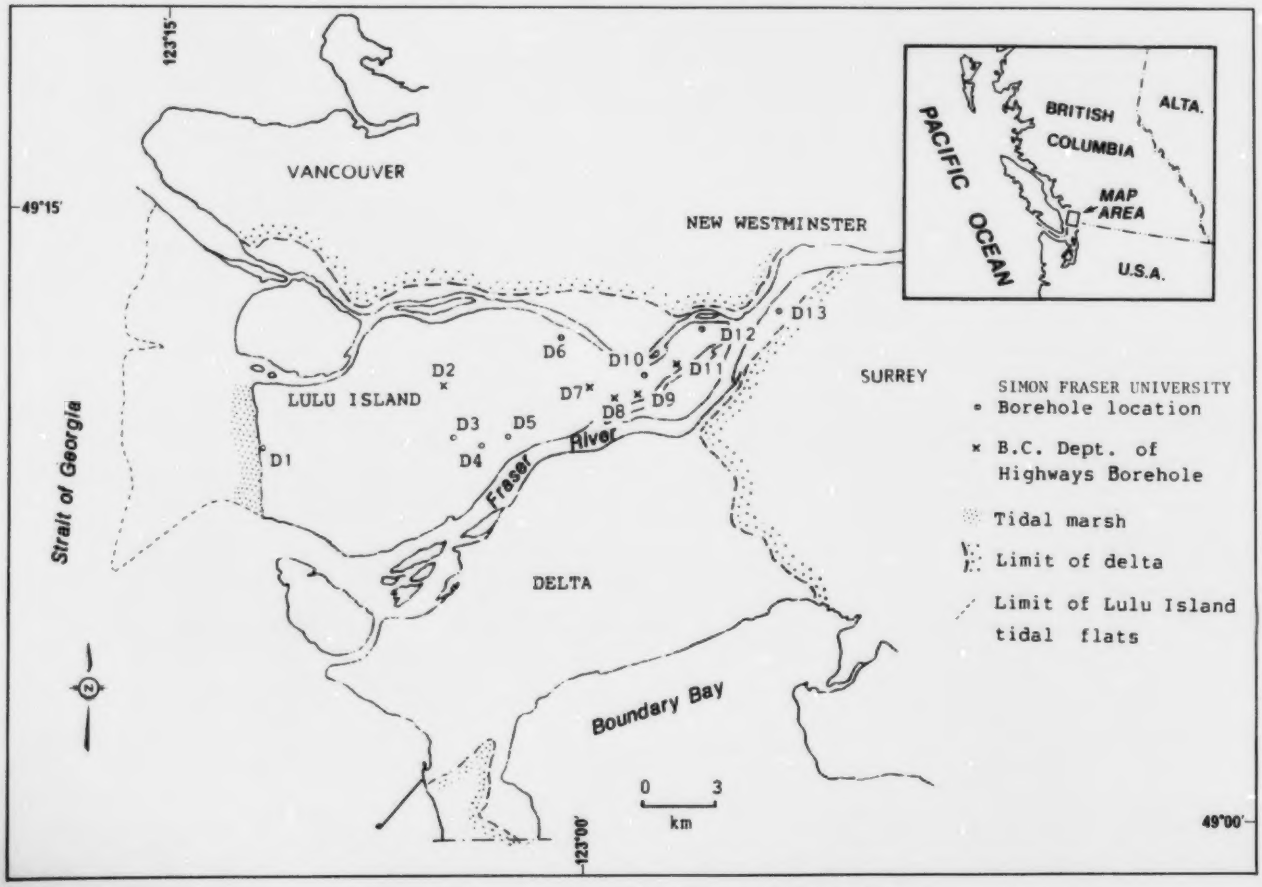

Figure 67.1. *Location of boreholes, Lulu Island, B.C.*

[1] Approximated by a straight line connecting site D1 and D9 and site D9 to D13. Boreholes were positioned along this line on the basis of their distance from site D9.

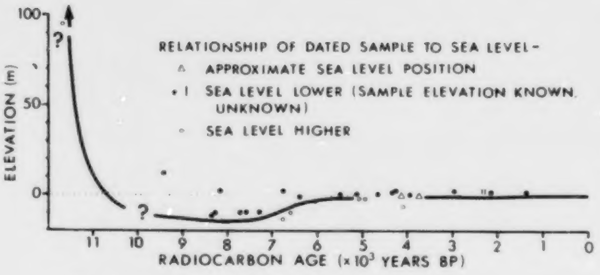

Figure 67.2. *Fraser Delta sea level curve (from Clague et al., 1982).*

borehole D10 confirmed the presence of volcanic glass fragments. The source of this tephra has not yet been determined, although a Mt. Mazama (Crater Lake, Oregon) origin seems probable.

Figure 67.4 shows the generalized biosedimentological zonation of the Lulu Island tidal flats. Borehole information from site D1 is included to illustrate the correspondence between the lateral succession of environments on the tidal flats and the vertical succession of deposits encountered in the drill cores.

Using Figure 67.4 as a guide, facies divisions were incorporated into the stratigraphic section across Lulu Island. Four facies types were tentatively identified[1]: subtidal delta front sands; lower and midtidal sands and silty sands; organic-rich tidal marsh and floodplain silts, and peat bog[2].

The most readily apparent division was the transition from organic-rich silts of tidal marsh and floodplain origin to the underlying lower and midtidal sands and silty sands. This transition corresponds to the base of the tidal-marsh zone in Figure 67.4.

On the basis of the present topographic profile of Lulu Island, a number of proposed paleosurfaces were added to the stratigraphic section (Fig. 67.5).

Discussion

It is proposed that the morphology of the tidal-marsh base in Figure 67.5 represents three major stages in the growth of Lulu Island during the past 10 000 years:

1. Prior to ca. 7700 BP the base of the tidal marsh was graded to a sea level 12 m lower than at present and extended to site D9 (Fig. 67.1). Overlying this base were presumably the subaerial deposits of a 'proto-delta'. To the west, the tidal flats of the 'proto-delta' would have extended to the vicinity of site D4[3].

2. Between ca. 7700 and 4700 BP the leading edge of the tidal-marsh zone continued its westward progradation and also rose vertically in response to the rise in sea level. The prevalence of organic-rich silts and lack of sandy deposits overlying the tidal marsh base suggests that no substantial marine transgression occurred during this period. A marine transgression resulting in a submergence of more than 2 m would presumably have caused the eastward migration of sandy tidal facies over the 'proto-delta' and yet no evidence of such an incursion has been found in the sediment column above the tidal marsh base.

   It would appear that facies existing on the 'proto-delta' underwent vertical accretion in response to the rise in sea level. The eastward migration of sandy tidal facies normally associated with a marine transgression was presumably confined to a marginal fringe.

   The average rate of vertical accretion, if the assumptions concerning the paleosurfaces (Fig. 67.5) are correct, is calculated at approximately 4 mm per year – which corresponds to the average rate of sea level rise during this period. The vertical accretion was apparently a direct response of the deltaic depositional system to the change in base level.

3. In the period ca. 4700 BP to present, Lulu Island continued to grow westward under fairly stable sea level conditions (Fig. 67.1). Consequently, the tidal-marsh base formed during this period is graded to present sea level (Fig. 67.5).

The proposed model of Lulu Island's evolution allows estimates of the rate of deltaic progradation to be made. On the assumption that the delta began to grown out from near site D13 about 10 000 BP, an average rate of 3.2 m per year would have been required to bring the leading edge of the tidal marsh to site D9 by 7700 BP.

During the next 3000 years the tidal marsh appears to have prograded another 8.5 km, despite the rising seal level, at an average rate of 2.8 m per year.

In the last 4700 years the base of the tidal marsh has extended a further 7.75 km to its present position – an average rate of 1.6 m per year.

These three rates have been incorporated into a model of the progradation rate of Lulu Island over the last 10 000 years (Fig. 67.6). The model suggests that growth has slowed considerably over this period. This finding is consistent with the concept of a progressive reduction in the Fraser Delta's growth rate due to progradation into deepening water, a lengthening delta front, and a reduction in sediment supply due to stabilization of drift-covered slopes following deglaciation (Clague and Luternauer, 1983; Mathews and Shepard, 1962).

Conclusions

1. The borehole data present, for the first time, direct evidence of the existence of a Fraser 'proto-delta' underlying eastern Lulu Island.

2. Vertical accretion of deltaic facies appears to have occurred over much of the 'proto-delta' in response to the rise in sea level between ca. 7700 and 4700 BP. Consequently, deposits formed during that time have considerably greater thickness than their modern analogues.

3. The vertical perpetuation of tidal marsh and/or floodplain facies above the former subaerial platform of the 'proto-delta' suggests that no marine transgression and submergence of more than 2 m occurred during the ca. 12 m rise in sea level between ca. 7700 and 4700 BP. This indicates that a landward migration of marine facies during a substantial rise in sea level, need not necessarily occur. The critical issue would appear to be the ability of the depositional system to maintain a sedimentation rate equal to the rate of sea level rise.

---

[1] The division between the first two facies was based mainly on estimated low tide levels in Figure 67.5.

[2] Part of the peat deposits on the Department of Highways borehole logs may in fact be organic-rich silts.

[3] This assumes that the slope of the tidal flats was not significantly different than now and that the paleosurfaces in Figure 67.5 are, in fact, correct.

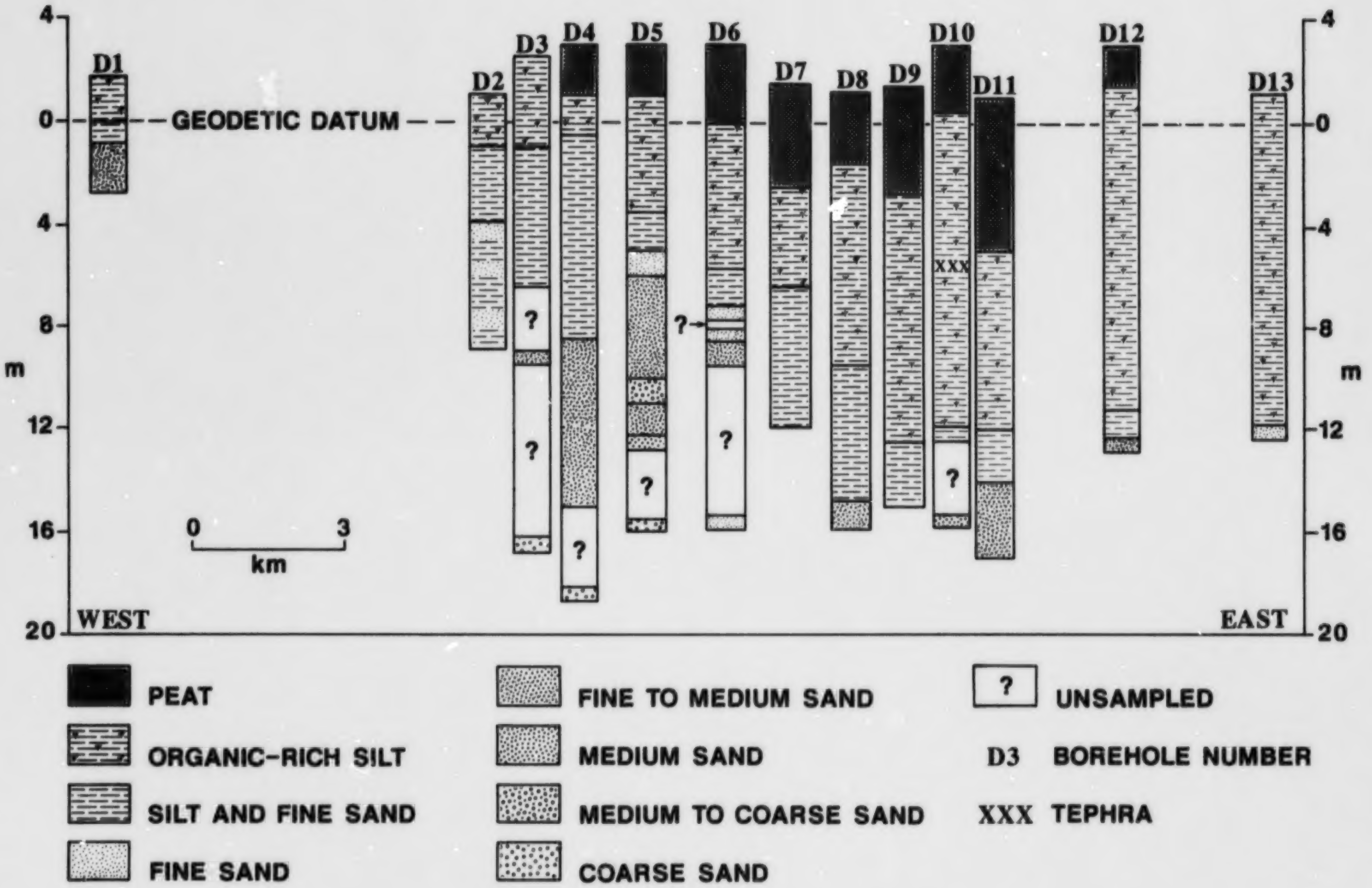

Figure 67.3. *East-west stratigraphic section, Lulu Island, B.C.*

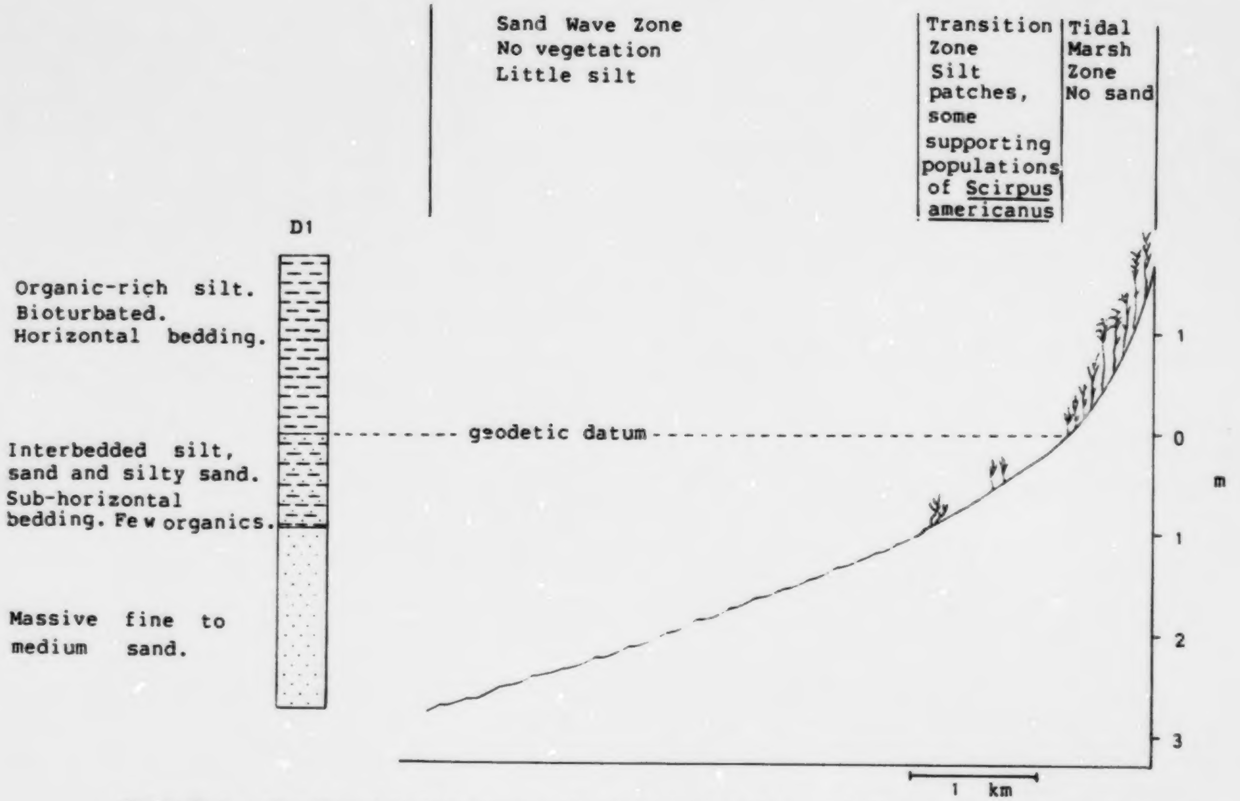

*Figure 67.4. Biosedimentological zonation of Lulu Island tidal flats. The tidal-marsh zone includes **Scirpus americanus, Scirpus maritimus, Carex lyngbyei, Potentialla pacifica, Distichlis spicata, Typha latifolia, Triglochin maritimum, Agrostis exarata**. Species density and diversity increases shoreward (distribution from Hutchinson, 1982).*

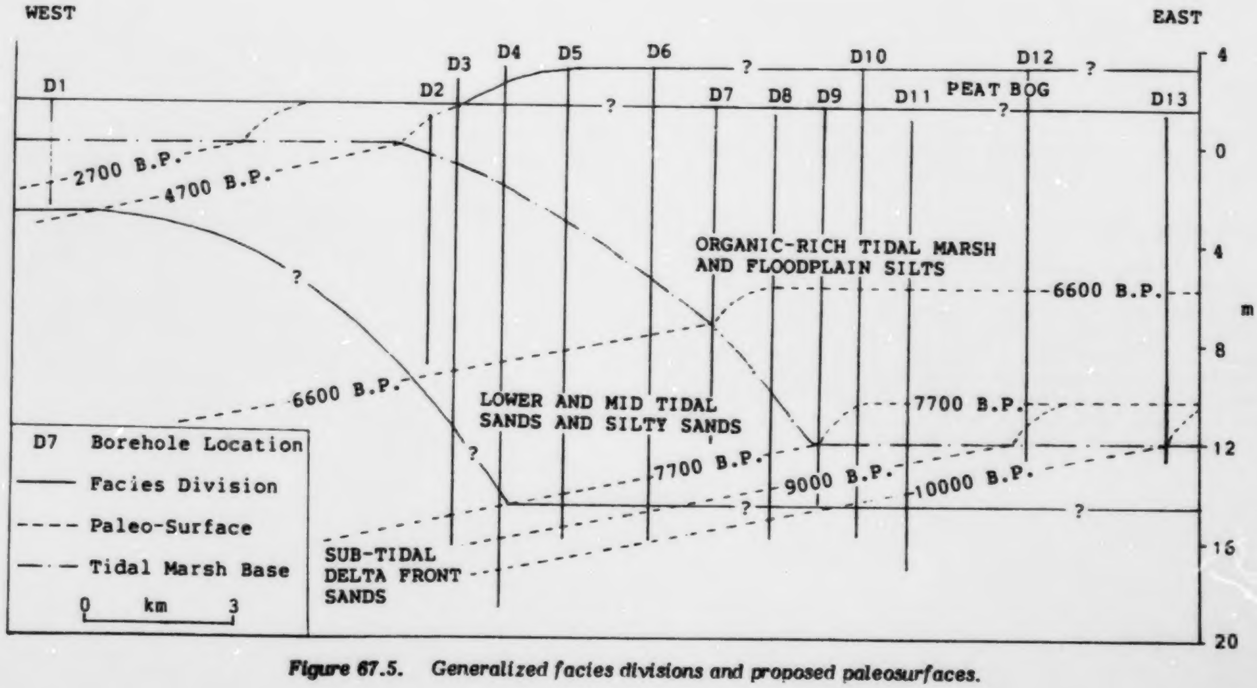

Figure 67.5. Generalized facies divisions and proposed paleosurfaces.

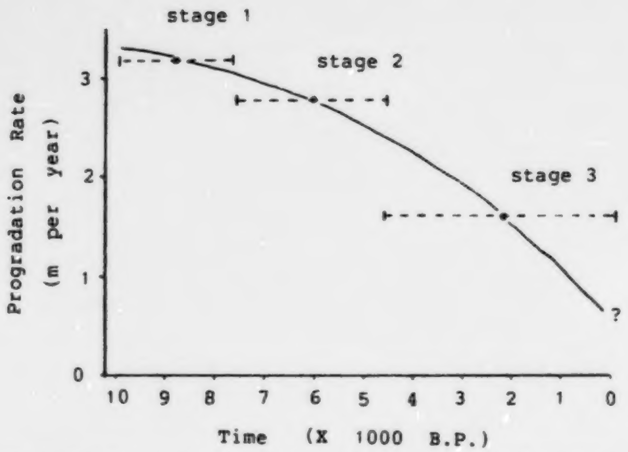

Figure 67.6. *A model of Lulu Island's progradation rates during the Holocene. Dashed line indicates time period associated with each stage of Lulu Island's growth.*

4. The model of Lulu Island's rate of growth into the Strait of Georgia, based on the westward migration of the leading edge of the tidal-marsh zone, is consistent with the concept of a progressive reduction of the Fraser Delta's progradation rate.

5. That vertical accretion of facies may occur in response to a rise in sea level, has important implications for other research concerned with coastal depositional environments. In many floodplain, estuarine and deltaic settings, the identification of vertically accreted facies may yield valuable information on the timing, magnitude and frequency of sea level changes.

Future work

Samples of organic matter collected from various depths within the organic-rich silt facies underlying borehole D10 have been submitted for radiocarbon dating. These dates will provide a more precise chronology of the development of Lulu Island. Detailed palynological analysis of this zone is also underway to provide a more accurate interpretation of depositional environments. Efforts are also progressing to identify the source and age of the tephra layer in borehole D10. It is planned to expand the area of investigation in the 1986 field season by additional drilling on Lulu Island and on the adjoining Fraser River floodplain.

Acknowledgments

The author is grateful to M.C. Roberts (Simon Fraser University) for supervision of the Ph.D. research, to John Luternauer and John Clague (Geological Survey of Canada) for critically reviewing an earlier version of this paper, and Bryan Kern (Ministry of Transporation and Highways) for provision of borehole logs. Field research was funded by an E.M.R. research grant awarded to M.C. Roberts and a Geological Society of America research grant awarded to the author and G.S.C. Project 790006.

References

Clague, J.J. and Luternauer, J.L.
1983: Late Quaternary geology of southwestern British Columbia; Geological Association of Canada, Mineralogical Association of Canada and Canadian Geophysical Union Joint Annual Meeting (1983), Field Excursion Guidebook, Field Trip 6, 99 p.

Clague, J.J., Luternauer, J.L., and Hebda, R.J.
1983: Sedimentary environments and post glacial history of the Fraser Delta and lower Fraser Valley, British Columbia; Canadian Journal of Earth Sciences, v. 20, p. 1314-1326.

Clague, J.J., Harper, J.R., Hebda, R.J., and Howes, D.E.
1982: Late Quaternary sea levels and crustal movements, coastal British Columbia; Canadian Journal of Earth Sciences, v. 19, p. 597-618.

Hutchinson, I.
1982: Vegetation-environment relations in a brackish marsh, Lulu Island, Richmond, B.C.; Canadian Journal of Botany, v. 60, p. 452-462.

Johnson, W.A.
1921: Sedimentation of the Fraser River; Geological Survey of Canada, Memoir 125, 46 p.

Luternauer, J.L.
1980: Genesis of morphological features on the western delta front of the Fraser River, British Columbia – status of knowledge; in Coastlines of Canada, ed. S.B. McCann; Geological Survey of Canada, Paper 80-10, p. 381-396.

Luternauer, J.L. and Murray, J.W.
1973: Sedimentation on the western delta front of the Fraser River, British Columbia; Canadian Journal of Earth Sciences, v. 10, p. 1642-1663.

Mathews, W.H. and Shepard, F.P.
1962: Sedimentation of Fraser River Delta, British Columbia (includes discussion by K. Terzaghi); American Association of Petroleum Geologists, Bulletin, v. 46, p. 1416-1443.

Styan, W.B.
1981: The sedimentology, petrography and geochemistry of some Fraser Delta peat deposits; unpublished M.Sc. thesis, University of British Columbia, Vancouver, B.C., 188 p.

Styan, W.B. and Bustin, R.M.
1984: Sedimentology of Fraser River peat deposits: a modern analogue for some deltaic coals; International Association of Sedimentologists, Special Publication, v. 7, p. 241-271.

Sediment transport during the 1985 freshet in the outer main channel of the Fraser River estuary, British Columbia

NSERC Operating Grant 677950 and Project 790006

R.A. Kostaschuk[1], J.L. Luternauer[2], and T.H. Millard[1]
Cordilleran Geology Division, Vancouver

Kostaschuk, R.A., Luternauer, J.L., and Millard T.H., Sediment transport during the 1985 freshet in the outer Main Channel of the Fraser River estuary, British Columbia; in Current Research, Part A, Geological Survey of Canada, Paper 86-1A, p. 565-570, 1986.

Abstract

A two year program to measure the bed and suspended load of the outer reach of the Main Channel distributary of the Fraser River Delta was initiated in 1985 as a first step towards defining the sediment budget of the delta front. Preliminary results indicate that suspended load increases with increasing river discharge and decreasing tidal elevation. A comparison of suspended load with a bed-load estimate based on bathymetric surveys indicates most sediment in the channel is transported in suspension. Future studies will more thoroughly examine transport under non-freshet conditions and vertical distribution in the water column of sand size particles which are essential to the maintenance of the adjacent, environmentally important, tidal flats.

Résumé

En 1985, un programme de deux ans a été entrepris en vue de mesurer le charge de fond et la charge en suspension du tronçon inférieur du chenal principal du delta du fleuve Fraser dans un premier effort pour établir le bilan des sédiments du front du delta. Les résultats préliminaires indiquent que l'augmentation de la charge en suspension est fonction de l'accroissement du débit du fleuve et de la diminution de la hauteur de la marée. Une comparaison entre la charge en suspension et une estimation de la charge de fond selon des levés bathymétriques indiquent que la majeure partie des sédiments dans le chenal est transportée en suspension. D'autres études traiteront en détail du transport en l'absence de veines d'eau douce et de la répartition granulométrique verticale du sable dans la colonne d'eau, facteurs qui sont essentiels au maintien des zones adjacentes, importantes pour l'environnement, soit les extrans.

[1] Department of Geography, University of British Columbia, Vancouver, B.C. V6T 1W5
[2] Pacific Geoscience Centre, Sidney, British Columbia V8L 4B2

Introduction

In a recent comprehensive review of sediment survey programs on the lower Fraser River for Environment Canada, Keilerhals (1984) suggested that the most pressing requirement is a detailed sediment budget of the delta because of the importance of this information to local environmental assessments. In response to this recommendation, a two-year study was intiated in 1985 to examine the patterns and mechanisms of sedimentation in the outer Main Channel between Steveston and Sand Heads (Fig. 68.1). This site was selected because it has been estimated that the Main Channel carries 80% of river discharge and 90% of the sediment load (Tywoniuk, 1973) and because measurements in this area will contribute to the interpretations of the sedimentary processes on the adjacent, environmentally important, tidal flats.

This report describes the first season's activities and offers a preliminary interpretation of the results. Final results of this study will have application to a variety of concerns such as the prediction of dredging requirements, design of self scouring channels and stabilization of the tidal flats and foreshore marshes.

Methods

Data were collected during three one-week cruises (April 22-28, May 20-26, and June 10-16) on the CSS **Richardson.** Suspended sediment sampling was carried out over a rising or falling tide as the vessel was anchored at stations at Steveston and Sand Heads (Fig. 68.2). Vertical profiles were taken at hourly intervals of suspended sediment concentration (using a pump sampler, P-61 sampler and pre-weighed 0.45 m filters), water temperature and salinity

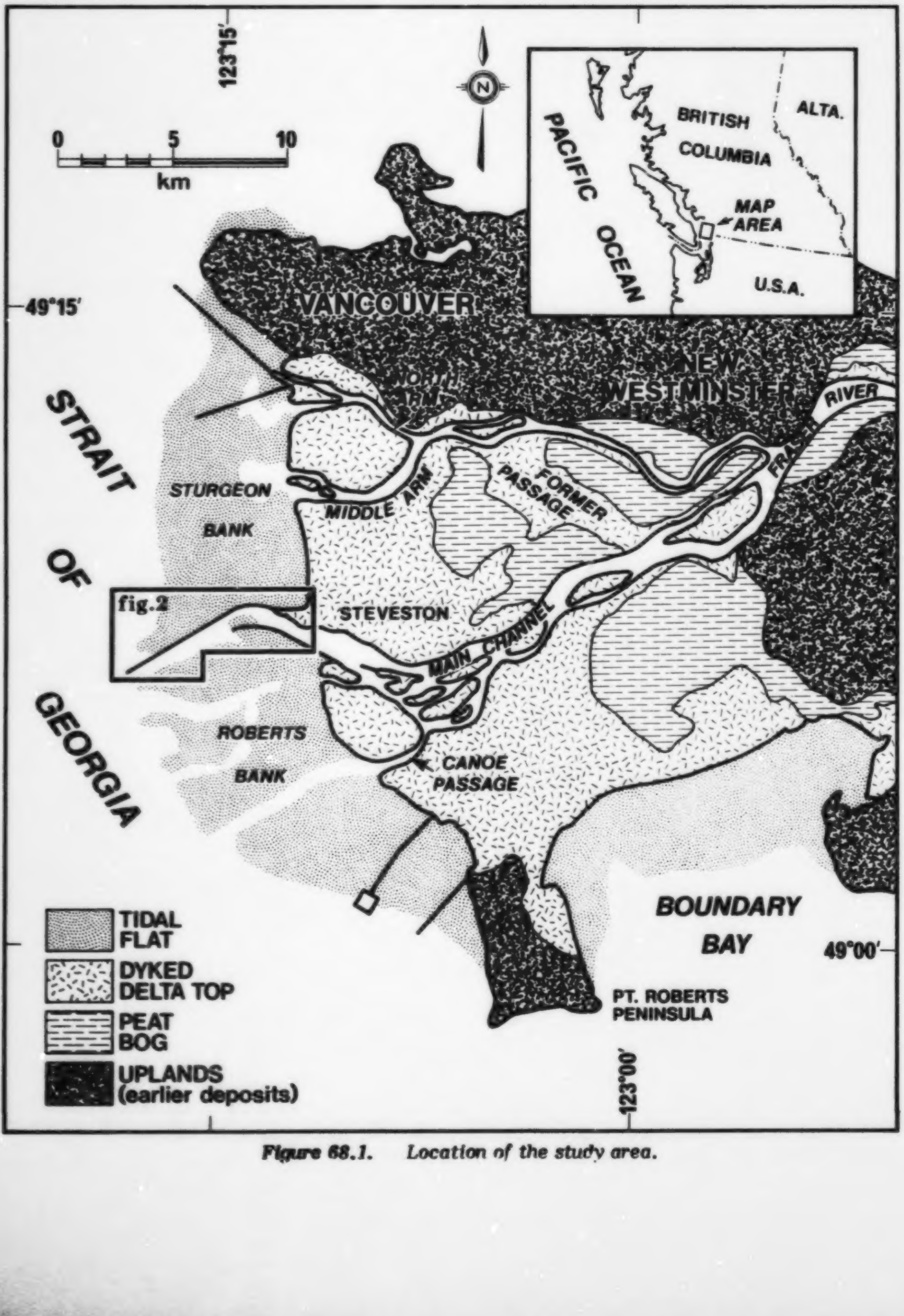

Figure 68.1. Location of the study area.

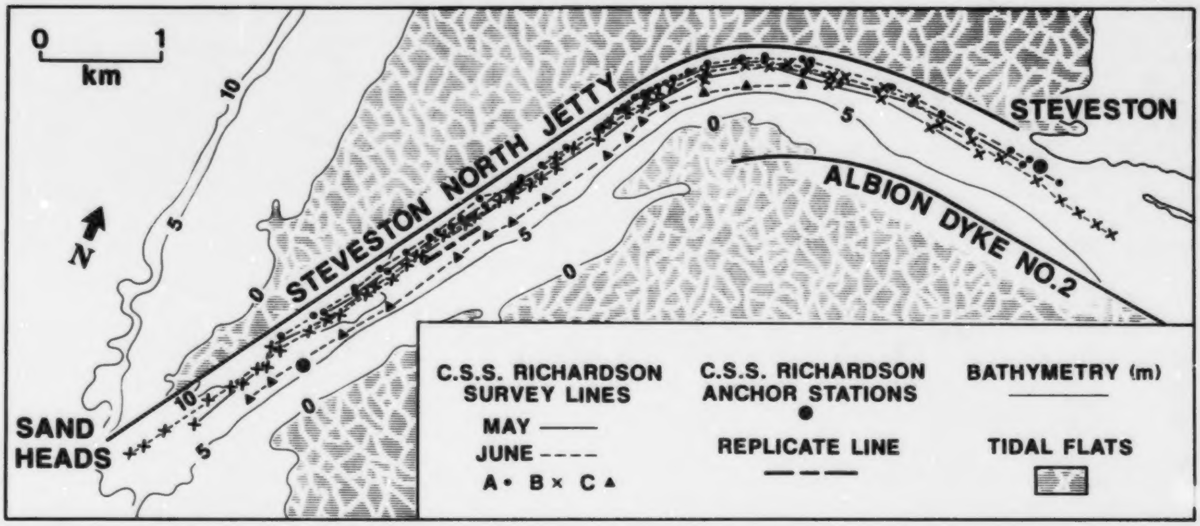

Figure 68.2. Survey lines and anchor stations in the study area. CSS **Richardson** *survey lines A, B and C were in the northern, central and southern sides of the channel, respectively. Bathymetry adapted from Canadian Hydrographic Service chart 3490 (Aug. 17, 1984).*

(using a YSI Model 33 S-C-T meter) and current speed and direction (using an N.B.A. Controls DNC3 velocity meter). The instrument array is shown in Figure 68.3.

For a variety of reasons (e.g. Gray, 1970) bed load transport is much more difficult to quantify than suspended load. For large rivers, such as the Fraser, the bed load can be estimated from repeated bathymetric surveys (Engel and Lau, 1980). Bedform configuration was monitored during the May and June cruises using a 100 kHz Klein Hydroscan sidescan sonar and shipboard echosounder, with positions determined using a Trisponder navigation system (lines A,B,C in Fig. 68.2). Migration rates of bedforms along a 500 m length of channel (Fig. 68.2) were determined from replicate echosounding profiles obtained from a small boat on June 19 and 20. Navigation during this procedure was accomplished using numerous shipping aids present in and along the channel.

Results

Suspended load

Water column characteristics at the anchored stations reflect the effects of fluctuations in river discharge and tidal stage. During April and May cruises instrument profiles were taken during large tidal ranges (2.4-3.1 m: Table 68.1). During both months a prominent salt wedge is apparent at Steveston and Sand Heads at high tide (Fig. 68.4). The upper portions of the water column are fresh, current speeds low and downstream directed, and sediment concentrations are low. Strong pycnoclines are present beneath the surface layers where salinity increases and, in this zone, the current begins to reverse direction and decrease in strength and sediment concentrations decline. Underlying this is the salt wedge where salinity is high (25-27‰), currents are generally low and upstream directed, and sediment concentrations are very low. During the June cruise the tidal range was much lower (0.6-0.9 m: Table 68.1) and the salt wedge, while present at Sand Heads, did not migrate to Steveston where the water column was fresh even at high tide.

As the tide ebbs, the salt wedge is flushed out of the channel and at low tide the entire water column becomes fresh and all currents are directed downstream (Fig. 68.4).

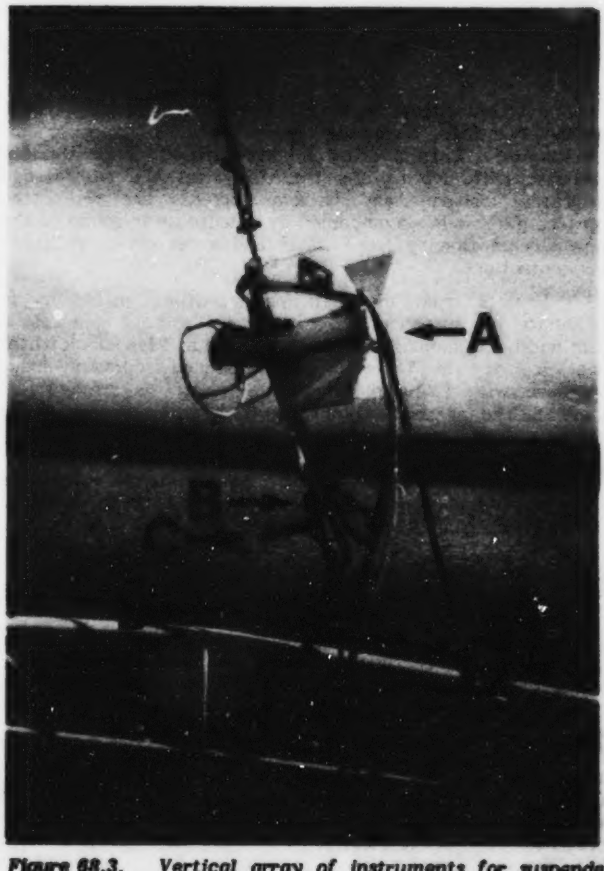

Figure 68.3. *Vertical array of instruments for suspended load determinations. A: N.B.A. Controls DNC 3 velocity meter; B: Yellow Springs Instrument Co. Model 33 S-C-T meter; C: pump sampler; D: P-61 river sampler.*

Table 68.1. Suspended sediment transport rates per unit width of channel at high and low slack water, for anchor stations at Steveston and Sand Heads. River discharge values are from Water Survey of Canada records of Agassiz and tidal values are from mathematical model predictions by Ages and Woollard (1985) calibrated to Hope discharges. Agassiz is 133 km upstream of Sand Heads, Hope is 160 km.

STATION	DATE	RIVER DISCHARGE ($m^3 s^{-1}$)	TIDAL HEIGHT (m)	SUSPENDED SEDIMENT TRANSPORT ($kg s^{-1}$)
STEVESTON	APRIL 25	2450	3.0	0.15
			0.6	1.83
	MAY 23	7830	3.2	0.47
			0.8	9.43
	JUNE 12	7790	2.6	0.72
			1.7	1.36
SAND HEADS	MAY 22	7160	4.0	0.26
			1.0	13.37
	JUNE 11	8170	3.1	0.43
			2.5	1.41

Sediment concentrations and downstream velocities increase as the tide falls, becoming highest 1-2 hours prior to low slack water. When the flow is non-stratified, concentrations increase with depth. As the tide rises the salt wedge migrates upstream and bottom currents are redirected upstream. This is accompanied by a decrease in speed of the downstream flowing fresh water and a decline in sediment concentrations.

Results from the instrument profiles enable us to calculate the suspended load in the water column across a 1 m width of channel (examples for high and low slack water are displayed in Table 68.1). Suspended sediment loads increase with rising discharge and display a strong tidal control. The larger the tidal range the greater the difference between high and low slack water loads during high discharges (May and June). Transport rates tend to be lower at Steveston than Sand Heads. However, these values are from single anchored stations and may not be representative of the entire channel cross-section.

Bed load

In April, when discharges were low, no bedforms were present on the channel floor. The May and June surveys, taken when discharges were much higher (Table 68.1), indicated that large bedforms had developed across the entire channel bed in the study area. Two distinct bedform types were apparent: very large, asymmetric, downstream oriented features with heights up to 4 m and wavelengths of 60 m and smaller, more symmetric forms of less than 0.5 m heights and 6 m wavelengths (Fig. 68.5). The smaller forms were often superimposed on the upper stoss sides (backs) of the larger features. The lower stoss sides of the large bedforms often lack the small waves and in some cases the large bedforms migrate up the backs of one another. The heights and wavelengths of large bedforms generally decrease in an upstream direction (Sand Heads to Steveston).

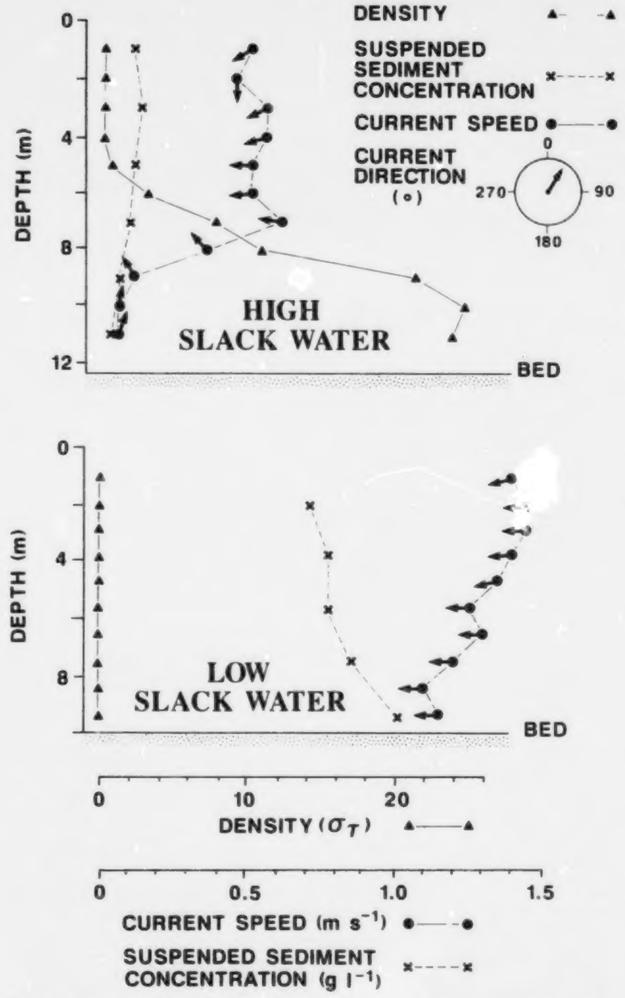

Figure 68.4. High and low slack water density (σ_T) suspended sediment concentration (mg l^{-1}) and current speed (m s^{-1}) and direction (o) for May 23 at the Steveston anchor station. The downstream current direction is 270°.

The lateral extent and form (planform geometry) of the large bedforms is difficult to assess because of generally poor sidescan resolution. Sonographs indicate, however, that the crests are moderately sinuous and continuous for distances in excess of 75 m. Recent, closely spaced, echo-sounding surveys by Public Works Canada suggest that some of the largest features are continuous for hundreds of metres (R. Richardson, personal communication, 1985). The small bedforms have irregular, often lunate crests with lateral extents of less than 20 m.

The ability to measure migration rates of bedforms depends on the reproducibility of survey lines and recognition of features from one survey period to the next. Reproducibility was tested by running each 500 m long survey profile a number of times in rapid succession (a few minutes apart). In all cases profiles were nearly identical, with a mean variation of 3 m in bedform positions. Migration rates were determined for the test site by comparing the profiles taken on June 19 and June 20 (Fig. 68.6), a period when discharges were waning (7260-6930 $m^3 s^{-1}$) and the tidal

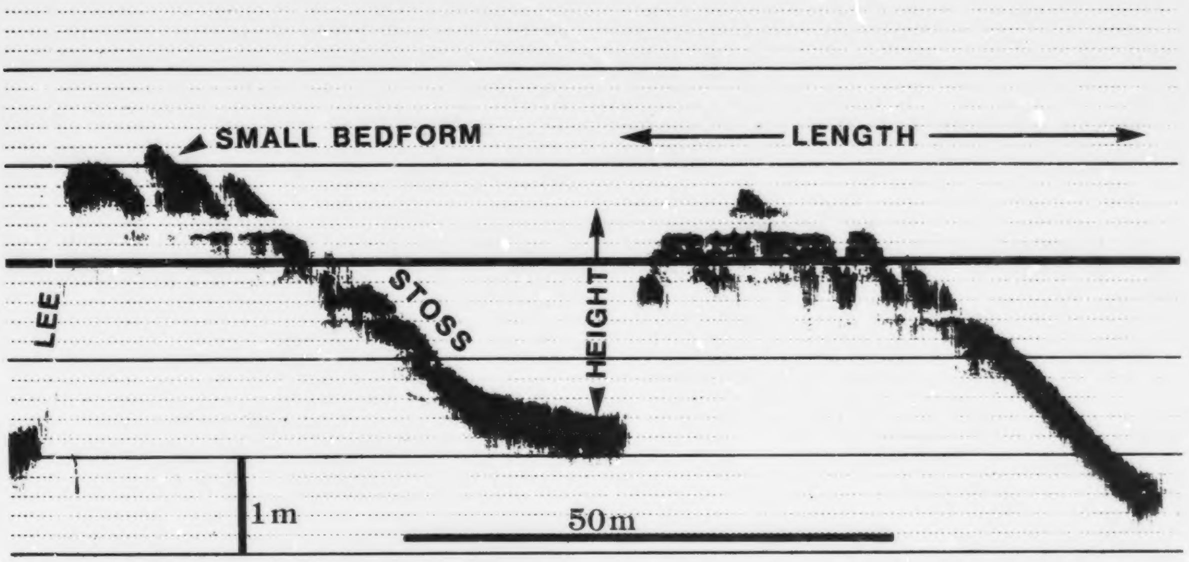

Figure 68.5. *Large, downstream-oriented asymmetric bedforms with smaller features superimposed on the stoss sides.*

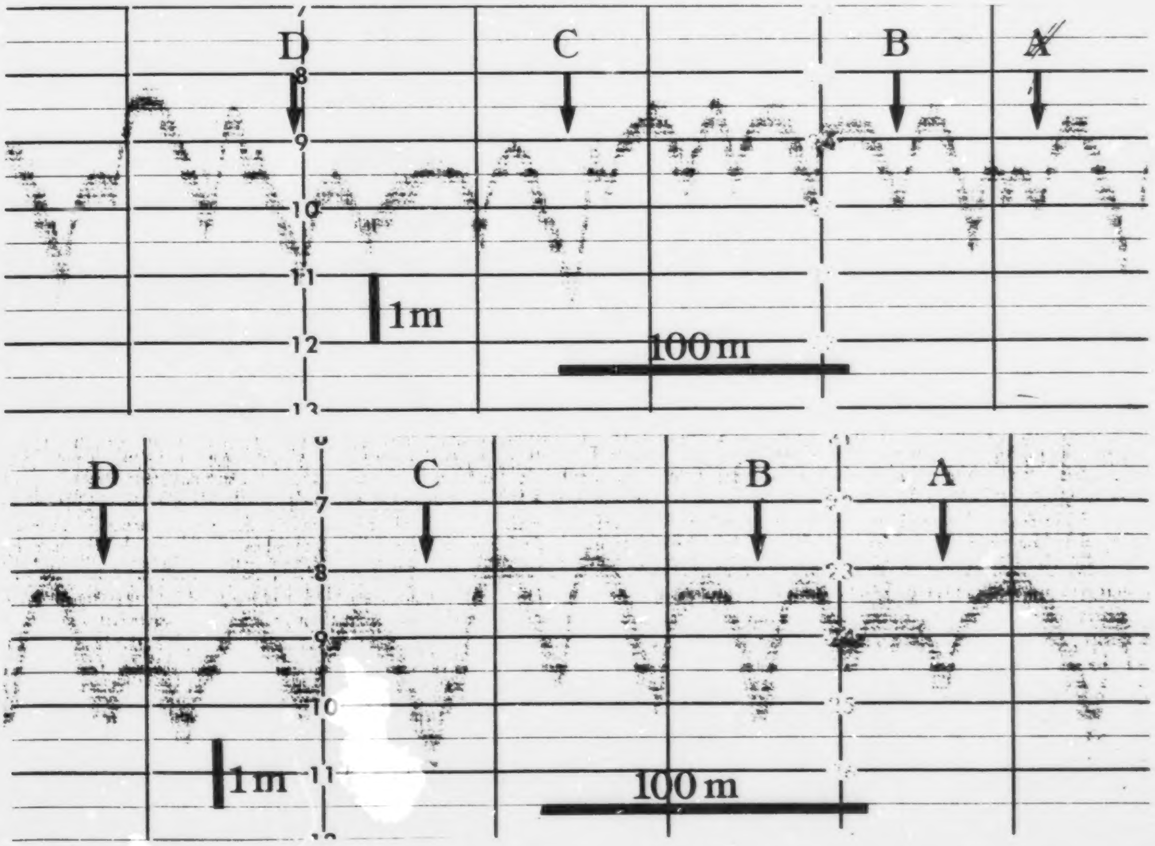

Figure 68.6. *Replicate echosounding profiles (Fig. 68.2) for June 19 (1323-1325) and June 20 (1320-1322). The "dirty" nature of the June 20 record reflects high concentrations of sediment in suspension.*

range was extreme (3.6 m). Some changes in bedform shape were evident between the two days, but specific features are easily identifiable from one profile to the other. Bedform migration rates were determined by tracing the downstream movements of 4 locations on the profiles (A-D). Movement rates varied between 27 and 38 m over the 23 hour 57 minute period, with an average migration of 31 $m \cdot a^{-1}$.

To determine the mean rate of bed load for the June 19-20 period, it is necessary to determine a representative volume for the bedforms. Assuming an idealized triangular shape for the bedform (Willis and Kennedy, 1975) and using a mean bedform height of 1.39 m, a mean length of 31.25 m, a migration rate of 31 $m \cdot a^{-1}$ and a saturated bulk density of 2000 $kg\text{-}m^3$ for the bed sediment (loose sand: Selby, 1982) at a transport rate of 0.56 $kg \cdot s^{-1}$ per 1 m unit width of channel is indicated for the 24 hour period surveyed. Because of the extreme tidal range, this would likely be the largest transport rate for this discharge.

Discussion

Although different sampling sites and procedures were used and tidal conditions differed, it is possible to make some general comparisons between our suspended load results for the 1985 freshet and those of Milliman (1980) for 1976 also determined during a freshet period. We noted similar discharge and tidal controls on suspended load, i.e. as discharge and tidal range increase so does the transport of material in suspension. Milliman (1980) noted that suspended concentrations at low tide were much higher at Sand Heads than Steveston and he drew the reasonable conclusion that this indicated bottom sediment was being resuspended and transported seaward. We also found higher transport rates at Sand Heads, although as suggested earlier, such comparisons must be viewed with caution.

There have been no prior attempts to estimate bed load in this portion of the estuary, although Pretious and Blench (1951) provide detailed freshet bedform geometry and migration rate information from Ladner reach upsteam of Steveston (Fig. 68.1). They found that when discharge at Hope was less than 9900 $m^3s{-}^1$, and there was a large tidal range, bedforms were in the order of 0.6 m high and 7 to 17 m long with migration rates of 7-17 $m \cdot a^{-1}$. Our measurements for June 19-20 indicate that during the 1985 freshet, when discharge was approximately 7000 m^3s^{-1} and the tidal range also was large, bedforms were larger and migrated more quickly. Pretious and Blench (1951) found that when discharge exceeded 9900 m^3s^{-1}, maximum bedform height, length and migration rates increased to 4.5 m, 150 m and 75 $m \cdot a^{-1}$ respectively. These are much higher value than those noted at Sand Heads during 1985 and suggest that bedforms in the Sand Heads reach might increase in both size and celerity as discharge increases. Bed load would increase accordingly.

Comparison of the bed load for June 19-20 with suspended loads earlier in the freshet (Table 68.1) shows that bed load is comparable to the high slack water suspended load. This suggests that most sediment in the estuary is transported in suspension, as is the case for the Fraser in general (Tywoniuk, 1973).

Although the 1985 investigation provides useful information on the logistics of data collection and synoptic details of sedimentation in the Steveston – Sand Heads reach, a more detailed, systematic investigation will be undertaken in 1986.

Acknowledgments

The authors wish to thank the officers and crew of the **CSS Richardson**, D. Duggan, J. Desloges, P. Matsushita and R. Lane for their able assistance, and E.J. Hickin and the Sediment Survey Office in New Westminster, B.C. (Environment Canada) for the loan of equipment. Special thanks are due M.A. Church for logistical (NSERC Operating Grant 677950) and technical support.

References

Ages, A. and Woollard, A.L.
1985: Tidal predictions, Fraser River estuary; Institute of Ocean Sciences, Sidney, B.C.

Engel, P. and Lau, Y.L.
1980: Computation of bed-load using bathymetric data; American Society of Civil Engineers Journal of the Hydraulics Division, HY3, p. 369-380.

Gray, D.M.
1970: Handbook on the Principles of Hydrology; National Research Council of Canada, Ottawa, p. 11.1-11.24.

Kellerhals, R.
1984: Review of sediment survey program, Lower Fraser River; Sediment Survey Section, Water Survey of Canada, Environment Canada, Ottawa, 51 p.

Milliman, J.O.
1980: Sedimentation in the Fraser River and its estuary, B.C.; Estuarine and Coastal Marine Science, v. 10, p. 609-633.

Pretious, E.S. and Blench, T.
1951: Final report on special observations of bed movement in Lower Fraser River at Ladner Beach during 1950 freshet, Canada; National Research Council, Fraser River Model Project.

Selby, M.J.
1982: Hillslope Materials and Processes; Oxford University Press, Oxford, 264 p.

Tywoniuk, N.
1973: Sediment budget of the Lower Fraser River in Canada; National Research Council, 9th Hydrology Symposium, University of Alberta, Edmonton, 1973, Proceedings, p. 624-638.

Willis, J.C. and Kennedy, J.F.
1975: Sediment discharge of alluvial streams calculated from bed form statistics; IIHR Report No. 202, Iowa Institute of Hydraulic Research, The University of Iowa, Iowa City, Iowa.

Airborne definition of suspended surface sediment and intertidal environments in the Fraser River plume, British Columbia

Project 790006

Arthur Roberts[1] and Jeffrey Liedtke[1]
Cordilleran Geology Division, Sidney, B.C.

Roberts, A. and Liedtke, J., Airborne definition of suspended surface sediment and intertidal environments in the Fraser River plume, British Columbia; in Current Research, Part A, Geological Survey of Canada, Paper 86-1A, p. 571-582, 1986.

Abstract

Most water-quality-related remote-sensing research has used satellite multispectral scanner imagery. Although these studies have successfully identified areas of sediment concentration they have been limited by scale and atmospheric problems. Airborne colour and colour infrared photography and multispectral video imagery were compared with satellite imagery of the Fraser River plume in the Strait of Georgia. Both the aerial photography and video imagery were capable of providing superior identification of surface sediment concentrations as well as littoral environmental targets (vegetation, soil particle size and near shore bottom reflectance).

These results are from preliminary stages of a more detailed research project which will include: (1) quantification of surface sediment concentrations from aerial photography and multispectral video imagery; (2) comparisons with Landsat 5 Thematic Mapper data; (3) corrections for atmospheric problems, and, corrections for specular reflection from sunlight.

Résumé

La plupart des travaux de recherche par télédétection sur la qualité de l'eau ont été faits à l'aide d'images produites par balayeurs multispectraux montés à bord de satellites. Bien que ces études aient bien identifié des zones de concentration de sédiments, elles ont été limitées par des problèmes d'échelle et des problèmes atmosphériques. Des photos aériennes en couleurs et infrarouges en couleurs ainsi que des images obtenues par magnétoscope multi-spectral ont été comparées à des images prises par satellite du panache du fleuve Fraser dans le détroit de Georgie. Les photos aériennes et les images magnétoscopignes ont su fournir une bien meilleure identification des concentrations de sédiments superficiels et des cibles environmentales littorales (végétation, granulométrie des particules de sol et réflectance du fond littoral).

Ces résultats proviennent des premières étapes d'un projet de recherche plus détaillé qui comprendra (1) la quantification des concentrations de sédiments superficiels à partir de photographies aériennes et d'images obtenues par magnétoscope multi-spectral; (2) une comparaison des données avec les données fournies par l'appareil de cartographie thématique du Landsat 5; (3) les corrections à apporter pour résoudre les problèmes présentés par les conditions atmosphériques et la réflexion spéculaire du soleil.

[1] Department of Geography, Simon Fraser University, Burnaby, British Columbia

Introduction

Most remote sensing water quality research has utilized multispectral satellite imagery and relatively large water bodies. As a result some general principles regarding reflectivity and multiband analytical procedures have been described. These mainly involved the utility of near infrared reflectance and spectral band ratioing procedures to determine some aspects of sediment loads and floral concentrations. Principal limitations have involved spatial resolution and atmospheric attenuation (Bowker et al., 1975; Aranuvachapun and LeBlond, 1981; Carpenter and Carpenter, 1983; Amos and Topliss, 1985; Lodwick and Harrington, 1985).

Clear water bodies absorb most incident energy in the reflected infrared (Fig. 69.1). Minor infrared reflectance is caused by mineral particles and chlorophyll components on or near the water surface. In general, water has a distinctly lower infrared reflectance than either vegetation or soil. Energy-matter interactions differ in the visible portion of the electromagnetic spectrum and transmittance for natural waters decreases as the level of turbidity increases (Fig. 69.2). In addition, the peak wavelengths for maximum transmittance/reflectance shift towards longer (red) wavelengths. The magnitude of this shift is dependent on the size, quantity and composition of the suspended particles.

Concentrations of chlorophyll (e.g. eelgrass and algae) in water affect the spectral response of a water body. As chlorophyll concentrations increase there is a corresponding increase in reflection from the green and infrared (if the chlorophyll concentrations are near the surface) spectral regions and a decrease in reflection from the blue spectral region. This can be an important indicator of littoral and submerged vegetation as well as primary productivity and eutrophication.

Johnson and Harriss (1980), Geraci et al. (1981) and Colwell (1983) reviewed relevant literature suggesting that suspended sediment and phytoplankton particles can be detected using optical techniques. Suspended particles affect general water clarity through scattering and absorption of incident energy. Different types of inorganic particulates, with various size and shape distributions, yield different absorption and scattering coefficients (Gupta and Ghovanlou, 1978). Consequently the relative and absolute strengths of the reflected residual radiance at different wavelengths can be used to determine the concentrations and some physical characteristics of the suspended material. Clear water reflects mainly blue light (450-500 nm); with the introduction of fine suspended particles this reflectance peak shifts to the blue-green (490-550 nm). As the particle size increases the colour of the peak reflectance will approach that of the material which forms the particle. As most sediment loads normally consist of heterogeneous particles

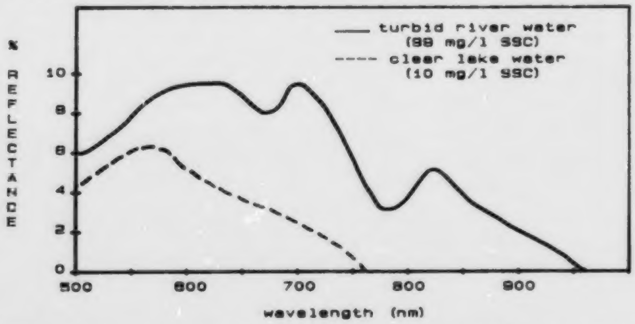

Figure 69.1. Spectral reflectance characteristics of turbid and clear water in the 500-1000 nm wavelength interval (after Swain and Davis, 1978).

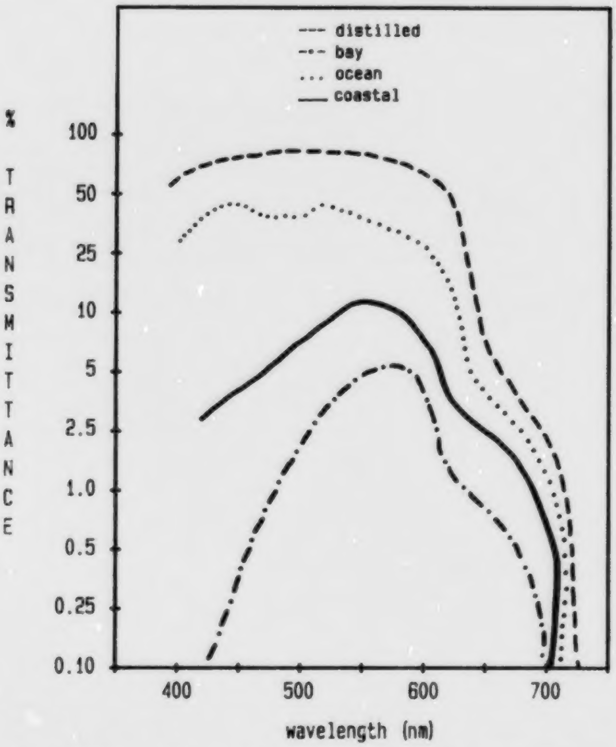

Figure 69.2. Spectral transmittance through 10 m of water with different turbidity levels (after Swain and Davis, 1978).

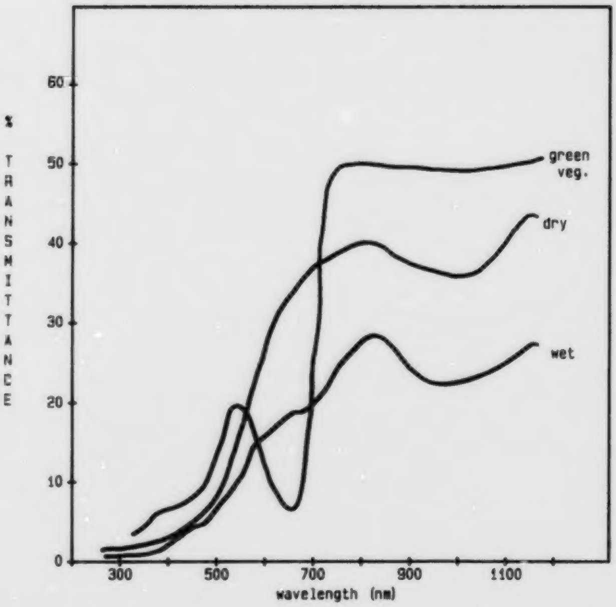

Figure 69.3. Reflection of wet and dry soil in relation to the response from healthy green vegetation (after Swain and Davis, 1978).

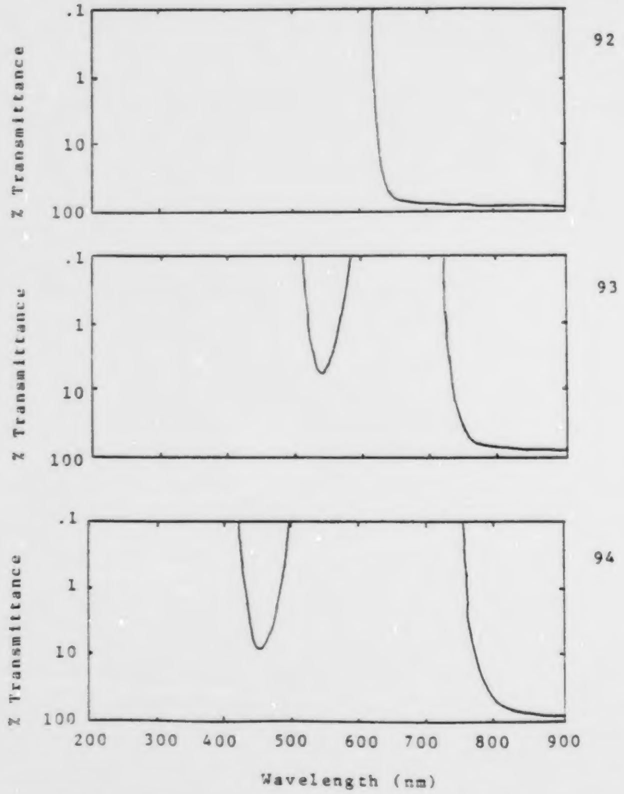

Figure 69.4. Transmittance by wavelength for Kodak Wratten red (92), green (93) and blue (94) filters (after Eastman Kodak Company, 1972).

and single spectral band measurements have limited utility for discerning concentrations and physical properties, multispectral analytical methods are required for most analyses.

Detection and measurement of suspended sediment has been successfully demonstrated in individual studies utilizing airborne (Johnson, 1975, 1978) and satellite (Bowker et al., 1975; Bowker and Witte, 1977; Alfoldi and Munday, 1978; Amos and Alfoldi, 1979; Aranuvachapun and LeBlond, 1981; Amos and Topliss, 1985; Lodwick and Harrington, 1985) multispectral scanners. Some general models have been developed to estimate sediment loads under a wide range of conditions and phenomena (Holyer, 1978; Munday et al., 1979). However, these models have been developed for high altitude platforms, or multi-date data comparisons where atmospheric alteration (noise) is an important term in the algorithms and is difficult to quantify. Correction for atmospheric scatter can be simplified, or eliminated, by the use of low altitude multispectral imagery (Miller et al., 1977). Low altitude aerial survey using multispectral photography and video imagery provides high spatial and spectral resolution, low noise, and intensive area coverage. The use of aircraft also allows the versatility of multi-date data to be collected (for temporal parameters) under a variety of weather conditions that would not permit satellite imaging.

By analyzing the spectral characteristics of a particular water body, reflectance (and attenuation) peaks can be identified and isolated by relatively narrow band filtration (to optimize information content of the reflected signal).

Table 69.1. Spectral regions and filter combinations used on the four airborne video cameras

Colour	Wavelength Band (nm)	Filter Combination
Blue	420-495	94/301 A
Green	510-585	93/301 A
Red	620-740	92/301 A
Infrared	735-900	87

The important spectral regions are:

1. 460 nm, where chlorophyll absorption is near maximum;
2. 560 nm, where chlorophyll absorption is low, and water penetration is optimum;
3. 670 nm, where reflection from suspended sediment is high, and chlorophyll absorption is high;
4. 750-800 nm, where water absorption is high, and reflection from organic and inorganic suspended sediment is evident.

Most soil moisture, remote sensing investigations use reflected electromagnetic energy from the soil surface. Visible and near-infrared reflectance is sensitive to differences in soil and plant surfaces (Condit, 1970). Albedo varies with wavelength, soil texture, surface roughness, organic content, mineral content, moisture, and illumination-geometry differences. Reflectance or density ratios obtained from multiple spectral bands can be used to delineate

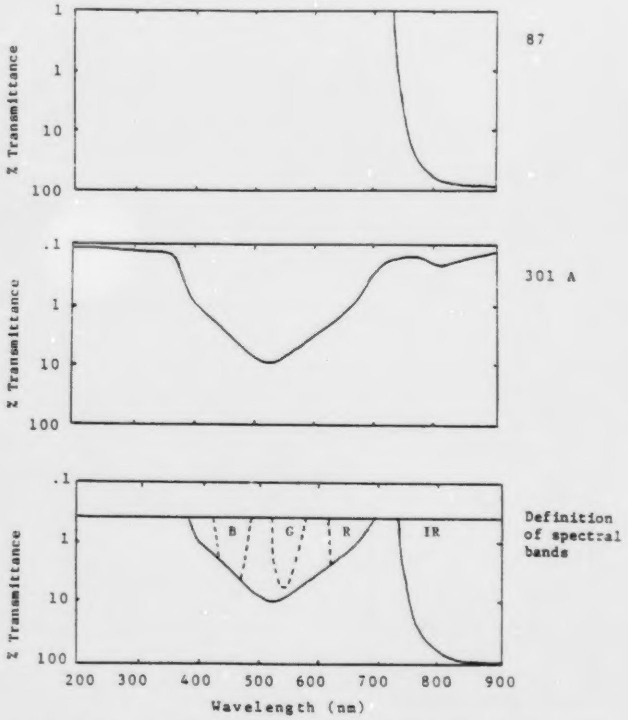

Figure 69.5. Transmittance by wavelength for Kodak infrared (Wratten 87) and infrared cutoff (301A) filters and illustration of the definition of the four bands (blue, green, red and infrared) resulting from various filter combinations (after Eastman Kodak Company, 1972).

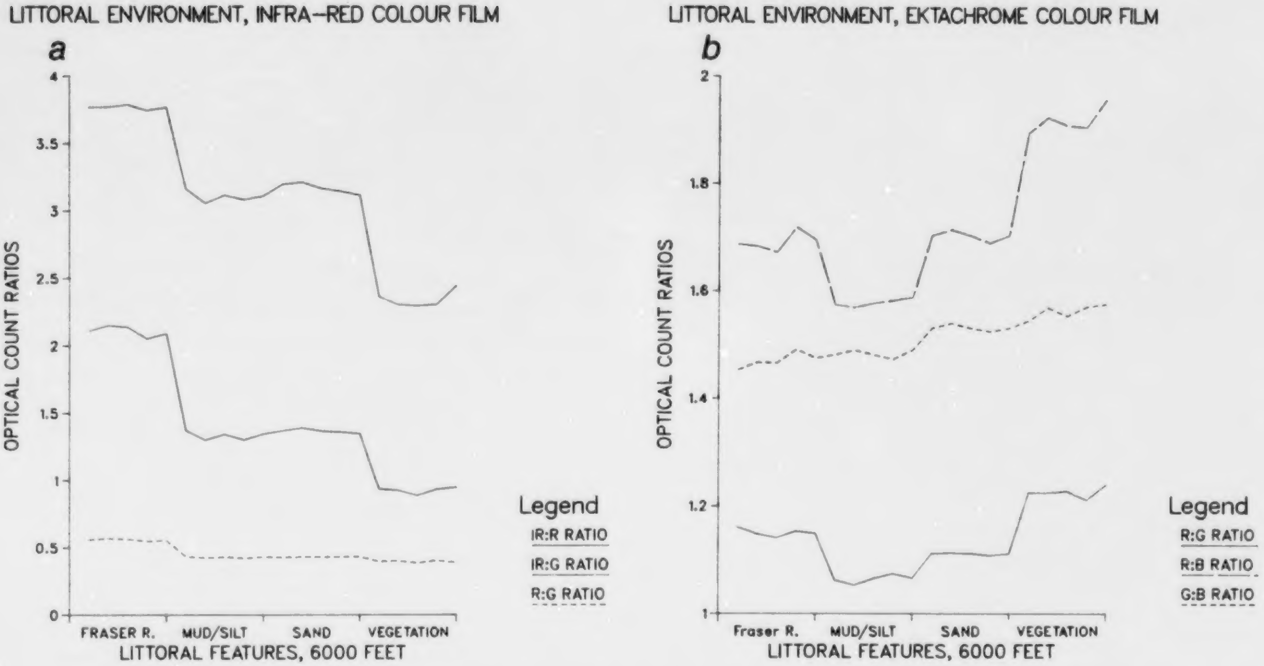

Figure 69.6. *Results of ratioed density readings (densitometer optical count ratios) from infrared colour (6a) and colour (6b) film of four target conditions within the littoral environment. At each location the infrared optical counts were divided by the red (IR:R ratio) and green (IR:G ratio) optical counts, and the red optical counts were divided by the green (R:G ratio) optical counts.*

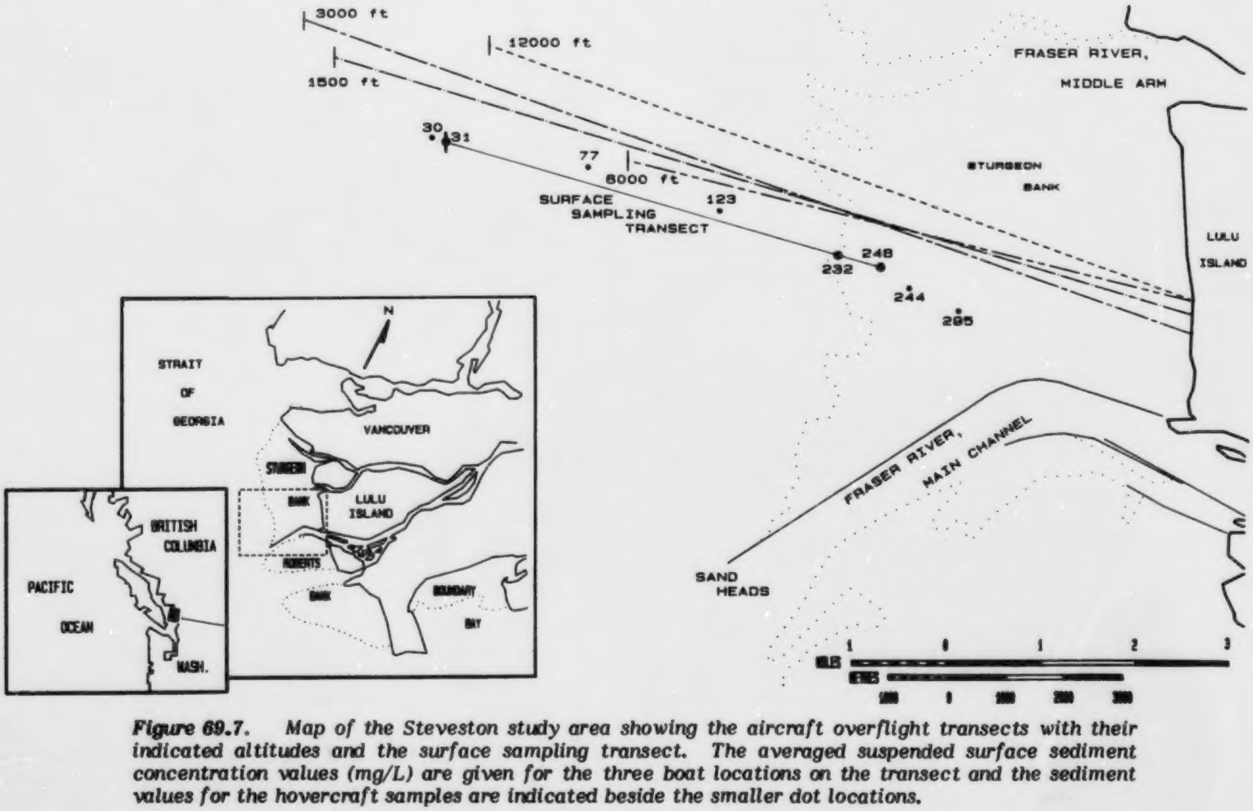

Figure 69.7. *Map of the Steveston study area showing the aircraft overflight transects with their indicated altitudes and the surface sampling transect. The averaged suspended surface sediment concentration values (mg/L) are given for the three boat locations on the transect and the sediment values for the hovercraft samples are indicated beside the smaller dot locations.*

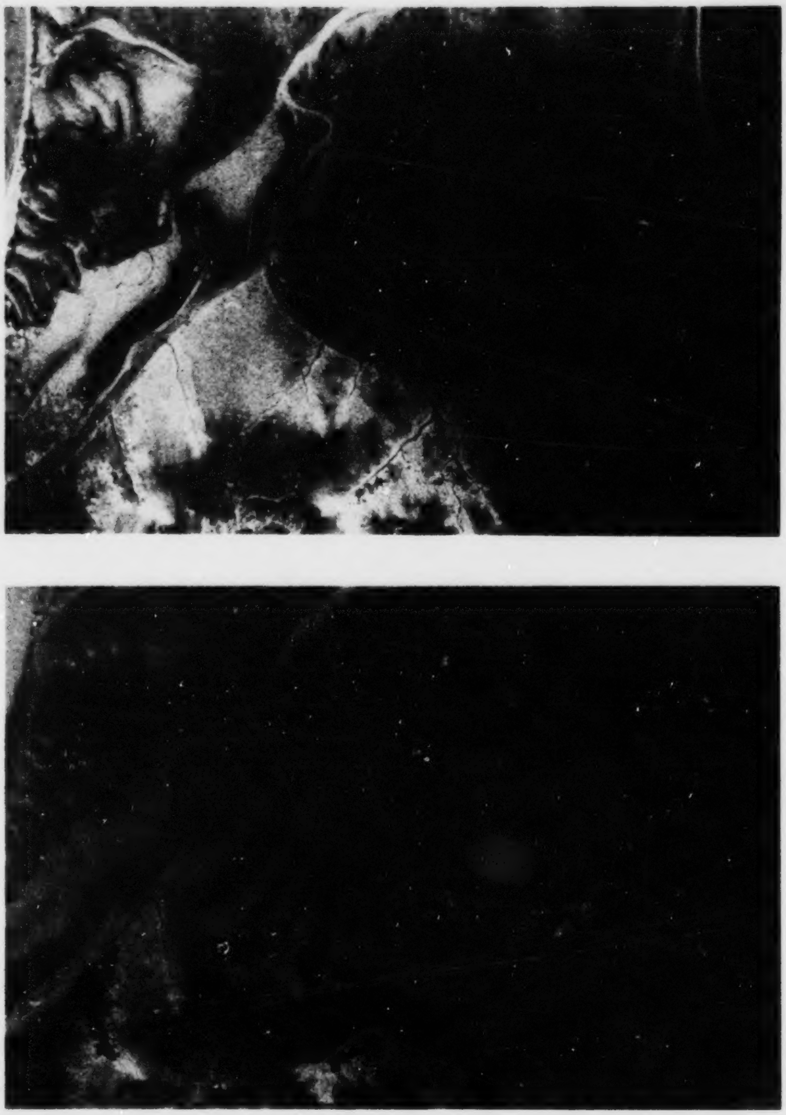

a

b

Figure 69.8

Black and white duplicates of the original colour infrared (8a) and colour (8b) aerial photographs of the Steveston area, taken from 6000 ft altitude. The Fraser River is visible in the upper left corner and an area of littoral vegetation is visible in the lower left corner on each image. The vegetation is seen as a relatively dark image on the colour photograph (8b) and as a medium grey image on the infrared photograph. On both images the mud-silt soils are light toned as are the drier well-drained sand bars; the sandy flats, however, are seen as darker grey images extending towards the upper right corner in each photograph. Although the sand bars can be visually confused with the finer soils, the wet sandy flats are visibly different. Analytically these targets were separated using ratioed density values (colour comparisons).

relative soil moisture and texture patterns. If a darker soil element has a greater red-to-blue density ratio than the lighter soil element, tonal variation between the soil elements is caused mainly by texture. If a darker soil element has a smaller red-to-blue density ratio, the soil elements differ in moisture content (Piech and Walker, 1974). Consequently, sand, silt and, clay have different spectral characteristics and are affected by colour, texture, and moisture. Infrared reflectance is particularly sensitive to moisture. If differences in soil surface-moisture content are present, changes in reflectance are most evident in the near-infrared portion of the photographic spectrum (Condit, 1970).

The low reflectance of leaves in the blue (460-500 nm), and red (630-680 nm) regions is generally attributed to chlorophyll absorption (along with other pigments). In the near-infrared (750-1300 nm), multiple scattering occurs, and reflectance of healthy vegetation is significantly higher (Gausman, 1974). Conversely, near infrared reflectance from water is very low and facilitates the spectral separation of vegetation and water. Soil reflectivity increases towards the green and red parts of the spectrum, as does water with high sediment load or bottom reflectance. As a result these features can be classified with the combined use of visible and near infrared spectral data. Figure 69.3 shows the spectral regions offering maximum discrimination of dry/wet soils and vegetation as 580-680 nm (yellow-red) and 725-1100 nm (near infrared). The green portion of the spectrum (520-550 nm) would be confusing while the blue (400-510 nm) shows moderate separation.

Aerial reconnaissance project

Because Landsat multispectral scanner (MSS) imagery consists of low resolution picture elements (79 m x 79 m), these pixels do not accurately represent ground values due to a large degree of spatial variability in coastal environments. Scene dynamics and smaller-scale features are masked or erased since pixel values are averages. Thematic Mapper (TM) imagery from Landsat 5 (pixel resolution of 30 m x 30 m) will be of assistance in determining spectral

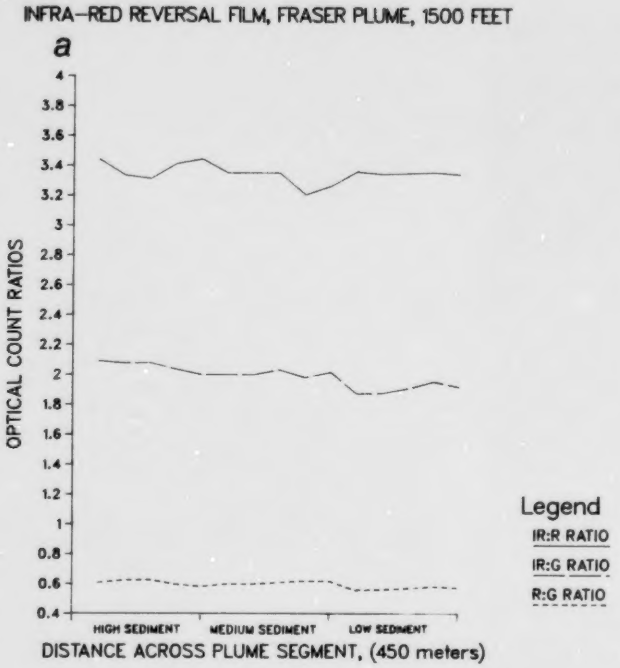

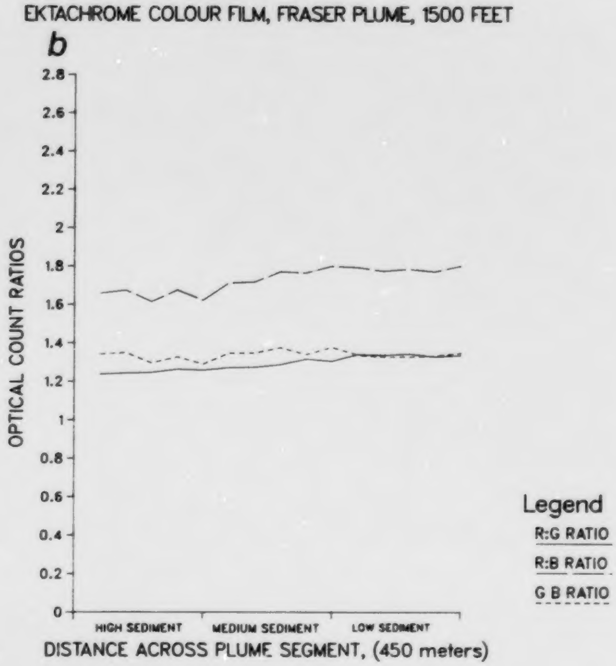

Figure 69.9. *Results of ratioed density readings (densitometer optical count ratios) from infrared colour (9a) and colour (9b) aerial photographs of three sediment conditions (high, medium and low extending from left to right to correspond with the three intervals on the X axis – see also Fig. 69.10). At each sample location across the photography the infrared optical counts were divided by the red (IR:R ratio) and green (IR:G ratio) optical counts, the red optical counts were divided by the green (R:G ratio), and blue (R:B ratio) optical counts, and the green optical counts were divided by the blue (G:B ratio) optical counts.*

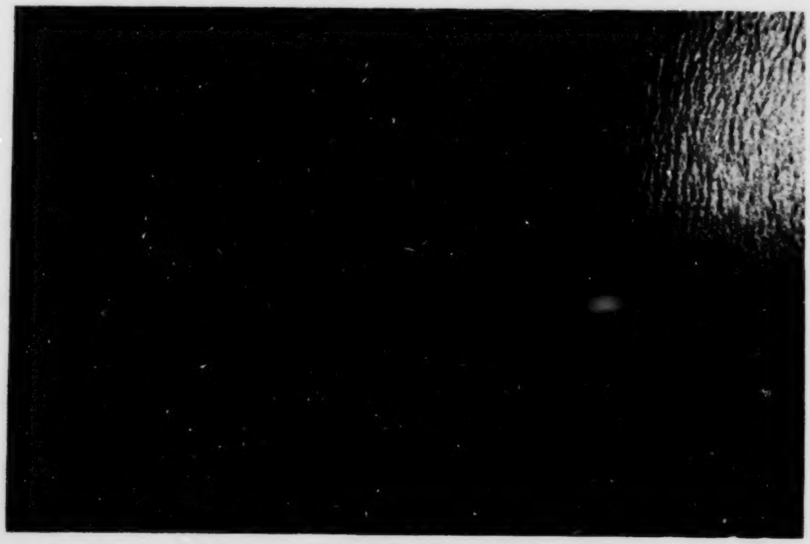

Figure 69.10

Black and white duplicate of a colour aerial photograph taken from 1500 ft and showing the sediment conditions measured in Figure 69.9. Suspended surface sediment conditions from left to right were designated as high, medium and low concentration areas. These areas are clearly visible on the colour photograph.

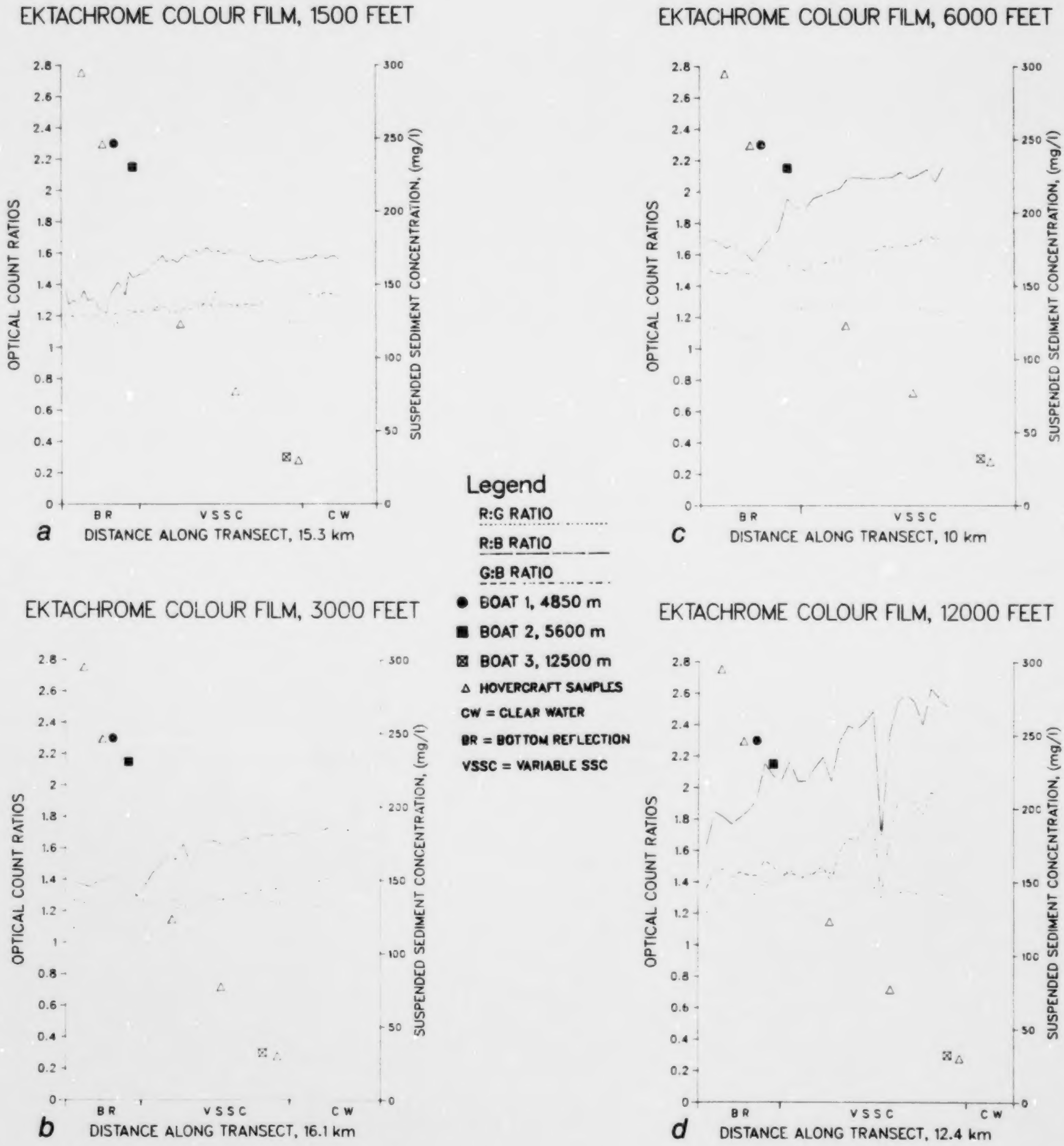

***Figure 69.11.** Results of ratioed density readings (densitometer optical count ratios) from a series of colour aerial photographs recorded along the four altitude transects illustrated in Figure 69.7. Suspended sediment concentrations for the three anchored sampling boat locations and hovercraft sampling sites are also shown for each graph: sites 1 and 2 are nearshore while site 3 is at the edge of the Fraser River plume in the Strait of Georgia. At each measured location across the photography, the red optical counts were divided by the green (R:G ratio) and blue (R:B ratio) optical counts, and the green optical counts were divided by the blue (G:B ratio) optical counts.*

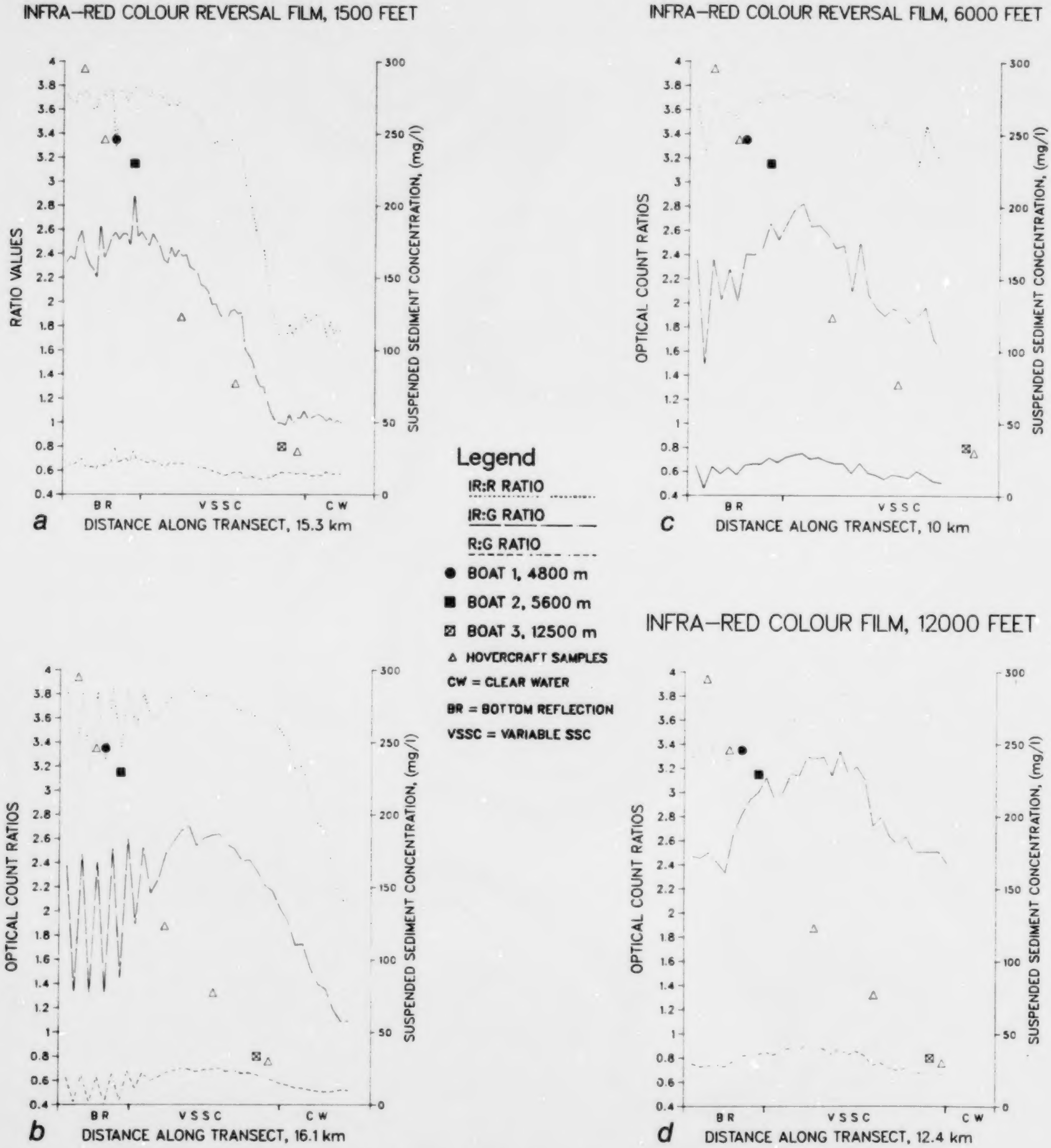

Figure 69.12. *Results of ratioed density readings (densitometer optical count ratios) from a series of colour infrared aerial photographs recorded along the four altitude transects illustrated in Figure 69.7. The three anchored sampling boat locations are also shown for each graph: sites 1 and 2 are nearshore while site 3 is at the edge of the Fraser River plume in the Strait of Georgia. At each measured location across the photography, the infrared optical counts were divided by the red (IR:R ratio) and green (IR:G ratio) optical counts, and the red optical counts were divided by the green (R:G ratio) optical counts.*

characteristics of land and tidal features for some applications. TM imagery may be adequate for estimating relative sediment concentrations in the Fraser River plume. However, problems of atmospheric attenuation remain, and orbital resolution is probably inadequate for specific site classifications since different alluvial deposits, vegetation, suspended sediment concentrations and geometric arrangements of scene elements cannot be accurately determined and evaluated.

To adequately map sediment loads in the plume of the Fraser River and categorize intertidal features, large scale (1:5000-1:250 000) reconnaissance aerial photography and multispectral video imagery were recorded. Infrared aerial photography was used for precision mapping and spectral identification of surface and submerged vegetation, suspended sediment, bottom reflection, and the land/water interface. Two reconnaissance cameras (Nikon F250 with Nikkor 24 mm f 2.8 lenses) were used with: (1) Kodak Infrared Aerochrome 2443 and a no. 22 filter for haze penetration and blue light removal, and (2) Kodak Ektachrome 5037 with an 85B filter for haze penetration and colour balance. Video cameras provided discrete spectral data for spectral classification mapping of different alluvial deposits (e.g. clay and sand), and sediment loads in the Fraser River plume. Three Sony CCD and one RCA Newvicon video cameras were used with narrow band optical filters and half inch video cassette recorders (VCR). Kodak Wratten filters (92, 93, 94 used with a Kodak infrared cutoff, 301-A, glass filter and 87 for infrared only) were used to separate the blue, green, red, and infrared spectral components of the sediment, bottom, and floral targets (Fig. 69.4, 69.5; Table 69.1).

Results from three reconnaissance flights from up to four different altitudes (1500, 3000, 6000 and 12 000 feet; approx. 450, 900, 1800 and 3600 m) at low tide conditions were analyzed. These results were subsequently compared with a Landsat 2 four-band MSS image of the Fraser Delta recorded on August 14, 1981. The digital data (video and MSS) was enhanced and analyzed using the Simon Fraser University image processing system (I^2S Model 70F4). The colour and colour infrared photography was analyzed using a Macbeth transmission densitometer.

Surface observations of sediment concentrations were taken at the time of each reconnaissance flight using water-sampling containers lowered to secchi disk disappearance depth (maximum visible depth) and raised to collect an integrated vertical column sample of water with suspended sediment.

Analytical results

Figure 69.6 shows the results of ratioed densitometer readings from colour and colour infrared photography taken at 6000 feet above Steveston (Fig. 69.7, 69.8) on July 29, 1985 at approximately 1000 h P.D.T. The infrared image (Fig. 69.6a, 69.8a) shows distinct separation between Fraser River water, bare soil and vegetation using both the infrared/red and infrared/green ratios. The red/green ratios show a weak separation between the river water and the soil and vegetation targets but cannot discriminate between the soil and vegetation. On the colour photography the red/blue ratio effectively discriminates wet mud-silt soils and vegetation but produces similar values for wet sandy soils and river water. When the mud-silt and sand soils are compared they are distinctly separated according to texture, as predicted. All four components, however, can be distinctly separated by comparing the red/blue ratio with the green/blue ratio: river water has the lowest green/blue density ratios while wet sandy soils have consistently higher green/blue density ratios.

Figure 69.9 illustrates the ratioed density values for three distinctly different sediment concentrations within the Fraser River plume. The infrared image (Fig. 69.9a) shows poorer discrimination between the high, medium and low sediment conditions. The colour image (Fig. 69.10) however, shows good discrimination using the red/blue density ratios. The red/green density ratio shows a weak effect (superior to the infrared image's red/green ratio) because of the increased blue sensitivity on the colour film's green sensitive emulsion layer. On the colour infrared film the complete elimination of any blue-green values on the green sensitive emulsion was due to the use of a Wratten 22 filter. Like the density ratios on the colour infrared film the green/blue density ratio on the colour film does not provide a satisfactory separation. When combined with either the red/green or red/blue density ratios, the resulting separation effect can be enhanced.

Figure 69.11 shows the ratioed colour film density values taken along a transect across the Fraser River plume (Fig. 69.7). Four altitude conditions are shown. The results clearly define areas with: (1) bottom reflectance; (2) varying sediment concentrations, and; (3) clear water. The ratioed density values for sediment concentrations are comparable with those in Figure 69.9. The area of bottom reflectance through high turbidity water is remarkably similar to the values for exposed wet soils and the highly turbid Fraser River illustrated in Figure 69.6. The 6000-foot-altitude colour density ratios in Figure 69.11, showing nearshore bottom reflectivity values are directly comparable with the 6000-foot colour density ratio values for river water and soils in Figure 69.6. The area of clear deep water at the end of the 1500-foot-altitude transect is identified by a distinct drop in red/green ratioed density values and a comparable increase in green/blue ratioed density values. Figure 69.12 shows four comparable, colour infrared ratioed density values of the same transect. The area of clear deep water stands out as depressed ratioed density values. The turbid shallow water shows the same high infrared ratioed density values as in Figure 69.6. The areas of bottom reflectance are clearly seen on these infrared ratioed values as sharp drops in density value. Figure 69.12 (3000-ft. altitude) shows recorded density values from alternating areas of deeper turbid water and shallow bottom reflectance near the shore. This resulted in a jagged "saw-tooth" plot of density values until the deeper turbid water prevented bottom reflectance. As the sediment plume thinned out the ratioed infrared density values dropped sharply to the clear water values. Table 69.2 gives the surface observation results of sediment concentrations taken

Table 69.2. Results of suspended surface sediment sampling transect using Canadian Coast Guard Hovercraft. The three site locations where samples were collected using anchored boats are also indicated. Values for suspended sediment concentrations were averaged over the duration of the overflight.

Distance from Steveston radio towers to sample site (metres)	Suspended sediment concentration (mg/L)	Sample site coordinates
2570	30	49°10.4'N; 123°22'W
2500 - Site 3	31	49°10.2'N; 123°21'W
2020	77	49°10'N; 123°20.2'W
1540	123	49°09.5'N; 123°18.4'W
1110 - Site 2	232	49°09.2'N; 123°16.8'W
960 - Site 1	246	49°09.0'N; 123°16'W
860	244	49°08.9'N; 123°15.6'W
680	295	49°08.8'N; 123°15'W

at the time of photography and indicated on Figures 69.11 and 69.12. There is a clear correspondence between these surface observations and the ratioed density values indicating sediment concentrations.

Figure 69.13 shows a density-ratioed Landsat MSS image of Vancouver with superimposed plotted density ratio values. This Landsat-2 image taken in August 1981 is spectrally comparable with colour infrared photography.

The illustrated image is composed from one infrared (band 7) one red (band 5) and one green (band 4) image. The transect was taken from the silt-laden Fraser River across the exposed shore and mud flats and out into the Fraser River plume in the Strait of Georgia. These ratioed density values show the differences between land and water but are unable to distinguish between varying sediment concentrations in the Fraser River and the plume in the Strait of Georgia. Unlike the densitometry values in Figures 69.11 and 69.12 the

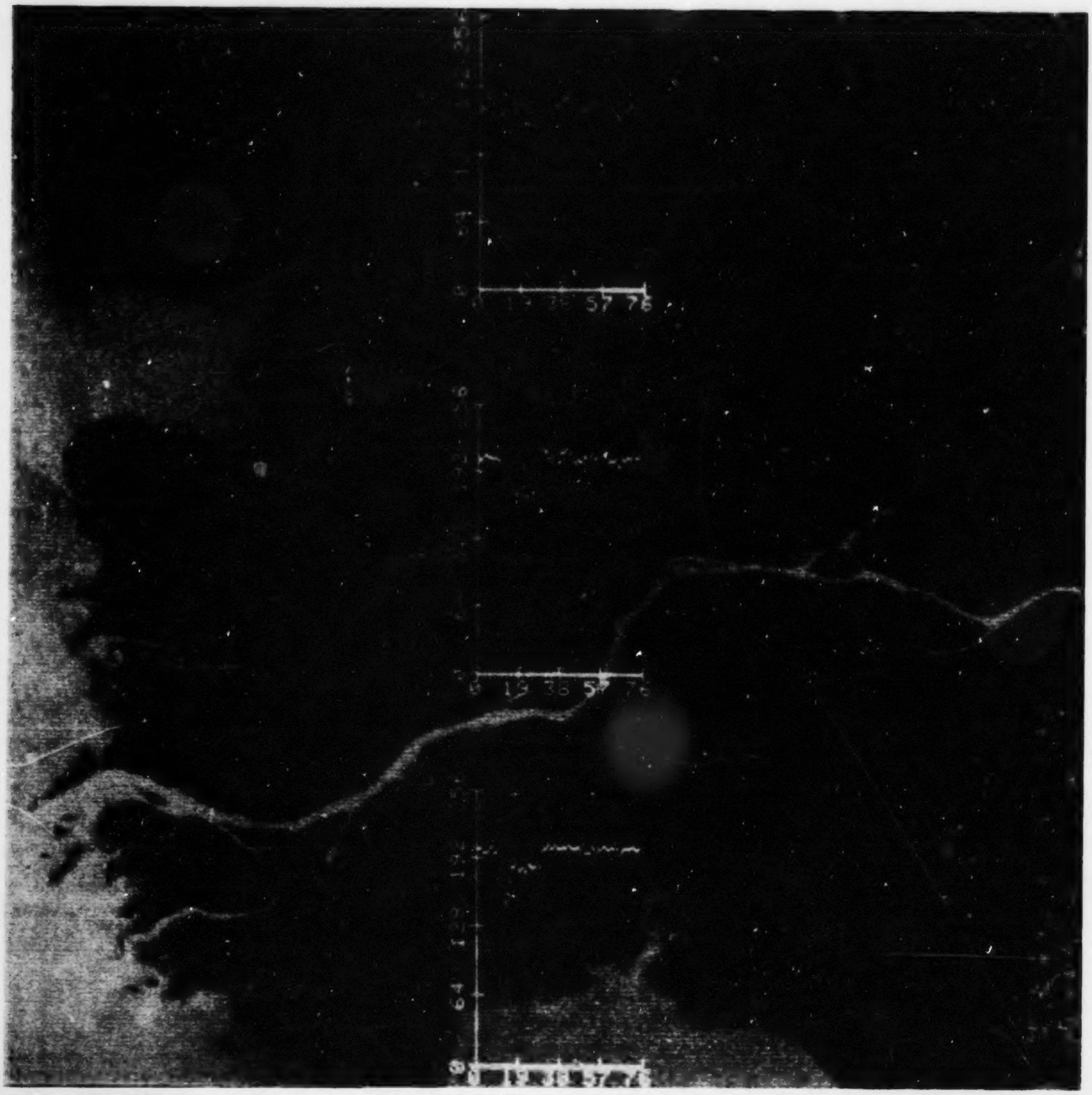

Figure 69.13. *A density ratioed Landsat-2 MSS image of the study area taken in August 1981. This is a black and white duplicate of a composite three band image composed of: band 1 (top graph) infrared density divided by red density; band 2 (middle graph) infrared density divided by green density; band 3 (bottom graph) red density divided by green density. The three graphs indicate these ratioed density values (0 to 256 indicated on the Y axis) for a total of 76 picture elements (pixels) indicated across the X axis. The 76 pixel transect indicated on the graphs (from left to right) extends across the Fraser River Main Stem (0-12), over a narrow band of vegetation (13-16), over the exposed tidal flats (17-28) and across the transect area in Figure 69.7 (29-76).*

satellite image is unable to clearly identify areas of bottom reflectance. Clear water can be defined but not with the same degree of resolution as the colour aerial photography (see Fig. 69.11).

This lack of spectral target resolution in the satellite image is principally a scale problem as the minimum cell resolution on this Landsat image is 6241 m^2 (79 m x 79 m). Such a ground scale makes fine resolution of areas with varying bottom reflectance conditions (i.e. sandbars and small channels) impossible except as boundary noise. Atmospheric attenuation of the reflected electromagnetic energy also results in some image degradation towards the blue end of the spectrum. For this reason a blue band was not incorporated into the Landsat sensor system. The superior radiometric identification of sediment concentrations, clear marine water and nearshore bottom reflectance from the airborne colour imagery (Fig. 69.11) is not available from orbital altitudes.

In addition to scale and atmospheric problems, incident sun angle produces specular reflectance from the water surface on all images. Under rough water conditions this is increased as some reflection results from each wave (see Fig. 69.10). In the Landsat image these rough water values are incorporated into the average reflectance values for each pixel. In the photographic image, densitometer readings can often be taken from wave surfaces not reflecting this specular glare to the image.

Figure 69.14 shows the results of a red/green density ratio transect across a video image of the three different sediment conditions illustrated in Figure 69.9. Considerable scatter is evident in the plot of density values as a result of specular reflectance of sunlight from the rough water. However, even with this scatter this red/green ratio is comparable to the photographic densitometer ratio derived in Figure 69.9. The video image exhibits a slightly steeper curve and indicates superior radiometric separation between the red and green images.

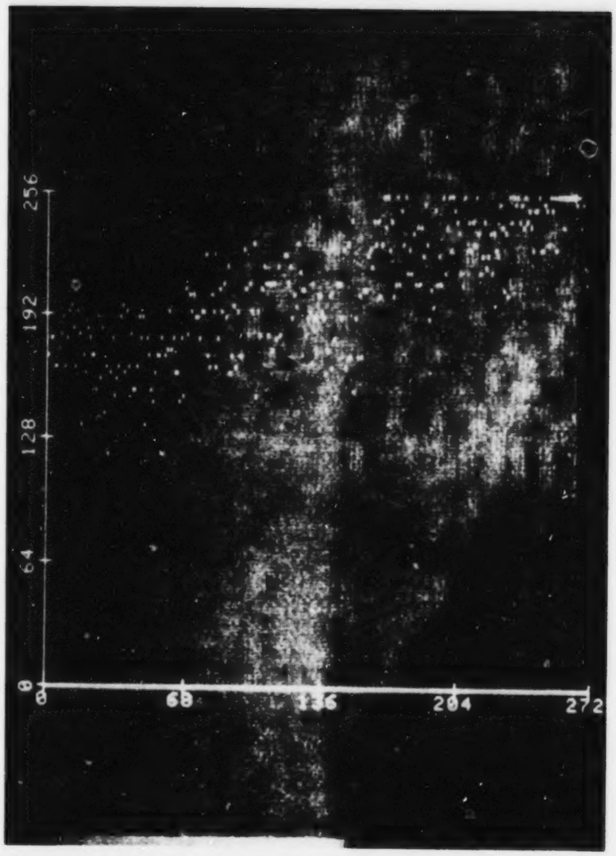

Figure 69.14. *Red divided by green (red/green ratio) video image of the high, medium and low surface sediment concentration conditions in Figures 69.9 and 69.10. The graph shows these ratioed density values (0-256 along Y axis) for a transect corresponding with the area slightly above the bottom line of the X axis across the image. Note the density increases as the plot crosses (left to right) the areas of high, medium and low sediment concentrations.*

Discussion

At this stage in the research it is apparent that both photographic and video airborne images are superior to orbital Landsat MSS images for identifying and characterizing areas of varying sediment concentrations. Variations in sediment concentrations from the surface samples closely correspond with imaged density values from both the colour infrared and normal colour images. Although the video imagery is not, as yet, fully analyzed the improved spectral resolution of this multispectral digital image system should provide superior results.

Presently the research is concentrating upon: (1) video-gain (electronic exposure control) adjustment in the multispectral video system; (2) image correction for atmospheric problems; (3) image correction for acute specular reflectance problems; (4) refinement of surface sampling procedures for sediment concentrations at the time of overflight, and; (5) comparison of airborne results with Landsat 5 thematic mapper multispectral imagery.

Conclusions

The densitometry results from the aerial photography indicate that the colour film (Ektachrome 5037 and 85B filter) provides better suspended surface sediment concentration identification than the colour infrared film (Infrared Aerochrome 2443 and no. 22 filter). The best results are obtained at the lowest altitudes (1500 ft.) but satisfactory results are possible from 12 000 feet. The photographic results are greatly superior to Landsat 2 MSS imagery. Although the multispectral video imagery has only received preliminary examination these results are promising. Spectral (colour) resolution and colour identification with the video system is superior to colour photography and it is predicted that the best results will be obtained with video imagery using a four band infrared, red, green and blue combination.

Landsat 5 TM imagery has not as yet been compared with the present data. The July 29 transect flight corresponded with a TM overpass and the time of photography and surface sampling was within twenty minutes. It is expected that the minimum spatial resolution (approximately 30 m x 30 m) of Landsat 5 TM imagery will still cause scale problems. Although TM imagery has more spectral bands (7) than MSS imagery (4), these additional spectral bands are mainly in the infrared spectral region and have little utility in remote sensing of surface-sediment concentrations due to the strong absorption of infrared energy by water.

It is predicted that airborne systems concentrating upon the visible spectrum but using some information from the near infrared spectrum (700 to 1100 nm) for vegetation and soils identification, will prove to be the most effective sensor systems for the remote sensing of surface sediment concentrations.

Acknowledgments

The authors wish to acknowledge the assistance of J. Luternauer, T. Forbes, D. Duggan and G. Julesbury (Geological Survey of Canada); and V. Cameron, D. Evans, L. Griswold, J. Karagatzides, J. MacDonald, J. Patchell, A. Schlecht, S. Smythe, J. Udell, G. Worthington and T. Yrjola (Department of Geography, Simon Fraser University). Without the assistance of the above persons this research would not have been possible.

References

Alfoldi, T.T. and Munday, J.C., Jr.
1978: Water quality by digital chromaticity mapping of Landsat data; Canadian Journal of Remote Sensing, v. 4, p. 108-126.

Amos, C.L. and Alfoldi, T.T.
1979: The determination of suspended sediment concentration in a microtidal system using Landsat data; Journal of Sedimentary Petrology, v. 49, p. 159-174.

Amos, C.L. and Topliss, B.J.
1985: Discrimination of suspended particulate matter in the Bay of Fundy using the Nimbus 7 Coastal Zone Color Scanner; Canadian Journal of Remote Sensing, v. 11, p. 85-92.

Aranuvachapun, S. and LeBlond, P.H.
1981: Turbidity of coastal water determined from Landsat; Remote Sensing of Environment, v. 84, p. 113-132.

Bowker, D.E., Witte, W.G., Fleishcher, P., Gosink, T.A., Hanna, W.J., and Ludwick, J.
1975: An investigation of the waters in the lower Chesapeake Bay; Proceedings of the Tenth International Symposium on Remote Sensing of the Environment, Ann Arbor, MI., p. 411-420.

Bowker, D.E. and Witte, W.G.
1977: The use of Landsat for monitoring water parameters in the coastal zone; Proceedings AIAA Joint Conference Satellite Applications to Marine Technology, American Institute Aeronautics and Astronomy, New Orleans, LA., p. 193-198.

Carpenter, D.J. and Carpenter, S.M.
1983: Modeling inland water quality using Landsat data; Remote Sensing of Environment, v. 13, p. 345-352.

Colwell, R.N. (Editor-in-Chief)
1983: Manual of Remote Sensing, v. 2, p. 1371-1496.

Condit, H.R.
1970: The spectral reflectance of American soils; Photogrammetric Engineering, v. 36, p. 955-966.

Eastman Kodak Company
1972: Kodak filters for scientific and technical users, Kodak Publication No. B-3, Rochester, N.Y. 14650.

Gausman, H.W.
1974: Leaf reflectance of near-infrared; Photogrammetric Engineering and Remote Sensing, v. 40, p. 182-191.

Geraci, A.L., Colwell, R.N., and Khorram, S.
1981: Remote sensing of water quality for estuarine environments; Matching Remote Sensing Technologies and their Applications, Proceedings of the Ninth Annual Conference of the Remote Sensing Society, p. 199-219.

Gupta, J.N. and Ghovanlou, A.H.
1978: Radiative transfer in turbid water; Society of Photo-Optical Instrumentation Engineers, Redondo Beach, CA., p. 132-147.

Holyer, R.J.
1978: Toward universal multispectral suspended sediment algorithms; Remote Sensing of Environment, v. 7, p. 323-338.

Johnson, R.W.
1975: Quantitative suspended sediment mapping using aircraft remotely sensed multispectral data; Proceedings NASA Earth Resources Survey Symposium, NASA Johnson Space Center, Houston, TX, p. 2087-2098.

1978: Mapping of chlorophyll – a distribution in coastal zones; Photogrammetric Engineering and Remote Sensing, v. 44, p. 617-624.

Johnson, R.W. and Harriss, R.C.
1980: Remote sensing for water quality and biological measurements in coastal waters; Photogrammetric Engineering and Remote Sensing, v. 46, p. 77-85.

Lodwick, G.D. and Harrington, R.D.
1985: Deriving sediment information for Lake Athabaska using principle components analysis of Landsat data; Canadian Journal of Remote Sensing, v. 11, p. 4-16.

Miller, R., Jain, S.C., and O'Neill, N.T.
1977: Interpretation of airborne spectral reflectance measurements over Georgian Bay; Remote Sensing of Environment, v. 6, p. 183-200.

Munday, J.C., Jr., Alfoldi, T.T., and Amos, C.L.
1979: Bay of Fundy verification of a system for multidata Landsat measurement of suspended sediment; Satellite Hydrology, American Water Resources Association, Minneapolis, MN., p. 622-640.

Piech, K.R. and Walker, J.E.
1974: Interpretation of soils; Photogrammetric Engineering, v. 40, p. 87-94.

Swain, P.H. and Davis, S.M.
1978: Remote Sensing: the Quantitative Approach; McGraw-Hill Inc., p. 252-259.

The Castlegar Gneiss Complex, southern British Columbia

Project 850001

David B. Halwas[1] and P.S. Simony[1]
Cordilleran Geology Division, Vancouver

Halwas, D.B. and Simony, P.S., The Castlegar Gneiss Complex, southern British Columbia; in Current Research, Part A, Geological Survey of Canada, Paper 86-1A, p. 583-587, 1986.

Abstract

The Castlegar Gneiss Complex is located on the south margin of the Valhalla Complex of southern British Columbia. It consists of the China Creek Gneiss, a heterogeneous assemblage of hornblende biotite gneisses laced with pegmatite sheets, and the Kinnaird Gneiss, a series of porphyritic quartz monzonite-to-granite sheets intruded into the Trail Gneiss and the metasediments of the Mount Roberts Formation. The Kinnaird Pluton was then deformed into gneiss. The Castlegar Gneiss Complex is younger than the Bonnington and Mackie quartz diorite/granodiorite plutons. Strain within the Castlegar Gneiss Complex is unevenly distributed and includes top-to-the-east simple shear that is weak above a gently dipping surface that passes under the Mackie, Bonnington, and Trail plutons. After being strained, the Castlegar Gneiss Complex was intruded by inclusion-laden mafic sheets, a young granite of the Mackie Plutonic Complex, Coryell syenite masses, and Eocene (?) basaltic and gabbroic dykes.

Résumé

Le complexe gneissique de Castlegar se situe sur la marge sud du complexe de Valhalla dans le sud de la Colombie-Britannique. Il comprend le gneiss de China Creek, association hétérogène de gneiss à hornblende et à biotite coupé de nappes de pegmatite, ainsi que le gneiss de Kinnaird, série de nappes de monzonite quartzifère porphyritique ou de granite pénétré par le gneiss de Trail et les métasédiments de la formation de Mount Roberts. Le pluton de Kinnaird a alors été déformé en gneiss. Le complexe du gneiss de Castelgar Lake date d'une époque plus récente que les plutons de diorite quartzeux et granodiorite de Bonnington et de Mackie. La déformation dans le complexe gneissique de Castelgar est inégalement répartie et comprend un cisaillement simple qui, en partant du haut, se dirige vers l'est; ce cisaillement est faible au-dessus d'une surface en pente douce qui passe sous les plutons de Mackie, de Bonnington et de Trail. Après avoir été déformé, le complexe gneissique de Castlegar a été pénétré par des nappes mafiques riches en inclusions, par un granite récent du complexe plutonique de Mackie, par des masses de syénite de Coryell et par des filons basaltiques et gabbroïques d'âge éocène (?).

[1] Department of Geology and Geophysics, University of Calgary, Calgary, Alberta T2N 1N4

Introduction

Field work in the summer of 1985 in the Castlegar Gneiss, on the southern margin of the Valhalla Complex just south of Castlegar, British Columbia (Fig. 70.1 – inset) mapped about 100 km^2 at a scale of 1:20 000. The objectives of the study are to describe the petrological and structural variations within the Castlegar Gneiss Complex, to define its contact relationships with the Trail Gneiss and the overlying Pennsylvanian Mount Roberts Formation in the south, the Mackie Plutonic Complex in the south and west, and the Bonnington Pluton on the east side. The intensity of strain within the Castlegar Gneiss Complex is also being studied.

Reconnaissance geological mapping in the area was carried out by Little (1960, 1962) for the Geological Survey of Canada. Simony (1979), Crowe (1981), and Corbett and Simony (1984) have worked in the area as part of an ongoing project of the University of Calgary. The southern part of the area is shown on the Rossland-Trail sheet (Little, 1982) and the Valhalla Complex (Reesor, 1965) is being restudied (Parrish, 1984; Parrish et al., 1985; Carr, 1985).

Lithologies

The Castlegar Gneiss Complex can be subdivided into two main phases; the Kinnaird Gneiss and the China Creek Gneiss (Fig. 70.1). The Kinnaird Gneiss is the more extensive unit. It is a light-grey weathering, medium grained quartz monzonitic to granitic orthogneiss with irregularly concentrated white weathering K-feldspar phenocrysts commonly 2 to 5 cm but ranging up to 12 cm in length. Euhedral hornblende phenocrysts, fine grained hornblende and minor biotite clusters comprise the mafic minerals. A Late Cretaceous age has been obtained for the Kinnaird Gneiss by R. Parrish (personal communication, 1985) using the U-Pb method on zircons.

A fabric of variable intensity present throughout the Kinnaird Gneiss, consists of both a foliation and a lineation (commonly the more strongly developed fabric element). The fabric is formed by the imperfect alignment of hornblende phenocrysts, mafic mineral clusters, ribbon quartz, and feldspar phenocrysts. In most places the feldspar phenocrysts have not been deformed into augen, but in some localities, especially in the southwestern portion of the area strain was sufficient to cause augen development.

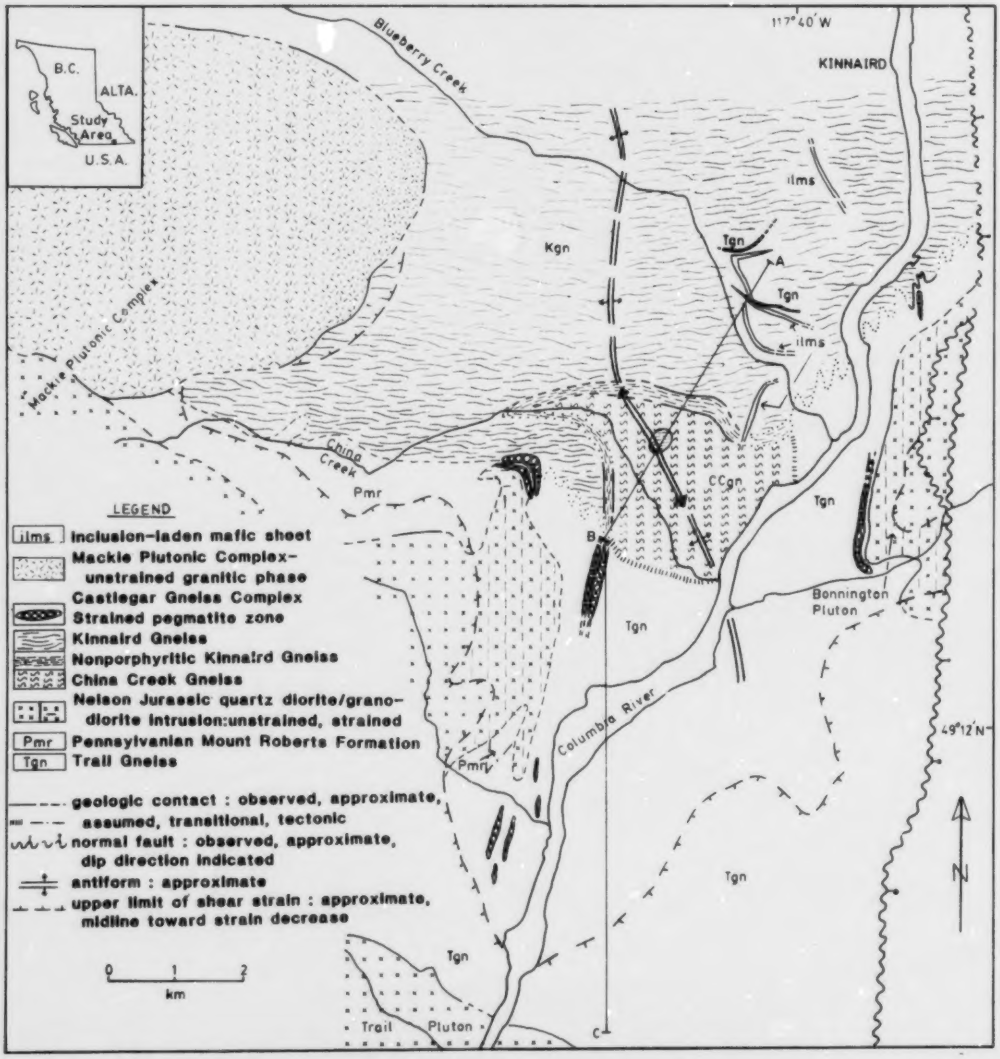

Figure 70.1. Geological map and regional geologic setting of the Castlegar Gneiss Complex.

The floor of the Kinnaird Gneiss is exposed in a structural culmination east of the sharp bend in China Creek (Fig. 70.1, 70.2). There, the basal 10 to 50 m consist of a sheeted equigranular granitic orthogneiss which differs from the rest of the Kinnaird Gneiss by having a low content of mafic mineral and a nonporphyritic to very sparsely porphyritic texture.

The China Creek Gneiss is a heterogeneous assemblage of rocks exposed structurally below the Kinnaird Gneiss and immediately north of the town of Genelle with an exposed thickness of approximately 350 m. It consists dominantly of highly strained, moderately foliated and lineated, pegmatitic veins ranging from less than 20 cm to several metres thick. The pegmatites are composed of K-feldspar crystals and augen up to 20 cm long, abundant ribbon quartz, variable concentrations of biotite clusters, almandine garnet, and locally magnetite and sillimanite. The pegmatites lace the other rocks of the China Creek Gneiss including: a dark grey, biotite granodiorite gneiss; a medium grained, light grey aplite; a dark hornblende-biotite gneiss with amphibolite layers; and several discrete thin calcsilicate layers. The last along with the enclosing gneiss probably belong to the lithologically complex Trail Gneiss (Simony, 1979) exposed in the southern part of the study area.

Rare thin screens and trains of inclusions of the China Creek Gneiss at low structural levels in the Kinnaird Gneiss suggest that the Kinnaird Gneiss postdates the China Creek Gneiss and at least some of the pegmatites that are associated with it. The pegmatites present a problem because other pegmatites of similar appearance intrude the Kinnaird Gneiss. The emplacement of the Kinnaird Gneiss and pegmatite injection may therefore have proceeded simultaneously.

The Trail Gneiss south of the Castlegar Gneiss Complex consists of a heterogeneous orthogneissic and paragneissic assemblage of melanocratic hornblende gneiss, biotite granodiorite gneiss, biotite-hornblende quartz diorite gneiss, quartzofeldspathic mica schist, amphibolite, calcsilicate and marble (Simony, 1979) (Fig. 70.1). Well developed foliation and lineation in the Trail Gneiss are continuous with the fabric scene in the Castlegar Gneiss Complex.

Along the east bank of the Columbia River and opposite Kinnaird, a southern suburb of Castlegar, is an excellent cliff exposure of an intrusive contact between the Kinnaird Gneiss and the Trail Gneiss. The outcrop reveals crosscutting relationships and the interfingering of apophyses of the Kinnaird Gneiss with the Trail Gneiss.

South of the main mass of the Castlegar Gneiss Complex extensive pegmatite sheets, each approximately 10 to 15 m thick, extend with a shallow tip from the Castlegar Gneiss Complex into the Trail Gneiss. They are lithologically similar to the pegmatites of the China Creek Gneiss, and extend approximately 2.5 to 3 km south of the main Castlegar Gneiss Complex, although roadside exposures indicate that similar pegmatite extends at least another 3 to 4 km farther south at valley floor level.

In the western part of the study area quartz-rich, psammitic and semipelitic paragneiss is intruded by the Kinnaird Gneiss (Fig. 70.1). This paragneiss is interpreted as a metamorphic equivalent of the Pennsylvanian Mount Roberts Formation identified farther south by Simony (1979). Although contact relationships are not exposed, the presence of paragneiss between extensive masses of the Kinnaird Gneiss suggests a similar interfingering intrusive relationship to that seen between the Kinnaird Gneiss and the Trail Gneiss. As well, rare quartz-rich paragneiss screens and inclusions found within the Kinnaird Gneiss support an intrusive relationship with the Mount Roberts Formation although some of the paragneiss inclusions may belong to the Trail Gneiss.

Along the southern and western parts of the study area, the Castlegar Gneiss Complex is in contact with the Mackie Plutonic Complex (Crowe, 1981) (Fig. 70.1). This plutonic mass actually consists of two separate assemblages of rocks; an older, possibly Jurassic, quartz dioritic/granodioritic phase and a younger, possibly latest Cretaceous or early Tertiary, granitic phase. Along the western portion of the study area the granitic phase clearly intrudes the Kinnaird Gneiss with foliated and lineated inclusions of Kinnaird Gneiss observed in the unstrained granitic phase.

Farther south, the contact between the quartz dioritic/granodioritic phase and the Castlegar Gneiss Complex is less easily defined. No direct contact was observed because it consists of an intervening zone of highly strained, well foliated and lineated, pegmatite sheets perhaps 100 m wide. They are lithologically similar to those seen intruding the Trail Gneiss at a lower elevation and they crosscut the strongly foliated basal part of the quartz dioritic/granodioritic phase of the Mackie Plutonic Complex (Fig. 70.2). It is therefore concluded that this part of the Mackie Plutonic Complex predates the Castlegar Gneiss Complex.

On the east side of the Columbia River valley, the part of the Bonnington Pluton west of the Champion Lake Fault (Corbett and Simony, 1984) has a gently east-dipping intrusive contact with the Trail Gneiss (Fig. 70.1). The lower part of the pluton is intruded by pegmatite sheets and is strained in a manner that resembles the quartz dioritic/granodioritic phase of the Mackie Plutonic Complex.

The Castlegar Gneiss Complex has been intruded by a swarm of shallowly east-to-northeast dipping mafic sheets with postductile deformation, located in a north-trending zone on the immediate west side of the Columbia River (Fig. 70.1). The sheets range from less than one to at least 40 metres thick and consist of 60 to 95 per cent angular-to-rounded, dioritic inclusions of several distinct types suspended in a fine grained granitic matrix. These mafic sheets were apparently emplaced as inclusion-laden intrusions into the Castlegar Gneiss Complex which had been previously deformed in a ductile manner.

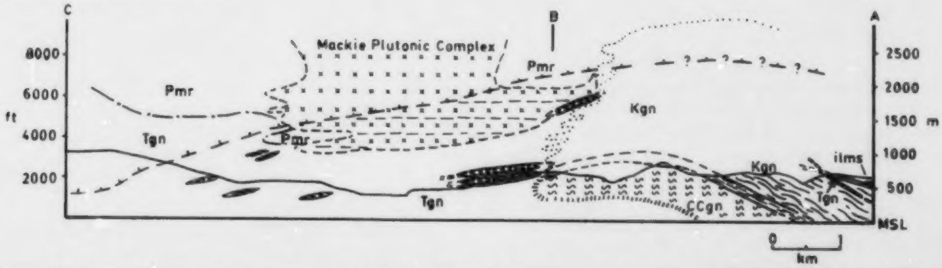

Figure 70.2. *Vertical cross-section ABC looking eastward. Line of section and legend are shown on geological map (Fig. 70.1). Geology shown above topographic surface is located by projection.*

Also intruding the Castlegar Gneiss Complex are an unstrained medium grained granite, dykes and small masses associated with the Eocene alkaline Coryell intrusions, and undeformed Tertiary basaltic-to-gabbroic dykes with northerly trends and steep east dips.

Mode of emplacement

The China Creek Gneiss appears to consist, at least in part, of Trail Gneiss injected by pegmatite that was subsequently highly strained. The Kinnaird Gneiss, on the other hand, consists of porphyritic granite which intruded the China Creek Gneiss, the Trail Gneiss and the Mount Roberts Formation as a series of parallel sheets. Screens of Trail Gneiss extending laterally more than 400 m, and zones of tabular inclusions as well as sharp planar contacts separate gently dipping, 50-to-200-m-thick sheets of porphyritic granite gneiss. Within each sheet, the size and abundance of phenocrysts remains constant but distinct variations in both parameters appear across contacts separating the sheets. Kinnaird Gneiss is seen in cliffs, some 100 m high, east of Kinnaird, to have intruded Trail Gneiss in a series of four parallel sheets that cut the layering in the Trail Gneiss at a small angle.

Kinnaird Gneiss is interdigitated with Trail Gneiss and China Creek Gneiss on the east and south sides of the Kinnaird orthogneiss. A similar interfingering relationship possibly exists with gneisses north of Castlegar (S. Carr, personal communication, 1985). The parent pluton of the Kinnaird Gneiss if it exists, was perhaps intruded from a source below or to the west.

Structure

Three phases of ductile deformation and one phase of brittle deformation were detected in the Castlegar Gneiss Complex. Phase-One deformation consists of localized, mesoscopic, inclined-to-recumbent, tight-to-isoclinal folding of the pegmatite veins in the China Creek Gneiss. Somewhat disharmonic, mesoscopic folds were also developed in the Trail Gneiss screens in several places in both the China Creek Gneiss and the Kinnaird Gneiss. Axes of all Phase-One folds trend approximately west with shallow east and west plunges depending on the dip of the foliation.

The original orientation of the mesoscopic Phase-One folds is undetermined because their present orientation is a result of rotation by strong Phase-Two deformation which led to a foliation and a lineation being imposed on the Castlegar Gneiss Complex as well as on adjacent lithologies. Phase-Two west-trending lineation is interpreted as stretching and is formed by elongate mafic mineral clusters and intense ribbon quartz development. The foliation appears to be largely due to simple shear since numerous types of "kinematic indicators" as outlined by Berthe et al. (1979), Simpson and Schmid (1983), and Hanmer (1984) were seen. They include asymmetric feldspar tails, sigmoidal feldspars, foliation fish, "turf" structures, and C-S fabrics. All the kinematic indicators showed top-to-east motion of simple shear parallel to the foliation.

The intensity of the foliation and lineation varies through the Castlegar Gneiss Complex, particularly in the Kinnaird Gneiss. At low structural levels the foliation is poorly to moderately developed whereas the lineation is well developed. The strain appears to be homogeneously distributed at the lower levels. At higher levels, as seen in the southwestern part of the area, lineation is strong and the foliation moderate with localized, but volumetrically significant mylonitic bands within the Kinnaird Gneiss. However, in the northwestern part of the area and apparently along strike with the highly strained Kinnaird Gneiss, the fabric is weak with only a faint lineation detectable in many places.

Despite the complex strain pattern within the gneiss package, an upper boundary of detectable strain can be mapped across the mountainsides and into Columbia River valley. This boundary cuts across the top of the Kinnaird Gneiss east of Mount Mackie, the lower part of the quartz diorite/granodiorite phase of the Mackie Plutonic Complex and the Bonnington Pluton, and presumably passes under the Trail Pluton north of Trail (Fig. 70.1, 70.2).

Phase-Three deformation resulted in the Castlegar Gneiss Complex being broadly arched along a north-trending axis, with the arch being outlined by the shallowly dipping foliation, shallowly plunging lineation, and the distribution of lithologies in the China Creek area (Fig. 70.1). There is a well defined, broad culmination situated just east of the sharp bend in China Creek where a small outlier of the Kinnaird Gneiss caps a hill of China Creek Gneiss (Fig. 70.2).

Phase-Four deformation consists of late, minor brittle faulting associated with activity along the east-dipping, east-side-down Champion Lake Fault on the eastern limit of the map area (Corbett and Simony, 1984; Corbett, personal communication, 1985). This late faulting is exhibited by scattered north-striking vertical zones showing little displacement but noticeable chlorite, epidote, and sericite alteration of the Castlegar Gneiss Complex.

Summary

The Castlegar Gneiss Complex within the study area consists of two phases, the Kinnaird Gneiss and the China Creek Gneiss. The Kinnaird Gneiss and the China Creek Gneiss pegmatites were intruded in a sheet-like manner into the Trail Gneiss, the Mount Roberts Formation, and the basal part of the quartz dioritic/granodioritic phase of the Mackie Plutonic Complex and the western lobe of the Bonnington Pluton. Several postdeformational intrusive events disrupted the Castlegar Gneiss Complex, including a young granitic phase of the Mackie Plutonic Complex, inclusion-laden mafic sheets, Coryell syenite dykes, and basaltic to gabbroic dykes.

Three phases of ductile deformation and one phase of brittle deformation affected the area. During Phase-Two deformation strong simple shear strained the Castlegar Gneiss Complex and the Trail Gneiss with top-to-the-east sense of motion. The essentially unstrained lithologies located above these gneisses, including the Mount Roberts Formation metasediments, the overlying Jurassic Rossland Group, the Mackie Plutonic Complex, and the Bonnington Pluton were probably transported eastward on this sheared zone.

References

Berthe, D., Choukroune, P., and Jegouzo, P.
1979: Orthogneiss, mylonite and non-coaxial deformation of granites: the example of the South Armorican Shear Zone; Journal of Structural Geology, v. 1, p. 31-42.

Carr, S.D.
1985: Ductile shearing and brittle faulting in Valhalla Gneiss Complex, southeastern British Columbia; in Current Research, Part A, Geological Survey of Canada, Paper 85-1A, p. 89-96.

Corbett, C.R. and Simony, P.S.
1984: The Champion Lake Fault in the Trail-Castlegar area of southern British Columbia; in Current Research, Part A, Geological Survey of Canada, Paper 84-1A, p. 103-104.

Crowe, G.G.
1981: The structural evolution of the Mackie Plutonic Complex, southern British Columbia; unpublished M.Sc. thesis, University of Calgary, Calgary, Alberta, 154 p.

Hanmer, S.K.
1984: The potential use of planar and elliptical structures as indicators of strain regime and kinematics of tectonic flow; in Current Research, Part B, Geological Survey of Canada, Paper 84-1B, p. 133-142.

Little, H.W.
1960: Nelson map area, west half, British Columbia; Geological Survey of Canada, Memoir 308, 205 p.

1962: Trail map area, British Columbia; Geological Survey of Canada, Paper 62-5.

1982: Geology of the Rossland-Trail map area, British Columbia; Geological Survey of Canada, Paper 79-26.

Parrish, R.
1984: Slocan Lake Fault: a low angle fault zone bounding the Valhalla Gneiss Complex, Nelson map area, southern British Columbia: 1984 field work; in Current Research, Part A, Geological Survey of Canada, Paper 85-1A, p. 81-87.

Parrish, R., Carr, S.D., and Brown, R.L.
1985: Valhalla gneiss complex, southeast British Columbia: 1984 field work; in Current Research, Part A, Geological Survey of Canada, Paper 85-1A, p. 81-87.

Reesor, J.E.
1965: Structural evolution and plutonism in Valhalla Gneiss Complex, British Columbia; Geological Survey of Canada, Bulletin 129, 128 p.

Simony, P.S.
1979: Pre-Carboniferous basement near Trail, British Columbia; Canadian Journal of Earth Sciences, v. 16, p. 1-11.

Simpson, C. and Schmid, S.M.
1983: An evaluation of criteria to deduce the sense of movement in sheared rocks; Geological Society of America Bulletin, v. 94, p. 1281-1288.

A regional east-dipping thrust places Hadrynian onto probable Paleozoic rocks in Cariboo Mountains, British Columbia

Project 820014

L.C. Struik
Cordilleran Geology Division, Vancouver

Struik, L.C., A regional east-dipping thrust places Hadrynian onto probable Paleozoic rocks in Cariboo Mountains, British Columbia; in Current Research, Part A, Geological Survey of Canada, Paper 86-1A, p. 589-594, 1986.

Abstract

A regional thrust overlaps distinctive terranes of Hadrynian to Paleozoic rocks in east-central British Columbia. Cariboo Terrane of the Cariboo Mountains is underthrust from the west by Barkerville Terrane along the Pleasant Valley Thrust. Paleozoic components of the Snowshoe Group of Barkerville Terrane underlie Pleasant Valley Thrust from Barkerville to east of Wells Gray Provincial Park where the hanging wall rocks are the Hadrynian Kaza Group. Part of the Paleozoic Snowshoe Group rocks are laterally equivalent to those mapped as Hadrynian Horsethief Creek Group in the southern Cariboo Mountains.

Résumé

Une poussé régionale chevauche des terrains caractéristiques de roches hadryniennes à paléozoïques dans la partie centrale est de la Colombie-Britannique. Le terrain de Cariboo a été sous-charrié de l'ouest par le terrain de Barkerville le long du chevauchement de Pleasant Valley. Des éléments paléozoïques du groupe de Snowshoe du terrain de Barkerville sont sous-jacents au chevauchement de Pleasant Valley à partir de Barkerville jusqu'à l'est du parc provincial de Wells Gray où les roches du groupe hadrynien de Kaza forment la lèvre supérieure. Certaines roches du groupe paléozoïque de Snowshoe sont latéralement équivalentes aux roches appartenant au groupe hadrynien de Horsethief Creek dans le sud des monts Cariboo.

Figure 71.1. *Pre-Jurassic terranes in an area of British Columbia shown by the inset map. Lines A to F refer to structural cross-section shown in Figure 71.2.*

Introduction

Mapping of Precambrian to Mesozoic bedrock units from Big Valley Creek southeast to Angus Horne Lake in east central British Columbia (Fig. 71.1) (Struik, 1982a; 1982b; 1983a; 1983b; 1985b; 1985c) has delineated four stratigraphically and tectonically distinct packages of rock (terranes). They are inferred to have thrust together and metamorphosed during the Jurassic, remetamorphosed during the mid-Cretaceous, and disrupted by dextral strike-slip and associated faults from the mid-Cretaceous to the early Tertiary. The terranes are included in, or are correlative to, terranes mapped the length of the North American Cordillera (Struik, 1985c).

The terranes are from east to west: Cariboo (continental shelf clastics and carbonates), Barkerville (continental shelf clastics, carbonates and volcanics), Slide Mountain (oceanic rift volcanics, intrusives and clastics), and Quesnel (island arc volcanics and clastics) (Fig. 71.1). The thrusts that separate the terranes are the east-dipping Pleasant Valley (placing Cariboo on Barkerville), flat Pundata (placing Slide Mountain on Barkerville and Cariboo), and west-dipping Eureka (placing Slide Mountain and Quesnel on Barkerville) (Fig. 71.1) (Struik, 1985a; 1985b; 1985c).

Within the Canadian Cordillera, Cariboo is a subterrane of Cassiar, Barkerville contains equivalents of Kootenay and Yukon-Tanana terranes and Slide Mountain and Quesnel are Cordillera-wide terranes.

Definition of Cariboo and Barkerville terranes

Cariboo Terrane is more completely defined as the Precambrian to Triassic? rocks of the Kaza, Cariboo and Black Stuart groups, Greenberry and Alex Allen formations and undifferentiated Permo-Triassic strata (Struik, 1985c) and underlies the Cariboo Mountains south to the headwaters of the North Thompson River. Herein, the Kaza Group is used as defined by Sutherland Brown (1963) and Murphy and Rees (1983); the Cariboo Group as described by Struik (1982a) as the Eastern Cariboo Group; the Black Stuart Group as described by Struik (1981) as the Black Stuart and Guyet formations; and the Greenberry and Alex Allen formations are described by Orchard and Struik (1985). Structures in the terrane plunge northerly exposing progressively older units to the southeast.

Struik (1982a) differentiated rocks of Cariboo Terrane (called Eastern Cariboo Group) from those of Barkerville Terrane (called Western Cariboo Group) on the grounds of stratigraphic differences and age, and recognized the Pleasant Valley Thrust which separates the two sequences. The Pleasant Valley Thrust is folded and its trace, north to south, cuts progressively downsection in the hanging-wall (Cariboo Terrane) and somewhat upsection in the footwall (Barkerville Terrane) (Fig. 71.2). Paleozoic units of the Snowshoe Group of Barkerville Terrane are everywhere directly overlain by the Pleasant Valley Thrust.

Barkerville Terrane consists of Precambrian to Permian rocks called Snowshoe Group and Sugar limestone as described by Struik (1985c). Regionally mappable units of the Snowshoe Group found from Cariboo Lake to Wells Gray Provincial Park are pre-, syn- and post-Downy succession (Fig. 71.3). The base of the Downey succession is marked by limestone and pyroclastic basalt and the top by the Bralco marble. The Downey and Bralco are assigned to the Paleozoic because they locally contain poorly preserved algae, echinoderm, byrozoan and ostracod(?) fragments (B.L. Mamet, personal communication, 1983) near Barkerville and Cariboo Lake. Pre-Downey rocks are mainly interpreted as Precambrian. The three fold division can be traced by means of the marbles and basalt to the eastern border of Wells Gray Park.

Stratigraphy at Wells Gray Park

The Snowshoe Group can now be traced in apparent continuity from Barkerville to Wells Gray Provincial Park, where it is equivalent to rocks mapped by Pell (1984) along the eastern border of the park as Horsethief Creek and Kaza groups. The equivalence, however, is a contradiction because the Horsethief Creek and Kaza groups are thought to be entirely Precambrian and the parts of the Snowshoe Group linked to them are Paleozoic.

The stratigraphy as mapped by Pell (1984) near Slide Mountain (Fig. 71.2, section F-F') east of Wells Gray Park consists of the semipelite and amphibolite, middle marble and upper clastic units ascribed to the Horsethief Creek Group (Fig. 71.3). The semipelite-amphibolite unit consists mainly of psammite, semipelite, pelite, and grit capped by orthoquartzite and pelite, ranging in metamorphic grade from garnet to kyanite. To the northwest it passes directly into the Downey succession of the Snowshoe Group. North of Azure Lake, as throughout the belt northwest to Barkerville, the base of the Downey succession is marked by a unit of interlayered carbonate, pelite, metabasalt, and quartzose rocks. Metabasalt (amphibolite where above garnet grade) is characteristic of the lower half of the Downey succession and in chlorite-grade rocks near Barkerville the protolith is pyroclastic basalt.

The middle marble unit consists of one to three, but principally two bands of light grey weathering marble separated by grit, psammite and semipelite. The marble bands generally contain a central layer of pelitic marble and the lower and upper contacts of the unit are commonly marked by quartzose marble (Fig. 71.3). The middle marble is equivalent to the Bralco marble of the Snowshoe Group as mapped in Wells Gray Park (Struik, 1985b) and to the northwest.

The upper clastic unit consists of semipelite, psammite and lesser amounts of grit and is capped by brown weathering thinly layered quartzose and pelitic marble. It is assumed to be equivalent to clastics which overlie the Bralco marble north of Azure River (Struik, 1985b) and between the North and East arms of Quesnel Lake (Struik, 1983b).

The Snowshoe Group through Wells Gray Provincial Park and northwest toward Barkerville is overthrust by the Cariboo and Kaza groups. East of Wells Gray Park, the Paleozoic part of the Snowshoe Group is the same as the upper clastic, middle marble and semipelite-amphibolite units of the Horsethief Creek Group (of Cariboo Mountains) of Pell (1984). The overlying Hadrynian Kaza Group is therefore inferred to be thrust onto the "Horsethief Creek Group" in the southeastern Cariboo Mountains along the easterly extension of the Pleasant Valley Thrust.

Pleasant Valley Thrust

The Pleasant Valley Thrust is inferred east of Wells Gray Park from the stratigraphic linkage of the Snowshoe Group with those rocks directly underlying the Kaza Group. Physical features which may mark the thrust include the presence of mylonites within the brown weathering dirty marbles at the top of the upper clastic unit along section F-F' (Fig. 71.2), local cutoffs of the thick bedded grit unit of the Kaza Group onto the mylonitic marble, and finally the apparent cutoff of an interval of the upper clastic unit under the thick bedded grit from the southeast to northwest.

At Slide Mountain (Fig. 71.2, section F-F') olive-grey grit in bundles of thick beds separated by olive-grey semipelite, assigned to the Kaza Group, directly overlies mylonitic marble of the upper clastic unit. The marble was mapped as Kaza Group carbonate by Pell (1984). In some places the grit beds are cut off at the contact with the marble. On the ridge southeast of Slide Mountain grey pelite,

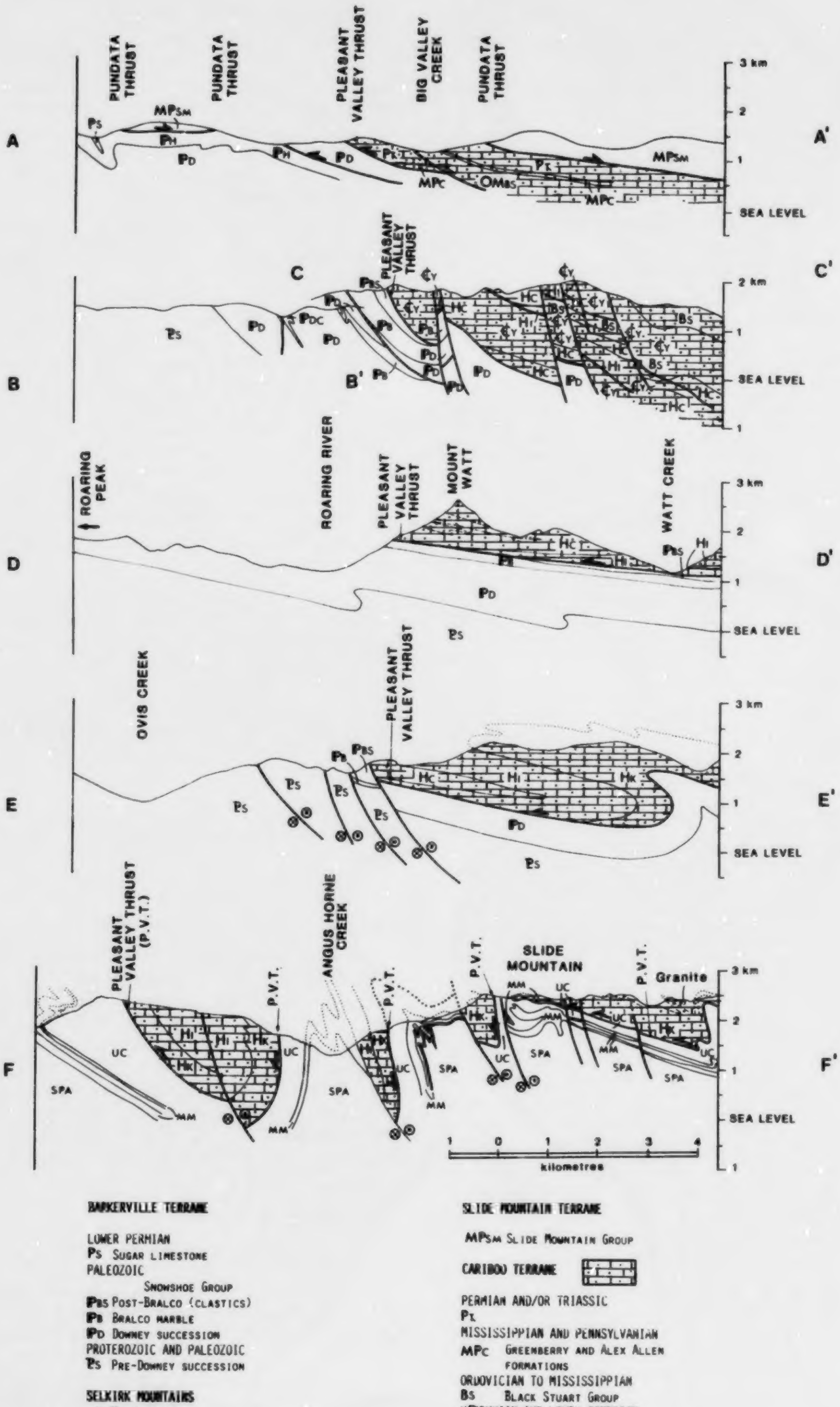

Figure 71.2. *Structural cross-sections emphasizing the Cariboo-Barkerville terrane boundary (Pleasant Valley Thrust) through the area of Figure 71.1.*

semipelite and light grey psammite lie between the Kaza Group grit and the marble. The grey rocks resemble more the upper clastic unit underlying the marble than they do the overlying Kaza Group grit sequence. The grey rocks may be an upper part of the upper clastic unit which is structurally cut out to the northwest. The cut-off of progressively lower units in the footwall of the Pleasant Valley Thrust is consistent throughout the exposure of the thrust to the northwest (Fig. 71.2).

Summary

Cariboo and Barkerville terranes are separated by the east-dipping folded Pleasant Valley Thrust. The thrust fault cuts down section in the hanging-wall Cariboo Terrane and somewhat upsection in the footwall Barkerville Terrane along its trace to the southeast. In the southernmost part of the map (Fig. 71.1) it is nearly parallel to bedding and places Kaza Group onto Snowshoe Group, an older over younger relationship. Rocks mapped as Hadrynian Horsethief Creek Group (Pell, 1984) east of Wells Gray Provincial Park are laterally equivalent to those mapped as Paleozoic Snowshoe Group.

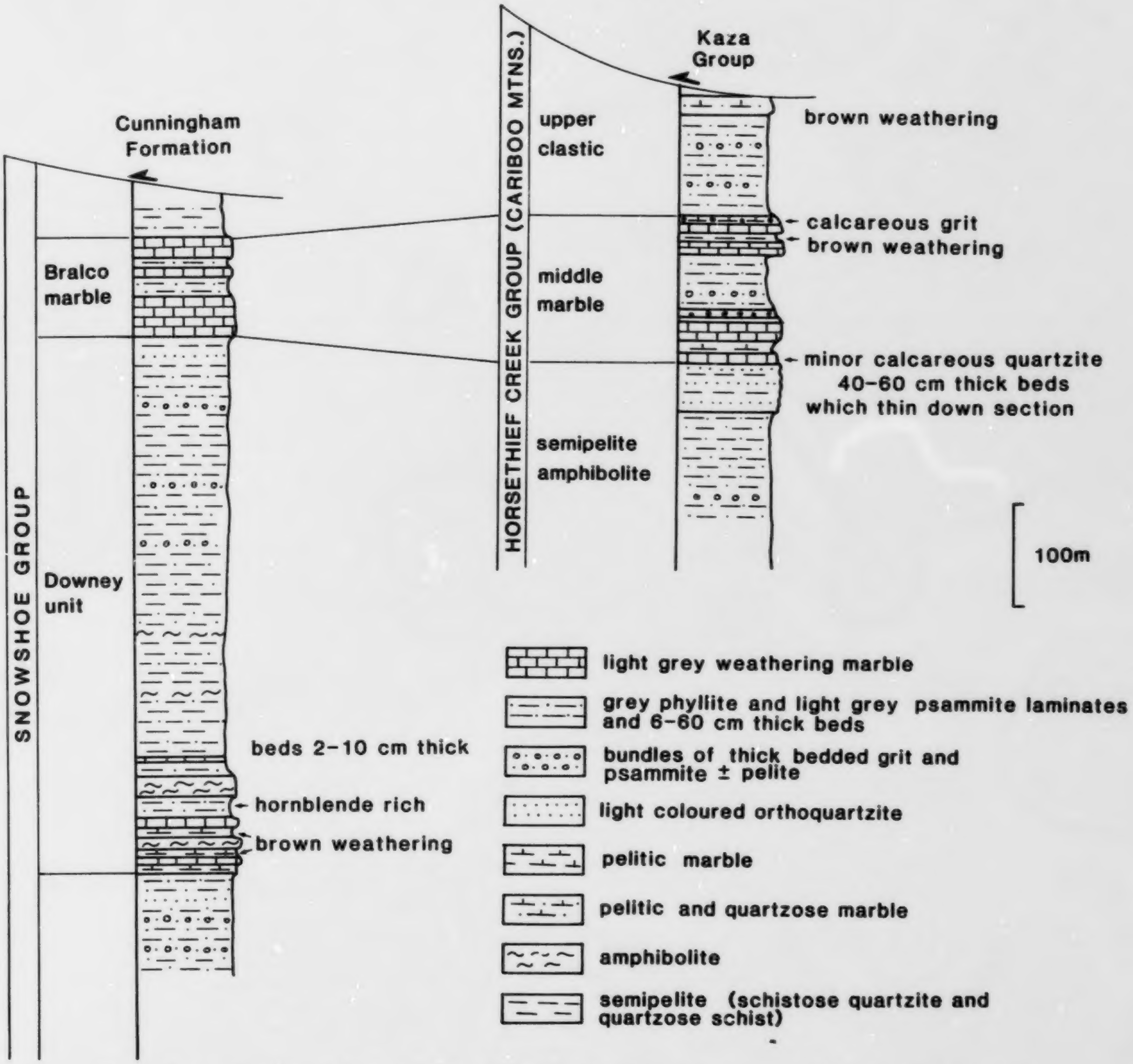

Figure 71.3. *Stratigraphic sections through the Snowshoe and Horsethief Creek groups. The Snowshoe Group section is an approximate compilation of sequences north of Azure Lake and the Horsethief Creek Group section represents the sequence south of structure section F-F' (Fig. 71.1, 71.2). The two sequences are essentially the same and are laterally linked; the Bralco and middle marbles can be traced into each other as can the upper part of the Downey and the semipelite-amphibolite units. The carbonate and amphibolite layers at the base of the Downey would correspond to the amphibolite bearing part of the semipelite-amphibolite unit, which Pell (1984) describes as downsection from the level displayed.*

References

Murphy, D.C. and Rees, C.J.
1983: Structural transition and stratigraphy in the Cariboo Mountains, British Columbia; in Current Research, Part A, Geological Survey of Canada, Paper 83-1A, p. 245-252.

Orchard, M.J. and Struik, L.C.
1985: Conodonts and stratigraphy of upper Paleozoic limestone of Cariboo gold belt, central British Columbia; Canadian Journal of Earth Sciences, v. 22, p. 538-552.

Pell, J.
1984: Stratigraphy, structure, and metamorphism of Hadrynian strata in southeast Cariboo Mountains, British Columbia; unpublished PhD Thesis, University of Calgary, 185 p.

Struik, L.C.
1981: A re-examination of the type area of the Devono-Mississippian Cariboo Orogeny, central British Columbia; Canadian Journal of Earth Sciences, v. 18, p. 1767-1775.

1982a: Snowshoe Formation (1982), central British Columbia; in Current Research, Part B, Geological Survey of Canada, Paper 82-1B, p. 117-124.

1982b: Bedrock geology of Cariboo Lake (93A/14), Spectacle Lake (93H/3), Swift River (93A/13) and Wells (93H/4) map areas, central British Columbia; Geological Survey of Canada, Open File 858.

Struik, L.C. (cont.)
1983a: Bedrock geology of Spanish Lake (93A/11) and parts of adjoining map areas, central British Columbia; Geological Survey of Canada, Open File 920.

1983b: Bedrock geology of Quesnel Lake (93A/10) and part of Mitchell Lake (93A/15) map areas, central British Columbia; Geological Survey of Canada, Open File 962.

1985a: Pre-Cretaceous terranes and their thrust and strike-slip contacts, Prince George east half and McBride west half, British Columbia; in Current Research, Part A, Geological Survey of Canada, Paper 85-1A, p. 267-272.

1985b: Dextral strike-slip through Wells Gray Provincial Park, British Columbia; in Current Research, Part A, Geological Survey of Canada, Paper 85-1A, p. 305-309.

1985c: Thrust and strike-slip faults bounding tectonostratigraphic terranes, central British Columbia; in Field Guides to Geology and Mineral Deposits in the Southern Canadian Cordillera, ed. D.J. Tempelman-Kluit; Geological Society of America, Cordilleran Section, p. 14.1-14.8.

Sutherland Brown, A.
1963: Geology of the Cariboo River area, British Columbia; British Columbia Department of Mines and Petroleum Resources, Bulletin 47.

Radiolarian ages from the Cache Creek and Bridge River complexes and from chert pebbles in Cretaceous conglomerates, southwestern British Columbia

Project 800029

F. Cordey[1]
Cordilleran Geology Division, Vancouver

Cordey, F., Radiolarian ages from the Cache Creek and Bridge River complexes and from chert pebbles in Cretaceous conglomerates, southwestern British Columbia; in Current Research, Part A, Geological Survey of Canada, Paper 86-1A, p. 595-602, 1986.

Abstract

Radiolarians from four localities in the Cache Creek Complex and from twelve localities in the Bridge River Complex range in age respectively, from Early Permian to Late Triassic and from Middle Triassic to Early Jurassic. Radiolarian chert pebbles from Cretaceous conglomerates in the region show the same Permian to Jurassic range.

Résumé

L'âge des radiolaires provenant de quatre emplacements dans le complexe de Cache Creek et de douze emplacements dans le complexe de Bridge River varie respectivement du Permien ancien au Trias récent et du Trias moyen au Jurassique ancien. L'âge des radiolarites provenant de conglomérats crétacés dans la région varie également du Permien au Jurassique.

[1] Université Pierre et Marie Curie, Laboratoire de Stratigraphie, 4, Place Jussieu, 75230 Paris Cedex, France

Introduction

The Cache Creek and Bridge River complexes in southwestern British Columbia comprise disrupted radiolarian chert, argillite, mafic volcanic and ultramafic rock and locally extensive bodies of carbonate. These rocks are inferred (e.g., Monger and Price, 1979) to be lower Mesozoic accretionary complexes of oceanic provenance. Prior to 1971 the only diagnostic fossils that had been reported were Permian fusulinids from the Cache Creek Complex. In 1971, Cameron and Monger extracted Middle Triassic conodonts from carbonates in the Bridge River Complex, which at that time was called Fergusson Group. In 1977, radiolarian cherts collected by Monger (personal communication) from the Bridge River Complex were sent to D.L. Jones of the United States Geological Survey, who suggested in a written communication with E.A. Pessagno, University of Texas, that the radiolaria range from Late Triassic to Early Jurassic. Later, D.L. Jones (oral communication, 1981) collected Permian and Triassic radiolaria from the Cache Creek Complex, and Orchard (1981, 1984, and personal communication) extracted Pennsylvanian, Permian and Triassic conodonts from the Cache Creek Complex, and Late Triassic conodonts from the Bridge River Complex.

The present study, funded by Centre National de la Recherche Scientifique-ASP 950078 (Paris), and supported in the field by the Geological Survey of Canada under Project 800029, was undertaken in part to determine the upper age limits of these accretionary complexes, because conodonts are not known in rocks younger than Upper Triassic. In addition, radioloarian-chert clasts in known and possible mid-Cretaceous chert-pebble conglomerates were sampled in order to clarify the provenances of the conglomerates. The study is not complete; this paper reports the results of field work during 1984.

Method

Radiolarians were identified first with a hand lens in the field prior to sampling. In the laboratory, the samples were dissolved in very dilute hydrofluoric acid (1 to 2%) for one week, using the extraction technique of Dumitrica (1970) and Pessagno and Newport (1972), as slightly modified by De Wever (1982). The chert pebbles from conglomerates were first cleaned with concentrated hydrofluoric acid to avoid risk of contamination (Seiders and Blome, 1984), and this was followed by separate etching of each pebble in dilute acid.

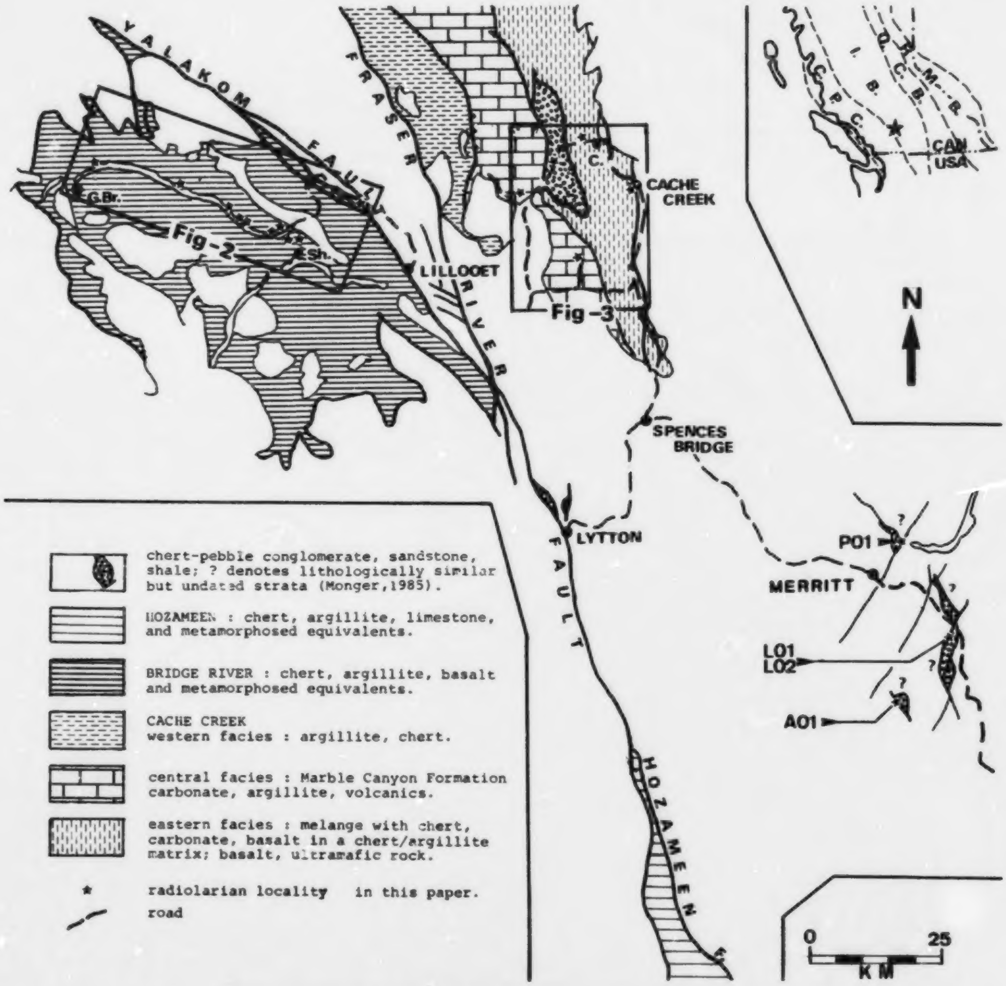

Figure 72.1. Lithological units and radiolarian localities, southwestern British Columbia.

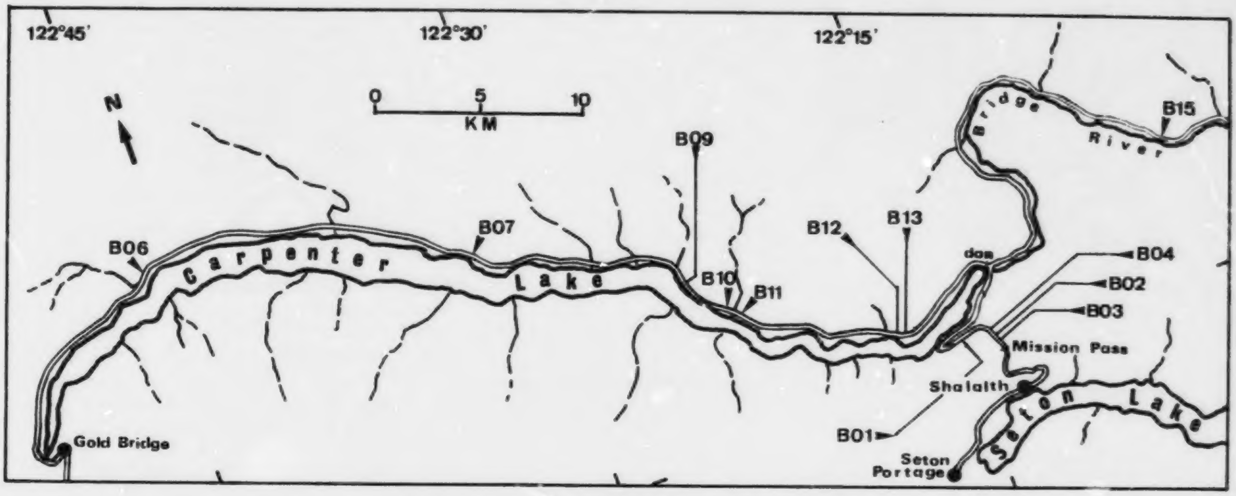

Figure 72.2. Radiolarian localities, Bridge River Complex, British Columbia.

Table 72.1. Bridge River complex localities (see also Fig. 72.2)

Locality	Longitude/Latitude	Grid reference	Location (kilometres by road given)
B01	122°15'20";50°46'00"	Bridge River 92J/16 52540	On road between Seton and Carpenter Lakes, 3.45 km from Mission Pass.
B02	122°14'13";50°45'21"	Bridge River 92J/16 539228	1.35 km north of Mission Pass.
B03	122°14'00";50°45'06"	Bridge River 92J/16 541223	0.50 km north of Mission Pass.
B04	122°14'10";50°45'28"	Bridge River 92J/16 536230	1.75 km north of Mission Pass.
B06	122°45'00";50°53'55"	Bralorne 92J/15 176384	10 km east of Gold Bridge (bridge), on north side of Carpenter Lake.
B07	122°32'00";50°51'50"	Bralorne 92J/15 324346	28 km from Gold Bridge, north side of Carpenter Lake.
B09	122°24'50";50°49'29"	Bridge River 92J/16 413303	39 km from Gold Bridge, 0.6 km east of Bighorn Creek, north side Carpenter Lake.
B10	122°23'26";50°48'19"	Bridge River 92J/16 429282	42 km from Gold Bridge, west of Fall Creek, north side Carpenter Lake.
B11	122°23'13";50°48'16"	Bridge River 92J/16 432281	43 km from Gold Bridge, east of Fall Creek, north side Carpenter Lake.
B12	122°17'16";50°46'02"	Bridge River 92J/16 502241	52 km from Gold Bridge, 0.7 km east of Viera Creek, north side Carpenter Lake.
B13	122°17'08";50°46'00"	Bridge River 92J/16 504240	0.9 km east of Viera Creek, north side of Carpenter Lake.
B15	122°04'05";50°48'47"	Bridge River 92J/16 657292	North side Bridge River Valley, 27 km from the Carpenter Lake dam toward Lillooet.

Table 72.2. Cache Creek Complex localities (see also Fig. 72.3)

Locality	Longitude/Latitude	Grid reference	Location (kilometres by road given)
C02	121°27'44";50°41'13"	Ashcroft 92I/11 086159	2.2 km south of fire lookout on Cornwall Hills.
C03	121°19'39";50°48'27"	Cache Creek 92I/14 179295	West side of settlement of Cache Creek.
C05	121°26'15";50°53'10"	Cache Creek 92I/14 099381	On the Highway 12, 3.0 km west of Highway 97.
C08	121°36'51";50°47'05"	Pavilion E 92I/13 977284	300 m north of Highway 12, 20.1 km west of Highway 97.

Table 72.3. Chert-pebble conglomerate localities (see Figures 72.1, 72.3)

Locality	Longitude/Latitude	Grid reference	Location (kilometres by road given)
C07	121°32'05";50°51'10"	Pavilion E 93I/13 032342	On Highway 12, 11.2 km from Cariboo Highway 97.
P01	120°42'47";50°10'00"	Merritt 92I/2 634595	5 km northeast of Merritt.
L01	120°36'42";50°00'32"	Merritt 92I/2 711422	0.2 km west from Highway 5 (elevation 3500 ft).
L02	120°36'57";50°00'08"	Merritt 92I/2 709415	0.6 km west of Highway 5 (elevation 4000 ft).
A01	120°46'25";49°54'30"	Aspen Grove 92H/15 598305	9.75 km east of Kingsvale; 1.5 km south of Vogt Creek Road

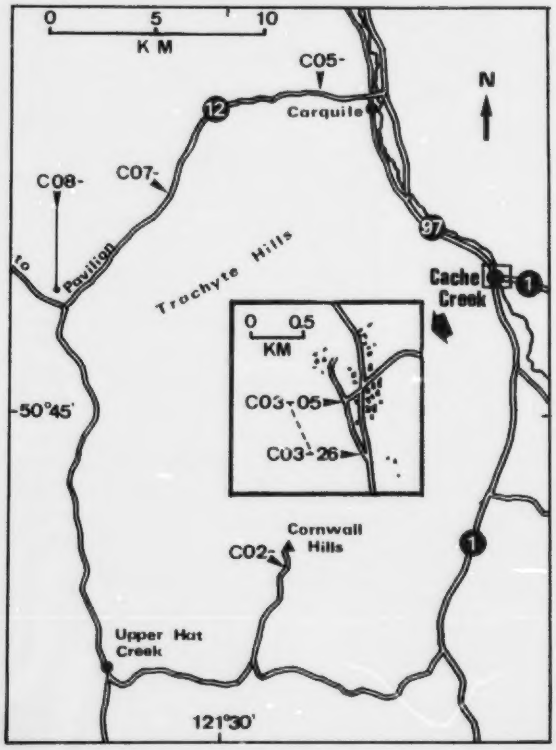

Figure 72.3. Radiolarian localities near Cache Creek, British Columbia.

In general, the radiolarians recovered from chert pebbles were found to be better preserved than those from the Cache Creek and Bridge River complexes. The recovery rate, namely, number of determinable radiolarians extracted/number of samples collected with visible radiolarians, ranged from 0 to 45% (average 20%) for cherts within the complexes, to 12 to 70% (average 50%) from chert pebbles in conglomerates.

Bridge River Complex

The Bridge River Complex, located west of Lillooet in the eastern margin of the Coast Plutonic Complex, is a Middle Triassic to Lower Jurassic melange comprising tectonically disrupted chert, argillite, basalt, alpine-type ultramafic rock and minor carbonate (Potter, 1983). Its probable south-southeasterly continuation, across the Fraser River Fault System, is the Hozameen Group (Fig. 72.1), which contains Permian to Lower, and possibly Middle Jurassic strata (R.A. Haugerud, in Monger and McMillan, 1984).

Radiolarian chert samples were collected along the road on the north side of Carpenter Lake, which lies 20 km west of the town of Lillooet (Fig. 72.2 and Table 72.1). There, ribbon chert probably forms more than half of the total outcrop, and consists of beds 1 to 10 cm thick that are commonly broken and highly disrupted; because of this it is not possible to measure sections.

Twelve ribbon chert outcrops provided radiolarians that were sufficiently well-preserved to permit the determinations given in Table 72.4. Seven locations are new (B01, 02, 03, 04, 06, 07, 09), and the remainder coincide with localities collected by Potter (1983). Ages range from Middle Triassic (B15) to Lower Jurassic (B07), with most in the Upper Triassic (Table 72.4). Ages generally become younger westward, with the exception of B06.

Table 72.4. Radiolarian associations and age of specimens from Bridge River Complex

B01-10 Bridge River Group age: Late Triassic (late Carnian to Norian)

Capnuchosphaera sp.	Late Triassic (late Carnian to early middle Norian)
Kahlerosphaera(?) sp.	Late Triassic
Poulpus phasmatodes De Wever	Carnian-Norian
Sarla sp. cf S. natividadensis Pessagno	Late Triassic (early Carnian to late Norian)
Stylosphaera(?) spinulosa (Nakaseko & Nishimura)	?Late Triassic
Stylosphaera(?) compacta (Nakaseko & Nishimura)	?Late Triassic
Tetraporobrachia sp.	known in late Carnian

B02-01 Bridge River Group age: Late Triassic

Capnodoce sp. cf C. venusta Pessagno	Late Triassic (late Carnian to early middle Norian)
Capnodoce sarisa De Wever	Late Triassic
Gorgansium sp.	Late Triassic to Late Jurassic
Sarla sp.	Late Triassic (early Carnian to late Norian)

B03-01 Bridge River Group age: Triassic

Emiluvia(?) sp. cf E.(?) cochleata Nakaseko & Nishimura	?Anisian to early Ladinian?
Staurocontium sp. cf S. minoense Nakaseko & Nishimura	?Late Triassic
Stylosphaera(?) helicata (Nakaseko & Nishimura)	?Late Triassic
Stylosphaera sp. cf S.(?) spinulosa (Nakaseko & Nishimura)	?Late Triassic

B04-03 Bridge River Group age: Late Triassic-Jurassic

Gorgansium sp.	Late Triassic to Late Jurassic
Kozurastrum sp.	Triassic-Early Jurassic (middle Jurassic?)

B06-02 Bridge River Group age: probably Late Triassic

Sarla sp.	Late Triassic (early Carnian to late Norian)

B07-01 Bridge River Group age: Early Jurassic

Canoptum anulatum Pessagno & Poisson	Early Jurassic (L.Pliens.) to Mid.Jurassic(Bajocian)
Canutus sp.	Early Jurassic (Sinemur. to Toarc./L.Pliensbachian)
Eucyrtidium(?) sp. C in YAO 1982	early Early Jurassic?
Hagiastrum sp.	Early Sinemurian to Early Cretaceous
Hsuum sp.	early Pliensbachian to late Valanginian
Lupherium sp.	Early Jurassic (Late Pliensbachian) to m. Jurassic
Parahsuum(?) sp. C in YAO 1982	early Early Jurassic?
Stichocapsa sp.A in YAO 1982	early Early Jurassic?
Trillus elkhornensis Pessagno & Blome	Pliensbachian to Bajocian

B09-01 Bridge River Group age: Late Triassic

Canoptum triassicum Yao	late Norian and Rhaetian
Capnodoce sp.	Late Triassic
Pentaspongodiscus(?) sp.	Late Anisian to Carnian
Sarla sp.	Late Triassic (early Carnian to late Norian)

B10-02 Bridge River Group age: Late Triassic

Canoptum sp.	Late Triassic (Carnian) to Middle Jurassic
Pantanellium sp.	Late Triassic (early Carnian) to Early Cretaceous
Sarla sp.	Late Triassic (early Carnian) to late Norian)

B11-04 Bridge River Group age: Late Triassic

Capnuchosphaera triassica De Wever	Late Triassic
Kahlerosphaera parvispinosa Kozur & Mostler	early Carnian
Praeorbiculiformella sp.	Triassic
Pseudoheliodiscus sp.	Triassic-early Jurassic
Spongostylus sp.	early Carnian
Stylosphaera(?) spinulosa (Nakaseko & Nishimura)	?Late Triassic
Tetraspongodiscus sp.	?Ladinian-early Carnian insofar as known

B12-02 Bridge River Group age: Late Triassic (Carnian to Middle Norian)

Capnodoce baldiensis Blome	Late Triassic (l.Carnian?-e.to l.Middle Norian)
Capnuchosphaera deweveri Kozur & Mostler	Late Triassic (Carnian to late Middle Norian)
Renzium sp.	Late Triassic (l.Carnian?-e.to l. Middle Norian)
Triassocampe nova Yao	Carnian to Norian

B13-01 Bridge River Group age: Late Triassic

Canoptum rhaeticum Kozur & Mostler	Late Triassic (Norian-Rhaetian)
Capnodoce sp.	Late Triassic
Kozurastrum sp.	Triassic-Early Jurassic (MiddleJurassic?)
Pantanellium sp.	Late Triassic to early Cretaceous
Sarla prietoensis Pessagno	Late Triassic (late Middle to early middle Norian)

B15-02 Bridge River Group age: Middle Triassic

Falcispongus calcaneum Dumitrica	late Anisian to early Ladinian insofar as known
Oertlispongus sp.	Anisian to Ladinian
Triassocampe deweveri (Nakaseko & Nishimura)	?Ladinian

Table 72.5. Cache Creek Complex – Radiolarian associations and age of specimens

C02-08 Cache Creek Group (central belt) age: Middle-Late Triassic (Middle Anisian(?) to Norian)

Eptingium sp. cf E. manfredi Dumitrica	Middle Anisian(?) to Norian
Staurosphaera(?) sp. B in Yao 1982	?Ladinian, so far as known
Stylosphaera(?) spinulosa (Nakaseko & Nishimura)	?Late Triassic
Triassocampe sp.	Middle Triassic (Ladin. to Late Triassic (Norian)

C02-14 Cache Creek Group (central belt) age: Middle-Late Triassic (Middle Anisian(?)-Norian)

Stylosphaera(?) japonica (Nakaseko & Nishimura)	?Ladinian-Norian
Baumgartneria retrospina Dumitrica	Late Anisian to Carnian, insofar as known
Eptingium manfredi Dumitrica	Middle Anisian(?) to Norian

C03-05 Cache Creek Group (eastern belt, matrix) age: Late Triassic (late Carnian to middle Norian)

Capnodoce kochi Blome	Late Triassic (l.Carn.(?); e.to l.Middle Norian)
Capnodoce sarisa De Wever	Late Triassic
Capnodoce sp. cf C. fragilis Blome	Late Triassic (l.Carn.(?); e.to l.Middle Norian)
Capnodoce sp. cf C. media Blome	Late Triassic (l.Carn.(?); e.to l.Middle Norian)
Capnuchosphaera sp.	Late Triassic (late Carnian to late Middle Norian)
Paleosaturnalis sp.	Late Triassic
Renzium sp.	Late Triassic (l.Carn.(?); e.to l.Middle Norian)

C03-09 Cache Creek Group (eastern belt, matrix) age: Middle-Late Triassic (Ladinian to Norian)

Stylosphaera(?) spinulosa (Nakaseko & Nishimura)	?Late Triassic
Triassocampe sp.	Middle Triassic (Ladin.) to Late Triassic (Norian)
Welirella sp.	Middle-Late Triassic

C03-13 Cache Creek Group (eastern belt, matrix) age: probably Middle Triassic (late Anisian to Ladinian?)

Gomberellus sp.	?Ladinian
Oertlispongus sp.	Late Anisian to Ladinian, insofar as known
Paroertlispongus sp.	Late Anisian to Ladinian, insofar as known
Paurinella sp.	Late Anisian to early Carnian, insofar as known
Tetraspongodiscus sp.	Late Anisian to Carnian

C03-20 Cache Creek Group (eastern belt, matrix) age: Middle Triassic-Late Triassic (Mid.Anis.(?) to Norian)

Eptingium sp. cf E. manfredi Dumitrica	Middle Anisian(?) to Norian
Gomberellus sp.	?Ladinian
Plafkerium longidentatum Kozur & Mostler	?Late Anisian-Ladinian insofar as known
Stylosphaera(?) japonica (Nakaseko & Nishimura)	?Ladinian-Norian

C03-23 Cache Creek Group (eastern belt, matrix) age: Middle-Late Triassic

Stylosphaera(?) spinulosa (Nakaseko & Nishimura)	?Late Triassic
Eptingium sp. cf E. manfredi Dumitrica	Middle Anisian (?) to Norian
Triassocampe sp. T. deweveri Kozur & Mostler	?Ladinian

C03-26 Cache Creek Group (eastern belt, matrix) age: Late Triassic (late Carnian to Middle Norian)

Canesium sp.	Late Triassic (l.Carn.(?); e.to l.Middle Norian)
Capnodoce fragilis Blome	Late Triassic (l.Carn.(?); e.to l.Middle Norian)
Capnodoce sarisa De Wever	Late Triassic
Capnodoce sp. cf C. malaca Blome	Late Triassic (l.Carn.(?); e.to l.Middle Norian)
Capnodoce sp. cf C. primaria Pessagno	Late Triassic (l. Carnian to l. Middle Norian)
Triassocampe sp.	Middle Triassic (Ladinian) to Late Triassic (Norian)
Xipha sp.	Late Triassic (l.Carn.(?); e.to l.Middle Norian)

C05-01 Cache Creek Group (central belt) age: probably Early Permian

Pseudoalbaillella scalprata Holdsworth & Jones	Early Permian
Pseudoalbaillella sp. cf Ps. longuscornis Ishiga & Imoto	Early Permian

C08-01 Cache Creek Group (central belt) age: Middle-Late Triassic (Middle Anisian(?) to Norian)

Stylosphaera(?) sp. cf S. spinulosa (Nakaseko & Nishimura)	?Late Triassic
Eptingium sp. cf E. manfredi Dumitrica	Middle Anisian (?) to Norian
Triassocampe sp.	Middle Triassic (Ladinian) to Late Triassic (Norian)

C08-09 Cache Creek Group (central belt) age: Triassic

Stylosphaera(?) compacta (Nakaseko & Nishimura)	?Late Triassic
Stylosphaera(?) japonica (Nakaseko & Nishimura)	?Ladinian-Norian
Triassocampe sp. cf T. deweveri (Nakaseko & Nishimura)	?Ladinian

Table 72.6. Chert-pebble conglomerates – Radiolarian associations and ages for specimens

C07-14 pebble from Cretaceous conglomerate, Highway 12	**age: Late Permian**
Follicuculus scholasticus Ormiston & Babcock	Late Permian
Follicuculus ventricosus Ormiston & Babcock	Late Permian
P01-22 pebble from conglomerate near Merritt	**age: Middle-Late Triassic**
Stylosphaera(?) sp. cf S. spinulosa (Nakaseko & Nishimura)	?Late Triassic
Tetraporobrachia sp.	early Carnian
Triassocampe(?) sp. cf T. deweveri (Nakaseko & Nishimura)	?Ladinian
Triassocampe(?) sp. G in YAO 1982	?Ladinian
P01-42 pebble from conglomerate near Merritt	**age: Early Jurassic**
Emiluvia sp.	Early Jurassic-Early Cretaceous
Hsuum sp.	Early Jurassic (e.Pliens.) to e.Cret.(Valongnian)
Parahsuum simplum Yao	early Early Jurassic?
Praeconocaryomma sp. cf P. immodica Pessagno & Poisson	Early Jurassic (Sinemurian-Pliensbachian)
Praeconocaryomma sp. cf P. media Pessagno & Poisson	Early Jurassic (?Pliensbachian?)
L01-01 pebble from conglomerate near Courtney Lake	**age: probably Late Permian**
Follicuculus sp. cf F. scholasticus Ormiston & Babcock	Late Permian
Nazarovella sp.	Late Permian
Pseudoalbaillella sp.	Carboniferous-Permian
Quinqueremis sp.	Late Carboniferous to Late Permian
L02-01 pebble from conglomerate near Courtney Lake	**age: Early Permian**
Pseudoalbaillella lomentaria Ishiga & Imoto	Early Permian
Pseudoalbaillella sp. cf Ps. u-forma Holdsworth & Jones	?Early Permian
Quinqueremis sp.	Late Carboniferous to Late Permian
L02-04 pebble from conglomerate near Courtney Lake	**age: Late Triassic (Norian)**
Canesium sp.	Late Triassic (l.Carn?; e.to l.Middle Norian)
Capnodoce antiqua Blome	Late Triassic (l.Carn.?; e.to l.middle Norian)
Capnuchosphaera sp.	Late Triassic
Corum sp.	Late Triassic (l.Carn.?; e.to l.Middle Norian)
Poulpus pansus De Wever	Late Triassic
Poulpus piabyx De Wever	Late Triassic (Norian)
Guasipetasus sp.	Late Triassic (l.Carn.?; e.to l.Middle Norian)
Renzium adversum Blome	Late Triassic (l.Carn.?; e.to l.Middle Norian)
Sarla sp. cf S. delicata Blome	Late Triassic (l.Carn.?; e.to l.Middle Norian)
Spongosaturnalis sp. cf S. elegans Kozur & Mostler	Late Triassic
Triassocampe nova Yao	Carnian-Norian
A01-02 pebble from conglomerate near Vogt Creek	**age: Middle-Late Triassic**
Pterospongus(?) sp.	Ladinian-Carnian
A01-08 pebble from conglomerate near Vogt Creek	**age: Early Permian**
Albaillella sp.	Carboniferous-Permian
Latentifistula crux Nazarov & Ormiston	Early Permian (Asselian insofar as known)
Latentifistula sp.	Early Carboniferous to Early Permian
Octatormentum sp. cf O. cornelli Nazarov & Ormiston	Early Permian
Guadriremis sp.	Late Carboniferous to Late Permian
A01-21 pebble from conglomerate near Vogt Creek	**age: Early Permian**
Pseudoalbaillella longuscornis Ishiga & Imoto	Early Permian (Wolfcampian insofar as known)
Pseudoalbaillella scalprata Holdsworth & Jones	Early Permian
Pseudotormentus kamigoriensis De Wever & Caridroit	Late Permian insofar as known
Quinqueremis sp.	Late Carboniferous to Late Permian
A01-28 pebble from conglomerate near Vogt Creek	**age: Early Jurassic**
Dictyomitrella sp. cf sp. C in YAO 1982	early Early Jurassic?
Hsuum sp.	early Pliensbachian to late Valanginian
Pantanellium sp. cf P. tanuense Pessagno & Blome	Rhaetian(?)-Hettangian
Pantanellium sp.	Late Triassic (early Carnian) to Early Cretaceous
Parahsuum simplum Yao	early Early Jurassic?
Parahsuum(?) sp. C in YAO 1982	early Early Jurassic?
Praeconocaryomma immodica Pessagno & Poisson	Early Jurassic to early Tithon.-late Kimmer.
A01-31 pebble from conglomerate near Vogt Creek	**age: Late Triassic**
Capnodoce sp.	Late Triassic (late Carnian to late Middle Norian)
Capnuchosphaera schenki Blome	Late Triassic (late Carnian to late Middle Norian)
Capnuchosphaera theloides De Wever	Late Triassic
Sarla sp.	Late Triassic (early Carnian to late Norian)

Cache Creek Complex

All radiolarians are from the central and eastern belt of the Cache Creek Complex (Monger and McMillan, 1984). The central belt comprises mid- to Late Permian and Triassic carbonates of the Marble Canyon Formation and minor thin-bedded chert, tuff and chert of Triassic age. The eastern belt is mélange containing blocks of Pennsylvanian and Early Permian limestone along with chert, basalt, ultramafic and acidic volcanic blocks, in a chert and argillite matrix of Late Permian to Late Triassic age (Orchard, 1984).

The central belt contains two new radiolarian localities (Fig. 72.3). The first, C08, is located near the road through Marble Canyon, and consists of a cliff of red ribbon chert and carbonates. Two red chert samples, one in place (C08-09), the other in the talus (C08-01) provided poorly preserved radiolarians respectively of Triassic and Middle to Late Triassic age. The second locality, C02, is situated on the Cornwall Hill road. The outcrop consists of alternating, thinly bedded, cherty carbonate and grey to white ribbon chert that contains clearly visible radiolarians, many of which are joined together, particularly at the tops and bottoms of chert beds. The radiolarians extracted were of Middle or Late Triassic age (C02-08) and of Late Ladinian to Early Carnian age (C02-14). The latter were associated with the conodont **Gondolella inclinata** Kovacs (determination by B. Vrielynck) which is Upper Ladinian to Lower Carnian. In the same general area, Orchard (1984; localities 21 and 22) obtained Early (?) Norian and Smithian ages.

Radiolarians were extracted from the matrix rocks at two main locaties in the eastern mélange belt. Locality C03 consists of a 500 m long roadcut in chert, cherty argillite and argillite with a variety of blocks on the west side of the settlement of Cache Creek (Fig. 72.3). Six stratigraphic levels were dated there (Table 72.5), ranging from Middle to Upper Triassic. Radiolarians from locality C05, (GSC locality C-087650, collected originally by K.R. Shannon, in Monger and McMillan, 1984) were recollected, and include Lower Permian forms.

Chert-pebble conglomerates

Small, isolated outcrops of chert-pebble conglomerate, sandstone and argillite are scattered across parts of Ashcroft (92I) and Hope (92H) map areas (Fig. 72.1). In places, these strata are known to be of mid- to Late Cretaceous age (Monger and McMillan, 1984) but elsewhere are undated, and are correlated solely on the basis of lithological similarity. Radiolarians in the chert pebbles had not been studied previously, but four collections were made in an attempt to obtain some idea of the provenances of the conglomerates (Tables 72.3, 72.6).

Exposed at one locality is the mid- to Late Cretaceous conglomerate that lies within the central belt of the Cache Creek Complex. The chert pebbles within it are slightly metamorphosed, and only one, Late Permian age (C07-14) was obtained (Table 72.6).

Chert pebbles were examined from three, undated conglomerates near the town of Merritt. Pebbles northeast of Merritt (Locality P01) ranged from Late Permian to Early Jurassic. Outcrops near Courtney Lake (Localities L01, L02) yielded Early Permian to Late Triassic fossils. Chert pebbles from conglomerate near Vogt Creek (Locality A01) ranged from Early Permian to Early Jurassic with some adjacent pebbles yielding very different ages.

Conclusion

At present, radiolarian faunas in the lithological packages containing abundant chert (Cache Creek and Bridge River complexes, Hozameen Group) are too poorly known to make any precise correlations; the presence of Jurassic pebbles in the conglomerates near Merritt favours their derivation from the Hozameen Group or Bridge River Complex, rather than the Cache Creek Complex.

Acknowledgments

I would like to thank B. Forman and M.J. Orchard for their help in the field, P. De Wever and M.J. Orchard for critical reading of the manuscript, and J.W.H. Monger for help in corrections and translation.

Selected bibliography

Cameron, B.E.B. and Monger, J.W.H.
1971: Middle Triassic conodonts from the Fergusson Group, northeastern Pemberton map-area, British Columbia; in Report of Activities, Part B, Geological Survey of Canada, Paper 71-1B, p. 94-96.

De Wever, P.
1982: Radiolaires du Trias et du Lias de la Tethys (Systématique, Stratigraphie); Société Géologique du Nord, Lille, Publication No. 7, 599 p.

Dumitrica, P.
1970: Cryptocephalic and cryptothoracic Nassellaria in some Mesozoic deposits of Romania; Revue Roumaine de Géologie, Géophysique et Géographie, Série de Géologie, Bucharist, v. 14, p. 45-124.

Monger, J.W.H. and McMillan, W.J.
1984: Bedrock geology of Ashcroft (92I) map area; Geological Survey of Canada, Open File 980.

Monger, J.W.H. and Price, R.A.
1979: Geodynamic evolution of the Canadian Cordillera – progress and problems; Canadian Journal of Earth Sciences, v. 16, p. 770-791.

Orchard, M.J.
1981: Triassic conodonts in the Cache Creek Group, Marble Canyon, southern British Columbia; in Current Research, Part A, Geological Survey of Canada, Paper 81-1A, p. 357-359.

1984: Pennsylvanian, Permian and Triassic conodonts from the Cache Creek Group, southern British Columbia; in Current Research, Part B, Geological Survey of Canada, Paper 84-1B, p. 197-206.

Pessagno, E.A., Jr. and Newport, R.L.
1972: A technique for extracting Radiolaria from Radiolarian chert; Micropaleontology, v. 18/2, p. 231-234.

Potter, C.J.
1983: Geology of the Bridge River Complex, southern Shulaps Range, British Columbia: a record of convergent tectonics; unpublished Ph.D thesis, University of Washington, 192 p.

Seiders, V.M. and Blome, C.D.
1984: Clast compositions of Upper Mesozoic conglomerates of the California Coast Ranges and their tectonic significance; in Franciscan Geology of Northern California, ed. M.C. Blake, Jr.; Pacific Section Society of Economic Paleontologists and Mineralogists, v. 43, p. 135-148.

Yao, A.
1982: Middle Triassic to Early Jurassic radiolarians from the Inuyama area, Central Japan; Journal of Geosciences, Osaka City University, Osaka, v. 25, no. 4, p. 55-70.

A shelf-to-basin transition in the Devonian Ogilvie Formation, Yukon Territory

Project 840016

M.P. Dubord[1], D.W. Morrow, and R.W. Macqueen
Institute of Sedimentary and Petroleum Geology, Calgary

Dubord, M.P., Morrow, D.W., and Macqueen, R.W., A shelf-to-basin transition in the Devonian Ogilvie Formation, Yukon Territory; in Current Research, Part A, Geological Survey of Canada, Paper 86-1A, p. 603-608, 1986.

Abstract

The Lower to Middle Devonian Ogilvie Formation thins markedly eastward between the Blackstone and Hart rivers, and at Hart River it passes abruptly into deep shelf margin (basin margin) deposits. Lithofacies analysis and conodont-derived biostratigraphic control indicate that Ogilvie deposition began on a rimmed shelf with stromatoporoid buildups forming the organic shelf rim. Toward the close of early Emsian time, the Ogilvie shelf was drowned, leading to the development of a distally steepened ramp with no distinct, shallow water, shelf-edge facies separating shallow water deposits from basin margin deposits farther east. A poorly developed shelf rim, inferred from the presence of intertidal deposits and the location of a zone of abrupt Ogilvie thinning, may have been re-established briefly in late Emsian time.

Résumé

La formation d'Ogilvie du Dévonien inférieur à moyen s'amincie considérablement vers l'est entre les rivières Blackstone et Hart; à Hart River, elle se transforme brusquement en dépôt de marge de plate-forme profonde (marge de bassin). L'analyse des lithofaciès et un contrôle biostratigraphique établi à partir de conodontes révèlent que la mise en place de cette formation a commencé par l'accumulation sur une plate-forme lisérée de stromatopores qui ont formé le rebord organique de la plate-forme. L'inondation de la plate-forme d'Ogilvie vers la fin de l'Emsien ancien a mené à la formation d'une rampe à faciès distal en pente brusque; aucun faciès distinct d'eau peu profonde et de marge de plate-forme ne sépare les dépôts accumulés en eaux peu profondes des dépôts de marge de bassin plus à l'est. La présence des dépôts intertidaux et la position d'une zone d'amincissement abrupt de la formation d'Ogilvie indique qu'un rebord de plate-forme mal développé aurait peut-être existé de nouveau pendant une courte période ves la fin de l'Emsien.

---

[1] Department of Earth Sciences, University of Waterloo, Waterloo, Ontario N2L 3G1

Introduction

The immediate purpose of this study was to investigate and define lithofacies within the Ogilvie Formation more systematically than had been done previously. To this end, a line of section was chosen along a structurally continuous panel of the Ogilvie Formation exposed between Blackstone and Hart rivers in the Hart River map area (NTS 116H) in the north-central part of the Yukon Territory (Fig. 73.1). This line of section was an advantageous choice, in that the original spatial relationships of facies within the Ogilive are preserved there. Additionally, it was discovered that the shallow water carbonates of this formation pass abruptly eastward to equivalent deep water sedimentary rocks at Hart River, providing an opportunity to investigate a structurally intact shelf-to-basin transition within the Ogilvie along this line of section.

Seven stratigraphic sections of the Ogilvie were measured (Fig. 73.1) with thicknesses ranging from 1068.5 m in Section 1 at Blackstone River to a minimum of 198.0 m in Section 7 at Hart River (Fig. 73.2).

This study supplements the regional studies of Perry et al. (1974), A.W. Norris (1968a,b), Perry and Lenz (1979) and Pugh (1983). A complete review of pertinent studies is contained in A.W. Norris (in press). Sections 1, 2 and 6 of the present study were measured previously and are reported originally in A.W. Norris (1968b) as sections 19, 18 and 14, respectively. The Ogilvie Formation has been mapped regionally by D.K. Norris (1982) in the Hart River map area. Lenz (1972), Perry and Lenz (1979) and A.W. Norris (in press) provided information on the regional paleogeographic setting of the Ogilvie Formation.

The preliminary data presented here were gathered during six weeks of fieldwork in the summer of 1984, and will form part of a Master of Science thesis by M. Dubord at the University of Waterloo. Conodont identifications were provided by T.T. Uyeno of the Geological Survey of Canada for six collections from the Ogilvie Formation (GSC locality numbers C-128454, C-128459, C-128472, C-128487, C-128504 and C-128523) and two collections from the Michelle Formation (GSC locality numbers C-128402 and C-128450). Further information concerning these collections is available on request.

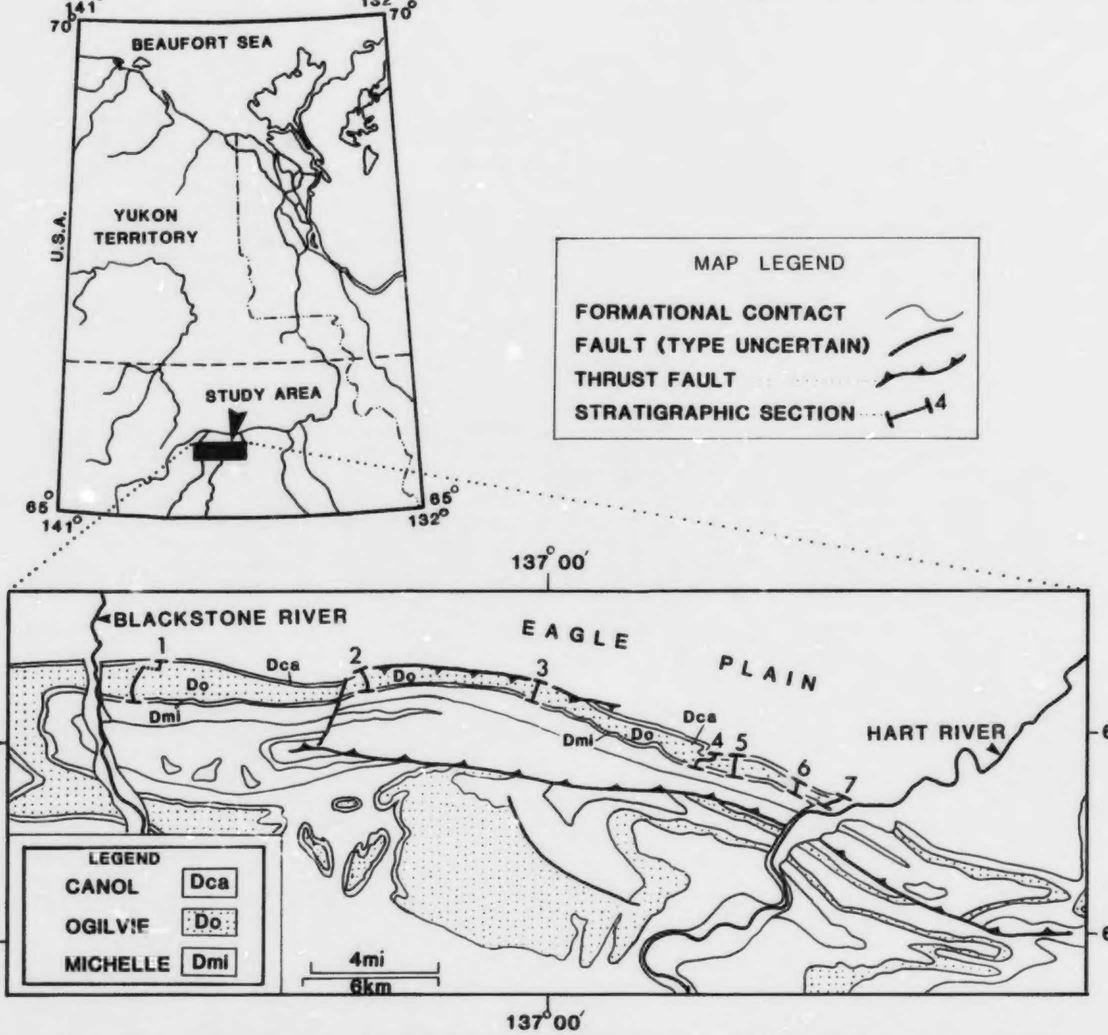

Figure 73.1. Index map showing location of study area between Hart and Blackstone rivers. Also shown are the locations of the seven stratigraphic sections of the Ogilvie Formation examined for this study. Geology is simplified from D.K. Norris (1982).

Lithostratigraphy and thickness variations

The Ogilvie Formation was originally defined as: "the Devonian carbonate succession overlying the Michelle and Gossage formations and underlying the Hare Indian Formation and tongue, unnamed shales of Middle Devonian and younger(?) ages, and clastic rocks of Carboniferous age" (A.W. Norris, 1968b, p. 28). The Gossage Formation was made obsolete by Pugh (1983). In the study area, the stratigraphic nomenclature is currently undergoing revisions (A.W. Norris, in press), but the terminology used here is consistent with that used for the Hart River map area

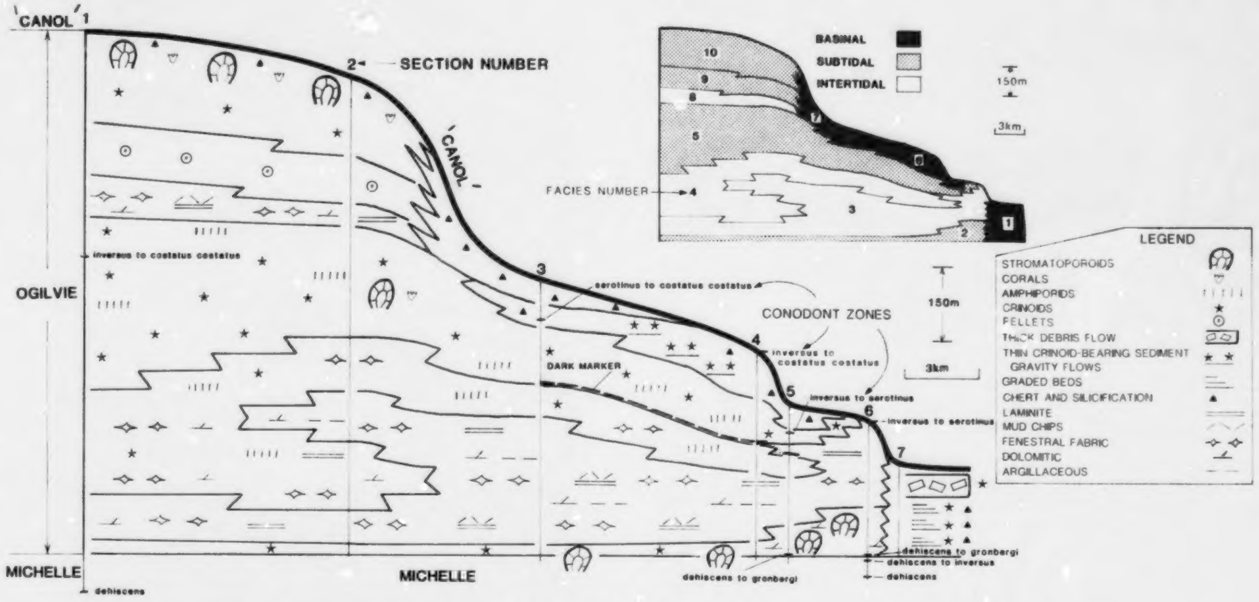

Figure 73.2. *A stratigraphic cross-section of the Ogilvie Formation and its 10 major lithofacies. The top of the Michelle Formation forms the cross-section datum. The rock type is uniformly limestone unless otherwise indicated. Two of the conodont zones shown here are derived from collections identified in Perry et al. (1974). Also shown is a summary interpretation of depositional environments of Ogilvie lithofacies.*

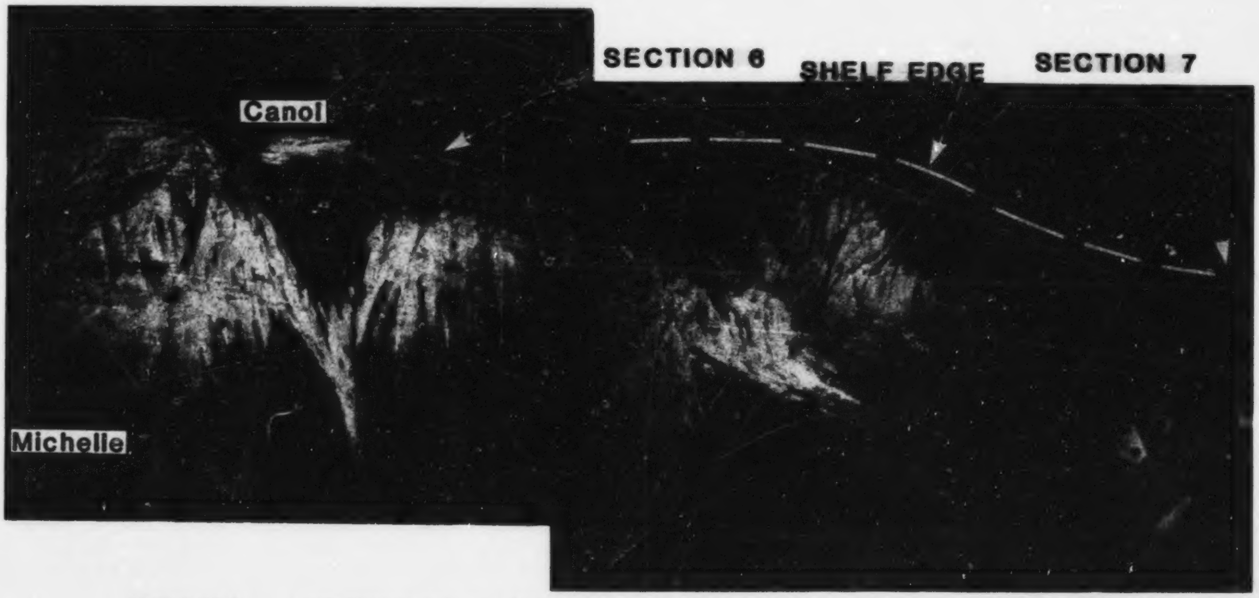

Figure 73.3. *A panoramic view of the Ogilvie Formation near Hart River. The transition from stromatoporoidal shelf edge strata to the basin margin strata of Section 7 occurs over a distance of less than a kilometre in this location.*

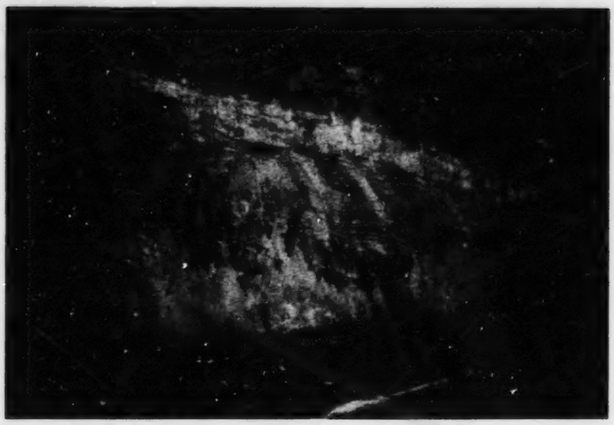

Figure 73.4. A closer view of the basinal Ogilvie strata at Section 7. The resistant rib is a large, 38.0 m thick limestone debris flow near the top of the "Ogilvie" Formation mapped at Hart River (D.K. Norris, 1982).

(D.K. Norris, 1982) in which the Ogilvie is overlain by the siliceous shales of the Canol Formation and is underlain by the argillaceous Michelle Formation.

General lithologic descriptions of the Ogilvie, Michelle and Canol formations can be found in articles by A.W. Norris (see references). Briefly, the Ogilvie consists of "medium brown to grey, aphanitic to fine grained, thin-bedded to massive, resistant, cliff forming limestone, weathering light to medium grey" (A.W. Norris, in press). Dolostones occur in the lower portions of the formation in the Hart River-Blackstone River area (Perry et al., 1974). The underlying Michelle Formation (A.W. Norris, 1968b) consists of fossiliferous, shaly limestones and limestones. The contact between the Ogilvie and Michelle formations is gradational over an interval of 1 to 3 m (this study). In Sections 3 through 6 (Fig. 73.2) the contact is well exposed. The overlying siliceous shales of the Canol Formation (Unnamed shale unit of Norris, in press) are recessive, and the Ogilvie-Canol contact was obscured in most cases although estimates of its position within ± 12 m can be made with confidence.

The following descriptions correspond to lithofacies identified in Figure 73.2. These descriptions are based on field observations and examination of hand samples and selected thin sections. A more complete description of these lithofacies will be presented at a future date.

Facies 1 - Limestone/cherty limestone: resistant, thin to thick, wavy-bedded, light to dark grey weathering; dark grey to black encrinites to crinoidal lime mudstone flows and breccias, commonly graded with clasts of encrinite and lime mudstone; silicification common and parallel to bedding, as black, discontinuous chert horizons; sporadic colonial corals and stromatoporoids, commonly in overturned positions, decreasing in abundance upsection; bases of flows are commonly scoured and grade upward into lime mudstones.

Facies 2 - Limestone/dolostone: basal unit of resistant, cliff forming, very thick to thick bedded, light to medium grey weathering, dark grey lime mudstone to wackestone, commonly with abundant stromatoporoid and crinoid debris, locally brecciated and/or dolomitized.

Facies 3 - Dolostone/calcareous dolostone: recessive, thin to medium bedded, platy; light yellow to orange grey weathering, medium to dark grey; common interbeds of dark grey, lime mudstones, local interbeds of yellow weathering, argillaceous, dolomitic lime mudstones; fenestral fabrics and intraclast breccias are common throughout; mottled in lower parts, rare exposure surfaces and rare dolomitized sedimentary breccias in lower part of unit; thicker bedded and more calcareous in eastern part of study area.

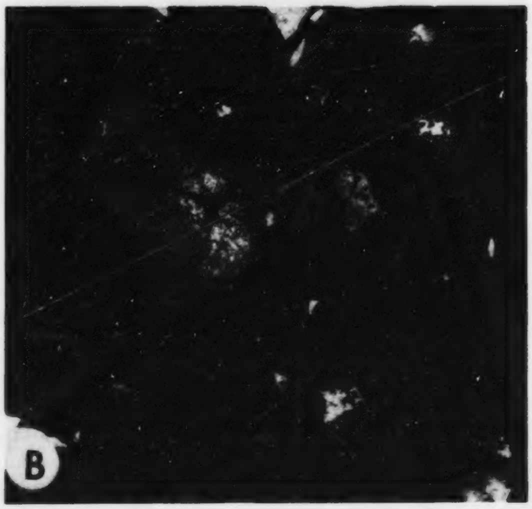

A. A close view of the thick debris flow shown in Figure 73.4. The debris flow rests on thin to medium bedded crinoidal wackestones that are probably sediment gravity flows.

B. Fragmental texture of the debris flow in Figure 73.5A, with subangular clasts of crinoidal wackestone and packstone in a crinoid wackestone matrix, forming a rubble floatbreccia.

Figure 73.5.

Facies 4 - Dolomitic limestone: moderately resistant; medium to thick bedded; medium to dark bluish grey and brownish grey weathering; dark grey dolomitic lime

Table 73.1. Correlation of late Early to early Middle Devonian conodont zones with stages of Europe and North America (from Klapper and Johnson, 1980, Figure 1, p. 403)

CONODONT ZONES	STAGES	
-------------------------	**Eifelian**	
costatus costatus		
-------------------------		**Couvinian**
patulus	-----------------	
-------------------------		-------- ? -------
serotinus		
-------------------------		**Dalejan**
inversus	**Emsian**	-----------------
-------------------------		
gronbergi		**Zlichovian**
-------------------------		
dehiscens		-----------------
-------------------------	-------- ? -------	**Pragian**

mudstone, mottled in lower half due to dolomitization; **Amphiporid** floatstone beds and crinoidal lime mudstones in upper half with local, flaggy weathering, laminated intervals containing fenestral fabric throughout.

Facies 5 - Limestone: moderately resistant; thick bedded cliff former at top and bottom of unit, thin to medium bedded in middle parts; medium to light grey weathering; brown grey to medium grey crinoidal lime mudstones and wackestones; local laminated intervals with **Amphipora** and mottling due to dolomitization in lower part; local stromatoporoids and colonial corals, **Moelleritia** in middle parts; black lime mudstone marker up to 2 m thick near base of unit in Sections 3 and 4; locally slightly argillaceous.

Facies 6 - Limestone: recessive; medium to thin irregularly bedded; dark grey weathering, black crinoidal lime mudstones and wackestones; debris flows common, with rare breccia beds, bases commonly scoured; **Alveolites, Amphipora** and solitary corals common; silicification of fossils abundant toward top of unit.

Facies 7 - Limestone: recessive; medium to thin bedded; medium grey to black weathering, black lime mudstone; unfossiliferous; abundant black chert nodules and stringers along bedding planes.

Facies 8 - Limestone/dolomitic limestone: slightly less resistant than Facies 9; thin to medium bedded; light to medium grey weathering; alternating laminated dolomitic lime mudstones and lime mudstones; local intraclast breccias within the laminated intervals in the west part (Section 1), grading to fenestral limestones in the east; lime mudstones locally mottled due to dolomitization; unfossiliferous.

Facies 9 - Limestone: resistant, forms a series of small ragged cliffs; commonly alternating thin to thick bedded; light grey weathering, light to medium brown lime mudstone and/or pelletal lime wackestone; unfossiliferous.

Facies 10 - Limestone: generally resistant; very thick to medium bedded; light grey weathering, light brown to dark grey crinoidal lime mudstone to wackestone, commonly with abundant hemispheroidal stromatoporoids and colonial corals; less fossiliferous beds are less resistant, forming series of 'ribbed' outcrops; fossils silicified near the Canol contact.

On the basis of these characteristics, facies 1, 6 and 7 are inferred to be basinal slope or basin margin deposits; facies 2, 5, 9 and 10, shallow subtidal deposits; facies 4, a mixture of subtidal and intertidal deposits; facies 8, an intertidal deposit; and facies 3 a mixture of intertidal and supratidal deposits. These interpretations are generalized in Figure 73.2.

The Ogilvie Formation thins dramatically from west to east (Fig. 73.1). In general, this corroborates the conclusions of Perry et al. (1974) concerning the change of thickness of the Ogilvie between Blackstone and Hart rivers. However, the lithostratigraphic data of this study provide a more complete characterization of this change. The eastward thinning of the Ogilvie occurs both as discrete steps where the Ogilvie becomes abruptly thinner (e.g. between Sections 4 and 5, or 2 and 3) and as more gradual thinning between these 'steps' (Fig. 73.2).

The most abrupt steps coincide with the transitions from shallow water carbonates in the west to laterally equivalent basin margin carbonates in the east (Fig. 73.2, 73.3). The transition between Sections 6 and 7 is typical in this regard, as 275 m of platform carbonates pass eastward in their entirety to about 198 m of basinal strata in Section 7. Thin to medium, graded beds of crinoidal wackestone and packstone (sediment gravity flows) form most of these strata, but one, spectacular, 38 m thick limestone debris flow deposit occurs near the upper contact of these strata with the Canol Formation (Fig. 73.4, 73.5a). Surface weathering has partially obscured the fabric of this breccia body, but talus blocks freshly spalled off the face of this deposit reveal it to be a polymictic rubble floatbreccia (Morrow, 1982), composed largely of poorly sorted, subangular to subrounded, subequant fragments of lime mudstone, crinoidal lime mudstone, wackestone and packstone and pieces of large stromatoporoids up to 30 cm across, set in a crinoidal wackestone matrix (Figs. 73.5a,b). The abrupt major thickness change between sections 2 and 3 also coincides with the eastward disappearance of facies 8, 9 and 10 into the possibly laterally equivalent basinal facies 7 (Fig. 73.2).

Between these zones of abrupt thickness changes, the Ogilvie appears to become thinner gradually, with no abrupt facies changes, reflecting the general thinning of all shallow water lithofacies from west to east (Fig. 73.2).

Perry et al. (1974) previously suggested a general two-fold division of the Ogilvie into a lower, shallow water carbonate sequence (i.e. facies 3, 4 and 5, Fig. 73.2) overlain by an upper, deeper water limestone sequence (i.e. facies 6-10, Fig. 73.2). Their generalization is substantiated by this study.

Discussion

Evidently the shelf edge of platform carbonate deposition remained in the region between the present Sections 6 and 7 during most of early Emsian or Zlichovian time (**dehiscens** to **inversus** zones, Table 73.1). The presence of abundant stromatoporoids in the lower part of Section 6 (Fig. 73.2) may indicate that the Ogilvie was first deposited as a rimmed shelf (Read, 1985). However, the lack of a definite shelf edge facies higher in the Ogilvie sequence suggests that the rimmed shelf was 'drowned' and evolved during later Emsian and early Eifelian time (**inversus** to **costatus costatus** zones) into a distally steepened ramp (Read, 1985) in which discrete, characteristic, shelf edge facies were not developed. This change in depositional style may explain the predominance of subtidal deposits higher in the sequence where the absence of a shelf edge rim implies more open marine circulation. The presence of the thin, intertidal zone represented by facies 8 at the base of the upper sequence of facies 8, 9 and 10 may imply that a poorly developed shelf edge rim was re-established between the present Sections 2 and 3 in mid-Emsian to Eifelian time (Fig. 73.2) and that, like its earlier counterpart, it was subsequently drowned. Based on their stratigraphic position within the Ogilvie Formation, and their lithologic characteristics, facies 9 and 10 appear to be lateral equivalents of the "Upper Ogilvie Reef Trend" as defined by Pugh (1983, p. 29). This trend is located to the north of this study area, and is found on the western margin of the Richardson Trough.

Conclusions

The conclusions of this study may be summarized as follows:

1. The Ogilvie Formation displays a pronounced eastward thinning between Blackstone and Hart rivers. This thinning culminates in the complete transition of platform carbonates into a thin basinal or basin margin sequence at Hart River.
2. Initially, the Ogilvie was deposited on a rimmed shelf that was later drowned to form a distally steepened ramp. A discrete shelf edge rim may have been re-established nearer the platform interior in mid-Emsian time but this rim was probably drowned near the end of the depositional period. Overall, the Ogilvie Formation along this line of section is a record of transgressive Emsian and Eifelian sedimentation.
3. The existence of a discrete shelf edge organic rim facies at Section 6 implies that similar potential reservoir facies may be found juxtaposed with basinal facies farther north in the subsurface beneath the Eagle Plain.

References

Klapper, G. and Johnson, J.G.
1980: Endemism and dispersal of Devonian conodonts; Journal of Paleontology, v. 54, no. 2, p. 400-455.

Lenz, A.C.
1972: Ordovician to Devonian history of northern Yukon and adjacent District of Mackenzie; Bulletin of Canadian Petroleum Geology, v. 20, no. 2, p. 321-361.

Morrow, D.W.
1982: Descriptive field classification of sedimentary and diagenetic breccia fabrics in carbonate rocks; Bulletin of Canadian Petroleum Geology, v. 30, p. 227-229.

Norris, A.W.
1968a: Devonian of northern Yukon and adjacent District of Mackenzie; in International Symposium on the Devonian System, ed. D.H. Oswald; Calgary, 1967, v. 1, p. 753-780.

1968b: Reconaissance Devonian stratigraphy of northern Yukon Territory and northwestern District of Mackenzie; Geological Survey of Canada, Paper 67-53, 287 p.

Norris, A.W.
– Stratigraphy of Devonian outcrop belts of northern Yukon Territory and northwestern District of Mackenzie (Operation Porcupine area); Geological Survey of Canada, Memoir 410. (in press)

Norris, D.K.
1982: Geology, Hart River, Yukon Territory; Geological Survey of Canada, Map 1527A, Scale 1:250 000.

Perry, D.G., Klapper, G., and Lenz, A.C.
1974: Age of the Ogilvie Formation (Devonian), Northern Yukon: based primarily on the occurrence of brachiopods and conodonts; Canadian Journal of Earth Sciences, v. 11, p. 1055-1097.

Perry, D.G. and Lenz, A.C.
1979: Emsian paleogeography and shelly fauna biostratigraphy of Arctic Canada; in Western and Arctic Canadian Biostratigraphy, ed. C.R. Stelck and B.D.E. Chatterton; Geological Association of Canada, Special Paper 18, p. 133-160 (1978).

Pugh, D.C.
1983: Pre-Mesozoic geology in the subsurface of the Peel River map area, Yukon Territory and District of Mackenzie; Geological Survey of Canada, Memoir 401.

Read, J.F.
1985: Carbonate platform facies models; American Association of Petroleum Geologists, Bulletin, v. 69, p. 1-21.

Petroleum source rock reconnaissance of southern Saskatchewan

Project 780003

K.G. Osadetz and L.R. Snowdon
Institute of Sedimentary and Petroleum Geology, Calgary

Osadetz, K.G. and Snowdon, L.R., Petroleum source rock reconnaissance of southern Saskatchewan; in Current Research, Part A, Geological Survey of Canada, Paper 86-1A, p. 609-617, 1986.

Abstract

Potential petroleum source rocks are present in the Mesozoic and Paleozoic strata of southern Saskatchewan. Type II marine source rocks are present in the Winnipeg (Ordovician), Duperow (Devonian), Bakken (Devonian-Mississippian), Watrous and Gravelbourg (Jurassic) formations and the Colorado Group (Cretaceous). Type III terrestrial sources are present in the Bakken Formation and the Mannville (Cretaceous) and Colorado groups. The maturation profile of this section is not yet understood. Ordovician sources are clearly thermally mature. The top of the oil window may coincide with the top of the Jurassic System, although intervening Devonian source rocks appear thermally immature.

Résumé

On trouve des roches mères potentielles dans des couches du Mésozoïque du sud de la Saskatchewan. On trouve des roches mères marines de type II dans les formations de Winnipeg (Ordovicien), de Duperow (Dévonien), de Bakken (Dévonien-Mississippien), de Watrous et de Gravelbourg (Jurassique) et dans le groupe de Colorado (Crétacé). On trouve des roches mères terrestres de type III dans la formation de Bakken et dans les groupes de Mannville (Crétacé) et de Colorado. On n'est pas encore arrivé à comprendre le profil de maturation de cette coupe. Les roches mères ordoviciennes présentent une nette maturité thermique. Le sommet de la fenêtre de pétrole pourrait correspondre au sommet du système jurassique, bien que des roches mères anciennes du Dévonien ne semblent pas avoir atteint la maturité thermique.

Introduction

The Institute of Sedimentary and Petroleum Geology has undertaken a comprehensive program of petroleum source rock identification and evaluation. The purpose of this program is to identify and characterize the potential of petroleum source rocks in selected portions of the Western Canadian Sedimentary Basin; specifically, at this time, the province of Saskatchewan. This will be accomplished by the analysis, using the RockEval pyrolysis technique, of both cutting and core samples.

Method of study

The RockEval pyrolysis technique allows the evaluation of shows of oil or gas, oil and gas generation potential, and thermal maturity, as well as providing an inference of the organic matter type in potential petroleum source rocks (Tissot and Welte, 1978, p. 443-447). The RockEval pyrolysis-organic carbon analysis gives five parameters: S1, S2, S3, TOC and Tmax. The S1 parameter is a measure of the free or adsorbed hydrocarbons that are volatilized at moderate temperatures during the pyrolysis experiment. The S2 parameter represents the quantity of hydrocarbons and hydrocarbon-like compounds that are liberated from the kerogen in the rock sample during the pyrolysis experiment. The S3 parameter is a measure of the CO_2 generated from the kerogen. All of these parameters are measured in milligrams of product per gram of rock sample, which is equivalent to kilograms of product per tonne of sample. The Total Organic Carbon TOC, is measured in weight per cent. Tmax is the temperature corresponding to the maximum of hydrocarbon generation, the S2 peak, during the pyrolysis experiment.

The source rock potential of a rock sample is determined by the amount of Total Organic Carbon as a function of lithology, and by the S2 parameter value (Table 74.1). Thermal maturity is determined by both the Tmax and the Hydrogen Index-Oxygen Index parameters (Macauley and others, 1985, p. 5). The Petroleum Potential of the samples, S1+S2, can be employed to rank the generative potential of different source rocks.

This initial survey represents the analysis of 619 well cutting samples from the Norcanols Parry No. 1 well (16-8-9-21W2M). Sampling was carried out at intervals of 40 feet (12.2 m) over the entire well section to a total depth of 9042 feet (2756.0 m). Potential source rock intervals identified by the inital survey were analyzed on a finer scale spacing (5-10 ft/1.5-3 m). Samples composed of homogenized collections of chips, as well as single chips, were analyzed. The analysis of ditch cuttings allowed the development of a continuous profile of pyrolysis parameters throughout the entire thickness of the well section, a determination particularly useful for the illustration of maturation gradients. This practice carries with it the danger that the analyses of caved or incorrectly logged samples will be entered out of place. Careful correlation of suspected samples with the sample descriptions, coupled with an examination of their thermal maturity in comparison with the maturation gradient of the entire well, identified most occurrences of out-of-place samples. Caving was not found to be a problem and samples were generally logged within one sample interval (1.5 m) of the reported depth.

Stratigraphy

The Norcanols Parry No. 1 well represents an almost complete penetration of the Phanerozoic sequence in Saskatchewan. All systems except the Permian and possibly the Triassic are represented. Other systems form lithostratigraphic sequences bounded by interregional unconformities. The regional stratigraphy of Phanerozoic rocks in Saskatchewan has been summarized by several authors (Christopher and others, 1971; McCrossan and Glaister, 1964). The stratigraphy of the Norcanols Parry No. 1 well is summarized in Table 74.2. The positions of many formation tops have been taken from other publications, which are referenced. Unreferenced formation tops have been picked by the authors of this report using the available literature.

Potential petroleum source rocks

Eleven of the thirty-five formations in the Parry No. 1 well have "fair" to "good" source rock potential. Source rocks are observed to occur within the following formations: Winnipeg, Duperow, Bakken, Watrous, Gravelbourg, Cantuar, Joli Fou/Skull Creek, Viking/Newcastle, Ashville, Favel and Niobrara (Table 74.3).

All potential source rocks exhibit an S2 peak greater than or equal to 2.0 mg/gm and, except for the carbonate source rocks of the Duperow Formation, a TOC content greater than or equal to 1.0 weight per cent. Carbonate source rocks with S2 greater than or equal to 2.0 contain TOC greater than 0.50 weight per cent. Only samples with TOC contents equal to or exceeding 0.50 weight per cent are reported in Table 74.3. Most potential source rocks have Oxygen indices of less than 150, allowing the assignment of an inferred organic matter type to potential sources. Only three samples with S2 greater than or equal to 2.0 cannot be so assigned. The low Hydrogen indices of these samples allow the reasonable inference that these three samples are Type III sources.

Table 74.3 displays the pyrolysis results from the Parry No. 1 well for all samples with TOC in excess of 0.50 weight per cent. The most notable trend in the well is the general increase of TOC in younger formations. Note that throughout most of the Paleozoic carbonates, the abundance of TOC does not exceed 0.50 weight per cent. The trend of increased organic carbon abundance reaches its maximum in the Favel Formation. Strata younger than the Colorado Group are characterized by a decreased abundance of organic carbon. The maturation parameter Tmax exhibits considerable scatter. Generally, Petroleum Potential and Hydrogen Index are observed to be positively, yet poorly related to TOC. These trends may be seen more clearly when the results are examined on a formation by formation basis.

Icebox Member, Winnipeg Formation

Shales of the Icebox Member of the Winnipeg Formation (Caradocian) show a progressive increase in both TOC content and S2 yield upward through the member. TOC increases from 0.02 weight per cent at 8595 feet (2620.0 m) to 1.51 at 8550 feet (2606.0 m). The corresponding S2 yields for these samples are 0.15 and 6.30 mg/gm, respectively. Inspection of Table 74.3 reveals that the results are reproducible in different sample runs. S1 yields are low (less than or equal to 0.24 mg/gm) as are the productivity indices [S1/(S1+S2)]. A strong linear correlation is observed between the TOC content and the Petroleum Potential of this unit. A yield of 4.2 kg/tonne/per cent organic carbon can be expected. Hydrogen and Oxygen indices suggest that the organic matter is Type II marine and that the formation is thermally mature. The average Tmax of samples from this shale is 436.33 degrees Celsius, just at the threshold of oil generation.

Duperow Formation

The Duperow Formation represents epeiric marine sediments equivalent to the Woodbend Group of Alberta (Frasnian). Two samples from the Duperow Formation

Table 74.1. Criteria for rating potential source rocks

Total Organic Carbon (TOC) value (weight per cent)		
%TOC in shales	Source rating	%TOC in carbonates
0.00-0.50	poor	0.00-0.12
0.50-1.00	fair	0.12-0.25
1.00-2.00	good	0.25-0.50
2.00-4.00	very good	0.50-1.00
4.00 and greater	excellent	1.00 and greater

S2 value (mg hydrocarbon/gm of rock)	
	Source rating
less than 2.00	poor
2.00-5.00	fair
greater than 5.00	good

exhibit the characteristics of petroleum source rocks. Results from one of the two sample intervals could be duplicated. The level of thermal maturity is consistent with the observed maturation gradient and the observed results are therefore inferred to be genuine. The findings suggest, however, that the potential source rocks may be present as thin horizons or partings. Source rocks are associated with evaporitic strata in rocks inferred to be equivalent to Dunn's Unit No. 3, underlying the region of the Flat Lake Halite (Dunn, 1975). Hydrogen and Oxygen indices and Tmax data indicate that these are thermally immature, Type II marine source rocks. Insufficient data were generated to establish a correlation between TOC and Petroleum Potential; however, yields of 6.8 to 7.8 kg/tonne/per cent organic carbon might be realized if none of the organic carbon is inert. It is possible that high yields could compensate for lack of source rock volume if suitably mature intervals exist.

Bakken Formation

The Bakken Formation comprises a widespread transgressive-regressive-transgressive triplet of Fammenian and Tournaisian age. In the Parry No. 1 well, potential petroleum sources are identified only within the Lower shale member (Fammenian). TOC contents and S2 yields show no progressive variation. One S1 yield exceeds 2.00 mg/gm, suggesting a very good oil show, although productivity index values are generally low. Thermal maturity indicators suggest that the formation is thermally immature. Hydrogen and Oxygen indices indicate that the Bakken Formation sources are mixed Type II and Type III. Petroleum potential is strongly correlated to TOC, and a yield of approximately 6.5 kg/tonne/per cent of organic carbon in excess of a threshold of 0.77 per cent inert organic carbon can be expected.

Watrous Formation

Grey and green marine shales occur above rock types characteristic of the lower Watrous Formation (Christopher, 1984). Age and correlation of this unit is uncertain (Poulton, 1984, p. 31, 32). Throughout this shale there is a general increase in TOC, although S2 yields are generally lower in this interval than in shales with lower TOC, occurring in the upper Watrous Formation. One sample at 4560 feet (1389.9 m) has a very promising organic carbon content and an S2 yield indicative of good source rock potential. Organic type suggests that it is a Type II source, and both Hydrogen and Oxygen indices and Tmax values suggest that it is marginally mature. All other shales in this interval are Type III sources, and were it not for the general improvement of TOC through this interval, and its marine environment of

Table 74.2. Table of formations

Norcanols Parry No. 1 (16-3-9-21W2M)

KB = 2547 feet (776.3 m)

Depth to (feet)	unit top (metres)	
370.0	(112.8)	Eastend Formation
390.0	(118.9)	Montana Group
		Bearpaw Formation
1790.0	(545.6)	Leapark Formation
2100.0	(640.0)	Eagle Shoulder
2580.0	(786.4)	Colorado Group
		Niobrara Formation
2640.0	(804.7)	Morden Formation
2690.0	(819.9)	Favel Formation
2828.0	(865.0)	Ashville Formation (Price, 1963)
		Belle Fourche Member
3027.0	(922.6)	Westgate Member
3173.0	(967.1)	Viking Formation (Price, 1963)
3209.0	(978.1)	Joli Fou Formation (Price, 1963)
3312.0	(1009.5)	Mannville Group
		Pense Formation (Price, 1963)
3375.0	(1028.7)	Cantuar Formation
		Atlas Member
3500.0	(1066.8)	Dimmock Member
3600.0	(1097.2)	McLeod Member
3680.0	(1121.7)	Vanguard Group (Price, 1963)
		Masefield Formation
3820.0	(1164.3)	Rierdon Formation
4045.0	(1232.9)	Shaunavon Formation
4220.0	(1286.2)	Gravelbourg Formation
4430.0	(1350.3)	Watrous Formation
4650.0	(1417.3)	Madison Group
		Charles Formation (MacDonald, 1956)
4887.5	(1490.0)	Mission Canyon Formation (MacDonald, 1956)
5350.0	(1630.7)	Lodgepole Formation (MacDonald, 1956)
5900.0	(1798.3)	Three Forks Group
		Bakken Formation (cf. MacDonald, 1956)
		Upper shale member
5925.0	(1805.9)	Middle sandstone member
5981.0	(1823.0)	Lower shale member
6038.0	(1840.4)	Torquay Formation
6061.0	(1847.4)	Saskatchewan Group
		Birdbear Formation (Nichols, 1970)
6330.0	(1929.4)	Duperow Formation (Dunn, 1975)
7020.0	(2139.7)	Manitoba Group
		Souris River Formation (Dunn, 1975)
7350.0	(2240.3)	First red bed
7360.0	(2243.3)	Dawson Bay Formation
7455.0	(2272.3)	Second red bed
7510.0	(2289.1)	Elk Point Group
		Prairie Formation (Holter, 1969)
7520.0	(2292.1)	Winnipegosis Formation (Holter, 1969)
7680.0	(2340.9)	Ashern Formation
7685.0	(2342.4)	Interlake Group Undivided
8060.0	(2456.7)	Big Horn Group (cf. Kendall, 1976)
		Stonewall Formation
8160.0	(2487.2)	Stoney Mountain Formation
8280.0	(2523.7)	Herald Formation
8370.0	(2551.2)	Yeoman Formation
8542.0	(2603.6)	Winnipeg Formation
		Icebox Member (Paterson, 1971)
8596.0	(2620.1)	Black Island Member (Paterson, 1971)
8760.0	(2670.1)	Deadwood Formation (Paterson, 1971)
9042.0	(2756.0)	Total Depth

Table 74.3. RockEval pyrolysis results for samples with TOC greater than or equal to 0.5 weight per cent

Depth in ft[1]	TOC	PI	S1+S2	TMAX	S1	S2	S3	HI	OI
TILL									
285	1.01	.15	.53	439	.08	.45	2.51	44	248
285	1.01	.15	.53	439	.08	.45	2.51	44	248
295	1.07	.22	.45	479	.10	.35	3.24	32	302
310	1.23	.07	.60	427	.04	.56	1.96	45	159
315	.65	.09	.22	496	.02	.20	2.28	30	350
335	.69	.16	.70	418	.11	.59	3.02	85	437
345	.68	.13	.46	427	.06	.40	2.20	58	323
BEARPAW FORMATION									
785	.56	.44	.09	318	.04	.05	3.32	8	592
815	.50	.42	.12	446	.05	.07	2.13	13	426
815	.56	.38	.08	457	.03	.05	3.23	8	576
860	.50	.33	.06	391	.02	.04	2.71	8	542
890	.65	.24	.33	427	.08	.25	3.23	38	496
910	.74	.17	.36	424	.06	.30	1.90	40	256
915	.72	.15	.46	431	.07	.39	1.72	54	238
935	.78	.22	.50	424	.11	.39	3.20	50	410
940	.74	.22	.69	430	.15	.54	3.14	72	424
960	.64	.11	.75	424	.08	.67	1.00	104	156
965	.65	.14	.79	582	.11	.68	1.76	104	270
985	.74	.50	1.08	368	.54	.54	3.00	72	405
990	.67	.28	.87	413	.24	.63	1.38	94	205
1010	.56	.32	.22	452	.07	.15	1.58	26	282
1035	.61	.55	.20	376	.11	.09	3.01	14	493
1040	.52	.50	.14	433	.07	.07	2.21	13	425
1060	.55	.41	.17	413	.07	.10	2.70	18	490
1065	.54	.40	.15	444	.06	.09	2.37	16	438
1085	.52	.60	.20	325	.12	.08	3.20	15	615
1090	.51	.59	.17	362	.10	.07	2.77	13	543
1115	.52	.15	.33	457	.05	.28	1.41	53	271
1135	.53	.13	.31	497	.04	.27	1.49	50	281
1160	.51	.16	.32	510	.05	.27	2.71	52	531
1315	.51	.12	.52	511	.06	.46	2.78	90	545
1340	.58	.26	.62	477	.16	.46	2.78	79	479
1360	.51	.06	.31	479	.02	.29	1.35	56	264
1365	.71	.11	.56	506	.06	.50	2.04	70	287
1385	.68	.11	.47	483	.05	.42	.92	61	135
1390	.76	.13	.61	472	.08	.53	1.70	69	223
1410	.58	.18	.34	445	.06	.28	1.30	48	224
1415	.63	.22	.37	475	.08	.29	2.72	46	431
1440	.71	.44	.48	479	.21	.27	2.94	38	414
1460	.50	.45	.29	489	.13	.16	3.70	32	740
1465	.56	.39	.33	494	.13	.20	2.60	35	464
1510	.64	.62	.13	446	.08	.05	4.50	7	703
1515	.53	.34	.29	477	.10	.19	2.79	35	526
1535	.67	.18	.22	453	.04	.18	3.15	26	470
1540	.67	.16	.31	504	.05	.26	2.52	38	376
1560	.52	.17	.23	500	.04	.19	2.16	36	415
1585	.53	.18	.22	425	.04	.18	2.81	33	530
1590	.55	.08	.37	511	.03	.34	1.30	61	236
1610	.52	.19	.27	490	.05	.22	2.02	42	388
1615	.51	.09	.45	485	.04	.41	1.56	80	305
1635	.50	.14	.14	508	.02	.12	2.73	24	546
1660	.57	.30	.23	442	.07	.16	4.59	28	805

Depth in ft[1]	TOC	PI	S1+S2	TMAX	S1	S2	S3	HI	OI
MORDEN FORMATION (cont.)									
2675	1.28	.17	.66	428	.11	.55	1.76	42	137
2680	1.28	.20	.50	429	.10	.40	1.88	31	146
2685	2.21	.04	3.44	427	.13	3.31	.27	149	12
FAVEL FORMATION									
2690	1.91	.29	.62	427	.18	.44	1.90	23	99
2695	1.49	.22	.40	426	.09	.31	2.81	20	188
2700	3.08	.10	2.30	431	.23	2.07	4.09	67	132
2705	2.43	.07	3.17	430	.21	2.96	1.90	121	78
2710	2.47	.07	2.69	425	.18	2.51	2.07	101	83
2710	3.03	.04	7.38	417	.32	7.06	2.41	233	79
2715	3.84	.15	2.26	427	.34	1.92	2.87	50	74
2720	2.89	.06	3.58	430	.23	3.35	3.22	115	111
2725	1.14	.25	.53	424	.13	.40	2.13	35	186
2730	2.31	.22	1.05	433	.23	.82	2.33	35	100
2735	1.85	.50	.70	467	.35	.35	2.12	18	114
2735	1.99	.70	.46	423	.32	.14	2.21	7	111
2740	4.90	.71	1.75	415	1.25	.50	2.77	10	56
2745	6.14	.14	10.32	427	1.41	8.91	4.78	145	77
2750	4.75	.04	34.32	415	1.29	33.03	5.26	695	110
2755	7.40	.12	6.42	424	.79	5.63	4.12	76	55
2760	2.94	.72	.46	402	.33	.13	3.61	4	122
2760	3.57	.43	.76	423	.33	.43	2.79	12	78
2765	4.86	.61	1.18	414	.72	.46	3.62	9	74
2770	3.98	.25	2.31	419	.58	1.73	3.25	43	81
2775	4.48	.05	7.97	414	.37	7.60	2.64	169	58
2780	1.93	.26	2.39	420	.61	1.78	3.94	92	204
2785	2.57	.77	.52	402	.40	.12	2.84	4	110
2785	4.39	.61	.88	424	.54	.34	3.28	7	74
2790	7.03	.24	2.09	423	.51	1.58	4.26	22	60
2795	5.19	.18	2.98	421	.55	2.43	4.31	46	83
2800	4.55	.22	4.81	413	1.08	3.73	6.26	81	137
2805	5.60	.16	4.44	424	.69	3.75	4.57	66	81
2810	2.69	.44	2.29	435	1.00	1.29	2.60	47	96
2810	2.97	.39	1.48	439	.57	.91	2.44	30	82
2815	4.66	.39	1.89	435	.74	1.15	3.41	24	73
2820	4.97	.05	21.70	417	1.03	20.67	3.43	415	69
2825	11.90	.03	67.50	416	2.16	65.34	3.54	549	29
2830	2.91	.21	1.13	434	.24	.89	2.46	30	84
2835	1.60	.30	.56	426	.17	.39	3.61	24	225
2835	2.56	.29	.58	430	.17	.41	4.76	16	185
2840	7.14	.08	9.80	426	.80	9.00	3.90	126	54
ASHVILLE FORMATION									
2860	1.13	.24	.21	483	.05	.16	3.96	14	350
2865	2.34	.20	1.14	432	.23	.91	2.75	38	117
2885	1.91	.31	.78	418	.24	.54	3.10	28	162
2910	1.58	.11	1.32	419	.14	1.18	2.44	74	154
2935	2.42	.57	.91	443	.52	.39	2.14	16	88
2960	1.99	.79	.47	351	.37	.10	2.62	5	131
2985	1.00	.81	.43	404	.35	.08	2.27	8	227
3010	1.85	.54	.56	414	.30	.26	2.50	14	135
3035	1.83	.34	.76	423	.26	.50	3.30	27	180

1685	.54	.26	.19	441	.05	.14	4.30	25	796
1690	.56	.13	.15	495	.02	.13	1.76	23	314
1735	.58	.14	.21	472	.03	.18	1.71	31	294
1755	.56	.09	.32	476	.03	.29	3.52	51	628
1785	.64	.18	.28	450	.05	.23	5.66	35	884
LEA PARK FORMATION									
1810	.55	.18	.22	427	.04	.18	4.19	32	761
1835	.54	.35	.20	448	.07	.13	6.00	24	1111
1860	.55	.35	.17	432	.06	.11	4.98	20	905
1885	.63	.36	.28	429	.10	.18	6.39	28	1014
1905	.60	.21	.24	432	.05	.19	2.45	31	408
1935	.58	.39	.36	422	.14	.22	6.06	37	1044
1960	.59	.39	.36	425	.14	.22	6.43	37	1089
1985	.74	.51	.73	474	.37	.36	8.03	48	1085
2010	.86	.23	.61	429	.14	.47	5.70	54	662
2035	.82	.23	.52	429	.12	.40	4.74	48	578
2060	1.18	.09	.87	430	.08	.79	3.91	66	331
2085	1.23	.00	.01	431	.00	.01	3.65	0	296
2110	.96	.11	.55	425	.06	.49	3.94	51	410
2135	.68	.38	.13	488	.05	.08	4.68	11	688
2155	.54	.43	.07	381	.03	.04	2.95	7	546
2210	.98	.67	.18	372	.12	.06	2.32	6	236
2230	.81	.38	.13	439	.05	.08	2.52	9	311
2260	.72	.22	.09	440	.02	.07	1.63	9	226
2285	.58	.25	.12	489	.03	.09	2.69	15	463
2305	.72	.24	.17	479	.04	.13	2.71	18	376
2330	.68	.28	.18	492	.05	.13	2.64	19	388
2355	1.31	.35	.34	438	.12	.22	2.59	16	197
2380	1.18	.10	.91	425	.09	.82	2.19	69	185
2405	1.35	.07	.97	426	.07	.90	2.47	66	182
2430	.70	.31	.16	483	.05	.11	2.77	15	395
2460	.64	.29	.14	491	.04	.10	2.28	15	356
2485	.96	.28	.25	484	.07	.18	1.84	18	191
2510	1.05	.19	.27	487	.05	.22	2.06	20	196
2535	1.31	.53	.43	505	.23	.20	2.32	15	177
2560	1.31	.33	.36	483	.12	.24	1.87	18	142
NIOBRARA FORMATION									
2585	2.11	.48	.75	439	.36	.39	2.38	18	112
2610	2.74	.47	1.02	434	.48	.54	2.74	19	100
2625	4.46	.04	16.96	421	.62	16.34	2.67	366	59
2635	2.34	.39	1.11	430	.43	.68	2.62	29	111
2635	2.45	.36	1.21	434	.44	.77	2.67	31	108
2640	2.53	.38	1.04	433	.40	.64	2.65	25	104
MORDEN FORMATION									
2645	2.59	.36	.89	429	.32	.57	3.51	22	135
2655	2.08	.18	1.22	432	.22	1.00	2.75	48	132
2660	1.12	.10	.39	427	.04	.35	1.79	31	159
2660	1.81	.15	.67	430	.10	.57	2.05	31	113
2665	1.36	.26	.35	458	.09	.26	1.64	19	120
2670	1.24	.11	.99	427	.11	.88	1.47	70	118

3060	2.70	.07	2.97	419	.22	2.75	3.39	101	125
3085	1.62	.11	.80	416	.09	.71	2.00	43	123
3110	1.28	.32	.31	402	.10	.21	3.82	16	298
3135	1.36	.04	1.14	420	.05	1.09	1.53	80	112
3160	1.10	.08	.61	425	.05	.56	2.46	50	223
VIKING FORMATION									
3185	1.17	.03	2.11	413	.06	2.05	1.03	175	88
JOLI FOU FORMATION									
3210	2.04	.15	1.40	402	.21	1.19	4.61	58	225
3210	4.28	.07	3.48	418	.26	3.22	3.67	75	85
3215	2.10	.09	1.96	426	.17	1.79	1.24	85	59
3220	1.61	.32	.69	421	.22	.47	3.20	29	198
3225	2.55	.19	1.13	425	.21	.92	2.88	36	112
3230	.85	.24	.63	420	.15	.48	3.03	56	356
3235	1.55	.09	1.21	418	.11	1.10	4.32	70	278
3235	1.96	.21	1.25	424	.26	.99	3.90	50	198
3240	1.78	.22	.77	421	.17	.60	3.30	33	185
3245	4.01	.19	3.18	423	.62	2.56	3.98	63	99
3250	2.89	.45	.89	430	.40	.49	3.91	16	135
3255	2.16	.21	1.15	425	.24	.91	4.16	42	192
3260	.81	.18	.17	424	.03	.14	3.43	17	423
3260	1.96	.14	1.04	430	.15	.89	3.60	45	183
3265	2.02	.19	.85	427	.16	.69	2.42	34	119
3270	1.22	.30	.46	437	.14	.32	2.26	26	185
3275	2.89	.15	1.11	428	.17	.94	1.53	32	52
3280	3.73	.20	3.79	422	.74	3.05	2.70	81	72
3285	1.72	.10	1.67	409	.16	1.51	2.97	87	172
3285	2.27	.10	1.74	421	.17	1.57	2.17	69	95
3290	2.53	.19	1.81	418	.34	1.47	2.89	58	114
3295	1.63	.22	1.47	421	.33	1.14	4.94	69	303
3300	2.02	.23	1.24	423	.28	.96	5.30	47	262
3306	.80	.41	.49	422	.20	.29	3.65	36	456
3310	.58	.03	.35	435	.01	.34	1.48	58	255
3310	1.53	.19	1.13	425	.21	.92	3.82	60	249
PENSE FORMATION									
3335	1.17	.06	1.60	427	.10	1.50	3.23	128	276
3360	.72	.14	.14	461	.02	.12	1.71	16	237
CANTUAR FORMATION									
3385	2.78	.29	1.24	411	.36	.88	4.32	31	155
3410	2.09	.14	1.42	408	.20	1.22	4.13	58	197
3410	2.85	.10	2.79	418	.29	2.50	3.49	87	122
3420	2.98	.17	2.04	423	.35	1.69	2.26	56	75
3430	1.34	.17	.77	428	.13	.64	1.26	47	94
3435	1.71	.09	2.42	415	.21	2.21	1.55	129	90
3440	1.09	.26	1.29	430	.34	.95	1.45	87	133
3450	1.36	.20	1.41	427	.28	1.13	1.59	83	116
3460	.77	.09	.65	422	.06	.59	1.63	76	211
3460	1.75	.08	2.26	423	.19	2.07	1.65	118	94

[1]The original measurements of core sample depths were made in feet; therefore, for reasons of accuracy, metric conversions are not given.

Table 74.3 (cont.)

Depth in ft[1]	TOC	PI	S1+S2	TMAX	S1	S2	S3	HI	OI
CANTUAR FORMATION (cont.)									
3470	.95	.13	1.04	427	.13	.91	.88	95	92
3485	1.73	.03	3.52	421	.12	3.40	2.07	196	119
3490	1.82	.07	2.02	424	.15	1.87	1.73	102	95
3500	1.09	.12	.75	426	.09	.66	2.56	60	234
3500	1.12	.21	.81	422	.17	.64	2.68	57	239
3510	2.83	.09	3.17	421	.27	2.90	3.16	102	111
3520	3.35	.03	7.53	421	.26	7.27	3.20	217	95
3525	1.81	.08	2.37	414	.20	2.17	3.45	119	190
3530	1.62	.13	1.35	427	.18	1.17	4.53	72	279
3540	1.73	.06	1.92	425	.12	1.80	1.58	104	91
3550	1.35	.19	.48	427	.09	.39	2.29	28	169
3550	1.40	.57	.21	359	.12	.09	2.64	6	188
3560	.99	.48	.21	436	.10	.11	2.95	11	297
3570	1.80	.36	.44	402	.16	.28	4.20	15	233
3575	.78	.33	.12	445	.04	.08	3.46	10	443
3575	1.32	.37	.38	427	.14	.24	3.94	18	298
3600	1.35	.20	.76	434	.15	.61	3.43	45	254
MASEFIELD FORMATION									
3680	1.61	.23	1.22	432	.28	.94	5.74	58	356
3705	1.78	.44	.63	406	.28	.35	4.90	19	275
3730	.83	.15	.26	416	.04	.22	1.44	26	173
3780	2.20	.41	.90	407	.37	.53	4.80	24	218
3805	1.60	.11	.98	425	.11	.87	1.57	54	98
RIERDON FORMATION									
3830	1.36	.30	.37	418	.11	.26	3.09	19	227
3855	.97	.04	1.00	424	.04	.96	1.51	98	155
3880	.98	.41	.22	407	.09	.13	3.74	13	381
3905	.81	.08	.38	424	.03	.35	2.74	43	338
3930	.80	.12	.65	432	.08	.57	3.58	71	447
3955	.97	.10	1.35	427	.13	1.22	3.26	125	336
3980	.70	.36	1.04	394	.37	.67	3.88	95	554
4005	1.47	.06	1.59	430	.09	1.50	2.63	102	178
4030	1.33	.27	.44	413	.12	.32	2.42	24	181
SHAUNAVON FORMATION									
4055	.51	.21	.28	429	.06	.22	2.74	43	537
4105	1.15	.13	.83	430	.11	.72	2.54	62	220
4125	.90	.16	.95	423	.15	.80	3.13	88	347
GRAVELBOURG FORMATION									
4225	.74	.15	.62	428	.09	.53	4.21	71	568
4250	.66	.14	.77	425	.11	.66	1.81	100	274
4253	2.28	.05	5.96	425	.32	5.64	1.94	247	85
4260	.67	.09	1.72	428	.15	1.57	1.99	234	297
4270	1.27	.17	1.00	424	.17	.83	2.47	65	194
4275	.68	.09	.88	425	.08	.80	1.92	117	282
4275	.78	.05	1.24	425	.06	1.18	2.80	151	358
4285	.76	.07	1.39	435	.10	1.29	2.81	169	369
4290	.53	.09	.66	428	.06	.60	1.80	113	339

Depth in ft[1]	TOC	PI	S1+S2	TMAX	S1	S2	S3	HI	OI
WATROUS FORMATION									
4450	.55	.09	.91	437	.08	.83	1.34	150	243
4485	.67	.23	.30	421	.07	.23	2.53	34	377
4505	.85	.05	1.77	427	.09	1.68	1.99	197	234
4510	.78	.21	1.30	428	.27	1.03	1.72	132	220
4520	.60	.37	.49	409	.18	.31	1.77	51	295
4530	.68	.43	.68	397	.29	.39	3.36	57	494
4530	.71	.38	.37	404	.14	.23	3.80	32	535
4540	1.09	.17	1.43	431	.24	1.19	2.06	109	188
4550	.53	.31	.45	421	.14	.31	1.55	58	292
4555	1.53	.15	1.14	416	.17	.97	2.27	63	148
4560	3.26	.03	12.76	434	.44	12.32	1.58	377	48
4570	1.09	.23	.71	430	.16	.55	1.60	50	146
4580	.73	.12	.99	427	.12	.87	3.51	119	480
4610	.70	.17	.84	427	.14	.70	2.93	100	418
4630	.55	.37	.43	400	.16	.27	3.05	49	554
4630	.90	.22	.51	430	.11	.40	4.19	44	465
4640	.62	.16	.89	430	.14	.75	1.36	120	219
CHARLES FORMATION									
4650	.54	.22	.55	422	.12	.43	1.10	79	203
4650	1.28	.08	1.27	432	.10	1.17	1.74	91	135
4775	.68	.06	2.01	436	.12	1.89	2.23	277	327
4875	1.57	.27	.81	409	.22	.59	3.20	37	203
MISSION CANYON FORMATION									
4900	.84	.16	.50	429	.08	.42	1.96	50	233
4925	.70	.26	.42	421	.11	.31	2.95	44	421
4975	.55	.20	.30	431	.06	.24	1.70	43	309
5025	.70	.43	.28	432	.12	.16	3.47	22	495
5050	.72	.10	.86	437	.09	.77	2.09	106	290
5075	.86	.08	1.49	429	.12	1.37	3.71	159	431
5200	.87	.63	.32	419	.20	.12	1.54	13	177
LODGEPOLE FORMATION									
5350	.56	.23	.53	429	.12	.41	2.04	73	364
5375	.52	.03	1.39	432	.04	1.35	.52	259	100
5605	.95	.36	.47	419	.17	.30	2.28	31	240
5655	.84	.55	.31	406	.17	.14	2.76	16	328
BAKKEN FORMATION									
5930	1.87	.26	1.08	450	.28	.80	.74	42	39
5980	1.52	.05	5.33	420	.24	5.09	.87	334	57
5995	.65	.37	.41	433	.15	.26	2.53	40	389
6005	1.66	.07	5.51	426	.40	5.11	2.43	307	146
6030	5.82	.07	32.81	421	2.28	30.53	2.16	524	37
TORQUAY FORMATION									
6055	.56	.57	.23	387	.13	.10	1.59	17	283

4295	2.63	.02	17.75	434	.30	17.45	1.53	663	58
4300	1.39	.04	4.27	435	.15	4.12	2.27	296	163
4300	2.41	.01	16.91	431	.13	16.78	1.70	696	70
4305	1.69	.03	6.42	434	.20	6.22	2.46	368	145
4325	1.72	.09	3.10	432	.28	2.82	2.84	163	165
4375	.69	.17	.36	430	.06	.30	2.37	43	343
4400	1.01	.13	.55	427	.07	.48	1.63	47	161

[1] The original measurements of core sample depths were made in feet; therefore, for reasons of accuracy, metric conversions are not given.

HERALD FORMATION									
8290	.50	.11	1.17	426	.13	1.04	.18	208	36
WINNIPEG FORMATION									
8545	1.27	.03	4.75	438	.13	4.62	.61	363	48
8550	1.41	.04	6.28	434	.24	6.04	.70	428	49
8550	1.51	.02	6.46	435	.16	6.30	.74	417	49
DUPEROW FORMATION									
6635	.89	.08	6.01	425	.51	5.50	.61	617	68
6685	.56	.03	4.23	428	.12	4.11	.22	733	39

deposition (belemnite fragments occur in cuttings), the possibility that this source represents cavings from the overlying Gravelbourg Formation would have to be considered.

Gravelbourg Formation

Potential petroleum source rocks in the Gravelbourg Formation occur in two zones. The lower zone spans the upper part of the Lower Gravelbourg limestone and the lower part of the Upper Gravelbourg shale. This interval is marked by a general increase in TOC and S2 yield. Pyrolysis results are reproducible between some runs. This zone contains interbedded Type II and Type III sources occurring discretely. S2 yields from Type II sources are very good (greater than 16.5 mg/gm). Type III sources have poor to fair yields. The second zone of potential source development occurs in shale beds associated with the shale to sandstone facies transition, which occurs at about 4255 feet (1296.9 m). Tmax for the formation is in the range 430-435 degrees Celsius, suggesting that the formation is marginally mature. This is a greater maturity than is indicated for the underlying, Paleozoic, marine, source rocks. The reason for this result is uncertain. It may be attributable either to the corruption of the sample from this interval or to a differing response of the Mesozoic sources to the pyrolysis experiment, as a result of a change in the nature of the source material. A similar greater maturity is exhibited by the marine source rocks of the Favel Formation. The reason for this anomaly is equally inexplicable. Type III sources show weak correlation of TOC and Petroleum Potential. Yields of 3.92 kg/tonne/per cent organic carbon in excess of an inert threshold of 0.46 weight per cent, are suggested. Type II sources may have yields of 6.75 to 7.02 kg/tonne/per cent of organic carbon if no inert material is present.

Cantuar Formation

Potential petroleum source rocks occur within the Dimmock Creek and Atlas members of the Cantuar Formation, Mannville Group. Total Organic Carbon increases upward through each of the two members. Within the Dimmock Creek Member there is a correlative increase of S2 yield with increasing TOC. The more arenaceous strata of the Atlas Member do not exhibit the same correlation of TOC and S2 yield, suggesting that a greater proportion of inertinitic materials may be present. S2 yield reaches its greatest value, 7.27 mg/gm, near the top of the Dimmock Creek Member. Type III organic matter forms the potential source in both members. Tmax and Hydrogen and Oxygen indices show the formation to be thermally immature. TOC and Petroleum Potential show no correlation for the formation as a whole and a poor positive correlation within the Dimmock Creek Member.

Lower Colorado Group

Potential petroleum source rocks are sparsely distributed throughout the Lower Colorado Group, occurring in the Joli Fou, Viking and Ashville formations. Within the Joli Fou Formation, a discernible trend of upward improvement in TOC and S2 yield is identified from 3305-3280 feet (1077.4-999.7 m) in the well. Similar but less marked trends occur from 3275-3245 feet (998.2-989.1 m) and 3240-3210 feet (987.5-978.4 m). These sequences correspond to discernible coarsening-upward cycles (shale to siltstone) reflected by the samples. Hydrogen and Oxygen indices indicate that Type III sources are present, and presumably the cyclic nature of the grain size and TOC abundance variations indicate an encroachment by both silt and terrestrial organic material into the area now penetrated by the well. All sources are immature. Tmax data show

considerable scatter; however, a value of 418.2 degrees Celsius is consistent with the maturation gradient for Type III, Mesozoic sources.

One potential petroleum source rock sample was obtained from near the top of the Viking Formation. It has a higher S2 yield per gram organic carbon than the underlying Type II sources and suggests an increased marine-source component associated with the termination of Viking sand desposition. This sample also is from an immature source rock.

The Westgate member of the Ashville Formation is marked by a single trend of improving TOC values upward throughout the member. S2 yields do not show a strong correspondence to TOC. All of the sources identified in the Westgate Member are immature Type III. A sample labelled as coming from the top of the Belle Fourche Member of the Ashville Formation has the same geochemical characteristics as the overlying Favel Formation. This sample is assumed to be either improperly lagged or to have caved (2840 ft, Table 74.3).

Upper Colorado Group

All three formations of the Upper Colorado Group exhibit some source potential. Sources are sparsely developed in the Niobrara and Morden formations and extensively developed in the Favel Formation. TOC is highest in the Niobrara Formation (2.77% on average) and similar in the Morden (1.66%) and Favel (1.66%) formations. In spite of this, the yield of sources in the Favel Formation is superior. Good and very good oil shows are recorded from seven samples confined to the Favel Formation (S1 yield) in spite of the immaturity of the source (Tmax). Hydrogen and Oxygen indices also suggest immaturity. Both discretely interbedded and intermingled Type II and Type III sources are present. Some inert organic carbon is present in the Type II sources (1.25 weight per cent) indicating a terrestrial component. Correlation of TOC with Petroleum Potential suggests that the Type III source would yield 2.39 kg/tonne/per cent of organic carbon in excess of 2.32 per cent inertinite. The yield of marine sources in excess of the 1.25 weight per cent inertinite threshold would be 6.67 kg/tonne/per cent organic carbon.

Discussion

The Parry No. 1 well occurs in the vicinity of oil production and of hydrocarbon shows in the Bighorn Group carbonates (Kendall, 1976). Several authors have suggested the kerogen-rich layers of the Upper Yeoman Formation as an indigenous source for the oils of the Bighorn Group (Red River Fm., Unit "C", Kohm and Louden, 1982; Kendall, 1976). Others have suggested that the source was the Icebox Member of the Winnipeg Formation, which was the source of the oil in Ordovician reservoirs (Meissner and others, 1984). Detailed descriptions of the correlation of Red River oils and potential sources remain to be made. Clearly, proof of the regional development of thermally mature sources in the Winnipeg Formation would be attractive as a potential source for oils in Ordovican and Silurian reservoirs. The thermally mature Type II source rock found in the interval 8542-8552 feet (2603.6-2606.6 m) of the Parry No. 1 well is a possible indicator of such a development.

The Duperow Formation represents deposits behind the main barrier reef complex of the Woodbend Group, in a setting somewhat analogous to the Muskeg and Keg River formations behind the Pine Point-Shekilie barrier. The evaporitic subbasins with indigenous sources similar to the Black Creek Basin must be considered the best hydrocarbon play. The association of thin yet rich marine source rocks and evaporitic strata of the Flat Lake Halite are encouraging. Although thermally immature in this well, similar geological sequences in zones of higher geothermal gradient or deeper Cretaceous burial could be mature.

Recently, considerable effort has been focused on the source potential of the Fammenian and Tournaisian shales of the Bakken Formation and laterally equivalent strata (Dembicki and Pirkle, 1985; Leenheer, 1984; Price and others, 1984; Webster, 1984; Schmoker and Hester, 1983). The present authors agree with previous investigations in assigning a high source rock potential to this formation. The lack of potential in cutting samples from the Upper shale member, however, is in contrast to the usual potential of both members recognized in the U.S.A. Despite its thermal immaturity, the Bakken Formation had a very good oil show in this well. Tracing of this formation to zones of enhanced maturity is also warranted.

The Jurassic sources in the Gravelbourg Formation are possibly equivalent to potential source rock intervals in the Sawtooth Formation (Clayton and others, 1982), although there is insufficient data at present to confirm such a correlation. The source interval within the Watrous Formation is a new discovery. However, it is such a thin development that it is of dubious significance regionally. The thermal maturity of Jurassic strata is anomalously high in comparison to the Tmax versus depth gradient obtained for the three, Paleozoic, Type II sources. This phenomenon is repeated in the Cretaceous Favel Formation. The reasons for this anomaly are not presently understood. The observed Tmax values of 430 to 435 degrees Celsius indicate that the Gravelbourg sources are marginally mature.

Immature Type III source rocks are present in both the Mannville and Colorado groups. Potential source rocks are absent from younger strata of the Pierre Formation of the Montana Group. Type II source rocks are developed in the Favel and Niobrara formations. These formations are immature as petroleum source rocks but prospective because they occur as oil shale at the outcrop (Macauley and others, 1985). Laterally equivalent strata of the Marias River shale are recognized as petroleum source rocks (Clayton and others, 1982).

This study is the result of the initial investigation of petroleum source rocks in Saskatchewan, derived from a single well. Further investigations will ascertain the source rock potential from other wells and thereby determine the lateral persistence of the source rocks identified in this study. Secondary investigations will then be made of the variation of source potential and thermal maturity of individual formations.

Acknowledgments

The authors appreciate the donation of well cuttings for this study by Suncor Inc. of Calgary, and thank Mr. Ed Schultz for arranging their delivery. This project was set up under the guidance of the O.E.R.D., 6.1.1., Government-Industry Review Committee, and the authors are grateful for this assistance.

References

Christopher, J.E.
1984: Depositional patterns and oil field trends in the Lower Mesozoic of the northern Williston Basin, Canada, in Oil and Gas in Saskatchewan, ed. J.A. Lorsong and M.A. Wilson; Saskatchewan Geological Society Special Publication No. 7, p. 83-102.

Christopher, J.E., Kent, D.M., and Simpson, F.
1971: Hydrocarbon potential of Saskatchewan; Saskatchewan Department of Mineral Resources, Report No. 157, p. 47.

Clayton, J.L., Mudge, M.R., Luceck, C., and Daws, T.A.
1982: Hydrocarbon source rock evaluation of the disturbed belt northwestern Montana; in Geologic studies of the Cordilleran thrust belt, Volume 2, ed. R.B. Powers; Rocky Mountain Association of Geologists, Denver, p. 777-804.

Dembicki, H., Jr. and Pirkle, R.L.
1985: Regional source rock mapping using a source potential rating index; American Association of Petroleum Geologists, Bulletin, v. 69, no. 4, p. 567-581.

Dunn, C.E.
1975: The Upper Devonian Duperow Formation in southeastern Saskatchewan; Saskatchewan Department of Mineral Resources, Report no. 179, p. 151.

Holter, M.E.
1969: The Middle Devonian Prairie Evaporite of Saskatchewan; Saskatchewan Department of Mineral Resources, Report no. 123, p. 134.

Kendall, A.C.
1976: The Ordovician carbonate successsion (Big Horn Group) of southeastern Saskatchewan; Saskatchewan Department of Mineral Resources, Report no. 180, p. 185.

Kohm, J.A. and Louden, R.O.
1982: Ordovician Red River of eastern Montana and western North Dakota: Relationships between lithofacies and production; in Fourth International Williston Basin Symposium Proceedings, ed. J.E. Christopher and J. Kaldi; Saskatchewan Geological Society, Regina, p. 27, 28.

Leenheer, M.J.
1984: Mississippian Bakken and equivalent formations as source rocks in the Western Canadian Basin; Organic Geochemistry, v. 6, p. 521-532.

Macauley, G., Snowdon, L.R., and Ball, F.D.
1985: Geochemistry and geological factors governing exploitation of selected Canadian oil shale deposits; Geological Survey of Canada, Paper 85-13, p. 65.

MacDonald, G.H.
1956: Subsurface stratigraphy of the Mississippian rocks of Saskatchewan; Geological Survey of Canada, Memoir 282, p. 46.

McCrossan, R.G. and Glaister, R.P.
1964: Geological history of Western Canada; Alberta Society of Petroleum Geologists, Calgary, 232 p.

Meissner, F.F., Woodward, J., and Clayton, J.L.
1984: Stratigraphic relationships and distribution of source rocks in the greater Rocky Mountain region; in Hydrocarbon source rocks of the greater Rocky Mountain region, ed. J. Woodward, F.F. Meissner, and J.L. Clayton; Rocky Mountain Association of Geologists, Denver, p. 1-34.

Nichols, R.A.H.
1970: The petrology and economic geology of the Upper Devonian Birdbear Formation in southeastern Saskatchewan; Saskatchewan Department of Mineral Resources, Report no. 125, p. 94.

Paterson, D.F.
1971: The stratigraphy of the Winnipeg Formation (Ordovician) of Saskatchewan; Saskatchewan Department of Mineral Resources, Report no. 140, p. 57.

Poulton, T.P.
1984: The Jurassic of the Canadian Western Interior, from 49°N latitude to Beaufort Sea; in The Mesozoic of Middle North America, ed. D.F. Stott and D.J. Glass; Canadian Society of Petroleum Geologists, Memoir 9, p. 15-41.

Price, L.C., Ging, T., Daws, T., Love, A., Pawlewicz, M., and Anders, D.
1984: Organic metamorphism in the Mississippian-Devonian Bakken shale, North Dakota portion of the Williston Basin; in Hydrocarbon source rocks of the greater Rocky Mountain region, ed. J. Woodward, F.F. Meissner, and J.L. Clayton; Rocky Mountain Association of Geologists, Denver, p. 83-134.

Price, L.L.
1963: Lower Cretaceous rocks of southeastern Saskatchewan; Geological Survey of Canada, Paper 62-29, p. 55.

Tissot, B.P. and Welte, D.H.
1978: Petroleum formation and occurrence; Springer-Verlag, Berlin, 538 p.

Schmoker, J.W. and Hester, T.C.
1983: Organic carbon in the Bakken Formation United States portion of Williston Basin; American Association of Petroleum Geologists, Bulletin, v. 67, no. 12, p. 2165-2174.

Webster, R.L.
1984: Petroleum source rocks and stratigraphy of the Bakken Formation in North Dakota; in Hydrocarbon source rocks of the greater Rocky Mountain region, ed. J. Woodward, F.F. Meissner, and J.L. Clayton; Rocky Mountain Association of Geologists, Denver, p. 57-81.

Geology of the northern Selwyn Range, western Main Ranges, Rocky Mountains, British Columbia: preliminary report

Project 850048

Michael R. McDonough [1] and Philip S. Simony [1]
Institute of Sedimentary and Petroleum Geology, Calgary

McDonough, M.R. and Simony, P.S., Geology of the northern Selwyn Range, western Main Ranges, Rocky Mountains, British Columbia: preliminary report; in Current Research, Part A, Geological Survey of Canada, Paper 86-1A, p. 619-626, 1986.

Abstract

Two mappable units are recognized within the Hadrynian Miette Group in the northern Selwyn Range. A sequence of sandstones and conglomerates, with lesser pelitic layers, is ascribed to the middle Miette. This sequence is underlain by a unit of pelite with thin quartzite layers, which may be correlated with lower Miette recognized elsewhere in the western Main Ranges. Shearing near the contact, however, suggests that a thrust fault may separate middle Miette from 'lower' Miette. Correlation of this 'lower' Miette with a sequence of pelite and quartzite that overlies basement gneisses in an area to the southwest is probable, and suggests that part of the lower Miette is missing above the basement. A basement 'high' is proposed to explain the missing section.

The structure of the northern half of the study area is dominated by the large, shallow-plunging Terry Fox Anticlinorium. To the south, the core of the anticlinorium is cut by a set of steep, west-dipping thrusts that thicken 'lower' Miette. Moderately inclined west-dipping thrust sheets constitute the west limb of Terry Fox Anticlinorium. A transition from reclined to upright structures in Packsaddle Thrust Sheet can be attributed to a single phase of thrust sheet motion up a steep ramp structure.

Résumé

On décrit deux unités de la carte géologique du groupe hadrynien de Miette dans la partie nord de la chaîne Selwyn. Une série de grès et de conglomérats avec quelques couches pélitiques appartiendrait au Miette moyen. Elle recouvre une unité pélitique qui renferme des couches minces de quartzite et qui pourrait être associée au Miette inférieur reconnu ailleurs dans la partie occidentale des monts Main. Un cisaillement près du contact indique cependant qu'un chevauchement séparerait le Miette moyen du Miette inférieur. Il est probable que le Miette inférieur soit associé à une série pélitique et quartzitique qui recouvre le socle gneissique dans un secteur au sud-ouest, ce qui indiquerait qu'une partie du Miette inférieur est absente au-dessus du socle. Un soulèvement du socle expliquerait l'absence de cette section.

La structure de la moitié nord de la région à l'étude est dominée par le grand anticlinorium de Terry Fox à faible plongement. Vers le sud, le noyau de l'anticlinorium est coupé par une série de failles inverses de fort pendage ouest qui épaississent le Miette inférieur. Des nappes de charriage modérément inclinées vers l'ouest constituent le flanc occidental de l'anticlinorium de Terry Fox. Le passage des structures subhorizontales aux structures verticales dans la nappe de charriage de Packsaddle peut être attribué à une phase unique de remontée des nappes de charriage le long d'une structure à forte pente.

[1] Department of Geology and Geophysics, University of Calgary, Calgary, Alberta T2N 1N4

Introduction and previous work

During the 1985 field season, an area of about 300 square km, between Bulldog and Swift creeks (Fig. 75.1) was mapped at 1:24,000 scale in order to elucidate the stratigraphy, structure and strain history of Hadrynian Miette Group rocks. The area lies east and southeast of Valemount, British Columbia, and forms part of the northern Selwyn Range of the Rocky Mountain Main Ranges subprovince.

Strata of the northern Selwyn Range have been assigned to the Miette Group of the Windermere Supergroup (Campbell, 1968). To the north, in the McBride map area, the Miette is informally divided into lower, middle, and upper units (Campbell et al., 1973). Carey and Simony (1985) described a section of the Miette Group from this area as having 380 m of lower Miette pelite and carbonate, 2.8 km of coarse grained middle Miette, and approximately 1.8 km of upper Miette pelite. At this locality, the middle Miette is dominated by thick layers of conglomerate and sandstone with lesser, interbedded pelite. In the southern Selwyn Range, a minimum of 1.5 km of lower Miette grits are overlain by about 2 km of lower pelite (Mountjoy, pers. comm., 1985). Mountjoy et al. (1985) found that this sequence underlies approximately 2.5 km of middle Miette grit, which is characterized by thick, coarse grained clastics consisting of relatively thick pelitic units separating the coarse, massive sandstone (grit) and conglomerate units.

In the study area, in the east half of the Valemount map area, a thick sequence of coarse grained clastics mapped by Mountjoy (see Campbell, 1968) appears to be similar to middle Miette grits typical of the western Main Ranges (Mountjoy et al., 1985). Mountjoy found that these coarse clastics outline a large antiform-synform pair, which forms part of a north plunging anticlinorium dominating the structure of the northern Selwyn Range. The anticlinorium is herein called the Terry Fox Anticlinorium, because its axial trace northwest of Swift Creek (Campbell, 1968) nearly intersects the summit of Mount Terry Fox (Fig. 75.1). Farther southeast, Mountjoy et al. (1985) mapped a large, doubly plunging anticlinorium in about the same structural position, called the Fraser River Anticlinorium. Numerous imbricate faults transect the traces of the two anticlinoria, and continuity is not clear.

Along the southwest edge of the central and southern Selwyn Range, southwest-dipping thrust sheets of basement and lower Miette cover are thrust northeast over middle Miette (Oke and Simony, 1981; McDonough and Simony, 1984; McDonough, 1984, 1985; Mountjoy et al., 1985).

Problematic transverse foliations found adjacent to the Rocky Mountain Trench have been reported by numerous workers (McDonough, 1984; Carey and Simony, 1985; Mountjoy et al., 1985). Transverse foliatons are penetrative adjacent to the Trench, and die out toward the northeast.

Stratigraphy

A maximum of 3850 m of Miette strata are exposed in the northern Selwyn Range (Fig. 75.2). That sequence can be divided into two lithologically distinct units. These are informally called the 'lower' and middle Miette (Fig. 75.2). Below stacked sandstones and conglomerates typical of the

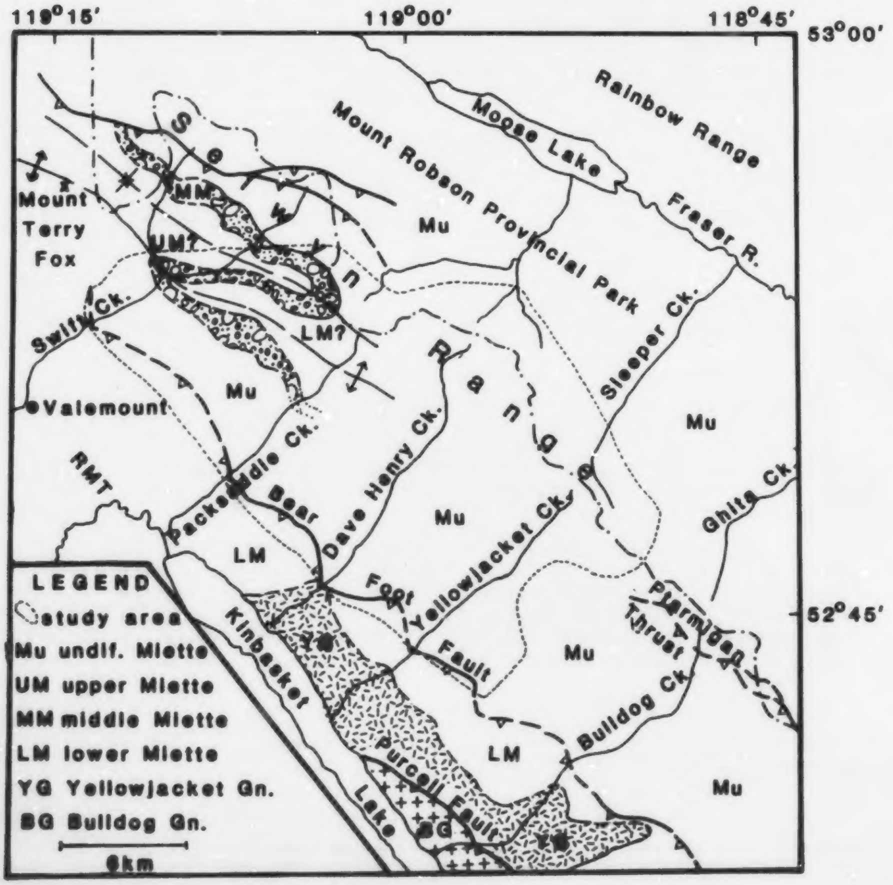

Figure 75.1

Location map and generalized geological map of the northern Selwyn Range. Modified from Campbell (1968); geology in southwest part from McDonough (1984); Ptarmigan Thrust from Mountjoy et al. (1985); RMT = Rocky Mountain Trench.

middle Miette, lies a unit of pelite with subordinate quartzite layers that tentatively is assigned to the 'lower' Miette. The 'lower' Miette has a maximum exposed thickness of 800 m, and the middle Miette has a maximum exposed thickness of 3050 m. These are minimum thicknesses, as neither the base of the 'lower' Miette nor the top of the middle Miette are exposed.

On the west limb of Swift Syncline (Fig. 75.3), the contact between 'lower' Miette pelite and coarse clastics of the middle Miette is a 40 to 50 m thick gradational zone. The base of this zone comprises silty pelites of the 'lower' Miette, which are overlain by pelites with lensoidal sandstone beds that become more numerous upward, and the strata then pass into the sandstone and conglomerate succession of the middle Miette. The gradational nature of the 'lower'/middle Miette contact suggests that the contact is conformable.

A flat-lying, pre-F_2 sheared zone in a single pelite outcrop, about 100 m below the base of the middle Miette, may be an indication, however, that the middle Miette and 100 m of 'lower' Miette are thrust over pelite that could be assigned to the upper Miette. This would require a major thrust, folded by Terry Fox Anticlinorium. However, evidence for a major thrust is lacking. Thus, the pelite is tentatively assigned 'lower' Miette status.

The 'lower' Miette consists mostly of recessive, dark grey to black, pyritic phyllites and phyllitic schists (schists at garnet grade) with dark brown to rust coloured weathered surfaces, and containing subordinate bands of white quartzite. These phyllites typically contain thin (1-2 mm thick) rhythmically bedded, white to light grey siltstone, as well as very fine grained, lensoidal, sandstone laminae that pinch out laterally within 10 to 30 cm. The stratigraphic spacing of siltstone laminae is 3 to 5 mm, imparting a finely banded character to fresh surfaces. Near the top of the 'lower' Miette, the phyllites become progressively sandier, and isolated, 1 to 3 m thick packages of pyritic, non- to slightly-argillaceous, medium grained, grey sandstone in 4 to 20 cm thick beds are found.

Resistant, cliff forming bands within the lower Miette are composed of mineralogically mature medium- to coarse-grained, white to tan quartzite in units 3 to 80 m thick, commonly with beds 10 to 40 cm thick. Feldspar and micas constitute <10 per cent of these very well cemented quartzites. Interbedded with the quartzite are lesser (0.5-1.0 m) thick beds of granule to pebble conglomerate. These conglomerates are sublitharenites containing 5 to 10 per cent feldspar clasts in a quartzite matrix, and are distinctly less argillaceous and less feldspathic than typical Miette conglomerates. They occur in fining-upward beds that grade into coarse and medium grained quartzites. The thickest and most continuous quartzite marker is 80 m thick and occurs 270 m below the base of the middle Miette. Its map pattern outlines the Terry Fox Anticlinorium across Packsaddle and Swift creeks (Fig. 75.3).

In Packsaddle and Dave Henry drainage areas, a 4 to 5 m thick, thinly bedded, black limestone marker is found 25 m above the quartzite marker. Limestone beds are 4 to 8 cm thick. Lesser, interbedded, black, calcareous siltstone and minor quartz-granule bearing, calcareous, black siltstone are present within black limestone. South and southeast of the termination of the Terry Fox Anticlinorium, against Sleeper Fault (Fig. 75.3), the quartzite marker is represented by at least four thinner, quartzite units, and the black limestone marker is absent.

Above the 'lower' Miette sequence lies an upright package dominated by thick conglomerate and sandstone units with subordinate, intervening green and/or brown pelite units. This sequence closely resembles the stacked conglomerates and sandstones typical of middle Miette of the central Main Ranges (Carey and Simony, 1985). Rare carbonates in this sequence occur as white marble and dolomitic sandstone, which contrast with the black limestone contained in the lower Miette grit beds described by Mountjoy et al. (1985). Bed thicknesses of up to 4 m also contrast with the thinner beds typical of lower Miette grit. The presence of white marble and the generally thicker bedding further suggest that this unit is more correctly assigned to the middle Miette.

Coarse clastics of the middle Miette are slightly argillaceous (rarely very argillaceous), immature, feldspathic wackes. Individual sandstone and conglomerate map units may be 520 m thick. Conglomerate beds commonly exhibit basal scours and upward-grading A-B and A-B-C Bouma sequences, providing excellent bedding-top indicators. A typical graded bed from the middle Miette comprises slightly argillaceous, small- to large-pebble conglomerate filling a scoured base, fining upward into slightly argillaceous to clean granule conglomerate (grit of other workers) and coarse grained sandstone, which in turn grade into planar laminated, medium grained sandstone. Reverse grading is very rare. Rare, trough crossbedding in 0.5 to 1.0 m thick granule conglomerate and coarse grained sandstone beds also indicates upright bedding orientation.

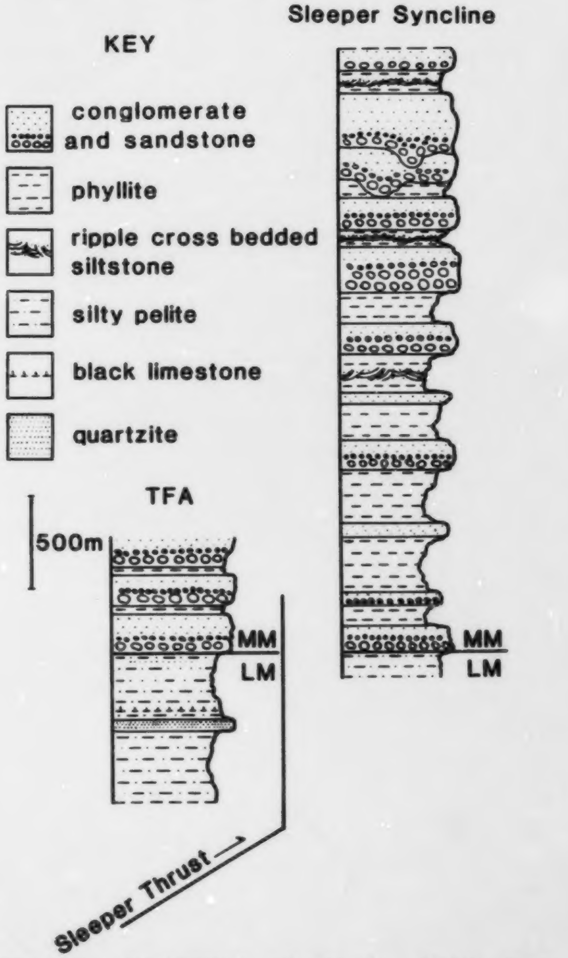

***Figure 75.2.** Stratigraphic columns for Miette Group; TFA = Terry Fox Anticlinorium, MM = middle Miette, LM = 'lower' Miette.*

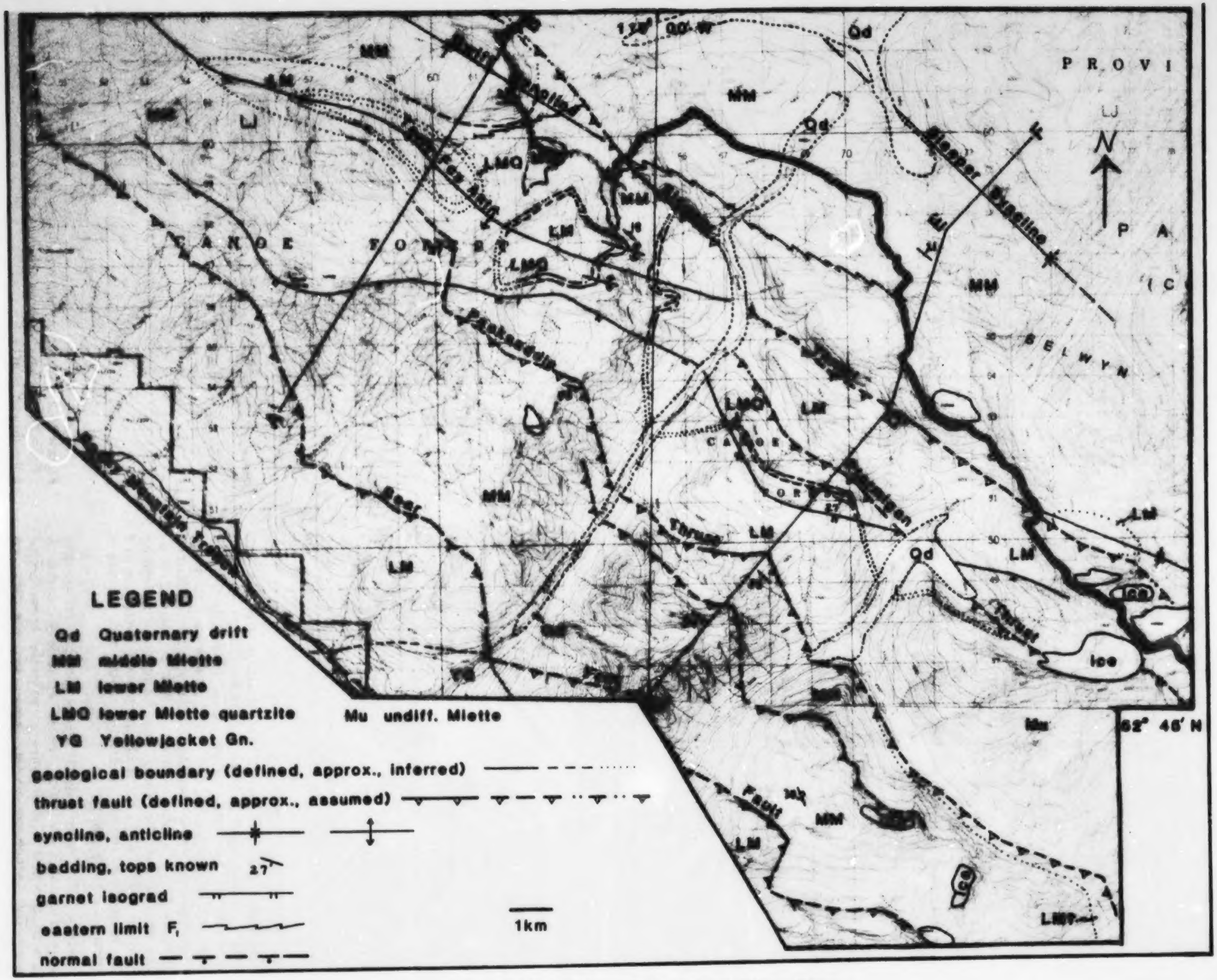

Figure 75.3. *Geological map of the northern Selwyn Range.*

North of Sleeper Creek, a thick conglomerate and sandstone unit forms a channel-like feature that cuts into and eliminates the underlying pelite unit. This coarse grained channel fill may imply fluvial processes. However, the thick pelites that occur between coarse clastic units in the section are too voluminous to represent overbank deposits, and are suggestive of deep water, probably marine, deposition. Thick conglomerates were deposited by mass gravity processes, and likely represent debris and grain flows that developed channel forms in an anastomosing submarine fan complex. Carey and Simony (1985) documented a submarine fan complex in the middle Miette near Cushing Creek, but they could not rule out the possibility of some deltaic influence.

Recessive map units within the middle Miette consist of green to brownish weathering pelites that individually have a maximum thickness of 300 m. A typical pelitic unit in the middle Miette has a tripartite character, with a middle section of bright green siltstone and chlorite-rich green phyllite, with or without dolomitic, medium- to coarse-grained, quartz sandstone. Siltstones are ripple cross-laminated and slightly argillaceous. Above the green horizon, a layer of light to medium grey phyllite is usually present. Locally, light coloured phyllite is missing and replaced by light brown to white marble with interbedded, amphibole bearing, calcareous schist. Below the green horizon, a sequence of medium to dark grey phyllite with lesser brown dolomitic sandstone is commonly found. Black, calcareous, granule conglomerate with load and flame structures occurs very rarely in the basal part. Some pelitic units lack green pelite and siltstone, and consist mostly of medium grey phyllite.

Southwest of the garnet isograd (Fig. 75.3) the phyllites give way to well foliated schists, and dolomitic sandstones are represented by grossular garnet- and hornblende-bearing, granoblastic calcsilicates. The occurrence of these calcsilicates led McDonough and Simony (1984) to suggest that some strata in the footwall of the Bear Foot Fault were lower Miette. However, these strata are interbedded with coarse clastics that can be mapped continuously into the west limb and around the core of the Terry Fox Anticlinorium, into what is probably middle Miette. Up-plunge, toward the southeast, these strata can be traced into strata called middle Miette by Mountjoy et al. (1985) on the west limb of Fraser River Anticlinorium, in the footwall of Bear Foot Fault.

Distinct markers that can be traced more than a few kilometres are lacking in the middle Miette of the northern Selwyn Range. Hence, middle Miette strata of the present study area can be correlated with those of other workers on the basis of gross lithological characteristics only (Fig. 75.4; Mountjoy et al., 1985). 'Lower' Miette pelite and quartzite can be correlated with a similar lower Miette pelite from the west limb of Fraser River Anticlinorium (Mountjoy et al., 1985), which also is a quartzite-bearing pelite succession (Fig. 75.4). 'Lower' Miette of this study is strikingly similar to the pelite and psammite reported as lower Miette from the cover rocks above the basement in the Bear Foot Thrust Sheet (McDonough, 1984). Correlation of these three sequences can be made on the basis of a similar percentage of interbedded quartzite, thickness of individual quartzite beds, and overall thickness of the quartzite-bearing unit.

The implication of these correlations is that a significant basement relief during middle Miette time is not required if all three sequences are lower Miette (Fig. 75.4). However, these correlations do require a relief on the basement sufficient to inhibit deposition of Mountjoy et al.'s (1985) lower grit. If middle Miette is thrust onto 'lower' Miette, then the 'lower' pelite would actually be upper Miette, and the cover to the basement in the Bear Foot Thrust Sheet would be upper Miette as well, requiring that the Malton Gneisses formed a high during Windermere time that had cumulative relief, inhibiting deposition of the entire middle and lower Miette. In each scenario, a 'high' is required to account for nondeposition of a minimum of 2 km of Miette strata.

Near the bottom of the middle Miette, on the ridge north of Yellowjacket Creek (Fig. 75.3), a small, tonalite sill is found within conglomerate and sandstone. The sill comprises plagioclase-rich, quartz, biotite, and chlorite augen gneiss, with a 4 to 5 cm thick alteration zone of dark green, chloritic, garnet schist at its base. The base is concordant to bedding in the host sediments, and the top of the sill is discordant to bedding, forming a small, 2 m wide by 0.5 m thick, lacolith-shaped intrusion. The first foliation in the country rock penetrates the sill, indicating that the tonalite is pre-tectonic.

Structural geology

The major structural elements of the northern Selwyn Range (Fig. 75.3) are: Bear Foot Fault (McDonough, 1984), Packsaddle Thrust, Sleeper Thrust, Sleeper Syncline, Swift Syncline, and Terry Fox Anticlinorium.

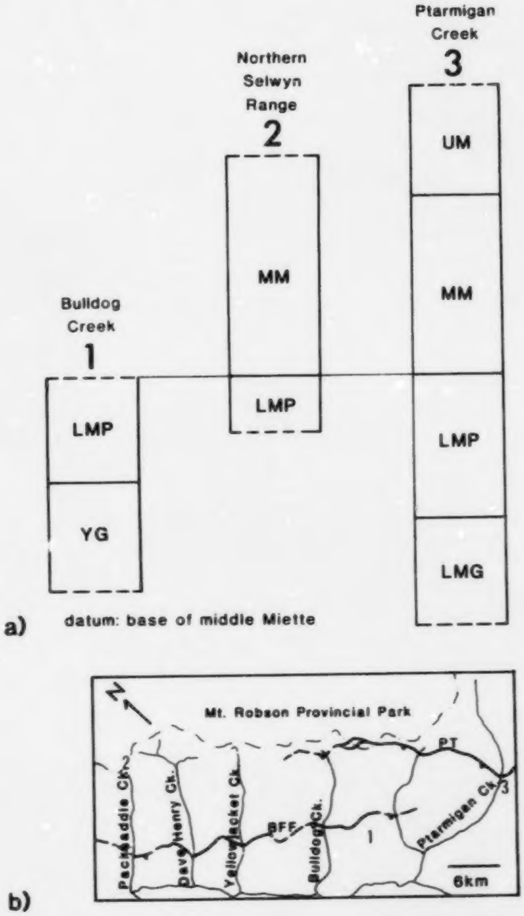

***Figure 75.4.** a) Stratigraphic correlation chart; YG = Yellowjacket Gneiss, LMG = lower Miette grit, LMP = lower Miette pelite, MM = middle Miette, UM = upper Miette. Data sources: McDonough (1984); this study; Mountjoy et al. (1985) and Mountjoy, pers. comm. (1985). b) Location map for sections in (a); PT = Ptarmigan Thrust; BFF = Bear Foot Fault.*

Two, coaxial, regional phases of folding (F_1 and F_2), and three phases of foliation development are found in association with three 'stages' of thrusting in the northern Selwyn Range. 'Stages' of thrusting can be viewed in terms of a continuum model of progressive deformation, where regional foliations are related to motion on thrust sheets (Sanderson, 1982). Superposed on these is a transverse set of minor folds and an accompanying transverse foliation (S_t). Faults in the Rocky Mountain Trench, which borders the study area on the southwest side, are interpreted as post-deformational, normal faults (McDonough, 1984).

The dark pelites of the lower Miette have a flat-lying schistosity parallel to siltstone laminae, which is the earliest tectonic foliation (S_1; structural equivalent of S_1 of McDonough and Simony, 1984) found in the westernmost Main Ranges. S_1 is cut by steeply dipping S_2 crenulation cleavage. Locally, S_2 is truncated by S_3 strain slip cleavage. In the 'lower'/middle contact zone, S_1 is refracted through the stratigraphy, but is continuous from bed to bed. It is oblique to bedding in phyllite, and is sigmoidal and at a high angle to bedding in interbedded sandstone. The continuity of S_1 from bed to bed indicates that a major F_1 thrust does not exist at that horizon.

Small scale F_1 isoclines and the low angle foliation (S_1) associated with them, which together represent the earliest deformation within each thrust sheet, die out to the northeast. An eastern limit of small-scale F_1 structures is located on Figure 75.3. East of this limit, S_1 is oblique to bedding in pelites and at a high angle to bedding in sandstones; large, upright, open to closed folds are the earliest structures present, because F_1 isoclines are not present. East of Sleeper Thrust (Fig. 75.3), sandstones and conglomerates of the middle Miette exhibit a weakly developed S_1 at an angle of 20° to 40° to bedding, and a well developed S_2 fracture cleavage. Fracture cleavage forms a convergent fan in large folds, remaining nearly perpendicular to bedding, and at the outcrop scale is continuous with S_2 crenulation cleavage in interbedded pelites. Thus, large folds in the footwall of Sleeper Thrust are related to S_2 in that thrust sheet.

A complex F_2 antiformal structure, the Terry Fox Anticlinorium, dominates the structure of the northern half of the study area. The anticlinorium has southwest verging structures on its northeast limb, which oppose northeast verging structures on its southwest limb (Fig. 75.5a). These structures plunge very gently to the northwest, and are accompanied by a nearly axial planar S_2 crenulation cleavage. Crenulation cleavage dips steeply southwest on the west limb, and dips steeply northeast on the east limb of the anticlinorium. In the core of Terry Fox Anticlinorium, the two crenulation cleavages are observed to alternately crosscut each other, suggesting that F_2 structures of opposing vergences formed synchronously.

On the northeast dipping limb common to Terry Fox Anticlinorium and Swift Syncline (Fig. 75.3), northeast verging F_1 isoclines with northeast dipping axial planar S_1 occur. The fact that the axial planes of F_1 are folded by the anticlinorium further substantiates an F_2 timing for Terry Fox Anticlinorium and related structures.

Middle Miette strata on the west limb of Terry Fox Anticlinorium are contained in a fold train of tight, slightly overturned, northeast verging, F_2 chevron folds with interlimb angles of 25° to 35°. In the core, and on the east limb of the anticlinorium, such structures are absent, and the stratigraphy passes into Swift Syncline (Fig. 75.5a), a broad, west verging syncline that has an interlimb angle of 110°. The greater shortening exhibited by F_2 chevrons on the west limb of the anticlinorium suggests that a detachment horizon may be present at the base of the fold train. In the field, discrete fault zone features, such as laterally truncated beds, are observable at the base of the middle Miette directly under the fold train.

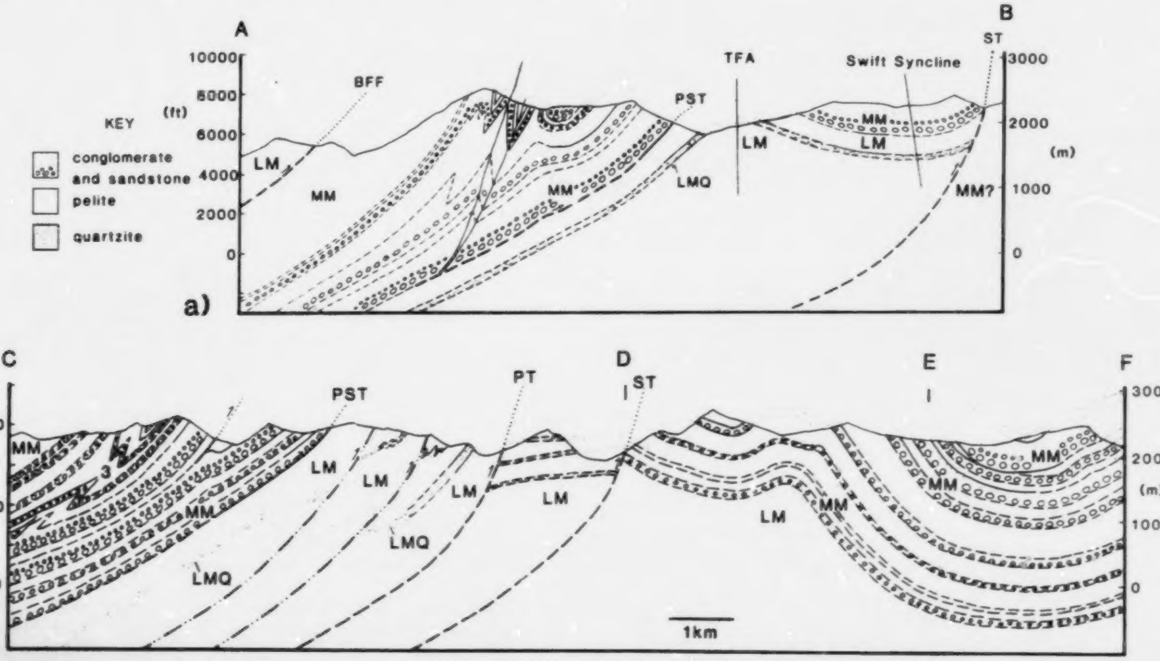

Figure 75.5. Cross-sections (1:1) along section lines A-B and C-D-E-F (see Figure 75.3 for location). Schematic minor folds in (b) are illustrative of scale and style of folds in 'lower' Miette; 3 = zone of Type 3 interference folds, TFA = Terry Fox Anticlinorium, BFF = Bear Foot Thrust, PST = Packsaddle Thrust, PT = Ptarmigan Thrust, ST = Sleeper Thrust, LM = lower Miette pelite, LMQ = lower Miette quartzite, MM = middle Miette.

Packsaddle Thrust (Fig. 75.3), located on the west limb of Terry Fox Anticlinorium, is the detachment that accommodates the shortening in the fold train discussed above. In Swift Creek, middle Miette strata are observed to pass unfaulted around the core of the anticlinorium. Stratigraphic and structural evidence presented above suggest that the thrust is not folded by Terry Fox Anticlinorium. Therefore, Packsaddle Thrust dies out to the northwest into the core of Terry Fox Anticlinorium, and is considered to be synkinematic to the anticlinorium. Packsaddle Thrust probably obeys the "bow and arrow" rule (Elliott, 1976), as it appears to gain displacement and cut downsection into 'lower' Miette to the southeast, away from its tip near Swift Creek (Fig. 75.3).

A modified Sanderson (1982) fold belt model can be applied to Packsaddle Thrust Sheet to explain a strike transition from reclined to upright folds. In the model, a flat-lying foliation, having an attitude nearly parallel to the fault, is developed in response to the imposition of simple shear boundary conditions (Sanderson, 1979, 1982). This foliation is roughly axial planar to the recumbent to reclined, tight to isoclinal folds that lie above the flat to moderately dipping portion of the thrust.

Continued thrust motion up a large, steep, ramp structure actuates rotation of the strain ellipsoid in such a way that an apparently younger crenulation cleavage overprints the 'earlier' foliation. This scenario can be attributed to a single phase of thrust motion. Younger faults can 'step out' toward the foreland in response to high stresses incurred by 'locking' of the hanging wall on a steep ramp.

The character of S_1 and S_2 foliations and their mutual textural relationships remains essentially the same from the Bear Foot Thrust Sheet in the west to the Packsaddle Thrust Sheet in the east. In both thrust sheets, S_1 is a gently to moderately southwest dipping schistosity that is probably associated with the earliest motion of the respective sheets, and is axial planar to F_1 folds. In the thrust sheet model under consideration, S_2 is an apparently younger crenulation cleavage formed by rotation of the strain ellipsoid during continued thrust motion up a steeper foreland part of the fault.

South of Yellowjacket Creek (Fig. 75.3), a hanging wall imbricate of Packsaddle Thrust truncates large, reclined, F_1 structures in a domain where large F_2 folds do not exist. To the northwest and downplunge, on the ridge between Yellowjacket and Dave Henry creeks, is a transitional zone where both F_1 and F_2 structures occur (Fig. 75.5b), showing Type 3 fold interference patterns. Farther downplunge, on the next two ridges north of Dave Henry Creek, large-scale, upright, F_2 folds predominate, and large F_1 folds are absent. This transition, from reclined F_1 folds to upright F_2 folds with a discrete zone of overlap, within the Packsaddle Thrust Sheet, is a function of structural level within the thrust sheet.

The upward transition from reclined to upright folds in the Packsaddle Thrust Sheet takes place northwestward, downplunge, across Yellowjacket Creek, and fits the Sanderson model well. Upright F_2 folds occur on the steeper foreland part of the thrust (the backlimb of Terry Fox Anticlinorium) and have a penetrative crenulation cleavage associated with them. To the southeast and up-plunge, crenulation cleavage is only weakly developed, and large, F_1 folds control the local structure. The transitional zone between the two fold domains, has Type 3 interference patterns, and has a vertical thickness of 200 m. This suggests that the domain of reclined F_1 folds has been carried up the steeper ramp section of the fault by that amount; that is, since the fault has a dip of 45°, displacement on Packsaddle imbricate is a minimum of 280 m.

The zone of imbricate faults in the hanging wall of Sleeper Thrust contains faults that truncate Terry Fox Anticlinorium, and therefore motion on them is younger than motion on Packsaddle Thrust. In this zone, a steeply southwest dipping, strain-slip cleavage (S_3) truncates west dipping S_2 crenulation cleavage, which also suggests that these faults postdate Packsaddle Thrust. The strain-slip cleavage (S_3) isolates foliation 'fish' (Hamner, 1984) of sigmoidal S_2 that consistently yield a shear couple in which the upper member is thrust up steeply to the northeast. Steep displacement indicators in outcrop are consistent with the steep attitude of the imbricate thrusts. These thrusts are considered part of a hanging wall imbricate fan in the Sleeper Thrust Sheet, and they represent the latest pulse of thrusting in the context of a local foreland progression. Ptarmigan Thrust (Mountjoy et al., 1985) can be traced into one of these imbricates, which dies out northward into Terry Fox Anticlinorium (Fig. 75.3).

Problematic transverse foliation (S_t) that crenulates S_1, is found adjacent to the Rocky Mountain Trench in pelites on either side of Bear Foot Fault. Transverse foliations have been reported near the Trench by many workers (Mountjoy et al., 1985; Carey and Simony, 1985; McDonough, 1984). They are penetrative adjacent to the Trench, and die out toward the east. If a transpression shear model (Wilcox et al., 1973) is applied to possible dextral strike slip faults in the southern Rocky Mountain Trench, the mean strike of 190° for the transverse foliation reported here would place it into the antithetic shear position. Dextral shear requires that the shear sense on the antithetic shear be sinistral. However, the sense of shear from more than 100 field observations is dextral, which is not compatible with a possible dextral system in the Trench. Thus, transverse foliations cannot be used to substantiate strike-slip faulting in the southern Rocky Mountain Trench. The preferred interpretation for the cataclastic crush zones on the east side of the Trench south of Dave Henry Creek is post-deformational, west-side down, normal faulting (Fig. 75.3).

Metamorphism and relative timing of deformation

Metamorphic grade in the northern Selwyn Range is recorded by Barrovian index minerals in pelites. To the southwest of the study area, a staurolite-kyanite isograd obliquely intersects the Rocky Mountain Trench (McDonough and Simony, 1984). North and east of this line is a garnet zone adjacent to the Trench that stretches northward from Dave Henry Creek to Swift Creek (Fig. 75.3). The garnet isograd shown in Figure 75.3 is oblique to the Trench as well. Here, garnet is indicative of the transitional greenschist-amphibolite facies, and represents maximum metamorphic grade in the western part of the study area. Garnets found along the isograd generally are small, retrogressed porphyroblasts contained within biotite-poor, phyllitic schists.

Metamorphic grade decreases to the north and northeast into a biotite zone with scattered chloritoid, and then into a chlorite zone farther to the east in Mount Robson Provincial Park. The biotite isograd is not shown on Figure 75.3 due to the sporadic occurrences of fine grained biotite. Careful mapping of the biotite isograd, through thin section analysis, is one objective of this project.

Chloritoid occurs sporadically in highly aluminous phyllites and schists throughout the study area. It is common in dark grey to black phyllites of the biotite zone near the top of the lower Miette, where it clearly truncates micas within S_2 crenulation cleavage. Thus, chloritoid is postkinematic with respect to S_2. These rocks probably represent low grade equivalents of staurolite schists found to the southwest of the study area.

Garnet porphyroblasts truncate micas oriented parallel to S_1, and are, therefore, considered to be postkinematic with respect to S_1. Their textural relationship to west dipping S_2 crenulation cleavage is not as clear cut, however. Garnets partially truncate, and in part are enveloped by micas in S_2, suggesting that the timing of garnet growth with respect to S_2 is pre- to syn-kinematic. Thus, metamorphic climax in the western part of the study area is interpreted to be pre- to syn-F_2. The relative timing of peak metamorphic conditions is slightly later than that for the basement and cover rocks of the westernmost Main Ranges, where peak metamorphism (staurolite-kyanite grade) is prekinematic with respect to F_2 (Oke, 1982; McDonough and Simony, 1984). There, garnet growth is syn- to post-S_1, and precedes S_2.

Discussion

Application of a modified Sanderson (1982) thrust and fold belt model to thrust sheets in the western Main Ranges raises some fundamental questions about correlation of structures across faults. If foliation development can be attributed to thrust sheet motion, then foliations of like structural character probably are not simply correlatives from thrust sheet to thrust sheet; that is, foliations may not have strict temporal correlatives beyond the thrust sheet they occur in. Thus, the presence of an early, moderately dipping foliation that is cut by a steeply dipping crenulation cleavage in both the Bear Foot and Packsaddle thrust sheets is probably a consequence of a similar internal structural style from sheet to sheet.

Existence of S_3 strain slip cleavage in the imbricate zone east of Packsaddle Thrust is indicative of a foreland progression of thrusting. The lack of early formed isoclinal folds (F_1) and the presence of a very weakly formed layer parallel 'S_1' foliation in the easternmost part of the area further substantiate a "younging" of deformation toward the northeast.

A minimum of 3.05 km of middle Miette strata are found above an 800 m thick unit of pelite and lesser quartzite in the northern Selwyn Range. The true stratigraphic position of this pelite unit is not yet known. Its upper contact with the overlying middle Miette is gradational on the east limb of Terry Fox Anticlinorium and in Swift Syncline. On the west limb of the anticlinorium, however, a fault is present at the base of the middle Miette, where it overlies the same pelite unit. Consequently, at this time, the pelite unit in question cannot unambiguously be assigned to either the lower or upper Miette. In this report, it is tentatively assigned to the 'lower' Miette pending further examination of the problem. Regardless of its true stratigraphic position, correlation of this unit with the predominantly pelitic unit above basement rocks of the Bear Foot Thrust Sheet reveals a minimum of 2 km of missing section above the basement. Thus, rocks of the Malton Gneiss complex probably formed a topographic high during Windermere time.

Acknowledgments

Special thanks are due Drs. D. Cook and M. McMechan of the Institute of Sedimentary and Petroleum Geology for arranging financial support. This work benefited greatly from the logistical support of Garry, Nikki and Todd of Yellowhead Helicopters, Valemount. The authors are most grateful to E.W. Mountjoy for continual discussion of western Main Ranges problems. Bruce Palmer provided field assistance during the summer months.

References

Campbell, R.B.
1968: Canoe River (83D), British Columbia; Geological Survey of Canada, Map 15-1967, scale 1:250,000 (part of GSC Open File Report 290).

Campbell, R.B., Mountjoy, E.W., and Young, F.G.
1973: Geology of the McBride map-area, British Columbia; Geological Survey of Canada, Paper 72-35, 104 p.

Carey, J.A. and Simony, P.S.
1985: Stratigraphy, sedimentology, and structure of late Proterozoic Miette Group, Cushing Creek area, B.C.; Bulletin of Canadian Petroleum Geology, v. 33, p. 184-203.

Elliott, D.
1976: The motion of thrust sheets; Journal of Geophysical Research, v. 81, p. 949-963.

Hamner, S.
1984: The potential use of planar and elliptical structures as indicators of strain regime and kinematics of tectonic flow; in Current Research, Part B, Geological Survey of Canada, Paper 84-1B, p. 133-142.

McDonough, M.R.
1984: Structural evolution and metamorphism of basement gneisses and Hadrynian cover, Bulldog Creek area, British Columbia; unpublished M.Sc. thesis, University of Calgary, Calgary, Alberta, 163 p.

1985: Basement involvement, Bulldog Creek area, southern Canadian Rockies; Geological Survey of America, Abstracts with Programs, v. 17, no. 7.

McDonough, M.R. and Simony, P.S.
1984: Basement gneisses and Hadrynian metasediments near Bulldog Creek, Selwyn Range, British Columbia; in Current Research, Part A, Geological Survey of Canada, Paper 84-1A, p. 99-102.

Mountjoy, E.W., Forest, R., and Leonard, R.
1985: Structure and stratigraphy of the Miette Group, Selwyn Range, between Ptarmigan and Hugh Allan creeks, British Columbia; in Current Research, Part A, Geological Survey of Canada, Paper 85-1A, p. 485-490.

Oke, C.
1982: Structure and metamorphism of precambrian basement and its cover in the Mount Blackman area, British Columbia; unpublished M.Sc. thesis, University of Calgary, Calgary, Alberta, 123 p.

Oke, C. and Simony, P.S.
1981: Basement gneisses of the western Rocky Mountains, Hugh Allan Creek area, British Columbia; in Current Research, Part A, Geological Survey of Canada, Paper 81-1A, p. 181-184.

Sanderson, D.J.
1979: The transition from upright to recumbent folding in the Variscan fold belt of southwest England: a model based on the kinematics of simple shear; Journal of Structural Geology, v. 1, p. 171-180.

1982: Models of strain variations in nappes and thrust sheets: a review; Tectonophysics, v. 88, p. 201-233.

Wilcox, R.E., Harding, T.P., and Seely, D.R.
1973: Basic wrench tectonics; Bulletin of American Association of Petroleum Geologists, v. 57, p. 74-96.

Lower Carboniferous lithostratigraphy and carbonate facies, upper Banff Formation and Rundle Group, east-central British Columbia

Project 810011

B. Beauchamp [1], B.C. Richards, E.W. Bamber, and B.L. Mamet [2]
Institute of Sedimentary and Petroleum Geology, Calgary

Beauchamp, B., Richards, B.C., Bamber, E.W., and Mamet, B.L., Lower Carboniferous lithostratigraphy and carbonate facies, upper Banff Formation and Rundle Group, east-central British Columbia; in Current Research, Part A, Geological Survey of Canada, Paper 86-1A, p. 627-644, 1986.

Abstract

In the Sukunka-Burnt River area of east-central British Columbia, the Lower Carboniferous succession comprises the upper Banff, Pekisko(?), "Shunda", Shunda, Turner Valley, and Mount Head(?) formations. This succession was deposited in the southern part of the Peace River Embayment. The upper Banff Formation consists of a recessive interval of middle to upper Tournaisian (Tn1 to Tn3), calcareous shale with subordinate lime mudstone to packstone, representing basin to relatively shallow water environments. In the southern part of the study area it is overlain by pelmatozoan lime grainstone of the upper Tournaisian (Tn3) Pekisko(?) Formation, which represents relatively high energy conditions. The overlying, upper Tournaisian (Tn3) "Shunda" formation comprises rhythmically bedded, mixed skeletal lime packstone and grainstone, deposited in shallow to moderately deep carbonate-ramp depositional environments. In the southeastern part of the study area, the "Shunda" is overlain by, and grades southeastward into the upper Tournaisian (Tn3) Shunda Formation, which is mainly composed of fenestrate, algal boundstone and calcisphere-algal lime wackestone to packstone of restricted shelf origin. The lower Viséan (V1) Turner Valley Formation comprises mixed-skeletal lime packstone and grainstone, of open shelf to upper slope origin. Hemicyclic, open- to restricted-shelf carbonates constitute the overlying, lower Viséan (V1) Mount Head(?) Formation.

Résumé

Dans le secteur hydrographique Sukunka-Burnt dans le centre-est de la Colombie-Britannique, la succession du Carbonifère inférieur est constituée des formations suivantes: Banff supérieur, Pekisko (?), "Shunda", Shunda, Turner Valley et Mount Head (?). Cette succession s'est déposée dans la partie sud de la baie de la rivière de la Paix. La formation de Banff supérieur consiste en un intervalle régressif d'argile schisteuse calcaire du Tournaisien moyen à supérieur (Tn1 à Tn3) accompagnée de mudstones et de packstones calcaires secondaires formant des couvettes et des dépressions d'eau relativement peu profondes. Dans la partie sud de la région à l'étude, cette formation est recouverte d'un grainstone calcaire à pelmatozoaire de la formation de Pekisko (?) du Tournaisien supérieur (Tn3) qui dénote des conditions énergétiques relativement intenses. La formation susjacente de "Shunda" du Tournaisien supérieur (Tn3) présente une sédimentation rythmique de packstones et de grainstones calcaires à squelettes mélangés qui se sont déposés sur des versants de carbonate peu à modérément profonds. Dans la partie sud-est de la région à l'étude, la formation de "shunda" est recouverte par la formation de Shunda du Tournaisien supérieur (Tn3) avec laquelle elle se confond progressivement au sud-est et qui est principalement constituée de boundstone fenestré à algues et de wackstone à packstone calcaire à algues calcisphères de plateau continental confiné. La formation de Turner Valley du Viséen inférieur (V1) est constituée de packstone et de grainstone calcaire à squelettes mélangés de plateau continental ouvert à talus supérieur. Des carbonates hémicycliques de plateau continental ouvert à confiné constituent la formation susjacente de Mount Head (?) du Vésien inférieur (V1).

[1] Department of Geology and Geophysics, University of Calgary, Calgary, Alberta T2N 1N4
[2] Département de Géologie, Université de Montréal, Montréal, Québec H3C 3J7

Introduction

Broad facies relationships within the Lower Carboniferous Banff Formation and Rundle Group of the Canadian Cordillera have been outlined in several, major, regional stratigraphic studies (Macauley et al., 1964; Bamber et al., 1984; Richards et al., in press). Few detailed sedimentological studies of these units have been published, however, and in many areas, precise facies relationships are unknown. A recent increase in hydrocarbon exploration in northern British Columbia, resulting in extensive subsurface studies of the Lower Carboniferous, has emphasized the need for equivalent surface assessment in the adjacent outcrop belt.

This paper provides a detailed account of four Lower Carboniferous stratigraphic sections measured in the Sukunka-Burnt River area, in the eastern Rocky Mountains of east-central British Columbia (Fig. 76.1, 76.3). The microfacies of the Banff, Pekisko(?), "Shunda", Shunda, Turner Valley, and Mount Head(?) formations are described, and lithostratigraphic correlations are made with the adjacent Monkman Pass area. The paper supplements a recent biostratigraphic study by Beauchamp and Mamet (1985), in which the foraminiferal zonation is presented and a brief discussion of the environmental significance of the algae is given.

Study area

The study area covers over 40 km, from the southeastern part of the Pine Pass map area (NTS 93O), to the southwestern corner of the Dawson Creek map area (NTS 93P) (Fig. 76.1). The four stratigraphic sections studied are: Watson Peak section (55°13'58"N, 122°05'07"W), North Burnt River section (55°14'30"N, 122°04'30"W), Burnt River section (55°12'00"N, 122°02'30"W), and Sukunka River section (55°01'30"N, 121°42'00"W). These four sections occur in the same thrust sheet and are more than ninety per cent exposed. At all four sections, the top of the Rundle Group is truncated beneath sub-Permian or sub-Triassic disconformities (Fig. 76.4).

Detailed stratigraphic logs, based on both field and microscopic observations, are provided in Figures 76.7 to 76.10. These figures show the distribution and relative proportions of carbonate grains, matrix, cement, dolomite, and fifteen types of allochems, including peloids, lithoclasts, lumps, mud-coated grains, and fossil fragments. In addition, the distributions and relative abundances of ten groups of calcareous algae are given. Accounts of previous work related to the study area and the adjacent Monkman Pass area can be found in Mamet et al. (in press) and Beauchamp and Mamet (1985).

Regional setting

The Lower Carboniferous of the eastern Cordillera and western Plains mainly comprises the Besa River and Banff formations and most of the Rundle Group (Fig. 76.2). Two major facies belts are recognized: an eastern belt of clastic and carbonate, slope to supratidal shelf facies (Fig. 76.5a,b); and a correlative, western belt of deeper water, basinal shale (Bamber et al., 1984). The lateral transition between these facies belts is a wide, irregular zone characterized by planar-laminated to rhythmically bedded spiculite, bedded chert, and cherty limestone to dolostone. These transitional deposits accumulated mainly in lower- to middle-slope environments on carbonate platforms and ramps (Fig. 76.5) having very low depositional slopes (Richards, 1983; Bamber et al., 1984; Richards et al., in press).

The lithostratigraphic units of Early Carboniferous age in the eastern Cordillera and western Plains reflect the depositional settings outlined above (Fig. 76.2). In general, the Besa River Formation is basinal shale, and the partly coeval Banff is a transgressive – regressive sequence of basin to supratidal, siliciclastics and carbonates. Carbonate-platform facies are present in the Banff, but most of the unit appears to comprise carbonate-ramp facies (Richards et al., in press). The overlying Rundle Group consists mainly of carbonate-platform facies deposited during several major transgressions and regressions, but carbonate-ramp deposits are locally important (Richards, in press; Richards et al., in press). Upper-slope to open-shelf lime-grainstone and packstone of the Pekisko Formation generally overlie the Banff and pass basinward into slope deposits of the "Shunda" (Fig. 76.3) and Banff (Richards et al., in press). In southwestern Alberta, shelf-margin to restricted-shelf carbonates (Fig. 76.5a) in the Shunda, Turner Valley, and Mount Head formations generally overlie the Pekisko and pass southwestward into shelf-margin to upper-slope grainstone of the Livingstone Formation (Fig. 76.2). To the north, the Pekisko is overlain in most areas by either the slope to shelf-margin deposits of the "Shunda" or the restricted-shelf carbonates of the Shunda (Fig. 76.2, 76.3). However, in southwestern District of Mackenzie and adjacent areas to the south, the Pekisko is also overlain by basinal shale of the Clausen (Fig. 76.2; Richards, 1983). The Shunda and its equivalents in the "Shunda" are mainly overlain by

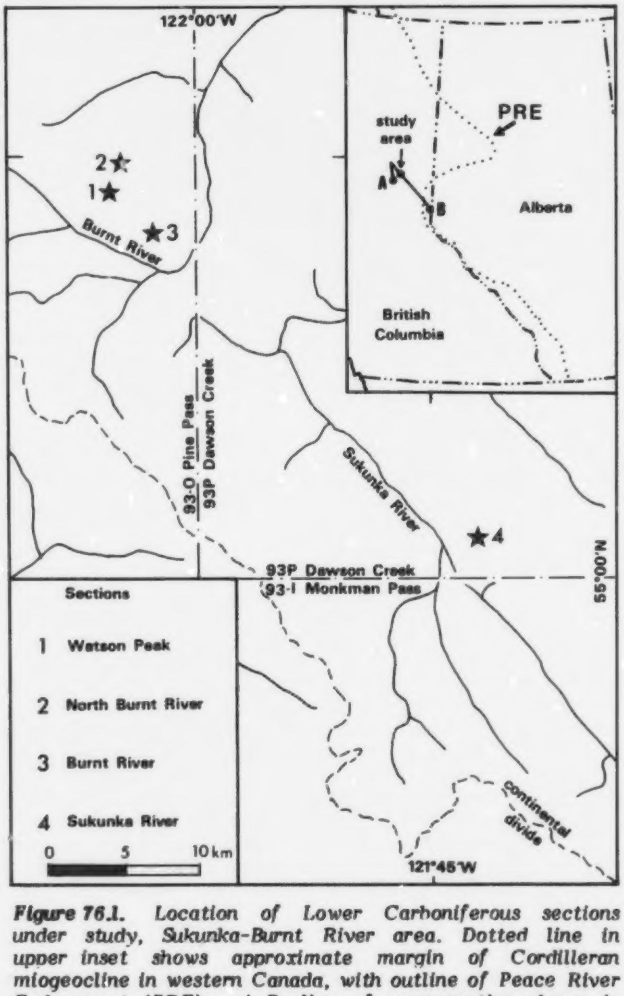

Figure 76.1. Location of Lower Carboniferous sections under study, Sukunka-Burnt River area. Dotted line in upper inset shows approximate margin of Cordilleran miogeocline in western Canada, with outline of Peace River Embayment (PRE). A-B, line of cross-section shown in Figure 76.3.

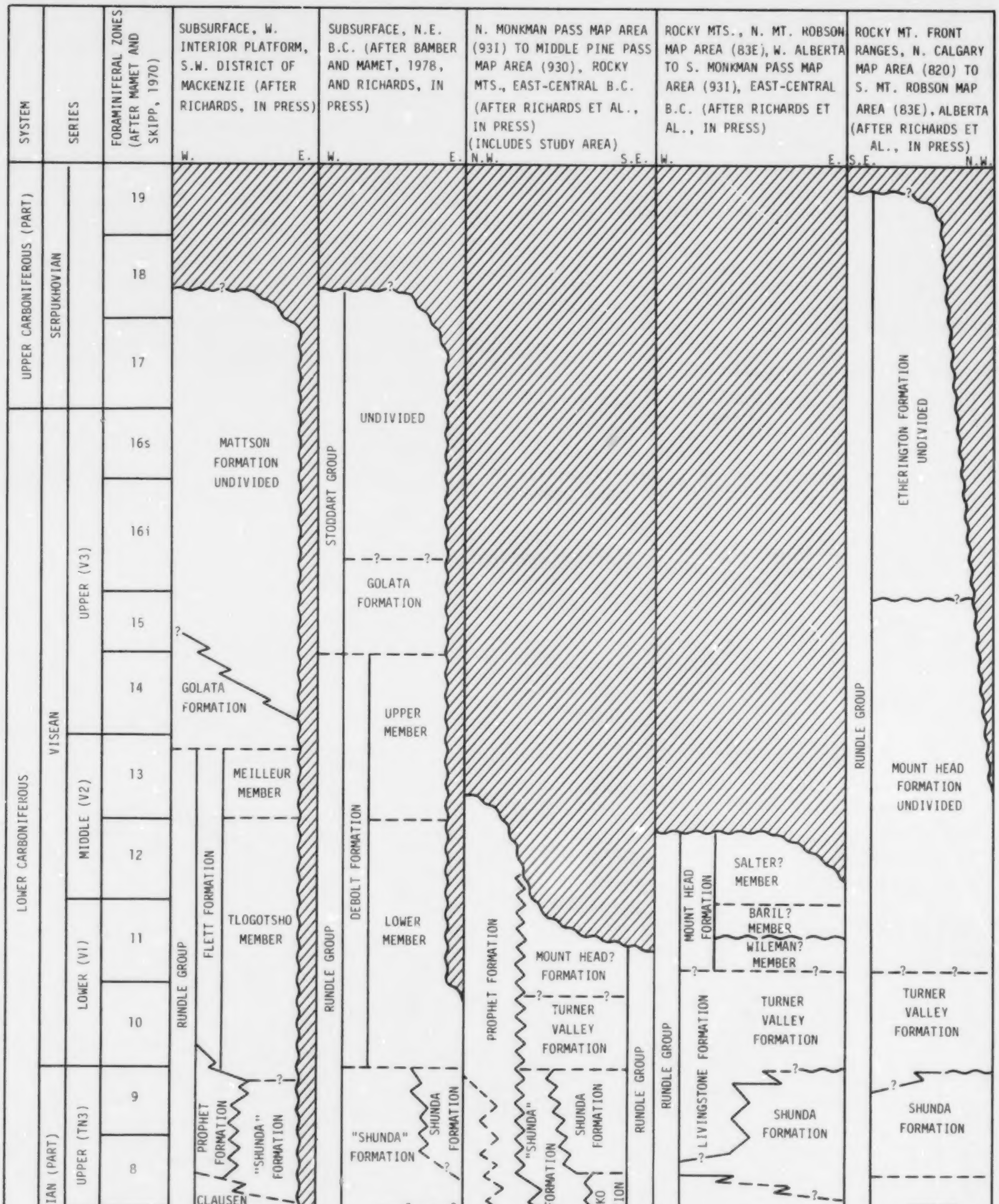

Figure 76.2. *Correlations of Lower Carboniferous formations, southwestern Alberta to southwestern District of Mackenzie.*

shelf-margin to restricted-shelf facies of the Turner Valley and Mount Head(?) in east-central British Columbia, and by middle-slope to restricted-shelf deposits of the Debolt to the north and in much of the area to the east. In east-central British Columbia, the "Shunda", Turner Valley, and lower Mount Head(?) pass basinward into the middle- to lower-slope facies of the Prophet (Fig. 76.3). A similar lateral facies change takes place to the north, where the "Shunda", Debolt, and Flett formations grade basinward into the Prophet.

In the Sukunka-Burnt River area, as in the adjacent Monkman Pass area, the Lower Carboniferous is represented by a wide range of basin and slope to shelf facies (Fig. 76.3; 76.5a,b). They were deposited near the southern margin of the Peace River Embayment, which developed during latest Devonian and Early Carboniferous time as an eastward extension of the Cordilleran miogeocline (Fig. 76.1; Richards et al., in press; see also Macauley, 1958 and Macauley et al., 1964).

Stratigraphy and facies in study area

The stratigraphic nomenclature used in this paper is mainly that of Richards et al. (in press). An exception is the unnamed unit informally referred to as the "Shunda" formation. This usage follows that of Bamber and Mamet (1978), who used the term "Shunda" for an open-marine unit that was deposited contemporaneously with the Shunda Formation, but lacks the restricted shelf facies characteristic of the latter. Richards et al. (in press) called the open-marine unit "unnamed formation F" and indicated that i passes into the Shunda and Pekisko formations (Fig. 76.2).

Banff Formation

Only the upper part of the Banff Formation outcrops in the study area. It occurs in all of the investigated sections, except the North Burnt River section, which is truncated at the base by a fault (Fig. 76.8). The upper Banff is best exposed at Watson Peak, where 50 m of the formation are exposed (Fig. 76.7). There, the formation comprises very calcareous, locally silty shale, with subordinate interbeds of lime mudstone and algal and mixed-skeletal lime packstone.

In the Burnt River section (Fig. 76.9), the Banff Formation is at least 49 m thick and consists mainly of noncalcareous shale with subordinate, nodular, lime mudstone. Thin bedded, algal-rich lime packstone is abundant in the uppermost part of the formation, which becomes more resistant.

Only the upper 20 m of the Banff Formation are preserved in the Sukunka River section (Fig. 76.10). Again, the formation consists of shale with rare siltstone and dolomitic limestone. Thin-bedded, brachiopod-bryozoan-echinoderm lime wackestone and packstone are also present.

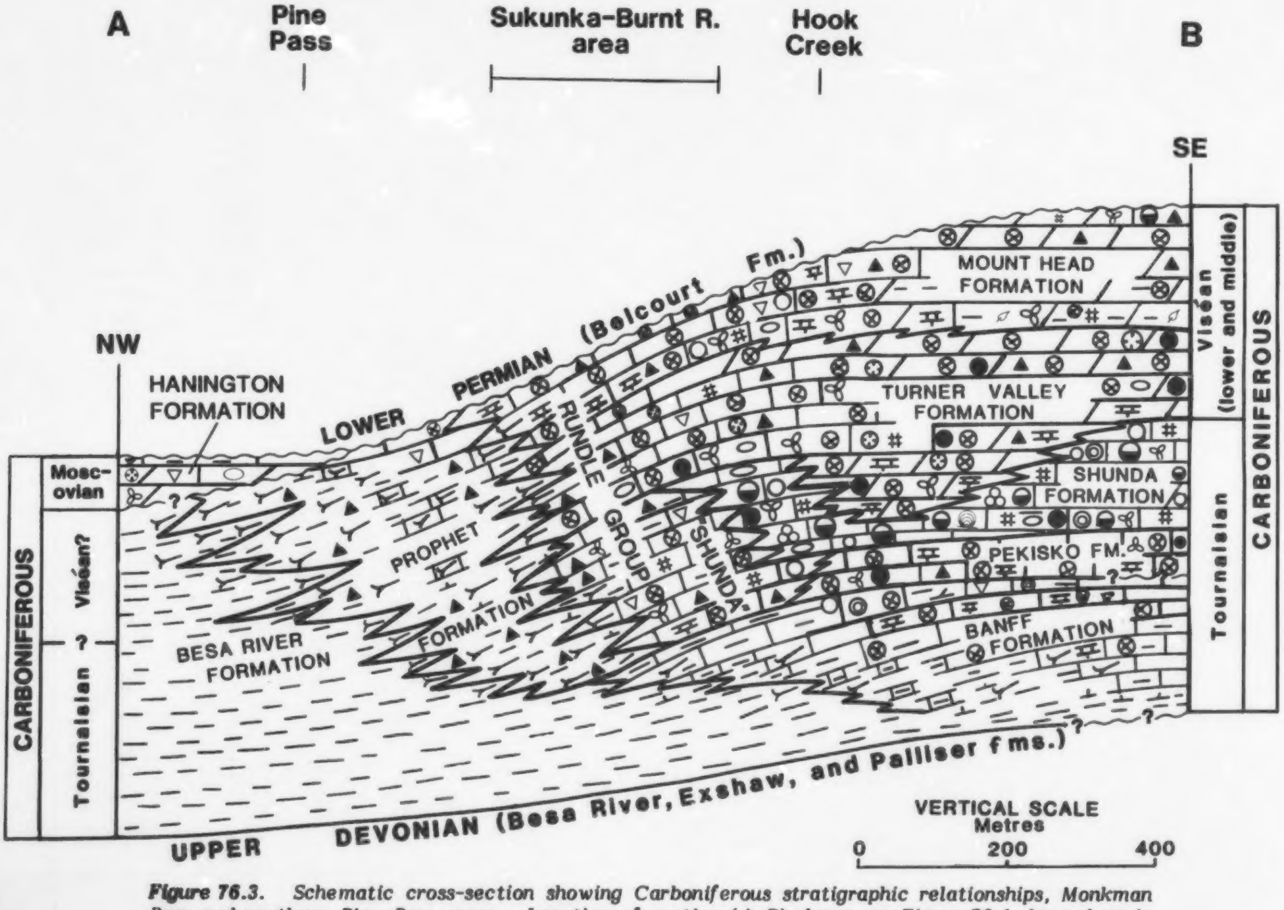

Figure 76.3. Schematic cross-section showing Carboniferous stratigraphic relationships, Monkman Pass and southern Pine Pass areas. Location of section (A-B) shown on Figure 76.1; legend as in Figure 76.5a.

The Banff is overlain by either the "Shunda" or by a unit provisionally assigned to the Pekisko. Resistant limestone of the lower "Shunda" abruptly overlies the Banff Formation at Watson Peak. At Burnt River, the formation is overlain by a covered interval that is 14 m thick and may contain either the Pekisko(?) Formation or the lower part of the "Shunda" formation. In the Sukunka River section (Fig. 76.10), the Banff is overlain by a grainstone-dominated unit that is possibly a tongue of the Pekisko Formation. The Banff Formation extends southeastward into the adjacent Monkman Pass area, where it comprises a thick (150-345 m) succession of basinal shale grading upward into limestone of slope to restricted-shelf aspect (Richards, pers. comm.). Toward the northwest, the Banff passes into basinal shale of the Besa River Formation (Fig. 76.4).

The depositional environments of the Banff Formation in the study area are not well established. At the outcrops studied, the predominance of dark shale containing few megafossils suggests that the upper Banff consists mainly of basin deposits. However, the uppermost Banff was probably deposited in relatively shallow water, because it commonly contains lime packstone rich in calcareous algae. Also, the uppermost Banff just north of the Hook Creek section

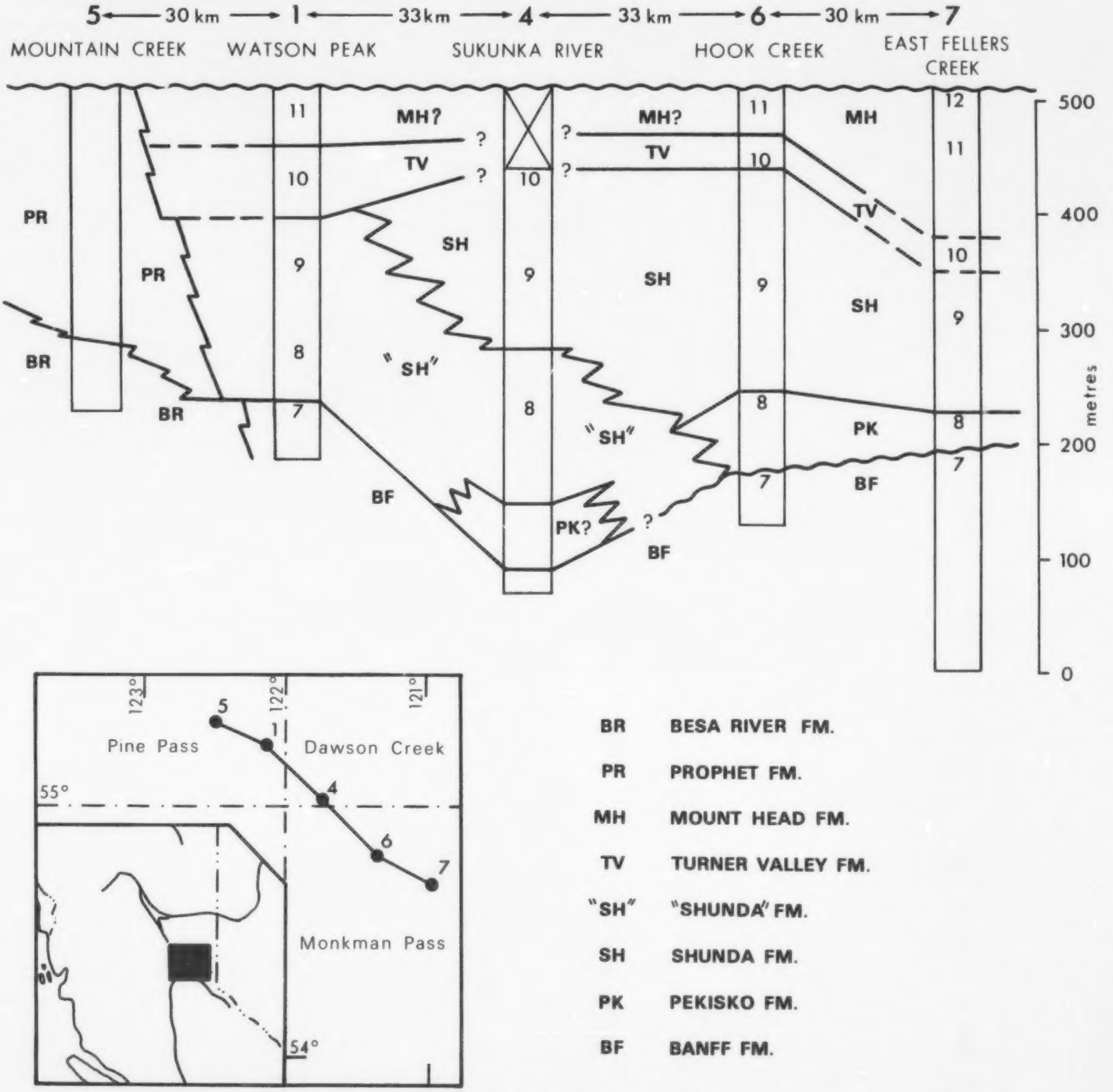

Figure 76.4. Lithostratigraphic correlations of Lower Carboniferous formations in study area (secs. 1, 4) and adjacent areas (secs. 5-7). Distribution of foraminiferal zones (7-12) as shown.

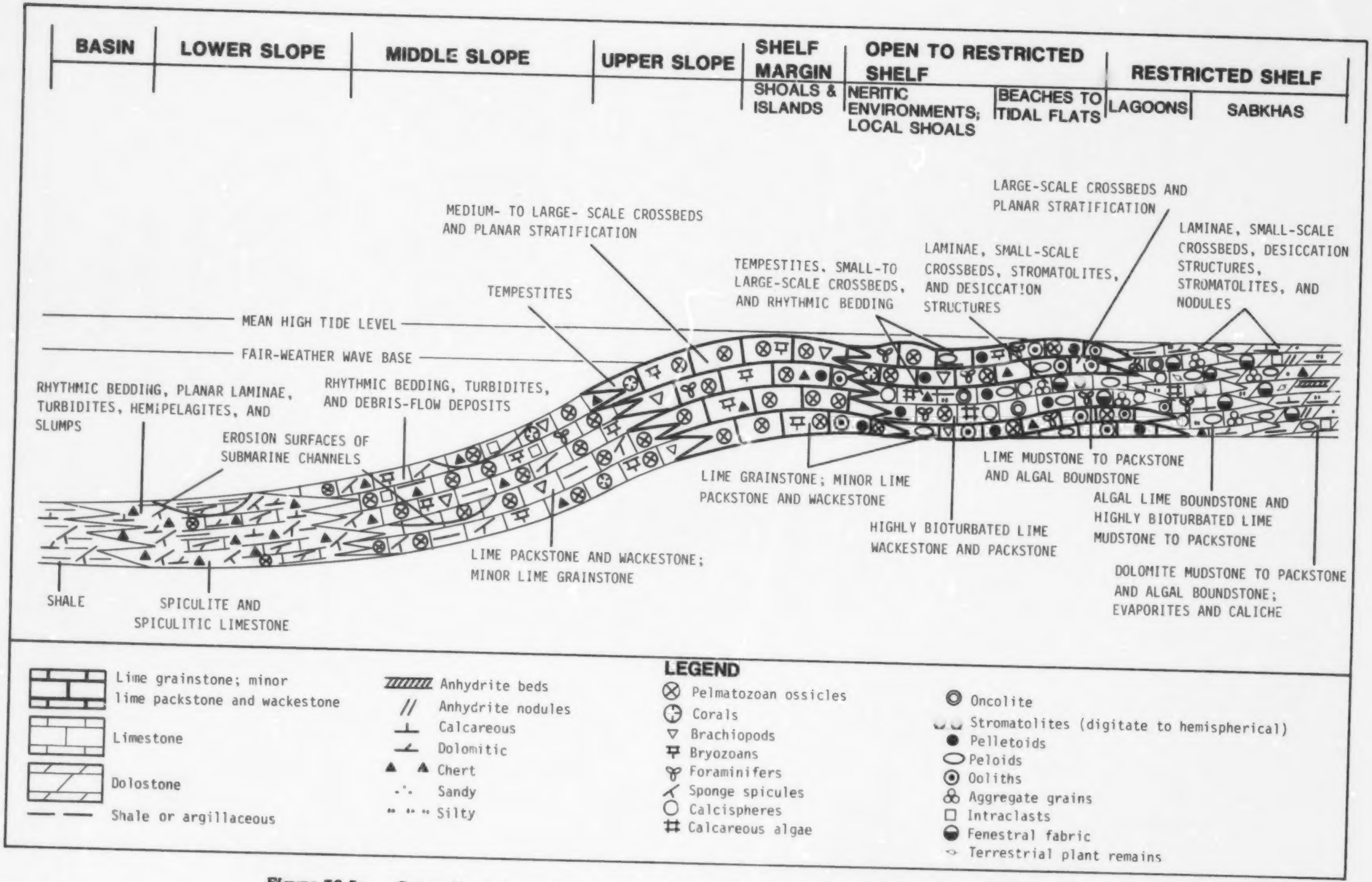

Figure 76.5a. *Generalized depositional model of a carbonate platform of Early Carboniferous age (from Richards et al., in press).*

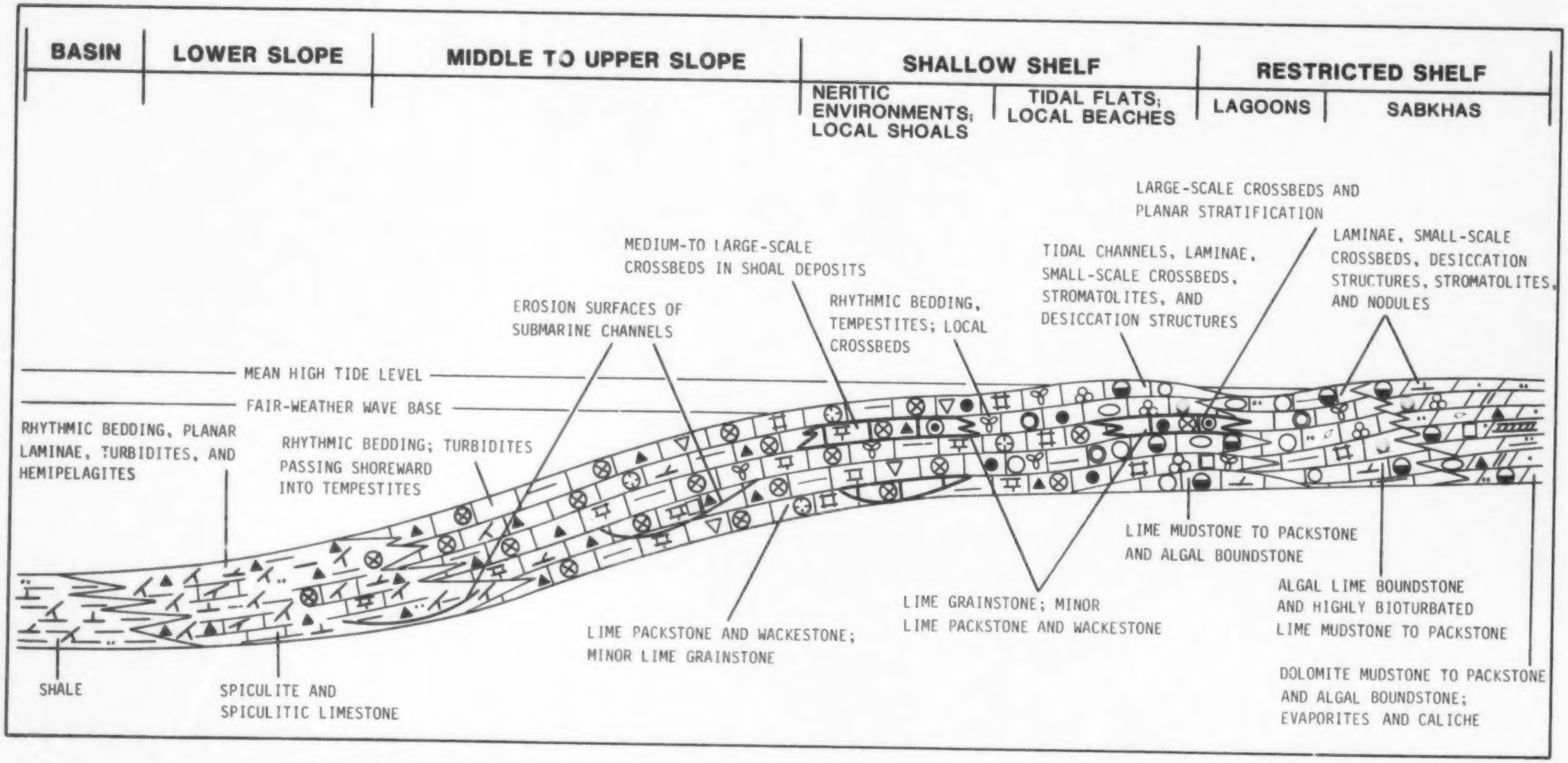

Figure 76.5b. *Generalized depositional model of a carbonate ramp of Early Carboniferous age (from Richards et al., in press).*

Figure 76.6a

Watson Peak section (Fig. 76.1, Sec. 1); BF – Banff Formation, "SH" – "Shunda" formation, TV – Turner Valley Formation.

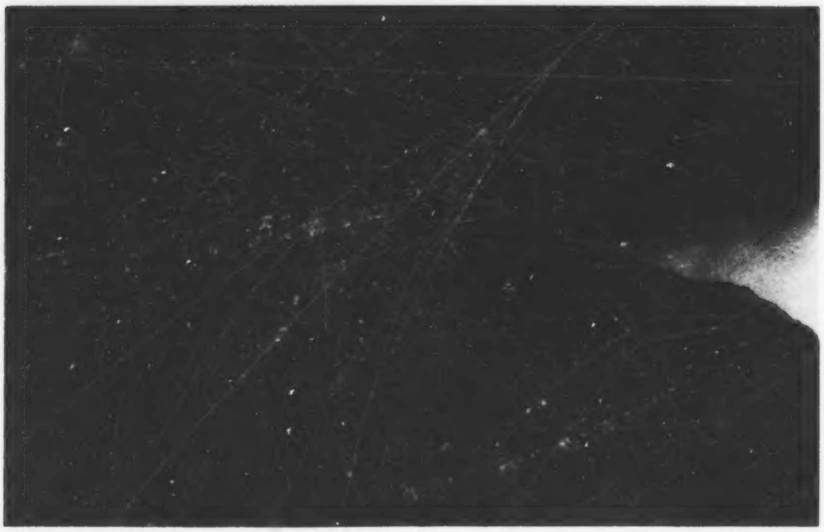

Figure 76.6b

Watson Peak section (Fig. 76.1, Sec. 1); "SH" – "Shunda" formation, TV – Turner Valley Formation, MH(?) – Mount Head(?) Formation, TR – Triassic. A thin bed of Permian conglomerate is present between the Mount Head(?) Formation and the Triassic.

(Fig. 76.4) contains beds with numerous oncolites. Deposition in relatively shallow water is also suggested by the presence of algal lime packstone in the overlying basal "Shunda" at Watson Peak (Fig. 76.7a).

Middle Tournaisian (Tn2) foraminiferal Zone 7 has been recognized in the upper part of the formation at Watson Peak (Figs. 76.4, 76.7a; see also Beauchamp and Mamet, 1985).

Pekisko(?) Formation

The Pekisko Formation is tentatively recognized in the Sukunka River section only. It is absent at Watson Peak and from the North Burnt River section, which is truncated by a fault at the base (Fig. 76.8). In the Burnt River section (Fig. 76.9) it may be represented by a covered interval immediately above the Banff Formation. The Pekisko is known to be very thin to absent in the area between the Hook Creek section and the Sukunka River section (Fig. 76.4; Richards, pers. comm.). The bryozoan-pelmatozoan grainstone assigned to the Pekisko at the Sukunka River section may be only a lens, completely separate from the Pekisko – hence the tentative assignment of the name Pekisko in this paper.

At the Sukunka River section, the Pekisko(?) Formation is overlain by the "Shunda" formation. The Pekisko-"Shunda" contact is gradational in terms of both outcrop profile and lithofacies. To the east and south of the study area, the Pekisko is conformably overlain by either the "Shunda" or the Shunda Formation.

In the adjacent Monkman Pass area, southeast of Hook Creek, the Pekisko Formation is generally well developed, and comprises mainly lime grainstone, deposited in shelf-margin to open-shelf environments on carbonate platforms (Fig. 76.3; Richards, pers. comm.). In most of that area, a minor erosional disconformity marks the Banff-Pekisko contact (Fig. 76.4). The Pekisko has not been recognized to the northwest, in the central and northern Pine Pass area, where correlatives of the Pekisko are in the "Shunda" and deeper water Prophet and Besa River formations (Fig. 76.3). At the Sukunka River section, the Pekisko(?) probably records deposition in a relatively shallow, high-energy, shoal environment on a carbonate ramp. Deposition under high energy conditions is suggested by the predominance of lime grainstone and by the occurrence of medium- to large-scale crossbeds. The lens-like aspect of the Pekisko(?) at this locality is suggestive of a shoal. The Sukunka section is on

the south side of the Peace River Embayment, where the lower part of the Rundle Group (Prophet, "Shunda", Pekisko, and Shunda) consists of carbonate-ramp deposits, rather than carbonate-platform deposits (Fig. 76.5b; Richards et al., in press). A ramp setting is suggested by the southeastward and eastward gradation of slope deposits of the Prophet and "Shunda" into supratidal Shunda facies with no intermediate, well-developed, shelf-margin grainstone facies like that characteristic of platform deposits (Fig. 76.3).

In the study area, the Pekisko(?) is probably of middle and early late Tournaisian (Tn2 and Tn3) age. Only nondiagnostic foraminifers were collected from the unit at the Sukunka River section (Beauchamp and Mamet, 1985), but at Hook Creek (Fig. 76.4), Bamber and Mamet (in press) recovered foraminifers assignable to Zone 7 and lower Zone 8.

"Shunda" formation

The "Shunda" formation is present in all four of the sections studied, and is most completely developed in the Pine Pass area (Fig. 76.1, 76.3). Where completely developed, the "Shunda" comprises two divisions. The lower division, which correlates with the Pekisko, is resistant. The upper division correlates with the Shunda, is commonly very recessive at its base, and generally becomes more resistant upward (Fig. 76.6).

At Watson Peak (Fig. 76.6), the "Shunda" is completely developed and consists of 160 m of thin to thick bedded deposits (Fig. 76.6, 76.7). With the exception of the Pekisko correlatives, which constitute the lower 31 m and become less resistant upward, the "Shunda" at this locality comprises multibed hemicycles that generally become more resistant upward. Dark, highly bioturbated, algal-foraminifer-echinoderm lime packstone and grainstone are common, and fine grained, algal-echinoderm lime packstone and grainstone are less abundant. In addition, units of algal lime packstone constitute much of the lower 31 m of the formation. The grainstone and packstone are commonly rhythmically interbedded with, and grade upward into, less resistant, argillaceous limestone and marlstone. Most beds resemble storm deposits, and have great lateral continuity (Fig. 76.6), sharp bases (commonly with load casts), and poorly developed normal grading. At this locality, the formation lacks restricted-shelf lithofacies, such as algal-calcisphere-peloid lime wackestone and packstone and fenestrate, algal boundstone. The "Shunda" at both Burnt River (Fig. 76.9) and north Burnt River (Fig. 76.8) closely resembles this unit at Watson Peak, but contains less lime grainstone.

At the Sukunka River section (Fig. 76.10), the "Shunda" consists of 180 m of thin to thick bedded, variably argillaceous and dolomitic limestone with a moderately recessive profile. The lowest part of the formation consists of brachiopod-bryozoan-echinoderm lime wackestone and packstone with minor grainstone, interbedded with spicule-rich lime wackestone and packstone. Higher in the section, the assemblage becomes more diversified, with the addition of foraminifers and tubular algae, mostly within the lime wackestone and packstone. Chert bands are moderately common throughout the lower part of the formation.

The "Shunda" is overlain by either the Shunda Formation or the Turner Valley Formation and grades southeastward into the Pekisko and Shunda (Fig. 76.3, 76.4; Richards, pers. comm.). In general, the boundary with the Pekisko and Shunda is a broad gradation, whereas that with the Turner Valley is sharp to gradational. Within the study area and in the Monkman Pass area to the south, strata in the "Shunda" that correlate with the basal Shunda extend farthest toward the east and southeast.

Toward the northwest, most of the "Shunda" appears to grade basinward into deeper-water slope deposits of the Prophet Formation (Richards et al., in press).

Lithofacies of the "Shunda" appear to have been deposited in carbonate-ramp environments (Fig. 76.5b) ranging from shallow and relatively restricted to open-marine and moderately deep (Richards et al., in press). For reasons given above, in the discussion of the depositional environments of the Pekisko(?), the "Shunda" of the study area is considered to comprise mainly carbonate-ramp deposits. Toward the northwest, deposition of the "Shunda" occurred at progressively greater depths, judging from its biofacies and lithofacies trends, and from its lateral relationships with the Prophet and Shunda formations.

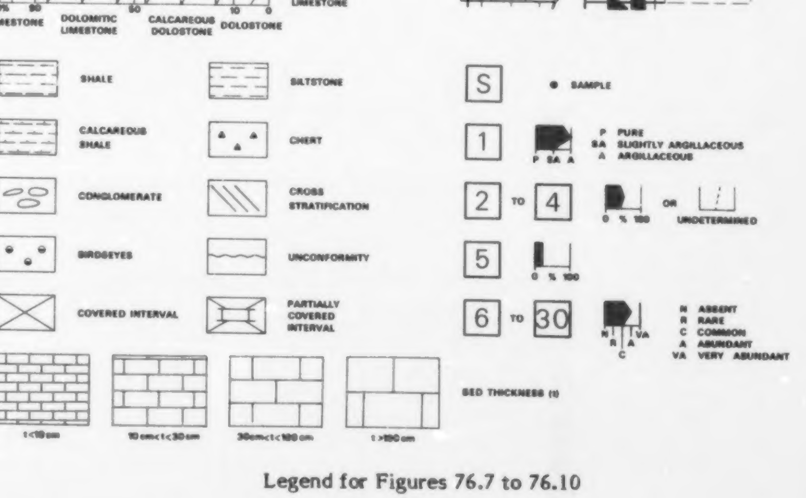

Legend for Figures 76.7 to 76.10

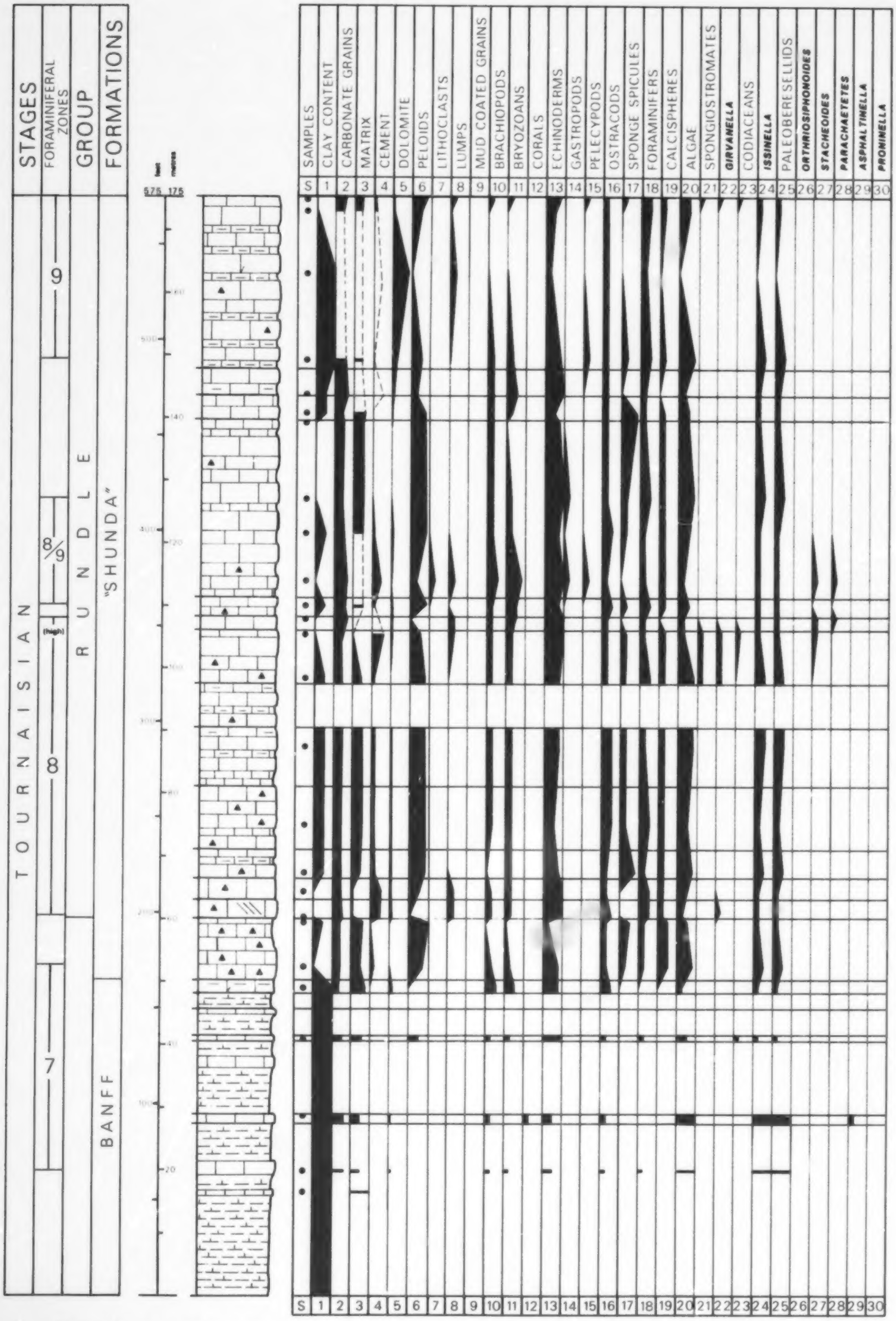

Figure 76.7a. *Watson Peak section, lower part: Banff (part), Pekisko(?), and "Shunda" (part) formations.*

The age of the "Shunda" formation has been well established using foraminiferal evidence (Beauchamp and Mamet, 1985). Late Tournaisian (Tn3) microfossils (zones 8, 9) have been recovered from most of the formation. The uppermost strata, however, contain an uppermost Tournaisian (Tn3) to earliest Viséan (V1) fauna (Zone 9/10).

Shunda Formation

The Shunda Formation is present only at the Sukunka River section. It is more than 140 m thick (Fig. 76.10), but faulting and lack of exposure at the top of the section prevent determination of the true thickness. The Shunda at this locality is recessive and medium bedded, and consists

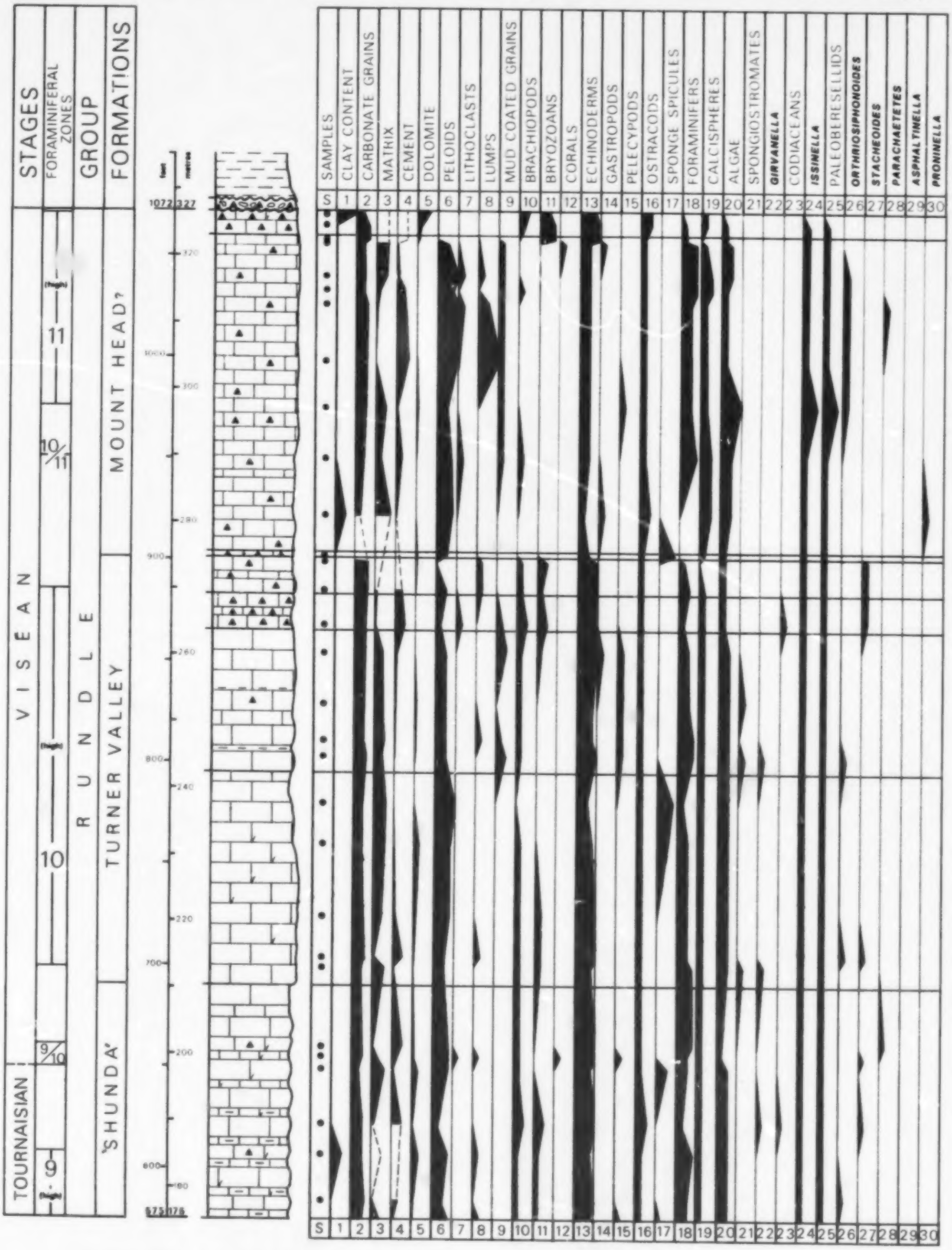

Figure 76.7b. Watson Peak section, upper part: "Shunda" (part), Turner Valley, and Mount Head(?) formations.

mainly of dark grey, argillaceous, peloid lime wackestone and packstone, rich in algae and calcispheres. Fenestrate, algal lime boundstone is also present. These carbonates are separated from the Pekisko by the "Shunda" formation, which is of more open-marine aspect, and comprises 180 m of moderately recessive, medium to thick bedded, argillaceous and dolomitic limestone.

The Shunda Formation is widespread in the adjacent Monkman Pass area. There, it consists mainly of carbonate

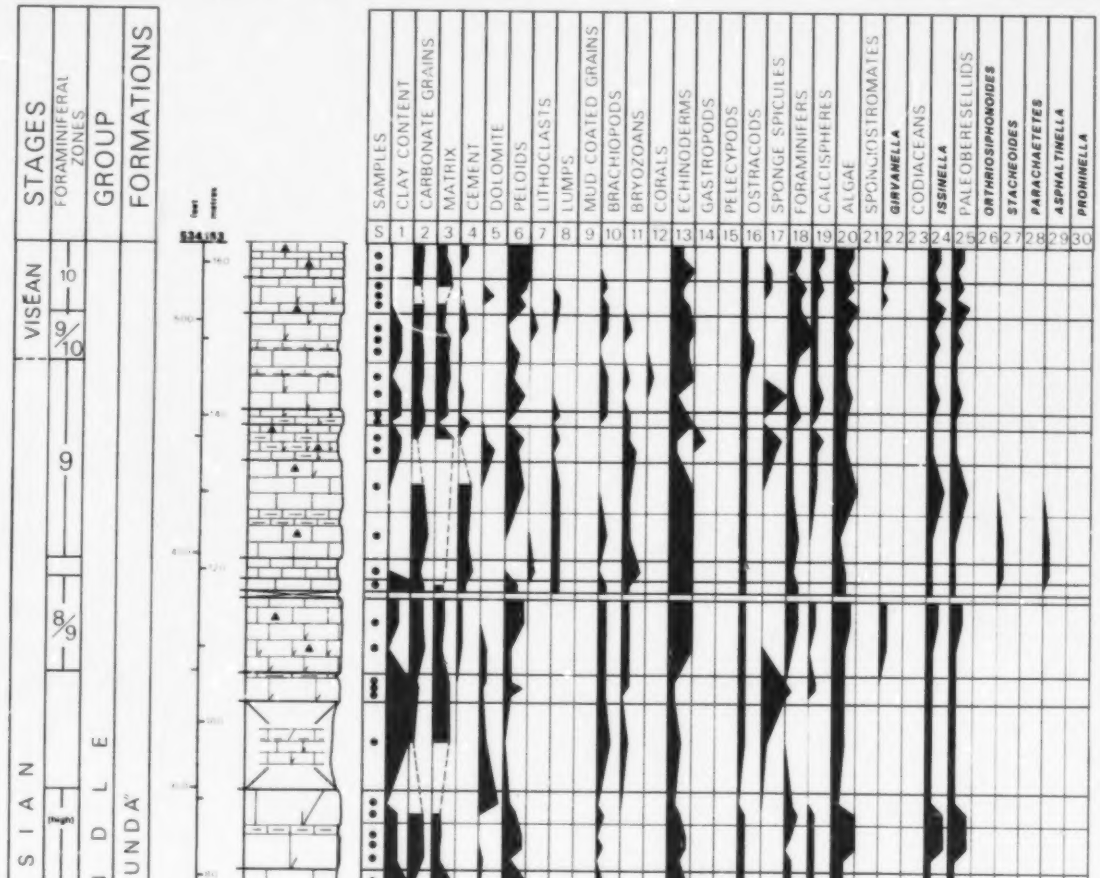

Figure 76.8a. North Burnt River section, lower part: "Shunda" formation.

facies that resemble those described above and were deposited on the restricted shelf of a carbonate platform (Fig. 76.5a; Richards, pers. comm.). Basinward, toward the northwest part of the study area (Fig. 76.4), the Shunda passes laterally into more open-marine deposits (mainly shallow-shelf and slope deposits, Fig. 76.5b) of the "Shunda". It grades into the latter without passing through a transitional shelf-margin grainstone belt (Fig. 76.3) like that preserved in coeval strata in the south (Richards et al., in press). Generally, the uppermost Shunda extends farthest toward the northwest.

In the study area, the Shunda is mainly composed of restricted-shelf lithofacies (Fig. 76.5b) that were probably deposited on a carbonate ramp. Deposition on the restricted shelf is indicated by the common occurrence of fenestrate algal boundstone and lime wackestone-to-packstone rich in foraminifers, calcispheres, and calcareous algae. A carbonate-ramp setting is favoured for reasons given above in the discussion of the depositional environment represented by the Pekisko(?) Formation.

A rich, late Tournaisian (Tn3), spinoendothyrid fauna, representing Zone 9, was recovered from the Shunda Formation (Beauchamp and Mamet, 1985). The lowest Viséan (V1) Zone 10 was also recognized from the uppermost 30 m of the formation, indicating that the upper age range of the Shunda at the Sukunka River section corresponds to that in southwestern Alberta (Mamet, 1984).

Turner Valley Formation

The Turner Valley Formation is present at the Watson Peak, North Burnt River, and Burnt River sections. In addition, it is locally exposed between the Sukunka River section and Burnt River.

At Watson Peak (Fig. 76.6, 76.7), the formation comprises 64 m of resistant, cliff-forming, thick bedded limestone, which is locally dolomitic and consists mainly of algal-foraminifer-echinoderm packstone. Subordinate amounts of algal-foraminifer-echinoderm lime grainstone and

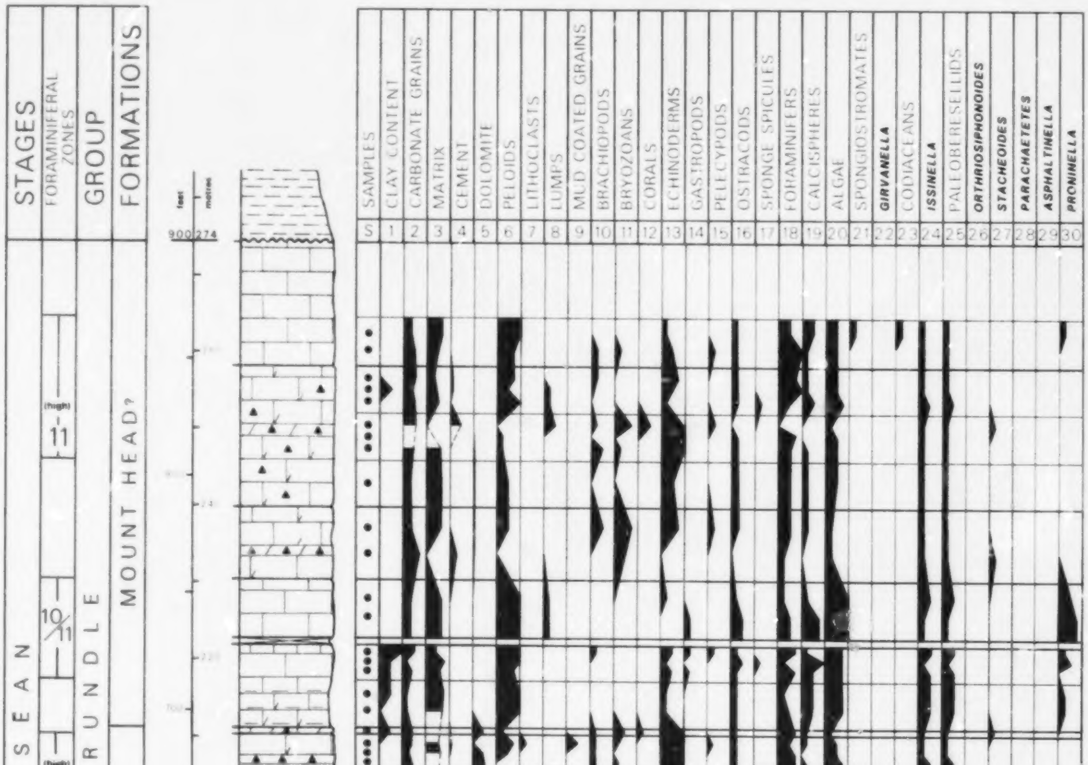

Figure 76.8b. North Burnt River section, upper part: Turner Valley and Mount Head(?) formations.

brachiopod-bryozoan-echinoderm grainstone are also present near the base and top of the formation. Chert is present in the uppermost beds.

Algal-foraminifer-echinoderm lime packstone and grainstone characterize the Turner Valley at North Burnt River (Fig. 76.8), where it is 53 m thick. There, it forms a resistant, thick to very thick bedded, cliff-forming unit. Minor dolomite and chert bands are also present.

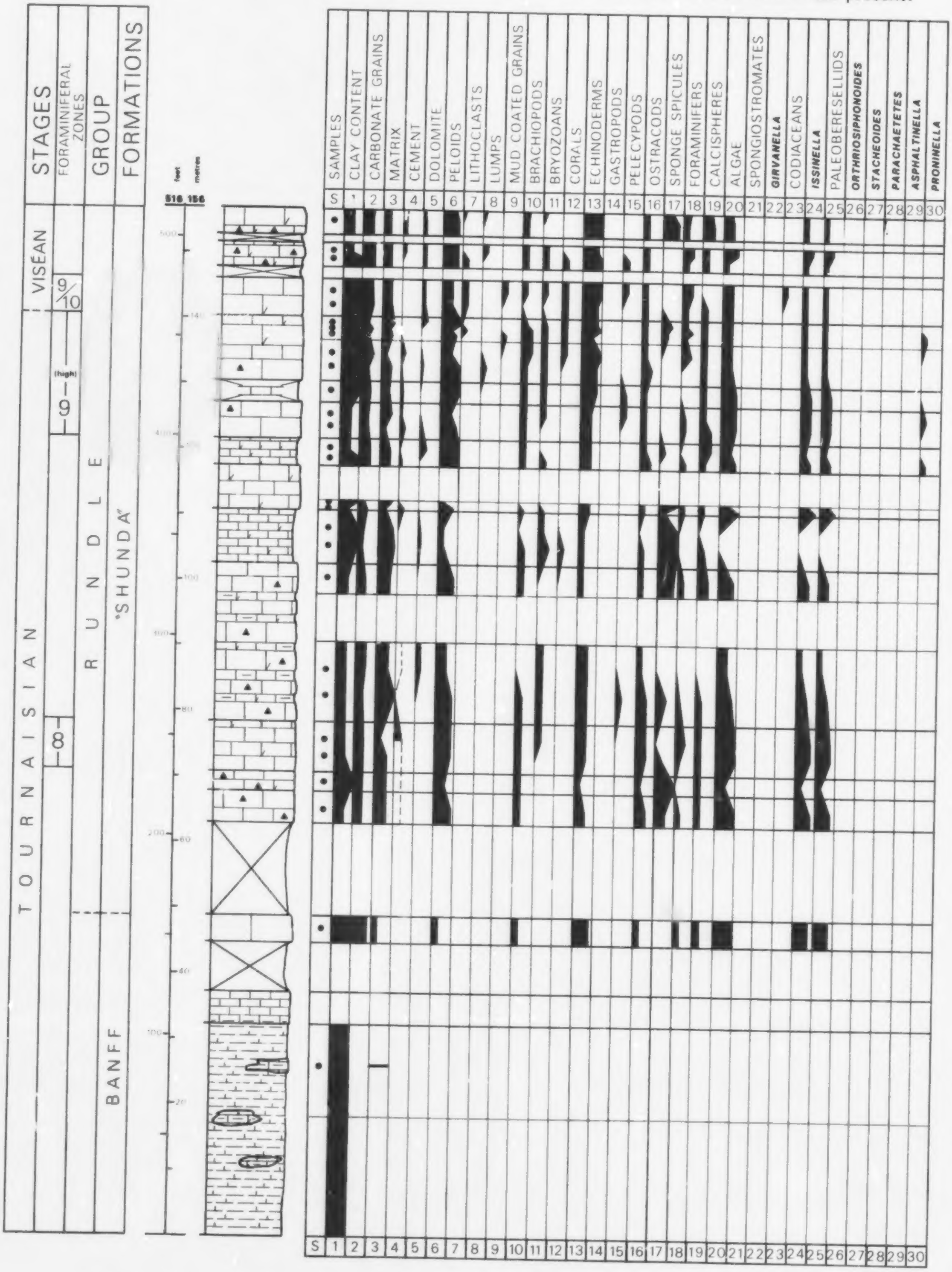

Figure 76.9a. Burnt River section, lower part: Banff (part) and "Shunda" formations.

At the Burnt River section (Fig. 76.9), the Turner Valley Formation is 65 m thick and consists mainly of thick to very thick bedded, algal-foraminifer-echinoderm lime grainstone and packstone.

In the study area, most beds of the Turner Valley Formation have sharp subplanar to gently undulose boundaries, are massive, and have great lateral continuity. However, beds with diffuse internal stratification are moderately common, and rare beds show medium-scale cross-bedding. At Watson Peak, the lower Turner Valley contains some normally graded beds resembling turbidites or some tempestites.

In the study area, strata assigned to the Turner Valley Formation are conformably overlain by a unit that is provisionally included in the Mount Head Formation (Fig. 76.4). The contact is placed at the top of a resistant grainstone and packstone unit that underlies more restricted, algal-rich facies. The Turner Valley Formation is present throughout much of the Monkman Pass area to the southeast, where it generally comprises shelf-margin to open-shelf lithofacies with subordinate, restricted-shelf lithofacies (Fig. 76.3, 76.5a; Richards, pers. comm.). Toward the northwest, this formation probably grades into the Prophet Formation (Fig. 76.4), but the details of this transition have not been established. On the western part of the Plains to the east of the study area, equivalents of the Turner Valley have been included in the lower Debolt by Macauley (1958) and Macauley et al. (1964).

The Turner Valley Formation of the study area is provisionally interpreted as comprising carbonate-platform lithofacies deposited in settings ranging from open shelf to upper slope. Deposition on a platform, rather than a ramp, is suggested by the presence of a thick and widespread grainstone lithofacies that: 1. is of upper-slope to shelf-margin aspect (Fig. 76.5a); 2. passes northwestward (basinward) into

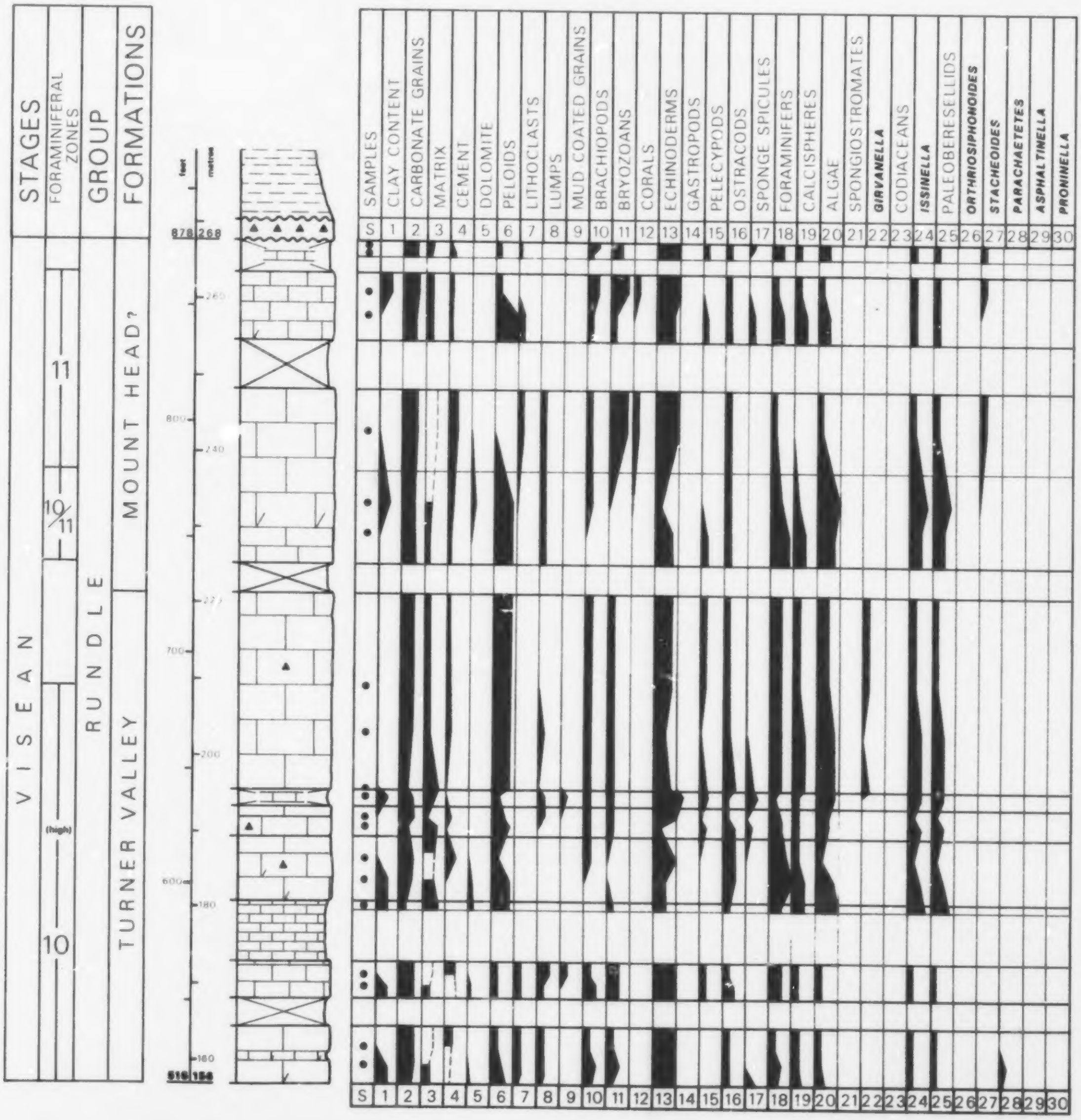

Figure 76.9b. Burnt River section, upper part: Turner Valley and Mount Head(?) formations.

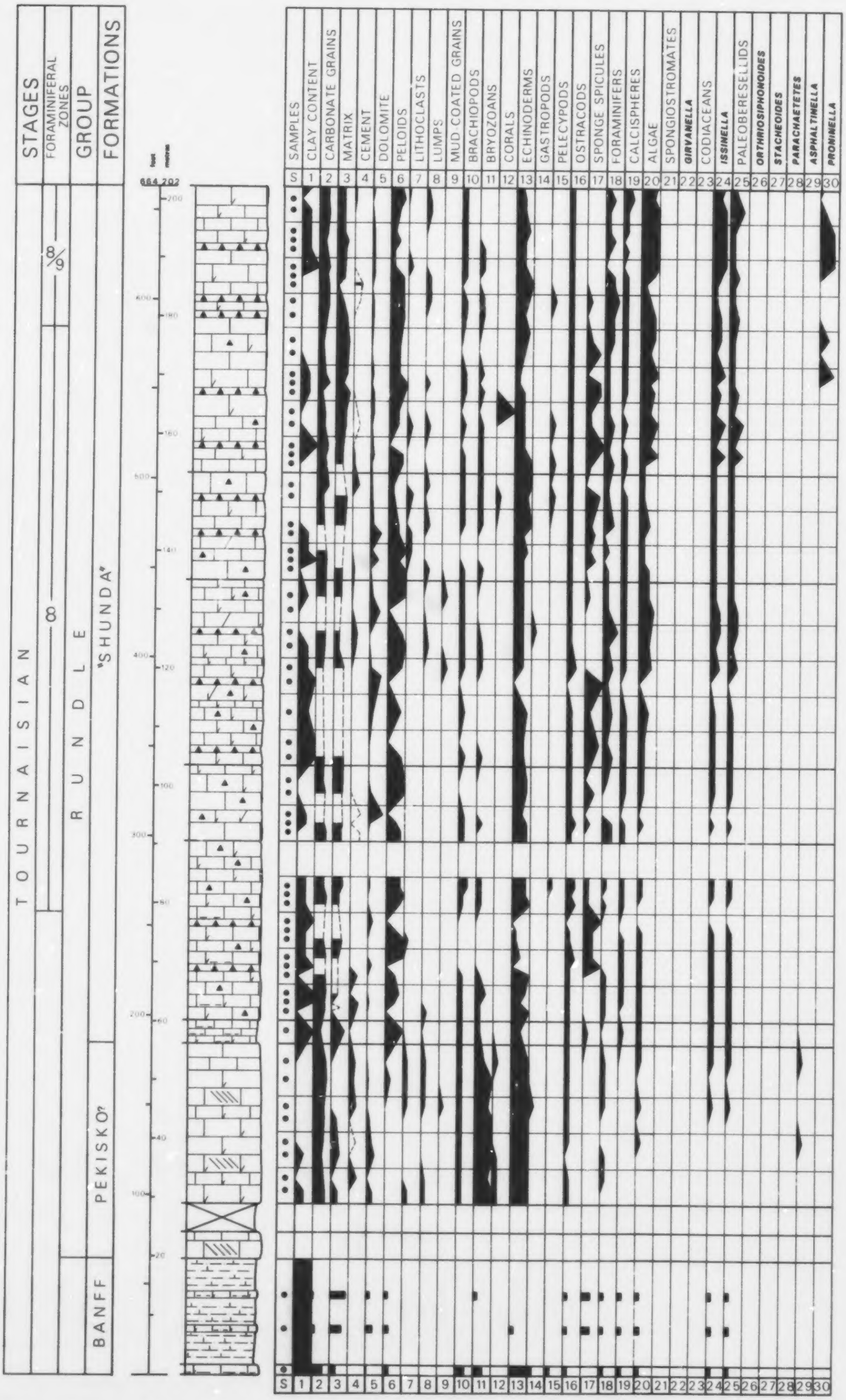

Figure 76.10a. *Sukunka River section, lower part: Banff (part), Pekisko, and Shunda (part) formations.*

deep-water deposits of the Prophet Formation; 3. grades southeastward (toward the paleoshore) into facies of open- to restricted-shelf aspect (Richards et al., in press).

Foraminiferal data indicate a late early Viséan (Tn1) age (Zone 10) for the Turner Valley Formation throughout the study area (Beauchamp and Mamet, 1985).

Mount Head(?) Formation

Strata identified as the Mount Head(?) Formation are present in sections 1, 2, and 3, located in the southeastern Pine Pass area (Fig. 76.1). The assignment of these strata to the Mount Head is provisional, because the relationships between this unit and the Turner Valley and Mount Head formations to the southeast are uncertain.

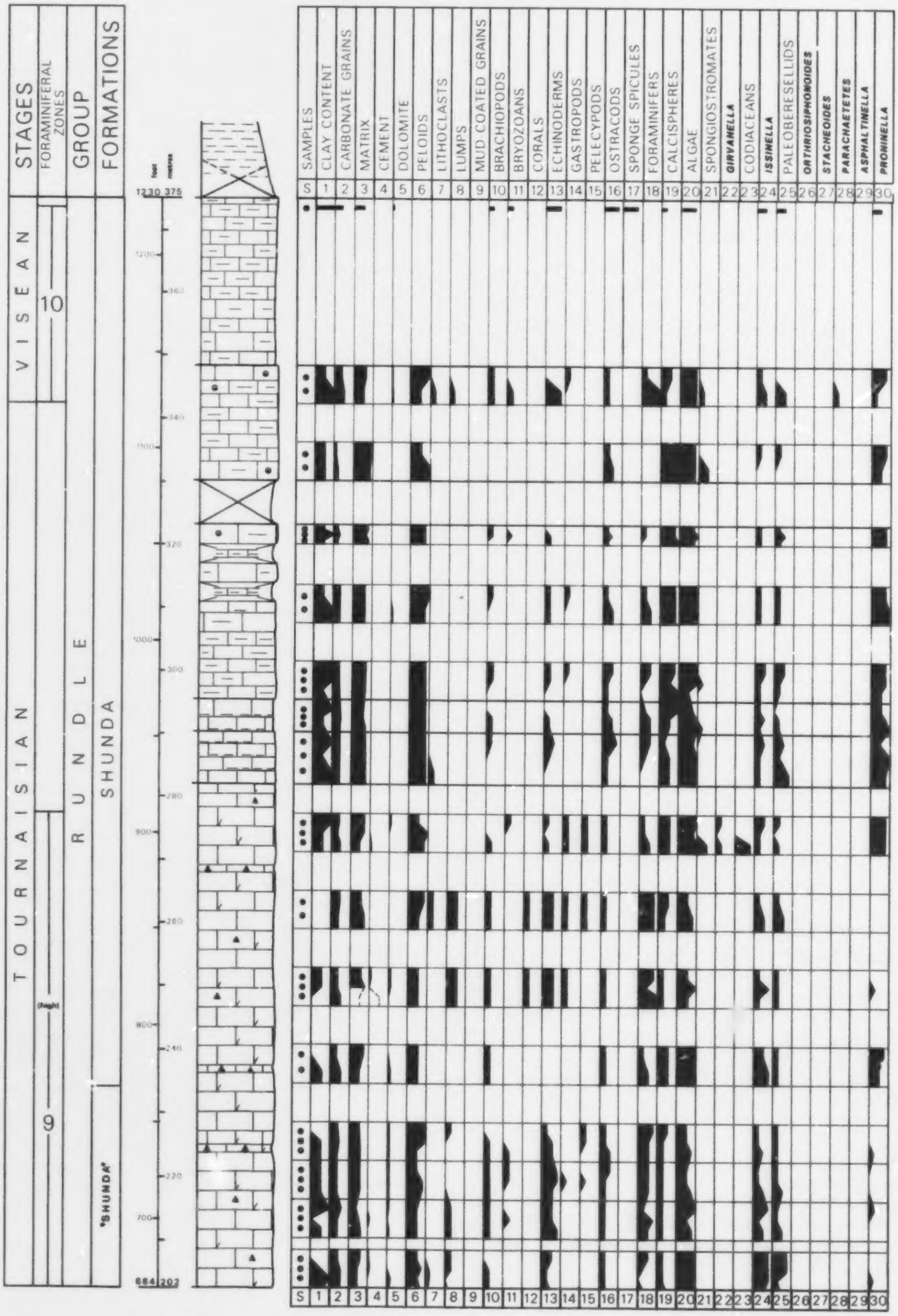

Figure 76.10b. *Sukunka River section, upper part: Shunda Formation (part).*

At Watson Peak (Fig. 76.7), the Mount Head(?) is 52 m thick, and consists of resistant, medium bedded, nonargillaceous to slightly argillaceous limestone alternating with intervals of more recessive carbonates. The formation comprises facies ranging from algal-calcisphere lime wackestone and algal-echinoderm packstone to foraminifer-algal-echinoderm packstone and grainstone and brachiopod-echinoderm-bryozoan grainstone. Lump-peloid-foraminifer lime grainstone is also present. In general, calcareous algae and other allochems characteristic of shallow, restricted-shelf environments (Fig. 76.5a) predominate in the lower 47 m of the Mount Head(?) Formation at this locality, whereas pelmatozoan ossicles and other open-marine bioclasts predominate in the upper 5 m.

A similar assemblage of lithofacies was observed within the Mount Head(?) Formation at North Burnt River (Fig. 76.8), where the formation is 62 m thick. Chert is present, as well as dolomitic limestone. The observed microfacies include lime wackestone through packstone and grainstone, containing various assemblages of tubular algae, calcispheres, foraminifers, echinoderms, brachiopods, bryozoans, and peloids.

At Burnt River (Fig. 76.9), the Mount Head(?) consists of a diversified assemblage of medium to thick bedded carbonates, including algal-echinoderm lime packstone and grainstone, algal-foraminifer-echinoderm lime packstone, and brachiopod-bryozoan-echinoderm lime grainstone and packstone.

At all localities in the study area, the Mount Head(?) Formation is truncated by regional unconformities beneath either Permian or Triassic strata. The formation is thicker and more completely developed southeast of the study area, where it consists mainly of lithofacies deposited in open- and restricted-shelf settings (Fig. 76.5a) during several transgressions and regressions (Richards et al., in press). On the western plains east of the study area, correlatives of the Mount Head(?) have been included in the Debolt Formation by Macauley (1958) and Macauley et al. (1964). Northwest of Watson Peak, it grades basinward into slope deposits of the Prophet Formation (Fig. 76.3, 76.4).

The Mount Head(?) Formation of the study area is provisionally interpreted to comprise carbonate-platform lithofacies deposited mainly in shallow water on either the restricted shelf or the open to restricted shelf (Fig. 76.5a). Deposition in relatively restricted environments is indicated by the allochems present. The echinoderm-rich beds in the uppermost Mount Head(?) probably were deposited in more open settings on the open shelf or seaward. Lithofacies of the Mount Head(?) are interpreted to be platform, rather than ramp deposits, because they appear to pass basinward (northwestward) into middle and lower-slope deposits through a transitional grainstone belt of upper-slope to shelf-margin aspect (Richards, pers. comm.).

Foraminiferal data indicate a late early Viséan (V1) age (Zone 11) for most of the Mount Head in the Sukunka-Burnt River area (Beauchamp and Mamet, 1985). Strata of middle Viséan (V2) age (Zone 12) have not been identified in the study area, but are widely distributed in the Mount Head of the Monkman Pass area. This indicates that pre-Permian erosion reached lower stratigraphic levels in the study area than to the south.

References

Bamber, E.W. and Mamet, B.L.
1978: Carboniferous biostratigraphy and correlation, northeastern British Columbia and southwestern District of Mackenzie; Geological Survey of Canada, Bulletin 266, 65 p.

Bamber, E.W., Macqueen, R.W., and Richards, B.C.
1984: Facies relationships at the Mississippian carbonate platform margin, western Canada; in Neuvième Congrès International de Stratigraphie et de Géologie du Carbonifère, E.S. Belt and R.W. Macqueen (eds.); Compte Rendu, v. 3, Southern Illinois University Press, Carbondale and Edwardsville, p. 461-478.

Beauchamp, B. and Mamet, B.L.
1985: Foraminiferal biostratigraphy, Rundle Group, Lower Carboniferous, east-central British Columbia; Bulletin of Canadian Petroleum Geology, v. 33, no. 2, p. 204-212.

Macauley, G.
1958: Late Paleozoic of Peace River area, Alberta; in Jurassic and Carboniferous of Western Canada, ed. A.J. Goodman; American Association of Petroleum Geologists, Allan Memorial Volume, p. 289-308.

Macauley, G., Penner, D.G., Procter, R.M., and Tisdall, W.H.
1964: Carboniferous; in Geological history of western Canada, ed. R.G. McCrossan and R.P. Glaister; Alberta Society of Petroleum Geologists, p. 89-102.

Mamet, B.L.
1976: An atlas of microfacies in Carboniferous carbonates of the Canadian Cordillera; Geological Survey of Canada, Bulletin 255, 131 p.

1984: Carboniferous small foraminifers and stratigraphy; in Neuvième Congrès International de Stratigraphie et de Géologie du Carbonifère, P.K. Sutherland and W.L. Manger (eds.); Compte Rendu, v. 2, Southern Illinois University Press, Carbondale and Edwardsville, p. 3-18.

Mamet, B.L., Bamber, E.W., and Macqueen, R.W.
– Microfacies of the Lower Carboniferous Banff Formation and Rundle Group, Monkman Pass map area, northeastern British Columbia; Geological Survey of Canada, Bulletin 353. (in press)

Mamet, B.L. and Skipp, B.A.
– Preliminary foraminiferal correlations of Early Carboniferous strata in the North American Cordillera; in Colloque sur la Stratigraphie du Carbonifère; Les Congrès et Colloques de l'université de Liège, v. 55, p. 327-348. (in press)

Richards, B.C.
1983: Uppermost Devonian and Lower Carboniferous stratigraphy, sedimentation, and diagenesis, southwestern District of Mackenzie and southeastern Yukon Territory (NTS 95B, C, and G); University of Kansas, Ph. D. thesis, 373 p.

Richards, B.C.
– Uppermost Devonian and Lower Carboniferous stratigraphy, sedimentation, and diagenesis, southwestern District of Mackenzie and southeastern Yukon Territory (NTS 95B, C, and G); Geological Survey of Canada, Bulletin. (in press)

Richards, B.C., Bamber, E.W., Higgins, A.C., and Utting, J.
– Carboniferous; in Sedimentary cover of the North American Craton: Canada, ed. D.F. Stott and J.D. Aitken; Geological Survey of Canada, Special Publication (Volume D-1 of the series "Decade of North American Geology"). (in press)

An occurrence of bitumen in the Interior Platform near Rengleng River, District of Mackenzie

Project 850044

D.K. Norris and A.R. Cameron
Institute of Sedimentary and Petroleum Geology, Calgary

Norris, D.K. and Cameron, A.R., An occurrence of bitumen in the Interior Platform near Rengleng River, District of Mackenzie; in Current Research, Part A, Geological Survey of Canada, Paper 86-1A, p. 645-648, 1986.

Abstract

A peculiar occurrence of solid bitumen exhibiting the grahamite to epi-impsonite level of maturation was discovered in the northern Interior Platform a few kilometres north of Rengleng River, District of Mackenzie. It may represent mobilized, strongly biodegraded hydrocarbons from a potential reservoir beneath or in association with the Upper Devonian Canol Formation and, correspondingly, improves the prospects for hydrocarbon exploration in the region.

Résumé

Une manifestation singulière de bitume solide présentant un niveau de maturation de la grahamite à l'épi-impsonite a été découverte dans la partie septentrionale de la plate-forme intérieure, à quelques kilomètres au nord de la rivière Rengleng, district de Mackenzie. Il pourrait s'agir d'hydrocarbures fortement bio-dégradés et mobilisés provenant d'un réservoir potentiel sous-jacent ou associé à la formation de Canol du Dévonien supérieur, améliorant ainsi les perspectives de recherche sur les hydrocarbures dans la région.

Introduction

A peculiar occurrence of coal-like material in the Interior Platform of western District of Mackenzie, NWT was first discovered by one of the authors (DKN) in 1983. However, it was not until after a second visit to the locality in 1985 by both authors, followed by detailed petrographic and chemical analyses, that the true nature of the material was ascertained. It is composed of two generations of solid bitumen; a brown, fluorescing one forming the matrix, and a dark orange fluorescing one forming inclusions in the matrix (F. Goodarzi, personal communication, 1985).

The occurrence is located in a borrow pit immediately west of the Dempster Highway (Fig. 77.1) about seven kilometres north of Rengleng River and slightly more than one kilometre north of a microwave tower, also beside the highway. It is located approximately at Kilometre 185, the posted distance along the highway from the boundary between Yukon Territory and Northwest Territories, at longitude 133°46.0'W and latitude 67°48.4'N, so that it falls within the Arctic Red River map area (Norris, 1981) on the west flank of Sitidgi Syncline. The location can be pinpointed precisely on National Air Photo Library vertical (coloured) air photograph A37501-100 at the following Cartesian co-ordinates, measured in centimetres from the centre of the picture, where the Y-axis coincides with the line joining the North and South fiducials and the positive Y direction points to the north side of the picture: X = -1.52 cm, Y = -4.71 cm.

The bitumen occurs as a sill-like mass, more or less parallel to bedding in the exposed hanging wall, in flyschoid, dark grey, fissile mudstone and platy to flaggy, fine grained sandstone of the marine, Upper Devonian Imperial Formation. The footwall is not exposed. The beds above the bitumen strike N30°E and are folded into a gentle, northeast-trending syncline that is completely exposed on the north (right) wall of the pit (Fig. 77.1). The beds on both flanks of the fold dip toward each other at about 15° so that the sill-like mass might be expected to surface at the near (east) side of the pit. The fact that this does not occur suggests that the bitumen intrusion must, on average, dip more steeply than bedding, or that it pinches out in an eastward direction. The conduit may be a northeast striking, high-angle fault, and its source may be a reservoir(s) at greater depth within the stratigraphic succession, perhaps beneath, or at least in association with, the underlying Upper Devonian Canol Formation.

Mudstones stratigraphically above the bitumen have been dated palynologically. Those immediately above the bitumen (GSC loc. C-92548) contain an extremely corroded spore assemblage of possible Frasnian age (D.C. McGregor and J. Utting, personal communication, 1985). Those in the ramp at the eastern approach to the pit (GSC loc. C-92547) contain a diverse assemblage of mid-Frasnian spores, including **Archaeoperisaccus opiparus** Owens, **Hymenozonotriletes deliquescens** Naumova, and **Hystricosporites furcatus** Owens (D.C. McGregor, Int. Rept., 1984). There is no evidence of reworking of these flora; thus, the early Late Devonian age indicated by them is considered to be the actual age of this part of the Imperial Formation which contains the bitumen.

The lateral limits of the bitumen sill have not been established. It is exposed continuously over a strike distance of about 20 m on the west wall of the pit. To the north it continues into the pit wall, whereas to the south it appears to lens out about half way across the pit (Fig. 77.1).

Figure 77.1. *View to northwest of bitumen occurrence in far (west) wall of borrow pit at Km 185 adjacent to Dempster Highway, near Rengleng River, NWT. Note syncline in interbedded sandstone and mudstone exposed on north wall of pit, GSC photo 2421-194.*

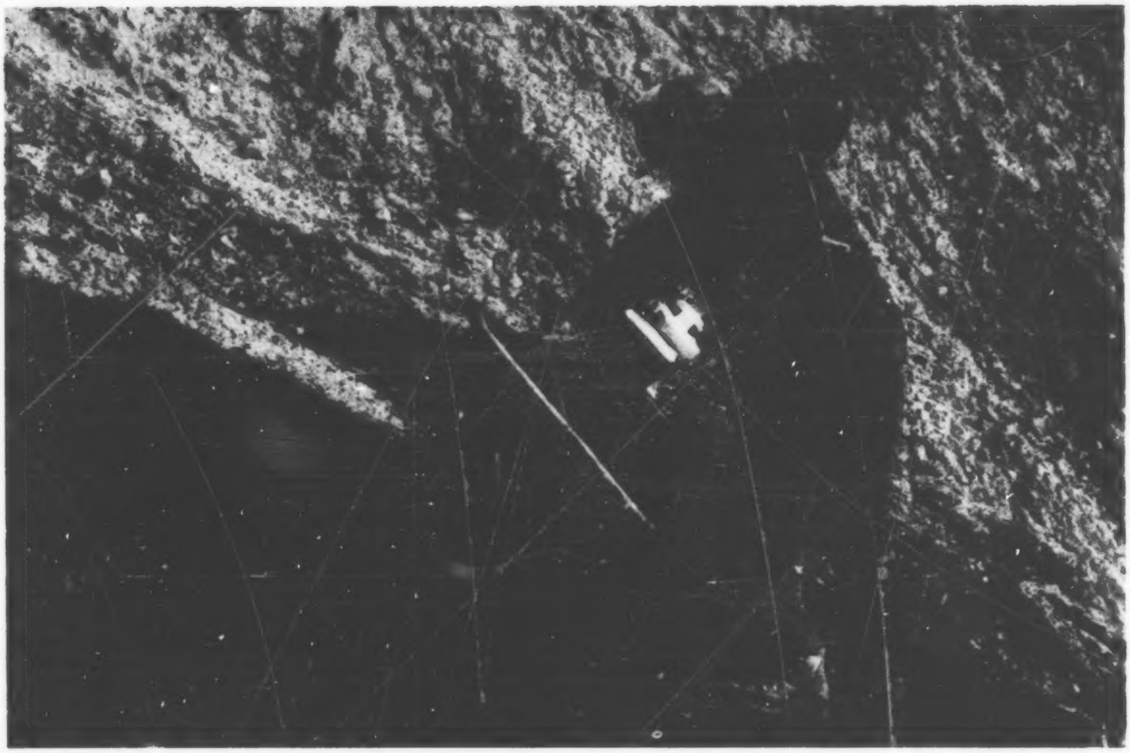

Figure 77.2. Drilling hole 90/83B with power auger in bitumen adjacent to north wall of borrow pit. GSC photo 2421-195.

In order to gain an appreciation of the thickness and extent of the sill, four 8-inch diameter holes were drilled with a power auger[1] perpendicular to bedding, and 8 m apart, beginning at water level near the southern limit of exposure of the bitumen (Hole 90/83A). The second hole (90/83C) was drilled 8 m up-dip from the first. The third and fourth holes were drilled 8 m and 16 m, respectively, on strike to the north of the second hole. The northernmost hole (90/83B) was drilled within 2 m of the north wall of the pit. Each hole was drilled to a depth of 1.22 m, the maximum limit of the equipment, without encountering the footwall of the sill. The true thickness of the sill where it was drilled is, therefore, unknown but it can be safely concluded that it is in excess of 1 m.

Macroscopically, the material is extremely bright and homogeneous. It is very friable and has a conchoidal fracture. In place it appears to be faintly laminated parallel to hanging wall bedding. It was not observed to contain any rock partings, although some chunks of sandstone similar to that occurring in the hanging wall appeared to be enclosed within the bitumen on the north wall of the pit, suggesting stoping during intrusion of the sill.

Samples representative of the part of the sill penetrated by the drill were recovered from two of the holes (90/83 A and 90/83 B; C-140251 and C-140252, respectively) and were analyzed petrographically and chemically. The results are presented in Tables 77.1 through 77.4. Reflectance measurements and chemical analyses were made according to procedures outlined by the American Society for Testing and Materials (ASTM, 1979). Pyrolysis data were determined by RockEval instrumentation as described by Espitalie et al. (1977) and Milner (1982). In addition, extracts of the samples were prepared by L.R. Snowdon at ISPG and analyzed by gas chromatography.

Microscopically, the material appears almost completely homogeneous, with no evidence of solubility in the immersion oil. When examined under reflected white light oil immersion, F. Goodarzi found that the two samples were in the grahamite to epi-impsonite (%Roil = 0.9 - 1.0, Jacob, 1981) level of maturation. Under fluorescent blue light he found the two generations of bitumen – the dark brown matrix and the inclusions of dark orange colouration. According to Goodarzi, these two bitumens are an end product of biodegradation of a mobile phase, perhaps originally gilsonite.

The mudstones from immediately above the bitumen (GSC loc. C-92548) contain rare spores which vary from medium brown, to dark brown, to brownish black on those with thick exines (J. Utting, personal communication, 1985). The colours suggest a Thermal Alteration Index of 3- to 3+ on the 5-point scale of Dow (1977), indicating a hydrocarbon potential in the lower part of the oil window.

Chemically, according to L.R. Snowdon (personal communication, 1985), the two samples have an intermediate atomic hydrogen to carbon ratio and Hydrogen Index, a very low oxygen to carbon ratio and Oxygen Index, a large amount of cyclic saturated hydrocarbons in the extracts (terpanes, steranes), and a level of thermal alteration lower than might be indicated by the bitumen reflectance (see Table 77.1). Total extracts were 6.1 and 10.5 mg/g for samples C-140251 and C-140252, respectively. Saturate fraction gas chromatograms contain substantial amounts of cyclic biomarker compounds but little or no normal alkanes or acyclic isoprenoids, indicating that the samples have undergone extensive biodegradation, and supporting Goodarzi's conclusions based on petrographic considerations.

As far as the authors are aware, the solid bitumen occurrence near Rengleng River is unique to the

[1] The authors are gratefully indebted to the Inuvik Scientific Resource centre for the loan of the auger.

Table 77.1. Reflectance data

Sample	%Ro Max		%Ro Random	
	Mean	Std. Dev.	Mean	Std. Dev.
C-140251	0.96	0.02	0.89	0.02
C-140252	0.97	0.02	0.84	0.02

Table 77.2. Proximate analysis data

Sample	Analytical basis	Moisture	Ash	Volatile matter	Fixed carbon	Calorific value MJ/Kg
C-140251	As rec'd DMMF[1]	0.30	4.20	35.00 35.88	60.50 64.12	36.1 38.0[2]
C-140252	As rec'd DMMF	0.50	6.00	34.00 35.50	59.50 64.50	35.3 37 9[2]

[1] DMMF = Dry, mineral-matter free
[2] Calorific value calculated on moist, mineral-free basis

Table 77.3. Ultimate analysis data

Sample	Analytical basis	Moisture	Ash	Carbon	Hydrogen	Nitrogen	Sulphur	Oxygen (by diff)
C-140251	As rec'd DAF[1]	0.30	4.20	82.27 86.15	6.03 6.31	2.54 2.66	2.57 2.69	2.09 2.19
C-140252	As rec'd DAF	0.50	6.00	80.76 86.37	6.00 6.42	2.40 2.57	2.41 2.58	1.93 2.06

[1] DAF = Dry, ash free

Table 77.4. Pyrolysis data (by RockEval method)

Sample	S_1	S_2	S_3	T max.°C
C-140251	6.82	202.49	0.16	439
C-140252	6.78	204.25	0.60	439

S values are mg yield/gm sample
T max is temperature of maximum yield of S_2
S_1 = Free hydrocarbon in sample
S_2 = Residual hydrocarbon potential
S_3 = CO_2 produced by pyrolysis

autochthonous stratigraphic succession of the northern Interior Platform. In the orogen, 210 km to the southwest, however, two albertite(?) dykes have been reported by Stelck (1944) in the lower canyon of the Peel River on the east flank of Richardson anticlinorium (Norris and Hopkins, 1977). These dykes also are hosted in the Imperial Formation and may well have had their source in the underlying, generally organic-rich Canol Formation.

A probable source for this Rengleng River bitumen is the Canol Formation, which is estimated to lie at a depth of 1600 m in the vicinity of the sampled outcrop (G.K. Williams, personal communication, 1985). At present, there is no way of determining when the bitumen migrated to its present location, and evaluation of the thermal history of the occurrence would be very speculative. At its present level of maturity (Ro Max 0.97) the bitumen probably has a slightly lower reflectance than associated vitrinite, which might be expected to have reflectances in the order of 1.0 to 1.1. The nearest site from which vitrinite reflectances have been published for Devonian strata was a well about 115 km northeast of Rengleng River. The values reported were 2.24 and 2.48 (Gunther and Meijer-Drees, 1977). These values are significantly higher than those determined on the Rengleng River samples and indicate a maturity level well above the upper limit of the "oil window". The reflectance of the Rengleng bitumen suggests a maturity level that is well within the "oil window", a conclusion supported by the fact that identifiable palynomorphs were recovered from the associated sediments, and also by the results of the chemical analyses (Snowdon, personal communication, 1985).

References

American Society for Testing and Material (ASTM)
1979: Annual Book of ASTM Standards-Part 26; American Society for Testing and Materials, Philadelphia, Pa.

Dow, G.W.
1977: Kerogen studies and geological interpretations; Journal of Geochemical Exploration, v. 7, p. 79-89.

Espitalie, J., Madec, M., and Tissot, B.
1977: Source rock characterization method of petroleum exploration; Proceedings of the 9th Offshore Technology Conference, Houston, Texas, p. 439-444.

Gunther, P.R. and Meijer-Drees, N.C.
1977: Devonian coal in the subsurface of the Great Slave Plain: a guide to exploration for oil and gas; in Report of Activities, Part A, Geological Survey of Canada, Paper 77-1A, p. 147-150.

Jacob, H.
1981: Mikroskopphotmetrische Analyse disperser Festbitumina in Sedimenten. Forschungsbericht (Research Report 232), Deutsche Gesellschaft fur Mineralolwissenschaft und Kohlechemie, Hamburg, West Germany, 123 p.

Milner, C.W.D.
1982: Geochemical analyses of sedimentary organic matter and interpretation of maturation and source potential; SEPM short course No. 7, p. 217-252.

Norris, D.K.
1981: Geology Arctic Red River District of Mackenzie; Geological Survey of Canada, Map 1521A.

Norris, D.K. and Hopkins, W.S., Jr.
1977: The geology of the Bonnett Plume Basin, Yukon Territory; Geological Survey of Canada, Paper 76-8, 20 p.

Stelck, C.R.
1944: Final geological report on "The Upper Peel River Area" Yukon Territory (Canada); Imperial Oil Ltd., Canol Project Assignment No. 23.

The Devonian rugose coral genera *Haplothecia*, *Kuangxiastraea* and *Scruttonia*

Project 680093

A.E.H. Pedder
Institute of Sedimentary and Petroleum Geology, Calgary

Pedder, A.E.H., The Devonian rugose coral genera **Haplothecia, Kuangxiastraea** and **Scruttonia**; in Current Research, Part A, Geological Survey of Canada, Paper 86-1A, p. 649-661, 1986.

Abstract

Haplothecia Frech, 1885, and **Kuangxiastraea** Yu and Kuang, 1983, are closely related but separable genera belonging to the Subfamily Hexagonariinae Bul'vanker, 1958, of the Family Columnariidae Nicholson, 1879. **Haplothecia** is known, with certainty, only from Frasnian rocks of Germany and the southern Urals. **Kuangxiastraea**, on the other hand, has been found in Eifelian and Givetian strata of China, Givetian limestones of Devon, England, and the Frasnian of Western Australia, China, the Rudny Altay region of the Soviet Union, Germany, and the Canadian Rocky Mountains. It is probably also present in the Frasnian of the Soviet Far East and the Urals. **Scruttonia** Cherepnina, 1975, and its possible senior synonym **Frechastraea** Scrutton, 1968, are assigned to the Phillipsastreidae Roemer, 1883. **Scruttonia**, strictly interpreted, is widely distributed in Frasnian rocks of Europe and Asia, but has not been found on other continents. **Kuangxiastraea julli** is established as a new species from Alberta.

Résumé

Haplothecia Frech, 1885, et **Kuangxiastraea** Yu et Kuang, 1983, sont des genres étroitement associés mais distincts, appartenant à la sous-famille des Hexagonariinae Bul'vanker, 1958, de la famille des Columnarridae Nicholson, 1879. **Haplothecia** n'est connu avec certitude que dans les roches du Frasnien en Allemagne et dans le sud de l'Oural. Par contre, Kuangxiastraea a été trouvé dans des couches de l'Eifélien et du Givétien en Chine, dans des calcaires du Givétien de Devon en Angleterre et dans le Frasnien en Australie occidental, en Chine, dans la région de Rudny Altay en Union Soviétique, en Allemagne et dans les Rocheuses au Canada. Il s'en trouve probablement aussi dans le Frasnien dans l'extrême est de l'Union Soviétique et dans l'Oural. **Scruttonia** Cherepnina, 1975, et son ancien synonyme possible **Frechastraea** Scrutton, 1968, sont associés à Phillipsastreidae Roemer, 1883. **Scruttonia**, au sens strict, est distribué partout dans des roches du Frasnien de l'Europe et de l'Asie et n'a pas été trouvé sur d'autres continents. **Kuangxiastraea julli** sp. nov. est établie comme une nouvelle espèce en Alberta.

Introduction and acknowledgments

The author first became interested in the European coral genus **Haplothecia** more than twenty years ago, while working on certain Australian Devonian phacellophyllid corals (Pedder, 1966). Knowing of this interest, the late R.K. Jull submitted a coral, which he thought might be a North American species of the genus, from beds transitional between the Perdrix and Cairn formations on the east side of Mt. Haultain in the Alberta Rocky Mountains.

Jull had polished a transverse face on the specimen, and is likely to have taken an acetate peel from it. On receiving the coral, the author prepared longitudinal and transverse thin sections. These revealed that the coral is thamnasterioid to astreoid, and lacks true intercorallite walls, such as occur in the cerioid type species of **Haplothecia**. Scrutton (1967, p. 271) admitted both cerioid and astreoid to thamnasterioid species to **Haplothecia**, but this interpretation was questioned by Hill and Jell (1971, p. 36), who thought that thamnasterioid species, otherwise similar to **Haplothecia**, might represent a distinct genus. In a review of Devonian rugose coral distribution, Oliver and Pedder (1979, p. 242) also questioned such a broad interpretation of **Haplothecia**, and placed similar astreoid to thamnasterioid species in a separate generic category, referred to as "**Haplothecia**" (astreoid). Shortly thereafter,

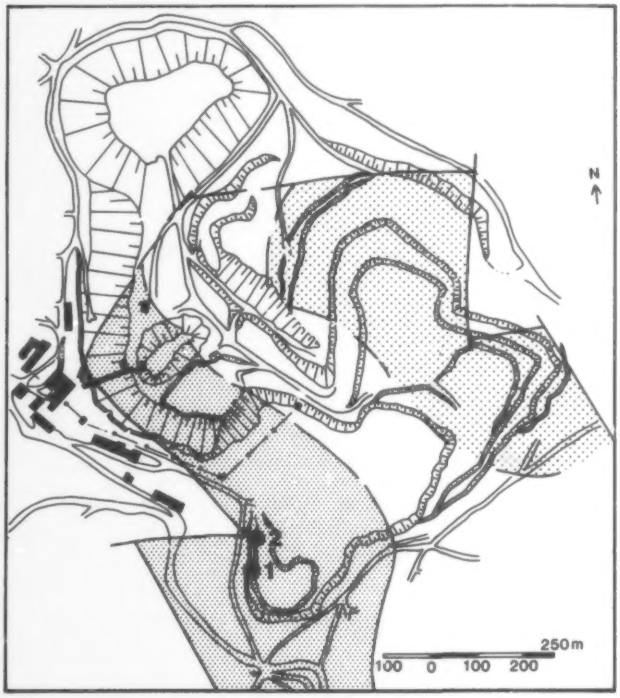

***Figure 78.1**. Plan of the Winterberg Quarry, Harz Mountains, West Germany. The centre of Bad Grund is 1.2 km south of the prominent road junction south of the quarry. Fine stippling indicates forereef; clear area inside the fault-bounded Iberg Limestone outcrop is fore-central reef; coarsely stippled area is back reef (after Franke, 1971, Fig. 3). Clear area outside the bounding faults is Carboniferous greywacke. Specimens of **Haplothecia filata** (Schlotheim) and **Scruttonia** sp. cf. **S. bowerbanki** (Milne Edwards and Haime), registered GSC 76343 and GSC 76346, were collected at Locality 1. The other specimen of **Haplothecia filata** (Schlotheim), GSC 76344, was collected at Locality 2.*

Yu and Kuang (1983, p. 255-256, 276) proposed a new subgenus, named **Haplothecia (Kuangxiastraea)**, for these forms.

Haplothecia filata, the type species of **Haplothecia**, is said to be a rare species (Birenheide, 1978, p. 98), and for a hundred years has been interpreted on the basis of only one specimen. One of the purposes of the present paper is to illustrate newly acquired material of this species to facilitate better appraisals of **Haplothecia**, and **Kuangxiastraea**, which is being elevated to full generic rank. Another purpose is to establish a new species based on Jull's specimen. The opportunity is also taken to review the problematic genus **Scruttonia**, because of similarities between transverse sections of its more carinate species and those of **Kuangxiastraea**.

The author is greatly indebted to the late R.K. Jull for allowing him to study a coral that Jull himself was interested in. The author is also much indebted to Prof. Dr. Peter Carls, Braunschweig University, for arranging access to the Winterberg Quarry, and to Dr. Herman Mader, Gottingen University, for guidance while collecting at the quarry.

Systematic paleontology

In this work, no consideration is given to the three problematic genera **Streptastraea** Sandberger and Sandberger (1854, legend to Pl. 37; spelled **Streptastrea** by the same authors in 1856, p. 416), **Pseudoacervularia** Schluter (1881, p. 84), and **Billingsastraea** Grabau (1917, p. 957).

The type species of **Streptastraea** is **S. longiradiata** Sandberger and Sandberger (1854, Pl. 37, figs. 3-3b; 1856, p. 416-417), from the Devonian Schalstein Conglomerate at Löhnberger Weg and Löhren, in the Lahn region of West Germany. There is no indication that the type specimen has ever been prepared for study. The Sandberger brothers believed **S. longiradiata** to be congeneric with **Astrea hennahi** Lonsdale, but were unaware that Lonsdale's species had become the type species of **Phillipsastrea** Orbigny (1849, p. 12), by designation of Milne Edwards and

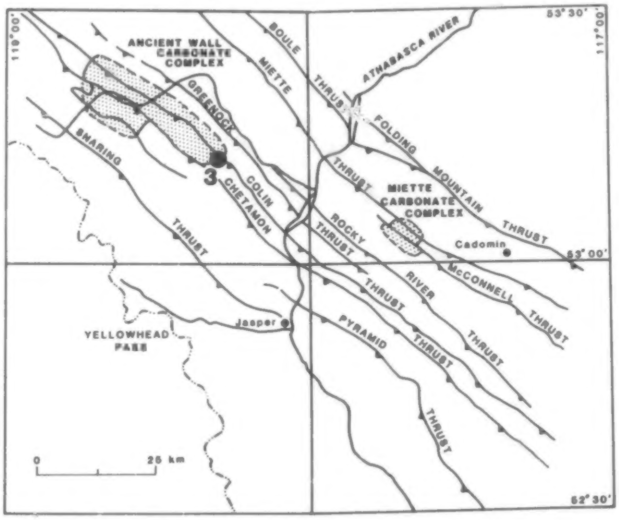

***Figure 78.2**. Location of the Ancient Wall Carbonate Complex, Jasper National Park, Alberta. Drawn from Mountjoy (1968, Fig. 2). The late R.K. Jull expressed the collection locality of **Kuangxiastraea julli** sp. nov., GSC 76345, shown here as Locality 3, in terms of this and Mountjoy's (1968) Figure 3a. See also Figure 78.3 of this work.*

Haime (1850, p. lxxi). Lang, Smith and Thomas (1940, p. 125), Scrutton (1968, p. 211, 215) and Hill (1981, p. 281), among many other recent authors, have regarded **Streptastraea** to be a junior subjective synonym, or a possible junior subjective synonym of **Phillipsastrea**.

Acervularia coronata Milne Edwards and Haime (1851, p. 416-417) from Barton, now a suburb of Torquay, Devon, England, is the type species of **Pseudoacervularia**, by designation of Lang, Smith and Thomas (1940, p. 108). The original specimens of **Pseudoacervularia coronata** are lost. In Scrutton's (1968, p. 213) opinion, they are almost certainly conspecific with **Phillipsastrea hennahi**, making **Pseudoacervularia** a subjective synonym of **Phillipsastrea**.

The type species of **Billingsastraea** is **Phillipsastrea verneuili** Milne Edwards and Haime (1851, p. 447-448, Pl. 10, fig. 5). Its derivation was originally given as "Dévonien, États-Unis: Wisconsin". Since the only Devonian outcrop area of Wisconsin, near Milwaukee, was not known before about 1860, and since no **Billingsastraea**-like form is known from it, **B. verneuili** was, for many years, assumed to be from glacial drift, and to have originated in the Onondaga or Bois Blanc beds of Ontario or Michigan. Oliver (1976, p. 89) has argued convincingly that this is not the case. More likely, **Billingsastraea verneuili** is a Silurian species of **Arachnophyllum** from the Hopkinton Dolomite, in an area that is now in northeastern Iowa, but was part of Wisconsin Territory from 1836 to 1838.

Family COLUMNARIIDAE Nicholson, 1879

Remarks. The author's current and tentative treatment of this family and its subfamilies was outlined in Pedder (1983, p. 228-231).

Subfamily HEXAGONARIINAE Bul'vanker, 1958

Genus **Haplothecia** Frech, 1885

Haplothecia Frech, 1885, p. 68.

Type species. **Madreporites filatus** Schlotheim, 1820, as restricted by Frech.

Diagnosis. Genus of cerioid columnariid corals. Septa in two orders, strongly carinate, typically with coarse yardarm carinae composed of bilaterally symmetrical monacanths.

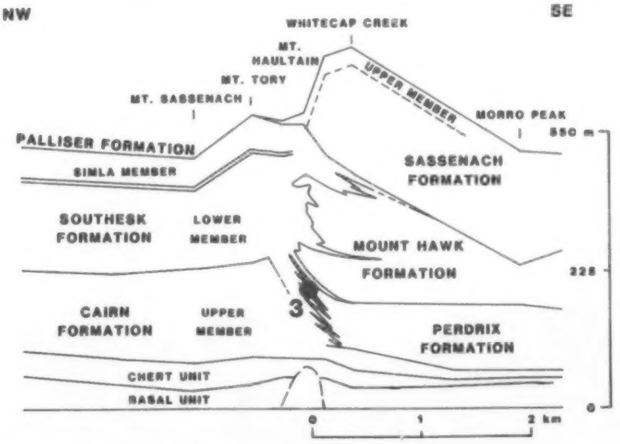

Figure 78.3. Schematic representation of the stratigraphic relationships of the Upper Devonian units in the Ancient Wall Carbonate Complex, Jasper National Park Alberta. Drawn from Mountjoy (1968), Figure 3a. Locality 3 represents the stratigraphic occurrence of ***Kuangxiastraea julli*** *sp. nov., GSC 76345, given by the late R.K. Jull.*

Commonly, septa curve in parallel groups through the dissepimentarium, locally, to such an extent that some septa are almost parallel to the intercorallite wall (Fig. 78.9). Peripherally, the septa may split into two or more lamellae (Fig. 78.8), or degenerate into discrete trabeculae (Fig. 11a of Pickett, 1967, Pl. 3). In longitudinal section, the long trabeculae and carinae display only slight radiation over most of the dissepimentarium (Fig. 78.4, 78.6). Dissepiments small, globose, numerous, forming flat to moderately everted dissepimentarial surfaces, except near the inner margin, where they are steeply inwardly inclined. Tabulae closely spaced, mostly incomplete and forming variable tabularial surfaces.

Remarks. This diagnosis differs from most previous diagnoses by excluding astreoid species. Scrutton's (1967, p. 271) diagnosis states that dissepimentarial surfaces are strongly reflexed, but this is not true, especially with respect to the type species (Fig. 78.13-78.16). Birenheide (1978, p. 97) wrote that the corallite walls are commonly translucent and are without a median line (axial plane of some authors). However, a line marking the axial plane is clearly visible in the holotype of **Haplothecia filata** (Pedder, 1966, Text-fig. 1; Pickett, 1967, Text-fig. 19; Scrutton, 1967, p. 272; Hill and Jell, 1971, p. 34) and in recently collected topotypes of the species (Fig. 78.8, 78.9).

Additional assigned species. **Haplothecia schlotheimi** Pickett (1967, p. 45-46, Pl. 3, figs. 11a, b; Text-fig. 1C). Frasnian, Iberg Limestone; Wirbelau near Weilburg, Lahn, West Germany (type locality), and near Elbingerode, Harz Mountains, East Germany (Weyer, 1971, p. 48, Pl. 2, fig. 2; Pl. 3, figs. 1-3).

Unnamed species, identified as **Phillipsastrea filata** by Soshkina (1951, p. 98-100, Text-fig. 36, Pl. 18, figs. 1a, b; also Soshkina, 1952, p. 101, Pl. 42, fig. 141). Unnamed Frasnian beds; River Bolshoi Nugush, below the village of Kosheli, western slope of the southern Urals.

Doubtful species. **Acervularia granulosa** F.A. Roemer (1855, p. 32, Pl. 6, figs. 21a,b). Frasnian, Iberg Limestone; near Grund, Harz Mountains, West Germany. From Roemer's brief description and crude figures this is a cerioid coral with weakly flexed outer walls and 14 x 2, distinctly curved septa, which consist largely of relatively coarse yardarm carinae in the dissepimentarium. Diameters of the tabularia and corallites are 2.0 mm, and 5.0 to 6.0 mm, respectively. Roemer described the inner wall as indistinct, and none is apparent in the figures. All these features are consistent with a small species of **Haplothecia**, but Frech (1885, Pl. 3, fig. 2) figured a transverse section of an "Originalexemplar" of **A. granulosa** Roemer. The diameters of the tabularia and corallites of this specimen appear to be 2.9 to 3.0 mm and 5.0 to 6.0 mm, respectively, and the septa are fusiform in the inner dissepimentarium. The overall morphology, as far as it is depicted, suggests a species of **Pseudoacervularia** in Różkowska's 1953 sense. Indeed, her synonymy (Różkowska, 1953, p. 49) for "**Pseudoacervularia**" **macrommata** (F.A. Roemer, 1855) includes Frech's, but not Roemer's figure of **A. granulosa**.

Rejected species. **Haplothecia** (?) **chinensis** Frech (1897, p. 195, Pl. 9, figs. 5, 5a; proposed as a new species again in Frech, 1911, p. 46, Pl. 9, figs. 5, 5a). Givetian, **Stringocephalus**-bearing beds; Hwaling-pu, western Sichuan Province, China. This species is unrecognisable, but it is not **Haplothecia**.

Haplothecia ogwellensis Scrutton (1967, p. 272-273, Pl. 41, figs. 3-6). Frasnian part of the East Ogwell Limestone; road cut 37 m west of Ransley Quarry, near Newton Abbot, Devon, England. The wall structure of this coral is unknown; should it prove to be pseudocerioid, the species would be better placed in **Frechastraea**.

4

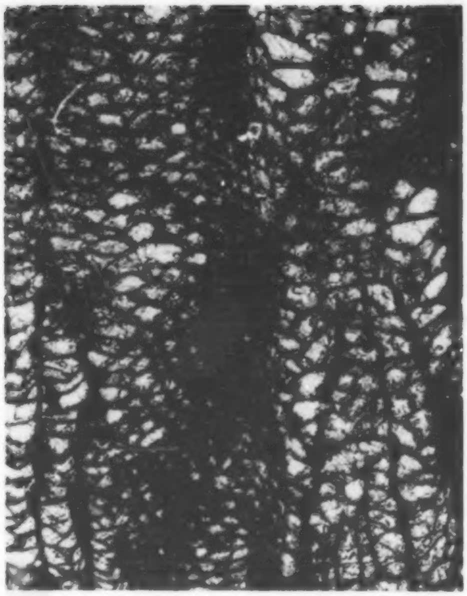

5

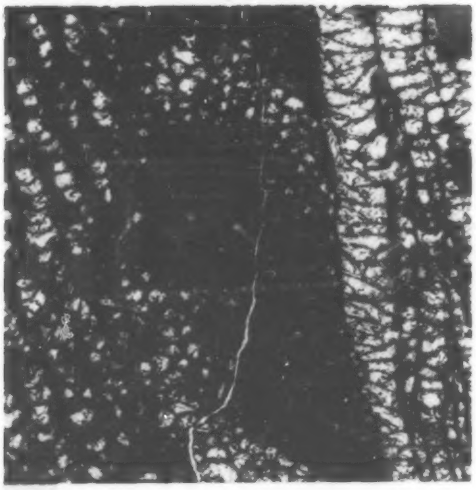

6

7

Figures 78.4–78.7. *Longitudinal thin sections, enlarged x10. Figures 78.4, 78.6,* ***Haplothccia filata*** *(Schlotheim), GSC 76344, forereef facies of the Iberg Limestone in Winterberg Quarry (see Figure 78.1). Figure 78.5,* ***Kuangxiastraea julli*** *sp. nov., GSC 76345, reef debris transitional between the Upper Cairn and Perdrix formations; Ancient Wall Carbonate Complex (see figures 78.2, 78.3). Figure 78.7,* ***Scruttonia*** *sp. cf.* ***S. bowerbanki*** *(Milne Edwards and Haime), GSC 76346, forereef facies of the Iberg Limestone in Winterberg Quarry (see Figure 78.1).*

Birenheide (1978, p. 100) wrote that "**Haplothecia**" **ogwellensis** Scrutton corresponds to **Phillipsastrea ananas** (Goldfuss) in almost all characters, but has more strongly developed carinae.

Haplothecia (?) **laciniosa** Hill and Jell, 1971. See below under **Kuangxiastraea.**

Haplothecia beichuanensis He (1978, p. 136, Pl. 67, figs. 1a, b). Eifelian, Yangmaba Formation; Beichuan County, Sichuan Province, China. The fine septa and zigzag carinae of this species suggest cyathophyllid affinities.

Haplothecia breviseptata Cao, 1982. See below under **Kuangxiastraea.**

Distribution. In addition to the rejected species listed above, and to the rejections from the type species listed below, corals assigned by Ivaniya (1981, p. 39-42) to **Haplothecia** are also removed from the genus. As **Haplothecia** is interpreted here, its known distribution is restricted to Frasnian rocks in Germany, the southern Urals, and possibly Moravia, Czechoslovakia (Galle, 1985, p. 62, 63).

Haplothecia filata (Schlotheim, 1820)

Figures 78.4, 78.6, 78.8, 78.9, 78.12-78.16

Madreporites filatus Schlotheim, 1820, p. 359, (in part) examples under heading "a" only.

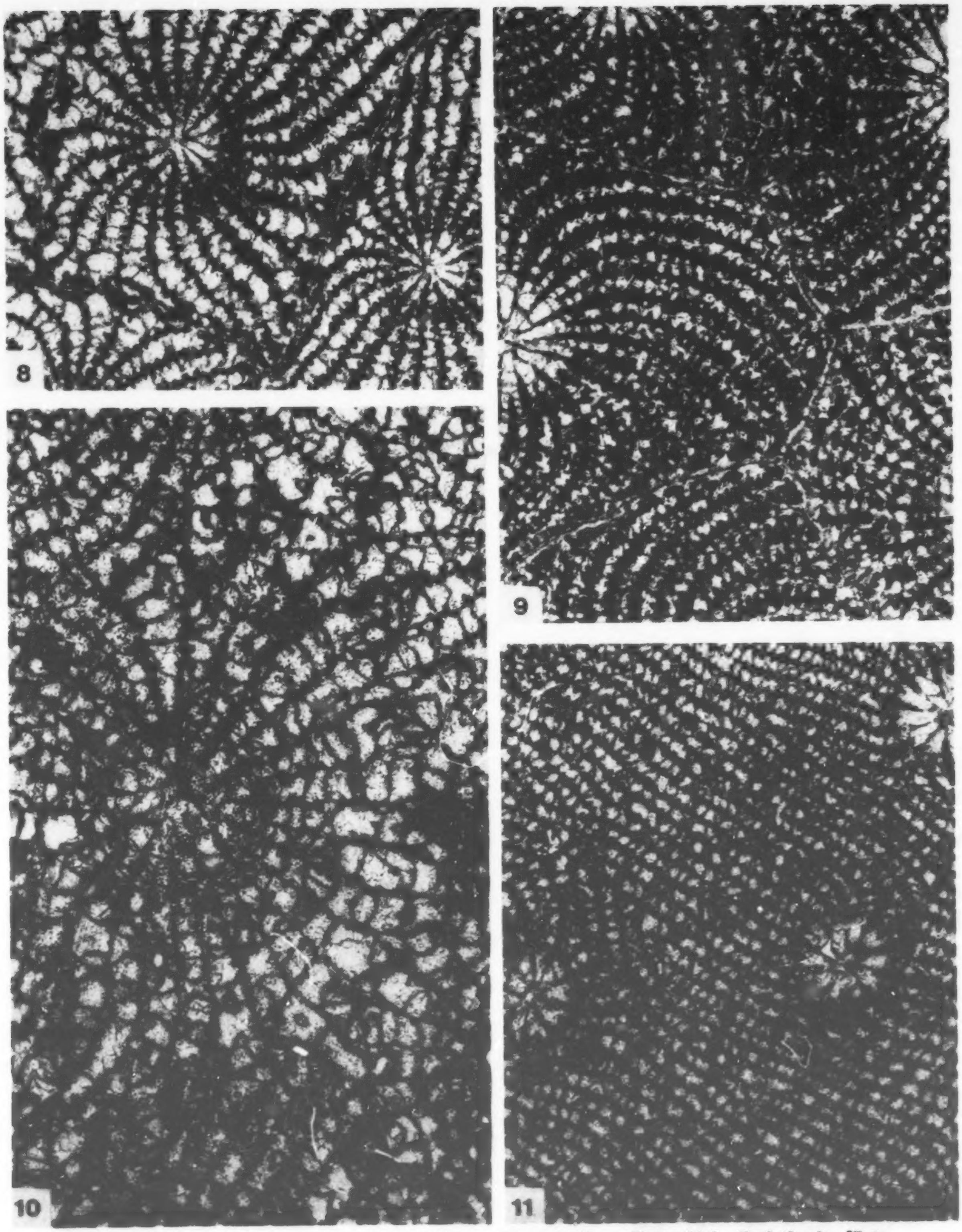

Figures 78.8–78.11. *Transverse thin sections, enlarged x10. Figure 78.8,* ***Haplothecia filata*** *(Schlotheim), GSC 76343, forereef facies of the Iberg Limestone in Winterberg Quarry (see Figure 78.1). Figure 78.9,* ***Haplothecia filata*** *(Schlotheim), GSC 76344, forereef facies of the Iberg Limestone in Winterberg Quarry (see Figure 78.1). Figure 78.10,* ***Kuangxiastraea julli*** *sp. nov., GSC 76345, reef debris transitional between the Upper Cairn and Perdrix formations; Ancient Wall Carbonate Complex (see figures 78.2, 78.3). Figure 78.11,* ***Scruttonia*** *sp. cf.* ***S. bowerbanki*** *(Milne Edwards and Haime), GSC 76346, forereef facies of the Iberg Limestone in Winterberg Quarry (see Figure 78.1).*

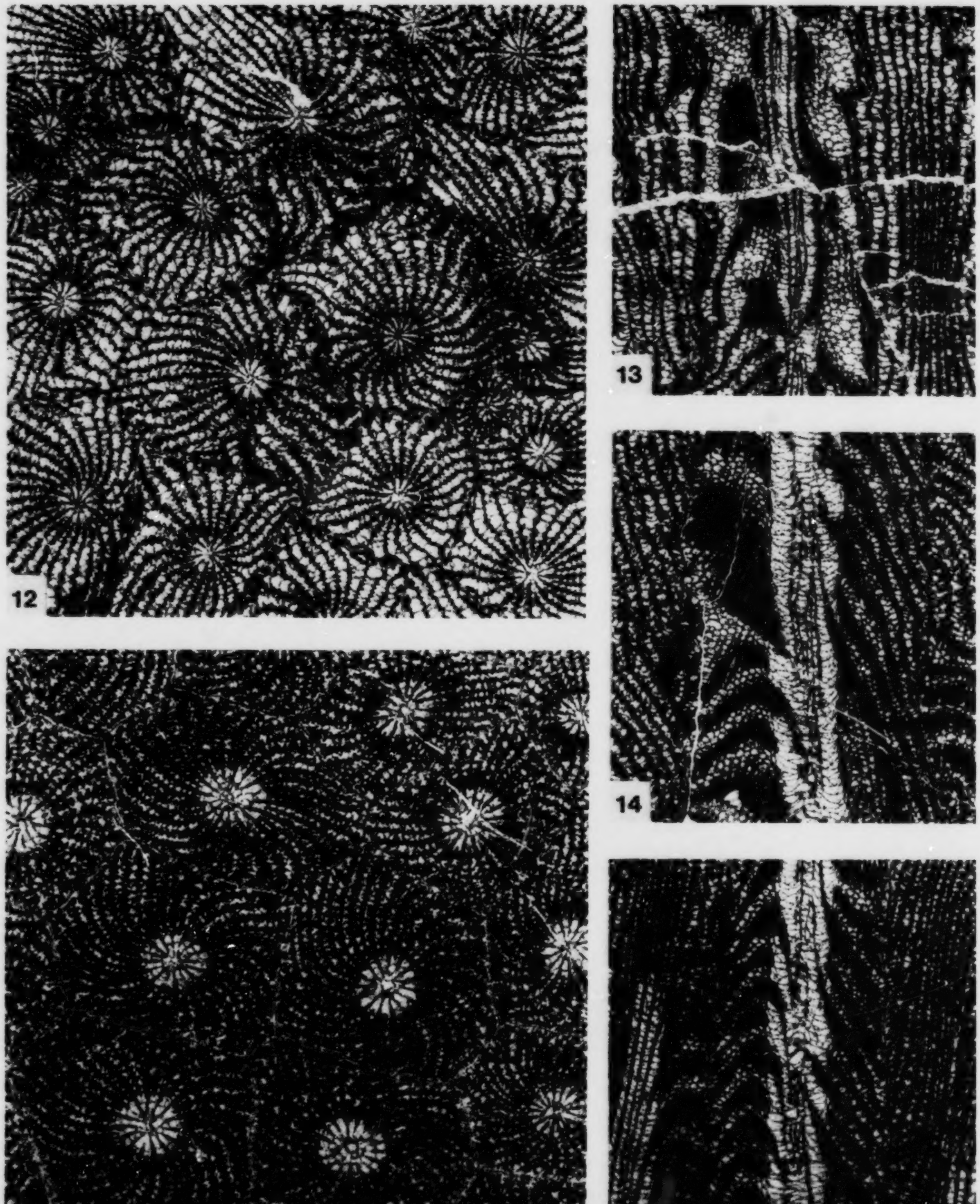

Figures 78.12–78.16. ***Haplothecia filata*** *(Schlotheim), all enlarged x5. Figures 78.12, 78.13, transverse and longitudinal thin sections, GSC 76343. Figures 78.14–78.16, two longitudinal and a transverse thin section, GSC 76344. Both specimens from the forereef facies of the Iberg Limestone in Winterberg Quarry (see Figure 78.1).*

Haplothecia filata (Schlotheim); Frech, 1885, p. 68-69, Pl. 4, figs. 7, 7a.

Haplothecia filata (Schlotheim); Hill, 1956, p. 280, figs. 191, 1a, 1b.

Haplothecia filata (Schlotheim); Pedder, 1966, p. 182-183, Text-figs. 1, 2, 4, 7.

Haplothecia filata (Schlotheim); Pickett, 1967, p. 24, Text-fig. 19, Pl. 6, fig. 23.

Haplothecia filata (Schlotheim); Scrutton, 1967, p. 271-272, Pl. 41, figs. 1, 2.

Haplothecia filata (Schlotheim); Hill and Jell, 1971, p. 34-35, Pl. 4, figs. 3a, b.

Haplothecia filata (Schlotheim); Hill, 1981, p. 275-276, figs. 176, 3a, 3b.

But not:

Phillipsastraea filata (Schlotheim); Soshkina, 1951, p. 98-100, Text-fig. 36, Pl. 18, figs. 1a, b (=**Haplothecia** sp. nov.).

Phillipsastraea filata (Schlotheim); Soshkina, 1952, p. 101, Pl. 42, fig. 141 (=**Haplothecia** sp. nov., as above).

Phillipsastraea filata (Schlotheim); Spasskiy, 1960, p. 66, Pl. 25, figs. 3, 4 (=**Kuangxiastraea** sp. nov.).

Billingsastraea filata (Schlotheim); Jia in Jia and others, 1977, p. 143-144, Pl. 48, figs. 1a, b (=**Kuangxiastraea** sp. nov.).

Haplothecia sp. cf. **H. filata** (Schlotheim); Birenheide, 1978, p. 240, Pl. 14, figs. 1a-c (="**Pseudoacervularia**" **roemeri** de Verneuil and Haime?).

Haplothecia filata (Schlotheim); He, 1978, p. 136, Pl. 67, figs. 2a, b (=**Kuangxiastraea** sp. nov.).

Haplothecia sp. aff. **H. filata** (Schlotheim); Rozkowska, 1979, p. 22, Pl. 2, figs. 5a, b (=indet. hexagonariinid coral).

Material. Institut für Paläontologie und Museum der Humboldt-Universität, Berlin, Q. Kat. A. 138, p. 1530. Iberg Limestone; Winterberg near Grund, Harz Mountains, West Germany. This is one of the original specimens of Schlotheim (1820) and following Frech's 1885 work, is technically the lectotype. When examined in 1964 it consisted of two small pieces and four transverse thin sections, including one figured by Frech. Frech's longitudinal section was missing, and as no other existed, the author was permitted to prepare a new one. All authentic figures of the species that have so far been published are either of the same transverse section, or of one of the two longitudinal sections.

The material used for this work consists of two specimens, registered GSC 76343 and 76344, collected by the writer in 1985 from the forereef facies of the Iberg Reef, exposed in the Winterberg Quarry. Although the type stratum and type locality of the species are not known precisely, for practical purposes these two specimens are topotypes. GSC 76343 consists of a hand specimen, one transverse and one longitudinal thin section, and comes from the 410-m level of the quarry. GSC 76344 consists of a hand specimen, one transverse and three longitudinal thin sections, and comes from the 385-m level. Figure 78.1 shows the collecting localities. Datings provided by Franke's (1973, Text-fig. 4 and Table 6) conodont samples 80 and 123, indicate that the newly collected specimens are Frasnian, and probably from the Lower **Palmatolepis gigas** Zone.

Diagnosis. Species of **Haplothecia** with well developed intercorallite walls, 1.5 to 3.5 mm thick. Diameters of adult corallites and tabularia 6.0 to 8.0 mm, and 1.3 to 2.3 mm, respectively. In most corallites the septal count is 12 x 2 to 15 x 2, the total range being 11 x 2 to 17 x 2. Septa abundantly carinate with coarse yardarm carinae. Locally, towards the periphery, septa may split into two or more lamellae. Dissepiments small, globose, numerous, forming essentially flat, or only slightly everted dissepimentarial surfaces. Tabulae closely spaced, incomplete, partly due to interruption by long major septa; morphology of tabularial surfaces variable.

Remarks. Transverse and longitudinal thin sections of a specimen of **Haplothecia** have been figured by Soshkina (1951, 1952) from Frasnian beds of the southern Urals. Soshkina identified the specimen as being conspecific with **H. filata**, although the generic identification was with **Phillipsastrea**. Pedder (1966, p. 182) upheld Soshkina's identification, whereas Scrutton (1967, p. 272) did not. The Russian specimen is larger, with corallite diameters of 10.0 to 11.0 mm, and has considerably more everted dissepimentarial surfaces. Neither of the two new authentic specimens of **Haplothecia filata** is any closer morphologically to Soshkina's specimen, so that it now seems probable that Scrutton was correct. Unless the Czechoslovakian form listed by Galle (1985, p. 62, 63) proves to be **Haplothecia filata**, the species is known only from the Winterberg in the Harz Mountains of West Germany.

Genus **Kuangxiastraea** Yu and Kuang, 1983

Kwangsiastraea Yu (MS.); Kong in Kong and Huang, 1978, p. 87 (**nomen nudum**).

"**Haplothecia**" (astreoid); Oliver and Pedder, 1979, p. 242.

?**Haplothecia** (**Lanceothecia**) Yu and Jiang in Jiang, 1982, p. 99 (**nomen nudum**).

Haplothecia (**Kuangxiastraea**) Yu and Kuang, 1983, p. 255-256, 276.

Type species. **Haplothecia (Kuangxiastraea) elegans** Yu and Kuang, 1983, p. 256-257, 276, Text-fig. 7, Pl. 2, figs. 1a-2b. Givetian, upper part of the Mintang Formation; near Liujing, Heng County, central Guangxi Province, China.

Diagnosis. Astreoid to thamnasterioid genus of hexagonariinid corals; any intercorallite wall that may be present is extremely fragmentary and entirely of septal origin. Septa in two orders, moderately to heavily carinate with yardarm and zigzag carinae. Toward the periphery, septa may split into more than one lamella, become retiform, or degenerate into isolated trabeculae that are only approximately aligned in the plane of the septum. Trabeculae radiate so as to be approximately normal to the moderately, or strongly arched inner dissepimentarial surfaces. Dissepiments small, numerous, globose, and steeply inwardly inclined against the tabularium. Tabulae abundant, only rarely complete. Tabularial surfaces variable, even within species.

Remarks. **Kuangxiastraea** is used somewhat tentatively at present, because it is not satisfactorily separated from **Sichuanastraea**, which was proposed by He (1978, p. 134-135) as a subgenus of **Billingsastraea**. **Sichuanastraea** is based on **S. crassiseptata** He (1978, p. 135, Pl. 66, figs. 4a, b; Pl. 67, figs. 4a, b) from the Givetian Guanwushan Formation at Shawozi and Ganxi, Beichuan County, Sichuan Province, China. Available figures of this species are not clear, but it appears to have considerably dilated septa that lack yardarm carinae, and its narrow dissepimentaria are not everted.

Additional assigned species. **Smithia pengellyi** Milne Edwards and Haime (1851, p. 422; originally misspelled **S. pengillyi**; revised by Scrutton, 1967, p. 274-275, Pl. 42, figs. 1-5; Pl. 43, figs. 1, 2). Givetian, Barton Limestone; Barton and Lummaton quarries, outskirts of Torquay, England, and possibly also in the Plymouth Limestone, Plymouth, Devon, England.

Haplothecia (?) **laciniosa** Hill and Jell (1971, p. 35-36, Pl. 5, figs. 1a, b). Frasnian, Sadler Formation; 4.3 km north of Mt. Krauss, Kimberley Division, Western Australia.

Billingsastraea trematophylloides Jia (in Jia and others, 1977, p. 144, Pl. 48, figs. 2a, b). Frasnian, Liujiang Formation; Tongwan and Xihoshan, Wuxuan County, Guangxi Province, China.

Haplothecia breviseptata Cao (in Cao and others, 1982, p. 88, Pl. 25, figs. 7a, b). Middle Devonian (Eifelian?), Lure Formation; Nanshimengou, Gansu Province, China.

Haplothecia (Lanceothecia) trematophylloides liuyangensis Yu and Jiang (in Jiang, 1982, p. 100, Pl. 56, figs. 4a, b). Frasnian, Yutianqiao Formation; Liuyang County, Hunan Province, China.

Kuangxiastraea julli Pedder sp. nov. Frasnian, beds transitional from the upper part of the Cairn Formation to the Perdrix Formation; Mt. Haultain, Alberta Rocky Mountains, Canada.

Unnamed species, identified as **Phillipsastraea filata** by Spasskiy (1960, p. 66, Pl. 25, figs. 3, 4). Frasnian, Nikolaev Beds; region of Nikolaev Mine, Rudny Altay, U.S.S.R.

Unnamed species identified as **Billingsastraea** sp. cf. **B. pengellyi** by Pickett (1967, p. 46-47, Pl. 1, fig. 1; Pl. 2, fig. 9). Frasnian, Iberg Limestone; Wirbelau near Weilburg, Lahn, West Germany.

Unnamed species, identified as **Billingsastraea filata** by Jia (in Jia and others, 1977, p. 143-144, Pl. 48, figs. 1a, b). Givetian, Donggangling Formation; Kejia, Chongzuo County, Guangxi Province, China.

Unnamed species, identified as **Haplothecia filata** by He (1978, p. 136, Pl. 67, figs. 2a, b). Eifelian, Yangmaba Formation; Ganxi, Beichuan County, Sichuan Province, China.

Doubtful species. **Phillipsastrea toupengensis** Yu (1947, p. 130, Pl. 3, figs. 1a, b). Givetian, Donggangling Formation; Toupengling and Litang, Xiangzhou County, Guangxi Province, China. This poorly illustrated species has very narrow dissepimentaria, lightly carinate septa that do not appear to be modified in any way near the periphery, and septa that scarcely penetrate the tabularia. It does not closely resemble other species of **Kuangxiastraea**, but, nevertheless, was unequivocally assigned to the genus by Yu and Kuang (1983, p. 255, 276). A coral identified as **Radiastraea toupengensis** (Yu) by Cao and others (1982, p. 87, Pl. 27, figs. 7a, b), from the Frasnian Cakuohe Formation at Larenguan in Gansu Province, China, may be a species of **Radiastraea**, but is certainly not **Kuangxiastraea**.

Phillipsastrea gropsicarina Ouyang (in Cao and others, 1982, p. 89, Pl. 28, figs. 2a, b). Frasnian, Lengshuihe Formation; Taoyuangou, Maoping, Zhen'an, Shaanxi Province, China. Ouyang's description mentions indistinct horseshoe dissepiments, but these are not visible in the figure of the longitudinal thin section; in all other respects the coral appears to be a small species of **Kuangxiastraea**.

Haplothecia (Kuangxiastraea) delicata Yu and Kuang (1983, p. 257-258, Pl. 1, figs. 9a, b). Givetian, upper part of the Mintang Formation; near Liujing, Heng County, central Guangxi Province, China. The carination and apparent lack of septal degeneration are not typical of the genus.

Unnamed species, identified as **Phillipsastrea pengellyi** (misspelled **P. pengelli**) by Soshkina (1951, p. 100-101, Pl. 19, figs. 2a, b; also Soshkina, 1952, p. 102, Pl. 41, fig. 146; Soshkina and Dobrolyubova, 1962, Pl. 20, figs. 4a, b). Unnamed Frasnian beds; River Bolshoi Nugush, below the village of Kosheli, on the western slope of the southern Urals. This form, which is represented by only one known specimen, seems better placed in **Kuangxiastraea** than in any other named genus, despite being locally pseudocerioid.

Unnamed species, identified as **Billingsastraea** sp. by Spasskiy and Kravtsov in Besprozvannykh and others (1975, p. 53, Pl. 7, figs. 2a, b). Unnamed Frasnian beds; River Kuranakh, Sette Daban Range, U.S.S.R.

Unnamed species, identified as **Haplothecia (Kuangxiastraea)** sp. cf. **H. (K.) elegans** by Yu and Kuang (1983, p. 257, Pl. 2, figs. 3a, b). Givetian, middle part of the Mintang Formation; near Liujing, Heng County, central Guangxi Province, China. As in **H. (K.) delicata**, the carination and apparent lack of septal degeneration are not typical of the genus.

Distribution. Eifelian strata of Sichuan Province and possibly Gansu Province, China. Givetian of Guangxi Province, China, and south Devon, England. Frasnian rocks of the Canning Basin, Western Australia, Hunan and Guangxi provinces of China, Rudny Altay region of the U.S.S.R., the Lahn Syncline of West Germany, and the Alberta Rocky Mountains. **Kuangxiastraea** is probably also present in the Frasnian of Shaanxi Province, China, the Sette Daban Range of the Soviet Far East, and the western slope of the southern Urals.

Kuangxiastraea julli sp. nov.

Figures 78.5, 78.10, 78.17-78.19

Type specimen. Holotype, GSC 76345. Frasnian reef slope beds transitional between the upper part of the Cairn Formation and the Perdrix Formation; stratigraphically equivalent to a level about 47.5 m below the top of the Cairn Formation. South wall of a cirque on the east side of Mount Haultain, Jasper National Park, Alberta (R.K. Jull, locality L196); approximately 53°11'30"N latitude, 118°17'00"W longitude. Collected by R.K. Jull, 1972.

Diagnosis. Essentially thamnasterioid species of **Kuangxiastraea** with small corallites (axes of adjacent adult corallites 0.8 to 14.0 mm apart) and slender tabularia (diameter 2.2 to 2.5 mm). Septa 13 x 2 to 16 x 2 in number, strongly carinate, but displaying little peripheral degeneration.

Description. The corallum was probably incomplete and certainly abraded before burial; no part of its exterior was visible before sectioning. The form of the colony is predominantly thamnasterioid with weak and only local development of pseudocerioid walls. Diameter of corallites about 10 mm (axes of adjacent corallites 0.8 to 14.0 mm apart); diameter of tabularia 2.2 to 2.5 mm.

Most adult corallites have 14 x 2 or 15 x 2 septa, the total range being 13 x 2 to 16 x 2. The septa are undifferentiated and strongly carinate in the dissepimentarium. Most of the carinae are of the yardarm type; a few are zigzag. Peripherally, there is some degeneration of the septa into separate divergent lamellae, which may form very imperfect intercorallite walls. Completely isolated carinae, however, are extremely rare. Minor septa are confined to the dissepimentarium. The attenuated, adaxial parts of the major septa are noncarinate and of variable length; some reach the axis, others terminate well short of it. Trabeculae, which are bilaterally symmetrical monacanths, are confined to, and responsible for, the carinae. They diverge over a broad zone in the inner dissepimentarium, and in longitudinal section many of them, in the major order of the septa, are seen to bifurcate close to the margin of the tabularium. This bifurcation concentrates the yardarm carinae and causes dilation of the major septa near the inner edge of the dissepimentarium.

The dissepiments are small, numerous and moderately well inflated. Near the periphery they are essentially horizontal, but toward the inner dissepimentarium they form weakly to moderately elevated dissepimentarial surfaces.

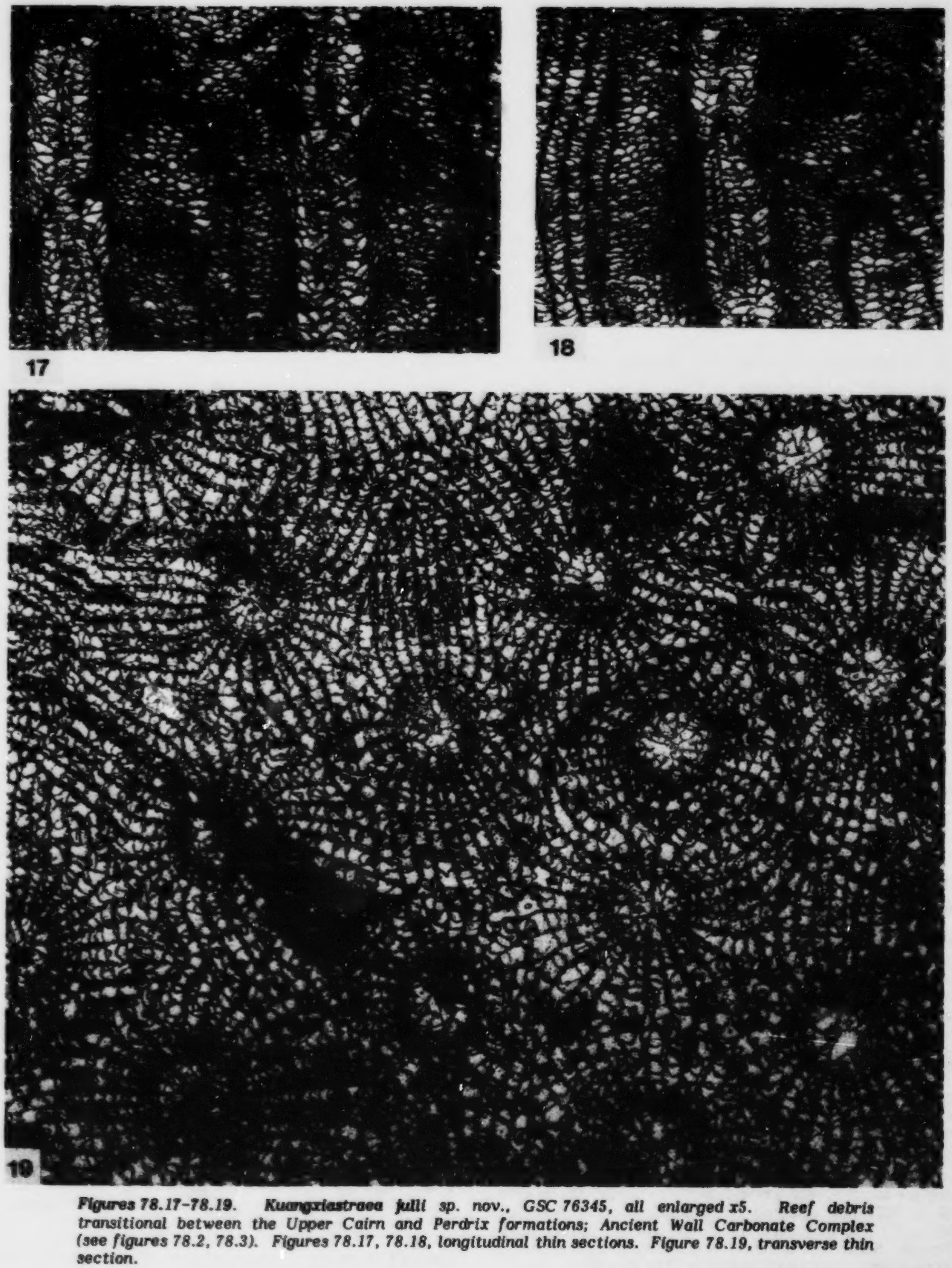

Figures 78.17–78.19. ***Kuangxiastraea*** ***fulli*** *sp. nov., GSC 76345, all enlarged x5. Reef debris transitional between the Upper Cairn and Perdrix formations; Ancient Wall Carbonate Complex (see figures 78.2, 78.3). Figures 78.17, 78.18, longitudinal thin sections. Figure 78.19, transverse thin section.*

Next to the tabularium they are steeply inclined inwards, and, on average, are smaller than those in other parts of the dissepimentarium.

One complete tabula is visible in one section; it is believed to be the result of rejuvenescence. All of the other tabulae are incomplete and many are distinctly vesicular. Typically, between 25 and 35 tabulae may be counted over a vertical distance of 10.0 mm. Morphology of the tabularial surfaces varies considerably.

Remarks. Of the previously named species of **Kuangxiastraea**, **K. trematophylloides** (Jia, 1977) most resembles the new species. It differs from **K. julli** in having narrower tabularia (diameter about 1.5 to 1.8 mm), much less carination in the inner dissepimentarium, and considerably more septal degeneration near the periphery of the corallites.

Derivation of name. The trivial name of the species is a patronym for the collector of its type specimen.

Family PHILLIPSASTREIDAE Roemer, 1883

Remarks. C.F. Roemer's (1883, p. 389) spelling of the family name Phillipsastraeidae is incorrect, because it is based on an unjustified emendation of **Phillipsastrea** Orbigny (1849, p. 12) [International Code of Zoological Nomenclature, edition 3, Article 32(c)(iii)]. A family-group name based on an unjustifiably emended generic name must be corrected [I.C.Z.N., edition 3, Article 36(d)(ii)]. A correction of this sort affects neither the authorship, nor the date of the family-group name.

Frechastraea Scrutton (1968, p. 231-232) and **Scruttonia**, which are referred to the Phillipsastreidae by most authors, including Hill (1981, p. 284), differ from other members of the family by having flat, or almost flat dissepimentarial surfaces, and by lacking, or having only rare, horseshoe dissepiments. A new subfamily is perhaps justified by these distinctions. Strongly carinate forms of **Scruttonia**, such as the Iberg Limestone coral figured in this work (Figs. 78.7, 78.11, 78.20-78.22), resemble **Kuangxiastraea** in transverse section. In longitudinal section, **Scruttonia** is distinguished by its narrow zone of trabecular divergence, confined to the inner part of an essentially flat dissepimentarium (compare Figs. 78.5 and 78.7). This feature is shared with **Frechastraea** and is the reason for placing these genera in the Phillipsastreidae.

Genus **Scruttonia** Cherepnina 1975

Scruttonia Cherepnina, 1975, p. 202.

Type species. **Smithia bowerbanki** Milne Edwards and Haime (1851, p. 423; species revised by Scrutton, 1968, p. 253-257, Pl. 11, fig. 3; Pl. 12, figs. 1-3; probable topotype figured by Rohart, 1982, Pl. 10, fig. 2). Frasnian part of the East Ogwell Limestone; vicinity of Ransley Quarry, near Newton Abbot, Devon, England. This species has been misidentified often, and many of its recorded occurrences are erroneous. Frasnian specimens from near Vodelée, in the Dinant Basin, Belgium, appear to be correctly identified (Coen-Aubert, 1980, p. 5-7, Pl. 1, figs. 1-3).

Diagnosis. Genus of phillipsastreid corals lacking horseshoe dissepiments, and differing from **Frechastraea** by being thamnasterioid rather than pseudocerioid.

Remarks. The distinction between **Frechastraea** and **Scruttonia** is slight, especially as some thamnasterioid species are locally pseudocerioid, and vice versa. Birenheide (1978, p. 102) has rejected **Scruttonia**, whereas Scrutton (1978, p. 49), Coen-Aubert (1980) and Rohart (1982) have adopted it. **Scruttonia** is tentatively accepted in this paper; the same position was taken by Hill in 1981 (p. 284).

Additional assigned species. **Smithia boloniensis** Milne Edwards and Haime (1851, p. 423; species revised by Rohart, 1982, p. 107-113, Text-figs. 2-6, Pl. 9, figs. 1a-4a, Pl. 10, figs. 1a-c, 3a-4b). Frasnian, Parisienne Member of the Ferques Formation; Ferques, Boulonnais area, northwest France.

Phillipsastrea sanctacrucensis Różkowska (1953, p. 59-60, Text-figs. 32, 33, Pl. 2, figs. 8-10). Unnamed Frasnian beds; Wietrznia Quarry, Holy Cross Mountains, Poland.

Phillipsastrea cordis Różkowska (1953, p. 61, 62, Text-fig. 34, Pl. 2, figs. 5-7). Unnamed Frasnian beds; Psie Górki Quarry, Holy Cross Mountains, Poland.

Phillipsastrea pentagona minima Scrutton (1968, p. 236-240; =**P. pentagona** var. **minima** Różkowska, 1953, p. 66-67, Text-figs. 36-38, Pl. 8, fig. 9). Unnamed Frasnian beds; Psie Gorki Quarry, Holy Cross Mountains, Poland.

Frechastraea dushanensis Kong (in Kong and Huang, 1978, p. 86, Pl. 30, figs. 2a, b). Frasnian, Wangchengpo Formation; near Dushan, Guizhou Province, China.

Scruttonia boloniensis minor Coen-Aubert (1980, p. 8-9, Pl. 1, figs. 4, 5). Frasnian, Upper **Polygnathus asymmetricus** Zone; Durbuy, Barvaux-sur-Ourthe, Han-sur-Lesse and Sautour, Dinant Basin, Belgium.

Scruttonia balconi Coen-Aubert (1980, p. 10-11, Pl. 2, figs. 1-4). Frasnian, Middle to Upper **Polygnathus asymmetricus** Zone; boreholes in the Beaumont and Silenrieux areas, Dinant Basin, Belgium.

Unnamed species, identified as **Billingsastraea** sp. cf. **B. bowerbanki** by Pickett (1967, Pl. 1, fig. 2; Pl. 6, fig. 24). Frasnian, Iberg Limestone; Winterberg Quarry, Harz Mountains, West Germany.

Unnamed species, identified as **Frechastraea pentagona minima** by Kong and Huang (1978, p. 87, Pl. 30, figs. 3a, b). Frasnian, Wangchengpo Formation; Jiyang near Majiang, Guizhou Province, China.

Unnamed species, identified as **Frechastraea bowerbanki** by Cao and others (1982, p. 90, Pl. 27, figs. 1a, b). Frasnian, Tieshan Group; Caodigou, Nanping County, Sichuan Province, China.

Doubtful species. **Astrea parallela** F.A. Roemer (1843, p. 5, Pl. 3, fig. 1). Frasnian, Iberg Limestone; near Grund, Harz Mountains, West Germany. This species is unrecognizable as presently described, but is quite possibly a species of **Scruttonia**. Frech (1885, p. 59) believed that it might be synonymous with **Phillipsastrea hennahi** (Lonsdale).

Acervularia seriaca Quenstedt (1852, p. 664, Pl. 60, figs. 3a, b). Frasnian, Iberg Limestone; near Grund, Harz Mountains, West Germany. Several authors have assumed this species to be conspecific with **S. bowerbanki**, but this has not been confirmed.

Phillipsastrea kunthi Frech (1885, p. 62, 63, Pl. 7, fig. 4). Frasnian, main limestone of Tietze (1870); near Ebersdorf, Klodzko (Glatz), southern Poland. Although no longitudinal thin section has been figured in publication, Rohart (1982, p. 106) refers the species to **Scruttonia**. Różkowska (1979, Table 1) identified a Frasnian coral from Pomerania, northwest Poland as **Frechastraea kunthi** (Frech).

Phillipsastrea focantiensis Tsien (1977, p. 206, Text-fig. 10). Frasnian, Fr1γ beds; Focant, Dinant Basin, Belgium. No figure of a longitudinal thin section is available. Tsien reported that the dissepiments are very small and numerous and likened the species to **"Phillipsastrea" bowerbanki**. Apparently, on these data, Rohart (1982, p. 107) assigned the species to **Scruttonia**. Birenheide (1978, p. 100) believed it to be synonymous with **"Phillipsastrea" ananas** (Goldfuss).

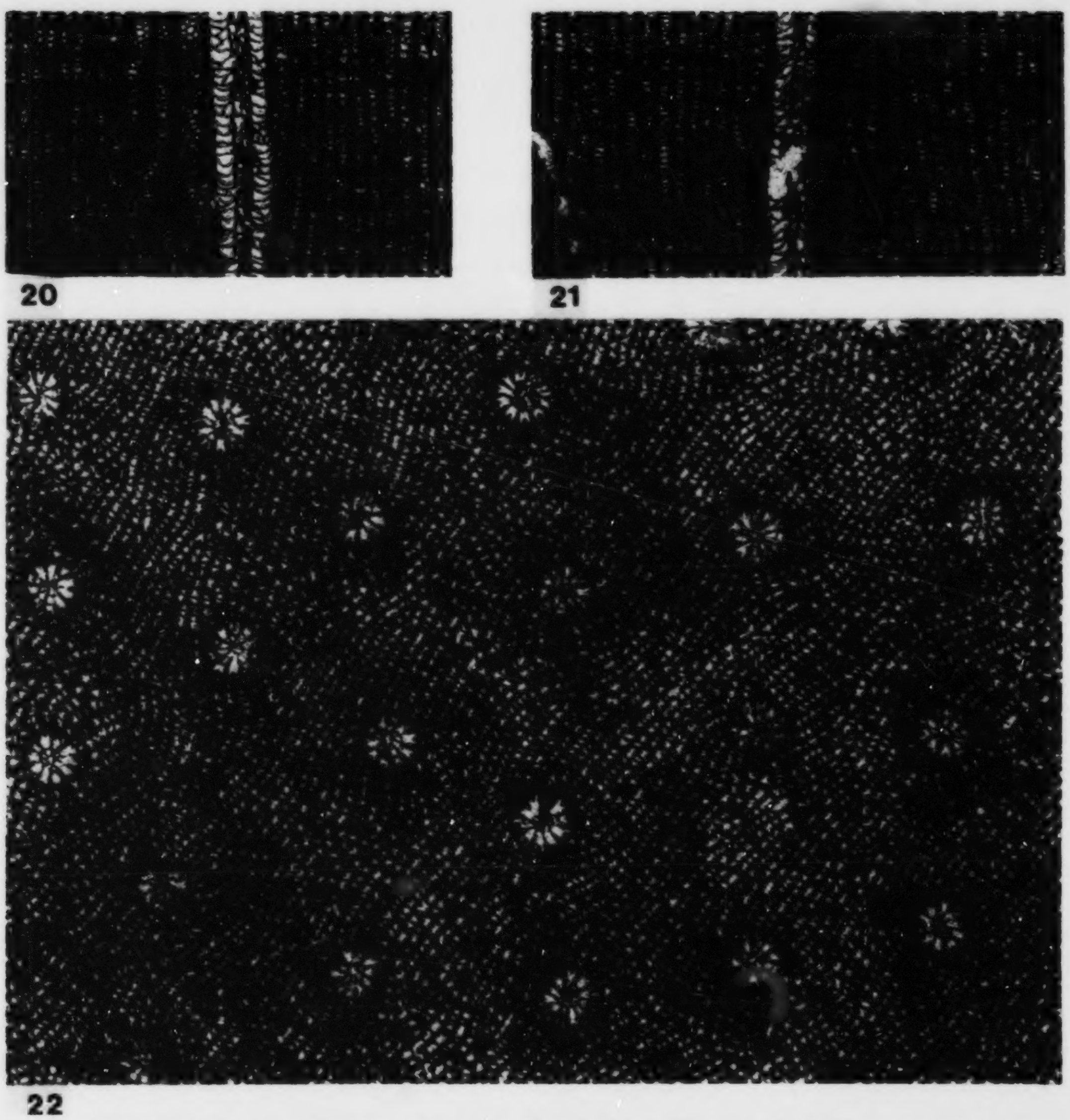

Figures 78.20–78.22. ***Scruttonia*** *sp. cf.* ***S. bowerbanki*** *(Milne Edwards and Haime), GSC 76346, all enlarged x5. Forereef facies of the Iberg Limestone in Winterberg Quarry (see Figure 78.1). Figures 78.20, 78.21, longitudinal thin sections. Figure 78.22, transverse thin section.*

Species identified as **Phillipsastrea bowerbanki** by Sun (1958, p. 6, 19, Pl. 10, figs. 1a, b). Frasnian, Shaitienchiao Formation; Hsianghsiang, Hunan Province, China. This specimen, which was the only one known from Hsianghsiang in 1958, may be of a species of **Frechastraea.**

Distribution. Frasnian strata only, in south Devon, England; northwest France; Dinant Basin, Belgium; Harz Mountains, Germany; Holy Cross Mountains, Poland; Sichuan (Cao and others, 1982, p. 90, Pl. 27, figs. 1a, b) and Guizhou provinces, China. There are indications that it may also be present in Frasnian rocks in the Pomeranian and Lower Silesian areas of Poland, the southern Ural Mountains (Soshkina, 1951, p. 89-90, Pl. 16, figs. 1-2b; 1952, p. 86, Pl. 21, fig. 75), and Hunan Province, China.

References

Besprozvannykh, N.I., Dubatolov, V.N., Kravtsov, A.G., Latypov, Yu. Ya., and Spasskiy, N.Ya.
1975: Devonskie rugozy Taymyro-Kolymskoy provintsii; Akademiya Nauk SSSR, Sibirskoe Otdelenie, Institut Geologii i Geofiziki, Trudy, vypusk 228, 172 p.

Birenheide, R.
1978: Leitfossilien. No. 2. Rugose Korallen des Devon; Gebruder Borntraeger, Berlin, Stuttgart, vi p.+ 265 p.

Cao Xuan-duo, Ouyang Xuan, and Jin Tong-an
1982: Rugosa; in Paleontological atlas of northwest China; Shaanxi, Gansu and Ningxia volume, Part 2, Upper Paleozoic; Xi'an Institute of Geology and Mineral Resources (ed.); Geological Publishing House, Beijing, p. 46-179, 565-593 (Chinese).

Cherepnina, S.K.
1975: K sistematike podotryada Phillipsastraeina A. Schouppé, 1958; in Drevnie Cnidaria, Tom 1, B.S. Sokolov (ed.); Akademiya Nauk SSSR, Sibirskoe Otdelenie, Institut Geologii i Geofiziki, Trudy, vypusk 201, p. 198-204 (imprint 1974).

Coen-Aubert, M.
1980: Représentants Frasniens du genre **Scruttonia** Tcherepnina, S.K., 1974 (Rugosa) en Belgique; Institute Royal des Sciences naturelles de Belgique, Bulletin, tome 51, no. 4, Sciences de la Terre, 15 p. (imprint 1979).

Franke, W.
1971: Structure and development of the Iberg/Winterberg Reef (Devonian to Lower Carboniferous, Harz, West Germany); in Sedimentology of parts of central Europe, ed. G. Müller; Guidebook to excursions held during the VIII International Sedimentological Congress 1971 in Heidelberg, Germany; Verlag Waldemar Kramer Frankfurt, am Main, p. 83-89.

1973: Fazies, Bau und Entwicklungsgeschichte des Iberger Riffes (Mitteldevon bis Unterkarbon III), NW-Harz, W-Deutschland; Geologisches Jahrbuch, Reihe A, Heft 11, 127 p.

Frech, F.
1885: Die Korallenfauna des Oberdevons in Deutschland; Deutsche geologische Gesellschaft, Zeitschrift, Band 37, p. 21-130.

1897: Palaeozoos Korállok; in Gróf Széchenyi Béla; Keletázsiai utazásának (1877-80) tudományos Eredménye, kötet. 3, Budapest, p. 195-199.

1911: China. Ergebnise eigener Reisen und darauf gegründeter Studien von Ferdinand Freiherrn v. Richthofen, Band 5, Verlag von Dietrich Reimer (Ernst Vohsen), Berlin, vii p.+ 289 p.

Galle, A.
1985: Biostratigraphy and rugose corals of Moravian Devonian (Czechoslovakia); Newsletters on Stratigraphy, v. 14, p. 48-68.

Grabau, A.W.
1917: Stratigraphic relationships of the Tully Limestone and the Genesee Shale in eastern North America; The Geological Society of America, Bulletin, v. 28, p. 945-958.

He Yuan-xiang
1978: Subclass Rugosa; in Atlas of fossils of southwest China; Sichuan Volume, Part 1, from Sinian to Devonian; Chengdu Institute of Geology and Mineral Resources (ed.), Geological Publishing House, Beijing, p. 98-179, 555-568 (Chinese).

Hill, D.
1956: Rugosa; in Treatise on invertebrate paleontology; Part F, Coelenterata, ed. R.C. Moore; The Geological Society of America and the University of Kansas Press, Boulder and Lawrence, p. 233-324.

Hill, D. (cont.)
1981: Treatise on invertebrate paleontology; Part F, Coelenterata, Supplement 1, Rugosa and Tabulata, ed. C. Teichert; The Geological Society of America and the University of Kansas Press, Boulder and Lawrence, v. 1, p. i-xl+ p. 1-378, v. 2, p. i, ii+ p. 379-762.

Hill, D. and Jell, J.S.
1971: Devonian corals from the Canning Basin, Western Australia; Geological Survey of Western Australia, Bulletin 121, 158 p. (imprint 1970).

Ivaniya, V.A.
1981: Devonskie chetyrekhluchevye korally Salaira i severnogo Kuzbassa (sistematika, biostratigrafiya, ekologiya); Izdatel'stvo Tomskogo Universiteta, Tomsk, 140 p. (imprint 1980).

Jia Hui-zhen, Xu Shou-yong, Kuang Guo-dun, Zhang Bu-fei, Zuo Zi-bi, and Wu Jin-shu
1977: Anthozoa; in Atlas of fossils of central and southern China, v. 2, Late Palaeozoic Era; Geological Science Research Institute, Hubei (ed.), Geological Publishing House, Beijing, p. 109-270, 764-789 (Chinese).

Jiang Shui-gen
1982: Anthozoa; in Atlas of paleontology of Hunan Province; Ministry of Geology and Minerals, Chinese People's Republic, Special Geological Publication 2, Stratigraphy and Paleontology no. 1, p. 81-162, 820-842 (Chinese).

Kong Lei and Huang Yun-ming
1978: Tetracoralla; in Atlas of the paleontology of the southwestern regions of China, Guizhou Section, v. 1, Cambrian to Devonian; Geological Science Research Institute, Hubei and other institutions (eds.), Geological Publishing House, Beijing, p. 35-161, 739-759 (Chinese).

Lang, W.D., Smith, S., and Thomas, H.D.
1940: Index of Palaeozoic coral genera; British Museum (Natural History), London, vii p.+ 231 p.

Milne Edwards, H. and Haime, J.
1850: A monograph of the British fossil corals. Part 1, Introduction and chapters I-VII; The Palaeontographical Society, London, p. i-lxxxv+ p. 1-71.

1851: Monographie des polypiers fossils des terrains paleozoiques; Archives du Muséum d'Histoire Naturelle, tome 5, v p.+ 502 p.

Mountjoy, E.W.
1968: Factors governing the development of the Frasnian, Miette and Ancient Wall reef complexes (banks and biostromes), Alberta; in International symposium on the Devonian System, Calgary, 1967, ed. D.H. Oswald; Alberta Society of Petroleum Geologists, Calgary, v. 2, p. 387-408.

Oliver, W.A., Jr.
1976: Noncystimorph colonial rugose corals of the Onesquethaw and Lower Cazenovia Stages (Lower and Middle Devonian) in New York and adjacent areas; United States Geological Survey, Professional Paper 869, v p.+ 156 p.

Oliver, W.A., Jr. and Pedder, A.E.H.
1979: Rugose corals in Devonian stratigraphical correlation; in the Devonian System, ed. M.R. House, C.T. Scrutton and M.G. Bassett; Special Papers in Palaeontology, no. 23, p. 233-248.

Orbigny, A.D.
1849: Note des polypiers fossiles; Victor Masson, Paris, 12 p.

Pedder, A.E.H.
1966: The Devonian tetracoral **Haplothecia** and new Australian phacellophyllids; The Linnean Society of New South Wales, Proceedings, v. 90, p. 181-189.

1983: New Dalejan (Early Devonian) rugose corals from the Blue Fiord Formation of southwestern Ellesmere Island, Northwest Territories; in Current Research, Part B, Geological Survey of Canada, Paper 83-1B, p. 223-236.

Pickett, J.
1967: Untersuchungen zur Familie Phillipsastreidae (Zoantharia rugosa); Senckenbergiana lethaea, Band 48, p. 1-89.

Quenstedt, F.A. von
1851-1852: Handbuch der Petrefaktenkunde; Verlag der H. Laupp'schen Buchhandlung, Tubingen, p. i-iv+ p. 1-528 (1851), 529-792 (1852).

Roemer, C.F.
1876-1883: Lethaea geognostica oder Beschreibung und Abbildung der für die Gebirgs-Formationen bezeichnenden Versteinerungen. 1. Theil. Lethaea palaeozoica; E. Schweizerbart'sche Verlagshandlung (E. Koch), Stuttgart, Atlas (1876), Textband, Erste Lieferung, 544 p. (1880), Zweite Lieferung, viii p.+ 688 p. (1883).

Roemer, F.A.
1843: Die Versteinerungen des Harzgebirges; Verlag der Hahn'schen Hofbuchhandlung, Hannover, xx p.+ 40 p.

1855: Beiträge zur geologischen Kenntnis des nordwestlichen Harzgebirges. Dritte Abtheilung; Palaeontographica, Band 5, p. i-iv+ p. 1-44, 163, 164.

Rohart, J.-C.
1982: Phillipsastraeidae (Rugosa) du Dévonien de Ferques (Boulonnais, France) 2. -**Scruttonia boloniensis** (M.E. et H., 1851). La Société Géologique du Nord, Annales, tome 101, p. 105-115.

Różkowska, M.
1953: Pachyphyllinae et **Phillipsastraea** du Frasnien de Pologne; Palaeontologia Polonica, no. 5, v p.+ 89 p.

1979: Contribution to the Frasnian tetracorals from Poland; Palaeontologia Polonica, no. 40, p. 3-56.

Sandberger, G. and Sandberger, F.
1850-1856: Die Versteinerungen des rheinischen Schichtensystems in Nassau; C.W. Kreidel's Verlag, Wiesbaden, p. 1-104, Pl. 1-13 (1850); p. 105-136, Pl. 14-18 (1852); p. 137-168, Pl. 19-23 (1853); p. 169-264, Pl. 24-39 (1854); p. i-xiv+ p. 265-564, 2 pl. (1856).

Schlotheim, E.F. Baron von
1820: Die Petrefaktenkunde auf ihrem jetzigen Standpunkte durch die Beschreibung seiner Sammlung versteinerter und fossilier Überreste des Thier- und Pflanzenreichs der Vorwelt erläutert; Becker Buchhandlung, Gotha, lxii p.+ 437 p.

Schlüter, C.
1881: Ueber einige Anthozoen des Devon; Deutsche geologische Gesellschaft, Zeitschrift, Band 33, p. 75-108.

Scrutton, C.T.
1967: Marisastridae (Rugosa) from south-east Devonshire, England; Palaeontology, v. 10, p. 266-279.

1968: Colonial Phillipsastraeidae from the Devonian of south-east Devon, England; British Museum (Natural History), Bulletin, Geology ser., v. 15, p. 181-281.

1978: Eastern south Devon; in A field guide to selected areas of the Devonian of south-west England, ed. C.T. Scrutton; The Palaeontological Association International Symposium on the Devonian System (P.A.D.S. 78), September 1978, London, p. 27-49.

Soshkina, E.D.
1951: Pozdnedevonskie korally Rugosa, ikh sistematika i evolyutsiya; Akademiya Nauk SSSR, Paleontologicheskiy Institut, Trudy, tom 34, 122 p.

1952: Opredelitel' devonskikh chetyrekhluchevykh korallov; Akademiya Nauk SSSR, Paleontologicheskiy Institut, Trudy, tom 39, 127 p.

Soshkina, E.D. and Dobrolyubova, T.A.
1962: Otryad Evenkiellida; in Osnovy paleontologii, tom 2. Gubki, arkheotsiaty, kishechnopolostnye, chervi, ed. B.S. Sokolov; Izdatel'stvo Akademii Nauk SSSR, Moskva, p. 333-339.

Spasskiy, N.Ya.
1960: Devonskie chetyrekhluchevye korally Rudnogo Altaya; Paleontologicheskoe obosnovanie stratigrafii paleozoya Rudnogo Altaya, vypusk 3, 143 p.

Sun, Y.C.
1958: The Upper Devonian coral faunas of Hunan; Palaeontologia Sinica, whole no. 144, new ser. B, no. 8, p. 1-28 (Chinese and English).

Tietze, E.
1871: Ueber die devonischen Schichten von Ebersdorf unweit Neurode in der Grafschaft Glatz, eine geognostisch-paläontologische Monographie; Palaeontographica, Band 19, p. 103-158.

Tsien, H.H.
1977: Rugosa massifs du Dévonien de la Belgique; Institut de Géologie, Université Catholique de Louvain, Mémoirs, tome 29, p. 197-229.

Weyer, D.
1971: Zwei neue Phillipsastraeidae (Anthozoa, Rugosa) aus dem Frasnium (Oberdevon) von Elbingerode und Rübeland (Harz); Deutsche Gesellschaft für geologische Wissenschaften, Berichte, Reihe A, Geologie und Paläontologie, Band 16, p. 45-51.

Yu, C.C.
1947: Some Devonian fossils from Kweilin and other localities in Kwangsi; Geological Society of China, Bulletin, v. 27, p. 123-140.

Yu Chang-min and Kuang Guo-dun
1983: Late Middle Devonian rugose corals from Liujing, Heng Xian, Guangxi and their paleoecological significance; Nanjing Institute of Geology and Palaeontology, Academia Sinica, Bulletin, no. 4, p. 241-278 (Chinese with English summary; imprint 1982).

Dioxycaris fritzi sp. nov. (Arthropoda, Phyllocarida) from the Pika Formation (Middle Cambrian, *Bolaspidella* Zone), Jasper National Park, Alberta

Project 720072

M.J. Copeland
Institute of Sedimentary and Petroleum Geology, Ottawa

Copeland, M.J., **Dioxycaris fritzi** sp. nov. (Arthropoda, Phyllocarida) from the Pika Formation (Middle Cambrian, **Bolaspidella** Zone), Jasper National Park, Alberta; in Current Research, Part A, Geological Survey of Canada, Paper 86-1A, p. 663-666, 1986.

Abstract

The carapace morphologies of the Middle Cambrian phyllocarid genera **Dioxycaris** and **Branchiocaris** are very similar. However, **Branchiocaris**, unlike **Dioxycaris**, is described from both carapace and soft body parts. Discovery of a second species of **Dioxycaris**, from the Pika Formation of western Alberta, permits additional taxonomic observations on the relationship of these genera.

Résumé

Les morphologies des carapaces des genres **Dioxycaris** et **Branchiocaris** de phyllocarides du Cambrien moyen sont très similaires. Cependant, **Branchiocaris** contrairement à **Dioxycaris** est décrit d'après sa carapace et les parties molles de son corps. La découverte d'une seconde espèce de **Dioxycaris** dans la formation de Pika, dans l'ouest de l'Alberta, a permis de faire d'autres observations taxinomiques sur la relation entre ces genres.

Introduction

Briggs (1976) presented a detailed discussion of three genera of Cambrian phyllocarids: **Protocaris** Walcott, 1883, **Branchiocaris** Briggs, 1976 and **Dioxycaris** Gurich, 1929. Two of these, **Protocaris** and **Branchiocaris,** based on soft body parts, may be contained within the Protocarididae Miller, 1889, but the third, **Dioxycaris,** is known only from the carapace and has been considered of uncertain family attribution. Based on carapace shape, **Protocaris** and **Branchiocaris** may be differentiated by the absence (**Protocaris**) or presence (**Branchiocaris**) of an oblique, pointed process on each of the cardinal extremities of the dorsal margin. **Dioxycaris,** like **Branchiocaris,** also bears these dorsal processes; thus, the two genera cannot be distinguished on carapace shape.

Systematic position

The systematic position of **Dioxycaris** is, therefore, in doubt. In 1886, Walcott described **Leperditia**? **Argenta** sp. nov. After several revisions, Gurich (1929) erected the genus **Dioxycaris** to which he assigned **D. argenta** (Walcott) as the type species. All subsequent authors have accepted this generic and specific terminology (see Briggs, 1976, p. 13). The suprageneric systematics have similarly been in doubt, depending on the taxonomic importance attributed to the fossilized hard parts versus the fossilized soft body parts. As Briggs pointed out, if **Dioxycaris** is placed in synonymy with **Branchiocaris** (based on similarity of carapace) both genera should probably be placed with other genera based on carapaces with pointed cardinal extremities, such as **Isoxys** and **Tuzoia** in the Isoxyidae Vogdes, 1893 (see also Brooks and Caster, 1956). However, if soft parts are the determining factor, **Branchiocaris** should remain with **Protocaris** in the Protocarididae. Pending another solution (i.e. the discovery of **Dioxycaris** specimens with generically distinct soft body parts) it is suggested herein that, because of the obvious similarity of the hard parts of **Branchiocaris** and **Dioxycaris, Dioxycaris** Gurich, 1929 be placed in the Protocarididae, with the possible implication that **Dioxycaris** may represent molted carapaces and **Branchiocaris** Briggs, 1976 may be a junior synonym.

Occurrences

The type species of both **Branchiocaris** and **Dioxycaris** are known only from Middle Cambrian strata, the former from the Stephen Formation (Burgess Shale, **Bathyuriscus-Elrathina** Zone) of British Columbia and the latter from the Ophir Shale (**Glossopleura** Zone) of Utah. Canadian specimens collected by C.D. Walcott and referred to the type species of **Dioxycaris** (**D. argenta** (Walcott), 1886) are contained within the United States National Museum collections (USNM 56514, 56518). They are recorded by Walcott (1908, 1912) and Briggs (1976, p. 13) from the Eldon Limestone, Mount Bosworth, British Columbia. These collections, from Walcott's locality 35g ("Eldon Limestone unit 2") are, based on lithology, now considered to be from 8 m (24 ft) above the base of the overlying Pika Formation (W.H. Fritz, personal communication, September 24, 1985).

In 1966, W.H. Fritz (GSC Report No. C8-1966-WHF) reported the occurrence of a phyllocarid (GSC loc. 72733) from a Cambrian sequence on the Chaba River, 8 km (5 mi) south of Fortress Lake, Jasper National Park (lat. 52°18'N, long. 117°47'W), Alberta. This specimen (part and counterpart), associated with the trilobite **Rowia** sp., is from 75 m (249 ft) above the base of the Pika Formation (**Bolaspidella** Zone) and is thus the youngest reported specimen of **Dioxycaris.** Its general morphology differs from that of **D. argenta** (Walcott) and it is described herein as a new species.

Systematic paleontology

Family Protocarididae Miller, 1889

Genus **Dioxycaris** Gurich, 1929

Type species. **Leperditia Argenta** Walcott, 1886.

Dioxycaris fritzi sp. nov.

Plate 79.1, figures 1-4

Description. Dioxycarid species with long, straight dorsal fold or hinge developed anteriorly and posteriorly into small processes. Curved anterior and posterior margins meet the line of the dorsum at about 110°. Suboval in outline, expanding posteriorly. Upper (right) portion (valve?) of the carapace does not appear to have marginal border although along anterior margin upper surface is broken, revealing lower part of the carapace with its anterior process. Large, scale-shaped area is slightly raised above general surface of specimen. Scale-shaped area extends, at mid-height of specimen, from 7 to 25 mm posterior of the anterior margin, and about 12 mm dorso-ventrally. This hemi-ovoid attachment or muscle area is relatively straight and oblique anteriorly. Surface of the carapace finely and somewhat linearly reticulate, with reticulae being somewhat rhomboidal in outline; that of the attachment area more coarsely so. Numerous, small, pore-like holes occur on surface of specimen; these are most numerous on area of attachment and just anterior of mid-length near the dorsum. Ventral part of the specimen bears compression wrinkles at 30° to 45° to the line of the dorsum.

Greatest length (near mid-height) 72 mm; greatest height (in the posterior third) 28 mm; length of dorsum and processes 67 mm.

Occurrence. GSC locality 72733, Chaba River, 8 km south of Fortress Lake, Jasper National Park, Alberta, lat. 52°18'N, long. 117°47'W, 75 m above the base of the Pika Formation, Middle Cambrian **Bolaspidella** Zone.

Type. Holotype, GSC 80999a, b (part and counterpart).

Remarks. The species is somewhat larger than the type species, being 72 mm at greatest length and 28 mm at greatest height vertical to the hinge (H/L=0.388). **D. argenta** is reported by Briggs (1976, p. 14) as 56 mm long and 30.4 mm high (H/L=0.542). Briggs chose to orient **D. argenta** with the less tapered end as anterior, but it is evident that in **D. fritzi** the attachment or muscle area in the tapering end of the specimen is anterior.

Briggs (1976, p. 13, 14) also pointed out the presence of pits on **D. argenta** and suggested that "These may be the result of nucleation caused by decaying organic matter...". These large pits are in the tapering end of **D. argenta** in the same area as the attachment or muscle area of **D. fritzi** that is here considered anterior. Brooks and Caster (1956) assumed the shell material of **D. argenta** to be chitinous, but no chemical analysis of the specimen has been made. A small piece (1.0 mm x 0.75 mm) of shell material was removed from the dorsal area of **D. fritzi,** and, after scanning electron microscope identification and X-ray powder defraction analysis was proved to be iron rich chlorite (possibly chamosite).

Walcott's original placement of **D. argenta** in the Leperditiidae may be disputed on several grounds: 1. The carapace material of **D. fritzi** was flexible (hence the ventral compression wrinkles). If it were a molted leperditiid carapace the shell material would have been rigid. A trilobite pygidium over which the phyllopod carapace is draped and other pygidia on the same slab (Plate 79.1, figure 4) are neither compressed nor fractured. They, like leperditiids, bore a hard exoskeleton (except possibly immediately after molting) and when subjected to pressure

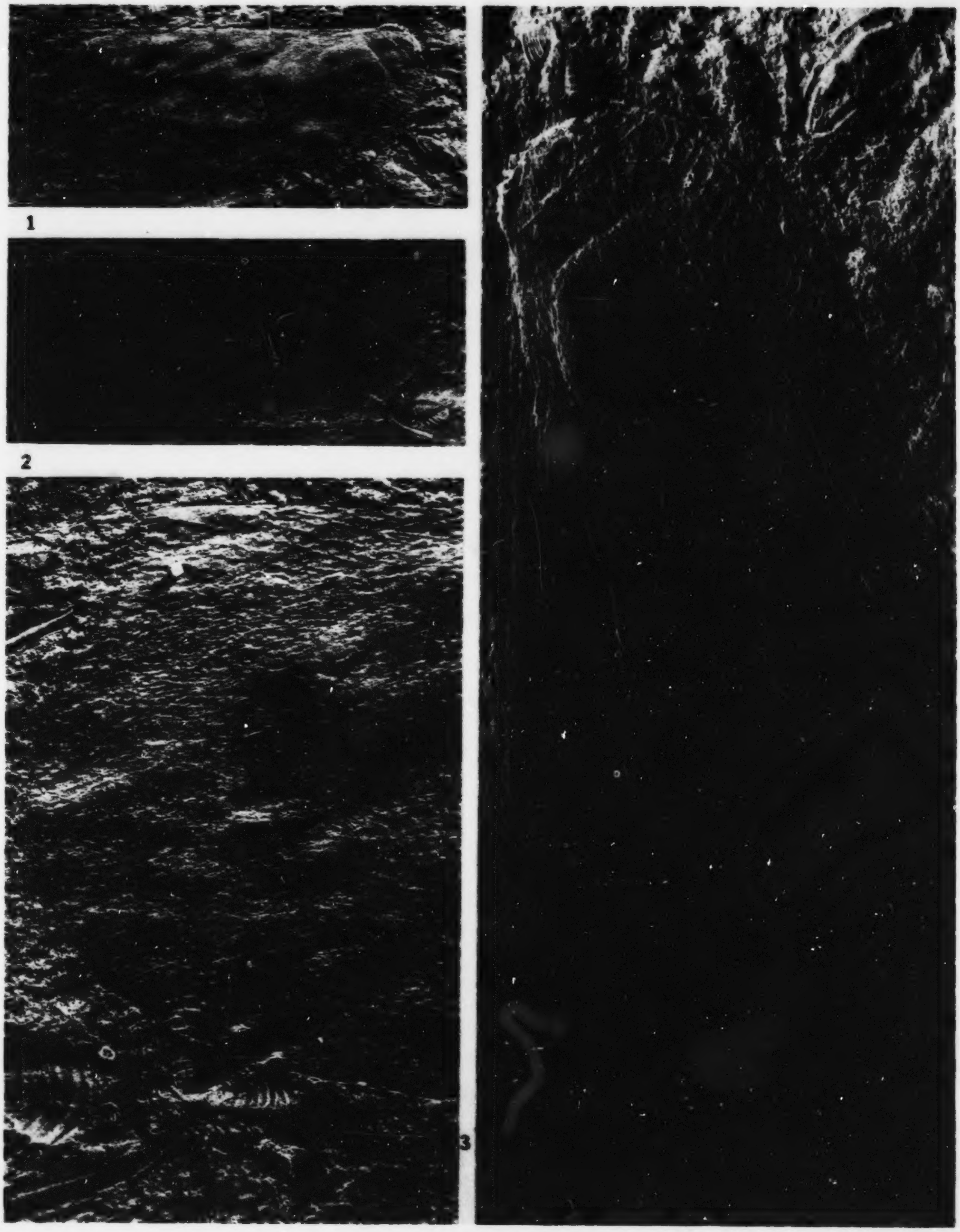

PLATE 79.1

Figures 1-4. **Dioxycaris fritzi** sp. nov.
1, 4. Lateral view of right side of carapace; x1 and x3; holotype; GSC 80999a.
2. Counterpart; x1; holotype; GSC 80999b.
3. Posterior end of right side of carapace showing posterior process; x4; holotype; GSC 80999a.

are usually observed in broken condition. 2. The attachment (muscle?) area of **D. fritzi** is extremely large even for the largest Devonian leperditiids. There is no apparent differentiation of the area into discrete scars, and the apparently linearly reticulate appearance of the shell surface may be ornamentation rather than reflection of inner adductorial scars. 3. The proportions of the shell of **D. fritzi** (H/L=0.388) are not leperditiid-like. They reflect a long bodied, phyllocarid-like arthropod, probably with exsert posterior segments, rather than a more compact ostracode body that was completely enclosed.

References

Briggs, D.E.G.

1976: The arthropod **Branchiocaris** n. gen., Middle Cambrian, Burgess Shale, British Columbia; Geological Survey of Canada, Bulletin 264, 29 p.

Brooks, H.K. and Caster, K.E.

1956: **Pseudoarctolepis sharpi** n. gen., n. sp. (Phyllocarida) from the Wheeler Shale (Middle Cambrian) of Utah; Journal of Paleontology, v. 30, no. 1, p. 9-14.

Fritz, W.H.

1966: Report on late Middle Cambrian and early Upper Cambrian fossils from the Chaba River section, 5 miles S. of Fortress Lake, Jasper National Park, Alta., Lat. 52°18' and Long. 117°47'; Geological Survey of Canada, Fossil Report, Palaeontology Section, Ottawa, May 18, 1966.

Gurich, G.

1929: Silesicaris von Leipe und die Phyllokariden uberhaupt; Mitteilungen aus dem Mineralogisch-Geologischen Staatsinstitut in Hamburg, Heft XI, p. 21-90.

Walcott, C.D.

1886: Second contribution to the studies on the Cambrian faunas of North America; Bulletin of the United States Geological Survey No. 30, 369 p.

1908: Cambrian sections of the Cordilleran area; in Cambrian geology and paleontology, 2; Smithsonian Miscellaneous Collections, [illegible]3, no. 5, p. 167-230.

1912: Cambrian Brachiopoda; United States Geological Survey, Monograph, v. 51, 872 p.

High grade metamorphic rocks of northwestern Melville Peninsula, District of Franklin

Project 840013

Mikkel Schau and M. Beckett
Precambrian Geology Division

Schau, M. and Beckett, M., High grade metamorphic rocks of northwestern Melville Peninsula, District of Franklin; in Current Research, Part A, Geological Survey of Canada, Paper 86-1A, p. 667-674, 1986.

Abstract

High grade metamorphic rocks are exposed in the Encampment Bay area. Preliminary results indicate that a tonalitic-granodioritic plutonic suite was intruded by granite and mafic dykes and later unconformably(?) overlain by sediments correlated with the 2.9 Ga Prince Albert Group. Shallow dipping slabs of dry basement and wet supracrustals were tectonically stacked and transported to deep levels within the crust where they were metamorphosed and partially melted under granulite and upper amphibolite conditions, probably during late Archean time. They were then uplifted possibly along the previous shallow dipping discontinuities. Northwest trending mafic dykes cut the rising mass and were metamorphosed to varying amphibolite facies grades probably conjointly with emplacement of a late pegmatite swarm in early Proterozoic time. Steep, east-west faults of Proterozoic age cut the region and late Proterozoic clastic sediments were deposited onto the basement after which faults, reactivated and new, cut the area. The region was peneplaned by early Ordovician time before the mid-Devonian uplift of the Melville Peninsula horst.

Résumé

Des roches fortement métamorphiques affleurent dans la région de la baie Encampment. Des résultats préliminaires indiquent qu'une série plutonique de tonalite et de granodiorite a été pénétrée par un granite et par des dykes mafiques et recouverte plus tard, en discordance (?) par des sédiments corrélés au groupe de Prince-Albert de 2,9 Ga. Des plaques de socle sec à faible pendage, et des roches supracrustales humides ont été empilées tectoniquement et transportées en profondeur dans la croûte, où elles ont été métamorphisées et partiellement fondues dans des conditions de granulites et d'amphibolites supérieures, probablement à la fin de l'Archéen. Ces plaques auraient été ensuite soulevées suivant les anciennes discordances à faible pendage. Des dykes mafiques de direction nord-ouest coupent le massif ascendant et ont été métamorphisés en divers faciès d'amphibolite, probablement au cours de la mise en place d'une nuée de pegmatite tardive au début du Protérozoïque. Des failles abruptes de direction est-ouest, du Protérozoïque, traversent la région; des sédiments clastiques du Protérozoïque supérieur se sont déposés sur le socle, après quoi des failles tant réactivées que nouvelles ont traversé la région. Cette dernière a été pénéplanée au début de l'Ordovicien avant le soulèvement du môle de la presqu'île de Melville au milieu du Dévonien.

Introduction

Mapping in the Encampment Bay map area (47C) in the 1985 season focused on problems in high grade terranes outlined in 1984 (Schau and Ashton, 1985) and extended to areas to the south and northwest (Fig. 80.1) but was limited by paucity of landing spots for a wheeled Twin Otter. Mapping was by foot traverse originating from main camps and backpack sites. A helicopter was available for two days in late June. The region is close to the magnetic north pole and sun compasses were used when possible. Brunton compasses were calibrated against true north daily to provide a means of measuring orientations during cloudy periods. Daily drift in magnetic declination was usually only a few degrees but on July 22, 1985 the azimuth of the magnetic pole, at one location, varied from 75°W to 41°W during the day.

The map area contains many glacial features which in part obscure the bedrock geology. Amphibolite grade rocks occur at higher elevations but are largely covered by felsenmeer, till, and other glacial debris. Granulites occur at lower elevations and are better exposed and present a more rugged topography since dykes, joints, and minor fractures have been preferentially excavated whereas granite, more easily eroded, forms lowlands.

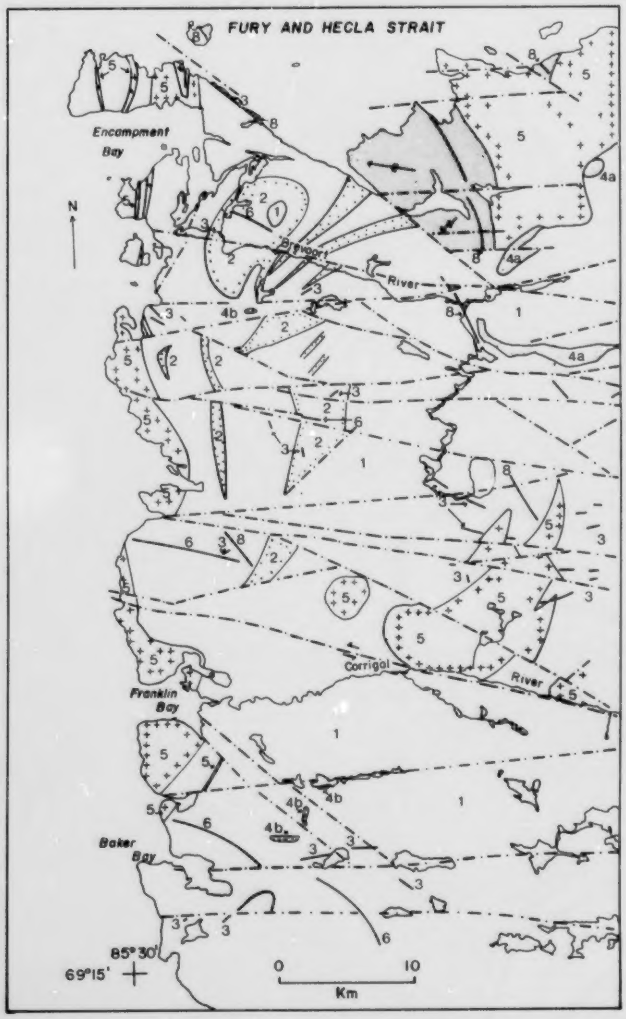

Figure 80.1. Geological sketch map of parts of NTS 47C.

The area is within the barren lands and there is only a sparse vegetational cover. Large lakes were ice covered until mid-July. Pack ice stayed in Committee Bay throughout the field season. Inclement weather in June was followed by good weather in July but extensive sweeping fog banks covered the area in August.

Description of lithological units

Tonalite-granodiorite orthogneiss suite (unit 1)

Unit 1, which underlies most of the area, consists of high grade orthogneisses formed from tonalitic to granodioritic intrusive rocks. Granulite grade orthogneiss comprises beige to olive weathering, grey to greenish blue coloured, quartzofeldspathic rocks with biotite, small amounts of orthopyroxene, and variable amounts of hornblende and/or clinopyroxene. The predominant rock is fine grained, foliated and lineated and is composed of quartz, feldspar, biotite, hornblende, pyroxenes and opaques. Textural variants include a "coarse-grained" type, in which centimetre-sized feldspar shapes are now composed of polygonitized feldspars and hornblende is more abundant than biotite; a streaky type, in which the relict fabric is medium grained and biotite is approximately equal to hornblende; a fine grained biotite variety in which a few relict feldspars persist giving a local seriate fabric; and a quartzose type in which the quartz is abundant and biotite is not. The granulites are generally homogeneous, but layered varieties with biotite-rich layers on the order of a centimetre in thickness, interlayered with leucocratic layers, do occur locally. In a few outcrops the typical fine grained gneiss has been intruded by the coarse type.

Similar rock types are encountered at amphibolite grade; these lack orthopyroxene, are grey in colour, and weather white or pink to red. Two localities at amphibolite grade studied in detail (Prevec, 1985) were found to be largely of granodioritic composition with hornblende, biotite, and opaques varying from 17 to 39 per cent and quartz ranging between 18 and 34 per cent. The alkali feldspar varies between 3 and 17 per cent and is largely untwinned perthitic orthoclase although most thin sections have small amounts of grid twinned potash feldspar as well. The plagioclase is calcic oligoclase to andesine. These variations are representative and although rocks poor in alkali feldspar are known, the relative proportions of each type await the completion of mapping.

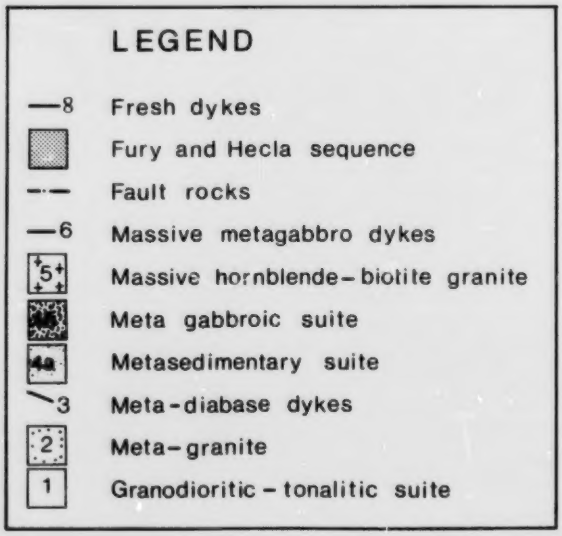

Foliations are generally shallow dipping and cast into local folds. At Baker Bay, for example, the foliation is folded into a broad open fold about a shallow northwest plunging axis. For other examples see Schau and Ashton, 1985. Only in localities such as south of Baker Bay where unit 3 dykes occur as passive markers can the foliation be shown to be axial planar to a previous relatively tight fold set. At Baker Bay early lineations are dispersed about a later shallow, northwest plunging lineation which is probably associated with the fold axis of a fold that affects the foliation. Lineations are not everywhere equally developed and several periods of lineation development are possible, but not proven, throughout the mapped region. Locally, poorly defined layers and aggregates of mafic minerals are tightly folded about horizontal axial planes defined by mafic clots and flattened quartz. Two poorly defined sets of sub-horizontal foliations that intersect at small angles were noted in several localities. One outcrop mapped in detail as typical of unit 1 near Baker Bay shows many minor structures and variable leucosome development. North of Corrigal River contacts between coarse- and fine-grained types in the form of planar 0.5 to 5.0 m thick alternating lithologies are transitional over a few tens of metres suggesting tectonic interleaving of the two units. Although foliations are generally subparallel, in a number of localities layering or gneissosity is intersected by a later foliation. If this foliation is associated with a fold set, then, since the layering is either steeper or shallower than the shallow to moderately dipping foliation it follows that some layers are overturned. On the other hand some layers are leucosome formed during deformation so they need not show a relative position of a fold limb (Fig. 80.2). On the whole the minor structures and the layering relations do suggest that, as yet unmapped, large, tight, overturned folds are present in the rocks of unit 1.

High grade metamorphism has affected the rocks of unit 1 as shown by regional development of orthopyroxene, over an area 10 to 20 km wide and in excess of 80 km long (Fig. 80.3). As detailed petrology is required before the reactions by which the orthopyroxenes formed can be identified the region shown as orthopyroxene zone is not bounded by isograds. To the west, near the Committee Bay coast amphibolite grade orthogneisses and migmatites grade eastward into granulite grade rocks. Figure 80.4 shows migmatite from this area. Near Brevoort Lake and Grinnel Lake amphibolite grade rocks predominate, although small patches of pyroxene-bearing orthogneisses occur locally. The age of this suite is unknown but they are considered the oldest rocks in the area.

Lineated granite (unit 2)

Unit 2 is a metagranite suite which occurs in stocks, sheets, and dykes of unit 2 cutting the granulite grade country rock in the western part of the region. Large bodies are slightly less resistant to erosion than the granulite host. The sheets have a shallow dip and are interleaved with the host in an intricate manner. Some of the smaller sheets have been omitted from Figure 80.1 for clarity.

Unit 2 consists of orange to pink weathering, pink to white, coarse to medium textured granite with characteristic flattened or lineated smoky quartz and polygonitized to sugary feldspar growth pseudomorphing coarse feldspar shapes. The colour index is about 5, mafic minerals consist of biotite and an opaque, generally magnetite. A thin section of the rock is seen to be a perthite rich granite with a trace of biotite partly altered to chlorite and a trace of magnetite. Variants include polygonitized, almost completely recrystallized and finer grained types. At contacts with unit 1 small granite dykes are particularly abundant , locally generating injection type gneisses, although local passive dykes and narrow gradational contact zones are found at contacts of many of the sills.

Foliation and local lineation in the metagranite is shown by quartz plates accentuated by small, irregularly oriented biotite flakes that cluster near the quartz. In less

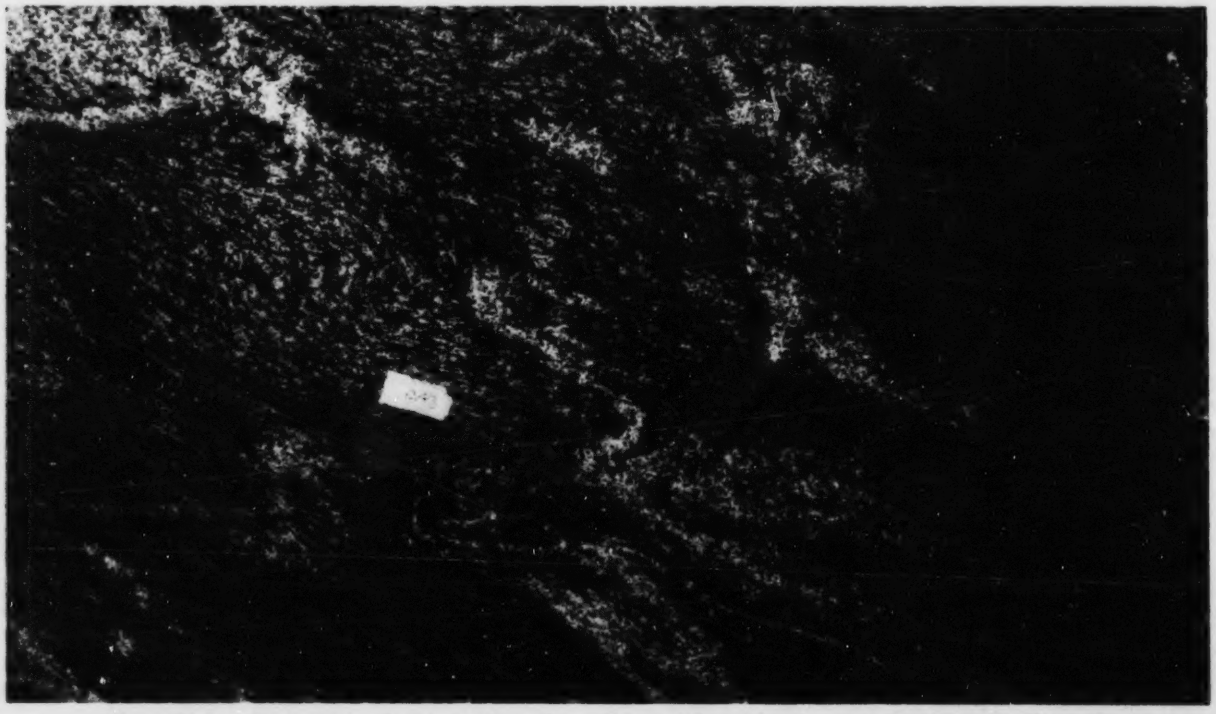

Figure 80.2. Photograph of unit 1 migmatite. Shows deformed unit 1 and development of unit 5 granite along axial plane. Tape is two cm across.

severely deformed rocks, in sections normal to foliation and the direction of lineation of the quartz grains, two intersecting foliations are distinguishable, and at two localities, relict feldspars show that they have been rotated in a dextral sense. These structures, although not common enough to characterize the deformation do indicate that shear was instrumental in producing the fabric. Thus, since grain size is demonstrably reduced by shear much of this unit can be considered as protomylonitic. The foliations so produced are generally shallow dipping and locally folded.

The mineral assemblage quartz, alkali feldspar, biotite, opaque with rare garnet and/or orthopyroxene is stable at high grades under moderately dry conditions. Dykes of unit 3 cut unit 2 and since unit 3 is locally metamorphosed to granulite grade the granite is likewise interpreted to have been affected by granulite metamorphism even though, as yet, only a few grains of orthopyroxene have been identified from the granite. The age of the granite is pre-unit 3, 5, and 6 and post-unit 1 and correlatives are not currently known.

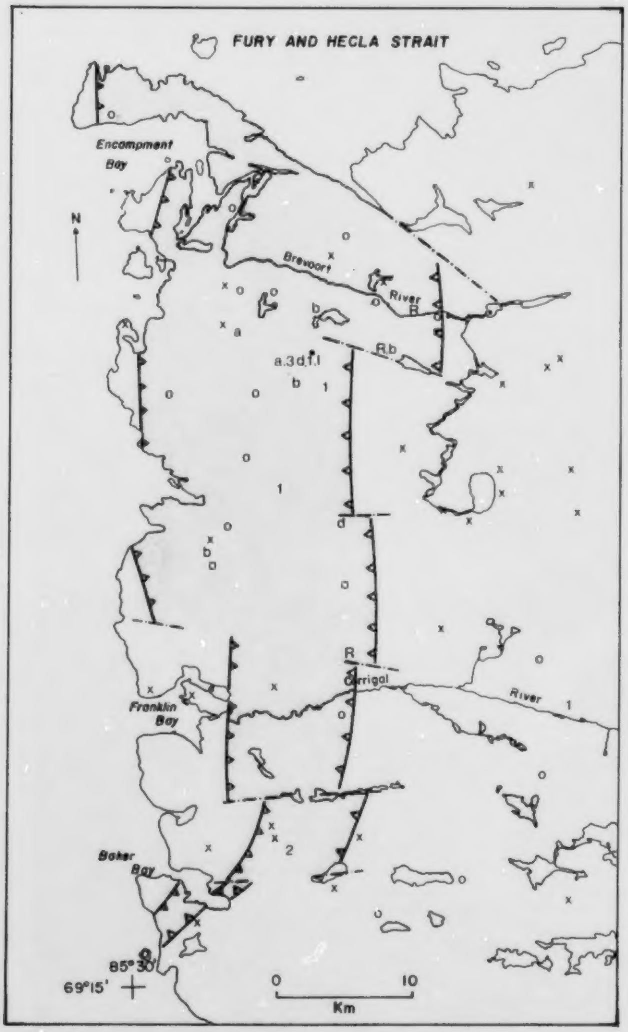

Figure 80.3. Sketch map of distribution of orthopyroxene zone. Note thin section distribution and assemblages reported therefrom. Letters and numbers correspond to those in Figure 30.5.

Lineated metabasic dykes (unit 3)

Foliated, lineated metadiabase dykes are well exposed in the cleared area southeast of the lake at the head of Brevoort River and are found in unit 1, and less abundantly in unit 2, throughout the area.

The dykes are 10 cm to 30 m wide and extend along strike for up to 6 km, but poor exposure and tectonic disruption combine to make most mapped dyke segments short.

In the amphibolite grade terrane the dykes are dark weathering, dark, fine- to medium-grained and consist of lineated hornblende and minor plagioclase whereas in the granulite terrane they are brown weathering, medium grained and contain pyroxenes and biotite as well as leucosome pods. Thinner dykes are fine grained and occur as satellites to nearby thicker medium grained dykes. The latter generally contain fist sized medium- to coarse-grained, feldspar-rich, pyroxene- and hornblende-bearing leucosomes. In the amphibolite grade region, the dykes are folded into upright, open, moderately northeast plunging structures with an internal lineation defined by elongate hornblendes. Dykes from the hypersthene zone lie along or at small angles to the foliation; at Baker Bay a large fold nose is fortuitously exposed and serves as an important marker in the sequence of geologic events. The fold is tight, has a steep plunge to the north-northeast and a moderately northwest dipping axial plane.

Dykes from the west consist of hornblende, orthopyroxene, clinopyroxene, plagioclase, quartz, biotite, and opaques which is consistent with granulite grade. In contrast, dykes from amphibolite grade country rocks are lineated, medium grained and contain sweats which, on the basis of one thin section consist of hornblende, clinopyroxene, plagioclase, quartz, biotite, opaque, and alkali feldspar, an assemblage consistent with the amphibolite grade of the country rock. We conclude that the dykes were emplaced prior to the high grade metamorphism that has affected the region.

The dykes cut units 1 and 2 and are cut by unit 5. The contact relations between units 3 and 4 have not been seen. There are three sets of deformed Archean dykes exposed to the southeast (GSC Open File 1046); the correlation of unit 3 with one of these three sets may be possible with further knowledge of field relationships and geochronological results.

LEGEND

Field data

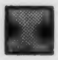 orthopyroxene zone

Thinsection data

l,1,2,3,a,b,d diagnostic assemblages see figure 5

o orthopyroxene bearing locality

x amphibolite grade assemblage

R retrograded opx? present in thinsection

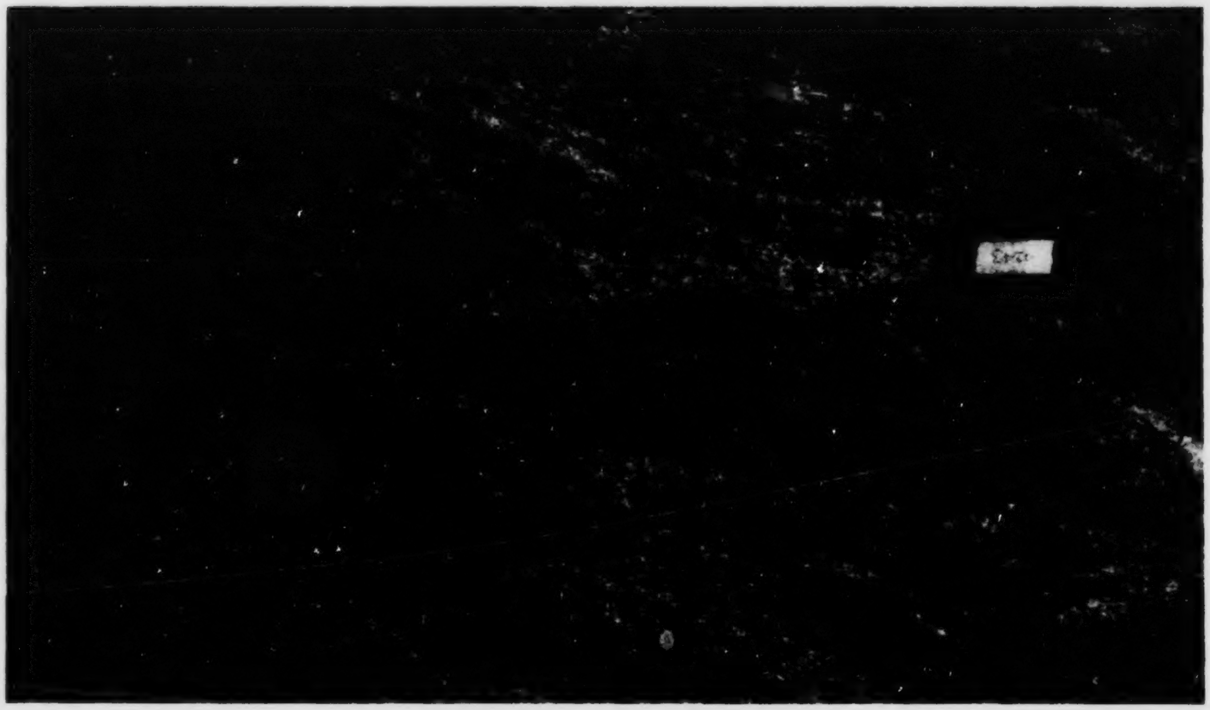

Figure 80.4. *Photograph of unit 5 migmatite. Shows fragment of unit 1 set in massive unit 5 granite. Photos (Fig. 80.2 and 80.4) were taken a few metres from each other.*

Metasedimentary suite (unit 4)

Small areas in the northern part of the map area are underlain by metasedimentary gneiss. Resistant units such as metaquartzite characteristically form hills whereas units such as sillimanite schist are recessive.

Rock types of the suite include gneiss, amphibolite, quartzites, sillimanite schist, and metapyroxenite. Hornblende- and biotite-bearing quartzofeldspathic gneisses grade into biotite-bearing quartzofeldspathic gneisses. The amphibolites are thin layers composed of hornblende and plagioclase and are locally garnetiferous. The quartzites are generally white but are locally red or green. They contain scattered muscovite and locally, chromiferous muscovite. They are fine- to medium-grained with abundant quartz veins and thin interbeds of mica- and sillimanite-bearing layers. Near the base, thin layers of strongly foliated quartzite pebble conglomerate and biotite, muscovite, and feldspar-bearing quartzite are interbedded with relatively pure quartzite and sillimanite schist. The schists generally contain muscovite, biotite, sillimanite and on occasion garnet and/or cordierite. Metre thick metapyroxenite dykes cut quartzites.

The unit outcrops in a crude U-shape, with the open end pointing to the east. In general, the foliations are shallow dipping and lineations have shallow plunges. The relationships of unit 4 with structurally underlying units is locally gradational, although pods of massive unit 5 granite occur throughout the contact region complicating relationships. The metasediments in contact with unit 1 are aluminous and grade into unit 1 with decreasing sillimanite and increasing hornblende contents. Nowhere is an intrusive relationship recognized between units 1 and 4. Instead we postulate that the aluminous metasediments are pelites and that the gradational part constitutes a metaregolith formed over an unconformity between units 1 and 4.

The metamorphic grade of the metasediment is upper amphibolite based on the coexistence of garnet and hornblende in the amphibolites and quartz and muscovite in the schist. An occurrence of garnet, cordierite, biotite, sillimanite schist suggests that metamorphic conditions were near highest amphibolite grade (cf. Froese, 1978). Metasedimentary rocks of unit 4 sit unconformably(?) on granodiorite of unit 1 and are cut by granite of unit 5. The association of chromiferous quartzites and iron rich (= garnetiferous) sediments is similar in lithology to the Prince Albert Group as described in adjacent areas (Frisch, 1982; Schau, 1977). We postulate that unit 4 can be correlated with the 2.9 Ga old Prince Albert Group.

Anorthositic metagabbro

Metamorphosed, small, layered sills of anorthositic gabbro are emplaced in the foliation of unit 1 northeast of Baker Bay. The metamorphism is characterized by grossularite, plagioclase and hornblende. These sills are not foliated although their layering is subparallel to the foliation. They are correlated with metagabbroic bodies of Archean age to the southeast (GSC Open File 1046). Metagabbroic stocks are irregularly distributed in the region and have been assigned to this unit.

Massive hornblende-biotite granite (unit 5)

Irregular stocks of fresh granite and dykes of pegmatite and aplite occur in areas underlain by amphibolite grade country rock. A large body underlies the north-central portion of the map area, smaller sheets are found along the west coast, and the small stock, outlined in 1984, is found in the central part of the map area. The granite is pink weathering, white to grey, medium grained, massive hornblende biotite granite. The aplites are pink and white

with only a small amount of biotite. A large proportion of the area marked unit 1, especially the region at amphibolite grade, contains about 15 per cent leucosome fraction of granite veins or pods. Gneissic rocks occur locally where sheets of granite intrude lit-par-lit fashion into tonalite gneiss of unit 1. Elsewhere, decimetre long, massive, unconnected pods of granite are set in tonalite and granodiorite. The composition of this leucosome is similar to larger bodies of granite. Migmatite with small blocks of unit 1 set in granite are locally well developed. Figure 80.4 is an example of this type. A working hypothesis is that the granite is the result of partial melting of tonalite granodiorite suite and, locally, of unit 2 granite, which occurred at deeper levels and possibly at presently exposed structural levels. Perhaps partial melting and the high grade metamorphism are coeval and/or cogenetic. The location of granite bodies in the amphibolite grade part of unit 1 may indicate the extent of higher partial pressures of water in the amphibolite grade rocks.

The granite cuts units 1, 2, 3, and 4 and is cut by fresh dykes and faults. The granite was exposed to erosion by time of deposition of Fury and Hecla sequence. Although the age of the granite is uncertain, and massive granites of both early to middle Proterozoic and late Archean age occur on Melville Peninsula to the south (GSC Open File 1046), a working hypothesis is that the granite and the high grade metamorphism are coeval and part of the Archean metamorphic event that affected the Prince Albert Group elsewhere on the peninsula.

Massive metagabbro dykes (unit 6)

West-trending, steeply dipping dykes of black weathering, fine- to medium-grained metagabbro cut granulite terrane. The dykes are less resistant to erosion than the country rock and are poorly exposed at edges of canyons or as small knobs on the canyon floor. Nevertheless they have been followed for many tens of kilometres along strike in several locations.

The dykes are hornblende-plagioclase rocks with white plagioclase phenocrysts locally rimmed by garnet suggesting that the dykes are metamorphosed. In thin section the rock is seen to be composed of hornblende, plagioclase, and opaques widely replaced by actinolite, chlorite, albite, and clinozoisite.

The dykes are cast into mesoscopic folds with shallow northwest plunges. The age and assignment of the dykes is not known. Other dyke swarms of similar appearance to the south on Melville Peninsula are Proterozoic in age.

Pegmatites (not on map)

Biotite bearing pegmatites cut unit 6. There are several sets of pegmatite which may be of differing ages, some containing hornblende others allanite?.

Fault rocks

Late faults are marked by linear zones of intensely altered rocks. The alteration is commonly quartz and hematite impregnation but epidosites are also common. Rusty patches are found as well. Where rare fabrics were observed, slickensides are nearly horizontal. The faults contain disrupted veins and have several episodes of movement and hence the fault rocks were probably formed at different times after the metamorphism. The east west faults and included fault rocks are part of a peninsula wide fault set of middle Proterozoic age (GSC Open File 1046).

Fury and Hecla sequence

Within the map area, this sequence outcrops along the south shore of Fury and Hecla Strait. A wedge mapped this year underlies 35 km^2 and is bounded to the west by a northwest striking, steeply dipping fault, to the south by an east-striking fault and to the east by an unconformity.

The sequence is 5 km thick as estimated from map pattern and measured dips. It consists of thick sequences of bedded quartzites and thinner interbeds of red siltstones.

Sedimentary structures include crossbeds which indicate current travelled from east to west and only rarely from south to north. Diagenetic discoloration have added fine purple patterns to the essentially white to tan quartzites. These patterns suggest massive water flow through the sediments probably precipitating newly oxidized iron hydroxides. The discoloration and local hematite veins indicate that oxidizing solutions which can transport uranium were active in this area during late Proterozoic time. Anomalous concentrations of uranium have been associated with this unit north of the strait (Chandler et al., 1980).

Secondary structures include fracture cleavage parallel to steep east-west faults that are apparently north side down. Two open synclines, a northern one with a shallow northwest plunge and a southern one with a southwest plunge also affect the sequence. The age of the sequence is late Proterozoic.

Fresh diabase dykes and sills (unit 8)

Brown weathering, black to greenish brown, very fine- to medium-grained diabase dykes with steep dips, a northwesterly trend, and widths of 5 cm to 45 m cut all units. The dykes are more resistant to weathering than the country rock but are more poorly exposed in the felsenmeer-covered amphibolite grade country rock. Linear magnetic anomalies (taken from GSC Geophysical Map Series 8304g) with similar trends and marked by diabase boulder trains probably indicate additional diabase dykes to those located in outcrop.

Although the dykes are linear on a map scale, in detail the contacts are irregular and metre-long blocks of country rock have been spalled from the walls of the dykes. The thinner dykes have irregular and angular shapes. At one locality an east-west trending steeply dipping fault offsets a fresh dyke with an apparent dextral offset of a few metres. The question of whether the fresh dykes belong to either of the major late Proterozoic northwest trending dyke swarms (i.e. the Franklin or Mackenzie sets), must await further work.

Sills in the Fury and Hecla sequence are up to 50 m thick and extend along strike for tens of kilometres. The sills are medium grained olivine-bearing gabbro, which locally along strike has been affected by deuteric alteration. The sills have been affected by some east-west faults. The age of the sills may be similar to the dykes.

Later events

Although no direct evidence of later depositional events is preserved in the region it is known that faulting affected the clastic rocks and the mafic dykes and sills. The region was then apparently peneplaned by early Ordovician time (Sanford, 1977). The uplift of Melville Peninsula in mid-Devonian time is the last structural event, save the isostatic adjustments to Pleistocene ice sheets.

Economic minerals

No interesting showings were located this year. Grab samples of rusty material with sulphides collected in previous seasons were assayed for Au, Ag, and As and returned values

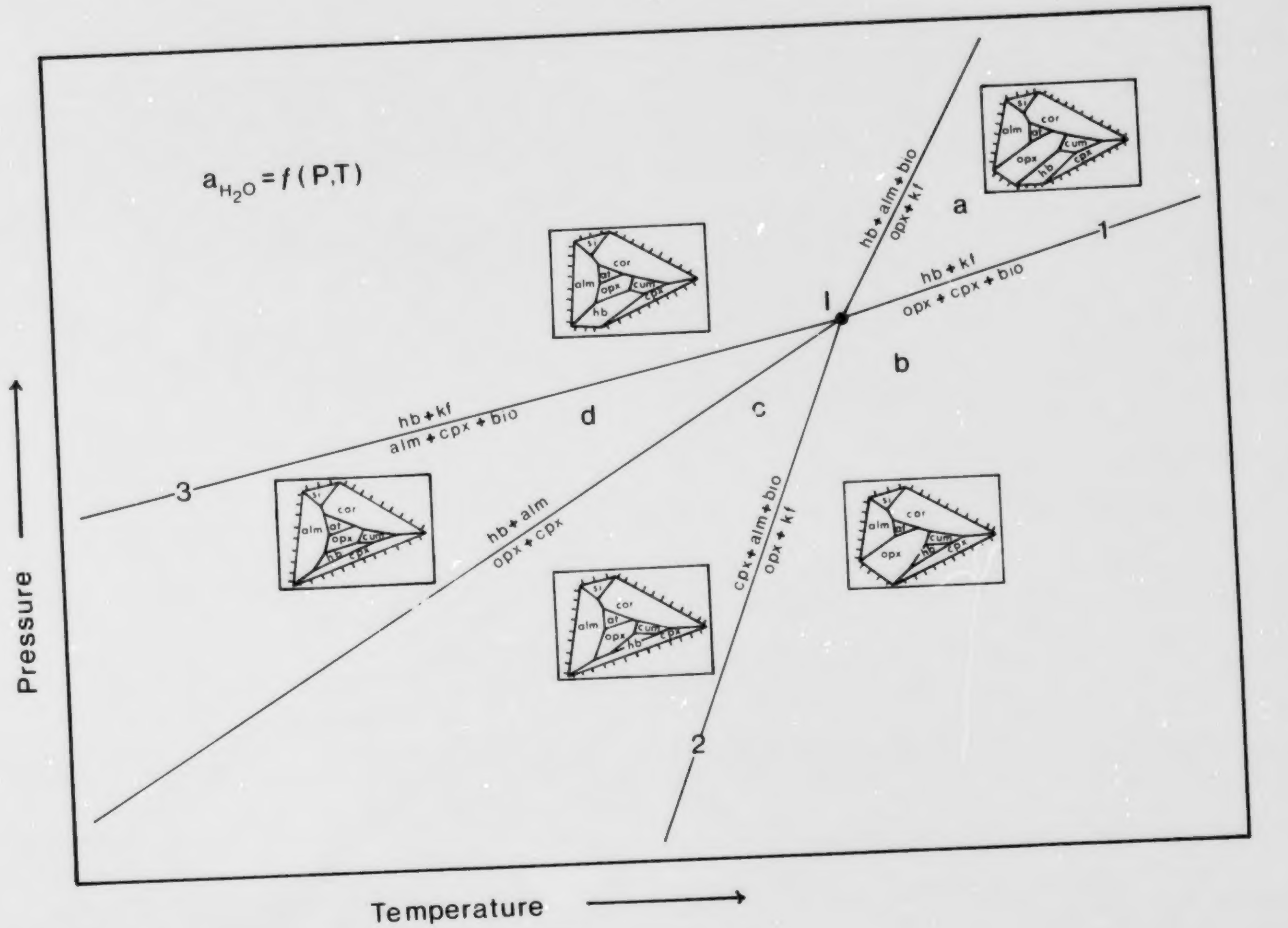

LEGEND

Abbreviations

si sillimanite
cor cordierite
alm almandine
at anthophyllite
cum cummingtonite
hb hornblende
opx orthopyroxene
cpx clinopyroxene
bio biotite
kf K feldspar

I invariant point
tie lines to K feldspar
1,2,3 univariant reactions
a,b,c,d divariant fields

Figure 80.5. Sketch showing granulite invariant point taken from Froese and Sen (1979). Numbers and letters correspond to those used on Figure 80.3. The compatible assemblages are shown on the biotite surface (Froese, 1978).

at or near detection limit. Although granites contain radioactive accessories no concentrations nor complex pegmatites were located.

Special problems

Metamorphosed fault zones by virtue of their strained nature and reduced grain size are recrystallized and hence difficult to identify in high grade metamorphic terranes. At one locality near Brevoort River a narrow shear zone is seen to have formed along a pegmatite dyke cutting unit 2 granite. Evidence that the zone is a fault zone is shown by relict amazonite crystals which have been rotated and reduced in size, z-shaped folds, and rare doubly plunging folds (sheath folds?) which only occur along the length of this 50 m by 0.5 m zone. The zone consists of quartzofeldspathic fine grained matrix interlayered with fine grained garnet-rich layers whereas the country rock is typical unit 2 granite. A longer zone, some 30 km long, and which traverses the deformed rocks of unit 1 being deflected only by the latest faults, is similarly composed of garnet, quartz, feldspar with local development of biotite and sillimanite. A third occurrence thought to be a fault zone is an aplite. In the Baker Bay area a thin unit of leucocratic, very fine grained granite can be traced across the area. The zone is subparallel to the foliation and is affected by the latest open

northwest plunging fold but not by the earlier northeast plunging folding. Locally near the edge of the aplite the country rock becomes more foliated and biotitic. Country rock on either side is unit 1 so offset is difficult to demonstrate. We believe this unit to be a shallow dipping fault possibly active in the later stages of the metamorphism and that the recrystallization took place when unit 6 was metamorphosed.

Another problem to be addressed is the extent of large fold structures. There is local evidence of folding on a sizable scale from minor structures and outcrop patterns from units 1 to 4 inclusive. The sparsity of marker horizons and the nature of the folded material (essentially homogeneous irregular masses of quartzofeldspathic rock) combined with the high grade of metamorphism which has partially melted or recystallized the rocks so as to remove the evidence, militate against proper definition of the folds. Nevertheless the possibility that slabs of basement and infolds of supracrustal units have been stacked in such a manner that the supracrustals have been lowered some five times their original thickness into the crust seems likely.

Schau and Ashton (1985) posed the question of whether granulites developed in unit 1 are "higher" grade than the surrounding amphibolite. The extent of the orthopyroxene zone as determined in the field is shown on Figure 80.3. Also shown are some locations of different mineral assemblages. These are keyed to the excerpt from Froese and Sen (1979) P-T diagram derived for biotite bearing mafic granulites (Fig 80.5). On the map the metamorphic conditions as deduced from the P-T diagram are not regular. Explanations for this irregularity include structural modification subsequent to peak metamorphism, variable extent of back reactions so that different quenching assemblages are preserved, or variable activity of water during metamorphism. There is local evidence supporting all three hypotheses, however the argument for the latter hypothesis is amplified below. Powell (1983) proposed phase relations for a model metabasic rock under high grade conditions. Powell (ibid.) shows the mineralogical evolution of a garnet, plagioclase, hornblende, and quartz assemblage under external buffering of water activity and contrasts it with the evolution of a similar assemblage under internal buffering. The sporadic occurrence of orthopyroxene with hornblende in the partial melts that constitute unit 5 supports the model of internal buffering of water activity. The occasional leucosome in which clinopyroxene is well developed would support externally imposed water activity. The relative importance of each of the processes is not known since the required mineral assemblages are not known to be widely distributed. Perhaps a competing reaction is more important. Percival (1983) suggested that biotite and hornblende react to form orthopyroxene, clinopyroxene, potash feldspar, and water. This assemblage is sporadically present and may have fixed the water activity instead of the Powell reactions. We conclude that water activity probably varied irregularly during metamorphism but that the processes responsible are not yet identified.

The proposal that hornblende bearing granite results from partial melting of crustal, albeit plutonic materials, recieves theoretical support from Powell (1985), and is analogous to that made by Kenah and Hollister (1983), as their explanation for high grade rocks in northwestern British Columbia.

Future work will focus on determining large scale structures and relating them to regions of higher and lower water activity. The processes whereby the high grade rocks reappear at the surface will be pursued.

Acknowledgments

We thank C. Williams, P. Blais, and G. Check for their assistance in the field and the staff of the Hudson Bay Company, Nordair and First Air for their assistance and service. S. Neufeld drafted figures and K. Card suggested improvements to an earlier version of the manuscript.

References

Chandler, F.W., Charbonneau, B.W., Ciesielski, A., Maurice, Y.T., and White, S.
1980: Geological studies of the Late Precambrian supracrustal rocks and underlying granitic basement, Fury and Hecla Strait area, Baffin Island, District of Franklin; in Current Research Part A, Geological Survey of Canada, Paper 80-1A, p. 125-132.

Frisch, T.
1982: Precambrian geology of the Prince Albert Hills, western Melville Peninsula, Northwest Territories; Geological Survey of Canada Bulletin, 346, 70 p.

Froese, E.
1978: The graphical representation of mineral assemblages in biotite bearing granulites; Current Research, Part A, Geological Survey of Canada, Paper 78-1A, p. 323-325.

Froese, E. and Sen, L.S.
1979: A reaction grid for biotite bearing mafic granulites; Current Research, Part A, Geological Survey of Canada, Paper 79-1A, p. 83-85.

Kenah, C and Hollister L.S.
1983: Anatexis in the Central Gneiss Complex, British Columbia in Migmatites, Melting and Metamorphism, ed. M.P. Atherton and C.D. Gribble; Shiva Publishing Edinburgh, p. 127-139.

Percival, J.A
1983: High grade metamorphism in the Chapleau-Foleyet Area, Ontario; American Mineralogist, v. 68, p. 667-686.

Prevec, S.A
1985: Petrology, geochemistry, and geochronology of some Precambrian rocks of the northwestern Melville Peninsula, Northwest Territories; unpublished Bachelor Thesis, McMaster University, 94 p.

Powell, R,
1983: Processes in granulite-facies metamorphism; in Migmatites, Melting and Metamorphism, ed. M.P. Atherton and C.D. Gribble; Shiva Publishing Edinburgh, p. 127-139.

Sanford, B.V
1977: Ordovician rocks of Melville Peninsula, southeastern District of Franklin; in geology of Ordovician rocks of Melville Peninsula region, southeastern District of Franklin; Bolton, T.E., Sanford, B.V., Copeland, M.J., Barnes, C.R., and Rigby, J.K.; Geological Survey of Canada Bulletin 269, p. 7-21.

Schau, M.
1977: "Komatiites" and quartzites in the Archean Prince Albert Group; in Volcanic Regimes in Canada, ed. by W.R.A. Baragar, L.C. Coleman, and J.M. Hall; Geological Association of Canada Special Paper 16, p 341-354.

Schau, M. and Ashton, K.E
1985: High grade metamorphic rocks of northwestern Melville Peninsula, District of Franklin; in Geological Survey of Canada, Current Research, Paper 85-1A, p. 527-532.

Northern extremity of the Humber Arm Allochthon in the Portland Creek area, western Newfoundland, and relationships to nearby groups

EMR Research Agreement 58/04/85

Peter A. Cawood[1] and Harold Williams[1]
Precambrian Geology Division

Cawood, P.A. and Williams, H., Northern extremity of the Humber Arm Allochthon in the Portland Creek area, western Newfoundland, and relationships to nearby groups; in Current Research, Part A, Geological Survey of Canada, Paper 86-1A, p. 675-682, 1986.

Abstract

The northern extremity of the Humber Arm Allochthon in the Portland Creek area consists of thrust imbricated slices of the Cow Head Group and overlying Lower Head formation[2]. The northernmost exposure of the Cow Head Group occurs east of Portland Hill and Lower Head sandstone extends to Portland Creek. Farther north, limestone breccias between Portland Creek and Daniels Harbour are assigned to the Cape Cormorant Formation and interpreted as part of the allochthon.

Sandstones that envelope the northern portion of the allochthon are correlated with the Goose Tickle Formation. They occur stratigraphically above the Table Head Group north of Daniels Harbour and extend southward to Southwest Feeder. In the vicinity of Portland Creek Pond, carbonates of the St. George and Table Head groups are thrust westward above the Goose Tickle Formation. Farther south, the carbonates are thrust above the Humber Arm Allochthon. The contact between the carbonate sequence and the Precambrian Long Range Complex is interpreted as a thrust that extends northward to Brians Pond.

Résumé

L'extrémité nord de l'allochthone de Humber Arm dans la région de Portland Creek est constitué d'écailles chevauchantes du groupe de Cow Head et de la formation susjacente de Lower Head. L'affleurement le plus septentrional du groupe de Cow Head se trouve à l'est de Portland Hill et les grès de Lower Head s'étendent jusqu'à Portland Creek. Plus au nord, des brèches calcaires, entre Portland Creek et Daniels Harbour, appartiendraient à la formation de Cap Cormorant et interprétées comme faisant partie de l'allochthone.

Les grès qui enveloppent la portion nord de l'allochthone correspondent à la formation de Goose Tickle. Stratigraphiquement, ces grès recouvrent le groupe de Table Head au nord de Daniels Harbour et s'étendent vers le sud jusqu'à Southwest Feeder. Près de l'étang Portland Creek, les carbonates des groupes de St. George et de Table Head chevauchent vers l'ouest la formation de Goose Tickle. Plus au sud, les carbonates chevauchent l'allochthone de Humber Arm. Le contact entre la série de carbonates et le comlexe précambrien de Long Range a été interprété comme une faille inverse qui se prolonge vers le nord jusqu'à Brians Pond.

---

[1] Department of Earth Sciences, Memorial University of Newfoundland, St. John's, Newfoundland, A1B 3X5

[2] lower case for informal formation names

Introduction

This report summarizes the results of field work carried out during the summers of 1984 and 1985 at the northern extremity of the Humber Arm Allochthon in the Portland Creek map area (NTS 12I/4, Fig. 81.1). It represents part of the final phase of a continued study to remap the entire Humber Arm Allochthon (Williams, 1973; 1985a,b; Schillereff and Williams, 1979; Williams and Godfrey, 1980; Williams et al. 1982; 1983; 1984; 1985; Quinn and Williams, 1983; Nyman et al., 1984).

The three distinct tectonic elements of western Newfoundland, i.e. the Humber Arm Allochthon, Cambrian-Ordovician carbonate sequence, and Precambrian Long Range Complex, have a clear morphological expression in the Portland Creek area. The Humber Arm Allochthon underlies a broad coastal lowland from Parsons Pond to Portland Creek Pond. Undulating hills to the east are underlain by the Paleozoic carbonate sequence. Highlands of the Long Range Mountains farther east consist of Precambrian granites and metamorphc rocks. Outcrop is poor throughout the western lowland, except for coastal sections. These are of limited use as the coast is parallel to the structural grain. More informative are the cross-sections of Parsons Pond and Portland Creek Pond, as these waterways were scoured by glacial ice that moved from east to west across the structural grain. Rock exposures improve eastward. Most inland traversing was done along streams.

Previous work in the Portland Creek area is limited to the stratigraphic studies of Schuchert and Dunbar (1934) and regional mapping by Johnson (1941a,b) and Oxley (1953). Schuchert and Dunbar (1934) defined the sequence of rock units in western Newfoundland and introduced the stratigraphic terminology that is still in wide usage. The work of Johnson and Oxley was tied in part to petroleum exploration and an attempt to assess the potential of oil seeps at Parsons Pond. Both Johnson and Oxley recognized the significance of thrusting in controlling repetition of rock groups and explaining relationships and setting of the carbonate sequence and Long Range Complex. Oxley's map at a scale of 1 inch to 2 miles covers most of the Portland Creek area. More recently, Knight (1985a,b) has mapped northern parts of the area as part of a study of the carbonate sequence in western Newfoundland.

General statement

The Portland Creek area contains Precambrian basement rocks, Cambrian to Middle Ordovician rocks of the west Newfoundland Paleozoic cover sequence, and Cambrian to Middle Ordovician rocks of the Humber Arm Allochthon. The Precambrian basement rocks are assigned to the Long Range Complex (Baird, 1960). Cambrian-Ordovician rocks of the cover sequence are separated into the Forteau and Hawke Bay formations (Schuchert and Dunbar, 1934), the St. George and Table Head groups (Schuchert and Dunbar, 1934; Klappa et al., 1980), and the Goose Tickle Formation (Cooper, 1937; Knight, 1985a), from oldest to youngest. The Humber Arm Allochthon contains rocks of the Cow Head Group (Kindle and Whittington, 1958; Williams et al., 1985), the Lower Head formation (Williams et al., 1985) and the Cape Cormorant Formation (Klappa et al., 1980).

Throughout most of western Newfoundland the Humber Arm Allochthon occurs structurally above the Paleozoic cover sequence, which in turn lies upon the Precambrian Long Range Complex with profound unconformity. Definition of the northern extremity of the Humber Arm Allochthon in the Portland Creek area is confused by several local conditions; (1) late thrusts bring the St. George and Table Head groups above the allochthon, (2) the Lower Head formation of the allochthon resembles nearby sandstones of the autochthonous Goose Tickle Formation, (3) carbonate breccias assigned to the Cape Cormorant Formation at Portland Creek Pond appear to be part of the allochthon, and (4) poor exposure throughout the critical area of Portland Creek Pond.

In the following account the Precambrian basement rocks and the Paleozoic cover sequence are described in order of decreasing age. This is followed by a description of rocks of the Humber Arm Allochthon and a concluding section on structural styles.

Autochthonous and parautochthonous rocks

Both the basement rocks and cover sequence are affected by thrust faults along the east margin of the area. They are therefore viewed as parautochthonous. North of Portland Creek Pond, thrusts are absent and the cover sequence may be autochthonous.

Basement rocks

Precambrian rocks of the Long Range Complex occur along the eastern side of the area in a structural inlier bounded on the west by the Long Range Thrust (Johnson, 1941b). The dominant rock type is pink, coarse grained granite. Most examples have a weak foliation defined by mica and tabular feldspars. Foliation is more pronounced in biotite-rich zones. A few examples are massive. Foliated and banded amphibolite and granodiorite (Hlr') outcrop along the eastern shore of Inner Pond. The contact with pink foliated granite is sharp, it is parallel to the regional foliation, and it has a marked topographic expression.

Paleozoic cover sequence

Rocks of the Paleozoic cover sequence occur as a narrow band bounded by thrusts between Parsons Pond and Brians Pond. Dips are moderately west, to steep and locally overturned. A wider area of cover rocks north of Portland Creek Pond has gentle dips and a uniform order of stratigraphic units that are younger to the southwest. There, the section appears to dip beneath the Humber Arm Allochthon.

The contact between the cover sequence and the Long Range Complex is interpreted everywhere as a thrust, although unconformable relationships are clearly defined both north and south of the area (Knight and Boyce, 1984; Knight, 1985a,b; Williams et al., 1985).

Basal units of the cover sequence, the Lower Cambrian Forteau and Hawke Bay formations, occur in a small wedge-shaped area near the east end of Parsons Pond and in an arcuate belt at Southwest Feeder Pond. The Forteau Formation consists of thin bedded grey-brown to green-brown shale and fine grained grey nodular limestone. A coarser grained and thicker bedded sequence containing calcarenites, oolitic grainstones and sandy limestones with intraformation rip-up clasts of shale occurs near the top of the formation to the south of Southwest Feeder Pond. The Hawke Bay Formation consists mainly of grey to pink quartzite.

The St. George and Table Head groups are the most extensive of the cover units and extend the full length of the area. The Port au Port Group of Middle to Upper Cambrian age (Knight and Boyce, 1984) is recognized locally beneath the St. George Group in the gorge draining Southwest Feeder Pond and along a woods-road 2 km to the south. The Port au Port Group is unseparated in Figure 81.1. It consists of laminated dolostone, thin bedded dolostone and argillite, limestone, lime mudstone and minor grainstone. Bioturbation and slumping locally disrupt bedding and produce breccia zones.

The St. George Group is well exposed along the gorge of Southwest Feeder and along the northeast shore of Portland Creek Pond. Well bedded and in places laminated cream to grey dolostones and grey limestones predominate. Thin brown-weathering chert bands, commonly disrupted by synsedimentary slumping occur in the lower and upper parts of the group. Bioturabation that produces a mottled appearance in the rocks is widespread. Gastropods occur in lower parts of the group along Southwest Feeder gorge. Dolostones in lower parts of the section are extremely hard in places, suggesting the presence of diagenetic silica. Dolostones are well developed on the north side of Portland Creek Pond. These rocks have a highly vuggy appearance and primary depositional features are masked by recrystallization.

The Table Head Group forms the top of the carbonate section and it is best exposed at Portland Creek Pond and along the coast in the northern portion of the area. Individual formations of the group, viz: Table Point, Table Cove, Black Cove and Cape Cormorant (Klappa et al., 1980) are recognized locally but no complete section is present. The Cape Cormorant Formation is absent in stratigraphic sections of the Table Head Group in the Portland Creek area. Breccias assigned to the Cape Cormorant Formation at Portland Creek Pond are interpreted as transported and part of the Humber Arm Allochton.

Fossiliferous thick bedded grey limestone of the Table Point Formation is well exposed on the north shore of Portland Creek Pond and in the low rolling hills to the north. Minor thin chert bands occur in the lower parts of the formation. Prominent gastropod- and nautiloid-bearing beds are found throughout the formation. Dolomitic zones, with sharp contacts against limestone beds, are extensive in some sections.

The contact between the St. George and Table Head groups is exposed on the north shore of Portland Creek Pond and on a small nearby island. Interbedded laminated dolostone and thin chert bands at the top of the St. George Group are disrupted into slump breccia with a dolomitic lime mudstone matrix. These beds are in abrupt contact with bedded pelletoidal fenestral limestone of the basal Table Point Formation. Bioturbation is widespread and the rocks locally show a well developed wavy lamination.

On the north shore of Portland Creek Pond, and in Bowing Brook, the Table Point Formation grades upward into thin bedded grey lime mudstone, nodular limestone, brown grey silty lime mudstone and grey shales of the Table Cove Formation. At both localities, an exposure gap to the west may correspond with the recessive black shales of the Black Cove Formation. Black shales conformably overlie Table Cove limestones in the Borax No 2 well near Bowing Brook and at Spudgels Cove, 5 km along strike to the north.

Clastics at the top of the cover sequence are assigned to the Goose Tickle Formation (Cooper, 1937; Tuke, 1968), following the lead of Knight (1985a). This unit is equivalent to the Norris Point formation of the Gros Morne area to the south (Williams, 1985a; Williams et al., 1985) and the Mainland Sandstone at the top of the cover sequence in the Stephenville area (Williams, 1985b). The Goose Tickle Formation conformably overlies the Black Cove Formation at Spudgels Cove and farther north at Table Cove. Carbonate breccias and shales of the Cape Cormorant Formation are absent at both localities.

The Goose Tickle Formation is well exposed along the coast at Spudgels Cove and along the lower to middle reaches of Southwest Feeder. It consists of green-grey to grey shale interstratified with well bedded green sandstone to granule conglomerate. Sandstones are graded and show well developed Bouma sequences, in places occurring as amalgamated beds up to a few metres thick. Towards the top of the section, the sandstone beds are thicker, more massive and coarser grained. Dewatering structures are common in the thicker beds.

Shales near the base of the formation on the north shore of Portland Creek Pond contain the following graptolites; **Climacograptus**, **Glossograptus**, and **Glypotograptus** or **Undulograptus**. These forms are suggestive of a Darriwillian (Da 2) to Gisbornian age (Llanvirn to early Caradoc, R.A. Cooper, personal communication, 1985). Reudemann (1947) assigned graptolites from a stratigraphically higher level within the formation at Southwest Feeder to the Normanskill (Caradoc). Additional material collected by L.A. Quinn and S.H. Williams in 1985 appear to confirm this late Middle Ordovician age.

Humber Arm Allochthon

The Humber Arm Allochthon consists of northeast-trending thrust slices of limestone breccia, platy limestone and shale of the Cow Head Group overlain stratigraphically by sandstones and conglomerates of the Lower Head formation. These rocks extend between Parsons Pond and Portland Creek Pond. A large area of limestone breccia between Portland Creek and Daniels Harbour is assigned to the Cape Cormorant Formation. These rocks appear to be a structural slice rather than a stratigraphic unit above the Goose Tickle Formation. Furthermore, because similar breccias are absent in nearby stratigraphic sections of the Table Head Group, the breccias are considered part of the Humber Arm Allochthon.

Middle Cambrian to Lower Ordovician rocks of the Cow Head Group are interpreted as a proximal to distal, eastern or continental slope facies of the shallow water, continental shelf, carbonate sequence (Williams et al., 1985). In its type area, the Cape Cormorant Formation occurs at the stratigraphic top of the carbonate sequence. Its age is early Middle Ordovician and its presence signals a disturbance of the carbonate shelf. Within the Humber Arm Allochthon, the Cape Cormorant Formation is viewed therefore as parautochthonous and incorporated during the latest phases of assembly and transport.

Stratal orientation within the Cape Cormorant Formation, although poorly defined, allows division into two structural blocks. One corresponds with the coastal outcrops where bedding trends north-northeast and dips 60° to the east. The second is the island in Portland Creek Pond where bedding strikes west-northwest and dips gently to the south. Bedding in the coastal block is consistent over a strike length of 7 km and parallels the strike of strata in the immediately adjacent Lower Head Formation of the Humber Arm Allochthon. However, it is markedly discordant to trends of strata in the nearby platformal sequence. This supports the notion that the Cape Cormorant Formation occurs as a series of tectonic blocks at the base of the Humber Arm Allochthon.

The Cape Cormorant Formation consists mainly of massive limestone breccia. Clasts range from granules to large blocks with the majority falling in the coarse pebble to fine cobble range. A single block at Cliffy Point measures 30 by 70 m. Rip-up clasts of poorly consolidated grey laminated shale and feldspathic sandstone up to 5 by 1 km are scattered throughout the unit. The lime mudstone matrix in places contains clastic debris derived from the partial disaggregation of intraformational shale and sandstone clasts.

Clast to matrix ratio is generally very high although at some localities, such as the northeast side of the island in Portland Creek Pond and south of Cliffy Point, there are

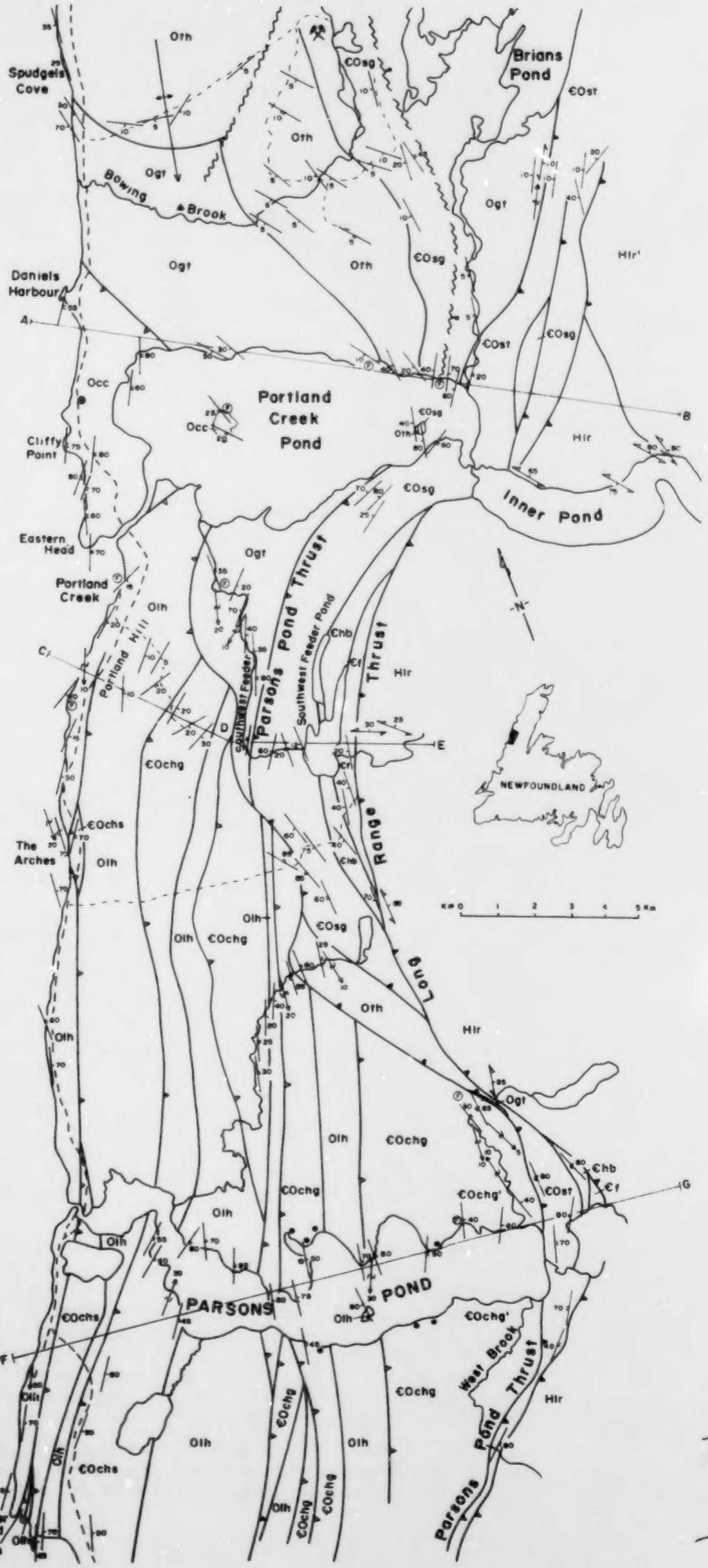

Figure 81.1

General geology of the Portland Creek area, western Newfoundland.

HUMBER ARM ALLOCHTHON

Lower to Middle Ordovician

Lower Head formation*

Olh Medium- to thick-bedded green sandstone, granule to pebble conglomerate and shale.

Middle Cambrian to lower Middle Ordovician

Cow Head Group

COch Pebble to coarse boulder limestone breccia and conglomerate, lime sandstone, thin bedded platy limestone, grey to black shale, green to black chert and buff dolomitic shale. Shallow Bay formation (COchs) contains abundant thick units of coarse limestone breccia and conglomerate; Green Point formation (COchg) has fewer and thinner units of mainly pebble to cobble limestone breccia and contains more shale; COchg', mainly shale and thin bedded limestone.

Middle Ordovician

Cape Cormorant Formation

Occ Pebble to boulder limestone breccia with clasts of Table Head limestone and intraformational sandstone and shale.

PARAUTOCHTHONOUS ROCKS

Middle Ordovician

Goose Tickle Formation

Ogt Thin- to medium-bedded grey shale and graded to massive grey green sandstone and granule conglomerate.

Upper Cambrian to Middle Ordovician

St. George and Table Head groups

COst Laminated to medium bedded grey dolostone, thin- to thick-bedded grey limestone, minor shale, grey to white marble adjacent to Long Range Structural Front. COsg, dolostones of St. George Group (includes Middle to Upper Cambrian carbonate rocks of Port au Port Group in vicinity of Southwest Feeder). Oth, thin- to thick-bedded grey limestone and vuggy dolostone of Table Head Group.

Lower Cambrian

Hawke Bay Formation

Chb Medium- to thick-bedded massive white to pink quartzite.

Forteau Formation

Cf Thin bedded grey, green to buff shale and grey nodular limestone, thick limestone beds at top of sequence, contains thin unit of red and green arkosic sandstone and granule conglomerate at base.

Precambrian (Helikian)

Long Range Complex

Hlr Foliated to massive pink granite, sheared pink to reddish and green granite; includes foliated to banded amphibolite and granodiorite (Hlr') at Inner Pond.

Stratigraphic contact, assumed in areas of poor exposure that are identifiable by a lack of structural symbols in Figure 81.1

Early thrust fault or tectonic contact beneath allochthonous slice or around large olistolith

Late or out-of-sequence thrust fault or high angle reverse fault

High angle fault, dot indicates downthrown side

Bedding, tops known, inclined, overturned

Bedding, tops unknown, inclined

Cleavage in sedimentary rocks, inclined

Foliation in plutonic rocks, inclined

Axes of minor folds with direction of plunge

Anticlinal axis with plunge

Petroleum exploratory well, Borax #2 well, water well

Fossil locality

Roads, paved, gravel or woods access

Daniels Harbour Mine (Zinc)

* lower case informal stratigraphic names

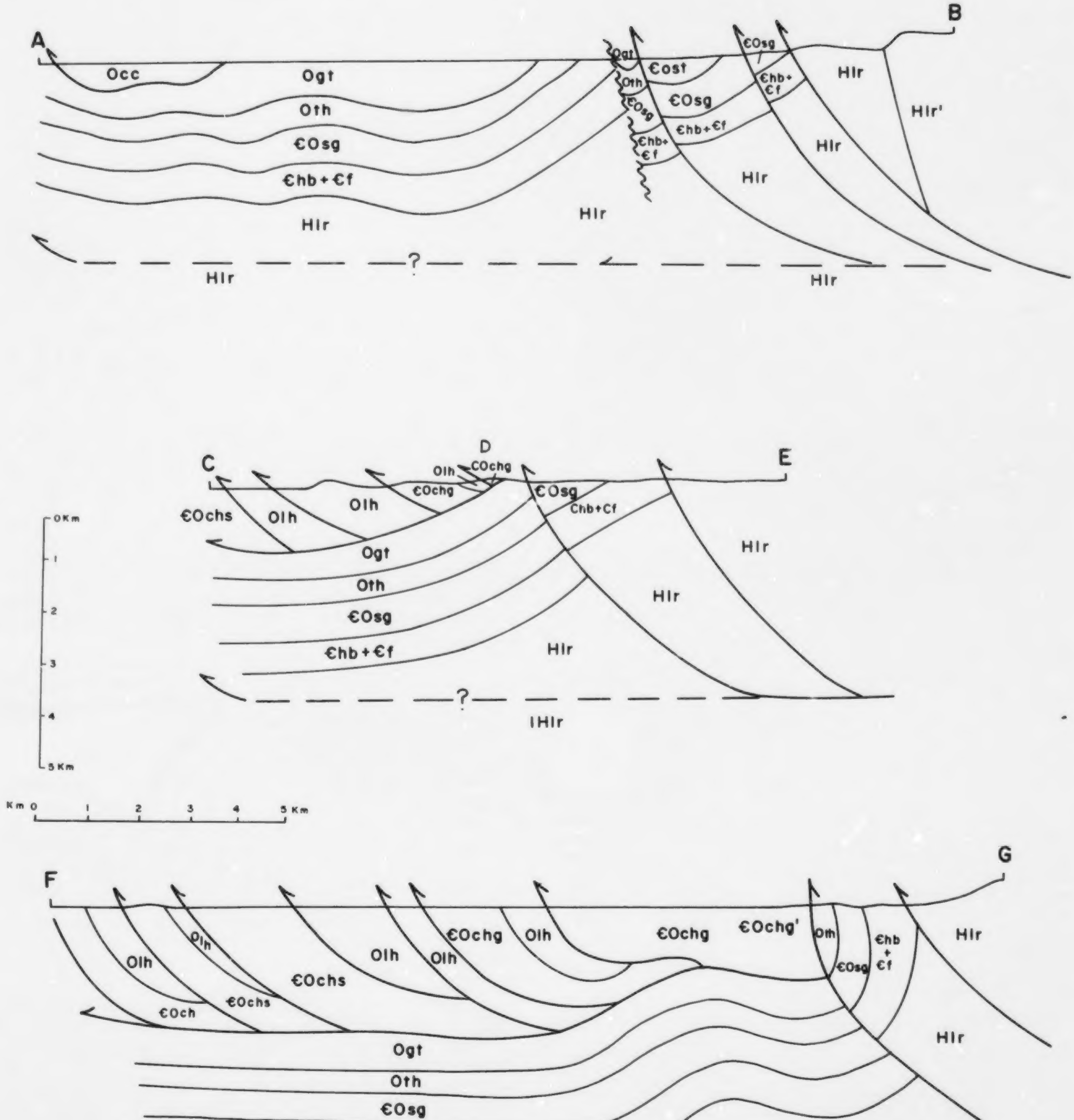

Figure 81.2. Interpretive geological cross-sections of Portland Creek area, western Newfoundland (see Fig. 81.1 for locations).

zones with a high proportion of matrix. In these areas the breccias approach paraconglomerates and the matrix is more shaly. At the island in Portland Creek Pond the shaly-matrix breccia directly overlies a sequence of bedded sandstone and shale, suggesting that the shale matrix was derived from intrabasinal material. Isolated lenses of shale-rich matrix within massive limestone breccia may have a similar origin and represent either completely disaggregated intraformational clasts, or shale beds totally incorporated and absorbed into the overlying breccias. Such zones may thus be useful in determining bedding within an otherwide massive monotonous sequence.

The lithological character and faunal content of breccia clasts between Eastern Head and Daniels Harbour indicate derivation of limestone debris from the Table Head Group (Schuchert and Dunbar, 1934; Klappa et al., 1980; James and Stevens, 1982; Williams et al., 1985). The largest limestone blocks within the formation consist of thin bedded limestone and shale probably derived from the Table Cove Formation.

Coastal outcrops of the Cape Cormorant Formation south of Cliffy Point are invariably massive and lack clear evidence of internal bedding. Bedding attitudes shown in Figure 81.1 are interpreted from the consistent orientation of clasts of platy Table Cove limestone and the pervasive development of a stylolitic fabric parallel to the clasts. If the steep bedding attitudes on the coast continue across strike, the coastal block has a minimum stratigraphic thickness of 1000 m. Facing criteria are unknown in any of the coastal sections.

A vertical water-well drilled within the coastal block north of Cliffy Point (Fig. 81.1) reveals only 60 m of limestone breccia underlain by 30 m of grey shale (Tom Lane, personal communication, 1985). This suggests that the block is a thin structural slice above shale.

At Daniels Harbour two 50 m zones of limestone breccia are separated by a recessive clastic horizon only a few metres thick. The western zone is a megabreccia, rich in blocks of thin stylobedded limestone up to 20 m long. Some of these blocks are contorted and partially disaggregated at their margins, suggesting they were not completely lithified when incorporated.

Bedding within the Cape Cormorant Formation is best seen on the north side of the island in Portland Creek Pond. Here massive breccia at least 10 m thick is overlain, or faulted against, 2 m of sandstone and 10 m of grey shale. The shale, in turn, is succeeded by a shale matrix-rich breccia with tabular limestone clasts overlain by massive breccia at least 15 m thick. Poorly preserved graptolites of Llanvirn aspect (R.A. Cooper and S.H. Williams, personal communication, 1985) were discovered by L.A. Quinn in the sandstone near the base of this sequence.

Bedding in the Cape Cormorant Formation on the island in Portland Creek Pond is parallel to bedding in the Goose Tickle Formation on the north shore of the pond. Beds face southwest at both localities. This situation is compatible with a stratigraphic contact between the two formations (Knight, 1985b).

Sandstones interstratified with the limestone breccias, as well as the lithologically identical intraformational sandstone clasts, are graded turbidites. This indicates that the Cape Cormorant limestone breccias accumulated below wave base in a relatively deep water basin.

The Cow Head Group (Schuchert and Dunbar, 1934; Kindle and Whittington, 1958) comprises a sequence of limestone breccias, thin bedded grey limestones, tan-weathering dolomitic lime mudstones, calcarenites and shales. The group is exposed along the shore of Parsons Pond and the creeks draining into the pond from the north. It extends as far north as the east side of Portland Hill.

Limestone breccia is the distinctive main lithology. It has pebbles to cobbles and boulders of platy limestone, similar in character to the interstratified thin bedded limestone. In addition, it contains a minor component of more equidimensional angular limestone clasts. Some are distinct from limestone interbeds and exotic to the basin of deposition. Breccia beds are generally less than 3 m thick.

The Cow Head Group was subdivided informally into the Shallow Bay, Green Point and Yellow Point formations, based on coarseness, thickness and abundance of limestone breccias (Williams et al., 1985). The Shallow Bay formation occurs along the western side of the allochthon and the Yellow Point formation along its eastern side. In the Portland Creek area the Shallow Bay formation is restricted to the southwest side of Parsons Pond. Northward along strike near Portland Hill, and within the same thrust slice, the breccias are finer and assigned to the Green Point formation. This suggests both along-strike and across-strike facies variations.

The more shaly sections assigned to the Yellow Point formation (Williams et al., 1985) at the east end of Parsons Pond resemble Cambrian beds at the base of the Green Point formation in its type area to the south. A rich fauna of rooted dendroids at Parsons Pond, including **Staurograptus dichotomus** (Schuchert and Dunbar, 1934) of probable Tremadocian age (S.H. Williams, personal communication, 1985), and the apparent absence of younger graptoloid forms, supports this correlation. Furthermore, the strata at the east end of Parsons Pond appear to be in the same structural slice as the Green Point formation farther south. Accordingly, the rocks are reassigned to the Green Point formation. The occurrence of rippled and laminated calcarenites of possible Cambrian age within this eastern thrust slice suggests that it contains the thickest and oldest, as well as themost distal parts of the Cow Head Group.

The Lower Head formation overlies the Cow Head Group with the contact defined by the appearance of the first sandstone bed. The formation is well exposed in coastal sections between Lower Head and Parsons Pond and between the Arches and Portland Creek. Both sections are contained in a single thrust slice. Lower Head sandstones in structurally higher thrust slices are exposed on the shore of Parsons Pond.

The formation consists of interbedded green sandstone and grey to green-grey shale. Limestone conglomerate occurs locally within the formation at Portland Hill. Thin grey limestone beds are interstratified with the shale immediately overlying the Cow Head Group at Lower Head and at an unknown stratigraphic level some 5 km farther north. No facies variation is evident among sandstones in the various thrust slices.

The sandstones are feldspatholithic and contain red and green chert and dark grey to black argillite fragments. Limestone clasts are less common, except near the base of some beds. However, a thick sequence of granule to cobble limestone conglomerate occurs at Portland Hill. There, the limestone clasts are embedded in a sandy matrix that appears more quartz-rich than elsewhere. Pebbly mudstone of probable intraformational slump origin occurs along the coast 2 km north of the Arches (Knight, 1985b). It contains sandstone, shale and minor limestone clasts in a predominantly shaly or sandy matrix.

Sandstones occur in graded to massive beds which commonly display water escape structures. These modify primary depositional fabrics. A few isolated paleocurrent determinations from ripple drift laminations in graded sandstones suggest a northerly source.

Graptolites occur within the Lower Head formation on the coast west of Portland Hill and at the northern end of Portland Creek village. Preliminary determinations are

Glossograptus and either **Climacograptus** or **Amplexograptus** at the southern locality and **Pseudoclimacograptus** and a small **Climacograptus** as well as **Dichograptid** stipe-fragments at the northern locality. Both faunas suggest a Darriwillian age, probably Da 2 to 3 (uppermost Arenig to basal Llandeilo, R.A. Cooper personal communication, 1985).

Structure

Structural styles and overprinting relationships within the Portland Creek area indicate a history of multistage thrusting and associated folding. Early thrusts developed during assembly and emplacement of the Humber Arm Allochthon. Later thrusts developed with regional compression of the allochthon and its underlying basement of carbonate strata and Precambrian crystalline rocks.

The Humber Arm Allochthon consists of a series of east-dipping and east-facing thrust slices, resulting in across strike repetition of the Cow Head Group and Lower Head formation. Large tectonic blocks of the Cape Cormorant Formation at the base of the allochthon indicate disruption and incorporation of some underlying strata during emplacement.

Early thrusts are confined to the allochthon. They have a linear north-northeast trend parallel to bedding. In the south at Parsons Pond, bedding dips steeply to the east. In the north at Portland Hill, dips are more gentle.

Individual imbricates are up to several kilometres wide. However, the wider imbricates show evidence of bedding reversals and small scale internal folding, indicating that widths do not reflect stratigraphic thicknesses. In areas of good exposure such as Lower Head, there is local repetition of stratigraphic units by anastomosing thrust faults. Local complications in such areas suggest that the portrayal of rock units in a relatively few broad slices, as depicted in Figures 81.1 and 81.2, is a gross oversimplification. Poor outcrop prevents a more rigorous interpretation of structural style.

Thrust contacts are rarely seen. At Lower Head the contact between the Lower Head formation and the overthrust Cow Head Group is marked by a zone of stratal disruption up to 20 m wide. Deformation is concentrated in the hanging-wall where the Cow Head Group displays shallow plunging, asymmetric, west-verging folds. A sequence of thin bedded limestones and shales in the contact zone pass conformably upward into breccia of the Cow Head Group and downward into a zone of progressive deformation and shearing. At the Lower Head contact, shales contain blocks of Cow Head and Lower Head lithologies. A similar zone of stratal disruption up to 40 m wide occurs in an unnamed creek north of Parsons Pond. It contains sandstone and limestone breccia blocks in a very fine grained, partly silicified, shaly matrix.

The relationships between the allochthon and underlying rocks are masked by later structures, except where the Cape Cormorant Formation is interpreted as blocks above the Goose Tickle Formation at Daniels Harbour.

South of Southwest Feeder, the sinuous Parsons Pond Thrust cuts across the imbricates within the allochthon and brings the Table Head and St. George groups above the Cow Head Group and Lower Head formation. North of Southwest Feeder this late thrust is confined to the cover sequence and brings carbonates of the St. George and Table Head groups above the Goose Tickle Formation. The Parsons Pond Thrust parallels the Long Range Thrust, which in turn brings the Long Range Complex against the carbonate sequence.

At Parsons Pond and immediately north, bedding in the thrust bounded carbonates is overturned and dips steeply to the east parallel to the orientation of the Parsons Pond and Long Range thrusts. Farther north, where the Parsons Pond and Long Range thrusts diverge, the platformal sequence dips moderately to gently westward.

Because Precambrian crystalline rocks form the hanging-wall of the Long Range Thrust, the décollement for late stage thrusting occurs at basement depths. The Parsons Pond Thrust marks the exposed western limit of this décollement. However, it is inferred to continue below the Humber Arm Allochthon (Fig. 81.2), perhaps extending beneath the Gulf of St. Lawrence. At Ten Mile Lake and Castor River approximately 100 km north of Portland Creek, Precambrian rocks occur 13 km west of the Long Range structural front (Williams, 1967; Knight, 1983). The Precambrian rocks are truncated along their western margin by a major break that marks the western side of the Highlands of St. John. The break is generally considered a high angle normal fault, downthrown on the west (Knight, 1983). However, it parallels the Long Range Thrust and could equally well represent an east-dipping thrust related to the same deep décollement. Its southern extension projects west of the Portland Creek area into the Gulf of St. Lawrence, implying that the carbonate sequence structurally underlying the Humber Arm Allochthon in the Portland Creek area is parautochthonous (Fig. 81.2).

Mesoscopic folds occur throughout the Portland Creek area. Although some folds, such as those in the hanging wall of the thrust plane at Lower Head, probably formed during initial assembly of the allochthon, most are later and affect the carbonate sequence. Mesoscopic fold axes in both the allochthon and the carbonate sequence plunge gently south to southwest.

Macroscopic folds also have a shallow south-southwest plunge and explain the termination of the Humber Arm Allochthon at Portland Creek Pond and the appearance of the structurally underlying carbonate sequence farther north. The folded allochthon-autochthon contact is truncated by the Parsons Pond Thrust south of Portland Creek Pond. Fold axes and late thrusts are subparallel, implying that folding took place during regional compression immediately prior to brittle facturing and overthrusting of the carbonate sequence and its crystalline basement. This agrees with the asymmetric west-verging style of the mesoscopic folds.

Few direct constraints are available on the age of deformation. The Middle Ordovician Goose Tickle and Lower Head formations are interpreted as a clastic wedge deposited in advance of the Humber Arm Allochthon (Stevens, 1970). Thus assembly and emplacment of the Humber Arm Allochthon is generally considered to have taken place during the middle-Ordovician Taconic Orogeny. There is no upper age limit on the time of later thrusting in the Portland Creek area. In the Stephenville area, at the southern end of the Humber Arm Allochthon, late stage thrusts are dated stratigraphically as Devonian (Williams, 1985b). A similar age is suggested for final deformation in the Portland Creek area.

Acknowledgments

We thank Alvin Crocker for his genial field assistance and his keen eye in fossil collecting. Roger Cooper and Henry Williams kindly provided preliminary graptolite identifications, and Winston Howell provided excellent drafting services. We thank Philippe Erdmer for helping with helicopter travel and Louise Quinn, Sheila Stenzel and Henry Williams for enjoyable discussions in the field. Support for

our work in western Newfoundland through the Natural Sciences and Engineering Research Council of Canada and the Department of Energy, Mines and Resources is greatly appreciated.

References

Baird, D.M.
1960: Sandy Lake (west half), Newfoundland; Geological Survey of Canada, Map 47-1959.

Cooper, J.R.
1937: Geology and mineral deposits of the Hare Bay area; Newfoundland Department of Natural Resources, Geology Section, Bulletin 9, 36 p.

James, N.P. and Stevens, R.K.
1982: Anatomy and evolution of a Lower Paleozoic continental margin; International Association of Sedimentologists, Guidebook, Excursion 2B, 75 p.

Johnson, H.
1941a: Paleozoic lowlands of northwestern Newfoundland; New York Academy of Science, Series 2, v. 3, p. 141-145.

1941b: Newfoundland, in Possible Future Oil Provinces of the United States and Canada; American Association of Petroleum Geologists, Bulletin, v. 25, p. 1558-1562.

Kindle, C.H. and Whittington, H.B.
1958: Stratigraphy of the Cow Head region, western Newfoundland; Geological Society of America, Bulletin, v. 69, p. 315-342.

Klappa, C.F., Opalinski, P.R., and James, N.P.
1980: Ordovician Table Head Group of western Newfoundland: a revised stratigraphy; Canadian Journal of Earth Sciences, v. 17, p. 1007-1019.

Knight, I.
1983: Geology of Cambro-Ordovician rocks in parts of the Castors River, St. John Island and Port Saunders map sheets; in Current Research. ed. M.J. Murray, P.D. Saunders, W.D. Boyce and R.V. Gibbons; Newfoundland Department of Mines and Energy, Mineral Development Division, Report 83-1, p. 1-10.

1985a: Port Saunders, Newfoundland, Mineral occurrence map; Newfoundland Department of Mines and Energy, Mineral Development Division, Map 85-30, scale 1:250 000.

1985b: Geological mapping of Cambrian and Ordovician sedimentary rocks of the Bellburns (12I/5 and 6), Portland Creek (12I/4) and Indian Lookout (12I/3) Map areas, Great Northern Peninsula, Newfoundland; in Current Research, ed. K. Brewer, D. Walsh and R.V. Gibbons; Newfoundland Department of Mines and Energy, Mineral Development Division, Report 85-1, p. 79-88.

Knight, I. and Boyce, W.D.
1984: Geological mapping of the Port Saunders (12I/11), St. John Island (12I/14) and parts of the Torrent River (12I/10) and Bellburns (12I/6) map sheets northwestern Newfoundland; in Current Research, ed. M.J. Murray, J.G. Whelan and R.V. Gibbons; Newfoundland Department of Mines and Energy, Mineral Development Division, Report 84-1, p. 114-124.

Nyman, M., Quinn, L., Reusch, D.N., and Williams, H.
1984. Geology of the Lomond map area, Newfoundland; in Current Research, Part A, Geological Survey of Canada, Paper 84-1A, p. 157-164.

Oxley, P.
1953: Geology of Parsons Pond - St Paul's area, west coast, Newfoundland; Newfoundland Geological Survey, Report No. 5, 53 p.

Quinn, L. and Williams, H.
1983: Humber Arm Allochthon at South Arm, Bonne Bay, west Newfoundland; in Current Research, Part A, Geological Survey of Canada, Paper 83-1A, p. 179-182.

Reudemann, R.
1947: Graptolites of North America; Geological Society of America, Memoir 19, 652 p.

Schillereff, H.S. and Williams, H.
1979: Geology of Stephenville map area, Newfoundland; in Current Research, Part A, Geological Survey of Canada, Paper 79-1A, p. 327-332.

Schuchert, C. and Dunbar, C.O.
1934: Stratigraphy of western Newfoundland; Geological Society of America, Memoir 1, 123 p.

Stevens, R.K.
1970: Cambro-Ordovician flysch sedimentation and tectonics in west Newfoundland and their possible bearing on a Proto-Atlantic Ocean; in Flysch Sedimentation in North America, ed. J. Lajoie, Geological Association of Canada, Special Paper No. 7, p. 165-177.

Tuke, M.F.
1968: Autochthonous and allochthonous rocks in the Pistolet Bay area in northernmost Newfoundland; Canadian Journal of Earth Sciences, v. 5, p. 501-513.

Williams, H., compiler
1967: Geological map, Island of Newfoundland; Geological Survey of Canada, Map 1231A, scale 1:1 000 000.

1973: Bay of Islands map area, Newfoundland; Geological Survey of Canada, Paper 72-34, 7 p.

1985a: Geology of Gros Morne map area, (12H/12), western Newfoundland; Geological Survey of Canada, Open File 1134.

1985b: Stephenville map area, north half, Newfoundland; Geological Survey of Canada, Map 1579A, scale 1:100 000.

Williams, H. and Godfrey, S.C.
1980: Geology of the Stephenville map area, Newfoundland; in Current Research, Part A, Geological Survey of Canada, Paper 80-1A, p. 217-221.

Williams, H., Gillespie, R.T., and Knapp, D.A.
1982: Geology of Pasadena map area, Newfoundland; in Current Research, Part A, Geological Survey of Canada, Paper 82-1A, p. 281-288.

1983: Geology of the Pasadena map area western Newfoundland; Geological Survey of Canada, Open File 928.

Williams, H., Quinn, L.A., Nyman, M., and Reusch, D.
1984: Geology of the Lomond map area, 12H/5, western Newfoundland; Geological Survey of Canada, Open File 1012.

Williams, H., James, N.P., and Stevens, R.K.
1985: Humber Arm Allochthon and nearby Groups between Bonne Bay and Portland Creek, western Newfoundland; in Current Research, Part A, Geological Survey of Canada, Paper 85-1A, p. 399-406.

Fossil ages and isotopic dates from the Paleozoic Sicker Group and associated intrusive rocks, Vancouver Island, British Columbia

Project 770006

M.T. Brandon [1], M.J. Orchard, R.R. Parrish [2], A. Sutherland Brown [3] and C.J. Yorath [1]
Cordilleran Geology Division, Vancouver

Brandon, M.T., Orchard, M.J., Parrish, R.R., Sutherland Brown, A., and Yorath, C.J., Fossil ages and isotopic dates from the Paleozoic Sicker Group and associated intrusive rocks, Vancouver Island, British Columbia; in Current Research, Part A, Geological Survey of Canada, Paper 86-1A, p. 683-696, 1986.

Abstract

The Late Silurian to Early Permian Sicker Group represents the oldest rocks of the Wrangellia terrane of Vancouver Island. This paper summarizes isotopic dates and fossil ages for the group and associated intrusives. The oldest unit, the Nitinat tuff, is preDevonian, possibly Silurian. It is intruded by Early Devonian quartz porphyry and granodiorite of the Saltspring Intrusions. In the Buttle Lake area, U-Pb dates for the Myra volcanics indicate a pre-Late Devonian age. Therefore, the Myra could be an extrusive equivalent of the Saltspring Intrusions. In the Cowichan Lake area, a chert that overlies the Nitinat tuff yielded Early Mississippian microfossils. No equivalents of the Myra volcanics occur in the Cowichan area. The highest unit in the Sicker is the Buttle Lake Limestone. New conodont ages span the interval early Middle Pennsylvanian (Atokan) through Early Permian (probably Sakmarian). The Sicker has been variably deformed in the early Mesozoic.

Résumé

Le groupe de Sicker du Silurien supérieur ou du Permien inférieur renferme les roches les plus anciennes du terrain de Wrangellia de l'île de Vancouver. Cette étude présente des datations isotopiques et des âges des fossiles du groupe et des intrusions associées. L'unité la plus ancienne, le tuff de Nitinat, date du pré-Dévonien et peut-être du Silurien. Elle est pénétrée par un porphyre quartzifère du Dévonien inférieur et une granodiorite faisant partie des intrusions de Saltspring. Dans le secteur du lac Buttle, la datation U-Pb des roches volcaniques de Myra indique un âge pré-Dévonien inférieur. Par conséquent, les roches de Myra pourraient être un équivalent extrusif des intrusions de Saltspring. Dans le secteur du lac Cowichan, un chert qui recouvre le tuff de Nitinat renferme des microfossiles du Mississippien inférieur. On ne trouve pas d'équivalent des roches volcaniques de Myra dans le secteur de Cowichan. L'unité la plus récente dans le groupe de Sicker est le calcaire de Buttle. Les âges de conodontes récents vont du début de Pennsylvanien moyen (Atokien) jusqu'au début du Permien (probablement le Sakmarien). Le groupe de Sicker a été plus ou moins déformé au début du Mésozoïque.

[1] Geological Survey of Canada, Pacific Geoscience Centre, P.O. Box 6000, Sidney, B.C. V8L 4B2
[2] Precambrian Geology Division, Ottawa.
[3] Consultant, 546 Newport Avenue, Victoria, B.C. V8S 5C7

Introduction

The Paleozoic Sicker Group comprises the oldest rocks of Wrangellia (Jones et al., 1977), a large allochthonous terrane that underlies most of Vancouver Island. This paper summarizes available fossil and isotopic data for the Sicker and associated intrusive rocks with the objective of providing a framework for ongoing stratigraphic and tectonic studies of the unit. One of the goals of these studies is to better resolve the origin of the Wrangellia terrane. The Sicker contains stratigraphic units ranging from at least Late Silurian through Early Permian, and therefore provides a long record, about 150 million years, of the early history of Wrangellia.

The Sicker Group was originally used by Clapp (1912) to refer to deformed volcanic and sedimentary rocks in the vicinity of Sicker Mountain on southern Vancouver Island (near N1 on Fig. 82.1). As presently defined (Fyles, 1955; Yole, 1969; Muller, 1980), the Sicker includes all stratified Paleozoic rocks of the Wrangellia terrane on Vancouver

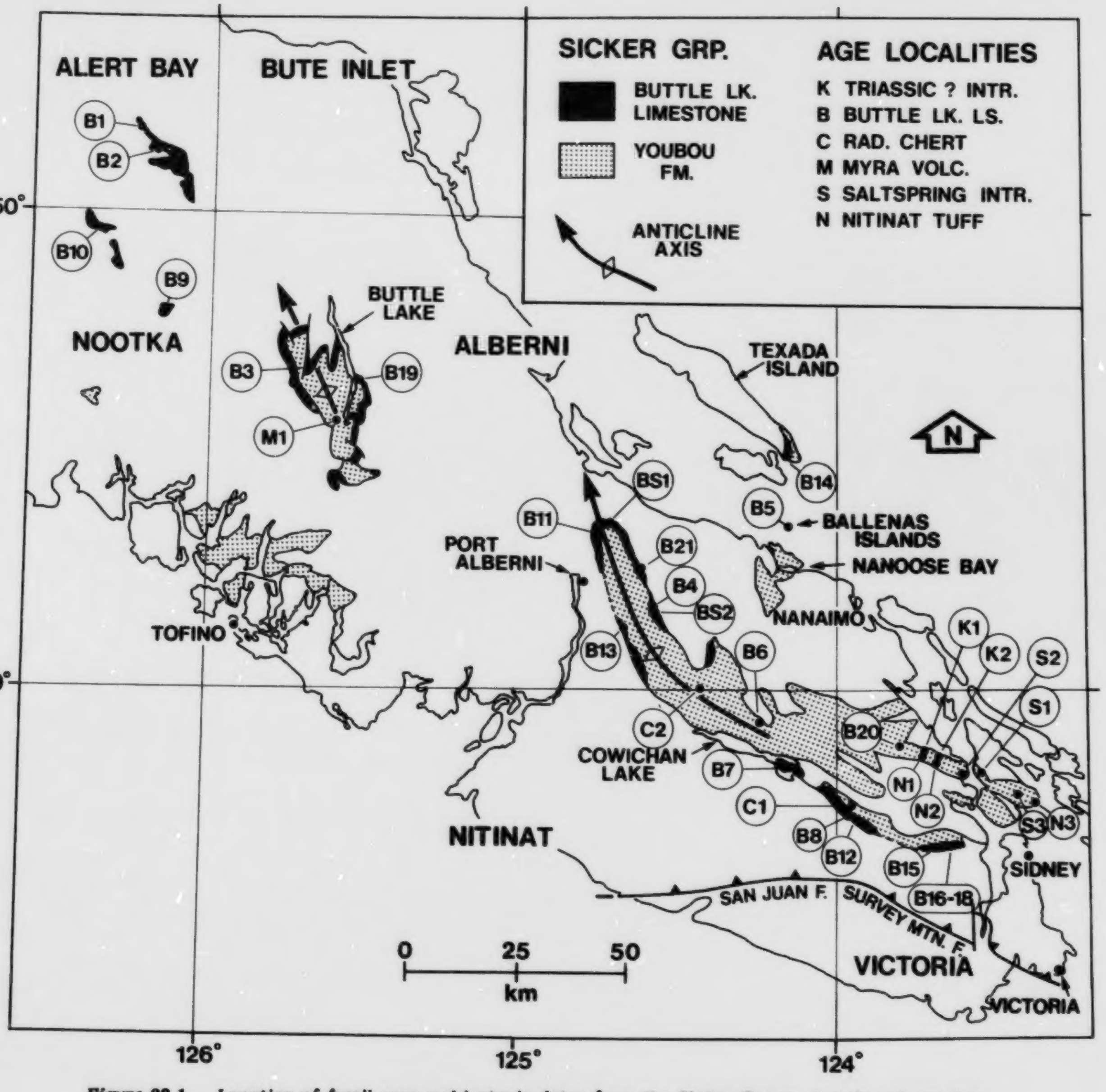

Figure 82.1. Location of fossil ages and isotopic dates from the Sicker Group. Labels refer to data summarized in Tables 82.1 and 82.3 through 82.6. BS1 and BS2 are localities where stratigraphic collections of conodont samples were made in the Buttle Lake Limestone (Table 82.5). The San Juan and Survey Mountain faults mark the southern limit of Wrangellia on Vancouver Island. The figure outlines the following GSC map areas: Alert Bay (Muller et al., 1974), Bute Inlet (Roddick and Woodsworth, 1977), Nootka (Muller et al., 1981), Alberni (Muller and Carson, 1969), Nitinat (Muller, 1982) and Victoria (Muller, 1983).

Table 82.1. Isotopic dates for lower Paleozoic rocks of the Sicker Group

No.	Rock type, Location (Sample no.)*	Dating method	Date** (Ma)	Ref.	Comments
NITINAT TUFF					
N1	Pyroxene crystal tuff. E of Mt. Sicker along Highway 1, Victoria map area. 48°51.3' 123°43.1' (UBC/Sicker 3)	K-Ar uralitic amphibole after pyroxene	421 ± 36	(1)	Date is a minimum age for the tuff and uralite alteration. The analyst noted that the date may be anomalous due to very low K content. Tuff in this outcrop is cut by quartz porphyry of the Saltspring Intrusions (Fig. 82.3).
N2	Pyroxene crystal tuff. Near Mt. Richards, SW of Crofton, Victoria map area. 48°50.9' 123°41.1' (UBC/E80-77 no. 24517M)	K-Ar uralitic amphibole after pyroxene	288 ± 28	(1)	Date is a minimum age for uralite alteration. This unit is intruded by Saltspring quartz porphyry on Mt. Richards (ref. no. 6).
N3	Pyroxene crystal tuff. Beaver Pt., Saltspring Is., Victoria map area. 48°46.10' 123°22.60' (UBC/28SM)	K-Ar uralitic amphibole after pyroxene	257 ± 20	(1)	Date is a minimum age for uralite alteration. The analyst noted that the very low K content of the amphibole is cause for concern. A nearby Saltspring quartz porphyry intrudes this tuff.
SALTSPRING INTRUSIONS					
S1	Quartz porphyry. Mt. Maxwell, Saltspring Is., Victoria map area. 48°50.05' 123°33.20' (GSC/MEZ-77-1)	U-Pb zircon	UI=393^{+25}_{-10} LI=92^{+120}_{-130} (n=5)	(2,3)	Discordant zircon dates. U-Pb dates define a good linear array (Fig. 82.4) which was used to calculate the intercept dates. UI date is presently the best estimate of the age of the Saltspring Intrusions.
S2	Schistose quartz porphyry. Arbutus Pt., Maple Bay, Victoria map area. 48°49.40' 123°35.60' (GSC/WN-19-74 for U/Pb, GSC/80-21 for K/Ar)	(a) U-Pb zircon	>370 (n=4)	(2,3)	Discordant zircon dates. Pb-Pb dates of 361-395 Ma indicate an approximate minimum age. Intercept dates are very poorly defined due to a lack of dispersion in U-Pb dates.
		(b) K-Ar muscovite	180 ± 8	(5)	Minimum age. Very low K content for muscovite, might be sericite.
S3	Granodiorite. Lake Stowell, Saltspring Is., Victoria map area. 48°46.90' 123°26.60' (GSC/MEZ-76-3)	U-Pb zircon	>370 (n=5)	(2,3)	Discordant zircon dates. Pb-Pb dates of 357-379 Ma indicate an approximate minimum age. Intercept dates are very poorly defined due to a lack of dispersion in U-Pb dates.
MYRA VOLCANICS					
M1	Quartz-feldspar porphyry. H-W mine(Westmin), Buttle Lake, Alberni map area. 49°34.25' 125°35.33' (GSC/P13-307-Sicker)	U-Pb zircon	>370 (n=2)	(7)	A minimum age base on preliminary analyses with Pb-Pb dates of 370 and 371 Ma.

* UBC = analysis at Univ. of British Columbia; GSC = analysis at Geol. Survey of Canada.
** Error limits are ±2 sigma (95% conf. interval). For U-Pb dates: UI = upper intercept date, LI = lower intercept date, n = no. of zircon analyses.

References: (1) Geochronology Data File of R.L. Armstrong (Univ. of British Columbia), writ. comm., 1985; (2) Muller, 1980; (3) see Table 82.7 in Appendix for analytical data; (4) unpublished results from GSC Geochronology Laboratory; (5) Stevens et al., 1982; (6) Eastwood, 1980; (7) Collected by R.V. Kirkham (GSC), analyzed by Parrish.

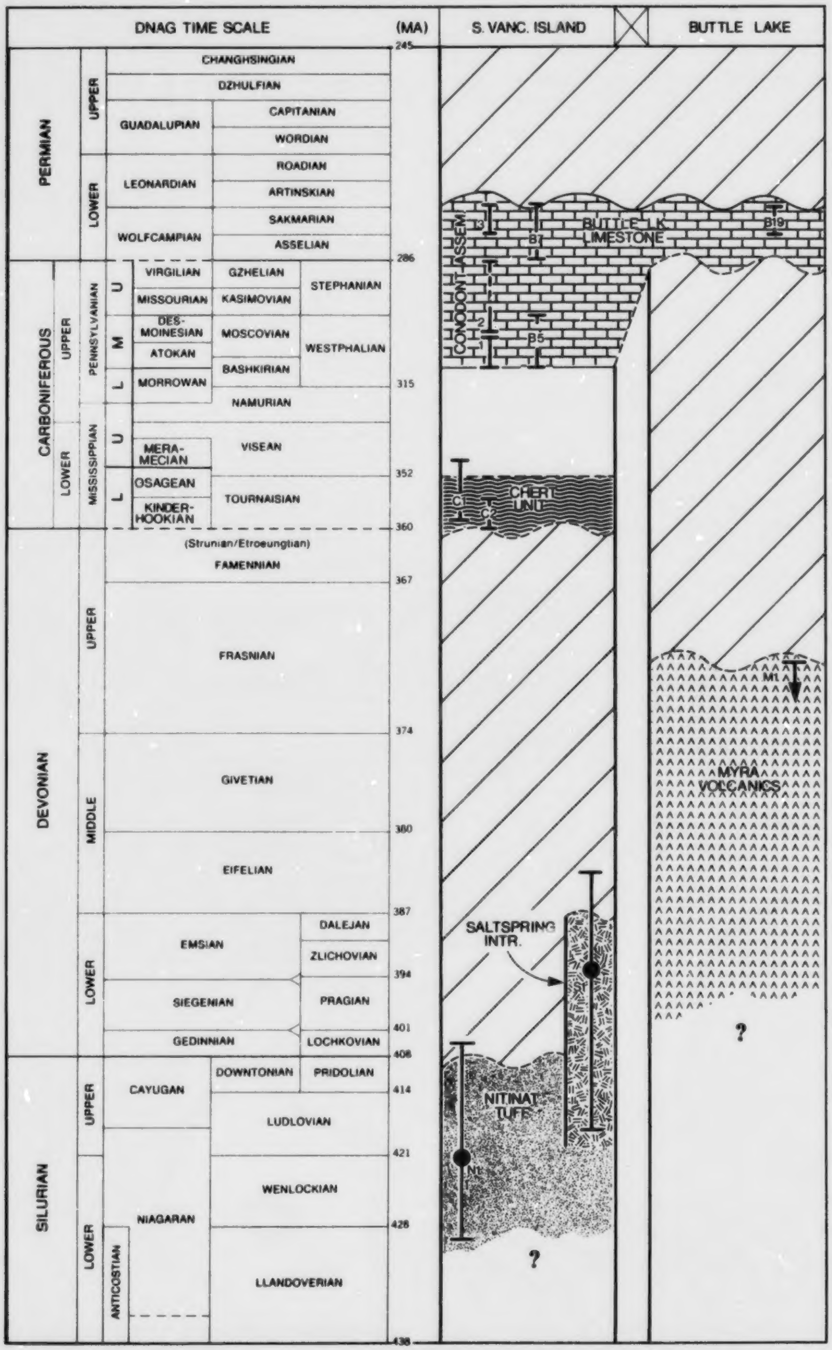

Figure 82.2. *Time stratigraphic summary of the Sicker Group on southern Vancouver Island and in the Buttle Lake area on the northern part of the island. Selected age data are portrayed with vertical bars which indicate the possible time range for each determination. The range for isotopic dates (N1, S1) is the 95% confidence interval. The arrow at M1 indicates a minimum age (Table 82.1). The preferred age range for each conodont fauna is shown with a solid line; the dashed line indicates the total possible range. The time scale is after that proposed for the Decade of North American Geology (DNAG) project (Harland et al., 1982; Palmer, 1983).*

Island (Insular Belt of Muller, 1977). The Sicker is exposed chiefly in three anticlinal uplifts (Fig. 82.1) located at Cowichan Lake, Nanoose Bay and Buttle Lake. Yole (1969) summarized previous stratigraphic studies of the Sicker Group and divided it into two formal units (Fig. 82.1):

1. An upper unit, called the Buttle Lake Formation, consists mainly of limestone with subordinate clastic rocks, and ranges from 30 to 470 m thick, although locally it is absent (Fig. 82.1; Yole, 1969).

2. A lower unit, called the Youbou Formation, comprises all stratified rocks beneath the Buttle Lake Formation. This lower sequence is dominated by volcanic and pyroclastic rocks with subordinate epiclastic sandstone, mudstone and radiolarian ribbon chert; its true thickness is unknown. Muller (1980) proposed to replace Yole's Youbou Formation with three new units, which, in order of increasing age, are: sediment-sill unit (informal name), Myra Formation and Nitinat Formation. As is shown below, there are significant problems with the definition and practicality of these new units. Therefore, in this paper Muller's units are considered as informal subdivisions of the Youbou Formation, applicable only in some areas. Nitinat tuff (Muller, 1980, p. 6) refers to a distinctive pyroxene-phyric tuff exposed in the Cowichan Lake uplift; Myra volcanics (Muller, 1980, p. 16; Fleming et al., 1983) refer to silicic pyroclastic rocks exposed in the Buttle Lake uplift.

The Sicker Group also is closely associated with two suites of intrusive rocks:

1. The Early Devonian Saltspring Intrusions of Muller (1980, 1983) which are apparently restricted to Saltspring Island (S1 and S3 in Fig. 82.1) and the area east of Cowichan Lake; and

2. Triassic(?) mafic intrusions which are widespread in the Sicker and are probably feeders to overlying Triassic basalts of the Karmutsen Formation. These intrusive rocks are important because they provide crosscutting relationships that can be used to determine stratigraphic ages and timing of deformation for the Sicker Group. These relationships are critical to our studies because conventional stratigraphic studies are hampered by the absence of reliable marker horizons and by structural complexities due to folding and faulting.

Tables 82.1 and 82.3 through 82.6 summarize available fossil and isotopic data, including a number of new conodont ages and U-Pb and K-Ar dates, for the Sicker Group and associated intrusions (some of these new isotopic dates are from R.L. Armstrong who has kindly allowed us to include them in our compilation. All isotopic dates were calculated using new decay constants (Harland et al., 1982). In addition to our own sampling, many of the localities of previous workers were re-examined in order to verify geological relationships exposed there (note that in some cases location descriptions have been corrected and therefore differ from the original sources). These data were used to construct the two time stratigraphic columns in Fig. 82.2, which focus on stratigraphic relationships amongst well-dated units of the Sicker. These units are discussed below, proceeding from oldest to youngest.

Nitinat tuff

The Nitinat tuff in the Cowichan Lake uplift is mainly pyroclastic with subordinate volcanic flows. Commonly, the tuff is agglomeratic with rounded, cobble-sized clasts of pyroxene-phyric volcanic rock comprising up to 20% of the rock. The unit is characterized by the conspicuous presence of stubby, black phenocrysts of augite which comprise up to 10% of the rock and which have been variably altered to actinolite (uralite). The Nitinat shows extensive development of static metamorphic assemblages of chlorite, epidote, actinolite and plagioclase indicating upper greenschist conditions. The main deformational fabric is a variably developed flattening foliation which is vertical and strikes northwesterly. Excellent descriptions of this unit are available in Clapp and Cooke (1917, p. 127-136) and Fyles (1955, p. 13-14) who described its occurrence in the southern part of the Cowichan uplift. In the northern part of the uplift, the Nitinat tuff is equivalent to units PS5, and possibly PS4, of Sutherland Brown and Yorath (1985).

The Nitinat tuff is clearly pre-Devonian because it is intruded in many places by Early Devonian porphyry of the Saltspring Intrusions. A particularly good example of this relationship is shown in Fig. 82.3. K-Ar dates for the Nitinat (Table 82.1, N1-N3) show a large scatter which is probably due to the fact that the dated mineral separates consisted of uralitized pyroxene and not hornblende. The two younger dates (N2, N3) are Permian and therefore clearly reset. The oldest date (N1) is Silurian and may approximate the actual age of the unit.

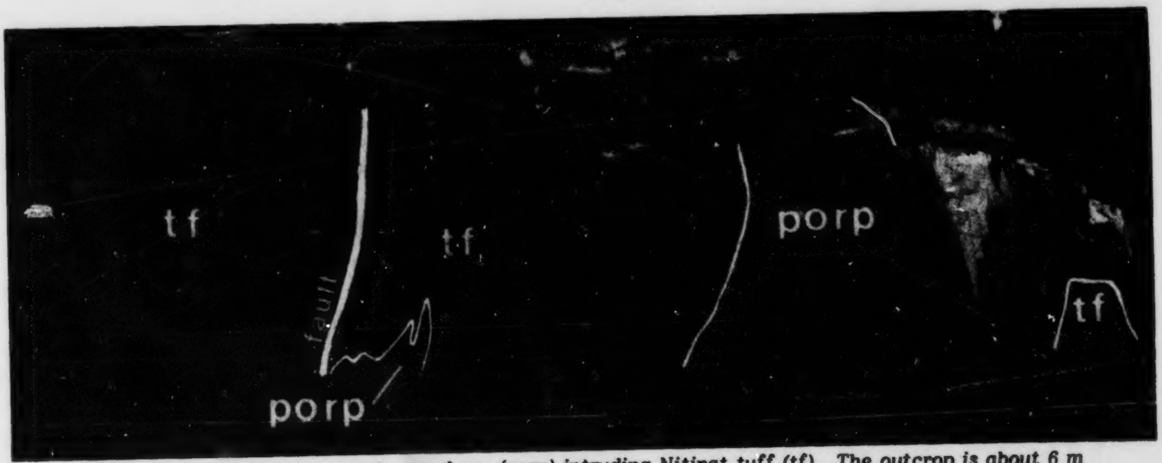

Figure 82.3. Saltspring quartz porphyry (porp) intruding Nitinat tuff (tf). The outcrop is about 6 m high and is located on the west side of Highway 1 about 2.3 km south of the Chemainus River (third outcrop south of river). Nitinat tuff from near this locality yields a 421 Ma K-Ar date (N1; 2.9 km south of river) on uralitized clinopyroxene which occurs as phenocrysts in the tuff.

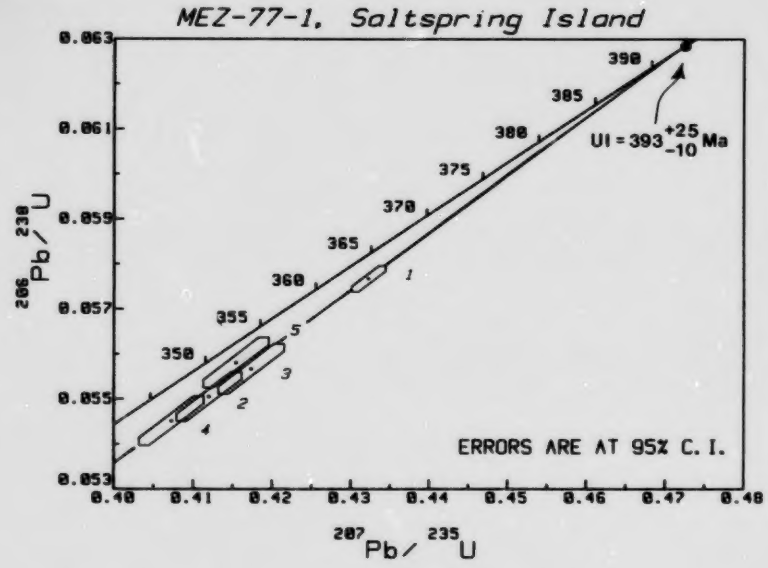

Figure 82.4

U-Pb concordia diagram for zircon dates from Saltspring quartz porphyry from Mount Maxwell, Saltspring Island (S1). Analytical data is summarized in Appendix A. The upper intercept date (UI) of 393 Ma is presently the best estimate of the igneous age of the Saltspring Intrusions.

Table 82.2. Stratigraphic sequence at the west fork of Shaw Creek

Approximate thickness (metres)	Rock type
	Top not exposed
60-90	Purplish volcanic breccia
400	Green tuffaceous greywacke.
80	Amygdaloidal basalt.
310	Thin and thick beds of tuffaceous greywacke.
240	Black feldspathic and argillaceous tuff, thin limestone lenses.
180	**Chert unit** (Early Mississippian and older?) Thin bedded cherty tuff, radiolarian ribbon chert.
	------------------ unconformity? ------------------
1400	**Nitinat tuff** (Silurian?) Massive green volcanic breccia.
	Base unknown

Note: After Fyles (1955, p. 18). This is the type section for the Youbou Formation of Yole (1969).

Saltspring Intrusions

The Saltspring Intrusions (Muller, 1980, 1983) occur on southern Saltspring Island and in the area east of Cowichan Lake, and include a suite of small quartz-feldspar porphyry intrusions and some larger stocks of granodiorite. This intrusive suite has previously been called Tyee quartz-feldspar porphyry by Clapp and Cooke (1917, p. 167-169, informal name) and Tyee Intrusions by Muller (1977). Muller (1980, 1983) introduced the new name Saltspring Intrusions, apparently to avoid conflict with the formally named Tyee Formation of Oregon. The following description of the unit is largely after Clapp and Cooke (1917, p. 167-169).

The Saltspring Intrusions typically occur as irregular bodies of porphyry with variable amounts of rounded quartz and lath-shaped feldspar phenocrysts. The larger stocks on Saltspring Island contain quartz, albitized plagioclase and potassium feldspar with minor mafic minerals now altered to chlorite and epidote (Muller, 1980). These intrusions show the same steeply dipping flattening foliation present in the Nitinat tuff, and locally are recrystallized to quartz-sericite schist.

U-Pb zircon analyses from three localites in the Saltspring Intrusions give a discordant set of dates (Table 82.1, S1-S3). Muller (1980), who reported on an early set of these U-Pb dates, concluded that the intrusions were Late Silurian or Devonian. Appendix A contains a table of the analytical results for these U-Pb dates, including several unpublished analyses. Zircon fractions from localities S2 and S3 are discordant but yield similar U-Pb dates so that a discordia line and intercept dates are very poorly defined. Pb-Pb dates indicate a minimum age of about 370 Ma (Late Devonian). For the Mount Maxwell locality (Table 82.1, S1), further dating of a handpicked, air-abraded fraction from the

Table 82.3. Microfossil ages for radiolarian chert from the Sicker Group

No.	Location (GSC locality no.)	Fossils identified	Age determination	Ref.
C1	South of Skutz Falls, Logging road S5K, Victoria map area. 48°45.37' 123°57.03' (no GSC locality)	radiolaria	Early to early Late Mississippian (middle Kinderhookian to early Meramacian)	(1)
C2	West of north Shaw Creek logging road (top of chert unit in Table 82.2), Alberni map area. 49°00.45' 124°26.28' (C127519-C127521)	conodonts	Early Mississippian (Kinderhookian)	(2)

References: (1) Muller, 1980, p. 23. Note the following corrections to Muller's text: Sample No. 79-42H, 48°45.37'N, 123°57.03'W, 3 km south of Skutz Falls. (2) Collected by Brandon, determined by Orchard.

original zircon separate allows a more precise age determination. When plotted on a concordia diagram (Fig. 82.4), the five zircon fractions define a good linear array with an upper intercept date of 393 Ma (Early Devonian). In this array, the handpicked fraction (no. 1 in Fig. 82.4) shows the least discordance which indicates that discordance is probably due to Pb-loss either from the surface of each zircon, which was removed by abrasion, or from the more highly cracked and metamict zircons, which were avoided by handpicking. This result precludes the possibility that the upper intercept date represents the age of an inherited zircon component assimilated in a younger pluton. Therefore, we conclude that the upper intercept date for the Mount Maxwell locality approximates the age of the Saltspring Intrusions. Further dating in progress should verify this conclusion.

Myra volcanics

In their type area on Myra Creek at the south end of Buttle Lake, the Myra volcanics of Muller (1980) underlie upper Paleozoic Buttle Lake Limestone (Fig. 82.2; Yole, 1969) and consist of a sequence of silicic pyroclastic rocks and related hypabyssal intrusions of dacite and quartz-feldspar porphyry (Fleming et al., 1983). The relationship of the Myra to the Nitinat tuff is not known at Buttle Lake since the base of the Myra is not exposed there. In general, metamorphic grade and deformation in the Myra at Buttle Lake are similar to that described above for the Nitinat tuff and Saltspring Intrusions (Fleming et al., 1983, p. 14).

Preliminary U-Pb determinations on two zircon fractions from quartz-feldspar porphyry in the type area of the Myra volcanics (M1 in Table 82.1) indicate a minimum age of 370 Ma (pre-Late Devonian). These dates suggest that the Myra volcanics may be the extrusive equivalents of the Saltspring Intrusions, a possibility originally suggested by Muller (1980, p. 16).

The pre-Late Devonian age of the Myra volcanics has another important implication. Muller (1980) argued that the Myra volcanics of Buttle Lake are equivalent to a sequence of volcaniclastic sandstone, cherty tuff and volcanic rock exposed in the Cowichan uplift. This sequence, which was mapped by Fyles (1955, p. 18) and is summarized in Table 82.2, lies above volcanic rock that is probably equivalent to the Nitinat tuff. As discussed below, a chert unit at the base of this sequence yielded Early Mississippian conodonts, which precludes a correlation with the Myra volcanics.

Chert unit

The chert unit corresponds to the thin bedded cherty tuff unit that Fyles (1955) described as a relatively continuous marker unit in the area north of Cowichan Lake. In the Shaw Creek area where it is best exposed (Table 82.2; C2 in Fig. 82.1), the chert unit consists of red and green radiolarian ribbon chert and thin-bedded green tuffaceous chert, and concordantly overlies pyroxene-phyric volcanic rocks (see map in Fyles, 1955) that are petrographically similar to, and probably correlative with, the Nitinat tuff. Northeast of Cowichan Lake, Clapp and Cooke (1917, p. 136-137) described three areas where similar stratigraphic relationships occur with thin bedded cherts overlying Nitinat-type volcanic rocks. This chert unit is also present in the northern part of the Cowichan uplift where it forms the base of unit PS3 of Sutherland Brown and Yorath (1985).

Radiolarian chert from near the top of the chert unit in the Shaw Creek area yielded the conodonts **Siphonodella** and **Pseudopolygnathus** (C2 in Table 82.3), which clearly are early Mississippian, Kinderhookian (approximately early and middle Tournaisian, Fig. 82.2). Radiolaria from chert in this area were too poorly preserved to be identified; however, southeast of Cowichan Lake, radiolaria from Sicker chert give a similar Mississippian age (C1 in Table 82.3). The geological setting of this locality is not known. Since the chert unit is relatively thick, and since only the top of the unit has been dated, it is likely that the unit could range down into the Devonian. Further systematic dating is needed.

The Early Mississippian age for the Shaw Creek chert unit has some important implications. If the chert unit does in fact rest depositionally on the Nitinat tuff, then, based on their pre-Late Devonian age and their dominantly pyroclastic character, the Myra volcanics cannot be equivalent to the sequence above the Nitinat tuff. Another possible implication is that the sequence overlying the chert unit (Table 82.2) is Mississippian and younger. One problem, however, is that in the Shaw Creek area, this sequence, at least locally, contains tight, outcrop-scale folds and, therefore, should not be considered a simple stratigraphic sequence. Fyles (1955, p. 25-26, also cross-sections on his map) also presented convincing evidence for larger, map-scale folds. The Shaw Creek sequence, however, also occurs in the northern part of the Cowichan uplift where it is relatively undeformed. With further work, that area may yield a more suitable type section for the Youbou Formation.

Table 82.4. Fossil ages for isolated outcrops of Buttle Lake Limestone

No.	Location (GSC locality no.)	Lat., Long.	Fossils identified*	Age determination**	Ref.
B1	NE of Schoen Lk., Alert Bay map area. (no GSC locality)	50°11.5' 126°14.0'	coral	Mississippian-Permian	(1)
B2	SE of Mt. Schoen, Alert Bay map area. (86301)	50°07.95' 126°10.87'	(a) coral	Mississippian-Permian	(1)
			(b) ostracods, foraminifera, conodonts	Pennsylvanian-Early Permian (prob. Late Pennsylvanian)	(2,1)
B3	W of Buttle Lake, Alberni map area. (no GSC locality)	49°41.65' 125°39.15'	(a) bryozoans	Permian	(3,4)
			(b) brachiopods	Pennsylvanian-Permian(4)	
B4	W fork of Cameron River, quarry at beginning of logging road E10, Alberni map area. (C-82857)	49°10.10' 124°32.90'	foraminifera	Permian (probably Early Permian)	(5)
B5	E side of North Ballenas Is., Alberni map area. (57588)	49°20.65' 124°09.35'	(a) fusulinids	Middle Pennsylvanian (prob. early Desmoinesian)	(6)
			(b) brachiopods	Pennsylvanian-Permian	(6)
B6	Mount Landalt, NE of Cowichan Lk., Nitinat map area. (no GSC locality)	48°56.90' 124°13.75'	no age-diagnostic fossil	age unknown	(7)
B7	Peninsula at E end of Cowichan Lake, Nitinat map area. (GSC locality unknown)	48°50.45' 124°08.15'	(a) brachiopods	Early Permian	(7)
			(b) fusulinids	Early Permian (Wolfcampian)	(7)
B8	E of Fairservice Crk. and NW of Waterloo Mtn., Victoria map area. (no GSC locality)	48°43.90' 123°58.00'	foraminifera	Pennsylvanian-Permian (probably Pennsylvanian)	(8)
B9	E side of McGee Crk., Nootka map area. (GSC locality unknown)	49°47.3' 126°08.4	foraminifera	Late Mississippian-Pennsylvanian (probably Early Pennsylvanian-	(9)
B10	SE of Vernon Lake, Nootka map area. (79150)	49°58.15' 126°19.00'	bryozoan, brachiopods	Ordovician-Permian	(9)
B11	W side of Horne Lake, Alberni map area. (no GSC locality)	49°20.0' 124°45.2'	fusulinids	probably early Middle Pennsylvanian	(10)
B12	E of Fairservice Creek and NW of Waterloo Mtn., Victoria map area. (C-86895)	48°43.85' 123°57.00'	algae	Mississippian or younger	(11)
B13	W of Douglas Peak, Alberni map area. (no GSC locality)	49°07.82' 124°39.81'	brachiopods	possibly Pennsylvanian or Permian	(12)
B14	SW coast of Texada Is., S of Mt. Dick, Alberni map area. (C-102163)	49°29.90' 124°09.35'	conodonts (CAI=5)	M. Pennsylvanian, Atokan (1)	(13)
B15	CNR railroad trestle, Koksilah River, Victoria map area. (C-087059)	48°40.75' 123°41.65'	conodonts (CAI=5)	M. Pennsylvanian, Atokan (1)	(13)
B16	Cobble Hill quarry, Victoria map area. (C-087058)	48°40.65' 123°38.15'	conodonts (CAI=5)	M. or L. Pennsylvanian, Desmoinesian to Virgilian (2)	(13)
B17	Cobble Hill quarry, Victoria map area. (C86308)	48°40.65' 123°38.15'	conodonts (CAI=6-7)	probably E. Permian (3?)	(13)
B18	Cobble Hill quarry, Victoria map area. (C-086309)	48°40.65' 123°38.15'	conodonts (CAI=6-7)	probably E. Permian (3?)	(13)
B19	Buttle Lake road, 3.3 km N of Ralph R., Alberni map area. (C-102165)	49°39.60' 125°31.45'	conodonts (CAI=6-7)	E. Permian, probably Sakmarian (3)	(13)
B20	Copper Canyon Chemainus River Victoria map area. (C-127506)	48°53.12' 123°47.45'	conodonts (CAI=6-7)	probably E. Permian (3?)	(13)
B21	S of St. Mary's Lk., Mt. Arrowsmith Regional Park, Alberni map area. (C-127712)	49°15.60' 124°37.60'	conodonts (CAI=6-7	probably E. Permian (3?)	(13)

* Conodont alteration index (CAI) is given for conodont localities.
** ( ) refer to conodont faunal associations discussed in text.

References: (1) Muller et al., 1974, p. 7; (2) B.E.B. Cameron (GSC), writ. comm., 1972 (GSC report no. P-2-1972-BEBC); (3) Fritz, 1932; (4) Yole, 1963 (see p. 143 in Yole for a discussion of revised age of brachiopods); (5) Muller, 1980, p. 23; (6) Muller and Carson, 1969, p. 9; (7) Fyles, 1955, p. 19; (8) Muller, 1971, p. 29, (no GSC locality or official report); (9) Muller et al., 1981, p. 8; (10) Sada and Danner, 1974, p. 250, 255, 262-263. Note that at this locality the age diagnostic fusulinid was not confidently identified; (11) unpublished locality of Muller, collected near B8 (GSC report no. 4-BM-1980, identified by B.L. Mamet); (12) Stevenson, 1945, p. A144; (13) Conodont determinations by Orchard on collections by Brandon, Muller, Sutherland-Brown and Yorath.

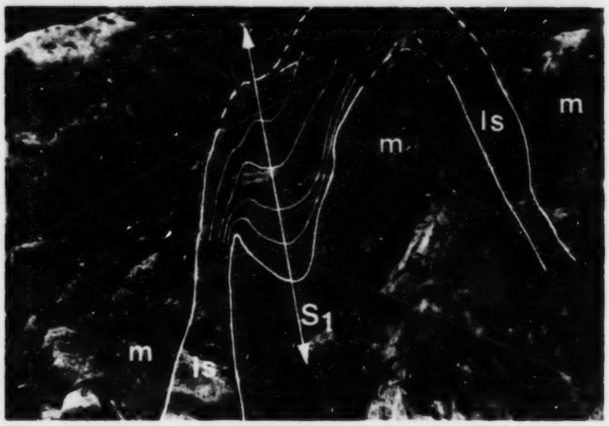

Figure 82.5. *Tight folds of Buttle Lake Limestone exposed in the Chemainus River at Copper Canyon. At this locality, the unit consists of interbedded limestone (ls) and black mudstone (m). The axial plane of these folds (S_1) is parallel to schistosity in nearby quartz-sericite schist and schistose metavolcanic rocks. Conodonts from the limestone (B20) are Early Permian and give a maximum age for Sicker deformation.*

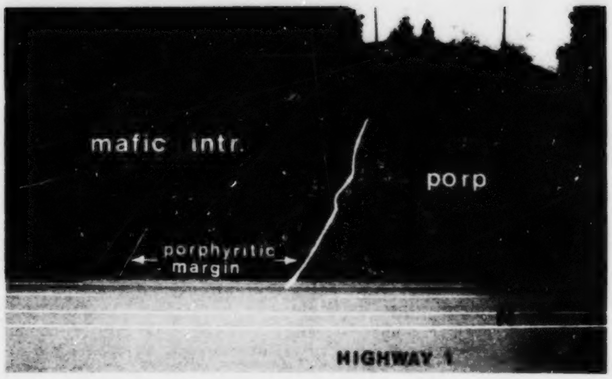

Figure 82.6. *Triassic mafic intrusion cutting Saltspring quartz porphyry (porp). The margin of the mafic intrusion is porphyritic near the intrusive contact. Concordant U-Pb zircon dates from this locality (K1) indicate a Late Triassic age for the intrusion. The outcrop is about 6 m high and is located on the west side of Highway 1 about 1.5 km south of the Chemainus River (second outcrop south of river).*

Buttle Lake Limestone

The highest unit in the Sicker Group is the Buttle Lake Limestone of Yole (1969). Yole (1969) described a section in the type area at Buttle Lake (B3 in Fig. 82.1) and two sections in the Cowichan Lake uplift (near BS1 and B8 in Fig. 82.1). The Buttle Lake typically consists of massive and bedded limestone with lenses and nodules of chert (Yole, 1969; Fyles, 1955); locally it also contains interbeds of siltstone and mudstone. In some areas, a thin clastic unit is present at the top of the Buttle Lake Limestone (PS1 of Sutherland Brown and Yorath, 1985). A gentle unconformity separates the Buttle Lake from overlying Triassic basalts of the Karmutsen Formation (Sutherland Brown and Yorath, 1985).

Based on extensive fossil collections (Tables 82.4 and 82.5), the age of the Buttle Lake is now known to range from Middle Pennsylvanian through Early Permian (Fig. 82.2). The macrofossil localities (B1-B13 in Table 82.4) generally give imprecise Pennsylvanian-Permian ages, although two fusulinid localities (B5, B7) do give more specific ages of Middle Pennsylvanian and Early Permian.

New conodont ages from twenty-one localities provide more complete data on the age and stratigraphy of the Buttle Lake Limestone. Table 82.4 summarizes eight isolated conodont localities (B14-B21); Table 82.5 shows ages for two stratigraphic collections, located at Mount Mark and on the Cameron River (BS1, BS2 in Fig. 82.1). The conodont collections are divided into three faunal associations (Fig. 82.2, Appendix B): (1) early Middle Pennsylvanian, Atokan; (2) late Middle or Late Pennsylvanian, Desmoinesian to Virgilian; and (3) Early Permian, probably Sakmarian. The stratigraphic collections, especially BS2, indicate that this age range is present, at least locally, in a single vertical section. This result contrasts with Yole (1963). Based on systematic sampling of macrofossils, he concluded that in its type area, the Buttle Lake Limestone is restricted to the Early Permian (Fig. 82.2), which is consistent with the one conodont age from the Buttle Lake area (B19). Further sampling for conodonts, however, is needed to determine the presence or absence of Pennsylvanian limestone at Buttle Lake.

The conodont alteration index (CAI; (Epstein et al., 1977) can be used to estimate the maximum temperature to which the Buttle Lake Limestone was exposed. CAI values for the Buttle Lake (Table 82.4 and 82.5) are all relatively high, ranging from 5 to 7; they indicate temperatures in excess of 300°C and are typical of conodonts from greenschist facies metamorphic rocks (Epstein et al., 1977). For comparison, Triassic limestones above the Sicker Group typically have CAI values of 3 to 4, indicating maximum temperature of about 200°C. In the Buttle Lake Limestone, there appears to be a general pattern of higher CAI values in younger parts of the unit (e.g., BS2 and B16-B18), which probably is due to high temperatures beneath the thick Triassic basaltic sequence that was erupted over the Buttle Lake Limestone (Muller, 1977). The CAI of the lower part of the Buttle Lake is probably related to the same greenschist metamorphism recorded in the underlying Youbou Formation.

One of the conodont localities in Table 82.4 comes from a newly discovered exposure of Buttle Lake Limestone in the Chemainus River at Copper Canyon. In this area, the Buttle Lake consists of interbedded limestone and mudstone which are highly deformed into a series of tight, upright folds (Fig. 82.5). Associated with these folded limestones are quartz-sericite schist and schistose mafic volcanic rocks, which probably correlate with the Saltspring Intrusions and Nitinat tuff, respectively. The foliation in these rocks parallels the axial plane of the folded limestones. Together these relationships indicate that all of these rocks were affected by the same deformational event. Schistose fabrics are common in the Sicker Group, but are more widely developed in the southeast part of the Cowichan uplift (Clapp and Cooke, 1917; Eastwood, 1980). One interpretation is that the more highly deformed rocks represent an older portion of the Sicker. The Copper Canyon locality, however, indicates that deformation of the Sicker occurred after the Early Permian. In fact evidence discussed below suggests that this deformation happened in the early Mesozoic. The more widespread occurrence of deformed Sicker rocks in the southeast part of the Cowichan uplift probably indicates that a deeper structural level is exposed there, which is consistent with the northwest plunge of the uplift.

Triassic(?) mafic intrusions

The Triassic(?) mafic intrusions occur as thick sills and dykes, typically with a porphyritic texture, and are composed of plagioclase and clinopyroxene (commonly altered to uralite) with minor skeletal ilmenite. These intrusions are fairly common in the Saltspring Island – Cowichan Lake area (gabbro-diorite porphyrite of Clapp and Cooke, 1917, p. 169-172; "hornblende shonkinite" of Eastwood, 1980; Franklin Creek intrusions of Fyles, 1955, p. 20-22). Muller (1980, p. 6) speculated that some of these intrusions may be related to the Nitinat tuff. A Triassic age, however, is preferred for the following reasons: (1) the intrusions are compositionally and texturally similar to the overlying Triassic Karmutsen basalts (Fyles, 1955, p. 20-22; Karmutsen basalts = Franklin Creek Volcanics of Fyles); (2) one of these intrusions yielded concordant U-Pb dates of about 220 Ma (Late Triassic; K1 in Table 82.6, Fig. 82.6); and (3) a mafic sill in the Copper Canyon area intrudes dated Buttle Lake Limestone (B20), and therefore must be post-Early Permian.

This conclusion is at variance with a K-Ar date of 363 Ma (Mississippian) reported by Eastwood (1983) for a mafic intrusion in the Mount Richards area (K2 in Table 82.6, Fig. 82.1). This intrusion, however, is identical, both in outcrop and in thin section, with the dated Triassic intrusion on Highway 1 (K1, Fig. 82.6). The dated sample at Mount Richards was obtained from a drill core, so that instead of mafic intrusion, Nitinat tuff may have been sampled accidently. Unfortunately, no thin section was made nor was any reference material retained. In any case, dating in progress of another sample from this locality should resolve this question.

Clapp and Cooke (1917) argued convincingly that the schist-producing deformation of the Sicker postdates the mafic intrusions and predates emplacement of Jurassic granitic plutons which are widespread in the outcrop areas of the Sicker Group (Fyles, 1955; Muller, 1983). Therefore, if the mafic intrusions are in fact Triassic, then deformation of the Sicker would be constrained to the early Mesozoic.

Table 82.5. Conodont ages for stratigraphic sections in the Buttle Lake Limestone

Metres above base of unit (GSC locality no.)	Age determination**	CAI*
BS1--Mt. Mark composite section, Alberni map area (49°21.60' 124°43.90')		
215 m (C127679)	E. Permian? (3?)	6-7
163 m (C127669)	M. Pennsylvanian- E. Permian (1-3)	5-6
69 m (C127674)	M. Pennsylvanian?, Atokan? (1?)	6-7
30 m (C127672)	M. Pennsylvanian, Atokan (1)	5
8 m (C127711)	M. Pennsylvanian, Atokan (1)	6-7
4 m (C127710)	M.Pennsylvanian?, Atokan? (1?)	6-7
2 m (C127660)	M. Pennsylvanian, Atokan (1)	6
0 m (C127670)	M. Pennsylvanian, Atokan (1)	6-7
BS2--Cameron River section, Alberni map area (49°10.30' 124°32.80')		
365 m (C127690)	E. Permian, probably Sakmarian (3)	6
200 m (C127688)	E. Permian, probably Sakmarian (3)	6
168 m (C127686)	E. Permian, probably Sakmarian (3)	6
79 m (C127683)	M. or L. Pennsylvanian, Desmoinesian to Virgilian (2)	5-6
67 m (C127681)	M. or L. Pennsylvanian, Desmoinesian to Virgilian (2)	5
*,** See Table 82.4		

Conclusions

The main conclusions are as follows:

1. The oldest known unit in the Sicker Group is the Nitinat tuff, which is definitely pre-Devonian, and possibly Silurian.
2. The Saltspring Intrusions, which intrude the Nitinat tuff, are Early Devonian.
3. Preliminary U-Pb dates indicate that the Myra volcanics of the Buttle Lake uplift are pre-Late Devonian, and therefore could be extrusive equivalents of the Saltspring Intrusions.
4. A Lower Mississippian chert unit is present in the Cowichan uplift and probably lies depositionally above the Nitinat tuff. Thus, in this area, rocks above the Nitinat tuff are not equivalent to the Myra volcanics as originally suggested by Muller (1980).
5. The Buttle Lake Limestone, which is the highest unit in the Sicker, ranges from Middle Pennsylvanian through Early Permian.
6. Deformation of the Sicker Group, which resulted in tight folds and a widespread schistose foliation, is definitely post-Early Permian, and probably early Mesozoic.

Acknowledgments

We are grateful and indebted to R.L. Armstrong of the University of British Columbia for access to his geochronology data file and for permission to use unpublished isotopic dates. We also thank K.J. Kveton of the University of Washington for helpful discussions about the geology of Saltspring Island.

Table 82.6. Isotopic dates for Triassic(?) mafic intrusions in the Sicker Group

No.	Rock type, location (sample no.)*	Dating method	Date** (Ma)	Ref.	Comments
K1	Pyroxene-phyric mafic dyke. East of Mt. Sicker along Highway 1 (Fig. 82.6), Victoria map area. 48°52.0' 123°42.6' (UBC/Sicker 1am)	(a) U-Pb zircon	217-222	(3)	Concordant U-Pb date, represents primary age of dyke.
		(b) K-Ar uralitic amphibole after pyroxene	190 ± 14	(1)	Minimum age of uralite alteration.
K2	Mafic rock of uncertain affinity. W of Crofton, N of Mt. Richards Victoria map area. 48°51.7' 123°40.4' (UBC/E80-24 no. 24566M)	K-Ar uralitic amphibole after pyroxene	363 ± 26	(1,2)	Minimum age of uralitic alteration. Sample was from a drill core and was identified as a mafic intrusion (ref. 2). Might be Nitinat tuff (no sample or thin section available).

*,** see Table 82.1.

References: (1) Geochronology data file of R.L. Armstrong (Univ. of British Columbia), writ. comm., 1985; (2) Eastwood, 1983; (3) Isachsen et al., 1985.

References

Baesemann, J.F. and Lane, H.R.
1985: Taxonomy and Evolution of the Genus **Rhachistognathus** DUNN Conodonta; Late Mississippian to Early Middle Pennsylvanian in Towards a Boundary in the Middle of the Carboniferous: Stratigraphy and Paleontology; ed. H.R. Lane and W. Ziegler; Courier Forschungsinstitut Senckenberg, v. 74, p. 93-135.

Bender, K.P.
1980: Lower and Middle Pennsylvanian conodonts from the Canadian Arctic Archipelago; Geological Survey of Canada, Paper 79-15, 29 p.

Clapp, C.H.
1912: Southern Vancouver Island; Geological Survey of Canada, Memoir 13, 143 p.

Clapp, C.H. and Cooke, H.C.
1917: Sooke and Duncan map-areas, Vancouver Island; Geological Survey of Canada, Memoir 96, 445 p.

Eastwood, G.E.P.
1980: Geology of the Mt. Richards area, Vancouver Island, British Columbia; British Columbia Ministry of Energy, Mines and Petroleum Resources, Preliminary Map 40, scale 1:15 625.

1983: Sicker project (92B/13); British Columbia Ministry of Energy, Mines and Petroleum Resources, Paper 1983-1, p. 46.

Epstein, A.G., Epstein, J.B., and Harris, L.D.
1977: Conodont color alteration – an index to organic metamorphism; U.S. Geological Survey, Professional Paper 995, 27 p.

Fleming, J., Walker, R., and Wilton, P.
1983: Mineral deposits of Vancouver Island: Westmin Resources (Au-Ag-Cu-Pb-Zn), Island Copper (Cu-Au-Mo), Argonaut (Fe); Geological Association of Canada, annual spring meeting of the Pacific section (Victoria), Field Trip Guidebook no. 9, 19 p.

Fritz, M.A.
1932: Permian bryozoa from Vancouver Island; Royal Society of Canada, Transactions, 3rd series, v. 26, sec. 4, p. 93-107.

Fyles, J.T.
1955: Geology of the Cowichan Lake area, Vancouver Island, British Columbia; British Columbia Department of Mines, Bulletin 37, 72 p.

Grayson, R.C., Jr.
1984: Morrowian and Atokan Pennsylvanian conodonts from the northeastern margin of the Arbuckle Mountains, southern Oklahoma; Oklahoma Geological Survey, Bulletin 136, p. 41-63.

Harland, W.B., Cox, A.V., Llewellyn, P.G., Pickerton, C.A.G., Smith, A.G., and Walters, R.
1982: A Geologic Time Scale; Cambridge University Press, London, 131 p.

Isachsen, C., Armstrong, R.L., and Parrish, R.R.
1985: U-Pb, Rb-Sr and K-Ar geochronometry of Vancouver Island igneous rocks; Geological Association of Canada, annual spring meeting of the Pacific Section (Victoria), Programme and Abstracts, p. 21.

Jones, D.L., Silberling, N.J., and Hillhouse, J.
1977: Wrangellia – a displaced terrane in northwestern North America; Canadian Journal of Earth Sciences, v. 14, p. 2565-2577.

Muller, J.E.
1971: Notes on the geology of southern Vancouver Island; in Report of Activities, Part A, Geological Survey of Canada, Paper 71-1A, p. 28-31.

1977: Evolution of the Pacific margin, Vancouver Island and adjacent regions; Canadian Journal of Earth Sciences, v. 9, p. 2062-2085.

1980: The Paleozoic Sicker Group of Vancouver Island, British Columbia; Geological Survey of Canada, Paper 79-30, 24 p.

Muller, J.E. (cont.)
1982: Geology of the Nitinat Lake map-area; Geological Survey of Canada, Open File 821, scale 1:125 000.

1983: Geology, Victoria, British Columbia; Geological Survey of Canada, Map 1553A, scale 1:100 000.

Muller, J.E. and Carson, D.J.T.
1969: Geology and mineral deposits of Alberni map-area, British Columbia (92F); Geological Survey of Canada, Paper 68-50, 52 p.

Muller, J.E., Northcote, K.E., and Carlisle, D.
1974: Geology and mineral deposits of Alert-Cape Scott map-area, Vancouver Island, British Columbia; Geological Survey of Canada, Paper 74-8, 77 p.

Muller, J.E., Cameron, B.E.B., and Northcote, K.E.
1981: Geology and mineral deposits fo Nootka Sound map-area, Vancouver Island, British Columbia; Geological Survey of Canada, Paper 80-16, 53 p.

Palmer, A.R. (compiler)
1983: The decade of North American geology, 1983 geologic time scale; Geology, v. 11, p. 503-504.

Roddick, J.A. and Woodsworth, G.J.
1977: Geology, Bute Inlet map-area, British Columbia (92K); Geological Survey of Canada, Open File 480, scale 1:250 000.

Sada, K. and Danner, W.R.
1974: Early and Middle Pennsylvanian fusulinids from southern British Columbia, Canada and northwestern Washington, U.S.A.; Palaeontological Society of Japan, N.S., Transactions and Proceedings, no. 93, p. 249-265.

Stevens, R.D., Delabio, R.N., and Lachance, G.R.
1982: Age determinations and geological studies, K-Ar isotopic ages, Report 15; Geological Survey of Canada, Paper 81-2, 56 p.

Stevenson, J.S.
1945: Geology and ore deposits of the China Creek area, Vancouver Island, British Columbia; Annual Report of the Minister of Mines of the Province of British Columbia, 1944, p. A142-A161.

Sutherland Brown, A. and Yorath, C.J.
1985: LITHOPROBE profile across southern Vancouver Island: geology and tectonics; Geological Society of America, Cordilleran section meeting, Vancouver, British Columbia, Field Trip Guidebook, p. 8-1 to 8-23.

Yole, R.W.
1963: An Early Permian fauna from Vancouver Island, British Columbia; Bulletin of Canadian Petroleum Geology, v. 11, p. 138-149.

1969: Upper Paleozoic stratigraphy of Vancouver Island, British Columbia; Geological Association of Canada, Proceedings, v. 20, p. 30-40.

APPENDIX A

U-Pb zircon dates from the Saltspring Intrusions

Table 82.7. U-Pb zircon results for Saltspring Intrusions

Sample/fraction[1]	Wt. (mg)	U (ppm)	Pb (ppm)	Pb isotopic abundance,[2] Pb 206 = 100			$^{206}Pb/^{204}Pb$ measured	Ratios and ages (Ma)[4]		
				208	207	204		$^{206}Pb/^{238}U$	$^{207}Pb/^{235}U$	$^{207}Pb/^{206}Pb$
MEZ-77-1	Mt. Maxwell, Saltspring Island									
[3]+200 HP, AB (1)	2.53	361.9	20.86	10.572	5.508	0.0050	6743	0.05767 (361.5)	0.4322 (364.8)	0.05435 (385.7)
-200 + 325 MAG (2)	3.06	549.9	30.37	11.021	5.511	0.0057	2038	0.05505 (345.5)	0.4120 (350.3)	0.05428 (382.6)
-140 + 200 NMAG (3)	9.48	470.0	27.61	13.742	6.7809	0.0920	121	0.05567 (349.2)	0.4174 (354.2)	0.05437 (386.5)
-200 + 325 NMAG (4)	14.37	474.0	25.82	10.784	5.421	0.0001	4162	0.05451 (342.1)	0.4073 (346.9)	0.05419 (378.8)
-140 + 200 MAG (5)	3.87	481.9	28.12	13.183	6.544	0.0783	888	0.05581 (350.1)	0.4154 (352.8)	0.05399 (370.6)
WN-19-74	Arbutus Point, Vancouver Island									
[3]+200 HP, ABR	1.89	502.9	29.13	11.404	5.435	0.0019	14067	0.05764 (361.3)	0.4298 (363.0)	0.05407 (374.2)
-200 + 250	9.39	594.3	35.01	13.405	5.538	0.0055	5108	0.05751 (360.5)	0.4327 (365.1)	0.05457 (394.8)
-250 + 325	19.25	623.3	36.75	14.184	5.737	0.0199	3133	0.05694 (357.0)	0.4276 (361.5)	0.05446 (390.1)
-100 + 140	2.81	465.0	27.06	12.491	5.938	0.0385	1253	0.05671 (355.6)	0.4204 (356.3)	0.05376 (360.8)
MEZ-76-3	Lake Stowell, Saltspring Island									
+200 HP	1.43	491.8	27.66	12.490	5.925	0.0382	2454	0.05480 (343.9)	0.4055 (345.6)	0.05367 (357.1)
-140 + 200 NMAG	18.66	485.0	27.16	11.768	5.592	0.0139	1542	0.05534 (347.2)	0.4112 (349.8)	0.05389 (366.6)
-140 + 200 MAG	11.47	563.6	31.30	12.546	5.895	0.0326	6126	0.05417 (340.1)	0.4047 (345.1)	0.05419 (378.9)
-200 + 230 NMAG	24.04	553.7	30.77	11.951	5.424	0.0015	3817	0.05503 (345.3)	0.4098 (348.8)	0.05401 (371.6)
-200 + 230 MAG	14.68	682.6	36.90	12.536	5.494	0.0077	730	0.05317 (334.0)	0.3946 (337.7)	0.05381 (363.2)

[1] Symbols refer to mesh size; HP = hand-picked; ABR = Abraded; MAG = magnetic fraction; NMAG = non-magnetic fraction; ( ) refers to numbers on concordia diagram in Fig. 4

[2] blank corrected

[3] 1983 analyses; these have smaller errors than other analyses

[4] Decay constants: $\lambda_{238} = 0.155125 \times 10^{-9}$/year; $\lambda_{235} = 0.98485 \times 10^{-9}$/year; $^{238}U/^{235}U = 137.88$

Isotopic composition of common Pb assumed to be ^{208}Pb:^{207}Pb:^{206}Pb:^{204}Pb = 37.93:15.60:19.11:1

APPENDIX B

Conodont faunas from the Buttle Lake Limestone

Twenty-one conodont collections recovered from the Buttle Lake Limestone can be grouped into three conodont faunal associations (Fig. 82.2) ranging in age from Middle Pennsylvanian (Atokan) through Early Permian (probably Sakmarian). None of the faunules is large, and several consist of only a few fragmentary specimens, so that it is not possible to determine many elements to species level. The faunal associations are described below. Ages and locality descriptions are summarized in Table 82.4 for locality numbers beginning with B and Table 82.5 for those beginning with BS.

(1) Middle Pennsylvanian (Atokan) fauna. This fauna occurs at B14 and B15 and at 0 m, 2 m, 8 m and 30 m above the base of the Mount Mark section (BS1); it may also be present at 4 m and 69 m in BS1.

Faunules from 0 m and 30 m in BS1 contain specimens that are homeomorphic after **Declinognathodus.** These elements resemble **Idiognathoides opimus** morphotype 2 described from the Canadian Arctic by Bender (1980) and **I. marginodosus** morphotype B described from Oklahoma by Grayson (1984), both of which are from strata of Atokan age. The faunule from 0 m in BS1 also contains a specimen of **Rhachistognathus minutus declinatus** Basemann & Lane; this subspecies ranges from the early (but not basal) Morrowan into at least early Atokan strata in western United States (Baesmann and Lane, 1985, p. 108-109.

Simple elements of **Idiognathoides** lacking accessory anterior nodes occur alone, or associated with fragments that may represent **Idioprioniodus,** in four or five faunules: at B14 and B15 and at 2 m, 8 m and possibly 69 m in BS1. Most of the specimens of **Idiognathoides** correspond to **I. marginodosus** Grayson morphotype C, or **I. opimus** morphotype 1 sensu Bender, indicating an early Middle Pennsylvanian, Atokan age.

The faunule at B14 also contains fragmentary specimens of the **Idiognathodus – Streptognathodus** plexus. This group, which ranges through much of the Upper Carboniferous and earliest Permian, is found alone at 4 m in BS1. The stratigraphic position of the latter implies it too is Atokan in age (Table 82.5).

(2) Middle or Late Pennsylvanian (Desmoinesian to Virgilian) fauna. This fauna occurs at B16 and at 67 m and 79 m above the base of the Cameron River section (BS2).

The most distinctive element of this fauna is a species of 'naked' Gondolella, although none of the elements recovered are complete. The species has a very narrow platform and simple, robust denticles; the character of the posterior termination is uncertain. Similar elements have been referred to **G. gymna** Merrill & King, a species of probable late Middle Pennsylvanian, Desmoinesian age. However, because of the uncertainty about the specific identity of the Sicker Group specimens, a Late Pennsylvanian age is also considered possible. Poorly preserved specimens of the long ranging **Idiognathodus** and **Adetognathus** are present.

(3) Early Permian (probably Sakmarian) fauna. This fauna occurs at B19 and at 168 m, 200 m and 365 m above the base of the Cameron River section (BS2) and probably is present at B17, B18, B20 and B21 and possibly at 215 m in the Mount Mark section (BS1). A faunule from 163 m in BS1 is also included with this assemblage, but its age is very poorly resolved.

Faunules from 168 m, 200 m and 365 m in the upper part of the Cameron River section (BS2), are characterized by typical Early Permian **Neogondolella** elements together with the long ranging **Adetognathus** sp. (at 200 m and 365 m) and/or **Hindeodus** sp., an association of probable Sakmarian age. Four or five other localities, B17, B18, B20, B21 and possibly 215 m in BS1, have yielded only **Neogondolella.** These localities may therefore be slightly younger than the Cameron River fauna or, alternatively, the difference may be ecological: **Adetognathus** is known to favour restricted shallow water conditions.

Faunules from B19 and 168 m at BS2 contain fragments of what are considered to be a new genus probably related to species of 'naked' Gondolella. One difference, however, is that these elements have laterally enlarged, icriodid-type denticles. Elsewhere in western Canada, the same species has been found in the Iskut River area of northwestern British Columbia and in the Nahanni map area of east-central Yukon, in both cases associated with conodonts of latest Pennsylvanian or earliest Permian age. In the faunule from 168 m in BS2, this new element is associated with **Neogondolella** and is therefore considered to be Early Permian in age, which is consistent with its stratigraphic position (Table 82.5). The same age is attributed to B19 from Buttle Lake, where the new element occurs with long-ranging **Hindeodus.**

A faunule from 163 m in BS1 only contains specimens of long ranging **Adetognathus** sp. and **Hindeodus**, and therefore has been assigned a Middle Pennsylvanian to Early Permian age (Table 82.5). However, the fact that these two genera are present in several of the Early Permian faunules (168 m, 200 m and 365 m in BS2) may suggest a similar age for the faunule at BS1.

Ice flow trends and drift composition, Flowers River area, Labrador[1]

Project 820039

R.A. Klassen and A.M. Bolduc
Terrain Sciences Division

Klassen, R.A. and Bolduc, A.M., Ice flow trends and drift composition, Flowers River area, Labrador; in Current Research, Part A, Geological Survey of Canada, Paper 86-1A, p. 697-702, 1986.

Abstract

Regional ice flow trends, representing the last phase of flow in the Flowers River area of central Labrador, vary from N55°E in the southeast to N85°E in the north. Farther west, the trends are generally eastward and, near major river valleys, appear topographically controlled. Evidence of an older, more northward phase (or phases) of flow (N10°E to N45°E) was found at several locations. Far travelled (>50 km) erratics of red sandstone occur throughout the area; although their specific bedrock source is not known, they appear derived from the Siamarnekh Formation, or unmapped outliers of it. Local scale (1 to 10 km) dispersal trains originating from a volcanic pile are defined by fine grained, porphyritic rock and by till geochemistry. Geochemically 'anomalous' till samples of unknown origin, defined by trace elements and rare earth elements, occur over the peralkaline granite batholith of the Flowers River Igneous Suite.

Résumé

Les directions régionales d'écoulement des glaces de la dernière phase d'écoulement dans le secteur de la rivière Flowers, dans le centre du Labrador, vont de N55°E au sud-est à N85°E au nord. Plus loin à l'ouest, les directions sont généralement est et, à proximité des grandes vallées fluviales, elles semblent être contrôlées par la topographie. On a trouvé, à plusieurs endroits, des indices d'une ou de plusieurs anciennes phases d'écoulement plus vers le nord (N10°E à N45°E). On trouve dans tout le secteur des blocs erratiques de grès rouge qui ont parcouru de longues distances (>50 km); bien que l'origine de ces blocs ne soit pas connue, ils semblent appartenir à la formation de Siamarnekh ou aux avant-buttes non cartographiées de cette dernière. Des trainées de dispersion restreinte (1 à 10 km) provenant d'un amas de roches volcaniques sont constituées de roches porphyriques à grains fins et sont apparentées à la géochimie des tills. Des échantillons de tills de géochimie "anomale", d'origine inconnue et caractérisés par des éléments à l'état de trace et des éléments de terres-rares recouvrent le batholite granitique et peralcalin de la série endogène de Flowers River.

[1] Contribution to Canada-Newfoundland Mineral Development Agreement 1984-89.
Project carried by Geological Survey of Canada.

Introduction

Patterns of glacier ice flow and drift composition in the Flowers River area of central Labrador (Fig. 83.1) are being used to develop models of glacial dispersal at regional (tens to hundreds of kilometres) and local (up to tens of kilometres) scales as part of the Canada-Newfoundland Mineral Development Agreement. The work represents a continuation of similar studies conducted in the Melody Lake (13J, 13K) and Churchill Falls (13E, 23H) areas (Klassen, 1983, 1984; Klassen and Bolduc, 1984). Fieldwork for the Flowers River area was completed during July 1984.

The Flowers River area was chosen for study because of its potential for economic mineralization associated with felsic volcanic and peralkaline intrusive rocks of the Flowers River Igneous Suite that are generally enriched in Ce, F, Nb, Pb, Y, Zn, and Zr (Hill, 1982). Lake sediments and waters in the area have been previously sampled and analyzed as part of a reconnaissance geochemical survey funded jointly by Canada and Newfoundland; data from the study indicate that the Flowers River area is geochemically 'anomalous' for Mo and Pb and, in the southeastern portion, for Cu and Zn (McConnell, 1984).

Geology and physiography

Geology of the Flowers River area has been mapped by Taylor (1979) at 1:250 000 as part of a reconnaissance study, and by Hill (1982) at 1:100 000. The area is underlain by Paleohelikian plutons of gabbroid to granitoid composition comprising the Nain Igneous Complex, and is bounded to the east by Archean banded gneisses, metagranite, and metagranidiorite of the Nain Structural Province, and to the southwest by Archean(?)-Aphebian gneisses and plutonic rocks of the Churchill Structural Province. The Paleohelikian plutons are intruded by rocks of the Neohelikian Flowers River Igneous Suite (FRIS). The suite consists of felsic volcanic rocks intruded by peralkaline granite, which includes a main batholith and smaller, satellitic plutons (Hill, 1982).

Volcanic rocks are rhyolitic and include felsite, tuff, porphyry, and breccia; they are enriched in Ce, La, Nb, Rb, Y, Zn, and Zr, compared with 'average' levels for rocks of similar composition and contain minor showings of lead and zinc (Hill, 1982). Peralkaline granite consists of three phases: a 'normal' phase having a medium- to coarse-grained equigranular texture and comprising the main lithology, a 'marginal' phase which is a less peralkaline variant of the main phase, and a 'chilled' phase around the pluton margin which includes a fine grained porphyritic variant. Mineralogical differences are evident among the phases, and the Flowers River Igneous Suite varies from weakly peralkaline granite to highly peralkaline felsite and tuff, possibly as a result of compositional zoning within the parental magma chamber (Hill, 1982, p. 86).

The Flowers River area occupies part of the Nain-George River Plateau (Greene, 1974). It is rugged, characterized by hills that extend to between 200 and 600 m a.s.l., and is crossed by large valleys occupied by Notakwanon, Flowers, and Hunt rivers. The valley floors, which are forested, commonly have significant (>10 m) thicknesses of stratified drift and outwash and, below 100 m a.s.l., marine sediments. The upper parts of hills are covered by thin (<3 m thick), continuous to discontinuous till and support tundra vegetation. No Quaternary geological studies of the area have been published.

Methods

Till samples were collected throughout the area at densities that varied from 1 per 5 km^2 to 1 per 10 km^2; sample density was greatest in areas underlain by the Flowers River Igneous Suite. Sampling density was considered sufficient to characterize gross compositional change in till and to have a reasonable chance of intersecting a dispersal train of the size associated with mineralization at Strange Lake (Batterson et al., 1985; R.N.W. DiLabio, personal communication, 1984). Till was collected from the base of pits dug to between 40 and 80 cm. In highland areas, where soil zonation is weakly developed, samples were commonly collected from mudboils. In areas where soil profiles were evident, effort was made to sample below the zone of obvious iron stain ('B' horizon) to avoid, as much as possible, the effects of secondary weathering on geochemical analysis.

The clay-size (<0.002 mm) fraction of the till samples was analyzed for Cu, Pb, Zn, Ni, Fe, and Mn by atomic absorption methods, and for U by delayed neutron activation; the clay plus silt-size (<0.063 mm) fraction was analyzed for Ce, Sr, Th, Nb, Y, and Zr by X-ray fluorescence. Analyses were done by Bondar-Clegg and Co. Ltd., Ottawa.

During the course of sample collection, the types of erratics present were noted and qualitative estimates made of their relative abundance. The orientations of striae and of other indicators of ice flow trends, such as streamlined landforms, were also noted. Particular effort was made to excavate and examine striated surfaces developed on the lee side of outcrops to determine ice flow trends that may have existed prior to the last phase of regional glaciation (cf. Klassen and Bolduc, 1984).

Ice flow directions

Ice flow trends vary in orientation between north-northeast and east-southeast (Fig. 83.1) and are thought to be the product of at least two distinct phases of ice flow. Across hilltops throughout the eastern part of the area, the most prominent flow directions, representing the last regional phase of flow, vary between N55°E in the south, and N85°E in the north. In the west, the most prominent flow directions are nearly eastwards, varying between N90°E and S70°E, and are recorded by striae and streamlined landforms on hilltops as well as valley floors. In the southwest there is an alignment of flow trends along main valleys, such as Adlatak River and Hunt River valleys, which suggests that the last phase of glacial flow in those areas may have been topographically controlled.

At five sites glacial striae predating those of the last regional phase were found on sheltered eastern (lee) sides of outcrop where the older striae were protected from erasure by later phases of ice flow. At all sites the older flow trends had a greater northward component than younger phases. The older striae are not considered to be the result of local ice moulding around obstacles because of the consistency of measured trends in the area from outcrop to outcrop and because the 'sheltered' surfaces can be, in fact, well exposed.

Indicator erratics

The most distinctive erractics derived from outside the study area are red to red-brown sandstones and pebble conglomerates. The erratics of sedimentary rock are widespread (Fig. 83.2) and, at some sites, constitute 1-2% by volume of the coarse fraction (visual estimate). For the most part, however, they are present at low levels and typically form much less than 1% of the glacial debris. The erratics of sedimentary rock are distinct in appearance from crystalline rock and are, consequently, easily seen despite their low level of abundance. The rocks are almost entirely quartz sandstones and arkosic quartz sandstones; clastic grains within them are commonly rounded, and have quartz overgrowths and sutured grain boundaries. Feldspar grains vary in abundance and some rocks are quartzitic. In hand specimens, some clasts contain ripple marks. Although erratics of

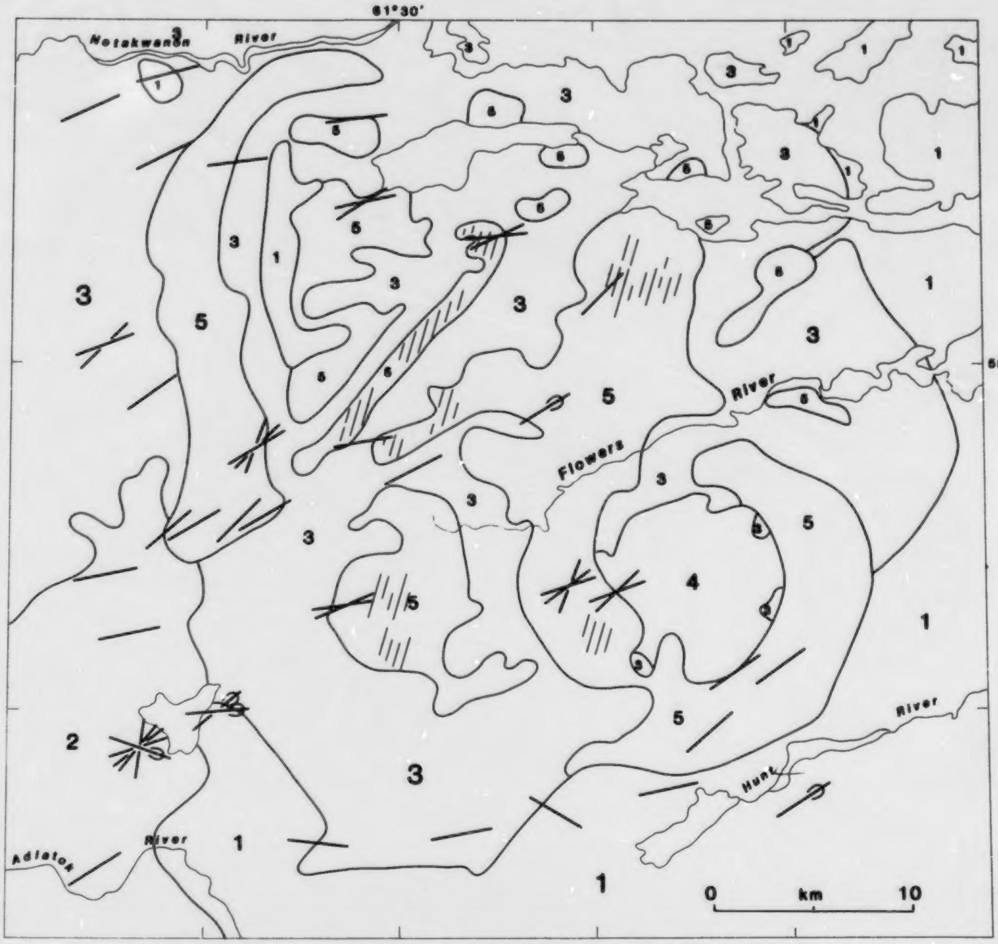

Flowers River Igneous Suite

5 Peralkaline granite ///porphyritic phase

4 Volcanic rock

Nain Igneous Complex

3 Gabbroid to granitoid plutonic rocks

Churchill Structural Province

2 Gneiss, plutonic rocks

Nain Structural Province

1 Gneiss, metagranite, metagranidiorite

Ice flow trends (direction known, unknown)...

Figure 83.1. *Flowers River area showing ice flow trends and generalized bedrock geology (after Taylor, 1979; Hill, 1982).*

sedimentary rock occur in the southern part of the study area and areas south of it, they are uncommon to absent in the northwest of the study area (Fig. 83.2).

Other distinctive erratics include coarse grained anorthosite, garnetiferous gneiss, rusty weathering graphitic quartz-feldspar gneiss, and fine grained porphyry. Most of the erratics have extensive bedrock sources either within or near to the western margin of the area and are of limited use in dispersal studies. An exception is the porphyritic rock of the volcanic pile which forms a glacial dispersal train trending generally northeastward, parallel to known local flow trends, and extending at least 10 to 20 km in a down-ice direction (Fig. 83.2). The full down-ice extent of the train has not yet been defined by fieldwork. An erratic of garnet-bearing gneiss, derived from bedrock of Churchill Structural Province in the southwest (F. Taylor, personal communication, 1984), was found at the western margin of the volcanic rocks and represents eastward glacial transport of 30-40 km (Fig. 83.2).

Till geochemistry

Preliminary interpretation of till geochemistry for lead and zinc at regional and local scales is presented here. In areas underlain by volcanic rocks and roof zones of the peralkaline granite batholith, till is generally enriched in lead and zinc and is characterized by scattered geochemical 'anomalies' of variable size. The regional geochemical patterns shown (Fig. 83.3) have been computer-contoured and, as such, the size and shape of the contours is strongly biased by variation in sample density and by the averaging effect of the contour search pattern. The patterns are

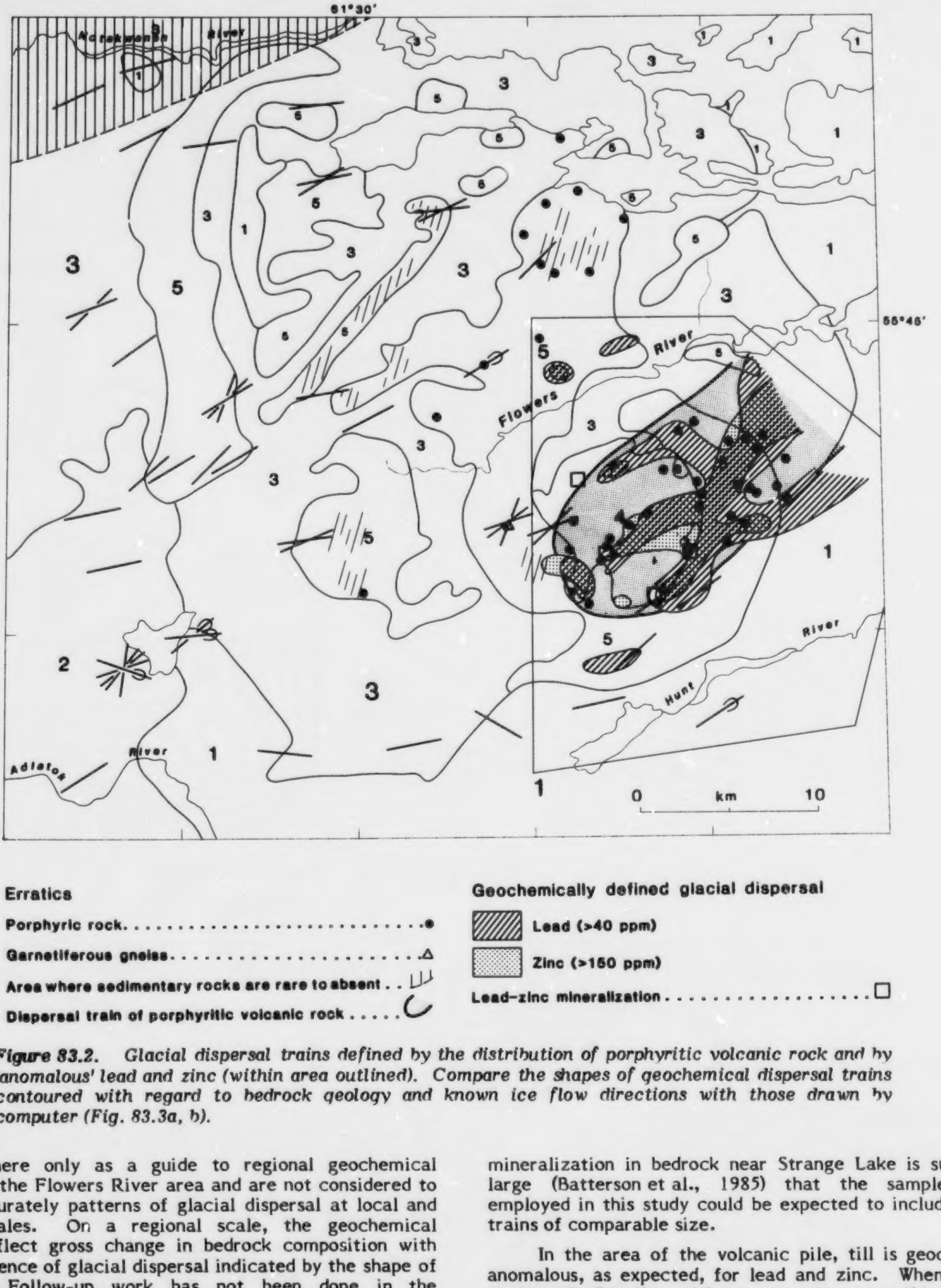

Figure 83.2. *Glacial dispersal trains defined by the distribution of porphyritic volcanic rock and by 'anomalous' lead and zinc (within area outlined). Compare the shapes of geochemical dispersal trains contoured with regard to bedrock geology and known ice flow directions with those drawn by computer (Fig. 83.3a, b).*

presented here only as a guide to regional geochemical variation in the Flowers River area and are not considered to portray accurately patterns of glacial dispersal at local and detailed scales. On a regional scale, the geochemical patterns reflect gross change in bedrock composition with limited evidence of glacial dispersal indicated by the shape of contours. Follow-up work has not been done in the geochemically anomalous areas and, except in the area of volcanic rock, the origins of the anomalies are not known. Some could be related to primary enrichment within marginal zones of the peralkaline granite batholith, as identified by Hill (1982), and others, particularly in the area of volcanic rock, could be related to bedrock mineralization. An 'anomalous' dispersal train from a site of rare earth element mineralization in bedrock near Strange Lake is sufficiently large (Batterson et al., 1985) that the sample spacing employed in this study could be expected to include parts of trains of comparable size.

In the area of the volcanic pile, till is geochemically anomalous, as expected, for lead and zinc. When data are contoured directly, without computer 'smoothing', glacial dispersal trains at a local-scale can be geochemically defined by lead and by zinc (Fig. 83.2). The trains extend northeastwards, and they are consistent in orientation with the last phase of regional ice flow and in size with the known glacial dispersal of porphyritic rock from the volcanic rocks. The down-ice extensions of the trains have not been fully

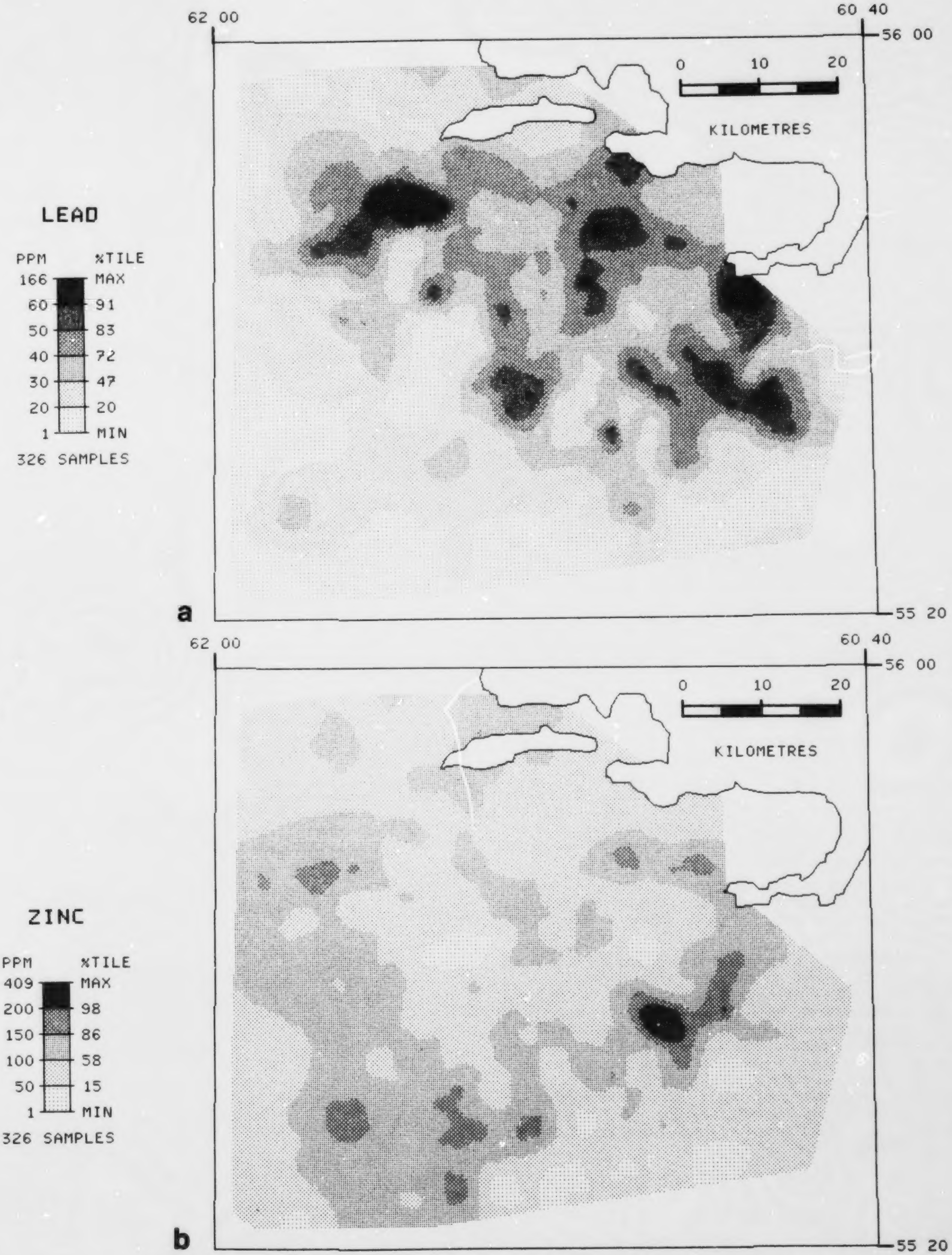

Figure 83.3. *Computer-drawn maps showing the distribution of* ***(a)*** *lead (>40 ppm) and* ***(b)*** *zinc (>150 ppm) in the clay fraction of till in the Flowers River area. Interpreted patterns indicating the character of glacial dispersal within the areas outlined are given in Figure 83.2.*

defined by fieldwork. The geologically interpreted patterns (Fig. 83.2) contrast with those drawn by computer (Fig. 83.3) by emphasizing known glacial trends and indicating more precisely the location of known bedrock sources. In contrast, computer-contoured patterns are oriented directly across the glacial trends due to the non-uniform sample distribution and to the strength of geochemical 'anomalies' associated with the volcanic rock. The occurrence of a number of isolated, geochemical 'highs' within the train suggests that at least part of the train may have been formed by glacial erosion of a number of separate, mineralized bedrock sources. Several sources have been mapped within the volcanic terrain by Hill (1982) and some appear located at the heads of the geochemically defined trains (Fig. 83.2).

Discussion and conclusions

Patterns of regional ice flow across Flowers River area vary from about N55°E in the southeast, to N85°E in the north and northeast. To the west, flow trends are nearly eastward. The alignment of flow trends with major valleys, such as Adlatok and Hunt rivers, indicates the last phase of flow may have been topographically controlled in some areas. Evidence of earlier phases of flow that varied between N10°E and N45°E has been found on protected bedrock surfaces at five locations. The earlier, more northward phase, or phases, of flow may correlate with trends having similar orientation and relative age found in the area of Schefferville (Kirby, 1961), Churchill Falls (Klassen and Bolduc, 1984), and Melody Lake (Klassen, 1984).

Erratics of sedimentary rock found in drift throughout the area are far-travelled (>50 km), although specific bedrock sources for them are not known. The rocks appear to have been derived from supracrustal sequences west of the area, which most likely include the Siamarnekh Formation and unmapped equivalents of it. Although no erratics from the Labrador Trough were found in the study area, cherty iron formation and specular hematite in drift to the west indicate that at least some of the sedimentary rock debris could have been potentially derived from the Labrador Trough. Such an interpretation would require regional ice flow patterns across the Labrador Trough, and central Labrador in general, that are markedly different from those recorded on the Glacial Map of Canada (Prest et al., 1968), although they would be consistent with older northeast trends recorded here, and by Kirby (1961) and by Klassen and Bolduc (1984). No volcanic or sedimentary rocks were found that can be shown to have been derived from Seal Lake Group, which occur southwest and south of the study area, indicating that the Seal Lake Group is not a principal source.

Local scale dispersal patterns defined by porphyritic volcanic rock record generally northeastward transport and are consistent with regional flow directions of about N55°E in the study area.

Trace element patterns defined by lead and zinc in till appear to be related to regional and local scale glacial dispersal from the Flowers River Igneous Suite. The dispersal patterns are most evident originating from the volcanic rocks and they are oriented parallel with striae trends. The origins of scattered geochemical 'anomalies' found in till overlying the peralkaline granite are not known, although they may reflect primary geochemical differentiation within the batholith. Whatever their source, it is suggested that the geochemical anomalies in till overlying the Flowers River Igneous Suite could indicate areas favourable for more detailed prospecting.

Acknowledgments

The capable field assistance of L. Newman, J. Oliver, and D. Fountain is gratefully acknowledged. F. Thompson is thanked for helpful discussions and contributions to fieldwork.

References

Batterson, M.J., Taylor, D.M., and Vatcher, S.V.
1985: Quaternary mapping and drift exploration in the Strange Lake area, Labrador; in Current Research, Part A, Geological Survey of Canada, Paper 85-1A, p. 4-10.

Greene, B.A.
1974: An outline of the geology of Labrador; Newfoundland Department of Mines and Energy, Information Circular 15.

Hill, J.D.
1982: Geology of the Flowers River-Notakwanon River area, Labrador; Department of Mines and Energy, Government of Newfoundland and Labrador, Report 82-6, 140 p.

Kirby, R.P.
1961: Movements of ice in central Labrador-Ungava; Cahiers de géographie de Québec, no. 10, p. 205-218.

Klassen, R.A.
1983: A preliminary report on drift prospecting studies in Labrador; in Current Research, Part A, Geological Survey of Canada, Paper 83-1A, p. 353-355.

1984: A preliminary report on drift prospecting studies in Labrador, Part II; in Current Research, Part A, Geological Survey of Canada, Paper 84-1A, p. 247-254.

Klassen, R.A. and Bolduc, A.
1984: Ice flow directions and drift composition, Churchill Falls, Labrador; in Current Research, Part A, Geological Survey of Canada, Paper 84-1A, p. 255-258.

McConnell, J.
1984: Reconnaissance and detailed geochemical surveys for base metals in Labrador; Department of Mines and Energy, Government of Newfoundland and Labrador, Report 84-2, 113 p.

Prest, V.K., Grant, D.R., and Rampton, V.N.
1968: Glacial Map of Canada; Geological Survey of Canada, Map 1253A.

Taylor, F.C.
1979: Reconnaissance geology of a part of the Precambrian Shield, northeastern Quebec, northern Labrador and Northwest Territories; Geological Survey of Canada, Memoir 393, 99 p.

Stratigraphy of placer gold deposits; overburden drilling in Chaudière Valley, Quebec[1]

Project 690095

W.W. Shilts and S.L. Smith
Terrain Sciences Division

Shilts, W.W. and Smith, S.L., Stratigraphy of placer gold deposits; overburden drilling in Chaudière Valley, Quebec; in Current Research, Part A, Geological Survey of Canada, Paper 86-1A, p. 703-712, 1986.

Abstract

Preliminary logs of recent, deep, overburden boreholes are correlated with stratigraphic sections and previous borehole data. The Rotasonic drill system used has proven to be superior to triple-tube methods in its ability to recover intact, large diameter core for stratigraphic studies.

Boreholes in the southern part of the area confirm the presence of three tills and associated thick glaciolacustrine sediments representing at least three glacial events. In the northern part of the area, the overburden is not so thick and in places appears to be older than any sediments encountered in upper Chaudière Valley.

Résumé

On a comparé des diagraphies préliminaires de sondages profonds réalisés récemment dans des morts-terrains, avec des coupes stratigraphiques et des données de sondages antérieurs. Le système de forage Rotasonic s'est révélé supérieur aux systèmes à trois tubes pour récupérer des carottes de grand diamètre intactes, à des fins d'études stratigraphiques.

Les sondages dans la partie sud de la région confirment la présence de trois tills et d'épais sédiments glociolacustres connexes, représentant au moins trois évènements glaciaires. Dans la partie nord de la région, les morts-terrains ne sont pas aussi épais et, par endroits, ils semblent plus anciens que tous les sédiments relevés dans la vallée du cours supérieur de la rivière Chaudière.

[1] Contribution to Federal Asbestos Initiatives, Geoscience Research Program 1984-87.

Introduction

In winter of 1984 and summer of 1985, two systems for drilling and continuously sampling deep overburden were tested in upper Chaudière River valley of the Eastern Townships, Quebec (Fig. 84.1). Selection of drilling sites, over areas of deepest overburden, was made from the study of hammer and dynamite refraction seismic profiles carried out in 1968 and 1984.

The objectives of this project, funded under the Federal Asbestos Initiatives, Geoscience Research Program, are 1) to test and compare new drilling methods in thick, stony, overburden typical of the Appalachian region; 2) to correlate glacial stratigraphy known from natural and man-made sections in upper Chaudière Valley with that in adjacent areas where overburden was mined for, or known to have high potential for gold, and; 3) to drill and sample known gold-bearing unconsolidated sediments to determine their stratigraphy, genesis, and the genesis of their gold. It is expected that the results of this project will contribute substantially to the rationalization and cost-effectiveness of gold exploration in this region long known for its buried and modern placer deposits.

Although the Quaternary history of Chaudière Valley and adjacent regions has been the subject of a great deal of research over the past two decades (Gadd, 1964, 1965a, 1971; McDonald, 1967; McDonald and Shilts, 1971; Gadd et al., 1972; LaSalle et al., 1976, 1979; Shilts, 1978, 1981; LaSalle, 1980) and a consensus has been reached regarding the major glacial events to affect the region (LaSalle, 1984), few attempts have been made to drill deep overburden to find older Quaternary deposits. In addition, the stratigraphy of the gold-bearing strata east of Saint-Georges has never been reconciled with modern Quaternary stratigraphy, the gold-bearing "gravels" being assigned a Tertiary age on the basis of their highly oxidized appearance (Boyle, 1979).

Glacial sedimentation and stratigraphy

Briefly, the glacial stratigraphy of Chaudière Valley (Fig. 84.2) comprises at least three glacial events represented by the Johnville, Chaudière, and Lennoxville tills (McDonald and Shilts, 1971), respectively, from oldest to youngest. At present all of these tills are thought to have been deposited during the Wisconsinan Stage.

Tills and sediments that were deposited in proglacial lakes or glacially fed streams in this part of the Appalachians are grey where fresh and contain abundant pyrite in the form of cubes, twinned cubes or broken cubes, as well as traces of other sulphides. Lennoxville Till, which forms the surface unit of most of the region, is commonly weathered to depths of 3-4 m, only the upper metre forming a true solum. Where weathered, Lennoxville Till and all associated and older glacial sediments are stained brown or tan by iron oxides formed as a result of oxidation of the abundant sulphides in the sand and finer sizes of the matrix (see Shilts, 1984, fig. 3). Where this oxidation occurs, sulphides and other labile minerals, such as siderite, are destroyed, making near-surface geochemical surveys using heavy mineral separates of drift or modern sediments derived from drift difficult to interpret. Oxidation is rarely noted in sections. Chaudière Till has never been observed to be oxidized, and although Johnville Till is oxidized at its surface where observed, it has only been seen exposed at two places in the Appalachians. Oxidation due to groundwater flow through permeable layers has been observed deep in some sections.

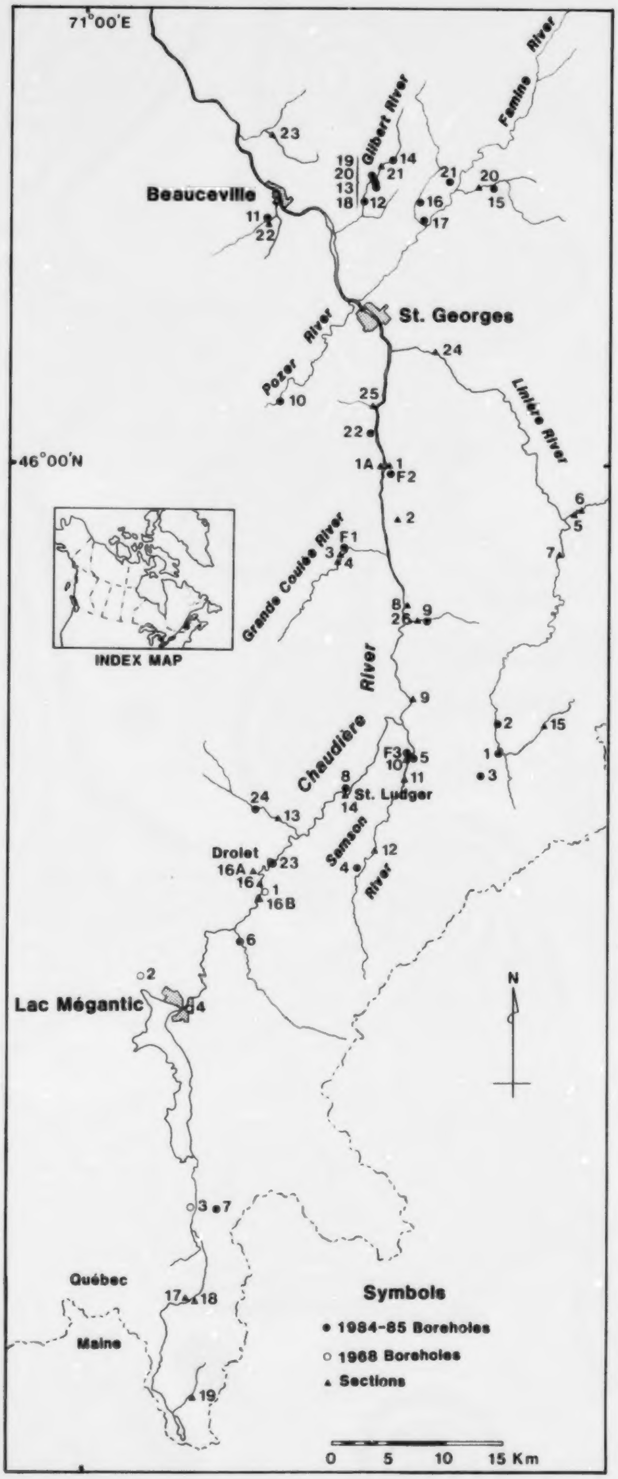

Figure 84.1. *Area of study in Eastern Townships, Quebec, showing locations of sections and boreholes.*

Sediments separating the till sheets are thick, laminated glaciolacustrine silty clay and fluvial gravel and silt. Whenever glaciers advanced into Chaudière Valley or retreated northward from the valley, the northward draining rivers were blocked, forming large lakes into which thick silty clay was deposited. When glaciers stood north of St. Lawrence River or disappeared altogether, allowing free northward drainage, fluvial gravels, sands, and floodplain deposits were formed in the Chaudière and its tributary valleys. Thus, a typical stratigraphic sequence for one glacial event might consist of fluvial sediments; overlain by thin laminated silty clay, which may or may not be deformed by glacial overriding; overlain by till, which commonly has thin (< 1 m) stratified lenses of sand or silty clay in it; overlain by thick laminated silty clay, commonly with till-like stony beds thought to be slumped from the retreating ice front in the form of turbidity current deposits. The common laminated facies of the glaciolacustrine deposits may grade into or be replaced by sandy to gravelly deltaic deposits where major streams entered the lakes or by ice-contact deltaic deposits where the ice front stood in one place in the lake for a time. It is important to understand these

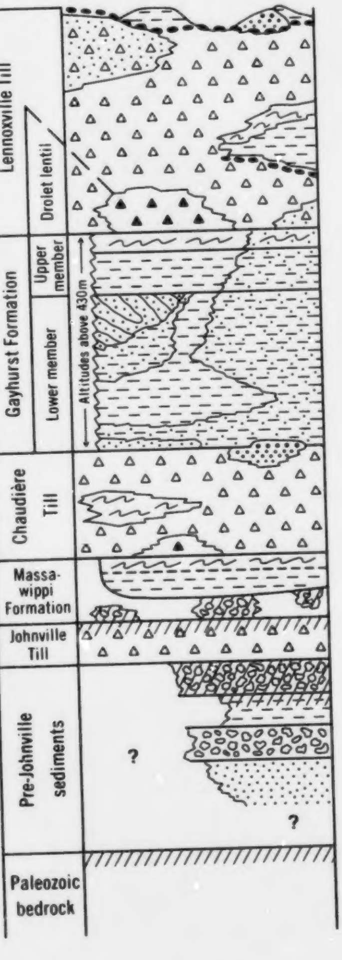

(Diagrammatic, not to scale)

Figure 84.2. *Composite section of Quaternary stratigraphy of upper Chaudière Valley (from Shilts, 1981).*

weathering and sedimentation models and the regional stratigraphy when interpreting the sedimentary facies encountered in the deep boreholes.

Preliminary observations

The stratigraphic drilling carried out in 1984-1985 intersected glacial units that generally can be fit into the stratigraphic framework proposed by Shilts (1981) (Fig. 84.3). In places, however, it appears that certain bedrock valleys were filled either with several glacial and nonglacial units early in the Pleistocene (Grande Coulée River, for example) or with an abnormal thickness of a single waterlain proglacial or subglacial unit (>40 m of ice contact gravel, sand, and silty clay in Samson River), forming a floor between bedrock sides of the valleys, over which several glaciers may have advanced without having much effect on the valley fill. If this actually happened, each glacier may have accomplished little more in these valleys than to rework and redeposit the upper few metres of sediment. Thus, there may be a significant unconformity between the surface till and older tills and associated sediments, particularly in valleys or depressions oriented or shaped in such a way that they were protected from the glacial erosion that stripped older unconsolidated sediments from less ideally located valleys. At present there is no way to judge how serious an impediment to correlation this situation may be.

Although Gadd (1965b) suggested that buried valleys may be found in the Beauceville area by study of aerial photographs, both seismic and drilling results indicate that significant buried valleys of more than 100 m depth may underlie slopes or modern alluvial plains with virtually no surface expression (Fig. 84.4). The only way that these valleys may be detected reliably is by geophysical or drilling techniques.

In many of these buried valleys in upper Chaudière River valley, the sediment fill comprises substantial thicknesses of silty clay deposited in glacial Lake Gayhurst. The Gayhurst Formation is a glaciolacustrine unit deposited in a large proglacial lake that filled the Chaudière and adjacent valleys to elevations of 396 to 427 m when the glacier that deposited Chaudière Till retreated northwestward and stood against the northwest slope of the Appalachian Highlands. When the glacier readvanced across Chaudière Valley, and eventually across New England, it deposited Lennoxville Till over Gayhurst sediments. North of Saint-Ludger, Gayhurst sediments are relatively thin because of glacial erosion or lower rates of deposition than south of Saint-Ludger where more than 90 m of laminated silt and clay were encountered in several boreholes, particularly near Drolet (see Fig. 84.1 for locations). These thick sediments form a significant part of the fill in upper Linière, Samson, and Chaudière valleys, and provide a major obstacle to mineral exploration and to exploitation of any old gold-bearing beds that might be found at depth. This problem should be recognized when planning an exploration program in valleys that were inundated by glacial Lake Gayhurst, including valleys to the west in the Saint-François River drainage basin.

Gilbert River gold deposits

Six holes were drilled to bedrock in the vicinity of the placer gold deposit in the buried valley along Gilbert River, just north of Saint-Georges. The appearance of the glacial units in these holes is generally quite unlike sediment encountered in any other of the 25 holes and 26 sections examined in Chaudière Valley (Fig. 84.5). Sediment at the base of the holes is so thoroughly oxidized and indurated that it was difficult in preliminary logging to tell its genesis or

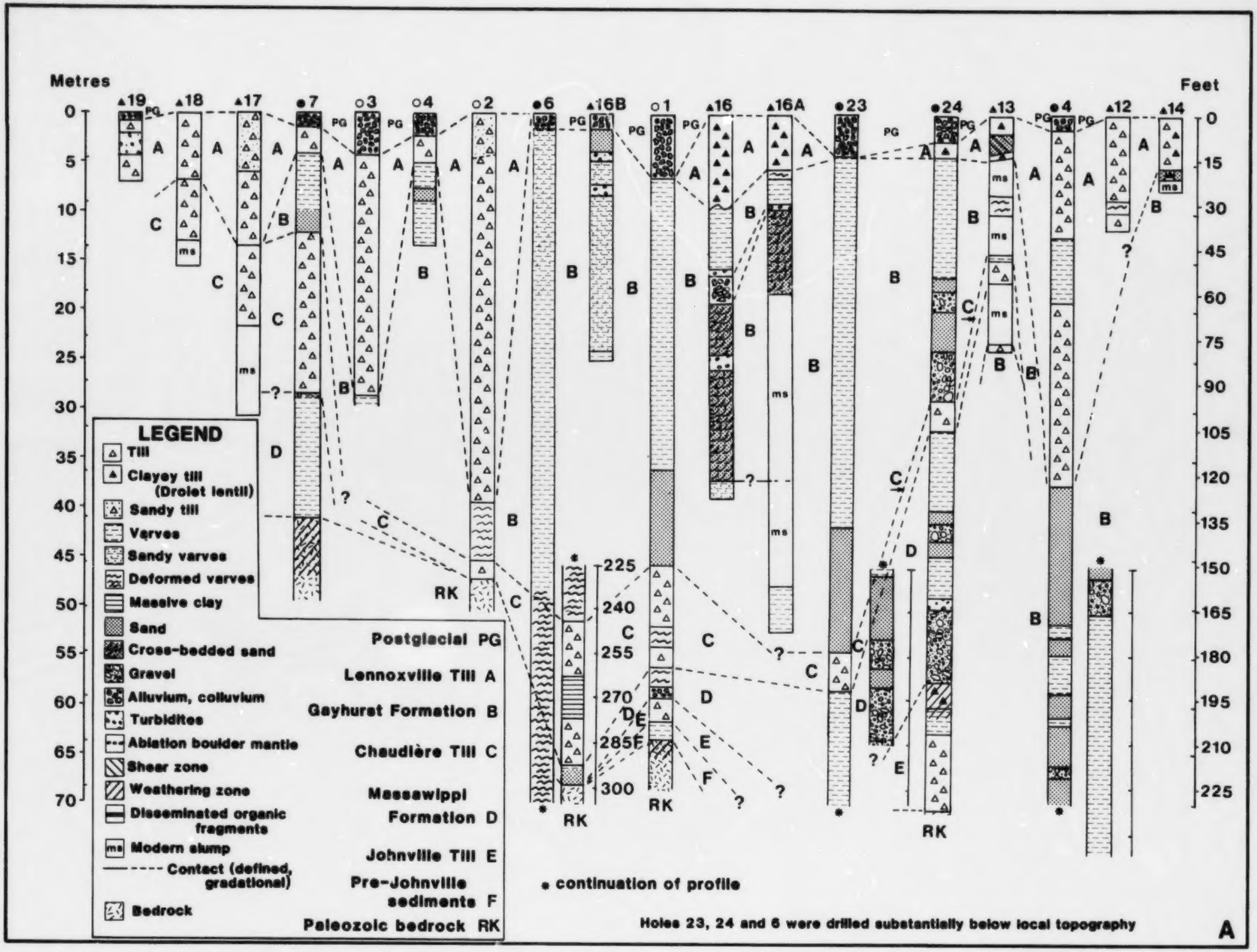

Figure 84.3. (A-C). Diagrams of measured stratigraphic sections and boreholes with assumed correlations along south to north cross-section of Chaudière River valley (see Fig. 84.1 for locations).

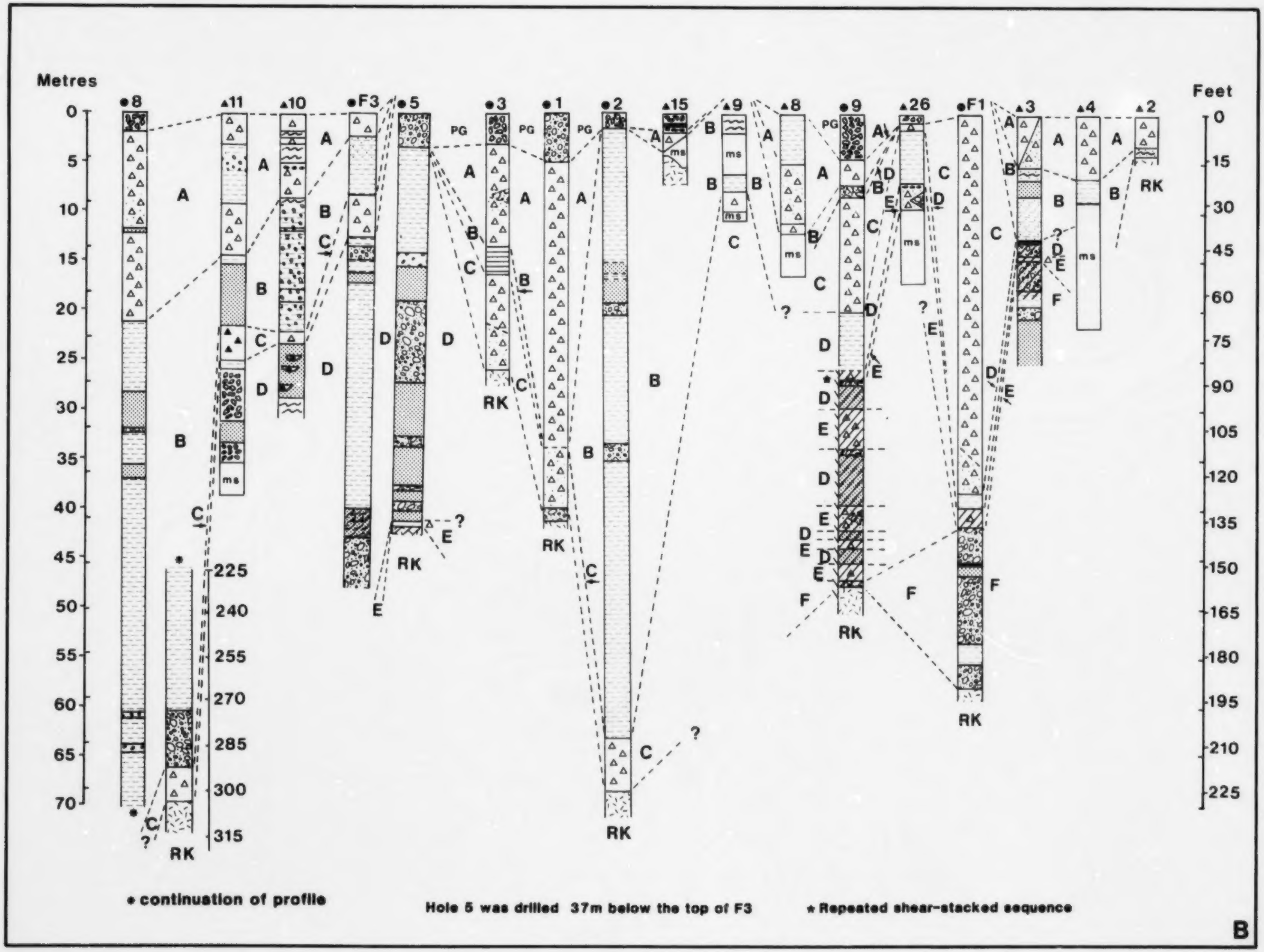
Metres
Feet
●8
▲11
▲10
●F3
●5
●3
●1
●2
▲15
▲9
▲8
●9
▲26
●F1
▲3
▲4
▲2
PG
RK
ms
• continuation of profile
Hole 5 was drilled 37m below the top of F3
* Repeated shear-stacked sequence
B

Figure 84.3b

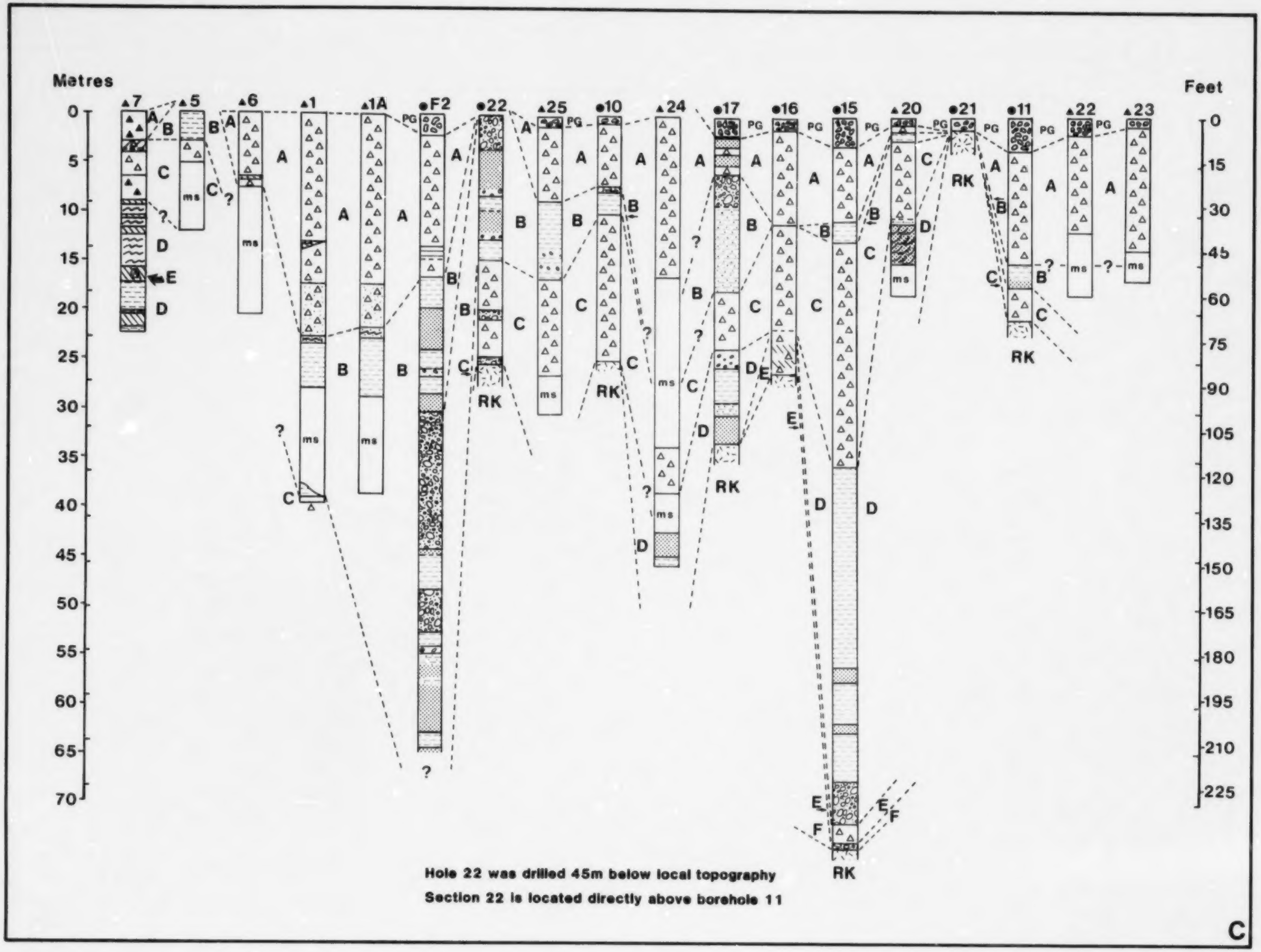
Metres
Feet
Hole 22 was drilled 45m below local topography
Section 22 is located directly above borehole 11
C

Figure 84.3c

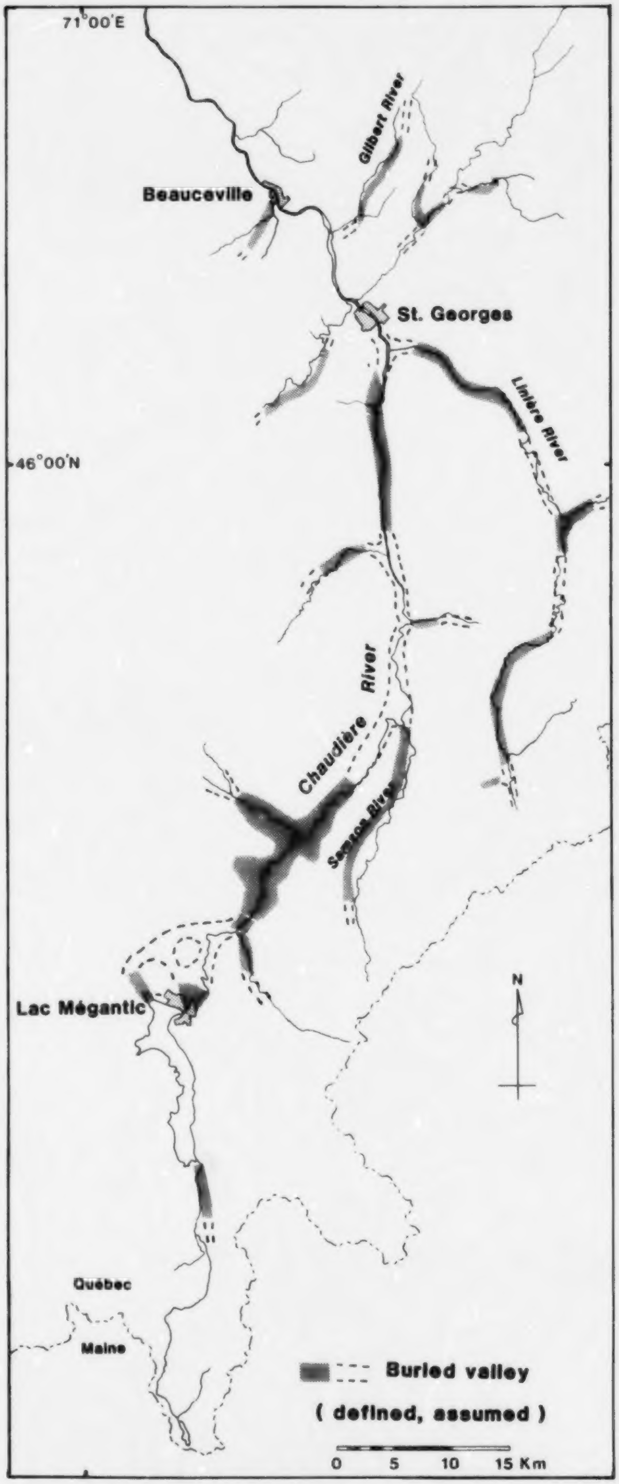

Figure 84.4. Approximate locations of buried valleys as determined by refraction seismic methods.

even to differentiate it from underlying, highly weathered bedrock. At present it is believed that till and colluvium overlie the weathered bedrock and are in turn overlain by a fluvial gravel which was the main pay zone sought in the placer operation. Near the axis of the buried valley up to 6 m of interlaminated grey and red silty clay with interbedded fine- to medium-grained sand overlies the gravel. These beds show few signs of oxidation and appear to be eroded away on the flanks of the buried valley. A till complex overlies the varves to the surface. Unlike tills of similar texture elsewhere in the region, these tills are brown, indicating deep oxidation or, more likely, that they contain a large amount of the highly weathered debris common at the base of the boreholes. This debris would have been eroded from adjacent areas and transported across the buried valley, filling it in. The tills in the boreholes and the surface till, well exposed along Gilbert River adjacent to the mine, contain ultramafic clasts transported from outcrops northwest of the buried channel. Because ultramafic provenance is detected easily by geochemical and mineralogical means, it should be easy to differentiate colluvial or preglacial units from glacial units at this site as well as Chaudière Till, which was deposited by westerly flowing ice that would not have crossed the ultramafic outcrops (Rencz and Shilts, 1980).

The upper till complex appears to comprise more than one till sheet, and in borehole 13 a highly altered zone within the complex has the appearance of a paleosol (Fig. 84.5). As many as three till sheets may be represented in borehole 13, suggesting that the varved sequence is much older than the Gayhurst Formation which it superficially resembles and which separates the youngest Lennoxville from older Chaudière Till in upper Chaudière Valley. Because of the importance of the Gilbert River site to modelling the source of buried and surficial placer gold in the region, a detailed sedimentological, mineralogical, and geochemical study will be made of these beds.

Drilling

A Rotasonic drill was used for the first time in the Eastern Townships in 1985 and proved to be superior to triple-tube methods tested previously. The Rotasonic drill utilizes high frequency vibration to drill, recovering an intact, 11 cm-diameter core to bedrock. Boreholes were cased to prevent collapse of material from the walls and subsequent sample contamination.

Access for drilling was by road, easily travelled by the six-wheel drive vehicle on which the drill head was mounted (Fig. 84.6). With only minor breaks for vehicle repair and maintenance, as well as a couple of days spent at borehole 4, the 24 holes, comprising 1091 m of continuous core, were drilled in one month.

Recovery averaged 90% but varied according to sediment cohesiveness. Compact or cohesive till and clay yielded as much as 100% recovery, slightly more than compact sand (85%). Loose sand and gravel commonly fell out of the core barrel unless blocked by underlying, more cohesive, sediment. Consequently, sand and gravel averaged 75% recovery and loose, soft, clay averaged below 60% recovery. In addition, soft sediment is squeezed and elongated by the drilling process.

Bedrock samples also were collected to depths of at least 1 m into bedrock, but soft, brittle shales that underlie most of the region were commonly powdered by the vibration.

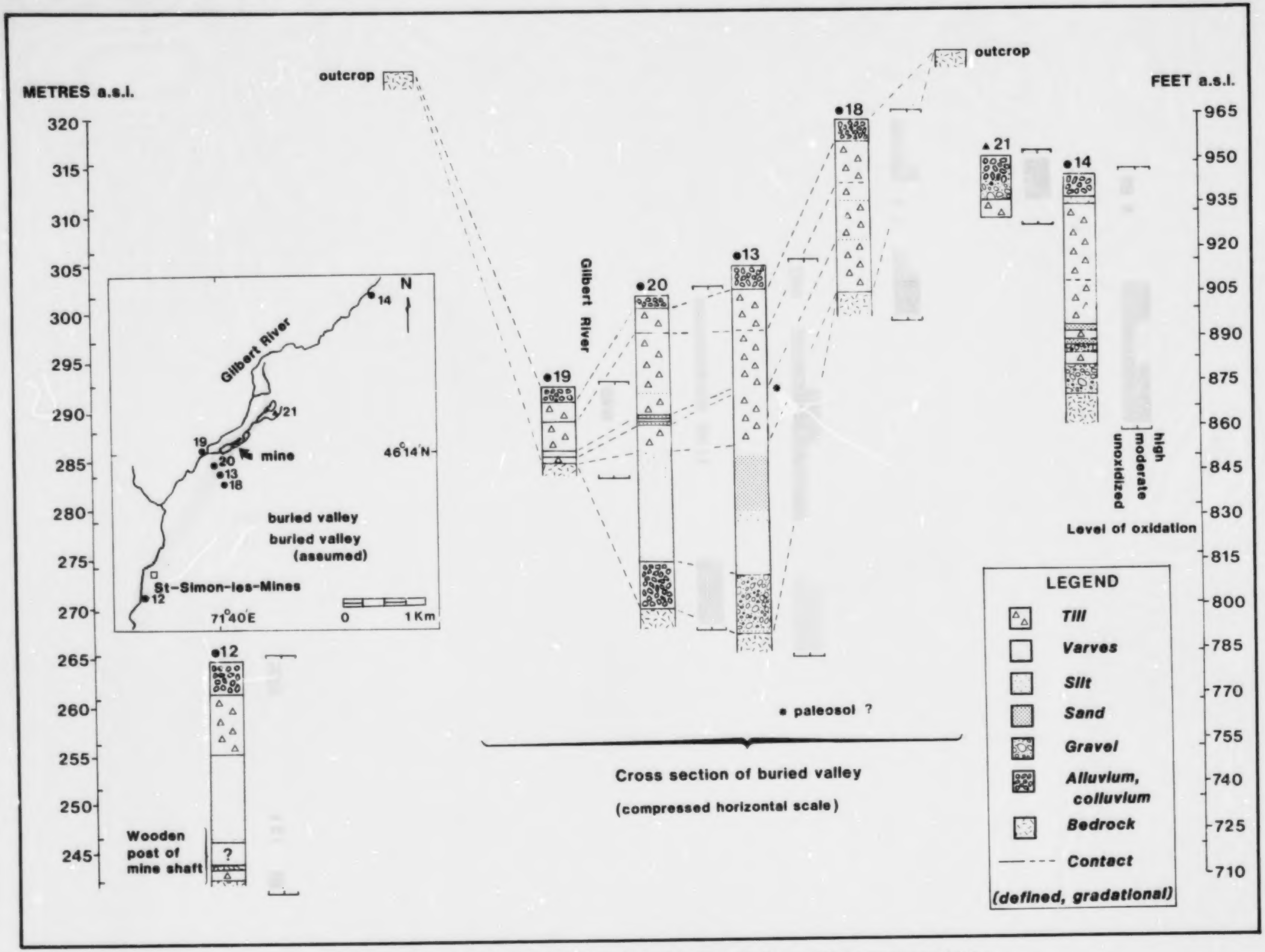

Figure 84.5. *Diagrams of boreholes and section along Gilbert River with assumed correlations.*

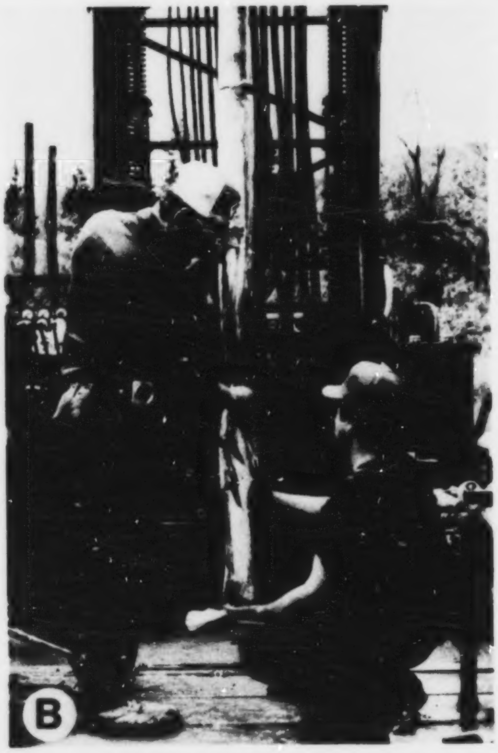

Figure 84.6. Drilling set-up (A) and close-up showing extrusion of core from core barrel (B).

Boreholes up to 96 m in depth were drilled with little difficulty except for borehole 4. Vibration of a thick sequence of clay and fine sand and gravel of the Gayhurst Formation(?) led to material settling around the casing, causing it to become stuck. Water pressure was ineffective to dislodge the casing because the water was able to flow freely away in sand and gravel units. Many pieces of metal casing had to be abandoned in the hole. A similar situation, also in thick Gayhurst sediments in borehole 23, was only avoided by not completing the hole.

Preliminary results

From seismic surveys and from results of the drilling program, it is obvious that whatever controlled local base level in Chaudière Valley before glaciation has been radically modified by glacial processes. Buried valleys have been found adjacent to most of the major rivers whose present channels are suspended, in many cases, as much as 100 m above the bedrock floor of the valleys they presently occupy. Although not much new stratigraphy has been identified in these buried valleys, further analysis of the sediment logs and quantitative data may lead to revision of the local stratigraphy as it has been deduced from the natural sections exposed above river level. For example, at least 100 m of unconsolidated sediment lies beneath the 40 m-high Samson River section (Shilts, 1978), which contains almost the entire known Quaternary sequence of Chaudière Valley.

Acknowledgments

The authors express their thanks to the crew from Midwest Drilling, Yves Harvey, Pierre Giroux, and Jean-Marc Lamothe of Roche Consulting Group, for setting up the logistics for the drilling program, and GPR Geophysics Inc. for the seismic profiles. Jacques Locat and François Gilbert of Coniagas Ltd. allowed access to the mining property around Saint-Simon-les-Mines, and kindly provided maps and information that assisted in locating drill sites. We gratefully acknowledge the efforts of Isabelle Proulx and Katharine Rodd in logging most of the drill core.

References

Boyle, R.W.

1979: The geochemistry of gold and its deposits; Geological Survey of Canada, Bulletin 280, 584 p.

Gadd, N.R.

1964: Surficial geology, Beauceville map-area; Geological Survey of Canada, Paper 64-12.

1965a: Surficial geology, Chaudière River valley; in Report of Activities, Geological Survey of Canada, Paper 65-1, p. 115-117.

1965b: Buried valleys and gold placers, Beauce County; in Report of Activities, Geological Survey of Canada, Paper 65-1, p. 117-119.

1971: Pleistocene geology of the central St. Lawrence Lowland (with selected passages from an unpublished manuscript "The St. Lawrence Lowland", by J.W. Goldthwait); Geological Survey of Canada, Memoir 359.

Gadd, N.R., McDonald, B.C., and Shilts, W.W.

1972: Deglaciation of southern Quebec; Geological Survey of Canada, Paper 71-47, 19 p.

LaSalle, P.

1980: L'or dans les sédiments meubles: Formation des placers, extraction et occurrences dans le sud-est du Québec; Ministère de l'énergie et des ressources du Québec, DPV-745, 26 p.

1984: Quaternary stratigraphy of Quebec: A review; in Quaternary Stratigraphy of Canada – A Canadian Contribution to IGCP Project 24, ed. R.J. Fulton; Geological Survey of Canada, Paper 84-10, p. 155-171.

LaSalle, P., Martineau, G., and Chauvin, L.
1976: Géologie des sédiments meubles d'une partie de la Beauce et du Bas Saint-Laurent, Québec; Ministère des richesses naturelles, DPV-438, 13 p.

1979: Lits de bryophytes du Wisconsin Moyen, Vallée-Jonction, Québec; Journal canadien des sciences de la terre, v. 16, p. 593-598.

McDonald, B.C.
1967: Pleistocene events and chronology in the Appalachian region of southeastern Quebec, Canada; unpublished Ph.D. dissertation, Department of Geology, Yale University, 161 p.

McDonald, B.C. and Shilts, W.W.
1971: Quaternary stratigraphy and events in southeastern Quebec; Geological Society of America Bulletin, v. 82, p. 683-698.

Rencz, A.N. and Shilts, W.W.
1980: Nickel in soils and vegetation of glaciated terrains; in Nickel in the Environment, ed. J.O. Nriagu; John Wiley and Sons. Inc., p. 151-188.

Shilts, W.W.
1978: Detailed sedimentological study of till sheets in a stratigraphic section, Samson River, Québec; Geological Survey of Canada, Bulletin 285, 30 p.

1981: Surficial geology of the Lac Mégantic area, Québec; Geological Survey of Canada, Memoir 397, 102 p.

1984: Till geochemistry in Finland and Canada; Journal of Geochemical Exploration, v. 21, p. 95-117.

Ice flow directions and drift composition, central Labrador[1]

Project 820039

F.J. Thompson and R.A. Klassen
Terrain Sciences Division

Thompson, F.J. and Klassen, R.A., Ice flow directions and drift composition, central Labrador; in Current Research, Part A, Geological Survey of Canada, Paper 86-1A, p. 713-717, 1986.

Abstract

Glacial striae over much of the study area are oriented east-northeast. Evidence from older striae indicates that a major northeast directed ice advance, which affected the entire study area, predates the east-northeast advance. Northeast oriented striae in the northeast part of the study area are attributed to this early advance. Striae trending east-southeast in the southern part of the area may reflect divergent flow during the east-northeast advance or a separate phase of flow. The distribution of glacial erratics shows broad fan-shaped eastward dispersal of 30 to more than 100 km from their bedrock sources. The transport of erratics and development of fan shapes are related to the multiple phases of flow recorded by striae. The complex history of glacial transport and difficulties in sampling till highlight the importance of scientific input for effective use of glacial debris as a prospecting medium in central Labrador.

Résumé

Des stries glaciaires recouvrant la majeure partie de la région d'étude sont orientées est-nord-est. Des anciennes stries indiquent qu'une important avancée glaciaire de direction nord-est, qui a modifié toute la région, a eu lieu avant l'avancée est-nord-est. Les stries nord-est dans la partie nord-est de la région sont attribuées à cette première avancée. Les stries est-sud-est dans la partie sud peuvent être le résultat d'un écoulement divergent pendant l'avancée est-nord-est ou d'une phase distincte d'écoulement. La répartition des blocs erratiques d'origine glaciaire indique une importante dispersion en éventail vers l'est, sur 30 à plus de 100 km à partir de leurs sources dans la roche en place. Le transport des blocs erratiques et leur dispersion en éventail sont associés aux phases multiples d'écoulement indiquées par les stries. L'histoire complexe du transport glaciaire et les difficultés dans l'échantillonnage des tills font ressortir le besoin de données scientifiques pour une utilisation efficace des débris glaciaires comme moyen de prospection dans le centre du Labrador.

[1] Contribution to Canada-Newfoundland Mineral Development Agreement 1984-89. Project carried by Geological Survey of Canada.

Introduction

This report presents the preliminary interpretation of Quaternary field work conducted during the summer of 1985 in the Snegamook Lake (13K) and Kasheshibaw Lake (13L) map areas of central Labrador (Fig. 85.1). The study is part of an ongoing project funded under Federal-Provincial mineral development agreements since 1982 (Klassen 1983, 1984; Klassen and Bolduc, 1984). The major objectives of the study are to determine the history of ice movement and the composition of glacial drift as a basis for developing techniques of drift prospecting. The compilation of geochemical results is in progress.

Physiography and bedrock geology

The study area is rugged, with hills commonly rising 200 m above valley floors, and is crossed by major valleys occupied by Kanairiktok and Naskaupi rivers. The low areas are heavily forested and on hilltops tundra vegetation is common.

The study area occupies parts of the Nain, Grenville and Churchill structural provinces in central Labrador. The bedrock (Fig. 85.2) comprises Archean gneiss and Paleohelikian anorthosite to the north, and Grenville gneiss and Paleohelikian granite to the south. The central part of the study area is underlain by supracrustal volcanics and sediments which include Aphebian Moran Lake Group, Paleohelikian Bruce River and Letitia Lake groups, and Neohelikian Seal Lake Group (Greene, 1970; Emslie, 1980; Baragar, 1981; Curtis and Currie, 1981; Thomas, 1981; Ryan, 1982a,b). The volcanics and sediments are part of the Central Mineral Belt, which is known to contain copper, zinc, uranium, and rare earth minerals (Douglas and Hsu, 1976; O'Driscoll and Noel, 1983).

Methods

Till was sampled throughout the area in order to establish regional variations in drift composition; approximately 600 samples were collected (Fig. 85.1) using a Bell 206B helicopter. Sample densities varied from 1-3 per 100 km^2 in areas with limited mineral potential, and from 8-12 per 100 km^2 within the Central Mineral Belt. In three areas of known mineralization, samples were collected on 50-200 m centres to determine glacial dispersal in till from a known bedrock source.

Pits were dug, by shovel, to depths of 30-70 cm depending on depth to bedrock and on difficulties in penetrating stony till. Samples were collected from the least oxidized and most organic-free section of the modern soil profile near the base of the pit. In areas of tundra vegetation, pits were dug in mudboils where soil zonation was absent or poorly developed due to periglacial churning (Shilts, 1977).

Sample sites were preferentially located on hilltops because valley bottoms are heavily forested, providing few landing sites, and because major valleys are commonly infilled with glaciofluvial deposits. Where more detailed work was necessary, swamps were used as landing sites to permit attempts at till sampling in low lying, tree covered areas.

Surficial geology

Till is the dominant glacial deposit in the area. It is generally thin (less than 2 m) to discontinuous in highland areas and locally thicker in valleys. The character of the till commonly reflects the character of the underlying bedrock. On bedrock units resistant to glacial erosion, such as Seal Lake Group quartzite and Archean gneiss, till is thin and has

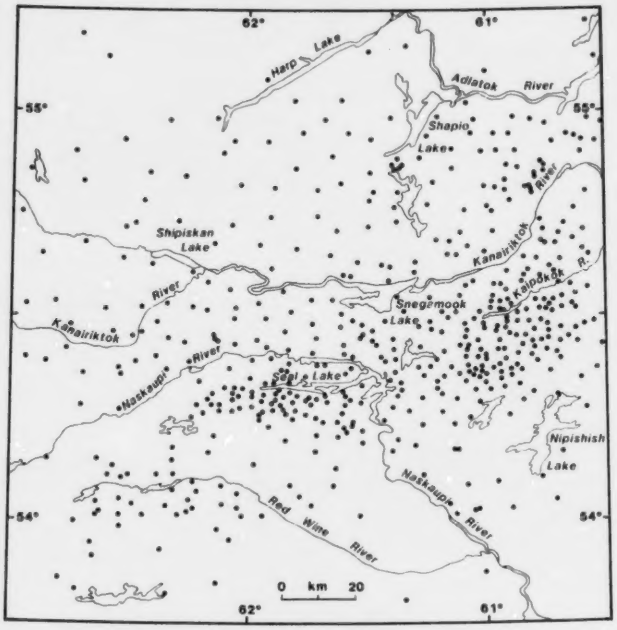

Figure 85.1. *Location map showing the distribution of sampling sites.*

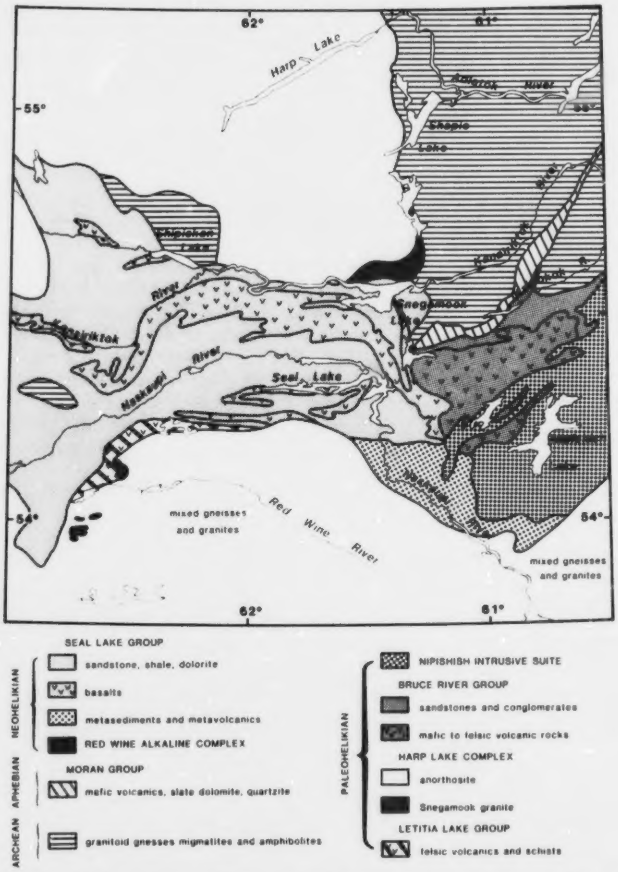

Figure 85.2. *Generalized geology (modified from Greene, 1979; Baragar, 1981; Ryan, 1982a, b).*

little fine matrix component. In areas of softer, more easily comminuted bedrock such as Seal Lake Group mudstone, till is generally thicker, has a greater component of fine material, and its colour reflects that of the underlying bedrock. Red and red-brown till is associated with red mudstone of the Seal Lake Group and contrasts with grey till which has a crystalline provenance. In areas underlain by Grenville gneiss, till is commonly sandy, relatively thick compared to till on Archean gneiss, and exhibits streamlined landforms suggesting that the Grenville rocks were more easily eroded by the ice. Till in areas of Nipishish Lake Intrusive Suite is characterized by large (1-4 m diameter), locally derived boulders, suggesting glacial incorporation of fracture or joint controlled bedrock blocks.

Extensive ice contact glaciofluvial deposits occur along Kanairiktok and Naskaupi rivers. Thick marine sand, silt, and clay sequences infill the Kaipokok, Kanairiktok, and Adlatok valleys below 100 m a.s.l. Marine silts and clays in the Kaipokok and Kanairiktok valleys are distinctly red, indicating that the source for these sediments is Seal Lake Group mudstone or till derived from these rocks.

Direction of ice movement

Most of the more than 200 striation observations were made on exposed surfaces on hilltops and are consequently thought to reflect the last regional phase of ice flow (Fig. 85.3). Striae trend east-northeast in the central part of the map area (area B, Fig. 85.3), northeast in the northeast part of the area (area A), and east-southeast in the south (area C). The sense of movement from rat tail and fluted features at outcrop scale is eastward and no evidence of westward flow has been recognized. Evidence from these striae is consistent with the generalized ice flow trends shown on the Glacial Map of Canada (Prest et al., 1968) and with streamlined landforms mapped by Fulton et al. (1980a, b, c, 1981).

Older striae occur on glacially faceted surfaces and on bedrock lows protected from erosion by the last ice advance. At sites in area B (Fig. 85.3) where relative ages are clearly shown, northeast trending striae generally predate the east-northeast striae. The older northeast striae are consistent in orientation and relative age with striae noted by Klassen and Bolduc (1984) in the Churchill Falls area and by Kirby (1961) in the Labrador Trough, and are considered to have been formed during a major phase of ice flow. It is not clear from the striae whether the northeast ice flow trends in area A are in fact contemporaneous with the older northeast striae in area B (Fig. 85.3) or are a product of diverging regional flow of a single glacial phase. There is evidence based on glacial dispersal patterns that would support the former interpretation. Interpretation of all northeast trending striae as "older" would indicate that area A was not glaciated during the last phase of regional ice flow.

At three sites in the south part of area B east-southeast striae predate east-northeast striae. There is insufficient evidence to demonstrate the significance of these older striae or their relationship with the east-southeast flow trends in area C.

Distribution of indicator clasts

The lithology and relative abundance of clasts were noted at most sample sites to help define how material was transported by the ice. The till is dominantly locally derived; generally less than 20 per cent of the coarse clasts have undergone transport of more than 5 km. Clasts that have been subjected to transport in excess of 50 km generally comprise less than 1 per cent of the till. Indicator clasts, those that are visually distinctive and have a restricted bedrock source area, usually occur in low concentrations but are useful in defining regional flow patterns.

The glacial dispersal patterns of indicator clasts, Red Wine alkaline complex rocks, Seal Lake Group basalt, and Snegamook granite demonstrate broad fan-shaped eastward dispersal of 30 to more than 100 km from their respective bedrock sources (Fig. 85.4, 85.5, 85.6). Transport of erratics and development of fan shapes appear to be related to the multiple phases of flow recorded by striae. The dispersal of Snegamook granite (Fig. 85.4) in area A (Fig. 85.3) indicates transport in the northeast phase of ice flow. The dispersal, in area B, of Snegamook granite and Seal Lake Group volcanic

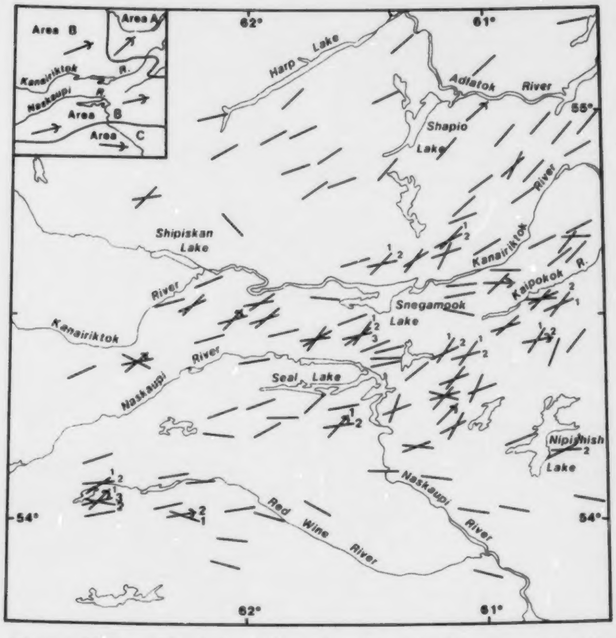

Figure 85.3. Glacial striae in the study area showing direction or trend of ice movement; numbers indicate relative age relationship (1, oldest). Inset map shows the dominant ice flow direction by area.

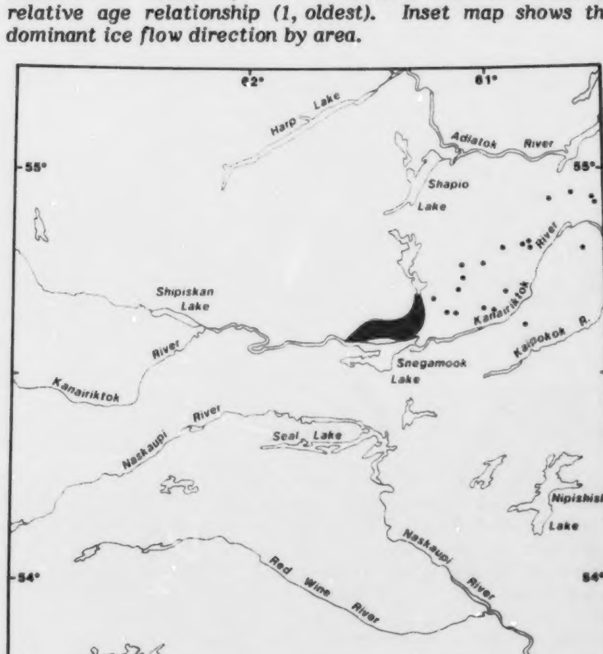

Figure 85.4. Area of outcrop and dispersal of glacial erratics of Snegamook granite.

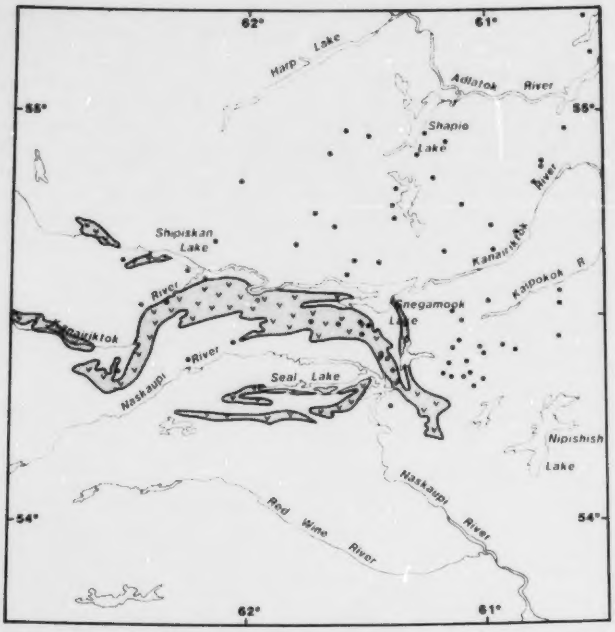

Figure 85.5. Area of outcrop and dispersal of glacial erratics of Seal Lake Group basalts.

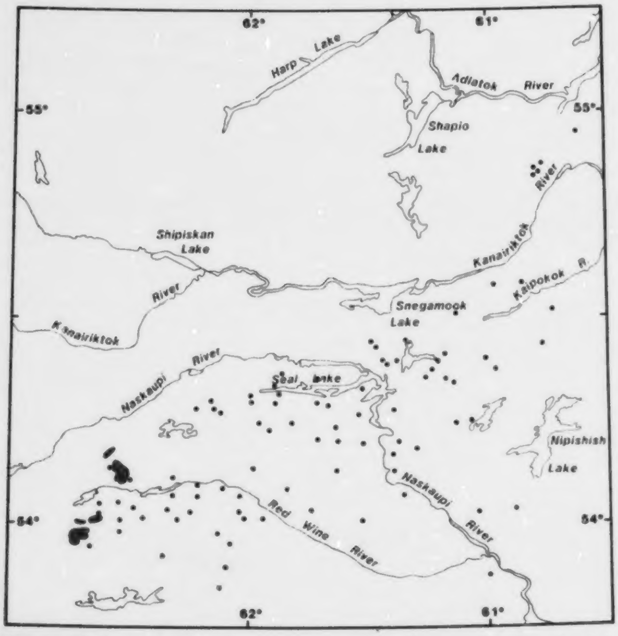

Figure 85.6. Area of outcrop and dispersal of glacial erratics of Red Wine alkaline complex.

rocks (Fig. 85.5) east from their respective source areas and the east-northeast trending northern limit of rocks derived from the Red Wine alkaline complex (Fig. 85.6) demonstrate transport in the east-northeast phase of ice flow. The presence of Seal Lake Group basalts in till northeast of the main bedrock source, which is in an area of east-northeast flow trends, suggests that part of their dispersal occurred during the early northeast-directed phase of ice flow. The presence of Red Wine alkaline complex clasts in area A, 150 km northeast of the bedrock source, would also indicate dispersal in the northeast phase of flow and would suggest that area A is a remnant of this early advance. The east-southeast trending southern limit of rocks derived from the Red Wine alkaline complex would indicate dispersal in the east-southeast directed ice flow; however, it is not clear whether debris was carried in a separate phase of flow or in a single advance which radiated both east northeast and east southeast from the complex.

Implication for drift prospecting

Drift prospecting conducted in central Labrador should be tailored to account for the complex history of glacial transport and the sampling problems particular to the area.

Till sampling in central Labrador is difficult. The area is rugged and heavily forested, and consequently mobility is restricted. Sampling sites are limited by areas of thin till and by swamps. The till is commonly compact and stony and is difficult to penetrate.

The data in this report demonstrate that bedrock debris can be traced over considerable distances in the till and can clearly indicate direction of ice transport. The information suggests that overall transport was the result of different phases of ice flow and consequently some of the glacial debris may have been subjected to a complex history of transport; for example, clasts of Seal Lake Group volcanic rocks appear to have been carried northeastward in the early phase of ice flow and then remobilized in the late phase. Furthermore, as yet unrecognized, topographically controlled local variations in ice flow direction, particularly in low areas or on hillsides, may have played an important role in the transport of glacial debris.

Conclusions

Within the Snegamook and Kasheshibaw map areas, striae are generally east-northeast in the central part of the area, northeast in the northeast, and east-southeast in the south. Evidence from older striae indicates that a major northeast directed ice advance predates the east-northeast phase of flow. The east-southeast flow trends may reflect either divergent flow in the east-northeast advance or a separate phase of flow. The distribution of indicator erratics demonstrates fan-shaped eastward transport consistent with the multiple phases of flow recorded by striae and suggests that till in the northeast part of the map area represents a remnant of this early advance.

Acknowledgments

B. Lane, G. McKenna, L. Newman, and B. Wener are thanked for assistance in the field and in compiling map data, and M. Kettles for her work as camp cook. Expediting services were capably provided by R. Watts. The helicopter pilot, L. Labadie, is thanked for his help and flying skills. The report benefited from critical reading by R.N.W. DiLabio.

References

Baragar, W.R.A.
1981: Tectonic and regional relationships of the Seal Lake and Bruce River Magmatic Provinces; Geological Survey of Canada, Bulletin 314.

Curtis, L.W. and Currie, K.L.
1981: Geology and petrology of the Red Wine alkaline complex, central Labrador; Geological Survey of Canada, Bulletin 294.

Douglas, C. and Hsu, E.
1976: Mineral occurrences, Kasheshibaw Lake; Mineral Development Division, Department of Mines and Energy, Government of Newfoundland and Labrador, Map 7644.

Emslie, R.F.
1980: Geology and petrology of the Harp Lake Complex, central Labrador: An example of Elsonian Magmatism; Geological Survey of Canada, Bulletin 293.

Fulton, R.J., Hodgson, D.A., Minning, G.V., and Thomas, R.D.
1980a: Surficial materials, Kasheshibaw Lake; Geological Survey of Canada, Map 28-1979.

1980b: Surficial materials, Snegamook Lake, Labrador; Geological Survey of Canada, Map 27-1979, scale 1:250 000.

1980c: Surficial materials, Goose Bay, Labrador; Geological Survey of Canada, Map 22-1979, scale 1:250 000.

1981: Surficial materials, Winokapau Lake; Geological Survey of Canada, Map 21-1979, scale 1:250 000.

Greene, B.A.
1970: Geological map of Labrador; Department of Mines, Agriculture and Resources, Province of Newfoundland and Labrador, scale 1:1 000 000.

Kirby, R.P.
1961: Movements of ice in central Labrador-Ungava; Cahiers de géographie de Québec, no. 10, p. 205-218.

Klassen, R.A.
1983: A preliminary report on drift prospecting studies in Labrador; in Current Research, Part A, Geological Survey of Canada, Paper 83-1A, p. 353-355.

Klassen, R.A. (cont.)
1984: A preliminary report on drift prospecting studies in Labrador, Part II; in Current Research, Part A, Geological Survey of Canada, Paper 84-1A, p. 247-254.

Klassen, R.A. and Bolduc, A.
1984: Ice flow directions and drift composition, Churchill Falls, Labrador; in Current Research, Part A, Geological Survey of Canada, Paper 84-1A, p. 255-258.

O'Driscoll, C.F. and Noel, N. (compilers)
1983: Mineral occurrences Snegamook Lake; Mineral Development Division, Department of Mines and Energy, Government of Newfoundland and Labrador, Map 83-36.

Prest, V.K., Grant, D.R., and Rampton, V.N.
1968: Glacial map of Canada; Geological Survey of Canada, Map 1253A, scale 1:5 000 000.

Ryan, B.
1982a: Geology of the Central Mineral Belt (central part – sheet 1); Mineral Development Division, Department of Mines and Energy, Government of Newfoundland and Labrador, Map 82-3.

1982b: Geology of the Central Mineral Belt (central part – sheet 2); Mineral Development Division, Department of Mines and Energy, Government of Newfoundland and Labrador, Map 82-4.

Shilts, W.W.
1977: Geochemistry of till in perennially frozen terrain of the Canadian Shield – application to prospecting; Boreas, v. 5, p. 203-212.

Thomas, A.
1981: Geology along the southwestern margin of the Central Mineral Belt; Mineral Development Division, Department of Mines and Energy, Government of Newfoundland and Labrador, Report 81-4.

Vegetation-geology-climate relationships of western Melville Island, District of Franklin

Project 760058

S.A. Edlund
Terrain Sciences Division

Edlund, S.A., Vegetation-geology-climate relationships of western Melville Island, District of Franklin; in Current Research, Part A, Geological Survey of Canada, Paper 86-1A, p. 719-726, 1986.

Abstract

Both surficial geology and climate closely control plant assemblages on western Melville Island. Vegetation falls into two broad categories: calciphilous communities on weakly to moderately alkaline substrates, and acetophilic communities on acidic substrates. Superimposed on this lithological control is the control imposed by climate. The region is subdivided into five bioclimate zones including a newly defined one – Zone 0 – unvegetated areas recently emerged from under neoglacial ice and snow.

An unusually vegetation-rich zone (Zone 4) covers a significant area of western Melville Island, making it the richest area of the central and western Queen Elizabeth Islands, comparable to the flora and communities in the Fosheim Peninsula region of Ellesmere Island. This zone may represent a disjunct of Mid Arctic vegetation into the region generally considered to be High Arctic.

Résumé

La géologie des formations en surface et le climat contrôlent étroitement les association végétales dans l'ouest de l'île Melville. La végétation dans cette région se répartit en deux grands groupes: des communautés calciphiles sur des substrats faiblement à modérément alcalins et des communautés acidophiles sur des substrats acides. Au contrôle lithologique s'ajoute le contrôle climatique. On divise la région en cinq zones bioclimatiques dont une zone nouvellement définie, soit la zone 0; il s'agit d'une zone sans végétation qui a récemment émergé de la glace et de la neige néoglaciaires.

Une zone exceptionnellement riche en végétation (zone 4) couvre une grande superficie de la partie ouest de l'île Melville, faisant de cette dernière la région la plus riche du centre et de l'ouest des îles de la Reine-Élisabeth, comparable par sa flore et ses communautés à la presqu'île Fosheim dans l'île d'Ellesmere. Cette zone peut être considérée comme un îlot isolé de végétation de l'Arctique moyen dans la région généralement considérée comme appartenant à l'extrême Arctique.

Introduction

Reconnaissance studies carried out on western Melville Island (Fig. 86.1) during the summers of 1984 and 1985 confirm the strong geological and elevational controls on the distribution of plant communities expected in a High Arctic environment (Edlund, 1983a). The landscape is dominated by plateaus and folded uplands, up to 776 m a.s.l., developed on relatively resistant Paleozoic clastic and carbonate rocks, whereas in the northern sector, lowlands and low cuestas occur on younger, generally recessive clastic sediments.

Geological control of vegetation

There is minimal soil development in this region, therefore the vascular plants root directly in the weathered rock which is the dominant surficial material. The chemistry of the bedrock therefore exerts a major influence on the vegetation. Most Quaternary surficial materials are locally derived, except at Bailey Point and Cape Hoare (Hodgson et al., 1984) and at Comfort Cove (D.A. Hodgson, personal communication, 1985) where a silty clay calacreous till was deposited by Late Pleistocene glaciers of continental origin. The strong correlation between vegetation and surface materials of Melville Island was first observed by Tozer and Thorsteinsson (1964). This study further refines their observations.

Preliminary pH studies show that the surficial materials can be grouped into two broad categories (Fig. 86.2), according to the types of plant communities they support (Fig. 86.3): (1) those with an alkaline pH, with calciphilic (lime-loving) vegetation and (2) those with an acidic pH, with accompanying acetophilic (acid-loving) or pH-indifferent vegetation. Near neutral soils show some overlap of both acid- and lime-loving species. Although the dominant and common species differ between these two broad divisions, the growth forms of the plants concerned are similar (dwarf shrubs, grass-like, herbaceous, lichen or moss).

Six subdivisions of the substrate, based on the degree of acidity/alkalinity and texture of the surficial materials, are shown in Table 86.1. Most materials are moderately to well drained, therefore the tundra and barrens vegetation dominate. Only on the silty clay till at Bailey Point is there extensive wetland vegetation. Accompanying vegetation is also described.

The densest and most diverse vegetation occurs on several members of the Ibbett Bay Formation found in the Canrobert Hills, which are recessive, black fissile shales that weather into thin, platy fragments. They are weakly to moderately alkaline, and moderately to well drained. At lower elevations these materials support dense, continuous dwarf shrub (**Dryas** and willow)-legume tundra and dwarf shrub-grass tundra, on all stabilized surfaces. At high elevations, grasses and purple saxifrage (herbaceous species) dominate.

Fluvial deposits (sand and silt) derived primarily from the Canyon Fiord Formation at the head of McCormick Inlet, also support dense and diverse calciphilous dwarf shrub-legume and dwarf shrub-grass tundra and barrens, although the parent formation is itself rather poorly vegetated. The lack of vegetation on weathered Canyon Fiord Formation may be due primarily to the instability of its surfaces.

The richest vegetation on weakly to moderately acidic surficial materials consists of willow-**Luzula** tundra, local arctic heather heathland, and **Luzula**-tundra, with a general absence of calciphilous species. The rubbly felsenmeer produced on the lower member of Hecla Bay Formation sandstone, although also weakly acidic, is too coarse for the rooting of vascular plants. Instead, cryptogamic (moss and lichen) communities are found, with crustose lichens on exposed rock facets, and mats of **Rhacomitrium** sp. moss, carpeting the sheltered junctions of boulders.

The poorest vegetation, both in species diversity and density of vascular plant cover, occurs in two general regions, the northern half of the Sproule Peninsula and Cape Grassy, and at elevations above 250-300 m on the plateaus and rolling hills. There the vascular plant species are entirely herbaceous, with purple saxifrage commonly dominant on the alkaline terrain and **Luzula** on the acidic ones. Wetlands are dominated by only grass species; sedges are absent.

Some materials do not support plant growth. Both the nearly pure carbonates of the Canrobert Formation and a Paleozoic carbonate inlier along Kitson River are devoid of plant life. These carbonate surfaces may weather too rapidly for crustose lichen attachment, and the fines lack sufficient other plant nutrients to buffer the overwhelming amounts of calcium and magnesium and thus are toxic.

The siliceous chert gravel facies of the Ibbett Bay Formation does not weather as rapidly as the carbonates and does support crustose lichen and **Rhacomitrium** moss communities.

Influence of climate on vegetation

In addition to the lithological control on plant communities, climate, probably through variations in summer warmth and the length of growing season, influences the diversity, abundance, and dominance of plant species and communities. This control cuts across lithological boundaries and shows a strong elevational trend and a weaker latitudinal trend, as was noted in the central Queen Elizabeth Islands (Edlund, 1983a).

Bioclimatic zones in this region (Fig. 86.3) are: Zone 1, with less than 35 vascular plant species, all of which are herbaceous; Zone 2 also dominated by herbaceous species, but an increase in diversity to between 35 and 60 vascular plant species, including the presence of sedges and woody plants; Zone 3, with woody species and sedges the dominant vascular plants and diversity between 60 and 100; and Zone 4 which is

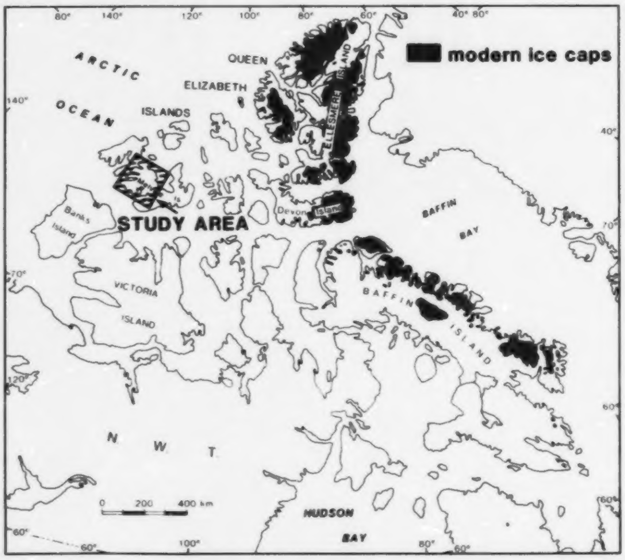

Figure 86.1. Location of study area, western Melville Island.

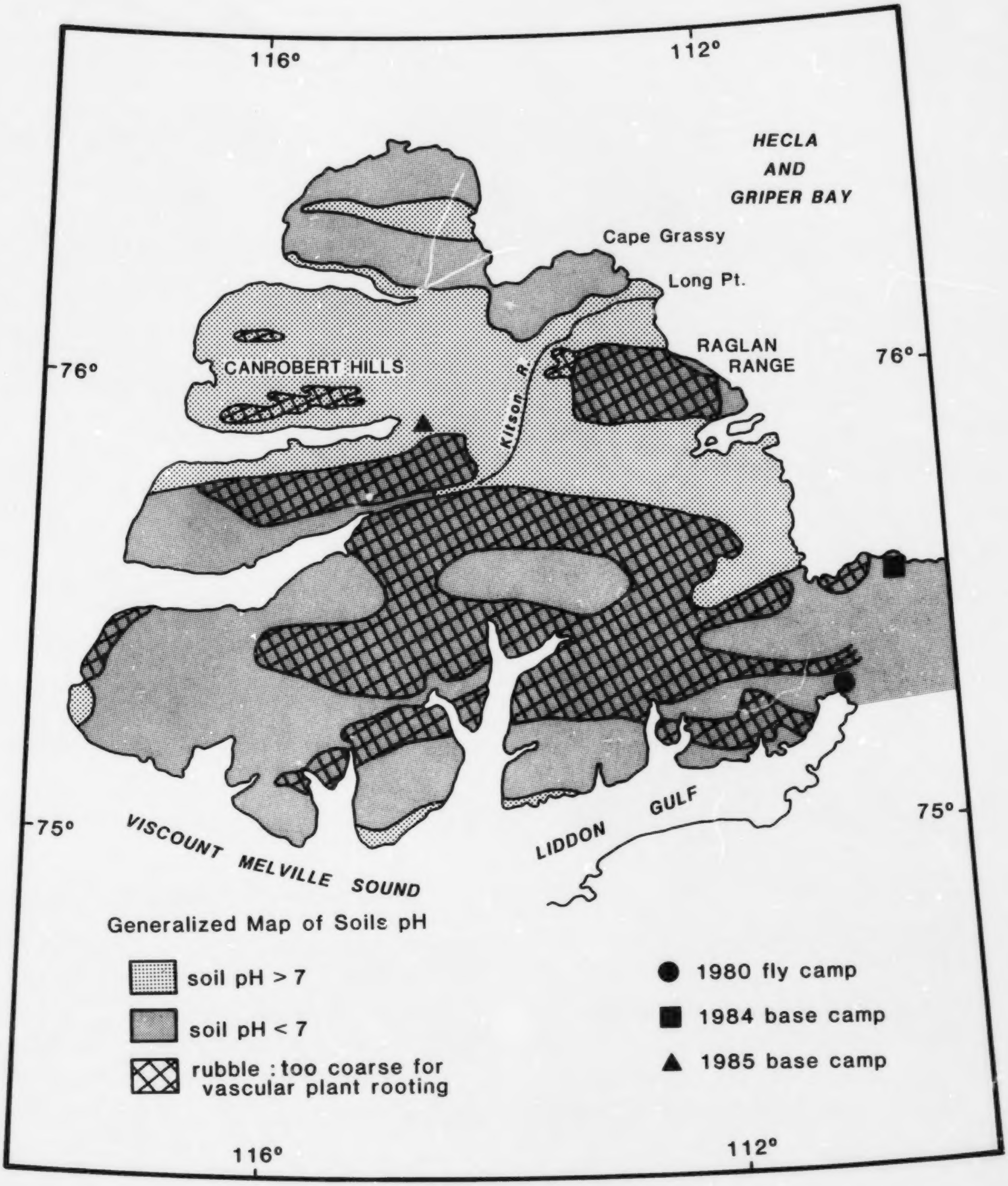

Figure 86.2. Generalized map of soil pH, western Melville Island.

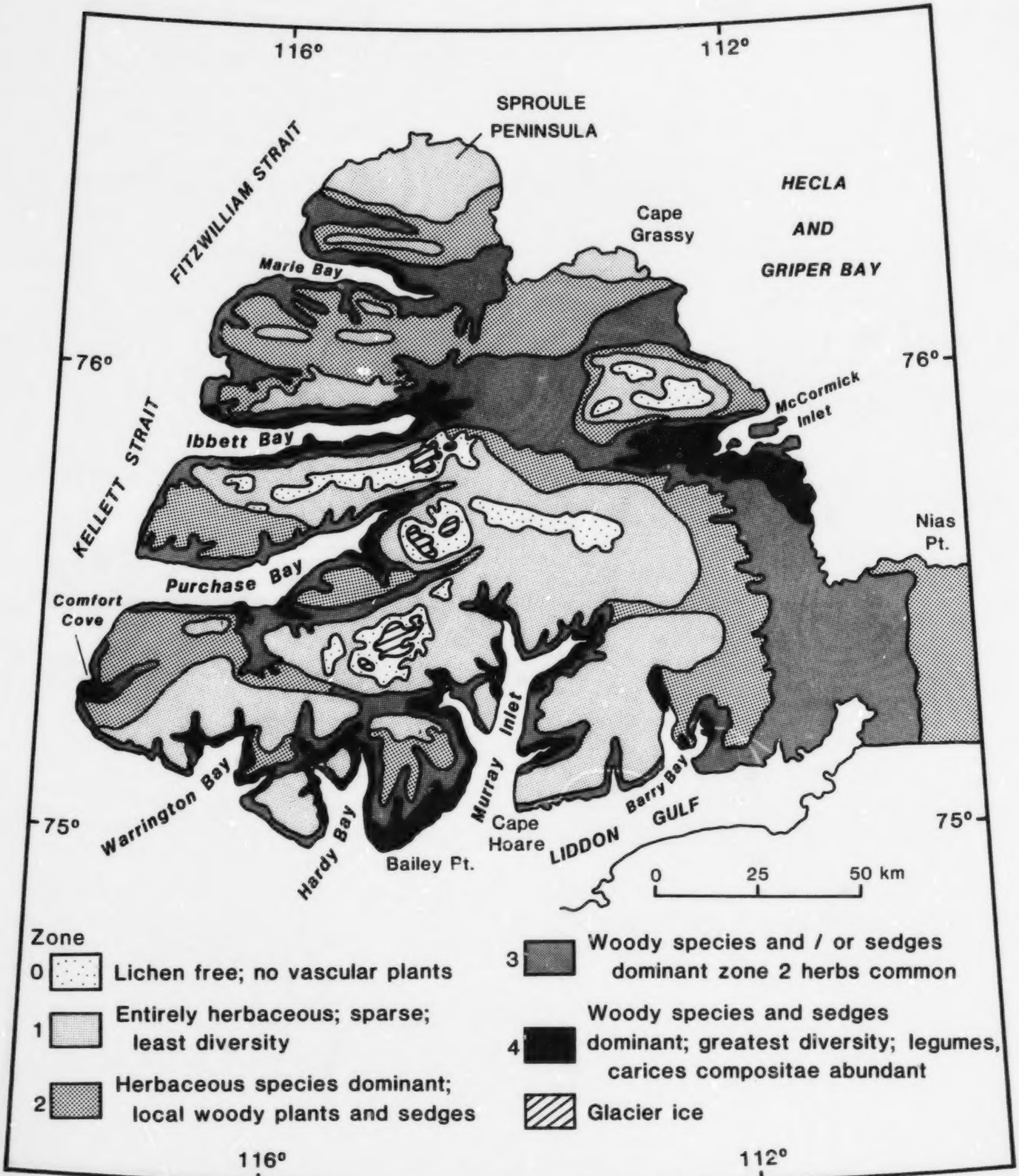

Figure 86.3. Bioclimatic zones of western Melville Island.

also dominated by woody species, including local heath, and sedges and has the greatest diversity of 120-125 or more vascular plant species.

All four bioclimatic zones described for the central Queen Elizabeth Islands occur on western Melville Island. On central and southern Melville Island (Edlund, 1982a, 1983a) the zone (Zone 4) of greatest density and diversity (>100 vascular plant species) is limited to a narrow strip along the southern coast and along the southern shore of western Liddon Gulf.

Zone 4

On western Melville Island Zone 4 occurs in valleys along the north side of Liddon Gulf and Viscount Melville Sound as well as along shores and sheltered valleys in the central part, a much more extensive coverage than predicted by Edlund (1983a). On weakly to moderately alkaline materials in this zone woody species, particularly **Dryas** (Arctic Avens) and **Salix arctica** (dwarf willow), dominate with the diameter of some willow clumps reaching more than 1 m. Common herbaceous associates include the legumes **Astragalus alpinus** (alpine milk-vetch) and **Oxytropis arctica**; other more southerly herbs **Geum Rossii**; a variety of compositae (Daisy family) including **Senecio congestus, Arnica alpina, Erigeron eriocephalus, E. compositus, Antennaria** sp.; **Crepis nana** (dwarf hawks beard), **Petasites frigidus** (Lapland butterbur), and four or five **Taraxacum** (dandelion) species; and local occurrences of the sedges **Carex nardina** and **C. rupestris** and grasses such as **Festuca rubra, F. baffinensis, Trisetum spicatum**, and **Agropyron violaceum**. Communities on acidic substrates include dense mats of **Salix arctica** and local heath of **Cassiope tetragona** (arctic white heather). Common herbaceous associates include **Luzula confusa** (northern woodrush), **L. nivalis**, and **Hierochloe alpina** and **Potentilla hyparctica**, and **Stellaria longipes**.

Wetlands in Zone 4 are dense with sedge and grass species: **Carex aquatalis** var. **stans; Eriophorum triste** and **E. scheuchzeri** (cotton grasses), and grasses **Arctagrostis latifolia, Dupontia Fisheri, Alopecurus alpinus**, and **Hierochloe pauciflora**. Dwarf woody species also occur on mossy hummocks in the wetlands.

Pond emergents include **Arctophila fulva**, a grass which locally fills shallow ponds, **Pleuropogon sabinei** (semaphore grass), **Caltha palustris** (marsh marigold), and tiny buttercups such as **Ranunculus hyperboreus** and **R. gmelini**. Halophytic (salt-loving) species along the ocean shore and in brackish lagoons include locally dense turfs of **Puccinellia phryganodes** (goose grass) and **Stellaria humifusa**, as well as unexpected occurrences of **Carex ursina** and **C. maritima**. An as yet unidentified caespitose Saxifrage was also found in tidal zones.

Zone 3

Zone 3, the more common "rich" zone of the High Arctic (60-100 vascular species) occurs up to 150 m a.s.l. It is also dominated by woody plant species and sedges as in Zone 4 but the diversity and per cent cover are less. Willow and arctic avens are common on weakly to moderately alkaline materials, but legumes, common in Zone 4, are rare and **Saxifraga oppositifolia** (purple saxifrage) and **Alopecurus alpinus** are common associates instead. On acidic materials **Cassiope** is restricted and generally absent. The Compositae family includes only **Petasites frigidus** and **Taraxacum** species. **Pleuropogon Sabinei** and **Ranunculus hyperboreus** are the common marsh emergents. Halophytes include only turfs of **Puccinellia phryganodes** and **Stellaria humifusa**.

Zone 2

In Zone 2 sedges and woody species are no longer dominant but are still present. It is dominated by herbaceous species, generally those that were common associates in Zone 3. Diversity (35-60 species) and per cent cover of vascular plant species decrease (generally less than 10% cover). Sedges and cotton grasses are rare; arctic heather, Compositae, and Leguminosae are absent. Purple saxifrage generally dominates on weakly to moderately alkaline materials, with grasses, generally **Alopecurus** and **Colpodium**, on the siltier aspects. Areas of acidic coarse sand to silt are dominated by **Luzula** (wood rush) species, with **Potentilla hyparctica** as a common associate; grasses, cruciferae, and **Papaver** (arctic poppy) occur on siltier sites. Vascular plants in wetlands are almost entirely dominated by grass species, particularly **Alopecurus** and **Dupontia**, with **Pleuropogon** as an occasional marsh emergent.

On western Melville Island Zone 2 vegetation occurs along the north coast and on the uplands and parts of the southern and central plateau, at elevations of ca. 150-200+ m a.s.l.

Zone 1

Zone 1, which has the most impoverished vegetation in the central Queen Elizabeth Islands, occurs primarily on the plateaus at elevations of generally more than 350 m a.s.l. This zone is entirely herbaceous and/or cryptogamic. There are generally less than 35 vascular plant species, and in places there is no clear dominance. There are no woody species sedges, compositae, or vascular cryptogams present in this zone. Vascular plant cover is generally less than 5 per cent. In some places communities are entirely cryptogamic.

Zone 0

Observations on western Melville Island indicate that another High Arctic bioclimatic zone is present. Zone 0 delineates areas that are devoid of vegetation due to its recent exposure from under ice and snow, rather than for reasons of toxic chemistry, lack of plant nutrients, or rapid weathering of the surficial materials. This zone covers several thousand square kilometres on the highest plateau surfaces of western Melville Island (ca. 500-700 m a.s.l., Edlund, 1985), as well as locally around the edges of permanent snowbanks otherwise lying in Zone 1 and rarely Zone 2.

Floristics

Most plant species observed on western Melville Island have already been reported from other parts of Melville Island (Porsild, 1955, 1964; Cody et al., 1976; Porsild and Cody, 1980; Edlund, in preparation); however, a few unreported species were found during fieldwork. One surprise was the occurrence of species of moss **Sphagnum subsecundum** in small wet meadows at 180 m a.s.l. near the east arm of Murray Inlet and again on the west side of Warrington Bay. **Sphagnum** is generally considered to be a species of the boreal bogs and rarely appears in the Low Arctic. It has not been included in modern flora in the High Arctic. The detection of modern **Sphagnum** on Melville Island may help to explain the seemingly anomalous occurrence of high levels of **Sphagnum** pollen from ice cores from a Melville Island ice cap (J. Bourgeois, personal communication, 1985).

Table 86.1. General types of substrates and accompanying vegetation, western Melville Island

SUBSTRATE CHEMISTRY AND TEXTURE	BIOCLIMATIC ZONES AND VEGETATION
ALKALINE MATERIALS (pH > 7.2)	CALCIPHILOUS VEGETATION
WEAKLY TO MODERATELY ALKALINE SILT, MINOR CLAY Includes Cape DeBray and Christopher formations; parts of Griper Bay, Weatherall Bay, Ibbett Bay, Blackley, Kitson River, Cape Phillips, Cape Fortune, and Canyon Fiord formations; silty calcareous till; Quaternary deposits derived from the above.	ZONES 4 and 3: Dwarf willow and arctic avens dominant; cover 10-50%; grasses, sedges, legumes, **Potentilla**, crucifers, purple saxifrage, composites common associates; sedge dominated wetlands. ZONES 2 and 1: grasses and/or purple saxifrage, herbs dominant; cover 2-10%; crucifers, Caryophyllaceae poppy, saxifrages common associates; grass dominated wetlands; no apparent dominant in some places.
WEAKLY TO MODERATELY ALKALINE SAND AND GRAVEL Gravel includes platy fissile shale fragments from Ibbett Bay, Cape DeBray, Kitson River, and Blackley formations; sand and gravel from Canyon Fiord, Trold Fiord, Assistance Bay and parts of Wilkie Point, Beverley Inlet formations; Quaternary deposits derived from the above.	ZONES 4 and 3: Arctic avens, and to a lesser extent, dwarf willow dominate; cover 10-50%; legumes, dryland sedges, grasses, composites, purple saxifrage common associates; sedge dominated wetlands. ZONES 2 and 1: Purple saxifrage dominant; cover 2-10%; grass dominated wetlands; no apparent dominant in some places.
STRONGLY ALKALINE FINES, GRAVEL, AND RUBBLE Parts of Cape Phillips, Thumb Mountain, Canrobert formations; Silurian carbonate inlier along Kitson River.	ZONES 4, 3, 2, and 1: Not vegetated
ACIDIC MATERIALS (pH 6.8-5.0)	ACETOPHILIC AND pH-INDIFFERENT VEGETATION
WEAKLY TO MODERATELY ACIDIC SILT AND/OR CLAY Local Weatherall Bay, Griper Bay, Beverley Inlet, Christopher formations; Kanguk Formation.	ZONES 4 and 3: Dominated by dwarf willow; cover 10-50%; grasses, particularly goose grass, foxtail grass Caryophyllaceae common associates; sedge dominated wetlands; arctic white heather locally dominant in Zone 4. ZONES 2 and 1: Dominated by grasses (foxtail grass, Colpodium, Phippsia); cover 1-10%; Caryophyllaceae and poppy common associates; grass dominated wetlands.
WEAKLY TO MODERATELY ACIDIC SAND AND GRAVEL Includes platy, fissile shale of Blackley and Weatherall Bay formations, Parry Island Group, and sand of Hecla Bay, Bjorne, Isachsen, Wilkie Point, Hassel formations, and local Quaternary deposits, and till and fluvial deposits derived from these formations.	ZONES 4 and 3: Dwarf willow dominated; cover 10-50%; arctic white heather locally dominant in Zone 4; common associates: woodrush, **Potentilla**, holy grass; sedge dominated wetlands; local **Sphagnum** moss. ZONES 2 and 1: woodrush and grass dominated; cover 1-10%; **Potentilla, Stellaria** common associates; grass dominated wetlands; no apparent dominants in some places.
NON ALKALINE GRAVEL AND RUBBLE WITH FEW FINES Includes upper member of Hecla Bay sandstone formation; local sandstone facies of Hecla Bay and Beverly Inlet formations; siliceous chert of Ibbett Bay Formation.	ZONES 4, 3, 2 and 1: Crustose and foliose lichens on exposed boulder facets; **Rhacomitrium** moss-lichen mats over sheltered rubble and in junctions of boulders.

A few vascular plant species new to Melville Island were also found: the halophytes **Carex maritima** and **Carex ursina**; the grass **Deschampsia pumila**; a possibly new **Festuca** sp. (S.G. Aiken, personal communication, 1985) and calciphilic species **Kobresia myosuroides**, **Antennaria canescens**; and the wintergreen **Pyrola grandiflora**, and dandelion **T. pumilum**. A nonflowering **Polemonium**, possibly **P. acutiflorum**, not previously reported from the Arctic Islands, occurred on several poorly drained organic deposits on extreme western Melville Island. All new species occurred in bioclimatic Zones 3 and 4 where summer temperatures are warmest.

Discussion

The diverse plant communities found in Zone 4 are more akin to plant assemblages farther south rather than to those of the central High Arctic. The calciphilous dwarf shrub-legume tundra communities at Ibbett Bay, McCormick Inlet, and Liddon Gulf have their counterpart in the broad zone of calcareous deposits of the Mid Arctic, on Banks Island (Vincent and Edlund, 1978) and Victoria Island (Edlund, 1983b). Similarly the dwarf shrub-heath tundra communities are comparable to Mid Arctic communities on acidic Precambrian Shield granites and gneisses of northern District of Keewatin (Edlund, 1982b) and Baffin Island.

Zone 4 seems to represent the sporadic occurrence of Mid Arctic vegetation in the western Queen Elizabeth Islands. The similarities between Zone 4 and Mid Arctic vegetation (National Atlas of Canada, 1971) in plant community common associates, colonizing species wetlands composition, emergent marsh species, and halophytes is striking. A difference between Zone 4 vegetation on western Melville Island and vegetation of the Mid Arctic is the absence in Zone 4 of woody species capable of erect and semi-erect shrub growth form, such as **Salix alaxensis**, **S. niphoclada**, and **S. lanata** var. **Richardsonii**. In the Mid Arctic, these woody species have adopted a prostrate growth form, similar to that of the genetically dwarfed, prostrate shrub **Salix arctica**; in the Low Arctic, however, these willow rise from 30 cm to 1 m or more above the ground.

The presence of Zone 4 vegetation in the Queen Elizabeth Islands is not restricted to southern and western Melville Island. Similar plant assemblages occur on the lowlands and sheltered slopes and valleys of Axel Heiberg and Ellesmere islands, up to at least 80°N (Waterston and Waterston, 1972). In the mountainous eastern Queen Elizabeth Islands, this seeming vegetation anomaly reflects a climate anomaly – the rain shadow effect. Major mountain ranges provide a barrier to low cloud moving in from the Arctic Ocean, thus many lowlands and valleys receive more direct sunlight than the low lying Queen Elizabeth Islands. This is illustrated best by a comparison of mean daily temperatures for July in several parts of the Queen Elizabeth Islands: Eureka (80°N), surrounded by mountains, has a mean daily July temperature of 5.4°C, whereas Isachsen (78°47'N) on low-lying Ellef Ringnes Island, has a mean daily July temperature of 3.2°C; Resolute (74°43'N), Cornwallis Island, 4.1°C; Rea Point (75°21'N), eastern Melville Island, 4.1°C; and Mould Bay (76°14'N), Prince Patrick Island, 3.1°C (Atmospheric Environment Service, 1975). The ridges and plateaus of western Melville Island may function as orographic barriers to southward moving systems off the Arctic Ocean in similar fashion to the mountainous eastern Queen Elizabeth Islands.

Along the north shore of Murray Inlet, Liddon Gulf some of the densest and most diverse heath and vegetation occur on small coastal plateaus at 150-180 m a.s.l., above the level of coastal fog and thus receiving more sunlight than the coastal strip.

The black shales and mudstones found in the Canrobert Hills, particularly where the Ibbett Bay Formation outcrops, support the most luxurious vegetation growth on Melville Island. No doubt several factors contribute to the richness of the vegetation there, including the occurrence of a wide range of plant nutrients and a source of carbon in the weathered rock. But so, too, the colour of the weathered rock may raise the temperature; the black, unvegetated, steep, unstable upper slopes and ridge tops absorb solar radiation and radiate it, to a much greater degree than the adjacent buff, grey, and white carbonate formations. The observations that vegetation on the black shales flowered and set seed 1-3 weeks earlier than on most of the rest of the island supports this hypothesis; temperatures recorded at the surface of the black shales were 7°C or more above the air temperature whereas temperatures on grey and light brown materials were less than 2°C above air temperature.

Acknowledgments

The author wishes to thank Polar Continental Shelf Project for logistics support during summers 1984 and 1985; D.A. Hodgson, as critical reader, suggested useful ways of improving the manuscript; S.G. Aiken (National Herbarium of Canada) and volunteer E. Robinson assisted in the curation of vascular plant specimens; R.R. Ireland (National Herbarium of Canada) identified the **Sphagnum** moss species.

References

Atmospheric Environment Service
1975: Canadian climate normals, Vol. 1, SI Temperature; Environment Canada, Downsview, Ontario.

Cody, W.J., Parker, G.R., and Lampert, D.B.M.
1976: Additions to the vascular flora of Melville Island, Franklin District, Northwest Territories; Canadian Field-Naturalist, v. 90, p. 70-72.

Edlund, S.A.
1982a: Vegetation of Melville Island, District of Franklin, N.W.T. (eastern and south-central Melville Island); Geological Survey of Canada, Open File 852, scale 1:250 000.

1982b: Plant communities on the surficial materials of north-central District of Keewatin; Geological Survey of Canada, Paper 80-33, 20 p.

1983a: Bioclimatic zonation in a High Arctic region: central Queen Elizabeth Islands; in Current Research, Part A, Geological Survey of Canada, Paper 83-1A, p. 381-390.

1983b: Reconnaissance vegetation studies on western Victoria Island, Canadian Arctic Archipelago; in Current Research, Part B, Geological Survey of Canada, Paper 83-1B, p. 75-81.

1985: Lichen-free zones as neoglacial indicators on western Melville Island, District of Franklin; in Current Research, Part A, Geological Survey of Canada, Paper 85-1A, p. 709-712.

– Vegetation of central Melville Island, Northwest Territories; relationships between vegetation and surficial materials; Geological Survey of Canada, Paper. (in preparation)

Hodgson, D.A., Vincent, J-S., and Fyles, J.G.
1984: Quaternary geology of central Melville Island, Northwest Territories; Geological Survey of Canada, Paper 83-16, 25 p.

National Atlas of Canada
1971: National Atlas of Canada: Vegetation; Ottawa, Canada.

Porsild, A.E.
1955: The vascular plants of the western Canadian Arctic Archipelago; National Museum of Canada, Bulletin, v. 35, 226 p.

1964: Illustrated flora of the Canadian Arctic Archipelago; National Museum of Canada, Bulletin 146, 218 p.

Porsild, A.E. and Cody, W.J.
1980: Vascular plants of the continental Northwest Territories; National Museum of Canada, Ottawa, 667 p.

Tozer, E.T. and Thorsteinsson, R.
1964: Western Queen Elizabeth Islands, Arctic Archipelago; Geological Survey of Canada, Memoir 332, 242 p.

Vincent, J-S. and Edlund, S.A.
1978: Extended legend to accompany preliminary surficial geology maps of Banks Island, Northwest Territories; Geological Survey of Canada, Open File 577.

Waterston, G. and Waterston, I.
1972: Report on wildlife, vegetation and environmental values in the Queen Elizabeth Islands, Ellesmere and part of Axel Heiberg, June 28-August 15, 1972; report to Canadian Wildlife Service, Ottawa, 54 p.

Fifty years (1935 to 1985) of coastal retreat west of Tuktoyaktuk, District of Mackenzie

Project 680047

J. Ross Mackay[1]
Terrain Sciences Division

Mackay, J. R., Fifty years (1935 to 1985) of coastal retreat west of Tuktoyaktuk, District of Mackenzie; in Current Research, Part A, Geological Survey of Canada, Paper 86-1A, p. 727-735, 1986.

Abstract

Coastal recession from 1935 to 1985 has been determined for four sites to the immediate west of Tuktoyaktuk, Northwest Territories. The 1935 shoreline position has been mapped from oblique air photographs and the positions of the shoreline from 1950 to 1985 from vertical air photographs and field studies. The mean rates of coastal retreat have been about: 8 m/year for high centre polygons underlain by a high ice content diamicton; 7 m/year for a tabular body of massive ice; 1 m/year or less for a sectioned pingo with a thick overburden of sands; and 1 m/year or less for sandy coastal bluffs. The rate of retreat is primarily a function of the amount of excess ice in the coastal bluffs and the severity of late summer storm surges. Where excess ice extends below sea level, some offshore thermokarst depressions have developed.

Résumé

On a déterminé la distance totale de recul du rivage de 1935 à 1985, en quatre endroits situés immédiatement à l'ouest de Tuktoyaktuk dans les Territoires du Nord-Ouest. On a porté sur une carte la position du rivage de 1935 à partir de photographies aériennes prises obliquement ainsi que les positions du rivage de 1950 à 1985 à partir de photographies aériennes prises verticalement et d'études sur le terrain. Les vitesses moyennes de recul du rivage ont été d'environ 2,8 m/a pour des polygones à centre surélevé recouvrant des diamictons riches en glace; de 7 m/a pour un corps tabulaire de glace massive; de 1 m/a ou moins pour un pingo tronqué, couvert de morts-terrains épais constitués de sables; et, de 1 m/a ou moins pour des falaises littorales de nature sableuse. La vitesse de recul dépend surtout de la quantité de glace en excès dans les falaises littorales et de l'intensité des ondes de tempêtes de fin d'été. Là où de la glace en excès avance en-dessous du niveau de la mer, il s'est formé au large des dépressions thermokarstiques.

[1] Department of Geography, University of British Columbia, Vancouver, British Columbia V6T 1W5

Introduction

Rapid coastal retreat has been reported from many arctic areas where the ice content of the coastal sediments is high. Rapid coastal retreat has been well documented for the Arctic Slope of Alaska (MacCarthy, 1953; Hume and Schalk, 1967; Hume et al., 1972; Reimnitz and Maurer, 1979); along the Yukon Coastal Plain (Mackay, 1963a; McDonald and Lewis, 1973; Lewis and Forbes, 1974); and along the Arctic Coastal Plain of the District of Mackenzie from Richards Island on the west to Cape Bathurst, Northwest Territories, on the east (Department of Public Works, 1971; Mackay, 1960, 1963b; Rampton and Mackay, 1971; Rampton and Bouchard, 1975; Shah, 1978). Coastal retreat is also rapid in some other areas of Arctic Canada (e.g. Harry et al., 1983). The literature on coastal retreat in permafrost areas of the U.S.S.R. is extensive (e.g., Are, 1983, 1984). This paper discusses coastal retreat for the past 50 years (1935 to 1985) in the area just to the west of Tuktoyaktuk, Northwest Territories (Fig. 87.1).

Acknowledgments

The field work has been supported by the Geological Survey of Canada, in part by Contract OS785-00150; the Polar Continental Shelf Project, Canada; the Natural Sciences and Engineering Research Council of Canada; and the Inuvik Scientific Resource Centre, Inuvik, Northwest Territories. Mr. C.P. Lewis has permitted use of an echo sounding bottom profile for one site. Mr. K. Rood has done the photogrammetric plotting for the 1935 coastline.

Methods

The coastal area under discussion was covered by oblique air photography in 1935. The location of the 1935 shoreline has been plotted photogrammetrically for two main areas west of Tuktoyaktuk, namely: 1) the Peninsula Point site (Fig. 87.1, site 1) and 2) the "Growing Pingo"[1] site farther west where rapid coastal retreat has resulted in lake drainage and the growth of four pingos (Fig. 87.1, site 2). Coastal retreat since 1950 has been delimited from vertical air photographs and field studies. The "Peninsula Point Pingo"[1] site has been studied in the field since 1954 and the Growing Pingo site since 1969.

Thermal erosion

The general processes associated with coastal erosion in high ice content coasts in the Arctic are well known (e.g., Are, 1983, 1984; McDonald and Lewis, 1973; Walker, 1983). The coastal area under discussion is on the south side of Kugmallit Bay at the east end of the estuarine mouth of the East Channel of Mackenzie River. Break-up of the winter ice commences first at the mouth of East Channel in late May or early June and by the end of June the southern part of Kugmallit Bay is mostly ice free (Giovando and Herlinveaux, 1981). Freeze-up of the largely fresh Mackenzie waters in the southern part of Kugmallit Bay is usually completed by the end of October. Thus, the open water period when wave action can be effective lasts about three months.

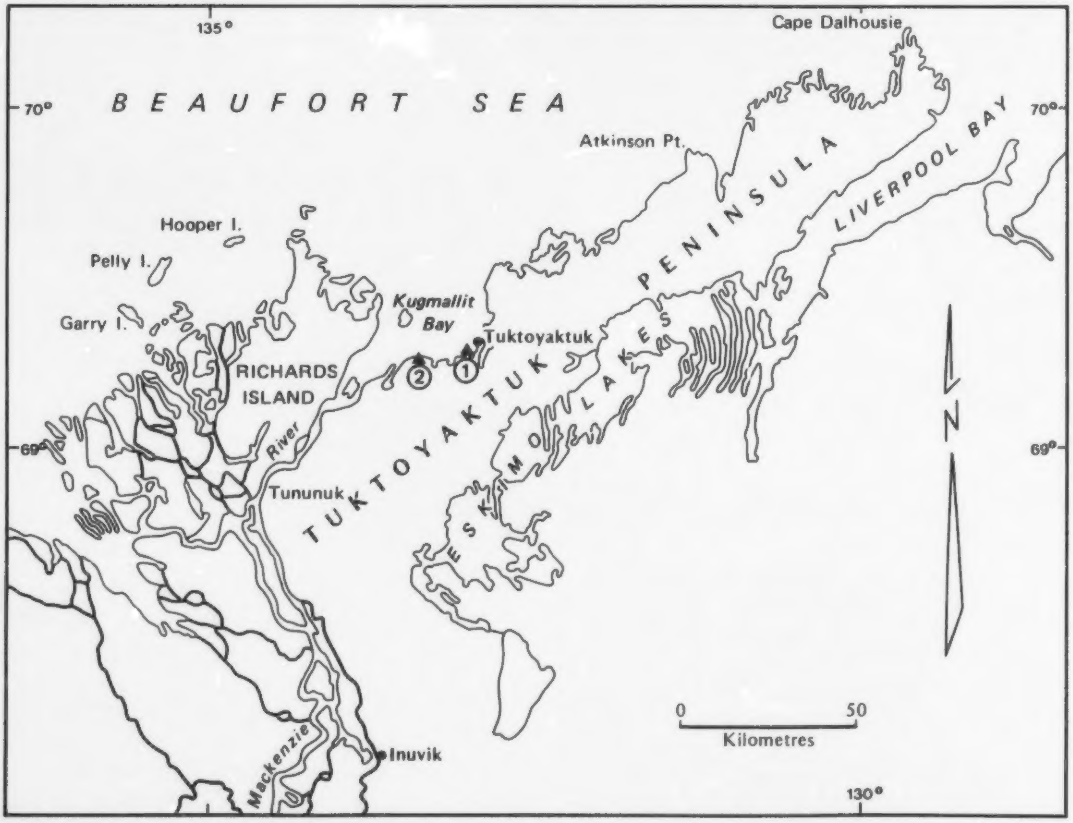

Figure 87.1. Location map. The Peninsula Point Pingo and massive ground ice sites are at location 1 and the Growing Pingo site is at location 2.

[1] Informal names

Kugmallit Bay is shallow. The water depth 10 km due north of the Growing Pingo site (Fig. 87.1, site 2) is only 2.5 m and it increases to only 5 m at 30 km to the north. The strongest winds are from the north and northwest so the fetch is limited by Richards Island and a small island (Hendrickson Island) to the north and northwest. The average tidal range at Tuktoyaktuk is 0.3 m thus tidal fluctuations are unimportant in coastal erosion. The most important water level changes are associated with storm surges.

Storm surges

Mean sea level in Kugmallit Bay can be raised 1 m or more during positive storm surges which are associated with westerly to northerly winds. Mean sea level can also be lowered by negative storm surges which are associated with easterly to southerly winds (Department of Public Works, 1971; Henry, 1975; Henry and Heaps, 1976). The positive storm surges are most frequent and severe in August and September. The upper limit of wave action can normally be delimited by the maximum height of stranded debris which can range in size from flotsam to logs 10 m long and 0.5 m in diameter. The height to which driftwood can be lodged depends primarily upon the exposure and the availability of lodgment sites. For example, along the Beaufort Sea coast of northern Alaska, where low-lying terrain can be inundated, driftwood from a 1970 storm was left in a line as much as 3.4 m above normal sea level and 5000 m inland (Reimnitz and Maurer, 1979). Along the Tuktoyaktuk coast, a mean sea level change of about 3 m has been reported for a 1944 storm surge (Giovando and Herlinveaux, 1981); a surge of at least 2.15 m has been cited for a 1970 storm (Department of Public Works, 1971); and a surge of about 1 m has been reported for a storm surge in 1972 (Henry and Heaps, 1976). The field evidence suggests that the eyewitness reports of many storm surges before water level records were available, such as the account of the 1944 surge of about 3 m, are exaggerated. The probable reason is a lack of distinction between the highest swash mark left by the run-up of storm waves and the actual mean sea level rise which cannot be determined visually. For example, Ibyuk Pingo is located 6 km south of Tuktoyaktuk and the pingo was fully exposed to storm surges since before the 1944 storm. In the summer of 1983, a detailed survey was made of the heights of the highest driftwood logs stranded on the lower slopes of Ibyuk Pingo. A few large logs, 0.3 m in diameter and as much as 10 m long, rested with the bottoms of the logs about 2.25 m above mean sea level. Inasmuch as the site was exposed to the 1944 storm surge, it seems likely that either the reported 3 m level was over-estimated or that no logs from the 1944 storm were left stranded on Ibyuk Pingo, which seems unlikely. To cite a second example, at the Growing Pingo site, the height of driftwood lodged on two pingos and on the coastal bluff has been surveyed since 1969. The maximum height of small driftwood lodged on the pingos is about 1.6 m above mean sea level despite the fact that the site was exposed to the severe surges of 1970 (Department of Public Works, 1971) and 1972 (Henry and Heaps, 1976). Although there was considerable coastal retreat after the 1970 and 1972 storms, there was no major shift in the height of pre-existing driftwood. To give a third example, a field site at Garry Island, Northwest Territories, has been occupied every summer from 1964 to 1985. As a result of the severe 1970 storm, many logs on the eroding northwest side of the island were stranded to a height of 3 m above mean sea level; however, in sheltered bays on the east coast the maximum height of fresh driftwood was only 1.5 m above mean sea level. Thus, during the 1964 to 1985 observation period at Garry Island and from 1969 to 1985 at the Growing Pingo site, any logs stranded higher than 1.6 m appear to have been lodged there by wave action, swash effect, and run-up on slopes rather than by a mean sea level rise of that magnitude. The same conclusion can be derived from a study of driftwood lodged on sandbars in the general Richards Island and Tuktoyaktuk Peninsula coastal zone.

***Figure 87.2.** A 1975 photograph of the massive ground ice site showing the ablating face of massive ground ice and the debris flow mud moving downslope from the foot of the ice slopes.*

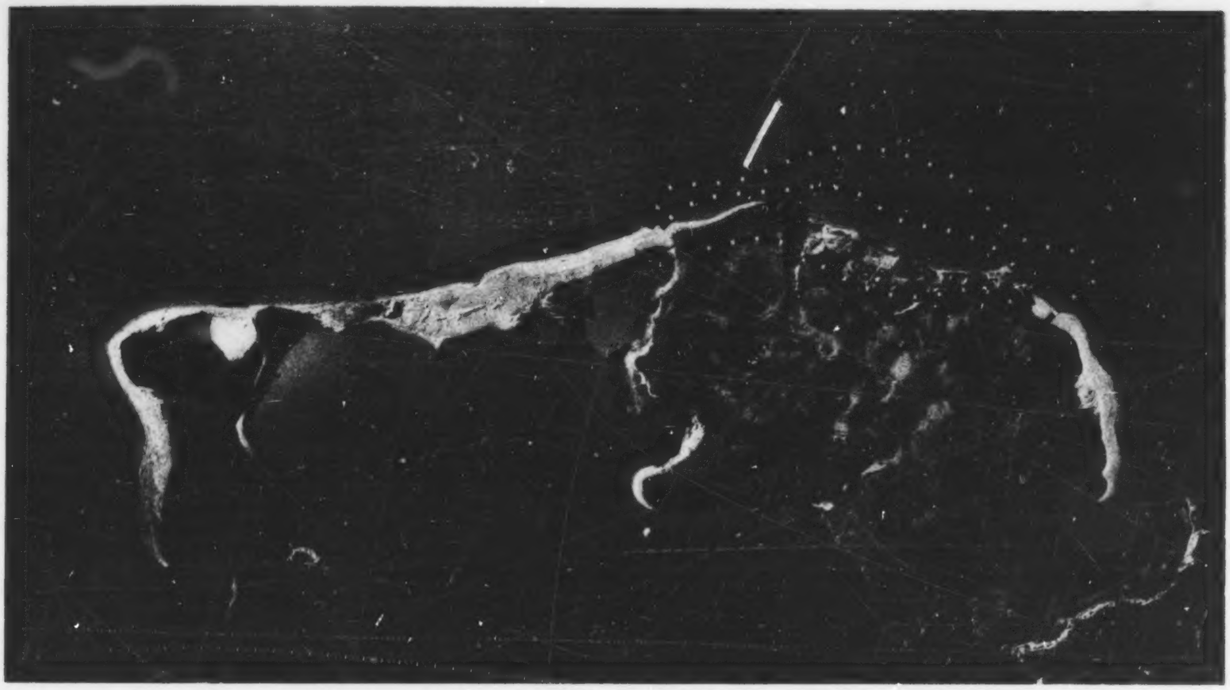

Figure 87.3. *A 1971 air photograph (A 22535-66) of Figure 87.1, location 1, showing the partially sectioned Peninsula Point Pingo on the left and the massive ground ice site on the right. The 1935, 1950, 1971, and 1985 shoreline positions are so indicated. For Peninsula Point Pingo coastal retreat, see Figure 87.7.*

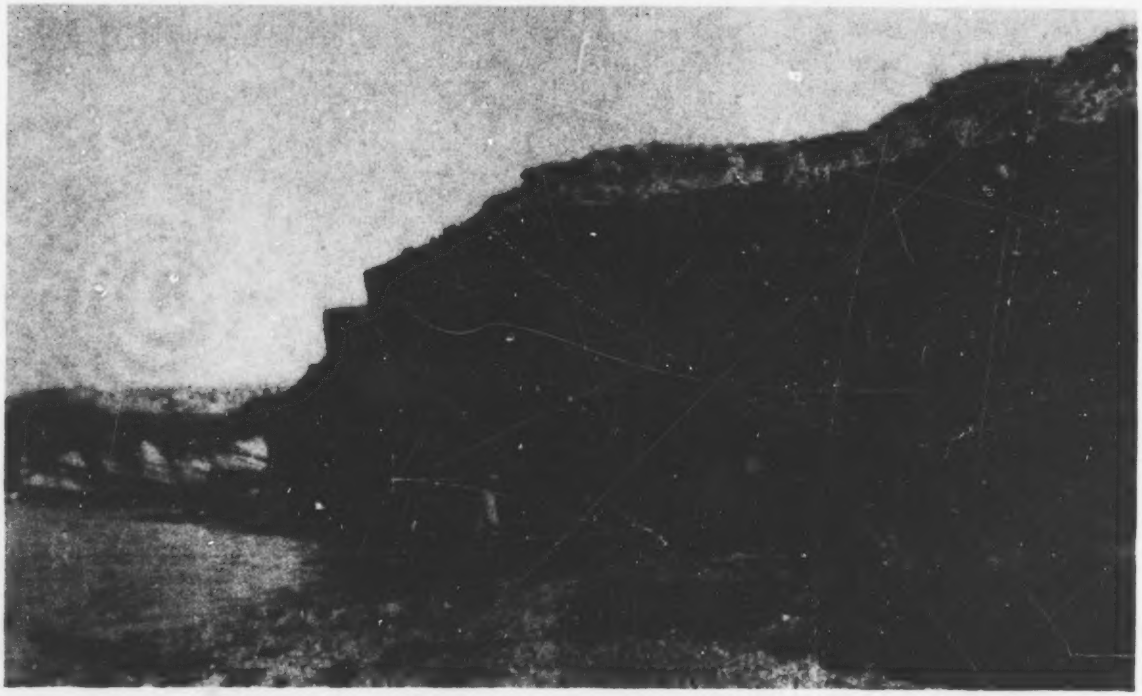

Figure 87.4. *Massive ground ice exposed at sea level in 1954 (see text).*

Peninsula Point Pingo and massive ground ice sites

On the east side of Peninsula Point there is a flat topped hill that is underlain by a horizontal tabular sheet of massive ground ice (Fig. 87.2). The area of the hill in 1935 was about 1 km^2 (Fig. 87.3). The massive ice is typical of the involuted hills of Tuktoyaktuk Peninsula (Mackay, 1963b, 1966, 1971). The site was covered by oblique air photography in 1935 and with vertical photography in 1950, 1967, 1971, 1972, 1973, 1976, and 1983, so the photographic record for mapping retreat is excellent. The position of the north coast is shown in Figure 87.3 for 1935, 1950, 1971, and 1985. In the 1935 to 1985 period, the maximum retreat was 350 m for a coastal recession of about 7 m/year.

The massive ground ice exposure was first examined in the summer of 1954 at which time wave erosion and thaw had produced a cave 40 m long, 15 m deep, and 5 m high (Fig. 87.4). The ice extended below sea level (Mackay, 1971). By the following summer of 1955, the ice cave had collapsed to give a coastal recession of about 10 m. During most of the period from 1954 to 1985, the steep headwall of the ablating massive ground ice receded more rapidly than the shoreline whenever the scarp was actively ablating (Fig. 87.3). The mean ablation rate has exceeded 7 m/year. This rate compares favourably with the 7.2 m/year ablation rate for massive ground ice at a site at Garry Island, Northwest Territories, for the 1964 to 1971 period (Kerfoot and Mackay, 1972). During periods of quiescence, coastal retreat would catch up to that of the massive ground ice scarp. The massive ground ice is covered by an overburden of diamicton whose thickness averages about 5 m. The massive ice is estimated to average about 10 m in thickness. As the massive ground ice melts, the overburden slides down the thawing ice face to the foot of the scarp and then moves downslope as a debris flow (Mackay, 1966; Rampton and Mackay, 1971). The debris flow usually comes to rest on pre-existing debris flows although some flows continue down to the sea (Fig. 87.5). Thus during a storm the available wave energy is usually expended first on eroding the mudflow debris which extends to sea level, rather than on eroding massive ground ice which is blanketed by the debris flows. In a major storm surge, the debris flow material that blankets a substantial part of the shoreline is soon eroded back to expose the underlying massive ground ice. The massive ground ice then recedes under the dual attack of wave erosion and ablation. A steep icy headwall develops and migrates inland, debris flows then transport material downslope (Fig. 87.2), and eventually a new cycle of stability is initiated (Fig. 87.5).

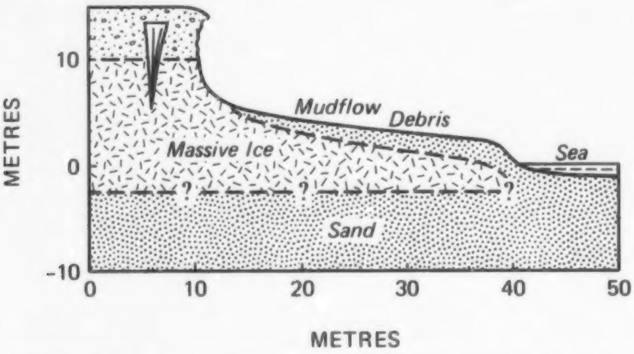

Figure 87.5. Schematic profile across the site shown in Figure 87.2. The extension of the massive ice below sea level is suggested by Figure 87.4.

Figure 87.6 shows a 1973 offshore profile (courtesy of C.P. Lewis) extending north from the middle of the massive ground ice exposure of Figure 87.3. Of particular interest is the 2.0 to 2.5 m relatively deep water that occurs in the first 160 m offshore from the 1973 shoreline. The mean maximum late winter thickness of salt and fresh water ice for the southern Kugmallit Bay area is about 1.7 m and the maximum thickness about 2.4 m (Allen, 1977). Thus, assuming the 1973 profile to be typical, the winter ice would rarely freeze to the bottom for the first 160 m offshore (Fig. 87.6). Therefore the mean temperature during the seven month ice-covered period would be slightly above 0°C. A portion of the Mackenzie River water that flows into Kugmallit Bay comes down East Channel past Inuvik, Northwest Territories, and the rest mainly from Middle Channel. For the 1963 to 1966 period, the water temperature of East Channel was above 10°C from 20 June to 10 September and above 15°C from 1 July to 15 August (MacKay and Mackay, 1974). Using the winter temperature of above 0°C and the summer temperatures for June to September, the mean annual sea bottom temperature for the first 160 m offshore should be of the order of about 2°C or even higher. Under these conditions, permafrost would degrade below the sea bottom as the coast recedes.

In the shallower offshore zone from about 180 to 300 m where the winter ice barely freezes to the bottom, the mean winter temperature might be just below 0°C. However, the summer temperatures would be warm, as in the area up to 160 m offshore, so the mean annual temperature should be positive. Therefore, the sea bottom should undergo seasonal freeze and thaw but because of the positive mean annual temperature, a talik of unknown depth should underlie the zone of seasonal freezing and thawing (cf. McDonald et al., 1973).

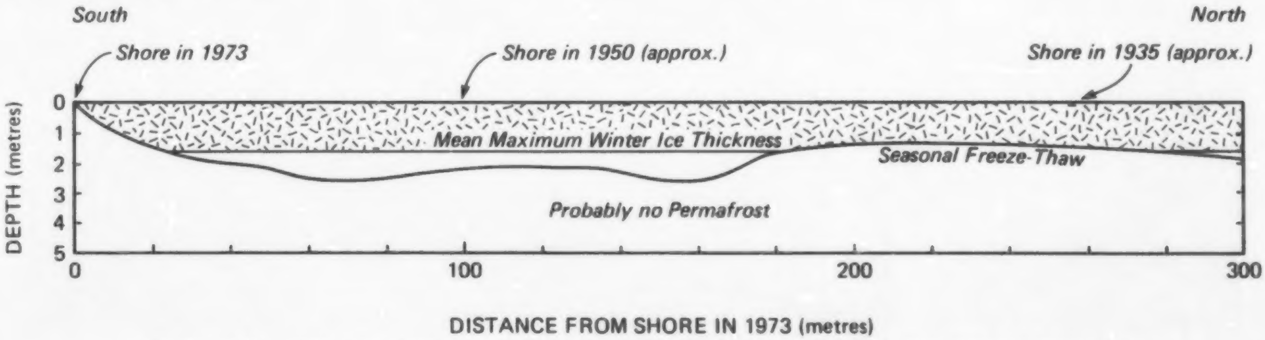

Figure 87.6. Offshore profile trending due north from the middle of the massive ground ice exposure of Figure 87.3. Data from echo sounding by C.P. Lewis in 1973.

Stefan's formula, which includes a number of simplifying assumptions, can be used to estimate the depth of thaw below the sea bottom:

$$z = \sqrt{\frac{2Tkt}{Q_L}} = b\sqrt{t} \qquad (1)$$

where z is the depth of thaw
T is the positive mean annual sea bottom temperature, 0°C
k is the thermal conductivity of the thawed material
t is time
Q_L is the volumetric latent heat of fusion required to thaw the soil

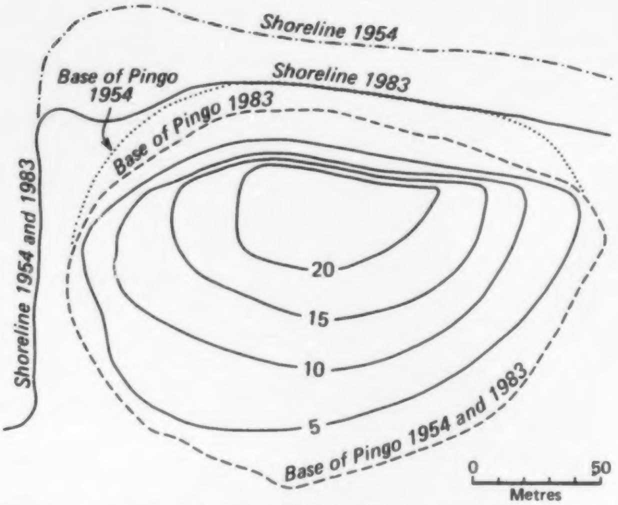

Figure 87.7. *Peninsula Point Pingo as surveyed in 1954 and 1983.*

When appropriate values for a high ice content soil and a low ice content frozen sand are substituted into equation (1), with a mean annual sea bottom temperature of 2°C, the value of b ranges from about 0.45 $m/year^{1/2}$ to about 0.9 $m/year^{1/2}$. If, during coastal retreat, the sea bottom is in direct contact with massive ice, thaw settlement of the sea bottom will correspond closely with the melting rate of the massive ice. If, on the other hand, the thawing sea bottom sediments have little excess ice, then there will be minimal thaw settlement and a progressively thick layer of saturated sediments will blanket the frozen soil at depth. In view of the fact that much of the sea bottom from the 20 to 160 m offshore zone (Fig. 87.6) has likely been exposed to positive mean annual sea bottom temperatures for decades, a deep talik probably underlies the sea bottom. Farther seaward, seasonal freezing probably occurs from the 180 to 280 m offshore distances but a talik probably occurs at depth.

Since the thickness of the overburden above the massive ice averages about 5 m, and the massive ice itself also contains at least 1 m of soil, all this soil must be removed seaward by wave action and sediment transport during coastal retreat. Thus, the offshore water depths are probably less than that due to thaw settlement of excess ice alone because of the probability of considerable sediment infilling from coastal erosion and Mackenzie River sedimentation.

Peninsula Point Pingo

Peninsula Point Pingo (Fig. 87.3) is joined to the large massive ground ice site by a sandspit. The 1935 air photographs show that the seaward side of the Peninsula Point Pingo was slightly truncated by wave erosion.

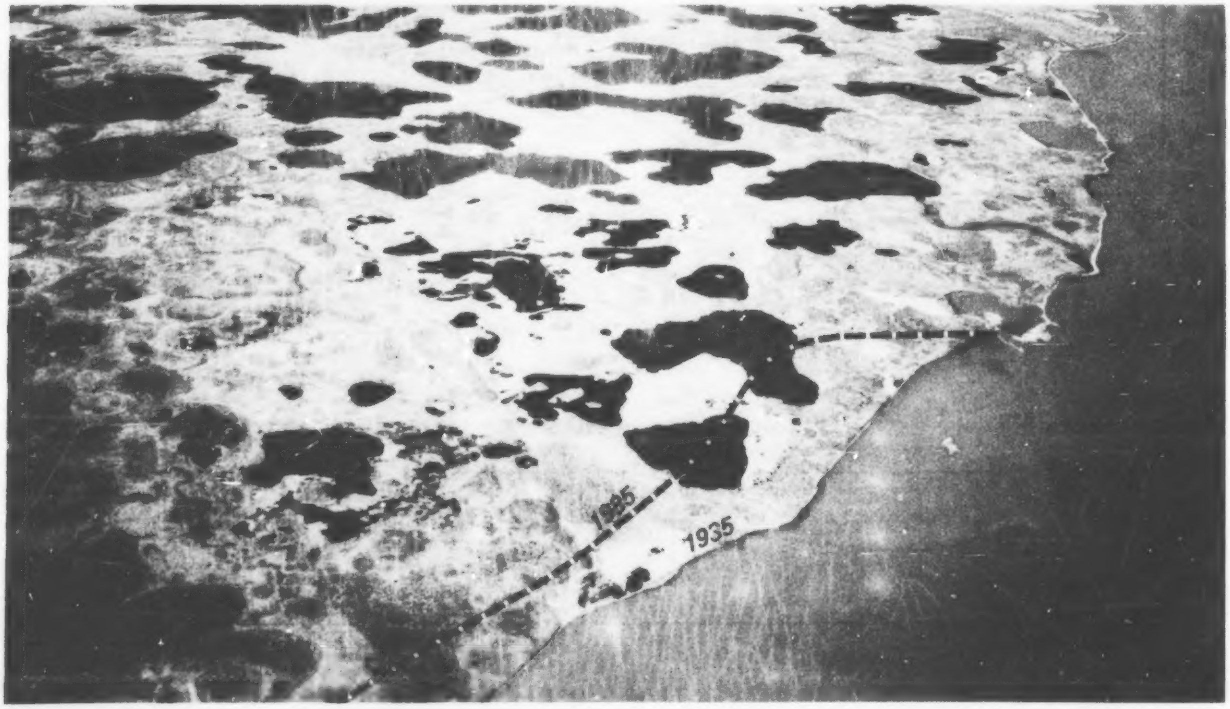

Figure 87.8. *A 1935 oblique photograph of the Growing Pingo shoreline (Figure 87.1, location 2) showing the 1935 to 1985 coastal retreat. (A 5026-35R)*

The pingo has been surveyed twice, first in 1954 and then again in 1983 (Fig. 87.7). In the intervening 29 years, the shoreline receded about 25 m southward but the sectioned bluff of the pingo receded only 15 m. The mean annual retreat of the sectioned pingo was then about 0.5 m/year. From 1954 to 1985 the sectioned pingo has been visited frequently and at no time has a good exposure of pingo ice been observed by the writer, although there have been unconfirmed reports that pingo ice has been exposed near sea level in an erosional niche following some storms.

Prior to erosion the pingo was about 200 m in basal diameter and the highest point was about 25 m above sea level. The overburden is sand. The slope of the cut bluff ranges from 30° to 45° so that in summer the thawed overburden sand constantly slumps from the top of the pingo to accumulate at the bottom to a thickness much greater than that of the active layer. Thus any pingo ice exposed at sea level by a storm would soon become buried by sand which upon freezing forms a protective blanket of frozen sand around the north face of the pingo. The result is that in the 1935 to 1985 period, pingo erosion has been less than 1 m/year in contrast to the 7 m/year for the massive ground ice exposure just to the east.

The sandbar that joins the Peninsula Point Pingo with the massive ground ice site has shifted back and forth some tens of metres from 1935 to 1985 but, in general, it has remained remarkably stable.

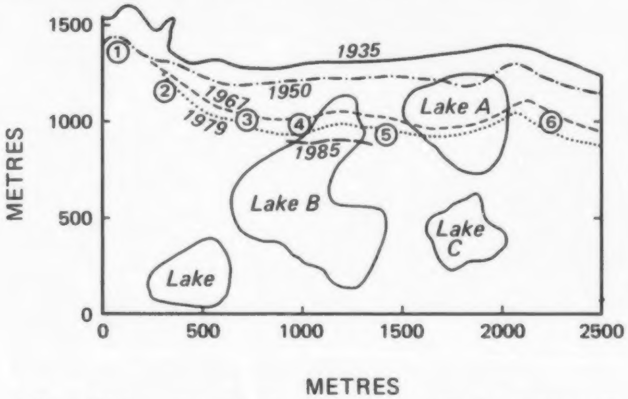

Figure 87.9. The Growing Pingo site with the 1935, 1950, 1967, 1979, and 1985 shoreline positions. See the text for locations 1 to 6. Lakes A, B, and C can be located on Figure 87.8.

Growing Pingo site

The Growing Pingo site has 1935 oblique photographic coverage (Fig. 87.8) and vertical coverage for 1950, 1967, 1971, 1973, 1975, and 1983 so the rate of coastal retreat is known in considerable detail. Field studies at the site have been carried out every summer from 1969 to 1985. For the 1969 to 1975 period, the coastal retreat was plotted directly on air photographs. In 1975, 12 stakes were placed 33 m from the shore and about 100 m apart along the coast due west of Lake B (Fig. 87.9). A 13th stake was located 47 m inland by Lake B. The distances of the stakes from the sea have been measured from 1975 to 1985 (Table 87.1).

The coastal retreat for the 1935 to 1985 period is shown in Figure 87.9. From 1935 to 1950 the total coastal retreat ranged from about 100 to 150 m depending upon the coastal section involved. By 1950, Lake A had been drained by coastal retreat and headward erosion had drained Lakes B and C. Four pingos have grown up in four residual ponds of Lake B (Mackay, 1973) so the site is referred to here as the Growing Pingo site. The coastal retreat for the 1950 to 1967 period (Fig. 87.9) was extremely rapid with some of the shoreline retreating as much as 200 m. The retreat from 1967 to 1985 has been less, averaging about 100 to 150 m. The average 1935 to 1985 retreat in the area of Lakes A and B has been about 400 m for an average retreat of about 8 m/year.

The material along the coast varies greatly in its susceptibility to erosion. The headland at location 1, in Figure 87.9, rises to about 10 m above sea level. The headland is composed of sands overlain by a diamicton in which there is some massive ice. The headland is partially protected from the most severe storm surges by a sand spit to the northwest, north, and northeast. The mean annual rate of retreat of the headland is less than 1 m/year. Locations 2, 4, and 6 of Figure 87.9 have high centre peaty polygons with the higher parts rising from 2 to 3 m above sea level. The surface layer is composed of peat from 0.75 to 1.5 m in thickness. The peat at the top of permafrost has a mean ice content (by weight) greater than 500 per cent. The peat is underlain by at least 2 m of an icy diamicton whose mean ice content exceeds 300 per cent. The ice wedges are 1 to 3 m in true width and the mean polygon diameters are about 10 m. In addition, there are numerous buried epigenetic ice wedges, small syngenetic ice wedges, and widespread "pool ice" which is formed by the infreezing of underground drainage channels that have carried a subsurface flow through the ice wedge systems. The combination of ice wedge and pool ice is so extensive that some coastal sections, more than 25 m in true

Table 87.1. Coastal retreat for 1975 to 1985 as measured by 13 stakes whose distances from the shore were known for the Growing Pingo site; all distances are measured to the shore.

Stake No.	1975 m	1977 m	1979 m	1980 m	1981 m	1982 m	1983 m	1984 m	1985 m	Comment
1	33	16	5	gone	gone	gone	gone	gone	gone	high centre polygon area
2	33	23	14	9	gone	gone	gone	gone	gone	high centre polygon area
3	33	25	22	22	6	6	6	gone	gone	high centre polygon area
4	33	26	23	22	11	11	11	8	1	diamicton over sands; large polygons
5	33	23	20	19	12	12	11	4	gone	diamicton over sands; large polygons
6	33	23	19	18	8	8	8	5	2	diamicton over sands; large polygons
7	33	30	26	25	16	16	16	15	13	diamicton over sands; large polygons
8	33	20	18	16	gone	gone	gone	gone	gone	high centre polygons
9	33	20	17	13	7	1	gone	gone	gone	high centre polygons
10	33	20	8	7	gone	gone	gone	gone	gone	high centre polygons
11	33	27	23	22	16	16	16	16	11	bluff, diamicton over sands
300	33	10	gone	gone	gone	gone	gone	gone	gone	high centre polygons
301	47	24	13	5	3	gone	gone	gone	gone	high centre polygons

section, show only peat overlying ice when freshly exposed after a storm. As an estimate, ice comprises about 70 per cent, on a volume basis, of the terrain above sea level. Consequently, when the water level rises during a storm surge, the waves soon remove any thawed soil and impinge directly upon the high ice content coastal exposures which results in a very rapid thermal erosion. As the peaty surface layer becomes undermined, however, large overhangs develop because the basal part of the peat is frozen, being still in permafrost. When the peaty overhangs collapse, the beach becomes armored with the peat if the water depth is too shallow for the peat mat to float (Fig. 87.10). As a result, the carpet of peat at the foot of such a bluff is remarkably absorbent of wave energy. Little erosion can result from the next storm until the peat can be floated away or else eroded bit by bit.

The offshore areas are extremely shallow. The water depth at the 1935 shoreline position, 500 m offshore, hardly exceeds 1 m. Because the mean maximum thickness of ice, as mentioned before, is about 1.7 m, the winter ice should freeze solidly to the sea bottom as far as the 1935 shoreline position and there should be an active layer in the bottom sediments. Figure 87.11 shows an offshore bottom profile as probed on 22 July 1979. For a distance of about 30 m from the beach, the bottom sediments are peat and mud, whereas farther offshore, the sediments are mainly mud. Because the active layer will continue to thicken until the end of August or early September, the depth of the active layer shown in Figure 87.11 might have increased as much as 20 to 30 per cent by the end of summer. Inasmuch as the bottoms of many ice wedges extend several metres below sea level in the coastal area, the roots of truncated ice wedges should be present at depth offshore as drawn schematically in Figure 87.11. As the shoreline recedes further, the bottom temperatures should increase as depths increase. At a water depth of about 1.5 m, the bottom temperature should become positive. Permafrost will then degrade and ice wedge pseudomorphs should develop, as they presumably are now developing in many of the deeper offshore areas.

Figure 87.10. Shoreline, just west of Lake B, showing the armoring of the beach with peaty debris fallen from overhangs.

In the areas where a diamicton overlies sands, as at locations 3 and 5 of Figure 87.9, the terrain is higher than in the high centre polygon areas and coastal retreat is less rapid than in the areas of peaty icy polygons.

Conclusions

Coastal retreat from 1935 to 1985 has been determined for three locations just west of Tuktoyaktuk, Northwest Territories, namely: an exposure of massive ground ice; a partially sectioned pingo; and a 2.5 km-long low coastal section composed mainly of high centre polygons but with some areas of sands overlain by a diamicton. The retreat of the coast with the massive ground ice has averaged about 7 m/year. The retreat of the ablating massive ice, as compared to the shoreline, exceeds about 7 m/year. The retreat of the Peninsula Point Pingo averages about 1 m/year or less. The retreat of the area of high centre polygons averages about 8 m/year. The ice content of the top of permafrost of the high centre polygon area averages in excess of 500 per cent by weight; the underlying icy diamicton generally averages in excess of 300 per cent; and ice wedge and pool ice are abundant. On a volume basis, about 70 per cent of the material above sea level is ice. If there is no armoring blanket of peat, resulting from the collapse of peat overhangs produced in a storm, coastal erosion can be rapid. A blanket of peat effectively protects the coast from wave action until the peat can be floated away or eroded bit by bit in the summer. The slowest rate of erosion, which averages less than 1 m/year, occurs on a sandy point, with a diamicton cover, where sandbars provide some shelter from the strong westerly and northerly winds.

The rate of coastal retreat west of Tuktoyaktuk is then highly variable. Coastal retreat is most rapid where high water levels associated with storm surges impinge directly on high ice content material and it is slowest where erosion is in low ice content sandy sediments. The 1935 to 1985 range in rate is from 8 m/year to less than 1 m/year. At Tuktoyaktuk, one of the most exposed headlands (Flagpole Point), retreated at an average rate of 4 m/year from 1935 to 1971 (Rampton and Bouchard, 1975). If present rates are representative of past rates, the south shore of Kugmallit Bay may have undergone several kilometres of coastal recession in the past 1000 years.

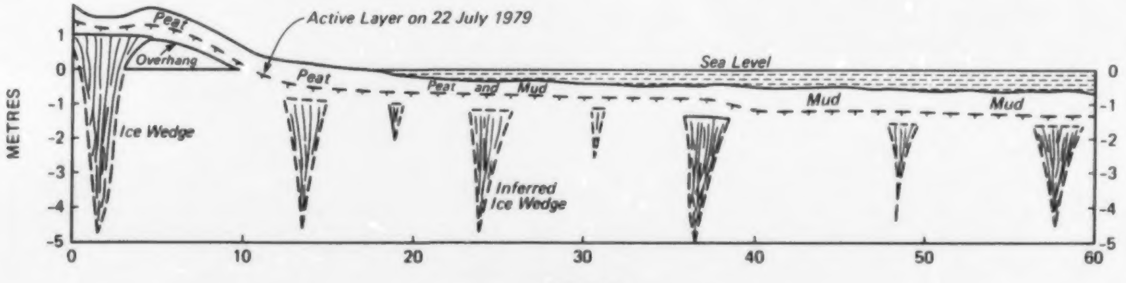

Figure 87.11. Offshore profile at the Growing Pingo Site, 22 July 1979, for the area just west of Lake B (see text).

The eyewitness accounts of high level storm surges, reported to reach 2 to 3 m, are probably over-estimated. The high levels probably result from swash and run-up effects, not a comparable rise in mean sea level. A survey of driftwood for the 1969 to 1985 period indicates no mean sea level rise as much as 2 m along the coast west of Tuktoyaktuk and no such rise for the 1964 to 1985 period at Garry Island, Northwest Territories.

In offshore areas where water depths exceed about 1.5 m, and the water is fresh, permafrost is probably degrading. If coastal retreat is across a low lying area, as at the Growing Pingo site, where the roots of ice wedges extend well below sea level, then coastal retreat, coupled with permafrost degradation, should now be producing ice wedge pseudomorphs.

References

Allen, W.T.R.
1977: Freeze-up, break-up and ice thickness in Canada; Atmospheric Environment, Fisheries and Environment Canada, Downsview, Ontario, CL1-1-77, 185 p.

Are, F.E.
1983: Thermal abrasion of coasts; Permafrost, Fourth International Conference, Proceedings, Washington, D.C., National Academy Press, p. 24-28.

Are, F.E. (Editor)
1984: Shore Processes in the Cryolithozone (in Russian); Novosibirsk, Nauka, 136 p.

Department of Public Works
1971: Investigation of storm, September 13-16, 1970; Engineering Programs Branch, Department of Public Works, Canada, 23 p.

Giovando, L.F. and Herlinveaux, R.H.
1981: A discussion of factors influencing dispersion of pollutants in the Beaufort Sea; Institute of Ocean Sciences, Department of Fisheries and Oceans, Sidney, B.C., Pacific Marine Science Report 81-4, 198 p.

Harry, D.G., French, H.M., and Clark, M.J.
1983: Coastal conditions and processes, Sachs Harbour, Banks Island, Western Canadian Arctic; Zeitschrift fuer Geomorphologie, N.F., band 47, p. 1-26.

Henry, R.F.
1975: Storm surges; Institute of Ocean Sciences, Department of the Environment, Victoria, B.C., Beaufort Sea Technical Report No. 19, 41 p.

Henry, R.F. and Heaps, N.S.
1976: Storm surges in the southern Beaufort Sea; Journal of the Fisheries Research Board of Canada, v. 33, p. 2362-2376.

Hume, J.D. and Schalk, M.
1967: Shoreline processes near Barrow, Alaska: a comparison of the normal and the catastrophic; Arctic, v. 20, p. 86-103.

Hume, J.D., Schalk, M., and Hume, P.W.
1972: Short-term climate changes and coastal erosion, Barrow, Alaska; Arctic, v. 25, p. 272-278.

Kerfoot, D.E. and Mackay, J.R.
1972: Geomorphological process studies, Garry Island, N.W.T.; in Mackenzie Delta Area Monograph, ed. D.E. Kerfoot; 22nd International Geographical Congress, Canada; published by Brock University, St. Catharines, Ontario, p. 115-130.

Lewis, C.P. and Forbes, D.L.
1974: Sediments and sedimentary processes, Yukon Beaufort Sea Coast; Environmental-Social Committee, Northern Pipelines, Task Force on Northern Oil Development, Report No. 74-29, 40 p.

MacCarthy, G.R.
1953: Recent changes in the shoreline near Point Barrow, Alaska; Arctic, v. 6, p. 44-51.

MacKay, D.K. and Mackay, J.R.
1974: Heat energy of the Mackenzie River; in Further hydrologic studies in the Mackenzie Valley; Environmental-Social Committee, Northern Pipelines, Task Force on Northern Oil Development, Report No. 74-35, p. 1-23.

Mackay, J.R.
1960: Notes on small boat harbors of the Yukon coast; Geographical Bulletin, No. 15, Ottawa, p. 19-30.

1963a: Notes on the shoreline recession along the coast of the Yukon Territory; Arctic, v. 16, p. 195-197.

1963b: The Mackenzie Delta Area, N.W.T.; Geographical Branch, Mines and Technical Surveys, Ottawa, Memoir 8, 202 p. (reprinted 1974 as Geological Survey of Canada Miscellaneous Report 23).

1966: Segregated epigenetic ice and slumps in permafrost, Mackenzie Delta area, N.W.T.; Geographical Bulletin, No. 8, Ottawa, p. 59-80.

1971: The origin of massive icy beds in permafrost, Western Arctic Coast, Canada; Canadian Journal of Earth Sciences, v. 8, p. 397-422.

1973: The growth of pingos, Western Arctic Coast, Canada; Canadian Journal of Earth Sciences, v. 10, p. 979-1004.

McDonald, B.C. and Lewis, C.P.
1973: Geomorphic and sedimentologic processes of rivers and coast, Yukon Coastal Plain; Environmental-Social Committee, Northern Pipelines, Task Force on Northern Oil Development, Ottawa, Report No. 73-39, 245 p. and maps.

McDonald, B.C., Edwards, R.E., and Rampton, V.N.
1973: Position of frost table in the near-shore zone, Tuktoyaktuk Peninsula, District of Mackenzie; in Report of Activities, Part B, Geological Survey of Canada, Paper 73-1B, p. 165-168.

Rampton, V.N. and Bouchard, M.
1975: Surficial geology of Tuktoyaktuk, District of Mackenzie; Geological Survey of Canada, Paper 74-53, 17 p.

Rampton, V.N. and Mackay, J.R.
1971: Massive ice and icy sediments throughout the Tuktoyaktuk Peninsula, Richards Island, and nearby areas, District of Mackenzie; Geological Survey of Canada, Paper 71-21, 16 p.

Reimnitz, E. and Maurer, D.K.
1979: Effects of storm surges on the Beaufort Sea Coast, northern Alaska; Arctic, v. 32, p. 329-344.

Shah, V.K.
1978: Protection of permafrost and ice rich shores, Tuktoyaktuk, N.W.T., Canada; Third International Conference on Permafrost, Proceedings, Ottawa, National Research Council of Canada, v. 1, p. 870-876.

Walker, H.J.
1983: Colville River Delta, Alaska; Fourth International Conference on Permafrost, Guidebook 2, Division of Geological and Geophysical Surveys, Department of Natural Resources, State of Alaska, Fairbanks, Alaska, 34 p.

Indurated deposits and possible plume bands in a hydrothermal mound, northeast Pacific

Project 820051

J.D. Adshead, B.D. Bornhold[1], and E.E. Davis[2]
Terrain Sciences Division

Adshead, J.D., Bornhold, B.D., and Davis, E.E., Indurated deposits and possible plume bands in a hydrothermal mound, northeast Pacific; in Current Research, Part A, Geological Survey of Canada, Paper 86-1A, p. 737-748, 1986.

Abstract

A hydrothermal mound ~400 m in diameter (heat flow anomaly 3 $W \cdot m^{-2}$; gradient $3^{o}C \cdot m^{-1}$) rises 60 m above flat-lying sediments filling the axial valley of the northern Juan de Fuca Ridge. A section of sedimentary core recovered from >2.4 m beneath the surface of the mound exhibits thin, soft brown bands (noncalcareous, high Ba, Mn, and organic carbon contents) that may be associated with episodes of hydrothermal plume sedimentation. Brown bands are interbedded with calcareous grey lutites in which noncalcareous indurated layers (and clasts) are present. Indurated deposits have higher Si and Mg contents than associated lutites.

The composition of brown bands and indurated layers is suggestive of late stage hydrothermal activity. The uncommon occurrence of episodic brown banding within the upper 2 m of mound sediment suggests that either plume sediments may be highly localized near vent sites or the mound may not have been actively venting Ba, Mn, and Si in recent times.

Résumé

Une colline hydrothermale d'environ 400 m de diamètre et de 60 m de haut (écoulement anormal de chaleur de $3W.m^{-2}$; gradient de $3^{o}C.m^{-1}$) surplombe la vallée axiale remplie de sédiments horizontaux dans la partie nord de la crête de Juan de Fuca. Une section d'une carotte sédimentaire récupérée à plus de 2,4 m au-dessous de la surface de la colline montre des intercalations brunes, minces et tendres (non calcaires et riches en Ba, Mn et carbone organique) qu'on peut associer à des épisodes de sédimentation du panache hydrothermique. Les intercalations brunes alternent avec des lutites calcaires de couleur grise qui renferment des couches (et des fragments) indurées non calcaires. Les dépôts indurés sont plus riches en Si et Mg que les lutites connexes.

La composition des intercalations brunes et des couches indurées semble témoigner d'une activité hydrothermale tardive. La rareté d'intercalations brunes épisodiques dans les 2 m supérieurs des sédiments de la colline semble indiquer, soit que les sédiments de panache peuvent être localisés extrêmement près des orifices, soit que la colline n'a pas évacué assez de Ba, de Mn, et de Si récemment.

---

[1] Geological Survey of Canada, Pacific Geoscience Centre, Sidney, British Columbia V8L 3S2
[2] Earth Physics Branch, Pacific Geoscience Centre, Sidney, British Columbia V8L 3S2

Introduction

In 1984, an acoustic and heat-flow survey of the sediment-filled axial valley at the north end of Juan de Fuca Ridge (Middle Valley; Fig. 88.1) revealed the presence of mound structures several hundred metres in diameter, rising tens of metres above the surrounding seafloor. One mound, approximately 400 m in diameter and 60 m in height had a heat flow gradient of $3°C \cdot m^{-1}$ and a heat flow anomaly of $3\ W \cdot m^{-2}$ (Fig. 88.2). A seismic profile recorded in 1985 indicates that the thickness of sediment underlying this mound is approximately 200 m. A gravity core from the mound (Fig. 88.3) was examined by geochemical and SEM-EDS techniques to determine whether hydrothermal processes suggested by the heat flow anomaly would be reflected in the composition of mound sediments. This information was supplemented by preliminary observations on sedimentary cores collected from the same mound in 1985.

Sampling

A gravity coring device was employed with an observed sediment penetration of approximately 3 m. Owing to a malfunction and blockage of the core head valve, however, the upper approximately 2.4 m of soft sediment was displaced by the corer until an indurated layer was encountered. The indurated layer and 57 cm of underlying sediment, including another indurated layer at the bottom of this short core, were subsequently recovered and form the basis of the present study.

Methods

The unopened core, which had been maintained in cold storage, was initially examined by X-radiography, then split, sampled for chemical analyses and photographed. Samples were dried at 60°C and gently crushed to remove pebbles. The <2 mm fraction was then ground and split for examination by inductively coupled plasma analysis (ICP: P, Ba, Cr, Mg, Al, Ca, Ti, Sr, Na, K, Si) and atomic absorption (Fe, Mn, Cu, Ni, Zn, Mo, Co). A nitric-perchloric-hydrofluoric dissolution was employed except for Si, for which a separate split of powder was processed by use of a tetraborate fusion-dissolution. Total carbon, carbonate carbon, and sulphur were determined on separate splits with a Leco analyzer; for carbonate carbon, acid-evolved CO_2 was measured with a Leco system fitted with a furnace bypass. Uranium was determined by neutron activation analysis.

Unidentified duplicates were used for the analysis of samples by each technique. Precision was estimated by the use of blind replicates (eight per special test sample used). Precision for ICP data was ±2 to 5% for Si, Mg, Na, Ti, Ba, Cr; and ±5 to 10% for Al, Ca, K, P, Sr. Precision for atomic absorption analyses was ±2 to 4% for all elements except Mo (±27%); for total and carbonate carbon ±6 to 7%, sulphur ±13%.

Polished sections of mud were prepared by repeated impregnation with araldite resin and polishing using a lead-bismuth surface. A Cambridge S-180 SEM was used with an energy dispersive system (Model 10,000 LINK systems).

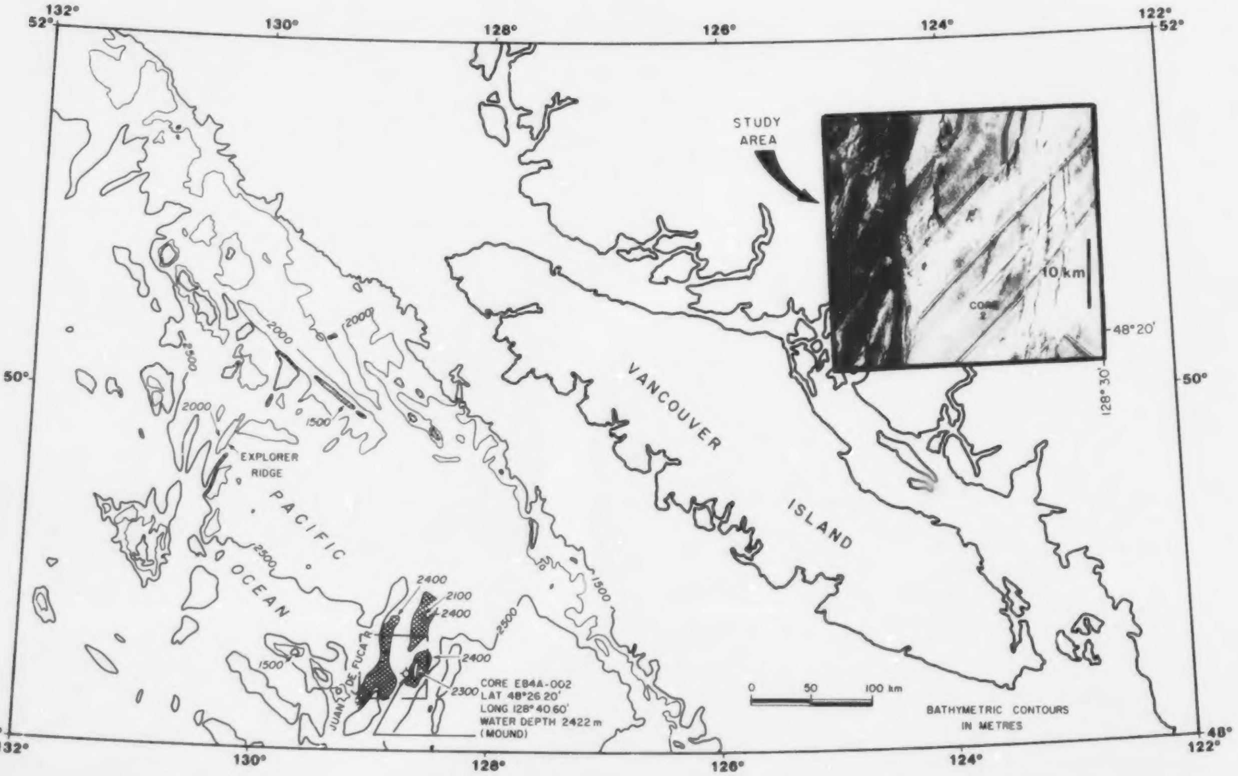

Figure 88.1. *Location of the hydrothermal mound in an area of flat-lying sediments filling the axial valley (Middle Valley) of the northern end of Juan de Fuca Ridge. Inset shows study area depicted by SeaMARC II side scan acoustic imagery.*

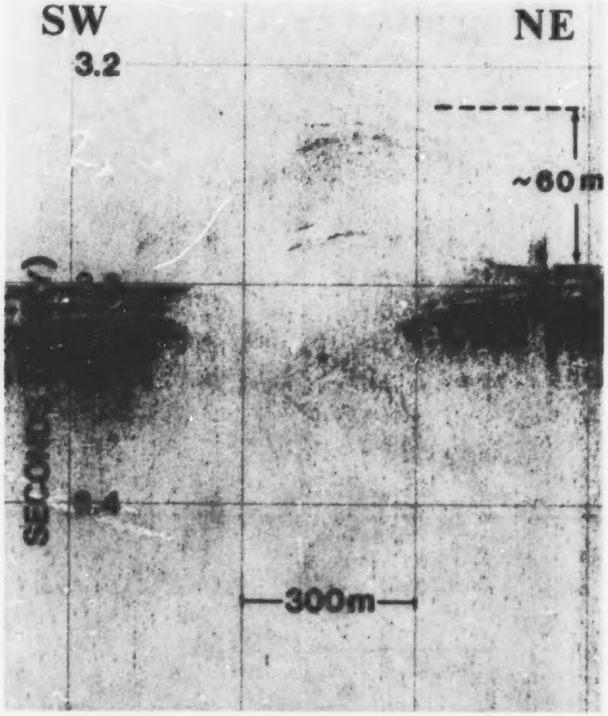

Figure 88.2. Subbottom profile (3.5 kHz) of hydrothermal mound.

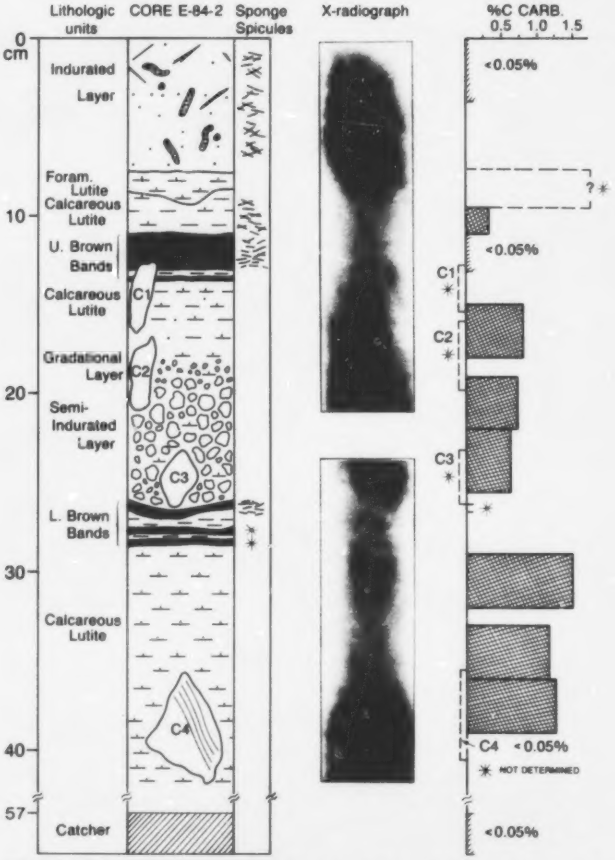

Figure 88.3. A core recovered from 2.4 m below the surface of the mound exhibits soft, dark brown colour bands, indurated (including the core catcher sediment) and semi-indurated sediment layers. Clasts of indurated sediment are present throughout the core. Clasts and zones of sediment induration appear dark on X-radiographs. Brown bands, indurated sediment, and clasts are noncalcareous when tested with HCl. Burrows are shown in the X-radiograph of the upper indurated layer which also exhibits black, fracture-filling Mn deposits.

Results

Lithology

The core comprises several lithological units (Fig. 88.3): (1) indurated sediment, olive grey; (2) semi-indurated sediment, olive grey; (3) clasts of sedimentary origin, olive grey; (4) nonindurated dark brown bands; and (5) lutite, olive grey. The results of semi-quantitative chemical examination (SEM-EDS) are incorporated into lithological descriptions.

Indurated sediment. Dark zones in X-radiographs correspond to intervals of indurated sediment (Fig. 88.3). Sedimentary clasts, also indurated, are evident throughout the core. Burrows (X-ray transparent) are present in the upper indurated layer, 0-7.5 cm, which forms a sharp contact with underlying lutite (Fig. 88.3). When freshly broken, the indurated layer exhibits burrows 1 mm in diameter (Fig. 88.4 A, B). Burrowing would have occurred prior to induration of the sediment. Burrows are lined with needles, possibly sponge spicules carried into burrows by deposit-feeding crustaceans (V. Tunnicliffe, personal communication, 1985). However, confirmation of needle composition was not made by SEM-EDS.

The 0-7.5 cm layer, when broken between the fingers, exhibits paper thin black films filling fractures inclined to the bedding. The black deposit is composed of manganese and exhibits the well developed box-work morphology characteristic of birnessite. Neither the indurated layer nor broken indurated material from the core catcher are calcareous (Fig. 88.3).

Semi-indurated sediment. A semi-indurated layer is present at 19.7-26 cm (Fig. 88.3). At its base this sediment comprises angular chunks up to 1 cm in size enclosed in soft mud. The bulk sediment is calcareous and has a blocky texture. The semi-indurated sediment grades upward (18-19.7 cm) into unlithified lutite. Blocky chunks, when washed free of adhering mud are easily broken and are noncalcareous indicating that carbonate in the bulk material is confined to the mud matrix.

Clasts. Clasts, encountered at several intervals in the core (Fig. 88.3) are noncalcareous, may be broken between the fingers, and are only slightly rounded (some terminations are subangular to angular). Clasts are texturally dissimilar but all are sedimentary in origin. Clasts 1 and 2 (C1, C2, Fig. 88.3) consist of lithified lutite, are flattened, and have some angular terminations. Clast 3 is composed of indurated silt and clast 4, which almost fills the core tube, exhibits well developed silt laminations (Fig. 88.3). A rust brown coating was observed on one face of the clast from 17-21 cm.

Dark brown bands. Clusters of several discrete dark brown unlithified bands are present at two levels in the core, 11-13.5 cm and 26-28.5 cm (variable in thickness; Figs. 88.3, 88.5A). The lower interval of brown band sediment comprises

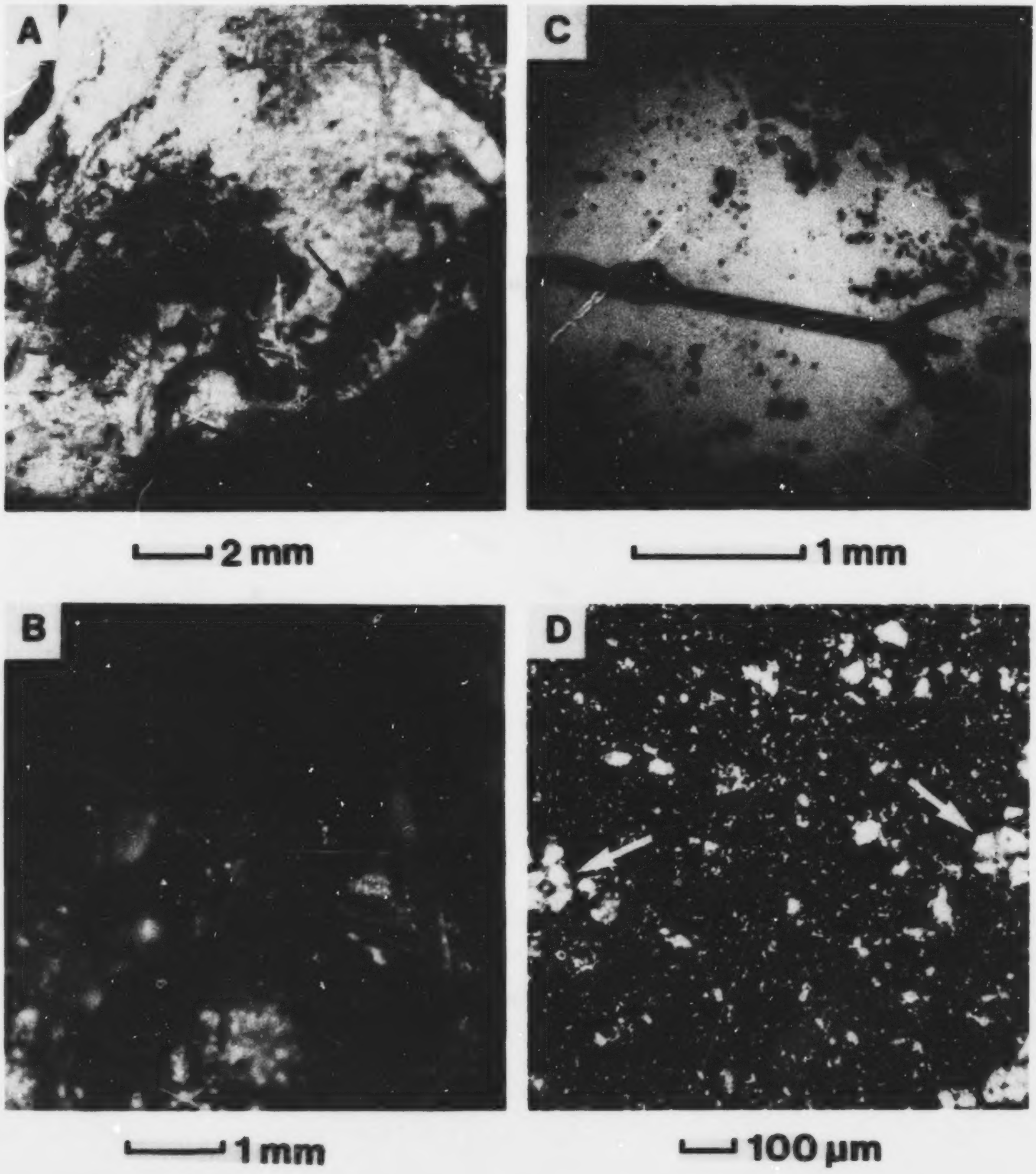

Figure 88.4. A. *The upper indurated layer contains burrows formed prior to sediment induration. A 1 mm-diameter burrow (arrows) leads to the holes shown in the centre of the micrograph.*
B. *Burrows are lined with spicules.*
C. *Sponge spicule from lutite (9.5-11 cm) above the upper brown band (sediment smear in oil).*
D. *Typical calcareous lutite (15-18 cm). The particle size is mainly <20 µm. Sand size foraminifera tests (arrows) are scattered through the sample (crossed nicols, sediment smear in oil).*

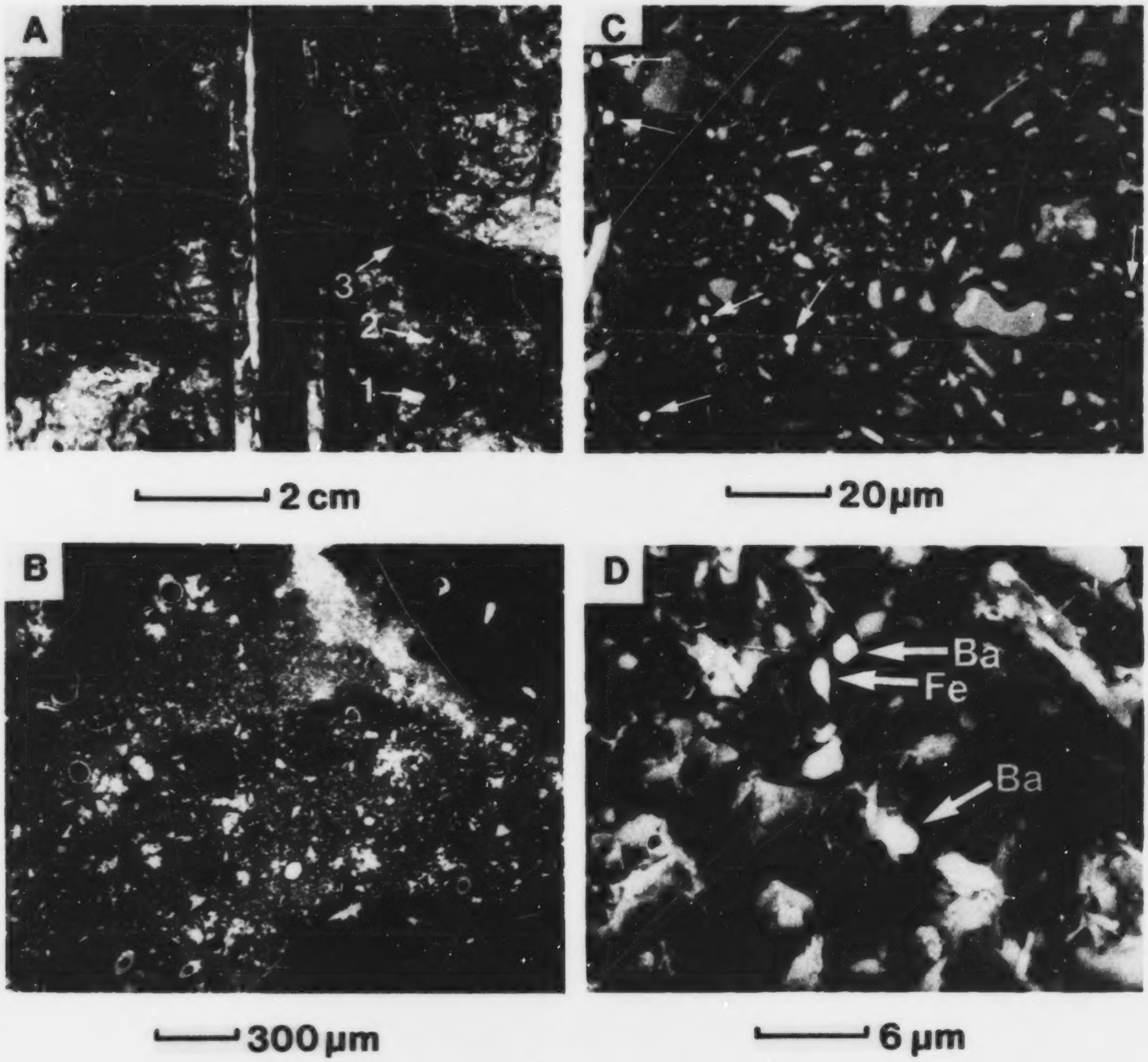

Figure 88.5. A. *Dark brown deposits occur as clusters of several discrete bands in core intervals of 2–3 cm. Three bands (1,2,3) are present in the lower zone (top at 26.5 cm). Bands have sharp upper and lower contacts.*

B. *The upper contact of the dark brown band at (26.5 cm) with overlying olive grey lutite is well defined. A large carbonate particle is present below the contact to the left of the arrow (polished section, SEM).*

C. *Barite particles ($\bar{x}$ 2 µm) some indicated by arrows, are scattered through the brown sediment. Grains are bright in back scattered electron image (polished section, SEM).*

D. *Upper and lower arrows indicate barite, middle arrow denotes an Fe particle (high atomic number elements appear bright in back scattered electron image). Flaky material is composed mainly of silicates.*

three dark brown layers interbedded with olive grey lutite. Upper and lower contacts of the brown bands are sharp (Fig. 88.5B). Sponge spicules are conspicuous in brown bands (Fig. 88.6) as is other siliceous biogenic debris (e.g. radiolarian tests), but carbonate is absent. Examination of the microtexture of brown bands (Fig. 88.4, 88.5, 88.6) revealed that most particles are in the clay and fine silt range (<20 μm). These detrital silicate particles are commonly angular and are associated with abundant flaky particles composed mainly of Si (Fig. 88.5D).

Barite crystals are common minor constituents of the brown layers (see Fig. 88.5C, D), easily identified in back scattered electron images of polished sections. These crystals are remarkably uniform in particle size, most being about 2 μm. Scattered particles of similar size contain only Fe (Fig. 88.5D).

The sharp upper contact of the main brown band at 26.5-27 cm is evident in Figure 88.6. Two zones of spicules are present, one located approximately 1 mm from the upper contact (Fig. 88.6) and a second approximately 1.5 mm below the upper zone. Spicules near the top of the 26.5-27 cm brown band are shown in Figures 88.6A, and 88.6C, where the spicule zone is several hundred microns in thickness.

Unusual coarser grains in which Fe is the principal constituent are present in brown bands. A fine sand-sized particle which appears shattered (Fig. 88.7), perhaps in preparation of the polished section, is in part composed of material with striking micromorphology identical with the micromorphology of an adjacent globular mass (Fig. 88.7A, B). Microspheres approximately 1 μm in diameter constitute the globular particle and part of the adjacent sand grain (Fig. 88.7A, B). The absence of filamentous structures in the globular particle suggests that microspheres may be purely inorganic in origin, but these spherical bodies resemble in some ways structures that could be produced by coccoid bacteria (J. W. Paden, personal communication, 1985). Microspheres, like the fragmented part of the sand grain, are composed primarily of Fe with minor Si; however, the content of Si is higher in microspheres. Calcium is a minor constituent of fragmented and microsphere parts of the sand grain (Ca is absent in the globular particle) and may reflect partial replacement of the grain by microsphere deposits. Brown bands also contain scattered red grains of sand size which have a radiating structure and are composed principally of Fe with minor Si and Ca (Fig. 88.7C). Ferruginous particles containing major Si and Fe were also noted in brown bands and may represent clay alteration products (Fig. 88.7D).

Lutite. Lutite is calcareous and similar in composition throughout the core except for sediment (9.5-11 cm) deposited immediately over the upper brown bands, where lutite composition is related to that of the underlying brown band (and also exhibits sponge spicules characteristic of upper and lower brown bands). Lutites are typically composed of particles <20 μm (Fig. 88.4D).

Chemical composition

Carbon and loss on ignition

Indurated sediment and brown bands are noncalcareous as are blocky lumps in the semi-indurated layer and all clasts (Fig. 88.3). The carbonate content of the lutite at 7.5-9.5 cm (Fig. 88.3) was not determined but would probably exceed carbonate contents for other lithologies in the core owing to the abundance of foraminifera tests observed in this interval. Lutites underlying brown bands have the highest carbonate carbon contents of samples tested (1-1.5%, Table 88.1).

Organic carbon values are generally similar for all lithological units, falling in the range 0.3-0.5%. Upper and lower brown bands have twice this organic carbon content (~1%). Lutites have the highest total carbon contents, 1.3-1.9%, while indurated layers (including the core catcher sample) and clasts have the lowest, 0.2-0.3% (Fig. 88.8, Table 88.1).

Loss on ignition (L.O.I.) values are closely related to carbonate carbon contents with lowest L.O.I. values being observed for indurated sediments and clasts (Table 88.1).

Fe, Mn, and trace elements

Highest Mn values are evident for the upper indurated layer and the upper and lower brown bands; these three deposits show a progressive decrease in Mn content from 4700 to 4200 to 2900 ppm, respectively (Fig. 88.9, Table 88.1). With the exception of the lower brown band, all sediments underlying the upper brown layer have closely similar Mn values, less than 1000 ppm. The depth distribution of Ni follows closely the pattern for Mn (Fig. 88.9). Highest values for Cu, Mo, and Zn are also found for the indurated upper layer (Table 88.1). Cobalt, although relatively uniform throughout the core, is lowest in the upper indurated layer, the core catcher indurated sediment, and in two of the clasts. Iron is distributed relatively uniformly, with most values falling in the range 4-4.6% (as %Fe; Table 88.1). Brown bands have iron contents similar to those of other lithologies in the core.

Upper and lower brown bands are distinguished by higher Ba contents (1900-2100 ppm; Table 88.1, Fig. 88.9) than the upper indurated layer, indurated core catcher material, the semi-indurated layer, and calcareous lutites where Ba contents of 500-800 ppm were observed. An exception is the lutite immediately overlying the upper brown layer which has intermediate Ba contents (Fig. 88.9).

Other major elements

The highest SiO_2 contents are observed for the upper indurated layer and indurated core catcher sediment (56-58%, Fig. 88.10) and for two clasts composed of indurated sediment (65-67%). Semi-indurated sediment and brown bands have intermediate SiO_2 contents of 50-53%, whereas lowest values are found for lutites below the upper brown band (47-50%).

The MgO content of core sediments is relatively uniform (3.4-4.0%) except for higher values for the upper indurated layer (4.6%) and indurated catcher material (6.2%). Two clasts composed of indurated lutite also have high MgO contents (6-9%, Table 88.1). Clasts and indurated layers lack carbonate; MgO is associated with silicates in these deposits. The low MgO and high SiO_2 content of clast 3 may be explained by its high silt composition (indurated silt rather than lutite). The distribution of other major elements is given in Table 88.1.

Discussion

A depositional setting for the mound based on observations made in this study may be constructed by assuming that calcareous lutite represents normal hemipelagic sedimentation in this area. This mode of sedimentation has been interrupted by the periodic influx of fine grained particulates represented by thin brown bands, and by the introduction of large clasts of indurated sediment whose angularity is indicative of a short distance of transport from their place of origin.

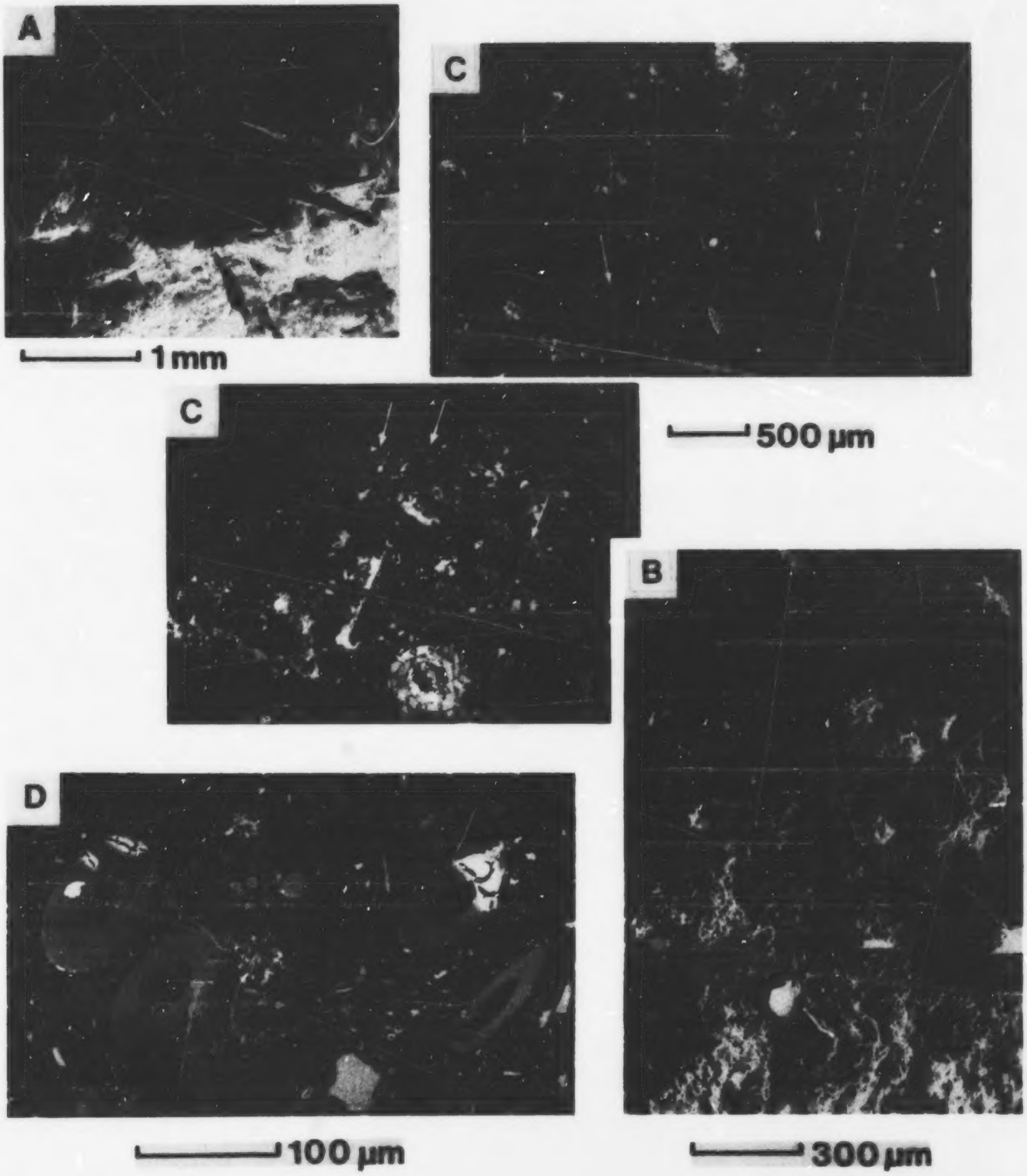

Figure 88.6. *Lower brown band, 26.5-27 cm.*

A. *Mud broken in wet state and air dried shows sponge spicules.*

B. *Air-dried mud scraped to remove salt coating reveals a concentration of sponge spicules in a zone 500-600 µm in thickness (SEM).*

C. *Scraped surface was repeatedly impregnated with resin and polished to outline the upper contact. Arrows show the location of two zones of sponge spicules. Spicules have accumulated with fine grained silicates and scattered radiolarian tests. A sand size grain of agglutinated detritus is present within the band in the lower micrograph (base of the brown band is not shown, SEM).*

D. *Sponge spicules in polished section (SEM).*

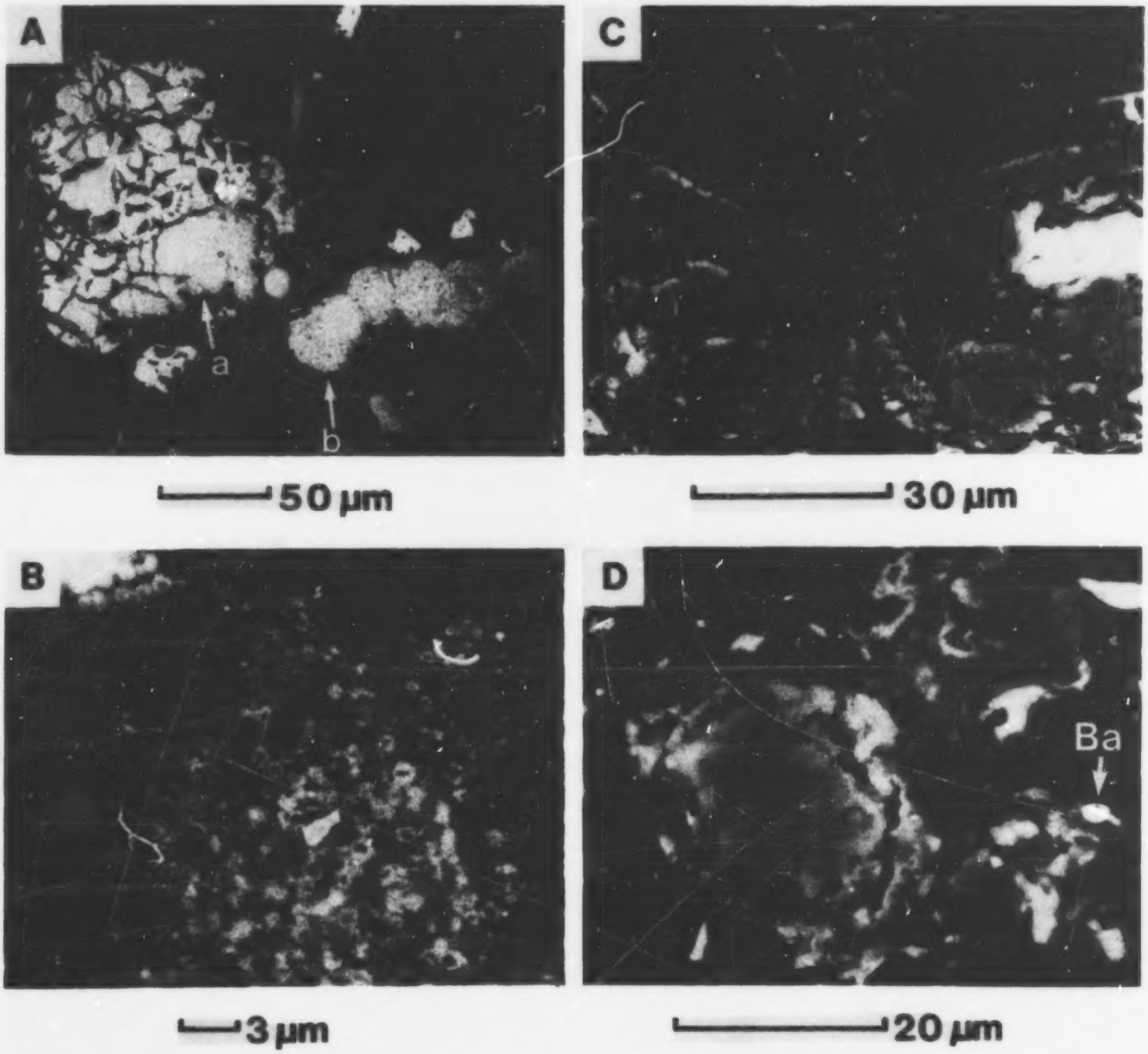

Figure 88.7. Iron-rich grains in lower brown band, 26.5-27 cm. All SEM micrographs are from a polished section.

- *A. The composition of the shattered sand grain on the left is major Fe, minor Si, Ca. A part of the grain appears altered (arrow a) but the composition of this part of the grain (a) is similar (slightly higher Si content) to that of the shattered grain. The globular particle (b) has a composition nearly identical with area (a) but lacks Ca. The microstructure of (a) and (b) is identical.*
- *B. Microstructure of (a) and (b) consists of spherical bodies 1 µm in diameter.*
- *C. Sand size grain with radiating structure consists principally of Fe (nonmetallic) with minor Si, Ca.*
- *D. Grain composed mainly of Si and Fe may be a clay alteration product. A barite particle lies to the right of the Si-Fe grain.*

Table 88.1. Chemical composition of sediments from mound site, core END84A002

Lithology				Oxides (%)								
Sample depth (cm)	Sediment	Colour Munsell 1973	HCl[a] test	SiO_2	Al_2O_3	TiO_2	CaO	MgO	Na_2O	K_2O	P_2O_5	LOI %
0-3.5	Indurated	5Y5/2 Olive grey	Noncalc.	58.0	15	0.80	1.2	4.6	3.4	2.4	0.21	7.9
7.5-9.5	Foram Lutite	2.5Y6/2 Lt. brown grey	Calc.	47.5	16	0.70	6.4	4.0	5.0	2.6	0.14	--
9.5-11	Lutite	5Y5/2 Olive grey[b]	Calc.	51.0	15	0.70	2.8	3.8	3.8	2.8	0.15	12.9
11-13	Brown bands	10YR3/3 Dk. brown	Noncalc.	52.5	15	0.75	1.8	3.6	4.0	2.8	0.19	12.3
26.5-27	Brown bands	10YR3/3 Dk. brown	Noncalc.	51.5	16	0.70	2.2	4.0	5.2	2.6	0.16	--
$\bar{X}_2$				52.00[c]	15.50	0.73	2.00	3.80	4.60	2.70	0.18	
15-18	Lutite	5Y5/2 Olive grey	Calc.	49.5	14	0.65	5.6	3.8	3.4	2.4	0.13	11.4
29-32	Lutite	5Y5/2 Olive grey	Calc.	47.5	13	0.60	7.8	3.6	3.2	2.4	0.13	13.2
33-36	Lutite	5Y5/2 Olive grey	Calc.	48.5	13	0.60	6.2	3.4	3.2	2.4	0.12	12.2
36-39	Lutite	5Y5/2 Olive grey	Calc.	48.5	14	0.65	6.6	3.8	3.4	2.8	0.14	12.1
$\bar{X}_4$				48.5	13.5	0.63	6.55	3.65	3.30	2.50	0.13	12.23
19-22	Semi-indurated	5Y5/2 Olive grey	Calc.[d]	50.0	16	0.70	5.0	4.0	3.4	2.8	0.14	11.0
22-25.5	Semi-indurated	5Y5/2 Olive grey	Calc.[d]	52.0	14	0.65	4.0	4.2	3.6	2.4	0.16	10.0
$\bar{X}_2$				51.00	15.00	0.68	4.50	4.10	3.50	2.60	0.15	10.50
12.5-16.5	Clast 1		Noncalc.	NSS	17	0.80	0.4	9.0	1.8	3.0	0.20	7.8
23.5-26	Clast 3		Noncalc.	67.0	13	0.65	2.8	3.4	3.8	1.4	0.13	--
35.5-41.5	Clast 4		Noncalc.	65.5	13	0.60	0.4	6.6	2.2	1.6	0.16	6.1
44.5-56.5			Calc.	49.5	12	0.55	5.2	3.8	3.2	2.0	0.13	8.4
Catcher[f]	Indurated		Noncalc.	55.5	13	0.65	0.6	6.2	3.0	1.6	0.15	5.8

Sample depth (cm)	% Fe	Mn (ppm)	Trace elements (ppm)									% S	Carbon (%)		
			Zn	Cu	Ni	Co	Mo	U	Ba	Sr	Cr		C_T[e]	C_{CARB}[e]	C_{ORG}[e]
0-3.5	4.2	4700	520	82	104	16	10	2.8	540	180	90	0.04	0.3	<0.05	.28
7.5-9.5	3.8	2200	164	78	62	20	4	1.2	1050	340	100	--	--	--	--
9.5-11	4.2	3200	200	80	87	21	6	1.5	1400	260	90	0.20	1.4	0.35	1.09
11-13	4.4	4200	205	80	86	22	4	1.9	2150	240	95	0.10	0.9	<0.05	.86
26.5-27	4.3	2900	198	72	71	23	6	1.6	1900	260	100	0.06	1.0	--	.99
$\bar{X}_2$	4.35	3550.00	201.50	76.00	78.50	22.50	5.00	1.75	2025.00	250.00	98.00	0.08	0.95		0.93
15-18	4.5	990	164	64	58	22	6	1.6	720	280	85	0.04	1.3	0.80	.48
29-32	4.1	660	156	70	52	22	6	1.5	700	320	80	0.04	1.9	1.50	.39
33-36	4.3	690	156	66	53	23	4	1.5	680	280	80	0.04	1.6	1.15	.44
36-39	4.3	650	160	68	56	22	6	1.5	740	300	90	0.04	1.6	1.25	.31
$\bar{X}_4$	4.30	747.50	159.00	67.00	54.75	22.25	5.50	1.53	710.00	295.00	83.75	0.04	1.60	1.18	0.41
19-22	4.5	690	172	64	56	23	4	1.2	760	280	90	0.04	1.1	0.75	.37
22-25.5	4.6	700	196	74	60	21	4	1.9	660	240	85	0.04	1.0	0.65	.38
$\bar{X}_2$	4.55	695.00	184.00	69.00	58.00	22.00	4.00	1.55	710.00	260.00	88.00	0.04	1.05	0.70	0.38
12.5-16.5	4.6	3100	280	64	70	23	6	3.2	1300	50	115	0.02	0.2	--	--
23.5-26	2.8	1000	122	42	28	14	4	1.2	800	260	80	--	--	--	--
35.5-41.5	2.9	440	104	22	26	10	2	1.6	460	50	95	0.02	0.2	<0.05	.16
44.5-56.5	4.1	710	138	64	46	15	2	1.7	600	260	75	0.02	1.4	1.02	.34
Catcher[f]	4.6	710	136	46	38	11	2	1.9	560	120	90	0.02	0.2	<0.05	.24

[a] Sample tested with concentrated HCl: Calcareo[illegible]s, slightly calcareous, noncalcareous.
[b] Black mottling present.
[c] Values shown to two decimal places as a result of calculation. See text for a discussion of reproducibility.
[d] Indurated fragments noncalcareous; unconsolidated matrix is calcareous.
[e] C_T = total carbon; C_{CARB} = carbonate carbon; C_{ORG} = organic carbon.
[f] See text for discussion of sample locations.

The unique characteristics of the brown bands suggest that these deposits may be associated with episodes of hydrothermal plume sedimentation. Specific compositional features supporting this suggestion include:

1. elevated Ba and Mn contents relative to enclosing sediments;
2. the common occurrence of Ba as clay-size particles $\lesssim 2$ µm;
3. organic carbon contents twice those of enclosing sediments and the concentration of sponge spicules, possibly reflecting favourable conditions for certain benthic fauna during periods of plume deposition;
4. the presence of Fe-rich sand-size grains in a sediment which is composed predominantly of silicates <20 µm in size;
5. the lack of carbonate.

It should be noted that the bulk chemical and mineralogical composition (predominantly silicates) of the brown bands, particularly the iron content, are not significantly different from the enclosing olive grey sediment. This similarity was confirmed by SEM-EDS assessment of integrated areas (120 µm^2) on polished sections of plastic-impregnated muds and by chemical analyses. The textural similarity of brown bands and enclosing olive sediment, both composed mainly of particles <20 µm in size is also apparent.

The results of this study suggest the importance of resedimentation of fine grained silicate sediments in the area surrounding a vent when hydrothermal fluids are vented at a sediment-covered mound site. Although samples of plume

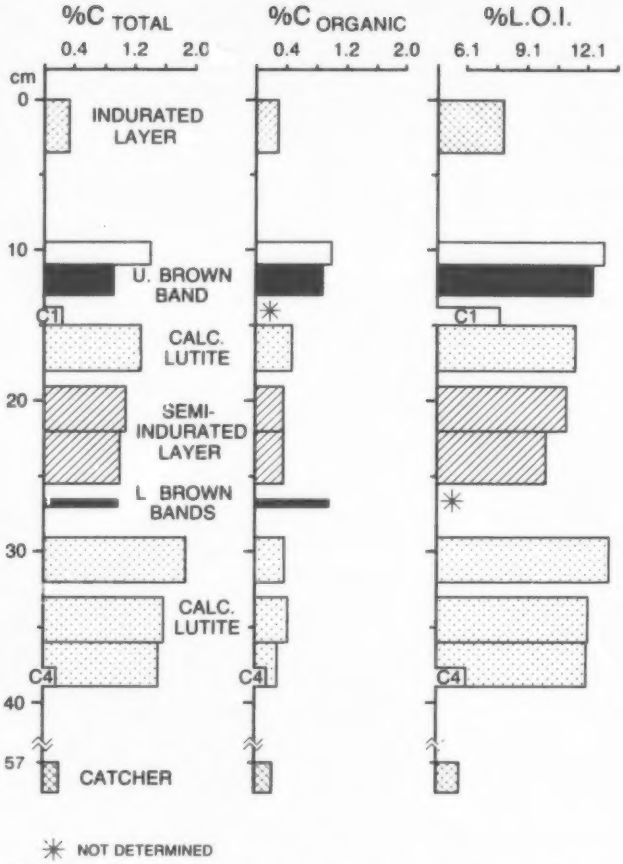

Figure 88.8. Distribution of carbon and loss on ignition values with depth in core. Note that organic carbon contents are highest for the brown bands and associated overlying lutite.

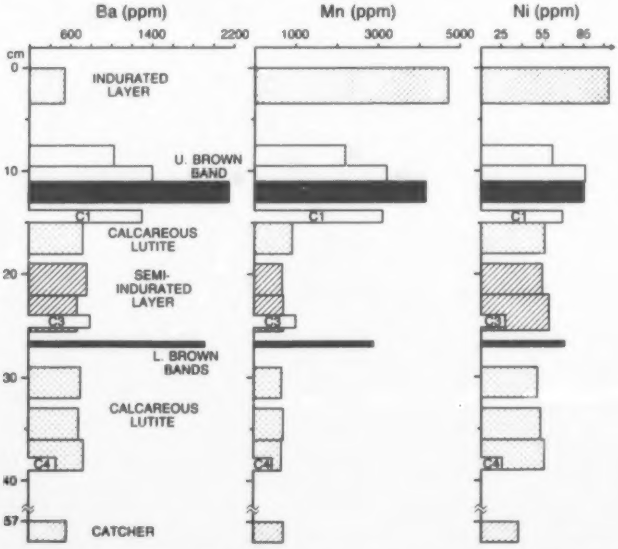

Figure 88.9. Distribution of Ba, Mn and Ni with depth in core. Ba and Mn contents are high in brown bands relative to adjacent sediment. Mn and Ni show characteristic metal diffusion profiles superimposed on initial metal contents, which were likely higher for brown bands than are now evident.

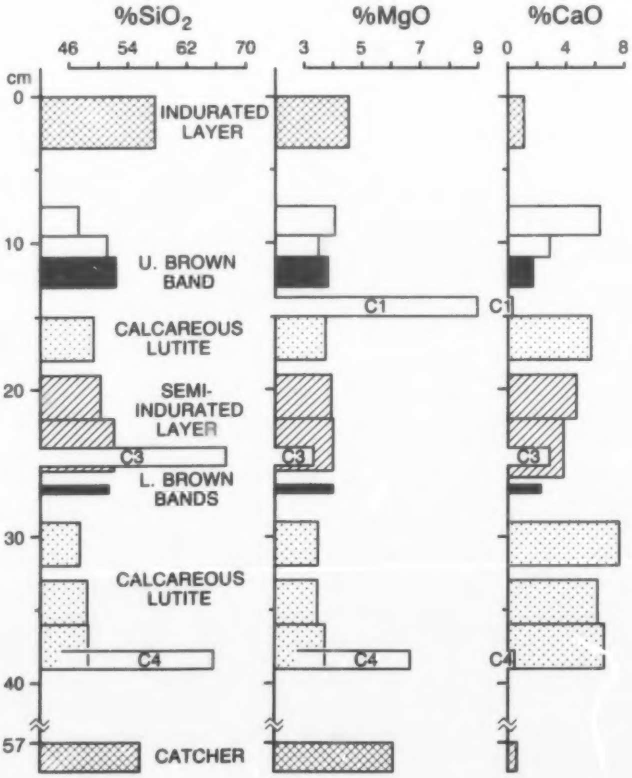

Figure 88.10. Distribution of SiO_2, MgO, and CaO with depth in core. Note higher SiO_2 and MgO and lower CaO values for indurated sediment (includes catcher material).

particulates may consist largely of chemical precipitates in fluids sampled over vents in rock terrain, e.g. the abundance of pyrrhotite crystals has been noted in samples from a vent on the East Pacific Rise (Oudin, 1979, p. 18-19), hydrothermal emanations in heavily sedimented areas may be expected to involve the mixing of hydrothermally derived particulates together with disturbed pelagic sediment near the vent site. Resuspended clays, diatom fragments, and organic matter occur with Mn and barite particles in hydrothermal plumes in the Guaymas Basin of the Gulf of California (Campbell et al., 1984; hydrothermal clouds are also enriched in dissolved barium). The results of the present study suggest that other forms of sediment transport may also occur. The presence of large clasts throughout the Juan de Fuca core indicates that indurated material from or near a vent conduit may be periodically released as debris to accumulate on the slopes of the mound.

Although carbonate grains were not detected in brown bands, except at the top of one band at the contact with overlying hemipelagic mud, siliceous tests of radiolarians were observed. Several speculative explanations may be offered to account for the lack of planktonic foraminifera tests in brown bands: (1) sedimentation of these deposits was rapid; (2) carbonate may have been dissolved at a local vent site (on the mound) upon mixing of hydrothermal fluid with resuspended hemipelagic sediment; (3) foraminifera tests may not have been as effectively resuspended or transported as the <20 μm silicates comprising the bulk of the brown deposits. In view of the presence of radiolarian tests in brown layers, it is difficult to explain their lack of carbonate by (1) or (3) above. Whatever the reason or combination of reasons for the carbonate relationship, all three explanations are compatible with a plume origin for the brown bands.

The depth distribution of Mn and related trace metals appears to follow normal diffusion patterns. Although upper and lower brown bands have higher Mn contents than enclosing sediments, the Mn contents of brown deposits when they formed at the surface may have been significantly higher than presently observed. Present Mn contents thus appear to reflect the effects of postdepositional diffusion processes. Mn and associated trace metals are present at highest levels in the core in fractures and cavities in the uppermost indurated layer where Mn oxides have been deposited as pore fillings. The distribution of Mn and related metals in clasts found at various levels in the core may reflect a depletion of these metals with depth in core (Table 88.1).

Of note is the periodic occurrence of indurated layers (three in the short core studied). A suggested mechanism contributing to sediment induration would involve the introduction of SiO_2 concomitant with the deposition of pelagic sediments. Postdepositional alteration effects likely involved the dissolution of calcium carbonate and possibly the precipitation of magnesium silicates in these sediments. The release of dissolved silica as a late stage of hydrothermal activity has been well demonstrated (Oudin, 1979). Although dissolved silica would be expected to precipitate within, at, or very close to a vent due to rapid cooling of hydrothermal fluids on mixing with seawater, a colloidal precipitate of silica or silica-bearing clay could be transported with other components of a turbid plume and be deposited at a greater distance from a vent site. Backer et al. (1985) suggested that elevated Si/Al ratios in surface sediments from the crest and western flank of the East Pacific Rise at 18.5°S could reflect a relatively widespread westward dispersion of silica in some form. Mineralogical examination of the core will be undertaken to supplement these chemical observations.

The relatively similar Fe content in the brown bands and also in the enclosing sediment (Table 88.1) suggests that Fe-bearing particulates were not important components of hydrothermal plumes affecting the site where the mound core was taken, possibly due to a low content of Fe particulates in the plume or to iron-mineral sedimentation closer to a hydrothermal vent.

On a ternary diagram (Fig. 88.11) Fe-Mn-(Cu+Ni+Co) after Rona (1978), the various lithologies from the hydrothermal mound fall near the iron-rich pole, within a field common to metalliferous and hydrothermal sediments (see Bornhold et al., 1981). The results of this plot, though useful for comparison with other studies, are inconclusive for differentiation of lithologies examined in the present study.

Preliminary appraisal of further coring carried out in 1985 at the same mound, which involved mainly the collection of shallow cores that sample the upper 2 m of mound sediment, indicated the presence of buried and episodic brown band accumulation in only one core. The core in question may have been fortuitously recovered from a site where the >2 m-thick veneer of olive grey sediment typical for this mound was very thin.

Although brown deposits were observed as sediment smears on the sides of core liners for most of the 1985 cores and appear to form surface deposits at the mound site at the present time, as well as occurring elsewhere in the region (Bornhold et al., 1981), these surface deposits may not necessarily reflect hydrothermal input.

These observations suggest that brown banding representing plume sedimentation may be more evident in sediments underlying the 2 m or more veneer of sediment now blanketing the mound (except in occasional sites where the veneer is thin).

Conclusions

Examination of a core collected from below the upper 2.4 m sediment veneer now covering a hydrothermal mound near Juan de Fuca Ridge reveals the presence of indurated layers (elevated SiO_2 content), and Ba- and Mn-rich brown bands of possible hydrothermal plume origin. As well, clasts of indurated sediment were deposited periodically on the mound surface. These features are suggestive of late-stage hydrothermal activity.

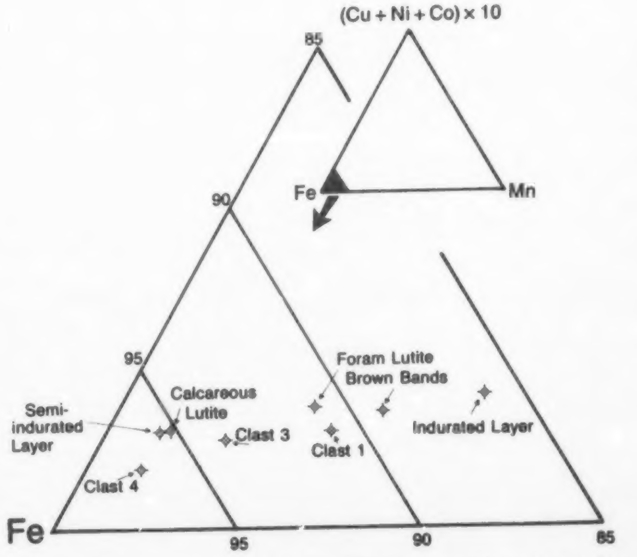

Figure 88.11. Ternary plot showing composition field for sediments from mound structure.

Because the mound is capped by >2 m of hemipelagic sediment in which dark brown bands and indurated layers are not generally observed, it is inferred that the mound may not have been actively venting manganese, barium, and silica-rich fluids in recent times. Moreover, it is possible that a series of deeper cores (>3 m) may reveal the episodic plume and induration banding that would permit reconstruction and dating of hydrothermal events at the mound studied. Alternatively, the deposition of plume sediments may be highly localized near vent sites and thus would be encountered in only a few cores.

Acknowledgments

We especially thank D.A. Walker for SEM assistance, R. Burke for preparation of polished sections, and S. Harper and K. Shrives for assistance with core X-radiography. D.C. Harris and J.L. Jambor provided microscope facilities and P. Dvorak kindly permitted use of X-radiography equipment. Support from V. Foster and S. Keddie is gratefully recognized. J.M. Franklin provided helpful suggestions for improvement of the manuscript. Uranium determinations were performed by Atomic Energy of Canada Limited; atomic absorption, inductively coupled plasma, carbon and sulphur analyses were provided by Chemex Labs. Ltd.

References

Backer, H., Lange, J., and Marchig, V.
1985: Hydrothermal activity and sulphide formation in axial valleys of the East Pacific Rise crest between 18 and 22°S; Earth and Planetary Science Letters, v. 72, pp. 9-22.

Bornhold, B.D., Tiffin, D.L., and Currie, R.G.
1981: Trace metal geochemistry of sediments, northeast Pacific Ocean; Geological Survey of Canada, Paper 80-25, 21 p.

Campbell, A.C., Gieskes, J.M., Chow, T.J., and Lonsdale, P.F.
1984: Geochemistry of hydrothermal clouds in the Guaymas Basin, Gulf of California; EOS, Transactions, American Geophysical Union, v. 65, p. 974.

Oudin, E.
1979: Étude minéralogique et géochimique des dépôts sulfurés sous-marins actuels de la ride est-Pacifique (21°N); Doc. B.R.G.M. 25, France, 141 p.

Rona, P.A.
1978: Criteria for recognition of hydrothermal mineral deposits in oceanic crust; Economic Geology, v. 73, p. 135-160.

Coastal characteristics, east-central Ellesmere Island, District of Franklin

Project 750063

M.T. Krawetz[1] and S.B. McCann[2]
Terrain Sciences Division

Krawetz, M.T. and McCann, S.B., Coastal characteristics, east-central Ellesmere Island, District of Franklin; in Current Research, Part A, Geological Survey of Canada, Paper 86-1A, p. 749-754, 1986.

Abstract

The coast of east-central Ellesmere Island is characterized by long fiords separated by bold headlands. The region is mesotidal with a semi-diurnal tidal oscillation. Wave activity is negligible due to restricted fetches and a short open water season; tidal and sea ice processes provide the principal dynamic activities in the shore zone. Coastal surveys from Baird Inlet to Copes Bay were completed, and a simplified coastal classification scheme was employed to describe backshore characteristics and to identify the occurrences of tidal flats in the intertidal zone. Three elements define the coastal expression: (1) bedrock, including Precambrian and Paleozoic exposures, (2) Quaternary deposits, and (3) tidewater glaciers. Tidal flats are found below till bluffs and moraines, fronting fiord head and fiord wall deltas, and at the heads of some embayments.

Résumé

La côte de la partie centre-est de l'île d'Ellesmere est caractérisée par de longs fjords séparés par des promontoires escarpés. Cette zone mésotidale est sujette à des marées semi-diurnes. L'activité des vagues est négligeable à cause des fetches limités et de la courte saison d'eaux libres. Les mouvements des glaces de mer et les marées s'avèrent les principales activités dynamiques dans la zone littorale. Des levés du littoral allant de l'inlet Baird à la baie Copes ont été réalisés; on a utilisé une méthode simplifiée de classification côtière pour décrire les caractéristiques de l'arrière-plage et pour identifier les estrans dans la zone intertidale. Trois éléments ont permis de définir les caractéristiques de la côte: 1) le socle rocheux, y compris des affleurements du Précambrian et du Paléozoïque, 2) des dépôts du Quaternaire et, 3) des glaciers d'eau de marée. Les estrans gisent sous des falaises de till et des moraines, devant des deltas au front et au pied des parois des fjords, ainsi qu'en amont de quelques baies.

[1] Department of Geography, University of Windsor, Windsor, Ontario N9B 3P4
[2] Department of Geography, McMaster University, Hamilton, Ontario L8S 4K1

Introduction

This report describes coastal conditions in east-central Ellesmere Island between latitudes 78°24'N and 79°32'N (Fig. 89.1). The data were obtained during a series of helicopter traverses made during the summers of 1981-84 in conjunction with an intensive study of tidal flat processess and morphology at Alexandra Fiord. There is little published information about the coast of the region though the bedrock geology is relatively well known (Christie, 1967; Frisch, 1982) and the late Quaternary history is being actively studied (Blake, 1977, 1982). The basic bathymetry of the fiords has been charted (Canadian Hydrographic Service, 1975); tidal predictions for Pim Island (Canadian Hydrographic Service, 1983) indicate that the region is mesotidal, with a semi-diurnal tidal oscillation and a mean range of 2.9 m expanding to 4.8 m at large tides.

High, steep, commonly vertical, glaciated rock slopes, in association with talus, are the dominant coastal landforms in this high relief, extensively glacierized region. The influence of wave action is negligible and there are no beaches. Fiord head and fiord wall gravel deltas and tidal flats with boulders constitute the depositional elements of the coast. Sea ice conditions are severe, with a short open water season, heavy concentrations of multiyear ice, and significant quantities of berg ice.

Coastal classification scheme

A simple classification scheme denoted by a letter code is used to depict the regional coastal characteristics (Table 89.1, Fig. 89.2, 89.3). The coast is initially divided into three primary classes or units (Table 89.1, Part I), depending on whether the material at the coast is bedrock (B), Quaternary sediments (Q), or tidewater glaciers (G). A series of modifiers (Table 89.1, Part II) is then employed to describe the conditions in the backshore. The modifiers for the bedrock coast indicate the rock type (Precambrian or Paleozoic), whether the coast is cliffed, and whether significant talus slopes occur; the modifiers for the Quaternary sediment coasts indicate the presence of deltas and the occurrence of erosional bluffs; the modifiers for the tidewater glacier coasts indicate the gradient of the glaciers, the presence of vertical ice cliffs, and whether a glacier is presently calving. The presence of raised shoreline features is also shown. The third part of the classification scheme (Table 89.1, Part III) reflects our particular interest and consists of a series of five descriptors for the bouldery tidal flats which occur at various locations in the region. The first and second descriptors concern the width and continuity of the tidal flats, the third describes the density of intertidal boulders, and the fourth and fifth denote the presence of a boulder barricade and indicate its degree of continuity.

Description of coastal types

The region can conveniently be divided into two zones – an inner fiord head zone consisting of a series of six fiords, and an outer zone consisting of Bache, Thorvald, and Johan peninsulas adjoining Kane Basin-Smith Sound (Table 89.2).

Inner fiord head zone (Fig. 89.2)

This zone occupies the northern portion of the study area from Copes Bay south to the head of Jokel Fiord. Lower Paleozoic rocks outcrop along the four northern fiords and Precambrian rocks outcrop in the south. The terrain is characterized by narrow fiords flanked by precipitous cliffs commonly rising 760 m a.s.l. The northern and southern uplands are extensively covered by ice but the central uplands either side of Flagler Bay are ice free. Of the 306 km of shoreline surveyed in the area, 71% is bedrock, 22% is Quaternary material, and 7% is tidewater glaciers.

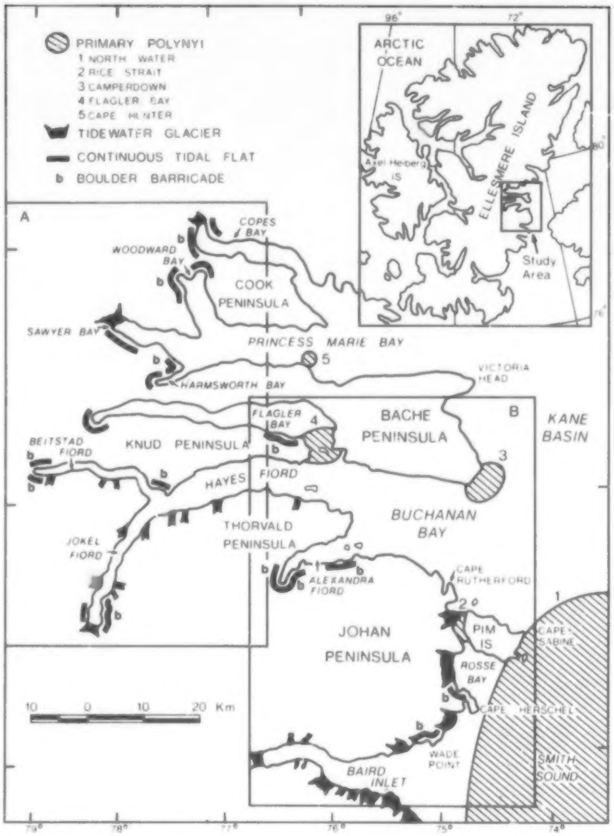

Figure 89.1. *Location map of the study area, east-central Ellesmere Island, showing the inner fiord head zone (A) and the outer zone (B).*

Wide fronted, low gradient fiord head glaciers occur in Copes Bay and Sawyer Bay in the north; the former is actively calving at the present time. Associated Quaternary deposits at the head of Copes Bay are fronted by moderately wide, bouldery tidal flats. Similar tidal flats also occur in association with Quaternary deposits around the two headward arms of Woodward Bay, where the glacier terminus is set back 1 km from tidwater. Continuous tidal flats with only a low concentration of boulders occur along both bedrock and Quaternary shores on the south side of Sawyer Bay. Boulder barricades are poorly developed in these areas. The rest of the coastline in these northerly fiords consists of a continuous talus apron developed below high, commonly vertical, cliffs in Paleozoic rocks. These are particularly spectacular in Harmsworth Bay. Raised shoreline features occur on the promontory separating the two heads of Woodward Bay and on the cape between Woodward Bay and Sawyer Bay.

Flagler Bay is shallow (less than 30 m deep in the central section; Canadian Hydrographic Service, 1975) but it is contained within high, steep bedrock cliffs and talus slopes. Along most of the northern side of Flagler Bay, however, a veneer of Quaternary deposits, both glacial and deltaic materials, masks the bedrock in the shore zone, and the coast is classed accordingly in Figure 89.2. Some of these deposits have been eroded into bluffs 30 m high. A narrow but relatively continuous tidal flat fringes the northern shoreline.

Beitstad and Jokel fiords, which are developed in Precambrian bedrock, are narrower (2-3 km) and deeper (greater than 200 m) than the previously mentioned fiords and the shore zone contains less Quaternary deposits. The well bedded, gently dipping sequence of Lower Paleozoic limestones and shales, which outcrop in the area to the north of Buchanan Bay and Hayes Fiord, are more susceptible to periglacial weathering processes than the Precambrian granites and gneisses which outcrop in the south. Thus, the original glacially eorded slopes have been modified to a greater degree. High vertical cliffs and long relatively continuous and uniform talus slopes characterize the Paleozoic outcrop. Broken discontinuous vertical cliffs and intermittent talus slopes characterize the Precambrian outcrop. Twelve steep gradient, cascading fiord wall glaciers enter the Beitstad-Jokel-Hayes Fiord system. In addition, there is a wide fronted, fiord head glacier in Jokel Fiord. Tidal flats occur at the head of and at the entrance to Beitstad Fiord and along the east shore near the head of Jokel Fiord. Boulder barricades are better developed than farther north and are continuous at the head of Beitstad Fiord.

Table 89.1. Coastal classification scheme

I Primary units	II Backshore modifiers				III Tidal flat descriptors				
	1	2	3	4	1	2	3	4	5
B	pЄ P	c	t	rb ri	N	c d s	l m h []	$\underline{B}$ $\overline{B}$	c d s
Q	d	b			M				
G	g s	v	x		W				

PART I PRIMARY COASTAL UNITS

Bedrock coast	B
Quaternary sediment coast	Q
Tidwater glacier	G

PART II BACKSHORE MODIFIERS

1. Type	pЄ P	Precambrian Paleozoic	d delta	g gentle s steep
2. Steepness	c b v	cliff (in bedrock) bluff (in Quaternary sediment) vertical front (in tidwater glacier)		
3. Slope form	t x	talus calving glacier front		
4. Raised shorelines	rb ri	raised beach raised intertidal platform or flat		

PART III TIDAL FLAT DESCRIPTORS

1. Tidal flat width	N M W	narrow medium wide	
2. Tidal flat continuity	c d s	continuous discontinuous sporadic	
3. Boulder density	l m h	low medium high	[] concentrated in mounds
4. Barricade	$\underline{B}$ $\overline{B}$	present intertidally present subtidally	
5. Barricade continuity	c d s	continuous discontinuous sporadic	

Outer zone (Fig. 89.3)

This zone extends from the entrance of Flagler Bay south to Baird Inlet. Glaciers cover most of the landscape in the region leaving only a narrow fringe of bedrock and glacial deposits along the coast. Large tidewater glaciers dominate the coast in the southern part of the zone whereas the northern coast is ice free. The Precambrian rocks outcrop as high precipitous cliffs and glacially sculptured lowlands. Of the 320 km of shoreline surveyed in the area, 74% is bedrock, 14% is Quaternary material, and 12% is tidewater glaciers.

The outer coasts of Knud and Thorvald peninsulas and the northern coast of Johan Peninsula are highly indented along the Precambrian lowlands. These embayments are commonly backed by Quaternary deposits; a thin veneer of glacial sediment covers the bedrock above the shore zone. Moderately wide, bouldery tidal flats occupy the embayments of Knud Peninsula. Boulder barricades and other boulder arrangements are well developed. Discontinuous, narrow tidal flats fringe the Thorvald and Johan peninsula shorelines. Raised shoreline features are prominent along the Knud and Johan peninsula coasts.

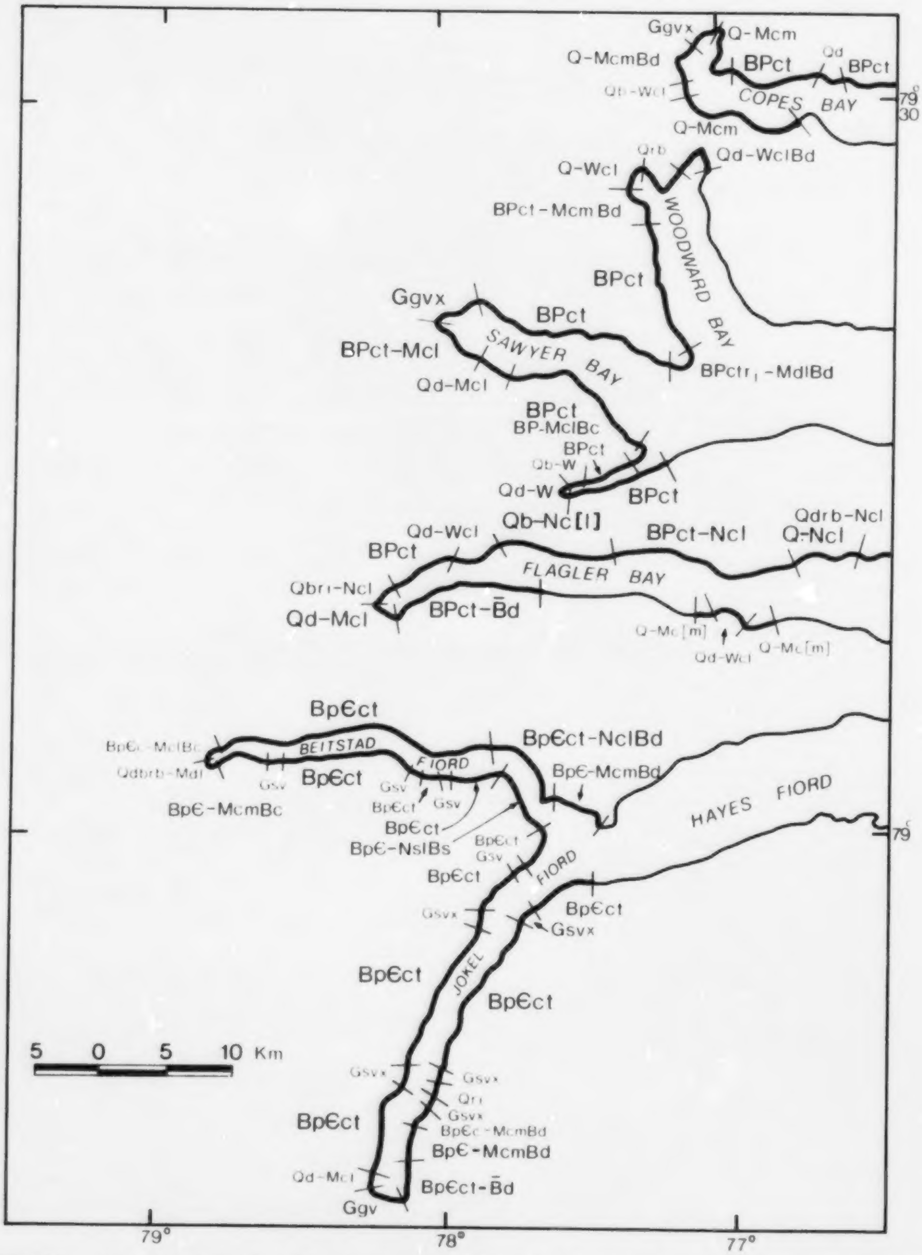

Figure 89.2. Coastal characteristics in the inner fiord head zone according to the classification scheme in Table 89.1.

Alexandra Fiord, a wide mouth fiord (7 km) narrowing to 1 km at the head, is contained by high bedrock cliffs along the north shore and bedrock lowlands along the south shore. The termini of the fiord head and fiord side glaciers are set well back from tidewater. Talus slopes extend below tidewater and are commonly eroded into low bluffs below broken Precambrian bedrock cliffs. Quaternary deposits around the head of the fiord and along extensive stretches of the south shore are fronted by moderately wide, bouldery tidal flats. A relatively continuous boulder barricade is well developed along this coast. Tidal flats are also developed in small embayments along the Precambrian lowlands of the south shore. Boulders form various arrangments in these embayments. The tidal flats are more common in Alexandra Fiord than elsewhere in the study area and constitute the major shoreline component.

The shoreline extending from Cape Rutherford south to Wade Point is characterized by high, precipitous Precambrian bedrock cliffs. Talus slopes along the base of these cliffs are especially well developed on Pim Island and Cape Herschel.

Figure 89.3. Coastal characteristics in the outer zone according to the classification scheme in Table 89.1.

Table 89.2. Coastal types

Location	Coastline surveyed km	Bedrock %	Quaternary deposits %	Tidewater glacier %
A. INNER FIORD HEAD ZONE				
Copes Bay	28.1	29.6	59.4	11.0
Woodward Bay	26.5	52.8	47.2	5.6
Sawyer Bay	41.6	80.8	7.0	-
Harmsworth Bay	16.0	83.1	16.9	-
Flagler Bay	59.1	52.4	47.6	12.2
Beitstad Fiord	69.5	91.7	2.7	-
Jokel Fiord	64.7	81.8	4.5	11.0
Total	305.5	71.0	22.2	6.8
B. OUTER ZONE				
Knud Peninsula	19.3	100.0	-	-
Thorvald Peninsula	19.0	100.0	-	-
Alexandra Fiord	57.6	74.8	25.2	-
Johan Peninsula (Buchanan Bay)	28.9	86.8	13.2	-
Johan Peninsula (Kane Basin)	103.9	66.6	14.9	18.5
Baird Inlet	91.2	66.1	11.7	22.2
Total	319.9	73.8	13.9	12.3
TOTAL	625.4	72.8	17.9	9.6

Six, low gradient tidewater glaciers enter the waters of the outer coast. The largest glacier, entering the head of Rosse Bay, has a high, vertical front and is actively calving at present, producing the largest icebergs in the study area. Tidal flats are best developed in the two bays which separate the Cape Herschel promontory from Johan Peninsula. The tidal flats are associated with Quaternary deposits which have been eroded into low bluffs yielding an abundant supply of boulders. The boulders are arranged in a variety of patterns – they occur singly, as mounds, armoured ridges, and barricades.

At Baird Inlet in the south there is a change in the overall character of the coast. The northern shore and the head of the fiord are similar to the fiords of the inner zone described previously, in particular Jokel Fiord. There is a calving fiord head glacier and four small, steep fiord wall glaciers separated by long stretches of high bedrock cliffs. Because of the bedrock type (Precambrian), talus slopes are poorly developed. In contrast, along the outer south coast of Baird Inlet six, wide (up to 6 km) tidewater glaciers occur separated by only very short stretches (1-2 km) of steep bedrock shoreline. The study area is essentially a bedrock coast with tidewater glaciers. The area to the south, beginning at Baird Inlet and continuing to Makinson Inlet in the south, is essentially a tidewater glacier coast with short stretches of bedrock.

Acknowledgments

W. Blake, Jr. introduced the authors to the area and has taken a keen interest in, and provided field support for, the work being undertaken by M.T. Krawetz as a doctoral dissertation at McMaster University. Logistical support from Polar Continental Shelf Project is gratefully acknowledged.

References

Blake, W., Jr.

1977: Glacial sculpture along the east-central coast of Ellesmere Island, Arctic Archipelago; in Report of Activities, Part C, Geological Survey of Canada, Paper 77-1C, p. 107-115.

1982: Coring of frozen pond sediments, east-central Ellesmere Island: A progress report; in Current Research, Part C, Geological Survey of Canada, Paper 82-1C, p. 104-110.

Canadian Hydrographic Service

1975: Field Sheet No. 3882; Princess Marie Bay-Buchanan Bay; Canadian Hydrographic Service, Ottawa.

1983: Canadian tide and current tables, 1983; Volume 4, Arctic and Hudson Bay; Fisheries and Environment Canada, Fisheries and Marine Service, 51 p.

Christie, R.L.

1967: Bache Peninsula, Ellesmere Island, Arctic Archipelago; Geological Survey of Canada, Memoir 347, 63 p.

Frisch, T.

1982: Reconnaissance geology of the Precambrian Shield of Ellesmere Devon, and Coburg Islands, Arctic Archipelago: A preliminary account; Geological Survey of Canada, Paper 82-10, 11 p.

Atikonak River massif, Labrador

Project 750011

R.F. Emslie, C. Lefebvre [1], B. Kjarsgaard [2], and R. Sherlock [3]
Precambrian Geology Division

Emslie, R.F., Lefebvre, C., Kjarsgaard, B., and Sherlock, R., Atikonak River massif, Labrador; in Current Research, Part A, Geological Survey of Canada, Paper 86-1A, p. 755-758, 1986.

Abstract

Atikonak River massif comprises a complex of troctolitic, noritic, and anorthositic rocks in southwestern Labrador. Spatially related pyroxene monzonites and coarse grained rapakivi granites typify this association as elsewhere in Labrador.

Magmatic structures and textures are well preserved in the basic rocks of the massif and clearly demonstrate that intrusion of the massif magmas was not accomplished as highly crystalline mushes. Widespread occurrence of mineral layering, including graded and crossbedded varieties, attests to the presence of substantial amounts of liquid at the time of their formation.

Evidence of subsolidus reaction between olivine and plagioclase is common in crystal cumulates of the massif. At present it is unclear to what extent such reactions may have taken place during cooling of the massif from magmatic temperatures or resulted from later regional metamorphism.

Résumé

Le massif d'Atikonak River, situé dans le sud-ouest du Labrador, est constitué d'un complexe de roches troctolitiques, noritiques et anorthositiques. Des monzonites à pyroxène et des granites rapakiviques à grains grossiers, qui sont liés géographiquement, caractérisent cette association comme ailleurs au Labrador.

Des structures et textures magmatiques, bien conservées dans les roches basiques du massif, démontrent nettement que des magmas n'ont pas pénétré le massif sous forme de boues fortement cristallines. Des couches minérales très étendues dont certaines présentent une sédimentation granoclassée et d'autre une stratification oblique, témoignent de la présence d'importantes quantités de liquide au moment de leur formation.

On trouve beaucoup de traces de réaction sub-solide entre de l'olivine et du plagioclase dans les cumulats de cristaux du massif. Actuellement, on n'est pas certain jusqu'à quel point ces réactions se seraient produites surtout pendant le refroidissement du magma ou à la suite d'un métamorphisme régional postérieur.

[1] Université de Quebec à Chicoutimi, Chicoutimi, Quebec
[2] University of Guelph, Guelph, Ontario
[3] McMaster University, Hamilton, Ontario

Introduction

Anorthositic massifs and associated intrusions constitute major components of the northeastern Grenville Province. Atikonak River massif forms the northern part of a much larger complex of anorthositic and related rocks that has been referred to as the Lac Fournier massif (Sharma and Franconi, 1975). The present mapping has shown that, in addition to forming a generally distinctive physiographic feature, the Atikonak River massif is almost completely isolated from similar rocks to the south by older paragneiss and younger granitic intrusions (Fig. 90.1). For these reasons, and to add precision to subsequent description, introduction of the new name was considered advisable.

Previous reconnaissance mapping of the northern part of the massif was done by Stevenson (1968). In a nearby area to the southwest, Blais (1960) has reported similar rock associations to those found during the present mapping. According to Thomas (1974) much of the Atikonak River massif is undistinguished by significant positive or negative Bouguer anomalies; this seems to imply that either olivine-bearing rocks at depth are less abundant than they appear at the surface or the massif is a relatively thin slab.

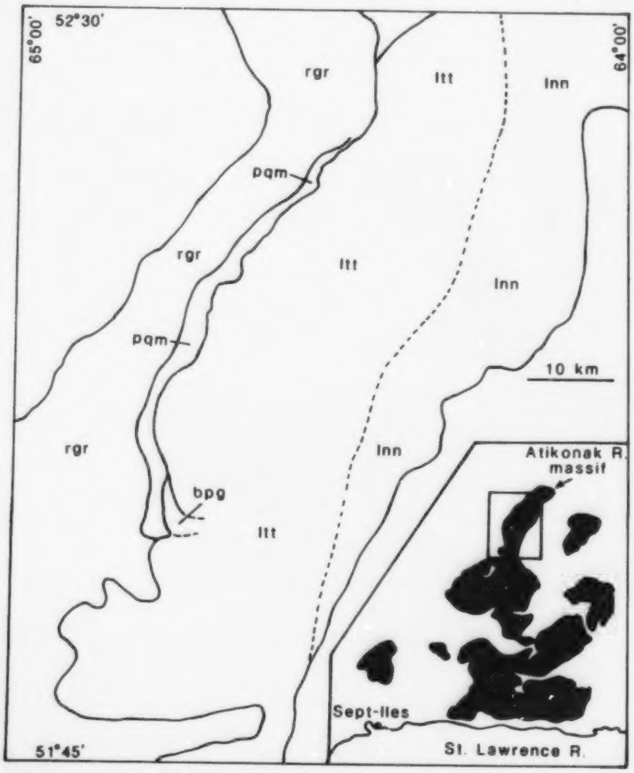

***Figure 90.1.** Major subdivisions of the Atikonak River massif and associated rocks. Leucotroctolite and troctolite with interlayered anorthosite (ltt) dominate the western part of the massif. Leuconorite and norite with interlayered anorthosite (lnn) are predominant in the east. Pyroxene quartz monzonite and monzonite (pqm) and coarse grained rapakivi granite (rgr) flank the massif to the northwest; the former unit intrudes ltt as dykes. Beaver Pond gabbro (bpg) comprises layered olivine gabbro, troctolite and gabbro in a lenticular, north to northeast dipping, layered intrusion. Inset shows relationship of Atikonak River massif to other major anorthositic massifs in the region.*

Rock units of the massif and associated intrusions

Major rock units of the Atikonak River massif include leucotroctolite (C.I.=10-25), troctolite (C.I.=25-50), leuconorite (C.I.=10-25), norite (C.I.=25-50), and anorthosite (C.I.<10). Olivine-bearing rocks are prominent in the better exposed part of the massif and exhibit a considerable variety of structures and textures. Mineral layering on scales of centimetres to at least several metres is widespread and is displayed particularly well in burned-over areas and along larger rivers. Troctolite and leucotroctolite, typically with more plagioclase-rich interlayers including anorthosite, form dominant rock types in the western part of the massif. Large masses of true anorthosite are distinctly subordinate members of the massif suite. Norite and leuconorite form separate large masses and tend to dominate the eastern sector (Fig. 90.1); these commonly also exhibit anorthositic interlayers. Substantial parts of all rock units are essentially massive with little variation in mineral proportions or grain sizes.

A medium grained layered intrusion containing olivine gabbro, troctolite, and gabbro has been named Beaver Pond gabbro (bpg, Fig. 90.1). It appears to intrude coarse grained leucotroctolite of the massif proper and is itself intruded by pyroxene monzonite. Local pyroxene and oxide rich pods or disrupted layers in the intrusion contain up to several per cent sulphides including pyrrhotite and chalcopyrite.

Immediately adjacent to the northwestern margin of the basic massif, and in intrusive contact with it, is medium- to coarse-grained pyroxene monzonite and pyroxene quartz monzonite. These rocks are typically brownish to rusty weathering commonly with colour index 20-30. Variable amounts of amphibole and biotite accompany, and may locally predominate over, pyroxenes in these rocks. Perthite megacrysts 1 to 3 cm in size become increasingly abundant away from the massif contact. Dykes of pyroxene monzonite from 1 to 30 cm thick intrude the basic massif up to 5 km or more from the northwestern contact.

A large mass of coarse grained biotite-hornblende granite with distinctive plagioclase-rimmed perthite ovoids up to 4 cm or larger (rapakivi texture) lies farther to the northwest; in several places this granite appears to be transitional into pyroxene-bearing monzonitic rocks. Large parts of the rapakivi granite are essentially massive with negligible deformation of original igneous textures (Fig. 90.2h). Distinct foliated and recrystallized zones occur within the granite but, for the most part, appear to be localized and relatively narrow.

Internal structures of the massif

Mineral layering, commonly accompanied by moderate to strong subparallel planar plagioclase lamination, is developed to some degree in nearly all of the basic rock types of the massif (Fig. 90.2a,b,c,f). In addition, textural layers defined by differences in plagioclase grain size and shape occur in association with mineral layers and independently. Examples of mineral graded, and grain size graded layers, crossbedded layers, and apparent slump features have all been observed in different localities. Modal contrasts between adjacent layers are commonly subtle, involving variations of less than 20% in amounts of mafic components present. Locally, however, stronger contrasts occur and melatroctolite and oxide-rich layers are present in a few localities.

Planar plagioclase orientation is frequently observed in rocks that lack mineral layering and is present in olivine- and orthopyroxene-bearing rocks as well as nearly pure plagioclase rocks. Where sections subparallel to dip surfaces are exposed it can be seen that plagioclase crystals are plate-like or discoidal, in places packed closely together like

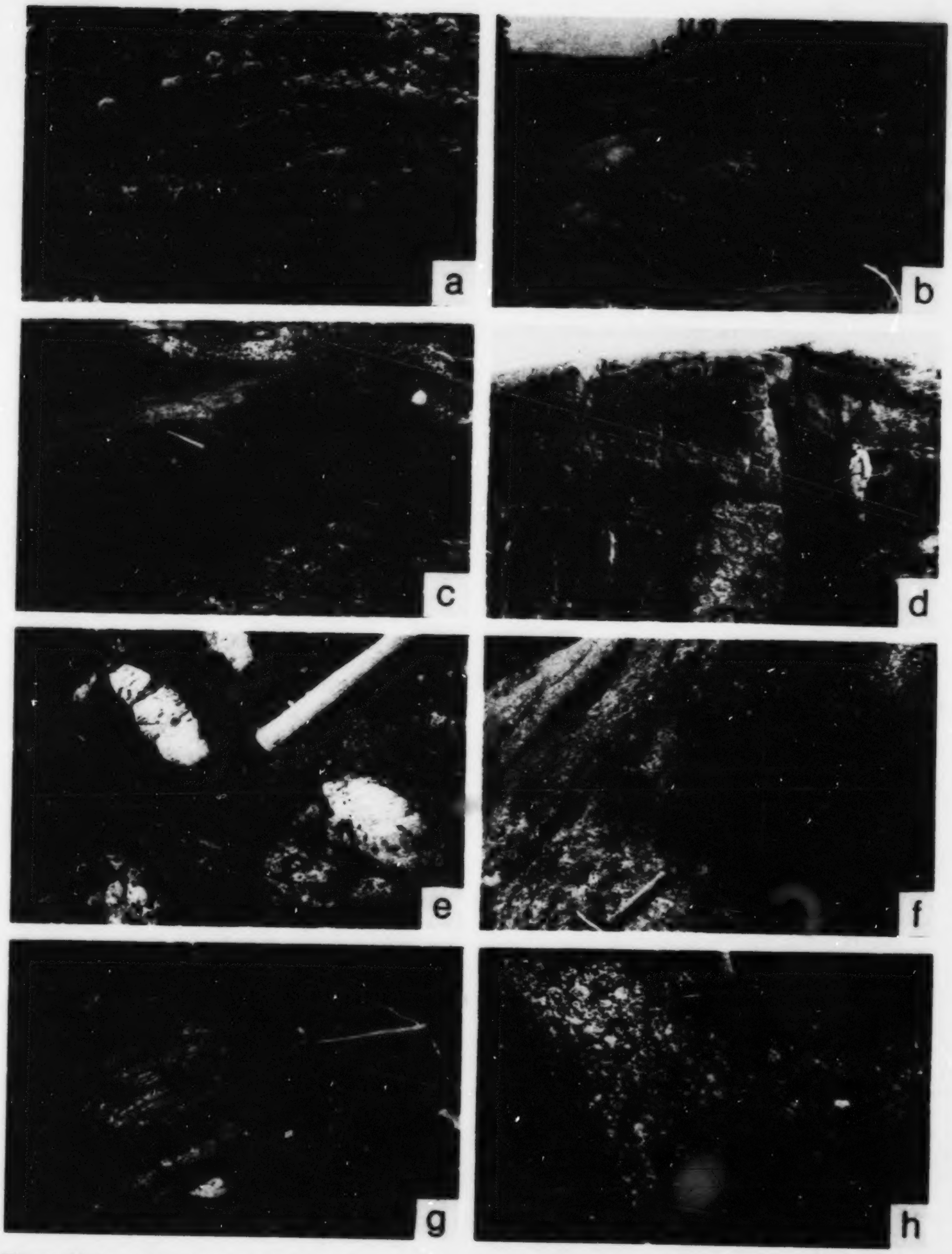

Figure 90.2. *Structures and textures of rocks of the Atikonak River massif and of associated rapakivi granite.*

a. Irregular centimetre-scale olivine-rich layers in troctolite; this is either a large xenolith or small intrusion surrounded by much coarser grained leucotroctolite.

b. Layered section of leucotroctolites dipping westerly at a moderate angle, Atikonak River.

c. Appendage from a thick anorthositic layer cuts across a layered section and dies out within it. Layers dip about 55° to the upper left (west); the relationship is consistent with a mild disturbance during bottom crystallization in which an overlying anorthositic cumulate penetrated already consolidated underlying cumulate rocks in a manner reminiscent of clastic dyke formation.

d. Highly irregular zones and masses of very coarse grained anorthosite occur within dominantly medium grained leucotroctolite.

e. Orthopyroxene megacrysts, many showing subhedral to rounded forms suggesting cumulus origin, occur in a large pod within leuconorite.

f. Strong planar plagioclase orientation in a coarse grained troctolite layer overlying a very coarse grained anorthosite layer also with marked planar plagioclase orientation.

g. Strong kink bands in a giant orthopyroxene crystal.

h. Coarse grained ovoid-rich massive rapakivi granite.

brickwork with only very small amounts of interstitial material. Planar plagioclase orientation occurs in rocks of grain sizes less than 1 cm to greater than 30 cm and may be present throughout a layered section or be limited to specific layers and be absent or much more weakly developed in intervening layers.

Oxide-rich pods, clots and layers occur locally and most are strongly magnetic, indicating a preponderance of magnetite over ilmenite. Disseminated grains of oxide are visible in many specimens. Clots of massive opaque oxide up to 30 cm across occur scattered through some noritic and leuconoritic outcrops, sometimes closely associated with coarse orthopyroxene and small amounts of sulphides.

Complex interrelationships occur among subunits on a local scale. A consistent relationship, however, is that xenoliths of coarse grained to very coarse grained anorthosite and leuconorite are present in many outcrops of troctolite and leucotroctolite (Fig. 90.2d). Xenoliths range in size from less than 1 m to at least 10 m across and probably much larger, their observed total extent being limited by the size of exposures.

Very coarse grained to 'giant' orthopyroxene crystals occur widely in the massif, commonly ranging to 30 to 60 cm across (Fig. 90.2e,g). These include both rounded or nodular shapes and crystals subophitically intergrown with plagioclase. Where these coarse orthopyroxenes are present within sections of olivine-bearing rocks, they are enclosed by very coarse grained anorthosite or leuconorite masses, commonly identifiable as xenoliths. Giant orthopyroxenes have not been found in direct contact with troctolite or leucotroctolite, implying that they were unstable in silica-deficient magmas at crustal pressures and survived transport only where they were armoured by an enclosing xenolith.

Although layered structures occur widely, the massif does not have an overall coherent pattern of layering. Areas up to 50 km^2 do show regular attitudes of layering but, because over considerable areas rock compositional changes are subtle, it is not possible to determine to what extent layer domains may represent discrete intrusions as opposed to disrupted, tilted or deformed parts of a larger intrusion. Because intrusive relations are visible on outcrop scales in many places, there is some support for interpreting the massif as a composite of numerous separate intrusions.

Metamorphism

Country rocks surrounding the Atikonak River massif are at regional amphibolite to granulite grade. Effect of metamorphic overprint is evident on rocks of the massif but its significance is not readily assessed. Reaction coronas separating olivine and plagioclase are nearly universal in olivine-bearing rocks but it is unclear whether these result from younger regional metamorphism or are a consequence of subsolidus cooling of a deep-seated intrusion. Typical coronas are narrow and extremely fine grained; details of petrography are not yet available but hand lens examination suggests two pyroxenes plus spinel are probably present. Locally, usually in proximity to altered shear zones or pegmatitic granite dykes, reaction rims and coronas become broader and their mineralogy changes to fibrous amphibole, chlorite, and other hydrous minerals; in places olivine is completely replaced although hydrous pseudomorphs can be readily identified.

Narrow, whitish-altered hairline fractures occur widely in the massif. Most show little or no offset but relative displacements up to a few metres can be seen in places. The distribution of these fractures is not uniform throughout the massif and they appear to be more abundant toward the northwest margin of the body.

Small amounts of garnet occur widely distributed in pyroxene monzonites and rapakivi granites. The garnet is commonly closely associated with opaque oxide grains and occurs in rocks that otherwise show little or no evidence of metamorphic or deformational overprint.

Discussion

The tectonic setting of the Atikonak River massif at the time of intrusion can be nothing more than speculation at present. The rock assemblage, however, is virtually identical to anorogenic associations in Labrador north of the Grenville Front. Basic rocks of the massif and the associated pyroxene monzonites and rapakivi granites lack extensive penetrative fabrics. Such fabrics are confined to relatively narrow shear zones that appear to entirely postdate crystallization of the rocks and may be much later (Grenvillian?). There is little doubt that the igneous suite intruded amphibolite to granulite grade rocks that had already been deformed in one or more previous events.

The complex variations in attitudes of layered sections in the massif coupled with widespread evidence of xenoliths and intrusive relations among units suggest that intrusion was prolonged and involved both partly crystallized rock and largely liquid magma. Proportions of each were probably variable at different times and locations within the massif. The extent to which different magma pulses are represented as opposed to successive intrusive events occurring through continuing movements of a single crystallizing magma batch cannot be assessed on field evidence alone. The common presence of well defined mineral layers is clear evidence that the massif cannot be regarded as a simple intrusion of plagioclase-rich crystal mush.

Xenoliths of country rock are rare in all of the major rock units. They are essentially absent from the basic rocks of the massif and only a few small inclusions of basic to intermediate composition were noted within pyroxene monzonite and rapakivi granite. The lack of country rock xenoliths suggests that magma stoping was not an important process of emplacement and constitutes permissive evidence in support of diapiric intrusion.

Acknowledgments

This project was carried out in co-operation with the Newfoundland Department of Mines and Energy. Generous assistance and geological consultation were furnished by G.A.G. Nunn, N. Noel, and S. Wells, who together with H. McCleave, M. Rice, J. Smyth, G. Wiseman and helicopter pilot M. Grechan shared in logistical support and provided excellent companionship during the field season.

References

Blais, R.-A.
1960: Wacouno-Waco area, Saguenay Electoral District; Quebec Department of Mines, Geological Report 96, 55 p.

Sharma, K.N.M. and Franconi, A.
1975: Magpie, St. Jean, Romaine Rivers area; Quebec, ministère des Richesses naturelles, Geological Report 163, 73 p.

Stevenson, I.M.
1968: Geology of Lac Joseph map area (23A), Newfoundland and Quebec; Geological Survey of Canada, Paper 67-62, 4 p.

Thomas, M.D.
1974: The correlation of gravity and geology in southeastern Quebec and southern Labrador; Earth Physics Branch, Ottawa, Gravity map series, 49 p., maps.

Relationships along the eastern margin of the Humber Arm Allochthon between Georges Lake and Corner Brook, western Newfoundland

EMR Research Agreement 58/04/85

Harold Williams[1] and Peter A. Cawood[1]
Precambrian Geology Division

Williams, H. and Cawood, P.A., Relationships along the eastern margin of the Humber Arm Allochthon between Georges Lake and Corner Brook, western Newfoundland; in Current Research, Part A, Geological Survey of Canada, Paper 86-1A, p. 759-765, 1986.

Abstract

A wide zone of carbonate breccias, thin-bedded grey limestones and shales occurs between rocks of the Humber Arm Allochthon and parautochthonous carbonate and metaclastic sequences in the vicinity of Pinchgut Lake, western Newfoundland. Grey sandstones and shales are imbricated with rocks at Pinchgut Lake. Toward the south at Georges Lake, shales and mélanges separate the Humber Arm Allochthon and carbonate sequence with boundaries marked by high angle faults. Toward the north at Corner Brook, the Humber Arm Allochthon and carbonate sequence are separated by a high angle fault.

Northwesterly dips of bedding, cleavage, axial surfaces of folds and thrust faults all indicate an important deformation of easterly polarity that followed the westward emplacement of the Humber Arm Allochthon. High angle faulting was a later event. These structures confuse original relationships between the Humber Arm Allochthon and nearby groups in this area.

Résumé

Une large zone constituée de brèches carbonatées, de calcaires gris et de schistes argileux en couches minces du groupe informel de Pinchgut se manifeste entre des roches de l'allochthone de Humber Arm et des séries de carbonates et de roches métaclasiques parautochtones de la région du lac Pinchgut, dans l'ouest de Terre-Neuve. Des grès gris et des schistes argileux de la formation de Whale Back sont imbriqués avec des roches du groupe de Pinchgut. Au sud, vers le lac Georges, des schistes argileux et des mélanges de la formation de Georges Lake séparent l'allochtone de Humber Arm et la série carbonatée entre lesquels les limites sont marquées par des failles à fort pendage. Au nord, vers Corner Brook, une faille à fort pendage sépare l'allochthone de Humber Arm et la série carbonatée.

Le groupe de Pinchgut est corrélé avec la formation cambrienne de Reluctant Head et est interprété comme un faciès oriental de la série carbonatée. Sa disposition semble indiquer qu'on est en présence d'un lambeau de poussée distinct, se trouvant à la base de l'allochthone de Humber Arm. La formation de Whale Back serait une unité clastique transgressive de l'Ordovicien, mise en place sur le sommet de la série carbonatée. La formation de Georges Lake est corréleé avec les schistes argileux et les mélanges de l'Ordovicien qu'on trouve ailleurs entre l'allochthone de Humber Arm et la série carbonatée.

Les pendages nord-ouest des plans axiaux, de stratification et de clivage des plis et des chevauchements indiquent une importante déformation de polarité vers l'est qui a suivi la mise en place à l'ouest de l'allochthone de Humber Arm. Les failles à fort pendage sont postérieures à cet événement. Ces structures embrouillent les relations originales qui existaient entre l'allochthone de Humber Arm et les groupes avoisinants de la région.

[1] Department of Earth Sciences, Memorial University of Newfoundland, St. John's, Newfoundland A1B 3X5

Introduction

The Humber Arm Allochthon of western Newfoundland was emplaced during the Middle Ordovician and it overlies an autochthonous Cambrian-Ordovician carbonate sequence. In most places an orderly succession of units marks the top of the carbonate sequence with thick bedded limestone of the Table Head Group (Klappa et al., 1980) overlain by limestone breccia and shale of the Cape Cormorant Formation and sandstone and shale of the Goose Tickle Formation and equivalents (Cooper, 1937; Williams et al., 1983; 1984; 1985; Williams, 1985a). These autochthonous rocks are separated from the overlying allochthon by a thin zone of shaly mélange, the Rocky Harbour, Gadds Point and equivalents (Williams, 1985a; Williams et al., 1984; 1985). Examples are well known at the southern margin of the allochthon in the Stephenville area (Williams, 1985b) and along its eastern margin in the Lomond (Williams et al., 1984) and Gros Morne (Williams, 1985a) areas. In other places this orderly pattern is disrupted or confused by one or more of the following: (1) omission of units by high angle faulting (Stephenville area, Williams, 1985b), (2) intervening structural slices of poorly known rocks separating the carbonate sequence from mélanges and better known rocks of the allochthon (Lomond area, Williams et al., 1984), (3) out-of-sequence westward thrusting of the carbonate sequence or its crystalline basement above the allochthon (Gros Morne area, Williams et al., 1985), and (4) folds and thrusts of southeast polarity (Pasadena area, Williams et al., 1982; 1983; Humber Arm area, Bosworth, 1985; Waldron, 1986).

The area between Georges Lake and Corner Brook is traversed by the Trans Canada Highway and frequently travelled. However, it is poorly known geologically and it is one of the more complex segments at the periphyry of the Humber Arm Allochthon. The first regional mapping of the area was done by Walthier (1949). He showed problematic rocks at Pinchgut Lake either as part of the carbonate sequence or as part of the Humber Arm "Series", which at that time was interpreted as autochthonous and stratigraphically above the carbonate sequence. Riley (1957) mapped the same area in reconnaissance fashion and assigned some of the Pinchgut rocks to the carbonate sequence and others to the Humber Arm Group. Most subsequent compilation maps are adaptations of Walthiers original work, showing a prominent bulge in the periphyry of the allochthon at Pinchgut Lake (e.g. Kennedy, 1981). Along the extreme eastern edge of the Stephenville map area, shales near Pinchgut Lake were included in the Humber Arm Allochthon, while limestone breccias were assigned to the Cape Cormorant Formation and interpreted as thrust westward above shales of the allochthon (Williams, 1985b). Farther south at Georges Lake, some dark shales were assigned to the Cape Cormorant Formation near the Trans Canada Highway and others where grouped with shales and melanges of the Humber Arm Allochthon to the west of the Trans Canada Highway (Williams, 1985b).

Present work was conducted to sharpen relationships and more clearly define rock units in the poorly known Corner Brook area. This work was also done in preparation for an imminent compilation of the geology of the entire Humber Arm Allochthon. Lithic similarities between rocks of the Pinchgut area and those of the newly defined Weasel slice (Williams et al., 1984) of the Lomond area suggested correlation and the likelihood of structural complications at Pinchgut Lake. The area was remapped at 1:50 000 scale using the latest coloured aerial photographs during a 5 week period in August and September.

Acknowledgments

We wish to thank Philippe Erdmer and Jean van Berkel for helping with helicopter travel and the Newfoundland Forest Protection Service for the use of their colour photographs. We also thank William Bosworth and John Waldron for the use of their unpublished reports and maps of the Humber Arm area, and Winston Howell for drafting services. Our work is part of an extended project in western Newfoundland, now near completion, to investigate and remap the entire Humber Arm Allochthon. We acknowledge support of this project by the Natural Sciences and Engineering Research Council of Canada and the Department of Energy, Mines and Resources through the Geological Survey of Canada.

General Geology

The distribution of rock units and relationships are shown in Figure 91.1. The problematic rocks of immediate interest in this report are assigned new informal names. Limestone breccias, thin-bedded limestones and shales in the vicinity of Pinchgut Lake are named the Pinchgut group, sandstones and shales associated with rocks of the Pinchgut group are called the Whale Back formation, and shales and mélanges between the Humber Arm Allochthon and carbonate sequence farther south are called the Georges Lake formation. Other units in the area include the well known Summerside, Irishtown and Cooks Brook formations (Stevens, 1970; Williams, 1975) of the Humber Arm Allochthon, undivided St. George and Table Head groups (Schuchert and Dunbar, 1934) and the Reluctant Head Formation (Lilly, 1963; 1967; Williams et al., 1982; 1983; Gillespie, 1983) of the carbonate sequence, and metaclastic rocks of the Mount Musgrave Group (McKillop, 1963; Williams et al., 1983) farther east. The outcrop pattern is largely controlled by easterly directed thrusts and high angle faults.

The stratigraphy of the carbonate sequence and of the established formations of the Humber Arm Allochthon is well known. Rocks of the Georges Lake formation, although bounded by high angle faults, comprise lithologies that are expectable and predictable in the contact zone between the carbonate sequence and allochthonous rocks. The Pinchgut group resembles the Cambrian Reluctant Head Formation and the position of the group between the Humber Arm Allochthon to the west and the carbonate sequence to the east is analagous to the setting of correlatives in the Weasel structural slice at the base of the Humber Arm Allochthon farther north (Williams et al., 1984). Sandstones and shales of the Whale Back formation are similar to Ordovician clastics at the top of the carbonate sequence elsewhere. Their occurrence among rocks of the Pinchgut group is controlled by later eastward thrusting and high angle faulting.

Rocks of the carbonate sequence and the Pinchgut group are affected by regional metamorphism that increases in intensity from northwest to southeast. Most noticable is a change from limestone to marble along a transitional boundary between Pinchgut Lake and Humber River (Fig. 91.1). This boundary has no obvious relationship to stratigraphy and structure where it crosses both the carbonate sequence and Pinchgut group along its course.

In the descriptions that follow, the parautochthonous rocks are treated first, then the newly defined units between the carbonate sequence and the Humber Arm Allochthon, and a brief mention of rocks and relationships within the allochthon. Structural setting and structural styles are summarized in a concluding section.

Parautochthonous rocks

The Mount Musgrave Group consists of metamorphosed mainly clastic sedimentary rocks that lie along the eastern margin of the area. It is part of the west Newfoundland metaclastic belt and is correlated with the Fleur de Lys Supergroup in the north (Kennedy, 1981; Williams et al., 1982; Hibbard, 1983). The group is considered late Precambrian (Hadrynian) to Early Cambrian in age. Quartz mica schist intercalated with lesser amounts of mica schist and quartzite are the principal local lithologies. Minor quartz-feldspar gneiss and associated amphibolite occur to the north of Corner Brook Lake.

The Mount Musgrave Group is separated from the carbonate sequence by the Corner Brook Lake Thrust (Kennedy, 1981). This fault and its continuation farther south, the Grand Lake Thrust (Williams, 1985b), are interpreted as segments of a major thrust that brings metaclastic rocks and Grenville basement against the carbonate sequence to the west. In the Corner Brook area the original thrust is modified by overturning, later easterly thrusting and high angle faulting.

The Cambrian Reluctant Head Formation represents the lowest stratigraphic unit of the carbonate sequence. It consists of thin-bedded to laminated light grey limestone and grey to buff dolomitic shale with green-brown phyllitic partings. The unit extends along the eastern side of the area and is best seen in the gorge of the Humber River. There its thickness is estimated at 250 m (Lilly, 1963). Limestone breccias are common in lower parts of the formation in its type area to the north (Lilly, 1963; Williams et al., 1982).

Thicker bedded limestones and dolostones of the St. George and Table Head groups overlie the Reluctant Head Formation. These make up the main section of the carbonate sequence. The rocks are well exposed along the Trans Canada Highway south of Corner Brook where thick-bedded limestones of the Table Head Group are faulted against other rocks to the west. Limestone breccias (Cape Cormorant Formation) and sandstones (Goose Tickle Formation and equivalents) that occur at the top of the carbonate sequence are absent in the Corner Brook area.

Problematic rocks between the Humber Arm Allochthon and carbonate sequence

The informal Pinchgut group and Whale Back formation constitute a parautochthonous assemblage of carbonates and clastics that are disrupted into an imbricate thrust stack. This structural pile occupies the position of the west Newfoundland carbonate sequence, which is hidden or missing at this locality. Toward the east, the Pinchgut group appears to be thrust against the Mount Musgrave metaclastic sequence. Toward the west it is both overthrust by, and structurally intercalated with, the Irishtown Formation of the Humber Arm Allochthon. Boundaries with the carbonate sequence to the northeast and southwest are high angle faults.

The informal Georges Lake formation lies between the carbonate sequence and the Humber Arm Allochthon in the vicinity of Georges Lake. It extends another 10 km southward along the Trans Canada Highway. Its boundaries with the carbonate sequence and the Humber Arm Allochthon are high angle faults.

The Pinchgut group is a distinctive sequence of thick-bedded to massive limestone breccias, thin-bedded platy limestones, dolostones and shales. It is best exposed in road cuts along the Trans Canada Highway northeast of Pinchgut lake, on forest access roads to the west, and along brooks in the general area. Metamorphosed equivalents are marbles, marble breccias and phyllitic schists in eastern parts of the group. Examples occur along Stag Hill Brook and its southern tributaries.

Interbedded grey limestones and buff-weathering dolomitic shales are common lithologies. Beds are generally less than 10 cm and locally contorted by soft sediment slumping. Green-grey shale bands of similar thickness are interstratified with the carbonate beds.

Limestone breccias occur in beds less than a metre to more than 10 m thick. They contain platy to rounded limestone clasts ranging from pebbles to cobbles and boulders. Most appear to be intraformational. The matrix is dolomitic lime mudstone or shale. Pelletoidal and oolitic grainstones are found locally as equidimensional clasts. Limy grey-green lithic sandstones are interbedded with the carbonate sequence near the top of thrust slices at Southwest Pond and north of Stag Lake.

No macrofossils were seen in the unit and its carbonate rocks are currently being processed for conodonts. Its rock types are similar to those of the Cambrian Reluctant Head Formation and the Weasel group of the Lomond area to the north (Nyman et al., 1984; Williams et al., 1984), although carbonate breccias are much more abundant in the Pinchgut group. Its structural setting between the Humber Arm Allochthon and carbonate terrane is like that of the Weasel group. These correlations suggest that the Pinchgut group is an eastern facies of the carbonate sequence and that it was emplaced originally as a slice at the base of the Humber Arm Allochthon.

Cleaved green-grey sandstones and shales of the Whale Back formation occur in three faulted slivers west of the Trans Canada Highway. Best exposures are in roadcuts and quarries and along the lower reaches of Whale Back Brook. Coarse clastic horizons are feldspatholithic and contain scattered clear angular quartz grains. Chemical analyses of the unit near Pinchgut Lake indicate low silica values and nickel and chromium concentrations (Dean and Meyer, 1985; Paul Dean, personal communication, 1985).

Sandstones and shales of the Whale Back formation resemble Middle Ordovician rocks of the Goose Tickle Formation (Cooper, 1937; Williams, 1985a). The formation may have been deposited therefore at the top of the carbonate sequence in response to the emplacement of the Humber Arm Allochthon. Its present structural setting is the result of a later episode of east-directed thrusting.

The Georges Lake formation consists mainly of dark shales with prominent shaly mélange zones. Intact shales are best exposed along its eastern margin in road cuts and gravel pits of the Trans Canada Highway. Shaly mélanges are best seen along the north shore of Georges Lake. The unit is narrower south of Georges Lake. Its eastern boundary with the carbonate sequence is a high angle fault with clear morphologic expression. Its western faulted boundary has less morphologic expression.

Shales of the Georges Lake formation are dark grey to black, graphitic and pyritic. Light grey and buff-weathering varieties are less common. Dark grey shales with thin brownish-weathering limy siltstone and quartz-rich beds are a common association. A distinctive conglomerate with contorted clasts of intraformational dark grey shale and brown-weathering quartzitic siltstone and a matrix of coarse quartzose greywacke occurs in a gravel pit on the Trans Canada Highway at the south edge of the area.

Chaotic zones vary from sections with slumped beds, to sections with rootless folds, to mélanges with blocks of greywacke, quartzite, thin-bedded shale and limestone, and limestone breccia. Mélange along the north shore of Georges Lake has lozenge-shaped lumps up to 5 m long. The resistent

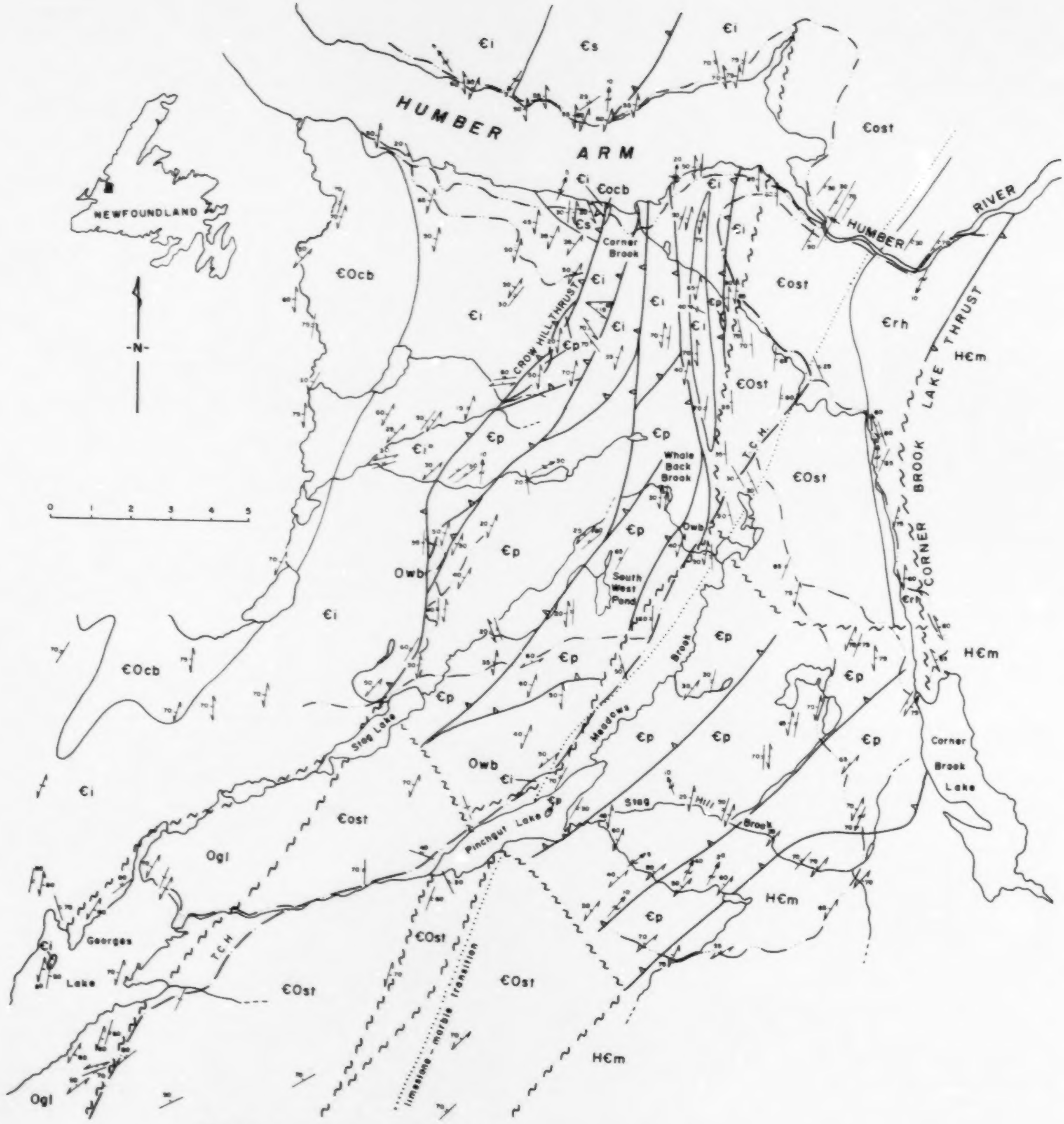

Figure 91.1. General geology of the area between Georges Lake and Corner Brook.

HUMBER ARM ALLOCHTHON

Middle Ordovician

Georges Lake formation

Ogl Dark grey shale with thin beds of buff limy sandstone and buff quartzite, mélange with scaly shale matrix and blocks of grey sandstone, thin bedded limestone and shale, and quartzite.

Middle Cambrian to Lower Ordovician

Cooks Brook Formation

€Ocb Thin bedded grey shale and platy limestone with limestone breccia units.

Lower to Middle Cambrian

Irishtown Formation

€i Dark grey to black shale with thick units of quartzite and local quartz pebble conglomerate. Ci', laminated green shale and thin bedded grey shale with lime mudstone and local quartzite at Watsons Brook. Ci", includes chaotic zones.

Lower Cambrian

Summerside Formation

€s Greywacke and quartz granule to pebble conglomerate, red and green shale.

PARAUTOCHTHONOUS ROCKS

(Pinchgut assemblage)

Middle Ordovician

Whale Back formation

Owb Green micaceous sandstone, siltstone and grey shale.

Cambrian(?)

Pinchgut group

€p Thin bedded limestone and dolomitic mudstone, grey to green shale, pebble to boulder platy limestone breccia; strongly deformed and regionally metamorphosed to greenschist facies in east.

(Carbonate sequence)

Upper Cambrian to Middle Ordovician

St. George and Table Head groups

€Ost Thick bedded grey limestone and dolomite, minor shale

Lower to Middle Cambrian

Reluctant Head Formation

€rh Thin bedded limestone and dolomitic mudstone, grey to green shale and platy limestone breccia.

Hadrynian to Lower Cambrian

Mount Musgrave Group

H€m Quartz mica schist, quartzite, mica schist, slate, minor amphibolite and quartz-feldspar gneiss.

Geological contact, approximate

Thrust fault, approximate

High angle fault, approximate

Bedding, tops known, inclined

Bedding, tops unknown, inclined, vertical

Dominant foliation, inclined

Axis of minor fold with direction of plunge

Roads, Trans Canada Highway, paved highway, woods road

Limestone-marble transition

blocks stand a metre above recessive shales in shoreline exposures. Blocks are a sampling of lithologies like those of the Pinchgut group, and quartzites of the nearby Irishtown Formation.

Dark grey shales, identical to those of the Georges Lake formation, occur conformably above thin- to medium-bedded limestones at the top of the carbonate sequence on the east side of Georges Lake. The preponderance of shale with local intraformational conglomerates along the eastern side of the Georges Lake formation, and mélanges along its western side, suggest a crude internal arrangement of units that bridge the gap from the top of the autochthon to the base of the allochthon. Thus shales along its eastern side may be equivalent to those at the stratigraphic top of the autochthon; associated wildflysch conglomerates are a harbinger to the arrival of the Humber Arm Allochthon; and mélanges toward the west and possible top of the unit result from overriding and emplacement of the allochthon.

Humber Arm Allochthon

Only the Summerside, Irishtown and Cooks Brook formations of the lower structural slices of the Humber Arm Allochthon are exposed in the area.

The Summerside Formation is restricted to a thin wedge that extends across Humber Arm near Corner Brook in the north. The formation consists of coarse quartz greywackes, quartz pebble conglomerates and red and green laminated shales. The formation underlies the Irishtown Formation with its top defined by the highest red shale horizon.

The Irishtown Formation in the western and northern parts of the area consists of dark grey shale with prominent white quartzite units, and local pebble to boulder conglomerates. Shales are laminated with local small scale cross lamination. Most are grey but a green shale unit occurs at the base of the formation, and silvery grey and green shales occur elsewhere. Quartzites are well-sorted, thick-bedded to massive. Conglomerates are well exposed in a large railway cutting at the railway yard of Corner Brook. These are coarse and polymictic with pebbles to large boulders of intraformational shale and quartzite, limestones, and medium- to coarse-grained massive to sheared and pyrophylitized granite. Quartz grains up to 5 cm in diameter occur in the matrix of this conglomerate.

Along Watsons Brook, the Irishtown Formation has laminated light and dark green shale with interbeded grey shale and buff-weathering lime mudstone (Ci' of Fig. 91.1). The Watsons Brook lithologies grade east and west into typical Irishtown grey shales.

In zones of strong deformation, quartzite beds are disrupted into boudins surrounded by dark shale. Examples occur in the city of Corner Brook especially behind the K-Mart shopping plaza. Broken formation that resembles mélange occurs in Big Feeder and Little Feeder Brooks (Ci" of Fig. 91.1).

The Cooks Brook Formation is the youngest unit of the allochthon in the Corner Brook area and consists of thin- to medium-bedded grey shale and limestone with limestone breccia units. It occurs in the axial zone of a regional syncline along the western margin of the area. A thin structural sliver of the formation is caught within the footwall of the Crow Hill Thrust on the south shore of Humber Arm. A conformable contact with the underlying Irishtown Formation is exposed in a road cut at this locality. The contact is marked by the appearance of thin-bedded light grey limestone above a sequence of dark shale. A thin horizon of pebbly limestone breccia occurs 5 m above the base of the formation in this locality.

Structure

The most pronounced structural feature in the Corner Brook area is a moderate to steeply-west-dipping cleavage that is axial planar to easterly-inclined folds. Thrust faults with westerly dips and easterly polarity, such as the Crow Hill Thrust, are related to this phase of deformation. High angle faults are later features.

Structures of eastern polarity in the type area of the Humber Arm Allochthon, which was emplaced from east to west, are enigmatic. These structures were of local concern to early workers (Stevens, 1965; Bruckner, 1966; Lilly, 1967) and they were noted along the east margin of the allochthon farther north (Williams et al., 1982, 1983). Structural styles at Humber Arm have been desrcibed recently by Bosworth (1985) and Waldron (1986). The structures affect the Humber Arm Allochthon and carbonate sequence alike. They therefore postdate the Middle Ordovician emplacement of the allochthon. An upper time limit is more difficult to ascertain.

Examples of easterly-inclined folds with related west-dipping axial-planar cleavage are best seen in roadcuts along the new industrial access between the Trans Canada Highway and Corner Brook. Folds are asymmetric with long shallowly-west-dipping upper limbs and short steep to overturned lower limbs. Axes are horizontal or plunge gently either north or south. Earlier cleavages, predating this phase of folding, are absent. Later folds that are upright to open affect bedding and cleavage. The syncline in the railway yard at Corner Brook is a good example.

Thrust faults vary from outcrop scale to regional features. They parallel the main cleavage with moderate dips. The Crow Hill Thrust is the best known of these features. Where exposed on the north side of Crow Hill, the thrust dips 35° southwestward and displays Summerside greywackes above Irishtown shales. The Irishtown of the footwall is in turn thrust upon a small wedge of Cooks Brook limestone and shale at the top of the section in the successively lower plate. Southward from Corner Brook the course of this fault is marked by slivers of Pinchgut group rocks and it is inferred to extend to Stag Lake.

Thrusts of similar orientation imbricate the Irishtown Formation and are responsible for repetitions of the Pinchgut group and Whale Back formation in the vicinity of Pinchgut Lake. One example east of Stage Lake is well exposed on a former logging road. It dips moderately west and brings limestone breccias of the Pinchgut group above shales and sandstones of the Whale Back formation. Shales are highly sheared in the thrust zone.

In the vicinity of Corner Brook Lake and southwestward, the Pinchgut group appears to structurally overlie metaclastics of the Mount Musgrave Group. The Corner Brook Lake Thrust (Kennedy, 1981) is interpreted as a conventional west-directed structure that is overturned and reoriented by later movements. This view stems from relationships to the north in the Pasadena area (Williams et al., 1982) where the continuation of the Corner Brook Lake Thrust is marked by a mylonite zone at the base of the upper plate overlain by an east-facing section, all overturned. The Corner Brook Lake Thrust is also affected by high angle faulting.

High angle faults postdate folding and thrusting. The omission of the carbonate sequence and the presence of the Pinchgut group are controlled by these vertical movements. High angle faults also juxtapose the Humber Arm Allochthon and carbonate sequence at Corner Brook, and the Georges Lake formation and the carbonate sequence at Georges Lake.

High angle faults in the Stephenville area to the south truncate folds that postdate emplacement of the Humber Arm Allochthon. Stratigraphic evidence there indicates that post emplacement folding and faulting are Devonian. A later generation of faults affect Carboniferous strata.

Structures that postdate the emplacement of the Humber Arm Allochthon have different polarities in different parts of the allochthon. In its northern portion between Bonne Bay and Portland Creek (Williams et al., 1985) and its southern portion between Port au Port Peninsula and Grand Lake (Williams, 1985b), post emplacement structures have westward polarity. In its central parts, structures have westward polarity in the west and eastward polarity in the east (Williams et al, 1982; 1984; Gillespie, 1983; Nyman et al., 1984). These structures, regardless of polarity, are viewed as manifestations of the same compressive stress regime. Logically, their controls originate in the east, or internal parts of the orogen.

References

Bosworth, W.
1985: East-directed imbrication and oblique-slip faulting in the Humber Arm Allochthon of western Newfoundland: structural and tectonic significance; Canadian Journal of Earth Sciences, v. 22, p. 1351-1360.

Bruckner, W.D.
1966: Stratigraphy and structure of west-central Newfoundland. in Guidebook, geology of parts of Atlantic Provinces, ed. W.H. Poole; Geological Association of Canada, Programme and Abstracts, p. 137-155.

Cooper, J.R.
1937: Geology and mineral deposits of the Hare Bay area; Newfoundland Department of Natural Resources, Geology Section, Bulletin 9, 36 p.

Dean, P.L. and Meyer, J.R.
1985: West coast shale projects; in Current Research, ed. K. Brewer, D. Walsh and R.V. Gibbons; Newfoundland Department of Mines and Energy, Mineral Development Division, Report 85-1, p. 74-78.

Gillespie, R.T.
1983: Stratigraphic and structural relationships among rock groups at Old Mans Pond, western Newfoundland; unpublished M.Sc. thesis, Memorial University of Newfoundland, 198 p.

Hibbard, J.P.
1983: Geology of the Baie Verte Peninsula, Newfoundland; Newfoundland Department of Mines and Energy, Mineral Development Division, Memoir 2, 279 p.

Kennedy, D.P.S.
1981: Geology of the Corner Brook Lake area, western Newfoundland; unpublished M.Sc. thesis, Memorial University of Newfoundland, 370 p.

Klappa, C.F., Opalinski, P.R., and James, N.P.
1980: Middle Ordovician Table Head Group of western Newfoundland: a revised stratigraphy; Canadian Journal of Earth Sciences, v. 17, p. 1007-1019.

Lilly, H.D.
1963: Geology of the Hughes Brook-Goose Arm area, west Newfoundland; Memorial University of Newfoundland, Geology Report No. 2, 123 p.

Lilly, H.D. (cont.)
1967: Some notes on stratigraphy and structural style in central west Newfoundland; in Geology of the Atlantic Region ed. E.R.W. Neale and H. Williams; Geological Association of Canada, Special Paper Number 4, p. 201-211.

McKillop, J.H.
1963: Geology of the Corner Brook area, Newfoundland, with emphasis on the carbonate deposits; Memorial University of Newfoundland, Geology Report No. 1, 102 p.

Nyman, M., Quinn, L., Reusch, D.N., and Williams, H.
1984. Geology of the Lomond map area, Newfoundland; in Current Research, Part A, Geological Survey of Canada, Paper 84-1A, p. 157-164.

Riley, G.C.
1957: Red Indian Lake (west half), Newfoundland; Geological Survey of Canada, Map 8-1957.

Schuchert, C. and Dunbar, C.O.
1934: Stratigraphy of western Newfoundland; Geological Society of America, Memoir 1, 123 p.

Stevens, R.K.
1965: The geology of the Humber Arm, west Newfoundland; unpublished M.Sc. thesis, Memorial University of Newfoundland.

1970: Cambro-Ordovician flysch sedimentation and tectonics in west Newfoundland and their possible bearing on a Proto-Atlantic Ocean; in Flysch Sedimentation in North America, ed. J. Lajoie; Geological Association of Canada, Special Paper No. 7, p. 165-177.

Waldron, J.W.F.
1986: Structural history of continental margin sediments beneath the Bay of Islands Ophiolite, Newfoundland; Canadian Journal of Earth Sciences.

Walthier, T.N.
1949: Geology and mineral deposits of the area between Corner Brook and Stephenville, western Newfoundland (Part 1); Geology and mineral deposits of the area between Lewis Hills and Bay St. George, western Newfoundland (Part 11); Newfoundland Geological Survey, Bulletin No. 35, 87 p.

Williams, H.
1975: Structural sucession, nomenclature, and interpretation of transported rocks in western Newfoundland; Canadian Journal of Earth Sciences, v. 12, p. 1874-1894.

1985a: Geology of Gros Morne map area, (12H/12), western Newfoundland; Geological Survey of Canada, Open File 1134.

1985b: Stephenville map area, north half, Newfoundland; Geological Survey of Canada, Map 1579A, scale 1:100 000.

Williams, H., Gillespie, R.T., and Knapp, D.A.
1982: Geology of Pasadena map area, Newfoundland; in Current Research, Part A, Geological Survey of Canada, Paper 82-1A, p. 281-288.

1983: Geology of the Pasadena map area, western Newfoundland; Geological Survey of Canada, Open File 928.

Williams, H., Quinn, L.A., Nyman, M., and Reusch, D.
1984: Geology of the Lomond map area, 12H/5, western Newfoundland; Geological Survey of Canada, Open File 1012.

Williams, H., James, N.P., and Stevens, R.K.
1985: Humber Arm Allochthon and nearby Groups between Bonne Bay and Portland Creek, western Newfoundland; in Current Research, Part A, Geological Survey of Canada, Paper 85-1A, p. 399-406.

SCIENTIFIC AND TECHNICAL NOTES
NOTES SCIENTIFIQUES ET TECHNIQUES

Marine geological program in the Byam Martin Channel — Lougheed Island region, District of Franklin

Project 820050

B. MacLean and G. Vilks
Atlantic Geoscience Centre, Dartmouth

MacLean B. and Vilks, G., Marine geological program in the Byam Martin Channel, Lougheed Island region, District of Franklin; in Current Research, Part A, Geological Survey of Canada, Paper 86-1A, p. 769-774, 1986.

Abstract

A seabed sediment sampling program was carried out through the ice in the Byam Martin Channel – Cameron Island – Lougheed Island region of the Canadian Arctic Archipelago in April and May 1985.

Sampling operations were carried out at 79 stations over a 23 200 km^2 area mainly with a 27 kg gravity corer. Maximum core recovery was approximately 1 m. Grab samples were obtained at 19 stations with a Dietz-Lafonde sampler.

Preliminary results indicate that the upper metre of seabottom sediments consists predominantly of silt or clay with variable amounts of coarser material. Foraminifera in the surface sediments indicate a distinct faunal break at 200 m water depth which is related to water mass characteristics.

Résumé

On a entrepris un programme d'échantillonnage de sédiments marins à travers la glace dans la région du détroit de Byam Martin, de l'île Cameron et de l'île Longheed de l'archipel Arctique, en avril et mai 1985. L'échantillonnage a été effectué dans 79 stations, couvrant une superficie de 23 200 km^2, à l'aide surtout d'un carottier à gravité de 27 kg. La longueur maximale de carotte récupérée a été d'environ 1 m. Des échantillons ont été prélevés au hasard dans 19 stations à l'aide d'un échantillonneur Dietz-Lafonde.

Les résultats préliminaires indiquent que le premier mètre des dédiments du fond marin est principalement constitué de silt ou d'argile qui renferment des quantités variables de matériau plus grossier. La présence de foraminifères dans les sédiments de surface indique une lacune faunique à 200 m de profondeur d'eau, reliée aux caractéristiques de la masse d'eau.

Introduction

During April 11 to May 14, 1985, the Atlantic Geoscience Centre carried out a field program to investigate the surficial geology of the Byam Martin Channel-Lougheed Island offshore region as part of studies of the inter island channels of the Canadian Arctic Archipelago supported by NOGAP (Northern Oil and Gas Action Program). The work consisted primarily of a through-the-ice sediment sampling operation to obtain regional information on the nature, distribution and history of the seafloor sediments in this area. Sampling operations were conducted at 78 stations over a 23 200 km^2 area (Fig. 1; Table 1). These were spaced to provide a regional coverage, as well as to include some bathymetric variations and nearshore areas (Fig. 1). The program was carried out from Panarctic Oils Ltd. Bent Horn camp on Cameron Island by means of a 206L helicopter of Quasar Helicopters Ltd., coordinated by Polar Continental Shelf Project (PCSP).

Methods

Sampling was conducted through 10" (25.4 cm) diameter holes drilled through the ice. Locations of the planned stations were locally adjusted in the field to utilize as favourable (thin) ice as possible, e.g. former leads, and to avoid very thick multiyear ice. Ice thickness at the stations attempted commonly was in the order of 2-2.5 m. Samples were collected mainly with a 60 lb. (27 kg) gravity corer fitted with a plastic liner that also served as a core barrel and modified core cutter and retainer assembly (Fig. 2). Maximum core recovery was approximately 1 m. Grab samples were obtained at 19 stations with a Dietz-Lafonde sampler. The sampling instruments were lowered to the seafloor by means of a tripod and small winch (Fig. 3). Both the sampling winch and the hole cutting augers were electrically driven from a portable 3000 W Honda generator.

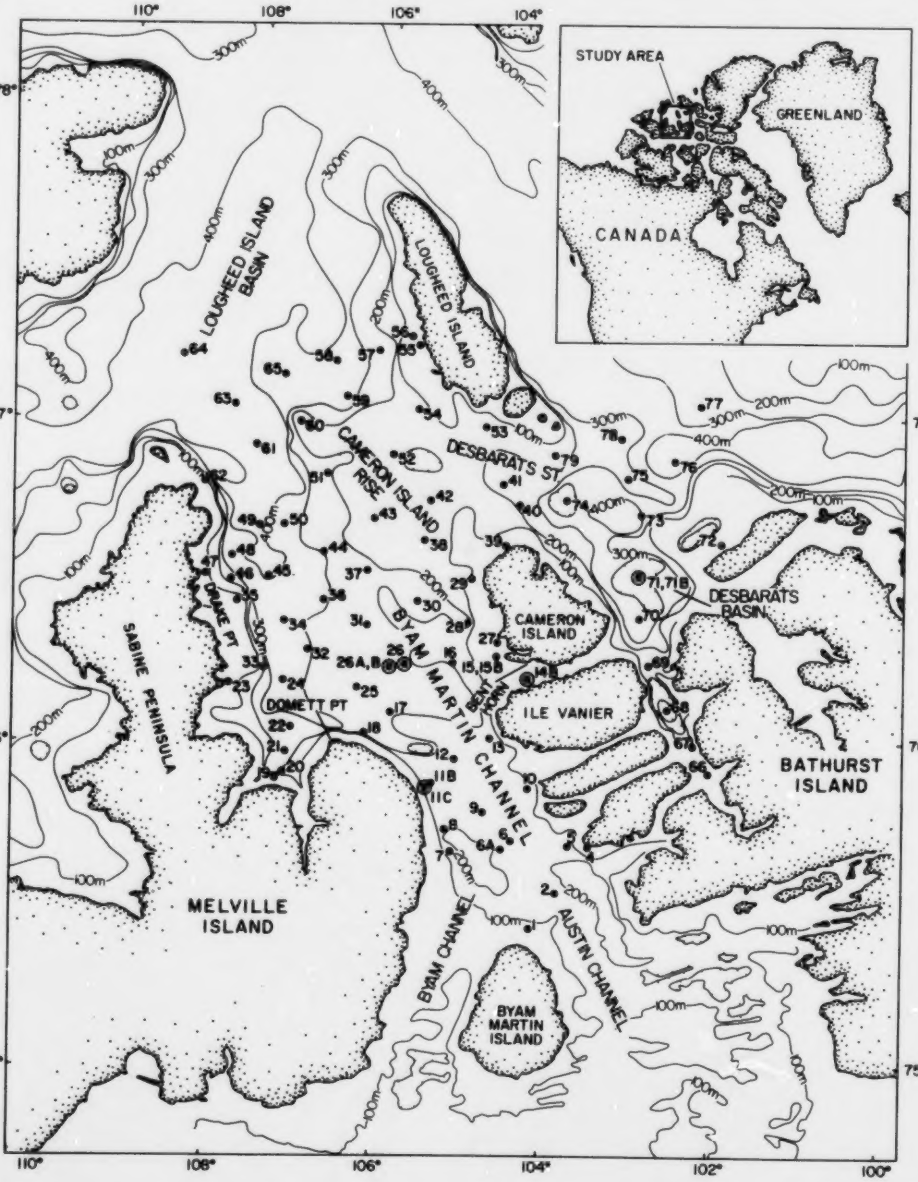

Figure 1. Index map showing sample station locations and general bathymetry. Circled stations indicate 3.5 kHz acoustic data points.

Table 1. 85-100 station data

STATION	LATITUDE	LONGITUDE	WATER DEPTH (Metres)	SAMPLE TYPE	CORE LENGTH (Cm)
1	75.48N	104.10W	99	GRAB	
2	75.59N	103.74W	154	CORE	0
4	75.74N	103.34W	79	GRAB	
5	75.74N	103.57W	129	CORE	53
6	75.76N	104.30W	161	CORE	90
6A	75.73N	104.44W	152	3.5 SEISMICS	
7	75.73N	105.07W	166	GRAB	
7B	75.73N	105.07W	166	CORE	0
8	75.80N	105.13W	247	GRAB	
8B	75.80N	105.13W	247	CORE	0
9	75.85N	104.69W	175	CORE	58
10	75.92N	104.09W	131	CORE	8
11	75.94N	105.33W	185	GRAB	
11B	75.94N	105.33W	185	CORE	0
11C	75.93N	105.38W	185	3.5 SEISMICS	
12	76.01N	105.02W	189	GRAB	
12B	76.01N	105.02W	189	CORE	0
13	76.08N	104.57W	179	CORE	20
14	76.26N	104.07W	40	CORE	76
14B	76.26N	104.07W	40	3.5 SEISMICS	
15	76.33N	104.48W	64	CORE	57
15B	76.33N	104.47W	50	3.5 SEISMICS	
16	76.31N	105.07W	189	CORE	0
17	76.15N	105.88W	236	CORE	46
18	76.09N	106.21W	221	CORE	71
19	75.93N	107.30W	126	CORE	59
20	75.96N	107.22W	140	CORE	58
21	76.02N	107.22W	157	CORE	87
22	76.10N	107.18W	292	CORE	95
23	76.23N	108.02W	35	GRAB	
23B	76.23N	108.02W	35	CORE	46
24	76.24N	107.29W	386	CORE	69
25	76.23N	106.31W	245	CORE	21
26	76.31N	105.71W	217	CORE	50
26B	76.30N	105.91W	245	3.5 SEISMICS	
27	76.38N	104.50W	64	GRAB	
28	76.44N	104.88W	89	GRAB	
29	76.57N	104.85W	69	GRAB	
30	76.50N	105.55W	240	CORE	32
31	76.42N	106.21W	260	*	
32	76.34N	107.00W	296	CORE	29
33	76.28N	107.57W	231	GRAB	
34	76.43N	107.34W	344	CORE	27
35	76.48N	107.95W	79	GRAB	
36	76.50N	106.81W	294	CORE	85

STATION	LATITUDE	LONGITUDE	WATER DEPTH (Metres)	SAMPLE TYPE	CORE LENGTH (Cm)
37	76.59N	106.25W	220	CORE	22
38	76.69N	105.46W	122	CORE	31
39	76.68N	104.37W	61	GRAB	
40	76.80N	104.20W	222	CORE	0
41	76.87N	104.39W	208	CORE	92
42	76.82N	105.40W	172	CORE	83
43	76.75N	106.15W	144	CORE	5
44	76.65N	106.84W	276	CORE	79
45	76.57N	107.56W	386	CORE	53
46	76.55N	108.11W	210	CORE	0
47	76.56N	108.43W	129	GRAB	
48	76.62N	108.09W	333	CORE	25
49	76.73N	107.72W	367	CORE	30
50	76.72N	107.38W	347	CORE	25
51	76.89N	106.82W	197	CORE	14
52	76.96N	105.93W	185	CORE	25
53	77.04N	104.61W	112	CORE	28
54	77.10N	105.58W	162	CORE	75
55	77.30N	105.61W	16	GRAB	
55B	77.30N	105.61W	16	CORE	0
56	77.32N	105.70W	48	CORE	28
57	77.28N	106.16W	252	CORE	
58	77.24N	106.76W	331	CORE	10
59	77.13N	106.62W	241	CORE	27
60	77.05N	107.23W	172	CORE	86
61	76.97N	107.82W	469	CORE	33
62	76.85N	108.52W	151	GRAB	
63	77.09N	108.16W	495	CORE	25
64	77.24N	108.94W	503	CORE	25
65	77.19N	107.46W	134	CORE	9
66	75.95N	101.77W	208	GRAB	
67	76.04N	101.92W	127	GRAB	
67B	76.04N	101.92W	127	CORE	0
68	76.15N	102.27W	386	CORE	100
69	76.30N	102.47W	139	CORE	23
70	76.44N	102.60W	255	CORE	23
71	76.58N	102.58W	460	CORE	70
72	76.66N	101.43W	104	GRAB	
73	76.76N	102.51W	193	CORE	91
74	76.81N	103.54W	301	CORE	52
75	76.88N	102.69W	266	CORE	89
76	76.93N	102.00W	461	CORE	99
77	77.09N	101.59W	237	CORE	35
78	77.00N	102.76W	263	CORE	93
79	76.95N	103.69W	150	*	

* Ice thickness was in excess of 3 metre hole cutting capability.

Figure 2

Photograph showing gravity corer being recovered with a sediment core in the plastic barrel.

Figure 4

X-radiograph of core interval 17-42 cm from station 2 illustrating layering of coarser particles in a sediment consisting predominantly of silt or clay. Random distribution of some coarse particles is also evident.

Figure 5

X-radiograph of core interval 17-42 cm from station 41 illustrating laminated fine sediments which underline mainly unstratified sediments that typically form the immediate seafloor.

Figure 3

Photograph illustrating sample station equipment including tripod, winch, generator, and ice augers. The rear of the 206L helicopter used to transport the equipment and personnel appears on the left of the photo.

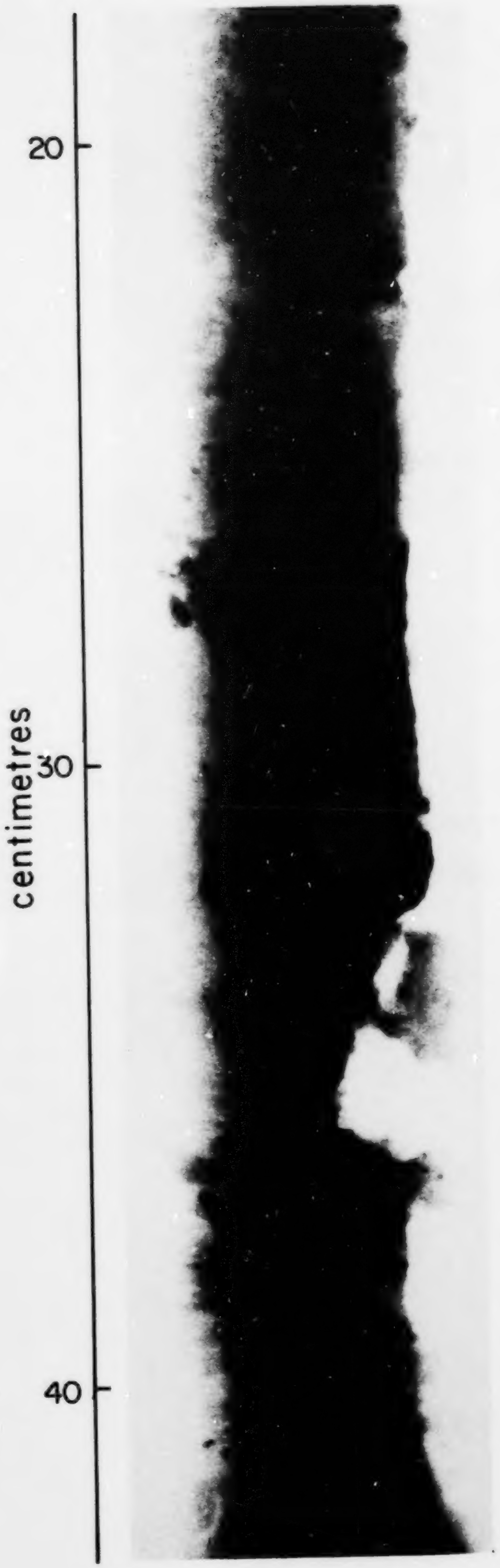

Figure 4

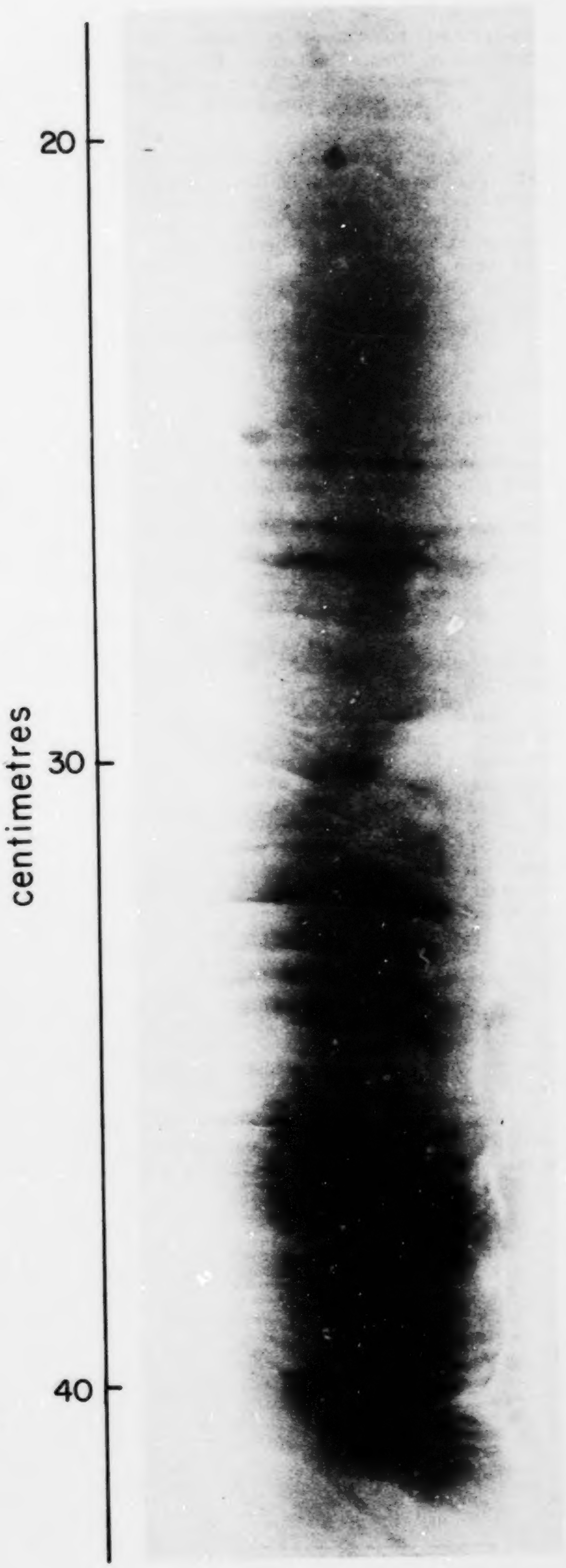

Figure 5

Aircraft navigation and station positioning was accomplished by Global Navigation System (GNS) and satellite navigation. The latter utilized a small onboard unit and an antenna set up on the ice and was used while on station to obtain good quality station positions and to update the GNS.

Acoustic experiments were conducted at six widely scattered localities (Fig. 1) using a single 3.5 transducer lowered through holes in the ice and recorded on a precision graphic recorder. These data suggest an acoustically transparent layer at the immediate seabed that is consistent with the mainly fine textural composition of the sediment samples collected in those areas. Further calibration and evaluation with ground truth information from longer cores and from other towed acoustic systems is required.

Results

Preliminary data from the cores indicate that the uppermost metre of sediments at the sample localities consists predominantly of silt or clay with variable lesser (often minor) amounts of particles in the sand or gravel size range. Where present, the coarser sediments appear to be more prevalent in the upper part of the cores and occur as scattered particles or bands (Fig. 4). Typically the upper 20-30 cm is a brown unstratified sediment underlain bv grey stratified sediments. At a few localities an interval of banded brown and grey sediment has been observed between the upper and lower units. Variations in the silt and clay fractions associated with the banding down core have been observed (Fig. 5).

Foraminifera in surface sediments consist of two different faunal assemblages; an arenaceous assemblage dominated by **Trochammina wana** and a calcareous assemblage dominated by **Cassidulina laevigata** or the planktonic **Neoglobogudrina pachyderma**. The distribution of the two assemblages is governed by water depth and access to the Arctic Ocean. In waters shallower than 200 m and in basins that are not directly connected to the Arctic Ocean with water deeper than 200 m, the sediment contains the arenaceous assemblage, for example, the basins in the southern Byam Martin Channel and the Desbarats Basin. The calcareous assemblage occurs in waters deeper than 200 m, except for the mid-channel Cameron Island Rise that faces the Arctic Ocean and where the calcareous assemblage dominates at waters slightly shallower than 200 m. The calcareous/arenaceous boundary in sediment cores is useful for paleo-water depth and paleo-oceanographic studies in the channels.

The textural composition of the cored sediments and core-top foraminiferal assemblages suggest that deposition of the sediments took place under generally quiet, but somewhat variable and in part possibly cyclical, marine conditions with some input of coarser sediments by ice rafting and possibly also from adjacent land sources.

The preliminary studies of the samples suggest that the sediments throughout much or all of the Byam Martin Channel-Cameron-Lougheed Island region are similar to adjacent areas, e.g. Prince Gustaf Adolf Sea, Hazen and MacLean straits to the north, west and east, previously investigated by Marlow and Vilks, 1963; and Marlow, 1968).

This initial program and preliminary analyses provide basic information on the seabed sediment types and distribution for future programs which will include geotechnical studies. Initial geotechnical analyses will be carried out on the several cores subsequently obtained from CCGS Des Groseilliers in August 1985 (Sonnichsen, 1985) which have been stored and transported under more optimum conditions than was possible during the April – May field program.

Acknowledgments

Financial support for this study was provided by the Northern Oil and Gas Action Program and is gratefully acknowledged. We also wish to thank the following organizations and individuals for their fine cooperation and assistance: Panarctic Oils Ltd., Calgary, K.G. Alexander in particular, and D. Smith and T. MacPike and other members of their staff at Bent Horn; G. Hobson, F. Hunt, B. Hough of Polar Continental Shelf Project and their staff. Special thanks are also extended to pilots J. Feaver and S. Kobayashi of Quasar Helicopters Ltd.; F. Jodrey and D. Locke of Atlantic Geoscience Centre for their excellent support in the field; and to D. Praeg and W. LeBlanc for laboratory support and to D. Piper and H. Josenhans for review of this manuscript.

References

Marlow, J.I.
1968: Sedimentology of the Prince Gustaf Adolf Sea area, District of Franklin; Geological Survey of Canada, Paper 66-29, 53 p.

Marlow, J.I. and Vilks, G.
1963: Marine geology, eastern part of Prince Gustaf Adolf Sea, District of Franklin; Geological Survey of Canada, Paper 63-22, 23 p.

Sonnichsen, G.
1985: Cruise Report – CCGS Des Groseilliers, cruise 85-071, August 16 – August 29, 1985; Atlantic Geoscience Centre, Bedford Institute of Oceanography, Dartmouth, N.S., Internal Report, 8 p.

Geotechnical investigation of seabottom sediments, Tuktoyaktuk area, District of Mackenzie

Project 820038

P.J. Kurfurst
Terrain Sciences Division

Kurfurst, P.J., Geotechnical investigation of seabottom sediments, Tuktoyaktuk area, District of Mackenzie; in Current Research, Part A, Geological Survey of Canada, Paper 86-1A, p. 775-778, 1986.

Abstract

Standard drilling equipment and a seismic cone penetrometer have been used to characterize seabottom sediments. The drilling and geotechnical equipment is described and examples of typical lithological sequences and sounding records obtained are presented.

Résumé

On a utilisé un équipement de forage ordinaire et un pénétromètre sismique conique pour caractériser des sédiments de fond marin. On décrit l'équipement de forage et l'équipement géotechnique et on présente des exemples de séries lithologiques caractéristiques et des enregistrements sismiques obtenus.

Introduction

A two-week experimental drilling and geotechnical testing program was carried out in late March and early April, 1985, in an area of seabottom sediments near Tuktoyaktuk, Northwest Territories. As part of this program, the proposed Polar Gas Pipeline crossing of the East Channel of Mackenzie River at Swimming Point was also drilled and tested. The drilling and sampling operation was handled by Foundex Explorations Ltd., Surrey, British Columbia, and the seismic cone penetrometer tests were performed by the In-situ Testing Group, Department of Civil Engineering, University of British Columbia; the entire program was overseen by personnel from the Regional Geophysics and Geochemistry and Terrain Sciences Divisions of the Geological Survey of Canada.

Equipment

The drill rig used was an HT-700 hydraulic top-drive rotary drill, totally enclosed in an insulated container, which was mounted on a sled for easy transportation. HW size wireline drill casing string, with latching tools, drill bits, and sampling equipment, was used throughout the drilling operation. The casing was advanced while rotating and pumping either water or drilling fluid down the inside of the casing. Shelby tube samples were taken intermittently during the drilling, at 1.5 m intervals and where required by change in lithology. A detailed description of the drilling equipment and techniques is given by Kurfurst (1984).

The geotechnical in situ borehole testing was performed using a research vehicle developed by the Civil Engineering Department, University of British Columbia. A complete description of the vehicle, its capacity, and controls, and full details of the design and operation of the seismic cone are given by Campanella and Robertson (1981). This research vehicle was used to perform seismic cone penetration tests (SCPT) in the seabottom sediments.

A pressure transducer, located inside the cone, measures the pore pressure immediately behind the cone tip. A temperature sensor and a slope sensor are also included in the cone to monitor temperature and verticality during penetration. Small velocity seismometers or accelerometers

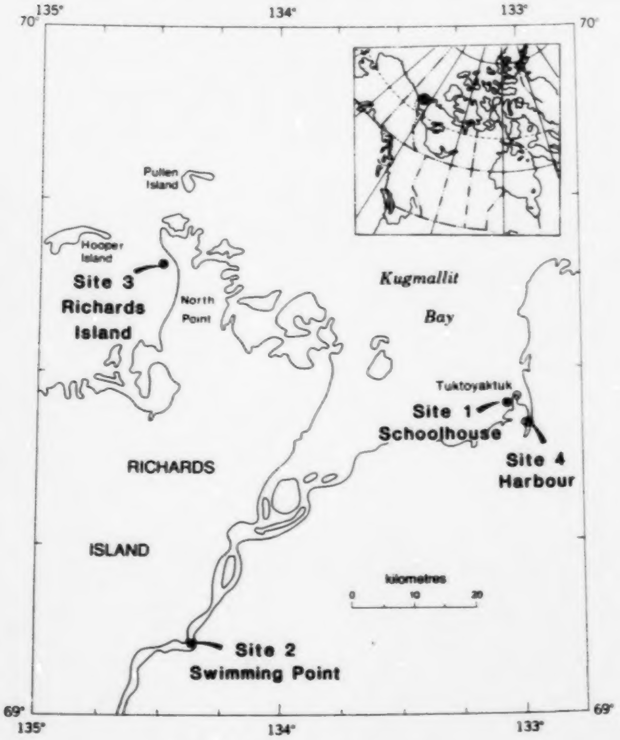

Figure 1. Site location map.

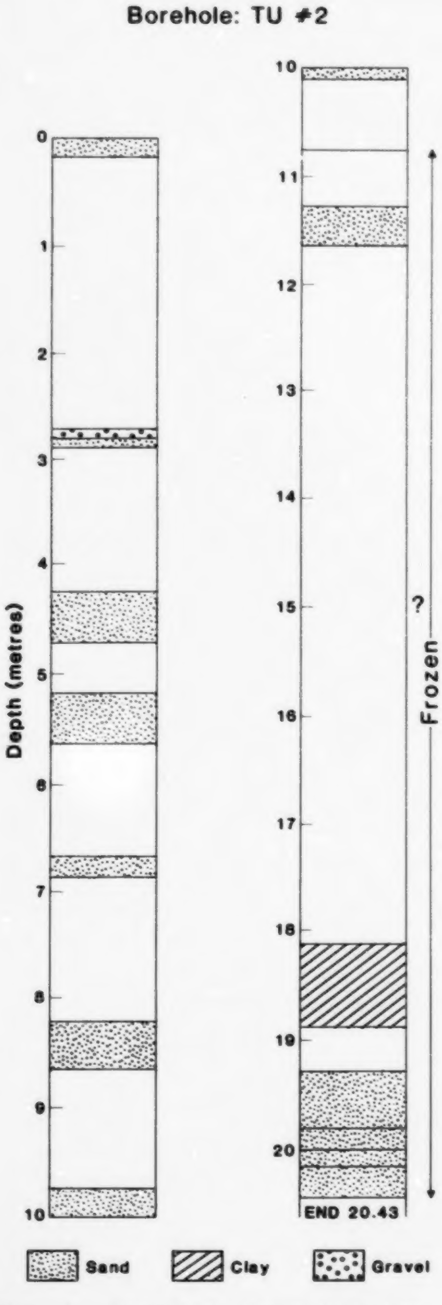

Figure 2. Example of a typical drilling log.

have been incorporated into the cone penetrometer to measure the seismic velocities; the seismic wave traces were observed on a digital oscilloscope and recorded on disk memory.

Several seismic sources were tested to evaluate their effectiveness in the generation of compressional and shear waves. Most commonly used were explosive caps, detonated at various water depths beneath the ice; caps were also placed on the seabottom with either a flat blade or a circular plate device. At locations where the sea ice extended to the seabottom, the seismic signal was generated by striking the rear support pads of the research vehicle with a sledge hammer.

Field Work

The field work was carried out between March 15 and April 3, 1985, at four sites in the Tuktoyaktuk area (Fig. 1). The depth of boreholes ranged from 13 to 30 m; the number of seismic soundings and cone penetration profiles at each site varied from one to five. The thickness of ice was about 2 m and the depth of water ranged from 0 to 5 m.

Site 1, "School house", was located in the nearshore area west of the hamlet of Tuktoyaktuk. Borehole TU-2 was drilled to a depth of 20.43 m through fine sand with interspersed thin layers of clay and gravel. Frozen material was encountered from 10.70 m to the end of borehole. A schematic diagram of the drilling record is shown in Figure 2. Five soundings were performed at this site in the vicinity of the borehole. The record of the measurements is presented in Figure 3.

Site 2, "Swimming Point", was located in East Channel of Mackenzie River, approximately 65 km southwest from Tuktoyaktuk. One borehole about 31 m deep and five soundings were made at this site.

Site 3, "Richards Island", was located in Beluga Bay, west of North Point, Richards Island. Two soundings were carried out in the area where boreholes were drilled during spring 1984 (Kurfurst, 1984).

Site 4, "Harbour", was located within the harbour at Tuktoyaktuk. One borehole was drilled to depth of 13 m and one sounding was carried out at this site.

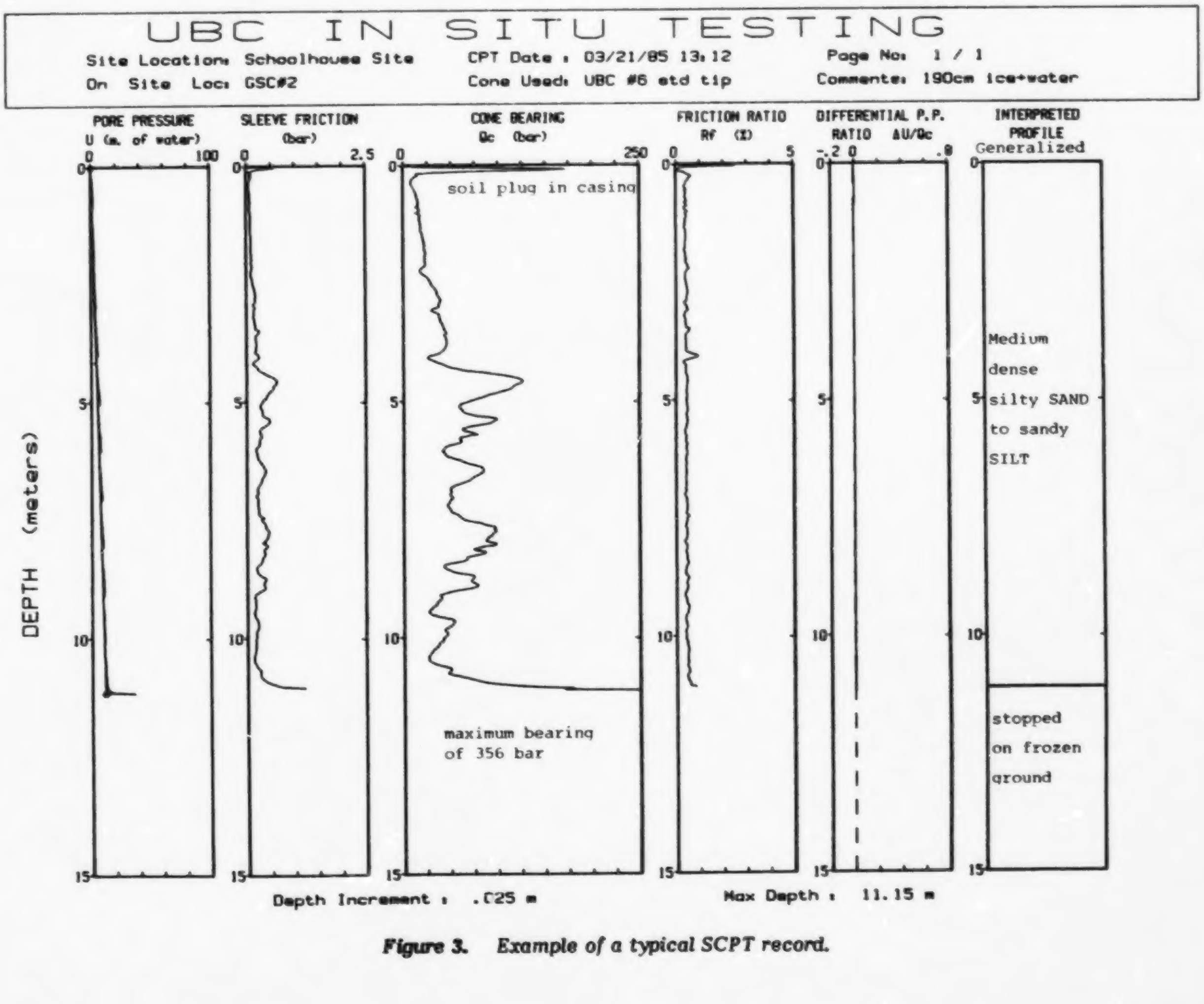

Figure 3. *Example of a typical SCPT record.*

The compilation of the geotechnical results from all sites, including the seismic records and their interpretation, is in progress.

Discussion

The seismic cone penetration test provides rapid continuous stratigraphic information with close vertical resolution. The stratigraphic interpretation is based on a calculated friction ratio, which is obtained by dividing the cone sleeve friction by cone bearing capacity (Fig. 3). Granular soils typically have low friction ratios and high cone resistance, whereas cohesive, fine grained or organic soils have high friction ratios and low cone resistance. Seismic velocities (compressional and shear waves) and temperature are the other parameters that can be measured directly by the seismic cone penetration test. Other geotechnical parameters which can be derived from the SCPT data include equivalent relative density, equivalent friction angle, equivalent Standard Penetration Test blow count, and undrained shear strength.

Detailed evaluation, interpretation, and discussion of the field results are in progress.

The seismic cone penetration equipment worked well in the harsh and cold environment and produced fast and reliable stratigraphic, seismic, and temperature data. It has several limitations, however. The cone will not penetrate coarse (gravelly) or frozen sediments, its performance is highly affected by quality and location of seismic sources, and the quality of the received signal is sometimes poor. Although the problem of penetrating coarse or frozen sediments cannot be eliminated because of the nature of the equipment used, alternate and improved seismic sources, improved types of accelerometers, and the introduction of filters can be expected to improve both the quality of data measured in situ and the derived parameters.

References

Kurfurst, P.J.
1984: Geotechnical investigations in the southern Beaufort Sea, spring 1984; Geological Survey of Canada, Open File 1078.

Campanella, R.G. and Robertson, P.K.
1981: Applied cone research; in Proceedings, Symposium on cone penetration testing and experience; Geotechnical Engineering Division, American Society of Civil Engineers, p. 343-362.

Gold concentrations in till, Great Island, northern Manitoba

Project 800024

L.A. Dredge and E. Nielsen [1]
Terrain Sciences Division

Dredge, L.A. and Nielsen, E., Gold concentrations in till, Great Island, northern Manitoba; in Current Research, Part A, Geological Survey of Canada, Paper 86-1A, p. 779-782, 1986.

Abstract

Gold analyses were run on the fine matrix fraction of till samples which were previously shown to have anomalously high arsenic values. Gold concentrations from 5 to 87 ppb were measured at six sites. Samples with the highest gold contents are underlain by, and probably derive from, the Great Island Group of metasediments and from Seal River volcanics.

Résumé

On a dosé l'or dans la fraction fine du ciment des échantillons de till dont la teneur en arsenic était anormalement élevée. On a trouvé des teneurs en or de 5 à 87 ppb dans six endroits différents. Les échantillons dont les teneurs en or sont les plus élevées reposent sur le groupe métasédimentaire de Great Island et les roches volcaniques de Seal River, qui en seraient la source.

[1] Manitoba Department of Energy and Mines, 535-330 Graham Avenue, Winnipeg, Manitoba R3C 4E3

Gold and arsenic concentrations

Till samples collected during the course of Quaternary geological mapping in northern Manitoba have been previously analyzed for base metals and uranium (Dredge, 1983a,b). The geochemical results from that study, which used the <2 µm fraction of the till matrix, indicated that the surface tills in the general vicinity of Great Island, and as far south as North Knife River (Fig. 1), had arsenic values well above the regional background, which was 6 ppm. One sample with a particularly high arsenic content is from about 5 km east of the eastern tip of Great Island.

Because of the arsenic anomalies, gold analyses have been run subsequently on 26 till samples in the Great Island-North Knife River area. Gold contents (in ppb) were determined by neutron activation techniques using the <63 µm fraction of till. Bondar-Clegg and Co. Ltd. of Ottawa analyzed the samples. Arsenic levels were also retested, using the <63 µm fraction and neutron activation technique. The new values obtained for gold and arsenic are shown in Table 1. The only anomalously high arsenic value on the samples retested lies east of Great Island, and corresponds to the highest gold value obtained (Fig. 2). However, gold values well above the detection limit (5 ppb) were measured at five other sites as well, all of which correspond to sites having high arsenic contents in the <2 µm fraction according to the original analysis.

Bedrock types

The bedrock geology of the area has been mapped by the Manitoba Department of Energy and Mines (Schledewitz, 1977; Fig. 3). The Seal River region, as shown

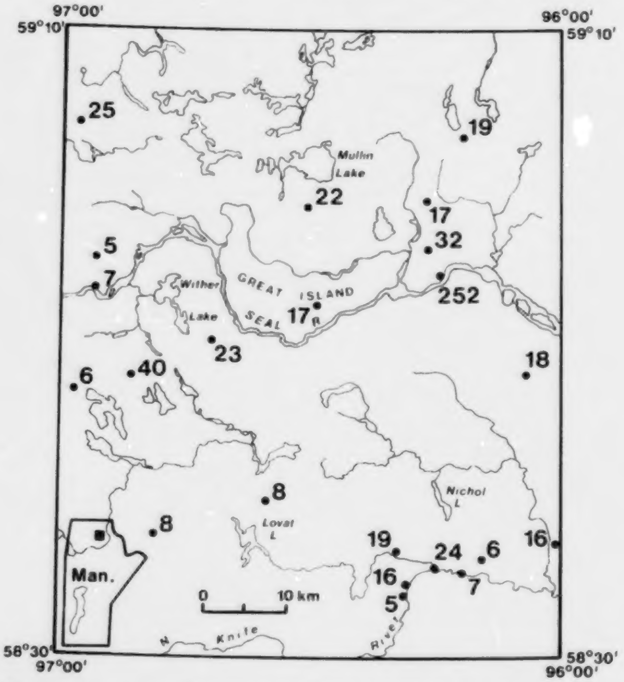

Figure 1. Arsenic concentrations (ppm) in the clay fraction of tills from the Great Island area (from Dredge, 1983b).

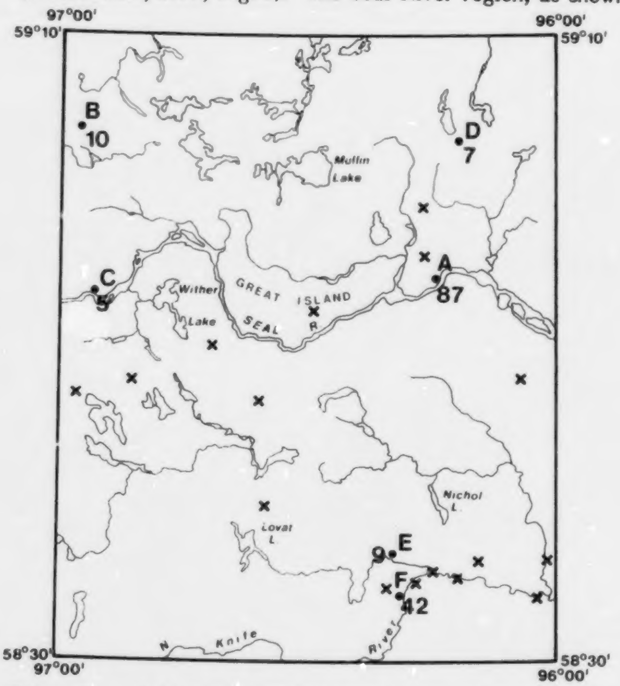

Figure 2. Gold concentrations (ppb) in till. X denotes sites with values less than 5 ppb.

Table 1. Data summary for till samples with gold content above detection limit (5 ppb)

Site	Field No.	Au (ppb)	As (ppm)[1]	As (ppm)[2]	Grain size[3]	Carbonate %	Underlying bedrock
A	311	87	252	122	10/49/38/3	4	quartzite, phyllite
B	379	10	25	8	8/65/24/3	2	pelitic gneiss/ monzonite
C	416	5	7	5	7/62/20/11	3	foliated quartz monzonite
D	350	7	19	2	13/63/20/2	2	tuff, andesite, and dacite
E	259	9	19	7	9/68/20/0	1	quartzite, phyllite
F	494	42	16	8	8/73/12/7	13	quartzite, phyllite

[1] <2 µm fraction, determined by colorimetry
[2] <63 µm fraction, determined by neutron activation
[3] percentage granules/sand/silt/clay

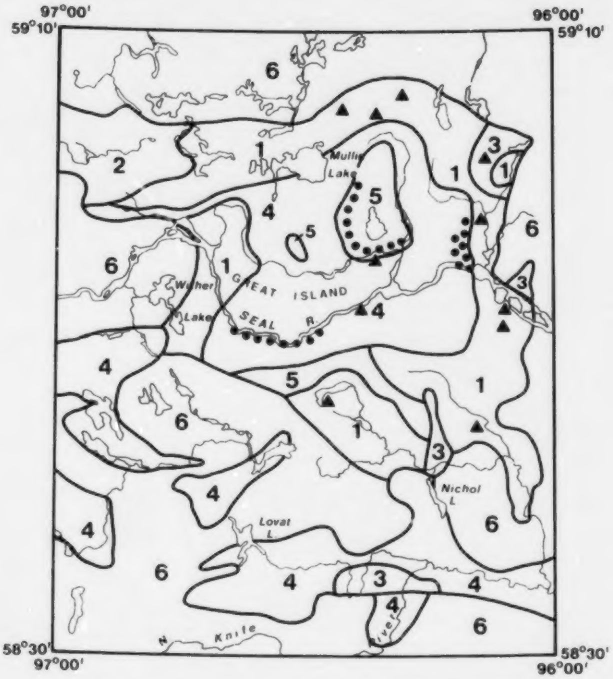

1 = *Seal River volcanic rocks (tuff, andesite, rhyolite and dacite)*
2 = *Semi-pelitic paragneiss*
3 = *Gabbro*
4 = *Great Island Group (quartzite and interlayered phyllite and schist)*
5 = *Great Island Group (conglomerate, dolomite, iron formation, greywacke, siltstone). Iron formation is denoted by rows of dots*
6 = *Quartz monzonite, minor granodiorite. Triangles give locations of sulphide showings.*

Figure 3. *Bedrock types (after Schledewitz, 1977).*

in Figure 3, is extensively underlain by volcanic and younger metasedimentary rocks, both of Proterozoic age. Most of the gold sites lie on these rock types. The Seal River volcanic rocks (e.g., site D, Fig. 3) consist of tuff, pillowed andesite, rhyolite, dacite, and related conglomerates, all of which have been intruded by gabbro stocks. Associated semi-pelitic gneisses underlie site B. Gabbro and quartzite-derived gneisses, which may belong to the Great Island Group, outcrop in the North Knife River area. Interlayered sequences of quartzite and andalusite-bearing phyllite underlie sites E and F. Sections of bedrock exposed along river banks near site F are intensely weathered. Site A also lies within the Great Island Group of metasediments, which includes quartzite, metadolomite, iron formation, argillite, and greywacke. Rocks in the vicinity of site A are chiefly interlayered sequences of quartzite, phyllite, and mica schist. Schistose iron formations outcrop nearby along Seal River and form an arc south of Meades Lake. Intrusive rocks, chiefly quartz monzonite (site C), form part of a batholithic body which surrounds the volcanics and metasediments. Schledewitz (1977) has reported pyrite, pyrrhotite, and chalcopyrite in the area (Fig. 3).

Glacial deposits and ice flow

The bedrock in the Seal River region is mantled by extensive glacial deposits and muskeg. The principal glacial deposits of this region are the sandy till blanket, which covers most of the region, and the network of eskers which trend in a south-southeasterly direction (Dredge et al., in press; Fig. 4). A veneer of marine sand covers some areas of till which lie below an elevation of 180 m. Silty till outcrops along North Knife River and interfingers with the sandier till there.

The six samples with measurable gold in the fine fraction are all from sandy till of northern provenance. Striations and streamlined glacial bedforms indicate that ice flow during the late Wisconsin maximum was towards the southwest and south-southeast. The strike of eskers suggests that ice flow during deglaciation was towards the south-southeast. The sample from site F, on North Knife River, was taken from the uppermost sheet of sandy till and is presumed to be of northern provenance, although most till exposed along the river is silty textured and has an eastern provenance. It is not known how far the till was transported before being deposited. Some of the samples came from compact structureless (basal?) till, whereas others are from looser tills with syngenetic bedding and are more likely ablation deposits. A study of garnet transport in similar tills to the west of the Great Island area indicated that most sand-sized debris moved less than 5 km down-ice from the source outcrops (Dredge, 1981). The till at site E, however, has a high percentage of volcanics in the pebble fraction. If the site E till derives from the volcanic bedrock to the north, then the fine fraction has possibly been transported as much as 15 km.

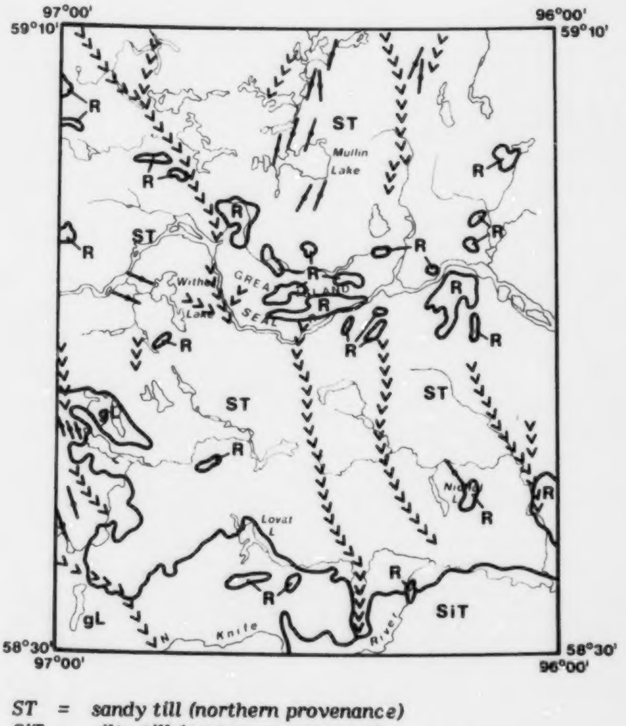

ST = sandy till (northern provenance)
SiT = silty till (eastern provenance)
gL = glaciolacustrine silts
R = rock outcrop
<<<< *Esker*
Streamlined glacial bedforms

Figure 4. *Surface materials (after Dredge et al., in press, Map 1608A).*

Comments

This report presents gold results from widely scattered till samples taken from the Great Island area. The till at site A yielded highest gold levels and lies within an area underlain by Proterozoic volcanic and metasedimentary rocks. The rocks, tills, and adjacent fluvial deposits in that general vicinity may be worth further investigation. Because of the scattering of gold showings over related rock types in other parts of the area, additional sampling on a denser grid than was used for the reconnaissance mapping may be useful.

References

Dredge, L.A.

1981: Trace elements in till and esker sediments in northwestern Manitoba; in Current Research, Part A, Geological Survey of Canada, Paper 81-1A, p. 377-381.

Dredge, L.A. (cont.)

1983a: Uranium and base metal concentrations in till samples from northern Manitoba; in Current Research, Part B, Geological Survey of Canada, Paper 83-1B, p. 303-307.

1983b: Uranium and base metal concentrations in till, northern Manitoba; Geological Survey of Canada, Open File 931 (11 maps).

Dredge, L.A., Nixon, F.M., and Richardson, R.J.

– Quaternary geology and geomorphology, northwestern Manitoba; Geological Survey of Canada, Memoir 418, Map 1608A. (in press)

Schledewitz, D.C.P.

1977: The Seal River area; Manitoba Mineral Resources Division, Open File Report 77-3, Maps 1977 S-1, S-2.

Notes on the geomorphology and Quaternary geology of northeastern Ungava Peninsula, Nouveau Québec

D.A. St-Onge and J.S. Scott
Terrain Sciences Division

St-Onge, D.A. and Scott, J.S., Notes on the geomorphology and Quaternary geology of northeastern Ungava Peninsula, Nouveau Québec; in Current Research, Part A, Geological Survey of Canada, Paper 86-1A, p. 783-785, 1986.

Abstract

Broad upland surfaces carved by wide shallow valleys suggest a mature preglacial landscape resulting from subaerial evolution during long periods of geological time. The history of these surfaces has not been studied, leaving long gaps in the geological history of the region. Glaciers later polished the rock surfaces leaving a generally thin veneer of drift, usually in the form of boulder fields. During deglaciation higher level glacial lakes occupied numerous depressions but, apparently, no extensive proglacial lakes occupied the area. Present geomorphic processes, such as solifluction and frost heave, contribute to landscape development but these processes have not significantly altered the pre-Quaternary landscape.

Résumé

De vastes surfaces de haute-terre, ravinées par de larges vallées peu profondes, indiquent l'existence d'un paysage pré-glaciaire parvenu à maturité, résultant d'une évolution sub-aérienne pendant de longues périodes géologiques. L'histoire de ces surfaces n'a pas été étudiée de sorte qu'il reste de grandes lacunes dans l'histoire géologique de la région. Plus tard, les glaciers ont poli les surfaces rocheuses, y laissant une couche de dépôts glaciaires généralement mince, habituellement sous forme de champs de blocs émoussés. Lors de la déglaciation, des lacs glaciaires, de niveau plus élevé, ont occupé de nombreuses dépressions, mais il semble qu'il n'y ait pas eu de grands lacs proglaciaires dans la région. Des processus géomorphologiques, comme la solifluxion et le soulèvement par le gel, contribuent actuellement à l'évolution du paysage, mais ils ont très peu modifié le paysage pré-Quaternaire.

Introduction

Little is known about the geomorphology and surficial geology of the Ungava Peninsula region of Nouveau Québec (Gangloff et al., 1976).

The authors took advantage of a Precambrian Geology Division field camp south of Kangiqsujuaq (Wakeham Bay) (Fig. 1) to carry out a preliminary survey in order to evaluate the requirements for Quaternary geology studies in this region. Although mechanical problems with a chartered helicopter resulted in a less extensive survey than originally planned, some significant preliminary results were obtained.

Preglacial landscape

As pointed out by Bird (1967, p. 59-60) little is known of the origin and age of the extensive upland of Nouveau Québec except that it "is an elevated peneplain" with broad areas lying between 460 and 600 m elevation, and that it includes "exhumed surfaces of sub-Paleozoic, sub-Proterozoic and possibly even an earlier age" (Bird, 1967, p. 60).

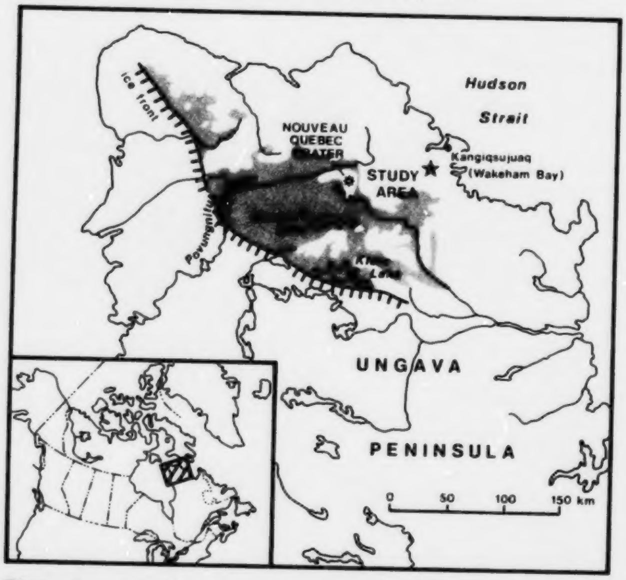

Figure 1. Location map showing the assumed glacial lake (shaded) as shown on the Glacial Map of Canada (Prest et al., 1968). Field camp location is shown by a star.

There is no doubt that this landscape of rolling uplands with accordant summit heights, broad valleys, and generally thin drift cover is preglacial in origin. Certainly subaerial denudation must have extended over long periods of geological time. Although no recent work has been done on the origin and age of these surfaces, the detailed topographic information required to reconstruct the surfaces is now available. This, joined with the now better known geological and tectonic history of surrounding sedimentary basins, should make it possible to construct a reasonably well documented history of the landscape.

Glacial landscape

The Glacial Map of Canada (Prest et al., 1968) shows a large glacial lake basin in the north-central part of Ungava Peninsula. This proglacial lake, covering the upper reaches of Povungnituk River and the present Nantais Lake (Fig. 1), was presumed to have been confined by ice to the southwest and by highlands to the northeast. Discussions with Prest indicate that the former presence of this lake was surmised from the study of airphoto mosaics which suggested the presence of extensive washed zones.

Detailed studies of aerial photographs reveal no substantial accumulation of unconsolidated sediments which could be related to a former lake level. This observation was also confirmed by bedrock geologists working in the area. The lack of fine sediments and the lack of high level deltas suggest there may never have been an extensive lake in this region. The 'washed zones' would appear to be a result of bedrock properties, particularly horizontal cleavages, which result in small benches being formed on the side of hills; these, particularly on airphoto mosaics, could easily be mistaken for former water planes or short lived beaches. There is evidence, however, for higher water levels along the valley sides of present lakes as pointed out by Taylor (1982, p. 4), particularly along the bedrock valley now occupied by Nantais Lake. It is likely that these terraces of apparently coarse material result from sedimentation at the margin of a stagnant ice mass which occupied the lowlands. Similar landforms and deposits are found above several unnamed lakes to the east of Nouveau Québec Crater. A systematic airphoto analysis of this region could likely yield a pattern that would help in defining phases in deglaciation.

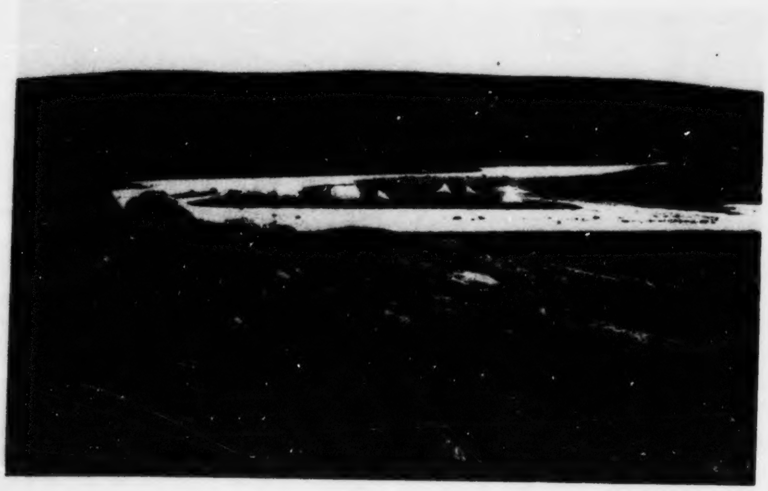

Figure 2

Erratic boulders on a bedrock surface in the vicinity of the field camp site.

Postglacial landscape

The whole region is mantled by a thin cover of drift, commonly in the form of a boulder field resting on a glacially polished bedrock surface (Fig. 2). Most of the boulders appear to be glacially transported erratics but, near ridge summits, frost heaved bedrock suggests that a felsenmeer is slowly developing. Solifluction is active in limited areas such as below perennial snowbanks where moisture and fines combine to make the material fluid. Even then this activity is relatively insignificant as demonstrated by the large number of bedrock outcrops which remain bare in spite of the existence of solifluction lobes above and below.

Accumulations of any substantial thickness of glacial and postglacial sediments are confined to the lower reaches of the main rivers draining into fiord valleys which indent the Ungava Bay coast. In such localities terraces formed from deltaic and deeper water sediments, as a result of postglacial isostatic rebound, should be examined to document the chronostratigraphy of the area since ice retreat. This would be important in attempting to model the history of the Laurentide Ice Sheet in the crucial Hudson Strait region (Dyke et al., 1982).

Conclusions

Our brief study raises more questions than it answers but it strongly suggests that an extensive glacial lake was not a feature in the deglaciation of the area. It highlights the need for a better understanding of the long history of the landscape of this region, and particularly for the late Quaternary, because of its bearing on the construction of deglaciation models for the Laurentide Ice Sheet.

References

Bird, J.B.
1967: The Physiography of Arctic Canada; John Hopkins Press, Baltimore, 336 p.

Dyke, A.S., Dredge, L.A., and Vincent, J.-S.
1982: Configuration and dynamics of the Laurentide Ice Sheet during the Late Wisconsin maximum; Géographie physique et Quaternaire, v. 36, p. 5-14.

Gangloff, P., Gray, J.T., et Hillaire-Marcel, C.
1976: Reconnaissance géomorphique sur la côte ouest de la baie d'Ungava, Nouveau-Québec; Revue de Géographie de Montréal, vol. 30, p. 339-348.

Prest, V.K., Grant, D.R., and Rampton, V.N.
1968: Glacial Map of Canada; Geological Survey of Canada, Map 1253A.

Taylor, F.C.
1982: Reconnaissance geology of a part of the Canadian Shield, northern Quebec and Northwest Territories; Geological Survey of Canada, Memoir 399, 32 p.

Felsic volcanic rocks in the Nonacho Group near Whitefish Lake, District of Mackenzie

Project 770055

S.M. Roscoe
Economic Geology and Mineralogy Division

Roscoe, S.M., Felsic volcanic rocks in the Nonacho Group near Whitefish Lake, District of Mackenzie; in Current Research, Part A, Geological Survey of Canada, Paper 86-1A, p. 787-789, 1986.

Abstract

Previously unrecognized phyric felsic volcanic rocks form a core up to 3.5 km wide and 35 km long, within a belt of sheared, but little metamorphosed, steeply dipping strata that extends 60 km southwesterly from the northwest arm of Whitefish Lake (62°25'N, 107°03'W) to Tent Lake within gneisses of the Churchill Province. Arkose and conglomerate along the south flank of the volcanic section and laminated siltstone at Tent Lake are similar to rocks that comprise the main belts of Nonacho Group strata to the southwest.

Résumé

Des volcanites felsique, preablement non reconnues, forment un noyeau atteignant 3.5 km, dans une ceinture de roche cisaillees mais faiblement meiamorphisees qui s'etend sur 60 km vers le sud-ouest du bras nord-ouest du lac Whitefish (62°25'N, 107°03'W) jusqu'au lac Tent dans les gneisses de la province de Churchill. Les arkoses et conglomerats formant le flank sud de la succession volcanique et les microgres lamines au lac Tent ressemblent aux roche qui forment les principales ceintures du group Nonacho au sud-ouest.

Introduction

A double pronged belt of strata correlated with the Nonacho Group is shown on Geological Survey of Canada Map 1216A (Wright, 1967) as extending 60 km southwesterly from the northwestern arm of Whitefish Lake (62°25'N, 107°03'W) to Tent Lake (Fig. 1) (75J/11). The two limbs of the belt are shown as flanked and separated by granitic gneiss. Wright noted only sedimentary rocks within the belt, but in 1984 the writer and R.F.J. Scoates found that felsic volcanic rocks were also present. In 1985, the writer and S.S. Gandhi discovered a zone of felsic volcanic rocks 3.5 km wide at Catholic Lake between the two limbs outlined by Wright. Minor bodies of probable Nonacho volcanic rocks have been mapped 50 km southwest of Tent Lake (Wright, 1952 and Geological Survey of Canada, 1968); however, the occurrences in the Whitefish belt are especially noteworthy because they may comprise the bulk of the strata in much of this belt, which represent the most northeasterly of the many widespread occurrences of rocks believed to be correlative with the Nonacho Group.

It was not possible, in the brief periods available for work in the area, to map or study the volcanic rocks and their relationships to other rocks. On four separate days, however, the writer together with Scoates or Gandhi, or assisted by A.K. Stordy, made some revelant observations in ten localities along the belt as outlined in this report.

Field observations

The general outline of the Whitefish belt as shown on Map 1216A (Wright, 1967) is illustrated in Figure 1. At locality 5, thin patches of sheared arkosic grit and polymict conglomerate containing flattened and elongated clasts of granite occur along the north-facing wall of a steep scarp, mainly in slump blocks and talus. Highly sheared sericitic rocks along the scarp grade southward into massive 'granite' and possibly represent paleosol. Bedrock exposures are lacking below the scarp but northward across a valley about 50 m wide they are plentiful through a cross-strike distance of about 200 m. The rocks are grey to pink and contain abundant to sparse grains of feldspar and quartz in a fine grained matrix which in some cases may have been tectonically milled and recrystallized. Sericite or chlorite and cleavage are developed locally. Steeply-dipping, compositionally varied layers, 10 cm to 1 m or more thick, are conspicuous in some outcrops, particularly southerly ones. Dark fiamme-like lenses and also fine laminae were noted locally. A small outcrop a few kilometres to the northeast at the shore of Whitefish Lake consists of fine grained mylonitic rock. Farther northeast (locality 10) near Zucker Lake sheared fragmental rock, probably conglomerate, is bordered by mylonitized granitoid gneiss. This occurrence suggests that belts of Nonacho rocks may extend farther northeast than previously realized.

Sheared conglomerate with subhorizontally stretched clasts is exposed in outcrops at locality 4 and at Catholic Lake (locality 3). Gritty feldspathic rock with steeply-dipping foliation at locality 2 on Catholic Lake was interpreted to be arkose. Similar, but less sheared, rocks were observed in extensive outcrops at locality 9. These include quartz and feldspar phyric, layered and massive varieties, like rocks at locality 5. Foliation was observed to truncate layering and laminations locally. The rocks are considered to be of volcanic and volcaniclastic origin and may include minor subvolcanic intrusions. Weak radioactivity was noted in this area and a grid outlined by small rock cairnes indicates that some prospecting was done here.

In a bay on the northeast side of Tent Lake (locality 6), steeply-dipping laminated and massive grey siltstones are well exposed on numerous large and small islands across a width of 1.5 km. No facing directions were discerned. Two sets of crenulations are present, one with axes dipping gently northeast, the other with axes pitching gently southwest. These indicate that deformation of the beds involved strain in the sense of northwest side up relative to the southeast side. Protomylonitic granite and augen gneiss outcrop on the north side of the bay. Relatively undeformed granite outcrops on islands southwest of the siltstone exposures and also along the southwest shore of the lake at locality 8, excepting along a narrow bay where there is a band of highly sheared rocks that includes probable conglomerate and arkose. A body of massive monzonite forms a prominent hill at the point of the lake (locality 7).

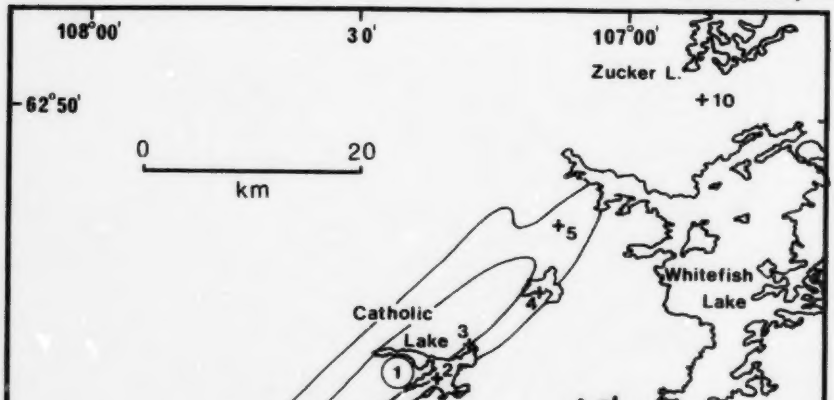

Figure 1

Outline of Whitefish Lake-Tent Lake belt of Nanacho Group as shown on Geological Survey of Canada Map 1216A, and locations of outcrop areas described in text.

The most interesting outcrop area examined is that along the south side of the west arm of Catholic Lake (locality 1) where a section of steeply-dipping phyric rhyolitic rocks extends about 3.5 km across most of the area between the two limbs of Nonacho sedimentary rocks that are shown on Map 1216A. Compositionally varied beds or flows are up to several metres thick and internal laminae are clearly discernible in some units. In places the strata show gradual or abrupt changes in strike, or are displaced by minor faults. Thin mafic flows or sills are present. Some relatively coarse porphyries may be intrusions. A large sample of quartz-feldspar porphyry near the northwest end of the section was taken for geochronological work. Thin chert layers are present in thinly bedded tuffs in the central part of the section, several containing very minor amounts of pyrite. A sample of one of these was analyzed for gold (Bondar Clegg & Co. Ltd.) and found to contain less than 1 ppb.

Discussion

The Whitefish Lake belt of Nonacho rocks appears to be composed mainly of a thick section of volcanic rocks overlying a thin layer of basal conglomerate and arkose. The absence of volcanic rocks at the southwestern end of the belt may be the result of faulting although there is no direct evidence of this. The extent of siltstones along the northwest edge of the belt is presently unknown and may be difficult to determine due to scarcity of outcrops. The Jones Lake Nonacho belt 12 to 41 km southwest of the Whitefish belt is composed almost entirely of slate and greywacke and is up to 6 km wide as shown on Map 1123A (Geological Survey of Canada, 1968). The two belts, separated by only 10 km, are likely structurally dismembered parts of a single basin the northeast part of which was filled with volcanic deposits and the southwest part with fine grained clastic sediments that may have been derived largely from volcanic ash and deposited in standing water dammed by volcanic rocks.

The Nonacho rocks as well as older gneisses are intensely sheared and in places mylonitized particularly along the north side of the Whitefish belt which is likely fault bounded. Disruptions of features shown on aeromagnetic maps (e.g. Geological Survey of Canada, 1981), together with topographic lineaments, reveal the existence of an important fault that strikes eastward from the McDonald Fault near Snowdrift to Tent Lake (Reinhardt, 1969). It transects northeasterly-trending magnetic trends displacing them dextrally. The fault curves northeasterly near Tent Lake and borders part of the northwest side of the Jones Lake belt. It probably converges at Tent Lake with a fault that borders the southeast of the Jones Lake belt and the northwest side of the Whitefish belt. The abrupt termination of the thick siltstone section at Tent Lake may be due to displacement at a branch of this fault system.

Wright (1967) noted that the strata in the Whitefish belt "appear to form a southwesterly plunging syncline". The discovery of volcanic strata rather than older granitic rocks and gneiss between the two previously mapped forks of the belt provides credibility for this idea. On the other hand, no repetitions of lithologies have been noted across the belt; nor was any evidence noted for a fold axis within bedded volcanic rocks in the central part. It seems likely therefore that the belt is homoclinal.

References

Geological Survey of Canada

1968: Geology, Reliance, District of Mackenzie; Geological Survey of Canada, Map 1123A.

1981: Magnetic Anomaly Map of Lockhart River, Northwest Territories; Geological Survey of Canada, Map 1566A.

Reinhardt, W.

1969: Geology of the Precambrian rocks of Thubin Lakes map-area in relationship to the McDonald Fault System, District of Mackenzie; Geological Survey of Canada, Paper 67-31.

Wright, G.M.

1952: Reliance, Northwest Territories; Geological Survey of Canada, Paper 51-26.

1967: Geology of the southeastern barren grounds, parts of the Districts of Mackenzie and Keewatin; Geological Survey of Canada, Memoir 350.

Efficient algorithms for computing the gravitational effect of rectangular prisms

Project 730081

K.G. Shih and Ron Macnab
Atlantic Geoscience Centre, Dartmouth

Shih, K.G. and Macnab, R., Efficient algorithms for computing the gravitational effect of rectangular prisms; in Current Research, Part A, Geological Survey of Canada, Paper 86-1A, p. 791-794, 1986.

Abstract

The reduction and interpretation of gravity data often calls for the repetitive calculation of the gravitational effects of rectangular prism. The exact expression for this effect is long and complex, and its implementation on a digital computer can consume a considerable amount of central processor time when large or complicated models are involved.

This note reviews the derivation of the rectangular prism formula, and describes shortcuts in its computer implementation that can achieve significant reductions in processing time with no degradation in accuracy.

Résumé

La réduction et l'interprétation des données gravimétriques exigent souvent le calcul répété des effets de gravitation d'un prisme rectangulaire. L'expression exacte de cet effet est longue et complexe; son calcul sur un ordinateur numérique peut exiger un temps extrêmement long de l'unité centrale lorsqu'il s'agit de grands modèles ou de modèles compliqués.

Dans cette note, on développe la formule du prisme rectangulaire et on décrit des raccourcis à prendre pour l'appliquer sur l'ordinateur et économiser beaccup de temps de traitement sans perte de précision.

Introduction

The equation for the gravity effect due to a rectangular prism has been derived and described by several authors (e.g. Grant and West, 1965; Nagy, 1966 and 1980; Talwani, 1973). The derivation involves the solution of a triple integral; the exact form of this integral does not appear in standard integral tables, however detailed descriptions of the solution procedures may be found in the literature.

The purpose of this note is twofold: a review briefly techniques for solving the triple integral, and to discuss some practical aspects of implementing this solution efficiently in a computer program.

Solution of the triple integral

From potential field theory, the vertical component of the gravitational effect of a rectangular prism (Fig. 1) can be expressed as:

$$g(0,0,0) = -G\rho \int_{x_1}^{x_2} \int_{y_1}^{y_2} \int_{z_1}^{z_2} \frac{z\,dx\,dy\,dz}{r^3} \qquad (1)$$

where $r = (x^2 + y^2 + z^2)^{1/2}$

For a gravitational constant $G = 6.6723 \frac{cm^3\ mgal}{g\ km}$, the attraction g will be expressed in milligals when X, Y and Z coordinates are in kilometres, and the density ρ is in grams per cubic centimetre.

Equation (1) can be decomposed into simpler integrals of the form:

$$\int \frac{du}{(a^2 + u^2)^{3/2}} = \frac{u}{a^2(a^2 + u^2)^{1/2}}$$

and

$$\int \frac{u\,du}{(a^2 + u^2)^{3/2}} = -\frac{1}{(a^2 + u^2)^{1/2}}$$

and then partially solved for X, Y or Z to yield:

$$g(0,0,0) = G\rho \int_{x_1}^{x_2} \ln(y + r) \Big|_{z_1}^{z_2} \Big|_{y_1}^{y_2} dx \qquad (2)$$

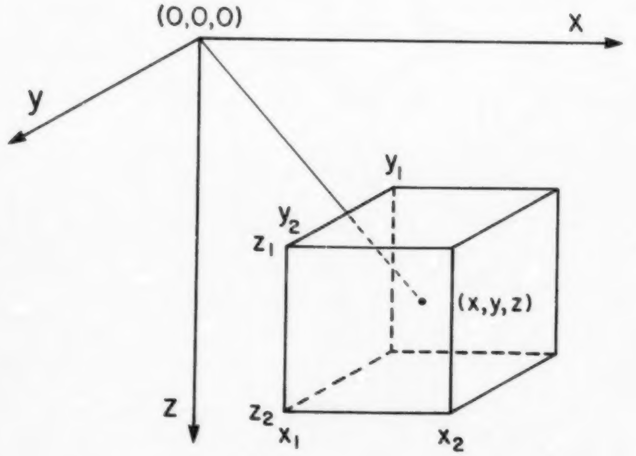

***Figure 1.** Coordinates of a rectangular prism.*

$$g(0,0,0) = G\rho \int_{y_1}^{y_2} \ln(x + r) \Big|_{z_1}^{z_2} \Big|_{x_1}^{x_2} dy \qquad (3)$$

$$g(0,0,0) = G\rho \int_{z_1}^{z_2} \tan^{-1}\left(\frac{xy}{rz}\right) \Big|_{x_1}^{x_2} \Big|_{y_1}^{y_2} dz \qquad (4)$$

A solution for (2) may be effected by substitution of the following:

$$\int \ln(y + r)dx = x \ln(y + r) + y \ln(x + r) - z \tan^{-1}\left(\frac{xy}{zr}\right) + x - \tan^{-1}\left(\frac{x}{z}\right) \qquad (5)$$

which yields:

$$g(0,0,0) = G\rho \left[x \ln(y+r) + y \ln(x+r) - z \tan^{-1}\left(\frac{xy}{rz}\right) \right] \Big|_{z_1}^{z_2} \Big|_{y_1}^{y_2} \Big|_{x_1}^{x_2} \qquad (6)$$

An identical solution may be effected by a similar substitution in equation (3).

An identical solution for (4) may be effected by substituting:

$$\int \tan^{-1}\left(\frac{xy}{zr}\right)dz = -x \ln(y + r) - y \ln(x + r) + z \tan^{-1}\left(\frac{xy}{zr}\right) + \frac{x}{2}\ln(x^2 + z^2) + \frac{y}{2}\ln(y^2 + z^2) \qquad (7)$$

Computer implementation

A full expansion of equation (6) leads to a lengthy and complicated expression. This can have a significant impact on computer execution times if a gravity model consisting of a large number of prisms is involved. It is therefore desirable to design an algorithm that will improve the efficiency of computation.

One simplifying assumption that will be used in the remainder of this note is that all prisms making up a given model are regular in their horizontal dimensions, but varying in the vertical, i.e. the prisms have the same length and width, but different depths. while this does not necessarily improve the execution speed of the actual computations, it does simplify the setting up of the model and the handling of the results, particularly in situations where observations (gravity measurements, height or depth) are available in gridded form. It also permits some rapid procedural improvements, as described later.

The most obvious way of speeding up computations is to combine parts of the expanded form of equation (6) in such a way that the computer code contains a minimum number of calls to time-consuming software functions. An even more effective procedure is to divide each prism into regular laminae, and then to extract the gravitational effect of each lamina from the lookup table. Both methods will be discussed and compared in the following sections.

Reformulation of the rectangular prism equation

The expanded form of equation (6) features sixteen logarithm terms and eight arctangent terms. The processing times required to evaluate these and other functions on a typical mainframe are listed in Table 1. Arctangents and logarithms require 65 and 60 microseconds, respectively, to evaluate. This is about half the time required to evaluate an exponential, but many times more than a simple operation (add, subtract, multiply, or divide).

An obvious strategy, then, is to combine log and arctan terms so that their coded implementation will invoke fewer calls to time-costly software functions, and more to simple operators.

Table 1. Approximate execution times of various functions on a Cyber model 173 mainframe

Operation	CPU time (microsec)
x ** y	125.
SIN (x)	80.
COS (x)	75.
ATAN (x)	65.
ALOG (x)	60.
SQRT (x)	35.
Simple IF	6.
ABS	2.
Simple operator (+, -, x, /)	0.2

These figures were derived by timing the duration of FORTRAN Do-loops where each operation was executed one million times.

Using the identities:

$$\ln(u) + \ln(v) = \ln(uv)$$
$$\ln(u) - \ln(v) - \ln(u/v)$$

and $\tan^{-1}(u) + \tan^{-1}(v) = \tan^{-1} \dfrac{u + v}{1 - uv}$

$$\tan^{-1}(u) + \tan^{-1}(v) = \tan^{-1} \frac{u + v}{1 - uv}$$

it is possible to reduce the sixteen log terms in the full expression to four, and the eight arctans to two. This shortens the length of the expression from twenty-four terms to six, and results in a roughly fourfold decrease in execution time.

Further simplification is possible by identifying the factor

$$r_{ijk} = (X_i^2 + Y_j^2 + Z_k^2)^{1/2}$$

that appears in both log and arctan terms. This need be pre-defined and calculated only once for each prism.

Laminae and lookup tables

If the rectangular prisms in a model are divided into horizontal laminae of uniform thickness, the lookup table method can offer a significant advantage in execution speed.

In the application being discussed here, the lookup table actually consists of a three-dimensional array stored in computer memory. The array represents the volume of a three-dimensional space, with elements of the array corresponding to laminae that fill the volume. For each lamina, there is a vertical gravitational attraction that can be sensed at the origin of the 3D space; the magnitude of this attraction is stored in the appropriate element of the 3D array.

The first step in applying the lookup table method involves calculating the gravitational effects of all the laminae in the 3D space, and storing them in the 3D array. Unit density is assumed for these calculations. It is not necessary to perform this calculation over all of the 3D spaces: in each octant, the gravitational attraction has X, Y and Z planar symmetry, so computations need be performed only over one eighth of the total volume. Similarly, it is not necessary to store the laminar attractions over the entire 3D space, but in one octant only; this can significantly reduce the memory requirement for the lookup table. Note also that laminar computation is a simple case of the general prism computation; the gravity formula in this case reduces to one arctan term. Use of the lookup table method should not therefore incur significant overhead costs in setting up and storing the table.

The second step in applying the lookup table method consists of examining a given model that has been expressed as an ensemble of rectangular laminae. For all the laminae that form part of the model, the appropriate elements in the lookup table are accessed, summed, and multiplied by a density factor to yield the total gravitational effect of the model.

The lookup table method derives its speed from the fact that simplified gravitational computations are only performed a limited number of times – at the beginning of the procedure, when the lookup table is being created – to be followed by the bulk of operations, which consist mainly of simple memory accesses and additions.

A comparison of execution times

From the information contained in Table 1, it is possible to estimate theoretically the lengths of time required to calculate the gravitational effect of a rectangular prism using the three different computer algorithms discussed in this note: the full expression with twenty-four terms, the reformulated expression reduced to six combined terms, and the lookup table method.

Tables 2, 3 and 4 list the number of software operations invoked in each case, and the theoretical time required. (For the purposes of this discussion, the category of "simple operator" includes the storage and retrieval of data from computer memory.) Exact figures will depend on how the algorithm is coded, but the information contained in these Tables is adequate for making general comparisons.

Table 4 requires some explanation, as it actually refers to an average theoretical time derived from the processing of three rectangular prisms that consist of one, ten, and twenty laminae. (Note that execution times are not proportional to the number of laminae that make up a prism.) This average time is used to more closely approximate a real-world situation, where prisms in a given model will usually consist of a varying number of laminae. Note also that these figures don't reflect the time required to compute the contents of

Table 2. Theoretical execution time for evaluation of the full expression

Type of Operation	Quantity	CPU time (microseconds)*
Simple operator	93	19
Square root	8	280
Logarithm	16	960
Arctangent	8	510
	Total	1769

*based on execution times listed in Table 1.

Table 3. Theoretical execution time for evaluation of the reformulated expression

Type of Operation	Quantity	CPU time (microseconds)*
Simple operator	135	27
Square root	8	280
Logarithm	4	240
Arctangent	2	130
IF statement	1	6
	Total	683

*based on execution times listed in Table 1.

Table 4. Theoretical time necessary to extract values from a lookup table

Type of Operation	Quantity	CPU time (microseconds)*
For a prism consisting of one lamina:		
Simple operator	9	2
IF statement	2	12
ABS	2	4
		Total 18
For a prism consisting of ten laminae:		
Simple operator	39	8
IF statement	11	66
ABS	2	4
		Total 78
For a prism consisting of 20 laminae:		
Simple operator	69	14
IF statement	21	147
ABS	2	4
		Total 165

Average for the three prisms: $\frac{18 + 78 + 165}{3} = 87$

*based on execution times listed in Table 1

Table 5. Measured execution times on a Cyber model 173 mainframe

Algorithm	Total Time (sec)
Full expression	376
Reformulated expression	192
Lookup table	43

the lookup table itself, but we have already seen that this operation is only performed once at the beginning of the computer run, and that it doesn't represent a serious penalty in overhead. (In fact, the penalty can be eliminated altogether in some circumstances, if the lookup table is saved from previous runs and loaded directly into memory.)

From the Tables, it can be seen that the theoretical execution times for the three different algorithms have the following ratios:

1769:683:87

i.e. the reformulated expression should take about a third as long to execute as the full expression, while the lookup table method should take about an eighth as long as the reformulated expression.

To verify these theoretical findings, computer code was created for all three algorithms and applied to a simple model. This consisted of 441 identical prisms arranged in a square 21 x 21 matrix; total gravitational effect of all 441 prisms was calculated at 400 points distributed over a 20 x 20 grid.

Results of these tests are shown in Table 5. It should be noted that the figures listed in this Table are total job execution times, which include operating system overhead (but not roll-out/roll-in times), input-output, and, in the case of the last method, calculation of the contents of the lookup table.

From Table 5, measured execution times have the following ratios:

376:192:43

Improvement in the real case is not as significant as the theoretical case: the reformulated expression takes about a half as long to execute as the full expression, while the lookup table method takes about a fifth as long as the reformulated expression. Part of this discrepancy could be attributed to the variability in execution times of some of the functions listed in Table 1; the arctan function, for instance, has an execution speed that is dependent on the value of its argument. Part could also be due to the clasification of memory accesses as "simple operators"; in the lookup table method, these would consist largely of fetching data stored in a three-dimensional array, which usually takes longer than fetching data addressed by a simple variable name.

Nevertheless, the lookup table technique still indicates a measured improvement factor of about 9 over the full expression (as opposed to a theoretical factor of about 20). In terms of the execution speed, therefore, the algorithm is clearly superior to the other two, and can result in significant savings of computer time in the processing of large models.

Software has been developed for execution of all three algorithms; copies of the code are available on request.

Acknowledgment

We are indebted to Fan Shouzhi (Institute of Oceanology, Academia Sinica, Qingdao, China) for discussions and helpful suggestions that contributed to the fulfillment of this project and to the preparation of this report.

References

Grant, F.S. and West, G.F.
1965: Interpretation Theory in Applied Geophysics; McGraw-Hill Book Company, N.Y., 581 p.

Nagy, D.
1966: The gravity attraction of a right rectangular prism; Geophysics, v. 31, p. 362-371.

1980: Gravity anomaly, deflections of the vertical geoidal highs for a three-dimensional model. Acta Geodaetica, Geophysica et Montanistica, Academia Scientiarum Hungarian, v. 15.

Talwani, M.
1973: Computer usage in the computation of gravity anomalies. In B.A. Bolt (Editor), Methods in computational physics, v. 13; Academic Press, N.Y., p. 343-389.

The Melville Project, 1984-85: progress report

Project 840048

R.L. Christie
Institute of Sedimentary and Petroleum Geology, Calgary

Christie, R.L., The Melville Project 1984-85: progress report; in Current Research, Part A, Geological Survey of Canada, Paper 86-1A, p. 795-799, 1986.

Abstract

A second field season of the two-year Melville Project, a field and laboratory study of Melville Island, has been completed. The project comprises a broad spectrum of research, and several reports are in preparation. A review of Melville Island geology in the light of accumulated information allows some new interpretations for potential hydrocarbon-bearing reservoirs.

Résumé

Dans le cadre du programme Melville de deux ans, une deuxième campagne d'étude sur le terrain et en laboratoire de l'île Melville a été effectuée. Le programme comprend toute une gamme de recherches, plusieurs rapports sont en préparation. Une étude de la géologie de l'île Melville, basée sur les renseignements accumulés, permet de jeter un nouvel éclairage sur les réservoirs éventuels d'hydrocarbures.

Introduction

A new field study of Melville Island, Arctic Archipelago, was begun in 1984 and completed in 1985 as part of the Geological Survey's ongoing program to map all parts of Canada at a scale of 1:250 000.

Melville Island includes parts of three Arctic geological provinces, each with petroleum potential: the Arctic Platform, the Franklinian Geosyncline (the Parry Islands Fold Belt), and the Sverdrup Basin (Fig. 1). Vigorous exploration for petroleum has taken place both on Melville Island and in the nearby offshore areas, and some 50 wells have been drilled. Both oil and gas fields have been delineated: Drake Point and Hecla fields are each estimated by the operator, Panarctic Oils Limited (1985), to contain more than 3 trillion cubic feet (84 billion m^3) of gas. In addition, a small but important discovery of oil was made in the Bent Horn well on Cameron Island (nearby, but outside the area discussed here).

Some features of the sedimentary rocks of the region were noted during early geographic exploration (outlined later in this paper). The initial, or reconnaissance geological surveys delineated the sedimentary basins and indicated their petroleum potential. The Arctic Islands' first wildcat well, Winter Harbour No. 1, tested, in 1962, noncommercial rates of gas flow (1700 m^3/day) from the Middle and Upper Devonian Weatherall and Hecla Bay formations. New concepts useful to exploration, and many prospective targets, were subsequently established through geophysical surveys and more detailed geological studies, and these led directly to the active phase of exploration drilling from 1970 to 1980.

Most of the drilling – and the success – has occurred in the Sverdrup Basin. The Melville Project provides an opportunity to review and restudy both surface and subsurface data on hand, and to collect new stratigraphic and sedimentological information. These data may be especially useful when dealing with the lower Paleozoic folded province, where new syntheses are required to arrive at models that account for facies distribution, structure, and geological history of this, a petroleum-prospective part of the Franklinian Geosyncline.

Field data and rock and fossil collections from 1984, 1985, and earlier field seasons are being studied at the Institute of Sedimentary and Petroleum Geology and at other centres, and reports are in preparation. This note is intended to call attention to ongoing work related to the Melville Project.

Melville Project, logistics and acknowledgments

Field work in 1984 was based at Nias Point, on the south shore of Hecla and Griper Bay. The base camp for the 1985 field season was located near Ibbett Bay, in the northwestern part of the island. The Panarctic Oils Ltd. airport and station at Rea Point was used as a shipping and transit point, and on occasion, as a base for fieldwork. Each field season began in late June and ended about mid-August. Air support was provided by Quasar Helicopters (Bell 206B Jet Ranger) and by Bradley Air Services (de Havilland Twin Otter), both services provided by contract through the Polar Continental Shelf Project of the Department of Energy, Mines and Resources. Drummed fuel for aircraft had been shipped by sea to Rea Point a year before each field season. Aviation fuel, in addition to considerable other materials for field support, was also purchased from Panarctic Oils Ltd. at Rea Point. Food for the field camps was supplied by Dorval Food Market Inc., Montreal, and by Star Meat and Fish Company Ltd., Edmonton.

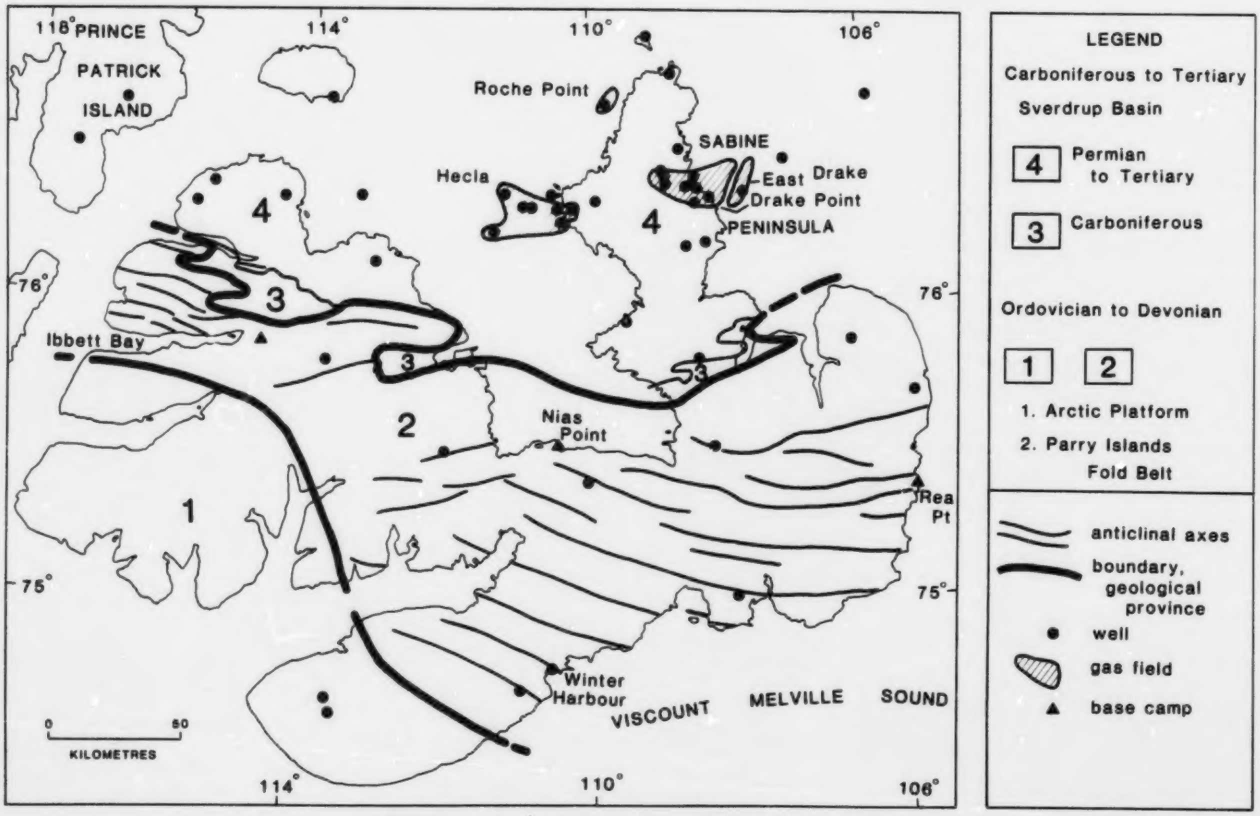

Figure 1. *Geological provinces of Melville Island.*

Helicopters were used for areal mapping and spot checking of geology during both field seasons; several traverses on foot also were made. Stratigraphic sections were measured from small 'fly' camps set out by helicopter.

A preliminary geological map had been completed from photo-interpretation (by J.C. Harrison) before the first field season. This map was continually refined through field checking and the addition of new interpretations. Some 50 stratigraphic sections were measured during the two-year project.

Stratigraphic studies were carried out by O.H. Goodbody (University of Alberta), R.L. Christie (Institute of Sedimentary and Petroleum Geology), and (in 1985) by C. Riediger (University of British Columbia). M.J. Robson (University of Western Ontario) studied lower Paleozoic 'shale basin' units on the northwestern part of the island. J.C. Harrison was responsible for structural-stratigraphic mapping.

Field assistance was provided in 1984, by Jane Bracken, Todd Cross, Sabine Feulgen, and Kathi Higgins; in 1985, by David Christensen, Sabine Feulgen, Linda Haid, Ben Lawson, and Rory McIntosh.

Other fieldwork supported by the project included: Jurassic biostratigraphy, T. Poulton (Institute of Sedimentary and Petroleum Geology); Pennsylvanian-Permian biostratigraphy, J. Utting, A.C. Higgins (Institute of Sedimentary and Petroleum Geology) and P. von Bitter (Royal Ontario Museum) in 1984; and collection of plesiosaur and other vertebrate remains, D.A. Russell and Clayton Kennedy (National Museum of Natural Sciences, Ottawa) in 1985. S.A. Edlund (GSC, Ottawa) completed geobotanical studies begun on the island in earlier years. D.A. Hodgson (GSC, Ottawa) and L. Dyke (Queen's University) studied aspects of surficial and glacial geology in 1985, with Gary Parkin and Suzanne Szojka, assistants.

Exploration and earlier geological studies

The first wintering by Europeans in the high Arctic Islands of Canada took place in 1819-20 at Winter Harbour, Melville Island. William Parry's was a remarkable achievement for the time; in the course of the first penetration of the islands by ship, he reached the northwestern part of the Arctic Archipelago.

Melville Island was explored by Parry and, along with Prince Patrick and nearby islands, was explored more fully in the 1850's, during the British Admiralty search for Sir John Franklin. The islands remained untouched for half a century following the Franklin search, until visits between 1906 and 1910 by Capt. J.E. Bernier in the **CGS Arctic**. Winter Harbour was again a haven for a ship - the **Arctic**, through the winter of 1908-1909 – and on this occasion the "whole Arctic Archipelago" was annexed to Canada in a formal ceremony, and a commemorative plaque was unveiled. Vilhjalmur Stefansson, leader of the Canadian Arctic Expedition of 1914-17, travelled the coasts of Melville and Prince Patrick islands en route to and returning from his exploration of more northerly islands. Melville Island was visited briefly by sledge, aircraft, and ship on occasion in the 1930's and 40's.

Systematic geological study of the region began in 1954, when E.T. Tozer explored parts of Prince Patrick, Eglinton, and Melville islands by dog team from Mould Bay Weather Station on Prince Patrick Island. Tozer mapped an area of Sabine Peninsula on Melville Island during the helicopter-supported project, Operation Franklin, and he and R. Thorsteinsson continued the mapping in 1958, using a Piper Super-Cub to cover the entire group of the Western Queen Elizabeth Islands (Tozer and Thorsteinsson, 1964). The stratigraphic nomenclature established by Tozer and Thorsteinsson has formed a basic framework for studies since that time.

Exploration for petroleum began in 1960, when geologists of the J.C. Sproule group began work in the Queen Elizabeth Islands. In 1962, the Arctic's first wildcat well, Dome Winter Harbour No. 1, was completed. A show of gas was obtained from Upper Devonian (Hecla Bay Formation) sandstone. H.P. Trettin studied the tar sands (Lower Triassic, Bjorne Formation) of northwestern Melville Island in 1964 (Trettin and Hills, 1966). The newly formed Panarctic Oils drilled its first hole on Melville Island in 1969, and in 1970 the company's Drake Point L-67 well came in – and blew out of control. Gas had been found in Jurassic sandstone (see Jones, 1981). Several gas fields have now been outlined in the northeastern part of the island and offshore (Fig. 1).

From stratigraphic studies and collections of ammonoids from Permian beds in 1964 and 1967, W.W. Nassichuk refined the correlations of Permian formations of Melville Island (Nassichuk, 1965, 1975).

Seismic exploration began on Melville Island in 1968, and the surveys were extended to offshore areas in the early 1970's. Some elements of the subsurface structure were reported and illustrated by Fox (1983, 1985) and by Texaco Canada Resources Ltd. (1983).

The stratigraphic nomenclature and the sedimentary environments of lower Paleozoic beds of Melville Island were described by Embry and Klovan (1976), and Embry (1976) after a study of the Middle and Upper Devonian 'clastic wedge' of the Arctic Islands. New stratigraphic divisions for the Middle Triassic to Lower Cretaceous beds of the Sverdrup Basin, which extends onto northern Melville Island, have been erected by Embry (1983; 1984a, b, c; 1985a, b) from the subsurface information now available from the many wells.

The surficial deposits and glacial features of parts of Melville Island were studied in 1962 by W.E.S. Henoch, and by several others since that time. A detailed account of the surficial materials of central Melville Island by Hodgson, Vincent, and Fyles (1984) includes a review of earlier studies of Quaternary material.

Mapping and reporting of the vegetative cover has been carried out by Edlund (1982).

Results of geological studies, Melville Project

Significant refinements or revisions in surface stratigraphic nomenclature that have been made over the past twenty years were reviewed by Harrison, Goodbody and Christie (1985), who also outlined some highlights of the regional mapping program of 1984. Robson (1985), Utting (1985), and Edlund (1985) have reported on aspects of the project. Following are further notes on activities by various researchers allied with the Melville Project.

Subsurface data obtained by petroleum exploration companies from wells and seismic surveys are being used in the Melville Project with two goals in mind: first, to elucidate the subsurface structures; and second, to relate subsurface and surface sedimentary units. Toward these ends, F.G. Fox (Panarctic Oils Limited, retired) and A.A. Densmore (Institute of Sedimentary and Petroleum Geology) have contributed a written study (see list of papers 'in preparation', below).

T. Poulton reports a "new" ammonite fauna in material he collected in 1984 at East Kitson River; the "new" fossil forms were found in the Opalinum Zone of the basal Aalenian (Wilkie Point Group).

Palynological collections from Silurian and Devonian beds are being studied by D.C. McGregor (GSC, Ottawa), and he has reported on collections by Goodbody, Christie, and Harrison. A notable feature of the material examined to date is an apparent absence of marine microfossils in shales of the Weatherall and Hecla Bay formations.

Palynological collections from upper Paleozoic beds are under study by J. Utting, who is making a systematic description of species from the Sabine Bay and Assistance formations. Carboniferous and Permian microfossils (conodonts) are being examined by A.C. Higgins and P. von Bitter. The work of Utting, Higgins, and von Bitter is dedicated to determining the relationship of upper Paleozoic stratigraphic units, both surface and subsurface, to the equivalent, well-documented units of Ellesmere Island.

Silurian conodonts are being worked on by A.D. McCracken (Ottawa), a Research Fellow with the Geological Survey of Canada.

Rock material from wells throughout the Arctic has been sampled by L. Brodylo, and measurement of the Thermal Alteration Index (TAI) of pollen and microfossils by J. Utting and J. Dougherty is in progress. Sampling of lower and upper Paleozoic beds is complete, and sampling of Triassic beds has begun. TAI measurement is also being carried out on surface samples collected during fieldwork. This work is being done in conjunction with F. Goodarzi (Institute of Sedimentary and Petroleum Geology).

The stratigraphy and sedimentology of the lower Paleozoic clastic units are being studied by Q. Goodbody (research fellow), and R.L. Christie. A report on the lower Paleozoic 'shale basin' is in preparation by J. Robson, under a Research Agreement. C. Riediger, research assistant, is working on stratigraphic material and data collected from Carboniferous and Permian beds in 1985.

The plesiosaur skeleton discovered in 1984 was examined by D. Russell who excavated and collected the skull in 1985. Two ichthyosaur 'bone-groups' were identified in nearby beds by the vertebrate paleontologists.

A report on the surficial deposits and glacial features of western Melville Island is in preparation by D.A. Hodgson; publication will follow completion of certain age-determinations.

J.C. Harrison's structural-stratigraphic studies on Melville Island are being carried out in collaboration with A.W. Bally and J.S. Oldow (Rice University, Houston, Texas), who are engaged in a wide-ranging project to test hypotheses concerning the opening of the Canada Basin. Both projects will combine surface, geological, and reflection seismic data to aid in interpretation of the kinematic-dynamic problems inherent in the geometry of the basin.

Structural and sedimentary geology, and implications for oil and gas exploration

The stratigraphic succession on Melville Island comprises some 2500 m of Lower Ordovician to Middle Devonian carbonates and equivalent basinal shales, 4500 to 5000 m of Middle and Upper Devonian clastic beds (Ellesmerian foreland basin, or 'clastic wedge'), and up to several kilometres of Carboniferous, Permian, and Mesozoic carbonates, evaporites, and clastic rocks.

The following points, in part speculative, are a result of the restudy and review of Melville Island geology, and draw attention to the potential for petroleum discoveries (J.C. Harrison, pers. comm., 1985).

1. Promising source and reservoir rocks of Silurian and younger Paleozoic ages clearly exist on Melville Island, but both the facies relationships and the tectonic history are more complex than previously thought, and this may account for the general lack of past success in petroleum exploration of these rocks.
2. Several formations, including both black shale and carbonate units of early Paleozoic age were confirmed as containing potential source beds judging by their generally organic or petroliferous characteristics.
3. Structural features in the southern marginal zone of the Parry Islands (Ellesmerian) Fold Belt were studied in 1985, and interpretation of these features is now in progress. It is possible that hydrocarbon reservoirs of the pre-Middle Devonian carbonate-to-basin transition belt, perhaps telescoped by thrust faults (a triangle zone?), may exist in the marginal zone.
4. Structural complexity in both the Canrobert Hills and the Weatherall Bay areas is evident from a study of slickenside lineations, en echelon giant carbonate veins, parasitic folds, thrust faults, and east-striking wrench faults. New interpretations of seismic data and well stratigraphy, in areas that include proven petroleum reservoir units, now seem possible.
5. Sedimentological and structural data for Carboniferous and Permian units of northern Melville Island suggest that a sequence of pull-apart basins developed along the southern margin of the Sverdrup Basin, and that faulting and transpressional folding (Melvillian Disturbance) took place.

References

Edlund, S.A.

1982: Vegetation of Melville Island, District of Franklin, Northwest Territories; Geological Survey of Canada, Open File 852, scale 1:250 000.

1985: Lichen-free zones as neoglacial indicators on western Melville Island; in Current Research, Part A, Geological Survey of Canada, Paper 85-1A, p. 703-712.

Embry, A.F.

1976: The Devonian clastic wedge of the Canadian Arctic Archipelago (Abs.); Geological Society of America, Abstracts, v. 6, p. 721-722; thesis, University of Calgary, Calgary, Alberta, Canada.

1983: The Heiberg Group, western Sverdrup Basin, Arctic Islands; in Current Research, Part B, Geological Survey of Canada, Paper 83-1B, p. 381-389.

1984a: Stratigraphic subdivision of the Roche Point, Hoyle Bay and Barrow formations (Schei Point Group), western Sverdrup Basin, Arctic Islands; in Current Research, Part B, Geological Survey of Canada, Paper 84-1B, p. 275-283.

1984b: The Wilkie Point Group (Lower-Upper Jurassic) Sverdrup Basin, Arctic Islands; in Current Research, Part B, Geological Survey of Canada, Paper 84-1B, p. 299-308.

1984c: The Schei Point and Blaa Mountain groups (Middle-Upper Triassic) Sverdrup Basin, Canadian Arctic Archipelago; in Current Research, Part B, Geological Survey of Canada, Paper 84-1B, p. 327-336.

1985a: Stratigraphic subdivision of the Isachsen and Chistopher formations (Lower Cretaceous), Arctic Islands; in Current Research, Part B, Geological Survey of Canada, Paper 85-1B, p. 239-246.

Embry, A.F. (cont.)
1985b: New stratigraphic units, Middle Jurassic to lowermost Cretaceous succession, Arctic Islands; in Current Research, Part B, Geological Survey of Canada, Paper 85-1B, p. 269-276.

Embry, A.F. and Klovan, J.E.
1976: The Middle-Upper Devonian clastic wedge of the Franklinian Geosyncline; Bulletin of Canadian Petroleum Geology, v. 24, p. 485-639.

Fox, F.G.
1983: Structure sections across Parry Islands Fold Belt and Vesey Hamilton Salt Wall, Arctic Archipelago, Canada; in Seismic expression of structural styles, v. 3, A.W. Bally (ed.); American Association of Petroleum Geologists, p. 3.4.1-54 to 3.4.1-72.

1985: Structural geology of the Parry Islands Fold Belt; Bulletin of Canadian Petroleum Geology, v. 33, p. 306-340.

Harrison, J.C., Goodbody, Q.H., and Christie, R.L.
1985: Stratigraphic and structural studies on Melville Island, District of Franklin; in Current Research, Part A, Geological Survey of Canada, Paper 85-1A, p. 629-637.

Hodgson, D.A., Vincent, J.-S., and Fyles, J.G.
1984: Quaternary geology of central Melville Island, Northwest Territories; Geological Survey of Canada, Paper 83-16.

Jones, G.H.
1981: Economic development – oil and gas; in A Century of Canada's Arctic Islands, 1880-1980, ed. M. Zaslow; Royal Society of Canada.

Nassichuk, W.W.
1965: Pennsylvanian and Permian rocks in the Parry Islands Group, Canadian Arctic Archipelago; in Report of Activities, Field, 1964, Geological Survey of Canada, Paper 65-1, p. 9-12.

Nassichuk, W.W. (cont.)
1975: Carboniferous ammonoids and stratigraphy in the Canadian Arctic Archipelago; Geological Survey of Canada, Bulletin 237.

Panarctic Oils Limited
1985: Seventeenth Annual Report, 1984.

Robson, M.J.
1985: Lower Paleozoic stratigraphy of northwestern Melville Island, District of Franklin; in Current Research, Part B, Geological Survey of Canada, Paper 85-1B, p. 281-284.

Texaco Canada Resources Ltd.
1983: Melville Island - Northwest Territories, Canada: Line No. 7; in Seismic expression of structural styles, v. 3, ed. A.W. Bally; American Association of Petroleum Geologists, p. 3.4.1.-73 to 3.4.1.-78.

Tozer, E.T. and Thorsteinsson, R.
1964: Western Queen Elizabeth Islands, Arctic Archipelago; Geological Survey of Canada, Memoir 332.

Trettin, H.P. and Hills, L.V.
1966: Lower Triassic tar sands of northwestern Melville Island, Arctic Archipelago; Geological Survey of Canada, Paper 66-34.

Utting, J.
1985: Preliminary palynological results from the Permian and lowermost Triassic of Sabine Peninsula, Melville Island, Canadian Arctic Archipelago; in Current Research, Part B, Geological Survey of Canada, Paper 85-1B, p. 231-238.

Lower Devonian Road River Formation on the north flank of Romanzof Uplift, northern Yukon Territory

Project 690005

D.K. Norris
Institute of Sedimentary and Petroleum Geology, Calgary

Norris, D.K., Lower Devonian Road River Formation on the north flank of Romanzof Uplift, northern Yukon Territory; in Current Research, Part A, Geological Survey of Canada, Paper 86-1A, p. 801-802, 1986.

Abstract

Late Early Devonian conodonts have been discovered in black shales and chert of the Road River Formation in the lower Firth River area, northern Yukon Territory. These shales are overlain with angular unconformity by the Upper Triassic Shublik Formation. The interregional sub-Upper Triassic unconformity, therefore, is now precisely defined at this point and the widespread nature of the lower and middle Paleozoic black shale basin in the northern mainland west of the Mackenzie Delta is further refined.

Résumé

On a découvert des conodontes de la fin du Dévonien inférieur dans des argiles schisteuses noires et des cherts de la formation de Road River, dans la région du cours inférieur de la rivière Firth, dans le nord du Yukon. Ces argiles schisteuses sont recouvertes en discordance angulaire par la formation de Shublik du Trias supérieur. Par conséquent, on s'attache actuellement à définir avec précision la discordance inter-régionale de la base du Trias supérieur à cet endroit et à mieux délimiter la vaste étendue du bassin d'argiles schisteuses noires du Paléozoïque inférieur et moyen se trouvant dans le nord de la terre ferme, à l'ouest du delta du Mackenzie.

In August, 1985 the author re-examined a well exposed section of the Upper Triassic Shublik Formation on the north flank of Romanzof Uplift almost directly across the Firth River from the Engigstciak archaeological site in the Herschel Island-Demarcation Point map area (Norris, 1981) of northern Yukon Territory. The section is located at longitude 139°33' West, and latitude 69°21' North. It may be pinpointed on National Air Photo Library vertical air photograph A13751-116 at the following Cartesian co-ordinates measured in cm from the centre of the picture, where the Y-axis coincides with the line joining the North and South fiducials and the positive Y-direction points to the north side of the photograph: X = -2.65 cm, Y = +1.54 cm.

At this location, the Shublik Formation rests with angular unconformity on acutely folded, black, fissile, variably calcareous shale, with thin interbeds of black, calcareous siltstone, argillaceous limestone and chert (Fig. 1). Both the shale unit and the overlying Shublik appear to be repeated on one or more south-verging, high-angle reverse faults on the southeast flank of Loney Syncline. The estimated maximum thickness of the deformed shale unit is 100 m.

The shale unit (GSC loc. C-112248) had been thought previously to be part of the Neruokpuk Formation and, therefore, to be Precambrian in age. It was recognized, however, to have many of the lithological and weathering attributes of the lower and middle Paleozoic Road River Formation. The writer, with the assistance of A.R. Cameron of the Institute of Sedimentary and Petroleum Geology and of I.L. Tailleur of the United States Geological Survey, made a most careful search for graptolites, only to be totally frustrated by the absence of these or any other macrofossils. Nevertheless, a representative sample of the rock types present in the outcrop was collected in search of conodonts and radiolaria. The sample contained an abundance of conodonts, including **Polygnathus serotinus** Telford and **P.** cf. **P. inversus** Klapper and Johnson which, according to T.T. Uyeno, are "most likely from the **serotinus** Zone and, therefore, late Emsian in age" (T.T. Uyeno, pers. comm., Oct., 1985). According to J. Dougherty (pers. comm., 1985) the conodonts have a Colour Alteration Index of 5, which suggests that the host rocks were subjected to temperatures greater than 300°C (Epstein et al., 1977).

The shale unit is a local remnant of the Road River Formation preserved below the interregional sub-Upper Triassic unconformity. Like the first reported occurrence (GSC loc. C-41895) of graptolite-bearing (latest Silurian) Road River Formation 30 km to the northwest (Norris, 1976), it is one of a widespread series of unconformity-bounded remnants preserved in structural or paleotopographic lows on the northern mainland west of the Mackenzie Delta (Norris and Yorath, 1981). Indeed, another possible occurrence of the Road River Formation was observed from the air on the opposite (northwest) side of Loney Syncline, beneath the Shublik and near GSC loc. C-11857 (see Norris, 1981). It was not examined on the ground. It was noted, however, that all three of these localities in Romanzof Uplift are collinear, and their northwest trend may well identify the orientation of the structural grain of the Ellesmerian (Late Devonian and Early Carboniferous) deformation in this segment of the northern Cordillera. The acute deformation of the Road River succession at the Firth River locality is presumed to be also Ellesmerian in age.

The high Colour Alteration Index (5) is in keeping with the anthracitic rank of the Early Carboniferous coals of the Kayak Formation (Norris, 1972) in Romanzof Uplift. It further substantiates the deep burial and high thermal alteration of this part of the supracrustal wedge up to and including Lower Cretaceous formations. The hydrocarbon potential of this part of the supracrustal wedge on the Arctic coastal plain and the adjacent continental shelf, therefore, is low.

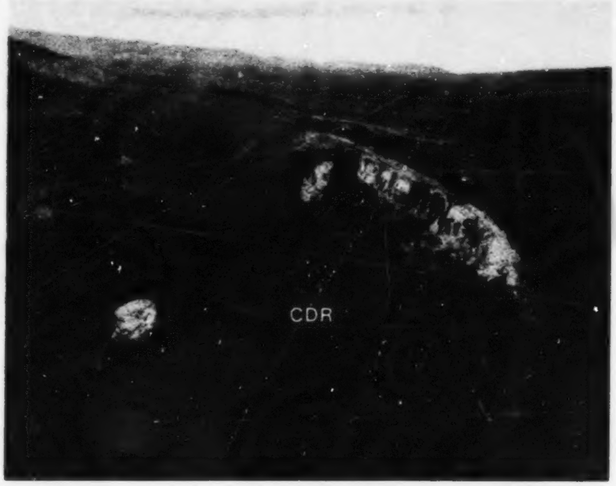

Figure 1. *Pale orange weathering limestones of the Upper Triassic Shublik Formation (TrS) rest with angular unconformity on black shales and chert of the Lower Devonian Road River Formation (CDR) on the southeast flank of Loney Syncline immediately west of lower Firth River. View is to the northwest from above Firth River. GSC photo 2421-206.*

The dating of the Road River Formation at this locality refines the definition of the hiatus separating Road River and Shublik strata there. The Road River formation is late Emsian (late Early Devonian). The overlying Shublik Formation is Upper Norian (Late Triassic) (E.T. Tozer, Int. Rept., 1973). Moreover no graptolites were found in the Road River Formation because the **serotinus** Zone is four conodont zones younger than the youngest graptolites!

References

Epstein, A.G., Epstein, J.B., and Harris, L.D.
1977: Conodont colour alteration – an index to organic metamorphism; United States Geological Survey, Professional Paper 995, 27 p.

Norris, D.K.
1972: Structural and stratigraphic studies in the tectonic complex of northern Yukon Territory, north of Porcupine River; in Report of Activities, Part B, Geological Survey of Canada, Paper 72-1B, p. 91-99.

1976: Structural and stratigraphic studies in the northern Canadian Cordillera; in Report of Activities, Part A, Geological Survey of Canada, Paper 76-1A, p. 457-466.

1981: Geology, Herschel Island and Demarcation Point, Yukon Territory; Geological Survey of Canada, Map 1514A.

Norris, D.K. and Yorath, C.J.
1981: The North American plate from the Arctic Archipelago to the Romanzof Mountains; in The Ocean Basins and Margins; v. 5, The Arctic Ocean, ed. A.E.M. Nairn, M. Churkin, Jr., and F.G. Stehli; Plenum Press, p. 37-103.

Gold occurrence in radioactive calc-silicate float at Sandybeach Lake, Nueltin Lake area, District of Keewatin

Project 840026

B.W. Charbonneau and S.S. Swettenham
Resource Geophysics and Geochemistry Division

Charbonneau, B.W. and Swettenham, S.S., Gold occurrence in radioactive calc-silicate float at Sandybeach Lake, Neultin Lake area, District of Keewatin; in Current Research, Part A, Geological Survey of Canada, Paper 86-1A, p. 803-808, 1986.

Abstract

Ground investigation of an airborne gamma-ray spectrometric anomaly characterized by high equivalent uranium and eU/eTh ratio has revealed boulders of white, chalky, tourmaline-bearing granite with up to 393 ppm eU contained mainly in uraninite. Adjacent to the granite is a well defined aeromagnetic anomaly where radioactive arsenopyrite-pyrrhotite-pyrite bearing calc-silicate float was found at two localities. These boulders contain significant gold concentrations (up to several ppm and with visible gold) and are enriched in U, W, Mo, and Co.

Résumé

Des recherches au sol, à la suite d'un levé aéroporté sur l'anomalie à l'aide de spectromètres à rayons gamma mettant en évidence un équivalent élevé d'uranium et du apport eU/eTh, ont révélées que des blocs erratiques granitiques à tourmaline, blancs, crayeux, ont une teneur de 393 ppm de eU présente en grande partie dans l'uraninite. Adjacente aux affleurements granitiques, une anomalie bien définie a été constatée dans des erratiques radioactifs calco-silicatés à arsénopyrite-pyrrhotite-pyrite trouvés à deux endroits. Ces blocs erratiques ont une teneur significative en or (jusqu'à plusieurs ppm d'or dont une certaine quantité est visible à l'oeil nu) enrichis en U, W, Mo et Co.

Introduction

During the summer of 1982 field work took place in southern District of Keewatin as a follow-up investigation of airborne gamma-ray spectrometer surveys (Geological Survey of Canada, 1978a, b; Charbonneau, 1982; Ford, 1982). The study area which contained highly radioactive granitic rocks is located to the west of Nueltin Lake (Fig. 1). The geology shown on Figure 1 is taken from Eade (1971, 1973) with modifications based on field observations during the 1982 field work and on interpretation of the airborne gamma-ray and aeromagnetic survey data.

Outcrop is scarce in the area. The terrain is generally flat, covered with a boulder till plain. Glacial direction is from slightly east of north.

Rock types in the area, from oldest to youngest, are 1) Archean? paragneiss, 2) meta-arkose which may include calc-silicates, 3) pre-Hurwitz quartz monzonite to granite including granodiorite gneiss, 4) Hurwitz Group including conglomerate, quartzite, greywacke, dolomite and limestone, 5) Aphebian granite-quartz monzonite, which varies from pink, massive, and medium grained to coarse grey, chalky, with abundant tourmaline, and 6) Helikian Nueltin Lake granite to quartz monzonite porphyry which is pink to grey, porphyritic, coarse grained, and commonly flourite-bearing.

Field work concentrated on three areas, indicated by arrows in Figure 1. Location 1 is a thoriferous veined portion of a Nueltin Lake porphyry body, where samples contained up to 460 ppm thorium and 0.2% rare earth elements. At location 2 samples of sulphide-bearing calc-silicate contained over 600 ppm uranium, 390 ppm molybdenum and 1.6 ppm gold (determined by neutron activation analysis). Samples from a quartz monzonite body at location 3 contained over 200 ppm uranium and 400 ppm molybdenum. Results of this work were presented at the 1985 GSC Current Activities Forum.

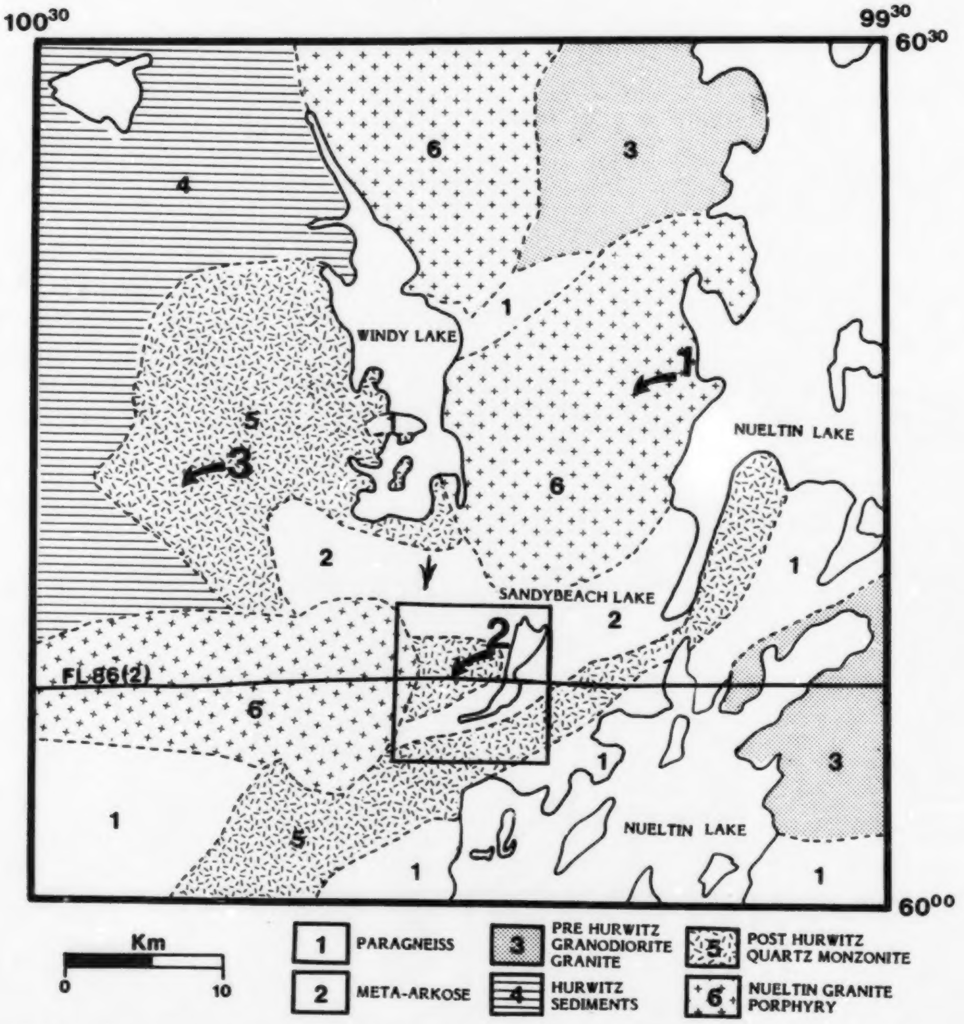

***Figure 1.** General geology, location of study area (box), and location of airborne gamma spectrometric flight line.*

Further field work in 1985 at location 2 located sulphide-bearing calc-silicate boulders containing visible gold, scheelite and greater than 1000 ppm equivalent uranium. Laboratory analysis by graphite furnace atomic absorption spectrometry indicated gold concentration of 12.6 ppm.

Figure 2 is an aeromagnetic map (Geological Survey of Canada, 1965a, b) of the area outlined at location 2 on Figure 1, showing geological contacts from Figure 1, and sites for three samples described below. Figure 3 is the gamma-ray spectrometric profile for flight line 86(2) which is indicated on Figures 1 and 2. The gamma-ray spectrometric profile shows a prominent anomaly in equivalent uranium and eU/eTh ratio which correlates with the granitic plug (unit 5) to the west of Sandybeach Lake. The adjacent metasediment unit (unit 2) has lower radioelement content but shows a well defined aeromagnetic anomaly. On the west, the body of Nueltin Lake granite porphyry (unit 6) is sharply defined by an increase in thorium.

Sample description

Samples of radioactive tourmaline-bearing granite (CZ-162-82) and auriferous sulphide-bearing calc-silicate (CZ-172-82 and CZ-4B-85) were collected from blocks of float with dimensions of about one metre.

CZ-162-82 is approximately 10% biotite, 3% white mica, 20% quartz, 35% microcline and 25% plagioclase. Accessory minerals, totalling 7%, include fluorite, amphibole, tourmaline, apatite, monazite, zircon, xenotime, molybdenite, pyrite and uraninite. Major element content/composition is 76.2% SiO_2, 4.83% K_2O, 2.40% Na_2O, 0.93% CaO, and 0.08% TiO_2. The sample contains 393 ppm eU, 150 ppm eTh, trace Mo, and 800 ppm F. Other samples of this rock contain up to 3200 ppm F. Figure 4 is an autoradiograph of the radioactive granite and shows the distribution of radioactive minerals including uraninite, monazite, zircon etc.

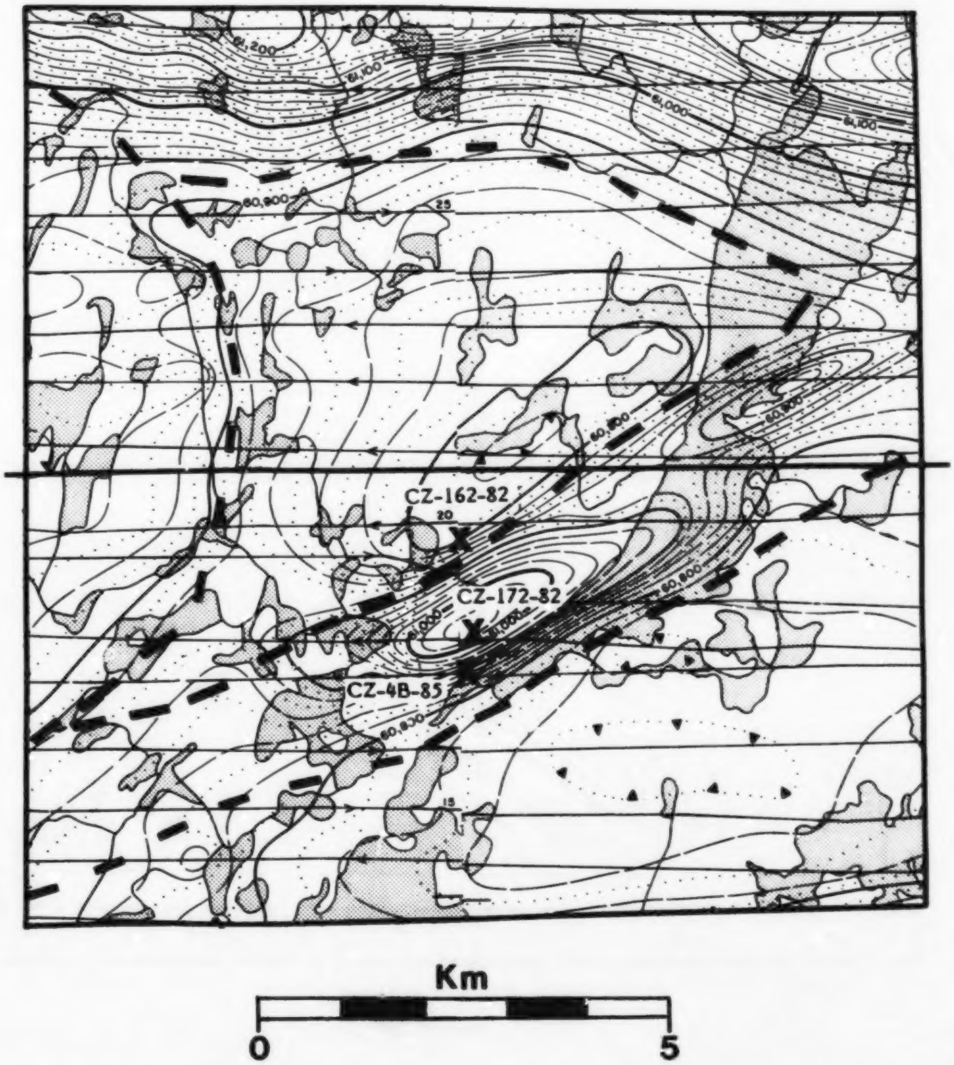

Figure 2. *Aeromagnetic map of study area (box from Figure 1) showing location of airborne gamma spectrometric flight line. Geological contacts from Figure 1 are superimposed.*

CZ-172-82 contains 50% plagioclase, 40% clinopyroxene and 5% pyrrhotite. Principal accessories and ore minerals amounting to 5% of the sample are amphibole, sphene, apatite, pyrite, molybdenite and uraninite with traces of cobaltite and chalcopyrite. The 1.6 ppm Au in this rock is mainly associated with pyrite and to some extent uraninite. Small inclusions of Au-Bi-Pb tellurides were noted in the pyrite. Pyrite concentrates were made which average 50 ppm gold. Microprobe analyses of some gold grains average 12.4% silver. Figure 5D shows the gold-pyrite relationship. Figure 4 is an autoradiograph from a cut face of sample CZ-172-82 and shows the distribution of uraninite sources both as discrete grains and veins.

CZ-4B-85 contains visible gold. The major minerals are 60% plagioclase with sericite alteration, 30% pyroxene and amphibole, and 5% biotite. The ore minerals, 5% in total, were identified as pyrrhotite, arsenopyrite, scheelite, with minor uraninite, molybdenite, native gold, tellurobismuthite, nickel telluride (melonite), lead telluride (altaite), chalcopyrite, cobaltite, ilmenite, and gold telluride (calaverite). Gold which averages 12.6 ppm in this sample occurs in uraninite (Fig. 5C), enclosed in pyrrhotite near arsenopyrite (Fig. 5B), and in gangue (Fig. 5A). No pyrite was identified in this sample and consequently this material is somewhat different from CZ-172-82.

Summary

This occurrence of gold at Sandybeach Lake is similar to the Gillander gold occurrence reported in the Northern Miner (Sept. 26, 1977) near Kasmere Lake in northern Manitoba. Both occurrences are in radioactive calc-silicates in proximity to radioactive granite. The Gillander occurrence was also outlined by follow-up investigation of federal-provincial airborne gamma-ray spectrometric surveys.

Although the Sandybeach occurrence is in float, the majority of the glacial drift in the area appears to be not far removed from its bedrock source. The granite plug and the entire northeast-trending belt of granite that runs through the study area towards Nueltin Lake are uraniferous and rich in tourmaline. The association of gold with tourmaline (Boyle, 1979) suggests that the contacts of these granite bodies with the metasedimentary belt (Fig. 2) may be favourable loci for gold occurrence.

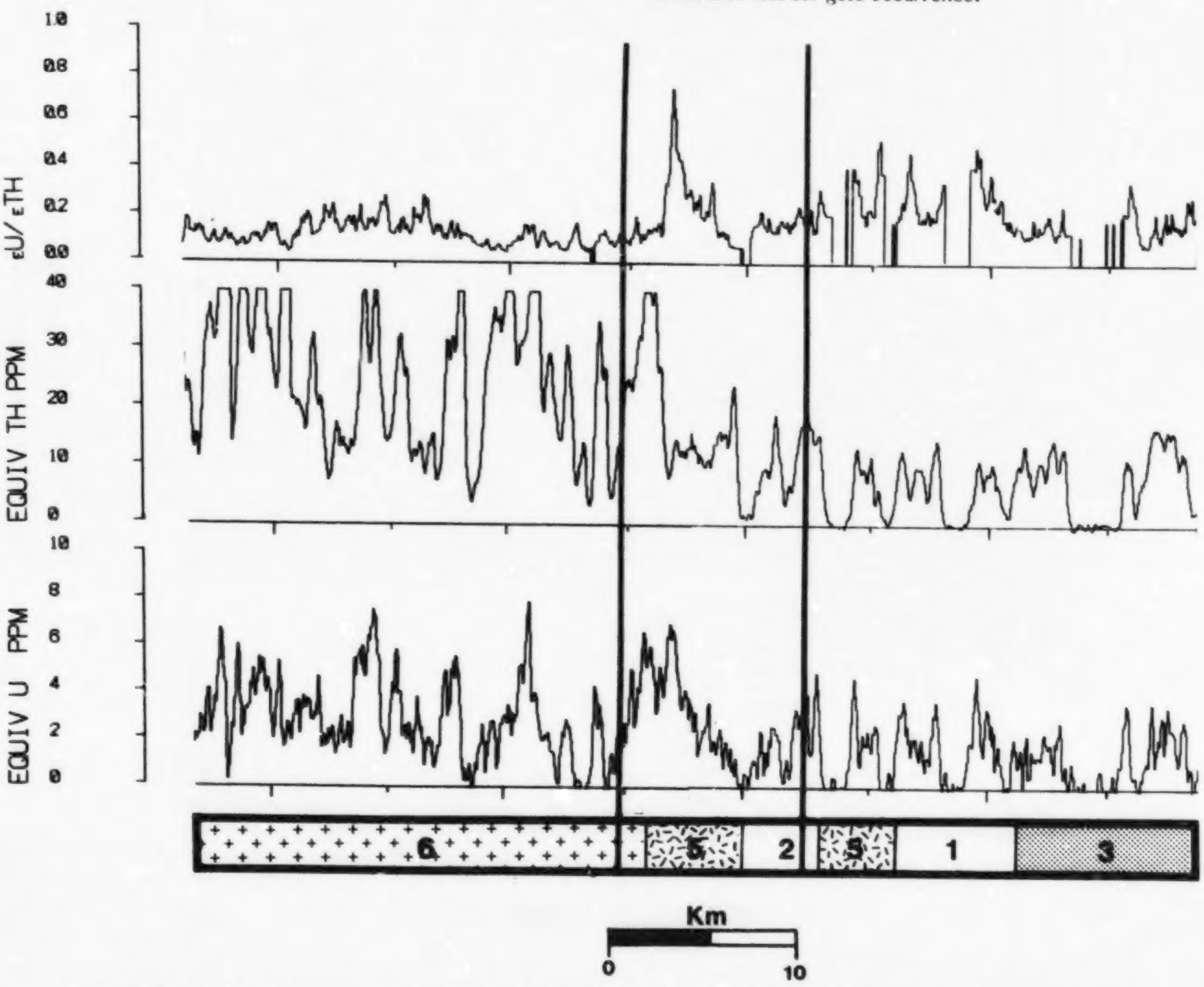

Figure 3. Airborne gamma spectrometric flight line 86(2) from Geophysical Series Maps 35265G and 35365G.

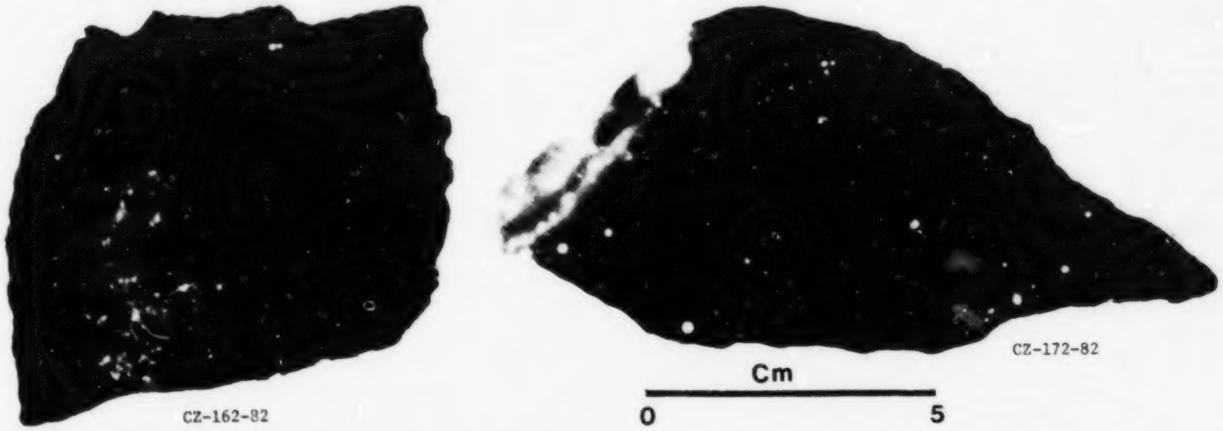

Figure 4. *Autoradiograph of cut faces of radioactive tourmaline-bearing granite CZ-162-82 and radioactive calc-silicate CZ-172-82.*

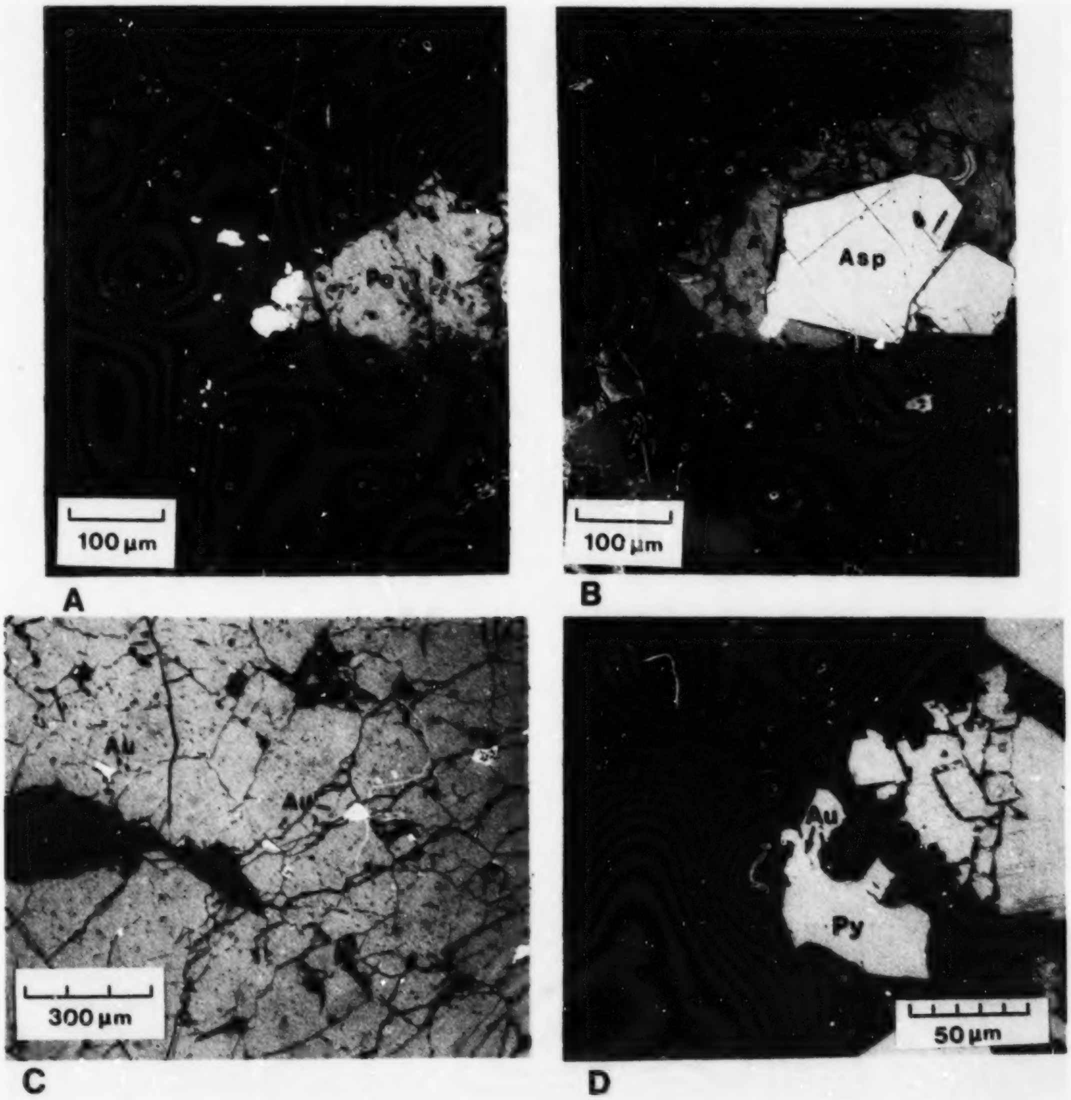

Figure 5. *Photomicrographs showing gold textural relationships.*

Acknowledgments

The authors are grateful for the contributions of GSC staff: R.W. Boyle for first suggesting the gold potential of the calc-silicate rocks, G.M. Lecheminant and D.C. Harris for detailed mineralogical reports, and G. Hall for gold analyses.

References

Boyle, R.W.
1979: The geochemistry of gold and its deposits; Geological Survey of Canada, Bulletin 280.

Charbonneau, B.W.
1982: Radiometric study of three radioactive granites in the Canadian Shield, Elliot Lake, Ontario; Fort Smith and Fury and Hecla, NWT; in Uranium in Granites, ed. Y.T. Maurice; Geological Survey of Canada, Paper 81-23, p. 91-99.

Eade, K.E.
1971: Geology of Ennadai Lake map area, District of Keewatin; Geological Survey of Canada, Paper 70-45.

1973: Geology of Nueltin Lake and Edehon Lake (west half) map area, District of Keewatin; Geological Survey of Canada, Paper 72-21.

Ford, K.L.
1982: Investigation of regional airborne gamma-ray spectrometric patterns in New Brunswick and Nova Scotia; in Current Research, Part B, Geological Survey of Canada, Paper 82-1B, pp. 177-194.

Geological Survey of Canada
1965a: Aeromagnetic Series Map 3136G.

1965b: Aeromagnetic Series Map 3137G.

1978a: Airborne Gamma-Ray Geophysical Series, Map 35265G Nueltin Lake, Northwest Territories.

1978b: Airborne Gamma-Ray Geophysical Series, Map 35365G Ennadai Lake, Northwest Territories.

A NORTHWARD FLOWING GLACIER IN CUMBERLAND, COLCHESTER AND PICTOU COUNTIES; GEOLOGICAL EVIDENCE AND EFFECTS ON TILL GEOCHEMISTRY*

R. R. Stea and P. W. Finck

ABSTRACT

Erosional and depositional glacial landforms indicate a major northward ice flow crossing the Cobequid Highlands in northern mainland Nova Scotia. Striations trending 001°-020° are found on the fine grained volcanic and metasedimentary rocks of the Cobequid Highlands. Sequences of ice contact stratified drift and outwash indicate northward paleoflow of meltwater streams. Distinctive plutonic and volcanic erratic boulders are dispersed northwards up to 6.2 miles (10 km) from the Cobequids Highlands onto the Carboniferous sedimentary Lowlands. Moraines parallel to the Highlands, and the northward termination of glaciofluvial sequences suggest a stillstand of the northward flowing glacier.

Element levels in the clay fraction of the reddish Lowland till sheet appear to have two controlling influences, provenance and weathering processes. Pb and Zn levels are strongly correlated, with anomalously high values of both elements commonly found in the same samples. Small Pb occurrences associated with grey coaly sandstones and conglomerates, may be the source of these high Pb and Zn values. A secondary influence to Zn levels is the amount of Fe in the till. This is especially significant in sandier tills, where Fe hydroxides form a large proportion of the clay fraction. Ca and Mg levels in the clay fraction of the surface till sheet may be controlled by the interaction of weathering processes and provenance. This study emphasizes the need to recognize till sheets in a mineral exploration program.

INTRODUCTION

This report presents further evidence for a late northward to northeastward ice flow which crossed the Cobequid Highlands and dispersed crystalline and metamorphic erratics over the northern Carboniferous Lowlands. The expression of the northward movement in terms of glacial erosional and depositional features and till geochemistry is also discussed.

The study area includes part of two physiographic regions, the Cumberland-Pictou Lowlands and the Cobequid Highlands (Fig. 1). The Cobequid Highlands are composed of plutonic, volcanic and metasedimentary rocks of Hadrynian to Early Carboniferous age (Donohoe and Wallace, 1978). The Cumberland-Pictou Lowlands are underlain by Early Carboniferous to Triassic age sedimentary rock.

---

*Canada-Nova Scotia Co-operative Mineral Program 1981-84
Canada-Nova Scotia Mineral Development Agreement
Mainly funded by Energy, Mines and Resources Canada

Originally published in Nova Scotia Department of Mines and Energy, Report 85-1, p. 69-84.

Camera-ready copy was provided by Nova Scotia Department of Mines and Energy.

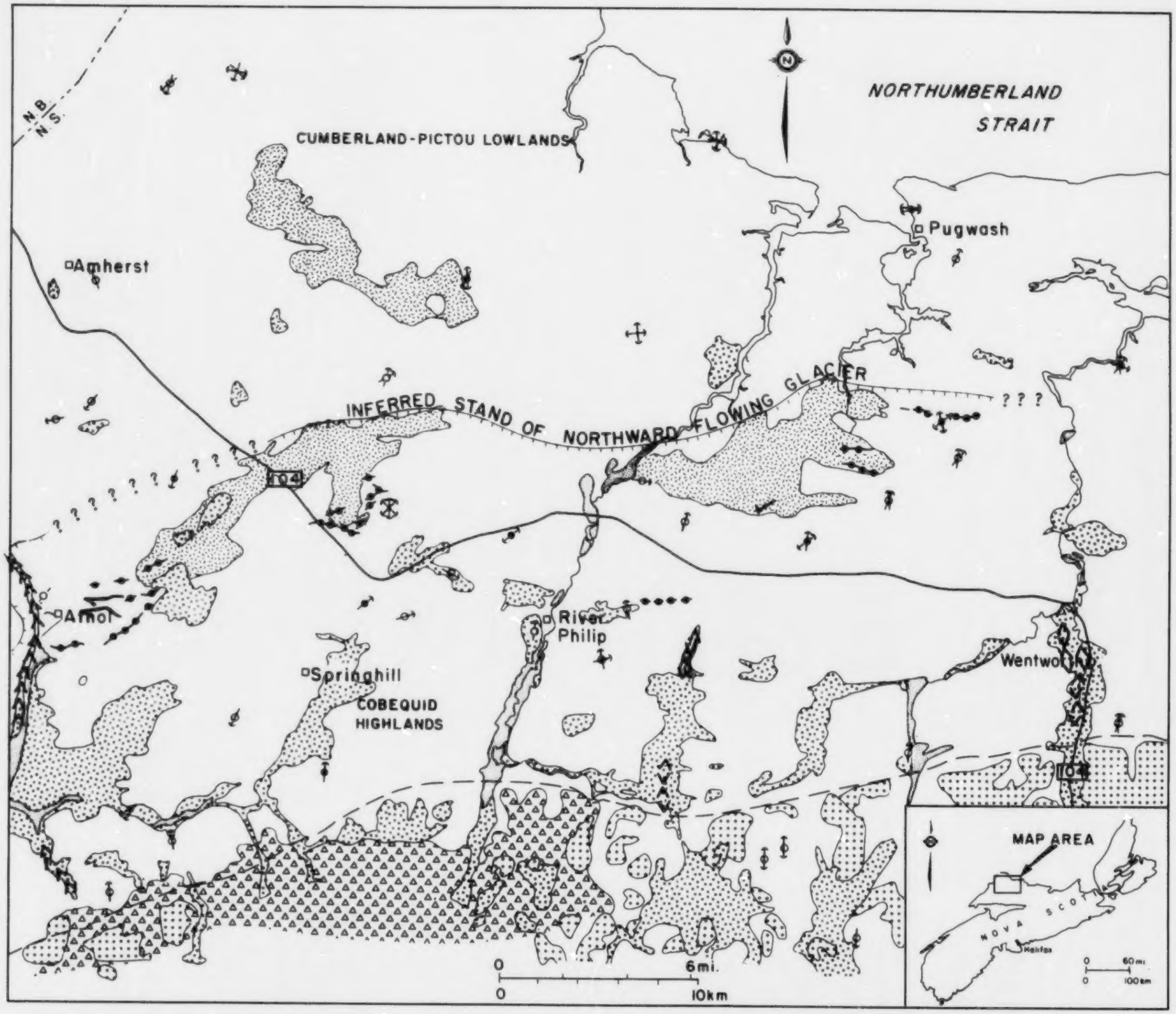

Figure 1. Surficial geology of the northern part of Cumberland and Colchester Counties.

LEGEND

OUTWASH : horizontally bedded, gravelly sand, forming a flat plain.

ICE CONTACT STRATIFIED DRIFT : bedded sand, gravelly sand and boulders, local faulting of strata, forming kame and kettle terrain.

ABLATION TILL : reddish brown, loose, stony, sandy partings and lenses, angular clasts; forming hummocky moraine

TILL : reddish brown, compact, stony, sandy, silt matrix, jointed, composed mainly of Carboniferous sandstone clasts, forming the ground moraine in the Cumberland-Pictou Lowlands

TILL : greyish brown, loose, sandy matrix, composed primarily of Cobequid Highlands plutonic and metamorphic clasts; forming the surface till on the Cobequid Highlands

Note : No stratigraphic order implied

ROCK : areas of barren rock, or thin (< lm) discontinous till cover.

SYMBOLS

Striations (direction known, unknown, striations from Chalmers (1895)) . . . .

Esker (direction of flow known, unknown) . . . .

Moraine . . . .

Meltwater channel . . . .

Northward transport of Cobequid Highlands erratics by ice action is not a new concept. Chalmers (1895) mapped northward to northeastward trending striations in the Cumberland-Pictou Lowlands. Poole (1890) and Prest (in Prest et al., 1972) noted the northward transported Cobequid erratics and Grant (1977) advocated a northward ice movement to explain Cobequid erratics near Pictou. Downey (1979), while mapping for Gulf Minerals southeast of Wentworth in the Cobequid Highlands, also described a northward ice flow.

Stea and Finck (1984) mapped and studied the glacial features and till stratigraphy in the study area. Preliminary results revealed a northward transport of Cobequid erratics (found in boulder piles in farmers' fields) onto the Lowlands. Two systematically divergent sets of striations were mapped on the Cobequid Highlands. A regionally consistent striation set trending 170-195° was mapped. The sense of ice movement was determined by northward-facing stoss surfaces and pressure shadows (mini crag and tail features). Striations trending 350° to 035° were also mapped and interpreted using the same criteria. The northward to northeastward trending striations were observed in the Lowland areas on southward facing stoss surfaces.

EROSIONAL INDICATORS OF ICE MOVEMENT

During the 1984 field season the authors revisited the Cobequid Highlands in the study area. Two reference areas for erosional indicators of the northward ice movement were found. At Economy Lake, south of the map area, well developed mini crag and tail forms or pressure shadows on a northward sloping outcrop indicate an 188° ice flow. A southward-sloping rock surface approximately 550 yards (500 m) south of that outcrop reveals mini crag and tail forms from carbonate-cored siliceous nodules that indicate a 001° ice movement. This site was originally discovered, and the northward flow noted, by S. Bradley of Gulf Minerals Canada Ltd. (D. R. Grant, personal communication, 1980). A similar outcrop south of Wentworth on the Cobequid Highlands reveals 165° grooves cut by younger striations trending 020°. In other areas the two striated surfaces meet along a distinct line or bevel.

DEPOSITIONAL INDICATORS OF ICE MOVEMENT

A morphosequence refers to a continuum of landforms composed of stratified drift deposited at and beyond the margin of a glacier while deposition was controlled by a specific base level (Koteff and Pessl, 1981). On the southern side of the Cobequid Highlands (west of the study area) morphosequences are characterized by ice contact stratified drift, moraines, and ice contact deltas which grade southward into outwash plains and marine Gilbert type deltas (Stea, 1983; Stea et al., in press).

North of the Cobequid Highlands, between River Phillip and Wentworth, the direction of ice retreat, as indicated by morphosequences, is reversed (Fig. 1). The esker south of Athol reveals northward dipping crossbeds and imbricated clasts which indicate northward flowing meltwater. This esker complex grades northward into an outwash plain (Fig. 1). Similar sequences are found at the mouths of major valleys in the Cobequid Highlands east of Springhill. The meltwater that produced these

deposits was derived from ice which retreated southward to the Cobequid Highlands.

A till sheet characterized by a sandy matrix and local Cobequid Highlands lithologies was found on top of a more compact reddish brown till on the northern edge of the Cobequid Highlands (Fig. 1). The sandy till was probably deposited by northward flowing ice because it contains virtually no Carboniferous erratics. It does not extend onto the Cumberland-Pictou Lowlands, but erratics of Cobequid Highlands provenance are found on the surface and in the upper metre of a compact reddish brown till which forms the surface till over much of the Lowlands. The dispersal of these erratics will be discussed in the following section.

INFERRED STAND OF NORTHWARD FLOWING ICE

Figure 1 shows an inferred stillstand of northward flowing ice based on the distribution of transverse moraine, hummocky moraine, meltwater channels and ice contact gravels. The area north of the limit is characterized by fluted and drumlinized till. South of the limit the terrain varies from flat and featureless to rolling closer to the Cobequid Highlands. The surface till sheet north and south of the inferred stand is visually indistinguishable except for the presence of crystalline erratics on the till surface south of the stand. Large areas south of the limit are covered by ice contact gravels grading distally into outwash plains. Near Athol the stand is defined by a series of east-northeastward trending moraines and a large body of ice contact stratified drift (Fig. 1). Near Springhill the stand is defined by ice marginal gravel deposits and a large arcuate area of hummocky moraine composed of a reddish sandy till. In the eastern part of the study area the stand is defined by a large body of ablation till and a series of small moraines (Fig. 1).

Striations mapped by the authors (Stea and Finck, 1984), which indicate a northward ice movement, are found exclusively south of the limit. Five isolated striation sites mapped by Chalmers (1895) indicate a northward movement in areas north of the stand of northward flowing ice.

DISPERSAL OF INDICATOR LITHOLOGIES

Pebbles from samples in the study area were counted and classified as plutonic, volcanic, metamorphic, red sedimentary, grey sedimentary, and other. The red and grey sedimentary clasts are derived from the Lowlands. The assemblages of the plutonic, volcanic, and metamorphic (crystalline) erratics suggest that they are of Cobequid Highlands provenance.

Figure 2 shows the percentage of crystalline erratics at each sample site and contours of the crystalline percentages. The contours show a decrease in the percentage of crystalline erratics with increasing distance northward from the Cobequid Highlands. The percentage of crystalline erratics decreases from 99 per cent to approximately 30 per cent within 2.5 miles (4 km) of the Highlands. The decrease in erratic percentages becomes more gradual with increasing distance from the Cobequid Highlands. Figure 3 shows the percentage of crystalline erratics versus distance northward from the contact of the Cobequid Highlands. The

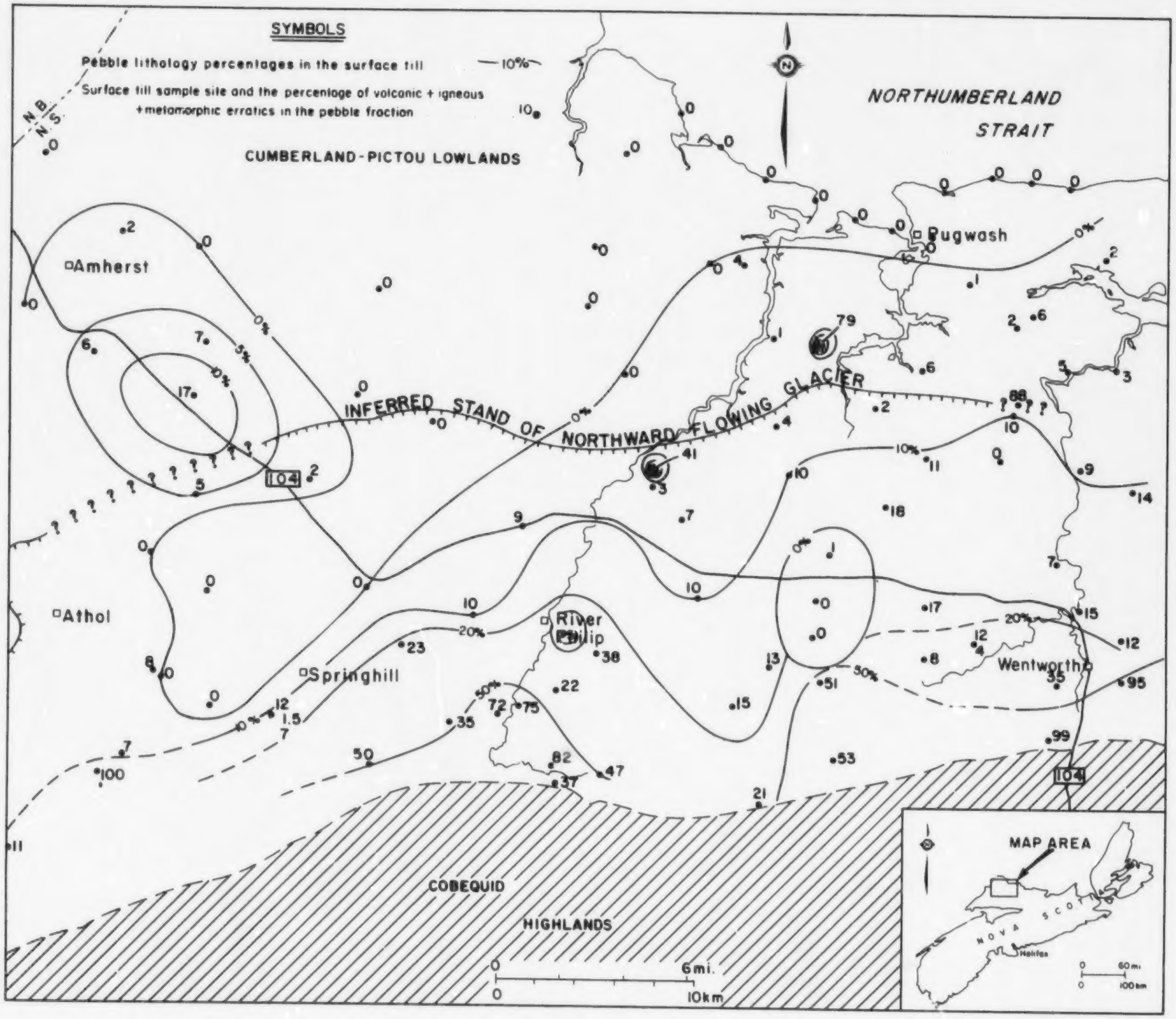

Figure 2. Contours of pebble lithology percentages, till sample locations, and the inferred stand of northward flowing ice based on morainal features and glaciofluvial morphosequences.

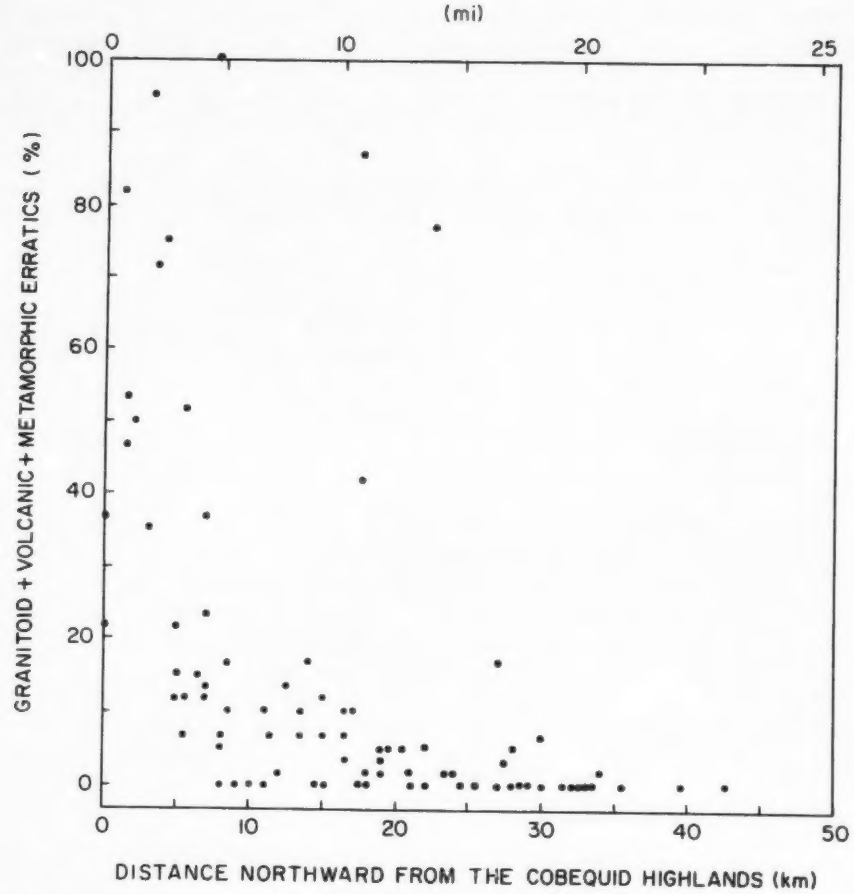

Figure 3. Plot of volcanic, metamorphic and intrusive pebble percentages with distance northward from the Cobequid Highlands massif.

decrease in erratics with increasing distance roughly conforms to the shape of a negative exponential curve which is a characteristic of glacial dispersal (Shilts, 1976). The Cobequid Highlands trend approximately east-west, perpendicular to ice flow inferred by glacial erosional features. Cobequid erratic dispersal is therefore parallel to the general trend of the northward ice flow and perpendicular to the source of indicator clasts.

In general the 0 per cent erratic pebble contour follows the inferred stand based on moraines (Fig. 2). This reinforces the concept that the moraines are an ice marginal feature. The northward deviation of the 0 per cent contour in the eastern area suggests that the ice may have at one point flowed beyond the inferred stand and retreated.

The distance ice flowed north across the Lowlands, as defined by the dispersal of crystalline erratics, generally increases from west to east. This may reflect a more vigorous northward ice flow in the eastern part of the study area (Stea and Finck, 1984). An erratic anomaly northeast of Athol (Fig. 1) and isolated striations suggest that a lobe of

ice may have advanced as far as Amherst. This glacier may have retreated to the postulated stand marked by ice contact statified drift near Athol.

EFFECTS OF NORTHWARD ICE FLOW ON TILL GEOCHEMISTRY IN THE CUMBERLAND-PICTOU LOWLANDS

The surface till in the Cumberland-Pictou Lowlands north of the Cobequid Highlands is primarily a reddish brown silty till derived from Carboniferous sedimentary rocks. It is believed to have been formed initially during a major southward to southwestward ice flow across the Carboniferous Lowland terrain (Stea and Finck, 1984). On visual examination, the colour and texture of the till sheet are similar north and south of the inferred glacier stand, although locally there are sandy tills which may represent ablation till related to the northward ice flow.

Ninety-seven surface till samples were collected from the Cumberland-Pictou Lowlands north of the Cobequid Highlands (Fig. 1). These samples were collected largely from the reddish silty till which represents the surface till sheet. Sandier and stonier till facies were also sampled, but only 7 samples were from the sandy ablation tills associated with hummocky moraine (Fig. 1). The samples were collected at an average depth of 4.9 feet (1.5 m) below the solum. The clay fractions (<2 µm) of these samples were analyzed for 14 elements including Cd, Ag, Cu, Ni, Pb, Zn, Co, Fe, Mn, Ca, Mg, Mo, U, As; heavy mineral separates of the medium to fine sand fraction were analyzed for Sn and W. The clasts in each till sample were examined and percentages of erratics determined. The analytical procedures are discussed in Stea and Fowler (1979) and Stea (1982).

The nonparametric Spearman Rank Correlation method was used to:

1. assess the effects of provenance related parameters including the northward distance from the Cobequid massif, and the percentage of erratics on levels of the analyzed elements;

2. determine the effects of provenance, weathering, and sampling depth on the analyzed elements by elemental associations.

Provenance-related Variations

Table 1 shows the significant (99.0% confidence level) correlations between distance from the Cobequid Highlands, erratic percentages and geochemical elements. A strong negative correlation (-0.73) is seen between the percentage of erratics in the surface till and distance from the Cobequid Highlands. The elements Cu, Ni, Pb, Mg and Ca are significantly correlated with the parameters relating to northward ice flow. Cu and Pb levels are negatively correlated with distance and Pb levels are positively correlated with the percentage of Cobequid Highlands erratics.

Pb and Zn levels are concomitant with a positive correlation coefficient of 0.62 (Fig. 4). Cu and As levels also vary accordantly with Pb and Zn levels. The Pb and Zn association is likely to be provenance

Table 1. Spearman Rank Correlation Coefficients (rho) between geochemical elements and sample parameters relating to northward ice flow.

Northward flow Parameter	**Sampling distance from Highlands (km)**		**Percentage Cobequid erratics (%CHe)**	
Element	**Correlation Coefficient (rho)**	**Significance**	**Correlation Coefficient (rho)**	**Significance**
Cd	-0.28	NS*	0.22	NS
Ag	0.03	NS	-0.07	NS
Cu	**-0.39**	S**	0.27	NS
Pb	**-0.48**	S	**0.43**	S
Zn	-0.22	NS	0.15	NS
Ni	0.27	NS	**-0.36**	S
Co	0.04	NS	-0.18	NS
Fe	0.09	NS	0.25	NS
Mn	0.02	NS	-0.19	NS
Ca	**0.46**	S	**-0.40**	S
Mg	**0.54**	S	**-0.40**	S
Mo	-0.19	NS	0.14	NS
U	-0.211	NS	0.15	NS
As	0.30	NS	0.19	NS
Sn	0.08	NS	-0.14	NS
W	0.07	NS	-0.10	NS
Distance (km)	-	-	**-0.73**	S
%CHe	**-0.73**	S	-	-

* NS = not significant
**S = significant

related because the mobilty of the two elements differs widely under oxidizing conditions (Rose et al., 1979, p. 25). Cu occurrences are widespread in the Cumberland-Pictou Lowlands (Chatterjee, 1983). Whole rock analyses of some of these occurrences show that Pb and Zn values are also elevated (above 500 ppm) (Ryan, in press). Pb occurrences in grey coaly sandstones and conglomerates have been discovered by recent mapping and exploration work in the region. The mineral commonly found is galena, but sphalerite and chalcocite are secondary components (Ryan, in press).

Figures 5 and 6 are scatter plots of the values of Cu and Pb and the distance northward from the Cobequid Highlands. Both plots show higher values (above 40 ppm) of Cu and Pb within the mapped stand of northward-flowing ice than beyond it. Peaks in Cu and Pb values are found in tills adjacent to the Cobequid Highlands and in tills north of the Cobequids up to the stand. Pb values vary accordantly with the percentages of erratics derived from the Cobequid Highlands and distance (Table 1). The Cobequid Highlands may be a source of Pb, but the pattern of decrease in Pb should be similar to the pattern of erratic dispersal (Fig. 3). A more plausible explanation is that mineralized Carboniferous bedrock sources within the limit were eroded and dispersed northward along with the Cobequid-derived erratics. Some of the elevated values of Pb in Figure 6 may be due to mineralization in the Boss Point Formation which has, in other areas, been known to carry Pb and Zn (R. J. Ryan, personal

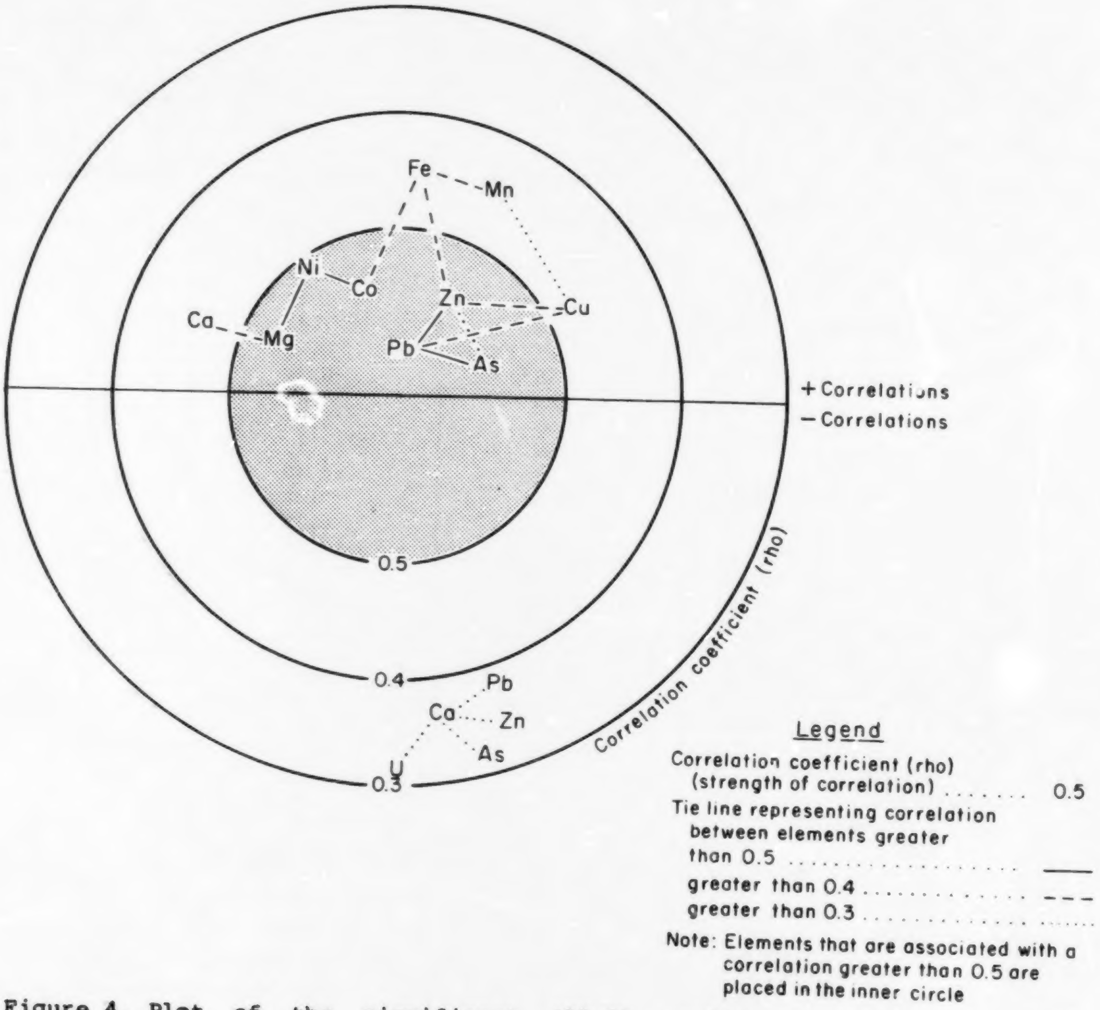

Figure 4. Plot of the significant (99.0% confidence level) elemental associations in the surface till.

communication, 1984). Till samples overlying the Boss Point Formation are circled. Many of these samples have Pb values over 90 ppm and Zn values over 200 ppm in the clay fraction. The highest Pb value in this suite of samples was 332 ppm accompanied by a 358 ppm Zn value. This sample was located southeast of River Phillip in bedrock of the Cumberland Group (Fig. 2). Some of the Pb anomalies further down-ice from the Boss Point outcrop may represent northward dispersal from this unit. R. J. Ryan (personal communication, 1984) noted distinct Pb-rich mineralized bedrock areas 9.3 miles (15 km) away from the Cobequid Highlands in the Tatamagouche Basin area. Figure 6 also shows Pb anomalies 8.7-9.9 miles (14-16 km) away from the Highlands. Fletcher (1905) postulated a Cu-rich zone running parallel to the Cobequid Highlands which falls within the limit of northward ice flow.

The reason for the negative correlation between Ca and Mg and erratic percentages is uncertain. The northward flow introduced some Cobequid Highland crystalline material into the Lowland till. This

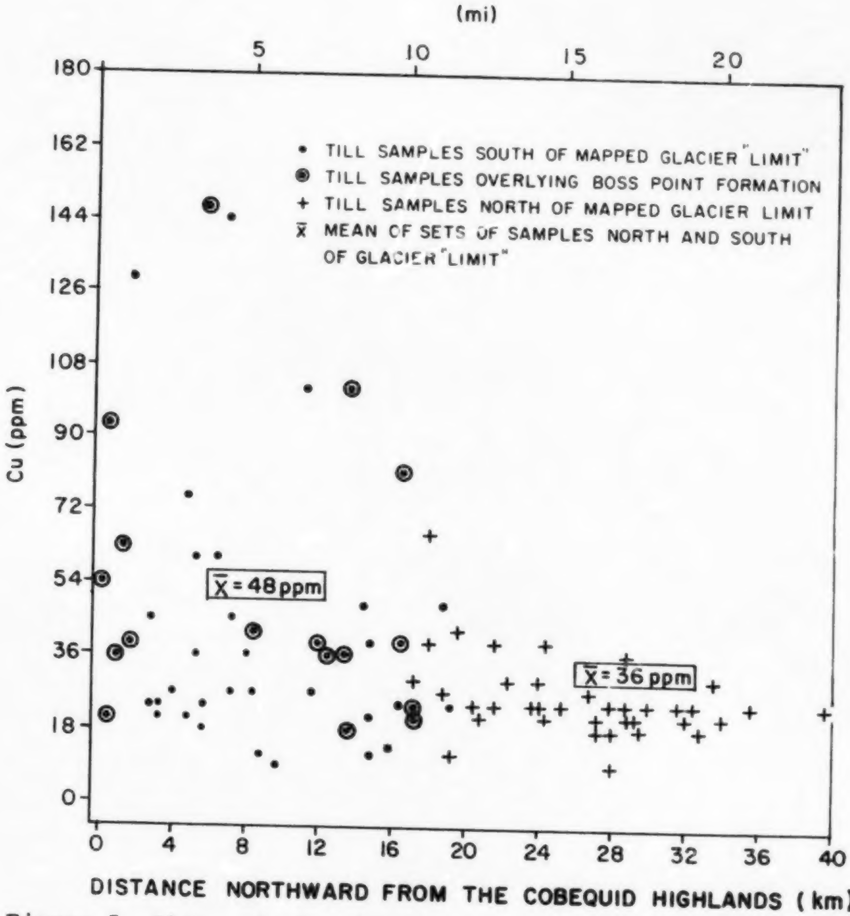

Figure 5. Plot of Cu levels in the surface till and distance northward from the Cobequid Highlands.

material may have diluted some of the calcium in the till matrix. The calcium and magnesium in the till fine fraction are largely derived from calcareous redbed sources in the Carboniferous Pictou and Cumberland Groups. Weathering of calcium and magnesium in the erratic-rich till samples may also explain this phenomenon. The erratic-rich samples may be slightly sandier than the erratic poor samples although they cannot be differentiated in the field. Figure 7 illustrates the inverse relationship of Ca to erratic pebble percentages. Depth of sample does not correlate significantly with either Ca or Mg levels.

Weathering Effects

Most of the samples were taken from a reddish silty till as stated earlier. This till has a substantial amount of clay-sized particles, up to 15 per cent of the total matrix. The fine fraction (<2μm) is composed largely of clay derived from red Carboniferous mudstones. Sandier till facies in the Lowlands, especially the ablation tills (Fig. 1), also have red clay in the matrix, but a larger proportion of these clay-sized particles may be present as Fe-Mn hydroxides, a result of in situ weathering or resedimented weathering products. Fe is moderately

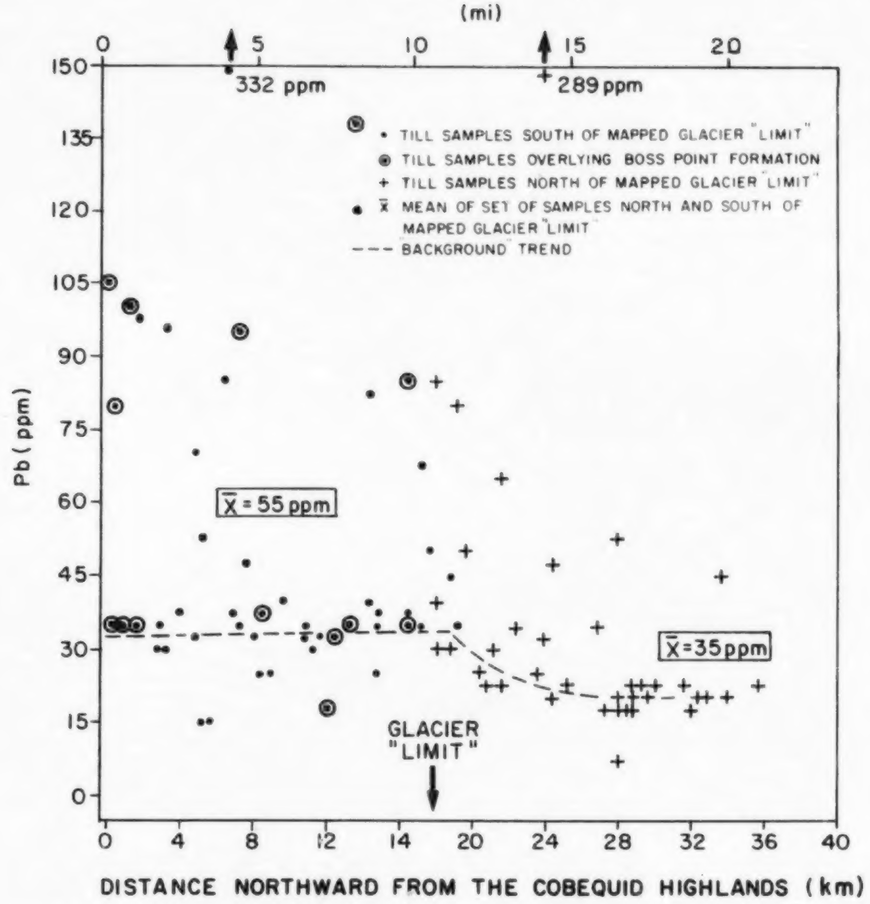

Figure 6. Plot of Pb levels in the surface till and distance northward from the Cobequid Highlands.

correlated with Zn (rho=0.40, Fig. 4) in the data set. A visual examination of the data shows that ablation till samples have generally higher Fe levels (>5% Fe-sandy samples, 3.3%-4.0%-silty samples) and Zn levels (>150 ppm-sandy samples, 80-130 ppm-silty samples). The ablation tills exhibited the highest Fe and Zn levels. The elevated Zn levels in the ablation tills may be due to adsorption or coprecipitation of Zn with Fe hydroxides. In this data set it is not difficult to separate weathering effects from those provenance-related element associations because the samples have been classified and the sandy tills mapped. Elemental associations can also help differentiate between these effects. The strongest correlation was between Pb and Zn levels (Fig. 4). An association of these two elements is unlikely if weathering processes were controlling element levels and creating false anomalies because these elements behave quite differently under oxidizing surficial conditions. In addition, Fe levels were not significantly associated with Pb levels. Samples that have anomalous Pb and Zn levels show normal Fe levels. Mapping conducted by the authors in an adjacent area (Stea et al., in press) has revealed texturally and lithologically distinct till sheets. These tills also show substantial differences in average element levels. A sandy till called the Shulie Lake Till has high average Fe and Zn values when compared to clay-rich tills.

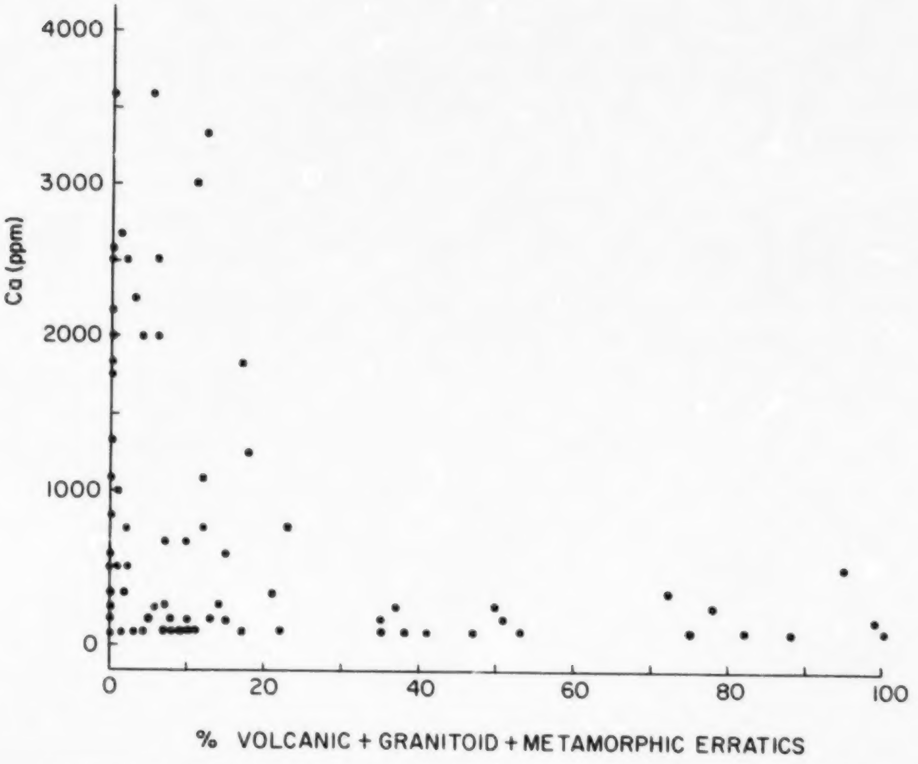

Figure 7. Plot of Ca levels and erratic pebble percentages in till samples north of the Cobequid Highlands.

CONCLUSIONS AND IMPLICATIONS FOR TILL PROSPECTING

Geological and geochemical evidence strongly suggest that ice flowed northward from the Cobequid Highlands onto the Cumberland-Pictou Lowlands. Morphosequences of hummocky moraine, ice contact stratified drift and outwash indicate a southward-retreating ice front. A local till sheet of Cobequid Highlands derivation overlies a reddish brown till sheet derived from rocks in the Carboniferous Lowlands. Striations on southward-facing stossed bedrock surfaces in the Lowlands indicate northward ice flow. A stillstand of this glacier is defined by moraines, ice contact stratified drift, and by the dispersion of Cobequid Highlands erratics on the Lowland till.

Element levels in the clay fraction of the reddish surface till sheet appear to have two controlling influences, provenance and weathering processes. Pb and Zn levels are strongly correlated, with anomalously high values of both elements commonly found in the same samples. Small Pb occurrences associated with grey coaly sandstones and conglomerates, may be the source of these high Pb and Zn values. Cu levels are also accordant with Pb and Zn levels in the till samples. Copper occurrences in the Cumberland-Pictou Lowlands have been found to have elevated Pb and Zn levels (Ryan, in press). All three elements are part of the same mineralizing process, which affected large areas of the Carboniferous basin and may have been responsible for the linear Cu zones described by Fletcher

(1905). A secondary influence to Zn levels is the amount of Fe in the till. This is especially significant in sandier tills, where Fe hydroxides form a large proportion of the clay fraction. Ca and Mg levels in the clay fraction of the surface till sheet may be controlled by the interaction of weathering processes and provenance. Both elements are negatively correlated with erratic percentages. The introduction of Cobequid Highlands erratic material into the Lowland till sheet by northward ice flow may have diluted the Ca and Mg levels directly, or indirectly reduced them by enhanced rates of weathering.

Care must be taken by exploration firms prospecting in areas within the northward ice flow terminus. The direction of transport of many surface boulders in this region is radically different from that north of the limit even though the surface till looks much the same. In the same way, geochemical anomalies in surface tills or soils may be displaced northward in this region. Figure 8 is a diagrammatic representation of the

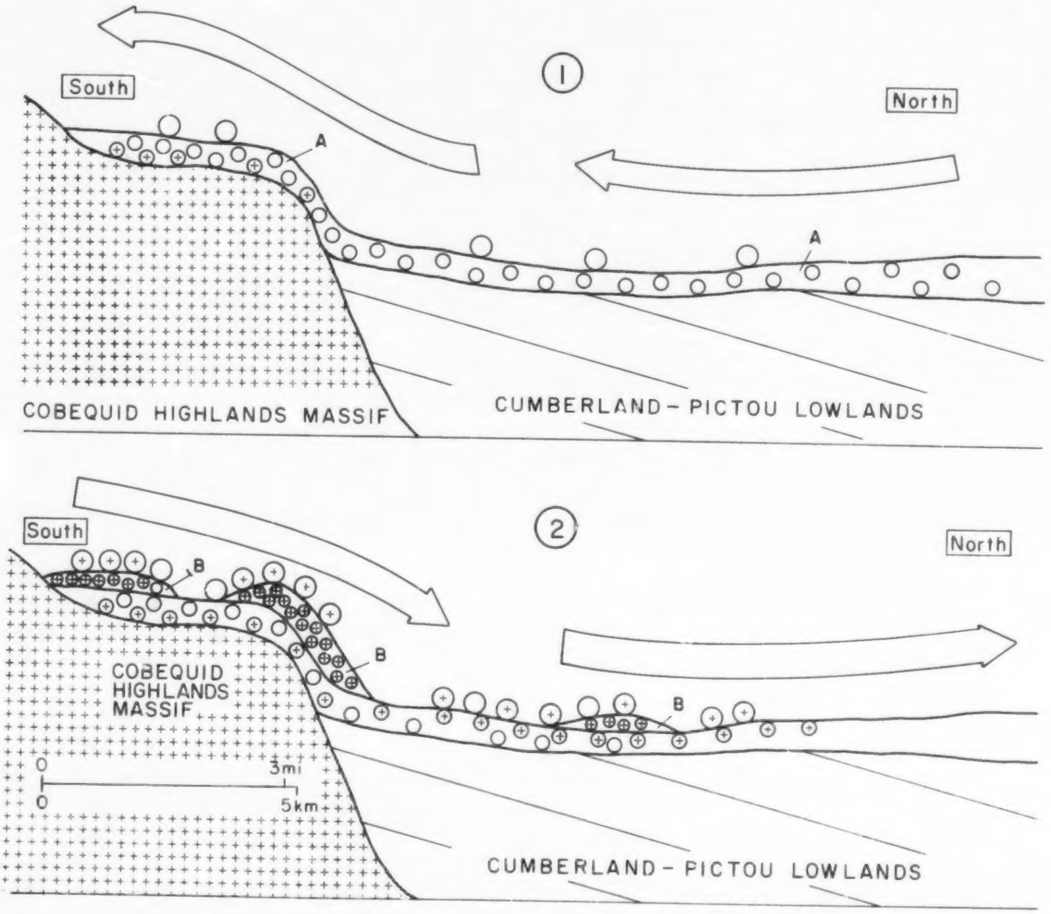

Figure 8. Diagrammatic representation of the sequence of ice flows and their deposits in the study area.
(1) Southward ice flow forming a red-brown silty till(A).
(2) North-northeastward ice flow forming a sandy local till(B) on the Cobequid Highlands and depositing Cobequid Highland erratics ⊕ on the previously formed till.

effects of the last two ice flows in the region. The first, southward flow, formed a reddish-brown till and dispersed Carboniferous bedrock-derived erratics on the Cobequid Highlands. The second, northward flow, formed a local till sheet on some areas of the Highlands, and transported boulders northward onto the Cumberland-Pictou Lowlands. These boulders may have been transported in an englacial position and deposited on the surface of the previously formed till, essentially a matrix-less melt-out till as envisioned by Shilts (1973).

The majority of the samples obtained in this study were from one till sheet. The few samples obtained from a mapped ablation till (Fig. 1) showed significant differences in Fe and Zn contents. Element levels can vary significantly between till genetic facies (Shilts, 1975) and tills of differing provenance related to distinct ice flows (Stea, et al., in press). This study has emphasized the need to recognize till sheets in a mineral exploration program through surface mapping of Quaternary deposits.

REFERENCES

Chalmers, R.
1895: Report on the surface geology of eastern New Brunswick, northwestern Nova Scotia and a portion of Prince Edward Island; Geological Survey of Canada, Annual Report, v. 1, no. 7, pt. M.

Chatterjee, A. K.
1983: Metallogenic map of the Province of Nova Scotia, scale 1:500,000; Nova Scotia Department of Mines and Energy.

Donohoe, H. V. and Wallace, P. I.
1978: Preliminary map of the Cobequid Highlands, scale 1:125,000; Nova Scotia Department of Mines, Map 78-1.

Downey, N.
1979: Cobequid Project: uranium assessment report Cobequid IV, Nova Scotia; Nova Scotia Department of Mines and Energy, Assessment Report 11E/12B 54-0-64(04).

Fletcher, H.
1905: Tatamagouche, Colchester and Pictou Counties, scale 1 mile: 1 inch; Geological Survey of Canada, Old Series Geological Maps, Sheet No. 59.

Grant, D. R.
1977: Glacial style and ice limits, the Quaternary stratigraphic record, and changes of land and ocean level in the Atlantic Provinces, Canada; Géographie Physique et Quaternaire, v. 31, no. 3-4, p. 247-260.

Koteff, C. and Pessl, F.
1981: Systematic ice retreat in New England; United States Geological Survey, Professional Paper 1179, 19 p.

Poole, H. S.
1890: Surface geology of the Pictou coal field; Proceedings and Transactions of the Nova Scotian Institute of Natural Science, v. 7, p. 388-393.

Prest, V. K., Grant, D. R., Borns, H. W., Brookes, I. A., MacNeill, R. H. and Ogden, J. G.
1972: Quaternary geology, geomorphology and hydrology of the Atlantic Provinces; 24th International Geological Congress, Montreal, Guidebook A61-C61, 79 p.

Rose, A. W., Hawkes, H. E. and Webb, J. S.
1979: Geochemistry in Mineral Exploration; Academic Press, London, 657 p.

Ryan, R. J.
in press: Geology of the Tatamagouche Syncline, Cumberland County, Nova Scotia, Canada; Geological Survey of Canada, Paper.

Shilts, W. W.
1973: Glacial dispersal of rocks, minerals and trace elements in Wisconsinan till, southeastern Quebec, Canada; *in* The Wisconsinan Stage, eds. R. P. Goldthwait and A. B. Willman; Geological Society of America, Memoir 136, p. 189-219.

1975: Principles of geochemical exploration for sulphide deposits using shallow samples of glacial drift; Canadian Mining and Metallurgical Bulletin, v. 68, no. 757, p. 73-80.

1976: Glacial till and mineral exploration; *in* Glacial Till, ed. R. F. Legget; Royal Society of Canada, Special Publication No. 12, p. 205.

Stea, R. R.
1982: Tin and tungsten data from tills sampled along the Eastern Shore region; Nova Scotia Department of Mines and Energy, Open File Report 480, 8 p.

1983: Surficial geology of the western part of Cumberland County, Nova Scotia; *in* Current Research, Part A; Geological Survey of Canada, Paper 83-1A, p. 197-202.

Stea, R. R. and Finck, P. W.
1984: Patterns of glacier movement in Cumberland, Colchester, Hants and Pictou Counties, northern Nova Scotia; *in* Current Research, Part A; Geological Survey of Canada, Paper 84-1A,

Stea, R. R., Finck, P. W. and Wightman, D. M.
in press: Quaternary geology and till geochemistry of the western part of Cumberland County, Nova Scotia; Geological Survey of Canada, Paper 85-17.

Stea, R. R. and Fowler, J. H.
1979: Minor and trace element variations in Wisconsinan tills, Eastern Shore region, Nova Scotia; Nova Scotia Department of Mines and Energy, Paper 79-4, 30 p.

Author Index/Index des auteurs

	Page
Adshead, J.D.	737
Ames, D.E.	205
Archer, A.	385
Avery, M.P.	489
Bamber, E.W.	627
Barr, S.M.	291
Barrie, J.V.	251
Beauchamp, B.	627
Beckett, M.	667
Bégin, N.J.	1
Bell, J.S.	489
Bell, R.T.	375, 385
Bell, T.	221
Bolduc, A.M.	697
Bornhold, B.D.	737
Bostock, H.H.	35
Brandon, M.T.	683
Brown, R.L.	81
Buchanan, J.R	275
Burden, E.T.	483
Calon, T.	471
Cameron, A.R.	645
Carter, R.W.G.	55
Cattalani, S.	365
Caudill, M.R.	343
Cawood, P.A.	675, 759
Chandler, F.W.	121
Charbonneau, B.W.	803
Christie, R.L.	795
Clark, J.I.	251
Coe, K.	159
Collins, W.T.	251
Copeland, M.J.	663
Cordey, F.	595
Coyle, M.	455, 499
Culshaw, N.	275
Currie, K.L.	333
Dabros, M.J.	107
Davis, E.E.	737
Dennis, F.A.R.	291
Dingwell, D.B.	455
Dredge, L.A.	779
Dubord, M.P.	603
Dunsworth, S.	471
Edlund, S.A.	719
Emslie, R.F.	755
Finck, P.W.	809
Forbes, D.L.	55
Forest, R.	177
Frarey, M.J.	43
Frith, R.A.	113
Furey, D.J.	461
Gall, O.	95
Galley, A.G.	205
Gao Ruixing	399
Gariépy, C.	265
Grant, A.C.	65
Graves, M.C.	423
Grotzinger, J.P.	95
Hall, G.E.M.	71, 89
Halwas, D.B.	583
Harris, D.C.	49
Haynes, S.J.	141
Henderson, J.B.	411
Henderson, J.R.	159
Henderson, M.N.	159
Hill, J.D.	185
Holloway, D.C.	483
Hope, T.L.	429
Insley, M.W.	259
Jackson, G.D.	541
James, D.T.	417
Jefferson, C.W.	159
Josenhans, H.W.	221
Journeay, M.	81
Kiely, L.A.	141
King, J.E.	21
Kjarsgaard, B.	755
Klassen, R.A.	697, 713
Kontak, D.J.	465
Kostaschuk, R.A.	565
Krawetz, M.T.	749
Krogh, T.E.	43
Kubli, T.	553
Kurfurst, P.J.	775
Langille, A.B.	483
LeCheminant, A.N.	159
LeCheminant, G.M.	531
Lee, K.	65
Lefebvre, C.	755
Levy, E.M.	65
Lewis, C.F.M.	251
Liedtke, J.	571
Linnen, R.L.	239
Loveridge, W.D.	113, 523
Lucas, S.B.	1
Luternauer, J.L.	565
Macfie, R.I.	411
MacInnis, I.	423
Mackay, J.R.	727
MacLean, B.	769
Macnab, R.	791
Macqueen, R.W.	603
Malpas, J.	471
Mamet, B.L.	627
Manojlovic, P.	275
Maurice, Y.T.	301, 307
McAlpine, K.D.	489
McCann, S.B.	749
McClay, K.R.	259
McDonough, M.R.	619
Mercier, M.M.	301
Millard, T.H.	565
Moffat, J.D.	65
Morrow, D.W.	603
Mountjoy, E.W.	177
Mudie, P.J.	107
Mulja, T.	423
Murphy, J.B.	445
Nance, R.D.	343, 351
Nielsen, E.	779
Norris, D.K.	645, 801
O'Brien, B.H.	439
Orchard, M.J.	683
Orford, J.D.	55
Osadetz, K.G.	609
Owen, J.V.	515

	Page
Paktunc, A.D.	327
Parrish, R.R.	683
Parrott, D.R.	251
Pedder, A.E.H.	649
Pelchat, J.C.	89
Poulsen, K.H.	205
Raeside, R.P.	291
Reilly, B.A.	141
Richards, B.C.	627
Roberts, A.	571
Rogerson, R.J.	221
Roscoe, S.M.	787
Ruzicka, V.	531
St-Onge, D.A.	783
St-Onge, M.R.	1
Sacks, P.E.	213
Samson, I.M.	239, 359
Sangster, A.L.	151
Sangster, D.F.	133
Saunders, C.M.	229, 319
Schau, M.	667
Scott, D.J.	1
Scott, J.S.	783
Sears, W.B.	483
Sherlock, R.	755
Shih, K.G.	791
Shilts, W.W.	703
Simony, P.S.	583, 619
Smith, S.L.	703
Snowdon, L.R.	609
Spethmann, D.	21
Stea, R.R.	809
Stevens, K.	435

	Page
Strong, D.F.	229, 319, 393, 455, 461, 465, 499
Struik, L.C.	589
Sutherland Brown, A.	683
Swettenham, S.S.	803
Swinden, H.S.	213
Taylor, R.B.	55
Thompson, F.J.	713
Thompson, P.H.	275
Thorpe, R.I.	385
Vaillancourt, P.D.	133
Vaive, J.E.	71
van Breemen, O.	113
van Staal, C.R.	193
Vilks, G.	769
Villeneuve, M.E.	21
Wallace, G.M.	507
Warner, J.B.	351
Whalen, J.B.	265, 297
White, C.E.	291
Wilcox, K.H.	21
Williams, H.	675, 759
Williams, H.F.L.	559
Williams-Jones, A.E.	239, 359, 365
Woodend, S.L.	429
Yeo, G.M.	399
Yorath, C.J.	683
Zaleski, E.	15
Zentilli, M.	423
Zwicker, E.J.	393

Erratum

Geological Survey of Canada, Paper 85-1B

Current Research, Part B

Report 16: Regional sedimentology of the Namewaminikan Group, northern Ontario: Archean fluvial fans, braided rivers, deltas, and an aquabasin: J.R. Devaney and P.W. Fralick.

p. 132: The following references were omitted.

Goodwin, A.M.
1977: Archean basin-craton complexes and the growth of Precambrian shields; Canadian Journal of Earth Sciences, v. 14, p. 2737-2759.

Hyde, R.S.
1980: Sedimentary facies in the Archean Timiskaming Group and their tectonic implications, Abitibi greenstone belt, northeastern Ontario, Canada; Precambrian Research, v. 12, p. 161-195.

Kehlenbeck, M.M.
1983: Structural studies in the Beardmore-Geraldton area; in Summary of Field Work, 1983, by the Ontario Geological Survey, ed. J. Wood et al.; Ontario Geological Survey, Miscellaneous Paper 116, p. 201-203.

1984: Use of stratigraphic and structural-facing directions to delineate the geometry of folded folds near Thunder Bay, Ontario; Geoscience Canada, v. 11, p. 23-32.

Langford, G.B.
1929: Geology of the Beardmore-Nezah gold area, Thunder Bay District; Ontario Department of Mines Annual Report, v. 37, part 4, 1928, p. 83-108.

Mackasey, W.O.
1975: Geology of Dorothea, Sandra, and Irwin Townships, District of Thunder Bay; Ontario Division of Mines, Geological Report 122, 83 p.

1976: Geology of Walters and Leduc Townships, District of Thunder Bay; Ontario Division of Mines, Geoscience Report 149, 48 p.

Mackasey, W.O., Edwards, G.R., and Cape, D.F.
1976: Legault Township, District of Thunder Bay; Ontario Division of Mines, Preliminary Map P 1191, Geological series, scale 1:15 840.